

Transactions

of the

A.S.M.E.

PLEASE INITIAL AND	NOTE ANSWER SEE ME RETURN
JAN 18 1945	
LUCKE	SCOTTEN
PARR	HAGLEY
HODGKINSON	
KAY, M.	
DUTCHER	
BAKER	
ENGLUND	LIBRARY
FULLER	DEPT. FILES
T. BAUMEISTER	

SOCIETY RECORDS—Part 3

(Including Indexes to Publications)

[Part 1 of Society Records for the year 1944 (containing Council and Committee Personnel and other general information) was issued as Section Two of the Transactions for February, 1944; and Part 2 (Membership List) as Section Two of the Transactions for July, 1944.]

Depositories for A.S.M.E. Transactions in the United States	RI-47
A.S.M.E. Transactions in Central and South America and Great Britain	RI-50
Indexes to A.S.M.E. Papers and Publications	RI-51
Regular Society Publications, 1944	RI-51
Publications Issued in 1944	RI-51
How to Find Papers Presented at 1944 A.S.M.E. Meetings	RI-51
Publications Developed by the Technical Committees	RI-51
Biographies	RI-53
Books on Special Subjects	RI-53
Index to <i>Mechanical Engineering</i> , 1944	RI-55
Index to Transactions, 1944	RI-63

JANUARY, 1945

VOL. 67, NO. 1

Transactions

of The American Society of Mechanical Engineers

Published on the tenth of every month, except March, June, September, and December

OFFICERS OF THE SOCIETY:

ALEX D. BAILEY, *President*

K. W. JAPPE, *Treasurer*

C. E. DAVIES, *Secretary*

COMMITTEE ON PUBLICATIONS:

E. J. KATES, *Chairman*

L. N. ROWLEY, JR.

H. L. DRYDEN

W. A. CARTER

J. M. JURAN

GEORGE A. STETSON, *Editor*

K. W. CLENDINNING, *Managing Editor*

ADVISORY MEMBERS OF THE COMMITTEE ON PUBLICATIONS:

N. C. EBAUGH, GAINESVILLE, FLA.

O. B. SCHIER, 2ND, NEW YORK, N. Y.

Junior Member

RICHARD S. BIDDLE, NEW YORK, N. Y.

Published monthly by The American Society of Mechanical Engineers. Publication office at 20th and Northampton Streets, Easton, Pa. The editorial department is located at the headquarters of the Society, 29 West Thirty-Ninth Street, New York 18, N. Y. Cable address, "Dynamic," New York. Price \$1.50 a copy, \$12.00 a year; to members and affiliates, \$1.00 a copy, \$7.50 a year. Changes of address must be received at Society headquarters two weeks before they are to be effective on the mailing list. Please send old as well as new address. . . . By-Law: The Society shall not be responsible for statements or opinions advanced in papers or . . . printed in its publications (B13, Par. 4) . . . Entered as second-class matter March 2, 1928, at the Post Office at Easton, Pa., under the Act of August 24, 1912. . . . Copyrighted, 1945, by The American Society of Mechanical Engineers. Reprints from this publication may be made on condition that full credit be given the Transactions of the A.S.M.E. and the author, and that date of publication be stated.

Depositories for A.S.M.E. Transactions in the United States, Including Territories and Dependencies

BOUND copies of the complete Transactions of The American Society of Mechanical Engineers will be found in the libraries in the United States and other countries which are listed on the following pages.

Alabama

Auburn.....Engineering Library, Alabama Poly. Inst.
Birmingham.....Public Library
University.....Library, University of Alabama

Arizona

Tucson.....Library, University of Arizona

Arkansas

Fayetteville.....Engineering Library, University of Arkansas

California

Berkeley.....Library, University of California
Long Beach.....Public Library
Los Angeles.....Public Library
University of Southern California
Oakland.....Oakland City Library
Teachers' Professional Library
Pasadena.....Library, California Institute of Technology
Santa Clara.....Library, University of Santa Clara
San Diego.....Public Library
San Francisco.....Engineers Club of San Francisco
Mechanics Institute
Public Library (Civic Center)
Stanford Univ....Library, Stanford University

Colorado

Boulder.....Library, University of Colorado
Denver.....Public Library
Fort Collins.....Colorado State College of Agriculture and
Mechanic Arts

Connecticut

Bridgeport.....Public Library
Hartford.....Public Library
New Haven.....Public Library and Yale University
Storrs.....University of Connecticut
Waterbury.....Silas Bronson Library

Delaware

Newark.....University of Delaware
Wilmington.....Wilmington Free Institute

District of Columbia

Washington.....George Washington and Catholic Universities; Library of 'Congress; National
Bureau of Standards Library; Scientific
Library, U. S. Patent Office

Florida

Gainesville.....University of Florida
Jacksonville.....Free Public Library
Miami.....Public Library
Tampa.....Public Library

Georgia

Atlanta.....Carnegie Public Library
Georgia School of Technology
Savannah.....Public Library

Hawaii

Honolulu.....University of Hawaii Library

Idaho

Moscow.....University of Idaho

Illinois

Chicago.....John Crerar Library; Library, Illinois
Institute of Technology; Museum of Science
and Industry; Public Library of
Chicago; Western Society of Engineers
Evanston.....Northwestern University
Moline.....Public Library
Peoria.....Public Library
Urbana.....University of Illinois

Indiana

Evansville.....Public Library
Fort Wayne.....Public Library
Indianapolis.....Public Library and Indiana State Library
Notre Dame.....Library, University of Notre Dame
Terre Haute.....Rose Polytechnic Institute
West Lafayette...Library, Purdue University

Iowa

Ames.....Iowa State College
Des Moines.....Public Library
Iowa City.....State University of Iowa

Kansas

Kansas City....Public Library, Huron Park
Lawrence.....Library, University of Kansas
Manhattan.....Kansas State College
Wichita.....Wichita City Library

Kentucky

Lexington.....University of Kentucky
Louisville.....Speed Scientific School
University of Louisville

Louisiana

Baton Rouge....Louisiana State University
New Orleans....The Howard-Tilton Memorial Library
Louisiana Engineering Society
Public Library
Tulane University

Maine

Orono.....University of Maine

Maryland

Annapolis.....United States Naval Academy
Baltimore.....Engineers Club of Baltimore
Johns Hopkins University
Public Library
College Park....Library, University of Maryland

Massachusetts

Boston.....Boston Public Library
Engineering Societies of New England
Northeastern University
Cambridge.....Harvard University (Engineering Library)
Massachusetts Institute of Technology
Fall River.....Public Library
Lynn.....Free Public Library
New Bedford....Free Public Library
Springfield....Springfield City Library
Tufts College....Tufts College
Worcester.....Free Public Library
Worcester Polytechnic Institute

Michigan

Ann Arbor.....University of Michigan
Detroit.....Cass Technical High School
Highland Park Public Library
Public Library
University of Detroit
East Lansing....Michigan State College
Flint.....Public Library
Grand Rapids....Public Library
Houghton.....Michigan College of Mining & Technology
Jackson.....Public Library

Minnesota

Duluth.....Public Library
Minneapolis....Minneapolis Public Library (Engineering
and Circulating Libraries)
University of Minnesota
St. Paul.....James Jerome Hill Reference Library

Mississippi

State College....Mississippi State College

Missouri

Columbia..... University of Missouri
 Kansas City..... Public Library
 Rolla..... Missouri School of Mines and Metallurgy
 St. Louis..... Engineers Club of St. Louis; Public Library;
 Washington University; Mercantile Library

Montana

Bozeman..... Montana State College

Nebraska

Lincoln..... University of Nebraska
 Omaha..... Public Library

Nevada

Reno..... University of Nevada Library

New Hampshire

Durham..... University of New Hampshire

New Jersey

Bayonne..... Free Public Library
 Camden..... Free Public Library
 Elizabeth..... Free Public Library
 Hoboken..... Stevens Institute of Technology
 Jersey City..... Free Public Library
 Newark..... Free Public Library
 Newark College of Engineering
 New Brunswick..... Rutgers University
 Paterson..... Free Public Library
 Princeton..... Princeton University
 Trenton..... Free Public Library

New Mexico

Albuquerque..... University of New Mexico
 State College..... New Mexico State College

New York

Albany..... New York State Library
 Brooklyn..... Polytechnic Institute
 Pratt Institute
 Brooklyn Public Library
 Buffalo..... The Grosvenor Library
 Engineering Society of Buffalo
 Buffalo Public Library
 Ithaca..... Cornell University
 Jamaica, L. I..... Queens Borough Public Library
 New York..... College of the City of New York
 Columbia University
 Cooper Union
 Engineering Societies Library
 New York Museum of Science and Industry
 New York University Library
 Public Library
 Potsdam..... Clarkson College of Technology
 Rochester..... Rochester Engineering Society
 Schenectady..... Union College
 Syracuse..... Public Library
 Syracuse University
 Troy..... Rensselaer Polytechnic Institute
 Utica..... Public Library

North Carolina

Chapel Hill..... University of North Carolina
 Durham..... Duke University
 Raleigh..... North Carolina State College

North Dakota

Fargo..... North Dakota State Agricultural College
 Grand Forks..... University of North Dakota

Ohio

Ada..... Ohio Northern University
 Akron..... Public Library
 University of Akron
 Canton..... Public Library
 Cincinnati..... Engineers Club of Cincinnati
 Public Library
 University of Cincinnati
 Cleveland..... Case School of Applied Science
 Cleveland Engineering Society
 Fenn College
 Public Library

Columbus..... The Ohio State Library
 Ohio State University
 Public Library
 Dayton..... Engineers Club of Dayton
 Toledo..... Public Library
 University of Toledo
 Youngstown..... Public Library

Oklahoma

Norman..... Oklahoma University
 Oklahoma City..... Public Library
 Stillwater..... Oklahoma A.&M. College
 Tulsa..... Public Library

Oregon

Corvallis..... Oregon State College
 Portland..... Portland Library Association

Pennsylvania

Allentown..... Free Library
 Bethlehem..... Lehigh University
 Easton..... Lafayette College
 Public Library
 Erie..... Public Library
 Lewisburg..... Bucknell University
 Philadelphia..... Drexel Institute
 Engineers Club
 Franklin Institute
 The Free Library
 University of Pennsylvania
 Pittsburgh..... Carnegie Free Library of Allegheny
 Carnegie Institute of Technology
 Carnegie Library (Schenley Park)
 Engineers' Society of Western Pennsylvania
 University of Pittsburgh
 Reading..... Public Library
 Scranton..... Public Library
 State College..... Pennsylvania State College
 Swarthmore..... Swarthmore College
 Villanova..... Villanova College
 Wilkes-Barre..... Public Library

Puerto Rico

Mayaguez..... University of Puerto Rico

Rhode Island

Kingston..... Rhode Island State College
 Providence..... Brown University
 Providence Engineering Society
 Public Library

South Carolina

Clemson College.. Library, Clemson College

South Dakota

Brookings..... South Dakota State College

Tennessee

Kingsport..... Public Library
 Knoxville..... University of Tennessee
 Memphis..... Goodwin Institute
 Nashville..... Vanderbilt University

Texas

Austin..... University of Texas
 College Station... Texas Agricultural & Mechanical College
 Dallas..... Public Library
 Southern Methodist University
 El Paso..... Public Library
 Fort Worth..... Carnegie Public Library
 Houston..... Public Library
 Rice Institute
 Lubbock..... Texas Technological College
 San Antonio..... Carnegie Library

Utah

Salt Lake City... University of Utah
 Public Library

Vermont

Burlington..... University of Vermont

Virginia

Blacksburg..... Virginia Polytechnic Institute
 Charlottesville... University of Virginia

SOCIETY RECORDS

RI-49

Lexington.....Virginia Military Institute
Norfolk.....Public Library
Richmond.....Virginia State Library

Washington

Pullman.....State College of Washington
Seattle.....Engineers Club
Public Library
University of Washington
Spokane.....Public Library
Tacoma.....Public Library

West Virginia

Morgantown.....West Virginia University

Wisconsin

Madison.....Library, University of Wisconsin
Milwaukee.....Marquette University
Public Library
Vocational School Library

Wyoming

Laramie.....Wyoming University

A.S.M.E. Transactions in Central and South America and Great Britain

Argentina

Buenos Aires.....Biblioteca de la Sociedad Cientifica

Australia

Adelaide.....Public Library of Adelaide
Melbourne.....Public Library of Victoria
Perth.....University of Western Australia Library
Sydney.....Public Library of Sydney

Brazil

Rio de Janeiro...Bibliotheca da Escola Polytechnica
Bibliotheca Nacional
São Paulo.....Bibliotheca da Escola Polytechnica

Canada

Kingston.....Queen's College
Montreal.....Engineering Institute of Canada
McGill University
Toronto.....University of Toronto, Library
Vancouver.....University of British Columbia

Chile

Santiago.....Universidad de Chile, Facultad de Ciencias
Fisicas y Matematicas (Engg. School)

Cuba

Havana.....Cuban Society of Engineers

England

Birmingham.....Birmingham Public Libraries
Bristol.....University of Bristol
Cambridge.....University of Cambridge
Leeds.....University of Leeds
Liverpool.....Liverpool Engineering Society
Public Library of Liverpool
London.....City and Guild Engineering College
Institution of Automobile Engineers

London (Continued)

The British Coal Utilization Research Association
The Institution of Mechanical Engineers
Institution of Civil Engineers
Institution of Electrical Engineers
The Junior Institution of Engineers
The Royal Aeronautical Society

Manchester.....Manchester Public Libraries (Reference Library)

Oxford.....Oxford University

Newcastle-upon-

Tyne.....The North-East Coast Institution of Engineers and Shipbuilders

Sheffield.....Sheffield Public Libraries

India

Bangalore.....Mysore Engineers Association
Calcutta.....Bengal Engineering College
Poona.....Poona College of Engineering
Rangoon.....University of Rangoon

Ireland

Belfast.....Queen's University of Belfast

Mexico

Mexico City.....Asociacion de Ingenieros y Arquitectos de Mexico
Library of the Escuela de Ingenieros Mecanicos y Electricistas

Scotland

Glasgow.....Royal Technical College
Mitchell Library

South Africa

Cape Town.....University of Cape Town
Johannesburg...South African Institute of Engineers

Wales

Cardiff.....Cardiff Public Library

The Missing Data on Coal Sampling

By B. A. LANDRY,¹ COLUMBUS, OHIO

Beginning with the crude attempts at coal sampling reported 100 years ago, the author reviews the slow progress made down to 1916, when Bailey's experimental work on sampling was incorporated in A.S.T.M. Designation D-21, Standard Method of Sampling Coal for Analysis. By this standard, which is still official, the gross sample taken must be not less than 1000 lb; a large number of increments are required involving considerable time and expense, which has led in many cases to taking smaller samples, causing uncertainty in representativeness of the samples. In 1930, Grumell and Dunningham, in England, modified the method to include the effect of ash content and size of piece on occurrence of impurities. Far less stringent sampling rules were subsequently formulated. Many studies were then commenced on this subject, and about 1934, Subcommittee XIII of A.S.T.M. Committee D-5 began to reconsider specifications for taking gross samples, and tentative standards (D492-43T) have been prepared. The present paper is devoted to classifying missing data on coal sampling which are needed to supply information on (a) consist; (b) variability of ash of pieces by float-and-sink method, and by direct analysis; (c) variability of ash of increments; supplemented by (d) collection and analysis of gross samples of specified number of increments of constant weight to give confirmation of established relations between variables involved. Four sampling experiments are described from which principles are developed to bring out one of the important characteristics affecting the sampling of coal. This is the degree of mixing of the coal at the point of sampling.

ATTENTION has recently been called (1)² to "A Report to the Navy Department of the United States on American Coals," by Walter R. Johnson, Washington, whose publication in 1844 makes it now 100 years old. The purpose of this 400-page report was to give the results of tests on the evaporative power of some 44 coals, and the occasion, of course, was the impending conversion of the Navy from sail to steam navigation.

A number of other properties of these coals were investigated and reported; among them was the "earthy matter" or ash percentage. For this determination, the procedure was to select two specimens, usually about 4-in. lumps, pulverize each one separately, place from 30 to 55 grains of the powder in thimbles and "incinerate" for 4 hours or more. Generally, four "trials" or thimble samples were ignited for each specimen sample, but sometimes as many as eight were run.

Table 1 shows a few of the results obtained. As would be expected, some of the pairs of ash contents determined were nearly the same; others differed considerably. The ignition method

appears to have been quite precise, however; thus four trials of specimen No. 1, Beaver Meadow anthracite, gave, respectively, 10.91, 11.09, 11.14, and 11.05 per cent ash. The variability of the results from different specimens does not seem to have caused concern except in the case of specimen No. 2 for the Henrico County coking bituminous coal; a third specimen was obtained, containing "purer plies," which was found to have 6.22 per cent ash and thus canceled the bad impression left by the 41.56 per cent ash of specimen No. 2.

The acceptance of such crude sampling methods must reflect the conviction of the times, that the ash content of pieces of coal was essentially such a variable quantity that nothing could or, possibly, need be done to improve the representativeness of the sample analyzed. The thought did occur that a larger sample would be more acceptable. Once, 40 lumps were taken and ground down, but this practice was not repeated.

Fifty-five years later, the necessity for taking larger samples had, however, become recognized. A report (2) to the American Chemical Society, in 1899, outlined a method of sampling cars whereby 18 increments (grabs) were to be taken, six scoop-shovelfuls (unspecified weight) along each side, and six through the center, at equal intervals, each taken "vertically down as deep as it (the scoop) will reach." The report added that "a more representative (gross) sample may be secured by taking shovelfuls of the coal at regular intervals during the loading or unloading of the car." No consideration was given to the fact that the variability of the ash content of the increments, as it might be related to the ash content of the coal or to the particular distribution of the ash in some coals, might sometimes require a larger number of increments for equal representativeness.

In fact, it is doubtful if the implications of the word "representativeness" were fully recognized. In a United States Government sampling specification (cir. 1909) mentioned by E. G. Bailey (3) we find that "...The sample taken is to be selected proportionately from the lumps and fine coal in order that it will in every respect truly represent the quantity of coal under consideration."

TABLE 1 PERCENTAGE ASH OF VARIOUS COALS, AS REPORTED BY W. R. JOHNSON: "A REPORT TO THE NAVY DEPARTMENT OF THE UNITED STATES," WASHINGTON, 1844

	U. S. Coals	Ash, per cent	
		Specimen 1	Specimen 2
1	Anthracite, Beaver Meadow No. 3, Pa.....	11.05	8.69
2	Anthracite, Peach Mountain, Pa.....	6.62	6.487
3	Non-Coking Bit. Coal, Cumberland, Md....	4.056	6.52
4	Non-Coking Bit. Coal, Blossburg, Pa.....	5.40	13.246
5	Coking Bit. Coal, Deep Run, Richmond, Va.	14.919	5.086
6	Coking Bit. Coal, Henrico County, Va.....	8.72	41.56
7	Coking Bit. Coal, Midlothian Coal Co., Va.	4.800	4.375
8	Coking Bit. Coal, Pittsburgh, Pa.....	4.17	3.26
Foreign Coals			
9	Bituminous Coal, Liverpool, England.....	1.120	2.940
10	Bituminous Coal, Scotland.....	12.325	14.870

The hope that a sample of such a heterogeneous material as coal could ever be truly representative of the average ash was dispelled by Bailey who saw that the ash content of accurate samples must still show variability, and proposed that acceptable representativeness be expressed as the probability or chance, not the certainty, that the ash found will be within a certain preassigned range around the true average being sought.

Bailey's experimental work on sampling, as reported (3), consisted of riffle tests with marked pieces of coal to designate pieces of high impurity. From the occurrence of divided samples containing more than their share of high impurities, he extra-

¹ Assistant Supervisor, Fuels Division, Battelle Memorial Institute. Mem. A.S.M.E.

² Numbers in parentheses refer to the Bibliography at the end of the paper.

Presented at the Joint Fuels Meeting of THE AMERICAN SOCIETY OF MECHANICAL ENGINEERS and the American Institute of Mining and Metallurgical Engineers, Charleston, West Va., October 30-31, 1944.

NOTE: Statements and opinions advanced in papers are to be understood as individual expressions of their authors and not those of the Society.

polated to the chance of such occurrences in the original coal and arrived at large weights of gross samples as the means of fulfilling acceptable requirements of representativeness.

These findings were incorporated by the American Society for Testing Materials, in 1916, through the adoption of A.S.T.M. Designation D-21, Standard Method of Sampling Coal for Analysis (4). By this standard, which is still official, the gross sample taken must not be less than 1000 lb. For small coals, increment may be 5 to 10 lb, so that from 200 down to 100 of them must be taken uniformly over the lot of coal sampled. For run-of-mine or lump, increments may be from 10 to 30 lb each, and thus from 100 to 34 increments must be taken, to make the 1000-lb gross sample.

There is no doubt that a large number of gross samples have been and, possibly, are now taken on the basis of A.S.T.M. D-21. However, the considerable expense and time involved undoubtedly also led to the taking, in many cases, of smaller samples. The consistency of the results so obtained eventually brought about an empirical acceptance of less stringent sampling procedures by coal samplers; but these were not uniform, nor even publicized, so that in sampling practice a situation potentially dangerous, because of the uncertain degree of representativeness of samples, was becoming the rule rather than the exception.

To Grumell and Dunningham (5), in 1930, belongs the credit of having reopened the question. While admitting the value of Bailey's work for gross-sample reduction to laboratory size, they were led to modify his extrapolation process to include the effect of ash content and of size of piece on the occurrence of impurities. These considerations brought about the formulation of far less stringent sampling rules than those of A.S.T.M. D-21. Since then, the British have done a considerable amount of investigation of the results obtained by these new sampling rules. Nevertheless, the present British Standard (6) is very nearly that first suggested by Grumell and Dunningham.

Following Grumell and Dunningham, many workers began studies of the theory and practice of coal sampling, and a substantial bibliography has accumulated. Important references can be found in Bushell (7), Morrow and Proctor (8), and Grumell (9). Around 1934, Subcommittee XIII, of A.S.T.M. Committee D-5, began to reconsider specifications for taking gross samples, and tentative standards have been prepared, of these the latest is designated D492-43T (10).

THE MAIN PROBLEM OF COAL SAMPLING

Starting with Bailey (3), all calculations for the number of increments (grab samples) required to give a gross sample of pre-assigned acceptable representativeness have been based on the use of a formula of the simple form

$$N = \frac{V^2}{v^2} \dots \dots \dots [1]$$

where N is the number of increments required, V is a measure of the variability of the ash percentage of all the increments in the coal when this is known, and v is a measure of the variability of the ash percentage of gross samples of acceptable representativeness. Sometimes, this formula has been expressed as

$$\sqrt{N} = \frac{V}{v}$$

or as

$$v = \frac{V}{\sqrt{N}}$$

but these are obviously equivalent forms. Various measures, all "precision measures," have been used for the variabilities V

and v . They are called "probable error," "average error," or "standard deviation." These variations in usage have caused a few misconceptions but, generally speaking, have not invalidated the method.

There has also been complete agreement on the method of determination of v , the variability of acceptable gross samples, although the American and the British standards of "acceptability," at present, differ somewhat.

The main problem, which has concerned workers in the field of coal sampling for the last 15 years, has been the investigation of the nature of V , the variability in ash percentage of the coal to be sampled, in order to make it possible to relate this variability to definite characteristics of the coal, such as the size of the pieces and the approximate average ash content, and to the main character of the increments, which is of course their weight.

The usual approach for this study has been rather empirical, however, and has not led, until recently, to specific and definite relations. Nevertheless, from the extensive sampling experience obtained, there has accrued a remarkable sense or estimate of the number of increments required for acceptable accuracy. Another way of expressing this thought is to say that the theoretical approach has lagged somewhat behind the experimental. For that reason some of the conclusions which could be derived from existing sampling experiments have been overlooked and specific directives for new experimental work have not been fully recognized. The object of this study is to inquire into the nature of these missing data on coal sampling in the light of recent developments in the theory of coal sampling.

REPRESENTATION OF VARIABILITY AND MEANING OF ACCEPTABLE VARIABILITY OR REPRESENTATIVENESS

The variability of the ash content of pieces of coal, or of increments, or of gross samples composed of a given number of increments, can be represented very simply. Fig. 1 shows, as an example, the variability of the ash content of 50 increments, of 8 lb weight each, of a raw nut-slack (0×2 -in.) coal from Western Pennsylvania (11). Each increment was analyzed separately, and the step curve shown was plotted after rearranging the ash percentages found in an ascending order. The scale of abscissas is arbitrary in length but, of course, the same length of step is assigned to each increment; multiple lengths of steps represent multiple increments of the same ash percentage.

Had a larger number of increments been taken and analyzed separately, the number of steps in the curve would have increased proportionately, but the chances are that the general shape would

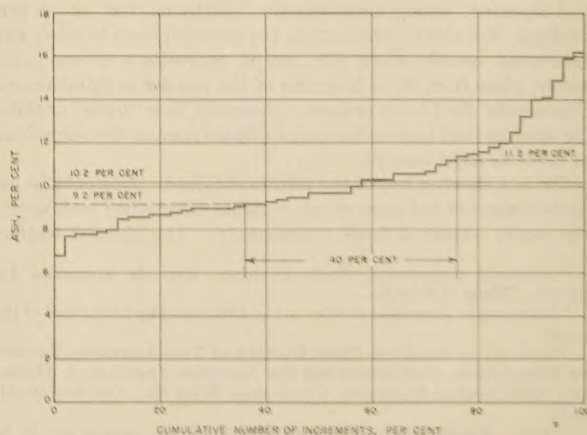


FIG. 1 VARIABILITY OF ASH PERCENTAGES OF FIFTY 8-LB INCREMENTS, FOR A 0×2 -IN. COAL, FROM WESTERN PENNSYLVANIA

have maintained itself, while becoming more smooth. Thus it can be assumed that the curve shown represents very nearly the variability associated with all possible 8-lb increments of the coal that was sampled.

The horizontal line shown intersecting the ordinate at 10.2 per cent ash represents the average ash of 50 increments. The two broken lines at 9.2 and 11.2 per cent ash thus define a range of variation of ± 1 per cent ash from the average, and the curve shows that of the 50 increments taken only 20, or 40 per cent, had an ash content within this range from the average.

If it is assumed that the curve, representing the variability of all possible 8-lb increments of this coal, also passes through these two points, then it is clear that only 40 per cent of all the increments in the coal would be expected to have ash percentages within the range 9.2 to 11.2 per cent.

Representativeness of an Increment. From the diagram, shown in Fig. 1, a clear idea of the meaning of the representativeness of a single sample can be obtained. Let an 8-lb increment be taken at random from the lot of coal considered and assume that the possibility of true random selection implies that the chance of taking a designated increment is the same as the chance of taking any other increment; it follows that the increment actually taken has an equal chance of being any one of all those represented by the curve. Therefore, the chance that the ash percentage found will be between 9.2 and 11.2 per cent ash is exactly 40 per cent.

Thus the representativeness of a single 8-lb increment from this lot of coal is said to be such that 40 times out of 100, in the long run, the ash percentage found will be within the range average ash ± 1 per cent ash.

Fundamental Law of Sampling. The fundamental fact upon which all sampling is based is that, if a number of increments of a specified weight are taken and combined together into a gross sample, then the representativeness of the gross sample will be increased as compared to that of the individual increments. In other words, the curve of variability of all such gross samples will be flatter than that of the increments and the chance will increase that the ash percentage found will be within a preassigned range about the true average.

Acceptable Variability or Representativeness. By taking a sufficiently large number of increments, it is possible to obtain a gross sample such that the probability of its ash content falling within a given range around the true ash content is as great as is desired, although, of course, certainty cannot be achieved.

Gross samples of low variability ordinarily have ash contents which are distributed very closely to a so-called normal law. Fig. 2 shows examples of variability curves for ash percentages of gross samples following normal-law distributions which have acceptable variability as defined by the British Standards Institution and by the American Society for Testing Materials (tentative, 1943).

Three sets of variability curves are shown for coals of 8, 10, and 15 per cent ash, respectively. For the British standard the specification calls for a number of increments such that gross samples composed of them will have 99 chances out of 100, in the long run, of having an ash content within ± 1 per cent ash of the true average independently of the ash percentage of the coal. Thus the three B.S.I. curves of Fig. 2 show the same variability.

The tentative A.S.T.M. standard calls for a lowering of accuracy or a permissible increase in variability as the average ash of the coal is higher in percentage and, conversely, an increase in accuracy as the percentage ash of the coal is lower. This is accomplished by defining the range as ± 10 per cent of the ash percentage. Consequently, as shown by the middle set of curves, the range is the same for both standards, for a 10 per cent ash coal,

since 10 per cent of 10 per cent is 1 per cent. But, for the 15 per cent ash coal, the range is ± 1.5 per cent and for the 8 per cent ash coal it is ± 0.8 per cent. In addition, in the A.S.T.M. tentative standard, the number of increments required is allowed to be such that the gross samples will have as few as 95 chances in 100 (instead of 99 for the British) of falling within the assigned range.

The relative compensations introduced by the A.S.T.M. definition of acceptable accuracy are such that, for a 7.6 per cent ash coal, the accuracy of both systems is the same. This is suggested in Fig. 2, by the fact that the two curves almost coincide for the 8 per cent ash coal. On the other hand, from the 15 per cent ash coal, a gross sample acceptable to the A.S.T.M. would have only 80 chances in 100 of falling within the British range of ± 1 per cent.

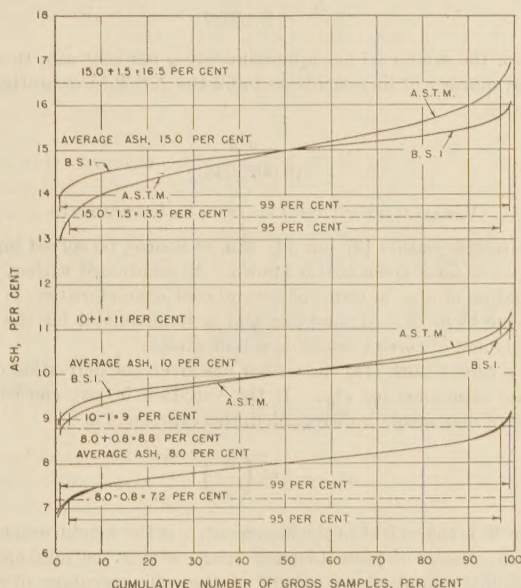


FIG. 2 COMPARISON OF ACCEPTABLE ACCURACY OF GROSS SAMPLES, BRITISH STANDARDS INSTITUTION AND AMERICAN SOCIETY FOR TESTING MATERIALS (TENTATIVE)

THE MEASURE OF VARIABILITY

The curves, shown in Figs. 1 and 2, to represent the variability of increments or of acceptable gross samples, can all be assigned a numerical value to represent quantitatively their respective variabilities. Mechanically speaking, this characteristic number is the moment of inertia of the curve about its average height (12). Statistically speaking, it is the square of the standard deviation of the points of the curves. For a given set of data, as in Fig. 1, this is calculated by the formula

$$(\text{Standard deviation})^2 = \sigma^2 = \frac{\sum y_i^2}{n} - \left(\frac{\sum y_i}{n} \right)^2 \dots [2]$$

when the y_i are the ash percentage of each increment, n the number of them, and Σ means the operation of summation. Performing this calculation on the data represented in Fig. 1 would give $\sigma^2 = 4.292$.

The (standard deviation)² of the curves of gross samples in Fig. 2 are calculated from an expression developed by LaPlace (13). They are, respectively, for the B.S.I. curves: $\sigma^2 = 0.15073$ and for the A.S.T.M. tentative curves: $\sigma^2 = (0.0026033)\bar{y}^2$, where \bar{y} is the average ash of the coal.

CALCULATION OF NUMBER OF INCREMENTS REQUIRED FOR GROSS SAMPLES OF ACCEPTABLE ACCURACY

As mentioned earlier, in connection with Equation [1], the number of increments required to give gross samples of acceptable accuracy can be calculated by

$$N = \frac{V^2}{v^2}$$

when V^2 is the (standard deviation)² of the increments, and v^2 is the (standard deviation)² of the acceptable gross samples. If we let σ_w^2 represent the variability of increments of weight W of a given coal, then the number of required increments for the B.S.I. standard is consequently given by

$$N = \frac{\sigma_w^2}{0.15037} \dots \dots \dots [3]$$

while if the same coal has approximately \bar{y} per cent ash, the required number of increments to fulfill the A.S.T.M. tentative is given by

$$N = \frac{\sigma_w^2}{(0.0020033\bar{y})^2} \dots \dots \dots [4]$$

VARIABILITY IN ASH CONTENT OF INCREMENTS

Neither Equation [3] nor [4] can, of course, be solved for N unless σ_w^2 for a given coal is known. As mentioned earlier, the evaluation of σ_w^2 , in terms of general coal characteristics, is the main problem of coal sampling and is fundamental for the establishment of correct sampling specifications.

In a recent work (14) the author has given the derivation of a general expression for σ_w^2 . If the variation in size consist of different increments is disregarded, this expression is

$$\sigma_w^2 = \sigma_u^2 \left(\frac{W}{\bar{w}} \right)^{a-1} \dots \dots \dots [5]$$

where W is the weight of the increment, \bar{w} is the weight-weighted average weight of piece (defined later), σ_u^2 is the measure of variability (standard deviation)² of the ash percentage of this average weight of piece, and the exponent $(a - 1)$ expresses the degree of randomness with which the ash is distributed throughout the lot of coal being sampled.

Equation [5] has the advantage that it can be linearized by writing it as

$$\log \sigma_w^2 = \log \sigma_u^2 + (a - 1) \log \frac{W}{\bar{w}} \dots \dots \dots [6]$$

This means that a log-log graph of the equation is a straight line, so that, as will be seen, the graphical use of this equation is greatly simplified.

Weight of Increment. Of the four variables contained in Equation [5], only one, the weight of increment W , is arbitrary. The rule in selecting the weight W is that it must be large enough, in comparison with the weight of the largest piece of coal in the lot to be sampled, that there will be little possibility of introducing bias in the sampling through the rejection of one of the large pieces present when several of them happen to be at the point of sampling; of course, the use of Equation [5] implies that the weight W used for the increment will be constant during the taking of each increment forming the gross sample as well as for all other gross samples so taken to meet the long-run requirement.

Average Weight of Piece. The average weight of piece \bar{w} of Equation [5], when the coal to be sampled does not have all of its pieces of the same weight, depends upon the consist or size distribution of the pieces. In addition, this average weight is not

the common average whereby the sum of the weights of the pieces present would be divided by the number of pieces, but rather it is a weight-weighted average given by the expression (15)

$$\bar{w} = \frac{\Sigma \bar{w}_i^2}{W} = \frac{\Sigma \bar{w}_i^2}{\Sigma \bar{w}_i}$$

where the \bar{w}_i are the individual weights of the pieces, Σ is the sign of summation, and $W = \Sigma \bar{w}_i$ is the sum of the weight of the pieces.

For example, if we assume a specific gravity of 1.3 and a uniform distribution of sizes between the 1-in. and the 2-in. sizes of a coal, then the simple average weight of piece for this range of sizes would be 0.111 lb. On the other hand, if we take the average consist of the 38 Appalachian coals reported by Malleis (16), and use same specific gravity, the value of the weight-weighted average weight of piece, for the same 1 × 2-in. interval (round hole) is $\bar{w} = 0.087$ lb, indicating how the effect of the consist and of the method of weighting bring out the importance of the smaller-size fractions within the range. Relatively simple means exist of calculating this average weight of piece for coals of known consist (17).

Variability of Ash Content of Pieces. The variability of the ash content of the pieces in a lot of coal is the direct result of the variability of the ash in the bed of coal. It is well known, of course, that the variability of ash contents of adjoining large portions of the bed is small. Thus if coal were quarried, so to speak, and each user was content to receive very large blocks of coal, there would be practically little difference between the average ash of each shipment, so long as operations were localized and portions of the formations extraneous to the bed were not included.

However, as the bed coal is broken into smaller pieces, the variability of ash content of the pieces usually increases more and more as the broken pieces are smaller. From one point of view, this is required because the ultimate particle would necessarily be either pure inorganic or pure organic and thus presents a maximum of variability. Exceptions to the rule occur when the basic ash distribution in the coal bed so affects the breakage of coal that impurities are more highly concentrated in certain sizes or when degradation of friable coals augments the proportion of low-ash pieces in the smaller sizes.

Fortunately for coal-sampling studies, the variability of ash content of single pieces of a given size can be determined rather easily without having to determine the ash percentage of each piece. This is owing to the fact that any disturbance in the arrangement of the pieces in the original lot of coal does not affect the variability of their ash content and, consequently, float-and-sink methods can be used. This is not true of the variability of increments since the particular arrangement or distribution of the pieces of variable ash, in the lot, affects the average ash content of the increments very materially, as will be shown later.

Fig. 3 is an example of the application of the float-and-sink method for the determination of the variability of the ash percentage of single pieces of coal. The step curve shown is a plot of the average ash content of successive floats and the final sink, against the cumulative weights of coal separated, multiplied by the inverse ratio of specific gravities, in order to pass from cumulative weights to cumulative number of pieces; thus the length of step for float at 1.4 specific gravity is proportional to the weight of floated material, multiplied by 1.3/1.4 to convert from cumulative weight to cumulative number of pieces, and so on.

Passing a curve through the steps on the basis of equality of areas included and excluded gives what may then be assumed to be a close representation of the actual ash percentage variability of the pieces. The coal in Fig. 3 was a raw coal, size $\frac{5}{16} \times \frac{3}{8}$

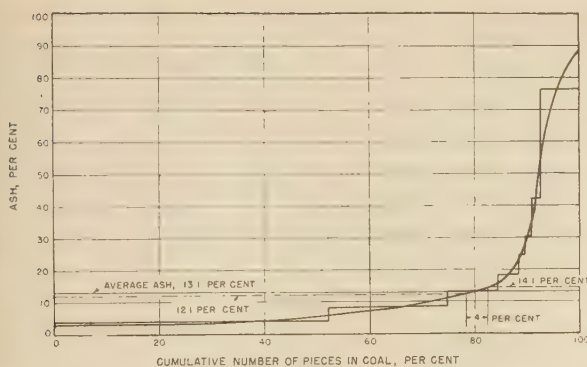


FIG. 3 FLOAT-AND-SINK VARIABILITY DATA OF SINGLE PIECES OF A $\frac{5}{16} \times \frac{3}{8}$ -IN. COAL FROM WESTERN PENNSYLVANIA

in., from Western Pennsylvania, with a $\bar{w} = 0.00096$ lb. From the curve, it is seen that a single piece of this weight from this coal would have about 4 chances out of 100 of falling within the range 12.1 to 14.1 per cent around the true average of 13.1 per cent. Calculation of the (standard deviation)² or $\sigma^2\bar{w}$ by taking the ash percentage at 50 equidistant points and applying Equation [2] gave $\sigma^2\bar{w} = 382$.

Available data from 15 raw coals, for which float-and-sink tests had been made on a number of close size ranges have been studied by this method (18). Only those coals which showed an increase in variability with decrease in size were included since the fulfillment of sampling requirements for them would obviously lead to safe oversampling rather than undersampling for other type coals.

From this study, it has been possible to arrive at relations between not only the variability of the ash of pieces of coals and the weight of piece but also between the variability and the average ash content of the coal.

Fig. 4 has been prepared from the relations obtained. The vari-

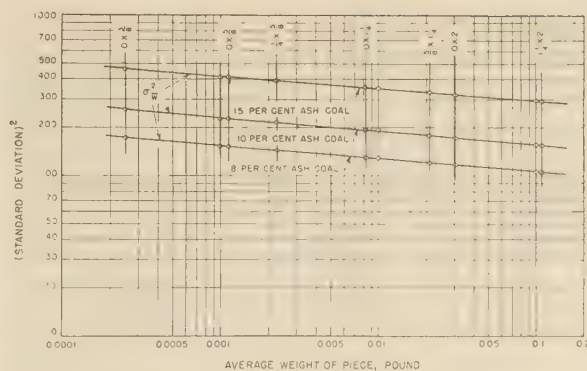


FIG. 4 RELATIONS OF VARIABILITY OF ASH PERCENTAGE OF SINGLE PIECES OF "AVERAGE" COALS OF DESIGNATED AVERAGE ASH PERCENTAGES TO WEIGHT OF PIECES

ability or (standard deviation)² of the ash percentages for single pieces of "average" 8, 10, and 15 per cent ash coal is given as a function of the weight of piece. The three curves show that the variability decreases with increase in weight of piece and increases with increase in the average ash of the coal. The latter relation, of course, would not be expected to continue indefinitely but to pass through a maximum at around 50 per cent ash since a "coal" having 100 per cent ash would have no more variability than a "coal" having zero per cent ash.

The size designations, represented by vertical intersections with the curves in Fig. 4 represent the weight-weighted average weights of pieces, calculated on the basis of the average consists established by Malleis (16, 17).

The curves in Fig. 4 have not been extended beyond a weight of piece of 0.16 lb, corresponding to about a 2-in. piece. Paucity of data beyond this size is such that extension is not thought permissible, although in the original publication on which this study is based, extension to 6-in. pieces was attempted (19).

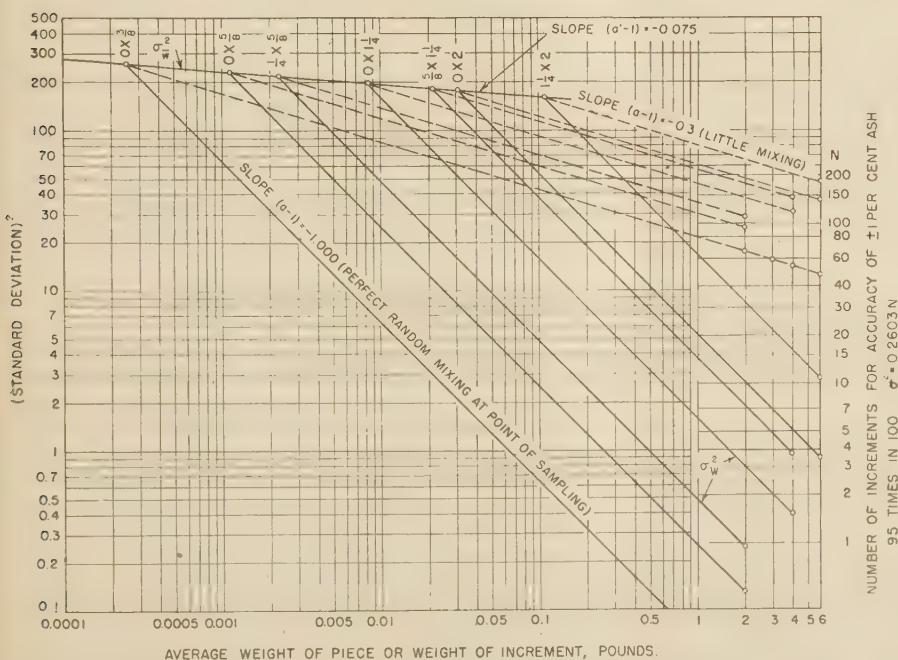


FIG. 5 EFFECT OF DEGREE OF MIXING OF BROKEN COAL FROM BED TO POINT OF SAMPLING ON VARIABILITY AND ON NUMBER OF INCREMENTS REQUIRED, "AVERAGE" 10 PER CENT ASH COAL

Effect of Mixing. The effect of coal mixing, subsequent to breakage, on the variability of ash content of increments and, consequently, on the number of them required for a gross sample of acceptable accuracy can probably be described best by the aid of Fig. 5. In this figure, it will be noticed that the lines shown are of three slopes.

First, the upper line, with attached size designations, represents the variability of the ash of pieces for an "average" 10 per cent ash coal and has been taken directly from Fig. 4. Note that the slope of the line is -0.075 ; this is the direct measure of the degree of initial mixing of pure coal and ash in the bed.

The full lines, with a slope of -1.000 , starting at each size designation indicate how the variability of increments, composed of the stated size of pieces of this coal, would decrease with increase in the weight of increment, if, beforehand, the coal

were mixed to perfect randomness. Perfect randomness of mixing (slope of -1.000) means that, given the ash content of a given piece, the possibility that the ash content of neighboring pieces in the increment will be similar depends upon an infinitesimally small chance. A reduction in the absolute value of the slope, toward the rather flat initial curve of slope -0.075 , means, on the other hand, that the chance that neighboring pieces will have similar ash contents becomes nearer and nearer to certainty. If small neighboring "regions" are substituted for neighboring pieces, then the evidence of face samples of coal beds confirms this statement (20).

The degree of mixing is then represented by the term $(a-1)$ of Equation [5], which is the slope of the variability relations. Between the original slope and the slope of -1.000 , representing the maximum degree of mixing obtainable with blind forces, there exists an infinity of slopes representing different degrees of mixing corresponding to the method of loading of the broken coal, screening operations, and coal-cleaning operations, which all effect changes in the relative positions of the pieces with respect to their initial position in the unbroken bed and bring on a greater measure of randomness. The broken lines of slope -0.300 represent just one of these different possible degrees of mixing.

Fig. 5 shows how important the factor of mixing is on the number of increments required for gross samples of acceptable accuracy for 10 per cent ash coals. The intersection of the sloped lines with the weight-of-increment ordinates at the bottom right-hand corner of the diagram gives the number of increments required (21), with the scale of increment numbers given by $\sigma^2 = 0.2603 N$ in accordance with the A.S.T.M. definition of accuracy. Thus a perfectly random-mixed $1/4 \times 5/8$ -in. "average" 10 per cent ash coal would require only one 2-lb increment; whereas, if the state of mixing corresponds to the slope of -0.3 , then about 120 increments of 2 lb each would be required for a gross sample of the same accuracy. Similarly, a perfectly random-mixed 0×2 -in. size from the same coal would require four 6-lb increments, while if only slightly mixed to a slope of -0.3 , the corresponding number of 6-lb increments would be about 140.

Incidentally, the diagram, Fig. 5, shows also the effect of increment weight on the number of increments required for gross samples of the same accuracy. For example, a $0 \times 3/8$ -in. size of this same coal, if mixed only to a slope of -0.3 , would require 68 two-lb increments, 60 three-lb increments, 55 four-lb increments, or 48 six-lb increments. Thus, in general, the total weight of gross sample increases with the weight of increment taken; so that the weight of increment should be as small as possible, but should not be so small as to cause bias from the noninclusion of all the larger pieces of coal that may present themselves to the scoop.

SAMPLING DATA SHOWING IMPORTANCE OF MIXING FACTOR

The following four sets of data, from sampling experiments, will illustrate the principles developed and show how the graphical method associated with Equation [6] can be used to bring out the important characteristics that affect the sampling of coal. These data have been collected and were supplied by a large Western Pennsylvania coal producer.

Coal 1. Hand-Loaded Conveyor Raw Coal, $0 \times 3/8$ In., Panhandle District of Western Pennsylvania, Pittsburgh Bed:

Fifty parallel gross samples, consisting each of 5 increments of approximately 2.5 lb weight each, were taken by cutting across the stream of coal at the sampling station. As each increment was taken, it was placed, in rotation, in one of the fifty receptacles provided. Thus each gross sample represented an "orderly" sample (22) over the lot of coal sampled. Each gross sample was then reduced to laboratory size and analyzed for ash.

The step curve in Fig. 6 represents the 50 ash percentages found, after rearranging in an ascending order. The average ash of the fifty samples was 10.51 per cent and the (standard deviation)

$\sigma^2 = 0.202$.

The smooth curve, shown in Fig. 6, represents the acceptable

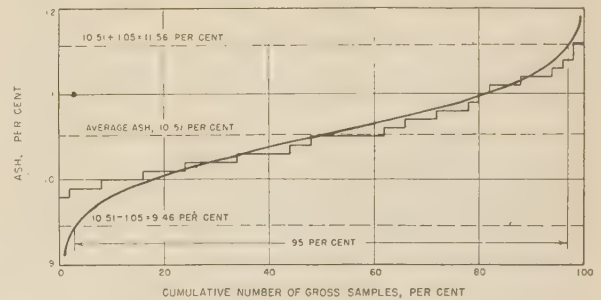


FIG. 6 VARIABILITY OF ASH PERCENTAGE OF 50 GROSS SAMPLES, EACH CONSISTING OF FIVE 2.5-LB INCREMENTS FOR A $0 \times 3/8$ -IN. RAW COAL, HAND-LOADED CONVEYER, FROM PANHANDLE DISTRICT OF WESTERN PENNSYLVANIA, PITTSBURGH BED

(Step curve, $\sigma^2 = 0.202$. Smooth curve is A.S.T.M. tentative standard of accuracy for gross samples of this coal $\sigma^2 = 0.287$.)

A.S.T.M. (Tentative) accuracy for gross samples from this coal. Its (standard deviation)² is given by

$$\sigma^2 = (0.0026033) (10.51)^2 = 0.287$$

and it is seen that 95 per cent of the gross samples, whose ash would be represented by this curve, would fall within the range (10.51 ± 1.05) per cent ash.

The step curve representing the sampling data had a lower (standard deviation)² and higher accuracy, since 98 per cent of the gross samples fell within the range. Thus the coal was slightly oversampled. The reason for this appears in Fig. 7.

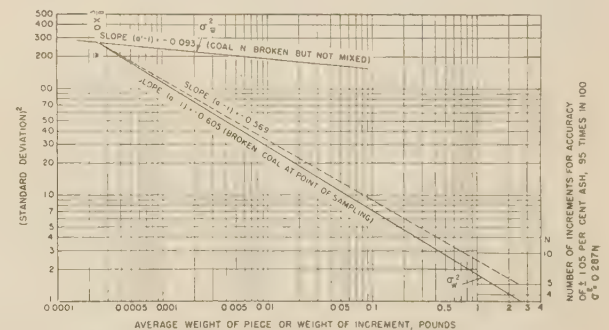


FIG. 7 VARIABLES AFFECTING SAMPLING OF COAL 1

Fig. 7 brings together the four fundamental variables affecting the number of increments required for a gross sample of acceptable accuracy for this coal. These are: (a) the average weight of piece for the $0 \times 3/8$ -size range; (b) the variability or (standard deviation)² of ash percentage of this weight of piece; (c) the degree of mixing at the point of sampling, represented by the slope of the full inclined line; (d) the arbitrary weight of the increments. The intersection of the sloping line with the vertical line at an increment weight of 2.5 lb shows that slightly less than four increments, would have been sufficient to sample this coal, instead of the five used. This conclusion was obtained as follows:

The variability of ash content of the broken coal in the bed was assumed to be that of coal N from Bureau of Mines data (18). This has been plotted as the upper curve of slope -0.093 . The "average" coal variability curve corresponding to those in Fig. 4,

for a 10.5 per cent ash coal, could however have been used just as well, as the two would have been practically superposed.

The assumption was then made that the average weight of piece for the $0 \times \frac{3}{8}$ -in. range was that which has been determined from Malleis' data (17). This is $\bar{w} = 0.000251$ and gives the point marked $0 \times \frac{3}{8}$ in the upper curve.

Now the original sampling data had been obtained by taking five 2.5-lb increments for each gross sample. Joining the point of intersection of 2.5-lb increments with the 5-increment line to the $0 \times \frac{3}{8}$ point gives the broken line of slope -0.569 shown. The fundamental assumption made in the sampling of this coal was therefore that the state of mixing corresponded to that shown by the broken line.

From the (standard deviation)² obtained for these gross samples of five increments, it is possible to calculate the true degree of mixing. Write Equation [1] as

$$v^2 = \frac{V^2}{N}$$

where v^2 is the (standard deviation)² obtained, N is the number of increments taken, and V^2 is given by Equation [5]

$$V^2 = \sigma_w^2 = \sigma_{\bar{w}}^2 \left(\frac{W}{\bar{w}} \right)^x$$

where σ_w^2 is the (standard deviation)² of the increments, $\sigma_{\bar{w}}^2$ is the (standard deviation)² of the pieces of average weight \bar{w} , W is the weight of increments, and x is the unknown degree of mixing or "slope." Combining these two expressions, solving for x , and replacing the letters by their numerical values gives

$$x = (a - 1) = \frac{\log \frac{(5)(0.0202)}{270}}{\log \frac{2.5}{0.000251}} = -0.605$$

This is the slope of the inclined full line in Fig. 7, giving the proper number of increments of any weight for gross samples of acceptable accuracy.

The result shows that the coal sampled was more effectively mixed, toward the random state, than had been assumed; this was the cause of the oversampling noted in connection with Fig. 6. The slight degree of oversampling, however, is due to the proximity of the assumed (broken line) and the actual (full line) slopes or degrees of mixing.

Coal 2. Mechanically (Wet) Cleaned Coal, $0 \times \frac{3}{8}$ In., Youghiogheny District of Western Pennsylvania, Pittsburgh Bed:

Fifty parallel gross samples, consisting each of four 2.5-lb increments, were taken by orderly cutting of a stream of $0 \times \frac{3}{8}$ -in. cleaned coal. The step curve in Fig. 8 represents the ash percentages of the 50 samples. All of the samples fell within the limits of (6.84 ± 0.68) per cent ash, although this does not mean that, in the long run, this would always happen. The (standard deviation)² of the step curve is $\sigma^2 = 0.0247$.

The smooth curve in Fig. 8, whose (standard deviation)² is given by $\sigma^2 = (0.00026033)(6.84)^2 = 0.1218$, represents the variability of acceptable gross samples from this coal by the A.S.T.M. standard. The coal was obviously oversampled.

Fig. 9 shows why the coal was oversampled. The upper line of slope -0.075 represents the relation of (standard deviation)² to weight of piece for an "average" coal of 6.8 per cent ash (23). Because this is a cleaned coal this line no longer represents the variability of the original coal as it existed in the bed, but rather of an "equivalent" coal, resulting from the effect of the cleaning operation on the ash variability of the pieces, if such a coal can be pictured restored to bed form.

The average weight of piece for the minus $\frac{3}{8}$ -in. cleaned coal was taken as equal to that of average raw Appalachian $\frac{3}{8}$ -in. resultant, on the assumption that the fines were returned to the cleaned coal to restore the consist, approximately.

The broken line of slope -0.600 represents the assumption made in the sampling experiment, whereby four 2.5-lb increments were used for each gross sample.

The full line of slope -0.768 was determined, as in Coal 1, by the following calculation

$$x = (a - 1) = \frac{\log \frac{(4)(0.0247)}{116}}{\log \frac{2.5}{0.000251}} = -0.768$$

The intersection of this line with the 2.5-lb increments vertical shows that a single increment would have been sufficient to give an acceptably accurate gross sample.

The departure of slopes of the full and broken lines represents the error in the estimate of mixing and, in a way, the measure of oversampling.

Coal 3. Mechanically Loaded Raw Coal, $0 \times \frac{5}{8}$ In., Panhandle District of Western Pennsylvania, Pittsburgh Bed:

The two examples given were of oversampled coals. This example refers to an undersampled coal. Fifty parallel gross samples, obtained in the manner described for Coal 1, were taken, each consisting of five 2.5-lb increments (approximately). The coal was a $0 \times \frac{5}{8}$ -in. mechanically loaded raw coal.

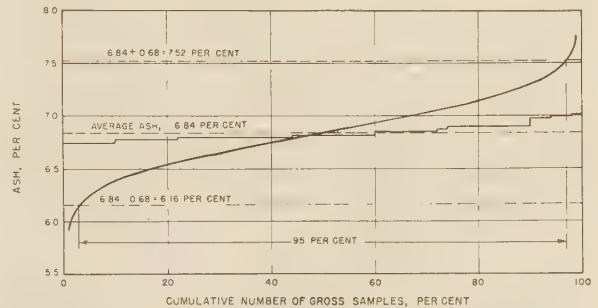


FIG. 8 VARIABILITY OF ASH PERCENTAGE OF 50 GROSS SAMPLES, EACH CONSISTING OF FOUR 2.5-LB INCREMENTS FOR A $0 \times \frac{3}{8}$ -IN. WET CLEANED COAL FROM YOUGHIOGHENY DISTRICT OF WESTERN PENNSYLVANIA, PITTSBURGH BED

(Step curve, $\sigma^2 = 0.0247$. Smooth curve is A.S.T.M. tentative standard of accuracy for gross samples for this coal; $\sigma^2 = 0.1218$.)

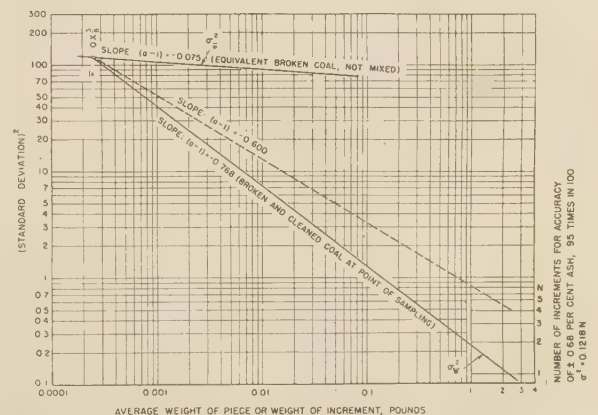


FIG. 9 VARIABLES AFFECTING SAMPLING OF COAL 2

The step curve in Fig. 10, shows the ash variability of the 50 gross samples. Only 28 per cent of the gross samples had ash percentages within the range (13.30 ± 1.33) per cent ash around the average. The (standard deviation)² of the step curve is $\sigma^2 = 6.272$.

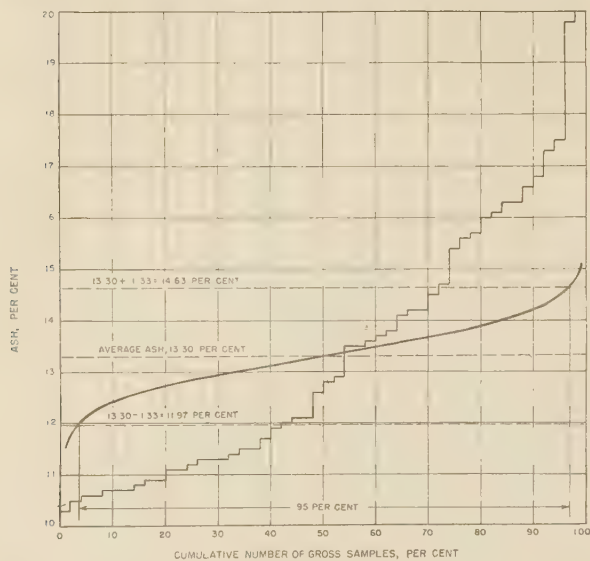


FIG. 10 CURVE OF VARIABILITY OF ASH PERCENTAGE OF 50 GROSS SAMPLES, EACH OF FIVE 2.5-LB INCREMENTS FOR A $0 \times \frac{5}{8}$ -IN. MECHANICALLY LOADED RAW COAL FROM PANHANDLE DISTRICT OF WESTERN PENNSYLVANIA, PITTSBURGH BED

(Step curve, $\sigma^2 = 6.272$. Smooth curve is A.S.T.M. tentative standard of accuracy for gross samples of this coal; $\sigma^2 = 0.461$.)

The smooth curve, shown in Fig. 10, represents what would be the acceptable variability (A.S.T.M.) for gross samples of this coal; its (standard deviation)² is given by

$$\sigma^2 = (0.0026033)(13.3)^2 = 0.461$$

The coal was obviously considerably undersampled.

Fig. 11 shows the correct number of increments required and the reason for the undersampling. For the variability of ash percentages of the broken coal, still in the bed, the relation given for coal K, from Bureau of Mines data (18), was used. This differs very little from that of the "average" coal of 13.3 per cent average ash content.

The designated average weight of piece for the $0 \times \frac{5}{8}$ -in. size range, 0.001126 lb, was as for the average Appalachian coals used for the previous examples. The broken line represents the assumed degree of mixing, implicit in the use of 5 increments of 2.5 lb weight, for the sampling of this coal. Calculation of the true degree of mixing, as for the previous coals, gave

$$x = (a - 1) = \frac{\log \frac{(5)(6.272)}{370}}{\log \frac{2.5}{0.001126}} = -0.321$$

which is the slope of the full line shown. Intersection with the 2.5-lb increment vertical shows that approximately 67 increments would have been required, instead of five, to give gross samples of acceptable accuracy. The coal was thus grossly undersampled, because so very little mixing took place between the face and the point of sampling. Comparison of loading and other handling

methods, for this coal, with corresponding mixing operations of Coal 1, should reveal interesting reasons for the considerable departure in degree of mixing for the two coals.

Coal 4. *Hand-Loaded Raw Coal, $0 \times \frac{1}{8}$ In., Panhandle District of Western Pennsylvania, Pittsburgh Bed:*

The sampling data for this coal are of interest because the origin of this coal is probably the same as that of Coal 3. However, the data for Coal 4 were obtained 2 years earlier than those for Coal 3.

Fifty parallel gross samples, each composed of 35 increments of 4 lb weight, were taken of the $0 \times \frac{1}{8}$ -in. size of this raw coal. The step curve in Fig. 12 shows the ash variability of the gross samples obtained. The (standard deviation)² of these experimental samples was $\sigma^2 = 0.286$.

The smooth curve whose (standard deviation)² is given by

$$\sigma^2 = (0.0026033)(12.8)^2 = 0.427$$

is less than that for the samples obtained. The coal was thus oversampled.

Fig. 13 gives the sampling characteristics of this coal. The relation of variability of ash of pieces to their weight was taken to be that of Coal K, as in Coal 3. The average weight of piece for the $0 \times \frac{1}{8}$ -in. range was taken as 0.00596 lb, in accordance with

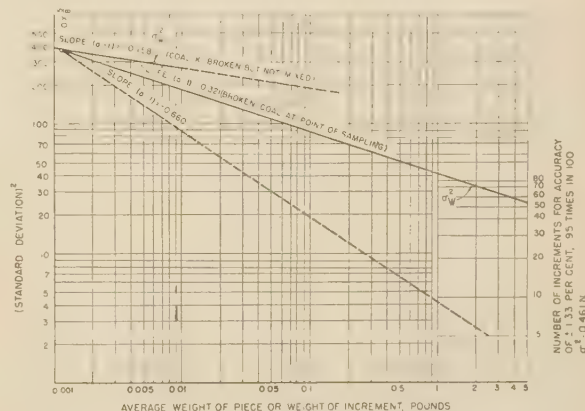


FIG. 11 VARIABLES AFFECTING SAMPLING OF COAL 3

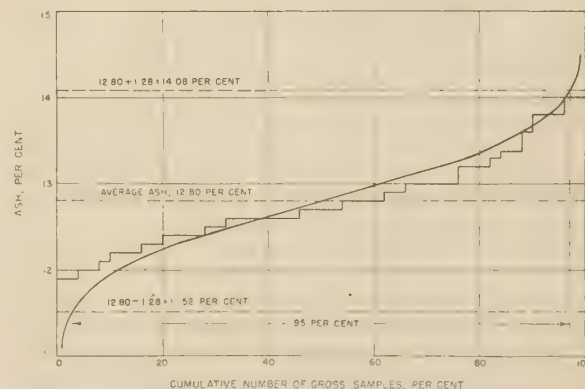


FIG. 12 CURVE OF VARIABILITY OF ASH PERCENTAGE OF 50 GROSS SAMPLES OF THIRTY-FIVE 4-LB INCREMENTS FOR A $0 \times \frac{1}{8}$ -IN. HAND-LOADED RAW COAL FROM PANHANDLE DISTRICT OF WESTERN PENNSYLVANIA, PITTSBURGH BED

(Step curve, $\sigma^2 = 0.286$. Smooth curve is A.S.T.M. tentative standard of accuracy for gross samples of this coal; $\sigma^2 = 0.427$.)

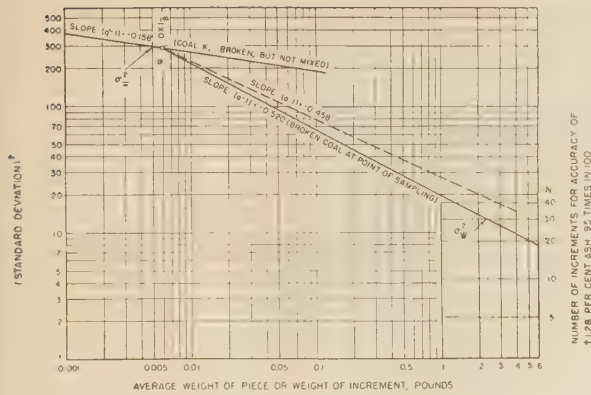


FIG. 13 VARIABLES AFFECTING SAMPLING OF COAL 4

the average Appalachian coals. The broken line of slope -0.458 represents the initial assumption of mixing, implicit in the use of 35 increments for this coal. The full line, whose slope was calculated to be

$$x = (a - 1) = \frac{\log \frac{(35)(0.286)}{295}}{\log \frac{4}{0.00596}} = -0.520$$

represents the actual degree of mixing of this coal. The intersection of this line with the 4-lb increment-weight vertical shows that only about 23 increments were necessary for an accurate gross sample of this coal; in other words, the actual mixing was more random than had been assumed; hand-loading of this coal probably accounts for the increased mixing, as compared to Coal 3.

ESTABLISHMENT OF SAMPLING SPECIFICATIONS

The foregoing developments show that the establishment of general sampling specifications is not an easy matter, if both oversampling and undersampling are to be avoided, but gross samples of preassigned accuracy are to be obtained.

It is believed, however, that Equation [5]

$$\sigma_w^2 = \sigma_w^2 \left(\frac{W}{w} \right)^{(a-1)} \dots \dots \dots [5]$$

and its simple logarithmic expression furnish the correct theoretical approach for the study of those variables which may be called the sampling characteristics of coals.

The examples given, however, were all concerned with only one of the four variables in the right-hand side of the equation, this being the exponent $(a - 1)$ representing the effect of mixing.

Two of the three other variables involved could also have been studied by the same method, had data been available. These are (a) the effect of consist on the average weight of piece, in a given size range, and consequently on the variability of the increments,

and (b) the effect of variability of the ash of the individual pieces of coal, in relation to the weight of the pieces and the average ash of the coal, on the variability of the increments.

Log-log plots used, such as Fig. 14, show, for example, that a modification of consist favoring the larger-size fractions would by displacing the size designation to the right require, with the same mixing effect, a larger number of increments. Conversely, a consist running toward the fine sizes, in a given range, would allow taking fewer increments, everything else being the same.

Similarly, a displacement upward of the curve of ash variability of the pieces would necessitate taking more increments, while a lower variability of pieces would lower the required number of increments.

The remaining factor of weight of increment has received some study from the point of view of the bias that may be introduced when using weights that are too small (24); this need not be discussed here.

Effect of Coal-Mixing Operations on Sampling Specifications. The four examples of sampling data, given previously, can be used to show how the matter of coal-mixing operations, during the course of mining, loading, screening, washing, crushing, and so on, may affect sampling specifications.

The four coals studied were found to have the following mixing "exponents:"

Coal	Degree of mixing at point of sampling
1	-0.605
2	-0.768
3	-0.321
4	-0.520

The exact causes for these different degrees of mixing could only be investigated at the mine and tippie. However, the fact that such variations in degree of mixing could occur is justification enough to show the result on sampling specifications. Figs. 14, 15, and 16 have been prepared for this purpose. Three possible slopes, representing approximately the extremes and the median degrees of mixing of the coals studied, were taken as -0.7 , -0.5 , and -0.3 ; the three figures being, respectively, for "average" coals of 8, 10, and 15 per cent ash. The size designations are the average Appalachian mentioned before.

The intersections of the inclined lines with the verticals at increment weights, give in the right-hand scale the corresponding required number of increments for the A.S.T.M. (tentative) accuracy. This follows from the fact that Equations [4] and [5], combined, can be written as

$$\sigma_w^2 = (0.0026033) \bar{y}^2 N = \sigma_w^2 \left(\frac{W}{w} \right)^{(a-1)} \dots \dots \dots [7]$$

Table 2 summarizes these results and brings them together for comparison with the present tentative A.S.T.M. specifications. The departures from the specification are quite large in many instances.

Of course, any single specification must be based on a compromise. One natural question is whether enough representative

TABLE 2 NUMBER OF INCREMENTS REQUIRED FOR AN ACCURACY OF ± 10 PER CENT OF AVERAGE ASH, 95 TIMES IN 100, IN THE LONG RUN. COMPARISON OF A.S.T.M. SPECIFICATIONS (D492-43T) WITH RESULTS OF THIS STUDY

Average ash of coal, per cent		8			10			15			
Number of increments by D492-43T		15			20			35			
Size range, in.	Weight of increments, lb	Degree of mixing									
		-0.7	-0.5	-0.3	-0.7	-0.5	-0.3	-0.7	-0.5	-0.3	
0 × 5/8	2	Number of increments by this study	5	22	96	5	21	88	4	16	75
1/4 × 5/8	2		8	29	115	7	27	110	7	22	85
0 × 1 1/4	4		11	35	128	9	34	120	8	28	92
5/8 × 1 1/4	2		18	52	150	17	50	140	15	43	120
0 × 2	4		17	51	146	16	47	137	14	40	115
1 1/4 × 2	6		37	84	180	36	76	175	30	67	160

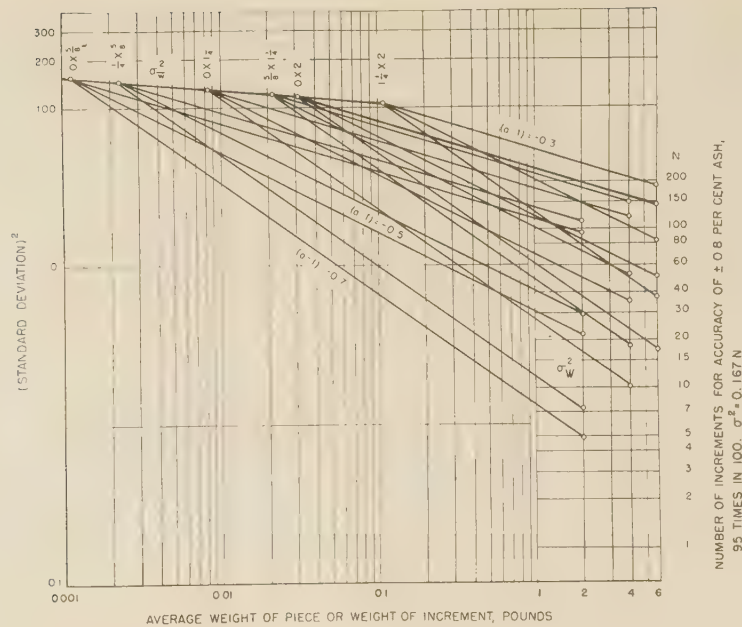


FIG. 14 RELATION OF NUMBER OF INCREMENTS REQUIRED TO DEGREE OF MIXING FOR AN AVERAGE 8 PER CENT ASH COAL

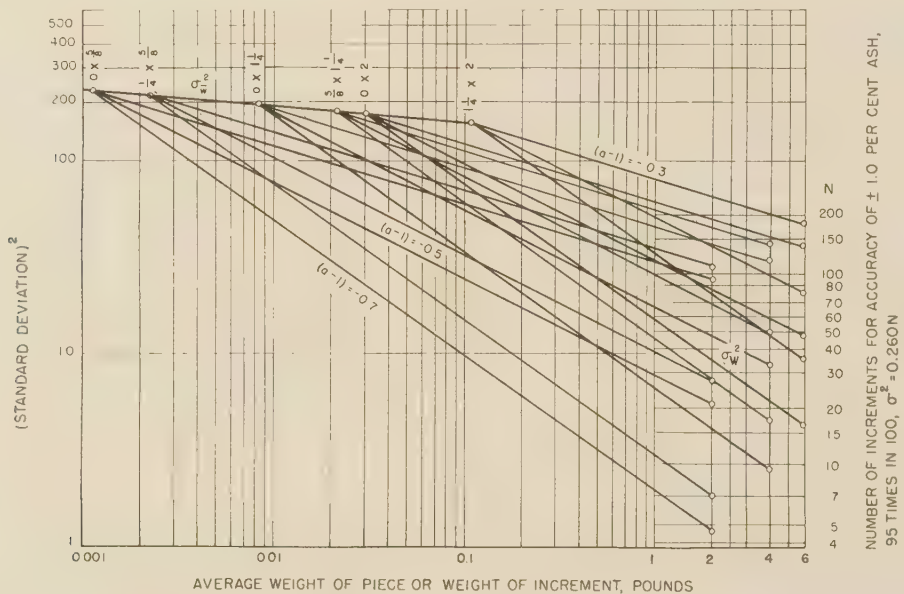


FIG. 15 RELATION OF NUMBER OF INCREMENTS REQUIRED TO DEGREE OF MIXING FOR AN AVERAGE 10 PER CENT ASH COAL

data have been collected to arrive at a median compromise. Another question is whether a number of classifications, reflecting methods of coal handling and preparation, should be made so as to lead to an equal number of compromises between sampling characteristics of similar coals.

Table 2 shows two interesting facts that have been mentioned earlier (25) and need not be emphasized here. One is that sized coals require a larger number of increments than resultant coals of the same top size. The other fact is that because of the increased laxity in accuracy, allowable by the specifications, the number of required increments decreases with increase in average ash content, everything else being equal.

CONCLUSIONS

The missing data on coal sampling fall under the classifications already discussed. Basic data, over a wide range of coals, are needed that will supply information (a) on consist; (b) on the variability of ash of pieces by the float-and-sink method and by direct analysis of pieces for confirmation of the method; (c) on the variability of the ash of increments, whereby a large number of increments, of a variety of specified large weights each, are taken to establish the degree of mixing directly, rather than by inference, as was done here; and, finally, (d) collection and analysis of gross samples of a specified number of increments of constant weight to

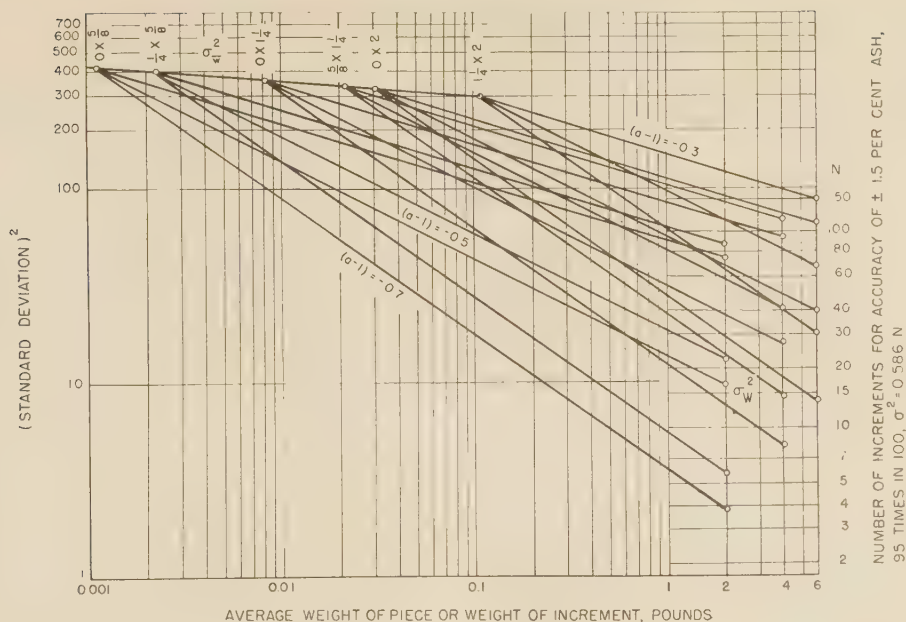


FIG. 16 RELATION OF NUMBER OF INCREMENTS REQUIRED TO DEGREE OF MIXING FOR AN AVERAGE 15 PER CENT ASH COAL

give over-all confirmation to the established relations between the variables involved.

In connection with the determined degree of mixing for any coal, a special effort should be made to relate this to mining and tippie operations.

Carried systematically, such a program would eventually rid coal sampling of much of its unpleasant surprises and reduce sampling costs to a minimum.

BIBLIOGRAPHY

- 1 "Coal Research a Century Ago," *Bituminous Coal Research*, vol. 4, no. 3, July, 1944.
- 2 Report of the Committee on Coal Analysis, *Journal of the American Chemical Society*, vol. 21, 1899, pp. 1116-1132.
- 3 "Accuracy in Sampling Coal," by E. G. Bailey, *Industrial and Engineering Chemistry*, vol. 1, 1909, pp. 161-178.
- 4 "Standard Method of Sampling Coal for Analysis," A.S.T.M. Standards, 1942, part 3, p. 11.
- 5 "The Sampling of Small Fuel Up to 3 Inches," by E. S. Grumell and A. C. Dunningham, British Standards Institution B.S.S. (Report) 403, 1930.
- 6 British Standard Methods for the Sampling of Coal and Coke, British Standards Institution, B.S.S. 1017, 1942.
- 7 "The Sampling of Coal," by L. A. Bushell, *Journal of the*

Chemical, Metallurgical, and Mining Society of South Africa, vol. 37, Feb., 1937, pp. 361-434; also *Journal of the Institute of Fuel*, vol. X, Aug., 1937, pp. 384-408.

8 "Variables in Coal Sampling," by J. B. Morrow and C. P. Proctor, *Trans. A.I.M.E.*, vol. 119, 1936, pp. 227-276.

9 "A Decade of Sampling," by E. S. Grumell, *Trans. A.I.M.E.*, vol. 139, 1940, pp. 11-52.

10 "Tentative Methods of Sampling Coals Classed According to Ash Content," A.S.T.M. Standards, 1943 Supplement, part 3, pp. 147-153.

11 "Fundamentals of Coal Sampling," by B. A. Landry, U. S. Bureau of Mines, Bulletin 454, table 18, p. 56.

12 Reference 11, p. 8.

13 Reference 11, p. 23.

14 Reference 11, pp. 100-105.

15 Reference 11, pp. 113-115.

16 "Screen Analysis of Nut-Slack Coals Taken at Mines While Loading," by O. O. Malleis, *Trans. Fuel Eng. Meeting, Appalachian Coals*, vol. 2, 1933, table 2, p. 161.

17 Reference 11, pp. 115-127.

18 Reference 11, pp. 61-67.

19 Reference 11, pp. 74-80.

20 Reference 8, p. 234.

21 Reference 11, p. 79.

22 Reference 11, p. 68.

23 Reference 11, p. 67.

24 Reference 11, pp. 46-60.

25 Reference 11, p. 78.

Electrical-Analogy Method for Fundamental Investigations in Automatic Control

By D. P. ECKMAN¹ AND W. H. WANNAMAKER,² PHILADELPHIA, PA.

The purpose of this paper is to demonstrate an approach to automatic-control investigation through the use of an electrical-analogy method. A complete description of the apparatus is included, each unit being related to a counterpart in an industrial control application. Diagrams and calibrations of the various units comprising the electrical process analog are given. For illustration of the manner of setting up a problem, the effect of controller scale span upon controller adjustment is shown.

INTRODUCTION

THE need for process simulation in the laboratory arises in the study of automatic-control methods. Testing automatic controllers in the field on actual control applications is often very difficult because of changing conditions over which there is no control. In addition, the introduction of intentional load changes, disturbances, or control-point shifts in order to determine the dynamic action of the control system is generally not permissible. Consequently, electrical, hydraulic, mechanical, and thermal analogies to controllable industrial processes have come into use for development testing of automatic-control methods (1, 2).³ The electrical capacitance-resistance analogy seemed to offer more advantages of versatility and was therefore selected by the authors.

Under simulated control conditions, the dynamic action of the control system may be observed. Any factor, either in the process or in the controller, may be readily altered. The electrical process analog therefore becomes a versatile means for the investigation of various phenomena in automatic control.

ELECTRICAL PROCESS ANALOG

Where a number of processes are to be studied and the variable must take numerous forms, the time-consuming analytical approach must be condensed to a minimum. Even then, it is generally desirable to have experimental means for checking analytical results. Where the experimental apparatus involves a portion of the system under investigation, less likelihood of error in the final result will be evidenced because of the simplified analytical data required.

If the results of a few trials of an experimental analogy bear close agreement to the performance characteristics of the actual process, we may rely on analogies for more complicated and less understood process-control problems. Such a study may lead to the simplest, most economical form of control, while the effect of precision, dependability, and ease of adjustment is easily determined.

¹ Development Engineer, Brown Instrument Company. Jun. A.S.M.E.

² Development Engineer, Brown Instrument Company.

³ Numbers in parentheses refer to the Bibliography at the end of the paper.

Contributed by the Industrial Instruments and Regulators Division and presented at the Spring Meeting, Birmingham, Ala., April 3-5, 1944, of THE AMERICAN SOCIETY OF MECHANICAL ENGINEERS.

NOTE: Statements and opinions advanced in papers are to be understood as individual expressions of their authors and not those of the Society.

Previous investigators have evolved techniques of applying control to simulated processes. These analogies were rather specialized and do not lend themselves readily to changes for duplicating a variety of multiple-capacity processes. The electrical analogy⁴ possesses extreme flexibility for duplicating numerous processes by altering the values of resistor and capacitor networks through plug-and-jack connections.

The physical constants may be calculated using well-known theory (3, 4, 7). In the electrical analogy, a direct relationship exists between electrical units and thermal units of a process. The time basis of the analogy may bear any chosen convenient ratio to that of the actual process, although an altered time relation may introduce complications when the control system involves integral and derivative functions.

Table 1 illustrates the similarity between thermal, hydraulic, and electrical units.

TABLE 1 ANALOGOUS UNITS

Quantity.....	Dimensional symbol	Electrical	Hydraulic	Thermal
Potential.....	P	Coulomb ^a	Cu ft	Btu
Time.....	T	Volt	Ft	Deg
Flow.....	W/T	Second	Min	Min
		Coul = amp	Cu ft	Btu
		Sec	Min	Min
Capacity.....	W/P	Coul = farad	Cu ft	Btu
		Volt	Ft	Deg
		Volt	Ft	Deg
Resistance.....	PT/W	Coul/sec = ohm	Cu ft/min	Btu/min

^a For purposes of this paper coulomb will be abbreviated "coul."

It must be assumed that the fundamental units in this table are based upon point values, in order to avoid the complicity of power functions. In view of the inviting aspects of the electrical analogy, an investigation into the problem of adapting its use to process control was made. In order to duplicate long thermal lags present in many processes, it is evident that large values of capacity are needed in the various networks, particularly if the time ratio is to remain near unity.

Although the process analogy itself is perhaps the most important single link in the control study, several other units must be used to complete the essential equipment. For example, equivalents for a fuel valve and fuel supply are required. There often is need for a means for simulating dead time in a process. There also must be an equivalent primary measuring element with means for introducing a lag in its response. These are discussed in the following section.

TEST EQUIPMENT

Most industrial controllers possess some form of pneumatic unit, electric contacting means, or power-set slider on a resistance slide-wire. The experimentation so far has been concerned chiefly with a single controller of the self-balancing potentiometer type, equipped with control devices of all the foregoing types,

⁴ This method of control application was developed after a study of existing published analogy data. Credit for the electrical analogy is due Dr. Victor Paschkis of Columbia University for applying electrical means developed by C. L. Beuken (5, 6) in the study of heat flow and allied problems.

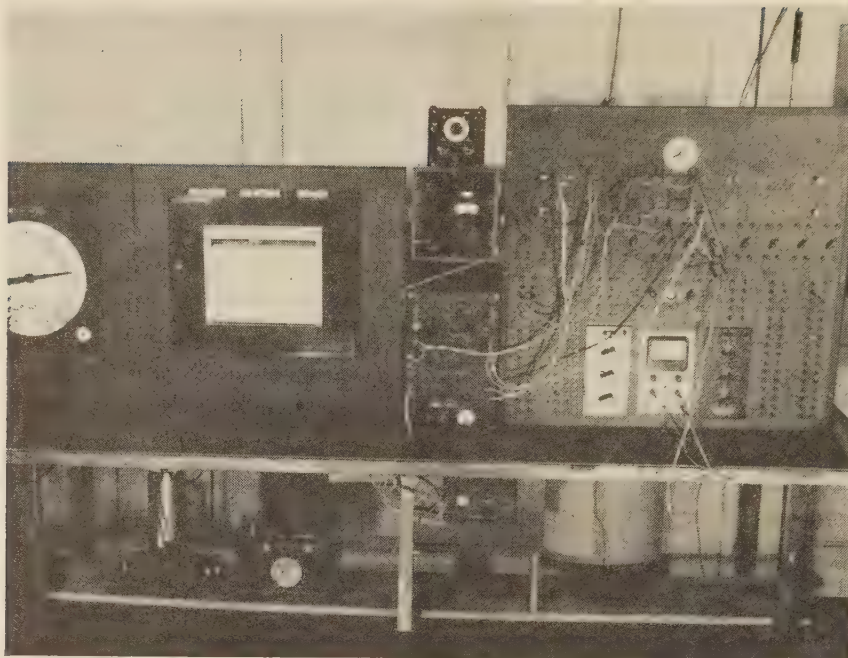


FIG. 1 PROCESS-CONTROL BOARD

any of which could be used as desired. The complete system is shown in Fig. 1.

Referring to Fig. 2, a closed-circuit control system of general form is shown. A self-balancing potentiometer, equipped with pneumatic control, causes the air pressure to a diaphragm motor to position a slider along a resistor. This determines the voltage passing through a dead-time unit to a current-input unit.

The valve slide-wire voltage actually charges each of a number of high-grade condensers one at a time by means of a 25-position ratchet-type multiple-contact switch. Its average speed of rotation is governed by means of an adjustable electronic-pulse circuit which causes the contact blades to advance one step at a time. The two blades are out of step by one position and are so wired that, in turn, each previously charged condenser applies its potential to the current-input unit for a period equal to the time between pulses. This effectively produces a dead time equal to 24 times the pulsing period.

The current-input unit then passes a current into the resistance-capacity mesh network, its value being a function of the voltage applied to the current-input unit. The mesh output-voltage simulates the temperature of the process under consideration. In order to measure the output voltage, a vacuum-tube voltmeter is used in conjunction with the potentiometer controller. This voltmeter serves as an impedance-matching device to permit the proper functioning of potentiometer controllers designed to work from low-voltage low-impedance circuits.

The controlled system having been described briefly, details of the equipment follow, and reference to Fig. 3 should be made:

The diaphragm motor positions the slider of the slide-wire, according to the applied air pressure. About 200 useful convolutions are used on this slide-wire, so that the number of valve positions are, in effect, limited to this number. More convolutions would probably require the use of a valve positioner, but this sensitivity has proved satisfactory particularly when used in conjunction with the dead-time unit with its step functioning.

The dead-time unit has certain limitations in that the equivalent fuel-supply rate is not a continuous function of controller

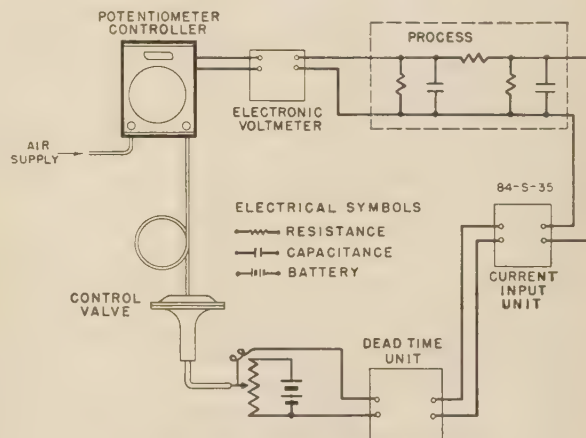


FIG. 2 CONTROLLED SYSTEM WITH PROCESS ANALOG

output, although the integrated amount of fuel closely follows it. In low-capacity processes where low rates of switching would be objectionable, dead time to any large degree is generally not met in actual practice, and the consequent fast pulsing of this controller provides a satisfactory dead time even for such low-capacity processes. A 25-position selector-switch assembly was chosen as the most feasible device to approximate delays of from zero to several minutes' duration. Its rotation is made in a series of steps, the time between each step being determined by an electronic pulse circuit. The condensers used with the switch may stand idle for the necessary periods without appreciable loss of charge, while the current drain during the period that each is connected to the current input unit is very small.

Most processes are nonregenerative. Burning fuel, for example, releases some given number of heat units regardless of the temperature within the firebox. If the fuel is reduced, heat does not flow back into the fuel supply as fuel. To simulate such a

burner, a controllable constant-current device, consisting of a high-gain direct-current amplifier, having considerable negative feedback, was used. For a fixed applied potential, a current will flow in the output circuit at a set value practically independent of the impedance into which it is working. When this load is composed of condensers and resistors, as in the mesh analog circuit, this flow of current simulates flow of heat, while the voltage in any portion of the mesh represents temperature. If the demand should go to zero, the input current may be made to go to zero. Current will not flow back into the source and alter the rate of heat dissipation. If some decrease in demand should occur, the input current will be reduced to some lower value in accordance with the demand. The complete current-supply system has been designed to approximate a semilogarithmic valve characteristic in its action.

The mesh circuit of the process analog makes use of ordinary dry electrolytic condensers. Their terminals are wired to colored jacks on a bakelite panel, and about 30,000 microfarads of capacity are used together with about 30 adjustable resistors. These may be connected by means of jumpers into jacks to form various types of mesh circuits. A built-in bridge circuit and null indicator is included for circuit-measuring purposes. The use of electrolytic condensers imposes limitations on the analog board. For example, a circuit calling for higher shunt resistances than are inherent in the condensers in the form of leakage may not be used. Variation of capacity and leakage, both with temperature and impressed voltage, must be taken into account. Even with those limitations, a real advantage is gained by the use of electrolytic condensers, since many industrial-process applications may be approximated satisfactorily with considerable savings in cost and space.

The vacuum-tube voltmeter is composed of a sharp cutoff type triode tube operated at a low plate voltage. A large series grid resistor is used to reduce grid current to a low value. The potential across an adjustable portion of the plate resistor furnishes the voltage to operate the potentiometer controller. In order to make the controller read upscale for an increasing negative voltage applied to the grid of the tube, an adjustable fixed potential is used to buck the voltage across a portion of the load resistor. Both the plate and the heater voltage supplies are regulated to reduce the effect of line-voltage variations. Two voltmeter units have been built into a single housing, one of which serves to actuate the controller and the other may be used to

actuate a recorder to show the demand, the actual fuel flowing, or may be used to indicate the voltage within any portion of the process mesh circuit.

An impedance measuring bridge is built into the process board with jacks for inserting leads from the various circuit components. An ordinary amplifier, rectifier, and electron-ray tube of the indicating type are used as a null indicator.

Typical performance characteristics of the various portions of the equipment described are shown in Fig. 4. Curves under *A* indicate the current flow into the process analog for values of impressed voltage on the current-input supply. It should be noted that the current value is practically independent of the dynamic impedance of the process mesh circuit, and that the sensitivity or equivalent valve size may be selected by changing the self-bias resistor value as shown in Fig. 3.

Part *B* in Fig. 4 shows the manner in which the dead-time unit delays the voltage from the valve slide-wire. Part *C* illustrates several different calibration curves obtainable with the voltmeter by which the equivalent of suppressed-range studies, for example, may be made.

SETTING UP PROCESS ANALOG FOR TEST

Although it is possible by means of electrical analogy to approximate a particular process through calculation of its resistance and capacity, it is only necessary to arrange certain combinations of capacity, transfer lag, and dead time to represent whatever particular characteristic is desired. In this manner the effect of various characteristics in automatic control may be investigated without actually attempting to set up specific processes. The principal application for the electrical analog therefore is to simulate process characteristics rather than to duplicate a specific physical process apparatus.

Suppose, for example, that we wish to investigate the effect of suppressed-range controller scale upon controller adjustment. A suitable process should be selected which approximates an actual process of the type on which a proportional-reset controller is used. For the purposes of this investigation dead time is not required and is accordingly omitted.

The process used in this case is shown in Fig. 5. A multiple-capacity process is desired and three RC networks are used. Each RC network is connected by a 40,000-ohm resistor to cause an equivalent temperature drop between capacitors. In order to obtain a fixed rate of temperature decrease, each capacitor is

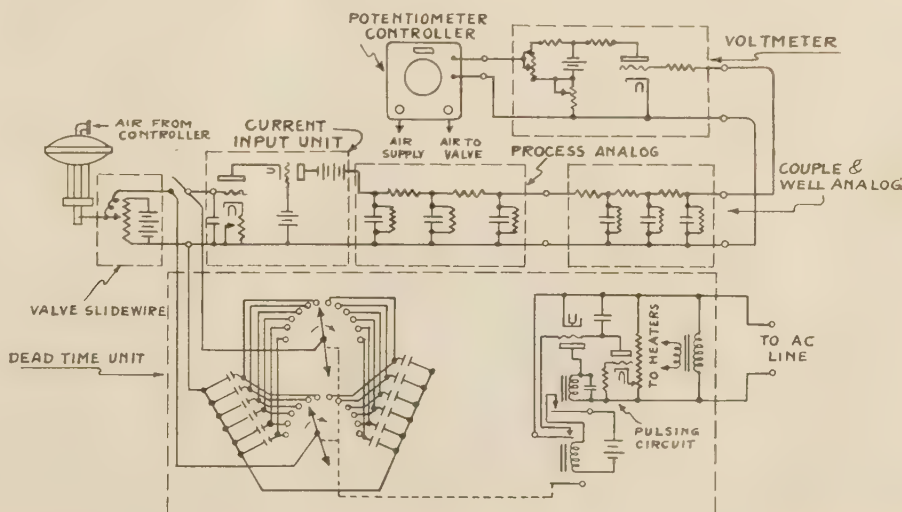


FIG. 3 SCHEMATIC DIAGRAM OF PROCESS CONTROL-BOARD EQUIPMENT

A potentiometer pneumatic controller was connected to the process previously described and adjustments of proportional band (throttling range) and reset rate selected for control of the process. The adjustments are based upon minimum area recovery from a supply change.

The supply change was introduced manually by a throw switch so that an additional bias voltage was inserted in the sliding-contact lead on the control-valve slide-wire. When the voltage is introduced, a 25 per cent increase in flow is caused with the actual valve position remaining unchanged. This corresponds to a change in upstream pressure at a control valve, causes a greater flow of control agent, and requires that the controller correct for this change.

The potentiometer controller was calibrated in turn to various spans, and the suppression adjusted so that the control point represents 3 v. The controller adjustments were then redetermined. Table 2 shows the results, while Fig. 6 shows the recovery curves under each condition.

TABLE 2 CONTROLLER ADJUSTMENTS

Controller calibration span, v	Proportional band, s, per cent scale	Reset rate, r, per min	Maximum deviation, v
6	22	0.51	0.40
5	32	0.48	0.42
4	38	0.47	0.42
3	44	0.43	0.42
2	52	0.39	0.42

From the theoretical standpoint, it would be expected that the proportional band would follow a reciprocal law such that, as the controller span is reduced by one half, the proportional band would be doubled. The results of these tests are in approximate agreement. The proportional band is smaller than expected, however, at the smaller scale spans.

These differences can only be explained by one or a combination of factors. If nonlinearities exist in the control system, it is possible that the greater deviation in per cent of scale, which, however, representing the same deviation in volts for various spans, may require a smaller proportional band in order to achieve the same stability in the recovery curve. Since the controller is calibrated for linear response of voltage input to air-pressure output, it is unlikely that this is the cause of the differences. The semi-logarithmic control valve characteristic probably influenced the test results.

A second cause may be the difference in apparent dead zone of the control system with respect to changes in voltage of the process when various controller spans are used. For example, a dead zone of 0.04 per cent of controller scale with a 6-v span would represent 0.0024 v, while at a 2-v span, the dead zone would represent 0.0008 v. Since the process possesses slight transfer lag, the decrease in apparent dead zone with smaller spans would allow a slightly smaller proportional band.

A third cause may be that controller adjustments were not set to the optimum values to produce a recovery curve having the smallest possible period. In fact, the recovery curves in Fig. 6 indicate that the period increased slightly as the span decreased. Controller adjustments were made in each case without changing the reset rate from the previous setting. It was found necessary in every test to decrease the reset rate in order to achieve the desired stability. Although the reset rate should be unchanged with various spans, the required decrease in reset rate may be in part due to the method of selecting controller adjustments.

In using any type of analog for investigations in automatic control, it is necessary to avoid imposing any limits on the operation of the analog under dynamic conditions. If the control valve is required to move to its limit of travel, if the process

reaches a potential beyond which it cannot go, or if the controller pen should attain full scale, the complete system is unable to follow adequately its own laws of operation. Such action in the system correspondingly influences the dynamic operation unless limits are required as in two-position control.

CONCLUSIONS

The electrical analogy method of simulating industrial processes lends itself readily to the selection of varying degrees of process characteristics. It is shown how such factors as process capacity, transfer lag, dead time, valve size, controller-scale range, and load changes are set up in the analog.

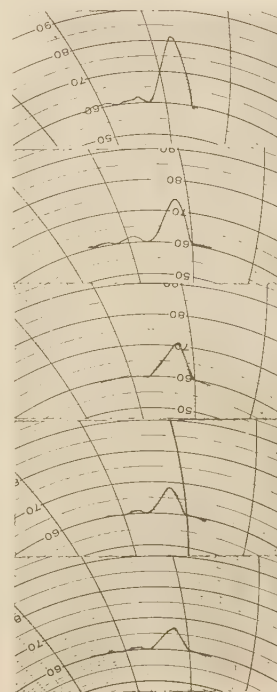
Various investigations of automatic control, particularly when actual control equipment is used, point out the necessity of taking into account such factors as measuring lag, controller lag, and dead zones in the measuring and controlling means. The results of the investigation of controller span indicate that these factors should not be neglected. Empirical methods of analysis of automatic control must generally be tempered by the influence of factors difficult to account for in mathematical methods.

ACKNOWLEDGMENT

The authors wish to acknowledge the valuable suggestions of Messrs. G. M. Muschamp and T. R. Harrison.

BIBLIOGRAPHY

- 1 "Quantitative Analysis of Process Lags," by C. E. Mason, Trans. A.S.M.E., vol. 60, 1938, pp. 327-334.
- 2 "Experimental Studies of Automatic Control," by J. C. Peters, Trans. A.S.M.E., vol. 64, 1942, pp. 247-255.
- 3 "A Method for Determining Unsteady State Heat Transfer by Means of an Electrical Analogy," by V. Paschakis and H. D. Baker, Trans. A.S.M.E., vol. 64, 1942, pp. 105-112.
- 4 "Periodic Heat Flow in Building Walls Determined by Electric



Prop. Band 52 %
Reset Rate .39 per min.
Span 2 Volts

Prop. Band 44 %
Reset Rate .43 per min
Span 3 Volts

Prop. Band 38 %
Reset Rate .47 per min
Span 4 Volts

Prop. Band 32 %
Reset Rate .48 per min
Span 5 Volts

Prop. Band 22 %
Reset Rate .51 per min
Span 6 Volts

FIG. 6 RECOVERY CURVES FOR VARIOUS SCALE SPANS

cal-Analogy Method," by V. Paschkis, Trans. American Society of Heating and Ventilating Engineers, vol. 48, 1942, pp. 75-90.

5 "Wärmeverluste bei periodisch betriebenen Elektrischen Öfen," by C. L. Beuken, *Elektrotechnik und Maschinenbau*, vol. 55, 1937, p. 232.

6 "Die Berechnung der Durchwärmungszeiten von Gutstücken auf der relativen Mindertemperatur," by V. Paschkis and C. L. Beuken, *Elektrotechnik und Maschinenbau*, vol. 56, 1938, pp. 98-100.

7 "Operational Circuit Analysis," by V. Bush, John Wiley and Sons, Inc., New York, N. Y., 1929.

Discussion

VICTOR PASCHKIS.⁵ Electrical analogs can be most useful in the study of different types of transients, such as expressed in heat flow, etc.

In describing the analogous units it is stated in the paper that these are based upon "point values." A definition would be desirable.

The impression is derived from the paper that the process analog is built and operated without reference to any given piece of equipment or process. The writer feels that this method of approach is a definite disadvantage perhaps made necessary by the use of the inexpensive and inaccurate electrolytic condensers. The time lag between the achievement of a given temperature in the equipment and the corresponding achievement in the thermocouple is one of the major causes of temperature oscillations. These oscillations would be insufficiently reproduced through the use of the "dead-time unit." It would be desirable if in the closure the authors would give a definition of what they call "dead time." This term is used by various authors with different meanings and should be defined. Moreover, a more complete description of the dead-time unit would be desirable.

By not representing actual equipment, e.g., furnace charge and thermocouple, the authors limit their investigation to that of a measuring and control instrument alone. The user of temperature control is primarily interested in the uniformity of the product and not in the uniformity of the temperature record.⁶

The uniformity in time refers to temperature fluctuations at any one given point in the equipment at which the measuring device happens to be located. Temperature uniformity in space can be very poor even with perfect uniformity in time. For example, cold spots can occur as a result of poor design or operation of the equipment and not be detected by the thermocouple.

⁵ Research Associate, Research Laboratories, Department of Mechanical Engineering, Columbia University.

⁶ "Relation of Uniform Pyrometer Records to Uniform Products," by J. A. Doyle, "Temperature—Its Measurements and Control." (Papers presented at Symposium of the American Institute of Physics, 1939), pp. 984-987.

There is another aspect of the uniformity in space referring to uniformity of temperature within the load itself. It is this latter with which the user of control is primarily concerned. The method as used by the authors is limited to problems of uniformity in time. By using higher-grade condensers, it could also be applied to even more important problems of uniformity in space (temperature distribution).

These three phases of uniformity tie in and really should not be investigated separately. This investigation of the three phases in one calls for higher-grade and more complete equipment than that covered in this paper.

However, it should be stated that the present investigation forms a very welcome start in a field of analysis so far insufficiently covered.

AUTHORS' CLOSURE

The discussion by Dr. Paschkis, whose heat- and mass-flow analyzer served as inspiration for the authors' work, is particularly welcome.

The analogous units given for thermal, hydraulic, and electrical systems are based on point values, that is, on a given system with static conditions of potential and resistance. In a thermal system, for example, resistance often varies with potential (specific heat varies with temperature). In a hydraulic system, flow may vary with the square root of potential. Other examples might be given. Consequently, in using any analogy, it is necessary to assume that the system is operating at a "point" or about an average point of capacity, resistance, and potential.

The remainder of Dr. Paschkis' comments are directed toward whether an analogy should be set up on the basis of physical process apparatus or upon process characteristics. If one is investigating the apparatus, the former method is appropriate; if one is investigating automatic control, the analogy may be more easily handled by choosing the desired characteristics of capacity, transfer lag, and dead time.

The use of electrolytic capacitors imposes no serious limitation to the study of automatic control other than the attainment of time constants greater than are inherent in the leakage characteristic. Reproducibility of results has been found to be practicable.

There is use, as Dr. Paschkis has found, for electrical-analogy apparatus adaptable to simulation of specific physical problems. The analog equipment described in this paper is used primarily for experimental work in connection with the study of automatic control.

Dead time is any pure time delay, expressible in units of time, existing either in the process or in the control system.

Stabilizing a Suction-Relief Valve

By ED S. SMITH,¹ TETERBORO, N. J.

Starting with a less than fully stable conventional valve in aircraft use, a simple analysis is presented which is based upon energy considerations under resonance conditions and involves a minimum of mathematics. This analysis led to the disclosed improvement which renders the valve stable under all installations except the worst, from an acoustic standpoint. A short appendix on acoustic systems is included for the convenience of control engineers who may need in advance to evaluate and, if necessary, correct acoustic difficulties of installations. The analysis of this paper amounts to an informal use of the Nyquist method.

THIS valve is required to maintain constant suction, i.e., depression below atmospheric pressure of an air-carrying line. A conventional regulator, as shown in Fig. 1, has a damped valve piston with a long compression spring having the

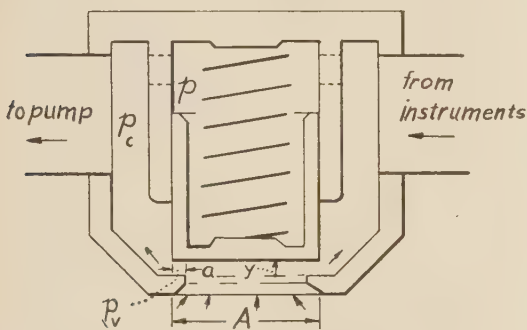


FIG. 1 FORMER TYPE VALVE WITH FLAT SURFACE AT a , TO MINIMIZE LEAKAGE WHEN SHUT

position of one of its ends adjustable to set the desired suction. The end of the piston seats against a flat rim seat a to minimize the leakage when the valve abuts its seat.

This valve is damped by friction between the valve piston and its cylinder whether due to rubbing, to coulomb friction, or to the shearing of a film of lubricant. Rubbing friction is preferably minimized since it is quite sensitive to clearances and generally tends to produce an objectionably large departure from the suction setting.

The use of lubricant friction also has disadvantages since the viscosity, and hence the damping, changes seriously with temperature. However, this may not be a bar since winterization requirements reasonably take into consideration the location of the valve and its function. Lubricant damping tends to seal the cylinder and hence trap an uncertain amount of air within the cylinder, which makes the setting unreliable. Consequently, when lubricant damping is relied upon, one or more holes (shown

dotted) into the cylinder are needed to admit the line pressure into it.

From the foregoing, it appears that there are practical disadvantages to these alternatives to air-damping between the piston and its cylinder wall. Air-damping is most effective when the clearance is small enough to provide a pumping action giving a relatively high velocity of air flow through the clearance and hence resistance to axial motion of the piston. This high velocity exists when the clearance is still large enough to allow the piston, without its spring, to rotate freely as in an air bearing when the piston is manually given a spin. In other words, the air-damping must be due to the leakage air flow rather than to the shear which results directly from the relative velocities of the piston and cylinder.

Since the air trapped in a cylinder acts as a spring which is much stiffer than the metal spring (or has a higher "rate"), the critical frequency of the valve is considerably raised due to the air spring action. Also affecting the critical or resonant frequency is the mass of the piston valve. If the valve is lightened (1)² the critical frequency is raised, possibly into the range of forcing or driving frequencies due to the pump, and the required damping is somewhat reduced.

METHOD OF ANALYSIS

The sort of analysis required for an investigation of damping depends upon whether it is used as a creative tool or merely for its own sake. An analysis by means of differential equations soon runs into nonlinearities that put considerable difficulties in the way of a formal solution and would be followed by relatively few readers.

Instead, the line of reasoning that led to the stabilization of these suction-relief valves may be of wider interest. It must be remembered in following such reasoning that, since it is difficult for most human minds to give attention to more than one control action at a time of several which are occurring simultaneously, differential equations are superior to such unaided consideration for this purpose since they continuously take account of such simultaneous relations.

However, the modern Fourier approach (1, 2),² in predicting control transients and performance directly makes use of the universality of differential equations without the labor of a formal solution but retaining the advantage that differential equations are "always true," while their solutions may have widely different forms for different coefficients and initial conditions. Such a Fourier approach involves the use of a known sinusoidal forcing function, and an investigation of the amplitude and phase of the response. By using small oscillations, any deviations from linearity may be neglected and this method extended from the linear system of Fig. 2 to the nonlinear systems of Figs. 1 and 6.

The performance with reference to stability of a simple regulator may be considered in a preliminary way from an elementary Fourier viewpoint by assuming that hunting exists at the resonant frequency of the valve itself, and investigating the phases of the force components relative to the velocity, since the phase relations usually determine whether or not positive damping exists. Of course, hunting is generally undesirable, and this assumption is made only as the initial step in this simple test for stability.

A stable valve may be considered as the damped sprung mass

² Numbers in parentheses refer to the Bibliography at the end of the paper.

¹ Research Engineer, Eclipse-Pioneer Division, Bendix Aviation Corporation. Mem. A.S.M.E.

Contributed by the Industrial Instruments and Regulators Division and presented at the Semi-Annual Meeting, Pittsburgh, Pa., June 19-22, 1944, of THE AMERICAN SOCIETY OF MECHANICAL ENGINEERS.

NOTE: Statements and opinions advanced in papers are to be understood as individual expressions of their authors and not those of the Society.

system, the 90-deg lag of the effect x behind the cause F indicates that this system is stable.

The flow over the outer face of the valve lowers the pressure near its edge, and especially so where there is a rim seat a . This has been loosely termed a "Venturi" effect although it might better be known as a "potentiometric" effect, since the average pressure over area a is approximately $(p_n + p_c)/2$ and conveniently considered as tied to pressure p_c rather than flow q . Since $p_c/2$ (taking the atmospheric pressure p_n as zero) acts on a portion of the outer (or opposite) face of the piston it may be represented by a vector $p_v = p_c/2$ extending in the opposite direction, or toward 12 o'clock. This is seen in Fig. 4 not to affect directly the stability, since it neither puts in nor takes out energy; in other words, p_c is no "damping" component since it has no component in phase with the velocity. However, the existence of the Venturi effect requires that the driving force F must shift toward x and hence cut down the stabilizing lag.

LINE CAPACITY APPRECIABLE

However, when the line capacity is appreciable, the line pressure p_c lags x by up to nearly 90 deg with the result, shown in Fig. 5, that the Venturi effect shifts from the 12 o'clock position to, say, approximately the 2 o'clock position, and has a powerful unstabilizing tendency. At the same time p has shifted from the 9 o'clock to the 11 o'clock position so that it has less damping effect. Hence the resultant of p and p_v shifts to the 1 o'clock position and the input force F , which must be opposite, shifts to the 7 o'clock position. The net result is that hunting can exist. In electrical parlance, a positive feedback now exists due to the Venturi effect. Since the effect x leads its cause F , instability exists according to the earlier stated simple phase test. The result is that there is an increase of the hunting amplitude, and hence the energy in the system.

While the unstabilizing Venturi effect can be reduced somewhat by using a truly conical seat and a very sharp square edge on the valve, the unstabilizing effects cannot certainly be fully overcome in view of damping piston-cylinder clearance variations resulting from necessary manufacturing and operating-temperature tolerances. To be positively stable, the valve requires an additional source of damping.

Additional damping can be provided, as in Fig. 6, by adding a rim b to the valve so that its seating area is larger than the piston area. Then, as shown in Fig. 7, p_c acting on the rim as p_{cr} at 8 o'clock has a powerful stabilizing effect which balances off the Venturi effect. This modification has the advantage that it produces no unstabilizing effect under any installation condition, e.g., when there is no appreciable line capacity C . All that one

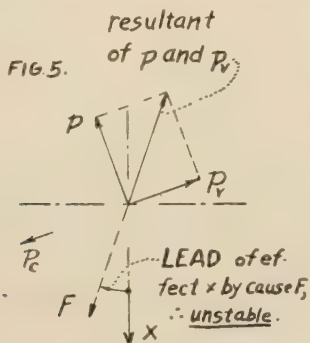


FIG. 5 NEGATIVE DAMPING DUE TO VENTURI ACTION p_v , SHOWN AS HAVING AN UNSTABILIZING EFFECT ON A PLAIN PISTON VALVE WHERE LINE CAPACITY IS APPRECIABLE, I.E., EFFECT x CAN LEAD CAUSE F

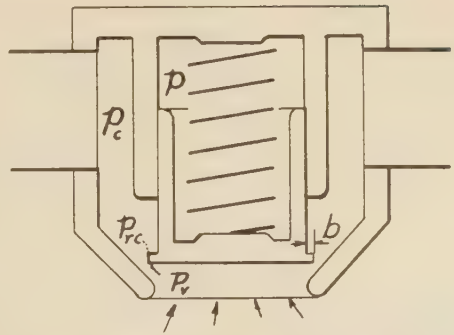
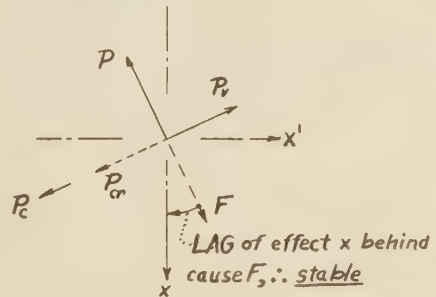


FIG. 6 IMPROVED RIM-HEAD VALVE WITH SHARP SQUARE EDGE AND WITH CONICAL SEAT



Courtesy of Dr. Harry F. Olson

FIG. 7 RIM FORCE p_{cr} , DUE TO p_c , EXERTS A FORCE THAT BALANCES VENTURI FORCE p_v REGARDLESS OF LINE CAPACITY

needs to do is to keep the size of the valve head down enough not to increase unduly either the inertia of the valve or its periphery, and hence sensitivity. The best results are obtained when the rim area is small, i.e., only large enough to provide substantial compensation and hence eliminate any appreciable feedback or reaction, i.e., to prevent feeding energy back into the valve as a result of its own oscillations.

ACOUSTIC EFFECTS

The aircraft suction pump is ordinarily of a type which creates pulsations. When these happen to be near the resonant frequency of the valve or a harmonic thereof, this tends to feed energy into the valve. In general, the tendency is to produce long-time beats during which hunting slowly builds up and dies away. However, with a reasonable valve clearance and a rim-head valve, the Venturi effect can be so well offset by the rim-damping that no objectionably large valve pulsations occur.

Another source of resonance that intensifies any hunting tendency is the suction line either to the instruments or to the pump when this line acts as a closed pipe of nearly the same frequency as the resonant frequency of the valve. Further, there is a Helmholtz resonator action in which the suction lines and the valve opening act, respectively, as the capacity and the nozzle.

Still another possible source of hunting due to resonance occurs when a filter pipe of considerable length, which is added to the valve inlet, acts as an open-pipe resonator. In any of these cases of acoustic resonance (except possibly when the filter pipe is more than 2 ft long), tests showed that hunting is not produced with a rim-head valve in which the unstabilizing Venturi effect is well balanced by the rim.

It is better thus to eliminate hunting difficulty, i.e., by modifying the valve itself to be less affected by line pulsations, than to

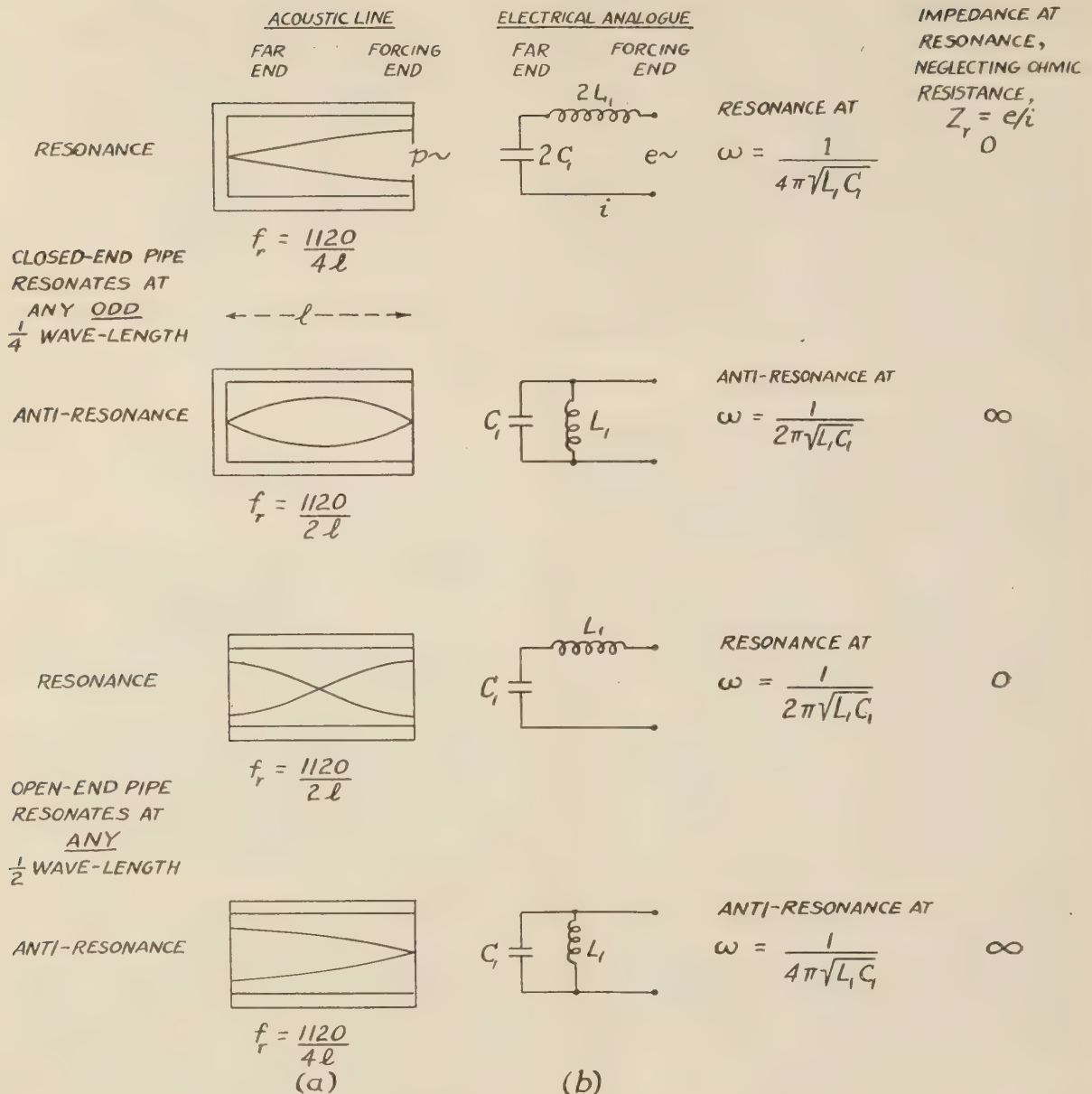


FIG. 8 (a) MODES OF ACOUSTIC OSCILLATION OF AIR IN PIPES, AND (b) ANALOGOUS ELECTRIC CIRCUITS

use a valve which is sensitive to them and become lost in the maze of additional damping gadgets that then become necessary. For example, while the effect of filter-pipe pulsations upon a plain cylindrical-piston valve can be reduced by adding a screen producing damping friction near the valve, the extra resistance of the screen tends to cause the valve characteristic to depart, upon a large change of flow, from the constant suction which is ideal.

While any valve must be a compromise, still the rim-head suction-relief valve with a conical seat in subsequent aircraft installations has exceeded any reasonable expectations, based upon earlier designs, for both accuracy and stability of operation under the range of required aircraft-installation conditions. This particular development has been described only to typify the advances obtainable in practice through the use of this general theoretical approach and technique.

Appendix

ACOUSTIC CONSIDERATIONS

In self-operated controllers for air, the air may participate regeneratively in any oscillations of either a control valve or a pump in the regulated system. Hence the motion and pressure of the air itself require consideration.

The velocity of a compressional wave in a fluid is

$$c = \sqrt{e/\rho}$$

where e is the volume elasticity and ρ is the density of the fluid. Since for gases the compression is adiabatic, the effective elasticity is k times that for constant temperature so that the relation becomes

$$c = \sqrt{k p / \rho}$$

where k is the specific-heat ratio and p is the pressure. The speed of sound in atmospheric air is about 1120 fps.

When a moving column of any fluid is slowed down by a valve, its loss of momentum is accompanied by a pressure which starts a compressional wave along the line with a reflection from its open or closed other end or from any discontinuity in the pipe wall.

With an open pipe end, the phase of a pressure wave is reversed, since the momentum tends to carry a slug of fluid from the pipe out into the ambient fluid, with the result that the wave length is about 4 times the length of the pipe plus an "end correction" of about 0.8 times the radius of the pipe. The enlargement at the nearest manifold may provide an effective open end.

These phenomena occur when the pulsation-forcing frequency of a valve or pump is near that of the line. In such a case and referring to Fig. 8, there can be resonance at frequencies around either $f_r = 1120/2l$ or $1120/l$ for a line having its far end open. The resonant frequency is around $1120/4l$ for the fundamental for a closed-end pipe, in which case resonance can occur at any odd quarter wave length. With complex systems, the response amplitude tends to vary less sharply with the frequency so that the resonance peaks are lower, and there is a higher response between the peaks.

While a better electrical analogue may be a long-distance transmission line, the situation, as regards the possibility of resonance, may be taken as roughly analogous to a tuned L - C series (inductance and capacitance) circuit whose impedance is

$$Z = e/i = \omega L - \frac{1}{\omega C}$$

where $\omega = 2\pi f$ radians per sec and f cycles per sec express the forcing-voltage frequency. At resonance, $Z = 0$ and the voltage across C or L may rise to many times the value of the forcing voltage. At resonance with this circuit

$$f_r = \frac{1}{2\pi\sqrt{LC}} \text{ radians per sec}$$

Electric networks may be set up analogous to complicated acoustical-mechanical-electrical systems and, for such networks, steady-state solutions reached by well-established electric-network techniques, i.e., using Kirchhoff's laws and the concepts of impedance, including "coupling" or "transfer" impedances; and using operational methods if transients are desired.

Resonance may also occur in a storage volume with a small opening as in Fig. 9(a). Where, as in Fig. 9(a), a storage volume V cm³ has a small opening of area S cm², it acts as a Helmholtz resonator of frequency

$$f_r = \frac{1}{2\pi\sqrt{MC_a}}$$

(Olson⁶) where

- $M = m/S^2$, inertance (Olson⁶), g per cm⁴
- $m = \rho v$, mass of accelerated fluid in opening, g
- v = volume of accelerated fluid in opening, cm³
- ρ = density of fluid accelerated, g per cm³
- $C_a = V/\rho c^2$ acoustical capacitance (Olson⁷), cm⁴ sec²/g
- c = velocity of sound, cm

The M and C_a , respectively, correspond with inductance L and capacitance C in a resonant electric circuit of negligible resistance.

For a circular thin-plate orifice, the length of the accelerated mass is roughly equal to the orifice diameter or, more closely, the

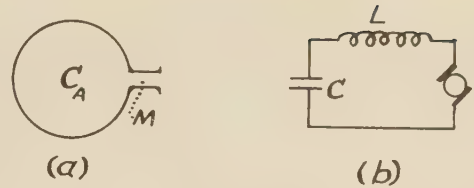


Fig. 9 (a) HELMHOLTZ' ACOUSTIC RESONATOR, AND (b) ITS ELECTRICAL ANALOGUE

volume is that of a sphere which will just pass through the opening. However, the volume may exceed several times this value where "smoke-ring" vortices are formed, as is possible where turbulence does not interfere and there is a space into which the vortices may be launched.

Even though one cannot always obtain precise solutions of acoustic problems analytically, still even a rough analysis often provides a reasonable starting point in design and indicates the essential variable to be experimentally investigated in seeking optimum performance.

Other references on acoustic problems are given as (6) and (7) of the Bibliography.

BIBLIOGRAPHY

- 1 "Analysis of Systems With Known Transmission-Frequency Characteristics by Fourier Integrals," by W. L. Sullivan, A.I.E.E. Symposium, 1941; *Electrical Engineering*, vol. 61, 1942, pp. 248-256.
- 2 "Analysis, Synthesis, and Evaluation of the Transient Response of Television Apparatus," by A. V. Bedford and G. L. Fredendall, *Proceedings I.R.E.*, vol. 30, 1942, pp. 440-457.
- 3 "Mechanical Vibrations," by J. P. Den Hartog, McGraw-Hill Book Company, Inc., New York, N. Y., second edition, 1940, pp. 61 ff.
- 4 "Automatic Control Engineering," by Ed S. Smith, McGraw-Hill Book Company, Inc., New York, N. Y., 1944, pp. 36 ff, 139-140, and 225-234.
- 5 "Dynamical Analysis," by H. F. Olson, D. Van Nostrand Company, Inc., New York, N. Y., 1943, recommended for electrical engineers who wish to apply their network-analysis techniques in acoustical and mechanical fields.
- 6 "Elements of Acoustical Engineering," by H. F. Olson, D. Van Nostrand Company, Inc., New York, N. Y., 1940.
- 7 "Acoustics, a Text on Theory and Application," by G. W. Stewart and R. B. Lindsay, D. Van Nostrand Company, Inc., New York, N. Y., 1930.

Discussion

H. L. MASON.⁸ The analysis presented by the author is a qualitative modification of known quantitative relations among the forces acting on a mass under forced vibration. It should be understood that the rotating vector representation of Fig. 3 expresses exactly the solution of the differential equation (linear by assumption) corresponding to Fig. 2. For the valve described, pneumatic forces give driving, damping, and spring effects, and the author approximates the phase angles of their vectors and draws conclusions concerning stability. The criterion of stability as a displacement lagging its cause seems to the writer to be of doubtful utility. Whether or not energy is removed from the system described depends, more fundamentally, on whether or not the resultant force vector has a component opposing the velocity, and this may be determined directly by inspection of the vector diagram. Moreover, in the presence of a pulsating driving pressure, small positive damping does not always eliminate oscillation of a controller, although it will hold it to a smaller amplitude. "Stable" as applied to such a system means only "having smaller vibratory motion."

⁸ Director of Research, Taylor Instrument Companies, Rochester, N. Y. Mem. A.S.M.E.

⁵ Ref. (5), p. 33.

⁶ Ibid. p. 16.

⁷ Ibid. p. 19.

AUTHOR'S CLOSURE

Dr. Mason has raised the two fundamental questions of the basic tests for a limited amplitude of oscillation and for stability of a regulated system. The first question has been answered for conservative systems by the statement of LeCorbeiller (8):⁹ "For any system to oscillate stably at a definite amplitude, it is necessary to involve some nonlinearity." For others, Dr. Mason's penultimate sentence is of course correct.

On the second point, Dr. Mason's approach is helpful for simple cases. However, for more complex cases, one may advantageously use the more general method of Nyquist which is well known among electrical engineers. An application of the Nyquist method to control recently appeared in a publication by Prinz (9). The test used in the present paper is a "free-hand" application of Nyquist's teaching to cases in which one must eliminate hunting of a regulator having a well-defined resonance peak.

In Nyquist's method, one *breaks* the system between, e.g., the control valve and its actuating stem and oscillates the valve at a number of different frequencies; a "cause." If, at some frequency, the "effect" be an oscillation of the stem of the same amplitude as that of the valve and lagging 360 deg, so that the effect in each cycle precisely equals the cause in the next, the *connected* stem and valve would theoretically continue to oscillate steadily at this frequency and amplitude. In other words, the over-all sensitivity (i.e., effect/cause in any cycle) of a steadily hunting regulated system is unity.

At 360 deg lag, sensitivities less and greater than unity result in stable and unstable operation, respectively, with the *connected* stem and valve. Since an increase of lag tends to produce instability, lags of more and less than 360 deg at a sensitivity of unity are accompanied by instability and stability, respectively, with any simple system.

Since with any actual physical system, the amplitude of the effect tends to approach zero as the forcing frequency increases indefinitely, the rule for instability may be made general by requiring either that the lag be more than 360 deg for the highest frequency at which the sensitivity is unity or that the sensitivity exceed unity at the highest frequency at which 360 deg lag exists. Hence, for instability, the 360-deg lag axis must be last traversed in the direction of increasing lag at a sensitivity of more than unity as the frequency increases. Since it is always present, the 180 deg for the basic control relation may be dropped as a matter of convenience in plotting the Nyquist sensitivity-lag loci for varying frequency, as in Fig. 10 of this closure, on which the critical point $(-1, j0)$ appears at a radius of unity and a lag of 180 deg.

Treating sensitivities and lags vectorially, the over-all sensitivity is equal to the product of the individual sensitivities of the several elements of the regulated system, and the total lag is the sum of the angular lags for the several elements.

It may help those unfamiliar with the use of the Nyquist method in process control to take the suction-relief valve of the present paper as an illustration, without however adjusting the coefficients to the numerical values necessary for consistency with the paper itself.

Starting with an oscillation of the valve at ω rad per sec that produces ≈ 1 psi change in the line pressure p_e , the pressure p changes due to flow through the piston-cylinder clearance so that the sensitivity-lag locus is the semicircle a (in Fig. 10) (10) on

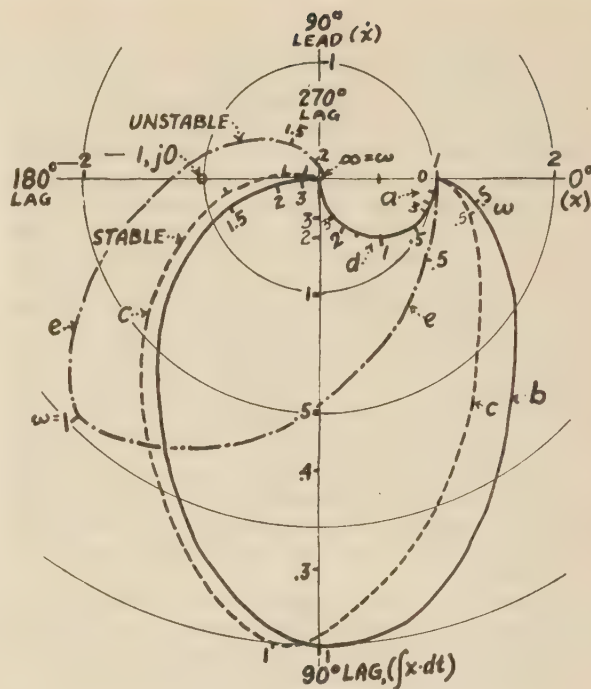


FIG. 10

which the inner numbers indicate ω 's for $\tau = 0.1/\omega_n$, where τ sec is the time-constant, and ω_n , rad per sec, is the natural frequency of the piston-valve itself. If of constant amplitude, ≈ 1 psi, pressure p acts on the piston to produce an oscillation of amplitude x with the sensitivity-lag locus b taking a constant of unity, e.g., at zero frequency (11). Then curve c shows the response of the regulated system with the over-all sensitivity $S = S_p \times S_x$ and the total lag $\phi = \phi_p + \phi_x$. Since this curve does not enclose the critical point $-1, j0$, this regulated system would be stable.

But if the line capacity is such that the response of the line pressure p to the oscillation of the valve is shown by the outer graduations of semicircle d (for $\tau = 1/\omega_n$), then that of the regulated system is shown by curve e . Since curve e encloses the critical point, this regulated system would be unstable.

The Nyquist approach takes advantage of the fact that steady sinusoidal oscillations produce others whose amplitude and lag may be used to determine stability. Empirical and/or operational techniques (9, 12) may be used as convenient. And the concept itself is valuable, even though loosely used as in the present paper.

BIBLIOGRAPHY (continued)

- 8 "Non-Linear Theory of Maintenance of Oscillations," by P. LeCorbeiller, Institute of Electrical Engineers, Wireless Section, vol. 11, 1936, p. 292.
- 9 "Contributions to the Theory of Automatic Controllers and Followers," by D. G. Prinz, *Journal of Scientific Instruments*, vol. 21, April, 1944, pp. 53-64; also June, 1944, pp. 110-111.
- 10 *Ibid.*, April, p. 57.
- 11 Reference (4), pp. 141 and 146, or Reference (3) pp. 62 and 68.
- 12 "Considerations in Servomechanism Design," by S. W. Herwald, A.I.E.E. Technical Paper 44-188, preprint July, 1944, (operational methods for handling transients).

⁹ Numbers in parentheses in this closure refer to Bibliography (continued) at end of closure.

Economic Thickness of Thermal Insulation for Intermittent Operation

By C. B. BRADLEY,¹ C. E. ERNST,² AND V. PASCHKIS³

Economic thickness of an insulation is defined as that thickness yielding the smallest sum of cost of heat loss and fixed cost of insulation. The difficulties in determining the economic thickness for intermittent operation are reviewed. By means of the electrical-analogy method, curves have been developed which permit the ready determination of the heat losses in intermittent operation for any temperature, any single-material wall, any intermittency, any length of period, and any film conductance. These curves permit the determination of the economic thickness for intermittent operation. The application of the curves is illustrated by an example. The influence of intermittency on the economic thickness is discussed for one specific case. The limitations of the method and prospect of obtaining results avoiding the limitations are considered.

THE PROBLEM

THE cost of operation of any piece of industrial equipment, whether it be in a chemical or similar process, or involved in an operation in the manufacture of a metal article, is of prime importance. When the operation of such equipment involves the application of heat or refrigeration, the application of thermal insulation to reduce heat transmission through the walls of the equipment becomes a major consideration.

The application of insulation obviously adds to the cost of the equipment. However, the reduced heat transmission, resulting from the application of insulation, gives an economic justification for the added cost. In other words, it can be demonstrated that the saving in heat energy will more than pay for a given amount of insulation.

As the thickness of insulation is increased, the cost of heat-energy loss per unit of time is obviously decreased, but the cost of the insulation (cost per unit of time determined by amortizing initial cost over a given number of time units) is increased. Therefore, the economic thickness is that thickness which gives the least sum of the two costs. The relationship between these two costs, and the way they affect the determination of economic thickness is visualized in Fig. 1.

It is to be noted that the first increment of thickness of a good thermal insulation effects a greater saving in heat energy than the second increment, the second increment a greater saving than the third and so on. Also, for similar cases of steady and unsteady state, the cost of heat loss and annual cost of insulation are, in general, both less for unsteady state.

Steady state is the process of heat flow where the temperature at any point in a wall structure is independent of time, and unsteady state is the process of heat flow where temperature varies with time.

When the heat flow through the walls of heated or refrigerated equipment takes place under steady-state conditions, the determination of the economic thickness of insulation is a relatively simple operation, as the heat flow is a function of only the conductivities of the materials in the wall and the equilibrium temperature gradient. The heat storage of the wall is only a factor in the initial heating up of the wall and has no bearing on the heat flow once a steady-state condition is attained.

For flat surfaces (single material), and steady state, this thickness may be determined (1)⁴ from the equation

$$X = \sqrt{\frac{ak}{b}} - Rk$$

in which X is the most economical thickness, k is the thermal conductivity of the insulation, b is the cost of insulation per inch thickness per year, R is the sum of the resistances of all of the other elements in the construction and

$$a = \frac{Y(t_1 - t_2)M}{1,000,000}$$

in which Y is hours of operation per year, t_1 is the temperature of the warmer surface of the wall, t_2 is the air temperature on the cooler side of the wall, and M is the value of the thermal energy in dollars per 1,000,000 Btu. This formula applies only when the time of continuous operation is sufficiently long to make the amount of stored heat negligible with respect to the total heat transmission.

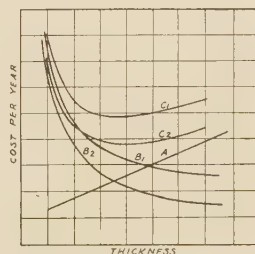


FIG. 1

A, Cost of insulation
B, Cost of heat-energy loss
C, Sum of A and B
Subscript 1, steady state
Subscript 2, unsteady state

Where the heat flow takes place under unsteady-state conditions, i.e., where the temperature varies with time, the determination of the economic thickness is complicated by the fact that the heat flow also varies with time, and it is therefore necessary to determine the average flow. The average heat flow is a function of the average temperature gradient through the

¹ Research Physicist, Johns-Manville Research Laboratory, Manville, N. J.

² Staff Engineer, Industrial Insulation Department, Johns-Manville, New York, N. Y.

³ Research Associate, Department of Mechanical Engineering, in charge of Heat Transfer Laboratory, Columbia University, New York, N. Y.

Contributed by the Heat Transfer Division and presented at the Semi-Annual Meeting, Pittsburgh, Pa., June 19-22, 1944, of THE AMERICAN SOCIETY OF MECHANICAL ENGINEERS.

NOTE: Statements and opinions advanced in papers are to be understood as individual expressions of their authors and not those of the Society.

⁴ Numbers in parentheses refer to the Bibliography at the end of the paper.

wall which is affected by the heat storage capacity (density \times specific heat), as well as by the conductivity.

For the purpose of this paper, it is assumed that the inside temperature follows a pattern or cycle of variation, where for a portion of the cycle the temperature difference across the wall is increasing and for the remainder of the cycle the temperature difference is decreasing. If, for each cycle, the temperature variation at any point in the wall duplicates that of the previous cycle, a state of cyclic equilibrium can be said to exist. The average heat flow of a typical cycle (after cyclic equilibrium is attained) is used as a basis for economic calculations.

In the selection of the most economic materials for composite walls in unsteady operation, it is necessary to take into account the maximum temperatures reached at the interface points within the wall. It is obvious that for many cases the maximum temperature for a given point in a wall will be appreciably less than the steady-state temperature, which means that for a given set of conditions a less expensive combination of insulating materials could be used for the unsteady state with a given maximum temperature on the hot side than for the steady state with the same maximum temperature.

METHOD OF APPROACH

So far there have been no formulas available for the determination of unsteady-state heat flow that compare with the calculations for steady-state flow in simplicity and economy of time. A rigorous mathematical analysis of the heat flow in cyclic operation would be ideal. This would, however, involve a solution of Fourier's differential equation of heat flow applied to the particular problem, and this is possible for only a few simple constructions and conditions. This has been done for sinusoidal temperature variation, considering a 24-hr period only (2).

The graphical method of Schmidt (3) presents a means of solving many unsteady-state problems, but it is very tedious and time-consuming and involves certain assumptions which limit its accuracy.

Probably the most useful mathematical method for solving unsteady-state heat-flow problems is the application of Christopherson and Southwell's relaxation method described by Emons (4). This method is applicable to a large variety of such problems and its accuracy is good. The time of calculation, especially for cyclic-heat-flow problems, is however long in comparison to the use of the curves described in this paper.

Direct determination of heat flow in the unsteady state by experimental means requires a degree of instrumentation and of testing technique, which is, in general, so time-consuming that it is usually quite out of the question. This has been pointed out in a previous paper by two of the authors (5). Perry and Berggren have published a very interesting extension of Schmidt's method for application on hollow cylinders (pipe insulation) exposed to a sudden change of temperature from the inside (6).

There has been a definite need for a short and accurate method of determining heat flow for intermittent heating or cooling operations but, since the development of such a method involved the accumulation of data from a vast number of wall constructions under actual operating conditions, it was a considerable, if not practically impossible, undertaking until the advent of the "Heat and Mass Flow Analyzer" at Columbia University.

A test program, designed to develop a short method, was instituted and carried out on the analyzer. The result of this work is a method which requires only the reading of values from curves and a small amount of arithmetic to determine the heat flow for any cyclic operation.

In describing the present method of determining heat flow, two characteristics have to be discussed:

1 The method of investigation (utilizing the heat and mass flow analyzer).

2 The method of presentation by means of dimensionless units which allow the simple procedure mentioned.

The entire program has been carried out by the electrical-analogy method. This method, described previously (7), is based on the identity of the equations for loading of a noninductive resistance-capacity circuit and those governing the heating or cooling of a wall initially at zero temperature difference. This identity leads to the following analogy:

Heat terms	Equivalent electrical terms
Temperature difference	Voltage
Rate of heat flow	Current
Thermal resistivity	Electrical resistivity
Volumetric specific heat	Electrical capacity

In order to utilize this method, a resistance-capacitance circuit must be built, the electrical properties of which are, by certain equations, related to the thermal properties of a wall. This circuit is then subjected to intermittent applications of voltage according to the intermittency and length of period in the thermal problem.

In carrying out the electrical experiments, it is not necessary to use the same time as in actual heat flow. By appropriate selection of the electrical properties a "time ratio" can be applied. The experiments were carried out with various time ratios, so selected to make the experiments as short as possible, and still give good reading on the instruments. Thick walls, with slow changes of temperature and heat flow from the cold surface, were investigated with low time ratio, i.e., by relatively short electrical experiments. Thin walls, with fairly rapid changes of temperature on the cold surface were investigated with high time ratio, i.e., by relatively long experiments.

The setting up of a large number of such circuits as required for a large number of walls is facilitated by using the heat and mass flow analyzer. This analyzer consists of a great number of resistors and condensers so arranged as to facilitate the setting up of a large variety of circuits. Recording voltmeters are provided which allow the recording of voltage-time curves, which are analogous to temperature-time curves; the current, read on milliammeters, can be translated into the rate of heat flow.

The end of the circuit representing the hot surface of the wall is connected for a period equivalent to the time "on" to a power supply held at a constant voltage equivalent to the inside temperature. After the time "on" has elapsed, the power supply is disconnected and the circuit starts to discharge. Following the basic assumption that no heat can be lost from the hot surface except that flowing through the wall, the circuit remains open at its "hot end." At the "cold-surface end," current continues to flow out of the circuit, equivalent to the heat flowing from the cold surface during the time "off." At the end of the time "off," the power supply is again connected. This procedure continues until "cyclic equilibrium" is reached.

In order to be able to present the results in a general way, certain simplifications had to be made which limit the accuracy. The possibility of eliminating some of these simplifications in future experiments is discussed later. Here a brief statement of the simplifications will be given in order that the method of presentation may be easily understood.

The main simplifications are as follows:

1 The insulated space is tight. The heat exchange takes place only through the wall with no by-pass such as stack loss.

2 No corner effect. Only walls of infinite size have been investigated.

3 The walls have been considered to be homogeneous. The influence of joints has not been considered separately. The prop-

bound to lie between these two limits. A set of curves as shown in Fig. 2 may therefore be expected.

The happenings become more clear, if cross curves to the curves of Fig. 2 are drawn, as in Fig. 3. The period P is plotted on the abscissa and FHF again on the ordinate. One curve is shown which holds for one intermittency. The curve starts at $FHF = 1$ for $P = 0$, then decreases with increasing P and approaches asymptotically a value of FHF which is equal to the f for which the curve holds.

A chart, such as the one exemplified in Fig. 2 or in Fig. 3, holds only for a given value of m . Inasmuch as m may be different for different conditions, there was the choice of a large number of graphs, following Figs. 2 and 3, for different values of m with interpolation between graphs for values of FHF , or a set of curves for $m = 0$ with correction factors for other values of m . It is believed that this second method results in easier handling of the graphs.

In order to use such curves, it is always necessary to determine first the steady-state heat flow; the curves show merely the fraction of this steady-state flow occurring under given conditions.

The presentation of results for the two-material wall was found to be more complex than the presentation for the single-material wall.

An analysis (as yet unpublished) made by Dr. M. Avrami of Columbia University showed that all two-material walls having the same characteristic figures behave in the same way. The characteristic figures are as follows

$$x_1 = \frac{L_1/k_1}{L_1/k_1 + L_2/k_2}$$

$$\tau = \frac{k_1 c_1 \rho_1 \left(\frac{L_1}{k_1} + \frac{L_2}{k_2} \right)^2}{P}$$

$$g = \frac{k_2 c_2 \rho_2}{k_1 c_1 \rho_1}$$

In these formulas the following notations are used:

L = thickness of one layer
 k = thermal conductivity
 τ = time ratio
 c = specific heat
 ρ = volumetric density
 P = length of period (time "on" plus time "off")
 g = characteristic wall figure
 x = relative resistance

In the equations, the subscripts 1 are used for all items referring to inside material, and the subscripts 2 are for all items referring to outside material.

Moreover, he suggested that the heat flows in a two-material wall, in so far as intermittent heating is concerned, can be approximated by those of a so-called "equivalent single-material wall," which is found by using the thermal properties of the inside material with an "equivalent thickness" L_e defined by

$$L_e = L_1 + L_2 \frac{k_1}{k_2}$$

In order to eliminate the error due to this approximation, a correction factor must be used. To obtain the FHF of a two-material wall, the FHF for the "equivalent single-material wall" must be multiplied by this correction factor.

RESULTS AND EXAMPLE

Fig. 4 shows a chart with correct figures drawn following the

scheme discussed in general in Fig. 2. Intermittencies are plotted on the abscissa, fractional heat flows on the ordinates, the individual curves hold for different values of P' . Fig. 4 is drawn for $m = 0$ or, in other words, for zero surface resistance. This means that the chart holds for the case where the outside surface of the wall is held at constant temperature.

It has been stated previously that the results hold accurately only for the case in which the inside surface reaches its final temperature immediately.

It has been mentioned that the main chart was made for a value of $m = 0$ and that correction charts have been prepared to take account of finite film conductances. It is impossible to show here all these correction factors. By way of example, Figs. 5 and 6 are shown giving the correction factor C_F for various values of

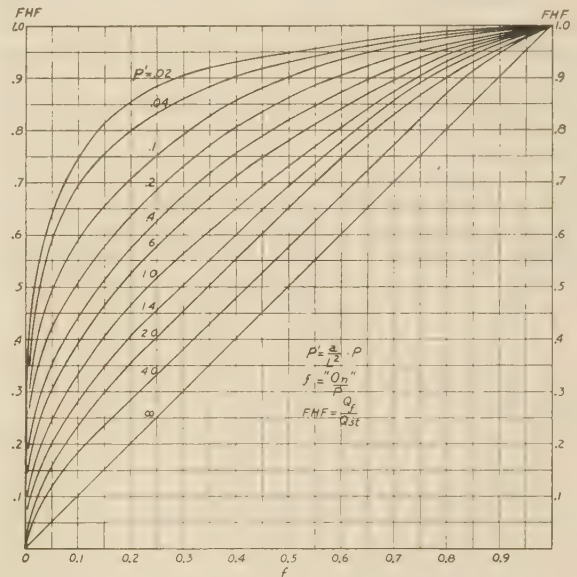


FIG. 4 FHF VERSUS f FOR VARIOUS VALUES OF P' , $m = 0$

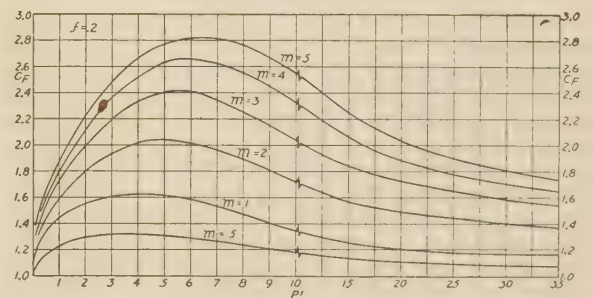


FIG. 5 CORRECTION FACTOR C_F FOR $f = 0.2$

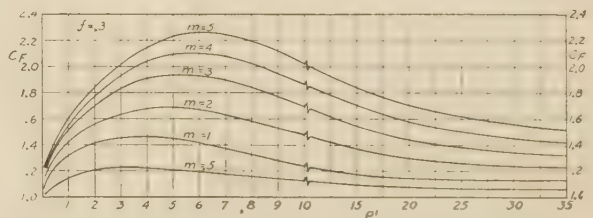


FIG. 6 CORRECTION FACTOR C_F FOR $f = 0.3$

P' and several values of m for intermittencies of $f = 0.2$ and $f = 0.3$.

A great many experiments were carried out in order to gather correction factors to be applied to the heat flow of the "equivalent single-material wall" to find the heat flow for two-material walls. Out of the large number of correction factors C_2 , a few are plotted by way of example in Fig. 7. Correction factors are closest to 1 for values of g near unity. For small g , the correction factors are very low, for high values of g , they become quite large. Inasmuch as the correction takes place by multiplication by the correction factor, low values of the latter as well as high ones indicate large correction. Necessary correction decreases with decreasing values of P' ; with increasing values of x_1 ; with increasing values of f ; with decreasing values of m .

It appeared desirable to know the temperatures within the wall, particularly for two-material walls. Dimensionless representation was again selected. Rather than attempting to plot temperatures directly, the temperatures for any point in the wall were plotted as fractions of the steady-state temperature for the same point (fractional temperature). However, as only the maximum temperatures are of interest, they only are plotted. Fig. 8 shows, by way of example, such a curve giving the fractional temperatures (maximum) versus P' for $m = 0.5$ and $f = 0.25$ (single-material wall).

An example of the difference in economic thickness determined on the basis of steady-state and unsteady-state heat flow is demonstrated in Table 1. The economic thickness for both steady and unsteady state is worked out in the manner shown because a formula, similar to that used for steady state, would be so complex as to be impractical for unsteady state, and it was desirable to have the two examples directly comparable. The example is for a wall of a high-temperature furnace, constructed of JM-20 insulating firebrick. Operating conditions are 8 hr "on" ($2\frac{1}{2}$ hr heating up; $5\frac{1}{2}$ hr holding at maximum temperature) and 16 hr "off;" maximum temperature 1900 F; outside air 100 F; and operating time 7200 hr per year. Costs are \$100 per thousand brick for material and labor, 15 per cent annual charge and 30 cents per million Btu for heat.

It is to be noted in this instance that the economic thickness for unsteady state falls between the $7\frac{1}{2}$ -in. and 9-in. thicknesses. However, owing to the flatness of the total-cost curve, a 5-in. thickness can be chosen as the economic thickness. This compares with the $13\frac{1}{2}$ -in. thickness for steady state. Also, as evidence that estimations of the intermittent rate of flow frequently used are unsafe, it should be pointed out that the fractional heat flow varies from 0.48 for the 5-in. JM-20 to 0.63 for the 9-in. JM-20. This is a change of better than 30 per cent.

To demonstrate the simplicity of determining the unsteady-

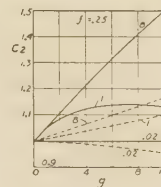


FIG. 7 CORRECTION FACTORS FOR TWO-MATERIAL WALLS FOR VALUES OF P' INDICATED ON THE CURVES (Solid line $X_1 = 0.2$; dashed line $X_1 = 0.5$.)

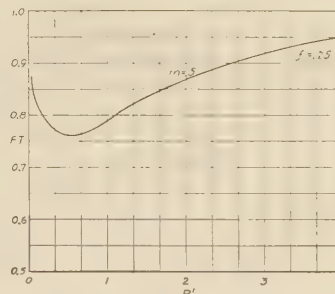


FIG. 8 MAXIMUM F_t VERSUS P' FOR OUTSIDE SURFACE OF A SINGLE-MATERIAL WALL ($m = 0.5$ and $f = 0.25$.)

state heat flow by the present method, the calculation for the 9-in. wall thickness is given as follows:

In order to average the properties over space and time, the temperature at which k and c are determined is

$$1900 \cdot \frac{1 + f}{4}$$

Assuming a linear temperature rise during the $2\frac{1}{2}$ -hr heating up period, the intermittency is taken as

$$f = \frac{\frac{2.5}{2} + 5.5}{24} = \frac{6.75}{24} = 0.281$$

Hence the properties are selected for the temperature

$$1900 \cdot 1.281/4 = 608 \text{ F}$$

At this temperature for JM-20 brick

$$k = 0.0875 \text{ Btu ft/hr sq ft F}$$

TABLE 1 DIFFERENCE IN ECONOMIC THICKNESS OF INSULATION FOR STEADY-STATE AND UNSTEADY-STATE HEAT FLOW

Thickness, in.	Btu per hr per sq ft	Million Btu per sq ft per year	Cost per year heat loss, dollars	No. brick per sq ft	Cost per year brick, dollars	Total cost per year, dollars
STEADY STATE						
5	401.8	2.893	0.868	7.12	0.107	0.975
7	291.3	2.098	0.629	9.96	0.149	0.778
$7\frac{1}{2}$	272.7	1.964	0.589	10.68	0.160	0.749
9	229.7	1.654	0.496	12.80	0.192	0.688
$9\frac{1}{2}$	217.9	1.569	0.471	13.52	0.203	0.674
10	207.7	1.496	0.449	14.24	0.214	0.663
$11\frac{1}{2}$	180.2	1.298	0.389	16.36	0.245	0.634
12	173.1	1.246	0.374	17.08	0.256	0.630
$12\frac{1}{2}$	166.4	1.199	0.360	17.80	0.267	0.627
$13\frac{1}{2}$	154.5	1.113	0.334	19.20	0.288	0.622
14	149.3	1.075	0.323	19.92	0.299	0.622
$14\frac{1}{2}$	144.4	1.040	0.312	20.64	0.310	0.622
16	131.1	0.944	0.283	22.76	0.341	0.624
UNSTEADY STATE						
5	166.1	1.196	0.359	7.12	0.107	0.466
7	146.8	1.057	0.317	9.96	0.146	0.466
$7\frac{1}{2}$	141.2	1.017	0.305	10.68	0.160	0.465
9	126.2	0.909	0.273	12.80	0.192	0.465
$9\frac{1}{2}$	122.2	0.880	0.264	13.52	0.203	0.467
10	118.1	0.850	0.255	14.24	0.214	0.469

$$c = 0.23 \text{ Btu/lb F}$$

$$\rho = 0.31 \text{ lb/cu ft}$$

A surface conductance of 2.13 Btu/sq ft/hr (0.47 surface resistance) is used

$$P' = \frac{24 \times 0.0875}{31 \times 0.23 \times 0.562} = 0.524$$

$$Q_{st} = \frac{1800}{\frac{0.75}{0.0875} + 0.47} = \frac{1800}{8.57 + 0.47} = 199.2 \text{ Btu/sq ft hr}$$

From Fig. 4 for $f = 0.281$ and $P' = 0.4$ $FHF = 0.657$
 $P' = 0.6$ $FHF = 0.609$

By direct interpolation for $f = 0.281$ and $P' = 0.524$
 $FHF = 0.627$

Using the film resistance of 0.47

$$m_0 = \frac{0.47 \times 0.0875}{0.75} = 0.055$$

The correction factor C_{FHF} is determined from Figs. 5 and 6

$$\text{For } f = 0.3 \quad C_{FHF} = 1.01$$

$$f = 0.2 \quad C_{FHF} = 1.02$$

By direct interpolation for $f = 0.281$ $C_{FHF} = 1.012$.

Therefore, the corrected $FHF = 0.627 \times 1.012 = 0.634$.

The average heat flow is then $199.2 \times 0.634 = 126.2 \text{ Btu/sq ft hr}$.

By way of demonstrating the accuracy of this method of determining the heat flow, the heat flow for the 24-hr period for the 9-in. JM-20 wall is $24 \times 126.2 \text{ Btu}$ or 3030 Btu per sq ft which compares with 3350 Btu per sq ft for a 9-in. JM-20 wall in actual test under similar conditions as reported in a previous paper by two of the authors (5).

It would be desirable to have general curves showing the economic thickness as a function of intermittency. However, the large number of variables involved makes the development of such curves impractical. Therefore, by way of example, the effect of intermittency on unsteady-state economic thickness is demonstrated by the curve in Fig. 9. This curve is based on JM-20

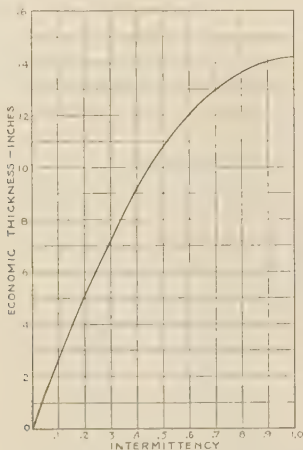


Fig. 9 ECONOMIC THICKNESS VERSUS INTERMITTENCY

brick using the temperature conditions, costs, etc., used in the examples just given. The end points of the curve must obviously be zero thickness for an intermittency of zero and the steady-state economic thickness for an intermittency of 1. The general

shape of the curve between these end points is a function of the various factors determining the economic thickness and would appear to hold for other similar curves covering other sets of conditions.

ACCURACY AND SIMPLIFICATIONS

As mentioned previously, the tests were based upon a number of assumptions which made a simple and fairly comprehensive presentation possible. A discussion of the limitations of the method and the prospects of eliminating some of them is therefore in order.

The accuracy of the analogy method depends upon a number of different items discussed in some detail in a recent paper (10). From these considerations, it can be estimated that the accuracy of the experiments was within 2 to 3 per cent as far as heat loss is concerned. The accuracy for the temperatures is less; this was accepted in order to keep the presentation simple. In view of the fact that the thermal properties of insulating materials are not known with any greater accuracy and, moreover, change with temperature, the achieved degree of accuracy was considered to be entirely sufficient.

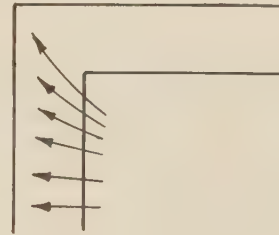


FIG. 10 EFFECT OF CORNERS ON HEAT FLOW

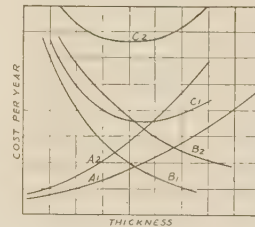


FIG. 11

A, Cost of insulation
 B, Cost of heat-energy loss
 C, Sum of A and B
 Subscript 1, without corners
 Subscript 2, with corners

The assumption of no corner effects leads to results which are sufficiently accurate for large enclosures. For small enclosures, however, considerable errors may occur; the smaller the enclosure the greater the error. This becomes evident from Fig. 10, which shows conditions for the two-dimensional corner; conditions in the three-dimensional corner are correspondingly aggravated. The total heat flow through the walls of a small enclosure, taking into account the corner effect, is higher than that of an enclosure insulated equally but discounting the corner effects. This holds for any intermittency and length of period. It is obvious that the volume of insulation per unit inside area is smaller than with corners. Therefore, the cost of the insulation increases more steeply if corner effects are considered than without them. The corner effect (shape factor) will decrease the economic thickness and increase the heat loss at that thickness (Fig. 11). Fortunately, the present investigations allow an approximation, which, except for extremely small furnaces, yields acceptable results.

Instead of introducing the thermal diffusivity of the materials actually employed, fictitious values are used which take into account the decrease of thermal resistance and the increase of thermal capacity due to the corner effects.

The "thermal conductivity" is increased by multiplying it by the ratio of the geometric-mean area to the inside area of the wall. This is equal to a ratio of the rate of heat flow with to that without corners.

Similarly, the "specific heat" is increased. Let V_s be the wall volume without corners, V_c the volume with corners, then instead of using the value c of specific heat, a value $\frac{V_s + V_c}{2V_s} \cdot c$ is used.

The density is not changed but is introduced at its actual value.

For single-material walls of extreme thickness and small inside dimensions, a further improvement can be made by dividing the thickness into two layers and treating the wall as a two-material wall, correcting the conductivity and specific heat for each of the two layers separately. If the enclosure is insulated in a different way on its six sides, each side has to be treated accordingly.

The assumption of no joints cannot be avoided in any general solution. A study by one of the authors of the influence of joints in one particular low-temperature steady-state application has been published (11). The electrical-analogy method lends itself easily to such studies.

The thermal properties of most insulating and refractory materials change to a considerable degree over the entire temperature range. Unfortunately, the changes are different for different materials. Consequently, it is not possible to obtain general curves. Moreover, the generality would be lost even for one material if it were used at different temperature ranges, say once for a furnace at 1800 F, and then for one at 1400 F. If for any one specific case of sufficient importance (e.g., the annealing furnaces for the lens of the Mt. Palomar observatory) it appears desirable, investigations taking account of the change of properties can be carried out on the analyzer. But for general purposes, it is necessary to use the curves based upon constant properties. Several tests based upon conductivity-temperature and specific heat-temperature curves were carried out and compared with an experiment in which the properties were held constant during the experiment. They showed that the differences were reasonably small, the ratio of the results not exceeding, even in the most unfavorable case, 1.075.

Preliminary tests showed that the assumption of infinite inside film conductance is, for all wall designs which may be reasonably expected, permissible. This is not surprising. An inside film conductance of 10 Btu/sq ft hr F would not add appreciably to the resistance of a well-insulated structure. In the relatively few cases where conditions of essentially still air and low temperature obtain, the error due to neglecting film conductance would be somewhat greater.

The assumption of an empty enclosure is not particularly desirable as many insulated spaces are heated or cooled together with a charge. However, there was again the choice to be made between generally applicable curves and curves which would be more true to practice but applying only to individual cases. The difficulty encountered in an attempt to get general solutions including load is that the total energy input is split. If the energy input is thought of as taking place at the inner surface of the structure, then part flows into the wall and part into the load. If the ratio between both were constant (as might be the case in a furnace with continuous flow of load), then general curves could be set up. But the curves are most important for cases where the flow of load is not constant (batch operations). In such cases,

the distribution between energy absorbed by the wall and energy absorbed by the load changes continuously as the saturation of the load proceeds. To make things worse, the distribution depends upon the temperature range at which the enclosure is operated as well as upon the shape, size, and material of the load and upon the nature and position of the temperature control. Again, individual cases can easily be investigated on the analyzer but no general curves should be expected. However, it would be possible to investigate the influence of the load on the selection of the insulation in some typical cases. It is not impossible that a more or less empirical rule might be found from such a set of experiments.

If the rate of energy input at the start of a cycle were infinite, then the assumption of "sudden temperature rise" would be correct. However, this assumption does not hold. Each "on" period is really composed of two parts: i.e., the first can be with sufficient accuracy considered to work with constant rate-of-energy input; during the second, the inside temperature is held constant. For heating up from cold to steady state, these conditions have been investigated and solved in a general way by one of the authors (12). For the intermittent operation covered by this paper, they have not been considered. It is possible to set up curves similar to Fig. 4 of this paper based, however, upon the assumption that during the first part of the "on" period up to the time at which the inside surface temperature reaches the final temperature, only n times the rate of steady-state heat flow at this temperature is available. The amount of experimental work involved would be quite appreciable.

In the meantime, the approximation used in the example given is advisable. For this purpose, one half of the time which the equipment needs to reach full temperature is deducted from the "on" period and added to the "off" period. For instance, in the example, a furnace which operates 8 hr "on" and 16 hr "off" was considered. The heating-up period takes $2\frac{1}{2}$ hr daily. Then, based upon the approximation, the "on" period would be counted as lasting only 6.75 hr; the "off" period as lasting 17.25 hr. The intermittency would then be $f = 0.281$. Preliminary experiments proved that this method of approximation yields fairly accurate results; accurate enough for the purpose of determining the economic thickness of insulation.

The assumption of a tight enclosure is probably reasonable for a great many cases. There would be no difficulty in developing more sets of curves similar to that in Fig. 4 of this paper, each holding for a different amount of leakage of heat from or to the inside of the enclosure. In order to obtain general curves, this leakage would have to be expressed as a multiple of the insulation of the wall, i.e., a leakage resistance equal to n times the resistance of the wall.

INSULATION APPLICATIONS TO INDUSTRIAL EQUIPMENT, INTERMITTENTLY OPERATED

The economic applications of insulation to industrial equipment under intermittent operation are found in large numbers. For example, in the medium- and high-temperature fields, there are various types of heat-treating furnaces such as annealing, malleablizing, and carburizing furnaces, blast furnaces, and core ovens. In the low-temperature field, there are test chambers for aircraft equipment and personnel. These are but a few of the examples of equipment whose operation is inherently intermittent. As a matter of fact, any equipment which does not operate 24 hrs a day should be considered as in intermittent operation. For instance, a continuous type of annealing oven which operates at a constant temperature throughout the work day but is shut down overnight would show a very different heat loss on this basis from that determined for steady-state operation.

BIBLIOGRAPHY

- 1 "Heat Transfer Through Insulation in the Moderate- and High-Temperature Fields; a Statement of Existing Data," by L. B. McMillan, Trans. A.S.M.E., vol. 48, 1926, pp. 1269-1317.
- 2 "Summer Comfort Factors as Influenced by the Thermal Properties of Building Materials," by C. O. Mackey and L. T. Wright, Jr., *Heating, Piping and Air Conditioning*, A.S.H.V.E., Journal Section, vol. 14, Dec., 1942, pp. 750-757.
- 3 "Beitrag zur Technischen Mechanik und Technischen Physik," by E. Schmidt, A. Foeppel-Festschrift, J. Springer, Berlin, 1924, p. 179. Abstracted in "Heat Transmission," by William H. McAdams, McGraw-Hill Book Company, Inc., New York, N. Y., 1942.
- 4 "The Numerical Solution of Heat Conduction Problems," by H. W. Emmons, Trans. A.S.M.E., vol. 65, 1943, pp. 607-615.
- 5 "Analyzing Heat Flow in Cyclic Furnace Operation—New Method Simplifies Determination of Economic Insulation Thickness," by C. B. Bradley and C. E. Ernst, *Mechanical Engineering*, vol. 65, 1943, pp. 125-129.
- 6 "Transient Heat Conduction in Hollow Cylinders After Sudden Change of Inner Surface Temperature," by R. L. Perry and W. P. Berggren, University of California Publications in Engineering, vol. 5, 1944, no. 3, pp. 59-88.
- 7 "A Method for Determining Unsteady-State Heat Transfer by Means of an Electrical Analogy," by Victor Paschkis and H. D. Baker, Trans. A.S.M.E., vol. 64, 1942, pp. 105-112.
- "New Heat-Transfer Research Tool," editorial in *Mechanical Engineering*, vol. 64, 1942, pp. 95-96.
- "Electrical Analogy Method for the Investigation of Transient Heat Flow Problems," by Victor Paschkis, *Industrial Heating*, vol. 9, 1942, pp. 1162-1170.
- "Establishment of Cooling Curves of Welds by Means of Electrical Analogy," by Victor Paschkis, *Welding Journal*, Welding Research Supplement, vol. 722, 1943, pp. 462-483 S.
- "Periodic Heat Flow in Building Walls Determined by Electrical Analogy Method," by Victor Paschkis, *Heating, Piping and Air Conditioning*, A.S.H.V.E. Journal Section, vol. 14, Feb., 1942, pp. 133-138.
- 8 "Dimensional Analysis," by P. W. Bridgman, Yale University Press, New Haven, Conn., 1922; revised 1937.
- 9 "Charts for Estimating Temperature Distributions in Heating or Cooling Solid Shapes," by H. P. Gurney and J. Lurie, *Industrial and Engineering Chemistry*, vol. 15, 1923, pp. 1170-1172.
- 10 "The Accuracy of Measurements in Lumped R-C Cable Circuits as Used in the Study of Transient Heat Flow," by V. Paschkis and M. P. Heisler, *Electrical Engineering*, Trans. Section, vol. 63, April, 1944, p. 165.
- 11 "Temperature Distribution on the Surface of a Brick Wall With Mortar Joints," by V. Paschkis, *Refrigerating Engineering*, vol. 47, June, 1944, p. 469.
- 12 "Heating Up Time and Energy Losses of Furnaces," by V. Paschkis, presented at the Semi-Annual Meeting, Pittsburgh, Pa., June 19-22, 1944, of THE AMERICAN SOCIETY OF MECHANICAL ENGINEERS.

Discussion

G. D. BAGLEY.⁵ The method of determining heat losses from intermittently operating equipment by setting up an analogous electrical circuit, as described in this paper, is a marked improvement over previous methods of making such measurements by direct thermal tests. Since the time involved in the electrical measurements is so short as compared with thermal methods, it should be possible to make a more complete study of each problem.

In order to apply the method, however, the thermal conductivity and heat capacity of the heat insulation must be determined, and these measurements must still be made by the old methods of direct thermal tests. Once these constants have been established for a given type of insulation, it should be a very simple matter to determine the optimum economic thickness for any given application by the method described in this paper.

The authors have made rather severe assumptions in order to simplify the formulas and make the electrical method applicable.

⁵ Research Engineer, Union Carbide and Carbon Research Laboratories, Inc., Niagara Falls, N. Y. Mem. A.S.M.E.

These assumptions appear to be amply justified when the method is used for the purpose of determining the optimum economic thickness of heat insulation, because the economic factors of depreciation and obsolescence and of the unit value of heat over a period of years are much less definitely known. The curves for the total cost, including cost of insulation and cost of heat energy lost, as shown in Fig. 11 of the paper, are usually rather flat at the minimum point, and the ordinary tendency is to choose a thickness of insulation slightly on the low side of the minimum. If obsolescence should retire the insulation in less than the assumed period of time, the saving in capital investment would more than balance the value of the extra heat loss, but if the period of use should extend beyond the assumed time, the increased energy lost would more than eliminate the saving in capital investment.

Simplification 4 in the paper assumes that the thermal properties of the wall do not change with temperature. Over relatively small temperature ranges, this assumption will not affect the result seriously, but when very high temperatures are involved, the thermal resistivity of the part of the insulation at the high temperature drops markedly, and the assumption will result in a thickness determination that is on the low side. If this effect were to be taken into account electrically, it would be necessary to set up a circuit in which the resistance varied with the voltage at any particular point in the circuit.

Simplification 7 assumes an instant increase in temperature on the internal furnace wall to the maximum value when the heat is turned on, and this in turn requires an infinite rate of energy input at the instant of heat application. This assumption does not appear to affect the results for intermittent applications when the time cycle is fairly long, but for short periods and for low values of f , as shown in Fig. 2, it leads to an anomalous result. For curve 1 in Fig. 2, where P is equal to infinity, the result is not affected by this assumption, but for curve 2 where P equals zero and at the point at which f also equals zero, the graph shows that the fractional heat flow is equal to the full normal value for constant operation even when the "on" period is zero. It appears that these curves should not be used for low values of f unless P is large.

This paper represents a valuable contribution to the methods of studying heat flow which has long been difficult and time-consuming. The clear definitions of the terms and symbols used in the paper are a valuable feature to the reader.

M. H. MAWHINNEY.⁶ The use of the heat and mass flow analyzer is showing increasing value as a means of reproducing thermal flow conditions for study, to avoid the almost impossible obstacles in the road of either mathematical or heat-test methods.

Even with this new method, a considerable number of assumptions must be made, as outlined in the paper. The writer agrees that all of these assumptions are unimportant to the result, with the exception of the first one, i.e., that the insulated space is tight. The first purpose of this discussion is to demonstrate that by-passing of heat should be considered in the case of industrial heating furnaces, in which the writer is particularly interested.

Referring to the example (with data in Table 1), the authors evidently mean that the cost of the fuel is \$0.30 per million Btu fired at the burner (for example, natural gas delivered at 30 cents per thousand cubic feet). Of this million Btu fired into the furnace at 1900 F internal temperature, about 460,000 Btu leave as latent heat in the flue gases, and only 540,000 Btu remain as useful heat for work and for heat losses through the walls. The cost of these heat losses is therefore actually 1.85 times that

⁶ Consulting Engineer, Salem, Ohio. Mem. A.S.M.E.

TABLE 2 COST OF HEAT LOSSES ON REVISED BASIS

At 1900 F furnace temperature, or 54 per cent efficiency—						At 1000 F furnace temperature, or 76 per cent efficiency—					
1	2	3	4	5	6	7	8	9	10	11	12
Thickness, in.	Yearly cost of brick, dollars	Yearly cost of heat loss, dollars	Total yearly cost, dollars	Net saved over 5-in. thick per year, dollars	Investment for brick per sq ft, dollars	Years to pay for increased investment over 5-in. thickness	Estimated Btu per sq ft per hr	Yearly cost of heat loss, dollars	Total yearly cost, dollars	Net saved over 5-in. thick per year, dollars	Years to pay for increased investment over 5-in. thickness
STEADY STATE											
5	0.107	1.610	1.717	...	0.712	...	174	0.495	0.602
7	0.149	1.165	1.314	0.403	0.996	0.705	127	0.360	0.509	0.093	3.06
7 1/2	0.160	1.090	1.250	0.467	1.068	0.762	122	0.348	0.508	0.094	3.79
9	0.192	0.918	1.110	0.607	1.280	0.935	103	0.293	0.485	0.117	4.85
9 1/2	0.203	0.873	1.076	0.641	1.352	1.000	98	0.278	0.481	0.121	5.29
10	0.214	0.831	1.045	0.672	1.424	1.060	94	0.267	0.481	0.121	5.88
11 1/2	0.245	0.720	0.965	0.752	1.636	1.225	83	0.237	0.482	0.120	7.70
12	0.256	0.693	0.949	0.768	1.708	1.282	79	0.226	0.482	0.120	8.21
12 1/2	0.267	0.667	0.934	0.783	1.780	1.365	76	0.216	0.483	0.119	8.96
13 1/2	0.288	0.619	0.907	0.810	1.920	1.491	72	0.204	0.492	0.110	11.00
14	0.299	0.598	0.897	0.820	1.992	1.580	70	0.198	0.497	0.105	12.20
14 1/2	0.310	0.578	0.888	0.829	2.064	1.635	68	0.193	0.503	0.099	13.67
16	0.341	0.524	0.865	0.852	2.276	1.836	63	0.179	0.520	0.082	19.10
UNSTEADY STATE											
5	0.107	0.665	0.772	...	0.712	...	Information not available				
7	0.149	0.586	0.735	0.037	0.996	7.66					
7 1/2	0.160	0.565	0.725	0.047	1.068	7.57					
9	0.192	0.505	0.697	0.075	1.280	7.56					
9 1/2	0.203	0.489	0.692	0.080	1.352	8.00					
10	0.214	0.472	0.686	0.086	1.424	8.28					

calculated on the basis of fuel cost at the burner. At 1000 F internal furnace temperature, 76 per cent remains as useful heat, and the cost is only 1.32 times the cost at the burner.

Table 2 has been prepared by the writer to show the cost of heat losses on this revised basis (columns 3 and 9), and the total cost including brickwork cost (columns 4 and 10) for furnace temperatures of 1900 F and 1000 F, and for the same thicknesses of JM-20 insulating brick as were used in Table 1 of the paper. It is immediately evident that much heavier insulation is now indicated for the steady state at 1900 F on the basis of this more expensive fuel figure.

This creates a question whether the assumption that the thickness which produces the least total cost is necessarily the best practical thickness, and the problem has been analyzed by the writer in another way in Table 2.

For each temperature, the net saving in heat-loss cost per year was obtained, as compared with the minimum thickness of 5 in. This was done by subtracting the increased brick cost above 5 in. thickness (15 per cent of the investment per square foot per year) from the increased savings per year over that for 5 in. thickness. The additional investment over that for 5 in. thickness was then divided by the annual net saving to determine the number of years required to return the initial additional investment.

By this method, the economical thickness of insulation at 1900 F for steady-state conditions would seem to be 9 1/2 in., if the investment is to be returned in 1 year, which is a measure commonly used in industry. By the same measure, no increase above 5 in. thickness would be indicated at the temperature of 1000 F. These conclusions are based on fuel cost after correcting for furnace efficiency, as has already been discussed, and therefore cannot be compared directly with the conclusions reached in the paper. On the basis of a fuel cost of \$0.30 per million Btu at the burner and with the assumption that additional investment is to be returned within 1 year, a thickness beyond 5 in. cannot be justified. The thickness of 13 1/2 in. arrived at by the authors' method in the paper for steady-state conditions would require 3.42 years to pay for itself.

For the unsteady state, the tabulation with a true valuation of fuel cost indicates a very heavy wall in place of the authors' selection of 5 in., arrived at by the method of total cost. By the method of determining return on the investment, it would appear that the minimum thickness permitted by structural considerations should be used. It is well known that light brick linings will save large quantities of fuel, particularly on inter-

mittent operation, but a minimum thickness is indicated because of the lower conduction losses with this type of operation.

In conclusion, it is the opinion of the writer that the development of a method of evaluation of heat losses for the infinite combination of possible conditions which are met in practice is a very real contribution. By the methods outlined in the paper, a great many problems will be solved which to date have resisted efforts by other methods, and future papers will be awaited by engineers interested in the many phases of heat transfer.

R. L. PERRY⁷ and W. P. BERGGREN.⁸ The authors are to be commended for making available their simplified solutions for a difficult and important heat-flow problem.

Analytical solutions for several transient cylindrical problems, which can be applied to pipe-line insulation, are given by Carslaw and Jaeger.⁹

The assumptions which limit the Schmidt method, in particular the use of average properties and subdivision of a wall into finite layers, also apply to the electrical-analogy apparatus. The principal disadvantage in the Schmidt method for cyclic problems is that, unless a fortunate estimate of temperature distribution at some point in the cycle is made, say, at the start of the "on" period, the graphical procedure must be carried through several cycles before a repetitive distribution is established. For particular examples, when general curves are not being attempted, the Schmidt and Emmons methods have not been superseded.

It should be pointed out that simplifications 1 and 4 do not influence the wall loss during the "on" period, because of simplification 7. They do affect the energy input required to approach simplification 7, and also affect the inner-wall temperature during the "off" period.

If the shape of the warming-up temperature curve can be predicted, a closer approximation than allocating one half of the heating-up time to "on" and one half to "off" can be made.

R. M. STUCHELL.¹⁰ The economics of any industrial process

⁷ Associate Professor of Agricultural Engineering, and Associate Agricultural Engineer in the Experiment Station, University of California, Davis, Calif.

⁸ Assistant Professor of Physics, and Assistant Physicist in the Experiment Station, University of California, Davis, Calif.

⁹ "Some Two-Dimensional Problems in Conduction of Heat With Circular Symmetry," by H. S. Carslaw and J. C. Jaeger, *Proceedings of the London Mathematical Society*, series 2, vol. 46, 1940, p. 361.

¹⁰ Mellon Institute of Research, Pittsburgh, Pa.

is often the major factor in its success or failure. Thus the contributions made by the authors in their present paper will find extreme usefulness in the many applications of insulation to temperature equipment under intermittent operation.

The problem has not been completely solved. Certain considerations must yet be worked out, and many assumptions must be justified or corrected. In 1913 Prof. Edwin F. Northrup stated, "the flow of heat is often difficult of calculation and is always difficult of precise measurement." Thirty years from now this same statement if repeated will no doubt be as much in order as it is today. Yet it is only through farsighted vision that we recognize the problem, approach a solution from a basic viewpoint, and finally arrive at a workable and practical answer. This the authors have done with the problem presented in their paper, and they are to be commended for it. The adaptability to all insulations of the fractional heat-flow curves for the determination of economic thicknesses should serve as a stimulus to insulation manufacturers. Research programs must be broadened to include further investigation of thermal-conductivity and specific-heat values in the extremely low- and high-temperature ranges along with the ever-increasing development of new insulation materials.

Dr. Irving Langmuir¹¹ was among the first to recognize the similarity between the flow of electrical and heat energies and made use of the analogy in the theoretical as well as experimental determination of shape factors for various geometrical designs. Many others have attempted to continue this work. With the inception of the heat and mass flow analyzer, present-day investigators have been given a new tool which may mean the discarding of time-consuming heat-flow measurements.

It is most interesting to note that the method provides a means of making a more economical choice of a combination of insulation materials. This point is important; for under certain conditions, as in the walls of a steelmaking furnace, the service life of which is relatively short, a substitution of less expensive materials may mean an appreciable saving.

In the light of their results, the authors point out the inadvisability of using estimated intermittent heat-flow values. As an example, we recall the insulation of a group of four 1-in.-diam copper tubes through which liquefied natural gas at a temperature of about -258°F was to be passed in regular cycles. After consultation the experts decided that 3 ft of insulation was necessary to prevent undue regasification of the liquid. However, when the insulation was to be put into place it was found that the copper tubes had been installed in such a manner that there was space enough for a thickness of only about 6 in. The 1-ft-diam enclosure did the job satisfactorily.

The increasing use of the electrical-analogy method of determining heat flow has brought into greater prominence the factor of thermal diffusivity. This is heartily applauded. The practice of basing the selection of an insulating material upon thermal-conductivity values alone is certainly not in keeping with other rigorously scientific procedures.

In the calculation of the illustrative problem, an explanation of the method for determining the average temperature would be appreciated. Is the formula, Maximum temperature

$\times \frac{(1 + \text{Intermittency})}{4}$, an empirical quantity? Has it been developed in a manner similar to the intermittency approximation?

In the section including an analysis of corner effects, the paper contains a so-called "fictitious" or equivalent specific-heat value. This is made up of the volume of the insulation without corners

plus the volume with corners multiplied by one half the normal specific heat. This would seem to be a misprint as the specific-heat value would obviously increase beyond reason.

Mr. Ludwig Adams¹² of our research organization has described some of the difficulties encountered in determining thermal conductivities of insulating material in ranges as low as -320°F . Those of us who have experienced these difficulties can appreciate the desire to eliminate any part of the tedious and time-consuming procedures involved in such investigations.

For this reason, the writer would like to know if the authors have ever attempted the determination of k values by means of the heat and mass flow analyzer? Using experimentally determined temperatures on the surfaces of a given thickness of insulation, could the electrical circuit resistances be varied until the voltage readings corresponded to the temperature factors? If this could be done, the conductivity k could then be readily calculated from the resistance obtained, along with the thickness and the heat capacity of the insulating material. A means of obtaining temperature gradients might be through the construction of a cubical metal box, approximately 1 ft along each edge, and with an open top. Five different types of insulations or five different thicknesses of the same insulation could be fastened to the five faces of the box. The box could then be filled with a constant-temperature medium such as boiling liquid nitrogen, liquid propane, or liquid butane and so maintained for a suitable period of time until temperature equilibrium was established. The temperatures through the insulation could then be measured along the center line normal to each face of the box by means of thermocouples placed at convenient locations. Attacking this problem along the experimental lines noted would mean that at least five conductivity determinations could be accomplished in the time previously required for one. The authors' comments upon this tentative suggestion will be greatly appreciated.

Again, we congratulate the authors upon work well done, and we hope that these studies will be continued to broaden even further the knowledge of economical thermal insulations for intermittent heat flow.

H. R. WILSON.¹³ This practical demonstration of a method for determining the economical thickness of refractories and insulation serves to establish further the merit of the electrical-analogy principles, as developed by Dr. Paschkis. The presentation is in a form facilitating general application to problems within the scope outlined and extension of the method to include more variables appears possible without undue complications. The simplifying assumptions appear to have been well taken, the relatively small loss in accuracy being compensated by increased utility.

AUTHORS' CLOSURE

A large part of the discussion deals with the various simplifications made in the paper and therefore these comments will be answered first.

Simplification 1 (Mr. Mawhinney) could be dropped but for the presentation by dimensionless charts, this would mean one more parameter, resulting either in a three-dimensional graph, or in a fairly large number of one-dimensional graphs. The (dimensionless) parameter to be introduced might be, e.g., in the form of a relative boundary resistance, active only during the off

¹¹ "Flow of Heat through Furnace Walls, and the Shape Factor," by Irving Langmuir, E. Q. Adams, and G. S. Meikle, Trans. American Electrochemical Society, vol. 24, 1913, pp. 53-84.

¹² "A Method of Determining Thermal Conductivities at Low Temperatures," by Ludwig Adams, paper presented at June 7, 1944, meeting of the American Society of Refrigeration Engineers published September, 1944, in *Refrigerating Engineering*.

¹³ Research and Development Laboratories, Diamond Alkali Company, Painesville, Ohio.

period: resistance of heat leak/resistance of the wall. The authors agree that it would be desirable to extend the graphs for such case, if time and funds permit.

Simplification 4. In the case mentioned by Mr. Bagley a simple and practical approximation would consist in considering the single layer wall to consist of two or more fictitious layers of different materials; the properties of each of these fictitious layers would be those of the true wall material, but selected for a different temperature range; the temperature ranges would conform to the estimated temperatures for the respective part of the wall. As mentioned in the paper, curves for the two-layer wall are available, whereas for three or more layer walls no general solutions are available as yet. The authors cannot agree with Messrs. Perry and Berggren's statement, that simplification 4 does not influence the "on period."

Simplification 7 (Mr. Bagley). The authors agree with the first part of Mr. Bagley's statement (regarding the necessary infinite rate of energy input). Regarding curve 2 in Fig. 2 it should be pointed out that this curve is introduced as "limit" which as such of course can never be reached; an infinitely short period is physically not obtainable. If more curves were put between curves 1 and 2, they would follow closely the ordinate axis and near the value "one" bend very sharply to follow almost the horizontal line "one" for *FHF*. Because of the lack of curves in the upper left corner of graph 3, however, extrapolations in this range would be rather inaccurate. The authors believe, that few practical cases, if any, call for curves in this region.

Two discussers (Mr. Bagley and Mr. Stutchell) bring up the problem of physical properties. It is agreed that the heat and mass flow analyzer is mainly a calculating device, which is accurate only to the extent to which the physical properties of the materials involved are known. However, it should be pointed out that the analyzer could be very helpful in determining properties by operating it, so to say, in reverse. It has been proposed to determine thermal diffusivities through experiments with transient heat flow; by heating or cooling a body and observing temperatures at two or more points, the diffusivity can be calculated. Calculation, however, is only possible if a number of conditions prevail: thermal conductivity and specific heat must be independent of temperature; the temperature or the heat input at the surface or some other characteristic point must follow a reasonably simple mathematical law and the shape of the body must be sufficiently simple to permit mathematical analysis. These conditions are mostly nonexistent or very hard to obtain. If the analysis of temperature-time observations is carried out on the heat and mass flow analyzer only the condition of simple shape need be retained, whereas the two other limitations do not apply. Thus by the use of the heat and mass flow analyzer the scope of the very promising method of determining the conductivity by the apparent detour of measuring temperature differences is greatly enhanced, and the experiments serving to establish the temperature differences are simplified.

Mr. Stutchell's suggestion to use the analyzer for the steady-state conductivity measurements is interesting. The authors understand the idea as follows: if the cubical box is covered on five sides with insulation of different values (conductivity and/or thickness), and if the inside temperature is the same, then due to lateral heat flow on the different sides a certain temperature pattern will evolve.

This pattern is characteristic for the conductivities involved. By trial-and error-method this pattern could be duplicated on the heat and mass flow analyzer, and thus the conductivities of the five materials could be found. Such procedure would be technically possible; but the authors doubt if it would offer advantages above and against the direct measurements of conductivity. The trial-and error-method on the analyzer would be quite lengthy; the maintenance of constant temperature on the inside of the body would be difficult; and the heat loss from the open top would be considerable.

Mr. Mawhinney's comments on the method of determining the economic thickness introduce the idea of "minimum thickness," probably on the basis of the requirements of mechanical strength. It appears to be more desirable to determine the economic thickness from the thermal point of view, and independent of that the minimum thickness from the viewpoint of mechanical design; the choice then will of course be determined by the larger value. Mr. Mawhinney moreover suggests as "normal" to introduce an annual charge of 100 per cent rather than 15 per cent. To the authors this appears to be exaggerated. The insulation thickness is thereby so reduced that the increased cost of heat lost every year of operation after the first would more than cover the cost of the greater thickness of insulation, calculated as "economic thickness." However, the charts presented in this paper allow any method of selecting the thickness, including the one proposed by Mr. Mawhinney.

Mr. Stutchell's request for an explanation of the use of the factor $\frac{1+f}{4}$ is answered as follows. It is assumed that the space (referring to space occupied by wall material) mean temperature is approximately equal to one half of the inside surface temperature; the latter is approximately proportional to *FHF*. *FHF* lies always between the limits $1 > FHF > f$. For many cases it is sufficiently accurate to put $FHF = \frac{1}{2}(1+f)$. Then the spaces time mean temperature is $\frac{1}{2} \cdot \frac{1+f}{2}$ or $\frac{1+f}{4}$ times the maximum inside surface temperature. If the approximation $FHF = \frac{1+f}{2}$ is not found to be sufficiently accurate, a step by step method can be applied.

In connection with the fictitious specific-heat value, there was a misprint in the preprint, which has been corrected in the final paper.

Shear Strength of Glue Joints as Affected by Wood Surfaces and Pressures

Including Data on Glue Penetration Into Wood and Relationship Between Glue Thickness and Shear Strength

By J. W. MAXWELL,¹ WALLINGFORD, CONN.

The study reviewed in this paper was initiated to determine accurately the pressures and types of surfaces that would insure the strongest glue joints. The prevailing idea that roughing wood prior to gluing has been proved to be faulty. As a result of this study, the author advocates the use of the smoothest type of surface that is practical to produce. Photomicrographs of the various types of glue joints studied are presented and discussed, while graphs and photographs give evidence of the conclusions drawn. A discussion on glue penetration is included, and conclusions are drawn concerning the possibilities of such a situation. A glue-film thickness and shear-strength relationship is also presented, with a brief discussion on the possible nature of adhesion.

INTRODUCTION

SINCE the inception of the war, the use of synthetic-resin-bonded wood has attained major importance in replacing scarce and strategic metals in the manufacture of airplanes, PT boats, and many other war products. The science of wood engineering, particularly as related to the fabrication and assembly of wooden members through the use of modern adhesives, is still in the experimental stage. It is unfortunate that the available data are nowise comparable to those at the command of engineers working with steel, the alloys of aluminum, etc. At the present time such engineers are metal-minded and logically so, largely because of a dearth of information on the superiority of wood over metal within its sphere of usefulness.

Since wood, unlike metal, is of organic origin and results from the growth of trees, from its very nature it is a variable material of construction. Its proper use is therefore contingent on the solution of many engineering problems not encountered with metal, the composition of which can be accurately decided upon in advance, to insure the properties required. In the use of wood, design which insures the greatest working efficiency of wood for a product such as an airplane may be quite different from that where metal is used. Aeronautical engineers versed in designing metal planes will do well to keep this ever in mind.

Wood has certain drawbacks as a structural medium, among which is the fact that it does not shrink equally in all directions, it varies in volume below the fiber saturation point with varying degrees of atmospheric humidity, etc. It does, however, have the advantage of relative cheapness and light weight in proportion to its strength. Furthermore, the objections traceable to the heterogeneity of wood can be largely overcome through the fabrication of plywood and laminated wooden members, using

modern methods of molding and synthetic-resin adhesives. The proper use of such adhesives in bonding wood to wood in making wooden members is a major problem in the woodworking industry today, a prime objective in the competition between wood and metal. This country has now arrived at the era of the refined use of wood. It will stand or fall in competition with metal only in so far as full advantage is taken of those peculiar properties which recommend it for certain purposes in lieu of metal.

PURPOSE, NATURE, AND DEVELOPMENT OF THE INVESTIGATION

The purpose of the present study from its inception has been to provide basic and accurate information relative to the bonding of wood. If the proper technique is used in making plywood, a material that is more homogeneous and stronger than solid wood will be the result. However, unless the bonding is as strong or stronger than that which holds the cells of wood together, the resulting product will be weaker than a piece of solid wood of the same dimensions. Strength of fabricated members at the glue lines therefore is of first importance; and gluing procedures that result in weak joints should be avoided. The subject research was initiated to determine accurately the pressures and types of surfaces that would insure the strongest glue joints, using a given kind of glue.

Many types of surfaces and pressures were considered for use in this research. The types of surfaces to be glued were chosen from those commonly used in industrial practice. Good and bad types were selected intentionally, to indicate the disadvantages or advantages accruing from the use of such surfaces. Glue companies and other agencies have advocated glue pressures approximating 200 psi.² It seemed desirable therefore to employ different pressures below and above this point, since it might be that pressures well under 200 psi would prove fully as effective in producing a strong joint as those above this figure.

The development of the problem necessitated a study of the pressure methods in use in the industry to hold the members of an assembly together while the glue is setting. In practice, it was found that C-clamps, nails, and screw presses were most commonly employed for secondary gluing.³ Such devices, once in use, do not allow for automatic readjustments to maintain the initial pressure, should this be dissipated to any extent.

Fortunately, this phenomenon of diminishing initial glue pressures was fully realized at the start of this research. Some means had to be found therefore to apply a given pressure within the range of those employed in the industry and to keep it constant throughout the gluing process. Only by such a procedure could comparative data of the efficacy of arbitrarily

¹ Wood Technologist, Plastics Division, American Cyanamid Co. Compiled from M.S. degree thesis at the New York State College of Forestry and contributed by the Wood Industries Division of THE AMERICAN SOCIETY OF MECHANICAL ENGINEERS.

NOTE: Statements and opinions advanced in papers are to be understood as individual expressions of their authors and not those of the Society.

² "Uformite CB-551 Cold Bonding Studies," Resinous Products and Chemical Company, Philadelphia, Pa., Bulletin No. 2, October, 1942, p. 5.

³ Secondary gluing is a term used to designate gluing of small parts in assembly work to larger parts that have been preformed. Many of the present plywood materials of war are glued this way. The cold-setting type of resin is most widely used for this type of work.

chosen pressures in force over a given period of time be obtained.

It was also necessary to set up certain other controls, in addition to that of insuring a constant pressure. These pertained to glue and wood.

The government specification AN-G-8 was followed very closely in setting up the experimental procedure. For example, sugar maple (*Acer saccharum* Marsh) was the wood used, since the maple shear block is an accepted method of testing the strength of glue joints in shear.

There are other factors connected with wood such as the "cut" (flat or quartered sawed), and the method of surfacing. The latter will be discussed subsequently.

The glue used was one of the many synthetic urea-formaldehyde dry adhesives now on the market. This type of glue was selected since it is one that has been commonly used throughout the field for secondary gluing. It was mixed and used according to the manufacturer's specifications. A small laboratory model of a roller-type glue spreader was used for spreading the test strips. It was adjusted to coat a film comparable to 24 g per sq ft of glue line (equivalent to 52.6 lb per 1000 sq ft). Double spreading was used throughout this research.

Other factors that were considered to be of importance as controls were the temperature of the glue room, the conditions of the storage room used for the conditioning of the final glued test blocks, the open assembly time, closed assembly time, and the length of pressing. The temperature of the glue room ranged between 75 to 85 F. No equipment was available for controlling the relative humidity, except in the conditioning room used for storing the pieces after pressing. Here the relative humidity was kept at 50 per cent and the temperature at 75 F.

MATERIALS AND EQUIPMENT USED IN INVESTIGATION

Materials. The glue, as stated previously, was of the urea-formaldehyde cold-setting type, from one source.

The wood, sugar maple, grade No. 1 common, was obtained from a local lumberyard and was kiln-dried stock that had been stored for some time in a shed. After purchase, the lumber was

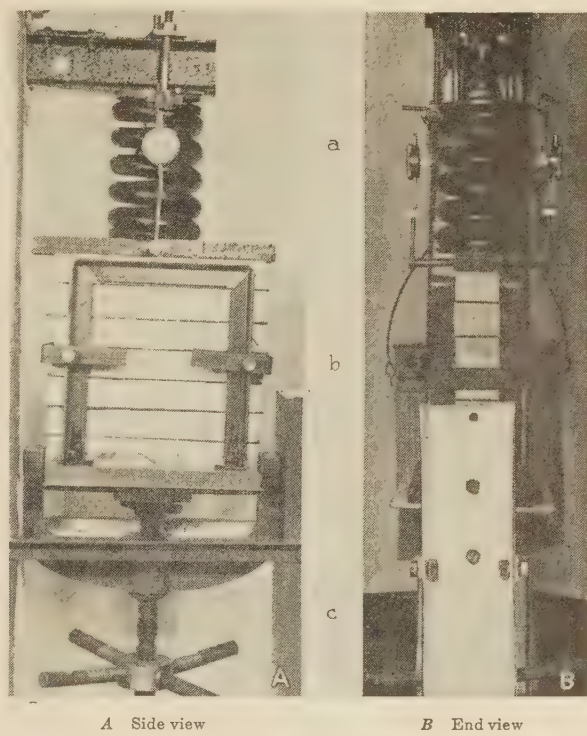


FIG. 2 PRESSURE HEAD CONSISTING OF LARGE COIL a, TEST-STRIP CRIB b, AND PRESSURE-ADJUSTING SCREW c

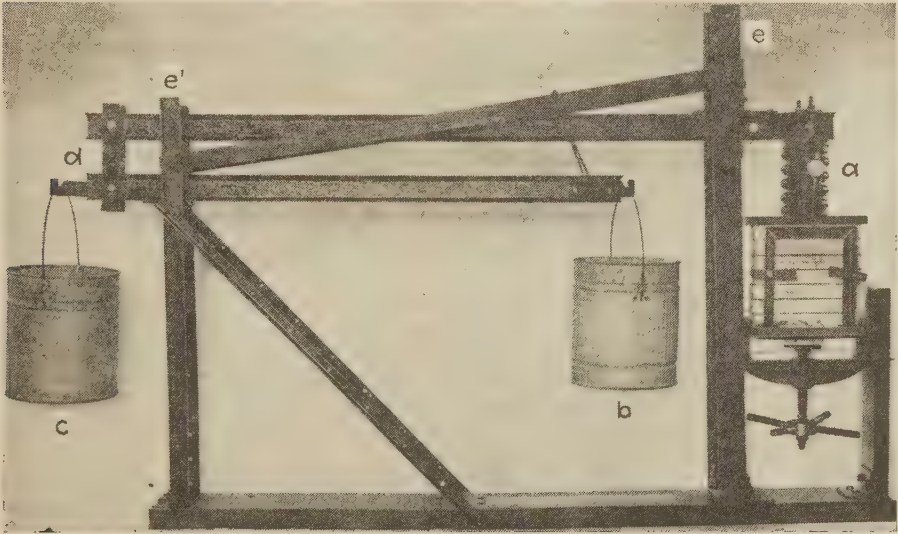
stored in the laboratory for a period of 1 month before use. Throughout the experiment, moisture-content determinations were made and at no time did these vary more than 1 per cent from an average of 10 per cent.

Equipment. The equipment consisted of the following:

- (a) Constant-pressure machine, shown in Figs. 1 and 2.
- (b) Glue spreader of the roller type, similar to that used in industry.
- (c) Woodworking machines which are commonly used in industry such as a jointer, sander, planer, and circular saw.
- (d) Riehle testing machine with a standard shearing tool. The rate of the load application was 0.013 ipm. The pressure was registered on the calibrated beam. Constant poise was maintained by special attachments added by the author.

METHODS OF PREPARING SURFACES

Planed. For this type of surface it was only necessary to plane the faces in a planer and then pass the surface to be glued over the jointing machine which was set for a thin cut.



a Pressure head
b Poise weight
c Counterbalance
d Coupling
e Front fulcrum support
e' Rear fulcrum support

FIG. 1 CONSTANT-PRESSURE MACHINE
(Made entirely from scrap metal.)

This tended to produce a smoother surface than the planer.

Sanded. In preparing this type, the pieces were treated as follows: Boards were planed and then sanded at 0.5 psi pressure. Care was taken to obtain a flat and even surface. The test strips were then cut to size for gluing.

Sawed. This type of surface was prepared by rip-sawing the face of a planed test strip so as to produce a sawed-surface effect.

Burnished. This surface was produced by passing the wood over a very dull planer at a slow speed. The effect achieved is that which occurs when a board sticks in a planer and the planer knives beat at one place until the wood is charred.

Combed or Tooth-Planed. This type of surface was secured by planing the wood with a hacksaw blade in place of the normal planer blade. The wood was deeply furrowed.

THE MAIN INVESTIGATION—EFFECT OF VARIATION OF PRESSURE AND SURFACE ON SHEAR STRENGTH OF GLUE JOINTS

Objectives Sought. The purpose of this study was to determine the pressures and the types of surfaces that would result in the strongest glue joints. To be sure many investigations have been made on the effect of pressure alone upon the shear strength of such joints.⁴ In others the surfaces were varied,⁵ but the pressures were kept constant for each series of tests. Both of these objectives were sought in this research. Seven constant pressures, namely, 5, 25, 50, 100, 150, 200, and 250 psi, and five types of surfaces were used.

Procedure. The test strips were sawed from selected wood and surfaces were prepared in the manner described previously. When one half of the working life of the glue had elapsed, the strips were spread and immediately placed together. This meant that the open assembly time was about 30 sec. As soon as six "sets" had been prepared, they were placed in the crib, with rubber cauls between each set. The side clamps of the crib were then tightened to prevent slippage. The pressure was applied, after which the side clamps were loosened slightly to prevent the sides of the crib from absorbing any of the pressure. The closed assembly period ranged from 10 to 15 min. A 12-hr pressure was used and then the glued strips were placed in a constant 50 per cent relative humidity room for a 10-day conditioning period. At the end of this time, the glued strips were band-sawed to approximately 2 in. width, then planed to the exact width, Fig. 3, and the end piece cut off in squaring. The side strips were saved for further studies of the glue joint. The test strip was then sawed into test blocks. This method warranted the assumption that the two ends were parallel and that the area of the contact face of the glue joint was 3 sq in.

The shear tests were made according to AN-G-8 specifications.

⁴ Uformite CB-551 Cold Bonding Studies," Resinous Products and Chemical Company, Philadelphia, Pa., Bulletin No. 2, October, 1942, pp. 5-6.

⁵ "Preliminary Experiments to Improve the Gluing Characteristics of Refractory Plywood Surfaces by Sanding," by F. H. Kaufert, Forest Products Laboratory, Bulletin No. 1351.

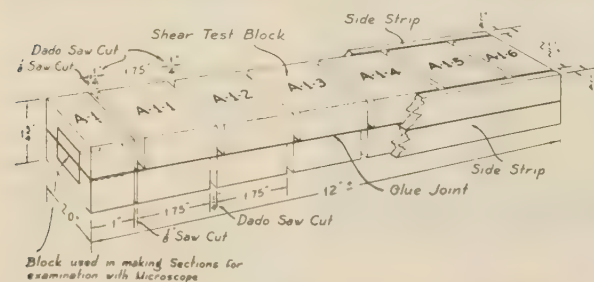


FIG. 3 SCHEMATIC DRAWING OF TEST STRIP AND METHOD OF TEST-BLOCK PREPARATION

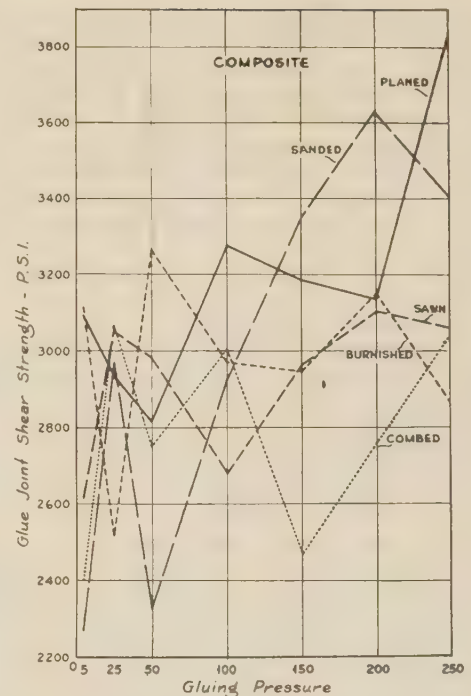


FIG. 4 COMPOSITE GRAPH OF AVERAGE SHEAR-STRENGTH VALUES FOR ALL SURFACES

Discussion of Shear-Test Data. It is difficult to arrive at any conclusions by simply scanning the shear values and the average shear values. In order to interpret the data so as to give some weight to the factor of "per cent fiber pull," the average shear values must be computed in terms of per cent fiber pull. The averages for the pieces between 50-0 per cent wood failure were used to plot graphs showing the effect of pressure of the shear strengths of the glued joints. These average values and the averages of all the tests are given in Table 1.

TABLE 1 AVERAGE SHEAR STRENGTHS OF GLUE JOINTS FOR VARIOUS SURFACES

Surfaces	Wood failure, per cent	Gluing pressures, psi						
		5	25	50	100	150	200	250
Planed	50-0	3092	2934	2815	3277	3182	3135	3837
	100-0	3116	2998	2813	3369	3224	3009	3757
Sanded	50-0	2274	2970	2331	2922	3353	3634	3406
	100-0	2357	2988	2342	2996	3378	3558	3422
Sawed	50-0	2616	3050	2985	2685	2961	3104	3061
	100-0	2690	3044	3003	2777	2988	3107	3078
Burnished	50-0	3112	2520	3268	2971	2949	3149	2863
	100-0	3143	2687	3268	2979	3051	3215	2893
Combed	50-0	2403	3068	2750	3004	2473	2760	3043
	100-0	2403	3062	2812	3004	2491	2795	3006

A composite graph, Fig. 4, was plotted, containing the curves of all the shear data for the various surfaces. These curves were quite irregular and were not especially illuminating. The data were again studied as a problem in correlation. New curves were then plotted on this basis, as shown in Fig. 5, the composite statistically treated graph. These new curves were straight and were understandable.

The composite statistically treated graph, Fig. 5, warrants the following deductions: Planed surfaces result in the strongest joints, followed by sanded, sawed, burnished, and combed, in the order listed. The coefficient of correlation (which can be determined from the graph by the rate of increase in shear value in proportion to increase in gluing pressure) was the greatest for sanded surfaces. This, the author believes, was due to the

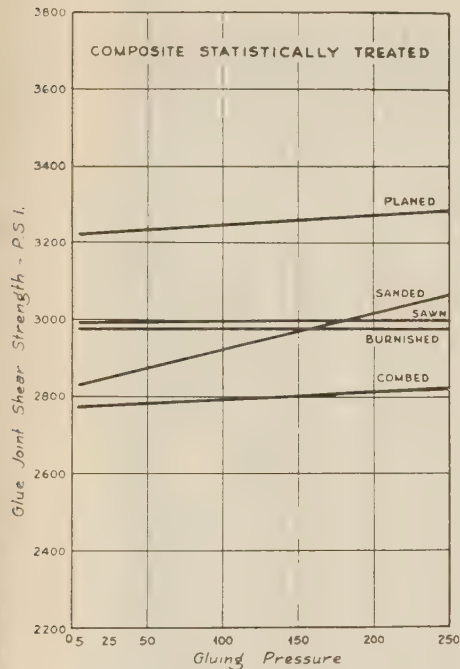


FIG. 5 COMPOSITE GRAPH OF STATISTICALLY TREATED VALUES FOR ALL SURFACES

nature of the surface and its relation to the phenomenon of adhesion.

Referring to Fig. 6, note should be made of the fact that the sanded surface appears splintered and that certain portions of the wood have been carried away by the grit, leaving more or less uniform striae. By contrast, in Fig. 6, the planed surface shows almost a complete absence of such striae. It is fairly easy to understand why a joint with faces surfaced by sanding will increase more in strength with increasing glue pressures than one with planed surfaces, when the nature of adhesion is considered.

Adhesion is due to attractive forces set up between unlike molecules. If two surfaces of wood could be forced together so that an infinitesimal distance remained between them the pieces would cohere, according to the conception of physicists. These conditions, in the case of wood, only exist in theory. The use of glue between two such surfaces, however, could permit of molecular linkage by adhesion, sufficient to hold the pieces together.

It is a well-known fact that the thinner the glue line, the stronger the bond.² Therefore, if the two surfaces that are being glued can be brought into closer proximity by pressure, a strong bond will result. This condition holds when the surfaces are planed. Granted, that a planed surface does have some irregularities due to the hitting of the planer blades (this is noticeable in Fig. 6F)—still these irregularities are not so deep as those in sanded wood. Consequently, an increase in the gluing pressure will not diminish the distance between planed wood surfaces to any appreciable degree, and the expense involved in

applying higher pressures is not justified. In contrast, sanded surfaces can be brought closer together by pressure, with a resultant proportionate increase in the strength of the glue bond as the thickness of the glue film becomes thinner.

The same theory may likewise be applied to sawed surfaces. On these there are many fibers that have been cut diagonally to their longitudinal axis, thereby weakening them as anchors for glue. The coefficient of correlation is very low in this case, owing to the poor surface contact of the glued pieces. This can readily be seen in Fig. 7C which illustrates a sawed type of glue joint. In this instance, too, high pressures are not capable of forcing the two surfaces sufficiently close together to result in joints as strong as those when the surfaces are planed.

Combed or tooth-planed surfaces may be considered as a cross between those that are planed and those that are deeply sanded. The reason for the higher value of the coefficient of correlation in these instances was probably due to the presence of planed portions which came into juxtaposition along the glue line. This increased the holding power of the joint as the surfaces were brought closer together with increasing pressure.

Burnished surfaces produced joints of uniformly low strength, with no tendency to increase with the higher pressures. This

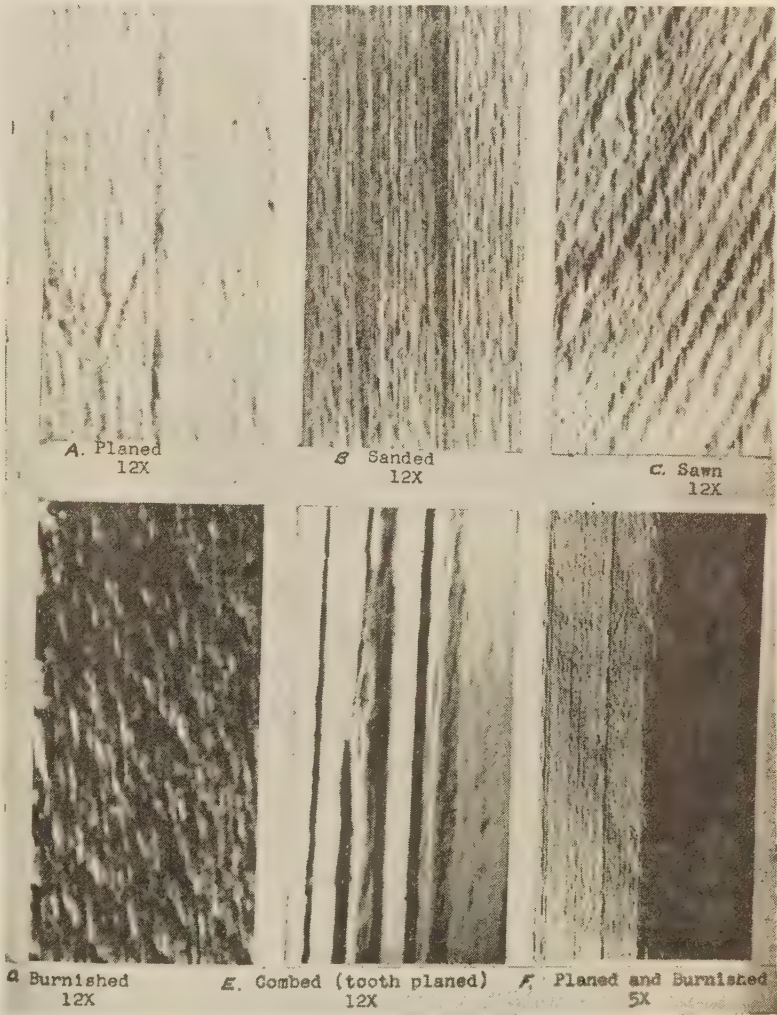


FIG. 6 VIEWS OF VARIOUS SURFACES

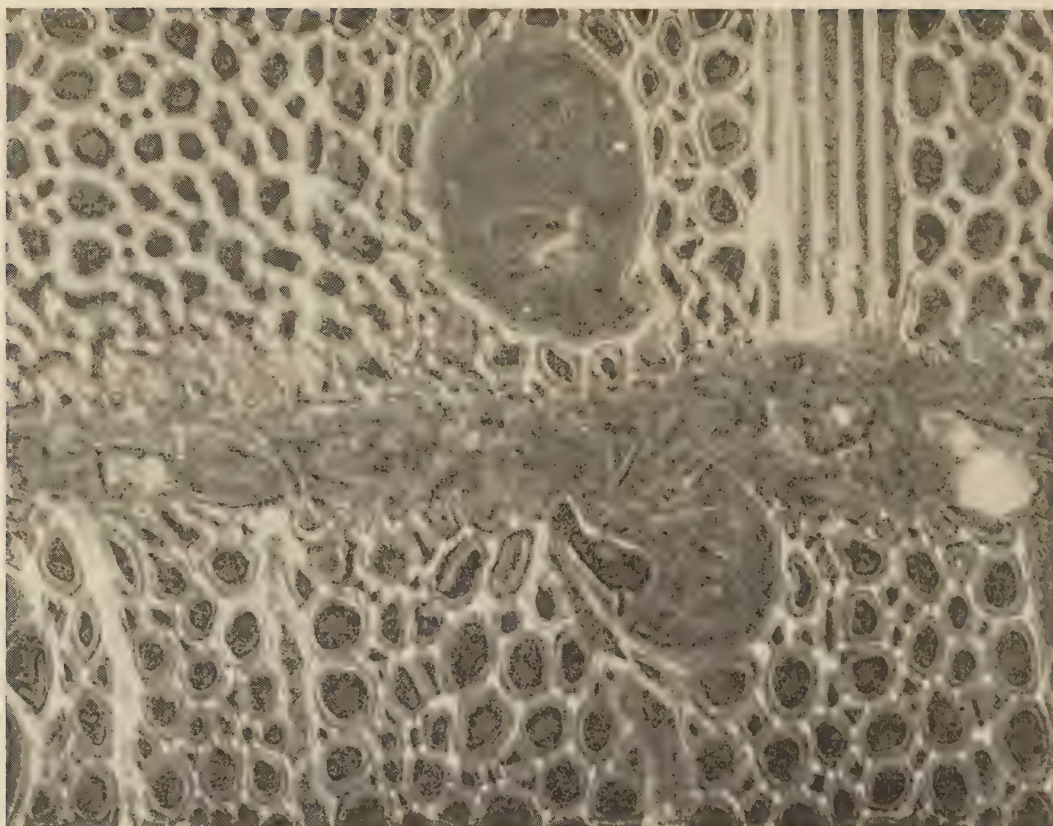


FIG. 8 PHOTOMICROGRAPH OF CROSS SECTION OF GLUE JOINT; $\times 500$

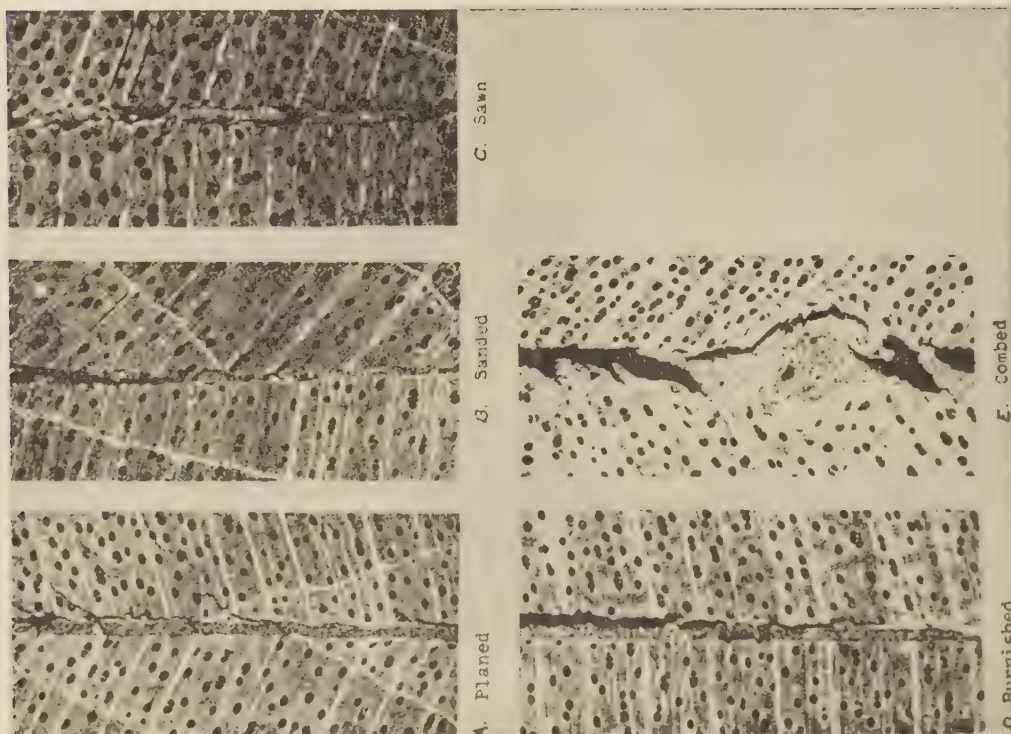


FIG. 7 PHOTOMICROGRAPHS OF CROSS SECTIONS CUT FROM TEST PIECES WITH VARIOUS SURFACES BUT GLUED AT SAME PRESSURE; $\times 30$

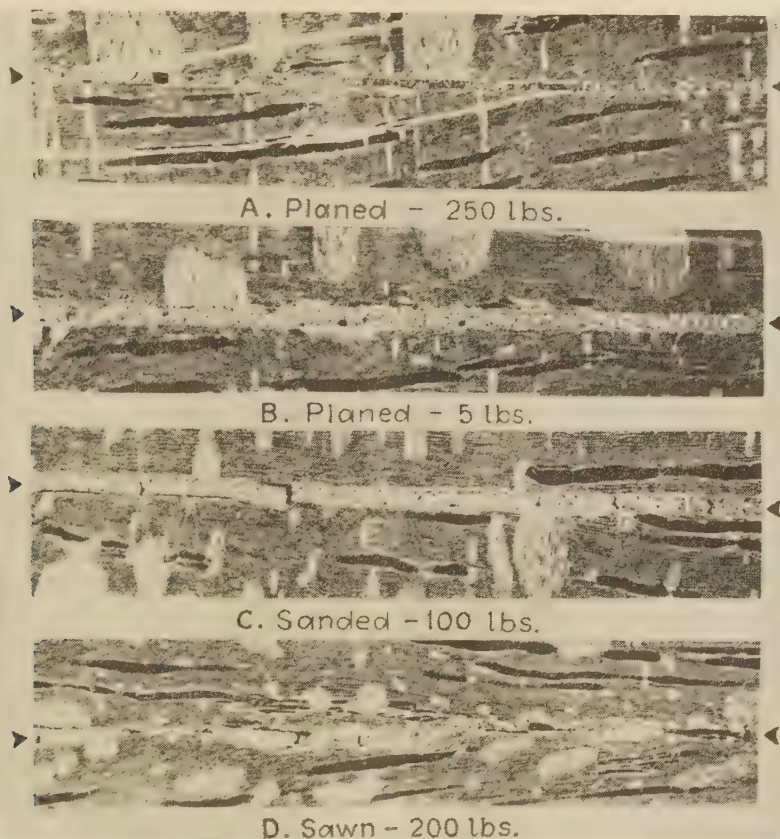


FIG. 9 PHOTOMICROGRAPHS OF RADIAL SECTIONS OF TEST PIECES GLUED AT VARIOUS PRESSURES AND WITH VARIOUS SURFACES; $\times 30$
(Note where the glue has streamed into the vessels as indicated by the arrow. Also note that in all four photomicrographs air bubbles are visible in the glue seams.)

was probably due (1) to the deposit of slightly charred wood on the surface which prevented the glue from adhering to the sound wood, and (2) to the nature of the even surface. The evenness approached that of planed surfaces.

EXAMINATION OF GLUE JOINTS AT HIGH MAGNIFICATION

These studies were initiated to determine whether pressure had any effect on glue penetration; to determine, if possible, the nature of adhesion between the glue and wood. The micro-technique involved in making mounts for such an examination presented some difficulties but these were surmounted.

A small block, $1\frac{1}{2}$ in. sq, was cut from the center of each of the end pieces reserved for this study at high magnification (see Fig. 3, and accompanying text). A sample was studied from each surface type and each pressure differential.

The blocks were softened by a water and acetone treatment and were then placed in a 12 per cent solution consisting of cellulose acetate butyrate dissolved in acetone for several days. Sections 15 to 20 microns in thickness were cut from these blocks with a sliding microtome. These were stained with Haidenhain's haematoxylin, followed by aqueous soluble safranin and mounted on slides with diaphane. Photomicrographs were taken and are presented in Figs. 7, 8, and 9.

Study of the sections and photomicrographs can lead to but one conclusion in so far as hard maple is concerned, namely, that pressure had little effect on glue penetration. Little penetration occurred other than into those vessels, fibers, and ray cells that opened immediately to the glue-spread surface. Glue

of the type used in this investigation does not pass through cell walls because of the size of semipolymerized glue molecules which are larger than the spaces between cellulose molecules. Fig. 8, which is a photomicrograph of the glue bond between wood, clearly shows the actual relationship that exists. The glue would have considerable difficulty in passing directly through the cell wall from one fiber cavity to another except by osmosis or absorption and this is not likely since the molecules of glue are macromolecular in size. Consequently, penetration can only take place through openings that result when the walls of such cells are cut or broken. Fig. 9D illustrates glue penetration where the cell cavities were exposed to the glue-spread surface. This is the only penetration that occurs other than into the minute porous irregularities of the wood surface which are opened on the surface by the various methods of machining.

ADHESION THEORY

In 1925, the Adhesive Research Committee of the Department of Scientific and Industrial Research, London, England, undertook an investigation into the nature of adhesion. As a result of its work several contributors⁶ have classified joints as (1) specific and (2) mechanical. The specific joint is that type which results when smooth surfaces such as those of metals, are joined; the mechanical type, in contrast, is produced when glue, through pressure, is squeezed into the depressions and minute cavities of a surface and forms projections and tentacles as it hardens. By

⁶ "Adhesives and Adhesive Action," by J. W. McBain and D. G. Hopkins, *Journal of Physical Chemistry*, vol. 29, 1925, p. 199.

this reasoning, it would appear that, in their opinion, the strength of a glue wood joint was due to the resistance by which such projections oppose the action of a shearing force. On the other hand, the smooth metal surface offered no such resistance and such opposition to shear must be considered to be due to specific attraction between the metal or wood molecules and those of glue.

Since the results obtained in this investigation coincide with those of previous investigators,⁷ the author agrees that (1) the thicker the seam the weaker the bond, and (2) if glue is not present in sufficient amount to fill the spaces between two surfaces, the joint is weak. He also wishes to state that the more irregular the glue film the weaker the bond.

The conditions as recorded should be kept in mind when the photomicrographs of the five types of glue seams discussed previously are subjected to re-examination. The discussion that follows pertains chiefly to the relationships that exist between the glue and surfaces of varying roughness.

Fig. 7A indicates that, when planed surfaces are glued, the adhesive forms a film of uniform thickness.

Fig. 7B illustrates a sanded surface and the manner in which the glue is distributed throughout the striae left by the sanding operation. It is obvious that enough of the adhesive is present to fill all the cracks and crevices. The nature of the failure between the glue and wood indicates that such a striated surface does not permit of the formation of as even a film and hence of as strong a bond as is true for planed surfaces. The sawed type shows this to an even greater degree, Fig. 7C.

Fig. 7D reveals that, although the glue film between the burnished surfaces is uniform, a desirable feature, the presence of charred wood on the surface results in poor adhesion. This is the reason that, in this series of illustrations, the glue film is shown separated from the wood.

The illustration of a combed or tooth-planed joint exhibits a very irregular glue line and an area devoid of glue.

The deductions made by the author, as a result of the critical examination of these photomicrographs, and others not presented, led him to a further investigation of the effect of glue-film thickness on the strength of a joint in shear. The side strips taken from the glued assemblies served as material for the following investigation:

The thickness of the glue film was measured in each strip. The figure obtained was assumed to indicate accurately the thickness of the film in the corresponding shear block for which shear data were available. The curve, Fig. 10, demonstrates the relationship that exists between the thickness of a glue film and the shear strength of a joint. It should be noted that the strength diminishes rapidly to a point where the glue-film thickness approaches 80 microns (0.0032 in.), beyond which it is relatively stable.

The explanation of this phenomenon, that a bond in a joint can be 200 to 1000 lb stronger than the glue itself, should be sought.⁸ Why the curve, as shown, changes abruptly several hundred pounds above the shear strength of the glue is intriguing; evidently it is the result of a factor as yet not understood.

In the past, investigators have avoided the discussion of this phenomenon. The emphasis in their studies has been rather on the nature and importance of specific adhesion, respectively. Solution of the problem projected would undoubtedly entail a study of the molecular forces that are responsible for the adhesion that exists between glue and wood. It may be that glue molecules have a greater attraction for wood molecules than for kindred glue molecules. Yet, according to chemists, a synthetic resin such as urea formaldehyde is actually a lone molecule that has

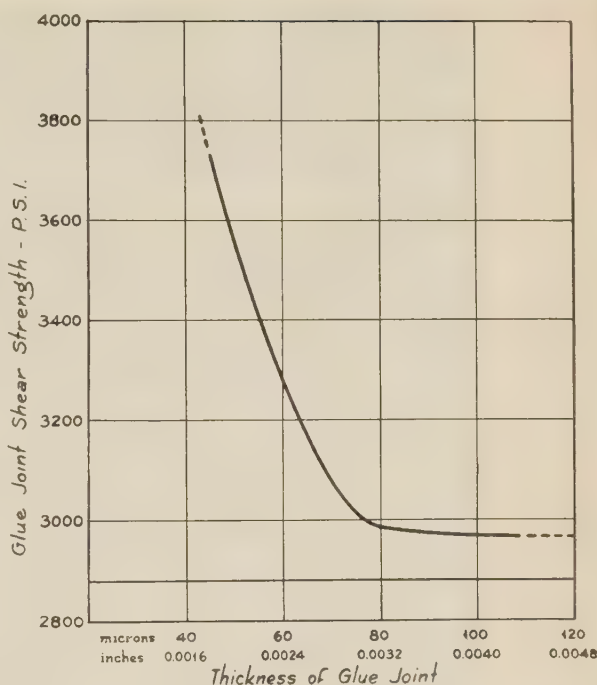


FIG. 10 GLUE-JOINT SHEAR-STRENGTH AND FILM-THICKNESS RELATIONSHIP FOR PLANED SURFACES

resulted from the polymerization of many smaller molecules. Reasoning thus, there is but one molecule of glue between the surfaces of a two-membered assembly and such a molecule is flanked on either side by innumerable wood molecules. It may be that the wood molecules are attracted by the outer bonds of the glue, which are free. Such free bonds are thought to exist because the number of urea and formaldehyde molecules which may enter into the formation of a lone molecule through polymerization is indefinite.

Further study of the nature of adhesion is imperative if the present procedures in bonding wood to wood, wood to metal, or any other combination of these are to be improved. It is hoped such investigations may be initiated in the near future.

CONCLUSIONS

- 1 Only minimum pressure would be necessary if optically smooth surfaces could be prepared for wood; just enough to squeeze the glue line down to a thin continuous layer.
- 2 Relatively smooth surfaces (planed) result in the strongest glue joints.
- 3 Splintery surfaces (sanded and sawed) provide poor anchorage for glue and should be avoided.
- 4 Weaker joints also result from splintery and irregular surfaces because they do not mesh well, hence the glue film is less even, and thicker.
- 5 Burnished surfaces, although smooth, do not produce good joints because of charring.
- 6 Cold-setting urea-formaldehyde glue does not penetrate into hard maple wood, except into those cells the cavities of which are open to the spread surface.
- 7 "Specific adhesion" and "mechanical adhesion" are largely responsible for the adhesive strength between glue and wood. Another phenomenon as yet unexplained requires further research. Why does a thin glue film result in a joint of greater shear strength than the shear strength of the glue itself?

⁷ "Adhesives and Adhesion," by J. W. McBain and W. B. Lee, *Journal of Physical Chemistry*, vol. 31, 1927, p. 1675.

⁸ Shear strength of glue was 2880 psi. See Fig. 10 at 2880 psi.

New Machines for Creep and Creep-Rupture Tests

By M. J. MANJOINE,¹ EAST PITTSBURGH, PA.

This paper describes two new creep-rupture machines. One combines eight conventional lever-arm creep machines into a single unit but with individual furnaces, controls, and recording equipment. The elongation of each test specimen is indicated by a revolution counter and can be read directly. The indicating counters for the eight specimens are brought to a single panel and photographed periodically to obtain a continuous record of the creep. The counters are driven by new extensometers which are attached to the test specimens. Two types of extensometers are used; one which gives readings over a 3-in. gage length in hundred thousandths of an inch for measuring small strains up to 2 per cent total strain, and a second extensometer which records in ten-thousandths inch for strains up to rupture. The second is a screw-driven creep-rupture machine in which the specimen is loaded through a stiff spring. A continuous elongation-time curve up to rupture is automatically recorded without the need of an extensometer on the test specimen. The machine has a capacity of 10 tons and occupies a floor space of only 15 × 15 in. It can also be used to make short-time tensile, constant-strain-rate, and relaxation tests. The latter test requires the use of an extensometer on the gage length of the test specimen. To illustrate the satisfactory operation of these machines, the results of creep-to-rupture tests on a cast 25 Cr 12 Ni alloy are presented. The data from these tests are summarized in "design curves" which serve to describe the behavior of a material at a given temperature.

INTRODUCTION

IN recent years great progress has been made in the development of alloys for high-temperature service, bringing about the need for new testing equipment. While the most universally accepted method for testing high-temperature alloys is the long-time creep test, short-time tensile tests (1)² are also widely used. More recently the constant strain-rate (2, 3) and the relaxation tests (4, 5) have been used to advantage as a rapid means of testing and comparing alloys. Some investigators (6, 7) have suggested that the service life of a high-temperature alloy be based upon a certain amount of deformation without rupture rather than on a given total deformation alone, such as 1 per cent in 10,000 hr, or on an allowable creep rate. These investigators have used the sustained-load rupture test to test and compare alloys.

¹ Research Engineer, Westinghouse Electric and Manufacturing Company. Jun. A.S.M.E.

² Numbers in parentheses refer to the Bibliography at the end of the paper.

Contributed by the Metals Engineering and Applied Mechanics Divisions and presented at the Semi-Annual Meeting, Pittsburgh, Pa., June 19-22, 1944, of THE AMERICAN SOCIETY OF MECHANICAL ENGINEERS.

NOTE: Statements and opinions advanced in papers are to be understood as individual expressions of their authors and not those of the Society.

The machines described in this paper were designed at the Westinghouse Research Laboratories to test alloys developed for high-temperature furnaces and other applications. Since the allowable strains may be rather large, the creep-to-rupture test was selected as the most suitable means of evaluating the alloys used in furnace constructions.

CREEP-RUPTURE MACHINES

In a creep-rupture test, a specimen is held at a constant load and temperature and allowed to elongate until rupture occurs. At high loads rupture may occur in a few hours while at a somewhat lower load the rupture time may extend to a few thousand hours. Since the time to rupture may vary over this wide range, two types of testing machines were designed, one for the long tests and the other for the shorter tests. The testing machine for the longer tests will be referred to as the lever-arm creep machine while the other will be called the screw-driven creep-rupture machine.

Lever-Arm Creep Machine. In the lever-arm creep machine, shown in Figs. 1 and 2, the specimen is loaded through a lever arm with weights. The specimen is attached by means of threaded heads to extension pieces which project out of each end of the furnace. The lower extension piece is anchored to the frame with a spherical seat and the upper extension piece is attached to the horizontal lever arm. Load is applied to the specimen by placing weights on the hanger at the end of a lever arm having the ratio 20 to 1. The maximum load which can be put on the hanger is 600 lb, giving a stress of 60,000 psf or a standard 0.505-in.-diam specimen. Four separate specimens are mounted in a common frame.

Each specimen has a separate electric furnace and power supply. The temperature of the furnace is controlled by an expansion rod located near the furnace winding. The difference in expansion of the rod in the furnace and an invar rod located outside the furnace wall is magnified by a 10-to-1 lever arm and used to operate an electric contact which controls the current in the furnace winding. An electronic control, Fig. 3, is used so that no contact pressure is necessary at the contacts. The average temperature can be held to within ± 2 deg F.

The standard creep specimen is shown in Fig. 4. The coupon on the end of the specimen is used for metallurgical studies. This coupon is cut into two parts. One part is retained as a sample of the material "as received." The other part is placed in the furnace with the specimen from which it was cut and undergoes the same temperature cycle; it is then studied to determine the effect of the temperature cycle on the material without stress. After the test a micrograph of a section of the specimen and the specimen itself are studied to determine the effect of stress, time, and exposure to temperature.

In designing this machine two types of tests were anticipated: (a) the creep test under a large constant load in which the specimen would be strained to rupture, and (b) the creep test under a comparatively small constant load in which the specimen would elongate less than 2 per cent total strain. To satisfy the require-

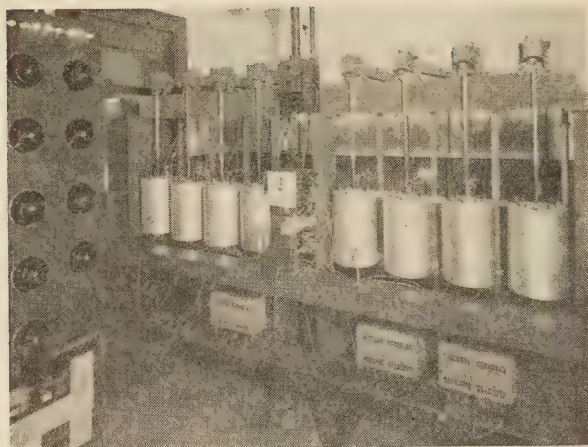


FIG. 1 LEVER-ARM CREEP MACHINE

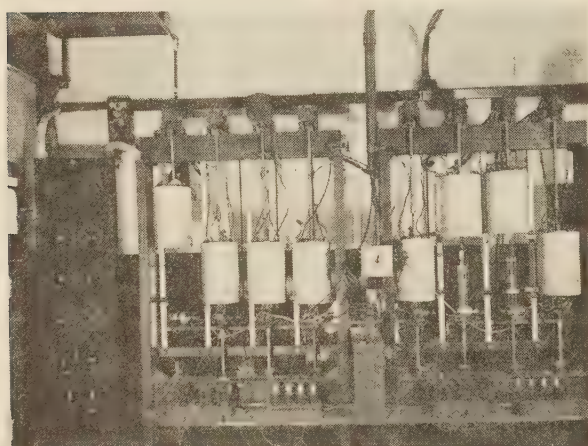


FIG. 2 LEVER-ARM CREEP MACHINE

ments of each type of test, two kinds of extensometers were built, a "creep-rupture" extensometer and a "sensitive" extensometer.

The creep-rupture extensometer is shown at the left in Fig. 5, and at the right in Fig. 6. The extension is measured from the heads of the specimen because the gage length undergoes considerable reduction of area when the test is carried to rupture, and therefore an extensometer cannot be clamped to the gage length. Since there may be some plastic flow at the fillet, the extension measured at the heads must be corrected to give the actual strain. This correction is found by putting an extensometer on the gage length and on the heads to find the "effective gage length" of the specimen. The effective gage length is the ratio of the deformation measured at the heads to the strain in the gage length. The extensometer is attached to the heads of the specimen by pins (see Figs. 5 and 6). Holes are drilled through the heads of the specimens for these pins which are about 0.1 in. diam. The comparison rods extend from the pin clamps out of the furnace and terminate in steel plates. The two plates are kept in the same relative sidewise position by a set of flat springs, as shown in Fig. 6. The comparison rods are made of a high-temperature alloy which has good dimensional stability at the temperature used. The movement caused by bending of the specimen or non-axial loading is taken up by the two pins and the reduced sections of the rods which are at right angles to the pins.

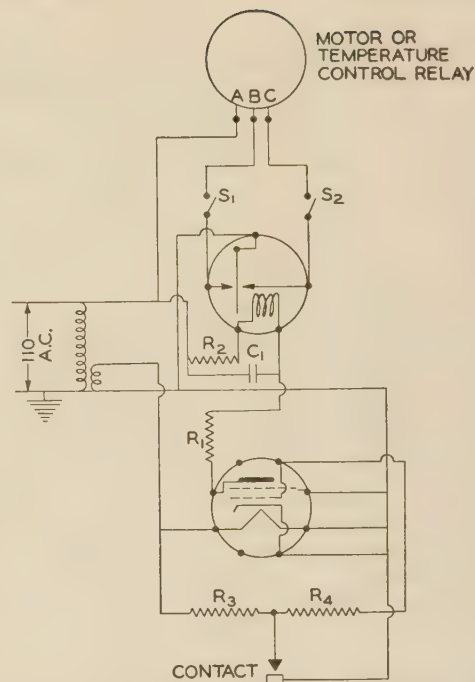


FIG. 3 CIRCUIT FOR EXTENSOMETER AND TEMPERATURE CONTROLS

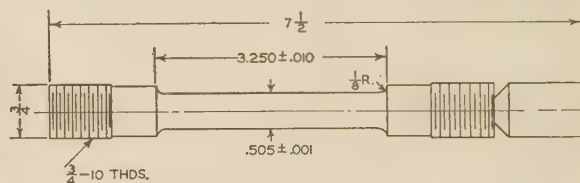


FIG. 4 HIGH-TEMPERATURE CREEP SPECIMEN

As the specimen elongates, the heads and plates separate an equal amount. The creep is therefore found by measuring the relative displacement of these plates with a motor-driven micrometer. To indicate the amount of extension or creep, a revolution counter is coupled to the micrometer-screw drive through a flexible shaft. To make the recording continuous, one electrical contact from the control is mounted on the upper plate and the other contact to the micrometer screw which is held in the lower plate. When no elongation takes place, the contacts are closed and the motor which drives the micrometer is stopped. As the specimen elongates, the contacts separate; this causes the motor to start and drive the micrometer until the contacts are closed. In this manner the micrometer follows up the creep of the specimen. The electronic control is shown in Fig. 3. Because of this control no pressure is necessary on the contacts. The micrometer screw is driven through a special gear drive, as shown in Figs. 5 and 6. The counter coupled to the gear drive reads in ten-thousandths of an inch. For the 3-in. gage length of the standard specimen (Fig. 4), this gives a least count for the extensometer of 3.3×10^{-5} in. per in.

The sensitive extensometer is shown on the right in Fig. 5 and on the left in Fig. 6. Since the strains are less than 2 per cent, this extensometer can be clamped to the gage length, Fig. 6. The pins are replaced by short wires from the clamps to the plates which carry the rods. In this extensometer the movement of the plates which hold the comparison rods is magnified by a 10-to-1 lever arm. This magnification is accomplished through a double cross-spring pivot which serves both to magnify the motion and

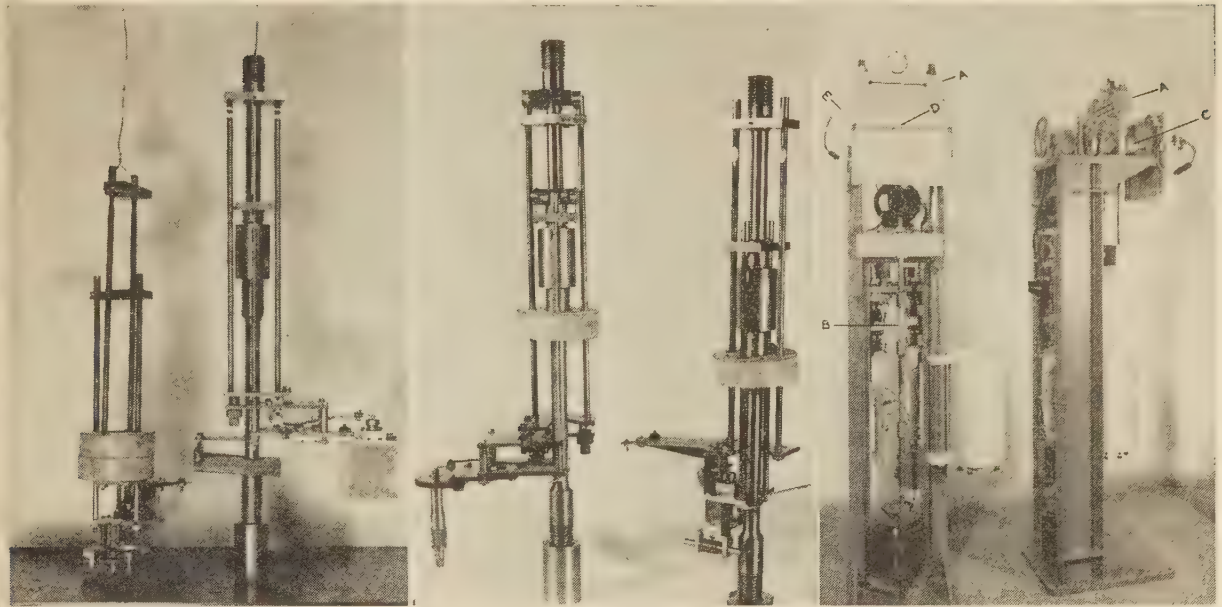


FIG. 5 HIGH-TEMPERATURE EXTENSOMETERS FIG. 6 HIGH-TEMPERATURE EXTENSOMETERS FIG. 7 SCREW-DRIVEN CREEP-RUPTURE MACHINE

to maintain the alignment of the plates. This pivot is very rugged and allows considerable mishandling without changing the calibration of the lever arm. However, because of the limited travel of the lever arm, this extensometer cannot be used for specimens which rupture. The electrical contacts are now placed on the lever arm and on the micrometer screw which is fastened to an extension of the lower plate. Either a motor-driven, Fig. 5, or a hand-driven micrometer, Fig. 6, can be used. When the motor-driven micrometer is used, the recording counter reads in hundred-thousandths of an inch or 3.3×10^{-6} in. per in. for a 3-in. gage length. The same least count can be obtained when the hand micrometer is used.

Eight of the lever-arm creep machines are assembled into a single unit. Illustrations of two of these units are shown in Figs. 1 and 2. Each specimen has its own furnace, recording, and control equipment. The electronic controls for the strain and temperature regulation are housed in the cabinets on the lower shelf of the machines. The eight counters which indicate the creep for the extensometer are brought to a single panel at the middle of the two machines. Another counter on the panel indicates the time. The camera at the middle of the unit is a motion-picture camera which takes a single-shot exposure of the counters every 4 hr. This camera film gives a continuous record of the creep of each specimen with time.

Above the camera is a thermocouple switch into which three thermocouples from each specimen can be plugged. The temperatures are read on a potentiometer by stepping from one thermocouple to the next. The stepping is done by remote control at the potentiometer. One thermocouple from each specimen is brought directly to the eight-point recorder shown at the extreme left in Fig. 2, for a permanent continuous record. The panel to the right of the temperature recorder contains a separate variable power supply for each furnace. The pilot lights at the top of the panel indicate if the furnace is heating.

Since some of the specimens elongate until rupture occurs, a contact is placed on a support beneath the weights of each machine so that the extensometer is shut off when the specimen breaks and allows the weights to fall on the support. As a check

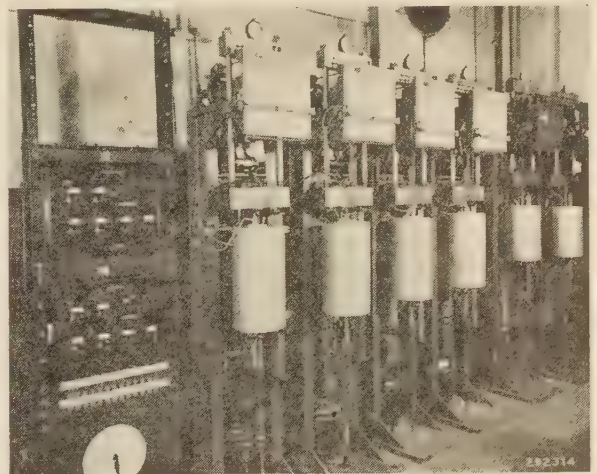


FIG. 8 CREEP-RUPTURE MACHINES IN OPERATION

on each test, daily readings are also taken of the counters and the thermocouples.

Screw-Driven Creep-Rupture Machine. In the shorter creep-rupture tests, the specimens elongate to rupture in a few hours. In these tests, the loads and strains are much larger than those of the creep tests. Since the tests are so short, readings of the elongation must be made every few minutes. To avoid these many readings, a machine was developed which automatically records the elongation of the specimen against time from start of test until rupture occurs. Since the strain is much larger in this short test, a less sensitive measurement can be used.

The machine is shown in Fig. 7 and consists of a stiff spring *A* in series with the test specimen *B*, which is loaded by a screw-driven jack *C*. The load is maintained by keeping a constant deflection of the spring *A*. The deflection of the spring is meas-

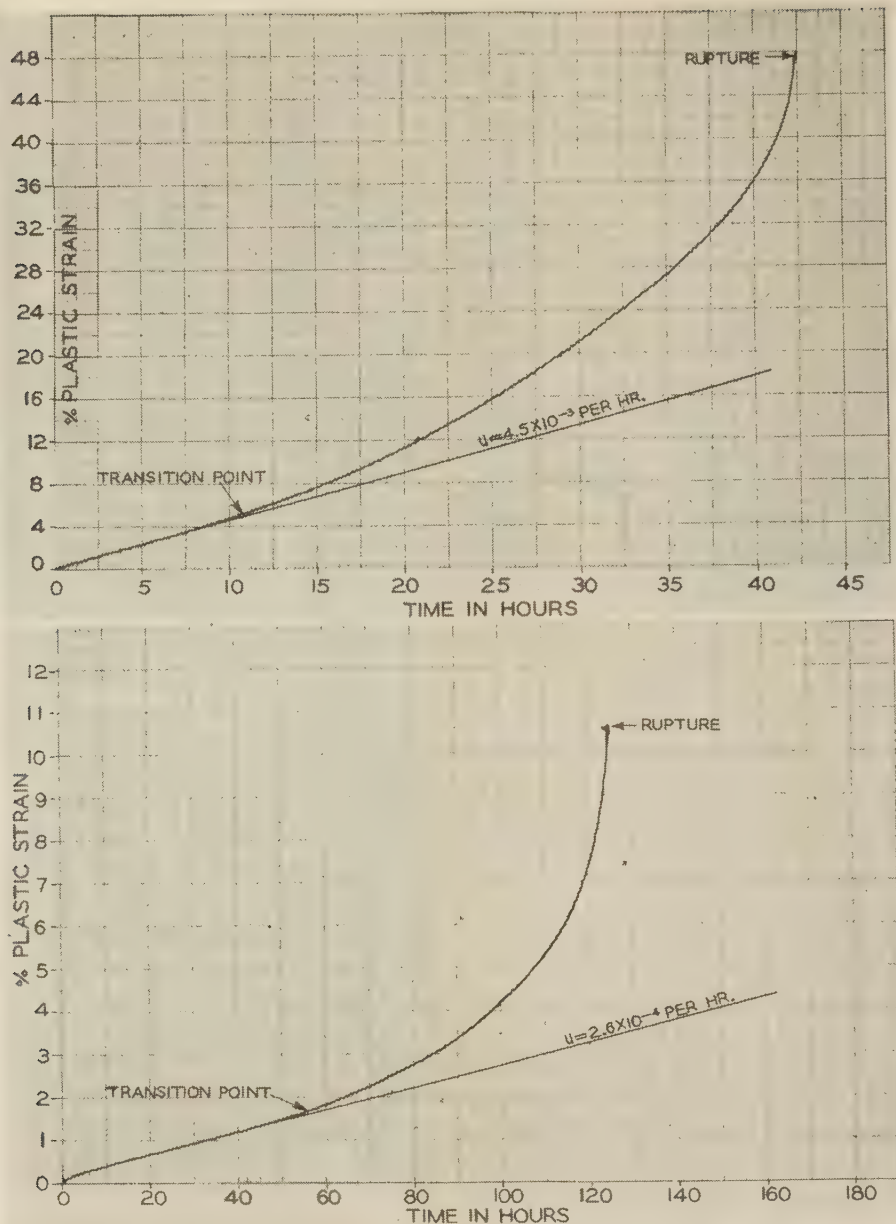


FIG. 9 ORIGINAL CURVES FROM CREEP-RUPTURE MACHINE

ured by a dial gage to which an electrical contact has been added. This electrical contact controls the motor which drives the jack to keep the load constant. The deformation of the test specimen is measured from the relative motion of the upper head of the machine and the stationary frame, that is, through the rise of the jack. This motion is magnified through a gear train and drives the pen of the recorder *D* vertically. A time clock *E* drives the pen horizontally. The recorder therefore plots a continuous elongation-time curve. The accuracy of this measurement of elongation depends upon the following conditions.

Since the load and temperature are held constant, the thermal and elastic deflections of the entire system are fixed. Therefore, the relative motions of the heads of the machine (the movement of the jack) are caused by the plastic flow of the parts of the system

which consist primarily of the extension pieces and the specimen. The cross-sectional area of the extension pieces in the hot zone of the furnace is over 4 times that of the gage length.

An inspection of the stress versus creep-rate curve, Fig. 12, will show that the creep rate in the extension pieces will be less than 0.01 per cent of that in the gage length. There are, however, parts of the specimen in which the stress is nearly as large as that in the gage length; these parts are the threads, heads, and fillets. The average stress in the minimum cross section in the threads is two thirds that of the gage length, and the stress at the heads is one half. The relative creep rates are, respectively, 2 per cent and 0.3 per cent that of the gage length (see Fig. 12). Because of the length of these parts, the relative plastic flow is much smaller. The largest plastic flow

outside the gage length takes place in the fillets. This flow, however, is nearly counterbalanced by the reinforcing effect of the heads. In order to compensate for the plastic flow outside the gage length, an "effective gage length" must be determined for each shape of specimen. This effective gage length is found by comparing the relative motion of the heads of the machine with the strain of the gage length, as follows:

$$\text{Effective gage length} = \frac{\text{Relative movement of machine heads}}{\text{Elongation of gage length per inch}}$$

The relative movement of the machine heads is the movement of the jack and is measured by the recorder. The elongation of the gage length is found by clamping an extensometer to the gage length. It has been found that the effective gage length depends primarily upon the shape of the test specimen and varies only slightly from alloy to alloy. Thus knowing the effective gage length of the test specimen, the strain of the gage length can be measured by the recorder without an extensometer on the gage length, and a continuous record of strain can be plotted against time. At the instant of rupture of the specimen, the machine is shut off by a control circuit which passes through the test specimen. In this manner the strain at rupture is more accurately determined than can be measured by matching the broken halves of the specimen.

The machine occupies a floor space of only 15×15 in. but has a capacity of 10 tons which gives a stress of 100,000 psi for the standard 0.505-in.-diam specimen.

To measure small loads as well as large loads, a special two-range spring is used which consists of two parallel beams cut from a single block of steel (see A, Fig. 7). When the lower beam is loaded, it deflects toward the second beam. At a load of about 4000 lb, it reaches the second beam, and then both beams carry the higher loads up to 20,000 lb. The flexibilities of the two beams are such that the dial gage makes a full revolution for each range.

The advantage of this machine lies in the fact that no extensometer is necessary on the specimen for creep-rupture tests, so that the only parts protruding from the furnace are the thermocouples and the extension pieces. No weights are necessary, and the rate of initial loading can be controlled.

A group of six of these machines is shown in Fig. 8. The temperature controllers are shown in the stand at the extreme left. Commercial controllers are used to short a resistance in series with the furnace. These controllers keep the temperature within ± 5 deg F. The dial of a stepping relay is shown at the bottom of the stand. Three thermocouples from each machine are brought to this relay, and individual readings can be made on a potentiometer. A six-point recorder is used to keep a continuous record of the temperature of each furnace. This recorder is placed at the top of the stand but was not installed at the time this view was photographed.

The recorded curves obtained from these machines have been very satisfactory. Two typical original curves plotted by one of these machines are shown in Fig. 9. The upper one presents a creep-rupture curve of a very ductile alloy. This alloy shows no first-stage creep. The transition point³ is indicated. The ripple in the curve is caused by the screw which drives the pen and not by fluctuations of temperature or load. This ripple has been eliminated by straightening the drive screw. Minimum creep rates as low as 10^{-5} per hr and as high as 0.1 per hr have been recorded. Normally stresses are used which give rupture lives greater than 10 hours and less than 400 hrs. The lower curve shows a creep-rupture curve of a less ductile alloy. This curve

³ Defined as that point in the third stage of creep at which the creep rate has increased 10 per cent over the minimum rate.

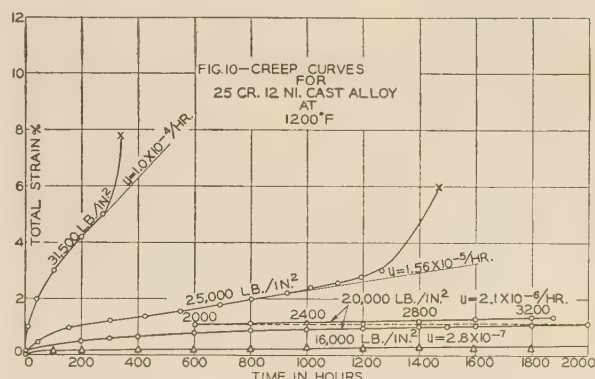


FIG. 10 CREEP CURVES FOR 25 Cr 12 Ni CAST ALLOY AT 1200 F

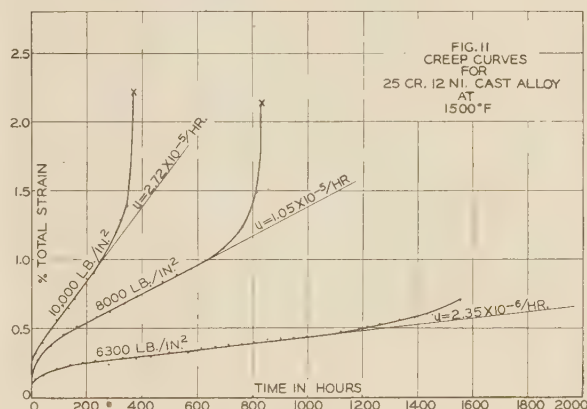


FIG. 11 CREEP CURVES FOR 25 Cr 12 Ni CAST ALLOY AT 1500 F

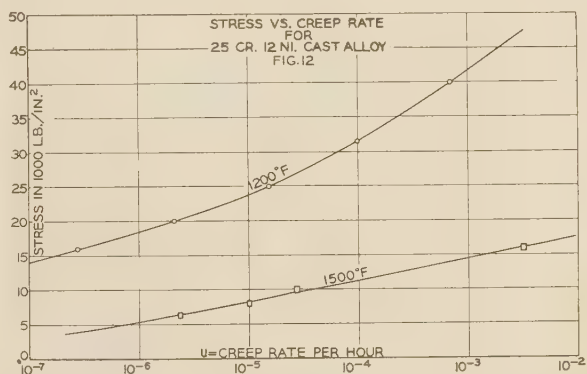


FIG. 12 STRESS VERSUS CREEP RATE FOR 25 Cr 12 Ni CAST ALLOY

has all three stages of creep. The first stage, or period of diminishing creep rate, is very short and is followed by a second stage where the rate is substantially constant. In the third stage, the rate increases until fracture occurs. The transition point is indicated at the start of the third stage.

Because of its simplicity and ease of operation, this machine has been used to compare alloys, to check the effect of heat-treatments, and to obtain creep-rupture data in the stress range which gives rupture lives from 1 to 300 hr.

Although the machine was designed for creep-rupture tests, other applications have been made. The machine can readily be used for constant-strain-rate or short-time tensile tests and

for relaxation tests. For constant-strain-rate and short-time tensile tests, the machine is run at a constant head speed and periodical readings are made of the load and strain. In a relaxation test, the extensometer, shown at the left in Fig. 6, is clamped to the gage length of the test specimen and the specimen is loaded. The total strain is then kept constant by setting the extensometer and using the control to regulate the load so that the extensometer contacts are kept in a fixed position. When plastic strain occurs in the specimen, the load must be lowered to decrease the elastic strain, thus keeping the total strain constant. The recorder in this type of test plots the decay of the load with time.

TEST RESULTS

To demonstrate the types of tests made on the two machines described, a high-temperature alloy was chosen. Tests were made in which the time to rupture varied over a wide range. The alloy selected is a cast 25 Cr 12 Ni iron-base alloy. This alloy is used for high-temperature parts in electric furnaces. Since such parts as baffles and trays are serviceable even after considerable plastic flow, the rupture life becomes an important limitation on the service life. The creep curves for the lower stresses are given in Figs. 10 and 11, for tests at 1200 and 1500 F, respectively.

For purposes of direct comparison among alloys, the stresses used in the creep-rupture tests are taken from the 10 series of preferred numbers. The minimum rate of the creep-time curve is used as a comparison between alloys and also as a means of predicting the deformation at very low stresses. Stress is plotted as a function of minimum creep rate $\dot{\epsilon}$ and is shown in Fig. 12.

A second method of representing the family of creep-rupture curves on a particular alloy at a given temperature is given by

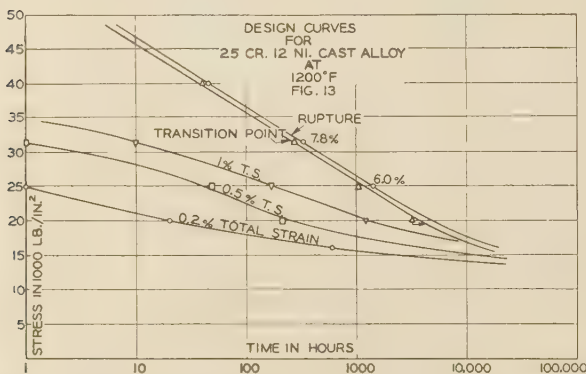


FIG. 13 DESIGN CURVES FOR 25 Cr 12 Ni CAST ALLOY AT 1200 F

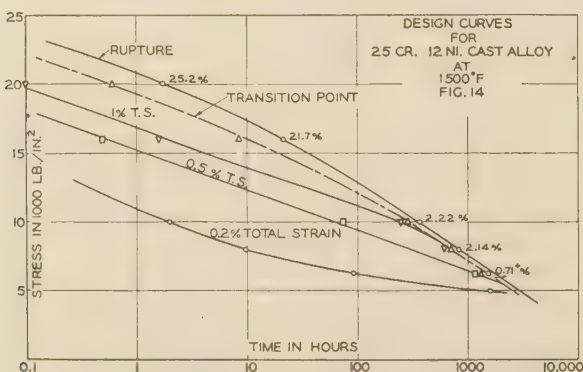


FIG. 14 DESIGN CURVES FOR 25 Cr 12 Ni CAST ALLOY AT 1500 F

the "design curves" (Figs. 13 and 14). In the "design curves" stress is plotted against the logarithm of time for several points of the creep-time curve. The following points are used: (a) 0.2 per cent, 0.5 per cent, and 1 per cent total strains; (b) the "transition point;" and (c) the rupture point. On this latter curve the total strain is shown adjacent to the test point.

The transition point is a measure of the useful life of an alloy and is defined as that point of the creep-time curve, in the third stage of creep, at which the creep rate has increased by a given percentage greater than the minimum rate. The allowable percentage increase depends upon the application.

In these curves the transition point represents the point at which the rate has increased 10 per cent over the minimum rate. An example of this point is shown in Fig. 10. From the design curves, the engineer can readily choose the stress for a given service life.

Since the curve for the transition point is practically parallel to the rupture curve, the long-time tests can be stopped when the transition point is reached and many hours of testing time can be saved.

CONCLUSIONS

Two new creep-rupture machines have been described. One, a lever-arm creep machine, combines the compactness of a multiple unit with the flexibility of an individual one. Each of the eight specimens of the machine is equipped with an extensometer which gives a direct reading of the extension on a counter. A continuous record of the elongation of all the specimens is made by photographing these counters periodically. Two types of extensometers are used; one which gives readings in hundred-thousandths of an inch for measuring small strains up to 2 per cent, and a second which records in ten-thousandths of an inch for strains up to rupture.

The other machine is a radically different type of creep-rupture machine which loads the specimen through a stiff spring and records a continuous creep-to-rupture curve without the use of an extensometer on the specimen. Occupying a space of only 15 X 15 in., this machine has a capacity of 10 tons. It can also be used for making short-time tensile tests, constant-strain-rate tests, and relaxation tests.

ACKNOWLEDGMENTS

The author expresses his appreciation to Dr. A. Nadai for suggesting the need for these machines, to Mr. E. A. Davis for assisting in their design, and to Dr. L. W. Chubb, Director of the Westinghouse Research Laboratories for permission to publish the results.

BIBLIOGRAPHY

- 1 Symposium on "Effect of Temperature on the Properties of Metals," A.S.M.E.-A.S.T.M., June, 1931.
- 2 "High-Speed Tension Tests at Elevated Temperatures—Parts II and III," by A. Nadai and M. J. Manjoine, *Journal of Applied Mechanics*, Trans. A.S.M.E., vol. 63, 1941, p. A-77.
- 3 "Constant-Strain-Rate Tests on 0.35 C Steel K20 at 850 F," by A. Nadai and E. A. Davis, Trans. A.S.M.E., vol. 59, 1937, pp. 447-450.
- 4 "Relaxation of Steels at Elevated Temperatures. A New Automatic Relaxation Machine," by A. Nadai and J. Boyd, Proceedings of the Fifth International Congress of Applied Mechanics, 1938, p. 245.
- 5 "Relaxation of Metals at High Temperatures," by W. E. Trumpler, Jr., *Journal of Applied Physics*, vol. 12, 1941, pp. 248-253.
- 6 "Rupture Strength of Steels at Elevated Temperatures," by A. E. White, C. L. Clark, and R. L. Wilson, Trans. A.S.M.E., vol. 26, 1938, pp. 52-80.
- 7 "Correlation of High Temperature Creep and Rupture Test Results," by R. H. Thielemann, Trans. A.S.M., vol. 25, 1941, pp. 355-372.

Some Thermal Effects in Oil-Ring Journal Bearings

By R. A. BAUDRY,¹ EAST PITTSBURGH, PA.

This paper discusses the design of oil-ring journal bearings from the thermal standpoint and gives a method for predetermining the operating temperature of air-cooled and water-cooled bearings. It is shown that at high temperatures the performance of a ring-lubricated bearing has a tendency to become unstable. The design features of a high-speed water-cooled and a forced-ventilated bearing are given.

NOMENCLATURE

The following nomenclature is used in the paper:

- a = area, sq in.
- b = axial length of bearing surface, in.
- d = journal-bearing diameter, in.
- f = coefficient of friction
- h_0 = minimum oil-film thickness, in.
- k = coefficient of heat transfer, watts per sq in. per deg C
- l = developed length of bearing surface, in.
- l = length of heat path, in.
- N = revolutions per minute
- P = unit bearing pressure on projected area, psi
- q = quantity of cooling liquid, gpm
- U = peripheral velocity of journal, ips
- R_L = leakage factor
- t = temperature, deg C
- V_L = side leakage, cu in. per sec
- S.U.V. = viscosity, Saybolt Universal
- Z = oil viscosity, centipoises
- η = radial clearance, in.
- ρ = specific thermal resistance, deg C per in. per watt

INTRODUCTION

Because of its simplicity and reliability, the oil-ring journal bearing is used on most of the rotating electrical equipment built today, and much effort is spent to improve its performance and extend its range of application.

The satisfactory performance of this type bearing is usually judged by its ability to dissipate the heat generated by the internal friction of the lubricant.

OPERATING TEMPERATURE

The predetermination of the operating temperature of the bearing involves two distinct problems:

1 Calculation of the friction losses.

2 Calculation of the thermal resistance to the flow of heat from the oil film to the cooling medium.

For many years numerous tests on various types of bearings have been conducted in research laboratories (1, 2).² These tests,

¹ Mechanical Engineer, Westinghouse Electric & Manufacturing Company. Mem. A.S.M.E.

² Numbers in parentheses refer to the Bibliography at the end of the paper.

Contributed by Special Research Committee on Lubrication and presented at the Annual Meeting, New York, N. Y., Nov. 27-Dec. 1, 1944, of THE AMERICAN SOCIETY OF MECHANICAL ENGINEERS.

NOTE: Statements and opinions advanced in papers are to be understood as individual expressions of their authors and not those of the Society.

with the help of theoretical work (3, 4, 5, 7, 9), published in recent years, make it possible to predetermine with a reasonable accuracy the performance of journal bearings.

The coefficient of friction of a bearing is usually given as a function of the characteristic number ZN/P , as shown in Fig. 1, which is discussed in Appendix 1.

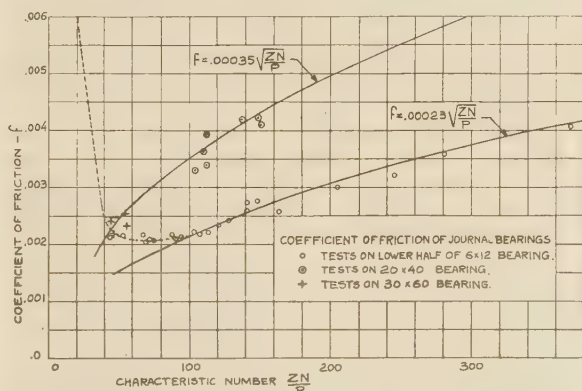


FIG. 1 COEFFICIENT OF FRICTION OF 90-DEG CENTRAL PARTIAL BEARING; $\eta = 0.0015$, $\frac{1}{d} = 2$

(Dotted line represents estimated friction near and below ZN/P critical for a 6×12 bearing.)

A convenient way of analyzing the performance of a bearing is to plot the friction loss for a given load and speed as a function of the oil-film temperature, as shown in Fig. 2, for oils having viscosities of 150, 200, and 300 S.U.V. at 100 F, respectively. The friction losses decrease with rising temperature until conditions corresponding to the critical value of ZN/P are reached, then they increase rapidly as shown in dotted lines in Fig. 2.

The heat dissipated from the bearing can also be plotted as a

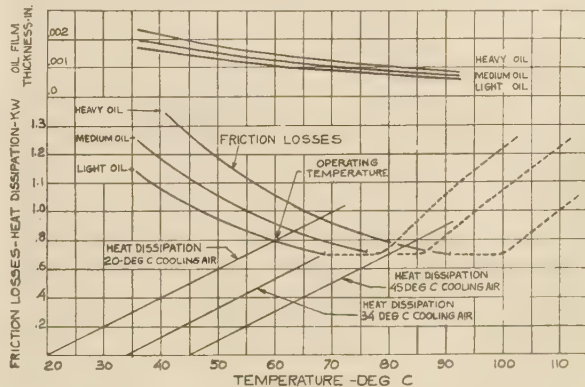


FIG. 2 OPERATING TEMPERATURE OF 6×12 BEARING

(Active length of bearing = $9\frac{3}{4}$ in., $P = 150$ psi, $N = 900$ rpm. Friction losses are given for light, medium, and heavy oils having viscosities of 150, 200, and 300 S.U.V. at 100 F, respectively. Solid line corresponds to $f =$

$0.00035 \sqrt{\frac{ZN}{P}}$ dotted line to dotted line of Fig. 1.)

straight-line function of the bearing-surface temperature intersecting the temperature axis at the temperature of the cooling medium, which in this case is air. The slope of this line is determined by the thermal resistance to the flow of heat through the bearing as discussed in Appendix 2. The intersection of the curves, representing the friction losses and heat dissipation, indicates the operating temperature of the oil film and gives the friction losses for the specified condition.

Critical Operating Temperature. It is seen that with the light oil, when the temperature of the cooling air attains 34 C, the critical ZN/P for this particular bearing is reached, and at higher temperature it will operate under condition of boundary lubrication. When the temperature of the cooling air reaches 45 C, the two lines do not intersect any more, and the friction losses increase faster than they can be dissipated from the bearing. There exists therefore an unstable condition which will cause seizure of the bearing. At this temperature only the heavy oil will give a sufficient factor of safety for this bearing. Furthermore, the increase in operating temperature with the heavy oil is relatively small.

Critical Starting Temperature. Most bearings used with electrical machines remain under constant pressure during the starting period, and for a short time during that period they operate under condition of boundary lubrication. The journal becomes supported on a perfect oil film at a speed which makes the characteristic number ZN/P larger than its critical value. The speed corresponding to this critical value varies with the temperature and viscosity of the oil, as shown in Fig. 3, which has been plotted for a 6×12 bearing loaded to 150 psi, having a critical value of ZN/P equal to 50.

At the beginning of the starting period, there will be an appreciable temperature rise of the bearing surface due to the high coefficient of friction corresponding to boundary lubrication, as shown in Fig. 3 by the line intersecting the temperature axis at the starting temperature. At low temperature this effect is very small but it becomes larger with increasing temperature until a point is reached at which a perfect oil film cannot be formed before normal speed is attained. This is shown in Fig. 3 for a light oil and a starting temperature of 65 C. With this temperature the heavy oil will permit formation of a perfect oil film before the normal speed is reached.

This critical condition indicates the necessity of starting a bearing under load at a conservative temperature and of selecting an oil of sufficient viscosity to meet the starting conditions.

CRITICAL OIL SUPPLY

The maintenance of a perfect oil film necessitates an adequate

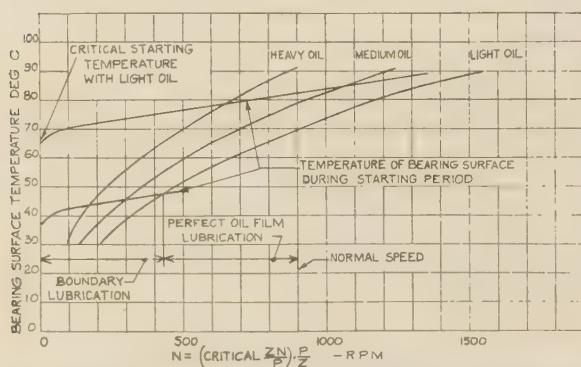


FIG. 3 SPEED AT WHICH PERFECT OIL FILM IS FORMED WHEN STARTING FROM REST UNDER LOAD

(Same conditions as in Fig. 2, except variable speed. Curves drawn for critical $ZN/P = 50$.)

supply of oil which under all operating conditions must be greater than the oil lost through side leakage (1, 10).

The side leakage of the large water-cooled bearing, described later in this paper, has been plotted as a function of the bearing temperature in Fig. 4 according to the data given in Appendix 3. It shows a slight increase of the oil requirements with increasing temperature.

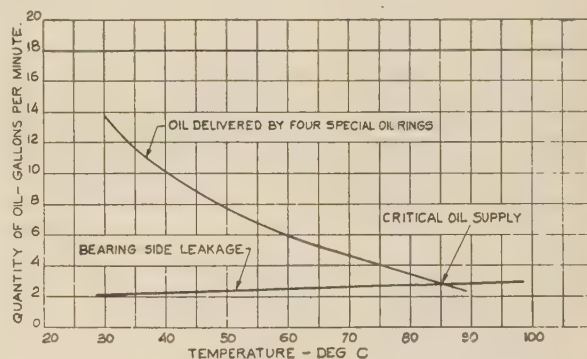


FIG. 4 CRITICAL OIL SUPPLY FOR 20×40 WATER-COOLED BEARING ($N = 720$; oil viscosity, 200 S.U.V. at 100 F.)

The oil supplied by oil rings has been the subject of several investigations (1, 10), which show a rapid decrease in the quantity supplied with an increase in temperature of the oil. The oil delivery, which is also shown in Fig. 4, was obtained from tests on a full-size model described in a previous paper (11). It is seen that above a temperature of 85 C there is not a sufficient quantity of oil supplied to maintain a perfect oil film; this will result in a thinner oil film, higher friction losses, and higher bearing temperatures, which in turn will cause a further decrease in oil delivery and a rapid failure of the bearing.

This critical operation of an oil-ring bearing at high temperature makes it necessary to provide an ample supply of oil in order to place the critical point beyond the normal operating temperature.

WATER-COOLED BEARINGS

An effective way to dissipate the friction losses from a bearing is to circulate water through ducts in the bearing shell. Many types of such bearings have been used, among which the most common is a cast-iron shell with water passages, or a conventional shell with a copper cooling tube embedded in the babbitt.

The friction losses for a large water-cooled oil-ring bearing are given in Fig. 5, as a function of the average oil-film temperature. For the speed at which this bearing operates, there is an appreciable difference in temperature between the oil film and the bearing shell which can be estimated as shown in Appendix 3 and used to plot the temperature of the bearing surface as a function of the friction losses. As in Fig. 2, the heat dissipated from the bearing is proportional to the difference in temperature between the bearing surface and the cooling water. This relationship can be represented by a straight line, the intersection of which with the bearing-surface-temperature curve indicates the operating temperature, as shown in Fig. 5, for several metals.

The use of a copper cooling lining results in a much lower oil-film temperature than is possible with other metals. In Fig. 6 is shown a copper lining for the large water-cooled bearing shown in Fig. 7. It is made of rolled copper plate into which holes have been drilled for the water passages. This lining is fastened to a heavy steel shell by a number of bronze screws, and covered

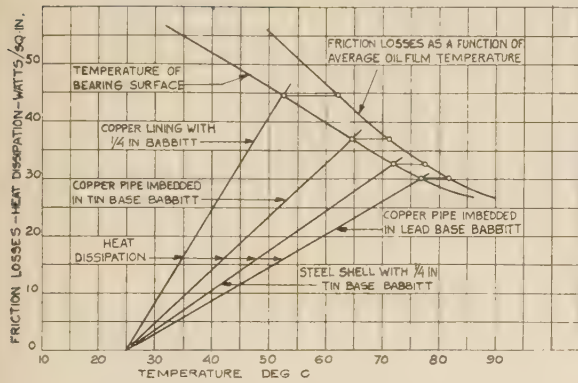


FIG. 5 OPERATING TEMPERATURE OF 20 X 40 WATER-COOLED BEARING

($N = 720$; oil viscosity, 200 S.U.V. at 100 F; temperature of cooling water, 25 C; heat dissipation taken from Fig. 11.)

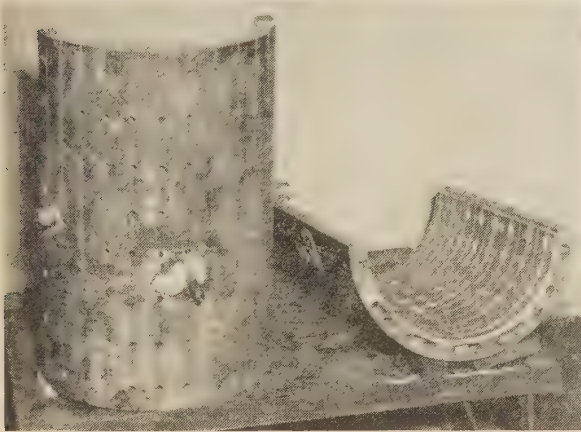


FIG. 6 COPPER LINING FOR 20 X 40 WATER-COOLED BEARING

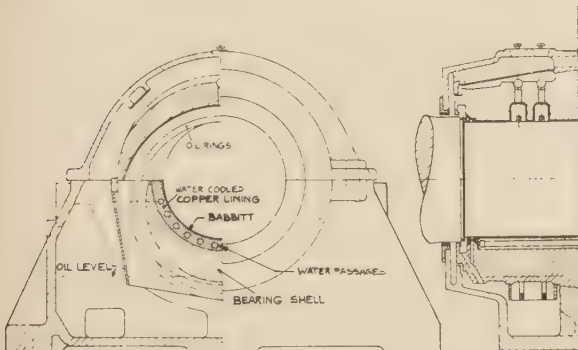


FIG. 7 CROSS SECTION OF 20 X 40 WATER-COOLED BEARING

with a thin layer of babbitt metal. The use of a copper lining reduces to a minimum the thermal stresses produced in the bearing. These stresses are of sufficient magnitude in certain cases to cause cracks in the babbitt when it is used in thick and uneven sections around the water passages.

This water-cooled bearing has been used very successfully on several large hydrogen-cooled units and was designed to operate at approximately 4000 fpm peripheral speed. For lower speeds,



FIG. 8 FORCED-VENTILATED OIL-RING JOURNAL BEARING ON 3600-RPM MOTOR

(Air, cooling the bearing, is circulated through large pipe passing under motor and connected to blower at rear end.)

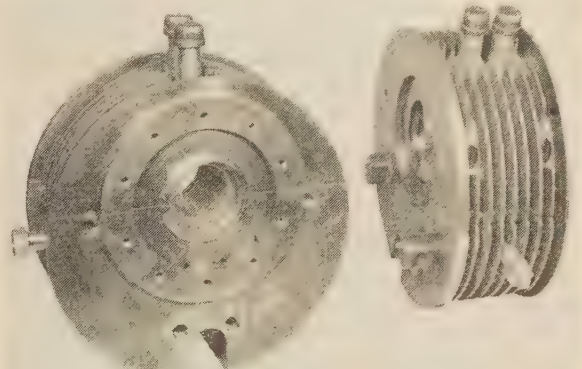


FIG. 9 HOUSING FOR FORCED-VENTILATED OIL-RING JOURNAL BEARING

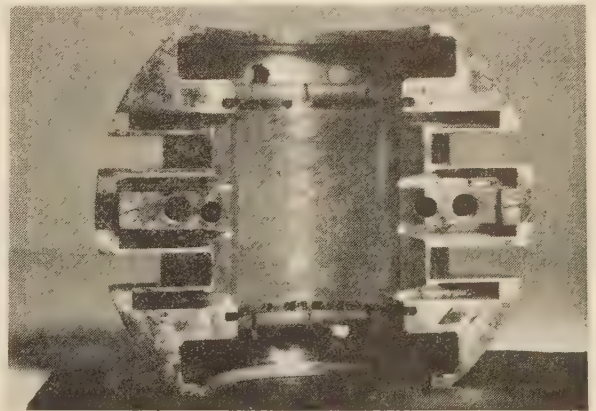


FIG. 10 LOWER BEARING SHELL FOR FORCED-VENTILATED OIL-RING JOURNAL BEARING

the friction losses make it possible to use copper pipes inserted in a steel shell, which gives the same advantage of strength as a copper shell, but at a lower cost.

FORCED-VENTILATED OIL-RING JOURNAL BEARING

Although water-cooling is a very effective way of cooling a bearing, water is not always available, and sometimes it becomes desirable to use an air-cooled bearing at higher speed than usual. In the conventional self-aligning oil-ring bearing, the largest resistances to the flow of heat from the oil film to the cooling air are at the joint between the bearing shell and the bearing housing and at the outer surface of the bearing housing where heat is dissipated to the ambient air. In Fig. 8 is shown a fan-cooled motor where part of the air used to cool the machine is circulated around the bearing housing (Fig. 9), which is provided with fins, thus obtaining a large cooling area and a high heat-transfer rate. The self-aligning spherical bearing shell (Fig. 10) has a large contact surface with the bearing housing and heavy sections of metal in order to facilitate the heat flow.

The thermal resistance of such a bearing can be calculated by a method similar to the one discussed in Appendix 2. The bearing shown in Figs. 8, 9, and 10 is 3 in. diam and operates continuously at 3600 rpm with a very low temperature rise.

CONCLUSION

With the use of available data the oil-film temperature of an oil-ring bearing can be predetermined with reasonable accuracy.

At high temperature, the performance of an oil-ring bearing becomes unstable. Depending upon the design and accuracy of manufacturing, there are several critical temperatures:

1. One at operating speed above which a steady temperature can never be reached.
2. One when starting, above which a perfect oil film cannot be formed before normal speed is reached.
3. One above which the oil rings supply less oil than required to maintain a proper oil film.

All the foregoing critical temperatures when reached will cause a continuous temperature rise of the bearing until failure results. An oil of higher viscosity increases slightly the temperature of the oil film but gives a larger margin between the operating and critical temperatures.

By a judicious choice of materials and lubricants, it is possible to design an oil-ring journal bearing which will operate at high speed with a reasonable factor of safety.

Appendix 1

FRICTION LOSSES

The coefficient of friction of a bearing is usually given as a function of the characteristic number ZN/P , and of other variables, such as the bearing angle, the clearance ratio, and the ratio length to diameter. For bearings of similar design, the coefficient of friction can be given as a function of only ZN/P , as shown in Fig. 1 for a 90-deg central partial bearing having an axial length equal to twice the diameter, and a clearance ratio of 0.0015. The lower curve in Fig. 1, obtained experimentally on a test rig consisting of two half shells of a bearing, gives values which agree with the hydrodynamic theory of lubrication. However, tests on large machines give consistently higher values, which are accounted for by the losses in the nonactive parts of the bearing, machining variations, deformations due to load and temperature, etc. These latter values of the coefficient of friction are shown on the upper curve in Fig. 1 and have been used to calculate the losses in the bearings discussed in this paper.

As found by tests (12) at low values of ZN/P , the coefficient of friction deviates from the value indicated by conditions of perfect lubrication, it decreases with ZN/P to a minimum value and then increases rapidly. This critical value of ZN/P is a function of the

design of the bearing shell and manufacturing conditions; it can be brought down to a very low value by a sturdier design which minimizes distortion, accurate machining or fitting and running-in, etc.

A critical value of ZN/P of 50 has been found for the experimental bearing in Fig. 1. To this value of ZN/P corresponds a minimum oil-film thickness of 0.0009. Since for a given value of ZN/P , the minimum oil thickness increases proportionately to the diameter of the journal, the critical value of ZN/P decreases with an increase in size of the bearing, as has been found by experience.

For this reason, a given critical value of ZN/P can be used to determine the performance of a bearing only if it has been obtained experimentally on the same size of bearing and under similar operating conditions.

Appendix 2

DISSIPATION OF HEAT FROM BEARING

In a self-cooled oil-ring bearing, the heat generated in the oil film is removed by conduction through the bearing shell and by the oil circulated by the oil rings, some of which passes through the oil film as end leakage. The heat then flows through different paths, by both conduction and convection to the outside surface of the housing and then to the ambient air. The different factors determining the rate of heat transfer between oil or air and metals have been found experimentally (1, 13) and can be used to determine the thermal resistance to the flow of heat from the oil film to the cooling medium. The flow of heat through a bearing and its housing can best be represented by using the electrical analogy (14) which is used very successfully to determine the temperature of electric machines.

The flow of heat in solids can be represented in the same form as that for the flow of electricity. If there is a flow of energy w in a path of cross section a , the temperature variation over a length l is

$$t = w\rho \frac{l}{a}$$

where ρ is the specific thermal resistance of the material expressed in deg C per in. per watt.

The transfer of energy from a cooled surface by radiation and convection is a greatly complicated phenomenon, but for practical purposes it is usually assumed that, for a flow of energy w across a surface of area a , the temperature difference between the cooled surface and the cooling medium is

$$t = w \frac{1}{ka}$$

Where k is the coefficient of heat transfer expressed in watts per sq in. per deg C of temperature difference.

When heat is removed by a cooling fluid circulated at a rate q , for a flow of energy w , the temperature rise of the fluid is

$$t = w \frac{\theta}{q}$$

Where θ is the temperature rise of a unit volume of the fluid corresponding to a unit flow of energy.

When the flow of the fluid is expressed in gpm (gallons per minute), and w in watts, $\theta = 0.0038$ for water, and 0.0095 for oil (for the average conditions obtained in bearings).

The foregoing thermal resistances $\rho \frac{l}{a}$, $\frac{1}{ka}$, $\frac{\theta}{q}$ can be combined in

parallel, in series, or in combination of both as electrical resistances and solved by the same methods.

In a water-cooled bearing, the path for the flow of heat from the bearing surface to the cooling water is quite simple and can be determined graphically, as shown in Fig. 11, where the thermal resistance of the complete path is also given for several combinations of materials.

For air-cooled oil-ring journal bearings, the path for the flow of heat is much more complicated, and the coefficients of heat

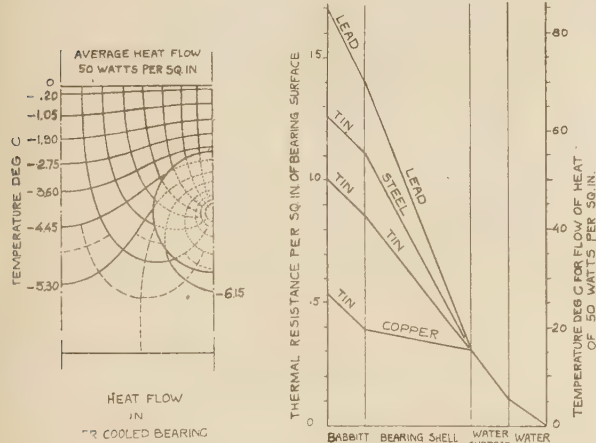


FIG. 11 WATER-COOLED OIL-RING JOURNAL BEARING. THERMAL RESISTANCE BETWEEN BEARING SURFACE AND COOLING WATER FOR VARIOUS METALS

(Specific thermal resistance of copper = 0.102
Specific thermal resistance of tin = 0.625
Specific thermal resistance of steel = 0.91
Specific thermal resistance of lead = 1.24
Flow of water for bearing = 10 gpm
Flow of water per sq. in. of bearing surface = 0.017 gpm
Coefficient of heat transfer from cooling water to bearing shell, 4 w per sq in. per deg. C.)

transfer between the various surfaces and oil or air have to be determined by tests duplicating operating conditions (1), as much as possible.

The thermal-resistance network for a 6 × 12 bearing of conventional design is shown in Fig. 12, as well as the flow of heat through the different paths.

Appendix 3

AVERAGE TEMPERATURE OF OIL FILM

With high friction losses, the temperature gradient through the thickness of the oil film becomes appreciable, i.e., it is 24 C through an oil film 0.001 in. thick for a rate of heat flow of 100 w per sq in. In a water-cooled bearing, most of the heat generated in the oil film flows to the bearing surface and only a negligible amount to the journal. For moderate speed where the rate of shear and viscosity are nearly constant through the thickness of the oil film, the average temperature of the latter above the surface of the bearing is independent of the oil-film thickness (4, 6) and equal to

$$t \text{ deg C} = 1.29 \times 10^{-6} ZU^2$$

Example: For a peripheral velocity of 750 ips, and an oil having a viscosity of 10 centipoises at 70 C, the average temperature of the oil film will be 7.25 deg C above the temperature of the bearing surface.

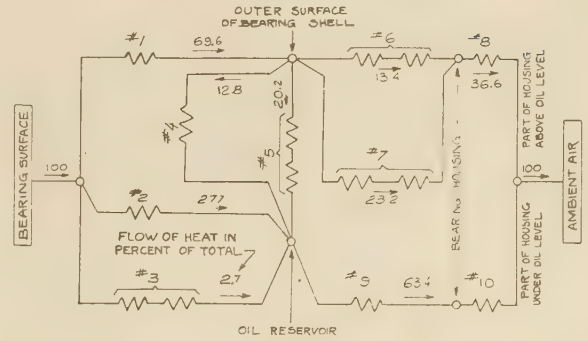


FIG. 12 AIR-COOLED OIL-RING JOURNAL BEARING. THERMAL RESISTANCE BETWEEN BEARING SURFACE AND AMBIENT AIR (The following numbers correspond to thermal resistance in diagram:

1 Bearing shell in radial direction

$$r_1 = \frac{l_1}{a_1 p_1} = \frac{2}{300} \times 0.78 = 0.0052$$

2 Oil end leakage

$$r_2 = \frac{0.0095}{q} = \frac{0.0095}{0.15} = 0.653$$

3 Oil at side relief

$$r_3 = \frac{1}{k_{23} a_3} + \frac{0.0095}{q} = \frac{1}{0.1 \times 17} + \frac{0.0095}{0.15} = 0.063$$

4 Bottom of bearing shell dipping in oil reservoir

$$r_4 = \frac{1}{k_{45} a_4} = \frac{1}{86 \times 0.1} = 0.116$$

5 Oil spray in oil-ring groove

$$r_5 = \frac{1}{k_{56} a_5} + \frac{0.0095}{q} = \frac{1}{290 \times 0.1} + \frac{0.0095}{0.3} = 0.0658$$

6 Outside of bearing shell to housing

$$r_6 = \frac{1}{k_{67} a_{67}} + \frac{1}{k_{68} a_{68}} = \frac{1}{750 \times 0.01} + \frac{1}{1070 \times 0.01} = 0.226$$

7 Outside of bearing shell to housing

$$r_7 = \frac{l_{71}}{a_{71} p_1} + \frac{l_{72}}{a_{72} p_7} = 0.131$$

8 Outside of housing to air

$$r_8 = \frac{1}{a_8 k_8} = \frac{1}{1070 \times 0.02} = 0.0467$$

9 Oil in reservoir to housing

$$r_9 = \frac{1}{a_9 k_9} = \frac{1}{1670 \times 0.02} = 0.03$$

10 Outside of housing to air

$$r_{10} = \frac{1}{a_{10} k_{10}} = \frac{1}{1670 \times 0.02} = 0.03$$

Over-all thermal resistance from bearing surface to air = 0.0553.)

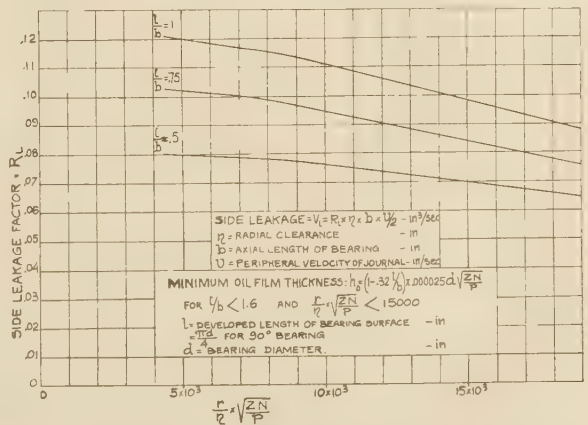


FIG. 13 SIDE LEAKAGE IN 90-DEG CENTRAL PARTIAL JOURNAL BEARING

Appendix 4

MINIMUM OIL-FILM THICKNESS AND END LEAKAGE

The oil-film thickness and the flow of oil in a bearing of finite width have been investigated by many authors (1, 3, 7). The data they have published have been discussed in a previous paper (2) and used to plot the values of the side leakage and of the oil-film thickness given in Fig. 13, which are in reasonable agreement with experimental values (10, 15).

BIBLIOGRAPHY

- 1 "Performance of Oil-Ring Bearings," by G. B. Karelitz, Trans. A.S.M.E., vol. 52, 1930, paper APM-52-5.
- 2 "Journal Bearing Performance," by R. Baudry and L. M. Tichvinsky, Trans. A.S.M.E., vol. 57, 1935, p. A-121.
- 3 "The Theory of Film Lubrication," by R. O. Boswall, Longmans, Green and Company, London, Eng., and New York, N. Y., 1928.
- 4 "Theory of Lubrication," by Mayo D. Hersey, John Wiley & Sons, Inc., New York, N. Y., 1938.
- 5 "Optimum Conditions in Journal Bearings," by A. Kingsbury, Trans. A.S.M.E., vol. 54, 1932, paper RP-54-7, pp. 123-148.
- 6 "Fundamentals of Automotive Lubrication," by H. C. Dickin-

son and O. C. Bridgeman, *S.A.E. Journal*, vol. 31, July, 1932, pp. 278-282, and 304.

7 "Effects of Side Leakage in 120-Degree, Centrally Supported Journal Bearings," by S. J. Needs, Trans. A.S.M.E., vol. 56, 1934, pp. 721-732.

8 Discussion by R. Baudry of (7), Trans. A.S.M.E., vol. 57, 1935, pp. 136-137.

9 "Graphical Study of Journal Lubrication," by H. A. S. Howarth, Trans. A.S.M.E., vol. 45, 1923, pp. 421-448; vol. 46, 1924, pp. 809-832; vol. 47, 1925, pp. 1073-1099. Combined reprint, under the title, "A Graphical Analysis of Journal-Bearing Lubrication," was published by the A.S.M.E. in 1928.

10 "Side Oil Flow in a 120-Degree Bearing," by G. B. Karelitz, *Mechanical Engineering*, vol. 57, 1935, pp. 292-293.

11 "Performance of Oil Rings," by R. Baudry and L. M. Tichvinsky, *Mechanical Engineering*, vol. 59, 1937, pp. 89-92.

12 "Friction of Journal Bearings as Influenced by Clearance and Length," by S. A. McKee and T. R. McKee, Trans. A.S.M.E., vol. 51, 1929, APM-51-15.

13 "The Basic Laws and Data of Heat Transmission," by W. J. King, *Mechanical Engineering*, vol. 54, 1932, pp. 190-194, 275-279, 296, 347-353, 410-414, 426, 492-497, and 560-565.

14 "Steady Flow of Heat in Large Turbine-Generators," by C. R. Soderberg, Trans. A.I.E.E., vol. 50, June, 1931, pp. 782, 801.

15 "Film Lubrication in Sleeve Bearings," by M. Stone, *Journal of Applied Mechanics*, Trans. A.S.M.E., vol. 57, 1935, p. A-59.

Effect of Aeration on Gear-Pump Delivery and Lubrication Ceiling

By P. H. SCHWEITZER,¹ STATE COLLEGE, PA.

Gear-pump delivery falls off with altitude and, above a certain point, it fails to provide the necessary engine lubrication. By deductive reasoning, an equation has been developed for calculating the gear-pump delivery with aerated oil and also the "lubrication ceiling." Charts are presented to show the effect on lubrication ceiling of (1) entrained air, (2) dissolved air, (3) pipe length, (4) pipe diameter, (5) tank height, pressure boost, valves, and ells, (6) oil viscosity, (7) pump speed. According to results obtained, a reduction of dissolved air and reduced pipe resistance between oil tank and pressure pump have relatively small effects on the lubrication ceiling. Effective ways to raise the ceiling are pressurizing the oil tank and reducing the pump speed.

GEAR pumps have been used almost exclusively in aircraft-engine lubrication systems and have given excellent service, except for difficulties experienced as a result of aeration, especially at high altitudes. A most common trouble caused by aeration is reduced pump delivery. It has been shown by Dolza² and Pigott³ that aeration at high altitude markedly reduces the delivery of the gear pump. It has also been pointed out that small-diameter pipes, sharp bends, valves, and reducers in the suction line, in combination with entrained and dissolved air in the oil, are harmful, and adverse conditions are aggravated by such factors as high oil viscosity and high pump speed.

The object of this paper is to enable the reader to predict gear-pump delivery with aerated oil under a variety of circumstances. A further object is to show how the "lubrication ceiling" is influenced by a number of factors.

NO AERATION

The gear pump is a positive-displacement pump, hence its delivery is constant except when the tooth space fails to fill up with liquid. However, even in an ideal gear pump, pumping liquid which is completely air and gas free, at a speed which assures that its rotors are completely filled, by reducing the inlet pressure progressively, a point is finally reached at which the liquid begins to vaporize. At that and lower pressures, cavitation sets in, and the tooth space will be filled partially with vapor. In consequence, below the cavitation point *C* in Fig. 1, the pump delivery decreases rather sharply, to become zero at zero absolute inlet pressure, when all of the tooth space is filled with vapor.

In the foregoing, pump losses such as "back delivery" and "slip" have been ignored. With an ordinary gear pump, such as shown in Fig. 2, there is an appreciable clearance volume between

the teeth. The amount of liquid contained in that clearance volume is taken from the discharge side and delivered back to the inlet side. Therefore, the pump delivery will be that much less. The geometric displacement is defined as

$$V_{geo} = 2NLH \dots\dots\dots [1]$$

where *N* is the number of gear teeth on one gear, *L* the effective length of the gears, *H* the tooth area, consisting of $(1/N)(D^2\pi/4 - G)$, *D*_o the outer diameter of the gear, *G* the cross-sectional area of the gear, including the hub cross section.

Referring to Fig. 3, borrowed from Pigott,⁴ the tooth space

⁴ "Some Characteristics of Rotary Pumps in Aviation Service," by R. J. S. Pigott, Trans. A.S.M.E., vol. 66, 1944, pp. 615-623.

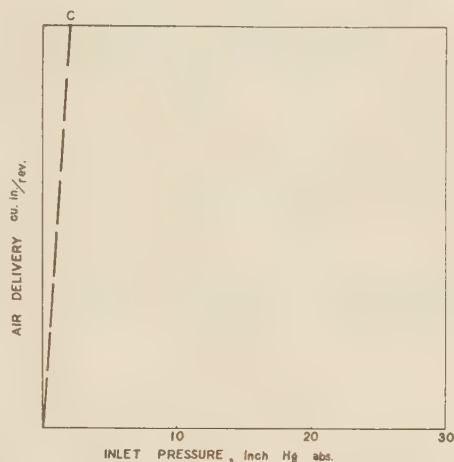


FIG. 1 GEAR-PUMP DELIVERY, IDEAL

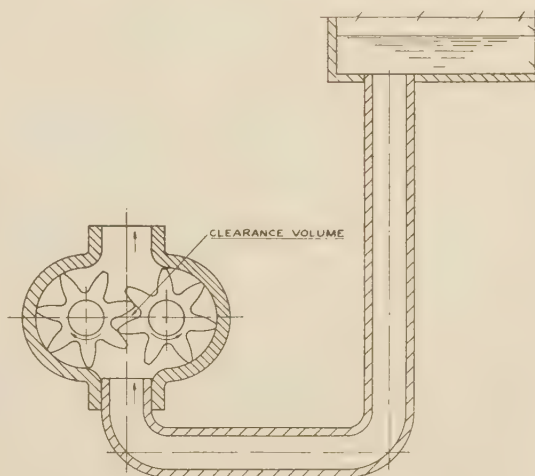


FIG. 2 ELEMENTS OF AN EXTERNAL GEAR PUMP

¹ Professor of Engineering Research, Pennsylvania State College. Mem. A.S.M.E.

² "Correlation of Ground and Altitude Performance of Oil System," by John Dolza, presented at S.A.E. meeting, June 8, 1942.

³ "Oil Aeration," by R. J. S. Pigott, S. A. E. Journal, March, 1944, pp. 73-84.

Contributed by the Oil and Gas Power and Aviation Divisions and presented at the Annual Meeting, New York, N. Y., Nov. 27-Dec. 1, 1944, of THE AMERICAN SOCIETY OF MECHANICAL ENGINEERS.

NOTE: Statements and opinions advanced in papers are to be understood as individual expressions of their authors and not those of the Society.

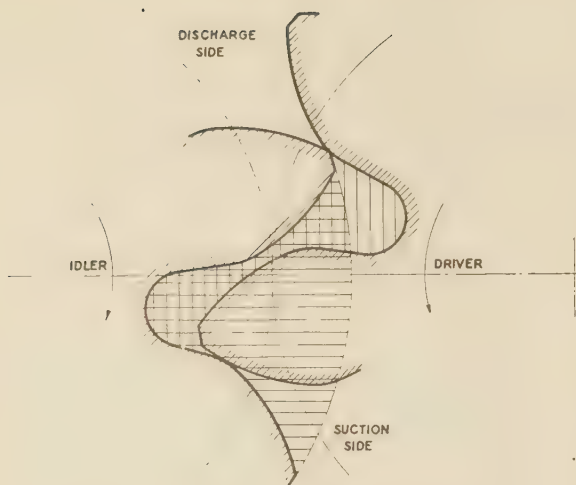


FIG. 3 TOOTH SPACE AND CLEARANCE VOLUME

(Horizontal shaded area represents tooth space; vertical shaded area represents clearance volume.)

corresponds to the horizontally shaded area H , the clearance volume to the vertically shaded area V . The back delivery B can then be expressed as

$$B = NLV \dots \dots \dots [2]$$

and the gear-pump delivery as

$$Q = n(V_{geo} - B) = n 2NL \left(H - \frac{V}{2} \right) \dots \dots \dots [3]$$

in cubic inches per minute.

It is convenient to express the gear-pump delivery in the form of volumetric efficiency η , defined as

$$\eta = \frac{Q/n}{V_{geo}} \dots \dots \dots [4]$$

with which

$$\eta = 1 - \frac{V}{V_{geo}} = 1 - \frac{V}{2H} \dots \dots \dots [5]$$

This permits the gear-pump delivery to be predicted by planimetry. If $V/H = 0.2$, the pump delivery will be reduced (due to back delivery) by 10 per cent.

Slip also reduces the pump delivery. Slip is the leakage of the liquid past the periphery, the face and the shaft of the gears. Slip is naturally dependent upon the machining clearances, the pressures, the liquid viscosity, and rotative speed. In aviation-type gear pumps, delivering lubricating oil, the slip is of the order of 3 per cent of the delivery but, under unfavorable conditions, it may be much more. In Fig. 4, the effect of slip is shown by the dash-dot line, which is drawn 3 per cent below the delivery line as already reduced by the clearance.

The cavitation point C in Fig 1 was related to the absolute inlet pressure. What really controls the cavitation, as well as aeration, is not the inlet pressure as it is measured at the pump flange but the pressure existing in the tooth space, Fig. 2. If there is neither a pressure drop between the pump entrance and the tooth space nor a pressure rise due to leakage from the discharge side, then the tooth-space pressure is equal to the pump-flange pressure, but ordinarily the former is lower. There are numerous losses in pressure resulting from the entry of the liquid into the

gear pump, the most important ones belonging to the following three categories:

1 Impact loss in the pump housing, due to changes in the cross section and direction of the flow, varies with the square of the flow quantity and can be calculated by the known hydraulic formulas. According to Pigott,⁵ the impact loss may be expressed as

$$\Delta p_i = 0.000108 \rho v^2 \dots \dots \dots [6]$$

where ρ for 180 deg S.A.E. 60 oil is 52.44 lb per cu ft and varies only slightly with the temperature.

* 2 Centrifugal loss: For entering the tooth space the liquid has to overcome the centrifugal force, which, as was shown by Dolza,² amounts to

$$p_c = \frac{1}{2} \omega^2 \rho (R^2 - r^2) \dots \dots \dots [7]$$

where ω = angular speed of gear, radians per sec

r = root radius, in.

R = addendum radius, in.

ρ = mass density of liquid, lb in.⁻⁴ sec²

p_c = centrifugal pressure upon liquid, psia

The product $\omega^2 \rho$ happens to be close to $\frac{\text{rpm}^2}{1,000,000}$ for lubricating oil.

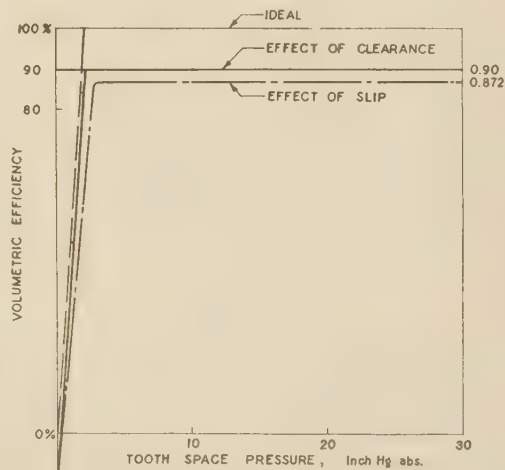


FIG. 4 GEAR-PUMP DELIVERY; EFFECT OF CLEARANCE AND SLIP

3 Acceleration pressure loss: This is spent on raising the velocity of the liquid from pump-flange velocity to peripheral velocity of the pump gear. If the liquid did not have a velocity equal to the gear tip when it is picked up, the liquid column would break and cavitation would set in. The acceleration pressure loss can be expressed as

$$p_a = \frac{\rho}{2} (v_t^2 - v_f^2) \dots \dots \dots [8]$$

where ρ is the mass density of liquid (lb in.⁻⁴ sec²), $v_t = R\omega$ the gear-tip velocity, and v_f the pump-flange velocity, both in in. per sec.

⁵ "Preliminary Calculations on Air-Oil Performance of Spur-Gear Pumps," Gulf Research and Development Company Report KG-00 of April 13, 1942, and Supplement File KG-00-I, of Jan. 17, 1944.

In a typical gear pump, described by Pigott,⁵ the respective values for normal delivery are as follows:

Impact loss in pump housing.....	$p_i = 0.353$ psi
Centrifugal loss.....	$p_c = 1.23$ psi
Acceleration pressure loss.....	$p_a = 1.85$ psi

making the total pressure loss in the pump 3.433 psi.

Considering the pressure difference between the pump flange and the tooth space, the delivery shown with dot-dash line in Fig. 4, plotted against the pump-flange pressure will appear as in Fig. 5. The point *C* (Fig. 1) moves 3.433 psi \cong 7 in. Hg to the right to *C'*. This point, frequently referred to as the knee point, break point, or fall-off point, is naturally determined by the pump losses and the vaporization pressure of the liquid.

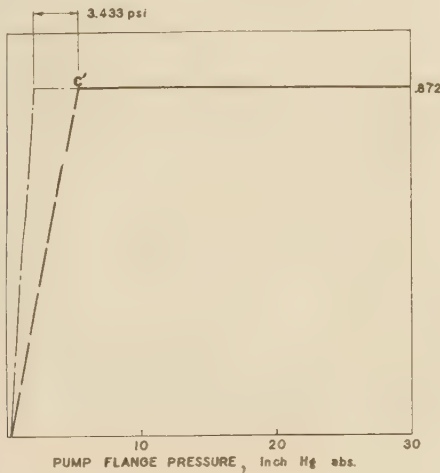


FIG. 5 GEAR-PUMP DELIVERY RELATED TO PUMP-FLANGE PRESSURE

The foregoing description of gear-pump behavior refers to an incompressible liquid medium that is completely air, gas, and vapor free, down to the vaporization pressure. Under such circumstances the pump volumetric efficiency will not be affected by such factors as liquid viscosity, pump speed, and absolute inlet pressure, except at inlet pressures below the fall-off point.

In reality, the lubricating oil always contains air and, frequently, also some vapor and gases. Air is present in the oil in two forms, entrained air and dissolved air.

Entrained air is in the form of bubbles. Large bubbles are very unstable as they quickly rise to the surface and either collapse or form foam. Small air bubbles make the oil lighter in color and opaque. They are more stable although given time they all settle out. Oil free from entrained air is transparent or translucent but it still contains a certain amount of dissolved air. Dissolved air is invisible and, since it only fills the intermolecular spaces, it does not increase the oil volume. In equilibrium, lubricating oil holds approximately 8 per cent air in solution under normal pressure and temperature conditions. We have found⁶ that the amount of air dissolved is proportional to the pressure. If the ambient pressure increases, the oil absorbs proportionately more air from the atmosphere; if it decreases, part of the dissolved air evolves in the form of bubbles. Under violent agitation, as in the gear pump, the evolution of air takes place very quickly.

While the amount of dissolved air in the lubricating oil is

⁶ "Air-Lock and Foaming in Aero-Engine Lubrication System," Report of May, 1943, from The Pennsylvania State College, Engineering Experiment Station, to the National Advisory Committee for Aeronautics.

small and varies but slightly, the amount of entrained air may be considerable and vary a great deal along the circuit. It generally enters the system in the engine crankcase. As the capacity of the scavenge pump usually exceeds the capacity of the pressure pump by a considerable margin, the difference is made up largely by entrained air. Therefore, the oil discharged by the scavenge pump contains 50 per cent or more entrained air and 8 per cent or so dissolved air. Most of the entrained air is eliminated (usually in the oil tank) before the oil enters the pressure pump, but 2 to 12 per cent or more may remain and affect the pressure-pump delivery unfavorably. The amount of entrained air remaining depends greatly upon the design of the oil tank. Some "hopper-type" tanks render a poor performance with respect to air separation.

Other gases may be present in the oil, originating from piston-ring blow-by, and vapor from gasoline dilution. Like air they may be entrained or dissolved and are controlled by similar laws. All air, gas, and vapor may be treated alike with respect to their influence on the delivery of the gear pump, and the term "aeration" is intended to cover all of them.

EFFECT OF AERATION ON GEAR-PUMP DELIVERY

Entrained Air. The amount of entrained air or gas in the oil may be expressed by its volume *NTP* (under 60 F temperature and 14.7 psia pressure) relative to the oil volume; which means that the amount of entrained air at ambient barometric pressure⁷ p_b is

$$V_{(pb)}^{NTP} = e V_{oil} \dots \dots \dots [9]$$

The volume of this air under tooth-space pressure is

$$V_{(pb)}^{(pt)} = \frac{p_b}{p_t} e V_{oil} \dots \dots \dots [10]$$

The tooth space is filled partly with oil and partly with entrained air, therefore

$$V_{geo} = V_{oil} + \frac{p_b}{p_t} e V_{oil} = V_{oil} \left(1 + e \frac{p_b}{p_t} \right) \dots \dots [11]$$

Dissolved Air. Any dissolved air that may be present in the oil occupies no volume therefore need not be considered in Equation [11]. On the other hand, any dissolved air that comes out of solution in the tooth space as a result of the reduced pressure must be considered. The next problem therefore is to determine how much dissolved air comes out of solution while the oil flows from the tank through the pipe and pump housing into the tooth space.

If the clear oil contains under *NTP* (sea level) condition *d* part of dissolved air in equilibrium

$$V_{(po)}^{NTP} = d V_{oil} \dots \dots \dots [12]$$

at a lower barometric pressure existing in the oil tank, the amount of the dissolved air will be

$$V_{(pb)}^{NTP} = \frac{p_b}{p_o} d V_{oil} \dots \dots \dots [13]$$

and at the still lower pressure existing in the tooth space, the amount of the dissolved air will be

$$V_{(pt)}^{NTP} = \frac{p_t}{p_o} d V_{oil} \dots \dots \dots [14]$$

⁷ Where terms p_b , p_t , and p_o appear as exponents or subscripts they will be given as (pb) , (pt) , and (po) , respectively.

Consequently, on its way from the oil tank to the tooth space (see Fig. 2) an amount of

$$V_r^{NTP} = V_{(pb)}^{NTP} - V_{(pt)}^{NTP} = \frac{p_b - p_t}{p_o} d V_{oil} \dots [15]$$

dissolved air will be released. This amount of air will occupy a greater actual volume at the lower p_t pressure

$$V_r^{(pt)} = V_r^{NTP} \frac{p_o}{p_t} = \frac{p_b - p_t}{p_t} d V_{oil} \dots [16]$$

or

$$V_r^{(pt)} = d V_{oil} \left(\frac{p_b}{p_t} - 1 \right) \dots [17]$$

This volume of air will augment the volume of entrained air contained in the oil and will displace a corresponding volume of oil from the tooth space. In consequence, the geometric delivery will include an additional member and, in place of Equation [11], we obtain

$$V_{geo} = V_{oil} + \frac{p_o}{p_t} e V_{oil} + \left(\frac{p_b}{p_t} - 1 \right) d V_{oil} \dots [18]$$

from which the oil delivery can be expressed as

$$V_{oil} = \frac{V_{geo}}{1 + e \frac{p_o}{p_t} + d \left(\frac{p_b}{p_t} - 1 \right)} \dots [19]$$

If V_{geo} is expressed in cubic inches, the oil delivery will be obtained in cubic inches per revolution. The oil delivery per minute is

$$Q = n \frac{V_{geo}}{1 + e \frac{p_o}{p_t} + d \left(\frac{p_b}{p_t} - 1 \right)} \dots [20]$$

and using the term volumetric efficiency, as defined by Equation [4]

$$\eta = \frac{1}{1 + e \frac{p_o}{p_t} + d \left(\frac{p_b}{p_t} - 1 \right)} \dots [21]$$

which is a measure of the pump performance, irrespective of its size.

In Equation [21] e denotes the amount of free air entrained in the oil, and d the amount of free air dissolved in the oil, in either case cubic feet of air NTP per cubic foot of oil. If the oil is at rest and accessible for sampling, e can be determined by weighing a known volume of the aerated oil or by allowing the sample to settle. The volume decrease after complete settling gives the air content under the actual barometric conditions which can be converted to NTP conditions by Boyle's law. The air content NTP divided by the remaining oil volume gives d .

If the oil is in motion, or is otherwise inaccessible for sampling, the "Ariometer," shown in Fig. 6, may be used. The operation of this instrument is based on the relation between compressibility and air content and has been fully described elsewhere.⁶

In a conventional lubrication system, as shown in Fig. 7, a considerable amount of air is taken into the engine sump as a result of the excess capacity of the scavenge pump over the pressure pump. In consequence, the entrained air e may be 50 per cent or more at the outlet of the scavenge pump. Most of that air escapes in the oil tank and what remains at the pressure-pump

inlet should not be expected to be more than 10 per cent. The design of the oil tank may help or hinder the air separation.

For the determination of dissolved air, the Okonite tester, described in a previous report,⁶ may be used. However, under NTP conditions, the dissolved air in lubricating oil is as a rule between 7 and 11 per cent and, by assuming it to be 8 per cent, no great error will be made.

With a typical gear pump, characterized by a total pressure, loss of 3.433 psi, and a total line loss of 0.7205 psi between the tank and pump under full delivery and 2600 rpm pump speed, Equation [21] gave the results shown in Fig. 8.

The calculation is not as simple as it may appear because of the presence of p_t in the denominator. The tooth-space pressure p_t is equal to the oil-tank pressure p_b plus tank height equivalent, less line loss, less pump loss. The line loss up to the pump flange can be calculated by the method described by Pigott.⁶ It depends upon the velocity of the flowing oil, $v = Q/F$, and consists of two kinds of losses, the vee losses, which under laminar flow comprise the pipe resistance, etc., and vee-square losses like impacts, cross-sectional changes, etc. The pump losses also consist of two sets of losses, the vee-square losses in the pump housing and the tooth-entry losses, which in turn are composed of

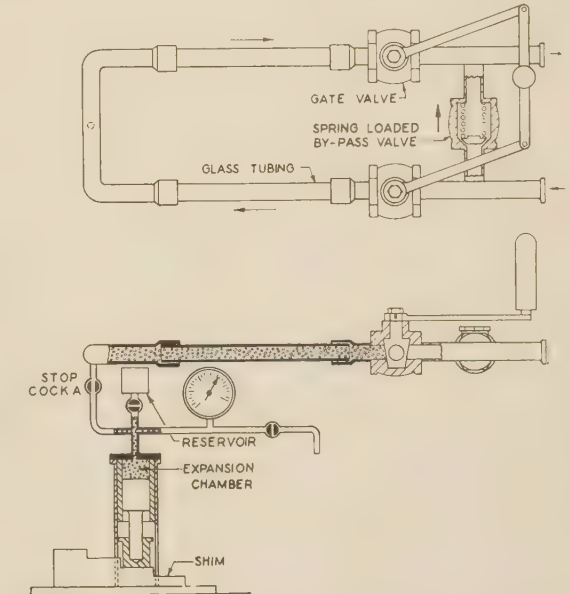


FIG. 6 ARIOMETER FOR DETERMINING ENTRAINED AIR CONTENT OF OIL

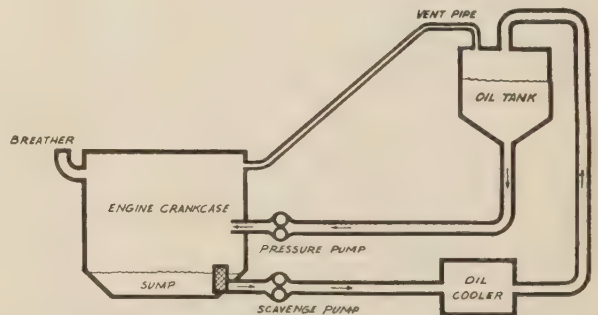


FIG. 7 BASIC COMPONENTS OF CONVENTIONAL LUBRICATION SYSTEM

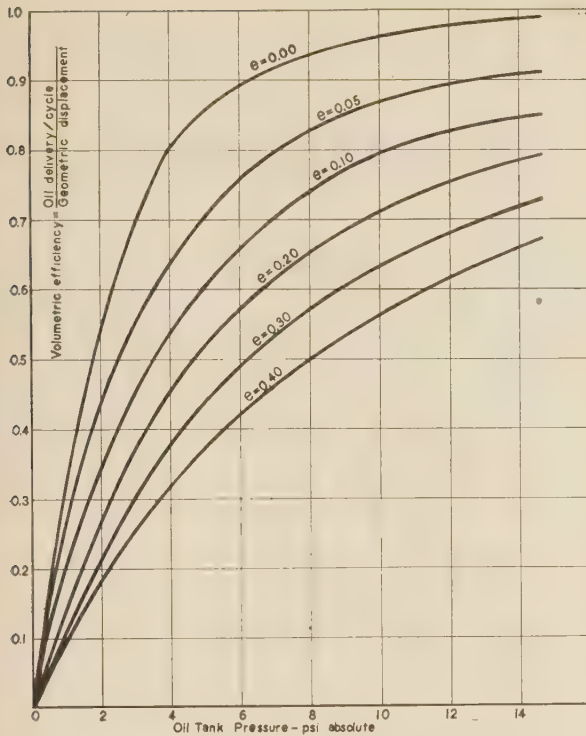


FIG. 8 CALCULATED DELIVERY FOR TYPICAL GEAR PUMP WITH 8 PER CENT DISSOLVED AIR AND VARYING AMOUNT OF ENTRAINED AIR

the centrifugal loss and the acceleration or pickup loss as previously described. Of these losses, the vee losses and vee-square losses vary with Q/F and Q^2/F^2 , respectively. The tooth-entry losses vary as the square of the pump rpm and as the first power of the oil velocity.

The dependence of p_t on the velocity $v = Q/F$ and velocity square $v^2 = Q^2/F^2$ makes a cubical Equation of [21], which, however, can be solved without higher algebra by convenient graphical methods.

Equations [20] and [21] permit the solution of a number of interesting problems which, hitherto, have been inaccessible to mathematical treatment. One of them pertains to the optimum pump speed. What speed of a given pump, pumping a given liquid at a given altitude, gives greatest delivery? With low pump speeds, the delivery obviously will increase approximately in proportion to the speed. When the speed becomes high, incomplete filling of the tooth space reduces the delivery. Above a certain speed, the negative effect of the incomplete filling resulting from aeration is greater than the positive effect of the speed increase, and the delivery will decrease.

Fig. 9 shows the oil delivery plotted against the pump speed for our typical gear pump at various altitudes. It shows that at sea level about 4000 rpm gives maximum delivery. At higher altitude the optimum pump speed will be lower; at 32,500 ft altitude less than 3000 rpm. The curve refers to aviation oil containing 10 per cent entrained air and 8 per cent dissolved air. Since it is in high altitudes where lubrication failure is likely to occur, gear pumps should be so designed as to give maximum delivery at high altitudes rather than at sea level.

In Equations [20] and [21], the slip and back delivery have been

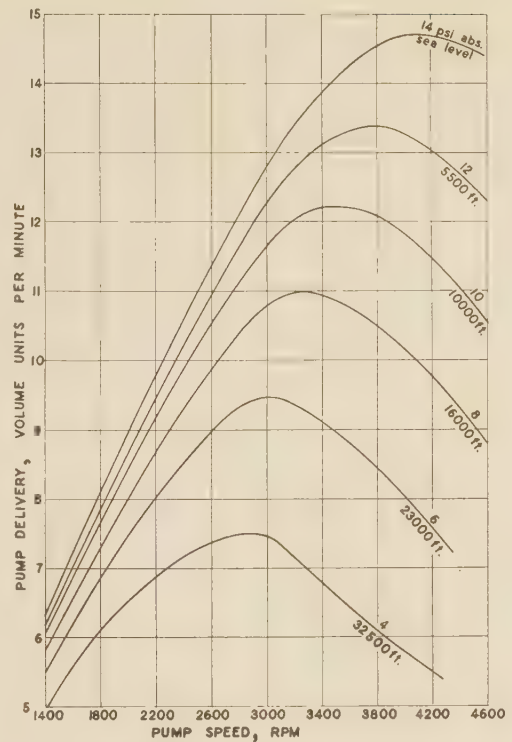


FIG. 9 OIL DELIVERY VERSUS PUMP SPEED AT VARIOUS ALTITUDES (Entrained air, 10 per cent; dissolved air, 8 per cent.)

ignored. Allowing for these, the oil delivery will be that much smaller

$$Q = n \frac{V_{geo}}{1 + e \frac{p_o}{p_t} + d \left(\frac{p_b}{p_t} - 1 \right)} - S - B \dots \dots [22]$$

The slip S , or leakage of oil between and around the gear teeth is a certain fraction of the total oil delivery, depending mainly upon the oil viscosity, discharge pressure, and machining clearances in the gear pump. In an aviation-type pump, pumping lubricating oil, it is of the order of 3 per cent. Generally it may be set as

$$S = s \frac{Q}{n} \dots \dots \dots [23]$$

The back delivery B , as just explained, is due to the clearance volume between the meshing teeth on the noncontacting side of the gear (See Fig. 3) and is a fraction of the geometric displacement and may be expressed as

$$B = b V_{geo} \dots \dots \dots [24]$$

Pumping air-free oil, b is constant and of the order of 16 per cent. With aerated oil, b will slightly decrease with aeration because the back-delivered oil also contains some air. However, in case of a pressure pump, where the inlet pressure is atmospheric or less and the discharge pressure is of the order of 100 psi, the volumetric air content in the back delivery is only a fraction of the air content of the oil fed, and its effect on b may be neglected for all practical purposes.

From Equations [22], [23], and [24], we obtain

$$\eta = \frac{1}{1+s} \left[\frac{1}{1 + e \frac{p_o}{p_t} + d \left(\frac{p_b}{p_t} - 1 \right)} - b \right] \dots \dots [25]^8$$

If we neglect slip and assume $b = 0.16$

$$\eta = \frac{1}{1 + e \frac{p_o}{p_t} + d \left(\frac{p_b}{p_t} - 1 \right)} - 0.16 \dots \dots [26]$$

which means that the effect of clearance can be provided for by a parallel translation of the volumetric-efficiency curves along the vertical axis. Fig. 10 shows the delivery of the gear pump, represented in Fig. 8, with 16 per cent back delivery.

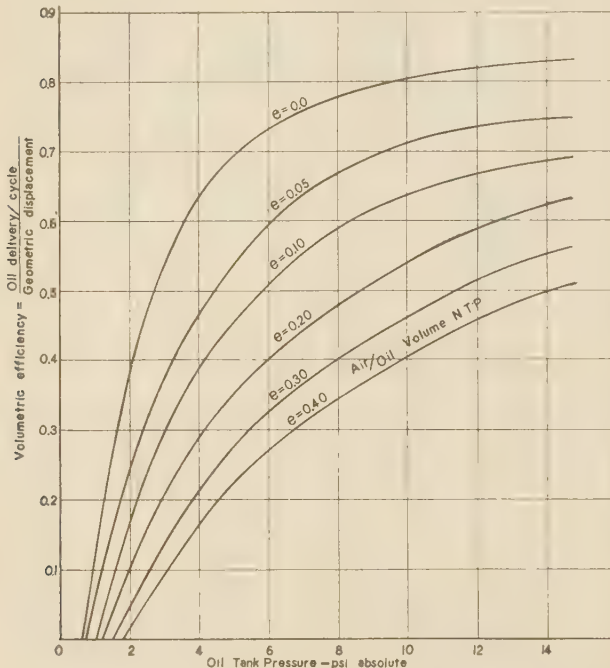


FIG. 10 CALCULATED DELIVERY FOR TYPICAL GEAR PUMP WITH VARIOUS DEGREES OF AERATION

(Pump: 1.5 in. OD; 0.963 in. root diam; 32 per cent clearance volume; 2600 rpm. Line: 1.134 in. ID; 17 in. long; one ell, three nipples, one valve. Dissolved air, 8 per cent of oil volume NTP; entrained air, as indicated.)

It will be noted that the delivery becomes zero before the inlet pressure becomes zero. This is not surprising since, at very low inlet pressures, all of the delivery is recirculated.

LUBRICATION CEILING

In aviation service, a pertinent question is: How high can a plane fly before the engine is distressed for lack of adequate oil supply? This problem would seem to be much more complicated than computing pump delivery but, actually, it turns out to be a great deal simpler.

Lubrication ceiling is reached when the delivery of the pressure pump drops below the tolerable minimum. If we stipulate that

⁸ Although Equation [25] has been obtained by deductive reasoning, its validity has been confirmed by test results obtained in the course of an experimental investigation on "Airlock and Foaming in Aero-Engine Lubrication System," sponsored by the National Advisory Committee for Aeronautics,⁶ at The Pennsylvania State College.

this tolerable minimum be one half of the maximum capacity of the pump, Equation [27] evolved in the Appendix, from Equation [26], is

$$p_b = PL(1 + d) + 14.7e \dots \dots [27]$$

where p_b is the absolute barometric pressure at the lubrication ceiling (psi), PL the total pressure loss from oil tank to tooth space (psi), d the ratio of the dissolved air volume (NTP) to oil volume, and e the ratio of the entrained air volume (NTP) to oil volume.

This equation refers to a pump with zero slip and zero back delivery. These assumptions have been made to simplify the formula. The general formula is given in the Appendix. But ignoring slip and back delivery, the effect of other factors on p_b is practically the same.

From p_b , by the known empirical relation, Fig. 11, the lubrication ceiling, L.C., can be determined. For purposes of this discussion, "lubrication ceiling" is defined as the altitude above which the pump delivery drops below the critical delivery, which is taken to be 50 per cent of the sea-level delivery. For another percentage Equation [27] is slightly different as seen in the Appendix.

The application of Equation [27] resulted in the charts, Figs. 12 to 18, which give both detailed facts and a perspective on the effects of various factors on the lubrication ceiling.

Only one variable was changed on each chart, the other variables being kept standard. The chosen standards were as follows:

Pump: W. A. external gear pump, 1.5 in. OD, 0.963 root diam, 2600 rpm, delivering normally 16 gpm of oil.

Oil: An S.A.E. 60 oil with 32.2 centipoises abs viscosity at 180 F and 1293 centipoises at 60 F.

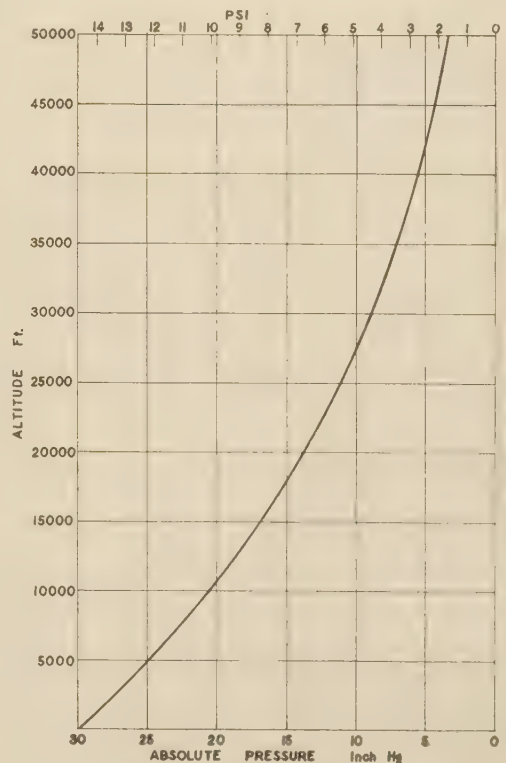


FIG. 11 RELATION BETWEEN BAROMETRIC PRESSURE AND ALTITUDE

Line from tank to pump and fittings identical to those described by Pigott⁴ with 1.134-in-ID \times 17-in. tubing, one ell, three nipples, and one valve.

Entrained air: 4 per cent of oil volume.
 Dissolved air: 8 per cent of oil volume.
 Pump speed: 2600 rpm.
 Oil temperature: 180 deg F.

These basic conditions correspond to those of a typical installation.

An inspection of these charts reveals some startling facts.

Fig. 12 shows the effect of entrained air and is in line with expectation. The L.C. is 46,000 ft with zero per cent entrained air and drops gradually to 24,000 ft with 24 per cent entrained air. The entrained air is in the pipe between tank and pressure pump; and, because most of the air gets out of the oil in the tank, it must be an unsatisfactory tank or cold oil if the entrained air is more than 8 per cent. Usually it is more likely to be 4 per cent, which gives 41,000 ft L.C. under basic conditions.

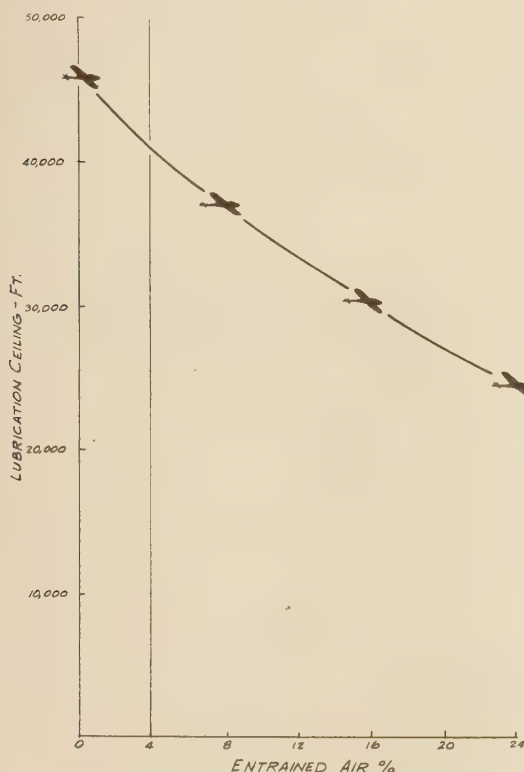


FIG. 12 EFFECT OF ENTRAINED AIR ON LUBRICATION CEILING

The effect of entrained air can be stated very simply: At about 40,000 ft altitude, every additional 1 per cent aeration reduces the lubrication ceiling by 1250 ft, and this irrespective of the pump and line resistance.

Fig. 13 shows the surprising fact that the effect of dissolved air is so slight as to be negligible. The L.C. changes only from 42,000 ft to 40,000 ft when the dissolved air increases from 0 to 12 per cent. The normal amount, according to our measurements, is 8 per cent. It must not be forgotten, however, that the effect of dissolved air would be greater if the pipe resistance were greater. The curve refers to 1.134 \times 17-in. pipe and fittings.

Fig. 14 shows the effect of pipe length and is in line with expectation. Very long pipe is not good.

The effect of pipe diameter is shown in Fig. 15 and is sur-

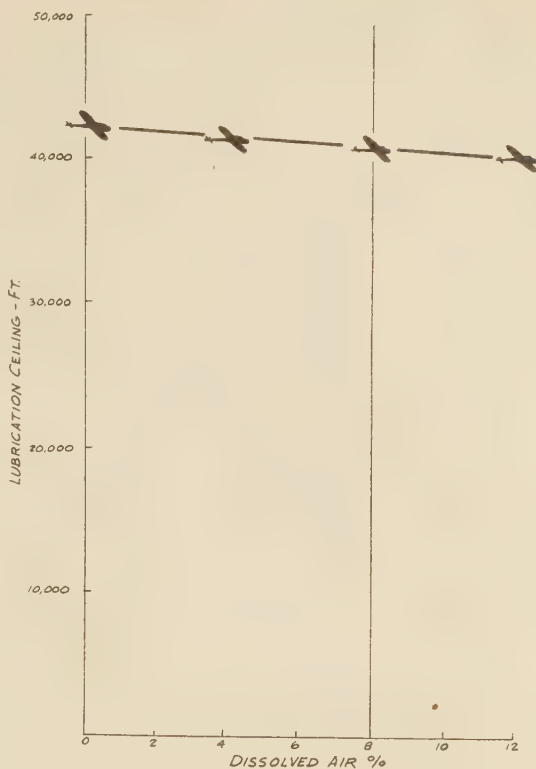


FIG. 13 EFFECT OF DISSOLVED AIR ON LUBRICATION CEILING

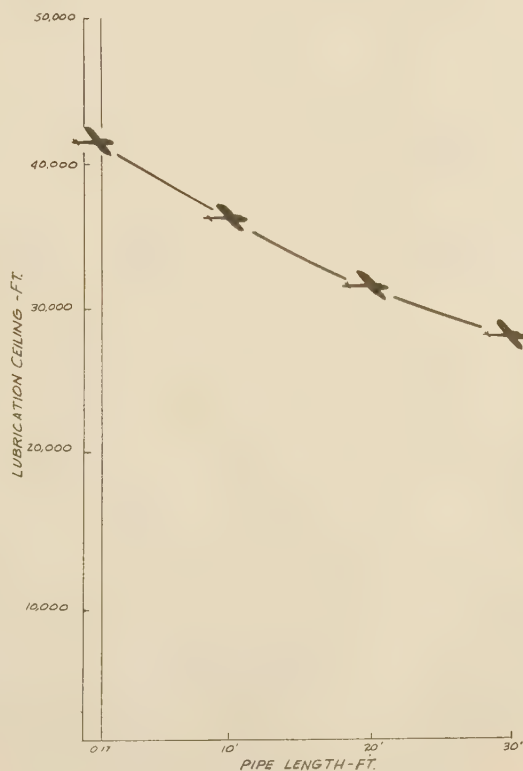


FIG. 14 EFFECT OF PIPE LENGTH ON LUBRICATION CEILING

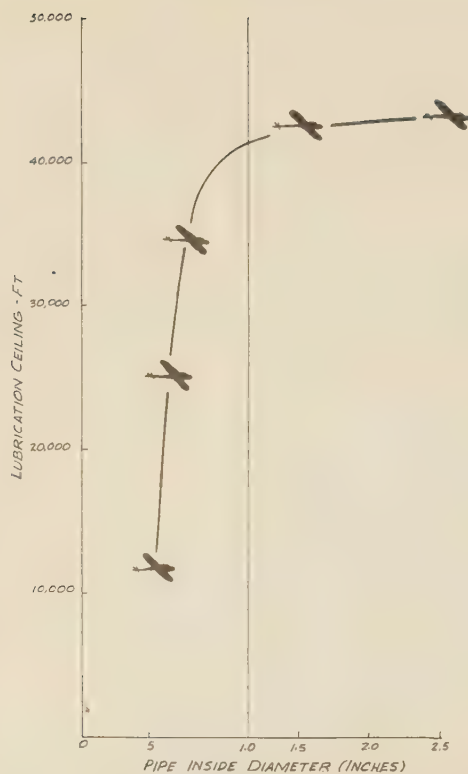


FIG. 15 EFFECT OF PIPE DIAMETER ON LUBRICATION CEILING

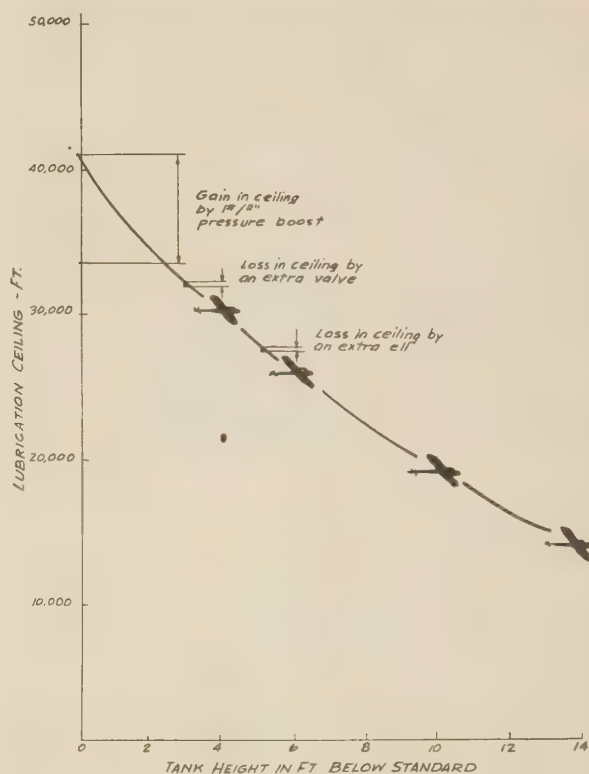


FIG. 16 EFFECT OF TANK HEIGHT, PRESSURIZED TANK, ELLS, AND VALVES ON LUBRICATION CEILING

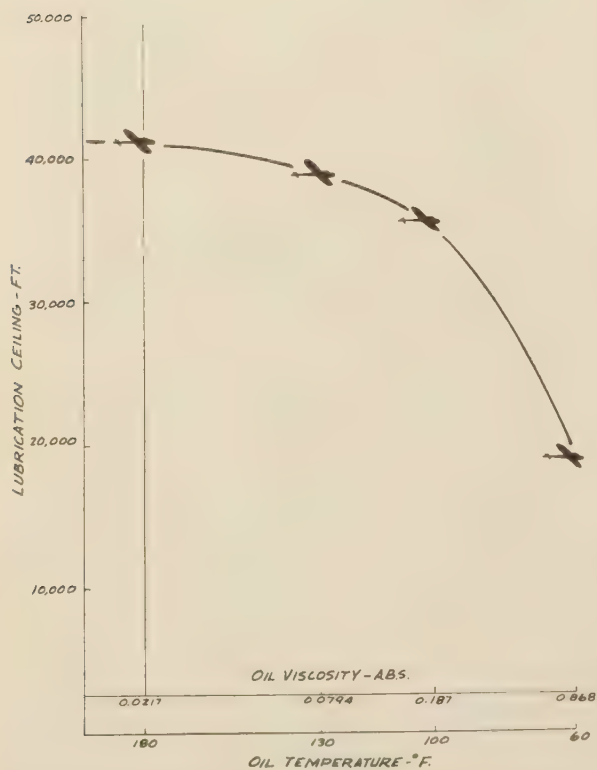


FIG. 17 EFFECT OF OIL VISCOSITY ON LUBRICATION CEILING

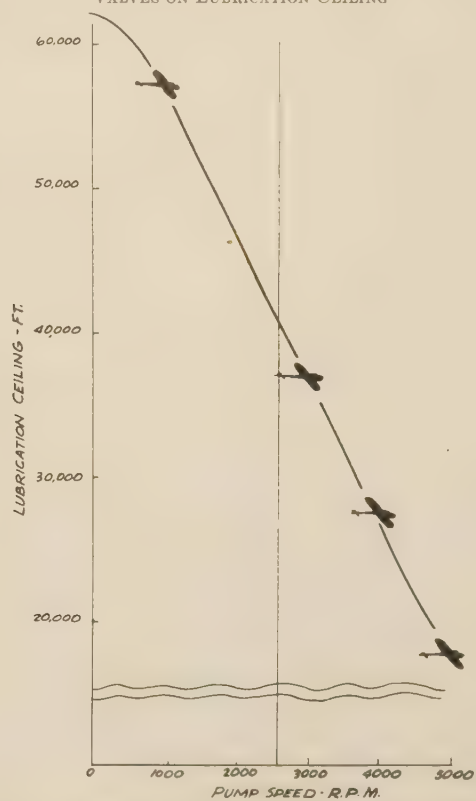


FIG. 18 EFFECT OF PUMP SPEED ON LUBRICATION CEILING

prisingly small in the normal region. By substituting 2½-in-ID for 1.134-in-ID tubing, the L.C. is raised from 41,000 ft only to 42,000 ft. Of course the fittings are supposed to be changed in proportion. The use of extra-large pipe is therefore not justified.

Fig. 16 shows the effect of tank height above the pump. Lowering the tank 2 ft lowers the lubrication ceiling by 6000 ft. It is immaterial whether the tank is lowered from 2 ft height to pump level or from pump level to 2 ft below pump level, the effect is practically the same. Of course, we are considering the L.C. with the pump in continuous operation. The fact that with a negative suction height one may have priming troubles is another story.

On the same chart the effect of an extra ell (90 deg) or an extra valve in the line is shown, both unexpectedly small. Neither of them reduces the ceiling by as much as 500 ft. Therefore, the avoidance at all price of ells and valves is not justified. On the other hand, pressurizing the tank to 1 psig raises the ceiling by 9000 ft, provided the air content of the oil remains the same.

Fig. 17 shows the effect of oil viscosity or temperature and is somewhat as would be expected, except that the effect of heating the oil above 160 F is insignificant.

The effect of the pump speed is shown in Fig. 18. When the pump speed is raised from 1000 to 4000 rpm, the L.C. drops from 52,500 ft to 27,500 ft. This is considerable, even though it is realized that, in order to have 16 gpm normal delivery with low speed, a larger pump must be provided.

On all charts a vertical line marks the basic conditions and corresponds to a lubrication ceiling of 41,000 ft.

The questions may be asked: What is the ceiling with a perfect pump? Is it infinite? First we must decide what we mean by perfect pump. If we define a perfect pump as one which has zero slip and zero tooth clearance (zero back delivery) then our charts already refer to a perfect pump, but the charts made up for an actual pump will not be much different. If, on the other hand, we define a perfect pump as one with zero slip, zero clearance, and zero pressure drop between pump flange and tooth space, the L.C. curves will be raised considerably. But the ceiling is still finite.

With all pump losses being equal to zero, the total pressure loss will be $PL = 0.231$ psi and

$$p_b = 1.08 \times 0.2315 + 0.04 \times 14.7 = 0.83 \text{ psi}$$

corresponding to a lubrication ceiling of L.C. = 65,000 ft. On the other hand, if the total line resistance from oil tank to the pump flange were zero, with a standard pump the pressure loss would be $PL = 0.8582$ psi, and

TABLE 1 LINE AND PUMP LOSSES

	At 16 gpm delivery, psi	At 8 gpm delivery, psi
Vee losses in line.....	0.2057	0.1028
Vee square losses in line.....	0.5148	0.1287
Total line loss.....	0.7205	0.2315
Vee-square losses in pump housing.....	0.3528	0.0882
Tooth entry (n^2) losses:		
Centrifugal loss.....	1.2300	0.6150
Pickup loss.....	1.8500	0.9250
Total pump loss.....	3.4328	1.6282
PL = Total pressure loss from tank and tooth space.....	4.1533	1.8597
Vee losses.....	0.2057	0.1028
PL -vee losses.....	3.9476	1.7569
Vee-square losses.....	0.8676	0.2169
PL -vee square losses.....	3.2957	1.6428
N^2 losses.....	3.0800	1.5400
PL - n^2 losses.....	1.0733	0.3197

NOTE: The figures in this table refer to the example calculated by Pigott (references 3 and 4), corresponding to the conditions specified. Flow of 16 gpm represents normal flow, while 8 gpm represents the critical flow, limiting the ceiling.

$$p_b = 1.08 \times 0.8582 + 0.04 \times 14.7 = 1.518 \text{ psi}$$

corresponding to a lubrication ceiling of L.C. = 52,000 ft.

A conclusion to be drawn from the foregoing analysis is that the greatest obstacle to raising the lubrication ceiling lies in the gear pump itself. This cannot be neutralized to any appreciable degree by minimizing line resistance or the percentage of entrained air.

Table 1 shows the pressure losses from oil tank to gear teeth for normal (16 gpm) and critical (8 gpm) pump delivery.

APPENDIX

According to Equation [25], the volumetric pump delivery is

$$\eta = \frac{1}{1+s} \left[\frac{1}{1+d \left(\frac{p_b}{p_t} - 1 \right) + e \frac{p_o}{p_t}} - b \right] \dots\dots [25]$$

When, due to altitude, the volumetric efficiency of the pump drops to a critical value η_{cr} , the plane has reached its lubrication ceiling.

Since the tooth-space pressure is equal to oil-tank pressure less pressure loss

$$p_t = p_b - PL \dots\dots\dots [28]$$

Equation [25] can be written as

$$\eta_{cr}(1+s) + b = \frac{1}{1+d \left(\frac{p_b}{p_b - PL} - 1 \right) + e \frac{p_o}{p_t}} \dots\dots [29]$$

or

$$1 + d \left(\frac{p_b}{p_b - PL} - 1 \right) + e \frac{p_o}{p_b - PL} = \frac{1}{\eta_{cr}(1+s) + b} \dots\dots [30]$$

which with some algebraic transformation yields

$$p_b = \frac{PL \left(1 - d - \frac{1}{\eta_{cr}(1+s) + b} \right) - e p_o}{1 - \frac{1}{\eta_{cr}(1+s) + b}} \dots\dots [31]$$

Assuming for the sake of simplicity that both slip and back delivery are zero, then with $s = 0$ and $b = 0$, from Equation [31]

$$p_b = \frac{PL \left(1 - d - \frac{1}{\eta_{cr}} \right) - e p_o}{1 - \frac{1}{\eta_{cr}}} \dots\dots\dots [32]$$

or

$$p_b = \frac{PL \left(\frac{1}{\eta_{cr}} + d - 1 \right) + e p_o}{\frac{1}{\eta_{cr}} - 1} \dots\dots\dots [33]$$

which gives the required barometric pressure for the critical pump delivery. Assuming that the pump delivery becomes critical when the volumetric efficiency of the pump drops to or below 0.5, which means one half of the pump's maximum capacity, then Equation [33] becomes

$$p_b = PL(1+d) + 14.7 e$$

which is identical with Equation [27] of the paper.

Discussion

W. L. WEEKS.⁹ While we may not agree with the author in his appraisal of the theoretical handicap on a pump, of 12 per cent dissolved air in its supply, it is comforting to realize the loss is theoretical. When at 42,000 ft, the importance to the pilot of another 2000 ft in either direction may be considerable. However, our research work with the Gulf Company has indicated that the practical effect of dissolved air in the power-plant oil system, on the pressure pump, is much less than would show by calculation. The principal reason for the gratifying discrepancy is that, in most installations, the oil simply does not have time to change condition as to dissolved-air content at the place it would have the greatest detrimental effect, namely, at the inlet zone of the pump rotors. Mr. Piggott assures us that a natural reluctance of the usual oil to release its dissolved air is a factor in this.

In the author's discussion of the calculation and actual measurement of entrained free air, he refers to and recommends the "Airometer" which he has developed and described in a previous report.⁶ With due respect to the clever design which this device shows, the writer feels that it is a mistake to recommend it or any other instrument which measures entrained air on the basis of volumetric displacement, without simultaneously stressing the prerequisite to its practical use, namely, that it be supplied a homogeneous mixture, as the sample. It is quite soundly established that accurate measurement of entrained air is more a problem of obtaining a truly representative sample than of evaluating the sample.

This line of experiment is very intriguing and there are so many possible ways of doing the displacement-measuring job on a static sample of oil/air mixture that many want to, and do, tackle it. It is quite easy to assume that the sample captured and taken aside to be tortured is representative in the per cent of air it contains, but the assumption is as likely to be wrong as it is easy to make.

The author's statement of the effect of inlet-pipe diameter is extremely misleading, as is its reference, Fig. 15, unless it is qualified by tying it in with the particular pump in the case. It so happens that the pipe line used with the pump was already large enough to cause small inlet pressure loss, at the normal pumping rate. That should be pointed out. In some other pump case (engine flow rate), a change of 0.25 in. in diameter of pipe from one which was too small to start with, might easily make a difference of a couple of thousand feet altitude.

Again, when the author discusses the effect of an extra ell (90 deg) or an extra valve in the line, the need for some qualification of statement is indicated. The effect on the oil pump of differences of inlet pressure vary, depending upon the altitude at which the comparison is being made. For instance, the "extra ell" is cited as costing somewhat less than 500 ft altitude (we make

it 585). This is true only at the particular altitude, shown as about 28,000 ft. The resistance of the fitting is known to be about 0.26 in. Hg. If the author were to try the effect of this pressure loss up half way in the altitude zone where he shows 1 psi "pressure boost" applied (33,000 to 42,000 ft), the cost of the "extra ell" will be found more significant. A loss of 0.26 in. Hg at that altitude or 37,500 ft costs roughly 720 ft in "ceiling."

In reference to this and the statement on effect of pipe diameter, the writer would like to mention the fact that Wright Aeronautical has been very active for the last 3 years in selling the small and seemingly detailed refinements in oil-inlet lines, as to size and fitting restrictions, as being important when accumulated in an installation. The airplane companies bought the idea, and it has paid off. We have applied it in new pump design. Now, along comes the author of the present paper to discount, perhaps unintentionally, the cumulative importance of the small factors in installation design.

AUTHOR'S CLOSURE

As to the dissolved air, the author fails to see the discrepancy mentioned by Mr. Weeks, between the calculated and practically observed effects, both being insignificant. According to theory, in the specified case, the lubrication ceiling decreases only 165 ft for each per cent increase of dissolved-air content. The practically observed effect can hardly be "much less." True, the calculations have been based on the assumption that dissolved air is released at the pump inlet in proportion to the pressure drop (Henry's law). It is believed that this is a close approximation of the truth. Our unpublished experiments show that air goes *into* solution reluctantly in oil but comes *out of* solution very readily even from a quiescent liquid and almost instantaneously when the oil is agitated. Even so, the calculation showed the effect of the dissolved air on lubrication ceiling to be negligible.

A feature of the "airometer" mentioned in the text is that it is a full-flow instrument, in distinction to those devices that handle a sample bled from the main flow. Handling the full flow, there cannot be any question about the mixture not being representative. The air content is of course measured on the volumetric basis and the results are therefore not identical with the per cent air content measured on the time basis, the latter being the ratio of the volumes of air and oil passing a given cross section of the pipe in, say, one second. Even that difference is insignificant unless slugs of air pass the line with a velocity greater than the velocity of the oil, a condition that rarely exists between the oil tank and the pressure pump.

The numerical effect of the inlet-pipe diameter, valves, and ells are true only for the example cited which represents a typical Wright Aeronautical installation described by Piggott.⁶ It certainly was not the intent of the author to discourage refinements and streamlining on oil-inlet lines, but the figures have shown to his own surprise that at least in certain cases effects are very small. The opposite is true of air entrainment, tank, pressurization, and pump speed.

⁹ Project Engineer, Lubrication Systems Unit, Wright Aeronautical Corporation, Paterson, N. J.

Boiler Nozzles and Valve Inlets for Maximum-Capacity Safety Valves

By E. K. FALLS,¹ ROCHESTER, N. Y.

This paper gives results of a developmental program for a safety-valve design which would be capable of discharging the greatest amount of fluid that could flow through a given size inlet, within the limitations imposed by entrance conditions of pressure, and either temperature or quality. Conditions were determined which would guarantee satisfactory performance, and also those which might possibly contribute to poor entrance conditions of the design developed, or any other design using the same inlet condition. Suggestions are made by the author for consideration when new Boiler Code rules are established for high-capacity valves: (a) Welding rings should be prohibited in boiler-safety-valve nozzles. (b) Rounded-surface entrances are requisite. (c) Welding metal should not interfere with flow at outside edge of entrance surface. (d) Minimum distances from entrance to other surfaces should be specified.

INTRODUCTION

THE present designs of safety valves commercially available have discharge capacities which are based upon areas of opening considerably less than that of the inlet connection.

Coefficients of discharge approaching unity, computed by Napier's equation for steam flow and based on the smallest cross-sectional flow area, are attainable with some of the commercial valves. For a given inlet size, the ratio of the smallest flow area to the area of the inlet may be considerably less than unity. Although such a safety valve may discharge practically the maximum theoretical possible quantity for the given flow area, an increase in the flow area may increase the capacity even though the total flow is considerably less than that theoretically possible.

The A.S.M.E. Boiler Code permits the use of safety valves which give any opening up to the full discharge capacity of the area of the opening of the inlet of the safety valve (1).²

A development program was pursued by the company with which the author is a consultant, for the purpose of developing a safety-valve design that for all practical purposes would be capable of discharging the greatest amount of fluid that could flow through a given size inlet for imposed entrance conditions of pressure, and either temperature or quality. The advantage to be gained is that the smallest total area of opening in the shell of a boiler or pressure vessel required to discharge the proper amount of fluid is obtained with this type of construction. As a part of the development, it was considered desirable to determine those conditions that would guarantee satisfactory performance, and also those that might possibly contribute to poor entrance

conditions of this design or any other design using the same type of inlet connection.

Sufficient consideration has not been given to the proper mounting of safety and relief valves in the past. Relief valves in particular are mounted incorrectly in many cases. At times designers specify long pipe lines with several turns or elbows to connect a relieving device with the pressure vessel to be protected. If the pressure drop due to friction in the entrance line is appreciable, faulty valve performance results. Boiler-safety-valve installations are much more closely controlled in this respect as a result of the various boiler-code rules prescribing acceptable means of installation, and yet, dry pipes or the like, placed within the boiler drum near the safety-valve inlet, can constitute a possible hindrance to flow, especially if the rate of flow through the boiler safety-valve nozzle approaches the maximum. At present there are no code rules covering the design of this part of a boiler installation.

Practically all present-day safety valves have capacities considerably less than the capacity possible through a nozzle having a throat diameter equivalent to the inlet size or entrance-piece diameter. The ideal design is capable of having a capacity that approaches the maximum capacity possible of attainment through an entrance nozzle, and yet, at the same time, maintaining satisfactory performance. Previous tests have been reported on nozzle-type safety valves which had throat areas equal to the boiler-nozzle areas (2), but the values of lift and capacity for this arrangement were not mentioned.

To produce capacities that are large relative to the entrance-piece diameter, the commercial product must have a flow passage that simulates the flow nozzle which has (a) a rounded-entrance converging section; (b) a short length of straight-tube section usually termed the throat; and (c) a diverging section beyond the throat of increasing cross-sectional area, assuming that expansion is incomplete at the throat of the safety-valve nozzle. Thus the performance of the design described herein is not determined solely by the constriction above the inlet flange or threaded inlet connection, but by the arrangement of the entire flow passage from the entrance within the boiler shell to the outlet connection.

The rounded-entrance flow nozzle is considered the ideal shape for the contour up to and including the throat, but because of mechanical requirements there must be marked departures from this simple shape in the final design. For example, the throat section of the ideal nozzle consists of a short tube about 1 diam long or less. This length in the new design is increased to approximately 5 diam, because the flow passage must pass through the safety-valve inlet flange and up to about the center line of the outlet connection. This length of throat section may introduce a noticeable increase in the amount of friction if the wall roughness is permitted to increase during the life of the safety valve. It is important then that the wall of this section be as smooth as is commercially feasible.

With ideal wall conditions, the rounded entrance could converge immediately to a throat size equal to that of the inlet diameter. However, a boiler safety-valve nozzle is usually welded or riveted to the boiler shell and is needed to provide a means for mounting or removal of the safety valve. Due to this

¹ Assistant Professor of Mechanical Engineering, University of Rochester, and Consulting Engineer, Consolidated Safety Valve Division, Manning, Maxwell & Moore, Inc., Bridgeport, Conn. Jun. A.S.M.E.

² Numbers in parentheses refer to the Bibliography at the end of the paper.

Contributed by the Power Division and presented at the Annual Meeting, New York, N. Y., Nov. 27-Dec. 1, 1944, of THE AMERICAN SOCIETY OF MECHANICAL ENGINEERS.

NOTE: Statements and opinions advanced in papers are to be understood as individual expressions of their authors and not those of the Society.

tube having a relatively rough wall compared with the throat, the desirability of a joint between the boiler and the safety-valve body, and the need of providing sufficient distance from the shell to the safety-valve body to make up this joint, the converging section is split into two parts; (a) a rounded entrance at the lower end of the boiler nozzle, and (b) a conical section immediately preceding the throat which produces a small reduction of diameter, and which is connected with the rounded entrance by a cylindrical passage. There should be no break in the wall surface of the second converging part, hence the joint is located at the discharge end of the boiler nozzle where the full diameter occurs. The large reduction of diameter at the rounded entrance of the flow nozzle is made to occur within the boiler drum in this design and is formed by turning a radius on the lower end of the tube.

APPARATUS AND EQUIPMENT

All development tests were performed at the Bridgeport Works of the company, with wet saturated steam as the fluid. Although many different combinations were tested during the period of development, the experimental work consisted primarily of two types of tests; (a) flow tests for which the capacity-lift relation was investigated as affected by various factors; and (b) pop tests for which the pop action, amount of blowdown, and lift at pop and accumulated pressures were determined.

A flowmeter installation, Fig. 1, was used for the flow tests. Saturated steam from boiler No. 1 was admitted to the flowmeter line through a 6-in. power-operated gate valve. The maximum pressure available from this boiler was 700 psi. A $\frac{3}{4}$ -in. by-pass line around the gate valve was used for close adjustment of the pressure during tests. This line also had a discharge connection to a returns tank.

The primary element of the flowmeter consisted of a stainless-steel orifice with pipe taps installed in a 4-in. horizontal line. Straightening vanes were located in the line ahead of the orifice,

leaving approximately 6 pipe diam of straight pipe between the vanes and the orifice. A recording flowmeter indicated the volume of flow. A set of seven range tubes permitted measurements of flow up to 25,000 lb per hr of saturated steam.

The inlet for supplying steam to the drum of the flowmeter installation was located at the middle of the drum, the outlet for mounting of the safety valves at the upper head concentric with the vertical longitudinal axis. Pressure taps were located at the drum and the meter line. The drum tap was connected to the drum above the inlet but 90 deg around the shell. A drain valve was attached to the lower head.

Quality was determined with a calibrated throttling calorimeter. Once flow was started through the apparatus, readings were not recorded until the quality was approximately 98 per cent.

Disk lift was regulated by manual adjustment of a threaded spindle which engaged a nut at the top of a special valve yoke. A 20-pitch thread on the spindle, and a lift wheel, attached to the upper end of the spindle, having an adjustable dial divided into 50 divisions, provided means for measuring 0.001-in. lift increments. The closed or zero lift position was determined by lowering the spindle and disk until the disk was seated, after first having heated the safety valve parts by discharging steam through the apparatus at test pressure. The dial was adjusted for zero reading at this setting.

Interchangeable throat tubes, Fig. 2, were made for insertion into a 2 $\frac{1}{2}$ -in. Type 1555 Consolidated safety-valve body to form the throat of the nozzle and the second converging section. A wall angle of 10 deg was used throughout to form the tapered converging section within the tubes, all of which were constructed with 1-in. throats. This constant throat size permitted the use of only one set of moving parts above the throat for all entrance tests, so that any change in flow, lifting force, or other performance factors was caused by the changes of contour introduced

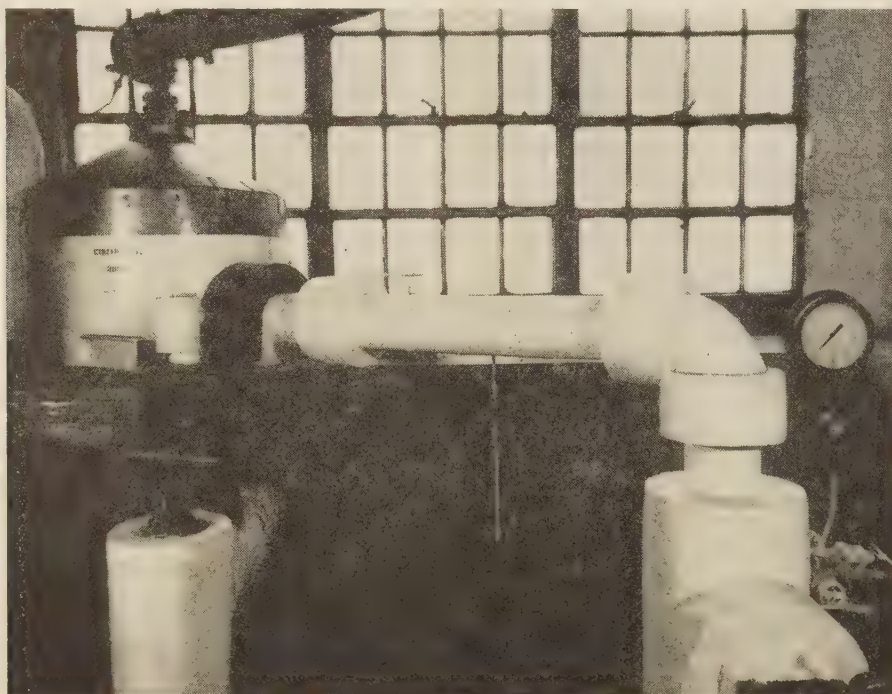


FIG. 1 600-PSI 25,000 LB PER HR FLOWMETER INSTALLATION FOR SAFETY-VALVE TESTING

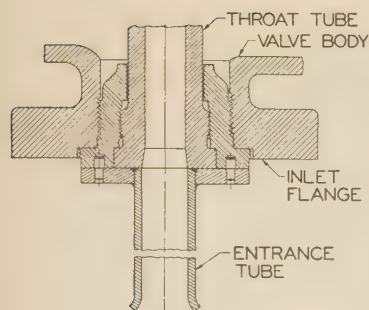


FIG. 2 ASSEMBLY OF THROAT TUBE IN 2 1/2-IN. TYPE 1555, CONSOLIDATED SAFETY VALVE

(1 1/8-in. rounded-surface entrance tube.)

tion at the converging section but also increased the length of the throat.

Flow passages formed by boiler safety-valve nozzles were simulated by manufacturing a number of entrance tubes, most of which were approximately the same length as commercial long-neck welding flanges of the same size used for boiler nozzles. However, in addition to a sharp-edged 90-deg turn for the entrance, as is common for boiler installations, a rounded-surface entrance construction, Fig. 2, was also used. The tubes were made of both brass and steel. A fine tool finish was machined on the inside surfaces except for those made of standard pipe. The outside diameter of the flange on all tubes was maintained constant so that they could be placed within the bolt circle and clamped between the flanges of the safety-valve base and the several test mountings. Locating pins served to center the entrance tubes with the various throat tubes.

The effect of throat ratio was investigated by varying the size of the inside diameter of the entrance tubes, which ranged from 1 5/16 in. down to 1-in. standard pipe size. One series of tubes was manufactured with square-edged entrances to investigate flow conditions similar to present practice. A second series was manufactured with rounded-surface entrances. The radii of the rounded surfaces of this second series were made sufficiently large to eliminate entrance losses at the entrance-tube inlets. Several of the surfaces were generated with two radii to approximate an ellipse, but in all cases the outside diameter of the lower end of the tubes was 2 1/2 in. or less which permitted them to be inserted into the mounting blocks.

The radius of the rounded entrance was investigated to determine how small a radius could be used without reducing the flow. A series of tubes having an inside diameter of 1 1/8 in. was made with radii of the rounded surface varying from zero for the straight sharp-edged tube to a maximum of 1 1/2 in. A circular arc was chosen for the generating curve of this surface to facilitate the manufacture of the entrance tubes.

All of the entrance tubes mentioned were made 9-in. long. One approved method of welding nozzles into boiler drums that is used at present permits the tube to project through the shell into the interior of the drum a short distance, which is relatively simple to manufacture. A few tubes of 12-in. length were made to determine whether this construction would produce an effect similar to a "Borda mouthpiece." The lower end of these tubes projected into the interior of the pressure vessel.

A flat circular plate, 3 3/4-in. diam \times 1/8-in. thick, attached to the inlet end of a 1 1/8-in.-diam rounded-surface entrance tube by means of two slotted supports, was used to simulate possible restrictions to flow, Fig. 3. The distance from the upper surface of the plate to the lower end of the tube was adjustable from the

within the entrance piece and throat tube. The large diameter of the conical section of the throat tube was made equal to that of the inlet connection. As the over-all length and throat diameter of all the throat tubes were the same, an increase of the ratio of throat diameter to inlet-connection inside diameter, termed the "throat ratio," not only reduced the amount of area reduction

contact position to a value greater than the tube inside diameter. The plate outside diameter was limited by the 4-in. valve-mounting outlet of the 700-lb drum of the flowmeter installation. A similar arrangement was used with a sharp-edged entrance tube. During the tests it was found necessary to provide additional means of support to prevent the steam forcing the plate against the end of the tube at relatively high rates of flow and small gap distances.

Pop tests were performed on No. 4 or No. 5 test drum, or on the test mounting of boiler No. 3 (3). No. 4 drum was approximately 3 ft diam \times 10 ft long, was designed for 700 lb pressure, and was provided with a 6-in. valve for mounting safety valves. Valves were set at pressures up to 1200 psi on boiler No. 3. A 4-in. gate valve, which was open during tests, connecting piping directly from the boiler, and an adapter block formed the entrance passage to the safety valve under test. A by-pass around the gate valve with a discharge connection to a returns tank, and the rate of firing (oil-fired) were used to control the pressure. The experimental models were first set for the desired pop pressure and the blowdown adjusted to within 4 per cent because access to the compression screw was prevented once the lift-measuring apparatus was attached.

Disk lift was measured with a Tabor indicator which had a 5:1 ratio of pencil movement to piston-rod movement; The indicator was supported above safety valve models by adapters on which it was mounted, and which carried setscrews to clamp the adapters to the top of the safety valves. A coupling screwed onto the upper end of the spindle together with 1/8-in.-diam connecting rods transmitted any disk motion to the indicator mechanism.

If the capacity of the drum or boiler No. 3 was sufficient to hold the safety valve model open at the set pop pressure and the accumulated pressure, the lift measurement was taken with the safety valve discharging at the desired pressure. But for capacities too large to be supplied by steady flow to the drums or by the boiler, the pop lift was recorded on the indicator at the instant of pop by imparting manually a reciprocating motion to the indicator drum. Accumulated lift was measured by holding the safety valve closed until the boiler or drum pressure reached 103 per cent of the gage popping pressure, then repeating the procedure used to record the pop lift. The closing pressure was observed on these tests to obtain the blowdown and also to determine whether the

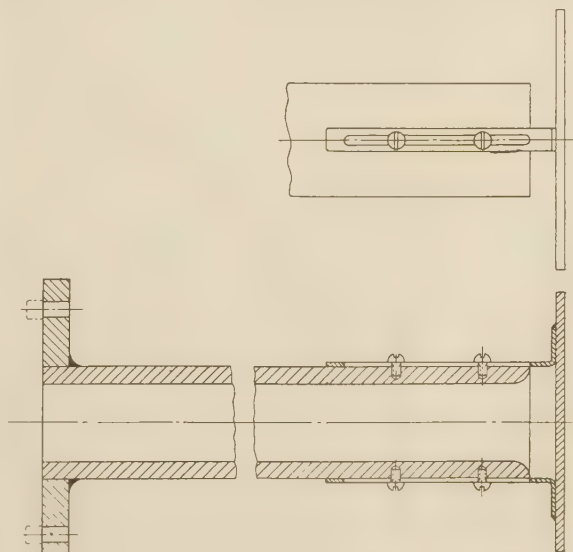


FIG. 3 ADJUSTABLE FLAT-PLATE ENTRANCE RESTRICTION

TABLE 1 RESULTS OF TESTS

SHARP-EDGED ENTRANCE TUBES							
Entrance tube diameter, in.	1.049	1 ¹ / ₁₆	1 ¹ / ₈	1 ¹ / ₄	1 ¹ / ₂	1 ³ / ₄	2 ¹ / ₈
Throat ratio	0.954	0.941	0.889	0.842	0.800	0.762	0.421
Lift, (maximum flow), in.	0.35	0.35	0.26	0.26	0.25	0.26	0.35
Meter pressure, psig.	198	198	198	199	198	198	197
Meter pressure, psia.	213.4	213.5	213.5	214.5	213.5	213.4	212.5
Calorimeter temperature, deg F.	273	294	286	296	272	272	280
Quality at meter, per cent.	98	99.2	98.8	99.4	98	99	98.5
Quality correction factor	1.000	0.994	0.996	0.993	1.000	0.995	0.998
Pressure correction factor	1.358	1.351	1.350	1.351	1.349	1.350	1.355
Range tube constant, lb per hr.	8000	8000	8000	8000	8000	8000	8000
Meter reading, per cent.	69	70	73	75.25	76	77.25	81.25
Meter flow, lb per hr.	7490	7530	7860	8070	8200	8300	8780
Calorimeter flow, lb per hr.	36.5	36	36	36	36	36	36
Valve flow, lb per hr.	7453	7494	7824	8034	8164	8264	8744
Inlet pressure, psig.	200	200	200	200	200	200	200
Inlet pressure, psia.	213.9	214.0	214.0	214.0	214.0	213.9	214.0
Throat diameter, in.	1	1	1	1	1	1	1
Coefficient of discharge, K_D	0.863	0.870	0.908	0.93	0.946	0.96	1.01
ROUNDED-SURFACE ENTRANCE TUBES							
Entrance tube diameter, in.	1 ¹ / ₃₂	1.049	1 ¹ / ₁₆	1 ¹ / ₈	1 ¹ / ₄	1 ¹ / ₂	1 ³ / ₄
Throat ratio	0.970	0.954	0.941	0.889	0.842	0.800	0.762
Rounded-surface radius, in.	1 ¹ / ₄	1 ¹ / ₂	1 ¹ / ₂	1 ¹ / ₂	1 ¹ / ₂	1 ¹ / ₂	1 ¹ / ₂
Lift, (maximum flow), in.	0.35	0.25	0.35	0.30	0.35	0.26	0.35
Meter pressure, psig.	197	197.5	197	198	198	198	198
Meter pressure, psia.	212.4	212.9	212.5	213.5	212.5	213.5	213.6
Calorimeter temperature, deg F.	281	272	288	282	292	282	285
Quality at meter, per cent.	98.5	97.9	98.9	98.5	99.0	98.5	98.7
Quality correction factor	0.998	1.0005	0.996	0.998	0.995	0.998	0.997
Pressure correction factor	1.355	1.357	1.356	1.351	1.358	1.351	1.351
Range tube constant, lb per hr.	8000	8000	8000	8000	8000	8000	8000
Meter reading, per cent.	77	74.75	77.3	78	78.25	78	79.7
Meter flow, lb per hr.	8310	8125	8340	8430	8460	8420	8540
Calorimeter flow, lb per hr.	36	36.5	36	36	36	36	36
Valve flow, lb per hr.	8274	8089	8304	8394	8424	8384	8544
Inlet pressure, psig.	200	200	200	200	200	200	200
Inlet pressure, psia.	213.9	213.9	214.0	214.0	214.0	214.0	214.0
Throat diameter, in.	1	1	1	1	1	1	1
Coefficient discharge, K_D	0.958	0.939	0.961	0.970	0.975	0.970	0.987

blowdown changed as a result of the disk lifting higher at the accumulated pressure. Manual operation of the recording mechanism was also used to determine the disk-lift position from which the safety valve closed.

RESULTS AND DISCUSSION

If ideal entrance conditions prevail and there is no interference beyond the throat, the maximum rate of discharge is governed by the throat area and the initial state of the fluid. Interference, as used here, is defined as any condition in the diverging section that can prevent the development of maximum nozzle flow. One combination which had nearly ideal entrance conditions and a discharge coefficient, based on Napier's rule³ (4) of 1.01, was constructed with a long 10-deg wall-angle conical entrance of 2³/₈-in. diam at the inlet end of the safety-valve-throat tube and a 1-in. diam at the junction with the throat of the tube. As the combination described likewise proved satisfactory with regard to lifting force and performance and developed practically full nozzle flow at a lift ratio⁴ of 0.25, no material change was made in the shape of the diverging-flow passage beyond the throat of the model safety valve that would decrease the rate of flow during the series of entrance tests. On the basis of this test the 10-deg wall angle was incorporated in the construction of all throat tubes used to investigate entrance characteristics.

Results of the throat-ratio tests are given in Table 1, which includes computed values for test points having the highest rate of flow for each combination. The coefficients of this table, based upon the throat diameter, are plotted in Fig. 4. The superiority of the rounded-surface entrance over the sharp-edged entrance is considerable at throat-ratio values near unity. It was assumed that both would have the same coefficient of 1.01 for the example just cited. The coefficients for several of the rounded-surface tubes, which had large entrance radii, may have been low with respect to the curve owing to an arc length less than 90 deg.

³ The maximum rate of flow of saturated steam through a nozzle is given approximately by Napier's rule as $W = PA/70$, where W = rate of flow, lb per sec, P = initial absolute pressure, psi, and A = throat or minimum cross-sectional area, sq in.

⁴ Ratio of disk lift to throat diameter.

The reduction of the value of the coefficient at approximately unit values of the throat ratio does not necessarily imply a decrease of flow with respect to the inlet diameter. The results of the rounded-surface-entrance tests were also represented by plotting the capacity factor F_c against the throat ratio, Fig. 5, where F_c was obtained by dividing the capacity at 0.25 lift ratio by the product of the absolute pressure P and the entrance tube diameter squared. These values are tabulated in Table 2 and were taken from capacity-lift curves of complete tests of each

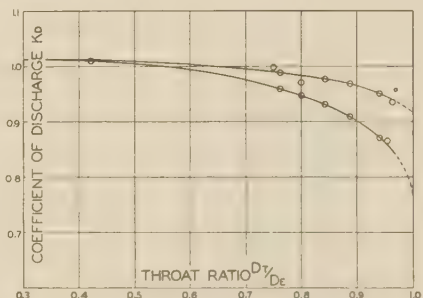


FIG. 4 EFFECT OF THROAT RATIO ON COEFFICIENT OF DISCHARGE (Upper curve: Rounded-surface entrance. Lower curve: Sharp-edged entrance.)

throat ratio, rather than from the actual test points for 0.25 lift ratio. For this reason the capacities do not agree with the maximum computed capacities of Table 1, where the apparent maximum occurred at 0.25 lift ratio. Curve 2 has been included to show the values that would be obtained if the coefficient of discharge remained constant at 1.01. It was assumed the two curves would coincide at a throat ratio of 0.421. This method of representing the results includes the coefficient-of-discharge factor and the entrance tube diameter.

Results of the tests to determine the minimum radius of the rounded surface are given in Table 3; coefficients have been plotted in Fig. 6, which indicates that if the ratio of the radius

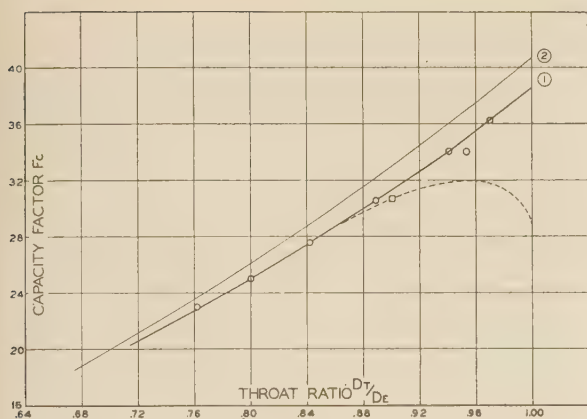


FIG. 5 CAPACITY FACTOR FOR ROUNDED-SURFACE ENTRANCE TUBES

$$\text{Curve 1 } F_c = K_D \times 51.43 \times 0.785 \times (D_7/D_8)^2$$

$$\text{Curve 2 } F_c = 1.01 \times 51.43 \times 0.785 \times (D_7/D_8)^2$$

D_8 = entrance tube diameter, in.

D_7 = throat diameter, in.

F_c = capacity factor

P = drum pressure, psia

W = capacity, lb per hr

of curvature at the inlet end of the entrance tube diameter is kept at a value not less than

$$\frac{1/4}{1 1/8} = 0.222$$

no reduction of flow occurs owing to the shape and size of the entrance edge. A full 90-deg arc can be turned on the lower end

TABLE 2 CAPACITY FACTOR AT 0.25 LIFT RATIO

Capacity taken from flow tests				Capacity factor = $40.75 (D_7/D_8)^2$	
1 Inlet diam D_8 in.	2 Capacity, W lb per hour	3 Throat ratio, D_7/D_8	4 Capacity factor, F_c	5 Throat ratio, D_7/D_8	6 Capacity factor, F_c
1.049	8075	0.954	34.35	1.00	40.75
1 1/32	8250	0.970	36.25	0.95	36.79
1 1/16	8225	0.941	34.05	0.90	33.00
1 1/8	8275	0.889	30.57	0.85	29.43
1 1/4	8300	0.842	27.50	0.80	26.07
1 1/2	8350	0.800	24.97	0.75	22.95
1 5/8	8475	0.762	23.00	0.70	19.97

P was considered as 214 psia.

$K_D = 1.01$ for column 6, then

$$W = 1.01 \times 51.43 \times 0.785 \times (D_7/D_8)^2 \times D_8^2 \times P = 40.75 (D_7/D_8)^2 D_8^2 P$$

of the entrance tubes to form the required entrance shape when a commercial long-neck welding flange is used for the boiler safety-valve nozzle as the wall thickness is greater than the rounded-surface radius.

Test results of the 12-in. tubes showed no appreciable change in the rate of flow even though the lower ends of these longer tubes projected slightly below the inside surface of the straight-run section of a 6-in. tee which served as the original flowmeter drum. This factor therefore was ignored in all subsequent tests.

Correct alignment of the conical converging passage at the valve inlet with the straight portion of the entrance tube is important. As the large diameter of the conical section is the same size as the straight tube diameter of the entrance tube, any eccentricity produces a sharp section projecting into the passageway which reduces the capacity. This effect was discovered accidentally when a 1-in. throat was assembled with a 1 1/4-in. entrance tube. An inspection of the combination showed 1/32 in. eccentricity of the two parts after test results indicated a flow less than what was expected. This was corrected by an accurate alignment of the two parts. The same

amount of eccentricity, for a combination having a smaller-diameter entrance tube and the same throat diameter, produced a greater disturbance as a result of higher velocities at the joint and a greater ratio of per cent reduction of area.

An attempt was made to allow for eccentricity by making the large diameter of the conical section larger than the diameter of the entrance tube. But even with concentric alignment, the rate of flow decreased as the difference of the diameters increased. The sudden expansion followed by recompression apparently introduced a pressure loss that reduced the rate of flow. A construction somewhat similar was investigated by Stodola (5). A rounded entrance on the throat tube rather than a conical section would not improve this condition as a flat surface perpendicular to the high velocity would be introduced. However, decrease of flow, introduced by increasing the safety-valve inlet diameter, may be exaggerated as the differences determined by the tests are within the experimental limits of accuracy of the apparatus.

The maximum capacity for a given inlet size may be computed by using the maximum value of the capacity factor of curve 1, Fig. 5. However, throat ratios near unit value can produce poor safety-valve performance. If the pressure loss due to friction in the converging section is sufficient to reduce the throat pressure to less than what it would be at the closing pressure for satisfactory performance, the safety valve will go into a chatter.

Lift ratios of 0.25 probably cannot be maintained throughout a spring range for conditions like those just described. Therefore

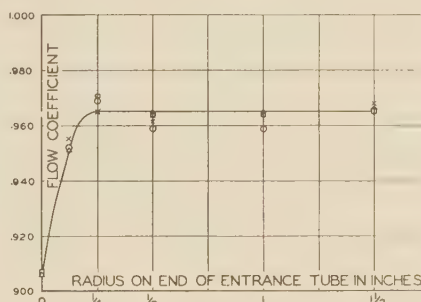


FIG. 6 DISCHARGE COEFFICIENT AS AFFECTED BY RADIUS OF ROUNDED-SURFACE ENTRANCE

Symbol	Lift
×	0.25
○	0.26
□	0.30
△	0.35

TABLE 3 COEFFICIENT OF DISCHARGE FOR VARIOUS RADII OF ROUNDED-SURFACE ENTRANCE

(1-in. throat, 1 1/8-in. entrance, 9-in. tube)

Radius, in.	Lift, in.	Pressure, psia	Flow, lb per hr	Coefficient of discharge, K_D
0	0.25	214.0	7814	0.905
0	0.26	214.0	7824	0.906
0	0.30	214.0	7824	0.906
0	0.35	214.0	7814	0.905
1/8	0.25	213.9	8244	0.953
1/8	0.26	213.9	8234	0.953
1/8	0.30	213.9	8224	0.952
1/8	0.35	213.9	8224	0.952
1/4	0.25	214.0	8344	0.965
1/4	0.26	214.0	8364	0.969
1/4	0.30	214.0	8394	0.971
1/4	0.35	214.0	8364	0.969
1/2	0.25	214.0	8314	0.963
1/2	0.26	214.0	8284	0.959
1/2	0.30	214.0	8324	0.964
1/2	0.35	214.0	8344	0.965
1	0.25	214.0	8284	0.959
1	0.26	214.0	8284	0.959
1	0.30	214.0	8324	0.964
1	0.35	214.0	8344	0.965
1 1/2	0.25	213.9	8364	0.969
1 1/2	0.26	213.9	8344	0.965
1 1/2	0.30	213.9	8344	0.965
1 1/2	0.35	213.9	8344	0.965

the capacity factor for actual safety valves designed for large throat ratios would probably be much less than shown by curve 1 in Fig. 5, at the upper end. The dotted curve may more nearly represent values of F_v to be expected at throat ratios near unity. In consideration of these difficulties, the throat ratio should be as large as possible and yet less than that at which these troubles may occur. A maximum constant ratio of 1 to $1\frac{1}{8}$ (0.889) was used for all the tests that determined the minimum required rounded-surface radius and the effect of the flat-plate obstruction.

The flat-plate test results, Table 4, were obtained by varying the clearance at the inlet end of the entrance tubes and also varying the disk lift for each setting of the plates. Capacities in per cent of maximum nozzle capacity, based upon the entrance tube inside diameter, were plotted against the ratio of plate clearance to the inside diameter, termed the plate-clearance ratio, Figs. 7 and 8. Curves connecting equal lift values then represent the effect of the plate position on the amount of flow that would normally occur through a constant-size orifice.

For each rate of unrestricted flow, the plate must be at some minimum distance from the tube. This distance as a ratio is represented roughly by the dashed straight line from the origin. Any condition to the left of this line represents a reduction of flow. Additional curves at increments of 5 per cent maximum nozzle flow have been located approximately among the experimental curves in this region. The advantage possessed by the rounded-surface over the sharp-edged entrance at equal plate distance ratios can be readily observed from the two graphs. The results of these tests are not limited to safety valves but are applicable to any steam flow entering a line from a vessel.

To check the experimental results of the development program, several $1\frac{1}{2}$ -in.-size commercial safety valves were designed and built, including $1\frac{1}{2}$ -in. entrance tubes to be adapted to larger-size mounting connections. A throat ratio of 0.90 was used, making a throat diameter of 1.35 in. The minimum requirement of 0.222 for the entrance-radius ratio was satisfied. Design features determined by tests in the first part of the development program were applied to flow passages and moving parts of these safety valves. All flow passages from rounded entrance to discharge connection were formed similar to those of development safety valves.

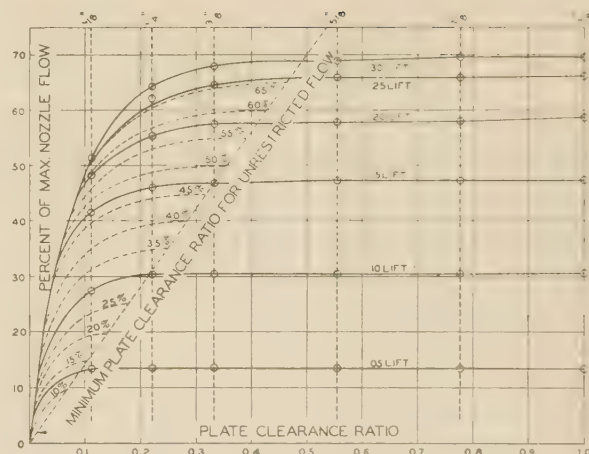


FIG. 7 CAPACITIES DEVELOPED WITH CIRCULAR FLAT PLATE AT ENTRANCE, SHARP-EDGED ENTRANCE TUBE

Pop tests on these safety valves were made at Bridgeport to set them for the proper opening pressure and amount of blowdown. Flow tests were performed at the Naval Boiler and Turbine Laboratory at the Philadelphia Navy Yard as a part of Navy acceptance-test requirements. The steam flow was measured by weighing the amount of feedwater, and the entire flow of steam was passed through the safety valve under test, all other outlets being closed.

The results of the test on the saturated-steam safety valve are given in Table 5. Although the lift ratio was only 0.242, a flow coefficient of 0.942 is comparable to those obtained during the de-

TABLE 5 TEST OF $1\frac{1}{2}$ -IN. VALVE, PHILADELPHIA NAVY YARD

Boiler-nozzle size, in.	$1\frac{1}{2}$	Lift ratio.....	0.242
Throat diameter, in.	1.35	Test pressure, psia.....	649.9
Throat ratio.....	0.90	Actual flow, lb per hr.....	44,789
Entrance radius ratio.....	0.222	Theoretical flow, lb per hr.....	46,426
Pop pressure, psig.....	616.7	Discharge coefficient.....	0.942
Blowdown, per cent.....	2.60	Capacity factor.....	30.65

TABLE 4 CAPACITIES WITH FLAT PLATE AT ENTRANCE, LB PER HR

1.125-IN-ID, SHARP-EDGED ENTRANCE TUBE, THROAT DIAMETER = 1.000 IN.								
Lift ratio.....	0.05	0.10	0.15	0.20	0.25	0.30	0.35	0.40
Valve flow.....	1358	3075	4825	5965	6745	7095	7065	7065
Per cent theoretical flow...	13.3	30.2	47.4	58.7	66.3	69.7	69.4	69.4
Valve flow.....	1365	3080	4805	5915	6705	7085	7085	7105
Per cent theoretical flow...	13.4	30.3	47.3	58.2	65.9	69.6	69.6	69.9
Valve flow.....	1363	3086	4805	5895	6705	7025	7025	7065
Per cent theoretical flow...	13.4	30.4	47.3	57.8	65.8	69	69	69.5
Valve flow.....	1363	3080	4745	5855	6565	6885	6865	6890
Per cent theoretical flow...	13.4	30.3	46.6	57.7	64.6	67.7	67.5	67.7
Valve flow.....	1365	3085	4725	5835	6525	6855	6835	6825
Per cent theoretical flow...	13.4	30.3	46.4	55.3	61.8	64.2	64.3	64.2
Valve flow.....	1365	2755	4225	4915	5205	5185	5205	5205
Per cent theoretical flow...	13.4	27.2	41.5	48.3	51.2	51	51.2	51.2
1.125-IN-ID, ROUNDED-SURFACE ENTRANCE TUBE, THROAT DIAMETER = 1.000 IN.								
Lift ratio, in.....	0.05	0.10	0.15	0.20	0.25	0.30	0.35	0.40
Valve flow.....	1367	3090	4865	6135	6965	7467	7500	7480
Per cent theoretical flow...	13.4	30.4	47.8	60.2	68.5	73.4	73.6	73.5
Valve flow.....	1615	3266	5006	6256	7206	7586	7586	7516
Per cent theoretical flow...	15.8	32	49.1	61.5	70.7	74.5	74.5	73.8
Valve flow.....	1616	3166	4916	6156	7026	7426	7421	7441
Per cent theoretical flow...	15.8	31	48.3	60.5	69.0	72.9	72.9	73.0
Valve flow.....	1618	3301	4976	6161	6986	7386	7371	7366
Per cent theoretical flow...	15.8	32.4	48.8	60.5	68.5	72.5	72.4	72.3
Valve flow.....	1600	3170	4875	6015	6780	7175	7185	7205
Per cent theoretical flow...	15.7	31.1	47.9	59.0	66.5	70.4	70.5	70.6
Valve flow.....	1595	3030	4255	4855
Per cent theoretical flow...	15.6	29.7	41.7	47.6

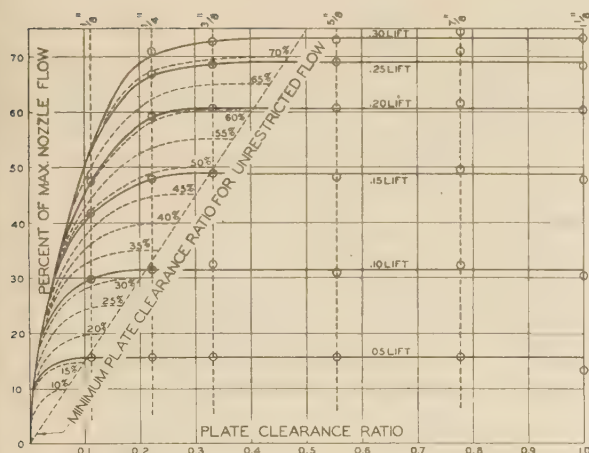


FIG. 8 CAPACITIES DEVELOPED WITH CIRCULAR FLAT PLATE AT ENTRANCE, ROUNDED-SURFACE ENTRANCE TUBE

velopment work. The capacity factor also is reasonably close to the curve in Fig. 5.

CONCLUSIONS

Although the coefficient of discharge for commercial safety valves must be based upon the throat diameter, which is held to close tolerances, the coefficient alone is not suitable as a criterion of the orifice efficiency when a high rate of discharge is required with respect to the size of the boiler nozzle. Rather the inside diameter of the boiler nozzle itself must also be used as a measure of the amount of flow. Both of these factors are included in the capacity-factor value represented in Fig. 5.

Boiler Code rules permit the throat diameter to be as large as the tube diameter used for the boiler nozzle, that is, a throat ratio of unity. But as the throat ratio is increased, a point is reached at which an actual safety-valve design does not have the desirable popping and reseating characteristics, and the high lift ratio is not maintained. As a result, the capacity factor may have a maximum value; performance at and near this value is poor so that the maximum area allowable by the code is not realized in the actual safety valve.

However, even with more conservative values of the throat ratio and correspondingly lower capacity factors, the results indicate that certain precautions in fabrication and assembly of the converging section of the flow passage must be exercised to realize the expected high capacities. Concentricity between the boiler nozzle and the throat tube must be maintained.

Projection of the boiler nozzle into the drum is not objectionable so long as no object near the entrance interferes with the flow. For a welded assembly, the approach of fluid, perpendicular to the nozzle axis and toward the outside circumference of the rounded entrance, is less apt to be interfered with when the nozzle does project into the drum than when the outside edge is flush with the inside surface of the drum, owing to rough welding metal around the end of the nozzle.

The greatest reduction of cross-sectional area of the flow passage is made to occur at the lower end of the nozzle. In order to reduce entrance losses to a minimum and secure high capacities, a minimum value of the rounded-surface radius ratio must also be maintained. This surface, of which the longitudinal crosssection is a full 90-deg arc, normally can be formed entirely on present commercial tubes and welding flanges, in particular on those for the higher pressures. If the cross section is not circular, the surface must still possess a gradual curvature.

Otherwise, additional entrance losses are introduced (6). Conical surfaces are not desirable at this location for this reason.

Surfaces of equipment entirely within the drum should not be placed too near the safety-valve inlet. The minimum distance is governed by the boiler nozzle diameter and the amount of flow. The effect of the flat-plate obstruction, although perhaps not typical of objects located within the steam drum near the safety-valve nozzle, provides a guide as to the amount of reduction to be expected. Present marine-boiler construction practice places equipment within the drum near the inlet to the safety-valve nozzle that, if close enough, can materially alter the ideal approach flow pattern.

In some installations, welding rings are used inside the boiler-safety-valve nozzle to weld the nozzle into the drum. This practice would affect seriously the entire performance of the new design and could not be permitted.

Greater capacities than in the majority of the top-guided-type safety valves installed at present are possible if these precautions are taken. At present the exercise of these precautions is not entirely within the control of the safety-valve manufacturer. Even if the ideal boiler-safety-valve nozzle were to be supplied with the safety valve by the safety-valve manufacturer, satisfactory performance would not be assured unless they were installed with the foregoing precautions being taken. New or revised Boiler Code rules covering the installation of maximum-capacity safety valves may be essential. It is suggested that the following items be considered in establishing new code rules for high-capacity safety valves:

- 1 Welding rings should be prohibited in the boiler-safety-valve nozzle.
- 2 Rounded-surface entrances are requisite.
- 3 Welding metal should not interfere with flow at the outside edge of the entrance surface.
- 4 Minimum distances from the entrance to other surfaces should be specified.

ACKNOWLEDGMENT

The author wishes to thank the management of Manning, Maxwell & Moore, Inc., for permission to use the test results given in the paper. The experimental work was initiated by Mr. C. H. Graesser, Vice-President in Charge of Engineering and carried on by Mr. J. L. Corcoran, Chief Engineer of the Consolidated Safety Valve Division, by the author, and by Mr. P. A. Ibold, Development Engineer of the Consolidated Safety Valve Division.

BIBLIOGRAPHY

- 1 "Power Boiler Code, 1943," THE AMERICAN SOCIETY OF MECHANICAL ENGINEERS, New York, N. Y.
- 2 "Fundamentals of Safety-Valve Design," by R. J. S. Pigott, *Power*, vol. 65, no. 16, April 19, 1927, pp. 580-583.
- 3 "The High-Pressure Steam Testing Laboratory," Manning, Maxwell & Moore, Inc., New York, 1925.
- 4 "Steam Air & Gas Power," by W. H. Severns and H. E. Degler, John Wiley & Sons, Inc., New York, N. Y., third edition, 1939, p. 73.
- 5 "Steam and Gas Turbines," by A. Stodola, translated by L. C. Loewenstein, McGraw-Hill Book Company, Inc., New York, N. Y., vol. 1, 1927, p. 107.
- 6 "Steam Turbines," by J. A. Moyer, John Wiley & Sons, Inc., New York, N. Y., sixth edition, 1929, p. 56.

Discussion

JAMES L. CORCORAN,⁵ The research work which Dr. Falls has described is worthy of discussion as to its significance to the users

⁵ Chief Engineer, Consolidated Safety Valve Division, Manning, Maxwell & Moore, Inc., Bridgeport, Conn. Mem. A.S.M.E.

of safety valves. The principles of design for maximum flow through the valve inlet fitting mean a greater utilization of the possible theoretical flow than has been the practice. This may mean, for one thing, the use of smaller diameters of fittings, and safety-valve inlets to match. The connection sizes may be reduced by at least one size and possibly more when compared with present-day practice. In this case, even considering the machining of a rounded entrance, there will very likely be a saving over present practice.

Secondly, the possibility of maximum flow through the valve inlet may be utilized with mounting connections of sizes comparable to present practice, in which case the capacity of one valve may be sufficient to take the place of several valves under present ratings. This of course will be dependent on considerations as to operating conditions, etc., which would be affected by valves of higher capacity than those now in use. The

ultimate solution to this question may depend on investigation along the lines of this work.

As Dr. Falls has stated, certain field tests have been conducted, using the principles set forth in the discussion. The conclusive answer to the question of maximum capacity will depend upon further work along these lines.

There is a question which might arise in regard to Dr. Falls's discussion, namely, that of the mounting of superheater valves.

It might be well to add that in connection with the field tests, a service test of a superheater valve built to the entrance specifications outlined by Dr. Falls was made. The valve performed satisfactorily both as to operation and capacity, though there were two sharp 90-deg bends ahead of the valve inlet. There would therefore not seem to be any difficulty in the way of mounting of superheater valves, in which case the practice is different from that of drum-valve mountings.

10,000-Kw Railway-Mounted Mobile Steam Power Plant for U. S. Navy Department, Bureau of Yards and Docks

By EDWIN LUNDGREN¹ AND L. R. BIGGS²

Well-established practice was followed in the design of equipment for the two mobile power plants so far constructed, within the limitations of railway clearances and need for increased ruggedness to meet road conditions. The units are intended for purposes of the Navy Department at stations on the East and West Coasts, wherever a breakdown in power supply or increased power demand occurs, where naval work is involved. Details are given of the six-car power plant which includes a boiler car, turbine car, switchgear car, transformer car, gondola car mounting auxiliary equipment, and a box car also containing pumps and miscellaneous equipment. A comprehensive description is given of the main steam generator, the turbogenerator equipment, and all auxiliaries.

IN the early part of 1940, the Bureau of Yards and Docks of the Navy Department investigated the possibilities of mobile power plants as a desirable part of the defense program for its various activities at the navy yards and naval stations. Hull-mounted plants were considered for sea transportation, and railway-mounted plants for land transportation.

The value of such plants, which would be located at strategic points for rapid transport, is self-evident. They could be moved to any location where a serious breakdown in power supply occurred or where a sudden demand for increased generating capacity was desired in important navy yards or naval stations.

Since this time, the recognition of the general idea has resulted in the construction of mobile power plants on barges and special trucks, and in the construction of a number of railway-mounted power plants for shipment to our Allies, particularly the Russians.

The Navy Department decided to build two railway-mounted mobile power plants each of 10,000-kw capacity, one unit to be stationed on the West Coast and one on the East Coast. A contract was authorized by the Secretary of the Navy, and the order placed with the General Electric Company for the equipment; the design to be under the general supervision of the Bureau of Yards and Docks and its Chief, Vice-Admiral B. Moreell, and the head of the Power Division, Capt. L. W. Bates.

The general plan was to follow well-established power-plant designs with well-tried commercial equipment and work toward dependability rather than high efficiency. Of main technical interest is the adaptation of this equipment within the narrow confines of the clearance limits of standard-gage railway systems. The principal dimension of a railroad car is its length; therefore,

the ordinarily square dimensions of a power plant had to be changed to a status of small height and width and great length.

Investigation of the routing from a central point to some 35 locations in various parts of the United States connected by the major railroads showed that a car width of 10 ft 1 $\frac{3}{4}$ in., and a height above rail of 15 ft 3 in. must not be exceeded.

Particular problems such as supporting the boiler, the turbine generator, the condenser, and auxiliaries were encountered and solved in a satisfactory manner. Distribution of the load uniformly on the axles to conform to the requirements of the railroad companies, maintaining clearance for minimum-radius curves, and keeping the center of gravity down to prevent overturning were some of the things that had to be considered.

Certain special designs were required for the main equipment to meet these limitations, the turbine exhausting horizontally to a special design of vertical condenser, and the boiler design being of the straight-through type as influenced by the limiting clearance dimensions. Fig. 1 shows the dimensions of the various cars.

A capacity of 10,000-kw for the plant was chosen from the viewpoint of desirable vital emergency requirements of many of the naval activities, and the approximate maximum size of commercial turbine equipment that could be installed within the clearance limits of the turbine car.

SIX CARS MAKE UP POWER PLANT

The power plant is made up of six cars as follows:

1 Boiler car containing the main steam boiler, the boiler feed pumps, forced-draft fan, deaerating heater, fuel tank and pumps, air compressors, water tank, and auxiliary boiler. Complete arrangement is shown in Fig. 2.

2 Turbine car (Fig. 3) containing the main turbine, generator, condenser, evaporator, 350-kw auxiliary generator, water-chilling equipment, lubricating-oil tank, surge protectors, and neutral pyranol reactor.

3 Switchgear car (Fig. 4) containing main and auxiliary switching equipment, 50-kw Diesel-engine generator, exciter set, storage battery, chemical laboratory, and cable reels.

4 Transformer car (Fig. 5) containing the 12,500-kva transformer, gas-sealing equipment, and cable reels.

5 Gondola car (Fig. 6) containing the circulating-water pump and motor, the strainers and suction hose, the hose for connecting up the circulating water, and the fuel-oil piping system.

6 Boxcar (Fig. 7) containing raw-water pump and hose, fuel-oil transfer pumps, oil hose, air-conditioning equipment, workbench and lockers, wrenches, and electrical jumper cables.

These six cars occupy a track length of approximately 386 ft. The length of the train in transit with additional cars, such as caboose, oil car, locomotive, etc., is approximately 634 ft. The train is designed for a speed of 40 mph maximum and for curves of 20 deg maximum, for the whole or unbroken train. Minimum-radius curve, 150 ft, requires special individual handling of the boiler car and the turbine car.

¹ Senior Mechanical Engineer, Bureau of Yards and Docks, Navy Department, Washington, D. C.

² Construction Engineering Department, General Electric Company, Schenectady, N. Y.

Contributed by the Power Division and presented at the Annual Meeting, New York, N. Y., Nov. 27-Dec. 1, 1944, of THE AMERICAN SOCIETY OF MECHANICAL ENGINEERS.

NOTE: Statements and opinions advanced in papers are to be understood as individual expressions of their authors and not those of the Society.

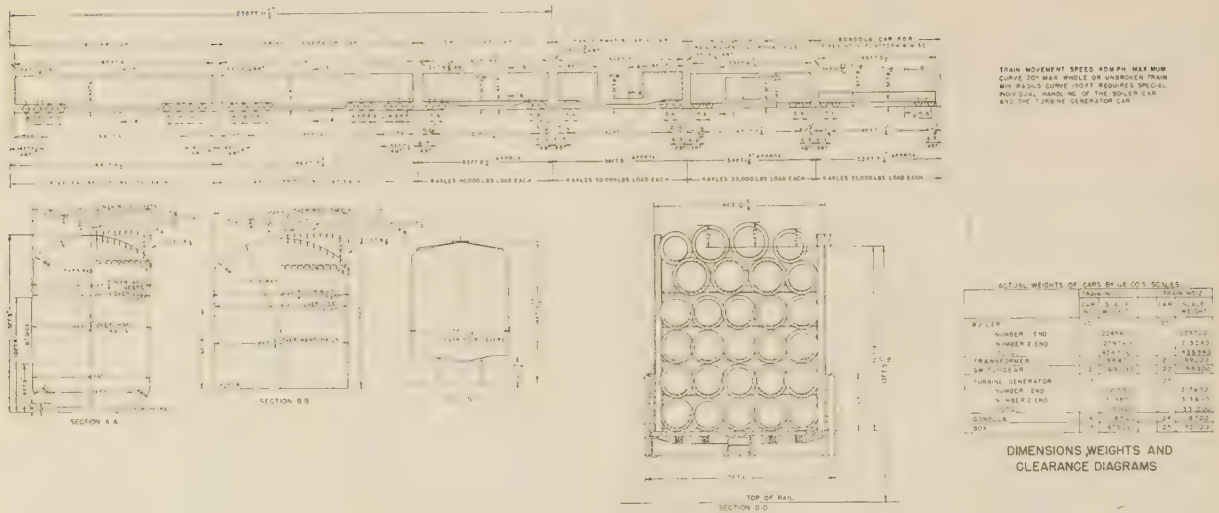


FIG. 1 CLEARANCE DIAGRAMS, WEIGHTS AND LENGTH OF TRAIN

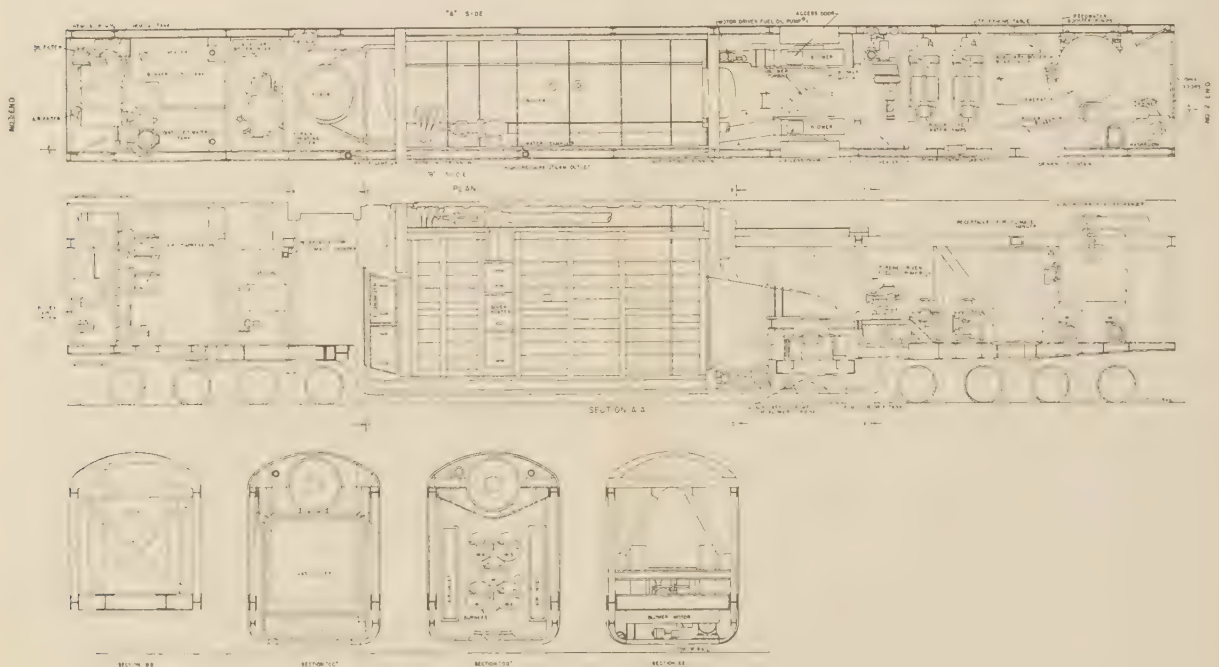


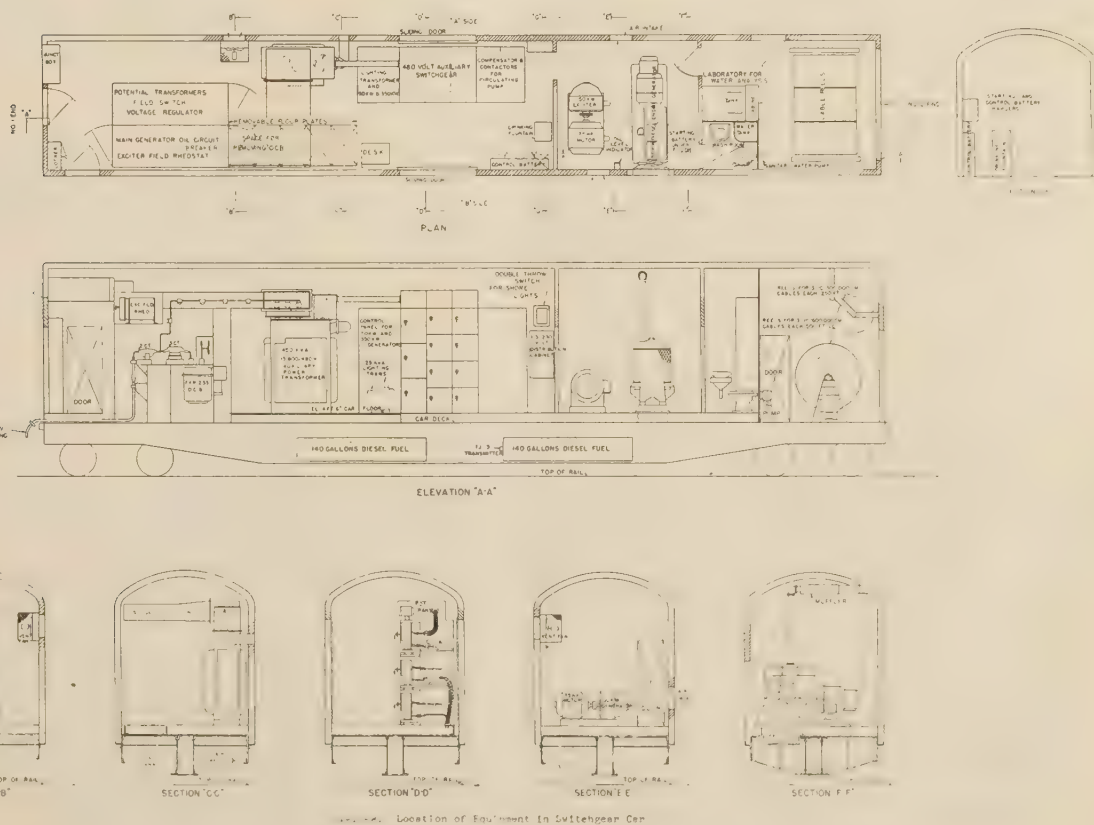
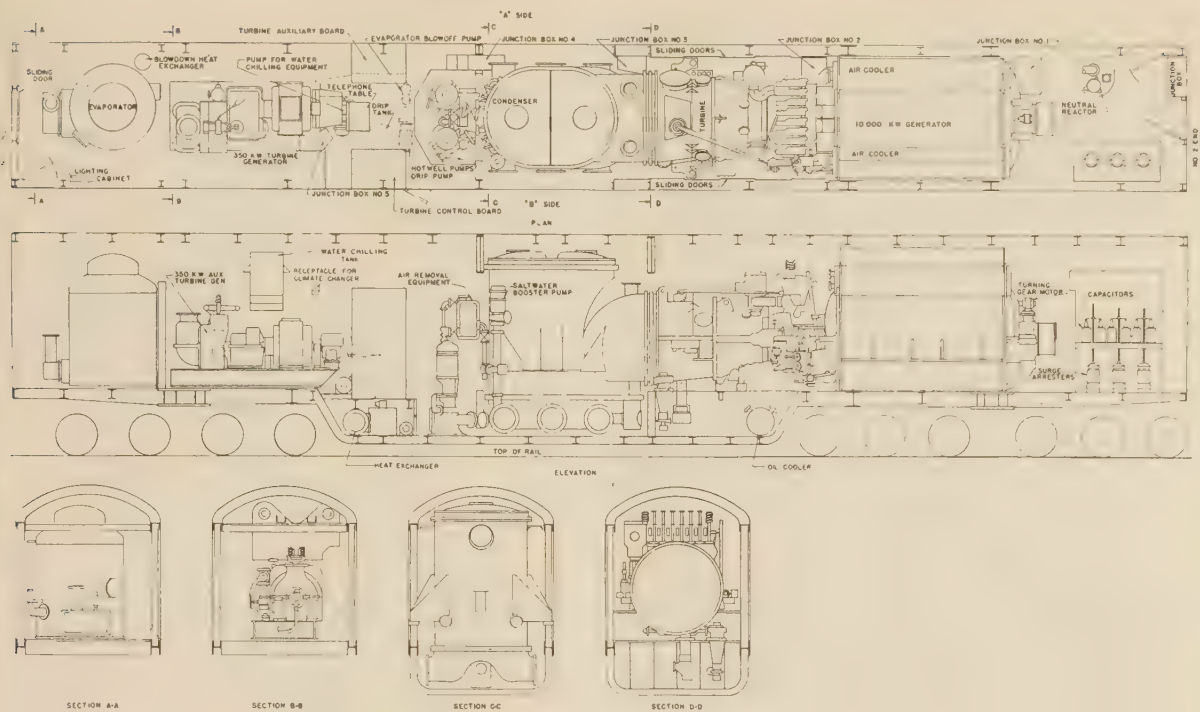
FIG. 2 LOCATION OF EQUIPMENT IN BOILER CAR

The boiler, turbine, switchgear, and transformer cars are of special design while the gondola and boxcars are of standard make. The boiler car complete with equipment weighs approximately 450,000 lb and is supported on eight axles. The over-all length from coupler to coupler is 89 ft 4 1/2 in. The turbine car weighs approximately 550,000 lb, has four axles on one end and six on the other, making a total of ten. The over-all length is 86 ft. The turbine car was designed with more axles on one end than the other because of the concentrated load of the generator which is inherent in such a piece of equipment. The switchgear car weighs approximately 160,000 lb, has an over-all length of 63 ft 6 in. and four axles. The transformer car weighs approximately 200,000 lb, has an over-all length of 56 ft 5 in. and also four axles.

CONSTRUCTION OF BOILER AND TURBINE CARS

The boiler and turbine cars are of special interest. The horizontal members forming the top and bottom chords of the side frame trusses were made by taking a wide-flange beam of large section and removing part of the web by slitting with acetylene torches then rewelding to obtain the desired section. Increased stability in the horizontal direction was thus obtained from the wider flanges and the inside clearance was kept to a maximum. The truss-web members of the cars were built from H-sections welded into place.

Both cars have a welded underframe supported from the lower chord. This is composed of H-sections and is trussed to increase the horizontal stability. Owing to the fact that the equipment occupies all of the space inside the framing, no cross bracing



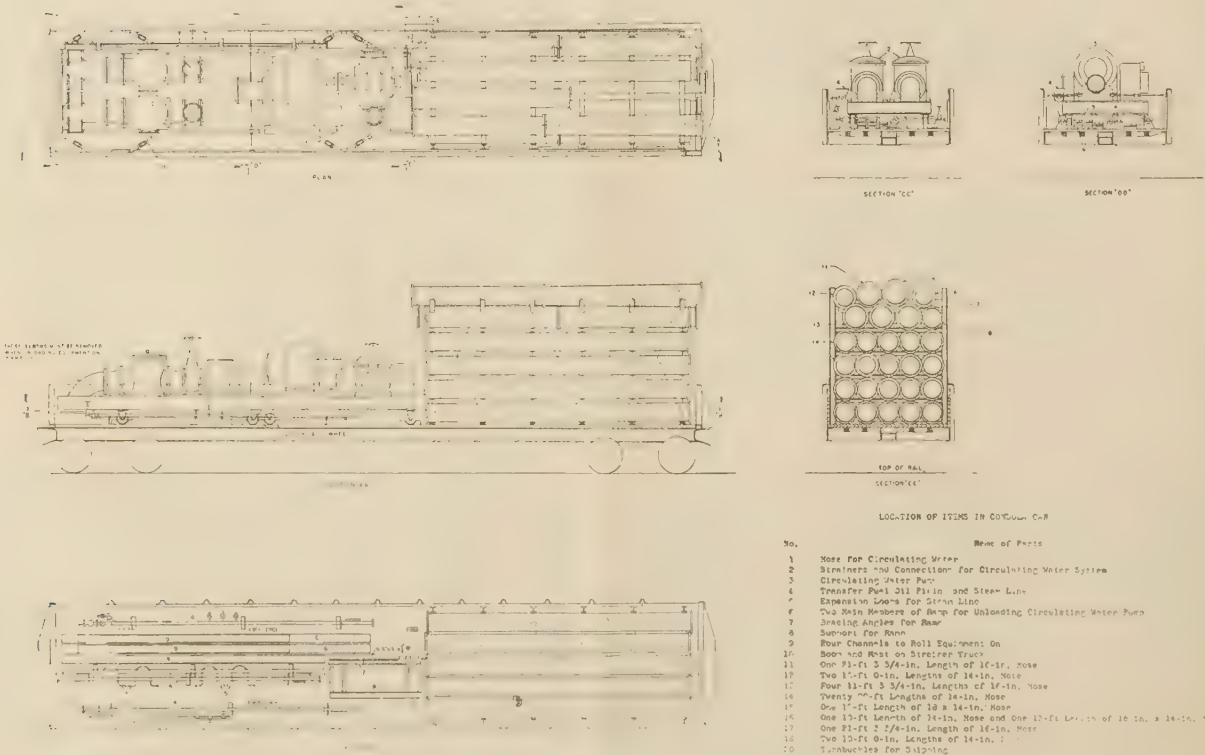
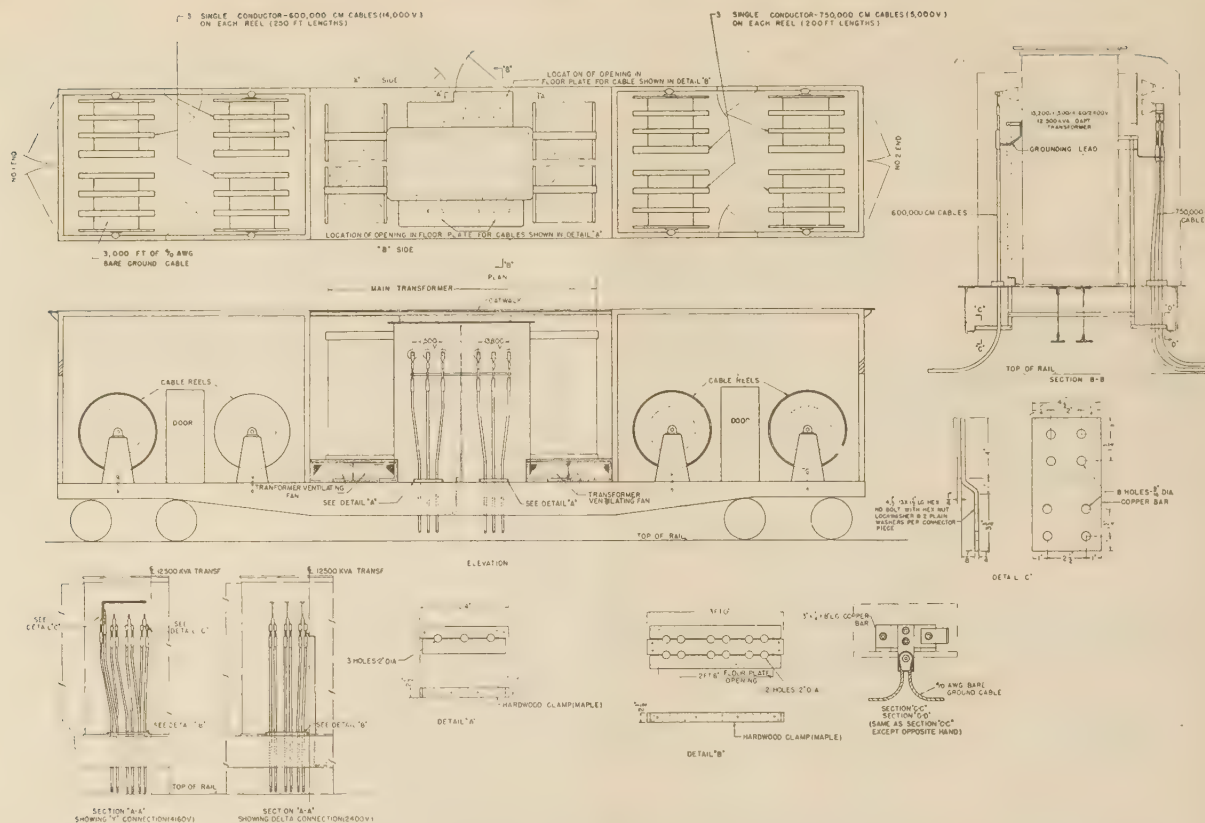
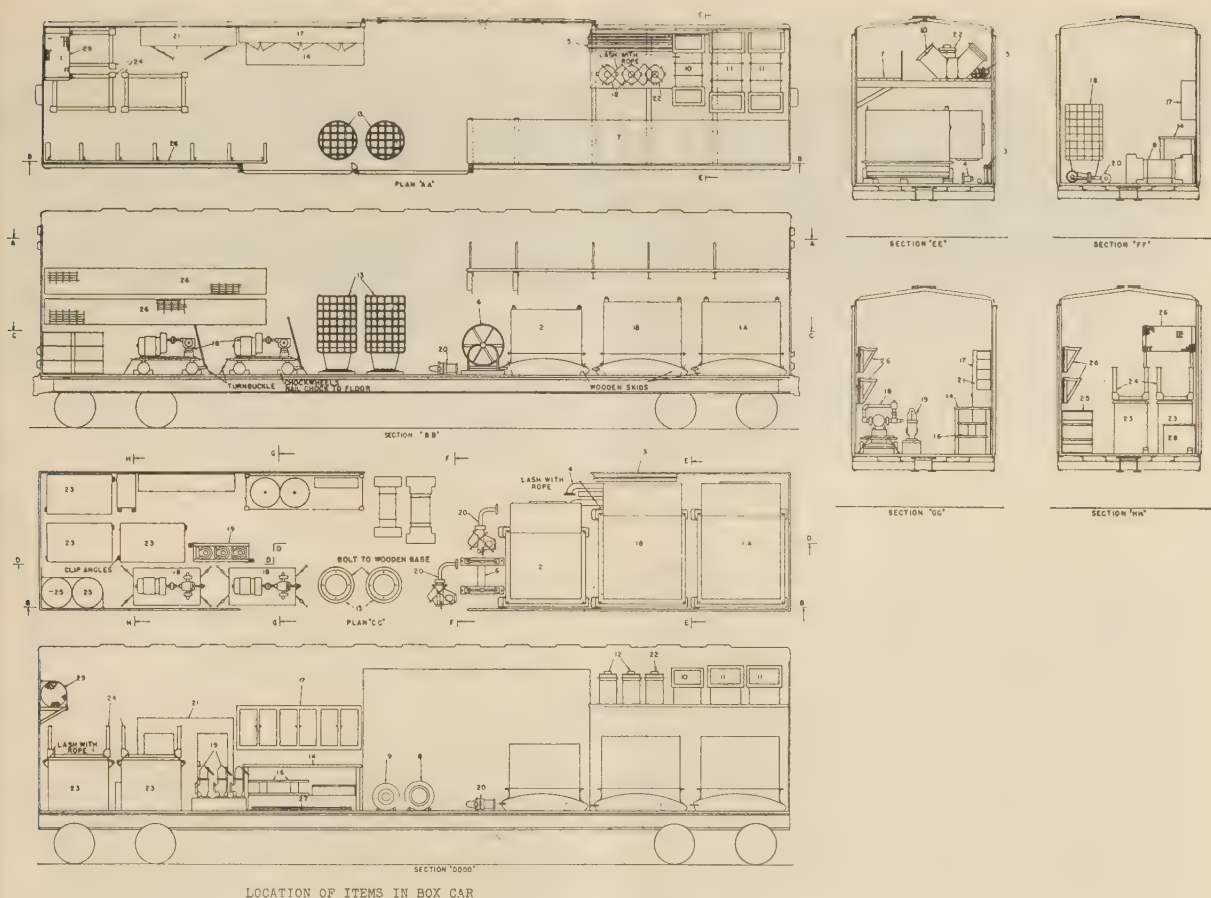


FIG. 6 LOCATION OF EQUIPMENT IN GONDOLA CAR



LOCATION OF ITEMS IN BOX CAR

No.	Name of Parts		
1A	No. 48-M Climate Changer for Boiler Car	15	Turbine Department Tool Box
1B	No. 48-M Climate Changer for Turbine Car	16	Cable Reels
2	No. 30-M Climate Changer	17	Cabinet
3	Ladder to Walkway on Turbine Car	18	Transfer Oil Pump
4	Piping for Relief Valves on Boiler	19	Relief Valves on Boiler
5	Connection Hose Between Cars to be Stored on Rack	20	Soot Blowers
6	Fire Hose Reel with 500 Feet of hose	21	Locker
7	Rack for Hose Which is Used Outside - Long Lengths	22	Spare Toilet Can
8	Connection for Exhaust Steam Between Cars	23	High Voltage Feeder Cables - Junction Box
9	Connection for High Pressure Steam Between Cars	24	Junction Box Supports
10	Discharge Duct for No. 30-M Climate Changer	25	Drums for Chemicals
11	Discharge Duct for No. 48-M Climate Changer	26	Walkway on Turbine Car
12	Toilet Cans for Boiler and Switchgear Cars	27	Forty 3/4-in. Diameter - 7 Feet Long - Grounding Rods
13	Suction Strainer on Circulating Water	28	Box for Bolts and Nuts on Circulating Water Hose
14	Work Bench	29	Spare Basket for Andale Strainer on Circulating Water Suction

FIG. 7 LOCATION OF EQUIPMENT IN BOXCAR

could be used where most effective, therefore the bottom and roof had to be utilized. The car bolsters were fabricated and welded from plate sections and then annealed before welding into the car framing. The work was done by the Greenville Steel Car Company. Tolerances were kept to $\pm 1/8$ in.

The problem of designing the cars so that equipment could be placed in them and later removed if necessary was solved by making the roof removable and bolting the side plates into place. Some details are shown in Figs. 8 and 9. Supporting structures and equipment were designed to stand a loading of $2\frac{1}{2}$ times gravity in the horizontal direction along the rails and 1 times gravity in the vertical direction. The wheel loading was limited to 55,000 lb per axle; the center of gravity in the vertical direction was kept to approximately 82 in. above the rail.

Owing to the length of the boiler and turbine cars, it was necessary to place the draft gear in the end of the span bolster

which connected the two sets of wheels together, instead of the standard practice of placing it in the car frame. This gave in effect two short cars upon which the body of the main structure was placed. As the bolsters were required to hold a tremendous weight, each casting was magnafluxed and X-rayed, then proof-tested by loading to $1\frac{1}{2}$ times the weight to be carried. The work was done at the plant of the Buckeye Steel Castings Company. Fig. 10 shows one of the 6-wheel trucks. Fig. 11 shows the completed boiler car and Fig. 12, the turbine car.

Brakes were of the Westinghouse "AB" type and all of the necessary equipment was mounted on the trucks thus making two sets of brakes for each car. Braking was designed for approximately 25 per cent.

The side plates on the turbine car were provided with ribs as an insurance against high-frequency vibration. The ribs were made by pressing ridges into the plate.



FIG. 8 BOILER CAR FRAME BEFORE INSTALLATION OF BOILER

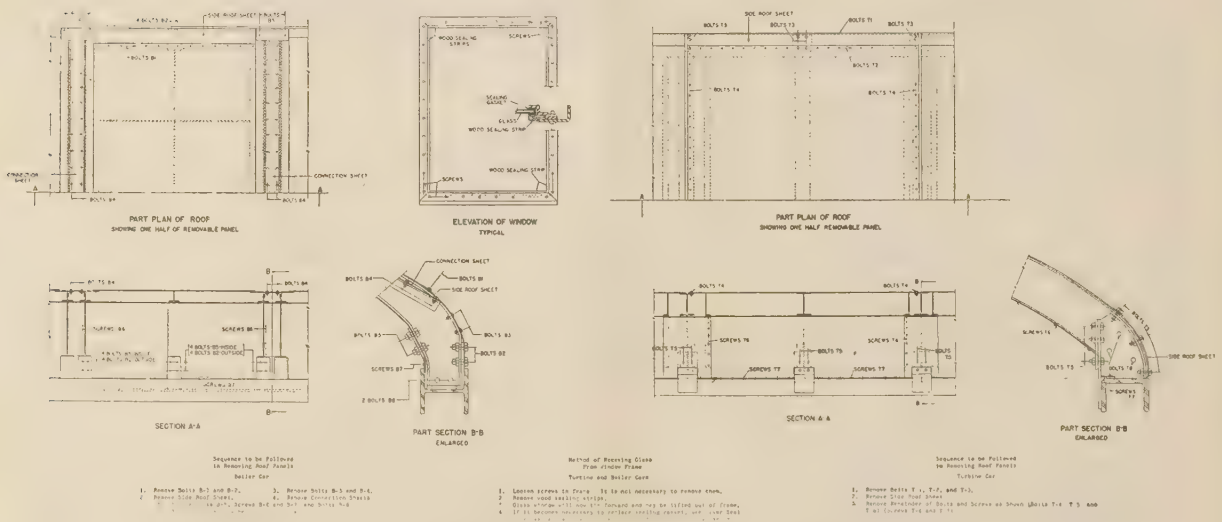


FIG. 9 DETAILS OF REMOVABLE ROOF AND WINDOWS

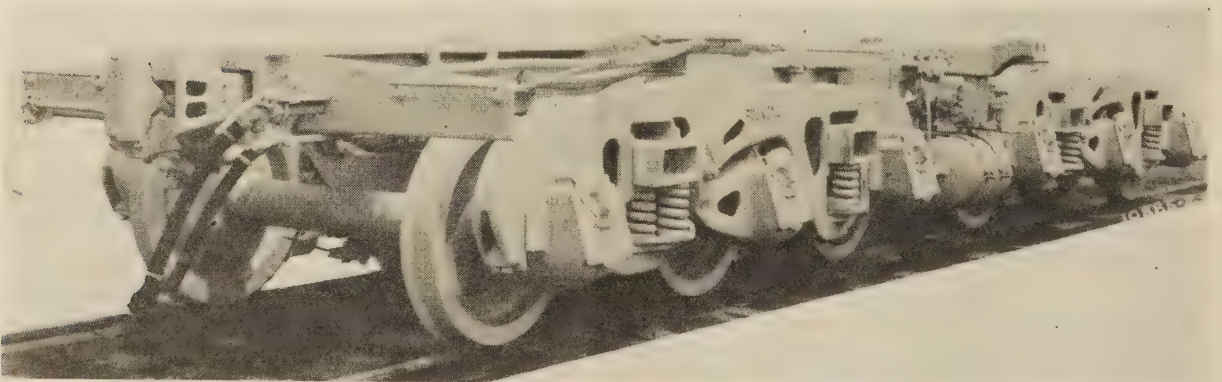


FIG. 10 6-AXLE TRUCK SHOWING COUPLER, AIR TANK, AND AIR-BRAKE EQUIPMENT

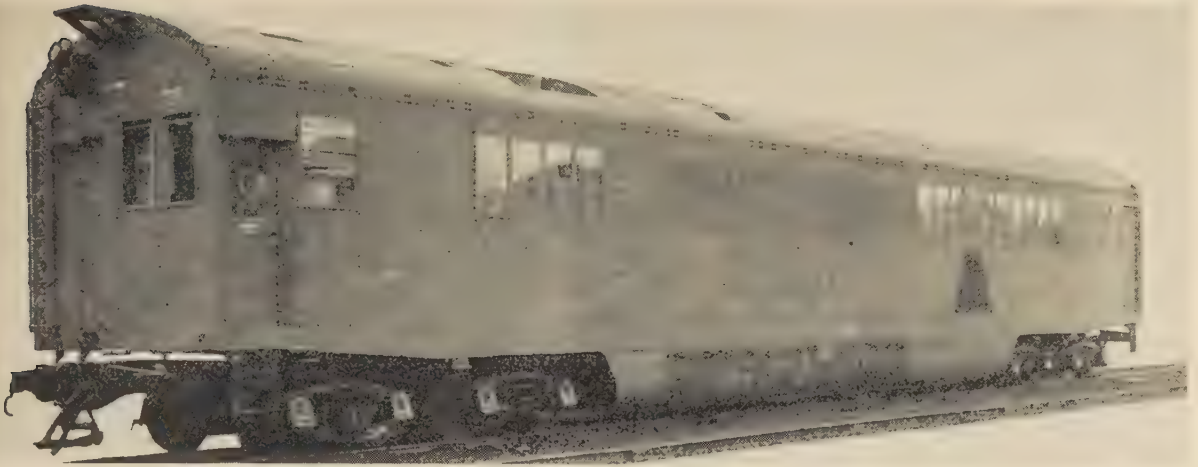


FIG. 11 BOILER CAR READY FOR TRANSPORTATION



FIG. 12 TURBINE CAR READY FOR TRANSPORTATION

The roof of the three main power-plant cars was insulated with approximately 4 in. of "stonefelt" and the side plates with a layer of asbestos millboard. The latter was done principally to avoid excessive condensation during cold weather.

The switchgear car was of conventional riveted construction with the draft gear located in the center sills.

STEAM-GENERATOR DETAILS

One Babcock and Wilcox natural-circulation boiler supplies the steam required to operate the power plant. This boiler is necessarily compact to meet the stringent space conditions imposed by railroad clearances. The designed full power condition is 120,000 lb of steam per boiler per hour at 560 psi pressure and 825 F total temperature at the superheater outlet; when generating 10,000 kw. The boiler design pressure is 650 psi and the feed temperature to the economizer is 220 F. One hundred thousand pounds of steam per hour passes to the main turbine,

the remaining 20,000 lb of steam per hour, desuperheated to 650 F in a pipe coil submerged below the water level in the main steam drum, is used for such auxiliary equipment as the forced-draft blower, feedwater pumps, and the oil-pump turbine. The maximum, designed, continuous output of the unit is 140,000 lb of steam per hour.

The arrangement of the boiler and its component parts is shown in Figs. 13, 14, 15, and 16.

The furnace is practically completely water-cooled to insure long life at the extremely high combustion rate of 416,000 Btu per cu ft of furnace volume at full power when delivering a total of 120,000 lb of steam per hour. The side walls and a portion of the roof of the furnace are of Babcock and Wilcox stud-tube construction with plastic chrome ore rammed between the studs. Note the crossed stud tubes in the roof arranged to protect the steam drum. Water cooling is provided at either side of the front wall by stud tubes. The water screen is at the rear of the

furnace. The only noncooled surfaces in the furnace are in the zone of the burners in the front wall and the floor.

In order to insure satisfactory combustion conditions at the extremely high rates of operation in the relatively cold furnace, heated combustion air is supplied to the burners. The air, delivered by the forced-draft fans, passes through the air ducts and over banks of finned-tube downcomers extending between the steam drum and the waterwall headers. The air is heated to 320 F at the full power rate of operation, and approximately 400 F at 2500 kw by the water at saturation temperature entering these downcomers. We believe that this is the first application of the finned-tube downcomer type of air heater in boiler work.

Steam mechanical atomization is employed, using five Babcock and Wilcox Iowa type oil burners, to assure satisfactory combustion conditions in the cold furnace especially at the low rates of operation, and to provide wide-range burner operation, which is desirable when full-automatic control is used, without changing sprayer plates from 2500 kw to the overload rate of operation. The range of operation of the burners is from 510 lb of oil per burner per hour, corresponding to 15 psi oil pressure, to 2530 lb of oil per burner per hour corresponding to 240 psi oil pressure. The steam is supplied to the burners at all oil pressures up to 100 psi with the steam pressure approximately 20 psi higher than the oil pressure. Straight mechanical atomization is used above 100 psi oil pressure. Number 6 fuel oil, Bunker "C," is used under all operating conditions except when lighting off under the cold condition when Diesel or No. 3 oil is used. An electric-driven fuel-oil pump of 2 gpm capacity is used for this purpose.

The boiler is so arranged that the combustion gases flow horizontally, parallel to the steam drum, through a nine-row water screen, consisting of four rows of widely spaced tubes and five rows of closely spaced tubes, before the superheater. The gases then flow through the convection-type superheater (537 sq ft) and the boiler convection bank and the stud-tube economizer (1772 sq ft) to the stack. The boiler heating surface is 3195 sq ft.

In addition to the circulation provided by the finned-tube downcomer air heaters, circulators are placed in the front wall and the boiler convection bank behind the superheater. Boxes, formed by stud-plated boiler tubes, shield the boiler-convection-bank downcomers from direct impingement of the gases of combustion.

Dry steam is assured by the installation of 18 Babcock and Wilcox cyclone separators in the 42-in. steam drum.

The entire boiler is suspended from the steam drum. The weight of the boiler is carried to the side trusses of the car by trunnions fitted over the ends of the steam drum. The trunnion at the front is securely anchored to take the entire buffer action of the boiler when the car is stopped and started. The trunnion at the rear supports the drum but allows it to slide in a fore and aft direction to provide for expansion. Provision is made to allow the heating surfaces to expand downward. The front ends of the side wall headers are anchored to take the buffer action.

Combustion air is supplied by forced-draft fans, no induced draft is provided, so that all of the boiler is under gas pressure relative to the surrounding atmosphere. Except for the closely bolted, gasketed panels for access to the superheater and economizer headers and tubes and waterwall headers, the boiler casings are entirely welded to prevent gas leakage.

The equipment for providing air for combustion consists of two forced-draft blowers operating in parallel on the same shaft, driven by a steam turbine. They are designed to deliver a total of 56,000 cfm of air against a static pressure of 55 in. The blower rotors, made of an aluminum alloy, are mounted as an overhung structure on the shaft extension of the turbine. The turbine is

rated at 740 hp, at 3000 rpm; is supplied with desuperheated steam of 530 psi pressure, 650 F; and operates at 5 psi back pressure. When starting the plant, the blower can be operated at 820 rpm from a 15-hp, 1200-rpm, 440-v induction motor, connected through gearing to the turbine shaft. The special turbine was built by the General Electric Co. and the rotors, housing, and base were built and the complete unit assembled at the shops of the Buffalo Forge Co. Five rotors were made and one was tested by overspeeding successfully to 5000 rpm.

MAIN AND AUXILIARY PUMPS AND HEAT EXCHANGERS

The main fuel-oil pumps consist of two Quimby gear-driven pumps, one motor- and one steam-driven. Each has a capacity of 35 gpm delivering oil at 350 psi at 1150 rpm. The turbine-driven pump is mounted over two Lummus Company high-pressure heaters having a capacity of heating 15,000 lb per hr of bunker C fuel oil from 120 deg to 204 deg F. The shell side of the heater is designed for 350 psi operating pressure. Steam at 5 psi is used for heating. The fuel-oil pumps take oil from the bunker C oil tank located at one end of the car, the oil passing through a Lummus suction heater preheating the oil from 80 deg F to 140 deg F.

The boiler car also contains the Cochran deaerating heater, having a capacity of 140,000 lb per hr. The oxygen content in the heated water does not exceed 0.01 cc per l at maximum capacity. The heater is of the spray type, the steam supply being at 5 psi. All water passing to the heater first goes through the continuous-blowdown heat exchanger. Water level is controlled by two float valves, one in the supply line from the distilled-water tank which is operated by the low-level float, and the other in the line from the condenser hot-well pump which is connected to the high-level float. With the evaporator in service, some water is always discharged to the distilled-water tank through the spring-loaded valve located in the condensate-return line.

The feedwater pumping equipment consists of two 356 gpm Ingersoll-Rand booster pumps each driven by a 15-hp 1750-rpm motor. The pumps operate with a positive suction head of 4 ft against a total head of 90 ft. These pumps discharge into two Ingersoll-Rand boiler feed pumps operating against a total head of 1793 ft with a suction head of 70 ft. The pumps operate at 5000 rpm and are driven by 290-hp turbines, actually requiring 270 bhp.

The telescoping smokestack, 3 ft 10 in. diam, can be raised to a height of approximately 34 ft above the rails when the boiler car is in service. During transit of the car and when secured, the telescoping sections are lowered below the clearance line of the car.

Other major equipment in the boiler car is the Vapor Clarkson recirculating-type steam boiler, manufactured by Vapor-Car Heating Company and used to provide initial steam for fuel-oil heating, heating the train, and for supplying steam for oil atomization at the main boiler when the plant is started in operation. It is a forced-circulation water-tube-(coil) type boiler, oil-fired with electric ignition, and is designed and equipped to operate automatically either for intermittent or continuous operation. Steam generation is almost immediate upon starting. Full steam-generating capacity is reached within 4 to 5 min from a cold start. Maximum evaporation is 1800 lb of water per hr at 240 psi, distilled or condensate water being used. Light fuel oil is used in the forced-draft burner.

Two air compressors and three air tanks are installed to supply the compressed air for the operation of various controls in the boiler, turbine, and switchgear cars, and for use in blowing out various pipe lines when the plant is secured. Each compressor is rated at 52 cfm and operates at 100 psi pressure. Two Milton-Roy chemical pumps and a chemical tank are installed to supply

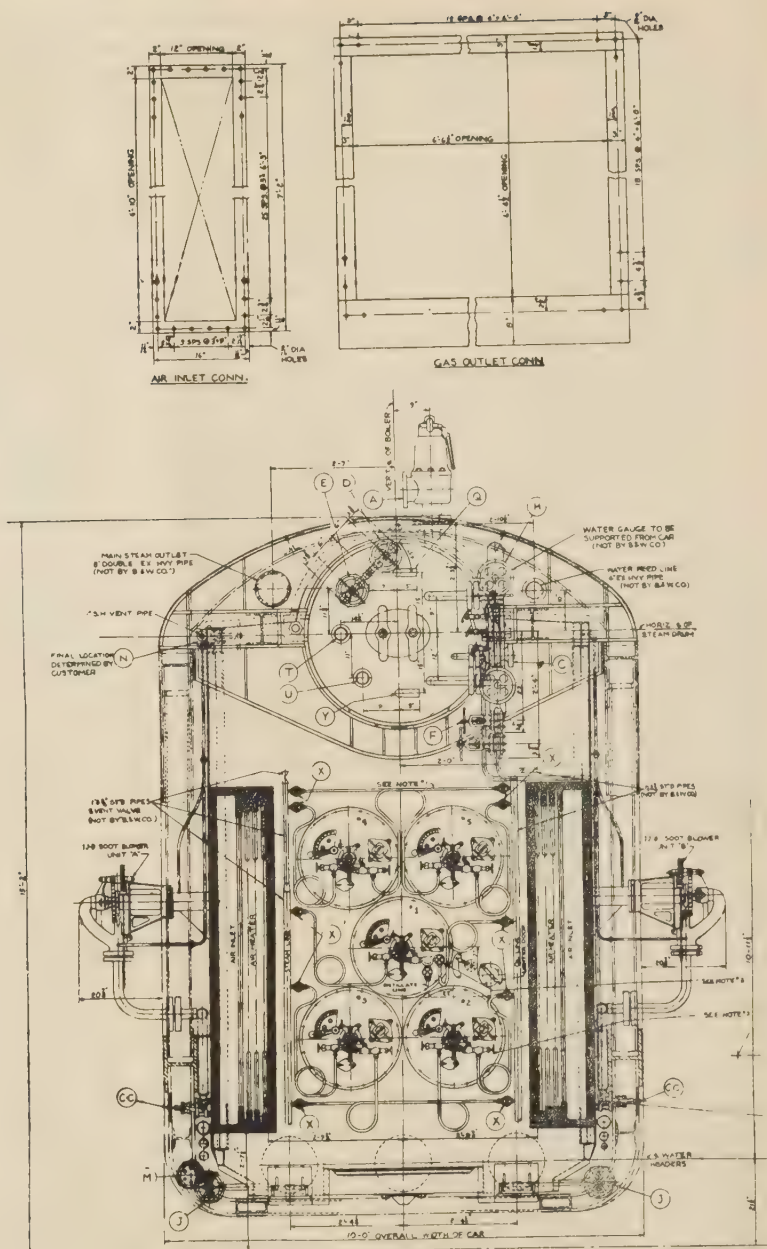


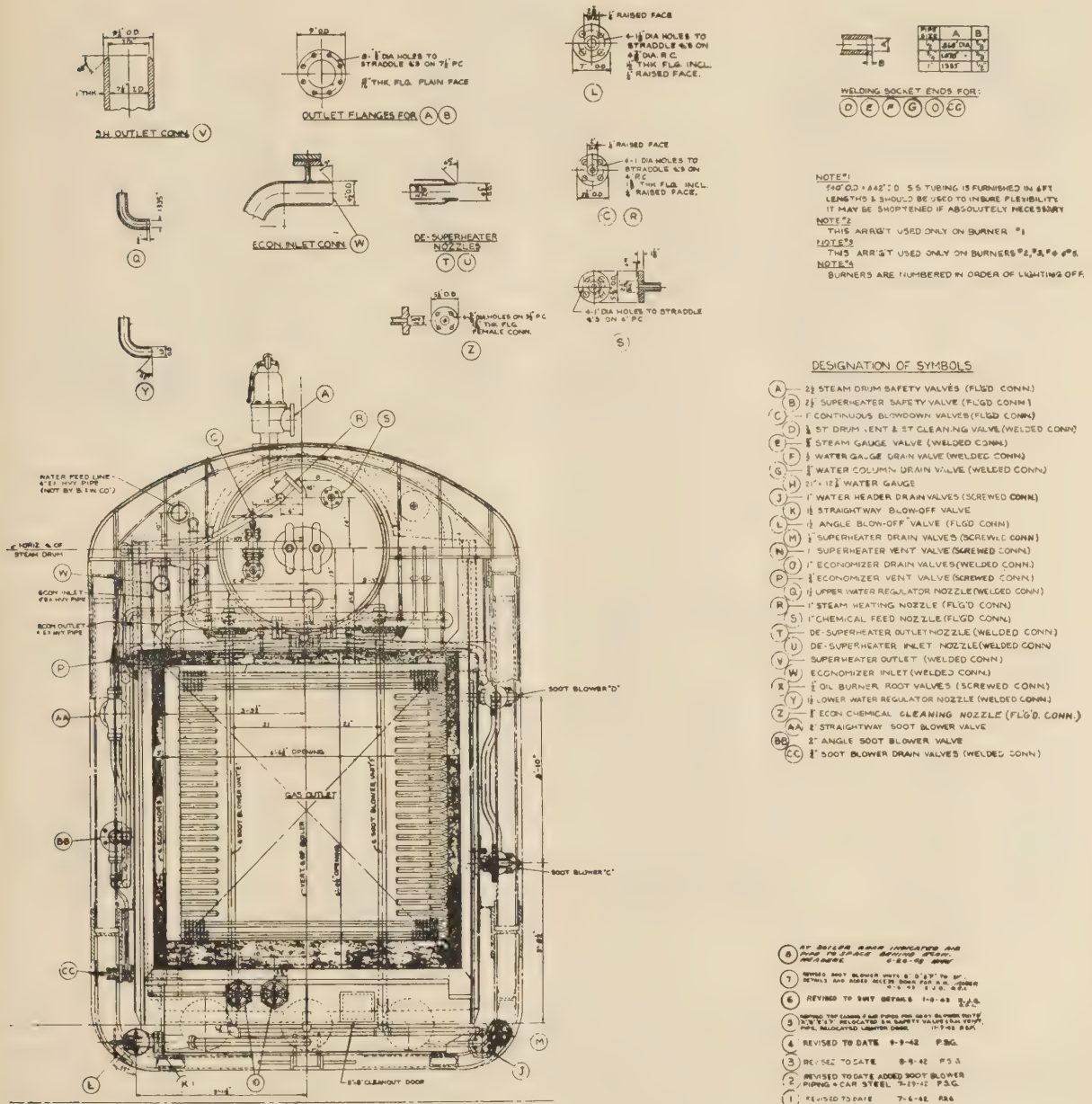
FIG. 14 GENERAL ARRANGEMENT

the chemical treatment of the boiler water at the boiler drum. The main boiler control board and two auxiliary boards for electrical control are also installed in this car. Water-sampling cooler and two 150-gpm motor-driven distilled-water pumps and the distilled-water tank are also included. A complete diagram showing the steam, water, and fuel-oil piping is shown in Fig. 17.

POWER-GENERATING EQUIPMENT

The main power-generating unit consists of a 10,000-kw, 14-stage, 3600-rpm turbine, connected to a 12,500-kva, 13,800-v, three-phase, Y-connected, 60-cycle generator of General Electric Company standard type. Operating conditions for the turbine are 550 psi 825 deg FTT at the throttle, and 3 in. mercury abs

back pressure at the exhaust outlet. It is of the single-cylinder design having 14 stages; the first stage being of double-row construction, the remaining 13 stages of single-row construction. The exhaust shell of this standard turbine is modified for horizontal discharge to accommodate the vertical condenser. For easy starting and to insure even cooling of the rotor, the turbine is equipped with a motor-driven turning gear and oil pump. The turbine is protected from overspeeding by an emergency governor and two trip valves. One of these trip valves operates through the hydraulic control mechanism to close the control valves, while the other functions to dump the oil from the operating cylinder of the stop valve, thereby closing this valve. Fig. 18 shows a cross section of the main turbine, and Figs. 19 and 20, a



FRONT AND REAR OF MAIN BOILER

cross section and end view, respectively, of the main generator.

The unit differs from the usual design in that the steam flow in the turbine is away from the generator instead of toward it. The turbine is connected to the generator frame through a ball-and-socket connection to allow the outboard or exhaust end to be adjusted to correct any misalignment of the shaft. There are three main bearings, two of which are supported by the generator frame and a third in the exhaust shell. The thrust bearing is a part of the middle bearing and is designed to take the buffer thrust of the rotor while in transportation. Expansion is toward the condenser, and a copper expansion joint is placed between the exhaust shell and the condenser inlet. Lack of space and complications of piping prevented the use of extraction

heating. The generator stator is anchored securely to the side frames of the car by body bound bolts and by welded chocks. The generator is air-cooled and is equipped with finned surface air coolers supplied with water from a circulating system.

The control of the turbine can be carried out almost entirely from the operating room inside the car. The mechanical and electrical control boards are located in this space. Pistol-grip type SB1 switches for control from the operating panel with light indication are provided for testing the emergency stop valve and for tripping the emergency oil trip valves, for tripping the emergency stop valve alone, and for resetting the oil trips. Control from the operating panel is provided for the motor-operated speed governor to permit synchronizing and for operation of the main steam-

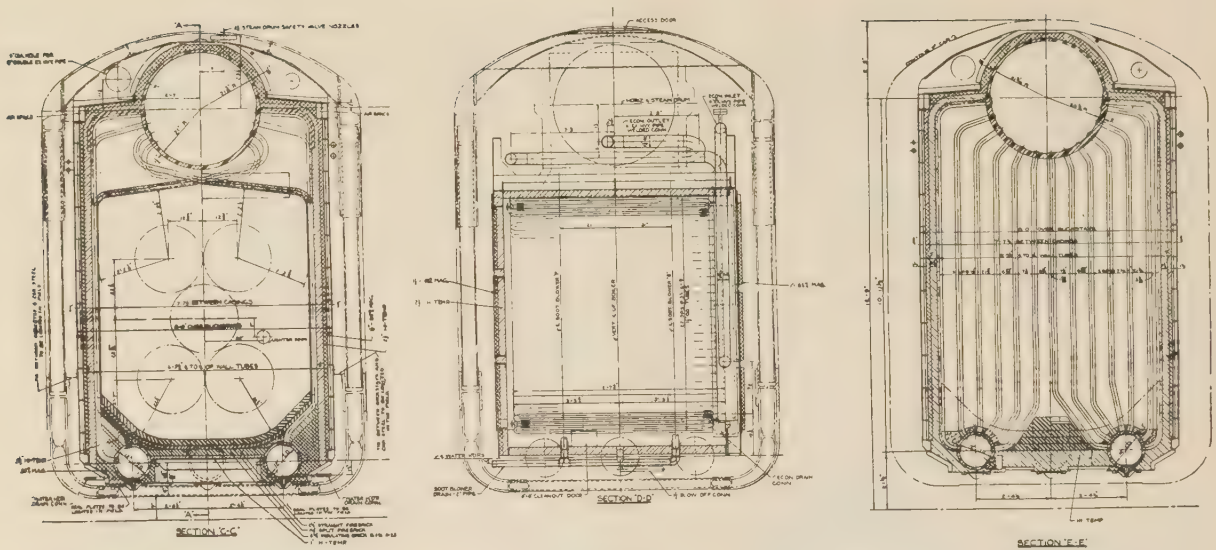


FIG. 15 SECTIONAL VIEWS OF MAIN BOILER AS INDICATED IN FIG. 14

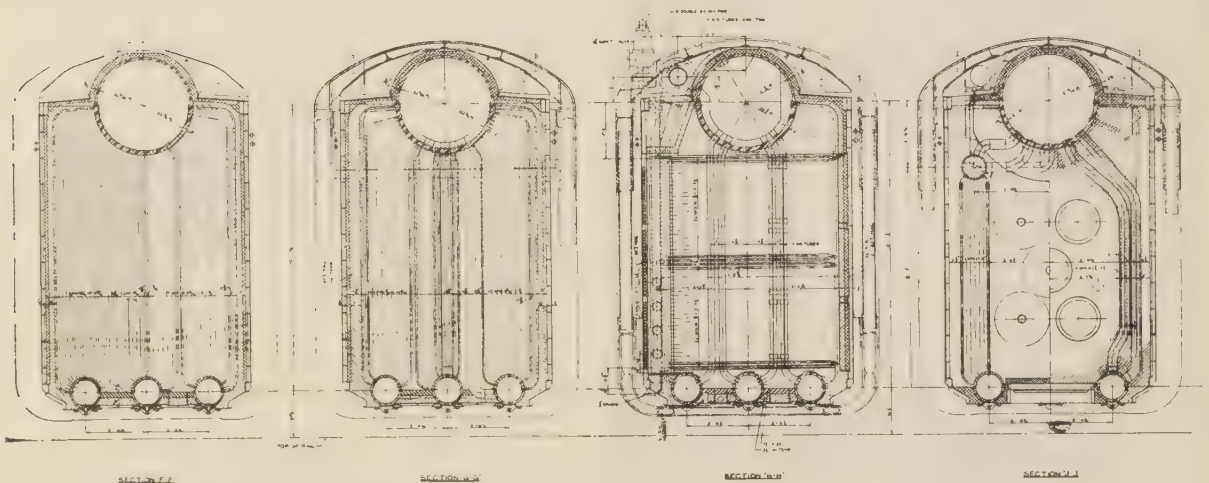


FIG. 16 SECTIONAL VIEWS AS INDICATED IN FIG. 14

control valves functioning through the auxiliary pilot valve. The mechanism which operates the turbine load-control valve can be operated at the turbine by hand or remote operation electrically at the control board in the turbine-operating room, or through transfer switches from the switchgear car. Selsyn indication on the control panel indicates the position of the valve and also indicates the load which is being carried. An electric tachometer is provided for use in indicating turbine speed for the warming-up cycle. Several other valves can be operated from the turbine room, such as live-steam supply valve for sealing high-pressure packing during starting, packing leak-off valve, above-seat and below-seat stop-valve drains, high-pressure water packing feed and drain valves, and low-pressure water packing feed valve. Control of the synchronizing motor is ordinarily switched to the generator board in the switchgear car from which the unit is synchronized. Fig. 21 shows the location of the controlling mechanism for the 10,000-kw turbine.

Other equipment installed in the turbine car includes the

following items: The evaporator for make-up water which is of the single-stage type using steam in the coil at 5 psi and exhausting at approximately 25 in. of mercury vacuum on the vapor side. A total of 7000 lb of raw water per hr can be evaporated. The vapor is condensed in the main condenser and is pumped back with the the general condensate. The Lummus Company steam-jet refrigerating unit, operating with two booster jets, has a capacity of 70 tons per hr. The chilled water is delivered at approximately 50 deg by a 180-gpm pump to the air-conditioning units on the boiler and turbine cars. The air-conditioning units are standard demountable types as manufactured by the Trane Company, and when in service are bolted to the roof of the cars. The units are also arranged for heating the ventilating air for winter service. Air conditioning was provided to make the plants suitable for operation in all kinds of climates from 110 F, to many degrees below zero; also for operating in bombproof or splinterproof shelters.

The condenser is designed for condensation of 112,000 lb per hr

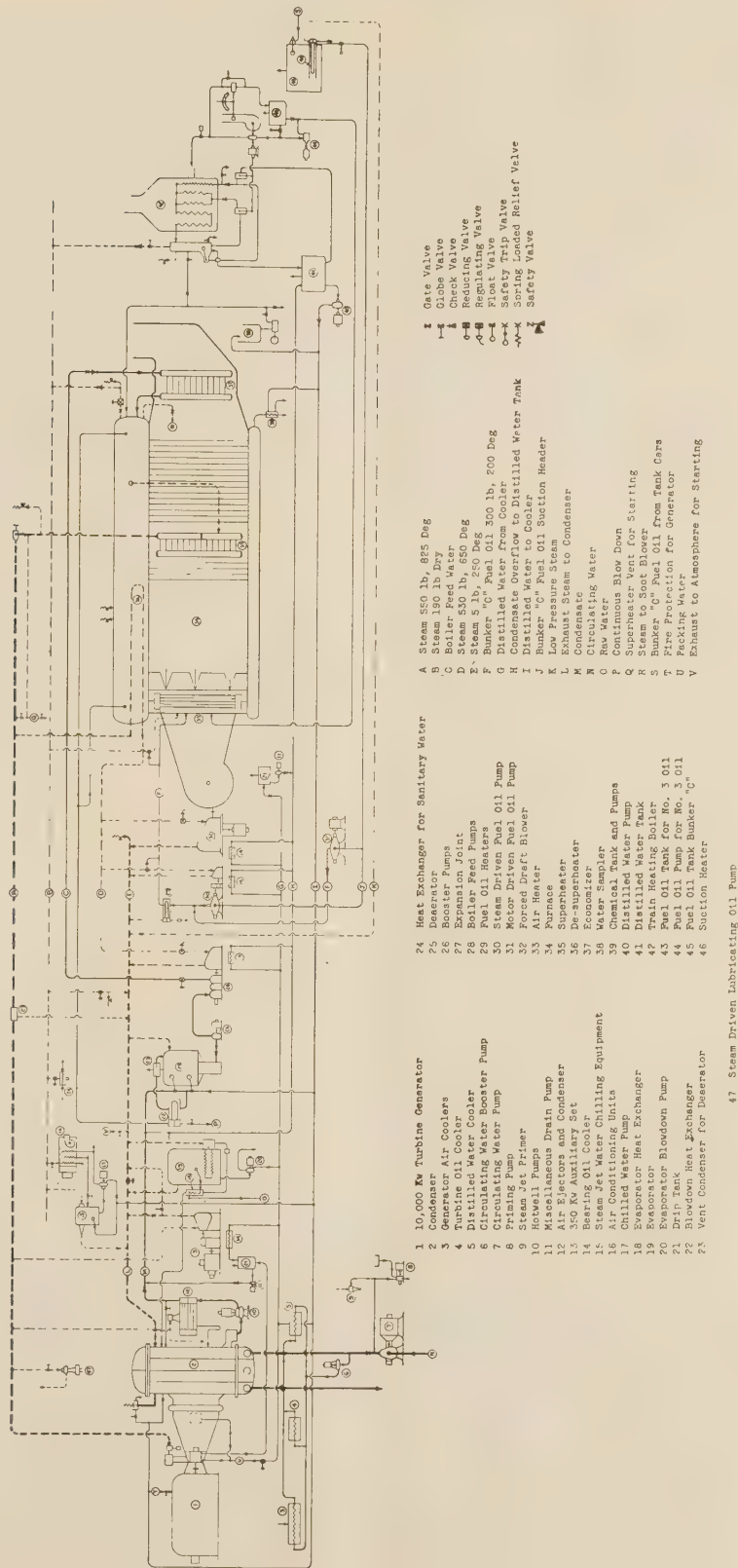


FIG. 17 PIPING DIAGRAM OF STEAM, WATER, AND FUEL-OIL INTERCONNECTIONS

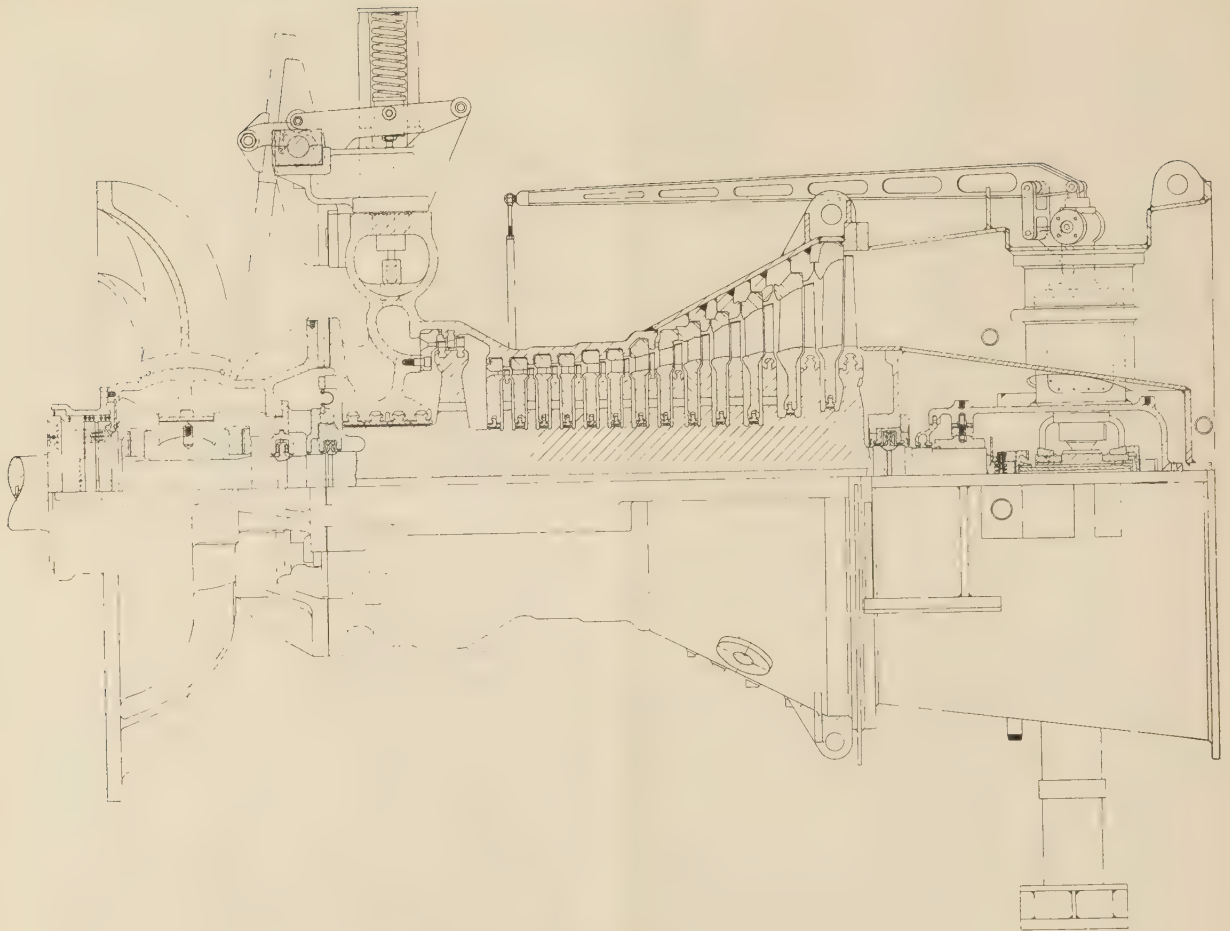


FIG. 18 CROSS SECTION OF MAIN TURBINE

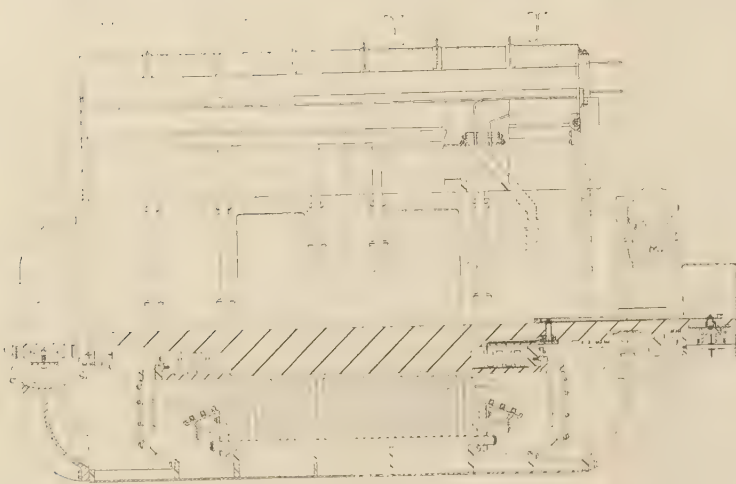


FIG. 19 CROSS SECTION OF MAIN GENERATOR

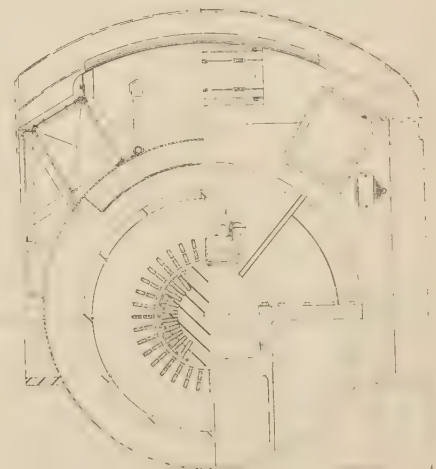


FIG. 20 END VIEW OF MAIN GENERATOR

steam with 70-deg F circulating water requiring 6420 gpm, design pressure 3 in. Hg abs. Approximately 4230 aluminum-brass tubes $\frac{3}{4}$ in. diam 18 Bwg, 9 ft $2\frac{1}{2}$ in. long are rolled at both ends in Muntz-metal tube sheets. The total effective tube surface is 7300 sq ft. There are four passes for the circulating water. Flanges for connecting the circulating-water line are provided on each side of the condenser to suit inlet and discharge requirements on the actual site where the plant is operating. The hot well is located at the steam-entrance end of the condenser. Fig. 22 shows a section and plan view of the condenser.

STEAM-DRIVEN AUXILIARY GENERATOR SET

The steam-driven auxiliary set consists of a 350-kw, 0.8-pf, 5645-rpm steam turbine, and a 1200-rpm generator with a 125-v direct-connected exciter. The set is rated 350 kw at normal steam conditions of 550 psi, 825 deg F total temperature at the throttle, and 3 in. abs back pressure at the turbine-exhaust flange. This set primarily furnishes power for the circulating-water pump when the plant is started in operation at any particular location. The set will also carry 275 kw with steam conditions of 550 psi, 825 deg F total temperature, 0 psi back pressure for operation of the pump until vacuum is established in the main condenser and the turbine can be shifted to condensing operation.

In addition, the turbine car also carries the evaporator blow-off pump, condensate drip pump, all auxiliaries for the condenser, such as air ejectors with inter- and after-coolers, two vertical condensate pumps, salt-water booster pump supplying cooling water to generator air coolers, turbine oil cooler, and

distilled-water cooler for bearing oil. The main turbine oil tank also included has a capacity of 800 gal.

DETAILS OF SWITCHGEAR CAR

The switchgear car is shown in Fig. 23. In this car is located the 13,800-v switchgear, consisting of a single oil circuit breaker of the vertical-lift removable type, rated 15,000-v, 1200-amp, 500-mva interrupting capacity. Here also are the control panels for the 10,000-kw turbine and generator, including such equipment as exciter-field rheostat, potential transformers, field switch, and voltage regulator. A 450-kva 13,800/480-v auxiliary power transformer for use after the plant is in operation is installed. The 50-kw exciter set for the main generator, and the 50-kw Diesel-engine generator set are included in this car. The 50-kw 0.8-pf, 60-cycle-480-v-1200-rpm Cummins Diesel-engine generator set is used when starting up the plant from a cold condition. This auxiliary power, as previously mentioned, is used for the starting oil pump, starting of the combustion blower, minor pumps, etc. The 350-kw steam-turbine generator set can later be synchronized with this Diesel set.

Electric power for starting up the plant can be obtained from three sources:

- 1 Shore power of 480 v where available can be plugged into the auxiliary bus.
- 2 Power of 13,800 v can be fed back from the substation through the transformer car into the switchgear car and stepped down to 480 v by the 450-kva auxiliary transformer.
- 3 The 50-kw Diesel-engine generator.

The 480-v auxiliary switchgear and a 25-kva lighting transformer are installed in this car. Where no power is available

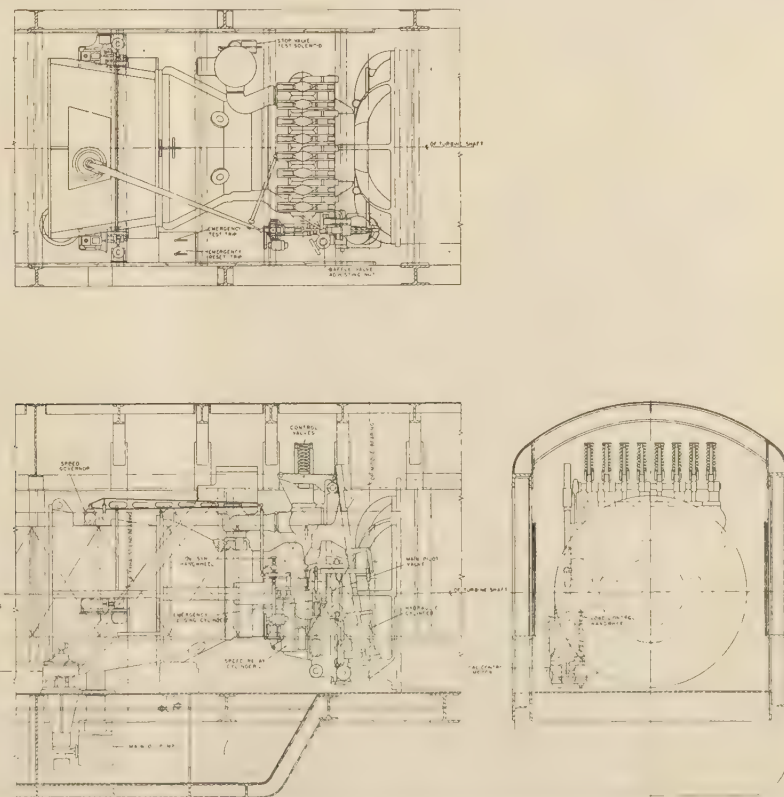


FIG. 21 CONTROLLING MECHANISM FOR 10,000-KW TURBINE

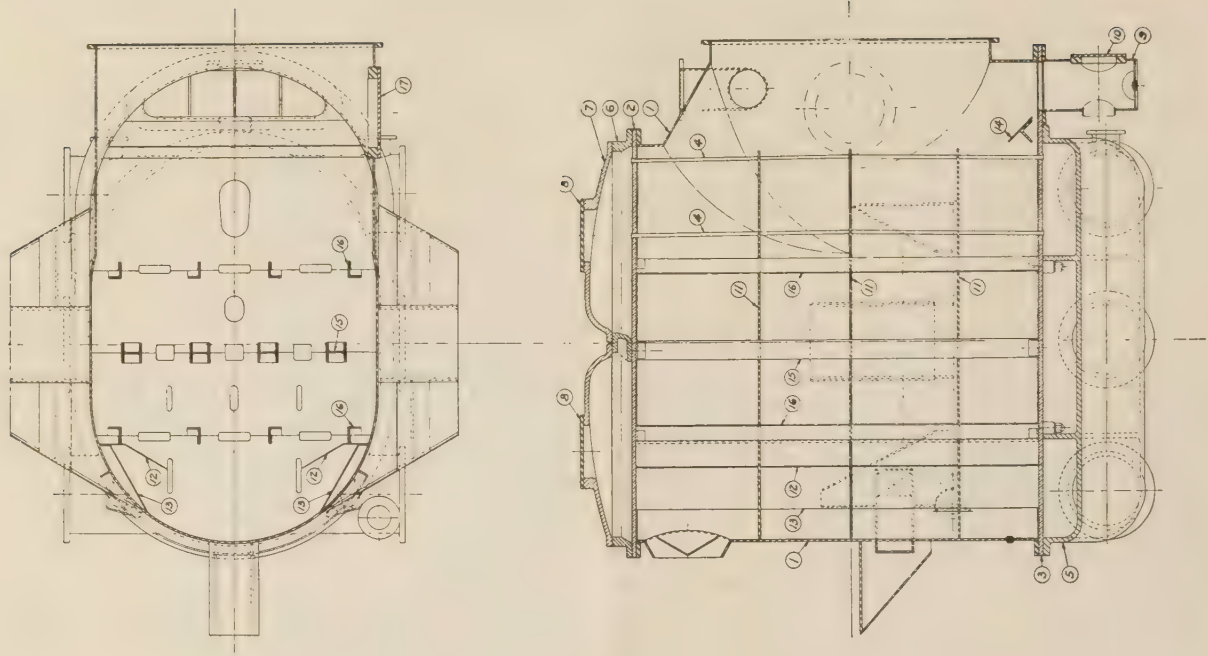


TABLE 1

Condenser

Steam condensed at 70 deg lbs hr	112,000
Design pressure absolute	3-in. Hg
Temp. of inlet water deg F	70
Water required GPM	6420
Friction loss through condenser	15.25
Effective surface sq ft	7300
No. passes	4
Shell thickness	1/2-in.
Water boxes material	CI
Tube heads thickness	1 1/8-in.
Tube heads material	Muntz
Tubes size	3/4-in. - 18 BWG
Tubes material	Aluminum brass
Approximate No. tubes	4230
Length overall	9 Ft 2 1/2-in.
Tube fastenings	Rolled both ends
Weight empty pounds	47910
Weight in service	63270
Weight flooded	85070

TABLE 2

Main Condenser

Part No.	Name of Part
1	Shell 1/2-in.
2	Top Tube Head
3	Bottom Tube Head
4	3/4-in. OD Tubes
5	Nozzle Head
6	Ring
7	Ring Head Cover
8	Ring Head H.H. Plate
9	Hot Well
10	Hot Well H.H. Plate
11	Support Plate
12	Baffle Plate
13	Cooler Plate
14	Deflector Plate
15	H-Beam Brace
16	Angle Brace
17	Shell Manhole Plate

FIG. 22 SECTION AND PLAN VIEWS OF WORTHINGTON CONDENSER

for lights before the Diesel engine is started up, emergency lights are supplied with current from the 48-v d-c control battery. The car also houses the cable reels for 3 single-conductor 600,000 CM cables each 500 ft long, and 3 single-conductor CM cables each 250 ft long. The reels are shown in Fig. 24.

EQUIPMENT IN TRANSFORMER CAR

The transformer car is shown in Fig. 25. This car contains the 12,500-kva transformer unit, consisting of a combined transformer and auto transformer of special design for mounting on the car. The transformer is the forced-air-cooled gas-seal type; the core and coils being specially braced in the tank to withstand the strains imposed by transportation over railroads. All high- and low-voltage bushings are brought out through the side of the transformer tank into fabricated-steel enclosures welded to each side of the tank. A large bank of cooling tubes is assembled at each end of the transformer tank. Located under each bank

of tubes are eight weatherproof fans mounted in a rack which is supported over an opening in the car floor. Doors made of heavy screening are located below the cooling tubes to provide protection for the fans.

The transformer can be operated as an autotransformer from 13,200 v to 11,500 v at 12,500 kva with forced-air cooling, or at 10,000 kva, self-cooled. It can also be operated as a straight transformer from 13,200 v to 2400 v delta, or 4160 v Y, at 12,500 kva with forced-air cooling, or at 10,000 kva self-cooled. The transformer can also be operated as a combined autotransformer and transformer carrying simultaneous loads at 11,500 v and 2400 or 4160 v, provided the arithmetical sum of the outputs does not exceed 12,500 kva forced-air-cooled, or 10,000 kva self-cooled. On the car are also mounted various cable reels for connection cables to the transformer, and the bare copper cable for grounding the system.

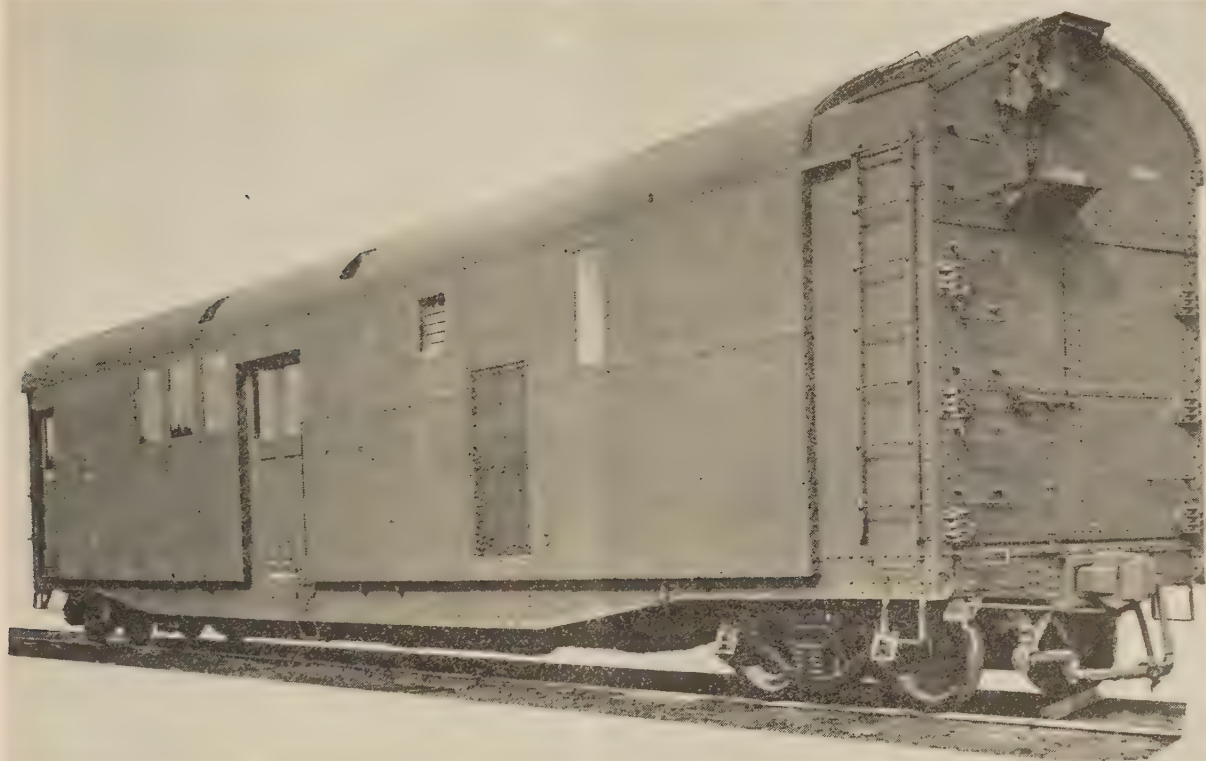


FIG. 23 SWITCHGEAR CAR READY FOR TRANSPORTATION

CIRCULATING-WATER PUMPING SYSTEM

The circulating-water pumping system consists of two sections, each mounted on a separate platform provided with wheels for mobility. Lugs are provided on each truck for lifting with a crane where one is available. Where a crane is not available, a ramp is provided for rolling the equipment down to rail level from the platform of the gondola car. A view of the car with equipment is shown in Fig. 29.

The first section of the system contains a 14-in. Worthington single-stage pump, driven by a 285-hp 440-v motor. A Nash vacuum pump for priming the system is provided for use in moderate weather, and a steam jet for extremely cold weather. The second section, which supports the vertical suction hose extending down into the supply of circulating water contains two Elliott type 105 strainers. Each strainer contains a basket having $\frac{1}{4}$ -in.-mesh openings. One spare basket has been provided for making a rapid change. The pressure drop at 7500 gpm is about 0.25 psi. Metal baskets with a larger mesh opening than in the strainer are provided for the bottom of the suction hose.

Two 20-ft lengths and two 10-ft lengths of 16-in. flanged rubber hose are provided to take care of variations in the water level at various sites where the plant may operate. The discharge line from the pump and discharge from the condenser can be made up from twenty lengths of 20 ft each, and five lengths of 10 ft each of 14-in.-discharge flanged rubber hose. Two sections 14 in. \times 18 in., 12 ft long, provide the connections at the condenser. All of the hose was specially manufactured by the United States Rubber Company, mechanical goods division, and is similar to that used by suction dredges. Fig. 27 shows the mechanical connections, and Fig. 28 shows the electrical connections for the

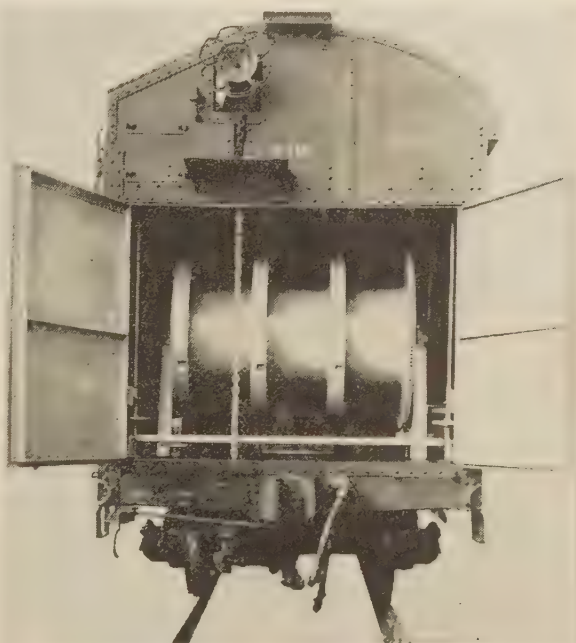


FIG. 24 SWITCHGEAR CAR SHOWING CABLE REELS

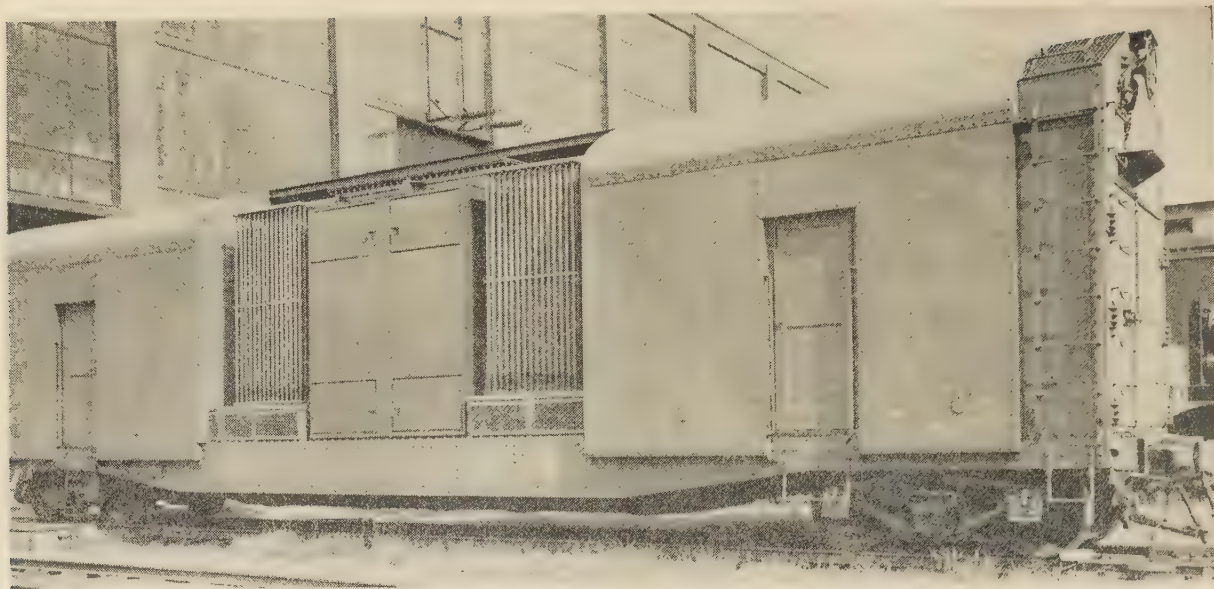


FIG. 25 TRANSFORMER CAR READY FOR TRANSPORTATION

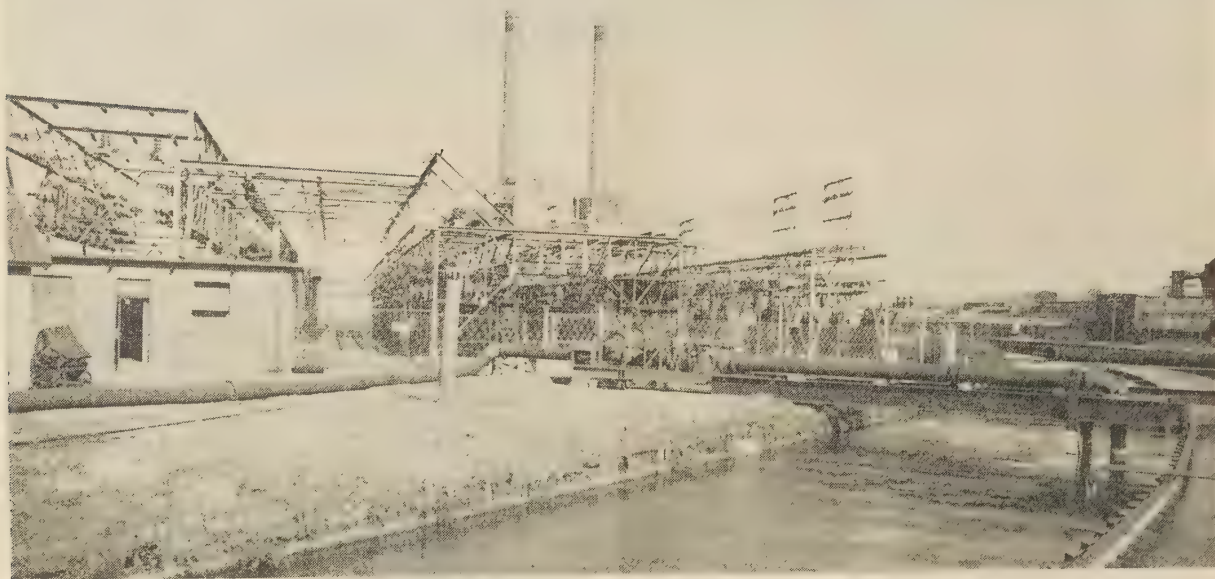


FIG. 26 CIRCULATING-WATER PUMP AND STRAINERS

circulating-water pump. The electrically heated enclosure of the priming pump should be noted. A view of the equipment is shown in Fig. 26.

Connections to be made between the boiler and turbine car are as follows: The 12-in. low-pressure steam line, connected through a corrugated expansion joint with standard flanges, the specially designed 6-in. high-pressure steam-loop connection (Figs. 30 and 31), the 4-in. condensate-return line, and cold- and hot-water service lines, distilled-water lines to and from the heat exchanger, service air line, $2\frac{1}{2}$ -in. air-conditioning water line, and jumper cables connecting the electrical circuits. A plan view is shown in Fig. 32.

The connections between the turbine and switchgear car consists of the two 480-v auxiliary power feeders, the field and control circuits, the 13,800-volt connections between the generator and switchgear, hot- and cold-water service connections.

COMMUNICATION SYSTEM

An internal telephone system has been provided with four permanent stations; two are in the boiler car, one is in the turbine car, and the other in the switchgear car. The permanent stations are splashproof sound-powered marine telephone systems, as manufactured by the Automatic Electric Sales Corporation. Two portable units have been provided for use where needed.

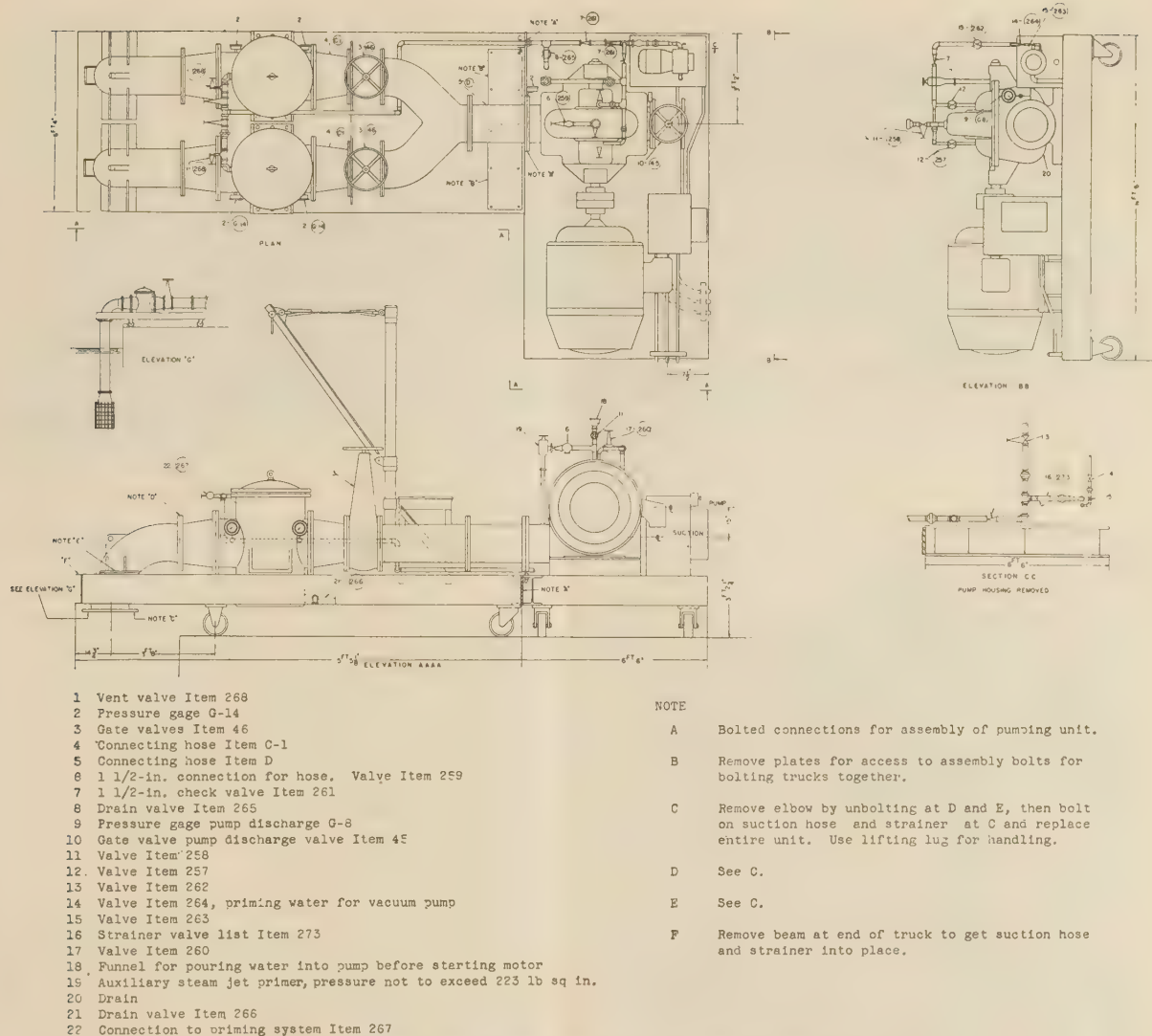


FIG. 27 MECHANICAL CONNECTIONS FOR CIRCULATING-WATER PUMP

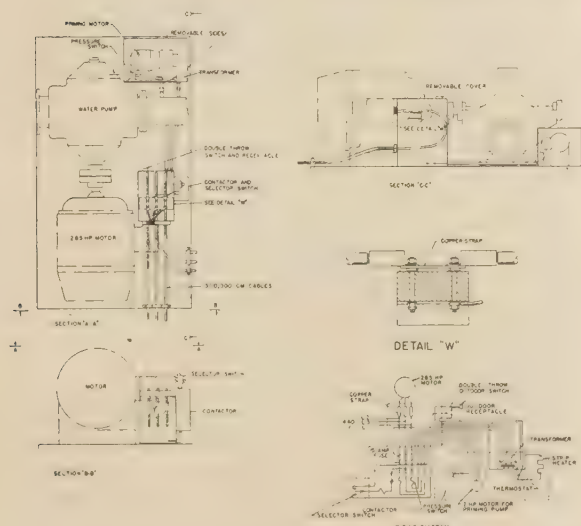


FIG. 28 ELECTRICAL CONNECTIONS FOR CIRCULATING-WATER PUMP

Plug receptacles are located at connection points which would be near the fuel supply and near the 10,000-kw turbine or which could be extended to the location of the circulating-water supply. A telephone of the dial type is located at the operating desk in the switchgear car. Outside connection to another telephone system can be made by this telephone.

There are seven control boards located in the various cars as follows: In the boiler car there is the main control board which contains the various metering, indicating, and recording instruments as supplied by the Bailey Meter Company for operating the boiler combustion-control equipment, three-element water-level control, fuel-oil supply, and speed control of the forced-draft blower. The Bailey electronic type recorders show steam flow from the boiler, air flow supplied for combustion, boiler drum water level, feedwater flow to the boiler, and also feedwater and steam temperature.

The Bailey steam pressure master controller controls the air-operated fuel-supply valve and forced-draft-fan speed as required to maintain the load. The forced-draft-fan speed is automatically readjusted to maintain the measured fuel-air ratio for the desired combustion efficiency. Feedwater supply pressure is automatically maintained by control of the steam sup-

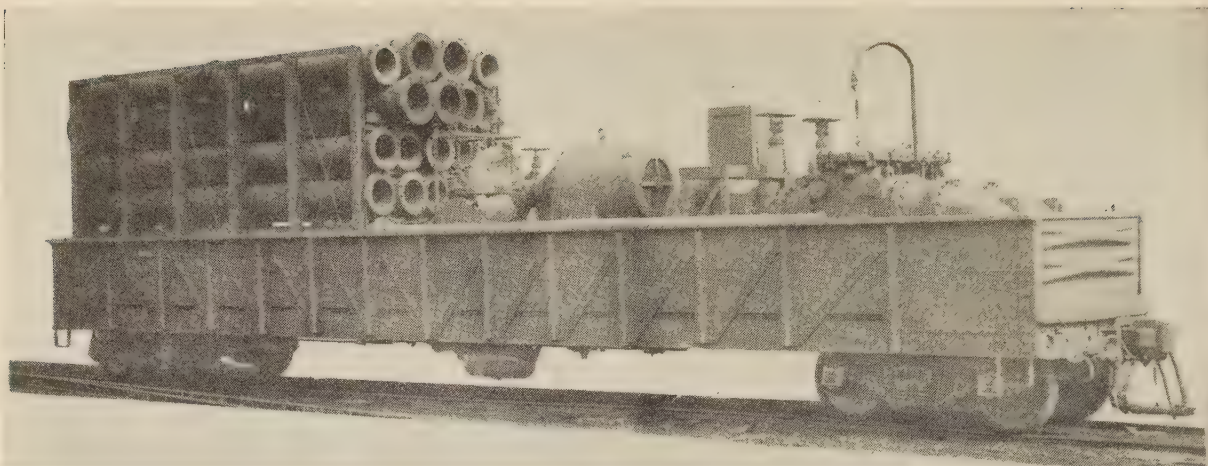


FIG. 29 GONDOLA CAR READY FOR TRANSPORTATION

Type AE-1A air circuit breakers are used on the feeders, and type CR-7006 magnetic contactors are used for control.

CONTROL AND INSTRUMENT PANELS

In the turbine car the Bailey board contains the flowmeters for main and auxiliary turbine generators, the Fulscope temperature controller, supplied by the Taylor Instrument Company for the generator air-temperature regulation, thermometers to indicate bearing oil temperatures, vacuum and pressure gages for various services, and a tachometer to indicate the speed of the main turbine. Various controls are also included, such as the emergency governor trip, stop-valve trip switch with indicating lights, load-limit-control switch, load-control transfer switch with indicating lights to show control from the turbine car or from the switchgear car, etc.

The turbine electrical auxiliary board, known as No. 3, is of the same design as the boiler boards, having two feeders with AE-1A breakers and magnetic-operated contactors for operating the motors of the hot-well pumps, booster, and chilled-water pumps, auxiliary oil pump and turning gear for the main turbine, as well as the alarm system. Lights to indicate which services are in operation are provided.

Two boards are located in the switchgear car. One controls the 13,800-v 12,500-kva generator, and the synchronizing and loading of the turbine. The equipment on the board consists of various relays such as overcurrent, differential protection, and reverse power. There are also the synchroscope and instruments to show the field and armature current, voltage, frequency, and reactive kva. A watt-hour meter totalizes the output of the plant. Provision is made at the back of this board to attach the three single-conductor 13,800-v outgoing power feeders.

The other board is called the 480-v auxiliary board and controls the auxiliary transformer, the exciter-set motor, the Diesel engine, and the 350-kw generator. The lighting transformer and shore power are attached to this board. The type CR-7890-Y1 automatic starting panel for the 285-hp circulating-pump motor is also part of this board. AE-1A and AE-1B hand-operated air circuit breakers of the draw-out type compose the main control equipment of the board.

Other facilities in the boiler and switchgear cars include a sanitary water system. A tank for the water and a small pump to maintain pressure and keep the water circulating so that it will not freeze are provided in the switchgear car. The water is pumped through the train to the boiler car where it is heated

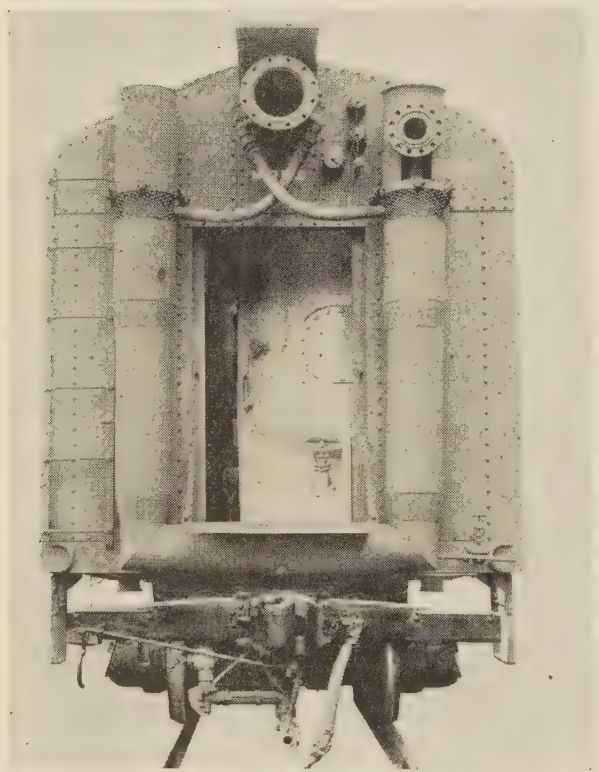
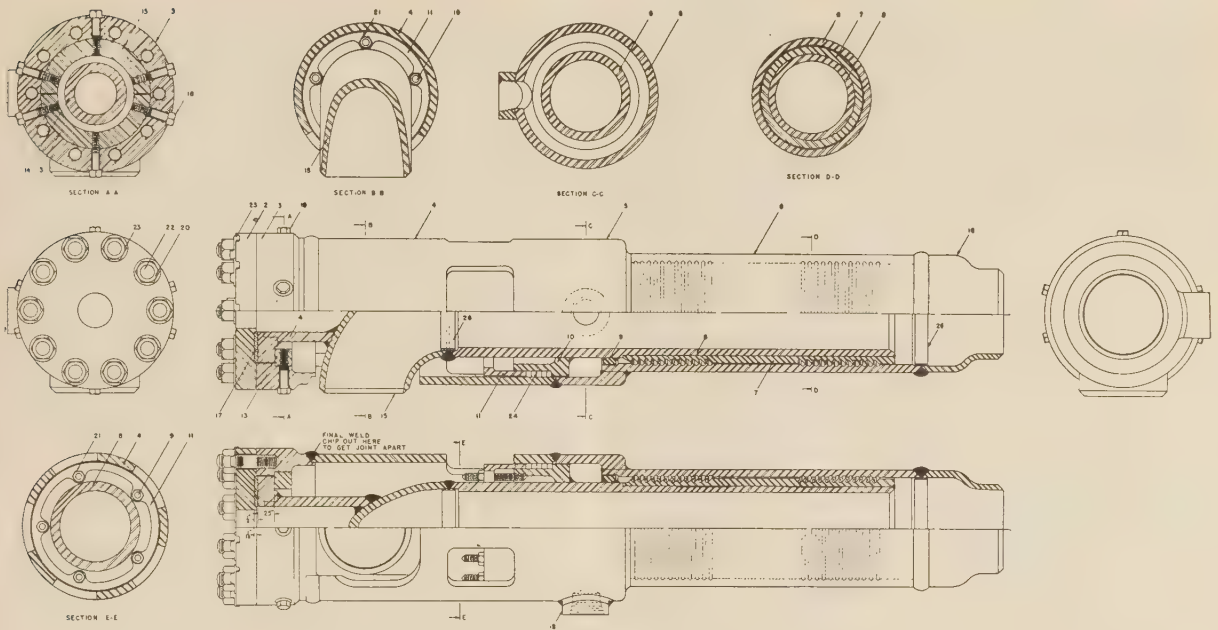


FIG. 30 VIEW OF HIGH-PRESSURE EXPANSION LOOP ON END OF BOILER CAR

plied to the feedwater pump turbines. The feedwater flow to the boiler is automatically maintained in direct proportion to the steam flow from the boiler, and the drum level is maintained within predetermined safe limits by Bailey three-element feedwater control. Two of the electrical auxiliary boards known as Nos. 1 and 2, used for controlling the electrical auxiliary equipment and the alarm circuits, are included. The alarms show on the Edwards annunciator and are connected to a klaxon horn.



PARTS LIST

Part No.	Name of Part	Drawing No. or Description			
2	Buffer Plange	719-42T - Part No. 1	14	Buffer	721-42T - Part No. 1
3	Joint Head	719-42T - Part No. 2	15	Tube-burn	721-42T - Part No. 5
4	Joint Body	719-42T - Part No. 5	16	Welding Reducer	721-42T - Part No. 6
5	Leakage Box	719-42T - Part No. 6	17	Bearing Ring	719-42T - Part No. 4
6	Joint Body	720-42T - Part No. 1	18	Cap Screw	Hex Head 1/2-in. - 13 x 2 1/2-in. long
7	Sealing Sleeve	720-42T - Part No. 2	19	Bolt Stud	720-42T - Part No. 6
8	Body Core	720-42T - Part No. 3	20	Bolt Stud	719-42T - Part No. 8
9	Stop Ring	720-42T - Part No. 4	21	Nut	Hex 1/2-in. - 13
10	Stuffing Box	720-42T - Part No. 5	22	Nut	Hex 1-in. - 8
11	Packing Gland	721-42T - Part No. 4	23	Lock Washer	719-42T - Part No. 9
12	Pipe Saddle	719-42T - Part No. 7	24	Packing	John Crane Style 6-AM, Size 3/8-in. x 2 Ft. 6 In.
13	Ring Segment	719-42T - Part No. 3	26	Chill Ring	721-42T - Part No. 7

FIG. 31 ASSEMBLY OF ROTATING EXPANSION JOINT

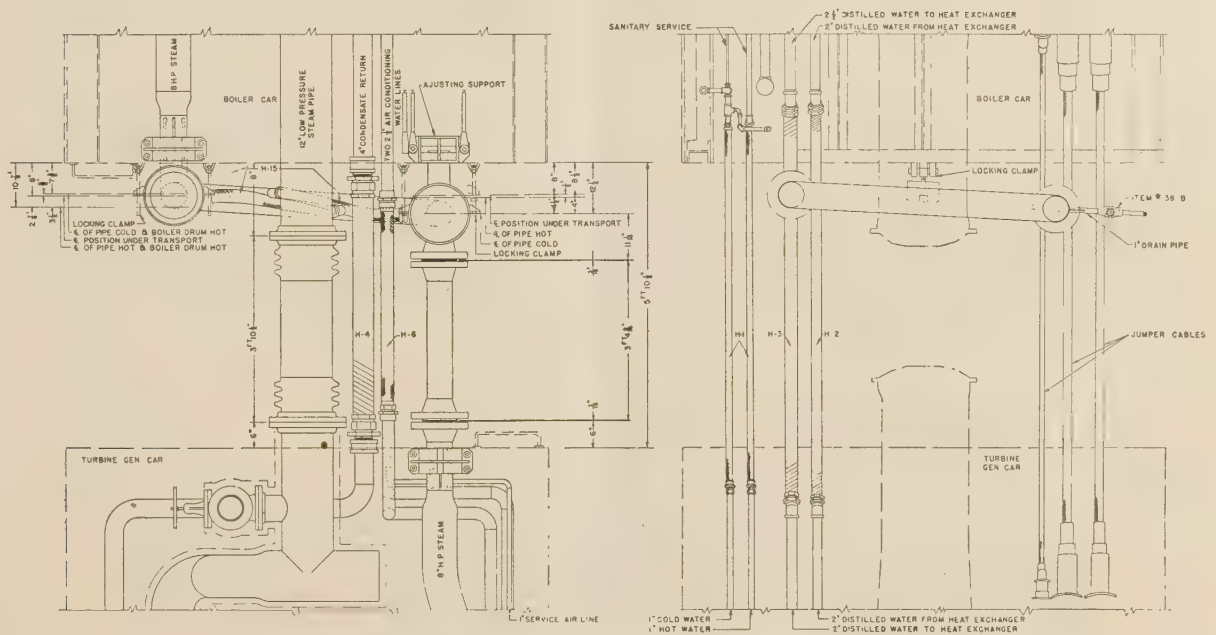


FIG. 32 PLAN VIEW OF CONNECTIONS BETWEEN TURBINE AND BOILER CARS

before returning to the tank. Cold and hot water are thus available for the washrooms, toilets, and drinking fountains in the boiler and switchgear cars, and for the chemical laboratory. The chemical laboratory is located in the switchgear car and is used for boiler-feedwater analysis. An operator's desk and chair are provided in each car.

The piping was prefabricated in so far as possible by the Blaw-Knox Company before final assembly. For the high-temperature steam, carbon-molybdenum steel pipe specification A.S.T.M. A-209-39 was used, and all joints were welded, except the one connection to the turbine stop valve and the thimble between cars. Other piping was carbon steel A.S.T.M. 106-39.

Insulation for the high-temperature piping consisted of a layer of Carey Hi-temp No. 12 under a layer of Carey multi-ply. For lower temperatures, a layer of multi-ply only was used. Where fire hazard existed, asbestos-cloth covering sewed on was used, and in other places 8-oz canvas. All covering was given a coat of fireproof paint.

Welding-type steel valves were used on the high-pressure steam, oil, and water lines. Cast-iron flanged valves were used on the exhaust-steam system operating at 5 psi pressure. The valves were manufactured and prepared for welding in the shops of the Crane Company, with the exception of one 8-in. valve which was supplied by Reading, Pratt, and Cady.

For the plant setup, the circulating-water pump, the transformer car and the oil-supply cars must be located within the limits of the hose, cable, and oil-transfer piping supplied with the power-plant unit. These distances are roughly as follows: Transformer car to load connection 250 ft; transformer car to switchgear car 1000 ft; turbine car to circulating-water supply 250 ft; fuel-oil supply to furthest tank car 200 ft; raw water 500 ft. The setup for delivering bunker C fuel oil to the boiler car, as shown in Fig. 33, consists of five sections, approximately 20 ft long of 2½-in. steel pipe for oil, insulated with a 1¼-in. pipe for steam. One 50-ft section and two 25-ft sections of 2-in. hose are provided.

Two fuel-oil transfer pumps, motor-operated, are furnished with hose for connection to the tank car and electrical cable connections to the boiler car. A float valve is provided in the bunker C fuel-oil tank to keep it full of oil.

BASIC DATA FOR MOBILE POWER PLANT

The basic requirements for the mobile power plant are as follows:

Heavy fuel oil (bunker C or Navy special) approximate quantities:

5000 kw.....	15420 gal per 24 hr
7500 kw.....	21900 gal per 24 hr
10000 kw.....	29400 gal per 24 hr
12500 kw.....	38900 gal per 24 hr

Light oil (No. 3 or Diesel fuel):

Train-heating boiler (at 1500 lb per hr).....	370 gal per 24 hr
Diesel engines (at 30 kw).....	64 gal per 24 hr
Main boiler (cold to steaming).....	140 gal

Electric power load (three-phase, 60-cycle):

Direct-connected.....	13800 v
With autotransformer.....	11500 v
With Y connection.....	4160 v
With delta connection.....	2400 v

Tank capacities (approx.):

Bunker C oil (boiler car).....	1200 gal
No. 3 oil (boiler car).....	400 gal
No. 3 oil (switchgear car).....	280 gal
Distilled water (boiler car).....	800 gal
Drinking water (switchgear car).....	150 gal

Water:

Circulating system, 6820 gpm (avg).....	7500 gpm (max)
Raw make-up 4 gpm (avg).....	75 gpm (max)
Sanitary water (drinking) 2 gpm (avg).....	10 gpm (max)

Shore power (optional):

Power feeder (three-phase).....	480 v
Lighting feeder (single-phase).....	240/120 v

OPERATING PLAN FOR SYSTEM

Fig. 33 shows a typical plan setup for operation of the plant. In general a level well-prepared track which will hold a wheel loading of 55,000 lb per axle without settlement will be satisfactory. On average soil, with a good rock ballast about 3 ft thick, the plant should run for a reasonable length of time. Where level-measuring devices on the turbine car show that excessive settlement has occurred, the plant will have to be removed from the siding and the track leveled.

Leveling devices are provided for checking both the vertical and horizontal alignment of the main turbine generator. The

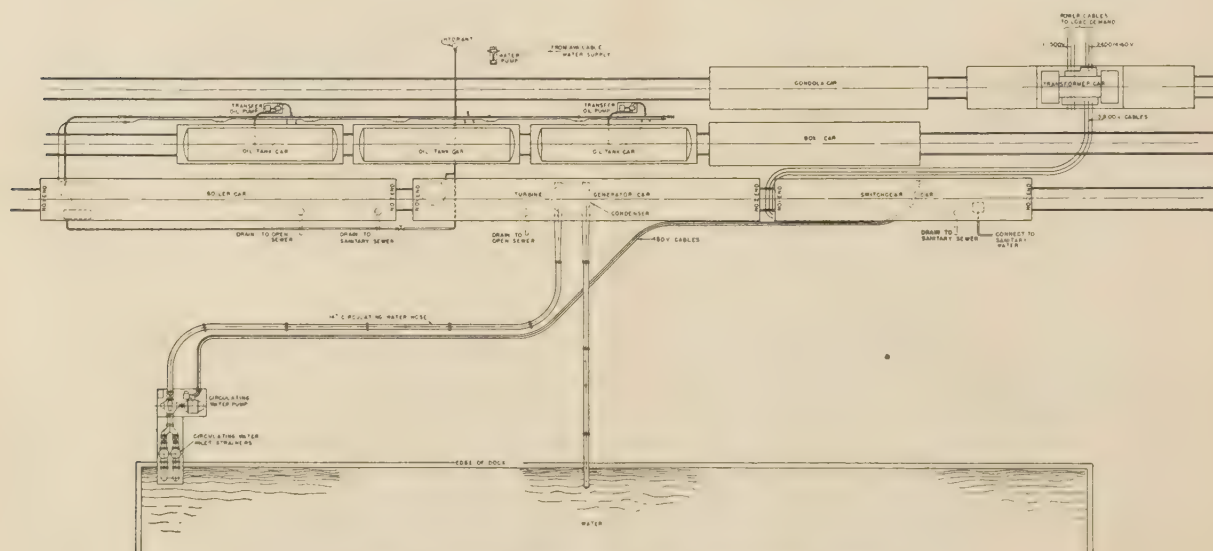


FIG. 33 TYPICAL PLAN OF SETUP FOR OPERATION OF PLANT

equipment for the vertical check consists of six liquid-level micrometers, details of which are shown in Fig. 34 and located as shown in Fig. 35.

The equipment for checking the horizontal alignment consists of a set of micrometer pulleys bolted to the side of the car and a steel wire with weight attached stretched between the pulleys. Measurements are made between the wire and pads provided on the bearing frame; details are shown in Fig. 34.

No. 1 power plant was operated under test for a total time of approximately 77 hr 45 min. Table 1 gives the time, various loads, and heat rates.

The test site on which the power plant operated consisted of a rock ballast approximately 3 ft thick on top of a cinder fill. The turbine operated satisfactorily on this type of track. However, it is not known whether the operation would continue to be successful if settlement occurred. For emergency operation over not too long a period of time, apparently any good railroad track

will be satisfactory. During test, the track settled under one set of wheels approximately $\frac{1}{2}$ in. without any apparent detrimental effect on the operation of the turbine. There was a change in the side alignment of 0 to 15 mils of the middle bearing, caused by the temperature difference from the sun shining on the car during the day. The vertical alignment changed from 0 to 20 mils with the middle bearing going up. This occurred during the starting and returned to normal when the turbine cooled off, thus indicating that it was a temperature condition. In spite of these conditions, the unit operated satisfactorily, both coming up to speed and during the active loading. The actual setup is shown in Fig. 36.

TEST AND SERVICE RESULTS OF SYSTEM

A test was conducted to determine the time required to place the mobile power plant in service after it arrived at a certain location. Two locomotive cranes and a total crew of 21 men were employed. Fourteen hours after arrival, the plant was placed in operation carrying 500 kw load, gradually increasing to 7500 kw. It is estimated that a crew of 40 men, including the specially trained skeleton crew assigned to each mobile power plant, could locate and start the plant within 8 hr.

Since the delivery of the units to the Navy Department the mobile plant located in the East has been used for emergency

TABLE 1 OPERATING DATA OF SYSTEM

Name of run in kw	Corrected net output, kw	Time		Heat rate, Btu/kwhr
		Hr	Min	
1500	1250	37	15	...
2500	2150	6	15	25200
5000	4500	3	00	18640
7500	7500	5	30	17560
10000	9850	5	30	17570
12500	12093	3	30	18400

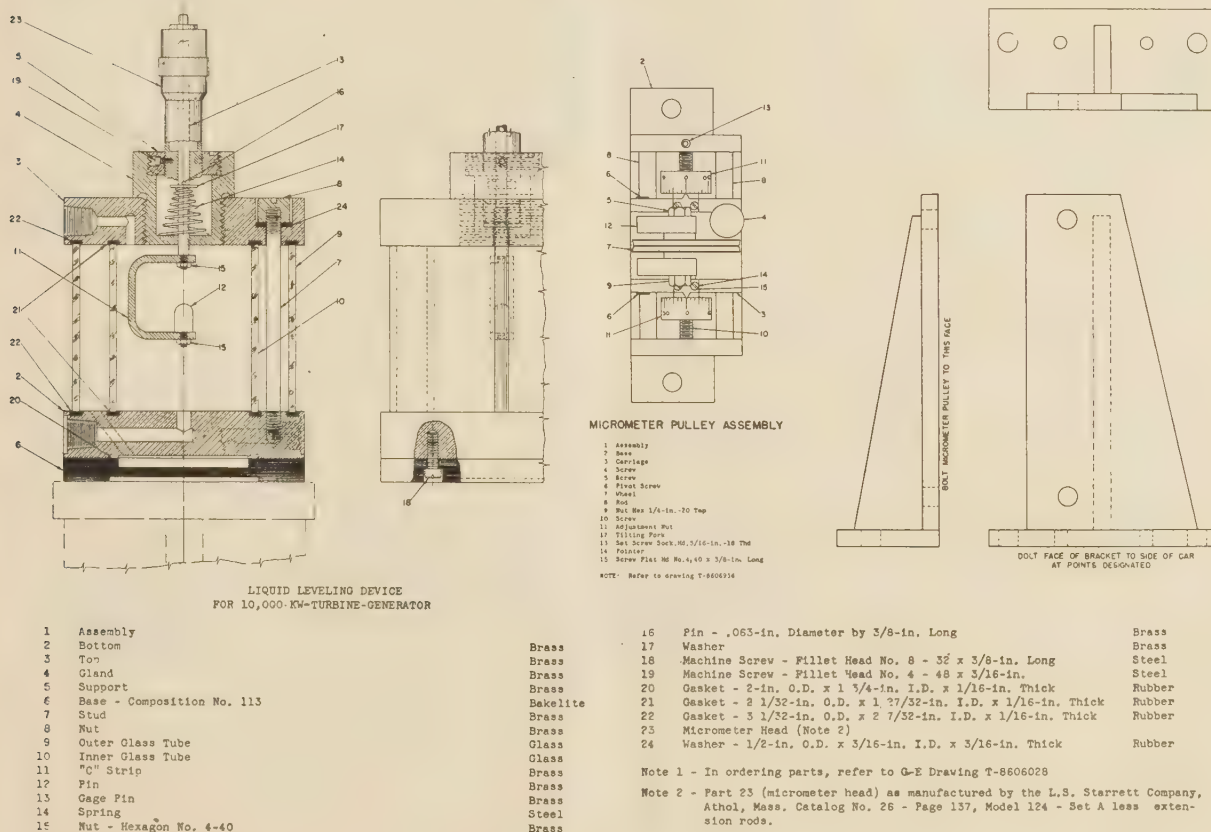


Fig. 34 DETAILS OF LEVELING MICROMETERS

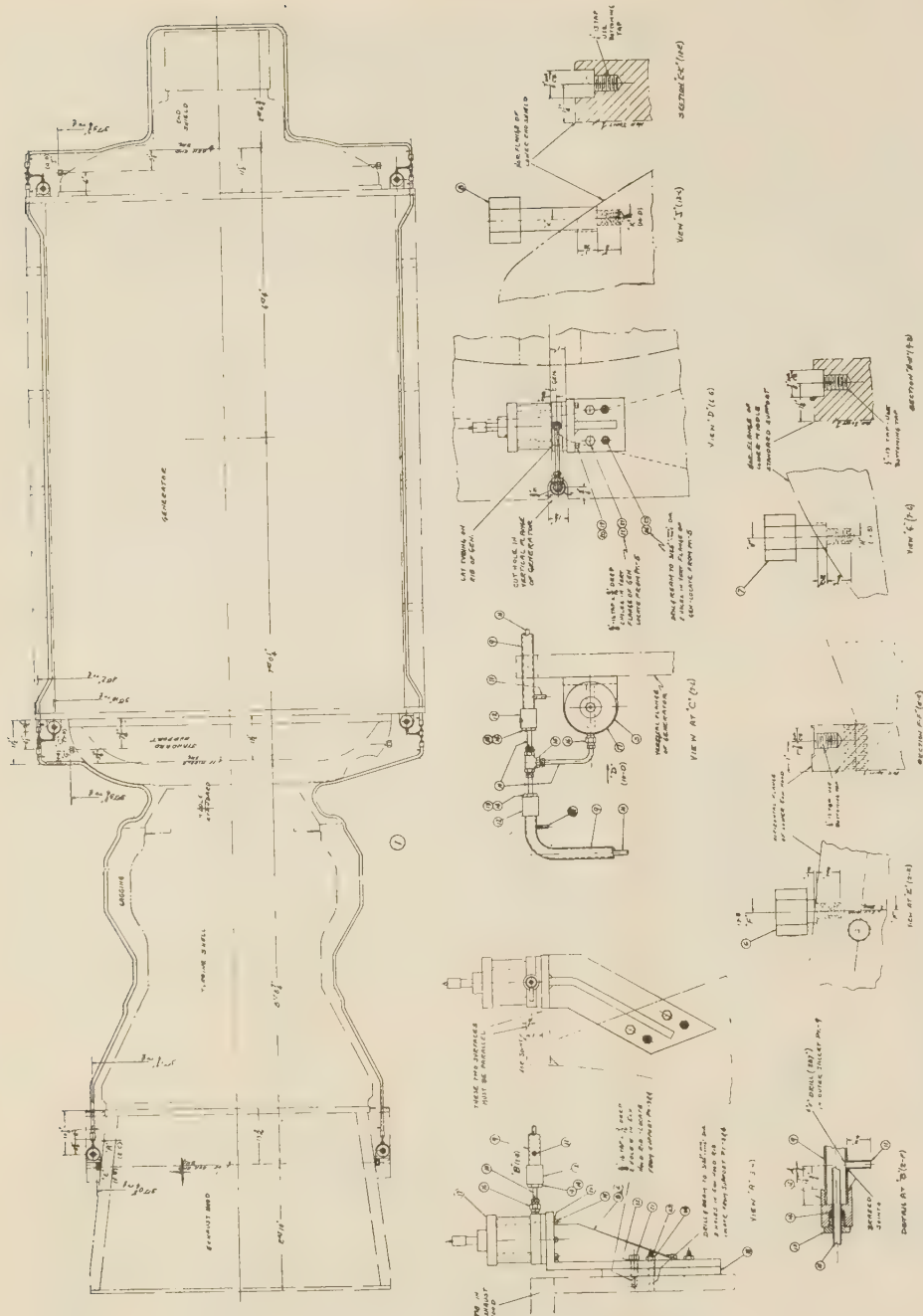


FIG. 35 LOCATION OF LIQUID MICROMETERS FOR LEVELING EQUIPMENT

Pt. No.	Name of Part	Drawing Number, Group or Part, or Description	Size of Material (Per Piece)
1	Assembly	ML-8603931-01	
2	Indicator Supports	T-8603931 Pt. 1	
3	Exhaust Hood Support	T-8603931 Pt. 2	
4	Generator Support	T-8603931 Pt. 3	
5	Gage Plug	T-8603931 Pt. 10	
6	Gage Plug	T-8603931 Pt. 11	
7	Gage Plug	T-8603931 Pt. 12	
8	Outer Jacket	3/4-in. OD x .065-in. Wall	
9	Inner Tubing	1/4-in. OD x .052-in. Wall	
10			
11	nipple		
12	Jacking Cap		
13	Packing Gland		
14	Packing		
15	Tubing Tee		
16	Liquid Level		
17	Locking Screw for 17		
18	Machine Screw for 19		
19	Lockwasher for 19		
20	Cap Screw for 21 and 5		
21	Lockwasher for 21		
22	Lockwasher for 21		
23	Screw		
24	Nut for 23		

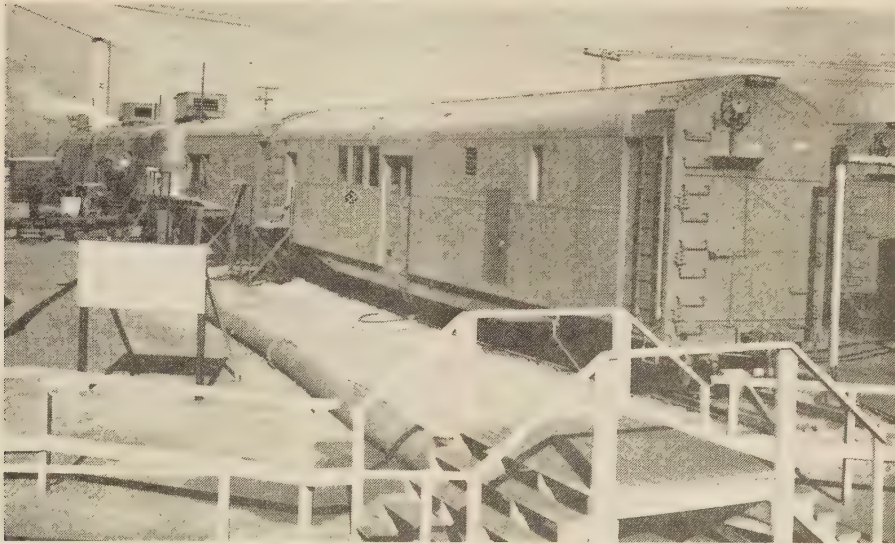


FIG. 36 ACTUAL SETUP ON A TEST SITE

purpose to supply steam at the rate of 100,000 to 120,000 lb of steam per hr at one of the Defense Corporation manufacturing plants for producing butadiene for the synthetic-rubber program. The boiler car alone was used for this purpose operating on condensate without difficulties of any kind. At this writing, the entire mobile power plant was moved to a southern city and placed in operation to supply emergency service for a public-utility plant supplying power to a naval activity. The other plant has been set up for stand-by service at one of the Navy's activities and has delivered power on various occasions.

Discussion

L. W. BATES.³ It would appear to be somewhat incongruous for the Navy to operate railway-mounted power plants and for the Army to operate floating power plants. The latter are 30,000-kw plants mounted on steel barges, several of which, it is understood, are destined for use in the European theater of operations.

The Bureau of Yards and Docks of the Navy Department was glad to have pioneered in the development of these railway power plants and much credit is due to Mr. Biggs and his associates for the excellent design under the difficult conditions imposed by railroad clearances. These plants are the largest railway plants which have been constructed. Many such plants of 1000, 3000, and 5000-kw capacity have since been built, principally for use overseas.

Aside from minor operating difficulties which would be ex-

pected in a new development of this character, operation of these units has been entirely satisfactory.

When the first plant was completed at Schenectady, representatives of the Navy were present to witness the trial run. Since the turbine appeared to be operating without noticeable vibration, a careful examination was made to determine whether it had been necessary to use jacks under the turbine car to correct vibration difficulties. No jacks were discovered and the only vibration noticeable was a vertical handrail on the outside of the car.

At the time the plants were completed there was no emergency power requirement to be met at any naval shore establishment. At the request of the Department of Commerce the boiler car of one plant was loaned to the Rubber Reserve Company, a subsidiary of the Defense Plant Corporation, to supplement the boiler capacity of a synthetic-rubber plant in West Virginia. More recently the entire power plant was transported to Florida where it is now being operated in parallel with an 80,000-kw central station pending extensive repairs to station boilers. This central station serves important naval activities and Maritime Commission shipyards in the vicinity.

Recently, an inspection was made of this mobile plant and it was found that it has been furnishing an average of 9000 kw for 24 hr a day and has been rendering good service. The track under the turbine car had settled slightly but this has apparently caused no increase in vibration.

The second of the mobile power plants is located at the large Navy yard near San Francisco where it is operated at intervals to insure its readiness for service for meeting power emergencies in the western part of the country.

³ Captain, U.S.N., Bureau of Yards and Docks, Navy Department, Washington, D. C.

Locomotor Mechanics and Occupation

By A. STEINDLER,¹ M.D., F.A.C.S., IOWA CITY, IOWA

RECENTLY, I had the privilege of appearing before a group of mechanical engineers on the question: "Can Mechanics of Locomotion Be Treated as a Special Case in Mechanics?" Today, as I follow Dr. Barnes' flattering invitation, the question is further expanded: "Can Time-and-Motion Study, which is an outgrowth of mechanics of locomotion, likewise be treated as a special case in mechanics?" I am confident that I can answer the first question in the affirmative; but I am not so sure of the second question, considering the complexity of the locomotor problems and the many factors outside of mechanical ones which influence the performances in refined and complicated industrial activities.

It is not the question of calculating a motor act as you calculate a machine; the question is whether a motor act already committed can be analyzed along lines of mechanics; and whether its performance has been in harmony with existing mechanical laws. The reasoning is deductive, not inductive. Even though the work of the engineer is committed to mathematical accuracy, I believe that human locomotion can be included as a special case of mechanics, even though it is necessary to make certain compromises and approximations. Such compromises consist in the fact that we are not dealing with an entirely homogeneous material in calculating unit stresses, breaking-point determinations, etc., and that we have to approximate the body parts to standard geometrical figures such as cylinders and truncated cones. Furthermore, we must accept average values for physical properties of tissues, although these physical properties change during action; for instance, a muscle will change its degree of tension during action as well as its rotary moment because of the change of the angle of application. To facilitate calculations, we adopt certain approximate values for the intrinsic physical properties of tissues. For instance, the radius of gyration for limbs is 0.35 of their diameter for length rotation, and 0.3 of their length for transverse rotation, Fig. 1.²

It is from this basis that the French physiologists, Amar³ and others, have calculated not only the radius of gyration but also the moments of inertia for the different portions of the human body, Tables 1 and 2. It appears that the force necessary to produce acceleration for rotatory movements about the length axis is surprisingly small, as compared with the effort necessary for the movement of a perpendicular axis.

This is of very definite practical value because on second thought it becomes clear that thousands of details characterizing the various phases and types of locomotor acts are explained thereby. We realize why the length rotatory movements of the body and the limbs play such an important part in the accumulation of momentum, since they are being carried out with such comparatively little effort. Instances of this are the twisting motion of the body in the gait in which the rotating body imparts acceleration to the extremities, Fig. 2,

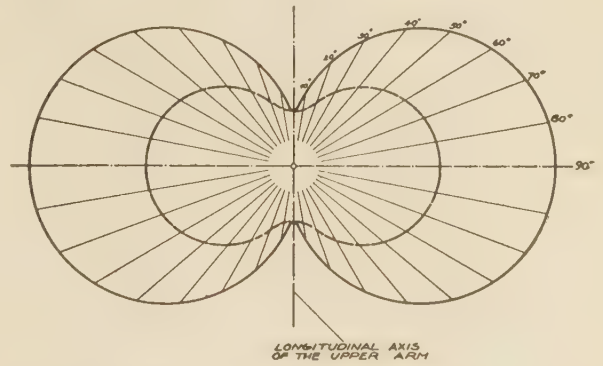


FIG. 1² RADII OF GYRATION OF UPPER ARM FOR ALL AXES GOING THROUGH CENTER OF THE HUMERAL HEAD, AT DIFFERENT ANGLES TO THE LONG AXES, ALL LYING IN THE SAME PLANE (BRAUNE AND FISHER)

the spin of the discus thrower, the twist of the golfer, or many other locomotor activities in everyday life.

Actually, the calculation of the forces and the work performed in certain locomotor acts has been possible to a rather close approximation. For instance, in the analysis of the normal walk, we divide it into the up and down movement, the forward propulsion, and the swing. The first component of this is determined by the weight of the body times the normal displacement times the coefficient which embodies the invisible work spent in the so-called restraint, which amounts per step, all told, to about 3.952 kg-m. The second part of the work, namely, that of forward propulsion, is determined by the formula $\frac{1}{2} \times mv^2$, also multiplied by the coefficient of restraint, which is 52 per cent of the propelling force, and one arrives at the figure 1.812 kg-m per step. The third pendulum movement equals $\frac{1}{2} w^2 I \pi$ and is determined as 0.281 kg-m per step, which gives a grand total of 6.045 kg-m work per step, or 7.712 kg-m per m; or, according to Amar's figure, a value of 0.119 kg-m per horizontal meter-kilogram, Table 3.³ This is an approximate evaluation of the work actually performed by the muscles during the gait. The values of Dr. McClintock and Paisley give the average cost somewhat higher, 0.23 kg-m for work per horizontal meter-kilogram.

Even with those variations, we see that an approximate idea of the actual work can be obtained. The same may be true in calculating the work for the ascending or descending walk, or the work at running. For instance, the calculation of the work in jumping, that is, the visible work performed, would be on the basis of work equals $\frac{1}{2} mv^2$, for a man weighing 65 kg, leaving the ground at a speed of 8 m per sec, and would amount to about 212 kg-m, or, in addition to the preparatory run, about 300 kg-m for a space of 6.5 m covered, or about 0.77 kg-m per meter-kilogram. This, of course, would show again that the work performed by jumping, Table 4, is much higher than that covering the same distances in the walk.

EFFICIENCY OF WORK PERFORMED

It is on this basis that kinesiologists have tried to establish the coefficients of efficiency for any work performed. The

¹ Professor, Orthopedic Surgery, State University of Iowa Hospitals.

² From "Mechanics of Normal and Pathological Locomotion in Man," by A. Steindler, Charles C. Thomas, Springfield, Ill., 1935. Reproduced through courtesy of the publisher.

³ From "The Human Motor," by Jules Amar, E. P. Dutton & Company, Inc., New York, N. Y., 1920.

Contributed by the Management Division and presented at the Spring Meeting, Davenport, Iowa, April 26-29, 1943, of THE AMERICAN SOCIETY OF MECHANICAL ENGINEERS.

TABLE 1² MOMENTS OF INERTIA OF DIFFERENT PARTS OF HUMAN BODY (FROM JULES AMAR³)

Adult weight $P = 65$ kg.				
Parts of the Body	Mass kg	Shape assumed for the Calculation and the manner in which the Calculation is done	Moment of Inertia I cm ² kg	
Bust (trunk and Head) 50% of tot. wt.	32.5 kg g	* Cylinder of height $h = .88$ m radius $r = .13$ m (axis of reference: axis through base of cylinder and axis of cylinder.)	8,600	
Upper Arm	2.20 kg g	Treated as truncated cone. Center of gravity, .145 m from shoulder; $h = 0.35$ m (height) $r = 0.047$ m. $r_1 = 0.040$ m.	33	
Forearm	2.04 kg g	Same as upper arm: Center of gravity 0.54 from shoulder; $h = 0.35$ m.; $r = 0.045$ m.; $r_1 = 0.027$ m.	37	
Fingers		Approximately	V 0.04 IV 0.12 III 0.14 II 0.12 I 0.06	
Whole upper Limb	4.20 kg g	Treated as truncated cone: Center of gravity 0.32 m from shoulder. $h = 0.70$ m; $r = 0.047$ m $r_1 = 0.027$ m	300	
Lower leg Whole Limb	4.4 kg g 12 kg g	** Treated as truncated cone: $h = 0.44$; $r = 0.062$; $r_1 = 0.038$ $h = 0.88$; $r = 0.086$; $r_1 = 0.038$	130 1460	

* Formula for moment of inertia for cylinder referred to axis perpendicular to axis of cylinder and thru base of the cylinder: $I = M/12(3r^2 + 4h^2)$

** The center of gravity in the lower limb of adult is 0.38 m from hip joint. The radius of gyration can be found from $I = M \cdot \rho^2$ which gives $\rho = 0.34$ m

TABLE 2² VALUES OF RADII OF INERTIA ρ_0 FOR AXES THROUGH CENTER OF GRAVITY FORMS ANGLE α WITH AXIS OF THE EXTREMITY (FROM 5° TO 5°), IN CM

Angle α of the Axis with Axis of Extremity	Thigh	Calf	Upper Arm	Lower Arm
0°	4.56	3.09	2.77	2.73
5°	4.65	3.19	2.84	2.88
10°	4.89	3.45	3.05	3.28
15°	5.28	3.85	3.36	3.85
20°	5.75	4.34	3.74	4.51
25°	6.29	4.86	4.17	5.21
30°	6.86	5.41	4.61	5.91
35°	7.44	5.96	5.05	6.61
40°	8.01	6.50	5.49	7.28
45°	8.56	7.00	5.90	7.90
50°	9.08	7.48	6.29	8.49
55°	9.56	7.91	6.64	9.02
60°	9.98	8.29	6.95	9.49
65°	10.35	8.63	7.23	9.89
70°	10.66	8.91	7.46	10.23
75°	10.90	9.12	7.64	10.49
80°	11.08	9.28	7.77	10.69
85°	11.18	9.38	7.84	10.80
90°	11.22	9.41	7.87	10.84

¹⁰ $I = m \rho^2 + m e^2$ for rotation about a joint axis perpendicular to the longitudinal axis of the limb.

problem becomes the more complex the more specified the motion. But, on the other hand, we can recheck the correctness of the locomotor act already performed in relation to its conformity to the accepted mechanical laws. The more efficient the motion, that is, the higher the efficiency quotient, the more it can be considered to be consistent and subservient to these laws.

The manner of determination of the efficiency belongs to the field of thermodynamics on the basis of Joule's thermodynamic equivalent, which is established as 1 kg-cal, equivalent to 427 kg-m of work. In the human body, which is also a combustion engine, part of the potential energy is transformed into kinetic energy, but the fate of this potential energy is fourfold. A small portion is lost in urine and feces; a larger portion appears as heat necessary for the function of the body; a third portion is transformed into kinetic energy; a fourth portion remains stored in the body as potential energy. Under these circumstances, obviously it is much more difficult to devise a



FIG. 2² BALL THROWING
(a, The wind-up. b, Delivery.)

balance sheet for any utilization. Nevertheless, even in the living motor, the efficiency degree can be determined by gasometric methods. Of course, we must make certain reservations as follows:

1 We will have to consider the expenditure of energy necessary to the maintenance of the vital functions, so-called basal metabolism, which amounts to 1450 to 1550 cal per 24 hr.

2 In addition, some portion of the energy consumed leaves the body unutilized through feces and urine; about 10 per cent.

3 A great deal of energy is expended on actual muscle work but is absorbed by postural attitudes, fixation, and stabilization of the extremities before any actual work is performed, Fig. 3.

TABLE 3³ COMPUTATION OF EXTERNAL WORK IN HUMAN GAIT, T

WEIGHT 65 kg., RESTRAINT 52%

T_1 Vertical Oscillation (40 mm.)

$$(W \times D) = 65 \times 0.04 \times 1.52 = 3.95 \text{ kgm/step}$$

T_2 Forward propulsion ($\frac{1}{2} m v^2$) $v_1 - v_0 = 0.6$ m.)

$$= \frac{1}{2} \times \frac{65}{9.8} \times 0.6^2 \times 1.52 = 1.81 \text{ kgm/step.}$$

T_3 (Swing, $\omega = 126^\circ$; $\frac{1}{2} \omega^2 I$) = 0.281 kgm/step.

$$T = 6.045 \text{ kgm/step} = 7.712 \text{ kgm/m} = 0.119 \text{ kgm/m kg.}$$

TABLE 4 WORK IN JUMPING

$W = 65$ kg., Distance 6.5 m., Speed 8 m/sec.

$$T = \frac{1}{2} m v^2 = \frac{1}{2} \times \frac{65}{9.8} \times 8^2 = 212 \text{ kgm.}$$

with preparatory run = 300 kgm.

$$= \frac{300}{65 \times 6.5} = 0.77 \text{ kgm/m kg.}$$

It is obvious that in certain motor acts in which the whole body takes part in the visible work, for instance, in walking or in climbing, the ratio between work and energy consumed is to be computed simply by subtracting the basal-metabolism expenditure plus about 10 per cent of the calories taken which pass through the body unutilized. If we assume that of the total heat energy available, 50 per cent is consumed in resynthesis of the metabolic products, we would place the maximum potential efficiency for any human act at about 50 per cent.

Such a maximum figure cannot be obtained in actual life, even in the most automatic and skillful motion such as walking, which has an efficiency coefficient of 33.5 per cent.

In this manner the efficiency of certain movements has been established under different working conditions. For instance, in the cranking of wheels of different sizes, weights, or heights, Fig. 4 and Table 5, we see a caloric value which varies with the arrangement, the lowest expenditure of gram-calories per meter-kilogram of physical work performed in this particular arrangement being about 18 per cent efficiency.

In this same manner we have established the optimum efficiency for all kinds of work; for example, filing (9.4 per cent), weight lifting (8.4 per cent), while cycling goes as high as 36 per cent.

It is taken for granted that in athletic performances the efficiency is high, because the work is skilled and well trained. In military activities, the efficiency maximum has been found by trial-and-error methods, just as it is being found in time-and-motion studies. However, it is remarkable how close the empiricism will come to accurate laboratory determinations. For instance, military experience establishes the optimum average marching velocity at 4.2 km per hr with a cadence of 115 steps per min, 78-cm step length, and a load of 35 to 50

TABLE 5² ENERGY EXPENDED IN SMALL CALORIES PER METER-KILOGRAM WORK CRANKING WHEELS OF DIFFERENT RADII, DIFFERENT WEIGHTS IN KILOGRAMS (6.5, 13.0, 26.0, 32.5 KG) AT DIFFERENT HEIGHTS FROM FLOOR (55.3, 82.7, 114.3, 162.2 CM). THE LOWEST FIGURES, GIVING THE SMALLEST CALORIC EXPENDITURE, GIVE THE HIGHEST EFFICIENCY (ATZLER⁴)

Elevation of Crank Axis above Floor in Centimeter	Radius of Crank	Work in Meter Kg. per Revolution				
		6.5	13.0	19.5	26.0	32.5
55.3	19.4	20.7	15.8	16.5	18.7	23.3
	28.4	22.3	14.6	13.2	13.8	17.1
	36.6	27.8	16.5	13.8	14.4	16.5
82.7	19.4	17.8	14.5	15.5	17.8	26.0
	28.4	19.4	15.0	12.5	14.2	15.7
	36.6	25.1	15.5	13.9	13.5	14.6
114.3	19.4	14.6	14.1	18.3	25.1	
	28.4	13.6	11.7	12.5	14.3	17.5
	36.6	17.0	13.5	12.4	12.1	14.2
162.2	19.4	14.5	17.4	23.5	28.0	
	28.4	30.3	19.2	19.0	22.6	33.5
	36.6	22.0	18.4	18.5	20.5	22.2

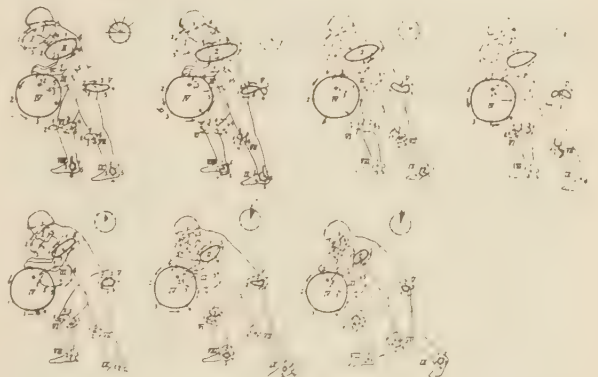


FIG. 4⁴ ENERGY EXPENDITURE IN CRANKING WHEELS OF DIFFERENT SIZES, WEIGHTS, AND HEIGHTS

by observation of the walk or by moving pictures, but these observation photographs and even movies represent always a concentrated momentary effort and give no information as to the real efficiency and endurance the patient has acquired by surgical means. It is therefore of interest to check up on the patient's performance by establishing the efficiency of the motor acts in terms of caloric expenditure. We know beforehand from observing the gait, particularly the greatly increased oscillations and swayings of the body in a spastic or scoliotic, in a case of infantile paralysis, or in a case of muscular dystrophy, that there is an inordinate amount of expenditure and that the gait is costly, Fig. 5a, b, c, d, e.

Much more accurate information will be gained by actual calculation of the increase in energy output of the particular patient over that which would be expended in the normal gait (for details see Tables 6 and 7).² For instance, in infantile paralysis, it is not unusual to find the expenditure for the gait on a treadmill to be increased 150 per cent, and in spastics even more. In muscular dystrophy we found it increased as much as 330 per cent above the normal caloric output in gram-calories per horizontal kilogram-meter.

It is obvious that the greater the percentage is which the actual visible work performed occupies in the total energy output, including the basal metabolism and wastes, the greater also will be the accuracy by which the efficiency of the par-

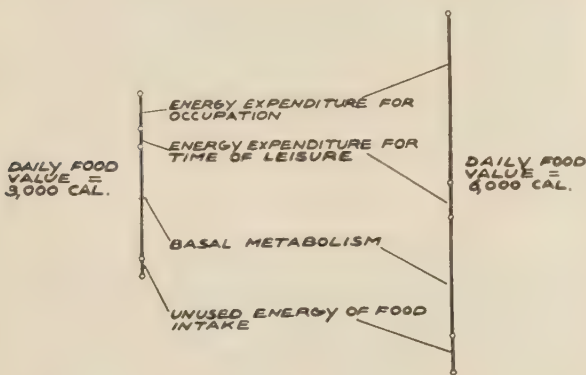
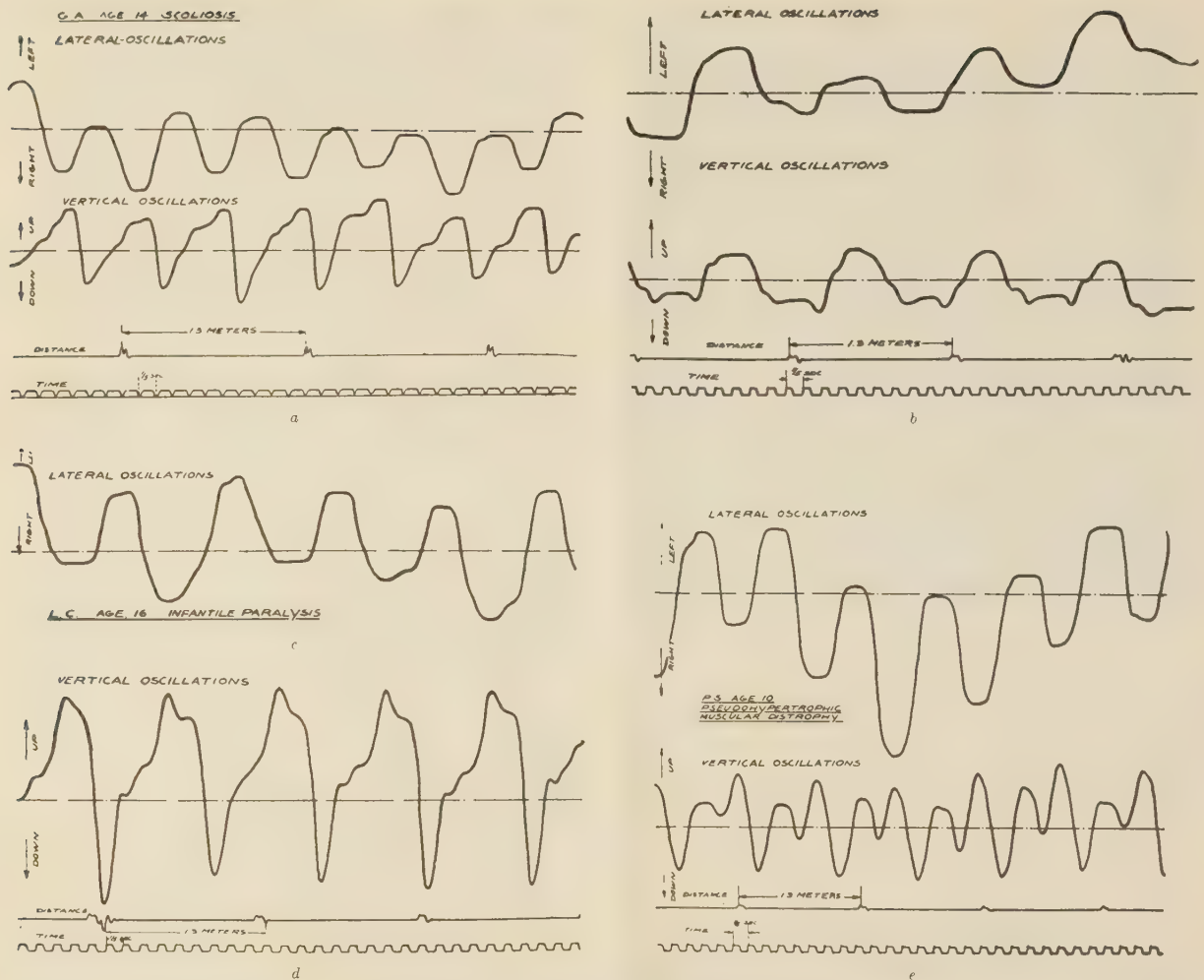


FIG. 3² RELATION OF BASAL METABOLISM, UNUSED FOOD ENERGY, ENERGY EXPENDITURE DURING LEISURE, AND ENERGY EXPENDITURE DURING WORK (ATZLER⁴)

lb. The physiologists, when they undertook the same problem, found a minimum energy consumption and therefore the maximum efficiency obtained at a speed of 4.2 km, load of 15 to 18 kg, findings which come extremely close to the empirical findings of the Army regulations.

This criterion of efficiency by which we can determine the standard skill is, of course, also applicable under pathological conditions, particularly so when we try to evaluate operative reconstruction. For example, let us take a case of congenital dislocation of the hip that has been reduced, or a flail limb that has been stabilized; usually the clinical evaluation is made

⁴ From "Körper und Arbeit," by E. Atzler, Leipzig, 1927.

FIG. 5² EXCESSIVE LATERAL AND VERTICAL OSCILLATIONS OF CENTER OF GRAVITY(a) Scoliosis
(b) Spastic case(c) Scoliosis
(d) Infantile paralysis

(e) Progressive muscular dystrophy

ticular motor act can be measured. To demonstrate this point, let us take the work of a lumberjack. If the intake of the lumberjack is 6000 cal per 24 hr, 2000 of which are used up in basal metabolism, and there may be another 600 to 1000 passing unutilized, it is obvious that the energy required for actual work is more than 50 per cent of the entire energy output. The movements carried out are simple and can be calculated, so that an efficiency index on the basis of the caloric value of the actual physical work performed, compared with the caloric values of energy consumed, will be comparatively easy and quite adequate.

As soon as the actual visible work, however, occupies only a lesser part of the entire energy output, we can see, of course, that these calculations will become increasingly inaccurate, especially in those occupations which require accuracy and which therefore postulate the preparatory assumption of certain rigid postures and attitudes. Two things seem to be deducible from these facts, (1) that a great deal of attention must be given to the preparatory attitudes such as sitting, standing height, bending height, etc.; and, (2) that, in the calculations of optimum conditions for finer work, we are

more and more dependent upon observational and empirical than on actual calculative methods.

ENDURANCE AND FATIGUE

It is common practice to measure the efficiency of the work by endurance, calculating that the longer a certain work can be carried out before signs of fatigue and exhaustion set in, the more economical and therefore the more efficient such motor acts must be. We should definitely distinguish between fatigue in the engineering and fatigue in the physiological sense. In the engineering term, it means that, after a great number of stresses, failure appears at the stress lower than the ultimate strength of material. Fatigue in the engineering sense is irreversible. But fatigue in the physiological sense is a reversible process, at least to a large extent, and the human motor forecasts excessive stresses and impending failure much sooner by signs of physiological fatigue. This results from the fact that the human motor is endowed with an extremely delicate and complicated system of sensory receptors which record stresses minutely in the brain, and thereby produce a premonitory

TABLE 6^{2,5} INCREASE IN ENERGY OUTPUT OVER THAT EXPENDED IN NORMAL GAIT IN CASES OF SCOLIOSIS, AND ARTHRITIS

A. FORM						
NAME	AGE		Total Gm. Cal. per H. Kgm.	Gm. Cal. for Normal	Difference in Gm. Cal.	Per Cent Above Normal
GROUP I—SCOLIOSIS						
R.H.	11	— brace + brace	.48418 .45694	.63366 .63366	.14948 .17672	-23.59 -27.89
M.C.	12	— brace + brace	.58271 .65875	.61661 .61661	.03390 .04214	-5.50 6.83
L.H.	13		.72904	.59672	.13232	22.17
C.S.	13		.51834	.59672	.07838	+13.14
G.A.	14		1.50580	.61678	.88094	44.16
V.B.	15		1.30289	.56262	.74027	131.58
A.L.	15	(aft. 9 mo.)	.97984 .96060	.56262 .56262	.08920 .39798	74.16 70.74
B. FUNCTION						
GROUP II—ARTHRITIS, CONGENITAL DISLOCATION OF THE HIP						
G.C.	15		.65182	.56262	.08920	15.85
E.C.	32		.99007	.51432	.47575	92.50
K.B.	47		1.01201	.49727	.51474	103.51

phenomenon of fatigue and incoordination. This applies particularly to the muscles.

The exertion of a muscle fortunately can now be recorded by means of action-current pictures much better and much sooner than was possible before Einthoven's discovery. At that time we knew little of the physiological properties of the muscle except that it possessed a certain degree of contractility, and that the strength of the muscle contraction depended upon the quantitative amount of muscle fibers which were simultaneously involved in contraction.

By means of these action-current pictures, we can follow up voluntary contractions of the muscle and demonstrate them on the living. We see that both resistance and speed modify the action-current curve, and that it is different according to whether motion is carried out loosely or in the free swing, or under a strain, as in the so-called directed motion, Figs. 6 and 7.

The free pendulum swing requires only a momentary impulse at the motor end plate, both in the synergistic and antagonistic muscle. The greater the impulse, the faster is the swing, and the sooner the antagonistic check to restrain motion appears at the proper time. Consequently, we see also in the co-ordinate and directed motion, which is the usual motion, that there is no such syncopation and alternation between synergistic and antagonistic muscle. The greater part of all muscular effort serves to produce stability as the foundation upon which the actual motor effort is superimposed; and, consequently, we see a continuous action-current play both in the synergistic and in the antagonistic muscle, Fig. 8.

When resisted motion is made more difficult by continually adding to the external load, the amplitudes of the action current not only become high but more and more irregular, and the discharges at the motor impulse resemble a peloton fire or a machine gun. The amplitudes go still farther until the limit

⁵ Tables 6 and 7 show in percentages of excess gram-calories per horizontal meter-kilogram great variations; from 6.83 per cent (scoliosis) to a maximum of 325 per cent (progressive muscular dystrophy, after exercise) above normal. This means that walking efficiency in these cases (all ambulatory) is decreased from 35 per cent normal to as low as 10 per cent.

TABLE 7^{2,6} INCREASE IN ENERGY OUTPUT OVER THAT EXPENDED IN NORMAL GAIT IN CASES OF INFANTILE PARALYSIS, SPASTIC PARALYSIS, AND MUSCULAR DYSTROPHIES

NAME	AGE		Total Gm. Cal. per H. Kgm.	Gm. Cal. for Normal	Difference in Gm. Cal.	Per Cent Above Normal
GROUP I—INFANTILE PARALYSIS						
L.J.	6		.84145	.72033	.12112	16.81
E.T.	8		1.09630	.68351	.41279	60.39
E.M.	9		.88632	.67283	.21349	31.73
C.H.	10		1.55052	.66082	.88970	134.64
H.T.	12		.93572	.61661	.31911	51.75
M.L.	13		1.28400	.59672	.68728	115.18
R.S.	13		.74091	.59672	.14419	24.16
G.H.	14		1.46095	.58251	.87844	150.80
W.G.	15		.77995	.60475	.17520	28.97
R.W.	15		1.20953	.60475	.60478	100.00
L.C.	16	— shoes + shoes	1.36744 1.14700	.59674 .59674	.77070 .55026	129.15 92.21
M.K.	19		1.29904	.52852	.77052	145.79
V.H.	20		.70231	.52426	.17805	33.96
GROUP II—SPASTIC PARALYSIS						
R.R.	9		1.73830	.67283	1.06547	158.38
F.H.	11		1.47206	.64880	.82326	126.89
V.H.	15		1.50481	.60475	.90006	148.83
V.S.	16		1.27578	.54699	.72879	133.24
GROUP III—MUSCULAR DYSTROPHIES						
P.S.	10		1.19749	.66082	.53667	81.21
E.K.	14		1.78972	.61676	1.17296	190.18
M.K.	17		1.96224	.58339	1.37885	236.35
F.G.	37	Bed rest Exerc. 2 days	.84692 2.16230	.50863 .50863	.33829 1.65367	66.51 325.12
C. COMBINED						
SCOLIOSIS AND SPASTIC PARALYSIS						
B.K.	13	— brace + brace	.74929 .68554	.59672 .59672	.15257 .08882	25.57 14.88
(after 9 m.)		— brace + brace	.97548 .72876	.59672 .59672	.37876 .12704	63.47 21.29

of muscle capacity is reached, that is, when one enters the threshold of exhaustion, it is noted that the muscle assumes chronic contraction, its amplitudes are high, and the impulses become more grouped so that the motor discharges resemble more the salvo type of firing, Fig. 9. The explanation is obvious because, to understand fatigue one must remember that prolonged contractions are only made possible by the arrangement of alternation in the activity of the individual constituents of the group of muscles. Each muscle fiber contracts at maximum, according to Sherrington's law, and only by alternating the different muscle-fiber groups in rotation is it possible that a sustained contraction may be obtained.

However, the action-current picture gives only one special feature of fatigue. There are many ways of measuring fatigue, including ergographic methods, manometric methods, etc. We generally consider fatigue as a completely reversible process which disappears when the lactic acid accumulation in the blood and in the muscle has been taken care of by increased subsequent oxidation, Fig. 10.

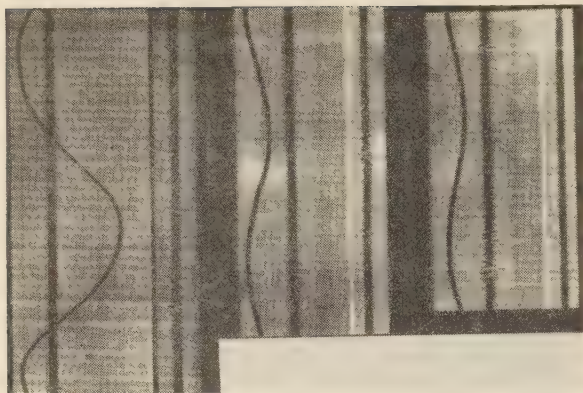


FIG. 6 ACTION CURRENT FROM ANTERIOR AND POSTERIOR PORTIONS OF THE DELTOID

(Top—Free forward and backward swing. Center—Complete alternation of current. Bottom—Short duration of motor impulses. From Wachholder.)

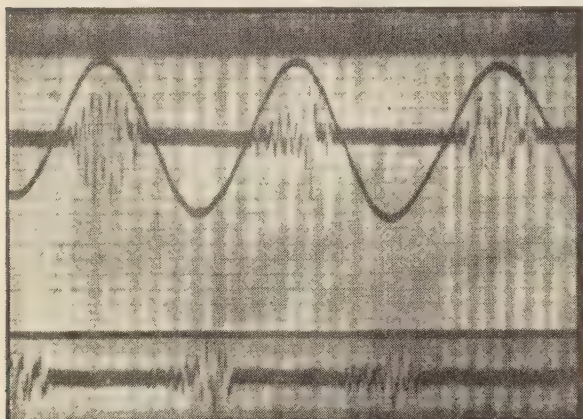


FIG. 7 ACTION CURRENT FROM ANTERIOR AND POSTERIOR DELTOID (Free forward and backward swing with increased velocity. Higher curves; precocious antagonistic action. Perfect alternation. From Wachholder.)

What makes it so difficult to evaluate fatigue is the fact that it is by no means entirely or even principally a muscular phenomenon. In so far as the muscles are concerned, we can get a measure of the degree of muscular effort from the action-current picture as well as from the chemical accumulations in the blood and in the muscles. If we define fatigue as a state in which a certain amount of work is carried out under increasing sense of difficulty and effort, and with constantly decreasing visible effect, this definition would of course include all kinds of ataxic deficiencies, clumsiness, etc. Evidently such a kind of fatigue is not based upon a state of muscle function alone but it also has a very definite cerebrospinal component.

In normal persons the fatigue of the muscle itself is only exceptionally the primary factor. The primary factor is usually fatigue or exhaustion of the motor ganglion cells. This interferes, above all things, with the independent and free innervation of the muscles, and it leads to mass innervation of muscles by which more and more of the neighboring muscles become engaged in performance of ordinarily simple and distinctive motions. Gilbreth conducted the analyses of motion by

kinematographic records to establish the time and rapidity of fatigue occurring under certain conditions, as well as the period necessary for a complete recovery, as it occurs under varied conditions of work. His criterion for fatigue always is that it involves engaging more muscle groups than are necessary for a specific work when performed under absence of fatigue.

We who are interested primarily in the pathological aspect of locomotion and in the reconstruction and recovery of locomotor efficiency have a good deal to learn from the engineering concept of and approach to the problem of time and motion. We are interested also in the phenomenon of fatigue and how its threshold can be raised.

TIME-AND-MOTION STUDIES

In time-and-motion studies, the objective is to find the most economical way to perform a certain motor operation. This is done by scientific study of the methods, material, tools,

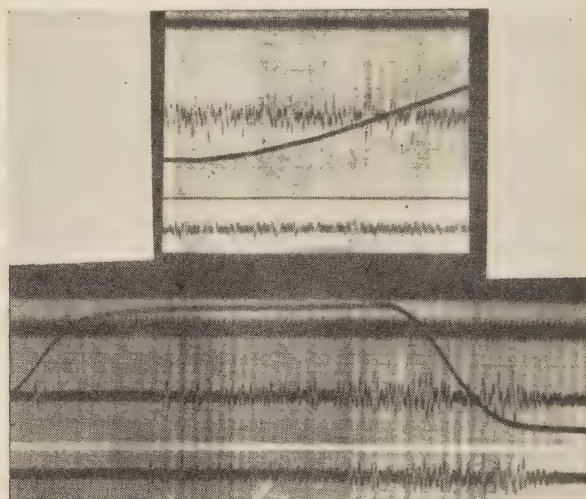


FIG. 8 ACTION CURRENT IN SLOW RIGID MOTION (Agonist and antagonist continually at work. No periodicity. From Wachholder.)

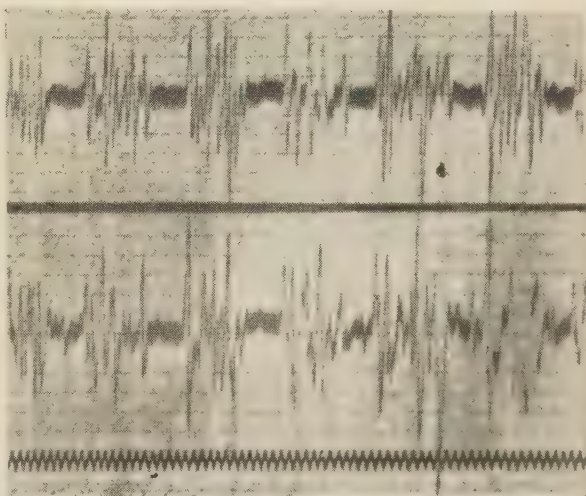


FIG. 9 ZONE OF EXHAUSTION WHEN MUSCLE ASSUMES CHRONIC CONTRACTION, WITH HIGH AMPLITUDES AND GROUPED IMPULSES

and equipment which are used. This, of course, presupposes a minute analysis of the movements made by the worker performing his task. Gilbreth, who is the father of the modern scientific way of establishing optimum performances, used for the purpose of time-and-motion study photographic and kinematographic registrations. It appears to me that several cardinal points become apparent in the course of these studies.

The gasometric method of determining an efficiency becomes more and more uncertain, to the degree that the motor acts under investigation form a smaller and smaller portion of the entire motor effort expended; that is to say, the greater the effort preparatory to the performance of the work, such as standing or attitude, etc., in comparison to the expenditure of the work itself, the greater naturally will be the inaccuracy in determining the efficiency of the particular kind of work. Thus we see that the actual work of the lumberjack who is using his whole body, or of a man walking or running, can be computed in regard to its efficiency in terms of energy expended over the actual visible work performed much more accurately than would be the case of a man who uses his hands for the performance of certain intricate tasks.

It is only natural, therefore, that time-and-motion studies have developed entirely along observational and empirical lines, and not upon calculative methods of mechanical or thermodynamic nature.

There are some situations in orthopedic reconstruction work which may serve as corollary. Probably one of the best examples is the spastic because here all operative interference to procure alignments of the body or to procure stabilization of the joints for static functions are merely episodes, and the treatment rests almost entirely upon efforts at substitution and re-education.

To this end we divide the static functions into their components; for instance, in the maintenance of the lordosis of the cervical spine by keeping the head erect, the maintenance of the lumbar lordosis by sitting, the upright position with the development of the gluteal and abdominal muscles and the extensors of the knee. These points are embodied in the first prerequisites for the restoration of function in the spastic, namely, the re-establishment of upright posture, Fig. 11. The second



FIG. 11 WALKING WITH SKIS IN CASE OF SPASTIC PARALYSIS

objective is to procure the stability of the weight-bearing joint, which means that alignment is not only accomplished but also maintained, Fig. 12. The third point is the control of active muscle equilibrium which presupposes voluntary muscle innervation and muscle co-ordination, Fig. 13. Finally, the fourth objective is the establishment of well-directed voluntary motion, and this depends entirely upon training and re-education. The principle under which training and re-education in spastics (and for that matter in other locomotor disorders) is carried out, has much in common, basically, with the development of occupational efficiency in the work of an individual.

The first principle of muscle training is that of relaxation. Relaxation means that in the attempt to maintain a posture, mass movements should be eliminated and only such muscles should be innervated as are necessary for the particular function. The principle of relaxation underlies all educational progress. We have special methods for very young children, especially babies.

The next principle is that of alternation, i.e., the principle of using independently the extremities or part of the extremities. It is often observed in spastics that the so-called concomitant movements dominate the locomotor acts, where a single extremity cannot be moved without the other moving with it. These concomitant movements may appear as full-fledged athetotic movements or they may appear in spasms. We have learned recently in the study of infantile paralysis that spasm is a widespread phenomenon even in apparently nonparalyzed muscles.

Afflicted children are taught the principle of alternation and with it the principle of rhythm. Very often we have to avail ourselves of the so-called conditioned reflexes, that is, alternation must be elicited, not by the inherent sense of rhythm which is often distorted and disturbed in the spastic, but by auxiliary senses, for instance, the eye or the ear. Consequently, we use counts, victrolas, etc., to aid in rhythmic motion.

The third principle which we observe in the re-education of spastics is the so-called principle of automatism, which is the most important of all. The premise of this principle is a satisfactory degree of (1) relaxation, and (2) alternation, such as we see in the gait. Here also, we have recourse to the introduction of conditional reflexes, auditory reflexes from phonographs, or regional reflexes which should substitute for the proprioceptive reflexes that normally operate in muscles and joints.

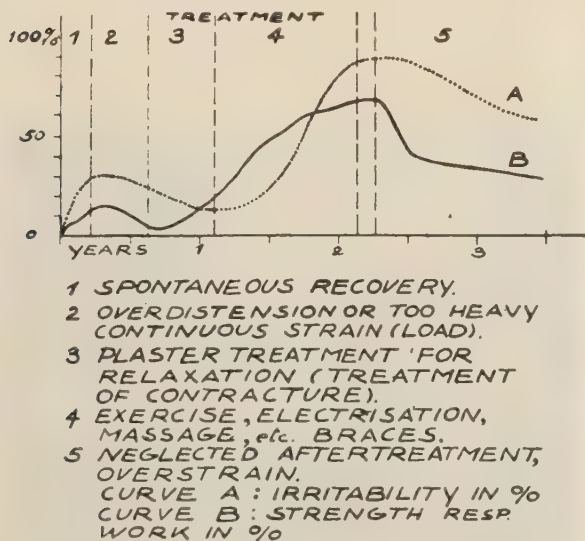


FIG. 10 FATIGUE IN A POLIOMYELITIC MUSCLE (PROEBSTER); EFFECT OF OVERSTRAIN OR NEGLECT



FIG. 12 SECURING STABILITY OF WEIGHT-BEARING JOINT

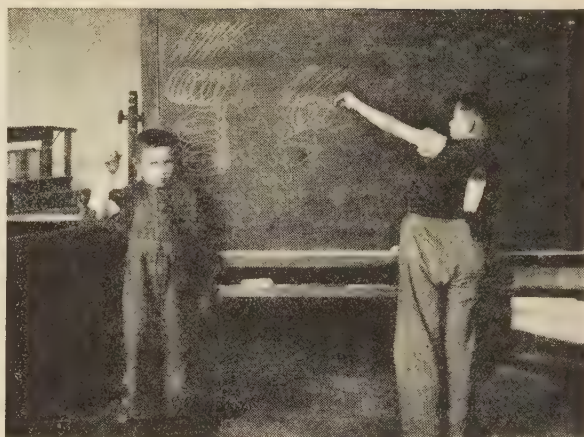


FIG. 15 BLACKBOARD EXERCISES FOR DEVELOPING SPEED AND ACCURACY IN MOTION

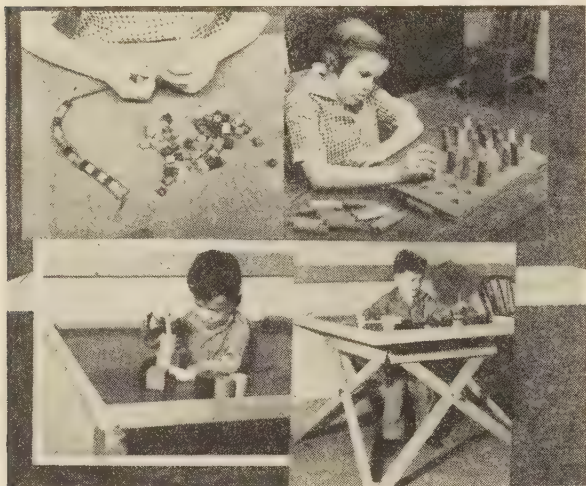


FIG. 13 EXAMPLES OF SECURING CONTROL OF ACTIVE MUSCLE EQUILIBRIUM



FIG. 16 PEGBOARD EXERCISE

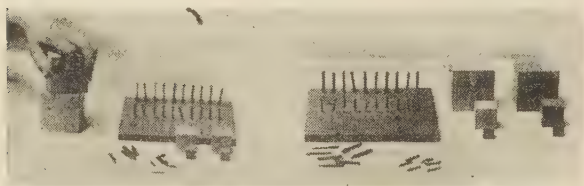


FIG. 14 PEG-AND-BLOCK METHODS FOR TIMING MOTION

The final point in training is the timing. First, the education progress itself must be timed. For instance, under 1 year it is recommended that gross motor co-ordination involving large joints should be tried in the preschool years to accomplish speech, standing, walking; in the primary school years, finer co-ordination such as roller skating, skipping ropes, should be tried in spastic cases.

Next, the motor act itself must be timed, because it becomes impractical and useless unless performed in reasonable time. So far as the timing of the specific motions is concerned, we have for many years instituted certain standard methods, such as peg



FIG. 17 BASKET, CHAIR, AND OTHER WEAVING EXERCISES

and drill methods, in order to ascertain and to develop speed and accuracy in motion. There is, of course, a tremendous possibility for variations and introduction of new factors, Figs. 14 to 19.

CONCLUSION

In conclusion, I believe that efficiency studies of human locomotion, whether they cover the field of physical training, indus-

trial efficiency, or orthopedic reconstruction, all stem from a common basic science, the mechanics of locomotion. It makes no difference whether the motor act is still within possibility of calculation or whether by its complexity or intricacy it has eluded mathematical computation and therefore depends for its solution upon trial-and-error methods. It may still become, someday, amenable to mathematical analysis; and it always will be a special case in mechanics.

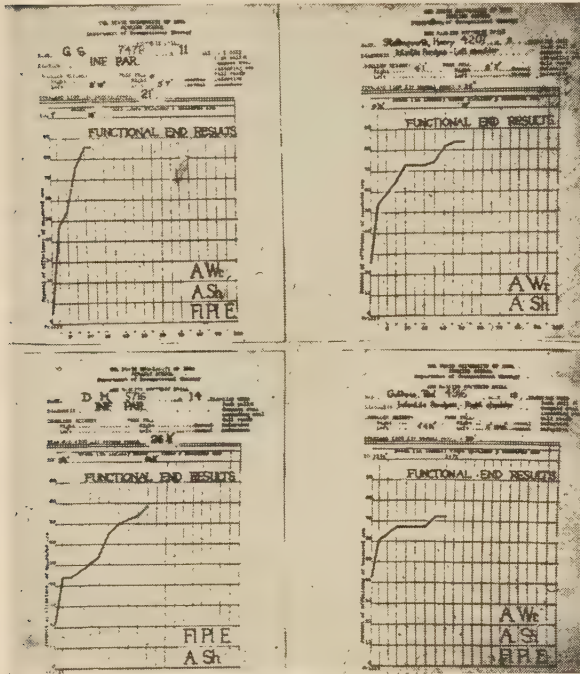


FIG. 18 FUNCTIONAL END-RESULT CHARTS FOR CASES OF INFANTILE PARALYSIS

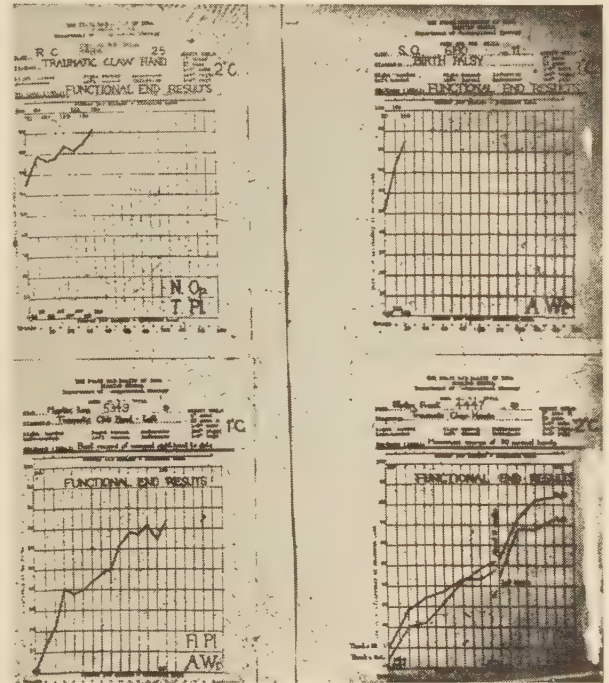


FIG. 19 FUNCTIONAL END-RESULT CHARTS FOR CASES OF TRAUMATIC CLAW, AND BIRTH PALSY

Lubrication Characteristics of Involute Spur Gears

A Theoretical Investigation

By E. K. GATCOMBE,¹ CAMBRIDGE, MASS.

In this paper the lubricating-oil wedge which separates the tooth surfaces of involute straight spur gears is analyzed mathematically. Expressions are derived for the pressure distribution, the maximum pressure, the minimum thickness, and the load-carrying capacity of the wedge for any phase of mating. The equation for the load-carrying capacity may give guidance to gear designers and to gear operators who are conscious of the importance of lubrication in their fields of work.

NOMENCLATURE

The following nomenclature is used in the paper:

$$G = \frac{12 \mu_a U \sqrt{2rh_0}}{h_0^2}$$

h = vertical distance between rotating cylinders

h_0 = minimum oil-wedge thickness

h^* = that value of h where $\frac{\partial p}{\partial x} = 0$

$k_0 = 1.30$

$K_1 = \frac{h^*}{h_0}$ by definition

p = pressure

P = pitch point

Q = flow across any cross section parallel to y direction

$$r = \frac{r_1 r_2}{r_1 + r_2}$$

r_1 and r_2 = radii of curvature of tooth profiles

R_1 and R_2 = pitch radii of gears

$$S = \tan^{-1} \frac{x}{\sqrt{2rh_0}}$$

S_1 = particular value of $S = 30$ deg

T = torque

U_1 and U_2 = peripheral velocities of rotating cylinders

¹ Staff member, Division of Industrial Co-Operation, Massachusetts Institute of Technology, Cambridge, Mass. (On leave of absence from Cornell University, Ithaca, N. Y.) Jun. A.S.M.E.

From a thesis submitted to Cornell University in partial fulfillment of requirements for the degree of Doctor of Philosophy.

Contributed by Special Research Committee on Lubrication and presented at the Annual Meeting, New York, N. Y., Nov. 27-Dec. 1, 1944, of THE AMERICAN SOCIETY OF MECHANICAL ENGINEERS.

NOTE: Statements and opinions advanced in papers are to be understood as individual expressions of their authors and not those of the Society.

$$U = \frac{U_1 + U_2}{2} \text{ by definition}$$

u, v , and w = co-ordinate velocity components

x_0 = effective width of band of contact

α = pressure angle

$$\nabla^2 = \frac{\partial^2}{\partial x^2} + \frac{\partial^2}{\partial y^2} + \frac{\partial^2}{\partial z^2} = \text{Laplacian operator}$$

μ = viscosity

μ_a = viscosity at atmospheric pressure and stated temperature

μ_x = value of μ with reference to the x direction

ω = angular velocity

ρ = density

$$\theta = \frac{\partial u}{\partial x} + \frac{\partial v}{\partial y} + \frac{\partial w}{\partial z} \text{ by definition}$$

INTRODUCTION

In general, experimental work on gears indicates the desirability of the establishment and maintenance of an oil wedge between gear-tooth surfaces for the mating period, if certain types of wear are to be minimized. In this paper we shall show, through the use of the hydrodynamic theory (subject of course to certain assumptions), that an oil wedge of a reasonable minimum thickness may be established for each mating phase. This wedge, the formation of which depends upon the combined action of several factors such as the viscosity of the oil, the tooth curvature, load, and velocity, may either partially or completely separate the tooth faces during the period of mating.

PROCEDURE

The general procedure shall be to state and to solve the equations of viscous fluid motion into which have been incorporated the combined effects of all the variables which govern the establishment of the wedge.

Specifically, we shall state the equations of viscous fluid motion in which the viscosity shall be considered a function of the pressure (the temperature assumed constant). These general equations, the complete solutions of which are difficult to obtain, shall be simplified by making certain assumptions and by neglecting certain relatively small terms. The resulting equations of motion shall then be solved and expressions obtained for (a) the pressure p at any point in the wedge, (b) the maximum pressure p_{\max} within the wedge for any particular phase, (c) an expression for the load-carrying capacity F of the wedge, (d) the minimum thickness h_0 of the wedge, (e) the effective width x_0 of the supporting band of contact. Experimental test data on gears which

have been recorded in the literature shall then be checked through the use of these expressions to show that an oil wedge existed and lubricated the tooth surfaces during the mating period.

EQUATIONS OF MOTION—VISCOSITY ASSUMED CONSTANT

Fig. 1 shows the elements of a pair of mating spur gears. Fig. 2 shows an elementary cube of oil of the wedge in Fig. 1, with the stresses indicated on the positive faces of the cube. The x and y axes are taken in the plane of rotation of the gear set, and

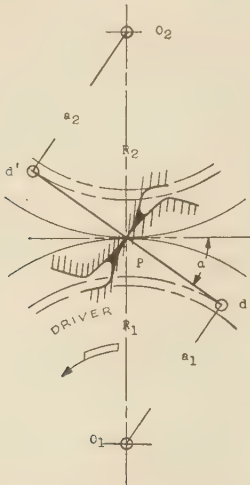


FIG. 1 ELEMENTS OF A PAIR OF MATING SPUR GEARS SHOWING ENTRAPPED OIL WEDGE

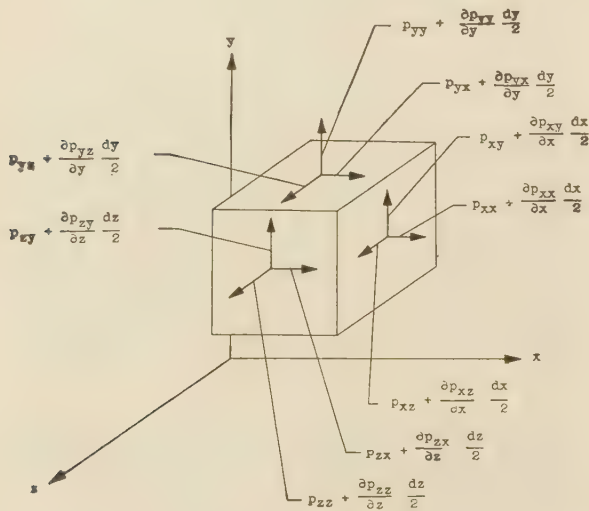


FIG. 2 ELEMENTARY CUBE OF OIL WITH INDICATED POSITIVE STRESSES

the z direction is at right angles to the plane of rotation of the gears.

The equations of viscous-fluid motion in which the viscosity μ is considered constant, have been developed in a number of reference books among which is one by Horace Lamb (1).² While these equations of motion are written here, the usual details of development have been omitted. The equations are as follows

² Numbers in parentheses refer to the Bibliography at the end of the paper.

$$\left. \begin{aligned} \rho \frac{Du}{Dt} &= \rho X - \frac{\partial p}{\partial x} + \frac{1}{3} \mu \frac{\partial \theta}{\partial x} + \mu \nabla^2 u \\ \rho \frac{Dv}{Dt} &= \rho Y - \frac{\partial p}{\partial y} + \frac{1}{3} \mu \frac{\partial \theta}{\partial y} + \mu \nabla^2 v \\ \rho \frac{Dw}{Dt} &= \rho Z - \frac{\partial p}{\partial z} + \frac{1}{3} \mu \frac{\partial \theta}{\partial z} + \mu \nabla^2 w \end{aligned} \right\} \dots\dots [1]$$

Equations [1] indicate the state of stress at each and every point throughout the fluid under consideration and must strictly apply to those problems in which there is no variation in μ , since in their development, μ is considered constant.

However, in many practical problems, there are large variations in the viscosity, since it may vary with temperature and pressure. Thus the development of the equations of motion in which μ is a function of the pressure shall follow.

EQUATIONS OF MOTION—VISCOSITY ASSUMED VARIABLE

If, in the development of the equations of motion, we consider μ a function of the pressure, we may write the following equations

$$\rho \frac{Du}{Dt} = \rho X - \frac{\partial p}{\partial x} + \frac{1}{3} \mu \frac{\partial \theta}{\partial x} + \mu \nabla^2 u - \frac{2}{3} \theta \frac{\partial \mu}{\partial x} + 2 \frac{\partial u}{\partial x} \frac{\partial \mu}{\partial x} + \left(\frac{\partial v}{\partial x} + \frac{\partial u}{\partial y} \right) \frac{\partial \mu}{\partial y} + \left(\frac{\partial u}{\partial z} + \frac{\partial w}{\partial x} \right) \frac{\partial \mu}{\partial z} \dots [2]$$

$$\rho \frac{Dv}{Dt} = \rho Y - \frac{\partial p}{\partial y} + \frac{1}{3} \mu \frac{\partial \theta}{\partial y} + \mu \nabla^2 v - \frac{2}{3} \theta \frac{\partial \mu}{\partial y} + 2 \frac{\partial v}{\partial y} \frac{\partial \mu}{\partial y} + \left(\frac{\partial v}{\partial x} + \frac{\partial u}{\partial y} \right) \frac{\partial \mu}{\partial x} + \left(\frac{\partial w}{\partial y} + \frac{\partial v}{\partial z} \right) \frac{\partial \mu}{\partial z} \dots [3]$$

$$\rho \frac{Dw}{Dt} = \rho Z - \frac{\partial p}{\partial z} + \frac{1}{3} \mu \frac{\partial \theta}{\partial z} + \mu \nabla^2 w - \frac{2}{3} \theta \frac{\partial \mu}{\partial z} + 2 \frac{\partial w}{\partial z} \frac{\partial \mu}{\partial z} + \left(\frac{\partial u}{\partial z} + \frac{\partial w}{\partial x} \right) \frac{\partial \mu}{\partial x} + \left(\frac{\partial w}{\partial y} + \frac{\partial v}{\partial z} \right) \frac{\partial \mu}{\partial y} \dots [4]$$

SIMPLIFICATION OF EQUATIONS OF MOTION

The following assumptions shall be made which will cause some simplification in the equations of motion:

- 1 Steady state.
- 2 Incompressible fluid.
- 3 Flow in the z direction is zero.
- 4 Temperature constant.
- 5 Inertia-force components are negligible, since they consist of product terms of relatively small quantities.

Further steps in the simplification of Equations [2], [3], and [4] may be gained by neglecting certain relatively small terms. Let us refer to Fig. 3, in which is represented the region of contact-surface profiles of two mating teeth. These profiles may, to the first order of approximation, be represented by circular arcs.

Let h be the vertical distance between the arc profiles for any phase of the mating period. Further, let x_0 be that value of x which is large compared with the corresponding value of h . Such values exist in these thin-film problems. It may now be seen from a consideration of streamline motion within the wedge that the ratio of v to u is of the same order of magnitude as the ratio of h to x_0 . Written symbolically

$$\frac{v}{u} \sim \frac{h}{x_0}$$

The following orders of magnitude may be written:

$$\frac{\partial u}{\partial x} \sim \frac{u}{x_0} \quad \text{and} \quad \frac{\partial^2 u}{\partial x^2} \sim \frac{u}{x_0^2}$$

$$\frac{\partial v}{\partial x} \sim \frac{v}{x_0} \quad \text{and} \quad \frac{\partial^2 v}{\partial x^2} \sim \frac{v}{x_0^2}$$

$$\frac{\partial u}{\partial y} \sim \frac{u}{h} \quad \text{and} \quad \frac{\partial^2 u}{\partial y^2} \sim \frac{u}{h^2}$$

$$\frac{\partial v}{\partial y} \sim \frac{v}{h} \quad \text{and} \quad \frac{\partial^2 v}{\partial y^2} \sim \frac{v}{h^2}$$

Thus

$$\frac{\partial^2 u}{\partial x^2} \sim \frac{h^2}{x_0^2}$$

The term $\frac{\partial^2 u}{\partial x^2}$ may therefore be neglected.

Similarly

$$\frac{\partial v}{\partial u} \sim \frac{h^2}{x_0^2}$$

Thus the term $\frac{\partial v}{\partial x}$ may be neglected.

Likewise the terms $\frac{\partial^2 v}{\partial x^2}$ and $\frac{\partial v}{\partial x}$ may each be neglected.

It is clear that there is a certain group of problems in which μ is constant. For this group

$$\frac{\partial p}{\partial y} \sim \frac{v}{u}$$

Further, it is clear that even with a variable viscosity, there is a second group of problems in which $\frac{\partial p}{\partial y}$ is small compared with $\frac{\partial p}{\partial x}$. The limits of this group become fixed once a specific meaning is attached to the word "small." The investigations carried out

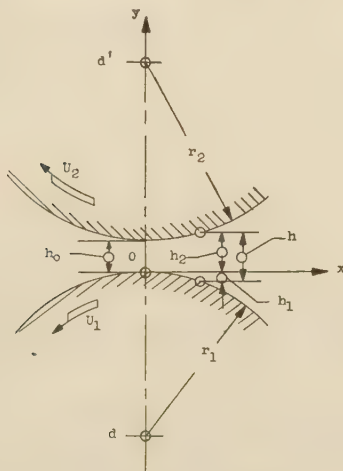


FIG. 3 TOOTH PROFILES ARE ARC-SHAPED IN REGION OF CONTACT

in this paper must be assumed to be those in which $\frac{\partial p}{\partial y}$ is small compared with $\frac{\partial p}{\partial x}$. It will then be seen that

$$\frac{\partial u}{\partial x} \frac{\partial \mu}{\partial x} \sim \frac{h^2 \mu_{x \max}}{x_0^2 \mu_{\max}}$$

But $\mu_{x \max}$ is approximately equal to μ_{\max} ; thus

$$\frac{h^2}{x_0^2} \frac{\mu_{x \max}}{\mu_{\max}} \sim \frac{h^2}{x_0^2}$$

Hence the term $2 \frac{\partial u}{\partial x} \frac{\partial \mu}{\partial x}$ may be neglected.

It is also seen that $\frac{\partial u}{\partial y} \frac{\partial \mu}{\partial x}$ and $2 \frac{\partial v}{\partial y} \frac{\partial \mu}{\partial y}$ may each be neglected.

The equations of motion may now be written in the following simplified form

$$\left. \begin{aligned} \frac{\partial p}{\partial x} &= \mu \frac{\partial^2 u}{\partial y^2} \\ \frac{\partial p}{\partial y} &= \mu \frac{\partial^2 v}{\partial y^2} + \frac{\partial u}{\partial y} \frac{\partial \mu}{\partial x} \\ \frac{\partial p}{\partial z} &= 0 \end{aligned} \right\} \dots \dots \dots [5]$$

Thus for that group of problems in which $\frac{\partial p}{\partial y}$ is small compared with $\frac{\partial p}{\partial x}$, the pressure p may be regarded as a function of x only.

PRESSURE BETWEEN TWO ROTATING CYLINDERS WHICH ARE SEPARATED BY AN OIL WEDGE

It will be recalled that circular arcs were assumed for the mating-tooth profiles in the region of contact for any particular phase of the mating period. We have assumed "steady-state conditions." This means that for any phase of contact we have substituted for the contact surfaces those circular cylindrical surfaces whose radii are the radii of curvature of the tooth profiles in the region of contact, and whose angular velocities are constant and equal to the angular velocities possessed by the gears.

Our problem is now reduced to that of finding (a) the expression for the pressure p in the wedge which separates two cylinders rotating at constant angular velocities, (b) the expression for the maximum pressure p_{\max} of the wedge, (c) its load-carrying capacity F , (d) its effective width of the supporting band of contact. We need to solve the first equation of Equation [5] to obtain the results desired in parts (a), (b), (c), and (d).

The first equation of Equation [5] is

$$\mu \frac{\partial^2 u}{\partial y^2} = \frac{\partial p}{\partial x}$$

the solution of which is

$$u = \frac{1}{\mu} \left[\left(\frac{\partial p}{\partial x} \right) \frac{y^2}{2} + C_1 y + C_2 \right] \dots \dots \dots [6]$$

The boundary conditions are as follows:

$$u = -U_1 \text{ at } y = -h_1$$

$$u = -U_2 \text{ at } y = +h_2$$

U_1 and U_2 being the peripheral velocities of the cylinders.

The solution now becomes

$$u = \frac{1}{2\mu} \left[y^2 + y(h_1 - h_2) - h_1 h_2 \right] \frac{\partial p}{\partial x} + \frac{y}{h} (U_1 - U_2) - \frac{U_1 h_2 + U_2 h_1}{h} \quad [7]$$

The flow across any cross section parallel to the y direction will be denoted by Q which is given by

$$Q = \int_{-h_1}^{h_2} u dy \quad [8]$$

By substituting in Equation [8] the value of u found in Equation [7] and performing the integration we find that

$$Q = -\frac{h^3}{12\mu} \frac{\partial p}{\partial x} - \frac{h}{2} (U_1 - U_2) \quad [9]$$

Upon rearranging terms we may write

$$\frac{1}{12\mu} \frac{\partial p}{\partial x} = - \left[\frac{Q}{h^3} + \frac{(U_1 + U_2)}{2h^2} \right] \quad [10]$$

Now, to the first order of approximation

$$h = h_0 \left(1 + \frac{x^2}{2rh_0} \right)$$

where

$$\frac{1}{r} = \frac{1}{r_1} + \frac{1}{r_2}$$

and r_1 and r_2 are the radii of the cylinders. Equation [10] now becomes

$$\frac{1}{12\mu} \left(\frac{\partial p}{\partial x} \right) = - \left[\frac{Q}{h_0^3 \left(1 + \frac{x^2}{2rh_0} \right)^3} + \frac{U_1 + U_2}{2h_0^2 \left(1 + \frac{x^2}{2rh_0} \right)^2} \right] \quad [11]$$

Now there is a value of x for which $\frac{\partial p}{\partial x} = 0$. At this value of x Equation [7] becomes

$$u = \frac{y}{h^*} (U_1 - U_2) - \frac{U_1 h_2 + U_2 h_1}{h^*} \quad [12]$$

Equation [12] shows that u is linear with y at the section where $\frac{\partial p}{\partial x} = 0$. Therefore

$$Q = \left(\frac{U_1 + U_2}{2} \right) h^* \quad [13]$$

where h^* is the value of h at the section where $\frac{\partial p}{\partial x} = 0$.

Upon substituting the value of Q from Equation [13] into Equation [11], we note that Equation [13] may be written as follows

$$\frac{1}{12\mu} \frac{\partial p}{\partial x} = \frac{\left(\frac{U_1 + U_2}{2} \right) h^*}{h_0^3 \left(1 + \frac{x^2}{2rh_0} \right)^3} - \frac{U_1 + U_2}{2h_0^2 \left(1 + \frac{x^2}{2rh_0} \right)^2} \quad [14]$$

Let the ratio $\frac{h^*}{h_0}$ be indicated by K_1 and let

$$U = \frac{U_1 + U_2}{2}$$

Equation [14] is then written as

$$\frac{1}{12\mu} \frac{\partial p}{\partial x} = \frac{U}{h_0^2} \left[\frac{K_1}{\left(1 + \frac{x^2}{2rh_0} \right)^3} - \frac{1}{\left(1 + \frac{x^2}{2rh_0} \right)^2} \right] \quad [15]$$

We may now make a change of variables by letting

$$x = \sqrt{2rh_0} \tan S \quad [16]$$

Equation [15] now becomes

$$\frac{1}{12\mu} \frac{\partial p}{\partial S} = \sqrt{2rh_0} \frac{U}{h_0^2} (K_1 \cos^4 S - \cos^2 S) \quad [17]$$

The viscosity μ is a function of the pressure in the fluid. Experiments by Hersey and Shore (2), the results of which are quoted by Needs (4), show that for pressures up to several thousand atmospheres

$$\mu = \mu_a (10)^{p\delta} \quad (\text{approx}) \quad [18]$$

Equation [18] indicates that the viscosity μ at any pressure p and temperature t is approximately equal to the viscosity μ_a at atmospheric pressure, and the same temperature t multiplied by $(10)^{p\delta}$. The symbol δ indicates the slope of the pressure versus logarithm of viscosity curve. Inserting $\mu = \mu_a (10)^{p\delta}$ in Equation [17], the following equation may be written

$$(10)^{-p\delta} dp = \frac{12\mu_a U \sqrt{2rh_0}}{h_0^2} (K_1 \cos^4 S - \cos^2 S) dS \quad [19]$$

now

$$(10)^{-p\delta} = e^{-p\delta \ln 10} \quad [20]$$

Equation [19] then becomes

$$\frac{dp}{e^{p\delta \ln 10}} = G (K_1 \cos^4 S - \cos^2 S) dS \quad [21]$$

Integration of Equation [21] yields

$$-\frac{(10)^{-p\delta}}{\delta \ln 10} = G \left[K_1 \left(\frac{1}{32} \sin 4S + \frac{1}{4} \sin 2S + \frac{3}{8} S \right) - \left(C_3 + \frac{1}{2} S + \frac{1}{4} \sin 2S \right) \right] \quad [22]$$

The constant C_3 is evaluated for the boundary conditions

$$p = 0 \text{ at } S = \pm \frac{\pi}{2}$$

It will be noted that the wedge pressure p is assumed to be zero at $S = \pm \frac{\pi}{2}$ rather than atmospheric. This assumption is valid since it is observed that the atmosphere would simply elevate the value of p throughout the wedge by a certain small value; this value will then be shown to be small compared with the pressure created in the wedge independently of the atmospheric action.

For $p = 0$ at $S = +\frac{\pi}{2}$ it is found that

$$C_3 = \frac{1}{G\delta \ln 10} + \frac{3\pi K_1}{16} - \frac{\pi}{4}$$

For $p = 0$ at $S = -\frac{\pi}{2}$, it is found that

$$C_3 = \frac{1}{G\delta \ln 10} - \frac{3\pi K_1}{16} + \frac{\pi}{4}$$

Thus

$$K_1 = \frac{4}{3} \quad \text{and} \quad C_3 = \frac{1}{G\delta \ln 10}$$

The expression for the pressure p now becomes

$$p = -\frac{1}{\delta} \log \left[G\delta \ln 10 \left(\frac{1}{G\delta \ln 10} - \frac{1}{12} \sin 2S - \frac{1}{24} \sin 4S \right) \right] \dots \dots [23]$$

The maximum pressure occurs at

$$S = S_1 = \frac{\pi}{6}$$

The maximum pressure is given by

$$p_{\max} = -\frac{1}{\delta} \log \left[G\delta \ln 10 \left(\frac{1}{G\delta \ln 10} - \frac{\sqrt{3}}{16} \right) \right] \dots [24]$$

WEDGING FORCE BETWEEN TWO ROTATING CYLINDERS WHICH ARE SEPARATED BY AN OIL FILM

The wedging force, created by the pressure in the film which separates two rotating cylinders, is given by the integral of the pressure function $p(x)$ (see Fig. 4), between the limits $-\infty$ and $+\infty$. However, experiments show that lubricants are incapable of creating or sustaining the tension stresses indicated by that portion of the graph below the x axis in Fig. 4.

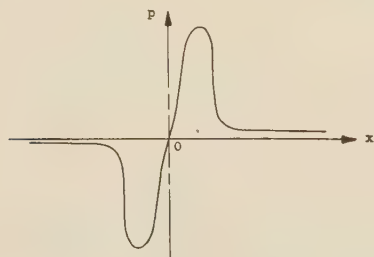


FIG. 4 HYPOTHETICAL PRESSURE-DISTRIBUTION GRAPH FOR SINGLE PHASE OF MATING PERIOD

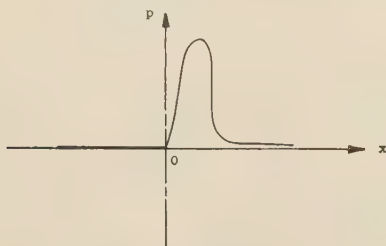


FIG. 5 THEORETICAL PRESSURE-DISTRIBUTION GRAPH FOR SINGLE PHASE OF MATING PERIOD

Thus, the absolute pressure will be atmospheric for any point in the interval $-\infty$ to zero. The wedging force will then be obtained by integrating the pressure function over the interval $0 = x = \infty$ (see Fig. 5).

Symbolically, the total wedging force is given by

$$F_n = \int_0^\infty p dx \dots \dots \dots [25]$$

We may express Equation [25] in terms of the variable S as follows

$$F_n = \int_0^{\pi/2} -\frac{\sqrt{2r h_0}}{\delta} \log \left[G\delta \ln 10 \left(\frac{1}{G\delta \ln 10} - \frac{1}{12} \sin 2S - \frac{1}{24} \sin 4S \right) \right] \sec^2 S dS \dots \dots [26]$$

Let

$$F(S) = -\frac{\sqrt{2r h_0}}{\delta} \log \left[G\delta \ln 10 \left(\frac{1}{G\delta \ln 10} - \frac{1}{12} \sin 2S - \frac{1}{24} \sin 4S \right) \right] \sec^2 S \dots \dots [27]$$

Then the expression for the wedging force is

$$F_n = \int_0^{\pi/2} f(S) dS \dots \dots \dots [28]$$

INTEGRATION OF EQUATION FOR WEDGING FORCE—APPROXIMATE SOLUTION

Considerable difficulty would be experienced if one attempted to obtain an exact analytical solution of Equation [28]. An approximate solution may be obtained by a number of methods, among which are (a) graphical, (b) interpolation. A detailed solution of Equation [28] by each of the methods (a) and (b) is given by the author (5). The solution of Equation [28] by the interpolation method is given herewith, the details employed being omitted. In general the steps employed are as follows:

Several characteristic features of the $f(S)$ function are observed, such as

$$(a) f(0) = 0$$

$$(b) f'(0) = \frac{G \ln 10 \sqrt{2 r h_0}}{3}$$

$$(c) f\left(\frac{\pi}{6}\right) = \psi \text{ where } \psi \text{ is maximum value of } f(S) \text{ which occurs at } S = +\frac{\pi}{6} \text{ (approx)}$$

$$(d) f'\left(\frac{\pi}{6}\right) = 0$$

$$(e) f\left(\frac{\pi}{2}\right) = 0$$

$$(f) f'\left(\frac{\pi}{2}\right) = 0$$

These features are then incorporated in several terms of a series, and in the terms of the derivative of the series.

The several linear equations containing the incorporated features are then solved to determine the unknown coefficients of the series terms.

An expression is next written for the function $f(S)$ in terms of the series.

A simple integration then yields the desired value of the integral. The approximate solution of Equation [28] is

$$F_n = \frac{\pi}{24} \left(\frac{81 \psi}{20} + \frac{\pi G \ln 10 \sqrt{2 r h_0}}{15} \right) \dots \dots \dots [29]$$

where

$$\psi = \frac{4}{3} \sqrt{2 r h_0} \cdot p_{\max}$$

LOAD-CARRYING CAPACITY OF FILM

Equation [29] indicates the load or force F_n which can be supported by the wedge that separates two rotating cylinders. It will be recalled that this force F_n is the force which maintains separation of the tooth surfaces during the mating period. Force F_n acts approximately along the line of action of the gear teeth. Thus, it has an effective torque force of $F_n \cos \alpha$. It is also seen that, in most sets of gears, more than one pair of teeth are mating at any given instant. For example, one pair may be beginning its mating period at the same instant another pair is at the pitch-point phase, and still another pair may be finishing its mating period. Now each mating pair of teeth has a supporting film which carries its certain share of the total gear torque. It will be found advantageous to express the average supporting action of the wedge (considering all phases of any mating period) in terms of the supporting action for the pitch-point phase. The author investigated a number of tooth profiles and found that the ratio of the average supporting action of the wedge to its value for the pitch-point phase, denoted by k_0 , was approximately 1.30.

The average number of pairs of teeth, interpreted in terms of average length of contact lines, denoted by L_c , making simultaneous mesh, can be found from the geometry of the gears.

Upon incorporating these three factors (a) effect of the pressure angle, (b) the ratio of the average supporting action of the wedge to that of the pitch-point phase, (c) the average length of contact lines of the teeth making simultaneous mesh, in Equation [29], we may write the following final expression for the load-carrying capacity of the wedge per unit face width of the set of gears

$$F = k_0 L_c \cos \alpha \frac{\pi}{24} \left(\frac{81 \psi}{20} + \frac{\pi G \ln 10 \sqrt{2 r h_0}}{15} \right) \dots [30]$$

In Equation [30] F is the pitch line component of the total supporting action of the oil wedge per unit face width of the set of gears. The value of k_0 may be taken as 1.30. Length L_c is the average length of contact lines of the teeth making simultaneous mesh; α is the pressure angle.

$$\psi = \frac{4}{3} \sqrt{2 r h_0} \times p_{\max}$$

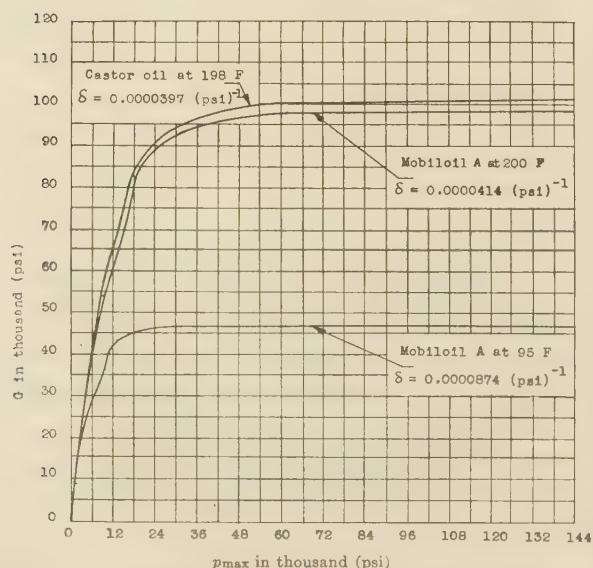


FIG. 6 GRAPHS INDICATING FUNCTIONAL RELATIONSHIP BETWEEN G , δ , AND p_{\max} FOR ANY PHASE OF CONTACT

where p_{\max} is the maximum pressure in the oil wedge for the pitch-point phase.

$$G = \frac{12 \mu_a U \sqrt{2 r h_0}}{h_0^2}$$

and

$$r = \frac{r_1 r_2}{r_1 + r_2}$$

Before citing an application of Equation [30], it will be found convenient to plot graphs (see Fig. 6), showing the functional relationship between the three quantities, G , p_{\max} , and δ .

Equation [24] shows that this functional relationship is

$$p_{\max} = -\frac{1}{\delta} \log \left[G \delta \ln 10 \left(\frac{1}{G \delta \ln 10} - \frac{\sqrt{3}}{16} \right) \right]$$

MINIMUM THICKNESS OF OIL WEDGE AND EFFECTIVE WIDTH OF BAND OF CONTACT

The minimum thickness denoted by h_0 of the oil wedge is its thickness (measured in the y direction) at $x = 0$. The following expression may be used to calculate h_0

$$h_0 = \sqrt[3]{\frac{2r(12 \mu_a U)^2}{G^2}}$$

It is shown by the author (5) that the pressure in the wedge dies off to a negligible quantity compared with p_{\max} (in computing supporting capacities) at a short distance (measured along the x axis) from the origin. Thus the effective width of the supporting band of contact may be taken as the distance from $S = 0$ to $S = 85$ deg, approximately.

The expression for the effective width of the supporting band of contact is then

$$x_0 = \sqrt{2 r h_0} \tan 85 \text{ deg}$$

PROCEDURE USED IN APPLYING EQUATION [30]

To check the load-carrying capacity of a pair of gears from the point of view of lubrication alone, Equation [30] is used as follows:

- 1 Select an oil of a known viscosity
- 2 Compute L_c from the geometry of the gears
- 3 Choose a value of the maximum permissible surface pressure, p_{\max} , and find the corresponding value of G from the graphs similar to those of Fig. 6
- 4 Compute the value of h_0 from

$$h_0 = \sqrt[3]{\frac{2r(12 \mu_a U)^2}{G^2}}$$

- 5 Compute the value of ψ from

$$\psi = \frac{4}{3} \sqrt{2 r h_0} \times p_{\max}$$

- 6 Solve Equation [30] for the load-carrying capacity of the pair of gears.

APPLICATION

PROBLEM No. 1

Data. The following straight spur pinion and gear have the same dimensions, physical properties, etc., as a pair of helical spur gears which are used on one of the gear-reduction units manufactured by the Westinghouse Electric and Manufacturing Company. This pair of gears when checked by Buckingham's

(6) "strength and wear equations" is found to be well designed and proportioned to transmit approximately 9 hp at a pinion speed of 1750 rpm.

Pinion:

3140 S.A.E. steel
Width of face = 1.625 in.
Pitch diameter $D_1 = 2$ in.
20 deg involute stub teeth
Diametral pitch $p'_d = 12$
Brinell hardness number = 325
Oil-quenched and drawn at 900 F

Gear:

1045 S.A.E. steel
Pitch diameter $D_2 = 10$ in.
Brinell hardness number = 250
Oil-quenched and drawn at 1000 F

Lubricating oil—Mobiloil A (see Hersey and Shore) (2) for which $\mu_a = 5.5 \times (10)^{-6}$ lb-sec/sq in. at 95 F and $\delta = 0.0000874$ (psi) $^{-1}$. Class-three gears are assumed.

Solution:

- 1 $\mu_a = 5.5 \times (10)^{-6}$ lb-sec/sq in. at 95 F
- 2 From geometry of gears, it is found that
 $L_e = 1.23$ in. per in. of face width
 $k_0 = 1.30$
- 3 Maximum permissible surface compressive stress of 56,000 psi will be selected for p_{\max}
- 4 $U = r_1\omega_1 = 0.342 \times 183.3 = 62.6$ ips

$$\frac{1}{r} = \frac{1}{r_1} + \frac{1}{r_2} = \frac{1}{0.342} + \frac{1}{1.71}$$

therefore

$$r = 0.29 \text{ in.}$$

$$h_0 = \left\{ \frac{2r(12\mu_a U)^2}{G^2} \right\}^{\frac{1}{3}}$$

$$= \left\{ \frac{2 \times 0.29 [12 \times 5.5 \times (10)^{-6} \times 62.6]^2}{(46,000)^2} \right\}^{\frac{1}{3}}$$

$$= 0.0000168 \text{ in.}$$

- 5 Maximum value of $f(S)$ is

$$f(S) = \psi = \frac{4}{3} \sqrt{2rh_0} \times p_{\max}$$

$$= \frac{4}{3} \sqrt{2 \times 0.29 \times 0.0000168} \times 56,000$$

$$= 232 \text{ lb per in.}$$

- 6 Load F is given by

$$F = k_0 L_e \cos \alpha \frac{\pi}{24} \left(\frac{81\psi}{20} + \frac{\pi G \ln 10 \sqrt{2rh_0}}{15} \right)$$

$$= 1.30 \times 1.23 \times 0.94 \times \frac{\pi}{24} \left(\frac{81 \times 232}{20} + \frac{\pi \times 46,000 \times 2.3 \times 0.0031}{15} \right)$$

$$= 197 \text{ lb per in. of face width}$$

$$F = 197 \times 1.625 = 320 \text{ lb for total face width}$$

This corresponds to a transmitted horsepower of

$$\text{Hp} = \frac{T \text{ rpm}}{63,030} = \frac{320 \times 1 \times 1750}{63,030} = 8.9 \text{ (approx)}$$

Thus, it is seen that the wedge can create within itself sufficient pressure (56,000 psi maximum) to transmit the required torque load, while maintaining a minimum wedge thickness of 0.0000168 in. This is a reasonable wedge thickness as was shown by Karelitz (7) in his research on heavily loaded bearing surfaces.

The effective width of the supporting band of contact for this example is

$$x_0 \sqrt{2rh_0} \times \tan 85 \text{ deg}$$

$$= 0.0031 \times 11.43$$

$$= 0.0355 \text{ in.}$$

If we now assume that this same set of gears transmits the same horsepower, namely, 9 (approximately) at a reduced pinion speed of, say, 1160 rpm we shall find that the minimum wedge thickness will be reduced and that the p_{\max} is approximately doubled, with a decrease in the effective width of the supporting band of contact.

PROBLEM No. 2

Data. Same as in Problem No. 1, but the pinion speed has been reduced to 1160 rpm.

Solution:

- 1 $\mu_a = 5.5 \times (10)^{-6}$ lb-sec per/sq in. at 95 F
 $\delta = 0.0000874$ (psi) $^{-1}$
- 2 From geometry of gears, it is found that
 $L_e = 1.23$ in. per in. of face width
 $k_0 = 1.30$
- 3 A maximum permissible surface compressive stress of 100,000 will be selected for p_{\max}
- 4 $U = r_1\omega_1 = 0.342 \times 121 = 41.4$ ips
 $h_0 = \left\{ \frac{0.58[12 \times 5.5 \times (10)^{-6} \times 41.4]^2}{(46,100)^2} \right\}^{\frac{1}{3}}$
 $= 0.0000127 \text{ in.}$
- 5 $\psi = 1.33 \sqrt{0.58 \times 0.0000127 \times 100,000}$
 $= 361 \text{ psi.}$
- 6 $F = 0.197 \left(\frac{81 \times 361}{20} + \frac{\pi \times 46,100 \times 2.3 \times 0.00271}{15} \right)$
 $= 300 \text{ lb per in.}$
 $F = 300 \times 1.625$
 $= 487 \text{ lb for total face width}$

This corresponds to a transmitted horsepower of

$$\text{Hp} = \frac{T \times \text{rpm}}{63,030} = \frac{487 \times 1 \times 1160}{63,030} = 9 \text{ (approx)}$$

The effective width of the supporting band of contact is now

$$x_0 = \sqrt{2rh_0} \times \tan 85 \text{ deg}$$

$$= \sqrt{2 \times 0.29 \times 0.0000127} \times 11.43$$

$$= 0.0311 \text{ in.}$$

We thus see that the maximum pressure in the wedge (assuming that the equations involved in the computations still hold for such high pressures) may be in the neighborhood of the surface endurance limit of the gear material.

It also will be of interest to show the following solution of this problem when a higher oil-wedge temperature is assumed:

PROBLEM No. 3

Data. Same as in Problem No. 1, except that the temperature of the Mobiloil A is now assumed to be 199 F.

Solution:

- 1 $\mu_a = 0.258 \times (10)^{-6}$ lb-sec/sq in. at 199 F
 $\delta = 0.0000414$ (psi) $^{-1}$
- 2 Average length of contact lines is

$L_c = 1.23$ in. per in. of face width

$k_0 = 1.30$

- 3 A maximum permissible surface compressive stress of 206,000 psi will be selected for p_{\max}

The corresponding value of G is

$G = 97,100$ psi

- 4 $U = r_1 \omega_1 = 0.342 \times 183.3 = 62.6$ ips

$r = 0.29$ in.

$$h_0 = \left\{ \frac{2r(12 \mu_a U)^2}{G^2} \right\}^{\frac{1}{3}}$$

$$h_0 = \left\{ \frac{2 \times 0.29 [12 \times 0.258 \times (10)^{-6} \times 62.6]^2}{(97,100)^2} \right\}^{\frac{1}{3}}$$

$= 0.00000132$ in. (A dangerously small value)

- 5 $\psi = \frac{4}{3} \sqrt{2rh_0} \times p_{\max}$

$$= 1.33 \sqrt{2 \times 0.29 \times 0.00000132 \times 206,000}$$

$= 239$ lb per in.

- 6 $F = k_0 L_c \cos \alpha \left(\frac{\pi}{24} \left(\frac{81\psi}{20} + \frac{\pi G \ln 10 \sqrt{2rh_0}}{15} \right) \right)$

$$F = 0.197 \left\{ \frac{81 \times 239}{20} + \frac{\pi \times 97,100 \times 2.3 \times \sqrt{0.000000765}}{15} \right\}$$

$= 198$ lb per in. of face width

$$F = 198 \times 1.625 = 324 \text{ lb for total face width}$$

This corresponds to a transmitted horsepower of

$$Hp = \frac{T \times \text{rpm}}{63,030} = \frac{324 \times 1 \times 1750}{63,030} = 9 \text{ (approx)}$$

It will be observed that the wedge is extremely thin for this high-temperature consideration, and that the maximum pressure is very high (206,000 psi). It is likely that the wedge would be broken down because of the extreme thinness of the wedge and to the tooth-surface roughness. This would suggest the use of a lubricating oil with a relatively higher viscosity.

Further insight into this lubricating problem may be gained if we show calculations for the foregoing calculated quantities based on castor oil as a lubricant.

PROBLEM No. 4

Data. Same as in Problem No. 1, except that the lubricant is now assumed to be castor oil at 92 C.

Solution:

- 1 $\mu_a = 0.35 \times (10)^{-5}$ lb-sec/in.²

$$\delta = 0.0000397 \text{ (psi)}^{-1}$$

- 2 Average length of contact lines per inch of face width

$L_c = 1.23$ in.

$k_0 = 1.30$

- 3 Maximum permissible surface compressive stress of 82,000 psi will be selected for p_{\max}

The corresponding value of G is

$G = 101,000$ psi

- 4 $U = r_1 \omega_1 = 0.342 \times 183.3 = 62.6$ ips

$r = 0.29$ in.

$$h_0 = \left\{ \frac{2 \times 0.29 [12 \times 0.35 \times (10)^{-5} \times 62.6]^2}{(101,000)^2} \right\}^{\frac{1}{3}}$$

$= 0.00000734$ in. (Film might not break down)

- 5 $\psi = 226$ lb per in.

- 6 $F = 200$ lb per in.

$$= 220 \times 1.625 = 325 \text{ lb for total face width}$$

This corresponds to a transmitted horsepower of

$Hp = 9$ (approx)

It is seen that the castor oil would provide a better wedge than would the mineral oil at this high temperature.

COMPARISON WITH OTHER RESEARCH WORK

In an anonymous paper (8), an investigation was reported of the lubricating wedge which separated the surfaces of an involute spur pinion mating with a straight sided rack tooth. The radius of curvature of the pinion tooth was 2.749 in. for the phase considered. The pressure angle of the tooth was $14\frac{1}{2}$ deg. The teeth were lubricated with an oil having a viscosity of 0.70 poises. The author did not give sufficient information for the exact calculation of δ for this oil, but an approximate value may be obtained from the work of Hersey and Shore (2), if we assume that its δ corresponded to that of Veedol medium, for which $\delta = 0.0000714$ (psi)⁻¹. The tooth load per inch of face width was 267 lb. The speed U with which the pinion tooth profile rolled over the rack tooth was 243.6 ips. The author, considering that the film of one pair of teeth carried the total load of 267 lb per in. of face width, found a minimum film thickness $h_0 = 0.000124$ in., and a maximum pressure $p_{\max} = 6376$ psi, with a width of the band of contact $x_0 = 0.3000$ in.

Sufficient information has now been given so that a comparison (Table 1) may be drawn between the results of the present paper and the earlier one (8).

PROBLEM No. 5

Solution:

- 1 $\mu_a = 0.70 \times 1.45 \times (10)^{-5}$

$$= 1.015 \times (10)^{-5} \text{ lb-sec/in.}^2$$

$$\delta = 0.0000714 \text{ (psi)}^{-1}$$

- 2 Average length of contact lines

$L_c = 1$ in. (load carried by one tooth)

$k_0 = 1.30$

- 3 Maximum permissible surface compressive stress of 7300 psi is selected for p_{\max} . The corresponding value of G is $G = 39,000$ psi.

- 4 $U = 243.6$ ips (stated roll speed)

$r = 2.749$ in.

$$h_0 = \left\{ \frac{2 \times 2.749 [12 \times 1.015 \times (10)^{-5} \times 243.6]^2}{(39,000)^2} \right\}^{\frac{1}{3}}$$

$= 0.000145$ in.

- 5 $\psi = 1.33 \sqrt{2 \times 2.749 \times 0.000145 \times 7300}$

$= 274$ lb per in.

- 6 $F = 1.30 \times 1 \times 0.968$

$$\times \frac{\pi}{24} \left(\frac{81 \times 274}{20} + \frac{\pi \times 39,000 \times 2.3 \times 0.0282}{15} \right)$$

$= 267$ lb per in. of face width.

- 7 Results of comparison.

TABLE 1 RESULTS OF METHOD COMPARISON

Author	h_0 (in.)	p_{\max} (psi)	x_0 (in.)
Ref. (8)	0.000124	6376	0.3000
This paper	0.000145	7300	0.3240

It is seen that the calculations based upon increased viscosity due to pressure gave a thicker wedge than did those of the author of the paper mentioned (8), his being based upon constant viscosity; this could be expected and partially explains why heavy loads may be carried by an oil wedge.

CONCLUSIONS

1 An oil wedge may be established between the tooth surfaces, and its minimum thickness depends upon several factors, such as viscosity, tooth curvature, load, and velocity.

2 The wedge may be broken down when its minimum thickness becomes approximately equal to the surface roughness.

3 The time element is important in the maintenance of a film in that it tends to govern the amount of end flow. Prof. E. Buckingham recently pointed out to the author that the time element for the pitch-point contact phase was a relatively long one. This fact might cause the film to become very thin or even broken down for the pitch-point contact phase, depending upon the length of period required for such a breakdown.

4 The maximum pressure in the wedge may approximate the value of the surface endurance limit of some gear materials.

5 This maximum pressure for any phase can be changed by altering any one or the combination of the following factors: Viscosity, tooth curvature, load, and velocity. For example, a low-viscosity lubricant will carry the same load as a high-viscosity lubricant only at the expense of a relatively thin wedge thickness and a relatively narrow band of contact, causing large maximum wedge pressures. Further, the relatively thin film thickness carries with it the danger of metal-to-metal contact. The involute internal gear might be cited as an example in which the effect of tooth curvature on the load-carrying capacity is important. In the internal-gear set, the lubrication problem is known to be a comparatively satisfactory one. The relative radii of curvature with convex-concave mating surfaces might well account for the relatively great width of the band of contact, relatively large minimum wedge thickness, low maximum wedge pressures, and thus satisfactory lubrication. This is not necessarily true for the cycloidal-gear set, because of the critical pitch-point contact phase with its small radii of curvature.

6 The author (5) investigated the load-carrying capacity of the wedge for involute helical spur gears and found that the helical spur gear could transmit approximately 1.18 times as much load as a similar straight spur-gear set, depending, of course, upon the physical dimensions of the set.

7 The temperature in the wedge may reduce the viscosity and thus increase the maximum pressure for any given set of conditions. Mr. M. D. Hersey points out that there may be an intensified viscosity of the lubricant near the boundary of such thin films. Both of these points require further investigation.

ACKNOWLEDGMENT

The author wishes to acknowledge the assistance of the members of his Special Committee on Graduate Work at Cornell University where parts of this paper were prepared. He also wishes to express appreciation for the suggestions which he has received on parts of this work from Dr. G. F. Carrier and M. D. Hersey of Cambridge, Mass.

BIBLIOGRAPHY

- 1 "Hydrodynamics," sixth edition, by Horace Lamb, Cambridge University Press, 1932, pp. 515-516.
- 2 "Viscosity of Lubricants Under Pressure," by M. D. Hersey and H. Shore, *Mechanical Engineering*, vol. 50, 1928, pp. 221-232.
- 3 "Die Druckabhängigkeit der Viskosität (The Effect of Pressure on Viscosity)," by S. Kiesskalt, *Petroleum Zeitschrift*, vol. 26, 1930, pp. M III 4 (348), M XII 17 (1924).
- 4 "Influence of Pressure on Film Viscosity in Heavily Loaded Bearings," by S. J. Needs, *Trans. A.S.M.E.*, vol. 60, 1938, pp. 347-358.
- 5 "Lubrication Characteristics of Involute Spur Gears," A Thesis by E. K. Gatcombe, Cornell University, 1944.
- 6 "Dynamic Loads on Gear Teeth," by Earle Buckingham, A.S.M.E. Research Publication, 1931.
- 7 "Oil Film Thickness at Transition From Semifluid to Viscous Lubrication," by G. W. Karelitz and J. N. Kenyon, *Trans. A.S.M.E.*, vol. 59, 1937, RP-59-3, pp. 239-246.
- 8 "The Lubrication of Gear Teeth," *Engineering*, vol. 102, 1916, pp. 119-121.

9 "Lubrication and Lubricants, A Treatise on the Theory and Practice of Lubrication," by Leonard Archbutt and R. Mountford Deeley, J. B. Lippincott Co., New York, N. Y., 1927, pp. 490-548.

10 "The Theory of Film Lubrication," by R. O. Boswall, Longmans, Green & Company, New York, N. Y., 1928, pp. 186-275.

11 "The Lubrication of Gear Teeth," by H. M. David, *Mechanical World and Engineering Record*, vol. 85, 1929, pp. 195-196.

12 "An Investigation of the Efficiency and Durability of Spur Gears," by C. W. Ham and J. W. Huckert, University of Illinois Engineering Experiment Station, Bulletin No. 149, vol. 22, 1925.

13 "The Hydrodynamical Theory of Lubrication," by W. J. Harrison, *Cambridge Philosophical Society Transactions*, 1912-1923, pp. 6-11.

14 "Zur Theorie der Flüssigkeitsreibung zwischen Gleit und Wälzflächen," by E. Heidebroek, *Zeit. V.D.I.*, vol. 80, 1936, pp. 54-55.

15 "Theory of Lubrication," by M. D. Hersey, John Wiley & Sons, Inc., New York, N. Y., 1936, pp. 43-54, second printing.

16 "Lubrication," by A. E. Norton, first edition, McGraw-Hill Book Company, Inc., New York, N. Y., 1942, pp. 78-125.

17 "Protecting Heavy-Duty Gears by Proper Lubrication," by Maurice Reswick, *Iron Age*, vol. 127, 1931, pp. 860-863.

18 "On the Theory of Lubrication," by Osborne Reynolds, *Philosophical Transactions of the Royal Society*, part 1, 1886, pp. 157-234.

19 "Steam and Gas Turbines," by Dr. A. Stodola, McGraw-Hill Book Company, Inc., New York, N. Y., vol. 1, 1927, pp. 470-499.

20 "Gear Tooth Pitting," by Stewart Way, *Electric Journal*, vol. 33, April, 1936, pp. 175-177.

Discussion

P. H. BLACK.³ The author has made an important contribution to the theory of gear-tooth action. It is shown in his paper that a pressure can be developed in the fluid film that is of sufficient magnitude to support the transmitted load, and that the calculated minimum thickness of the film compares favorably with experimental results.

The minimum film thickness in the examples is of an order of magnitude that may be found in the accumulated deviations of an actual gear tooth from the ideal form assumed in the paper, so that boundary conditions may replace those of a fluid film. The deviations may be due to surface roughness, unequal tooth spacing, or tooth deflections, and may be aggravated by dynamic loads. In addition, the effect of temperature rise in the film due to the friction of relative motion of the mating surfaces may be so high that the viscosity of the lubricant is reduced materially. The effect of this reduction in viscosity would, as the author infers in his conclusions, further reduce the film thickness. It has been reported by H. Blok⁴ that for boundary-lubrication conditions the temperature may rise an average of 170 deg F above the mean level of the temperature of the teeth.

A theoretical treatment including the foregoing actual conditions may be impractical so that an experimental approach to a study of the conditions existing in lubricated gear teeth may be the logical step to complete the author's very valuable theoretical analysis.

J. T. BURWELL, JR.⁵ The substitution for the actual gear-tooth surfaces of circular cylindrical surfaces whose radii are the radii of curvature of the tooth profiles in the region of contact and whose angular velocities are constant and equal to the angular velocity of the gears themselves, appears to be an ingenious

³ Associate Professor of Machine Design, Cornell University, Ithaca, N. Y. Mem. A.S.M.E.

⁴ "Theoretical Study of Temperature Rise at Surfaces of Actual Contact Under Oiliness Lubricating Conditions," by H. Blok, *General Discussions on Lubricants*, vol. 2, The Institution of Mechanical Engineers, 1937, pp. 222-235.

⁵ Lieutenant Commander, U.S.N., Office of Co-Ordinator of Research and Development, Executive Office of the Secretary, Navy Department, Washington 25, D. C.

method of solving analytically an otherwise complicated problem.

Several of the problems which are worked out in the paper as applications of the theory show that the required torque load can be maintained by the gear teeth with a reasonable minimum oil-film thickness. However, the definite improvement in performance which can be obtained through the use of extreme-pressure additives whose mechanism of operation is not hydrodynamic indicates that even in this range of oil-film thickness certain nonhydrodynamic factors must be considered.

In his conclusions the author notes that the time element is important in the maintenance of a film. In this connection A. F. Underwood⁶ recently presented a paper before the Society on the contribution of so-called "squeeze oil films" to the load-carrying capacity of dynamically loaded bearing surfaces. It would seem that due to the motion of the point of contact along both the gear-teeth surfaces during the mating phase, the "squeeze film" concept should also be applied here and it would be of interest to include in this analysis calculation of the time taken to squeeze out the oil which is caught between the two teeth surfaces.

A final point concerns the μ_a , which is defined in Equation [18] of the paper as the viscosity of the lubricant at atmospheric pressure and temperature T . In the analysis it is assumed that μ_a is a constant, i.e., independent of the space variables x and y . Actually, heat will be developed locally in the oil as it enters the wedge due to compression and shearing action and the temperature will rise locally with a resultant reduction in μ_a as x decreases to the point of minimum wedge thickness. Consequently, the viscosity in the wedge although increased by pressure will not be as great as calculated in the present analysis and the theoretical load capacity will probably not be as great. This is a difficult problem to treat analytically but it is believed that a better approximation than that of constant μ_a could be made.

The present paper work is, however, a very good beginning in a relatively new field and further work in the direction of more completeness of the present analysis and of extension to other types of gears is much needed.

HARRY ENGVALL⁷ AND ALEXANDER HAMMER.⁸ The method developed in the paper makes possible the calculation of the minimum thickness of the oil wedge and the maximum pressure existing within the wedge, as well as the effective width and load-carrying capacity.

Because of uncertainty as to the actual temperature of the oil and therefore of its viscosity, the values calculated by means of this method must not be treated as absolute but only as relative values, and it is necessary to relate them in some way to past experience. For this purpose it would seem possible to tie them in with the conventional " K factor," now widely used as a

basis for design, K being equal to $\frac{F}{D} \times \frac{R+1}{R}$, where F denotes tooth pressure per inch of face width, D the pitch diameter of the pinion, and R the reduction ratio. Assuming a reasonable temperature for the oil wedge and assuming that the maximum pressure within the wedge is equal to the surface endurance limit of the material used in the gear, a corresponding K factor can be calculated which would then represent the maximum permissible K .

⁶ "Rotating-Load Bearings," by A. F. Underwood, presented at the Annual Meeting, New York, N. Y., Nov. 27-Dec. 1, 1944, of THE AMERICAN SOCIETY OF MECHANICAL ENGINEERS.

⁷ Assistant Chief Engineer, Helical Gear Division, De Laval Steam Turbine Company, Trenton, N. J. Mem. A.S.M.E.

⁸ Research Engineer, De Laval Steam Turbine Company, Trenton, N. J. Mem. A.S.M.E.

In an effort to obtain this correlation a number of specific cases were investigated at 150 F oil-wedge temperature. It was found that for the same pressure in the wedge, a high-speed gear had a distinctly higher permissible K than a low-speed gear. This would indicate that, for instance, in the case of a double-reduction gear, the first reduction could be designed for a substantially higher K factor than the second reduction. In confirmation of this, experience has shown that wear and pitting are more prevalent in the second reduction gears than in the first reduction when designed to approximately the same K values, and the tendency has therefore been, purely on an empirical basis, to allow higher K factors in high-speed gears.

There is one detail in the author's examples which calls for some clarification. The value of δ in problem No. 3 is given as $0.0000414 (\text{psi})^{-1}$. Study of the Hersey and Shore data⁹ leads to a value of $0.0000759 (\text{psi})^{-1}$ for 93 C or 200 F, as can be easily checked from Fig. 7 of this discussion, which is reproduced from reference (2),⁹ with an added curve for 150 F interpolated by the writers. The difference in these values has a serious effect on

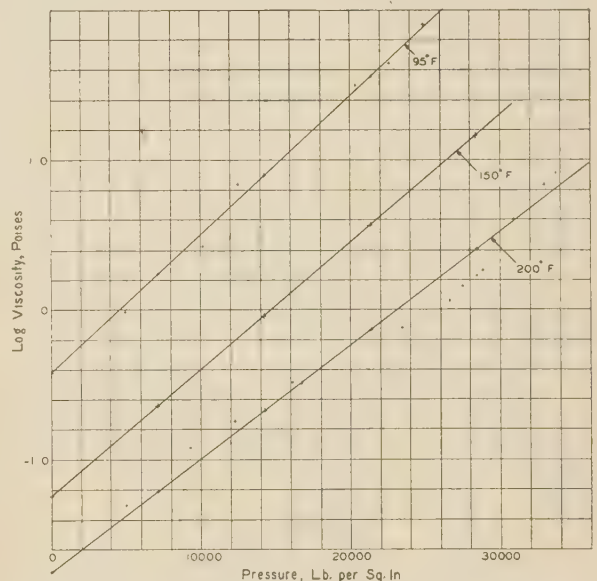


FIG. 7 VISCOSITY OF MOBILIL A UNDER PRESSURE

the results of the calculations and if, as appears to be the case, the author's value is incorrect his results are also invalid. The corresponding curve in his Fig. 6 is then incorrect also.

This point is brought up simply because this paper is of real value and for the sake of those who may study it in the future, all the details should be correct. With further study and correlation with experience, possibly by means of empirical factors, the author's method offers real promise of being an important design tool.

D. D. FULLER.¹⁰ The author in this contribution to the hydrodynamic theory of lubrication includes in his analysis the effect of pressure on viscosity. Stanton¹¹ was one of the first to report on this phenomenon in his account of a very interesting experiment where the pressure distribution was measured in a heavily loaded journal bearing.

⁹ Author's Bibliography (2).

¹⁰ Department of Mechanical Engineering, Columbia University, New York 27, N. Y. Jun. A.S.M.E.

¹¹ "Friction," by T. E. Stanton, Longmans Green & Co., New York, N. Y., 1923, pp. 102-104.

Plotting these pressures against θ , the angular distance around the bearing, a curve was obtained from which several values of $\frac{dp}{d\theta}$ were determined. Then using Harrison's equation¹²

$$\frac{dp}{d\theta} = \frac{6\mu\omega}{m^2} \left[\frac{c(\cos\theta - \cos\theta^*)}{(1 - c \cos\theta)^3} \right]$$

as applied to journal bearings of infinite width (with the usual assumptions of constant viscosity, etc.) simultaneous equations were found which evaluated such unknowns as C , eccentricity of the journal in the bearing, and μ , the viscosity. In one typical test the average value of the viscosity obtained in this manner was 25 per cent greater than the viscosity computed on the basis of temperature change alone.

Since that time this concept has been included in a number of theoretical analyses, the most recent ones known to the writer being an investigation of oil flow through capillary glands by P. G. Exline¹³ and the present paper.

The film thicknesses computed by the author in problems Nos. 1 through 4 show values ranging from 0.0000168 in. down to 0.00000132 in. These appear to be less than the thickness generally considered as the minimum to maintain fluid-film lubrication between highly finished surfaces. Stanton¹¹ computed the least distance between surfaces of journal and bearing to be 0.000054 in.

Needs¹⁴ measured the film thickness between optically plane, parallel plates forced together for 8 hr or more. This oil-film thickness approached values of from 0.00003 to 0.00004 in.

Karelitz¹⁵ computed the minimum film thickness for various bearing metals on steel to be from 0.00003 to 0.00006 in. A photomicrograph through the cross section of one of these bearing blocks showed the height of asperities to be of this same order of magnitude.

The film thicknesses as computed by the author are definitely less than the foregoing and offer no guarantee that fluid-film conditions will be maintained between the gear teeth. Such low values only serve to emphasize the ease with which an oil film between gears can be destroyed, even during normal operation.

The fact that this analysis indicates that film thicknesses will be found considerably smaller than those usually accepted as minimum for maintenance of surface separation might be construed as a prediction that oil-film breakdown will occur. Such a prediction serves as a rough qualitative check on the accuracy of the paper itself for it is recognized that most gears wear, and wear is indisputable proof (with uncontaminated oil) that film breakdown does actually occur. Here then is a rational explanation of an observed phenomenon.

Through the medium of this paper the tools are finally available that will permit the designer to adjust the pertinent variables until satisfactory gear lubrication is attained.

For this significant contribution to machine design and to the hydrodynamic theory of lubrication the author is to be congratulated.

MAYO D. HERSEY.¹⁶ Can the author briefly outline the main

¹² "Friction," by T. E. Stanton, Longmans Green & Co., New York, N. Y., 1923, Equation 10, p. 91.

¹³ "Formulas for Leakage in Capillary Seals," by P. G. Exline, Gulf Research and Development Company, Pittsburgh, Pa., Nov. 6, 1944.

¹⁴ "Boundary Film Investigations," by S. J. Needs, Trans. A.S.M.E., vol. 62, 1940, pp. 331-345.

¹⁵ "Oil Film Thickness at Transition From Semifluid to Viscous Lubrication," by G. B. Karelitz and J. N. Kenyon, Trans. A.S.M.E., vol. 59, 1937, pp. 239-246.

¹⁶ Research Associate in Mechanical Engineering, Massachusetts Institute of Technology, Cambridge, Mass. Fellow, A.S.M.E.

steps in his derivation of the general equations for variable viscosity?

The solutions for Problems Nos. 1 to 4 may be plotted as a family of curves in dimensionless co-ordinates from the data given in Table 2 of this discussion. Here h_0 is the film thickness at point of nearest approach, D the pinion diameter, Z_1 the film viscosity at atmospheric pressure (elsewhere denoted by μ_a), N the pinion speed in revolutions per unit time, and P the tooth load per unit of projected area, this being taken as the ratio of F to the product of face width into the pitch diameter of the pinion. The factor b_1 denotes the pressure coefficient of viscosity (fractional increase in viscosity per unit increase of pressure) evaluated at atmospheric pressure, or 2.3 δ .

TABLE 2 FILM-THICKNESS RELATIONS

Problem	h_0/D	Z_1N/P	b_1P
1	8.4	98	2.0
2	6.4	43	2.0
3	0.7	4.6	0.94
4	3.7	61	0.91

The data for Table 2 have been expressed in the most convenient units, h_0 in microinches, D in inches, Z_1 in newtons (millionths of a pound-second per square inch), N in revolutions per minute, P in pounds per square inch, and b_1P in per cent.

From the chart so obtained it appears that the film thickness increases almost in proportion to the square root of Z_1N/P , as if the action were similar to that of thrust-bearing shoes. Two curves may be plotted at constant values of b_1P , each passing through the origin. One curve is drawn for b_1P equal to 2 per cent, the other for a mean value of 0.93 per cent. The curve for the higher value of b_1P lies approximately twice as high up as the other, showing the importance of the viscosity-pressure effect in augmenting load capacity.

The same chart is applicable to all pairs of gears that are geometrically similar regardless of size, provided elastic deformations and temperature inequalities are negligible to the approximation required.¹⁷ Other performance ratios, such as p_{\max}/P , for example, could be plotted in the same way. Thus the author's method of solution by which the change in viscosity of oils under pressure is taken into account opens a new and useful approach to the theory of gear lubrication.

AUTHOR'S CLOSURE

The welcomed comments set forth in the discussions of this paper indicate a real interest in lubrication problems.

Professor Black injects the question of surface roughness. This factor must receive more and more attention in our future problems in lubrication.

Commander Burwell has, in effect, stated that the mechanism of operation of extreme-pressure lubricants is not covered by the hydrodynamic theory. The author believes that this is only partly the case. In the hydrodynamic theory, we assume that there is "perfect adhesion" between the lubricant and metal surface, i.e., no slippage. Probably this "perfect adhesion" never exists, but the extreme-pressure lubricant may give less surface "slippage" than do the ordinary lubricants, and thus a better lubricating action, at least, in some cases. R. G. Larsen and G. L. Perry¹⁸ observed this adhesive action in their experiments on additive-containing mineral oils. Thus, while the hydrodynamic theory does not possess the power of correction for this surface "slippage," it may correct for certain yet unobserved "rate-of-distortion" effects (the fundamental distinguishing basis

¹⁷ Author's Bibliography (15), p. 90.

¹⁸ "Investigation of Friction and Wear Under Quasi-Hydrodynamic Conditions," by R. G. Larsen and G. L. Perry, Trans. A.S.M.E., vol. 67, Jan., 1945, pp. 45-50.

upon which the hydrodynamic theory is propounded), and so it would be unwise to state that the theory's corrective measures were nil. Commander Burwell scored another point when he mentioned the importance of the "time element" in his reference to the recent work of A. F. Underwood. This time-effect problem or "nonsteady state" problem is a most interesting one; it is interesting because it has never been solved, except for certain limited cases where the restrictions are most severe. It has been the dream problem of the mathematicians for years. However, the author believes that if carefully conducted experimental research work were closely correlated with theoretical work on such problems, worth-while results could be accomplished. Commander Burwell, and this is stated in all seriousness, the field is wide open.

Messrs. Engvall and Hammer propose that a correlation be made between the physical dimensions of the gears, the design factor K , and the findings of this work on lubrication. Such a correlation is highly desirable. With reference to their (Engvall and Hammer) comments on the K value for reduction gearing, it can be added that, in this paper on the lubrication of the gears, no mention has been made of the "dynamic loads" on the film. Such loads must be considered when choosing the proper K value. Engvall and Hammer ask for a clarification of the value of $\delta = 0.0000414 \text{ (psi)}^{-1}$ used by the author in problem No. 3. The value of δ is found through experimentation. Theoretically it should be constant but actually for this particular case, it ranged in value from $\delta = 0.0000410 \text{ (psi)}^{-1}$ to $\delta = 0.0000906 \text{ (psi)}^{-1}$, as can be seen from an examination of Table 4 of reference (2). The author intentionally selected a low value (yet within the range) of δ to throw emphasis upon certain points which he wished to stress in problem No. 3. However, he agrees with Engvall and Hammer that for future references to this paper, one should have this graph plotted for more nearly an average

value of δ , namely, $\delta = 0.0000759 \text{ (psi)}^{-1}$. Such a graph is found in Fig. 8 of this closure.

The author cannot quite agree with Mr. Fuller's statement that "most all gears wear." Tests made on gears running under normal load making millions of contacts have shown no measurable amount of wear as long as they were well lubricated, yet these same gears become worn out in a matter of a few hours when deprived of a lubricant. The lubricant just plainly does something.

Mr. Hersey has asked for a brief outline of the steps required in the derivation of the variable-viscosity equations. Such steps are given here for the x -component equation only. The fundamental basis upon which the hydrodynamic theory is founded is that resistance to distortion depends upon the "rate" of change of shape. It may be seen that the x -component (p_{xx}) of the normal stress of an elementary cube of fluid can be expressed in terms of the "rate" of distortion components as follows

$$p_{xx} = -p - \frac{2}{3}\mu \left(\frac{\partial u}{\partial x} + \frac{\partial v}{\partial y} + \frac{\partial w}{\partial z} \right) + 2\mu \frac{\partial u}{\partial x} \dots [31]$$

The x -component of the equation of dynamical equilibrium is

$$\rho \frac{Du}{Dt} = \rho X + \frac{\partial p_{xx}}{\partial x} + \frac{\partial p_{yx}}{\partial y} + \frac{\partial p_{zx}}{\partial z} \dots [32]$$

Now, if we differentiate Equation [31] with respect to x , treating μ as a function of x , we shall have an expression for $\partial p_{xx}/\partial x$ which may be inserted into Equation [32]. Similarly, expressions may be gained for $\partial p_{yx}/\partial y$ and $\partial p_{zx}/\partial z$. Upon substituting these expressions into Equation [32], the variable viscosity, Equation [2] of the paper is formulated. It is interesting to note that similar variable-viscosity equations recently appeared in a German publication. Mr. Hersey has shown how the very important tool "dimensionless co-ordinates" may be used to a decided advantage.

Messrs. Black, Burwell, Engvall and Hammer, and Fuller call attention to the fact that temperature variation would alter these results. This is true, but the constant-temperature assumption was clearly stated. More work in which the temperature is considered variable may be forthcoming.

As a final comment, the author suggests that the oil wedge may have a decided "cushioning effect" on the dynamic loads on gear teeth. The present-day electrical apparatus is so highly developed that this "cushioning effect" might well be detected and measured through the use of condenser plates; such a method has recently been employed in measuring the thickness of the lubricating-oil wedge in journal bearings. Thus the author proposes that it might be desirable to begin a new series of tests on gears.

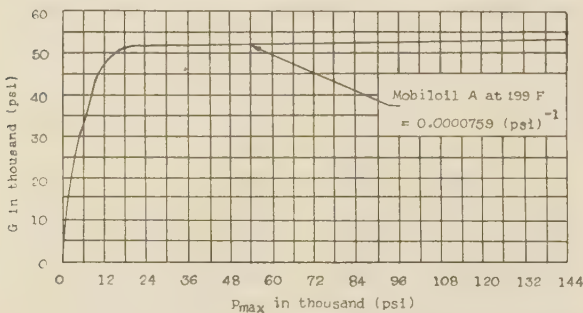


FIG. 8 GRAPH INDICATING FUNCTIONAL RELATIONSHIP BETWEEN G AND p_{max} FOR ANY PHASE OF CONTACT

Relation of Surface-Roughness Readings to Actual Surface Profile

By L. P. TARASOV,¹ WORCESTER, MASS.

Studies of surface finish have shown the desirability of relating profilometer roughness readings to actual peak-to-valley distances of the type that a micrometer measures. Approximate multiplying factors for converting profilometer readings into peak-to-valley roughness have been obtained from taper sections of a variety of abrasive-finished steel surfaces with profilometer roughness in the range of 1 to 100 microinches rms. For cylindrical ground surfaces, the factor can be taken as about $4\frac{1}{2}$; for other types of fixed-abrasive finishes, as 6 or 7; and for loose-abrasive-lapped surfaces, as 10. These are mean values and individual factors may deviate by as much as one third of the mean value. The factors quoted give values for "predominant peak" roughness; they should be doubled to obtain "deepest maximum" roughness, this being a second way of describing the peak-to-valley roughness. No evidence was found of any increase in the factor for a given type of finish with a decrease in the profilometer roughness, even for the finest surfaces studied.

TYPES OF ROUGHNESS MEASUREMENTS

It has become a well-established practice in this country to specify the roughness of a surface in terms of a special kind of average distance, which is the root-mean-square deviation of the surface irregularities from the mean surface. This distance is shown in Fig. 1, which represents the magnified profile curve of an idealized surface. The rms roughness can be read directly by the profilometer, or it can be calculated from the graphical record made by the Brush surface analyzer.

The question arises from time to time as to the physical significance of such a reading. In other words, how far below the peaks are the deepest valleys for an ordinary surface whose rms roughness is known? This question has always been of interest because one can visualize the peak-to-valley distance in terms of the type of reading obtainable with a micrometer, whereas it is extremely difficult to visualize an rms value in terms of the details of the surface profile.

The unit for roughness measurements is the microinch. This is merely 0.000001 in. and is just the same kind of a unit for linear measurements as is 0.001 in. The fact that profilometer roughness measurements are expressed in rms microinches, which are not readily visualizable, does not mean that the linear microinch itself is such a unit. It is the purpose of this paper to show how roughness measurements can be converted to linear microinches that can be readily visualized and are handled in the same manner as any other linear dimension.

As the subject of surface finish is developing, attention is being paid to waviness, which comprises irregularities more widely spaced than those making up roughness, the limit between the two having been arbitrarily set at 0.040 in. The two types of

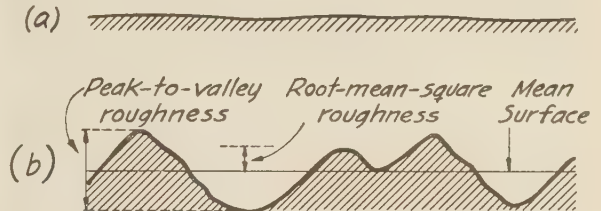


FIG. 1 SECTIONS ILLUSTRATING A TYPICAL SURFACE
(a, True profile section magnified equally in horizontal and vertical directions. b, Exaggerated appearance of same section by further magnification of 25 times in vertical direction only, horizontal magnification remaining the same as in a.)

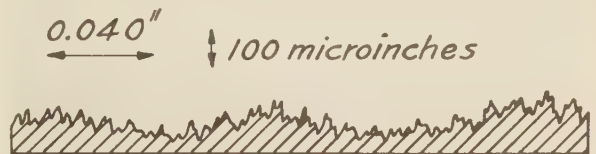


FIG. 2 SECTION OF A SURFACE SHOWING BOTH ROUGHNESS AND WAVINESS IRREGULARITIES

(Vertical magnification 125 times greater than horizontal magnification. Roughness, consisting of the fine irregularities, is superimposed on waviness, which comprises the gradual curvature with a wave length greater than 0.040 in.)

surface irregularities² are depicted schematically in Fig. 2. Since waviness is always expressed in terms of total height, any worthwhile comparison of the waviness and the roughness of a surface requires that both be expressed in the same type of units. Here again it is found desirable to convert the rms roughness (h_{rms}) to the peak-to-valley roughness (h_{max}).

Such a conversion must be made empirically for two distinct reasons. In the first place, every surface contains a considerable proportion of roughness irregularities smaller in magnitude than the largest ones. All the roughness irregularities contribute to the rms value, and therefore the rms value is necessarily smaller than if it were calculated on the basis of the larger irregularities alone. Thus the ratio of h_{max} to h_{rms} depends on the detailed characteristics of the surface. Furthermore, an rms value of the roughness obtained by a tracer-type instrument is not that for the roughness profile itself but rather for the profile as interpreted by the instrument. The tracer point and the electrical and mechanical characteristics of the instrument enter into the interpretation. The distinction between the actual profile and the interpreted version is particularly important when the roughness irregularities are such that their bottoms cannot be reached by the tracer point, whose radius of curvature at the spherical tip is 500 microinches (0.0005 in.) in both the profilometer and the Brush surface analyzer. These matters are discussed in some detail by Way.³

¹ Research Laboratories, Norton Company.

Contributed by Special Research Committees on Cutting Fluids and Metal Cutting Data and Bibliography and presented at the Annual Meeting, New York, N. Y., Nov. 27-Dec. 1, 1944, of THE AMERICAN SOCIETY OF MECHANICAL ENGINEERS.

NOTE: Statements and opinions advanced in papers are to be understood as individual expressions of their authors and not those of the Society.

² "Proposed American Standard for Surface Roughness, B46," published by the A.S.M.E., 1940; also "Surface Finish," by L. H. Milligan, *Grits and Grinds* (Norton Company publication), vol. 34, no. 10, Oct., 1943, pp. 1-10.

³ "Description and Observation of Metal Surfaces," by Stewart Way, *Proceedings of the Special Summer Conference on Friction and Surface Finish*, Massachusetts Institute of Technology, Cambridge, Mass., June, 1940, pp. 44-75.

EXISTING DATA ON CONVERSION FROM ONE TYPE OF ROUGHNESS MEASUREMENT TO ANOTHER

Some information on the quantity h_{\max}/h_{rms} has appeared in the literature. For a simple sine wave, this is of course equal to $2\sqrt{2}$ or 2.8. For profile records of actual surfaces, however, the ratio is likely to be from 3 to 5, according to Abbott, Bousky, and Williamson,⁴ who obtained their values of both h_{\max} and h_{rms} from tracer-point measurements. To the extent that the tracer point was unable to reach the bottoms of the roughness irregularities, the recorded values of h_{\max} were lower than those actually present. Thus the ratio of the real value of h_{\max} to the tracer-point value of h_{rms} could in such cases be greater than 5.

Much higher ratios than those of Abbott were found by Way^{5,6} for cylindrically ground surfaces, for which the h_{rms} values were known from profilometer readings, while h_{\max} was obtained by the straightedge shadow method. In this method, the irregularities in the surface cause corresponding irregularities in the shadow of a straightedge in contact with the surface, the shadow being viewed through a microscope. Way's results indicate that the ratio increases from 3 for extremely rough surfaces to about 10 for commercial finishes and to as high as 25 or 30 for very finely ground surfaces.

A third set of ratios can be obtained from Nelson's work on taper sections of steel surfaces prepared by various abrasive operations.⁷ A taper section is one taken at a small angle to the surface so that the surface irregularities are magnified much more in depth than in width. An optical magnification of 100 diam, superimposed on a vertical magnification of 25 due to taper sectioning, has been found convenient, this combination giving a horizontal magnification of 100 and a vertical one of 2500.

A photomicrograph of such a section is capable of furnishing the most accurate picture of the true depths of the surface irregularities. Nelson's values of h_{\max} , which he determined from the taper sections, together with the corresponding profilometer values of h_{rms} , lead to ratios that are in general intermediate to those found by Abbott and those found by Way, but there is a great deal of scatter.

Thus we have the situation that a factor for converting an rms roughness reading to total roughness depth can apparently be chosen to suit one's taste. Actually, as will be shown in this paper, there is good reason to believe that the uncertainty in the ratio of h_{\max} to h_{rms} is much less than the foregoing would indicate, provided proper consideration is paid to the type of finish involved and to a clear definition of just what is meant by h_{\max} .

PREPARATION OF SPECIMENS USED IN PRESENT STUDY

The present work is based upon a detailed examination of Nelson's taper sections, of which only a few were published. The surfaces in question were all finished by various abrasive methods, the specimens being S.A.E. 6150 steel hardened and tempered to approximately Rockwell C42. Both cylindrical and flat specimens were used. The profilometer readings for the cylindrical specimens were taken along the axial direction, the highest values being obtained in this manner for the reason that the lay of the surface, in those cases in which it was unidirectional, was perpendicular to the axial direction. The flat specimens were measured in analogous manner relative to the lay. The surfaces had been

carefully prepared to have certain profilometer readings in connection with a general study of the effect of surface finish upon frictional properties,⁷ but with no thought of obtaining the type of data to be described herein. Since no attempt was made to control the conditions of preparation such as might have been made if the specimens had been finished primarily with the present study in mind, the surfaces can be taken as representative of good abrasive-finishing practice and not involving any unusual restrictions on the method of preparation. For this reason, the ratios of h_{\max} to h_{rms} obtained for these surfaces should be generally applicable to hardened and tempered steels finished by abrasive methods to corresponding profilometer readings, and the spreads in the ratios should be about the same as would occur in practice.

The methods used for preparing the surfaces included grinding, hyprolapping,⁸ sandpapering, superfinishing,⁹ and loose-abrasive lapping. Details of the methods by which most of the surfaces were obtained have been described elsewhere.^{6,7} There is no advantage in repeating these details here inasmuch as the final results can be correlated only with the type of finish and not with the particular size or kind of abrasive that happened to be used.

"PREDOMINANT PEAK" AND "DEEPEST MAXIMUM" ROUGHNESS

Careful examination of the taper sections revealed that most of the surfaces could best be visualized in terms of two sorts of peak-to-valley roughness. One of these, the roughness that occurs more or less uniformly over the whole surface, we are designating as "predominant peak" roughness. The other, here termed "deepest maximum" roughness, comprises the deepest irregularities occurring at intervals that are large compared to the width of the irregularities themselves but, occurring closer than 0.040 in., are still too close together and too numerous to be disregarded as flaws.

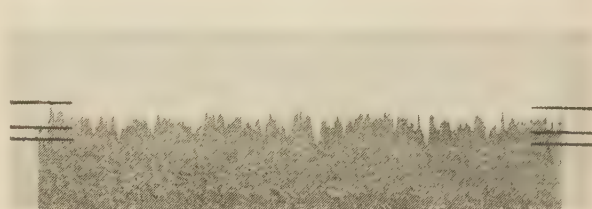


FIG. 3 TAPER SECTION OF CYLINDRICAL SURFACE FINISHED BY GRINDING

(Profilometer reading was 12 microinches rms. The dark portion is the steel while the white is the nickel plate protecting the steel surface. Horizontal magnification is 100X; vertical magnification is 2500X. The upper and middle black lines define the predominant peak roughness while the upper and lower lines define the deepest maximum roughness.)

The two types are well illustrated in Fig. 3, which depicts a taper section, at a horizontal magnification of 100 and a vertical magnification of 2500, of a ground surface that reads 12 microinches rms on the profilometer. The predominant peak roughness is measured between the upper and middle lines while the deepest maximum roughness extends, in half a dozen spots, from the upper to the lower line. Only the ends of the lines are drawn because, if the full lines were shown, the roughness irregularities would be obscured. It is to be noted that the same upper line is chosen for both predominant peak and deepest maximum roughness. It is appropriate to measure both kinds of roughness from

⁴ "The Profilometer," by E. J. Abbott, S. Bousky, and D. E. Williamson, *Mechanical Engineering*, vol. 60, 1938, pp. 205-216.

⁵ Way's ratios are also discussed briefly in "Surface Finish," by G. Schlesinger, American edition published by the Society, 1942, pp. 29-30.

⁶ "Taper Sectioning as a Means of Describing the Surface Contour of Metals," by H. R. Nelson, Proceedings of the Special Summer Conference on Friction and Surface Finish, Massachusetts Institute of Technology, Cambridge, Mass., June, 1940, pp. 217-238; also *American Machinist*, vol. 85, 1941, pp. 743-747.

⁷ "Surface Finish of Journals," by R. W. Dayton, H. R. Nelson, and L. H. Milligan, *Mechanical Engineering*, vol. 64, 1942, pp. 718-726.

⁸ Hyprolapping is a Norton mechanical process similar to machine lapping except that bonded abrasive disks are substituted for the cast-iron plates and loose abrasive used in machine lapping.

⁹ Superfinishing is a Chrysler process employing reciprocating bonded-abrasive sticks at low pressures.

a common line along which contact would first be made with an ideal mating surface.

The location of the base line for the determination of predominant peak roughness is chosen visually through the use of a transparent straightedge superimposed on the section showing the surface profile. This line is located by trial and error in a position to serve as a base for the roughness irregularities extending as peaks above it. As the straightedge is raised from a low position, this is the level at which valleys begin to be intersected at frequent intervals. The distance from the base line for the predominant surface irregularities to the highest portions of the surface defines the predominant peak roughness.

For some surfaces the predominant peak roughness and the deepest maximum roughness are the same. Usually, however, there are deep scratches occurring often enough to be classified as roughness and not as waviness or flaws, and yet not often enough to represent a true base line for the surface irregularities themselves.

Predominant peak roughness is considered significant because the general frictional behavior of an ordinary abrasive-finished surface in original contact with another is most likely to be determined by the roughness irregularities present everywhere rather than by the widely separated deep irregularities constituting deepest maximum roughness. There is little reason to expect that an increase in the depth of the deepest irregularities will affect the contact behavior if the predominant peak roughness remains unchanged.

Usually it is not difficult to decide upon a value of predominant peak roughness that is reasonably reproducible, say within a range of one fourth of its numerical value. Greater accuracy could perhaps be obtained by specifying that the lower line bounding the region of predominant peak roughness intersect the peaks and valleys at such a level that only some small fraction of the line would be situated in the valleys. An analogous method has been used by Abbott and Firestone to construct depth versus bearing-area curves from tracer-point profile records.¹⁰ For the purposes of the present study, however, it is felt that sufficient accuracy is obtained by estimating visually, with the aid of a transparent straightedge, the position of the lower line for the predominant peak roughness.

REPRESENTATIVE TAPER SECTIONS

Various typical taper sections together with the lines defining the predominant peak and deepest maximum roughness are shown in Figs. 3 to 9. All the taper sections, except Figs. 6 and 9, have a horizontal magnification of 100 diam and a vertical one of 2500; for Fig. 6, the corresponding magnifications are 500 and 10,000; while for Fig. 9 they are 20 and 500.

The sandpapered surface of Fig. 4 resembles the ground surface of Fig. 3 and requires no comment. Fig. 5 shows a super-finished surface having a profilometer reading of 1.6 microinches rms. Although the roughness irregularities are barely visible in the reproduction, it was possible to draw satisfactory lines and to measure the distance between them by performing the operations under a binocular microscope at 10 diam. A taper section at a higher magnification of a different portion of the same surface is shown in Fig. 6, and here the surface irregularities are clearly visible. In this particular case, the same values of predominant peak and deepest maximum roughness were obtained at 10,000 vertical magnification as at 2500; in two other cases, however, the higher magnification appeared to give a much lower peak-to-valley distance than did the lower magnification, but this was evidently because the extremely short length of the surface appearing in the high magnification taper section was not repre-

sentative of the surface as a whole. Even for very fine surfaces, it appears that a horizontal magnification of 100, which results in a vertical magnification of 2500, is more useful than a higher one, unless the length of the photomicrograph is correspondingly increased for the higher horizontal magnification.

A loose-abrasive-lapped surface is shown in Fig. 7, and a hypolapped one in Fig. 8, in both of which the distinction between predominant peak and deepest maximum roughness is very clear. The roughness irregularities do not actually undercut the surface but appear to do so in these taper sections because the individual abrasive grain marks are not parallel to the direction of the slope of the taper section.

A surface for which it is difficult to determine the predominant peak roughness is the very rough-ground one in Fig. 9, having an average profilometer reading of 105 microinches rms. Examination of this taper section shows it to consist of a coarse roughness superimposed on a fine roughness. The fine roughness characteristic is evidently due to the scratches cut by individual abrasive grains, whereas the coarse roughness has resulted from the cutting action of groups of abrasive grains. Since the wave length of coarse irregularities in this case is less than 0.040 in., we are dealing by present definition with coarse roughness and not with waviness.

For this unusual type of surface, how should the values for predominant peak and deepest maximum roughness be chosen? In deciding this question, the type of reading obtained with the profilometer should be considered, the tracer point of which mainly measures the coarse roughness.

Therefore, it is logical to conclude that the predominant peak roughness should be measured for the gradual large-scale variations of the coarse roughness, rather than for the fine irregularities in this taper section. The calculation of predominant peak roughness is justified for the large-scale variations because their spacing apart is similar to their width. To qualify as deepest maximum roughness, the spacing must be many times greater than the width of the roughness irregularities.

PEAK-TO-VALLEY ROUGHNESS VERSUS PROFILOMETER ROUGHNESS

The results of such measurements of predominant peak roughness for a variety of cylindrical surfaces are plotted in Fig. 10 as a

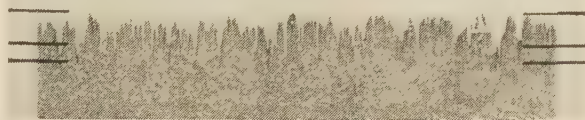


FIG. 4 TAPER SECTION OF CYLINDRICAL SURFACE FINISHED BY SANDPAPERING

(Profilometer reading was 8 microinches rms. Horizontal magnification is 100X, vertical magnification is 2500X.)

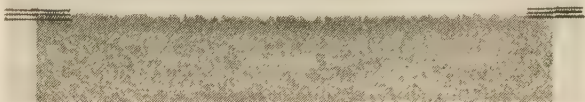


FIG. 5 TAPER SECTION OF CYLINDRICAL SURFACE FINISHED BY SUPERFINISHING

(Profilometer reading was 1.6 microinches rms. Horizontal magnification is 100X, vertical magnification is 2500X.)

¹⁰ "Specifying Surface Quality," by E. J. Abbott and F. A. Firestone, *Mechanical Engineering*, vol. 55, 1933, pp. 569-572.

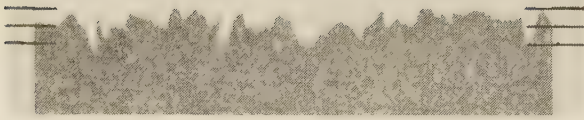


FIG. 6 ANOTHER TAPER SECTION OF SUPERFINISHED SURFACE SHOWN IN FIG. 5, BUT AT A HIGHER MAGNIFICATION (Horizontal magnification is 500X, vertical magnification is 10,000X.)



FIG. 7 TAPER SECTION OF CYLINDRICAL SURFACE FINISHED BY LOOSE-ABRASIVE-LAPPING (Profilometer reading was 3.5 microinches rms. Horizontal magnification is 100X, vertical magnification is 2500X.)

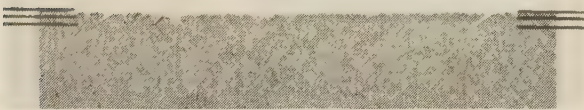


FIG. 8 TAPER SECTION OF CYLINDRICAL SURFACE FINISHED BY HYPROLAPPING (Profilometer reading was 2.3 microinches rms. Horizontal magnification is 100X, vertical magnification is 2500X.)

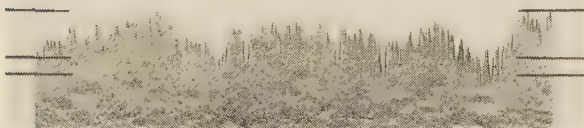


FIG. 9 TAPER SECTION OF CYLINDRICAL SURFACE FINISHED BY ROUGH-GRINDING (Profilometer reading was 105 microinches rms. Horizontal magnification is 20X, vertical magnification is 500X, both considerably lower than in any of the other taper sections.)

function of the profilometer reading. For the predominant peak roughness, the ground surfaces lie close to a straight line such that the ratio, h_{\max}/h_{rms} , is constant along that line. Thus this ratio, which is the multiplier for converting profilometer readings into peak-to-valley roughness, is essentially the same for ground cylindrical surfaces ranging from the smoothest (1.6 microinches rms) to the roughest (105 microinches rms). This represents the range of roughness values normally encountered in ground surfaces. The points representing the other types of abrasive finish lie a little above this line, indicating that the ratio h_{\max}/h_{rms} is somewhat higher for them than for ground surfaces.

It now becomes convenient to discuss the results for the various surfaces in terms of the ratio h_{\max}/h_{rms} and they are tabulated on that basis in Table 1, which also includes the results for flat surfaces. The ratios have been calculated for both predominant peak and deepest maximum roughness and are listed in the order of decreasing profilometer reading for each type of finish. The

values of h_{\max}/h_{rms} for the predominant peak roughness of cylindrical ground surfaces are practically the same for the whole range of roughness studied, the comparatively small variations being of a random nature. For these same surfaces, h_{\max}/h_{rms} for the deepest maximum roughness is higher for the smooth finishes than for the medium or rough ones. The corresponding data for the flat ground surfaces show a greater scatter in the ratios.

The cylindrical surfaces that were hyprolapped, sandpapered, or superfinished, all show a decrease in the ratio with decreasing profilometer reading, and this is true of both the predominant peak and the deepest maximum roughness. The same can also be said of the flat surfaces that were sandpapered or superfinished. This behavior is opposite to the general assumption that the finer the finish, the greater the ratio h_{\max}/h_{rms} . The decrease actually observed in the ratio is very likely real since it occurred in a number of instances. In the case of the cylindrical sandpapered surfaces, the taper sections showed that the width of the individual irregularities remained more or less the same while their depth became considerably less as the finish improved; thus the tracer point was enabled to come relatively closer to the bottoms of the irregularities and the difference between h_{\max} and the measured value of h_{rms} diminished. Probably the same thing happened in the other cases in which the ratio was less for the smoother finishes.

The values of h_{\max}/h_{rms} for the loose-abrasive-lapped surfaces vary irregularly with respect to the profilometer readings and the scatter is considerable.

A comparison of the ratios for the various types of surfaces is facilitated by considering only their average values, as is done in

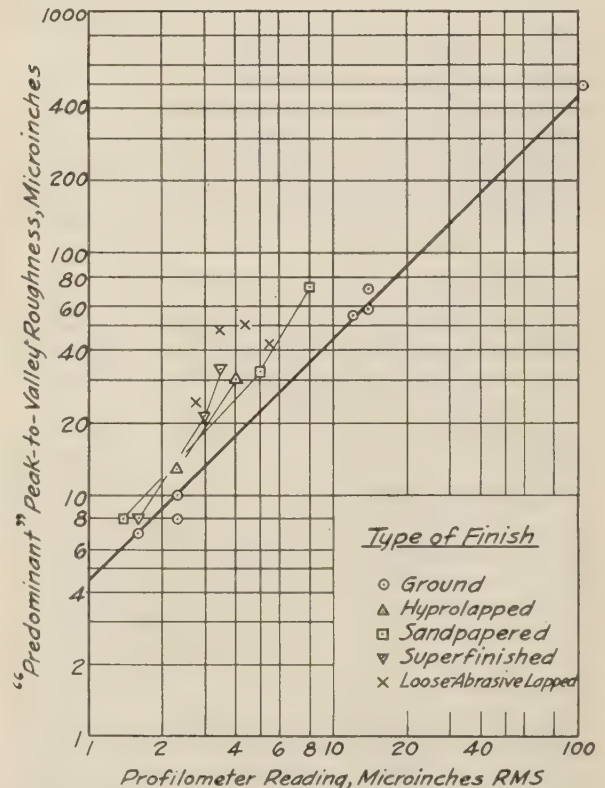


FIG. 10 PLOT OF PREDOMINANT PEAK ROUGHNESS FOR CYLINDRICAL SURFACES, FINISHED BY VARIOUS METHODS, VERSUS PROFILOMETER READINGS

TABLE 1 RATIO OF PEAK-TO-VALLEY ROUGHNESS (h_{\max}) TO PROFILOMETER READING (h_{rms}) FOR VARIOUS CYLINDRICAL AND FLAT SURFACES

Type of finish	Cylindrical surfaces			Flat surfaces		
	Profilometer reading, microinches, rms	h_{\max}/h_{rms} for "Predominant peak" roughness	h_{\max}/h_{rms} for "Deepest maximum" roughness	Profilometer reading, microinches, rms	h_{\max}/h_{rms} for "Predominant peak" roughness	h_{\max}/h_{rms} for "Deepest maximum" roughness
Ground	105	$4\frac{1}{2}$	$6\frac{1}{2}$	11	5	7
	14	5	$8\frac{1}{2}$	4.5	8	15
	14	4	$7\frac{1}{2}$	1.9	$7\frac{1}{2}$	11
	12	$4\frac{1}{2}$	7
	2.3	$4\frac{1}{2}$	10
Hyprolapped	2.3	$3\frac{1}{2}$	10
	1.6	$4\frac{1}{2}$	10
	4.0	$7\frac{1}{2}$	14	2.5	$5\frac{1}{2}$	$9\frac{1}{2}$
Sandpapered	2.3	$5\frac{1}{2}$	13	1.2	$6\frac{1}{2}$	21
	8	9	13	5.0	$7\frac{1}{2}$	19
	5.0	$6\frac{1}{2}$	10	3.3	$6\frac{1}{2}$	14
Superfinished	1.4	$5\frac{1}{2}$
	3.5	$9\frac{1}{2}$	16	10	$7\frac{1}{2}$	12
	3.0	7	12	8	$5\frac{1}{2}$	9
	1.6	5	11	2.5	$3\frac{1}{2}$	9
Loose-abrasive-lapped	5.5	$7\frac{1}{2}$	18	5.5	$5\frac{1}{2}$	12
	4.4	11	20	3.0	13	17
	3.5	13	23	3.0	11	22
	2.8	$8\frac{1}{2}$	15

TABLE 2 AVERAGE VALUE AND RANGE OF VALUES OF h_{\max}/h_{rms} FOR VARIOUS TYPES OF FINISH (SUMMARY OF TABLE 1)

Type of finish	h_{\max}/h_{rms} for Cylindrical surfaces				h_{\max}/h_{rms} for Flat surfaces			
	"Predominant peak" roughness		"Deepest maximum" roughness		"Predominant peak" roughness		"Deepest maximum" roughness	
	Average value	Range of values	Average value	Range of values	Average value	Range of values	Average value	Range of values
Ground	$4\frac{1}{2}$	$3\frac{1}{2}$ - 5	$8\frac{1}{2}$	$6\frac{1}{2}$ - 10	7	5 - 8	11	7 - 15
Hyprolapped	$6\frac{1}{2}$	$5\frac{1}{2}$ - $7\frac{1}{2}$	13	13 - 14	6	$5\frac{1}{2}$ - $6\frac{1}{2}$	15	$9\frac{1}{2}$ - 21
Sandpapered	7	$5\frac{1}{2}$ - 9	12	10 - 13	7	$6\frac{1}{2}$ - $7\frac{1}{2}$	17	14 - 19
Superfinished	7	5 - $9\frac{1}{2}$	13	11 - 16	$5\frac{1}{2}$	$3\frac{1}{2}$ - $7\frac{1}{2}$	10	9 - 12
Loose-abrasive-lapped	10	$7\frac{1}{2}$ - 13	19	15 - 23	10	$5\frac{1}{2}$ - 13	17	12 - 22

Table 2. The cylindrical surfaces can be separated into three groups according to the average value of the ratio h_{\max}/h_{rms} for the predominant peak roughness of each group. This quantity is $4\frac{1}{2}$ for the ground surfaces, close to 7 for the hyprolapped, sandpapered, or superfinished ones, and 10 for the loose-abrasive-lapped ones. The corresponding average ratios for the deepest maximum roughness are almost exactly twice as great.

Turning to the flat surfaces, the average ratio for the predominant peak roughness places the ground surfaces in the same group as the hyprolapped, sandpapered, and superfinished ones, for all of which the quantity in question is in the vicinity of 6. The loose-abrasive-lapped surfaces again have a definitely higher average ratio than the rest. The average ratios for the deepest maximum roughness of the flat surfaces are erratic when compared to the corresponding figures for the predominant peak roughness, being anywhere from 50 to 150 per cent greater than the latter.

The various ratios that have been quoted are, of course, averages for all the specimens with a given type of finish. The actual ratios for the individual specimens may be anywhere from one third less to one third greater than the average ratios, as is revealed by an inspection of the ranges of values included in Table 2. This applies to both predominant peak and deepest maximum roughness.

The physical significance of these findings can be summarized in the following manner: For cylindrical surfaces finished to a given profilometer reading, a ground surface is likely to be slightly smoother in terms of peak-to-valley roughness than a hyprolapped, sandpapered, or superfinished one, while a loose-abrasive-lapped surface will probably be rougher than the three just mentioned and will almost certainly be rougher than the ground surface. For flat surfaces finished to the same profilometer reading as just mentioned, a ground surface will have about the same peak-to-valley roughness as any of the other surfaces except the loose-abrasive-lapped one, which will probably be rougher. Comparing cylindrical and flat surfaces finished by the same method to the same profilometer reading, a ground surface will very likely be smoother when it is cylindrical than when it is flat, while for the other types of finishes it will be immaterial whether the sur-

face is cylindrical or flat. Of course, it should be kept in mind that the ground and the sandpapered surfaces are unidirectional and were studied across the lay, whereas the hyprolapped, superfinished, and loose-abrasive-lapped surfaces have substantially no directional characteristics.

At first glance, it may appear that the range of values of h_{\max}/h_{rms} is so broad for a given type of finish that calculations involving the average ratio listed in Table 2 are not likely to be of practical use. However, even a possible error of one third is not too large when it is considered that in shop practice the classes of roughness progress by factors of 2.

The values of the ratio h_{\max}/h_{rms} for predominant peak roughness are higher for most types of finish than the values of 3 to 5 proposed by Abbott,⁴ the one outstanding and very important exception being that of cylindrical ground surfaces, the ratio for which agrees satisfactorily with Abbott's. However, even for deepest maximum roughness, the ratios are much lower than most of the ratios deduced from Way's study by the straightedge shadow method³ of cylindrical ground surfaces. Since the taper sections showed no evidence of any increase in the ratio with decreasing roughness, such as was found to a marked extent by Way, it appears that the very high ratios for the finer surfaces may have been caused by experimental difficulties in getting an undistorted shadow of very fine and shallow irregularities.

To illustrate how the average ratios of Table 2 can be applied, we can assume that the profilometer reading is known for a given type of surface. Multiplying this reading by the corresponding average ratio in the predominant-peak-roughness column gives us the roughness in terms of the predominant peak-to-valley height, a distance that is easy to visualize and one that is well suited for comparisons of roughness and waviness. The occasional deep irregularities, if needed, are obtained similarly by the use of the average ratio in the deepest-maximum-roughness column.

The converse problem, that of establishing a likely value of the profilometer reading if h_{\max} is given, requires a knowledge of whether or not the deepest maximum irregularities were excluded from consideration when h_{\max} was established. If they were ex-

cluded, as is likely to be the case, the ratio for predominant peak roughness should be used, but if h_{\max} is based upon the most pronounced irregularities, the ratio for deepest maximum roughness should be used. In all these examples, the degree of uncertainty in the calculated quantity can be obtained by substituting the extreme values for the average value given in Table 2.

SUMMARY

Although roughness is generally expressed in terms of a special kind of average distance from the mean surface, h_{rms} , such as is read on a profilometer, it can also be expressed in terms of the peak-to-valley height of the irregularities, h_{\max} . It is desirable to be able to convert from one to the other, but the available results in the literature have not been in agreement. The present results have been compiled from a careful examination of numerous taper sections of cylindrical and flat surfaces of hardened and tempered steel finished by various abrasive methods and for which values of profilometer roughness were known. In most of these taper sections, it was found desirable to distinguish between two types of peak-to-valley roughness, predominant peak and deepest maximum.

For cylindrical surfaces finished by grinding, the ratio h_{\max}/h_{rms} for predominant peak roughness was practically the same even though the profilometer roughness ranged from 1.6 to 105 microinches rms. The average value of this ratio for all of these surfaces was $4\frac{1}{3}$. The corresponding figure for cylindrical surfaces finished by hyprolapping, sandpapering, or superfinishing was around 7, while those finished by loose-abrasive-lapping had the highest average of 10. The individual values differed from the average by as much as one third of the average value itself except for the ground surfaces, which varied less from the average. The corresponding ratios for deepest maximum roughness were in each case just about double those for predominant peak roughness. For cylindrical surfaces finished to a common profilometer reading, one that has been ground is likely to be somewhat smoother, i.e., have a lower peak-to-valley roughness than a hyprolapped, sandpapered, or superfinished surface, while a loose-abrasive-lapped one is likely to be rougher than any of the others.

When the surfaces were flat instead of cylindrical, the average ratio h_{\max}/h_{rms} for predominant peak roughness was practically the same for ground surfaces as for hyprolapped, sandpapered, or superfinished ones, being about 6 for all these finishes. The loose-abrasive-lapped surfaces again had a higher ratio than any of the others, this ratio being 10, the same as for cylindrical surfaces with this type of finish. The individual values of the ratios for the various flat surfaces deviated from the average values to the same extent as in the case of the cylindrical surfaces.

These ratios enable a reasonably satisfactory conversion to be made for several types of abrasive-finished surfaces from profilometer reading to peak-to-valley roughness or vice versa.

ACKNOWLEDGMENT

The author wishes to express his appreciation to Dr. L. H. Milligan of Norton Company for his advice in the preparation of this paper.

Discussion

A. H. DALL.¹¹ The author is to be commended for his clear analysis of finish interpretation based on the comparison of the electrical-measuring method and the taper-sectioning method of finish evaluation. His statement, in effect, that "predominant peak" roughness is more significant in performance than "deepest maximum" roughness should find universal agreement. It is to

¹¹ Research Engineer, Cincinnati Milling Machine Company, Cincinnati, Ohio.

be noted that no explanation for the high ratios of h_{\max}/h_{rms} is attempted by the author. It is the purpose of this comment to suggest a possible reason for these high ratios on the better types of finish.

A study of Table 1 of the paper reveals that, in every case except the loose-abrasive type of finish and the highest-quality ground finish, the ratio for each type declines as the quality of finish improves. The fact that grinding finishes, in general, show ratios nearer to the theoretical values may be significant, since the grinding operation usually generates an entirely new surface, while the other operations rework a ground surface to a greater or lesser degree. It is suggested, therefore, that the previous history of the surfaces which are superfinished, hyprolapped, etc., may be a determining factor in the ratios indicated. In loose-abrasive lapping, particularly, the abrasive particles may cut on the sides and bottoms of the deep grinding scratches as well as on the elevated regions. As the appearance of a surface is governed by the distribution of the light reflected therefrom, and this in turn is determined largely by the character of the finish on the sides of the ridges and valleys of the surface asperities, a surface may often appear to have been lapped so as to eliminate all grinding imperfections, when actually this is not so. In several instances it has been found that a lapped surface on which no grinding scratches were visible exhibited a definite grinding-scratch pattern again after light superfinishing.

This raises the question whether each of the hyprolapped, sandpapered, superfinished and loose-abrasive-lapped surfaces listed in Table 1 had actually been worked to a point where every vestige of the original ground surface had been eliminated.

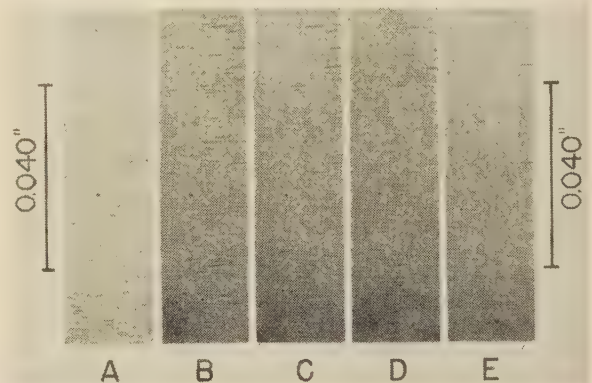


FIG. 11 PHOTOMICROGRAPHS OF SURFACE WORKED BY SPECIAL SUPERFINISHING TECHNIQUE

A	3.5 microin. rms	D	1.0 microin. rms
B	1.4 microin. rms	E	0.9 microin. rms
C	1.1 microin. rms		

Fig. 11 of this discussion shows a series of bright field photomicrographs of a surface which was worked by a special superfinishing technique using extremely fine stones and an effective cutting fluid. The original ground surface A was 3.5 microin. rms, and successive members of the series B, C, D, and E show the same spot on the workpiece after superfinishing for 15 sec, 30 sec, 45 sec, and 60 sec, respectively. In C, the frequency of the scratches remaining from the grind would be sufficient to influence the appearance of the taper section, as with this method of investigation it is inherent that the depths of occasional scratches are magnified more than their distribution. Thus these scratches would also be used in the calculation of predominant peak roughness ratio, but their frequency is not sufficiently high to affect the profilometer reading appreciably,

as the fidelity of such readings decreases with decreasing frequency. The profilometer reading for C averaged 1.1 micron. rms.

It is quite possible on this finish that the "predominant peak" measurement would be only slightly different from the original grind. The predominant peak roughness ratio would therefore be of the order of 12.

It would therefore seem possible that the reason for the high values of predominant peak roughness ratio obtained with the loose-abrasive-lapping method may not be due so much to an inherent characteristic of this type of finish, as to the incomplete removal of deep scratches produced in a preliminary grinding operation. At the present time with most commercial methods of finishing, it is quite difficult to determine when all such scratches have been eliminated.

It will also be noted from the photomicrographs that the frequency of the residual grinding scratches varies from one area to another; thus the roughness indication of a taper section may vary in accordance with the particular area in which this section happened to be taken.

D. E. WILLIAMSON.¹² The present paper is a comparison of two widely different means of designating the roughness of surfaces finished with abrasives. One striking difference in the two methods is that, whereas the "tracer method" gives a non-destructive test, taper sectioning renders the sample unsuitable for future examination or use. For this reason, the tracer method is so attractive that we may well examine its possible disadvantages.

The principal objection to the tracer method seems to be that a 0.0005-in-radius tracer point is suspected of failing to bottom the valleys of the roughness to such a degree that readings obtained are reasonably reduced. An extension of this feeling is that profile records made by the tracer method are likewise unreliable, this usually without consideration as to whether the profile records were made with a 0.0005-in-radius point or one many times sharper. Although tracer-point radius studies have been made, published, and talked about for years, most of this work (and certainly the selection of a suitable standard radius) has been done by the instrument manufacturers and is therefore suspected of prejudice.

Another source of confusion is a result of the convenience of showing profile records with greatly different horizontal and vertical magnification. It just does not seem possible that a tracer point could be made to bottom these greatly sharpened valleys. And then there is the added fact that a 0.0005-in-radius point does indeed fail to bottom an occasional valley.

In view of the foregoing, it is the writer's belief that faith in the tracer method would be strengthened if some impartial experimenter would attempt to determine just how faithfully a point of a given shape can be expected to reproduce surfaces of various characters. In this work the experimenter should pin his faith on logic and the scientific method, and not on an arbitrarily adopted standard of perfection. One of the tests which he might make would be to prepare graphs of average roughness reading (ordinate) versus tracer-point radius (abscissa). If any portion of this curve is horizontal, it might be concluded that readings are independent of tip radius in that range.

Also, in comparison studies, such as that reproduced herewith, it would be interesting to compute the average roughness by graphical means in an attempt to ascertain whether or not apparent anomalies are due to the tracer point. For instance, it is suggested that the tendency of the profilometer to indicate the larger irregularities in Fig. 9 of the paper is due to the

squared element in a "root-mean-square" average, and not because the tracer point fails to enter the smaller irregularities. In fact it appears, from rather superficial examination of the half-tone reproductions, that a 0.0005-in-radius point would bottom essentially all of the irregularities shown in the paper.

The determination of the ratio of h_{max}/h_{rms} here given may well prove more useful than the factors previously published. The difference between the author's values and those referred to as published by Abbott, Bousky, and Williamson⁴ is probably due to the difference in what was meant by h_{max} . The earlier value was obtained from profile records made with a 0.00005-in-radius (approx) diamond point, and profilometer readings taken using a 60-deg, 0.0005-in-radius point. Even though a different definition of h_{max} was used, it was recognized that ratios of greater than 5 frequently occurred.

A point of interest is that the present data are based on the shop practice used in preparing Nelson's specimens,⁶ and it would be interesting to ascertain if these results would compare favorably with data from samples prepared elsewhere. If so, this would indicate that the words "grinding," "hyprolapping," "sandpapering," etc., are also descriptive of surface character.

The author is to be commended on his treatment of the experimental data and preparation of this paper, and it is to be hoped that more work along these lines will be forthcoming.

AUTHOR'S CLOSURE

The author appreciates the additional information and comments offered by the discussers and is pleased to find that the distinction set up between the two kinds of roughness, predominant peak and deepest maximum, appears to serve a useful purpose.

Mr. Dall has presented some very interesting evidence that abrasive operations other than grinding may not completely eliminate the deepest scratches left by the preceding operation. The question of how the presence of residual scratches may affect the ratio h_{max}/h_{rms} , i.e., the conversion factor, is a very important one and deserves detailed consideration. First, we have to determine what this effect may be; and second, we have to see to what extent residual scratches may have been present in the surfaces for which the conversion factors were calculated in this paper.

The spacing of the grinding scratches in the superfinished surfaces shown in Fig. 11 can be taken as characteristic of residual scratches in general. If we had a taper section through any of the superfinished surfaces, we would find that the grinding scratches left after superfinishing are spaced far apart compared to their own width; consequently, they contribute to the deepest maximum roughness. The predominant peak roughness, by definition and by measurement method, is composed of the closely spaced and comparatively shallow superfinishing scratches covering the rest of the surface and therefore is not affected by the widely spaced scratches remaining from grinding.

This means that in so far as predominant roughness of abrasive-finished surfaces other than ground ones is concerned, neither the observed high values of the conversion factors nor their decrease with improved finish can be explained by reference to any residual scratches that may be left from the preceding operation. The explanation given in the paper (in the paragraph of the second column that is next to Fig. 7), which is based on the approximate constancy of the widths of the valleys as their depths decreased with improved finish, appears to be the most satisfactory that can be proposed at the present time.

We can now turn to the conversion factors for deepest maximum roughness. Since occasional irregularities either may be left from the preceding operation or may be introduced during the final one, it is necessary to consider the depth to which the

¹² Research Engineer, Lincoln Park Industries, Inc., Lincoln Park, Mich.

material was removed from the actual specimens during the final abrasive operation.

Highly accurate measurements of the material removed, made during the preparation of the cylindrical specimens, showed that enough was removed to get below the deepest scratches likely to have been present except in the case of the superfinished cylindrical surfaces and here it is probable that residual scratches contributed to the deepest maximum roughness. The reason for eliminating residual scratches as far as possible was to obtain surfaces representative of the final abrasive operation only. This was done by continuing, when necessary, the abrasive operation beyond the time that might be considered usual in commercial practice.

As regards the flat specimens, our records show that residual scratches from the preceding operation were definitely present in the finer hypolapped surface, in both sandpapered ones and in the finest superfinished one; there is also a possibility that the same was true for the other two superfinished surfaces. In all other cases, it is certain that enough stock was removed to eliminate all residual scratches.

To the extent that commercially prepared surfaces do contain residual scratches, the conversion factors reported in this paper for deepest maximum roughness may be low. Since the depth of the residual scratches obviously depends on the manner in which the surface was prepared prior to the final operation, it is not possible to predict how the conversion factor for deepest maximum roughness should be corrected in such cases. This, however, is not particularly important inasmuch as even in the absence of residual scratches there is considerable uncertainty concerning the importance of the deepest maximum roughness, a quantity that does not appear to be a true characteristic of a surface. The main purpose in listing the deepest maximum conversion factors was to show why such high values of h_{\max} have been reported by others for very smooth surfaces. The thing to be kept in mind is that one of the really significant characteristics of a surface, the predominant peak roughness, is not affected by residual scratches, so that the corresponding conversion factors are likewise not affected.

The author is in general agreement with the comments made by Mr. Williamson, especially about the desirability of further work, the present study being essentially of an exploratory nature. One idea that this paper should dispel is the widely prev-

alent one that commercial instruments for measuring roughness, furnished with tracer points of 0.0005-in. radius, lose their sensitivity below approximately 10 microinches rms, thus causing the conversion factor to increase very rapidly with decreasing meter reading. Absolutely no evidence was found to substantiate this belief, as will be seen by referring to Table 1 in the paper, where conversion factors are listed for obtaining predominant peak roughness from profilometer readings. Thus in the second numerical column in that table it is seen that for surfaces finished by a given method there is no tendency for smoother surfaces to give higher conversion factors. In fact, for those methods of finish which show any trend at all, whatever trend there is, is in the opposite direction. The results also show that the method of producing the surface affects the relationship between meter reading and peak-to-valley distance.

For anyone who wishes to study in detail the extent to which the valleys in a surface are actually bottomed by the tracer point of a profilometer, it is suggested that he draw the vertical section of a 0.0005-in-radius tracer point at a magnification of $100\times$ horizontal and $2500\times$ vertical, and after cutting around its outline superimpose it on the taper sections of Figs. 3 and 4, which have this same magnification.

To aid in construction such a tracer-point section, its dimensions are:

Vertical distance from tip of tracer point	Corresponding total width of tracer point
0.000 in.	0.00 in.
0.025	0.02
0.05	0.03
0.10	0.04
0.25	0.06

When this tracer point is moved along the taper sections it is seen that the point can approach the bottoms of the valleys much more closely and frequently for the ground surface of Fig. 3 than for the sandpapered surface of Fig. 4. The degree to which the bottoms of the valleys can be approached is consistent with the predominant-peak conversion factors of $4\frac{1}{2}$ and 9 found for these ground and sandpapered surfaces respectively, assuming that a taper section capable of being bottomed completely would give a conversion factor of about 3.

Carry-Over in Locomotive Boilers

By ARTHUR WILLIAMS,¹ EAST CHICAGO, IND.

While tremendous advances in feedwater treatment to protect boiler heating surfaces from scale, corrosion, and embrittlement have been made, the methods commonly used on railroads have been accompanied by an increasing degree of foaming troubles. According to statements of the American Railway Engineering Association, the introduction of alkaline sodium compounds, while reducing the scale problem, has increased the foam-producing capacity of the water supplies. This paper approaches a solution to the problem of carry-over by discussing the mechanisms which cause other than dry steam to leave the boiler. The most important type of carry-over is probably that due to foaming. Carry-over by effervescence is also discussed. The effects of carry-over and methods of prevention are treated in detail. In the study of the problem and its correction numerous tests have been conducted by the author's company, and by the A.R.E.A., and individual railroads. These are reported at some length, the results showing that proper control of feedwater treatment will help minimize foaming. Antifoam compounds increase the concentrations that may be carried in the boiler, but concentration must be controlled either manually or by automatic blowing. Apparatus of various types for this purpose is described, as well as a suitable design of steam separator, which is essential to separate the carry-over from the steam, and discharge the carry-over to the atmosphere.

INTRODUCTION

THIS paper deals mainly with carry-over in locomotive boilers, its causes, effects, and prevention. It is proper to make some mention first of feedwater treatment since this has a great deal to do with the amount of carry-over that may take place. The main objectives of feedwater treatment are to protect the boiler and its heating surfaces from scale, corrosion, and embrittlement. It is not the purpose of this paper to cover the chemistry of feedwater treatment. Water-treatment engineers, working with the highly specialized knowledge available, have accomplished results without which the locomotive could not hope to approach its present state of maximum power output with high availability.

There is no standard treatment for feedwater and each case must be studied by those with the proper knowledge and experience. There is still a great deal to be learned about the reactions that take place inside a boiler using treated water, and new advances are continually being made in the art. However, there is no question as to the excellent results obtained from recognized treatments for locomotive-boiler feedwater in general use at the present time.

The details of the various chemical processes employed, the practical application, and the supervision necessary have been widely covered in the literature, outstanding among which are papers and reports presented before this Society, the American Railway Engineering Association, and other organizations.

¹ Chief Engineer, The Superheater Company. Mem. A.S.M.E.

Contributed by the Railroad Division and presented at the Annual Meeting, New York, N. Y., Nov. 27-Dec. 1, 1944, of THE AMERICAN SOCIETY OF MECHANICAL ENGINEERS.

NOTE: Statements and opinions advanced in papers are to be understood as individual expressions of their authors and not those of the Society.

Unfortunately, with the methods commonly used on railroads for prevention of scale, the troubles with foaming have increased in proportion to the rate at which the scale deposits on the boiler heating surfaces have decreased. This is clearly illustrated by the following statement made in a recent American Railway Engineering Association (A.R.E.A.) bulletin (1):² "A generation or so ago, with little water treatment, the major action of dissolved solids was to form scale, and foaming was not a problem. By proper treatment of water supplies, scale is no longer a problem, but the introduction of alkaline sodium compounds has increased the foam-producing capacity of the water supplies."

CAUSES OF CARRY-OVER

In this paper, carry-over is defined as any substance leaving the boiler other than dry steam. This includes moisture in any form, regardless of the mechanism which caused it to enter the steam path, and also suspended solids.

It is conceivable that carry-over could be caused by a mechanical action due to the natural circulation in the boiler and attributable only to the boiler design. In such a case, carry-over would occur with any water, no matter how pure it might be. In general, this is not thought to be the case with locomotive boilers of conventional design. It is well known that identical locomotives will have different characteristics with respect to carry-over when operated in different districts with different water. It would seem therefore that carry-over in locomotive boilers must be associated with the water in the boiler and its characteristics due to the nature and quantity of dissolved and suspended solids. It is not meant to infer that the extent of carry-over resulting from foaming is not influenced by the design and details of the boiler, but that the carry-over is primarily due to the condition of the water.

The most important type of carry-over is probably that due to foaming. There is also some evidence that a carry-over can occur which is not due to the presence of a dense foam. A theory has been advanced that this is caused by the bursting of bubbles on the steam surface.

FOAMING OF BOILER WATER

There has been considerable discussion regarding the influence of dissolved solids and suspended solids on foaming characteristics. With water treatments in general use on railroads, both are increased, so that it is not possible to draw any conclusions in this respect. The question as to the effect of suspended solids in the foaming of boiler water is covered thoroughly in a report by Foulk (2) presented by the Joint Research Committee on Boiler Feedwater Studies in 1935.

In the early part of this century the general belief seemed to be that suspended solids were necessary for foaming to occur. This appears to be based mainly on a report by Koyl on the foaming of water in locomotive boilers, which has been referred to and quoted in a number of papers and textbooks. A paper by Foulk in 1924 (3), reported tests at atmospheric pressure which demonstrated the production of a persistent foam due to the stabilizing action of solid matter. In 1927, a paper by Joseph and Hancock (4) reported certain tests which for the particular conditions investigated indicated no effect by suspended solids on foaming.

² Numbers in parentheses refer to the Bibliography at the end of the paper.

Further tests by Hancock (5) in 1930 confirmed these conclusions, with tests at 160 psi pressure.

In 1932 the first of a series of three papers by Foulk and others was published. The first paper (6) covered experiments at atmospheric pressure and showed that different kinds of solid matter exhibited widely varying degrees of foam-stabilizing ability, and that this stabilizing power was lost in some cases on prolonged boiling. The second paper (7) reported tests made at 100 to 150 psi and showed that solids which have lost their foam-stabilizing effects may actually reduce foaming because of the greater smoothness of boiling induced. In this series of tests the work done by Joseph and Hancock was duplicated as closely as possible, and a good agreement was obtained with their results.

The third paper (8) reports experiments at 250 psi pressure with calcium carbonate formed inside the boiler in different ways. Calcium carbonate, precipitated inside the boiler by the decomposition of calcium bicarbonate, reduced the foaming. Calcium carbonate, precipitated by pumping sodium-carbonate solution into the calcium chloride in the boiler, gave inconclusive results. Calcium carbonate, precipitated by pumping calcium-chloride solution into sodium carbonate in the boiler, increased the foaming but, after several hours of contact with the hot water in the boiler, this last form of calcium carbonate lost its effect on foaming. It was also established that magnesium hydroxide, precipitated along with calcium carbonate in an excess of sodium carbonate in the boiler, counteracted the tendency of the carbonate to increase the foaming. On the basis of the foregoing it seems that solid matter may or may not increase foaming, depending upon the physical nature of the matter.

The paper by Joseph and Hancock (4) reports tests with pressures from 70 to 165 psi indicating a decrease in foaming with increasing pressure. The tests by Foulk and Whirl (7) show that the effect of solid matter on foaming is less at 150 psi than at lower pressures. While these two series of tests indicate a trend, it would not be safe to assume a continued decrease in foaming with increasing pressure without further data.

There seems to be a general agreement that most types of oil or organic matter will increase foaming. Foulk and Hansley (6) reported tests at atmospheric pressure in which the removal of oil from boiler scale greatly reduced its foaming tendencies. Hancock (5) reported tests with river water showing definitely the effect of organic matter. With the water at a concentration of 1000 ppm (58 grains per gal) and 25 ppm (1.5 grains per gal) organic matter, the carry-over observed in a laboratory boiler was 50 per cent. After removing the organic matter, the carry-over was reduced to zero under the same test conditions.

Undoubtedly, the quantity and kind of dissolved solids in the boiler water have a great influence on foaming. In the tests referred to, a great number of salts in solution have been investigated. In general, these cover the salts found in practice in boilers. In most cases experiments were made with only one salt in solution at a time.

The A.R.E.A. bulletin (1), for example, gives a very interesting report by the Subcommittee on Mechanics of Foaming and Carry-Over in Locomotive Boilers. A number of tests were run at atmospheric pressure with a concentration of 2570 ppm (150 grains per gal) and varying proportions of sodium sulphate, sodium carbonate, and sodium hydroxide. Water was evaporated in glass tubes, and the rate of evaporation was adjusted so that the volume of steam produced per square foot of water surface was the same as for a locomotive operating at 285 psi. The height of foam produced was measured for each solution tested and the results plotted so that the foam height could be determined for all proportions of the three sodium salts. Although all tests were run with same concentration, foam height varied from practically nothing to 17 in., depending upon proportions of the three salts.

There is general agreement that the rate of evaporation and the height of the water level in the boiler will have a marked influence on the amount of carry-over. This is true regardless of the method by which carry-over may be produced. Even more important than the rate of evaporation is a sudden change in the rate. This is referred to in several of the papers on this subject and has been demonstrated in locomotive road tests that will be described later in this paper.

The average rate of evaporation of a modern locomotive boiler is of the order of 350 to 450 lb per sq ft of total water surface per hr, with the boiler evaporation at its maximum. The rate of evaporation will vary considerably at different points in the boiler. A typical example is shown in Fig. 1, in which the total evaporation was taken from test results. The evaporation in the firebox was calculated by subtracting the total heat in the gases at the back tube sheet from the total heat released in the firebox. Knowing the evaporation from the entire boiler and from the firebox, and the heat absorbed by the superheater, it was possible to determine the evaporation from the flues and tubes. The relative heat absorbed by different parts of the firebox was based upon consideration of the combustion conditions in the firebox. The variation in gas temperature between the back and front tube sheets was calculated, and the amount of heat absorbed at any point made proportional to the mean-temperature difference between the gases and the heat-absorbing surface. The highest liberation rate is at the back head where the back head, side sheets, and arch tubes are all releasing steam. As would be expected, there is a second high point at the back tube sheet, where there is a substantial concentration of heating surface at a high gas temperature.

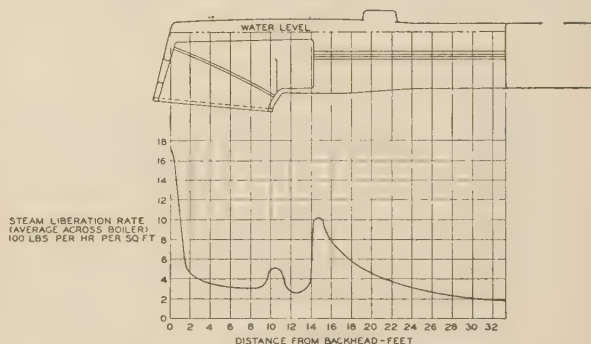


FIG. 1 STEAM-LIBERATION RATES IN LOCOMOTIVE BOILER

As noted in Fig. 1, the liberation rates shown are the average across the boiler at any point between the back head and the front tube sheet. At points along the firebox, the liberation rates will be higher at the sides than in the center.

Since the rate of foaming depends upon the combination of salts in solution, the working pressure, and the rate of evaporation, it is difficult to correlate the various investigations that have been made. In the tests by Joseph and Hancock (4), the pressures varied from 125 to 155 psi and the rate of evaporation from 50 to 100 lb per sq ft of water surface per hr. In the tests by Foulk and Brill (8), the boiler pressure was 250 psi, and the rate of evaporation 1150 lb per sq ft per hr. The tests reported by the A.R.E.A. bulletin (1) were at atmospheric pressure with a rate of evaporation of 29 lb per sq ft per hr, giving the same volume rate as 500 lb per sq ft per hr at a pressure of 285 psi.

FOAMING TESTS CONDUCTED

In approaching the problem of carry-over in locomotive boilers, some tests were made in the laboratory of the author's company

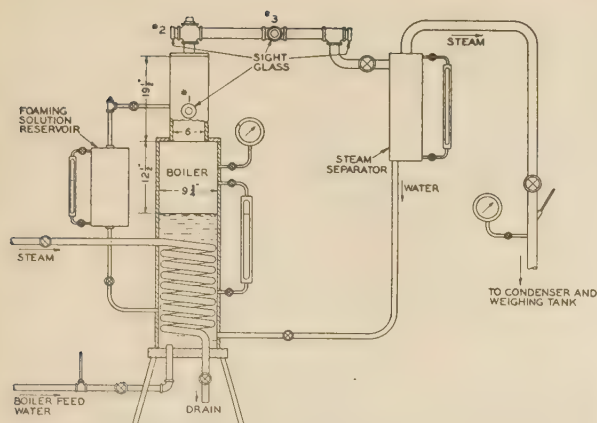


FIG. 2 APPARATUS FOR TESTS WITH FOAMING SOLUTIONS

at East Chicago, Ind., in 1939. A diagram of the test apparatus is shown in Fig. 2. The boiler had an inside diameter of $9\frac{3}{4}$ in., and was operated at 180 to 190 psi pressure, steam being generated by passing steam from an outside source through coils in the boiler. The steam and water leaving the boiler were led to a steam separator. The steam leaving the separator was throttled to a low pressure, and the moisture in the steam determined by observations of the temperature and pressure after throttling. This moisture was never greater than 0.8 per cent. The steam was then condensed and weighed. The water leaving the separator was returned to the boiler. A reservoir with a foaming solution was connected to the boiler and the slight quantity of solution necessary to correct for the moisture in the steam leaving the separator was fed to the boiler so that the concentration was maintained constant during a run. The boiler was fed with Lake Michigan water which was heated nearly to saturation temperature before entering the boiler. The quantity of water returned from the separator to the boiler was determined by closing a valve in the return line for a short period and observing the increase in water level in the separator. Sight glasses were located in the top of the boiler and in the line between the boiler and the separator so that visual observation could be made of the foam produced.

The results are shown in Table 1, each line being the average of several tests. Test series Nos. 1 and 2 were made with a soap solution, and Nos. 3 and 4 with sodium salts, using 80 per cent sodium sulphate and 20 per cent sodium chloride. Test series Nos. 1 and 3 were made with liberation rates of 800 to 1000 lb per sq ft per hr and may be considered as representing conditions which could be found in a locomotive boiler when there is a sudden increase in the rate of evaporation. In test series No. 1, a liberation rate of 998 with a solution of 5000 ppm (292 grains per gal) soap gave 58 per cent carry-over, and in test series No. 2,

increasing the liberation rate to 2470 with the same solution gave 81 per cent carry-over. Test series No. 3 with a liberation rate of 814 and 1400 ppm (82 grains per gal) sodium salts gave 47 per cent carry-over. Test series No. 4 was made under extreme conditions with a liberation rate of 3460 and 2800 ppm (163 grains per gal) concentration of sodium salts and resulted in 91 per cent carry-over. Observations through the sight glasses were very interesting. With all of the tests reported in Table 1, sight glass No. 1 showed the top of the boiler to be full of foam. Sight glass No. 2 at the top of the pipe leaving the boiler showed the foam to be partly collapsed, and sight glass No. 3 showed that the foam at this point was almost completely collapsed into a liquid. These tests showed that, under conditions approximating the worst that may be found in locomotive operation, it was possible for foam to carry a very high percentage of moisture, and that it should not be difficult to collapse this foam. This would indicate the desirability of an apparatus to collapse the foam and to be capable of discharging large amounts of moisture.

In 1938, a series of investigations was started by the Electro-Chemical Engineering Corporation and Dearborn Chemical Company to study visually the behavior of the water and steam in a locomotive boiler. Tests made on the St. Louis-San Francisco, Texas and Pacific, and Kansas City Southern Railways led to an elaborate investigation on the Missouri Pacific Railroad. These investigations are reported in a paper by Carrick (9).

In the Missouri Pacific tests the inside of the steam dome was illuminated with special light bulbs and visual observations made of conditions inside the boiler through six sight glasses in the steam-dome cover. Sufficient illumination was furnished so that motion pictures could be made with the boiler operating under foaming conditions. One series of tests was made with the engine standing, and a second series with the locomotive in road service. The observations indicated that foam would rise in the boiler until the high-velocity steam would carry the foam into the dry-pipe entrance. The foaming of the water could not be gaged by the boiler-water concentration or by the water level in the gage glass in the cab. Under the worst conditions, the foam would completely fill the dome. As a result of these tests, the "Electromatic" foam-collapsing system was developed. This device will be described later in the paper.

CARRY-OVER BY EFFERVESCENCE

It is possible for a small particle of liquid to be thrown upward due to the bursting of a bubble on the surface of a liquid. This condition has been investigated in detail by Seniff and reported in a bulletin of the American Railroad Engineering Association (10). The investigation showed that, in the absence of a foam layer, bubbles would burst almost instantly on reaching the surface of the water, and in bursting throw up a small particle of water. The size of the particle depended apparently upon the size of the bubble, and the height to which it was thrown de-

TABLE 1 TESTS WITH FOAMING SOLUTIONS

Test series no.	Boiler pressure, psi	Water temp entering boiler, deg F	Quantities leaving boiler lb per hr			Liberation rate, lb per hr per sq ft water surface	Moisture from boiler, per cent	Remarks
			Total steam and moisture	Dry steam	Moisture			
1	194	368	518	216	302	998	58.3	5000 ppm (292 grains per gal) soap
2	192	348	1280	238	1042	2470	81.4	5000 ppm (292 grains per gal) soap
3	182	363	422	223	199	814	47.2	1400 ppm (82 grains per gal) sodium salts; 80 per cent sodium sulphate, 20 per cent sodium chloride
4	181	365	1797	159	1638	3460	91.2	2800 ppm (163 grains per gal) sodium salts; 80 per cent sodium sulphate, 20 per cent sodium chloride

TABLE 2 ANALYSES OF SCALE IN SUPERHEATER UNITS

Sample	1	2	3	4	5	6	7	8	9	10	11
Oil.....	0.05	0.05	0.08	0.33	0.06	Per cent 0.03	2.25	1.40	1.01	23.90	Present
Other organic and volatile.....	1.67	...	1.30	6.04	5.20	...	4.12	0.40	11.26	13.05	32.80
Silica.....	16.23	39.35	51.05	37.07	31.36	37.62	33.80	9.70	7.38	12.10	6.85
Calcium carbonate.....	22.42	14.70	4.60	3.16	17.82	37.07	37.93	19.55	50.88	24.10	41.80
Lime ^a	3.27	...	17.11
Calcium sulphate.....	...	0.88	Trace	0.56	12.08	Trace	1.30	0.88	0.06	6.47	...
Magnesia.....	0.60	2.91	24.84	3.04	1.89	15.35	10.58	4.49	4.65	5.75	10.53
Iron oxide.....	5.02	17.6	10.82	3.62	10.00	4.00	5.62	40.00	4.50	9.20	2.49
Alumina.....	47.94	21.16	7.00	16.70	20.64	5.70	4.00	23.00	19.53	2.40	2.00
Sodium chloride.....	0.31	1.75	...	0.18	0.40	...	0.21
Sodium sulphate.....	3.43
Alkalies.....	2.64	10.00	0.58	...	3.03	3.55
Oil and other organic matter.....	1.7	0.05	1.4	6.4	5.3	0.08	6.4	1.8	12.4	37.0	32.8
Silica and alumina.....	64.2	60.5	58.1	53.8	52.0	43.3	37.8	32.7	26.9	14.5	8.9

^a In combination with other oxides.

pended upon the film tension and resulting internal pressure of the bubble. One series of observations was made in a test boiler with pressure similar to that in use on locomotives. A special lighting technique was used so that the extremely small particles could be seen. It was found that, under the particular test conditions used, the larger particles which were quite visible to the eye were only a small part of the total being projected into the steam space by the bursting bubbles. Some of these particles were so small that they remained suspended in the steam. With low boiler-water salt concentrations below 1000 ppm (58 grains per gal), there was a preponderance of the smaller-size particles. At higher concentration with a foam layer present, there were more of the larger-size particles.

Other tests were made with air bubbles produced in water at atmospheric pressure and temperature, the results being similar to those observed in the boiler under steam pressure. While there may be some question as to the exact relationship between foaming and effervescence, it is a fact that under road-operating conditions, the carry-over from the boiler can have different degrees of density as determined by its electrical conductivity and by visual observation.

Later in this paper, tests are described in detail of a steam dryer, with a discharge to the atmosphere, operating on a locomotive in road service. Certain of the observations made during these tests relate to the nature of carry-over. An electrode was located in the dome cover with the end close to the entrance of the tangential steam dryer. Through a relay this would light an electric bulb in the cab when foam was present of sufficient density to complete the circuit. Observation of action of the discharge valve from the steam dryer showed when carry-over was occurring. There were times when the dome electrode circuit did not light the cab signal, but the dryer discharge valve was operating, indicating that carry-over was taking place. In these same tests, visual observations were made of conditions inside the boiler with sight glasses. At times the foaming was so bad that nothing could be seen through the sight glass except a dense opaque mass completely filling the dome. At other times, the substance in the boiler steam space appeared to be hazy or semitransparent. It was not possible to observe the exact nature of the water and steam mixture under such conditions. It can, however, be definitely stated that the nature of carry-over will vary considerably with respect to its average density as determined by its electrical conductivity and by visual observations.

EFFECTS OF CARRY-OVER

The effects of carry-over will of course depend upon the nature of the substances leaving the boiler. The greater part of carry-over is usually moisture but it is possible to have an appreciable amount of solid matter. Table 2 gives the analyses of scale found in superheater units from eleven different railroads in all

parts of the country. It can be assumed that some of this matter would find its way into the multiple throttle, valve chests, and cylinders. In most cases, there is a high proportion of silica and alumina. With such substances being carried into the valve chests and cylinders, it can easily be understood why carry-over will cause rapid wear of bushings and packing. At the same time, lubrication will be adversely affected and wear of reciprocating parts accelerated. The analyses are arranged in descending order as to the percentage of silica and alumina taken together. It is interesting to note that, as the percentage of these two substances decreases, the amount of oil and other organic matter increases.

Probably the worst effect of carry-over is in relation to the superheater. The superheater is designed to take steam with no appreciable amount of moisture and raise its temperature so that the maximum efficiency can be obtained when the steam does its work in the cylinders. Any moisture that is in the steam will reduce the steam temperature at the cylinders. For a given operating condition the amount of heat taken up by the superheater units is fixed, and the moisture entering the superheater will reduce the final steam temperature, since some of the heat will be required to evaporate this moisture before superheating can begin. Steam tables show that for the same heat absorbed per pound of steam, there is a decrease in superheat of approximately 15 deg for each 1 per cent moisture entering the superheater. A loss of 15 deg steam temperature means a decrease of 1.5 to 2 per cent decrease in cylinder efficiency with a corresponding increase in water and fuel consumption. A severe carry-over will result in the loss of all the superheat, so that saturated steam and water will enter the cylinders.

Tests made many years ago showed that the use of superheated instead of saturated steam resulted in an increase of 25 to 30 per cent in efficiency and power. These tests were made with relatively low superheat. With the high steam temperatures obtained on modern steam locomotives, the loss of power due to loss of superheat can be even greater.

Fig. 3 illustrates the relation between locomotive steam rates and superheat. The values given are for 250 psi.³ An increase in the steam rate means either a decrease in cylinder horsepower or an increase in fuel and water consumption.

With large sums of money being spent for fuel it is readily seen that carry-over may cause an appreciable increase in the fuel bill. There is also an effect on the general railroad operation. The carry-over is likely to occur when the locomotive is being worked at its hardest. This means that, at a time when the maximum power output of the locomotive is required so that train movements may be made with maximum efficiency, the carry-over takes place and decreases the power output of the locomotive.

³ Taken from Table 25 of "The Steam Locomotive," by Johnson (11).

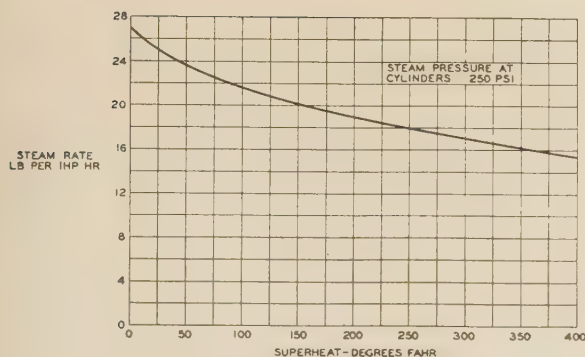


FIG. 3 LOCOMOTIVE STEAM RATES IN RELATION TO SUPERHEAT

Continued carry-over may result in the failure of the superheater units in service. The superheater-unit metal transfers heat from the hot flue gases to the steam inside the tubing. The temperature which the metal reaches depends upon the heat-transfer conditions, so that an equilibrium is established between the heat received by the metal from the flue gases and transferred from the metal to the steam. These conditions depend upon the temperatures of the gas and the steam, and the heat-transfer coefficients at the outside and inside surfaces. For a given pressure and temperature, the heat-transfer coefficient between the metal and the steam depends upon the velocity of the steam. The lower this velocity, the less the pressure drop through the superheater, but the lower the heat-transfer coefficient. Proper design of superheater units will insure that, under various operating conditions, the relations between steam velocity and heat transfer are such that metal temperatures will not be in excess of a safe figure. The maximum metal temperatures are always at the back end of the superheater unit, and it is at this point that failures occur. When the back end of the unit is heavily coated with scale, it is obvious that the failure is due to the scale deposits. It is not so easy to understand those failures which occur in actual practice when the metal is practically free from scale at the point where the failure has occurred.

Assume that a locomotive is being worked at high capacity, which means a high temperature of the gases at the back tube sheet and a high gas velocity in the superheater flues; under these conditions, there should be a correspondingly high steam velocity inside the superheater-unit tubing. Now assume that in one unit the steam flow is restricted, such as would occur if there were a scale deposit at any point in the tubing between the entrance and exit. One effect is that the steam temperature leaving this particular unit will increase because there is a reduction in the weight of steam, and therefore an increase in the heat added per pound of steam. Furthermore, the decrease in the steam velocity will lower the heat-transfer coefficient at the inside surface of the tubing. Both these effects increase the metal temperature. The relation between the steam and metal temperatures at the back end of a superheater unit for various steam velocities and with constant flow and temperature of gases at the back tube sheet are shown in Fig. 4. In making the calculations for Fig. 4, corrections have been made for the decrease in mean temperature difference between the flue gases and the steam as the steam temperature increases, and an increase in radiation from the superheater-unit metal to the flue in which it is located due to the increase in metal temperature.

It can be seen that a reduction in the proper steam velocity will give an appreciable increase in the metal temperature. With a steam flow approximately 50 per cent of normal, the metal temperature reaches 1015 F, and with 23 per cent of normal, the

metal temperature is 1200 F. At such temperatures, there is a rapid attack on the steel by steam. This is described in an article by Corey (12). At temperatures of 1000 F, some oxygen is available from the thermal decomposition of steam. Corey states that the partial pressure of oxygen from this source at such temperatures is too low to account for the rapid attack on the steel, and that a reaction takes place directly between the steel and the steam. The reaction results in the formation of magnetic oxide and hydrogen.

A number of investigations have been made at Purdue University to determine the corrosion rate of various steels in contact with steam at elevated temperatures. The results for mild steel show a slight amount of corrosion at 1000 F. At 1050 F, the corrosion rate starts to increase rapidly. At 1200 F, the corrosion rate is 15 times greater than that at 1050 F.

In comparing laboratory tests with the results obtained under service conditions, consideration must be given to the effect of alternating thermal and mechanical stresses in the metal which tend to cause fissures through which the steam can reach the metal.

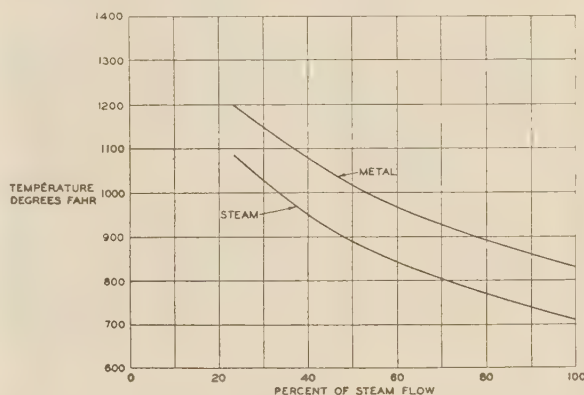


FIG. 4 METAL AND STEAM TEMPERATURES AT BACK END OF SUPERHEATER UNIT WITH RESTRICTED STEAM FLOW

In this respect, the conditions in a locomotive superheater are perhaps the worst that can be imagined. Every change in the locomotive operating conditions results in a change in the temperatures and stresses in the superheater-unit metal. It is the combination of elevated metal temperatures and alternating stresses which results in the rapid deterioration of superheater units reported in a number of cases. The failure may occur in the superheater-unit return bend or in the tubing close to the return bend.

Fig. 5 shows a return bend that has failed in service. For comparison, a new return bend made by the same process and of identical material is also shown. The black material at the inside edge of the failed return bend is magnetic oxide. Comparison of the inside contours of the two return bends indicates the continual process of formation of magnetic oxide and subsequent breaking away of part of the layer. The process continues until the metal becomes sufficiently thin for steam pressure to rupture the metal.

With the metal at elevated temperatures, there will also be corrosion of the steel by the oxygen in the flue gases in contact with the outside of the unit. The extent of this corrosion will depend upon the condition of the outside surface of the unit. It will usually be less when coal is used as a fuel than with oil. This is because there is usually some slag formation at the back end of the unit with coal. With an oil burner the sanding of the flues will keep the metal surface clean and allow increased contact between the steel and the oxygen.

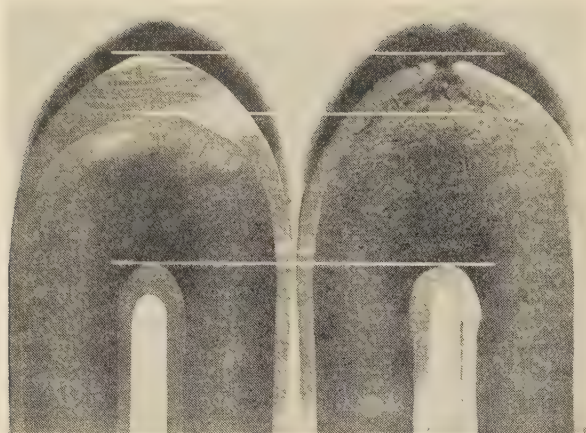


FIG. 5 NEW AND FAILED SUPERHEATER-UNIT RETURN BENDS

It has been shown that the corrosion of the superheater-unit metal at elevated temperatures is due to a restriction in the steam flow. Since such restriction is caused by deposits in the superheater-unit tubing which result from carry-over, it is the carry-over which must be held responsible for the effect of superheater-unit failures on the efficiency of railroad operation.

A superheater unit that fails in road service may cause a delay in train movement. The replacement of the unit means a delay in the roundhouse with time out of service for the engine. There is a direct expense chargeable to the actual work done in replacing the superheater unit. Even more important is the expense, owing to the fact that the large amount of money invested in the locomotive is not available for the production of revenue to the railroad.

PREVENTION OF CARRY-OVER

The prevention of carry-over may be accomplished by control of the foaming, the removal of the foam after it is formed, or a combination of the two methods. In the first group are feedwater treatment, antifoam compounds, and control of concentration for the particular operating conditions. It is obvious that anything that can be done with feedwater treatment to reduce the dissolved and suspended solids in the boiler water and decrease the amount of organic matter will be beneficial with respect to foaming. Any control in this direction must of course be considered with relation to prevention of scale, corrosion, and embrittlement.

ANTIFOAM COMPOUNDS

There are various antifoam compounds which are effective in controlling foaming. For a number of years the benefits obtained from castor oil in some form has been known. The suggestion has been made by Foulk (3) that the destruction of foam is due to the destruction of the stabilizing action of the solid matter rather than to any change in the surface tension of the liquid. This theory is perhaps supported by the statement in the A.R. E.A. bulletin (1) that there is no evidence that the action of antifoam compounds is based on surface tension changes. In recent years, amide types of antifoams have been found to give better results than the castor-oil compounds.

CONTROL OF CONCENTRATION IN BOILER

For given operating and feedwater conditions, the most general method for controlling carry-over is by blowing down the boiler to reduce the concentration of solids. Since this reduces both

the dissolved and suspended solids it does not make a great deal of difference which is the more important in the production of foam. The blowing down may be done in any of three following ways:

- 1 With manual control by the engine crew. If the boiler-water concentration is controlled by this method only, it is necessary for the supervisory forces to give proper instructions to the engine crews so that the blowing is in correct relation to the feedwater and operating conditions. It is also essential that a proper control be established to be sure that the instructions are carried out. The most common method of control in use on railroads is to take samples of the boiler water at the beginning and end of each run and to keep records of the concentrations.

- 2 By a continuous blowdown. With this type of equipment, a predetermined quantity of water is continuously discharged to the atmosphere while the locomotive is working. The blowdown valve is automatically opened in response to steam-chest pressure. The quantity that is to be discharged is determined by the nature of the feedwater used, the type of feedwater treatment, and the engine operation for the territory in which the engine runs. An orifice is then used so that this particular rate of blowdown will be maintained. The discharge from the blowdown valve is taken to a separator from which the steam is discharged to the atmosphere so that only the sludge and water are discharged to the ground.

- 3 Intermittent blowdown, automatically operated by the conditions existing in the boiler at the time. This is accomplished by a device known as the "signal foam-meter." An electrode is mounted in the steam space in the boiler at a distance above the normal water level determined by locomotive operating conditions. When the foam in the boiler rises and contacts the electrode, an electrical circuit is completed which, through a relay, opens a solenoid valve. The solenoid valve admits air pressure to a piston which opens a blowoff valve connected to the boiler. In this way the amount of blowing is proportional to the foam-producing characteristics of the water in the boiler. A second shorter electrode in the boiler, when contacted by foam, lights a warning signal in the cab and indicates to the engineer that the foaming is too much for the automatic blowoff cock to control and that the manual blowoff cocks should be opened, and possibly the rate of working of the locomotive reduced.

REMOVAL OF CARRY-OVER FROM STEAM

It is possible to prevent carry-over from leaving the boiler by an apparatus designed to separate the moisture and solids from the steam and blow them to the atmosphere. Such an apparatus must take care of any kind of foam or effervescence leaving the boiler. One such device, known as the "Electromatic Foam-Collapsing System," is shown in Fig. 6. A trough is located in the boiler in the vicinity of the steam dome and dry pipe, the top of the trough being located above the water level in the boiler. If foaming takes place, the foam level will rise until it reaches the top of the trough. The foam will then collapse and the water

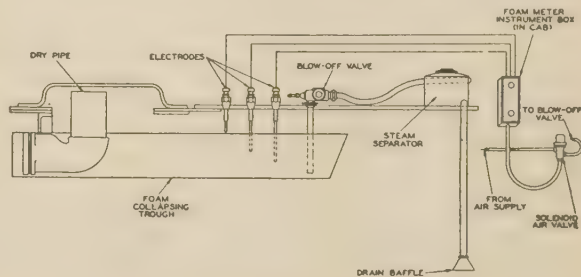


FIG. 6 ELECTROMATIC FOAM-COLLAPSING SYSTEM

and solids in the steam will fall into the trough. When the water contacts the medium-length electrode, a circuit is completed and an air-operated blowoff valve is opened in the same way as described in connection with the foam-meter. The blowoff valve discharges the contents of the trough to the atmosphere through a steam separator and will remain open until the water level is below the longest electrode. The third and shortest electrode operates a warning signal light in the cab.

STEAM-SEPARATOR SYSTEM TESTS

Another system consists of a steam separator in the boiler connected to a discharge valve on the outside of the boiler so that any carry-over is blown to the atmosphere. The development of this device called for a large number of tests to be made in road service under foaming conditions and resulted in a great deal of valuable information. The arrangement of the apparatus is shown in Fig. 7.

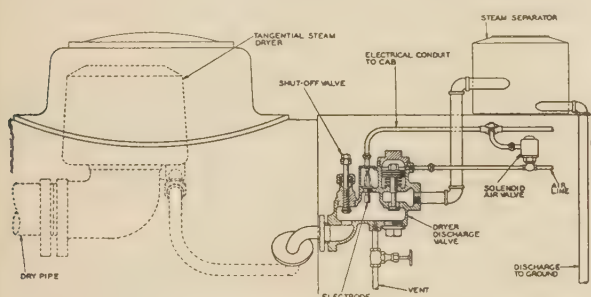


Fig. 7 STEAM DRYER WITH DISCHARGE TO ATMOSPHERE

Previous investigations had shown the possibility of large quantities of moisture being carried over under foaming conditions. Considerable development work resulted in a design of steam separator known as the "tangential dryer," which is extremely efficient at all steam velocities and is capable of handling high percentages of moisture.

Referring to Fig. 7, the tangential dryer is located at the dry-pipe entrance. The discharge from the dryer through which the separated moisture is delivered is connected to a discharge valve mounted on the outside of the boiler. When any moisture is carried into the discharge valve, an electrical circuit is completed through an electrode to operate a relay which opens a solenoid valve. This admits air to the piston which operates the discharge valve. The discharge from the valve is connected to a separator on top of the boiler so that the steam is discharged to the atmosphere and only hot water to the ground. A vent pipe with a small orifice leads from the discharge valve to a point of lower pressure, such as a superheated-steam auxiliary pipe. The small quantity of steam which flows through the orifice keeps the discharge valve free of air and establishes a flow condition which insures the prompt action of the valve as soon as moisture enters the steam dryer.

To determine the performance of the dryer discharge valve, tests were run on a western railroad which was known to have very bad foaming conditions. During the tests the boiler evaporation was from 70,000 to 100,000 lb of steam per hr. The tangential dryer was fitted to a 9½-in. dry pipe, and the 2-in. dryer discharge valve had a capacity of 40,000 lb per hr of saturated water at boiler pressure. The performance of the dryer discharge system was determined by comparative tests made with the system turned on and shut off. The test results are given in Figs. 8 to 11, inclusive. These four tests were run over the same territory on three successive days, with the last two series being run on the same day, so that as far as possible

the tests with the system turned on and shut off were made under the same conditions.

The steam temperature was taken in the steam pipe and also leaving a No. 1 shape superheater unit. This is in the top row of units and is connected into the header at a point nearest to the dry-pipe entrance. Moisture naturally flows first into this shape unit and its presence is indicated by the difference between the temperature of the steam leaving the unit and the steam-pipe temperature. The moisture in the dry pipe was measured by two throttling calorimeters. One was connected to a standard A.S.M.E. sampling tube across the center of the dry pipe. Since the tangential dryer imparts a whirling action to the steam, a second calorimeter was connected to a sampling tube, consisting of a piece of 1/2-in. pipe extending into the bottom of the dry pipe for a distance of 1/4 in., with the side toward the direction of flow cut away.

The four readings mentioned gave an indication as to the extent of carry-over into the superheater. Sight glasses were installed in the dome cover so that visual observation could be made of the conditions inside the boiler. Readings were taken of the water level and the exhaust pressure, the latter being a measure of the rate of working of the locomotive. A record was made of the number of seconds in each minute of testing that the dryer discharge valve was open. It was explained earlier in the paper that a short electrode mounted in the dome cover would operate a signal light in the cab when the water-and-steam density was sufficient to complete an electrical circuit.

The results are given in the form of curves showing the change in the various observations for each minute of testing. The first test, shown in Fig. 8, does not include all of the readings taken in subsequent tests, but is reported because it illustrates a very bad condition of carry-over. With the boiler under foaming conditions, readings were taken for the first 11 min, recorded in Fig. 8, with the dryer discharge system shut off. The steam temperature in the steam pipe was at boiler saturation temperature, and water was being thrown out of the stack and through the cylinder cocks, which were open. After 11 min, the dryer discharge system was turned on. The discharge valve opened and blew steadily for 3 min and at short intervals thereafter. At the end of 3 min, the steam temperature had increased from 400 to 660 F, and 19 min

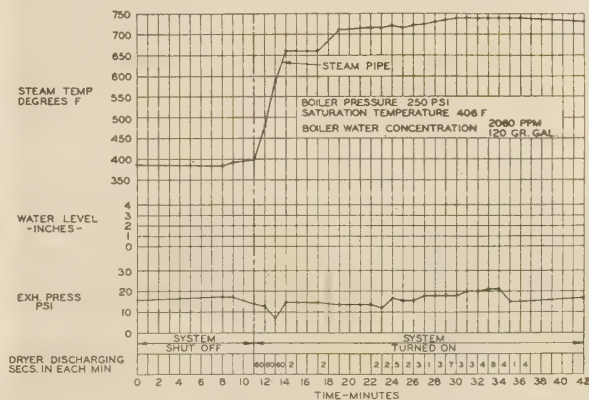


Fig. 8 TEST OF STEAM DRYER WITH DISCHARGE TO ATMOSPHERE

after the dryer discharge valve had been opened the steam-pipe temperature had reached 740 F. From the 22nd min to the 37th min, the dryer was discharging for intervals varying from 1 to 8 sec per min, showing that carry-over into the dryer was still occurring, and that the moisture and solids were being separated and discharged to the atmosphere.

STANDARD TESTS ESTABLISHED

After this test, it was realized that it would be better to produce a standard test condition so that the locomotive operation with and without the dryer discharge valve in action could be determined. Fig. 9 shows how this was done. The locomotive was operated at approximately 10 lb exhaust steam pressure and, when conditions were steady, several readings were recorded. The rate of evaporation from the boiler was then suddenly increased by increasing the cutoff, and observations were made of the results of the carry-over.

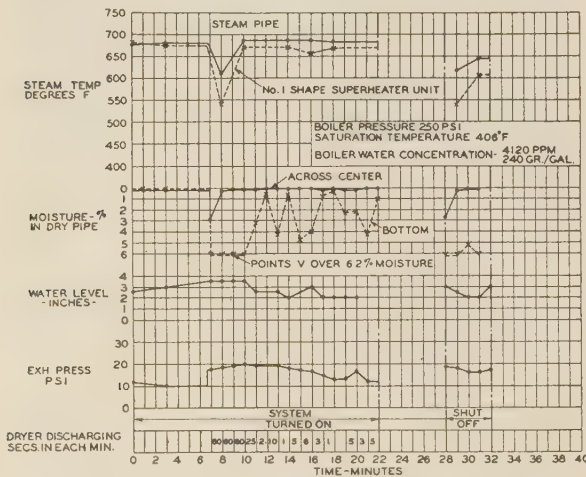


FIG. 9 TEST OF STEAM DRYER WITH DISCHARGE TO ATMOSPHERE

Referring to Fig. 9, the rate of evaporation was suddenly increased just before the 7th min as indicated by a rise in the exhaust pressure from 10 to 18 psi. Immediately, carry-over started and the dryer discharge valve opened. For $3\frac{1}{2}$ min the dryer discharge valve was open continuously. There was a momentary drop in the steam temperatures and increase in the dry-pipe moisture, but after 3 min the steam-pipe temperature was back to normal, and the steam temperature leaving the No. 1 shape unit showed only a slight amount of moisture. The calorimeter connected to the center sampling tube showed dry steam, and that connected to the bottom showed some moisture.

It should be pointed out that, while the moisture readings are represented as actual quantities, they should not be interpreted too literally. It is only possible to obtain a true sample when the steam-and-water mixture is homogeneous, and this is not possible in a dry pipe after the steam has left a dryer which has subjected the steam and water to a centrifugal action. At the end of the test shown in Fig. 9, a few more readings were taken with the dryer discharge system shut off. These readings show moisture entering the superheater as indicated by the steam-temperature and calorimeter readings.

Fig. 10 gives a series of readings taken with the dryer discharge system shut off, thus showing what can occur if no steps are taken to control the carry-over into the dry pipe. As before, the test was started by increasing the rate of evaporation suddenly. The temperature of the steam leaving the No. 1 shape unit dropped to boiler saturation temperature and there was a considerable drop in the steam-pipe temperature. Both calorimeters show moisture in the dry pipe. After 9 min, the observations indicated that the carry-over decreased. This was probably due to the fact that concentration of both dissolved and suspended solids in the boiler had been reduced by the amount carried away. At 18 min,

the carry-over became worse again but not to so great an extent as the first occurrence.

The next series of tests, shown in Fig. 11, was made with the dryer discharge system both turned on and shut off for practically continuous locomotive operation. The test was started with the discharge system shut off, and a foaming condition was created by increasing the exhaust pressure from 10 to 20 psi. Considerable carry-over immediately resulted. The steam-temperature and calorimeter readings show the same alternations in severity of carry-over as pointed out for Fig. 10. At 20 min, the dryer discharge system was turned on. Five minutes later both calorimeters indicated zero moisture and both steam temperatures were together at 675 F. With such readings, it must be assumed that the steam in the dry pipe was practically dry. The dryer discharge valve continued to blow intermittently showing that carry-over into the dryer was still occurring. The train then went through a siding slowly but did not actually stop. After getting back to the main line, readings were continued with the dryer discharge system shut off. With 18 psi exhaust pressure, the steam-temperature and calorimeter readings show a severe carry-over. At 60 min of the test, when both steam temperatures were at the boiler saturation temperature, the dryer discharge system was turned on. The steam temperatures immediately started to increase and moistures indicated by the calorimeters approached zero. At the end of 62 min, the engine came to a stop and the test was ended.

All during these tests, the observations made through the sight glasses were interesting. At the very beginning with good water in the boiler, the surface of the water appeared relatively clear. Later, when the water was in a foaming condition, the surface of the water would usually appear to be a grayish color. When in this condition, an increase in the rate of evaporation would cause the foam level to rise and, when it approached the entrance to the dome, the steam would carry it up so that the dome would be entirely filled. As stated earlier in this paper, the degree of foaming would vary from a condition where the dome was completely filled, and nothing but a dark mass could be seen through the sight glasses, to a hazy or semitransparent condition.

RELATION BETWEEN CARRY-OVER ON WORKING RATE OF ENGINE

One of the most significant results obtained from these tests is the relation between carry-over and a change in the rate of working of the engine. It is always true that foaming will increase when the rate of evaporation is increased, but the effect is very

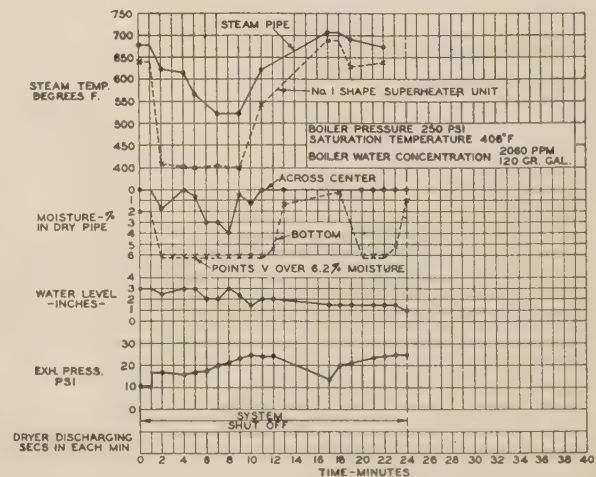
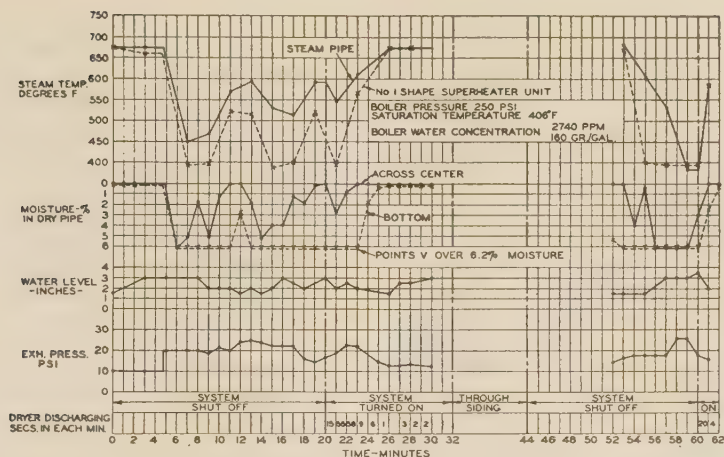


FIG. 10 TEST OF STEAM DRYER WITH DISCHARGE TO ATMOSPHERE



much worse when the rate is changed suddenly. The tests show directly what occurs when there is a sudden increase in the rate of working, as indicated by the increase in the exhaust pressure.

It is possible for carry-over to be sufficiently severe for the engine crew to notice it, as for the conditions illustrated in Fig. 8. Frequently, carry-over is taking place with no indications to the engine crew. Figs. 9 to 11, inclusive, do not show any change in the water level that can be attributed to anything but the normal variations obtained due to track conditions and operation of the boiler feed pump. The condition of the water in the glass during these tests was good at all times. In spite of this, the readings proved that sufficient carry-over was taking place to impair the efficiency of the locomotive and, over a period of time, to result in the failure of superheater units.

SUMMARY

It seems probable that the major cause for carry-over in locomotive boilers is due to foaming. Various investigators in the past have produced evidence both for and against the theory that suspended solids increase foaming. With the feedwater treatments commonly used on railroads, locomotive boilers have to operate with both dissolved solids and suspended solids in appreciable amounts and with as high a concentration as may be permitted so that the amount of heat blown away is at a minimum.

The effects of carry-over are extremely injurious, particularly with respect to wear of valve and cylinder bushings and packing, decrease of cylinder efficiency by the reduction in superheat, and failure of superheater units due to scale restriction.

Proper control of feedwater treatment will help to minimize foaming. Usually, antifoam compounds will increase the concentrations that may be carried in the boiler. The control of the concentration in the boiler is extremely important and may be done manually or by continuous or automatic blowing.

Even with everything possible being done to prevent foaming in the boiler it seems desirable that means should be taken to separate carry-over from the steam and discharge the carry-over directly to the atmosphere. This may be done by means of a suitable design of steam separator connected to an automatically controlled outside-discharge valve.

BIBLIOGRAPHY

- 1 "Mechanics of Foaming and Carry-Over in Locomotive Boilers," American Railway Engineering Association Bulletin 441, Nov., 1943, pp. 58-62.

- 2 "Suspended Solids in the Foaming and Priming of Boiler Water," by C. W. Foulk, *Mechanical Engineering*, vol. 58, 1936, pp. 372-374.
- 3 "Foaming of Boiler Water," by C. W. Foulk, *Industrial and Engineering Chemistry*, vol. 16, 1924, pp. 1121-1125.
- 4 "The Priming of Saline Waters," by A. F. Joseph and J. S. Hancock, *Journal of the Society of the Chemical Industry*, Transactions Section, vol. 46, 1927, pp. 315T-321T.
- 5 "Observations on the Priming of Saline Waters," by J. S. Hancock, *Journal of the Society of the Chemical Industry*, Transactions Section, vol. 49, 1930, pp. 369T-374T.
- 6 "Solid Matter in Boiler-Water Foaming—I," by C. W. Foulk and V. L. Hansley, *Industrial and Engineering Chemistry*, vol. 24, 1932, pp. 277-281.
- 7 "Solid Matter in Boiler-Water Foaming—II," by C. W. Foulk and S. F. Whirl, *Industrial and Engineering Chemistry*, vol. 26, 1934, pp. 263-266.
- 8 "Solid Matter in Boiler Water Foaming—III," by C. W. Foulk and H. C. Brill, *Industrial and Engineering Chemistry*, vol. 27, 1935, pp. 1430-1435.
- 9 "A Motion Picture Study of Locomotive Boiler Foaming," by O. W. Carrick, *Brotherhood of Locomotive Firemen and Engineers' Magazine*, January and February, 1941.
- 10 "Steam Contamination by Aquaglobejection," by R. W. Seniff, American Railway Engineering Association, Bulletin 446, June, July, 1944, pp. 57-76.
- 11 "The Steam Locomotive," by R. P. Johnson, second edition, Simmons-Boardman Publishing Corp., New York, N. Y., 1944, pp. 166.
- 12 "Corrosion by Hot Gases," by R. C. Corey, *Combustion*, vol. 15, 1943, pp. 34-39.

Discussion

R. A. CARR.⁴ The author and his associates have made a comprehensive study of the water carry-over problem. Serious work of this nature is appreciated by everyone interested in the betterment of the steam locomotive.

In his outline of the causes of boiler-water foaming, a distinction must be drawn between the types of organic matter which aggravate foaming. Decayed vegetation in surface waters and sewage or industrial-waste pollution in streams are the principal offenders. Tannin extract, however, also comes under the general term of organic matter and it is widely used as a valuable constituent of locomotive-boiler-water treatment. In addition to other useful characteristics, certain grades of tannin act to reduce foaming.

The specially prepared amines and amides which form the

⁴ President, Dearborn Chemical Company, Chicago, Ill.

basis of the newest antifoam water treatments are also classified chemically as organics and they are definite foam inhibitors.

The visual studies of the interior of a working locomotive boiler made by the Electro-Chemical Engineering Corporation and the writer's company in 1938 are believed to be the first such studies ever made. They forcibly brought out the fact that the foam-creating substances in the boiler water could be removed much more effectively by skimming the contamination from the surface of the boiling water than by depending upon the conventional mud-ring blowoff which is located about as far as possible from the foaming region of the boiler.

At the time foaming develops in a working boiler there is a definite flotation effect taking place. Oil and suspended sludge are carried to the top of the boiler in the foam bubbles, and the quickest way to settle the foaming water by blowdown is to remove this floated contamination. The author has included in his presentation of the carry-over problem the "Electromatic Foam-Collapsing Blowoff System" which was developed from the original "Electromatic Signal Blowoff" as a result of our foaming boiler-water investigations. By operating a blowoff valve from the foam-collapsing trough, and a blowoff valve from the mud ring, through the same electrical circuit, test samples of boiler water have been taken simultaneously from the top and bottom of a foaming boiler. The collapsed foam and water, blown from the trough at the water surface, has contained 137 grains of sludge per gal, while water blown from the mud ring has contained 42 grains of sludge per gal.

Anything which will prevent water carry-over is an improvement in the steam-locomotive boiler. Some sort of automatic blowing is needed, either with or without chemical antifoaming water treatment, and when automatic blowing is combined with means for entrapping and removing water from the steam space, worth-while progress is being made.

J. R. JACKSON.⁵ Having in mind experience with locomotive-boiler waters west of the Mississippi for a number of years past, the writer knows foaming as an increasingly serious operating problem, and that the carry-over of the quality of boiler waters with which we have to deal in many sections of the country is a current major problem which must be solved if the development of the steam locomotive is not to become static. There is no doubt but that the seriousness of the carry-over problem has been increasing during the past few years and that with the extended use of chemically treated water and the gradual increase in size of locomotive boilers, carry-over is adversely affecting efficiency of operation and also increasing maintenance costs in many instances.

As indicated in the paper, there appear to be two ways of controlling carry-over within the present conventional design of locomotive boiler: (1) to correct it at the source through treatment to provide solid water, and (2) to provide mechanical means for preventing carry-over into the superheater if and when foaming occurs.

Being responsible for water treatment on the Missouri Pacific Lines for some 12 years past, the writer has had to answer for foaming delays and mechanical upkeep of locomotives in so far as water is or may be involved. Approximately 75 per cent of the water supplied locomotives on our railroad is chemically treated. On some divisions we have foaming water the year around, on other divisions, seasonally. Some 5 years ago we started to learn something about the development of foam within locomotive boilers and to study means for controlling carry-over. The author has mentioned that part of our work related to the development of the Electromatic Foam-

Collapsing System. This work was in collaboration with the Electro-Chemical Engineering Corp., Chicago, which has since placed this device on the market and now has many installations in service on the railroads of the country.

Parallel with the development of this mechanical means for carry-over control, we carried on extensive service studies of antifoam additives in an endeavor to correct the trouble at its source. The considerable progress we have made in this direction is the basis for belief in water treatment in preference to mechanical means for controlling carry-over in locomotive boilers of present conventional design.

As an example of what can be accomplished by the use of antifoam additives will be mentioned the record of a through 910-mile trip in freight service during May, 1941, between St. Louis, Mo., and Pueblo, Colo. During this test trip the antifoam additives were handled by a water chemist at all points where water was taken en route, eighteen watering points in all. A total of 157,735 gal of water were consumed, of which 1780 gal were blown out at the intermediate terminal-servicing points passed through. Starting with a water change at St. Louis, the boiler did not indicate a condition of foaming water during the entire 910-mile trip; total dissolved solids (grains per U. S. gallon), 28 leaving St. Louis and 620 arriving Pueblo. Without the use of the antifoam additives it would have required from 15 per cent upward on-line blow to control foaming with the feedwaters available, and there could have been carry-over at numerous times during the last 500 miles of the trip.

As a result of extensive experimentation with foam-control additives during 1940, 1941, and 1942, we equipped our Colorado Division with automatic plants for supplementary treatment at key watering points on the 338-mile division and operated successfully on a locomotive mileage-service contract with the Dearborn Chemical Company for a period of 2 years. We also have an experimental plant at St. Louis and have experimented with a powder form of antifoam additive handled manually over the entire railroad with generally satisfactory results. We cannot say that we yet have an antifoam material that is universally effective with all combinations of locomotive-boiler waters on our system or that the treatment is entirely foolproof, but we are making progress and feel that we are working in the right direction.

As for the phenomenon of carry-over and the best means of prevention from a mechanical standpoint, we have spent hours on top of a locomotive boiler in road service, looking down through sight glasses in the dome cap into an illuminated space beneath the dome and have observed all conditions from solid water and a clear steam space to a frothy foam completely filling the dome and being carried over into the dry pipe. We believe that once the foam has filled the dome and is being carried over into the dry pipe, it is too late to prevent carry-over into the superheater where a relatively small quantity of highly concentrated carry-over can dry out, deposit on the relatively hot interior surfaces of the superheater, or carry through as dust to affect lubrication of valves, cylinders, or appurtenances on the locomotive using superheated steam. From personal experience the writer believes that the best way to prevent carry-over in a locomotive boiler is to keep the dome as free from obstructions as possible and to maintain as great a free height as possible between the top surface of the foam and interior of the boiler shell around the dome entrances. The increasing size of locomotive boilers within fixed overhead-clearance limitations has resulted in reducing the steam dome to little more than a flange for the manhole cover, thus increasing the desirability for solid water to prevent carry-over.

That other investigators are thinking and working along

⁵ Engineer of Tests, Missouri Pacific Lines, St. Louis, Mo. Mem. A.S.M.E.

the same lines is evidenced by a recent report⁶ to the Master Boiler Makers' Association. The following statements are made in this report:

"It is hoped that sufficient knowledge of the chemistry and physics of foaming and spray will soon be gained to permit its control either by chemical or physical means. We should all do more thinking about the subject from the foam-control angle, keeping in mind that foaming is not a function of the quantity of dissolved solids but rather their quality. We can carry terrific concentrations of dissolved solids without foaming under certain specific conditions. When we have learned to apply this under any and all conditions we will have found the answer to the foam problem.

"The chemical treatment of feedwater for scale and corrosion prevention is commonplace but there is still room for further improvement in purifying the steam before it enters the dry pipe of the locomotive. The elimination of the foaming of the boiler water is a prime requisite for satisfactory locomotive operation.

"Moisture carry-over of a subtle nature by so-called effervescence remains a major problem on many railroads. It is responsible for encrusted superheater units, cut-out valve bushings, destruction of cylinder packing, and serious impairment of the lubrication of valves and cylinders. This is a water problem which can be overcome by proper chemical treatment of the water."

It may be added that this same committee recommends that the crown sheet in locomotive boilers be lowered to provide more steam space, suggests a change in construction whereby this may be accomplished in existing boilers, and that observations be made to determine whether or not beneficial results are obtained in the control of carry-over.

It is believed that the mechanical-engineering profession should give detailed study to the problem of carry-over from the standpoint of steam space and steam take-off and delivery in the locomotive boiler, more particularly as applying to locomotive boilers to be built during the years ahead.

V. E. McCoy.⁷ For many years the writer's company has supported research programs at Ohio State University and at other laboratories as well as carrying out research work in its own laboratory to determine the causes of foaming, the various forms of foam and carry-over, and developing special treatments which eliminate foam formation. Some of the reports quoted in this paper are the product of this program.

We have recognized that under all conditions of locomotive operation there is a small amount of carry-over, and we have made our recommendations to our railroad customers as to treatment and blowdown schedules with this in mind in order to protect the superheaters as much as possible from scale formation and also to protect the locomotive engine from damage due to impairment of lubrication.

This paper indicates that a mechanical device can be incorporated between the steam dome and the superheater that will at least reduce if not entirely eliminate the moisture from the steam and thus prevent damage to the superheater and the engine from this cause. We feel this is an important development and are in agreement with the principle involved. However, we would like to add a word of caution in case some might think that a device of this nature can be depended upon to take care of all the blowdown requirements in locomotive-boiler operation.

Blowdown is required to keep the build-up of dissolved solids

below some predetermined figure and also to keep the amount of solid matter normally in suspension in the boiler water from concentrating to such a point that the normal water circulation can no longer hold this solid matter in suspension. It is then precipitated out of the water in the form of mud banks that may cause overheating of the boiler steel and consequent difficulty.

We would recommend, in cases where a mechanical device of this kind is installed to eliminate moisture from the steam, that it should be maintained solely for that purpose and that normal blowdown practice be continued to avoid foam formation and prevent too great concentrations either of suspended solids or dissolved solids in the boiler water.

It seems desirable to clarify one point. A quotation is made regarding organic matter. In the particular instance quoted, the specific organic matter (probably sewage) did contribute to foaming. However, there are thousands of organic compounds a great many of which have antifoam properties. In fact the very best of the so-called "antifoam" materials are organic. Practically all water-treatment materials in use today provide organic materials of one kind or another which are required in some fundamental aspect of the treatment program. We want to point out these facts as otherwise all organic materials might be considered to be harmful to boiler performance and that is definitely not the case.

We feel that devices of the type tested and reported upon in this paper will be of great benefit to locomotive performance and take this opportunity of commending the author on his presentation.

R. M. OSTERMANN.⁸ Within the last 30 years, the approximate period during which the writer, in his association with The Superheater Company, has witnessed at close range the fight which railroad mechanical men, water chemists, and the company's engineers have waged against the growing menace of carry-over in locomotive boilers, the latter's steam-generation duty has not only vastly increased but they have also become more and more handicapped in rendering their duty in a normal manner. While the necessity of having to move ever heavier trains at ever higher speeds created a market for locomotives with a greater and greater maximum-horsepower output, the railroads' clearance profiles could, of course, not be similarly expanded nor could most railroads sufficiently increase the strength of their tracks and bridges so as to allow a substantial increase of driving-axle loads.

The general result has been that our more modern steam locomotives have had to be equipped with boilers which mainly derive their enlarged steaming capacity from longer fireboxes, larger combustion volumes, and larger grate areas on which an enlarged amount of coal can be burned with reasonable combustion efficiency. The diameter of the boiler barrel could rarely be sufficiently increased to provide a steam space and a steam-liberating surface commensurate with the large increase of steam-generation capacity. It is thus that we have come to face the tremendous carry-over problem which the author has so ably dealt with in his paper. Had it not been for the substantial decrease of the steam consumption per horsepower which we have attained by raising the superheat to the very maximum that is practicable with a reciprocating locomotive, our predicament would have been still greater when handling some of our highly treated feedwaters.

It is thought that the idea of separating the carry-over from the steam and of getting rid of it before the steam reaches the superheater, which idea the author has described and made practical, is eminently sound. The realization of this idea un-

⁶ "Treating Boiler Feedwater," Master Boiler Makers' Association Proceedings, Topic no. 2, 1944, pp. 63-69; also *Railway Mechanical Engineer*, vol. 118, 1944, pp. 496-497.

⁷ Chief Engineer, National Aluminate Corporation, Chicago 38, Ill. Mem. A.S.M.E.

⁸ Vice-President, The Superheater Company, Chicago 3, Ill. Mem. A.S.M.E.

questionably represents the most logical and direct attack upon the problem. Credit should be also given for the development of the "Signal Foammeter" and of the electromatic blowoff foam-collapsing trough, both of which have undoubtedly paved the way for the author's latest development.

W. A. POWNALL.⁹ The author has briefly described results from water treatment and emphasized the fact that an unfortunate result is the increased foaming tendency of treated water, with the resultant carry-over of water and suspended matter into superheater units and into the valves and cylinders. Whether this foaming be due to dissolved solids, suspended solids, a combination of the two, or to other causes, is of no special importance except for the effect of these causes on the development of corrective measures. The primary object is so to control the water in the boiler that the carry-over will not occur. With waters of low to moderate alkali salts this can be done by systematic use of the blowoff cock and, except for very bad waters, the use of an antifoaming compound in combination with the blowoff cock will accomplish the desired results. These points are also well covered by the author.

A modern large locomotive carries a 5000-hp boiler with water level subject to considerable disturbance at high speeds; and because of clearance limitations this boiler has limited steam space and steam liberation per square foot of water surface is rapid. Under these conditions, even with a good measure of foaming control, there may be occasional carry-over of water.

When a locomotive that by using superheated steam has increased its efficiency 20 to 25 per cent is affected by water carry-over, it loses that extra efficiency and approaches a saturated-steam locomotive in performance. In essence the carry-over has changed the superheater into an ordinary boiler, with a resultant reduced capacity of the locomotive as well as increased fuel and water consumption.

The foam-collapsing trough is of advantage in providing additional steam space directly under the throttle and it acts as a blowing-off device to remove the concentrated water at the critical time. The steam separator functions, not as a preventer of foaming, but to remove water from the steam before it reaches the superheater units. The tests of the steam dryer quoted in the paper indicate definite removal of carry-over water. Neither device apparently permits of any increase in concentration of dissolved solids before foaming occurs.

The removal of water and entrained solids from the steam before entering the superheater unit is quite worth while in improved superheater and cylinder performance and in preventing stopping and burning of superheater units.

Serious thought should be given to changes in boiler design with a view to increasing the steam space, improving dome design, getting a most favorable dome location, baffling; in fact, any change to keep the throttle as high above the water level as possible and slow down the movement of steam to the throttle.

J. L. RYAN.¹⁰ The lines of the writer's employer are so located that the well-known mid-western and southwestern boiler-water conditions are encountered, and the performance of an equipment for removing the moisture in the dry pipe to prevent its carrying through to the superheater is of more than passing interest.

The character of the tests, Figs. 8 to 11 of the paper, and the component parts of the equipment, Fig. 7, are familiar, these lines having conducted tests in 1935, with a steam separator applied to discharge the moisture carry-over to the atmosphere. However, the equipment had less capacity than that of the pres-

ent equipment and was without the electric automatic control of the water discharge. Visual observations were made in 1938, of the action of the steam and water within the boiler through sight glasses installed in the dome cap. The solenoid valve and blowoff separator or muffler are standard equipment as parts of the electromatic blowoff apparatus.

The test results in Figs. 8 and 11, showing the effectiveness of the tangential steam dryer with electric automatic control of the water discharge to the atmosphere in correcting bad carry-over conditions, are encouraging and justify tests by those having superheater-unit maintenance problems and valve- and cylinder-lubrication difficulties.

In addition to presenting the foregoing test results, the author also supplies basic data on design and operation that are too often neglected. Two of these are the influence that the height provided in the boiler above the mean water level has upon operation at high work rates, and the steam-liberation curve, Fig. 1 of the paper. Both should be given major consideration when designing a boiler.

Regarding the height provided in the boiler above the mean water level, i.e., the height that is available for steam, it has been the writer's experience that in addition to providing maximum height at the steam dome consistent with balanced design, it can be continued throughout the length of the boiler to an operating advantage, as maximum steam space is important in providing favorable performance at high work rates and in cushioning violent increases in the rates. Weight limits, however, frequently govern the boiler that may be provided.

A calculated steam-liberation curve similar to that shown in Fig. 1 should be studied for each boiler when designed. The peak directly ahead of the back tube sheet would no doubt influence placing the steam dome forward of some of the older practices. The U.S.R.A. light Mikadoes have the steam dome placed with the center line 30 in. ahead of the back tube sheet and the entrance at the back only 15 1/4 in. ahead of the back tube sheet. The writer favors extended wagon-top construction and the steam dome placed 7 to 8 ft ahead of the back tube sheet.

A record of the steam space at various water levels and the steam-liberation curve for maximum evaporation for the important classes on a railroad are of value in connection with operation and its problems.

The temperature curves, Fig. 4, for metal and steam, where the superheater unit has its full area, and the curves are carried upward showing the temperatures for severe area restriction, provide a clearer understanding of the failure of return bends as represented by the one shown in Fig. 5 of the paper.

With reference to the matter of controlling the concentration in the boiler by blowing; of the three methods, manual, continuous, and automatic intermittent, the writer considers the latter supplemented by manual means to be the most practical where locomotives are run through over a number of divisions having different water conditions.

The author's statement that one of the most significant results obtained from these tests is the relation between carry-over and a change in the rate of the working of the engine is well substantiated by the data in Figs. 8 to 11, inclusive. However, the writer does not find in these data entirely clear substantiation for the author's statement that it is always true foaming will increase when the rate of evaporation is increased, but the effect is very much worse when the rate is changed suddenly. The effect of sudden increase in work rate on carry-over can be checked to best advantage from the data when the separator blowoff was turned off, which was the first 11 min, Fig. 8; the 28th to 32nd min, inclusive, Fig. 9; the entire test, Fig. 10; the first 20 min, Fig. 11, and 52nd to 60th min, inclusive, Fig. 11. The test period, Fig. 8, was made with exhaust pressure of 16 to 18 psi. There

⁹ Wabash Railroad Company, Decatur, Ill.

¹⁰ Mechanical Engineer, St. Louis-San Francisco Railway Company, Springfield, Mo.

was no appreciable variation in the exhaust pressure for the period 28th to 32nd min, inclusive, of test, Fig. 9; Fig. 10 contains data for two gradual increases from 17 to 24 psi. However, there are no data for comparison where the work rate was changed suddenly from 17 to 24 psi. The work rate was gradually increased 15 to 26 psi exhaust pressure in the period from the 52nd to 58th min of test, Fig. 11, the branch-pipe temperature decreasing from 675 F to that of the saturated steam.

Positive information on the extent of the carry-over that occurs when making given work-rate increases, when the change is sudden and when it is gradual, would be of value to the railways for educational purposes with their enginemen. It would necessarily vary for some classes owing to the difference in the proportions of boilers.

One cannot entirely avoid these sudden increases in the work rate in locomotive operation, particularly on single-track main lines. An excellent example is an approach to an order board with a locomotive eased off and then the immediate high work rate that frequently follows receiving a few minutes' additional time that permits making a close meet.

When familiar by experience with the influence that carry-over has on the immediate performance of a locomotive, one cannot but take exception to the author's statement that it is possible for carry-over to be sufficiently severe for the engine crew to notice it, as in the case of the conditions illustrated in Fig. 8. Continued operation with the conditions that existed for the first 11 min of this test would have been practically impossible, as the steam-pipe temperature was that of the saturated steam. This would result in 30 to 35 per cent reduction in the cylinder work rate or, if maintained, an increase in steam demand of approximately 50 per cent. The influence of the carry-over in Figs. 10 and 11 would be definitely observable by seasoned enginemen.

It is possibly fitting to add that the operating and maintenance departments of many of the carriers will indeed be indebted to the one who provides the solution to the problem of "carry-over." The test results presented by the author are such that the writer is inclined to the opinion that the author and his fellow workers have made a long stride in providing this solution.

R. W. SENIFF.¹¹ The ever-increasing demands being placed on steam-locomotive performance greatly enhance the value of information such as that presented in this paper. The data from the tests are convincing and contribute valuable knowledge of the art of locomotive-boiler operation.

It is gratifying to read a paper where the vague (the writer would like to say obsolete) word "priming" is not used and where there is such an excellent choice of specific, clearly defined, descriptive terms. The only possible exception appears to be in the use of the term "effervescence," the definition of which is not descriptive of the phenomenon referred to.

The author is to be congratulated for his broad view of the problem which is typified by one of his opening statements, "There is no standard treatment for feedwater and each case must be studied . . . , " and again in his summary where he recognizes the various aspects of the locomotive-boiler carry-over control problem.

Nowhere in the power-boiler field are so many variables encountered. On a single railroad operating division the variables introduced by the number of water supplies of differing qualities, the number of treating plants, the number of boilers, the number of different operators handling the boilers, complicated further by the erratic boiler-operating conditions peculiar to railroading, make the problem of precise control of feed- and boiler-water conditions much more complex than that encountered

in stationary or marine service. These erratic variables which make precise control difficult also make precise and responsive control more essential. The tangential steam dryer appears to fulfill this requirement by reacting quickly and in a positive manner. It seems to the writer that the principal advantage of the steam dryer is its ability to prevent carry-over from sudden cases of foaming of short duration such as those which occur when sudden maximum steam demand is made while accelerating a train. He agrees with the author that the major responsibility for control of foaming rests on water treatment and adequate but efficient partial blowdown. It is obvious that the steam dryer cannot serve as a practical foam indicator or blowoff device because foam must fill the steam space of the boiler before it will function in that capacity.

If the steam dryer will remove aquaglobes and foam spray from steam, and it appears that it should, a report of its performance in that respect would be of interest because there are districts where this type of carry-over causes more superheater, valve, and cylinder damage than foam carry-over does on most railroads.

The author's remarks on relation of carry-over to working rate of the engine are interesting, and, although outside of the immediate scope of the paper, the cause of the violence of the carry-over on sudden increase in working rate would be of interest to the water chemist. Answers to the following questions, if available, would be of value to him in that connection. What was the foaming point of the boiler water used in the tests; that is, at what concentration does this water produce foam carry-over when the engine is worked normally at maximum steam demand with constant boiler steam pressure and a half-glass of water? A boiler-water concentration is given for the graphs. Is this at the beginning of the carry-over period, the end, or an average? Was any blowoff done during the test and was there any drop in steam pressure during the first few minutes following the sudden increase in working rate when the excessive carry-over was observed?

The writer's experience has been that very violent foam carry-over is encountered upon sudden steam demand if the boiler water is above the foaming point (or near the foaming point if accompanied by a drop in boiler steam pressure); that carry-over has the same effect as an equivalent amount of blowdown toward reducing the boiler-water concentration and will therefore rapidly reduce the concentration to the foaming point where a much smaller amount of carry-over is encountered. This is indicated by the dryer discharge in seconds accompanying the author's graphs (Figs. 8, 9, and 11) where the dryer appears to be acting as a blowoff device in reducing the foam height in the boiler by reduction in boiler-water concentration. The writer feels that the violent carry-over on sudden steam demand is simply a function of the evaporation rate and boiler-water concentration and that the sudden change in rate of working has no other result than to make the effect of these factors appear suddenly. Under such conditions foam carry-over ceases just as suddenly when the steam demand is reduced, indicating a like reaction in both directions. Perhaps this is what the author has in mind but, if he has evidence of some other factor which increases the carry-over out of proportion to evaporation and concentration effect, it would be of interest.

J. C. SOMERS.¹² The outline of mechanical methods to prevent foaming is interesting but such methods in wartime involve purchase and installation of equipment which must be considered in comparison with application of antifoaming agents which are also mentioned favorably by the author in the paper. Because

¹¹ Engineer of Tests, The Alton Railroad, Bloomington, Ill.

¹² Industrial Products Engineering Company, Long Island City, N. Y. Mem. A.S.M.E.

of continued heavy locomotive loads and no letup in wartime restrictions on labor and equipment, such available antifoaming materials, it seems to the writer, deserve consideration since they evidently can be delivered promptly. The obvious success of colloidal type of antifoam agents needs to be brought to the attention of operators in view of the elementary principles involved in preventing foaming. Recent publications can explain much more scientifically how this occurs, notably a paper by Jean de Frank,¹³ discussing organic colloids.

P. B. PLACE.¹⁴ Mr. Williams has presented a very complete discussion of the characteristics and causes of carry-over from locomotive boilers, and described methods and equipment for control of foam carry-over. It is of interest to note that, in general, the problem of carry-over from locomotive boilers is similar in many respects to that from stationary water-tube boilers.

Foam carry-over, or foamover as it may be termed, constitutes by far the greater percentage of carry-over problems and is particularly troublesome because it is difficult to predict or correlate with known factors. Although foaming is primarily a function of the boiler-water concentration, the ratios of constituent salts, alkalinity, presence of small amounts of oil or organic matter, water level, rating, changes in rating, type of firing, and boiler circulation are all factors of sufficient influence to make duplication, correlation, and interpretation of foam carry-over difficult.

The inconsistency of rating and concentration as criteria of satisfactory steam purity is shown in Table 3.

TABLE 3

Example	Drum diam	Pressure	Rating, Sq ft	lb per hr Ft. width	Safe concentration limit, ppm
A	60	960	3000	15000	700
B	54	800	2800	12500	5000
C	60	890	2000	10250	1500
D	66	425	1700	9450	4000
E	48	410	1000	4100	2500
F	48	575	975	3900	1500

The boilers listed are all single-drum units having similar drum internals. Note that the ratings in terms of liberation per sq ft of water surface are considerably higher than for the average locomotive boiler and that the safe limits of boiler water concentration show no relation to operating pressure, boiler rating, or drum diameter. All of these units were likely to give foam carry-over at concentrations above the limits given. The most troublesome case, F, was very conservatively rated and the foaming was traced to presence of oil and organic matter in the boiler water.

In general, boiler waters with concentrations less than 600 ppm seldom give trouble with foam carry-over. Higher concentrations do not necessarily, however, induce excessive foaming and isolated cases are known where boiler-water concentrations are maintained continuously at 10,000 to 15,000 ppm without trouble.

Experimental work on steam purification and control of foaming has been in progress for some time in our laboratory and much of the mystery of the mechanics of carry-over has been eliminated. Using a short section of a simple water-tube boiler having lights and windows installed in the heads of the 54-in-diam drum to give full visibility within the drum, it has been possible to observe the physical characteristics of foam and the effectiveness of various methods of controlling it. Although the test unit is operated at atmospheric pressure, correlation of the

observations with field tests of pressure units suggest that, qualitatively at least, the low pressure observations are a valuable guide in the analysis and solution of carry-over problems.

It is difficult to compare the performance of locomotive and water-tube boilers of the same total output and operating pressure, because of the difference in method of rating the boilers and difference in design.

The established methods of rating boilers are based primarily on velocity of steam flow. Thus locomotive boilers are rated in terms of steam liberation per sq ft of water surface. This is a logical system as the steam is actually liberated from the water surface and vertical velocity must be kept low to avoid entrainment of spray. On the other hand, water-tube boilers do not, as a rule, liberate their steam from the water surface, but deliver the riser mixtures to the drum above the water level and depend on various designs of baffles to obtain separation.

Stationary boilers have the advantage over locomotive boilers of greater available drum space for installation of separation and drying equipment and in most cases, can distribute the steam offtakes over the length of the drum rather than concentrate the steam flow through a steam dome. In such boilers, the available drum volume becomes a better measure of potential rating than the area of the water surface and a common method of rating water-tube boilers is in terms of steam output per foot of drum length, with drum diameter as an additional factor.

Where foaming is involved, carry-over is induced, not so much by steam velocity as by the fact that the foam simply accumulates in the available drum space until it piles up to the steam outlet and is swept out of the drum by the steam flow. In such cases, the amount of drum space available for foam accumulation becomes a major factor and boilers with small available drum space may foam over at relatively low ratings.

The limited space available in locomotive boilers calls for a dynamic type of separator rather than the ordinary baffle or filter type of separator used in many water-tube-boiler drums. The tangential dryer, described by Mr. Williams, utilizes available velocities to accelerate separation and with automatic and positive drainage, this equipment appears to be both logical and satisfactory by test.

AUTHOR'S CLOSURE

All of those taking part in the discussion have emphasized the importance of the present-day carry-over problem. Their contributions discuss the subject from all angles and will be valuable in approaching an answer to the problem.

There is general agreement that every effort should be made to control or prevent foaming by the use of proper feedwater treatment, by proper blowdown, and by the use of antifoam treatment where such is necessary. The steam separator with an outside discharge valve should be considered as an additional precaution against carry-over leaving the boiler when conditions are such that foaming or effervescence takes place in spite of all that has been done in an attempt to prevent such an occurrence. Agreement with this view is expressed directly by Messrs. Carr, McCoy, Pownall, and Seniff. Mr. Seniff points out the difficulty of controlling carry-over by chemical means and by blowing due to the great number of variables that enter into railroad operation.

The increase of foaming in recent years due to improved feedwater treatment is confirmed by Messrs. Jackson and Pownall. Messrs. Ostermann and Ryan comment particularly on the increase in carry-over due to the harder working of locomotive boilers demanded by modern operating conditions with no increase in the boiler size.

Mr. Jackson states that he believes that once the foam has filled the dome it is too late to prevent carry-over into the superheater.

¹³ "Internal Feedwater Treatment of Locomotive Boilers," by Jean de Frank, Master Boiler Makers' Association Proceedings, 1944, pp. 69-78; also "Colloidal Organic Boiler Feedwater Treatment," by Jean de Frank, *Railway Mechanical Engineer*, vol. 118, 1944, pp. 555-557, 566.

¹⁴ Research and Development Engineer, Combustion Engineering Co., Inc., New York, N. Y. Mem. A.S.M.E.

The results given in the paper show that under such conditions, the apparatus tested reduced the moisture entering the superheater units to a very small amount and in some cases eliminated it entirely. For instance, the results given in Fig. 11 from the twenty-sixth minute to the thirtieth minute indicate dry steam entering the superheater. During this and other tests, observations through the sight glasses showed that the dome was entirely filled with foam as stated by Mr. Jackson from his observations.

Mr. Ryan comments on the relation between carry-over and a change in the rate of the working of the engine. The test periods commented on by Mr. Ryan were for more or less constant rate of working. The effect on carry-over of a sudden change in the rate of working is best shown by those times when the rate of working was suddenly increased so that a test under foaming conditions could be started. Such times are at the seventh minute in Fig. 9, the first minute in Fig. 10, and the fifth minute in Fig. 11. In each case, the sudden change in the rate of working as indicated by the increase in exhaust pressure from 10 to 17 or 20 psi produced immediately a foaming condition. It is true that during these tests the water was in a condition extremely susceptible to foaming and it should not be inferred that foaming will always occur when the rate of working of an engine is suddenly increased. Whether or not this happens will depend on the condition of the boiler water. Mr. Ryan also comments on the possibility of carry-over being noticed by the engine crew. For the results recorded in Fig. 8 there was no question as to the carry-over being noticeable. For the other tests there were no variations in the water level or condition of the water in the glass that would indicate foaming. It is possible that the influence of a small amount of carry-over on the power output of the locomotive would be noticed by an experienced engineman. This would of course depend to a great extent upon the individual and the conditions under which the locomotive is operating.

Mr. Seniff raises some specific questions with regard to the tests. The boiler-water concentration given in Figs. 8 to 11 was that of a sample taken at the end of the run. The exact foaming point of the boiler water used in the tests is not known. Reference to Figs. 8 and 10 will show that there was considerable foaming with a boiler-water concentration of 120 grains per gallon. During all of the tests the boiler was worked at a high rate of evaporation with a constant boiler steam pressure and normal water level in the glass. Normally antifoam compound was used in the territory where the tests were made, but this was not done during the tests so that the foaming conditions of the water would be as bad as possible. For the same reason the blowoff cocks were never used. There was no noticeable drop in the boiler steam pressure during the times when excessive carry-over was observed. Mr. Seniff's feeling that the violent carry-over on sudden steam demand is simply a function of the evaporation rate and boiler-water concentration is probably correct, as is also the statement that carry-over can be stopped by reducing the steam demand.

Mr. Place's comments are extremely interesting since they indicate that locomotive boilers are not the only type which are subject to troubles from carry-over. The table included in Mr. Place's discussion indicates the difficulty of determining the possibility of foaming in relation to boiler design and water concentration. It is evident that when everything possible has been done to prevent foaming it is still desirable to have a device which will prevent carry-over from the boiler when conditions occur which cannot be anticipated in advance.

Both Mr. Carr and Mr. McCoy were correct in pointing out that while certain types of organic matter will aggravate foaming, it is also true that other types of organic matter such as tannin extract, and the amines and amides which form the basis for the newest antifoam water treatments, are definite foam inhibitors.

On Fatigue Failure Under Triaxial Static and Fluctuating Stresses and a Statistical Explanation of Size Effect

By F. H. FOWLER, JR.,¹ CALDWELL, N. J.

The purpose of this paper is to develop a framework for establishing a criterion of safe fatigue characteristics of manufactured units. In addition a statistical theory of fatigue has been indicated. Provision can be made for a study of combined stresses, static and vibratory stresses, and variations in amplitude. Interesting explanations of scale effect and stress gradient effect are given. It is hoped that this will provide a useful framework to improve the designer's judgment and upon which to build additional work on fatigue.

INTRODUCTION

IN establishing a criterion of safe fatigue characteristics of manufactured units, decisions are necessary concerning the required degree of safety, required operating conditions, and basic theory of failure. Also the stress history of each point and the properties of the material must be determined. After these decisions are made and these data are determined, computations as outlined in this paper can be made to determine whether or not a design is safe.

Definition of "Safe Design." A safe design is one which requires a properly manufactured, installed, used, and serviced example of that design to have a probability of premature failure less than a maximum permissible amount. The decision as to the maximum permissible probability of failure must be based upon individual design requirements. In this paper primary consideration will be given to "safe designs" with a positive probability of premature failure.

Assumed Operating Requirements. If the use to which a product is to be put calls for varied distributions of operating time among specified permissible operating conditions, there may be considerable differences among individual units in the severity of the fatigue loads. Therefore, for the use of the designer there should be specified a standard history of operating conditions rather than merely a list of severest operating conditions. Also, for the individual customer, guarantees should be based upon histories similar to and more severe than those required of his particular unit.

BASIC THEORY OF FAILURE

A basic theory of failure is recommended modifying Orowan's (1)² work for the case of variable stress amplitude, for the case of triaxial stress, and for the case of both static and vibratory loads.

Orowan's theory of fatigue failures is as follows: Materials

¹Senior Structures Engineer, Propeller Division, Curtiss-Wright Corporation. Jun. A.S.M.E.

²Numbers in parentheses refer to the Bibliography at the end of the paper.

Contributed by the Aviation and Applied Mechanics Divisions and presented at the Annual Meeting, New York, N. Y., Nov. 27-Dec. 1, 1944, of THE AMERICAN SOCIETY OF MECHANICAL ENGINEERS.

NOTE: Statements and opinions advanced in papers are to be understood as individual expressions of their authors and not those of the Society.

contain imperfections which cause stress concentrations. Under static loading, these stress concentrations are reduced by plastic flow. However, in the fatigue process, successive cycles work-harden the material in the neighborhood of the imperfection, thereby continually diminishing the reduction in stress concentration due to plastic flow. This continues until a condition is approached in which there is no plastic flow because either the yield point is sufficiently increased or because the true ultimate strength of the material is exceeded. In the latter case, a fatigue failure takes place. This theory is reviewed by Prof. Frederick Seitz (2). It is interesting that in addition to its ability to account for the difference between ultimate strength and endurance limit, this theory is indirectly confirmed by its ability to predict the shape of the $S-N$ diagram.

One of the points of Orowan's theory is that the effect of the static stresses in fatigue is insignificant and that only the vibratory stresses are important. If it is possible to so work-harden the material that no local plastic flow occurs during the unloading cycle, none will occur during the reloading cycle. The range of stress determines, practically independently of the static stresses, whether or not this takes place. Consequently, the range of stress alone should determine whether or not a fatigue failure should take place. On the other hand, there is the possibility that the static stresses might influence the severity of the imperfections and hence might affect the range of the local vibratory stresses. J. O. Smith has gathered considerable data on fatigue (3). Looking at this theory in the light of these data, it would seem that under certain circumstances the static stresses are important and under others they are not.

For combined stresses where the number of cycles before damage is important, the situation becomes more complicated. There remains the problem of the probable effects of static stresses upon the severity of irregularities. In addition, the effect of the fluctuating stresses has to be divided into two elements. The first is the rate at which work-hardening will take place under various conditions of fluctuating stress. The second is the condition of combined stress which will cause fracture after work-hardening has resulted in increasing the stresses. Thus for the general case of fatigue, decisions are necessary concerning the assumed laws of the effect of static stresses upon irregularities, of the rate of work-hardening under combined stress, and of fracture under combined stress.

PROPERTIES OF THE MATERIAL

To simplify the problem of properties of the material, assume a true stress-strain diagram shaped as in Fig. 1. There is a straight line of slope E from the origin O to the yield point A . There is a straight line of slope σ' from A to the breaking point Z . Unloading curves have the slope E . Symmetry also exists between the tensile and compressive diagrams about the strain intercepts of the unloading-loading lines (e.g., O, C, E). Note how the yield point has been increased by cold work from the stress corresponding to B to the stress corresponding to F . It is hoped that the foregoing simplifications will prove satisfactory for prac-

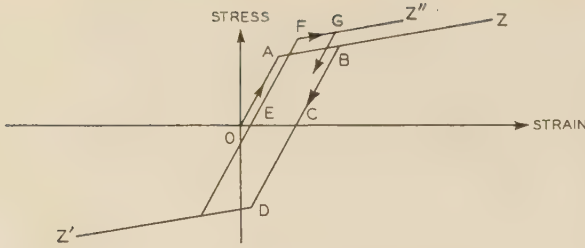


FIG. 1 ASSUMED STRESS-STRAIN DIAGRAM

tical application. If not, their use will simplify this explanation and the additional complications introduced by their replacement will not alter this general pattern.

Using these assumptions, probability distributions of several properties are required. These properties are the existence of an irregularity of stress-concentration factor K , in a unit volume of material, and for each point the true ultimate strength σ_f , the slope σ' , the modulus of elasticity E , and the original yield point σ_0 . Note that K has a minimum possible value of 1. It is reasonable to assume that any irregularity must have a finite radius of curvature at any of its corners and hence that K has a maximum possible value. Also it is reasonable to assume that σ_f has a maximum and minimum value. It also seems reasonable that the other properties would have a finite range of values.

Stress History. A knowledge of the stress history of each point is required. It is possible that exact values of this can be obtained. However, it is more likely that there will be an error in the stated stress. Hence to avoid either timidity or rashness in an estimate of the probability of failure, it is necessary to replace stresses with a distribution curve giving the probability of every possible stress at a given point at a given time. By stress here is meant the stress, ignoring irregularities. When the effect of irregularities is considered, the term local stress or local strain will be used.

PROBABILITY OF FAILURE IN UNIT VOLUME

The first computation required is a computation of probability of failure in a unit volume subjected to the stress history of a given point. This probability is required for every point.

Consider the case where there are p periods of time during each of which the fluctuating stress is constant; let

- S_i = amplitude of fluctuating elastic stress during i th period
- ϵ_i = local plastic strain, first quarter-cycle of i th period
- $\sigma_{(i-1)}$ = yield point before i th period
- σ_i = yield point after i th period
- n_i = number of cycles during i th period
- K = stress-concentration factor
- E = modulus of elasticity
- σ' = slope of stress-strain diagram in plastic range

To obtain S_i it is necessary to postulate a type of irregularity; then

$$\epsilon_i = f(S_i, \sigma_{(i-1)}, K, \sigma', E)$$

From Equations [2] of Orowan's paper (1), the increase in yield point during the i th period is given by the formula

$$\sigma_i = S_i K \left[1 - e^{\left(-4n_i \frac{\epsilon_i}{S_i K} \right) \sigma'} \right] + \sigma_{(i-1)} e^{-4n_i \left(\frac{\epsilon_i}{S_i K} \right) \sigma'} \quad [1]$$

Then if each n_i is constant, successive application of Equation [1] gives

$$\sigma_p = F(S_1, S_2, \dots, S_p, \sigma_0, K, E, \sigma') \quad [2]$$

It is interesting to note that the order in which the stresses occur is significant; let

$P(\sigma_p) d\sigma_p$ = probability of a yield point after p th period between σ_p and $\sigma_p + d\sigma_p$

$P(S_i) dS_i$ = probability of a stress during the i th period between S_i and $S_i + dS_i$

$P(\sigma_f) d\sigma_f$ = probability of a true ultimate strength between σ_f and $\sigma_f + d\sigma_f$

$P(\sigma_0) d\sigma_0$ = probability of an original yield point between σ_0 and $\sigma_0 + d\sigma_0$

$P(\sigma') d\sigma'$ = probability of a slope of true stress-strain diagram beyond yield point between σ' and $\sigma' + d\sigma'$

$P(E) dE$ = probability of a modulus of elasticity between E and $E + dE$

$P(K) dK$ = probability that the most severe irregularity in a unit volume has a stress-concentration factor between K and $K + dK$

Then

$$P(\sigma_p) d\sigma_p = \int P d\tau \dots \dots \dots [3a]$$

where

$$P = P(\sigma_0) P(\sigma') P(E) P(K) \pi \prod_{i=1}^p P(S_i) \dots \dots \dots [3b]$$

$$d\tau = d\sigma_0 d\sigma' dE dK \pi \prod_{i=1}^p dS_i \dots \dots \dots [3c]$$

and the integration is carried out over the $(p + 4)$ dimensional volume between the $(p + 4)$ dimensional surfaces

$$F = \sigma_p \dots \dots \dots [3d]$$

and

$$F = \sigma_p + d\sigma_p \dots \dots \dots [3e]$$

Now the probability that the true ultimate strength is less than σ_f is given by the formula

$$P_f(\sigma_f) = \int_0^{\sigma_f} P(\sigma_f) d\sigma_f \dots \dots \dots [4]$$

The probability that the final yield point lies between σ_p and $\sigma_p + d\sigma_p$, and that such a final yield point will result in failure, is given by the expression

$$P_f(\sigma_p) P(\sigma_p) d\sigma_p$$

and the probability of failure in a unit volume is given by the formula

$$P_v = \int_0^\infty P_f(\sigma_p) P(\sigma_p) d\sigma_p \dots \dots \dots [5]$$

PROBABILITY OF FAILURE IN UNIT

The next step is to consider the final problem of whether there will be a failure in the unit.

1 — P_v = probability of no failure in a unit volume

q = probability of no failure in a volume dv , or the probability of no failure at a given point

$1/dv$ = number of volumes dv per unit volume

As the probability of no failure in a unit volume is the probability of no failure in all the volumes dv comprising it, or the product of the probabilities of no failure in all of these elementary volumes

$$(q)^{1/dv} = 1 - P_v$$

$$q = (1 - P_v)^{dv}$$

Therefore

$(1 - P_v)^{dv}$ = probability of no failure at a given point having a volume dv

As P_v is now considered known for every point in the solid, the probability of there being a point in this solid at which a failure will occur can be calculated as follows:

Let P = probability of a failure in the entire unit
then

$$1 - P = \prod_{i=1}^{v/dv} (1 - P_v)^{dv_i}$$

and

$$\ln(1 - P) = \sum \ln(1 - P_v)^{dv} = \sum \ln(1 - P_v) dv$$

$$P = 1 - e^{\int \ln(1 - P_v) dv} \dots \dots \dots [6]$$

This statistical procedure has been used and checked experimentally by Weibull (4) for brittle materials. In place of Equation [6], Weibull uses the approximate formula

$$P = 1 - e^{-\int P_v dv}$$

Weibull distinguishes between materials for which a crack will propagate until failure of the unit takes place and materials for which no such propagation takes place. As most cases of fatigue of metals involve situations where cracks will propagate, the second case has not been considered.

SCALE EFFECT

If two pieces of different size are geometrically similar and subjected to the same stress distributions, the probability distribution of failure is changed.

In Equation [6] let

$$B_0 = e^{\int \ln(1 - P_v) dv_0}$$

where

$$v_0 = \text{volume of small piece}$$

for the small piece. Note that $1 - P_v$ is always less than 1, hence $\ln(1 - P_v)$ is always negative and B_0 is never more than 1. Let

$$B_1 = e^{\int \ln(1 - P_v) dV_1} = B_0^{V_1/V_0}$$

where

$$V_1 = \text{volume of large piece}$$

as

$$V_1 > V_0, \quad B_1 < B_0$$

Hence, for the large piece, P is always greater than for the small piece unless B_0 is 0 or 1. If the endurance limit is regarded as the fluctuating stress for which a fatigue failure and no fatigue failure are equiprobable, then the endurance limit becomes, for geometrically similar pieces, a function of the diameter of the piece.

The curve of endurance limit as a function of diameter should have the shape given in Fig. 2.

The upper flat portion approaches a constant stress equal to the maximum possible true ultimate strength divided by minimum possible stress-concentration factor due to irregularities. The lower flat portion is asymptotic to a constant stress equal to the minimum possible true ultimate strength divided by the maximum possible stress-concentration factor. A plot indicating the lower flat portion can be found in the appendix of A.S.T.M. report (5).

Stress-Gradient Effect. The stress-gradient effect is conceived as similar to the scale effect in that there are differences in the volume of materials for which the greatest probability of failure per volume exists.

Certainties. This problem becomes very much simplified when $P_v = 0$. In that case no failure will occur in the unit. Pre-

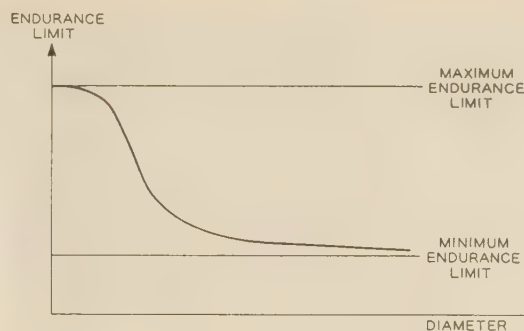


FIG. 2 ENDURANCE-LIMIT CURVE

sumably, in this case no scale effect or stress-gradient effect would be observed.

SUMMARY

While the general framework for a theory of fatigue has been proposed, there remains considerable research to be done before a quantitative application to design can be made. However, it emphasizes the desirability of deciding whether to use large enough specimens in testing for endurance limit to avoid the possibility of failure or to evaluate the probability that a failure will occur. It also provides the index P_v which can be used if not quantitatively at least qualitatively in co-ordinating stress-distribution data and material data in determining the severity of the stresses at any point. It is therefore hoped that this paper will prove to be of guidance to the designer. Furthermore, it is hoped that this discussion will stimulate further research in the undeveloped phases of this field.

BIBLIOGRAPHY

- 1 "Theory of Fatigue of Metals," by E. Orowan, Proceedings of the Royal Society of London, series A, vol. 171, 1939, pp. 79-106.
- 2 "Physics of Metals," by F. Seitz, McGraw-Hill Book Company, Inc., New York, N. Y., 1943.
- 3 "Effect of Range of Stress on the Fatigue Strength of Metals," by J. O. Smith, University of Illinois, Engineering Experiment Station, Bulletin No. 334, 1942.
- 4 "The Phenomenon of Rupture in Solids," by W. Weibull, Ingeniors Vetenskaps Akademien Handlingar No. 153, 1939.
- 5 "Progress Report on the Effect of Size of Specimen on Fatigue Strength of Three Types of Steel," by H. F. Moore and D. Morkovin, Proceedings of the A.S.T.M., vol. 42, 1942, pp. 150-151.

Discussion

R. E. PETERSON.³ This paper points in a direction which is certain to receive considerable attention in the future.

We have attempted to apply Weibull's statistical analysis to materials testing and found it useful in connection with static strength of porcelain, but thus far have not been successful with application to the fatigue strength of ductile materials.

According to Weibull, the volume of material under test may be viewed as an important variable. To test this, it is desirable to vary volume without changing stress gradient; this can be done by keeping diameter constant and changing length. The writer can recall only two cases of this kind. Horger and Maubetsch⁴ tested 0.3-in.-diam 0.45 per cent C steel specimens with contour radii of 5 in., 97/8 in., and infinity (straight section

³ Manager, Mechanics Department, Westinghouse Research Laboratories, East Pittsburgh, Pa. Mem. A.S.M.E.

⁴ "Increasing the Fatigue Strength of Press-Fitted Axle Assemblies by Surface Rolling," by O. J. Horger and J. L. Maubetsch, *Journal of Applied Mechanics*, Trans. A.S.M.E., vol. 58, 1936, p. A-97.

17/16 in. long). The same endurance limit was found for all cases, although the upper branch of the $S-N$ diagram differed. Kenyon⁵ found a lower endurance range in testing long wires, but there is some question if the tests, carried out on different types of machine, are strictly comparable.

The author's sketch of endurance limit versus diameter is quite interesting. Actually we do obtain a hump at small diameters, i.e., for medium-carbon steel, a 0.3-in.-diam specimen was found to be 5 to 10 per cent higher than a 1/2-in.-diam specimen.⁶ It is hoped that the author will show the degree to which the theoretical curves fit the foregoing data as well as those recently published by the A.S.T.M. Research Committee on Fatigue of Metals.⁷

AUTHOR'S CLOSURE

The author wishes to thank Mr. Peterson for the interest taken in this paper. The data of Horger and Maubetsch⁴ cited provide information on only three failed specimens of each type. While all but two of the failed specimens failed at points on the $S-N$ diagram related to one another in a manner regarded as the most probable by the principles stated in the paper, there is insufficient data to provide more than a qualitative confirmation of the principles. The data of Kenyon⁵ because of differences in machines cannot be applied to this problem with confidence. The curve of the A.S.T.M. Research Committee on Fatigue of Metals cited in the discussion does not provide much more than qualitative confirmation because of the meagerness of the data.

⁵ "A Pulsating Tension-Fatigue Machine for Small-Diameter Wire," by J. N. Kenyon, Proceedings of the A.S.T.M., vol. 40, 1940, p. 768.

⁶ "Two- and Three-Dimensional Cases of Stress Concentration and Comparison With Fatigue Tests," authors' closure to discussion, by R. E. Peterson and A. M. Wahl, *Journal of Applied Mechanics*, Trans. A.S.M.E., vol. 58, 1936, p. A-150.

⁷ Second Progress Report (Appendix) on Effect of Size of Specimen on Fatigue Strengths of Three Types of Steel, Proceedings of the A.S.T.M., vol. 43, 1943, p. 119.

However, the conclusion of an endurance limit for large diameters is in line with that of a minimum possible endurance limit.

The curves of endurance limit vs. diameter⁶ cited in the discussion provide real interest. Further discussion of them has been carried out between Mr. Peterson and the author as follows: The existence of a maximum point as shown in the curves is contrary to predictions made based upon the principles developed in this paper alone. This could be because of relative grain size effects which were neglected in this paper. For the smallest specimens used, the number of grains in a cross section becomes very low and hence these smallest specimens might be expected to behave in some respects similar to a single crystal. This would tend to cause a reduction in strength, possibly to such an extent as to change the rate of change of strength with respect to cross sectional area from positive to negative. Also, the effect of variations in conditions at or near the surface can be expected to assume even greater importance for the very small specimens. On the other hand, it might be possible to explain the maximum point on the basis of a certain discontinuity in some of the tests. The sources of two of the curves has been examined. There it was found that in both cases the maximum point represented the results of a rotating beam tests whereas all the others represent results of rotating cantilever tests. A comparison of the $S-N$ diagrams for the different diameter specimens of one of these curves has been published.⁸ It can be noted that the upper branches of $S-N$ curves for all rotating cantilever specimens tend to converge toward a single point. However, the upper branch of the $S-N$ diagram for the rotating beam specimens diverges from the point. This tends to strengthen the possibility that the use of a rotating beam specimen is the cause of the maximum points. The author regrets that rotating cantilever tests at this diameter are not available to clarify this matter.

⁸ "Fatigue Tests of Small Specimens With Particular Reference to Size Effect," by R. E. Peterson, American Society for Steel Treating (now American Society for Metals), Transactions, vol. 18, 1930, p. 1043.

Influence of Applying Cutting Fluids at Different Temperatures When Turning Steel

By O. W. BOSTON,¹ W. W. GILBERT,² AND R. E. MCKEE³

This paper presents the results of an investigation to determine the influence on cutting speed, tool life, chip formation, and other pertinent factors, of a cutting fluid applied at each of several different constant temperatures, ranging from 55 F to 150 F. A sulphurized mineral oil and an emulsion, consisting of 1 part soluble oil and 20 parts water, were used as cutting fluids.

MATERIAL CUT

THE material cut in the tests to determine the influence of the application of cutting fluids at different temperatures was an S.A.E. 3140 annealed steel originally in the form of a forging 4 ft long and 12 in. diam. The chemical composition was C, 0.39 per cent; Mn, 0.72 per cent; P, 0.025 per cent; S, 0.022 per cent; Si, 0.20 per cent; Ni, 1.11 per cent; Cr, 0.72 per cent. The scleroscope hardness was 24 to 26, and the Brinell hardness was 207. A tensile specimen taken at a radius of 4 in. showed the following physical properties: Ultimate strength, 105,600 psi; yield point, 60,300 psi; reduction in area, 46.5 per cent; elongation, 23 per cent in 2 in.

The large steel forging was mounted in a 30-in.-swing engine lathe, Fig. 1, being chucked at the spindle end, and mounted on a live center in the tailstock. This 12-speed geared-head lathe was driven by an alternating-current motor, through a mechanical variable-speed-drive unit so that desired cutting speeds could be maintained as the diameter of the work was reduced by machining.

CUTTING TOOLS

The cutting tools were tool bits $\frac{3}{8}$ in. square \times $3\frac{1}{2}$ in. long, of Red Cut Superior (18-4-1) high-speed steel ground to the shape of 8 deg back rake, 14 deg side rake, 6 deg end relief, 6 deg side relief, 6 deg end-cutting-edge angle, 15 deg side-cutting-edge angle, and $\frac{3}{64}$ in. nose radius. This tool is designated as 8-14-6-6-15- $\frac{3}{64}$ (Fig. 2). It was held in a solid-block tool holder approximately $1\frac{1}{2}$ in. wide, $2\frac{5}{8}$ in. high, and 4 in. long. The tool bit was clamped by one setscrew in the holder with a back slope of $10\frac{1}{2}$ deg. These tool bits were ground on a special tool grinder in which a Norton Company abrasive wheel of 3846J5BE type was used so that the finish was very good at $3\frac{1}{2}$ microin. parallel to the abrasive marks which were at right angles to the cutting edge. The surface parallel to the cutting edge measured $5\frac{1}{2}$ microin.

CUTTING FLUIDS

A commercial all-purpose industrial fluid cooler was used in

addition to the regular cutting-fluid tank on the lathe so as to maintain the larger quantity of cutting fluid, some 40 gal in all, at a constant temperature for each series of tests. A discharge of cutting fluid on the tool of 5 gpm from a $\frac{25}{32}$ -in-ID nozzle was maintained in all tests. A 2100-watt electric heating coil was installed in the tank of the cooler so that the oil could be heated up to the temperature at which each test was to be run. The cooler prevented the temperatures from rising during the tests. A dial-type thermometer reading from 50 F to 250 F was installed in the tank beside the centrifugal pump of the cooler. This

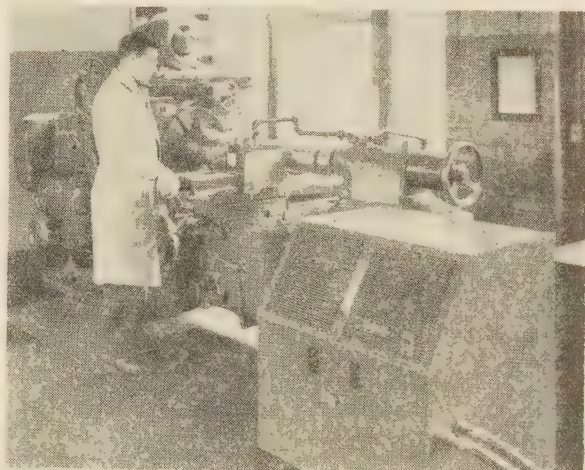


FIG. 1 THE INFINITELY VARIABLE SPEED LATHE AND CUTTING-FLUID COOLER AS SET UP FOR THE CUTTING-FLUID EVALUATION TEST

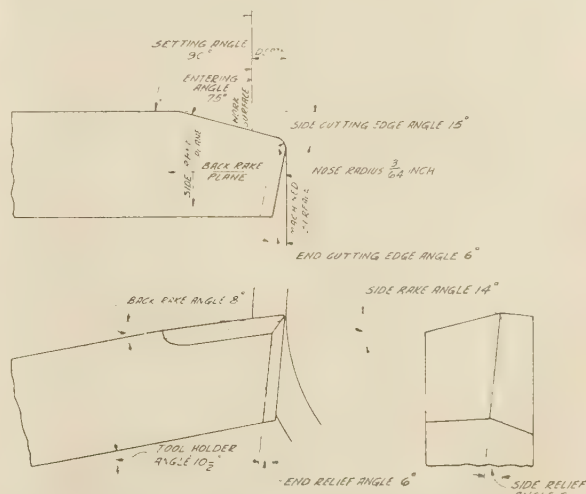


FIG. 2 TOOL-BIT NOMENCLATURE AND SHAPE
(Tool designation 8-14-6-6-15- $\frac{3}{64}$.)

¹ Professor of Metal Processing and Chairman of the Department of Metal Processing, University of Michigan, Ann Arbor, Mich. Fellow A.S.M.E.

² Associate Professor of Metal Processing, University of Michigan. Jun. A.S.M.E.

³ Instructor in Metal Processing, University of Michigan.

Contributed by the Research Committees on Cutting Fluids and Metal Cutting Data and Bibliography and presented at the Annual Meeting, New York, N. Y., Nov. 27-Dec. 1, 1944, of THE AMERICAN SOCIETY OF MECHANICAL ENGINEERS.

NOTE: Statements and opinions advanced in papers are to be understood as individual expressions of their authors and not those of the Society.

was the controlling temperature at which the cutting fluids were applied to the tool.

The cutting oil consisted of a sulphochlorinated petroleum oil which had viscosities at the 7 temperatures at which it was used as follows:

Temperature, F	Saybolt Universal, seconds
55	530
70	320
85	205
100	145
115	110
130	85
150	66

The sulphochlorinated mineral oil referred to is a mixture of a sulphochlorinated fatty-oil base with a mid-continent neutral petroleum oil. Its analysis shows approximately 0.6 per cent sulphur and 0.5 per cent chlorine.

The second series of tests was carried out with an emulsion. This emulsion was made by mixing 1 part of a standard soluble oil with 20 parts by volume of distilled water. Inasmuch as this liquid did not increase in viscosity for the lower temperatures, a low temperature of 40 F was added to the 7 at which the oil was used. The soluble oil used in making the emulsion is of the petroleum-sulphonate-soap type and from appearances and routine tests was an exceptionally well-made product.

CUTTING-SPEED TOOL-LIFE TESTS WITH OIL

As noted, the first series of tests was run with a sulphochlorinated mineral oil. For each of the constant temperatures of the oil, a number of cutting-speed tool-life tests were run. Every third or fourth test was run dry at a given cutting speed of 135 fpm to furnish points for the dry-cutting line and also provide a means of checking the uniformity of the machinability of the test log throughout the tests.

Three or more tests were run with the oil at each of the 7 temperatures, using a depth of cut 0.100 in. and a feed of 0.0125 in. per revolution. These cuts were maintained in all tests. In Fig. 3 ten circles are shown plotted on log-log paper. Each circle represents the tool life obtained in a test run at its corresponding cutting speed. Erratic results were obtained, as indicated by the fact that the points, particularly at the shorter values of tool life, do not lie uniformly on the line. The line shown was taken to represent these data, however. The equation of this line had previously been determined to be $VT^m = C$, in which V is the cutting speed in feet per minute at which the test was run, T is the resulting tool life in minutes, as indicated by the complete breakdown of the tool, n represents the tangent of the angle of slope made between the line and the horizontal line of the graph sheet, and C is a constant depending on the tool material, tool shape, material cut, size of cut, cutting fluid, etc. This line represents the performance of the cutting oil under these conditions in two ways: (1) by its height or vertical displacement as indicated by C (which equals the cutting speed for a 1-min tool life); or (2) by V_3 , which is the cutting speed for a 3-min tool life, or V_{30} , the cutting speed for a 30-min tool life, or T_{135} , which is the tool life for a cutting speed of 135 fpm, etc. Values of V and T for any tool life or speed can be taken, depending on the comparative information desired. The table in Fig. 10 shows these values of C , n , V_3 , V_{30} , and T_{135} .

Figs. 4 to 9 represent corresponding cutting-speed tool-life lines obtained from experimental data shown plotted as circles with a similar tabulated record of the line characteristics. These lines are all grouped for better comparison in Fig. 10. Here the circles representing the various tests in Figs. 3 to 9, inclusive, are omitted to relieve congestion and give emphasis to the lines

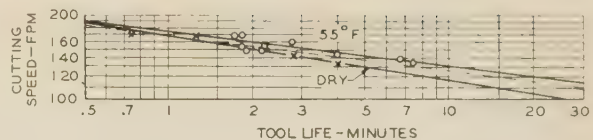


FIG. 3 CUTTING-SPEED TOOL-LIFE LINE ON LOG-LOG PAPER FOR TURNING ANNEALED S.A.E. 3140 STEEL WITH A SULPHURIZED MINERAL OIL MAINTAINED AT A TEMPERATURE OF 55 F AND WHEEL CUTTING DRY

(High-speed steel tool bits $\frac{3}{8}$ in. square were used, ground to a shape of 8-14-6-6-15- $\frac{3}{4}$; depth of cut was 0.10 in. and feed was 0.0125 in. The dots and the light dashed lines represent points of preliminary failure.)

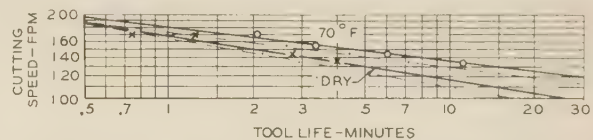


FIG. 4 CUTTING-SPEED TOOL-LIFE LINE WHEN THE OIL IS MAINTAINED AT 70 F
(Other conditions are as given in Fig. 3.)



FIG. 5 CUTTING-SPEED TOOL-LIFE LINE WHEN TURNING STEEL WITH THE OIL MAINTAINED AT 85 F

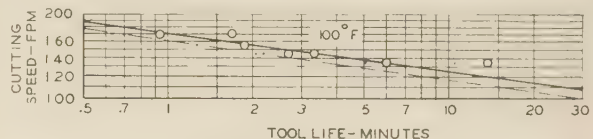


FIG. 6 CUTTING-SPEED TOOL-LIFE LINE WHEN TURNING STEEL WITH THE OIL MAINTAINED AT 100 F

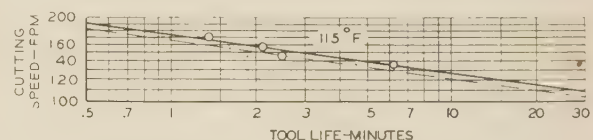


FIG. 7 CUTTING-SPEED TOOL-LIFE LINE WHEN TURNING STEEL WITH THE OIL MAINTAINED AT 115 F

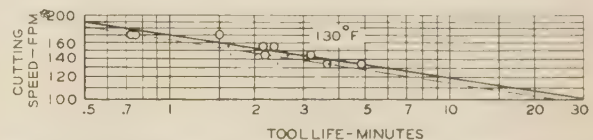


FIG. 8 CUTTING-SPEED TOOL-LIFE LINE WHEN TURNING STEEL WITH THE OIL MAINTAINED AT 130 F

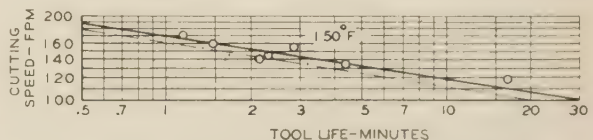


FIG. 9 CUTTING-SPEED TOOL-LIFE LINE WHEN TURNING STEEL WITH THE OIL MAINTAINED AT 150 F

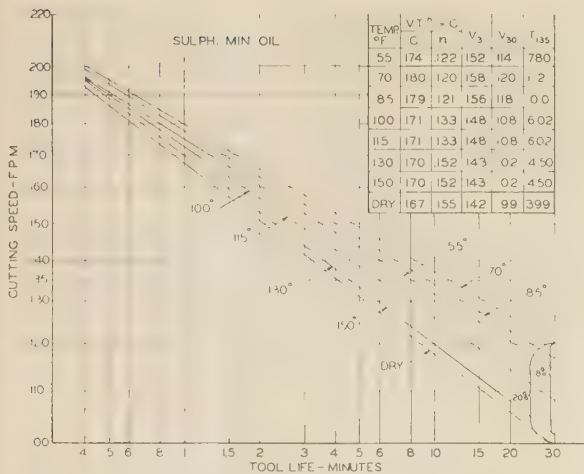


FIG. 10 SUMMARY CHART OF CUTTING-SPEED TOOL-LIFE LINES FOR SULPHURIZED MINERAL OIL AT VARIOUS CONSTANT TEMPERATURES (High-speed steel tool bits of a shape 8-14-6-6-15-3/64 were used to turn an annealed S.A.E. 3140 steel, using a depth of cut of 0.10 in. and a feed of 0.0125 in. The enclosed table gives the characteristics of each line for comparative purposes. The vertical scale of the log-log graph is 5 times that of the horizontal.)

themselves. In Fig. 10, the vertical scale is 5 times that of the horizontal scale, the better to magnify the vertical displacements between the several lines. Any values read from these curves, except that of n (slope), are correct, however. Values of C , n , V_3 , V_{30} , and T_{135} for all curves are also summarized in the table at the upper right in Fig. 10. In Fig. 10, it is clear that the line for the 70 F oil temperature is highest on the graph. This indicates that the cutting speed is highest for any given value of tool life when the cutting fluid is maintained at 70 F. The value of C is 180 fpm, V_3 is 158 fpm, V_{30} is 120 fpm, and T_{135} is 11.2 min. These are the highest values in the table.

The 85 F line is next highest on the graph, indicating probably less cooling effect of the oil. For some reason the line for 55 F is next in height. This position probably results from the fact that at this temperature the viscosity of the oil is 530 SSU, very high—too high to allow the oil to flow freely and act effectively as a coolant. The lines for the temperatures of 100 and 115 F are practically identical and next in height on the chart. Also the line for the 150 F temperature was found to be substantially equal to that of the 130 F. They lie between the line for the 100 and 115 F temperatures and that for dry cutting. The fact that the 150 F line is not lower than the 130 F line may indicate that a high temperature is reached such as 130 F, beyond which little cooling takes place, but that the cutting speed for a given tool life is slightly above that for dry cutting because of the lubricating effect of the oil in reducing the energy required to form the chip. This lubrication probably takes place in the fissures on the outside of the chip. The viscosity of the oil at 150 F is only 66 SSU.

Figs. 11 and 12 summarize the data shown in the table of Fig. 10 and emphasize the value and relationship of the results. Fig. 11 shows viscosity of the oil at different temperatures plotted over the oil temperature, as a solid line. The viscosity is reduced from 530 SSU at 55 F to 66 SSU at 150 F. The dashed line shows T_{135} , the tool life for a cutting speed of 135 fpm; this shows clearly how tool life is low at 7.8 min for the oil at a temperature of 55 F, a maximum of 11.2 min at or a little above 70 F, and then falls off to the lowest value of 4.5 min for the highest temperature of 150 F. It drops further to 3.99 min for dry cutting. This line shows that the best temperature for

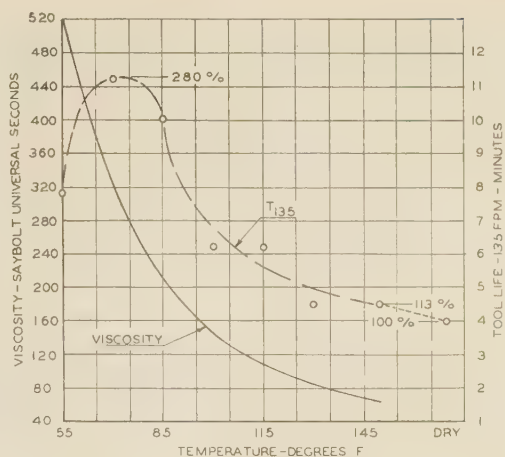


FIG. 11 VALUES OF VISCOSITY, SSU, AND T_{135} OR TOOL LIFE FOR 135 FPM, WHEN TURNING S.A.E. 3140 STEEL WITH A SULPHURIZED OIL AT VARIOUS CONSTANT TEMPERATURES

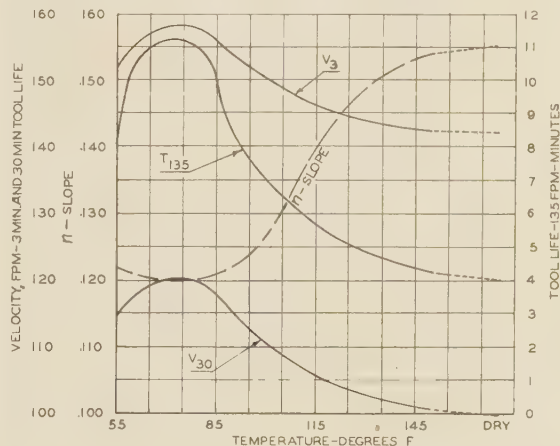


FIG. 12 VALUES OF n , SLOPE, V_3 , V_{30} , AND T_{135} WHEN TURNING ANNEALED S.A.E. 3140 STEEL WITH HIGH-SPEED STEEL TOOLS (Tools ground to a shape of 8-14-6-6-15-3/64 at 0.100 in. depth and 0.0125 in. feed with a sulphurized mineral oil at each of several constant temperatures.)

longest tool life is at or slightly above 70 F. If the value of T_{135} of 3.99 min for dry cutting represents 100 per cent, then the 4.5 min for the 150 F temperature is 113 per cent, and the 11.2 min for the 70 F temperature is 280 per cent. This shows the very effective result of refrigerating the oil.

Fig. 12 gives the summary lines representing V_3 , V_{30} , n , and T_{135} , plotted over the temperature of the oil. If V_3 for dry cutting is 142 fpm and represents 100 per cent, then the value of V_3 of 143 fpm at 150 F is 100.5 per cent, and the 158 fpm for the 70 F temperature is 111 per cent. Again, if 99 fpm is V_{30} for dry cutting and represents 100 per cent, then the 102 fpm for 150 F is 103 per cent, and the 120 fpm for 70 F is 121 per cent.

The values of n , which represent the slope of the lines in Figs. 3 to 9, are low (beneficial) for the low temperatures; this indicates that the line is more nearly horizontal. The values of n are high for the high temperatures and represent lines of greater slope. This indicates that cooling causes a beneficial change in slope of the line from 0.155 for the steep slope of dry cutting and high oil temperatures to the shallow slope 1.2 for the lines for the low-temperature oils. The important significance of the low

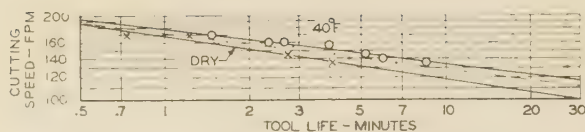


FIG. 13 CUTTING-SPEED TOOL-LIFE LINE ON LOG-LOG PAPER FOR TURNING ANNEALED S.A.E. 3140 STEEL WITH AN EMULSION, CONSISTING OF 1 PART SOLUBLE OIL AND 20 PARTS DISTILLED WATER MAINTAINED AT A TEMPERATURE OF 40 F AND WHEN CUTTING DRY (High-speed steel tool bits $\frac{3}{8}$ in. square were used, ground to a shape of 8-14-6-6-15- $\frac{1}{4}$; depth of cut was 0.10 in. and feed was 0.0125 in. The dots and the light dashed lines represent points of preliminary failure.)

values of n is that the lines for different oil temperatures diverge from some common point at the left of the figure and become more widely spaced for the longer values of tool life. Therefore, for commercial cutting speeds such as V_{480} (the cutting speed for an 8-hr tool life) the differences in cutting speeds would become much greater and be in favor of the lower cutting-fluid temperatures.

CUTTING-SPEED TOOL-LIFE TESTS WITH EMULSION

A second series of tests was carried out to observe the influence of an emulsion at each of the several temperatures, when applied to a turning tool under the same conditions as those listed for the oil. The temperatures used were 40, 55, 70, 85, 100, 115, 130, and 150 F. The emulsion consisted of a commercial soluble oil mixed with 20 parts, by volume, of distilled water.

The experimental data, representing the various tests for the emulsion at 40 F, are shown plotted as circles on log-log paper in Fig. 13. These seven points indicate quite definitely a straight line. Similar lines for the emulsion at other temperatures are shown in Figs. 14 to 20, inclusive, in which the relationship between each line and its experimental data are shown. These lines on log-log paper are then grouped in Fig. 21, so their position with respect to each other may be more clearly observed. The vertical scale of Fig. 21 is logarithmic but elongated to equal 5 times that of the horizontal scale to emphasize the vertical displacements.

In Fig. 21 the line for dry cutting is shown to be the lowest and steepest. Its slope n is 0.155, V_3 is 142 fpm, V_{20} is 99 fpm,

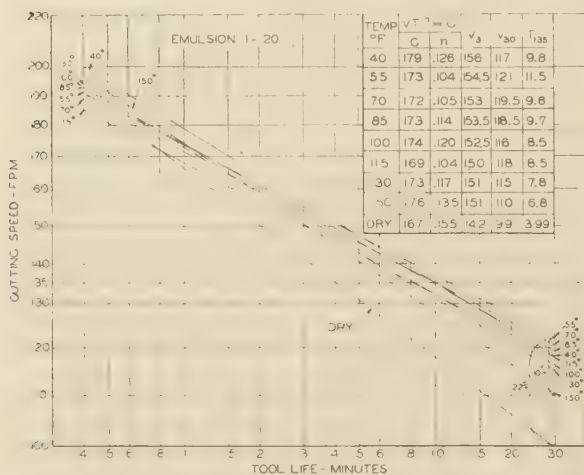


FIG. 21 SUMMARY CHART OF CUTTING-SPEED TOOL-LIFE LINES FOR EMULSION 1-20 AT VARIOUS CONSTANT TEMPERATURES

(High-speed steel tool bits of a shape 8-14-6-6-15- $\frac{1}{4}$ were used to turn an annealed S.A.E. 3140 steel, using a depth of cut of 0.10 in. and a feed of 0.0125 in. The enclosed table gives the characteristics of each line for comparative purposes. The vertical scale of the log-log graph is 5 times that of the horizontal.)

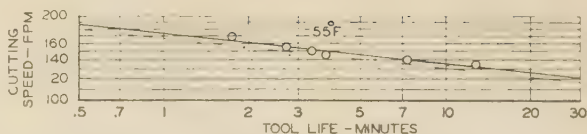


FIG. 14 CUTTING-SPEED TOOL-LIFE LINE FOR EMULSION MAINTAINED AT 55 F; OTHER CONDITIONS SAME AS IN FIG. 13

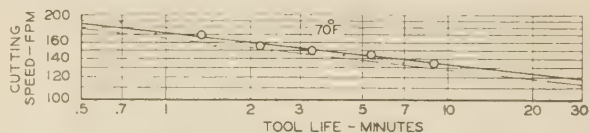


FIG. 15 CUTTING-SPEED TOOL-LIFE LINE WHEN MAINTAINING EMULSION AT 70 F

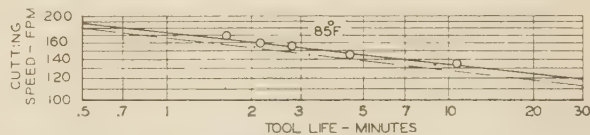


FIG. 16 CUTTING-SPEED TOOL-LIFE LINE WITH EMULSION AT 85 F

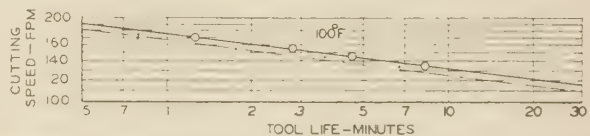


FIG. 17 CUTTING-SPEED TOOL-LIFE LINE WHEN TURNING STEEL WITH EMULSION AT 100 F

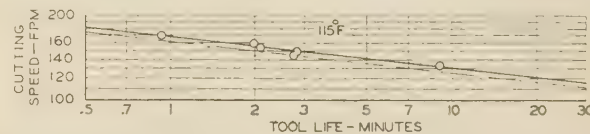


FIG. 18 CUTTING-SPEED TOOL-LIFE LINE WITH EMULSION AT 115 F

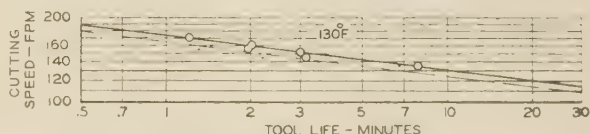


FIG. 19 CUTTING-SPEED TOOL-LIFE LINE WITH EMULSION AT 130 F

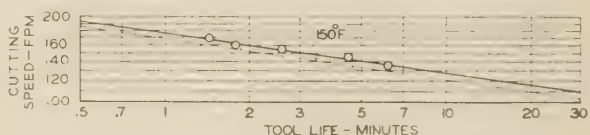


FIG. 20 CUTTING-SPEED TOOL-LIFE LINE WITH EMULSION AT 150 F

and T_{138} is 3.99 min. Corresponding values for the emulsion at each of the eight different temperatures are also given in the table of Fig. 21. The lowest line when an emulsion is used is for the emulsion at 150 F. The highest line is for the emulsion at the lowest temperature of 55 F, while the three next highest lines in order are for 70, 85, and 115 F, respectively.

The line for the 40-deg temperature is highest for all cutting speeds above 150 fpm, but due to its steeper slope, it does not perform so well at lower speeds. At this low temperature the material cut was thoroughly chilled and this may have made it more difficult to machine. The lines for the higher temperatures are shown to have the greatest slope, while the lines for the 55 and 70 F temperatures have the lowest slope. Low values of slope accompanied by high vertical placement on the chart represent the most favorable metal-cutting conditions.

Values of T_{135} (tool life for a speed of 135 fpm) for the emulsion are shown plotted as circles in Fig. 22. The smooth solid line

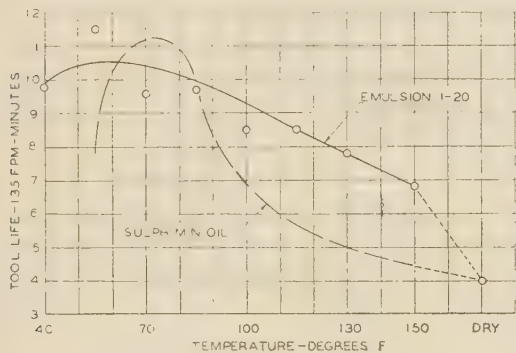


FIG. 22 VALUES OF T_{135} OR TOOL LIFE FOR 135 FPM CUTTING SPEED, PLOTTED FOR EMULSION AS A SOLID LINE, AND SULPHURIZED MINERAL OIL FROM FIG. 11, AS A DASHED LINE OVER TEMPERATURE OF CUTTING FLUID IN DEG F

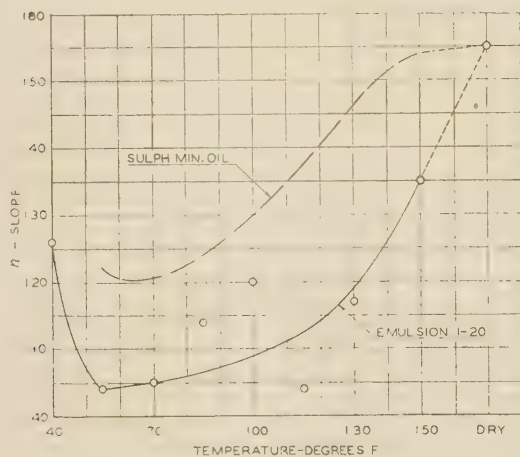


FIG. 23 VALUES OF n SLOPE OF CUTTING-SPEED TOOL-LIFE LINE, FOR EMULSION AS TAKEN FROM FIG. 21, SHOWN AS A SOLID LINE, AND FOR SULPHURIZED MINERAL OIL AS TAKEN FROM FIG. 10, AS THE DASHED LINE, PLOTTED OVER CUTTING FLUID AT VARIOUS TEMPERATURES

represents a mean average. The short dashed line at the right simply connects the solid line with the value of T_{135} for dry cutting. The circles for the temperatures of 70 and 100 F are shown to lie below the solid line and similarly the point for the 55 F temperature appears to be high, but the curve was drawn through the mean values. The long dashed curve represents corresponding values for the oil, as brought forward from Fig. 11, for the sake of comparison. These two curves clearly show that the cooling effect of the emulsion is greater than that for the oil, for all temperatures above 85 F. From these average curves, it appears that the oil is superior to the emulsion for temperatures

between 60 and 85 F. For temperatures below 60 F, the emulsion is superior because of the extremely high viscosity of the oil at these low temperatures.

Values of n (slope) are shown plotted as circles for the emulsion in Fig. 23. The values of slope for the lines for the temperatures of 85 and 100 F seem excessively high, while that for

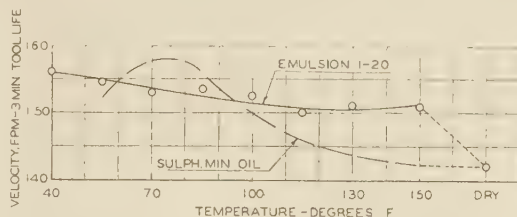


FIG. 24 VALUES OF V_3 , CUTTING SPEED FOR A 3-MIN TOOL LIFE, FOR EMULSION SHOWN AS A SOLID LINE, AND FOR SULPHURIZED MINERAL OIL SHOWN AS A DASHED LINE, PLOTTED OVER TEMPERATURE OF CUTTING FLUID

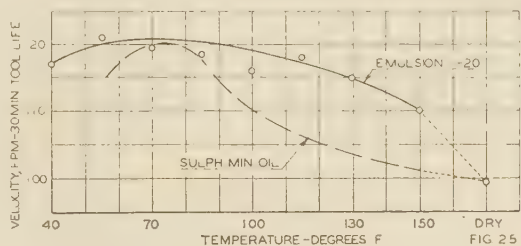


FIG. 25 VALUES OF V_{30} , CUTTING SPEED FOR A 30-MIN TOOL LIFE, FOR EMULSION AND SULPHURIZED MINERAL OIL PLOTTED OVER TEMPERATURE OF CUTTING FLUID

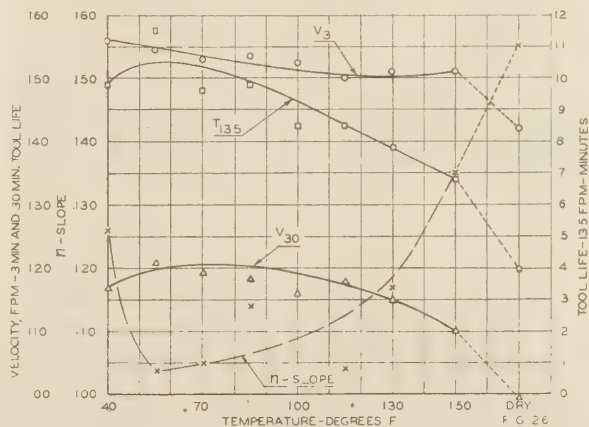


FIG. 26 SUMMARY CURVE CORRELATING VALUES OF T_{135} , V_3 , V_{30} AND n WHEN MACHINING ANNEALED S.A.E. 3140 STEEL WITH HIGH SPEED STEEL TOOL BITS GROUND TO A SHAPE OF 8-14-6-6-15-1/64 USING AN EMULSION OF 1-20 AT EACH OF SEVERAL CONSTANT TEMPERATURES

the 115-deg line is low, with respect to the solid line which is drawn to represent an average. It is not clear why the value of n for the 40-deg temperature line is so high, as the experimental data of Fig. 13 seem to indicate favorably the line shown there. The light dashed line in Fig. 23 again shows the values of n for the oil, as brought forward from Fig. 11 for comparison. The general trends are similar, but the emulsion has in general lower values of slope.

Values of V_3 , the cutting speed for a 3-min tool life, for the several temperatures are shown in Fig. 24 as a heavy solid line,

which indicates that the lowest temperatures give the highest cutting speeds. Again the light dashed line represents corresponding values of V_s for the oil, as brought forward from Fig. 12, for comparison. In the temperature range of 60 to 95 F, the cutting speeds V_s are higher for the oil than for the emulsion.

Values of V_{30} , the cutting speeds for 30-min tool life, for each of the temperatures of the emulsion are shown in Fig. 25. The corresponding line for the oil, as brought forward from Fig. 12, is shown for comparison. Because the emulsion gives lower values of slope in general than the oil, values of V_{30} for the emulsion are higher at all temperatures than for those of the oil. It is clear, however, that the values of V_{30} for the emulsion and oil are nearly equal for the temperature range of 70 to 80 F.

The curves representing T_{135} , n , V_s , and V_{30} , as shown for the emulsion in Figs. 22 to 25, inclusive, are summarized in Fig. 26, for better comparison. The fact that the V_s and V_{30} lines are not similar in shape results from the irregularity of the slopes of the lines.

HEAT COLOR OF CHIPS

The first chip coming from the tool point in the tests on the emulsion at each of the various temperatures gives an indication of the effect of temperature control of the emulsion in relation to heat transfer at the cutting edge of the single-point tool. During the tests using the emulsion, observations were made as shown in Table 1.

TABLE 1 TEMPERATURE OF THE CHIP DURING TESTS WITH EMULSION

Temperature of emulsion, F	Oxide color of chip	Approximate temperature of the chip, F
40	Natural	400 or below
55	Light straw	440
70	Medium straw	460
85	Dark straw	490
100	Purple	540
115	Purple	540
130	Blue	580
150	Blue	580
Dry	Blue	580

The data of Table 1 indicate that emulsions kept at the lower temperatures give more cooling effect on the chip, and those at the higher temperatures allow more heat at the tool point, thus causing shorter tool life and more tool grinds per piece.

CONCLUSIONS

The following conclusions may be drawn from the tests as described:

1 For the sulphochlorinated mineral oil, the tool life in minutes for a 135-fpm cutting speed T_{135} is maximum when the oil is maintained at the temperature of 75 F. Apparently the relationship between viscosity and temperature is most effective then. The maximum value of T_{135} at 75 F is 11.2 min (100 per cent), at 55 F it is 7.8 min (70 per cent), and at 150 F, it is 4.5 min (40 per cent). Dry cutting gives a value of 4 min (35.7 per cent).

2 For the emulsion the maximum value of T_{135} for 60 F is 10.5 min (100 per cent), for 40 F it is 9.8 min (93 per cent), for 150 F it is 6.8 min (64.7 per cent), and for dry cutting it is 4 min (38 per cent).

3 For the oil (the cutting speed for a 30-min tool life) V_{30} for the 75 F is 120 fpm (100 per cent), for the 55 F is 114 fpm (95 per cent), for the 150 F is 101.5 fpm (84.7 per cent), and for dry cutting it is 99.0 fpm (82.5 per cent).

4 For the emulsion, V_{30} for the 75 F is 120.6 fpm (100 per cent), for 40 F is 117 fpm (97 per cent), for 150 F is 110 fpm (91.4 per cent), and for dry cutting it is 99 fpm (82 per cent).

5 For the oil, the slope n of the cutting-speed tool-life lines is low (0.12) for the low range of temperatures and high (steep) (0.155) for the high range and dry cutting.

6 For the emulsions, the slope is low (0.104 to 0.115) for the temperature range of 55 to 130 F, inclusive, but high for other temperatures, as 0.125 for 40 F, 0.135 for 150, and 0.155 for dry cutting.

7 It appears that the high viscosity of the oil at the temperatures below 70 F is detrimental and that cooling is impaired. At the high temperatures, the viscosity of the oil is low but its ability to carry heat away is reduced. The cutting speed for a 30-min tool life at the high temperatures of the oil is only about 2.2 per cent above that for dry cutting. The increase in cutting speed because of the cooling of the oil is about 18 per cent for cooling the emulsion 10 per cent.

8 The most effective operating temperature of the oil is from 70 to 75 F, whereas the emulsion was most effective at a temperature of 55 to 70 F.

9 In general, the slope of the cutting-speed tool-life lines for the emulsions is below those for the oil at corresponding temperatures.

ACKNOWLEDGMENT

This work has been done as an Engineering Research Project at the University of Michigan, sponsored by the Gray-Mills Company of Evanston, Ill. Model No. 400 industrial fluid cooler of that company was used to keep the oil and emulsions at the constant low temperatures.

Discussion

W. A. ALEXANDROFF⁴ AND Z. LETELLIER.⁵ The writers believe that the temperature of a cutting fluid plays an important part not only on the tool life but on the finish as well. It is felt that the authors of this paper have done a good job on a very important phase of metal turning as the writers have always observed a difference in tool life for different temperatures of cutting fluid.

The tool life is different on a machine that has stood idle for some time, thus allowing the cutting fluid to cool, than it is after the machine has been run long enough to heat up the fluid. Owing to the fact that no cooling apparatus is provided for cutting fluids on commercial machines, it often results that a higher-viscosity oil is used than would otherwise be necessary. This is done because at the higher temperatures, the heavier oil is about the correct viscosity, its flash is generally higher, and by its use smoking is avoided. However, at the elevated temperatures, the oil cannot carry away the heat as it should. On the other hand, when this heavy oil is cooled, as when the machine has been standing idle, its viscosity is entirely too high, and again the heat is not properly removed. Therefore, it appears that the body of the oil with respect to temperature or its viscosity index, as commonly called, becomes an important factor.

The oil used for the test in this paper has a viscosity of 85 sec at 130 F, and 530 sec at 55 F. Thus for a temperature change of 75 F, the oil changed viscosity by 445 sec. Such a rapid thickening of the oil as it is cooled would quickly offset the cooling effect due to the lower temperature, by the inability of the oil to scrub the surface and properly remove the heat.

The paper indicates that the best temperature for an oil coolant is 70 to 75 F, and for the emulsion type of coolant is between 55 and 70 F.

We believe that much better results would be obtained on the oil at the temperature between 55 and 70 F (the same as the emulsion), provided a change is made in the oil to one of a lighter body and one that does not thicken so much when cooled, i.e., an oil

⁴ Technical Adviser, Pate Oil Company, Milwaukee, Wis. Mem. A.S.M.E.

⁵ Vice-President, Pate Oil Company, Milwaukee, Wis.

with high viscosity index. By using an oil with higher viscosity index, its body in the temperature range of 55 to 70 F would then be about the same as the body of the oil used at 70 to 75 F.

This change would allow, in the lower temperature range, a more satisfactory viscosity plus the added advantage of greater cooling as a result of the lower temperature of the oil.

It would have been interesting had the authors noted the shape and size of the chips formed at the various test temperatures, as this might have thrown light on the theory sometimes advanced that the functions of a cutting fluid are not only that of carrying away the heat from the work and its lubricating value, but also its chilling action on the upper surface of the chip which causes it to shrink and form short curling chips.

The authors' observation of the color and temperature of the chips and their relation to tool life when using a water emulsion is interesting. The writers have recently encountered a case that seems to substantiate their findings. When turning an S.A.E. 1025 steel forging $3\frac{1}{2}$ in. long and $2\frac{1}{2}$ in. diam on a Cabolite single-spindle lathe with a Vascology steel tool, it was observed that the tool life did not conform with other machines performing the same operation, and that the chips were much darker in color. On investigating it was found that the temperature of the water emulsion used was much higher than the emulsion on the other machines. Further investigation showed that the operator had allowed the volume of the solution in the reservoir to drop to a minimum. When the volume of the solution was restored, the temperature of the solution dropped considerably, tool life returned to normal, and the color of the chips became noticeably lighter. It is unfortunate that the circumstances at the time did not allow for more detailed information.

The effect of the temperature of a cutting fluid on various machining operations on steel has undoubtedly come to the attention of many investigators. An interesting case of this nature has recently been brought to the writers' attention. While it does not deal with the turning of steel, it does bring out the points the authors of this paper wish to convey, i.e., that the temperature of the cutting fluid has a bearing on tool life. The case deals with the drilling of a blind 0.72-in. hole 12.56 in. deep in a 1.8-in.-diam AMS 62-53 stainless-steel forging on a special Davis-Thompson horizontal drilling machine. A Carboly-tipped gun drill with a $\frac{1}{16}$ -in. oil hole was used, traveling at 600 rpm. Numerous cutting oils were tried, tolerances could not be held, and tool life was very poor. Water emulsions were also tried with no appreciable improvement. The oil temperature rose to 110 F during the operation. It was therefore decided to investigate the effects of the temperature of the cutting fluid on the operation. A 200-gal coiled tank and pump were installed and city water was passed through the coils, the temperature of the oil being controlled by the flow of the water through the coils. The oil was pumped through the drill under a pressure of 325 psi. Beneficial results were immediately obtained. Tests were taken at several temperatures from 110 F to 70 F, and best results were obtained in the 70 to 80 F range. The oil is now maintained at 72 F, and expected tool life and tolerances are obtained with a conventional-type cutting oil.

The writers question the supposition that the low-tool-life results obtained with the water emulsion at the 40 F test temperature could be caused by the chilled condition of the test piece, because it is not believed that the hardness of the metal would be increased to any degree with such a small drop in temperature. In order to verify this, the hardness of a disk of S.A.E. 3140 steel 3 in. diam $\frac{1}{2}$ in. thick was determined at several steel temperatures with the following results:

At 75 F, Brinell hardness = 217
At 55 F, Brinell hardness = 217
At 40 F, Brinell hardness = 217

It is agreed that hardness is not the sole criterion of the machinability of a steel, but under the excellent controlled conditions used by the authors of this paper in their tests, it is felt that, in this case, the hardness does indicate the machinability, and therefore the writers do not believe that the poor results obtained on the 40 F test can be attributed to the effects of the temperature on the machinability of the test piece.

JOSEPH GESCHELIN.⁶ The department of metal processing, University of Michigan, is noted for its contributions to the art of metal cutting, and its work, in combination with others doing fundamental research in this field, should go far to mold the advanced practice in metal cutting and in the utilization of cutting fluids.

It is to be regretted that industry in general has not appreciated the vital role of the cutting fluid in metal cutting. Much progress has been made in that direction, some of it possibly due to the influence of the committee with which many of us are associated. Unquestionably the work done by the authors will have a great deal to do with improved methods and more economical metal removal.

The present paper is extremely valuable. It focuses attention upon an important phase of metal cutting, namely, the refrigeration of the cutting fluid as an aid to better metal removal and longer tool life. During the war, some manufacturers have adopted this practice. However, the subject is not widely understood nor appreciated, and it is hoped that this paper and other work along the same line in the future will result in better understanding of the principle and its practical applications.

F. W. LUCHT.⁷ It would be interesting to know what kind of results the authors would have obtained if they had substituted a suitable steel-cutting grade of cemented carbide for the 18-4-1 high-speed steel and operated the lathe at cutting speeds ranging between 200 and 400 surface fpm. It might have been necessary also to use slightly different rake angles on the tool. It might have been necessary to check the size of the motor in their machine because their feed of 0.0125 in. when operating at increased revolutions might have placed an added burden on it. This results from the fact that the rate of metal removal would have been doubled or tripled. The carbide industry does not have any tangible data similar to that which the authors have compiled, and would welcome it. Have the authors done any such work with cemented carbides?

All indications to date, as a result of plenty of experience, are that the longest tool life would have resulted from the runs mentioned, when cutting dry, because it is questionable if at a cutting speed of 200 fpm and greater the coolant would have reached the point of the tool. The main reason for this is that the chip would have developed at such a high rate of speed that the coolant would never have been permitted to reach the immediate surface being cut, unless the velocity of the coolant was great enough and was directed at the tool point underneath the curling chip.

Our experience indicates that pure water with only enough soluble oil added to it to prevent the rusting of the machine parts serves as one of the finest coolants when turning steel with carbides. Many times we are forced to use such a coolant to maintain work tolerance when much better tool life might be obtained cutting dry. The main hazard when using a coolant is to keep the tool sufficiently cool at all times so that the tool will not be chilled too quickly when it comes out of the cut.

We are sorry to say that cutting oils, as developed to date,

⁶ Chairman, Independent Research Committee on Cutting Fluids; Detroit Editor, Chilton Publications, Detroit, Mich.

⁷ Development Engineer, Carboly Company, Inc., Detroit, Mich. Mem. A.S.M.E.

have never seemed to contribute much to the life of carbide tools when operating at the more efficient higher carbide cutting speeds. It is difficult to keep the flow of the oil on the work and within the confines of the machine when operating at these high cutting speeds. It also makes what might be termed a messy job.

We have also found that, even though there is a sufficient volume of oil to flood the entire cut in the vicinity of the tool, the moment the chips emerge from the oil stream and drop into the chip pan they create a new problem. A dense cloud of objectionable vapor rises from the pile of chips and many operators do not care to work anywhere near it.

We are glad to say that cutting oils are used successfully with cemented-carbide-tipped gun drills. In this particular application, an ample volume of oil is used which cools the chips within a confined space before they contact the air.

Any kind of a cutting fluid would be welcome which could be used with cemented carbides for turning steel at the lower cutting speeds, and reduce or even eliminate the built-up edge which is so troublesome at these lower speeds.

W. H. OLDACRE.⁸ Once again Dr. Boston and his associates have brought us a well-documented well-organized report on a specific research in metal cutting. This report will be very valuable if properly understood and clearly correlated with the complete metal-cutting picture, but much harm is almost certain to result from poor correlation and misunderstanding.

Too often consideration of metal-cutting problems suffers from attempts at oversimplification. Crowding the many complexities and perplexities of the behavior of metals, the mechanisms of lubrication, the relationships of tool and work materials, and the chemical effects of cutting fluids into the mold of our limited understanding, we toil busily, recapturing the spill but making poor progress toward comprehensive clarification.

The effects of temperature change are universal. Therefore, in appraising the results of this investigation and applying them to everyday metal cutting, generalizations must be carefully avoided.

In any particular case, what is the effect of temperature on the material of the tool and the workpiece? Most materials become stiffer on cooling. With some this improves machinability, with others it does not. The viscosity of oils changes greatly with temperature; this in turn affects velocity of flow and heat-transfer characteristics. Undoubtedly, chemical activity plays an important part in the functioning of sulphurized, chlorinated, and other special oils frequently used in metal cutting. Chemical activity is accelerated at higher temperatures. Whether greater or less activity is desirable depends upon specific conditions.

Equilibria in multiphase emulsions and soap-oil systems fluctuate with temperature, and performance is thereby affected but just how is not apparent.

Undoubtedly, temperature regulation will play an important part in tomorrow's machining processes but there is little basis for the assumption that cooling alone will be a panacea.

AUTHORS' CLOSURE

The authors are pleased with the amount of interest that the subject matter of this paper has aroused. While the scope of the paper was limited, it obviously has pointed directly to the primary value of cooling the tool in order to increase tool life. These results have been confirmed in a number of letters re-

ceived from manufacturing plants. As Messrs. Alexandroff and LeTellier have pointed out in their discussion, the application of cutting oils at lower temperature is more advantageous providing the viscosity is not increased, disadvantageously. It is doubtful, however, if it would be commercially practical to operate oils at temperatures below that of 70 deg or so because of the possible influence on the composition of the oils as brought out by Mr. Oldacre in his discussion and because of the chilling effect on the tools.

The authors did observe, not only in these tests but in others, that chips coming from the tool at high speeds and with inadequate cooling are blue, whereas either a drop in speed or better cooling will cause the chips to be removed at lower temperatures and retain the steel-like color. These and similar results have been reported previously in other papers.

It has been found that simply by chilling the steel test log the tool life has been increased. For example, in one test conducted several years ago, a 6-in-diam \times 24-in-long test log of annealed 3140 steel when turned under standard conditions with a high-speed steel tool bit gave the equation $VT^{0.0645} = 125$ when the test log was heated to 200 F and cutting was done dry; $VT^{0.0856} = 140$ when the test log was at a temperature of 65 F when cutting dry, and $VT^{0.103} = 149$ when the test log was chilled for 24 hours at 0 F. This means that the slope (tangent) of the cutting-speed (V) tool-life (T) line for the test log at 200 F was 0.0645 and the cutting speed for a 1-minute tool life was 125 fpm. For the test log at 65 F the slope was 0.0856 and the cutting speed for a 1-minute tool life was 140 fpm. For the test log chilled to 0 F, the slope was 0.103 and the cutting speed for a 1-minute tool life was 149 fpm. When cutting the same log at room temperature, cooling the tool with an emulsion, the slope of the line was 0.107 and the cutting speed for a 1-minute tool life was 157 fpm. For a 30-minute tool life, cutting speeds would be 100.3, 104.5, 105, and 109, respectively. It is therefore seen that by chilling the log even to 0 F, the tool life is not as long as when using an ordinary emulsion as a cooler. The statement in the paper to the effect that the steel is harder at lower temperatures is obviously incorrect.

Mr. Lucht has raised the question of value of a coolant on carbide tools when turning. He then proceeds to answer the question, stating that cutting fluids do not seem to contribute much to the life of carbide tools, that the cutting fluids become messy by splashing and vaporizing at these high speeds, and that there is danger of cracking the tipped tools of carbide through the possible sudden changes in temperature caused by intermittent cooling. The authors agree with these conditions in general but have no further information to offer on the subject. Mr. Lucht further states that any cutting fluid which would tend to reduce or eliminate the built-up edge in the lower range of cutting speeds would be welcome. Probably one of the chief virtues of carbide tools is that they can withstand high cutting speeds, and high cutting speeds in themselves are believed by the authors to be the principal medium of reducing the size of the built-up edge. Even at the normal cutting speeds associated with high-speed steel cutting tools, it is evident that the built-up edge is better when the tools are operated at the higher speeds.

Mr. Oldacre raises the question as to the chemical stability of the oils when operated at temperatures above or below normal operating temperatures. This is, of course, a problem constantly being met but on which little constructive data are available at the present time. Undoubtedly this subject alone would profit by further research.

⁸ President and General Manager, D. A. Stuart Oil Company, Chicago, Ill. Mem. A.S.M.E.

A Thermal-Balance Method and Mechanical Investigation for Evaluating Machinability

By A. O. SCHMIDT,¹ W. W. GILBERT,² AND O. W. BOSTON³

The first section of this paper reports on the results of an investigation of a calorimetric process for the determination of drilling forces. Tests were run on a drill press which was provided with a dynamometer for registering torque and thrust. The calorimetric setup was mounted on the accurately calibrated dynamometer. The temperature rise of 50 cc of water which surrounded the tool and test bar during the cutting operation was determined. Horsepower was computed from the torque and thrust registered on the dynamometer and was found to agree substantially with the power determined from the temperature changes in the calorimeter due to cutting. The results of another series of tests run on a different machine using calorimetric apparatus of slightly changed design are also given. The second section of this paper gives a description of the machine used and the tests made prior to the investigation with the calorimetric apparatus. In these experiments a tubular test bar was cut by a tool mounted in a special holder in a drill press spindle. The feeding of the tool was effected by a weight. Because of chip interference during the cutting of magnesium alloys, these penetration tests were discontinued in favor of the calorimetric tests.

DISCUSSION OF PREVIOUS INVESTIGATIONS

THE problem of the machinability of metals and other engineering materials is encountered daily in every machine shop. Since this problem varies with each material, cutter, and machine tool, and also with many other factors, numerous investigations have been conducted. Even if each of them gave the answer to a particular question, so far it has not been possible to sum them up in a "comprehensive philosophy of metal cutting." This statement was made by O. W. Boston (1)⁴ in a discussion of the results of his own work and those of other research workers in the field of metal cutting. He lists nine methods used in the investigation of machinability, of which the determination of tool life, power consumption, and surface finish are now recognized as the most representative machinability tests.

Since it is necessary to have a considerable amount of experience and also special equipment in order to conduct and evaluate these tests, other and simpler methods have been devised in an attempt to gain an easier and more rapid method of finding the relative machinability of various materials.

¹ Research Engineer in Charge of Metal Cutting Research, Kearney & Trecker Corporation, Milwaukee, Wis. Mem. A.S.M.E.

² Associate Professor of Metal Processing, University of Michigan, Ann Arbor, Mich. Mem. A.S.M.E.

³ Professor of Metal Processing, Chairman of Department, University of Michigan, Ann Arbor, Mich. Mem. A.S.M.E.

⁴ Numbers in parentheses refer to the Bibliography at the end of the paper.

Contributed by Special Research Committees on Cutting Fluids and Metal Cutting Data and Bibliography and presented at the Annual Meeting, New York, N. Y., Nov. 27-Dec. 1, 1944, of THE AMERICAN SOCIETY OF MECHANICAL ENGINEERS.

NOTE: Statements and opinions advanced in papers are to be understood as individual expressions of their authors and not those of the Society.

The penetration test on the drill press, in which a standardized drill works under a constant load and speed for a definite time, was used by Boston (2) and Kessner (3). This method assumes that the drill makes a hole with a depth proportional to the machining properties of the metal tested. Because there exists a great deal of friction on the margin and chisel-edge point of the drill, the penetration tests have not been found reliable. The same can be said of the sawing test, mentioned by A. S. Kenneford (4), in which the time required to saw a test bar with a power hacksaw is measured. Here, again, the high amount of friction developed at the hacksaw blade is a varying factor, and therefore the cutting time does not give a true measure of machinability. Boston (5) measured the effect of cutting fluids on the performance of a hacksaw and found large variations in the time required to cut off 1½-in-square sections of eight different metals when applying various cutting fluids.

Hardness tests, for which definite relationships to other physical properties are established, Boston (2) found to be remote and also misleading as a measure of machinability, when he tested 18 ferrous and 21 nonferrous metals. Changes in the structure of the metal are caused by the tool pressure. E. G. Herbert (6) investigated this problem and found that metals are work-hardened ahead of the cutting edge. This hardness of the test log is affected by (a) ductility or brittleness, and (b) its capacity for work-hardening. Sorenson and Gates (7) collected machining data on more than 100 different S.A.E. steels and established machinability ratings on the basis of volume of material removed in a given time. It was found that to some extent decreasing hardness and tensile values gives an increase in machinability, but there are also wide divergencies.

Several investigations with the purpose of measuring the temperature during the metal-cutting operation have been carried out. Boston and Gilbert (8) conducted tests to determine the cutting temperatures developed by single-point turning tools. They used the tool-work thermocouple method in which the cutting tool and the test log acted as the two elements of the thermocouple. In their tests they measured a maximum temperature of approximately 980 F for certain conditions, but came to the conclusion that the temperatures as measured with the tool-work thermocouple may be affected by changed electrical properties of the metal in the test log, which is compressed and deformed by the tool point. E. G. Herbert (9) in England also used this method, and K. Gottwein (10) in Germany used it while investigating the relation of tool temperature to chip cross section in turning.

Friedrich Schwerd (11) questioned which part of the tool gains the maximum temperature and developed an optical arrangement which directs the heat rays from a point on the chip to a highly sensitive thermoelement. Boston and Gilbert (8) think that it is doubtful whether the maximum or even proportional temperatures could be obtained by Schwerd because his setup allows the measurement of the temperature distribution on the surface only. They found that the temperature of the tool is also dependent upon the built-up edge. This built-up edge is formed on the tool by compressed layers of ductile materials

and is influenced by numerous factors which are discussed by Hans Ernst (12).

Although these various investigations were conducted to determine cutting temperatures, only a part of the temperature was recorded in each case and a large amount of the heat was not measured. During each cutting operation, heat is lost by the conduction of the tool, toolholder, and workpiece, as well as by radiation and convection.

A test which was carried out to determine the amount of heat generated during a metal-cutting operation was reported by Count Rumford (13) to the Royal Society on January 25, 1798. With a blunt boring tool he machined a brass cannon barrel submerged in a box filled with water, Fig. 1. The experiment was conducted as an inquiry concerning the source of heat, and it constitutes the first recorded research to measure the heat generated by friction during the cutting operation of a machine tool.

Joule (14) made several investigations of the mechanical equivalent of heat. In one of these, he used beveled cast-iron wheels pressed against one another while revolving under water and observed the increase in temperature. A similar arrangement was employed by Favre (15) who used a copper disk rotating in a partitioned ring which steel springs forced to contract. In this case, the friction was used to heat a mercury calorimeter. Hirn (16) performed a number of experiments on the friction and deformation of metals for the determination of the mechanical equivalent of heat. He also measured the heat generated while boring metal but did not give any description of the equipment.

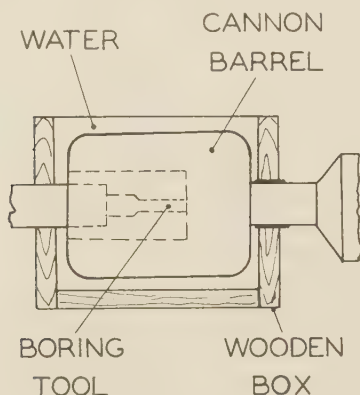


Fig. 1 CALORIMETRIC TEST SETUP AS USED AND ILLUSTRATED BY COUNT RUMFORD

(On left-hand side is an iron bar to the end of which a blunt boring tool is fixed which is forced against bottom of bore in cannon. Tool and workpiece are submerged in a wooden box filled with water.)

Brackenbury and Meyer (17) conducted a few calorimetric tests to determine the heat in the chips and in the test bar. A lathe was used and the chips were collected in a pan filled with water. The temperature rise of this water and the temperature rise in another quantity of water into which the test bar was dropped at the end of the test, were used in the computation of the power required to cut the test bar. Similar tests were conducted by Friedrich (18) who stated that the temperature of the chips increases with the cutting speed when the cross section of the chips remains the same.

Sawwin (19) arranged a calorimeter and dynamometer on a lathe. He used a two-lip cutter similar to a milling cutter to cut a tubular test bar. Although, with this setup, he tested mainly the cooling and lubricating effect of cutting oils and emulsions, he had found in earlier experiments that the work expended in metal cutting was transformed into heat.

CALORIMETRIC PROCESS APPLIED TO DETERMINATION OF TOOL FORCES

In the reported tests water is employed as a means of measuring the quantity of heat generated by a combination of friction and deformation during the cutting operation. To measure the quantity of heat thus generated, the tool and workpiece are submerged during the cutting operation in a specified quantity of distilled water. The temperature of the water at the beginning and end of the cutting operation is read by a thermometer. Rate of cooling is observed and used for the determination of the temperature which would have been attained at the end of the cutting operation if no radiation, conduction, and convection had taken place. When work is transformed into heat, or heat into work, a quantity of work is the mechanical equivalent of a quantity of heat. Thus by observing the temperature changes of the water surrounding the tool and workpiece during the cutting operation, it is possible to study the power requirement for the cutting of different materials and the effect of tools upon the power consumption by changes in tool design.

The test specimen and the cutting tool are arranged in a container so that both will be covered by water. Therefore, to obtain a correct computation of horsepower, the water equivalent of the container, test specimen, and all the other parts which are immersed in water must be considered with the water in the container. The time of cutting is constant; it can be chosen to suit the particular test and made short enough to eliminate noticeable heating through agitation of the water. To minimize the influence of the surrounding temperature, the water and all parts of the equipment should be at room temperature at the beginning of the experiment. All the necessary values are therefore available for the determination of the horsepower required in the cutting of metals or other materials from the heat generated in the cutting operation.

The calorimeter can be taken as one body of weight W with a temperature t which has a mean specific heat c_m . A change of temperature dt of this body brings about a change dQ of the heat in the body

$$dQ = Wc_m dt$$

The quantity of heat which this body absorbs when being heated from room temperature t to a higher temperature t_h is

$$Q = W \int c_m dt$$

Since c_m can be considered as constant in this case and all parts of the calorimeter as having attained the same temperature

$$Q = Wc_m (t_h - t)$$

PROCEDURE AND EQUIPMENT FOR CALORIMETRIC TESTS ON DRILL PRESS

The calorimetric apparatus is shown in Fig. 2. Two centering pins protruding from the top surface of the dynamometer fit into holes in the finished base plate. It is thus assured that the test bar is always centered with the drill. The test bar has an outside diameter of 0.375 in. and is 1.625 in. long. The pilot hole in the center is 0.110 in. diam and $1\frac{1}{4}$ in. deep. The thread at the bottom is $\frac{3}{8}$ in. N.C. and $\frac{1}{2}$ in. long. To insure uniform cutting conditions, the test bars are countersunk at the top with a $\frac{7}{16}$ -in. drill. The container is of sheet metal 0.012 in. thick and can be removed from the rubber gasket to permit easier mounting and removal of the test bar. A $\frac{5}{8}$ -in.-thick felt insulation is wrapped tightly around the container. The drill is $\frac{7}{16}$ in. diam with a helix angle of 30 deg, a point angle of 118 deg, and 12 deg relief angle. It is held in the universal chuck of the drill press on the table of which the dynamometer is mounted.

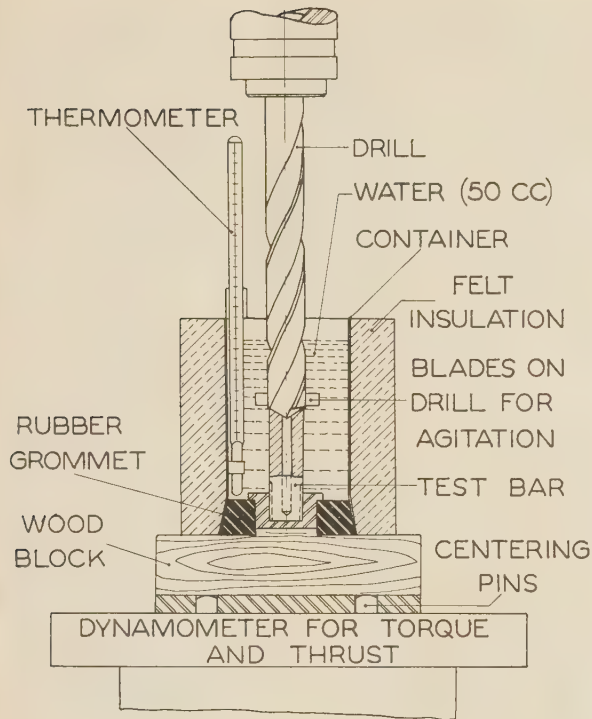


FIG. 2 CALORIMETRIC APPARATUS FOR DRILLING TESTS MOUNTED ON A DYNAMOMETER FOR REGISTERING TORQUE AND THRUST SIMULTANEOUSLY

(The calorimeter is located on top of dynamometer by two centering pins. Test bar is threaded at lower end and screwed into a holder.)

After the test bar is screwed into the holder, the container with the felt insulation is put in place and the calorimeter is set upon the dynamometer. With a pipette, 50 cc of distilled water is measured into the container. This water completely covers the test bar and the drill for a height of $\frac{3}{4}$ in. when the point of the drill touches the test bar before cutting has started. The thermometer is put in the container and is held in place by braces. Water temperature is taken before cutting begins (it should be about equal to the room temperature). Feed is stopped after 1 in. of the test bar has been cut. Water temperature is noted again when the maximum temperature has been reached, about 2 sec after the drill has stopped cutting. The drill is kept running in the water during this time. To effect a better stirring action, the drill is provided with two blades of sheet metal, 0.012 in. thick, which are soldered to the land. The blades extend $\frac{3}{16}$ in. from each side of the drill. They pass the thermometer without interference and the water is churned but not thrown out of the container. The chips cut from the test bar do not sink to the bottom but are kept floating by the turbulence of the water. The thermometer used is graduated in 1-deg increments and is read with a reading glass.

Nine Dowmetal alloys were used for these tests, the drill press spindle making 700 rpm and having a feed of 0.0025 in. per revolution. A number of tests were made with varying feeds on test bars of the same extruded Dowmetal. On another drill press, with a different speed and feed, a three-jaw chuck clamped on the table was used to hold a test bar of the same design but with a length of $2\frac{5}{16}$ in., Fig. 3. A $\frac{7}{16}$ -in. drill which had blades soldered on for better stirring action did the cutting.

Spindle speed was 510 rpm with a feed of 0.004 in. per revolution. All of the different magnesium alloys were tested in this

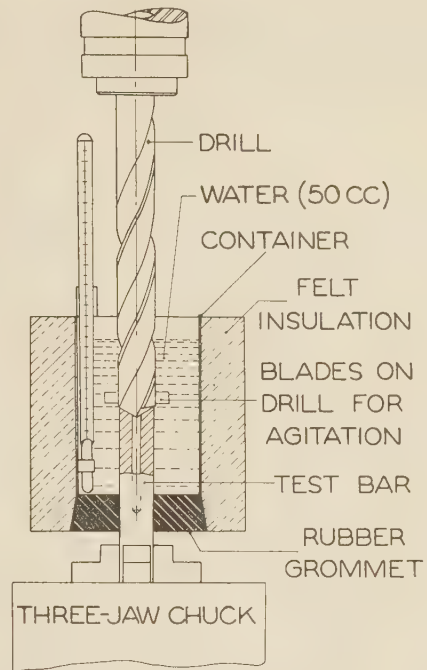


FIG. 3 CALORIMETRIC APPARATUS FOR DRILLING TESTS
(Test bar is held in a three-jaw chuck which is mounted directly on table of drill press.)

manner, and the results were in agreement with those of the first setup. The same agreement was found with test bars made of steel and brass when cut on either machine.

A series of tests was conducted with a room temperature of 55 F, as compared to 70 F, when the other tests were made. The difference in temperature in the calorimeter was the same in each case.

The felt insulation was removed during a number of tests. As a result, the temperature difference was between 5 per cent and 10 per cent lower, depending upon the surrounding temperature which was changed by opening doors and windows.

DISCUSSION AND INTERPRETATION OF RESULTS

The main advantage of this testing method is that it shows even small differences in the cutting properties of various metals and alloys. In order to measure the heat generated during the cutting operation as accurately as possible, using only 50 cc of water in these tests is expedient. A larger volume of water causes smaller temperature rises. This makes the differences in thermometer readings less pronounced and also necessitates the use of a correspondingly larger agitator.

Readings of torque and thrust were taken simultaneously for each test bar as it was cut in the calorimeter. In order to obtain accurate readings of torque and thrust on the dynamometer, the drill was ground with a slight brass point. This of course increased the power values but resulted in cutting without vibration and permitted true readings of the dial gages, which registered torque and thrust with a high degree of accuracy. The values are given in Tables 1, 2, and 4 and are the averages of 10 recorded tests with each metal.

Magnesium alloys were all cut with the same drill, and the differences measured in temperature were within ± 0.2 deg F for each alloy (see Table 3). Care was taken to keep the felt insulation dry as otherwise a marked change in temperature

TABLE 1 TABLE OF TEST DATA FROM DYNAMOMETER AND CALORIMETER, FIG. 2^a

Material Cut	No.	Temp. Difference in Degrees F.	Torque in lb ft	Thrust in lb	Horsepower from Torque and Thrust	Horsepower per cu in. per min (Torque + Thrust)	Horsepower from Heat	Horsepower per cu in. per min	Ratio in Per Cent Horsepower from Heat Torque + Thrust	Hardness Brinell	Tensile Strength lb per sq in.	Composition of Alloy
Downmetal Extruded	1	13.00	.605	83.5	.0810	.458	.0789	.446	97.4	53	40,000	3 Al 1 Zn
Downmetal Extruded	2	13.80	.631	94.4	.0846	.478	.0838	.474	99.5	65	43,000	6 Al 1 Zn
Downmetal Extruded	3	11.6	.534	65.8	.0714	.404	.0702	.397	98.3	40	40,000	1.5 Mn
Downmetal, As Cast	C	13.85	.631	95.0	.0846	.478	.0839	.475	99.2	60	24,000	9 Al 2 Zn
Downmetal, Heat Treated	C	13.85	.631	95.0	.0846	.478	.0838	.475	99.2	60	39,000	9 Al 2 Zn
Downmetal, Heat Treated and Annealed	C	13.85	.631	95.0	.0846	.478	.0838	.475	99.2	75	39,000	9 Al 2 Zn
Downmetal, As Cast	H	13.85	.640	100.0	.0852	.482	.0839	.478	98.4	50	27,000	6 Al 3 Zn
Downmetal, Heat Treated	H	14.95	.695	104.0	.0927	.525	.0902	.510	97.2	50	38,000	6 Al 3 Zn
Downmetal, Heat Treated and Annealed	H	13.50	.629	98.0	.0842	.476	.0818	.464	97.5	62	38,000	6 Al 3 Zn
Free Turning Brass	21		.993	110.0	.1326	.750	.129	.729	97.3	140	30,000	3.5 Pb 35 Zn
Low Carbon Steel	SAE1030	49	2.34	185.0	.312	1.765	.303	1.715	97.1	145	70,000	SAE 1030
High Carbon Steel	SAE1090	95	4.52	260.0	.603	3.421	.586	3.321	97.2	260	150,000	SAE 1090

^a Spindle speed, 700 rpm; feed 0.0025 in. per revolution; $\frac{7}{16}$ -in. drill with brass point; time of cutting, 0.57 min.

TABLE 2 TABLE OF TEST DATA FROM DYNAMOMETER AND CALORIMETER, FIG. 2^a

Material Cut	Feed in./rev	Time of Cutting min	Temp. Difference in Degrees F	Torque in lb ft	Thrust in lb	Horsepower		Horsepower		Ratio in per cent hp/Heat	hp/Torque + Thrust	Hardness Brinell	Tensile Strength lb per sq in.	Composition of Alloy
						From Torque & Thrust	Per cu in. per min	From Heat	Per cu in. per min					
Downmetal No. 2 Extruded	.0025	.57	13.80	.631	94.4	.0846	.478	.0838	.474	99.5	65	43,000	6 Al 1 Zn	
Downmetal No. 2 Extruded	.0034	.42	12.40	.772	100.0	.1034	.431	.1025	.427	99.3	65	43,000	6 Al 1 Zn	
Downmetal No. 2 Extruded	.0057	.25	9.23	.949	110.0	.1265	.314	.1280	.318	101.0	65	43,000	6 Al 1 Zn	
Downmetal No. 2 Extruded	.0074	.193	8.14	1.091	122.0	.1455	.278	.1463	.280	100.6	65	43,000	6 Al 1 Zn	

^a Spindle speed, 700 rpm; feed 0.0025, 0.0034, 0.0057, 0.0074 in. per revolution; $\frac{7}{16}$ -in. drill with brass point.

occurred. Provision was made to stop the feed of the drill in exactly the same place each time by putting a collar on the drill press spindle. At the beginning of the cut, the height of the test bar was checked with a vernier height gage with which the depth of cut was also measured.

Since the increase in temperature when cutting steel bars is several times greater than that for magnesium, tests were made in which the length of cut was $\frac{1}{2}$ in. and/or $\frac{1}{4}$ in. The resulting temperature increase was one half or one quarter of that for a 1-in. length of cut, and horsepower per cubic inch per minute was the same in each case.

The thermometers used had a 1-deg graduation from -40 to 120 F and from -10 to 100 C.

Prior to each test, the container and drill were dried with a piece of cloth. Before the cutting operation was started, the temperature of the water was taken after it had been stirred by the drill in the container for 1 min. No heating effect could be observed in the water through the stirring action of the drill, even with chips in the water, after a 3-min period. To keep heat losses at a minimum, the time of cutting was kept at 0.57 min or less.

In a previous investigation of cutting oils (20) a twist drill and test bars with a pilot hole were employed. These tests showed that cutting such a test bar with a twist drill eliminates the friction and squeezing action at the chisel-edge point and margin which always occur in the drilling of holes. Nine different cut-

ting fluids, including distilled water, had no effect on the cutting forces when a tubular test bar was used. It can therefore be stated that in the tests reported here there was no change in the cutting forces due to the fact that tool and workpiece were surrounded by distilled water.

SAMPLE COMPUTATION OF VALUES IN TABLE 1

Horsepower required for cutting extruded Dowmetal I:

$$Hp_{\text{Torque}} = \frac{2 \times \pi \times 700 \times 0.605}{33,000} = 0.08063$$

$$Hp_{\text{Thrust}} = \frac{700 \times 0.0025 \times 83.5}{12 \times 33,000} = 0.00037$$

$$Hp_{\text{Total}} = \frac{0.08063}{0.00037} = \frac{0.08100}{0.00037}$$

The water equivalent of the calorimeter (Fig. 2) was determined as 16.73 g by using the following values:

	Grams
Container (steel).....	30.00
Holder for test bar (steel).....	40.00
Screws (steel).....	8.20
Drill, part in water (steel).....	19.00

	Grams
All steel parts.....	$97.20 \times 0.110^a = 10.69$
Part of thermometer in water....	$4.20 \times 0.200 = 0.84$
Rubber gasket.....	$8.63 \times 0.480 = 4.14$
Dowmetal test bar.....	$4.25 \times 0.249 = 1.06$

$$\text{Water equivalent} = 16.73$$

When cutting a test bar of steel, the water equivalent is 17.52 g.

When cutting a test bar of brass, the water equivalent is 17.68 g.

Horsepower from heat:

Water equivalent of container, etc.....	16.73 g
Water.....	50.00 g
	66.73 g

$$\frac{66.73}{453.6} = 0.1471 \text{ lb}$$

Temperature difference = 13.00 deg F

$$\text{Time of cutting} = \frac{1 \times 400}{700} = 0.5714 \text{ min}$$

$$0.1471 \times 13.00 = 1.9123 \text{ Btu per } 0.5714 \text{ min}$$

$$\frac{1.9123}{0.5714} = 3.3467 \text{ Btu per min}$$

$$\frac{33,000 \text{ ft-lb per min}}{778.76 \text{ ft-lb per Btu}} = 42.44 \text{ Btu per min}$$

$$1 \text{ hp} = 42.44 \text{ Btu per min}$$

$$\text{Horsepower from heat} = \frac{3.3467}{42.44} = 0.079$$

The rate of fall of temperature of the calorimeter is 0.1 deg F per min at a temperature of 83.60 F, which is almost the maximum reached at the end of cutting. No correction for conduction, radiation, and convection has therefore been made, as heat

^a For specific heat compare Marks' "Mechanical Engineers' Handbook," p. 300, Table 9; and Kent's "Mechanical Engineers' Handbook" II, Power, pp. 3-20, Table 6.

TABLE 3. TYPICAL TEMPERATURE READINGS AS TAKEN IN TESTS FOR EXTRUDED DOWMETAL FROM CALORIMETER, FIG. 3^a

No. of Test	Temperature at Begin. of Cutting °F	Temperature at End of Cutting °F	Temperature Difference °F
1	71.2	78.4	7.2
2	71.4	78.5	7.1
3	71.5	78.3	6.8
4	71.5	78.7	7.2
5	72.0	78.9	6.9
6	72.4	79.3	6.9
7	72.4	79.2	6.8
8	72.5	79.5	7.0
9	72.8	79.9	7.1
10	72.8	79.8	7.0
Ave.			7.0

^a Maximum temperature difference = 7.2 deg F

Minimum temperature difference = 6.8 deg F

Average temperature difference used for computation = 7 deg F

losses amount to less than 0.4 per cent. The time of cutting is only 0.57 min, and the sum of all uncertainties including those of the dynamometer is not more than 3 per cent.

Cubic inches of metal cut per minute = area \times feed per revolution \times rpm

$$= \frac{(0.375^2 - 0.110^2)\pi}{4} \times 0.0025 \times 700$$

$$= 0.1768$$

Horsepower per cubic inch of metal cut per minute:

$$\text{From heat} = \frac{0.079}{0.1768} = 0.446$$

$$\text{From torque and thrust} = \frac{0.0810}{0.1768} = 0.458$$

Ratio in per cent of

$$\frac{\text{Horsepower per cu in. per min from heat}}{\text{Horsepower per cu in. per min from torque thrust}} =$$

$$\frac{0.446}{0.458} \times 100 = 97.4$$

It was assumed that the felt on the outside of the container acted as a perfect insulator and that the wood block did not become heated during the test. That the foregoing assumptions conform in a sufficient degree of accuracy to the action of the calorimeter during a cutting time from 0.193 to 0.57 min can be seen from the dynamometer values in Tables 1 and 2. With equal accuracy, it can be stated that the heat increase in 50 cc of water in the setup in Fig. 2 constitutes 75 per cent of the total heat generated during the cutting period.

It is not always possible to use a dynamometer simultaneously with the calorimeter. However, a similar approximation of the water equivalent can be made in other cases and will suffice for metal-cutting operations. Differences in the cutting properties of metals require different tool forces, and therefore gen-

erate different amounts of heat. The better the cutting properties of a metal the less heat will be generated while it is being cut.

SAMPLE COMPUTATION OF VALUES IN TABLE 4

The water equivalent of the calorimeter in Fig. 3 was computed as 18.46 g when cutting magnesium.

When cutting a steel test bar the water equivalent was 20.07 g.

When cutting a brass test bar the water equivalent was 19.75 g.

Water equivalent of container, etc. = 18.46 g

Water = 50.00 g

68.46 g

$$\frac{68.46}{453.6} = 0.1506 \text{ lb}$$

Temperature difference = 7.5 deg F

$$\text{Time of cutting} = \frac{1 \times 250}{510} = 0.491 \text{ min}$$

$$0.1506 \times 7.5 = 1.130 \text{ Btu per } 0.491 \text{ min}$$

$$\frac{1.130}{0.491} = 2.305 \text{ Btu per min}$$

$$\text{Horsepower from heat} = \frac{2.305}{42.44} = 0.0544$$

Horsepower per cubic inch of metal cut per minute

$$\frac{0.0544}{0.1768} = 0.308$$

RECOMMENDATIONS FOR FURTHER STUDY

More than 300 tests were conducted with the calorimeter shown

in Fig. 2, and 200 with that shown in Fig. 3. The most noteworthy feature in these tests was the ability to duplicate the results with each magnesium alloy taken from the same rod within very close limits. For general testing purposes the setup as shown in Fig. 3 is better because it is more rigid.

The calorimetric process can be applied to other types of machine tools. In most cases, the test specimen will be arranged in a container filled with a definite quantity of distilled water or any other fluid whose specific heat is known. The cutting or forming tool will operate while it and the test specimen are covered with water, and the rise in temperature of the water, as brought about by the cutting or forming operation during a definite time period, will be measured. The correction for radiation, conduction, and convection, and for the water equivalent of the container, test specimen, tool, and thermometer must be made before computing the final power values. To minimize the influence of the surrounding temperature, the water and all parts of the equipment should be at room temperature at the beginning of the operation. The rise in temperature of the calorimeter can be used as an indicator. It will be possible to study the power requirements for the cutting and forming of different materials, and the effect of tools upon the power consumption and surface finish, by changes in tool design and tool material. In cases where there is not enough stirring effect by the movement of the tool or workpiece a special agitator should be provided so that the temperature readings represent the mean temperature of the water.

An application of the calorimetric principle was made for the determination of tool forces in high-speed milling by A. O. Schmidt (21). The test bars were cut dry and only the heat in chips was measured.

When using various types of cutting fluids, oils, and emulsions in place of distilled water to cover the tool and test specimen, their cooling effect as well as their influence on power con-

TABLE 4 TABLE OF TEST DATA FROM CALORIMETER, FIG. 3^a

Material Cut	No.	Temp. Difference in Degrees F	Horsepower		Brinell Hard- ness	Tensile Strength (lb per sq in.)	Com- position of Alloy
			from Heat	per cu in. per min.			
Dowmetal Extruded	1	7.0	.0508	.287	53	40,000	3 Al 1 Zn
Dowmetal Extruded	2	7.5	.0544	.308	65	43,000	6 Al 1 Zn
Dowmetal Extruded	3	6.25	.0453	.256	40	40,000	1.5 Mn
Dowmetal Cast	C	7.5	.0544	.308	60	24,000	9 Al 2 Zn
Dowmetal Cast, Heat Treated	C	7.5	.0544	.308	60	39,000	9 Al 2 Zn
Dowmetal Cast, Heat Treated & Annealed	C	7.5	.0544	.308	75	39,000	9 Al 2 Zn
Dowmetal Cast	H	7.24	.0525	.297	50	27,000	6 Al 3 Zn
Dowmetal Cast and Heat Treated	H	7.93	.0575	.326	50	38,000	6 Al 3 Zn
Dowmetal Cast, Heat Treated & Annealed	H	6.95	.0504	.285	62	38,000	6 Al 3 Zn
Free Turning Brass		10.00	.0740	.419	140	50,000	3.5 Pb 35 Zn
Low Carbon Steel	SAE 1020	28.00	.2080	1.118	145	70,000	SAE 1030
High Carbon Steel	SAE 1090	49.00	.3640	2.059	260	150,000	SAE 1090

^a Spindle speed, 510 rpm; feed, 0.004 in. per revolution; 7/16-in. drill.

sumption can be studied by measuring the difference between the beginning temperature and the temperature at the end of the cutting operation.

CONCLUSIONS

1 A comparison of the values of horsepower from torque and thrust with those from the heat generated during cutting shows that the calorimetric method gives results comparable to those of a well-calibrated dynamometer.

2 The calorimetric setup is simpler than other methods used for the determination of tool forces, such as the dynamometer, and its sensitivity permits the accurate determination of those small differences which occur in various magnesium alloys in a short time and with a small amount of material.

3 In the calorimetric test, when steel test bars or other materials requiring large cutting forces are used, the amount of metal cut may be one half or one quarter of that of magnesium. There is still a high increase in temperature, and the final result is of the same order.

PENETRATION TESTS

Before the calorimetric investigation was carried out, other tests were made. Their object was to find a more reliable method for a rapid determination of machinability than the drill-penetration and sawing tests. Boston (2) and Kessner (3)

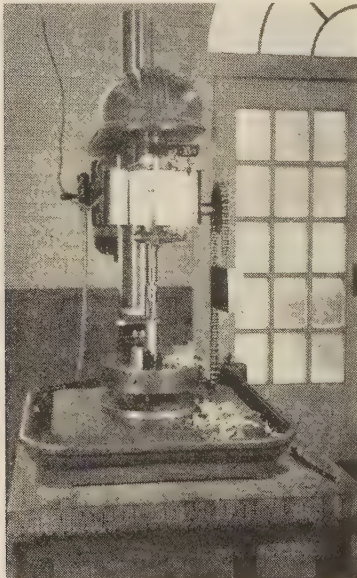


FIG. 4 ARRANGEMENT OF TEST EQUIPMENT FOR PENETRATION TESTS

had used the penetration test with the twist drill. Boston had found it of little value because of the difficulties encountered in regrinding a drill with exact angles. This difficulty was eliminated by using a special single-point tool which could be reground accurately. A tool bit was rotated in a spindle under a constant load, at the same time cutting a stationary tubular test bar. The penetration was recorded on a chart from which certain deductions about the machinability of the test-bar material with relation to the tool could be made.

A somewhat similar tool-steel testing machine, designed by E. G. Herbert (22), also used a tubular test bar of standard dimensions and properties which was rotating against a stationary tool. It was intended to measure the durability of the tool by

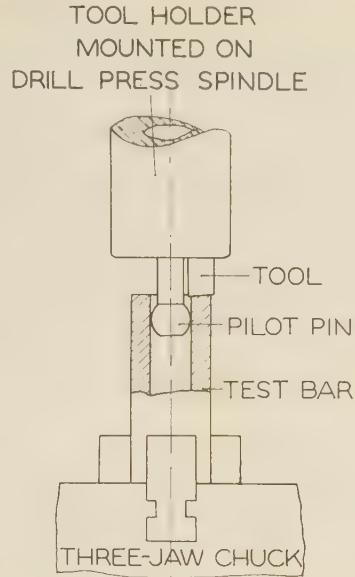


FIG. 5 TOOL AND TEST BAR AT BEGINNING OF CUT IN PENETRATION TEST

the amount of material removed from the standard test bar before the tool had worn a definite amount.

Since the new arrangement was simpler than the ones used before, it was thought worth while to carry out an investigation.

PROCEDURE AND EQUIPMENT

For these tests a bench-type, Delta drill press was used. It was equipped with a recording instrument consisting of a Leich motor making 1 rpm, mounted in a housing, and pulling "Waxon" recording paper across the face of the housing with a speed of 2 ipm. A special toolholder for the single-point tool was designed, and a three-jaw chuck was mounted on the table of the drill press concentric with the spindle. A sprocket wheel over which ran a weighted chain provided the feed, Fig. 4.

At the lower end of this spindle was mounted a toolholder which carried a single-point tool. In the center of the toolholder was a pilot pin which rotated in the cylindrical hole of the test bar. The test bar was held stationary in a three-jaw chuck mounted rigidly upon the table of the machine and was centered in such a way that the pilot pin rotated in the hole without rubbing on the walls. The tool cut the walls, thus reducing the length of the test bar. Amount of reduction of the test bar was dependent upon the material, cutting speed, load applied, tool angle, and surface quality of the tool. A scriber made the same vertical movement as the spindle and registered a line on the recording sheet which moved horizontally at a constant speed. As long as the tool was cutting at a uniform rate, the scriber had a uniform motion and thus made a straight line. When the rate of penetration changed, the slope of the line made by the scriber also changed. The depth of cut was affected by the material used for the test bar and by the tool angles. These factors also entailed different slopes of the line made by the scriber.

Making the tool bit wider than the wall thickness of the test bar permitted a simultaneous comparison of the cutting edge before and after cutting since a short distance on either side of the active cutting edge was left unaffected. To assure centering of the $\frac{1}{2}$ -in. pilot pin in the test tube, it was reamed with a 0.500-

in. reamer when mounted in the three-jaw chuck before the test was run.

DISCUSSION OF TESTS

A number of tests were run with test bars of aluminum, brass, and magnesium, each of which had an outside diameter of 1 in., a center hole of 0.500 in. diam, and a length of 5 in. A Rex high-speed tool bit, $\frac{5}{16}$ in. square, with a 4-deg rake angle and an 8-deg relief angle was used first on aluminum and then on brass. An 8-lb weight was used to pull the chain. Spindle speed was 590 rpm and gave a cutting speed of 140 fpm. The angle of the line made with the horizontal on the chart by the scribe was different for these two metals because of the varying rate of penetration of the tool.

The same arrangement was used for cutting a test bar of Dow-metal except for a larger rake angle (14 deg) and an increased relief angle (12 deg).

When cutting magnesium, the penetration was very fast at the start but stopped almost completely after approximately 1 sec because the ribbonlike magnesium chips interfered and packed solidly in front of the tool. This packing did not occur when magnesium was cut with the tool used for brass and aluminum.

CONCLUSIONS AND RECOMMENDATIONS

There are several possibilities of error with this penetration test. It is questionable whether the feed is always positive, and some provision should be made to keep the spindle from being affected because of irregularities encountered by the cutting tool. The downward feed of the spindle must be checked carefully since any difference in the bearing friction affects the registered line on the recording paper. When the pilot pin is used in the tubular test bar, there is varying friction in different metals. This can be avoided by employing a twist drill as the test tool or a toolholder with two accurately ground cutting tips. The spindle should have a positive drive to prevent the belt from slipping. Disturbing chatter occurs unless the machine is sturdy and well mounted.

ACKNOWLEDGMENT

The work covered in this paper was done by A. O. Schmidt in partial fulfillment of the requirements for the degree of Doctor of Science (Mechanical Engineering) in the University of Michigan, 1943, under the direction and with the co-operation of Professors O. W. Boston and W. W. Gilbert.

The tests were continued in the machine-tool laboratories of the Colorado State College of Agriculture and Mechanic Arts, and the University of Illinois.

The magnesium alloys used in the experiments were furnished by the Dow Chemical Company through Mr. H. W. Schmidt.

BIBLIOGRAPHY

- 1 "Machinability of Metals," by O. W. Boston, Trans. American Society for Steel Treating, vol. 13, 1928, pp. 49-50.
- 2 "Methods of Tests for Determining the Machinability of Metals in General, With Results," by O. W. Boston, Trans. American Society for Steel Treating, vol. 16, 1929, pp. 659-710.
- 3 "A Method for Determining the Resistance of Metals to Drilling and Its Application to the Investigation of the Machinability of Metals," by A. Kessner, *Testing*, April, 1924, pp. 270-285.
- 4 "A Laboratory Test for Machinability," by A. S. Kenneford, *Metal Progress*, vol. 39, 1941, pp. 354 and 356. Abstract from Paper No. 849, British Institute of Metals, 1939.
- 5 "Metal Processing," by O. W. Boston, John Wiley & Sons, Inc., New York, N. Y., 1941, p. 210.
- 6 "Work-Hardening Properties of Metals," by E. G. Herbert, Trans. A.S.M.E., vol. 48, 1926, pp. 705-748.
- 7 "Machinability of Steels," by James Sorenson and Wallace Gates, *Product Engineering*, vol. 10, 1939, pp. 12-14.
- 8 "Cutting Temperatures Developed by Single-Point Turning Tools," by O. W. Boston and W. W. Gilbert, Trans. American Society for Metals, vol. 23, 1935, pp. 703-726.
- 9 "The Measurement of Cutting Temperatures," by E. G. Herbert, Proceedings of The Institution of Mechanical Engineers, vol. 1, 1926, pp. 289-329.
- 10 "Die Schneidentemperatur beim Drehen in Abhaengigkeit von der Form des Spanquerschnittes," by K. Gottwein, *Maschinenbau*, vol. 5, 1926, pp. 505-506.
- 11 "Über die Bestimmung des Temperaturfeldes beim Spanablauf," by Friedrich Schwerdt, *Zeitschrift des Vereines deutscher Ingenieure*, vol. 77, 1933, pp. 211-216.
- 12 "Physics of Metal Cutting," by Hans Ernst, published by American Society for Metals, in "Machining of Metals," Cleveland, 1938, pp. 1-34.
- 13 "Essays—Political, Economical, and Philosophical," by Benjamin Count of Rumford, first American edition, David West, Boston, 1799. An article entitled, "An Inquiry Concerning the Source of the Heat Which Is Excited by Friction," appears on pp. 469-496 of vol. 2 of this work.
- 14 "On the Mechanical Equivalent of Heat," by J. P. Joule, Philosophical Transactions of the Royal Society of London, 1850, pp. 61-82.
- 15 "Recherches sur l'équivalent mécanique de la chaleur," by P. A. Favre, Comptes Rendu de l'Academie des Sciences, Paris, vol. 46, 1858, pp. 337-340.
- 16 "Théorie mécanique de la chaleur," by G. A. Hirn, third edition, Gauthier-Villars, Paris, vol. 1, 1875, pp. 91-118.
- 17 "The Heat Generated in the Process of Cutting Metal," by H. I. Brackenbury and G. M. Meyer, *Engineering*, vol. 91, 1911, pp. 39-40.
- 18 "Über die Wärmevergange beim Spanschneiden und die vorteilhaften Schnittgeschwindigkeiten," by H. Friedrich, *Zeitschrift des Vereines deutscher Ingenieure*, vol. 58, 1914, pp. 379-383, 417-422, and 454-459.
- 19 "Die Kuehlung des Werkzeuges," by N. N. Sawwin, Dingler's *Polytechnisches Journal*, vol. 327, 1912, pp. 88-90, 103-105, and 121-125.
- 20 "Correlation of Coefficient of Friction With Drilling Torque and Thrust for Different Types of Cutting Fluids," by A. O. Schmidt, W. W. Gilbert, and O. W. Boston, Trans. A.S.M.E., vol. 64, 1942, pp. 703-709.
- 21 "Determining Tool Forces in High-Speed Milling by Thermoanalysis," by A. O. Schmidt, *Mechanical Engineering*, vol. 66, July, 1944, pp. 439-442.
- 22 "Tool Steel Testing Machine," by Edward G. Herbert, Ltd., Manchester, England, catalogue section F, June, 1914.

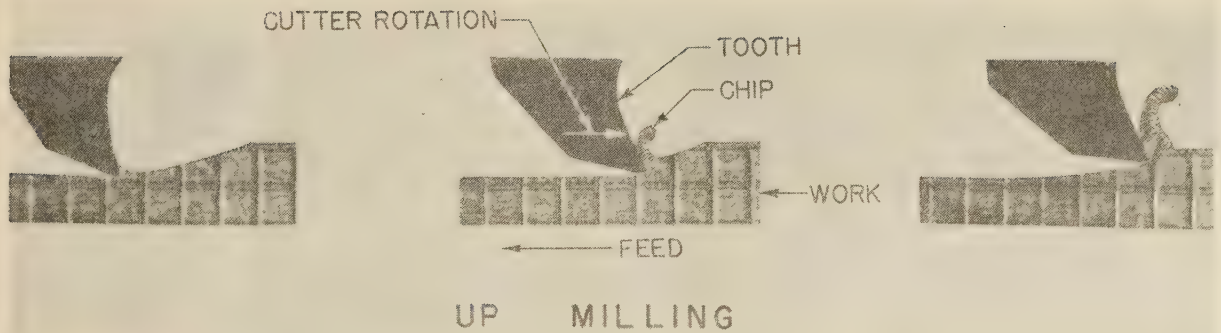


FIG. 1 MILLING CHIP AT DIFFERENT STAGES OF FORMATION IN UP MILLING

An Analysis of the Milling Process,¹ Part II—Down Milling

By M. E. MARTELOTTI,² CINCINNATI, OHIO

The method of milling here described as down milling is compared with up milling on the basis of geometric characteristics such as length of tooth path, radius of curvature, thickness of the undeformed section of the chip, chip formation, character of the milled surface, power required in cutting S.A.E. 1112 steel and cast iron, and intensity of vertical and horizontal components of the cutting force obtaining for various depths of cut. Typical mechanical backlash-eliminating devices for the feeding mechanisms of milling machines to permit down-milling operations are described. Results obtained in actual application of down milling are given together with information on cutter life and production. The analytical and factual data presented permit a comparison of the advantages and disadvantages inherent in both methods of milling. It is shown that the power required at the cutter not including the feed is slightly more in down milling than in up milling. The total power supplied to the machine, however, is slightly less in down milling than in up milling. Actual intensities of horizontal and vertical components of the forces on the cutting edge are given for both methods of milling. Down milling, known for many years but not generally used in milling operations until recently, finds an ever-widening field of application.

INTRODUCTION

FOR a number of years, up milling, also known as "conventional milling" and "milling against the feed," has been used almost exclusively in milling operations, Fig. 1. In

¹ "An Analysis of the Milling Process," by M. E. Martellotti, Trans. A.S.M.E., vol. 63, 1941, pp. 677-700.

² Research Engineer, Cincinnati Milling Machine Company. Mem. A.S.M.E.

Contributed by the Production Engineering Division and presented at the Annual Meeting, Nov. 27-Dec. 1, 1944, of THE AMERICAN SOCIETY OF MECHANICAL ENGINEERS.

NOTE: Statements and opinions advanced in papers are to be understood as individual expressions of their authors and not those of the Society.

this method, the workpiece is fed in the direction opposite to that of cutter rotation.

Another method of milling, herein described as down milling, Fig. 2, and variously called "climb milling" and "milling with the feed," known since the early 1880's when it enjoyed a considerable popularity, has not been generally used in milling operations. In this method, the work is fed in the direction of cutter rotation.

In recent years, however, down milling has received a great deal of attention. In some instances it has provided simplification in fixture design and in the manufacture of parts difficult to hold properly. It also has generally improved the quality of machined surfaces, increased cutter life between grinds, provided smoother operation of the machine and higher production.

In milling machines of the screw-feed type, down milling has been made possible by the development of adequate means for eliminating backlash between the lead screw and nut. If down milling is performed on milling machines not equipped with a backlash eliminator, the motion of the table will be unsteady and characterized by a series of jerks. Eventually this will lead to the building up of forces of high intensity between cutter and work, and damage to cutter and work with possible serious injury to the operator may result.

A backlash eliminator alone, however, is not sufficient to secure positive control of the table. It is also necessary to eliminate play at the point where the screw is anchored to the table or understructure of the machine.

Furthermore, the cutter must be keyed to the arbor and securely held thereon with a minimum of deflection, and every sliding member of the machine must be maintained in the closest sliding fit with its mating part. The machine should be kept in good repair, and every possible precaution should be taken in setting it up to insure safe operation.

In up milling, owing to the existence of separating forces between cutter and work opposing the motion of the table rather than favoring it, these requirements are desirable but not necessary to insure a satisfactory operation of the machine.

BACKLASH ELIMINATORS

Elimination of backlash involves a tight engagement between

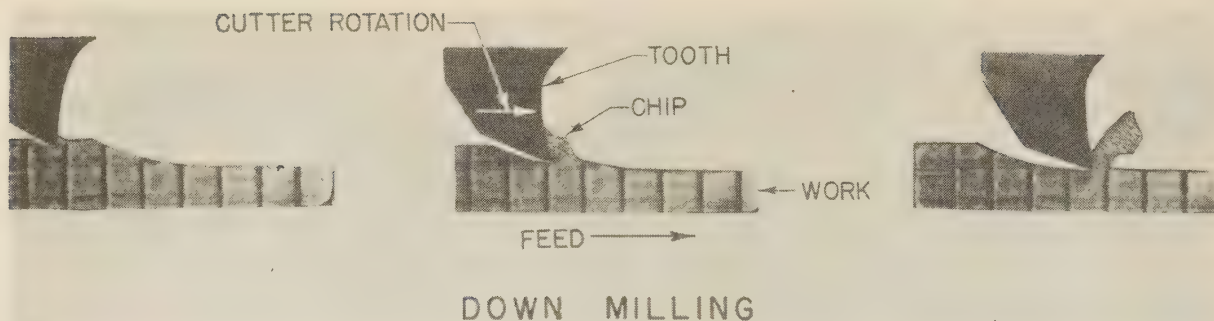


FIG. 2 MILLING CHIP AT DIFFERENT STAGES OF FORMATION IN DOWN MILLING

the screw and the nut. There are various types of backlash eliminators, a few examples of which will be given.

In order to minimize wear between nut and screw, a backlash eliminator should be in operation only during the working cycle and released during the idle movement of the table. A backlash eliminator having these characteristics, Fig. 3, consists of a nut *A*, movable axially but prevented from rotating by a key extending from cylinder head *D*, and a fixed nut *C* of conventional design. Oil under pressure operating on one end of nut *A* provides the necessary load on the screw *B* and fixed nut *C* to eliminate backlash in the direction of feed.

When the table is rapid-traversed in either direction or it is moved by hand, or when the machine is operated in up milling, a valve connects the two ends of the cylinder, eliminating the preload on nut *C*. The table then operates in the usual manner.

A backlash eliminator, controlled directly by the load change on the machine table, is shown in Fig. 4. This backlash eliminator consists of two nuts mounted for free rotation on the lead screw and connected by a crown gear, for opposite hand of rotation. A very light preload is applied on nuts *A* and *B* by a spring acting on a rack engaging a pinion on the crown-gear hub.

The frictional torque, developed by the light preload between the threads of the screw and the nuts, is small and no undue effort is required on the part of the operator when operating the table manually. The preload, however, can be released when the table is operated by hand for long periods of time.

When the table is moved by power, the frictional torque between the threads of screw and nut *A*, for example, is increased by the thrust required to overcome the frictional resistance opposing the table motion, and nut *A* is rotated in the direction of the screw, while nut *B* is rotated in the opposite direction. This reduces the frictional torque between the threads of nut *B* and lead screw, and nut *A* will operate as the ordinary driving nut.

In up milling, when idle-feeding and rapid-traversing the table, no change takes place in the position of the two nuts. In down milling, the load shifts from nut *A* to *B*. The resulting increase in frictional torque causes nut *B* to rotate with the screw, and to turn nut *A* in the direction which effects a tight engagement of both nuts with the screw, thus eliminating backlash.

The degree of tightness varies with the intensity of the cutting force. When the load is off, the nuts *A* and *B* readjust themselves to the conditions obtaining when feeding idle.

These types of backlash eliminators are operative in either direction of table movement.

KINEMATICS OF MILLING

Milled surfaces are generated with single- or multiple-tooth rotating cutters, which progressively remove from the workpiece

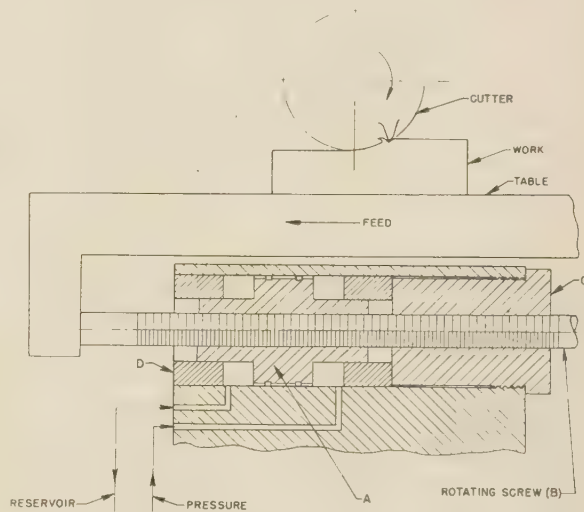


FIG. 3 HYDRAULICALLY OPERATED BACKLASH ELIMINATOR

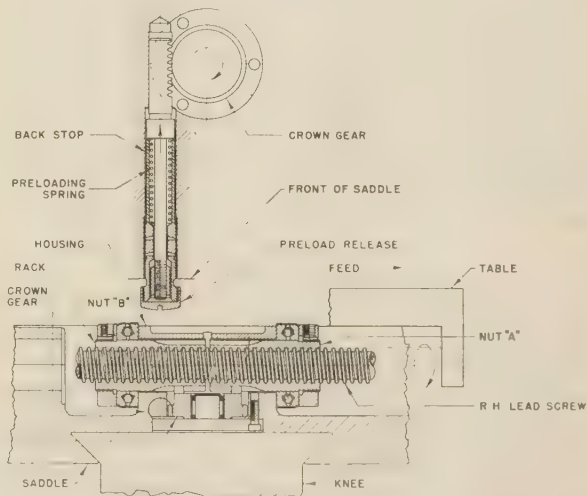


FIG. 4 BACKLASH ELIMINATOR, FOR APPLICATION TO ROTATING LEAD SCREW, AUTOMATICALLY OPERATED BY FORCES DEVELOPED DURING WORKING CYCLE OF MACHINE

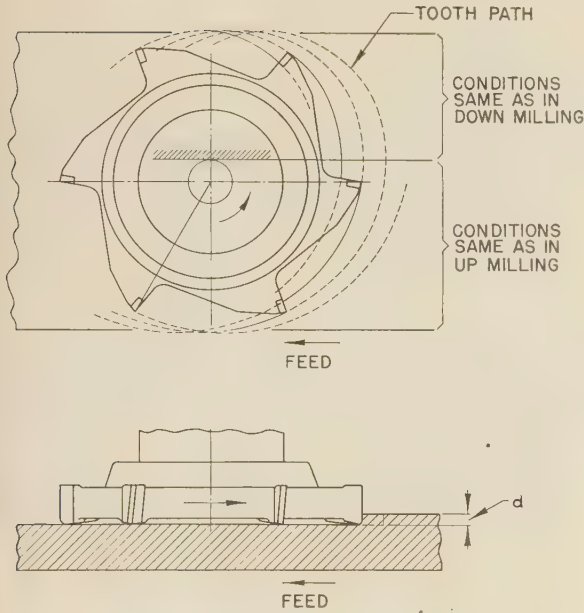


FIG. 5 PATH GENERATED BY A FACE-MILL TOOTH

a predetermined amount of material in the form of small chips. The diversity of milling operations performed with innumerable types and sizes of milling cutters may be classified in the following groups:

(a) *Peripheral Milling.* The milled surface is generated in a plane generally parallel to the axis of cutter rotation, as for example in milling with a helical mill.

(b) *Face Milling.* The milled surface is generated at right angles to the axis of cutter rotation as in milling with face mills.

"Peripheral-milling" operations can be performed either in up milling or down milling, while in "face milling" the two methods are usually combined, since in general the feeding motion is partly with and partly against the direction of cutter rotation, Fig. 5.

PATH GENERATED BY A MILLING-CUTTER TOOTH

The path generated by a milling-cutter tooth in the process of removing metal from the workpiece is an arc of a looped proctoid¹ of the following parametric equations, Figs. 6 and 7

$$\left. \begin{aligned} x &= \pm ra + R \sin a \\ y &= (1 - \cos a) \end{aligned} \right\} \dots\dots\dots [1]$$

which by eliminating the parameter a can be reduced to the Cartesian form

$$x = r \cos \frac{R - y}{R} \pm (2Ry - y^2)^{1/2} \dots\dots\dots [2]$$

The plus and minus signs apply to up milling and down milling, respectively. In face milling, y is the width of cut.

For any given condition, the tooth path can be reproduced by an arrangement similar to that shown in Figs. 6 and 7, by rotating the cutter in the direction of the arrow M . The pinion Q (attached to the cutter) rolls on the rack Z , and the cutting edge of the tooth (2) describes path AN' , Fig. 6, and AN , Fig. 7, which together with the paths generated by tooth (1) determine the undeformed section of the chip obtained in up milling and down milling, respectively.

The feed rate is a function of the dimension of the pinion as

expressed in the following relation

$$F = 2\pi rn \dots\dots\dots [3]$$

By expressing the feed rate as a function of the feed per tooth F_t inch (increment of feed per tooth), number of teeth T , and the revolutions per minute of the cutter

$$F = F_t T n \dots\dots\dots [4]$$

and then combining Equations [3] and [4], the pinion radius r can be obtained from the given feed per tooth and number of teeth as follows

$$r = \frac{F_t T}{2\pi} \dots\dots\dots [5]$$

But the product $F_t T$ is the feed per revolution F_r , hence

$$r = \frac{F_r}{2\pi} \dots\dots\dots [6]$$

When this expression for r is substituted in Equations [1] or

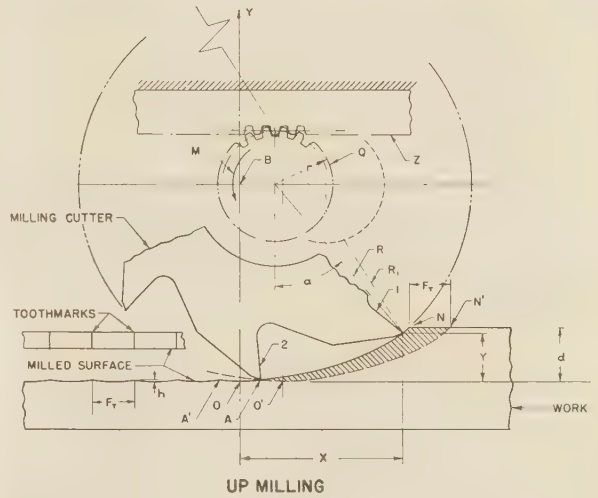


FIG. 6 PATH GENERATED BY PLAIN-MILLING-CUTTER TOOTH IN UP MILLING

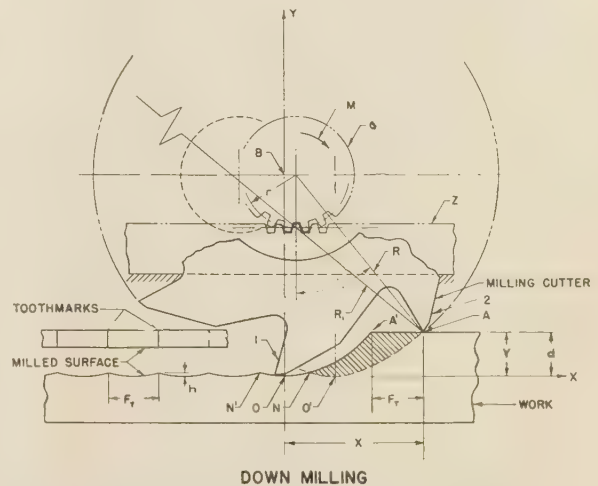


FIG. 7 PATH GENERATED BY PLAIN-MILLING-CUTTER TOOTH IN DOWN MILLING

[2], it will be apparent that in peripheral milling, as well as in face milling, the important variables affecting the tooth path and, consequently, the undeformed section of the chip, are the feed per revolution F_r , the cutter diameter or radius R , and the depth of cut d or y in peripheral milling, and the width of cut w or y in face milling.

For values of F_r used in practice, r is usually a small quantity, but it cannot be generally disregarded, however, without impairing the analytical accuracy of the derivations obtained when comparing the two methods of milling. If r is considered a negligible quantity, and is therefore eliminated from Equations [1] and [2], these become the equations of a circle, and the tooth path becomes an arc of a circle with a radius equal to the cutter radius, which is not true in practice. Actually the radius of the tooth path or radius of curvature varies with the depth of cut and also with the radius R of the cutter and radius r of the pinion (or feed per revolution), as indicated in the following equation

$$R_1 = \frac{[r^2 + R^2 \pm 2r(R - y)]^{1/2}}{R^2 \pm r(R - y)} \dots \dots \dots [7]^3$$

where

- R_1 = instantaneous radius of curvature, in.
- y = instantaneous value of depth of cut, in.
- R = radius of cutter, in.
- r = radius of pinion, in.
- $+$ = up milling
- $-$ = down milling

From Equation [7], it will be found that under the same operating conditions, the radius of curvature is greater than the radius of the cutter in up milling, while in down milling it is smaller than the radius of the cutter. As a result, for given conditions, the generated tooth-path length is longer in up milling than in down milling.

LENGTH OF TOOTH PATH

The length of tooth path is a measure of the length of surface milled by a tooth in each engagement with the workpiece, but only a small fraction of this surface, approximately equal to the feed per tooth F_t , is actually used, Figs. 6 and 7.

In up milling, Fig. 6, when tooth (2) has completed the path AN' , it will remove the amount AN of the tooth path generated by tooth (1) and leave the amount AA which is equal to NN and to the feed per tooth.

In down milling, Fig. 7, tooth (2), after completing its path, leaves on the workpiece an amount $N'N$ of the surface milled by tooth (1), also equal to the feed per tooth.

The feed per tooth is a small quantity in comparison with the actual length of tooth path, and it is therefore desirable for the economy of the operation to reduce the length milled by a tooth to a minimum. This can be done by proper selection of cutter diameter, feed per revolution, and method of milling. A reduction in the total surface milled by each tooth produces a corresponding increase in cutter life which is affected by the amount of work done per tooth.

The following expression of tooth-path length for "peripheral milling" (obtained from Equation [1]) is sufficiently accurate for values of feed per revolution, cutter diameter, and depth of cut used in practice

$$L = \frac{\pi}{180} R \cos^{-1} \left(\frac{R-d}{R} \right) \pm \frac{F_r}{2\pi R} (2Rd - d^2)^{1/2} \dots [8]^4$$

where

L = tooth path length, in.

³ See Appendix, section 1.

⁴ See Appendix, section 2.

R = cutter radius, in.

d = depth of cut, in.

F_r = feed per revolution, in.

Equation [8] shows that the tooth-path length is longer in up milling (+) than in down milling (—). A saving therefore in the actual amount of surface milled can be obtained by using the latter method. In face milling, the tooth-path length is the sum of the length generated in up milling and down milling.

When the width of cut is nearly equal to the cutter diameter the tooth-path length is

$$L = \frac{\pi}{90} R \cos^{-1} \left(\frac{R - w/2}{R} \right) \dots \dots \dots [9]$$

In this equation the width of cut w replaces the depth of cut d of Equation [8]. Owing to the compensation in tooth-path length between up milling and down milling, the saving obtained under comparable conditions in face milling is not as great as in down milling.

A greater approximation in the evaluation of tooth-path length in face milling can be obtained by means of the following formula

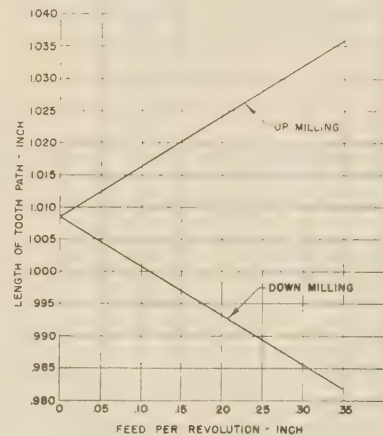


FIG. 8 LENGTH OF TOOTH PATH VERSUS FEED PER REVOLUTION (Plain milling cutter, 4 in. diam, 10 T, depth of cut $1/4$ in.)

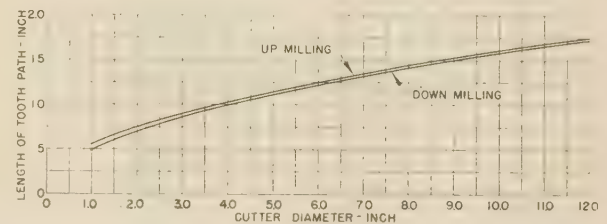


FIG. 9 LENGTH OF TOOTH PATH VERSUS CUTTER DIAMETER (Plain milling cutter, feed per revolution 0.200 in., depth of cut $1/4$ in.)

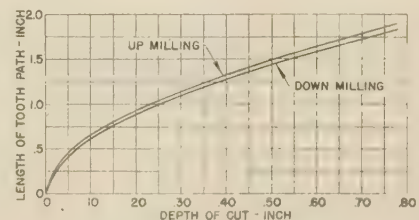


FIG. 10 LENGTH OF TOOTH PATH VERSUS DEPTH OF CUT (Plain milling cutter, 4 in. diam, 10 T, feed per revolution 0.210 in.)

which results from the use of additional terms of the series shown in the Appendix, section 2

$$L = \frac{\pi}{90} (r^2 + R^2)^{1/2} \left[\left(1 - \frac{r^2}{4R^2} \right) \cos^{-1} \frac{R - w/2}{R} \right] \dots [10]$$

This indicates that a shorter tooth-path length than that given by Equation [9] may be obtained at high feeds per revolution. Calculated values of tooth-path length versus feed per revolution, cutter diameter and depth of cut for given conditions in peripheral milling are shown in Figs. 8, 9, and 10.

The difference in tooth-path length between up milling and down milling is usually small, but when the total number of tooth engagements and number of pieces milled are considered, the saving in milled surface may be considerable. For example, if the length to be milled on a workpiece is 12 in., the feed per revolution 0.200 in., the depth of cut $1/4$ in., and the cutter used is a 10-tooth, 4-in-diam, plain milling cutter, the number of engagements per tooth per piece is $(12 \div 0.20 = 60)$. From Fig. 8, the length of tooth path in up milling and down milling, corresponding to a feed per revolution of 0.200 in., is 1.024 and 0.993 in., respectively, and the difference in surface milled per piece in favor of down milling is

$$(1.024 - 0.993) 60 = 1.86 \text{ in.}$$

If the number of pieces to be milled is 100, a total saving of 186 in. will be obtained, by using the down-milling method.

Greater savings can be obtained with either milling method by

using a cutter of smaller diameter. If the 4-in. cutter is replaced with a 3-in-diam cutter, the tooth-path lengths (up milling) are, respectively, 1.430 in. and 1.245 in., Fig. 9, and the saving per piece in favor of the 3-in-diam cutter is

$$(1.430 - 1.245) 60 = 11.10 \text{ in.}$$

or 1110 inches, per 100 pieces milled.

Similar analysis can be made for the depth of cut. This should be kept as small as possible in relation to design and method of fabrication of the part being milled.

A modification of Equation [8], giving the total length L_T (inches) of milled surface corresponding to N_p parts, L_p inches long, milled at cutting speed C feet per minute, and feed rate F inch per minute, is the following

$$L_T = L_p N_p \left[\frac{c}{30F} \cos^{-1} \left(\frac{R - d}{R} \right) \pm \frac{(2Rd - d^2)^{1/2}}{2\pi R} \right] \dots [11]$$

The plus sign applies in up milling and the minus sign applies in down milling. The graphic relationship between L_T , F , and C when $N_p = 1$ is shown in Fig. 11. From an inspection of this chart, the following conclusions may be drawn:

1 For any given cutting speed:

(a) As the feed rate is increased, the length of surface milled per tooth and per piece decreases.

(b) In down milling, a progressively shorter surface is milled than in up milling.

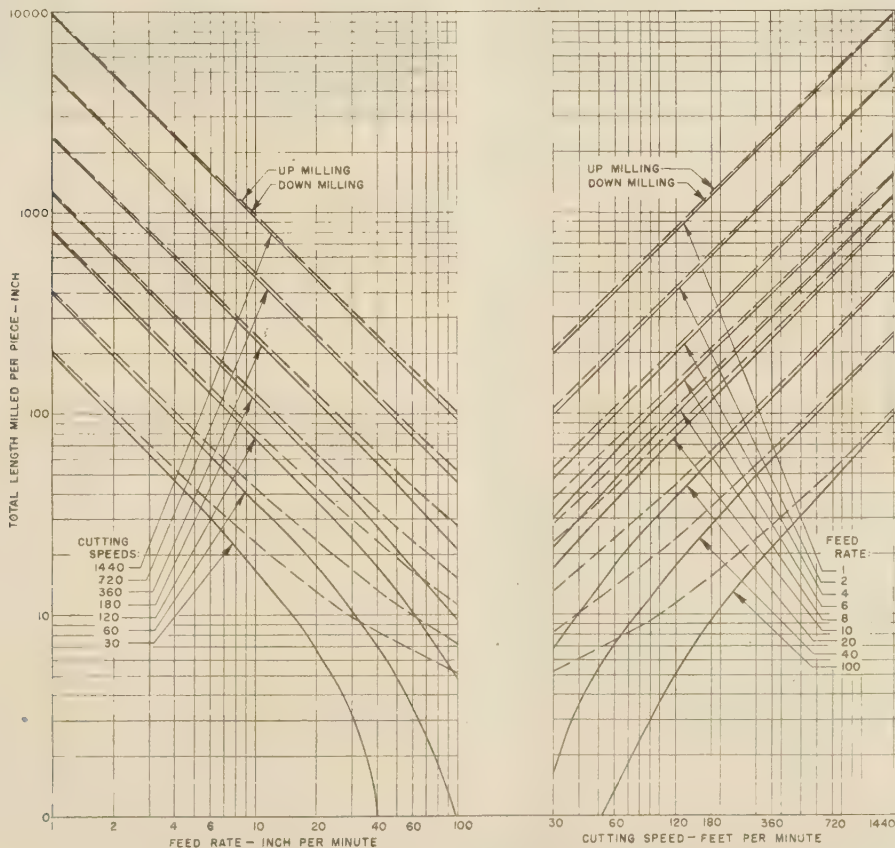


FIG. 11 LENGTH OF SURFACE MILLED PER PIECE VERSUS FEED RATE AND CUTTING SPEED
(Plain milling cutter, 4 in. diam, 8 T, $1/4$ in. depth of cut, workpiece 10 in. long.)

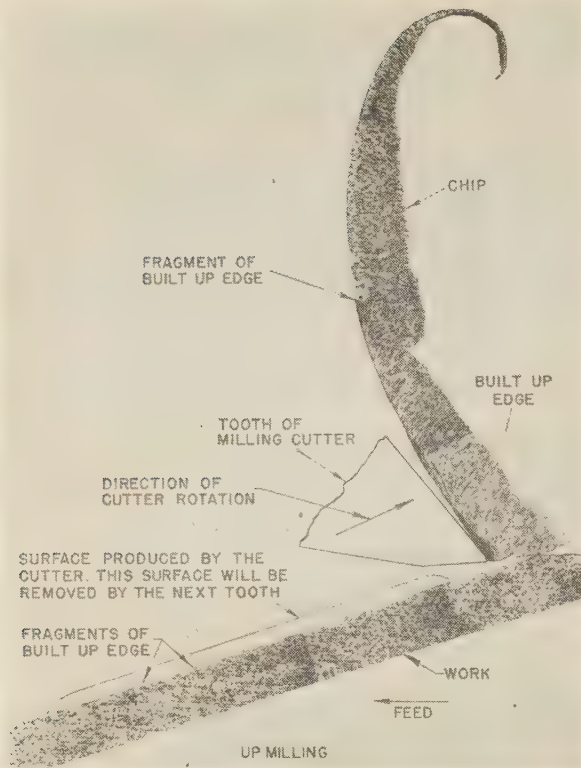


FIG. 12 COMPLETE UP-MILLING CHIP

(Material, S.A.E. 1112; feed rate, $6\frac{1}{4}$ ipm; depth of cut, $\frac{1}{8}$ in.; cutter, plain milling cutter, 10 T, 4 in. diam; cutting speed, 40 fpm. Magnification $\times 43$.)

2 For any given feed rate:

- (a) As the cutting speed is increased, the length of surface milled per tooth and per piece increases.
- (b) The difference in surface milled in favor of down milling decreases.

3 The length of surface milled per piece and per tooth can be maintained constant by changing both the cutting speed and the feed so that their ratio remains constant.

4 Down milling shows a greater saving in milled surface at higher than at lower feed rates.

CHIP THICKNESS

A comparison of Figs. 6 and 7 reveals that the undeformed chip section in up milling is more elongated and, on the average, thinner than in down milling, although the areas are the same in both cases. The cross sections of two complete milling chips, obtained under identical conditions, are shown considerably enlarged in Figs. 12 and 13, respectively.

It is also confirmed by the fact that the average chip thickness, i.e., the ratio between the area of the cross section and the length of tooth path, is greater in down milling than in up milling because the tooth-path length is shorter in down milling than in up milling, Fig. 14, namely

$$t_D = \frac{F_d d}{L_d} > t_U = \frac{F_u d}{L_u} \dots \dots \dots [12]$$

For a given depth of cut, the maximum chip thickness is also greater in down milling than in up milling, and the difference between the values of t_U and t_D , obtained in up milling and down milling, increases with the feed per revolution.

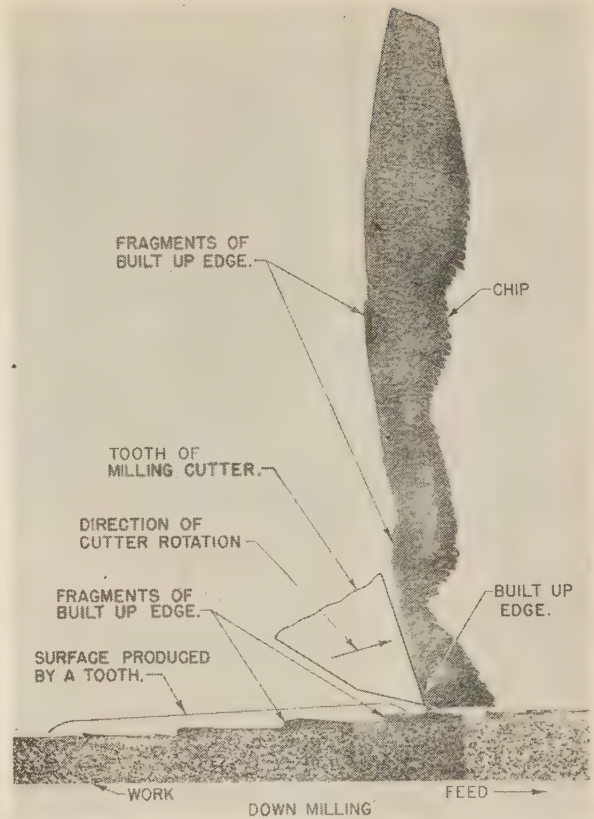
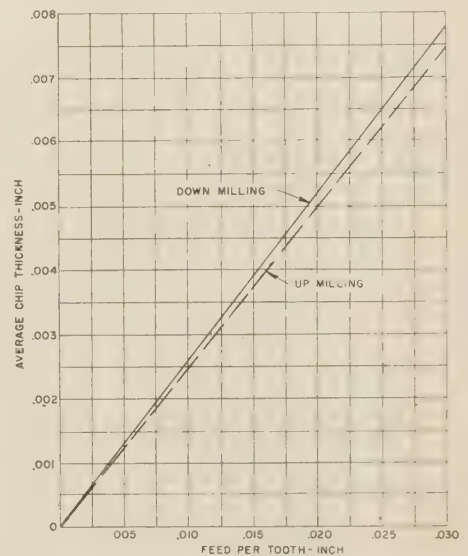


FIG. 13 COMPLETE DOWN-MILLING CHIP

(Material, S.A.E. 1112; feed rate, $6\frac{1}{4}$ ipm; depth of cut, $\frac{1}{8}$ in.; cutter, plain milling cutter, 10 T, 4 in. diam; cutting speed, 40 fpm. Magnification $\times 50$.)

FIG. 14 AVERAGE CHIP THICKNESS VERSUS FEED PER TOOTH
(Plain milling cutter, 4 in. diam, 10 T, depth of cut $\frac{1}{4}$ in.)

The maximum chip thickness is the portion AD_1 of the radial line R_1 (normal to the tooth path) included between the paths of

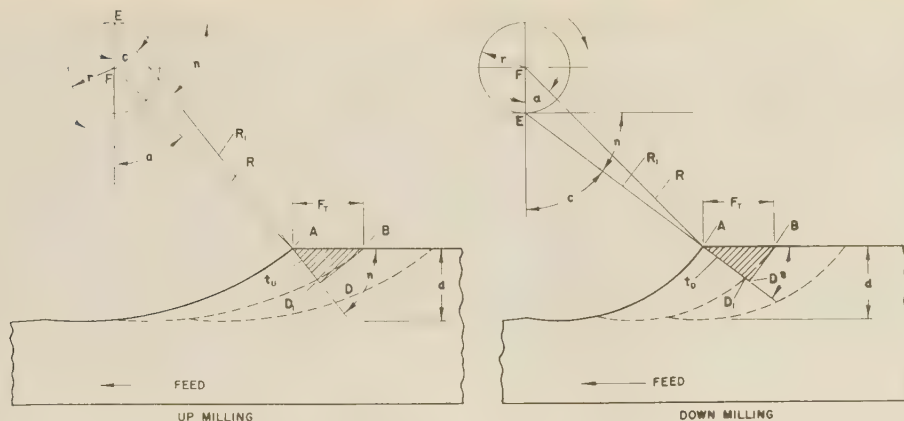


FIG. 15 MAXIMUM CHIP THICKNESS IN UP MILLING AND DOWN MILLING

two consecutive teeth. Assuming $AD_1 = AD$, Fig. 15, from the triangles FEA and ABD , the following relation is obtained

$$t_{U,D} = F \left[\frac{d(2R - d)}{(R \mp r)^2 \pm 2rd} \right]^{1/2} \quad [13]$$

In the denominator, the upper signs apply in down milling and the lower signs in up milling.

Since each of the maximum thicknesses, t_U and t_D is a function of depth of cut, cutter radius, and feed per revolution, it is a truer indication of the tooth load than the feed per tooth.

QUALITY OF FINISH OF MILLED SURFACES

Quality of finish of a machined surface is generally affected by:

1 Toolmarks, which depend on the geometry of the machining process used.

2 Marks of microscopic dimensions resulting from the plastic flow of the material during the formation of the chip.

Toolmarks: Tooth and Revolution Marks. In up milling, tooth marks such as A , Fig. 6, result from the engagement of a tooth with the work material. In down milling, a similar mark N' , Fig. 7, is generally produced which is the outline of the intersection of the plane of shear with the surface of the work along which the material of the chip yields prior to severance from the work, Fig. 13. In down milling, therefore, an element of the machined surface is generally not produced by the direct action of the cutting edge on the work material, as in the case of up milling, and the quality of the machined surface is affected by the type of chip obtained. Under certain conditions, however, definite marks are produced on a surface generated in down milling, Fig. 17.

A milled surface therefore may be generally considered as the result of innumerable elements of the tooth path of a length approximately equal to the feed per tooth. The uniformity of the spacing depends on the location of the points such as AA' and NN' , Figs. 6 and 7, where the teeth intersect the path generated by the preceding teeth.

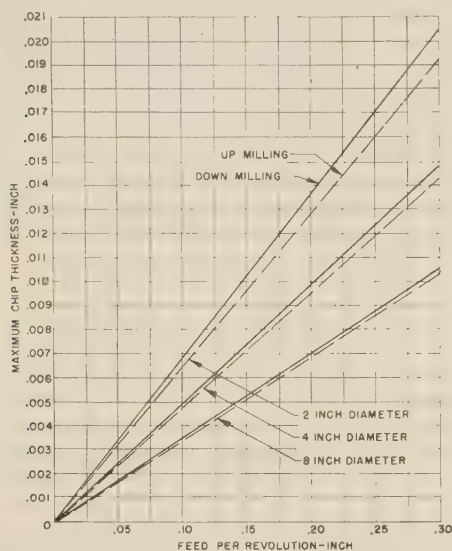
Any variation in the instantaneous radius of curvature of the tooth path, Equation [7], will affect the width and the depth of the tooth marks.

Within the range of tooth path determined by the feed per tooth and forming an element of the finished surface, the radius of curvature is maximum in up milling and minimum in down milling, hence a flatter arc of trochoid will be obtained in up milling than in down milling. On this basis a better finish will result in up milling, since the height h , between the cusps corresponding to the tooth marks and the point O , is less in up milling than in down milling, as shown by the following equation

$$h = \frac{R}{8} \left(\frac{F_r}{R \mp r} \right)^2 \quad [14]$$

where h = height of tooth mark above point O of lowest level, in.

The value of h for the case shown in Fig. 17, in which a 0.118-in. feed per tooth, and an 8-tooth 3.894-in.-diam plain milling cutter were used, is 0.000775 and 0.00105 in. for up milling and down milling, respectively. The actual readings are plotted in Fig. 18.

FIG. 16 MAXIMUM CHIP THICKNESS VERSUS FEED PER REVOLUTION AND DIFFERENT PLAIN-MILLING-CUTTER DIAMETERS; DEPTH OF CUT $1/4$ IN.

If the feed per revolution is kept constant, the maximum thicknesses t_U and t_D increase as the diameter of the cutter is decreased, Fig. 16. In order to maintain t_U and t_D constant with a change in cutter diameter, the feed per revolution should be correspondingly increased. Since the feed per revolution is equal to the feed per tooth times the number of teeth, this can be accomplished by increasing the feed per tooth or the number of teeth, or both.

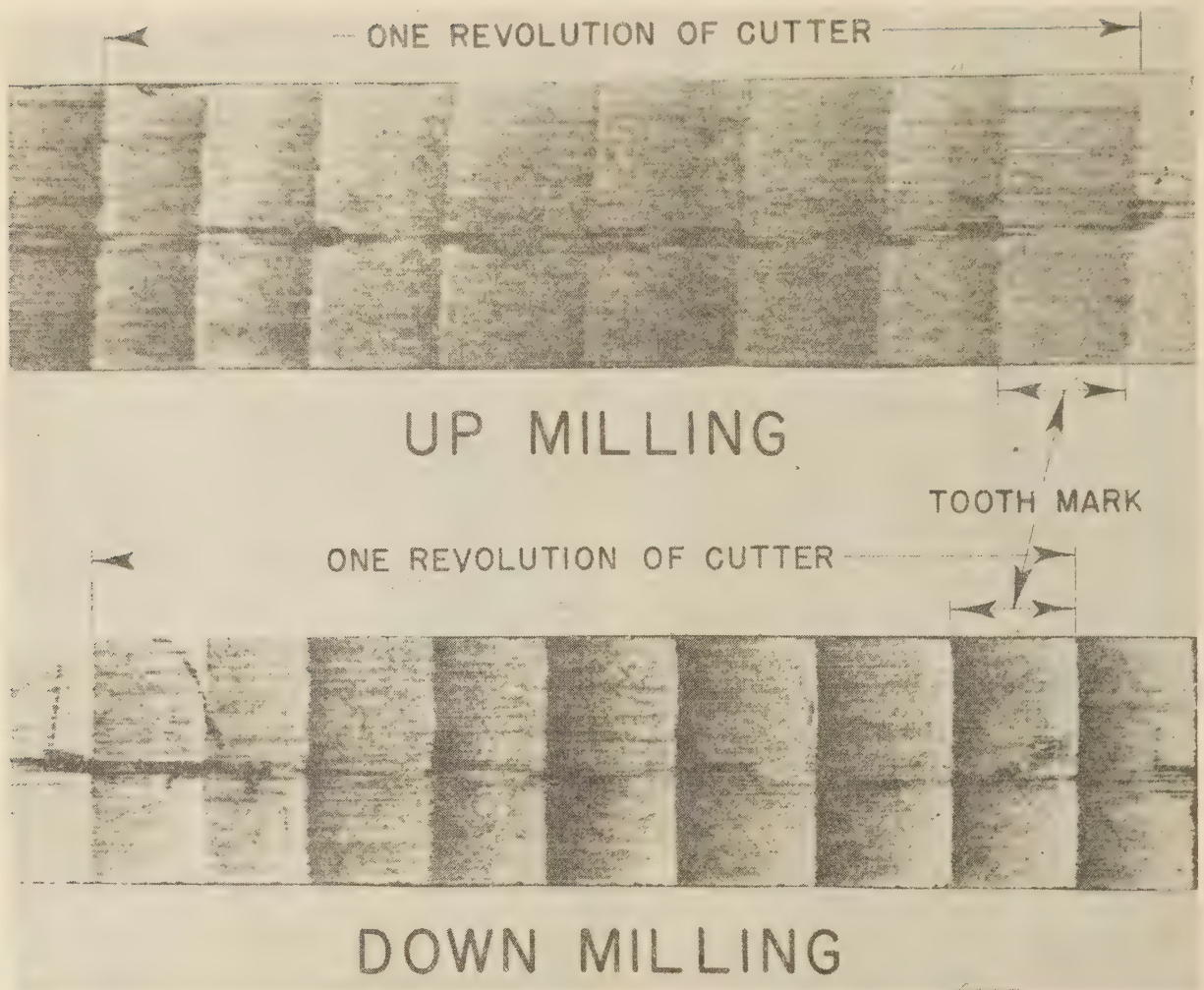


FIG. 17 TOOTH MARKS PRODUCED ON A MILLED SURFACE IN UP MILLING AND DOWN MILLING

(Material, brass; plain milling cutter; 3.894 in. diam, 8 T, 38 rpm; helix angle, 35 deg; feed rate, 38 ipm; depth of cut, $1/32$ in. Magnification $\times 6$.)

In addition to the tooth marks, a surface milled with a plain milling cutter may show periodic variations having a wavy appearance, and recurring with the frequency of the cutter revolutions per minute. The amplitude or height of the revolution mark is a function of the eccentricity of the cutter and arbor, the tooth marks, the so-called "high tooth," and the periodic variation in the deflection of the arbor, caused by the presence of the keyway and possible uneven conditions on the arbor supports. These various conditions are graphically reproduced in Fig. 19. In the case shown in Fig. 18, the average height of revolution mark is 0.004 in. and 0.0045 in. in up milling and down milling, respectively. The tooth marks follow the undulation of the revolution marks. The presence of one or the other or both types of marks alters the geometric conditions of the surface and, consequently, the quality of finish.

The height of the tooth marks can be reduced by increasing the radius of the cutter and decreasing the feed per tooth. The revolution marks can be prevented by grinding the cutter teeth within close limits and making sure that the runout of the cutter and arbor is reduced to the lowest possible value. In down milling, there is the additional advantage that both revolution

and tooth marks are usually obliterated by the material of the chip yielding in almost tangential direction as the tooth approaches the finished surface of the work. The finished surface has a dull appearance, free from the characteristic parallel markings of a surface produced in up milling.

Marks Produced in Formation of Milling Chip. The deterioration of a milled surface along the tooth path for up milling and down milling is shown in Figs. 20 and 21, respectively.

For a short distance after the cutting edge contacts the work, the surface machined by both methods is shiny in appearance and of uniformly good finish. The extent of this surface depends on the material being cut, chip thickness and rake angle, and also on the presence on the cutting edge and adjacent surfaces of a film of molecular dimensions which prevents the chip material from bonding to the tooth and forming the built-up edge.

The wiping action of the chip and the temperature of cutting soon reduce the effect of this film and the built-up edge begins to form. Fragments of built-up edge are periodically sloughed off as the tooth continues in its travel through the work, and are found on the milled surface.

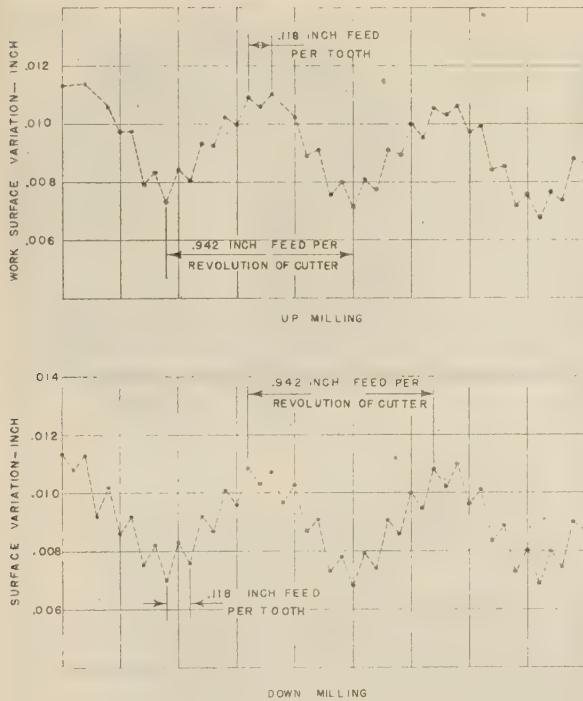


FIG. 18 ACTUAL VALUES OF TOOTH AND REVOLUTION MARKS ON A MILLED SURFACE

(Material, brass; plain milling cutter, 8 T, 3.89 in. diam; 38 rpm; helix angle 35 deg; feed rate, 36 ipm; depth of cut, $1/32$ in.)

In up milling, the element of smooth surface produced at the beginning of chip formation is an element of the final surface. This condition insures a surface of generally good finish and free from fragments of the built-up edge.

In down milling, an element of the final surface is produced when the built-up edge is fully developed, hence the surface, owing to the presence of fragments of built-up edge, is rougher and of a poorer quality than that produced in up milling. This, however, is not generally true, particularly when the surfaces of different kinds of work materials are compared, Fig. 22.

The quality of surface finish also may sometimes be affected by chip fragments adhering to the teeth and being dragged into the work in subsequent engagements.

ANGLE OF APPROACH

There is a fundamental difference between the two methods of milling in the manner in which a tooth engages the work. In down milling, a tooth engages the work on the unmachined or rough surface of the workpiece at a distance equal to the feed per tooth from the path generated by the previous tooth and, after forming a chip leaves the workpiece in an almost tangential direction. In up milling, a tooth engages the work in a nearly tangential direction on the surface milled by the previous tooth, and at a distance from the point of engagement of the previous tooth equal to the feed per tooth, Fig. 23. However, the point where contact actually begins is indefinite, owing, for example, to variations in center distance of the teeth. It is also evident that the thickness of the chip in the early stage of chip formation in down milling is considerably greater than in up milling, Figs. 24 and 25.

The relative conditions of tooth engagement in up milling and down milling are affected by the variables of the cut, as indicated by the value of the angle q , Fig. 23, made by the tangent to the

tooth path with a line parallel to the milled surface and given by the following formula

$$q = \tan^{-1} \left[\frac{2\pi(2Rd - d^2)^{1/2}}{2\pi(R - d) \pm F_d T} \right] \dots \dots \dots [15]$$

The negative sign in the denominator applies in down milling, and the positive sign in up milling.

For a given cutter diameter, the angle q in down milling changes with the feed per revolution and depth of cut. With a constant depth of cut, the angle q increases with the feed per revolution. This effect, however, is usually small. With a constant feed per revolution, q varies with the depth of cut, and large values of q may be obtained when the depth of cut is great. At the point of tooth contact with the work, q has always a definite and relatively large value in down milling, while in up milling, q is very small, Fig. 23.

From this, it follows that in down milling as a tooth begins to cut, the load, being generally normal to the cutting edge, produces compressive stresses on the cutting material, while in up milling, on account of the nearly tangential direction of tooth engagement with the work, bending stresses result on the cutting edge of the tooth.

The load conditions in down milling are particularly advantageous when using high feed rates and in high-speed milling. In this case, the carbide material can more favorably resist the destructive effects of the cutting force.

It should be remembered, however, that in down milling the angle q is not constant. It varies with the depth of cut and

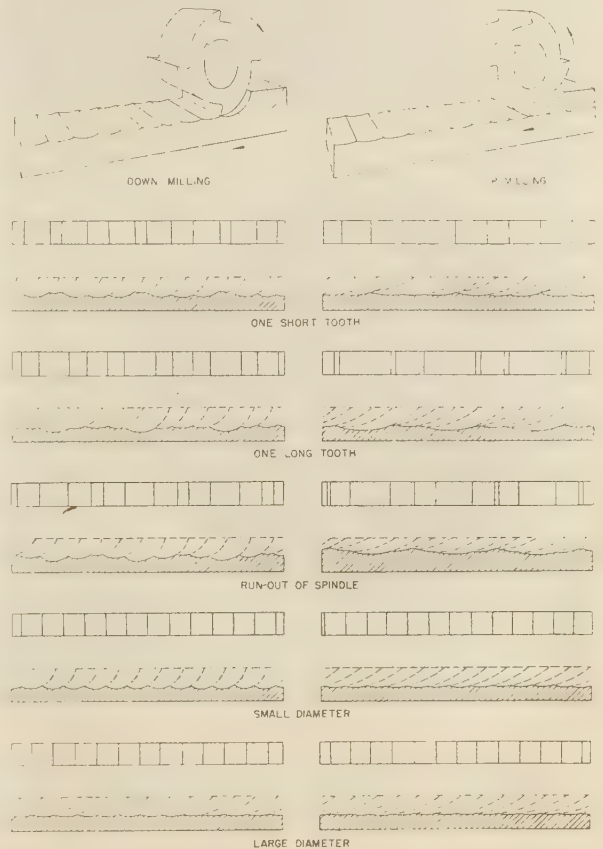
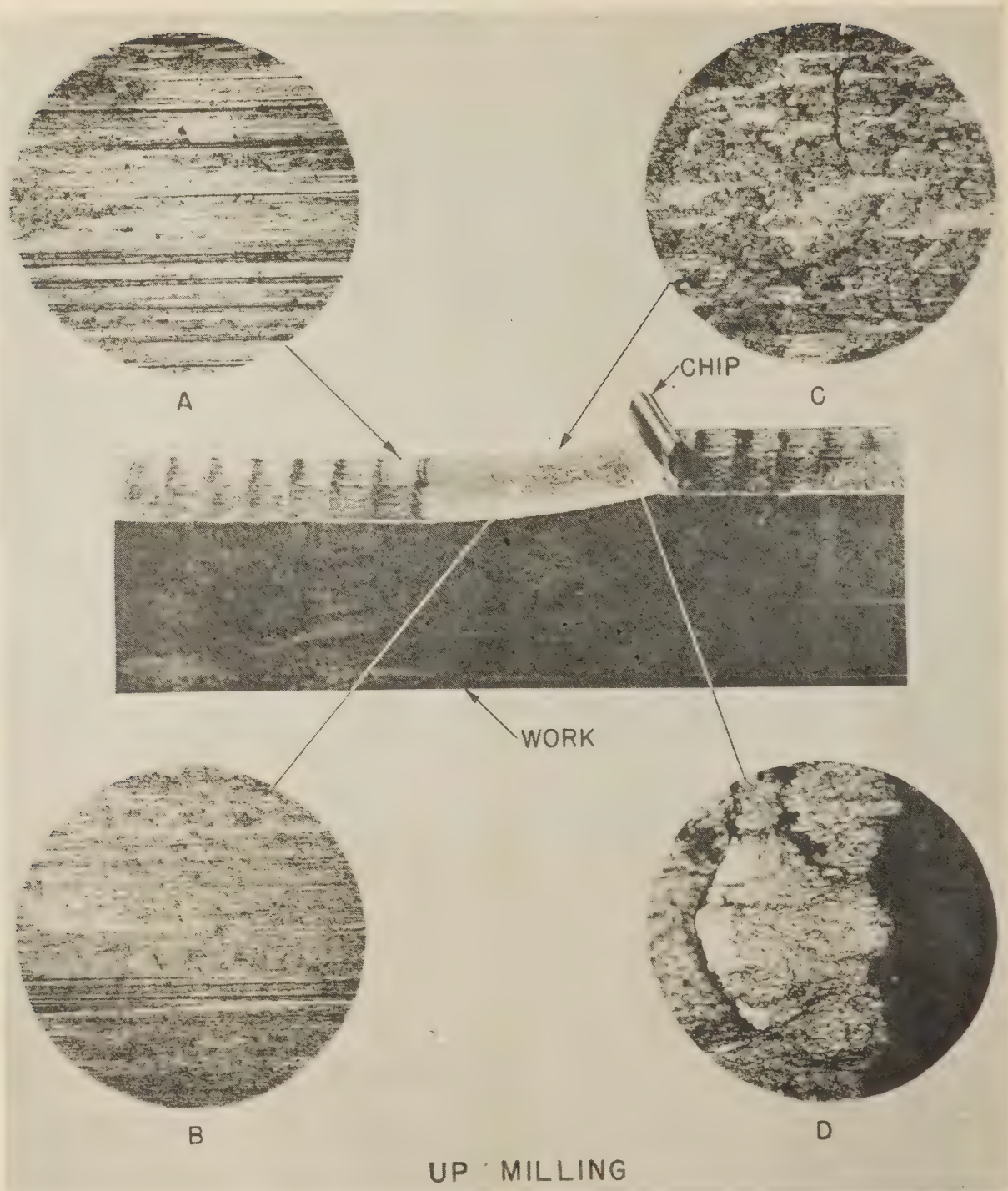
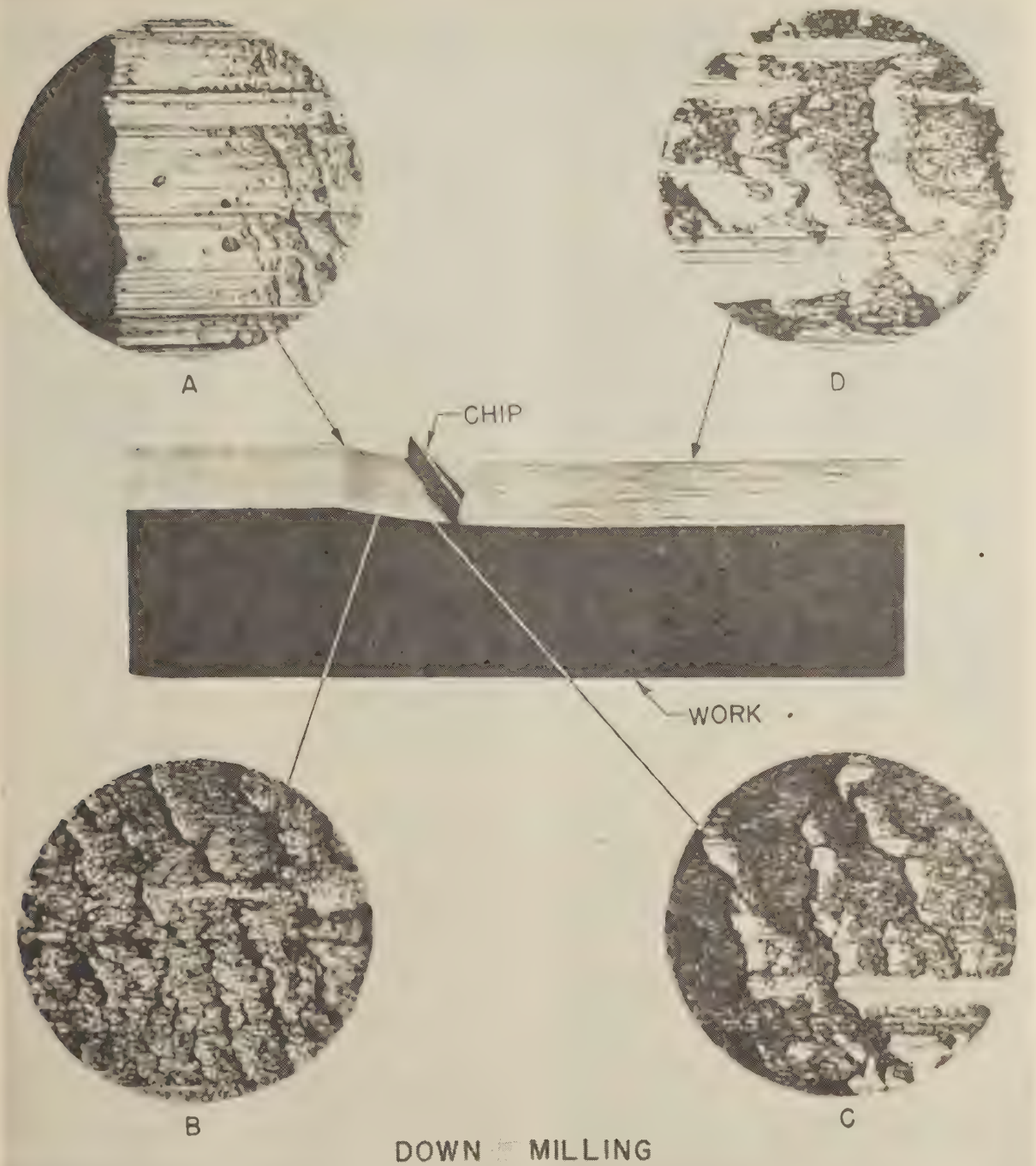


FIG. 19 GREATLY ENLARGED OUTLINE OF A MILLED SURFACE PRODUCED GRAPHICALLY FOR DIFFERENT ASSUMED CONDITIONS



A, Final Surface; B and C, Middle of Tooth Path; D, End of Tooth Path

FIG. 20 PHOTOMICROGRAPHS SHOWING CHANGE IN QUALITY OF MILLED SURFACE ALONG TOOTH PATH IN UP MILLING
(Material, S.A.E. 1112; feed rate, $6\frac{1}{4}$ ipm; depth of cut, $\frac{1}{8}$ in.; plain milling cutter, 4 in. diam, 10 T; cutting speed, 40 fpm; cutting fluid, soluble oil and water; photomicrographs $\times 100$, workpiece $\times 8$.)



A, Beginning of tooth path; *B* and *C*, Middle of tooth path; *D*, Final surface

FIG. 21 PHOTOMICROGRAPHS SHOWING CHANGE IN QUALITY OF MILLED SURFACE ALONG TOOTH PATH IN DOWN MILLING
 (Material, S.A.E. 1112; feed rate, $6\frac{1}{4}$ ipm; depth of cut, $\frac{1}{8}$ in.; plain milling cutter, 4 in. diam, 10 T; cutting speed, 40 fpm; cutting fluid, soluble oil and water; photomicrographs $\times 100$, workpiece $\times 8$.)



FIG. 22 QUALITY OF SURFACES OBTAINED IN UP AND DOWN MILLING VARIOUS KINDS OF WORK MATERIALS
(Materials, S.A.E. 3115 steel, stainless steel, "Rezistal;" cutting fluid, soluble oil and water; depth of cut, $1/16$ in.; width of cut, $1/4$ in.; feed rate 3 ipm; plain milling cutter, 4 in. diam, 10 T; cutting speed 63 fpm. Materials, duralumin, brass, cut dry; depth of cut, $1/16$ in.; width of cut, $1/4$ in.; feed rate, $6 1/4$ ipm; plain milling cutter, 4 in. diam, 10 T; cutting speed, 230 fpm.)

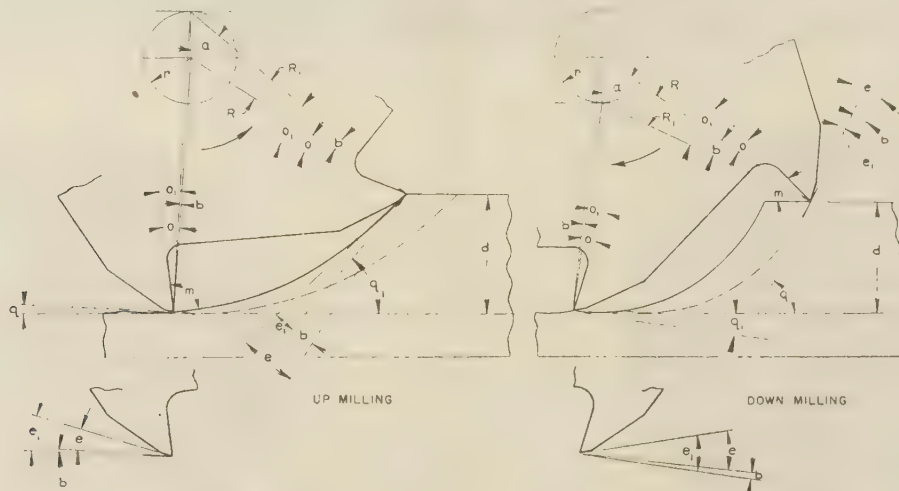


FIG. 23 ANGLE OF APPROACH, RAKE AND CLEARANCE ANGLES IN UP MILLING AND DOWN MILLING

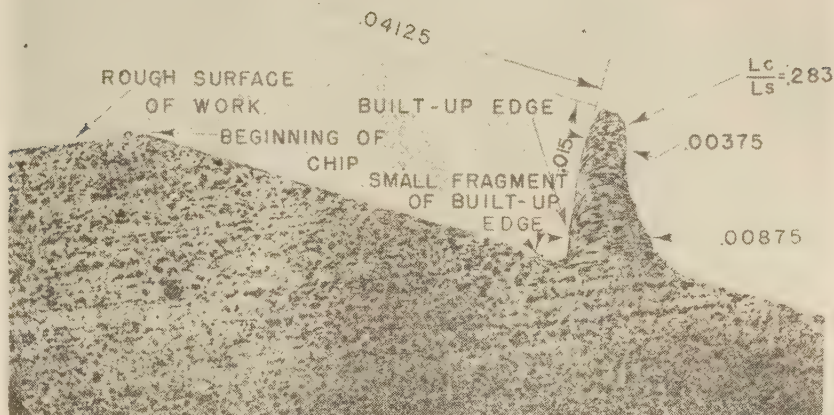
although it may be the same in any given job, it will be different in different jobs. The minimum value of q_1 occurs at the point where the tooth leaves the work. At this point the value of d in [15] is equal to h , Equation [14]. The change in depth of cut causes wide variations in the angle $m = 90 - q + O$, included between the face of the tooth and the rough surface of the work. Therefore, proper consideration should be given to its value in order to limit the intensity of tooth impact, which depends upon the rate of increase of the chip thickness to its maximum value. This is especially important when using small-diameter milling cutters in deep cuts. If the angle m is too small, the intensity of the impact may be sufficient to break the cutter. A certain de-

gree of control of tooth impact may be obtained by increasing rake angle O , or reducing the feed rate, or both.

In up milling, q is small at the point of tooth engagement with the work, and it can be considered to remain practically constant under all conditions (the depth of cut being at this point equal to h , Equation [14]), although it varies somewhat with the feed per revolution. The maximum depth of cut has no effect on the value of q , except in the initial stages of tooth engagement with the work, where q_1 assumes the maximum value q_1 , corresponding to the maximum depth of cut d . In up milling the angle $m = 90 - q + O$ therefore is large and nearly the same in every job. This produces uniform conditions of tooth engage-

FIG. 24 PHOTOMICROGRAPH OF WORK AND CHIP AT BEGINNING OF CUT IN DOWN MILLING

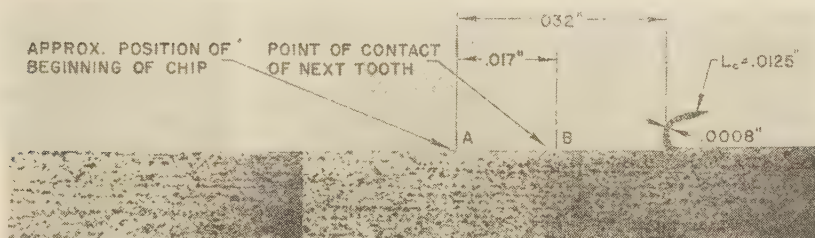
(Material, S.A.E. 1112 steel, $\times 50$; feed rate, $6\frac{1}{4}$ ipm; depth of cut, $\frac{1}{8}$ in.; plain milling cutter, 4 in. diam, 10 T; cutting speed, 40 fpm; cutting fluid, soluble oil and water.)



DOWN MILLING

FIG. 25 PHOTOMICROGRAPH OF WORK AND CHIP AT BEGINNING OF CUT IN UP MILLING

(Material, S.A.E. 1112 steel, $\times 50$; feed rate, $6\frac{1}{4}$ ipm; depth of cut, $\frac{1}{8}$ in.; plain milling cutter, 4 in. diam, 10 T; cutting speed, 40 fpm; cutting fluid, soluble oil and water.)



UP MILLING

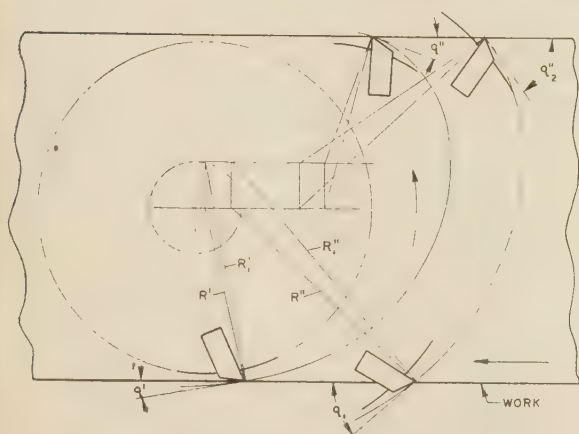


FIG. 26 ANGLE OF APPROACH IN FACE MILLING

ment, furthermore the gradual increase of chip thickness results in a considerable reduction in tooth impact.

In face milling the value of the angle of approach q is greatly influenced by the relative dimensions between cutter diameter and work width, and also cutter location with respect to the work. If for example, the cutter diameter is slightly larger than the work width, the angle q is small, but a large value of q may be obtained if the cutter overlaps the work, Fig. 26.

The angle q can be obtained from Equation [15] by substituting for the depth of cut d the amount which the cutter overlaps the work on the side which the tooth enters the work.

RELATIVE VELOCITY ALONG TOOTH PATH

The relative velocity along the tooth path is given by the following expression

$$V = 2\pi n[(R \pm r)^2 \pm 2ry]^{1/2} \dots \dots \dots [16]$$

The upper signs apply in up milling and the lower signs in down milling. In practical milling applications, the relative velocity V is nearly equal to the peripheral speed of the cutter. Equation [16], however, indicates that V varies with the position of the tooth on the tooth path as given by y .

In up milling when the tooth enters the work and the depth of cut is nearly zero, V assumes a maximum value, which decreases as the tooth progresses along the tooth path. In down milling, V has a minimum value when the tooth leaves the work and somewhat higher value when the tooth enters the work.

RAKE AND CLEARANCE ANGLES

In milling, both the rake and clearance angles vary along the tooth path. The rake angle O_1 is the angle determined by the tooth face and the normal to the tangent at the tooth path at the point being considered. This angle may be called the actual rake angle. It is the sum of the rake angle O , normally provided on a milling cutter, and the angle b , which can be obtained from the following expression, Fig. 23

$$b = \sin^{-1} \left[\frac{F_r(2Rd - d^2)^{1/2}}{2\pi R \sqrt{\left(R \pm \frac{F_r}{2\pi}\right)^2 \mp \frac{F_r d}{\pi}}} \right] \dots \dots [17]$$

Since b is a small angle, the sine of the angle can be assumed equal to the arc, hence

$$b = \frac{180}{\pi} \left[\frac{F_r(2Rd - d^2)^{1/2}}{2\pi R \sqrt{\left(R \pm \frac{F_r}{2\pi}\right)^2 \mp \frac{F_r d}{\pi}}} \right] \dots \dots [18]$$

and

$$O_1 = \pm O + \frac{180}{\pi} \left[\frac{F_r(2Rd - d^2)^{1/2}}{2\pi R \sqrt{\left(R \pm \frac{F_r}{2\pi}\right)^2 \mp \frac{F_r d}{\pi}}} \right] \dots \dots [19]$$

In the denominator, the lower signs apply in down milling, and the upper signs in up milling. The negative sign of O is used when O is negative.

In up milling, at the beginning of tooth engagement with the work, the actual rake angle is nearly equal to O and increases to a maximum O_1 when the tooth leaves the work. In down milling; the actual rake angle is a maximum at the beginning of tooth engagement, and a minimum nearly equal to O when the tooth leaves the work.

The minimum clearance angle at any point of the tooth path is the angle b included between the cutter radius and radius of curvature. If the path were circular, the radius of curvature R_1 would coincide with the radius R of the cutter, and the angle b would be zero. The minimum clearance can be calculated from Equation [18].

The actual clearance angle e_1 at any point of a tooth path is the difference between the clearance angle e ground on the flank of a cutter tooth and the minimum clearance angle b

$$e_1 = e - \frac{180}{\pi} \left[\frac{F_r(2Rd - d^2)^{1/2}}{2\pi R \sqrt{\left(R \pm \frac{F_r}{2\pi}\right)^2 \mp \frac{F_r d}{\pi}}} \right] \dots \dots [20]$$

except at the beginning of the tooth path in up milling and at the end of tooth path in down milling where the actual clearance angle is the sum of e and b , Fig. 23.

In up milling therefore at the beginning of chip formation, the actual clearance angle e_1 is equal to the given clearance angle e . As the tooth assumes different positions along the tooth path, the actual clearance angle e_1 decreases, and rubbing on the flank of the tooth will eventually result, if the depth of cut is such as to make the minimum clearance b greater than the given clearance

angle e . In down milling, the actual clearance e_1 is a minimum at the beginning of the chip formation and a maximum nearly equal to e when the tooth leaves the work.

Thus under identical cutting conditions, the actual rake angle O_1 is greater in down milling than in up milling, while the actual clearance angle is greater in up milling than in down milling. In order to avoid interference and rubbing on the tooth flank, it is necessary to provide a clearance angle greater than the maximum value of the angle b .

POWER REQUIRED IN MILLING

In order to determine the power required in up milling and down milling, blocks of S.A.E. 1112 and cast iron were milled with an 8-tooth $3^{39}/_{32}$ -in-diam plain milling cutter. Two machines were used, one being provided with independent motors for the spindle and feed drive, while the other was a standard machine driven by an electric dynamometer which replaced the regular motor.

With the first machine, the power required by the spindle and feed drive was measured separately, while with the second machine was measured the total power consumption. The data obtained in these tests indicate the following:

1 The total power input into the machine, corresponding to given values of feed rate and different depths of cut is higher in up milling than in down milling, Figs. 27 and 28.

2 The efficiency of metal removal, measured in cubic inches per minute per horsepower, and based on the net power input to the machine (including the power for the feed drive), is higher in down milling than in up milling, Figs. 29 and 30.

3 The power required by the cutter alone is higher in down milling than in up milling, Fig. 31.

4 The power required by the feed drive is higher in up milling than in down milling, Fig. 32.

The foregoing results may be explained as follows:

In down milling, the component of the cutting force, acting parallel to the table and in the direction of the feed, helps to propel the table, thus producing a corresponding decrease in the power required to feed the table. In up milling, the component of the cutting force, acting parallel to the table but against the direction of the feed, causes a proportional increase in the power required to feed the table, Fig. 32.

The higher power required by the cutter in down milling may be attributed to the fact that the thickness of the chip is greater in down milling than in up milling, Figs. 14 and 15. When the power input to the machine is considered, however, this difference is not sufficiently great to compensate for the reduction in the power used in the feed drive, and the final result is a lower power and correspondingly a higher efficiency of metal removal in down milling than in up milling.

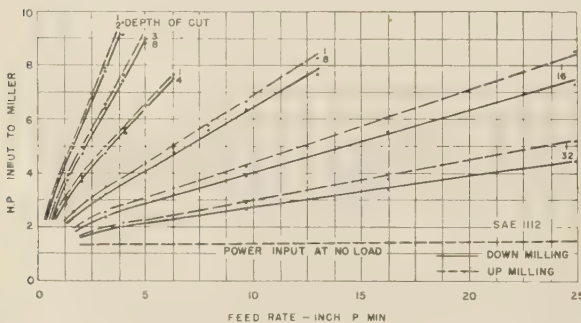


FIG. 27 HORSEPOWER INPUT TO THE MACHINE VERSUS FEED RATE, UP MILLING AND DOWN MILLING.

(Material, S.A.E. 1112 steel; cutting fluid, soluble oil and water; width of cut, 4 in.; plain milling cutter, 4 in. diam, 8 T; cutting speed, 60 f.p.m.)

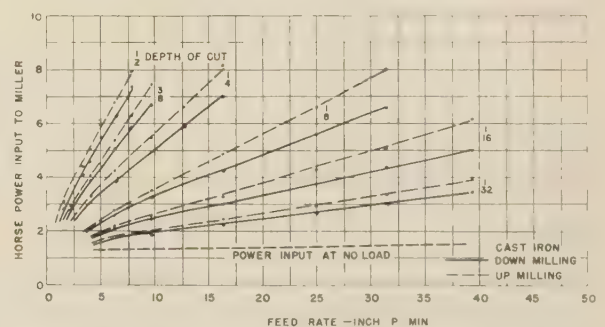


FIG. 28 HORSEPOWER INPUT TO THE MACHINE VERSUS FEED RATE, UP MILLING AND DOWN MILLING

(Material, cast iron, cut dry; width of cut, 4 in., plain milling cutter, 4 in. diam, 8 T.)

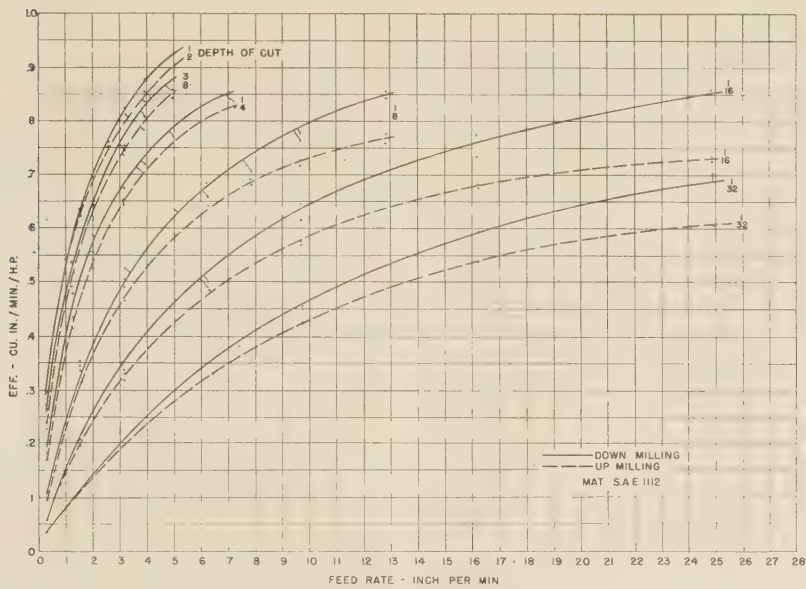


FIG. 29 EFFICIENCY OF METAL REMOVAL IN UP MILLING AND DOWN MILLING, S.A.E. 1112 STEEL
(Cutting fluid, soluble oil and water; cutter, plain milling cutter, 4 in. diam, 8 T; width of cut, 4 in.; cutting speed, 60 fpm.)

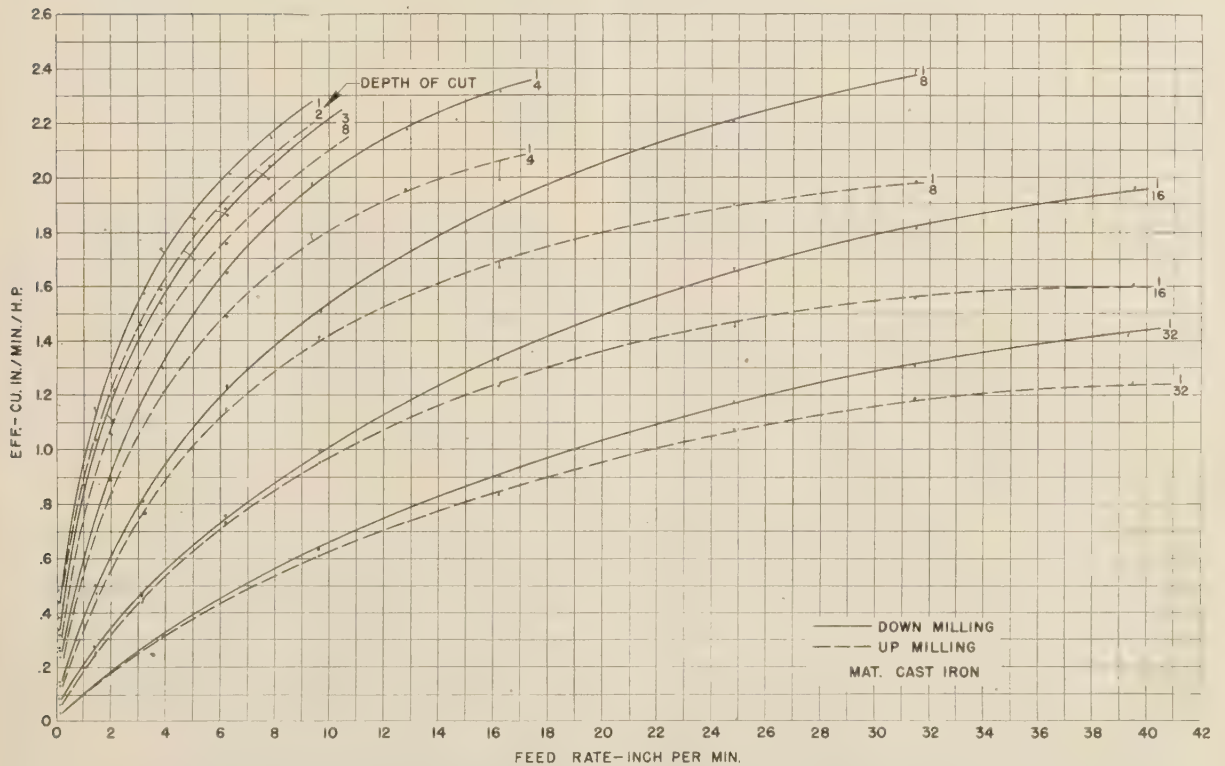


FIG. 30 EFFICIENCY OF METAL REMOVAL IN UP MILLING AND DOWN MILLING CAST IRON
(Cut dry; plain milling cutter, 4 in. diam, 8 T; width of cut 4 in.; cutting speed, 60 fpm.)

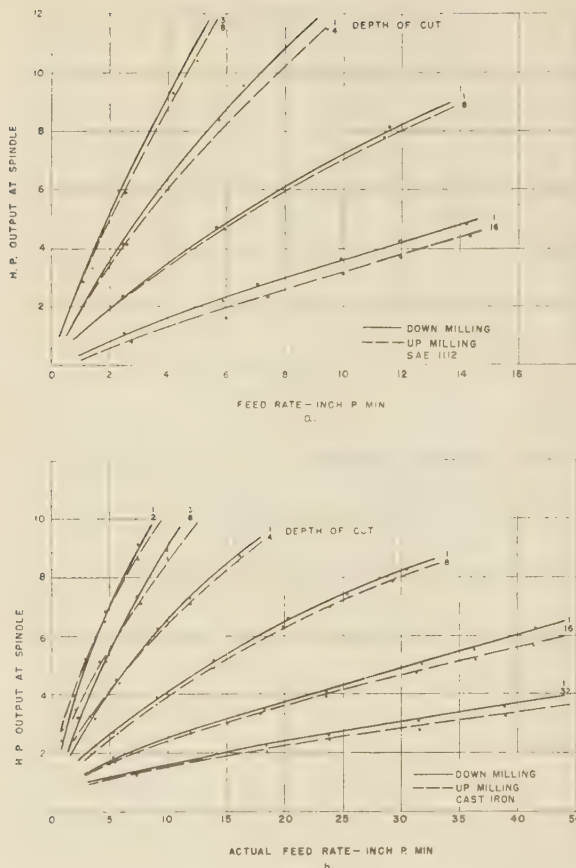


FIG. 31(a) NET POWER REQUIRED AT THE SPINDLE VERSUS FEED RATE, INCHES PER MINUTE, IN UP MILLING AND DOWN MILLING (Material, S.A.E. 1112 steel; cutting fluid, soluble oil and water; plain milling cutter, 5 in. diam, 8 T; 5 in. width of cut; cutting speed, 80 fpm.)

FIG. 31(b) NET POWER REQUIRED AT THE SPINDLE VERSUS FEED RATE, INCHES PER MINUTE, IN UP MILLING AND DOWN MILLING (Material, cast iron, cut dry; width of cut, 4 in.; plain milling cutter, 4 in. diam, 8 T; cutting speed, 60 fpm.)

Horizontal and Vertical Components of Cutting Force. The horizontal and vertical components of the cutting force were measured by calibrating with known loads the structure of the milling machine on which these tests were conducted.

A combination of plain right- and left-hand-helix milling cutters was used to neutralize the axial thrust.

From the data shown in Fig. 33, it is apparent that comparable intensities of the horizontal component are obtained in both methods of milling. The vertical component, however, is small in up milling, its intensity tending to decrease as the depth of cut is increased. A reversal in the direction of the vertical component may occur when the depth of cut is great. This may result in lifting the workpiece out of the fixtures in some milling operations requiring deep cuts.

In down milling, there is no reversal of the vertical component as the depth of cut is increased. Actually the intensity of the vertical component increases with the depth of cut, thus helping to keep the workpiece securely in its fixture.

The forces acting near and along the cutting edge of a milling-cutter tooth and the chip being formed can be assumed to be represented by a force N normal to the face of the tooth and a frictional force F acting along the face of the tooth opposing the

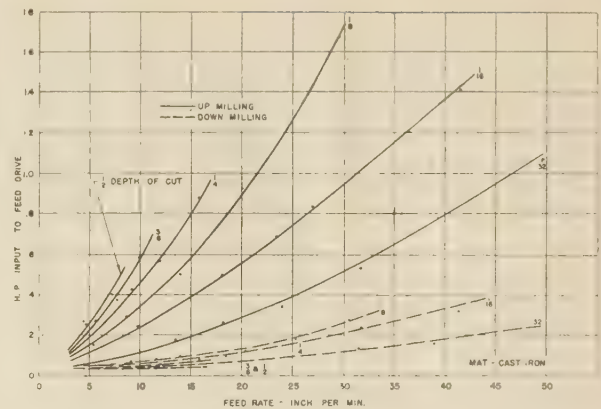


FIG. 32 HORSEPOWER INPUT TO THE FEED DRIVE VERSUS FEED RATE, INCHES PER MINUTE, IN UP MILLING AND DOWN MILLING (Material, cast iron, cut dry; width of cut, 4 in.; plain milling cutter, 4 in. diam, 8 T; cutting speed, 60 fpm.)

flow of the chip. The resultant R of these forces is the force required to form a chip, Fig. 34. The projection T of the resultant along the tangent and at any point of the tooth path multiplied by the velocity at that point is the power required to form a chip at that point.

The conditions obtaining in up milling and down milling with positive and negative radial rake angles are expressed in the following relation

$$TV = R \cos (f \pm O_1) V \dots \dots \dots [21]$$

where

V = instantaneous velocity obtained from Equation [16]

f = angle of friction measured between R and N

The \pm signs apply with negative and positive rake angles, respectively.

Since the projection of the resultant is equal to the sum of the projections of the components, Equation [21] can be written as follows

$$TV = (N \cos O_1 \mp F \sin O_1) V \dots \dots \dots [22]$$

(— sign for negative and + sign for positive rake angles)

It can be seen that when the rake angle is negative, the frictional force F , which is always opposed to the motion of the chip along the face of the tooth, provides a component along the tangent which tends to reduce the power required to form a chip. This also indicates that if the power consumed and the frictional force are assumed to be the same, then the force N is higher with negative than with positive rake angles. With negative rake angles, a reduction in the frictional force will increase the power consumed if a corresponding reduction does not take place in the normal force N .

RESULTS OBTAINED IN DOWN-MILLING APPLICATIONS

The characteristic difference between the two milling methods has been found particularly advantageous in various classes of work. It is often possible to use a substantially higher feed rate in down milling than in up milling with a corresponding increase in production as, for example, milling the sides and bottom of the cast-iron part shown in Fig. 35. In up milling, the maximum feed rate that could be used to avoid the cutter lifting the work out of the fixture, was $3\frac{1}{8}$ ipm. By changing to down milling, the feed rate was safely increased to $7\frac{1}{4}$ ipm.

A considerable increase in cutter life was recorded in milling the cast-iron part shown in Fig. 36. This operation consists in milling from solid the top, sides, and bottom surfaces of the T-

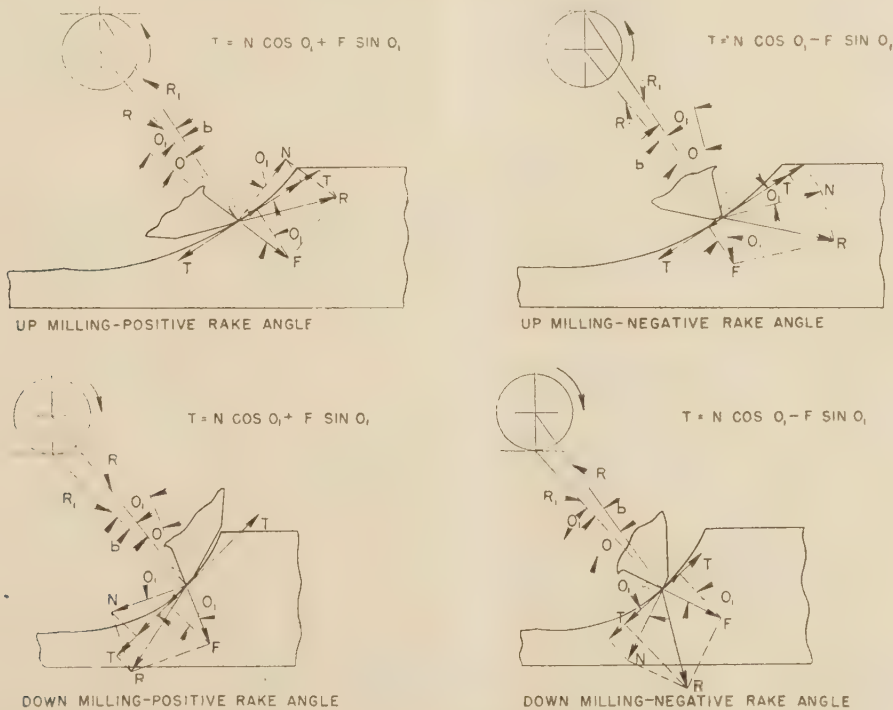
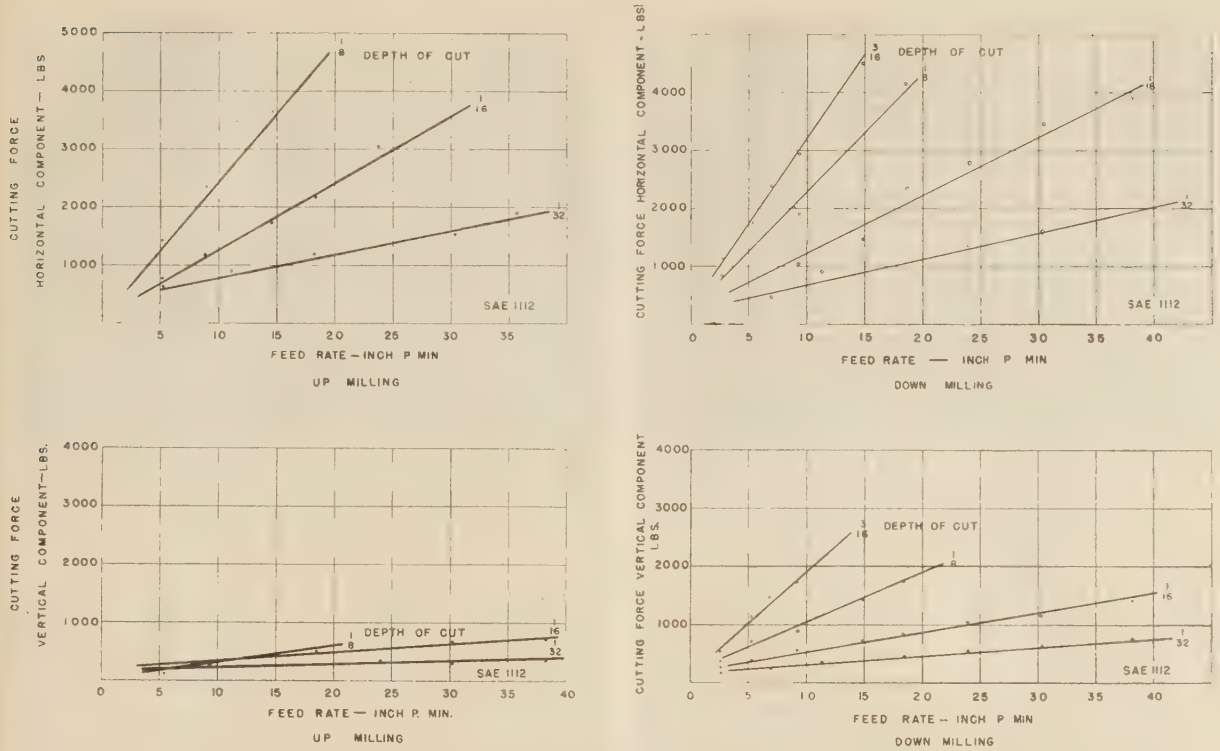


FIG. 34 FORCES ON A MILLING CUTTER TOOTH IN UP MILLING AND DOWN MILLING AND WITH POSITIVE AND NEGATIVE RAKE ANGLES

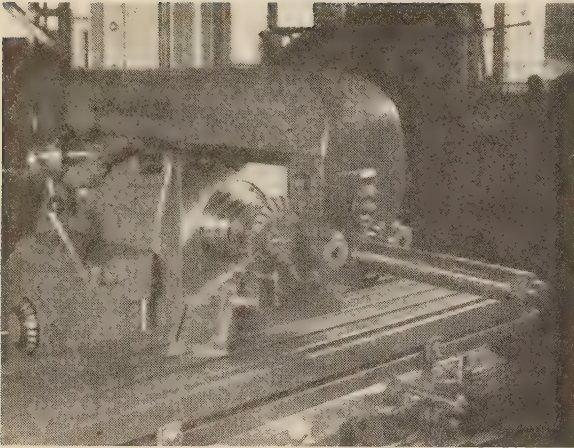


FIG. 35 SETUP USED IN DOWN MILLING A CAST-IRON PART ON MACHINE EQUIPPED WITH BACKLASH ELIMINATOR
(Material, cast iron; operation, straddle-milling sides, peripheral-milling top and bottom. Down milling permitted increase in feed rate from $3\frac{1}{8}$ ipm to $7\frac{1}{4}$ ipm, thus production was increased 116 per cent.)

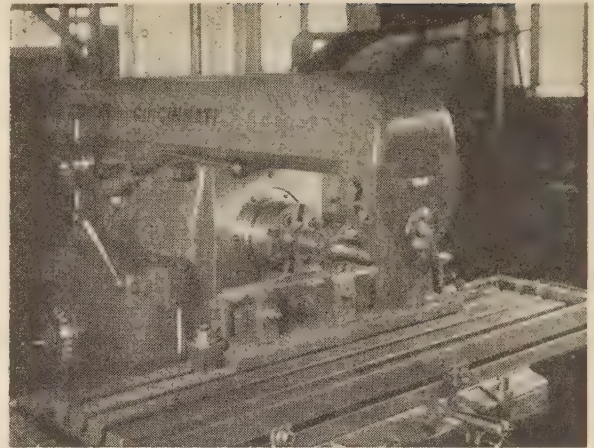


FIG. 36 SETUP USED IN DOWN MILLING FROM SOLID T-SECTION ON MILLING MACHINE EQUIPPED WITH BACKLASH ELIMINATOR
(In this job, cutter life was increased 68 per cent by changing from up to down milling.)

section. The number of pieces per grind was 93 in up milling, and 156 in down milling, with an increase of 68 per cent in cutter life between grinds.

In milling parts made of S.A.E. 4150, Brinell hardness 190-210, the life of the interlocking slotting cutters with a 20-deg radial rake angle was from 2 to 3 times that obtained with cutters having a 10-deg rake angle, and with a considerable saving in the actual power consumed. The reduced work of deformation of the chip and lower temperature at the cutting edge permitted also an increase in cutting speed from 40 to 100 fpm, which for the same feed per tooth gave a corresponding increase in production rate.

Down milling is also used successfully in milling turbine blades, since among other advantages, it produces a milled surface, free from revolution marks, which can be easily and quickly polished.

Thin slotting cutters and saws have less tendency to deflect sideways when used in down milling.

In high-speed milling, down milling provides a better load condition and, consequently, an increase in the resistance of carbide tips to the destructive effects of the cutting force.

In down milling, however, the cutting edge begins to cut on the rough surface of the work and the presence of sand or scale is detrimental to cutter life. In up milling, the cutting edge engages the workpiece on the surface milled by the previous tooth, and the condition of the outer surface of the workpiece has generally no appreciable effect on cutter life.

In down milling the danger of the work being dragged under the cutter is also present. If this occurs, expensive cutters, fixtures, and the machine itself may be seriously damaged, and the operator exposed to injury. It is therefore important to make sure that every possible precaution has been taken in setting up the machine and that the machine is kept in good repair.

CONCLUSION

From the data presented in this paper, the respective advantages of both methods of milling are summarized as follows:

- | DOWN MILLING | UP MILLING |
|--|---|
| 1 Possibility of simplified fixtures, and of milling parts that cannot be easily held. | 1 Does not require backlash eliminator. |
| 2 Milled surface not affected by revolution marks, and | 2 Safer operation due to separating forces between cutter |

- | | | | | |
|--|---|---|---|--|
| can be easily polished. | 3 | Lower power consumption which permits increased metal removal of the machine for a given motor capacity. | 3 | Less wear on screw and nut threads due to absence of preload. Repair and replacement of parts not as frequent. |
| 4 Smoother operation of the machine; less tendency to chatter. | 4 | Use of larger positive rake angles with high-speed steel cutters which lessen work of deformation on material of chip, lower cutting temperature and longer tool life; better load condition on carbide tips in high-speed milling. | 4 | Looseness in moving parts not detrimental to cutting action and performance of machine. |
| 5 Higher cutting speeds and feeds. | 5 | Less surface milled per piece. | 5 | Fragments of built-up edge absent from milled surface. |
| 6 | 6 | | 6 | Life of cutter not affected by scale or sandy surfaces. |
| 7 | 7 | | 7 | Tooth engagement with work generally the same on all jobs, and remote possibility of cutter breakage due to variation in depth of cut. |

Down milling has increased the usefulness of the milling process and is finding an ever-widening field of application.

The selection of one or the other methods of milling, however, should be dictated by a proper consideration of the job on hand and the various factors contributing to its economic production

Appendix

1 RADIUS OF CURVATURE

Substituting in the following expression for the radius of curvature

$$R_1 = \frac{\left[\left(\frac{dx}{da} \right)^2 + \left(\frac{dy}{da} \right)^2 \right]^{1/2}}{\frac{dx}{da} \frac{d^2y}{da^2} - \frac{dy}{da} \frac{d^2x}{da^2}}$$

in the numerator and denominator, the expression obtained from Equation [1] results

$$R_1 = \frac{[r^2 + R^2 \pm 2rR \cos a]^{1/2}}{\pm rR \cos a + R^2}$$

but

$$\cos a = \frac{R - y}{R}$$

hence

$$R_1 = \frac{[r^2 + R^2 \pm 2r(R - y)]^{1/2}}{\pm r(R - y) + R^2}$$

2 LENGTH OF TOOTH PATH

From the differential of the arc

$$dL = \left[\left(\frac{dx}{da} \right)^2 + \left(\frac{dy}{da} \right)^2 \right]^{1/2} da$$

and Equation [1]

$$dL = (R^2 + r^2)^{1/2} \left(1 \pm \frac{2rR}{R^2 + r^2} \cos a \right)^{1/2} da$$

and

$$L = (R^2 + r^2)^{1/2} \int_0^a \left(1 \pm \frac{2rR}{R^2 + r^2} \cos a \right)^{1/2} da$$

Let

$$m = \frac{2rR}{R^2 + r^2}$$

and developing in series

$$L = (R^2 + r^2)^{1/2} \left[a \left(1 - \frac{m^2}{16} \right) \pm \left(1 + \frac{m^2}{8} \right) \frac{m \sin a}{2} \right. \\ \left. - \frac{m^2 \sin 2a}{32} \mp \frac{m^3 \sin 3a}{48} \right]$$

The upper signs apply in up milling and the lower signs in down milling.

Creep Properties of Molded Phenolic Plastics at Elevated Temperatures

By W. J. GAILUS¹ AND DAVID TELFAIR²

To augment the small amount of published data on the creep properties of thermosetting materials, the authors undertook a study of the behavior of molded phenolic plastics at approximately 192 F. Tension creep data are reported up to 1000 hr, and recovery data up to 250 hr. Modulus-of-elasticity values were obtained at the beginning and end of the 1000-hr tests. Studies included the effect of moisture content on creep properties.

INTRODUCTION

MOLDED phenolic plastics have long been used in applications where stability at fairly high temperatures is of prime importance. Numerous studies have been made of the effects of different temperatures on such physical properties as tensile strength, flexural strength, compressive strength, shear strength, modulus, etc., with one exception. Comparatively little has been done to increase our fund of information on the creep properties of thermosetting materials. The papers which have been published on this subject cover only a small range of stress values and are on tests of fairly short duration. Practically no data exist on the creep of phenolics at high temperatures.

The work reported herein was undertaken to complement the investigation previously reported by Telfair, Carswell and Nason, (1),³ and to obtain a more definite understanding of the behavior of phenolics at high temperatures. The research reported here concerned itself with the behavior of molded phenolic plastics at approximately 192 F.

Tension creep data up to 1000 hr are reported, with recovery data up to 250 hr. Values of modulus of elasticity were obtained at the beginning and end of the 1000-hr tests. Effect of moisture on creep properties was studied.

DETAILS OF INVESTIGATION

Materials. The materials investigated included molded phenolics with wood flour, chopped canvas (rag), cotton cord, asbestos, and mica fillers, unfilled phenolic resin, and two types of paper laminate (both cross-laminated). The filled materials contained approximately 50 per cent phenol-formaldehyde resin and 50 per cent filler, with the exception of the asbestos-filled material, which contained approximately 40 per cent resin, 45 per cent asbestos filler, and 15 per cent wood-flour filler (to improve molding properties).

The wood-flour-, asbestos-, and mica-filled molding compositions were prepared by rolling the resin and filler in the usual manner for the preparation of general-purpose phenolic molding

compositions. The cotton-cord and chopped-canvas fillers were blended with the resin in a wet-mix process. The wet resin filler was dried and the resin further polymerized to give a moldable composition. A special technique was developed to produce satisfactory molding powder for specimens of pure resin compound.

Specimens. Standard A.S.T.M. (D638-42) tensile specimens of these materials were compression-molded, using approximately a 10-min cure at 165 C and a pressure on the specimen of approximately 4000 psi. The specimens were cooled to below 85 C before removal of pressure. The paper-laminate specimens were machined from sheets supplied by the Forest Products Laboratory of Madison, Wis. The sheets were made of high-strength paper, cross-laminated, using two different phenolic resins.

Baldwin Southwark SR-4 strain gages were mounted on opposite sides of each specimen with phenolic cement. "Dummy" specimens, for use as the balancing arm in the Wheatstone-bridge circuit, were made up in the same manner. In addition, special "standard" dummies were made by mounting SR-4 gages on unglazed porcelain.

Definitions. The terms "elastic deformation," "creep" or "delayed deformation," "elastic recovery," "delayed recovery," and "permanent set" were defined and illustrated in the earlier paper (1). It may be well for the reader at this point to refer to Fig. 1, which illustrates the meaning of the additional terms "shrink," "effect of stress," and "behavior," as they will be used in this paper.

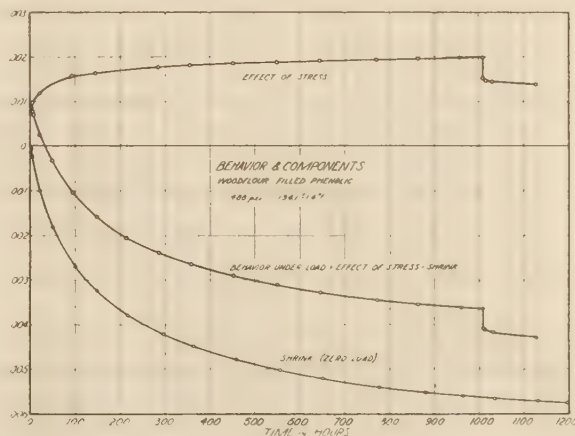


FIG. 1

¹ Research Engineer, Plastics Division, Monsanto Chemical Co., Springfield, Mass. Jun. A.S.M.E.

² Physicist, Plastics Division, Monsanto Chemical Co., Springfield, Mass.

³ Numbers in parentheses refer to the Bibliography at the end of the paper.

Contributed by the Rubber and Plastics Division and presented at the Annual Meeting, New York, N. Y., Nov. 27-Dec. 1, 1944, of THE AMERICAN SOCIETY OF MECHANICAL ENGINEERS.

NOTE: Statements and opinions advanced in papers are to be understood as individual expressions of their authors and not those of the Society.

Testing Equipment and Procedure. A special technique was developed to study the creep phenomena at this temperature (192 F). The electrical-measuring system used is shown as a circuit diagram in Fig. 2. More detail concerning the testing equipment may be found in the earlier paper (1).

With this setup, it was possible to obtain: (a) Effect-of-stress data; all effects of thermochemical reaction within the specimen were automatically canceled out by balancing a virgin specimen against a virgin-specimen dummy (assuming, of course, that

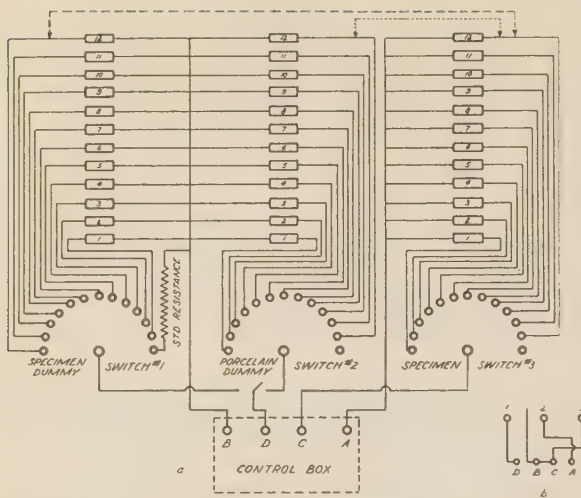


FIG. 2 SWITCHING ARRANGEMENT
(a, Specimen versus specimen or porcelain dummy. b, Porcelain versus specimen dummy.)

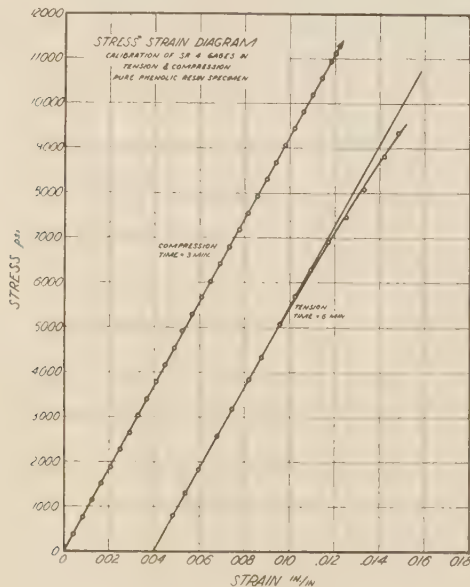


FIG. 3

the thermochemical reaction within the specimen is the same without stress as it is with stress). (b) Behavior data, i.e., a measure of the absolute deformation under the conditions imposed, were obtained by balancing a specimen against a "standard" porcelain dummy. (c) Shrink data (zero load) were obtained by balancing a porcelain dummy against a specimen dummy. The stability of the porcelain dummies was checked periodically against a standard resistance (Fig. 2). In order to increase the accuracy of the measurements, slight changes were made in the SR-4 control-box circuit so that it would operate as an adaptation of the Kelvin bridge, in effect reducing to a minimum errors caused by switch resistances.

Constant longitudinal loads were applied, as before, in the form of lead weights in convenient increments. The loads applied to each material varied from zero to values which caused fracture in less than 1000 hr. Results are reported only for speci-

mens that stood up for 1000 hr (except in the case of unfilled resin). Strain readings were taken for each load increment and the results were used for obtaining modulus data. The extension due to the application of the load was measured as a function of time over a period of 1000 hr. The loads were then removed in increments and strain readings were again taken. The contraction due to removal of load was then measured as a function of recovery time over a period of about 250 hr. The effect of moisture on the creep properties of these materials was studied by taking specimens which had been subjected to test for 1250 hr, soaking them in water at 50 C for 48 hr, and once more subjecting them to the original test procedure.

The SR-4 gages were calibrated in tension and compression (see Fig. 3). The gages were mounted on a pure phenolic-resin specimen so that practically a straight stress-strain curve would be obtained. The deviation of the curve in tension was probably caused by creep and cold flow since the time interval of testing was so much longer than that taken for the compression curve.

EXPERIMENTAL RESULTS

The results of creep measurements for the six molded and two cross-laminated phenolic compositions have been plotted in Figs. 4 to 17, inclusive. These materials, in general, possess the same type of creep and recovery curves. From Fig. 1, it can be seen that the creep at high temperatures consists of a balance between the opposing actions of strain due to load, and shrink due to molecular transformation. The technique used in this work permitted a separation of these components so that each might be studied individually. Rectangular co-ordinate plotting has been used to enhance clarity of interpretation. (Log-log plotting was used in Fig. 27, to show special characteristics of the materials.) The "shrink" data obtained by using the SR-4 gages were further confirmed by results obtained from virgin specimens with mechanical strain gages attached which were placed in an oven maintained at 192 F.

The first group of curves (Figs. 4 to 9, inclusive), shows how these materials would behave under stress action alone, thermochemical effects being ignored. All of the materials showed an extremely large amount of nonrecoverable flow. A rough comparison of the stress required to produce a total strain (elastic plus inelastic) of 0.003 in. per in. during a 1000-hr test at 192 F, as against room temperature (25 C) is presented in Table 1.

TABLE 1 COMPARISON OF STRESSES REQUIRED TO PRODUCE A TOTAL STRAIN OF 0.003 IN. PER IN. IN 1000 HR

	At room temperature, psi	At 192 F, psi
Cord filled.....	2150	...
Rag filled.....	2100	700-800
Wood-flour filled.....	2400	800
Resin compound.....	2100	...
Asbestos filled.....	2700	1600
Mica filled.....	4800	1400
Paper laminate.....	...	2600

The unfilled resin compound would not bear a stress as low as 100 psi for more than 370 hr at this temperature. Only one set of data is presented for the paper laminate, since both materials proved to have identical creep characteristics.

The second group of curves (Figs. 10 to 16, inclusive) shows the actual behavior of the materials; a summation of the physical and thermochemical forces acting on the specimens. A survey of the data plotted for zero stress gives an idea of the effects of thermochemical reaction within the specimen; it compares the materials on the basis of shrink. Mica-filled phenolic, unfilled resin compound, paper laminate, asbestos-filled phenolic, rag-filled phenolic, wood-flour-filled phenolic, and tire-cord-filled phenolic array themselves in that order when compared on this basis, mica shrinking least and tire cord most. It is only

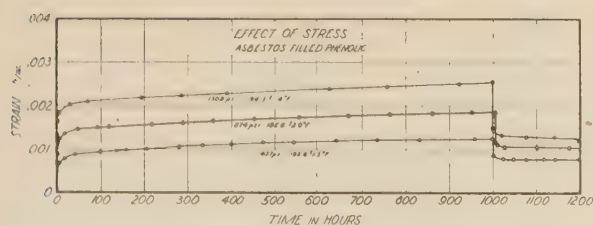


FIG. 4

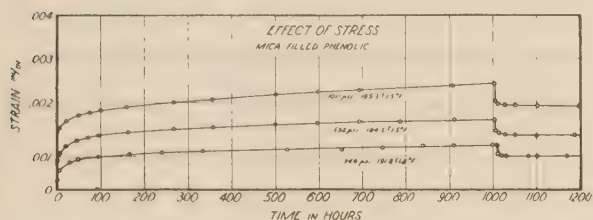


FIG. 5

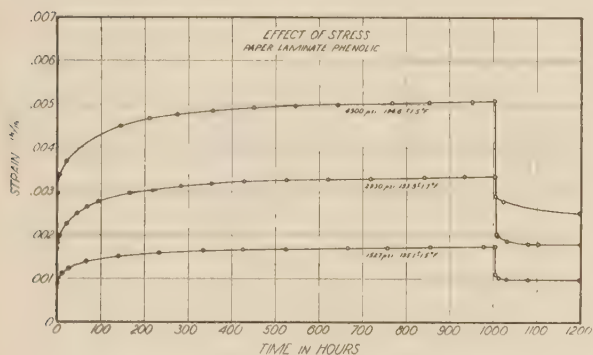


FIG. 6

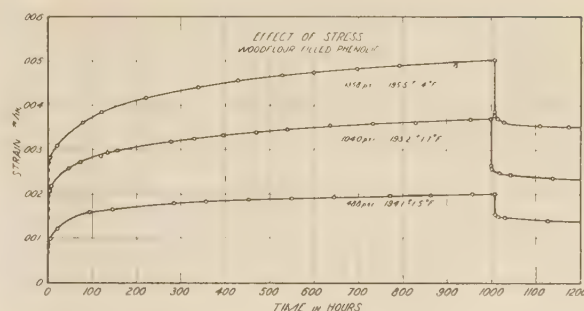


FIG. 7

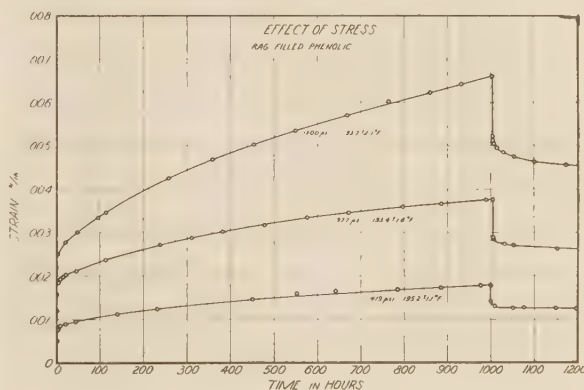


FIG. 8

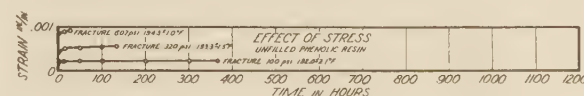


FIG. 9

reasonable that the temperature employed throughout this investigation would show little effect on such a heat-insensitive filler as mica, while it is well known that cellulosic materials shrink considerably when subjected to heat (2, 3, 4). The somewhat strange behavior of the asbestos-filled phenolic is explained by the fact that 15 per cent of the "asbestos"-filled molding powder was wood flour. Fig. 17 shows the average total deformation (elastic plus inelastic) after 1000 hr of constant load at 192 F, as measured by the two separate methods employed, plotted against stress. The ordinate distance between the two plots of each material is a measure of the amount of shrink.

Modulus data before and after the 1000-hr period under load are shown in Figs. 18 to 23, inclusive, and in Table 2.

TABLE 2 MODULUS DATA BEFORE AND AFTER 1000-HR TEST

Material	Average modulus of elasticity at beginning of test (192 F), psi	After 1000 hr under load (192 F), psi	Difference, per cent
Tire cord.....	710000	898000	26.5
Rag.....	807000	1053000	30.5
Mica.....	1580000	2347000	50.4
Asbestos.....	987000	1243000	25.9
Wood flour.....	746000	1083000	45.0
Paper laminate.....	1700000	2227000	31.0

The effect of continued heating on the modulus of these materials is readily apparent. Figs. 15, 24, 25, and 26 present the data obtained from a study of moisture effects. The curves tend to show that moisture does affect the creep characteristics of

phenolics with cellulosic fillers but that it does not in any way affect the behavior of phenolics with mineral fillers. Findley found that paper-laminated phenolic tended to shrink when humidity decreased (5). Table 3 presents a comparison of the long-time tensile strength at 192 F with both the long-time and short-time tensile strengths at room temperature.

TABLE 3 COMPARISON OF LONG-TIME TENSILE STRENGTH AT 192 F WITH BOTH LONG-TIME, AND SHORT-TIME STRENGTHS AT ROOM TEMPERATURE

	Short-time tensile strength A.S.T.M. D638-42, 25 C, 50 per cent RH, psi	Long-time tensile strength—estimated limiting stress		
		At 25 C, 50 per cent RH, time at 25 C, psi	At 192 F, psi	Per cent of short-time at 25 C
Cord filled.....	6000	2400-2800	43	900-1200 18
Rag filled.....	6100	2400-2800	43	1200-1400 21
Woodflour filled.....	6100	2600-2800	44	1300-1400 22
Resin compound.....	8900	<100
Asbestos filled.....	5700	2800-3200	53	1300-1400 24
Mica filled.....	5400	2200-2400	39	1200-1500 25
Paper laminate.....	2800	4900-5200 18

DISCUSSION OF RESULTS

The high-temperature data presented in the earlier paper (1) are somewhat in error inasmuch as they do not resolve the stress effects and thermochemical effects. It is to be noted that the high-temperature curves of that paper appear to lie between the effect-of-stress and behavior curves presented in this work. This

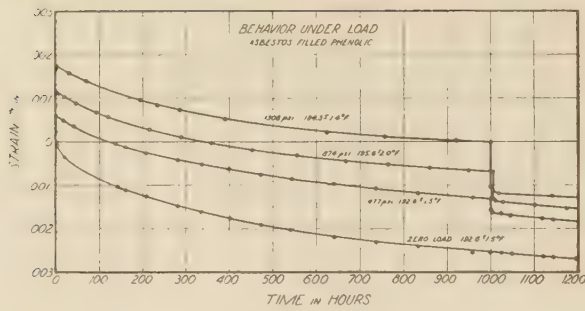


FIG. 10

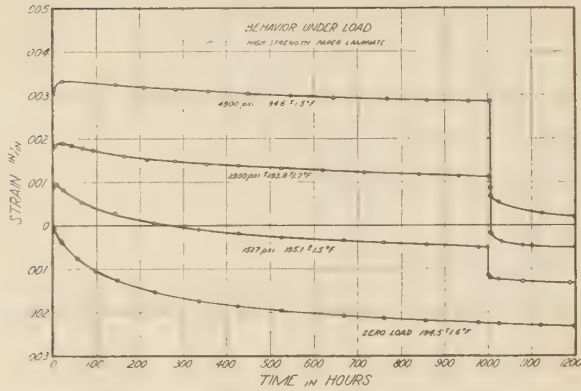


FIG. 12

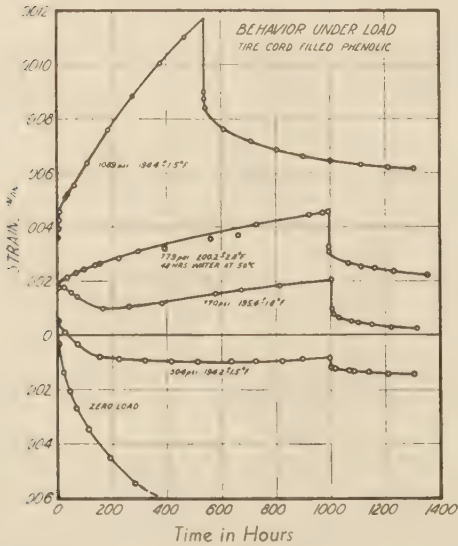


FIG. 15

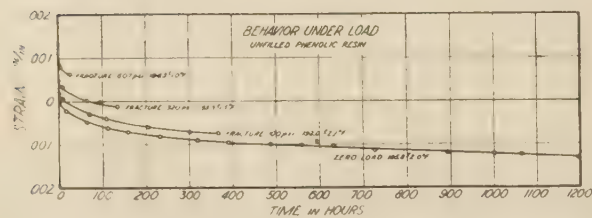


FIG. 16

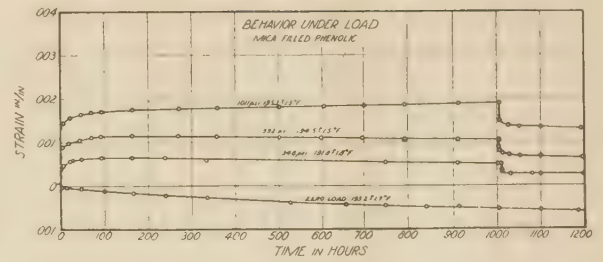


FIG. 11

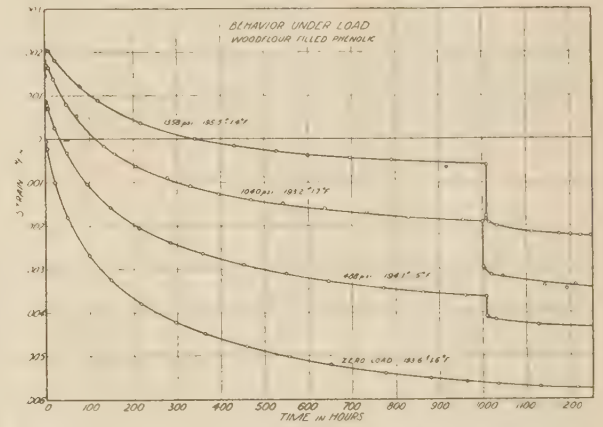


FIG. 13

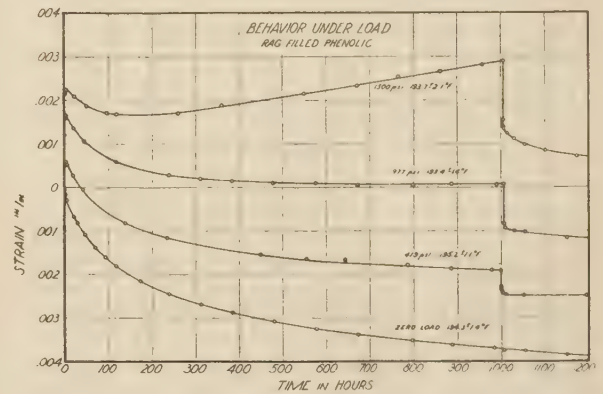


FIG. 14

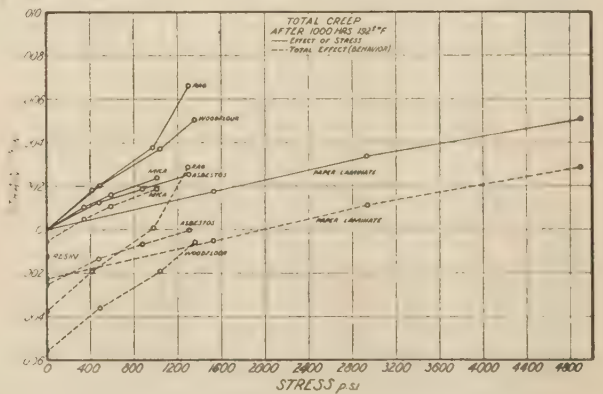


FIG. 17

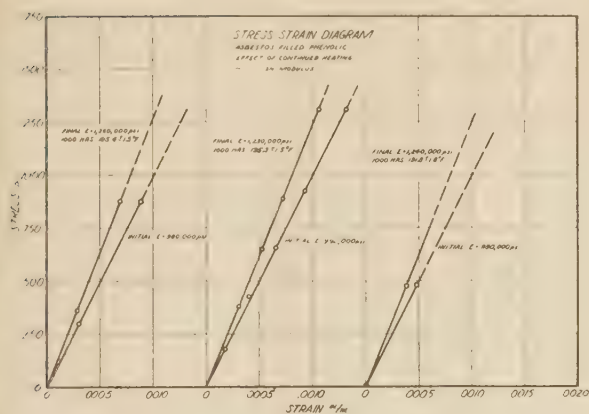


FIG. 18

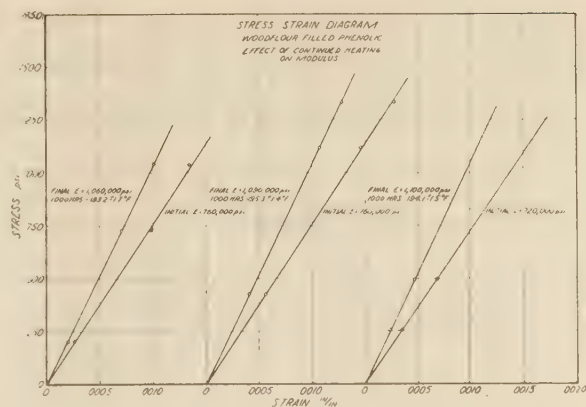


FIG. 21

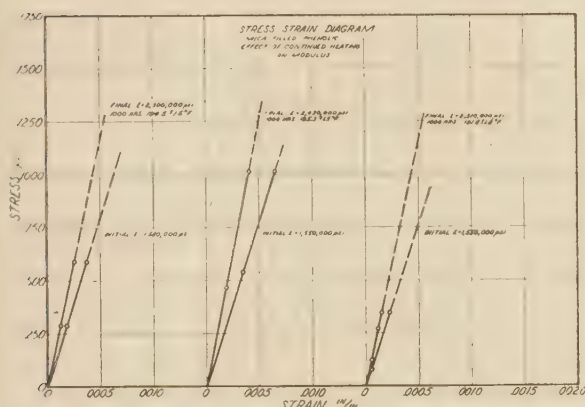


FIG. 19

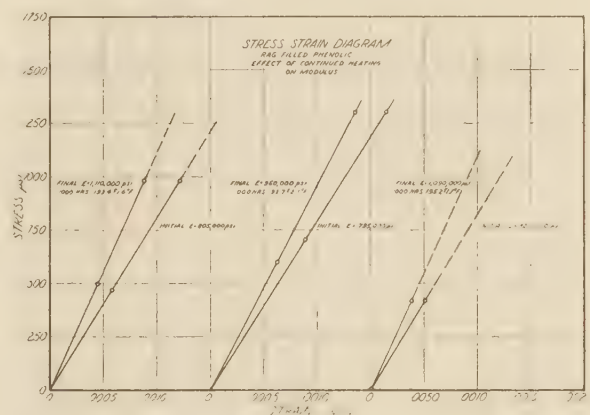


FIG. 22

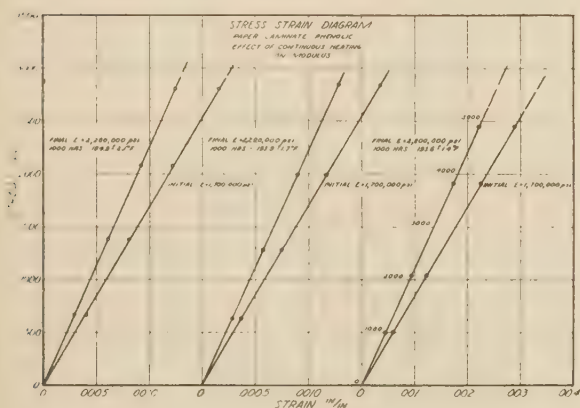


FIG. 20

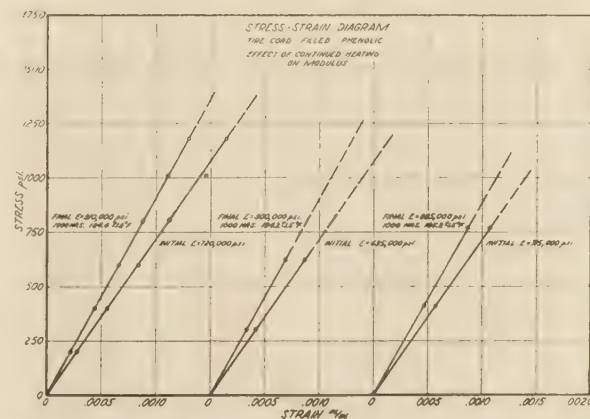


FIG. 23

phenomenon is readily explainable in that the same specimen dummies had been repeatedly used in those tests and had already "shrunk" to varying degrees in the first run. In succeeding tests, the dummies would therefore tend to act partially as virgin-specimen dummies and partially as porcelain dummies.

The change in properties of phenolics after being exposed to heat is presumably connected with a continuation of the condensation reaction. It is well known that in the curing of thermosetting resins, as in other chemical processes, the reaction of

the constituents is practically never complete. The specimens used in this work were molded at a temperature of 165 C, with a cure time of about 10 min. As a general rule, a chemical reaction doubles in speed for each 10-deg-C rise in temperature. Thus while the reaction during molding proceeded about 181 times as fast (estimated) as it did at the testing temperature (90 C), the total time of molding was only $\frac{1}{6000}$ of the time the specimens were subjected to test. It is only reasonable to pre-

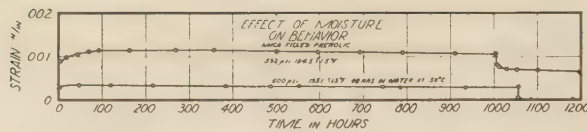


FIG. 24

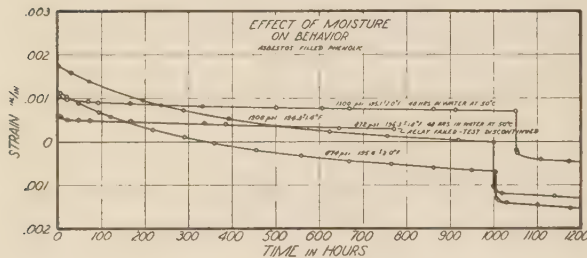


FIG. 25

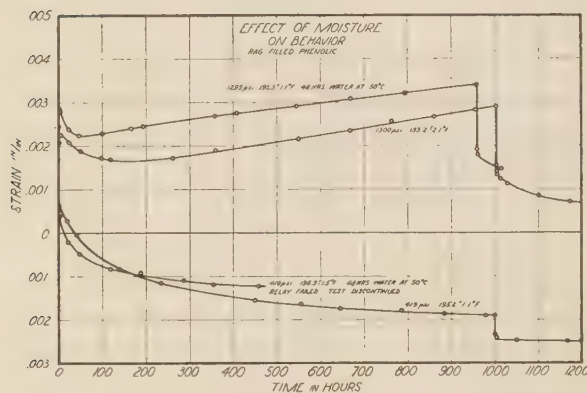


FIG. 26

sume that the materials continued to cure slowly during the tests. Data taken on phenolic resin before and after molding showed that specific gravity changed about 1 per cent. The shrink observed for phenolic resin during the creep test was 0.00123 in. per in., which corresponds to a density increase of 0.369 per cent. If this shrinkage were entirely due to continued condensation, this would lead to the estimate that about $\frac{1}{3}$ as much reaction takes place during a long-time creep test as during molding.

An attempt was made to see whether the hyperbolic-sine (6, 7, 8) or the logarithmic method would best express the relations between stress and creep rate of these materials at constant temperature. Fig. 27 is a plot of creep rate in per cent per 1000 hr versus stress. (The data were obtained from the "effect-of-stress" curves.) It was found, tentatively, that the straight-line relation of the log-log plot best expressed the relation between stress and creep rate for the mineral-filled materials but that the hyperbolic-sine relation is better suited for the cellulose-filled materials.

CONCLUSIONS

1 The total creep in 1000 hr and creep rate (in per cent per 1000 hr) depend to a considerable degree upon the type of filler used in molded phenolic plastics. The creep of inorganic materials is much less than that of materials with organic fillers of the cellulose type.

2 Continued heating has tremendous effects on the creep properties of phenolic plastics. Extension due to load is largely

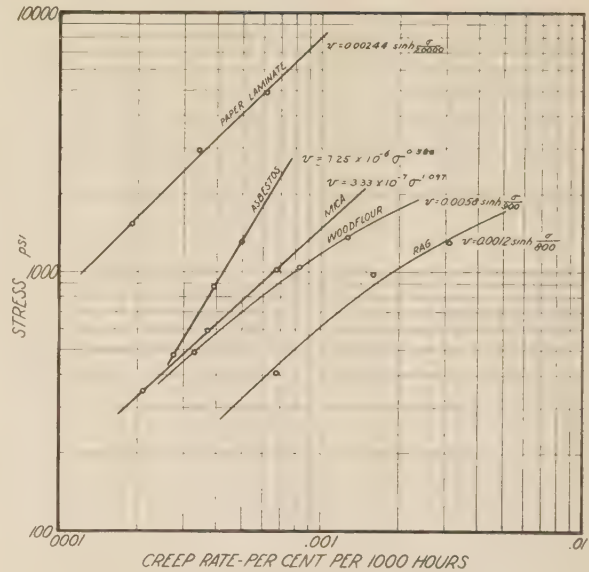


FIG. 27

compensated by contraction due to shrink. Cellulose-filled materials show an especially large amount of shrink.

3 The long-time tensile strength at 192 F varies roughly from 18 to 25 per cent of the short-time tensile strength at room temperature, depending upon the filler used.

4 Modulus of elasticity in tension increases 25 to 50 per cent after continued heating at 192 F for 1000 hr, depending upon the type of filler used.

5 The straight-line relation of the log-log plot apparently best expresses the relation between stress and creep rate for the mineral-filled phenolics but the hyperbolic-sine method is better suited as a simple method of expressing this relation for the cellulose-filled phenolics.

6 By using the technique presented in this paper, a more definite knowledge of the behavior of phenolics at high temperatures can be obtained.

ACKNOWLEDGMENT

The suggestions of Dr. Turner Alfrey on the interpretation of the shrink phenomena are greatly appreciated.

BIBLIOGRAPHY

- 1 "Creep Properties of Molded Phenolic Plastics," by David Telfair, T. S. Carswell, and H. K. Nason, *Modern Plastics*, Feb., 1944, pp. 137-144, 174, and 176.
- 2 "Fatigue of Fabrics," by W. F. Busse, E. T. Lessig, D. L. Loughborough, and L. Larrick, *Journal of Applied Physics*, vol. 13, 1942, pp. 715-724.
- 3 "Permanence of the Physical Properties of Plastics," by J. Delmonte, *Modern Plastics*, vol. 17, June, 1940, pp. 65-68, 84, and 86.
- 4 "Elastic and Creep Properties of Filamentous Materials," by H. Leaderman, Textile Foundation, Washington, D. C., 1943.
- 5 "Short Time Static Tests and Creep Tests of a Paper Laminated Plastic," by W. N. Findley and W. J. Worley, A.S.T.M., 1944 preprint, No. 90.
- 6 "The Influence of Time Upon Creep—the Hyperbolic Sine Creep Law," by A. Nadai, Stephen Timoshenko Anniversary Volume, The Macmillan Company, New York, N. Y., 1938, pp. 155-170.
- 7 "Creep of Metals at Elevated Temperatures—The Hyperbolic-Sine Relation Between Stress and Creep Rate," by P. G. McVetty, *Trans. A.S.M.E.*, vol. 65, 1943, pp. 761-769.
- 8 "Hyperbolic-Sine Chart for Estimating Working Stresses of Alloys at Elevated Temperatures," by A. Nadai and P. G. McVetty, *Proceedings of the A.S.T.M.*, vol. 43, 1943, pp. 735-748.

Effect of Some Environmental Conditions on the Permanence of Cellulose-Acetate and Cellulose-Nitrate Sheet Plastics

By T. S. LAWTON, JR.,¹ AND H. K. NASON¹

The effect of outdoor exposure, both in Florida and in Massachusetts, on the tensile properties, impact strength, optical properties, and shrinkage of cellulose-acetate and cellulose-nitrate sheet plastics is shown in detail, and the general nature of these effects is summarized. The effect of outdoor exposure on the composition of these plastics and on the molecular weight of the base cellulose esters is shown quantitatively. Moisture pickup and dimensional change upon immersion in water are reported.

THE use of plastics in engineering applications has been accentuated because of the demand for these materials by the Armed Forces. For the intelligent engineering application of any material, a knowledge of its properties under all environmental conditions which may be encountered in service is essential. A summary of recent progress in this field has been published (1).²

Such data on cellulose acetate and cellulose nitrate have been scarce until recently. A paper describing the effect of environmental conditions on the mechanical properties of cellulose acetate and cellulose nitrate was recently published (2). The work reported in the present paper covers the effect of environmental conditions such as weathering, ultraviolet-light exposure, moisture exposure, heat exposure, etc., on the permanence of cellulose-acetate and cellulose-nitrate plastic sheets.

MATERIALS USED

The cellulose-acetate sheets used in this investigation were 2050 TVA Fibestos. They were manufactured by the sheeter process (3, 4), and the surfaces were given an "HH" (polished) finish in a planish press under the conditions customarily employed for such materials. The residual solvent-and-water content was less than 1.5 per cent as received. These materials are of the type customarily furnished for transparent enclosures on aircraft and similar applications, and meet all requirements of Air Corps Specification 12025-B (5), Navy Aeronautical Specification P-41c (6), and A.S.T.M. Specification D786-44T (7). These materials are of the same composition as those studied by Findley (8, 9, 10).

The cellulose-nitrate sheets were manufactured from medium-viscosity pyroxylin of approximately 11 per cent nitrogen content and were plasticized with approximately 25 per cent camphor. Processing was by the sheeter method and was similar to that employed for the cellulose-acetate sheets. Residual solvent and water content was less than 1 per cent as received. These

materials meet all requirements of A.S.T.M. D701-44T, Type 1 (11), U. S. Army Specification 95-12008B (12), and Federal Specification GG-T-671 (13).

All materials used for these tests were taken from regular production lots.

TEST PROCEDURES

A.S.T.M. standard test methods were used wherever possible; specific reference to test methods is made in the following section.

The desired number of test specimens was cut from a single plastic sheet and mixed thoroughly to minimize geometric variables. All samples were preconditioned for 48 hr at 50 C (122 F), to eliminate moisture, and were stored in a desiccator over anhydrous calcium chloride until needed. All tests were made at 25 C (122 F), 50 per cent relative humidity (rh), unless noted otherwise.

The outdoor weathering samples were exposed both in Miami, Fla., and Springfield, Mass., at 45 deg to the vertical and facing south. The specimens were not confined in a frame but were supported on the edges only. After the desired exposure time, the specimens were rinsed lightly with warm water to remove all surface dirt and other extraneous matter. The desired test samples were then cut out of the 12-in. × 12-in. exposed specimens.

To determine the effect of ultraviolet exposure on the permanence of these materials, test specimens were exposed under a General Electric S-1 sun lamp as specified in A.S.T.M. Designation D620-41T (14), at a distance of 6 in. from the bottom of the bulb. Samples were so placed on the turntable that each received the same light intensity. Only S-1 bulbs which had been burned more than 50 and less than 500 hr were used.

To determine the effect of heat on the permanence properties, samples were exposed in a circulating-air oven operating at 50 C.

The type of apparatus used has been described previously (2).

Reported values represent the arithmetic mean of at least five determinations, and the plus or minus limits shown represent the arithmetic-mean deviation of the individual values from the mean.

GENERAL EFFECTS OF WEATHER EXPOSURE

The general effects of outdoor exposure on cellulose ester plastics may be summarized as follows:

- 1 The base cellulose ester is degraded. Both saponification and molecular degradation due to breaking of the cellulose chain, with the formation of lower-molecular-weight fractions, may occur. The latter reaction is usually the more important; the extent of saponification is different for different cellulose esters. Thus considerable denitration of cellulose nitrate takes place during weathering, but relatively little deacetylation of cellulose acetate has been observed. The degree of degradation is dependent upon the length of exposure and upon the intensity of the incident radiation.

- 2 Plasticizer is lost by evaporation and by leaching.

¹ Research Department, Monsanto Chemical Company, Plastics Division, Springfield, Mass.

² Numbers in parentheses refer to the Bibliography at the end of the paper.

Contributed by the Rubber and Plastics Division and presented at the Annual Meeting, New York, N. Y., Nov. 27-Dec. 1, 1944, of THE AMERICAN SOCIETY OF MECHANICAL ENGINEERS.

NOTE: Statements and opinions advanced in papers are to be understood as individual expressions of their authors and not those of the Society.

3 The color of the material may be changed due to darkening or bleaching of added colorants, or, in the case of plastics containing no added color, to darkening or bleaching of the plastic material itself. Uncolored cellulose-acetate plastics usually bleach and become lighter in color upon prolonged exposure, but cellulose-nitrate formulations usually yellow and become darker.

4 Because of loss of plasticizer and degradation of the base plastic, shrinkage usually occurs upon prolonged exposure, and this may be accompanied by warping also.

5 Fine surface cracks, known as crazing (21), and deeper cracks, penetrating nearly through the sheets, form after extended exposure. These are the result of shrinkage and general deterioration of mechanical properties of the plastic. Crazing nearly always occurs first, because both shrinkage and degradation are most severe at the surface of the sheet. The deeper cracks usually occur only after prolonged exposure. Crazing is generally taken as the criterion of failure for materials whose use is optical in nature.

6 Stress frozen in the plastic by the particular manufacturing process used, and other imperfections, are usually released upon extended exposure, thus impairing the surface quality of the object.

TENSILE PROPERTIES

Tensile properties were determined by the method specified in A.S.T.M. Designation D638-44T (15); the method specified by Federal Specification L-P-406a (16) is identical. Stress-strain data were determined at a crosshead speed of 0.20 ipm.

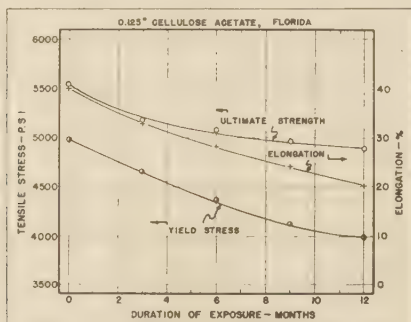


FIG. 1 EFFECT OF EXPOSURE TO WEATHER AT MIAMI, FLA., ON TENSILE PROPERTIES OF CELLULOSE-ACETATE SHEET PLASTIC

Effect of Subtropical Exposure. The effect of exposure at Miami, Fla., on the tensile strength (ultimate), yield stress, and elongation is shown graphically in Fig. 1, for the cellulose-

acetate, and in Fig. 2, for the cellulose-nitrate sheets. Fig. 3 shows graphically the effect of Florida exposure on the modulus of elasticity of these two materials.

Table 1 summarizes the effect of Florida exposure on the modulus of elasticity, yield stress, tensile strength, and elongation (at break) of the cellulose-acetate sheet plastic. Table 2 summarizes similar data for the cellulose-nitrate sheets.

Effect of Temperature Exposure. The effect of exposure at Springfield, Mass., on the tensile strength (ultimate), yield stress, and elongation (at break) is shown graphically in Fig. 4 for the cellulose-acetate, and in Fig. 5, for the cellulose-nitrate sheets. Fig. 6 shows the effect of such exposure on the modulus of elasticity of these two materials.

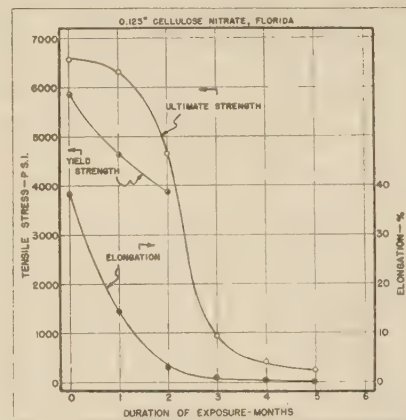


FIG. 2 EFFECT OF EXPOSURE TO WEATHER AT MIAMI, FLA., ON TENSILE PROPERTIES OF CELLULOSE-NITRATE SHEET PLASTIC

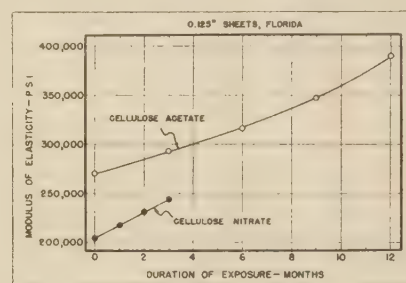


FIG. 3 EFFECT OF EXPOSURE TO WEATHER AT MIAMI, FLA., ON MODULUS OF ELASTICITY OF CELLULOSE-ACETATE AND CELLULOSE-NITRATE SHEET PLASTICS

TABLE 1 EFFECT OF FLORIDA AND MASSACHUSETTS EXPOSURE ON TENSILE PROPERTIES OF CELLULOSE-ACETATE SHEET PLASTIC

Exposure time, months	Modulus of elasticity, psi $\times 10^4$		Yield stress, psi		Tensile strength, psi		Elongation, per cent	
	Florida	Mass.	Florida	Mass.	Florida	Mass.	Florida	Mass.
Original	2.70 \pm 0.03	2.70 \pm 0.03	4970 \pm 75	4970 \pm 75	5540 \pm 80	5540 \pm 80	40 \pm 5	40 \pm 5
3	2.93 \pm 0.02	2.80 \pm 0.04	4650 \pm 80	4800 \pm 93	5175 \pm 75	5310 \pm 96	33 \pm 5	35 \pm 2
6	3.16 \pm 0.04	2.96 \pm 0.03	4360 \pm 95	4520 \pm 111	5080 \pm 68	5130 \pm 76	28 \pm 4	30 \pm 3
9	3.46 \pm 0.04	3.11 \pm 0.02	4120 \pm 73	4340 \pm 56	4980 \pm 110	5030 \pm 68	24 \pm 3	27 \pm 4
12	3.88 \pm 0.05	3.41 \pm 0.05	3990 \pm 110	4300 \pm 61	4890 \pm 95	5010 \pm 79	20 \pm 3	24 \pm 3

NOTE: Specimens, 0.125 in., preconditioned 48 hr at 50 C, and stored in desiccator. Tested at 0.2 ipm crosshead speed.

TABLE 2 EFFECT OF FLORIDA AND MASSACHUSETTS EXPOSURE ON TENSILE PROPERTIES OF CELLULOSE-NITRATE SHEET PLASTIC

Exposure time, months	Modulus of elasticity, psi $\times 10^4$		Yield stress, psi		Tensile strength, psi		Elongation, per cent	
	Florida	Mass.	Florida	Mass.	Florida	Mass.	Florida	Mass.
Original	2.04 \pm 0.01	2.04 \pm 0.01	5840 \pm 64	5840 \pm 64	6570 \pm 115	6570 \pm 115	38 \pm 2	38 \pm 2
1	2.17 \pm 0.02	2.12 \pm 0.03	4610 \pm 87	5730 \pm 80	6310 \pm 65	6410 \pm 63	14 \pm 3	27 \pm 3
2	2.30 \pm 0.02	2.20 \pm 0.01	3880 \pm 79	5430 \pm 71	4650 \pm 96	6160 \pm 81	3.1 \pm 0.20	17 \pm 2
3	2.44 \pm 0.03	2.28 \pm 0.01		5090 \pm 76	936 \pm 36	5800 \pm 93	1.0 \pm 0.07	9 \pm 1
4		2.37 \pm 0.02		4310 \pm 57	430 \pm 19	5000 \pm 79	0 \pm 1	4 \pm 1
5		2.45 \pm 0.03			260 \pm 23	3270 \pm 52	0 \pm 1	1.0 \pm 0.06
6						1520 \pm 33		

NOTE: Specimens, 0.125 in., preconditioned 48 hr at 50 C, and stored in desiccator. Tested at 0.2 ipm crosshead speed.

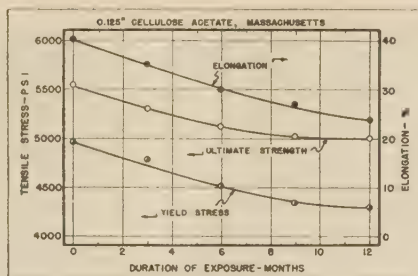


FIG. 4 EFFECT OF EXPOSURE TO WEATHER AT SPRINGFIELD, MASS., ON TENSILE PROPERTIES OF CELLULOSE-ACETATE SHEET PLASTIC

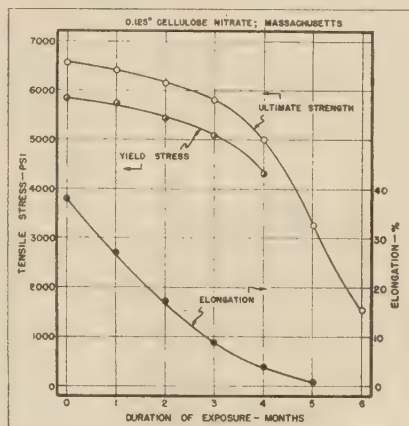


FIG. 5 EFFECT OF EXPOSURE TO WEATHER AT SPRINGFIELD, MASS., ON TENSILE PROPERTIES OF CELLULOSE-NITRATE SHEET PLASTIC

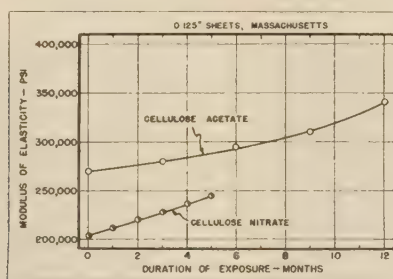


FIG. 6 EFFECT OF EXPOSURE TO WEATHER AT SPRINGFIELD, MASS., ON MODULUS OF ELASTICITY OF CELLULOSE-ACETATE AND CELLULOSE-NITRATE SHEET PLASTICS

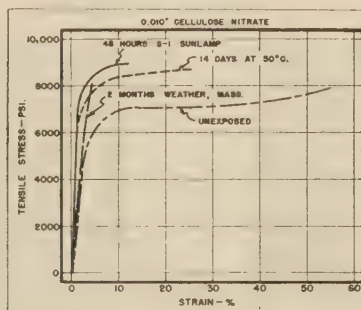


FIG. 7 EFFECT OF HEAT, LIGHT, AND EXPOSURE TO WEATHER AT SPRINGFIELD, MASS., ON STRESS-STRAIN PROPERTIES OF CELLULOSE-NITRATE SHEET PLASTIC

Table 1 summarizes the effect of Springfield exposure on the modulus of elasticity, yield stress, tensile strength, and elongation of the cellulose-acetate sheets. Table 2 summarizes similar data for the cellulose-nitrate sheets.

Effect of Various Accelerated Aging Environments. Cellulose-nitrate plastic (0.010 in.) was subjected to various accelerated aging tests, namely, (a) 48 hr under an S-1 sun lamp at a distance of 6 in., (b) 14 days in a circulating-air oven at 50 C, and (c) 2 months' outdoor exposure at Springfield. At the end of the designated exposure time, stress-strain data were determined. These tests were run on a Scott IP-4, tilting-table tensile tester at 600 rpm. Stress-strain relationships after the various exposures are shown graphically in Fig. 7.

This material was of the same composition as that used in the rest of this work, but taken from a different production lot.

EFFECT ON GENERAL PROPERTIES

Impact Properties. Impact properties were determined by the Charpy method, in accordance with the procedure described in A.S.T.M. Designation D256-43T (17). Specimens 0.125 in. thick, 0.5 in. wide, and 5 in. long were notched with a single-tooth milling cutter at 400 rpm, and wire-bound together in groups of four to give the correct aggregate width (0.5 in.).

The effect of Florida and Massachusetts exposure on impact strength for both the cellulose-acetate and cellulose-nitrate plastics is shown graphically in Fig. 8. These data are summarized in Tables 3 and 4.

Light Transmission and Haze. Light transmission and haze

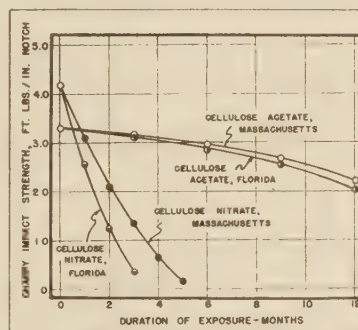


FIG. 8 EFFECT OF EXPOSURE TO WEATHER AT SPRINGFIELD, MASS., AND MIAMI, FLA., ON IMPACT STRENGTH OF CELLULOSE-ACETATE AND CELLULOSE-NITRATE SHEET PLASTICS

TABLE 3 EFFECT OF FLORIDA AND MASSACHUSETTS EXPOSURE ON IMPACT STRENGTH OF CELLULOSE-ACETATE SHEET PLASTIC

Exposure time, months	Impact strength, ft-lb per in., notch - Florida	Massachusetts
Original	3.28 ± 0.09	3.28 ± 0.09
3	3.04 ± 0.11	3.14 ± 0.13
6	2.81 ± 0.17	2.93 ± 0.24
9	2.51 ± 0.09	2.67 ± 0.17
12	2.01 ± 0.19	2.20 ± 0.18

NOTE: Specimens preconditioned 48 hr at 50 C, and stored in desiccator. Specimens comprised four 0.125-in. plates, broken edgewise.

TABLE 4 EFFECT OF FLORIDA AND MASSACHUSETTS EXPOSURE ON IMPACT STRENGTH OF CELLULOSE-NITRATE SHEET PLASTIC

Exposure time, months	Impact strength, ft-lb per in., notch - Florida	Massachusetts
Original	4.13 ± 0.08	4.13 ± 0.08
1	2.56 ± 0.13	3.07 ± 0.12
2	1.21 ± 0.14	2.09 ± 0.11
3	0.33 ± 0.02	1.32 ± 0.09
4	0.62 ± 0.07
5	0.15 ± 0.01

NOTE: Specimens preconditioned 48 hr at 50 C, and stored in desiccator. Specimens comprised four 0.125-in. plates, broken edgewise.

were determined by the Bowen-Kline method, in accordance with the procedure described in A.S.T.M. Designation D672-42T (18). Specimens 0.125 in. thick, 3 in. square were used.

The effect of Florida and Massachusetts exposure on the light transmission of both cellulose-acetate and cellulose-nitrate plastics is shown graphically in Fig. 9. These data are summarized in Table 5 and Table 6.

The effect of Florida and Massachusetts exposure on the haze of both cellulose-acetate and cellulose-nitrate plastics is shown graphically in Fig. 10. These data are summarized in Table 5 and Table 6.

Figs. 11 and 12 show the general appearance of cellulose-acetate and cellulose-nitrate sheets, respectively, after various lengths of exposure in Florida.

Shrinkage. Shrinkage was determined by scribing marks 10 in. apart in both directions of the 12-in. \times 12-in. plastic sheets. The distance between marks was measured to within 0.01 in. before and after exposure. The percentage of shrinkage reported

was calculated by dividing the difference in length between marks before and after exposure by the original length. The values reported are the average of the two directions.

The effect of Florida and Massachusetts exposure on the shrinkage of both cellulose-acetate and cellulose-nitrate plastic sheets is shown graphically in Fig. 13. These data are summarized in Table 7 and Table 8.

Abrasion Resistance. The abrasion resistance of cellulose-acetate and cellulose-nitrate sheet plastics was determined by the Boor abrader, in accordance with A.S.T.M. Designation D673-42T (19). Specimens 0.125 in. thick and 2 in. square were used. The specimens were preconditioned 48 hr at 50 C and stored in a desiccator prior to testing.

The effect of the amount of abrasive on the percentage of original gloss for both cellulose-acetate and cellulose-nitrate sheet plastic is shown in Fig. 14. Data are summarized in Table 9.

Water Absorption. The percentage of water absorption for cellulose-acetate and cellulose-nitrate sheet plastics was determined in accordance with A.S.T.M. Designation D570-42 (20). In addition, long-time water-absorption tests were run to determine the time for the plastic to reach equilibrium.

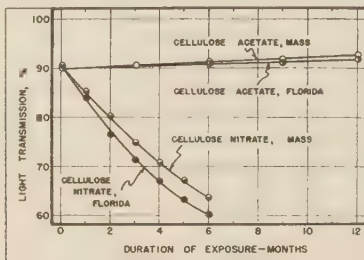


FIG. 9 EFFECT OF EXPOSURE TO WEATHER AT SPRINGFIELD, MASS., AND MIAMI, FLA., ON LIGHT TRANSMISSION OF CELLULOSE-ACETATE AND CELLULOSE-NITRATE SHEET PLASTICS

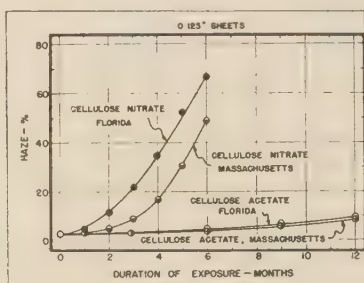


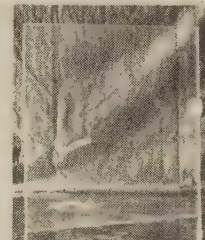
FIG. 10 EFFECT OF EXPOSURE TO WEATHER AT SPRINGFIELD, MASS., AND MIAMI, FLA., ON HAZE OF CELLULOSE-ACETATE AND CELLULOSE-NITRATE SHEET PLASTICS

TABLE 5 EFFECT OF FLORIDA AND MASSACHUSETTS EXPOSURE ON LIGHT TRANSMISSION AND HAZE OF CELLULOSE-ACETATE SHEET PLASTIC

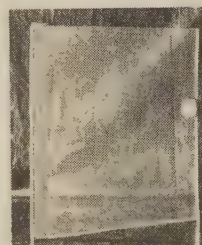
Exposure time, months	Light transmission, per cent—		Haze, per cent—	
	Florida	Mass.	Florida	Mass.
Original	89.9	89.9	3.1	3.1
3	90.1	90.2	3.6	3.4
6	90.3	90.9	5.0	4.6
9	90.9	91.4	7.3	6.4
12	91.2	92.1	9.8	8.7

TABLE 6 EFFECT OF FLORIDA AND MASSACHUSETTS EXPOSURE ON LIGHT TRANSMISSION AND HAZE OF CELLULOSE-NITRATE SHEET PLASTIC

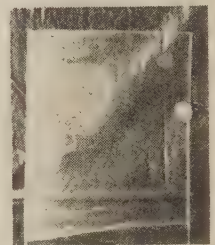
Exposure time, months	Light transmission, per cent—		Haze, per cent—	
	Florida	Mass.	Florida	Mass.
Original	90.1	90.1	2.5	2.5
1	83.8	85.1	4.5	3.0
2	78.3	80.1	11.9	4.3
3	71.0	74.7	22.0	8.9
4	66.9	70.8	35.1	17.2
5	63.0	67.1	53.1	30.8
6	60.0	63.5	66.6	49.5



ORIGINAL



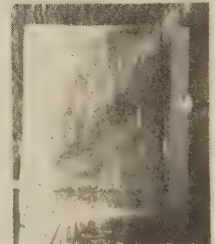
3 MONTHS



6 MONTHS



9 MONTHS



12 MONTHS

FIG. 11 EFFECT OF FLORIDA EXPOSURE ON CELLULOSE-ACETATE SHEET PLASTIC

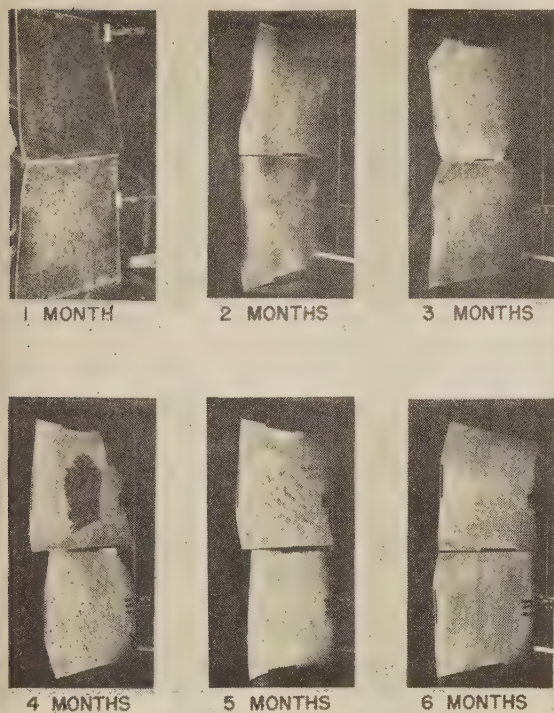


FIG. 12 EFFECT OF FLORIDA EXPOSURE ON CELLULOSE-NITRATE SHEET PLASTIC

TABLE 7 EFFECT OF FLORIDA AND MASSACHUSETTS EXPOSURE ON SHRINKAGE OF CELLULOSE-ACETATE PLASTIC

Exposure time, months	Shrinkage, per cent	
	Florida	Mass.
Original		
3	0.03	0.01
6	0.58	0.33
9	1.42	0.96
12	2.18	1.62

TABLE 8 EFFECT OF FLORIDA AND MASSACHUSETTS EXPOSURE ON SHRINKAGE OF CELLULOSE-NITRATE PLASTIC

Exposure time, months	Shrinkage, per cent	
	Florida	Mass.
Original		
1	0.12	0.09
2	0.28	0.22
3	0.48	0.37
4	0.71	0.56
5	0.96	0.76
6	1.21	0.98

TABLE 9 EFFECT OF AMOUNT OF ABRASIVE ON PERCENTAGE OF ORIGINAL GLOSS FOR CELLULOSE-ACETATE AND CELLULOSE-NITRATE SHEET PLASTICS

Grams of abrasive	Per cent of original gloss	
	Cellulose acetate	Cellulose nitrate
200	94.8	94.1
400	89.0	88.4
800	81.4	77.3
1200	69.0	67.1
1600	64.3	60.8

NOTE: Boor abrader used. Samples preconditioned 48 hr at 50 C, and stored in desiccator.

The effect of immersion time on the total water absorption is shown graphically in Fig. 15, for cellulose-acetate, and in Fig. 16 for cellulose-nitrate plastic. The effect of immersion time on percentage of solubles lost is shown graphically in Fig. 17 for

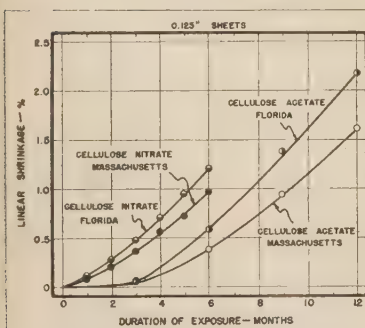


FIG. 13 EFFECT OF EXPOSURE TO WEATHER AT SPRINGFIELD, MASS., AND MIAMI, FLA., ON LINEAR SHRINKAGE OF CELLULOSE-ACETATE AND CELLULOSE-NITRATE PLASTIC SHEETS

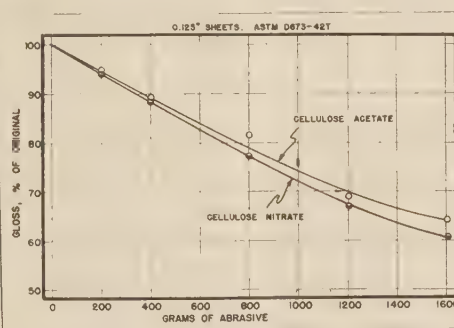


FIG. 14 ABRASION RESISTANCE OF CELLULOSE-ACETATE AND CELLULOSE-NITRATE PLASTIC SHEETS

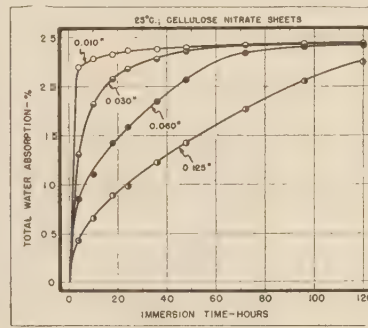


FIG. 16 WATER ABSORPTION OF CELLULOSE-NITRATE PLASTIC SHEETS

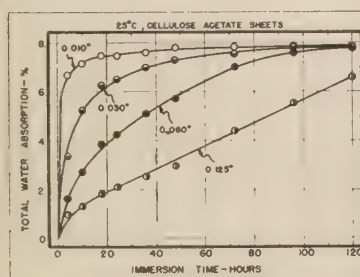


FIG. 15 WATER ABSORPTION OF CELLULOSE-ACETATE PLASTIC SHEETS

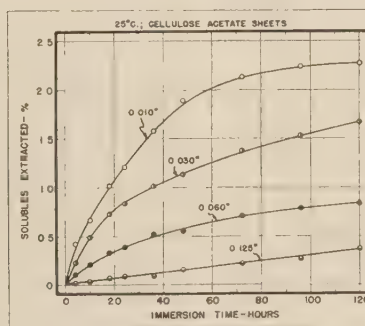


FIG. 17 SOLUBLE MATTER EXTRACTED FROM CELLULOSE-ACETATE PLASTIC SHEETS UPON IMMERSION IN WATER

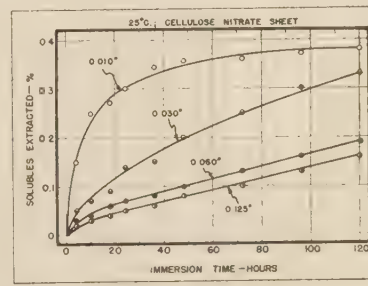


FIG. 18 SOLUBLE MATTER EXTRACTED FROM CELLULOSE-NITRATE PLASTIC SHEETS UPON IMMERSION IN WATER

cellulose-acetate, and in Fig. 18, for cellulose-nitrate plastic. These data are summarized in Table 10 and Table 11.

Viscosity and Molecular Weight. The effect of Florida exposure on the viscosity and molecular weight of the base cellulose esters in cellulose-acetate and cellulose-nitrate sheet plastic was determined. Viscosity measurements were made at $25\text{ C} \pm 0.02\text{ deg}$ using Fenske pipettes. The exposed plastic was dissolved in anhydrous acetone, and the cellulose acetate or cellulose nitrate was precipitated with a nonsolvent, washed, and dried. The dried ester was dissolved in anhydrous acetone, and concentrations to give $\eta_r = 1.2\text{--}1.3$ were chosen.

Viscosity was determined both on the whole plastic sheet and on the surface portion only. In the latter case, the surface was

cellulose acetate and cellulose nitrate is shown in Fig. 19. These data are summarized in Tables 12 and 13.

DISCUSSION OF RESULTS

The effects of temperature, humidity, and testing speed on the mechanical properties of cellulose-acetate and cellulose-nitrate sheet plastics have been pointed out previously by Lawton, Carswell, and Nason (2). The data presented herein show the effect of some environmental conditions on the permanence of these two plastic materials.

Cellulose acetate is moderately resistant to outdoor aging, whereas cellulose nitrate tends to degrade and lose its properties rather rapidly. Cellulose acetate is more sensitive to moisture

TABLE 10 EFFECT OF IMMERSION TIME ON TOTAL WATER ABSORPTION OF CELLULOSE ACETATE AND CELLULOSE-NITRATE PLASTICS

Immersion time, hr	Total water absorption, per cent							
	0.010 in.		0.030 in.		0.060 in.		0.125 in.	
	Cellulose acetate	Cellulose nitrate	Cellulose acetate	Cellulose nitrate	Cellulose acetate	Cellulose nitrate	Cellulose acetate	Cellulose nitrate
4	6.69	2.22	3.36	1.31	1.61	0.85	1.04	0.43
10	7.18	2.29	5.27	1.83	2.73	1.10	1.32	0.65
18	7.50	2.32	6.28	2.08	3.86	1.43	1.83	0.89
24	7.43	2.36	6.52	2.19	4.25	1.59	2.08	0.98
36	7.60	2.38	7.01	2.28	5.13	1.85	2.53	1.23
48	7.80	2.40	7.32	2.37	5.74	2.07	2.99	1.43
72	7.81	2.43	7.57	2.40	7.00	2.36	4.41	1.77
96	7.85	2.43	7.83	2.43	7.69	2.41	5.58	2.05
120	7.87	2.44	7.85	2.43	7.85	2.43	6.85	2.25

TABLE 11 EFFECT OF IMMERSION TIME ON SOLUBLES LOST FOR CELLULOSE-ACETATE AND CELLULOSE-NITRATE PLASTICS

Immersion time, hr	Solubles lost, per cent							
	0.010 in.		0.030 in.		0.060 in.		0.125 in.	
	Cellulose acetate	Cellulose nitrate	Cellulose acetate	Cellulose nitrate	Cellulose acetate	Cellulose nitrate	Cellulose acetate	Cellulose nitrate
4	0.43	0.15	0.24	0.05	0.11	0.04	0.02	0.02
10	0.67	0.25	0.50	0.07	0.21	0.05	0.04	0.03
18	1.02	0.27	0.74	0.08	0.33	0.06	0.07	0.04
24	1.21	0.30	0.83	0.14	0.38	0.07	0.09	0.05
36	1.58	0.35	1.01	0.15	0.51	0.08	0.09	0.06
48	1.91	0.36	1.13	0.20	0.53	0.09	0.16	0.08
72	2.14	0.36	1.36	0.25	0.69	0.13	0.22	0.10
96	2.24	0.37	1.54	0.30	0.77	0.16	0.26	0.13
120	2.26	0.38	1.68	0.33	0.82	0.19	0.38	0.16

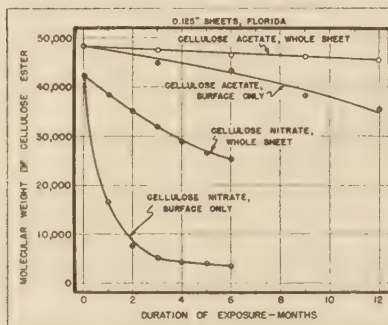


FIG. 19 EFFECT OF EXPOSURE TO WEATHER AT MIAMI, FLA., ON MOLECULAR WEIGHT OF BASE CELLULOSE ESTER IN CELLULOSE-ACETATE AND CELLULOSE-NITRATE SHEET PLASTICS

scraped off and then dissolved and precipitated.

Molecular weight was calculated by the equation

$$MKc = \ln \eta_r$$

where M = weight average molecular weight

K = Staudinger's constant:

$K = 10.25 \times 10^{-4}$ for cellulose acetate

$K = 11.00 \times 10^{-4}$ for cellulose nitrate

c = concentration, unit moles per liter

η_r = relative viscosity

The effect of Florida exposure on the molecular weight of

TABLE 12 EFFECT OF FLORIDA EXPOSURE ON MOLECULAR WEIGHT OF CELLULOSE ACETATE

Exposure time, months	Molecular weight, whole plastic	Molecular weight, surface of plastic
Original	48100	48100
3	47300	44600
6	46600	43100
9	46100	37500
12	45200	35200

TABLE 13 EFFECT OF FLORIDA EXPOSURE ON MOLECULAR WEIGHT OF CELLULOSE NITRATE

Exposure time, months	Molecular weight, whole plastic	Molecular weight, surface of plastic
Original	42100	42100
1	38200	16800
2	35100	7400
3	31900	5100
4	28900	4400
5	26600	4100
6	25400	3500

than cellulose nitrate, whereas the effect of temperature is about the same for both.

Tensile strength, elongation, and yield stress for both cellulose acetate and cellulose nitrate decrease with increasing outdoor exposure time, until the material eventually degrades so badly that mechanical properties cannot be measured. The modulus of elasticity increases with increasing exposure time as long as the material remains sufficiently coherent to be tested.

Approximately three times as long is required to degrade cellulose acetate as is required for cellulose nitrate. The degradation of cellulose nitrate appears to start soon after exposure, whereas, in cellulose acetate, a more gradual change is noted.

Two months of outdoor exposure is a more severe test for

cellulose nitrate than 2 weeks at 50 C, or 48 hr under an S-1 sun lamp.

The impact strength for both cellulose acetate and cellulose nitrate decreases with increasing exposure, whereas haze, light transmission, and shrinkage increase. The increase in light transmission of cellulose acetate upon exposure is thought to be due to a bleaching action. With cellulose nitrate, light transmission decreases with increasing exposure, as would be expected.

Exposure in Miami, Fla., is more severe than at Springfield, Mass. To obtain the same effect as 1 year exposure in Florida, approximately 15 months' exposure in Massachusetts is required. This ratio appears to be the same for both cellulose-acetate and cellulose-nitrate sheet plastic.

The degradation from outdoor exposure can be measured by change in viscosity. Viscosity measurements showed that for both cellulose-acetate and cellulose-nitrate sheet plastic most of the degradation was on the surface. As the exposure time increases the degradation penetrates deeper into the sheet. Cellulose nitrate shows a much greater decrease in molecular weight than does cellulose acetate for the same exposure time.

After 12 months in Florida, the cellulose-acetate plastic sheet lost approximately 20 per cent of its plasticizer, whereas the cellulose-nitrate sheet lost 33 per cent plasticizer after 6 months' exposure in Florida. Since the center of the plastic sheets appeared to be unchanged, undoubtedly the plasticizer was lost from the surface of the sheets.

Water-immersion tests showed that cellulose nitrate is more resistant to moisture than cellulose acetate. On continual immersion, both materials appear to approach equilibrium.

The data given in this report are for typical production materials and are known to be representative. Since they are based on a limited number of tests and on only a few samples of materials, they should not be regarded as minimum values for design or specification purposes. A much larger number of tests should be made and evaluated statistically before any such values are set up.

ACKNOWLEDGMENT

The authors are indebted to Mr. J. H. Watt and Miss Dorothy L. Woodruff for assistance with much of the test work, to Mr. M. Ziembra for handling the outdoor-exposure samples, and to Dr. C. K. Bump for the photographs. The interest and encouragement of Mr. T. S. Carswell is gratefully acknowledged.

BIBLIOGRAPHY

- 1 "Effect of Environmental Conditions on the Mechanical Properties of Organic Plastics," by T. S. Carswell and H. K. Nason, paper presented at A.S.T.M. Symposium on Plastics, Philadelphia, Pa., Feb. 22, 1944; *Modern Plastics*, vol. 21, June, 1944, pp. 121-126, 158, and 160, and vol. 21, July, 1944, pp. 125-130, 160, and 162.
- 2 "Effect of Environmental Conditions on Cellulose Acetate and Nitrate Sheets," by T. S. Lawton, Jr., T. S. Carswell, and H. K. Nason; paper presented before the Rubber and Plastics Division, A.S.M.E., Pittsburgh, Pa., June 22, 1944; *Modern Plastics*, vol. 22, Oct., 1944, pp. 145-152, and 188.
- 3 "1943 Plastics Catalog," Plastics Catalog Corporation, New York, N. Y., pp. 290-291.
- 4 "Handbook of Plastics," by H. R. Simonds, C. Ellis, and M. H. Bigelow, D. Van Nostrand Company, New York, N. Y., 1943, pp. 510-513.
- 5 "Plastic, Sheet, Cellulose-Acetate Base," Air Corps Specification No. 12025-B, issued Nov. 19, 1940, amended Sept. 27 1943. Materiel Division, U.S.A.A.F., Wright Field, Dayton, Ohio.
- 6 "Plastic, Transparent, Flame-Resisting Sheet," Navy Aeronautical Specification P-41c, Feb. 22, 1943.
- 7 "Proposed Tentative Specifications for Cellulose Acetate Plastic Sheets," A.S.T.M. Designation D786-44T. A.S.T.M. 1944 preprint no. 84, report of Committee D-20 on plastics, pp. 45-47.
- 8 "Mechanical Tests of Cellulose Acetate," by W. N. Findley, Trans. A.S.T.M., vol. 41, 1941, pp. 1231-1245; *Modern Plastics*, vol. 19, Sept., 1941, pp. 57-62, and 78.

9 "Mechanical Tests of Cellulose Acetate. Part II on Creep," by W. N. Findley, Trans. A.S.T.M., vol. 42, 1942, pp. 914-922; *Modern Plastics*, vol. 19, Aug., 1942, pp. 71-73, and 114.

10 "Mechanical Tests of Cellulose Acetate—III," by W. N. Findley, Trans. A.S.M.E., vol. 65, 1943, pp. 479-487; *Modern Plastics*, vol. 20, March, 1943, pp. 99-105, and 138.

11 "Proposed Revised Tentative Specifications for Cellulose Nitrate (Pyroxylin) Plastic Sheets, Rods, and Tubes," A.S.T.M. Designation D701-44T. A.S.T.M. 1944 preprint, Report of Committee D-20 on plastics, pp. 66-70.

12 "Plastic Sheet, Cellulose-Nitrate Base," U. S. Army Specification 95-12008B, Materiel Division, U.S.A.A.F., Wright Field, Dayton, Ohio, Dec. 28, 1940.

13 "Triangles, Pyroxylin," Federal Specification GG-T-671, Washington, Sept. 4, 1934.

14 "Tentative Method of Test for Colorfastness of Plastics to Light," A.S.T.M. Designation D620-41T, A.S.T.M. Standards, 1942, part III, pp. 1223-1225.

15 "Tentative Method of Test for Tensile Properties of Plastics," A.S.T.M. Designation D638-44T, proposed revision. A.S.T.M. 1944 preprint no. 84, Report of Committee D-20 on plastics, pp. 8-9.

16 "Plastics, Organic, General Specifications, Test Methods," Federal Specification L-P-406a, Government Printing Office, Washington, D. C., Jan. 24, 1944.

17 "Tentative Methods of Test for Impact Resistance of Plastics and Electrical Insulating Materials," A.S.T.M. Designation D256-43T, A.S.T.M. Standards, 1943 Supplement, Part III, pp. 249-254.

18 "Tentative Method of Test for Haze of Transparent Plastics by Photoelectric Cell," A.S.T.M. Designation D672-42T, A.S.T.M. Standards, 1942, part III, pp. 1260-1262.

19 "Tentative Method of Test for Mar Resistance of Plastics," A.S.T.M. Designation D673-42T, A.S.T.M. Standards, 1942, part III, pp. 1263-1267.

20 "Standard Method of Test for Water Absorption of Plastics," A.S.T.M. Designation D570-42, A.S.T.M. Standards, 1942, part III, pp. 400-402.

21 "Tentative Descriptive Nomenclature for Objects Made From Plastics," A.S.T.M. Designation D675-43T, A.S.T.M. Standards, 1943 Supplement, Captions part III, pp. 364-368.

Discussion

M. L. MACHT.³ The facts which the authors have so ably presented lead one to the obvious conclusion that the proper selection of a plastic for any specific application is a compromise based on the selection of characteristics which are essential for the particular job. For example, it is obvious from a reference to Figs. 1 and 8 that the tensile and impact strengths of cellulose-nitrate plastics deteriorate more rapidly on outdoor exposure than do those of cellulose acetate. On the other hand, reference to Figs. 15 and 16 shows conclusively that the water absorption of cellulose acetate, and hence moisture sensitivity, is higher by a ratio of approximately 4 to 1 for cellulose acetate. Consequently, one would select cellulose nitrate for an application in which the finished article is used indoors. Thus for a drawing instrument, where warpage and dimensional change due to variations in atmospheric humidity are of importance, it would be ideal. On the other hand, cellulose acetate would be preferred over nitrate for applications in which outdoor exposure must be encountered. This difference in moisture sensitivity has been borne out in practice time and again for indoor applications, in which cellulose-nitrate sheeting has been shown to lie flatter and warp less than do cellulose-acetate sheets.

In order that misconceptions do not arise, the apparently anomalous results reported in Fig. 3, in which modulus of elasticity increases as a result of exposure, are deserving of some further discussion. The increase in modulus of elasticity is of course obviously due to plasticizer loss. However, it is accompanied by

³ E. I. du Pont de Nemours & Company, Plastics Department, Arlington, N. J.

such a marked decrease in impact strength and in tensile strength that it would not be wise to count on the increase in any design calculations which might be based on these figures.

AUTHORS' CLOSURE

Mr. Macht's remarks are well taken and we agree on the points he has emphasized.

Properties and Development of Papreg—A High-Strength Laminated Paper Plastic

By E. C. O. ERICKSON¹ AND G. E. MACKIN²

Papreg the new paper-base laminate which has recently found application in aircraft and other strength structures resulted from research at the Forest Products Laboratory. Having more than twice the tensile strength and improved mechanical properties compared with the best earlier paper-base laminates, papreg also lends itself to low-pressure molding techniques and can be formed to moderate double curvature without special treatment. This paper reviews the development work, the characteristics, properties, and service experience with papreg.

INTRODUCTION

AS the result of research at the Forest Products Laboratory, a laminated paper plastic is now being produced with more than twice the tensile strength and with improvement in most other mechanical properties over the best conventional paper-base laminates formerly available. This new paper plastic, termed "papreg," has attracted the attention of aircraft and other manufacturers because of its higher strength characteristics. It has a density about one half that of aluminum and can be produced as a comparatively uniform product. It has a smooth hard surface and reasonable moisture and decay resistance. It has been molded to moderate double curvature without special treatment, and slight taper or gage variations are readily achieved. It lends itself to low-pressure molding techniques, and has been satisfactorily postformed to moderate double curvature.

Prior to the development of papreg, laminated plastics, because of insufficient strength, had found acceptance only in limited fields. Typical applications included electrical-insulation panels, table tops, and other nonstructural uses. With the attainment of higher strength in the new material, a wider use of paper-base laminates is now realized in aircraft and other products.

The development work covered investigations on (a) the suitability of several species of wood, pulped by several processes such as the sulphate and sulphite, and in a limited way on other materials, such as cotton, flax, and rag; (b) fiber properties and pulp-processing variations; (c) special papermaking procedures; (d) impregnation of paper with resin; (e) molding of the laminated sheets; and (f) evaluation of the plastic in terms of its physical and mechanical properties (1).³ During this development, the Forest Products Laboratory has consulted with pulp and paper manufacturers, impregnators, resin manufacturers, and laminators in the analysis of the separate process problems of each.

DEVELOPMENT OF PAPREG

Analysis of the components of laminated paper plastics showed

¹ Engineer and Industrial Specialist, respectively, Forest Products Laboratory, Forest Service, U. S. Department of Agriculture, maintained at Madison, Wis., in co-operation with the University of Wisconsin.

² Numbers in parentheses refer to the Bibliography at the end of the paper.

Contributed by the Rubber and Plastics Division and presented at the Annual Meeting, New York, N. Y., Nov. 27–Dec. 1, 1944, of THE AMERICAN SOCIETY OF MECHANICAL ENGINEERS.

NOTE: Statements and opinions advanced in papers are to be understood as individual expressions of their authors and not those of the Society.

the major strength-producing factor to be the base paper, and since the properties of paper are to a large extent affected by the type of fibers used, a survey of available pulps representing different kinds of fibers was initiated early in the work. Modifications of standard pulping, fiber-processing, and papermaking procedures were developed using the Laboratory's experimental pulp- and papermaking equipment to achieve the superior properties.

Several hundred experimental papers were made during this work. It was found that papers giving the highest-strength papreg are those obtained from pulps, either sulphate, acid sulphite, or neutral sulphite, produced with a minimum of cooking required for making a well-fiberized pulp, and a minimum of bleaching, beating, and jordaning, all of which tend to reduce the native strength of the individual fiber. From a study of the papermaking requirements investigated, it was found that papers having the following properties are suitable for high-strength laminated plastic:

Ream weight (25 × 40 — 500).....	25 to 40 lb
Thickness.....	0.001 to 0.004 in.
Density.....	0.60 to 0.75 g per cc
Minimum tensile strength:	
In grain.....	10000 psi
Cross-grain.....	4000 psi
Porosity (Gurley densometer, 100 cc) less than	30 sec

The papermaking experiments showed that high tensile strength in one direction could be obtained by alignment of fibers during the formation of the sheet and that the relatively high density could be obtained by employing high wet-press pressure without reducing the absorbent characteristics of the sheet below that required for satisfactory impregnation (2). It was also found that densification of the sheet by calendaring was advantageous, since in this way equal or higher strengths than when uncalendered paper was used (3) could be obtained in laminates molded at lower pressures.

Impregnation of paper with resin involves a number of factors that greatly affect the physical properties of the ultimate plastic. Among the important factors recognized are the resin and volatile content of the treated paper, the temperature of drying the impregnated sheet, time of absorption of resin, kind of resin diluent, and kinds of resin. Although many different resins were investigated in the development of papreg, considerations of availability as well as resultant properties led to the selection of spirit-soluble phenolic-type resins for this purpose.

Results showed that there is an optimum resin content for the production of desired plastic properties for each type of fiber and for the particular molding pressure used. Relatively high resin content imparts better water resistance to the finished papreg, but some strength properties are lowered. For laminating pressures of approximately 250 psi, a resin content of 30 to 40 per cent is most desirable for over-all optimum properties. Fig. 1 shows the effect of resin content of the impregnated sheet on the properties of papreg, laminated under standard conditions. Within the indicated range of resin contents and provided the volatile content is maintained constant, the strength properties of the plastic are not greatly affected by variations of the resin content (4).

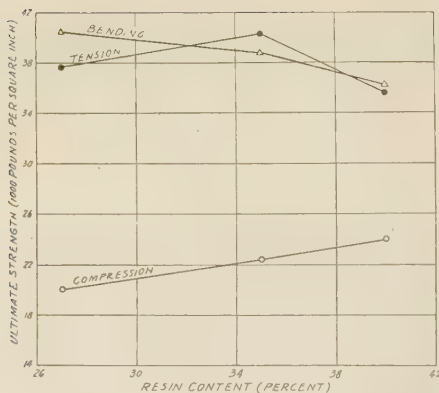


FIG. 1 EFFECT OF RESIN CONTENT ON CERTAIN PROPERTIES OF PAPREG

Properties of the papreg are considerably affected by the volatile content of the resin-treated paper (4). High volatile content (about 7 per cent) causes greater flow of the resin under the heat and pressure of laminating and results in lower strength values of the plastic than those obtained with treated paper having a volatile content of about 4 per cent.

In order to avoid the necessity of using steel dies and to utilize low-capacity presses for laminating, 250 psi was fixed as the upper limit of pressure to be used. However, the effects of using both higher and lower pressures were investigated (4). Fig. 2 shows the effects of laminating pressure on the properties of papreg.

PROPERTIES OF PAPREG

The development work previously discussed resulted in a decision to adopt as a standard the product resulting from a certain combination of materials and processing procedures, and to carry out a series of tests to determine the basic engineering properties of this standardized product (designated "Improved Standard, June, 1943"). Some data on high-strength paper laminates have appeared in publications during the past 2 years (5, 6, 7).

Although satisfactory materials were produced from other species such as balsam fir and Western hemlock, processed by the previously mentioned pulping methods, evaluations for basic properties made at the Forest Products Laboratory were confined to a standardized papreg made from spruce Mitscherlich-type sulphite paper impregnated with a phenolic-type thermosetting resin. The resin content was about 36 per cent, and the volatile content was 4.5 per cent. The material for test consisted of parallel-laminated and cross-laminated flat panels, approximately 11 in. square, some $\frac{1}{8}$ in. and others $\frac{1}{2}$ in. in thickness. The $\frac{1}{8}$ and $\frac{1}{2}$ -in.-thick panels were molded from approximately 70 and 280 sheets of treated paper, respectively, and were pressed for 12 and 25 min, respectively, at 250 psi. The temperature of the hot-press platens was 325 F. The panels were removed from the press immediately after pressing and allowed to cool in air at room temperature. Material constituted and processed in this way is identified as Improved Standard, June, 1943. The specific gravity, based upon weight and volume after conditioning at 75 F and 50 per cent relative humidity, is 1.4.

Although the material tested was produced under laboratory controlled conditions, its properties are believed to be representative of those of products of similar composition when produced by commercial laminators employing the same conditions and manufacturing procedure. The base materials are commercially available, and impregnated paper and molded stock are now being produced on a commercial scale.

Except where otherwise noted, properties of papreg here re-

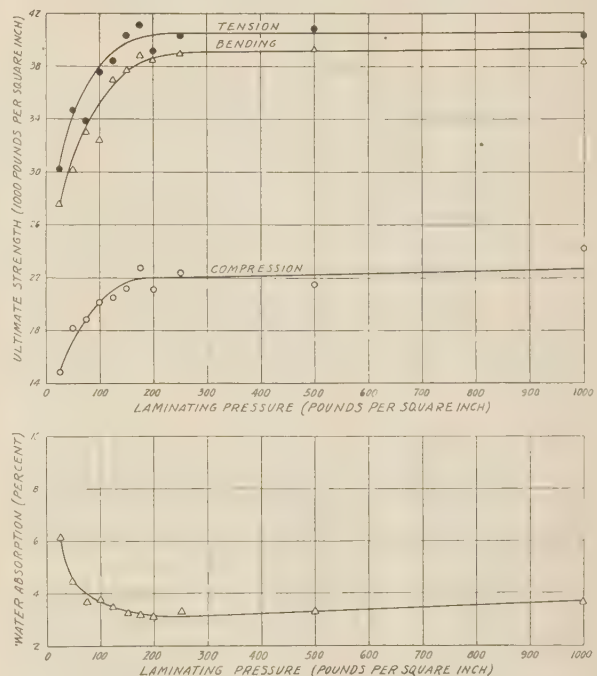
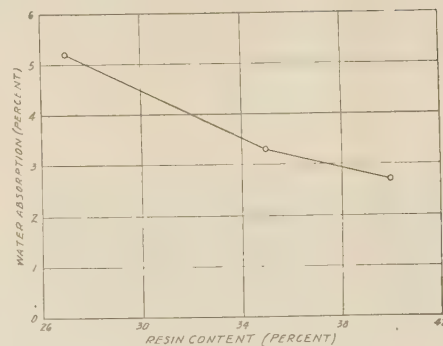


FIG. 2 EFFECT OF LAMINATING PRESSURE ON CERTAIN PROPERTIES OF PAPREG

ported were obtained from specimens prepared, conditioned, and tested in accordance with Federal Specification L-P-406 for Plastics, Organic; General Specifications (Methods of Tests) dated December 9, 1942. The specimens were machined with high-speed steel tools in such a manner as to be virtually free from toolmarks or any evidence of overheating and therefore were not otherwise finished prior to test.

Results of tests at room temperature on nominal $\frac{1}{8}$ -in. and $\frac{1}{2}$ -in. material are presented in Tables 1 and 2, respectively.

In these tables "flatwise" refers to load applied to a surface of the original material, that is, in the direction of molding pressure. "Edgewise" refers to load applied on the edges of the laminations, that is, in a direction perpendicular to that of the molding pressure. Lengthwise or crosswise refers to the orientation of the predominant direction (machine direction or "grain" direction) of fibers in the constituent sheets of paper with respect to the length of the specimen. Consequently, parallel-laminated

specimens are either lengthwise or crosswise, whereas cross-laminated specimens are designated "lengthwise and crosswise." Thus values of shear for "lengthwise" and "crosswise" are, respectively, perpendicular and parallel to the predominant fiber directions. Actually, for cross-laminated papreg, the fiber direction of the face plies was lengthwise in one half the specimens and crosswise in the other half. Because results did not differ significantly, the values for the two directions are combined in Tables 1 and 2.

Average values represent the arithmetic average of the indicated number of tests, composed of not more than two tests from any one panel in each of the directions indicated. The standard deviation for each property is also presented to provide a measure of the variability or the range of values that can be expected from stock sheet materials of this type.

Parallel-laminated papreg has average tensile and flexural strengths of about 36,000 psi lengthwise, and tensile and flexural strengths of about 20,000 and 24,000 psi crosswise, respectively. For cross-laminated papreg, the tensile and flexural strengths are 27,000 and 30,000 psi, respectively, or intermediate between those for the two principal directions of the parallel-laminated type. This relationship exists among all tensile and flexural properties, and to a lesser degree among most other properties.

The average ultimate compressive strength (edgewise) varied between 19,000 and 23,000 psi. Only in the crosswise direction of parallel-laminated material were the tensile and compressive properties about equal. Young's moduli of elasticity in compression and flexure were essentially the same, and were from 15 to 25 per cent less than the tensile modulus. Yield strengths in compression were likewise considerably less than in tension. The similarity of compressive ultimates for the two directions, together with the disparity in tension between these directions suggested that the resin is the major factor in strength in compression.

In general, failures in compression were characterized by two shear failures at one end of the specimen extending at 45 deg across the edges of the lamination in the form of a V, with subsequent delamination near the center of the thickness of the specimen forming a Y. Strength in interlaminar shear varied between 800 and 3000 psi, depending on the type of test and the orientations of the specimen. Tensile-type shear on kerfed specimens ranged from 800 psi (crosswise) to 1100 psi (lengthwise). Block-type shear values ranged from 1300 psi, lengthwise, to 1600 psi, crosswise. On the other hand, cylindrical specimens tested in double shear (Federal specification L-P-406) produced values on the order of 3000 psi.

TABLE 1 STRENGTH AND RELATED PROPERTIES OF NOMINAL 1/8-IN. PAPREG AT NORMAL TEMPERATURE, 75 F \pm 5 DEG F

Test and properties	Parallel laminated				Cross laminated	
	Lengthwise		Crosswise		Lengthwise and crosswise	
	Av.	Standard deviation	Av.	Standard deviation	Av.	Standard deviation
	:	:	:	:	:	:
Specific gravity	1.41	1.41	1.41
Tension						
Ultimate strength	psi : 35,610	2,321	20,010	853	27,160	1,591
Yield strength at 0.2 percent offset	psi : 32,780	2,575	14,560	838	23,160	1,665
Yield strength at 0.7 percent strain	psi : 23,090	2,223	10,860	980	16,760	706
Proportional limit stress	psi : 14,480	3,011	7,880	856	9,760	1,072
Secant modulus at 0.2 percent offset	psi $\times 10^3$: 2,951	147	1,352	174	2,177	111
Modulus of elasticity	psi $\times 10^3$: 3,645	377	1,713	261	2,692	181
Elongation immediately before fracture	Percent : 1.20	0.16	1.88	0.30	1.29	0.14
Static bending - (flatwise)						
Modulus of rupture	psi : 36,590	1,171	24,300	785	30,540	1,153
Proportional limit stress	psi : 15,900	1,473	10,510	1,148	12,240	1,325
Modulus of elasticity	psi $\times 10^3$: 3,016	99	1,481	51	2,241	58
Bearing - 1/8-in. dia. pin (tensile loading)						
Bearing strength (4 to 6 tests)	psi : 24,920	22,940	25,920
Ultimate bearing stress	psi : 35,060	31,300	34,280
Shear - (Johnson-type shear tool)						
Shearing strength (flatwise)	psi : 16,980	700	14,010	733	15,550	415
Modulus of rigidity	psi $\times 10^3$: 909	29	887	33
Indentation hardness (Rockwell)	M-numbers : 110	110
Loss in weight on drying at 221° F. for 24 hours						
Loss in weight (2 \times 2 in. spec.)	Percent : 1.99	2.60
Water absorption (24 hours immersion 2 \times 2 in. spec.):						
Increase in weight	Percent : 2.21	2.36
Increase in length	Percent : .0103
Increase in width	Percent : .0602
Increase in thickness	Percent : 1.67	1.82

NOTE: Values for indentation hardness and those properties for which standard deviation is reported, represent the average of 32 tests. Loss in weight on drying and water absorption percentages for parallel and cross-laminated papreg are based on 16 and 9 tests, respectively.

TABLE 2 SOME STRENGTH PROPERTIES OF NOMINAL 1/2-IN. PAPREG AT NORMAL TEMPERATURE, 75 F \pm 5 DEG F

Test and properties	Parallel laminated				Cross laminated	
	Lengthwise		Crosswise		Lengthwise and crosswise	
	Av.	Standard deviation	Av.	Standard deviation	Av.	Standard deviation
Specific gravity	1.41		1.41		1.41	
Compression (edgewise) (20 - 20 - 32) ¹						
Ultimate strength	psi : 22,530	727	psi : 19,430	729	psi : 20,790	911
Yield strength at 0.2 percent offset	psi : 14,040	421	psi : 9,730	462	psi : 11,290	439
Yield strength at 0.7 percent strain	psi : 14,130	407	psi : 8,590	321	psi : 11,340	320
Proportional limit stress	psi : 7,910	884	psi : 4,280	629	psi : 5,430	841
Tangent modulus at 0.7 percent strain	psi x 10 ³ : 773		psi x 10 ³ : 833		psi x 10 ³ : 785	
Secant modulus at 0.2 percent offset	psi x 10 ³ : 2,049	86	psi x 10 ³ : 1,139	46	psi x 10 ³ : 1,621	52
Modulus of elasticity	psi x 10 ³ : 2,913	166	psi x 10 ³ : 1,496	96	psi x 10 ³ : 2,279	95
Compression (flatwise) (3 - 0 - 3) ¹						
Ultimate strength	psi : 42,200				psi : 45,600	
Static bending (flatwise) (10 - 10 - 16) ¹						
Modulus of rupture	psi : 31,710	1,371	psi : 19,540	2,489	psi : 28,710	1,622
Proportional limit stress	psi : 14,410	920	psi : 7,850	1,201	psi : 11,000	1,068
Modulus of elasticity	psi x 10 ³ : 2,847	60	psi x 10 ³ : 1,418	35	psi x 10 ³ : 2,061	97
Static bending (edgewise) (10 - 10 - 16) ¹						
Modulus of rupture	psi : 28,870	1,502	psi : 20,790	1,239	psi : 26,590	1,319
Proportional limit stress	psi : 14,960	884	psi : 7,940	1,039	psi : 8,240	1,092
Modulus of elasticity	psi x 10 ³ : 2,726	138	psi x 10 ³ : 1,402	64	psi x 10 ³ : 2,184	105
Shear (Johnson-type shear tool) (20 - 20 - 32) ¹						
Shearing strength (edgewise)	psi : 20,500	581	psi : 17,840	684	psi : 18,670	922
Impact strength (Izod) (20 - 20 - 32) ¹						
Flatwise, notch on face	Ft. lb. per in. of notch : 4.69		Ft. lb. per in. of notch : 2.43		Ft. lb. per in. of notch : 3.82	
Edgewise, notch on edge	Ft. lb. per in. of notch : .67		Ft. lb. per in. of notch : .60		Ft. lb. per in. of notch : .66	

¹Numbers in order indicate the number of tests of parallel-laminated lengthwise, parallel-laminated crosswise, and cross-laminated papreg, respectively.

A few tests to determine the tensile strength normal to the plane of the laminations averaged 600 psi. The bonding strength (Federal specification L-P-406a) was about 1000 psi. This value represents the force required to rupture the bond of a 1-in-square \times 1/2-in-thick specimen by edgewise loading through the medium of a 10-mm steel ball.

The shear strength of parallel-laminated and cross-laminated papreg by the Johnson-type double-shear method was about 20 per cent greater edgewise than flatwise; and both edgewise and flatwise shear strength for parallel-laminated papreg was 15 to 20 per cent greater perpendicular to the fiber direction than parallel to the fiber direction.

The modulus of elasticity in shear, or the modulus of rigidity G (the modulus associated with shear distortions in the surfaces of the sheet and in planes parallel thereto) is about 900,000 psi.

The bearing strength of 1/2-in. papreg, determined from tensile-type tests of standard specimens having a hole diameter of 1/8 in., is approximately 25,000 psi. Tests of standard 4 3/4-in. \times 1 1/2-in. specimens, having a hole of 1/4 in. diam and centered in the width at a distance of 3/4 in. from one end of the specimen, failed in tension across the net section before the specified 4 per cent deformation of the hole diameter occurred. For these tests, the average deformation of hole diameter at failure and corresponding ultimate stresses were 3.65 per cent and 28,000 psi, respectively, for parallel-laminated (lengthwise) papreg, and 3.69 per cent and 26,500 psi, respectively, for cross-laminated papreg.

Papreg has a flatwise Izod strength of from 2 to 6 ft-lb per in. of notch; whereas edgewise values are on the order of 0.5 to 0.7.

Typical tensile and compressive stress-strain diagrams are presented in Figs. 3 and 4. Each curve presents actual load-deformation data for individual specimens that have properties in close agreement with the average of the group. The material exhibits good elastic behavior up to a well-characterized proportional or elastic limit stress, but upon further stressing shows a plastic behavior or nonlinear relationship between stress and strain. Papreg, not unlike many thermosetting plastics, has comparatively little ductility, and ultimate failures in tension occur without a marked yield point and at relatively small strains.

Directional properties of papreg, based on a limited number of tests, are presented in Table 3. These results indicate that the cross-laminated material is essentially isotropic in the plane of the sheet. In general, the 45-deg properties of the cross-laminated material are equal to or slightly better than the lengthwise or crosswise values, whereas the values of the parallel-laminated material at 45 deg are essentially intermediate between those at 0 and 90 deg to the fiber direction.

Fatigue. Constant-strain flexural-fatigue studies were conducted in a room maintained at 80 F, and 50 per cent relative humidity. Test specimens were of 1/2-in. papreg, similar in shape to that specified in Federal Specification L-P-406, except for slight modifications in dimensions found necessary in order to employ existing fittings of available Krouse flat-plate fatigue machines.

The flatwise flexural-fatigue strength for completely reversed bending stress at 100,000,000 cycles was about 7000 psi for cross-laminated (lengthwise) papreg; and 7700 and 5800 psi for papreg parallel-laminated lengthwise and crosswise, respectively. Fatigue limits of papreg at higher induced stresses are indicated in the S-N diagram, Fig. 5.

Fatigue limits were determined by the deflection method (5), wherein specimens are considered as having failed when the deflection produced by the reapplication of the initial load shows a marked increase in its rate of change.

The greatest increase in specimen temperature above the ambient temperature was 60 deg F at 14,000 and 12,000 psi for cross-laminated and parallel-laminated crosswise specimens, respectively. Temperature increases at a fatigue limit of approximately 10,000,000 cycles were: Cross-laminated, 11 deg F at 8000 psi; parallel-lengthwise, 10 deg F at 9800 psi; and parallel-laminated papreg, crosswise 15 deg F at 6700 psi. Temperature increases at the 100,000,000-cycle limits were only 2 to 3 deg F, except for the parallel-crosswise, which increased 10 deg F above the ambient temperature. Fatigue strengths, shown in Fig. 5, were not corrected to include any calculated reductions due to thermal effects.

Flammability. Flammability or rate-of-burning tests of $1\frac{1}{2}$ -in. \times 6-in. specimens of $\frac{1}{8}$ -in. papreg indicated the material to be self-extinguishing. The average flaming and glowing time which persisted following removal of the Bunsen burner after the second application was 1 and 2 min, respectively. The maximum spread of char did not exceed $\frac{3}{4}$ in. The charred end increased about 50 per cent in thickness.

Abrasion. Abrasion-wear tests of papreg of 1.4 specific gravity were conducted on a Taber abraser employing CS-17 wheels and a 1000-g load. One thousand revolutions produced a loss in weight of 0.0168 g.

Thermal Expansion. The coefficients of linear thermal expansion of papreg were greater in the direction of compression perpendicular to the laminations than in the plane of the laminations. Test specimens were heated for 24 hr at 105 C, and then stored in a desiccator over phosphoric anhydride, prior to test. Results of a few measurements made on 1-cm square specimens, (1 cm long for the measurements in the direction of compression normal to the laminations, 3 cm long for the linear measurements

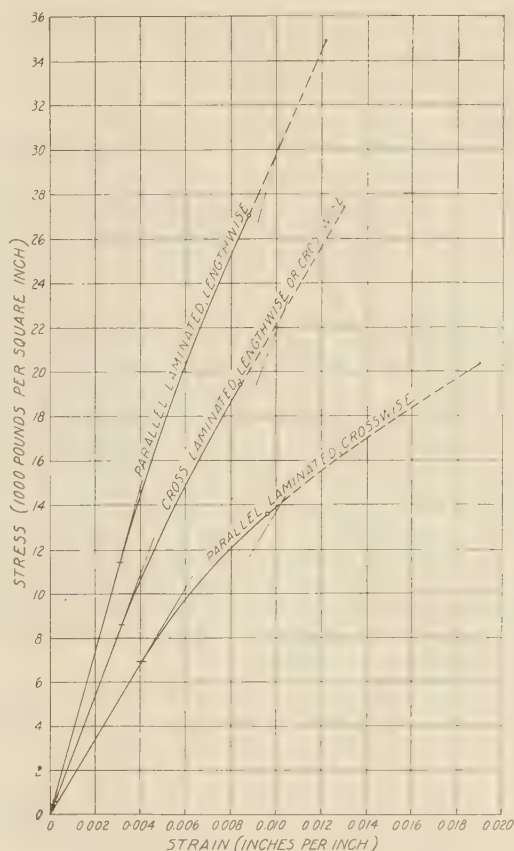


FIG. 3 TYPICAL TENSILE STRESS-STRAIN CURVES FOR PAPREG AT NORMAL TEMPERATURE; $75^{\circ}\text{F} \pm 5^{\circ}\text{F}$

in the plane of the laminations other than those parallel to the fibers in the parallel-laminated material, and 10 cm long for the lengthwise measurement of the parallel-laminated papreg) be-

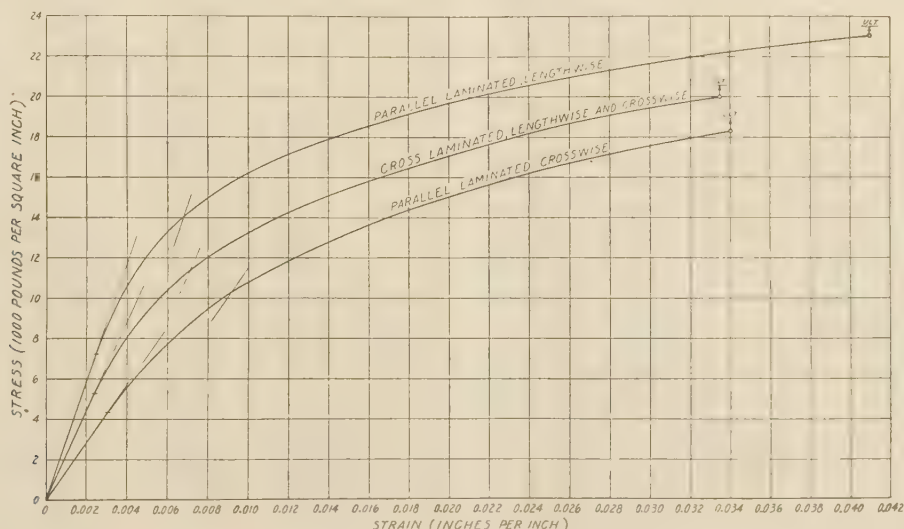


FIG. 4 TYPICAL COMPRESSIVE LOAD APPLIED EDGEWISE, STRESS-STRAIN CURVES FOR PAPREG AT NORMAL TEMPERATURE; $75^{\circ}\text{F} \pm 5^{\circ}\text{F}$

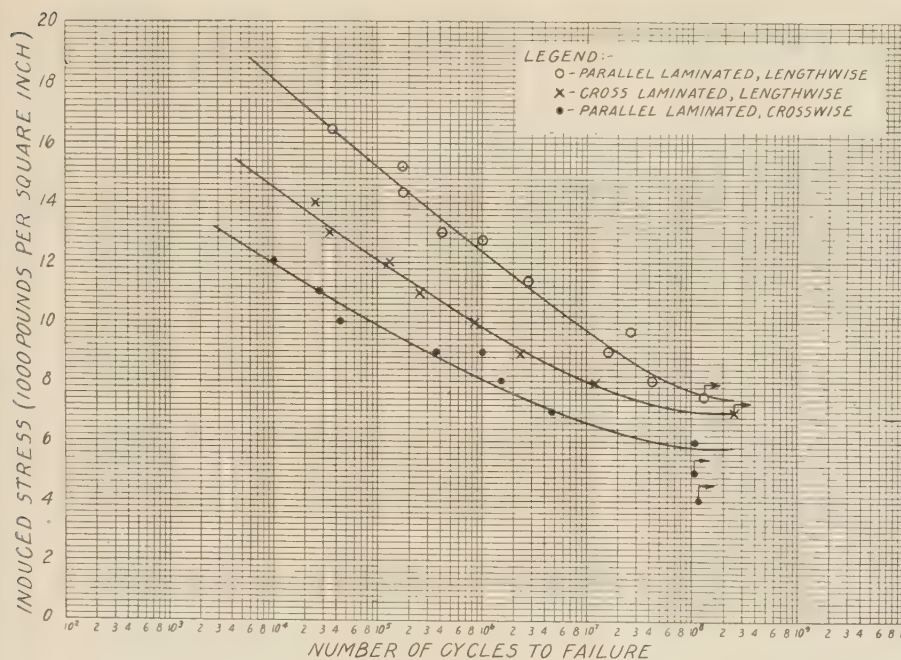


FIG. 5 CONSTANT-STRAIN FLEXURAL FATIGUE STRENGTH OF PAPREG AT 80 F AND 50 PER CENT RELATIVE HUMIDITY

follow this general behavior but indicated, instead, a slight decrease in strength with respect to normal temperatures at both temperature extremes.

The subzero tests were conducted in a room maintained at $-69\text{ F} \pm 3\text{ deg F}$, at the Army Air Forces Materiel Command, Wright Field, Dayton, Ohio, by the personnel of the Materials Laboratory and on specimens supplied by the Forest Products Laboratory from the same material as was used for tests at other reported temperatures. Specimens tested at -69 F were exposed to that temperature for at least 4 hr prior to test. Specimens tested at normal temperature were conditioned at 75 F , and 50 per cent relative humidity for approximately $2\frac{1}{2}$ weeks prior to test. Those tested at 158 F were conditioned at 158 F and 20 per cent relative humidity for 24 hr, and those at 200 F , were heated, prior to test, for 24 hr in an electric oven maintained at 200

F and essentially zero per cent relative humidity. The high-temperature (158 and 200 F) tests were conducted in a thermostatically controlled heat chamber, but without control of humidity.

It is recognized that in consequence of the conditions to which specimens were subjected prior to and during test, factors other than temperature, such as differences in dryness, may have affected the results shown in Fig. 6. These data agree substantially with temperature-strength data⁸ of paper-base laminates of the same composition impregnated with other phenolic resins (11).

Moisture. Studies to determine the moisture-strength relationship of papreg indicated that exposure to increased humidity with consequent moisture absorption results in a definite decrease in strength properties, as well as increase

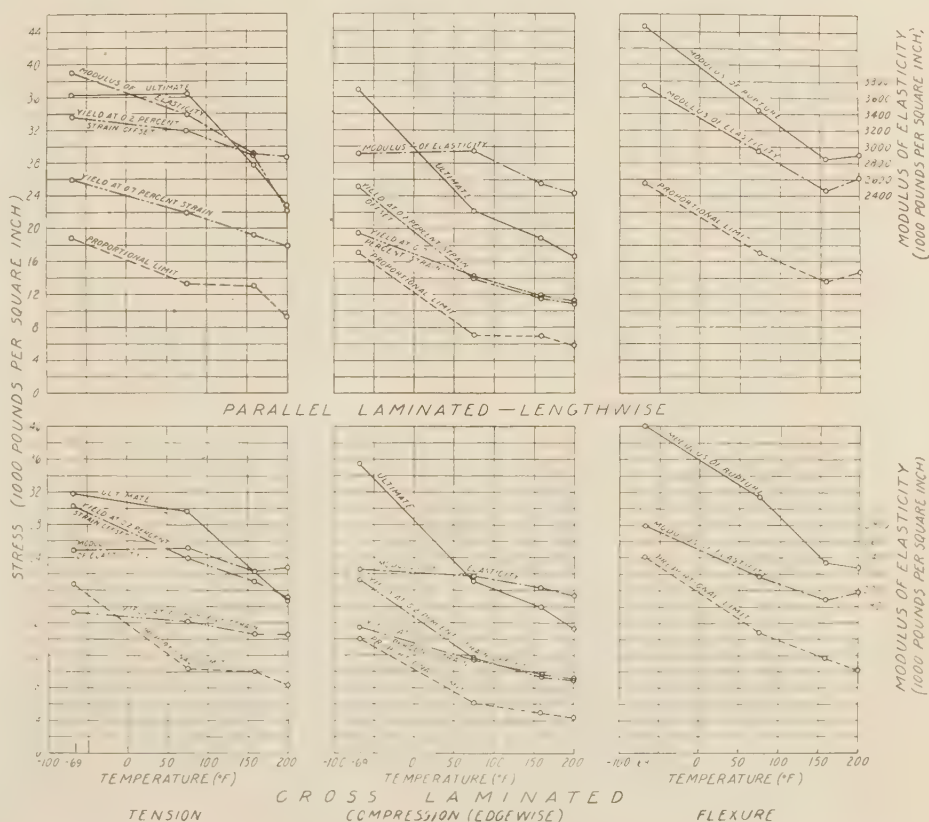


FIG. 6 TEMPERATURE-STRENGTH RELATIONSHIPS OF PAPREG

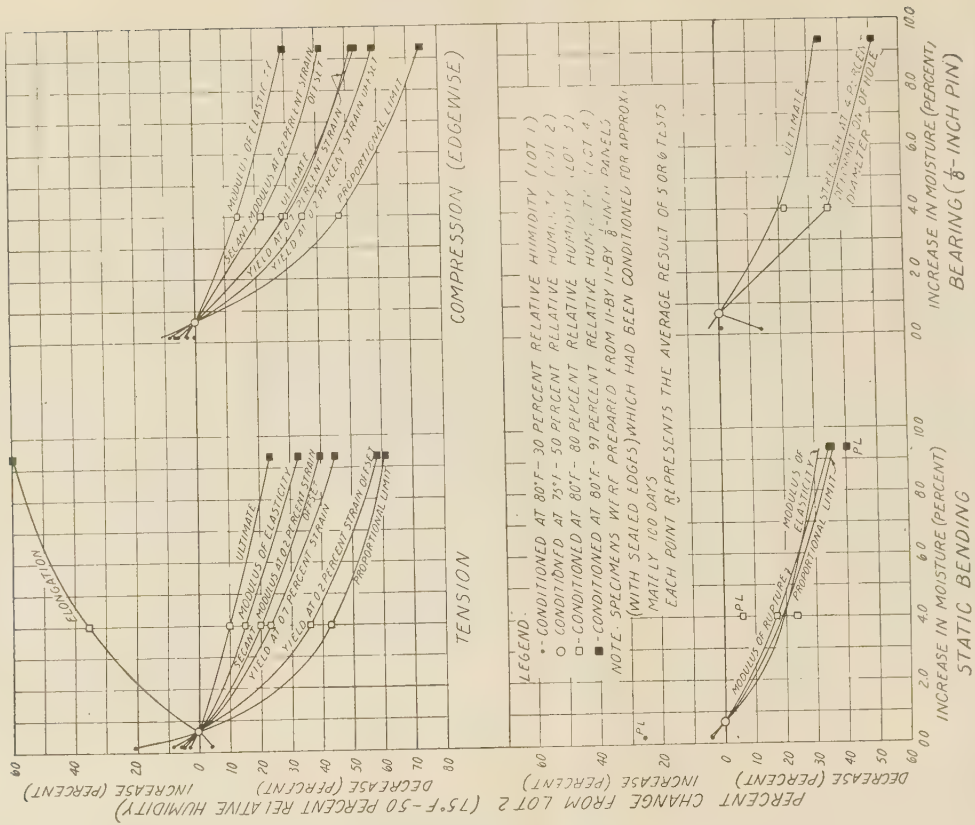


Fig. 8 MOISTURE-STRENGTH RELATIONSHIP OF CROSS-LAMINATED PAPREG, EXPRESSED AS A PERCENTAGE OF STRENGTH PROPERTIES AT 75 F AND 50 PER CENT RELATIVE HUMIDITY (Points show changes based on average results of the test data, whereas curves show changes based on the average relationship among the several humidities.)

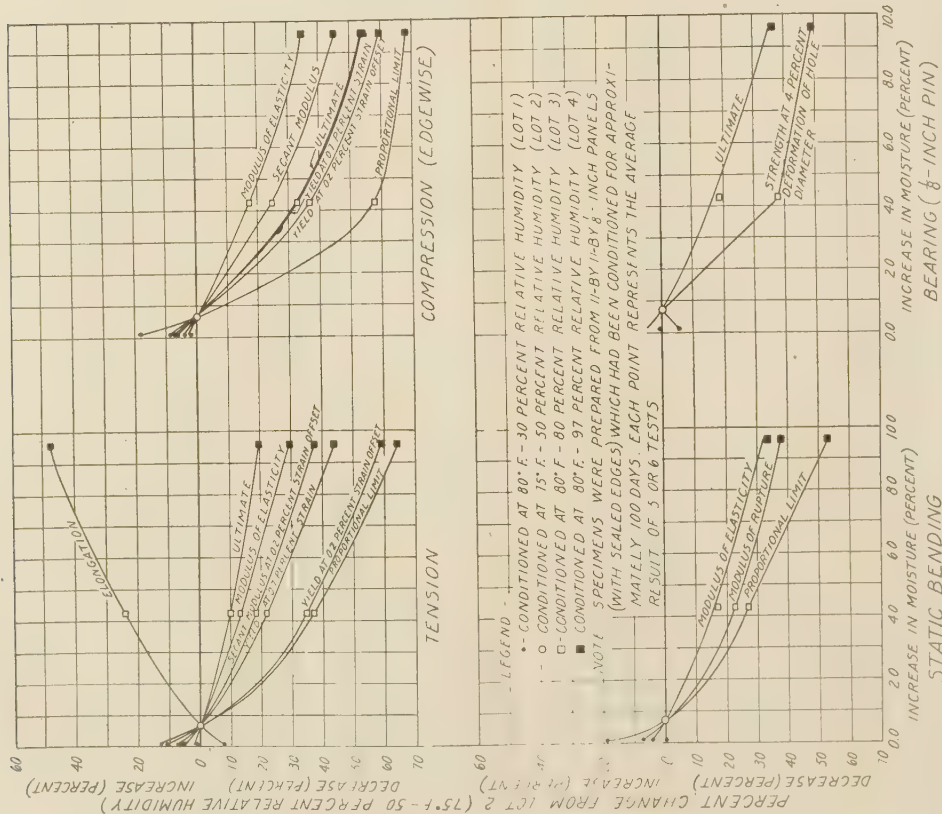


Fig. 7 MOISTURE-STRENGTH RELATIONSHIP OF PARALLEL-LAMINATED PAPREG IN LENGTHWISE DIRECTION, EXPRESSED AS A PERCENTAGE OF STRENGTH PROPERTIES AT 75 F AND 50 PER CENT RELATIVE HUMIDITY

in dimensions. These characteristics are common to cellulose compositions. Tension, compression, static-bending, and bearing tests were made on specimens taken from $\frac{1}{8}$ -in. panels of parallel- and cross-laminated papreg, conditioned for 100 days to approximate equilibrium at 75 F and 50 per cent relative humidity, and at 80 F and relative humidities of 30, 80, and 97 per cent, and from panels immersed in distilled water at 75 F.

The moisture-strength relationships of parallel-laminated (lengthwise) and cross-laminated papreg, expressed as a percentage of the strength properties at 75 F and 50 per cent relative humidity, are indicated in Figs. 7 and 8, respectively. The data show that the modulus of elasticity is least affected by moisture; and proportional or elastic limit, the most affected; also, that parallel-laminated and cross-laminated materials differ but little with respect to the effects of increase in moisture. The two types of papreg exhibited similar reductions in tensile and compressive properties at corresponding moisture levels, except in ultimate strength. The percentage reduction in compressive strength was approximately 2 or 3 times that produced on the tensile strength for a given increase in moisture. Decreases in static bending and bearing strength due to moisture increases were less than those in tension and compression.

A few tests made to determine the effect of moisture on the hardness of papreg by the standard Rockwell indentation tests indicated a decrease in M values from 108 for material conditioned at 30 per cent relative humidity to 65 for material conditioned at 97 per cent relative humidity.

A few shear modulus tests (G) on $\frac{1}{8}$ -in. \times 5-in. \times 5-in. specimens, conditioned at 97 per cent relative humidity and tested wet, indicated a modulus of rigidity of 677,000 psi for parallel-laminated papreg and 707,000 psi for cross-laminated papreg. This indicated a loss in shear modulus with respect to values at 50 per cent relative humidity of approximately 20 to 25 per cent due to moisture increases of approximately 10 per cent.

Typical tensile and compressive stress-strain diagrams, for papreg under various humidity and immersion conditions, are shown in Figs. 9 and 10. Each curve represents actual load-deformation data for an individual specimen whose properties are in close agreement with the average of the group.

The curves show that papreg in approximate equilibrium with high humidity and immersion conditions exhibits a plastic type of behavior throughout the greater portion of its stress range, with a limited elastic range.

Fig. 11 shows the rate of moisture gain of 12-in.-square panels of $\frac{1}{8}$ -in. papreg used in the moisture-strength evaluations. The conditioning time in days is plotted against the per cent increase in moisture or weight rather than against moisture content, because the actual moisture content was not determined. An approximation, based on extrapo-

lation methods, indicated a decrease in weight of approximately 0.5 per cent between 30 and 0 per cent relative humidity.

Data for panels conditioned in 30 per cent relative humidity are not shown because the change in weight was approximately 0.1 per cent. Hence papreg having a volatile content of 4.5 per cent before molding was found to be in equilibrium with 80 F and 30 per cent relative humidity conditions after molding. Panels exposed to 50 per cent relative humidity reached weight equilibrium in 100 days and had increased less than 1 per cent in weight. Those panels exposed to 80 and 97 per cent relative humidities for strength evaluations reached only 85 and 90 per cent of weight equilibrium, respectively, in 100 days. These percentages were based on the behavior of companion panels retained in these humidities until weight equilibrium was reached after 200 to 250 days. Approximate weight increases for these panels at equilibrium were 5 per cent at 80 per cent relative humidity, and 10 to 11 per cent at 97 per cent relative humidity. Panels immersed in water also reached approximate weight equilibrium in 250 days and had increased approximately 17 per cent in weight. Consequently, the strength relations indicated for papreg, exposed to 80 and 97 per cent relative humidity,

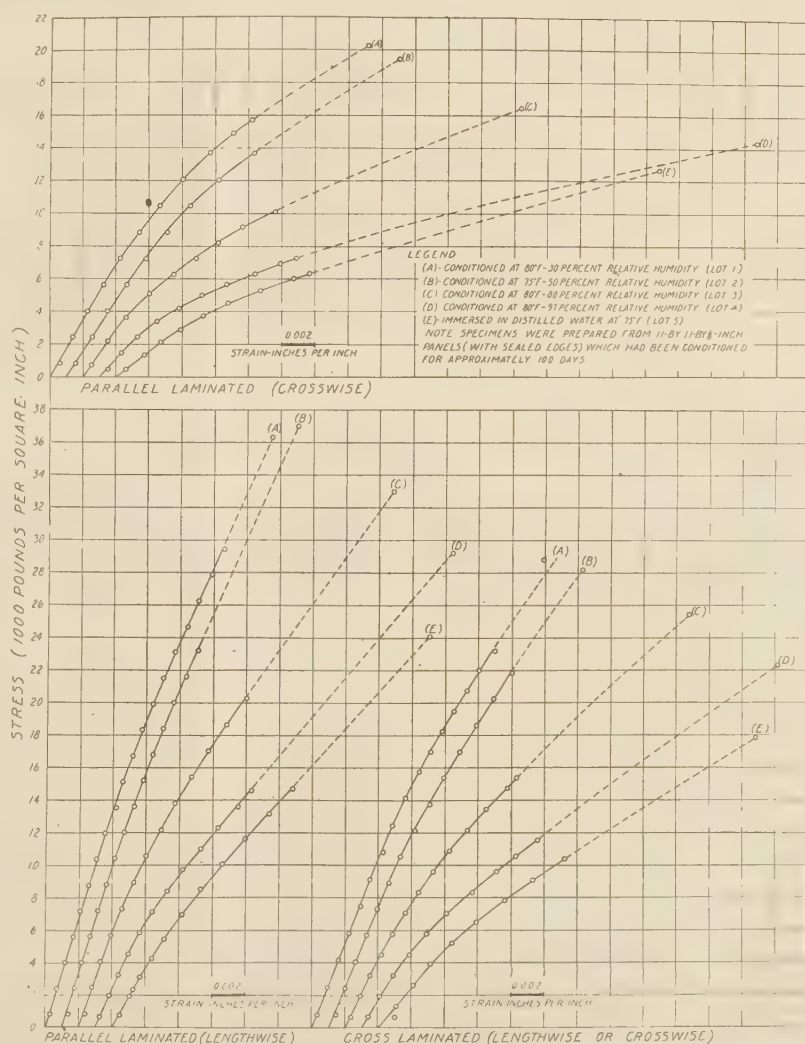


Fig. 9 TYPICAL TENSILE STRESS-STRAIN CURVES FOR PAPREG UNDER VARIOUS HUMIDITY AND IMMERSION CONDITIONS

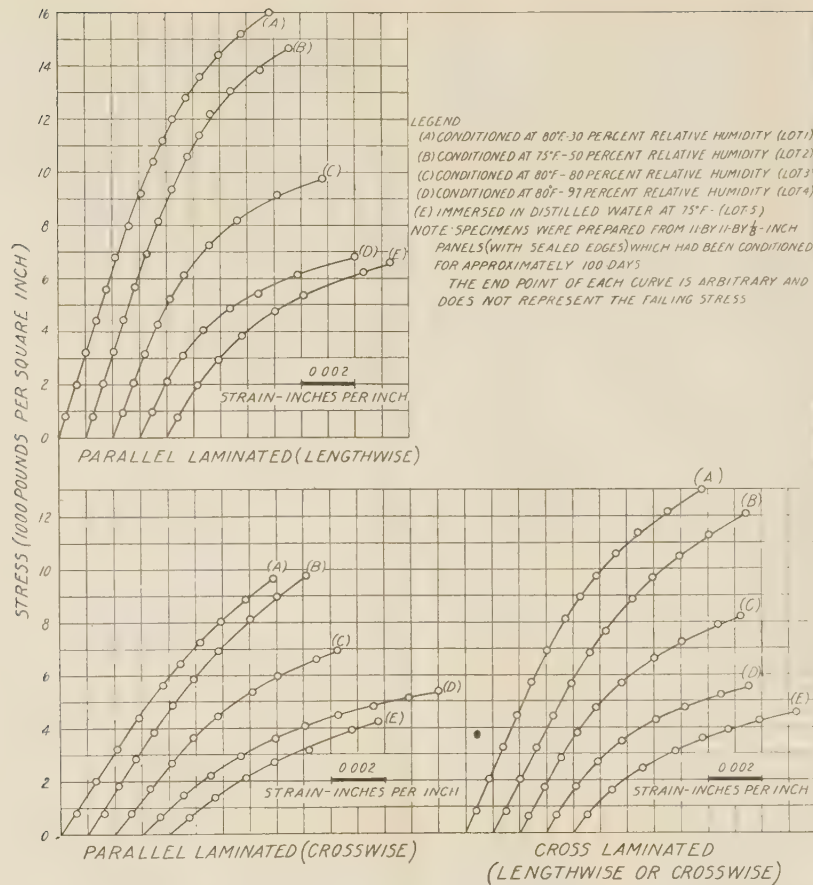


FIG. 10 TYPICAL COMPRESSIVE STRESS-STRAIN CURVES FOR PAPREG UNDER VARIOUS HUMIDITY AND IMMERSION CONDITIONS

are slightly higher than may be expected at equilibrium moisture content.

The principal dimension change of papreg, incident to increase in weight due to moisture gain, is in thickness (direction of molding pressure). The increases in thickness and in weight, expressed as percentages of the original values, are approximately equal. From a relatively dry condition (24 hr at 122 F) to equilibrium at 97 per cent relative humidity, $\frac{1}{16}$ -in. parallel-laminated papreg increased 0.09 per cent in length, and 0.48 per cent in width; $\frac{1}{16}$ -in. cross-laminated papreg increased 0.22 per cent in length and 0.18 per cent in width.

Freezing and Thawing. Freezing and thawing investigations of papreg, exposed to the moisture conditions previously described, did not indicate significant effects on strength beyond those attributed to moisture. The freezing-and-thawing cycle employed consisted of 1 hr of freezing at -30 F, followed by 1 hr of thawing at 80 F, in the respective chambers in which the material was conditioned. Strength tests were conducted following 36 and 95 cycles of exposure.

Accelerated Weathering. Papreg $\frac{1}{8}$ in. thick, exposed to ten 24-hr cycles of irradiation and wetting (sun lamp and fog) in accordance with Federal Specification L-P-406, showed an increase in certain strength properties, as compared to papreg conditioned at 75 F, and 50 per cent relative humidity. In tension, for instance, the improvement based on average values was 4 to 13 per cent in ultimate strength, 4 to 7 per cent in Young's modulus, and 4 to 6 per cent in yield stress at 0.7 per cent strain. In com-

pression, the improvement was 5 to 10 per cent in ultimate strength, and 2 to 3 per cent in Young's modulus.

The physical changes resulting from the exposure were a decrease of approximately 2 per cent in weight, between 1 and 2 per cent in thickness, and a color change from a light-yellow-brown to a mottled dark-reddish-brown. No checking, warping, blooming, crazing, or delamination was apparent. To all

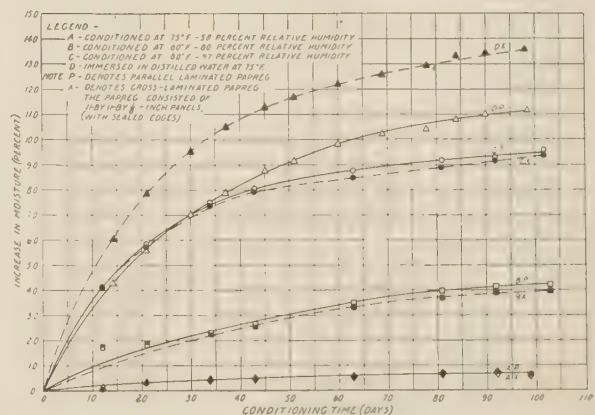


FIG. 11 MOISTURE GAIN OF PAPREG DURING CONDITIONING IN VARIOUS RELATIVE HUMIDITIES AND DURING IMMERSION

appearances, the simulated sunlight had no deteriorating effect. Instead, irradiation had a drying effect which resulted in increased strength.

Natural Weathering. Outdoor exposure tests of 11-in-square panels of $1/16$, $1/8$, and $1/4$ -in-thick papreg were conducted at Madison, Wis. The panels were mounted flatwise on exposure racks facing south and inclined 45 deg. During 15 months of continuous exposure, the appearance of the exposed surface changed from a glossy yellow-brown to a dull gray-brown. There were no indications of blooming, crazing, or delamination. Changes in strength properties attributed to weathering have not yet been determined.

BIBLIOGRAPHY

- 1 "High-Strength Laminated Paper Plastics for Aircraft," U. S. Forest Products Laboratory, Mimeograph no. 1395, revised April, 1943.
- 2 "Certain Properties of Papreg Affected by Wet Press Pressure on Mitscherlich Base Paper," by G. E. Mackin, R. J. Seidl, and P. K. Baird, Forest Products Laboratory, Mimeograph no. 1575, July, 1943.
- 3 "Certain Properties of Papreg Affected by Calendering Pressure on Mitscherlich Base Paper," by G. E. Mackin, R. J. Seidl, and P. K. Baird, Forest Products Laboratory, Mimeograph no. 1389, July, 1943.
- 4 "Certain Properties of Papreg as Affected by Laminating Pressure, Resin Content, and Volatile Content," by R. J. Seidl, G. E. Mackin, and P. K. Baird, Forest Products Laboratory, Mimeograph no. 1394, revised October, 1943.
- 5 "Basic Physical Properties of Laminates," by P. M. Field, *Modern Plastics*, August, 1943, pp. 91-102, 126, 128, and 130.
- 6 "Engineering Properties of Plastics," by F. B. Fuller, *Modern Plastics*, June, 1943, pp. 95-97 and 130.
- 7 "Evaluation of High-Strength Plastics," by Henry Sang and P. M. Field, *Modern Plastics*, October, 1943, pp. 107-109 and 142.
- 8 "Effect of Environmental Conditions on Mechanical Properties of Organic Plastics, Part I," by T. S. Carswell and H. K. Nason, *Modern Plastics*, June, 1944, pp. 121-126, 158, and 160; Part II, *Modern Plastics*, July, 1944, pp. 125-130, 160, and 162.
- 9 "Temperature Versus Strength for Phenolics," by T. S. Carswell, D. Telfair, and R. U. Haslanger, *Modern Plastics*, July, 1942, pp. 65-69.
- 10 "Effect of Moisture on the Physical Properties of Paper-Base Plastics," by A. H. Croup, *Paper Trade Journal*, vol. 118, May 18, 1944, pp. 43-46.
- 11 Unpublished special report on "The Influence of Temperature on the Physical Properties of High-Strength Paper Laminate," by D. Telfair and R. U. Haslanger. Summarized in Forest Products Laboratory Mimeograph no. 1321.

External Corrosion of Furnace-Wall Tubes—I

History and Occurrence¹

By W. T. REID,² R. C. COREY,³ AND B. J. CROSS⁴

Since 1942, many large central-station boiler furnaces burning pulverized coal and removing the ash as molten slag have experienced external corrosion of furnace-wall tubes. In a few cases the loss of metal was so severe as to cause failure of tubes during operation, in others, seriously thinned tubes had to be replaced to prevent unexpected interruption of service. Because the rate of corrosion under certain conditions may be so high as seriously to weaken the tubes between normally scheduled inspections, operators charged with the continuous production of power under wartime emergency conditions have been greatly concerned over prevention of further corrosion. To expedite the solution of the problem, a co-operative investigation was instituted between the Bureau of Mines and the Combustion Engineering Company. This report gives the results of the preliminary study of the occurrence of external corrosion, 16 furnaces in 13 stations being examined. Corrosion was found to occur when the temperature of the tube metal was in the normal range for boiler furnaces, usually not exceeding 700 F, while the maximum temperatures observed were less than 900 F. Deposits in corrosion areas are shown to be of two types, one having the appearance of a bluish-white porcelain enamel, being largely soluble in water in which it produces an acid reaction, and consisting principally of sodium and potassium sulphates in a complex form. The second type is iridescent blue or black, is insoluble in water, may contain significant amounts of carbon, and consists primarily of iron sulphide. Because of the greater incidence of the sulphate deposit, its study was made first and is reported in detail in a following report.⁵

INTRODUCTION

LOSS of metal externally from wall tubes has, in recent years, been one of the major problems facing the operators and manufacturers of pulverized-coal-fired slag-tap furnaces. Although tube failures definitely identified as resulting from this type of corrosion have been rare lately, largely because seriously affected tubes have been located by frequent inspections and

have been replaced before actual failure occurred, earlier losses of tubes may have been caused by external corrosion although attributed at the time to other conditions, such as internal deposits or faulty circulation.

Since early 1942, when it was demonstrated conclusively that external corrosion was resulting in a decrease in the thickness of furnace-wall tubes, the efforts of many investigators were directed toward determining means of preventing further loss of metal and studying the reactions involved. Because of the war, many central stations were operating under exceptionally heavy load demands, and excessive outages for repairs made the problem acute. As a result, in a few furnaces where the rate of corrosion was high, various engineering changes were made which resulted in arresting further active corrosion. However, it was believed that fundamental studies to identify the materials causing corrosion and to understand the mechanism of the action would be required before any real control of external corrosion would be possible. It was realized that such data might not in themselves indicate feasible methods of preventing corrosion but that, by pointing out the factors most important in causing loss of tube metal, the effectiveness of various corrective procedures could be evaluated before their application.

Because it was recognized early that external corrosion was associated with the deposits of slag on wall-tube surfaces (corrosion occurring apparently only under slag deposits), the Bureau of Mines became interested in the problem as part of its continuing study of the properties of coal-ash slags at high temperatures. Previously, the Combustion Engineering Company had been intensively investigating external corrosion in the field, and because it appeared that a mutual study would result in a more effective solution of the problem a co-operative investigation was begun in June, 1942. This report and others⁵ in this series present the results of this co-operative study.

HISTORICAL REVIEW

Although considerable work has been done on the corrosion of air heaters, economizers, and other units at temperatures where condensation of sulphuric acid is possible, few references have been found in the literature to the occurrence of external corrosion at the higher temperatures existing in furnaces. The earliest recorded account is by Stromeyer,⁶ who in 1917 described the decrease in thickness from $7/16$ in. to $3/32$ in. of boiler-shell plates, the corrosion area being covered with a scale consisting principally of ferric oxide and a sulphate, which he described as dehydrated iron sulphate. Although he explained the loss of metal as occurring during idle periods from the action of sulphuric acid, formed by condensation from the flue gases, he also mentions that when the examination was made there was not the least indication of moisture or of apparent corrosion due to dampness. Further, this sulphate scale was found to be present over most of the heating surface of the boiler, suggesting that it may have been deposited during operation when temperatures were too high to permit condensation of sulphuric acid.

The first instance of external corrosion on which direct informa-

¹ Published by permission of the Director, Bureau of Mines, United States Department of the Interior, Washington, D. C., and the Combustion Engineering Company, Inc., New York, N. Y.

² Supervising Engineer, Fuel Section, Bureau of Mines, Pittsburgh, Pa. Mem. A.S.M.E.

³ Research Chemist, Combustion Engineering Company, Inc., New York, N. Y.

⁴ Research Engineer, Combustion Engineering Company, Inc., New York, N. Y. Mem. A.S.M.E.

⁵ Part II of this study appears on page 289 of this issue of the Transactions.

Contributed by the Pittsburgh Experiment Station, U. S. Bureau of Mines, and presented under the auspices of the Research Committee on Furnace Performance Factors in co-operation with the Fuels and Power Divisions at the Annual Meeting, New York, N. Y., Nov. 27-Dec. 1, 1944, of THE AMERICAN SOCIETY OF MECHANICAL ENGINEERS.

NOTE: Statements and opinions advanced in papers are to be understood as individual expressions of their authors and not those of the Society.

⁶ "Memorandum by Chief Engineer for the Year 1917-1918," by C. E. Stromeyer, Manchester Steam Users' Association, 1918, pp. 13-15.

tion is available for this report occurred in September, 1934, in the No. 13 boiler at Springdale Station, when an unusual failure of a wall tube led to close inspection of the furnace. It was found that many of the tubes in the walls adjacent to those in which the opposed burners were located had flattened surfaces and that as much as 0.12 in. of metal had been lost externally in some locations. Although consideration was given to the possibility that the metal had been lost by abrasion, the appearance of the surface was such as to indicate that some form of chemical attack had been taking place. Also, the inspection showed that the flattened surfaces were arranged in an elliptical pattern beginning at about the 5th tube from the corner, gradually increasing to a length of about 7 ft at the 12th tube, and decreasing rapidly to the 19th tube. Since this occurred from each corner on the side walls, only about 5 tubes in the center of each wall were unaffected. Additional tube failures in November, 1934, and March, 1935, led to the replacement of all the corroded tubes.

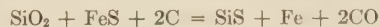
Because the importance of this type of corrosion was not then apparent, it being considered that the loss of metal had been gradual over the 5 years the furnace had been in service, no profound study of the problem was made. A sample of the slag deposit on the tube showed the presence of iron sulphide, and the explanation at that time, without knowledge of the actual tube-metal temperature, was based on the solubility of the tube metal in molten ferrous sulphide. Another inspection of the furnace in April, 1942, showed that the tubes, installed as replacements in 1934, were in good condition and that further corrosion apparently was not occurring. At the same time the original tubes in the burner walls were examined, and a maximum loss of 0.06 in. of metal was noted in one location, again indicating that loss by abrasion through flame impingement was not a primary factor. However, since these tubes had been in continuous service for 13 years, this loss was not considered significant.

As described in a report of the Edison Electric Institute,⁷ external corrosion was observed first in furnaces at the Schuylkill Station of the Philadelphia Electric Company in December, 1939, but the significance of the attack again was not recognized, the loss of metal being attributed to other factors involved in operational difficulties. A similar type of corrosion also was observed in November, 1940, at the 12th Street Station of the Virginia Electric and Power Company. In November, 1941, inspection of the Schuylkill furnaces showed that rapid corrosion had been occurring since an examination made 3 months earlier and the condition then was recognized as being extremely serious. Thereafter, furnaces in other stations were examined as they became available and external corrosion was found to be occurring in many installations. Additional information on the Schuylkill furnaces was reported by Gethen,⁸ who also stressed the importance of controlling the admission of secondary and tertiary air so as to maintain oxidizing conditions over the tube surface. Like the Springdale furnace, corrosion usually was found in definite patterns associated with direction of the flame, and it was observed that a deficiency of air generally occurred in these zones. In a recent survey,⁹ Weisberg and Harlow each described briefly the loss of metal by external corrosion in different types of furnaces.

External corrosion of wall tubes has been observed in this country to a serious extent only in slag-tap furnaces; no references by foreign investigators to similar effects have been found, either because of the few such furnaces installed abroad or be-

cause the condition has not been recognized as yet. However, data on the failure by external corrosion of a radiant-superheater tube in a furnace equipped with a traveling-grate stoker has been made available from England. This superheater, installed in front of a water-cooled wall, the tubes of which were coated with plastic refractory, raised the steam temperature approximately to 625 F. Loss of metal externally from the elements was noted after one tube had failed in service, several other tubes being thinned almost to the bursting point. Analysis of deposits from the corrosion areas showed the presence of appreciable amounts of alkali-metal sulphates and iron oxide. Examination and scaling tests of the tube metal indicated that the metal had not been overheated in service and that the loss of metal resulted from chemical action with the alkali sulphates, although the reactions leading to the loss of metal were not understood.

Investigations by others directed toward determining the composition of deposits adhering to heat-receiving surfaces also have been made and, because of the obvious relation to external corrosion, will be mentioned briefly. External deposits of silicon sulphide have been described by Lessnig,¹⁰ who suggested that the reaction of silica with pyritic sulphur according to the equation



would be particularly objectionable because it would produce a sticky surface to which fly ash or slag could adhere easily. Kleeberg¹¹ mentions a deposit containing greatly increased magnesium oxide and alkalies over that in the coal ash and believes that these constituents are responsible for its objectionable nature. Because this deposit is found as a hard sintered mass he suggests the formation of a hydraulic cement through reaction of moisture with silica, alumina, and lime, although such an explanation neither takes into account the high temperatures in deposits on tube surfaces during operation nor the presence of alkalies and sulphates in moderately large quantities.

Recent work in England has developed interesting results. Although no mention is made of external corrosion, interest being solely in the formation of deposits on furnace and boiler tubes, the similarity in the materials described¹² to those found on corroded wall tubes in this country is striking, usually being white, about 50 per cent water-soluble, and containing a high percentage of alkali-metal sulphate. Because these deposits were found on the tubes of furnaces equipped with chain-grate stokers, attempts were made to control deposition of the material by changes in burning conditions, and it was shown that factors such as thickness of fuel bed, rate of air supply, and tendency to produce blowholes were important.

As the result of tests made in a small laboratory furnace, it was stated that no simple correlation between the production of deposits and the fuel-bed temperature could be obtained as measured by a platinum-rhodium thermocouple. However, it appears that some relationship must exist, for the deposits were produced in the small underfeed furnace after the plane of ignition had reached the grates, which is the beginning of the period of highest fuel-bed temperatures.

Attempts to prevent the formation of deposits by chemically treating the coal were unsuccessful, deposits continuing to form despite the addition of either acidic or alkaline substances. In this study it was also observed that, during the period when de-

⁷ "Furnace Tube Corrosion," Publication K-3, Edison Electric Institute, March, 1943.

⁸ "Tube Corrosion of Furnace Walls," by G. S. Gethen, *Power Plant Engineering*, vol. 47, Oct., 1943, pp. 74-78.

⁹ Symposium on Furnace Performance Factors, THE AMERICAN SOCIETY OF MECHANICAL ENGINEERS, May, 1944.

¹⁰ "Chemical Action in the Fouling and Clinkering of Boiler Plant and Gas Producers," by R. Lessnig, *Feuerungstechnik*, vol. 28, 1940, pp. 145-149.

¹¹ "Salts in Raw Brown Coal Which Are Harmful for Boiler Firing," by W. Kleeberg, *Braunkohle*, vol. 39, 1940, pp. 94-97.

¹² "Deposits on External Heating Surfaces of Water-Tube Boilers," Biennial Report, British Coal Utilities Research Association, 1940-1941, pp. 19-36.

TABLE 1 FURNACES EXAMINED FOR EXTERNAL TUBE CORROSION

Station	Boiler no.	Type	Pressure, psi	Rated capacity, lb per hr	Type of fuel	Combustion rate, Btu per hr per cu ft	Heat release, Btu per hr per sq ft	Severity of corrosion ^a
Buzzard Point	3	Continuous slag-tap	690	425000	Medium-volatile bituminous coal	25600	150500	Very severe
Chester	20	Continuous slag-tap	1350	600000	Medium-volatile bituminous coal	28700	63200	Slight
Firestone	21	Intermittent slag-tap	1285	300000	High-volatile A bituminous coal	28800	138500	Moderate
Kearny	..	Dry-bottom	140	(Mercury boiler)	Medium-volatile bituminous coal	18540	91950	Slight
"L" Street	76	Dry-bottom	1200	375000	Medium-volatile bituminous coal	27600	153000	Negligible
Northeast	14	Continuous slag-tap	1275	300000	High-volatile C bituminous coal	28600	147500	Moderate
Northwest	1-7	Continuous slag-tap	1325	425000	High-volatile C bituminous coal	24800	114500	Very severe
12th Street	17	Intermittent slag-tap	900	450000	Medium-volatile bituminous coal	27100	131000	Severe
Reeves Ave.	21	Intermittent slag-tap	850	450000	Medium-volatile bituminous coal	30200	138000	Slight
Schuylkill	23	Continuous slag-tap	1350	600000	Medium-volatile bituminous coal	29400	170000	Moderate
	24							Moderate
Springdale	13	Intermittent slag-tap	375	300000	High-volatile A bituminous coal	25000 ^b	90000 ^b	Moderate
Waterside	42	Continuous slag-tap	1350	500000	Medium-volatile bituminous coal	30200	168500	Moderate
	61 and 62		1350	615000		28700	169500	Moderate
Windsor	72 and 82	Continuous slag-tap	1350	750000	High-volatile B bituminous coal	24300	144300	Severe

^a Negligible..... <0.025 in.

Slight..... 0.025-0.050

Moderate..... 0.050-0.100

Severe..... 0.100-0.150

Very severe..... >0.150

^b Estimated.

posits were forming, a characteristic spectrum appeared in the secondary flame, and that spectroscopic methods could be used to indicate the presence of conditions resulting in the formation of deposits. This suggests that such methods might be applicable in developing a detector to predict the occurrence of conditions permitting wall tubes to corrode in any given furnace.

In a continuation of this work,¹³ analysis of the water-soluble portion of these deposits confirmed that it was largely a mixture of sulphates. The low melting point of mixtures of several sulphates as determined in the laboratory suggested that the water-soluble fraction of the deposits was responsible for its low sintering temperature and, consequently, its objectionable nature. Because of possible connection between segregation of ash constituents and the formation of tube deposits, further work on this interesting phase is being conducted.

Although at first glance these investigations may not appear to be closely related to the problem of external tube corrosion in pulverized-coal-fired furnaces, the deposits described probably are of the same fundamental origin, and information on their possible control, as by treating the coal chemically, would have tremendous importance. That such control methods were not found to be effective in chain-grate operation suggests the futility of attempting similar fuel modifications in furnaces burning pulverized coal.

SCOPE OF INVESTIGATION

The objectives of this investigation have been (1) to determine the conditions under which external corrosion occurs in actual operating furnaces, (2) to identify the materials causing corrosion and to learn their source, (3) to discover the mechanism by means of which corrosion occurs, (4) to duplicate corrosion in relatively small-scale laboratory tests under controlled conditions, and (5) to develop feasible methods of preventing further loss of metal. This report describes the occurrence of corrosion in the field and illustrates briefly the conditions associated with loss of metal.

FIELD STUDIES

Examination of Furnaces. The early part of this study was concerned with factors related to the occurrence of corrosion; thus inspections were made of 16 furnaces in 13 stations to determine the loss of metal that had occurred and to obtain information on conditions at the surface of the tube, such as metal temperature and gas composition. In most cases, samples of deposits from the corrosion areas also were obtained for laboratory

examination and analysis. These data not only helped to determine the extent of corrosion in individual furnaces and the effectiveness of early corrective measures but also served as a guide for the later laboratory experimentation. For instance, data obtained on the temperature of tube metal under the usual range of operating conditions showed that studies of reactions occurring at temperatures much in excess of 1000 F obviously would not be applicable; thus the field data outlined the range of temperatures over which laboratory experimentation should proceed. Similarly, data on the composition of deposits in contact with the corroding surface and gases adjacent to the slag covering also were necessary to indicate the ranges of these variables associated with corrosion.

The furnaces examined are listed in Table 1. All are fired with pulverized coal; two use dry-bottom ash removal and the remainder slag-tap. Pressures on the units range from 375 to 1350 psi, the majority being at the higher pressure; the corresponding saturated-steam temperatures range from 438 F to 582 F. The Kearny mercury boiler is unusual in that alloy tubes are involved, and the metal temperature is considerably higher than that of steam-generator tubes. As noted later, the type of corrosion existing in this unit is different from the other furnaces examined. The rated capacity of the boilers varies from 300,000 to 750,000 lb of steam per hr; consequently, these units are representative of the size of boiler commonly in use in central-station power plants. For the steam-generating units, the design rates of combustion range from 24,300 to 30,200 Btu per hr per cu ft of furnace volume. The heat release, expressed as Btu per hour per square foot of furnace surface, varied between 114,500 and 170,000 for the tangentially fired units and was 63,200 for the open-pass furnace at Chester Station. The fuel burned varied from high-volatile C bituminous coal to medium-volatile bituminous coal. The lower-rank coals were of particular interest because they contained greater quantities of sulphur, but no relationship could be detected between the sulphur content of the fuel and the occurrence or extent of corrosion.

An approximate indication of the severity of corrosion is given by the maximum observed loss of metal at the time the furnace was inspected. Because the time interval over which this loss occurred was seldom known, the rate of corrosion cannot be deduced except in a very general way, but, based on routine periodic inspections in most cases where severe loss of metal took place, it appears that the period of active corrosion was short and, consequently, that the rate was high.

Cross sections of typically corroded furnace-wall tubes are shown in Fig. 1. Although none of these tubes failed while in service, inspection of the furnace disclosed thinning, and sections

¹³ "Deposits on External Heating Surfaces of Water-Tube Boilers," Annual Report, British Coal Utilities Research Association, 1942, pp. 18-32.

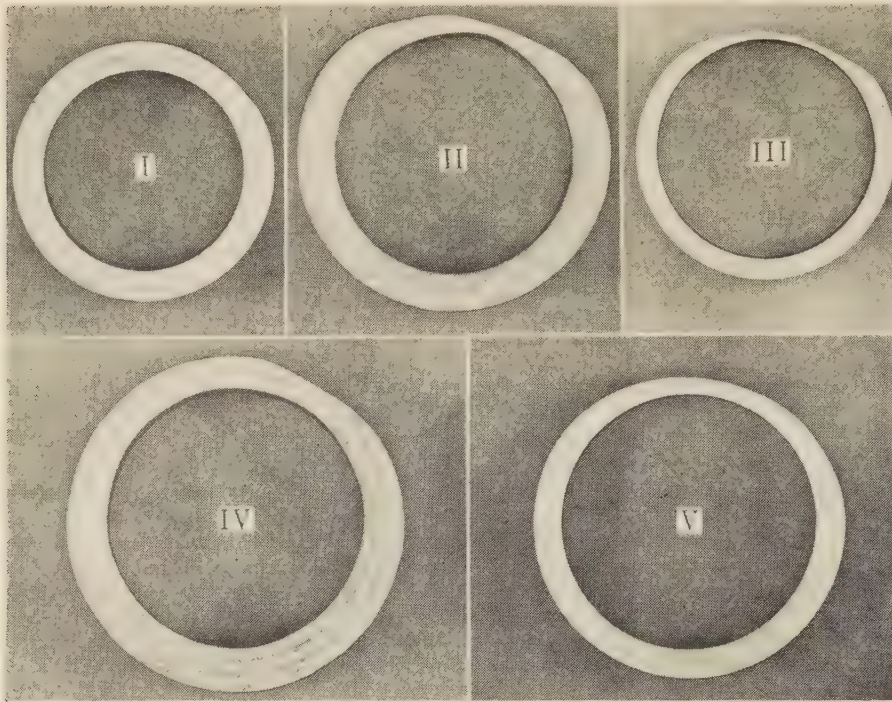


FIG. 1 CROSS SECTIONS OF TYPICALLY CORRODED FURNACE-WALL TUBES

(From: I, Schuylkill, II, Windsor, III, Buzzard Point, IV, Firestone, V, 12th Street Stations.)

of the tubes were removed for examination. It is obvious in some that additional loss of metal would allow failure. No unusual internal conditions that might have resulted in excessive metal temperatures or other interference with normal behavior were revealed in any of the specimens.

Tube-Metal Temperature. Measurement of the surface temperature of wall tubes was obtained by peening thermocouples into the tube along the center line of the normal surface exposed to the furnace; the lead wires were protected by thin cover plates welded to the tube. Being located no deeper than $1/64$ in. below the surface, these thermocouples furnished information on the temperature of the metal at the point where corrosion could occur. A survey of an installation of 17 such thermocouples in one wall of the No. 24 boiler at Schuylkill Station, together with the pattern of the corrosion area, is shown in Fig. 2. Observed temperatures ranged from 590 to 710 F; the maximum temperature at any time was 860 F, 6 hours after lighting off; this temperature gradually decreasing to approximately 700 F.

As shown in the upper part of Fig. 2, the average temperatures at the 4-ft elevation were higher in the area where no corrosion occurred. This suggests that the influence of temperature on external corrosion may not be too important in the range 600 to 1000 F. Inspection of furnaces when cold often discloses slag adhering tightly to the tube metal in corrosion areas, whereas elsewhere normal contraction on cooling may cause the slag to loosen and drop off. Consequently, a lower average temperature in corrosion areas may result from differences in the manner in which the slag layer adheres.

In Fig. 3, the temperature of point A in the corrosion area and point B outside it, which are at approximately the same elevation, are compared over a period of 30 hr, the temperature of A being less than that of B except for a short period before deslagging, probably as the result of a temporary, unusually thin slag deposit at point A. After a 2-hr period of reduced load (at about 50 per cent of rating) to permit deslagging, the temperature of A again was less than that of B, confirming the fact that aver-

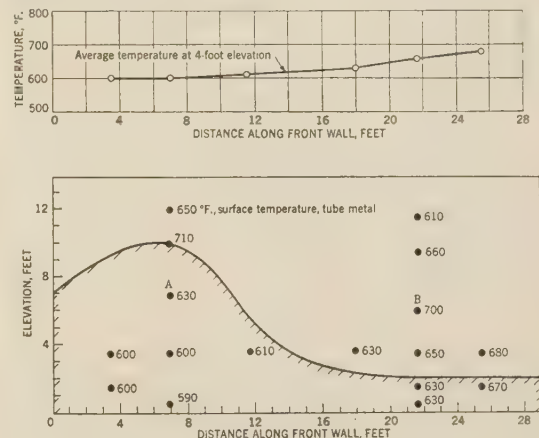


FIG. 2 CORROSION AREA AND TUBE-METAL SURFACE TEMPERATURES IN BOILER NO. 24, SCHUYLKILL STATION

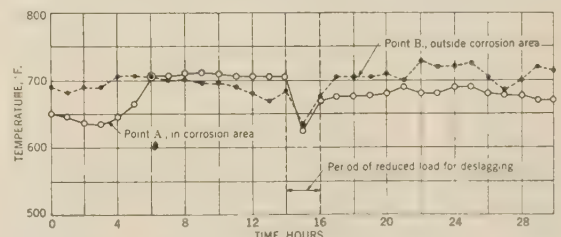


FIG. 3 COMPARISON OF TEMPERATURE OF SURFACE OF TUBE IN CORROSION AREA WITH THAT OF UNAFFECTED TUBE

age temperatures may be lower in tubes that are being corroded than in near-by unaffected tubes.

Metallographic examination of a corroded tube from this same

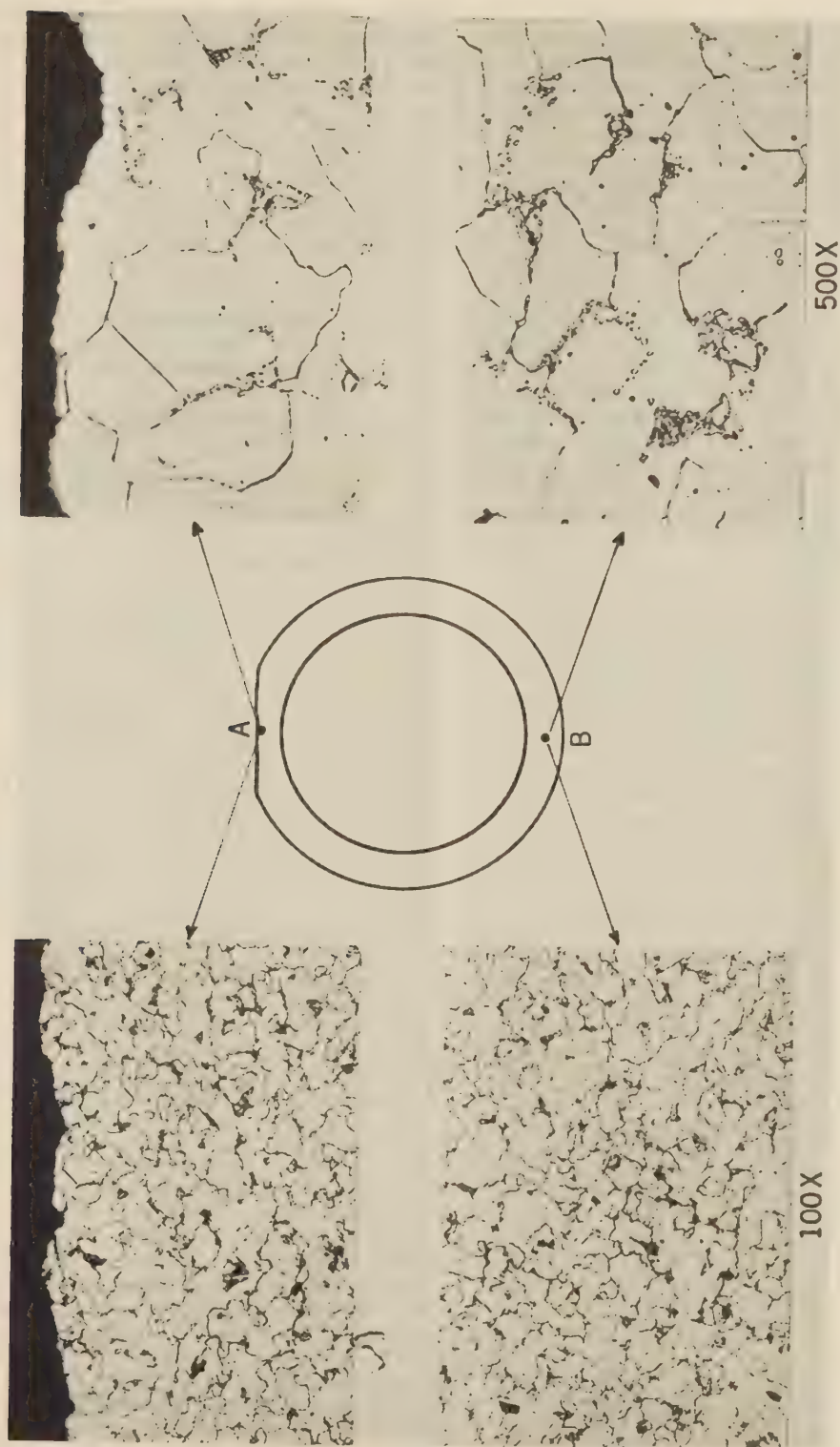


FIG. 4 MICROSTRUCTURE OF FURNACE-WALL TUBES, NITAL ETCH
(A, Adjacent to corroded surface. B, Center of tube on cool side.)

station shows no perceptible differences in microstructure between the metal at the point of corrosion and the metal at the rear face of the tube where the temperature must have been approximately at the saturated-steam temperature, 585 F. Microstructures of this tube at magnifications of 100X and 500X are shown in Fig. 4. It is obvious that no unusual changes have occurred in the metal in the corrosion area, as compared to the remainder of the tube. No decarburization has occurred at either position, and there is no intergranular penetration of oxides; this is typical of most tubes studied metallographically in this investigation. However, at the 12th Street Station, some intergranular penetration has been observed in badly thinned tubes. Also, the extent of spheroidization is the same in both specimens shown in Fig. 4, indicating that it resulted from temperatures involved in fabrication of the tube rather than from excessive temperatures during service, in which case the cool side of the tube would have shown pronouncedly less spheroidization than the hot side. That it did not do so is additional evidence that where corrosion occurred the tube metal had not been overheated. Studies of tubes from other installations show similar results, in no case indicating that the decreased wall thickness resulted from oxidation caused by excessive temperature. It is also interesting to note that no intergranular penetration was observed in the corrosion areas, except at 12th Street, as previously noted, and that there was no evidence of the presence of eutectics of the system iron-sulphur.

As the result of these studies, it was apparent that corrosion could occur at metal temperatures of less than 1000 F, and that active corrosion often was present at temperatures as low as 600 F. As noted previously, these studies aided in establishing the limits of the laboratory investigation so that particular emphasis was placed on reactions occurring between 600 and 1000 F.

Composition of Furnace Gases; (a) Carbon Monoxide. Prompted by the visual observation that flame often was coming in contact with the tubes or their adherent slag, surveys of various furnaces were made early in the study to determine the composition of the products of combustion adjacent to the slag covering in the corrosion area. Such studies showed that carbon monoxide usually was present, occasionally being as high as 6.5 per cent, and that in areas where carbon monoxide was absent no corrosion could be detected. A typical case where carbon monoxide in contact with the slag covering is shown in relation to the corrosion area appears in Fig. 5, for the same boiler but for the opposite wall for which temperatures were reported in Fig. 2. It will be noted that carbon monoxide ranged from 0.9 to 4.9 per cent in the corrosion area. In an adjacent zone where 2 to 3 per cent carbon monoxide was present, some loss of metal may have occurred, but it is obvious that there would be no sharp line of distinction between corroded and unaffected tubes. When carbon monoxide was absent consistently, or present only occasionally in quantities not greater than 0.2 per cent, corrosion was not observed. These findings are substantiated by similar

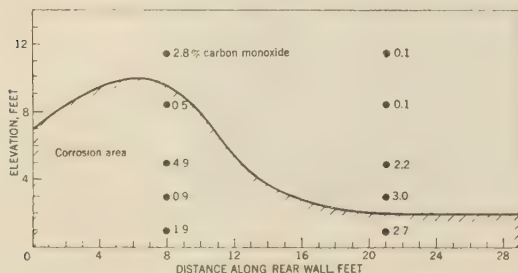


FIG. 5 CARBON MONOXIDE IN FURNACE GASES IN CORROSION AREA, BOILER NO. 24, SCHUYLKILL STATION

studies made on other furnaces at Windsor, Reeves Avenue, Waterside, and Northeast stations. Because no means were available for sampling the gas actually in contact with the metal surface, there is no assurance that these gas analyses were truly representative of the composition of the products of combustion at the point where corrosion was occurring.

(b) *Sulphur Dioxide.* Because the analysis of deposits from corrosion areas showed that compounds of sulphur always were present, the occurrence of this element in furnace gases also was investigated in the No. 24 boiler at Schuylkill Station. Fig. 6 shows the amount of total sulphur expressed as sulphur dioxide

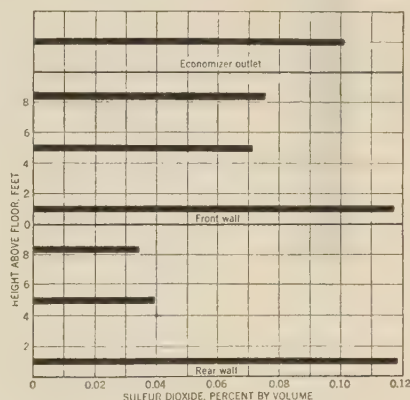


FIG. 6 COMPARISON OF QUANTITY OF SULPHUR DIOXIDE IN FURNACE GASES AT DIFFERENT POSITIONS IN FURNACE, BOILER NO. 24, SCHUYLKILL STATION

present at various locations in the furnace. At both front and rear walls, the SO_2 was highest near the floor of the furnace. At higher elevations, the SO_2 concentration at the front wall was approximately twice that of the rear wall, but the extent and severity of corrosion of both walls were about the same. Because of its low concentration, not exceeding 0.118 per cent by volume at any point, the effect of SO_2 in causing increased loss of metal by direct oxidation is negligible, as will be shown in the report following.⁵

The method of analysis used, which consisted of absorbing the sample of gas in a dilute sodium-hydroxide solution containing benzyl alcohol and determining the sulphur forms by a double titration, indicated that sulphur trioxide was present only at the economizer outlet. However, these data are useful in showing the maximum amount of SO_3 from the furnace gases that could be present in contact with the surface of the tube had all the SO_2 been oxidized as the result of lower temperatures and the presence of an active catalyst. As will be shown in the next report,⁵ the presence of SO_3 is necessary to permit one type of corrosion to occur, and the maximum quantity that can exist, as just described, is of considerable importance.

Rate of Heat Transfer. An additional factor is the rate of heat transfer, which has been considered important because it may affect the temperature of both the tube metal and the adhering deposit. Kreisinger and Patterson¹⁴ measured this property in a furnace in which active corrosion was occurring, one of their test units being mounted directly in a corrosion area in the No. 18 boiler at the 12th Street Station in Richmond. A comparison between the heat absorbed in this position as compared to other zones in the furnace where no corrosion occurred is given in

¹⁴ "Heat Transfer to Water-Cooled Furnace Walls," by H. Kreisinger and R. C. Patterson, Furnace Performance Factors Symposium, THE AMERICAN SOCIETY OF MECHANICAL ENGINEERS, May, 1944, pp. 71-78.

Fig. 7, which is based on their data. Although the rate of heat absorption is higher in the corrosion area than at other elevations of the same furnace wall, the difference is not striking, the rate being approximately 30 per cent greater than in the next higher position, where no corrosion has been observed.

The importance of the rate of heat transfer would depend largely upon its effect on the temperature of the tube metal and on the temperature gradient through any deposits adhering to the tube. As already shown, the tube-metal temperatures in service, as measured with thermocouples, seldom exceed 700 F, nor are any data available indicating that temperatures greater than 900 F have occurred, even for short periods. For the tubes at the 12th Street Station, the maximum measured heat-absorption rate of 108,000 Btu per sq ft per hr would result in a temperature gradient of only 86 F through the tube wall. Assuming no gradient through the steam film inside the tube, this would result in a tube-metal temperature of only 615 F. Even had the heat rate been increased to twice that observed, the tube-metal temperature could still have been but 701 F. Impaired circulation might have resulted in higher temperatures, but it is apparent that normal variations in the rate of heat transfer will have only a moderate effect on tube-metal temperature and that under no conceivable operating conditions in which circulation was adequate would the metal temperature exceed 1000 F.

With respect to oxide films on the tube, the closely adherent thin layers caused by normal oxidation at temperatures in the range of 600 to 1000 F would not show large temperature gradients, but this item will be considered in greater detail in the next report⁶ in discussing the effect of slag.

COMPOSITION OF DEPOSITS

During the earlier part of the investigation, samples of the

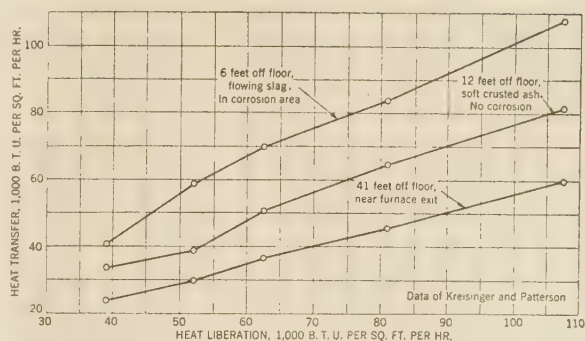


FIG. 7 RATE OF HEAT TRANSFER IN CORROSION AREA AS COMPARED TO OTHER LOCATIONS IN A SLAG-TAP FURNACE

deposits on furnace wall tubes in corrosion areas were taken from most of the furnaces examined. Later when it became apparent that only two distinctive types of materials were being obtained, samples were taken only when it appeared that an unusual condition existed or when the loss of metal was unusually great.

All available analyses have been tabulated and are listed in Table 2. It is evident that the number of samples analyzed for a given furnace is not a direct indication of the severity of corrosion being experienced in that unit, largely because of the difficulty of obtaining representative specimens from some installations, or because it was felt desirable to direct attention largely to typical samples rather than to all those obtained during an inspection. Thus considerable time was spent on the samples from the 12th Street Station because they were easily obtained in large quantities, whereas at Schuylkill difficulty in obtaining satis-

TABLE 2 ANALYSIS OF DEPOSITS IN CORROSION AREAS

1	2	3	4	5	6	7	8	9	10	11	12	13	14	15	16	17	18	19	20	21	22
Station	Boiler No.	Extent of corrosion in sample area, inches.	Sample No.	Total moisture	Total iron computed as								Solubility in H ₂ O, percent.							pH	
					SiO ₂	Al ₂ O ₃	Fe ₂ O ₃	FeO	Fe	Fe ₂ O ₃	CaO	MgO	SO ₃	S	Na ₂ O	K ₂ O	Cu	Cr ₂ O ₃	Carbon		
Chester	20	(f) 0.02	C-64 C-63	0.3 0.6	5.3 2.5	4.1 3.7	- -	- -	- 57.2	4.9 -	0.6 0.2	0.1 0.0	49.2 0.1	0.0 32.3	35.5(b) 3.4(b)	- -	- -	- -	- 0.97	- -	3.3 5.0
Firestone	21	0.08 (d)	C-70 F-3	- -	7.2 3.2	4.2 3.6	- -	- -	15.9 57.8	- -	0.2 -	0.0 -	47.5 19.3	0.0 -	22.7(e) -	- 0.2	0.5 -	- -	- -	87.7 2.3	4.0 -
Kearny	-	(f) (f) (f)	C-60 C-61 C-62	- - -	8.0 4.7 7.4	4.9 3.1 5.5	58.4 73.9 60.7	25.4 11.0 18.6	- 86.1 81.4	86.6 0.2 0.1	0.4 0.2 0.1	1.3 3.7 4.3	0.0 0.0 0.0	- -	- -	- -	- -	3.0 5.2 5.7	- -	- -	- -
"L" Street	76	0.02 (f)	C-21 C-22	- -	2.1 3.5	2.7 14.4	- -	- -	55.3 26.6	- -	1.5 1.4	0.3 0.7	3.4 31.9	23.7 0.0	- 21.5(b)	- -	- -	- -	0.5 -	3.9 53.8	6.0 4.6
Reeves Ave.	21	0.02 0.01	C-16 C-17	- -	4.2 10.1	5.5 6.6	- -	- -	20.3 14.9	2.8 4.6	0.6 1.1	40.5 36.9	0.0 0.0	26.1(b) 25.8(b)	- -	- -	- -	- -	- -	70.0 64.0	4.0 4.0
Schuylkill	24	(d)	C-36	-	1.2	2.9	-	-	78.1	-	-	-	11.1	0.0	-	-	-	-	-	16.4	6.1
"12th" Street	17	0.06 0.02 (d) (e)	C-3 C-4 C-9 C-9A	0.3 1.1 0.2 0.9	2.6 4.0 8.3 9.5	5.3 2.0 6.2 0.2	- - - -	- - - -	1.5 5.1 16.6 0.5	1.8 2.0 2.7 1.9	0.0 0.0 0.2 0.3	54.4 54.0 36.5 52.4	0.0 0.0 0.0 0.0	14.7 13.1 28.7(b) 42.0(b)	20.0 17.8 0.15	- -	- 0.6 0.5	- -	- -	96.0 97.4 50.8 (100)	3.5 1.0 3.6 3.5
	18	0.03 0.09 0.10 (d)	C-5 C-6 C-7 C-8	- - - -	6.1 7.9 6.2 7.3	(a) (a) (a) 0.4	- - - -	- - - -	43.0 14.0 8.0 27.7	1.5 3.7 3.3 5.1	0.0 0.0 0.0 0.8	26.3 44.5 48.2 33.7	0.0 0.0 0.0 0.0	10.8 15.1 19.2 25.0(b)	12.8 14.0 16.0	0.15 0.15 0.16	- -	- -	- -	49.7 71.6 89.0 62.2	4.8 3.2 3.2 4.9
Waterside	61	0.02 0.06 0.01	C-24 C-27 C-28	- - -	8.6 6.3 4.8	3.7 11.3 4.7	- - -	- -	38.3 42.1 47.6	- -	1.6 1.4 2.9	0.3 0.5 0.4	29.7 14.2 2.5	16.5 16.5 21.2	- -	17.8(b)	- -	- -	- -	44.1 3.7 2.4	3.7 6.0 6.1
	62	0.01 0.10	C-29 C-30	- -	10.2 8.2	8.2	- -	- -	65.7 22.4	1.3 -	0.6 -	9.9 -	0.0 12.8	3.5(b)	- -	- -	- -	- -	- -	13.6 8.8	4.9 4.3
Windsor	72	0.10	C-46	-	-	-	-	-	52.0	-	-	-	-	20.2	-	-	-	-	3.1	0.7	6.1
	82	0.03	C-48	-	-	-	-	-	37.5	-	-	-	-	21.5	-	-	-	-	4.0	1.8	6.1

(a) Included with Fe₂O₃.

(b) Total alkalis, by difference.
(c) Total alkalis, computed as Na₂O.

(d) From 4 walls of furnace, in corrosion track.

(e) Water-soluble portion of sample C-9.

(f) Less than 0.010 inch loss.

factory samples discouraged quantitative analysis, most of the tests therefore being qualitative in nature. Moreover, for some stations no analyses are reported, either because no samples were obtained, or because upon examination they appeared to be of slight value in the study.

Although the extent of corrosion observed in the area sampled is given in column 3, such data are only approximate and may vary widely from point to point. Furthermore, no completely satisfactory method has been devised as yet for measuring the loss of metal from tubes without removing sections of them from the furnace, which obviously is not practical in most instances. In all the cases reported, the surface of the tube in place was cleaned as well as possible by chipping and scraping, feeler gages then being used in conjunction with a "C" gage having the same diameter as the original tube. Because of the difficulty of cleaning the tube surface completely, these measurements were not always consistent, but the loss of metal reported is considered reasonably accurate.

The analyses of the deposits (columns 5 to 20) were made by standard methods but not always for the same constituents because of obvious differences in the deposits. In addition, the method of expressing data was adapted to individual conditions. Thus column 10 was used to express the quantity of iron in the sample in terms of equivalent metallic iron when that seemed justified, whereas in column 11, the equivalent iron was expressed as Fe_2O_3 for other samples. In the case of forms of sulphur, no such recalculation was made, the reported values in columns 14 and 15 representing the actual quantity of sulphate or sulphide sulphur, respectively, in the sample. Alkalies, shown in columns 16 and 17, were determined directly only on a few samples, largely because of the difficulty of the analysis, but also because in most cases where the analysis otherwise was complete the alkalies could be determined by difference with sufficient accuracy. Early in the investigation, the pale greenish-blue color of one type of deposit was attributed to the presence of copper, and column 18 shows the copper content of several samples. Later it was evident that no significance need be attached to the small quantity present, and no further analyses for copper were made. Because of the black appearance of some specimens and other evidence that they came from strongly reducing areas, analyses were made for carbon on a few selected samples and are shown in column 20. It is apparent that, in some deposits, the presence of carbon may be significantly large. To distinguish between different types of deposits, their solubility in water is a useful guide, column 21 showing the solubility of most of the samples taken. A further important property is the acidity of the deposits in aqueous solution, not because corrosion occurs as the result of damp surfaces during periods when the boiler is cold, but because it is an indication of the presence of materials radically affecting the corrosive properties of the deposit at operating temperatures. This acidity is shown in column 22, which expresses the pH of a solution containing 1 g of the deposit in 100 ml of distilled water, or nominally a 1 per cent solution.

CHARACTERISTICS OF DEPOSITS

With the exception of the Kearny mercury boiler, the deposits found in corrosion areas are of two distinct types, differing widely in characteristics and existing under different conditions. These two may be described briefly as the sulphate type and the sulphide type.

Sulphate Deposit. This type of deposit occurs most often in areas where external corrosion has been observed and usually is found beneath a layer of slag. Because generally it has a glossy surface and closely resembles a fired-porcelain coating, it has often been referred to as "enamel." Its color varies from an "off" white through greenish blue to pale blue and usually has more of a

bluish tint than green. The thickness of such deposits varies widely, ranging from only a few thousandths of an inch in some cases to as much as $1/16$ in. in others. Usually adhering strongly to the tube, thin layers may be moderately difficult to remove unless underlaid by a weak layer of iron oxide, in which case fracture can occur in the oxide itself. Thicker layers usually can be removed easily by chipping. For example, about 2 lb of a typical thick deposit was removed from the walls of the No. 17 furnace at the 12th Street Station to make up sample C-9.

Reference to Table 2 indicates the wide occurrence of this type of deposit. Of the 11 furnaces for which samples were analyzed, 4 showed the presence of sulphate deposits exclusively, and 5 more showed it to be present in significant amounts on the wall tubes, although sulphide deposits also were found in other areas. Thus sulphate deposits were present in more than 75 per cent of the furnaces examined.

Of these deposits, those found in furnaces of the 12th Street Station were considered typical, and most attention was given to their study. Sample C-4, for instance, can be considered representative of this type. The relatively small amounts of SiO_2 , Al_2O_3 , and CaO undoubtedly result from particles of fly ash or slag that have become entrapped in the deposit, while the iron content, computed as equivalent to 5.1 per cent Fe_2O_3 , probably comes both from slag and from the corrosion of the tube. The presence of large amounts of SO_3 and of Na_2O and K_2O indicates that the deposit must consist of some form of Na_2SO_4 and K_2SO_4 , although the alkalies present account for only 32 per cent SO_3 , whereas the analysis indicated that 54 per cent was present. As might be expected, the sample is highly soluble in water. Further, the water solution is highly acid, the pH of a 1 per cent solution being only 3.0.

Other samples of sulphate deposits are similar in nature, although considerable variance in composition may occur. Thus in obtaining some samples, flakes of iron oxide adhered strongly to the deposit with the result that the iron content of the sample might have been high, and the amount soluble in water consequently was decreased. In such cases the iron oxide was considered an end product of the corrosion reaction, and the composition of the effective material causing corrosion, that is, the water-soluble sulphate deposit, was little changed. For example, although sample C-9 contained 16.6 per cent equivalent Fe_2O_3 and only 36.5 per cent SO_3 , the water-soluble portion (sample C-9A) was nearly identical with samples C-3 and C-4 from the same furnace. Basically, all samples of the sulphate deposits have been found to be alike, characterized by a large amount of SO_3 , moderate amounts of Na_2O and K_2O , pronounced solubility in water, and an acid reaction in water. Because no known reactions could explain the effectiveness of this material in causing loss of metal under the limitations of temperature already described, its study was considered the first objective of the experimental work to be performed in the laboratory, the results of which are given in detail in the report following.⁶

Sulphide Deposits. The other type of deposit commonly found in corrosion areas is characterized by the presence of sulphide sulphur, usually present as ferrous sulphide. Although occurring less commonly than the sulphate deposit, nevertheless, under the proper conditions, it is accompanied by a serious loss of tube metal. Typically it consists of an insoluble, iridescent, bluish-black material, occasionally having a brilliant dark-blue sheen, best described as "peacock blue." Distinguished easily by its appearance and color, its presence can be checked by its reaction with acids to liberate hydrogen sulphide. It occurs in layers of varying thickness, in some cases being so thin as to be indistinguishable from a heat scale and in others as much as $1/8$ in. thick.

Of the furnaces examined, only the two at Windsor showed the

presence of sulphide deposits exclusively, no sulphate deposits being found. In addition, 5 other furnaces showed the sulphide type to be present, sulphate deposits also being found in other areas. In two cases, at "L" Street and at Waterside Stations, both sulphide and sulphate characteristics existed in the same deposit, but the quantity of sulphate present was small and could be detected only by chemical analysis.

Although corrosion accompanied by sulphide deposits resulted in severe loss of metal at Windsor Station, its investigation has been delayed until the completion of the study of sulphate corrosion.

Oxide Deposits. An additional source of loss of metal may be oxidation resulting from operation of tubes at high temperatures. As already demonstrated, such conditions do not occur normally with furnace-wall tubes in steam generators. However, where a metal or alloy is subjected to higher temperatures or to other conditions than those for which it was designed, oxidation may be a significant item. Because such a condition was believed to be present in the mercury boiler at Kearny, it was examined to determine if actions were taking place similar to those found in other units.

The tubes used in the mercury boiler are of Sieromo 5MS alloy containing 1.5 per cent silicon, 5 per cent chromium, and 0.5 per cent molybdenum and operate at a working temperature of about 1250 F. During the first 2 years of operation, during which the boiler was fired with oil about one half of the time and the remainder with coal, the observed loss of metal was about 20 times that predicted from laboratory oxidation tests, the loss being greater on the fire side of the tube than on the cool side. Because the inorganic residue in oil has been considered definitely corrosive under certain conditions, this loss of metal may be attributed to it rather than to actions resulting from the burning of coal; thus these data are not conclusive.

Examination of the surface of a new tube installed since oil was last burned shows a slightly roughened surface, with so little loss of metal as to make exceedingly difficult any accurate measurement without removing a section of tube. However, a layer of oxide thick enough to indicate active corrosion was found; its analysis is given as C-60 in Table 2. A deposit from the adjoining tube, which has been in service since the furnace was first installed was also analyzed and is reported as sample Q-61, while a deposit from a tube on the opposite side of the furnace where carbon monoxide was present in low concentrations was analyzed as sample C-62. There is no essential difference in any of these deposits, their analysis showing them to be that expected from the oxidation of this steel. The absence of alkalis in significant amounts indicates that corrosion of the sulphate type is not occurring, and the fact that no sulphide sulphur could be detected shows that loss of metal in this manner is negligible. Thus it appears that, if excessive loss of metal still is occurring in this unit, the action of corrosion is by accelerated oxidation and no explanation of such metal loss is yet available.

EFFECT OF SLAG

Composition of Slag. As already noted, corrosion usually occurs beneath a layer of slag, but in areas where the ash exists on the tubes in a light fluffy form loss of metal normally does not occur. This agrees with the observed facts that corrosion may be serious in slag-tap furnaces but, if it occurs, is insignificant in dry-bottom furnaces. From these observations it might appear that the slag was itself the corroding medium, but consideration of the physical properties of slag indicates that this is extremely unlikely, principally because the lowest temperature at which slag exists in the liquid state is very much higher than that known to exist at the surface of the tube. This has already

been discussed elsewhere,¹⁵ the conclusions being that the temperature of the slag at the boundary between tube and slag deposit will be many hundred degrees cooler than the temperature of critical viscosity, with the result that the slag will be completely in the solid state and without ability to react with the materials with which it is in contact.

Analyses of samples of slag taken from the walls of furnaces in corrosion areas show no essential difference from the slag in other locations. Table 3 gives the composition of slags from the No. 18 furnace at 12th Street Station.

TABLE 3 COMPOSITION OF SLAG

Sample	A	B
SiO ₂	29.3	40.7
Al ₂ O ₃	24.0	24.7
Fe ₂ O ₃	17.6	21.2
FeO.....	21.5	4.7
Fe.....	0.0	0.0
CuO.....	4.1	4.5
MgO.....	1.4	1.2
SO ₂	0.2	0.2
Alk. by diff.....	1.9	2.8
Ferric percentage.....	42	80
Viscosity at 2600 F, poises.....	2.4	17
Predicted temperature of critical viscosity, deg F.....	2550	2500

Description:

Sample A: From tubes in corrosion area, mildly reducing conditions; slag 1/8 in. thick, dense, highly vitrified. Solid phase present on cold face.

Sample B: From tubes outside corrosion area, definitely oxidizing conditions; slag 1 in. thick, vitrified on hot face, solid phase present near center, unsintered where in contact with tube.

The differences in composition are attributed to segregation of ash in the furnace and to variations in the surrounding atmosphere. The decreased thickness of sample A results from a higher rate of heat transfer in that area and a low viscosity. Both samples have about the same temperature of critical viscosity, indicating that both will be solids at about the same temperature, and reactions between each slag and other solids at temperatures below about 2200 F are considered extremely unlikely.

Reactions between metallic iron and slag, even at high temperatures when both are in the liquid state, depend almost entirely upon the state of reduction of the slag. Thus metallic iron can exist in equilibrium with slag at temperatures where the slag is fluid only by imposing strongly reducing conditions so that the ferric percentage of the slag is very low. When the molten slag is allowed to oxidize somewhat, for example, by limited exposure to air, the metallic iron disappears as such and is converted to an oxide which reacts with the slag to increase its flux content. However, this reaction is known to occur only at temperatures exceeding about 1800 F and is not rapid below 2200 F for slags of usual composition; thus in the case of external corrosion such actions are quite improbable. Further, in the case of sample A, had the increased content of iron oxide been attributed to metal removed from the tube rather than to segregation of ash in the furnace, the high rate of flow of this very fluid slag would have been capable of causing failure of the tube in an extremely short period, certainly not more than a few days. But because a solid layer of slag must exist at the tube surface where the temperatures are low, such reactions do not occur and the role of slag in causing loss of tube metal must be explained by some other mechanism.

Dry-Bottom Furnaces. Although slag-tap furnaces have been the only ones in which severe corrosion of wall tubes has been observed, it has been suspected that loss of metal has occurred under dissimilar conditions in other fuel-burning applications. The failure of superheater elements already discussed may be

¹⁵ "Factors Affecting the Thickness of Coal-Ash Slag on Furnace-Wall Tubes," by W. T. Reid and P. Cohen, Trans. A.S.M.E., vol. 66, 1944, pp. 685-690.

such a case, but without further data on slag accumulations, metal temperatures, and composition of the gases, this cannot be evaluated properly. Also, failure of metal components of gas producers has been suggested as an instance of the same type of corrosion, but attempts to obtain definite information on such failures have not been successful.

Because no positive loss of metal in pulverized-coal-fired dry-bottom furnaces had been reported by any operators, it was believed that this type of equipment was immune to external corrosion. Consequently, when it was heard that corrosion was suspected in such equipment at the L Street Station, an inspection was made. This showed that conditions on the side walls in close proximity to the turbulent horizontal burners were not radically unlike those occurring in slag-tap furnaces, despite the fact that no flowing layer of slag was present. Perceptible roughening of the tube surface existed in a region on both side walls ranging over about 18 tubes near the burner wall, and over a maximum vertical distance of about 4 ft. In this area, the maximum observed loss of metal was 0.025 in., and averaged about 0.010 in., but it is significant that most of this loss occurred on the tube quadrant facing the burner. Sample C-21 of Table 2 shows the deposit in this area to be of the sulphide type, and it was bluish black and of a hard brittle nature. Particular attention should be paid to the fact that this deposit contained 0.5 per cent carbon, indicating the presence of highly reducing conditions. In the quadrant away from the burner, the adherent deposit was gray to greenish white in color and was of the sulphate type as shown by analysis C-22.

Thus although dry-bottom furnaces are considered relatively free from external corrosion, some slight and normally unobserved loss of metal may occur under conditions where flame can impinge directly on the tubes. This loss may be insignificantly small but suggests the possibility of serious corrosion under unusually unfavorable conditions.

CONTROL OF CORROSION

Although it is not within the scope of this report to include detailed results of corrective measures applied in the field to prevent further serious loss of metal, a brief discussion is warranted. Such measures were based on preventing reducing conditions at the surface of the wall tubes, as evidenced by the presence of carbon monoxide in the furnace gases, and by the observation that no corrosion was being experienced in zones where a plentiful supply of air was available. For this purpose, burner changes were made so as to blanket the wall with a stream of air, and in some cases, "air belts" were installed which admitted air between the tubes in the corrosion area. When the atmosphere was controlled satisfactorily, active corrosion was arrested, but difficulties in maintaining these conditions have not all been solved satisfactorily as yet.

The relationship between the presence of carbon monoxide and active corrosion is not obvious except in the case of the sulphide deposits where strongly reducing conditions are known to be necessary. With the sulphate deposits, it appears more likely that carbon monoxide is only an indication of other unfavorable conditions, such as the presence of the flame envelope in contact with the furnace walls, and that the addition of air serves simply as a diluent to decrease the concentration near the tubes of other constituents which may be responsible for corrosion. Thus the added air may serve only to ventilate the surface of the tubes, and, in the case of sulphate deposits, the fact that carbon monoxide is

also removed in the process may be of no importance. This will be discussed at some length in the next report.⁶

CONCLUSIONS

External corrosion of wall tubes in pulverized-coal-fired slag-tap furnaces has been observed in a large number of installations, severe enough in some instances to result in failure of tubes, and in many others in tube replacement for security reasons. Although this type of corrosion has been recognized only since early 1942, evidence exists that earlier troubles associated with tube maintenance may have resulted from the same actions.

Field studies included the inspection of 16 furnaces, most of which showed appreciable loss of metal from wall tubes. In addition, studies of tube-metal temperatures, gas composition, and rate of heat transfer were made in some instances to determine the conditions accompanying corrosion. It was shown that (1) tube-metal temperatures did not exceed 900 F in any area at any time, and usually were less than 800 F; (2) tube-metal temperatures may be lower in corrosion areas than in adjacent locations where corrosion does not occur; (3) active corrosion usually occurs in zones where the furnace gas over the slag covering contains appreciable amounts of carbon monoxide; (4) the amount of sulphur dioxide in the furnace gas where corrosion is occurring is not excessive; and (5) the rate of heat transfer in corrosion areas is not significantly greater than in other parts of the furnace.

Deposits existing in corrosion areas are shown by chemical analysis to be of two types. The most common consists principally of sodium and potassium sulphate, is usually greenish blue, and strongly resembles a porcelain enamel in appearance, has a strongly acid reaction, and is highly soluble in water. The second contains large amounts of ferrous sulphide, is usually bluish black but occasionally is a brilliant "peacock blue," is insoluble in water, and may contain up to 5 per cent carbon. Usually these deposits exist separately, but instances where they are found together are noted.

Data on the physical properties of coal-ash slags show that they are solids at temperatures lower than about 1800 F. Thus it is believed that slag does not react directly with the tube metal or its oxide coating, despite the fact that corrosion usually occurs beneath a layer of slag.

ACKNOWLEDGMENTS

This investigation has been conducted under the authorization, for the U. S. Bureau of Mines, of A. C. Fieldner, Chief, Fuels and Explosives Branch; and for the Combustion Engineering Company, of Henry Kreisinger, Engineer in Charge, Development and Research Department. Grateful thanks are due many members of the staffs of both organizations for their suggestions and help, particularly to W. C. Schroeder and W. J. Vogel. The assistance of executives and operating personnel of the many power plants from which data and samples were obtained also is gratefully acknowledged; without their generous help and support the earlier field investigations would have been impossible. Many of the chemical analyses were made in the Miscellaneous Analyses Section of the Bureau under the direction of W. A. Selvig, and the metallographic examinations were made by Richard Akin of the Superheater Company. Finally, the Special Research Committee on Furnace Performance Factors of The American Society of Mechanical Engineers, under whose sponsorship this paper is being presented, aided the investigation by their encouragement and suggestions.

External Corrosion of Furnace-Wall Tubes—II Significance of Sulphate Deposits and Sulphur Trioxide in Corrosion Mechanism¹

By R. C. COREY,² B. J. CROSS,³ AND W. T. REID⁴

The external corrosion of furnace-wall tubes of slag-tap furnaces became a problem to operators and manufacturers in 1942. Since that time, in order to determine the mechanism of corrosion so that rational protective measures could be developed, an extensive laboratory study has been in progress on the sulphate, or "enamel," deposits found on the tubes in areas where external corrosion occurs. These deposits are greenish-white to reddish-brown in color and are soluble in water, in which they produce an acid reaction. X-ray diffraction studies show them to consist primarily of a solid solution of sodium and potassium sulphates and alkali-metal ferric trisulphates, such as $K_3Fe(SO_4)_3$. Experiments under controlled laboratory conditions with actual and synthetic "enamels" have shown that, at temperatures of 1000 F, sodium and potassium sulphates will react readily with iron oxide in an atmosphere containing a low concentration of sulphur trioxide to form the same alkali-metal ferric trisulphates that occur in "enamels." However, under the same conditions of temperature and concentration of SO_3 neither iron oxide nor the alkali-metal sulphates alone will react with SO_3 . These reactions suggest the mechanism of corrosion to involve the removal of the normally protective oxide on the furnace tubes by (a) the condensation on the relatively cool tubes of alkali-metal oxides which are converted to the corresponding sulphates by the SO_3 in the furnace, and (b) the subsequent reaction of the iron oxide on the tubes and the alkali-metal sulphates with the SO_3 evolved as the result of the slagging reactions in the coal ash deposited mechanically on the "enamel." Thus conditions are afforded for the removal of the iron oxide on the tube with the formation of alkali-metal ferric trisulphates. Deslagging causes thermal decomposition of these compounds, and the cycle is repeated. It is suggested that prevention of corrosion by this process can be achieved by ventilating the surface of the tubes with air so as to decrease the concentration of SO_3 below that necessary for the formation of the complex iron sulphates. Also,

because the alkali metals required for the reaction are believed to originate principally from the flame, the addition of such air decreases the rate of deposition of alkalis. These findings are in agreement with field observations in which the maintenance of oxidizing conditions prevented further corrosion.

INTRODUCTION

ANALYTICAL data already have been presented⁵ showing that two characteristic types of deposits on furnace-wall tubes are associated with external corrosion. The most prevalent type is a greenish-white to reddish-brown glazed material that is appreciably soluble in water in which it produces an acid reaction, and which contains a relatively large percentage of sodium and potassium sulphate. In other cases the deposit is dark-blue or black, magnetic, insoluble in water, and rich in ferrous sulphide. The present paper is concerned with corrosion occurring in the presence of the sulphate type of deposit; and because this deposit resembles in appearance a ceramic enamel it will be convenient hereafter to designate it as "enamel" to distinguish it from the iron-sulphide deposit.

It is well known that considerable information may be obtained about the mechanism of corrosion of metals at high temperatures if a critical examination is made of the products of corrosion, or of any deposits which occur at the site of corrosion.^{6, 7, 8, 9} With this as a premise in the present investigation, considerable significance was attached to the exact chemical nature, and behavior under controlled conditions, of actual and synthetic enamel deposits. The results of these studies suggested that unusual chemical reactions at temperatures between 600 to 1000 F were involved in the mechanism of corrosion. Inasmuch as the technical literature afforded no clue to the type of reactions believed to be pertinent to the problem, it was necessary to supplement the work with considerable fundamental experimental study.

The foregoing factors form the basis of the laboratory studies and follow partly the four primary objectives of the investigation, which were as follows:

- 1 To determine the factors involved in corrosion associated with enamel deposits.
- 2 To determine the mechanism of corrosion.
- 3 To reproduce this type of corrosion under controlled laboratory conditions.

⁵ Part I of this study appears on page 279 of this issue of the Transactions.

⁶ "Resistance to Furnace Atmospheres of Heat-Resisting Steels," by A. Quarrel, *Journal of the Iron and Steel Institute*, Special Report No. 24, 1941.

⁷ "The Corrosion of Alloy Steels by High-Temperature Steam," by G. A. Hawkins, J. T. Agnew, and H. L. Solberg, *Trans. A.S.M.E.*, vol. 66, 1944, pp. 291-295.

⁸ "The Constitution of Scale," by L. B. Pfeil, *Journal of the Iron and Steel Institute*, vol. 123, 1931, pp. 237-258.

⁹ "Corrosion by Hot Gases," by R. C. Corey, *Combustion*, vol. 15, Nov., 1943, pp. 34-39.

¹ Published by permission of the Director, Bureau of Mines United States Department of the Interior, Washington, D. C., and the Combustion Engineering Company, Inc., New York, N. Y.

² Research Chemist, Combustion Engineering Company, Inc., New York, N. Y.

³ Research Engineer, Combustion Engineering Company, Inc., New York, N. Y. Mem. A.S.M.E.

⁴ Supervising Engineer, Fuel Section, Bureau of Mines, Pittsburgh, Pa. Mem. A.S.M.E.

Contributed by the Pittsburgh Experiment Station, U. S. Bureau of Mines and presented under the auspices of the Research Committee on Furnace Performance Factors in co-operation with the Fuels and Power Divisions at the Annual Meeting, New York, N. Y., Nov. 27-Dec. 1, 1944, of THE AMERICAN SOCIETY OF MECHANICAL ENGINEERS.

NOTE: Statements and opinions advanced in papers are to be understood as individual expressions of their authors and not those of the Society.

4 To devise means for retarding the rate of corrosion to a negligible rate, or arresting it completely, in operating furnaces.

This paper is intended to present the results of laboratory work performed to date on the enamel deposits as related to these objectives. Inasmuch as no work of a similar nature has been reported elsewhere, numerous approaches to the problem were necessary before the present theory was developed. Considering the plausibility of certain of these ideas, they will be mentioned briefly and reasons for rejecting them will be discussed.

It is contended that the reporting of negative results in an investigation of this kind is equally as important as the positive results, as they serve to delineate the scope of the investigation and to indicate the least probable, or impossible, interpretations.

SCOPE OF INVESTIGATION

The experimental work will be presented in two separate parts as follows:

(a) Preliminary studies of various factors believed to be directly involved in, or related to, the mechanism.

(b) The effect of alkali-metal sulphates and sulphur trioxide, as determined by experiments under closely controlled conditions in small electrically heated tube furnaces and in a small gas- and coal-fired furnace that was operated under conditions closely simulating actual furnace conditions.

These phases of the work follow a more or less chronological order as it was only after the preliminary work had eliminated certain factors from consideration that other chemical and physical properties appeared to be related to the problem.

PRELIMINARY STUDIES

Oxidation of Steel at High Temperatures. It is desirable at this point to present briefly a few facts concerning the fundamental mechanism of the oxidation of plain low-carbon steel at temperatures up to 1200 F, as any discussion of such corrosion proc-

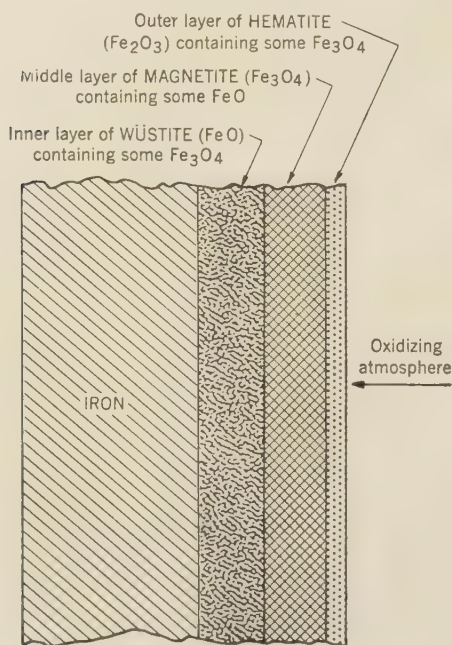


FIG. 1 SCHEMATIC VIEW OF OXIDE PHASES FORMED ON IRON AT HIGH TEMPERATURES

esses must consider the sequence of events at the surface of steel in contact with hot gases.

The oxidation of steel by oxygen or water vapor produces a scale that consists of three separate phases as shown in Fig. 1. Nearest the metal is a phase known as wüstite, of the nominal formula FeO , which contains 75 to 77 per cent by weight of iron. Chemically it is a solid solution of iron in magnetite (Fe_3O_4).¹⁰ The middle phase consists primarily of magnetite, which contains 72.3 per cent by weight of iron and is strongly magnetic. The outer phase is ferric oxide, Fe_2O_3 , which is reddish-brown and nonmagnetic and contains 70 per cent of iron. It is more commonly known as hematite. The relative proportions of these three phases vary greatly, depending upon the temperature and the composition of the gas. The mechanism causing this heterogeneity in the scale is well established on experimental and theoretical grounds as the result of the diffusion of iron atoms from the metal *outward* through the scale. It is upon this phenomenon that the most recent mechanism of high-temperature corrosion is based and not, as formerly believed, on the diffusion of oxygen atoms *inward* through the scale to the metal-oxide interface.

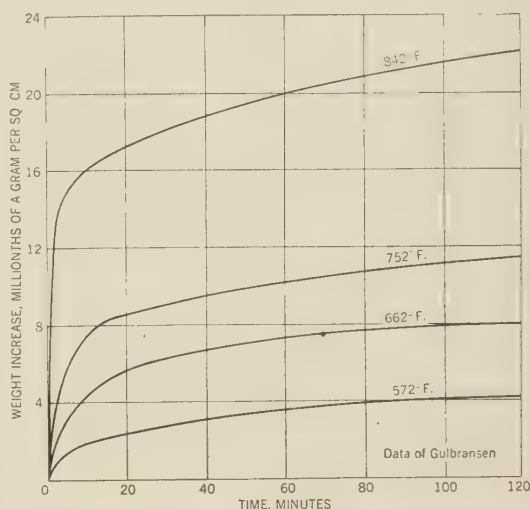


FIG. 2 OXIDATION OF IRON AT VARIOUS TEMPERATURES IN 10 PER CENT OXYGEN

The scaling of steel in the temperature range 550 to 850 F occurs parabolically with time,¹¹ as shown in Fig. 2, and may be represented by the following equation

$$y^2 = k_1 t \dots \dots \dots [1]$$

where y = thickness of scale, k_1 = constant for the conditions under which oxidation is taking place, and t = time. Thus for a given temperature, the rate of scaling decreases with the thickness of the scale as follows

$$\frac{dy}{dt} = \frac{k_1}{2y} \dots \dots \dots [2]$$

In the normal range of furnace-wall-tube temperatures, say, from 650 to 800 F, for high-pressure boilers, the oxidation of low-carbon steel takes place at a relatively low rate, and the tube walls

¹⁰ "The Crystal Structures of Fe, FeO, and Fe_3O_4 and Their Interrelations," by H. J. Goldschmidt, *Journal of the Iron and Steel Institute*, vol. 146, 1942, pp. 157-180.

¹¹ "The Transition State Theory in Oxide Films," by E. A. Gulbransen, *Trans. Electrochemical Society*, vol. 83, 1943, pp. 301-317.

would not be thinned materially during the expected life of the unit. Any factors, however, that interrupt the normal growth of the scale, such as spalling, cracking, recrystallization, or removal of the oxide by chemical reaction with some other material, materially increase the rate of scaling at a given temperature. In the case of the corrosion of furnace tubes, numerous factors were considered from this viewpoint, i.e., that whatever the mechanism of corrosion, the primary reaction was one involving removal of the normal oxide on the metal either mechanically or by chemical reaction.

Rate of Corrosion of Steel in Sulphur Dioxide. Because of the fact that the corrosion areas in each furnace followed a unique pattern that could be related to flame conditions, consideration was given early in the investigation to the possibility that the concentration of SO_2 at the surface of the tubes could become quite high as the result either of local concentration of combustion products from flame impingement or from the decomposition of solid products adhering to the tube, such as incompletely oxidized pyrites or ash during the slag-forming reactions.

Accordingly, the rate of corrosion of steel specimens cut from boiler tubes was determined over a range of temperatures in air and in pure sulphur dioxide. The results, given in Fig. 3, show that, in the temperature range attained by furnace tubes, sulphur dioxide does not have a materially greater effect than air. These results are corroborated by the data of Hatfield¹² shown in Fig. 4.

Although the lowest temperature at which his work was done exceeds by about 500 F that of a furnace tube, the results show that below 1000 F the effect of various gases is about the same. For these reasons, the effect of sulphur dioxide as such was given no further consideration.

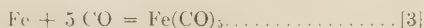
Effect of Carbon Monoxide on Bare Steel. Reports were received that a similar type of corrosion had been found in water-cooled gas producers and was believed to be due to reaction of the carbon monoxide with the steel to form an iron carbonyl. Inasmuch as relatively high concentrations of carbon monoxide are found in areas where corrosion is active, it was considered as a possible factor.

Table 1 shows the properties of three common iron carbonyls.¹³

TABLE 1 PHYSICAL PROPERTIES OF IRON CARBONYLS

	$\text{Fe}(\text{CO})_5$	$\text{Fe}_2(\text{CO})_9$	$\text{Fe}(\text{CO})_4$
Form at room temperature	Pale yellow liquid	Orange hexagonal crystals	Green prismatic crystals
Melting point, deg. C....	20	Dissociates	Dissociates
Boiling point, deg. C....	102	Dissociates	Dissociates
Effect of heating.....	Decomposes at 180 C to Fe + CO	Decomposes at 100 C to $\text{Fe}(\text{CO})_5$, Fe and CO	Decomposes at 140 C to $\text{Fe}(\text{CO})_5$, Fe and CO

Fieldner and Jones¹⁴ state that the formation of the pentacarbonyl, which is the most stable form, takes place mainly in the temperature range 100 to 300 C (212 to 572 F); the reaction is shown in Equation [3]



reversing by an increase in temperature and decrease in the concentration of carbon monoxide.

It was apparent therefore that at the metal temperatures prevailing at normal operating conditions, and the concentrations of carbon monoxide associated with corrosion in slag-tap furnaces, direct combination of the steel with the carbon mon-

¹² "Heat Resisting Steels," by W. H. Hatfield, *Journal of the Iron and Steel Institute*, vol. 115, 1927, p. 483.

¹³ "Iron Oxide Reduction Equilibria," by O. C. Ralston, U. S. Bureau of Mines, Bulletin 296, 1929, p. 285.

¹⁴ "Iron Carbonyls; Their Physical and Chemical Properties," by A. C. Fieldner and G. W. Jones, *American Gas Association Monthly*, vol. 6, 1924, pp. 439-447.

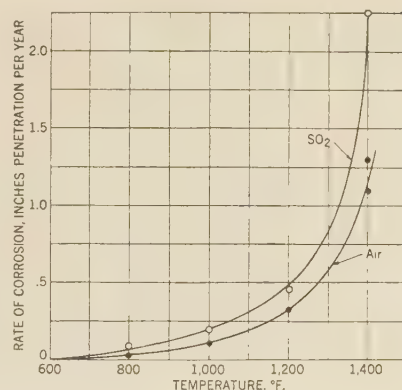
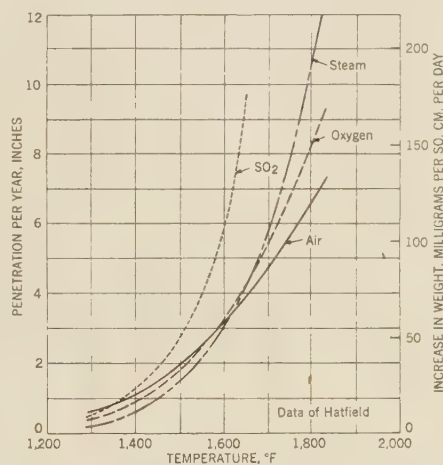
FIG. 3 RATE OF CORROSION OF BOILER-TUBE STEEL IN AIR AND IN SO_2 FOR TEST DURATION OF 24 HR

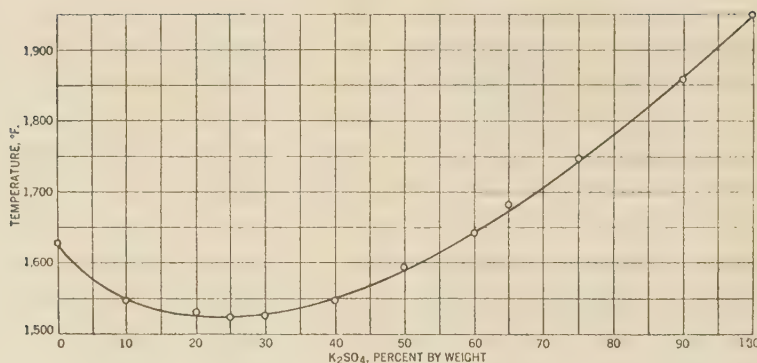
FIG. 4 RATE OF CORROSION OF 0.17 PER CENT CARBON STEEL IN VARIOUS ATMOSPHERES FOR TEST DURATION OF 24 HR

oxide to form volatile iron carbonyls was not a factor in corrosion.

Effect of Molten Alkali-Metal Sulphates on Steel. The enamel deposits contain a high percentage of sodium and potassium sulphate. Therefore, the possibility was considered that the temperature of the deposit might exceed the melting point of the alkali-metal sulphates and the molten salt consequently would attack the tubes. The melting point of mixtures of sodium and potassium sulphates depends upon the ratio of the salts and may vary from a minimum of 1530 F, for a 75 per cent Na_2SO_4 , 25 per cent K_2SO_4 mixture, to 1950 F for pure K_2SO_4 , as shown in Fig. 5.

Corrosion tests were made by placing cleaned and weighed specimens of boiler steel in a molten mixture of alkali-metal sulphates whose melting point was 1530 F, and the temperature was maintained at 1600 F. The tests were conducted both in air and in nitrogen containing less than 0.2 per cent oxygen. To provide a reference point, the rate of corrosion of the same steel in air, without contact with the molten salt, also was determined.

The results given in Fig. 6 show that the steel corrodes at a much higher rate in the molten salt than in air alone. The initial condition of the steel, that is, whether it was clean or had an appreciable oxide scale, had no effect on the results. Subsequent work, to be described later, showed that molten alkali sulphates do not attack iron oxide, therefore, in these experi-

FIG. 5 MELTING-POINT CURVE FOR SYSTEM $\text{Na}_2\text{SO}_4\text{-K}_2\text{SO}_4$

ments the scale apparently was removed mechanically, permitting the molten salt to attack the bare metal.

Two adverse factors caused this mechanism of attack to be rejected from further consideration. An examination of the product of the test in nitrogen showed it to be strongly alkaline in water and to contain a large amount of sulphide sulphur, probably combined as sodium ferrous pentasulphide, $\text{FeS}\cdot 4\text{Na}_2\text{S}$, or the corresponding potassium salt. In the test with air over the molten salt, the product was somewhat less alkaline but contained considerable iron sulphide. These characteristics are opposite to those of furnace-tube enamels, which do not contain sulphides and which produce an *acid* reaction in water. The other factor concerns the temperature necessary to effect the corrosion of the steel, being a minimum of 1530 F to permit melting of the salt. Subsequent work indicated that the temperature of the enamels probably does not exceed 1100 to 1200 F, and as this is considerably below the melting point of the alkali sulphates, no reaction will occur.

Action of Molten Alkali Sulphates on Magnetite. The protectiveness of the normal oxide on steel depends upon its inertness toward substances with which it is in contact and also upon its physical structure remaining undisturbed. For example, spalling or cracking of the oxide as the result of changes in its density would permit the corroding gases to reach the metal. The possibility was considered that a decrease in the density of the scale might result from diffusion of aluminum atoms, which are a constituent of the enamel, into the scale.

The basis for this action is as follows:

Magnetite, a constituent of the normal oxide on steel, belongs to a class of compounds known as spinels,¹⁵ which bear the general formula $\text{M}''\text{O}\cdot\text{M}_2'''\text{O}_3$ where M'' is a divalent and M''' a trivalent metal. In the case of magnetite, Fe_3O_4 , which is represented more properly by $\text{FeO}\cdot\text{Fe}_2\text{O}_3$, the metals are the same, ferrous and ferric iron, respectively. A characteristic of spinels which is important to the present case is that they can take certain elements into solid solution, aluminum being a notable example, and a change occurs in the size of the unit cell of the spinel which is reflected by a change in its density. If, for example, aluminum atoms diffused from the enamel into the oxide on the tube, a maximum contraction of 15.6 per cent in the unit cell of the magnetite could occur, the density changing from 5.20 to 4.39 g per cu cm, and cracking or fissuring of the scale could occur.

The effect of aluminum on magnetite was determined by tests in which 1:1 mixtures of powdered magnetite with powdered samples of (a) 67.5 per cent Na_2SO_4 , 22.5 per cent K_2SO_4 , 10 per

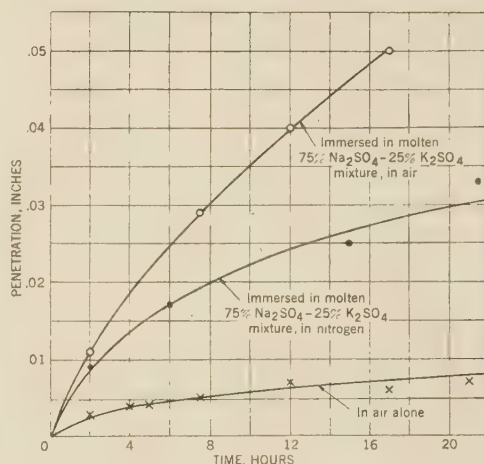


FIG. 6 CORROSION OF LOW-CARBON STEEL AT 1600 F UNDER VARIOUS CONDITIONS

cent Al_2O_3 and (b) enamel deposit from the 12th Street Station were heated at 1600 F for several days in an inert atmosphere. At this temperature the alkali-metal sulphates were molten, a purposely rigorous condition to effect any possible reactions in a short time. An X-ray diffraction pattern was made of the products to determine if solid solution of aluminum, or other changes, had occurred in the magnetite.

The results showed that the magnetite remained unchanged and that it did not react with the molten salt, therefore these possibilities were considered no further.

Effect of Slag. In the early phases of the investigation, the slag immediately overlaying the corroded tubes was given some attention, as it was logical to suspect that it was directly involved in, or contributory to, the action.

Two conditions must be fulfilled if corrosion is to occur as the result of chemical reaction of the slag with the normal oxide on the tube; (1) there must be direct contact of the slag with the oxide, and (2) the temperature at the oxide-slag interface must be at or near that at which a liquid phase can form. There are two factors to be considered relative to the temperature at the oxide-slag interface, i.e., the heat-transfer coefficient of the oxide on the tube and the ability of coal-ash slags to react with the oxide layer at that temperature.

Considering first the temperature at the interface, the schematic diagram in Fig. 7, shows a sheet of slag in contact with the normal oxide on the tube. If the coefficient of thermal con-

¹⁵ "A Study of a Group of Spinels," by C. W. Parmelee, A. E. Badger, and G. A. Ballam, Bulletin No. 248, University of Illinois, June 17, 1932.

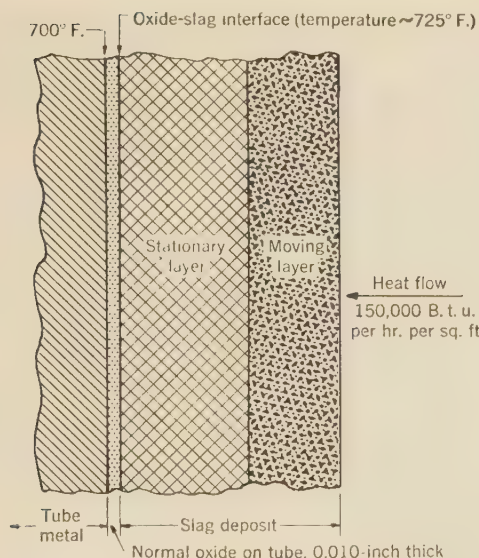


FIG. 7 SCHEMATIC VIEW OF IDEALIZED SLAG DEPOSIT IN DIRECT CONTACT WITH NORMAL OXIDE ON TUBE

ductivity k and the thickness of the oxide were known, it would be a simple matter to calculate the temperature at the oxide-slag interface for a given metal temperature and rate of heat transfer. Neither of these factors, however, is known with certainty, although a reasonable estimate of the thickness of the oxide may be obtained from high-temperature corrosion data.

It is possible, however, to estimate the magnitude of k for iron oxide scale from data that were published recently.¹⁶ Table 2 shows these data in familiar units.

TABLE 2 THERMAL CONDUCTIVITY OF IRON OXIDES

Material	$k = \text{Btu/hr-ft-deg F-in.}$
Single crystal of hematite, Fe_2O_3	93.5
Massive hematite.....	16.7
Massive magnetite, Fe_3O_4	8.3-20.8

The difference between the value of k of a single crystal of hematite and that of the massive form is the result of a difference in density between the two materials, the latter being an aggregate of small crystals. It is to be noted that k for massive magnetite is of the same magnitude as that of massive hematite. It is a reasonable assumption, therefore, that k for a single crystal of magnetite is of the same order as that of a single crystal of hematite and for the purpose of this discussion it will be assumed to be $k = 100$.

The normal oxide formed on steel at high temperatures is dense and, depending upon the conditions under which it is formed, may consist of large or small crystals of hematite and magnetite. The value of k therefore probably will lie between 21 and 100. For the present purposes, a mean value of $k = 60$ will be used, as it will be seen that, regardless of whether a mean value or the minimum value is used, the maximum temperature at the interface will not be affected seriously.

At a tube-metal temperature of 700 F, the normal oxide would not exceed a thickness of 0.010 in. over a reasonable period of normal service. Moreover, it would be in such close contact with the steel surface that it can be assumed that no temperature gradient would exist between the metal and the oxide. There-

fore, assuming a heat-transfer rate of 150,000 Btu per sq ft per hr through the tube, the temperature gradient through the oxide would be

$$t = \frac{(150,000)(0.010)}{60} = 25 \text{ deg F}$$

resulting in a temperature of 725 F at the oxide-slag interface under these conditions.

Regarding the temperature at which the liquid phase can form at the oxide-slag interface, it is necessary to discuss briefly some of the properties of coal-ash slags. Although the chemistry of such slags is complex, owing to the many constituents involved, it is possible to establish with reasonable accuracy the lowest temperature at which a liquid phase can form. In addition, experimental work on the fusibility and viscosity of coal-ash slags also is available to indicate the minimum temperature at which slags have fluid properties.

Coal ashes contain compounds of silicon, aluminum, iron, and calcium, with smaller amounts of magnesium and the alkali metals, sodium and potassium. In addition, insignificant amounts of titanium and phosphorus also are present. At temperatures where slag forms, complicated reactions occur in the ash to produce complex silicate phases, and the variables which affect the formation of these phases are (a) the original composition of the ash (including the petrographic form of the constituents), (b) the temperature at which they are formed, (c) the time that the slag is maintained at this temperature, and (d) the ratio of oxidizing to reducing constituents in the surrounding atmosphere.

A petrographic or an X-ray diffraction analysis of the slag shows definitely the primary solid phases which crystallize from the slag during cooling and are embedded in a glassy matrix. For example, in a slag that is low in calcium and magnesium, such as occurs with most eastern bituminous coals, and belongs essentially to the $\text{SiO}_2\text{-Al}_2\text{O}_3\text{-FeO}$ system, the following crystalline phases may be found:

Mullite	Al_2SiO_5
Hercynite	FeAl_2O_4
Fayalite	Fe_2SiO_4
Magnetite	Fe_3O_4

A photomicrograph of a typical thin section of slag, as viewed by transmitted light, is shown in Fig. 8 and illustrates the crystalline phases mullite and hercynite in a glassy matrix.

The phase diagram of the $\text{SiO}_2\text{-Al}_2\text{O}_3\text{-FeO}$ system¹⁷ is shown in Fig. 9. Its essential features, for the present discussion, are the minimum temperatures in the system at which the eutectics and the peritectics will melt, as it is at these temperatures that liquid phase first will be formed on heating. It is to be noted that this minimum melting point in the $\text{SiO}_2\text{-Al}_2\text{O}_3\text{-FeO}$ system is 1963 F, occurring at a composition where hercynite, fayalite, and tridymite all are in equilibrium. Results of cone-fusion determinations of coal ashes confirm this fact experimentally, initial deformation temperatures never being observed at less than about 1800 F. Values this low probably result from the presence of feldspars or alkali-metal salts, which explains the decreased temperature compared to the $\text{SiO}_2\text{-Al}_2\text{O}_3\text{-FeO}$ system. Further, viscosity measurements show that the minimum temperature at which any liquid can be detected in coal-ash slags is also about 1800 F, and that most slags containing any liquid phase have a viscosity of more than 100,000 poises at these low temperatures. Thus, for this application, coal-ash slags can be considered to be solids at temperatures less than 1800 F.

¹⁶ "Handbook of Physical Constants," by F. Birch, J. F. Schairer, and H. C. Spicer, Geological Society of America, Special Paper No. 36, 1942.

¹⁷ "The System $\text{CaO-FeO-Al}_2\text{O}_3\text{-SiO}_2$: I. Results of Quenching Experiments on Five Joints," by J. F. Schairer, *Journal of the American Ceramic Society*, vol. 25, no. 10, 1942, pp. 241-274.



FIG. 8 THIN CROSS SECTION OF SLAG UNDER TRANSMITTED LIGHT; MAGNIFICATION $\times 25$

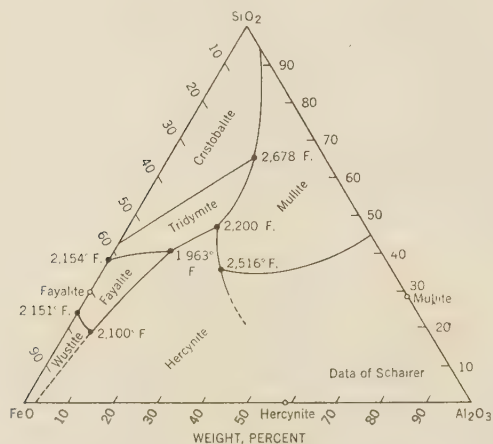


FIG. 9 EQUILIBRIUM DIAGRAM OF THE $\text{SiO}_2\text{-Al}_2\text{O}_3\text{-FeO}$ SYSTEM

Therefore, if the premise is correct that before reaction can occur between the slag and the oxide, the temperature at the interface must be at or slightly below that at which liquid phase will form in the slag, the temperature at the oxide-slag interface is far too low for such reactions to occur.

Effect of Fe-FeS or FeO-FeS Eutectics. The possibility was considered that corrosion occurred as the result of iron sulphide deposits on the tubes reacting with the tube metal or its oxide to form eutectics of low melting point which then progressively attacked the metal, probably by intergranular penetration.

A metallographic examination was made of a number of corroded tubes for evidence of eutectic phases. The photomicrographs in Fig. 10 show the microstructure of the metal in the corroded section of tubes from three stations where the enamel deposit was prevalent and one station where sulphide deposits occurred. The microstructure of the FeO-FeS eutectic also is shown for comparison. No evidence of eutectic phases is to be found in any of the tube samples.

Brief consideration of the chemistry of the FeO-FeS and the

Fe-FeS systems will show that the temperatures prevailing at the surface of the tubes are too low for the formation of eutectics of this type.

It has been shown experimentally¹⁸ and by free-energy data¹⁹ that the reaction



will not proceed below about 1850 F. Preece²⁰ states, "At tempering and hardening temperatures, i.e., 650° C (1202° F) to slightly below 900° C (1652° F) there is no formation of the oxide-sulphide complex—and there is little or no tendency for sulphide penetration along the grain boundaries. At temperatures above 900° C the sulphide forms a molten oxide-sulphide complex at the scale-metal interface, which penetrates into the metal along the grain boundaries."

An explanation for the temperature required for the formation of Fe-FeS,^{21, 22} and FeO-FeS²³ eutectics is afforded by the equilibrium diagrams for both systems, which are shown in Fig. 11. It is apparent that for molten Fe-FeS eutectic to form at the surface of the tube the temperature would have to be 1805 F, and for the FeO-FeS eutectic it would have to be 1724 F.

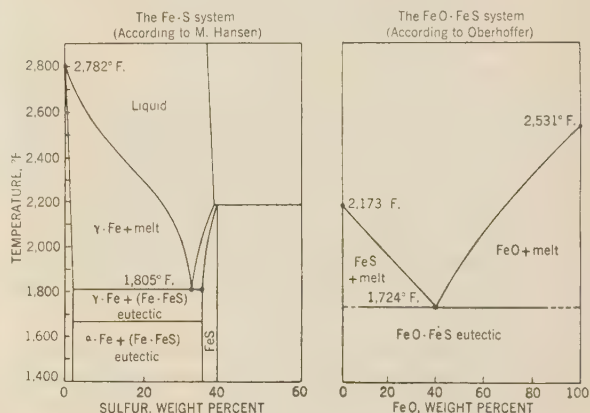


FIG. 11 EQUILIBRIUM DIAGRAMS OF Fe-S AND FeO-FeS SYSTEMS SHOWING EUTECTIC POINTS

REACTIONS OF ALKALI-METAL SULPHATES AND SULPHUR TRIOXIDE

The Chemical and Physical Properties of Enamels. Attention next was directed toward a critical examination of the enamel deposits. It was logical to suspect that they played an important part in the mechanism, inasmuch as this type of deposit always was found where corrosion was active. It should not be inferred, however, that corrosion always was found under an enamel deposit; rather, its presence indicated a potentially corrosive state that would become active under certain conditions.

¹⁸ "The Reaction Between Magnetite and Ferrous Sulfide," by F. S. Wartman and G. L. Oldright, Bureau of Mines Report of Investigations, no. 2901, 1928, pp. 1-14.

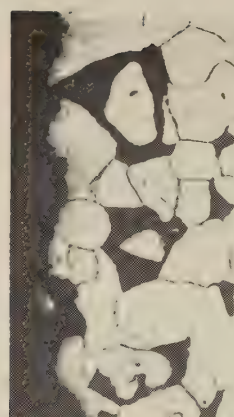
¹⁹ "Reactions Between Iron Sulfide, Sulfur Dioxide, and Iron Oxides in the Metallurgy of Copper," by A. C. Halferdahl, *Industrial and Engineering Chemistry*, vol. 22, 1930, pp. 956-963.

²⁰ "Removal of Sulfur From Gaseous Fuels," by A. Preece, *Engineering*, vol. 155, 1943, pp. 405-406.

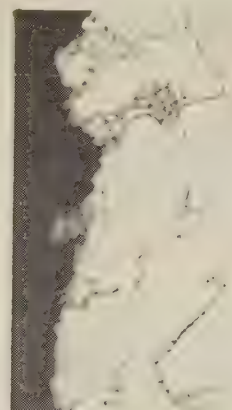
²¹ "Der Aufbau der Zweistofflegierungen," by M. Hansen, Julius Springer, Berlin, 1936, p. 723.

²² "Pyrrhotite—Melting Relation and Composition," by E. Jensen, *American Journal of Science*, vol. 240, 1942, pp. 695-709.

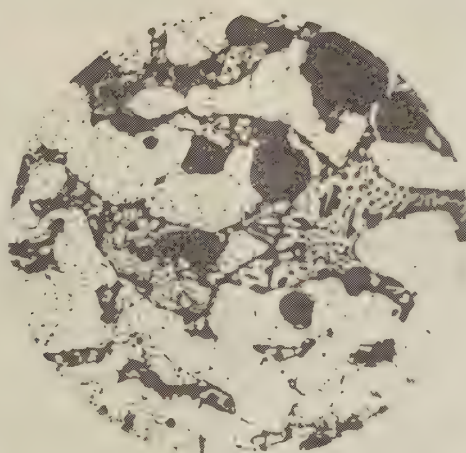
²³ "Das Technische Eisen," by P. Oberhoffer, Julius Springer, Berlin, second edition, 1925, p. 98.



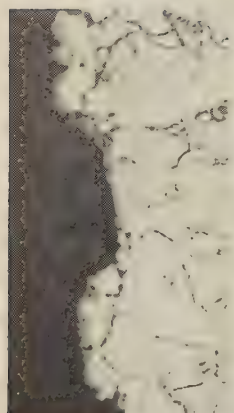
Firestone



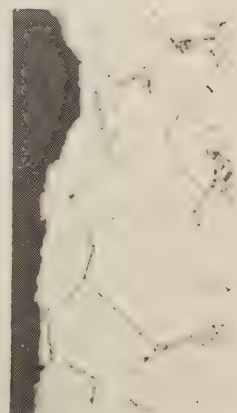
Windsor



Typical FeO-FeS
eutectic in low carbon steel



Buzzards Point



Schuylkill

FIG. 10 MICROSTRUCTURE OF FURNACE-WALL TUBES, NITAL ETCH; $\times 500$. WITH TYPICAL FeO-FeS EUTECTIC PHASE FOR COMPARISON

To afford a basis for the experimental work that is to be described, it is desirable to examine the chemical composition and physical properties, given in Table 3, of the typical sample of enamel that was removed from the wall tubes of No. 17 boiler of the 12th Street Station.

TABLE 3 EXAMINATION OF ENAMEL DEPOSIT, SAMPLE C-9

Chemical analysis:	Per cent
Silica, SiO_2	8.3
Aluminum calculated as Al_2O_3	6.2
Total iron calculated as Fe_2O_3	16.6
Calcium calculated as CaO	2.7
Magnesium calculated as MgO	0.2
Sulphur trioxide, SO_3	36.5
Alkali metals calculated as Na_2O	28.7
Copper, Cu.....	0.6
Solubility in water.....	53.5
pH of 1 per cent solution in water—3.3	
Loss of weight in 24 hr at:	
220 F.....	0.7
1000 F.....	1.4
1100 F.....	3.4

Melting point:

Not sharp; became semimolten at 1200 F; solidified as temperature was increased; then became semimolten again at 1500 F.

Physical appearance in "as-received" condition:

Brittle, greenish-white to reddish-brown glazed flakes, A, in Fig. 12. Average thickness, 0.020 in. Side in contact with tube generally had a thin layer of iron oxide tightly bonded to it, B in Fig. 12. When the deposit was ground and added to cold distilled water, it produced an acid reaction. When the solution was filtered rapidly to remove insoluble materials, filtrate assumed a brownish opalescence which, with heating, became a reddish-brown flocculent precipitate, indicating that the sample contained a soluble iron compound which hydrolyzed to an insoluble iron oxide.

The outstanding characteristics typical of all enamel samples were the relatively low pH which they produce in water, the presence of a water-soluble iron compound, the evolution of sulphur trioxide when heated, and an indefinite melting point. These characteristics suggested the following questions:

(a) How are the sodium sulphate and potassium sulphate combined?

(b) How is the iron combined?

(c) What changes occur upon heating them?

(d) What causes the enamels to produce an acid reaction in water?

An X-ray diffraction analysis was made of the enamel to determine the compounds present. This method of analysis is unique for this purpose, as it is impossible to determine the compounds present in a complex mixture by ordinary analytical methods. All X-ray diffraction analyses were made by the Debye-Scherrer-Hull method, using filtered copper radiation produced at 35 kv and 20 ma. The samples were mounted by the wedge technique in quadrant cassettes of 20.35 cm radius.

The X-ray patterns, shown in Fig. 13, indicate that the sodium and potassium sulphates do not exist independently in the enamel but are in solid solution in the weight ratio of 3 K_2SO_4 :1 Na_2SO_4 , a composition corresponding closely to that of the



FIG. 12 FLAKES OF TYPICAL "ENAMEL" DEPOSIT; MAGNIFICATION $\times 10$
(A, Furnace side. B, Side in contact with tube showing adherent magnetite.)

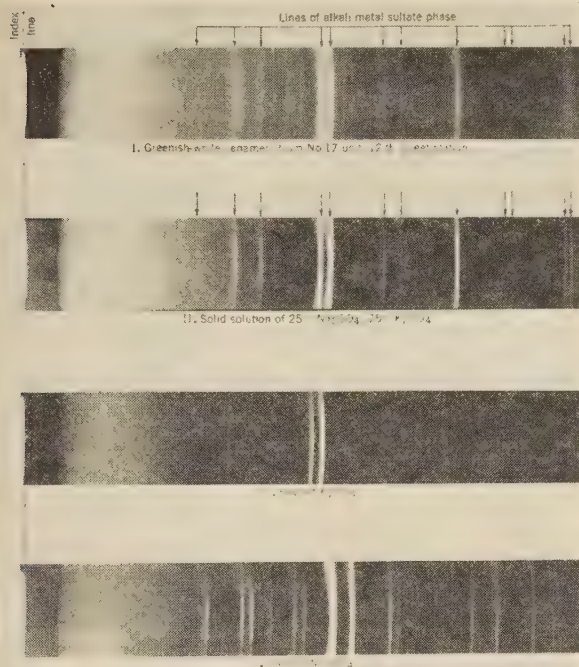


FIG. 13 X-RAY DIFFRACTION PATTERNS OF "ENAMEL" DEPOSIT AND ALKALI-METAL SULPHATES

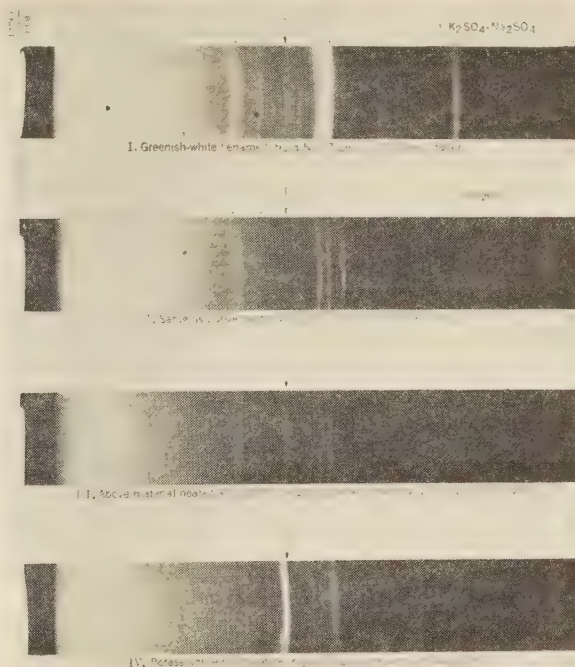


FIG. 14 X-RAY DIFFRACTION PATTERNS OF "ENAMEL" DEPOSIT AND POTASSIUM FERRIC TRISULPHATE

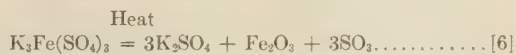
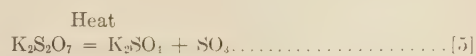
mineral glaserite,²⁴ which has a nominal formula $K_3Na(SO_4)_2$. The fact that the alkali sulphates are in solid solution is shown by the correspondence of the lines with a synthetic solid solution of 75 per cent K_2SO_4 and 25 per cent Na_2SO_4 . It is to be noted that the lines in Fig. 13 (II), correspond closely with those in Fig. 13 (III), which is pure K_2SO_4 , except that the lines of the former are shifted slightly to the right. This shift is characteristic of the formation of solid solutions, arising from the fact that the dimensions of the unit cell of the potassium sulphate, which is the solvent in this case, are changed as sodium sulphate, the solute, is taken into solid solution. The change in cell dimensions of the solvent is reflected in shifts in its diffraction angles which are proportional to the amount of solute present.

Fig. 14 (I) is an X-ray photograph of the 12th Street enamel. The next photograph, Fig. 14 (II), is that of the same sample after heating at 1400 F for several hours. It is to be noted that the diffraction line under the arrow in (I) has disappeared and that lines of Fe_2O_3 have become more pronounced in the heated sample. This indicates that there was a complex iron compound in the deposit which was decomposed by heat to form Fe_2O_3 . It will be shown later that, when the enamels are heated above about 1000 F, sulphur trioxide (SO_3) is evolved. Therefore, it was believed that the iron was combined with sulphur trioxide in some manner, although not as ferric or ferrous sulphate, as no lines for these compounds were found in the X-ray pattern. It was reasoned, therefore, that if SO_3 and Fe_2O_3 occurred as the result of heating the enamel, then by placing the heated enamel in an atmosphere of SO_3 the line which had disappeared from the original sample should reappear. Accordingly, the sample was heated at 1000 F in an atmosphere containing

about 1 per cent by volume of SO_3 . The next photograph, Fig. 14 (III), is that of the product after this treatment. It is to be noted that the line has reappeared and the lines of Fe_2O_3 have disappeared, thus confirming the fact that the iron in the enamel was combined mainly as a sulphate compound.

Inasmuch as the X-ray diffraction literature on inorganic compounds did not show any iron compound with a strong line corresponding to that of the unknown, it was necessary to synthesize a number of likely compounds in the laboratory and to compare their X-ray diffraction patterns with that of the sample. It was found from this work, which will be described in detail later, that the iron is combined in the enamel as potassium ferric trisulphate, $K_3Fe(SO_4)_3$. It is to be noted from its X-ray photograph, Fig. 14 (IV), that it has an intense line corresponding to the unknown line in the enamel. This line corresponds to an interplanar spacing of $d = 3.25$ Angstrom units. The terminology of X-ray diffraction data is described elsewhere.²⁵

In Table 3, it is noted that upon heating, the enamel lost weight and sulphur trioxide was evolved. This loss of weight could result from the loss of water or from the decomposition of alkali-metal pyrosulphates or potassium ferric trisulphate, sulphur trioxide being evolved as follows

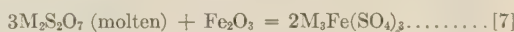


Although the X-ray pattern of the enamel did not show the presence of pyrosulphates, which might be formed by reaction of sulphur trioxide with the sodium and potassium sulphates, there was the possibility that they might be present in amounts up to about 5 per cent, in which case the diffraction lines would not be strong enough to be detected.

²⁵ "X-Ray Diffraction—A New Industrial Research and Control Technique," by R. Corey, *Combustion*, vol. 16, July, 1944, pp. 48–55.

²⁴ "On the Formation and Inversion of Mix-Crystals and Double Salts in the Binary Systems of Dimorphous Sulfates of Lithium, Sodium, Potassium, and Silver," by R. Naeken, *Neues Jahrbuch für Mineralogie, Geologie und Paläontologie, Beilageband*, vol. 24, 1907, pp. 1–68 (see *Chemical Abstracts*, vol. 1, 1907, pp. 2345–2347.)

The presence of pyrosulphates in the enamel is important from the standpoint that molten pyrosulphates attack iron oxides very rapidly according to the following equation



where $M = Na$ or K .

From qualitative observations of the behavior of the enamel on heating, it did not appear that pyrosulphates were present to any considerable extent. In order, however, to determine more precisely the behavior of the enamel, it was heated in air for 24 hr at various temperatures, the loss of weight being determined at frequent intervals during this period.

For comparison with the enamel, $K_3Fe(SO_4)_3$ and a mixture of potassium pyrosulphate and potassium sulphate were heated under the same conditions; similar tests were made with the sodium salts.

The $K_3Fe(SO_4)_3$ and $Na_3Fe(SO_4)_3$ were synthesized by heating together stoichiometric amounts of ferric sulphate and the respective alkali-metal sulphate in evacuated, sealed tubes at 1000 F for 24 hr. An X-ray diffraction pattern of the products showed that complete reaction had occurred to form the desired compounds. The tests were made in a vertical electrically heated

It has been noted that a 1 per cent solution of the enamel in water has a pH of 3.3. Some of this acidity may result from the small amount of pyrosulphate present, but an acid reaction also occurs when the complex iron compounds $K_3Fe(SO_4)_3$ and $Na_3Fe(SO_4)_3$ are dissolved in water. This results from hydrolysis of the salt by the water, liberating free sulphuric acid as follows:



A synthetic enamel was made by mixing $K_3Fe(SO_4)_3$ and $Na_3Fe(SO_4)_3$ in various percentages with a synthetic solid solution of $3K_2SO_4-Na_2SO_4$. A 1 per cent solution in water then was made of the mixture, and the pH was measured with a glass electrode. The results obtained are given in Table 4.

TABLE 4 ACIDITY OF MIXTURES OF ALKALI-METAL FERRIC TRISULPHATES AND $3K_2SO_4-Na_2SO_4$

Quantity in mixture, per cent— $K_3Fe(SO_4)_3$	$Na_3Fe(SO_4)_3$	pH of 1 per cent solution
5	..	3.45
10	..	3.05
15	..	3.00
..	5	3.30
..	10	3.15
..	15	2.95

These pH values are of the same magnitude as that produced by the enamel.

As a result of these studies, it is known that enamel deposits (a) contain sodium and potassium sulphates in solid solution; (b) contain a small amount of alkali-metal pyrosulphate; (c) contain iron combined primarily as the compound $K_3Fe(SO_4)_3$ or $Na_3Fe(SO_4)_3$; (d) are acid in an aqueous solution because of hydrolysis of the pyrosulphates and the complex iron compounds; and (e) decompose when heated, the pyrosulphate breaking down at about 600 F, and the complex iron compound at temperatures over 1000 F.

REACTIONS BETWEEN ALKALI-METAL SULPHATES, IRON OXIDE, AND SULPHUR TRIOXIDE AT 1000 F

The most significant characteristic of the enamel is the manner in which the iron is combined, as the mechanism of corrosion is based on the reactions involved in the formation of the complex iron compounds. Thus if the iron oxide on the tube, the sodium and potassium sulphates in the enamel, and the sulphur trioxide in the gases in contact with the enamel react at operating temperatures according to the equation

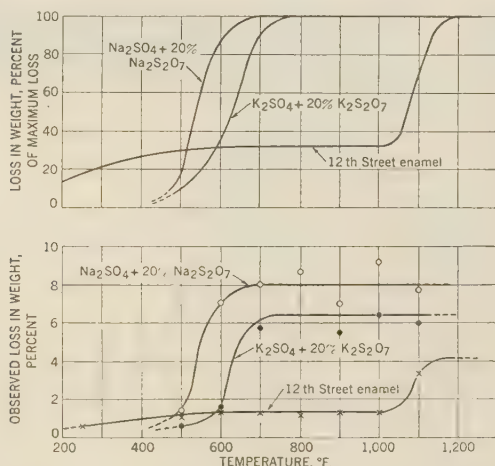


FIG. 15 DECOMPOSITION OF "ENAMEL" DEPOSIT AND OF MIXTURES CONTAINING PYROSULPHATES, FOR TEST DURATION OF 24 HR.

tube furnace the temperature of which was controlled to $\pm 5^\circ$ deg F. The velocity of air over the specimens was maintained at a low constant rate for all determinations.

The results for the enamel and the pyrosulphates are given in Fig. 15. The lower graph gives the absolute loss of weight at various temperatures, and the upper graph, a different plot of the same data, shows the percentage of the total loss of weight of the materials at various temperatures. For the enamel, these data may be summarized as follows:

- 1 The 0.7 per cent loss at 250 F represents water.
- 2 The additional loss of 0.7 per cent between 250 and 600 F represents decomposition of pyrosulphate, which begins at about 600 F for potassium pyrosulphate and 500 F for sodium pyrosulphate. This represents approximately 2 per cent of pyrosulphate in the enamel.
- 3 The sharp increase in the loss of weight between 1000 and 1100 F represents decomposition of the $K_3Fe(SO_4)_3$ in the enamel, which is shown in Fig. 16, to begin decomposing according to Equation [6] at about 1100 F. Calculation shows approximately 10 per cent of $K_3Fe(SO_4)_3$ to be present.

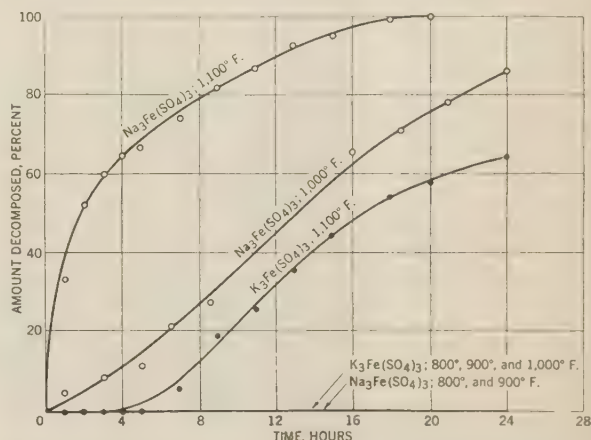
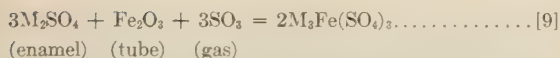


FIG. 16 DECOMPOSITION OF $K_3Fe(SO_4)_3$ AND $Na_3Fe(SO_4)_3$ IN AIR AT VARIOUS TEMPERATURES



then removal of the normal oxide on the tube could occur until the enamel was converted completely to the complex iron compound, resulting in a higher rate of corrosion of the metal than if the enamel were not present. Consequently, a series of experiments was directed toward determining the conditions necessary for the formation of the alkali-metal ferric sulphate found in the enamel.

Essentially, the procedure followed was to pass dry mixtures of sulphur trioxide and air over weighed amounts of powdered alkali sulphates, iron oxide, and intimate mixtures of these substances, the gas and samples being maintained at 1000 F, and the tests lasting 24 hr. The samples then were weighed, the increase in weight representing the amount of sulphur trioxide that reacted with the material. A temperature of 1000 F was selected for these tests as representing an average temperature of the enamel deposit on the furnace tubes. Lower temperatures would result in a difference in degree rather than in kind of reaction. The pH of these residues was determined, and an X-ray diffraction pattern was made when it was desirable to determine the phase that had been formed.

The sulphur trioxide was prepared by mixing the required amount of sulphur dioxide with air in 20-liter bottles, using a saturated brine solution as a retaining fluid. By using a layer of mineral oil over the brine, any solution of the gas largely was prevented. This mixture of gases, after being dried, was then passed at the constant rate of 0.75 liter per hr over a platinum catalyst maintained at 750 F, at which temperature maximum conversion to sulphur trioxide occurs. The catalyst was packed into one end of a 1-in-diam \times 26-in-long pyrex tube, separate electrically heated furnaces being used to heat the catalyst and the reaction sections of the tube. Being continuous, there were no cool surfaces between the catalyst and the specimens, thus no condensation of sulphur trioxide could occur to decrease the concentration in the vapor phase below that desired. Platinum-platinum-rhodium thermocouples were used to measure temperatures, which were controlled automatically to ± 5 deg F.

In Table 5 are shown the qualitative data obtained under these conditions. A plus sign indicates that an increase of weight occurred due to the reaction of sulphur trioxide with the material in question, and a minus sign indicates that no reaction occurred.

TABLE 5 REACTION OF SO_3 WITH VARIOUS MATERIALS AT 1000 F

Material	SO ₃ , per cent by volume								Phase formed when reaction occurs
	0.025	0.05	0.1	0.3	0.5	1.0	2.5	5.0	
Na ₂ SO ₄	—	—	—	—	—	—	—	—	No reaction
K ₂ SO ₄	—	—	—	—	—	+	+	+	K ₂ S ₂ O ₇
Fe ₂ O ₃	—	—	—	—	—	+	+	+	Fe ₂ (SO ₄) ₃
Mixtures of:									
Na ₂ SO ₄ and Fe ₂ O ₃ ...	+	+	+	+	+	+	+	+	Na ₂ Fe(SO ₄) ₃
K ₂ SO ₄ and Fe ₂ O ₃	+	+	+	+	+	+	+	+	K ₂ Fe(SO ₄) ₃

The significant facts from these experiments may be summarized as follows:

- 1 Sodium sulphate will not react with sulphur trioxide to form sodium pyrosulphate at concentrations of 5 per cent by volume, or less, of sulphur trioxide.
- 2 Potassium sulphate will not react with sulphur trioxide to form potassium pyrosulphate at concentrations of 0.5 per cent by volume, or less, of sulphur trioxide. Molten potassium pyrosulphate begins to form at approximately 0.8 per cent by volume of sulphur trioxide, which corresponds to a partial pressure of 6 mm Hg.
- 3 Ferric oxide will not react with sulphur trioxide to form ferric sulphate at concentrations of 0.5 per cent by volume, or less, of sulphur trioxide.

4 Mixtures of sodium sulphate or potassium sulphate and ferric oxide react with sulphur trioxide to form sodium ferric trisulphate, $\text{Na}_2\text{Fe}(\text{SO}_4)_3$, and potassium ferric trisulphate, $\text{K}_2\text{Fe}(\text{SO}_4)_3$, respectively, at concentrations as low as 0.025 per cent of SO_3 corresponding to a partial pressure of 0.2 mm Hg. The residue dissolved in water has a pH of 2.8 to 3.3.

Thus under conditions where neither iron oxide nor the alkali-metal sulphates *alone* will react with sulphur trioxide at 1000 F, mixtures of these materials will combine definitely to form complex alkali-metal ferric sulphates.

The relative reactivity of various mixtures toward different concentrations of SO_3 is given in Fig. 17, in which the percentage of the theoretical increase of weight in 24 hr, and the concentration of SO_3 are plotted. To determine the effect of the amount of ferric oxide present in a mixture, various ratios of alkali-metal sulphate and ferric oxide were used. In addition, the effect of varying the ratio of sodium to potassium sulphate was determined by mixing the ferric oxide with solid solutions of the sulphates. All mixtures are expressed on a mol rather than a weight basis for convenience in calculating the maximum amount of SO_3 that would react with a given mixture.

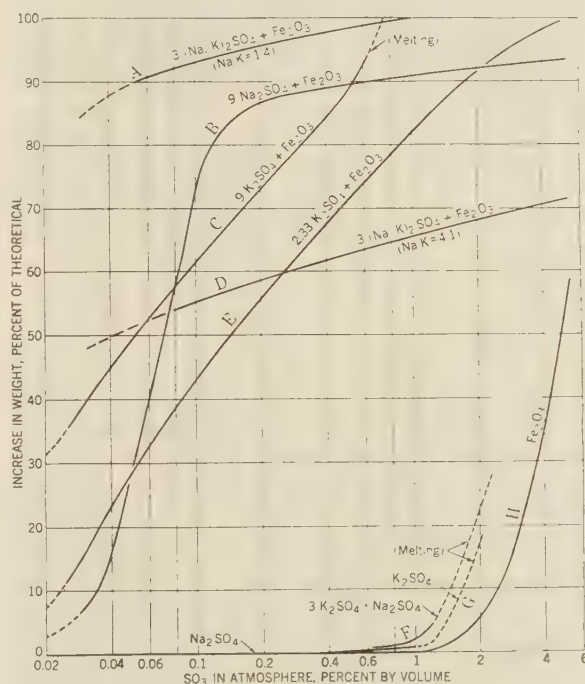


FIG. 17 EXTENT OF COMPLETION OF REACTION BETWEEN VARIOUS MATERIALS AND SO_3 AT 1000 F FOR PERIODS OF 24 HR

The significant facts to be noted from Fig. 17 may be summarized as follows:

- (a) Neither K_2SO_4 , solid solutions of K_2SO_4 and Na_2SO_4 , nor Fe_2O_3 react with concentrations of SO_3 less than about 0.7 per cent, and Na_2SO_4 does not react in concentrations up to 5 per cent. (Curves F, G, H.)
- (b) Above 0.025 per cent SO_3 , the relative reactivity of the oxide-sulphate mixtures increases rapidly with SO_3 . (Curves A to E.)
- (c) The relative reactivity, for a given concentration of SO_3 , is greater for mixtures having a low iron oxide content than when the iron oxide is high. (Curves C and E.)
- (d) Increasing the ratio of K_2SO_4 to Na_2SO_4 , for a given mix-

ture of alkali-metal sulphate and Fe_2O_3 , and concentration of SO_3 increases the relative reactivity of the mixture. (Curves A and D.)

(e) In all mixtures containing more than 3 mols of K_2SO_4 to 1 mol of Fe_2O_3 , the stoichiometric ratio required to form $\text{K}_3\text{Fe}(\text{SO}_4)_3$, excess K_2SO_4 forms $\text{K}_2\text{S}_2\text{O}_7$ when the SO_3 is higher than approximately 0.7 per cent. If a sufficient amount of $\text{K}_2\text{S}_2\text{O}_7$ is formed, the mixture becomes fluid (curve C), and the reactivity increases rapidly. This does not occur, however, with Na_2SO_4 in the range of SO_3 concentrations that was studied. (Curve B.)

A pH determination and an X-ray diffraction pattern were made of the final product of a number of the mixtures of alkali-metal sulphates and Fe_2O_3 . Although the pH varied somewhat with the amount of SO_3 that was absorbed, it was found to lie between 2.6 and 3.0, thus these materials had about the same pH as enamels. The question arose as to whether a disulphate, $\text{KFe}(\text{SO}_4)_2$, in which the ratio of K_2SO_4 to Fe_2O_3 is 1, would be formed as the Fe_2O_3 content of the mixture was increased. The X-ray patterns of a series in which the ratio of K_2SO_4 to Fe_2O_3 was varied are given in Fig. 18 and show beyond doubt that, under the conditions of these tests, $\text{K}_3\text{Fe}(\text{SO}_4)_3$ is formed regardless of the K_2SO_4 - Fe_2O_3 ratio. Although the $1\text{K}_2\text{SO}_4 + 1\text{Fe}_2\text{O}_3$ mixture is capable of forming a product containing 75 per cent $\text{K}_3\text{Fe}(\text{SO}_4)_3$, and the $9\text{K}_2\text{SO}_4 + 1\text{Fe}_2\text{O}_3$ mixture only 47 per cent, the density of the predominant lines for $\text{K}_3\text{Fe}(\text{SO}_4)_3$ in Fig. 18, made with the same X-ray exposure in each case, shows that increase in the iron oxide content of the mixture decreases the fraction of the theoretical amount of the compound that can be formed in a given time. Thus the relative reactivity increases as the iron oxide content decreases, corroborating the data in Fig. 17. The same results were obtained for a Na_2SO_4 - Fe_2O_3 series, in which $\text{Na}_3\text{Fe}(\text{SO}_4)_3$ was the only complex iron phase formed.

In all of the tests which have been described, the mixtures were prepared by mixing intimately powdered samples of alkali-metal sulphates and ferric oxide, thus providing a physical condition of maximum surface of contact between the two solid phases. In the case, however, of a deposit on a furnace tube, the point of contact is a "plane" comprising the interface between the oxide on the tube and the deposit. In such a case, the rate of reaction depends upon the rate of diffusion of SO_3 inward through the enamel to the interface or the rate of diffusion of the products of the reaction outward through the enamel, the slower process governing the rate of reaction. Therefore, to simulate a deposit on a furnace tube, solid oxide scale obtained from heavily scaled low-carbon steel was cut into pieces, measuring 0.5 in. \times 0.2 in. \times 0.05 in., which were dipped momentarily into a molten mixture of 75 per cent K_2SO_4 and 25 per cent Na_2SO_4 , producing on each flake a layer approximately 0.015 in. thick of a fused solid solution of alkali-metal sulphates.

The coated flakes then were placed in the tube furnace and heated to 1000 F in an atmosphere of SO_3 , O_2 , and N_2 . It was noted during the test that the salt became brownish, indicating that iron was dissolving. Specimens were removed at intervals, the salt being dissolved from each specimen with hot water, and the iron determined by a Zimmerman-Rheinhardt permanganate titration. A pH determination and an X-ray diffraction pattern were made of the coating on two specimens which were included in the test solely for these purposes.

The results of the iron determinations, expressed as iron dissolved per square centimeter of specimen, are plotted in Fig. 19, for 0.1 per cent and 0.5 per cent SO_3 . It is apparent from these results that reaction of iron oxide with alkali-metal sulphates and SO_3 will occur readily where there is a plane of contact be-

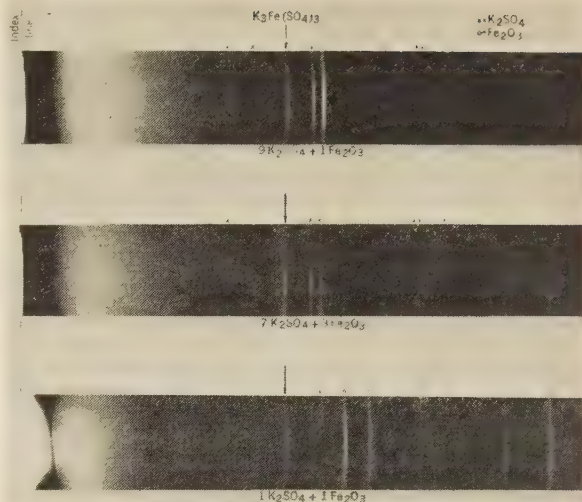


FIG. 18 X-RAY DIFFRACTION PATTERNS OF K_2SO_4 - Fe_2O_3 MIXTURES IN PRESENCE OF SO_3 AT 1000 F

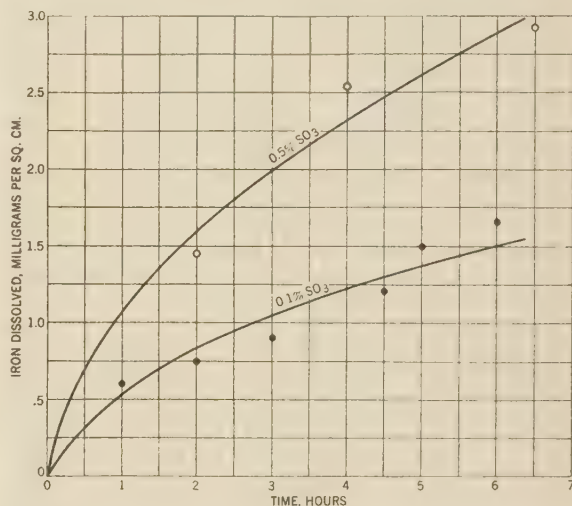


FIG. 19 CORROSION OF SOLID MAGNETITE COATED WITH FUSED ALKALI-METAL SULPHATES, IN THE PRESENCE OF SO_3 AT 1000 F

tween the salt and the oxide, and, under the conditions of these tests, the rate of removal of the oxide at 0.5 per cent SO_3 is approximately twice that at 0.1 per cent SO_3 . The pH of the coating, dissolved in sufficient water to make a 1 per cent solution, was 2.8. Strong lines of the compound $\text{K}_3\text{Fe}(\text{SO}_4)_3$ appeared in the X-ray diffraction pattern.

MECHANISM OF CORROSION

As the result of these studies of the chemical and physical properties of enamel, and of the behavior of synthetic deposits under controlled laboratory conditions at 1000 F, in atmospheres containing SO_3 , it is believed that corrosion occurs during operation of the furnace as the result of a chemical reaction between (a) the normal iron oxide on the furnace tubes, (b) the alkali-metal sulphates composing the deposit in contact with the oxide, and (c) the SO_3 in the atmosphere in contact with the enamel. This reaction results in the formation of the com-

compound $K_3Fe(SO_4)_3$ or $Na_3Fe(SO_4)_3$, which is found in the enamel. Corrosion will not occur to any appreciable extent in the absence of alkali-metal sulphates, or under conditions when the concentration of SO_3 is less than about 0.02 per cent, even though alkali-metal sulphates are present.

The sequence of events, assuming that a furnace with clean tubes is placed in operation, is shown schematically in Fig. 20 and may be described as follows:

Step A. As the result of normal oxidation between 600 and 800 F, a thin layer of oxide forms on the tube metal. The rate at which this oxide grows decreases with its thickness, and in the absence of adverse conditions, a more or less limited thickness is approached.

Step B. A layer of alkali-metal sulphates forms on the oxide. This is believed to result from the deposition on the tubes of alkali-metal oxides which originate from the flame and from the molten slag on the hearth by volatilization, subsequent reaction with SO_3 in the surrounding atmosphere forming alkali-metal sulphates.

Step C. As the layer of alkali sulphates thickens, the surface temperature increases to the point where it becomes somewhat sticky, and ash particles begin to adhere to it. As a consequence of a porous structure, the initial deposit of ash has a low thermal conductivity, therefore, as it thickens, the outside temperature ultimately increases to the point where the ash begins to form a layer of slag. During this process, SO_3 is evolved as the result of reactions in the ash during the melting process.

Step D. The SO_3 diffuses through the alkali-metal sulphates and reaction occurs at the oxide-sulphate interface forming $K_3Fe(SO_4)_3$ or $Na_3Fe(SO_4)_3$, thus reducing the thickness of the oxide. The metal then will oxidize further to renew the oxide layer. At the same time, the thickness of the slag layer increases and reaches equilibrium, the temperature at the surface of the enamel deposit decreasing because of the low thermal conductivity of the slag.

Step E. Deslagging increases the temperature of the enamel, causing a portion of it to exceed the decomposition temperature of the $K_3Fe(SO_4)_3$ and $Na_3Fe(SO_4)_3$, and SO_3 is released, part of which diffuses to the oxide-sulphate interface and reacts with the oxide and the excess K_2SO_4 and Na_2SO_4 . Meanwhile, more alkali-metal sulphate is depositing on the enamel until another layer of slag forms and the cycle is repeated.

The mechanism of the formation of alkali-metal sulphates on the furnace-wall tubes (Step B) and of the SO_3 from the slagging reactions (Step C) requires further explanation.

Regarding the alkali-metal sulphates, it has been noted in glass-melting furnaces²⁶ that Na_2SO_4 may be deposited on relatively cool surfaces in the furnace, despite the fact that the glass charge contains no Na_2SO_4 . These furnaces were fired with producer gas from coal having 1.7 to 3.2 per cent sulphur, hence it appears that the Na_2O which volatilizes from the glass charge and condenses on the cooler parts of the furnace reacts with the small amount of SO_3 in the furnace gas and forms Na_2SO_4 . At the operating temperatures of these furnaces, the amount of SO_3 present should be a small fraction of the SO_2 , as is also the case in pulverized-coal-fired furnaces. The alkali-metal sulphates are relatively stable compounds, the sodium salt for example decomposing to a negligible extent at 2550 F,²⁷ thus implying that they can form at lower temperatures in the presence of extremely small concentrations of SO_3 .

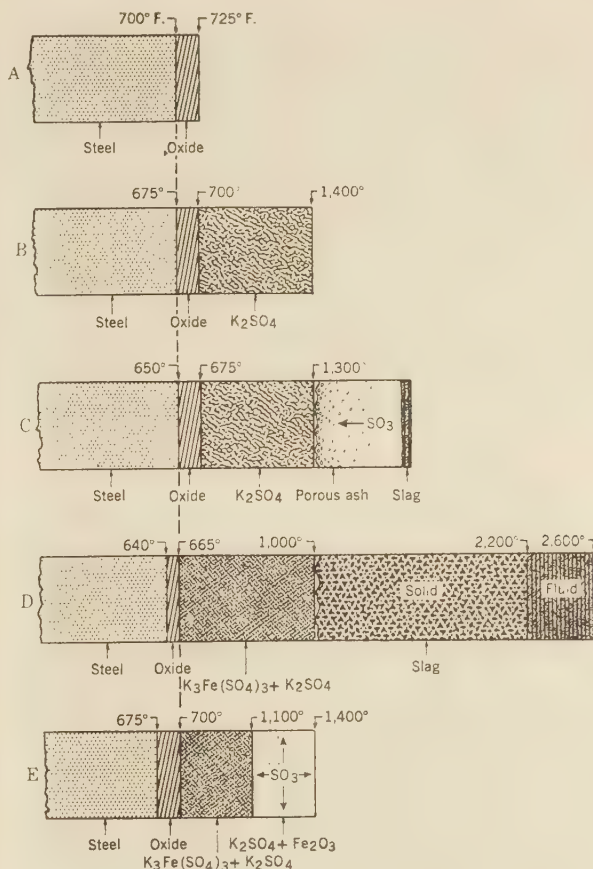


FIG. 20 MECHANISM OF CORROSION OF WALL TUBES BY SULPHATE DEPOSITS

Although laboratory tests conducted in a gas-fired furnace, containing molten slag to which sodium sulphate was added, showed that perceptible amounts of alkalis were volatilized (as shown by their condensation on a steel surface at 800 F), and other smaller scale tests of the salts alone, melted in platinum crucibles showed that volatilization of alkalis was evident at 2400 F for Na_2SO_4 and 1650 F for Na_2CO_3 , it is not believed that the loss of alkalis from the hearth of slag-tap furnaces is of great consequence. No information is available on the loss of alkalis from molten slag, but data on the rate of volatilization of alkalis from glass have been reported by Bradley.²⁸ The small amount lost at 2640 F from a soda-lime-silica glass containing no SO_3 , 0.07 lb per sq ft per day, indicates that the total amount of alkalis volatilized per day from the hearth of a slag-tap furnace may be insignificant, and that excessively long periods would be required to condense sufficient alkalis on the wall tubes to form enamel. Thus the principal source of alkalis appears to be the flame itself, where the temperatures are high and the small particles of ash suspended in the burning gases have a large surface per unit weight. Under these conditions, it is reasonable to believe that the concentration of alkalis in the flame is high compared with that volatilized from the hearth; thus the impingement of this flame directly on tubes probably contributes alkalis at a higher rate than any other method of transfer.

²⁶ "Formation of Sodium Sulfate in Glass Furnaces and Defects Arising Therefrom," by W. E. S. Turner, *Journal of the Society of Glass Technology*, vol. 17, 1933, pp. 22-24.

²⁷ "Pyrogenetic Decomposition of Sodium Sulfate," by K. I. Losev, N. I. Nicolskaya, and T. G. Guseva, *Journal of Applied Chemistry* (U.S.S.R.), vol. 4, 1931, pp. 743-756.

²⁸ "Fume or Vapors From Molten Glasses," by C. A. Bradley, Jr., *Bulletin, American Ceramic Society*, vol. 23, no. 10, Oct. 15, 1944, pp. 379-381.

The availability of SO_3 is an important part of the mechanism. It is evident that the concentration of SO_3 in the furnace gases will be low as a result of the high temperatures involved, although, as was just shown, sufficient SO_3 exists at similar high temperatures in glass-melting furnaces to form Na_2SO_4 . An additional source of SO_3 is from reactions occurring during the formation of slag from coal ash, as shown in Step C. When coal ash melts, the sulphur it contains is released almost quantitatively, analyses of many slags from slag-tap furnaces showing the total sulphur content to be less than 0.1 per cent, computed as SO_3 . Whether the sulphur is evolved as SO_2 or SO_3 depends upon the form in which it occurs in the ash, but in either case O_2 also usually is present from thermal decomposition of ferric-iron compounds, so that any SO_2 released is capable of being oxidized to SO_3 while in contact with the porous ash. The presence of these gases is evident in any examination of slag from wall tubes, bubbles showing that gases were formed during melting of the slag.

SMALL-SCALE FUEL-FIRED FURNACE

One of the ultimate aims of the investigation is to reproduce this type of corrosion in the laboratory under conditions that simulate as closely as possible those in a slag-tap furnace. After a number of trials, a design of furnace was developed which meets the requirements. It consists of a refractory combustion chamber 9 in. square and 26 in. high, fired with either natural gas or pulverized coal. There are two burners, arranged so that the flame can be made to impinge directly upon a water-cooled low-carbon-steel specimen which is mounted in one wall 8 in. above the hearth, the heat-receiving surface being flush with the wall. To maintain an even temperature on the surface of the specimen and to prevent the transfer of heat from the adjacent refractory, a guard ring surrounds the specimen. The thickness of both specimen and guard ring is adjusted so that the surface of the metal is at a temperature of 800 to 1000 F, at a heat-transfer rate of approximately 200,000 Btu per hr per sq ft. Thermocouples at different depths in the specimen permitted extrapolation of temperatures to that of the surface. A radiation pyrometer was used to indicate furnace temperature, and the composition of furnace gases, which was easily controlled for any degree of oxidation or reduction, was determined in an Orsat apparatus, the sampling tube being water-cooled. The pulverized-coal feeder constructed in the laboratory also could be used for adding finely ground slag or various salts. As the specimen can be removed quickly for examination and measurement, and test conditions are under complete control, the maximum facility in conducting tests is possible.

Fig. 21 shows the log of a typical test in which slag and Na_2SO_4 were added alternately. The decrease in the rate of heat transfer following slagging of the specimen is evident, as is its gradual increase during the addition of Na_2SO_4 , probably because this salt acted as a flux to decrease the thickness of slag. Later, when slag was again added, the heat-transfer rate decreased only slightly, the fluxing effect of the Na_2SO_4 remaining on the specimen still being evident.

Although, in the relatively few tests made so far, it has not been possible to obtain corrosion deposits closely resembling those found in large furnaces, it is believed that the ability to reproduce large-scale conditions has been achieved and that further experimentation will furnish satisfactory results.

CONCLUSIONS

The results of laboratory experimentation have shown that external corrosion of furnace-wall tubes is the result of the com-

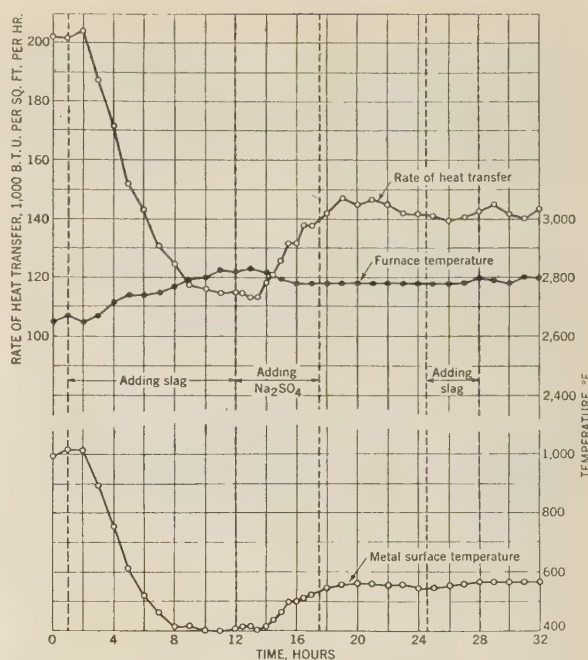


FIG. 21 LOG OF TYPICAL TEST IN GAS-FIRED FURNACE TO DUPLICATE CORROSION CONDITIONS

bined action on the tube surface of alkali-metal sulphate deposits and sulphur trioxide. Absence of either of these materials effectively prevents corrosion, neither material by itself being corrosive under normal furnace conditions.

From these considerations, it appears that prevention of corrosion will depend on establishing conditions at the tube surface such that alkali-metal sulphates cannot deposit on the tube, or the concentration of sulphur trioxide is reduced below that capable of reacting with alkali-metal sulphates and iron oxide to form $\text{K}_3\text{Fe}(\text{SO}_4)_3$ and $\text{Na}_3\text{Fe}(\text{SO}_4)_3$. This suggests that reducing the amount of alkali-metal oxides or sulphur trioxide in the gas phase in contact with the tube by the addition of air along the tube surface should effectively prevent further corrosion, thus corroborating field observation in which it was shown that the maintenance of oxidizing conditions near the tubes by means of burner changes or "air-belt" effectively stopped further loss of metal. Thus the addition of air serves only to ventilate the tube surface, the role of such air being considered to be that of a diluent, and the fact that carbon monoxide disappears in the process is not in itself important where "enamel" deposits are concerned.

ACKNOWLEDGMENTS

In addition to those whose help has been previously acknowledged,⁵ the authors express their gratitude for the efforts of the following in the laboratory work:

Robert C. Patterson, mechanical engineer, Combustion Engineering Company, assisted in the analytical and experimental work.

Florence Feicht, Physicist of the Health and Safety Branch, U. S. Bureau of Mines, made numerous X-ray diffraction analyses.

Edward C. Chapman, metallurgist, Combustion Engineering Company, and Richard Akin, metallurgist, the Superheater Company, made numerous photomicrographs of boiler tubes.

Helical Taper Reamers Milled With Constant Helix Angle

By THOMAS F. GITHENS,¹ CLEVELAND, OHIO

The author explains the process of milling helical flutes on a taper reamer so that the flute will have a constant helix angle of 45 deg at every point along the length of the reamer. The problem is solved by the development of a former or master cam cylindrical in shape and bearing upon its lateral surface a helical groove such that, as the cylinder turns on its axis with constant angular velocity, the whole former advances in the direction of its own axis at a controlled but variable feed. The milling cutter is mounted so that its plane forms a constant angle with an element of the taper blank being machined to form the reamer. The advantage of the method described is its adaptability to a quick practical solution either mathematically or by graphical means.

INTRODUCTION

THE problem is to mill helical flutes on a taper reamer so that they will have a constant helix angle of 45 deg at every point along the length of the reamer. Fig. 1 shows a helical taper pin reamer.



FIG. 1 HELICAL TAPER PIN REAMER

In the present discussion, the helix angle at any point on the helix is defined as the angle made by the tangent to the helix with the element through the point. It is defined mathematically by the equation: $\text{Tangent of the helix angle} = \text{circumference} / \text{lead}$. This definition is illustrated in Fig. 2.

On a cylinder, a helix with constant lead will have a constant helix angle, because of the relations existing in the formula just given.

On a cone, however, such as the surface of the taper reamer, the circumference varies with the distance from the apex or point; therefore, if the lead is constant, the tangent of the helix angle will vary with the circumference.

In order to obtain a constant helix angle on the cone, we must vary the lead with the circumference, so that (tangent of the helix angle = circumference/lead = a constant), i.e., circumference and lead must both vary.

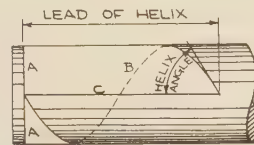
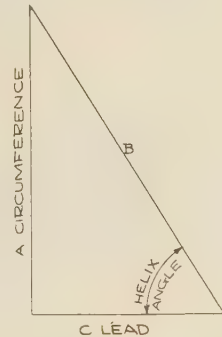
The problem is, with what lead must the helical flutes of the taper reamer be milled to secure a constant helix angle; or, in other words, the problem is that of finding a combination of circumference and lead so that the ratio is constant.

In Fig. 3 is shown a constant-lead helix on a cone. It is interesting to note that the horizontal projection of this helix is the "spiral of Archimedes." This is the spiral traced by a point

¹ Mechanical Engineer, Cleveland Twist Drill Company. Mem. A.S.M.E.

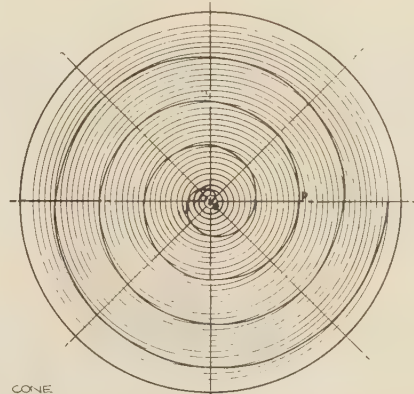
Contributed by Special Research Committee on Metal Cutting Data and Bibliography and presented at the Annual Meeting, New York, N. Y., Nov. 27-Dec. 1, 1944, of THE AMERICAN SOCIETY OF MECHANICAL ENGINEERS.

NOTE: Statements and opinions advanced in papers are to be understood as individual expressions of their authors and not those of the Society.



$$\text{TAN. HELIX ANGLE} = \frac{A}{C} = \frac{\text{CIRCUMFERENCE}}{\text{LEAD}}$$

FIG. 2 HELIX ANGLE



GIVEN CONE
TO FIND HELIX WITH CONSTANT LEAD
CONSTRUCTION: HORIZONTAL PROJECTION IS SPIRAL OF ARCHIMEDES.
DEFINED AS PATH TRACED BY POINT P WHICH, STARTING AT O,
MOVES WITH UNIFORM VELOCITY ALONG RAY OP WHILE RAY
ITSELF REVOLVES WITH
UNIFORM ANGULAR VELOCITY
ABOUT O. EQUATION IN
POLAR FORM: $P = K\theta$
WHERE P = RADIUS VECTOR
 θ = ANGLE OF
ROTATION (RADIAN'S)
K = CONSTANT

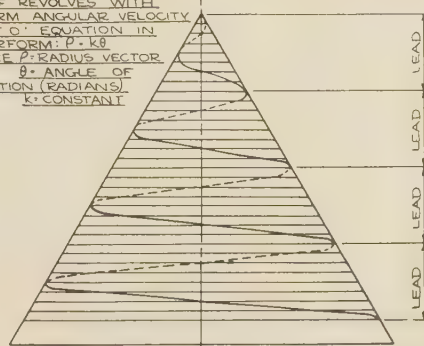


FIG. 3 HELIX ON CONE WITH CONSTANT LEAD

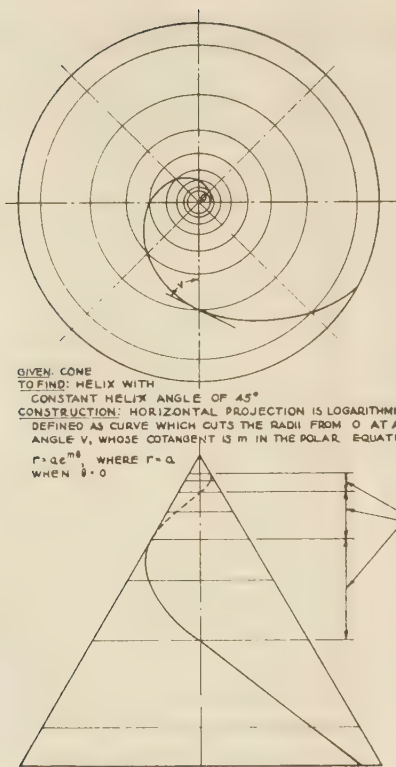
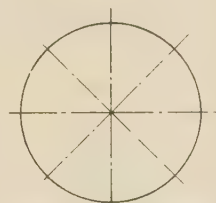


FIG. 4 HELIX ON CONE WITH CONSTANT HELIX ANGLE



GIVEN CYLINDRICAL FORMER
TO FIND: "INCREASED TWIST HELIX"
WHOSE LEAD AT EACH POINT IS THE
SAME AS THAT OF A 45° CONSTANT
ANGLE HELIX ON A GIVEN CONE
(TAPER PIN REAMER)
CONSTRUCTION BY PROJECTION

FIG. 5 HELIX ON CYLINDER WITH INCREASED TWIST

which, starting from the origin, moves with uniform velocity along a ray while the ray itself revolves with uniform angular velocity about the origin. In Fig. 4 is shown a constant-angle helix on a cone. This is the helix which presented the problem. How can this helix be calculated and drawn? In Fig. 5 is shown an increasing "twist" or lead helix on a cylinder. This helix has the same "leads" as the one shown in Fig. 4 and will produce the constant-angle helix on the cone there shown.

METHOD OF MILLING HELICAL TAPER REAMER

In Fig. 6 is shown diagrammatically the method of milling a helical taper reamer. The sketch shows the former or master cam cylindrical in shape, and bearing upon its lateral surface a helical groove, such that, as the cylinder turns on its axis with constant angular velocity, the whole former shall advance in the direction of its own axis at a controlled but variable feed.

There is also shown the milling cutter mounted so as to have its plane form a constant angle (45° deg in practice) with an element of the taper blank to be transformed into a reamer. From this diagram it will be seen that the lead of the reamer flutes is obtained from the "former" or guide. The problem resolves itself into the question: With what increasing or varying lead (increased twist helix) shall the grooves on the cylindrical former be cut to secure a groove of constant helix angle on the conical reamers?

The method of solution was to find the relation between the value of the axial distance from the vertex Z , see Fig. 7, and radius ρ of the cone for any point on the helix such as P , and the angle of rotation θ .

MATHEMATICAL ANALYSIS

For the method of analysis consider Fig. 7:

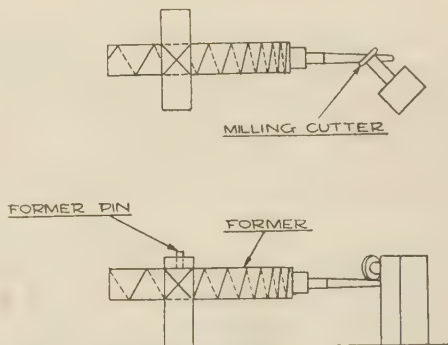


FIG. 6 METHOD OF MILLING A TAPER REAMER

(a) The angle between the axis and an element of the cone (angle β of the figure) is a constant.

(b) Let P be a representative point on the conical helix; APQ the corresponding element of the cone; TPT' a tangent to the conical helix and making with APQ a constant angle α , located in the tangent plane through the element APQ .

(c) Let $CP = \rho$ be the perpendicular distance of P from the axis of the cone.

(d) Since plane ACP is always perpendicular to the tangent plane APT' and since AP , the intersection of the two planes, makes constant angles with both CP and TPT' , the angle between CP and TPT' is also constant.

Consequently, the projections of CP or ρ and of TPT' , namely, OM and TM , on the x, y -plane, will always form a constant angle ψ of the figure.

(e) Consider the direction of $T'PT$ to be kept constant while the cone, to an observer looking from base to apex, rotates in a clockwise direction, thus causing point P to move relatively in a counterclockwise direction toward the base of the cone and away from the axis.

It is evident that the projection M of point P upon the xy -plane, i.e., upon any plane perpendicular to the axis of the cone, will travel in a spiral curve such that ρ is the radius vector of a representative point and MT , the xy -projection of the tangent $T'PT$, is always tangent to it. Our problem is now resolved into the finding of the equation of the spiral in the xy or any parallel plane in terms of the vectorial angle θ of the figure and the constants that are known; and, in obtaining a relation which will give the distance of P from a reference plane through a parallel to plane xy for any and every value of θ and of ρ .

Any standard textbook in calculus² derives the formula for the

$$\log C\rho = \frac{\sin \beta \theta}{\tan \alpha} = (\sin \beta \cot \alpha) \theta$$

This in exponential form is

$$C\rho = e^{(\sin \beta \cot \alpha) \theta}$$

or

$$\rho = \frac{1}{C} e^{(\sin \beta \cot \alpha) \theta}$$

$$\text{Let } R = \frac{1}{C} = \text{const}$$

$$\therefore \rho = R e^{(\sin \beta \cot \alpha) \theta} \dots \dots \dots [1]$$

when $\theta = 0$, $\rho = \frac{1}{C} = R$, where R is the initial value of the radius vector for the value of $\theta = 0$. This is the equation of the curve known as the "logarithmic spiral." By definition this is a curve which cuts radii from the origin at a constant angle.

Again, from Fig. 7, let the distance of P from a reference plane, through the vertex A parallel to plane xy , namely, AC , be called z , then

$$\frac{AC}{CP} = \frac{z}{\rho} = \cot \beta, \text{ i.e., } z = \rho \cot \beta \dots \dots \dots [2]$$

since $CP = OM = \rho$ is a representative radius vector.

The foregoing Equations [1] and [2] fully define the motion styled a conical helix.

In Equation [2], we can substitute the value of ρ given in Equation [1] and get

$$z = \cot \beta (R) e^{(\sin \beta \cot \alpha) \theta} \dots \dots \dots [3]$$

In this equation there are two unknowns z and θ . All the other values are constants given by the problem. To construct the helix, assume values for θ and compute the corresponding values of z . The former itself may then be laid out in a milling machine by turning the former through the required angle θ with an index head and then measuring off the distance z by means of the micrometer measuring screw.

The curve may also be plotted on a piece of paper, abscissas being distances around the circumference (θ), and ordinates being the distances z . This paper may then be wrapped around the cylindrical former thus getting the helical curve.

SAMPLE CALCULATIONS

Sample calculations from these formulas are as follows:

Taper of reamer $1/4$ in. per ft.

Diameter of reamer at small end is 0.075 in., radius (R) is 0.0375 in.

Helix angle required is 45 deg.

From this

$$\tan \beta = \frac{1/2 \times 1/4}{12} = \frac{1}{96} = 0.0104167$$

$$\cot \beta = 96$$

$$\therefore \beta = 0^\circ 35' 48\frac{1}{2}''$$

$$\therefore \sin \beta = 0.0104160$$

$$\cot \alpha = \cot 45^\circ = 1$$

$$R = 0.0375$$

$$e = 2.71828$$

Substituting in Equation [3], we get

$$z = (96) (0.0375) 2.71828^{(0.0104160 \theta)}$$

$$= (3.6000) 2.71828^{(0.0104160 \theta)}$$

$$\log z = \log 3.6000 + 0.0104160 (\theta) \log 2.71828$$

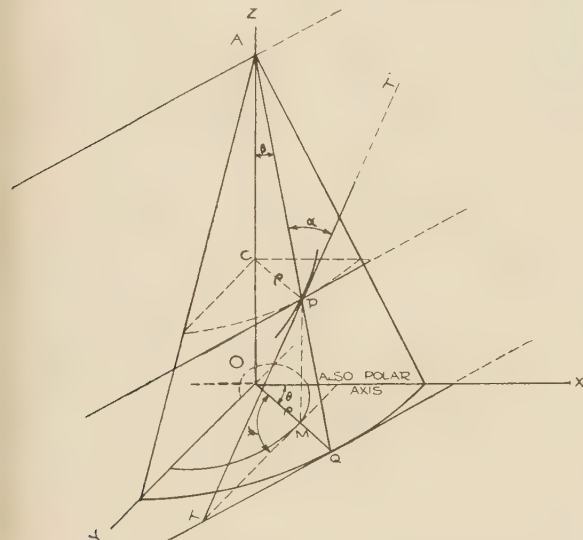


FIG. 7 MATHEMATICAL DIAGRAM

angle between the radius vector of a curve, whose equation is in polar co-ordinates, and the corresponding tangent to the curve. The formula is

$$\cot \psi = \frac{1}{\rho} \frac{d\rho}{d\theta}$$

Applying this

$$\frac{1}{\rho} \frac{d\rho}{d\theta} = \cot \psi = \cot (OMT) = \frac{MQ}{QT}$$

$$= \frac{PQ \sin (MPQ)}{PQ \tan \alpha} = \frac{\sin \beta}{\tan \alpha}$$

Since β and α are definite angles, $\sin \beta$ and $\tan \alpha$ are constants. By separation of the variables

$$\frac{d\rho}{\rho} = \frac{\sin \beta d\theta}{\tan \alpha}$$

By integration

$$\log \rho + \log C = \frac{\sin \beta \theta}{\tan \alpha}$$

that is

² See for example, "Elements of the Differential and Integral Calculus," by W. H. Granville, Ginn and Company, Boston, Mass., 1911, p. 144.

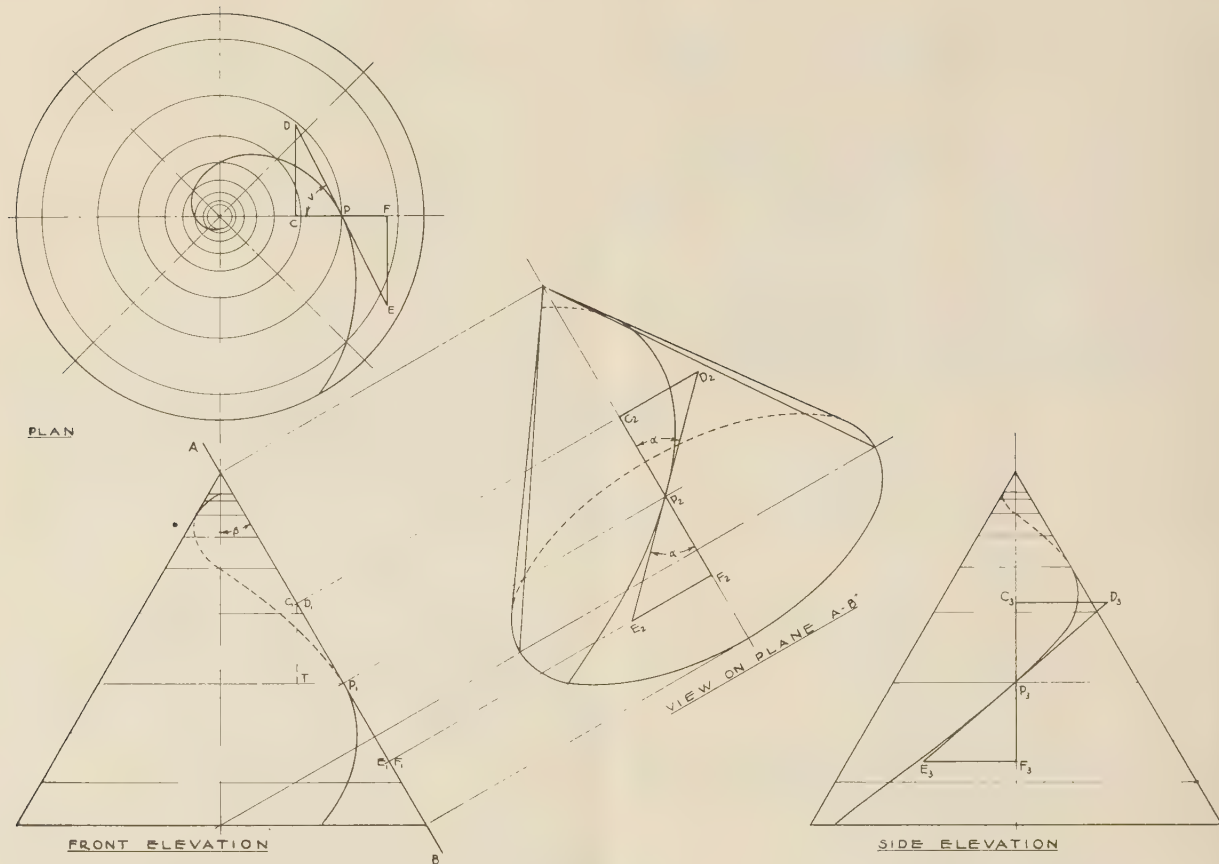


FIG. 8 GRAPHICAL ILLUSTRATION

Therefore

$$\log z = 0.5563025 + 0.0045236 (\theta)$$

Substituting various values for θ , we can calculate z as given in Table 1.

TABLE 1 CALCULATING VALUES FOR z

θ	z	Increase
$1/2 \pi$ or $1/4$ revolution	3.6594	
π or $1/2$ revolution	3.7198	0.0604
$1 1/2 \pi$ or $3/4$ revolution	3.7811	0.0613
2π or 1 revolution	3.8435	0.0624
$2 1/2 \pi$ or $1 1/4$ revolutions	3.9069	0.0634
3π or $1 1/2$ revolutions	3.9713	0.0644
$3 1/2 \pi$ or $1 3/4$ revolutions	4.0368	0.0655
4π or 2 revolutions	4.1034	0.0666
$4 1/2 \pi$ or $2 1/4$ revolutions	4.1711	0.0677
5π or $2 1/2$ revolutions	4.2399	0.0688

For a graphical solution of the problem refer to Fig. 8; in this figure we have data as follows:

Given: The vertex angle of the cone (β) and the helix angle of the helix (α).

To find: The constant angle v of the logarithmic spiral, which is the horizontal projection of the helix, in terms of β and α :

$$r = ae^{m\theta} \text{ is equation of logarithmic spiral}$$

$$a = 0.0375 \text{ for smallest reamer } (\theta = 0)$$

$$m = \cot v \text{ (see footnote}^3\text{)}$$

To illustrate the method of finding m :

- 1 Draw cone in plan, elevation, and the two end views
- 2 Assume point P , find projections P_1, P_2, P_3
- 3 The tangent to the helix at P will lie in the plane AB , which is tangent to the cone
- 4 Assume P_1D_1 and P_1E_1 convenient equal lengths
- 5 Draw D_2E_2 so that $E_2P_2F_2$ equals helix angle
- 6 Draw horizontal projections CD, EF , and $DPE, CD = C_2D_2$.
- 7 Draw side elevation C_3D_3, E_3F_3 , and $D_3P_3E_3, C_3D_3 = C_2D_2$

$$m = \cot v = \cot CPD = \frac{CP}{CD} = \frac{TP_1}{C_2D_2} = \frac{C_1P_1 \sin \beta}{C_2D_2}$$

$$\frac{C_1P_1}{C_2D_2} = \frac{C_2P_2}{C_2D_2} = \cot \alpha$$

$$\therefore m = \sin \beta \cot \alpha$$

$$\text{When } \alpha = 45^\circ, \cot \alpha = 1$$

$$\therefore m = \sin \beta$$

$$\therefore r = ae^{(\sin \beta)\theta}$$

$$a = 0.0375$$

$$e = 2.71828$$

$$\sin \beta = 0.0104160$$

$$(\tan \beta = 1/8 \div 12 = 1/96 \\ = 0.0104167)$$

$$\therefore r = 0.0375 \times 2.71828^{(0.0104160 \theta)}$$

³ "Mechanical Engineers' Handbook," by Lionel S. Marks, fourth edition, McGraw-Hill Book Company, Inc., New York, N. Y., 1941, p. 155.

CONCLUSIONS

When the tangent to a helix on a conical surface makes a constant angle with the element of the cone through the point of tangency, then the projection of the helix on a plane perpendicular to the axis of the cone is a logarithmic spiral. From the equation of the logarithmic spiral can be readily found the radius vector of the point on the helix corresponding to any particular angle of rotation. This radius vector is trigonometrically related to the axial distance from the vertex of the given cone.

Knowing the axial distance from the initial position of the helix on the cone, a cylindrical former for producing that helix can be laid out having an increased twist helix on its surface, any point of which is at the same axial distance from its initial position as the point on the conical helix for the same angle of rotation.

The advantage of this method is its adaptability to a quick practical solution either mathematically or by graphical means.

ACKNOWLEDGMENT

The author is indebted for the method given in the "Mathematical Analysis" section to Charles F. Thomas, Professor of Mathematics of Case School of Applied Science, Cleveland, Ohio.

Discussion

E. A. RATZEL.⁴ The author has presented an extremely interesting means of machining taper reamers with a constant helix angle. He shows clearly the procedure to be followed for a particular angle and taper. There is an implication, however, that each size and shape of reamer requires a special former.

The following discussion shows that a former designed for one reamer can be used to machine all reamers regardless of size, taper, or helix angle. Either a milling machine or a lathe can be used. A lathe will prove more satisfactory if production is sufficient to warrant almost continuous use of one machine. Substitution of a former for the lead screw of a lathe is all that is required.

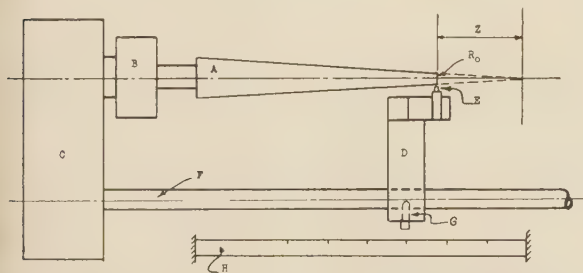


FIG. 9 DIAGRAM SHOWING FORMER SUBSTITUTED FOR LEAD SCREW OF LATHE TO MAKE REAMERS OF ANY SIZE, TAPER, OR HELIX ANGLE

Fig. 9 of this discussion illustrates the application. A graduated scale H for R_{fl} is fixed relative to the former F . The position of the saddle D is adjusted until the former pin G is at a value of R_{fl} , calculated from

$$R_{fl} = R_0 \frac{\cot \beta}{\cot \beta_f}$$

The cutting tool E , which has been ground to the shape of the flute desired, is set at the end of the taper by using the compound rest at 90 deg, or by adjusting the taper in the chuck. The taper attachment of the lathe is used in the ordinary manner.

The ratio of the speed of the chuck to the speed of the former $\frac{\theta}{\theta_{fl}}$ is calculated from

$$\frac{\theta}{\theta_{fl}} = \frac{\sin \beta_f \cot \alpha_f}{\sin \beta \cot \alpha}$$

The taper reamer will then be cut with a constant helix angle.

The two formulas just given have been determined by equating the relation between Z and θ for a taper reamer requiring α , β , and R_0 to the relation between Z_f and θ_f of the former designed for α_f and β_f . Here θ_{fl} is measured from a point at which $R = R_{fl}$.

A, Tapered shaft	E, Cutting tool
B, Lathe chuck	F, Former substituted for lead screw
C, Geared drive	G, Former pin
D, Saddle	H, Graduated scale for R_{fl}

F. W. LUCHT.⁵ The writer has had occasion to assist in the tooling up of many taper-reamer jobs where it was considered advisable to have reamer flutes milled at a 45-deg helix angle to obtain a smooth finish in the taper hole in finish-reamed parts. Most of these jobs did not have a slight taper of $1/4$ in. per ft as is used on taper pin reamers but had increased tapers of $3/4$ in. per ft, $1 1/2$ in. per ft, and even larger. This made the problem even more difficult to handle than that cited by the author.

The best we could do when we milled the flutes in the reamer was to select a lead which would give an average helix angle of 45 deg in the portion of the reamer which would do the most work. This meant that we obtained a helix angle less than 45 deg as we approached the small end of the reamer, and a helix angle greater than 45 deg as we milled the flutes nearer to the large end of the reamer. The deviation from the required 45-deg helix angle would become even greater for reamers which had increased tapers.

It was also found that when these taper reamers were put into operation, one end of the reamer would sometimes leave a much better finish in the hole than the other end. When this happened, we frequently had to make more than one taper reamer until we found one which would meet the requirements.

Such a method as described by the author will permit a taper reamer to be made with some definite degree of spiral which it is known will give the best results. This reamer will give a uniformly smooth finish for the full length of the taper hole in the work when it is new. It should also give a uniformly smooth finish in the taper hole for the successively different axial positions as the reamer is sharpened to the final position where it becomes undersize in diameter.

Owing to the fact that a former is required for this method of milling a taper reamer, is it possible that this method can only be applied to reamers having definite sizes and tapers? It would seem that a former can be developed for each size taper, for example, one for $1/4$ TPF, one for $3/4$ TPF, one for $1 1/2$ TPF, etc., and when a particular reamer has to be milled, a definite portion of the former can be used. In other words, if the small diameter of $3/4$ TPF reamer is $1 1/4$, the flute length is 6 in., and its large diameter is $1 5/8$, one portion of the former will be used. If the small diameter of another $3/4$ TPF reamer is $1 1/2$, the flute length is 7 in., and the large diameter of the reamer is $1 15/16$, another portion of the former will be used.

There is no reason why this analysis cannot be applied to helix angles other than 45 deg.

AUTHOR'S CLOSURE

The author is grateful to Mr. Ratzel for his valuable suggestion

⁴ Associate Engineer, Armour Research Foundation, Chicago, Ill.

⁵ Development Engineer, Carboly Company, Inc., Detroit, Mich.

which makes it possible to adapt one former to any size, taper, or helix angle.

In the machine set up as shown in Fig. 6, the one former has actually been used for a large range of reamer sizes by starting the former at various points along its axis; but the former can be used for only those combinations of taper and helix angles as will make $\sin \beta \cot \alpha = 0.0104160$; see sample calculations following Equation [3]. For other tapers and helix angles it would be necessary to make a new former. Mr. Ratzel ingeniously uses one former as a lead screw and by the proper gearing as shown in his equation secures another increased lead which will fit any combination of size, taper, and helix angle. This cannot be done in a machine of the type shown in Fig. 6 where

the former directly turns and moves the work forward, without the use of change gears.

The experiences related by F. W. Lucht are very interesting and show that there are practical problems for which this method will supply the solutions. As Mr. Lucht says, one former will mill a large range of sizes of a given taper and helix angle; for example, for a taper of $1/4$ inch per foot and a helix angle of 45 deg one former was actually used for milling all sizes from about 0.0966 in. to 0.3540 in. This was done by using the part of the curve in Figs. 4 and 5 near the apex for small sizes, and the part near the base for larger sizes. The exact place to start on the former can be calculated by substitution of the correct value of R in Equation [3].

Silica Deposition in Steam Turbines

By F. G. STRAUB² AND H. A. GRABOWSKI,² URBANA, ILL.

Laboratory and power-plant tests have been conducted to determine the cause of silica deposition in steam turbines. The tests indicate that the silica leaves the boiler as vaporized silicic acid which later crystallizes on the blades in the lower-pressure stages of the turbine. When the silica in the steam is below 0.1 ppm, no appreciable deposits are found in the turbines. Two methods of preventing deposits are suggested; (1) maintain the silica in the boiler water below 5 ppm; (2) remove the silica from the steam by scrubbing with a pure-grade water.

TURBINE-blade deposits have been the cause of much trouble in the steam-power plant. In recent years almost parallel with the increase in steam pressures, a new type of deposit appears to be forming in steam turbines. When the upper steam pressures were about 600 psi, the deposits which formed were water-soluble and could readily be removed by a water wash. The average type of deposit was mainly the sodium salts such as chlorides, sulphates, and silicates together with sodium hydroxide.

Since the increase of steam pressures to around 1400 psi and the installation of topping turbines, the type of deposit formed in the high-pressure end of the topping turbine is similar to older types and is water-soluble. However, at the low-pressure end of the topping unit and in the low-pressure machines, a deposit insoluble in water is formed. This deposit consists mainly of silica (SiO_2) in its various crystalline forms. It may be removed by mechanical cleaning or by washing with sodium hydroxide.

It has been rather difficult to give a logical explanation of how the silica present in the boiler water as sodium silicate is transported through the high-pressure turbine and deposited on the low-pressure machines as a crystalline silica. Splittgerber³ presented experimental data which showed that silica could be vaporized from silicic acid in appreciable amounts at 100 atm steam pressure. These results showed that the silica in the steam increased with increasing silica concentration in the boiler water. As the pressure increased, the silica in the steam increased. The addition of NaCl , Na_2SO_4 , NaOH , and Na_3PO_4 to the boiler water caused the silica in the steam to decrease. The values given by Splittgerber were not readily correlated with data available from boiler operation.

If this work of Splittgerber could be carried further and additional data collected as to the feasibility of silica leaving the boiler as vaporized silicic acid, a logical explanation would be available to account for the deposition of the silica crystals in the low-pressure turbines. If silicic acid has an appreciable vapor pressure at higher steam pressures, the sodium silicate in the boiler would hydrolyze, and silicic acid would be present in the

steam in amounts depending on the mole concentration of the silicic acid in the boiler water and the vapor pressure of silicic acid at that temperature. Since the concentration in boiler water of the silicates is very low, the amount in the steam would be much lower than that corresponding to the true vapor pressure of silicic acid. When superheated steam containing this amount of silicic acid is dropped in pressure and temperature, a point will be reached where the silicic acid in the steam becomes greater than the amount corresponding to the vapor pressure of solid silicic acid. When this point is reached, the silicic acid in the steam will leave the superheated steam and deposit as a hydrated-silica deposit. If the steam reaches the saturation point before this occurs, the silicic acid being slightly soluble in water will be dissolved in the condensate and no deposit will form.

Since this appeared to be a logical approach to this problem, laboratory work parallel with power-plant tests was inaugurated in order to see if Splittgerber's method of approach was applicable to the problem of silica blade deposits. The laboratory work was conducted along two lines as follows:

- 1 The relationship between silica in the steam and silica in the boiler water at various pressures.
- 2 The relationship between solid silicic acid and the silica in the steam at various pressures and temperatures.

The power-plant tests were conducted to find the following:

- 1 The relationship between the silica in the steam and silica in the boiler water.
- 2 The changes occurring in the silica in the steam as it passed through the turbines.

LABORATORY INVESTIGATION

RELATIONSHIP BETWEEN SILICA IN STEAM AND SILICA IN BOILER WATER AT VARIOUS PRESSURES

The silica in the steam cannot be considered as being mechanically carried into the steam as the soluble silicate occurring in the boiler water. If it were being mechanically carried, the salts in the steam entering the superheater should be present in the same relative proportions as they are in the boiler water. Thus, with a total dissolved-solids content of 500 ppm and SiO_2 30 ppm in the boiler water, a steam having 0.30 ppm of SiO_2 should have 5 ppm of soluble solids present, if the silica were present as a mechanical carry-over from the boiler water. Since the total solids in the average steam, as indicated by conductance measurements and evaporation tests, are well below 1 ppm, the presence of such a large percentage of silica would indicate that there was a selective concentration of silica in the steam.

If the silica were being vaporized as silicic acid, such concentrations could occur in the absence of mechanical carry-over. In order to obtain data as to the possibility of such vaporization, tests were started using a high-pressure laboratory boiler, Fig. 1. This boiler was designed to prevent any mechanical entrainment of boiler water in the steam. It also prevents any condensation of steam prior to leaving the boiler and thus gives a representative sample of the steam in equilibrium with the boilerwater.

The steam from the boiler was condensed under pressure, the pressure reduced to atmospheric, and passed through a conductivity cell and a glass electrode to determine the conductance and pH value before exposure to air. In order to check the amount of

¹ Data from research conducted at the University of Illinois in co-operation with the Utilities Research Commission of Chicago and released by permission of both organizations.

² Engineering Experiment Station, University of Illinois.

³ "The Volatility of Silicic Acid," by A. Splittgerber, *Archiv. für Wärmewirtschaft*, vol. 22, 1941, p. 66.

Contributed by the Joint Research Committee on Boiler Feedwater Studies and presented at the Annual Meeting, New York, N. Y., Nov. 27-Dec. 1, 1944, of THE AMERICAN SOCIETY OF MECHANICAL ENGINEERS.

NOTE: Statements and opinions advanced in papers are to be understood as individual expressions of their authors and not those of the Society.

entrainment of boiler water in the steam, the boiler was operated at 600 F (1540 psi) with 1200 ppm NaCl in the boiler water. The steam contained less than 0.01 ppm of NaCl. Tests with sodium hydroxide gave similar results. These tests showed that the mechanical entrainment of boiler water was less than 0.001 per cent.⁴

The boiler was then operated with varying amounts of sodium silicate in the boiler water by adding crystalline $\text{Na}_2\text{SiO}_3 \cdot 5\text{H}_2\text{O}$ or a solution $\text{Na}_2\text{O} \cdot 2\text{SiO}_2$, or NaOH to distilled water. The conductance, pH value, and silica content of the steam were determined. The silica content was determined colorimetrically.⁵ Table 1

TABLE 1 RELATION OF COMPOSITION OF SOLUTION IN BOILER TO STEAM LEAVING BOILER

Temp. of Sat. Steam	Solution in Boiler			Steam			Ratio in % $\frac{\text{SiO}_2 \text{ Steam}}{\text{SiO}_2 \text{ Soln.}}$
	SiO_2 ppm	pH	NaCl ppm	SiO_2 ppm	Sp. Cond. Micromhos	pH	
550	4.4	8.8	----	0.02	0.33	7.35	0.45
550	3.8	10.2	----	0.02	0.31	7.65	0.52
550	20.4	10.2	----	0.07	0.35	7.60	0.35
550	20.2	10.1	700	0.07	0.37	7.50	0.35
550	20.2	10.1	1460	0.06	0.42	7.50	0.30
600	4.4	8.8	----	0.06	0.43	6.50	1.36
600	3.8	10.2	----	0.04	0.30	7.40	1.05
600	12.8	10.3	----	0.14	0.32	7.70	1.10
600	21.4	10.5	----	0.22	0.29	7.60	1.05
600	21.0	10.1	1580	0.17	0.42	7.20	0.82
600	18.8	10.2	3160	0.16	0.56	7.20	0.85
600	19.6	11.1	3160	0.09	0.60	7.30	0.46

gives the results of these tests. The results indicated that at 550 F (1045 psi), there was a measurable amount of SiO_2 in the steam which increased as the silica in the boiler water increased; at 600 F (1540 psi), the SiO_2 in the steam reached an amount equal to about 1 per cent of the silica in the boiler water when the pH value of the boiler water was around 10. The addition of sodium chloride to the boiler water decreased the silica in the steam a small amount. However, increasing the pH value of the boiler water from 10.2 to 11.1 had a much greater effect in reducing the silica in the steam than the addition of 3160 ppm of NaCl had on the SiO_2 content. Another interesting observation was that, as the silica in the steam varied, the conductance and pH value of the steam remained practically constant. This indicated that the silica was present in a form which would not affect the pH value or conductance of water to any marked degree for such low concentrations.

Table 2 shows the results of tests run at 600 F (1540 psi) with potassium hydroxide, silicate, and chloride in the boiler water. The results indicate that the ratio of the silica in the steam to the silica in the boiler water is the same as when the sodium salts were present. As the pH of the boiler water increases, the SiO_2 in the steam decreases. The addition of KCl also decreases the SiO_2 in the steam.

In order to vary the silica content of the boiler water and to study the effect of solids present in the boiler water, the procedure of testing was changed. Steam generated from distilled water in the boiler, shown in Fig. 1, was passed into a bomb, Fig. 2, so constructed that the steam bubbled through a solution kept at the same temperature as the steam. The composition of the solution could be varied as desired by adding chemicals. The advantage of the use of the bomb was that it could be easily taken apart and cleaned when different solutions or solids were used.

Table 3 gives the results of tests conducted at 600 F (1540 psi), in which varying amounts of silicates were in solution in the bomb at different pH values. The results obtained are in good agree-

TABLE 2 RELATION OF COMPOSITION OF SOLUTION IN BOILER TO STEAM LEAVING BOILER

Temp. of Sat. Soln.	Solution in Boiler		Potassium Salts Used in Boiler			Ratio in % $\frac{\text{SiO}_2 \text{ Steam}}{\text{SiO}_2 \text{ Soln.}}$
	SiO_2 ppm	pH	SiO_2 ppm	Sp. Cond. Micromhos	pH	
600	1.9	8.0	0.03	0.27	7.22	1.58
600	5.2	8.2	0.06	0.27	7.22	1.15
600	17.0	8.8	0.23	0.27	7.22	1.36
600	17.2	9.6	0.20	0.25	7.20	1.16
600	19.2	10.7	0.16	0.26	7.20	0.84
600	19.8	11.1	0.12	0.27	7.20	0.61
600	6.0	10.8 (1)	0.03	0.36	7.20	0.50
600	19.4	11.0 (2)	0.10	0.35	7.17	0.53

(1) Solution also had 1000 ppm KCl present.

(2) Solution also had 1880 ppm KCl present.

ment with those obtained in the tests reported in Tables 1 and 2 and show that apparently the bomb tests are similar to the boiler tests.

Table 4 gives the results of tests conducted at temperatures between 400 F (250 psi) and 600 F (1540 psi), with high concentrations of silica and lower pH values. Table 5 gives the results of tests run between 500 and 600 F, with pH values similar to those encountered in steam-boiler operation.

When the ratio of the SiO_2 in the steam to the SiO_2 in the solution is plotted against the pH value of the solution, Fig. 3, it is shown that this ratio varies inversely with the pH value. With a

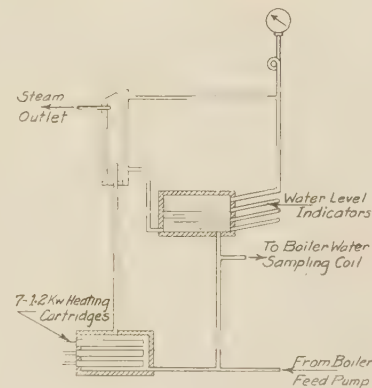


FIG. 1 HIGH-PRESSURE BOILER

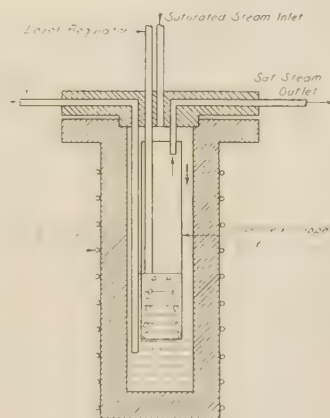


FIG. 2 BOMB USED TO HOLD SILICA SOLUTIONS

⁴ "Solubility of Salts in Steam at High Pressures," by F. G. Straub, Proceedings, Third Water Conference, Engineering Society of Western Pennsylvania, 1942.

⁵ "Photometric Determination of Silica in Condensed Steam in Presence of Phosphates," by F. G. Straub and H. A. Grabowski, *Industrial and Engineering Chemistry, Anal. Ed.*, vol. 16, 1944, p. 575.

TABLE 3 RELATION OF COMPOSITION OF SOLUTION IN BOMB TO STEAM LEAVING BOMB

Temperature 600°F (1545 psi)

Solution in Bomb		Steam		Ratio in %	
SiO ₂	pH	SiO ₂	Sp. Cond.	SiO ₂ Steam	SiO ₂ Soln.
ppm		ppm	Microhms		
8.6	8.4	0.12	0.25	7.10	1.40
3.6	8.8	0.03	0.28	6.80	0.83
41.7	9.6	0.40	0.23	7.60	0.96
6.4	9.7	0.04	0.27	7.05	0.74
6.4	9.8	0.05	0.26	6.95	0.78
51.0	9.8	0.49	0.26	7.60	0.96
5.4	9.9	0.06	0.36	7.07	0.93
7.0	10.0	0.06	0.28	7.00	0.85
6.9	10.0	0.06	0.35	7.13	0.87
36.6	10.0	0.37	0.28	7.72	1.00
48.6	10.0	0.48	0.24	7.26	1.00
7.1	10.2	0.07	0.28	7.00	1.00
42.2	10.2	0.44	0.31	6.95	1.02
52.0	10.2	0.52	0.29	6.95	1.00
41.8	10.5	0.36	0.29	7.06	0.86
3.8	10.6	0.01	0.22	7.50	—
22.8	10.8	0.20	0.23	6.88	0.88
30.2	10.8	0.23	0.22	6.95	0.76
0.7	11.6	0.01	0.33	7.15	—
39.0	11.7 (1)	0.27	0.70	7.50	0.69
16.4	11.8	0.08	0.24	6.90	0.49
18.0	11.8	0.08	0.38	7.25	0.44
42.5	11.8 (1)	0.22	0.31	7.10	0.52
43.9	11.8 (1)	0.25	0.36	7.17	0.67
30.2	11.9	0.13	0.28	7.05	0.43
32.2	11.9	0.13	0.23	7.00	0.41
63.0	12.0	0.33	0.25	7.08	0.52
23.6	12.1	0.10	0.26	7.10	0.42

 (1) Solution also had 1400 ppm Na₂SO₄ present.

TABLE 4 RELATION OF COMPOSITION OF SOLUTION IN BOMB TO STEAM LEAVING BOMB

 High Silica in Bomb
Solution with pH Low.

Solution in Bomb		Steam		Ratio in %	
Temp. of Sat. Steam	SiO ₂	SiO ₂	Sp. Cond.	SiO ₂ Steam	SiO ₂ Soln.
F	ppm	ppm	Microhms		
400	600	8.1	0.02	0.37	7.80
450	600	8.1	0.10	0.28	7.75
500	665	6.8	0.55	0.28	7.25
500	336	8.6	0.16	0.40	7.80
550	435	8.6	0.80	0.38	7.10
550	500	6.8	1.80	0.34	6.85
550	735	9.8	0.66	0.36	7.90
600	465	7.6	6.90	0.44	6.20

TABLE 5 RELATION OF COMPOSITION OF SOLUTION IN BOMB TO STEAM LEAVING BOMB

Silica in Bomb with Average pH Values

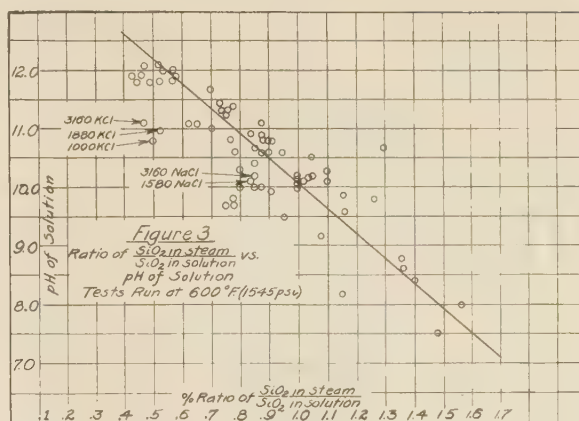
Solution in Bomb		Steam		Ratio in %	
Temp. of Sat. Steam	SiO ₂	SiO ₂	Sp. Cond.	SiO ₂ Steam	SiO ₂ Soln.
F	ppm	ppm	Microhms		
500	6.4	9.2	0.00	0.00	0.00
500	25.	10.1	0.00	0.00	0.00
500	17.	11.1	0.01	0.06	0.06
500	99.	11.0	0.04	0.04	0.04
550	6.4	9.2	0.02	0.31	0.31
550	25.	10.1	0.04	0.16	0.16
550	99.	11.0	0.12	0.12	0.12
550	97.	11.2 (1)	0.16	0.16	0.16
600	25.	10.1	0.20	0.80	0.80
600	24.	10.3 (2)	0.19	0.80	0.80
600	66.	11.1	0.44	0.65	0.65

(1) Solution also had 1550 ppm NaCl present.

(2) Solution also had 424 ppm NaCl present.

low pH value in the solution, the silica content of the steam is greater than when the pH value is high.

The silica present in the steam is of a very high order of magnitude when compared to the sodium hydroxide or sodium chloride found in the steam. At 600 F (1540 psi), saturated steam from the hydroxide or chloride solutions showed less than 0.001 per cent of the sodium salts in the steam. However, when silicates were present in the solution, the silica in the steam varied between 0.4 and 1.6 per cent of the silica in the solution. This variation in silica from 0.4 to 1.6 per cent was due to the change in pH of the solution. Thus the silica is present in the steam in such large amounts as to preclude the possibility of its being mechanically entrained in the steam. Furthermore, the lack of


 FIG. 3 RATIO OF $\frac{\text{SiO}_2 \text{ IN STEAM}}{\text{SiO}_2 \text{ IN SOLUTION}}$ VERSUS pH OF SOLUTION
(Tests run at 600 F (1545 psi).)

much change of conductance or pH value of the steam with increasing silica content indicated that the sodium salts of silica are not present.

With a solution having a pH value around 10 to 11, the amount of silica in the steam is about 0.05 per cent of the silica in the solution at 500 F (681 psi); 0.15 per cent at 550 F (1045 psi); 1.0 per cent at 600 F (1540 psi); 1.6 per cent at 625 F (1854 psi); 3.3 per cent at 650 F (2211 psi).

The variation of SiO₂ in the steam with the change of pH in the boiler water, its rapid increase with temperature increase above 500 F (681 psi), combined with the lack of a marked effect on the conductance and pH value of the steam, all indicate that the silica is not present in the steam as the sodium silicate. If the silica leaves the boiler water in another form than the sodium silicate, it may be in some form of silicic acid, such as H₄SiO₄ or H₂SiO₃. Sodium-silicate solutions hydrolyze and at some temperature around 500 F could liberate silicic acid. This reaction would be influenced by the pH value of the solution and, since silicic acid is a very weak acid, it would in turn have only a slight influence on the pH value or conductance of the condensed steam.

RELATIONSHIP BETWEEN SOLID SILICIC ACID AND SILICA IN STEAM AT VARIOUS TEMPERATURES AND PRESSURES

If silicic acid is being vaporized, solid sodium silicate in contact with superheated steam should be present in the steam in amounts equal to its vapor pressure. In order to determine the action of these solids in contact with superheated steam, the test procedure was changed. Steam from the laboratory boiler was passed through the bomb shown in Fig. 4. The salts to be studied were pumped into the bomb in solution or suspension, and the temperature of the bomb, being above the saturation temperature, gave superheated steam in contact with the solid materials to be studied. Copper spirals were placed on the plates in the bomb in order to increase the contact surface. The steam leaving the bomb passed through a stainless-steel tube 1/4 in. OD × 20 gage about 10 ft long to a double coil (stainless-steel 1/4 in. × 20 gage inside coil) condenser. The rate of flow was controlled by a needle valve on the outlet end of the condenser. Thus the steam was cooled while under pressure with no throttling of the steam.

The bomb was partly filled with a solution of sodium silicate made from crystals of Na₂SiO₃·5H₂O and heated with the removal of steam until the steam was superheated, and then steam in the bomb kept superheated. This allowed superheated steam to be in contact with the solid sodium silicate. When steam at

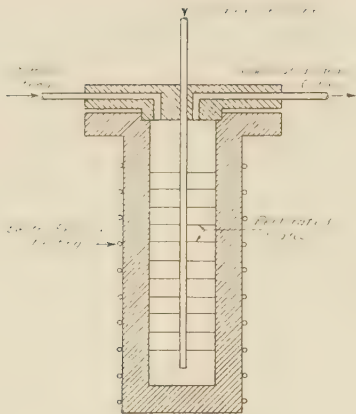


FIG. 4 BOMB USED TO SUPERHEAT STEAM IN CONTACT WITH SOLIDS

681 psi (500 F) was passed through and heated to 600 F in contact with the solid sodium silicate, the steam contained 0.02 ppm SiO_2 .

In the next test a similar solution of sodium silicate was put in the bomb, and while under steam pressure, sulphuric acid was added until the solution in the bomb became neutral. This would form silicic acid and sodium sulphate in the bomb. The solution was then slowly evaporated under pressure, and steam from the boiler passed through the bomb, which in turn superheated the steam in contact with the silicic acid. Purified silicic acid was also pumped into the bomb while under steam pressure for additional tests.

Table 6 gives the results obtained on tests run under these conditions. There was a marked variation in the silica content of the steam with change in rate of steam flow and at the same time very little variation with change in temperature. The condenser being so far from the bomb would not give samples of steam representative of that leaving the bomb. In order to check the effect of the location of the condenser, it was moved so as to be within a few inches of the bomb outlet. Table 6 shows the results of this change and indicates that the results were more consistent. However, even under this condition, the results were still slightly inconsistent.

The bomb was heated at the lower portion, and the top received its heat only by heat transfer through the metal or by heat from the superheated steam; consequently, the steam leaving the bomb would be at a lower temperature than the steam in

contact with the silicic acid. This would not give true values for the silica over silicic acid at the control temperature.

In order to obtain true values, the apparatus was changed to that shown in Fig. 5. Superheated steam was passed through a stainless-steel tube ($1/4$ in. OD \times 20-gage wall) inside a steel tube about 2 in. ID and 95 in. long. The space inside the larger tube was filled with copper spirals to increase the contact surface. The large tube was heated by means of electric-resistance wiring wrapped around the pipe. Thermocouples (constantan) were attached to the middle of the tube and at the outlet at the top.

The superheated steam was passed down through the small inner tube up around the copper spirals and out the top of the tube. The steam was superheated by passing through an electrically heated superheater before passing through the tubes. Thus the only heat added to the larger tube was that necessary to counterbalance radiation loss. When the tube was at the desired temperature, a suspension of pure silicic acid alone was pumped into the top of the big tube. The silicic acid was prepared by adding hydrochloric acid to a solution of $\text{Na}_2\text{O} \cdot \text{SiO}_2 \cdot 5\text{H}_2\text{O}$ in distilled water. The precipitated silicic acid was filtered and washed with distilled water until free of chloride. This deposited the silicic acid on the spirals. The superheated steam leaving the tube should contain an amount of silicic acid corre-

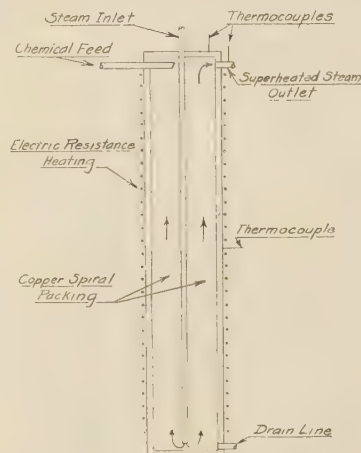


FIG. 5 APPARATUS USED TO SUPERHEAT STEAM IN CONTACT WITH SILICIC ACID

sponding to the vapor pressure at the temperature and pressure used. In order to prevent silica deposit due to any temperature drop after leaving the tube, the condenser was placed at the outlet of the tube.

Table 7 gives the results of tests run, using this equipment. The silica content of the steam was the same for rates of flow from 2 to 10 lb per hr. This indicated that the silica present in the steam represented the equilibrium condition between the silica in the steam and the vapor pressure of the silicic acid. Fig. 6 shows the silica in the superheated steam at various pressures and superheat temperatures. In Fig. 7, the concentration of the silica in the superheated steam (log scale) is plotted against the reciprocal of the absolute temperature. This results in a series of straight lines for the various pressures. This relationship indicates that the silica present in the steam is the result of vapor pressure of silicic acid.

DISCUSSION OF LABORATORY TESTS

The laboratory tests show that sodium silicate in boiler water at steam pressures above 700 psi will liberate silica, presumably

TABLE 6 TESTS RUN USING BOMB SHOWN IN FIG. 4

Pressure P.s.i., <i>gage</i>	Superheat Temp., °F	Rate of Flow lbs. per hr.	SiO_2 in Steam p.p.m.	
150	410	10	0.04-0.06	Silicic acid in bomb, Con- denser about 10 ft. from bomb.
150	420	10	0.04-0.04	
150	460	10	0.03-0.04	
150	550	10	0.11-0.14	
150	650	10	0.14-0.17	
150	750	10	0.23-0.57	
150	750	10	0.21-0.45	
150	750	5	1.70-1.07	
150	750	3	2.7-2.7	
150	750	1.3	10.0-3.9	
150	720-610	1.3	2.9-2.7	
150	800	5	0.19-0.29	Place conden- ser within about 4" of bomb out- let.
150	600	10	0.15-0.21	
150	600	2	0.23-0.25	
150	800	6	0.21-0.41	
150	600	2	0.34-0.46	
150	500	5	0.08-0.23	
150	500	2	0.14-0.16	
150	400	2	0.06-0.07	
150	400	5	0.03-0.04	
150	400	1.2	0.07-0.17	
150	400	5	0.04-0.04	
50	400	1.2	0.01-0.04	
50	400	2.0	0.01-0.01	
50	400	5.0	0.01	
50	400	1.2	0.03-0.03	

TABLE 7 TESTS RUN USING APPARATUS SHOWN IN FIG. 5

Pressure p.s.i., gage	Temperature of			Rate of Steam Flow lbs. per hr.	SiO ₂ ppm
	Steam Leaving Superheater	Wall	Outlet		
50	530	530	500	5	0.04-0.04
50	640	640	600	5	0.10-0.12
50	430	430	400	5	0.00-0.00
150	520	540	500	5	0.13-0.13
150	520	540	500	10	0.13-0.13
150	550	550	500	2	0.10-0.12
150	540	540	500	5	0.14-0.15
150	680	630	600	5	0.28-0.32
150	640	640	600	10	0.30-0.31
150	700	690	650	5	0.49-0.50
250	540	540	500	5	0.27-0.30
250	640	640	600	5	0.65-0.67
250	680	680	650	5	0.92-0.98
400	530	530	500	5	0.62-0.66
400	640	630	600	5	1.41-1.45
400	640	630	600	5	1.41-1.45
400	680	670	650	5	2.04-2.06

as silicic acid, in appreciable amounts without mechanical entrainment of boiler water. This amount increases rapidly with pressure increase. It also increases as the pH value of the boiler water is decreased.

When superheated steam is passed over solid silicic acid at various pressures and temperatures, definite amounts of silica are present in the steam corresponding to the temperature and pressure. No silica occurs in the superheated steam when it is passed over solid sodium silicate ($\text{NaO} \cdot \text{SiO}_2 \cdot 5\text{H}_2\text{O}$ before being superheated).

These results indicate that solid silicic acid has an appreciable vapor pressure at temperatures above 400 F. When the silica is present in solution in the boiler water as sodium silicate, the mole concentration of the silicic acid is very low, consequently the vapor pressure over the solution does not become appreciable until pressures around 1200 psi are reached. The vapor pressure of the silicic acid over the boiler water will be low due to the small mole concentration and the high pH value of the boiler water. Thus the concentration in the steam will be much lower than that corresponding to the true vapor pressure of the solid silicic acid at the higher temperature and pressure in the superheater and the higher-pressure end of the turbine. However, as the temperature and pressure of the steam drop as it passes through the turbine, a point will be reached where the silicic-acid concentration in the steam becomes greater than the silicic-acid content corresponding to the vapor pressure over solid silicic acid. When this occurs, silicic acid will deposit. Thus the higher the silica content of the steam leaving the boiler, the higher up in the turbine the deposits will start forming, and the greater the amount of deposit which will form in the turbine. If the silica in the boiler water is kept below certain values, the deposit forming in the turbines should be negligible.

POWER-PLANT TESTS

RELATIONSHIP BETWEEN SILICA IN STEAM TO SILICA IN BOILER WATER

Studies have been made in three power plants having boilers operating around 1250 psi to determine the ratio between the silica in the steam and that in the boiler water. All three of these plants use evaporator make-up, have phosphate treatment, and use fresh water for surface condensers.

In plant A, the pH value of the boiler water was between 10.9 and 11.1. Daily analyses for silica were made on the superheated steam from each of the three boilers and on the combined steam from the main header. Silica was also determined in the boiler water from each boiler.

The silica in the boiler water averaged 8 ppm with a minimum of 4 ppm and a maximum of 13 ppm. The silica in the steam averaged 0.05 ppm with a minimum of 0.02 ppm, and a maximum of 0.10.

The ratio of the silica in the steam to that in the boiler water was between 0.5 and 0.8 per cent. The specific conductance of the degassed steam was about 1 micromho.

In plant B, the pH value of the boiler water was between 10.7 and 11.2. Daily analyses for silica were made in a similar manner to plant A.

The silica in the boiler water averaged 9 ppm with a minimum of 5 ppm, and a maximum of 14 ppm. The silica in the steam averaged 0.05 ppm with a minimum of 0.03 ppm, and a maximum of 0.10 ppm. The ratio of the silica in the steam to that in the boiler water was between 0.5 and 0.7 per cent. The specific conductance of the degassed steam was about 1.2 micromho.

In plant C when the pH value of the boiler water was between 11.0 and 11.3, the silica in the steam was between 0.01 and 0.05 ppm. The boiler water had a silica content between 2 and 5 ppm.

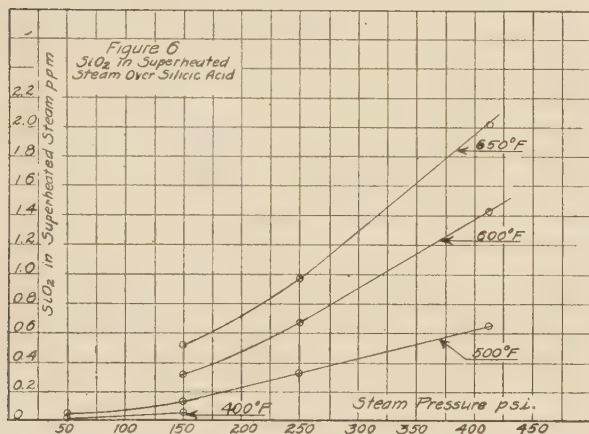
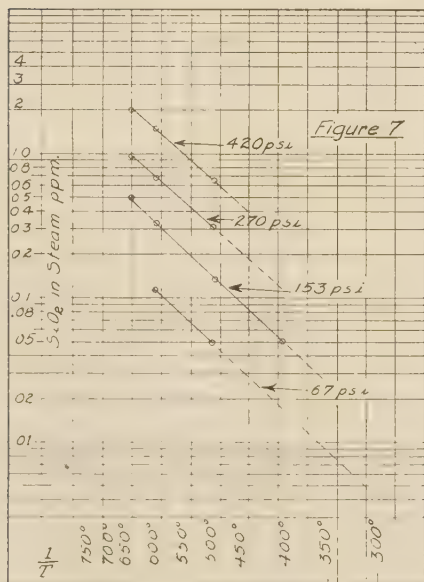
FIG. 6 SiO₂ IN SUPERHEATED STEAM OVER SILICIC ACID

FIG. 7 CONCENTRATION OF SILICA IN SUPERHEATED STEAM VERSUS RECIPROCAL OF ABSOLUTE TEMPERATURE

This gave a ratio of silica in the steam to that in the boiler water around 0.8 per cent with a maximum of 1 per cent.

CHANGES OCCURRING IN STEAM AS IT PASSES THROUGH TURBINES

In plants A and B, no data are available on the silica content of the low-pressure steam or the condensate. This was due to the fact that the deposits forming on the low-pressure units were of a small order of magnitude. Thus in plant B, the low-pressure unit at the end of 2 years when examined on scheduled outage showed a small amount of deposit. However, this soft and easily removed deposit was forming in the temperature range from 400 to 250 F. It contained from 30 to 71 per cent SiO_2 . The silica was present as cristobalite and chalcedony, both crystalline forms of silica. The rest of the deposits consisted mainly of iron oxides (red and black).

In plant C, prior to the time when the values reported were obtained, much difficulty was experienced with turbine-blade deposits in the low-pressure units. At the time these deposits were forming the silica content of the boiler water varied between 10 and 40 ppm. The silica in the steam leaving the boilers varied between 0.1 and 0.4. The steam condensate from the low-pressure machines contained about 0.1 to 0.2 ppm SiO_2 . This showed a loss of up to 0.2 ppm SiO_2 in the steam passing through the low-pressure units, a definite indication of silica deposition in the units. At the same time, the stage pressures indicated deposits were forming. When the conditions of operation were changed so that the silica in the boiler water was kept below 5 ppm, the silica in the high-pressure steam was the same as that in the condensate from the low-pressure units. This indicated no silica deposition in the units. At the same time, the stage pressures showed no indications of deposits forming.

From the study made in this plant, it was concluded that, when the silica in the steam became higher than 0.1 ppm, there was a probability that deposits would form in the low-pressure turbines. When this value has been kept below 0.05 ppm, the units have operated over 1½ years with no indications of deposits forming.

During these plant tests, it was noticed that the silica content of the boiler water in plants A, B, and C (during the days of higher silica content) increased whenever the boilers came on the header after being on bank. At the same time the silica content of the steam also increased. These values returned to average shortly after the boiler was in normal operation. This appears to be connected with so-called "hideout."

PREVENTION OF SILICA BLADE DEPOSITS

The plant tests have indicated that when the silica in the boiler water is kept below 5 ppm and the pH of the boiler water around 11, no appreciable silica deposits form in the turbines. When the silica in the steam becomes greater than 0.1 ppm deposits will form.

This indicates that, in order to prevent this type of deposit, it is essential that the silica in the steam be kept very low. This may be accomplished either by keeping the silica in the boiler water very low or by removing it from the steam before superheating.

Studies have been made in the laboratory relative to reducing the soluble silica in the boiler water by the addition of chemicals which will precipitate the silica as an insoluble sludge.

Fig. 2 shows the bomb used for these tests. Steam was passed through the solution in the bomb. The procedure followed was to add sodium silicate and NaOH to get the desired silica and pH value of the solution in the bomb. Known amounts of $\text{MgSO}_4 \cdot 7\text{H}_2\text{O}$ (Epsom salts) were put in solution and pumped into the bomb. The steam and a sample of the bomb solution were then analyzed. This procedure was followed until a constant low

value for silica was reached. Table 8 gives the results of a test run under these conditions. The addition of the magnesium reduced the soluble silica from 82.5 ppm to around 2 ppm. Since Epsom salts is acidic, it was necessary to add an equivalent amount of sodium hydroxide in order to maintain the desired pH value. The soluble silica remained around 2 ppm even after an excess of magnesium salt had been added. These results indicate that it is possible to reduce the soluble silica to around 2 ppm by the addition of magnesium and that the silica is retained in the sludge.

TABLE 8 EFFECT OF MAGNESIUM ON SILICA IN SOLUTION

Tests Run at 600° F (1545 p.s.i.)				
Solution in Bomb SiO_2 ppm	pH	SiO_2 in Steam ppm	Chemical Added	Amount Added in Grams
8.3	9.2	0.09		
82.5	11.0	0.70	$\text{Na}_2\text{SiO}_3 \cdot 5\text{H}_2\text{O}$	0.20
31.0	10.1	0.34	$\text{MgSO}_4 \cdot 7\text{H}_2\text{O}$	0.15
27.0	10.7	0.26	NaOH	0.065
14.0	10.6	0.15	$\text{MgSO}_4 \cdot 7\text{H}_2\text{O}$	0.10
8.0	10.4	0.13		
11.0	10.5	0.13		
10.0	10.5	0.11		
4.3	9.9	0.05	$\text{MgSO}_4 \cdot 7\text{H}_2\text{O}$	0.10
4.1	10.8	0.03	NaOH	0.125
2.3	10.5	0.01	$\text{MgSO}_4 \cdot 7\text{H}_2\text{O}$	0.10
1.6	10.3	0.01	$\text{MgSO}_4 \cdot 7\text{H}_2\text{O}$	0.10
1.9	10.8	0.005	NaOH	0.12
2.4	11.4	0.005		
1.5	11.1	0.005	$\text{MgSO}_4 \cdot 7\text{H}_2\text{O}$	0.20

Since the concentration of the silica in the steam is a function of the silica concentration of the solution in contact with the steam, the silica in the steam could be reduced to a low value by bringing the saturated steam in contact with a water having a very low silica content. This would involve the scrubbing of the saturated steam with a fairly pure water low in silica. Such a procedure should also reduce mechanically entrained boiler water to a low value and stop soluble as well as insoluble deposits.

Discussion

C. E. IMHOFF.⁶ The authors are to be congratulated for filling in some of the vacant spaces in our knowledge of the behavior of silica in high-temperature high-pressure steam. Having assisted in a similar study of the solvent action of superheated steam on "fiberglass" (95 per cent SiO_2), the writer can affirm the difficulties the authors encountered in their study. As they point out, it is absolutely necessary to reduce the length of piping between the bomb and the condenser to a minimum and to condense the sample under full steam pressure.

In order to understand completely the mechanism of silica deposition, one must know just how the silica gets into the steam in the first place, whether it enters into any reactions within the steam as it passes through the turbine, in what form it exists in solution, what is the medium of solution, and how crystallization takes place from this solvent. The authors have shown one way in which silica may exist in solution in the steam. The theory of steam as a solvent explains almost all of the characteristics of precipitation of quartz and amorphous silica, but the mechanism for the crystallization of sodium disilicate is more complex. It is, however, theoretically possible for the deposition of silica and silicates to take place from droplets, and the mechanical-entrainment theory, therefore, should not be completely discarded, in spite of the greater plausibility of the solubility theory.

⁶ Feedwater Treating Department, Allis-Chalmers Manufacturing Company, Milwaukee, Wis.

For a number of years the constitution of turbine-blade deposits has been studied by means of X-ray diffraction in the laboratories of the writer's company. The various compounds have been charted according to the temperature zones in which they occur. The most common forms of silica thus far found in the study are those of amorphous silica, alpha quartz, and sodium disilicate.

The mechanism of turbine-blade-scale formation will be clarified if the observations regarding scale constituents can be correlated with the solubility data. For this purpose the data in the authors' Fig. 7 have been replotted as is shown in Fig. 8 of this discussion. These data are extrapolated down to the saturation temperature for each pressure and on the other side of the curve extrapolated up to 950 F. The shaded area in Fig. 8 covers the ordinary ranges of pressures and temperatures which are encountered in the intermediate- and low-pressure stages of modern steam turbines. The lower part of this shaded area is labeled alpha quartz and the upper part is labeled sodium disilicate. Below the alpha-quartz area there is a notation for amorphous silica. These notations designate the temperature ranges in which these three forms of silica are most often found in turbine-blade deposits. The boundaries shown in Fig. 8 are not as sharp as indicated, for there is some overlapping of the various constituents on either side of the border lines as shown. By far the greater percentage of amorphous-silica deposits, however, are found at temperatures below 300 F. In fact, amorphous silica often occurs in the saturated-steam zone. Alpha quartz is found between 300 and 500 F and sodium disilicate exists largely between 500 and 700 F.

It is of interest to note the solubility values of silica in the ranges of temperature and pressure indicated for these three forms of silica. At the pressure and temperature existing in the turbine where quartz deposits are found, the solubility of silica ranges between 0.005 ppm to about 0.25 ppm, and amorphous silica is found where the equilibrium solubility is below 0.005 ppm. If these data are interpreted correctly, silica deposits will occur with lower concentrations of silica in the steam than has normally been thought the case. It should be kept in mind, however, that it is quite probable that silica exists in a high degree of supersaturation as it passes through these lower temperature zones in the turbine and that crystallization lags considerably behind the true saturation point. For example, according to the curve, quartz should start to crystallize when the solubility of silica in the steam falls below 0.25 ppm. It is quite possible, however, that the silica concentration may actually be higher than this at the point of crystallization owing to the high degree of supersaturation.

The solubility data also give us some explanation as to why we find amorphous silica at the lower end of the turbine following alpha quartz. Normally, those compounds which precipitate in an amorphous state are those which have a very low degree of solubility and in which precipitation takes place at a rapid rate. In the zone where amorphous silica is commonly found, the solubility of silica is extremely low, and the temperature is changing very rapidly, causing the separation from the soluble phase to take place also at an extremely rapid rate. The silica therefore changes over into the solid state before it has time to be oriented into a crystalline configuration.

Considering the zone for sodium disilicate, it is apparent that the solubility of silica is considerably above what we would normally expect to find in any high-pressure steam. The formation of sodium disilicate, therefore, probably takes place according to a different mechanism from that of alpha quartz and amorphous silica. The temperature range for crystallization corresponds rather closely to that for sodium hydroxide and suggests that there may be a reaction in the steam between

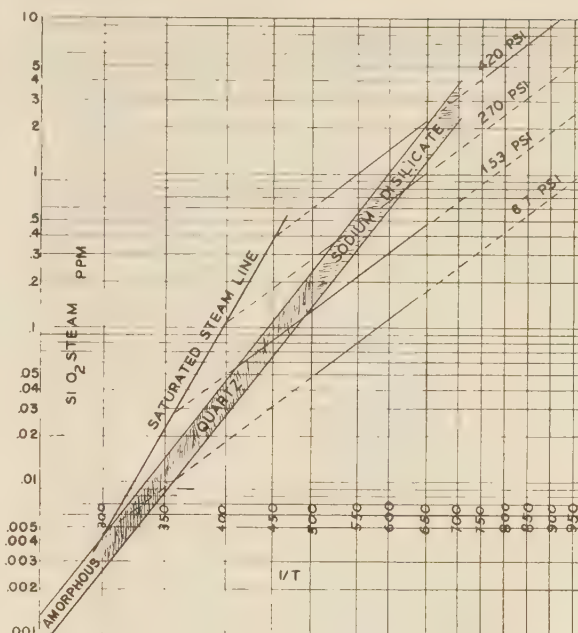
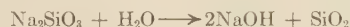
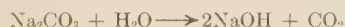


FIG. 8

sodium hydroxide and dissolved silica; and that crystallization proceeds from droplets in which this reaction and subsequent precipitation occur. In none of the silica deposits thus far studied has there ever been any evidence of sodium hydroxide being present from the X-ray diffraction patterns. The same is true for sodium metasilicate. It is quite possible that many deposits which, on the basis of chemical analysis, were previously thought to be composed of sodium hydroxide, were actually composed of sodium disilicate. During titration, the alkalinity of sodium disilicate behaves as though the compound were caustic soda. One can therefore be easily misled on the basis of chemical titration only.

It has been theorized that silica is present in the steam as H_2SiO_3 , and there are some reasons why this could be true. However, if one draws an analogy between sodium silicate and sodium carbonate, it can be argued that silica is present as SiO_2 . Equilibrium conditions for this comparison can be represented by an equation showing SiO_2 as one of the components where it behaves similarly to CO_2 in the sodium carbonate equilibrium



Whether silica is present as dissolved H_2SiO_3 or SiO_2 is important, because it has a bearing on how silica is deposited. X-ray diffraction patterns of blade deposits show that the silica is in the anhydrous form, whether it be alpha quartz or amorphous silica. If the deposition is in the form of silicic acid it must be followed by a dehydration to account for the anhydrous form found in deposits. The authors used silicic acid for the solid phase. However, in the writer's experiments, the solid phase was anhydrous silica glass and this went into solution apparently as readily as silicic acid. In this case anhydrous silica went into solution in superheated high-pressure steam to the extent of between 3.6 and 14.6 ppm. If the silica were present as H_2SiO_3 , it would have to be preceded by a hydration of the SiO_2 when it went into solution. From the standpoint of the crystallization products and from the solubility behavior of anhydrous silica in steam, it would seem

somewhat more plausible to consider the dissolved form of silica to be SiO_2 rather than H_2SiO_3 .

The authors' observation that silica contributes but little to the specific conductance of a condensed sample was verified in some of this writer's tests on the solubility of fiberglass. In one instance, when the bomb was allowed to fill with hot condensate, the silica content of the sample was 285 ppm, whereas the specific conductance was only 3 micromhos.

The authors have made a significant generalization in regard to the amount of silica found in the steam at different pressures. According to their findings, one would expect that there would be 20 times as much silica in steam generated at 1540 psi as there would be in steam generated at 680 psi. with the same silica

concentration in the boiler water. From this it can be easily seen why it is so important to keep the silica concentration low in high-pressure boilers and why silica turbine-blade deposits are so much more likely to be found in the higher-pressure machines.

Is any significance attached to the fact that the pH values in most of the tests are above 7, while the assumption is that the silica is present as H_2SiO_3 ? Both specific conductance and pH measurements indicate extremely low degrees of ionization, and yet the silica can be readily determined colorimetrically. Any slight degree of ionization, however, should tend to produce a pH value below 7.

History of Potassium Boiler-Water Treatment at Springdale

By L. E. HANKISON¹ AND M. D. BAKER²

Results are given in considerable detail of 2 years' experience in the treatment of boiler water at Springdale Station, West Penn Power Company, with potassium compounds which were substituted for sodium salts for water conditioning of both the high- and low-pressure boilers. This change in treatment was started August 25, 1942, in an endeavor to prevent the formation of silica scale in the boilers and also to minimize if possible deposits of silica on the turbine blades.

THE use of potassium salts instead of sodium salts for boiler-water conditioning at Springdale Station, West Penn Power Company, was started August 25, 1942. This change in treatment was made in an endeavor to prevent the formation of silica scale in the boilers and also possibly to minimize the deposition of silica on the turbine blades. The basic theory for believing potassium salts superior to sodium for this purpose is the increasing solubilities of potassium-silicate compounds with increase in temperature and pressure, as described by Morey,³ compared to sodium-silicate compounds which decrease in solubility with increase in temperature and pressure. The application of Morey's information to boiler waters has been described by Hall.⁴

Since discussion of Hall's paper last year, we have received many inquiries regarding details on application of the treatment, conditions existing, and technique employed in the control of the potassium boiler-water treatment. This presentation will go into greater detail than might normally be considered necessary, but it is based on the many questions that have been asked and is given in order that all may benefit from the 2 years' experience with potassium compounds for boiler-water treatment at Springdale. Potassium salts were substituted for sodium salts for water conditioning of both the high- and low-pressure boilers in the Springdale Station.

DESCRIPTION OF BOILER

The boiler plant is composed of three 1350-psi steam generators each rated at 475,000 lb of steam per hr and operated at maximum capacity; and eight 350-psi boilers, each capable of generating 160,000 lb of steam per hr. Serious trouble with analcite scale had always been experienced in the high-pressure boilers, and loss of capacity was observed and thought to be caused by a deposition of silica scale in various sections of the boiler. The low-pressure boilers had some analcite scale in the upper rows of tubes

¹ Superintendent, Efficiency Department, West Penn Power Company, Pittsburgh, Pa. Mem. A.S.M.E.

² Chief Chemist, West Penn Power Company, Springdale, Pa.

³ "The Ternary System $H_2O-K_2SiO_3-SiO_2$," by G. W. Morey, *Journal of the American Chemical Society*, vol. 39, 1917, pp. 1173-1229.

⁴ "A New Approach to the Problem of Conditioning Water for Steam Generation," by R. E. Hall, *Trans. A.S.M.E.*, vol. 66, 1944, pp. 457-488.

Contributed by the Joint Research Committee on Boiler Feed-water Studies and presented at the Annual Meeting, New York, N. Y., Nov. 27-Dec. 1, 1944, of THE AMERICAN SOCIETY OF MECHANICAL ENGINEERS.

NOTE: Statements and opinions advanced in papers are to be understood as individual expressions of their authors and not those of the Society.

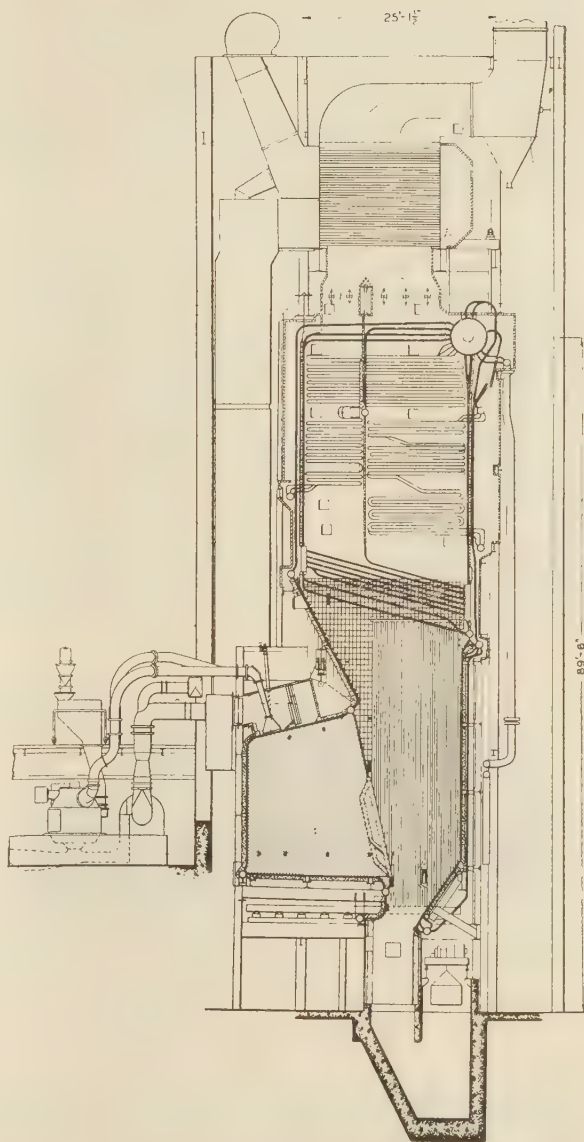


Fig. 1 CROSS-SECTIONAL VIEW OF A HIGH-PRESSURE BOILER

but there were no tube failures. The detrimental effect of scale in these low-pressure boilers was confined to loss in efficiency and capacity. This discussion therefore exclusively describes experiences with the high-pressure boilers. Fig. 1 is a cross-sectional view of a high-pressure boiler.

A description of the high-pressure boilers requires mentioning the many water circuits or individual boilers included in each generating unit. Forty more or less complete circuits are con-

nected in common to one drum. Each circuit has its own characteristics regarding circulation, heat absorption, sludge deposition, etc. The location where the largest sludge deposits occur is in the twenty-eight sections composing the horizontal tube area of each boiler. Each section is an individual boiler made up of a downcomer from the drum which supplies a sectional header, which in turn supplies water to five and one half steam-generating tubes. The half tube extends part way across the boiler and then ascends vertically, forming a baffle wall. The five full-length tubes discharge into an uptake sectional header where the volume of steam and water mixture from the lower rows tends to restrict the flow in the top rows of tubes. This restriction causes sluggish circulation and results in sludge accumulations in these upper rows. Some corrections to this circulation have been made so that at present most of the sludge deposits only in the top full row of tubes. Silica scale forms under the sludge.

MECHANISM OF SCALE FORMATION

The boiler water in the sludge is boiled off into steam and new water filters through the sludge to the tube surface, carrying additional soluble solids which form a concentrating film of boiler water. Under this condition, high concentrations develop which are not diluted by an inflow of boiler water as the inflow is only sufficient to replace the water that is evaporated. The high alumina content of most of the silica scales indicates many thousands of concentrations. The localized concentrations of sludge which permit scale formation cannot be corrected by water conditioning except by the complete elimination of the scale-forming elements from the water.

The silica-scale trouble, with one exception, was entirely confined to the tubes in the generating or horizontal section of the boilers. This one exception was during a period when some compounded oil contaminated the feedwater system. This incident will be described later.

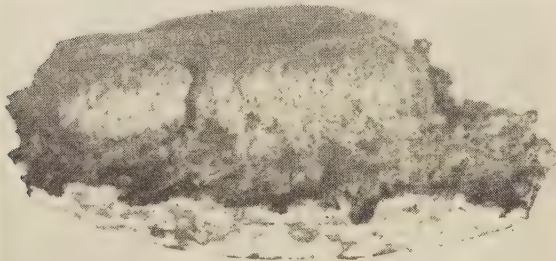


FIG. 2 TYPICAL SCALE FORMATION FOUND IN PARTS OF BOILER WHERE CIRCULATION IS SLUGGISH

Fig. 2 shows a typical scale formation that is found in parts of the boiler where the circulation is sluggish. The upper portion of loose deposit has been removed by water washing and, consequently, is not shown. This loose deposit is usually 5 to 10 times the volume of the other two deposits. The view shows the copper-colored semiaherent portion and the hard layer of silica scale that is tightly adherent to the tube. The chemical analyses of the loose and semiaherent deposits do not vary greatly, both being high in iron oxide and containing appreciable amounts of phosphates, calcium, and copper, but with very little aluminum, potassium, or sodium. The hard adherent scale is high in silica, iron, aluminum, and potassium. Table 1 gives the chemical analyses of these separate deposits.

Table 2 gives the suggested combined form of the hard deposit

TABLE 1 ANALYSES OF DEPOSITS ILLUSTRATED IN FIG. 2

	Loose deposit, per cent	Semi-adherent, per cent	Hard scale, per cent
Sulphur trioxide, SO_3	Trace	Trace	1.0-1.5
Phosphorus pentoxide, P_2O_5	7-8	7-8	2-3
Silica, SiO_2	3	2	25.2
Iron oxide, Fe_2O_3	59	63	27.0
Iron oxide, Fe_3O_4	20.0
Aluminum oxide, Al_2O_3	1-2
Calcium oxide, CaO	7-8	Less than 5	1-2
Magnesium oxide, MgO	2-3	1-2	Low
Sodium oxide, Na_2O	21
Potassium oxide, K_2O	2.7
Copper, Cu.....	10.4	15.0	0.9
Ignition loss.....	6.0	4.9	..

TABLE 2 SUGGESTED COMBINED FORM OF HARD SCALE IN TABLES 1 AND 11

	Hard scale, per cent Table 1	Hard scale, per cent Table 11
Hydroxyapatite, $3\text{Ca}_3(\text{PO}_4)_2\text{Ca}(\text{OH})_2$	2.5	6.1
Magnesium phosphate, $\text{Mg}_3(\text{PO}_4)_2$	1.7	1.1
Magnesium aluminate, MgAl_2O_4	2.6
Potassium sulphate, K_2SO_4	2.2	..
Potassium-aluminum tetrasilicate, $\text{K}_2\text{OAl}_2\text{O}_3\cdot 4\text{SiO}_2$	26.3
Potassium-aluminum disilicate, $\text{K}_2\text{OAl}_2\text{O}_3\cdot 2\text{SiO}_2$	62.2	12.7
Potassium-iron disilicate, $\text{K}_2\text{OFe}_2\text{O}_3\cdot 2\text{SiO}_2$	5.0	..
Magnetic iron oxide, Fe_3O_4	46.4
Iron oxide, Fe_2O_3	24.9	..
Copper, Cu.....	2.7	2.4
Ignition less combined water.....	0.8	2.2

TABLE 3 TYPICAL ANALYSIS OF BOILER WATER WHILE ADDING SODIUM SALTS

A reading, ppm.....	3.4*	Phosphate, PO_4 , ppm.....	161
B reading, ppm.....	2.3	Chloride, Cl, ppm.....	74
Sulphite, SO_3 , ppm.....	7	Silica, SiO_2 , ppm.....	3
Sulphate, SO_4 , ppm.....	554	Total solids, ppm.....	1274

* A Reading: Titration of the sample to the end point of phenolphthalein. B Reading: Addition of barium chloride to the sample followed by its titration to the end point of phenolphthalein.

TABLE 4 TYPICAL ANALYSIS OF BOILER DEPOSITS WHILE ADDING SODIUM SALTS

	Loose deposit, per cent	Semi-hard deposit, per cent	Hard scale, per cent
Sulphur trioxide, SO_3	Trace	4.5	..
Phosphorus pentoxide, P_2O_5	30 or more	11.5	..
Silica, SiO_2	Less than 1	20.4	25.1
Iron and aluminum oxides, R_2O_3	10-12
Iron oxide, Fe_2O_3	14.4	..
Aluminum oxide, Al_2O_3	15.1	..
Calcium oxide, CaO	20+	4.8	..
Magnesium oxide, MgO	20+	2.4	..
Sodium oxide, Na_2O	18.3	..
Copper, Cu.....	17.1	6.1	..
Total ignition loss.....	None	1.8	3.3

Microscopic examination:

Loose Deposit. Crystalline calcium phosphate and crystalline magnesium phosphate, copper, and a small amount of Fe_3O_4 .

Semiaherent Deposit. Principally analcite with a small amount of calcium sulphate. A fair amount of metallic material, and a fair amount of a phosphate compound which is probably calcium phosphate. A fair test was obtained for the presence of a very acid-soluble magnesium compound.

Hard Scale. A deposit of analcite and calcium phosphate with a very small amount of calcium sulphate, a rather fair amount of acid-soluble magnesium compound.

in Table 1 and the hard deposit in Table 11. The compound formed depends upon the amount of silica present and no doubt follows the general rule that it is the highest containing silicate that can form with the amount of silica available. These potassium-aluminum-silicate compounds will disintegrate in a hydrochloric-acid solution.

CONDITIONS WHEN USING SODIUM SALTS

The sodium chemicals that formerly had been used for water conditioning were flake caustic soda, anhydrous disodium phosphate, and santosite (alkaline sodium sulphite). The make-up was evaporated, and chemical treatment was needed because of condenser-water leakage and evaporator carry-over. A typical analysis of the boiler water during the period when using sodium salts is given in Table 3. A chemical and microscopical analysis of the loose sludge, semihard scale, and also the hard scale adhering to the tube surfaces during this period are given in Table 4. The increase in the silica content of the various deposits as

they approach the tube surface illustrates the mechanism of deposit formation. The top layer contained very little silica, not sufficient aluminum to separate it from the iron, no sodium, and it was easily removed. As the water evaporated, the concentrated layer caused the formation of the sodium-aluminum-silicate scale on the tube surface. This scale requires turbinizing for removal. The 25.1 per cent silica is equivalent to 42.2 per cent analcite.

Analcite scale formed on the tubes in amounts varying from a layer that was just visible, to a deposit about $\frac{1}{4}$ in. thick. This material was formed in patches of maximum width about half the lower inside circumference of the tube and in length up to 12 in., and it was always found under large amounts of loose deposit. Each of the heavier analcite deposits required 4 hr of turbinizing for removal. Normal intervals between turbinizings were about 3 months, but when the boiler came off for other reasons there was one interval of only 14 days between turbinizings. The formation of analcite scale, the resultant frequent turbinizing, and loss in capacity of the boilers were the principal reasons for changing from sodium to potassium treatment.

SUBSTITUTION OF POTASSIUM SALTS AND CONTROL

The potassium salts substituted for sodium salts were potassium pyrophosphate, potassium hydroxide, and potassium sulphate. The change from sodium to potassium treatment of the boiler water required no change in the plant control or analytical methods. The only additional testing required is to determine the ratio of potassium to sodium. With sodium treatment the amount of potassium present in the boiler water was generally less than 1 per cent of the sodium. With potassium treatment, the ratio is usually 6 or more of potassium to 1 of sodium expressed in ppm. Best conditions are obtained in the boilers when the ratio of potassium to sodium is 8 to 1 or higher. As the contamination that enters the system contains sodium compounds, the amount of sodium is a definite measure of the amount of contamination. During a time when the contamination was excessive, the ratio of potassium to sodium dropped to 1.3 to 1.

Gasket Failure. The first trouble that could be attributed to potassium was the failure of handhole cap gaskets. Monel-clad asbestos gaskets were used. Before introducing potassium these gaskets had started to fail as was shown by the number of gaskets that had to be replaced during boiler outages. No boiler outage could be attributed to gasket failure while using sodium treatment but the hydrostatic tests made during shutdowns showed caps to be leaking. With sodium treatment, failures that might have occurred in service were largely self-sealing. With the introduction of potassium, gasket failures made it difficult to keep all three boilers in service at the same time. Any seals that had been established with the sodium-treated water were dissolved and this caused numerous shutdowns. This condition existed until the boilers were entirely regasketed. During this time, delivery of gaskets was very slow, so for a period of weeks the gaskets on hand were only sufficient to fix the caps that were leaking and not enough to completely regasket a boiler. The seals that had been made on all rolled tubes that had not been perfectly fitted were dissolved and leaks developed, making it necessary to reroll a large number of tubes. After regasketing and getting all tubes properly rolled, this type of trouble has practically disappeared. Potassium-conditioned water will not seal even the smallest leak.

An analysis of boiler water collected at the time of gasket trouble is given in Table 5. During this time it was necessary to add approximately double the amount of potassium hydroxide that was calculated to be sufficient to maintain excess hydroxide in the boiler water. This fact together with the low amount

of silica found in the boiler water (Table 5) and boiler deposits (Table 6) together with the removal of silica from the boiler metal has not been satisfactorily explained.

Inspections of the boilers made at this time showed soft deposits in the generating tubes of the boiler, but there was no hard scale under these deposits. Table 6 gives an analysis of the sludge deposits found. All sludge deposits sampled at this time contained less than 3 per cent silica.

Magnetic-Iron-Oxide Scale. From the second to the sixth month of potassium treatment, the amount of Fe_3O_4 in the boiler deposits gradually increased from about 3 per cent to more than 50 per cent. Also, instead of a soft powdery deposit in the boiler tubes, pieces of iron-oxide scale (Fe_3O_4) were found. This loose scale gradually increased until it was necessary to remove the boilers from service to clean out the headers. A possible explanation for this scale is that a layer of acmite scale had formed over large areas in the waterwall tubes when using sodium treatment. The potassium had leached out the silica, made the scale porous, and caused the magnetic-iron-oxide scale to loosen. The scale retained only sufficient silica to cement the particles of Fe_3O_4 together.

Table 7 gives a comparison of the analyses of the acmite-analcite scale found in the boilers with sodium treatment and the loose magnetic-iron-oxide scale found after potassium treatment had been in use 6 months.

pH Values Lowered to Reduce Fe_3O_4 . Another thought regarding the increase of Fe_3O_4 in the boiler deposits was caustic attack of the boiler iron in areas of high heat input. The alkalinities of the boiler waters were considered high, the pH value being in excess of 11. As an experiment, the alkalinities were dropped and the pH values were carried between 10 and 10.5. The effect of the lowered alkalinities was quickly noticed. After 2 months of operation, the sludge in the boiler had changed from

TABLE 5 BOILER-WATER ANALYSIS AT TIME OF GASKET FAILURES

pH reading.....	11.7
A reading, ppm.....	3.5
B reading, ppm.....	1.5
Sulphite, SO_3 , ppm.....	3
Sulphate, SO_4 , ppm.....	274
Phosphate, PO_4 , ppm.....	269
Chloride, Cl, ppm.....	21
Nitrate, NO_3 , ppm.....	1
Dissolved silica, SiO_2 , ppm.....	5
Aluminum, Al, ppm.....	2
Sodium, Na, ppm.....	39
Potassium, K, ppm.....	505
Total solids, ppm.....	1292
Ratio K/Na, ppm.....	7.6/1

TABLE 6 ANALYSIS OF SLUDGE DEPOSIT AT TIME OF GASKET FAILURES

	Per cent
Sulphur trioxide, SO_2	0.3
Phosphorus pentoxide, P_2O_5	11.8
Silica, SiO_2	2.2
Iron oxide, Fe_2O_3	55.7
Aluminum oxide, Al_2O_3	4.2
Calcium oxide, CaO	7.7
Magnesium oxide, MgO	5.2
Sodium oxide, Na_2O	5.1
Copper, Cu.....	5.4

Microscopic examination: Major constituents of this deposit are Fe_3O_4 , calcium phosphate, and copper. The minor constituents are magnesium phosphate and an isotropic silica or silicate.

TABLE 7 IRON-SILICA SCALE BEFORE AND AFTER POTASSIUM TREATMENT

	Sodium treatment, per cent	Potassium treatment, per cent
Sulphur trioxide, SO_3	2.5	Trace
Phosphorus pentoxide, P_2O_5	8.9	10.7
Silica, SiO_2	13.3	1.3
Iron oxide, Fe_3O_4	45.9	60.3
Aluminum oxide, Al_2O_3	10.7	0.4
Calcium oxide, CaO	5.2	7.3
Magnesium oxide, MgO	1.5	6.2
Sodium oxide, Na_2O	9.2	0.0
Copper, Cu.....	1.1	8.1
Net ignition loss calc.....	2.9	2.2

a soft powdery deposit to a deposit that contained many small pieces of scale. Also, the boiler tubes were coated with a deposit that resembled hard dried sludge. The color of the deposit changed from black to gray. Because of the condition of the boiler tubes, the alkalinities were again raised to their former levels and the deposits became soft and the tubes free of adhering deposits. When the alkalinities were raised, potassium chloride was added to the boiler waters to prevent caustic attack. There was no change in the color of the deposits as the chlorides (Cl) were always maintained higher than the hydroxide (OH).

The analysis of a sample of hard scale that was formed at the time of low alkalinities is shown in Table 8.

TABLE 8 DEPOSIT FORMED DURING PERIOD OF LOW pH VALUES

	Per cent
Sulphur trioxide, SO ₃	0.0
Phosphorus pentoxide, P ₂ O ₅	7.9
Silica, SiO ₂	13.6
Iron oxide, Fe ₂ O ₃	38.0
Aluminum oxide, Al ₂ O ₃	10.2
Calcium oxide, CaO.....	6.3
Magnesium oxide, MgO.....	3.7
Sodium oxide, Na ₂ O.....	Not determined
Potassium oxide, K ₂ O.....	More than 10
Copper, Cu.....	10.6
Net ignition loss.....	2.0

Microscopic examination: The major constituent is iron oxide as magnetite with some hematite. The minor constituents are calcium phosphate (hydroxyapatite), metallic copper, fair amount of potassium, and an unidentified isotropic material.

Addition of Chloride to Prevent Caustic Attack. The reason for adding chloride is for dilution of the caustic concentration. When a small bubble of steam forms on an evaporating surface, a certain amount of superheat is formed on the under side of the bubble. This theory was described in detail by Hall⁴ as the Δt_s function. In areas of high heat input, the amount of superheat is usually sufficient to cause deposition of the phosphate and sulphate salts that are in solution in the boiler water. Under this condition, the remaining soluble salts, hydroxides, chlorides, and some silicates will concentrate to form a 5 per cent plus solution of molecules. A 5 per cent solution of hydroxide at elevated temperatures and pressures will readily attack iron. The introduction of the chloride ion does not change the molecular concentration of the superheated solution but does change the percentage of hydroxide available for attack. The addition of chlorides reduces the percentage concentration of hydroxide. A 5 Cl to 1 OH ratio in a 5 per cent solution has 0.83 per cent of OH and 4.17 per cent of Cl. Hence the effect of the caustic is reduced by that amount.

An analysis of the boiler water prior to the time potassium chloride was started is given in Table 9. At that time the ratio was 1 of Cl to 2.7 of OH.

TABLE 9 BOILER-WATER ANALYSIS AT START OF CHLORIDE TREATMENT

A reading, epm.....	4.2
B reading, epm.....	1.9
pH value.....	11.4
Sulphate, SO ₄ , ppm.....	395
Sulphite, SO ₃ , ppm.....	0
Phosphate, PO ₄ , ppm.....	256
Chloride, Cl, ppm.....	26
Nitrate, NO ₃ , ppm.....	1
Dissolved silica, SiO ₂ , ppm.....	9
Aluminum, Al, ppm.....	8
Sodium, Na, ppm.....	85
Potassium, K, ppm.....	595
Organic.....	7
Total dissolved solids, ppm.....	1550
Cl/OH, epm.....	1.0/2.7
K/Na, epm.....	4.1/1

Following the introduction of the chlorides, the iron content of the deposits gradually decreased over a period of several months, and the boiler deposits had either a gray or a copper color. The amount of copper found in the sludge was in pro-

TABLE 10 BOILER-WATER ANALYSIS AT TIME OF SLIGHT SLUDGE DEPOSIT

pH value.....	11.0
A reading, epm.....	2.0
B reading, epm.....	0.8
Sulphate, SO ₄ , ppm.....	249
Sulphite, SO ₃ , ppm.....	1
Phosphate, PO ₄ , ppm.....	127
Chloride, Cl, ppm.....	193
Dissolved silica, SiO ₂ , ppm.....	8
Sodium, Na, ppm.....	8
Potassium, K, ppm.....	581
Total solids.....	1260
Cl/OH, epm.....	6.7/1
K/Na, epm.....	42.5/1

portion to the amount of ammonia in the feedwater. Adherent deposits were not formed and most of the loose material was removed when a boiler was drained so that it was not necessary to clean the tubes in the generating section during each boiler outage.

A typical boiler-water analysis made during this period is given in Table 10.

Potassium Sulphite Discontinued. Potassium sulphite treatment was discontinued in September, 1943, as the small amount of oxygen in the feedwater should normally affect only the economizers and they were protected by the recirculation of boiler water. Any oxygen that might enter the boiler drum is rapidly liberated and expelled with the steam. To date, with 14 months' operating experience, there have been no noticeable effects from the discontinuance of the sulphite treatment.

OIL CONTAMINATION

During the first 4 months of 1944, heavy sludge deposits were found in the boilers and there were several boiler outages due to tube failures. The reason for this trouble was severe contamination from evaporator carry-over, and the presence of a lead-compounded oil in the feedwater. The total amount of oil in the boiler water amounted to 15 to 20 ppm by ether extraction. The amount of lead in the deposits was rarely more than a trace, but the lead plus the oil were sufficient to cause the sludge to adhere to the interior surfaces of the boiler where it first came in contact with large heat input. The presence of this sludge started the cycle for concentrating the boiler water and the formation of potassium-aluminum-silicate scale. This period was the only time sludge deposits on the vertical surfaces of the boiler caused tube failures. The analyses of the sludge layer and the hard scale under the sludge that was removed from a tube that failed in the primary furnace wall are given in Table 11. The

TABLE 11 DEPOSITS REMOVED FROM FURNACE-WALL TUBE AT TIME OF OIL CONTAMINATION

	Loose deposit, per cent	Hard scale, per cent
Phosphorus pentoxide, P ₂ O ₅	10-15	3.2
Silica, SiO ₂	1.7	19.3
Iron oxide, Fe ₂ O ₃	22.0	46.4
Aluminum oxide, Al ₂ O ₃	11.4
Calcium oxide, CaO.....	...	3.4
Magnesium oxide, MgO.....	...	1.9
Sodium oxide, Na ₂ O.....	...	0.2
Copper, Cu.....	52.6	2.4
Potassium oxide, K ₂ O.....	...	8.6
Lead.....	0.005	...
Oil.....	Present	Present
Net ignition loss.....	...	2.3

TABLE 12 BOILER-WATER ANALYSES DURING AND AFTER CORRECTION OF CONTAMINATION

Sample date.....	1/10/44	3/7/44	5/8/44	6/5/44
pH value.....	11.3	11.8	11.5	11.3
A reading, epm.....	3.9	6.5	4.2	5.4
B reading, epm.....	1.9	4.0	3.1	3.1
Sulphate, SO ₄ , ppm.....	266	89	151	163
Phosphate, PO ₄ , ppm.....	224	254	119	216
Chloride, Cl, ppm.....	255	191	167	251
Sodium, Na, ppm.....	210	90	20	10
Potassium, K, ppm.....	470	600	530	780
Dissolved silica, SiO ₂ , ppm.....	6	12	18	13
Total solids.....	1660	1488	1274	1692
K/Na, epm.....	1.3/1	3.95/1	15.1/1	45.0/1
Cl/OH, epm.....	3.8/1	1.35/1	1.5/1	2.3/1

boilers were acid-cleaned with hydrochloric acid which caused the potassium aluminum silicate to disintegrate and be removed by flushing with water.

Table 12 gives a series of boiler-water analyses which were made in January, March, May, and June, 1944. These analyses show that during the period of severe contamination the potassium-sodium ratio was 1.3 to 1 and in the last analysis the ratio was 45 to 1.

MAGNESIUM-PHOSPHATE SLUDGE

Magnesium phosphate was always present in the sludge accumulations and seemed to be the agent that caused the sludge to form into gummy adherent masses. To prevent the precipitation of magnesium phosphate, potassium silicate, when needed, is added to the boiler to maintain the silica at 1 to 1.5 per cent of the boiler-water solids. Also, the phosphate which had been 10 to 15 per cent of the boiler-water solids was reduced so that the maximum now carried is 5 per cent.

The maintenance of these concentrations should permit the precipitation of the magnesium as a silicate which can be easily removed from the boilers and not serve as a bond to hold the other deposits. This practice has been in effect about 8 weeks, and boiler inspections indicate favorable results, but sufficient time has not elapsed to allow a definite statement to be made.

CONCLUSIONS ON BOILER CONDITIONS

When using potassium salts for boiler-water treatment all

TABLE 13 TURBINE-BLADE DEPOSITS

Impulse	Sodium treatment	Temperature, deg F	Potassium treatment
1st row	Sodium and magnesium-chloride phosphate, sulphate, some silica	700	Potassium chloride and sulphate
2nd row	Sodium and magnesium-chloride phosphate and sulphate, some silica, quartz ^a		Potassium chloride, phosphate, and sulphate
Reaction			
1st row	Magnetic iron oxide, sodium silicate, phosphate ^a	635	Potassium chloride, sulphate, some silica ^a
2nd row	Same as 1st row ^a		Ferric oxide, potassium chloride, sulphate, silica
3rd row	Ferric oxide, sodium silicate ^a		Potassium chloride, sulphate, silica
4th row	Same as 3rd row ^a		Potassium chloride and sulphate, potassium tetrasilicate ^a
5th row	Quartz, sodium disilicate, magnetic iron oxide		Potassium chloride, potassium tetrasilicate, ferric oxide
6th row	Quartz, sodium phosphate ^a		Potassium tetrasilicate, potassium chloride, ferric oxide ^a
7th row	Quartz, trace of chloride and sulphate		Potassium tetrasilicate, potassium chloride, ferric oxide
8th row	Quartz, trace sodium salts ^a	460	Potassium tetrasilicate, potassium chloride, ferric oxide
9th row	Quartz, trace sodium salts ^a		Potassium tetrasilicate, amorphous silica, trace sulphate, chloride, ferric oxide
10th row	Quartz, trace phosphate, and magnesium		Quartz, potassium chloride ^a
11th row	Quartz, and amorphous silica ^a		Amorphous silica, ferric oxide, potassium salts
12th row	Amorphous silica, some quartz		Amorphous silica, ferric oxide, trace potassium salts
13th row	Amorphous silica ^a		Amorphous silica, ferric oxide, potassium salts
14th row	Amorphous silica		Amorphous silica, ferric oxide, potassium salts
15th row	Amorphous silica		Amorphous silica, ferric oxide, potassium salts
16th row	Amorphous silica ^a	235	Amorphous silica, ferric oxide, potassium salts
17th row	Amorphous silica ^a		Amorphous silica, ferric oxide, potassium salts
18th row	Amorphous silica ^a		Amorphous silica, ferric oxide, potassium salts
19th row	Amorphous silica, magnetic iron oxide		Amorphous silica, ferric oxide, potassium salts
20th row	Amorphous silica, magnetic iron oxide	134	Amorphous silica, ferric oxide, potassium salts
21st row	Amorphous silica, and magnetic iron oxide ^a		Amorphous silica, ferric oxide, potassium salts
22nd row	Magnetic iron oxide ^a		Amorphous silica, ferric oxide, potassium salts
23rd row	Magnetic iron oxide		Amorphous silica, ferric oxide, potassium salts
24th row	Magnetic iron oxide ^a		Amorphous silica, ferric oxide, potassium salts

^a X ray as well as microscopic analyses of deposit.

surfaces where sludge does not accumulate are clean. With sodium treatment, a film of silica scale was often present. Potassium silicate will not deposit as a scale but potassium-aluminum silicate and potassium-iron silicate will form under sludge deposits where the boiler water can concentrate. The indications are that the amount of scale is not as heavy with potassium as with sodium, and also that the potassium scales will disintegrate in hydrochloric acid. When the epm ratio of potassium to sodium is less than 8 to 1, the condition of the interior boiler surfaces are similar to those found when using sodium treatment.

TURBINE-BLADE DEPOSITS

The normal carry-over in the steam from the high-pressure boilers at Springdale is about 0.3 ppm. Under these conditions high-pressure-turbine-blade deposits do not exist. When the carry-over is higher than this, some water-soluble deposits accumulate on the turbine blades. In the low-pressure turbines, silica deposits cause a loss in capacity and efficiency of the turbines. When using sodium treatment, these deposits had to be cleaned off by sandblasting or other similar means. Caustic washing was never tried, but water washing would restore approximately 30 per cent of the lost capacity. A recent water washing of a turbine, on which blade deposits had accumulated since using potassium treatment, restored 90 per cent of the lost capacity. Water-washing of another turbine on which blade deposit accumulated during the same interval of time failed to restore any appreciable amount of the lost capacity. Further studies and more washings will have to be made before any definite statements can be made on this subject.

A tabulation of the deposits found on the turbine blades with both sodium and potassium treatments is given in Table 13.

Discussion

THOMAS FINNEGAN.⁵ The Oswego Station of the Central New York Power Corporation has two 80,000-kw condensing turbines, each with its own boiler delivering 900,000 lb of steam per hr at 1250 psi and 900 F at the turbine inlet. The Huntley station of the Buffalo Niagara Electric Corporation has a single high-pressure unit resembling those at Oswego, except that the Huntley boiler is an open-pass boiler while those at Oswego are the radiant type. All three turbines are 17-stage machines with extraction points after the 1st, 3rd, 6th, 9th, 12th, and 14th stages.

Potassium treatment was substituted for sodium treatment at Huntley in August, 1943, following a scheduled shutdown of the boiler for inspection and maintenance. At the same time, chloride was added to the boiler water in order to establish the ratio of chloride to alkalinity which had been recommended as a possible preventive of the formation of magnetic-oxide deposits. During the shutdown the Huntley boiler was acid-cleaned.

When the turbine was first started following the shutdown, some trouble with sticking valves was noticed and, when a few days later it was brought up to speed and put on the line, several control valves and the turbine stop valve stuck, necessitating an immediate shutdown of the unit. A heavy soluble deposit had formed on the first few stages of the turbine. This deposit was primarily chloride. The turbine was washed with wet steam and put back in service with the boiler under sodium treatment.

After 4 months' operation under sodium treatment during which a slight increase in stage pressure occurred, it was decided to try potassium treatment again with the hope that it might

⁵ Buffalo Niagara Electric Corporation, Buffalo, N. Y. Mem. A.S.M.E.

prevent the deposition of silica in the turbine. This was done without a repetition of the rapid fouling of the machine which had occurred when potassium treatment was first used.

During the 10 months in which potassium treatment has now been used, the turbine first-stage pressure has increased more rapidly than when sodium treatment was used, indicating a deposition of material in the turbine. The deposit is soluble and can be removed by washing with wet steam. This is done about once a month at which time the first-stage pressure increases about 5 per cent since the last washing.

The condensed steam has a conductivity of about 1 micromho. The conductivity drops to about 0.7 micromho when the steam is degassed with a Straub degasifier. This indicates that the solid content of the steam is of the order of 0.5 ppm or less.

At Oswego, potassium treatment was started in one boiler in April, 1944, and in the other in June, 1944, following the annual shutdown of these units. During the 2 years on sodium treatment since the previous overhaul of the turbines, the pressure for four highest extraction points had increased an average of 7 per cent for No. 1 unit and 4 per cent for No. 2 unit. During the 7 months that potassium treatment has been used in No. 1 unit, these pressures have shown little or no increase; but during the 5 months it has been used in No. 2 unit, they have increased about the same as in the previous 2 years under sodium treatment.

The purity of the steam from both boilers is about the same as at Huntley. About 3 months after starting operation with potassium treatment, leaks were found at the locations where two of the tubes were rolled into the upper drum in No. 1 boiler. These joints were rerolled and no additional leaks were found in this boiler.

A few weeks after starting potassium treatment in No. 2 unit, thirteen leaks of this type were found, and during the following 2 months a total of forty-three such leaks occurred. There are 167 tubes entering the upper drum. The entire number of tubes were rerolled and no further leaks have occurred.

Hideout had always been present in these boilers under sodium treatment, especially in No. 2 boiler at Oswego. Since starting potassium treatment, hideout has been practically eliminated.

While there has been an increase in the rate of deposit of soluble material in the front end of the turbine, it is not as yet known whether there has been any change in the rate of deposition of the insoluble silica which has been found at about the 9th stage.

It has not been established that potassium treatment is responsible for the soluble deposits. Another modification of the water-conditioning process was made at the same time that potassium treatment was started, namely, the addition of chloride to establish the chloride ratio. Some time prior to starting potassium treatment, but nevertheless recent enough to make it a factor to be considered, was the discontinuance of sulphite treatment. The boiler-water solids, which at one time had been several hundred ppm, are now at about 100 to 200 ppm.

A study of the complete problem is now in progress in which all these factors will be investigated.

E. B. POWELL.⁶ Dr. Hall's 1943 paper,^{4,7} presenting a record from preliminary results of great promise at Springdale Station dealt basically with laboratory data from the literature and with

⁶ Consulting Engineer, Stone & Webster Engineering Corporation, Boston, Mass. Mem. A.S.M.E.

⁷ This is a discussion also of the following papers, presented at the Annual Meeting, New York, N. Y., Nov. 27-Dec. 1, 1944: "Experience With Potassium Treatment at Windsor Station," by W. L. Webb; "Experience With Sodium and Potassium Chemicals for Boiler-Water Conditioning at Montaup Electric," by G. U. Parks; and "Embrittlement Cracking in Waters Containing Potassium Salts," by A. A. Berk and N. E. Rogers.

theoretical considerations in support of his "new approach to the problem of conditioning water for steam generation." It is fortunate to have at such early date these summaries of operating experiences under the widely different conditions of the three separate high-pressure boiler plants, and also to have the Bureau of Mines test results on the embrittling characteristics of compounds associated with potassium treatment.

None of the authors from the power field considers his experience with potassium chemicals to have covered sufficient time or scope for derivation of really comprehensive conclusions but each is able to record evidence of definitely favorable trend within his observations. More specifically, under certain circumstances potassium treatment has proved capable of giving a less obstructed heating surface in the boilers under discussion than so far obtainable with the usual sodium treatment under the same circumstances. It would appear that appropriate predominance of potassium over sodium salts in the boiler waters of the three high-pressure plants, together with appropriate conditions of boiler-water alkalinity, has given properties of less tendency to adherence, or greater fluidity, in precipitated solids and, particularly in the Montaup Electric plant, greater solubility in the simple 2-ion potassium compounds, hydroxides, phosphates, and sulphates. On the other hand, the control of silica reactions seems rather uncertain and the experience would also indicate that, under some circumstances at least, the desirable properties of high solubility in the simpler potassium compounds and lower tendency to adherence on boiler surfaces in the precipitated solids may have quite equal sensitivity to alkalinity control as encountered with sodium treatment.

Obviously, there is altogether too little known of the properties of silica in the combinations encountered and formed in boiler waters. Under the conditions recorded by the present papers, silicate scale has occurred with potassium treatment where the overlying deposit is of character to impose sufficient interference in transfer of heat from the tube surface or transfer of water to the tube surface. Possibly, the ratios of potassium to sodium, or the concentrations of potassium, were not sufficiently high for the desired control. The potassium-sodium ratios for most favorable boiler-water conditioning may be governed to some degree by the nature and proportions of solids in the boiler water and may also bear some relation to the temperature of water and heat-transferring surfaces within the boiler.

The possibilities of potassium treatment seem very real and the limitations equally real, both needing further exploration.

Messrs. Berk and Rogers refer to the use of nitrate as offering promise of successfully inhibiting tendency to boiler-plate embrittlement, which apparently is to be expected from potassium hydroxide in the presence of silicate to about the same degree as from sodium hydroxide under like conditions. The following two sentences quoted from the paper would seem, however, somewhat disconcerting to the prospective user of nitrate:

"Nitrate tends to react with the metal of the autoclave and piping under the conditions of the test."

"Nitrate, although comparatively inert in dilute alkaline solution (boiler water), appears to react rapidly with metal and metal-oxide surfaces in concentrated caustic solutions."

These sentences might readily be interpreted as a warning that, if the fabrication of the pressure vessel has left a seam or other crevice in which concentration of alkaline boiler water might take place to the degree necessary for embrittling attack, nitrate in the water in the nitrate-to-hydroxide ratio used in the Bureau of Mines research reported would cause serious corrosion on the metal walls of the crevice. I believe that it would be helpful if the authors presented such pertinent detail of their observations as may be available, to make clear particularly whether the nitrate reaction with the steel is actually of the

continuously progressive type such as would result ultimately in serious loss of metal or, on the contrary, is rapidly checked and causes no practical damage.

J. D. YODER.⁸ This paper describing results obtained in more than 2 years' treatment of boiler water at Springdale is an important contribution to the recent knowledge on the subject of boiler-feedwater treatment. It gives a practical measure of this treatment, the theory of which has been so ably presented by Dr. Hall.⁴ It is a subject in which all engineers concerned with efficient operation of boilers are much interested.

The paper is helpful because it reports not only on data to substantiate the value of the method, but it outlines the troubles encountered with its use. The value of the paper is increased because it reports many typical analyses of water and scale which will be helpful to other engineers and chemists interested in similar problems. In this respect, it would have been helpful if there had been more consistency in the method of reporting the analyses of the boiler water. The alkalinities and ratios of potassium to sodium are reported in epm, while the solids in solution are generally reported in ppm. Again, the alkalinities are reported in the colloquial expressions of "A" and "B" readings which might suggest different values to different people. Since some of the analyses are reported in their equivalents, it would have been helpful if all of the ions had been reported in their equivalents possibly in terms equivalent to calcium carbonate, which terms are frequently used and well understood by the engineering fraternity.

The analyses of boiler water do not show any carbonate ions, but it seems evident from the character of the make-up water that some carbonates were present. A knowledge of the quantity of carbonates present might be of value.

Their experience in operating with low alkalinities is not in agreement with Purcell and Whirl,⁹ who reported that both scale and embrittlement could be prevented with no hydroxide alkalinity other than that given by trisodium phosphate. The authors found it necessary to maintain a substantial hydroxide alkalinity in excess of that produced by trisodium phosphate.

This paper indicates that the prevention of silica scale remains related to boiler design. Even with the sodium-phosphate treatment, silica scale did not form in all of the tubes but was found only in the horizontal tubes where the circulation was sluggish. Unfortunately, from the standpoint of determining the value of the potassium treatment, some corrections were made in circulation during the time of the test. This raises the question of how much the improved results were due to improvement of circulation and how much to potassium treatment. The authors finally conclude that "potassium iron silicate will form under sludge deposits when the water concentrates." This means when the circulation is not good.

One is impressed with the high solids in the boiler water considering that the feed comes from surface condensers with evaporators for make-up. The solids would not need to be greater if the make-up water were softened and not evaporated. This possibility is further emphasized because the authors observed improvement when adding chlorides to the water. A similar result might often be obtained if the make-up water were softened by Zeo-Karb-H which is a zeolite treatment operated on the hydrogen cycle. This removes the sodium, calcium, and magnesium from the water, but leaves the chlorides and sulphates to give a slight acidity proportional to the chlorides and sulphates

present. This acidity may then be neutralized with potassium hydroxide to give the desirable potassium chloride in the feed-water. Such treatment might avoid the need for evaporators and make available a simple and more desirable hookup from the standpoint of the feedwater-heating cycle.

AUTHORS' CLOSURE

We are in agreement with both Mr. Finnegan's and Mr. Powell's position that both time and scope of observation are still too limited to permit comprehensive conclusions regarding potassium treatment. Following the suggestion in Mr. Yoder's discussion, we have added a footnote to Table 3 defining A and B readings as used. As noted by Mr. Yoder, our alkalinities are higher than those of the Purcell-Whirl co-ordinated phosphate control curve. However, it is our experience that if sludge tends to be a problem, higher alkalinities than those of this control curve are essential to keep the sludge in suspension. Mr. Yoder's reasoning regarding use of Zeo-Karb-H in preparation of make-up waters seems sound.

Definitely, as pointed out by Mr. Parks in his discussion, potassium treatment is effective in minimizing hide-out of boiler-water salts, particularly the sulphates and phosphates. This is in accord with the fact that potassium sulphate is slightly more soluble than sodium sulphate at higher pressures and temperatures, and potassium phosphate is tremendously more soluble than sodium phosphate, steadily increasing in solution with increasing temperature as pointed out by Kaufman.¹⁰

Where high concentration of boiler water occurs, as in the concentrating film boiler water under sludge, potassium aluminum silicate forms, but is far more friable and easily removed than the sodium aluminum silicate forming under similar conditions. Presumably, this means that the potassium aluminum silicate is more soluble than sodium aluminum silicate, and the fact of its ready decomposition by hydrochloric acid further affirms this assumption, since sodium aluminum silicate is very difficult to decompose. The significance of this last fact is that acid-washing of the boiler should be much easier with potassium-aluminum-silicate deposits than with those of sodium aluminum silicate.

In his paper¹¹ Professor Straub has shown that silica (SiO_2) is carried to the steam by volatilization of the silica in the boiler water. This seems reasonable by analogy to known facts. Thus carbon dioxide is vaporized into the steam as follows



Again, sodium sulphite at higher temperatures undergoes auto-oxidation as follows



The required temperature is supplied especially in regions of steam blanketing and concentrating-film boiler water, and consequently, any maintenance of sulphite in boilers having such characteristics is attended with uncertainty. Under these conditions, hydrogen sulphide is vaporized into the steam thus



By analogy, the vaporization of silica would be as follows



Dr. Morey,¹² however, has shown that the sodium oxide volatil-

⁸ Manager of Boiler Feedwater Division, The Permutit Company, New York, N. Y. Mem. A.S.M.E.

⁹ "Embrittlement of Boiler Steel—Experiences With the Schroeder Detector," by T. E. Purcell and S. F. Whirl, Trans. A.S.M.E., vol. 64, 1942, pp. 397-402.

¹⁰ Discussion by C. E. Kaufman of paper by R. E. Hall,⁴ Trans. A.S.M.E., vol. 66, 1944, pp. 478-479.

¹¹ "Silica Deposition in Steam Turbines," by F. G. Straub and H. A. Grabowski, published in this issue of the Transactions, pp. 309-316.

¹² "Solubility of Solids in Water Vapor," by G. W. Morey, Proceedings of the American Society for Testing Materials, vol. 42, 1942, p. 987.

izes as well as the silica, and in considerable quantities at temperatures from 707 to 932 F, and at pressures ranging up to 16,500 psia. The quantity vaporized increases more markedly with pressure than with temperature increase.

As noted in Table 13 of the paper, identification of the turbine deposits by petrographic microscope and X ray shows that sodium silicate is deposited in the high-pressure stages, then sodium disilicate or potassium tetrasilicate at lower pressures, next quartz, and finally, amorphous silica. This process of silica enrichment in passage through the turbines has been dis-

cussed by Hall¹³ and is in accord with the vaporization data of both Morey and Straub. Apparently, an answer must be awaited to the question of whether the sodium or potassium chloride, sulphate, and phosphate, also iron oxide, are carried to the turbine in vapor form, or as customary mechanical carry-over. In the latter case, of course, at least some of the silica or silicate found in the turbine is similarly derived.

¹³ "A New Approach to the Problem of Conditioning Water for Steam Generation," by R. E. Hall, Trans. A.S.M.E., vol. 66, 1944, footnote p. 470.

Experience With Potassium Treatment at Windsor Station

By W. L. WEBB,¹ NEW YORK, N. Y.

Under conventional sodium treatment and with hardness, alumina and silica in quantity entering the cycle through condenser leakage, wall-tube losses in two 1350-psi boilers were extensive. Upon establishment of potassium treatment in these boilers under the then controlled equilibria, tube losses continued. A direct comparison of sodium versus potassium treatments was started in these boilers after solvent-cleaning them. This test has been under way only 7 months during which no wall-tube failures have occurred.

POTASSIUM treatment developed by Hall² as a new approach to the problem of boiler-water conditioning has been employed experimentally at the Windsor Station of the Beech Bottom Power Company in an effort to prevent boiler-tube losses which had occurred previously under conventional sodium treatment.

About 1 year after starting the new treatment in two boilers whose wall-tube surfaces were not free of analcite scale layed down previously under sodium treatment, extensive tube losses again occurred. These boilers which receive the same feedwater were then chemically cleaned, and one was put on potassium treatment and the other on sodium treatment. This latter test has been under way only 7 months and no wall tube has failed. As a result, only tentative conclusions can be drawn from this latter comparison. However, the presentation of the data from both tests may help to broaden the knowledge of the merits and limitations of a treatment which is now receiving widespread attention.

SODIUM TREATMENT

From the initial operation in late 1941, until April, 1943, boilers 82 and 84 at Windsor Station were operated on conventional sodium treatment under supervision of the Hall Laboratories. These boilers are similar in design, both being rated 750,000 lb per hr, 1350 psi, and 925 F steam temperature. They are 3-drum, bent-tube, tangentially fired, wet-bottom boilers which, along with two other boilers of the same rating, supply steam to two 60,000-kw topping turbines exhausting to six 30,000-kw 230-psi 550 F condensing units.

Because of high condenser leakage which only can be eliminated by steps which will require outages longer than can be afforded, considerable Ohio River water enters the cycle, carrying with it hardness and, during turbid river conditions, large quantities of silica and alumina. Suspended matter as high as 4000 ppm has been observed, its composition averaging about 23 per cent SiO_2 , 42 per cent Al_2O_3 , 23 per cent Fe_2O_3 , and 10 per cent

organic matter. Condenser leakage is greatest at times of most rapid change in river-water temperature, and, occasionally, highest leakage and maximum suspended matter occur simultaneously. Under these conditions, it was and is difficult or impracticable to maintain the silica in the boiler waters at a low value by blowdown and to hold concentrations of treating chemicals at the desired values.

During the 16-month period of initial operation of the boilers, furnace-wall-tube wastage developed to a serious degree. In the wastage zones many tubes blistered and a number developed leaks in longitudinal cracks usually located in slight bulges. The removal of tube specimens revealed thin hard deposits of analcite scale which turbinizing failed to remove. Sludge deposits were extremely heavy on steam-scrubber and downcomer surfaces and only slightly less so in riser tubes.

Starting early in 1942, at the time of highest condenser leakage under turbid river conditions, water-insoluble deposits occurred in the 30,000-kw low-pressure turbines at such a rate as to cause capacity losses of 3000 kw per unit in 4 to 6 months. These units were periodically caustic-washed,³ restoring outputs and stage differential pressures to normal.

The foregoing operating difficulties, namely, boiler sludge and analcite-scale deposits and water-insoluble turbine deposits, were problems which potassium treatment appeared to be designed to solve. As a result, early in April, 1943, potassium treatment was started in boilers 82 and 84. This was done even though fundamental data were not available and, in so far as the author knows, are not available, to show the advantages of potassium over sodium in the prevention of aluminum-silica complex scales.

POTASSIUM TREATMENT IN BOILERS 82 AND 84

When the decision was made to use potassium treatment in the two boilers, it was recognized that the fire sides of wall-tube internal surfaces were not free of hard scale even though these tubes had been cleaned with turbine-driven cutters. The jobs put to potassium, therefore, were to remove old scale as well as to prevent new scale and sludge deposits from forming and, in so far as possible, to prevent capacity losses resulting from turbine deposits. That this proved to be more than potassium treatment could accomplish was shown by the following wall-tube damage:

Boiler 82:

May 3, 1943—2 tube leaks in longitudinal cracks in furnace-wastage areas
Oct. 9, 1943—1 leaking tube and 6 bulges
March 29, 1944—1 leaking tube

Boiler 84:

March 1, 1944—7 leaks and 9 bulges
March 20, 1944—9 leaks and many bulges in wall tubes requiring welding-in 19 new tube sections, 7 window welds, and numerous surface welds

Periodic inspections of boiler-drum surfaces and internals, and the visible portions of tubes and headers indicated somewhat reduced sludge deposits from those experienced under sodium

¹ Engineering Department, American Gas and Electric Service Corporation.

² "A New Approach to the Problem of Conditioning Water for Steam Generation," by R. E. Hall, Trans. A.S.M.E., vol. 66, 1944, pp. 457-488.

Contributed by Joint Research Committee on Boiler Feedwater Studies and presented at the Annual Meeting, New York, N. Y., Nov. 27-Dec. 1, 1944, of THE AMERICAN SOCIETY OF MECHANICAL ENGINEERS.

NOTE: Statements and opinions advanced in papers are to be understood as individual expressions of their authors and not those of the Society.

³ "Removal of Water-Insoluble Turbine Deposits by Caustic Washing," by W. L. Webb and R. G. Call, Trans. A.S.M.E., vol. 65, 1943, pp. 713-717.

treatment, but the relative amount of sludge appeared to be affected more by the extent and character of condenser leakage than by the type of treatment. Turbine deposits continued at rates substantially the same as before.

The tube losses in March, 1944, followed a period of high condenser leakage and river turbidity such as to make proper coagulation of the raw water impossible, resulting in extremely poor evaporator vapor quality. The extent of these tube failures made it imperative that remedial steps be taken immediately. The first step called for was to remove the hard scale from the boilers by means of suitable solvents. The next was to limit condenser leakage in so far as possible. This was done by the installation of wood-slat bracing to reduce tube-cracking at the tube sheets. The third step was to improve the raw-water treating facilities. Finally, a decision had to be made as to whether to return to sodium treatment which had already demonstrated its inability to prevent analcite scale, making necessary periodic use of solvent cleaning methods, or to continue with potassium treatment for determining its merits when used on a clean boiler.

Early in April, both of the boilers were cleaned under Dowell supervision using a solvent consisting of 10 per cent hydrochloric acid, 5 per cent ammonium bifluoride, and Dowell's inhibitors and wetting agents. Following the cleaning operation, representative tube specimens indicated satisfactory removal of deposits from one boiler but complete removal had not occurred in the other. The remaining scale, however, had been loosened by the solvent and was removed by means of turbine cutters.

The middle course was chosen with respect to treatment, boiler 82 being put on sodium treatment and boiler 84 on potassium treatment. As the boilers are similar in design, are normally loaded substantially equally, and both receive the same feedwater, they present as nearly an ideal situation as possible for direct comparison of the two methods of treatment under conditions in which considerable alumina enters the cycle.

COMPARISON OF Na AND K TREATMENTS

After cleaning the boilers involved, a comparison of treatments was started in mid-April, 1944. Since that time, internal inspections and removal of tube specimens for examination occurred in June and October. During this entire operating period up to and including October, 1944, condenser leakage has been relatively low and river conditions abnormally good. The real merits of the two treatments, therefore, have not been put to the crucial test. Fortunately, no wall-tube losses have occurred.

Critical examination of tube specimens from both boilers

showed no hard scale deposits. At the October shutdown, sludge deposits in the potassium-treated No. 84 boiler on scrubber hoods and downcomer tubes were substantially nil and deposits on wall-tube specimens examined were entirely absent. A considerable quantity of sludge, however, had accumulated in the bottom of the scrubber drum and lower drum.

The scrubber hoods and visible portions of the downcomer tubes of the sodium-treated No. 82 boiler were coated with sludge having an average thickness of $\frac{1}{8}$ in. and a maximum thickness on some areas of $\frac{3}{8}$ in. The riser-tube specimens showed coatings of less than $\frac{1}{64}$ in. It appeared that, roughly, the same amount of sludge had accumulated in each boiler, but in the potassium-treated boiler it was very much less adherent.

BOILER-WATER CONDITIONS

In Table 1 are indicated the average boiler-water conditions maintained initially under sodium treatment (column 1), when the two boilers were on potassium treatment (columns 2 and 3), and under the present comparison of sodium and potassium (columns 4 and 5).

It will be noted in comparing the present control of potassium treatment to that formerly used (columns 3 and 5 of Table 1) chlorides are higher and phosphate values are lower than previously. The present conditions requested by Hall Laboratories and the indicated reasons therefore are as follows:

- Condition A—K/Na (epm)—3 or greater to permit operating mainly under potassium equilibria
- Condition B— SiO_2/OH (epm)—0.5 or less to assist in keeping silica in a soluble form in the boiler and turbine
- Condition C— Cl/OH (epm)—Preferably 10 or at least 5 to limit the concentration of caustic in areas where film-boiling occurs to reduce the production of iron oxide in the boiler
- Condition D— PO_4 (ppm)—10 to 30 or not higher than 40 favoring the precipitation of magnesium as the silicate rather than the phosphate.

As shown by column 5 of Table 1, water control was such that condition B only was rigidly met. Conditions A and D were only partially met, and condition C was seldom met. The problem would be much simpler in the absence of condenser leakage, but as long as it exists to the extent it does, it is desirable to maintain sufficient soluble phosphate in the boiler water to precipitate all incoming calcium hardness as sludge and so to control treatments and blowdown to limit boiler-water total solids to about 800 ppm from the standpoint of steam quality.

Putting conditions A to D, inclusive, in simpler terms calls for:

- 1 A high feed of potassium chemicals, particularly chloride

TABLE 1 AVERAGE BOILER-WATER ANALYSES AND TREATMENTS

Column no.	(1)	(2)	(3)	(4)	(5)
Treatment	Sodium	Potassium		Sodium	Potassium
Boiler no.	82 and 84	82 and 84	82 and 84	82	84
Period	Start up to April '43	April, 1943	April '43 to April '44	April '44 to Nov. '44	April '44 to Nov. '44
Boiler-water conditions:					
OH (ppm)	15	5 to 15	15	10 to 30	10 to 30
PO_4 (ppm)	40	25 to 50	40	25 to 50	20 to 40
SO_4 (ppm)	150	50 to 150	150	50 to 150	30 to 100
Cl (ppm)	15	50 to 100	100	100 to 150	100 to 170
Na_2SO_3 (ppm)	5 to 10	0	0	0	0
SiO_2 (ppm)	10	7 to 40	8	5 to 10	5 to 10
Total solids (ppm)	400	350 to 700	600	350 to 700	400 to 800
pH	10.8	10.0 to 10.8	10.8	10.7 to 11.0	10.7 to 11.0
Cl/OH (epm)	0.5	3+	3+	2+	3+
SiO_2/OH (epm)	0.4	0.5 to 2.0	0.5	0.2 to 0.5	0.1 to 0.5
K/Na (epm)	...	1 to 2	2	...	2 to 5
Average condenser leakage (per cent of feedwater)					
	0.1	0.2	0.1	0.1	0.1
Treating chemicals:					
(Average per million lb feedwater)					
NaOH (lb)	0.15	0.15	...
Na_2HPO_4 (lb)	0.2	0.2	...
Na_2SO_3 (lb)	0.2	0	...
NaCl (lb)	0.3	...
KOH (lb)	...	0.2	0.5	...	0.4
KCl (lb)	...	0.3	0.5	...	0.7
KH_2PO_4 (lb)	...	0.3
H_3PO_4 , 75 per cent (lb)	0.4
$\text{K}_4\text{P}_2\text{O}_7$ (lb)	0.3

TABLE 2 TYPICAL BOILER DEPOSITS

Column no.	(1)	(2)	(3)	(4)	(5)	(6)	(7)
Treatment	Sodium		Potassium			Sodium	Potassium
Period	Start up to April '43		April '43 to April '44			April to Oct. '44	April to Oct. '44
Boiler no.	84	84	84	84	84	82	84
Sampling date	4/2/43	5/18/42	11/20/43	11/20/43	3/1/44	10/17/44	10/12/44
Deposit	Sludge	Scale	Sludge	Scale	Scale	Sludge	Sludge
Source	Scrubber	Wall	Wall	Wall	Wall	Wall	Drum
Chemical analysis (per cent):							
Sulphur trioxide (SO ₃)	Nil	1.4	Trace	0.5	Nil	0.8	<1
Carbon dioxide (CO ₂)	Nil	Nil	Nil	Nil	Nil	Nil	Nil
Phosphorous pentoxide (P ₂ O ₅)	30	11.5	16.1	8.1	9.2	18.2	25
Silica (SiO ₂)	0.3	24.2	1.6	14.1	17.6	0.9	<1
Iron oxide (Fe ₂ O ₃)	15	24.8	21.4	41.2	36.1	30.5	31
Aluminum oxide (Al ₂ O ₃)	Nil	9.0	1.3	4.0	9.4	Nil	Present
Calcium oxide (CaO)	>40	8.2	14.1	5.6	8.0	17.6	25
Magnesium oxide (MgO)	7-8	3.3	5.9	4.4	4.1	7.2	8
Sodium oxide (Na ₂ O)	Nil	14.5	2.9	6.2	1.8	N.D.	N.D.
Potassium oxide (K ₂ O)			<0.5	<0.5	>3.3	0	1
Copper (Cu)	Slight	Nil	35.0	12.0	6.1	21.4	2
Net ignition loss (calculated)	..	4.7	1.9	3.0	3.7	4.0	4
Oil	Nil	Nil	..	Nil	..
	>93	99.6	100.7	99.6	99.3	100.6	98
Compounds shown by chemical, X-ray and petrographic analysis, per cent:							
Sodium sulphate, Na ₂ SO ₄	2.5	14.4
Hydroxyapatite, 3Ca ₃ (PO ₄) ₂ · Ca(OH) ₂	11.5	(a)	(a)
Sodium phosphate, Na ₃ PO ₄	14.0	5.7
Magnesium phosphate, Mg ₃ (PO ₄) ₂	0.3
Serpentine, 3MgO · 2SiO ₂ · 2H ₂ O	7.0	3.9
Magnesium aluminate, MgAl ₂ O ₄	3.6	(b)	..
Magnesium aluminum silicate, MgAl ₂ O ₄ · 4SiO ₂	15.3
Leucite, K ₂ Al ₂ O ₄ · 4SiO ₂	..	(a)	(a)	..	8.7
Analcite, Na ₂ Al ₂ O ₄ · 4SiO ₂ · 2H ₂ O	38.9	(a)	(a)	..	4.2
Acmite, Na ₂ Fe ₂ O ₄ · 4SiO ₂	..	(a)	(a)	..	34.8
Magnetite, Fe ₃ O ₄	24.8	(a)	(a)
Hematite, Fe ₂ O ₃	..	(a)	6.1
Copper, Cu	Nil	(a)	2.6
Ignition loss (less combined water)	0.6

(a) Probably present but identity masked by presence of magnetite.

(b) Microscopic analysis shows magnetite, copper oxide, and rod-shaped calcium phosphate.

and sufficient blowdown to hold the sodium concentration at a low level.

2 A high hydroxide-silica ratio from the standpoint of keeping silica soluble, but low hydroxide and phosphate values and a relatively high silica value to permit precipitating magnesium as the silicate rather than the phosphate or hydroxide.

3 A low hydroxide-chloride ratio for reduction of iron oxide produced from the boiler metal.

In other words, chloride must be higher than hydroxide, and hydroxide must be higher than silica, but silica must be enough higher than phosphate and hydroxide to satisfy magnesium.

For the sake of discussion, let us assume a cycle having very low condenser leakage and evaporator carry-over with no low limit on boiler-water total solids. To assure magnesium being precipitated as silicate might require a soluble SiO₂ value of at least 15 ppm. To assure calcium being precipitated as phosphate likely would require a soluble PO₄ value of 10 ppm. With these values fixed and meeting conditions B to D, inclusive, and at the same time being well on the potassium side with a K/Na (epm) ratio of 10:1, the boiler-water conditions would be approximately as follows:

SiO ₂ (ppm)	15
PO ₄ (ppm)	10
OH (ppm)	17
Cl (ppm)	350
K/Na (epm)	10:1

The 10:1 K/Na ratio would permit the presence of about 25 ppm of sodium. Such a limitation, particularly with sea-water condenser cooling, might require abnormally high blowdown. The total soluble solids in the boiler water under this condition would be approximately 900 ppm.

The foregoing example is given to show the requirements of the relatively tight cycle and to indicate the difficulties of the plant chemist in attempting to maintain the desired boiler-water conditions during periods of high condenser leakage, while at the same time juggling blowdown and limiting total solids to give acceptable steam quality.

It is not the intention of the author to discourage the pros-

pective user of potassium treatment but rather to give a clearer conception of the requirements for boiler-water control.

BOILER DEPOSITS

In Table 2 are given the analyses of representative scale and sludge samples taken from boilers 82 and 84 under the various treatments. Sludges from the steam scrubbers and drums were sampled directly from the surfaces involved. Prior to 1944, it was common practice to obtain wall-tube deposits by collecting them in a cloth bag at the lower end of the tube while passing a turbine-driven cutter through the tube. That portion of the collected sample which passed a 20-mesh sieve was then termed "sludge," and that retained on the sieve was termed "scale." This procedure usually gives interpretable analyses, but the removal of tube specimens permitting direct sampling of sludge and scale is a preferable procedure and is the one now being followed wherever practicable.

Column 1 of Table 2 indicates that the sludge under initial sodium treatment is mainly calcium and magnesium phosphate and iron oxide. This same condition exists today under sodium treatment (column 6), giving a sludge that is quite adherent. Deposits are less heavy on the riser tubes than on the steam scrubber and downcomer surfaces, but under conditions where large quantities of hardness enter the cycle the sludge accumulations during relatively short operating periods are unquestionably detrimental. The same situation exists under potassium treatment (column 7), but to a considerably lesser degree. Why this is so is not apparent. Magnesium is still precipitated as phosphate rather than silicate.

The scales under initial sodium treatment were predominantly analcite with additional complexes containing aluminum. The analysis given in column 2, Table 2, is of particular interest in that it indicates the presence of some of the least soluble boiler-water salts, namely, sodium sulphate and sodium phosphate. This suggests hide-out which has been observed on a number of occasions. No scales have been found during the present test of sodium treatment on boiler 82.

During the April, 1943-April, 1944, period of operation of both

boilers on potassium treatment, several periods of high condenser leakage under turbid river conditions were experienced. Sludge deposits were heavy on scrubber and downcomer surfaces although somewhat less so than previously under sodium treatment. The quantity of deposit turbed from wall tubes in some cases ranged between 5 and 6 g per linear ft of tube. Although this was as high as previously observed under sodium treatment, the effects of the respective amounts of condenser leakage under the two treatments are not readily determinable. These sludges, of which the analysis in column 3, Table 2, is typical, were comparable to those prevailing under sodium treatment.

The wall-tube scales under potassium treatment, columns 4 and 5, are similar to those under sodium treatment in that they contain alumina and silica. However, now sodium is present in a lesser amount, and potassium and iron have entered the complexes.

In attempting to interpret scale analyses during the April, 1943–April, 1944, period, it must be kept in mind that potassium treatment was not started with the boiler heating surfaces clean. The effect of the old scale may have had a definite bearing on the character of deposits observed.

MISCELLANEOUS

In November, 1943, while boiler 82 was under potassium treatment, hydrogen measurements by means of a Cambridge hydrogen recorder were made in the saturated steam. Tests in which the OH and the Cl/OH values were varied gave the following average results:

OH (ppm)	Cl (ppm)	Cl/OH (epm)	H ₂ (ppm)
13	26	1.00	0.0020
45	26	0.28	0.0036
45	155	1.67	0.0041

With low chlorides an increase in caustic resulted in a slight increase in the hydrogen value. With the higher caustic value, an increase in chlorides (to give only a Cl/OH ratio in epm of 1.67, as compared to 5 or 10 as now suggested by Hall Laboratories) caused the hydrogen value to increase further. Inasmuch as the hydrogen is subject to some normal fluctuation, it is possible that such tests, if conducted over longer periods and at a greater Cl/OH value, would have shown the effect of high chlorides in retarding the production of iron oxide in the boiler as measured by hydrogen evolution.

Early in June, 1944, oil in considerable quantity and definitely identified as turbine oil reached boilers 82 and 84 and one of the other high-pressure Windsor boilers. At one time boiler 82 saturated steam contained in excess of 100 ppm of oil, and 1/2 in. or more of oil appeared in the water columns of several boilers. The boiler-water alkalinities were promptly lowered and the affected boilers were given heavy and prolonged blowdown. Oil was detected in and removed from a number of surge tanks, with the result that it disappeared from the steam about 2 days later.

The inspection of boilers 82 and 84 later in June showed substantially no indication of oil, but collected deposits showed some evidence of it. So far as is known the oil contamination caused no direct harm. It is perhaps fortunate that this condition occurred at a time when tube losses were not being experienced as it might have obscured the real causes of the failures.

At no time under potassium treatment has there been difficulty with leaks in rolled tube ends or in gaskets as was experienced by others. Flexitallic handhold gaskets are used throughout.

Governed principally by changing rates of condenser leakage, the boiler-water-sampling and analysis schedules for both sodium and potassium treatment call for determining OH and PO₄ four times, and the other usual constituents once per 24 hr per boiler.

The cost of chemicals for potassium treatment is 3 to 6 times that for sodium treatment and at Windsor averages about 10 to 12 cents per million pounds of feedwater.

CONCLUSIONS

Although the direct comparison of potassium and sodium treatments now under way has been carried on for too short a period to permit drawing more than preliminary conclusions, the author's conclusions with respect to the entire Windsor experience are as follows:

1 Following the usual start-up periods, boiler waters are substantially free of turbidity under both sodium and potassium treatments. This indicates in both cases that substantially all sludge-forming material entering the boilers with the feedwater remains in the boilers as sludge and/or scale.

2 No information has come to our attention to show how sodium treatment can be controlled to prevent deposition of analcite scale when alumina in quantity reaches the boiler.

3 When both boilers 82 and 84 were operated under potassium treatment with a K/Na ratio of 2 and an SiO₂/OH ratio of 0.5, both in epm:

(a) This treatment did not prevent the failure of wall tubes on which analcite had already been layed down. These tube losses presumably resulted from the deposition of additional aluminum-silica complexes containing both sodium and potassium.

(b) The rates of accumulations of deposits in 30,000-kw low-pressure turbines receiving steam from these boilers were substantially the same as under sodium treatment. These deposition rates caused capacity losses of about 3000 kw per unit in periods of 4 to 6 months.

4 The direct comparison of Na and K treatments in two boilers receiving the same feedwater for a period of 7 months, during which condenser leakage was low and river conditions were good, has been of too short duration to permit drawing conclusions other than that the sludge in the potassium-treated boiler is less adherent than in the sodium-treated boiler. No hard-scale deposits have been observed in either boiler.

Embrittlement Cracking in Waters Containing Potassium Salts^{1, 2}

By A. A. BERK³ AND N. E. ROGERS,⁴ WASHINGTON, D. C.

On behalf of Subcommittee No. 6 of the Joint Research Committee on Boiler Feedwater Studies, the embrittlement characteristics of waters containing potassium-hydroxide alkalinity have been studied. The embrittlement detector was used to test dilute solutions in the range of concentrations encountered in boiler operation. The effect of potassium-hydroxide solutions on stressed steel was also determined with concentrated solutions in a tension-testing device. It was found that potassium-hydroxide solutions could cause intercrystalline cracking of stressed steel. At 250 C a small concentration of silica in the solutions greatly accelerated the attack. Potassium nitrate and quebracho extract both proved to be effective inhibitors. No cracks were obtained with solutions of pure tripotassium phosphate, potassium metasilicate, or potassium disilicate, indicating that these alkaline potassium salts would not cause embrittlement cracking of boiler seams. Potassium hydroxide is therefore very similar to sodium hydroxide with respect to embrittlement.

THE use of potassium salts in place of sodium salts to condition boiler waters has led to continuation of the investigation of embrittlement cracking⁵ sponsored by Subcommittee No. 6 of the Joint Research Committee on Boiler Feedwater Studies. Specific questions to be answered were whether potassium hydroxide, like sodium hydroxide, could cause the intercrystalline corrosion that led to the cracking and, if so, whether inhibitors such as potassium nitrate and quebracho extract⁶ could prevent the attack. A third question, whether tripotassium phosphate or the potassium silicates could be used in a "zero caustic alkalinity" treatment^{6, 7} is of special importance to the operators of high-pressure boilers.

APPARATUS AND PROCEDURE

Testing equipment consisted of five embrittlement detectors

¹Prepared by permission of the Director, Bureau of Mines, U. S. Department of the Interior.

²This investigation was conducted under a co-operative agreement between the Joint Research Committee on Boiler Feedwater Studies and the Bureau of Mines. It was supervised by a subcommittee of which J. H. Walker is chairman and was carried out at the Washington, D. C., laboratories of the Bureau of Mines.

³Chemist-in-Charge, Boiler Water Research, Bureau of Mines, Washington, D. C.

⁴Chemist, Bureau of Mines, Washington, D. C.

⁵"Caustic Embrittlement Research Brings Results," by J. H. Walker, *Mechanical Engineering*, vol. 64, 1942, pp. 891-893.

⁶"A Practical Way to Prevent Embrittlement Cracking," by A. A. Berk and W. C. Schroeder, *Trans. A.S.M.E.*, vol. 65, 1943, pp. 701-711.

⁷"Protection Against Caustic Embrittlement by Co-Ordinated Phosphate pH Control," by T. E. Purcell and S. F. Whirl, *Trans. Electrochemical Society*, vol. 83, 1943, pp. 343-359.

Contributed by the Joint Research Committee on Boiler Feedwater Studies and presented at the Annual Meeting, New York, N. Y., Nov. 27-Dec. 1, 1944, of THE AMERICAN SOCIETY OF MECHANICAL ENGINEERS.

NOTE: Statements and opinions advanced in papers are to be understood as individual expressions of their authors and not those of the Society.

and a tension-testing device. Much of the apparatus had been used for the embrittlement work with sodium salts,⁸ and such new parts as were required were duplicates of the original units. The tests were run in the same manner and for the same length of time as were the previous tests with sodium-hydroxide solutions.

The embrittlement detectors (Fig. 1) were mounted on small autoclaves, as shown in Fig. 2. The temperatures of the testers

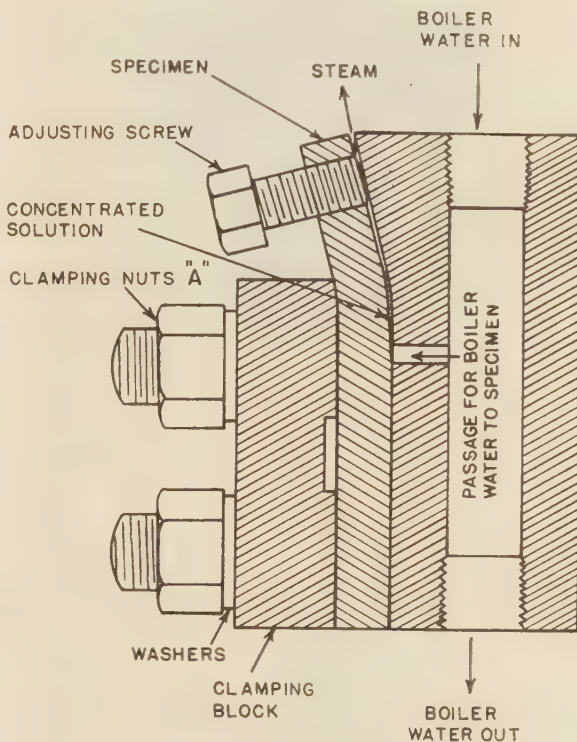


FIG. 1

were controlled through individual air thermostats. Hot dilute solutions, containing chemicals in concentrations such as might exist in boiler waters, circulated as a result of thermal effects through the piping to the detectors. Part of each solution was diverted to the stressed surface of the test specimen where concentration occurred by evaporation against atmospheric pressure. The American Society for Testing Materials method D-807-44T was followed in making adjustments of the rate at which evaporation occurred. Hot-rolled-steel specimens were used until it was established that cracking could be produced in the potassium-hydroxide solutions; cold-rolled specimens were used from then on.

The tension-testing device is shown in Fig. 3. The hollow test

⁸"Inter-crystalline Cracking of Boiler Steel and Its Prevention," by W. C. Schroeder and A. A. Berk, *Bureau of Mines Bulletin* 443, 1941.

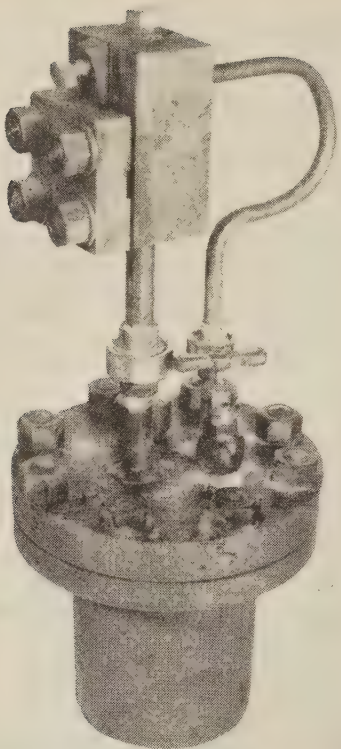


FIG. 2

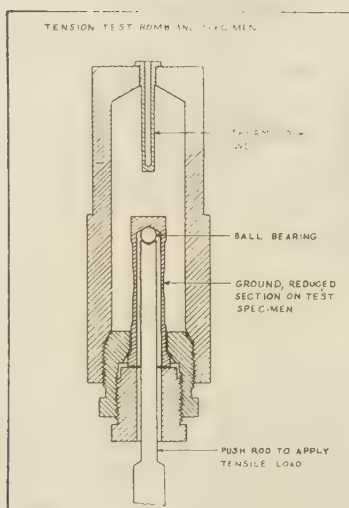


FIG. 3

specimen of boiler-flange steel seals a bomb that contains the hot concentrated solution. A known load, obtained with a lever system, is applied to the tubular specimen by a push rod passing through its center and bearing on its closed end while the bomb is held firmly in a rigid frame. The specimen has a reduced section which is ground concentrically on the outer or solution side. The smallest diameter of the reduced section is 0.6 in., and the inside diameter of the specimen is 0.5 in. A heating jacket acts as an air thermostat, and the heat input is adjusted with a

variable-voltage transformer in accordance with the temperature indicated by a thermocouple in the wall of the bomb.

All solutions were prepared from standard chemically pure reagents and distilled water. Concentrations were checked by analysis before each test and were rechecked in all tests where the solution was not lost through the detector or because of the failure of the tension-test specimen. The cracking of detector specimens did not appear to be affected by the number of times the autoclaves went dry and had to be refilled during the test.

TESTS WITH THE EMBRITTLEMENT DETECTOR

Table 1 shows that potassium hydroxide, like sodium hydroxide, can cause the intercrystalline corrosion responsible for boiler-seam cracking. Eight specimens were cracked in the fourteen tests run with uninhibited potassium-hydroxide solutions at 200 and 250 C (corresponding to 210 and 560 psi, respectively). Cracks in sections cut from five of the specimens were found to be almost completely intercrystalline.

No cracks were found in six of the specimens. In these, however, the area exposed to the concentrating solution was covered with a dense, yellow, crystalline deposit instead of the normal black-oxide film. Although the bombs were washed thoroughly before each test, they had been used for many runs with boiler waters as well as synthetic solutions. Apparently the hot potassium-hydroxide solutions dissolved the scales that had built up in the bombs, and the yellow coatings were formed on the test specimens from the contaminated solutions. Deposits, removed from some of the specimens by stretching the base metal, were subjected to petrographic, spectrographic, and X-ray analysis. The only compound identified with certainty was potassium carbonate. The spectrograph, however, revealed that potassium, sodium, iron, silicon, calcium, and magnesium were major constituents in most samples (at least 5 per cent of each was present).

The tendency for the yellow protective coating to form appeared to be greater at higher starting concentrations of potassium hydroxide, which presumably were more active in dissolving scale from the bomb. The protective coating was not effective at 250 C, possibly because of the greater penetrating power of concentrated potassium-hydroxide solutions at this higher temperature. Deposits were most serious in the earlier runs (five of the first eight specimens were not cracked) when those specimens which did fail cracked at the edge of the yellow coatings. There was little or no evidence of such interference in later tests.

Table 2 shows the effect of potassium nitrate on embrittlement-detector tests with potassium-hydroxide solutions at 200 and 250 C. No cracks were found in any of the five test specimens. The concentration of nitrate as NO_3 was approximately one half the alkalinity as OH in the solutions (a potassium nitrate to potassium hydroxide ratio of 0.26). This ratio has proved effective as a nitrate treatment of boiler waters containing sodium-hydroxide alkalinity. No attempt has been made to determine the minimum ratio of nitrate to hydroxide required to prevent cracking in waters treated with potassium salts.

Nitrate tends to react with the metal of the autoclave and piping under the conditions of the test. To prevent the concentration of the inhibitor from falling too low during the 30-day period, the solutions for these tests were renewed every 10 days. Tests K22 showed that similar renewal of an uninhibited potassium-hydroxide solution did not affect cracking of the specimen.

Table 3 shows the effect of quebracho extract⁹ as an inhibitor of

⁹ The Argam Brand quebracho extract used for these tests was part of the sample obtained and used for the work with sodium hydroxide.

TABLE 1 EMBRITTLMENT-DETECTOR TESTS WITH POTASSIUM-HYDROXIDE SOLUTIONS; 30-DAY TESTS

Test no.	Temp, deg C	Steel	Solution composition			Result of test	Residual solution		
			Ppm	KOH As OH, ppm	Epm		Total alkalinity as KOH, ppm	"Free" ^a KOH, ppm	SiO ₂ , ppm
K13	200	Cold rolled	82	25	1.5	..	86	64	25 ^c
K12	200	Cold rolled	165	50	2.9	..	224	171	19 ^c
K17	200	Cold rolled	165	50	2.9	Bomb dry	..
K22	200	Cold rolled	263	80	4.7	.. ^d	290	201	15 ^c
K6	200	Hot rolled	330	100	5.9	..	336	277	12 ^c
K32	200	Cold rolled	330	100	5.9	..	297	230	12 ^c
K11	200	Cold rolled	330	100	5.9	..	616 ^f	448	23 ^c
K10	200	Cold rolled	660	200	11.8	..	722	621	37 ^c
K7	200	Hot rolled	660	200	11.8	..	688	632	27 ^c
K8	200	Hot rolled	660	200	11.8	50	955 ^f	780	37
K9	200	Hot rolled	660	200	11.8	50	..	370 ^e	40
K14	250	Cold rolled	165	50	2.9	..	224	128	38 ^c
K15	250	Cold rolled	330	100	5.9	..	395	293	25 ^c
K16	250	Cold rolled	660	200	11.8	.. ^d	890 ^f	662	60 ^c

^a Determined by strontium-chloride method using phenolphthalein indicator.^b Cracking confirmed as intercrystalline.^c No silica added; that found in solution must have been dissolved from the walls of the bomb.^d 20 ppm KCl also present in solution.^e Solution dark colored by leachings from bomb.^f Indicates loss of steam from bomb and concentration of the dilute solution.

TABLE 2 EMBRITTLMENT-DETECTOR TESTS WITH NITRATE IN POTASSIUM-HYDROXIDE SOLUTIONS; 30-DAY TESTS WITH COLD-ROLLED-STEEL SPECIMENS

Test no.	Temp, deg C	Solution composition			Result of test	Residual solution averages ^a				
		Ppm	KOH As OH, ppm	Epm	Ppm	Total alkalinity as KOH, ppm	"Free" ^b KOH, ppm	KNO ₃ , ^b ppm	SiO ₂ , ^c ppm	Ratio KOH to KNO ₃ , ^e Ppm
K18	200	165	50	2.9	41	168	101	8	14	0.15
K23	200	263 ^d	80	4.7	86	263	184	50	13	0.26
K33	200	330	100	5.9	99	330	234	83	18	0.28
K19	250	330	100	5.9	114	445	302	25	62	0.18
K20	250	660	200	11.8	224	720	603	96	61	0.23

^a All bombs were refilled with fresh solution every 10 days; the solutions removed after each 10-day period were analyzed and the data averaged for this table.^b Determined by the standard strontium-chloride procedure.^c In this ratio KOH is the total alkalinity in terms of KOH. The sodium nitrate to sodium hydroxide ratio of 0.3, which has been found completely successful for preventing cracking of specimens in detectors attached to stationary boilers, corresponds to a KNO₃ to KOH ratio of 0.26 (0.14 if the concentrations are expressed in ppm).^d Solution also contained 20 ppm KCl.^e No silica in any of these solutions at start of tests.

TABLE 3 EMBRITTLMENT-DETECTOR TESTS WITH QUEBRACHO EXTRACT IN POTASSIUM-HYDROXIDE SOLUTIONS; 30-DAY TESTS WITH COLD-ROLLED-STEEL SPECIMENS

Test no.	Temp, deg C	Solution composition			Result of test	Residual solution averages ^a				
		Ppm	KOH As OH, ppm	Epm	Quebracho, ppm	Total alkalinity as KOH, ppm	"Free" ^c KOH, ppm	Quebracho, ppm	SiO ₂ , ^d ppm	Ratio ^b Quebracho to KOH to OH
K28	200	165	50	2.9	48	170	59	14	9	0.18
K27	200	263	80	4.7	76	244	138	20	24	0.19
K31	200	330	100	5.9	95	280	158	40	12	0.22
K26	250	330	100	5.9	95	310	152	20	23	0.18
K21	250	660	200	11.8	190	636	382	34	..	0.17

^a All bombs were refilled with fresh solution every 10 days; the solutions removed after each 10-day period were analyzed and the data averaged for this table.^b In this ratio KOH is the total alkalinity in terms of KOH. The quebracho extract to sodium hydroxide ratio of 0.4, which has been used with considerable success to inhibit cracking of test specimens in embrittlement detectors attached to stationary boilers, corresponds to a quebracho to KOH ratio of 0.3 (0.94 to OH).^c Determined by the standard strontium-chloride method.^d No silica was added to the solutions for any of these tests.

cracking in potassium-hydroxide solutions. No cracking resulted in the five tests run at 200 and 250 C. The concentration of quebracho extract approximately equaled the alkalinity as OH in these solutions (a quebracho-to-potassium hydroxide ratio of 0.3). This ratio has been used with considerable success for the quebracho-extract treatment of stationary-boiler waters. As in the tests with nitrate, solutions were renewed every 10 days to maintain the inhibitor concentration at the desired level.

Table 4 contains four tests in which the solution was alkaline but contained no "free" potassium hydroxide. As the water evaporated from these solutions in the detector, a concentrated solution of a potassium salt was formed instead of a concentrated solution of potassium hydroxide. Two tests were run with tripotassium phosphate, and one each with potassium disilicate and potassium metasilicate. None of the specimens was cracked, indicating that the "zero caustic" treatment with potassium salts should be effective with respect to embrittlement cracking.

TENSION TESTS

In the tension tests, the specimen is subjected to a known ten-

sile stress at a known temperature while it is acted on by a concentrated solution of known composition. No assumptions are made as to how a boiler water may concentrate to attain the composition of the test solution. In that sense the results are therefore not controversial.

On the other hand, the concentration of hydroxide used for the tension test may not provide the most aggressive attack on the grain boundaries of the stressed-steel specimen. It would thus be possible to demonstrate that an inhibitor prevented cracking in a series of hydroxide solutions without establishing the effectiveness of the inhibitor and its required concentration with respect to the most severe cracking conditions. For these tests with potassium hydroxide, a concentration of 35 g per 100 g of water was used. This solution contains exactly as much hydroxide (OH) as the solutions containing 25 g of sodium hydroxide per 100 g water, which were used in previous work. While reagent-grade chemical was used, it is possible that traces of impurities were present in the solutions and had some effect on the results. All tension tests were run at 250 C.

Table 5 shows that at this temperature silica greatly acceler-

TABLE 4 DETECTOR TESTS WITH ALKALINE POTASSIUM SALTS IN THE ABSENCE OF "FREE" CAUSTIC; 30-DAY TESTS WITH COLD-ROLLED-STEEL SPECIMENS AT 250 C

Test no.	Salt used	Concentration		Result of test	Residual solution		
		Ppm	Epm		"Free" OH, ^a ppm	SiO ₂ , ppm	PO ₄ , ppm
K25	Tripotassium phosphate	150 ^a	4.7	Not cracked	8	...	128
K30	Tripotassium phosphate	300 ^a	9.5	Not cracked	1	5	290
K24	Potassium disilicate	300 ^c	5.0	Not cracked	..	210	...
K29	Potassium metasilicate	300 ^c	10.0	Not cracked	..	Autoclave dry	...

^a As PO₄.^b Determined by the standard strontium-chloride method, using phenolphthalein indicator.^c As SiO₂.

ates the attack of potassium-hydroxide solution on the test specimen. "Pure" potassium-hydroxide solution caused a specimen stressed at 70,000 psi to fail in 10 days, but apparently did not affect a specimen stressed to 60,000 psi. The addition of a very small quantity of silica to the solution decreased the load-carrying ability of the specimens, causing relatively rapid failure at loads of 60,000 and 50,000 psi. The cracks produced by "pure" caustic were wide and transcrystalline, while those resulting in the solution containing silica were narrow, and some were largely intercrystalline. Silica has a similar accelerating effect on the tendency of sodium-hydroxide solutions to cause intercrystalline cracking.¹⁰

Runs T8 and T10 in Table 6 indicate that potassium nitrate is an effective inhibitor of cracking in potassium hydroxide-silica solutions. The relative concentration of nitrate used in these tests was very low compared to the ratio used in the detector tests. It was also noted that at the conclusion of the 10-day tests the solutions contained no nitrate. Apparently a protective coating was formed on the specimen before the nitrate was decomposed in the concentrated caustic solution. The specimen did not fail, because the coating was not disturbed and broken during the remainder of the run.

This hypothesis was checked by test T9, for which the load was applied after the solution had been in the bomb at the operating temperature for 3 days. The specimen failed, showing that there was not sufficient nitrate in solution at that time to repair the protective coating that must have been broken when the steel was stressed beyond its elastic limit. Nitrate, although comparatively inert in dilute alkaline solution (boiler water), appears to react rapidly with metal and metal-oxide surfaces in concentrated caustic solutions.

Runs T6 and T7 in Table 7 indicate that quebracho extract is also a good inhibitor of cracking in concentrated potassium-hydroxide-silica solutions. As in similar tests with sodium hydroxide,¹¹ a relatively low concentration of quebracho extract gave satisfactory protection in the concentrated caustic solution. Much higher ratios are used for the detector tests of simulated boiler waters to allow for the loss of tannin, which apparently occurs during concentration.

SUMMARY AND CONCLUSIONS

All of the tests run during the project are included in Tables 1 to 7, inclusive. Five tests, numbered K1 through K5, were begun and then abandoned when it became necessary to postpone the work several months. Table 8, therefore, summarizes all the data that were obtained with respect to the embrittlement characteristics of waters in which potassium salts are used.

Potassium-hydroxide solutions produced intercrystalline crack-

TABLE 5 FAILURE OF TENSION SPECIMENS IN CONCENTRATED POTASSIUM-HYDROXIDE SOLUTIONS; ALL TESTS WITH BOILER-FLANGE STEEL AT 250 C

Specimen no.	Applied stress, ^a psi	Solution composition		Failure, hr	No failure, days
		KOH, g/100 g H ₂ O	SiO ₂ , g/100 g H ₂ O		
T1	70000	35 ^f	0	220 ^b	..
T2	60000	35	0	..	9 ^c
T3	60000	35	0.2	59 ^d	..
T4	50000	35	0.2	..	1 1/2 ^e
T5	50000	35	0.2	69 ^d	..

^a Load applied after specimen reached test temperature.^b Specimen failed at one side of reduced section and solution was lost; the cracks were wide, and little or no intercrystalline cracking could be found.^c A pinhole leak developed in the reduced section of the specimen after 9 days, and the solution was lost. There were no cracks, intercrystalline or otherwise.^d Microscopic examination of the broken specimens showed that some of the finer cracks were predominantly intercrystalline.^e A pinhole leak developed in the wall of the specimen within 24 hr of the application of the load. No cracks were found.^f Equal to 25 g of NaOH per 100 g of H₂O.

TABLE 6 EFFECT OF NITRATE ON CRACKING OF TENSION SPECIMENS IN CONCENTRATED POTASSIUM-HYDROXIDE SOLUTIONS; ALL TESTS AT 250 C

Test no.	Applied ^a stress, psi	Solution composition			Failure, hr	No failure, days
		KOH, g/100 g H ₂ O	SiO ₂ , g/100 g H ₂ O	KNO ₃ , g/100 g H ₂ O		
T3	60000	35 ^d	0.2	...	59 ^b	..
T5	50000	35	0.2	...	69 ^b	..
T8	80000	35	0.2	1.0 ^e	..	10
T9	60000 ^c	35	0.2	1.0	51 ^b	..
T10	60000	35	0.2	1.0	..	12

^a Load applied after specimen reached test temperature.^b Cracks confirmed as intercrystalline.^c Load applied after solution had been at test temperature 3 days.^d Equal to 25 g NaOH per 100 g H₂O.^e Equal to 0.84 g NaNO₃ per 100 g H₂O.

TABLE 7 EFFECT OF QUEBRACHO EXTRACT ON CRACKING OF TENSION SPECIMENS IN CONCENTRATED POTASSIUM-HYDROXIDE SOLUTIONS; ALL TESTS AT 250 C

Test no.	Applied ^a stress, psi	Solution composition			Failure, hr	No failure, days
		KOH, g/100 g H ₂ O	SiO ₂ , g/100 g H ₂ O	Quebracho, g/100 g H ₂ O		
T3	60000	35 ^c	0.2	...	59 ^b	..
T5	50000	35	0.2	...	69 ^b	..
T6	60000	35	0.2	1.8	..	11
T7	60000	35	0.2	1.8	..	10

^a Load applied after specimen reached test temperature.^b Cracks intercrystalline.^c Equal to 25 g NaOH per 100 g H₂O.

TABLE 8 SUMMARY OF EMBRITTLEMENT TESTS WITH POTASSIUM SALTS

Solution used	Type of test	Specimens	
		cracked	not cracked
KOH (without inhibitor).....	Detector	8	6
KOH-K ₂ SiO ₃ (without inhibitor)....	Tension	2	0
KOH-KNO ₃	Detector	0	5
KOH-K ₂ SiO ₃ -KNO ₃	Tension	1	2
KOH-quebracho extract.....	Detector	0	5
KOH-K ₂ SiO ₃ -quebracho.....	Tension	0	2
No "free" KOH.....	Detector	0	4

^a Load applied after solution had been at test temperature 3 days.

¹⁰ "Action of Solutions of Sodium Silicate and Sodium Hydroxide at 250° C on Steel Under Stress," by W. C. Schroeder and A. A. Berk, Trans. American Institute of Mining and Metallurgical Engineers, vol. 120, 1936, pp. 387-400.

¹¹ "Protecting Steel Against Intercrystalline Attack in Aqueous Solution," by W. C. Schroeder, A. A. Berk, and R. A. O'Brien, Trans. A.S.M.E., vol. 60, 1938, pp. 35-42.

ing in stressed-steel specimens both in the embrittlement detector and in the tension tests (in the latter a small quantity of silica was required under the test conditions). It is unfortunate that there was so much interference from impurities in the first eight detector tests to be run. Hindsight indicates that new equip-

ment should have been used. Cracking undoubtedly was prevented by impervious coatings formed on the specimens from impurities in the caustic solutions. It is quite possible that the tendency for such coatings to form often may be the controlling factor as to whether boiler-seam cracking occurs in boilers operated with scale-forming waters.

The tests with nitrate and with quebracho extract show that the practical inhibitors of embrittlement cracking in solutions containing sodium-hydroxide alkalinity are also effective in potassium-hydroxide solutions. No attempt has been made to determine the inhibitor ratios required to prevent cracking. The apparatus available was unsuited to such determinations, and the data can be obtained much more readily in embrittlement detectors attached to operating boilers. Also it would be a most unusual boiler water that contained no sodium salts. The ratios found suitable for sodium-hydroxide alkalinity would therefore probably be required in most cases.

No tests were run at temperatures corresponding to the higher operating pressures. Several specimens, however, have been cracked in embrittlement detectors mounted on boilers operating with potassium-salt treatment at 1250 and 1350 psi. The tests that showed the effect of "zero caustic" treatment should be of special interest, therefore. Tripotassium phosphate apparently can be used as effectively as the now widely used "co-ordinated" sodium-phosphate treatment. The potassium silicates also caused no cracking, but whether a boiler can be operated with high silicate concentrations without serious scaling and turbine-fouling troubles is beyond the scope of this project.

Discussion

C. E. KAUFMAN,¹² When Dr. Hall¹³ first formulated his ideas on potassium equilibrium in boiler waters, work was started in our laboratories with embrittlement-detector installations in order to investigate the characteristically different waters produced.

In general our experiments, run from 30 to 60 days at 250 C (482 F, 577 psia), parallel and confirm those of the authors. Inhibition with nitrate and tannin was successful, and maintenance of alkalinity with either K_3PO_4 or K_2SiO_3 alone resulted in no cracking of hot- or cold-rolled test bars. In fact, with no inhibitor present, potassium-salt solutions containing free hydroxide in appreciable quantity caused an even lesser percentage of cracking than the authors found, although, again, deposition of complex substances derived from previous tests may have been an important factor.

Mixtures of sodium and potassium salts with free hydroxides present were intermediate in their tendency to produce cracking, exhibiting less aggressiveness than sodium salt-caustic solutions and greater action than exclusively potassium salt-hydroxide solutions.

T. E. PURCELL¹⁴ AND S. F. WHIRL¹⁵ The results of two embrittlement-detector tests, one of 58 days' duration, the other of 90 days' on a boiler operating at 900 psi, substantiate the findings of this research investigation that alkalinity produced by potassium-phosphate salts, with no caustic alkalinity present, will not cause embrittlement cracking of the detector specimens.

In this investigation, the authors used pure tripotassium phosphate. Our tests, the first of which was reported before this Society,¹³ were run with co-ordinated phosphate pH control,^{16, 17, 7} wherein the pH of the boiler water was maintained slightly on the acid side of the stoichiometrical neutral point of pure tripotassium phosphate. A typical boiler-water analysis is given in Table 9 of this discussion.

TABLE 9 TYPICAL ANALYSIS OF BOILER WATER; NO. 1 BOILER, F. R. PHILLIPS POWER STATION

pH: determined.....	10.77
From phosphate-pH curve.....	11.05
Sp. cond., micromhos.....	944
Dissolved salts, ppm.....	566
Phosphate, PO_4 , ppm.....	130
Sulphate, SO_4 , ppm.....	220
Sulphite, SO_3 , ppm.....	—
Chloride, Cl, ppm.....	16
Hydroxide, OH, ppm ^a	0

^a By modified Winkler method, using strontium chloride and phenolphthalein.

The authors are to be commended for presenting all of their data instead of only that portion which fits the present general pattern of thinking. In research investigations, it is often the seemingly undesirable data which eventually prove to be the most significant. Of particular interest are the preliminary results with potassium hydroxide in the old bombs. At first thought they are somewhat surprising, but a little reflection and study give quite a clear picture. For example, approximately 3 years ago, one of our boilers was treated with quebracho tannin for a test period of 1½ years. Since the discontinuance of this treatment, the boiler has evaporated approximately 800,000,000 lb of water and has been drained and refilled with condensate five times, but still the characteristic wine color produced by the quebracho remains in the boiler water. It is readily conceivable, as the authors point out, that deposits laid down on boiler surfaces may be a controlling factor as to whether boiler-seam cracking will occur later.

AUTHORS' CLOSURE

The authors are grateful to the contributors of the three written discussions. Both C. E. Kaufman, and T. E. Purcell and S. F. Whirl have presented corroborating data that are always welcome. E. B. Powell¹⁸ has suggested that the action of nitrate on steel be discussed in greater detail. A summary of the observed behavior of this chemical during plant and laboratory tests does appear appropriate because of its increased use in boiler-water conditioning.

Nitrate in hot dilute alkaline solution is a relatively stable substance; for example, it does not appear to react with sodium sulphite at boiler temperatures (observations have been made at 200 to 700 psi). Specially prepared metals can reduce nitrate quantitatively to ammonia in such solutions, however, and this property is the basis for the evolution method for its determination.

The loss of nitrate from hot dilute solutions in laboratory autoclaves is thought to be due to its electrochemical reduction at especially active areas in the steel surface. Such areas tend to lose their activity during the reduction reaction, and decreasing quantities of the chemical are lost during successive tests in the same apparatus. Plant experience is similar in that, when ni-

¹² Research Engineer, Hall Laboratories, Inc., Pittsburgh, Pa.

¹³ "A New Approach to the Problem of Conditioning Water for Steam Generation," by R. E. Hall, Trans. A.S.M.E., vol. 66, 1944, pp. 457-474.

¹⁴ General Superintendent of Power Stations, Duquesne Light Company, Pittsburgh, Pa. Mem. A.S.M.E.

¹⁵ Chief Chemist, Power Stations Department, Duquesne Light Company, Pittsburgh, Pa.

¹⁶ "Embrittlement of Boiler Steel—Experiences With the Schroeder Detector," by T. E. Purcell and S. F. Whirl, Trans. A.S.M.E., vol. 64, 1942, pp. 397-402.

¹⁷ "Protection Against Caustic Embrittlement by Co-Ordinated Phosphate pH Control," by T. E. Purcell and S. F. Whirl, Third Annual Water Conference, Engineering Society of Western Pennsylvania, 1942, pp. 45-60.

¹⁸ See p. 322 of this issue for Mr. E. B. Powell's written discussion

trate treatment is first added to a boiler, the concentration found in the boiler water is usually substantially lower than that expected. The boiler surfaces seem to be conditioned in 2 or 3 weeks, however, and no further reduction or loss of chemical appears to occur. As with any other stable salt, the concentration in the boiler water can then be predicted on the basis of feedwater, blowdown, and carry-over relationships.

In hot concentrated hydroxide solutions such as those that may exist in boiler seams, nitrate is much more reactive with respect to steel and the ordinary oxides of iron. The product of the reaction appears to be a higher oxide, which tends to remain at the original steel or oxide surface as an adherent coating. The formation of the coating tends to limit the extent to which the base metal can be attacked. Thus the embrittlement-detector specimens tested in nitrate solutions are generally colored red where the coating is heavy, but the quantity of metal lost is no greater than when the inhibitor is absent. It would be incorrect to state that nitrate prevents embrittlement by increasing

the general corrosion activity at the steel surface. More probably, no intercrystalline attack can occur because the grain boundaries as well as the grains are covered with an unbroken passivating film or coating.

Confusion also exists with regard to the use of nitrate as an inhibitor when its concentrated solutions are known to produce intercrystalline cracking very rapidly in stressed steel. Experiments have shown that nitrate in alkaline solution will not produce cracking. The explanation is derivable from the observed reactivity of the chemical. In hot alkaline solutions it corrodes steel very rapidly until a protective oxide coating is produced. Hot concentrated neutral solutions are not generally corrosive; and the attack, if any, is limited to the material at the grain boundaries. Thus hot alkaline nitrate solutions protect steel by coating it with an adherent oxide; while hot concentrated neutral solutions may cause stressed steel to crack as the result of intercrystalline corrosion.

Experience With Sodium and Potassium Chemicals for Boiler-Water Conditioning at Montaup Electric

By G. U. PARKS,¹ FALL RIVER, MASS.

Since its installation in June, 1942, the high-pressure forced-circulation boiler at Somerset Station of the Montaup Electric Company, which is designed to produce 650,000 lb of steam per hr at 1950 psi, has been of considerable general interest, because of certain unique features in power-plant practice. Operation for the first 9 months, using standard sodium chemical treatment for water conditioning, was unsatisfactory. A potassium treatment was evolved, which corrected the adverse conditions. Today the Somerset Stations' high pressure boiler is in every respect an excellent commercial steam generator.

INTRODUCTION

IN June, 1942, a new high-pressure forced-circulation boiler was placed in operation at this company's Somerset Station. This boiler is designed to produce 650,000 lb of steam per hr at 1950 psi at the steam-drum outlet. Final steam temperature is 960 F. The boiler contains a 400-lb reheat section with a capacity of 537,000 lb of steam per hr. Details of this boiler and related generating and electrical equipment were previously presented in a paper by Clark, Rosencrants, and Armacost.²

This high-pressure steam-generating unit has certain features which were unique in American stationary-plant practice at the time of installation. Some of these features should probably be mentioned as they undoubtedly have relation to boiler-water conditions. These special features are high-pressure pumps circulating boiler water from the wet-drum downcomers at boiler-water temperature and pressure to the bottom headers supplying the two side-wall and rear-wall tubes, and also the circuit of tubes which comprises the floor, front wall, and roof; strainers which are 1-in. tubes so placed in the supply headers that entry of boiler water is obtainable only through a number of $\frac{3}{16}$ -in.-diam perforations; orifices at the upper ends of the strainers of either 0.34 in. or 0.40 in. diam, depending upon the tube circuit supplied, each of these orifices supplying water to a pair of 1 $\frac{1}{4}$ -in.-OD furnace-wall tubes (bifurcated tube construction); over-all ratio of boiler water circulated to steam generated of 4:1 at full load.

Feedwater to this boiler consists of condensate from two turbine condensers with an average of about 2 $\frac{1}{2}$ per cent make-up water supplied from evaporators. Raw water is from Coles River, which is the drainage source of a typical New England country watershed. Condensing water is from the Taunton

River, which is a tidewater river, and contains substantial amounts of sewage.

RESULTS DURING TREATMENT WITH SODIUM CHEMICALS

A series of boiler inspections during the first 9 months of operation with the use of standard sodium chemicals (phosphate, hydroxide, and sulphite) for boiler-water conditioning consistently showed internal conditions which were unsatisfactory. Analyses of the various deposits showed these to consist largely of magnetic oxide of iron with appreciable quantities of calcium and magnesium phosphates also present. In some of the samples the magnesium actually exceeded the calcium in percentages. Small amounts of copper were also found in many of the deposits.

While some of the magnetic oxide of iron present during this period was undoubtedly mill scale, this did not account for all of this material. Examination of tube sections also showed that under the coating of magnetic oxide on the tubes, quite a little pock-marking or pitting existed, which gave some concern. Dissolved oxygen in the feedwater was naturally one of the first things to be checked, but tests on the feedwater generally showed negative results with traces of oxygen being found only occasionally. Furthermore, even though small amounts of oxygen could have been present in the feedwater, this could hardly be a significant factor in the corrosion of the boiler tubes for the increase in temperature of the feedwater as it reached the boiler drum and extremely low partial pressure of oxygen in the steam would tend to remove the oxygen with the steam leaving the boiler, before the water reached the downcomers located at the two ends of the wet-steam drum.

Sodium sulphite was also used as a chemical oxygen scavenger. However, it was found that this chemical was unstable in our unit, and when maintained at more than a few parts per million in the boiler water, considerable contamination of steam with hydrogen sulphide occurred.

After a few months' operation, it was also noted that considerable hide-out of sodium phosphate and sodium sulphate occurred, as indicated by boiler-water tests when dropping load

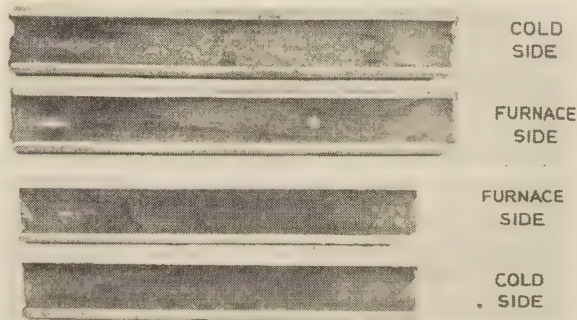


FIG. 1 TUBE SECTIONS AFTER SIX MONTHS' OPERATION WITH SODIUM CHEMICAL TREATMENT

¹ General Manager, Montaup Electric Company. Mem. A.S.M.E.

² "1825-Pound-Pressure Topping Unit With Special Reference to Forced-Circulation Boiler," by F. S. Clark, F. H. Rosencrants, and W. H. Armacost, Trans. A.S.M.E., vol. 65, 1943, pp. 461-477.

Contributed by the Joint Research Committee on Boiler Feedwater Studies and presented at the Annual Meeting, New York, N. Y., Nov. 27-Dec. 1, 1944, of THE AMERICAN SOCIETY OF MECHANICAL ENGINEERS.

NOTE: Statements and opinions advanced in papers are to be understood as individual expressions of their authors and not those of the Society.

Condition of tubes after 6 months' operation with sodium chemical treatment is shown in Fig. 1.

POTASSIUM TREATMENT

In March, 1943, Dr. R. E. Hall called the attention of our consultants, the Stone & Webster Engineering Corporation, and ourselves, to certain data which he had developed, showing the possibilities of certain advantages which might be obtained by maintaining potassium rather than sodium equilibria in boiler waters. Details of this development have also been presented in a paper³ by Dr. Hall.

It was decided that we would try this new approach, and arrangements were made to get the necessary chemicals which included potassium phosphate, potassium hydroxide, potassium sulphite, potassium chloride, and potassium silicate. Before instituting the new treatment, plans were made to clean the boiler thoroughly, inasmuch as considerable accumulation of deposits was present. The cleaning was done about the middle of April, 1943, using inhibited hydrochloric acid, supplied by Dowell, Inc.

Operation of the boiler was resumed on April 22, 1943, using the potassium chemicals mentioned.

After a few relatively short runs, followed by internal inspections of the boiler, the results were decidedly encouraging, as measured by reduction in deposit formation. Therefore, the boiler was placed in operation at full design pressure and load increased to about 75 per cent of design, whereas, during the greater part of the operating period with sodium chemicals, it had been deemed advisable to operate at lower pressure and load, until improvement in internal conditions could be obtained.

One of the first encouraging features of the new treatment was the sharp decrease in the extent of chemical hide-out found on dropping boiler load. In fact, no hide-out at all could be obtained with the potassium chemicals used for boiler-water conditioning when simply dropping load. Once the furnace fires were actually out, slight amounts of phosphate and silicate hide-out were indicated. A typical comparison of hide-out test results are given in Table 1.

TABLE 1 CHEMICAL HIDE-OUT IN BOILER WATER WHEN TAKING BOILER OUT OF SERVICE

	During sodium treatment		During potassium treatment	
	Start	Finish	Start	Finish
Phosphate as PO_4 , ppm.....	20	175	40	45
Phosphate increase, PO_4 , ppm....				
Sulphate as SO_4 , ppm.....	90	223	35	15
Sulphate increase, SO_4 , ppm.....		133		0
Silica as SiO_2 , ppm.....	Not determined		7	12
Silica increase, ppm.....	Not determined		5	
Chloride as Cl, ppm ^a	39	24	270	115
Phosphate increase, corrected for dilution, ppm.....		265		12
Sulphate increase, corrected for dilution, ppm.....		272		0
Silica increase corrected for dilution, ppm.....	Not determined			21

^a Decrease in chloride gives a measure of the dilution of the boiler water with feedwater as the load on the boiler is decreased and the unit taken out of service.

While with potassium treatment, the hide-out of sulphate had been completely eliminated, and that of phosphate reduced to an almost negligible factor, the small amount of silica hide-out came as somewhat of a surprise. We have since learned that in other high-pressure boilers, operating on sodium treatment, silica hide-out is not at all uncommon, but inasmuch as tests for silica were not made during hide-out tests on our boiler during the

period of sodium treatment, we have no knowledge of the extent to which this could have occurred.

As a result of the silica hide-out, the silicate feed was reduced so that the boiler-water silica concentration was generally maintained at about 5 to 6 ppm. After a boiler inspection in July, 1943, when some magnesium phosphate was found in the deposits, it was decided to increase the silica feed with the object of favoring the precipitation of magnesium as magnesium silicate which would be expected to be less adherent to the internal boiler surfaces. The increased feed of silica was begun in August, 1943. However, within about 30 days or so, it was noted that capacity of the condensing turbines was dropping off, and thrust-bearing temperatures were also increasing, indicating turbine deposits. As the result of these undesirable turbine conditions, the silica feed was again reduced to the former level. Inspection of one of the condensing turbines showed deposits of insoluble silica present, which were removed by mechanical cleaning. The other condensing unit was restored to full capacity with normal thrust-bearing temperatures by washing with caustic soda and saturated steam.

An inspection of the high-pressure boiler during the latter part of October, 1943, showed quite good internal conditions, as had become customary since the institution of potassium treatment. Therefore, it was decided to put the boiler back on the line and increase the load to full design operation. Shortly after

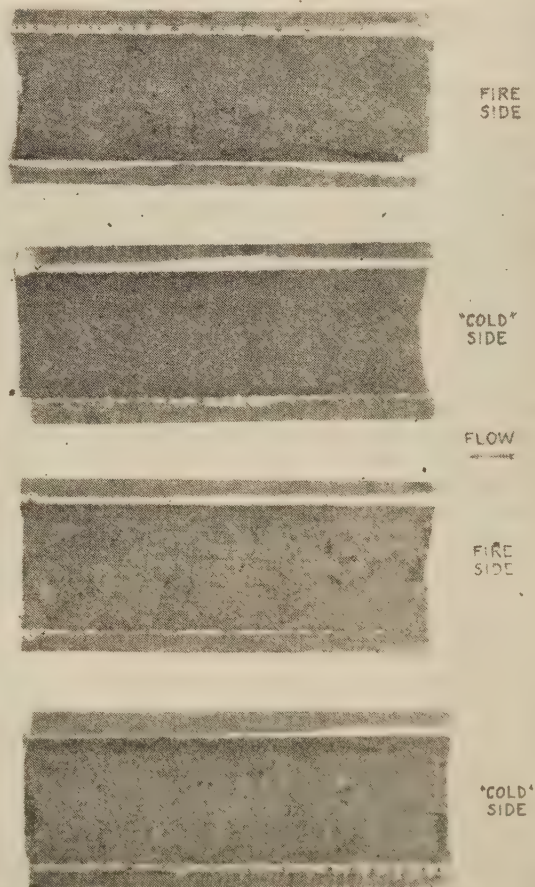


FIG. 2 TUBE SECTIONS AFTER SEVEN MONTHS' OPERATION WITH POTASSIUM CHEMICAL TREATMENT

³ "A New Approach to the Problem of Conditioning Water for Steam Generation," by R. E. Hall, Trans. A.S.M.E., vol. 66, 1944, pp. 457-488.

TABLE 2 COMPARISON OF INTERNAL BOILER CONDITIONS, SODIUM VERSUS POTASSIUM

	Sodium treatment, June, 1942, to April 15, 1943	Potassium treatment, during periods subsequent to April 22, 1943
Economizer outlet tubes	Deposits showing magnesium phosphate and magnetic oxide of iron as major constituents.	No deposits.
Downtake screens	Heavy deposits showing calcium phosphate and magnetic oxide of iron as major constituents. Screen openings found as much as 40 per cent plugged.	Similar deposits in decreased amount. Screens seldom found more than 10 per cent plugged.
Waterwall supply headers	Considerable deposits showing calcium phosphate, magnesium phosphate, and magnetic oxide of iron as major constituents. Large quantities of these deposits found in definite "scaly" pieces.	Very small quantities of deposits, mainly magnetic oxide of iron and some copper.
Strainers supplying orifices	Considerable deposits showing magnetic oxide of iron, magnesium phosphate, and calcium phosphate as major constituents. Strainer openings found as much as 50 per cent plugged at times.	Very little deposits, mainly magnetic oxide of iron. Seldom find strainer openings as much as 10 per cent plugged.
Boiler tubes	Considerable deposits with magnetic iron oxide as major constituent. Minor constituents found present were water-soluble sodium salts, calcium phosphate, magnesium phosphate, and ferric oxide. Considerable action on tubes under deposits.	Generally find some deposits, of about the same composition as found under sodium treatment, but quantities are considerably less. Some action on tubes under deposits.
Reversing hoods (Through which boiler water and steam generated discharges in the steam drum)	Deposits showing crystalline calcium phosphate and magnetic oxide of iron as major constituents, with magnesium phosphate, and water-soluble sodium salts present as minor constituents.	No deposits.
Wet-steam drum	Considerable deposits showing magnetic oxide of iron and copper as major constituents, with calcium and magnesium salts present as minor constituents.	Very small quantities of deposits found, consisting mainly of magnetic oxide of iron and some copper, with calcium and magnesium phosphates as minor constituents.

midnight on December 7, 1943, with a load of 630,000 lb per hr on the boiler, the No. 2 roof tube, counting from the north wall, failed, necessitating taking the unit out of service. This was the first tube failure since the institution of potassium treatment, although several similar failures had occurred during the period of sodium treatment. Inspection of the unit showed that the failure was unquestionably due to a build-up of sludge, mostly iron oxide, in the north end of the rear bottom header which supplies water to this tube circuit, consisting of floor, front-wall, and roof tubes. This condition of iron-oxide accumulation at the ends of the rear header was corrected by the boiler manufacturer by connecting these ends to the west ends of the side-wall headers through collecting chambers, to permit boiler-water circulation instead of stagnation at the header ends. The continuous-blowdown collection system was also improved.

During the boiler outage, starting December 7, 1943, a number of tubes were cut out and split for internal examination (Fig. 2). The deposits on the tubes were found to be greater than had previously been seen since the institution of potassium treatment. Most of the coating was found to be iron oxide, but under this, on the internal surface of the tube area exposed to the heat of the furnace, a thin band of acmite, sodium-iron silicate, was found. To clean the boiler tubes thoroughly, before returning the unit to service, acid cleaning by Dowell Inc., was done, using inhibited hydrochloric acid supplemented by a fluoride. The fluoride was included to obtain removal of the silicate deposit.

In case of any question as to the source of the sodium on the acmite which had been found in the boiler tubes, the answer to this lies in the fact that tidewater for condenser cooling is used at the Somerset station. While condenser leakage is kept relatively low, a little does occur, and the sodium-salt content of this condenser leakage, which goes into the feedwater system is naturally quite high. Thus to keep boiler-water blowdown and chemical feed within reason, it is necessary to operate normally with a potassium-to-sodium ratio, expressed in equivalents of about 3 to 1, and during periods of relatively high condenser leakage this ratio is but 2 to 1. If the station were located so that fresh water could be used for condenser cooling, providing a considerably higher ratio of potassium to sodium to be readily maintained, it is possible that the danger of acmite formations in the boiler, with the silica concentrations which were used, might not exist.

When the boiler was returned to service, the use of silicate was discontinued, but the other potassium chemicals previously mentioned were continued in use as the sole water-conditioning chemicals. The silica feed had been used to try and maintain "captive alkalinity," as well as for the separation of magnesium as the silicate, as discussed in Dr. Hall's paper.³ As a substitute for the "captive alkalinity," the potassium-chloride feed was increased to reduce the hydroxide concentration which could develop in case of localized evaporation. This chloride-to-hydroxide ratio control is based upon solution-concentration limits determined by the Δt developed of solutions⁴ of alkali chlorides and hydroxides which show increasing solubility with temperature increase, beyond the critical temperature of water. This relationship is also discussed in Dr. Hall's paper.³

The 25,000-kw back-pressure turbine, which receives its steam from the high-pressure boiler, was dismantled in August, 1944, for internal examination and general repairs. No blade deposits were found, other than a slight film of iron oxide.

During 1944, we found that, from time to time, there was substantial carry-over from the evaporators. This has been corrected by the installation of steam scrubbers. Condenser leakage, never relatively high, has been further reduced by retubing one of the two surface condensers. Studies inaugurated during 1944 demonstrated that a certain part of the iron oxide found in the boiler sludges comes from the feed system. The results of several tests run recently indicate that deposits on the boiler tubes are loosely held together, and that approximately 75 per cent of these deposits can be placed in suspension and expelled through the blowdown system by operating the boiler at a drum pressure of approximately 400 lb for not more than 24 hr.

A summary showing general results as observed at various boiler inspections, during the periods of sodium and potassium boiler-water conditioning, is given in Table 2.

CONCLUSIONS

From our operation since 1942, we may draw the following conclusions:

1 The forced-circulation boiler at Somerset Station is now an excellent commercial steam generator.

2 With introduction of the potassium treatment, water conditions improved immediately, and the quantity of the sludges

⁴ Δt is the temperature difference between the saturated steam in the boiler and the boiler-water film on an evaporative surface.

has decreased substantially. Some part of this improvement, undoubtedly, was occasioned by changes in the feed system, but we feel a substantial amount can be credited to the change in boiler-water treatment.

3 Since conditions remain so satisfactory without the feed of potassium silicate, and since there was some trouble while potassium silicate was being fed, we see no reason for its use in the future

The Coefficient of Herschel Type Cast-Iron Venturi Meters

By W. S. PARDOE,¹ PHILADELPHIA, PA.

IN the past the A.S.M.E. Research Committee on Fluid Meters has published several plots of coefficients of Herschel Venturi Meters deduced by the author from experiments conducted in the Hydraulic Laboratory of the Civil Engineering Department of the University of Pennsylvania. On each occasion the curves were based on experiments to date. The accompanying curves, Figs. 1 and 2, are based upon eighty-six tests made during the years 1928 to 1943.

The coefficient (C) of the Venturi meter is defined by the formula

$$V_2 = \frac{C}{\sqrt{1 - \beta^4}} \sqrt{2gh_v}$$

in which C is the coefficient; V_2 is throat velocity in feet per second; β = ratio d_2/d_1 ; and h_v Venturi head in feet.

If the frictional loss expressed as $k \frac{V_2^2}{2g}$ be included in Bernoulli's theorem, and α_1 and α_2 be coefficients of the corresponding velocity heads to allow for the excess kinetic energy per pound

$$V_2 = \frac{1}{\sqrt{\alpha_2 - \alpha_1 \beta^4 + k}} \sqrt{2gh_v}$$

Equating these expressions for V_2

$$C = \sqrt{\frac{1 - \beta^4}{\alpha_2 - \alpha_1 \beta^4 + k}}$$

As the velocity at the throat V_2 is quite uniform, the pipe factor is close to unity, and α_2 may be assumed unity; α_1 will vary with the pipe factor of the upstream pipe which is a function of f , the friction factor. If the pipe is smooth and $f = \frac{0.3164}{Rn^{1/4}}$, after

Blasius, the pipe traverse follows the seventh-root law, the pipe factor being 0.817, and $\alpha_1 = 1.056$ as this is a factor of β^4 a small number for usual ratios, α_1 will also be assumed unity. This reduces the formula to the simple expression

¹ Professor, Department of Civil Engineering, University of Pennsylvania.

Contributed by Special Research Committee on Fluid Meters and the Industrial Instruments and Regulators Division and presented at the Annual Meeting, New York, N. Y., Nov. 27-Dec. 1, 1944, of THE AMERICAN SOCIETY OF MECHANICAL ENGINEERS.

NOTE: Statements and opinions advanced in papers are to be understood as individual expressions of their authors and not those of the Society.

$$C' = \sqrt{\frac{1 - \beta^4}{1 - \beta^4 + k}}$$

or

$$k = \frac{1 - \beta^4}{C'^2} - (1 - \beta^4)$$

the effect of α_1 being absorbed in k .

The eighty-six tests are presented herewith in reverse chronological order. The pertinent data obtained from these curves² are shown in Table 1:

Column 1, size diameter of main and throat in inches.

Column 2, ratio $d_2/d_1 = \beta$

Column 3, coefficient, C when constant.

Column 4, value of Reynolds number at which C becomes constant.

Column 5, values of k from Fig. 3.

In Fig. 4, the value of k is plotted as ordinate and the throat diameter in inches as abscissa on log-log paper. Limiting lines are drawn and the arithmetic average gives the equation

$$k = 0.0435/d^{1/4}$$

Table 2 shows values of k and C for the various sizes in Figs. 1 and 2.

In Fig. 4 is also plotted the relation between throat diameter and Reynolds number for constant coefficient giving the equation

$$R_n = 115000d^{0.69}$$

The fourth column in Table 2 is obtained from this plot and the corresponding velocity for Temp = 68 F computed.

The 1936 Oklahoma 4 × 2-in. tests gave information up to Reynolds number 2500. The curves between this and the flat parts were obtained by plotting about a dozen curves going to fairly low values and using them as guides in the connecting curves.

Figs. 5 and 6 are typical curves of the 86 tests shown in Table 1.

It may be suggested that the d - k curve in Fig. 3 is an area and not a curve but, as an error here of 50 per cent makes only an error of 1/2 of 1 per cent in C , it is fairly accurate at that.

² Data for Table 1 was obtained from 86 curves similar to those shown in Figs. 5 and 6.

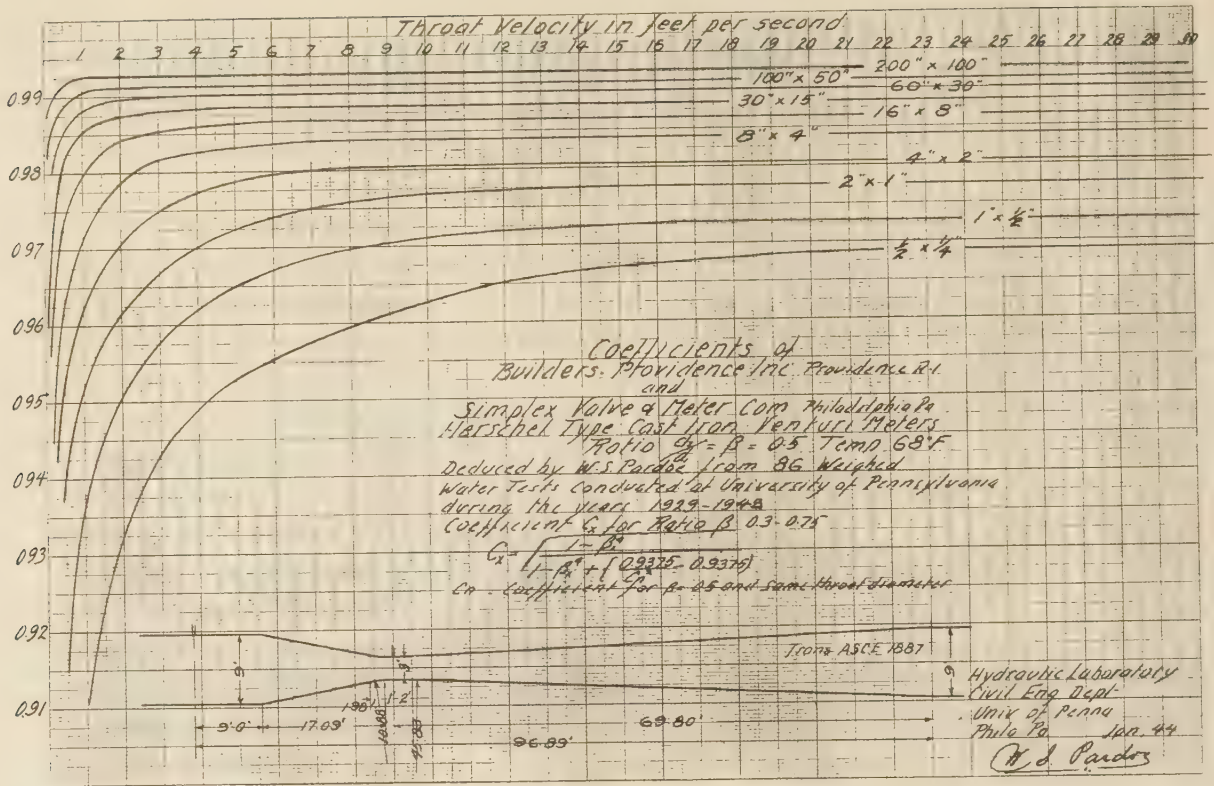


Fig. 1

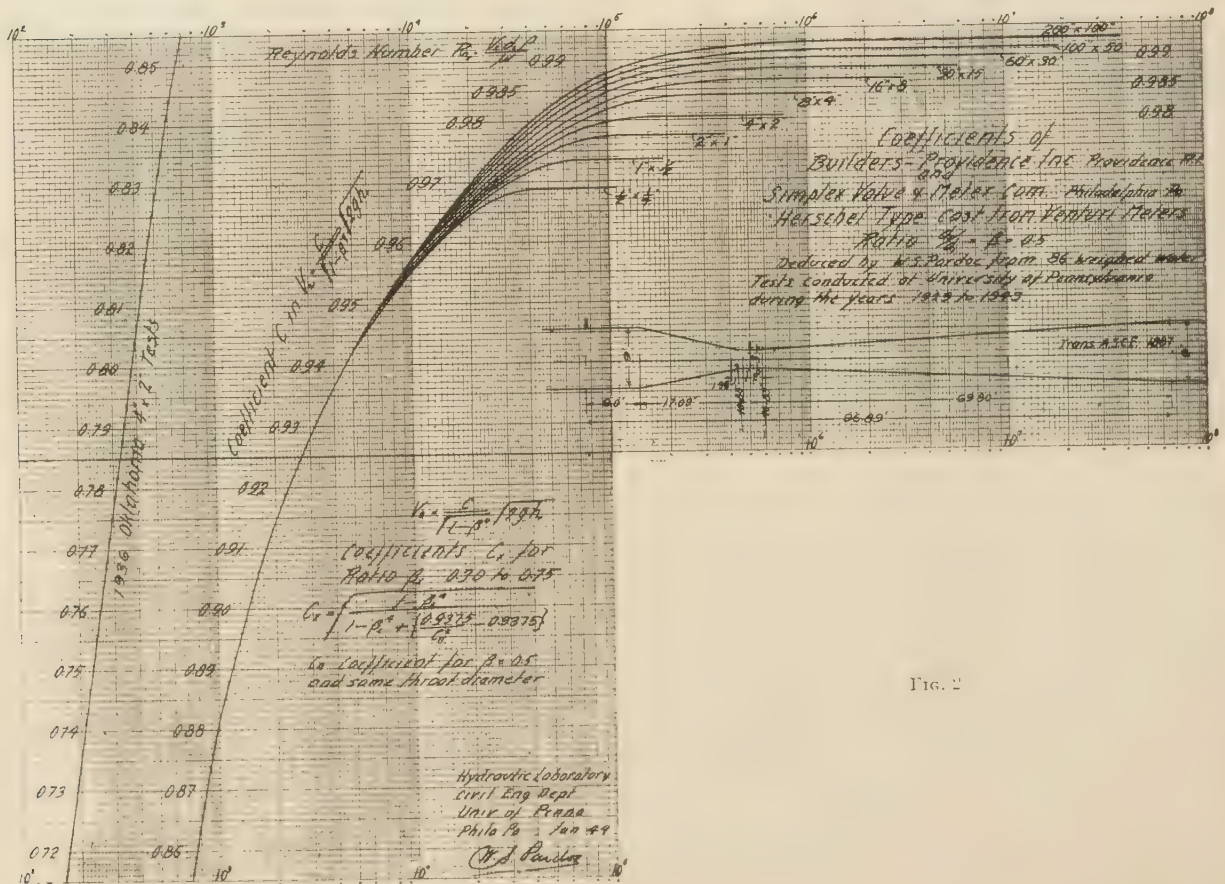


Fig. 2

TABLE 1 DATA OBTAINED FROM TESTS

SIZE IN INCHES	Flow G.P.	C	R_n	K
19.226 x 12.00	0.003	0.282	1000000	0.0320
30.14 x 17.991	0.007	0.285	690	0.0295
13.992 x 7.999	0.007	0.2815	440	0.0335
2.023 x 1.5015	0.007	0.277	100	0.0223
7.9132 x 5.0035	0.011	0.281	380	0.0222
2.022 x 1.5019	0.011	0.289	490	0.0217
2.50 x 1.875	0.011	0.282	100	0.0231
2.882 x 1.252	0.011	0.279	250	0.0436
3.984 x 2.248	0.011	0.289	330	0.0174
0.752 x 0.457	0.011	0.280	360	0.0192
3.814 x 2.3075	0.011	0.281	380	0.0337
3.818 x 2.3234	0.011	0.2815	"	0.0330
0.752 x 0.457	0.011	0.280	200	0.0162
1.625 x 0.946	0.011	0.280	225	"
3.818 x 2.3482	0.011	0.282	175	0.0334
3.818 x 2.3477	0.011	0.282	390	0.0298
4.267 x 2.372	0.011	0.286	180	0.0359
4.02 x 2.00	0.011	0.284	165	0.0302
4.024 x 2.4283	0.011	0.281	210	0.0262
2.8235 x 2.0029	0.011	0.281	335	0.0280
0.013 x 0.5738	0.011	0.284	370	0.0272
2.029 x 1.5223	0.011	0.282	0.95	0.0335
0.007 x 0.5018	0.011	0.288	"	0.0217
1.827 x 0.4025	0.011	0.285	225	0.0289
1.829 x 0.4026	0.011	0.285	"	0.0292
10.084 x 1.054	0.011	0.281	285	0.0266
2.9954 x 2.5223	0.011	0.287	185	0.0234
2.016 x 2.219	0.011	0.276	145	0.0474
2.982 x 1.2513	0.011	0.281	195	0.0298
0.766 x 0.4928	0.011	0.280	380000	0.0208
7.9435 x 3.4446	0.011	0.280	250	0.0294
2.823 x 2.4284	0.011	0.282	352	0.0253
7.957 x 3.446	0.011	0.280	260	0.0294
6.011 x 2.2983	0.011	0.283	260	0.0288
16.956 x 6.2286	0.011	0.2825	200	0.0278
5.024 x 2.0712	0.011	0.280	150000	0.0305

(K. J. Pardoe)

SIZE IN INCHES	Flow G.P.	C	R_n	K
3.010 x 3.5958	0.011	0.284	100000	0.0314
0.038 x 3.6008	0.011	0.285	370	0.0304
4.035 x 2.0733	0.011	0.285	270	0.0316
3.068 x 2.2932	0.011	0.285	450	0.0262
4.008 x 2.3018	0.011	0.287	300	0.0219
2.216 x 2.1138	0.011	0.282	440	0.0240
12.003 x 2.198	0.011	0.285	450	0.0236
3.1754 x 3.7427	0.011	0.280	400	0.0294
12.380 x 2.2564	0.011	0.280	380	0.0193
3.260 x 2.2566	0.011	0.285	350	0.0272
2.045 x 0.2891	0.011	0.285	180	0.0290
12.024 x 2.1966	0.011	0.285	350	0.0204
9.032 x 2.1564	0.011	0.287	"	0.0246
3.012 x 2.6048	0.011	0.285	450	0.0204
3.253 x 2.0765	0.011	0.286	250	0.0293
12.38 x 2.2464	0.011	0.285	450	0.0242
3.010 x 2.2408	0.011	0.285	300	0.0217
2.860 x 2.688	0.011	0.283	350	0.0243
6.025 x 2.5403	0.011	0.287	250	0.0234
14.022 x 2.2465	0.011	0.285	300	0.0233
10.075 x 2.2993	0.011	0.283	275	0.0217
4.025 x 2.2993	0.011	0.285	270	0.0288
9.014 x 2.7342	0.011	0.283	350	0.0290
2.032 x 2.3432	0.011	0.2825	270	0.0245
3.870 x 2.502	0.011	0.285	400	0.0236
2.860 x 2.0023	0.011	0.289	"	0.0209
12.125 x 2.5967	0.011	0.284	600	"
12.051 x 2.0015	0.011	0.284	300	0.0208
14.06 x 2.0032	0.011	0.287	400	0.0250
14.034 x 2.9993	0.011	0.283	350	0.0236
7.995 x 2.5701	0.011	0.285	250	0.0265
6.025 x 2.000	0.011	0.282	100	0.0290
12.00 x 2.00	0.011	0.287	350	0.0256
2.810 x 2.458	0.011	0.283	200	0.0250
12.038 x 2.1235	0.011	0.282	350	0.0256
8.0713 x 3.3534	0.011	0.283	150000	0.0332

(K. J. Pardoe)

TABLE 1 (continued)

SIZE IN INCHES	Flow G.P.	C	R_n	K
5.482 x 3.392	0.011	0.286	300000	0.0244
6.130 x 2.7258	0.011	0.287	220	0.0253
6.0706 x 2.1001	0.011	0.287	220	0.0246
4.075 x 2.4953	0.011	0.286	200	0.0210
3.1015 x 2.0012	0.011	0.285	200	0.0263
2.904 x 2.280	0.011	0.285	150	0.0212
2.504 x 2.8484	0.011	0.286	200	0.0217
3.980 x 2.8482	0.011	0.286	200	0.0225
3.4985 x 2.8488	0.011	0.2845	200	0.0241
12.022 x 2.050	0.011	0.282	350	0.0264
4.070 x 2.1182	0.011	0.285	180	0.0218
0.00 x 2.00	0.011	0.284	150	0.0238
7.982 x 2.404	0.011	0.285	250	0.0227
6.866 x 2.084	0.011	0.286	350000	0.0267

Table II Results				
SIZE IN INCHES	Flow G.P.	C	R_n	K
2.00 x 1.00	0.0137	0.2927	3100000	0.04
1.00 x 0.50	0.164	0.2913	1850000	0.09
0.50 x 0.25	0.186	0.2932	1320	0.72
0.25 x 0.125	0.222	0.2884	800	6.98
0.125 x 0.0625	0.258	0.2865	515	8.37
0.0625 x 0.03125	0.300	0.284	312	10.15
0.03125 x 0.015625	0.376	0.2805	190	12.34
0.015625 x 0.0078125	0.436	0.2775	115	14.95
0.0078125 x 0.00390625	0.517	0.2756	68	18.05
0.00390625 x 0.001953125	0.616	0.2688	42000	21.85

Hydraulic Laboratory
Civil Eng. Dept.
Univ. of Penna.
Phila. Pa. 19104
K. J. Pardoe

TABLE 2 VALUES FOR VARIOUS SIZES OF VENTURI METERS

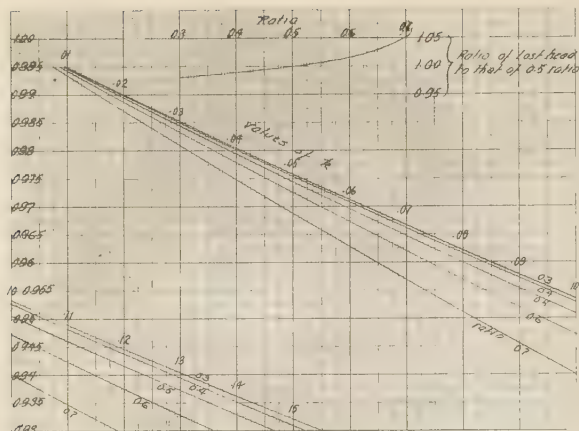


FIG. 3

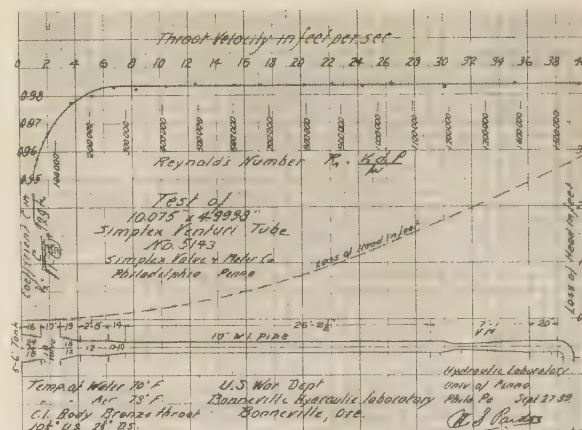


FIG. 5



FIG. 4

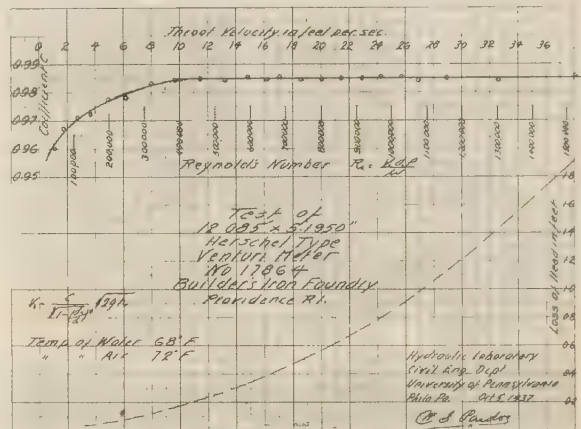


FIG. 6

Discussion

M. M. BORDEN.³ Since laboratory tests of the Venturi tubes referred to in the paper are of necessity limited to those of usual size, the paper is of further particular value for the estimation of C for other sizes and ratios which have not or cannot be tested. The lesser change of C for the increasingly larger sizes is important.

The trifling divergence of the test points from the curves for the two tubes whose ratings are shown reflects the accuracy of the test methods and operations.

Since those conditions and details which determine the inherent performance of the Venturi tube are all contained within its structure, its manufacturer may guarantee its C with its tolerance value.

Nevertheless, due regard for the effect of upstream conditions upon C remains a mutual responsibility of the user as well as the maker.

The author's earlier paper¹ on effect of installation contains information of greatest value in this matter.

Manufacturers and users of such Venturi tubes are greatly indebted to the author of the paper; the former for his critical

and painstaking investigation of those matters which determine the value of C , and the latter for the unbiased information as to coefficient and effects thereupon of conditions ahead of its entrance.

The Venturi-tube proportions of the Company's production have been adhered to closely throughout the entire range of sizes constructed by it. Their surface roughness is practically the same, being controlled by the core material and finish.

W. A. CARTER.⁵ Great credit is due for this excellent paper establishing the coefficient for the Herschel type of Venturi tube. It represents a tremendous amount of painstaking work and is of great value.

It should be understood that at least two American manufacturers of Venturi tubes build cast-steel units that do not conform to the Herschel design and whose coefficient curves do not conform to those given in this paper.

It is hoped that the author will conduct further tests on this other style of Venturi tube and report the results as completely as he has done in this case.

I. O. MINER.⁶ It has been customary ever since head meters

³ Vice-President, Department of Engineering, Simplex Valve & Meter Company, Philadelphia, Pa. Mem. A.S.M.E.

⁴ "Effect of Installation on the Coefficients of Venturi Meters," by W. S. Pardoe, Trans. A.S.M.E., vol. 58, 1936, pp. 677-684.

⁵ Technical Engineer of Power Plants, The Detroit Edison Company, Detroit, Mich. Mem. A.S.M.E.

⁶ Chief Engineer, Builders-Providence, Inc., Providence, R. I. Mem. A.S.M.E.

were first used to calculate flow by means of a formula taking into account increase of velocity as a fluid passes from a pipe through a restriction and to provide a coefficient which takes into account all other effects.

Various formulas have been proposed from time to time to segregate some of the factors in the coefficient. The author has given us formulas taking into account the variation in velocity across a section of the conduit and frictional loss between the upstream and the throat taps. He has correlated his formulas with the results of tests on 86 Venturi meters. He has done a great service to those interested in the manufacture and development of Venturi meters because he has given us a better insight into the reasons why Venturi tubes behave as they do.

As pointed out in the paper, α_1 , the factor taking into account the effect of uneven velocity distribution in the upstream pipe, is multiplied by the factor β^4 , and since the latter is quite small the error caused by assuming the pipe factor to be unity is extremely small. Furthermore, the constriction in a Venturi tube causes the velocity distribution at the throat to be nearly uniform, and if the pipe factor at the throat is assumed to be unity, the error is extremely slight.

The latter effect is particularly interesting to the writer's company because on special tubes made for installations with limited available space we have found that a special shape designed to give uniform velocity at the throat within very small limits produces much more consistent results than does the semi-elliptical shape of the A.S.M.E. long-radius nozzle. Unfortunately, we have not calibrated a sufficient range of sizes and throat-to-diameter ratios to make publication of results seem advisable as yet. However, more Venturi tubes of this special shape are being calibrated, and it is hoped that a full range will have been covered in another year or two.

The author concludes with the statement, "It may be suggested that the d - k curve in Fig. 3 is an area and not a curve but as an error here of 50 per cent makes only an error of $1/2$ of 1 per cent in C , it is fairly accurate at that."

If the author had had data from a sufficiently large number of tests he undoubtedly could have reduced the scattering of his plot in Fig. 4. The factor k represents the loss of head between the inlet and the throat. Certainly it is to be expected that as β varies, the coefficient k will also vary. If we take all of the tests reported in this paper for tubes having

$$\beta = 5/8 \text{ or above}$$

we find that with one exception the points in Fig. 4 lie below the line

$$k = 0.0435/d_2^{0.25}$$

If we pick out the points for tubes having ratios below $3/8$, we find that they all lie on or above the line

$$k = 0.0435/d_2^{0.25}$$

Data from several hundreds of tests would be required to establish curves for k for several different ratios.

We believe that if a sufficient number of curves were available to plot the experimental values of k for a series of β 's we should also find it advantageous to include α_1 and α_2 . As already mentioned, α_1 is multiplied by a small quantity and therefore has relatively little effect. However, to offset this fact k , the quantity in which we are interested, is also small so that even though the product $\alpha_1 \beta_1^4$ is small it still has an appreciable effect on k .

As for α_2 , we are quite in agreement with the author that at small β 's this can be assumed to be unity, but as β is increased the point must come where α_2 can no longer be considered unity without causing k to appear different from its actual value.

It is hoped that when the urgency of meeting war requirements

is past we shall be able to conduct experiments to study flow patterns with various roughnesses, inlet shapes, and upstream pipe conditions. If this opportunity ever occurs, we shall find this paper of great assistance in analyzing our results and we may be able to employ sufficient refinements to pin k down to a very narrow band even though we are dealing with differences of small quantities, making the job extremely difficult.

The question has been raised as to whether the results are any different from what would be obtained if the Venturi tubes had but a single tap upstream and at the throat. It seems obvious that there would be no difference as long as upstream piping conditions are good. However, if one refers to the previous work of Professor Pardoe on the effect of installation on the coefficients of Venturi meters,^{4,7} and to the joint A.G.A.-A.S.M.E. Committee report on orifice coefficients,⁸ he will find that the required piping upstream of a Venturi meter is much less than that with an orifice. The accompanying table shows representative values.

Upstream fitting	β	Diameters of straight pipe required upstream	
		Venturi	Orifice
Decreaser	0.5	4 ¹ / ₂	7 ¹ / ₂
	0.8	12 ¹ / ₂	15
Increaser	0.5	2	7 ¹ / ₂
	0.8	7	15
Elbow	0.5	1	7
	0.8	4 ¹ / ₈	20

The author warns us to use caution in applying his summary curves from which the values for Venturi tubes were taken, but the evidence is pretty conclusive that with increasers or decreasers considerably less straight piping is required for Venturi tubes than for orifices, and that for elbows the difference is in the same direction but much greater.

The fact that with increasers and decreasers less straight pipe is required ahead of the Venturi than ahead of the orifices indicates that symmetrical abnormal velocity distribution has less effect with the Venturi, probably mainly because the "vena-contracta" is established mechanically and has a definite diameter. On the other hand, with the orifice not only do α_1 , α_2 , and k vary but also the diameter and location of the vena-contracta probably vary.

The fact that with an elbow upstream of the Venturi the reduction in required straight piping caused by the substitution of a Venturi tube for an orifice is so much greater than with an increaser or decreaser, may well be accounted for by the multiple vents. It is the writer's belief that the number of vents in the upstream annular chamber of a Venturi tube should not be reduced below present practice but that the number of vents at the throat is superfluous. A single vent at the throat is sufficient up to

$$\beta = \text{about } 0.5 \text{ or } 0.6$$

and at higher β 's two vents diametrically opposite are sufficient. The writer feels strongly that an investigation of the required number of vents is long overdue. A great deal of labor in an accurate Venturi tube is put into the making of the throat vents sharp without burrs or other defects. If one or two vents are sufficient then no more should be provided. The reason for believing that one or two vents at the throat are sufficient is, of course, the effect of the reducing section of the Venturi tube in causing the throat velocity to be nearly uniform.

⁷ Discussion of W. S. Pardoe's paper (ref. 4), Trans. A.S.M.E., vol. 59, 1937, pp. 750-756; also see "Effect of Installation on the Coefficients of Venturi Meters," by W. S. Pardoe, Trans. A.S.M.E., vol. 65, 1943, pp. 337-349.

⁸ Report by the Joint A.G.A.-A.S.M.E. Orifice Coefficient Committee, Nov., 1935.

AUTHOR'S CLOSURE

Mr. Borden brings out the fact that in extrapolating results for larger Venturi meters the author cannot be far wrong as the coefficient cannot approach unity even for very large meters.

Mr. Carter's plea for similar curves for short steel Venturi nozzles is quite understandable but the author regrets that it will be a long time at present rate of testing such meters before he will have sufficient data. In the meantime each such meter should be calibrated if a high degree of accuracy is desired.

Dr. Miner brings out the effect of ratio very nicely. The author has suggested the theoretical formula

$$C_x = \sqrt{\frac{1 - \beta_x^4}{1 - \beta_x^4 + \left\{ \frac{0.9375}{C_n^2} - 0.9375 \right\}}}$$

as of use temporarily for values of β other than 0.5. He regrets he has insufficient data on which to base a practical imperial formula for the effect of ratio on the coefficient, but it is very small up to $\beta = 0.625$.

Values of β above 0.75 should be used with much caution and always should be calibrated with the upstream pipe used in the permanent setup.

The author agrees with Dr. Miner with regard to multiple

upstream vents but must disagree with his conclusions about throat vents. Recent unpublished experiments on the diameter of six throat vents varying from $1/8$ in. to 1 in. in a 10×5 -in. Venturi meter indicate that the correct diameter of the vents is zero; hence if for no other reason than to get sufficient area he would use multiple vents not over $1/8$ in. diam. With this small diameter the task of getting them flush, square, and sharp should be much easier.

The author desires to thank Messrs. Borden, Carter, and Miner for their constructive discussions. Also thanks for "them" kind words about his contributions.

At this time he would like to suggest the following names for these meters:

The *Venturi meter* for those which conform in the upstream section to the proportions laid down by Mr. Clemens Hirschel as published in the Transactions of the American Society of Civil Engineers, 1887.

The *Venturi nozzle* for meters of other shapes and proportions using an expanding downstream section.

The *Insert Venturi nozzle* for those having expanding downstream sections and inserted between pipe flanges.

The *Flow nozzle* for meters using no expanding downstream section with either throat or wall taps.

Piping Arrangements for Acceptable Flowmeter Accuracy

By R. E. SPRENKLE,¹ CLEVELAND, OHIO

The author correlates data previously published on metering fluid flow through pipe lines and analyzes the requirements for piping arrangements, according to interpretations developed from many actual field installations. Most of the recommendations given in the literature are based on standards of piping requirements established by the Joint A.G.A.-A.S.M.E. Committee on Orifice Coefficients. These standards as well as others obtained since that report was published in 1935 are shown in this paper in the form of seven schedules covering the use of "Orifices and Flow Nozzles," and an eighth schedule, applying to "Venturi Tubes" only. These schedules serve as the basis for developing typical piping layouts which are designed to interpret and clarify the principles involved from a practical application standpoint.

IN metering any fluid through a pipe line, it is most important that the flow approach the orifice, flow nozzle, Venturi tube, Pitot tube, or other type of primary element, in a normally turbulent state. It must not be influenced by swirls, crosscurrents, eddies, or other disturbances which create helical paths of flow. Nor can there be any disturbance following the primary element, which would in any way cause interference with the static-pressure measurement at that point.

These conditions can best be controlled by providing adequate lengths of straight pipe on both sides of the orifice or other primary element. The necessity for doing this has long been recognized in fluid-flow literature (1, 2, 3, 4, 5, 6, 7, 8).²

It is interesting to note that most of the recommendations given in these several papers and articles have been based on the standards of piping requirements established by the Joint A.G.A.-A.S.M.E. Committee on Orifice Coefficients, which appear as sketches 1 to 5 of its 1935 Report.

In general these standards have been found quite satisfactory when properly used. It is only natural though that in their application to specific meter installations, many questions of interpretation should have arisen. Furthermore, additional data have been obtained from researches at the author's company, at the University of Pennsylvania, at the Case School of Applied Science, and at other sources, which both add to and make more clear these original standards.

It is the purpose of this paper therefore not only to correlate these data with those previously published but also to furnish a reasonable interpretative analysis of these requirements as reflected by results obtained from many actual field installations.

In doing this, however, the author hastens to disclaim any intention of implying that everything is now known about suitable piping recommendations for any and all combinations of fittings,

bends, and turns with straight and curved pipe sections. On the contrary, this paper should be considered only as a progress report based on experiences gained thus far both in the laboratory and in the field. As a matter of fact, this subject well merits a great deal more research and field investigation before we can be sure all the standards established and the interpretations thereof can be considered as fully proved and beyond reproach. It is sincerely hoped that when such additional data are obtained they will be made public at first opportunity.

PIPING-REQUIREMENT STANDARDS

For convenience in presenting the piping-requirement standards published in the A.G.A.-A.S.M.E. Report in 1935, together with the additional data obtained since then, eight piping groups or schedules have been set up, as shown in Fig. 1. The first seven schedules cover the use of orifices and flow nozzles, while the eighth applies only to Venturi tubes. Each schedule, except the eighth, shows the minimum lengths of straight pipe required for that particular piping arrangement, both on the inlet and on the outlet sides of the orifice or flow nozzle. Alternately, it also shows the lengths of straight pipe required on the inlet side when straightening vanes must be used in lieu of the longer runs of straight pipe.

PIPING ON INLET SIDE

(a) *Orifices and Flow Nozzles.* It will be apparent at once on examining Schedules 1 to 7, that the minimum required lengths of straight pipe on the inlet side of the primary element increase rapidly with (a) the diameter ratio of the primary element, and (b) with the complexity of the piping arrangement preceding the straight run. On the other hand, the length of straight pipe on the outlet side varies but little with these or any other factors.

The simplest arrangements, shown in Schedule 1, may include any fitting such as an elbow, tee, Y-fitting, drum or tank, separator or strainer, expansion joint, long-radius bend, etc. In the case of tees and Y-fittings, the flow can enter either one end or the side, provided the other end is blanked off. Also note, a second fitting cannot be closer than 6 diam to the first and in the same plane, except in the case of large-diameter vessels or separators.

When two or more fittings, producing a change in direction of fluid flow, are adjacent to each other, and in the same plane preceding the straight pipe ahead of the primary element, somewhat longer runs of straight pipe are required on the inlet side of the primary element. These are shown in Schedule 2. Note that elbows or tube turns require slightly more straight pipe than long-radius bends. In this schedule can be included all expansion bends and U-bends, since the directional changes thereby produced are in the same plane even though the bend itself may be a single fabricated section.

Schedules 3 and 4 show that considerably longer runs of straight pipe are required when two preceding fittings are at right angles with each other. When the fittings are separated by at least 10 diam of straight pipe, the disturbance created by the first fitting is partially eliminated by this pipe before reaching the second. Therefore, shorter lengths can be used, as indicated in Schedule 3, as compared with the longer lengths required when

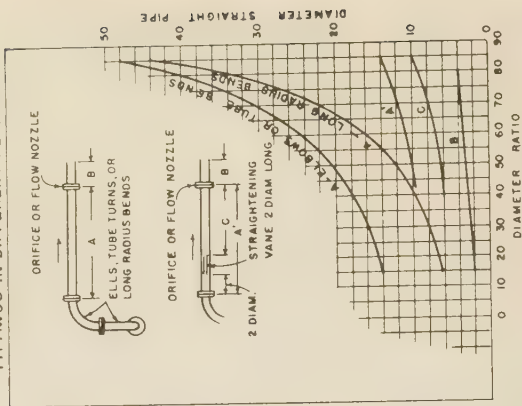
¹ Hydraulic Engineer, Bailey Meter Company. Mem. A.S.M.E.

² Numbers in parentheses refer to the Bibliography at the end of the paper.

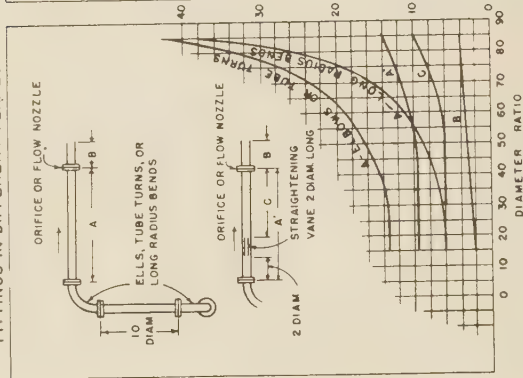
Contributed by Special Research Committee on Fluid Meters and the Industrial Instruments and Regulators Division and presented at the Annual Meeting, New York, N. Y., Nov. 27-Dec. 1, 1944, of THE AMERICAN SOCIETY OF MECHANICAL ENGINEERS.

NOTE: Statements and opinions advanced in papers are to be understood as individual expressions of their authors and not those of the Society.

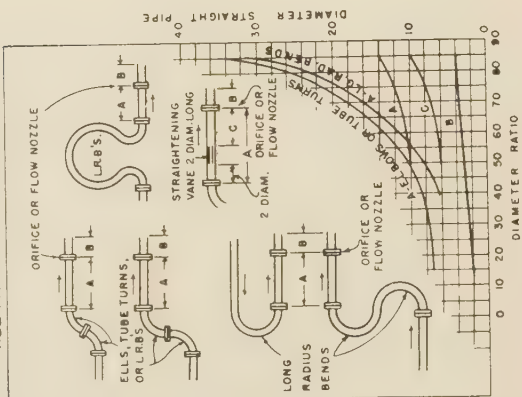
SCHEDULE 4 FOR ORIFICES AND FLOW NOZZLES FITTINGS IN DIFFERENT PLANES.



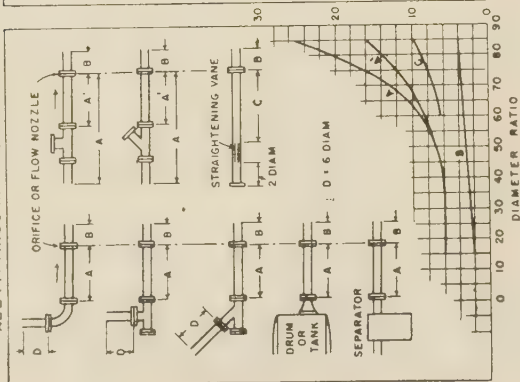
SCHEDULE 3 FOR ORIFICES AND FLOW NOZZLES FITTINGS IN DIFFERENT PLANES



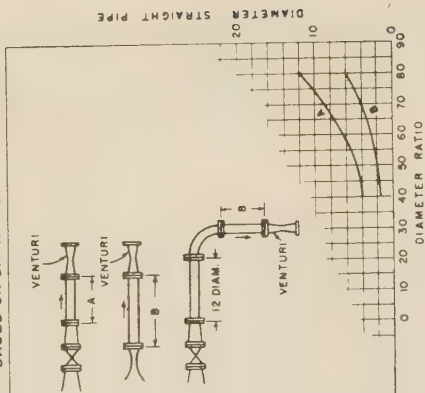
SCHEDULE 2 FOR ORIFICES AND FLOW NOZZLES ALL FITTINGS IN SAME PLANE



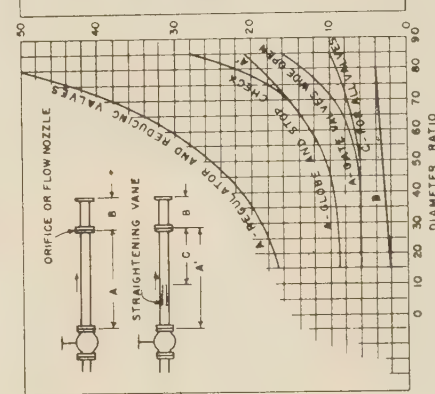
SCHEDULE 1 FOR ORIFICES AND FLOW NOZZLES ALL FITTINGS IN SAME PLANE



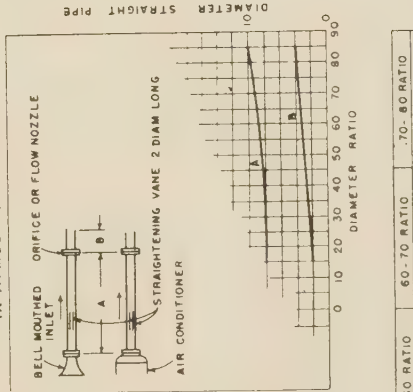
SCHEDULE 8 FOR VENTURI TUBES BASED ON DATA FROM W.S. PARDOE



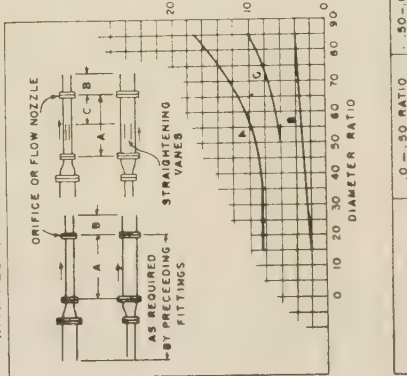
SCHEDULE 7 VALVES



SCHEDULE 6 FOR ORIFICES AND FLOW NOZZLES IN ATMOSPHERIC INTAKE



SCHEDULE 5 FOR ORIFICES AND FLOW NOZZLES WITH REDUCERS AND EXPANDERS.



PIPING REQUIREMENTS FOR ORIFICES, FLOW NOZZLES AND VENTURI TUBES.

	0-50 RATIO	50-60 RATIO	60-70 RATIO	70-80 RATIO
FITTINGS ALLOWED ON OUTLET SIDE IN PLACE OF STRAIGHT PIPE.	1. TEES 2. 45° ELLS 3. GATE VALVES 4. SEPARATORS 5. Y-FITTINGS 6. EXPANSION JTS	1. TEES 2. EXPANSION JTS 3. GATE VALVES 4. Y-FITTINGS 5. SEPARATOR (IF INLET NECK IS ONE DIAM. LONG)	1. GATE VALVES 2. Y-FITTINGS 3. SEPARATOR (IF INLET NECK IS ONE DIAM. LONG)	1. GATE VALVE 2. LONG RADIUS BEND

FIG. 1 PIPING REQUIREMENTS FOR ORIFICES, FLOW NOZZLES, AND VENTURI TUBES

the fittings are immediately adjacent, as illustrated in Schedule 4.

Because of the abrupt change in direction produced by two elbows or tube turns at 90 deg to each other, compared with the more gradual change caused by two long-radius bends, considerably more straight pipe is required on the inlet side for elbows and tube turns than for long-radius bends. This is true whether there is straight pipe between these turns or bends, or whether they are immediately adjacent to each other.

Research so far has been entirely confined to turns or bends in the same plane, and at 90 deg to each other. Until such time as additional data are forthcoming, we recommend that the piping requirements of Schedules 3 and 4 be followed, when the bends are not in the same plane.

Attention should be called in Schedule 5 to the fact that the lengths shown apply only to the lengths of the increased- or decreased-diameter pipe and not to their required over-all lengths of straight pipe. Such over-all or total lengths depend entirely on the nature of the fittings, valves, etc., which precede. For example, in the case of expanding an 8-in. pipe to 10 in., a 75 per cent diameter ratio orifice located in the 10-in. line would require 14 diam of 10-in. pipe, as shown in Schedule 5. If, however, two adjacent long-radius bends of 8-in. pipe, at right angles to each other, precede the expanded section, the total length of straight 8-in. and 10-in. pipe would be determined from Schedule 4, which in this case would be 26 diam. Thus there would be required a total of 14 diam of 10-in. pipe, plus a sufficient length of 8-in. pipe to make up an equivalent total length of 26 diam of 10-in. pipe.

When air is being measured in an atmospheric intake, the orifice or flow-nozzle installation should be made as indicated in Schedule 6. To avoid undue fluctuation of the meter or manometer, straightening vanes should be installed as indicated, although if a tubular air conditioner is used at the atmospheric inlet, a straightening vane may not be required. To avoid excessive entrance losses, it is also best to provide a bellmouthed inlet.

Regulators and reducing valves, illustrated in Schedule 7, require more straight pipe between them and the primary element than any other type of valve of which we have knowledge; in fact the preferable location for any regulating valve is 6 or more diameters following the primary element, rather than preceding it. In this connection, also, other fittings cannot immediately precede a wide-open gate valve if only the short length *A* is available between the gate valve and the primary element.

(b) *Venturi Tubes.* As indicated, the data on Venturi-tube piping requirements, as shown in Schedule 8, was obtained entirely from Prof. W. S. Pardoe's papers (8). His last paper supplied figures³ which were cross-plotted on the basis of diameter ratio versus the lengths of pipe required to eliminate all disturbances created by fittings preceding the straight pipe. Since the piping arrangements used by Professor Pardoe were not exactly the same as indicated in Schedules 1 to 7, they are shown separately in Schedule 8, together with the lengths of straight pipe required for each.

(c) *Pitot Tubes.* While no specific research and very little actual field experience have come to the author's attention covering piping requirements for Pitot tubes, it is reasonable to assume, until proved to the contrary, that piping requirements for this type of primary element should be at least as stringent as for orifices and flow nozzles. In fact there is some field evidence to indicate even longer runs of straight pipe are desirable on the inlet side, unless traverses are run to determine the point of average velocity, etc. More research and field experience are obviously needed to clarify this point.

STRAIGHTENING VANES

While straightening vanes are shown as alternative arrangements in each schedule, permitting shorter lengths of straight pipe on the inlet side, they should not always be considered as entirely equal to the longer runs of straight pipe in reducing flow turbulence. Especially is it desirable to limit their use to moderate line velocities, pressures, and temperatures, since application to high-pressure and high-temperature service involves special designs and materials to provide a safe installation. The preferable arrangement, no matter what the operating conditions may be, is to provide whenever possible the lengths of straight pipe specified in the schedules described, without resorting to the use of straightening vanes.

The recommended general design of straightening vanes is shown in Fig. 2. On cross section it resembles an "egg crate," with the spacings between plates not more than from $\frac{1}{3}$ to $\frac{1}{4}$ the inside pipe diameter. In measuring air in the atmospheric intake, as shown in Schedule 6, this spacing should be $1\frac{1}{2}$ in. to 2 in., regardless of pipe size.

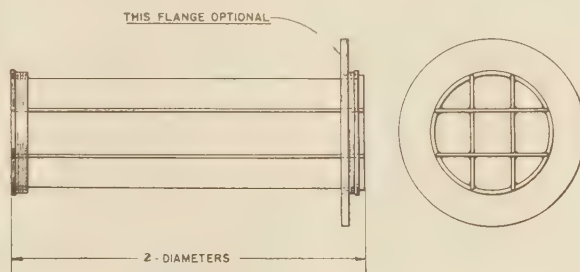


FIG. 2 BAILEY METER STRAIGHTENING VANE

PIPING ON OUTLET SIDE OF ORIFICES AND FLOW NOZZLES

From 2 to 4 diam of straight pipe are normally sufficient on the outlet side, as shown in Schedules 1 to 7, assuming a fitting, bend, or wide-open gate valve follows these 2 or 4 diam. Should a control valve, regulator, stop check valve, or partly throttled gate valve closely follow the primary element, then at least 5 and preferably 6 diam should follow the orifice or the nozzle.

From the table in Fig. 1, it will be noted certain fittings can replace the straight pipe on the outlet side. While this list includes the use of seven different fittings up to a 50 per cent diam ratio, only wide-open gate valves and long-radius bends can immediately follow the orifice or nozzle at ratios in excess of 70 per cent. Incidentally, however, due to lack of physical clearances, it is impossible to install flow nozzles at the inlet to gate valves unless the face-to-face dimension is at least 18 in. In any case, it should be remembered that the preferable arrangement is the use of straight pipe immediately following the primary element.

THERMOMETER WELLS, NIPPLES, ETC.

All thermometer wells, bulbs and sockets, thermocouples, resistance elements, etc., must be located at least 6 diam following the orifice or nozzle on the outlet side, or not less than 15 diam preceding it on the inlet side. The preferable location is on the outlet side.

When thermocouples are embedded in the pipe wall in such a way as not to protrude into the pipe area, they may be located wherever desired.

GENERAL

Attention is called again to the fact that the lengths of pipe indicated in Schedules 1 to 8 are the *minimum* required in each case, and not the maximum. For best accuracy in metering, it is

³ Reference (8) Trans. A.S.M.E., vol. 65, 1943, pp. 337-349.

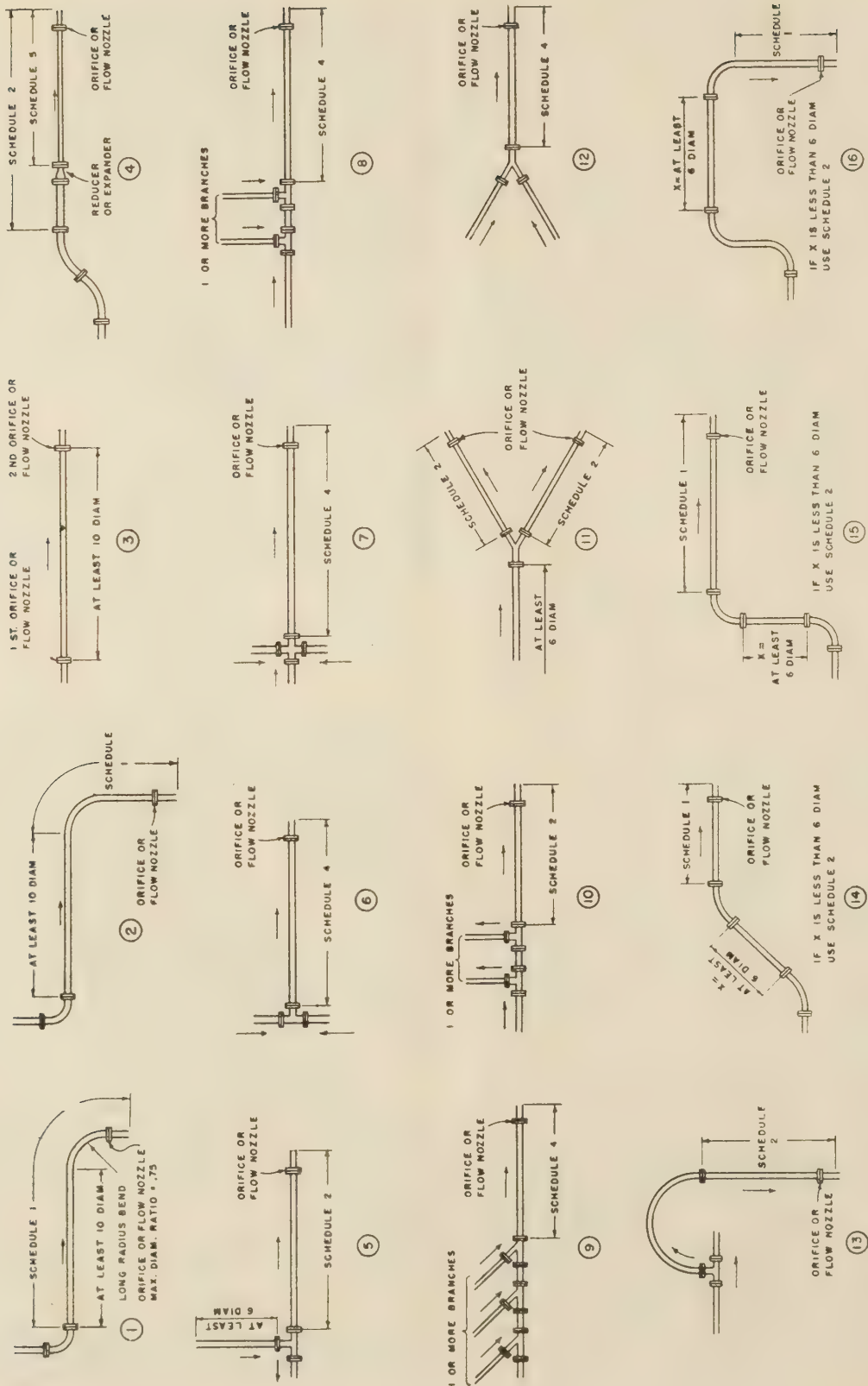


FIG. 3 TYPICAL PIPING ARRANGEMENTS WITH FITTINGS OR BENDS IN SAME PLANE
Refer to Fig. 1, for schedule specifications.)

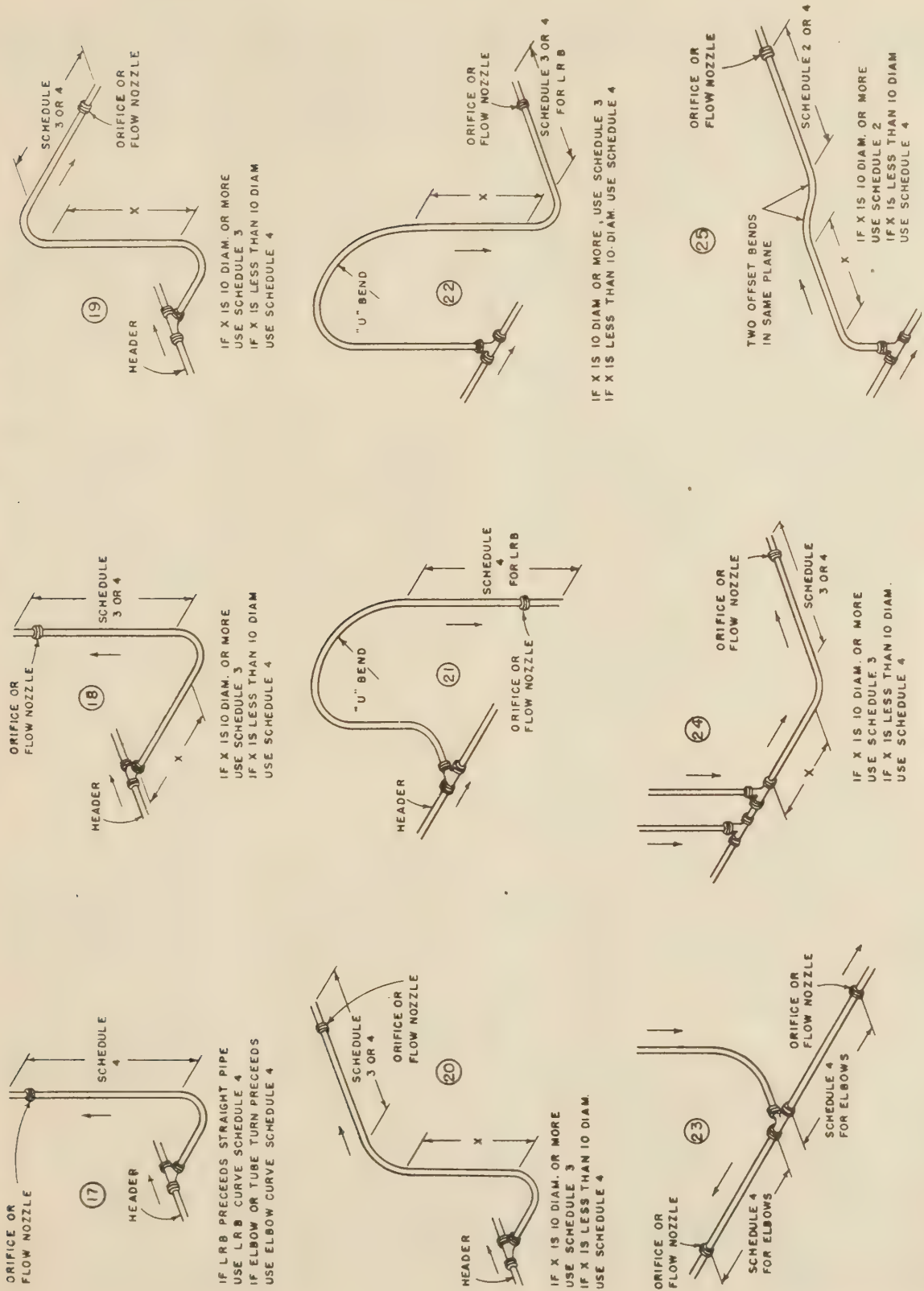


FIG. 4 TYPICAL PIPING ARRANGEMENTS WITH FITTINGS AND BENDS NOT IN SAME PLANE
(Refer to Fig. 1, for schedule specifications.)

always desirable to provide the longest lengths of pipe possible, especially when the complete piping system on the inlet side includes a number of bends or fittings in different planes. It must be remembered that it is impossible, from a metering standpoint, to provide too much straight pipe.

TYPICAL PIPING ARRANGEMENTS

Experience has indicated that the "Piping Requirement Standards," as shown in Schedules 1 to 7, are not sufficiently complete and precise in themselves to enable one always to choose the correct location of an orifice or a flow nozzle in any particular piping layout. Further clarification or interpretation thus appears desirable in order to translate these standards into typical cases. To this end the author believes the diagrammatic sketches shown in Figs. 3, 4, and 5 will be helpful, particularly if the meter engineer is given the opportunity of assisting in laying out the piping before it is purchased and erected.

A few pertinent comments regarding some of these arrangements may be of assistance in understanding their application fully.

From arrangements Nos. 1 and 2, Fig. 3, it will be noted that a long-radius bend can itself be considered as so much developed straight pipe under Schedule 1, only if it is preceded by at least 10 diam of straight pipe. It cannot be so considered if it is preceded within a short distance by any fitting or valve or by another long-radius bend. Also note that in arrangement No. 1, an orifice or nozzle of a diameter ratio of 75 per cent or less can be placed at the outlet of a long-radius bend.

Arrangements Nos. 5 to 12, inclusive, emphasize the necessity of having long lengths of straight pipe when there are multiple-entrance flows or when the flow divides into one or more streams ahead of the primary element. Multiple-entrance flows in particular are quite apt to produce swirls or disturbances which are particularly difficult to eliminate. In a few instances, it has been found necessary to use a combination of these long lengths together with straightening vanes to obtain entirely satisfactory metering conditions.

Nos. 14, 15, and 16 illustrate the fact that with at least 6 diam of straight pipe between two long-radius bends, elbows, or tube turns in the same plane, the required lengths of straight pipe following the last fitting need be only that corresponding to Schedule 1. On the other hand, if the second fitting immediately or very closely (less than 6 diam) follows the first fitting, then Schedule 2 applies, as shown in arrangement No. 13.

The isometric views in Fig. 4 depict a few typical arrangements where the component bends are not in the same plane. All of these require lengths of pipe corresponding to Schedule 3 or 4, depending upon whether there is sufficient straight pipe between the preceding bends or not.

A number of typical boiler outlets are shown in Fig. 5, both coming directly off the boiler drum, and starting with the superheater outlet.

Since these boiler leads usually are rather short in length, it is necessary to start the study of the piping layout at the drum or superheater outlet. This is particularly true of those cases where the steam-flow orifice or nozzle must be located in the outlet from the boiler drum, as shown in Nos. 26 to 31, inclusive.

Note that in all cases when bends or turns closely follow the angle stop check valve, as in Nos. 28, 29, and 30, this valve is considered as having the same effect as an elbow, thus requiring the lengths of straight pipe as called for under Schedules 2, 3, or 4, as the case may be; whereas when straight pipe immediately follows the valve as in No. 27, and when the orifice or nozzle can be located in this straight pipe, the requirements of Schedule 7 for stop check valves apply.

When the angle stop check valve follows the superheater outlet in a plane at right angles to the outlet, the requirements of Schedule 4 apply, regardless of the fact that the orifice or nozzle can be located in the straight pipe immediately following the stop-check valve. This is shown in arrangement No. 34, as contrasted with No. 27 in which Schedule 7 applies, because the angle check valve is not preceded by a bend or elbow, but by the boiler drum.

CONCLUSION

Of course it must be realized that the Piping Requirement Standards, Schedules 1 to 8, supplemented by the typical arrangements shown in Figs. 3, 4, and 5, cannot possibly cover every conceivable installation. We trust, however, they will illustrate the principles involved with sufficient clarity and completeness, and that, with the exercise of a little imagination and common sense, the engineer can project any specific case into one or the other of these schedules or diagrammatic arrangements with reasonable assurance of obtaining a satisfactory meter installation.

BIBLIOGRAPHY

- 1 "The Effects on Orifice Meter Indications of Various Pipe Fittings Near the Orifice Plate," by H. S. Bean, *Western Gas*, vol. 5, 1929, pp. 30-32.
- 2 "Durchflussszahlen von Düsen und Stauranden," by R. Witte, in *Technische Mechanik und Thermodynamik*, vol. 1, 1930, pp. 34-41; 72-85; 113-120.
- 3 "History of Orifice Meters and the Calibration, Construction, and Operation of Orifices for Metering," Report of the Joint A.G.A.-A.S.M.E. Committee on Orifice Coefficients, 1935.
- 4 "Influence of Steam Flow Metering Equipment on Piping Design," by R. M. Van Duzer, Jr., *Mechanical Engineering*, vol. 60, 1938, pp. 834-836.
- 5 "Flow-Measurement—1940," Report of Instruments and Apparatus Committee No. 19, A.S.M.E. Power Test Codes.
- 6 "Installation Requirements for Head Meters," by H. S. Bean, *Heating, Piping and Air Conditioning*, vol. 13, 1941, pp. 741-746.
- 7 "Selection and Installation of Flow Meters," by R. E. Sprenkle, *Instruments*, vol. 15, 1942, pp. 75-82.
- 8 "The Effect of Installation on the Coefficients of Venturi Meters," by W. S. Pardoe, *Trans. A.S.M.E.*, vol. 58, 1936, pp. 677-684; discussion, vol. 59, 1937, pp. 750-756; vol. 65, 1943, pp. 337-349.

Appendix

DETERMINATION OF DIAMETER RATIO

Since all piping-requirement schedules, as well as all other considerations of fluid-flow problems, involve the use of diameter ratio B , it is necessary that the prospective user be able to determine what the approximate ratio will be for any particular case.

Diameter ratio B is the ratio of the diameter of the orifice, flow nozzle, or Venturi-tube throat d , to the internal pipe diameter D ,

or $\frac{d}{D}$, and is an approximate function of capacity factor E . This

factor in turn depends on the desired flow capacity, pressure, temperature, specific gravity, meter differential head, and pipe size, which factors are expressed by flow Equations [1] and [2] as follows

For steam

$$E = \frac{W}{\sqrt{\frac{h_w}{\text{Sp. vol.}} D^2}} \dots \dots \dots [1]$$

For air, gases, and liquids

$$E = \frac{W}{\sqrt{h_w \times \rho D^2}} \dots \dots \dots [2]$$

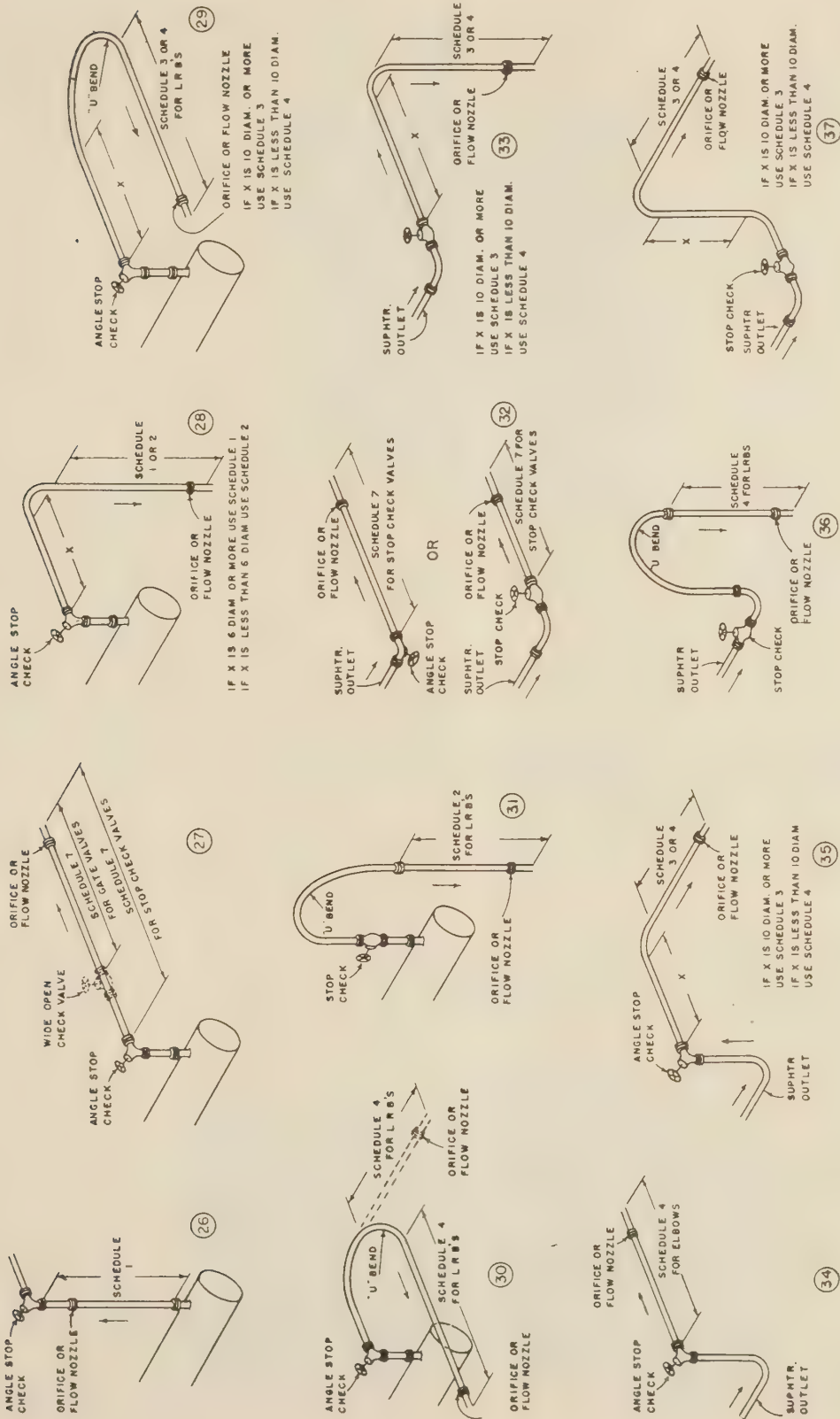


FIG. 5 TYPICAL BOILER-OUTLET ARRANGEMENTS
(Refer to Fig. 1, for schedule specifications.)

in which

E = capacity factor

W = weight of flowing fluid, lb per hr

h_w = differential head of meter in inches of water at 68 F

ρ = the density of the flowing fluid, lb per cu ft

D = internal pipe diameter, in.

Sp. vol. = specific volume of steam

The approximate relation between "diameter ratio" and "capacity factor E ," for vena-contracta pressure connections, is shown in the right-hand logarithmic curve included as a part of Figs. 6, 7, and 8. Note that, for a given diameter ratio, the value of capacity factor E is considerably greater for a flow nozzle than for an orifice. Conversely, for any given value of capacity factor E , the diameter ratio B of a flow nozzle is lower than that of an orifice. This means that for the same capacity, pipe size, and all other conditions, the flow nozzle requires shorter lengths of straight pipe preceding, because of its smaller diameter ratio, or again it may permit the use of either a smaller-size pipe, smaller differential-head meter, or of the measuring of a higher maximum flow.

On the other hand, the thin-plate orifice is considerably cheaper, especially in the larger sizes, is easier to replace with another plate in the event of a capacity or other change, and its accuracy is of the highest order because of its thorough investigation by many experimenters. The orifice should be used, therefore, whenever and wherever possible.

USE OF DIAMETER-RATIO DIAGRAMS

While the capacity factor E can be calculated by either Equations [1] or [2], and the corresponding approximate diameter ratio $\frac{d}{D}$ of either the orifice, flow nozzle, or Venturi tube can be obtained from the right-hand section of Figs. 6, 7, and 8, it is usually more convenient and quicker to use the complete nomogram diagrams included with these figures. It should be understood, however, that these equations or diagrams should not be used for final design of any orifice, flow nozzle, or Venturi tube, but for estimates of approximate sizes only.

While each diagram is complete with examples illustrating its use, the following supplemental information may be found helpful.

Pressures intermediate to those shown on the curves at the left of the V-scale in Fig. 6 can be plotted linearly between adjacent curves. Or, if preferred, the specific volume for any pressure and temperature condition can be obtained from steam tables,⁴ from which these curves were derived, and spotted on the V-scale for use in solving the particular problem.

The curve showing densities of water was taken from an A.S.M.E. research report,⁵ and the curve showing petroleum-oil densities was plotted from data published by the Kansas City Laboratory.⁶

The lines of specific gravity for variation in temperature, shown at the bottom of the density curves, were taken from the same publication⁷ and are reproduced herewith with the publisher's permission.

The extension of the density line from 62.37 to 80 lb per cu ft allows the use of the nomogram for oils and liquids having specific gravities greater than 1.

In solving any air- or gas-flow problem, first determine the

density from the nomogram, Fig. 9. Note that in applying the pressure component in this figure, only the absolute pressure scale P is used in determining the density of dry gas. However, when fully saturated gas is being metered, it is necessary to use the temperature-versus-gage-pressure curves to the right of the absolute-pressure scale P , disregarding the numerical values on the absolute-pressure scale itself. Linear interpolation between adjacent pressure curves is satisfactory for intermediate-pressure values.

The W or flow scale in Fig. 8 is based on a specific gravity of 1.00. It is necessary therefore to multiply the desired capacity in cubic feet per hour by the specific gravity of the gas and apply the resulting figure to the W scale in using this nomogram.

It must also be understood that this diagram can be used only when the air or gas volume W is referred to standard conditions of 30 Hg and 60 F.

Note that the temperature-versus-pressure curves to the right of the PT scale in Fig. 8 are used only with saturated gas and that the value of 1.00 on the PT scale is the only one used with dry gas or air.

In the event the gas is partially saturated, proportional interpretation between dry gas and 100 per cent saturated-gas capacity factor E is sufficient. For example, if in example 1, Fig. 8, the gas were 50 per cent saturated, first proceed exactly as shown in example 1. Then determine the capacity factor E as if the gas were dry, as in example 2. The correct capacity factor

E for 50 per cent saturated gas would then be $\frac{138 + 128}{2}$ or 133.

DIAMETER-RATIO LIMITS

It will be noted that the curve for orifices stops at a maximum diameter ratio of 85 per cent. In like fashion the flow-nozzle curve stops at 81 per cent, and the Venturi curve at 75 per cent. Due both to the lack of complete and reliable coefficient data for ratios higher than these and to the much increased sensitivity of primary elements to preceding piping arrangements, higher ratios than these limits are not recommended.

SELECTING THE METER DIFFERENTIAL

In solving the nomograms or Equations [1], [2], it is necessary first to determine the differential head h_w of the meter, required to handle that particular flow problem.

The standard differentials for which Bailey meters for steam and water are built are 13 $\frac{1}{4}$ in., 53 in., 120 in., 212 in., and 331 in. of 68 F H₂O. These are shown in larger type on the h_w scales in Figs. 6 and 7. The differentials most commonly used are 53 in. and 120 in. The selection in most cases should thus tentatively start with the 53-in. differential.

Similarly the standard differentials for Bailey gas and air meters are 2 in., 4 in., 6 in., 8 in., 14.3 in., 57.2 in., and 129.6 in. of 68 F water, as shown in Fig. 8. The differentials used commonly are 2 in., 4 in., and 8 in.

If, in the case of a 53-in. differential steam or water meter, the orifice ratio exceeds 85 per cent but the flow-nozzle ratio is less than 81 per cent, then the engineer has the option either of using the flow nozzle or of increasing the meter differential to 120 in. and using an orifice. If both orifice and flow nozzle exceed their maximum diameter-ratio limits, then it will be necessary to use either a 120-in. meter with a flow nozzle, if this combination gives a diameter ratio of 81 per cent or less, or an even higher head meter such as a 212 in. or 331 in. if required.

In this connection, it is important to point out that the net unrecovered pressure loss due to metering increases both with an increase in differential head, and with a decrease in diameter ratio. Such losses can be determined for orifices and flow nozzles from the L scale on the extreme right-hand side of Figs. 6, 7, and

⁴ "Steam Tables," by J. H. Keenan and F. G. Keyes, A.S.M.E., New York, N. Y., 1930.

⁵ A.S.M.E. Research Report on Fluid Meters, part 1, 1937, Fig. 59.

⁶ Handbook of Petroleum Asphalt and Natural Gas, Bulletin No. 25, 1928 revision, Kansas City Laboratory.

⁷ Ibid., Fig. 137.

EXAMPLE:- REQUIRED TO MEASURE A MAXIMUM FLOW OF 300,000 POUNDS OF WATER AT 395°F. 50 PSI. THRU A 55" I.D. PIPE.



SOLUTION:- REFER TO DIAGRAMMATIC SKETCHES ① ② ③
 1. FROM 395° ON WATER TEMPERATURE SCALE, PROJECT VERTICALLY UPWARD TO WATER DENSITY CURVE, THEN GO HORIZONTALLY TO RIGHT TO DENSITY SCALE. ANSWER: 54.00 LBS. PER CU. FOOT.
 2. FROM 50 ON DEGREES A.P.I. SCALE, DROP VERTICALLY DOWN TO OIL DENSITY CURVE, THEN GO HORIZONTALLY TO RIGHT TO DENSITY SCALE. ANSWER: 48.6 LBS. PER CU. FOOT.
 3. CONNECT THIS POINT OF 83.50 ON "S" SCALE WITH 5.6" ON "I.D." SCALE, AND EXTEND LINE TO "E" SCALE. THIS "E" VALUE IS 184. IF A FLOW NOZZLE OR VENTURI IS USED, ITS DIA. "B" = .68. THE FLOW NOZZLE IS 392% X .53" = 20.8".

1. FROM 395° ON WATER TEMPERATURE SCALE, PROJECT VERTICALLY UPWARD TO WATER DENSITY CURVE, THEN GO HORIZONTALLY TO RIGHT TO DENSITY SCALE. ANSWER: 54.00 LBS. PER CU. FOOT.
 2. FROM 50 ON DEGREES A.P.I. SCALE, DROP VERTICALLY DOWN TO OIL DENSITY CURVE, THEN GO HORIZONTALLY TO RIGHT TO DENSITY SCALE. ANSWER: 48.6 LBS. PER CU. FOOT.
 3. CONNECT THIS POINT OF 83.50 ON "S" SCALE WITH 5.6" ON "I.D." SCALE, AND EXTEND LINE TO "E" SCALE. THIS "E" VALUE IS 184. IF A FLOW NOZZLE OR VENTURI IS USED, ITS DIA. "B" = .68. THE FLOW NOZZLE IS 392% X .53" = 20.8".

EXAMPLES OF DENSITY CALCULATION

- FIND DENSITY OF H₂O AT 395°F.
 SOLUTION:- FROM 395°F ON TEMPERATURE SCALE ON BOTTOM, PROJECT VERTICALLY UP TO WATER DENSITY CURVE AND THEN GO HORIZONTALLY TO RIGHT TO DENSITY SCALE. ANSWER: 54.00 LBS. PER CU. FOOT.
- FIND DENSITY OF OIL AT 50 DEGREES A.P.I. (OR BAUME).
 SOLUTION:- FROM 50 ON DEGREES A.P.I. SCALE, DROP VERTICALLY DOWN TO OIL DENSITY CURVE AND THEN GO HORIZONTALLY TO RIGHT TO DENSITY SCALE. ANSWER: 48.6 LBS. PER CU. FOOT.
- FIND DENSITY OF OIL AT 495°F HAVING A SPECIFIC GRAVITY OF 98 AT 60°F.
 SOLUTION:- FOLLOW 98 LINE OF SPECIFIC GRAVITY LOWER FAMILY FROM 495°F ON TEMPERATURE SCALE ON BOTTOM GO HORIZONTALLY TO REFERENCE CURVE, AND PROJECT INTERSECTION VERTICALLY UPWARD TO OIL DENSITY CURVE AND GO HORIZONTALLY TO RIGHT TO DENSITY SCALE. ANSWER: 51.8 LBS. PER CU. FOOT.

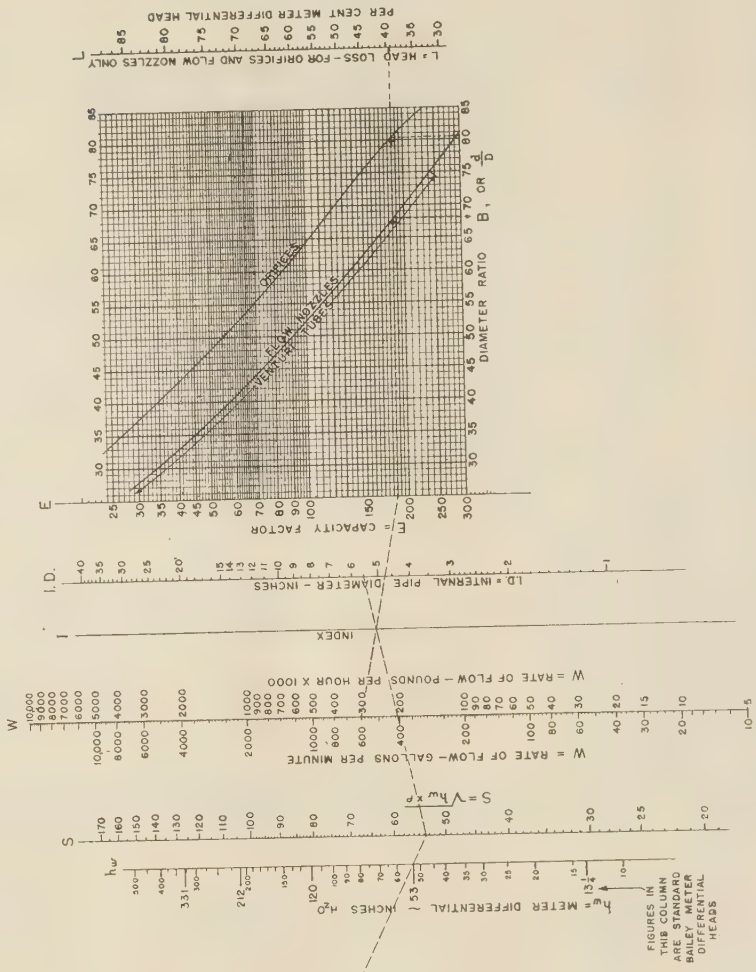
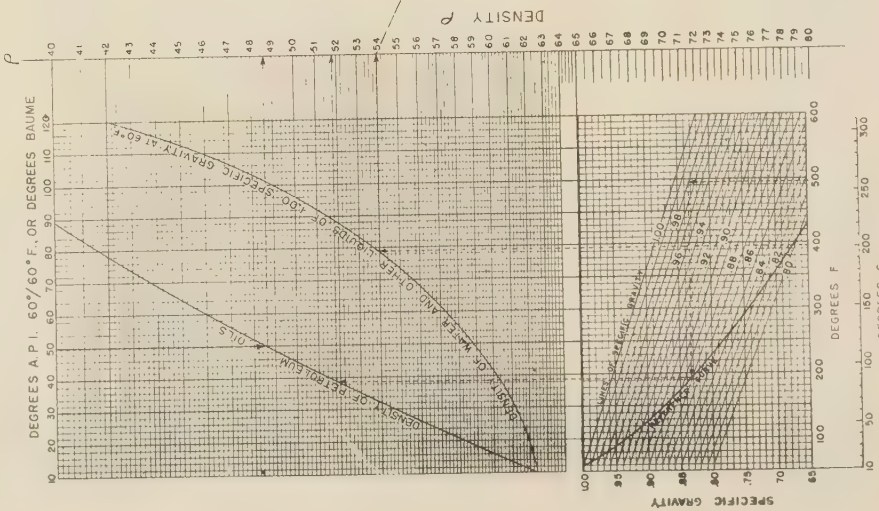


Fig. 7 APPROXIMATE DIAMETER-RATIO CALCULATION DIAGRAM FOR WATER AND LIQUID FLOW

EXAMPLE 1—SATURATED GAS

REQUIRED TO MEASURE A MAXIMUM FLOW OF 100,000 CUBIC FEET OF SATURATED GAS PER HOUR AT STANDARD CONDITIONS OF 30" BAROMETER 60°F, SPECIFIC GRAVITY .40, BUT FLOWING AT A PRESSURE OF 5 LB GAGE 125°F, SPECIFIC GRAVITY .40, 100 PER CENT SATURATED, THRU 12.00" I.D. PIPE.

SOLUTION—

- A—DETERMINE DENSITY OF DRY GAS PART OF MIXTURE FROM DENSITY CALCULATION DIAGRAM. THIS IS .666 LB PER CUBIC FOOT.
- B—REFER TO DIAGRAMMATIC SKETCHES (1), (2), (3) AND (4) AT LEFT, ASSUME MAXIMUM METER DIFFERENTIAL IS 6" H₂O AND CONNECT .066 ON "P" SCALE, .125 ON "W" SCALE, EXTENDING STRAIGHT LINE TO INTERSECT "S" SCALE ON INDEX I.
- 2—CONNECT .628 ON "S" SCALE WITH 12.00 ON "I.D." SCALE, AND THRU POINT OF INTERSECTION ON INDEX I, SCALE, DRAW A LINE TO 100,000 X .8 OR 80,000 ON "W" SCALE, EXTENDING LINE TO INTERSECT INDEX II SCALE.
- 3—PROJECT HORIZONTALLY TO THE "PT" SCALE THE INTERSECTION OF 5 LB GAGE PRESSURE CURVE WITH 125°F LINE, CONNECT THIS POINT, OR 1.035, WITH 100,000 ON "W" SCALE, EXTENDING LINE TO INTERSECT INDEX II SCALE.
- 4—PROJECT HORIZONTALLY FROM INDEX II SCALE TO EITHER ORIFICE OR FLOW NOZZLE CURVE, AND DROP VERTICALLY TO DIAMETER RATIO SCALE.

RESULT—

IF AN ORIFICE IS TO BE USED, ITS DIAMETER RATIO B .513 WITH A NET UNRECOVERED LOSS OF 47.2" H₂O = 1.285"

IF A FLOW NOZZLE OR A VENTURI TUBE IS TO BE USED, ITS DIAMETER RATIO IS .40 THE FLOW NOZZLE WOULD HAVE A NET UNRECOVERED LOSS OF 24.2" H₂O = .675"

EXAMPLE 2—DRY GAS

REQUIRED TO MEASURE A MAXIMUM FLOW OF 200,000 CUBIC FEET OF DRY GAS PER HOUR AT STANDARD CONDITIONS OF 30" BAROMETER 60°F, SPECIFIC GRAVITY .80, BUT FLOWING AT A PRESSURE OF 5 LB GAGE 125°F, SPECIFIC GRAVITY .80, THRU 12.00" I.D. PIPE.

SOLUTION—

- A—DETERMINE DENSITY FROM DENSITY CALCULATION DIAGRAM. THIS IS .073 LB. PER CUBIC FOOT.
- B—REFER TO DIAGRAMMATIC SKETCHES (1), (2), (3) AND (4) AT LEFT, ASSUME MAXIMUM METER DIFFERENTIAL IS 6" H₂O AND CONNECT .073 ON "P" SCALE, .125 ON "W" SCALE, EXTENDING STRAIGHT LINE TO INTERSECT "S" SCALE AT .622.
- 2—CONNECT .622 ON "S" SCALE WITH 12.00 ON "I.D." SCALE, POINT OF INTERSECTION ON INDEX I SCALE, DRAW LINE TO 200,000 X .8 OR 160,000 ON "W" SCALE, EXTENDING LINE TO INTERSECT INDEX II SCALE.
- 3—CONNECT 1.00 ON "PT" SCALE WITH POINT OF INTERSECTION ON INDEX II SCALE, THE INTERSECTION OF THIS LINE WITH THE "E" SCALE AT 1.8 IS THE CAPACITY FACTOR FOR THE FLOW NOZZLE, AND 1.8 ON "E" SCALE, EXTENDING LINE TO INTERSECT INDEX II SCALE, AND DROP VERTICALLY TO DIAMETER RATIO SCALE "B".

RESULT—

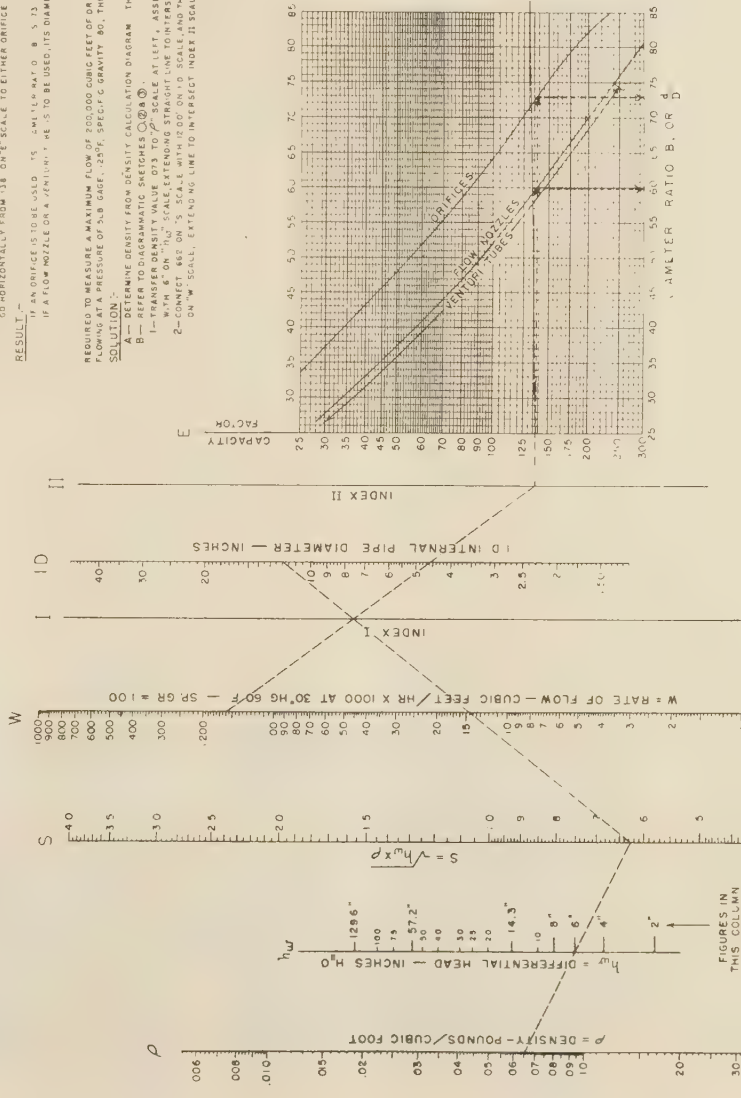
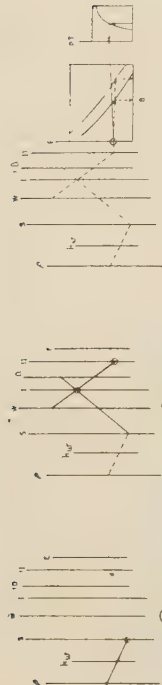
IF AN ORIFICE IS TO BE USED, ITS DIAMETER RATIO "B" IS .711,

WITH A NET UNRECOVERED LOSS OF 50 X 6" = 300" H₂O.

IF A FLOW NOZZLE OR VENTURI TUBE IS TO BE USED,

UNRECOVERED LOSS FOR THE FLOW NOZZLE WOULD

BE 50 X 4" = 200" H₂O.



EXAMPLE 1—ILLUSTRATED ABOVE

FIGURES IN
THIS COLUMN
ARE STANDARD
BAILEY METER
DIFFERENTIAL
HEADS

FIG. 8 APPROXIMATE DIAMETER-RATIO CALCULATION DIAGRAM FOR AIR AND GAS FLOW

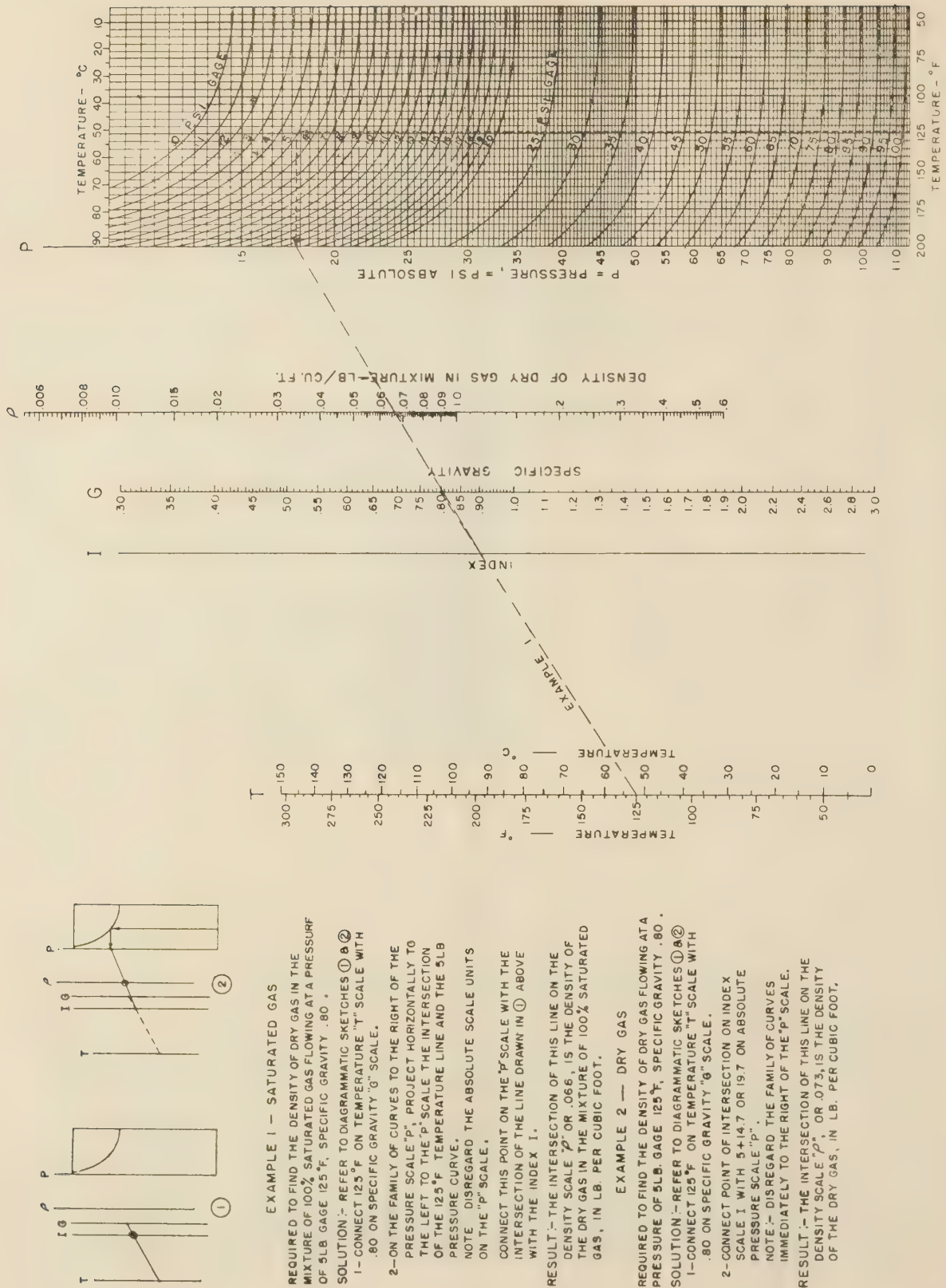


Fig. 9 DENSITY-CALCULATION DIAGRAM FOR AIR AND GAS

8. For example, if a 212-in.-head meter were selected instead of a 53 in., in the example given in Fig. 7, the resulting orifice diameter ratio would have been approximately 62 per cent. By projecting horizontally to the right on the L scale, the net unrecovered pressure loss at maximum capacity would be 60×212 or 127.2 in. H_2O or 4.6 lb.

While the diameter ratio of the orifice using the 53-in. head meter is approximately 80.5 per cent, the net unrecovered loss is considerably less, since it would be 39.2×53 or 20.8 in. H_2O or $\frac{3}{4}$ lb. If the 4.6 lb were not prohibitive and if the piping layout were such as not to allow the use of a higher diameter ratio than 62 per cent, then the 212-in. meter could be used. Should it be desirable to limit the loss to not more than $\frac{3}{4}$ to 1 lb and if the piping layout permitted the use of an 80.5 per cent ratio orifice (or a 68 per cent ratio flow nozzle), then the 53-in. meter should be used.

When there is a choice between two different head meters or between an orifice or a flow nozzle, the ultimate decision in most cases will depend upon the cost involved. In general, the higher the meter differential the higher is the cost. Similarly, flow nozzles are more expensive than thin-plate orifices. Naturally, therefore, the lower-differential-head meters and thin-plate orifices are chosen whenever possible.

When they are inadequate to handle the specific problem at hand, then it is a question of determining which combination of higher head meter, with an orifice or with a flow nozzle, will cost the least and still meet all requirements for a satisfactory installation.

Discussion

S. R. BEITLER.⁸ This paper presents the first discussion of a problem which has been bothering many measurement engineers for a long time and which has not been covered in previous work of this sort, that is, the effect of two upstream disturbances. It is apparent on studying the effect of disturbances on meters that, if the disturbances are some distance apart, they will have a different effect than if they are close together. It has been difficult to get data on the effect of multiple disturbances because of the extremely large number of possible arrangements of these disturbances. This paper represents a start in this direction, and the data that are presented will enable the measurement engineer to determine whether or not it will be possible to make accurate measurements for piping conditions where previous knowledge would indicate that these measurements could not be made.

Attention might be directed to matters such as (a) a definition of the condition which has been called "normally turbulent state of flow;" and (b) the effect of straightening vanes. In some cases the flow in a pipe line may be quite different from others, owing to the effect of pipe roughness and of piping conditions in the line to the meter so that the boundary layer may be considerably thicker for one condition than it is for another. The thickness of this layer undoubtedly has considerable effect on the measurement.

Straightening vanes, if improperly installed, or installed after improper fittings are applied, may increase rather than decrease the length of straight pipe required. It can readily be seen that, if the flow is such that there is a high velocity on one side of the pipe parallel to its axis, the effect on the straightening vanes will be to cause this irregular flow to continue on down the pipe line.

Because of this fact, straightening vanes are at times a hindrance rather than a help in getting better measurement conditions, and considerable judgment is required in deciding whether or not they should be installed.

The nomographic charts which are a part of this paper are certainly an aid in computing measurement problems and their publication should be of great interest to the industry.

W. A. CARTER.⁹ The author is to be commended for his thorough treatment of the subject, and it is recommended that it be printed in pamphlet form in order that it may be put in the hands of piping designers. Such a guide has been needed for a long time in order to avoid the installation of piping systems that are ill-suited to the accurate measurement of fluid flow.

The writer would ask: Are the recommended lengths of straight pipe ahead of orifice plates, flow nozzles, and Venturi tubes dependent upon the Reynolds number of the fluid stream?

W. S. PARDOE.¹⁰ This paper should prove to be of great use to layout engineers.

In his Schedule 8, the author gives in part some deductions from the work of the writer. He did not include the results shown in Figs. 13 and 14, being the effect of two elbows in planes at right angles with and without cross-straightening vanes.

At no point does the author give any values of errors involved if the flowmeter is set with less than the prescribed length of straight pipe ahead of it. Figs. 10 to 14, inclusive, of this discussion give such values for Venturi meters of the Herschel type. They should be reasonably correct for all flow nozzles with throat taps. Note that the cross-straightening vane used in Fig. 14 is quite effective when compared with Fig. 13.

Fig. 15, herewith, shows the effect of vortex flow at various angles on the coefficient of a 2-in. \times 1-in. special Venturi meter. The setup is shown in Fig. 16.

In Fig. 16, a single straightening vane 2 in. \times $\frac{1}{8}$ in. \times 12 in. long removed the vortex and brought the coefficient back to normal for all angles of whirl. Also a vane 2 in. \times $\frac{1}{8}$ in. \times 3 in. long was not entirely effective.

Fig. 17 shows in a dotted line the effect of a partially opened gate valve 2 in. ahead of the Venturi meter. If the distance is increased to 12 in. (6 diam), there is no effect on the coefficient. This is as might be expected for a Venturi ratio $\beta = 0.5$.

Fig. 18 shows that a gate valve may be placed immediately after an 8-in. \times 5-in. Venturi meter (a large ratio β) without in the least affecting the coefficient. The full line shows the normal coefficient, and the points the various openings of the 8-in. valve.

In Fig. 19 is shown the coefficient of the 2-in. \times 1-in. Venturi meter for various angles of whirl plotted from Fig. 15. The coefficient falls as the angle decreases. Also in this figure is shown a similar curve for a 2-in. \times 1-in. orifice. Note that the coefficient rises, becomes normal at 45 deg, and then falls off as does that of the Venturi meter. This is probably due to the centrifugal force enlarging the vena contracta thus getting a greater flow although a lower axial velocity.

Fig. 20 is a test of the Bailey Meter Company and University of Pennsylvania straightening vanes. They are both equally effective in destroying the 50-deg vortex and returning the coefficient of the Venturi meter to normal. It would appear that the latter is the simpler construction.

⁹ Technical Engineer of Power Plants, The Detroit Edison Company, Detroit 26, Mich. Mem. A.S.M.E.

¹⁰ Professor, Department of Civil Engineering, University of Pennsylvania, Philadelphia, Pa.

⁸ Professor of Hydraulic Engineering, Ohio State University, Columbus, Ohio. Mem. A.S.M.E.

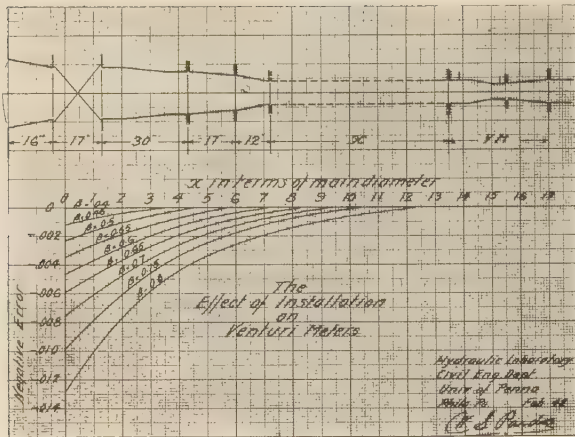


Fig. 10

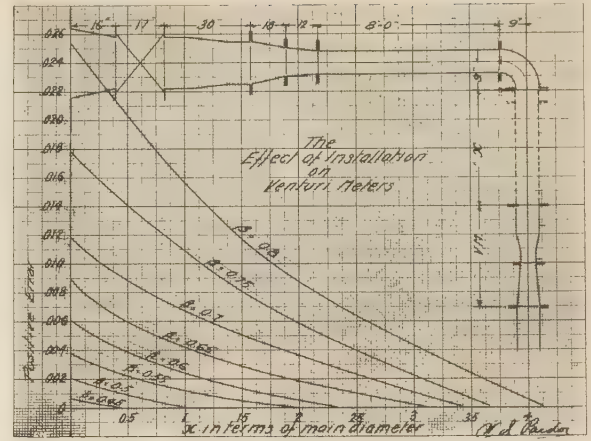


Fig. 12

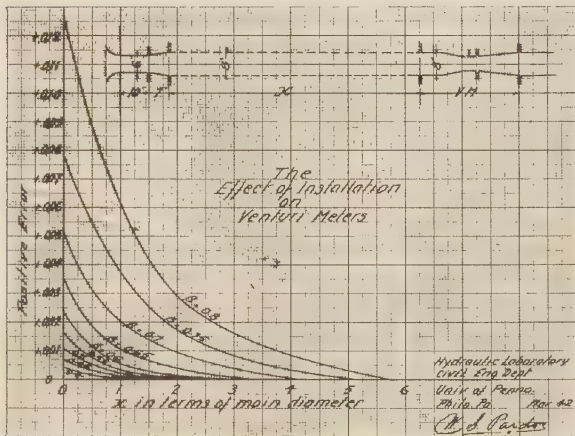


Fig. 11

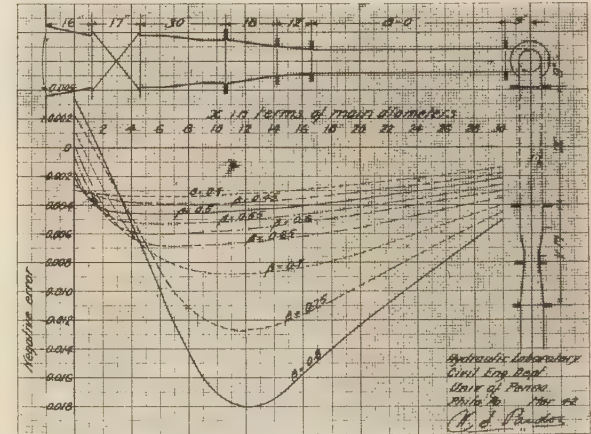


Fig. 13

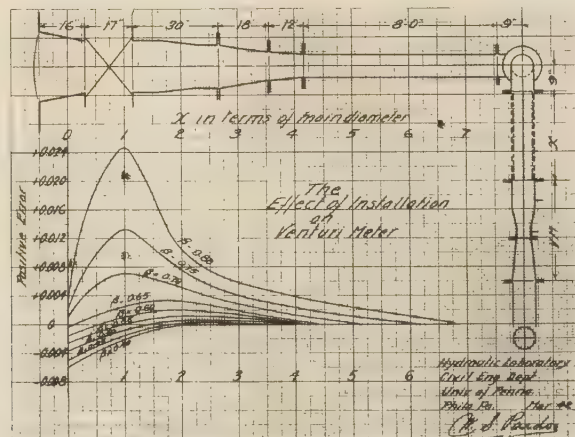


Fig. 14

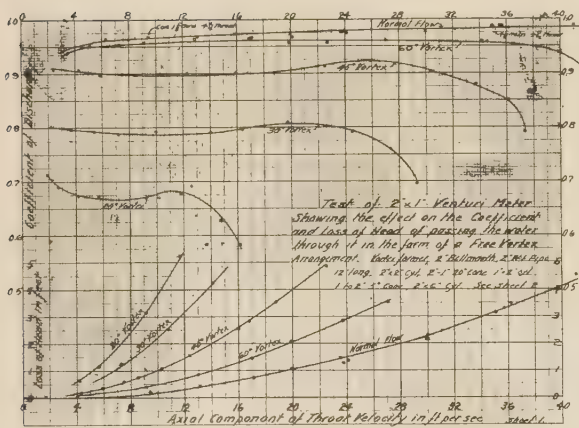


FIG. 15

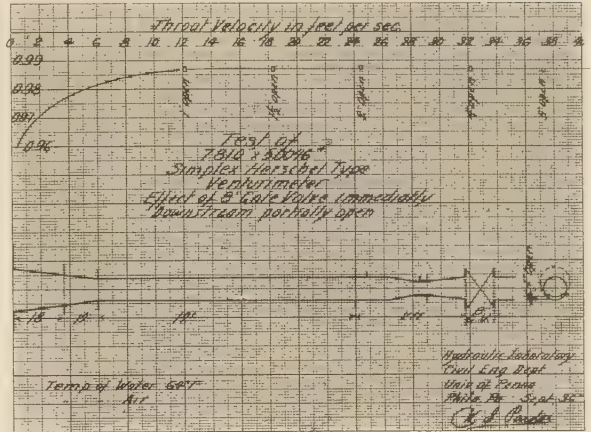


FIG. 18

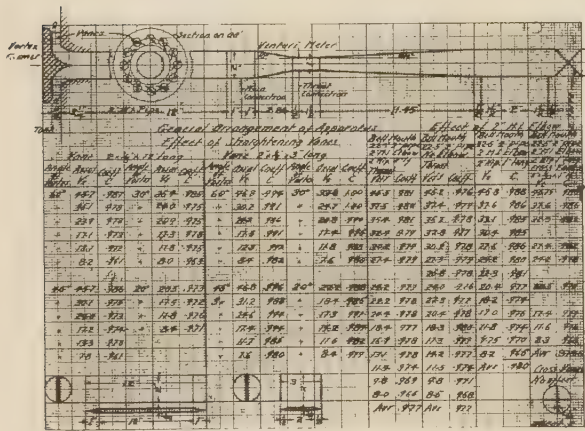


FIG. 16

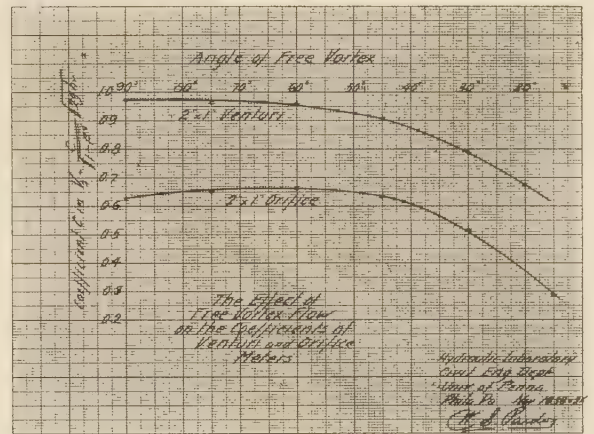


FIG. 19

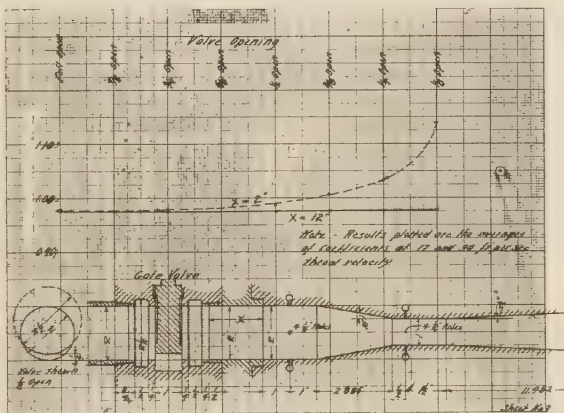


FIG. 17

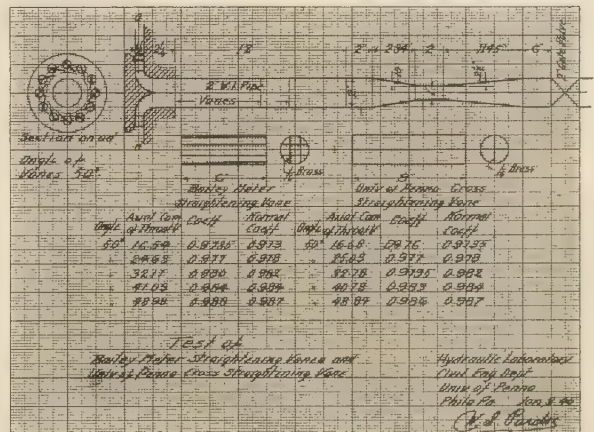


FIG. 20

R. J. S. PIGOTT.¹¹ When the purchaser of a meter buys a Venturi tube, nozzle, or disk orifice, plus a recording secondary instrument of some kind, he is not in any case buying the entire meter but only the primary and secondary elements. He provides the rest of the meter in the piping when he installs it. It cannot be said too often or too emphatically that the accuracy of the meter will be influenced considerably by the character of the piping with which it is associated. It is quite obvious that, although a very considerable amount of money has been spent both by organizations like our own and by individual users and manufacturers, our knowledge of the effect of piping additions is as yet incomplete, and we must work as well as we can with the material that is available. We have advanced a considerable distance in the last 30 years. In the early days after the introduction of orifice meters as a commercial business in this country, there were many cases where an orifice or a nozzle might be placed on the side outlet of a tee. We now know better.

Perhaps it should be said that the approach to the meter should be normal in turbulence and not in any way distorted. Actually there is no change in average turbulence in the approach to a meter with any of the piping systems described. What does happen, however, is that the local turbulences which vary across the section of pipe change their value and their position. Perhaps another way of putting it would be to say that the approach to the meter should have, as nearly as possible, the normal velocity traverse of flow in a straight pipe.

With regard to straightening vanes these have been useful in the majority of cases as an aid to producing normal flow ahead of the meter primary element. Basically their major purpose is to eliminate rotational effects or helical swirls, and theoretically at least they would have little effect in eliminating a distorted velocity traverse such as occurs directly after an elbow. However, any resistance does tend to average out even this type of distortion, and all of the straightening vanes have some friction resistance which is higher than that of the pipe in which they are placed. We have found in particular cases that one of the best devices for suppressing distortion is an eccentric disk orifice placed at the outlet of an elbow causing the disturbance. Obviously, the use of such a device is specific and not general, since offhand the amount of eccentricity required to render the flow symmetrical again cannot be predicted beforehand.

The author's work is a summation of practically all the reliable information we have on the subject, collected from a very wide range of sources. While it is not in the form of a report from the Fluid Meters Committee, it is without doubt the best material available at this time and carries with it the authority of this committee. In time this material will be, without doubt, incorporated in the reports of the committee.

AUTHOR'S CLOSURE

The author deeply appreciates the valuable contributions

¹¹ Chief Engineer, Gulf Research and Development Company, Pittsburgh, Pa. Fellow A.S.M.E.

made to this paper in the several discussions offered. Both Professor Beitler and Mr. Pigott emphasize the need of having more data on piping arrangements; a thought which is entirely in accord with that expressed by the author in his introductory remarks. Manifestly, the data in this paper are but the beginning of a compilation which must be greatly expanded before the needs of industry as a whole can be satisfied. For this reason the author is particularly grateful to Professor Pardoe for the additional data on Venturis with particular regard to the use of partially opened gate valves both preceding and following the Venturi. It is sincerely hoped that much additional data of a similar nature will be forthcoming in the near future.

Professor Beitler is correct in his statement that straightening vanes may under certain conditions be more of a hindrance than a help, particularly where the velocity traverse in the pipe shows distorted flow on one side of the pipe as compared with the other. The most effective use of straightening vanes is to eliminate helical flows or whirls which are caused by combinations of bends or turns preceding the primary element.

It is believed that the second paragraph and, in particular, the last sentence thereof of Mr. Pigott's discussion, quite aptly answers the request of Professor Beitler for a better definition of normally turbulent flow.

In answer to Mr. Carter's question of the possible effect of Reynolds numbers on the recommended length of straight pipe, the author can only say that all the explorations which have come to his attention have been made within a rather narrow band of relatively high Reynolds numbers. There was no appreciable change in the lengths of piping required within this range. As to what might happen at ranges beyond this band—as, for example, within the viscous-flow range—the author would hesitate to predict with any degree of certainty.

Professor Pardoe points out that no errors were given which result when the prescribed lengths of straight pipe were not used. Such errors varied with the type and size of primary element used, and with the piping arrangement. To have shown such variations in detail would have required a separate graph of every diameter ratio size and type of primary element, and for every piping arrangement specified. Quite obviously, this would have involved the inclusion of far too great a quantity of data in this particular paper. The author would be glad to discuss quantitative errors found for shorter than recommended lengths of piping for any specific case in mind, within the limit of the available experimental data, if such inquiry is directed to him.

The type of straightening vane shown in Fig. 2 is essentially the form prescribed in the A.S.M.E.-A.G.A. 1935 Report and which has been found quite satisfactory through a number of years' service. Obviously, Professor Pardoe's cross type of vane is simpler, and if it were demonstrated to be as efficient for all types of fluids and with all types of primary elements as it is with water and with Venturis, it would be the type to use. More study should be made of this particular type of straightening vane before changing the recommendations now in force.

Water-Hammer Analysis by the Laplace-Mellin Transformation

By G. R. RICH,¹ KNOXVILLE, TENN.

The author supplements the pioneer work of Prof. F. M. Wood in applying operational methods to the study of water-hammer phenomena. The Heaviside calculus is replaced by the Laplace-Mellin transformation together with the elementary theory of functions of a complex variable. This substitution facilitates interpretation of a much wider range of operators, is believed to be better adapted to problems starting from a steady-state system in motion, and permits working directly with total pressures and velocities instead of surge pressures and velocities. This third feature operates to eliminate ambiguity concerning reflection coefficients at junction points in branched-conduit problems. When the effect of friction is not included, results are given in the form of simple trigonometric series of rapid convergence. When the abscissas of the two terminal sections of the conduit are inserted in these formulas, the resulting expressions are, in many cases, Fourier representations in the time variable of well-known periodic step or saw-tooth functions. In such instances, almost no computation work is required; it is unnecessary to sum the series, as the value of the summation may be taken at a single reading from a graph of the function, one plot of such a function serving for all particular cases within its domain. In cases where the effect of friction is included, a standard table of Bessel functions, used in conjunction with the formulas developed, affords easy and comparatively rapid solution.

INTRODUCTION

THE role of operational methods in water-hammer analysis² has been ably defined by Professor Wood, to whom the author is indebted not only for the general features of the application, but also for the basic hydraulic principles of representing conduit friction by an equivalent linear law with respect to the velocity, and of prescribing the conduit discharge velocity rather than the gate motion as one of the given boundary conditions. Both of these deviations from conventional practice result from the inability of either operational method to solve any but linear differential equations. At first thought, the second of these two limitations appears to impose a serious penalty on the operational approach; but on the basis of the examples given, the author is inclined to regard specification of the efflux velocity as a more rational and flexible basis for over-all design.

Because of space limitations and the current availability of several outstanding books^{3,4,5,6} written particularly for engineers,

¹ Chief Design Engineer, Tennessee Valley Authority. Mem. A.S.M.E.

² "The Application of Heaviside's Operational Calculus to the Solution of Problems in Water Hammer," by F. M. Wood, Trans. A.S.M.E., vol. 59, 1937, pp. 707-713.

³ "Operational Methods in Applied Mathematics," by H. S. Carslaw and J. C. Jaeger, Oxford University Press, New York, N. Y., 1941.

Contributed by the Hydraulic Division and presented at the Annual Meeting, New York, N. Y., Nov. 27-Dec. 1, 1944, of THE AMERICAN SOCIETY OF MECHANICAL ENGINEERS.

NOTE: Statements and opinions advanced in papers are to be understood as individual expressions of their authors and not those of the Society.

the purely mathematical manipulation will be given in skeleton form, and references will be made to these texts. The first book will be designated in the notes simply as Carslaw³ and the second as McLachlan.⁴ However, in using these works in combination, a word of caution is necessary. Carslaw states the basic theorem as follows

If

$$\bar{x}(p) = \int_0^{\infty} \bar{e}^{pt} x(t) dt \quad R(p) > 0 \quad (\text{Carslaw p. 71})$$

then

$$x(t) = \frac{1}{2\pi i} \int_{\gamma-i\infty}^{\gamma+i\infty} e^{\lambda t} \bar{x}(\lambda) d\lambda$$

McLachlan's statement of the same theorem is as follows

If

$$\phi(p) = p \int_0^{\infty} \bar{e}^{pt} f(t) dt \quad R(p) > 0 \quad (\text{McLachlan p. 116})$$

then

$$f(t) = \frac{1}{2\pi i} \int_{Br_1}^{\infty} \frac{e^{zt} \phi(z)}{z} dz$$

This means that all the operators, $\bar{x}(p)$, tabulated in Carslaw will be less than the corresponding operators tabulated in McLachlan by a factor p . McLachlan's reason for adopting the second form is that it makes the Heaviside unit function equal to the value 1, as compared with $1/p$ for the first form. The operators tabulated in Doetsch and in Churchill are in the same form as those given in Carslaw. In this article the Carslaw notation and statement of the inversion theorem will be employed. The section on impulse functions given in McLachlan is particularly valuable, but in applying the impulse charts to the Carslaw form, particular care is necessary to avoid confusion regarding this factor p . McLachlan's treatment of the practical method of determining residues also is excellent, while Churchill gives an exceptionally clear treatment of the basic theory.

NOTATION

The derivation of the basic differential equations is given in admirable form by Professor Wood and will not be repeated. The same notation will be retained in this paper, with the exception that no relation whatever is postulated between p and the operator $\frac{d}{dt}$; p is considered simply as an inversion parameter in the basic Laplace-Mellin theorem.

⁴ "Complex Variable and Operational Calculus," by N. W. McLachlan, Cambridge University Press, The Macmillan Company, New York, N. Y., 1939.

⁵ "Modern Operational Mathematics in Engineering," by Ruel V. Churchill, McGraw-Hill Book Company, Inc., New York, N. Y., 1944.

⁶ "Theorie und Anwendung der Laplace Transformation," by Gustav Doetsch, Dover Publications, New York, N. Y., 1943 (formerly published by Julius Springer, Berlin, 1937).

D = diameter of pipe, ft
 L = length of pipe, ft
 A = area of pipe, sq ft
 P = total pressure (surge plus steady state), psf
 V = total velocity (surge plus steady state), fps; positive in positive direction of x
 x = distance of section along axis of pipe, ft; measured from origin at reservoir
 K = volume modulus of compression of water, ft units
 b = thickness of pipe walls, ft
 E = modulus of elasticity of pipe wall, ft units
 f = friction coefficient
 w = weight of unit volume of water, lb per cu ft
 g = acceleration of gravity, ft per sec per sec
 k_f = friction factor of linear approximation to friction pressure

$$W = \frac{w}{g}$$

$$Q = \frac{1}{K} + \frac{D}{bE}$$

p = inversion parameter

t = time variable, sec

λ = complex variable in Bromwich-Mellin complex inversion integral (Carslaw p. 71)

$$a = \frac{1}{\sqrt{WQ}} = \text{wave velocity, fps}$$

$$\bar{V} = \text{Laplace transform of } V = \int_0^\infty e^{pt} V dt$$

$$\bar{P} = \text{Laplace transform of } P = \int_0^\infty e^{pt} P dt$$

$\int_{B_{r_2}}$ denotes integration along second alternative Bromwich contour. This path consists of a straight line from $-i\infty$ to $+i\infty$ (displaced a sufficient distance γ to the right of the axis of imaginaries to include all singularities of the integrand) and a circle of infinite radius centered at the origin to complete the contour. The only singularities of the integrands occurring in this paper are poles; there are no branch points. Consequently, integration along B_{r_2} is equal to $2\pi i$ times the summation of residues at the poles.

F = friction-pressure-loss coefficient per unit length of pipe and per unit cross section of water area in pipe. This factor is to be applied to the first power of the velocity and is proportioned to give the best approximation to the conventional loss of

$$\frac{4fw}{D} \times \frac{V^2}{2g} \text{ by means of the assumption}$$

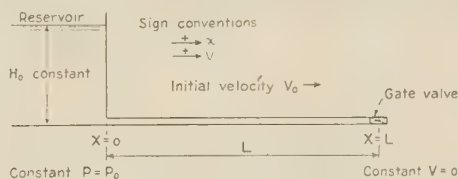
$$FV = \frac{2fwV^2}{gD} = \frac{2fw}{gD} (k_f V_m) V = \left(\frac{2fw}{gD} k_f V_m \right) V$$

EXAMPLE 1

The elementary case of the simple conduit, with instantaneous gate closure and with friction neglected, is included as an introduction to the use of the Laplace-Mellin method and the step function⁷ diagram of the Fourier series⁸ to avoid the computational labor of summing the infinite series. When the abscissas

EXAMPLE 1

SIMPLE CONDUIT - FRICTION NEGLECTED - INSTANTANEOUS GATE CLOSURE



$$a^2 \frac{\partial^2 P}{\partial x^2} = \frac{\partial^2 P}{\partial t^2} \quad (1)$$

Multiply through by e^{-pt} and integrate from 0 to ∞ : {Carslaw p. 143}

$$a^2 \frac{\partial^2}{\partial x^2} \int_0^\infty e^{pt} P dt = \int_0^\infty e^{pt} \frac{\partial}{\partial t} \left(\frac{\partial P}{\partial t} \right) dt = \int_0^\infty e^{pt} \frac{\partial}{\partial t} \left(\frac{\partial P}{\partial t} \right) dt$$

$$a^2 \frac{\partial^2}{\partial x^2} \bar{P} = \left[e^{pt} \left(\frac{\partial P}{\partial t} \right) \right]_0^\infty + p \left[e^{pt} P \right]_0^\infty + p^2 \int_0^\infty e^{pt} P dt$$

$$= - \left[\frac{\partial P}{\partial t} \right]_{t=0} - p \left[P \right]_{t=0} + p^2 \bar{P} - 0 - p P_0 + p^2 \bar{P}$$

$$\frac{\partial^2 \bar{P}}{\partial x^2} - \frac{p^2 \bar{P}}{a^2} + \frac{p P_0}{a^2} = 0$$

$$\text{Solving } \bar{P} = A \cosh \frac{px}{a} + B \sinh \frac{px}{a} + \frac{P_0}{p} \quad (2)$$

$$- \frac{\partial \bar{P}}{\partial x} = W \frac{\partial V}{\partial t} \quad (3)$$

Multiply through by e^{-pt} and integrate from 0 to ∞

$$- \frac{\partial}{\partial x} \int_0^\infty e^{pt} P dt = W \int_0^\infty e^{pt} \frac{\partial V}{\partial t} dt = W \int_0^\infty e^{pt} \frac{\partial V}{\partial t} dt$$

$$- \frac{\partial \bar{P}}{\partial x} = \left\{ \left[e^{pt} V \right]_0^\infty + p \int_0^\infty e^{pt} V dt \right\} W$$

$$- \frac{\partial \bar{P}}{\partial x} = \left\{ - \left[V \right]_{t=0} + p \bar{V} \right\} W = - W V_0 + W p \bar{V}$$

$$- \frac{\partial \bar{P}}{\partial x} = - W V_0 + W p \bar{V} \quad (4)$$

Boundary Conditions: When $x=0$, $P=P_0$ and $\bar{P} = \int_0^\infty e^{pt} P_0 dt = \frac{P_0}{p}$, so $A=0$

When $x=L$, $V=0$ and $\bar{V} = \int_0^\infty e^{pt} V_0 dt = \frac{V_0}{p}$

$$\text{From (2) and (4)} \quad B = \frac{W V_0}{p \cosh \frac{pL}{a}}$$

$$P = \frac{P_0}{2\pi i} \int_{B_{r_2}} \frac{e^{\lambda t} d\lambda}{\lambda} + \frac{W V_0}{2\pi i g} \int_{B_{r_2}} \frac{e^{\lambda t} \sinh \left(\frac{\lambda x}{a} \right) d\lambda}{\lambda \cosh \left(\frac{\lambda L}{a} \right)} \quad (5)$$

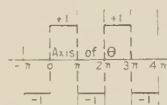
$$V = \frac{V_0}{2\pi i} \int_{B_{r_2}} \frac{e^{\lambda t} d\lambda}{\lambda} - \frac{V_0}{2\pi i} \int_{B_{r_2}} \frac{e^{\lambda t} \cosh \left(\frac{\lambda x}{a} \right) d\lambda}{\lambda \cosh \left(\frac{\lambda L}{a} \right)} \quad (6)$$

$$P = P_0 + \frac{W V_0}{g} \frac{4}{\pi} \sum_{n=1}^{\infty} \frac{(-1)^{n-1}}{(2n-1)} \sin \frac{(2n-1)\pi at}{2L} \sin \frac{(2n-1)\pi x}{2L} \quad (7)$$

$$V = V_0 \frac{4}{\pi} \sum_{n=1}^{\infty} \frac{(-1)^{n-1}}{(2n-1)} \cos \frac{(2n-1)\pi at}{2L} \cos \frac{(2n-1)\pi x}{2L} \quad (8)$$

For P

When $x=L$ (at gate) $\frac{4}{\pi} \sum$ is given by:



Step function $y = \frac{4}{\pi} \left(\sin \theta + \frac{1}{3} \sin 3\theta + \frac{1}{5} \sin 5\theta \right)$

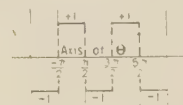
$$\theta = \frac{\pi at}{2L}$$

$y=0$ at dotted lines

Reference Bromwich p. 357

For V

When $x=0$ (at reservoir) $\frac{4}{\pi} \sum$ is given by:



Step function $y = \frac{4}{\pi} \left(\cos \theta - \frac{1}{3} \cos 3\theta + \frac{1}{5} \cos 5\theta \right)$

$$\theta = \frac{\pi at}{2L}$$

$x=0$ for V , and $x=L$ for P , together with the time t , are designated, the value of the summation is given by the diagrams and the values of P and V follow immediately. For values of intermediate sections the series will be found to converge rapidly. It will also be found that the functions of the higher multiple

⁷ "An Introduction to the Theory of Infinite Series," by T. J. I'a Bromwich, The Macmillan Company, New York, N. Y., 1942, p. 357.

⁸ "Fourier Series and Spherical Harmonics," by W. E. Byerly, Ginn & Company, 1893.

CHART FOR
EXAMPLE 1

CONDUIT ——— { VELOCITY $V_0 = 12' / \text{sec}$
DIAMETER $D = 15'$
LENGTH $L = 5000'$

PRESSURE WAVE ——— { VELOCITY $a = 3000' / \text{sec}$
TIME $\frac{2L}{a} = 3.33 \text{ sec}$

INSTANTANEOUS CLOSURE:

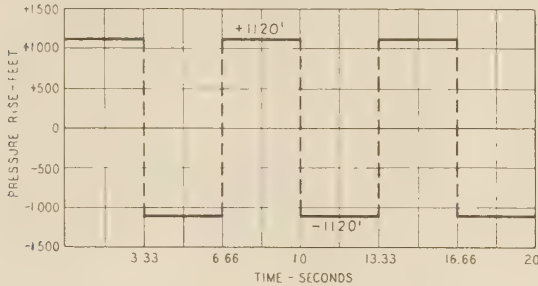
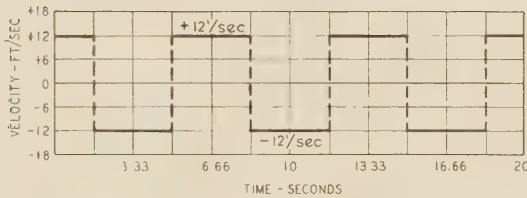
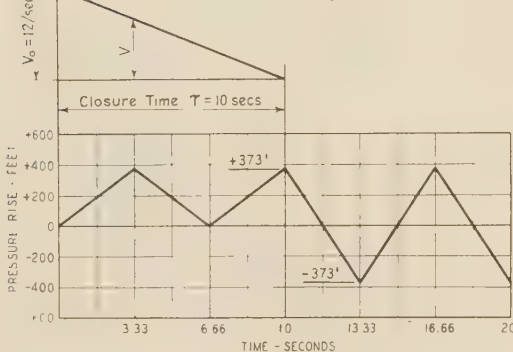
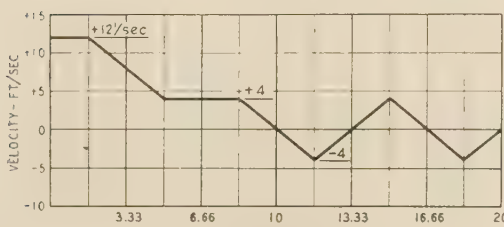

 PRESSURE RISE AT GATE
($x = L$)

 VELOCITY AT RESERVOIR
($x = 0$)

 CHART FOR
EXAMPLE 2

CONDUIT - SAME AS IN EXAMPLE 1

PRESSURE WAVE ——— { VELOCITY $a = 3000' / \text{sec}$
TIME $\frac{2L}{a} = 3.33 \text{ sec}$


 PRESSURE RISE AT GATE
($x = L$)

 VELOCITY AT RESERVOIR
($x = 0$)

EXAMPLE 2

 SIMPLE CONDUIT - FRICTION NEGLECTED
VALVE CLOSURE REDUCING VELOCITY LINEARLY TO ZERO

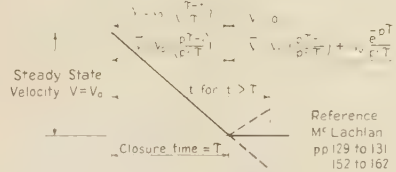
 From Example 1 Eq (2) $\dot{P} = B \sinh \frac{px}{a} + \frac{P_0}{p}$

 From Example 1, Eq (4) - $\frac{\partial \bar{P}}{\partial x} = -WV_0 + W_0 \bar{V}$

 Boundary Condition When $x=L$ $V=V_0 \left(\frac{T-t}{T} \right)$; T = closure time

$$P_0 = \frac{W_0 V_0}{p} \left(1 - \frac{p}{p^2 T} \right) \quad (3)$$

$$P = \frac{W_0 V_0}{p} \left(1 - \frac{p}{p^2 T} \right) \left(\frac{e^{-px/a}}{cosh \frac{pL}{a}} \right) \quad (4)$$


 First Stage $0 < t < T$

$$B = \frac{W_0 V_0}{p} \left\{ 1 - \frac{p}{p^2 T} \left(\frac{e^{-px/a}}{cosh \frac{pL}{a}} \right) \right\}$$

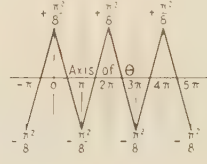
$$P = \frac{P_0}{2\pi i} \int_{Br_2} \frac{e^{\lambda t} d\lambda}{\lambda} + \frac{W_0 V_0}{2\pi i g T} \int_{Br_2} \frac{e^{\lambda t} \sinh \frac{\lambda x}{a} d\lambda}{\lambda^2 \cosh \frac{\lambda L}{a}} \quad \text{Carslaw p138} \quad (5)$$

$$V = \frac{V_0}{2\pi i} \int_{Br_2} \frac{e^{\lambda t} d\lambda}{\lambda} - \frac{V_0}{2\pi i T} \int_{Br_2} \frac{e^{\lambda t} \cosh \frac{\lambda x}{a} d\lambda}{\lambda^2 \cosh \frac{\lambda L}{a}} \quad (6)$$

$$P = P_0 + \frac{W_0 V_0}{g T} \left\{ \frac{x}{a} - \frac{8L}{\pi^2 a} \sum_{n=1}^{\infty} \frac{(-1)^{n-1}}{(2n-1)^2} \cos \frac{(2n-1)\pi a}{2L} \sin \frac{(2n-1)\pi x}{2L} \right\} \quad (7)$$

$$V = V_0 - \frac{V_0}{T} \left\{ t - \frac{8L}{\pi^2 a} \sum_{n=1}^{\infty} \frac{(-1)^{n-1}}{(2n-1)^2} \sin \frac{(2n-1)\pi a}{2L} \cos \frac{(2n-1)\pi x}{2L} \right\} \quad (8)$$

 For P

 When $x=L$ (at gate) Σ is given by:

 Values of $y = \cos \theta + \frac{1}{3^2} \cos 3\theta + \frac{1}{5^2} \cos 5\theta$

 For $\theta = -\pi$ to 0 $y = \frac{8}{\pi^2} (\pi^2 + 2\theta)$

 For $\theta = 0$ to π $y = \frac{8}{\pi^2} (\pi^2 - 2\theta)$
 $\theta = \frac{\pi a t}{2L}$

Reference Bromwich p 360

 Second Stage $t > T$

Zone of "Afterwaves"

$$B = \frac{W_0 V_0}{g} \left\{ 1 - \frac{p}{p^2 T} \left(\frac{e^{-px/a}}{cosh \frac{pL}{a}} \right) \right\} \quad (9)$$

$$P = \frac{P_0}{2\pi i} \int_{Br_2} \frac{e^{\lambda t} d\lambda}{\lambda} + \frac{W_0 V_0}{2\pi i g T} \int_{Br_2} \frac{e^{\lambda t} \sinh \frac{\lambda x}{a} d\lambda}{\lambda^2 \cosh \frac{\lambda L}{a}} - \frac{W_0 V_0}{2\pi i g T} \int_{Br_2} \frac{e^{\lambda(t-T)} \sinh \frac{\lambda x}{a} d\lambda}{\lambda^2 \cosh \frac{\lambda L}{a}} \quad (10)$$

$$V = \frac{V_0}{2\pi i} \int_{Br_2} \frac{e^{\lambda t} d\lambda}{\lambda} - \frac{V_0}{2\pi i T} \int_{Br_2} \frac{e^{\lambda t} \cosh \frac{\lambda x}{a} d\lambda}{\lambda^2 \cosh \frac{\lambda L}{a}} + \frac{V_0}{2\pi i T} \int_{Br_2} \frac{e^{\lambda(t-T)} \cosh \frac{\lambda x}{a} d\lambda}{\lambda^2 \cosh \frac{\lambda L}{a}} \quad (11)$$

$$P = P_0 - \frac{W_0 V_0}{g T} \left\{ \frac{x}{a} - \frac{8L}{\pi^2 a} \sum_{n=1}^{\infty} \frac{(-1)^{n-1}}{(2n-1)^2} \cos \frac{(2n-1)\pi a}{2L} \sin \frac{(2n-1)\pi x}{2L} \right\} \quad (12)$$

$$V = V_0 + \frac{V_0}{T} \left\{ (t-T) - \frac{8L}{\pi^2 a} \sum_{n=1}^{\infty} \frac{(-1)^{n-1}}{(2n-1)^2} \sin \frac{(2n-1)\pi a}{2L} \cos \frac{(2n-1)\pi x}{2L} \right\} \quad (13)$$

angles have the same numerical values as the lower orders, and that the only variations are a change in algebraic sign and division by a progressively larger numerical coefficient.

EXAMPLE 2

This case is to be considered as an intermediate step in the progressive development of the theory and as an introduction to Example 3. It is emphatically not advocated as an optimum type of closure but is of interest in studying the effect of various modes of extinguishing discharge upon the shape of the water-hammer curve. Its salient feature is the method of formulating the boundary condition at the gate. The conventional procedure, using the graphical or arithmetic integration methods, is to specify the gate opening, discharge coefficient, and time rate of gate closure, and to calculate V at the outlet as part of the water-hammer computation, proportional to $\sqrt{H_0 + h}$, where h is the water-hammer head. In this example the efflux velocity and its time variation are prescribed. The resultant pressures and velocities in the conduit are then determined without reference to the gate characteristics. With the head at the outlet thus established by the water-hammer calculation and the outlet velocity prescribed in advance, the design and rate of operation of the gate, pump, or turbine to conform are handled as a separate problem. The relation of the head to the discharge, whether proportional to $\sqrt{H_0 + h}$ or some more suitable relation, may then be selected according to the judgment of the valve designer, preferably on the basis of extensive tests on the particular type of outlet mechanism. Discussion of this mode of attack will be extended under Example 3.

In applying the formulas of this example to pumps instead of turbines, it is important to remember that the initial steady-state velocity is opposite in direction to positive x and should therefore enter the formulas as $-V_0$ instead of $+V_0$. The same principle is to be applied in Examples 3 and 4.

EXAMPLE 3

The hydraulic concept underlying this example is based on an earlier article by S. Logan Kerr,⁹ in which attention is directed to the possibility of securing any desired shape of water-hammer curve by properly varying the efflux velocity. One practical mechanical means of accomplishing this result in turbine installations is mentioned.

Example 3 indicates the method of synthesizing nonuniform outlet-velocity rates to approach any characteristic shape of water-hammer curve that may be desired. For the sake of simplicity in explanation of the method, a two-segment rate is discussed; but three or more segments or any other suitable continuous curve may be substituted if desired. The mode of attack is to select trial values of V_0 , τ , V_β , and β , and continue the trial-and-error process until a satisfactory form of water-hammer diagram is obtained. V_β and β may be selected so as to lie either above or below the dotted line representing uniform rate of velocity decrease; the formulas given will be found correct for either case.

With the outlet velocity prescribed in advance, and the pressure at the outlet established by the water-hammer calculations, the valve- or outlet-mechanism design and rate of operation to give the prescribed velocity step-curve is segregated as a second separate problem in which the designer is afforded complete latitude to exercise his best judgment regarding the head-discharge relation ($\sqrt{H_0 + h}$ or otherwise) and to use whatever relation

EXAMPLE 3

SIMPLE CONDUIT - FRICTION NEGLECTED WITH VARIABLE RATE OF EXTINGUISHING GATE DISCHARGE VELOCITY

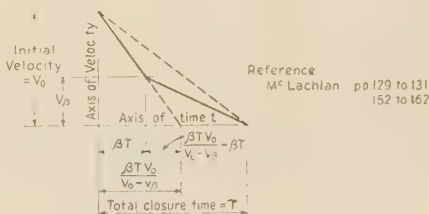
Boundary Conditions When $x = L$ (at gate)

$$\text{For } t = 0 \text{ to } t = \beta T: \quad V = (V_0 - V_\beta) \left(\frac{\beta T - t}{\beta T} \right) + V_\beta$$

$$\bar{V} = \frac{V_0}{\beta} - \frac{(V_0 - V_\beta)}{\beta^2 \beta T} \quad (1)$$

$$\text{For } t = \beta T \text{ to } t = T: \quad V = V_\beta - V_\beta \left(\frac{t - \beta T}{T - \beta T} \right) = V_\beta \left(\frac{T - t}{T - \beta T} \right)$$

$$\bar{V} = \frac{V_0}{\beta} - \frac{(V_0 - V_\beta)}{\beta^2 \beta T} + e^{\beta A T} \frac{(V_0 - V_\beta)}{\beta^2 \beta T} - \frac{e^{\beta A T} V_\beta}{\beta^2 (T - \beta T)} \quad (2)$$



Assumed Outlet Velocity Rate

First Stage $0 < t < \beta T$

$$B = \frac{w a}{g} (V_0 - V_\beta) \frac{1}{\beta^2 \beta T \cosh \frac{p L}{a}} \quad (3)$$

$$P = \frac{P_0}{2 \pi i} \int_{\beta T}^{\frac{1}{\lambda}} \frac{e^{\lambda t} d \lambda}{\lambda} + \frac{w a (V_0 - V_\beta)}{2 \pi i \beta T} \int_{\beta T}^{\frac{1}{\lambda}} \frac{e^{\lambda t} \sinh \frac{\lambda x}{a} d \lambda}{\lambda^2 \cosh \frac{\lambda L}{a}} \quad (4)$$

$$V = \frac{V_0}{2 \pi i} \int_{\beta T}^{\frac{1}{\lambda}} \frac{e^{\lambda t} d \lambda}{\lambda} - \frac{(V_0 - V_\beta)}{2 \pi i \beta T} \int_{\beta T}^{\frac{1}{\lambda}} \frac{e^{\lambda t} \cosh \frac{\lambda x}{a} d \lambda}{\lambda^2 \cosh \frac{\lambda L}{a}} \quad (5)$$

$$P = P_0 + \frac{w a}{g} (V_0 - V_\beta) \left\{ \frac{x}{a} - \frac{8 L}{\pi^2 a} \sum_{n=1}^{\infty} \frac{(-1)^{n-1}}{(2n-1)^2} \cos \frac{(2n-1) \pi x}{2L} \sin \frac{(2n-1) \pi \beta T}{2L} \right\} \quad (6)$$

$$V = V_0 - \frac{(V_0 - V_\beta)}{\beta T} \left\{ t - \frac{8 L}{\pi^2 a} \sum_{n=1}^{\infty} \frac{(-1)^{n-1}}{(2n-1)^2} \sin \frac{(2n-1) \pi x}{2L} \cos \frac{(2n-1) \pi \beta T}{2L} \right\} \quad (7)$$

For Values of Σ for P when $x = L$ and for V when $x = 0$ refer to diagrams Example 2

Second Stage

For $t = \beta T$ to $t = T$

$$B = \frac{w a}{g} \left\{ \frac{V_0 - V_\beta}{\beta^2 \beta T \cosh \frac{p L}{a}} - \frac{e^{\beta A T} (V_0 - V_\beta)}{\beta^2 \beta T \cosh \frac{p L}{a}} + \frac{e^{\beta A T} V_\beta}{\beta^2 (T - \beta T) \cosh \frac{p L}{a}} \right\} \quad (8)$$

$$P = \frac{P_0}{2 \pi i} \int_{\beta T}^{\frac{1}{\lambda}} \frac{e^{\lambda t} d \lambda}{\lambda} + \frac{w a (V_0 - V_\beta)}{2 \pi i \beta T} \int_{\beta T}^{\frac{1}{\lambda}} \frac{e^{\lambda t} \sinh \frac{\lambda x}{a} d \lambda}{\lambda^2 \cosh \frac{\lambda L}{a}} - \frac{w a (V_0 - V_\beta)}{2 \pi i \beta T} \int_{\beta T}^{\frac{1}{\lambda}} \frac{e^{\lambda t} \cosh \frac{\lambda x}{a} d \lambda}{\lambda^2 \cosh \frac{\lambda L}{a}} + \frac{w a V_\beta}{2 \pi i (T - \beta T)} \int_{\beta T}^{\frac{1}{\lambda}} \frac{e^{\lambda t} \sinh \frac{\lambda x}{a} d \lambda}{\lambda^2 \cosh \frac{\lambda L}{a}} \quad (9)$$

$$V = \frac{V_0}{2 \pi i} \int_{\beta T}^{\frac{1}{\lambda}} \frac{e^{\lambda t} d \lambda}{\lambda} - \frac{(V_0 - V_\beta)}{2 \pi i \beta T} \int_{\beta T}^{\frac{1}{\lambda}} \frac{e^{\lambda t} \cosh \frac{\lambda x}{a} d \lambda}{\lambda^2 \cosh \frac{\lambda L}{a}} + \frac{(V_0 - V_\beta)}{2 \pi i \beta T} \int_{\beta T}^{\frac{1}{\lambda}} \frac{e^{\lambda t} \sinh \frac{\lambda x}{a} d \lambda}{\lambda^2 \cosh \frac{\lambda L}{a}} - \frac{V_\beta}{2 \pi i (T - \beta T)} \int_{\beta T}^{\frac{1}{\lambda}} \frac{e^{\lambda t} \cosh \frac{\lambda x}{a} d \lambda}{\lambda^2 \cosh \frac{\lambda L}{a}} \quad (10)$$

$$P = P_0 + \frac{w a (V_0 - V_\beta)}{g \beta T} \left\{ -\frac{8 L}{\pi^2 a} \sum_{n=1}^{\infty} \frac{(-1)^{n-1}}{(2n-1)^2} \sin \frac{(2n-1) \pi x}{2L} \cos \frac{(2n-1) \pi \beta T}{2L} \right. \\ \left. + \frac{8 L}{\pi^2 a} \sum_{n=1}^{\infty} \frac{(-1)^{n-1}}{(2n-1)^2} \sin \frac{(2n-1) \pi x}{2L} \cos \frac{(2n-1) \pi (T - \beta T)}{2L} \right\} \\ + \frac{w a V_\beta}{g (T - \beta T)} \left\{ \frac{x}{a} - \frac{8 L}{\pi^2 a} \sum_{n=1}^{\infty} \frac{(-1)^{n-1}}{(2n-1)^2} \cos \frac{(2n-1) \pi x}{2L} \sin \frac{(2n-1) \pi (T - \beta T)}{2L} \right\} \quad (11)$$

$$V = V_0 - \frac{(V_0 - V_\beta)}{\beta T} \left\{ t - \frac{8 L}{\pi^2 a} \sum_{n=1}^{\infty} \frac{(-1)^{n-1}}{(2n-1)^2} \cos \frac{(2n-1) \pi x}{2L} \sin \frac{(2n-1) \pi \beta T}{2L} \right. \\ \left. + \frac{8 L}{\pi^2 a} \sum_{n=1}^{\infty} \frac{(-1)^{n-1}}{(2n-1)^2} \cos \frac{(2n-1) \pi x}{2L} \sin \frac{(2n-1) \pi (T - \beta T)}{2L} \right\} \\ - \frac{V_\beta}{\beta T} \left\{ (T - \beta T) - \frac{8 L}{\pi^2 a} \sum_{n=1}^{\infty} \frac{(-1)^{n-1}}{(2n-1)^2} \sin \frac{(2n-1) \pi x}{2L} \cos \frac{(2n-1) \pi \beta T}{2L} \right\} \quad (12)$$

For Values of Σ for P when $x = L$ and for V when $x = 0$ refer to diagrams Example 2 with $\theta = \pi a(t - \beta T)$ as required

Extension for "afterwaves" may be developed by using shift operator $e^{-\beta A T}$ second branch at $(t - T)$ similar to procedure employed in Example 2

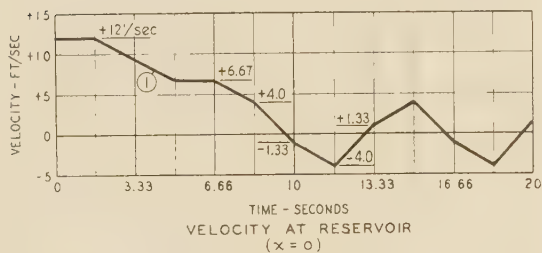
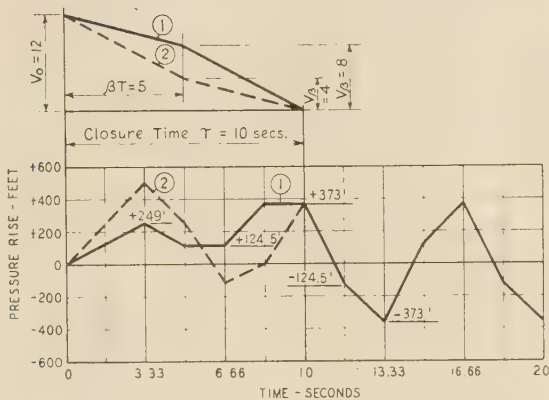
⁹ "New Aspects of Maximum Pressure Rise in Closed Conduits," by S. Logan Kerr, Trans. A.S.M.E., vol. 51, 1929, paper HYD-51-3; subheading on "Ideal Gate Motion," p. 21.

CHART FOR
EXAMPLE 3

CONDUIT - SAME AS IN EXAMPLE 1

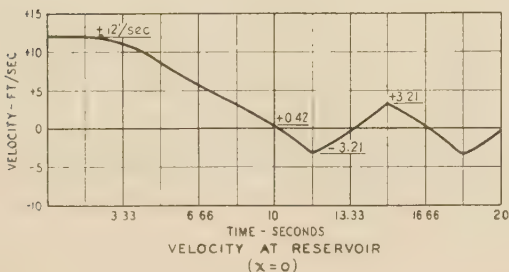
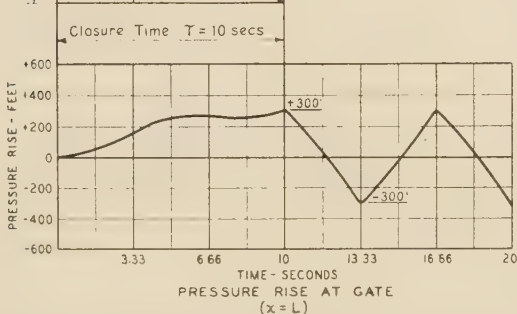
 PRESSURE WAVE — VELOCITY $a = 3000'$ /sec
TIME $\frac{2L}{a} = 3.33$ sec

 VELOCITIES: $V_0 = 12'$ /sec $V_B = 8'$ /sec $V_0 - V_B = 4'$ /sec

 TIME: $T = 10$ sec $\beta T = 5$ sec

 CHART FOR
EXAMPLE 4

CONDUIT - SAME AS IN EXAMPLE 1

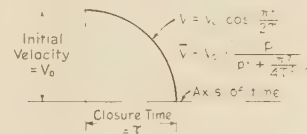
 PRESSURE WAVE — VELOCITY $a = 3000'$ /sec
TIME $\frac{2L}{a} = 3.33$ sec

 $V = V_0 \cos \frac{\pi t}{2T}$
Closure Time $T = 10$ secs


EXAMPLE 4

 SIMPLE CONDUIT-FRICTION NEGLECTED
VALVE, TURBINE OR CENTRIFUGAL PUMP AT DISCHARGE END
VELOCITY EXTINGUISHED ACCORDING TO COSINE FUNCTION

Derivation same as Example 1 through Equation 4



Boundary Conditions:

 when $x=0$, $P = P_0$, $\bar{P} = \frac{P_0}{P}$ and $A = 0$

 when $x=L$, $\bar{V} = V_0 \left(\frac{P}{P_0} - \frac{P}{P_0} \right)$

$$B = \frac{\omega a V_0}{g \rho \cosh \left(\frac{g L}{a} \right)} = \frac{\omega a V_0}{g \rho \cosh \left(\frac{g L}{a} \right)} \left(\frac{P}{P_0} - \frac{P}{P_0} \right)$$

$$P = \frac{P_0}{2\pi i} \int_{-\infty}^{\infty} \frac{e^{\lambda t}}{\lambda} d\lambda + \frac{\omega a V_0}{2\pi i g} \int_{-\infty}^{\infty} \frac{e^{\lambda t} \sinh \left(\frac{\lambda L}{a} \right)}{\lambda \cosh \left(\frac{\lambda L}{a} \right)} d\lambda = \frac{P_0}{2\pi i} \int_{-\infty}^{\infty} \frac{e^{\lambda t}}{\lambda} d\lambda + \frac{\omega a V_0}{2\pi i g} \int_{-\infty}^{\infty} \frac{e^{\lambda t} \sinh \left(\frac{\lambda L}{a} \right)}{\lambda \cosh \left(\frac{\lambda L}{a} \right)} d\lambda$$

$$\frac{\partial P}{\partial x} = -\frac{P_0}{2\pi i} \int_{-\infty}^{\infty} \frac{e^{\lambda t}}{\lambda} d\lambda - \frac{\omega a V_0}{2\pi i g} \int_{-\infty}^{\infty} \frac{e^{\lambda t} \cosh \left(\frac{\lambda L}{a} \right)}{\lambda \cosh \left(\frac{\lambda L}{a} \right)} d\lambda$$

$$P = P_0 + \frac{\omega a V_0}{g} \frac{4}{\pi} \sum_{n=1}^{\infty} \frac{(-1)^{n-1}}{(2n-1)} \sin \frac{(2n-1)\pi a t}{2L} \sin \frac{(2n-1)\pi x}{2L}$$

$$+ \frac{\omega a V_0}{g} \frac{\sin \frac{\pi t}{2T} \sin \frac{\pi x}{2T}}{\cos \frac{\pi L}{2Ta}}$$

$$+ \frac{\omega a V_0}{g} \frac{4a^2 T^2}{\pi} \sum_{n=1}^{\infty} \frac{(-1)^{n-1} (2n-1)}{(2n-1)^2 a^2 T^2} \sin \frac{(2n-1)\pi a t}{2L} \sin \frac{(2n-1)\pi x}{2L}$$

$$V = V_0 - V_0 \left\{ 1 - \frac{4}{\pi} \sum_{n=1}^{\infty} \frac{(-1)^{n-1}}{(2n-1)} \cos \frac{(2n-1)\pi a t}{2L} \cos \frac{(2n-1)\pi x}{2L} \right\}$$

$$+ V_0 \frac{\cos \frac{\pi t}{2T} \cos \frac{\pi x}{2T}}{\cos \frac{\pi L}{2Ta}}$$

$$+ V_0 \frac{4a^2 T^2}{\pi} \sum_{n=1}^{\infty} \frac{(-1)^{n-1} (2n-1)}{(2n-1)^2 a^2 T^2} \cos \frac{(2n-1)\pi a t}{2L} \cos \frac{(2n-1)\pi x}{2L} \quad (7)$$

 Expression for afterwaves may be developed by using shift operator to cut off cosine function at $t = T$ similar to procedure employed in Example 2

best fits the available test data for the particular mechanism under study.

EXAMPLE 4

The purpose of this example is to indicate how the efflux velocity may be specified to vary in conformity with almost any desired continuous curve. The function selected in this case,

 $V_0 \cos \frac{\pi t}{2T}$, will be found to give results almost identical with the so-called standard Allievi method, in which the rate of decrease of gate opening is prescribed and the efflux velocity calculated as proportional to $\sqrt{H_0 + h}$.

EXAMPLE 5

 This example, including the effect of conduit friction, furnishes a good illustration of the power and range of the Laplace-Mellin transformation. Equations [13] and [14] of Example 5 are derived in the standard manner by calculating the residues of the integrands in Equations [11] and [12]. Equations [13] and [14] are perfectly correct and convergent; but the rate of convergence after the first two terms is so slow that results must be obtained by averaging terms in blocks of from $n = 0$ to $n = 100$, $n = 100$ to $n = 500$, and so on until the additional terms become negligible.

EXAMPLE 5

SIMPLE CONDUIT-INSTANTANEOUS CLOSURE
FRICTION INCLUDED

$$\frac{\partial P}{\partial x} + FV + \frac{W}{g} \frac{\partial V}{\partial t} = 0 \quad (1)$$

$$\frac{\partial V}{\partial x} + Q \frac{\partial P}{\partial t} = 0 \quad (2)$$

$$\frac{\partial^2 V}{\partial x^2} = WQ \frac{\partial^2 V}{\partial t^2} + \frac{FQ}{g} \frac{\partial V}{\partial t} \quad (3)$$

Multiply through by \bar{e}^{pt} and integrate from $t = \infty$ to $t = 0$

$$\frac{\partial^2 \bar{V}}{\partial x^2} = WQ \left\{ -\left[\frac{\partial V}{\partial t} \right]_{t=0} - p \left[V \right]_{t=0} + p^2 \bar{V} \right\} + FQ \left\{ -\left[V \right]_{t=0} + p \bar{V} \right\}$$

$$\frac{\partial^2 \bar{V}}{\partial x^2} - \bar{V} pQ (Wp + F) + V_0 Q (Wp + F) \quad (4)$$

$$\bar{V} = A \sinh (\sqrt{WQp^2 + FQ} x) + B \cosh (\sqrt{WQp^2 + FQ} x) + \frac{V_0}{p}$$

For convenience let $\beta = \sqrt{WQp^2 + FQ}$, then

$$\bar{V} = A \sinh (\beta x) + B \cosh (\beta x) + \frac{V_0}{p} \quad (5)$$

$$\frac{\partial \bar{V}}{\partial x} = -Q \frac{\partial P}{\partial t} \quad (6)$$

Multiply through by \bar{e}^{pt} and integrate from $t = \infty$ to $t = 0$

$$\frac{\partial \bar{V}}{\partial x} = -Q \left\{ -\left[P \right]_{t=0} + p \bar{P} \right\}$$

$$\frac{\partial \bar{V}}{\partial x} = QP_0 - FQV_0 x - Qp\bar{P} \quad (7)$$

Boundary Conditions when $x=0$ $P=P_0$ and $\bar{P} = \frac{P_0}{p}$ From (5) and (7) $A=0$

$$\text{Equation (5) becomes } \bar{V} = B \cosh (\beta x) + \frac{V_0}{p} \quad (8)$$

When $x=L$ $V=0$ and $\bar{V}=0$

$$\text{From (8) } B = \frac{-V_0}{p \cosh (\beta L)}$$

$$\bar{V} = \frac{V_0}{p} - \frac{V_0 \cosh (\beta x)}{p \cosh (\beta L)} \quad (9)$$

From (7)

$$\bar{P} = \frac{P_0}{p} - \frac{FV_0 x}{p} + \frac{\beta V_0 \sinh (\beta x)}{Qp^2 \cosh (\beta L)} \quad (10)$$

$$P = \frac{P_0}{2\pi i} \int_{\beta_1}^{\beta_2} \frac{e^{\lambda t} d\lambda}{\lambda} - \frac{FV_0 x}{2\pi i} \int_{\beta_1}^{\beta_2} \frac{e^{\lambda t} d\lambda}{\lambda} + \frac{V_0}{2\pi i Q} \int_{\beta_1}^{\beta_2} \frac{e^{\lambda t} \sinh (\beta x) d\lambda}{\lambda^2 \cosh (\beta L)} \quad (11)$$

$$V = \frac{V_0}{2\pi i} \int_{\beta_1}^{\beta_2} \frac{e^{\lambda t} d\lambda}{\lambda} - \frac{V_0}{2\pi i} \int_{\beta_1}^{\beta_2} \frac{e^{\lambda t} \cosh (\beta x) d\lambda}{\lambda \cosh (\beta L)}$$

where β becomes $\pm \sqrt{WQ\lambda^2 + FQ}$

$$P = P_0 - \frac{V_0 \pi^2 \alpha^2}{4LQ} \sum_{n=1}^{\infty} \frac{(-1)^{n-1} (2n-1)^2 e^{\frac{Ft}{2W}} \sin \frac{(2n-1)\pi x}{2L} \left\{ \frac{2FV_0}{W} \cos \psi t + \frac{F^2}{2W^2} \sin \psi t - 2\psi^2 \sin \psi t \right\}}{\psi \left(\frac{F^2}{4W^2} + \psi^2 \right)^2} \quad (13)$$

$$V = \frac{V_0 \pi^2 \alpha^2}{4L} \sum_{n=1}^{\infty} \frac{(-1)^{n-1} (2n-1)^2 e^{\frac{Ft}{2W}} \cos \frac{(2n-1)\pi x}{2L} \left\{ \frac{F}{W} \sin \psi t - 2\psi \cos \psi t \right\}}{\psi \left(\frac{F^2}{4W^2} + \psi^2 \right)^2} \quad (14)$$

$$\psi = \sqrt{\frac{(2n-1)^2 \pi^2}{4L^2} - \frac{F}{W}}$$

This form of solution is interesting but the rate of convergence is so slow that it is tiresome for practical computation

(Continued)

EXAMPLE 5 (Cont.)

For an alternative solution having rapid convergence make the following substitutions in Equations (11) and (12)

$$\text{In (11) } \frac{\beta \sinh (\beta x)}{\lambda^2 \cosh (\beta L)} = \sum_{m=0}^{\infty} (-1)^m \frac{\beta}{\lambda^2} \left[\frac{e^{\beta(L-x+2mL)}}{e^{\beta(L+x+2mL)}} \right] \quad (16)$$

$$\text{In (12) } \frac{\cosh (\beta x)}{\lambda \cosh (\beta L)} = \sum_{m=0}^{\infty} (-1)^m \frac{1}{\lambda} \left[\frac{e^{\beta(L-x+2mL)}}{e^{\beta(L+x+2mL)}} \right] \quad (17)$$

Carslaw p 103

These afford the following standard solutions in Bessel functions:

$$P = P_0 - FV_0 x + \frac{W\alpha V_0}{g} \sum_{m=0}^{\infty} (-1)^m \left\{ \begin{aligned} & \frac{F}{2W} I_0 \left(\frac{F}{2W} \sqrt{t^2 - \frac{(L-x+2mL)^2}{a^2}} \right) \\ & + \frac{F}{W} \int_0^t \frac{F}{2W} I_0 \left(\frac{F}{2W} \sqrt{t^2 - \frac{(L-x+2mL)^2}{a^2}} \right) dt \\ & - \frac{F}{2W} I_0 \left(\frac{F}{2W} \sqrt{t^2 - \frac{(L+x+2mL)^2}{a^2}} \right) \\ & - \frac{F}{W} \int_0^t \frac{F}{2W} I_0 \left(\frac{F}{2W} \sqrt{t^2 - \frac{(L+x+2mL)^2}{a^2}} \right) dt \end{aligned} \right\}$$

McLachlan p 217
Churchill p 331-No 37
p 300-No 88

For first two terms in $\left\{ \right\}$ $t > \frac{L-x+2mL}{a}$ and for the second two terms in $\left\{ \right\}$ $t > \frac{L+x+2mL}{a}$ $I_0 \left(\frac{F}{2W} \sqrt{t^2 - \frac{(L-x+2mL)^2}{a^2}} \right)$ denotes the modified Bessel function of the first kind, of order zero, and having the argument $\left(\frac{F}{2W} \sqrt{t^2 - \frac{(L-x+2mL)^2}{a^2}} \right)$.

in series form this function is:

$$I_0(\theta) = J_0(i\theta) = \sum_{r=0}^{\infty} \frac{\left(\frac{1}{2} \theta \right)^{2r}}{(r!)^2} = 1 + \frac{\left(\frac{1}{2} \theta \right)^2}{(2!)^2} + \frac{\left(\frac{1}{2} \theta \right)^4}{(4!)^2} + \frac{\left(\frac{1}{2} \theta \right)^6}{(6!)^2} + \dots = 1 + \frac{\theta^2}{64} + \frac{\theta^4}{2304} + \dots$$

Tables of this function are given in Jahnke and Emde p 226 and Gray & Matthews p 303.

For the velocity:

$$V = V_0 - V_0 \sum_{m=0}^{\infty} (-1)^m \left\{ \begin{aligned} & \frac{F}{2W} I_1 \left(\frac{F}{2W} \sqrt{t^2 - \frac{(L-x+2mL)^2}{a^2}} \right) \\ & + \frac{F}{2W} \left(\frac{L-x+2mL}{a} \right) \int_0^t \frac{F}{2W} I_1 \left(\frac{F}{2W} \sqrt{t^2 - \frac{(L-x+2mL)^2}{a^2}} \right) dt \\ & + \frac{F}{2W} I_1 \left(\frac{F}{2W} \sqrt{t^2 - \frac{(L+x+2mL)^2}{a^2}} \right) \\ & + \frac{F}{2W} \left(\frac{L+x+2mL}{a} \right) \int_0^t \frac{F}{2W} I_1 \left(\frac{F}{2W} \sqrt{t^2 - \frac{(L+x+2mL)^2}{a^2}} \right) dt \end{aligned} \right\} \quad (19)$$

For first two terms in $\left\{ \right\}$ $t > \frac{L-x+2mL}{a}$ and for the second two terms in $\left\{ \right\}$ $t > \frac{L+x+2mL}{a}$ $I_1 \left(\frac{F}{2W} \sqrt{t^2 - \frac{(L-x+2mL)^2}{a^2}} \right)$ denotes the modified Bessel function of the first kind, of order one, and having the argument $\left(\frac{F}{2W} \sqrt{t^2 - \frac{(L-x+2mL)^2}{a^2}} \right)$.

In series form this function is:

$$I_1(\theta) = -J_1(i\theta) = \sum_{r=0}^{\infty} \frac{\left(\frac{1}{2} \theta \right)^{1+2r}}{r! \Gamma(r+2)} = \left(\frac{1}{2} \theta \right) + \frac{\left(\frac{1}{2} \theta \right)^3}{2(6)} + \frac{\left(\frac{1}{2} \theta \right)^5}{2(6)(24)} + \dots = \frac{\theta}{2} + \frac{\theta^3}{384} + \frac{\theta^5}{147456} + \dots$$

Tables of this function are given in Jahnke and Emde p 227 and Gray & Matthews p 306.

An alternative derivation in Bessel functions proceeds directly and easily from the basic wave method of attack with a minimum of labor as compared with the tediousness of expanding the radicals by the binomial theorem and then expanding the exponentials in power series.¹⁰ In using jointly the tables of operators in Churchill and McLachlan for this problem, attention is again called to the fact that all operators in McLachlan are greater than those in Churchill by a factor p , owing to a difference in statement of the fundamental inversion theorem.

It is unfortunate that the integral terms are necessary in Equations [18] and [19]; but when the Bessel-function argument is substituted in the corresponding power series, cancellations reduce the solution to the simplest of elementary integrals. Rapid convergence of the power series makes it unnecessary to employ more than the first few terms.

The nonintegral terms are simply picked from a standard table of Bessel functions.^{11,12,13}

The effects of the direct and reflected waves are easily identified, the direct wave contribution being associated with the expression $(L - x + 2mL)$ and the reflected wave component with $(L + x + 2mL)$.

Some explanation of the process intended by Equations [18] and [19] may be necessary, and for convenience let us select the section at the gate $x = L$. The first contribution consists of the direct wave alone (identified by $L - x + 2mL$). The formulas permit calculating this component at any time between $0 < t \leq \frac{2L}{a}$; so for convenience take $t = \frac{2L}{a}$. Next, the second component consists of the direct wave contribution with $m = 1$ and $(-1)^m = \text{minus}$, and the reflected wave contribution with $m = 0$ and $(-1)^m = \text{plus}$, so that the final pair of signs for the second component will be $(- \text{ and } -)$. The time permitted by the formulas for the second component will be $\frac{2L}{a} < t \leq \frac{4L}{a}$ for both the direct

and reflected wave effects, so we shall use $t = \frac{4L}{a}$. Similarly, for the third component pair of waves the final signs will be $(+ \text{ and } +)$ with $m = 2$ direct wave, $m = 1$ reflected wave, and $t = \frac{6L}{a}$ both waves. The total effect at any time t is the sum of all component wave effects up to and including that time. With this interpretation it will be found that for $F = 0$ the equations give the same results as Example 1, and for $t = 0$ the steady-state condition prior to closure of the valve.

Excellent charts summarizing the results obtainable by this example are given in Professor Wood's paper² and will not be repeated here.

It will be noted that, when the effect of friction is included, the pressure is not a maximum at the instant of gate closure but increases progressively as the primary wave travels up the conduit. This is, of course, due to the fact that, as the steady-state velocity is reduced to zero, the cumulative friction-head loss is manifested as a regain at the gate section. This effect tends to confirm Professor Wood's point that the only basis for assuming

¹⁰ "Operational Circuit Analysis," by Vannevar Bush, John Wiley and Sons, Inc., 1937, New York, N. Y., chap. 12, pp. 213-263.

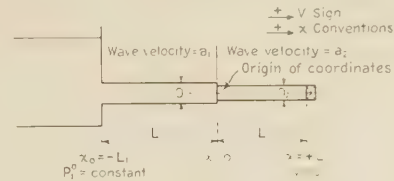
¹¹ "Tables of Functions With Formulas and Curves," by Eugen Jahnke and Fritz Emde, B. G. Teubner, Leipzig and Berlin, and G. E. Stechert and Co., New York, N. Y., 1938, p. 227.

¹² "A Treatise on Bessel Functions," by Andrew Gray, G. B. Mathews, and T. M. MacRobert, Macmillan & Co., Ltd., London, Eng., 1931, p. 303, et seq.

¹³ "A Treatise on the Theory of Bessel Functions," by G. N. Watson, Cambridge University Press, 1922, new edition in printing, The Macmillan Co., New York, N. Y., p. 698.

EXAMPLE 6

COMPOUND PIPE - INSTANTANEOUS VALVE CLOSURE
FRICTION NEGLECTED



Basic Equations - See Example (1)

$$\begin{aligned} P_1 &= A_1 \cosh \frac{pX}{a_1} + B_1 \sinh \frac{pX}{a_1} \\ P_2 &= A_2 \cosh \frac{pX}{a_2} + B_2 \sinh \frac{pX}{a_2} \\ V_1 &= -\frac{A_1}{\omega a_1} \sinh \frac{pX}{a_1} - \frac{B_1}{\omega a_1} \cosh \frac{pX}{a_1} \\ V_2 &= -\frac{A_2}{\omega a_2} \sinh \frac{pX}{a_2} - \frac{B_2}{\omega a_2} \cosh \frac{pX}{a_2} \end{aligned}$$

When $x = +L$, $V_2 = 0$

$$P_1 = \frac{P_0}{2\pi i} \int_{\gamma_1} \frac{e^{\lambda t} d\lambda}{\lambda} + \frac{\omega a_1 V_0}{2\pi i g} \int_{\gamma_1} \frac{e^{\lambda t} \cosh \frac{\lambda L}{a_1} \cosh \frac{\lambda L}{a_2} + a_1 D_1' \cosh \frac{\lambda L}{a_1} \sinh \frac{\lambda L}{a_2}}{\lambda \left(a_1 D_1' \sinh \frac{\lambda L}{a_1} \sinh \frac{\lambda L}{a_2} + a_1 D_1' \cosh \frac{\lambda L}{a_1} \cosh \frac{\lambda L}{a_2} \right)} d\lambda$$

With similar expressions for V_1 and V_2

In Equation (2) replace the hyperbolic by exponentials; multiply numerator and denominator by $e^{-\frac{\lambda L}{a_1} - \frac{\lambda L}{a_2}}$

$$P_1 = P_0 + \frac{\omega a_1 V_0}{2\pi i g} \int_{\gamma_1} \frac{e^{\lambda t} \left(e^{-\frac{\lambda L}{a_1} - \frac{\lambda L}{a_2}} - e^{\lambda \left(t - \frac{2L}{a_1} - \frac{L}{a_2} - \frac{\lambda}{a_1} \right)} \right)}{\lambda \left(1 + e^{-\frac{2\lambda L}{a_1} - \frac{2\lambda L}{a_2}} \right)} d\lambda$$

$$+ \frac{\omega a_2 V_0}{2\pi i g} \int_{\gamma_2} \frac{e^{\lambda t} \left(e^{-\frac{\lambda L}{a_1} - \frac{\lambda L}{a_2}} - e^{\lambda \left(t - \frac{2L}{a_1} - \frac{L}{a_2} - \frac{\lambda}{a_2} \right)} \right)}{\lambda \left(1 + e^{-\frac{2\lambda L}{a_1} - \frac{2\lambda L}{a_2}} \right)} d\lambda$$

(Continued)

discharge proportional to $\sqrt{H_0 + h}$ is to compensate for the regain of friction-head loss.

EXAMPLE 6

Example 6, showing one of the more elementary cases of the compound pipe, is included to illustrate the general procedure for formulating equations at the junction points for all types of compound and branched systems. At such junctions, the total combined pressure (steady state plus water hammer) at any instant is the same for each of the tributary branches, and the algebraic sum of the discharges is zero, flow toward the junction point being taken as positive and flow away from the junction point negative.

For this particular example, at least, the wave-type solution, in which the hyperbolic functions are converted to exponentials, appears to require less labor than the alternative trigonometric-series solution. The wave solution also gives a clearer picture of the physical action, since, as one of its essential features, it identifies each component wave and reflection by its own particular starting time.

CONCLUSION

It is believed that the examples submitted demonstrate that

the Laplace-Mellin transformation affords a practical and sufficiently rapid means of analyzing water-hammer phenomena in simple conduits for any desired boundary conditions. By means of the shift operator and the proper combination of linear or curved segments, the action of any mechanism at the discharge end of the conduit may be closely simulated.

Because of space limitations, only one example of the compound or branched-system type has been given. However, these problems do not differ in principle from the simple conduit cases. At the junction points, there is a common total pressure and the algebraic sum of the discharges is zero. The Laplace-Mellin transformation, dealing directly with total pressure and total velocities, expresses this condition simply and directly, since there is no need for calculating surge-reflection coefficients. The process of setting up the solution for branched-conduit problems is no more difficult than for the simple cases; the difficulty is due to the sheer weight of the algebraic detail, and much of this may be eliminated by inserting the numerical values for the particular problem at the early outset and making no attempt to develop general formulas.

The simultaneous determination of tank levels and water hammer in surge-tank and pipe-line, or tunnel problems, without major qualifying approximations, can be accomplished only by the graphical or the arithmetic integration method. For such cases, the author prefers to separate the mass-acceleration and the water-hammer elements and to determine the former by arithmetic integration. For the section of the tunnel upstream from the penstock all the designer usually requires is the value of the maximum water hammer, and this can be obtained by an obvious elementary calculation. Water-hammer pressures in the penstock downstream from the tank are obtained with sufficient accuracy simply by considering the surge tank as a fixed reservoir, neglecting the portion of the pressure wave passing up the tunnel, and using simple conduit formulas. If greater refinement is desired for research investigations, the system may be calculated as a branched group of three elements with tank level constant at the initial elevation. Water-hammer pressures will be a maximum at this time because the water in the tank has not yet been accelerated appreciably and, consequently, affords the maximum resistance or, conversely, the minimum relief to the pipe line and penstock. In short, the author sees no practical need for formulating solutions of the combined mass-acceleration and water-hammer problem.

The various supplementary problems appearing in the current literature, including the effect of hunting in turbine governors or the chattering of valves, may be solved directly by the Laplace-Mellin method, using a process similar to Example 4.

ACKNOWLEDGMENT

The author acknowledges substantial assistance in the preparation of this paper from Mr. Adolf A. Meyer, Head Civil Design Engineer; Mr. Alf Grini, Associate Civil Engineer; and Mr. John W. Hammacher, Assistant Office Engineer, of the Tennessee Valley Authority.

EXAMPLE 6 Cont.

$$\text{in which } C = \frac{a_1 D_1^2 - a_2 D_2^2}{a_2 D_1^2 + a_1 D_2^2}$$

Segregate the terms $\left(e^{\lambda(t - \frac{L_1}{a_1} + \frac{x}{a_1})} - e^{\lambda(t - \frac{2L_1}{a_1} - \frac{L_2}{a_2} + \frac{x}{a_2})} \right)$ and $\left(e^{\lambda(t - \frac{L_1}{a_2} - \frac{x}{a_1})} - e^{\lambda(t - \frac{2L_1}{a_1} - \frac{L_2}{a_2} + \frac{x}{a_2})} \right)$. By means of the series

$$\frac{1}{1+\theta} = 1 - \theta + \theta^2 - \theta^3 + \theta^4 \dots \text{ for } \theta^2 < 1$$

The remaining expression becomes

$$\left\{ \sum_{n=0}^{\infty} \frac{(-1)^n e^{-\lambda \frac{2nL_1}{a_1}}}{1 + e^{-\lambda \frac{2nL_1}{a_1}}} + e^{-\lambda \frac{2nL_1}{a_1}} \right\} \left\{ \sum_{n=0}^{\infty} (-1)^n e^{-\lambda \left(\frac{2nL_1}{a_1} + \frac{2nL_2}{a_2} \right)} \right\}$$

Neglecting terms of order C^2 and higher this becomes

$$\left\{ 1 - Ce - \frac{\lambda L_1}{a_1} - \frac{\lambda L_2}{a_2} + \frac{\lambda L_1}{a_1} + \frac{\lambda L_2}{a_2} - \frac{\lambda L_1}{a_1} - \frac{\lambda L_2}{a_2} + \dots \right\} \times \left\{ 1 - e^{-\lambda \left(\frac{L_1}{a_1} + \frac{L_2}{a_2} \right)} + e^{-\lambda \left(\frac{L_1}{a_1} + \frac{L_2}{a_2} \right)} - e^{-\lambda \left(\frac{L_1}{a_1} + \frac{L_2}{a_2} \right)} + \dots \right\} \quad (4)$$

Now by Churchill No 61 p 298

$$\int_{B_1}^{\infty} \frac{e^{-\lambda(t-k)}}{\lambda} d\lambda = \begin{cases} 0 & \text{when } 0 < t < k \\ 1 & \text{when } t > k \end{cases} \quad (5)$$

So the integrals in Equation (3) reduce to integrals of the product of each of the four segregated exponentials and the series Equation (4). By means of basic Equation (5) these all reduce to the very simple form $+1, -1, +C$ or $-C$ since the terms in C^2 and higher orders may be neglected. Attention is directed to the requirement that each wave increment starts at the instant $t > k$ in accordance with Equation (5). This solution is rapid and simple with the added advantage of affording a clear picture of the physical action.

Alternative Form of Solution

By the methods of Example (1) we may also obtain solutions in the form

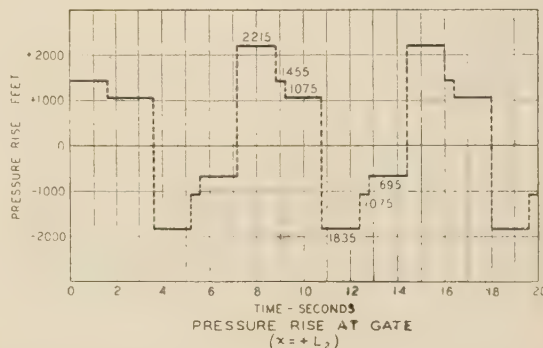
$$p = p_0 + \frac{1}{g} \sum_{n=1}^{\infty} \frac{1}{\beta_n} \sin \beta_n t \left[a_1 D_1^2 \sin \frac{\beta_n L_1}{a_1} \cos \frac{\beta_n x}{a_1} + a_2 D_2^2 \cos \frac{\beta_n L_1}{a_1} \sin \frac{\beta_n x}{a_2} - a_2 D_2^2 \left[\frac{L_1}{a_1} \sin \frac{\beta_n L_1}{a_1} \cos \frac{\beta_n L_2}{a_2} + \frac{L_2}{a_2} \cos \frac{\beta_n L_1}{a_1} \sin \frac{\beta_n L_2}{a_2} \right] + a_1 D_1^2 \left[\frac{L_1}{a_1} \cos \frac{\beta_n L_1}{a_1} \sin \frac{\beta_n L_2}{a_2} + \frac{L_2}{a_2} \sin \frac{\beta_n L_1}{a_1} \cos \frac{\beta_n L_2}{a_2} \right] \right]$$

in which β_n are the positive intersections obtained by plotting the curves $Z = \cot \frac{\beta L_1}{a_1}$ and $Z = \frac{a_1 D_1^2}{a_2 D_2^2} \tan \frac{\beta L_2}{a_2}$ with the ordinates Z and abscissas β . (6)

Many examples of this type require solution a table may be prepared by plotting a few representative curves, and the values of β obtained from the table with sufficient accuracy by interpolation.

CHART FOR
EXAMPLE 6
INSTANTANEOUS VALVE CLOSURE

$L_1 = 3000'$ $V_1 = 12'/\text{sec}$ $D_1 = 12'$
 $a_1 = 3000'/\text{sec}$ $L_2 = 2000'$ $V_2 = 18.75'/\text{sec}$
 $D_2 = 15'$ $a_2 = 2500'/\text{sec}$ $C = 0.13$



Discussion

R. W. ANGUS.¹⁴ The writer's long interest in water-hammer problems causes him to welcome any new contribution to the subject, particularly when the approach is from a new angle. The paper presents a mathematical discussion, which is an addition to the arithmetical and graphical solutions available and will help to clarify the latter, so that the author is to be commended for his paper.

The writer thinks the paper has been too greatly condensed and that some further discussion of the formulas would be helpful. He hopes that at a later date the author will also supplement his paper by tables or curves which will aid in the solution of the equation.

B. A. BAKHMETEFF.¹⁵ The author extends further the pioneer suggestions of F. M. Wood² in applying "transform" methods to water-hammer phenomena. It could be contended rightfully that in the particular cases selected as examples, the previous methods lead to simpler and easier solutions. The intent of the paper, however, is obviously educational, aiming to illustrate new possible approaches. It may so happen, in the course of further development, that operational techniques will prove to be particularly useful in the more complicated instances, such as nonuniform or branched conduits, where the procedures hitherto used become cumbersome and unhandy. The verdict regarding the practicability of the transform method will be rendered in time by the practicing profession. For the present, engineering science is indebted to the author for fascinating and provocative exploring.

The specific purpose of the transform technique is to substitute the regular methods of solving differential equations by simpler mathematical operations. It stands to reason, as a general principle, that no procedure intended as a substitute, may yield more by way of disclosure than the original method which it is called upon to replace. Accordingly, the transform method cannot dispense with any of the physical or dynamical facts, required for setting up boundary conditions in the earlier procedures.

Certain misgivings arise in this connection in regard to the pressure-rise chart in Example 2, based on the premise of a linear extinction of velocity. For proper perspective, it should probably be mentioned that the procedure of prescribing a velocity-extinction law instead of a gate-closure rule, as originally done by Allievi, is not new. Indeed, it has been common practice among engineers overseas since the early days of water hammer. In this connection, reference is made to an earlier publication of the writer,¹⁶ in which linear velocity extinction was used as the basis of the analysis.

The fact is, that operating with a prescribed law of velocity change makes the application of the traditional Joukowski-Allievi theory especially simple. Indeed, the "direct" pressure wave front simply copies the velocity change law ($V_0 - V$) to the scale a/g , which in the author's case No. 2 would result in a straight line OB , Fig. 1, of this discussion. By the same token the negative wave, reflected from the open end and reaching the gate at $t = 2L/a$, is represented by $O'B'$. In the traditional treatment, the resulting pressure rise, until the time of final closure at $t = T$, was taken to be the difference of the aforesaid direct and

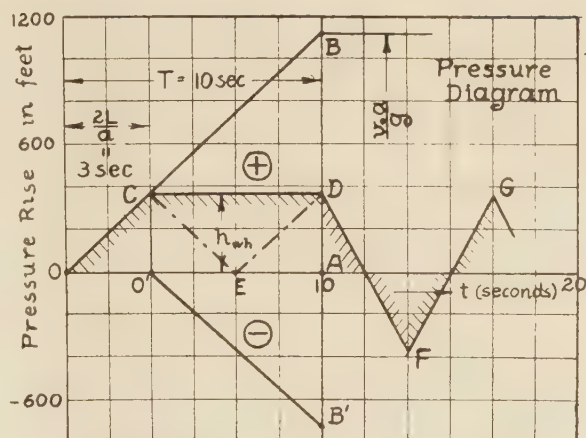


FIG. 1

reflected waves, making the water-hammer pressure for the period constant, as evidenced by the line CD with

$$h_{u-h} = \frac{2V_0L}{gT} \quad [1]$$

This pressure implies a certain margin over the Allievi linear gate solution. Furthermore, the whole treatment is particularly simple. Accordingly, the Relation [1] was considered particularly convenient for thumb-rule appraisals. Obviously, the closure of the gate causes an abrupt change in the regimen, as hereafter the direct wave pressure ceases, while the dead solid end causes the indirect wave to suffer complete reflection without change of sign. This doubles the angle of the pressure line and results in the pendulations indicated by $DFC \dots$

There is no difference between the author's chart, Example 2, and Fig. 1 herewith, for the period preceding $t = 2L/a$, and for the time $t > T$ after closure. On the other hand, for the interval $2L/a < t < T$, the author's diagram exhibits the zigzag outline CED in Fig. 1, as against the constant parallel line CD . The zigzag pressure outline would follow from the Allievi method, were one to assume that during the period of closure ($t < T$), the indirect negative wave front $O'B'$ experiences at the gate the same full reflection, as it is expected to do after the gate is completely closed. Inasmuch as the transform and the previous methods should give identical results for the same boundary conditions, it can be surmised that in applying the operational procedure to Example 2, the same set of boundary premises, in so far as reflection at the gate end is concerned, were used throughout the whole analysis, making no distinction whether the valve was still partly opened or was fully closed.

The difference in result, mentioned, raises an interesting and quite pertinent question, regarding the physics of shape reflection at a partly open gate. One may contend that the reflection mechanism under the circumstances is not as simple as heretofore assumed. The fact remains, nevertheless, that full reflection without change of sign at the completely closed end is conditioned physically by the fact that the interposed solid barrier permits no axial displacement in the elastic fluid media, thus imposing the boundary limitation of zero deformation and zero velocity. Obviously, no such limitations exist as long as the gate remains open, so under all circumstances there is bound to be a brusque change in boundary conditions at the $t = T$ moment. Also, with all possible doubts relating to the reflection mechanics at a partially open gate, which has been arrested in the course of closure, it would stand to reason that during the time the gate is being

¹⁴ Professor Emeritus of Mechanical Engineering, University of Toronto, Toronto, Ont., Can. Hon. Mem. A.S.M.E.

¹⁵ Professor, Columbia University, New York, N. Y. Mem. A.S.M.E.

¹⁶ "Introduction to the Study of Variable Motion of Liquids" (in the Russian Language), by Boris A. Bakhmeteff, St. Petersburg, 1915, p. 93.

negligible error, but such may not be the case for high friction heads, or low wave velocities.

It is evident from the solutions of Example 5 that the expression $F/2W \cdot 2L/a$, which reduces to $2fk_f V_m/aD$, may be used as a modulus for the effect of friction. Two pipe lines for which this expression is the same will have identical surges, if we use as the unit of time the period $2L/a$, and as the unit of pressure, the maximum surge for frictionless flow wV_m/g . This expression $F\mu/2W$ might be called the "friction modulus."²⁰ A set of graphs or tables for values of the modulus ranging between zero and unity, and extending up to the tenth period could be constructed to facilitate future studies.

Examples 3 and 4 show the possibilities of this method for a wide variety of boundary conditions, provided these are functions of the time variable, however arbitrarily chosen. Solutions are possible when either the velocity or pressure, or both, enter into these boundary conditions, specified at any desired point along the pipe, or at the ends.

As pointed out by the author, if the aim of a certain study is to impose certain restrictions on the pressure or velocity surges, it would seem logical to solve first for the necessary boundary conditions, and then to adjust the operation of the controlling machinery (gate, pump, turbine, etc.), in accordance with their particular characteristics, to give these boundary conditions.

AUTHOR'S CLOSURE

The able discussion of Professor Bakhmeteff, to whom the writer is indebted for valuable suggestions during preparation of the paper, deals with the pertinent question of partial reflections at the open valve during gradual closure. By means of the arithmetic integration, Table 1, and its verification by the appropriate Angus diagram, Fig. 2(b) of this closure, the author will attempt to demonstrate in figures for a representative case (that of initial head = 1000 ft) that the transform method has, like the Angus diagram, the virtue of making the requisite compensation automatically for the effect of such partial reflection. The Angus diagram has purposely been drawn for the case of initial head = 500 ft instead of 1000 ft, to show that when the velocity extinction pattern is specified as a boundary value, the water-hammer superpressures are, contrary to results obtained by the conventional method, invariant with respect to the initial head.

In performing arithmetic integration for the conventional method, the time rate of decrease of valve area is prescribed as one of the given boundary conditions, and we solve for the unknowns Δh and ΔV . In our case, the time rate of extinction of efflux velocity is prescribed in steps ΔV , and we solve for Δh and the time rate of decrease of valve area. In the sense that Δh and the relative valve opening are obtained directly with no necessity for trial-and-error computation, the process is not true arithmetic integration.

Now let us examine in detail the line of integration for the time $t = 4.17$ sec. At this instant the positive increment $\Delta h = +93.7$ ft initially generated at time $t = 0.83$ sec, returns to the valve from the reservoir as a negative reflection -93.7 ft. By the particular method of accounting we have chosen to adopt, all waves, when once generated, are carried forever in the tabulation at the original magnitudes and are given the correct algebraic sign corresponding to the number of transits of the pipe line that each has made. By this same method of accounting we double this negative reflection to -187.4 ft in column 7 and then proceed to show that the requisite correction for partial reflection of the wave -93.7 ft returning up the conduit to the reservoir is included in the value of the nascent wave Δh , column 8.

²⁰ See footnote 2 of paper, p. 712.

To make this demonstration, let us suppose that no negative reflection had yet arrived at $t = 4.17$ and let us calculate by the conventional method the corresponding magnitudes of Δh and ΔV , assuming the gate motion to be given as 0.516, column 9. This time we are employing true arithmetic integration and must establish by successive trial and error that value of Δh that will give identical results for column 6 and column 10. We obtain $\Delta h = 55.7$ ft instead of 93.7 ft, a difference of +38 ft. It is this excess of +38 ft that effects the requisite decrease in the magnitude of the negative wave traveling up the pipe line after partial reflection, and in actual amount this becomes $-93.7 + 38 = -55.7$ ft. The percentage reflection is accordingly $\frac{55.7}{-93.7} =$ about 60 per cent.

By the same type of analysis we find that at time $t = 6.67$, the percentage reflection with the valve opening at 0.333 is 71 per cent, which is in the increasing direction as would reasonably be expected. We have therefore shown that Table 1 makes specific provision for partial reflection at the control valve.

But the transform method, in which no explicit mention whatever is made of any reflections, gives pressures and velocities identical with Table 1 and Fig. 2(b). We therefore conclude that the proper orders to the transform mechanism are implicit in the specified velocity-extinction pattern and that the transform method may be relied upon to make proper compensation for the effect of partial reflection at the control valve automatically. The valve motion corresponding to column 9 is of course nonlinear and possibly even impracticable, but we qualified our original Example 2 at the outset in the original paper as merely an academic step leading to the definitely practical Example 3.

In defense of his use of a prescribed boundary condition which is not "self-dependent," the author cites the practice of assuming a locus for the deflected elastic line in the Rayleigh method of computing gravest frequencies of natural vibration and least critical buckling loads. The assumed equation of elastic line frequently bears only "shape" resemblance and not necessarily any algebraic similarity to the theoretically perfect deflection curve; but the results are obtained in surprisingly short time and to a satisfactory degree of accuracy. As a parallel case, we as engineers perform water-hammer computations for two primary purposes, (1) to determine maximum and minimum values of total steady-state plus water-hammer head, and (2) to estimate speed variations in turbo-machines. As Mr. Nagler pointed out so forcefully during the oral discussion, we have no great interest in establishing the absolutely correct shape of water-hammer curves, except in so far as this feature affects the desired degree of accuracy of determination of head and speed, and we generally find that no economy in capital cost is sacrificed if our computations for these variables are not carried to closer than 5 or even 10 per cent. It is just this practical latitude which permits us to develop by the transform method reasonably simple workable formulas for even the more complicated problems.

In response to the incisive comment of Professor Wood, the author has prepared a chart to accompany Example 5 for the particular case of friction factor $F = 0.05$ and conduit reflection

time $\frac{2L}{a} = 10$ sec. The effect of the term FV_0L has purposely

been included in the plotting to demonstrate that the wave decays in steps generally symmetrical about the reservoir elevation as would naturally be expected; but it should be carefully noted that inclusion of this term limits theoretically the applicability

of the chart to conduits having a reflection time $\frac{2L}{a} = 10$. At

some subsequent date, when time permits, the author will under-

TABLE 1 ARITHMETIC INTEGRATION—SIMPLE CONDUIT—FOR LINEAR DECREASE OF EFFLUX VELOCITY

Conduit length $L = 5000$ ft
 Conduit diameter = 15 ft
 Conduit area = 177 sq ft
 Valve closure time = 10 sec

Initial conduit velocity $v = 12$ fps
 Wave velocity $a = 3000$ fps
 Initial head = 1000 ft
 Initial $Q = 2120$ cfs

$$\text{For } \Delta t = 0.83 \text{ sec, } \Delta h = \frac{\Delta V \times 2500}{32.2 \times 0.83} \text{ or Column 3} = \frac{\text{Column 4} \times 2500}{32.2 \times 0.83}$$

Column 8 = previous $(H_0 + h)$ plus column 3 plus Column 7

$$\text{Column 9} = \frac{\text{Column 10} \times \sqrt{1000}}{2120 \times \sqrt{\text{Column 8}}}$$

Note on calculation of reflection: Reflected wave component at time $t = 4.17$ seconds equals direct wave component at time $t = 0.83$ seconds multiplied by minus 2.

Reflected wave component at time $t = 7.50$ seconds equals direct wave component at time $t = 0.83$ seconds multiplied by plus 2, added to direct wave component at time $t = 4.17$ seconds multiplied by minus 2.

Reflected wave component at time $t = 11.67$ seconds equals minus twice the sum of the direct wave component at time $t = 0.83$ seconds plus the direct wave component at time $t = 1.67$ seconds; plus twice the sum of the direct wave component at time $t = 4.17$ seconds plus the direct wave component at time $t = 5$ seconds; minus twice the sum of the direct wave component at time $t = 7.50$ seconds plus the direct wave component at 8.33 seconds.

		COLUMN 7									
		2 Δh		REFLECTED		COLUMN 8		COLUMN 9		COL. 11	
COL. 1	COLUMN 2	COLUMN 3	COLUMN 4	COLUMN 5	COLUMN 6	FROM	TOTAL HEAD	COLUMN 9	COL. 10	COL. 8 -	
TIME	Δt	AT VALVE	ΔV	V	$Q = 177V$	RESERVOIR	$H_0 + h$	VALVE	CFS	1000	
SEC	SECONDS	FT	FPS	FPS	CFS	FT	FT	OPENING		FT	
0.00	—	—	—	12.000	2120	—	1000.0	1.000	2120	0'	
0.83	0.83	93.7	- 1.000	11.000	1950	—	1093.7	0.882	1950	93.7	
1.67	0.84	93.7	- 1.000	10.000	1770	—	1187.4	0.766	1770	187.4	
2.50	0.83	93.7	- 1.000	9.000	1590	—	1281.1	0.666	1590	281.0	
3.33	0.83	93.7	- 1.000	8.000	1415	—	1374.8	0.570	1415	374.8	
4.17	0.84	93.7	- 1.000	7.000	1238	- 187.4	1281.1	0.516	1238	281.0	
5.00	0.83	93.7	- 1.000	6.000	1060	- 187.4	1187.4	0.460	1060	187.4	
5.83	0.83	93.7	- 1.000	5.000	885	- 187.4	1093.7	0.397	885	93.7	
6.67	0.84	93.7	- 1.000	4.000	708	- 187.4	1000.0	0.333	708	0	
7.50	0.83	93.7	- 1.000	3.000	531	0	1093.7	0.229	531	93.7	
8.33	0.83	93.7	- 1.000	2.000	344	0	1187.4	0.149	344	187.4	
9.17	0.84	93.7	- 1.000	1.000	177	0	1281.1	0.074	177	281.1	
10.00	0.83	93.7	- 1.000	0.000	0	0	1374.8	0	0	374.8	
11.67	1.67	Valve closed at time $t = 10$ seconds				-374.8	1000.0			0	
13.33	1.66					-374.8	625.2			- 374.8	
15.00	1.67					374.8	1000.0			0	
16.67	1.67					374.8	1374.8			+ 374.8	
18.33	1.66					-374.8	1000.0			0	
20.00	1.67					-374.8	625.2			- 374.8	
21.67	1.67					374.8	1000.0			0	
23.33	1.66					374.8	1374.8			+ 374.8	

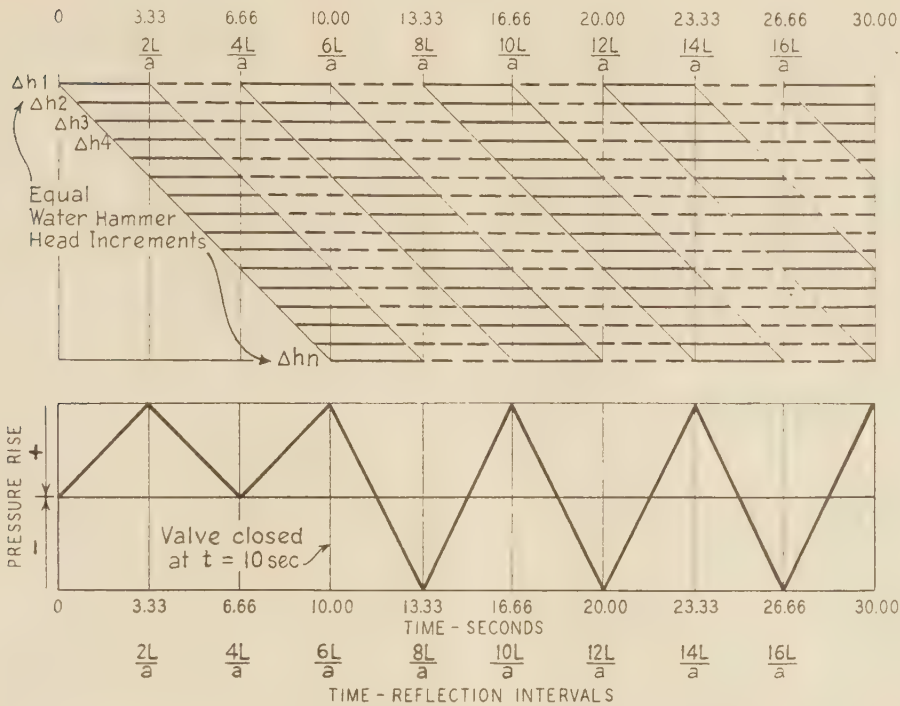


FIG. 2 (a) ILLUSTRATING SYNTHESIS OF PRESSURE RISE FOR UNIFORM LINEAR VELOCITY EXTINCTION AT OUTLET

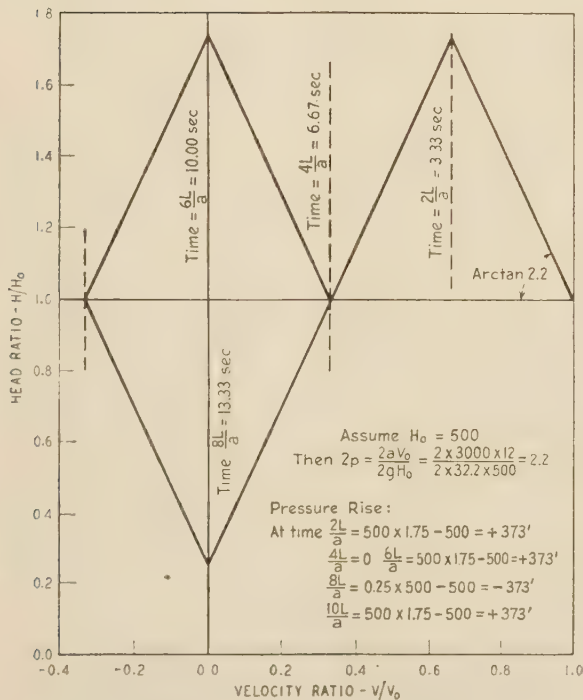


FIG. 2 (b) SUPPLEMENTARY CHART, EXAMPLE 2, BY ANGUS GRAPHICAL METHOD

take to compute charts in which, for several assumed representative values of friction modulus, the ordinates consist simply of the third term of Equation [18]. As Professor Wood points out, such charts will have perfect generality so as to be applicable to all cases having the same value of friction modulus $\frac{F}{2W} \cdot \frac{2L}{a}$.

In computing the chart for Example 5, the author found that with respect to the integral terms, Equation [18], convergence of the Bessel function series was so rapid that only the first term was necessary. With this simplification, Equation [18], for $x = L$ at the valve, reduces to

$$P = P_0 - FV_0L + \frac{\omega a V_0}{g} \left\{ e^{-\frac{Ft}{2W}} I_0 \left(\frac{Ft}{2W} \right) + \frac{F}{W} \int_0^t e^{-\frac{Ft}{2W}} dt \right\} + \frac{2\omega a V_0}{g} \sum_{n=1}^{\infty} (-1)^n \left\{ e^{-\frac{Ft}{2W}} I_0 \left(\frac{Ft}{2W} \right) + \frac{F}{W} \int_0^t e^{-\frac{Ft}{2W}} dt \right\} \dots \dots \dots (18a)$$

In using Equation [18a] the third term is computed for $t = 0$ and $t = \frac{2L}{a}$; then the fourth term is computed successively for $m = 1, t = \frac{2L}{a}$ and $t = \frac{4L}{a}$; $m = 2, t = \frac{4L}{a}$ and $t = \frac{6L}{a}$, and so on. Then taking $t = \frac{2L}{a}$ as an example, the upper value is given

EXAMPLE 1

(HEAVISIDE WAVE ALTERNATE)

From Equation (5) Original Example 1:

$$p = \frac{P_0}{2\pi i} \int_{Br_2} \frac{e^{\lambda t} d\lambda}{\lambda} + \frac{\omega a V_0}{2\pi i g} \int_{Br_2} \frac{e^{\lambda t} \sinh \left(\frac{\lambda x}{a} \right) d\lambda}{\lambda \cosh \frac{\lambda L}{a}}$$

In the second integrand replace the hyperbolic by exponentials and multiply numerator and denominator by $e^{-\frac{\lambda L}{a}}$.

$$p = P_0 + \frac{\omega a V_0}{2\pi i g} \int_{Br_2} \frac{e^{\lambda t} e^{-\frac{\lambda L}{a}} \left(e^{\frac{\lambda x}{a}} - e^{-\frac{\lambda x}{a}} \right) d\lambda}{\lambda \left(1 + e^{-\frac{2\lambda L}{a}} \right)} \quad (9)$$

$$\text{But } \frac{1}{1 + e^{-\frac{2\lambda L}{a}}} = 1 - e^{-\frac{2\lambda L}{a}} + e^{-\frac{4\lambda L}{a}} - e^{-\frac{6\lambda L}{a}} + e^{-\frac{8\lambda L}{a}} - \dots \text{ Provided that } e^{-\frac{4\lambda L}{a}} < 1 \quad (10)$$

Substituting (10) in (9).

$$p = P_0 + \frac{\omega a V_0}{2\pi i g} \int_{Br_2} \frac{\left\{ e^{\lambda \left(t - \frac{L}{a} + \frac{x}{a} \right)} - e^{\lambda \left(t - \frac{L}{a} - \frac{x}{a} \right)} - e^{\lambda \left(t - \frac{3L}{a} + \frac{x}{a} \right)} + e^{\lambda \left(t - \frac{3L}{a} - \frac{x}{a} \right)} \dots \right\} d\lambda}{\lambda} \quad (11)$$

By Churchill! No 61 p 296

$$\frac{1}{2\pi i} \int_{Br_2} \frac{e^{\lambda(t-k)} d\lambda}{\lambda} = \begin{cases} 0 & \text{when } 0 < t < k \\ 1 & \text{when } t > k \end{cases} \quad (12)$$

Integrating (11) term by term

$$p = P_0 + \frac{\omega a V_0}{g} \left\{ 1 - \frac{1}{t > \frac{L-x}{a}} - \frac{1}{t > \frac{L+x}{a}} - \frac{1}{t > \frac{3L-x}{a}} + \frac{1}{t > \frac{3L+x}{a}} \dots \right\} \quad (13)$$

$$p = P_0 + \frac{\omega a V_0}{g} \sum_{n=1}^{\infty} (-1)^{n+1} \left\{ 1 - \frac{1}{t > \frac{(2n-1)L-x}{a}} - \frac{1}{t > \frac{(2n-1)L+x}{a}} \right\} \quad (14)$$

At gate section when $x=L$:

$$p = P_0 + \frac{\omega a V_0}{g} \left\{ 1 - 2 \sum_{n=1}^{\infty} (-1)^n \frac{1}{t > \frac{2nL}{a}} \right\} \quad (15)$$

EXAMPLE 3

(HEAVISIDE WAVE ALTERNATE)

First stage similar to Example 2 (Heaviside Wave Alternate):
Proceeding from Example 3 (Original) - Equation 4.

$$p = P_0 + \frac{\omega a (V_0 - V_d)}{g \beta T} \sum_{n=1}^{\infty} (-1)^{n+1} \left\{ \frac{1}{t > \frac{(2n-1)L-x}{a}} - \frac{1}{t > \frac{(2n-1)L+x}{a}} \right\} \quad (13)$$

At gate section when $x=L$

$$p = P_0 + \frac{\omega a (V_0 - V_d)}{g \beta T} \left\{ 1 - 2 \sum_{n=1}^{\infty} (-1)^n \frac{1}{t > \frac{2nL}{a}} \right\} \quad (14)$$

Second stage $t = \beta T$ to $t = T$ (Heaviside Wave Solution)

Proceeding similar to Example 2. (Heaviside Wave Alternate)

$$p = P_0 + \frac{\omega a (V_0 - V_d)}{g \beta T} \sum_{n=1}^{\infty} (-1)^{n+1} \left\{ \frac{1}{t > \frac{(2n-1)L-x}{a}} - \frac{1}{t > \frac{(2n-1)L+x}{a}} \right\} - \frac{\omega a (V_0 - V_d)}{g \beta T} \sum_{n=1}^{\infty} (-1)^{n+1} \left\{ \frac{1}{t > \beta T + \frac{(2n-1)L-x}{a}} - \frac{1}{t > \beta T + \frac{(2n-1)L+x}{a}} \right\} \quad (15)$$

When $x=L$ at gate

$$p = P_0 + \frac{\omega a (V_0 - V_d)}{g \beta T} \left\{ 1 - 2 \sum_{n=1}^{\infty} (-1)^n \frac{1}{t > \frac{2nL}{a}} \right\} - \frac{\omega a (V_0 - V_d)}{g \beta T} \left\{ 1 - 2 \sum_{n=1}^{\infty} (-1)^n \frac{1}{t > \beta T + \frac{2nL}{a}} \right\} \quad (16)$$

EXAMPLE 2

(HEAVISIDE WAVE ALTERNATE)

From Equation (5) Original Example 2:

$$p = \frac{P_0}{2\pi i} \int_{Br_2} \frac{e^{\lambda t} d\lambda}{\lambda} + \frac{\omega a V_0}{2\pi i g T} \int_{Br_2} \frac{e^{\lambda t} \sinh \frac{\lambda x}{a} d\lambda}{\lambda^2 \cosh \frac{\lambda L}{a}} \quad (5)$$

Using procedure similar to Example 1 (Heaviside Wave Alternate):

$$p = P_0 + \frac{\omega a V_0}{2\pi i g T} \int_{Br_2} \frac{\left\{ e^{\lambda \left(t - \frac{L}{a} + \frac{x}{a} \right)} - e^{\lambda \left(t - \frac{L}{a} - \frac{x}{a} \right)} - e^{\lambda \left(t - \frac{3L}{a} + \frac{x}{a} \right)} + e^{\lambda \left(t - \frac{3L}{a} - \frac{x}{a} \right)} \dots \right\} d\lambda}{\lambda^2} \quad (14)$$

Now by Churchill! No. 62 p 298

$$\frac{1}{2\pi i} \int_{Br_2} \frac{e^{\lambda(t-k)} d\lambda}{\lambda^2} = \begin{cases} 0 & \text{when } 0 < t < k \\ t-k & \text{when } t > k \end{cases} \quad (15)$$

Integrating (14) term by term:

$$p = P_0 + \frac{\omega a V_0}{g T} \left\{ \frac{1}{t > \frac{L-x}{a}} - \frac{1}{t > \frac{L+x}{a}} - \frac{1}{t > \frac{3L-x}{a}} + \frac{1}{t > \frac{3L+x}{a}} \dots \right\} \quad (16)$$

$$p = P_0 + \frac{\omega a V_0}{g T} \sum_{n=1}^{\infty} (-1)^{n+1} \left\{ \frac{1}{t > \frac{(2n-1)L-x}{a}} - \frac{1}{t > \frac{(2n-1)L+x}{a}} \right\} \quad (17)$$

At gate section when $x=L$

$$p = P_0 + \frac{\omega a V_0}{g T} \left\{ 1 - 2 \sum_{n=1}^{\infty} (-1)^n \frac{1}{t > \frac{2nL}{a}} \right\} \quad (18)$$

For zone of "Afterwaves!" Use similar procedure on Equation (10)
Original Example 2:

$$p = P_0 + \frac{\omega a V_0}{g T} \sum_{n=1}^{\infty} (-1)^{n+1} \left\{ \frac{1}{t > \frac{(2n-1)L-x}{a}} - \frac{1}{t > \frac{(2n-1)L+x}{a}} \right\} - \frac{\omega a V_0}{g T} \sum_{n=1}^{\infty} (-1)^{n+1} \left\{ \frac{1}{t > \beta T + \frac{(2n-1)L-x}{a}} - \frac{1}{t > \beta T + \frac{(2n-1)L+x}{a}} \right\} \quad (19)$$

At gate section when $x=L$

$$p = P_0 + \frac{\omega a V_0}{g T} \left\{ 1 - 2 \sum_{n=1}^{\infty} (-1)^n \frac{1}{t > \frac{2nL}{a}} \right\} - \frac{\omega a V_0}{g T} \left\{ 1 - 2 \sum_{n=1}^{\infty} (-1)^n \frac{1}{t > \beta T + \frac{2nL}{a}} \right\} \quad (20)$$

by $t = \frac{2L}{a}$ from the third term and the lower value by $t = \frac{2L}{a}$ fromthe fourth term. For $t = \frac{4L}{a}$ the lower value is given by $m = 1$, $t = \frac{4L}{a}$ and the upper value by $m = 2$, $t = \frac{4L}{a}$. In making up

the summations care must be taken not to mix these two groups

of values: In one group we have values for t just greater than 0,plus t just greater than $\frac{2L}{a}$, plus t just greater than $\frac{4L}{a}$, and so on;while in the second group we have values for t just less than $\frac{2L}{a}$ t just less than $\frac{4L}{a}$, and so on. In other words, we never sumvalues that are not separated by an entire interval $\frac{2L}{a}$ un-

diminished even by infinitesimals of time.

It will of course be immediately apparent that the value of

friction factor $F = 0.05$ has been purposely magnified many

times over the value normally encountered in practice, in order

to give substantial drops in intensity for each succeeding wave.

A friction value $F = 0.01$ would in all probability be heavier

EXAMPLE 4 (HEAVISIDE WAVE ALTERNATE)

Equation (3) Example 4 (Original):

$$P = \frac{P_0}{2\pi i} \int_{Br_2} \frac{e^{\lambda t} d\lambda}{\lambda} + \frac{\omega a V_0}{2\pi i g} \int_{Br_2} \frac{e^{\lambda t} \sinh(\frac{\lambda x}{a}) d\lambda}{\lambda \cosh(\frac{\lambda L}{a})} - \frac{\omega a V_0}{2\pi i g} \int_{Br_2} \frac{e^{\lambda t} \lambda \sinh(\frac{\lambda x}{a}) d\lambda}{(\lambda^2 + \frac{\pi^2}{4T^2}) \cosh(\frac{\lambda L}{a})} \quad (13)$$

Treatment of the first two integrals is identical with Example 1 (Heaviside Wave Alternate - Equation 14):

In the third integral replace the hyperbolics by exponentials and multiply numerator and denominator by $e^{-\frac{\lambda L}{a}}$

$$\int_{Br_2} \frac{e^{\lambda t} \lambda \sinh(\frac{\lambda x}{a}) d\lambda}{(\lambda^2 + \frac{\pi^2}{4T^2}) \cosh(\frac{\lambda L}{a})} = \int_{Br_2} \frac{\lambda e^{\lambda t} e^{-\frac{\lambda L}{a}} (e^{\frac{\lambda x}{a}} - e^{-\frac{\lambda x}{a}}) d\lambda}{(\lambda^2 + \frac{\pi^2}{4T^2}) (1 + e^{-\frac{2\lambda L}{a}})} \quad (8)$$

$$\text{But } \frac{1}{1 + e^{-\frac{2\lambda L}{a}}} = 1 - e^{-\frac{2\lambda L}{a}} + e^{-\frac{4\lambda L}{a}} - e^{-\frac{6\lambda L}{a}} + e^{-\frac{8\lambda L}{a}} \dots \text{Provided that } e^{-\frac{4\lambda L}{a}} < 1 \quad (9)$$

Substituting (9) in (8):

$$\int_{Br_2} \frac{\lambda}{(\lambda + \frac{i\pi}{2T})(\lambda - \frac{i\pi}{2T})} \left\{ e^{\lambda(t - \frac{L-x}{a})} - e^{\lambda(t - \frac{L+x}{a})} - e^{\lambda(t - \frac{3L-x}{a})} + e^{\lambda(t - \frac{3L+x}{a})} + \dots \right\} d\lambda \quad (10)$$

But by the theory of residues:

$$\frac{1}{2\pi i} \int_{Br_2} \frac{e^{\lambda(t-k)} d\lambda}{\lambda^2 + \beta^2} = \begin{cases} 0 & \text{when } 0 < t < k \\ \cos[\beta(t-k)] & \text{when } t > k \end{cases} \quad (11)$$

The integral (10) then becomes:

$$\left\{ \cos\left[\frac{\pi}{2T}\left(t - \frac{L-x}{a}\right)\right] - \cos\left[\frac{\pi}{2T}\left(t - \frac{L+x}{a}\right)\right] - \cos\left[\frac{\pi}{2T}\left(t - \frac{3L-x}{a}\right)\right] + \cos\left[\frac{\pi}{2T}\left(t - \frac{3L+x}{a}\right)\right] + \dots \right\} \quad (12)$$

and the entire Equation (3) equals:

$$P = P_0 + \frac{\omega a V_0}{g} \sum_{n=1}^{\infty} (-1)^{n+1} \left\{ 1 - \cos\left[\frac{\pi}{2T}\left(t - \frac{(2n-1)L-x}{a}\right)\right] + \cos\left[\frac{\pi}{2T}\left(t - \frac{(2n-1)L+x}{a}\right)\right] \right\} - \frac{\omega a V_0}{g} \sum_{n=1}^{\infty} (-1)^{n+1} \left\{ \cos\left[\frac{\pi}{2T}\left(t - \frac{(2n-1)L-x}{a}\right)\right] - \cos\left[\frac{\pi}{2T}\left(t - \frac{(2n-1)L+x}{a}\right)\right] \right\} \quad (13)$$

When $x=L$ at gate:

$$P = P_0 + \frac{\omega a V_0}{g} \left\{ 1 + 2 \sum_{n=1}^{\infty} (-1)^{n+1} \cos\left[\frac{\pi}{2T}\left(t - \frac{2nL}{a}\right)\right] \right\} - \frac{\omega a V_0}{g} \left\{ \cos\left[\frac{\pi}{2T}t\right] + 2 \sum_{n=1}^{\infty} (-1)^n \cos\left[\frac{\pi}{2T}\left(t - \frac{2nL}{a}\right)\right] \right\} \quad (14)$$

than is likely to be encountered in economical pipe-line design, but for this more common case the rate of attenuation is hardly perceptible for the limited number of intervals that could be accommodated on the diagram. The fact that this difference between succeeding waves is so small is of course the very reason why friction is not a relevant consideration in most practical problems.

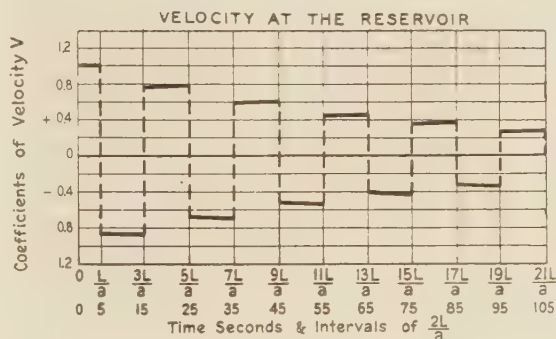
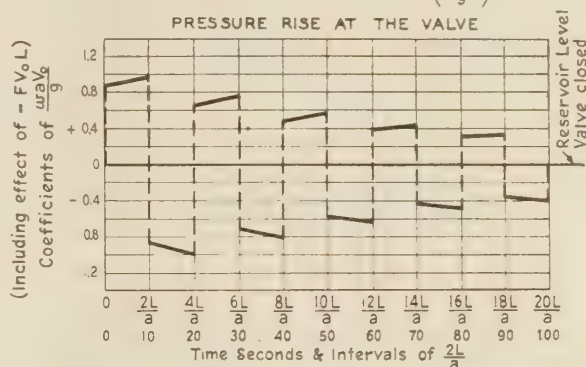
Mr. Roberts' interesting discussion has an important bearing on water-hammer fundamentals. His mention of item 3, the provision of rate-setting cams for a prescribed nonuniform gate motion, may be taken as practical confirmation of the author's thesis that it is entirely feasible for the consulting engineer to establish in advance the optimum velocity-extinction pattern consistent with most favorable over-all project economy and leave to the manufacturer's engineers the corresponding design of terminal mechanism.

The valve designer could develop the requisite closure rate by a procedure essentially similar to that employed in the arithmetic integration of Table 1, column 9, or, as an alternative method, by trial-and-error shifting of the valve-discharge parabolas of the Angus diagram.

With respect to Mr. Roberts' and Professor Angus' mention of the desirability of condensing water-hammer results in tabular form, the author suggested in his oral presentation that the Water-Hammer Subcommittee undertake the preparation of a handbook in which compact workable formulas be collected for the rapid solution of 50 or 60 representative problems, including

CHART TO ACCOMPANY EXAMPLE 5 SIMPLE CONDUIT-INSTANTANEOUS VALVE CLOSURE CONDUIT FRICTION INCLUDED-VELOCITY HEAD NEGLECTED

$$\begin{aligned} \frac{2L}{a} &= 10 \text{ sec} & FV_0 L &= 5FV_0 a \\ F &= 0.05 & &= \frac{5Fg}{\omega} \left(\frac{\omega a V_0}{g} \right) \\ & & &= 0.125 \left(\frac{\omega a V_0}{g} \right) \end{aligned}$$



all current types of terminal mechanism and operation, and the desired compound- and branched-system cases. This is obviously too extensive a task for any one individual and consequently it was the author's intention that these problems be parceled out to about 25 technicians throughout the country, assigning each one or two cases. These problems could then be exchanged and verified, and the entire task brought to completion within a reasonably short time. In the interim preceding organization of this undertaking on a large-scale basis, the author will continue to derive as many additional representative cases as his somewhat limited time will allow.

During the oral presentation of the original paper, the author submitted alternative solutions by the Heaviside wave method as well as the trigonometric-series method for each of the illustrative examples. In response to the interest that appeared to develop during the subsequent discussion, the fundamental steps of these Heaviside alternatives are given in the supplementary examples accompanying this closure.

In connection with the manipulation of Equations [4] and [5], original Example 6, it is believed that some word of amplification will be worth while. In preparing the chart for Example 6 of the original paper, the author's primary purpose was to indicate how the refinements of the method might be dispensed with if it is desired to obtain an estimate of the peak instantaneous value of the water hammer and only a very rough idea of the wave pattern. In line with this purpose, all terms of order C^2 and higher were dropped in Equation [4] and the pattern was based solely on what occurred during the first two or three intervals. Be-

EXAMPLE 6 - ALTERNATE (INCLUDING EFFECT OF TERMS IN C^2)

In Equation (4) Example 6 (Original), include terms in C^2 :

$$\left\{ \begin{aligned} &1 - C^2 \frac{2\lambda L_1}{a_1} - C^2 \frac{2\lambda L_2}{a_2} + C^2 \frac{4\lambda L_1}{a_1} - 2C^2 \frac{2\lambda L_1}{a_1} \frac{2\lambda L_2}{a_2} + C^2 \frac{4\lambda L_2}{a_2} - C^2 \frac{4\lambda L_1}{a_1} \frac{2\lambda L_2}{a_2} \\ &+ C^2 \frac{2\lambda L_1}{a_1} \frac{4\lambda L_2}{a_2} - 2C^2 \frac{6\lambda L_1}{a_1} \frac{2\lambda L_2}{a_2} - 4C^2 \frac{4\lambda L_1}{a_1} \frac{4\lambda L_2}{a_2} - 2C^2 \frac{2\lambda L_1}{a_1} \frac{6\lambda L_2}{a_2} \\ &- C^2 \frac{6\lambda L_1}{a_1} \frac{4\lambda L_2}{a_2} - C^2 \frac{4\lambda L_1}{a_1} \frac{6\lambda L_2}{a_2} + 3C^2 \frac{8\lambda L_1}{a_1} \frac{4\lambda L_2}{a_2} + 6C^2 \frac{6\lambda L_1}{a_1} \frac{6\lambda L_2}{a_2} \\ &+ 3C^2 \frac{4\lambda L_1}{a_1} \frac{8\lambda L_2}{a_2} + C^2 \frac{8\lambda L_1}{a_1} \frac{6\lambda L_2}{a_2} + C^2 \frac{6\lambda L_1}{a_1} \frac{8\lambda L_2}{a_2} \dots \end{aligned} \right\} \quad (6)$$

Solve integrals in Equation (3) Original Example by using Churchill No 61 p 298

$$\int_{Br_2}^{\lambda(t-k)} \frac{e^{-\lambda} d\lambda}{\lambda} = \begin{cases} 0 & \text{when } 0 < t < k \\ 1 & \text{when } t > k \end{cases} \quad (7)$$

At gate section $x = L$ this reduces to:

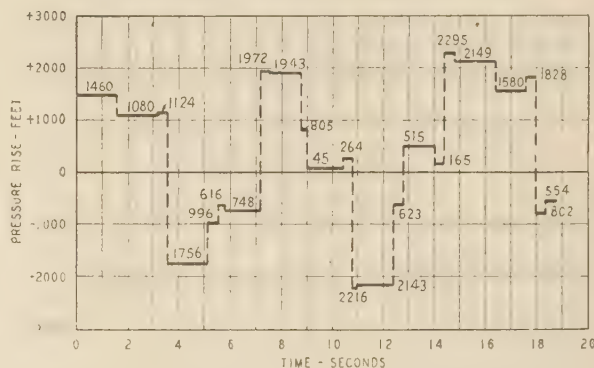
$$\begin{aligned} P_2 = P_2^0 + \frac{\omega a V_2^0}{g} \sum_{n=0}^{\infty} (-1)^n (1 - [n+1] C^2) &\left\{ 1 - \frac{2nL_1}{a_1} + \frac{2nL_2}{a_2} - 1 \right\} t > \frac{(2n+2)L_1}{a_1} + \frac{(2n+2)L_2}{a_2} \\ + \frac{C\omega a V_2^0}{g} \sum_{n=1}^{\infty} (-1)^n n &\left\{ 1 - \frac{(2n-2)L_1}{a_1} + \frac{2nL_2}{a_2} - 1 \right\} t > \frac{(2n-2)L_1}{a_1} + \frac{(2n+2)L_2}{a_2} \\ &+ \frac{C\omega a V_2^0}{g} \sum_{n=0}^{\infty} (-1)^n n &\left\{ 1 - \frac{(2n+2)L_1}{a_1} + \frac{2nL_2}{a_2} - 1 \right\} t > \frac{2nL_1}{a_1} + \frac{(2n+2)L_2}{a_2} \\ &+ \frac{C^2 \omega a V_2^0}{g} \sum_{n=1}^{\infty} (-1)^n n &\left\{ 1 - \frac{(2n-2)L_1}{a_1} + \frac{(2n-2)L_2}{a_2} - 1 \right\} t > \frac{(2n-2)L_1}{a_1} + \frac{(2n+2)L_2}{a_2} \\ &+ \frac{C^2 \omega a V_2^0}{g} \sum_{n=1}^{\infty} (-1)^n \frac{n(n+1)}{2} &\left\{ 1 - \frac{(2n+4)L_1}{a_1} + \frac{2nL_2}{a_2} - 1 \right\} t > \frac{2nL_1}{a_1} + \frac{(2n+4)L_2}{a_2} \\ &- 1 &\left\{ 1 - \frac{(2n+2)L_1}{a_1} + \frac{(2n-2)L_2}{a_2} - 1 \right\} t > \frac{(2n+2)L_1}{a_1} + \frac{(2n+2)L_2}{a_2} \end{aligned} \quad (8)$$

cause of the mounting importance of terms in C^2 as the series progresses, confusion will result if this short-cut is applied to later intervals.

For the cases in which more accurate delineation of wave pattern as well as the peak pressure is of importance, the attack

CHART FOR EXAMPLE 6 - ALTERNATE INSTANTANEOUS VALVE CLOSURE INCLUDING EFFECT OF TERMS C^2

$$\begin{aligned} L_1 &= 3000' & V_1^0 &= 12'/\text{sec} & D_2 &= 12' \\ a_1 &= 3000'/\text{sec} & L_2 &= 2000' & V_2^0 &= 18.75'/\text{sec} \\ D_1 &= 15' & a_2 &= 2500'/\text{sec} & C &= 0.13 \end{aligned}$$



should be modified as indicated in the subsequent supplementary example. Terms of order C^2 should be retained as indicated in Equation [5] of the following alternative solution. These results may be accurately applied to succeeding later stages of the phenomenon.

The author appreciates the comment of Professor Angus and trusts that the foregoing discussion and closure will to some extent compensate for the admitted brevity of the original paper. In this connection, Professor Angus, as a successful teacher of long experience, is of course well aware that the only effective means of mastering any theory is to follow the precept enunciated by Newton centuries ago and work many representative examples by its use. It is hoped that the basic material presented in condensed form in the article will, with the references given, furnish background for such an approach.

In conclusion, the author expresses thanks to those who have participated in the discussion.

Water-Hammer Problems in Connection With the Design of Hydroelectric Plants

By E. B. STROWGER,¹ BUFFALO, N. Y.

A review is given of the subject, based upon previously published papers, and in addition Allievi charts, which have been extended to include practically all problems an engineer may consider, are presented. The review covers, among other things, a simple statement of the fundamentals of the problem as usually encountered in hydroelectric plants, an explanation of the arithmetic-integration and graphical methods, and the solution of the surge-tank problem. Other aspects of the subject, such as the influence of gate motion, pressure conditions along the pipe, etc., are discussed. Emphasis is placed upon presenting to the designing engineer definite and useful procedures for the solution of some of the more common and simpler water-hammer problems in connection with hydroelectric plants. The arithmetic-integration method is set forth because it is a useful method per se and is a prerequisite to a ready understanding of the graphical method. The solution of the surge-tank problem is given by reference to the Calame and Gaden approximate formulas. These formulas, as published in English at the present time, contain several typographical errors and, consequently, may be misapplied. For this reason, the author has included them herein after checking them against the original French version. Several typical examples of various problems are used as illustrations in order to make the methods of computation clear.

DEFINITION OF WATER HAMMER

WATER hammer is defined as the change in pressure, above or below normal pressure, caused by sudden changes in the rate of flow of water in closed conduits. Because of sudden changes in the demand for water during load fluctuations, it occurs at all points in pipe lines between the forebay and the turbines, but to a less extent in the pipe line between the reservoir and the surge tank and to a greater extent in the penstock.

Accompanying a rather sudden decrease in load on a hydroelectric plant, the turbine gates operate to close and the hydraulic gradient moves up from AJ to AB , as shown in Fig. 1. This position is called the positive water-hammer gradient. At the instant the turbine-gate movement ceases, the supernormal pressure then existing becomes unstable, and the gradient AB begins to swing to AC . The pressure then fluctuates between positive and negative until damped out by friction.

Accompanying a rather sudden increase in load on a hydroelectric plant, the turbine gates operate to open, and the hydraulic gradient moves down from EJ to EG , as shown in Fig. 2. This position is called the negative water-hammer gradient. After the gate movement ceases, the negative pressure EG swings to positive pressure EF .

¹ Hydraulic Engineer, The Niagara Falls Power Company. Mem. A.S.M.E.

Contributed by the Hydraulic Division and presented at the Annual Meeting, New York, N. Y., Nov. 27-Dec. 1, 1944, of THE AMERICAN SOCIETY OF MECHANICAL ENGINEERS.

NOTE: Statements and opinions advanced in papers are to be understood as individual expressions of their authors and not those of the Society.

The penstock should be designed to withstand at every point an internal pressure corresponding to the maximum positive water-hammer pressure AB . The negative water-hammer gradient AC or EG , whether caused directly by gate opening or by the swing of pressure from positive to negative after gate closure, should not be below the top of the penstock at any point, as at K . If it is, a partial vacuum will occur within the pipe with possibility of collapse of the shell. Air-inlet valves to prevent vacuum in this case are not recommended, as they may not operate quickly enough to prevent collapse.

GENERAL DISCUSSION

If the turbine gates of the installation, shown in Fig. 1, are at a fixed position, as when the governor is operating on load limit, the rate of flow through the turbine orifices is constant and the hydraulic gradient remains in a fixed position. If, however, the turbine gates are regulating, i.e., causing the orifice area to open and close alternately, the column of water is accelerated and decelerated, and the hydraulic gradient changes in position. During this perturbed regimen of flow, the phenomenon of water hammer occurs. During a closure or an opening of the gates, kinetic energy is converted to potential energy or vice versa and the pressure existing at any instant could readily be computed from Newton's laws of motion if it were not for the effect of elasticity of the pipe walls and of the water itself. As the pressure changes occur, the water is compressed or relieved of pressure, the pipe is expanded or contracted, and water-hammer waves travel along the pipe as the whole liquid column vibrates.

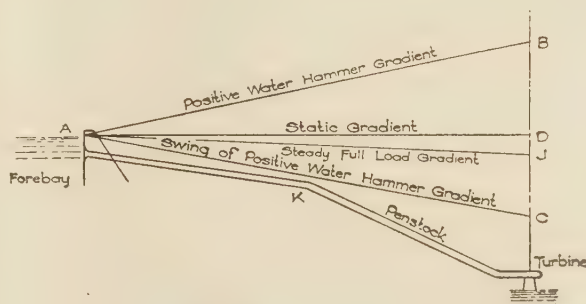


FIG. 1 POSITIVE WATER-HAMMER GRADIENT

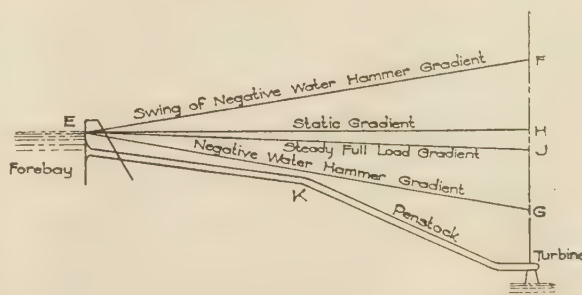


FIG. 2 NEGATIVE WATER-HAMMER GRADIENT

Velocity and pressure at any instant thus are dependent upon the elastic characteristics of pipe and water, as well as upon the initial conditions of head and velocity, the length of pipe, the velocity change, and the character of the gate motion.

FUNDAMENTAL RELATIONS

As the turbine gates start closing, a positive pressure wave starts to travel up the penstock to the forebay. A given motion of the gates may be considered to consist of a great number of small motions, each one of which is instantaneous. Considering one of these small instantaneous motions of the gates in the closing direction, the positive wave resulting therefrom travels up the penstock to the forebay and, upon reaching the forebay, it is reflected back from the open end of the pipe as a negative wave which travels back to the turbine and which has the same magnitude as the positive wave. The time of one round trip of the wave is designated as μ and is called "time of one interval" or the "critical time" of the pipe. It is expressed (in seconds) as

$$\mu = \frac{2L}{a} \quad [1]$$

where L is the length of the penstock in feet and a is the velocity of the pressure wave in feet per second.

Joukovsky (1)² proved that the maximum water hammer produced in a pipe is equal to

$$h_{\max} = \frac{a \Delta v}{g} \quad [2]$$

where

h_{\max} = maximum pressure rise, ft
 Δv = velocity destroyed, fps
 g = acceleration due to gravity, ft per sec per sec

This pressure rise is produced when a velocity of Δv feet per second is destroyed instantaneously, or in a time less than the critical time of the pipe. Equation [2] is the fundamental equation upon which all water-hammer studies are based.

If the pipe is of variable diameter, the effective velocity v should be used in Equation [2] and should be calculated as follows

$$v = \frac{l_1 v_1 + l_2 v_2 + \text{etc.}}{L} = \frac{\Sigma lv}{L} \quad [3]$$

The formula developed for the velocity of the pressure wave is given by

$$a = \frac{12}{\sqrt{\frac{w}{g} \left(\frac{1}{k} + \frac{d}{Ee} \right)}} = \frac{4660}{\sqrt{1 + \frac{kd}{Ee}}} \quad [4]$$

where

d = diameter of pipe, in.
 e = thickness of walls of pipe, in.
 k = voluminal modulus of elasticity of water, 294,000 psi
 E = modulus of elasticity of material of pipe walls, approximately 29,400,000 for steel, psi
 w = weight of 1 cu ft of water, lb

For steel pipes commonly encountered in practice, this formula becomes

² Numbers in parentheses refer to the Bibliography at the end of the paper.

$$a = \frac{4660}{\sqrt{1 + \frac{d}{100e}}} \quad [5]$$

For a pipe concreted in solid rock, the fraction $\frac{kd}{Ee}$ in Equation [4] becomes infinitesimal, and the limiting value of 4660 is reached for a , this being the velocity of sound in water.

The value of a for wood-stave pipes depends not only upon the modulus of elasticity of the wood making up the staves and that of the steel of the bands, but also upon the deflection of the staves between bands, the degree the bands have been embedded in the staves, and perhaps other factors.

In general, however, the value of a for wood-stave pipes is low, how low it is impossible to foretell. This would make the problem of water hammer in such pipe indeterminate if it were not for the fact that, in many cases, it makes little difference what value of a is selected since, with a given time of closure of the turbine gates, the higher the value of a the greater the number of intervals within the closure period. This tends to lower the pressure rise and more or less to compensate for the greater magnitude of the water-hammer wave. Thus if a is increased, the factor a/g in Equation [2], converting velocity change to pressure change, is increased, but the number of intervals (see Equation [9]) increases due to a smaller value of $2L/a$, and these two factors tend to offset each other in the result. It is suggested that the following formula be used to determine a tentative value of a , and that several lower values be used to investigate what effect a change in a has upon the result

$$a_w = \frac{4660}{\sqrt{1 + \frac{KD}{E_w b + E_s \phi}}} \quad [6]$$

where

a_w = velocity of pressure wave in wood-stave pipe
 K = modulus of elasticity of water in compression
 $= 42,400,000$ psf
 D = diameter of pipe, ft
 E_w = modulus of elasticity of wood staves. For the usual kinds of wood used in the construction of wood-stave conduits, the moduli of elasticity are as follows:
 B.C. fir or Douglas fir 230,000,000 psf
 Redwood or cypress 192,000,000 psf
 White pine 100,000,000 psf
 For old staves deteriorated by use and the action of the elements, these values should be reduced considerably, for instance, tests on B.C. fir have shown that the value of 230,000,000 psf may be reduced to as low as 60,000,000 psf.
 b = stave thickness, ft
 E_s = modulus of elasticity of steel bands in tension
 $= 4,230,000,000$ psf
 ϕ = total cross-sectional area of steel bands in sq ft per linear ft of pipe

For concrete pipe and buried pipe, the value of a usually runs high with a possible upper limit of 4660 fps.

ALLIEVI'S WATER-HAMMER CHARTS

Allievi's chart (2) for the solution of the maximum pressure of water hammer when the velocity is destroyed at a uniform rate to zero is reproduced in Fig. 3. The range of this chart has been extended considerably beyond that of charts heretofore published, in order to cover many cases of water hammer involving

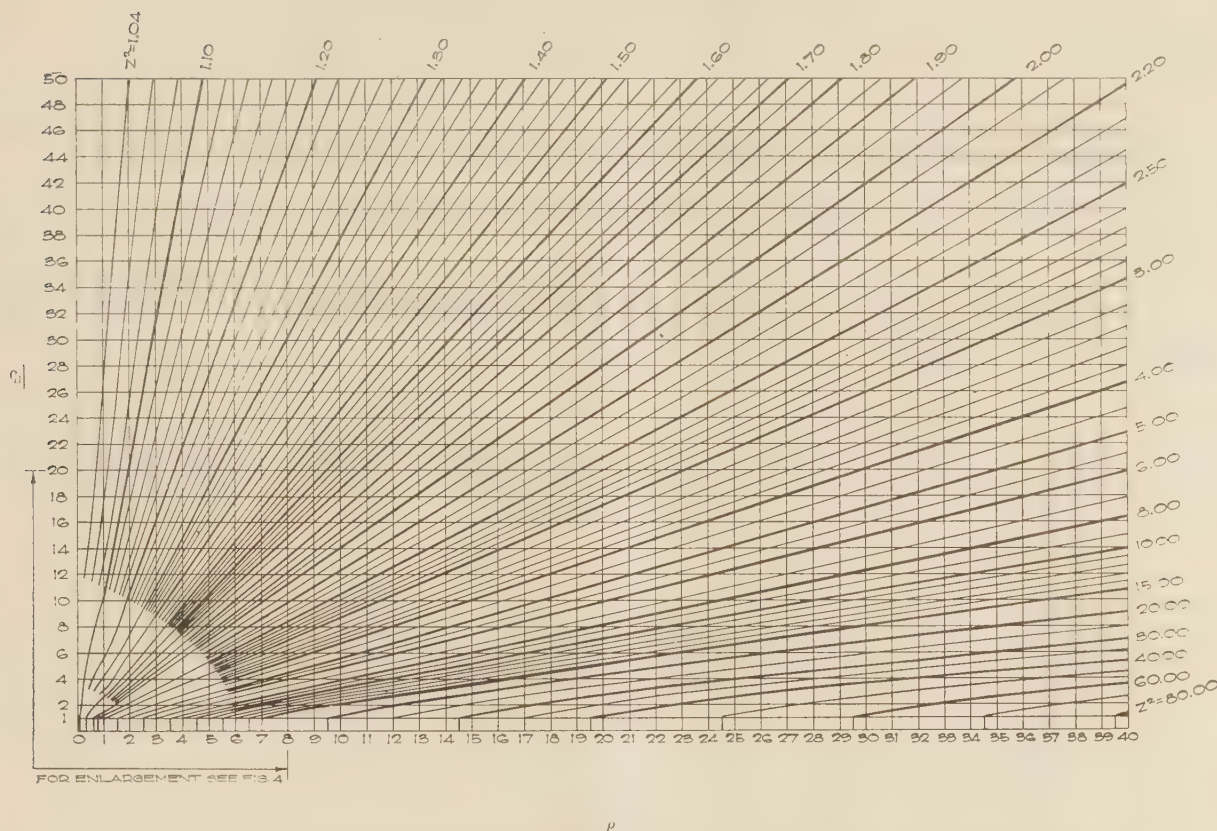


FIG. 3 CHART FOR DETERMINING MAXIMUM PRESSURE RISE FOR UNIFORM GATE MOTION AND SIMPLE CONDUITS
(For large values of ρ and/or θ .)

pipe lines whose physical characteristics are outside of the values for which these charts were designed. The uniform rate of velocity decrease assumes a uniform speed of closure of the gate and a straight-line relation between discharge and gate opening. The lines on the chart converge at low values of ρ and θ and, because of this, only a few have been carried through to the ρ axis. Fig. 4 has been prepared to show the detail of the chart at low values of ρ and θ .

Allievi's chart for the minimum pressure due to uniform increase in velocity is shown in Fig. 5. Here also, simple conduits are assumed. The chart is made for opening the turbine gates from a closed position to any desired degree of opening and at any speed of operation.

The ordinates of the charts are dimensionless numbers or parameters and are designated as ρ and θ . The parameter ρ is called the "characteristic" of the conduit and is expressed by the equation

$$\rho = \frac{av_0}{2gH_0} \quad [7]$$

where

H_0 = static head at lower end of pipe, in feet (of water), measured from forebay level or from elevation of water in surge tank at beginning of gate movement to tailrace level, and other symbols are as previously given.

The parameter θ is called the "time parameter" and is the ratio of the total time of gate operation to the time of one interval as given by Equation [1], i.e., it is the time of gate operation expressed in intervals and may be written

$$\theta = \frac{aT}{2L} = \frac{T}{\mu} \quad [8]$$

where

T = time of gate operation as obtained in the following section.

The symbol Z is a measure of the water hammer. Symbol Z^2 is defined as the ratio of the maximum total head to the initial head

$$Z^2 = \frac{H_0 + h_{\max}}{H_0} \quad [9]$$

The curves S in Fig. 4 indicate the time, in terms of μ , which elapses from the beginning of closure to the instant of the occurrence of the maximum pressure. An example giving the use of Allievi's charts is given later.

The charts are for pipes having a constant value of a throughout their lengths and, therefore, apply to pipes of uniform wall thickness and diameter, classed as simple conduits by the A.S.M.E. Water Hammer Committee (3). Where the closing time is relatively long and the gate motion is approximately uniform, the Allievi charts may be used for approximate results in problems involving complex conduits. To apply the chart, the complex conduit must be reduced to an equivalent simple conduit. In this case a value of a should be determined for each section of constant diameter and thickness, and the effective value of a should be determined from the following equation

$$\frac{L}{a} = \frac{L_1}{a_1} + \frac{L_2}{a_2} + \frac{L_3}{a_3} + \text{etc.} \quad [10]$$

³ A conduit having variable thickness and diameter.

In addition to the Allievi chart, the Quick chart (4) is also recommended for the determination of the maximum pressure rise for uniform gate motion and simple conduits.

GATE MOTION

The time of governor action is not necessarily proportional to the percentage of gate motion, owing to the fact that certain time elements enter into the problem caused by the physical limitations of the governor itself. A typical curve of percentage of time of full stroke, corresponding to the percentage of gate travel, obtained on the test of a modern turbine, is shown in Fig. 6.

The penstock velocity at any particular gate opening may be expressed by an equation in the form of one representing the velocity through an orifice as follows

$$V_0 = C \frac{A_0}{A_p} \sqrt{2g} \sqrt{H_0} \dots \dots \dots [11]$$

where

V_0 = penstock velocity at gate opening A_0 , fps

C = coefficient of discharge of turbine

A_p = the area of the penstock, sq ft

H_0 = head operating on turbine

This equation may be written

$$V_0 = B_0 \sqrt{H_0} \dots \dots \dots [12]$$

where

$$B_0 = C \frac{A_0}{A_p} \sqrt{2g} \dots \dots \dots [13]$$

Knowing the characteristics of the turbine the value of B_0 may be readily determined and for any gate opening A and any head H we may write

$$V = C \frac{A}{A_p} \sqrt{2g} \sqrt{H} = B \sqrt{H} \dots \dots \dots [14]$$

Where uniform motion of the turbine gates is assumed, the relation between time and the gate-opening factor B may be expressed by

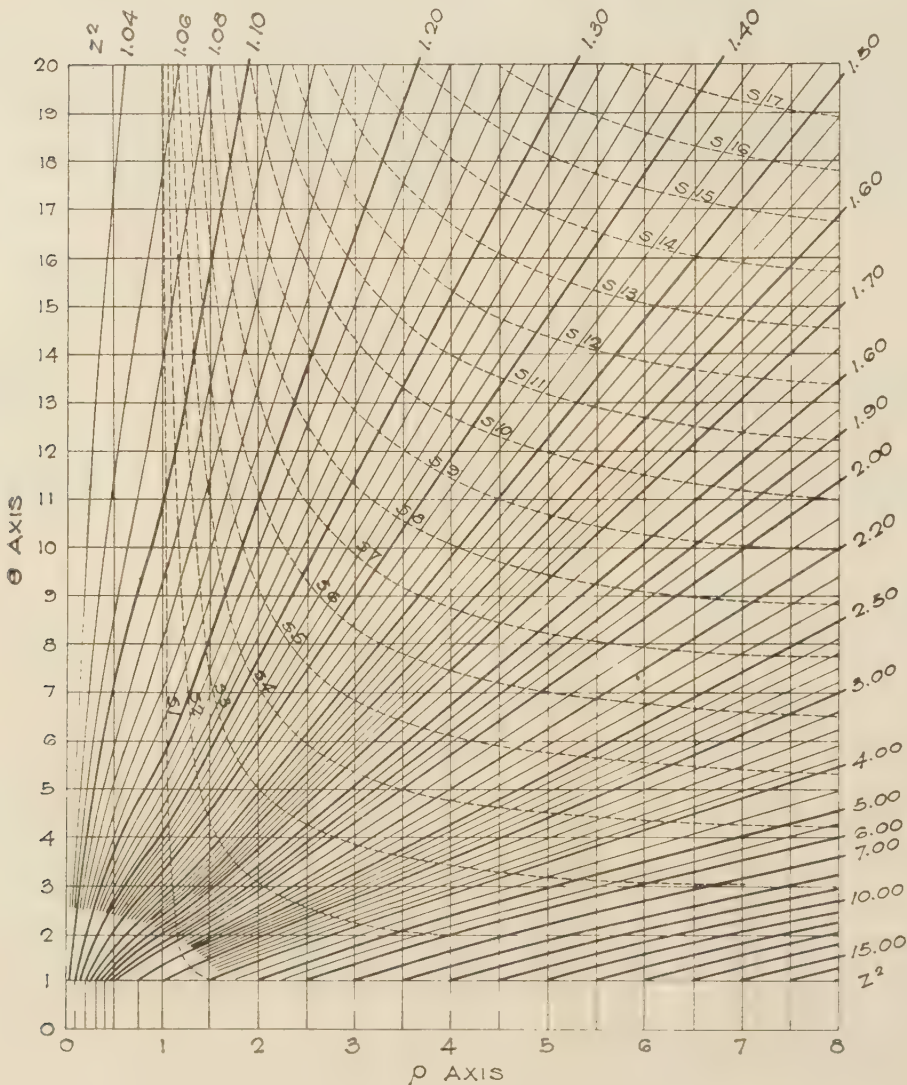


FIG. 4 CHART FOR DETERMINING MAXIMUM PRESSURE RISE FOR UNIFORM GATE MOTION AND SIMPLE CONDUITS
(For small values of ρ and θ .)

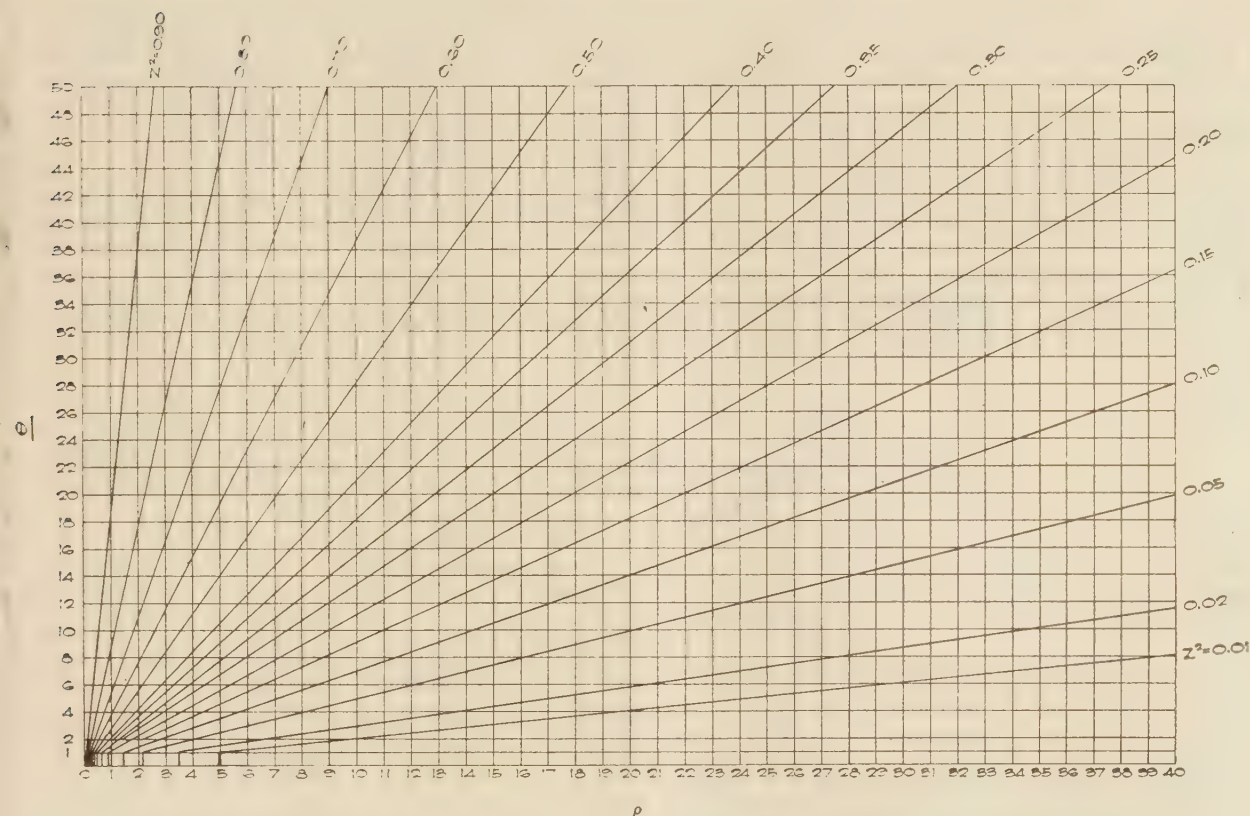
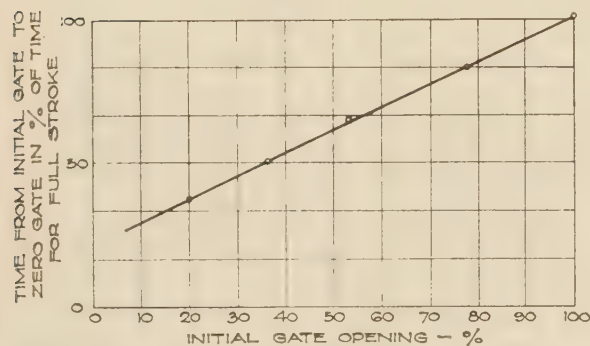


FIG. 5 CHART FOR DETERMINING MAXIMUM FALL IN PRESSURE FOR UNIFORM GATE MOTION AND SIMPLE CONDUITS

FIG. 6 TYPICAL RELATION BETWEEN AMOUNT OF GATE TRAVEL AND TIME OF TRAVEL FOR HYDRAULIC TURBINE
(Per cent time; per cent full stroke to zero.)

$$B = \left(1 - \frac{t}{T}\right) B_0 \dots \dots \dots [15]$$

where T is the total time of closure and B_0 the initial gate-opening factor.

The usual movement of the turbine gates with respect to time, however, is not uniform as the mechanism has an inertia effect at the beginning of the stroke, and a cushioning effect may be present at the end of the stroke. A curve of typical gate motion with respect to time is compared with uniform movement in Fig. 7. This curve may be considered sufficient for preliminary examination, but the final curve should be furnished by the turbine manufacturer. Also the relationship between gate opening

and discharge in practical cases is not a straight-line relationship, as is illustrated by the curve in Fig. 8.

To simplify the solution of water-hammer problems, by means of the Allievi chart, it is possible to secure a value of "equivalent time" for cutting off the flow to represent the time which would be required to close the gates from the wide-open position if they moved uniformly at the maximum rate existing at any portion of the entire movement. Fig. 9 illustrates one method of obtaining "equivalent time."

If the variation of discharge with respect to gate opening is also nonuniform, a correction must be applied to the gate opening to secure the "equivalent gate opening" for full quantity being cut off uniformly. This equivalent gate opening must then be used as a percentage of full gate opening, and a corresponding additional reduction must be made in the "equivalent time," resulting in the net equivalent time T , for use in Equation [9], as shown in Fig. 9 (see reference 3).

It should be noted that results thus obtained are approximate and if an exact solution is desired, the arithmetic-integration method or the graphical method, as described in later sections, should be employed.

CRITICAL GOVERNOR TIME

Although the total time of closure in the ordinary hydraulic turbine from full gate is much larger than μ , it is evident that there is a closure from a partial gate opening with a timing approximating the critical time. The pressure rise from such a gate closure is obtained from Equation [2] and may be greater than the pressure rise occurring when closure from full gate is made. Consequently, it is desirable to investigate closures from part gate positions as well as closures from full gate to obtain

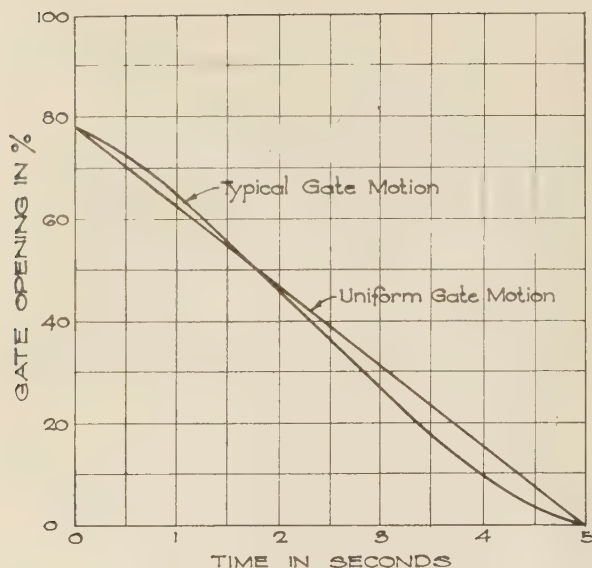


FIG. 7 TYPICAL GATE MOTION-TIME CURVE FOR HYDRAULIC TURBINE FOR CLOSURE FROM 77 PER CENT GATE OPENING TO ZERO

the maximum pressure rise to which the penstock may be subjected (5).

PRESSURE CONDITIONS ALONG PIPE

If closure occurs instantaneously, the pressure wave will travel undiminished up the conduit to the intake or point of relief. For closures which take place in a time greater than zero but less than one interval $\left(T > 0 < \frac{2L}{a}\right)$, the maximum pressure rise will be transmitted along the pipe to a point where the distance to the intake is equal to $\frac{Ta}{2}$. From that point to the intake, the pressure reduces uniformly to zero. When the duration of uniform closure is equal to or greater than the critical time $\frac{2L}{a}$, the maximum rise of pressure occurs at the gate, and in the case of a pipe of constant diameter and thickness, from there to the forebay, reduces to zero uniformly along the length of the pipe. If the pipe is of varying diameter, as shown in Fig. 10, it is usually assumed that the magnitude of the maximum superpressure or depression found at the gate diminishes from the gate to the point of open water and has a value at any point k , equal to that given in Equation [16]. For fast closures, this equation may not give results which are sufficiently exact, and for this case the graphical method should be used (7, 8).

$$h_k = \frac{h(l_1v_1 + l_2v_2 + \dots + l_kv_k)}{LV} = \frac{h \sum_0^k l_0v}{LV} \dots [16]$$

where

- h_k = water hammer at point k
- h = water hammer at turbine
- V = effective velocity for whole pipe from Equation [2]
- L = total length of pipe
- $l_1, l_2, l_3 \dots l_n$ = successive lengths of pipe having constant velocity values of $v_1, v_2, v_3 \dots v_n$, respectively

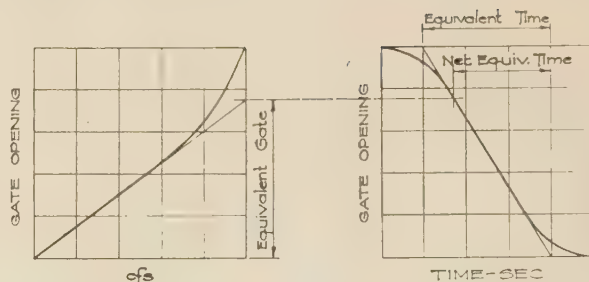


FIG. 8 RELATION BETWEEN GATE OPENING AND DISCHARGE

FIG. 9 SHAPE OF TIME-GATE CURVE AND DETERMINATION OF "NET EQUIVALENT TIME"

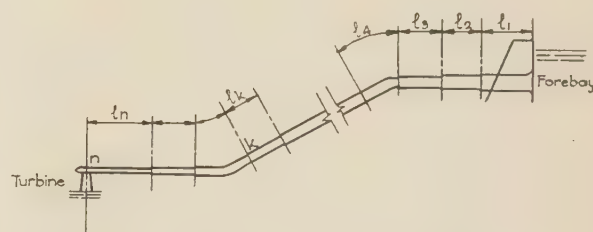


FIG. 10 PENSTOCK OF VARIABLE DIAMETER

Using n to denote the penstock at the turbine and referring back to Equation [3], we may write Equation [16] as follows

$$h_k = \frac{h \sum_0^k l_0v}{\sum_0^n l_0v} \dots [17]$$

ARITHMETIC-INTEGRATION METHOD OF COMPUTATION

The arithmetic-integration method (6), as considered here, applies to simple pipes and is included for the purpose of bringing out certain fundamental concepts of the subject which will facilitate the presentation of the graphical method of computation.

The water hammer resulting from a gate movement can readily be calculated by using Equation [2] to determine and tabulate the pressure rise (or fall) due to the velocity change during each interval of time of $\frac{2L}{a}$ seconds and by combining properly these tabulated values of pressure rise (or fall) considered as supernormal and subnormal pressure waves. Considering a gate closure, and letting V_1 be the velocity destroyed during the first interval, V_2 the velocity destroyed during the second interval, etc., the pressure rise during the first interval is

$$\Delta h_1 = \frac{a}{g} \Delta V_1 \dots [18]$$

and the pressure existing at the end of the first interval is

$$h_1 = h_0 + \Delta h_1 \dots [19]$$

During the second interval, the pressure rise due to the velocity change ΔV_2 is

$$\Delta h_2 = \frac{a}{g} \Delta V_2 \dots [20]$$

but during this interval the pressure wave formed during the first interval is reflected and starts to travel from the valve or gate as a subnormal wave. At the end of the second interval, the magnitude of this subnormal wave is $-\Delta h_1$ instead of $+\Delta h_1$, and the pressure existing at this time is

$$h_2 = h_1 + \Delta h_2 - 2\Delta h_1 \dots \dots \dots [21]$$

At the end of the third interval Δh_2 has become subnormal and Δh_1 has become supernormal so that at this time the pressure existing at the turbine is

$$h_3 = h_2 + \Delta h_3 - 2\Delta h_2 + 2\Delta h_1 \dots \dots \dots [22]$$

Accordingly, the pressure existing at the end of the n th interval is

$$h_n = h_{n-1} + \Delta h_n - 2\Delta h_{n-1} + 2\Delta h_{n-2}, \text{ etc.} \dots \dots \dots [23]$$

From these relations, the ordinary water-hammer problem may be solved by means of arithmetic integration. To illustrate the method, the solution of the following problem is presented:

Assuming a penstock area of 55.66 sq ft, and the following conditions

$$\begin{array}{ll} L = 1000 \text{ ft} & g = 32.2 \text{ ft per sec per sec} \\ V_0 = 10.78 \text{ fps} & T = 2.66 \text{ sec} \\ H_0 = 200 \text{ ft} & a = 3005 \text{ fps} \end{array}$$

calculate the maximum pressure rise at the turbine for a gate closure to zero at a rate as shown by the gate-time curve in Fig. 19. Assume that the turbine gate-discharge relation is as shown

in Fig. 19. The time of one interval, Equation [1], is $\frac{2 \times 1000}{3005} = 0.665$ sec. The computation is shown in Table 1; and the following procedure is used:

1 The time in terms of intervals and seconds is recorded in columns 1 and 2 in Table 1.

2 The initial gate-opening factor B_0 is calculated from Equation [12] or $V_0 = \frac{10.78}{\sqrt{200}} = 0.7623$ and recorded in the first line of column 3.

3 The initial values of head and velocity are set down in the columns 4 and 5, respectively.

4 The remaining values of B in column 3 are then set down, using Fig. 19, as follows: Entering curve A (Fig. 19) with the value of time at the end of the first interval, i.e. 0.665 sec, the gate-opening position of 80 per cent is found. Entering curve B with a gate-opening value of 80 per cent, a discharge of 541 cfs is found. This corresponds to a velocity of $\frac{541}{55.66} = 9.724$ fps

and therefore the value of B at the end of the first interval is $\frac{9.724}{\sqrt{200}} = 0.6876$. Similarly the values of B at the end of the second, third, etc., intervals are obtained.

5 The change in velocity during the first interval is then estimated. Since there are four intervals in the closure, this velocity change would be not greater than $\frac{10.78}{4} = 2.695$ fps, due to the slow motion of the gate at the start. Accordingly, the value selected would be somewhere between 0 and 2.695. Estimating this change at 0.330, the pressure rise during the first interval would be $\frac{3005}{32.2} \times 0.330 = 93.32 \times 0.330 = 30.79$ ft. This is entered in column 7 as h_1 .

6 The total head at the turbine at the end of the first interval is then calculated as $200 + 30.79 = 230.79$ and entered in column 4.

7 The velocity remaining at the end of the first interval is $10.780 - 0.330 = 10.450$ which is entered in column 5.

8 The value of B , corresponding to a head of 230.79 and a velocity of 10.450, is then calculated from Equation [14],

$$B = \frac{10.450}{\sqrt{230.79}} = 0.6876 \text{ and, if this value checks the one already}$$

recorded in column 3, the estimate of velocity change, i.e., 0.330, is correct. If this value of B does not check the one already recorded, a new estimate of velocity change is then made and the steps outlined are again taken, until a satisfactory check is obtained.

9 Similarly the remaining figures in the table are filled out, remembering that Equation [23] should be used to obtain h_i , i.e., the h_i at the end of the third interval is calculated as follows:

$$h_3 = 175.36 + 481.00 - 2 \times 206.15 + 2 \times 30.79 = 305.64$$

TABLE 1 ARITHMETIC INTEGRATION

(1) Time Intervals	(2) Seconds	(3) Gate B	(4) Head H	(5) Velocity V and ΔV	(6) $\Delta h =$ 93.32 ΔV	(7) h_i
0	0	0.7623	200.00	10.780		0
1.0	0.665	0.6876	230.79	0.330 10.450	30.79	30.79
2.0	1.33	0.4253	375.36	2.209 8.241	206.15	175.36
3.0	2.00	0.1372	505.64	5.155 3.086	481.00	305.64
4.0	2.66	0.0000	182.26	3.086 0.000	287.90	-17.74

GRAPHICAL METHOD OF ANALYSIS

The graphical method (7, 8) of determining the water-hammer pressure in pipes is convenient for use in solving many problems which, with analytical methods, would require considerable time and labor. In general, the method involves the plotting of sets of simultaneous equations relating flow or velocity to head, and taking the form of a series of straight lines and a series of parabolas, the straight lines representing the pressure due to the direct and indirect water-hammer blows, and the parabolas representing discharge through the turbine gates, considered during the disturbed regimen as a series of orifices under varying heads. The orifice relation is given by Equation [14] and, assuming that the penstock from turbine to forebay is uniform in thickness and diameter, as illustrated in Fig. 11, the water-hammer equation is given by

$$\begin{aligned} H_{AT1} - H_{Bt^{1/2}} &= + \frac{a}{g} (V_{At1} - V_{Bt^{1/2}}) \\ H_{Bt^{1/2}} - H_{At1} &= - \frac{a}{g} (V_{Bt^{1/2}} - V_{At1}) \end{aligned} \dots \dots [24]$$

where

$$\begin{aligned} H_{AT1} &= \text{head, in ft, at the gate end of the penstock at time } t_1 \\ H_{Bt^{1/2}} &= \text{head, in feet, at forebay end of penstock at time } t_1/2 \\ &\quad (1/2 \text{ interval}) \\ V_{AT1} &= \text{velocity, in ft per sec, at gate end of penstock at time } t_1 \end{aligned}$$

Using the zero subscript to indicate initial conditions, and lower-case letters primed to indicate head, velocity, etc., in terms of relative values, thus

$$v' = \frac{V}{V_0}, h' = \frac{H}{H_0}, \text{ and } \tau' = \frac{B}{B_0} \dots \dots \dots [25]$$

then Equation [14] becomes

$$v' = \tau' \sqrt{h'} \dots \dots \dots [26]$$

and Equation [24] becomes

$$\left. \begin{aligned} h'B_{1/2} - h'A_1 &= -2\rho(v'B_{1/2} - v'A_1) \\ h'A_1 - h'B_{1/2} &= +2\rho(v'A_1 - v'B_{1/2}) \end{aligned} \right\} \dots [27]$$

where ρ is the parameter as given by Equation [7].

To solve Equations [26] and [27] graphically, a diagram as illustrated in Fig. 12 is constructed. The family of parabolas starting from the origin is first constructed. One parabola is made for each interval of time (or fraction of interval). In the diagram, the curve $\tau' = 1$ gives the relation between h and v for the initial gate opening as in Equation [26], the curve

$$\tau' = \left(1 - \frac{2L}{aT}\right) = 1 - \frac{1}{\theta} = \frac{\theta - 1}{\theta}$$

for the gate opening at the end of the first interval, etc. From the point 1, 1 a line of slope (-2ρ) is drawn which intersects $\tau' = 1 - \frac{1}{\theta}$ at A_{11} . This line represents the first straight line of Equation [27]. Then a line is drawn through A_{11} with a slope of $(+2\rho)$ which intersects the line $h = 1$ at $B_{11/2}$, etc. The co-ordinates of the points A_{11} , A_{12} , etc., indicate the head and velocity conditions at the turbine end of the penstock at the end of intervals 1, 2, etc., and the co-ordinates of the points $B_{11/2}$, $B_{12/2}$, etc., indicate the head and velocity conditions at the forebay end of the penstock at the end of intervals $\frac{1}{2}$, $\frac{1}{2}$, etc. The pressure-time curve for the turbine end of the penstock is obtained by plotting the values of head at the points A_{10} , A_{11} , A_{12} , etc., against $0, \frac{2L}{a}, \frac{4L}{a}$, etc., seconds, respectively.

Where friction is an appreciable quantity in relation to the total head on the turbine, it should be taken into account. This may be done graphically by assuming that the friction acts as though it were concentrated at one or more points along the pipe. The greater the number of points selected for concentrating the friction, the greater the accuracy obtained. Usually it is sufficiently accurate to assume that all of the friction is concentrated at the gate or valve.

Fig. 13 illustrates the method of taking account of friction on the assumption that it acts at the turbine end of the conduit. The parabolas, representing the discharge-head relations for the various gate positions at interval points during the closure, are first drawn and then the line OA is drawn below the X axis by the amount of the friction loss in the conduit. The diagram is then begun at the point C which is located on the X axis and directly above the point B which is at the intersection of the parabola for the initial gate opening and the friction curve. The line DC is drawn through C with the slope of -2ρ , and then the line EB is drawn below DC by the amount of the friction loss. This line intersects the parabola for the end of the first interval at F . A vertical line through F intersects DC at the point G which gives the velocity and head conditions at the end of the first interval. The same procedure is followed for succeeding intervals, as shown by the diagram.

APPROXIMATE EQUATIONS FOR WATER HAMMER IN PENSTOCK WITH SURGE TANK

In the case of a hydroelectric plant supplied with a surge tank, the water-hammer pressures which may take place in the penstock or pipe line, due to tripping the load off the station, may be determined by close approximation by the formulas of Calame and Gaden (9), and (10). By the ingenious use of a number of parameters or "relative values," these authors have reduced con-

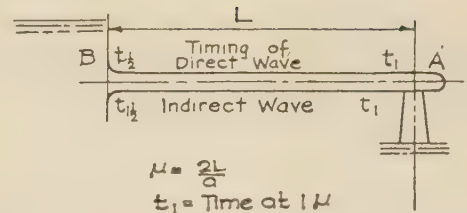


FIG. 11 PENSTOCK SHOWING TIMING OF DIRECT AND INDIRECT WAVES

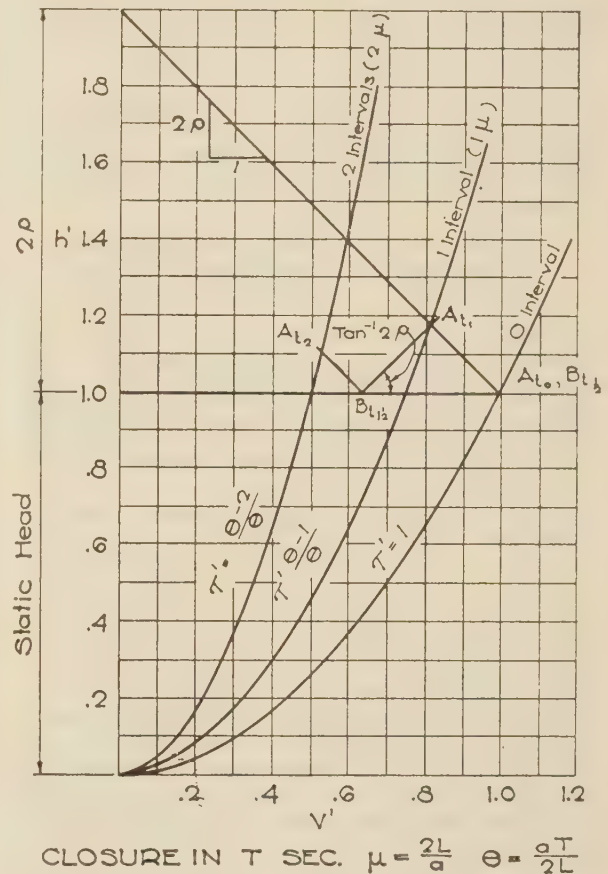


FIG. 12 GRAPHICAL CONSTRUCTION FOR SOLUTION OF WATER HAMMER PROBLEMS OF PRESSURE RISE IN PENSTOCKS

siderably the work formerly required for a solution of this problem.

The water-hammer pressures in the system should not be confused with the more or less gradually changing pressures caused by the mass oscillation of the water which takes place over a much longer period than that associated with the normal timing of the gate stroke. The pressure rise due to mass oscillation may be larger or smaller than that due to water hammer and should also be investigated to see which is controlling for the proper design of the pipe.

In the following analysis, it is assumed that the governor time is greater than the period of the penstock (μ_c). Also the effect of friction is neglected.

Fig. 14 shows a typical surge-tank installation, with pipe line a , tank b , penstock c , and turbine d . The following list of sym-

bolds refers to this diagram. If there is more than one penstock, the group may be considered to be reduced to a single penstock with equivalent values of a_e , V_{c0} , etc.

Let

L_a = length of pipe line along its axis from forebay to surge tank, ft

L_b = length of surge tank along its axis measured from intersection of axes of riser and pipe line to initial water surface in tank, ft

L_c = length of penstock along its axis from surge tank to turbine, ft

a_a = velocity of pressure wave in pipe line, fps

a_b = velocity of pressure wave in surge-tank riser, fps

a_c = velocity of pressure wave in penstock, fps

V_{a0} = initial velocity in pipe line, fps

V_{b0} = velocity in riser of surge tank corresponding to initial flow in pipe line, fps

V_{c0} = initial velocity in penstock, fps

μ_a = period of pipe line, (sec) = $\frac{2L_a}{a_a}$

μ_b = period of surge tank, (sec) = $\frac{2L_b}{a_b}$

μ_c = period of penstock, (sec) = $\frac{2L_c}{a_c}$

$K_a = \frac{a_a V_{a0}}{2g H_{b0}}$

$K_b = \frac{a_b V_{b0}}{2g H_{b0}}$

$K_c = \frac{a_c V_{c0}}{2g H_{b0}}$

$K_d = \frac{a_c V_{c0}}{2g H_0}$

$Z_{d \max}^1 = \frac{H_0 + h_{d \max}}{H_0}$ = ratio of maximum total head at turbine with respect to initial head on turbine

$(Z_{d \max}^1 - 1) = \frac{h_{d \max}}{H_0}$ = maximum pressure rise at turbine in terms of total head H_0

T = governor time, sec

$N_c = \frac{T}{\mu_c}$

$M_b = \frac{K_a}{K_b}$

$M_c = \frac{K_a}{K_c}$

$Z_{bm}^1 = \frac{H_{b0} + h_{bm}}{H_{b0}}$ = ratio of maximum total head at surge tank with respect to initial head at tank

Subscript 0 refers to initial conditions, subscript a to the pipe line, b to the tank, and d to the turbine.

The pressure rise at the lower end of the penstock is determined approximately as follows:

1 If $K_d < 1$, the pressure rise is a maximum during the first interval of μ_c and

$$(Z_{d \max}^1 - 1) = \frac{2K_d/N_c}{1 + K_d(1 - 1/N_c)} \dots \dots \dots [28]$$

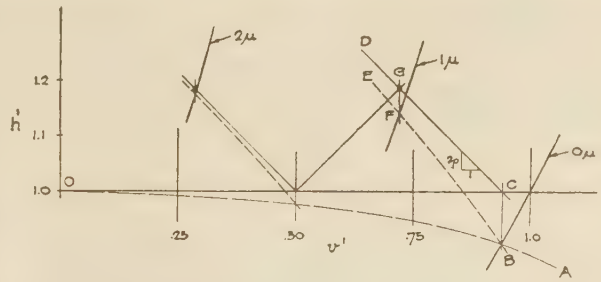


FIG. 13 GRAPHICAL CONSTRUCTION TAKING FRICTION INTO ACCOUNT

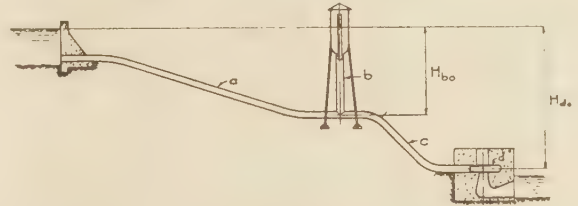


FIG. 14 TYPICAL SURGE-TANK INSTALLATION

2 If $K_d > 1$, the pressure rise tends toward a maximum of

$$(Z_{d \max}^2 - 1) = \frac{K_d/N_c}{1 - K_d/2N_c} \dots \dots \dots [29]$$

The value of $Z_{d \max}^2$ in Equations [28] and [29] for a particular installation may be evaluated by reference to Figs. 15 and 16, respectively.

The pressure rise at the base of the surge tank may then be calculated as follows:

1 If $M_b - M_c - 1 > 0$, the maximum rise occurs during the first interval and may be expressed as

$$(Z_{b1}^2 - 1) = \frac{2K_a \mu_b}{K_c \mu_c} \left(\frac{Z_{d \max}^2 - 1}{M_b + M_c + 1} \right) \dots \dots \dots [30]$$

2 If $M_b - M_c - 1 < 0$, the maximum rise occurs during subsequent intervals, and the maximum pressure rise may be calculated from

$$(Z_{bm}^2 - 1) = \frac{K_a \mu_b}{K_d \mu_c} \left(\frac{Z_{d \max}^2 - 1}{M_b} \right) \dots \dots \dots [31]$$

NUMERICAL EXAMPLES

Example 1. Pressure Rise With Uniform Gate Motion Friction Neglected.

Assuming uniform gate motion and a straight-line relation between gate opening and discharge, find the rise in pressure at the turbine if the penstock velocity is reduced to zero with the following initial conditions and physical constants given. Also, plot the pressure-time curve to cover the duration of closure and the first few afterwaves.

L = length of penstock = 805 ft

V_0 = penstock velocity = 8 fps

H_0 = head = 160 ft

T = time of closure = 4 sec

a = 3220 fps

From Equation [1]

$$\mu = \frac{2L}{a} = 0.5 \text{ sec}$$

from Equation [9]

$$\theta = \frac{T}{\mu} = \frac{4}{0.5} = 8$$

and from Equation [8]

$$\rho = \frac{aV_0}{2gH_0} = \frac{3220 \times 8}{2 \times 32.2 \times 160} = 2.5 \quad 2\rho = 5$$

1 Solution by Allievi chart for maximum pressure rise (Fig. 4):

The maximum pressure is found by obtaining the value of Z^2 when $\theta = 8$, and $\rho = 2.5$ and, from Equation [10], is

$$H_0 + h_{\max} = 1.363 \times 160 = 218.1 \text{ ft}$$

The maximum pressure rise is therefore

$$h_{\max} = 218.1 - 160 = 58.1 \text{ ft, or } 36.3 \text{ per cent}$$

This pressure occurs between the 5th and 6th intervals, as determined by the S lines on the chart.

2 Solution by graphical method (see Fig. 17):

Compute the parabolas determined by Equation [26] for values of τ' of 1, 0.875, 0.75, 0.50, 0.375, 0.25, and 0.125. These curves are marked 0μ , 1μ , 2μ , etc. The series of straight lines is drawn with alternate slopes of $+5$ and -5 , and intersect the parabolas and the line $h = 1$ at the working points. The points 1, 2, 3, 4, etc., indicate the values of h at the turbine at the end of intervals 1, 2, 3, 4, etc., respectively. The maximum pressure is shown to be

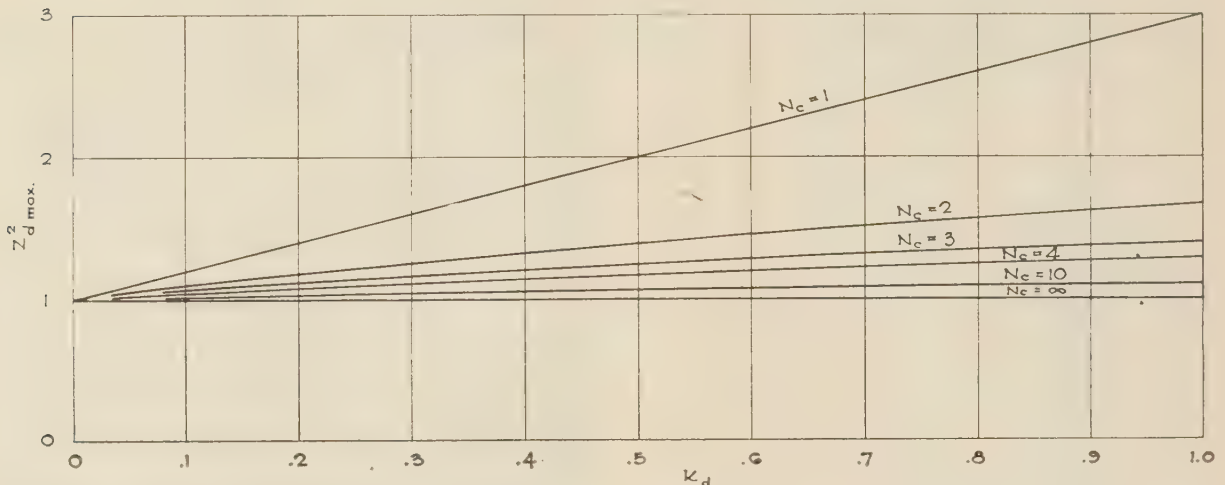


Chart solution of Equation (28) $(Z_{d \max}^2 - 1) = \frac{2K_d/N_c}{1 + K_d(1 - \frac{1}{N_c})}$ where $K_d < 1$

FIG. 15 CHART SOLUTION OF EQUATION [28]

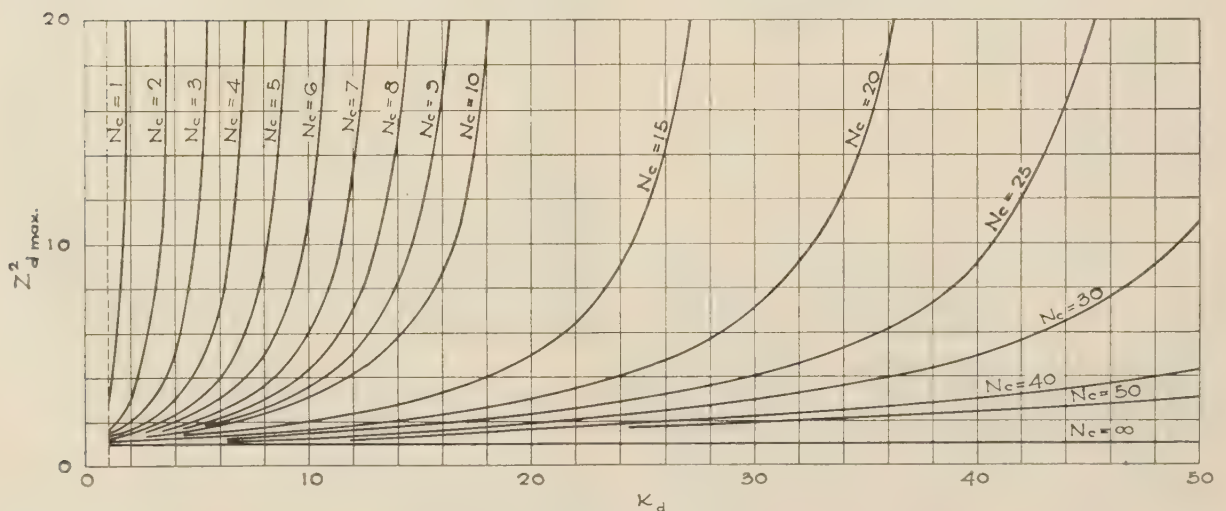


Chart solution of Equation (29) $(Z_{d \max}^2 - 1) = \frac{K_d/N_c}{1 - K_d/2N_c}$ where $K_d > 1$

FIG. 16 CHART SOLUTION OF EQUATION [29]

$$1.365 \times 160 = 218.4 \text{ ft}$$

and the maximum pressure rise is

$$218.4 - 160 = 58.4 \text{ ft or } 36.5 \text{ per cent}$$

The maximum pressure is shown to occur between the fifth and sixth intervals. Fig. 18 shows the relation of pressure at the turbine and time during, and for a short time after, the gate closure. The time and pressure values are taken from the upper set of working points in Fig. 17. It should be noted that the points 8, 9, 10, 11, etc., are for conditions immediately following the gate closure and show the afterwaves of the pressure diagram.

Example 2. Pressure Rise With Nonuniform Gate Motion, Friction Neglected.

With a rate of gate closure and a discharge-gate relationship, as shown in Fig. 19, find the maximum pressure rise at the turbine for full load thrown off in 2.66 sec, assuming a flow of 600 cfs corresponding to full load, a head of 200 ft operating at the turbine, and the penstock conditions given in Table 2.

TABLE 2 PENSTOCK CONDITIONS FOR EXAMPLE 2

Section of penstock.....	1	2	3	4
Diameter, <i>d</i> , ft.....	9	9	8.5	8
Length of section, ft.....	100	200	300	400
Thickness, <i>e</i> , in.....	1/2	3/4	3/4	3/4
<i>d/e</i>	216	144	136	128
<i>a</i>	2625	2990	3050	3100
Area, sq ft.....	63.6	63.6	56.7	50.3
Velocity for <i>Q</i> = 600 cfs.....	9.44	9.44	10.58	11.93

From Equation [3]

$$V_0 = \frac{300 \times 9.44 + 300 \times 10.58 + 400 \times 11.93}{1000} = 10.78 \text{ fps}$$

From Equation [10]

$$\frac{1000}{a} = \frac{100}{2625} + \frac{200}{2990} + \frac{300}{3050} = \frac{400}{3100}$$

$$\text{Average } a = 3005 \text{ fps}$$

$$\mu = \frac{2L}{a} = \frac{2000}{3005} = 0.665 \text{ sec}$$

$$\theta = \frac{2.66}{0.665} = 4$$

The values of τ' (see Equation [26]) are first obtained for as

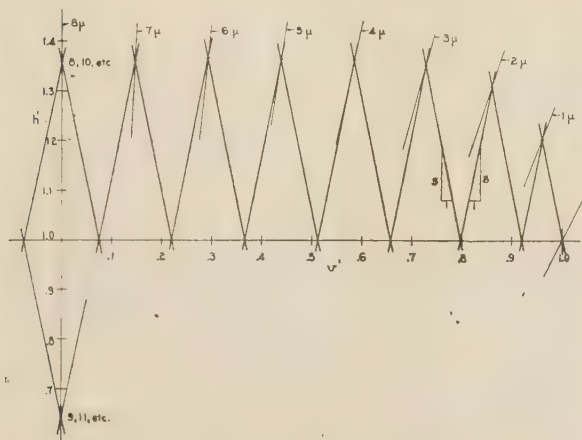


FIG. 17 GRAPHICAL SOLUTION OF PROBLEM 1

many points along the gate curve as desired, in order to plot the parabolas shown in Fig. 20. These values are obtained, as shown in Table 3, for every half interval of time during the closure. With these values of τ' the family of parabolas as shown may be drawn, and then the straight lines of slope plus and minus

$$2\rho = \frac{3005 \times 10.78}{32.2 \times 200} = 5.026$$

are drawn.

TABLE 3 VALUES OF τ' FOR HALF INTERVALS DURING GATE CLOSURE

Time Interval	Sec	Gate opening, per cent (from Fig. 19)	Cfs (from Fig. 19)	V	τ'
0	0	100	600	10.78	1.000
0.5	0.333	93	586	10.50	0.975
1.0	0.665	80	542	9.72	0.902
1.5	1.00	63	455	8.16	0.757
2.0	1.33	46	335	6.01	0.558
2.5	1.66	29	210	3.77	0.350
3.0	2.00	15	108	1.94	0.180
3.5	2.32	5	35	0.63	0.059
4.0	2.66	0	0	0.00	0.000

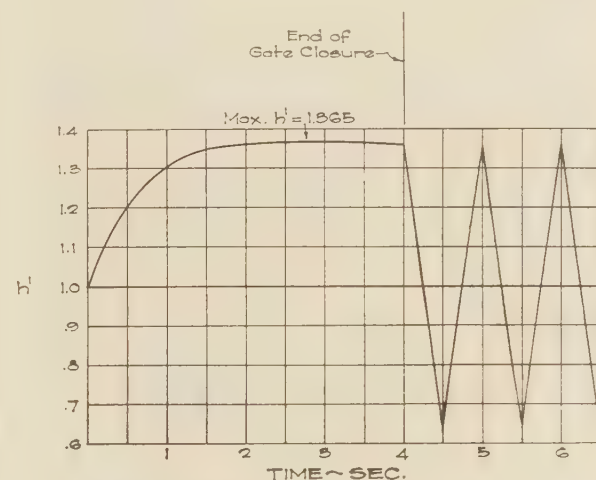


FIG. 18 PRESSURE-TIME CURVE FOR PROBLEM 1

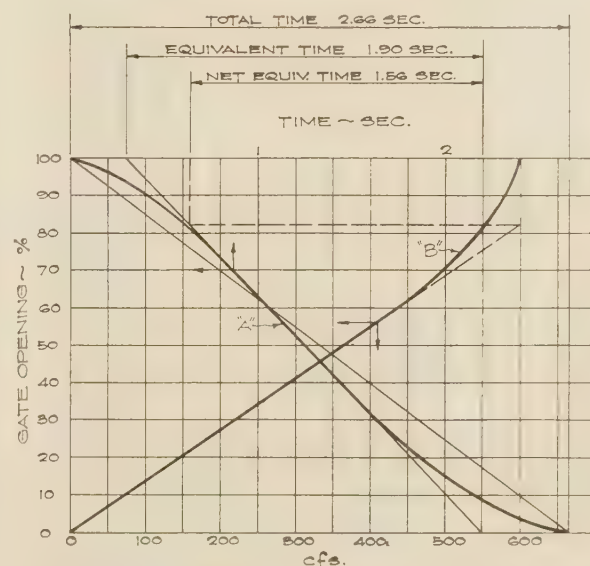


FIG. 19 CHARACTERISTIC CURVES FOR PROBLEM 2

The maximum pressure is shown to be

$$2.525 \times 200 = 505 \text{ ft}$$

The maximum pressure rise is 305 ft or 153 per cent.

It should be noted that, if the Allievi chart is used to determine the pressure rise by using the "net equivalent time" of gate closure, as shown in Fig. 19, and as discussed in the section on "Gate Motion," we obtain

$$\theta = \frac{1.56}{0.665} = 2.346$$

$$\rho = \frac{3005 \times 10.78}{64.4 \times 200} = 2.514$$

and a pressure rise of 400 ft (instead of 305 ft) which is considerably on the safe side for design purposes. This particular example was chosen to emphasize the statement made under "gate motion" that the use of the approximation of "net equivalent time" gives an approximate result and that, if an exact answer is required, the rigorous solution as just shown should be used.

Example 3. Pressure Drop With Uniform Gate Motion and Friction Neglected.

Assuming uniform gate motion and a straight-line relation between gate opening and discharge, find the fall in pressure at the turbine if the penstock flow is increased from zero to 600 cfs in the case of the turbine installation described in Example 2. Assume

$T = 3.66$ seconds for the opening stroke of the governor

The maximum fall in pressure may be found by obtaining the value of Z^2 in Fig. 5, for the proper values of θ and ρ . In this case $\theta = \frac{3.66}{0.665} = 5.5$, and $\rho = 1.513$. Term Z^2 is therefore 0.58; the minimum pressure $0.58 \times 200 = 116$ ft; and the fall in pressure 84 ft or 42 per cent.

Example 4. Pressure Rise at Turbine and at Base of Surge Tank.

Data: Head at turbine = 266.3 ft

Head at base of tank = 213.2 ft

Initial flow = 1650 cfs

Closing time = 6 sec

Pipe line	Surge tank	Penstock
$L_a = 11850 \text{ ft}$	$L_b = 213.2$	$L_c = 250$
$a_a = 2400 \text{ fps}$	$a_b = 2400$	$a_c = 2400$
$D_a = 14 \text{ ft}$	$D_b = 10' - 8''$	$D_c = 13' - 9''$
$A_a = 153.94 \text{ sq ft}$	$A_b = 89.42$	$A_c = 151.98$
$V_{a0} = 10.72 \text{ fps}$	$V_{b0} = 18.45$	$V_{c0} = 10.86$
$\mu_a = 9.88 \text{ sec}$	$\mu_b = 0.178$	$\mu_c = 0.208$
$K_a = \frac{a_a V_{a0}}{2g H_{b0}}$	$K_b = \frac{a_b V_{b0}}{2g H_{b0}}$	$K_c = \frac{a_c V_{c0}}{2g H_{b0}}$
$= \frac{2400 \times 10.72}{64.4 \times 213.2}$	$= \frac{2400 \times 18.45}{64.4 \times 213.2}$	$= \frac{2400 \times 10.86}{64.4 \times 213.2}$
$= 1.874$	$= 3.225$	$= 1.898$

$$N_c = \frac{T}{\mu_c} = \frac{6}{0.208} = 28.85 \text{ number of intervals}$$

$$K_d = \frac{a_c V_{c0}}{2g H_0} = \frac{2400 \times 10.86}{64.4 \times 266.3} = 1.520$$

$K_d > 1$, therefore the pressure rise at the lower end of the penstock is determined by using Equation [29] or Fig. 16.

$$(Z^2_{d \max} - 1) = \frac{K_d/N_c}{1 - K_d/2N_c} = \frac{1.520/28.85}{1 - 1.520/2 \times 28.85} = \frac{0.0527}{0.9737} = 0.0541$$

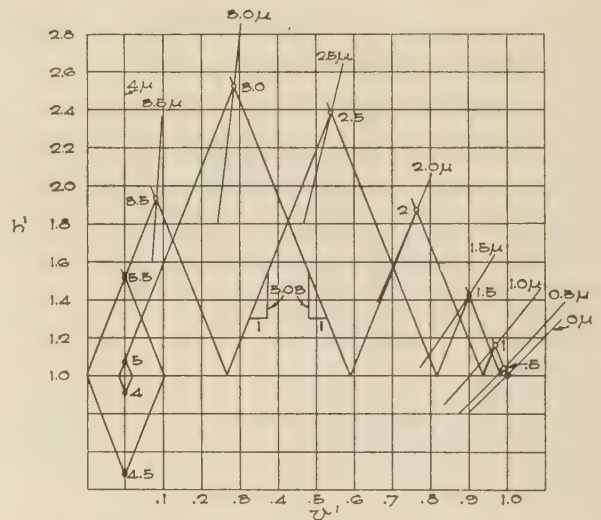


FIG. 20 GRAPHICAL SOLUTION OF PROBLEM 2

$$M_b = \frac{K_a}{K_b} = \frac{1.874}{3.225} = 0.581$$

$$M_c = \frac{K_a}{K_c} = \frac{1.874}{1.898} = 0.987$$

$$M_b - M_c - 1 = 0.581 - 0.987 - 1 = -1.406$$

$M_b - M_c - 1 < 0$, therefore the pressure rise at the base of the tank is determined by using Equation [31]

$$(Z^2_{bm} - 1) = \frac{K_a \mu_b}{K_d \mu_c} \left(\frac{Z^2_{d \max} - 1}{M_b} \right) = \frac{1.874 \times 0.178}{1.520 \times 0.208} \times \frac{0.0541}{0.581} = 0.0982$$

The pressure rise at the lower end of the penstock is $0.0541 \times 266.3 = 14.4$ ft, and the pressure rise at the base of the tank $0.0982 \times 213.2 = 21.0$ ft.

BIBLIOGRAPHY

- "Water Hammer," by Joukovsky, translated by Miss O. Simin, Proceedings of the American Water Works Association, vol. 24, 1904, pp. 341-424.
- "Theory of Water Hammer," by L. Allievi, translated by E. E. Halmos, Garroni, Rome, 1925.
- "Symposium on Water Hammer," A.S.M.E. Committee on Water Hammer, published by A.S.M.E., 1933.
- "Comparison and Limitations of Various Water Hammer Theories," by R. S. Quick, Mechanical Engineering, vol. 49, 1927, pp. 524-530.
- "New Aspects of Maximum Pressure Rise in Closed Conduits," by S. L. Kerr, Trans. A.S.M.E., vol. 51, 1929, HYD-51-3, pp. 13-30.
- "Pressures in Penstocks Caused by the Gradual Closing of Turbine Gates," by N. R. Gibson, Trans. A.S.C.E., vol. 83, 1919, pp. 707-775.
- "Water Hammer in Pipes, Including Those Supplied by Centrifugal Pumps; Graphical Treatment," by R. W. Angus, Proceedings of The Institution of Mechanical Engineers, vol. 136, 1937, pp. 245-331.
- "Etude des variations de regime dans les conduites d'eau. Solution graphique generale," by L. Bergeron. Comptes Rendus des Travaux de la Societe Hydrotechnique de France.
- "Théorie des Chambres D'Équilibre," by J. Calame and D. Gaden, Gauthier-Villars, Paris, 1926.
- "The Effect of Surge Tanks on the Magnitude of Water Hammer in Pipe Lines," by E. E. Halmos, A.S.M.E. Water Hammer Symposium, 1933, pp. 72-80.

Discussion

R. W. ANGUS.⁴ Early in the paper the author refers to the changes in velocity in the part of the system between the forebay and the surge tank as causing water hammer, but there is a distinction between what happens in the "conduit" just referred to and the penstock. In the former, a mass movement of the water always takes place, and it is always possible to treat the water and pipe walls as inelastic, except in the unfortunate case where the surge tank is separated from the conduit by a long small pipe; in the penstock for complete closure there is no mass movement and the elasticity of the parts must be allowed for. While a similar treatment may be applied to both parts of the plant, there is a distinct difference in the principles involved.

The author's Equations [3] and [10], respectively, for preliminary values of effective pipe velocity and effective wave velocity in tapered pipes, are in common use and save a great deal of time in such cases, but the writer knows of no proof of their accuracy and asks if the author does. No matter what method is used in computing water-hammer pressures, it is always tedious to take accurate account of changes in diameter, and these formulas enable the pipe to be treated as a simple one; for accurate results, however, the complete calculation should be made.

The writer has checked the accuracy of Equations [3] and [10] in case of the compound pipe discussed in a paper by Billings, Dodkin, Knapp, and Santos, and published in the Symposium on Water Hammer.⁵ The pipe had a horizontal axis and consisted of 354 ft of pipe 0.655 ft diam attached to a reservoir and joined at its outer end to 1630 ft of pipe 0.394 ft diam; the outlet of the smaller pipe was equipped with a control valve, the head was 328 ft, and friction was neglected. The steady velocities in the pipes were 0.91 fps and 2.52 fps, respectively, and the values of a were 4440 fps and 4180 fps in the large and small pipes, respectively.

Using the Equations [3] and [10] of the paper, the "equivalent simple pipe" would have a velocity $(0.91 \times 354 + 2.52 \times 1630) / 1984 = 2.233$ fps, and a value of a of $1984 / (354 / 4440 + 1630 / 4180) = 4224$ fps; its length would be 1984 ft and the pressure-wave interval $2 \times 1984 / 4224$, or 0.939 sec, while ρ would be 0.447.

The closing of the gate is linear in 2.20 sec in each case.

In Fig. 21 of this discussion, the writer has plotted in solid lines the results he obtained on the pressure rise at the gate for the "equivalent simple pipe," and in dotted lines the values given in the previous paper⁶ for the actual pipe. The agreement is exact for the maximum pressure and is fairly close for all the lengths of the curves.

The writer has never found it necessary to try to establish a "net equivalent time" of gate closure where the latter moves in an irregular way, as shown in Fig. 9 of the paper. It is always a simple matter to take account of any type of gate motion, and it should be done, since the pressure rise is very sensitive to the shape of the "time-gate" curve. In the numerical calculations made by the author, there is no difficulty in using the actual, instead of the modified form of gate-closure curve.

The writer does not think the Allievi diagrams in Figs. 3, 4, and 5 of the paper are very helpful in practice with our present knowledge of water hammer. Nobody has greater admiration than the writer for the work of Lorenzo Allievi and for the contributions he has made; he entered a practically unknown field and left a series of elegant solutions to a difficult problem. Allievi confined his attention to the simple pipe and to uniform gate closure, and the writer has found that with beginners this method is instructive and lends itself to a series of diagrams such as the

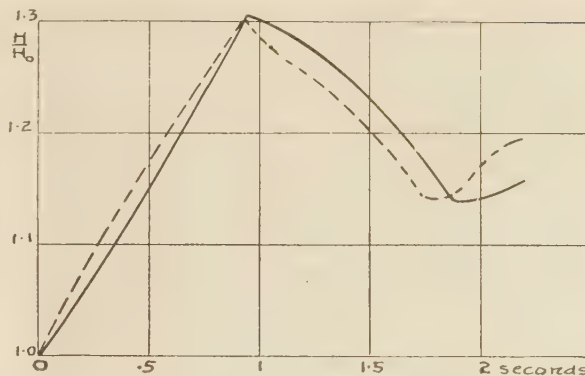


FIG. 21 PRESSURE RISE AT GATE
(Dotted curve is for actual compound pipe, and the curve in solid line is for the "equivalent simple pipe.")

author has included. They stimulate interest in the subject, and are of great importance if for no other reason. But Allievi's assumptions are rarely, if ever, realized in practice, and the type of gate closure has a very great effect. Further, the graphical method⁶ enables a problem to be solved (if Equations [3] and [10] are used) in a few minutes, with a high degree of accuracy, with any possible type of gate motion.

The author has shown that, in his Example 2, the charts indicate a pressure rise of 400 ft, while he estimates the correct rise to be 305 ft, so that the chart is quite inaccurate in this case.

It hardly seems desirable, therefore, to bring out these charts again even for preliminary work. With a small drafting board, or a pad of cross-section paper, the correct diagram for each case is easily drawn, although attention should be given to scales if acute intersections of lines are to be avoided.

Equations [28] to [31] of the paper are based on the deductions of Allievi and apply to linear gate closure, so that they also should be accepted with reserve. The solution of this problem with any type of gate motion may be made by the graphical method, as explained previously by the writer.⁷ While convenient solutions are available it does not seem desirable to use methods limited to special cases different from those being examined. In so far as formulas are used to give preliminary sizes of tanks, they are of great value, since otherwise the true size can be found only by repeated trials, which is a very slow process.

The graphical solutions given by the author have been published in various other papers and a fairly complete bibliography is given in the Water Hammer Symposium,⁸ and in a paper of the writer,⁶ among other sources. The writer hopes that the Water Hammer Symposium will be reprinted in revised form, and that before too long the principal papers dealing with this subject will be available in one publication.

In considering water hammer in power plants, the effects in the draft tubes may be serious, relative to those in the penstocks. Cases are not unknown where the entire rotating element has been lifted by the pressure rise in the draft tube, and therefore the penstock and draft tube should be considered at the same time. The writer has shown one method of dealing with this matter.⁷

C. R. MARTIN.⁸ For many years the writer's company has used the arithmetic-integration method for solving the problem

⁶ Refer to author's Bibliography (7).

⁷ "Water Hammer Pressures in Compound and Branched Pipes,"

by R. W. Angus, Trans. A.S.C.E., vol. 104, 1939, p. 340.

⁸ Engineer, Hydraulic Department, Allis-Chalmers Manufacturing Company, Milwaukee, Wis. Mem. A.S.M.E.

⁴ Professor Emeritus of Mechanical Engineering, University of Toronto, Toronto, Ont., Can. Honorary Mem. A.S.M.E.

⁵ Refer to author's Bibliography (3).

of pressure changes and speed regulation as developed originally by Mr. Gibson and later further explained by Mr. Strowger, Mr. Kerr, and other commentators.

It is our practice to prepare a complete table for each calculation of pressure and speed rises, with the addition of one extra column to show the unit speed at 1-ft head for each interval of time. The unit-speed column is for the purpose of correcting the turbine efficiency for changes above and below normal speed.

As pointed out by the author, it is necessary to consult with the turbine manufacturer for final curves to show the relationship between gate motion, discharge, horsepower, and efficiency all based upon time in seconds. It is considered necessary only to use that portion of the gate motion between the synchronous-speed no-load gate and the maximum gate opening. With present turbine designs, the gate motion is identical with the stroke of the servomotor. A rate-limiting device used in connection with the governor can always be set to produce this relationship.

Governor regulating valves, in most cases, are made to respond immediately to a change in speed, or at least within 0.01 per cent, which is the governor sensitivity obtained with present-day governors. The top portion of the curve, as shown in Fig. 7 of the paper, can be constructed on the basis of allowing $1/4$ sec to obtain the rate of travel as specified for the governor-operating time. If a straight line is drawn from this point of intersection for 100 per cent gate opening and $1/4$ -sec time to the intersection of the gate opening at synchronous speed no-load and the full governor operating time, a correct relationship will be established between these points. The top portion of the curve can be constructed by drawing in an arc of a circle tangent to the straight line and passing through the 100 per cent gate opening, locating the center of the arc on the zero line for time in seconds. The interval of time between the actual speed change and the start of the servomotor stroke is so small that it need not be considered in speed-regulation calculations. The gate position for synchronous speed no-load is one that must be furnished by the turbine manufacturer, as this may vary from 2 per cent as the lower limit to as much as 30 per cent of full-load gate position, depending upon the type of turbine and the variation in head under which the turbine will operate. The lower figure would apply to high-head turbines, while the higher figure is commonly experienced with propeller-runner installations.

In speed-regulation and pressure-rise calculations, the governor operating time should be defined as "the time consumed in moving the gates from synchronous speed no-load to full gate opening," and vice versa, for the reason that it is necessary to throttle the discharge from the servomotor between the synchronous-speed no-load gate position and final closure to avoid slamming of the gates. Otherwise, it would not be possible to carefully design a predetermined breaking point in the gate linkage. This slow travel does not affect pressure rise and speed regulation and can safely be disregarded. The time consumed in the final closure may equal or exceed the total governor-operating time.

Where extreme head-water elevations are encountered, pressure-rise and speed calculations should be made to cover the entire range of head variation. For example, if the governor time is set for 5 sec for normal operating-head conditions, it sometimes happens that the maximum head may be 50 per cent greater, and the governor-operating time may be reduced for the higher head condition. We may have a 3-sec governor closing time as the gate opening may be only 60 per cent of the full gate. Many times the normal rating is fixed at approximately best efficiency under normal head in order to provide for greater unit power under low-head conditions. Most of our high-head plants as now built must be designed to operate under wide range of head. The result is that we have a change in governor time and penstock

velocity for the different head conditions, which should be given consideration.

The manufacturer has found that pressure changes must be considered at three different points, namely, pressure change on the penstock, at the contraction of the speed-ring throat, and on the discharge side of the runner. The penstock manufacturer wants to know the pressure rise pertaining only to the penstock, and the waterwheel designer must design for the maximum pressure rise in the speed ring. The maximum pressure effect on the runner must be calculated to determine the horsepower input and corresponding speed rise for load-off conditions. To obtain this figure, the vacuum produced in the draft tube must be carefully analyzed and due consideration given to the surge effect or the negative pressure created to absorb the momentum of the water column. This consideration has led to further study in the matter of draft-tube design. It is quite possible that the short form of draft tube, of the straight conical type with flaring discharge, as exemplified by the hydracone, could be profitably used for some of our low-head-turbine installations.

While it is true that the change in the velocity of the wave does not materially affect pressure rise, it should be pointed out that with a lower value of a , we shall have a lower pressure rise for instantaneous gate movements and therefore less possibility of destructive pressure rises.

By making the complete calculations for pressure rise and speed regulation, we can plot curves for pressure rise, velocity, and speed change. Electrical designers are now requiring that they have information on the rate of speed change, as this rate affects the design of the generator-excitation system. When full load is thrown off the generator, they have the problem of limiting the maximum voltage, and therefore must know the speed characteristics of the unit.

Regulation guarantees are based upon load thrown off from the fixed gate opening to the synchronous-speed no-load gate position. This does not mean that the same speed rise would be obtained for throwing off fractional loads, starting at full gate opening. For example 25 per cent load-off from approximately 25 per cent gate position to synchronous-speed no-load position may only mean 2 per cent rise in speed, but this same amount of load thrown off from full-gate position to approximately 75 per cent gate may in extreme cases mean a 10 per cent rise in speed. Generally speaking, it is only practical to take on a maximum of 50 per cent load with a unit operating alone.

The writer feels that the author and his associates have done a great service to the hydraulic-engineering fraternity in so ably analyzing the problem of pressure changes and speed regulation. The turbine manufacturer is concerned only with the turbine design and is therefore in no position to furnish information beyond that for his own particular turbine. The economy of a hydroelectric plant is so involved in the full consideration of pressure changes and speed regulation that a complete solution can only be effected by engineers skilled in this work.

L. F. MOODY.⁹ This paper should be of value to the engineer who has not specialized in water-hammer theory. The literature on the subject is so scattered that a concise explanation of the application of the principles to problems of frequent occurrence is a most useful contribution. One of the most helpful publications in this field was the Symposium on Water Hammer.⁸ It would be a useful project for our Water Hammer Committee to bring it up to date, amplify it, and republish it. The present paper also contains some new material, particularly a convenient extension of the Allievi charts for uniform closure.

The writer notes a few minor points which may be worth con-

⁹ Professor of Hydraulic Engineering, Princeton University, Princeton, N. J. Fellow A.S.M.E.

sidering: Under "Fundamental Relations," the third sentence may not convey to some readers a clear idea of the nature of the "reflection" of the pressure wave. It states that upon an instantaneous closing motion of the gate at the outlet of a pipe—"the positive wave resulting therefrom travels up the penstock to the forebay and, upon reaching the forebay, it is reflected back from the open end of the pipe as a negative wave which travels back to the turbine and which has the same magnitude as the positive wave." The action may be viewed as a negative wave superposed on the initial positive wave; or it may be explained as follows: On reaching the forebay the pressure rise is released into the forebay and extinguished, and a wave of zero pressure rise and negative velocity change is propagated back to the gate. When this wave of pressure extinction reaches the gate, the negative velocity change is suddenly stopped and a pressure drop occurs which has the same magnitude as the original pressure rise. The result at the gate is a reversal of the pressure rise, as stated. At an intermediate point between forebay and gate, however, the pressure rise is not immediately reversed or "reflected," but an intermediate interval of zero pressure rise occurs.

The method of arithmetic integration illustrated in the paper was perhaps selected as requiring a minimum of explanation. It will be noted, however, that at one point—"the change in velocity ... is then estimated," thus requiring a guess and successive approximations at each step. Probably, with the author's skill and experience, he can make a close approximation at each point. It would greatly improve the procedure to carry out the graphical method first, and then the arithmetic integration would serve to check or to amend the graphical values in case the graphical work had not been carried out with sufficient accuracy.

If a purely arithmetic method is to be used, the writer prefers the Quick method,¹⁰ which gives a complete algebraic solution at each step without approximation, and requires only a limited number of steps. However, the graphical method, adequately explained in the paper, has so many advantages in simplicity of use and in visualizing the process and results, that its use is urged as the primary method. It requires careful construction, just as the arithmetic methods require close calculation, but it is simple to apply and is readily adapted to many special problems, as shown by Professor Angus in a number of papers. It is of interest to mention that this method was originally developed and published by Dr. Robert Lowy.¹¹

The paper covers many engineering applications such as problems involving wood-stave pipes, turbine-governor control of gate motion, and systems containing surge tanks. The numerical examples are particularly helpful, as are the author's methods of handling complex features by satisfactory simplifying assumptions. Naturally, some of the details may be open to argument or refinement; but this does not detract from the usefulness of the contribution.

AUTHOR'S CLOSURE

The paper was intended as a review of the subject of water hammer with emphasis on the practical requirements of the engineer in solving expeditiously some of the simpler water-hammer problems occurring in hydroelectric work, either where the final design of the project is being considered or in connection with rough estimates of projects where no detailed information is as yet known of the turbine characteristics.

The author is indebted to Professor Angus for pointing out the distinction between what happens in the conduit above the surge tank and in the penstock and for thus amplifying the author's statement as to avoiding confusion between the mass oscillation

of the water (between forebay and surge tank) and the water hammer in the system.

It is reassuring to know of the close check Professor Angus has obtained on the accuracy of Equations [3] and [10] in the case he has cited. Proof of Equation [3] comes from Newton's second law of motion applied to the momentum of the water flowing in a pipe of variable section and the impulse required to produce this flow. The equation is employed to arrive at the proper value of initial velocity to be used for the pipe as a whole in treating it as a simple conduit. Equation [10] is based on adding the time of travel of the wave in each section to obtain the total time of travel for the whole length of pipe and is used to arrive at the composite value of the velocity of the pressure wave. It seems to the author that the possible error in treating the pipe as a simple conduit comes from assuming the lower end of the pipe as of the same diameter as the upper end, thus showing for the usual case of tapered penstock too slow a pressure build-up (as indicated in Fig. 21) and from ignoring the partial reflections taking place from points of change in section. Where there are marked changes in v or a and where the governor time is very short, it is desirable for accurate work to use the graphical method. For ordinary "governor times" the author has found the agreement close enough for the cases he has investigated to warrant the use of the equivalent pipe method.

It is always desirable, where extreme accuracy is required, to use the actual gate motion as shown by the author's example. Also where this accuracy is required other factors such as those pointed out below should be taken into account. The graphical work can usually be done in the office but where manufacturers are making preliminary proposals for projects or where the engineer in the field is called upon to make a quick calculation of water hammer, the "net equivalent time" method is useful, particularly when the time of gate stroke is of normal value. The use of the net equivalent time results in conservative values of water hammer and allows for such factors as: (a) The influence of the speed-discharge characteristic of the runner; (b) the possible increased part gate discharge due to abnormally high heads; (c) possible change in governor characteristics due to wear, etc. The approximate answer of 400 ft in Example 2 was accordingly a result of the conservative method used in order to arrive at a practical answer taking into account the vagaries of the gate stroke rather than to any inaccuracy in the Allievi charts. It might be pointed out that if one is looking for a close check with the theoretical application of the charts without making allowance for these factors, the equivalent time should be used. The result, however, may be somewhat on the low side.

Referring to the Allievi charts, the author has found them to be very useful in estimating work where no detailed information was as yet available on the gate stroke. In these cases the charts determine the basic result to which a percentage may be added if desired to allow for nonuniform gate stroke and for other factors.

Professor Angus quite properly points out that Equations [28] to [31] of the paper are based on linear gate closure and that their value is more or less limited to use in connection with the determination of preliminary tank sizes. As just pointed out, due allowance may be made in the computations for the final design for nonuniform gate motion and other factors.

Professor Angus has succeeded in extending the application of the graphical method beyond the simple case to many problems which would be very difficult to solve analytically. One of these is in connection with the pressure changes in the draft tube where the length of draft tube is relatively great such as is frequently the case with propeller-runner installations.

Mr. Martin, as a turbine builder, very aptly reminds us of several factors to be taken into account when dealing with a practical installation. One of these is the correction of turbine

¹⁰ See author's Bibliography (4).

¹¹ "Druckschwankungen in Druckrohrleitungen," by Robert Lowy, Julius Springer, Vienna, 1928.

efficiencies for changes above and below normal speed referred to by speed-discharge characteristic of the runner. As the turbine speeds up upon rejection of load, the discharge is modified in accordance with the turbine discharge speed-characteristic, or to state it more technically, the change in speed changes the ϕ or rpm values and affects the rate of change in discharge. In many cases the effect of the change in speed is not very large but there are cases when it may be of considerable importance. For a more complete discussion of this factor, reference is made to a former paper¹² by the author.

Mr. Martin gives us a practical method of constructing the gate motion-time curve and points out the necessity of determining the gate position for the synchronous speed no-load point, particularly for propeller runners where the speed-no-load point may be as high as 30 per cent of full load position. The definition given by Mr. Martin of the governor operating time is useful in showing how one manufacturer has determined the time factor for design purposes.

As mentioned previously, the influence of the critical head condition should be kept in mind. In the case of the plant with a large reservoir drawdown, it is desirable to investigate the pressure rise for the complete range of heads for the governor timing specified or anticipated.

Mr. Martin points out several other factors of design influenced

¹² Relation of relief value and turbine characteristics in the determination of water hammer, by Earl B. Strowger, Trans. A.S.M.E. vol. 59, 1937, pp. 701-705.

by the water-hammer characteristics of the installation to which designers and manufacturers are giving their attention. One of these is the surge effect in the hydraulic system caused by load changes, including the negative surge in the draft tube, particularly in low-head installations. Another is the design of the excitation system on the basis of the prime-mover speed characteristic upon rejection of load. This is in the field of regulation but involves the determination of water-hammer pressure.

The author quite agrees with Mr. Martin that the complete solution of pressure changes and speed regulation is the responsibility of the engineers in charge of the design of the project.

The author is indebted to Professor Moody for clearing up the description of the phenomenon of pressure waves, i.e., by introducing the concept of pressure-wave extinction followed by a pressure drop.

The author also recommends the Quick method of computing water hammer and has used it in many instances and in general prefers it to the arithmetic-integration method. In writing a treatise on the subject instead of a short article, the Quick method should certainly be included. The arithmetic-integration process was used in the paper in order to explain the phenomenon of water hammer step by step and as an introduction to the graphical method.

The author wishes to thank the discussers for their useful contributions and also to thank Dr. Robert Lowy for presenting the paper at the meeting in New York.

Electronic-Type Instruments for Industrial Processes

By P. S. DICKEY¹ AND A. J. HORNFECK,² CLEVELAND, OHIO

This paper describes a new type of measuring and controlling instrument for general process work. The authors discuss the use of electronic equipment in fields of measurement where mechanical or electromechanical instruments have previously been employed. Typical measuring circuits for different problems are illustrated. Equipment for automatic computation of the results obtained from several primary measurements is discussed. Simplification and standardization of instruments for process control through the use of electronic devices is stressed as the important advantage of the equipment described.

IN discussing this subject, it is first necessary to define and describe the class of instruments suitable for measurement and control of industrial processes. All manner of measuring devices have been employed to improve the productive capacity and productive efficiency of the industrial machine which provides the necessities and the luxuries of our living. However, it is usually possible to make a distinction between those instruments which because of their complexity, delicate construction, or susceptibility to external disturbances must be classified as laboratory equipment and the more sturdy class of industrial instruments which are used as continuous operating guides.

The industrial instruments can be identified by the following important design features:

- 1 Sturdy construction.
- 2 Reliable performance.
- 3 Continuous operation for long periods.
- 4 Permanence of calibration.
- 5 Simple and inexpensive maintenance.
- 6 Adaptability to automatic control.

Instruments involving electronic devices, if properly designed, fulfill the foregoing requirements admirably and in addition provide many other desirable features for general process-control work.

1 As a result of extensive developments over the years, standard electronic tubes and associated devices are available which are capable of withstanding severe vibration, shock, and other deleterious external effects. Particularly as a result of aircraft, military, and naval requirements of the last few years, electronic devices have become available which are capable of withstanding not only vibration but a very wide range of ambient temperature and humidity conditions.

2 The extensive use of, and complete dependence upon electron devices by the armed forces is ample proof that this equipment is reliable enough for general process-control work. Men who

have staked their lives on proper performance of electronic devices will use this equipment with confidence in industrial work.

3 Much of the auxiliary equipment used with electronic devices will outlast the instrument mechanism in normal service. Electronic tubes have a limited life; but if the design is conservative, these tubes may be expected to operate for several years without replacement. In equipment designed independent of the tube characteristics the performance of the instruments will not be adversely affected by gradual deterioration of the tubes. During their working life it is possible at any time to predict the approximate tube life remaining by simple tests.

4 Electronic instruments using the null-balance system, as described later in this paper, can be expected to maintain a high degree of calibration accuracy over long periods even though service conditions are severe.

5 Electronic devices are adaptable to design involving packaged units of similar construction. Many of these units can be arranged for plug-in connection so that replacement requires only an easy exchange of simple and inexpensive parts. Thus maintenance does not require superskilled technicians and does not involve costly repairs or extended periods of outage of the equipment. Many of the component parts are used extensively in other electronic devices and as a result are available at electrical supply houses. High volume production of these parts makes their cost low.

6 Electronic-type instruments are especially well adapted to automatic-control problems because of the high speed with which measurements can be made. No mechanically or hydraulically actuated instrument mechanism can compare in speed of response with the control of electron flow in the electron tube. It is conceded that where motor-actuated balancing slidewires are used the full-scale deflection time is limited by the inertia of rotating parts in the system. However, since the basic measuring and controlling elements are free of inertia or friction no time lag is introduced because of these factors, as in the case of mechanical and hydraulic devices. Special designs of electronic amplifiers involving antihunt feedback are available to give high-speed full-scale deflection where necessary.

Pneumatic or hydraulic control systems are often actuated by electronic instruments where it is convenient or otherwise advantageous. This is inherently sound since the measuring apparatus is faster in response than the control system. Likewise, electrically operated or electronically operated control systems can readily be connected to electronic-operated instruments with the advantage that the same class of equipment is used throughout.

An added advantage of the electronically actuated instrument for general process work is that it is a simple matter to transmit measurements over considerable distances without serious sacrifice in accuracy or speed of response. Multiple receivers at different locations can be used to indicate or record the measurement of a single primary measuring element without loss of efficiency.

Combinations of several variables to obtain totals, differences, ratios, etc., are quite simple measurements with this class of equipment and do not involve any special design of the units which make up the instrument.

¹ Chief Engineer, Bailey Meter Company. Mem. A.S.M.E.

² Research Engineer, Bailey Meter Company.

Contributed by the Industrial Instruments and Regulators Division and presented at the Annual Meeting, New York, N. Y., Nov. 27-Dec. 1, 1944, of THE AMERICAN SOCIETY OF MECHANICAL ENGINEERS.

NOTE: Statements and opinions advanced in papers are to be understood as individual expressions of their authors and not those of the Society.

MEASURED OR CONTROLLED FACTORS

A great many kinds of measurements are required for proper regulation of different industrial processes. Few industrial plants can be operated successfully without one or more measurements of the following factors: Temperature; pressure or vacuum; fluid flow; liquid level; gravity or density; motion or position; light or color; viscosity or turbidity; conductivity or hydrogen-ion concentration; gas analysis; moisture content; calorific value; vibration or sound; stress or strain; hardness or internal structure; elapsed time.

Without intending to discredit any of the many ingenious devices which have been built for measurement of the factors just cited, it is noted that practically any of these measurements can be made with the standard electronic-type instruments to be described. While primary devices for these measurements must be designed for the individual problem, the advantage of a single type of recording instrument requiring a few standard assemblies is obvious.

The electronic amplifier and motor-control unit as described later, has ample sensitivity and stability for use in an instrument for most of the various measurements listed. Furthermore, an instrument of this type can be of sufficiently sturdy construction to permit installation in unfavorable surroundings. It is reliable enough to be used for continuous measurement or control.

MEASURING SYSTEM—AUTOMATIC NULL BALANCE

The electronic instruments described in this paper are basically of the same general class. It is realized that electronic-actuated instruments of the null-balance type are electromechanical as well as electronic. However, the commonly accepted meaning of the term "electronic" is used here to describe instruments which depend in a basic way upon electron tubes for their operation. Fig. 1 is an elementary diagram of the fundamental system.

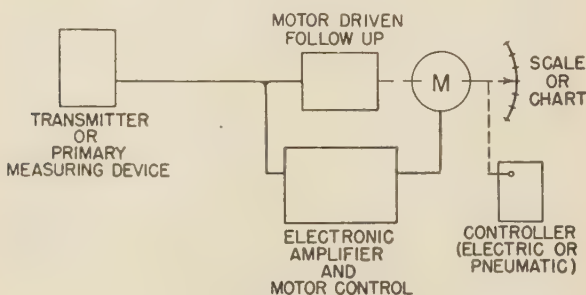


FIG. 1 ELEMENTARY DIAGRAM OF NULL SYSTEM

In this class of electronic instruments measurements are made by automatic and continuous balance of the null-type measuring circuit. The quantity is measured in terms of a reference potential, current, calibrated resistance, or impedance. The transmitter and the motor-driven follow-up together comprise the measuring circuit which may be a Wheatstone resistance bridge, an impedance bridge, or a potentiometer network. The quantity being measured is converted into a proportional electrical variable at the transmitter. For example, temperature is translated into resistance by means of a platinum coil, or into a direct-current voltage by means of a thermocouple. The motor-driven follow-up may be a slidewire, a variable inductor, or a variable capacitor. The specific instruments described in this paper use a resistance slidewire as the balancing unit.

The electronic amplifier detects and amplifies unbalanced voltages of the measuring circuit as produced by a change in the measured quantity. The amplified voltage applied to the motor-

control circuits causes the slidewire motor to rotate in such a direction as to rebalance the measuring circuit. Simultaneously the motor may drive any or all of the following devices: An indicator, a recording pen, an integrating device, or a pneumatic or electric control.

This type of measuring system has the following characteristics:

1 The null-balance principle of measurement makes the accuracy and stability dependent only upon the calibrated components of the measuring circuit. Variations and aging of amplifier and motor-control-circuit components have negligible effect on the calibration.

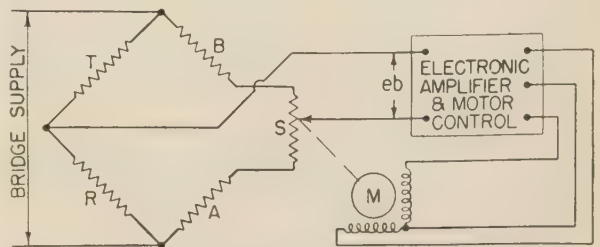
2 The electronic amplifier and balancing-motor control circuit are continuously operative and respond instantly to changes in the measured quantity. Also, the speed of the balancing motor is approximately proportional to the amplifier input so that the recording pen or indicator pointer moves smoothly and in synchronism with changes in the measured quantity.

3 The power actuating the recording pen, indicator, or controller is many times greater than the power expended in the measuring element. This power gain may be as great as 10^{12} and makes possible the measurement of electrical or mechanical quantities at an extremely low energy level. For example, an unbalance of 10^{-8} v in the direct-current potentiometer circuit results in a power input to the converter of 10^{-12} w and a motor power output of about 2 w. Since full torque is developed by the motor with a change of 1 per cent or less in the measured quantity, the accuracy of the system is practically independent of load or friction applied to the follow-up recording or indicating mechanism.

MEASURING CIRCUITS

Resistance Bridge. One of the most common circuits employed is a modified Wheatstone bridge as shown in Fig. 2. The primary measuring device is arranged to vary the value of resistance T in proportion to changes in the factor being measured. Fixed resistances R , A , and B are designed to provide the proper range of measurement. The adjustment of the slidewire contact on resistor S subtracts resistance from A and adds resistance to B , or vice-versa. Thus the bridge is balanced by adjusting the ratio of the bridge arms and since the slidewire contact does not carry bridge current, its resistance does not affect the calibration.

An alternating-current supply is used for the bridge which eliminates the need for a battery source of bridge voltage. Standard voltage cells and voltage standardization equipment are not required. The alternating-current bridge supply is taken from a transformer which is fed from the main power supply for the instruments.



T = TEMPERATURE SENSITIVE PLATINUM RESISTANCE
A, B & R = FIXED RESISTORS M = SLIDEWIRE DRIVE MOTOR
S = SLIDEWIRE

FIG. 2 WHEATSTONE-BRIDGE MEASURING CIRCUIT

The foregoing circuit or some modification of it is ideal for measurement of temperature using resistance-temperature detectors, vacuum using the thermal-conductivity principle, conductivity, gas analysis, and many other factors where the condition being measured can be proportioned to a variable resistance.

Impedance Bridge. A second circuit which is commonly employed is the impedance bridge, one type of which is shown in Fig. 3. In this case an adjustable transformer whose primary is supplied from the line is used as a transmitter. The core of this transmitter is moved by the factor being measured and the position of the core determines the magnetic-flux linkage between the primary windings and the two secondary windings E_1 and E_2 shown in the diagram. The voltage induced in each of the secondary windings by the primary depends upon the magnetic-flux linkage from the primary, and the voltage ratio is thus proportional to the displacement of the core from the center position.

An electrical bridge is formed by the two secondary coils of the transmitter and the resistance on either side of the slidewire contact at the receiver. By using proper values of the slidewire S and fixed resistors A and B , any desired proportionality between motion of the transmitter core and motion of the slide wire contact can be obtained.

By using the electronic amplifier and motor control to drive the motor which balances the slidewire, a very limited current flow is required in the measuring circuit. Thus connecting wires can be small and can be run for a considerable distance. Of greater importance is the fact that practically no force is exerted by the core of the transmitter so that there is no restraint against the primary measuring element.

Since the bridge circuit obtains its alternating-current supply from the power source for the instruments, no other source of voltage is required.

Extensive tests have shown that this circuit will accurately measure motions of the transmitter core as small as 0.00005 in.

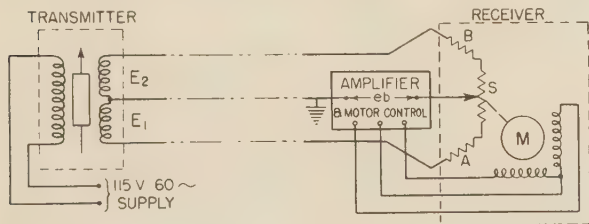


FIG. 3 IMPEDANCE-BRIDGE MEASURING CIRCUIT

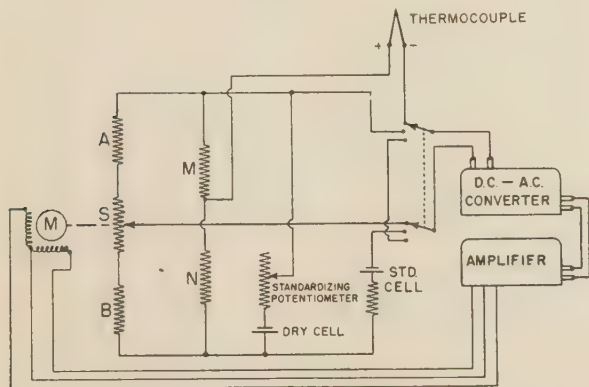


FIG. 4 DIRECT-CURRENT POTENTIOMETER CIRCUIT

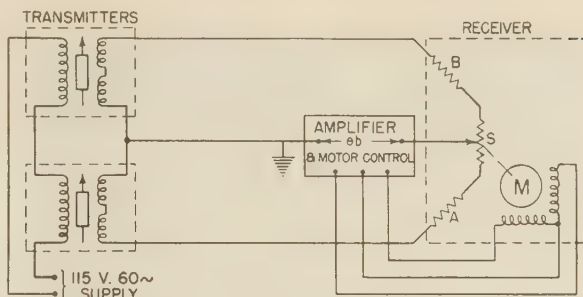


FIG. 5 IMPEDANCE BRIDGE FOR MEASURING RATIO

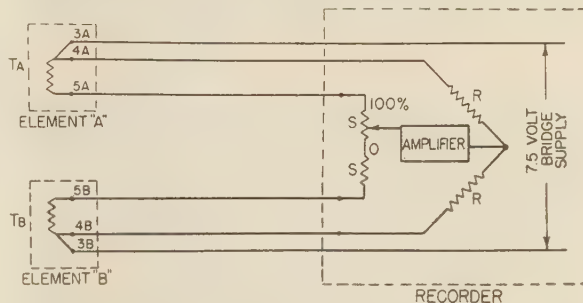


FIG. 6 CONNECTION DIAGRAM FOR MEASUREMENT OF DIFFERENCES

It is therefore ideally suited to measurement of pressure, moisture content, and stress, using displacement-type transmitters, or to any factor which can be translated in terms of position. Since the movable core can be inside a pressure housing and the transmitter coils on the outside of the housing, the circuit is especially adapted to determination of differential pressures, as for example, in the measurement of fluid flow, liquid level, viscosity, and other factors.

For measurement of variables which are translated into direct-current potentials, the conventional potentiometer circuit shown in Fig. 4 is employed. The usual battery source of bridge voltage and the standard cell and standardizing circuit are incorporated. The direct-current unbalance of the bridge is converted by means of a saturable-core-type direct-current to alternating-current converter and the resulting alternating-current voltage is applied to the input of the standard alternating-current amplifier and motor-control system. As a result of amplification obtained in the converter and the high degree of amplification available in the alternating-current amplifier, sensitivity is obtained equal to or greater than that available with galvanometer-type industrial instruments without any sacrifice in the sturdy construction of the unit.

This circuit is most commonly employed for measurement of temperature, using thermocouples or radiation-type primary elements. Modified circuits are employed for the measurement of vacuum, speed, light or color, turbidity, smoke density, and other factors.

Modifications of the circuits described are available for automatic computation of the results obtained from a number of primary measurements. For example, a simple modification of the impedance bridge described is illustrated in Fig. 5, by which the ratio of two independent variables can be automatically and continuously determined. A similar simple modification can be used to obtain a continuous total of any reasonable number of independent variables.

Fig. 6 shows a modification of the alternating-current resistance bridge to permit continuous determination of difference between

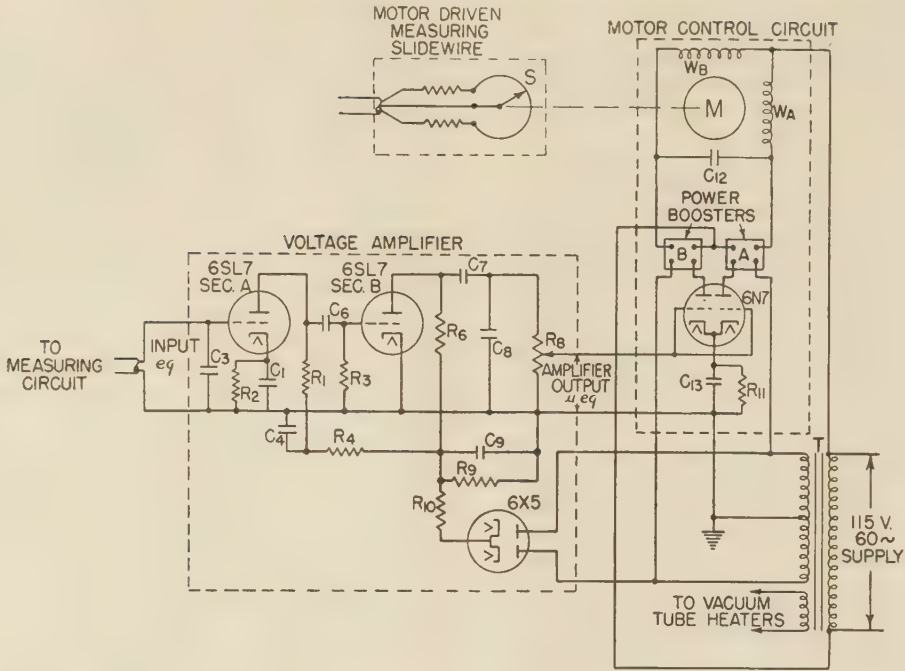


FIG. 8 SCHEMATIC DIAGRAM OF ELECTRONIC AMPLIFIER AND MOTOR-CONTROL CIRCUIT

two independent variables. Similar modifications are available for continuous determination of the product of two independent variables.

It is believed that there is a great field for such automatic calculating devices in the operation of industrial processes. This equipment not only eliminates the necessity for trained operators to summarize and compute the results from daily records and log sheets, but provides the necessary information auto-

AMPLIFIER AND MOTOR CONTROL

Fig. 7 shows the electronic-amplifier unit which detects and amplifies the unbalance of the measuring circuit. Electrically the unit consists of an amplifier section and a motor-control section. These are arranged into a compact assembly which is suited to quantity production. The assembly and testing are reduced to a number of simple operations which can be performed by relatively unskilled help.

The electronic amplifier is standardized in both mechanical and electrical design and is used on all 60-cycle alternating-current measuring circuits whether for measuring temperature, flow, level, etc. The same amplifier is also used on direct-current potentiometric circuits with the addition of the converter which transforms reversing polarity unbalance into reversing phase alternating current of 60-cycle frequency. Furthermore, the instrument calibration is unaffected by variations between amplifiers so that complete interchangeability is obtained.

The amplifier has an over-all voltage gain of 2500. This means that a 0.001-v unbalance from the measuring circuit produces an output voltage of 2.5 v for application to the motor-control tube. Since the slidewire-drive motor responds to voltages as low as 1-v input to the motor-control tube, it is sensitive to about 0.0004-v input to the amplifier. This is ample for the average application. This sensitivity is specifically illustrated in Table 1, in terms of voltage output or unbalance of measuring circuit.

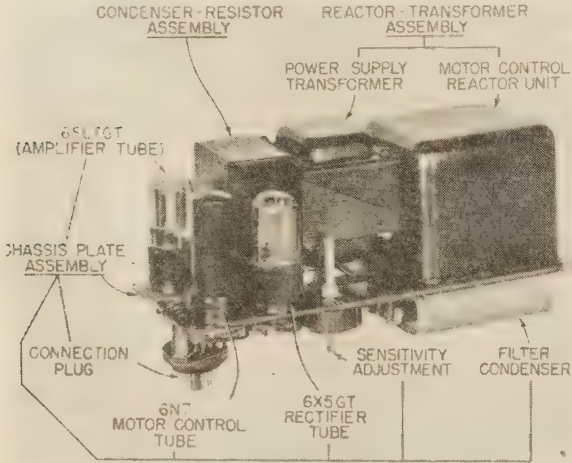


FIG. 7 ELECTRONIC AMPLIFIER UNIT

TABLE 1 SENSITIVITY OF SLIDEWIRE-DRIVE MOTOR IN RELATION TO AMPLIFIER INPUT

Input to amplifier	Minimum voltage to which motor will respond
Alternating-current systems:	
1 Direct connection.....	0.0004 a-c volt
2 Transformer coupling to amplifier input.....	0.00003 a-c volt
Direct-current systems.....	2×10^{-8} d-c volts (or 1×10^{-8} amperes)

ELECTRICAL DESIGN

The electrical design is based upon the requirement that in-

matically and continuously to those responsible for the operation. It is believed that in many cases great benefit is possible by having such computed information available instantly as an operating guide instead of after a delay of several hours or several days when this work must be done by technicians.

dustrial instruments must operate continuously and with unimpaired accuracy over long periods of time with a minimum of maintenance and often under adverse conditions. For this reason the design of the unit and the rating of components including tubes, capacitors, resistors, and transformers, are more conservative than in most communication and radio equipment. Also, to obtain maximum reliability, the number of circuit elements is held to a minimum consistent with good performance. Special or complicated features to obtain some peculiar operating characteristic for a specific application are avoided.

The elementary wiring diagram of the complete amplifier unit is shown in Fig. 8. The amplifier section is Class A of conventional design consisting of two stages of resistance-coupled amplification. A 6SL7 amplifying tube consisting of two triodes in one envelope is used. The alternating-current voltage obtained by unbalance of the measuring circuit is applied to the grid of the first section and is amplified about 50 times in each triode so that the total voltage gain is about 2500. Phase shift is negligible so that output voltage which appears across R8 is a magnified image of the input voltage.

The direct-current plate supply for the amplifier is obtained from a simple full-wave rectifier using a 6×5 vacuum tube and a capacitor resistance filter to provide smooth direct-current voltage.

OPERATION OF MOTOR-CONTROL CIRCUIT

All or part of the amplified voltage, depending upon the sensitivity required and determined by the adjustment of R8, is applied to the motor-control circuit which in turn determines the direction of rotation and speed of the reversing motor which drives the slidewire. Motor *M* is a "capacitor-run" type having two identical windings W_A and W_B 90 electrical deg apart on the stator. The operation is similar to that of a two-phase motor and rotor torque is developed by displacing the currents in the windings W_A and W_B in time phase relative to each other. The direction of rotation is determined by whether the current in W_A is leading or lagging the current in W_B . Consequently, the speed with a constant load is proportional to the magnitude of the winding currents and the phase displacement between them. This motor is of special design to permit rapid braking when the winding currents are brought into phase.

The voltage applied to the 6N7 plates is obtained from a center-tap secondary winding of the supply transformer. The grids are connected together and receive their voltage from the measuring or control circuit through a voltage amplifier. It is a fundamental requirement that the plate supply for the 6N7 be obtained from the same source and phase as the grid-input signal. For this application the source is the 115-v 60-cycle supply to which the motor is connected. However, the power supply to the motor can be entirely divorced from the control circuit. Since the plates of the 6N7 are 180 deg out of phase with each other and the grids are in phase, the plate currents of the two sections of this tube are selectively controlled by phase relation between the grid voltage and the plate voltage.

The plate circuits of the motor-control tube are coupled to the motor power circuit through power-boosting devices *A* and *B*. The tube-plate currents determine the torque and direction for rotation of the motor. If the unbalance of the measuring circuit is such as to give an amplified voltage in phase with the plate of triode *A*, this section will pass more plate current and triode *B* less current than at balance. Consequently, motor current will flow through power booster *A* directly through winding *A* and through the motor capacitor and winding *B*. This phase relationship of winding currents will cause the motor to rotate in a direction to rebalance the measuring circuit. By the same analysis, unbalance in the opposite direction will produce an amplified voltage in phase with triode *B* and resulting motor ro-

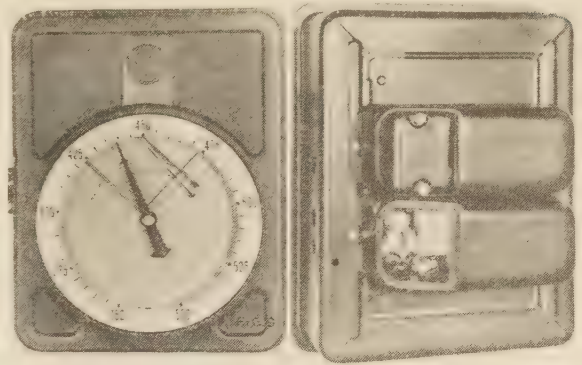


FIG. 9 RECTANGULAR-CASE INSTRUMENTS

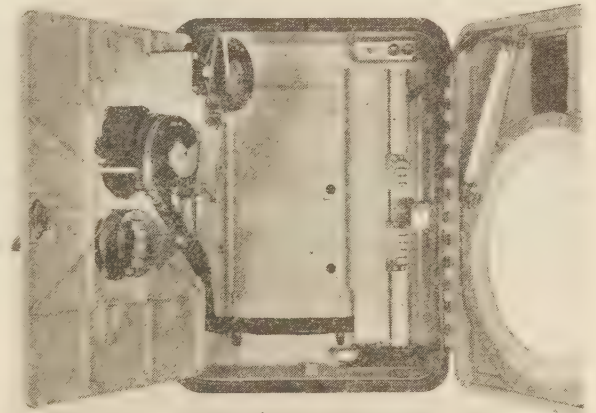


FIG. 10 RECTANGULAR-CASE INSTRUMENT SHOWING INTERNAL MECHANISM

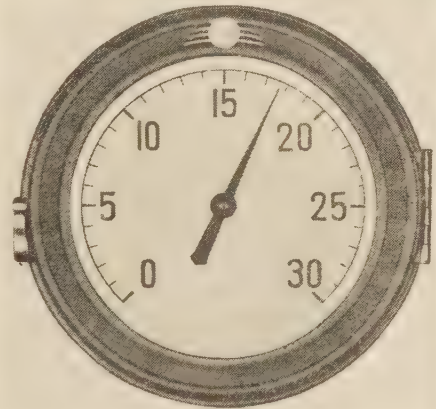


FIG. 11 ROUND-CASE INSTRUMENT

tation opposite to what it was before but again in such a direction to restore balance.

In general, the sensitivity of the system is sufficient to develop about 75 per cent of the maximum motor torque with about 0.002-v input to the amplifier.

INSTRUMENT CONSTRUCTION

To obtain the most flexible construction for the various types

of problems which must be handled the instruments have been developed in two general forms. The rectangular case instruments illustrated in Figs. 9 and 10 provide from one to four completely independent measuring systems. In every case the measuring circuit, the motor-driven slidewire, and the electronic amplifier and motor control are entirely independent for each system so that failure in any one measuring system does not affect the remaining units in any way.

The round pattern chart has been selected since it is the most economical means of recording the results and since the recording mechanism is extremely simple and does not take up space within the case which can be used for additional measuring or controlling devices.

The instruments can be equipped with one large dial indicator which can be operated by any of the different factors measured in the same instrument. The construction of the instrument is such that different basic measuring circuits can be employed in the same case giving a wide variety of combinations of measurements available on the same recording chart.

Two independent control systems of either the electrically operated or automatic types can be incorporated in the same case.

The amplifier unit is enclosed in a dust- and moisture-resistant housing normally mounted on the back of the receiver casing as shown at the right in Fig. 9. Electrical connections to the internal meter circuits are made by a plug and socket connector. Where such mounting is impossible the amplifier may be mounted remotely and connections made by means of a plug and cable. The vacuum tubes and the electrolytic condenser assembly which may require periodic check or replacement are made

accessible by removal of the sub cover. This packaged unit construction facilitates quick removal of the entire amplifier unit or of component parts for inspection or repair.

Round Case. Where recorded results are not desired a smaller round pattern case, as shown in Fig. 11, is employed. This unit incorporates one measuring system operating a large indicator or may incorporate one controller of the electrically operated or pneumatically operated type.

CONCLUSION

The authors are fully aware of the recent tendency to propagandize electronics as the panacea for all engineering problems. Therefore a few words of caution are in order. If electronic equipment is to be successful in process-control work manufacturers must design and build conservatively. Designs which are hastily conceived and poorly executed will tend to discredit all equipment of this type.

For many measuring problems today and new problems ahead the electronic equipment offers the only practical solution. However, there is a large field of measurement which can be handled with mechanical, electrical, or electronic-type instruments. The principal advantage of the electronic type of instrument in this field is standardization of design.

Mechanically operated instruments have economic advantages in certain applications. However, since a different mechanical instrument is usually required for each type of measurement, the standardization and resultant advantages possible with electronically operated equipment is not possible where a great variety of measurements is required.

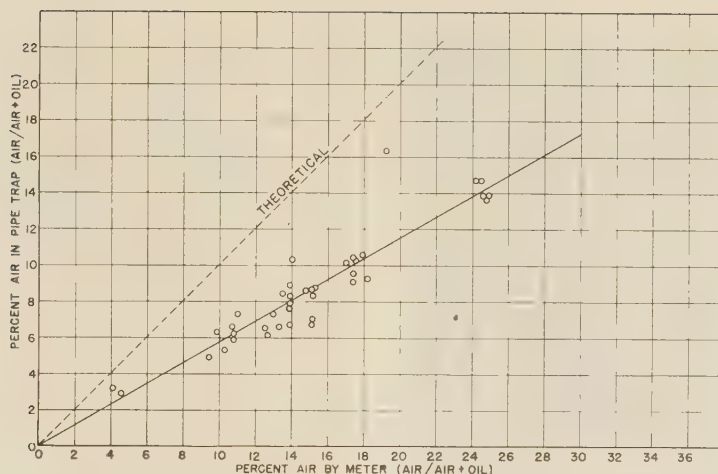


FIG. 1 Air-Oil Measurements

An Instrument for Indicating the Amount of Gas in Gas-Liquid Mixtures

By B. R. WALSH¹ AND G. S. PETERSON,² PITTSBURGH, PA.

The instrument described in this paper was developed by the authors' company at the instigation of the Wright Aeronautical Corporation, which early foresaw the need for clarifying the entire problem of satisfactory operation of an airplane-power-plant lubrication system if the increased demands of military-airplane performance were to be met. One of the major objectives was the development of an instrument which would make possible a quantitative measurement of the amount of entrained air in lubricating oil, because air present in the oil reduces the delivery of oil from the pump; the reduction of delivery is greater the higher the altitude for the same percentage of air at the intake to the pump. This reduction of delivery may be so great as to limit the safe ceiling of the plane, from failure to lubricate the engine. All such pumps, being the positive-displacement type, can deliver only displacement minus slip; as volume of air in the pump increases, obviously, the oil delivery must decrease since the sum of air and oil handled is substantially a constant.

DEVELOPMENT OF INSTRUMENT

IN the development of an instrument to indicate the amount of gas in gas-liquid mixtures, consideration was first given to the use of condensers, selenium cells, and mechanical traps, but tests conducted on these devices disclosed difficulties

inherent with these methods which made them not only unreliable but impractical. The use of a condenser for measuring the change in dielectric strength with change in the amount of entrained air was unstable owing to the segregation of air and oil, and the presence of foreign particles and water. A selenium cell was used to measure the variation in the amount of light transmitted through a column of oil in a transparent section of tubing with varying amounts of entrained air. It was found that the amount of light transmitted was a function of the number of oil films in the light path and, since a large number of small bubbles constituted a large number of oil films, compared to an equal amount of air in large bubbles, this method was not satisfactory.

Extensive tests made on several types of pipe traps showed this method to be impractical because of segregation of the air and oil. With striation of the air, the velocity of the oil is much lower than that of the air and therefore the air percentage as indicated by a pipe trap is lower than the actual amount, as shown in Fig. 1. In addition, this device would not be suitable for flight application since an indicating instrument is needed to determine the percentage of entrained air under different operating conditions. Numerous calibration tests on various sizes of positive-displacement pumps, used with different aircraft engines, showed a consistent relationship between the oil-flow rate and increased volume of air entrainment, which could be readily calculated when the displacement and clearance volume of the pump were known.

The engine-pressure pump cannot be used to indicate directly the amount of air entrainment because it is provided with a pressure-regulating valve which normally by-passes oil from the discharge to the pump inlet, which disturbs the normal oil-air relationship. The instrument, shown in Fig. 2, was therefore designed. This instrument is merely a small positive-displacement pump, direct-connected to a 24-v, d-c $\frac{1}{10}$ -hp aircraft-type

¹ Engineering Division, Gulf Research & Development Company.

² Engineering Division, Gulf Research & Development Company. Mem. A.S.M.E.

Contributed by Industrial Instruments and Regulators Division and presented at the Annual Meeting, New York, N. Y., Nov. 27-Dec. 1, 1944, of THE AMERICAN SOCIETY OF MECHANICAL ENGINEERS.

NOTE: Statements and opinions advanced in papers are to be understood as individual expressions of their authors and not those of the Society.

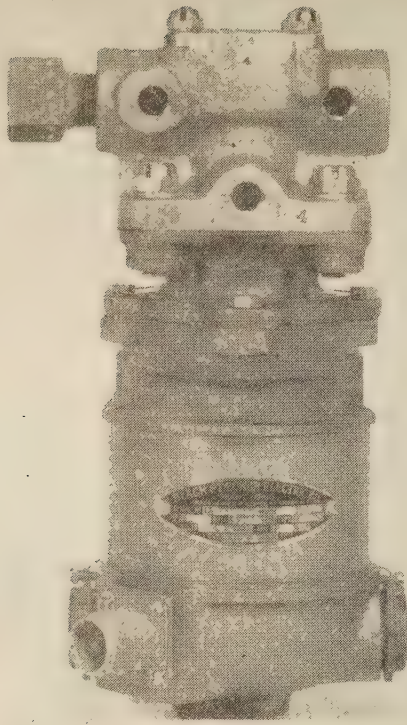


FIG. 2 WRIGHT-GULF AIR INDICATOR, FLIGHT MODEL

electric motor. The pump has a capacity of approximately 1 gpm and the assembled unit weighs 5 lb. The instrument is identified commercially in its present form as the "Wright-Gulf Air Indicator."

PRINCIPLE OF OPERATION

The instrument, shown in Fig. 3, is provided with a sharp-edged orifice placed on the discharge side of the pump. A pressure gage is connected at point *A* for indicating the pump discharge or upstream-orifice pressure. A second pressure gage is connected at point *B* for indicating the inlet pressure. Since

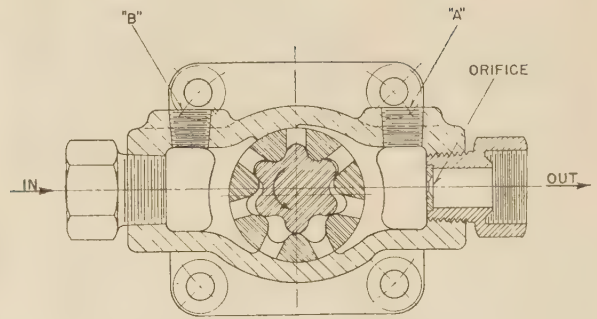


FIG. 3 CROSS SECTION OF INDICATOR

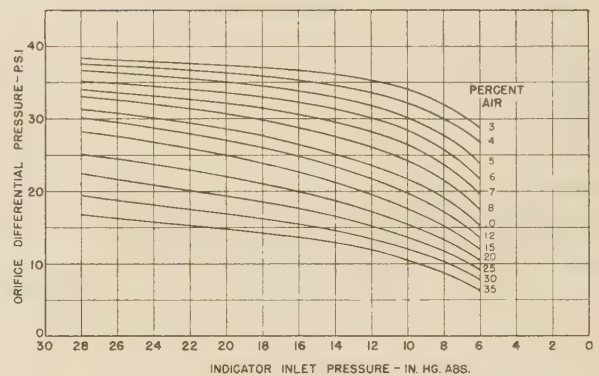


FIG. 4 CALIBRATION OF AIR INDICATOR

the pressure drop across a sharp-edged orifice provides a reliable measurement of fluid-flow rate through the orifice, the pressure at point *A* is a direct indication of the pump-delivery quantity, the pressure on the downstream side of the orifice being substantially equal to ambient pressure. The sharp-edged orifice was selected because variation of viscosity has the least effect on the coefficient of any primary element; for most operating ranges the effect is negligible, and therefore one possible variable is eliminated.

Thirty per cent air at pump inlet, for example, reduces pump-delivery quantity more than 30 per cent. But on the discharge side, where the orifice is located, this 30 per cent may be compressed to 3 to 5 per cent. Further, since even this compressed

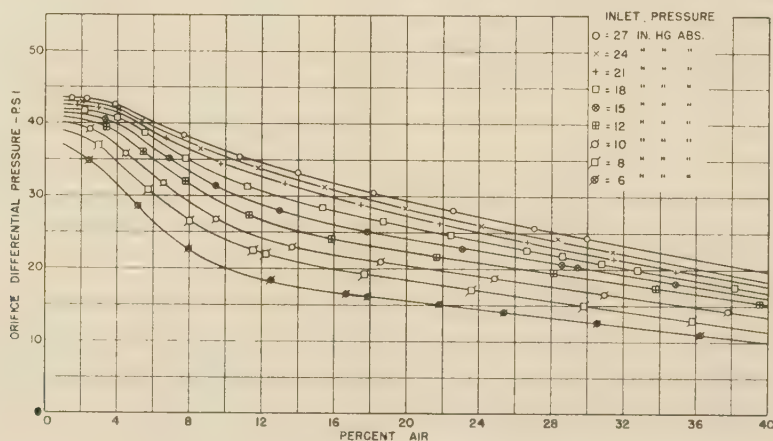


FIG. 5 ORIFICE DIFFERENTIAL PRESSURE VERSUS PER CENT AIR

air is still very low in density, the orifice responds almost entirely to the liquid flow and therefore does actually measure the liquid delivery consistently and accurately. This makes it possible to plot curves of orifice pressures at known percentages of air entrainment versus pump-inlet pressure. These curves, determined by test, are shown in Fig. 4 and constitute the calibration of the unit. It is to be noted that these curves were determined by cross-plotting from curves of orifice differential pressure versus per cent air for constant pump-inlet pressures for the sole purpose of saving time in calibrating. Fig. 5 shows these curves plotted through the test points.

In the calibration of the instrument, a voltage regulator is used which maintains a constant voltage on the motor terminals. The variation in the speed of the electric motor, due to a change of output resulting from reduction of pressure under conditions of air entrainment, is automatically taken care of in the calibration of the unit. While it is not the purpose of this paper to elaborate upon the method of calibrating the unit, it should be stated that this is accomplished by use of a displacement chamber into which the entire air-oil mixture handled by the pump is delivered. The mixture in the displacement chamber is allowed to stand until the entrained air has completely separated from the oil. The displacement chamber is shown in Fig. 6. The per cent of entrained air is determined by dividing the volume of air measured in the visisage *A* by this volume, plus the volume of oil as determined by means of the weigh scale *B*.

APPLICATION

The successful application of the instrument depends upon securing a sufficiently accurate sample of air-oil mixture flowing in the system to be analyzed. This does not impose any new obstacle on the use of the instrument because any method indicating the per cent of gas flowing in a gas-liquid mixture so far considered involves the problem of obtaining a correct sample.

Two successful sampler devices have been developed jointly by Wright Aeronautical and Gulf Research. The sampling chamber, shown in Fig. 7, is used where it is anticipated that the percentage of entrained air will not exceed 15 per cent, but in systems where the air entrainment exceeds this value, the orifice-type sampler, shown in Fig. 8, is applied. During the development of a sampler suitable for sampling air-oil mixtures obtaining in airplane lubrication systems, it was found that the air striates very quickly in mixtures containing more than 15 per cent air. In view of this, the sampler, shown in Fig. 7, is used only for

sampling mixtures containing less than 15 per cent air. Several schemes using different types of baffling for mixing the air and oil at the point of sampling were tested, none of which proved satisfactory.

Fortunately, one practical method of mixing air and oil to permit sampling was discovered. This method requires sufficient increase in velocity of the mixture to raise the turbulence to a Reynolds number in the order of 1500 or above. The objection to this method for use in an airplane application was the increase

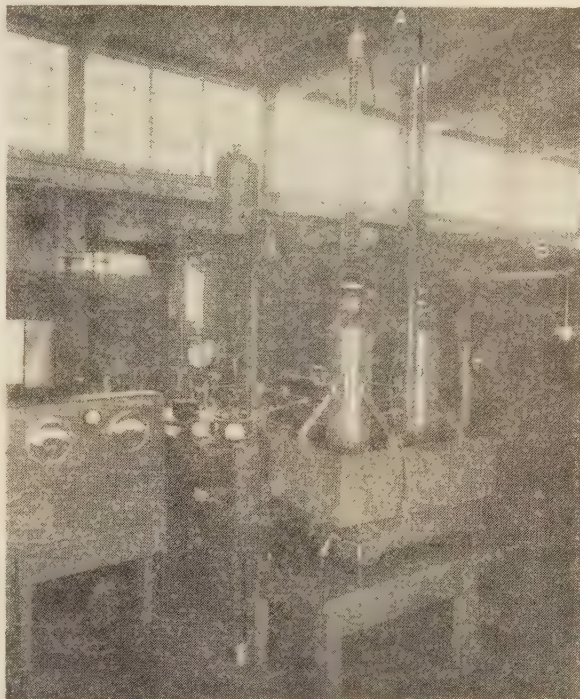


FIG. 6 DISPLACEMENT-CHAMBER SETUP USED FOR CALIBRATING INDICATORS

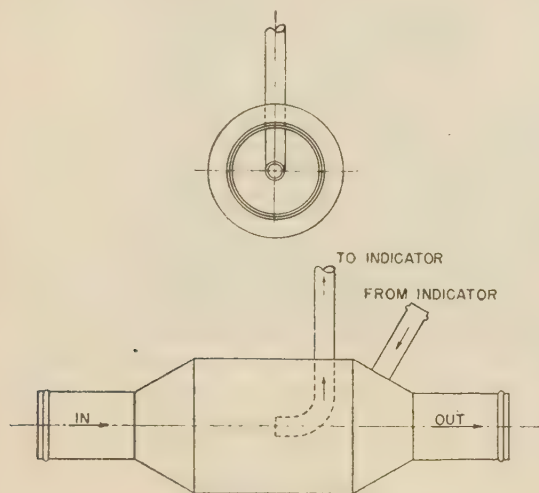


FIG. 7 STANDARD SAMPLING CHAMBER

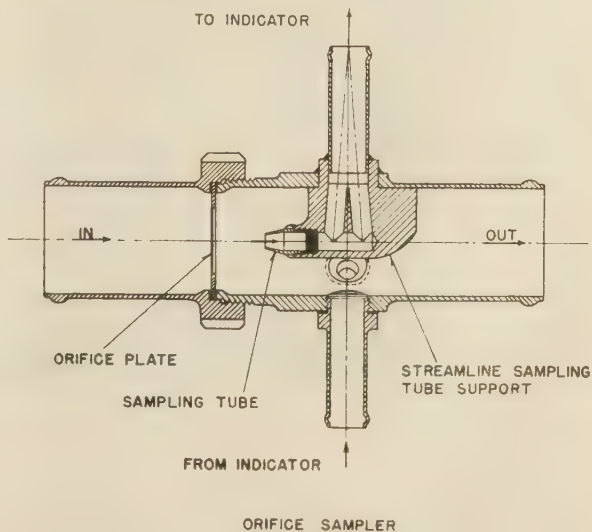


FIG. 8 ORIFICE SAMPLER

in pressure drop imposed by the sampler. Any appreciable increase in the pressure drop in the line between the oil-supply tank and the engine-pressure pump would impose, in effect, a higher altitude condition on the pump. In view of this condition, the first means tried was a Venturi tube with a sampling tube located in the throat section, as shown in Fig. 9.

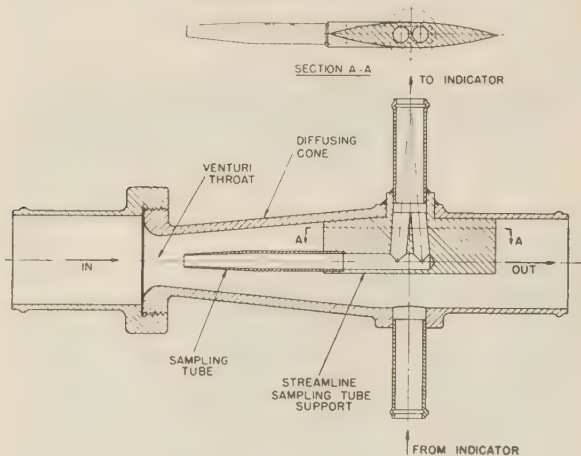


FIG. 9 VENTURI SAMPLER

It was thought that the Venturi tube would result in a minimum over-all pressure drop for a given turbulence, owing to its excellent reconversion of velocity to static head when handling one fluid. However, tests showed that the pressure drop was much higher than anticipated. This may be explained by the fact that the usual pressure-drop recovery in a Venturi diffusion tube does not hold for gas-liquid mixtures at low Reynolds numbers because wall separation occurs. In addition, the friction loss in the Venturi tube is a major part of the total loss at low Reynolds numbers.

In view of the high pressure drop encountered with the Venturi-type sampler, tests were conducted on an orifice-type sampler, as shown in Fig. 8. Tests showed a recovery of pressure drop across the orifice when flowing air-oil mixtures to be in accordance with the pressure-drop recovery for a single fluid, so that the over-all pressure drop across the orifice sampler was approximately 60 per cent of that obtained across the Venturi type.

The orifice sampler, when properly applied with respect to orifice diameter and size of sampling tube, will give satisfactory sampling for air percentages up to 35 per cent. Even though the orifice sampler gives good results at low air percentages, it is generally preferable to use the standard sampler, shown in Fig. 7, in view of the negligible pressure drop with this type of sampler.

It is important that the liquid viscosity be known for each application because, while a calibration curve determined for the instrument on, for example, S.A.E. 60 oil at 185 F is good for a range of temperatures from 160 to 225 F, it would not be applicable if the operating temperature of the oil were, for example, 140 F. In this case the instrument should be calibrated on 140 F oil. One reason for this is the effect of the high viscosity of the oil on the speed of the motor. Another effect of the viscosity at temperatures of 140 F or below is the change in coefficient of the orifice.

For Reynolds numbers above 800 to 1000, the curve of orifice coefficients versus Reynolds numbers is nearly flat; however, for Reynolds numbers below 800 to 1000, there is a noticeable change in coefficient with decreasing Reynolds numbers. The range of

temperature from 160 to 225 F for S.A.E. 60 oil covers the usual range encountered in aircraft engines during flight so that one calibration curve has been satisfactory for aircraft applications. In this case, the error in the calibration varies from ± 0.5 to ± 1.5 per cent air for increasing air percentages up to 35 per cent. Where greater accuracy in bench-testing is required, the use of a displacement chamber is recommended; but, for flight tests of airplane lubrication systems, the accuracy of this instrument is satisfactory and certainly exceeds that of any other known flight-type device for measuring entrained air.

Fig. 10 is a schematic diagram of an indicator installation on a typical aircraft lubrication system. An important item to note is that the performance of the lubrication system is unaffected by use of the instrument because the 1 gpm withdrawn by it is returned to the sampler. A relief valve is provided with the instrument to protect the motor from overload in the event the disk orifice becomes plugged with foreign matter. The discharge line from the relief valve may be connected back to the supply line being sampled, or to any low-pressure source.

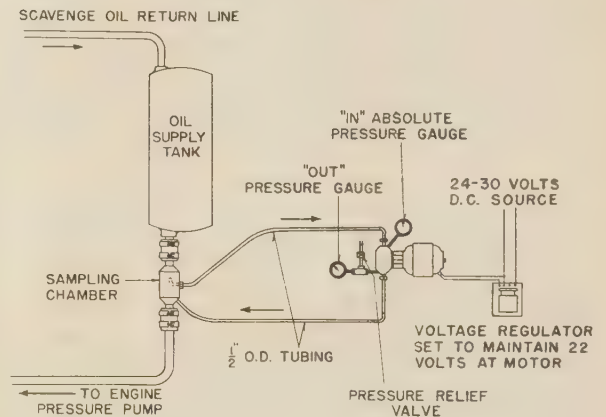


FIG. 10 TYPICAL AIRCRAFT INSTALLATION DIAGRAM

Fig. 11 shows the indicator installed on an airplane for flight test. Fig. 12 shows the installation of a standard sampler for use with the indicator shown in Fig. 11. In the development of this instrument, tests were conducted which showed that its accuracy was unaffected by the position in which it was mounted, and was only slightly affected by change in ambient temperature.

USE OF INDICATOR

In Figs. 11 and 12, the instrument was used to determine the amount of air entrained in the oil in the supply tank at different altitudes. While it was pointed out that the calibration curve, shown in Fig. 4, is plotted with the inlet pressure of the instrument as the abscissa, it is to be noted that the percentage of air indicated by each curve is based upon the volume of air at inlet pressure. It may be seen from the schematic installation diagram that this pressure will differ from the altitude barometric pressure by the amount of pressure drop in the lines between the oil-supply tank and the inlet tap on the instrument. It is necessary, therefore, that the air percentage, determined from the calibration curve, be converted to that corresponding to supply-tank pressure. (This may differ from the altitude barometric pressure, depending upon whether or not a pressurized tank is used.)

OTHER APPLICATIONS

To date the instrument described has been or is being used

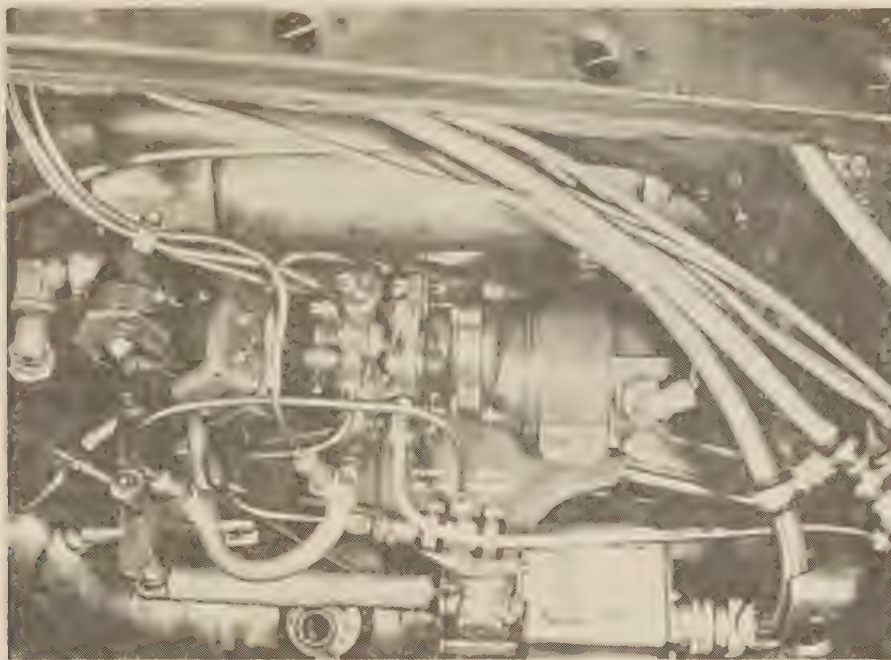


FIG. 11 AIR INDICATOR INSTALLED FOR FLIGHT TEST

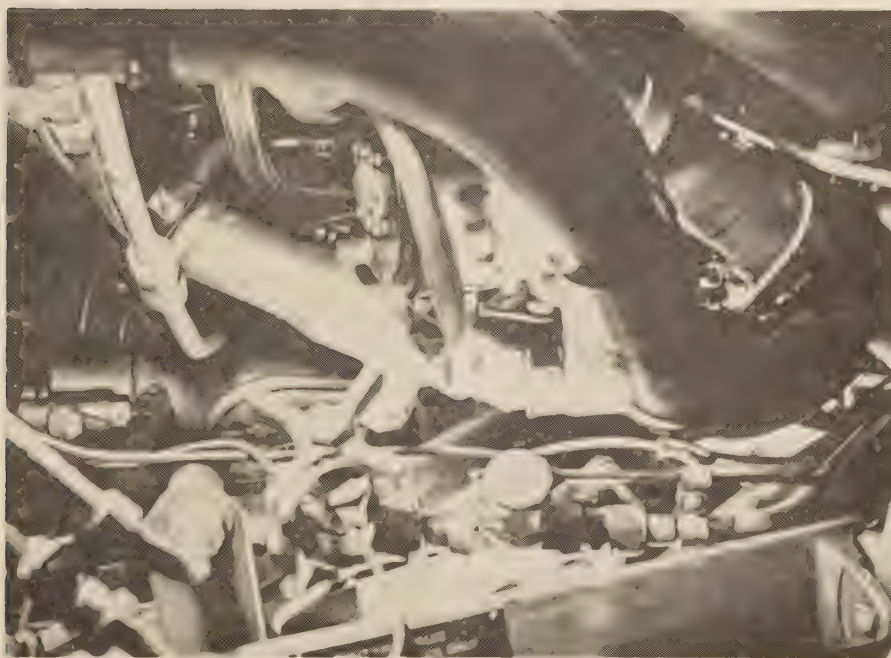


FIG. 12 SAMPLING CHAMBER INSTALLED FOR FLIGHT TEST

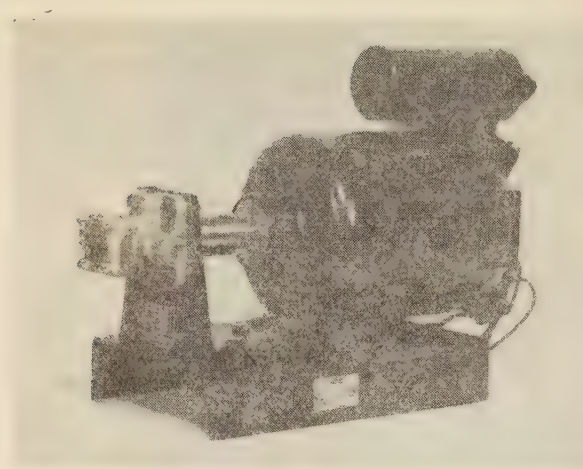


FIG. 13 BENCH MODEL OF AIR INDICATOR

by three aviation-engine manufacturers and six airplane manufacturers.

In addition to the flight-type instrument, a bench model has been prepared. On this model, a 110-v, a-c $\frac{1}{4}$ -hp electric motor is used, as shown in Fig. 13. To date, instruments of this type have been calibrated for, and used by, several manufacturers and the authors' laboratory for indicating the percentage of air in air-oil mixtures in various types of lubrication systems.

Because the device is a comparatively recent development and has not been in commercial production, its availability is probably known only to the aircraft industry for which it was developed. As a result, no applications of the instrument for indication of gas-in-liquid other than the indication of air-in-oil have been made. There appears to be no reason why the instrument cannot be used for indicating the percentage of gas entrained in any liquid-gas mixture capable of being pumped, and of which a correct sample can be obtained. It could therefore be used on gas-water mixtures, air-glycol mixtures, etc., as well as air-oil mixtures.

Use of Anthracite Fines in By-Product Coke Production

Factors Influencing the Relative Suitability of Different Anthracites for Blending

By J. D. CLENDENIN,¹ K. M. BARCLAY,¹ AND C. C. WRIGHT²

The blending of carbonaceous materials, particularly Pennsylvania anthracite, with coking coals as a means of mitigating the acute war shortage of certain types of metallurgical coke, has received considerable emphasis in recent months. However, the desirability of blending anthracite fines with coking coals for by-product coke production has been a matter of considerable controversy. To settle the differences of opinion and judgment, an attempt has been made as reported in this paper to evaluate, at least relatively, some of the variables encountered in the case of anthracite fines. The investigation in question was conducted at the Mineral Industries Experiment Station of The Pennsylvania State College, and was sponsored jointly by the Anthracite Institute and the Commonwealth of Pennsylvania.

THE blending of various types of carbonaceous and non-carbonaceous materials with coking coals has been the subject of laboratory and plant-scale experimentation for many years. The results of some of these investigations, in particular the effect of these more or less inert materials on the nature, properties, and characteristics of the several carbonization products have been reported (1)³ in numerous technical publications. Undoubtedly there has been other work of this nature the results of which have never been published, with a consequent loss to organized research in fuel technology.

With the increased demand for metallurgical coke and the shortage of certain types of coking coals as a result of the war, a new impetus has been given to the blending of carbonaceous materials, especially Pennsylvania anthracite, with coking coals as one means of mitigating the acuteness of these two problems. Some controversy has developed, however, concerning the desirability of blending anthracite fines with coking coal for by-product coke production and as a consequence it appeared desirable to examine some of the points of difference and to attempt to evaluate, at least relatively, some of the variables encountered in the use of anthracite fines. In this paper some of the more important points and variables are enumerated and discussed.

ANTHRACITE FINES USED FOR BLENDING

Considerable emphasis, and rightly so, has been placed upon

¹ Research Assistant in Fuel Technology, Mineral Industries Experiment Station, The Pennsylvania State College, State College, Pa.

² Professor of Fuel Technology, The Pennsylvania State College, State College, Pa.

³ Numbers in parentheses refer to the Bibliography at the end of the paper.

Contributed by the Mineral Industries Experiment Station of The Pennsylvania State College and presented at a Joint Meeting of the Fuels Division of THE AMERICAN SOCIETY OF MECHANICAL ENGINEERS and the American Institute of Mining and Metallurgical Engineers, Coal Division, Charleston, West Va., Oct. 30-31, 1944.

NOTE: Statements and opinions advanced in papers are to be understood as individual expressions of their authors and not those of the Society.

the importance of the size consist and the top and bottom sizes of the anthracite fines used for blending. There is general agreement concerning the detrimental effect of appreciable percentages of material larger than about 10-mesh size on the strength of the resultant coke. It is well known that discrete shale or other inert particles of appreciable size, as $1/4$ -in. or even smaller, in straight bituminous coking coals exert a detrimental effect on the strength of the resultant coke, and although numerous plants are pulverizing their coking coals to 90 per cent through $1/8$ -in.-sq mesh, this obviously permits the presence of shale or inert particles of appreciable size which can form centers of weakness in the final coke. Consequently, the presence of about 5 per cent of anthracite fines containing 1 to 5 per cent of plus 10-mesh material, which is the rule for most No. 5 buckwheat anthracites, will probably not exert as great a detrimental effect on the final coke as will the oversize in the bituminous coal itself.

Regarding the size consist and degree of fineness of the anthracite fines to be used, there are two main groups of thought. One, dating at least as far back as the work of Markle (2, 3), first reported in 1921, believes that anthracite fines for blending should be finely pulverized. One coke-plant operator who is using anthracite fines at the present time, has said that in his experience with inerts, the best structured cokes were produced when the added material contained the largest percentages of minus 50-mesh size. The other group, presumably of more recent origin, suggests that the presence of finely pulverized material in the anthracite is undesirable, and it is recommended that the anthracite be sized to 20×100 -mesh as nearly as possible.

Recently, and doubtless through misinterpretation of descriptions of the characteristics of anthracite fines suitable for blending, the idea has sprung up that specific gravity and volatile-matter content, per se, of an anthracite are sufficient criteria to use in selecting anthracite fines for blending, and other characteristics being similar, an anthracite of low volatile matter, about 6 per cent or less, and high specific gravity, about 1.7 or greater, would be more suitable than one possessing a somewhat lower gravity and higher volatile content. Ostensibly, this idea grew originally from observations made to the effect that anthracites which have proved to be most suitable were of the hard, lustrous, nonfriable variety, showing conchoidal fracture and having a high specific gravity and low volatile-matter content.

Some confusion concerning the specific gravity of the anthracites used in by-product blends has resulted from the fact that in Turner's (4) classification of anthracites, the specific gravity of face samples, crushed to minus $1/4$ in., are reported on the dry, ash-free basis, while specific gravities reported for the anthracites used in by-product blends have been determined on No. 5 buckwheat samples ground usually to 200 mesh and reported on the dry basis. In Turner's classification a wide variety of anthracites from the four producing fields are reported to have specific gravities ranging from 1.41 to 1.66, whereas the specific gravities reported by by-product plants have usually been 1.70 or higher. In part, the difference is due to the generally higher specific

gravities resulting from the higher ash content of the buckwheat samples as compared to face samples, in part to the higher gravities resulting from the use of the dry rather than dry ash-free basis and possibly also, in part, to the increase in gravity that has been observed in some cases when minus 1/4-in. samples are ground to minus 200 mesh.

Similarly, the data for volatile matter have been reported on different bases such as, as received, dry, dry ash-free, and dry mineral-matter-free. The latter method, which was not used by Turner (4), because it was not yet generally accepted at that time, but which is now widely accepted as the basis for classification of anthracites, appears to be the most reliable for the larger sizes of anthracite, but for the sizes smaller than about 1/4 in. is of questionable value. In general, the ash content of anthracite increases in the finer sizes, and due to the nature of the mineral matter, the generally used A.S.T.M. corrections to the mineral-matter-free basis are not reliable. This is illustrated in the proximate analyses given in Table 1, on a silt sample from a Northern Field colliery.

TABLE 1 PROXIMATE ANALYSES OF SCREEN FRACTIONS OF A NORTHERN FIELD, ANTHRACITE SILT

Screen fraction	Proximate analysis, per cent, air-dry basis				Dry, mineral-matter-free basis ^a	
	Moisture	Ash	Volatile matter	Fixed carbon	Volatile matter	Fixed carbon
Plus 10 mesh	1.5	8.1	5.4	83.0	4.9	95.1
10 × 20 mesh	1.3	10.1	5.4	83.3	5.7	94.3
20 × 30 mesh	1.3	17.3	6.3	75.1	5.7	94.3
30 × 40 mesh	1.1	17.2	6.4	75.3	5.7	94.3
40 × 60 mesh	1.3	23.9	7.0	67.8	6.3	93.7
60 × 100 mesh	1.5	29.1	7.9	61.4	7.6	92.4
100 × 200 mesh	1.4	32.9	8.2	57.5	7.8	92.2
200 × 325 mesh	1.7	43.7	9.2	45.4	9.6	90.4
Minus 325 mesh	1.7	45.6	8.7	44.0	8.5	91.5

^a A.S.T.M. approximation formula:

$$\text{Dry, mineral-matter-free FC} = \frac{\text{FC}}{100 - (M + 1.1A + 0.1S) \times 100}$$

The misinterpretation of the significance of the specific-gravity and volatile-matter-content data as a basis for selecting an anthracite for blending tends to create erroneous conclusions regarding the suitability of different anthracites. This can be illustrated in part by an examination of the data shown in Fig. 1, which are adapted from work on anthracites and semianthracites of Pennsylvania reported by Turner (4). The wide range in the friability of the anthracites of less than about 6 per cent volatile-matter content (dry ash-free basis) is clearly evident.

It is of interest to note that of the low-volatile high-gravity coals shown in Fig. 1, none has an apparent specific gravity greater than 1.68 on the air-dry basis, and the average ash contents (dry basis) vary from about 9 to 13 per cent. However, on the dry basis the apparent specific gravities are 1.7 or greater in several cases.

TESTS ON BUCKWHEAT SIZES OF PENNSYLVANIA ANTHRACITES

In order to examine and perhaps clarify some of these divergent ideas it was decided to test fine buckwheat sizes of anthracite from the four fields of the Pennsylvania anthracite region, and to investigate such factors as the relative physical and thermal stability of the different fine sizes, their volatile-matter content, apparent specific gravities, size consists, the extent of any inter-relationship between these factors, and to determine what, if any, correlation exists between these variables and the relative strength and size of the cokes produced in a small-scale oven when the anthracites are blended with a coking coal. In addition, some preliminary tests are outlined in order to observe the effect of changing the nature of the coking coal. It was also deemed of interest to obtain information from coke-plant operators using anthracite, regarding the relative suitability of the anthracites they have tested. Samples of a coking-coal blend

containing anthracite fines and regular by-product coke made from the blend were secured for purposes of comparison.

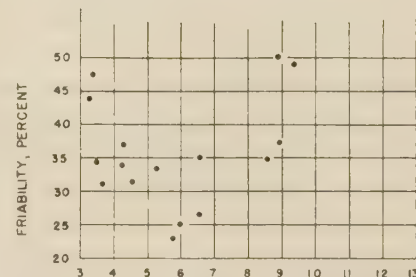
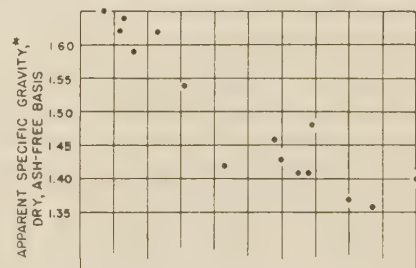
A number of samples of No. 4 and No. 5 buckwheat anthracite were obtained from various collieries located in the four major anthracite fields. The proximate analyses, apparent specific gravities, and size consists down to 40 mesh of the original buckwheat samples are given in Table 2. The specific gravities were determined in duplicate with the precision indicated by means of the pycnometer method using distilled water with 25-ml pycnometers and approximately 10-g portions of anthracite.

The size analyses shown in Table 2 were determined by the use of a "Ro-Tap" and U. S. S. sieves.

Preliminary graphical representation of the specific gravity-volatile matter data of Table 2 showed the same trend as do Turner's results in Fig. 1, when tried on all the commonly used bases, i.e., as received, dry, dry ash-free, and dry mineral-matter-free. Although there is some tendency in the direction of higher gravity with higher ash content, the specific gravity-ash content data, on the as-received and dry bases, showed a fairly typical "shotgun pattern." As a result none of these relationships for the data of Table 2 is presented graphically.

The next step was to gain some idea of the relative physical stability, or what may be called the relative "inherent" strength of the buckwheat anthracites in the raw state. After consideration of possible methods, the microstrength test apparatus, originally described by Blayden, Noble, and Riley (5), was chosen. The apparatus is shown in Fig. 2. The sample cylinders are so constructed that the ends can be tightly closed after placing 12 small steel balls and a weighed portion of a closely sized sample to be tested in each one. The cylinders are rotated for 800 revolutions at the rate of 25 rpm. Anthracite samples of 4 g

SPECIFIC GRAVITY AND FRIABILITY VS VOLATILE MATTER CONTENT OF PENNSYLVANIA ANTHRACITES AND SEMIANTHRACITES



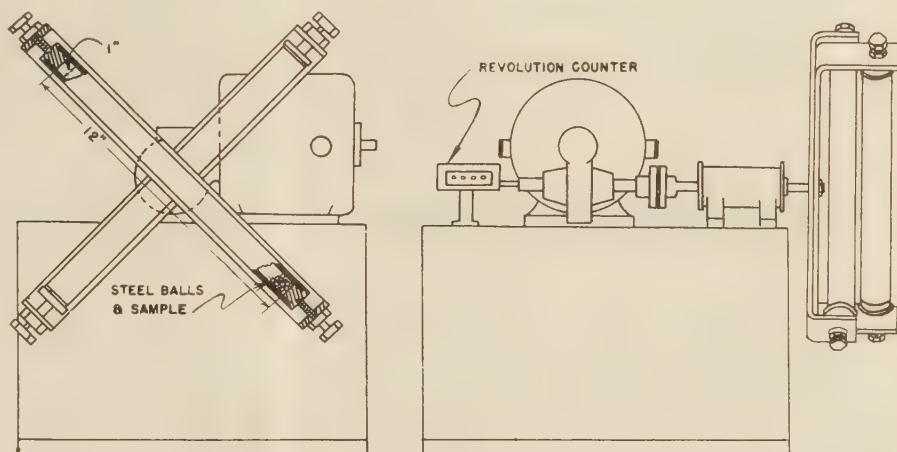
VOLATILE MATTER CONTENT, DRY, ASH-FREE BASIS (FACE SAMPLES)

* DETERMINED ON SAMPLES CRUSHED TO 100% MINUS 1/4 INCH

FIG. 1

TABLE 2 PROXIMATE ANALYSES, APPARENT SPECIFIC GRAVITIES, AND SCREEN ANALYSES OF NO. 4 AND NO. 5 BUCKWHEAT ANTHRACITES; AS-RECEIVED, AIR-DRY BASIS

Field and sample no.	Size and designation	Proximate analysis			Apparent specific gravity	Screen analysis (U. S.)			
		Moisture, per cent	Volatile matter, per cent	Ash, per cent		+10 mesh	+20 mesh	+30 mesh	+40 mesh
Northern	1 Buckwheat no. 4	1.7	7.2	21.8	1.66 ± 0.01	11.6	82.6	94.5	97.5
	2 Buckwheat no. 4	2.2	6.4	9.4	1.58	5.1	85.2	94.7	97.4
	3 Buckwheat no. 4	2.6	5.3	6.2	1.58	5.4	95.9	99.4	99.6
	4 Buckwheat no. 4	3.3	5.9	7.8	1.57	0.2	70.3	90.2	96.7
	5 Buckwheat nos. 4 and 5	3.3	6.1	9.1	1.59	0.2	50.6	75.9	88.9
Western Middle	6 Buckwheat no. 5	2.8	8.9	11.2	1.53	0.3	31.6	68.2	83.8
	7 Buckwheat no. 4	3.4	6.2	12.2	1.63	9.2	78.7	91.6	95.8
	8 Buckwheat no. 4	1.4	8.3	10.2	1.52	5.4	84.8	95.0	97.8
	9 Buckwheat no. 5	1.8	10.0	11.9	1.52	0.1	28.2	61.0	79.4
	17 Buckwheat no. 4	3.0	5.6	12.9	1.64	3.6	69.9	88.8	95.9
	24 Buckwheat no. 4	1.8	10.9	9.9	1.48	9.8	91.9	97.8	99.3
	31 Buckwheat no. 5	2.5	5.8	9.6	1.67	0.8	44.1	78.4	91.6
Eastern Middle	10 Buckwheat no. 4	3.2	3.8	8.8	1.65	32.4	96.7	99.5	...
	11 Buckwheat no. 4	2.9	4.1	8.8	1.65	33.0	96.0	99.5	...
	14 Buckwheat no. 5	4.6	6.2	10.8	1.67	3.1	54.2	81.4	93.1
	19 Buckwheat no. 4	2.8	4.4	14.0	1.70	13.5	81.7	94.0	97.8
	22 Buckwheat no. 4	2.7	5.5	17.1	1.69	5.7	92.4	98.8	99.4
	29 Buckwheat no. 5	4.3	4.9	11.3	1.67	4.5	68.5	87.3	95.2
	30 Buckwheat no. 5	4.4	7.7	12.0	1.70	5.6	48.3	68.9	80.5
	12 Buckwheat no. 4	1.5	7.0	13.2	1.60	5.9	80.3	91.6	96.7
Southern	13 Buckwheat no. 4	3.1	7.5	12.0	1.67	2.0	60.4	83.9	93.6
	15 Buckwheat no. 4	1.9	4.0	12.4	1.70	21.8	90.6	97.1	99.0
	16 Buckwheat no. 4	2.2	8.9	15.2	1.53	0.7	36.3	59.9	76.7
	18 Buckwheat no. 5	1.9	4.3	13.1	1.72	0.2	35.8	72.5	89.1
	20 Buckwheat no. 4	2.6	5.4	13.8	1.72	5.9	85.8	96.2	98.0
	21 Buckwheat no. 5	3.7	5.0	15.5	1.74	0.8	48.1	73.2	87.4
	23 Buckwheat no. 4	4.4	9.2	13.5	1.62	5.1	90.1	97.1	98.5



were used rather than the 2-gram samples originally specified for testing coles, in order that the anthracite would occupy about the same volume as the coke. In preparing carefully sized samples of fines, 16 × 30-mesh fractions, made up to a standard size consist, were used. The 16 × 30-mesh fraction corresponds closely to the size specified for coles as originally described in the test. The arbitrary standard size consist used in the present work is based upon the average of the size consists of the 16 × 30-mesh fractions of all of the samples tested, the average size consist being as follows: 16 × 18 mesh, 26.7 per cent; 18 × 20 mesh, 33.4 per cent; 20 × 25 mesh, 18.6 per cent; 25 × 30 mesh, 21.3 per cent. Proximate analyses and apparent specific gravities of the standard 16 × 30-mesh fractions of the different No. 4 and No. 5 buckwheat sizes are shown in Table 3. In Fig. 3 the degree of correlation existing between the apparent specific gravities (dry ash-free basis) of the original buckwheat sizes and the corresponding standard 16 × 30-mesh fractions is shown.

After the 4-g portions of the standard 16 × 30-mesh samples have been subjected to the prescribed treatment in the microstrength tester, the coal is carefully removed from the cylinders and the breakdown deduced from the amounts remaining on a 30-mesh and a 70-mesh screen. The microstrength index of the coal is expressed as the cumulative per cent on 30 mesh over the

TABLE 3 PROXIMATE ANALYSES AND APPARENT SPECIFIC GRAVITIES OF STANDARD 16 × 30-MESH FRACTIONS OF DIFFERENT RAW NO. 4 AND NO. 5 BUCKWHEAT ANTHRACITES; AS-RECEIVED (AIR-DRY) BASIS

Field and sample no.	Proximate analysis, per cent			Apparent specific gravity
	Moisture	Volatile matter	Ash	
Northern	1 2.0	7.1	20.9	1.69
	2 2.7	6.3	10.2	1.58
	3 2.9	5.4	9.4	1.61
	4 2.7	6.6	8.7	1.58
	5 2.8	6.7	8.2	1.58
Western Middle	6 2.1	9.2	8.6	1.51
	7 2.6	6.5	13.1	1.64
	8 1.6	8.9	12.7	1.53
	9 2.2	8.5	8.8	1.49
	17 3.6	5.8	15.8	1.67
	24 1.9	12.4	14.0	1.53
	31 2.3	5.3	8.8	1.61
Eastern Middle	10 3.0	4.6	13.6	1.64
	11 3.4	4.7	12.6	1.61
	14 4.6	6.5	10.7	1.53
	19 2.6	4.7	16.8	1.63
	22 2.6	6.1	19.1	1.69
	29 3.7	5.2	11.7	1.67
	30 4.7	7.4	9.6	1.66
Southern	12 2.3	6.9	13.1	1.59
	13 4.2	7.5	11.1	1.65
	15 2.6	4.3	16.7	1.52
	16 2.5	8.9	13.6	1.57
	18 2.4	4.4	9.2	1.66
	20 3.8	5.8	15.8	1.72
	21 3.4	5.3	16.4	1.74
	23 4.7	10.4	16.1	1.64

APPARENT SPECIFIC GRAVITY OF NO. 4 & NO. 5
BUCKWHEAT ANTHRACITES* VS. APPARENT
SPECIFIC GRAVITY OF THE CORRESPONDING
STANDARD CONSIST 16 X 30 MESH* FRACTIONS
(DRY, ASH-FREE BASIS)

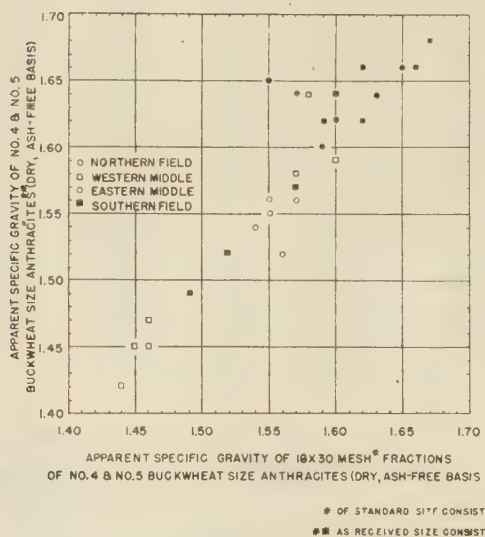


FIG. 3

RELATIVE "INHERENT" STRENGTH VS APPARENT
SPECIFIC GRAVITY OF ANTHRACITE

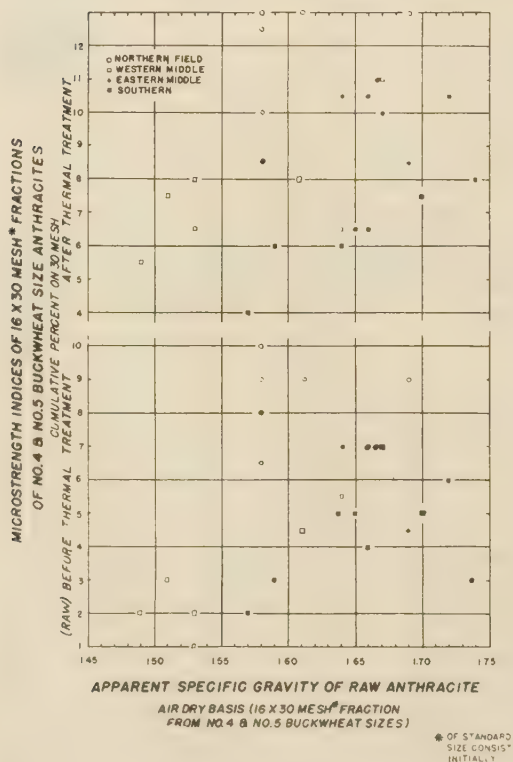


FIG. 4

cumulative per cent on 70 mesh, e.g., 5/50. In general the microstrength test was run in duplicate and for indexes in the vicinity of 10/60 the average deviation is $\pm 0.35/0.55$; for those in the vicinity of 6/40 it is $\pm 0.30/0.50$; and for those around 2/25 it is $\pm 0.35/1.25$.

The microstrength indices versus the apparent specific gravity (air-dry basis) of the raw standard 16 X 30-mesh fractions of the different No. 4 and No. 5 buckwheat anthracites are shown graphically in the lower part of Figs. 4 and 5; expression of the gravities on either the dry, dry ash-free, or dry mineral-matter-free basis did not alter the general nature of the relationship, and no advantage was evidenced from replacing specific gravity with volatile-matter content. The cumulative per cent on 30-mesh part of the index is shown on the lower half of Fig. 4, while on 70-mesh part is shown in the corresponding position in Fig. 5. To express a microstrength index as a single integer is not satisfactory, because it would thereby lose most of its significance.

An examination of these two figures shows that, just as was the case in Fig. 1, the highest-gravity coals in the raw state are not necessarily the coals which possess the highest physical stabilities as expressed by the microstrength indexes. It should be borne in mind, however, that one cannot set up definite categories on the basis of these relative stabilities which are determined only on a selected fraction of the fines. Nevertheless, it is clear that in the fine sizes, coals from different fields possess similar stabilities in some cases, while in others, coals from the same fields possess different stabilities which is in accord with experience in the use of the larger sizes of anthracite.

RELATIVE "INHERENT" STRENGTH VS APPARENT
SPECIFIC GRAVITY OF ANTHRACITES

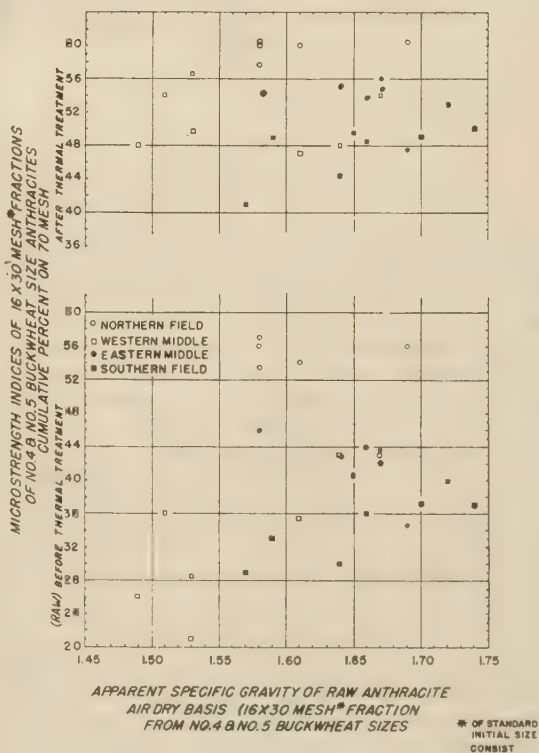


FIG. 5

EFFECT OF HIGH-TEMPERATURE THERMAL TREATMENT ON ANTHRACITE FINES

Since it has been generally observed as well as reported in several cases (6) that many anthracites show increased strength after being subjected to thermal treatment at elevated temperatures, it seemed reasonable to investigate the effect of high-temperature thermal treatment on the relative "inherent" strengths of the different anthracite fines. Likewise, it was desirable to obtain some estimate of the thermal stability or simply resistance to thermal shock of the different anthracite fines. Some preliminary experiments with the 16 × 30 fraction of a buckwheat No. 5 anthracite demonstrated that the necessary thermally treated samples for both tests could be prepared simultaneously by heating 40 to 50 g of coal in a covered fireclay crucible placed in an electric muffle furnace, the temperature of which was initially at 1000 C. At the end of 1 hr of heating in the furnace the temperature of the center of the coal charge in the crucible was found to be approximately 900 C. Heating the sample longer than 1 hr in the furnace, with subsequent cooling of the sample in the covered crucible, was found to effect no further significant change in the stability, or relative "inherent" strength, of the anthracite as determined by means of the microstrength tester. Similarly, most of the size breakdown of the 16 × 30-mesh fraction of fines due to thermal shock was accomplished by 1 hr of heating. Therefore, 1 hr was chosen as the optimum time of thermal treatment of the test samples when the temperature of the muffle furnace was initially at 1000 C.

Duplicate samples of 40 to 50 g each of the standard 16 × 30-mesh fractions of the different No. 4 and No. 5 buckwheat anthracites were subjected to thermal treatment in the manner already described. Upon removal of the covered crucibles from the furnace they were allowed to become cool to the touch before the lids were removed from the crucibles so as to eliminate ashing-over of the coal in the top of the crucible. After cooling, the samples were carefully weighed and subjected to a size analysis into 16 × 18-mesh, 18 × 20-mesh, 20 × 25-mesh, and 25 × 30-mesh fractions using the Ro-Tap. The shaking time was held to a minimum but was long enough so that no appreciable quantity of material could be shaken from one screen to the next by additional time on the Ro-Tap. The duplicate samples showed reasonably close agreement, except in the case of the 16 × 18-mesh fraction. However, even in this fraction the differences or similarities between samples appeared to be real rather than apparent. The results of the thermal breakdown tests on the selected fraction of the No. 4 and No. 5 buckwheat anthracites are shown graphically in Fig. 6, as relative resistance to thermal shock versus apparent specific gravity. In this figure only the cumulative percentages remaining on 20 mesh and 30 mesh after thermal treatment are shown, as an examination and comparison of the data for the different fractions suggested that these two sizes adequately represent the relative thermal stability of the different units of the 16 × 30-mesh fractions as measured by the procedure outlined here.

Comparing the results shown in Fig. 6 with those shown in Fig. 4 for the strength of the original coals, it will be noted that the relative positions of many of the samples with respect to each other are shifted. It appears that, in general, except for two samples of lowest gravity, a coal of low gravity may be as likely to possess a high thermal stability as a coal of high gravity.

The physical stabilities of the thermally treated samples, which are shown in the upper part of Figs. 4 and 5, were determined by the use of the microstrength test apparatus in the manner already described for the raw 16 × 30-mesh fraction before thermal treatment. The different fractions resulting from the "thermal-breakdown" size analysis were mixed thoroughly before being tested in the microstrength apparatus. The 5 to 10 per cent of

RELATIVE RESISTANCE TO THERMAL SHOCK VS APPARENT SPECIFIC GRAVITY OF ANTHRACITES

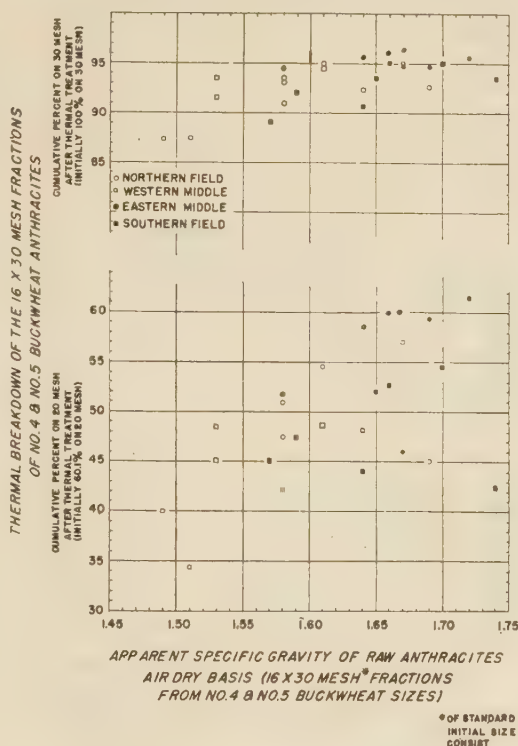


Fig. 6

minus 30-mesh material present in the thermally treated fractions was left in the samples to be tested for relative physical stability in the microstrength apparatus, and no correction was applied to the observed or apparent microstrength indexes of the various thermally treated samples, because the correction causes no appreciable change in the relative positions of the indexes with respect to each other, although it does cause a small change in the magnitude of the apparent or observed value of the various indexes.

Examination of the results depicted in Figs. 4 and 5 for the relative "inherent" strengths of standard 16 × 30-mesh fractions after thermal treatment shows that, in general, the physical stability of the 16 × 30-mesh fraction is increased as a result of the thermal treatment, and the increase is less, generally, for coals having the higher stability in the raw state. Certainly there is no clear-cut trend, albeit there is some tendency for the high-gravity coals to possess the greater stability. It is evident that, as previously implied, each coal must be judged on its individual merits and for the particular purpose.

In conclusion and as a summary of the work on the properties of anthracite fines, Fig. 7 has been prepared. In it the results of the work on the thermal stability, apparent specific gravity, and microstrength index or relative "inherent" strength of the 16 × 30-mesh fractions are plotted against the dry, ash-free volatile-matter content of the fractions; Fig. 7 is analogous to Fig. 1. It will be noted that below 11 per cent volatile-matter content, similar tendencies or trends are apparent, the clearest being in thermal breakdown (thermal stability) versus volatile matter.

As previously suggested, rather erroneous conclusions may result regarding the suitability of an anthracite for a particular

THERMAL STABILITY, APPARENT SPECIFIC GRAVITY AND RELATIVE "INHERENT" STRENGTH VS VOLATILE MATTER CONTENT OF 16X30 MESH FRACTIONS OF ANTHRACITE FINES

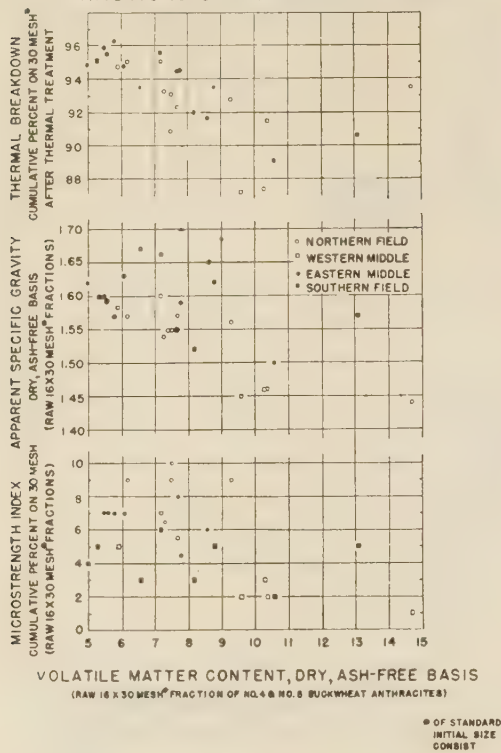


Fig. 7

purpose by placing too much emphasis on the data of specific gravity and volatile matter. The change in the relative positions of the different fines with respect to each other is rather illuminating. For example, it will be noted that the Northern Field fines, ranging in volatile content from 6 to 9.5, show the highest relative inherent strength in the raw state as measured by the microstrength indexes, while the same coals have only medium gravities and medium relative thermal stability measured by the cumulative per cent on 30 mesh in the thermal-breakdown test. The Eastern Middle Field fines ranging in volatile content from 5 to 8.5 per cent, and in gravity from medium to high, possess in general the highest thermal stability and medium relative "inherent" strength. The fines from both the Western Middle and Southern Fields are more variable as would be expected, and only in the microstrength test do they, generally, fall below the fines from the other two fields.

LABORATORY-SCALE COKING TESTS

The laboratory-scale coking tests with the exception of several preliminary experiments were all made using a bituminous coking coal from the Pittsburgh seam having the following proximate analysis: Moisture, 1.7 per cent; ash, 8.3 per cent; volatile matter, 36.3 per cent; and fixed carbon, 53.7 per cent. The anthracite fines used in conjunction with the coking coal are indicated in subsequent paragraphs. In general, only No. 5 buckwheats were used, with the exception that in one series of tests a Northern Field anthracite silt was used.

The coals and coal blends were carbonized in a small, two-wall heated, gas-fired oven that has been described previously (7); coal charges of about 7 lb were used. The coking time was

approximately 100 min when the oven flue temperatures were maintained at about 1100 C. At the end of 100 min, the center of the coke had reached a temperature of about 950.

The relative bulk density of the coal charge was hardly affected by the presence of 5 per cent of No. 5 buckwheat anthracite, and the differences observed with the different No. 5 buckwheats were generally within the limits of error in the measurement of the relative bulk density. However, with the addition of 5 per cent of a No. 5 buckwheat pulverized to minus 100-mesh size, a very small but apparently significant increase in the relative bulk density of the charge was observed. The coals as carbonized were in the air-dry condition.

In general, the coking tests were conducted at least in duplicate, and the yield of plus 2-in. coke was reproducible to within about ± 4 per cent of the average, while the yield of plus $1\frac{1}{2}$ -in. coke was reproducible to within about ± 2 per cent of the average.

The biggest problem was that of evaluating the relative strengths of the various blend cokes. Experiments indicated that the microstrength test apparatus was unsatisfactory as a means of deducing or inferring the relative macrostrengths of the different cokes, and that under the circumstances the usual test procedures for macrotesting of commercial cokes were hardly feasible. Since the primary interest was that of distinguishing differences in the relative strengths of the blend cokes, it was decided, finally, to make use of the rather vigorous and regular motion of a Tyler Ty-Lab tester which is ordinarily used for screening work.

The tester was used in two different ways and both seemed to permit the detection of differences in the relative strengths of the various blend cokes. In the first the 2, $1\frac{1}{4}$, and $\frac{3}{4}$ -in. screens were placed on the tester pan and the lid clamped on top, with the result that the maximum distance of travel of a piece of coke was about 4 in. In the second and preferred procedure, a blank screen frame was placed on the pan and the lid clamped on top over the blank frame, with the result that the maximum distance of travel of a piece of coke was about 8 in. The tester, charged with approximately 2000 g of coke, was operated for successive increments of time from 5 min up to a total of 80 min, and it was found that starting initially with plus 2-in. or plus $1\frac{1}{2}$ -in. coke, the cumulative percentages remaining on both the $1\frac{1}{4}$ -in. and the $\frac{3}{4}$ -in. screens after 15 and 80 min of treatment gave a reasonable measure of the relative strength of the different blend cokes.

In general, the relative-strength tests were performed in duplicate and at the end of 15 and 80 min the cumulative per cent remaining on $1\frac{1}{4}$ in. was reproducible to within about ± 2.5 per cent of the average; and the cumulative per cent on $\frac{3}{4}$ in. to within about ± 1.5 per cent of the average. Variations of a few hundred grams in the amount of coke taken for testing appeared to exert no significant effect on the relative-strength results.

BEST COKE FROM FINELY PULVERIZED ANTHRACITE

It was mentioned in a previous section that of the two groups of thought regarding the size and size consist of anthracite for blending, one believes the use of more or less finely pulverized anthracite produces the best coke. In order to examine this thesis a series of experiments was conducted using buckwheat anthracite sample No. 29. Some 2 kg of the original buckwheat, the nominal top size of which was 8 mesh, was divided into five representative fractions; the first was untouched, the second pulverized to minus 20 mesh, the third to minus 40 mesh, the fourth to 60 mesh, and fifth to 100 mesh. In each case the material passing the given screen was first screened out and the oversize pulverized to pass through the screen. Of each size, 5 per cent was blended with 95 per cent of the Pittsburgh seam coal for the coking tests.

The results for this set of experiments are shown graphically in

Figs. 8 and 9. In the former, the relative blockiness of the blend cokes as represented by the yield of plus 2-in. coke is shown as a function of the nominal top size of the anthracite fines used in the original coal blend. At the left of the figure the yield of plus 2-in. coke from the straight coking coal is shown above "No Anthracite." The effect of the relative coarseness of the anthracite on the blockiness is rather obvious. In the latter the relative strength of the blend cokes, as represented by the cumulative percentages remaining on $1\frac{1}{4}$ -in. and on $\frac{3}{4}$ -inch screens after both 15 and 80-min treatment in the Ty-Lab tester, is shown as a function of the nominal top size of anthracite used in the original coal blend.

It will be noted that the trend of the relative strength versus top size or relative coarseness of the anthracite is in a direction opposite to that evident for blockiness in Fig. 8. The effect of increasing coarseness of the anthracite on the relative strength of the blend coke is unmistakable. It appears that finely pulverized anthracite is not wholly detrimental to the quality of the coke, and when the top size of the anthracite is between about 20 to 60 mesh there is some enhancement of the coke strength. The results shown in Figs. 8 and 9 suggest that, as a generalization, there is some justification for the observation previously cited to the effect that the larger the percentage of inerts passing 50 mesh, the better the structure of the coke.

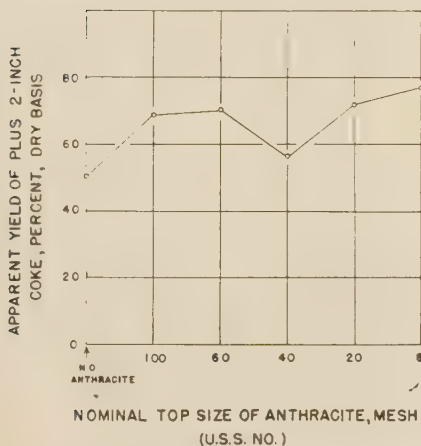
It was evident from the results of the foregoing experiments that it would be desirable to examine the effect of 5 per cent each of specific size fractions of anthracite fines on the relative strength and blockiness of blend cokes made with the same bituminous coal. Consequently, experiments, the results of which are shown graphically in Figs. 10 and 11, were conducted using the sized fractions indicated. Even a cursory examination of these two figures shows that the general relationships that exist in Figs. 8 and 9 between the size of the anthracite and the strength and blockiness of the blend coke, also exist in these figures. The same marked changes in the strength and blockiness in the

vicinity of 40 to 60 mesh are also evident. The effect of 5 per cent of the composite 12×200 -mesh anthracite is noteworthy. In general, the results for this composite are in accord with the results obtained with the individual fractions from which the composite was made up. The striking behavior of the sizes and fractions in the vicinity of 40 and 60 mesh suggests that more intensive study should be conducted in order more clearly to define that behavior.

In the light of the results observed in the foregoing experiments, the results of the work shown in Figs. 12 and 13, in which 5 per cent each of ten different No. 5 buckwheats were used, are of special interest. Fig. 14 in which the volatile-matter contents, specific gravities, and size consists of the ten buckwheat anthracites appear, should be used in conjunction with Figs. 12 and 13. Mental superposition of these three figures will show again the same general trend that is evident in Figs. 8, 9, 10, and 11; namely, that coarseness of size consist of the anthracite tends to enhance the relative blockiness of the blend cokes, while fineness tends to enhance their relative strengths. It will be noticed in Fig. 14 that generally those buckwheats having the coarser size consist also happen to possess higher specific gravities and lower volatile-matter contents.

Two of these No. 5 buckwheat samples, Nos. 18 and 31, are being used for blending in the production of foundry coke with apparent satisfaction. In Fig. 12 it will be seen that both of these samples show up well with regard to relative blockiness, but not quite so well in relative strength in Fig. 13. It will be seen from Fig. 14 that both anthracites have low volatile-matter contents and high gravities. Three other of these No. 5 buckwheat samples, Nos. 6, 14, and 30, are reported to be used for blending at

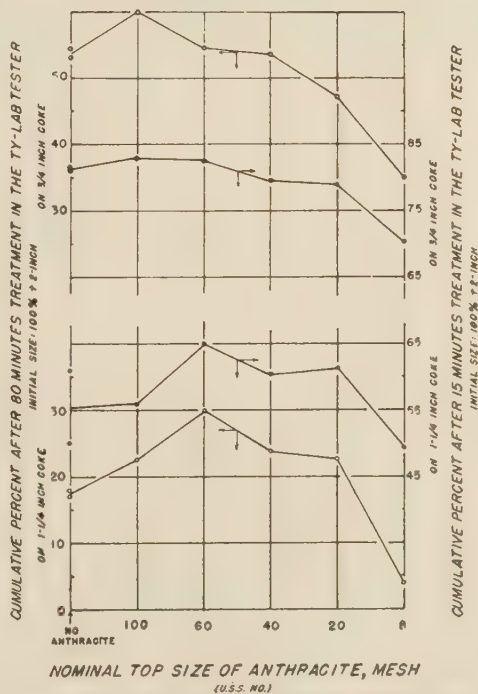
EFFECT OF BLENDING FIVE PERCENT OF THRU-MESH SIZES OF AN ANTHRACITE ON THE RELATIVE BLOCKINESS OF COKE



COALS USED: (1) COKING BITUMINOUS, PITTSBURGH SEAM;
(2) ANTHRACITE, EASTERN MIDDLE FIELD

FIG. 8

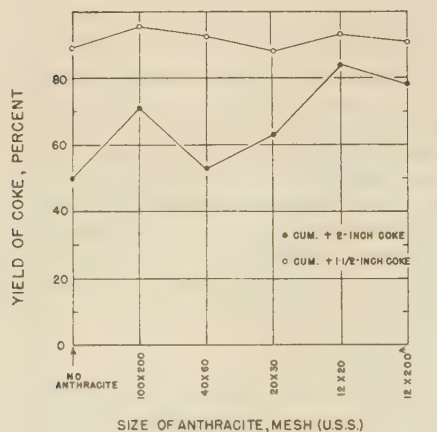
EFFECT OF BLENDING FIVE PERCENT OF THRU-MESH SIZES OF AN ANTHRACITE ON THE RELATIVE SHATTER-ABRASION STRENGTH OF COKE



COALS USED: (1) COKING BITUMINOUS, PITTSBURGH SEAM; (2) ANTHRACITE, EASTERN MIDDLE FIELD

FIG. 9

EFFECT OF BLENDING FIVE PERCENT OF DIFFERENT FRACTIONS OF AN ANTHRACITE ON THE RELATIVE BLOCKINESS OF THE COKE**

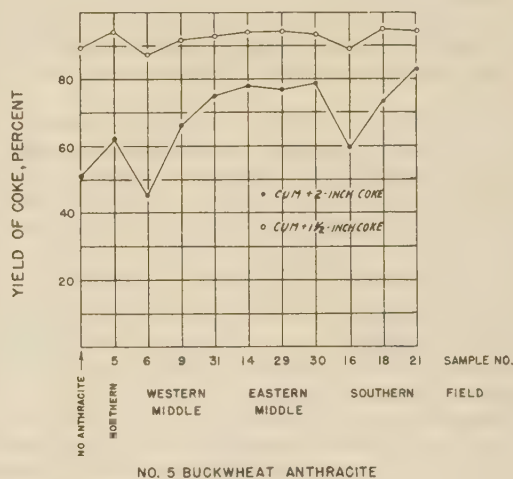


* SIZE CONSIST: 12X20 MESH 44.6 %
 (BASED ON THE AVERAGE SIZE CONSIST OF THE NO. 6 BUCKWHEAT ANTHRACITES IN TABLE 2) 20X30 27.4
 40X60 23.7
 100X200 4.3

** COALS USED: (1) COKING BITUMINOUS, PITTSBURGH SEAM;
 (2) ANTHRACITE, NORTHERN FIELD BILT

Fig. 10

EFFECT OF FIVE PERCENT OF DIFFERENT NO.5 BUCKWHEAT ANTHRACITES ON THE RELATIVE BLOCKINESS OF COKE

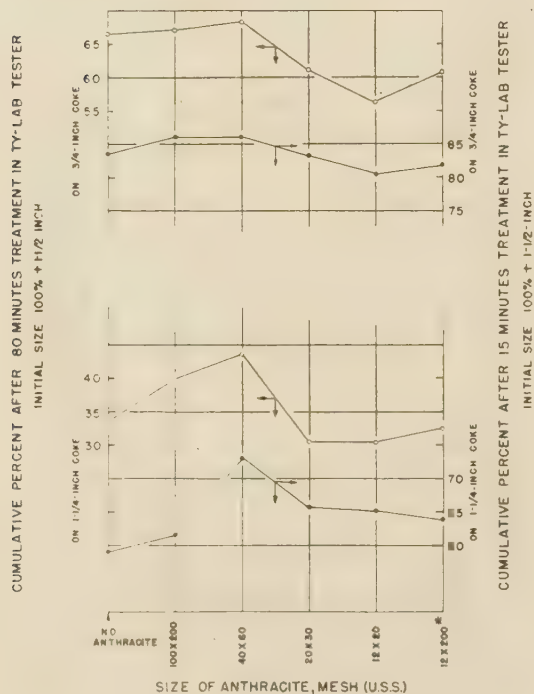


NO. 5 BUCKWHEAT ANTHRACITE

COALS USED: (1) COKING BITUMINOUS, PITTSBURGH SEAM;
 (2) ANTHRACITES, AS SHOWN

Fig. 12

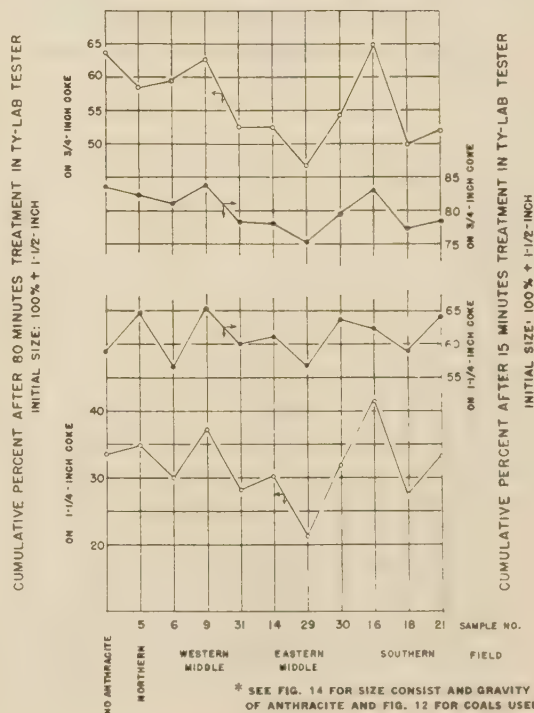
EFFECT OF BLENDING FIVE PERCENT OF DIFFERENT FRACTIONS OF AN ANTHRACITE ON THE RELATIVE SHATTER-ABRASION STRENGTH OF THE COKE*



* SEE FIG. 10 FOR DATA ON SIZE CONSIST OF 12 X 200 FRACTION AND COALS USED

Fig. 11

EFFECT OF FIVE PERCENT OF DIFFERENT NO.5 BUCKWHEAT ANTHRACITES ON THE RELATIVE SHATTER-ABRASION STRENGTH OF THE COKE*



* SEE FIG. 14 FOR SIZE CONSIST AND GRAVITY OF ANTHRACITE AND FIG. 12 FOR COALS USED

Fig. 13

coke plants, but it will be observed that the characteristics of these three buckwheats differ considerably as do their blend cokes. The results with sample No. 16 are rather unique. The relative blockiness of the blend coke is low while its relative strength is high, yet the specific gravity of the anthracite used is low and its volatile content is high.

An examination of the various data for the ten No. 5 buckwheat anthracites suggested that some relationships should exist between certain characteristics of these buckwheat anthracites and the relative strengths of their blend cokes, as represented by the cumulative percentage of coke remaining on $\frac{3}{4}$ in. after 80-min treatment in the Ty-Lab tester. In Figs. 15 and 16 are shown several apparent correlations. In the former the specific gravities and volatile-matter contents of the ten original No. 5 buckwheat anthracites are shown on the ordinate while the relative strengths of the blend cokes containing 5 per cent each of the ten different anthracites are shown on the abscissa. In the latter the percentage of 40×60 -mesh material in the ten original No. 5 buckwheat and the thermal breakdown, i.e., thermal stability, of the standard 16×30 -mesh fractions of the ten No. 5 buckwheats are shown on the ordinate while the relative strengths of the blend cokes are on the abscissa. The correlations are reasonably clear and somewhat at odds with certain prevailing ideas regarding the relative suitability of anthracites for blending.

No such apparent correlations between some characteristics of the buckwheat anthracites and the relative blockiness of the corresponding blend cokes could be readily ascertained, except for the general trend, already pointed out, of increasing blockiness of the coke with increase in the coarseness of the anthracite fines.

VOLATILE MATTER CONTENT, APPARENT SPECIFIC GRAVITY AND SIZE CONSIST OF NO. 5 BUCKWHEAT ANTHRACITES USED IN COKING TESTS

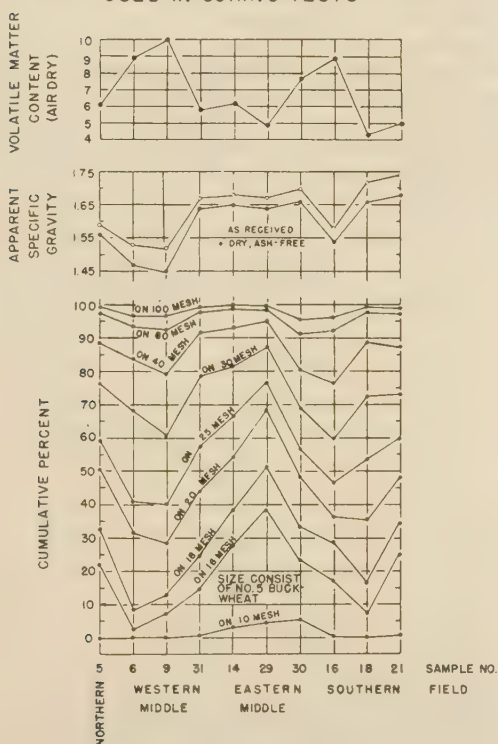


FIG. 14

SOME CHARACTERISTICS OF NO. 5 BUCKWHEAT ANTHRACITES VS RELATIVE STRENGTH OF BLEND COKES*

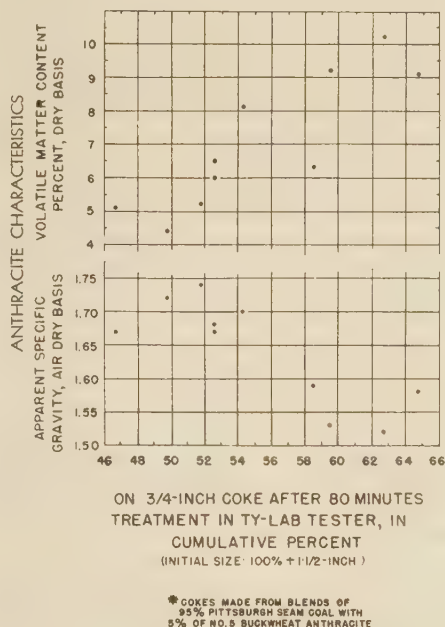


Fig. 15

SOME CHARACTERISTICS OF NO. 5 BUCKWHEAT ANTHRACITES VS RELATIVE STRENGTH OF BLEND COKES*

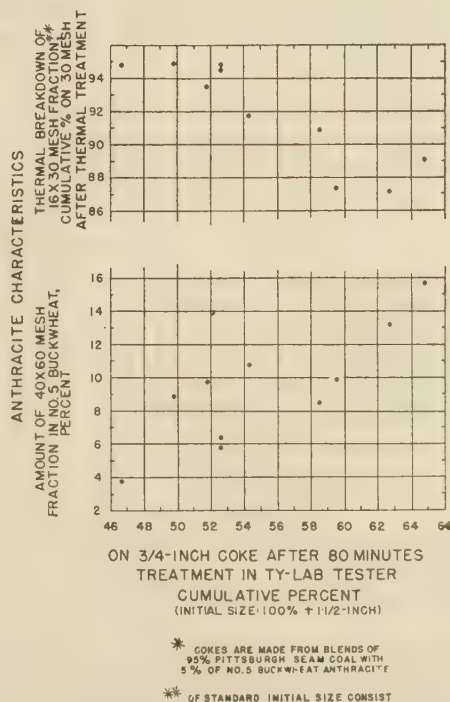


FIG. 16

In order to demonstrate the effect of using different types of coking coal and increasing the amount of anthracite on the relative blockiness and strength of the coke, several preliminary experiments the results of which are compiled in Table 4, were conducted. Perhaps the most unique thing in the entire set of tests is the remarkable difference in the relative strengths of the blend cokes made from the two different coking coals each blended with 15 per cent of No. 5 buckwheat in its original size consist, as contrasted with the strikingly similar strengths of the blend cokes made from these coking coals but with 15 per cent of No. 5 buckwheat pulverized to minus 100 mesh. In contrast with this, the relative blockiness of the blend cokes, as yield of +2-in. coke, does not differ to any great extent.

As a matter of interest a sample of a standard commercial coking blend containing 6 per cent of No. 5 buckwheat anthracite with high- and low-volatile coals in the ratio of 60-40, was secured. The yield and relative strength of the coke from this blend, after carbonization in the laboratory oven, are shown in Table 4. The relative strength appears to be about the same as the strengths observed on the two cokes made with 15 per cent of minus 100-mesh anthracite in the coal blend.

A sample of regular by-product coke made from this blend was also secured. The results of testing this coke in the Ty-Lab tester are shown in Table 4, and by means of A.S.T.M. drop shatter in the footnotes. This coke was also subjected to multiple-drop shatter and mathematical analysis for rate of degradation (8), the final results of which are also presented in the footnotes of Table 4.

Since particle shape has also been suggested as a factor which may be significant in the selection of buckwheat anthracites for blending, the ten No. 5 buckwheats used in the coking tests were examined with this in mind. Three different observers, using naked-eye observation as well as a low-power binocular, were in reasonable agreement regarding the shapes of the particles which were predominantly rhombic, rhomboidal, or cuboid, with some platelike or needlelike particles also present. But no correlation, the degree of which was as significant as those correlations already shown, could be deduced between particle shape and the characteristics of the blend cokes.

CONCLUSIONS

It has become evident as a result of the foregoing work that anthracites of high specific gravity and low volatile-matter con-

tent are not necessarily more suitable for blending than low-gravity, high-volatile anthracites, although it has been reported recently that high-gravity, low-volatile anthracites are most suitable for blending in small amounts in the manufacture of by-product coke.

In this small-scale carbonization work there was a discernible tendency toward increased blockiness and decreased strength of the blend cokes made with anthracite fines of coarser size consist, while with buckwheat anthracites of finer size consist the tendency was reversed. This would suggest that an anthracite for blending must be chosen, at least in part, on the basis of the use value of the resultant coke, e.g., in foundry coke blockiness is prized more highly than in blast-furnace coke. There is a reasonable indication from the results of the relative-strength tests on the blend cokes, in particular the cumulative per cent of coke remaining on $\frac{3}{4}$ in. after 80-min treatment in the Ty-Lab tester, that increased strength of the coke is favored by the use of anthracites of lower specific gravity and higher volatile-matter content, at least with the ten No. 5 buckwheat anthracites used. It appears that breeze production, of which the minus $\frac{3}{4}$ -in. coke resulting in the 80-min Ty-Lab treatment might be taken as a measure, tends to be lessened by the use of No. 5 buckwheat anthracites of finer size consist, lower specific gravity and higher volatile-matter content.

In these tests there is evidence that pulverization before blending of a No. 5 buckwheat of higher gravity and lower volatile content, which originally is of relatively coarse size consist, will result in improved strength of the blend coke over that of the coke made with the anthracite in its original size consist.

These laboratory tests indicate that the plus 20-mesh material in a No. 5 buckwheat, which in the ten No. 5 buckwheats tested varied from 28 per cent to 68 per cent, may be more detrimental to the strength of the blend cokes than would any appreciable amount of minus 100-mesh material. However, it was evident that the presence of plus 20-mesh material was conducive to increased blockiness of the blend cokes.

No significant correlation could be deduced between the particle shape of the ten No. 5 buckwheat anthracites and the characteristics of the corresponding blend cokes.

The laboratory investigation of the various No. 4 and 5 buckwheat anthracites indicated the following apparent relationships for the anthracites alone:

1 In general, buckwheat anthracites of higher volatile-matter

TABLE 4 MISCELLANEOUS EXPERIMENTS

Coals used	Anthracite	Relative bulk density of coal, lb per cu ft	Coke yields, per cent			Relative strength of coke as measured in Ty-Lab tester. Initial size: 100 per cent + $1\frac{1}{2}$ -in. Cumulative per cent remaining				Apparent specific gravity of coke
			Total	+2 in.	+ $1\frac{1}{2}$ in.	After 15 min— On $1\frac{1}{4}$	After 15 min— On $\frac{3}{4}$	After 80 min— On $1\frac{1}{4}$	After 80 min— On $\frac{3}{4}$	
100 per cent, Pittsburgh seam, high volatile	45.5	64	51	89	60.3	83.8	31.8	63.0	0.79
100 per cent, Lower Kittanning seam, low volatile	48.0	81	45	83	62.3	84.9	39.8	67.0	0.86
85 per cent, Lower Kittanning seam, low-volatile	15 per cent No. 29 original No. 5 buckwheat	48.0	81	90	98	75.4	83.2	48.3	60.6	0.83
85 per cent, Pittsburgh seam	15 per cent No. 29 original No. 5 buckwheat	46.2	72	96	98	38.9	46.1	0.7	10.4	0.81
85 per cent, Pittsburgh seam	15 per cent No. 29, 100 per cent minus 100 mesh	51.8	68	85	96	75.7	85.8	54.3	67.9	0.88
85 per cent, Lower Kittanning seam	15 per cent No. 29, 100 per cent minus 100 mesh	51.8	77	82	97	72.8	84.0	56.5	70.0	0.80
Standard commercial by-product blend $\frac{1}{2}$ (60-40, high-volatile-low-volatile) with 6 per cent of No. 5 buckwheat carbonized in small-scale oven		49.9	75	66	92	71.1	88.1	52.9	74.9	0.87
Anthracite blend coke made in a standard by-product oven from the blend above containing 6 per cent of No. 5 buckwheat			(3 \times $1\frac{1}{2}$ -in. initially)			94.0	94.6	83.0	84.5	0.92

^a Lower Kittanning seam coal of the following proximate analysis: Moisture, 1.1 per cent; ash, 13.0 per cent; volatile matter, 17.9 per cent; fixed carbon, 68 per cent.

^b Air-dried before coking in the laboratory oven.

^c This coke was made on a coking time of 18.4 hr in a 20-in. oven. The A.S.T.M. Standard 2-in. shatter index for this coke is 86 while the $1\frac{1}{2}$ -in. index is 94, both of which are significantly higher than is the case for straight bituminous cokes generally. Using the multiple-drop procedure (8) of the Coal Research Laboratory of Carnegie Institute of Technology, the rate of degradation of this anthracite-blend coke is —1.24 per 10 drops, as contrasted with values of —0.74 to —1.39 for three commercial blast-furnace cokes from straight bituminous coal as reported by the Coal Research Laboratory.

content and lower specific gravity possess lower thermal stability than do anthracites of lower volatile content and higher gravity.

2 High-temperature thermal treatment of the buckwheat anthracites increases their physical stability or relative "inherent" strength as measured in the microstrength test apparatus. The buckwheats showing the lower physical stability before thermal treatment often show a greater increase of strength as a result of thermal treatment than do those possessing the greater stability before thermal treatment.

3 For the buckwheat anthracites tested there was, in general, no satisfactory correlation between the physical stability of the raw anthracites, as measured in the microstrength tester, and the specific gravity of the anthracites. There was, however, some tendency toward higher-gravity anthracites possessing greater physical stability than lower-gravity anthracites. The degree of relationship with volatile-matter content is similar.

4 For the 27 No. 4 and No. 5 buckwheat anthracites tested there was no clear or distinct correlation between the specific gravity and the volatile-matter content of the anthracites; however, there was some tendency for the samples of higher volatile-matter content to possess lower specific gravity.

Finally, the selection of an anthracite for blending in by-product coke manufacture should be on the basis of the use value of the coke, keeping in mind that a higher-gravity, lower-volatile anthracite will not necessarily prove more suitable than a lower-gravity, higher-volatile anthracite. In addition, No. 5 buckwheat anthracite should be selected, the size consist of which will result in the desired strength and blockiness characteristics.

ACKNOWLEDGMENTS

This investigation was jointly sponsored by the Anthracite Institute and the Commonwealth of Pennsylvania under the terms of the O'Neill-Kowalski Bill of the 1943 Legislature, and carried out under the supervision of Richard Maize, Secretary, Pennsylvania Department of Mines.

The authors wish to express their appreciation to the several anthracite producers who furnished the samples of coal used in these investigations, to the personnel of the by-product plants who have furnished information concerning their experiences with the use of anthracite, and to the members of the Anthracite Research Advisory Committee for their co-operation and advice.

The authors gratefully acknowledge their indebtedness to their colleagues for assistance and advice, and especially to John Teti and Harold I. Tarpley, Jr., for material help in performing much of the routine testing of the anthracites and cokes, to J. W. Eckerd for assistance in calculating the data, to H. D. Mumper for assisting with the preparation of the figures, and to R. J. Grace and C. D. Nuebling for the coal analyses herein reported.

BIBLIOGRAPHY

1 "The Utilization of Anthracite Duff," by G. Cellan-Jones, *Coke*, March, 1944, pp. 46-48.

"Production and Use of Low-Temperature Char as a Substitute for Low-Volatile Coal in the Production of High-Temperature Coke," by J. D. Price and G. V. Woody, A.I.M.E., T.P. no. 1745, 1944.

"The Technical and Economic Aspects of the Use of Anthracite Fines in By-Product Coke Production," by J. D. Clendenin, K. M. Barclay, and C. C. Wright, Mineral Industries Experiment Station, Pennsylvania State College, Circular 16, 1944.

"Effect of Acids and Alkalies Upon Carbonization Products of Coal," by R. E. Brewer, U. S. Bureau of Mines, R.I. 3726, 1943.

"Increasing the Percentage Production of Large-Size Coke at Fast Coking Rates," by I. M. Roberts, A.I.M.E., T.P. no. 1612, 1942.

"Praktische Ergebnisse bei Kohlenauswahl, Kohlenmischung und Koksverbesserung für die Hochtemperaturverkokung" ("Practical Results in Coal Selection, Coal Blending and Coke Improvement in High-Temperature Coking"), by F. L. Kühlwein and C. Abramski, *Glückauf*, vol. 75, 1939, pp. 865-874, and 881-890.

"The Quality of Coke," by R. A. Mott and R. V. Wheeler, Iron and Steel Industrial Research Council, Midland Coke Research Committee, Report no. 2, 1939.

"Anthracite Blends," by I. J. Lane and J. W. Cobb, *Gas Journal*, vol. 222, 1938, p. 165.

Group of articles on "Effect on Coke of Adding Coke Breeze to Regular Coal Mixture," by F. J. Pfluke, A. C. Sedlachek, and A. B. Huyck, A. G. A. Proceedings, 1936, pp. 771-792.

"Investigations Into the Influence of Coke Quality on Blast-Furnace Operations," by W. J. Brooke, H. R. B. Walshaw, and A. W. Lee, *Journal of the Iron and Steel Institute*, vol. 134, 1936, no. 2, pp. 287P-325P.

"The Washing, Blending and Carbonization of Coal," by J. Mendelsohn, *Fuel*, vol. 13, 1934, pp. 140-154.

"Coke for Blast Furnaces," by R. A. Mott and R. V. Wheeler, Iron and Steel Industrial Research Council, Midland Coke Research Committee, Report no. 1, 1930.

"Process of Coking Coal-Dust for Manufacturing Fuel and Gas," by J. W. Pittinos, U. S. Patent no. 279,796, June 19, 1883.

"Note on the Manufacture of Anthracite Coke in South Wales," by W. Hackney, *Journal of the Iron and Steel Institute*, 1875, pp. 523-526; discussion, pp. 527-539.

2 "The Technical and Economic Aspects of the Use of Anthracite Fines in By-Product Coke Production," by J. D. Clendenin, K. M. Barclay, and C. C. Wright, Mineral Industries Experiment Station, Pennsylvania State College, Circular 16, 1944, p. 55.

3 "Anthracite," by D. Markle, *Trans. A.I.M.E.*, vol. 66, 1921, pp. 535-549.

4 "Anthracites and Semianthracites of Pennsylvania," by H. G. Turner, *Trans. A.I.M.E. (Coal Division)*, vol. 108, 1934, pp. 330-343.

5 "The Influence of Carbonizing Conditions on Coke Properties," by H. E. Blayden, W. Noble, and H. N. Riley, *Journal of the Iron and Steel Institute*, vol. 136, 1937, no. II, pp. 47P-76P.

6 "Thermoanthracite as a New Type of Metallurgical Fuel," by G. K. Mirochnichenko, *Vestnik Standartizatsii*, vol. 13, 1938, no. 11, p. 5; no. 12, p. 7.

"Thermoanthracite as a Substitute for Coke in the Smelting of Cast-Iron in the Cupola Furnace," by S. A. Skomorochov, *Novosti Tekhniki*, vol. 7, 1938, no. 7, p. 3.

"The Resistance of Anthracite to Mechanical and Thermal Shock," by C. C. Wright, L. L. Newman, and A. W. Gauger, Mineral Industries Experiment Station, Pennsylvania State College, Bulletin 31, 1941.

7 "Studies Concerning the Pressure Developed During the Carbonization of Coal," by Walter Fuchs, A. G. Sandhoff, J. A. Taylor, and A. W. Gauger, Mineral Industries Experiment Station, Pennsylvania State College, Bulletin 34, 1941.

8 "Properties of Blast Furnace Cokes," by H. H. Lowry and M. A. Mayers, *Iron and Steel Engineer*, vol. 20, February, 1943, pp. 39-40.

Blending Coals Reflects Greater Uniformity of Product

By R. F. STILWELL,¹ CLEVELAND, OHIO

Coal consumers look for three qualities in their fuel, suitability for their requirements, uniformity in shipments, and proper heating value, as well as suitable chemical and physical characteristics. The present paper gives a broad picture of the part that blending plays in the attainment of these qualities, discussing methods and equipment which have given the best results. Case examples are cited of the improvements achieved by suitable blending practices. Metallurgical engineers have had much wider experience in blending raw materials than have coal-preparation engineers; and the author has incorporated notes on "bedding" or blending with reference to coal, by A. J. Boynton, an authority on the subject. Suitable bin designs for blending purposes are included in the paper.

THERE are three things which all coal consumers look for when they burn coal, these are: (1) suitability for their particular requirements and burning equipment, (2) uniformity of shipments, and (3) quality, as expressed by heating value and other chemical and physical tests.

Suitability or proper application is determined generally from previous buying experience. It is a function of (a) the reliability and integrity of the shipper and distributor, (b) of a certain coal field or seam, and (c) of uniformity and quality.

Quality is limited by the location and geology of the seam and mine, the mining and preparation methods and equipment, and the knowledge and ability of the personnel.

Uniformity of shipments is in many ways the most important factor in coal selection. Lack of uniformity in chemical quality, size consist, and treatment causes most of the customer complaints which are the fault of the coal shipper. Lack of uniformity destroys suitability and quality standards, causing a large customer turnover, and greatly increases sales expense as well as reduces the net return to the operator.

Oil and gas fuels enjoy a greater uniformity of quality than solid fuels and there will be more gas and oil competition for coal markets after this war than before because the size of their market is a direct function of the dimensions of their pipe lines which have been greatly increased during the war.

Present mechanical coal-cleaning equipment based on gravity concentration has gone a long way toward giving us a coal of uniform ash content. The chart, Fig. 1, by Hebley² shows the greater uniformity of washed coal as compared to raw coal with respect to ash content. Wide variation in the nature and amount of ash in the coal feed to the washer results in a coal of nonuniform ash content. Mechanical cleaning equipment does not "understand" such terms as ash-softening temperature,

coking properties, size consist, and sulphur content. Unless the feed to the washer is uniform the washed coal will probably not be uniform.

Table 1 shows the ash, sulphur, and ash-softening temperature of two mines in the Pittsburgh bed, both raw and washed, loaded over the same tippie; also No. 3 and No. 4 Pocahontas seams both raw and washed, loaded over the same preparation plant. It is obvious that they must be blended or loaded separately if a uniform product is to be obtained.

WHY IS BLENDING NECESSARY?

It was natural for the captive-tonnage operators producing by-product coals to recognize the necessity for blending raw coals of different quality and coking characteristics. They have had many years of experience with blending high-, low-, and medium volatile coals at their oven plants. They have found that careful blending gives them a coke of more uniform quality and better structure. Coals which could not be coked successfully by themselves could be blended with other coals to produce a satisfactory coke. They have found that the better coke produced resulted in greater furnace capacity and lower-cost pig iron and steel. It is significant that all of their recently installed coal-preparation plants include elaborate blending plants.

Operators supplying the commercial market have been slow to adopt blending as a part of their preparation plants; probably as Hebley² states, because of its intangibility, uniformity does not fully reflect its importance to the coal-mine operator who is supplying consumers of steam coal.

There are many reasons why blending is necessary. Some of these are as follows:

1 Variation in quality over large areas. The prospecting of any large area containing one or more coal beds by diamond drilling and outcrop openings usually shows wide variation in ash and sulphur and may show wide variation in ash-softening temperature. The rapid exploitation produced by mechanical loading will probably bring quality changes more quickly than by hand loading.

2 Loading two or more seams over one tippie. Many mines in the steep mountainous regions of West Virginia, Virginia, Pennsylvania, and Kentucky, and at least one operation in Illinois load two or more seams of coal over the same tippie. In some cases these seams have wide differences in chemical analyses, physical properties, appearance, and coking properties. It is more economical to blend these seams and load them together, if a market is available, and provided that they can be blended uniformly.

3 Where mechanical cleaning equipment is installed wide variations in the washer feed make it difficult if not impossible to keep the washer in continuous operation. Careful blending may eliminate the necessity for a washer in low-ash-coal beds.

4 Blending through bins is about the only method available for producing a nut and slack coal of uniform size consist and for varying the proportion of one or another size necessary for obtaining the best results with various types of burning equipment.

5 Some mines use two or three different methods of mining;

¹ Fuel Engineer, North American Coal Corporation.

² "Economics of Preparing Coal for Steam Generation," by H. F. Hebley, TRANS.-A.I.M.E., vol. 130, Coal Division, 1938, pp. 79-99.

Presented at a Joint Meeting of the Fuels Division of THE AMERICAN SOCIETY OF MECHANICAL ENGINEERS and the Coal Division of the American Institute of Mining and Metallurgical Engineers, Charleston, West Va., Oct. 30-31, 1944.

NOTE: Statements and opinions advanced in papers are to be understood as individual expressions of their authors and not those of the Society.

TABLE 1 EFFECT OF WASHING WITHOUT BLENDING ON UNIFORMITY

	Pittsburgh bed				Pocahontas No. 3 and No. 4			
	Raw (1)	Float 1.55 (2)	Raw (1)	Float 1.55 (2)	Raw no. 3 no. 4	Raw no. 3 no. 4	Float 1.55 no. 3 no. 4	Float 1.55 no. 3 no. 4
Ash, per cent.....	8.4	7.4	6.4	5.6	9.8	9.6	6.3	6.7
Sulphur, per cent.....	2.3	1.8	2.0	1.6	0.7	0.5
Ash-softening temperature, deg F.....	2500	2600	2720	2460

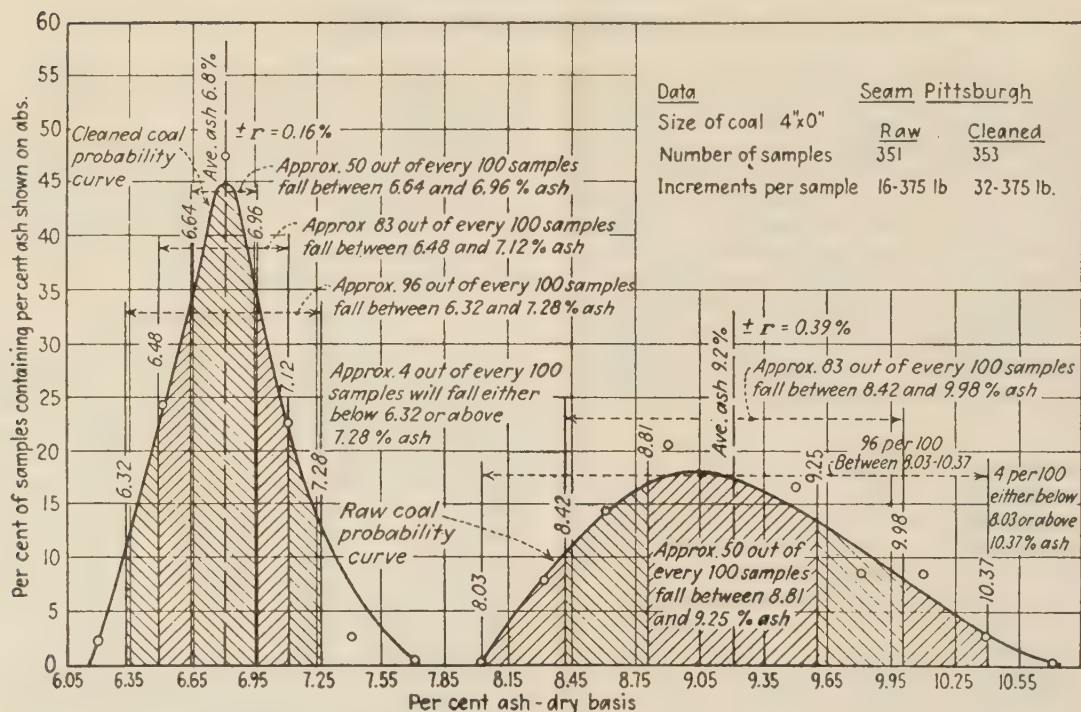


FIG. 1 COMPARISON OF UNIFORMITY BETWEEN RAW AND WASHED COAL

for instance, hand loading, mobile loading, and conveyer loading in the same mine. Blending is necessary under these conditions in order that a more uniform product may be loaded.

The upper and lower Cedar Grove beds in Mingo County, West Virginia, have an interval of about 70 ft between them. Both are of good quality and are generally mined together and loaded over the same tippie. Sometimes they are loaded separately while at other mines they are blended. Table 2 shows significant differences in the sulphur content, ash-softening temperature, and coking properties which are borne out in actual plant tests. The difference in the amount of splint and bright coal is noticeable in the domestic block or lump sizes if it is not uniformly blended and brings complaints from dealers asking for more of "that green coal" because of the green cast which forms on the bright coal band in the lower Cedar Grove bed upon exposure to air.

VALUE OF UNIFORM QUALITY, SIZE, AND APPEARANCE

Steel-company plant tests show that a change of 1 per cent in the ash content of the coal charged to their ovens will affect the rate of production from 3 to 6 per cent. If the ash content of their coal varied from 6 per cent one day to 9 per cent the next, one can well imagine the reaction of the management. Iron production is definitely limited today because of an increase in the ash and sulphur content of coal since the war began, and a lack of uniformity of coke because of variability in the ash, sulphur, and moisture content of coal. Variation in the sulphur content of coal may easily vary the cost of steel \$1 per ton or more.

TABLE 2 EFFECT OF BLENDING UPPER AND LOWER CEDAR GROVE BEDS

Bed	Upper Cedar Grove	Lower Cedar Grove	Blending as mined
Moisture, per cent.....	2.9	3.0	3.0
Volatile matter, ^a per cent.....	35.6	34.0	34.5
Ash, ^a per cent.....	7.5	6.4	6.7
Sulphur, ^a per cent.....	2.0	0.9	1.4
Btu, ^a	13640	13870	13750
Ash-softening temperature, ^a deg F.....	2400	2650	2510
Ash-softening temperature, ^b deg F.....	2250	2400	2275
Fines, ^b	26	25	...
Agglutinating index (15:1) ^c	7.6	6.8	...
Friability, ^c per cent.....	20.5	26.4	23.0
Bright coal, ^c per cent.....	29.0	63.0	46.0
Splint coal, ^c per cent.....	32.0	30.0	31.0
Semisplint, ^c per cent.....	39.0	7.0	23.0

^a Size 2 × 0 in.

^b Size 1/4 × 0 in.

^c Run of mine.

When melting malleable iron with pulverized coal any variation in the moisture, ash, and sulphur content of the coal is reflected in longer melting time, which results in increased labor and supply costs, thus increasing the cost of manufacture. If the sulphur becomes too high the metal may be lost entirely. A uniformly high temperature must be maintained with nearly constant CO₂-CO ratio in the furnace, which means that the coal must have a uniform Btu content and be fed at a constant rate. Variations in the ash and moisture content change the rate of delivery of heat to the furnace.

Variation in coal quality causes just as much trouble for the steam-coal consumer as it does for the by-product and metallurgical user. In addition to this the steam-coal consumer is

TABLE 3 EFFECT OF MOISTURE, ASH, AND SIZE VARIATION ON EVAPORATION, EFFICIENCY AND COAL COST, BURNING CEDAR GROVE SEAM (2 × 0-IN.) SCREENINGS ON MULTIPLE-RETORT STOKERS^a

Moisture, per cent	Ash, per cent	Btu as received	Fines $\frac{1}{4} \times 0$ in., per cent	Evaporation from and at 212 F	Efficiency, per cent	Coal cost along-side plant, per ton, dollars	Burning rate, lb per hr	Ash, lb per 24 hr
3.0	6.0	13875	25	10.7	75.0	5.50	40	10750
6.0	6.0	13420	25	10.3	74.8	5.71	41	11160
6.0	9.0	12975	40	9.7	73.0	6.07	44	12000

^a Load = 200 per cent rated capacity; burning rate 5600 lb, 13,875-Btu coal per hr, or 40 lb per sq ft grate per hr.

very much interested in a uniform size consist. The steam-coal consumer should have every consideration by the commercial shipper for he pays just as much for his coal in normal times (and often more) than the coke-oven operator.

Tests show that a variation of 1 per cent in ash content of coal from the same mine of the same size on the same boiler, under the same load, equipped with underfeed or chain-grate stokers, alters the boiler efficiency from 0.10 to 0.60 per cent in efficiency with an average of 0.34 per cent. A variation of 3 per cent ash in the same coal, which is common today, means a Btu variation of about 450 for a high-rank bituminous coal. The same variation in Btu occurs with a corresponding variation in the moisture content as occurs with a variation in ash content. One per cent of moisture or ash reduces the Btu value by 1 per cent.

Free or surface moisture up to about 5 per cent may actually result in an increase in boiler efficiency where chain-grate or underfeed stokers are the firing equipment. Free moisture always results in a lower burning efficiency where boilers are pulverized-coal-fired.

Variation in the size consist of coal on stoker fuel beds for coal from the same mine may cause a variation of from 1.5 to 2.5 per cent in burning efficiency for a coking coal. If the ash and moisture increase as the size decreases there is a much greater variation in efficiency. Table 3 shows the effect on coal costs of variations in ash, moisture, and size consist of a Cedar Grove seam coal.

Table 3 is based on an average industrial stoker-fired boiler plant in Detroit which normally burns District No. 8 Southern high-volatile coal. An increase of 3 per cent moisture alone increases the coal cost by 21 cents per ton. An increase of 3 per cent ash, plus 3 per cent moisture, and 15 per cent in the ($\frac{1}{4} \times 0$ in.) fines increases the coal cost by 57 cents per ton. These figures are not generally appreciated by the coal operator. The table shows that considerable investment could be made by an operator for washing and blending coal for this market if he had variations in quality and size shown in the table. In this particular coal increases in ash content and lower ash-softening temperature occur with an increase in the percentage of ($\frac{1}{4} \times 0$ in.) fines. Table 3 also shows the increased burning rate which follows an increase of moisture or ash which may mean a steam failure if the stoker is running wide open. It also shows the greater amount of ash which must be handled because of increases in ash and burning rate.

Variations in the fusing point of the coal ash are troublesome in steam generation. The suitability or the market for a certain coal is limited to a rather narrow fusing-point range. In the case of the Cedar Grove coals of Table 2 a much wider range of markets is available if they are properly blended because of the ash-fusing and coking characteristics. The upper Cedar Grove coals, if loaded separately, give good results in wet-bottom pulverized-coal-fired furnaces and on side-dump stokers and dead-plate types where the ash is removed in the form of clinker. However, in its fusing range this coal is in competition with large tonnages of low-fusing-ash coals on lower freight rates.

The lower Cedar Grove is limited to high-fusing applications and to larger stokers carrying heavy loads, where its stronger coking feature is not a factor. Blending produces a coal of 2500 deg ash-softening temperature which meets the specification of the high-fusion customer and permits the coal to satisfy much of the lower-fusing-ash and less strongly coking market.

Domestic coals are generally sold on appearance and physical structure with chemical quality taking a secondary role. Blending out variations in color and structure will eliminate dealer complaints and rebates. Mines having pillar sections which have been under pressure, or hand- and machine-loading sections, can make excellent use of blending for the domestic market. In the case of the Cedar Grove coals or other mines loading two seams together, careful blending must be practiced to avoid having two grades of coal of the same size selling at different prices at the same mine. If not carefully blended they should be loaded separately.

METHODS OF BLENDING

Blending at a mine is generally done by one of three methods or combinations of two or more of these methods, namely, (1) layer loading, (2) dumping mine cars of one grade of coal in definite ratios with cars of another grade, and (3) by means of bins. Blending at the face of two or more benches of coal in the seam having different analyses could be done fairly well in hand loading but is not practical with mechanical loading. Machine cuttings could be fairly well distributed over the day when hand loading, but this procedure does not seem to be feasible with machine loading.

Layer loading is a procedure for placing coal in railroad cars in horizontal layers by shutting from one to six railroad cars, hooked together, past the loading boom two or three or more times by means of a combination hoist and car retarder. It will smooth out many of the variations in moisture, structure, and chemical quality which occur in different sections of a mine. It is effective also in minimizing segregation of coarse and fine coal when loading nut and slack, or run-of-mine or resultant sizes. It is also effective in reducing the amount of breakage in loading domestic sizes. Fig. 2 is a chart prepared by Castanoli³ showing a comparison of layer and conventional loading. Care should be taken to hook together enough railroad cars to accommodate the various sections of the mine. For a mine loading two seams of coal at a rate of 300 tons per hr of which one seam supplies 200 tons per hr, loading 15 per cent lump, 20 per cent egg, 15 per cent stove, and 50 per cent nut and slack, then at least 3 cars should be hooked together on the nut and slack track, while only one car on the lump, egg, and stove tracks might be sufficient.

Layer loading will not always eliminate size variations and depends on trips coming out of the mine in a systematic and regular routine which is not always possible. It has been most effective in loading domestic sizes of unwashed coal. It may result in too many partly loaded cars which may be finished out by

³ "Layer Loading," by A. F. Castanoli, American Mining Congress, Washington, D. C., 1935, p. 270.

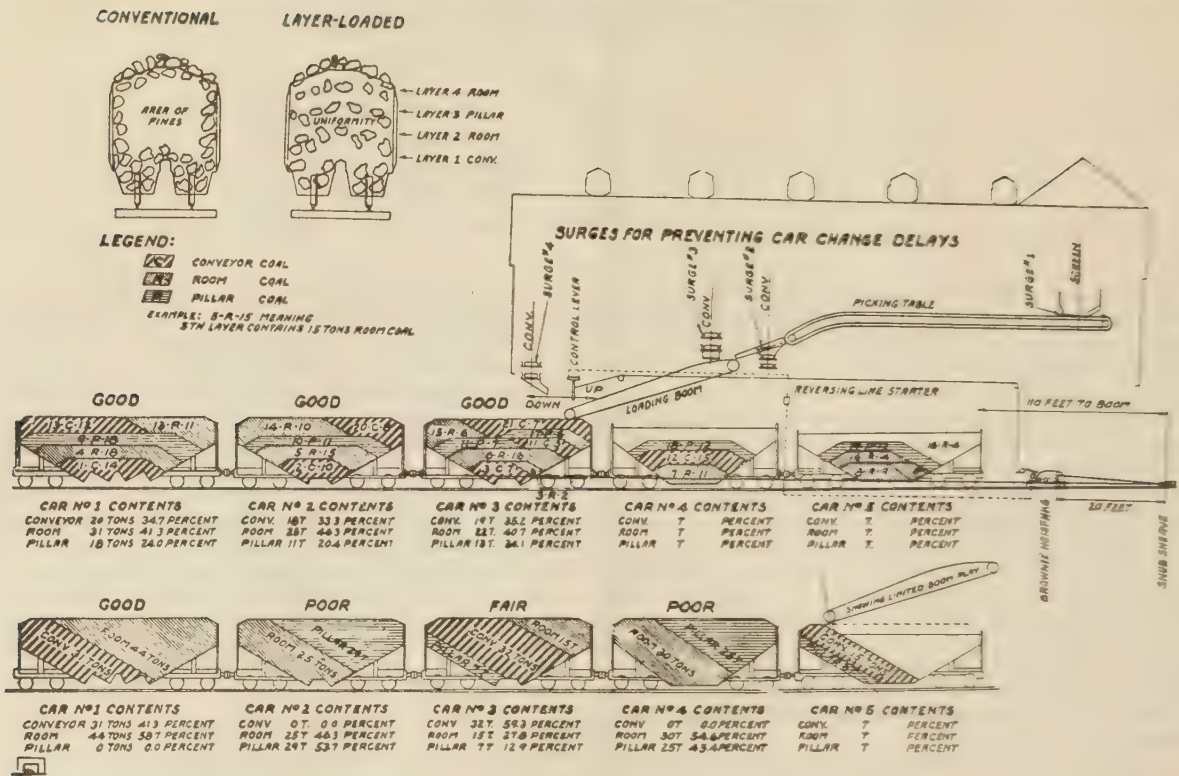


FIG. 2 LAYER LOADINGS VERSUS CONVENTIONAL LOADING

conventional loading. Many operators look upon layer loading as a means of reducing breakage rather than a means of blending but the blending possibilities are greater than generally realized in older mines which do not justify more expensive equipment.

Dumping mine cars of one grade of coal in definite ratios with cars of another grade is used effectively at many mines. It is often employed where coal washers have been installed without blending bins. It is used in the Pocahontas field when loading two different seams through a common washing plant. It is used in the Elkhorn field for blending hand-loaded (low-ash) and Joy-loaded (high-ash) coal for a common washing plant. It is used in eastern Ohio for blending strip and deep-mine coal for a common washer. When there are great differences in the washing characteristics, as at a southern Illinois mine loading the No. 5 and No. 6 sizes through the same plant, one seam is loaded on one shift and the other on the second shift. The washer is adjusted at different gravities for each seam. Partly loaded cars are pulled back through the tipple and held for the next day by the railroad.

Loading mine cars in definite ratios requires extra mine cars and may slow up production. It requires a special track layout and dumping equipment. It is usually impractical in older mines or where there may be three or four or more different grades of coal loaded over the same tipple.

The necessity for a uniform feed to a coal washer is something the operator sees and understands more clearly than the necessity for a uniform product for the consumer. Therefore it may be assumed that coal washing will bring much greater uniformity to the consumer than the washer itself will provide by gravity concentration.

Storing different grades of coal in bins would be the ideal system of blending if it were not for segregation and breakage of

the coal in bins. Anyone interested in blending coal should read the paper on this subject by David R. Mitchell⁴ and discussion by E. W. Davis.⁵

Blending through bins would seem to be impractical for domestic sizes of soft semibituminous coal on account of breakage. For most bituminous coals it is practical and many mines are storing and blending the run-of-mine coal. Bins at southern West Virginia mines sometimes serve a dual purpose; two grades or seams are either loaded separately or blended together depending on the specifications or uses of the consumer. This feature increases the market range of a mine.

Bins provide considerable flexibility in mining operations as well as continuous operation of the preparation plant. At one mine (perhaps more) two shifts are worked in the mine while the preparation plant operates one shift.

The number of bins to employ for a blending job and their size must be carefully determined after all of the quality variations have been carefully determined by analysis as well as the desired product uniformity. For commercial mines, variations in moisture, volatile matter, ash, sulphur, Btu coking properties, and ash-softening temperature are all very important.

One large bin will do the job if proper mixing is assured and segregation eliminated by correct stocking and reclaiming methods such as outlined by Boynton⁶ later in this paper.

For smaller mines and old mines where expensive equipment is not justified a number of small bins equal to the numbers of

⁴ "Segregation in the Handling of Coal," by David R. Mitchell, Trans. A.I.M.E., vol. 130, 1938, pp. 107-128.

⁵ Discussion of reference (4), by E. W. Davis, Trans. A.I.M.E., vol. 130, 1938, pp. 134-142.

⁶ "Notes on Bedding Practice," by A. J. Boynton, A. J. Boynton & Company, Chicago, Ill.

TABLE 4 RESULT OF BLENDING TWO LOW-VOLATILE COALS ON ASH-SOFTENING TEMPERATURE

	Ash, per cent	Ash-softening temperature, deg F
100 per cent Coal A.....	8.3	2650
100 per cent Coal B.....	5.3	2500
25 per cent A—75 per cent B.....	7.5	2510
50 per cent A—50 per cent B.....	6.8	2380
75 per cent A—25 per cent B.....	6.0	2300

grades of coal produced might be the best solution. Smaller bins are subject to less breakage and size segregation than larger ones. The smaller bins should be cubical or cylindrical and equipped with baffles, as recommended by Davis,⁵ in order to minimize segregation of sizes. Blending bins must be kept full or nearly full by stocking and reclaiming simultaneously if they are to be efficient.

The new Geneva mine in Utah supplying coal for the Columbia Steel Company is designed for 10,000 tons of coal per day. The coal is crushed to minus 3 in. and stored in 16 blending bins. These are used to give a uniform product as the coal comes from different portions of the mine.

Another steel company, producing about the same tonnage (12,000 tons per day), uses four large (500-ton) cylindrical bins in which the coal is kept at four different levels. Segregation of coarse and fine coal is at different stages at the four levels and as equal portions are taken from the four bins the effect of segregation is lessened. The feed is 4 in. \times 0 in. Blending is done to provide a coal of uniform sulphur content.

A commercial by-product mine in West Virginia blends No. 2 gas and Powellton seams through bins. The No. 2 gas seam is crushed to 1 in. and loaded into a 700-ton reinforced-concrete bin with a 45-deg sloping bottom. It is filled by means of a rubber belt and tripper. The Powellton is loaded into a 300-ton silo and blended by means of a feeder into the No. 2 gas on a conveyor belt in whatever proportion is necessary to maintain a required ash and sulphur content.

At one mine in Kentucky the No. 4 and No. 7 Hazard seams are about 70 ft apart. They are loaded over the same tippie which is a very old wooden structure. Block, egg, stove, and nut and slack are loaded. It was found several years ago that this coal could not be sold at a good market price without blending owing to differences in ash-softening temperature and coking properties. Both seams are low in ash and with hand loading a washer is not required. There was room for only one small bin (70 tons) for the No. 7 steam. By keeping a steady flow of No. 4 seam coal to the tippie and feeding No. 7 from the bin into it in the ratio in which it is mined a uniform product is loaded. This is an example of what may be done at a small tonnage (1000 tons per day) mine. Layer loading was tried here and was found to be unsatisfactory. There is no appreciable segregation or breakage at this plant.

A mine in West Virginia, mining the Island Creek and Chilton seams, loads the Chilton into a 500-ton bin sloping 45 deg from each end toward the center, equipped with double feeders. The bin is loaded from drop-bottom mine cars. The Chilton is either blended into the Island Creek for steam and domestic use or loaded separately for by-product use. Blending is used here to prepare a coal of more uniform sulphur and ash-softening temperature and for preparing a better stoker coal.

Another mine has blended the Alma and Eagle seams through small hillside-type bins for several years for the purpose of making a satisfactory stoker coal. Recently large bins (200 tons) of another design have been installed to care for larger capacity. This plant reports very little breakage loading through the bins. Lump, egg, stove, nut, stoker, and slack are loaded.

A mine in Virginia loading the Marker and Taggart beds at the same plant load each seam separately in the plus 2-in. size. The

coals are low in ash content and are not washed. The (2-in. \times 10-mesh) size is binned in two 100-ton cylindrical steel bins (one bin for each seam) and blended as loaded from the bins by adjustable feeders. Blending is controlled by chemical analysis. This mine produces about 1800 tons per day. Another feature of this plant is that a high-grade stoker coal is produced by blending through two 100-ton bins a high-ash high-ash-fusing coal (not marketable itself) with a low-ash low-fusing-ash coal. Feeders are adjusted according to chemical analyses of regular routine sampling. This stoker coal is of premium grade.

A very large mine in Illinois, perhaps the largest commercial mine in the world, has had an elaborate blending plant for nut and slack sizes for years. The plant is designed to produce stoker coals of nearly constant size consist and uniform quality. The management has recently installed washers to reduce the ash and sulphur content of No. 6 bed coal.

It is common practice in many mines to wash coal in the size range of (5 in. \times $\frac{1}{4}$ in.). In one operation the resultant ($\frac{1}{4}$ \times 0-in.) pulverizer runs 8 per cent ash in part of the feed and 12 per cent ash in another part. Unless the 12 per cent ash coal is mechanically cleaned it would be folly to load all of the ($\frac{1}{4}$ \times 0 in.) into a common bin and worse still to blend it back as mined into the washed nut coal on a conveyor. There is a difference of 600 Btu between the 8 per cent and 12 per cent ash coal which amounts to about 20 cents per ton in the market. If blended through two bins with a resultant 10 per cent ash coal it is doubtful if mechanical cleaning would be necessary.

The fusing point of ash of the resultant blend of two or more grades of coal cannot be accurately predicted. Tests must be made before blending to determine this feature. Table 4 shows the result of blending two low-volatile coals for lake shipment on the ash-softening temperature. Serious clinker trouble developed from this shipment at a plant in Minneapolis where either coal by itself had previously proved satisfactory.

BIN DESIGN

Fig. 3 shows roughly the "hillside" type bin. This is the cheapest and simplest type of bin where coal beds outcrop on mountainsides. It is subject to more segregation of sizes and breakage than any other type per cubic foot of capacity because its length permits more time for rolling friction. The movement of coal in this type bin is similar to the movement down the side of a conical storage pile. Like all bins, it should be kept as full as possible at all times.

An improvement of the hillside-type bin is the twin sloping-end bin, Fig. 4, used a great deal in southern West Virginia, where two seams of coal are loaded over the same preparation plant. It is usually loaded from drop-bottom mine cars. After it is once filled it can be loaded with a small amount of segregation and breakage according to reports from the field. It is usually constructed of wood for tonnages from 100 to 200 tons. The sloping bottom is covered with sheet metal. The slope is usually about 45 deg.

Another common type of bin is the silo, constructed of monolithic reinforced concrete or concrete staves, tongued and grooved. It is reported to be cheaper than wood bins in capacities ranging from 500 to 1000 tons. One operator uses this type bin equipped with ladders for lowering mine-run coal into the bin for reducing

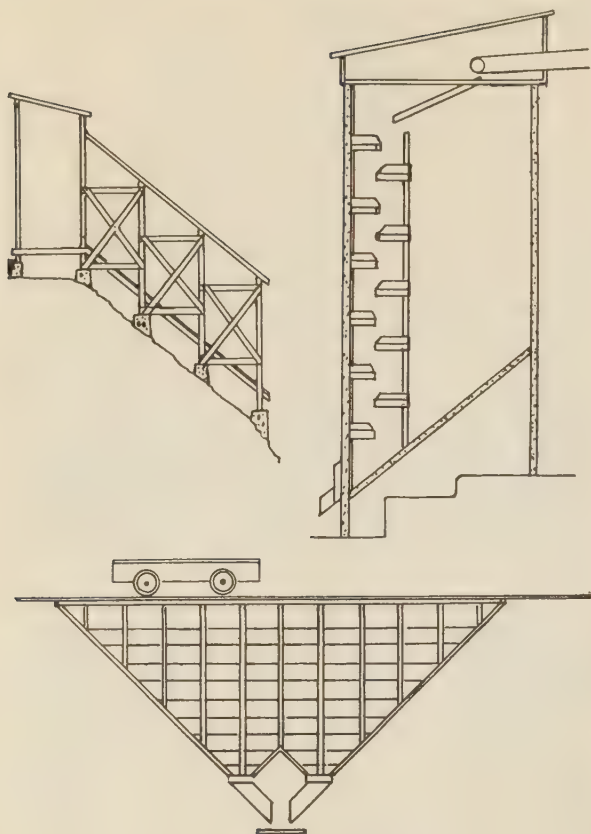


FIG. 3 (Top, left) HILLSIDE BIN

FIG. 4 (Bottom) SLOPING-END BIN, WOOD CONSTRUCTION

FIG. 5 (Top, right) SILO WITH LADDER

breakage. There is a great deal of segregation of sizes in removing coal from a silo even if it is placed in the silo without segregation but some form of ladder or avalanche chute will reduce the amount of segregation and breakage. A spiral chute has little value.

The author visited about twenty coal-preparation plants in 1943, investigating methods of storing and blending through bins. All bins examined were subject to considerable size segregation, particularly where mine-run or resultant sizes of coal were binned. This means considerable variation in the quality of the coal as well as overloading and blinding of screens, just the drawbacks which the blending was intended to prevent. In many cases, however, there was a decided improvement in quality and uniformity of product as compared to loading directly from mine cars to the screens or washer.

Metallurgical engineers have had a great deal more experience in blending raw materials than coal-preparation engineers. They use the term "bedding" instead of "blending" for averaging the composition and quality of raw materials so that a uniform product may be reclaimed. The term "bedding" results from the methods of piling ore in beds in layers such as the Robins-Messiter system.

NOTES BY BOYNTON⁶ ON "BEDDING" COAL

A. J. Boynton,⁶ metallurgical engineer, has written some interesting notes on bedding, with reference to coal, and gives

sketches illustrating bin design for eliminating many of the bad features of present bins. The following notes and sketches are by Boynton:

Enough experience has by this time been made public to show that averaging the composition and qualities of metallurgical raw materials by bedding confers a major technical benefit. The practical question which confronts the engineer is how to secure this benefit at the least cost.

The scale of the bedding operation may vary in two principal respects. One of these is the rate at which material is bedded and reclaimed and the other is the size of the bedding unit.

It is desirable that the contents of a bed shall include all the variations which are known to be likely to occur, provided these variations will presumably show themselves within a tonnage or interval of time small enough to permit inclusion in one bed.

Where the rate of use is high and the material flows freely, gravity handling through a bin is worthy of attention.

A complete averaging of quality by bedding may be considered as depending on the number of samples simultaneously taken in the reclaiming process as well as the number of tons in the bed.

Long piles and large bedding units obtained by lengthening the pile increase the probability that all the variations in composition of the materials are represented in the bed but do not increase the number of samples represented in the reclaimed cross section. The ideal bedding form would be one in which the three dimensions are as nearly equal as possible.

Many variations have characterized the construction and scheme of operation of bins built and used for bedding. Of these the least effective is the combination of silos . . . due to the failure to mix accurately and effectively by the acts of stocking and reclaiming.

Reclamation by gravity from a bin is preferably carried out by vertical flow of the material. This can only be carried out by simultaneous withdrawal of material from end to end of the bin at an equal rate for each unit of its length. . . . If bedding is carried out along an inclined plane extending the length of the bin, with the angle of deposition less than the angle of repose, a system will exist which has the following characteristics:

- 1 There will be no uncorrected size segregation and bulk density will be constant.
- 2 Bedding and reclaiming may be carried out simultaneously and continuously in a single unit.
- 3 The horizontal or sampling face will be of maximum length.
- 4 The bedding unit or mass which is being sampled in reclaiming is twice that of the contents of the triangular section of the bin.

Flow of Material in Bins. Flow is at a maximum rate directly over the discharge opening.

With a sufficiently large bin and a single (discharge) opening, the flow proceeds so that any downward movement disturbs the surface contour, evidence that the action sought in bedding is not being realized.

By increasing the number of outlets and thereby limiting the horizontal cross section of the column above each outlet, it is feasible to bring material down through the bin in a mass and to cause it to move without disturbing the surfaces, Fig. 6.

A bin as shown may have a width of about 42 ft, which means that each column width is 7 ft. The construction necessary to employ is shown in Fig. 7. This arrangement divides the bin into sections which are square horizontally in the same way that might be done by partitions, and more accurately because of friction of material on walls.

Reclaiming Feeders. In order to obtain the accuracy of mixture desirable in a bedding operation it is necessary to discharge

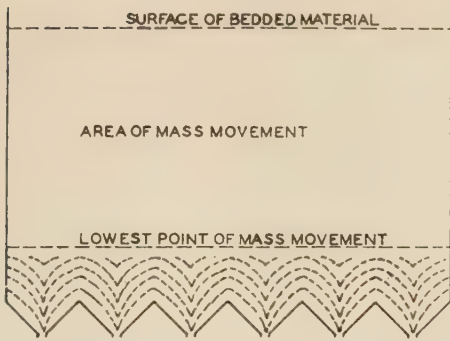


FIG. 6 IDEALIZED CROSS SECTION OF BEDDING BIN
(Boynton, reference 6, Fig. 21.)

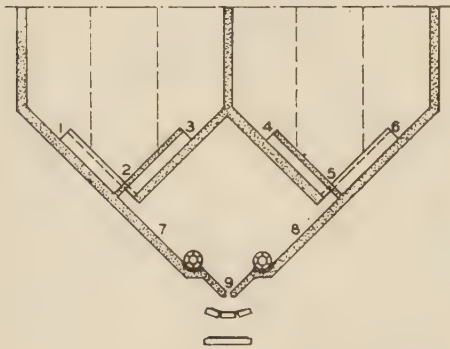


FIG. 7 BIN CONSTRUCTION, ELEVATION SECTION
(Boynton, reference 6, Figs. 22 and 23.)

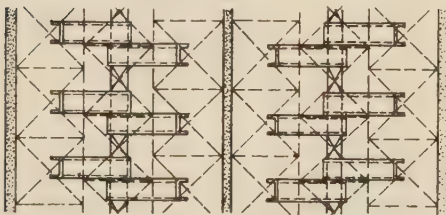


FIG. 8 BIN-CONSTRUCTION PLAN
(Boynton, reference 6, Figs. 24 and 25.)

not only in equal amounts per unit of length from end to end of the bin, but to discharge at a given rate per unit of time, continuously and regularly rather than intermittently. An intermittent discharge will not load the reclaiming conveyor uniformly, and an accurate means of composition will not be secured.

The feeder suited to accomplish these objectives is a modification of the star feeder shown in Fig. 8.

The feeder motors are arranged for variable speed. In the case of large bins (more than one shaft), the motors are electrically synchronized. One control will regulate the speed of all sections.

Longitudinal Bedding Bin. If a bedding bin of the shape shown in Fig. 9 is used, it is necessary to distribute the material lengthwise, by means of a conveyor and tripper working on an angle on the slope. For this bin (42 ft wide) two distributing conveyers are used.

Transverse Bedding Bin. The alternative form in which material is distributed down the slope by gravity in a bin is shown in Fig. 10. No mechanical means of longitudinal distribution is

used here as in Fig. 9, but a smooth inclined gliding platform is provided above the bed to insure uniform longitudinal distribution. This platform has a slope somewhat greater than the angle of repose of the material. It distributes accurately by means of its shape. Transverse distribution is by means of belt and tripper. The bedding angle is a little less than the angle of repose in order to prevent segregation down the slope.

The rate of flow of material down the slope may be regulated and prevented from becoming too rapid, particularly with respect to lumps, by chains or drag gates suspended across the slope.

The bin for transverse bedding and gravity flow costs less to build and to maintain and is simpler to operate.

Such an installation should include a mechanical sampling plant in connection with the reclaiming system for control of the operation.

Storage. A continuous bedding bin provides no storage in the

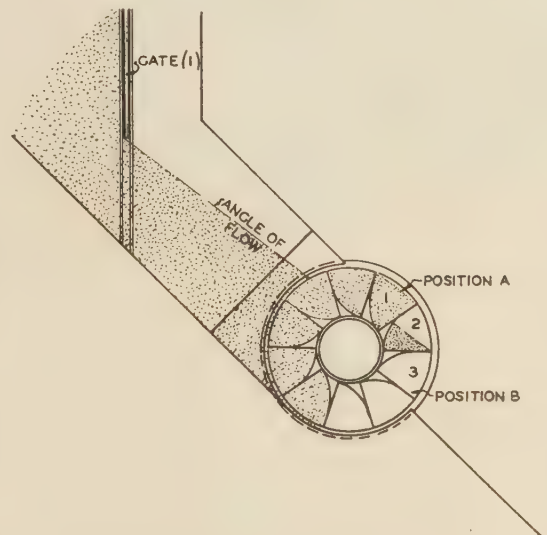


FIG. 9 STAR-TYPE FEEDER, ELEVATION SECTION
(Boynton, reference 6, Fig. 28A)

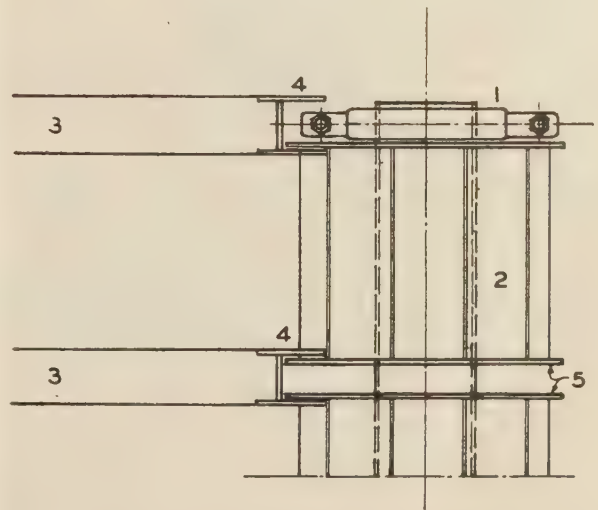


FIG. 10 STAR-TYPE FEEDER, PLAN VIEW
(Capacity, 5000 tons; bedding unit, 10,000 tons. Boynton, reference 6, Fig. 28B.)

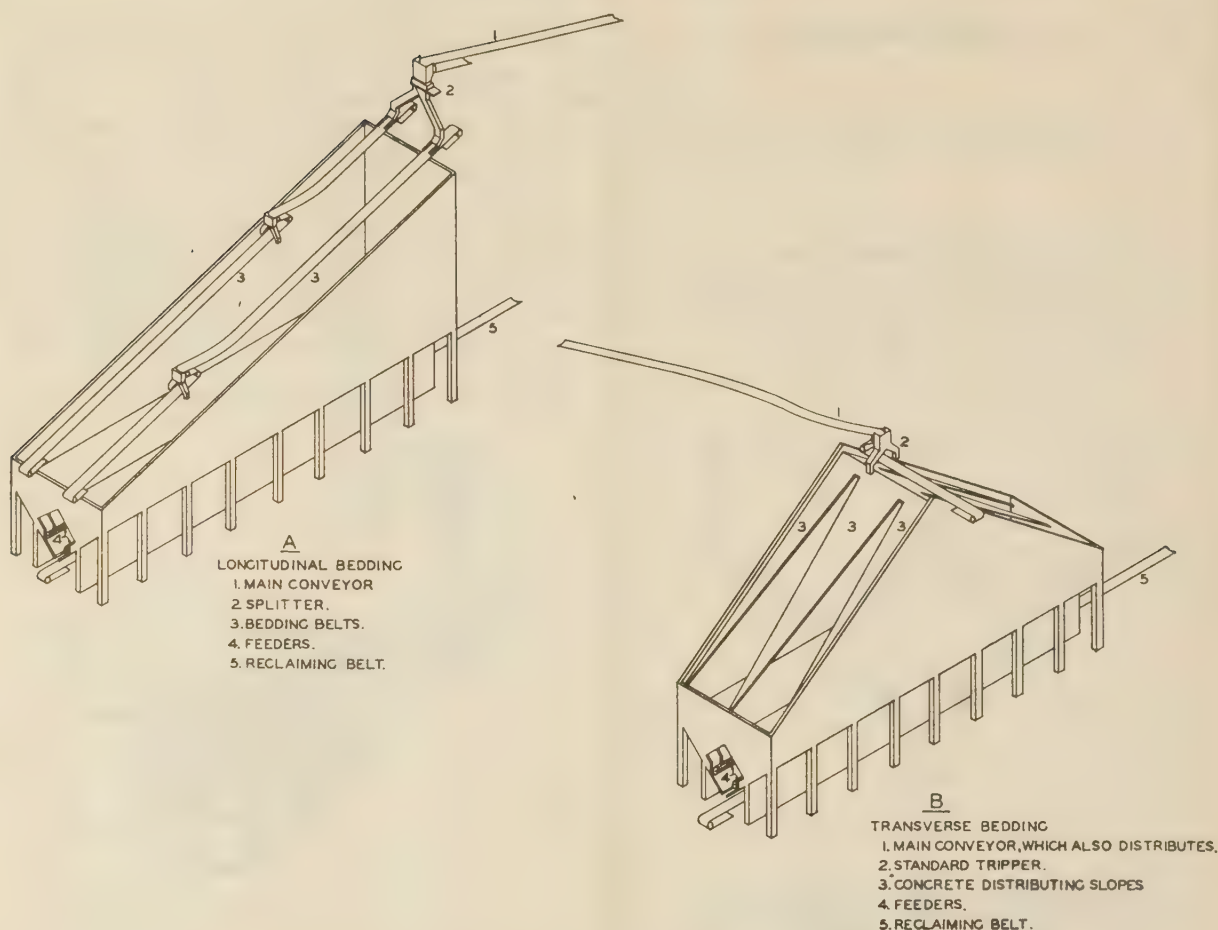


FIG. 11 ISOMETRIC VIEWS OF BINS FOR (A) LONGITUDINAL BEDDING AND (B) TRANSVERSE BEDDING

ordinary sense of the word. The bin remains full at all times. In any bedding system the amount reclaimed must be replaced continuously.

Economy. We estimate the cost of the bin shown in Fig. 10 to be \$410,000. It has a handling capacity of 10,000 tons per 8 hr, and a bedding unit of the same size. It will handle 3,000,000 tons of coal in 300 days of 8 hr each, and the fixed charges at 12.5 per cent amount to \$0.0171 per ton of coal handled. Two men form a crew for bedding and reclaiming operations.

Conclusions. We believe that the bedding and reclaiming operations for material such as coal, if required to be done at a rate of 250 tons per hr or more, are most economically carried on by means of a bin system. Where the circumstances of operation are adapted to continuous bedding, the system shown in Fig. 10 costs less to build and gives lowest over-all cost. It will produce a uniformity which with any considerable variation in the material (coal) will be worth much more than it costs.

COMBINATION BEDDING METHODS USED

The new Robena mine of the H. C. Frick Coke Company blends high- and low-sulphur coal by a combination of methods. Coal from high- and low-sulphur sections of the mine which are controlled by face sampling, are mixed by dumping mine cars in definite ratios. Next the coal is screened and the larger heavier pieces of refuse removed on a picking table. The coal is then crushed to 3 in. and bedded by means of a belt and tripper in an 18,000-ton horizontal bin of 168 compartments before going to the washing plant. The compartments are $7\frac{1}{2}$ ft wide \times 11 ft long \times 56 ft deep. Note the relatively small cross-sectional area.

It would appear to be advisable at a commercial mine where domestic sizes are loaded to separate the lump (plus 5-in. to 7-in. size) by screening and blend it by layer loading, or to blend at the dumping point rather than through bedding bins.

Ignition Through Fuel Beds on Traveling- or Chain-Grate Stokers¹

By E. P. CARMAN² AND W. T. REID³

Within recent times as part of its exhaustive studies on the burning of solid fuels on grates, the Bureau of Mines has investigated the factors affecting the burning of fuels on the cross-feed principle. Small-scale laboratory experiments, where the many variables could be closely controlled, have furnished information on the behavior of various fuels on traveling-grate stokers. Out of the wide range of results obtained, the present paper is limited generally to the study of ignition travel through a fuel bed and to important factors affecting it. Later reports will cover other phases of the investigation.

SINCE its inception, the Bureau of Mines has made many studies of the fundamentals affecting the burning of solid fuels on grates, beginning with the early investigations by Kreisinger⁴ and his co-workers on the principles of overfeed combustion and continuing with the work of Nicholls⁵ on underfeed burning processes. As a natural development, the factors affecting the burning of fuels on the cross-feed principle have been investigated more recently. This study furnished important information on the behavior of various fuels on traveling-grate stokers and was conducted in relatively small-scale laboratory apparatus where the many variables involved were subject to close control.

Initial ignition of the surface of the fuel bed by heat transferred by radiation, including determination of the absolute radiant heat received by the fuel, the travel of ignition through the bed, and burning after ignition reaches the grate have been studied. The resistance of the fuel beds to the flow of air has been measured, and its effects have been analyzed. Records have been obtained of the temperatures of experimental fuel beds and grates, and the factors that influence these temperatures have been determined. The effects of water tempering and of a limited number of chemical treatments also have been studied, and tests of a coal prepared with varying ash content have given data on the effect of ash on initial ignition, on the rate of ignition travel through the bed, and on burning rates. Measurements have been made of the effect of preheating primary air and of using secondary air, and relative smoke densities were determined for a wide variation in fuels and test conditions.

The large number of variables studied cannot be presented

¹ Published by permission of the Director, Bureau of Mines, United States Department of the Interior, Washington, D. C.

² Fuel Engineer, Bureau of Mines, Washington, D. C.

³ Supervising Engineer, Combustion Research Section, Bureau of Mines, Pittsburgh, Pa. Mem. A.S.M.E.

⁴ "Combustion in the Fuel Bed of Hand-Fired Furnaces," by Henry Kreisinger, F. K. Ovitcz, and C. E. Augustine, Technical Paper 137, Bureau of Mines, 1916; "Low-Rate Combustion in Fuel Beds of Hand-Fired Furnaces," by Henry Kreisinger, C. E. Augustine, and S. H. Katz, Technical Paper 139, Bureau of Mines, 1918.

⁵ "Underfeed Combustion, Effect of Preheat, and Distribution of Ash in Fuel Beds," by P. Nicholls, Bulletin 378, Bureau of Mines, 1934.

Contributed by the Fuels Division and presented at the Annual Meeting, New York, N. Y., Nov. 27-Dec. 1, 1944, of THE AMERICAN SOCIETY OF MECHANICAL ENGINEERS.

NOTE: Statements and opinions advanced in papers are to be understood as individual expressions of their authors and not those of the Society.

adequately in a single paper; consequently, this report will be limited generally to the study of ignition travel through a fuel bed and to important factors affecting it, and later reports will cover other phases of this investigation.

TYPES OF FUEL BEDS

The type of burning in a fuel bed is determined by the relative direction of flow of fuel and air, as described by Nicholls.⁶ In overfeed beds, Fig. 1, the fuel and air travel in opposite directions; and, assuming a "plane of ignition" where the incoming fuel becomes heated to the ignition point, this plane will travel through the unignited portion of the bed in the same direction as the air. Usually in this type bed, the fuel is fed from the top, the air enters at the bottom and travels up through the bed, and the plane of ignition moves upward with the air and the products of combustion into the green fuel.

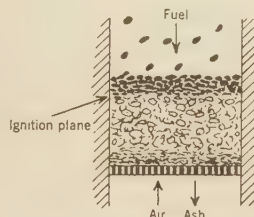


FIG. 1 DIAGRAMMATIC OVERFEED FUEL BED

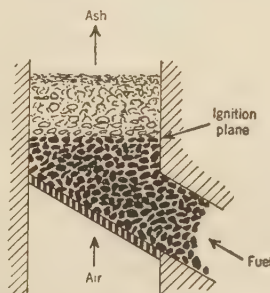


FIG. 2 DIAGRAMMATIC UNRESTRICTED-IGNITION UNDERFEED FUEL BED

In underfeed beds, Fig. 2, the fuel and air travel in the same direction, while the plane of ignition moves in the opposite direction. Usually the fuel and air are fed from the bottom and move upward while the plane of ignition moves downward, but in the downdraft furnace these directions are reversed.

In a pure cross-feed bed, Fig. 3, the fuel would move across the air stream at substantially a right angle, and the plane of ignition would move in the opposite direction into the incoming green fuel. With the traveling-grate stoker, Fig. 4, however, ignition occurs across the top of the incoming fuel, either by radiant heat, conduction from hot gases, or by deposition of ignited fuel blown from the rear, and the ignition plane travels in a direction nearly opposite to that of the air flow. Therefore,

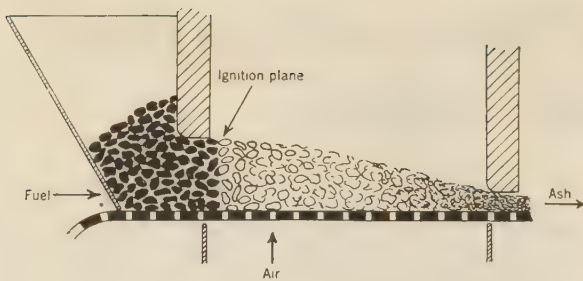


FIG. 3 DIAGRAMMATIC CROSS-FEED FUEL BED

during the length U , up to the point where the ignition plane touches the grate, the burning is essentially underfeed. After ignition reaches the grate and following a short change-over period, that is, during travel through length O , the burning is cross-feed, or overfeed which is similar when the plane of ignition is not involved. The traveling-grate stoker is quite commonly referred to as a type of overfeed stoker, but fundamentally the fuel is igniting and burning essentially underfeed during a considerable portion of the length of the bed, since volatile products evolved at the ignition plane must travel through ignited fuel to reach the combustion chamber.

OTHER INVESTIGATIONS

Many attempts have been made to determine ignition and burning rates in traveling-grate fuel beds, but many difficulties are involved in studying moving beds. One of the most interesting attempts was made by J. D. Maughan and reported by E. S. Grumell.⁶ In these tests a removable grid was fed into a traveling-grate stoker along with a regular fuel bed, and when the grid and fuel had been completely fed into the furnace, the grid was quickly removed and the fire quenched. Grumell and Dunningham⁷ have studied the burning of English coals on traveling-grate stokers in an apparatus much smaller than, but having some points of similarity to that used in these tests.

DESCRIPTION OF APPARATUS

The apparatus used in this investigation is shown in Fig. 5. It was designed with the view of obtaining carefully controlled, reproducible test conditions, in which small variations could be observed and their causes determined. The furnace proper was of welded steel construction with insulating refractory lining. The fuel-bed opening was 20 in. sq. and bed depths up to 10 in. could be used without blocking the peephole in the front wall of the furnace. Two interchangeable covers or hoods were used, and these were supported on corner posts resting on hydraulic jacks. One hood had six (subsequently changed to eight) "Glo-bar" resistor elements mounted under a carborundum backing plate. These Glo-bars could be heated electrically to 2800 F and the applied voltage could be controlled very closely by means of variable transformers, giving smooth variation of power input from 0 to 70 kw. During the heating-up period before the start of a test, this hood rested on a support at the side of the furnace, and the Glo-bars and heating surfaces were exposed to a water-cooled "cold box" of substantially the same dimensions as the furnace with fuel bed laid, the purpose being to duplicate the cold furnace and fuel bed from the standpoint

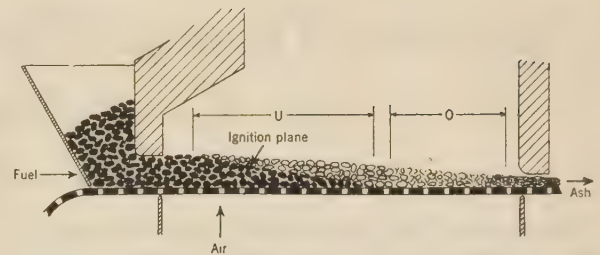


FIG. 4 DIAGRAMMATIC REPRESENTATION OF FUEL BED ON A TRAVELING-GRATE STOKER

of heat absorption. Thus no change in temperature conditions in the hood occurred during the start of the test when the previously heated hood was moved into position over the furnace.

The other hood was refractory-lined steel, and it rested on a small gas-fired furnace at the side of the test furnace, where it was preheated before the start of the tests. When the top of the fuel bed was thoroughly ignited by the Glo-bar igniting hood, both hoods were raised, the ignition hood was returned to its original position, and the refractory hood was transferred to the test furnace for the remainder of the test. This saved the Glo-bars from excessive heat and contamination by ash and smoke during the latter part of the tests.

In most tests only primary or undergrate air was used, and this was supplied by a fan capable of delivering up to 1000 lb of air per hr per sq ft of furnace area, at a static pressure of 3.7 in. of water. Close control of the quantity of air used was provided by a regulating valve, operated by a mechanism actuated by the pressure differential across a measuring orifice in the air line. By this means it was possible automatically to maintain a fixed air rate throughout a test.

A tubular heat exchanger in the air line between the orifice and the furnace permitted use of preheated air in some of the tests. Heat was supplied by a gas burner in a refractory combustion chamber beside the heat exchanger. A mixer and air distributor in the ash pit insured even distribution of the preheated air at the grate.

The furnace had a side-outlet stack which was used when the Glo-bar hood was over the furnace, but it was capped off when the refractory hood was in use, as this hood had a center stack. Both stacks had nipples for insertion of the Bureau's standard water-cooled gas samplers, modified to take samples across the stack rather than only at one position near the center. Gas samples were collected over mercury and analyzed in a water Orsat. A photoelectric smoke meter was installed on the side-outlet stack. When this was in use, the center stack of the refractory cap was closed, and only the side stack was used.

Initial ignition of the top of the fuel bed, the travel of ignition through the bed, and bed temperatures were determined by thermocouples inserted at vertically spaced intervals in the bed and connected, in order, to recording potentiometers. Observations of initial ignition of the bed top and of bed conditions during the test were made through a peephole in the front wall of the furnace.

In this furnace, the grate and bed were stationary. The transfer of the hot igniting hood over the fuel bed was comparable to emergence of the green fuel on a traveling-grate stoker into the furnace. Clocks were started at the time of this transfer, and the condition of the bed at any given elapsed time thereafter was comparable to the condition of a thin slice across a traveling bed at similar elapsed time after it entered the furnace. It was thus possible to follow the progress of ignition through the bed and to determine bed temperatures by means of the thermo-

⁶ "The Evaluation of Fuel from the Consumers' Viewpoint; Appendix, the Mechanism of Burning Coal on a Chain-Grate Stoker," by E. S. Grumell, *Journal of the Institute of Fuel*, vol. 5, no. 24, August, 1932, pp. 366-370.

⁷ "Combustion of Fuel on a Traveling Grate," by E. S. Grumell and A. C. Dunningham, *Journal of the Institute of Fuel*, vol. 12, no. 62, December, 1938, pp. 87-95.

TABLE 1 FUELS TESTED

Classification by rank	Source State, County, Mine, Bed	Proximate analysis as received, per cent				Heat value Btu per lb., as received
		Moisture	Volatile matter	Fixed carbon	Ash	
High-temp coke (sized coke).....	Penna., Neville Is. Plant of Pittsburgh Coke & Iron Co.	4.2	1.4	85.0	9.4	12280
High-temp coke (breeze).....	Penna., Neville Is. Plant of Pittsburgh Coke & Iron Co.	2.1	1.0	86.2	10.7	12400
Anthracite (pea and rice sizes).....	Penna., Schuylkill (Locust Summit Breaker)	2.0	6.1	82.4	9.5	13290
Anthracite, barley.....	Penna., Schuylkill (Locust Summit Breaker)	2.0	5.7	81.9	10.4	13140
Anthracite, No. 4 buckwheat.....	Penna., Schuylkill (Locust Summit Breaker)	3.2	6.1	80.9	9.8	13040
Anthracite, variable-ash:						
A.....	Penna., Schuylkill (St. Nicholas Breaker)	1.6	3.5	90.4	4.5	14000
B.....	Penna., Schuylkill (St. Nicholas Breaker)	2.6	4.6	83.0	9.8	13010
C.....	Penna., Schuylkill (St. Nicholas Breaker)	2.1	4.1	77.1	16.7	11980
D.....	Penna., Schuylkill (St. Nicholas Breaker)	2.3	4.7	68.6	24.4	10680
E (residue).....	Penna., Schuylkill (St. Nicholas Breaker)	1.1	81.3	..
High-volatile A bituminous.....	Penna., Allegheny Montour No. 10 Pittsburgh	1.6	37.2	55.8	5.4	14090
High-volatile C bituminous.....	Ill., Franklin, No. 2, Ill. No. 6	6.7	34.4	52.6	6.3	12630
Subbituminous B.....	Colo., Weld, Washington, Laramie	21.6	30.6	43.4	4.4	9900
Lignite.....	N. Dak., Mercer, Knife River	36.0	26.9	31.2	5.9	7140

couples, to note bed height by a depth gage extending through the refractory hood, and to determine the rate of burning from gas samples and the recorded rate of air supply.

FUELS TESTED

The fuels used in this investigation varied from high-temperature coke and anthracite to lignite and were chosen to represent reasonable differences in rank, rather than from consideration of their commercial usefulness on traveling-grate stokers. Actually all of the fuels tested are burned on this type of equipment, although strongly coking coals usually are considered less suitable. The analysis and source of each fuel tested are shown in Table 1.

EFFECT OF FACTORS, OTHER THAN RANK, ON RATE OF IGNITION

As was shown in Fig. 4, the direction of ignition travel through

the bed in traveling-grate stokers is substantially opposite to that of the air and the products of combustion, resulting in essentially unrestricted underfeed ignition. As noted in a previous bulletin,⁵ ignition and burning rates in beds of this type reach a maximum at some optimum air rate, with most fuels, after which ignition and burning rates decrease with increased supply of air. Consequently, above a certain point it is impossible to increase the rate of ignition and of burning by increasing the air rate. This same limitation applies to the underfeed-ignition portion of traveling-grate fuel beds and imposes operating limitations during the time ignition is traveling through the bed. This will be illustrated by the ignition curves of the various fuels tested, which follow later.

Ignition rates in fuel beds of traveling-grate stokers are affected by such factors as speed of "initial ignition," or ignition of the top layer of fuel, moisture on the fuel, size consist of the fuel,

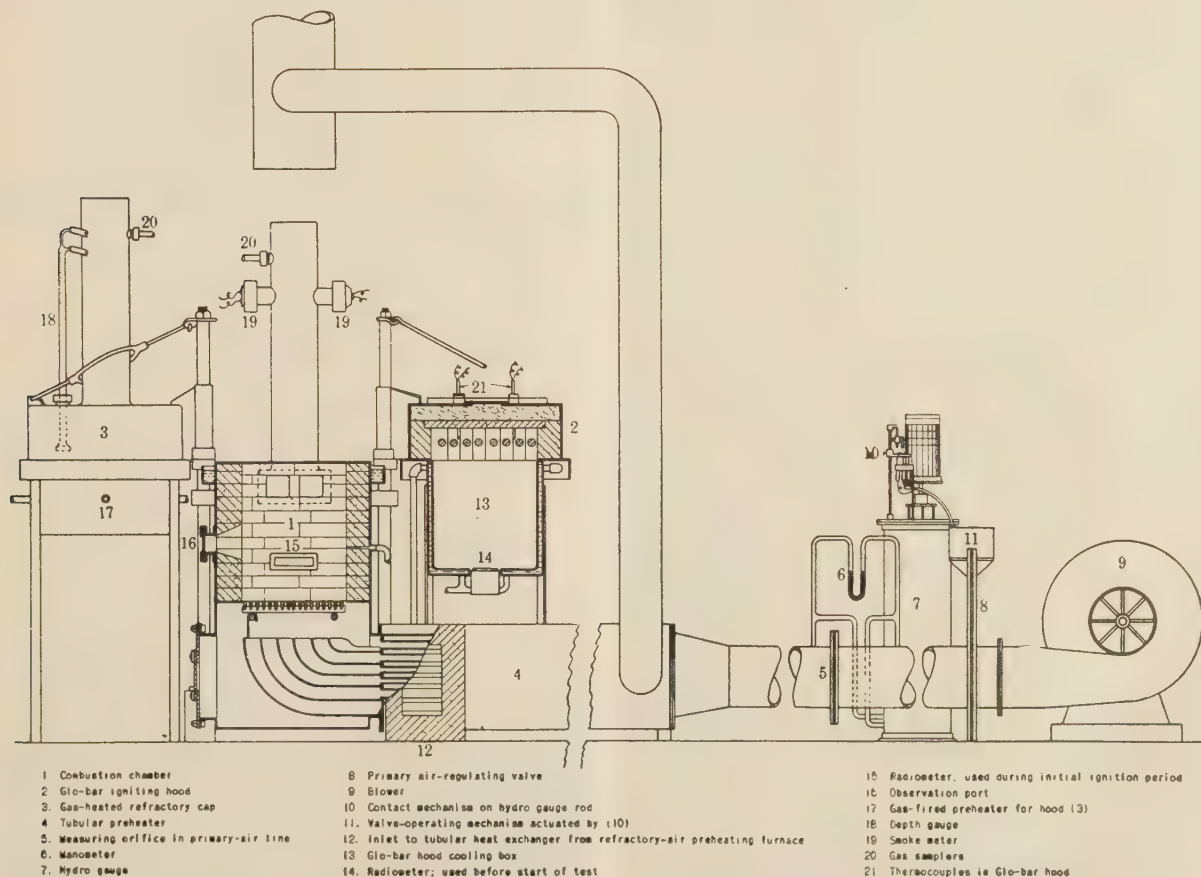


FIG. 5 CROSS SECTION AND DIAGRAMMATIC ARRANGEMENT OF FURNACE AND AUXILIARY APPARATUS

temperature of primary air, and ash content of the fuel, as well as by change of rank of fuel. These will be discussed in the order given.

Slow Initial Ignition. There are two phases in what may be called "igniting the bed." The first is initial ignition or the establishment of burning of the top layer of fuel, obtained either by radiant heat, or convection from hot gases, or from preignited fuel blown forward onto the entering green fuel. When ignition has been firmly established in the top layer and the reaction there has become exothermic, the second phase, "ignition through the bed," begins. Each phase involves problems affecting traveling-grate-stoker operation, and it has been found that these phases are to some extent interdependent.

Slow initial ignition was found to have a definite retarding effect on the rate of ignition travel. It was expected that slow ignition of the top layer of fuel would have only a very temporary effect and that with a fixed air rate a definite rate of ignition travel would be established quickly, regardless of the speed of initial ignition. This has not proved to be the case, however, with thin beds as used on traveling-grate stokers. The delaying effect of slow initial ignition on rate of ignition travel was pronounced in the top third or more of the bed and usually persisted to some degree throughout the bed. In most cases when it took 3 min or longer to establish an exothermic combustion reaction in the top layer of fuel, the rate of travel of ignition into the bed was much lower than in similar tests with rapid initial ignition, especially in the top third or half of the bed. In tests with slow initial ignition, the rate of ignition usually did increase as the plane of ignition traveled through the bed, and it appears probable that if the beds had been sufficiently deep, the delaying effect of slow initial ignition would ultimately have disappeared. However, in the thin fuel beds used on this type stoker, slow initial ignition has a definite retarding effect on the average rate of ignition travel.

In the figures that follow, showing the travel of the plane of ignition, low ignition-rate points from tests with slow initial ignition are indicated by the subscript *S*. Even greater local variations in rate of ignition travel than are indicated by these *S* points may be expected when initial ignition conditions are allowed to vary widely, since many of the ignition rates so shown were taken from the bottom two thirds of the bed, where the retarding effects of slow initial ignition are less pronounced than in the upper third of the bed.

Moisture. The effect of moisture on fuel on the rate of travel of the plane of ignition was determined in the tests with coke breeze, but with a single exception, one or more tests with each of the other fuels confirmed these data.

A typical coke breeze, designated "Breeze A," was made up from closely screened sizes of high-temperature coke by mixing thoroughly 4 per cent by weight of $\frac{3}{4}$ in. \times $\frac{1}{2}$ in., 20 per cent of $\frac{1}{2}$ in. \times $\frac{1}{4}$ in., 24 per cent of $\frac{1}{4}$ in. \times $\frac{1}{8}$ in., 18 per cent of $\frac{1}{8}$ in. \times $\frac{1}{16}$ in., and 34 per cent of $\frac{1}{16}$ in. \times 0. Without water tempering, this breeze is extremely unstable on the grate even at very low air rates. With varying percentages of added moisture, however, air rates up to 350 psf* and hr were successfully used, as shown in Fig. 6 (A and B).

About 10 to 12 per cent moisture is indicated as optimum for a breeze of this size consist. While faster rates of ignition travel are obtainable for given air rates when the moisture content is lower, as shown by the dotted 8 per cent moisture curve, this drier breeze makes much less stable beds. The resultant instability is liable to lead to maldistribution of air, with consequent rapid ignition travel in some areas and slow in others, as

indicated by the low point at the 150-lb air rate for the 8 per cent moisture test, in which considerable bed instability was noted.

Increase of moisture content to 16 per cent resulted in decreasing rates of ignition travel for given air rates, indicating that optimum conditions prevailed when the moisture content was the least that could be used and still maintain reasonable bed stability. To confirm this, tests were run with beds laid with breeze containing 16 per cent moisture and then predried before the start of the test. The delaying effect of added moisture is indicated by the difference between the curve for the predried

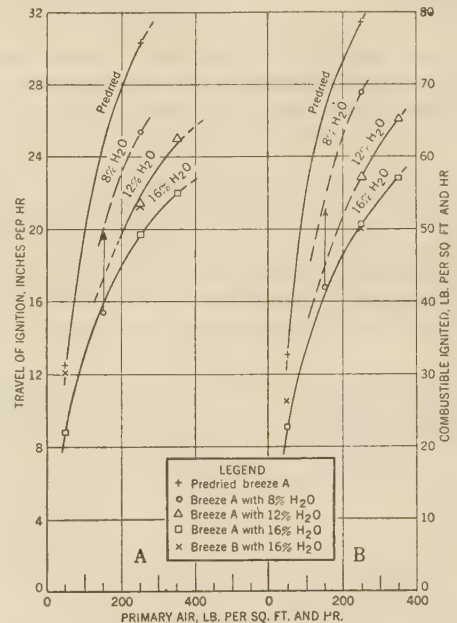


FIG. 6 A, RATE OF TRAVEL OF PLANE OF IGNITION, AND B, RATE OF IGNITION IN 6-IN-DEEP BEDS OF HIGH-TEMPERATURE COKE BREEZE WITH VARYING AMOUNTS OF MOISTURE

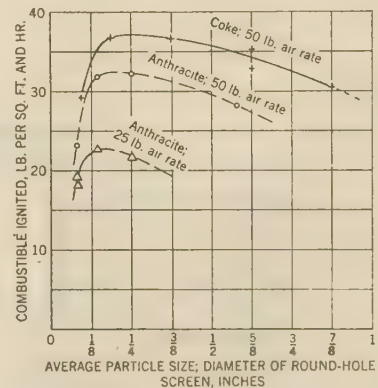


FIG. 7 RATE OF IGNITION OF HIGH-TEMPERATURE COKE AND ANTHRACITE OF DIFFERENT PARTICLE SIZE

beds and that for the breeze with 16 per cent moisture; ignition through the bed is much slower with the moist breeze. Preliminary trials indicated that the moisture content of the predried beds would be about 1 per cent.

Size of Fuel. With fuels larger than approximately $\frac{1}{2}$ in. avg diam, an increase of ignition rate with decrease of size had been observed. Data from the tests with coke breeze indicated

* This abbreviation follows the terminology used in American Standard Abbreviations for Scientific and Engineering Terms and means pounds per square foot.

that this trend might not continue into the very small sizes; therefore, tests were made with coke and anthracite to determine ignition rates for the smaller sizes. The data are shown in Fig. 7. Maximum rates of ignition travel were obtained with coke of $1/4$ in. avg diam, and with anthracite of $3/16$ in. avg diam, with a slight variation indicated for variation of air rate. Some of the decrease in ignition rate for sizes below the optimum must be ascribed to the effects of increased tempering moisture needed to give bed stability, but since such tempering is necessary, it is the over-all effect that is significant. The sharp drop in ignition rate below the optimum size indicates possibilities of operating difficulties due to slow rates of ignition with small sizes of coke and anthracite, effects that are entirely independent of the physical difficulties of maintaining relatively uniform and stable beds.

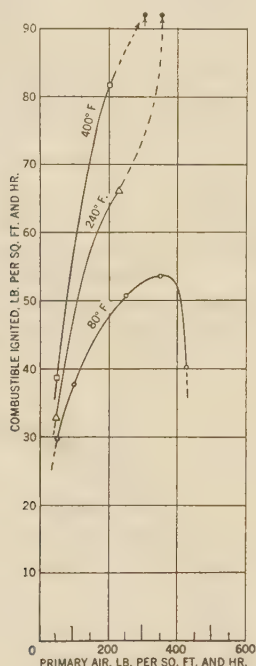


FIG. 8 EFFECT OF PRIMARY-AIR RATE AND PREHEAT ON RATE OF IGNITION OF ST. NICHOLAS BARLEY ANTHRACITE

This decrease of ignition rate with decrease of size below an optimum value was noted with high-temperature coke, the higher-rank coals, and lignite but was not found with high-volatile C bituminous coal nor with the subbituminous B coal.

Preheated Primary Air. Preheated primary air was used with beds of St. Nicholas barley anthracite and gave materially increased rates of ignition, the increase being almost linearly proportional to the amount of preheat used. In the first tests, both air and fuel were heated to the desired temperature before initial ignition to eliminate effects of variable heating of the fuel as the test proceeded. Fig. 8 illustrates the effects of preheat in increasing ignition rates under these test conditions. Although there was substantial increase of the rate of ignition at the 50-lb air rate, there was a much greater increase proportionately at the 200-lb air rate, and at still higher air rates extremely rapid ignition was obtained by mechanical mixing of ignited and unignited fuel in "boiling" beds. The proportional increase of ignition rate over the rate with air and fuel at approximately 80 F is shown in Fig. 9. With the 50-lb air rate, and fuel and air preheated to 240 F, an increase of only 11 per cent in ignition

rate is obtained; whereas with the 200-lb air rate, the increase in ignition rate over that obtained at 80 F was 35 per cent. Increase in rate of ignition with preheated primary air was therefore much more pronounced at high than at low air rates.

In subsequent tests simulating actual traveling-grate-stoker operation, where cold fuel is fed into the preheated air stream, the tests were started with a cold bed. In these tests with beds 4 in. thick, the ignition plane traveled downward through the top 2 in. of fuel at an average rate only slightly greater than that obtained without preheat; whereas in the bottom 2 in. the ignition rate approached that obtained when both coal and air were at preheat temperature. The fundamental curves obtained with air and coal at room temperature, and with both at preheat temperature give therefore the minimum and maximum

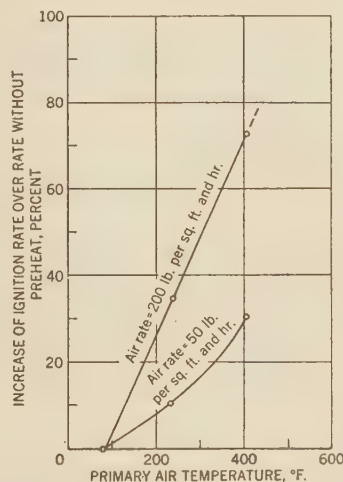


FIG. 9 PERCENTAGE INCREASE OF IGNITION RATE WITH PREHEATED PRIMARY AIR

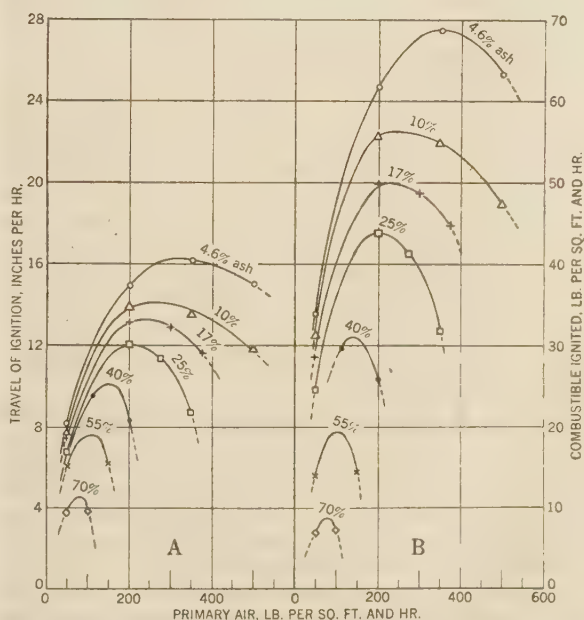


FIG. 10 A, RATE OF TRAVEL OF PLANE OF IGNITION, AND B, RATE OF IGNITION IN 4-IN-DEEP BEDS OF ST. NICHOLAS RICE ANTHRACITE WITH VARYING ASH CONTENT

limits, respectively, of the varying rate of ignition travel through fuel beds on traveling-grate stokers supplied with preheated air.

Variable Ash Content. Variation of ash content has a pronounced effect upon the rate of ignition of anthracite, as shown in Fig. 10. A special batch of St. Nicholas rice anthracite was separated by the float-and-sink process into fractions containing 4.6, 10.0, 17.0, 25.0, and 82.2 per cent ash, as shown on the moisture-free basis, Table 2.

TABLE 2 CHARACTERISTICS OF BATCH OF ST. NICHOLAS RICE ANTHRACITE

Fraction designation.....	A	B	C	D	E
Ash, moisture-free basis.....	4.6	10.0	17.0	25.0	82.2
Moisture- and ash-free:					
Volatile matter.....	3.7	5.2	5.0	6.4	..
Fixed carbon.....	96.3	94.8	95.0	93.6	..

The four fractions A, B, C, and D, Table 2, were tested first, giving the four upper curves in Fig. 10. The results were sufficiently interesting to justify preparation of higher-ash batches by appropriate mixtures of D and E fractions to give blends containing 40, 55, and 70 per cent ash.

Three definite effects of increase in the ash content of anthracite were found. The first was a decrease in ignition rate at all air rates. The second was a decrease in the range of air rates giving high ignition rates. The third was a decrease in the optimum air rate giving maximum ignition rate. For example, at an air rate of 200 psf and hr, the anthracite containing 25 per cent ash ignited at only 43.8 psf and hr of combustible, compared to 61.8 lb for the lowest-ash coal, a ratio of approximately 0.7:1.0. With the low-ash coal, however, at 200 lb, the ignition curve was still rising rapidly, and increase of air rate up to 325 lb gave increasing ignition rates, whereas for the 25 per cent ash coal the 200-lb air rate was the optimum.

The limitations of air rate with increase of ash content have even greater significance. An ignition rate of 40 psf and hr or more of combustible can be obtained with the 25 per cent ash coal only with air rates between about 125 and 290 psf and hr, but with the 17 per cent ash coal, a range of about 100 to 425 lb can be used, and with the 4.6 per cent ash coal, a range of 60 to 600 lb can be used. Low ash content is therefore a definite aid to stoker operation, in so far as rapid bed ignition and ability to use a wide range of air rates are concerned.

However, other factors affect stoker operation, and, to avoid a misleading picture, it is necessary to analyze not only the ignition data but the burning data for these tests of anthracite with variable ash content. A series of curves was drawn showing burning rates throughout the tests for various air rates, similar to those shown in Fig. 11 for the 200-lb air rates. These curves were corrected for slight differences in initial ignition conditions and were not extended beyond a 5-lb burning rate; then the areas under the curves were measured by a planimeter. The burning was underfeed before ignition had reached the grate (as indicated by the vertical lines on the curves between 22 and 26 min elapsed time), and was overfeed after ignition to the grate. Beds 4 in. thick were used in all tests.

Average burning rates were calculated from the areas of the curves and are shown in Fig. 12, as a function of primary-air rate. Up to a 350-lb primary-air rate, there was relatively little difference in over-all average burning rate between the 4.6, 10, and 17 per cent ash coals. For ash contents exceeding 17 per cent, a sharp drop in average burning rate with increase of ash was indicated, especially at the higher air rates.

Although the lower-ash coals had much higher rates of ignition travel than those with higher ash content, rates of burning were not substantially affected by variation of ash up to 17 per cent. As shown in Fig. 11, the lowest-ash coal developed a higher rate of underfeed burning than the others and started to develop a

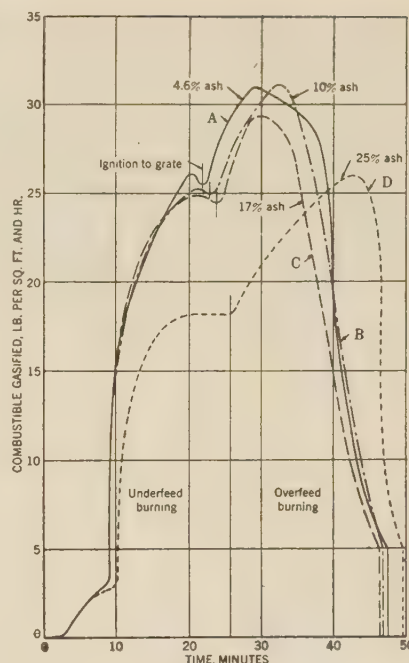


FIG. 11 RATE OF BURNING OF ST. NICHOLAS RICE ANTHRACITE WITH VARYING ASH CONTENT
(Initial ignition at 50 psf per hr.; burning at 200 psf and hr.)

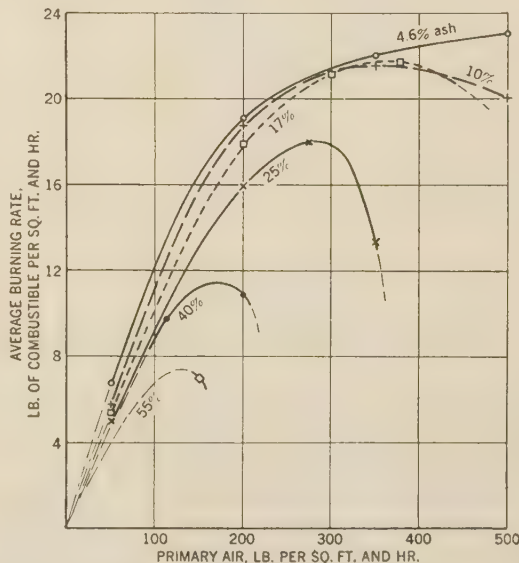


FIG. 12 EFFECT OF ASH ON AVERAGE BURNING RATE OF $\frac{5}{16} \times \frac{3}{16}$ -IN. ST. NICHOLAS ANTHRACITE, FOR BURNING RATES GREATER THAN 2 LB FOR 50-LB AIR RATE, AND 5 LB FOR HIGHER AIR RATES

higher overfeed-burning rate, but as the coal burned down and the pieces became smaller and the bed thinner, with little ash to impart stability and depth, blowholes and maldistribution of air developed and adversely affected the burning rates. The same conditions, but to a lesser degree, prevailed with the 10 per cent ash coal. As a result, the over-all average burning rates were very close for the three lowest-ash coals up to primary-air rates of 350 lb, despite rather distinct differences in ignition rate, as shown in Fig. 12. There was a substantial decrease in

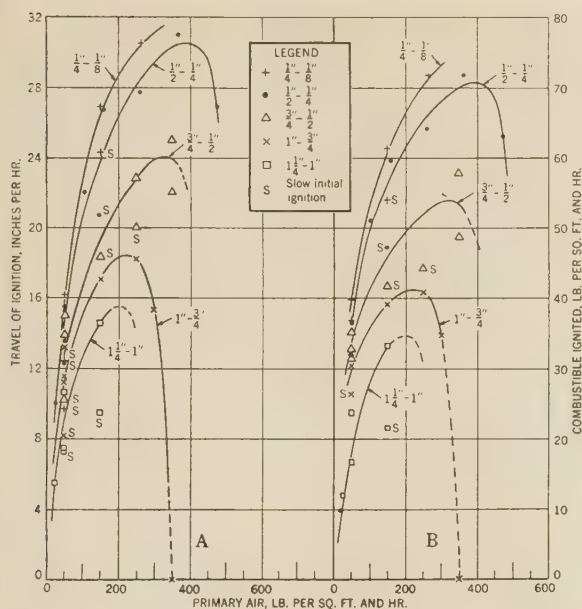


FIG. 13 EFFECT OF SIZE OF FUEL ON A, RATE OF TRAVEL OF PLANE OF IGNITION; AND B, RATE OF IGNITION IN 6-IN.-DEEP BEDS OF HIGH-TEMPERATURE COKE

both ignition and burning rates with increase of ash above 17 per cent.

EFFECT OF RANK OF FUEL ON RATE OF IGNITION

High-Temperature Coke. High-temperature coke was used in the early tests as the most convenient fuel for investigating principles of burning, since it is free-burning and smokeless, and the gas analyses are relatively simple. Fig. 13 (A) shows rate of ignition travel, in inches per hour, in beds of high-temperature coke, and Fig. 13 (B) shows rate of ignition in pounds of combustible per square foot and hour. Beds 6 in. thick were used in the tests plotted.

There is a fairly regular increase of ignition rate with decrease of size down to $1/2$ in. \times $1/4$ in., but relatively less change below this. In addition, there is an increase in the optimum air rate for maximum ignition rate as the size decreases. This means that not only will decrease of average size of piece, within certain limits, give faster rates of ignition for a given air rate, but also that higher air rates can be used to increase rate of ignition travel.

Increasing the air rate above that which gives the maximum rate of ignition causes a rapid decrease of ignition rate with high-temperature coke, as may be noted from the curves for the 1-in. \times $3/4$ -in. size. Increasing the air rate by only about 120 psf and hr above the optimum amount results in stopping ignition of the fuel completely. If part of the bed ignites because of a temporarily low air rate, increasing the air rate to 350 lb will stop further ignition because the fuel will not burn at a rate high enough to ignite more fuel.

In tests where initial ignition was rapid, that is, occurring in less than 3 min, ignition traveled through the bed at a constant rate. With slow initial ignition, however, the rate varied from relatively very slow to approaching that obtained with rapid initial ignition.

Coke Breeze. Curves of ignition rates for a typical coke breeze, Breeze A, were given in Fig. 6. Two observations regarding the use of this coke breeze should be noted as follows:

1 It was not found possible to go to air rates high enough to reach or exceed the maximum rate of ignition travel, as higher

air rates than those used blew the bed off the grates. In practical operation therefore with breezes of size consist similar to Breeze A, the maximum rate of ignition will be fixed by the highest air rate that does not cause excessive loss of fines or maldistribution of air. It would be expected that with a breeze having a smaller proportion of fines and with which air rates exceeding 400 psf and hr could be used, a peak of ignition travel would be reached beyond which increase of air rate would give decrease of ignition travel, as with the closely sized coke.

2 More uniform bed conditions prevailed at high than at moderate air rates. While there was more vigorous and widespread "boiling" of ignited fuel pieces across the top of the bed at high air rates than at lower rates, this action was more uniformly distributed at the higher air rates, and there was less tendency to form blowholes that would destroy uniformity of air distribution.

TABLE 3 SIZE CONSIST AND BULK DENSITY OF COKE BREEZE

Size, in.	Per cent by weight, dry coke		
	Breeze B	Breeze A	Breeze C
$3/4$ - $1/2$	6.06	4.0	2.0
$1/2$ - $1/4$	30.30	20.0	10.0
$1/4$ - $1/8$	36.36	24.0	12.0
$1/8$ - $1/16$	27.28	18.0	9.0
$1/16$ -0.....	0.00	34.0	67.0
Bulk density, lb per cu ft as laid in fuel bed.....	100.00	100.0	100.0
	35.7	43.0	46.9

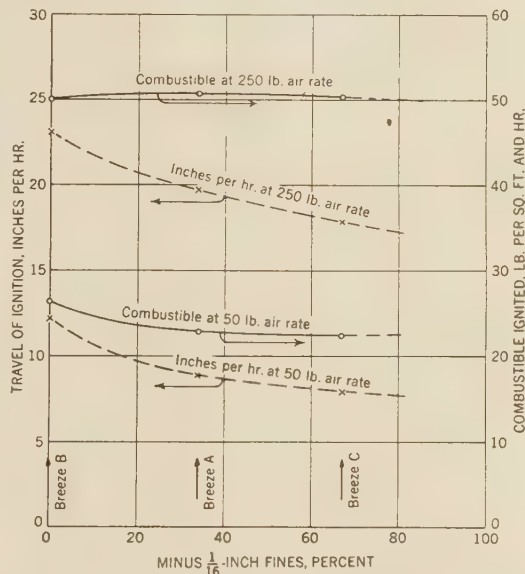


FIG. 14 RATE OF TRAVEL OF PLANE OF IGNITION IN COKE BREEZE OF VARYING PERCENTAGES OF MINUS- $1/16$ -IN. FINES; 16 PER CENT MOISTURE IN ALL TESTS

The effect of change in size consist on rate of ignition travel is shown in Fig. 14. The size consist of the fuels is given in Table 3, arranged according to percentage of $1/16$ -in. to 0 fines. As the percentage of fines was increased, the bulk density increased, and the rate of ignition travel, in inches per hour, decreased. On the basis of combustible ignited per square foot and hour, however, there was remarkably little change in the rate of ignition travel with change of size consist, indicating that the ignition data for the tests with Breeze A could be used with reasonable accuracy for other breezes having a wide range of size consist.

This does not mean that all coke breezes can be ignited and burned with equal operating ease, however, as the physical difficulties of maintaining uniform bed conditions and air distribution increased with the percentage of fines in the fuel.

Anthracite. Ignition data for a rice ($5/16$ -in. \times $3/16$ -in.) and a

substandard pea ($1\frac{1}{16}$ -in. \times $\frac{1}{2}$ -in.) anthracite are shown in Fig. 15. Travel of ignition, in inches per hour, is much slower than for the nearest comparable coke sizes, but on the basis of pounds of combustible ignited per square foot and hour, they are quite similar. Due to the large difference in bulk density, about the same amount of combustible can be ignited and burned in a 4-in. bed of anthracite as in a 6-in. bed of coke of comparable size, and the time for ignition to reach the grate will be approximately the same in either case.

The optimum air rate to secure the maximum rate of ignition travel was about the same for anthracite as for coke, namely, 350 to 400 psf and hr, but the anthracite showed a more gradual transition from increasing to decreasing rate of ignition, indicating a broader range of air rates for high rates of ignition.

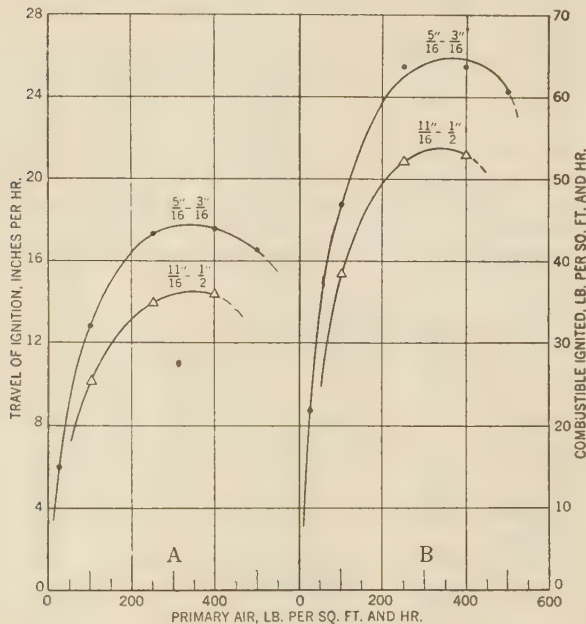


FIG. 15 EFFECT OF SIZE OF FUEL ON A, RATE OF TRAVEL OF PLANE OF IGNITION; AND B, RATE OF IGNITION IN 6-IN-DEEP BEDS OF ANTHRACITE

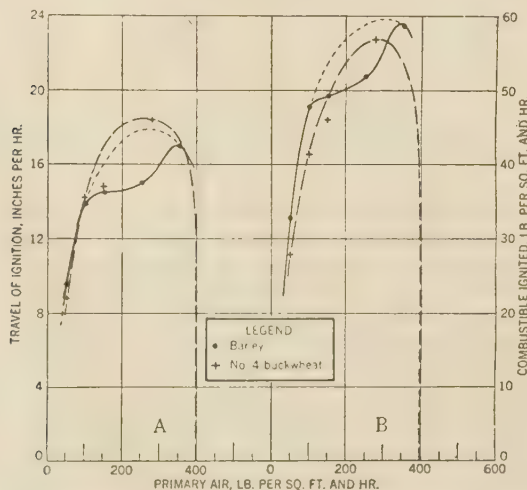


FIG. 16 EFFECT OF SIZE OF FUEL ON A, RATE OF TRAVEL OF PLANE OF IGNITION; AND B, RATE OF IGNITION IN 4-IN-DEEP BEDS OF LOCUST SUMMIT BARLEY AND NO. 4 BUCKWHEAT ANTHRACITE

Results of tests with barley and No. 4 buckwheat anthracite are shown in Fig. 16. Analyses indicate that these coals were similar in volatile matter and fixed-carbon content to those used for the pea and rice tests described, but the ignition rates for the barley coal are lower than for the rice, and those for the No. 4 buckwheat are lower still. This is a further illustration of the decrease in rate of ignition travel with decrease in size below the optimum of approximately $\frac{1}{4}$ in. avg diam, as mentioned previously.

The curves for the barley anthracite emphasize the observation made in connection with coke breeze, that more difficulty is often met in maintaining uniform air distribution and bed conditions with small fuels at moderate than at high air rates. Up to the 100-lb air rate, the bed was entirely stable; at the 150- and 250-lb air rates, there was irregular blowing and "boiling" of the coal at scattered areas in the bed, with resulting maldistribution of air. At the 350-lb air rate, however, while there was "boiling" (so-called because the bed top resembled a vigorously boiling fluid), this boiling was evenly distributed across the bed, which burned down very evenly. The broken curve for the barley anthracite indicates the ignition rates that normally would be expected with this fuel, but the solid line shows rates that are much more liable to be found with uneven bed conditions.

Nominal water tempering aids in maintaining stable fuel beds with No. 4 buckwheat anthracite as with other small-sized fuels.

High-Volatile A Bituminous Coal. Five close sizes and two mixtures or "slack" sizes of high-volatile A bituminous coal from the Pittsburgh bed were used as given in Table 4. Ignition rates for this fuel are shown in Fig. 17. The curves are characterized by high ignition rates over a much wider range of air rates than was found possible with the anthracites and cokes.

TABLE 4 SIZES OF HIGH-VOLATILE A BITUMINOUS COAL TESTED

Size, in.	Percentage composition—	
	Mix A	Mix B
$1\frac{1}{2}$ - $\frac{3}{4}$	20	10
$\frac{3}{4}$ - $\frac{3}{8}$	20	15
$\frac{3}{8}$ - $\frac{1}{8}$	30	20
$\frac{1}{8}$ - $\frac{1}{16}$	20	25
$\frac{1}{16}$ - $\frac{1}{32}$	10	30

Definite evidence of a decrease in ignition rate with increase of air rate for the sized coals was obtained only after increasing

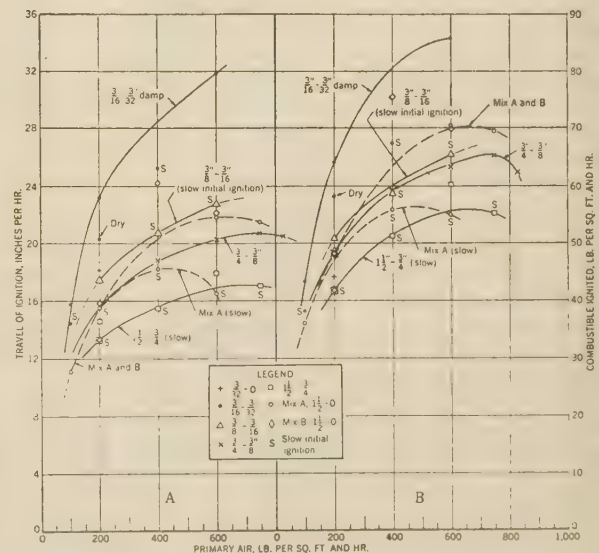


FIG. 17 A, RATE OF TRAVEL OF PLANE OF IGNITION; AND B, RATE OF IGNITION IN 6-IN-DEEP BEDS OF HIGH-VOLATILE A COAL FROM PITTSBURGH BED

the air rate to more than 750 psf and hr, indicating the possibility of using very high air rates to secure high ignition and burning rates with this coal. The mixed sizes, particularly mix B with 30 per cent fines, lacked bed stability at high air rates; and variable rates of ignition were obtained, as indicated by the high point for mix B at the 400-lb air rate. With this exception, the two slack mixtures had substantially identical ignition rates.

Slow initial ignition resulted in slow travel of ignition through the bed, as previously noted. This is indicated by the relatively low positions of the curves for the $1\frac{1}{2}$ -in. \times $\frac{3}{4}$ -in. and the $\frac{3}{8}$ -in. \times $\frac{3}{16}$ -in. sizes, and by the lower curve for mix A.

After ignition had proceeded 2 to 3 in. into the bed at air rates of 200 lb and lower, swelling and caking so interfered with air distribution that the rate of ignition in the bottom portion of the bed was extremely low at the bed center where the thermocouples were located; ignition rates shown for these tests therefore were taken from the upper portions of the bed. When burning highly caking coals, such as that from the Pittsburgh bed, more uniform fuel-bed conditions would be expected at moderate or low air rates with thin beds, 2 to 3 in. deep, and high stoker speeds, than with deeper beds and slower stoker speeds.

A bed of dry $\frac{3}{16}$ -in. \times $\frac{3}{32}$ -in. coal ignited more slowly than the damp coal containing 12 per cent moisture, although initial ignition was reasonably rapid; however, caking of the bed, possibly more rapid with the dry than with the damp coal, may have been responsible. This is the only instance in this investigation where a dry coal ignited more slowly than when damp.

Two tests with the fine size, $\frac{3}{32}$ -in. \times 0, gave ignition rates substantially less than those for the next larger size, confirming the previously described decrease in ignition rate for fuel below some optimum size, which for this coal appears to be about $\frac{1}{8}$ in. avg diam.

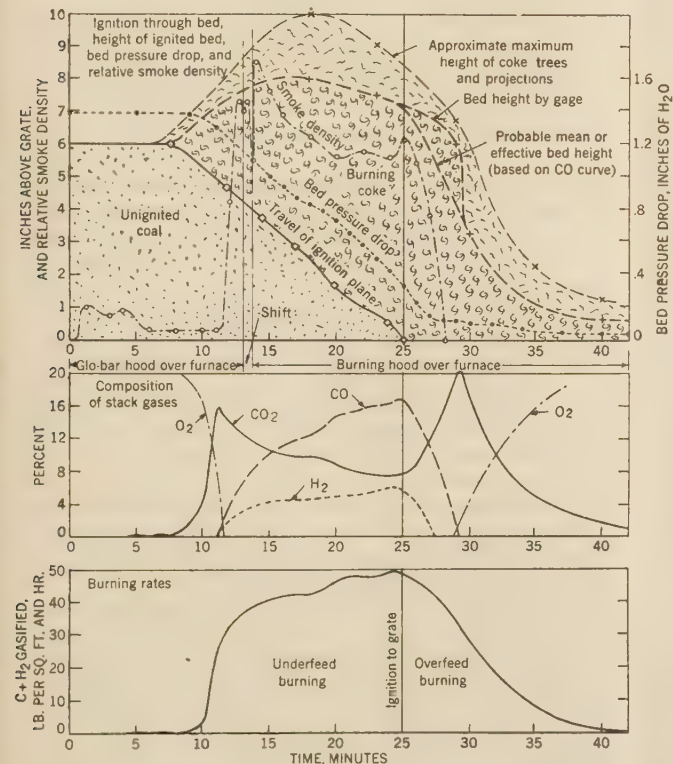


FIG. 18 LOG OF TEST WITH $\frac{3}{8} \times \frac{3}{16}$ -IN. HIGH-VOLATILE A COAL FROM PITTSBURGH BED AT AN AIR RATE OF 400 PSF AND HR

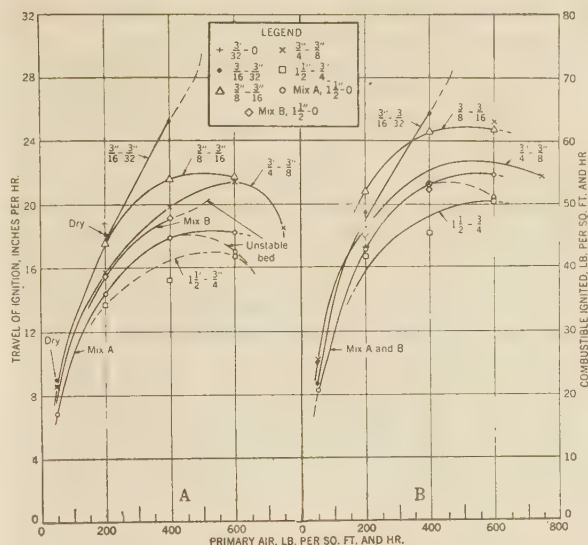


FIG. 19 A, RATE OF TRAVEL OF PLANE OF IGNITION, AND B, RATE OF IGNITION IN 6-IN.-DEEP BEDS OF HIGH-VOLATILE C BITUMINOUS COAL FROM ILLINOIS

A typical log of a test with $\frac{3}{8}$ -in. \times $\frac{3}{16}$ -in. coal from the Pittsburgh bed is shown in Fig. 18. At the 400-lb air rate used in this test, initial ignition was slow.

High-Volatile C Bituminous Coal. Rates of ignition in 6-in. beds of a high-volatile C bituminous coal from the Illinois No. 6 bed are shown in Fig. 19. The same sizes and size consists were used as with the high-volatile A bituminous coal. A much smaller variation of ignition rate with size was found with this coal than with the higher-rank coals and coke. Ignition rates for the two largest sizes of Illinois coal were even found to be higher than those for the corresponding sizes of the higher-rank Pittsburgh coal, in inches per hour, but in pounds of combustible per square foot and hour, the rates were lower since the average combustible in Illinois coal was only 75.3 per cent, compared to 82.8 per cent for the Pittsburgh coal. Considering this difference in combustible, however, the ignition rates of all sizes of the Illinois coal were relatively high.

As would be expected with a less strongly caking coal, there was less difficulty with caking and poor air distribution with the Illinois coal than with the Pittsburgh coal at the lower air rates, while air rates of 400 lb and higher gave ignition and burning with relatively little caking.

With this coal it was possible to burn the preignited bed at a higher rate than the remainder of the green fuel was igniting; this is the first fuel tested in which the burning rate exceeded the rate of ignition, even for short periods. Due to heat-output limitations of the igniting hood, it was necessary to secure initial ignition at moderate air rates in all tests, then to raise the air rate after the hoods had been shifted, thus simulating a zoned stoker. At the time of starting the high air rate therefore there was approximately 1 in. of preignited fuel at the top of the bed. With the Illinois and lower-rank coals, the high air rate burned this preignited layer at a faster rate than the fuel beneath was igniting, thereby rapidly diminishing the thickness of the burning layer. As this layer burned thin, an increase was noted in the ignition rate, giving a curve of rate of

travel of ignition having two distinct slopes. The reasons for this appear to be as follows.

Thermocouple records, gas analyses, and instantaneous CO_2 indications by meter definitely have indicated a thin zone of high-temperature burning immediately above the ignition plane. In this primary oxidation zone the oxygen is almost, if not entirely, converted to carbon dioxide. Above this relatively thin, high-temperature, high CO_2 zone, CO begins to appear as the percentage of CO_2 and the temperature of the fuel bed drops, that is, when certain temperatures and burning depth or time of contact are established in the primary oxidation zone, reduction of CO_2 to CO by reaction with the hot carbon of the fuel at the upper edge of the zone lowers the fuel temperature there to some relatively stable narrow range which prevails in the remainder of the bed above the hot zone. When relative equilibrium has been established between this hot zone and the cooler reducing zone above it, ignition into the green fuel will be a function of the temperature of the hot zone.

If the reactivity of the fuel is such that the cooler reduction zone is burned off, leaving a layer of ash rather than hot carbon

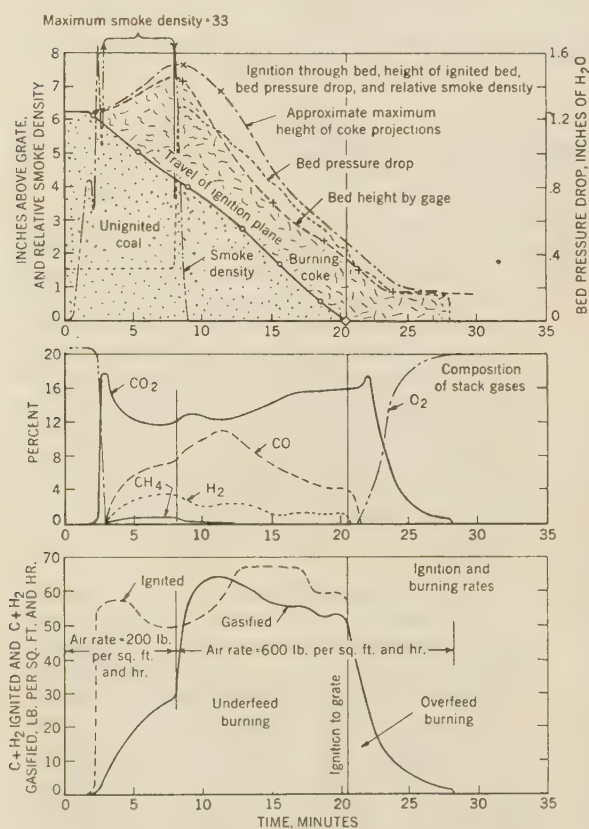


FIG. 20 LOG OF TEST WITH $3/4 \times 3/8$ -IN. HIGH-VOLATILE C BITUMINOUS COAL FROM ILLINOIS

above the primary oxidation zone, CO of course will not be formed, the temperature of the hot zone will not be restricted by the reduction reaction, and the hot zone and ash above it will increase in temperature if furnace temperatures are high enough to prevent excessive radiation from the ash layer. Then the rate of ignition, being a function of the temperature of the primary oxidation zone, will increase, giving ignition curves

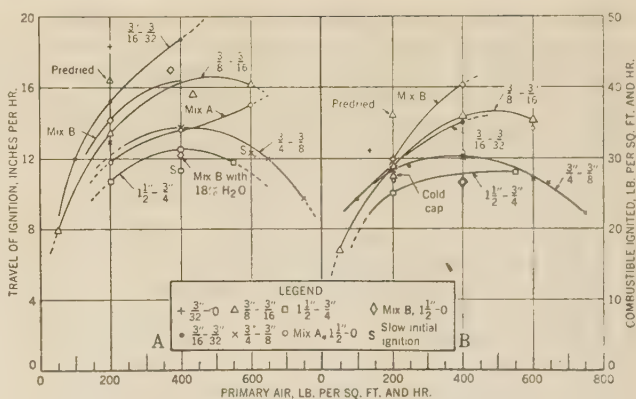


FIG. 21 EFFECT OF SIZE ON A, RATE OF IGNITION TRAVEL; AND B, RATE OF IGNITION IN 6-IN.-DEEP BEDS OF SUBBITUMINOUS B COAL

with two slopes. While this effect was first noted in a few tests with the Illinois coal, it became very pronounced with lower-rank coals.

The log of a test using $3/4$ -in. \times $3/8$ -in. Illinois coal with initial ignition at a 200-lb air rate and ignition through the lower two thirds of the bed with a 600-lb air rate is shown in Fig. 20. It should be noted that, as the depth of burning bed decreased, CO_2 increased, CO decreased, and the ignition rate increased slightly.

Subbituminous B Coal. Ignition rates for 6-in beds of Colorado subbituminous B coal are shown in Fig. 21. Effect of decrease in rank and in percentage of combustible are evident, as practically all the rates of ignition are below 20 in. per hr and 40 psf and hr of combustible ignited.

The curves shown are applicable only for 6-in-thick beds, however, as the rate of ignition varies during travel through the bed except at very low air rates. This fuel, being more reactive than higher-rank fuels, burns to a very thin bed at moderate as well as at high air rates, as previously described, after which the rate of ignition depends largely upon temperature of the surfaces to which the fuel bed loses heat. If such surfaces are hot, and radiation from the bed top therefore is not excessive, the rate of ignition will increase when the bed burns thin, giving an ignition curve with two slopes, in which ignition in the lower portion of a 6-in. bed will be at a more rapid rate than in the top. Under these conditions, the most rapid average rate of ignition will be obtained with deep beds, and, since the burning layer is very thin, there will be little fuel to be burned after ignition reaches the grate. It appears, therefore, that most satisfactory operation with low-rank fuels should be obtained in refractory-lined furnaces with deep beds and with stoker speeds slowed to give ignition to the grate just ahead of the rear bridge wall. Best results with low-rank fuels would be expected in a refractory-lined furnace with a long, low, refractory rear arch.

A comparison of the strikingly different conditions of ignition and burning in beds of $3/8$ -in. \times $3/16$ -in. high-volatile A bituminous coal and of subbituminous B coal is given in Fig. 22, which shows ignition and maximum underfeed burning rates for these fuels. Up to an air rate of 600 lb, ignition rate exceeds burning rate for the high-volatile coal, and therefore the depth of burning fuel would tend to increase as ignition proceeded through the bed. With the subbituminous coal, however, equilibrium burning, that is, ignition and burning at the same rate, is reached at an air rate of 250 lb; therefore, at air rates in excess of this, burning can proceed at a higher rate than ignition only if preignited fuel is available. This accounts for the thin layers of burning fuel in beds of this coal when using moderate to high air rates.

The higher reactivity of the subbituminous coal, as compared to the high-volatile A bituminous coal, is indicated by the higher burning rates of this coal at air rates below 250 lb, that is, in the range where the burning rate is not affected by ignition rate.

Lignite. Raw lignite, the lowest-rank fuel used in this investigation and containing only 43.4 per cent combustible, gave ignition rates under 20 in. per hr and 30 psf and hr of combustible ignited, as shown in Fig. 23. Under the test conditions, no gain is indicated for the use of air rates in excess of 250 psf and hr for the raw lignite, although no sharp drop in the rate of ignition is indicated at higher air rates. This fuel is more reactive than the subbituminous coal, and there is less difference between ignition

and burning rates with the lignite than with the subbituminous coal, even at air rates under 200 psf and hr. Since ignition and burning proceed at nearly the same rate, even at low air rates, an appreciable layer of preignited fuel is not developed at the initial air rate, as was the case with the higher-rank fuels. Consequently, when the air rate is increased, there is little, if any, preignited fuel to burn off at high "overequilibrium" burning rates, and the rate of ignition travel therefore is not accelerated by such high burning rates and by the hot furnace walls resulting from them. Instead of an ignition curve having two distinct slopes, therefore, as found with subbituminous coal, the lignite gave two general types of ignition curves at moderate to high air rates. In one type, enough heat was generated during the test to increase the temperature of the furnace walls gradually, and the hotter the furnace, the more rapid the ignition rate became. In the other type, ignition and burning were just barely maintained in a thin layer, but the amount of energy available was not enough to raise the furnace walls to visible red heat. In this type, ignition proceeded at a substantially constant rate.

The first type of ignition curve indicates that in a continuously operating traveling-grate furnace, where refractories can be brought up to and maintained at a high temperature, substantially higher ignition rates can probably be obtained than were possible under the test conditions, where the furnace walls initially were relatively cold.

The steam-dried lignite did not have a much more rapid rate of ignition travel, in inches per hour, than did the raw fuel, but the ignition rate of the dried lignite in pounds of combustible ignited was roughly double that of the raw lignite. Unfortunately, only a few tests could be made with the limited quantity of dried lignite available. Since, with this highly reactive fuel, burning rates are limited by the rate of ignition at moderate to high air rates, doubling the ignition rate will permit a proportional increase in burning rates.

CONCLUSIONS

Ignition through fuel beds on traveling-grate stokers is essentially unrestricted underfeed; therefore, until ignition reaches the grate, ignition and burning proceed according to unrestricted underfeed principles. At constant air rate, underfeed ignition proceeds through the bed at a steady rate unless certain factors alter air distribution or bed characteristics. These factors include: Development of blowholes, with consequent maldistribution of air; turbulence or "boiling" of the bed, which may give mechanical mixing of ignited and unignited fuel; slow initial ignition; drying of moist coal before ignition; heating of coal with preheated primary air; and burning of highly reactive fuels in very thin burning layers.

After ignition reaches the grate, burning is overfeed, and increase of air rate will give proportional increase of burning rate, at least within the range where stable bed conditions prevail.

Slow initial ignition of the top layer of fuel on traveling-grate stokers is followed by relatively slow rates of ignition travel through the bed, being slowest at the top, increasing with progress of ignition into the bed, and tending to approach, as ignition nears the grates, the steady, higher ignition rates found with rapid initial ignition.

Moisture is necessary to "temper" small-size fuels and, by agglomerating the fines, increase bed stability, but such moisture tends to retard the rate of ignition. The amount of "tempering" moisture added should therefore be held to the minimum necessary to obtain adequate bed stability.

There is an optimum size of particle which will give maximum rate of underfeed ignition with the higher-rank fuels. As shown in this investigation, the average round-hole screen size for this optimum ranges between $1/8$ in. and $5/16$ in. diam.

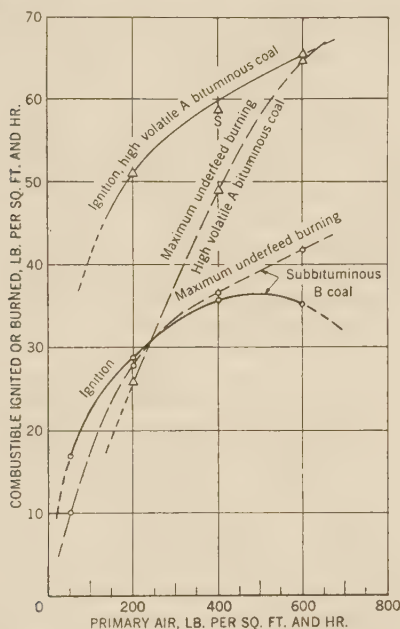


FIG. 22 RATES OF IGNITION AND MAXIMUM UNDERFEED BURNING WITH 6-IN-DEEP BEDS OF HIGH-VOLATILE A BITUMINOUS AND SUBBITUMINOUS B COALS, $3/8 \times 3/16$ IN.

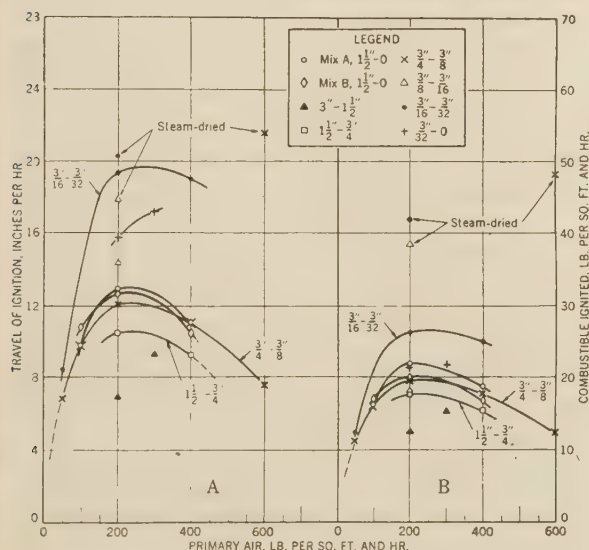


FIG. 23 A, RATE OF TRAVEL OF IGNITION; AND B, IGNITION RATE IN 6-IN-DEEP BEDS OF RAW AND STEAM-DRIED LIGNITE

Rate of underfeed ignition is increased by preheating the primary air approximately in proportion to the rise in temperature of the fuel. Such increase is proportionately greater at high than at low air rates. With preheated air, extremely high ignition rates are possible at air rates high enough to give physical mixing of ignited and unignited fuel, once a layer of fuel has been ignited.

Coal of low ash content has higher rates of ignition travel than similar coal of high ash content, and high ignition rates may be obtained with a much wider range of air rates with the low-ash coal. Burning rates, however, are not materially affected by moderate variation of ash content, and there is some indication that a nominal amount of ash tends to increase bed stability after ignition reaches the grates. Consequently, average burning rates do not vary widely for the usual variation of ash content at normal air rates.

High underfeed rates of ignition may be obtained with high-temperature coke, but only over a relatively narrow range of air rates. Ignition rates drop very rapidly with increase of air rate over the optimum.

Ignition rates as high as those with high-temperature coke may be obtained with anthracite, and the range of air rate giving high ignition rates is broader.

High-volatile bituminous coals give high ignition rates over a very wide range of air rates, but the highly caking types give trouble with air distribution at low air rates.

Subbituminous coals and lignite may be used with a wide range of air rates, but ignition rates are substantially lower than those of the higher-rank fuels. Because the layer of burning fuel tends to become very thin with these fuels, their ignition and burning rates are affected by thermal conditions in the furnace; therefore, maximum rates would be expected in refractory-lined furnaces operated with high wall and arch temperatures.

ACKNOWLEDGMENTS

This problem was initiated in 1938, by the late P. Nicholls, former supervising engineer of the Fuel Section, Bureau of Mines, to whom the authors are greatly indebted for the design of the apparatus, and for supervision and guidance in the early phases of the work. They are also indebted to A. C. Fieldner, Chief, Fuels and Explosives Branch, Bureau of Mines, for his continued interest in and support of the investigation, to David Buslik, Paul Cohen, and J. J. Pfeiffer for assistance in conducting the tests, to Catherine Spargo Barkley for her aid in calculating burning rates, and to Joseph P. Stein for continued work throughout the project in assembling and maintaining apparatus and assisting with the tests. Acknowledgments are given to the Philadelphia & Reading Coal and Iron Company, Philadelphia, Pa., the Pittsburgh Coke & Iron Company, Pittsburgh, Pa., the Bell & Zoller Coal Company, Chicago, Ill., the Pittsburgh & Midway Coal Company, Pittsburgh, Kan., the Clayton Coal Company, Denver, Colo., and the Knife River Coal Mining Company, Beulah, N. D., who contributed fuels used in the tests, and to Dean L. C. Harrington, of the University of North Dakota, who arranged for steam-drying some of the lignite.

Discussion

J. H. KERRICK.⁸ The paper is undoubtedly the most valuable contribution to the study of ignition since the splendid work of Nicholls⁵ and it is certainly to be hoped that the study may be pursued without delay.

⁸ Fuel Engineer, Philadelphia & Reading Coal & Iron Co., Philadelphia 5, Pa. Mem. A.S.M.E.

The following remarks have reference to that part of the work covering anthracite:

The ignition and burning of anthracite on traveling- or chain-grate stokers is perhaps more sensitive to furnace and arch design than any other method of burning, and it would appear that a complete ignition study would necessarily require considerable investigation in the direction of arch and throat design.

Much of the thinking until recent years considered arch design as primarily a provider of radiant heat to the fuel-bed surface. Conclusive evidence now supports the belief that arch design primarily provides control of the travel of the incandescent particles from the rear to the top of the bed of inflowing raw fuel and of the lean gases of combustion for proper intermixture with the rich volatile gases evolved from the raw fuel during the period of temperature rise to the point of ignition.

It would appear that any influence which might aid initial ignition and correspondingly improve the rate of ignition travel would improve the bed conditions in the burning area. Study is now being made of certain design changes as a means of aiding initial ignition with presently indicated favorable results.

While it is recognized that the temperature at which fuels reach their ignition point varies with the ignitibility of the particular fuel, it is important that the initial ignition should not be "pulled away" from the front of the furnace by improper control of flow of ignited particles toward the front of the furnace. Where this condition obtains, there develops a gradual loss of temperature in the bed until ignition is lost completely.

Particularly with reference to anthracite, there is a considerable variation in ignition characteristics. All of the range of ignitibility however is above other coals. It is therefore to be hoped that, in the further study indicated in the paper, some opportunity will be had to examine the range of anthracite ignitibility and its effect on initial ignition.

HENRY KREISINGER.⁹ The paper describes a study of ignition of the fuel on a stationary grate by applying heat by radiation from glo-bar elements. The principal factor studied was the penetration of the ignition from the surface of the fuel bed toward the grate. The apparatus was ingeniously designed so that the rate of heating and the rate of penetration of ignition could be determined accurately. The authors state that the results obtained apply to ignition on traveling-grate stokers.

The question is: To what extent are the results so obtained applicable to commercial installations of traveling-grate stokers? In practically all the traveling-stoker furnaces of recent design the heat for ignition is supplied to the incoming fuel bed by convection. In most cases the radiation factor is negligible and in some cases entirely absent. The arch extends from the rear end of the grate about two thirds of the way to the point where the fuel enters the furnace. The arch functions as a baffle directing the hot gases from the burning fuel toward the front end of the grate where the fuel enters the furnace. The incoming fuel is heated by the sweeping of the hot gases over the surface of the fuel bed and also by particles of burning fuel carried by the hot gases and dropped on the incoming fuel.

The old traveling-grate furnaces had refractory arch over the front part of the grate where the fuel comes in. The arch had to be heated to a bright-red heat before satisfactory ignition was obtained, and there was always the danger of losing the ignition when greater load had to be picked up.

With the rear-arch design the arch does not have to be heated. In fact, in some cases it is completely water-cooled, that is, it is constructed of bare tubes with continuous metal surface with no refractory exposed to the fire. With this design of furnace stable

⁹ Engineer in Charge of Research and Development, Combustion Engineering Company, New York, N. Y. Mem. A.S.M.E.

ignition is maintained at all loads because the faster the fuel is fed to the furnace the more intense is the scrubbing of the hot gases over the incoming fuel and also more burning particles of fuel are carried by the gases and dropped on the front part of the fuel bed.

The fuels usually burned on the rear-arch traveling-grate furnace are small sizes of anthracite, which usually have high moisture content, coke breeze and high-moisture fuels, such as lignites and subbituminous coal. All these fuels are usually difficult to ignite. In the rear-arch furnaces, ignition of these fuels is easily obtained.

RALPH A. SHERMAN.¹⁰ This paper carries on for the Bureau of Mines in the fine tradition of sound work established by Kreisinger, Blizard, and Nicholls. It is a natural corollary to the work on underfeed burning.

One could wish that the work had been available 25 years ago when the traveling-grate stoker was widely in favor, but even now the information can be of much value to those charged with the design and application of these stokers. The optimum rate of air supply in the ignition zone and the length of this zone can be deduced. The steep slopes of the rate-of-ignition curves on either side of the maximum for cokes and anthracite show the desirability of zoning of the air. The extremely variable gas composition over the length of the grate, as shown by Figs. 18 and 20, confirm the work of Shoudy and Mumford and the necessity of a rear arch to mix the oxygen-rich and combustible-rich gases.

Many mysterious effects have been claimed for tempering water, and it is interesting to note that the beneficial effect appears to be from the agglomeration of the fines. There is the suggestion also that the moisture was of some benefit with the Pittsburgh bed coal in reducing the rate of coking. Further discussion of this by the authors would be desirable. This has been suggested by others who have less opportunity to make careful measurements than did the authors in their well-designed equipment.

All will look forward to the publication of the Bureau bulletin on this piece of research as that will include many data impossible to include in the limited space of this paper.

AUTHORS' CLOSURE

The authors are grateful to the discussers for their assistance in pointing out certain phases of this problem that require further explanation.

The importance of ignition of the incoming fuel on traveling-grate stokers by the burning particles blown from the rear to the front end of the stoker is stressed by Mr. Kerrick, who points out that modern considerations of furnace design have led to long flat rear arches to accentuate this effect. In addition, he mentions that the influence of radiation from the front arch in securing initial ignition is now considered of minor importance. Mr. Kreisinger concurs in this belief and states further that in recent designs the heat transferred by convection from the burning gases is chiefly responsible for ignition of the incoming fuel. The authors are well aware of such effects and pointed out early in the paper that ignition occurs either by radiant heat, convection from hot gases, or by deposition of ignited fuel blown from the rear.

In making investigations such as the one reported in this paper, it is always necessary to control as many variables as possible, and to vary those under study in a controllable and logical manner. Further, since an attempt is being made to

place the burning of fuel on the level of a science rather than an art, it is necessary that wherever possible each variable be measured with reasonable exactness. In the case of ignition by the deposition of previously ignited fuel, the experimental difficulties involved in controlling and measuring such a factor would be enormous; when ignition is considered as occurring by heat transferred by convection or conduction from a high temperature stream of gases moving over the surface of the green fuel the difficulties involved in measuring the amount of heat transferred also would be great. However, by utilizing radiant energy, relatively simple laws fix the amount of heat transferred per unit of time and it is possible not only closely to control this energy but also to make fairly accurate measures of the amount received by the igniting fuel. Actually, it is energy that results in raising the temperature of the fuel to the point where ignition occurs, and the source of such energy is unimportant. Thus instead of stating that the igniting hood had a temperature of T degrees to result in a certain igniting effect, we could say that its equivalent of Q Btu per square foot per hour had been transferred to the fuel, and as far as the fuel is concerned this heat energy could have been received by conduction, by convection, or by radiation.

In that part of the study reported here, the amount of heat transferred to the fuel is unimportant except in so far as normal ignition or slow ignition occurred, since it deals with the travel of the plane of ignition through the fuel once ignition at the surface has begun. However, in other studies to be published later, certain variables such as the time for initial ignition are dependent upon this factor, and the points discussed here are directly applicable. Incidentally, it is interesting to note that even in a furnace having a water-cooled arch, radiation from the flame itself may be a significant factor in transferring heat to the incoming fuel, since the column of burning gases passing upward between the front and the rear arch may have sufficient thickness to radiate with a high emissivity. The position of this column of flame usually is such as to be "seen" by the incoming raw fuel.

With reference to Mr. Kerrick's question regarding the ignitability of various anthracites and its effect on initial ignition, that point will be covered in considerable detail in the forthcoming Bulletin of the Bureau of Mines reporting on all the phases of this investigation. Measurements of reactivity by the CIT ignitability method were made on each of the fuels tested, but the correlation with actual ignition characteristics is complex and will be reserved for the future.

The authors agree with Mr. Sherman regarding the desirability of having had these data available during the period when the traveling-grate stoker was being developed most rapidly. However, all the problems involved in the industrial burning of fuels by this method have not been solved, and it is hoped that this information may result in a better understanding of the actions occurring in relatively thin beds. He is correct in that the beneficial effects of tempering moisture result from the agglomeration of the fines, but this subject will be more thoroughly developed in the Bulletin already mentioned.

The suggestion that tempering moisture may have been beneficial in reducing caking with the Pittsburgh bed coal was offered as the most plausible explanation for the fact that, of all the fuels tested, only this particular coal gave a lower rate of ignition travel when dry than when moistened. Because of the many variables involved, only a few tests bearing directly on the effect of moisture were possible, and the complicating effects of caking with this coal added further difficulties. If time permitted, it would be of considerable interest to investigate this phase of water tempering, as the results would be of interest to operators of many types of furnaces.

¹⁰ Supervisor, Fuels Division, Battelle Memorial Institute, Columbus, Ohio. Mem. A.S.M.E.

Prediction of Centrifugal-Pump Performance

By R. J. S. PIGOTT,¹ PITTSBURGH, PA.

The author states that the selection of impeller, diffuser, and volute shapes of centrifugal pump designs are largely empirical, because the theory, based mostly upon the classical centrifugal theory, has been incorrect or at least incomplete. In the prediction of performance of small multistage deep-well pumps, some time ago, the author found another course of analysis which gave promise of excellent results. Essentially, the centrifugal pump does not operate as such except at shutoff but does behave as a radial-flow turbine. Consequently, the performance can be more truly analyzed and the hydraulic losses can be treated as if the pump were a pipe with a shock loss at the pickup edge of the blades and a recirculation loss. This method of prediction is explained and illustrated in the course of the paper.

PRIOR METHOD

IN the long period of centrifugal-pump development the selection of impeller, diffuser, and volute shapes has been largely empirical. The reason is that the theory of action, based mostly upon classical centrifugal theory, has been incorrect or at least incomplete. Professor Sherzer drew attention to this condition (1),² and pointed out that the generally published theory gave a value of shutoff head above what the pump actually yields, and a straight-line decrease to zero at a value beyond the failing value on test.

Some years ago the author had occasion to attempt prediction of performance of small multistage deep-well pumps and found that another course of analysis gave promise of excellent results. It was noted that with the exception of the Rees "Roturbo" design, no so-called centrifugal pump operates as such except at shutoff but does behave as a radial-flow turbine. As a result the performance can be much more truly analyzed and the hydraulic losses can be treated as if the pump were a pipe with a shock loss at the pickup edge of the blades and a recirculation loss, which is akin to a shock loss.

PIPE-FLOW-TYPE LOSSES

Referring to Figs. 1 and 2, the skin friction and bend losses are similar to those occurring in a pipe and respond to the same formulation. We can regard the pipe losses as occurring independent of rotation. Similar calculations made on axial flow in sleeve bearings or in rotary pumps checked by tests show that these losses are substantially unaffected by rotation.

The items to be calculated are as follows:

- 1 Velocity pressure, inlet.
- 2 76-deg bend in eye of impeller.
(a) Rotation loss, hub up to blades.
- 3 Blade passage, friction loss.
- 4 76-deg bend at rim to volute.
- 5 Rotation loss, at rim.

¹ Chief Engineer, Gulf Research & Development Company, Fellow A.S.M.E.

² Numbers in parentheses refer to the Bibliography at the end of the paper.

Contributed by the Hydraulic Division and presented at the Annual Meeting, New York, N. Y., Nov. 27-Dec. 1, 1944, of THE AMERICAN SOCIETY OF MECHANICAL ENGINEERS.

NOTE: Statements and opinions advanced in papers are to be understood as individual expressions of their authors and not those of the Society.

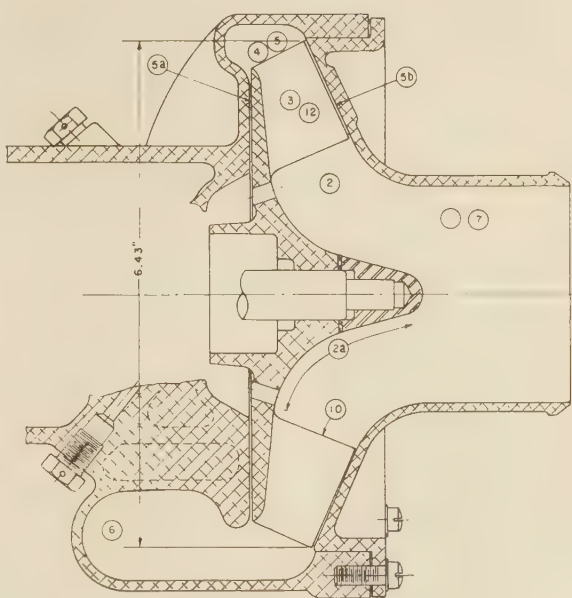


FIG. 1 AXIAL SECTION OF TEST PUMP

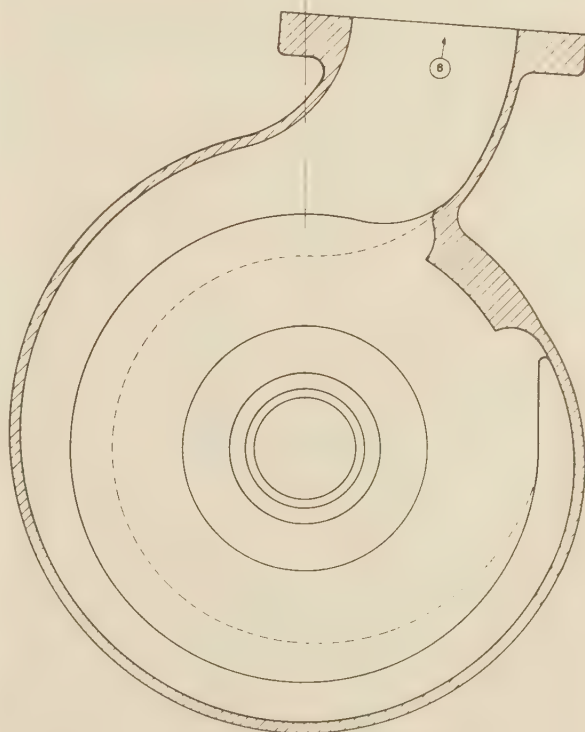


FIG. 2 VOLUTE OF PUMP TESTED

TABLE 1 DETAILS OF PUMP SHOWN IN FIGS. 1 AND 2

Air-free water							
Delivery, gpm.....	0	61.9	165.0	247.5	350.0	450.0	550.0
Circulation.....	28.0	89.4	191.4	273.0	374.2	472.4	569.6
Friction loss:							
Items 2, 3, 4, and 7.....	0.004	0.06	0.33	0.70	1.34	2.06	3.16
Pressure loss:							
50 per cent of pickup shock.....	9.12	7.34	4.82	3.21	1.73	0.82	0.49
Total pressure loss.....	9.12	7.40	5.15	3.91	3.07	2.88	3.65
100 Per cent air release in suction reabsorbed in volute							
Air factor.....	1.00	1.00	1.00	1.00	0.956	0.892	0.735
Friction loss:							
Items 2, 3, 4, and 7.....	0.004	0.06	0.33	0.70	1.40	2.35	4.30
Pressure loss:							
50 per cent of pickup shock.....	9.12	7.34	4.82	3.21	1.81	0.92	0.67
	9.12	7.40	5.15	3.91	3.21	3.27	4.97
Velocity pressure, outlet 8.....	0	0.21	1.51	3.39	6.79	11.21	16.75
Velocity pressure, inlet 1.....	0	0.08	0.56	1.27	2.53	4.18	6.24
Net difference.....	0	0.13	0.95	2.12	4.26	7.03	10.51

- (a) Rotation loss, between shroud and case.
- (b) Rotation loss, between open side of impeller and case.
- 6 Volute friction.
- 7 Outlet-elbow loss.
- 8 Outlet-velocity pressure.
- 9 Kinetic head for flow.
- 10 Pickup shock.
- 11 Static-pressure difference.
- 12 Recirculation loss.
- 13 Leakage.
- 14 Bearing and packing loss.
- 15 Blade-edge rotation loss.
- 16 Compression of released air.

The pipe losses up to the rim of the impeller shown in Figs. 1 and 2 are as follows:

- (a) Inlet-pipe friction from flange to impeller; usually, negligible
- (b) Impeller-blade passage, Item 3
- (c) Bend losses, impeller eye, throat turn, Items 2, 4, and 7.
- (d) Pressure drop due to pickup shock, Item 10.

SHOCK-TYPE LOSSES

There are two principal shock-type losses. The first (Item 10) occurs at the pickup edge of the blades in the eye of the impeller and is occasioned partly by an incorrect angle of blade for any but one flow at each speed and partly by the discontinuity imposed by a finite number of blades.

This loss has not been measured directly and probably cannot be. We can be assured that it is close to the energy loss represented by the difference of the squares of the absolute velocities just before and just after entering the blade passages. It is certain from test data that this energy loss appears partly as a pressure depression at lower flows, the remainder as a torque in the impeller. It is also apparent that it should be highest at shutoff, decrease nearly to zero at that delivery for which the pickup angle is correct, and at higher deliveries increase again. It is probable that for flows larger than the "optimum" this loss would appear only as a torque on the impeller, since there is deceleration on entering the blades instead of acceleration. All this is speculation but we find that some reasonable guesses as to the fractions lost give good correlation.

The only way apparent at this time to account for the remainder of the brake-horsepower input to a centrifugal pump at lower flows than rating, is to assume some recirculation in the blade passages. It is assumed that the impeller tends to pump the optimum delivery, probably that for the best efficiency. It is then assumed that the difference between best flow and actual flow recirculates from the rim toward the eye chiefly on the underside of the blades, as in Fig. 3. This recirculation is not a single closed eddy but returns to the outflow stream in increments distributed down part of the length of the blade. Consequently, the energy loss will be some fraction of that required if the recirculation amount were actually pumped against the full head. For the pump used as an example, 15 per cent was employed in calculating Item 12.

KINETIC HEAD

The kinetic head, or "throwoff" pressure, is simply the vector sum of the blade-flow speed and the rim speed. It is obvious that the radial components of velocity both at the pickup edge and eye are determined by the delivery only and are independent of speed of rotation. Referring to Fig. 4, the throwoff velocity is determined by

$$v_t = \sqrt{(v_r - v_b \cos \alpha)^2 + v_b^2 \sin^2 \alpha} \dots \dots [1]$$

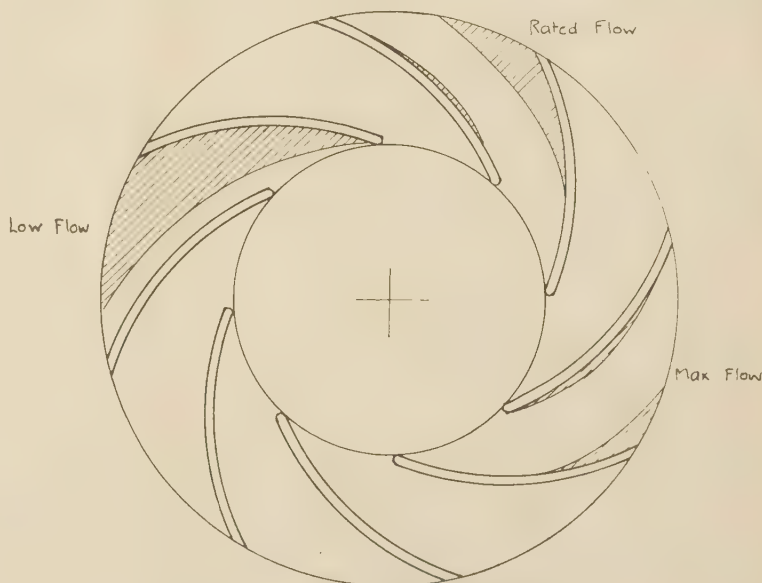


FIG. 3 RECIRCULATION CONDITIONS
(Shaded areas, recirculation; clear areas, delivered flow.)

Throwoff pressure is

$$p_t = 0.000108\rho [(v_r - v_b \cos \alpha)^2 + v_b^2 \sin^2 \alpha] \dots\dots [2]$$

$$v_r = \pi d N$$

$$v_b = \frac{Q}{a}$$

Reducing Equation [1]

$$v_t = \sqrt{\left(v_r - \frac{Q \cos \alpha}{a}\right)^2 + \left(\frac{Q \sin \alpha}{a}\right)^2} \dots\dots\dots [3]$$

where

- v_t = throwoff speed, fps
- v_r = rim speed, fps
- v_b = blade-flow velocity
- ρ = density of liquid, lb per cu ft
- p_t = throwoff pressure, psi
- d = rim diameter of impeller, ft
- N = rotational speed, rps
- Q = flow, cfs
- a = total blade opening area at rim perpendicular to flow

Fig. 5 shows the plot of throwoff pressure versus flow through a section of the impeller. This formulation differs from those given in most of the textbooks which usually include a subtraction of the energy at the pickup edge of the blade, which gives too small a value except at flow for which the blade angle is correct. It is obvious that the impeller is the only source for adding energy, and the only other energy of the liquid is that of the absolute static and kinetic pressure in the inlet of the pump. The maximum energy is at the rim of the wheel. Therefore the total differential added by the impeller will be the difference between that due to the absolute velocity leaving the rim, less the total energy at the inlet pipe. Fig. 5 shows the plot of throwoff pressure, the total internal flow losses (except for the volute), and the static differential pressure, Item 11. Table 1 gives the detail material for the pump shown in Figs. 1 and 2.

VOLUTE EFFECTS

If we now consider that the volute has a friction loss, it becomes evident that the flow through various sections of the

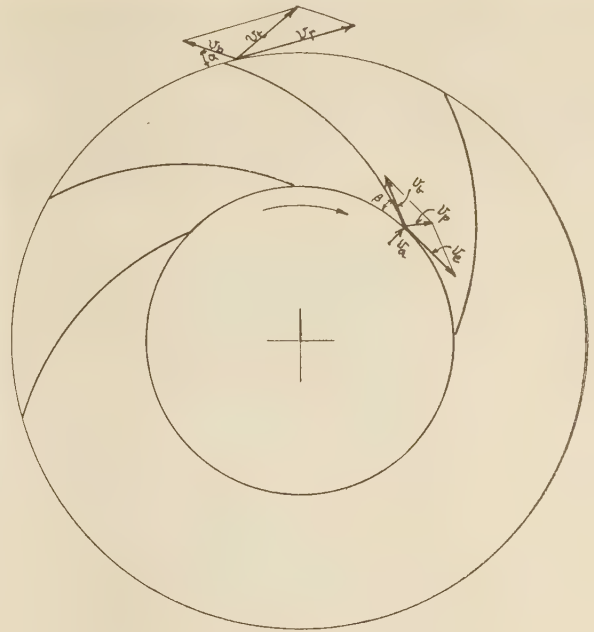


FIG. 4 THROWOFF VELOCITY AND PICKUP SHOCK

impeller cannot be uniform but must begin at a value lower than the mean; and as the pressure falls toward the outlet, the flows through succeeding sectors of the impeller continue to increase toward the outlet. In short, the friction loss in the volute controls the rate of flow from different sections of the impeller and therefore the flow around the impeller cannot be uniform unless the volute friction were zero.

It will be noted that the volute friction is missing from the list of losses previously given, because it occurs *after* throwoff. The first section has to flow against nearly the whole of the volute friction; the second section, against smaller value, and so on. In brief, the volute friction lowers the final outlet head. If the distribution of flow were uniform and the diameter of the volute were

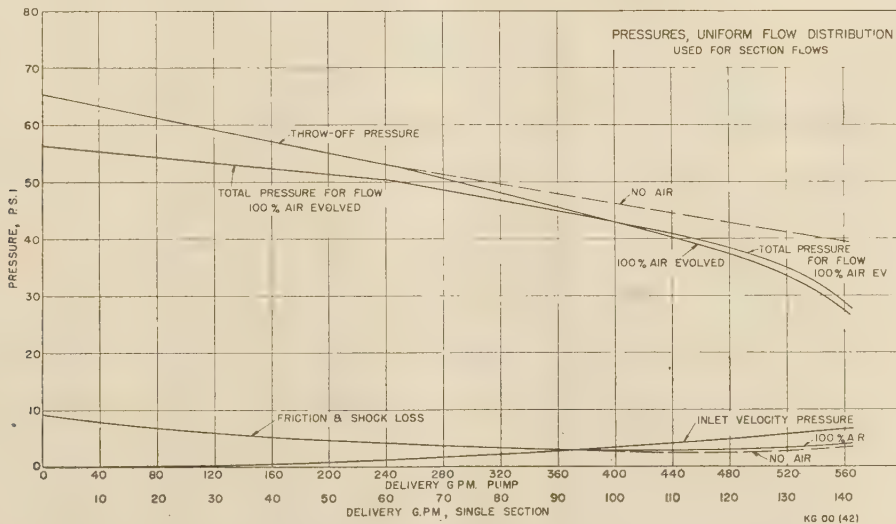


FIG. 5 PRESSURES, UNIFORM FLOW DISTRIBUTION
(Used for section flows.)

a definite function of the angle from the dam, integration to get pressure drop in the volute is not difficult. But we do not know the actual flow distribution beforehand; and such volutes as the author has examined do not appear to be designed on any consistent function of angle or length of volute.

In the pump chosen, for example, the volute equivalent diameter varies as $\frac{\theta}{330}$ for the first 120 deg, and as $\sqrt{\frac{\theta}{330}}$ for the remainder.

The convenient answer for the present is to break up the volute into sections (four appear to be enough), calculate the friction for each section on uniform flow distribution, and use these values in a step-by-step build-up of the flow distribution. Such friction curves for sections are shown in Fig. 6, and the calculation of flow, in Table 2.

A flow is assumed for section 1, concentrated at the middle of the section, and the net kinetic pressure taken from Fig. 5. The friction for this flow from the middle of section 1 to section 2 is ob-

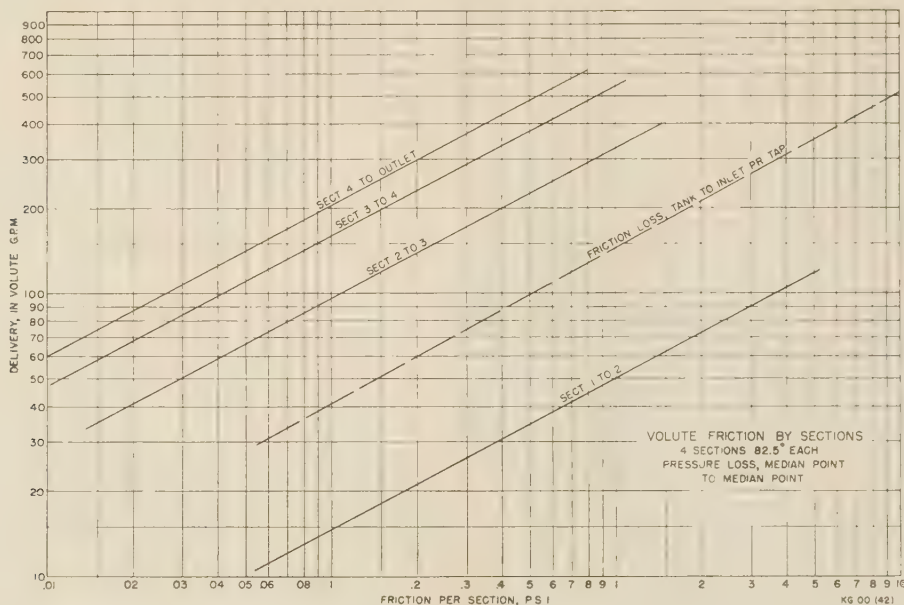


FIG. 6 VOLUTE FRICTION BY SECTIONS
(Four sections 82.5 deg each. Pressure loss, median point to median point.)

TABLE 2 CALCULATION OF FLOW DISTRIBUTION AND PRESSURES

From Fig. 5	No air release				100 Per cent air release			
	Gpm section	Kinetic pressure	Gpm volute	Volute friction, psi	Gpm section	Kinetic pressure	Gpm volute	Volute friction, psi
Section 1	15.0	54.85	15.0	0.11	15.0	54.85	15.0	0.11
	30.0	53.30	30.0	0.39	30.0	53.30	30.0	0.39
	40.0	52.26	40.0	0.66	40.0	52.26	40.0	0.66
	60.00	50.12	60.0	1.42	60.0	50.12	60.0	1.42
	80.00	48.07	80.0	2.44	80.00	46.58	80.0	2.44
	100.00	46.10	100.0	3.70	100.00	42.72	100.0	3.70
Section 2	120.00	44.15	120.0	5.18	120.00	37.60	120.0	5.18
	16.0	54.74	31.0	0.01	16.0	54.74	31.0	0.01
	33.8	52.91	63.8	0.05	33.8	52.91	63.8	0.05
	47.0	51.60	87.0	0.09	47.0	51.60	87.0	0.09
	73.8	48.80	133.8	0.19	73.8	48.80	133.8	0.19
	94.5	46.63	174.5	0.31	93.3	44.14	173.3	0.31
Section 3	139.5	42.40	239.5	0.56	115.5	39.02	215.5	0.47
	16.2	54.73	47.2	0.01	133.5	32.42	253.5	0.64
	34.3	52.86	98.1	0.04	16.2	54.73	47.2	0.01
	47.8	51.51	134.8	0.07	34.3	52.86	98.1	0.04
	75.0	48.61	208.8	0.17	47.8	51.51	134.8	0.07
	98.0	46.32	272.5	0.28	75.0	48.61	208.8	0.17
Section 4	144.0	41.84	383.5	0.53	94.5	43.83	268.1	0.27
	16.3	54.72	63.5	0.01	117.3	38.55	337.8	0.41
	34.8	52.82	132.9	0.05	135.0	31.78	388.5	0.54
	48.8	51.44	169.6	0.07	16.3	54.72	63.5	0.01
	76.3	48.44	285.1	0.19	34.8	52.82	132.9	0.05
	100.8	46.04	373.3	0.32	48.8	51.44	169.6	0.07
Outlet	149.5	41.31	533.0	0.62	76.3	48.44	285.1	0.19
	Gpm	Kinetic pressure	Velocity head	Static pressure	96.0	43.56	364.1	0.31
	63.5	54.71	0.22	54.59	118.5	38.14	455.3	0.46
	132.9	52.77	1.00	51.77	138.3	31.24	526.8	0.60
	169.6	51.37	1.61	49.76				
	285.1	48.25	4.55	43.70				

tained from Fig. 6, subtracted from the kinetic pressure of section 1 to get the pressure subsisting at the center of section 2. The corresponding flow for this pressure is taken from Fig. 5, this flow added to that from section 1, and the friction for this sum found in Fig. 6, for section 2 to 3, and so on to the outlet. This method, while it is an approximation, seems to give quite good correlation with more elaborate methods. It will be noted that the pressure difference available between inlet and outlet is always less than that found merely by assuming uniform flow as in Fig. 5 (used for sections individually).

PICKUP SHOCK

As previously stated, total pickup shock is calculated as the difference in energy between absolute radial velocity in the eye entering the blades, and absolute velocity in the blades immediately at pickup. Referring to Fig. 4, the formulation is the usual one for obtaining absolute velocity in the entry and need not be restated here.

DISSOLVED AIR OR GASES

Little attention has hitherto been paid to the possible effects of evolved air on the head-capacity curve of the pump. Water dissolves about 16 per cent of air by volume N.T.P., and most water handled by centrifugal pumps arrives at the pumps saturated. The cases where practically no gas is present would be those of hot-well or boiler-feed pumps on deaerated water. It appears that the release of this dissolved air has quite an important effect in reducing the head developed by the pump at flows beyond rated capacity and also increases most of the losses.

It has been proved that in turbulent flow the following relation holds: Flow of liquid plus gas

$$\Delta p = \frac{0.000108 \rho v^2 (1 + a)}{d}$$

where a is the air as fraction of liquid volume present. Since velocity will rise as $(1 + a)$ and ρ falls as $\frac{1}{1 + a}$, the effect in the liquid formula for the same flow of liquid is $\frac{(1 + a)^2}{(1 + a)}$ or $(1 + a)$.

Consequently, all passage frictions and bend losses increase as $(1 + a)$. The head developed should fall as $\frac{1}{1 + a}$ and if the entire blade passage flowed full there would be a further reduction of head in a back-laid blade due to the blade-velocity effect on throwoff velocity. But we do not know just what changes do take place although we know that in general, the outlet from the blades does not flow full. In any case the effect is rather slight and for the present has been disregarded.

In the region of air evolution, generally beyond rated flow, the normal liquid head, air free, multiplied by the air factor has been used. Fig. 7 shows the air factor $\left(\frac{1}{1 + a}\right)$ plotted against absolute pressure at 90 F temperature. Temperature is not important except as to vapor pressure, as the solubility of oxygen and nitrogen in water or petroleum oil is not much affected by temperature. Incidentally, the solubility of air in petroleum oils from heavy to light lube oils is about 9 per cent. In gasoline it varies from about 15 to 20 per cent, being highest where aromatics are present. Inspection of Fig. 5 will show that the effect of this evolved air is quite pronounced. The assumptions used in applying the air factor are: No release from 14.7 psi down to 12 psi in inlet (supersaturation); below 12 psi, complete release in the presence of turbulence. No effect on inlet velocity head as no air is yet evolved. No effect on outlet velocity head as all released

air, being in the form of fine bubbles, will be redissolved in the volute under the high pressure.

LEAKAGE

It would seem that leakage can be rather easily calculated. Looking at the leakage path down the back of the impeller shroud, Fig. 1, it is seen that there is a long capillary seal, followed by a chamber with relief holes to suction.

Taking

p_1 = pressure drop across capillary seal, psi

p_2 = pressure drop across relief holes, psi

$p = p_1 + p_2$ = static pressure difference across pump, psi

b = clearance back of shroud, ft

r_1 = outer radius of capillary seal, ft

r_2 = inner radius of capillary seal, ft

a = total area of relief holes, sq ft

$$\rho = \frac{0.000108 f l \rho v^2}{2b} \text{ for a flat slot.} \dots \dots \dots [4]$$

$$v = \frac{Q_1}{a} = \frac{Q_1}{2\pi r b}$$

$$d_p = \frac{0.000108 f \rho Q_1^2}{8\pi^2 b^3 r^2}$$

Integrating

$$p_1 = \frac{1.370 \times 10^{-6} f \rho Q_1^2}{b^3} \left(\frac{1}{r_2} - \frac{1}{r_1} \right) \dots \dots \dots [5]$$

For the relief holes which are sharp-edged, we can use a coefficient $c = 0.60$; then

$$p_2 = 0.000108 \rho v^2 = \frac{0.000108 \rho Q_1^2}{(0.60 a)^2}$$

$$p = p_1 + p_2 = \frac{1.370 \times 10^{-6} f \rho Q_1^2}{b^3} \left(\frac{1}{r_2} - \frac{1}{r_1} \right) + \frac{0.000108 \rho Q_1^2}{(0.60 a)^2} \dots \dots \dots [6]$$

$$Q = \sqrt{\frac{p}{\frac{1.370 \times 10^{-6} f \rho \left(\frac{1}{r_2} - \frac{1}{r_1} \right)}{b^3} + \frac{1.08 \times 10^{-4} \rho}{(0.6 a)^2}}} \dots \dots \dots [7]$$

For a given pump where all dimensions required are known and the passage is small so that $f = 0.054$, this becomes merely

$$Q = K \sqrt{\Delta p}$$

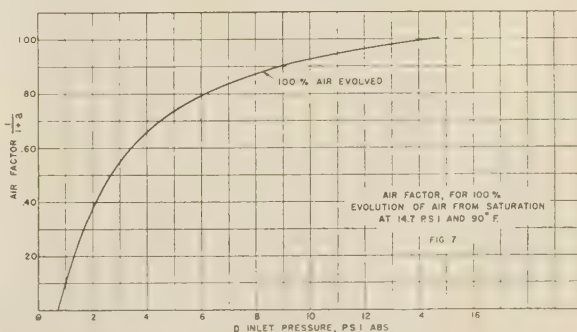


FIG. 7 AIR FACTOR FOR 100 PER CENT EVOLUTION OF AIR FROM SATURATION AT 14.7 PSI AND 90 F

Similar setups can be made for any other physical arrangement. For sealing rings, likely the flow may get into the viscous region and the appropriate formulas should then be used. The open side of the impeller does not afford a leak as the velocity developed in the pump impeller opposes it. If the pump impeller is shrouded on both sides there will be two leak paths. Both must then be calculated.

INPUT HORSEPOWER

The input horsepower consists of the following:

- 1 Water horsepower (Whp) on delivery plus leakage, (displacement).
- 2 Rotation losses, Items 2(a), 5, 5(a), 5(b).
- 3 Remainder of pickup shock energy not accounted pressure drop, Item 10.
- 4 Work done by blunt edge of blades, Item 15.
- 5 Recirculation, Item 12.
- 6 Compression of released air, Item 16.
- 7 Bearings and packing, Item 14.

Water horsepower on delivery is calculated on the pressures and flow, Table 2, by sections, as the water horsepower calculated on total flow and pressure difference between inlet and outlet is too low, especially at the higher flows.

Rotation losses are calculated for both sides of the impeller, for the breadth of the rim and the hub by the following formulas

$$\text{Disk: } \text{Hp} = 6.885 \times 10^{-5} f \rho N^3 (d_1^5 - d_2^5) \dots [8]$$

$$\text{Cylinder: } \text{Hp} = 6.885 \times 10^{-4} f \rho w d^4 N^3 \dots [9]$$

where

N = rotational speed, rps

ρ = density, lb per cu ft

f = friction factor

d_1 = outer diameter disk, ft

d_2 = inner diameter disk, ft

d = diameter cylinder, ft

w = width of cylinder face, ft

Inspection of Equation [9] shows that since b , the clearance, does not appear directly, the rotation loss of front and rear sides of the impeller will differ only because of difference in f . It is well known that

$$f = \frac{C}{R^n} \text{ and } R = \frac{2bv\rho}{\mu} \text{ for a slot}$$

so that f does change from shroud to open side. The value of b is very small behind the shroud but quite large for the open blade passage. For the example given in Fig. 1, at 3585 rpm:

	b , ft	hp	R	f
Shroud side.....	0.00167	1.244	74000	0.054
Open side.....	0.050	0.737	2443000	0.0191
Rim.....	0.0546	0.800	2594000	0.0142
Hub.....	0.0735	0.001	596000	0.0170
Total.....		2.782		

To split hairs, we should integrate for Equation [8], with the value $\frac{C}{R^n}$ substituted for f , but it is not worth the trouble. Most of the work is done near the outer diameter of the disk and a value of f from R at the outer diameter is good enough.

One half the pickup shock was treated as a pressure drop affecting head losses, the other half can be obtained simply by multiplying the remaining imaginary pressure by gallons per minute circulation and by 0.0005833 which will yield horsepower.

TABLE 3 CALCULATED RESULTS COMPARED TO TEST VALUES

	For sections						
Delivery, gpm.....	0	61.9	165	247.5	350	450	550
Leakage.....	28.0	27.5	26.4	25.5	24.2	22.4	19.6
Total flow.....	28.0	89.4	191.4	273.0	374.2	472.4	569.6
	No air released						
Throwoff pressure at outlet.....	65.54	62.14	56.80	52.66	47.82	43.63	39.85
Losses.....	9.12	7.40	5.15	3.91	3.07	2.88	3.65
Impeller differential.....	56.42	54.74	51.65	48.75	44.75	40.75	36.20
Inlet velocity pressure.....	0	0.08	0.56	1.27	2.53	4.18	6.24
Net kinetic pressure for flow.....	56.42	54.82	52.21	50.02	47.28	44.93	42.44
	100 Per cent air released						
Throwoff pressure.....	65.54	62.14	56.80	52.66	45.92	38.90	29.28
Losses.....	9.12	7.40	5.15	3.91	3.21	3.23	4.97
Impeller.....	56.42	54.74	51.65	48.75	42.71	35.67	24.31
Velocity head.....	0	0.08	0.56	1.27	2.53	4.18	6.24
Net pressure for flow.....	56.42	54.82	52.21	50.02	45.24	39.85	30.55
	Outlet pressures as reduced by nonuniform distribution and 100 per cent air released						
Net pressure for flow.....	56.42	54.74	51.88	49.46	44.04	38.00	26.20
Outlet velocity head.....	0	0.21	1.51	3.39	6.79	11.21	16.75
Static differential.....	56.42	54.53	50.37	46.07	37.25	26.79	9.45
Test.....	55.9	54.9	51.5	46.6	38.2	25.9	6.0
Difference.....	+ 0.52	- 0.4	-1.1	-0.5	-0.9	+0.9	+3.5

TABLE 4 HORSEPOWER INPUT, 100 PER CENT AIR RELEASE

	0	61.9	165	247.5	350	450	550
Delivery, gpm.....	0	61.9	165	247.5	350	450	550
Displacement horsepower.....	1.07	3.10	6.38	8.67	10.56	11.68	11.54
Rotation loss.....	2.78	2.77	2.76	2.76	2.75	2.62	2.38
Blade.....	0.19	0.19	0.19	0.19	0.19	0.17	0.14
Bearings and packing.....	0.50	0.50	0.50	0.50	0.50	0.49	0.49
Pickup shock.....	0.15	0.38	0.54	0.51	0.38	0.23	0.16
Recirculation.....	1.59	1.28	0.80	0.45	0.17	0.0	0.0
Air compression.....	0.30	0.78	1.10
Total.....	6.28	8.22	11.17	13.08	14.85	15.97	15.81
Test.....	6.30	8.15	11.11	13.03	14.78	15.88	15.45
Difference.....	-0.02	+0.07	+0.06	+0.05	+0.07	+0.09	+0.36
Delivery water horsepower.....	0	1.98	4.94	6.96	8.47	8.88	6.40
Efficiency, calc.....	0	24.0	44.2	53.2	57.1	55.6	40.5
Efficiency, test.....	0	24.3	45.4	53.9	58.7	54.5	34.4
Difference.....	0	-0.3	-1.2	-0.7	-1.6	+1.1	+6.1

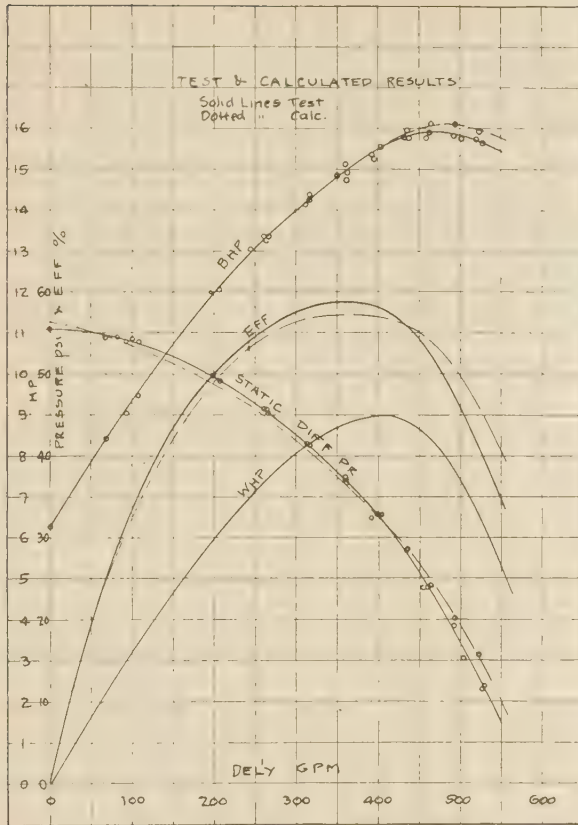


FIG. 8 TEST AND CALCULATED RESULTS
(Solid lines, test; dotted lines, calculated.)

The edges of the blades, while rounded, nevertheless have a finite section and must be ploughed through the liquid at eye-diameter speed; this resistance will add a torque to the impeller.

For recirculation calculation, the best flow was guessed at 450 gpm as being probable. It turned out from tests completed later that the best point of efficiency is about 375 gpm, highest water horsepower at 400 gpm. Water horsepower, calculated for each flow as described, was subtracted from the 450-gpm value, and 15 per cent of this difference was used as the recirculation horsepower. Inspection of Thoma's pictures and consideration of many tests indicated that in reasonable designs the recirculation loss cannot be much higher, and for large pumps may be less.

When air is released it is at the suction-side pressure and must be compressed to the pressures subsisting in the volute. The usual isothermal formula was used, since the air is in intimate contact with the liquid. The horsepower required is surprisingly large but the released air at 550 gpm and 5 psia inlet is about 36 per cent of the liquid volume.

Many diagrams of pressure through pump impellers, based on centrifugal force, indicate a considerable rise of pressure in the impeller toward the rim. We cannot subscribe to this idea because the curvature and absolute velocity of the water are always much less than that of the impeller rotation, with a laid-back blade. With the analysis adopted herein, there should be no appreciable rise of pressure in the impeller as the energy addition is all kinetic. There should therefore be little or no rise until the volute converts the throw-off speed to pressure.

Bearings are estimated from Dr. Styri's data on ball bearings

not flooded with liquid and the packing is a Cook seal type calculated on a friction coefficient of 0.005.

Tables 3 and 4 give the calculated results compared to test values, and Fig. 8 shows the comparative plot.

All the foregoing estimates of losses might appear rather drastically empiric; but so have the preceding usual methods. So far as head is concerned, it appears much closer to calculate the head on radial-turbine methods than on an inaccurate use of centrifugal force. Obviously, water horsepower is more accurately calculated on the real difference in pressure in different parts of the volute, on a realistic distribution of flow, than on assumed uniform distribution, and no recognition of the very considerable loss in the volute. Rotation loss and leakage do not seem to have received any but empirical attention. The formulas for rotation loss and leakage given herein are rigorous. The recognition of evolved air effects accounts for the sharp fall-off at high flows.

In so far as pressure drop due to pickup shock is concerned, we get a good check on the value by test. It will be noted that the pickup edge angle as designed is not yet correct at maximum flow. We designed a propeller mounted on the hub and designed

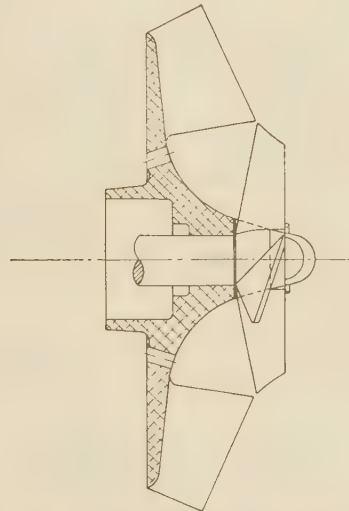


FIG. 9 AUXILIARY PICKUP IMPELLER

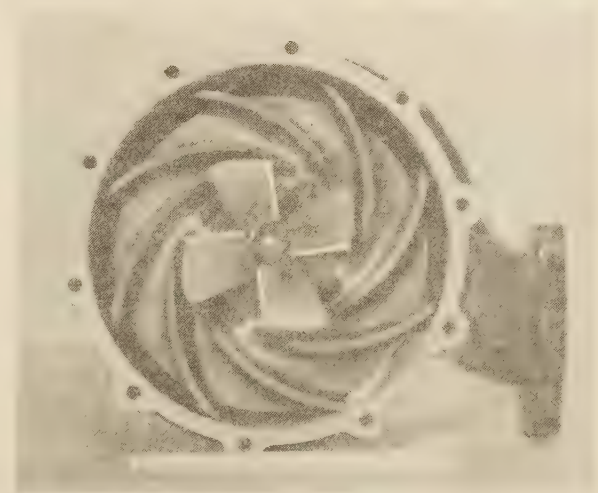


FIG. 10 PROPELLER ADDITION

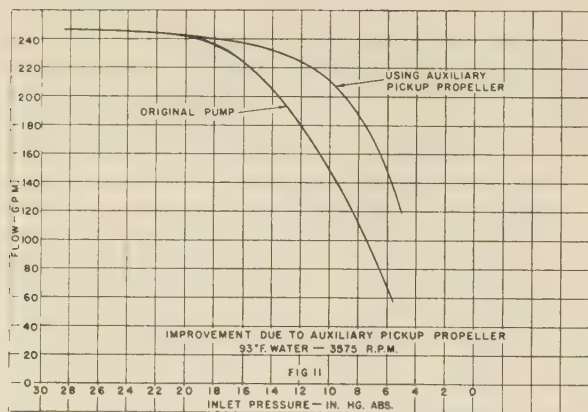


FIG. 11 IMPROVEMENT DUE TO AUXILIARY PICKUP PROPELLER
(93 F, Water; 3575 rpm.)

for correct angle at 247.5 gpm delivery. Figs. 9 and 10 show the general arrangement. Fig. 11 shows that the gain was 5 in. hg, or just under 2.45 psi for the cavitation point, and the calculated loss was 3.21 psi.

This method was tried out in rougher form on several pumps, but on the example chosen we had very complete tests and could make a fairly close check.

Some points for design are evident from this method of attack:

- 1 The pickup edge of the blades has an important effect upon the cavitation point, of value in the design of hot-well or high-altitude circulating pumps for aviation.
- 2 It should be possible to determine the optimum number of blades with less uncertainty.
- 3 The volute needs careful study for lower losses; most of those examined are much too small in area at the early sections.
- 4 A reasonable amount of research on impellers should fix the recirculation losses.
- 5 No doubt high-grade designers know most of what is given in this paper but the evidence is that a large number of commercial centrifugal pumps are still designed by the "whittle" method.

We propose to check pumps as opportunity occurs, as undoubtedly much more evidence to establish the value of some of the factors is needed. But in this case the correlation was good enough to encourage the author to present the method for what it may be worth.

BIBLIOGRAPHY

- 1 "New Theory for the Centrifugal Pump," by Allen F. Sherzer, Trans. A.S.C.E., vol. 93, 1929, p. 15.
- 2 "Centrifugal Pump Performance as Affected by Design," by R. T. Knapp, Trans. A.S.M.E., vol. 63, 1941, pp. 251-260.
- 3 "Investigations of the Flow Conditions in a Centrifugal Pump," by K. Fischer and D. Thoma, Trans. A.S.M.E., vol. 54, 1932, pp. HYD-54-8, pp. 141-155.
- 4 "A New Method of Separating the Hydraulic Losses in a Centrifugal Pump," by M. D. Aisenstein, Trans. A.S.M.E., vol. 50, 1928, HYD-50-2, pp. 1-7.
- 5 "A Method of Analyzing the Performance Curves of Centrifugal Pumps," by J. Lichtenstein, Trans. A.S.M.E., vol. 50, 1928, HYD-50-3, pp. 1-16.

Discussion

R. W. ANGUS.³ This paper attacks the centrifugal-pump problem from an unusual angle and gives some matters for consideration. The pump used in the experimental work was of a

design from which high efficiency could not be expected; and it actually gave less than 60 per cent. under test. Under such conditions the writer does not believe any theory can be satisfactorily checked, because the losses are so high. Perhaps the author will report later on an efficient pump.

The author casts doubt on the accuracy of generally accepted theories of the centrifugal pump, because he says the calculated results do not agree with the test ones, and cites the shutoff pressure as an example. It should be pointed out that the theory is based on certain conditions assumed to exist in the pump and if these assumptions are wrong, then the application of the fundamental laws of dynamics to the case will lead to a wrong result. But to take the case of the shutoff pressure, no one knows what happens in a pump with the discharge valve shut, and without such knowledge it is impossible to apply any laws to calculate the pressure reached.

Many years ago the writer worked out a theory which took into account the conditions in the pump when delivering at any rate of flow, whether the most efficient one or not. Starting with the well-known equation, usually attributed to Euler, then the power per pound of discharge per second, put into the water is $(c_2 u_2 - c_1 u_1)/g$ where u_2 and u_1 are, respectively, the rim speeds at the exit and entry of the impeller, and c_2 and c_1 are, respectively, the circumferential components of the absolute water velocities just before exit from and entry to the impeller.

By adding this head, having due regard to signs, to the friction losses in the suction pipe, impeller, guide ring, and spiral casing, and to the shock losses throughout the pump, a very simple relationship, in the form of a quadratic equation, is found between the physical dimensions of the pump and its speed, discharge, and head. The writer hesitates to give this somewhat long expression. The shock losses are not, of course, given by the author's method of taking the square of the difference of the absolute velocities, but the square of the vector difference of these velocities. This method of approach may be found in some old books on centrifugal pumps.

That the designers of pumps are working on satisfactory theory is proved by their product and the writer has found that the so-called classical theory has, when properly applied, given accurate results in many cases he has tried.

The writer can hardly conceive of the state of affairs referred to under the first paragraph on "Volute Effects." The word "dam" seems quite appropriate to the obstruction which prevents the water leaving the impeller at this point but few pumps have such a dam and there seems no reason for it. The accelerations and retardations of the water leaving the impeller, if the author's theory is correct, would undoubtedly produce vibration and trouble.

There are two sources of loss in the volute; the first is a shock loss due to the change in water velocity and direction, and the second is the friction loss in a bent channel. Some years ago the writer was engaged on the problem of design of an intake for a power plant and a brief statement of some of the work done is given in a paper by the writer.⁴ One form tried was a long, straight, submerged pipe, tapered at the outer end, and having a slot parallel to the pipe axis along about three quarters of the outer length of one side, through which the water entered the tube. The entire discharge left through the inner end of the pipe. By arranging guide vanes along the slot, and properly proportioning the latter, the draft per foot length was practically constant throughout the entire length of the slot. The case is exactly analogous to the volute and if the design of it is properly made the combination of shock and friction losses will make the

³ Professor, Head of Mechanical Engineering Department, University of Toronto, Toronto, Canada. Honorary Mem. A.S.M.E.

⁴ "Intakes for Power Plants," by R. W. Angus, Trans. A.S.M.E., vol. 46, 1924, pp. 1131-1164.

flow per linear inch of opening practically constant, which it doubtless is in good pumps.

Under "Leakage" the author discusses flow through the so-called "capillary seal," which does not exist in most pumps. There is usually considerable clearance between the casing and the back of the impeller, and doubtless water is whirling in this space producing variable pressures through it. These must affect the leakage but there seems little chance of evaluating these pressures. Experience is by far the best guide in this matter.

The general turbine theory furnishes a good basis for pump design and recent papers read before the Society show that the same machine may often be used as a pump or as a turbine, without much change in efficiency. From many tests made by the writer he is convinced that the designers of good pumps work along reliable theoretical lines; he finds it difficult to work up much interest in manifestly inefficient pumps.

R. M. WATSON.⁵ In his paper the author presents an interesting method of predicting the performance of a centrifugal pump. It is, as he says, highly empirical. It appears, however, to involve considerably more work than is usually applied using the so-called more rational methods based on the classical theory.

It is fortunate that occasionally individuals do rise to challenge the design methods based on the classical theory of Euler; such challenges force the designers into a more critical analysis of the basis of the theory and its use.

In the introductory paragraph the author states that the classical theory is incorrect or at least incomplete. Unfortunately, this concept has been fostered even by many centrifugal-pump and compressor designers who have blindly applied the formulas developed for an idealized flow to the actual pump or compressor, without consideration of the points of deviation which occur. For instance, the classical Euler theory sets up a relation between the energy transferred between the impeller and the fluid, based on the rate of change of moment of momentum of the fluid from the inlet to the discharge of the impeller. The relation is based on the actual absolute velocities and radii of the fluid and impeller at the inlet and discharge. This relation is absolutely correct, whether the hydraulic machine is a turbine, a centrifugal pump, a centrifugal compressor, or an axial-flow-type machine.

Unfortunately, many engineers have applied or rather misapplied this theory by assuming that the fluid flow follows the vane angle at discharge and that the velocity distribution is uniform across the vane channel, conditions which obviously could hold only for an infinite number of vanes. For a finite number of vanes, the pressure difference across the flow channel in the impeller, which results from the energy transfer between the impeller vanes and the fluid flowing, would naturally deflect the flow at discharge in such a direction as to reduce the absolute velocity and, consequently, the head at discharge. Refer to Figs. 12, 13, and 14 of this discussion in illustration of these points. This was predicted, based on the Euler theory, by Daugherty⁶ more than 20 years ago. This deflection was measured and verified by the investigations of Knapp and Binder in their work at the California Institute of Technology.⁷

Attempts have been made to give mathematical expression to the magnitude of this deflection principally based on the

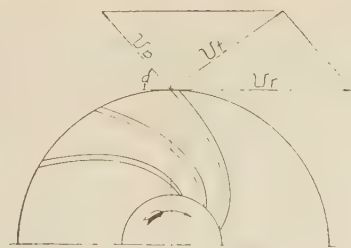


FIG. 12

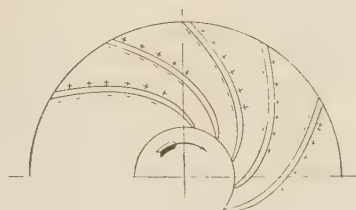


FIG. 13

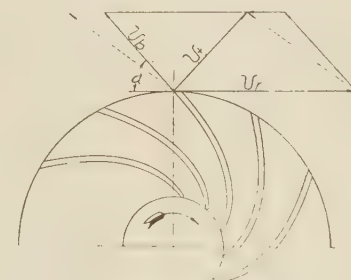


FIG. 14

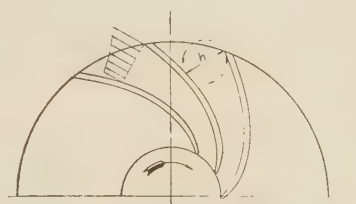


FIG. 15.

assumption that the flow in a centrifugal pump is irrotational, see Fig. 15 of this discussion. Probably the expression developed by Stodola is most usable. At other than the design conditions of the hydraulic machine, the Euler theory could still be applied were one to know the true flow conditions rather than, as is the usual practice, making simplifying assumptions for the purpose of easing the mathematics involved.

Unfortunately, at a given speed, any design is correct for only one rate of flow. As pointed out by the author, the rate of change of volute area is either too slow for rates of flow greater than design, or too rapid for rates of flow less than the design rates. This accounts to a large extent for the rather sharp peak at the design point which occurs in the efficiency curve for a pump. Incidentally, many designers, in an attempt to make a pump useable over a wide range of capacities, frequently depart from volute designs which would follow a simple law, to produce efficiency curves which are flat over a relatively wide range of flow rates. This, in many designs, would account for the difficulty the author

⁵ Chief Engineer, Centrifugal Division, Worthington Pump and Machinery Corporation, Harrison, N. J. Mem. A.S.M.E.

⁶ "Centrifugal Pumps," by R. L. Daugherty, McGraw-Hill Book Company, Inc., New York, N. Y., 1915.

⁷ "Experimental Determinations of Flow Characteristics in Volute Centrifugal Pumps," by R. C. Binder and R. T. Knapp, Trans. A.S.M.E., vol. 58, 1936, pp. 649-661.

had in finding a consistent mathematical expression which the volute areas would follow from the tongue to the discharge.

It is interesting to note that it is frequently easier over a wide range of flow to develop an empirical formula to fit the characteristic of an inefficient pump than that of an efficient pump. This is because of the relatively high state of turbulence in an inefficient pump which irons out the sudden changes in flow patterns in the pump inlet and volute which tend to occur with changing rates of flow. Assuming that the tests of the pump shown in the author's Fig. 8 were run at 3585 rpm, we could expect about 75 per cent efficiency for a pump properly designed for the conditions of service shown rather than the 59 per cent produced by the pump analyzed.

The inefficient pump thus produces a head-capacity curve which is much easier to express by empirical mathematics than one which is so efficient that the sudden flow changes show up in the shape of the characteristic curves as abrupt changes of shape.

For instance, it is believed that it would be difficult by the author's method or Professor Sherzer's theory, to which paper (1) the author refers, to predict or explain the performance of pumps giving the curves of the types shown in Fig. 16 of this discussion.

While it is not easy to predict the performance from shutoff to maximum capacity, a proper understanding and application of the classical theory combined with modern theory of fluid flow does offer an excellent means for explaining the phenomena observed and for adopting design features which will produce, within limits, various characteristics as desired.

It should be emphasized here that the classical Euler theory is developed for the impeller only. For the uniform discharge around the periphery of the impeller, and the normal flow angles to be realized, it is important that for each rate of flow the inlet angles of the impeller blades should match the actual flow angles, and the rate of area change in the volute should match the rate of flow. For any actual pump this can occur at only one rate of flow and for carefully designed inlets. To apply the Euler theory under any other conditions is to ignore the departures from the usually assumed flow angles and uniform flow rate which are impressed on the flow by the unmatched volute and inlet angles.

Unfortunately, the paper does not include dimensional data on the pump analyzed. This makes the reasoning somewhat difficult to follow.

Equation [1] in the paper is merely the trigonometric relation between the various vectors drawn at the discharge of the impeller. It expresses the absolute velocity at discharge in terms of the impeller areas, the rate of flow, and the peripheral velocity of the impeller. From this relation the author computes the "throw-off pressure" as a velocity head multiplied by the density. This seems to be the only part of the head developed which the author is willing to recognize. This impression is strengthened by later comments to the effect that no rise of pressure should occur, by the author's analyses, in the impeller. However, in a well-designed normal impeller, the absolute velocity at discharge is only about 50 per cent of the peripheral velocity of the impeller. By the Euler theory this would mean that the head produced by the impeller as velocity head only would be only 25 per cent of the total head developed. This is confirmed by many pump tests of the volute pressure at the periphery of the impeller and by the investigations of Knapp and Binder⁷ previously mentioned. It is also partially confirmed by the observed deformation between vanes of impeller shrouds which are too thin.

Due to the absence of numerical data and actual test readings, the writer has been unable to follow the analysis in detail to determine where the head actually developed came from. Although the efficiency of the pump was low and the application of the author's Equation [1] seems to have neglected the fact that the relative flow departs considerably from the actual vane angle,

even then when corrected, it is difficult to conceive of the throw-off pressure computed from Equation [2] agreeing as closely with the measured values as indicated by the author's figures.

The author's analysis of the effects of the evolution of air are interesting. As he comments, the effect on the pump performance is dependent to a considerable degree on the extent to which the pump designer considers this factor when laying out the pump-inlet passages and shaping the impeller-inlet vanes. This evolution of a gaseous phase not identical in nature to cavitation must be recognized by designers of process pumps for petroleum-refinery applications. Most petroleum products as pumped by centrifugal pumps are composed of fractions ranging from very heavy liquid fractions to very light dissolved gaseous components, in varying proportions. The release of these gases within the impeller at the inlet is the rule rather than the exception and must be considered in the pump design.

The introduction of a propeller in the pump inlet, particularly to improve operation where the energy in the incoming liquid in excess of the vapor pressure is low, is interesting. The improvement resulting from its introduction is understandable as the inlet design of the pump illustrated is particularly bad. As the pressure drop and the losses at the inlet are proportional to the square of the relative velocity between the impeller and the liquid, all other factors being equal, one would naturally expect the considerable improvement in performance due to the reduction of vane velocity at inlet.

The separate impeller construction was used many years ago in some critical applications because the open construction permitted careful cleaning and accurate shaping of the cast vanes at inlet, an important factor in hot-well-type pumps. However, as foundry technique improved, this corrective type of design was abandoned 15 to 20 years ago and the separate inlet vanes incorporated with the impeller. That impellers can operate under exceedingly difficult inlet conditions is illustrated by the results

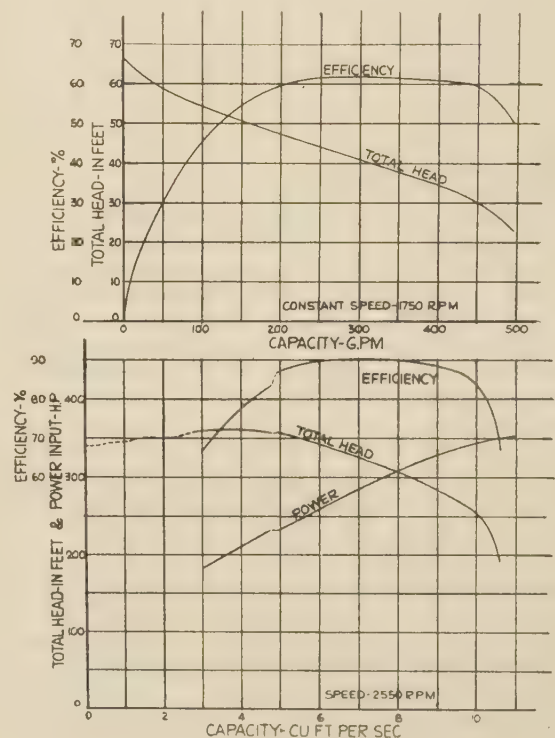


Fig. 16

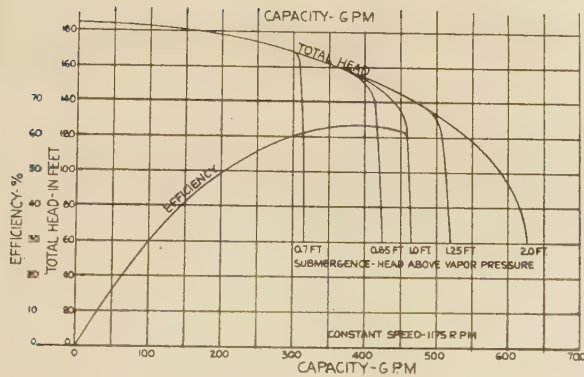


FIG. 17

shown in the designs developed for hot-well service aboard ships. There, suction specific speed values in excess of 26,000 (based on gpm units for capacity) have been reached, see Fig. 17.

It is unfortunate that the author appears to have been misled by Professor Sherzer's erroneous attack on the classical pump and turbine theory. However, his paper does serve to call attention to the fact that pump design is still, to a considerable degree, an art rather than a science. It should serve also, through the discussion it should evoke, to direct more careful attention to the application of the classical pump and turbine theory of Euler rather than to an attack on the theory itself.

AUTHOR'S CLOSURE

Answering similar points in both Mr. Watson's and Professor Angus's discussion, the author should perhaps have made himself clearer. He is not attacking the classical theory, only the way it has hitherto been applied in many cases, and particularly as it is applied in most of the texts on the subject. The author does not believe he has been misled by Professor Sherzer's remarks on the classical pump-turbine theory, because he is fully aware that his proposal for solving the problem was equally erroneous, but he

did bring up some points in the discussion indicating how the application of the classical theory will get us into trouble.

The author's purpose, as explained, is simply to get the designers to loosen up on what it is they actually do in allowing for the changes of behavior from the unadjusted classical theory because he cannot find it in the textbooks, and this paper was an attempt to needle some of the designers into telling us just what they think is right. The author also finds, in the literature, complete divergence of opinion in the theoretical treatments as to whether flow through impeller blades must be treated as rotational or irrotational. So far as he can learn, neither of the methods of approach has, at least in published prints, given us the complete answer.

With regard to the efficiency of the pump used as the single example in this case, it might be remarked that the method was applied actually to two other pumps and at different speeds, and still gave quite a reasonable check.

With regard to the efficiency of the particular model, the author is well aware that much higher efficiencies are obtainable in pumps and has in past years tested some of them, but the fact remains that pumps of the size under discussion, and as sold commercially, are as a rule not any better than the example given here. For example, a 300-gal pump, 60 per cent; 125-gal, 50 per cent; 40-gal, 30 per cent. These are all commercial pumps bought in the open market from different makers, and were supposed to be fitted to the jobs they were to do. There is not much gained by talking about high efficiency when the bulk of the pumps sold for ordinary purposes do not reach these values in this group of sizes. Therefore the pump in question is not a poor-efficiency pump—it is on a level with most of the stuff of this size being sold. Of course when one gets to a boiler-feed pump, or a large circulating pump, the picture is quite different and he should expect to get, and does generally get, efficiencies of around 72 to 75 per cent for the 1000-gal boiler-feed pump, and maybe 78 per cent for the circulator. But the fact remains that the small pumps are not usually within a considerable distance of these values. The author has seen tests on a pump of about the same dimensions as the one given in the example, and used for the same purposes, in which the efficiency was 78 per cent. This pump was really designed for high efficiency.

A Study of the Theory of Axial-Flow Pumps

By G. F. WISLICENUS,¹ HARRISON, N. J.

The essential aim of this paper is to present the theory of axial-flow pump runners in as simple a form as possible. The results are fairly conclusive in so far as the determination of the flow conditions in individual cylindrical stream surfaces is considered. In addition, it has been found possible to eliminate the controversy between the one-dimensional and the two-dimensional theories. The question of the method to be employed in building up the performance of the machine as a whole is still controversial and has been presented in this form.

INTRODUCTION

EXISTING publications on the theory of axial-flow pumps or turbines show a sharp distinction between the classical or one-dimensional approach and the "airfoil" or two-dimensional approach to this problem. It will be the principal aim of this paper to demonstrate that the results of these two methods of calculation are essentially the same, provided that certain well-established theoretical corrections are applied to the two-dimensional equations, in order to take into account the interaction of the vanes in the system. It is hoped that the natural correlations between these corrections and the familiar one-dimensional theory will tend to increase confidence in the theory to which they apply.

Another point of discussion will be the method of building up the performance characteristics of the machine as a whole from the head vs. through-flow characteristics of the individual cylindrical stream surfaces. Several recent publications calculate the head as the weighted average of different head values applying to the individual stream surfaces. The author has encountered certain logical difficulties connected with this method, and has therefore used the method of summing up the flow under the assumption that the pump head remains the same for all stream surfaces. In spite of practical difficulties connected with this method, a sufficient agreement with test results has been obtained to warrant using this latter method.

The theory of axial-flow machines will first be discussed strictly on the basis of frictionless flow; that is to say, the influence of the vane drag will be considered separately, at the end of this paper. The principal reason for this departure from the conventional form of presentation is that a simpler and at the same time more complete presentation becomes possible, since the theory of frictionless flow permits the determination of the flow for given vane systems, as well as the familiar derivation of the vane shape from given flow conditions.

The usual application of the theory to the design of new runners from given operating conditions is of unquestioned value. But it is not for this reason alone that the theory of axial-flow runners merits investigation. The theory is an indispensable instrument for obtaining information on the flow conditions in the machine. The relation between theory, flow conditions, and the development of new design forms is based on the simple consideration that any reasoning on the hydraulic design

of the machine, as well as any theory of the flow in the machine, requires a mental picture of the flow and of the action of the runner on the flow. Since the theory predicts the performance of the machine, it follows that the agreement or disagreement between the theoretical predictions and test results proves or disproves the validity of the mental picture of the flow. A flow picture thus corroborated can then be used as the basis for the improvement of existing forms and the development of new designs. It is for this reason that the theoretical determination of the flow and operating characteristics from the form of an existing test runner is considered as the most important object of the theory of such runners.

The present investigation is in agreement with most publications on the same subject, with regard to the fact that the flow is assumed to proceed through the runner along coaxial cylindrical stream surfaces. Only under this condition is it possible to consider, in the absence of friction, the relative flow along these stream surfaces as an irrotational fluid motion. This means that the relative flow through the moving vane system can be treated in the same manner as the absolute flow through a corresponding stationary system of vanes.

Of the various points of difference between the one-dimensional and the two-dimensional approaches to the theory of axial-flow runners, the outstanding contrast involves the amount of guidance assumed to be exerted by the vanes. The one-dimensional approach is defined by the fact that the flow on the discharge side of the vane system is, in the ideal case, assumed to be parallel to a suitably defined average direction of the discharge portion of the vane. In contrast to this approach, the two-dimensional theory is characterized by the calculation of the force action between the vane and the average flow, on the basis of theoretical or wind-tunnel data pertaining to a single vane in an infinitely extended stream. From this force action can be calculated the change of the flow and the head of the machine.

TWO-DIMENSIONAL THEORY

The two-dimensional procedure is exemplified in Fig. 1, where the average relative velocity is defined as the vectorial mean between the incoming and the discharging flow, and is designated by v_∞ . If L is the force-action normal to this average flow, then for unit span

$$L = C_L \frac{\rho v_\infty^2}{2} l \dots \dots \dots [1]$$

From theory, confirmed by wind-tunnel data

$$C_L = 2\pi \sin \alpha \dots \dots \dots [2]$$

where α is the angle of attack measured from the direction of zero lift.

For vanes which do not overlap, a sufficient approximation of the zero-lift direction can be obtained by drawing a straight line through the trailing edge and through the point A in Fig. 1. If the point of maximum camber lies in the leading half of the vane, this point A is the point of maximum camber,² otherwise point A is to be located at the center of the mean camber line of the vane.

¹ Research Engineer, Worthington Pump and Machinery Corporation. Mem. A.S.M.E.

Contributed by the Hydraulic Division and presented at the Annual Meeting, New York, N. Y., Nov. 27-Dec. 1, 1944, of THE AMERICAN SOCIETY OF MECHANICAL ENGINEERS.

NOTE: Statements and opinions advanced in papers are to be understood as individual expressions of their authors and not those of the Society.

² Defined as the point where the distance from the mean camber line to the chord reaches a maximum. The mean camber line and chord are understood to be drawn in accordance with the established practice of the N.A.C.A.

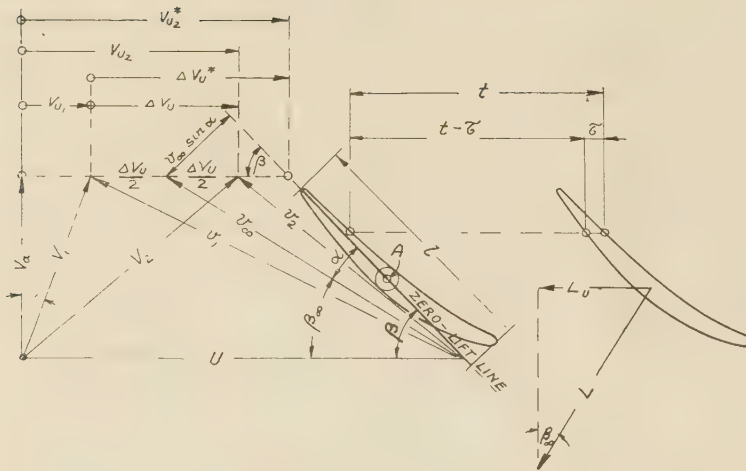


FIG. 1

If the vanes overlap, the leading part of the vane has less effect on the vane action than it would have if the vanes were widely spaced. This fact can be taken into account to some extent by drawing the zero-lift line according to the simple rule exemplified in Fig. 2.

From the change of the peripheral momentum of the flow

$$L_U = \Delta V_U V_{\infty} \rho t \dots \dots \dots [3]$$

where L_U is the peripheral component of L for unit span.

It is seen that

$$L_U = L \frac{V_a}{v_{\infty}} \dots \dots \dots [4]$$

consequently

$$C_L = \frac{2\Delta V_U}{v_{\infty}} \frac{t}{l} = 2\pi \sin \alpha \dots \dots \dots [5]$$

This equation relates the deflection ΔV_U to the average flow v_{∞} , to the ratio of vane spacing to vane length, t/l , and to the inclination α of the vane to the average relative flow.

Since only t/l and α represent the form of the vane system, the latter may be replaced, hydraulically, by a system of straight and parallel vanes, related to the actual vane system, as shown in Figs. 1 and 2. With this simplification in mind, it is then possible to compare the two-dimensional theory, Equation [5], with the one-dimensional assumption that the relative discharge velocity v_2 is parallel to this straight vane. The logical basis of the comparison is that the two theories must not give contradictory results. More specifically: the results of the two-dimensional theory must consistently approach those of the one-dimensional theory as t/l approaches zero.

Here an apparently paradoxical situation is encountered. If Equation [5] is rewritten in the form

$$\Delta V_U = v_{\infty} \sin \alpha \frac{l}{t} \dots \dots \dots [6]$$

it is seen that for infinitely close vane spacing, i.e., for $t = 0$, α must also become zero, since otherwise the deflection ΔV_U would become infinite. However, $\alpha = 0$ means that v_{∞} and not v_2 has the direction of the vane; and that the flow is deflected, according to the two-dimensional theory, more than predicted by the one-dimensional theory.

In order to eliminate this contradiction, and thereby bridge

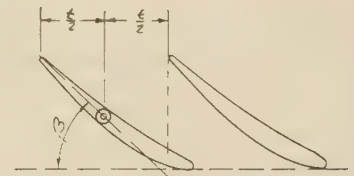


FIG. 2

the gap between the two-dimensional and the one-dimensional approaches, the foregoing equations must be changed. Physically, it is most natural to reason that the vane in the system cannot have the same characteristics as the same vane in the corresponding position in an infinitely extended stream. This means that Equation [2], which applies to the latter case, must be changed to apply to the vane in the system. The change is expressed by the 'lattice-effect coefficient' K , defined by the relation

$$C_L = 2\pi K \sin \alpha \dots \dots \dots [7]$$

Then Equation [5] becomes

$$2\pi K \sin \alpha = \frac{2\Delta V_U}{v_{\infty}} \frac{t}{l}$$

or

$$\frac{v_{\infty} \sin \alpha}{\Delta V_U} = \frac{t}{l} \frac{1}{\pi K} \dots \dots \dots [8]$$

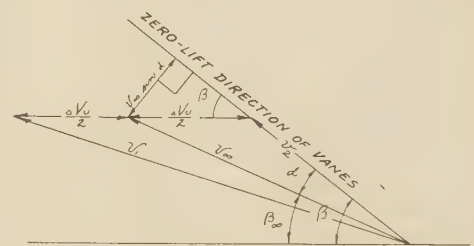


FIG. 3

For the limiting case represented by the identity of v_2 and the direction of the vanes, Fig. 3, the relation

$$\lim_{\frac{t}{l} \rightarrow 0} \left(\frac{v_{\infty} \sin \alpha}{\frac{\Delta V_U}{2}} \right) = \sin \beta \dots \dots \dots [9]$$

may be derived; and, by comparison with Equation [8], it is seen that

$$\lim_{\frac{t}{l} \rightarrow 0} \left(\frac{t}{l} \frac{2}{\pi K} \right) = \sin \beta$$

$$\lim_{\frac{t}{l} \rightarrow 0} K = \frac{t}{l} \frac{2}{\pi \sin \beta} \dots \dots \dots [10]$$

Equations [9] and [10], when written in the forms

$$v_{\infty} \sin \alpha = \frac{\Delta V_U}{2} \sin \beta \dots \dots \dots [9a]$$

$$K = \frac{t}{l} \frac{2}{\pi \sin \beta} \dots \dots \dots [10a]$$

may be considered as the one-dimensional approximation for the flow conditions in systems of straight and parallel vanes. This approximation for the lattice-effect coefficient K is represented graphically by the straight lines in Fig. 4, but is obviously correct only for small values of t/l . The actual shape of the curves of K as a function of t/l may now be estimated by the condition that these curves must approach their one-dimensional approximations for small values of t/l , and the line $K = 1$ for large values of t/l . This reasoning is confirmed by the exact K curves which are shown in Fig. 4, for $\beta = 20^\circ$ and $\beta = 70^\circ$, in relation to their one-dimensional approximations. A complete set of K curves, whose theoretical derivation is given by Weinig (1),³ is given in Fig. 5.

It is of interest to note that the exact theoretical values of K are never higher than their one-dimensional approximation. This means, physically, that the flow through a system of straight and parallel vanes is never deflected more than predicted by the one-dimensional theory. The strict proof of this important fact lies, of course, in the theoretical derivation of the K curves. A far simpler and more plausible demonstration, however, may be derived from the well-established "Joukowski condition" which states that the flow about a vane or airfoil is deflected to such a degree that it leaves the trailing end of the vane smoothly, i.e., in the direction of that part of the deflecting surface.

It is then clear that, in the immediate vicinity of the trailing edge, the theoretical direction of v_2 always coincides with the direction of the vane, and the local value of ΔV_U can be determined by that condition. The deflection ΔV_U , however, is produced by the vane, and must therefore be expected to be lower at a greater distance from the vane. Consequently, the average value of ΔV_U will be smaller than its local value at the vane discharge edge, so that the average flow is deflected from its initial direction, v_1 , somewhat less and never more than dictated by the direction of the trailing edge of the vane. The deflection, calculated by the one-dimensional condition that the average flow leaves the system in the direction of the vane, is therefore the greatest possible deflection and is reached only as a limit for very closely spaced vanes. The K value, which according to Equation [8] is proportional to the average deflection ΔV_U , is therefore less than, or for small vane spacing equal to, but never greater than its one-dimensional approximation. This confirms the theoretical results for K .

³ Numbers in parentheses refer to the Bibliography at the end of the paper.

The foregoing considerations, and the diagram in Fig. 5, show that the correction of the lift coefficient by the lattice-effect coefficient K is a matter of importance and cannot be disregarded even for approximate calculations. In the first place, the departures of K from unity are quite large, in particular in the vicinity of $t/l = 1$. Then, even according to their one-dimensional approximation, the K values are, within a large range of practical importance, well below unity, which means that in this range the assumption $K = 1$ would lead to greater deflections than the one-dimensional theory. This, however, is the very case which was shown to be incompatible with the Joukowski condition.

Form of Vane System. It is generally known that the foregoing equations can readily be used for finding the form of the vane system from the flow or operating conditions. The method of solving this problem is essentially the following:

The vane thickness can be taken into account by the following simple approximation: A "thickness reduction ratio" C_i , which is assumed to be constant throughout the system, is derived from the relation

$$C_i = \frac{t - \tau}{t} \dots \dots \dots [11]$$

where τ is a mean value of vane thickness, measured as shown in Fig. 1. Then, if V_a is the through-flow velocity between the vanes, and V_{a0} is the velocity before and in back of the vanes

$$V_a = \frac{V_{a0}}{C_i} \dots \dots \dots [12]$$

where V_{a0} is calculated from the continuity relation

$$V_{a0} = Q / (D_o D^2 - D_h^2) \frac{\pi}{4}$$

Here D_{oD} is the outside diameter, D_h the hub diameter, and Q is the rate of through-flow in volume per unit of time.

For all subsequent considerations, however, it is possible to make the simplifying assumption

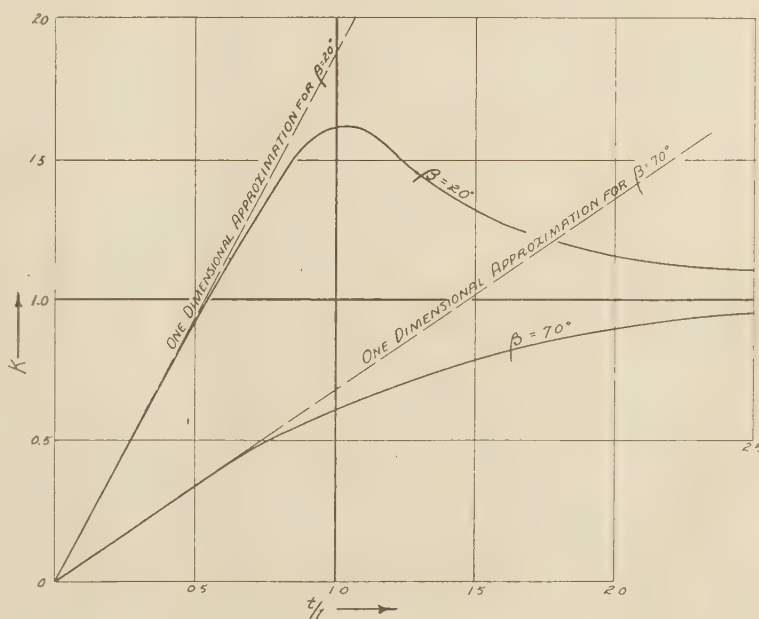


FIG. 4

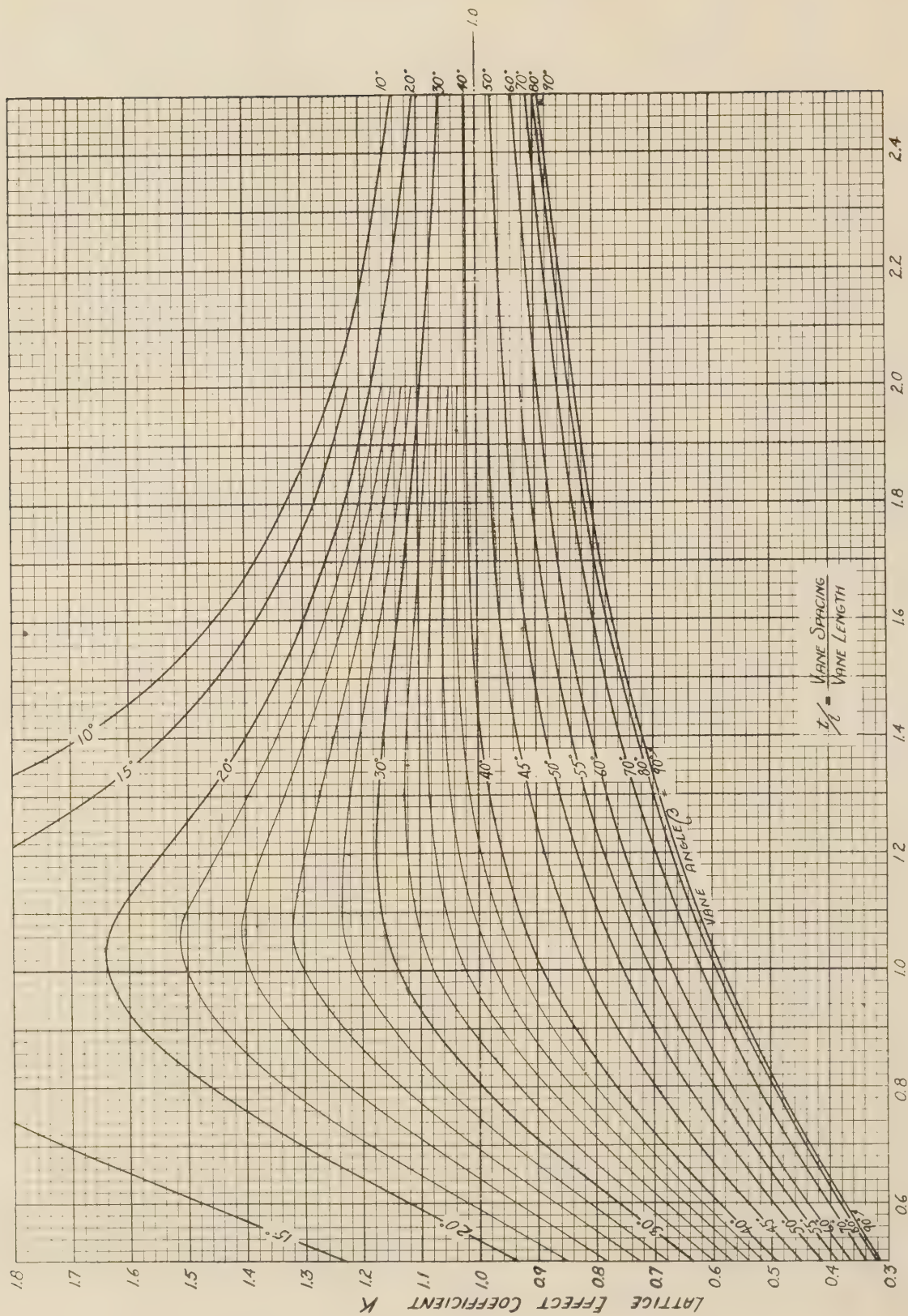


FIG. 5

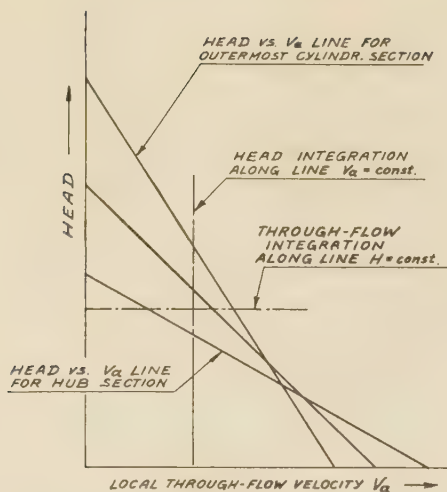


FIG. 7

where V_{U2}^* is defined by the fact that the corresponding relative velocity is parallel to the direction of the discharge portion of the vane (see Fig. 1). In general, this correction factor is determined empirically. It is, however, also possible to determine it on the basis of the results of the two-dimensional theory, in analogy with the method of determining K .

The first approximation of K was obtained by equating the results of the two-dimensional theory to those of the one-dimensional theory, putting the correction factor of the latter, C_H , equal to unity. This first approximation of K , however, was improved by the exact solution of the two-dimensional flow through a system of straight and parallel vanes. With these improved K values, it is then possible to determine the correction factor C_H of the one-dimensional theory, that is, by the inverse of the process by which the first approximation of K was originally obtained.

Equation [18] may be written in the form

$$\frac{H}{\eta_h} = C_H \Delta V_{U2}^* \frac{U}{g} = \Delta V_U \frac{U}{g} \dots \dots \dots [19]$$

where $\Delta V_{U2}^* = V_{U2}^* - V_{U1}$, while ΔV_U is the corresponding actual value of the change of the peripheral fluid velocity. But by using Equations [15] and [19], it is seen that

$$C_H = \frac{2}{\frac{t}{l} \frac{2}{\pi K \sin \beta} + 1} \dots \dots \dots [20]$$

The results of this equation are plotted in Fig. 8. It is seen that for low values of t/l the correction factor approaches unity, which is logically consistent with the fact that friction is not taken into account, so that the limiting case of $t/l = 0$ represents the ideal one-dimensional case.

Since these C_H values are derived from the two-dimensional theory by using theoretical K values, it follows that they apply directly only to systems of straight and parallel vanes, because only for this case are the theoretical K values strictly applicable. It is possible, however, to use these C_H values for other vane forms, provided that the average direction of the discharge portion of the vane is chosen to be equal to the zero-lift direction, as in Figs. 1 and 2.

The C_H diagram shows clearly that the one-dimensional theory in the form just stated applies with little or no correction

as long as $t/l < 1$. For wider vane spacing, this theory is less advantageous, but can still be employed when using the C_H factors given in the diagram. This does not mean that the two-dimensional theory becomes unnecessary, because the C_H values were derived on the basis of the two-dimensional theory. Using the K factors and the C_H factors, respectively, the two-dimensional and one-dimensional equations yield exactly the same results.

DERIVATION OF HEAD-CAPACITY CURVES OF MACHINE FROM CHARACTERISTIC LINES OF INDIVIDUAL FLOW SECTIONS

It has been shown that apparently conflicting theoretical treatments of the flow in the individual sections can be brought into satisfactory agreement. The resulting theory is not only simple and logically consistent, but it also is in reasonably good agreement with test results. No such satisfactory statement can be made as yet concerning the problem of deriving from the characteristics of the individual flow sections the performance of the machine as a whole.

At this point, it is well to consider the fact that the head may vary as a function of two variables, namely, the rate of through-flow and the distance r from the center of rotation in the runner. (This fact is demonstrated by Figs. 10 and 11.) Variations as a function of the rate of through-flow were previously discussed, while in the following sections the variations as a function of r are of major importance. "Constant head" or "variable head" therefore refers in the following discussion to the latter variation over the cross section:

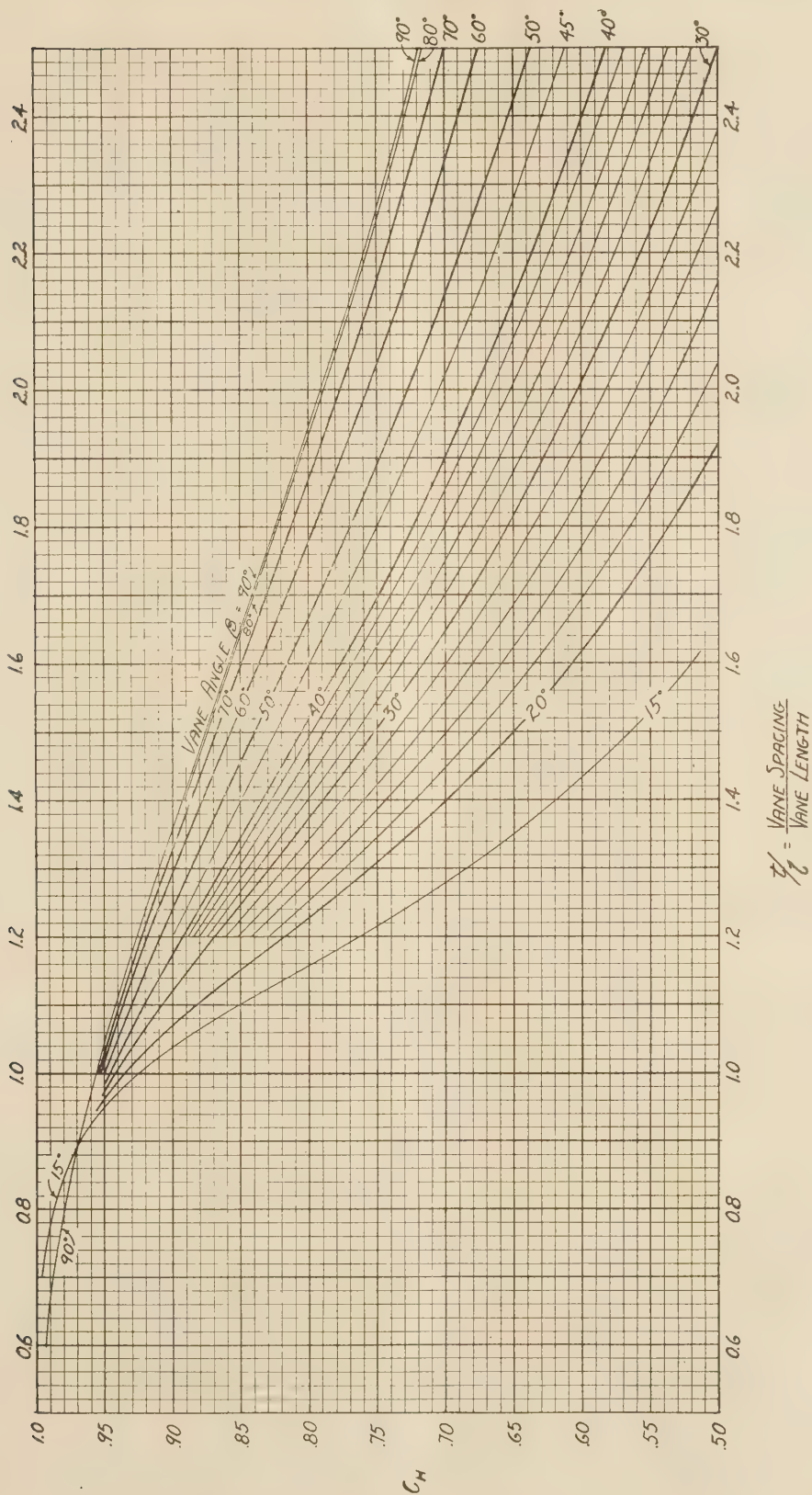
In some publications, notably those by O'Brien and Folsom (2), and by Wattendorf (3), the head of the machine is calculated as the average of different head values produced by the various cylindrical sections through the runner; only at the "design point" are these values assumed to be equal at the same through-flow velocity, V_a . Away from this point, the head is averaged, by multiplying each local head value by the narrow ring cross section to which it applies.

$$\pi (r_{OD}^2 - r_{hub}^2) H = \int_{hub}^{OD} H_a da = \int_{hub}^{r_{OD}} H_a 2\pi r dr \dots [21]$$

The through-flow velocity is assumed to be constant over the impeller cross section. This approach can best be represented by a vertical section through the bundle of local head vs. through-flow curves in Fig. 7.

The differences in pump head which are averaged by Equation [21] may be quite large. For approximately constant energy distribution at the inlet side of the runner, correspondingly large head or energy differences must be assumed to exist in the stream leaving the impeller. If the capacity differs appreciably from the design conditions, these theoretical energy differences may well exceed the velocity head of the average through-flow. In this case it becomes difficult to understand how this stream can form, further away from the runner, a flow of approximately constant energy. While such head differences between the individual vane sections have been observed by means of pitot-tube measurements, the resulting head of the machine did not seem to be consistent with the results obtained according to Equation [21].

A more serious difficulty arises from the question of whether the variations in pump head assumed by this theory are compatible with the requirement that the differences in static pressure over the cross section must be in equilibrium with the centrifugal forces of the rotating fluid masses. It will now be demonstrated that for a flow of constant angular momentum at one side of the runner (this includes the case of zero rotation), the requirement of equilibrium of radial forces is satisfied only if the



$$\frac{s}{l} = \frac{\text{VANE SPACING}}{\text{VANE LENGTH}}$$

FIG. 8

head produced along all the cylindrical stream surfaces of the runner is the same. The only exception to this rule will be seen to be the fictitious case that the fluid leaves the runner at a rotational velocity equal to the runner velocity ($V_{U2} = U$); that is, the whole mass of fluid leaving the runner rotates as a solid body at the velocity of the runner. This case, however, is not realized in axial-flow pumping machinery.

Assuming cylindrical flow, any differences in static pressure between various cylindrical sections must be caused by or be in equilibrium with the centrifugal forces of the fluid rotating about the axis of the machine. With reference to Fig. 9, the equilibrium

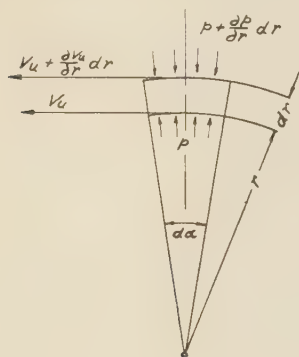


FIG. 9

between the radial pressure increase and the centrifugal force may be expressed

$$\left(p + \frac{dp}{dr} dr\right) (r + dr) d\alpha - p dr d\alpha - pr d\alpha = \rho r d\alpha dr \frac{V_u^2}{r}$$

or

$$\frac{dp}{dr} = \frac{\rho V_u^2}{r} \quad [22]$$

Dividing both sides by γ gives the change from pressure to static head. Then at the impeller inlet

$$\frac{dh_{st1}}{dr} = \frac{V_{U1}^2}{gr} \quad [23]$$

and at the discharge

$$\frac{dh_{st2}}{dr} = \frac{V_{U2}^2}{gr} \quad [24]$$

Therefore

$$\frac{d(h_{st2} - h_{st1})}{dr} = \frac{d\Delta h_{st}}{dr} = \frac{V_{U2}^2 - V_{U1}^2}{gr} \quad [25]$$

The total head H is the sum of the static head change Δh_{st} and the velocity-head change Δh_v .

$$\Delta h_v = \frac{V_2^2 - V_1^2}{2g}$$

but

$$V_2^2 = V_a^2 + V_{U2}^2 \\ V_1^2 = V_a^2 + V_{U1}^2$$

Consequently

$$\Delta h_v = \frac{V_{U2}^2 - V_{U1}^2}{2g} \quad [26]$$

so that

$$\Delta h_{st} = H - \frac{V_{U2}^2 - V_{U1}^2}{2g} \quad [27]$$

Then

$$\frac{d\Delta h_{st}}{dr} = \frac{dH}{dr} - \left(\frac{V_{U2}}{g} \frac{dV_{U2}}{dr} - \frac{V_{U1}}{g} \frac{dV_{U1}}{dr} \right) = \frac{V_{U2}^2 - V_{U1}^2}{gr} \quad [28]$$

For each cylindrical section, the Euler equation becomes

$$H = \frac{r\omega}{g} (V_{U2} - V_{U1})$$

and

$$\frac{dH}{dr} = \frac{\omega}{g} (V_{U2} - V_{U1}) + \frac{\omega}{g} r \left(\frac{dV_{U2}}{dr} - \frac{dV_{U1}}{dr} \right) \quad [29]$$

By substituting the last expression into Equation [28], it is seen that

$$\frac{\omega}{g} (V_{U2} - V_{U1}) + \frac{dV_{U2}}{dr} \left(\frac{\omega r}{g} - \frac{V_{U2}}{g} \right) - \frac{dV_{U1}}{dr} \left(\frac{\omega r}{g} - \frac{V_{U1}}{g} \right) = \frac{V_{U2}^2 - V_{U1}^2}{gr}$$

$$\frac{V_{U2}}{r} (\omega r - V_{U2}) - \frac{V_{U1}}{r} (\omega r - V_{U1}) + \frac{dV_{U2}}{dr} (\omega r - V_{U2}) - \frac{dV_{U1}}{dr} (\omega r - V_{U1}) = 0$$

$$\left(\frac{dV_{U2}}{dr} + \frac{V_{U2}}{r} \right) (U - V_{U2}) - \left(\frac{dV_{U1}}{dr} + \frac{V_{U1}}{r} \right) (U - V_{U1}) = 0 \quad [30]$$

This equation describes the condition for equilibrium between the centrifugal forces and the pressures in axial-flow machinery, under the restriction that the equilibrium must be satisfied on one side of the runner (see Equations [23] and [24]).

For constant angular momentum at the inlet

$$V_{U1}r = \text{const}$$

Consequently

$$d(V_{U1}r) = 0$$

$$r \frac{dV_{U1}}{dr} + V_{U1} = 0$$

$$\frac{dV_{U1}}{dr} + \frac{V_{U1}}{r} = 0 \quad [31]$$

With the exception of the fictitious case mentioned previously it can be said that

$$U - V_{U2} = v_{U2} \neq 0$$

Substitution of Equation [31] into Equation [30] therefore leads to the relation

$$\frac{dV_{U2}}{dr} + \frac{V_{U2}}{r} = 0 \quad [32]$$

By subtracting Equation [31] from Equation [32], it is seen that

$$\frac{d(V_{U2} - V_{U1})}{dr} + \frac{V_{U2} - V_{U1}}{r} = 0$$

$$\frac{d\Delta V_U}{dr} + \frac{\Delta V_U}{r} = 0$$

so that by integration

$$\log_e \Delta V_U + \log_e r = \text{const} \\ \Delta V_U r = \text{const}$$

Consequently

$$H = \text{const}$$

It is thus clear that under the assumption of cylindrical flow and for constant angular momentum (including the case of zero rotation) at the inlet or discharge side of the runner, the equilibrium of pressure differences and centrifugal forces demands a constant value of the pump head.

In view of this result and the previously mentioned difficulties connected with the assumption of constant through-flow velocity but differing pump heads for the various flow surfaces, the author has investigated the calculation of the pump performance on the basis of a constant pump head for all cylindrical stream surfaces. This approach may be characterized by using horizontal sections through the bundle of local head vs. through-flow curves in Fig. 7. It is seen that for all capacities away from the design point, the through-flow velocity V_a will vary appreciably over the runner cross section. This fact has already been pointed out by Pfeleiderer (4) and Spannhake (5).

The resulting head-capacity curves are obtained by an integration of the through flow with a constant head for the entire cross section of the runner

$$Q = \int_{\text{hub}}^{OD} V_a 2\pi r dr = \int_{\text{hub}}^{OD} \pi V_a d(r^2) \dots \dots \dots [33]$$

and may therefore be obtained as the area under the curve of V_a plotted against r^2 .

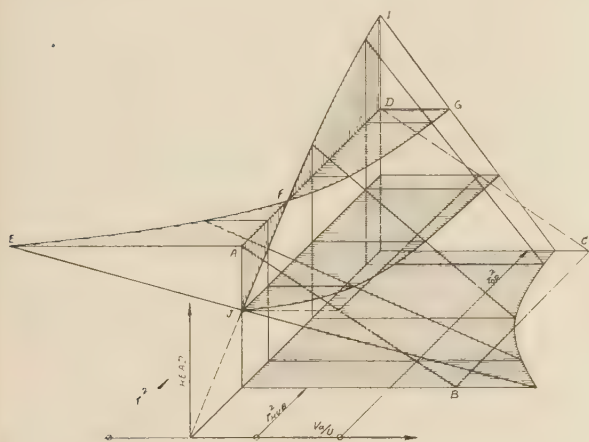


FIG. 10

In order to establish the total head-capacity curve, this process is carried out for two different head values, as shown in Fig. 10.⁴ For practical reasons of integration, the larger head value is selected as the head produced at the hub at $V_a = 0$; the smaller value is chosen as zero head. Through the two points obtained in this manner can be drawn the ideal straight-line characteristic of the machine. The fact that straight-line characteristics for the individual impeller sections lead to a straight-line characteristic for the impeller as a whole can be proved by considering that the local changes in V_a for a constant change in head are the same for every point along the local head vs. through-flow curves. Consequently, the average change in V_a for a given change in head is constant along the average head-capacity curve,

⁴ This represents a three-dimensional plot whose co-ordinates are V_a/U , the head at any particular cylindrical section, and the radius squared.

since it may be obtained by integration of the local changes in V_a plotted against r^2 .

The method described here encounters serious difficulties in the case of horizontal or rising-head vs. through-flow curves for the individual flow sections. Such a rising curve is obtained with conventional vane design only with a strong prerotation of the fluid against the runner motion. It may be concluded from Fig. 6 that, if the inlet-flow angle θ becomes larger than the angle $90^\circ - \beta$, then ΔV_U increases instead of decreasing with increasing V_a . Such a condition would presumably occur near the hub, where U is a minimum and, according to the momentum law, V_U is a maximum. If in the outer sections the local head vs. through-flow curve is falling, and near the hub it is rising, somewhere there exists a radius r_∞ at which the curve is horizontal. The difficulty of solution is connected with the fact that for all head values which differ from that of this horizontal curve, the through-flow velocity V_a at that radius becomes infinite. The determination of the average value of V_a therefore involves an integration over a region of infinite values, as shown, for instance, for zero head in Fig. 11. In many cases, such an integration is theoretically quite possible because of the cancellation of the positive and negative areas. But the result has no physical meaning, since the actual through-flow curve in this range cannot be even approximated by the theoretical curve.

The only possibility of practical calculations consists of assuming for the region inside of an arbitrarily chosen radius r_c , greater than r_∞ , an average through-flow velocity. The location of r_c relative to r_∞ must be considered as an empirical coefficient, to be determined by comparison with test results. Reasonable results have been obtained by giving to the ratio $(r_c^2 - r_\infty^2)/r_{OD}^2$ values in the vicinity of 0.06; but the data available are as yet insufficient. The average velocity assumed in the region inside of r_c is the average velocity obtained by integrating over the region outside of r_c .

It is preferable to carry out the determination of the average V_a value for $H = 0$ and $H = H_{r_\infty}$, as shown in Fig. 11; the latter being the only value for which the V_a integration can be carried out with finite values of V_a over the entire impeller area.

There exists another difficulty in connection with prerotation (fluid rotation at the inlet side) with or against the direction of the runner motion. Unless the fluid is guided by vanes up to the immediate vicinity of the runner, the distribution of the peripheral velocity of the fluid must be derived by theoretical means, for instance, by the law of constant angular momentum. The axial velocity component, on the other hand, is determined by the runner action and its distribution is assumed to vary for different capacities. The ratio between the peripheral and axial components of the inlet velocity V_1 and, therefore, the direction θ

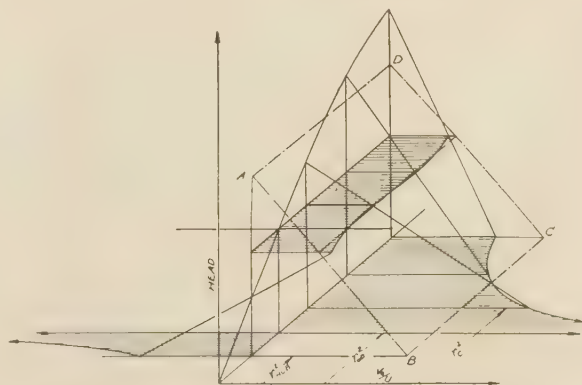
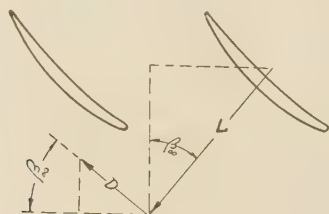


FIG. 11

of this velocity must, consequently, be different for different operating conditions.

Since the theoretical determination of the runner action requires a knowledge of the direction of the incoming flow, it is necessary to determine first the direction θ of V_1 , under the assumption of a uniform distribution of V_a , and to assume that this direction is constant for all operating conditions. The error introduced thereby is not serious in the vicinity of the point of normal operation, where V_a does not vary a great deal over the cross section of the runner. Under other operating conditions, however, it becomes necessary to approach the final result by a method of iteration. In this case, the velocity distribution obtained under the assumption of a constant value of θ constitutes the first approximation and can be used to determine the variations of θ under the assumption that V_{U1} satisfies the law of constant angular momentum. The θ values, thus determined, will lead to a new distribution of V_a , which forms the second approximation. Sometimes, however, this process does not converge. In this case it is necessary to estimate the θ value to be somewhere between the first and second approximations, and to check whether the estimated θ value is reasonably consistent with the resulting V_a values.

In concluding this part of the discussion, it must be noted that the two methods of building up the total head-capacity curve do not yield the same results. It can be seen in Fig. 10, that the plane surface, $ABCD$, represents the average head-capacity curve, according to the method which consists of averaging the through-flow. In the uppermost horizontal section shown, the negative area AEF must, under this assumption, equal the positive area DFG . Since the local head vs. through-flow curves are not parallel, so that, for instance, the ratio AE/AJ is not equal to the ratio DG/DI , it follows that the area AJF cannot cancel out against the area FDI . Consequently, if the line AFD represents the average of the V_a values, it cannot at the same time represent the average of the head values. Merely for simplicity of representation, this is shown in the diagram for the shutoff head; but it could have been demonstrated in the same manner for any other point of the resulting head-capacity curve.



According to the foregoing relations, the efficiency of the runner is

$$\eta = \frac{H_F}{H_0} : \frac{M_F}{M_0} = \frac{1 - \frac{C_D}{C_L} \tan \beta_\infty}{1 + \frac{C_D}{C_L} \cot \beta_\infty} \dots \dots \dots [39]$$

which is the well-known Prandtl formula for propeller efficiencies.

No complicated calculations are justified for obtaining a better approximation for the influence of friction in pump runners, since the flow conditions, in particular the boundary conditions, are different from those in the wind tunnel. For example, the existence of a radial motion of the boundary layer has been demonstrated by Weske (7). The motion is likely to have a significant effect on the drag coefficient of the vane section considered. Values of C_D/C_L obtained in the wind tunnel can at best be considered as a very crude approximation for the conditions in the runner. If, on the other hand, the ratio C_D/C_L is determined by means of Equations [34] and [38] from pump test data and theoretical analyses giving H_0 and M_0 , then these equations become part of the definition of C_D/C_L , thus determined. This condition eliminates to a large extent the approximate character of the equations derived here.

Since accurate calculations on friction do not seem possible, one is also justified in applying Equations [34], [38], and [39] to only one cylindrical stream surface of average radius, where

$$r_{0D}^2 - r_{av}^2 = r_{av}^2 - r_{hub}^2$$

hence

$$r_{av}^2 = \frac{r_{0D}^2 + r_{hub}^2}{2}$$

and in applying the results containing H_F/H_0 , M_F/M_0 , and η to the runner as a whole.

If there is reason to consider the velocity head due to friction, its effect can be expressed by a correction coefficient in Equation [38], in the form

$$\frac{H_F}{H_0} = 1 - K_F \frac{C_D}{C_L} \tan \beta_\infty \dots \dots \dots [38a]$$

where, according to the theoretical consideration of the momentum relations involved

$$K_F = 1 - \cot^2 \beta_\infty \frac{V_{U2} + \frac{\Delta V_U}{2} \frac{C_D}{C_L} \cot \beta_\infty}{v_\infty} \dots \dots [40]$$

It is seen that this coefficient can theoretically become negative, which means that the increase in velocity head due to friction outweighs the reduction in static head, as expressed by the Prandtl formula.

COMPARISON BETWEEN THEORY AND TEST RESULTS

The theoretical approach discussed here has been compared with a large number of test results. The runners used for the comparison included three widely differing vane shapes with a varying number of vanes, as well as modifications of the vane steepness. Fig. 13 shows a typical comparison. The essential result is represented by the difference Δ between the ratio H/H_{th} and the measured efficiency η . Part of the difference between the actual head H and the theoretical head H_{th} may of course be explained by the head losses in the machine. The ratio H/H_{th} would be the efficiency if these losses were the only losses in the machine and if the theory were to represent the flow conditions (without losses) exactly. The actual efficiency η , on the other and, expresses the head losses in addition to the leakage losses

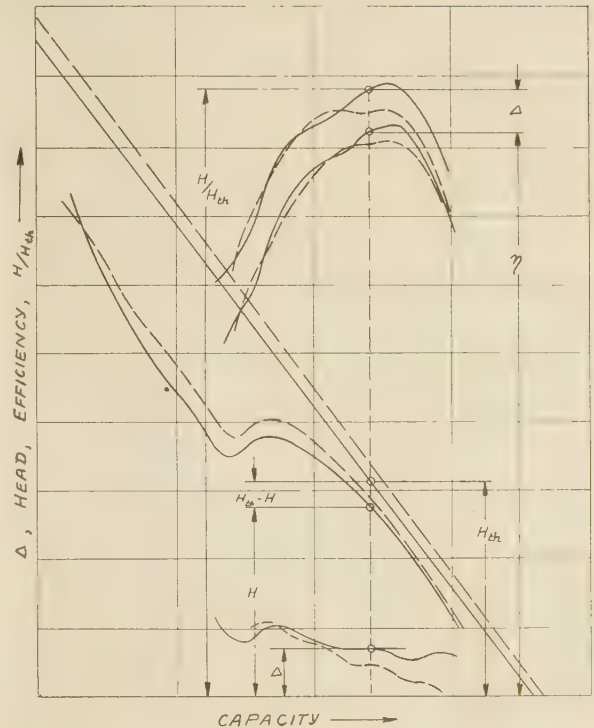


FIG. 13

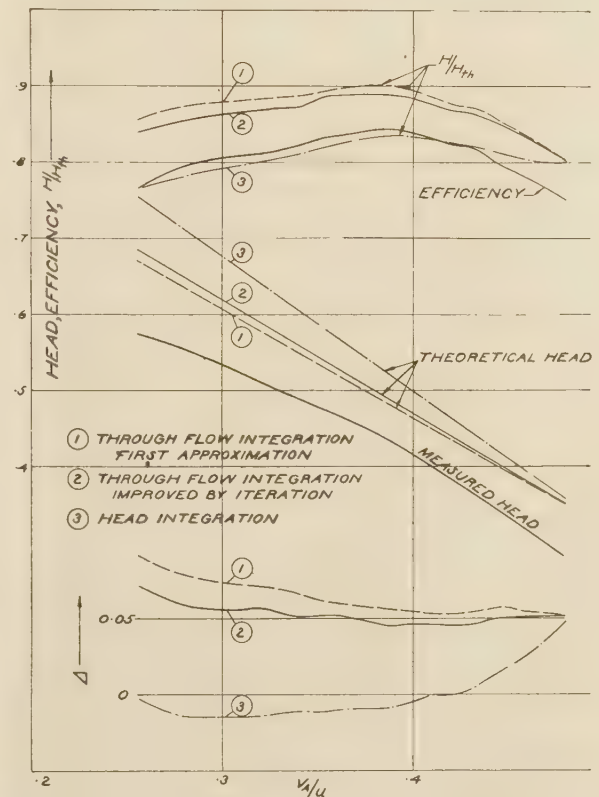


FIG. 14

and that part of the shaft torque which is not converted into hydraulic head. The difference Δ between the ratio of actual head to theoretical head and the efficiency, consequently, describes those losses which are not head losses, i.e., those losses which are primarily due to an increase in torque beyond what is really used for pumping. Shortcomings of the theory are also reflected in the value of Δ . Under the assumption that the losses, other than head losses, do not vary a great deal, it appears justified to judge the consistency of the theory by the consistency of the Δ curves.

The variations in the Δ curves constitute a confirmation of the theory, to the extent that these variations are in percentage smaller than the theoretical variations of the lattice-effect coefficient K used in the derivation. The agreement becomes progressively poorer with rotation at the inlet side of the runner, in particular with negative prerotation, where singular velocity conditions are encountered near the hub. Where there is prerotation, successive improvements of the agreement are obtained by the process of iteration previously discussed. This relation is demonstrated in Fig. 14, which shows the comparison between test results and the first and second approximations based on the integration of the through-flow, as well as the theoretical line obtained by integrating the head. The difference between these approaches is clearly expressed by the form of the resulting Δ curves.

The case represented in Fig. 14 appears to confirm the method of through-flow integration rather than that of head integration, particularly because of the negative Δ values obtained by using the latter method, indicating imperfections of the theory. This conclusion, however, is in no way final. In the first place, the Δ curves obtained by the through-flow integration are not always as consistent as those obtained in this case. As a matter of fact, the comparison of the over-all performance, Fig. 14, showed a marked contrast to the comparison between the theoretical velocity distribution and that obtained by Pitot-tube measurements of the same runner, as shown in Fig. 15. Here the change in the peripheral velocity ΔV_U is shown for the two methods discussed, and compared with test results. It is seen that the actual velocity distribution approaches the theoretical curve obtained under the assumption of constant through-flow distribution and, consequently, different head values for the different cylindrical stream surfaces. This result, in contrast to the previously mentioned comparison of the over-all performance, was the basis for the earlier statement that in at least one case the measured velocity distribution confirmed the assumption of different local head values, but that the resulting head does not confirm the method of integration expressed by Equation [21].

It must be noted that comparisons between theoretical and actual velocity distributions do not always have the characteristics shown in Fig. 15. For instance, in Fig. 16 are shown corresponding results obtained with a different runner. Here the comparison between test results and theoretical results, derived under the assumption of constant head for all stream surfaces, is carried out for two different pump-head values. In this case, the agreement is close, with the exception of the outermost stream surface, where the test value of ΔV_U abruptly increases to a higher value than the theoretical value. This section is quite close to the outer periphery, and the discrepancy may be caused by the end conditions of the vanes, for instance, the influence of friction on the casing walls, or the radial motion of the boundary layer.

It is of considerable interest that the differences between the theoretical discharge velocities and those actually observed by pitot-tube measurements are reasonably well in line with the theoretical direction of the relative flow of the particular vane section considered. In other words, present results seem to

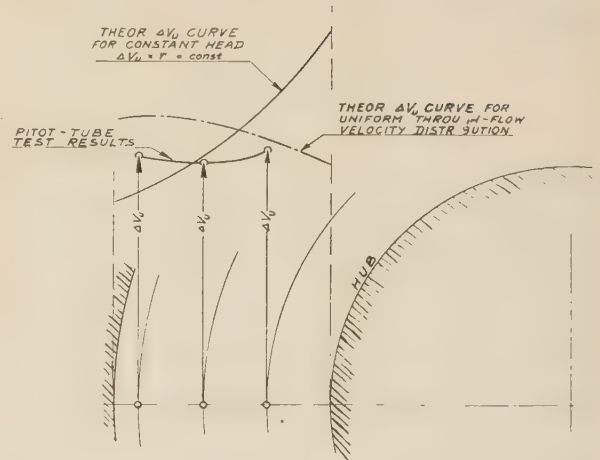


FIG. 15

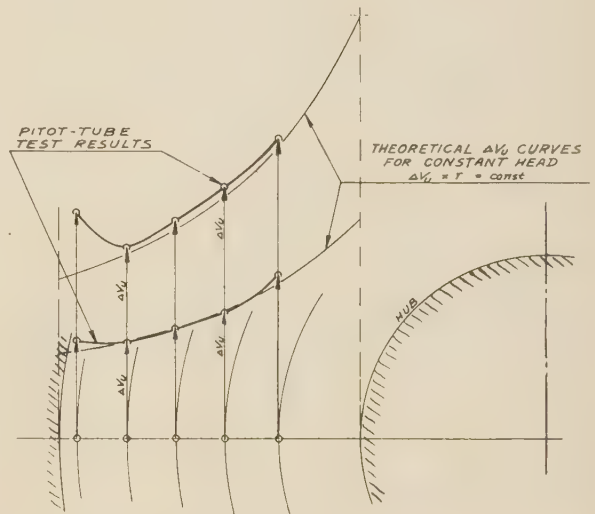


FIG. 16

indicate that the individual cylindrical stream surfaces actually operate very close to their theoretical head vs. through-flow characteristics. The discrepancy between the theory and test results appears to be connected mainly with the combination of the action of the individual flow sections into the performance of the pump as a whole. This situation seems to be in complete agreement with the fact that the flow of a frictionless fluid through the individual cylindrical sections can be handled theoretically in a rather conclusive manner, while the theoretical problem of combining these characteristics into the three-dimensional flow picture of the machine as a whole presents considerable difficulties.

ACKNOWLEDGMENTS

The experimental work for the present investigations was carried out under the direction of Mr. C. Collar and Mr. A. Oschwald, assisted by various members of the research and development department of the Worthington Pump and Machinery Corporation. The theoretical analysis of the test results and most of the work connected with writing this paper were in the hands of Mrs. H. Kaltenbacher.

The author would like to thank Prof. R. L. Daugherty for a number of helpful and constructive suggestions concerning the final arrangement of the paper. These suggestions have been used in preparing the final draft and it is hoped that a number of possible misunderstandings have been eliminated.

BIBLIOGRAPHY

- 1 "Die Strömung um die Schaufeln von Turbomaschinen," by F. Weinig, J. A. Barth, Leipzig, 1935.
- 2 "The Design of Propeller Pumps and Fans," by M. P. O'Brien and R. G. Folsom, University of California Publications in Engineering, vol. 4, no. 1, 1939.
- 3 "The Ideal Performance of Curved-Lattice Fans," by F. L. Wattendorf, Th. von Kármán Anniversary Volume, California Institute of Technology, 1941.
- 4 "Die Kreiselpumpen," by C. Pfeiderer, J. Springer, Berlin, 1932.
- 5 "Kreiselsräder als Pumpen und Turbinen," by W. Spannake, J. Springer, Berlin, 1931.
- 6 "Abriss der Strömungslehre," by L. Prandtl, F. Vieweg & Son, Braunschweig, 1935.
- 7 "Investigation of Blade Characteristics," by J. R. Weske, Trans. A.S.M.E., vol. 66, 1944, pp. 413-420.

Discussion

W. H. CHURCH.⁵ Having checked the equations given in this paper, the writer finds that they seem to be mathematically correct. It may be of interest to those not familiar with F. Weinig's booklet⁶ to have equations from which the lattice-effect coefficient K , as given in curve form (Fig. 5 of the paper) can be calculated. First calculate α_{ST} from the formula

$$\tan \alpha_{ST} = \cot \beta \frac{R^2 - 1}{R^2 + 1}$$

where R can be considered as an arbitrary parameter greater than unity (radius to some point outside the unit circle). Next calculate l/t by means of the following formula

$$l/t = \frac{1}{\pi} \left\{ \sin \beta \cdot \log_e \frac{(R^2 + 1) + 2R \cos \alpha_{ST}}{(R^2 + 1) - 2R \cos \alpha_{ST}} + 2 \cdot \cos \beta \cdot \tan^{-1} \frac{2R \sin \alpha_{ST}}{R^2 - 1} \right\}$$

using the same values of R assumed for the first formula given. Finally K is calculated from the formula

$$K = \frac{2}{\pi} \cdot t/l \cdot \frac{2R}{R^2 + 1} \cdot \frac{\cos \alpha_{ST}}{\sin \beta}$$

using the assumed values of R and the values of t/l calculated from the preceding formula.

$$\text{For } \beta = 0 \text{ deg } K = \frac{2}{\pi} \cdot t/l \cdot \tan \left(\frac{\pi}{2} \cdot l/t \right)$$

$$\text{For } \beta = 90 \text{ deg } K = \frac{2}{\pi} \cdot t/l \cdot \tan h \left(\frac{\pi}{2} \cdot l/t \right)$$

Assuming R values of 1.01, 1.1, 1.2, 1.5, 1.8, 2, 2.2, 2.5, and 5 cover the range of K values shown on the curves, Fig. 5. These calculations are repeated for various values of β , then values of K plotted against t/l for constant values of β .

It is interesting to compare the values of K , as given by Weinig with those of K_a or K_p given by F. Numachi. For $\beta = 90$ deg there is almost perfect coincidence. For $\beta = 45$ deg at t/l

$= 0.5$ and 2.5 there is good agreement but at $t/l = 1.0$, Numachi is 9 per cent higher than Weinig. For $\beta = 30$ deg again there is agreement at the extreme points but at $t/l = 1$, Numachi is 27 per cent higher than Weinig. For values of β below 30 deg at $t/l = 1$, there seem to be even greater differences. It is probable that Weinig's values are the more reliable, however.

R. G. FOLSOM.⁷ This paper presents some new approaches to specific theoretical design problems in connection with propeller or axial-flow pumps. When using the airfoil theory, one must remember that the airfoil characteristics are based on experimental investigations of a single airfoil in a uniform fluid stream without pressure gradient. In an axial-flow pump or turbine, the blade design may be based primarily on these single airfoil characteristics, but several correction factors must be applied so that the theoretical design will predict accurately the final machine performance. These corrections are made for the following:

- (a) Mutual interference of blades.
- (b) Pressure gradient through runner and guide vanes.
- (c) Velocity distribution before the propeller.
- (d) Velocity distribution after the propeller and guide vanes.
- (e) Curvature and change in section radially along the blade.

Although the author has presented material on these correction factors, much work remains to be done on all of them. For example, the results of the use of the author's ingenious method of averaging heads (item *d* of corrections) to obtain the head-capacity performance indicates that additional fundamental work must be accomplished before energy transfers during passage of water through a pump are clearly understood.

It should be noted that Equation [2] of the paper is for very thin airfoils only. This limitation is not important as experiments have shown that the characteristics of all useful airfoils can be expressed as

$$C_L = C \alpha$$

where C is a constant. Substitution of this relationship for Equation [2] would generalize the results of the analysis.

The performance of axial-flow machines is very sensitive to blade shapes and angles. Thus in reporting experiments of the type covered by the paper, it is desirable to indicate what measurements were made to ascertain the correspondence between actual pump elements and design drawings.

Recent University of California velocity-distribution measurements made at sections just downstream from a propeller-guide vane combination show the author to be correct in raising the question regarding "the amount of guidance assumed to be exerted by the vanes." The deflection of the flow at the trailing edges of the stationary guide vanes appears to be less than the amount predicted by the airfoil theory with simple mutual interference corrections.

R. LOWY.⁸ The author should be commended for attempting to correlate the one- and two-dimensional theories of axial pumps with the results of practical tests. Such studies are to be greatly appreciated, because it is essential to examine how the current theories correspond with the practical tests.

It cannot, however, be overlooked that all theories are based on certain fundamentals, and that it is not sufficient to rectify the theory in consequence of practical tests, if an inaccurate stipulation of fundamentals renders a theory inadequate.

⁷ Associate Professor of Mechanical Engineering, University of California, Berkeley, Calif. Mem. A.S.M.E.

⁸ Engineer, Baldwin Locomotive Works, Eddystone, Pa. Mem. A.S.M.E.

⁵ Worthington Pump and Machinery Corporation, Harrison, N. J.

⁶ Reference (1) of the author's Bibliography.

The author presents the principles of the one-dimensional and the two-dimensional theories: The one-dimensional theory presumes that all filaments on a cylindrical surface are identical; the two-dimensional theory consists of the conception of flow through a lattice of vanes corresponding to the development of cross sections on cylindrical surfaces. In both cases the cross sections on all cylindrical surfaces are hypothetically independent of each other.

Starting with these theories, the author evaluates the axial velocity at the outlet of the wheel and finds a more or less considerable difference with the practical measurements. The reason for this condition lies in the assumed independence of the cross section which actually causes the discrepancy.

Among the different facts which can be given in this connection to explain these circumstances, the following two should be considered in detail.

1 The wheel is not completely defined through independent cylindrical cross sections. An infinite number of wheels exist, all showing the same kind of cylindrical cross sections, and differing in their relative positions. It is obvious that numerous vanes can be constructed corresponding to the same cylindrical cross sections. The calculation is now based only on the cross sections; therefore one calculation would be applicable to an infinite number of vanes. Actually the characteristics and the efficiencies for different vane forms are not identical, and the distribution of the axial velocities is influenced essentially by the relative position of the cross section.

These circumstances are analogous to the case of pumps with medium specific speed (axial-radial impellers), whose outlet edge is arranged on a cylindrical surface. For instance, an improvement in efficiency can be obtained if the outlet edge is put on a helix instead of on a straight line. The independence of the cross sections, as used in the customary theory of axial-flow pumps, is therefore absolutely inadequate.

2 In general, it is presumed that pumps have a pure axial inflow, but it is also known that there exists a prerotation. Professor Hancock of the University of Liege made extensive studies concerning the prerotation and found that it attained a distance 6 to 7 times that of the wheel inlet diameter. The prerotation fundamentally influences the flow through the pump and also in a certain sense causes a mutual dependence on the vane cross sections.

All these circumstances show clearly that the customary one- and two-dimensional theory is not sufficient to explain the axial velocity distribution on an axial-pump wheel. By introducing such dependence, we are in the field of three-dimensional evaluation, in which sphere such considerations truly belong.

Considering these circumstances in the interpretation of the results obtained, the paper will be valuable for further investigation of axial pumps.

L. F. MOODY.⁹ One of the most valuable features of this paper is the correlation it establishes between the one-dimensional analysis based on the Euler principle, and the two-dimensional airfoil method. In starting with the Euler principle the author is on firm ground. The Euler equation represents merely a balance of moments of forces derived from the momentum principle and Newton's second law. It is as unassailable as the balance of forces on a free body in equilibrium.

It is most unfortunate that fallacious arguments inconsistent with this principle, such as those Scherzer advanced some years ago,¹⁰ continue to reappear and to becloud the picture. The dif-

ficulties encountered in the use of the Euler principle are mainly due, in the writer's view, merely to its misapplication. It is naturally necessary to apply it to actual flow velocities; and not to assumed velocities coinciding with the vane directions, presupposing an infinite number of impeller vanes, and neglecting the two-dimensional effects of variations of flow from one vane to the next.

Another method of formulating the correlation between airfoil theory and the Euler principle was that proposed for turbines by the late Professor Thoma,¹¹ who expressed the relation in the form that the sum of the circulations around the individual blades is equal to the difference between the circulations of the whole flow in the entrance and discharge spaces.

That the author's airfoil method of treatment, leading to a somewhat elaborate theoretical structure, can be shown to be reducible to the Euler relation is satisfying evidence that it meets the test of theoretical consistency. The comparison with actual experimental results is a still more valuable test of its practical value.

The author's simplification of the airfoil theory by the introduction of the sine law for the lift coefficient is a useful step, which leads to workable relations in fairly simple form in a field of much complexity. He clearly states his other simplifying assumptions such as the treatment of the flow as in parallel cylinders, to provide a reasonable starting point. The use of constant pumping head for the various subdivisions of the flow, rather than constant meridian velocity, seems a reasonable basis of procedure, leading to sufficiently simple relations. In developing a theoretic structure including coefficients to be determined by experiment, the writer has a strong predilection, in a field as complicated as this, for the simplest possible theoretic relations, with refinements and limitations to be dictated by tests; and he is inclined to favor those preliminary assumptions which lead to the simplest relations, provided they are reasonable and consistent—a pragmatic point of view.

To give some idea of the complexity of the flow problem in such machines as this, the writer might point out that use is made either expressly or implicitly of the relations for theoretic potential flow. This is almost unavoidable in the first steps of such an analysis. Thus the flow between the impeller blades is here treated as "irrotational" (fifth paragraph) and Weinig's theory for the K curves, Fig. 5 of the paper, is based on such flow.

A difficulty which plagues the hydraulic engineer in attempting to analyze the flow through passages even of simple form is the limitation inherent in the use of potential field theories involving the irrotational flow of that mathematical abstraction and physical paradox, the "ideal fluid." It is the viscous forces in a fluid which tend to stabilize it in "stream-line" flow. When these forces are overpowered by inertia forces, as in the majority of engineering problems, the flow is inherently unstable and turbulent, so that the less the viscous forces, and the more the fluid approaches the "ideal," the less does it conform to the streamlines of the mathematical theory. The most we can say is that, while the flow is essentially unsteady, the time-average velocities may approximate the theoretic behavior.

A factor of primary importance, however, is one which is not sufficiently emphasized in some fluid-mechanics textbooks, namely, separation. The flow lines cannot be arbitrarily assumed to follow the wall contours of a hydraulic passage. With converging flow, increasing velocity, and gradual curvature they will usually do so; but, in an elbow or diverging tube, the flow forms

⁹ Professor of Hydraulic Engineering, Princeton University, Princeton, N. J. Fellow A.S.M.E.

¹⁰ "A New Theory for the Centrifugal Pump," by A. F. Scherzer, Trans. A.S.C.E., vol. 93, 1929, pp. 1-29.

¹¹ "Neuere Anschauungen über die Hydrodynamik der Wasserturbine," by D. Thoma, in "Vorträge aus dem Gebiete der Hydraulischen Aerodynamik," by Th. von Kármán and Levi Civita, Julius Springer, 1924, p. 240. See also, "Hauptströmung und Ringwirbel," by M. Schilhansl, in "Hydraulische Probleme," V.D.I. Verlag, 1926, p. 79.

its own boundary which "separates" from the walls leaving circulating or eddying flow, or even backward flow, between.

The foregoing note is not intended as a criticism of the paper, the author of which is as aware of the problem as the writer. It is mentioned merely as a reminder to those applying similar methods to other problems. It has this specific application, however. In treating the flow in the impeller passages as irrotational, an approximation is involved. This flow actually occurs between somewhat diverging and curving walls, and is decelerating, as in a diffuser or draft tube, with tendencies toward turbulence and even separation, which are intensified under partial-capacity operation. The treatment should therefore be recognized as an approximation which is probably satisfactory so long as experimentally determined coefficients can be applied.

It will probably occur to some readers that the method of the paper should be applicable to propeller-type hydraulic turbines. This extension may require rather laborious study since the conditions are even more complex than in the pump.

The discrepancies noted in the last section of the paper between the theoretic velocity distribution and that observed by Pitot tube may be intensified with increased residual whirl in the turbine, as required by optimum conditions, as compared to the small or zero prewhirl more usual in a pump. A more difficult complication, however, is introduced by the turning of the entering flow from radial to axial, mostly in the transition space, and this requires not two-dimensional, but three-dimensional treatment.

With symmetrical or "spreading" types of draft tubes, the draft-tube subdivision of the turbine can be simply cared for at or near normal gate operation on the basis of free vortex flow; but this element of the problem is confused when the usual elbow draft tubes are used. The writer is not too optimistic of an early solution of the turbine problem; but by judiciously neglecting variables of minor effect and adopting reasonable simplifying assumptions some useful advances may be developed.

In conclusion, it is believed that the author has made a definite advance in the simplification of the "airfoil" or two-dimensional theory and its application to the propeller pump; and that his method meets the tests of both internal consistency and good agreement with the results of experiment. The theoretic and actual performances, compared in Fig. 13 of the paper, show striking consistency in the region of normal discharge; and to anyone experienced in hydraulic experimentation the agreement is unexpectedly good.

H. E. SHEETS.¹² The author has solved the problem of predicting the characteristics of an axial-flow machine. The proposed method has the advantage of simplicity. However, it might be of advantage to analyze the accuracy of some of the assumptions in order to predict the accuracy with which the proposed method may be applied to individual cases.

Equation [2] of the paper gives the lift coefficient of an individual airfoil as a function of $\sin \alpha$, α being the angle of attack from the direction of zero lift. This equation is a good assumption when α approaches zero. For good accuracy, this equation should be limited to small values of α . For the larger values of α , above 12 deg, the lift coefficient of this equation becomes too high. The maximum of this function is at $\alpha = 90$ deg, whereas the maximum lift of the actual airfoil is of considerably smaller values of α . Perhaps Equation [2] could be replaced by a Fourier series, the first member of which is Equation [2], having also a constant factor so that the maximum lift of airfoil used and the maximum of the function have the same values. It should be pointed out that the author uses the lift-coefficient

function in Equation [16] for zero capacity, i.e., where the lift coefficient has its largest values and $\alpha = \beta$. Therefore, only for grids having β equal to or smaller than 12 deg is Equation [16] sufficiently accurate. These grids are rarely encountered in practice.

The lift coefficient of the impeller is given in Equation [7], which is derived from Equation [2] by multiplying with the "lattice-effect coefficient" K . Coefficient K is derived by replacing the impeller vanes with a system of straight and parallel vanes related to the actual vanes system, as shown in Figs. 1 and 2 of the paper. These two figures show the method of determining the line for zero lift. The use of this factor K has been thoroughly discussed in a paper by Y. Shimoyama,¹³ who made a large number of tests on the subject in the range of small β up to $27\frac{1}{2}$ deg. From his paper, it is evident that the theoretical results obtained for a row of flat plates cannot be used directly for a row of airfoils with some thickness and camber. It may be used only if the line of zero lift is determined with sufficient accuracy. These facts have been taken from test data published in Shimoyama's paper.

Therefore, it may be suggested that the author's simple methods of determining the zero-lift line, as shown in Figs. 1 and 2, may be replaced by a more accurate method given in Shimoyama's paper. It shall be noted that the influence of the thickness of an airfoil is such that there is a different zero-lift line, depending on whether the airfoil cascade operates in accelerated flow or decelerated flow. This method of calculation should be used only from zero lift to the stalling point of the blades. At zero capacity, there exists secondary flow from the hub to the tip of the blades creating pressure by centrifugal action. Then the flow in the impeller is three-dimensional and cannot be calculated accurately with the two-dimensional theory.

This discussion has been given in order to show how the author's basic method may be modified when higher accuracy is required.

A. J. STEPANOFF.¹⁴ The author's presentation of the airfoil theory of axial-flow pumps differs in several respects from that of several previous publications: (a) The author uses the zero-lift line of the vane rather than chord as a reference line for angles of attack. This simplifies the theoretical formulas for the lift coefficient. (b) He treats the discharge end of the vane separately from the suction end, thus leading to the design of the vane instead of a selection from the available airfoil wind-tunnel-tested profiles. This removes one of the objections to the airfoil theory. The most complete collection of the airfoil data by N.A.C.A. is limited to cambers of 0, 2, 4, and 6 per cent, while in practice intermediate and higher cambers are in use. (c) The author does not try to supersede the classical Euler's theory but attempts to establish a common ground between the Euler and airfoil theories. (d) This paper presents difficulties and inconsistencies of the airfoil theory, also gives examples of disagreement of the tests with the assumed pattern of flow, thus leaving room for opinions and pattern flow different from his own.

Pumps have been designed with good success in a continuous series of specific speeds from very low centrifugals up to the straight propeller pumps. The theoretical reasoning, mental pattern of flow, and design method should be continuous for pumps of all specific speeds within the range mentioned. The airfoil theory of axial-flow pumps is handicapped by the fact that it becomes less accurate for lower-specific-speed propeller pumps, and fails entirely for mixed-flow and centrifugal impellers.

¹² Research Engineer, Elliott Company, Jeannette, Pa. Jun. A.S.M.E.

¹³ "Experiments on Rows of Aerofoils for Retarded Flow," by Y. Shimoyama, Trans. Society of Mechanical Engineers of Japan, vol. 3, Nov., 1937, pp. 334-344.

¹⁴ Development Engineer, Ingersoll-Rand Company, Phillipsburg, N. J. Mem. A.S.M.E.

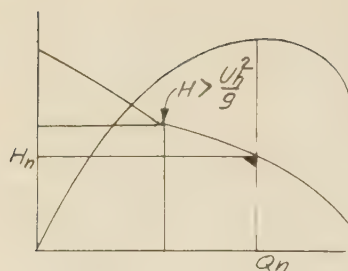


FIG. 17 ACTUAL HEAD EXCEEDS THEORETICAL AT HUB

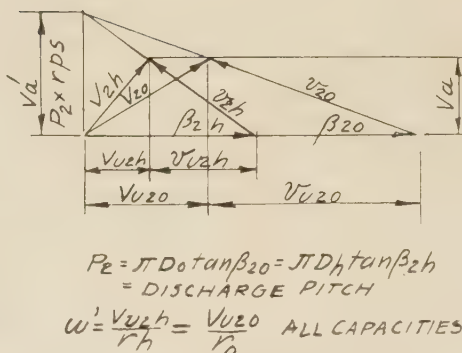


FIG. 18 DISCHARGE TRIANGLE

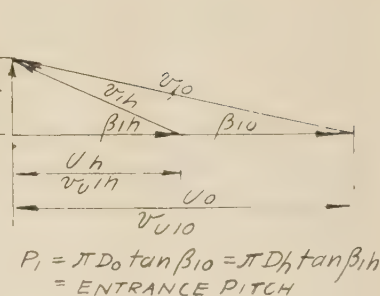


FIG. 19 ENTRANCE TRIANGLE AXIAL INLET

The object of the airfoil theory is to establish the shape of the impeller-vane profile and the chord-spacing ratio. A number of vital design elements have to be determined experimentally to complete the design of an impeller. Among these are: (a) Selection of a proper specific speed; (b) impeller diameter; (c) axial velocity; (d) hub ratio; (e) number of vanes for a given chord-spacing ratio. All of these design elements, expressed as dimensionless ratios, form a continuous function of specific speed. The progress in theory of centrifugal and axial-flow pumps was much slower than the development of actual designs. As a result, designers had to adopt some "geometrical" method of arriving at impeller-vane profiles according to their assumed mental pattern of flow. These too had to be continuous for all pumps, centrifugal, mixed, and axial flow.

As a prerequisite of the condition that there should be no cross-flows from one stream cylinder to another, the author, like all previous investigators, assumes that

$$\Delta V_u r = \text{const} \dots \dots \dots [41]$$

which is the same as

$$\frac{\Delta V_u U}{g} = H = \text{const} \dots \dots \dots [42]$$

or that equal heads are produced at all radii. The flow pattern represented by Equation [41] of this discussion is known as a "free vortex." The tangential velocity at discharge from the impeller ΔV_u increases toward the hub inversely as the radius, resulting in the absolute discharge flow revolving at higher angular velocity at the hub than at the periphery. A similar pattern of flow is assumed at the impeller suction. With an impeller revolving at constant speed between these two regions, such a pattern of flow is difficult to visualize.

The author points out that the condition represented by Equation [42] of this discussion can be fulfilled only at the design point. This equation is impossible to satisfy at capacities below or above the normal. Moreover, even at the best efficiency point, Equation [42] holds for one vane setting only. If the vane is turned a few degrees, velocity triangles representing Equation [42] are destroyed, although actual efficiency and head remain unchanged. Finally, at partial capacities, the condition represented by Equation [42] leads to an absurdity, as partial-capacity conditions are soon reached where the actual head is higher than the maximum possible theoretical head at the hub (Fig. 17 of this discussion).

$$H_{\text{hub}} = \frac{U_h^2}{g} < H \text{ actual} \dots \dots \dots [43]$$

All these drawbacks are eliminated in a pattern of flow represented by

$$\frac{\Delta V_u}{r} = \omega' = \text{const for all radii} \dots \dots \dots [44]$$

This is known as a "forced vortex"¹⁶ and is free from crossflows from one stream cylinder to the other.¹⁸

The flow leaves the impeller with a constant absolute angular velocity ω' . The same regime prevails at all capacities, ω' increasing as capacity decreases, reaching the impeller speed at zero capacity. Zero head and zero capacity are reached by all stream cylinders at the same time (Fig. 19 of this discussion). The forced-vortex pattern of flow is realized with impellers having vanes of constant pitch for all radii, the pitch increasing from entrance to discharge, Figs. 18 and 19. The increasing vane angle is necessary to produce "impelling action" on the water, as no power can be applied to the water if its axial velocity is exactly equal to the pitch of the vane-screw surface. This type of flow pattern requires a constant axial velocity. With a constant-pitch impeller, a constant axial velocity is maintained in practice throughout a wide range of capacities.

Evidently, in a forced-vortex pattern of flow, the Euler's head is lower at the hub and higher at the periphery, and the pump theoretical head is an integrated average over the whole area swept by the impeller. This is equal to the arithmetical average of the heads at the hub and periphery of the impeller. Attention is called to the fact that, although the head at the hub is lower than the pump total head, this part of the impeller contributes continuously to the pump total integrated head. This is illustrated graphically in Figs. 21 and 22 of this discussion.

The Euler head equation can be transformed so that the forced-vortex action will be apparent. Thus, for an axial inlet

$$H = \frac{\Delta V_u U}{g} = \frac{\Delta V_u^2}{2g} + \frac{v_{u1}^2 - v_{u2}^2}{2g} \dots \dots \dots [45]$$

The first term in Equation [45] represents the static pressure due to the absolute forced vortex at discharge, while the second is the difference in relative forced vortices at entrance and discharge. The axial component of flow does not appear in the foregoing ex-

¹⁶ The flow patterns represented by Equations [41] and [44] are special cases of a general flow regime $V_r^m = \text{const}$. With different values of m , different flow patterns result, all of which are stable or free from crossflows, giving different pressure and angular-velocity distribution along the radius.

¹⁸ "Hydraulics and its Applications," by A. H. Gibson, D. Van Nostrand Company, Inc., New York, N. Y., 1928, p. 101.

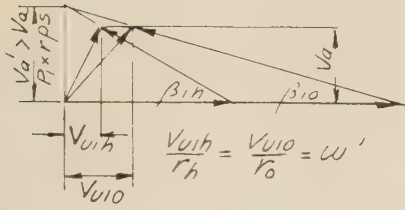


FIG. 20 ENTRANCE TRIANGLE PREROTA-TION ALLOWED

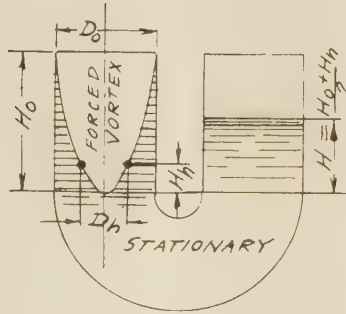


FIG. 21 HYDRAULIC INTEGRATION

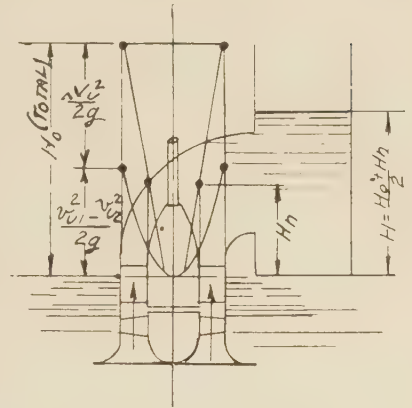


FIG. 22 AXIAL-FLOW PUMP

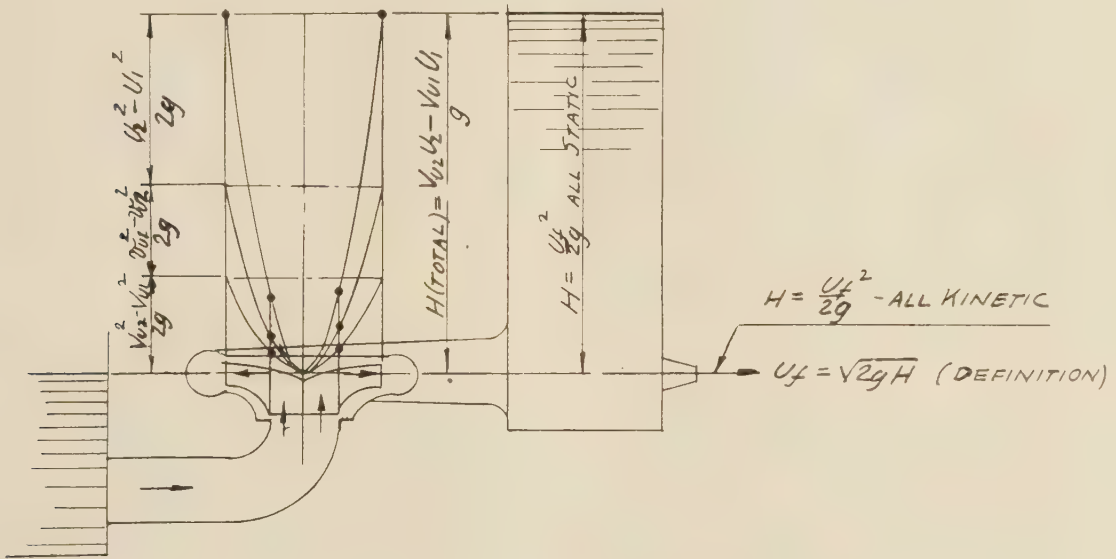


FIG. 23 CENTRIFUGAL-PUMP HEAD

pressions. The forced-vortex flow pattern, theoretical reasoning and the vane-layout geometry remain when applied to mixed-flow or straight centrifugal pumps. Taking Euler's equation in a most general form and applying the same transformations, we obtain the following

$$H = \frac{V_{u2}U_2 - V_{u1}U_1}{g} = \frac{V_{u2}^2 - V_{u1}^2}{2g} + \frac{v_{u1}^2 - v_{u2}^2}{2g} + \frac{U_2^2 - U_1^2}{2g} \dots [46]$$

This is of the same nature as Equation [45], except the third term is added to account for head increase due to water particles moving from inlet diameter to the outlet diameter. Note only tangential components of all velocities appear in Equation [46], and the radial velocities at the inlet and outlet (not equal in general) cancel out. All transformation of energy takes place in the plane of impeller rotation for both axial- and radial-flow impellers. Figs. 22 and 23 of this discussion show diagrams of total head for a centrifugal and axial-flow pump, expressed in terms of forced vortices, as given by Euler's Equation [46].

In a general case, where some prerotation is allowed ahead of the impeller, the velocity triangle, Fig. 19, is changed to Fig. 20 of this discussion. This shows that a forced vortex is formed in the impeller suction, as observed on occasions in practice.

The impeller-vane design method, based on this theory, has been in use for over 15 years by several pump and water-turbine designers for both axial- and mixed-flow impellers. One of the earliest examples on the record is that by Schmidt.¹⁷ His theory and pattern of flow the writer never has been able to understand, but his vane-design method, arrived at entirely in an experimental way, can be explained now by the forced-vortex reasoning. Terry¹⁸ recently described a Kaplan water-turbine design which fits into the forced-vortex pattern of flow.

The writer has applied forced-vortex reasoning and vane-layout geometry based on it to mixed-flow propeller pumps with very gratifying results.

¹⁷ "Some Screw Propeller Experiments With Particular Reference to Pumps and Blowers," by H. F. Schmidt, *Journal, American Society of Naval Engineers*, vol. 40, 1928, pp. 1-26.

¹⁸ "Development of the Automatic Adjustable-Blade Type Propeller Turbine," by R. V. Terry, *Trans. A.S.M.E.*, vol. 63, 1941, pp. 395-409.

It is interesting to note that now it is possible to bring about a closer agreement in the bitter and prolonged controversy aroused by Scherzer¹⁹ some time ago who claimed that the forced vortex is the only way head can be produced by a centrifugal impeller. He repudiated the Euler equation, and credited the impeller only with the head $H = \frac{U_2^2}{2g}$. Equation [46] of this discussion shows that it is possible to think of the pump head as produced by a forced-vortex action, but its value is still given by Euler's equation which shows that $U_2^2/2g$ is only a portion of the total vortex. Equation [46] can be written in a simpler form

$$H = \frac{V_{u2}U_2 - V_{u1}U_1}{g} = \frac{U_f^2}{2g} \dots \dots \dots [47]$$

where $U_f = \sqrt{2gH}$ by definition, its numerical value being equal to the velocity of a free jet under head H . Equation [47] represents a forced vortex with a peripheral velocity U_f which is a sum of the several vortices shown in Equation [46]. The velocity U_f does not exist at any part of the pump. The H on Fig. 23, and in Equation [47] of this discussion, is the total head and not a static head. This head is split differently between static and kinetic for pumps of different specific speed. If discharged into an open vessel (no losses), it will be all static. If discharged freely into the atmosphere, it will be all kinetic, Fig. 23.

The author takes an agreement between the predicted performance and actual test as a proof of soundness of the theoretical reasoning and the assumed pattern of flow. The quoted examples of Schmidt, Scherzer, and a more recent one by Pigott²⁰ disprove such belief. Among engineers, each theory can be judged on its own merit.

The best hydraulic performance may be an indication of a "preferred" pattern of flow. In this connection, it would be interesting to know which of the two designs referred to in Figs. 15 and 16 of the paper, was more efficient hydraulically?

T. H. TROLLER.²¹ This discussion refers to that part of the paper dealing with the interaction of the vane sections at various co-axial cylinders, and its effect on the pressure-volume characteristic.

The designer has at his disposal an arbitrary determination of the lift coefficient C_L and the width l whose product only is given by the requirements to be met for one design point of a characteristic. It is possible to a certain degree to use this degree of freedom for the vane or blade design in such a form that a desired co-ordination of the action of various vane elements is assured over a reasonable range of working conditions.

A derivation of such a relation is given in a paper on axial-flow fan design by the writer.²²

Starting with the proposition that the circulation about the rotating blade should in the ideal case remain constant for all co-axial cross sections of the rotor at any one point of the pressure-volume point, a condition in full agreement with the author's description of the ideal flow through a pump, one arrives at the following formula for the distribution of vane widths along the radial extent of the vane

$$l_r/l_R = \frac{\cos \beta_R}{\cos \beta_r} + \frac{C_{LR}}{C_{Lr}'} (R^2/r^2 - 1) \tan \beta_R$$

¹⁹ See L. F. Moody discussion, reference 10.

²⁰ "Prediction of Centrifugal Pump Performance," R. J. S. Pigott, paper presented at A.S.M.E. Annual Meeting, 1944, preprint no. 75.

²¹ LaDel Conveyor and Manufacturing Co., New Philadelphia, Ohio, and Daniel Guggenheim Airship Institute, Akron, Ohio. Mem. A.S.M.E.

²² "The Design of Axial-Flow Fans," by Th. Troller, Abhandlungen aus dem Aerodynamischen Institut, Aachen, no. 10, 1931, pp. 43-47.

(The symbols are the same as used by the author. In addition:

$C_L' = \frac{dc_L}{d\alpha}$, R = outside radius, r = any radius of the blades.

The indexes refer to the location of the section.)

This formula is entirely practical for axial-flow fan design for many cases, and the fact that unconsciously the condition given by this formula is often met by the designer is in the opinion of this writer responsible for a good bit of the successful operation over a wide range of many axial-flow machines.

Many designers (e.g., Ruden) prefer, for reasons beyond those stated in the theory presented by the author, to use shapes different from that given by the formula presented here; and there is no question that a different reasoning for the vane design is indicated in those cases where vane friction or tip leakage as non-ideal inflow conditions are of importance. Nevertheless, the formula is of great practical usefulness in many design problems.

F. L. WATTENDORF.²³ This paper is a welcome contribution to axial-flow pump or fan theory in that it gives a physical picture of the relationship between one-dimensional theory of guided flow for closely spaced blades and two-dimensional theory, used when the blades are so widely spaced that the elements behave essentially as single airfoils. One-dimensional theory is usually employed for ratios of blade chord to spacing greater than unity, and two-dimensional theory for ratios essentially less than unity. However, there is an increasing number of fan, pump, and compressor problems at the present time in which the spacing ratio varies from somewhat less than unity to somewhat greater than unity. For such problems as these, the present paper is a help to the designer.

AUTHOR'S CLOSURE

The author is indebted to W. H. Church for calling attention to an inaccuracy in a partially graphical solution for the plotting of the K and the C_H diagrams. These diagrams as presented in the paper were recalculated according to the equations which Church has quoted from the book by Weing (1). It may be of interest that in these equations the parameter R is, in the plane of conformal representation, the distance from the origin to the two singularities (vortex-sources) which represent the regions plus and minus infinity of the physical plane containing the vane system. The vane is represented by the unit circle; and the angle α_{ST} is the angular distance of the stagnation points on the unit circle from the real axis.

The comments by R. G. Folsom are of particular value since his earlier publication on the same matter (item 2 of Bibliography) stimulated to a considerable extent the present investigations of the author. The equation quoted by Folsom for the lift coefficient requires the determination of the constant C on theoretical or experimental grounds. It was, of course, the intention of the present paper to avoid the complications involved in considering the variations in C . In other respects, the equation quoted by Folsom is the same as Equation [2] of the paper, since for small values of α , the angle and its sine are proportional to each other.

The author agrees with Folsom regarding the significance of an exact determination of the blade shapes and angles. In recognition of this fact, the theoretical analyses reported here were based entirely on the dimensions of the test runner as determined by a special measuring device.

R. Lowy correctly points to the theoretical and physical limitations of the theory used by the author. It is unquestionably true that the problem is really a three-dimensional one. Therefore, even for an ideal fluid, considerations as represented by the

²³ Headquarters, Army Air Forces, Washington, D. C.

turbine theory by Lorenz are in order.²⁴ This problem has been outlined more recently by Spannhake at the Fifth International Congress for Applied Mechanics. The theoretical difficulties connected with such a more rigorous approach are so great as to cast some doubts on its practical usefulness. It must be remembered in particular that any departure from the admittedly fictitious picture of the flow along cylindrical surfaces makes the present simple approach to the two-dimensional problem impossible. This is due to the fact that the relative flow does not remain irrotational if it has a radial component. There can be no doubt that more detailed considerations of the three-dimensional problem will be necessary in order to answer some of the problems which have been left open by this paper.

The question of prerotation as raised by Lowy was answered by a test setup permitting a reliable control of this element of the flow. An influence on the incoming flow by the runner was observed only as a consequence of a lack of agreement between the flow and the vane design as, for instance, in the range of low capacities.

The author would like to express to Prof. L. F. Moody his appreciation for constant advice and encouragement over many years.

The method of Thoma can be related to that in the present paper by considering that the circulation around an individual vane has the value $\Gamma = \Delta V_U t$, while the circulation in front of runner is

$$\Gamma_1 = 2\pi r V_{U1} \dots \dots \dots [48]$$

and on the discharge side of the runner

$$\Gamma_2 = 2\pi r V_{U2} \dots \dots \dots [49]$$

The change in circulation with respect to the axis of rotation is therefore equal to the sum of the vane circulations

$$\Gamma_2 - \Gamma_1 = z\Gamma$$

The author certainly finds himself in agreement with Moody's point of view. With particular reference to the problem of the "ideal fluid," Moody clearly touches on the most difficult phase of the fluid mechanics of this type of machinery. Since a theory based on an "ideal fluid" cannot account for the losses in a machine, it is obvious that the problem of improving the design cannot be attacked without considering the characteristics of a real fluid, as, for instance, separation. The theoretical difficulties connected with this problem are well appreciated from other fields of fluid mechanics. Their solution with respect to the complicated flow conditions in turbomachinery must be considered as an essential element of future developments in this field.

The author does not believe that the application of the present theory to propeller-type turbines would differ essentially from that mentioned for pumps, since the "residual whirl" at the discharge from a turbine runner can be considered in the same manner as prerotation of the pump runner. In the case of a turbine, the rotation on the high-pressure side of the runner must be assumed to be prescribed by the guide apparatus and the whirl on the discharge side results from the action of the runner. It is true, however, that the space between the guide apparatus of a propeller turbine and its runner is likely to cause departures from the ideal velocity distribution at the runner inlet.

H. E. Sheets has called attention to an important limitation in the paper, which applies not only to this particular application of the theory of ideal fluids, but to any other based on the same assumption. From a physical point of view, the limitation of α

is simply the separation or stalling limit of any vane or airfoil, which must, of course, be taken into account in order to avoid outright contradictions between theory and physical facts. The theoretical use of α for a wider range than is physically permissible merely has the significance of a theoretical tool to establish the direction of the theoretical head-capacity characteristics. The relation between theory and physical facts is rational only for capacities larger than that of the familiar break in the actual head-capacity curve. For capacities below that limit, the flow picture is known to be radically changed and bears no resemblance to the assumptions made in this paper.

The author regrets that he did not have an opportunity to examine the apparently interesting paper by Shimoyama,¹³ referred to in the discussion.

We are greatly indebted to A. J. Stepanoff for a thorough discussion of this subject and shall try to answer only its most important points. At the outset, it must be realized that the basic reason for the fact that radial- and mixed-flow runners cannot be treated in the same manner as axial-flow runners is the previously mentioned fact that the relative flow in the former type of runner is not irrotational.

There appears to be a slight misunderstanding concerning the fact that Equation [42] of the discussion was applied by the author only to the design point. By averaging the rate of through-flow rather than the head, the author has assumed that this equation is satisfied at all times. This does not mean that Equation [42] is necessarily satisfied under the actual flow conditions in the pump, but merely that its application does not lead to logical inconsistencies. In this connection, Stepanoff's suggestion of using the law of a forced vortex furnishes a very interesting example of the significance of the derivations leading to Equation [30] of the paper. Substituting the law of a forced vortex

$$V_{U1} = r\omega_1 \text{ and } V_{U2} = r\omega_2 \dots \dots \dots [50]$$

into Equation [30] of the paper, one obtains

$$2\omega_2(r\omega - r\omega_2) = 2\omega_1(r\omega - r\omega_1)$$

or

$$\omega\omega_2 - \omega_2^2 = \omega\omega_1 - \omega_1^2 \dots \dots \dots [51]$$

Consequently, the angular velocity of the two forced vortices at the inlet and discharge ω_1 and ω_2 are the two roots of a quadratic equation, and as such have the relation

$$\omega_1 + \omega_2 = \omega \dots \dots \dots [52]$$

where ω is the angular velocity of the runner. This condition, however, is seldom if ever satisfied in axial-flow pumps.

One can obtain an independent check on the validity of Equation [30] of the paper by substituting the law of a forced vortex into the more fundamental Equation [22] of the paper, which expresses the equilibrium between pressures and centrifugal forces in a radial plane. The integration yields the relation

$$p - p_0 = \frac{\rho}{2} V_U^2 \dots \dots \dots [53]$$

where p_0 is the static pressure at the center of rotation if the law of a forced vortex were maintained that far. Equating the static-pressure differences between the two forced vortices to the static-pressure increase through the runner along the cylindrical stream surface, one obtains

$$\frac{\rho}{2} (V_{U2}^2 - V_{U1}^2) = \rho \left[U(V_{U2} - V_{U1}) - \frac{V_{U2}^2 - V_{U1}^2}{2} \right] \dots [54]$$

²⁴ "Neue Theorie und Berechnung der Kreiselr der," by Hans Lorenz, R. Oldenbourg, Munich and Berlin, 1906.

which may be simplified to

$$V_{U_2} + V_{U_1} = U \dots \dots \dots [55]$$

The latter, however, applying to one cylindrical stream surface has for forced vortices the same meaning as the previous Equation [52].

The conclusion to be drawn from these derivations is that with the exception of the flow conditions expressed by Equations [52] and [55], the assumption of a forced vortex flow at entrance and discharge of the runner is dynamically incompatible with the assumption of cylindrical stream surfaces through the runner. The problem answered by these considerations is not one concerning the existing flow but one of theoretical consistency of the assumptions employed. It is in this light that the derivations leading to Equation [30] of the paper have to be viewed.

The author would be greatly interested in learning more of the background of the relation suggested by T. H. Troller; in particular, the underlying variation of the lift coefficient as a function of the radius. This problem of design certainly warrants independent study, and it is to be hoped that there will be significant additions to the literature in this field.

F. L. Wattendorf's comments were greatly appreciated, particularly since his earlier work furnished much of the incentive for this paper. His remarks, in common with other contributions

to the discussion, seem to express the fact that essentially there is agreement on the main points of the paper, in so far as it goes.

The author wishes to thank Prof. John R. Weske for some interesting and encouraging comments which unfortunately were received too late to be published with the other discussions. Among various facts, Professor Weske points out that the first term in the denominator of Equation [20] is the inverse ratio of K to its one-dimensional approximation, i.e. the ratio between the ordinates of the straight lines and the curves in Fig. 4. This fact further illustrates the close relation between the correction factors K and C_H of the two- and the one-dimensional theories. Professor Weske is generally in agreement with the paper and expresses the opinion that it furnishes "a foundation from which the three-dimensional problems can be attacked with greater confidence."

The gratifying number of discussions received demonstrate that the subject is one of timely interest. What has been achieved may be considered only as groundwork. Obviously, the more difficult aspects of the problem are yet before us; for example, the three-dimensional approach mentioned by Lowy, and the problem of the "real" vs. the "ideal" fluid, suggested by Moody. The experimental evidence and the contributions received indicate that the theory presented, while far from complete, does contain what may be termed a significant relation to reality.

Optimum Compression Ratios for a High-Speed Diesel Engine

By W. P. GREEN,¹ COLLEGE PARK, MD.

Optimum compression ratios must give smooth and reliable ignition. They are high enough to procure maximum fuel economy. They are determined from data presented to show the effect of compression ratio upon the combustion and performance characteristics of a high-speed (2000-rpm) 3.25 × 4.5-in. single-cylinder compression-ignition engine equipped for varying the precombustion-chamber volume. These data show an optimum range of compression ratios varying with the indicated mean effective pressure. Compression ratios should be increased as the indicated mean effective pressure (imep) decreases. Optimum performance of the engine under test was obtained in the range of compression ratios from 16 to 1 to 24 to 1. Structural strength-weight requirements and cylinder wear may dictate the use of lower values of the compression ratio than does fuel economy.

A fundamental property of an internal-combustion engine is the compression ratio and the dependent expansion ratio. For the compression-ignition engine, it is also necessary that the compression ratio be high enough to insure certain and smooth ignition. The optimum compression ratio will be high enough to meet ignition requirements and give maximum fuel economy. Other factors, such as cylinder wear, ring wear, mechanical repairs, and cost of building the engine strong enough to withstand the stresses and temperatures which accompany high compression ratios were not considered to come within the scope of this paper.

To determine the compression ratios which insure ignition and give maximum thermal efficiency at any given load, it is necessary to know the major performance characteristics of an engine over a wide range of compression ratios. Since past published investigations of the effect of compression ratio on high-speed Diesel-engine performance have been limited in extent and performed on several types of engines not readily comparable, (1, 2, 3, 4, 5),² it was decided to measure the major performance characteristics of a high-speed CFR Waukesha Diesel engine equipped with a head having adjustable precombustion-chamber volume.

Data were taken for computing the performance characteristics, listed in Table 1, over a range of compression ratios from 12:1 to 31:1.

TEST EQUIPMENT

Major test equipment is shown in Fig. 1, while Fig. 2 shows schematically the arrangement of all equipment.

The engine used was a standard CFR single-cylinder evaporative-cooled engine of 3.25 in. bore and 4.5 in. stroke as pre-

TABLE 1 PERFORMANCE CHARACTERISTICS MEASURED OVER A WIDE RANGE OF COMPRESSION RATIOS

- (a) Friction horsepower and friction mean effective pressure
- (b) Brake horsepower and brake mean effective pressure
- (c) Indicated horsepower and indicated mean effective pressure
- (d) Volumetric efficiency
- (e) Maximum explosion pressures
- (f) Efficiencies, thermal and mechanical, on a brake-horsepower and indicated-horsepower basis
- (g) Exhaust appearance
- (h) Injection-advance-angle range
- (i) Combustion characteristics as shown by indicator cards
- (j) Heat rejection to coolant

Other operating variables, listed in Table 2, were maintained constant throughout the tests.

TABLE 2 STANDARD OPERATING CONDITIONS

- (a) Engine speed, 2000 rpm
- (b) Intake-air temperature, 140 F plus or minus 1 deg F
- (c) Intake-air pressure, atmospheric pressure plus or minus 1/2 in. of water
- (d) Exhaust pressure, atmospheric pressure plus 6 in. of water
- (e) Lubricating oil, S.A.E. 30
- (f) Lubricating-oil temperature, 170 F plus or minus 2 deg F
- (g) Cooling-water temperature, 212 F
- (h) Injection pressure, 2000 psi
- (i) A single commercial Diesel fuel of known specifications for all tests; 50 cetane number used
- (j) Angle of injection advance setting to obtain maximum fuel economy for a given load

viously noted. It was equipped with a Diesel conversion cylinder head allowing infinitely variable compression ratios between 12:1 and 31:1. The compression ratio was changed by varying the volume of a cylindrical precombustion chamber with a movable plunger in such a way as not to affect materially the combustion characteristics.

The cylinder and variable-compression-ratio head were mounted on a high-speed crankcase equipped with balanced pistons. The engine piston was of cast iron and was provided with three compression rings and one oil ring.

Fuel was supplied from a 5-gal tank above the engine panel-board to a weighing tank placed upon an accurate set of balances as shown in Fig. 2. After being weighed, the fuel entered a Bosch injection pump and was then injected into the cylindrical precombustion chamber through a Bosch pintle-type injector.

A contact device, attached to the injector and operated by the opening of the injector-nozzle pin, was used in conjunction with a neon indicator on the engine crankshaft to observe the crank-

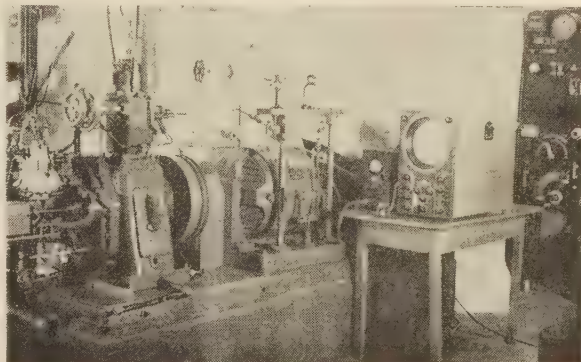


Fig. 1 MAJOR TEST EQUIPMENT

¹ Associate Professor of Mechanical Engineering, University of Maryland. Mem. A.S.M.E.

² Numbers in parentheses refer to the Bibliography at the end of the paper.

Contributed by the Aviation and Oil and Gas Power Divisions and presented at the Annual Meeting, New York, N. Y., Nov. 27-Dec. 1, 1944, of THE AMERICAN SOCIETY OF MECHANICAL ENGINEERS.

NOTE: Statements and opinions advanced in papers are to be understood as individual expressions of their authors and not those of the Society.

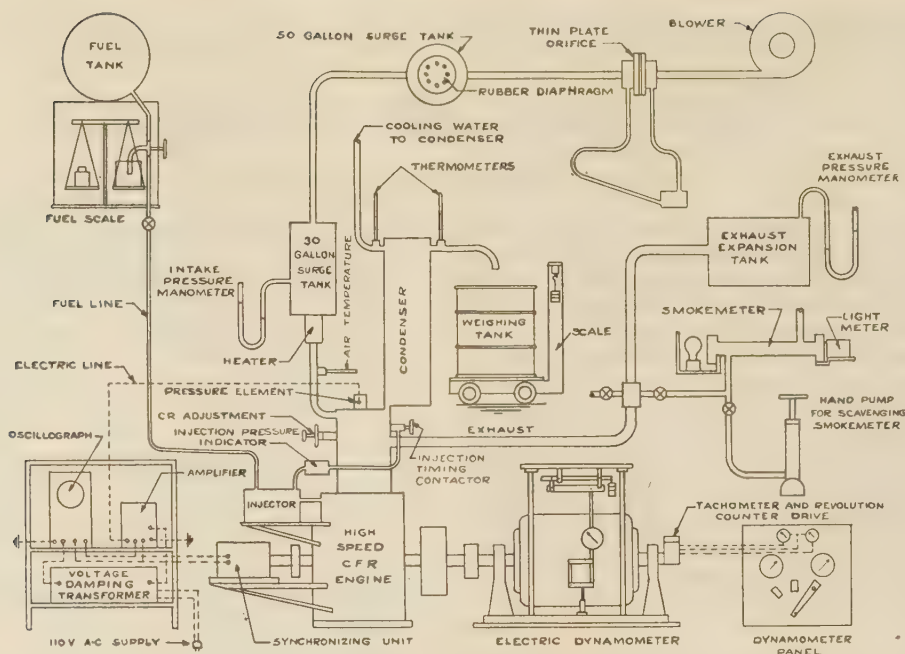
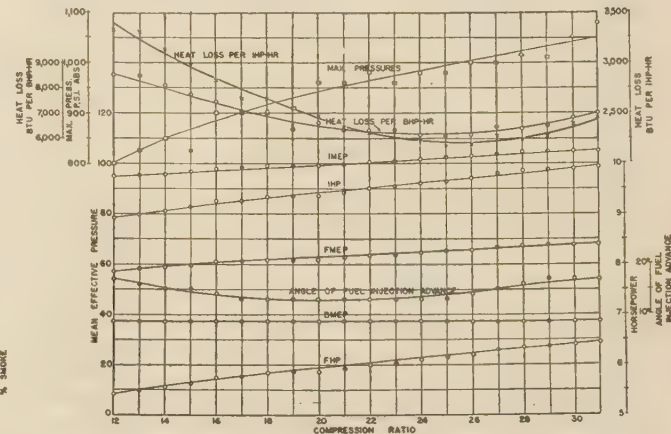
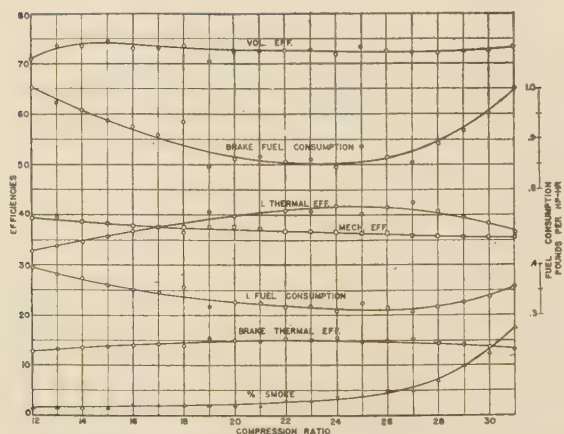


FIG. 2 SCHEMATIC LAYOUT OF ALL TEST EQUIPMENT

FIGS. 3 AND 4 PERFORMANCE CHARACTERISTICS OF A CFR WAUKESHA DIESEL ENGINE, OPERATING AT 2000 RPM AND $3\frac{1}{2}$ BHP

angle position at which fuel was first injected into the precombustion chamber.

Air to the engine passed through a small blower, a metering orifice, two surge tanks, and an air heater before entering the engine.

The blower supplied the air under pressure to a $\frac{5}{8}$ -in. Meriam orifice. Pressure taps from the orifice were connected to an inclined manometer for reading accurately the quantity of air flowing. In order to avoid pulsating flow through the orifice, a 50-gal steel drum, equipped with a rubber diaphragm in one end, was used as a surge tank. In addition, a small 30-gal drum was mounted above the air heater on the intake manifold of the engine. The pressure in this drum was maintained atmospheric within $\frac{1}{2}$ in. of water.

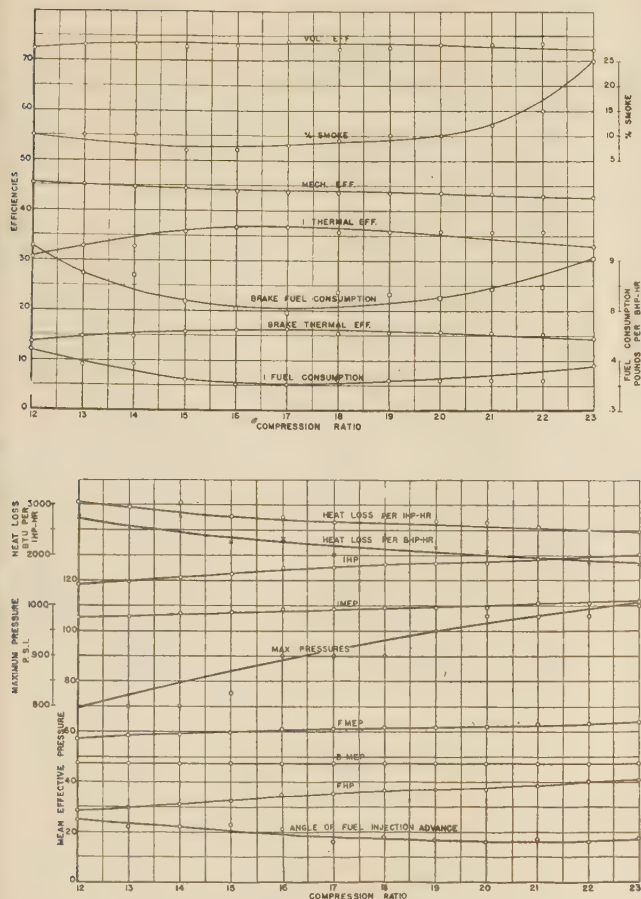
By means of this equipment a steady flow of metered air was delivered to the engine at 140 F and atmospheric pressure.

Exhaust gases passed from the engine cylinder through 20 ft

of $1\frac{1}{2}$ -in. pipe to a 10-gal expansion tank, and then into the laboratory exhaust main. Provision was made at the first 90-deg elbow 20 in. from the engine (see Figs. 1 and 2) to sample the exhaust gases for exhaust-appearance tests. The sample of gases was carried through tubing to a smokemeter where its appearance was evaluated. Smoke appearance was evaluated as described by Schweitzer (6).

A conventional type of cradle dynamometer was used for motoring and loading the engine. The engine speed was maintained at 2000 rpm by means of an electric-indicating tachometer. An electric revolution counter was also in operation for all fuel-consumption and power tests.

The pressure-crank-angle diagrams were photographed from the screen of a 9-in. cathode-ray oscillograph. A piezoelectric-crystal pickup mounted in the precombustion chamber of the engine was used in conjunction with an amplifier and the oscillograph to measure all pressures. It was calibrated by the manu-



FIGS. 5 AND 6 PERFORMANCE CHARACTERISTICS OF A CFR WAUKESHA DIESEL ENGINE, OPERATING AT 2000 RPM AND 4 1/2 BHP

facturer several times during the tests, and calibrations were checked with a balanced-diaphragm type of maximum-pressure indicator (7, 8). A modification of the Taylor and Draper pressure element was used.

Thermometers inserted in the inlet and outlet water lines of the condenser on the evaporative cooling system were read to determine the temperature rise of the cooling water. Water leaving the condenser outlet was weighed in a 50-gal drum mounted on scales.

OPERATING PROCEDURE

Having determined the proper angle of injection advance, tests were run in the following manner:

The engine was operated for a period of at least 2 hr until readings indicated standard conditions had been reached. Then readings were taken every 5 min during a 15-min period of the engine speed, of engine revolutions, time for the consumption of a given weight of fuel, angle of injection advance and injection pressure, cooling-water and oil temperatures, injector temperature, weight of condenser water, inlet and outlet condenser-water temperatures, dynamometer-scale readings, inlet-air temperature, inlet-air rate of flow, inlet air pressure, exhaust pressure and per cent smoke in the exhaust. During the test interval, pictures were taken of pressure-crank-angle cards on the screen of the oscillograph. After test data had been completed, the compression ratio was changed, 1/2 hr being allowed for stabilization of operating conditions, and the procedure was repeated in

duplicate for each compression ratio between 12:1 and 31:1. However, at a load of 4 1/2 hp the maximum compression ratio which gave good continuous operation was 23:1.

In some instances, it was impossible to obtain the indicator cards and smoke-meter readings during the original performance tests. Check tests were run later to obtain these data.

The engine was motored in order to determine the friction horsepower at the end of each test run. Since it was found that this procedure interrupted regular tests owing to a very poor laboratory direct-current power supply for metering purposes, the friction horsepower were determined during check runs under the same conditions of engine operation.

It should be mentioned that the mechanical condition of the engine was found to be of utmost importance. It was found necessary to clean the piston rings and injector after 8 to 10 hr of operation if best results were to be ob-

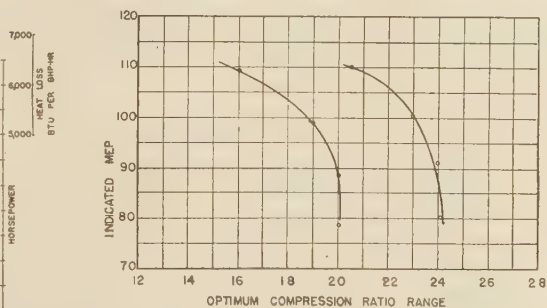


FIG. 7 OPTIMUM COMPRESSION RATIO RANGE FOR A CFR WAUKESHA DIESEL ENGINE AT VARIOUS INDICATED-MEAN-EFFECTIVE PRESSURE VALUES; 2000 RPM

tained. Operation for longer periods of time always resulted in a loss of power due to sticking of the top piston ring. With rings and grooves clean, a check of the blowby even at highest compression ratios indicated that it was considerably less than 3 per cent.

TEST RESULTS

The results of performance tests are shown by the curves in Figs. 3 and 4, for a load of 3 1/2 bhp. Figs. 5 and 6 show the same characteristics for a load of 4 1/2 bhp. It should be noted that for this horsepower the maximum compression ratio for continuous operation was 23 to 1.

The curves, based on performance at a wide range of compression ratios, show a number of interesting trends in compression ratios above 16:1. Friction horsepower increases with compression ratio. Indicated mean-effective-pressure values of 109 psi were obtainable without excessive smoke. Smoke increased rapidly and became excessive at mean-effective-pressure values above 115 psi.

Brake and indicated fuel consumption curves have a concave upward shape. They reveal decreasing fuel rates until the range of optimum compression ratios is reached. Fuel rates then increase.

Volumetric efficiency remains constant within 2 per cent over the range of compression ratios covered. Exhaust appearance becomes smokier with increases in compression ratio above 20 to 1. Heat losses to the coolant decrease with compression ratio, reaching a minimum value in the compression-ratio range from 23:1 to 28:1. Further increases in compression ratio lead to slightly increased heat losses.

OPTIMUM COMPRESSION RATIOS

From the data included in Figs. 3, 4, 5, and 6, and from tests at lower horsepower ratings, Fig. 7 was constructed. It shows the optimum compression ratios for the range of imep values studied with this precombustion-chamber-type Diesel. Fig. 7 brings out the fact that the maximum values of the imep as well as brake and indicated horsepower decrease with an increase in compression ratio after a ratio high enough for smooth ignition is reached.

It should be pointed out that while the range of compression ratios indicated gives maximum fuel economy, the curves of indicated fuel consumption versus compression ratio (see Figs. 3 and 5) are relatively flat for this type of engine. The range of compression ratios considered optimum might therefore be lowered considerably if such factors as engine wear and structural strength and weight are considered.

ACKNOWLEDGMENT

The author is indebted to the National Advisory Committee for Aeronautics for permission to incorporate in this report data obtained during an investigation at the University of Maryland which was sponsored by the National Advisory Committee for Aeronautics.

BIBLIOGRAPHY

- 1 "Prechamber Compression-Ignition Engine Performance," by C. S. Moore and T. H. Collins, Jr., Technical Report No. 577, N.A.C.A., 1937.
- 2 "Combustion in a High-Speed Compression-Ignition Engine," by A. M. Rothrock, Technical Report No. 401, N.A.C.A., 1931.
- 3 "Influence of Several Factors on Ignition Lag in a Compression-Ignition Engine," by H. C. Gerrish and F. Voss, Technical Note 434, N.A.C.A., November, 1932.
- 4 "Some Effects of Injection Advance Angle, Engine Jacket Temperature, and Speed on Combustion in a Compression-Ignition Engine," by A. M. Rothrock and C. D. Waldron, Technical Report No. 525, N.A.C.A., 1934.
- 5 "Effects of Air-Fuel Ratio on Fuel Spray and Flame Formation in a Compression-Ignition Engine," by A. M. Rothrock and C. D. Waldron, Technical Report No. 545, N.A.C.A., 1935.
- 6 "Smokemeter of Simple Design Tests Diesel Combustion," by P. H. Schweitzer, *Automotive Industries*, vol. 79, 1938, p. 238.
- 7 "The Measurement of Maximum Cylinder Pressures," by C. W. Hicks, Technical Report No. 294, N.A.C.A., 1928.
- 8 "A New High-Speed Engine Indicator," by E. S. Taylor and C. S. Draper, *Mechanical Engineering*, vol. 55, 1933, pp. 169-171.
- 9 "Correcting Diesel Engine Performance to Standard Atmospheric Conditions," by C. F. Taylor, *S.A.E. Journal*, vol. 41, 1937, pp. 312-314.
- 10 "The Effect of Compression Ratio Upon the Combustion and Heat Loss Characteristics of a Compression-Ignition Engine," by W. P. Green, unpublished, N.A.C.A. Project Report, 1943.

Discussion

H. H. FOSTER.³ As far as the writer knows, a compression ratio of 31:1 is considerably higher than has heretofore been reported. Apparently the author's test procedure and equipment were such that a maximum of information was obtained with a minimum of effort. The difficulty of carrying out rigorously an investigation of this kind is recognized and appreciated, for it is seemingly impossible to obtain a large change in the compression ratio of a Diesel engine without a resulting unpredictable change in the fuel and air mixing. From a practical viewpoint, perhaps, it is not feasible or entirely desirable to investigate engine performance at different compression ratios, independently of the variation in fuel and air mixing, but rather to choose for the investigation a combustion chamber such that the variation in mix-

ing is a minimum and the results have the greatest practical application.

It is quite likely that the author's test results were affected by variables, other than the compression ratio, which are not discussed in his paper. In any investigation of Diesel-engine performance at different compression ratios, the investigator is confronted with the problem of how to obtain the necessary change in combustion-chamber volume without a consequent change in combustion efficiency.

Unlike the gasoline spark-ignition engine in which the fuel and air mixture is homogeneous and therefore unaffected by changes in the combustion-chamber shape, the Diesel-engine fuel and air mixing is affected by differences in degree of fuel-spray impingement, and by changes in the relative positions of the fuel sprays and the mass of the combustion air. Fig. 8 of this discussion has been prepared to show the relative combustion-chamber lengths in the CFR engine used by the author for compression ratios of 12:1 and 31:1. The change in length is from about 1½ in. to about ½ in. Obviously, there will be considerably more spray impingement when the nozzle tip is ½ in. from the chamber wall than when it is 1½ in. away. It seems reasonable to believe that the combustion would be poorest when the spray impingement is the greatest. This belief is in agreement with the writer's experience and seems to be borne out by the trend of the curves in the paper, that is, the thermal efficiency decreases and the exhaust smoke increases at the upper end of the compression-ratio range. It is suggested that, if further work is contemplated, a combustion chamber of a different form be considered.

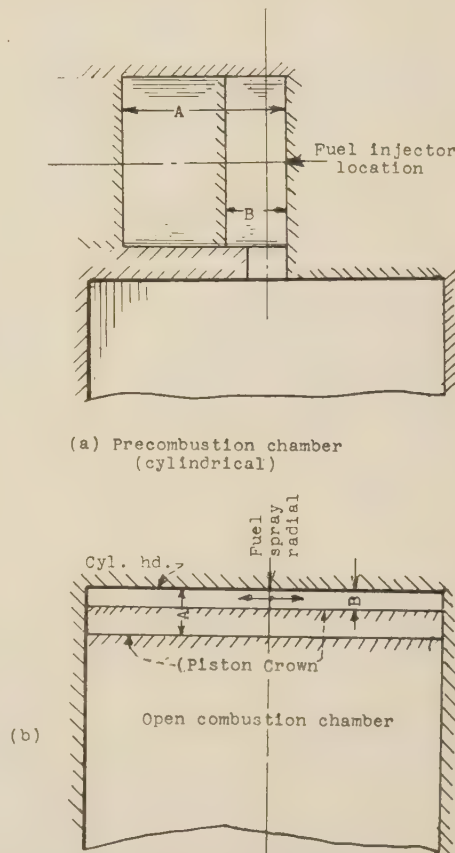


FIG. 8 COMPARISON OF CHANGE IN COMBUSTION-CHAMBER SIZE AND SHAPE IN A CFR DIESEL TEST ENGINE FOR A COMPRESSION-RATIO RANGE FROM 12:1, (a), TO 31:1, (b), IN OPEN-TYPE AND PRECHAMBER-TYPE COMBUSTION CHAMBERS

³ Engineer, Engine Research Division, Aircraft Engine Research Laboratory, N.A.C.A., Cleveland, Ohio.

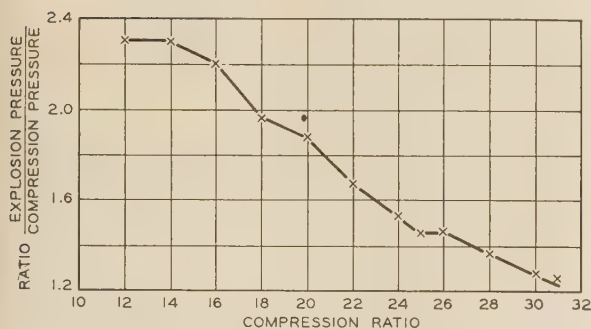


FIG. 9 PRESSURE-RISE RATIO FOR BEST FUEL ECONOMY IN CFR DIESEL TEST ENGINE
(Data from Table 1, reference 10, of paper.)

Fig. 8(b) herewith, shows an open-type chamber for the CFR engine for the foregoing compression-ratio range, 12:1 to 31:1. It is believed the open chamber formed between the piston crown and cylinder head with a central radial fuel spray should affect the combustion efficiency considerably less than the pre-chamber shown in Fig. 8(a) for equal changes in compression ratio.

In the section on operating procedure, the author mentions a "proper" injection-advance angle without defining it. In reference (10) of the paper, however, it is stated that "the angle of injection which would maintain engine output for the lowest rate of fuel injection was noted." (The lowest rate of total fuel flow rather than the lowest rate of injection presumably is meant.) From data in reference (10), the writer has prepared a plot, Fig. 9, of the ratio of explosion pressure to compression pressure versus compression ratio to show the large decrease in pressure-rise ratio with increase in compression ratio for these "proper" advance angles. The decrease is certainly greater than might have been expected and, from a practical viewpoint, is very fortunate: otherwise the upper range of the investigation would have been limited by maximum cylinder pressures.

The author states that the compression ratio should increase with a decrease in indicated mean effective pressure. Conversely, then, for high indicated mean effective pressure the compression ratio should be low. The latter seems to be in agreement with the present trend of thought in connection with compounding where extremely high boost pressures necessarily, from a practical standpoint, mean correspondingly low compression ratios.

W. J. King,⁴ The author has tackled a difficult experimental project and has contributed some interesting data. However, the difficulty of the problem is illustrated by the statement:

"The compression ratio was changed by varying the volume of a cylindrical precombustion chamber with a movable plunger in such a way as not to affect materially the combustion characteristics."

It is almost inconceivable that this could be accomplished, as it is more plausible to suppose that the volume of the precombustion chamber must necessarily have a significant effect upon combustion. This appears to be reflected in Figs. 3 and 5 of the paper, which show rapid increases in per cent smoke at the higher compression ratios. It is possible, therefore, that the decreased thermal efficiencies at the higher ratios are due primarily to the abnormal impairment of combustion. Perhaps the shape of the curves would be different if the compression ratio had been varied by changing the stroke without disturbing the combustion chambers.

⁴ Supercharger Engineering Division, General Electric Company, Lynn, Mass. Mem. A.S.M.E.

RALPH MILLER,⁵ The data plotted in Fig. 5 of the paper confirm the theoretical work of other investigators, with respect to the effect of clearance volume on volumetric efficiency.

The volumetric efficiency of a 4-cycle Diesel engine does not change with the volume of the clearance space nor is it affected by the temperature of the residual gases remaining in the clearance space after the end of the exhaust stroke. Volumetric efficiency is affected by wire drawing or pressure drop through the inlet valve but in moderate-speed engines this pressure drop is negligible, and the volumetric efficiency is almost entirely fixed by the heating of the fresh air charge from hot surfaces during the suction stroke. Obvious as it is, this theory is not generally recognized. The change in volumetric efficiency should therefore follow the line of total heat loss to the water jackets.

Optimum compression ratio with constant combustion pressure would have been of greater practical value to the designer because maximum pressure is usually fixed by design, whereas compression ratio can be changed.

In the method used by the author the volume of the combustion chamber is changed to change compression ratio. This variation of volume, which greatly influences combustion efficiency, could be eliminated by changing the stroke and maintaining constant the combustion-chamber shape and volume.

P. H. SCHWEITZER,⁶ Carefully conducted investigations on a specific problem of a limited scope, like the one presented, have their place and may yield very useful results if the instrumentation and procedure are correct, and the results are properly interpreted. The instrumentation set up by the author was complete, and the readings were taken with apparent care. Yet some of the results obtained appear questionable.

While the writer finds himself in complete agreement with the final conclusion that the engine power generally decreases with an increase in compression ratio after a ratio high enough for smooth ignition is reached, he finds insufficient data in the reported results upon which to base this conclusion. Running smoothness has not been reported by such scale as the maximum rate of combustion-pressure rise or by any other scale. Figs. 3 and 5 of the paper show best fuel consumptions at 23 and 17 to 1 compression ratios, but being plotted for constant brake horsepower they do not show what ratios give maximum power. What Fig. 7 represents is not clear to the writer.

The lowest specific fuel consumptions are shown as 0.85 and 0.81 lb per bhp-hr and the mechanical efficiency at full load varied between 35 and 40 per cent. These are at variance with our observations⁷ which show 0.65 lb per bhp-hr and mechanical efficiencies of the order of 65 per cent. The difference in speed (1200 rpm against 2000 rpm) can hardly account for that great a difference in fuel consumption. Plotting the values for compression pressure might be helpful as the movable plunger and other parts may not have been tight at compression ratios as high as 31:1.

The appearance of the curves, showing variations of indicated horsepower, friction horsepower, fuel consumption, maximum pressure, and smoke, agree with those observed by the writer, but numerically some of them show differences greater than attributable to the difference in engine speed or to experimental error. The complete report no doubt would shed some light on the discrepancies.

⁵ Chief Engineer, Worthington Pump and Machinery Corporation, Buffalo, N. Y. Mem. A.S.M.E.

⁶ Professor of Engineering Research, The Pennsylvania State College, State College, Pa. Mem. A.S.M.E.

⁷ "Oxygen-Boosting of Diesel Engines for Take-Off," by P. H. Schweitzer and E. R. Klinge, The Pennsylvania State College, Engineering Experiment Station Bulletin, No. 54 1941

AUTHOR'S CLOSURE

The author feels highly complimented by the interest exhibited by the engineers who have discussed this paper. The discussion has not only served to add information on a number of points in the paper but also to bring out some of the difficulties involved in an investigation of this type.

Messrs. Foster and King bring out in their discussion the effect of changes in combustion-chamber size and shape on combustion efficiency and point out that the type of chamber used undergoes such changes. The author was aware of these changes but felt that the increased pressure and density of the charge at higher compression ratios tended to offset changes in combustion-chamber shape, size, and surface-volume ratio. As noted, however, the performance curves indicate a definite falling off in combustion efficiency at very high compression ratios. Some of this was due to increased impingement as suggested by Mr. Foster. A number of tests were run varying the injection pressure and very little measurable effect was noted on the combustion efficiency. At higher injection pressures, greater impingement was to be expected. It is likely that another factor also affected the combustion efficiency greatly. A considerable portion of the total clearance volume at high compression ratios is in the passageway from the precombustion chamber to the cylinder and in the clearance space between piston and cylinder head. This means that the fuel-air ratio in the precombustion chamber at the start of combustion is greater at high compression ratios than at low ones. A greater portion of the burning would therefore have to take place in the cylinder. This would offer possibilities for less efficient combustion.

It is felt that Messrs. King and Miller's suggestion of using a fixed combustion-chamber shape and volume and varying the compression ratio by changing the length of stroke would give constant combustion efficiency. Lack of equipment for such an approach to the problem made this method untenable.

Mr. Foster's interpretation of the "proper" injection-advance angle is entirely correct. The pressure-rise ratios given by Mr. Foster in Fig. 9 offer further interesting data regarding the pressures encountered during combustion.

Mr. Miller's comments on volumetric efficiency explain why volumetric efficiency was relatively constant throughout tests. The entering air was heated to a high temperature so that there was very little change in charge temperature during the suction stroke although total heat loss to the evaporative cooling system varied with engine output.

Mr. Miller also suggests that optimum compression ratio with constant combustion pressure would have been of greater practi-

cal value to the designer. In running the tests the author aimed to do this and made an effort to set the maximum pressure at 1150 psi. Unfortunately, the injection equipment and engine characteristics only allowed this pressure to be maintained throughout a portion of the tests. For those on which data are given in this paper 1050 psi is approximately the maximum value. Since a very high maximum pressure could not be maintained constantly, results were taken at the maximum pressure obtainable with the injection equipment and combustion-chamber design used.

Professor Schweitzer questions the meaning of Fig. 7. By those curves the author intended to enclose the optimum range of compression ratios to be used with the test engine at any value of indicated mean effective pressure. For instance, at an Imep of 80 psi, optimum fuel economy would be obtained for a compression ratio between 20 and 24 since the efficiency curve against compression is relatively flat in this range.

The brake specific fuel rates and mechanical efficiencies obtained at full loads on these tests do not agree with those obtained by Professor Schweitzer in his work at Pennsylvania State College, using a CFR Diesel. The values in this paper show higher brake specific fuel rates and lower mechanical efficiencies. Since the tests given in the paper were made using a CFR engine with high-speed crank case while those run by Professor Schweitzer were made on a CFR engine with a low-speed crank case, these differences were to be expected. The engine with the high-speed crank case has a three-throw crankshaft and uses two balance pistons in the crank case in order to provide dynamic balance at speeds above 1200 rpm. The friction horsepower is increased by the balance pistons, resulting in a lower mechanical efficiency than would be obtained using the low-speed crank case. Increased friction horsepower also leads to higher brake specific fuel-consumption values. Indicated performance characteristics of the two engines would be more comparable since the engines differed greatly in mechanical efficiency.

Fig. 9 submitted by Mr. Foster in his comments gives some of the additional data requested by Professor Schweitzer. No measurements of rates of pressure rise were made. In reference (10), however, indicator cards are given for all tests run. These cards indicate very high rates of pressure rise since high thermal efficiency rather than smoothness of running was the criterion chosen for the tests.

It is noted that the general trends and appearance of the curves agree with those of other observers who have made tests over more limited ranges of compression ratio.

Elastic Properties of Plastic Materials

By JOHN DELMONTE,¹ LOS ANGELES, CALIF.

Unlike most metals, the average plastic material does not have a sharp break in the stress-strain curve to denote the yield strength or elastic limit. Usually experience or even conjecture is the guide to determining working stresses. An advance toward the solution of this problem is made by the author, who describes beam-deflection methods of obtaining elastic-limit stress data which have special significance in practical applications. A curve-deviation method is also suggested by means of which elastic limits are more accurately determined than by conventional stress-strain technique.

A specific characteristic of organic plastic materials seldom referred to in technical literature or in tabulations of physical properties is the elastic limit of plastic materials. This has left the determination of working stresses for plastics a matter of conjecture or of experience. The reason for this apparent gap in technical data may be explained by the difficulty of evaluating elastic limit from the tensile stress-strain curves of a plastic material. Unlike most metals, the average plastic material does not have a sharp break in its stress-strain curve to denote the yield strength or the elastic limit. In fact, as brought out in this paper, values of yield strength and elastic limit which have been reported vary considerably, leaving the designer confused as to safe limits of working stress.

Various definitions have been proposed for the elastic limit of plastic materials and related values of proportional limit. For example, the A.S.T.M. Specification D 638-42T offers the following definition:

"Elastic limit" is the greatest tensile stress which a material is capable of carrying without a permanent deformation remaining upon complete release of stress.

More recently tests which have been reported for various plastics show preference for proportional limit (tangential) and offset yield strength (1, 2).² These are defined in A.S.T.M. Standard E 6-36 as follows:

"Proportional limit" is the greatest stress which a material is capable of developing without a deviation from the law of proportionality of stress to strain (Hooke's law).

"Yield strength" is the stress at which a material exhibits a specified limiting permanent set (0.01 per cent and 0.2 per cent offset values have been reported for organic plastics).

STRESS-STRAIN CURVES OF PLASTIC MATERIALS

The proportional-limit and yield-strength values are just as difficult to evaluate as the elastic limit, as reference to Fig. 1 will demonstrate. These stress-strain curves may be found in references (2) and (3). A typical thermosetting and thermoplastic compound are plotted, with arrows vaguely pointing to the proportional limit. The straight lines offset a specified amount will not necessarily give concise data because of the gradual sloping of these stress-strain curves.

¹ Technical Director, Plastic Industries Technical Institute. Mem. A.S.M.E.

² Numbers in parentheses refer to the Bibliography at the end of the paper.

Contributed by the Rubber and Plastics Division and presented at a meeting of the Aviation Division, Los Angeles, Calif., June 8, 1944, of THE AMERICAN SOCIETY OF MECHANICAL ENGINEERS.

NOTE: Statements and opinions advanced in papers are to be understood as individual expressions of their authors and not those of the Society.

The problem is further complicated by the fact that what should be a specific physical property of an organic plastic material is in fact a function of the rate of applying stress. Specifications for the tensile or compression testing of plastics carefully define the rate of crosshead travel of the testing machine (4). In many instances this is specified as 0.05-ipm rate of crosshead travel in loading the test specimens of rigid plastics when stress-strain data are required, although this rate is greatly increased to 20 ipm when the plastics resemble rubberlike elastomers (5).

The variation of the stress-strain characteristics of plastic materials with rates of loading is to be expected because plastic materials have been observed to creep at very low values of stress (6). This implies that creep will take place during the normal application of load in testing, even at values far below the apparent elastic limit.

Experimental data on the variation of stress-strain characteristics of cellulose acetate with time of applying load have been shown in earlier literature (7, 8). In fact, the proportional limit may be observed anywhere from 1000 psi to 3800 psi, depending on the speed of testing. More recent data on the influence of rate of loading on the stress-strain curve have also been reported for polyvinyl butyral (9). Data on the effect of rate of strain on yield strength of brass, aluminum, copper, and S.A.E. 1020 and 1045 steel have already been reported, although the effect appears much less pronounced than for organic plastics (11).

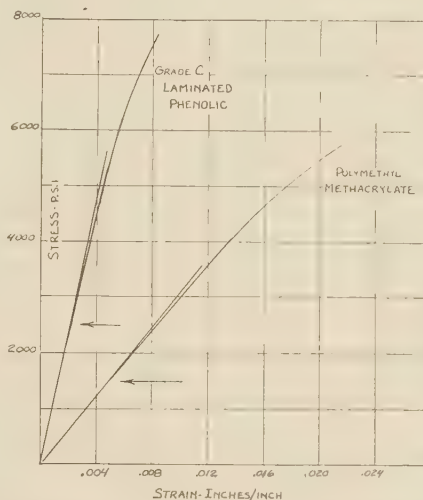


FIG. 1 STRESS-STRAIN CURVES OF TYPICAL THERMOSETTING AND THERMOELASTIC COMPOUNDS

There are various methods which may be employed for analyzing the elastic properties of materials. Contrary to popular impressions, elasticity is not necessarily determined by the amount of stretch or the amount of deformation but rather by the ability of a material to recover its original dimensions once it has been deformed. Thus, for example, a piece of steel may be more elastic than a piece of rubber in its greater ability to spring back to size upon removal of stress.

TWO-PHASE CHARACTER OF ORGANIC PLASTICS

In analyzing the physical behavior of organic plastics, one

will be impressed by the fact that he is dealing with a two-phase system and by analyzing it from this point of view, the anomalies of the elastic properties may be better understood. The two-phase character of plastics can be identified from the following salient facts:

- 1 Most molding compounds consist of resin-filler or resin-plasticizer combinations.
- 2 Most organic plastics possess an average molecular weight. There are low, medium, and high molecular-weight portions, varying in chemical and physical properties.
- 3 Laminated plastics consist of a resin binder and a reinforcing material.
- 4 There is evidence that some thermoplastics possess crystalline and amorphous phases, as evidenced by discrete spots in certain X-ray diffraction photographs.

In the light of physical behavior we may employ simple expressions in defining the two phases of an organic plastic (6):

Phase 1—Elastic portion: This portion permits instantaneous deformation under load and instantaneous recovery.

Phase 2—Plastic portion: This portion permits the plastic to continue deformation even after load has been applied for a period of time (creep).

TEST METHOD FOR EVALUATING ELASTIC PROPERTIES

In order that we may determine characteristics of the elastic portion we must employ experimental techniques which will permit evaluation of only the elastic properties. Such an experimental technique should be predicated upon substantially instantaneous phenomena before the results are clouded by deformation occurring in the time-dependent plastic portion. This would rule out the use of a universal testing machine in favor of a testing method where fixed loads and instantaneous deformation of the plastics can be observed. Such a technique is possible by means of apparatus already described in references (6) and (10). The simple cantilever beam is preferred for the following reasons: (a) Load is applied at that portion where stress concentration is minimum; and (b) the mechanical advantage of a simple cantilever beam in revealing small deformations is excellent. Of course tensile and compressive stresses are present, varying from maximum at the point of support to minimum at the end. However, the gradient is uniform, and the results express a performance more applicable to practical application than if the test were performed under pure tension or compression.

The testing technique consists of applying carefully a fixed weight at the end of the beam for a 1-min interval, removing the load, and allowing recovery to take place for 3 min; loading once again, etc., repeating this cycle 3 times. Deformation is read with an accuracy of ± 0.001 ; although the time interval during the first 30 sec may have varied as much as plus or minus 2 sec during observation of the deformation. The cycle is repeated 3 times largely to check readings and to observe changes in comparing one cycle with another.

The weights chosen were calculated to give certain maximum fiber stresses from the well-known formula, $M = SI/c$, where M is the maximum fiber stress and I/c the section modulus. The maximum fiber stress is recorded on each chart shown herewith. The technique could be improved through the use of an automatic electronic deflection-recording mechanism which did not contribute to the weight at the end of the beam. No corrections were made for the unsymmetrical tension and compression stress distribution but, rather, results are reported in the light of their integrated behavior.

All tests were conducted at temperatures varying from 75 to 80 F, and upon removal from a 50 per cent relative humidity

conditioning box. Prevailing humidities at time of tests were 35 to 50 per cent.

Analysis may be predicated on the assumption that instantaneous deflection substantially equals the instantaneous recovery within the elastic limit of the material. We may also detect the elastic limit through the drift of the zero point, indicating the attainment of permanent set. Other factors which were observed to indicate the elastic limit were: (a) Initial rate of creep recovery exceeds the initial rate of deformation under constant load (dR/dt to dD/dt) exceeds '1, where R is the recovery and D the deformation. (b) The elastic limit is readily indicated by the drift or deviation in deformation-time curves of adjacent cycles. This latter method provided the most positive index of the elastic limit and is described more fully later.

MATERIALS TESTED

- 1 Molded phenolic, rag-filled, $1/8$ in. thick; Monsanto Chemical Company, see Figs. 2 and 3.
- 2 Cellulose-acetate sheet, $1/8$ in. thick, Figs. 4 and 5.
- 3 Laminated phenolics, cloth, 8 oz per sq yd; resin content, 49 per cent; Grade C; laminated at 1500 psi and 330 F; $1/8$ in. thick, see Figs. 6 and 7.
- 4 Phenolic molding compound, woodflour-filled, $1/8$ in. thick; Monsanto Chemical Corporation, Fig. 8.
- 5 Polymethyl methacrylate sheet; $1/8$ in. thick, Fig. 9.

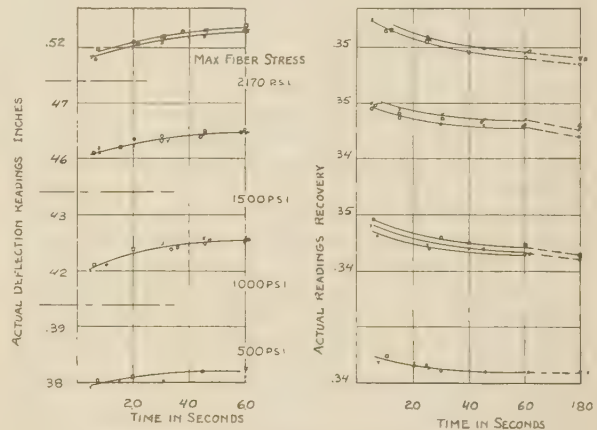


FIG. 2 TIME-DEFORMATION CURVES OF RAG-FILLED MOLDED PHENOLIC PLASTICS

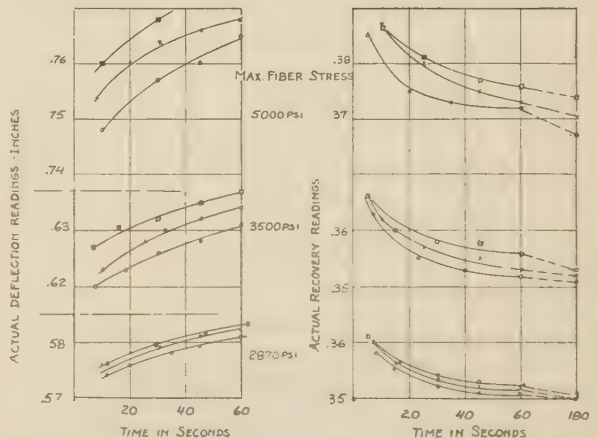


FIG. 3 TIME-DEFORMATION CURVES OF RAG-FILLED MOLDED PHENOLIC PLASTICS

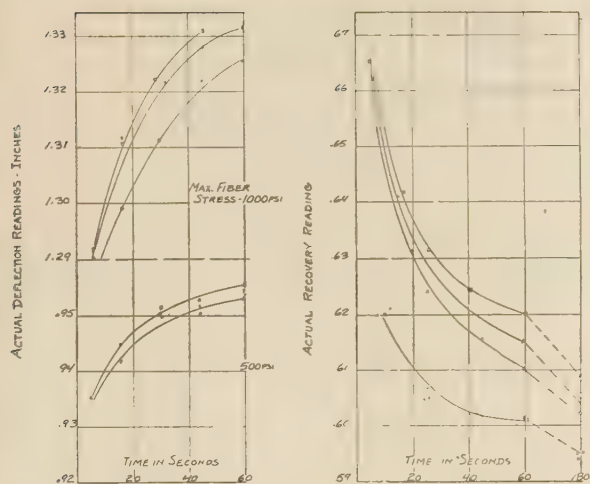


FIG. 4 TIME-DEFORMATION CURVES OF CELLULOSE-ACETATE SHEET

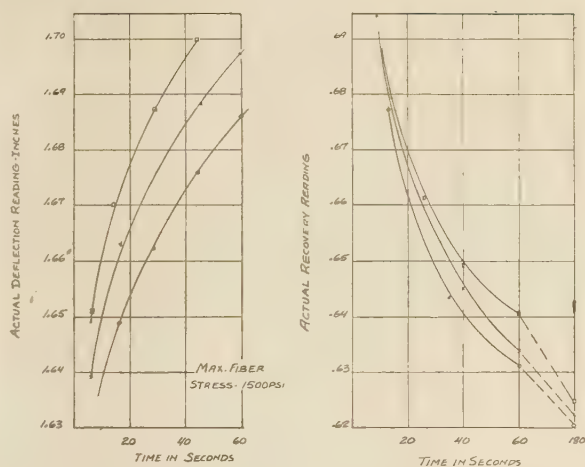


FIG. 5 TIME-DEFORMATION CURVES OF CELLULOSE-ACETATE SHEET

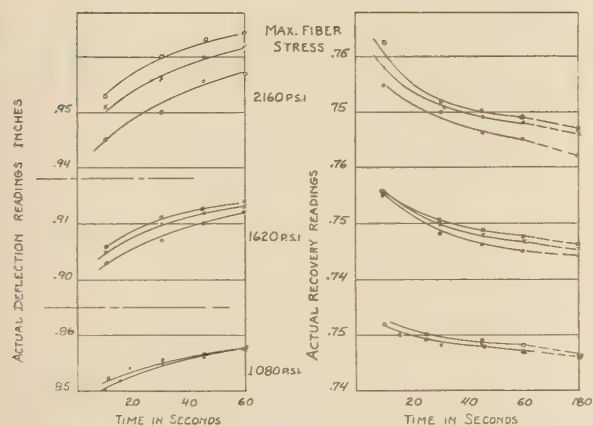


FIG. 6 TIME-DEFORMATION CURVES OF LAMINATED PHENOLIC CANVAS

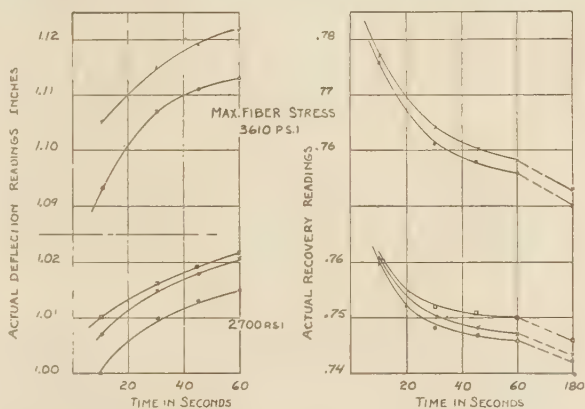


FIG. 7 TIME-DEFORMATION CURVES OF LAMINATED PHENOLIC CANVAS

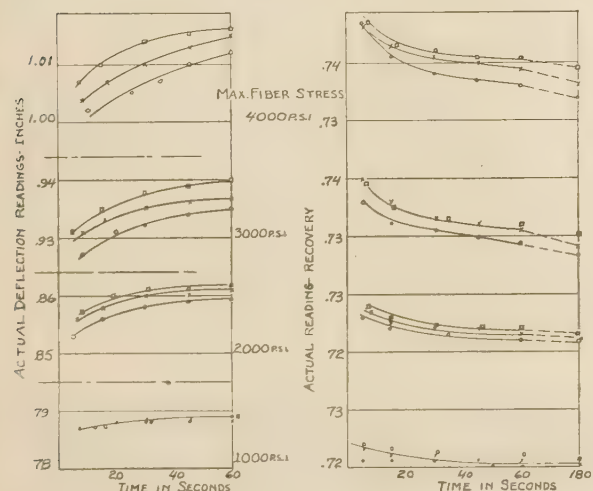


FIG. 8 TIME-DEFORMATION CURVES OF WOODFLOUR-FILLED MOLDED PHENOLIC PLASTICS

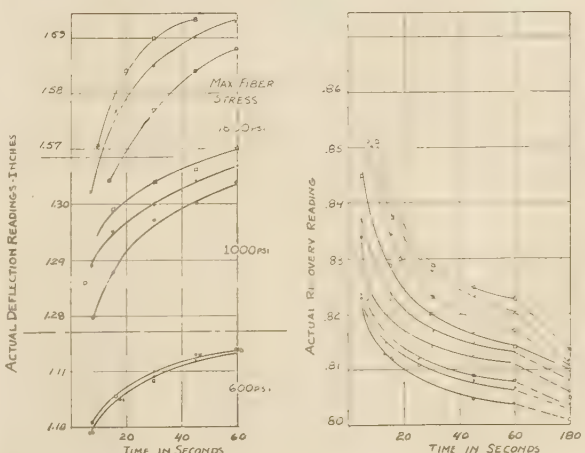


FIG. 9 TIME-DEFORMATION CURVES OF ACRYLIC PLASTIC SHEET

All materials were conditioned for at least 48 hr at 50 per cent relative humidity prior to test.

EXPLANATION OF CHARTS

In all the charts showing test results, deformation under constant load is shown during the first 60 sec. The actual deformation readings are plotted, although the same scale is maintained throughout and one set of curves may be visually compared with another set. In order to magnify the results, the actual elastic deformation under load (instantaneous deformation), and the actual elastic recovery (instantaneous recovery) are not plotted because they are so much greater than the short-time creep curves shown. Nevertheless, they may be estimated as follows:

Initial elastic deformation = deformation reading extrapolated to zero time, minus constant-recovery reading at 180 sec. (Interpolation to zero time is practically impossible for a material such as plasticized cellulose acetate, where the initial creep rate is quite rapid)

The constant-recovery reading at 180 sec is approximately equal to initial zero point. Only where elastic limit is exceeded for an appreciable time will there be an appreciable permanent set.

Initial elastic recovery = deformation when load was removed (at 60 sec), minus recovery-reading curve extrapolated to zero time axis

The circled points represent the first cycle of loading and the crossed points the second cycle, while the squared points are the third cycle; the error in deflection and recovery readings is plus or minus 0.001 in., the early time error is plus or minus 2 sec.

DISCUSSION OF CHARTS

It is at once apparent how thermoplastic materials differ from thermosetting materials by the steep gradient of their time-deformation curves. The more pronounced creep characteristics of thermoplastics are well known already for long time intervals (12), although not known for short applications of stress. These are the first comprehensive data on short-time creep of organic plastics.

The charts also reveal how difficult it is to obtain accurate data on initial elastic deformation and initial elastic recovery (R), as the elastic limit is approached and passed, because of the sharp slope of the curves. Approximations are possible, however,

TABLE 1 INITIAL ELASTIC DEFORMATION AND INITIAL ELASTIC RECOVERY OF PLASTICS TESTED

Material	Maximum fiber stress, psi	Initial elastic deformation, in.	Initial elastic recovery, in.	Elastic limit
Phenolic, rag-filled	1500	0.112	0.112	←
	2170	0.170	0.169	
	2870	0.220	0.215	
	3500	0.267	0.257	
Cellulose acetate	500	0.335	0.330	←
	1000	0.670	0.650	
	1080	0.102	0.103	
Laminated phenolic	1620	0.156	0.153	←
	2160	0.203	0.197	
Phenolic, woodflour-filled	1000	0.065	0.065	←
	2000	0.130	0.130	
	3000	0.198	0.193	
Polymethyl methacrylate	600	0.293	0.292	←
	1000	0.474	0.465	

by extrapolating the curves to the zero time axis. However, the earlier expressed theory that elastic limit is reached when initial elastic deformation exceeds the initial elastic recovery is borne out (see Table 1.)

An even more satisfactory method for arriving at the elastic limit of a plastic material is illustrated in Fig. 10. It is proposed that the elastic limit for plastics be determined from the per cent deviation of adjacent time-deformation curves on repeated cycles of stress. The maximum stress where the percentage deviation of time-deformation curves is zero is proposed as the elastic limit. This analysis admits the possibility of creep below the elastic limit, though the elastic limit is not attained until the material fails to recover fully from creep. At values above the elastic limit the absence of full recovery of deformation is noted experimentally as per cent deviation of the time-deformation

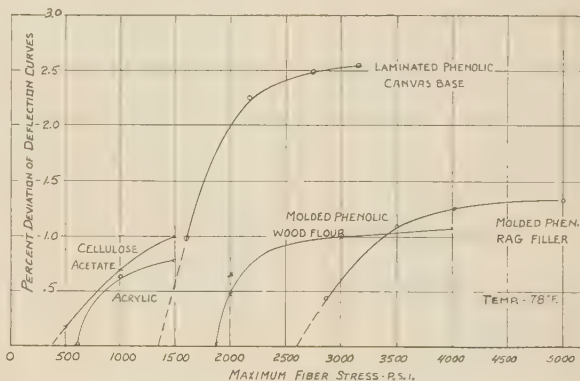


FIG. 10 METHOD OF DETERMINING ELASTIC LIMIT FROM PER CENT DEVIATION OF TIME-DEFORMATION CURVES OF PLASTICS TESTED

curves. As Fig. 10 brings out, the apparent elastic limit is approached sharply.

In securing data for Fig. 10, the average spacing between the curves for the different cycles of stress is divided by the initial elastic deformation. This gives the percentage deviation. For example, at a maximum fiber stress of 2870 psi for rag-filled phenolic composition, the average separation or deviation of the deflection curves is 0.0010 in. This divided by the initial elastic deformation of 0.220 in. and multiplied by 100 to convert to per cent equals 0.45 per cent (see point in Fig. 10). By this analysis the elastic limit is effectively located. The values of elastic limit are listed in Table 2.

It is also interesting to note that the experimental phenolic molding compounds provided through the courtesy of Monsanto Chemical Company were the same materials employed to determine the long-time tensile strength (12). The long-time tensile strength of the molded phenolic, woodflour-filled, was reported to lie within 2000-2500 psi, and the value for the molded phenolic, rag-filled, was reported to be 2400-3000 psi. Compare these values with the results for apparent elastic limit in Table 2. On the other hand, the proportional limit reported in another reference yields values which, in the opinion of the author, are too high for working stresses.

CONCLUSION

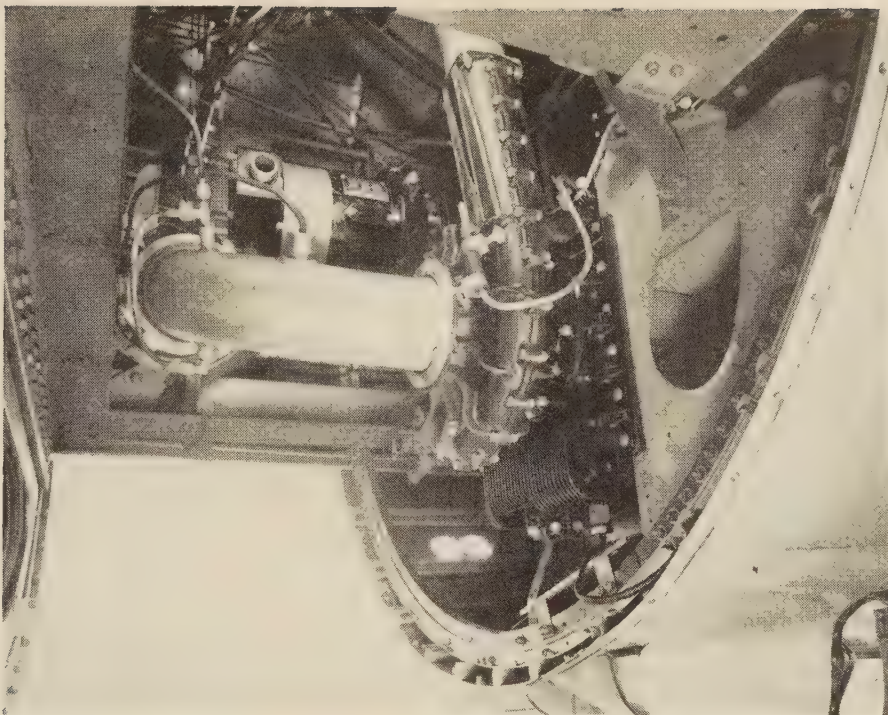
In conclusion, the author wishes to re-emphasize that elastic-limit stress data obtained by beam-deflection methods hold special significance in the practical applications. Elastic limits, as determined by the curve-deviation method suggested herein, appear to be more accurately arrived at than the more conventional stress-strain technique.

TABLE 2 VALUES OF ELASTIC LIMIT FOR PLASTICS TESTED

Material	Apparent elastic limit, psi (Fig. 10)	Long-time tensile strength, psi	Tangential proportional limit, psi	Proportional limit 0.01 per cent offset, psi	Reference
Molded phenolic, rag-filled..	2600	2400-3000	2200	3000	(12)
Laminated phenolic, cloth...	1400	2900	3200	(1)
Cellulose-acetate sheet,....	400	3300	3600	(1)
Polymethyl methacrylate,...	600	(1)
Molded phenolic, woodflour-filled.....	1900	2000-2500	(12)

BIBLIOGRAPHY

- 1 "Mechanical Properties of Plastics at Normal and Subnormal Temperatures," by T. P. Oberg, R. T. Schwartz, and D. A. Shinn, *Modern Plastics*, vol. 20, April, 1943, pp. 87-100, 122, 124, 126, and 128.
- 2 "Engineering Properties of Plastics," by F. B. Fuller, *Modern Plastics*, vol. 20, June, 1943, pp. 95-97 and 130.
- 3 "Technical Data on Plastic Materials," Plastic Materials Manufacturing Association, May, 1943, Washington, D. C.
- 4 "Method of Testing Tensile Properties of Plastics," A.S.T.M. D638-42T, A.S.T.M. Standards, 1942, Part 3, pp. 1241-1250.
 "Plastics, Organic (Methods of Tests), Fed Spec., L-P-406.
 "Method of Test for Compressive Strength of Plastics," A.S.T.M. D695-42T, A.S.T.M. Standards, 1942, Part 2, pp. 1268-1275.
- 5 "Methods of Tension Testing of Vulcanized Rubber," A.S.T.M. D412-41, A.S.T.M. Standards, 1942, Part 3, pp. 408-414.
- 6 "Permanence of the Physical Properties of Plastics," by J. Delmonte, *Trans. A.S.M.E.*, vol. 62, 1940, pp. 513-524.
- 7 "Mechanical Tests of Cellulose Acetate," by W. N. Findley, *Proceedings of the A.S.T.M.*, vol. 41, 1941, pp. 1231-1245.
- 8 "Elasticity, Plasticity, and Structure of Matter," by R. Houwink, Cambridge University Press, 1937, p. 258.
- 9 "Stress Elongation of Polyvinyl Butyral," by C. C. Zimmerman, A. Takacs, and D. M. Lovelee, *Plastics Trends*, vol. 4, May 15, 1944, pp. 5-6.
- 10 "Factors Influencing Creep and Cold Flow of Plastics," by J. Delmonte and W. Dewar, A.S.T.M. Bulletin No. 112, October, 1941, pp. 35-42.
- 11 "Effect of Rate of Strain on Yield Strength, etc., in Tension Tests," by H. E. Moore and P. G. Jones, *Proceedings of the A.S.T.M.*, vol. 41, 1941, pp. 488-491.
- 12 "Creep Properties of Molded Phenolic Plastics," by D. Telfair, T. S. Carswell, and H. K. Nason, *Modern Plastics*, vol. 21, Feb., 1944, pp. 137-144, 174, and 176.



CABIN SUPERCHARGER ON PERFORMANCE TEST IN DC-4 AIRPLANE ENGINE NACELLE

Presentation of Centrifugal-Compressor Performance in Terms of Nondimensional Relationships

By B. E. DEL MAR,¹ SANTA MONICA, CALIF.

The common difficulties encountered in handling performance information on centrifugal compressors or superchargers are overcome by a new and novel form of performance presentation introduced in this paper. Nondimensional coefficients which embody measured test quantities are derived and performance presentation is made using values of these coefficients on a single combined chart. From this chart the pressure, temperature, flow, speed, and power quantities, associated with a given blower, may be predicted over a broad range of inlet and discharge conditions. Particular facility is offered for orientation with respect to operation at peak efficiencies, for avoidance of surge limits, and for direct performance comparison among different compressors.

¹ Assistant to the Mechanical Design Engineer, Douglas Aircraft Company, Inc. Jun. A.S.M.E.

Presented at a meeting of the Aviation Division, Los Angeles, Calif., June 5-9, 1944, of THE AMERICAN SOCIETY OF MECHANICAL ENGINEERS.

NOTE: Statements and opinions advanced in papers are to be understood as individual expressions of their authors and not those of the Society.

PERFORMANCE data obtained from tests on centrifugal compressors often require presentation in some manner which will make possible prediction of operating results under conditions differing considerably from those of the tests. When a wide variation of inlet conditions is to be encountered, as is typical of superchargers on aircraft, in addition to the usual variation of conditions at discharge, then this manner of presentation must be arranged to satisfy a particularly large number of variables.

To serve the purpose of predicting operating results under conditions differing widely from those of test, it is common practice to plot performance curves rather than to specify any predetermined operating points. To justify the large number of variables present when inlet conditions vary over a considerable range, these performance curves can be greatly simplified through presentation as functions of nondimensional quantities. It is the purpose of this paper to outline an improved means of presenting compressor performance in terms of nondimensional relationships; whereby test results can be plotted to form more closely defined characteristics curves, and whereby the engineer with a minimum of interpretation and calculation can analyze the

merits of a blower and design its drive even when intended for operation throughout a broad range of inlet and discharge conditions.

PERFORMANCE-DATA REQUIREMENTS

For design work in conjunction with any compressor the resultant basic information usually desired for any set of operating conditions within the expected operating range is that of torque, discharge temperature, and operating speed. The first of these functions may also be expressed as power or efficiency and the second may also be expressed as temperature rise or temperature efficiency. At least three conditions must be determined to define the performance, and three sets of curves may therefore be expected in the performance presentation.

A further object can be accomplished by the compressor-performance presentation if characteristics are given in terms of compressor size. Temperature, speed, and efficiency can then be compared for small variations in impeller size, and comparison can even be made between blowers differing somewhat in general size and configuration.

EFFECT OF VARYING INLET CONDITIONS

A common practice in plotting the performance characteristics of commercial fans and ventilating blowers is that represented in Fig. 1 wherein the pressure head, power, and efficiency are plotted as a function of flow for various parameters of speed. Where inlet conditions of temperature and pressure are variable as in air turboblowers, and particularly variable over a broad range as in aircraft applications, such a plot would make no consideration for the performance decrease accompanying higher compression ratios which are encountered with inlet pressure and density decrease even though pressure head is maintained constant.

If a plot is made as a function of compression ratio, as shown in Fig. 2, one of the shortcomings noted for the previous plot is removed but each speed parameter still applies to only one inlet temperature, and separate curve sheets must therefore be supplied for any one inlet temperature in order to represent speed performance correctly. In view of these shortcomings and in order to provide comparison between compressors of different size, a presentation of performance which is soundly based on dimensional analysis may be noted as definitely desirable. Development and discussion of several different forms for such presentation are included in this paper.

DIMENSIONAL APPROACH

As a first step in preparing a dimensional background the physical quantities related to blower performance are to be noted. These physical quantities define the following:

- (a) The fluid.....Velocity, density, pressure, temperature, viscosity, and the ratio of specific heats
- (b) The rate of fluid flow...Mass intake per unit of time
- (c) The compressor.....Size, and speed of rotation
- (d) The power.....Compressor shaft power
- (e) Flow distortion.....A factor or factors defining any change in compressor performance influenced by nonlinear shock waves or geometric distortion in blower passages
- (f) Heat loss:.....Quantity of heat lost per unit time from compressor case

Since we are concerned herein with a compressible fluid, the values of the physical quantities associated with the fluid under (a) must be considered at both inlet and discharge from the compressor.

In the interest of simplicity it is desirable to eliminate any of those quantities noted which have a negligible influence upon the

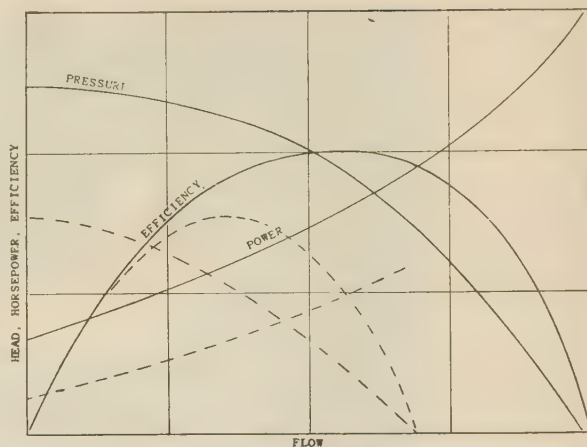


FIG. 1 CONVENTIONAL BLOWER CURVES
(Performance at a high and a low speed is indicated by the solid and dotted curves, respectively.)

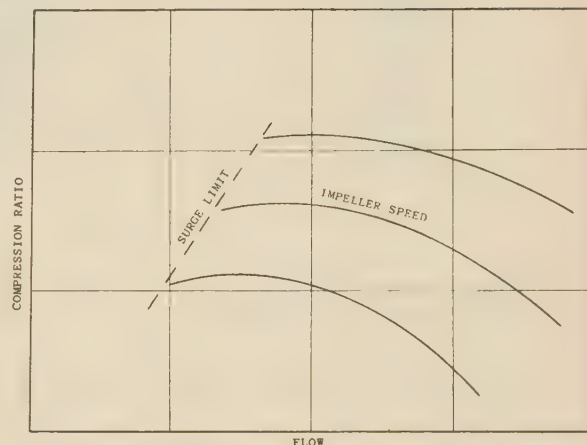


FIG. 2 CONVENTIONAL COMPRESSION-RATIO PERFORMANCE PLOT
(Performance at three different speeds is noted together with typical surge limit for a centrifugal compressor. This plot applies to one particular compressor at one particular inlet temperature only.)

performance characteristics. Velocity at inlet and discharge can thus be discarded from the quantities defining fluid flow in (b), for we shall assume either that the compressor is inspiring and discharging from relatively large reservoirs, respectively, or that we define pressure as total pressure at inlet and discharge, thereby including the velocity component.

Temperature may be omitted from the initial dimensional analysis since it is adequately defined by the two quantities density and pressure. Likewise velocity may be conveniently expressed only as a function of a linear dimension of the blower impeller and its rotational speed.

It is reasonable to expect that some influence on compressor performance might result from aerodynamic distortions which do not follow obvious physical laws. For example, if compressor clearances change as a result of considerable temperature distortion, then the resulting change in internal compressor leakage will affect performance. If a nonuniform growth of shock waves is created through the approach to sonic velocity within the passages, or if operation is attempted at or near stall conditions such as are common to centrifugal compressors, then compressor performance will be affected. These factors will be discarded from this analysis by qualifying the compressor as one of conven-

tional rigid design in which temperature distortions, shock distortions, and clearance changes are small, and by qualifying the performance presentation as intended only for the stable range of compressor operation.

Finally, we shall discard the effect upon compressor performance of heat lost from the blower case by assuming that any blower is operated under test conditions of temperature and heat transfer adjacent to the compressor similar if not identical to those under which performance prediction is to be made. Substantiation for the omission of these variables in the manner noted will be borne out by the results obtained in applications of this analysis noted later and by a review of the test data and conclusions of reference (1).²

DIMENSIONAL ANALYSIS

The actual quantities in which we are necessarily interested are given in Table 1.

TABLE 1 QUANTITIES USED IN COMPRESSOR ANALYSIS

Quantity	Definition	Dimensional units (<i>m</i> , mass; <i>t</i> , time; <i>l</i> , length)
<i>M</i>	= mass of fluid inspired in unit time	$\frac{m}{t}$
<i>p</i> ₁ and <i>p</i> ₂	= pressures at intake and delivery	$\frac{m}{l^2}$
ρ_1 and ρ_2	= densities at intake and delivery	$\frac{m}{l^3}$
ν	= kinematic viscosity of fluid	$\frac{l^2}{t}$
<i>k</i>	= ratio of specific heats of fluid (dimensionless)	
<i>N</i>	= rate of rotation of compressor rotor	$\frac{1}{t}$
<i>D</i>	= linear dimension of compressor (impeller diameter)	<i>l</i>
<i>P</i>	= power required to operate compressor less that dissipated in bearing friction	$\frac{ml^2}{t^3}$

Subscripts 1 and 2 indicate conditions at compressor inlet and discharge, respectively.

From the ten terms given in Table 1, the flow through the compressor is completely defined by the independent quantities

$$M, p_1, \rho_1, \nu, k, D, N$$

leaving as dependent quantities

$$p_2, \rho_2, P$$

The three dependent quantities represent the performance data which must be presented in the form of performance curves.

In order to develop a functional equation relating the performance quantities for the many combinations of forces acting in a centrifugal compressor it is convenient to make use of the π theorem relating to mathematical functions. Any physical equation, if complete, expresses the relation between all of the different physical quantities which control the physical phenomenon in question. Let these quantities be designated as $Q_1, Q_2 \dots Q_n$ if there be *n* kinds. If several quantities of the same kind appear, let these be represented by ratios with respect to one of them as Q, r', r'' . Then an equation may be written

$$f(Q_1, Q_2 \dots Q_n) f_2(r', r'') = 0 \dots \dots \dots [1]$$

The ratios *r* are nondimensional and may be excluded only in such cases where we wish to restrict ourselves to geometrically similar systems.

The π theorem of dimensional relationships states with respect to such quantities as follows: If a relation of $f(Q_1, Q_2 \dots Q_n) = 0$ exists among *n* physical quantities $Q_1, Q_2, \dots Q_n$ each of which is a function of *m* primary quantities (such as force, length, time, temperature), there is also a relation among *m* minus *n*

independent dimensionless products formed from the *Q*'s, (4).

Now applying the π theorem to these ten quantities, we may build up the seven independent quantities into $7 - 3 = 4$ non-dimensional quantities, taking care that each of the seven quantities enters at least once into the group of four. The three dependent quantities may then be converted to nondimensional form and each expressed as a function of the four independent nondimensional variables.

In grouping these independent quantities, as many of the non-dimensional force laws of dynamical similarity should be represented as possible. Where viscous forces, gravity (or acceleration) forces, or pressure forces are expected to exist, then Reynolds, Froude, and Mach criteria of dynamical similarity, respectively, should be represented and may be stated as follows (3):

Dimensionless number	Ratio of forces	Representation
Reynolds number	$\frac{\text{Inertia force}}{\text{Friction force}}$	R
Froude law	$\frac{\text{Inertia force}}{\text{Gravity force}}$	F
Mach number	$\left(\frac{\text{Inertia force}}{\text{Pressure force}} \right)^{1/2}$	M

Other similarity laws of Thompson, Cauchy, and Weber which are related to attractive forces, elastic forces, and surface tension forces, respectively, are obviously not applicable to the centrifugal compressor.

Adding the following symbols to our nomenclature:

W = weight flow of fluid per unit time
Q = volume flow of fluid per unit time
V = impeller-tip velocity
A = area for flow
V_e = velocity of sound in compressor fluid
g = acceleration of gravity
T = absolute temperature of compressor fluid
D = compressor-impeller diameter
 μ = absolute viscosity of fluid
R = gas constant in perfect gas law
 $C = \left(\frac{\text{Total inertia force}}{\text{Centrifugal inertia force}} \right)^{1/2}$

Then the following dimensional equations may be written representing the similarity laws

$$R = \frac{A \rho V^2}{A \mu \frac{V}{D}} = \frac{V D \rho}{\mu} = \frac{V D}{\nu} \dots \dots \dots [2]$$

Since $V \propto ND$ then: **R** may also be expressed as

$$R \propto \frac{ND^2}{\nu} \dots \dots \dots [3]$$

$$C = \left[\frac{A \rho V^2}{A \rho N^2 D^2} \right]^{1/2} = \frac{V}{ND} = \frac{Q/A}{ND} = \frac{Q}{ND^3} \dots \dots \dots [4]$$

Since $Q = \frac{W}{\rho g}$ and $W = gM$, then *C* may also be expressed as

$$C = \frac{M}{\rho ND^3} \dots \dots \dots [5]$$

$$M = \left[\frac{A \rho V^2}{A \rho V_e^2} \right]^{1/2} = \frac{V}{V_e} \dots \dots \dots [6]$$

Since $V_e \propto \sqrt{T}$ and from the perfect gas law $\frac{p}{\rho} = gRT$ then

² Numbers in parentheses refer to the Bibliography at the end of the paper.

M may also be expressed as

$$\mathbf{M} = \frac{V}{\sqrt{T}} = \frac{ND}{\sqrt{T}} = ND \sqrt{\frac{\rho}{p}} \dots \dots \dots [7]$$

The dimensionless quantity *C* is created here for use in place of Froude's law. Term *C* is defined in the nomenclature as a force ratio. Actually this is an expression of continuity of fluid flow within the compressor passages, the physical quantities in radial flow being thereby directly related to rotor angular velocity. Perhaps a name should be given to this dimensionless number. Froude's law is not directly applicable to the centrifugal compressor because gravity forces, as such, are negligible when pumping a compressible fluid.

Returning now to the development of nondimensional quantities; from the independent quantities of Table 1 we can see that the requirements of the π theorem may be satisfied by four nondimensional quantities, three of which are from Equations [3], [5], and [7], respectively, and the fourth is singularly nondimensional. These quantities are

$$\frac{M}{\rho_1 ND^3}, ND \sqrt{\frac{\rho_1}{p_1}}, \frac{ND^2}{\nu}, k$$

Three nondimensional quantities may be developed from the dependent quantities of Table 1 by simple relations between discharge and inlet density and pressure, and between kinetic rotor energy of the fluid at impeller-tip velocity (*T*), as compared to power *P*, previously defined. These quantities are

$$\frac{p_2}{p_1}, \frac{\rho_2}{\rho_1}, \frac{MN^2 D^2}{P}$$

A dimensional equation which fully satisfies the dimensional analysis may now be written

$$\frac{p_2}{p_1}, \frac{\rho_2}{\rho_1}, \frac{MN^2 D^2}{P} = f \left[\frac{M}{\rho_1 ND^3}, ND \sqrt{\frac{\rho_1}{p_1}}, \frac{ND^2}{\nu}, k \right] \dots \dots [8]$$

REDUCTION OF FUNCTIONAL QUANTITIES

To make possible a simple plot of the relation between any one of the dimensionless quantities such as pressure ratio on the left-hand side of Equation [8] and the dimensionless functional quantities on the right, it is desirable that the number of functional quantities be reduced by eliminating those not absolutely necessary to the analysis. The ratio of specific heats *k* may be deleted from the dimensional equation by qualifying the desired performance presentation to be applicable only to operations with the same fluid, the diatomic gases, or fluids of equivalent *k* value. The working fluid is of course generally air. Furthermore $\frac{ND^2}{\nu}$, Reynolds number, may be omitted from the dimensional equation because the viscous forces acting on the walls of centrifugal-blower passages are generally small in comparison with the centrifugal forces and pressure forces. In this respect the centrifugal compressor differs from the centrifugal fan. Omission of Reynolds number from the performance analysis can be well justified for centrifugal compressors which have smooth-surfaced passage boundaries in all operations above a Mach number of 0.25. For blowers with complicated guide-vane or return-flow passages this omission may be justified only above a somewhat higher value of Mach number. For centrifugal fans operating below a Mach number of approximately 0.25 (tip velocities less than 10,000 fpm), a performance presentation which applies Reynolds number as a parameter rather than Mach number, should be adopted because viscous forces are therein generally predominant over compressibility forces.

Graphic presentation of the relations between remaining terms in Equation [8] can now be conveniently made by simply plotting values of any one of the dimensionless dependent quantities as a function of the two remaining functional independent quantities and using the other functional dependent quantity as a parameter. Examples of such presentation will be given.

ALTERNATE QUANTITIES IN DIMENSIONAL EQUATION

Certain alternate terms, as follows, may be developed to those in Equation [8] which may be of special value in presenting compressor performance:

1 An alternate term to the density ratio ρ_2/ρ_1 is the temperature ratio T_2/T_1 in conformance with the perfect-gas law. Another alternate is the term η , the adiabatic temperature efficiency.

2 For various power ratios a number of components for the numerator or denominator are reasonable. One such component is the adiabatic compression energy, the power which would be necessary for true isentropic or reversible adiabatic change of state of the gas. The adiabatic energy per pound of fluid may be expressed as

$$P_k = \int_{p_1}^{p_2} V dp = \frac{k}{k-1} RT_1 \left[\left(\frac{p_2}{p_1} \right)^{\frac{k-1}{k}} - 1 \right] \dots \dots [9]$$

where *R* is the perfect-gas constant. Defining now the following

$$Y = \left[\left(\frac{p_2}{p_1} \right)^{\frac{k-1}{k}} - 1 \right] \dots \dots \dots [10]$$

c_p , c_v = specific heats at constant pressure and constant volume, respectively

J = mechanical equivalent of heat, a constant
The total adiabatic power may then be expressed as

$$P_k W = \frac{k}{k-1} RT_1 Y W \dots \dots \dots [11]$$

Since for diatomic gases $c_p - c_v = \frac{R}{J}$ and $k = \frac{c_p}{c_v}$ then

$$P_k W = c_p J T_1 Y W \dots \dots \dots [12]$$

The following components for the numerator or denominator of the power term are reasonable:

- (a) $c_p J T_1 Y W$, the adiabatic power
- (b) *P*, blower-drive power less bearing friction
- (c) *P_s*, blower-drive power including bearing friction
- (d) $(T_2 - T_1) c_p J W$, actual temperature-rise power
- (e) $\frac{W N^2 D^2}{g}$, impeller energy or power

Using these components in simplified fractional relationships, we may define

$$\frac{T_1 Y}{T_2 - T_1} = \eta, \text{ adiabatic efficiency} \dots \dots \dots [13]$$

$$\frac{P}{P_s} = \eta_m, \text{ mechanical efficiency} \dots \dots \dots [14]$$

$$\frac{c_p J T_1 Y W}{P_s} = \eta_s, \text{ adiabatic shaft-power efficiency} \dots \dots [15]$$

$$\frac{c_p J T_1 Y g}{N^2 D^2} = \eta_p, \text{ pressure-energy coefficient} \dots \dots \dots [16]$$

Obviously other combinations of the components (a), (b), (c), (d), and (e), are possible.

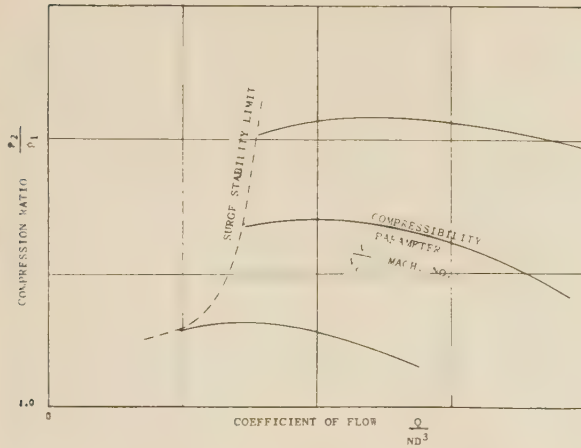


FIG. 3 COMPRESSION-RATIO PERFORMANCE PLOT REFERRED TO INLET-VOLUME FLOW AND MACH NUMBER

(Performance at three values of Mach number is noted. Presentation is dimensionally correct but uses quantities of indirect measure.)

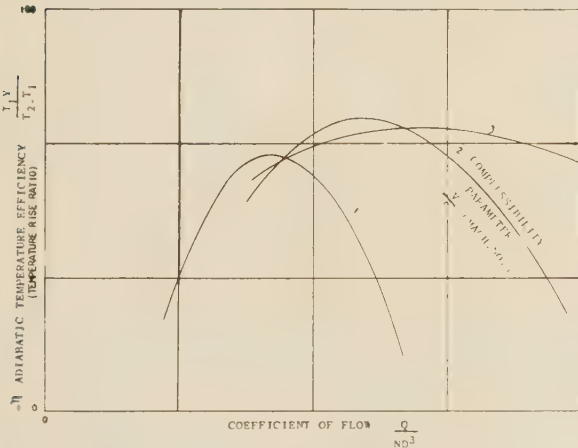


FIG. 4 ADIABATIC-TEMPERATURE PERFORMANCE PLOT REFERRED TO INLET-VOLUME FLOW AND MACH NUMBER

(Performance curves for three widespread values of Mach number are shown in typical form. Low, medium, and high values are noted 1, 2, 3, respectively. Presentation is dimensionally correct but uses quantities of indirect measure and is not readily determinate for speed due to use of speed quantities in more than one of the nondimensional coefficients.)

3 For the compressibility term in Equation [8], which is $ND\sqrt{\frac{p_1}{p_2}}$, one alternate $\frac{V}{V_c}$ may be found from Equation [6] and still another $\frac{ND}{\sqrt{T_1}}$ from Equation [7].

4 For the remaining centrifugal forces term in Equation [8], which is $\frac{M}{\rho_1 ND^3}$, one alternate form $\frac{Q}{ND^3}$ may be noted from Equation [4]. Other forms which are dimensionless and still satisfy the π theorem in derivation of the term are

$$\frac{M}{D^2\sqrt{\rho_1 p_1}}, \quad \frac{MN}{p_1 D}, \quad \frac{M}{v \rho_1 D}, \quad \frac{M \rho_1 D N^3}{p_1^2}, \quad \frac{M p_1}{\rho_1^2 N^3 D^2}$$

$$\frac{M N^2 D}{v p_1}, \quad \frac{M \sqrt{\rho_1 p_1}}{\rho_1^2 N^2 D^4}, \quad \frac{M N^2 \sqrt{\rho_1 p_1}}{p_1^2}$$

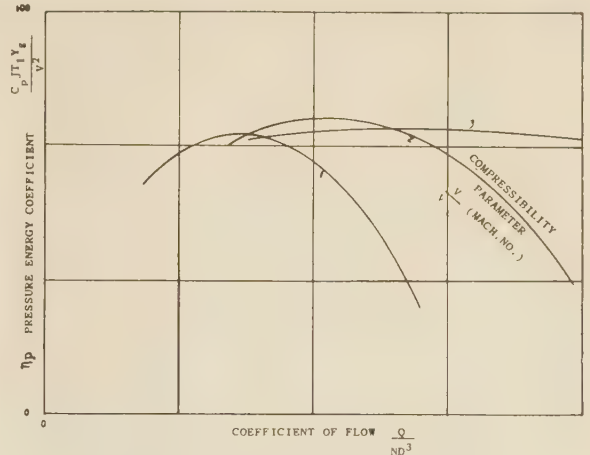


FIG. 5 PRESSURE-ENERGY PERFORMANCE PLOT REFERRED TO INLET-VOLUME FLOW AND MACH NUMBER

(Performance curves for three widespread values of compressibility parameter are shown in typical form. Low, medium, and high values of Mach number are noted 1, 2, 3, respectively. Quantities are of indirect measure and the form of flow coefficient is such as to cause confinement of curves in a somewhat congested range.)

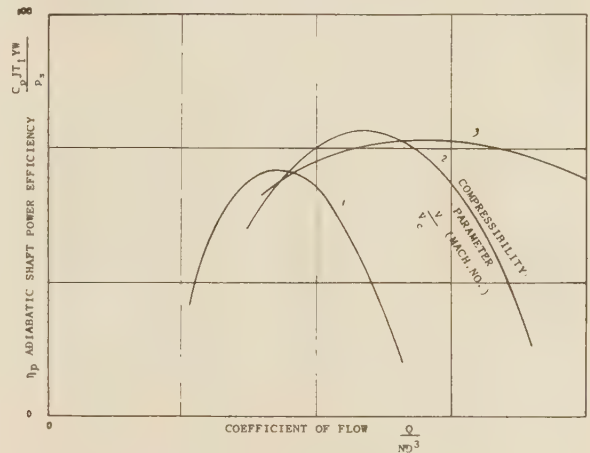


FIG. 6 ADIABATIC-SHAFT-POWER PERFORMANCE PLOT REFERRED TO INLET-VOLUME FLOW AND MACH NUMBER

(Refer to notes under Figs. 4 and 5.)

CURRENT USE OF TERMS IN DIMENSIONAL EQUATION

In the design and testing of centrifugal compressors considerable use has been made of nondimensional quantities conforming to the manner of presentation which is shown in Figs. 3, 4, 5, and 6. The dimensional equation for this presentation is as follows

$$\frac{p_2}{p_1}, \quad \frac{T_1 Y}{T_2 - T_1}, \quad \frac{c_p J T_1 Y g}{V^2}, \quad \frac{c_p J T_1 Y W}{P_s} = f \left[\frac{Q}{ND^3}, \quad \frac{V}{V_c} \right] \quad [17]$$

All terms of this equation have been previously identified and substantiated. Explanation of the graphic presentation of Equation [17] is made under Figs. 3, 4, 5, and 6.

A presentation of compressor performance in graphic form is shown in reference (1), conforming to the following dimensional equation

$$\frac{p_2}{p_1}, \quad \frac{T_1 Y}{T_2 - T_1}, \quad \frac{c_p J T_1 Y W}{P_s} = f \left[\frac{W}{\sqrt{p_1 \rho_1}}, \quad \frac{N}{\sqrt{T_1}} \right] \quad [18]$$

Substantiation of the first three terms has been made previously. For the latter two, $\frac{W}{\sqrt{p_1 \rho_1}}$ may be derived from $\frac{M}{D^2 \sqrt{p_1 \rho_1}}$ where $\frac{W}{\rho}$ is substituted for M and then the constant g and dimension D are omitted; and $\frac{N}{\sqrt{T_1}}$ may be derived by omission of D from the corresponding term in Equation [7].

In the same manner that D was omitted in the foregoing, use is often made of the term $\frac{Q}{N}$ rather than $\frac{Q}{ND^3}$ and furthermore, a single ND curve rather than a multiple-curve parameter such as $\frac{ND}{V_c}$ is occasionally used. Regarding these forms, it must be noted that omission of the dimension D from the performance presentation is not incorrect but only prevents direct comparison of results between compressors of different sizes. Omission of the compressibility parameter cannot be substantiated, however, except for certain limited-range test work.

Some serious disadvantages are present in these current methods of performance presentation. What is actually desirable is the following:

- Use of measured quantities.
- Use of rotational speed in only one functional quantity.
- Clarity and spread of plotted results.
- Well-defined limits of operation and surge.

That these aims have not and cannot be achieved by the current methods has bared the need for improvement.

FINAL CHOICE OF TERMS FOR DIMENSIONAL EQUATION

Density is measured through temperature and pressure. The effect of humidity on density is so small as to substantiate this substitution. Therefore the latter terms should be used in the graphic plots. Use of kinematic viscosity ν , mass rate of flow M , and density ρ is not convenient. The directly measurable quantities on test (2) are W , p_1 , p_2 , T_1 , T_2 , N , and P_s , all of which have been defined previously.

Power P is not a directly measured quantity, since by our original definition, bearing friction is not included. It is to our advantage to use the factor P_s denoting power to operate the

compressor at the impeller shaft rather than power P , since in the prediction of operating characteristics for conditions other than those of test as well as in comparisons between different blowers, the actual torque and power, which can be tested and must be furnished by the drive, is of first importance. In other words, test results on a blower with poor bearings and high seal drag should generally be made to show up to its disadvantage in the performance curves. It is to be noted that a small power error may be introduced if performance prediction is to be made for operations wherein the bearing fits, shaft-seal loads, and lubrication temperatures are different than they are on test. It will be assumed here that the test does simulate these particular operating conditions. Where slight differences cannot be prevented, the resulting influence on power input is still very small.

The flow coefficient or abscissa of the performance plot should not contain the quantity N , since speed of rotation is the primary variable in centrifugal-compressor operation. Of the available forms previously noted for this term only the nondimensional quantity $\frac{M}{D^2 \sqrt{p_1 \rho_1}}$ is free of N and ν . This quantity may now be easily converted to include only the desired measured quantities so that the result is $\frac{W \sqrt{T_1}}{g D^2 p_1}$. The fact that N has been eliminated in this flow coefficient results from the following derivation

$$\left. \begin{aligned} C \times M &= \frac{Q}{ND^3} \times \frac{ND}{\sqrt{T_1}} \\ &= \frac{W}{\rho g ND^3} \times \frac{ND}{\sqrt{T_1}} \\ &= \frac{WT_1}{p_1 g ND^3} \times \frac{ND}{\sqrt{T_1}} \\ &= \frac{W \sqrt{T_1}}{g D^2 p_1} \end{aligned} \right\} \dots \dots \dots [19]$$

The constant g may be omitted for simplicity. A final dimensional equation in the desired form for compressor performance presentation may be written

$$\frac{p_2}{p_1}, \frac{T_2}{T_1}, \frac{c_p J T_1 Y W}{P_s} = f \left[\frac{W \sqrt{T_1}}{D^2 p_1}, \frac{ND}{\sqrt{T_1}} \right] \dots [20]$$

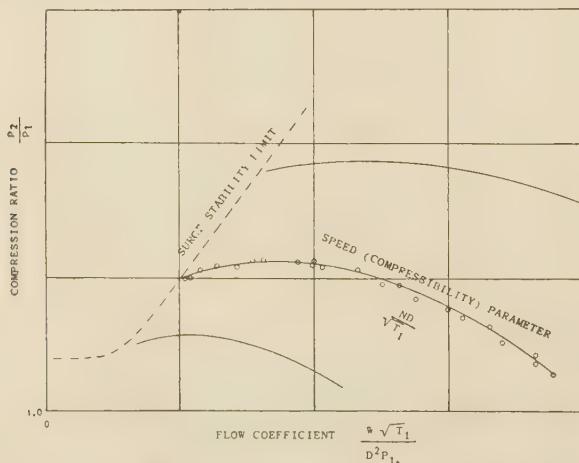


FIG. 7 COMPRESSION-RATIO PERFORMANCE PLOT DEVELOPED FOR APPLICATION TO CENTRIFUGAL COMPRESSORS

(Performance curves for three widespread values of compressibility parameter are shown in typical form. Typical uniform track of test points is also shown. Clarity results from spread of curves and use of measured values.)

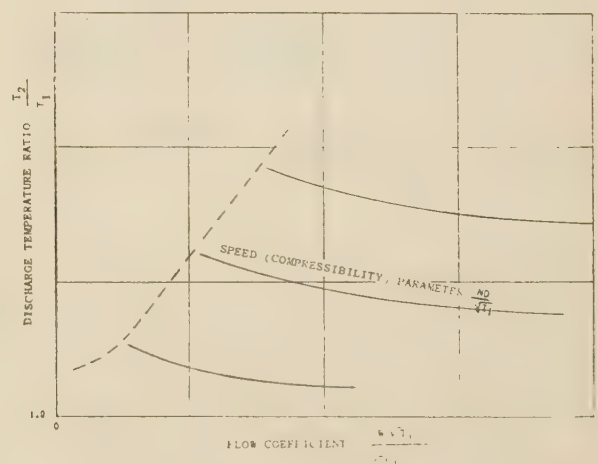


FIG. 8 TEMPERATURE-PERFORMANCE PLOT DEVELOPED FOR APPLICATION TO CENTRIFUGAL COMPRESSORS
(Refer to note under Fig. 7.)

COMPRESSOR-PERFORMANCE PLOT

Shown in Figs. 7, 8, and 9, are the characteristics curves of a typical centrifugal supercharger presenting quantity relations in the form shown in Equation [20]. These curves were developed from actual test data on a typical centrifugal supercharger.

One particular reason for the clarity of curves in the form of Figs. 7, 8, and 9, is the spread of values of the flow coefficient produced through multiplication by Mach number as noted in Equations [19]. The units, constants, and definitions which have been used in this performance presentation are shown in the following:

- $p_0 = 29.92$ in Hg, absolute pressure of standard atmosphere
- $p_1 =$ absolute value, in. mercury, of total pressure at compressor inlet
- $p_2 =$ absolute value, in. mercury, of total pressure at compressor discharge
- $T_0 = 459.6$ F absolute temperature of standard atmosphere at sea level
- $T_1 =$ absolute temperature deg F of fluid at compressor inlet
- $T_2 =$ absolute temperature deg F of fluid at compressor discharge
- $k =$ adiabatic exponent $= \frac{c_p}{c_v} = 1.3947$ for "normal air" (5)
- and $\frac{k-1}{k} = 0.283$
- $c_p =$ specific heat at constant pressure, Btu per lb per deg F $= 0.243$ for "normal air" (5)
- $Y = \left[\left(\frac{p_2}{p_1} \right)^{\frac{k-1}{k}} - 1 \right]$ ratio of temperature rise to absolute temperature in adiabatic compression
- $W =$ weight of fluid inspired, lb per min
- $P_s' =$ shaft horsepower $= \frac{P_s}{33,000}$
- $D =$ impeller diameter, in.
- $N =$ impeller speed, rpm
- $g =$ acceleration of gravity, 32.2 fpsps
- $J = 778$ ft-lb per Btu, the mechanical equivalent of heat
- $V =$ impeller-tip velocity, fps

From the constants and definitions given the following power terms may be reduced for general reference when air is the fluid:

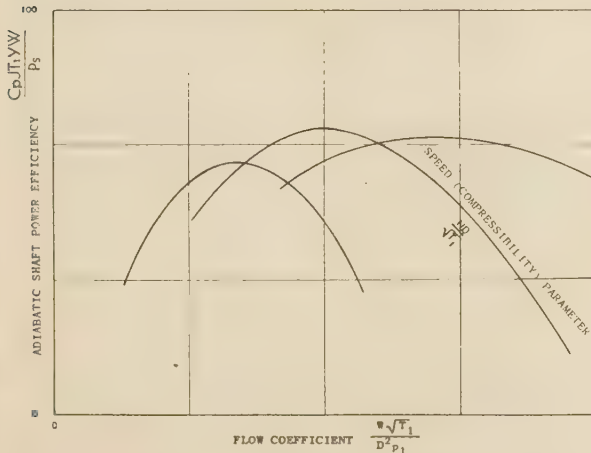


FIG. 9 POWER PERFORMANCE PLOT DEVELOPED FOR APPLICATION TO CENTRIFUGAL COMPRESSORS
(Refer to note under Fig. 7.)

$$\text{Adiabatic horsepower} = \frac{c_p J T_1 Y W}{33,000} = 0.00573 T_1 Y W \dots [21]$$

$$\begin{aligned} \text{Actual temperature-rise horsepower} &= \frac{(T_2 - T_1) c_p J W}{33,000} \\ &= 0.00573 (T_2 - T_1) W \dots \dots \dots [22] \end{aligned}$$

$$\text{Impeller horsepower} = \frac{W N^2 D^2 \pi^2}{12^2 g 60^2 \cdot 33,000} = 1.80 \times 10^{-11} W N^2 D^2 \dots \dots \dots [23]$$

$$\text{Pressure-energy coefficient, } \eta_p = \frac{3.18 \times 10^8 T_1 Y}{N^2 D^2} = \frac{6083 T_1 Y}{V^2} \dots \dots \dots [24]$$

The following power-efficiency equation may be reduced for evaluation of compressor power requirements from Fig. 9

$$\text{Adiabatic shaft horsepower efficiency, } \eta_s = \frac{0.00573 T_1 Y W}{P_s'} \dots [25]$$

A COMBINED PERFORMANCE PLOT

A number of additional advantages may be obtained in the compressor performance plot if the characteristics shown in Figs. 7, 8, and 9, can be consolidated into one chart. This may be accomplished, as shown in Fig. 10, by plotting the adiabatic shaft-power efficiency and adiabatic-temperature efficiency as contours on the compression-ratio performance chart. Individual contours for temperature and power efficiency may be shown, but these two functions have been found so similar in pattern and position that single contours with dual evaluation have been considered more practical.

As an example of typical use of the performance chart in Fig. 10, assume that inlet and discharge pressure, fluid-flow rate, fluid-inlet temperature, and impeller diameter are known; find the required speed, power, and the discharge temperature. From the compression ratio and flow coefficient a point may be located on the chart which by interpolation between compressibility parameters defines the required speed. From the adiabatic efficiency contour T_2 may be found by the equation

$$T_2 = T_1 \left(1 + \frac{Y}{\eta} \right) \dots \dots \dots [26]$$

Values of Y , Equation [10], may be most conveniently evaluated for any given compression ratio by the tables developed in reference (5). From the adiabatic shaft-power-efficiency contours, drive horsepower may be found by the equation

$$P_s' = \frac{0.00573 T_1 Y W}{\eta_s} \dots \dots \dots [27]$$

Drive torque, in inch-pounds, may be found from the equation

$$\text{Torque} = \frac{12 \times 33,000 P_s'}{2\pi N} = \frac{361 T_1 Y W}{N \eta_s} \dots \dots [28]$$

Characteristics curves on the combined performance chart are confined only within the following bounds: (a) To the surge stability limit on the left; (b) to the minimum compression ratio for unloaded conditions along the bottom; (c) to the maximum speed along the top; and (d) to the maximum power or torque on the right in Fig. 10.

CONCLUSION

The methods of performance presentation in terms of non-dimensional relationships discussed in this paper apply particularly to centrifugal compressors or superchargers, but it may be

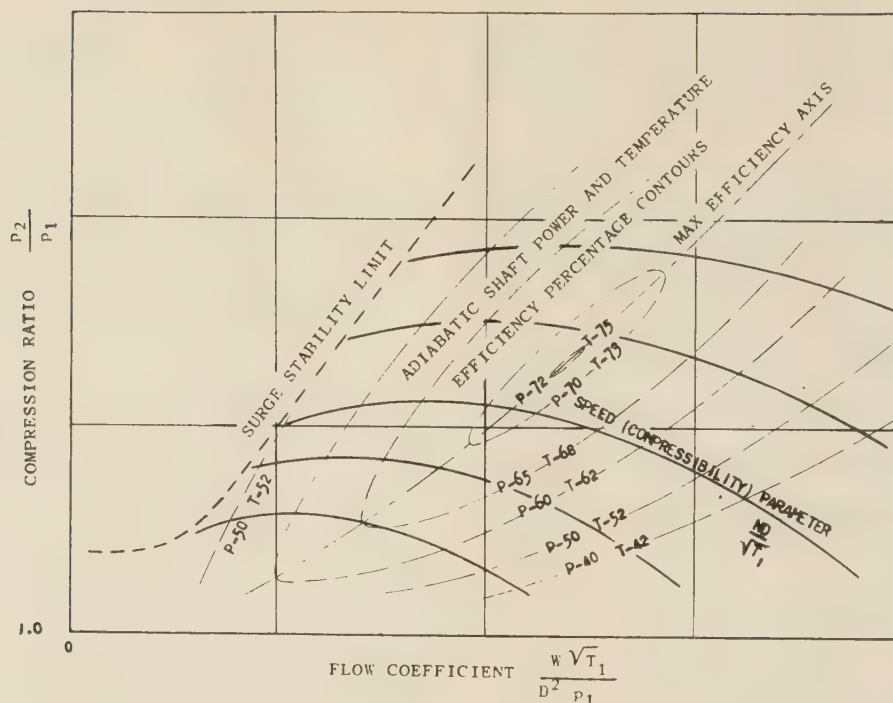


FIG. 10 COMBINED PERFORMANCE PLOT DEVELOPED IN PAPER FOR APPLICATION TO CENTRIFUGAL COMPRESSORS

(Performance in combined form is shown for a typical centrifugal compressor. The advantages of performance presentation in this form are obvious. From this one chart the speed, power, and temperature relations may all be determined. Power- and temperature-efficiency contours are combined and noted by P and T , respectively, but may be shown separately when so desired. Nomenclature is as follows: N = rpm; D = impeller diameter, in.; W = fluid flow, lb per min; p_1 = inlet pressure, in. Hg; p_2 = discharge pressure, in. Hg; T_1 = inlet temperature, deg F abs.)

reasonable to assume that application to other types may in certain cases be desirable and permissible. This presentation is perhaps most useful in conjunction with the aeronautical sciences where operation and orientation of performance with respect to peak efficiencies yields the greatest returns. Use of the combined performance chart may prove particularly useful in correlating performance of centrifugal superchargers with that of dependent or semidependent systems such as supercharger power drives, supercharged cabin pressures, engine-manifold pressures, and the like.

Since conditions in test commonly differ from those in actual operation and the inlet conditions encountered are so often variable over a broad range, it is increasingly important for the compressor designer-manufacturer submitting his product for use in these specialized fields to present performance information in a form which makes possible a precise analysis of performance suitability and drive requirements. It is desirable that future work on blower standards and test codes should eventually be extended to include consideration of these conditions.

BIBLIOGRAPHY

- 1 "The Application of Dimensional Relationships to Air Compressors With Special Reference to the Variation of Performance with Inlet Conditions," by R. S. Capon and G. V. Brooke, Reports and Memoranda no. 1336, British Research Committee, London, England, June, 1930.
- 2 "Test Code for Centrifugal Compressors, Exhausters, and Fans," by A.S.M.E. Power Test Code Committee, THE AMERICAN SOCIETY OF MECHANICAL ENGINEERS, New York, N. Y., 1935.
- 3 "Applied Hydro- and Aeromechanics," by O. G. Tietjens, McGraw-Hill Book Company, Inc., New York, N. Y., 1934.
- 4 "Dimensional Analysis and Similitude in Mechanics," by J. C. Hunsaker, Theodore von Kármán Anniversary Volume, Pasadena, Calif., California Institute of Technology, 1941, pp. 21-48.
- 5 "Engineering Computations for Air and Gases," by S. A. Moss and C. W. Smith, Trans. A.S.M.E., vol. 52 (Paper APM-52-8), 1930, pp. 93-102.
- 6 "Air Compression With Temperatures Above Adiabatic, With Special Reference to Airplane Superchargers," by S. A. Moss, Trans. A.S.M.E., vol. 55, (Paper AER-55-5), 1933, pp. 35-43.
- 7 "Energy Transfer Between a Fluid and a Rotor for Pump and Turbine Machinery," by S. A. Moss, C. W. Smith, and W. R. Foote, Trans. A.S.M.E., vol. 64, 1942, pp. 567-597.

A Pneumatic Piston-Ring Gage for Radial-Pressure Measurement

By P. G. EXLINE,¹ PITTSBURGH, PA.

This paper describes an instrument for indicating the radial pressure distribution of piston rings. The piston ring is supported at eighteen equally spaced points by flat-faced pins located around the circumference of a circle of the same size as the engine cylinder. The force exerted on each pin by the ring is measured by a self-balancing pneumatic device which simultaneously indicates all the forces on a row of eighteen manometers. The rapidity with which the measurements can be made makes the instrument suitable for production inspection.

THE principal functions of piston rings in internal-combustion engines are to prevent passage of combustion gases past the piston and to control the flow of lubricating oil from the crankcase to the combustion chamber. In the development of high-output engines, the piston ring is sometimes the limiting factor in increasing the power, since failure of the ring itself will cause failure of the entire engine. Much work is being done to improve the performance of piston rings, and one of the fundamental research problems is that of determining the optimum radial pressure which should exist between the piston ring and the cylinder wall. As part of this research, it is necessary to have an instrument for measuring this pressure for any given ring. This paper describes an instrument which was developed for this purpose.

Very little work on ring wall-pressure instruments has been described in the literature, although several different types have been constructed for experimental work.² In general, the ring is supported in a cylinder of the same bore as the engine cylinder and a force applied at a point on the ring just sufficient to lift it from the surface. The ring is then rotated several degrees and the measurement repeated. A polar diagram of the observations as a function of their angular location on the ring will then give a characteristic pattern of that ring, called the ring pattern. Such a method suffers from several disadvantages. It is quite slow, making the time to examine a production lot of rings prohibitive. It requires both force and displacement measurement, the displacement measurement being tedious because of the small magnitudes involved.

OPERATION SPEEDED BY INSTRUMENT MEASURING AIR PRESSURE

The device described in this paper combines the force and displacement measurement into a single measurement of air pressure. Air at constant pressure enters a cylindrical chamber through a fixed orifice. The end of the chamber is machined to a narrow edge and is closed by a flat disk which transmits the force, developed by the air pressure against its inner face, to a point on the piston ring under examination. The piston ring will then deform elastically, causing the disk to separate a distance h from the end of the chamber. Equilibrium is established

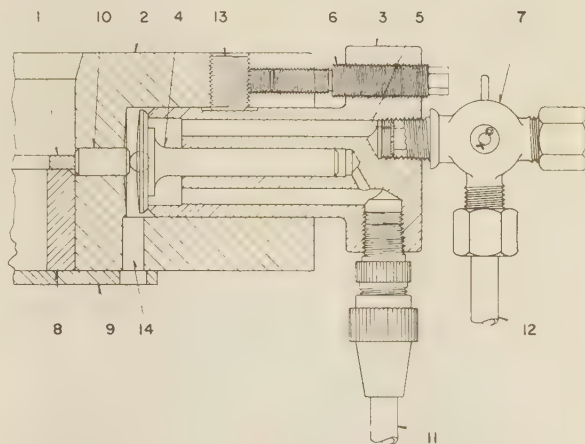


FIG. 1 CROSS SECTION THROUGH PISTON-RING GAGE

when the opening of the annular orifice is such that the air flow through it is equal to that through the fixed orifice. The pressure drop across the fixed orifice is then $P_s - P$, where P_s is the source pressure and P the back pressure. The drop across the annular orifice is $P - P_A$, where P_A is the atmospheric pressure.

The piston ring gage is composed of a heavy ring with eighteen measuring units radially mounted in it at 20-deg intervals. A cross section through one of the units is shown in Fig. 1. The piston ring 1, is mounted in the gage ring 2, which is bored to an inside diameter equal to that of the engine cylinder in which the ring is used. The body of the measuring unit 3, is mounted in a radial hole in the gage ring. The open end of the chamber is closed by the valve 4, whose stem is guided in an axial hole drilled in the measuring-unit body. Constant-pressure air enters at 12, passes through the three-way cock 7, and the fixed orifice 5, before entering the chamber. Force is transmitted to the piston ring through a steel ball and pin 10. Pressure in the chamber is measured by a mercury manometer attached at 11. Radial location of the measuring unit is obtained by the differential screw 6, and fixed by the clamping screw 13.

The ends of all pins are ground flat and perpendicular to the axis of the pin. This permits examination of aircraft-engine rings which have the outer face formed into a single or double cone of small angle. Use of a spherical ended pin, in this case, would require extreme exactitude in the vertical positioning of the piston ring.

A view of the instrument is given in Fig. 2. Air from the line is passed through an air regulator and cleaner and then into a manifold located under the table top. From this manifold, eighteen lines lead to the measuring units in the gage ring. The corresponding manometers for indicating the chamber pressures are mounted against a ruled board behind the gage ring. The pressure gage indicates the source pressure in the manifold.

The measuring units are numbered 1 to 18 clockwise around the ring, beginning at the point nearest the operator. The manometers are numbered correspondingly, beginning at the left. The ring under examination at the time the view, Fig. 2, was taken was located with its gap midway between units 1 and 18.

¹ Section Engineer, Gulf Research & Development Company. Mem. A.S.M.E.

² Refer to the Bibliography at the end of the paper.

Contributed by the Industrial Instruments and Regulators Division and presented at the Annual Meeting, New York, N. Y., Nov. 27-Dec. 1, 1944, of THE AMERICAN SOCIETY OF MECHANICAL ENGINEERS.

NOTE: Statements and opinions advanced in papers are to be understood as individual expressions of their authors and not those of the Society.

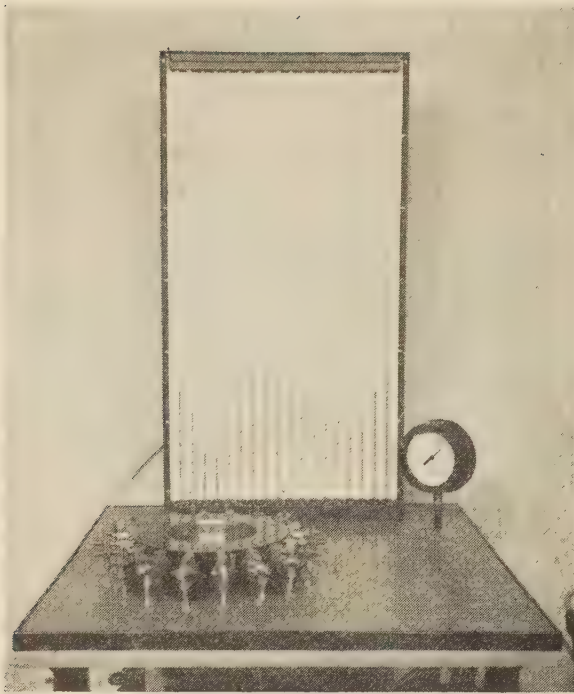


FIG. 2 PISTON-RING GAGE IN OPERATION

THE INSTRUMENT IN USE

The first step in preparing the instrument for use is to adjust the position of the measuring units so that ends of the pins 10 are all equidistant from the center of the gage ring when all slack is taken up. There are two methods of doing this. A solid disk, accurately ground to the cylinder diameter, can be placed in the gage ring and all units adjusted to give the same reading on the manometers. Next, a piston ring having a mark scribed opposite the gap can be placed in the gage with the mark lined up with one of the measuring units. That unit is then adjusted to give an arbitrarily chosen pressure on the manometer. The ring is then rotated 20 deg, and the adjacent unit adjusted to give the same pressure. This process is repeated until all units have been adjusted. This first adjustment is made with air flowing through all units. It is necessary to repeat the entire procedure one, or preferably two times, as a change in the position of one unit will influence the ring force on the adjacent units.

The choice of proper initial adjustment will depend on the area of the valve face exposed to the pressure, the area of the primary orifice, and the magnitude of the source pressure. It is necessary that the ring be entirely supported during a measurement by the eighteen pins. If it touches the cylinder wall at one or more points, part of the radial force will be exerted against the gage ring and false readings will result.

In order to measure the lift of the valve under different loads and with a range of source pressures, one of the measuring units was mounted with its axis in a vertical position so that a known force could be applied to the embedded ball, and the movement of the valve could be observed. The details of this arrangement are shown in Fig. 3. The measuring unit 1 was rigidly clamped to a fixed support. A beam 4, balanced on the ball 5 supported a weight pan suspended below the unit. A bridge 9, was rigidly attached to the valve head and passed over the beam. One leg of a three-legged optical lever rested on the center of this bridge.

The other two legs rested on two posts rigidly attached to the fixed support. The three legs were made by pressing three steel balls into a steel bar to form an isosceles triangle, the ball at the apex resting on the movable bridge. The two balls resting on the fixed posts were about 3 in. apart while the other was 0.2 in. from the line joining their centers. A plane mirror 11 reflected light from a scale 289 in. away to a telescope mounted vertically above. The magnification was such that a lift of 13.6×10^{-6} in. of the valve was equivalent to 1 mm change in scale reading. That part of the weight of the optical lever which rested on the bridge was considered as part of the total load. Air was applied through the tube 7, of the same length as used in the instrument, and an effort was made to duplicate all other conditions.

Results of some of the measurements are shown in Figs. 4, 5, and 6. All the data in Fig. 4 were obtained with a source pressure of 15 psi, with six fixed orifices ranging from 0.0135 in. diam to 0.0860 in., and with loads of 1.24, 2.74, 3.74, 4.74, 5.74, and 6.74 lb. In Figs. 5 and 6, the source pressures were 20 and 55 psi, respectively, the same orifices and loads being used.

The inside diameter of the counterbore in the end of the measuring unit was 0.796 in. to give an area of 0.500 sq in. The valve seat was of finite width averaging 0.016 in., so that pressure over the area of the seat would also help support the weight. The total area including that of the seat was 0.538 sq in. It would be expected then that the pressure necessary to support a weight w would lie between $w/0.500$ and $w/0.538$. In general, the data indicated that the effective area was but slightly greater than 0.500 sq in.

With the larger orifices and at the higher source pressures, there

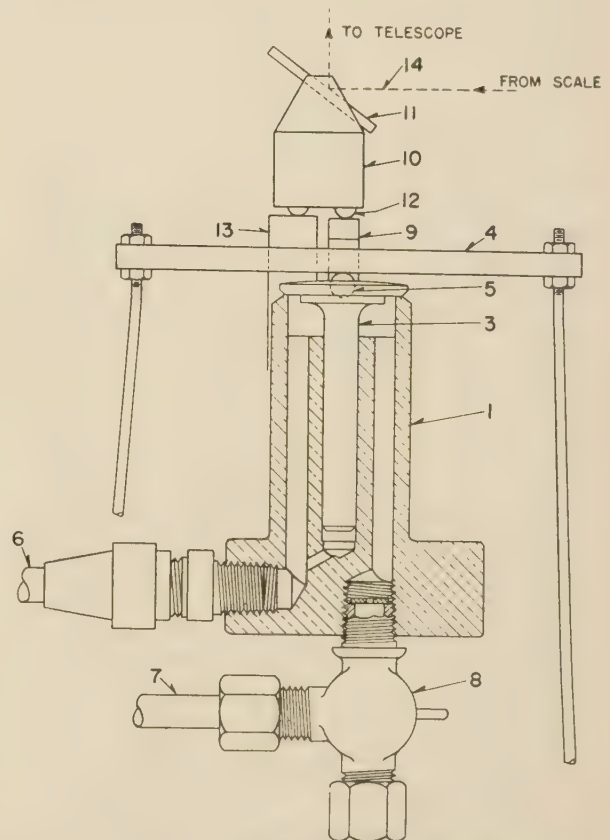


FIG. 3 VALVE-LIFT MEASURING APPARATUS

appears to be a tendency for the effective area to become less than 0.500 sq in. The cause of this cannot be stated with much assurance, but it is thought that the air flow in the chamber is such that the manometer no longer indicates the true average pressure below the valve head.

It is quite evident that with the 0.0135-in. orifice some of the back pressures indicated are substantially less than those necessary to support the loads, Figs. 4 and 5. Since the discrepancies occurred with valve lifts between 25 and 75 microinches, it is believed that the valve was not entirely separated from the seat and that part of the load was carried by the seat. The valve had been lapped to the seat with fine abrasive, but annular ridges of that order of magnitude had been left on both parts. It is also possible that a slight warping of the valve head or a cocking of the entire valve could place part of the load on the seat at low lifts. If the valve were cocked by an amount of 0.002 in. per ft, one edge of the valve could rest on the seat with the center lifted 75 microinches.

The instruments which were placed in use prior to the date of preparation of this paper were provided with 0.0625-in. orifices and have been used with source pressures from 15 to 25 psi. These conditions were chosen somewhat arbitrarily, and the valve-lift measurements were made with different orifices to determine if other orifices and source pressures would be likely to provide better operation.

RESULTS OF TESTS

Referring to Fig. 4, it can be seen that the back pressure, with the 0.0625-in. orifice, was proportional to the load with little er-

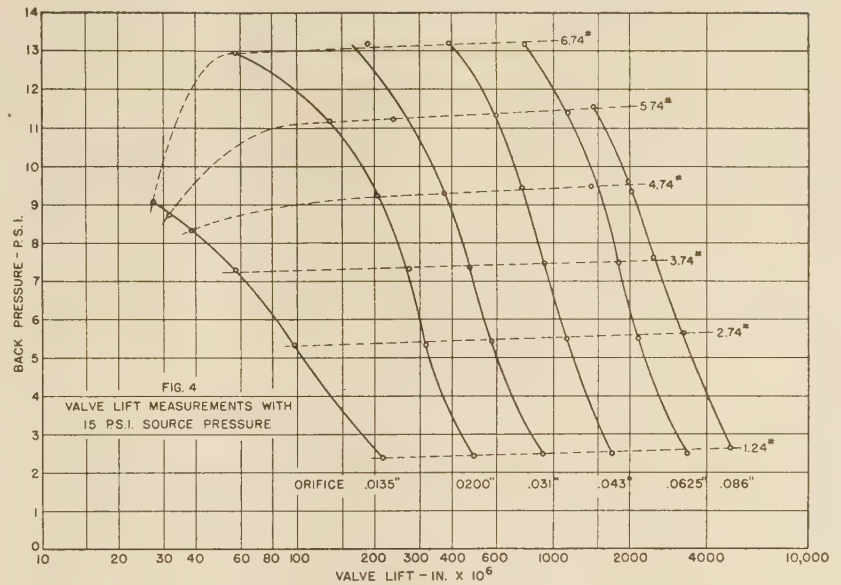


FIG. 4 VALVE-LIFT MEASUREMENTS WITH 15 PSI SOURCE PRESSURE

ror. The valve lift varied from 780 microinches at 13.2 psi to 3400 microinches at 2.5 psi back pressure. This curve can be used to find the values of valve lift for each unit in a piston-ring gage from the observed manometer readings. However, such values will not indicate the actual radial movement of the piston ring unless the valve is closed when the end of the force-transmitting pin, 10 in Fig. 1, is tangential to the surface of the gage ring. In general, the initial setting of the measuring unit leaves a small clearance between the valve and seat which can be determined only by placing a solid cylindrical plug in the gage ring with no clearance and applying the air.

During the measurement shown in Fig. 2, the back pressure was approximately 5 psi at points 7, 8, and 18. Since this was made with a source pressure of 20 psi, Fig. 5 must be used to determine that the valve lifts were 2800 microinches. At point 16, the back pressure was 2.6 psi corresponding to a valve lift of 3800 microinches. Point 16 on the piston ring was then forced in toward the center 1000 microinches farther than points 7, 8, or 18. The reason for the greater deflection at point 16 was that the elastic stiffness of the segment of piston ring resisting this pin was less than that of the segment at point 8, for example. The indications are thus a function of the stiffness of the various ring segments and give the characteristic ring pattern.

Had it been possible to measure the force at point 16 with no greater deformation than occurred at point 18, the indication would have been less than that actually observed since the elastic force continued to increase during the additional 1000-microinches deflection. It is obvious that all observations are in error by the amount of the

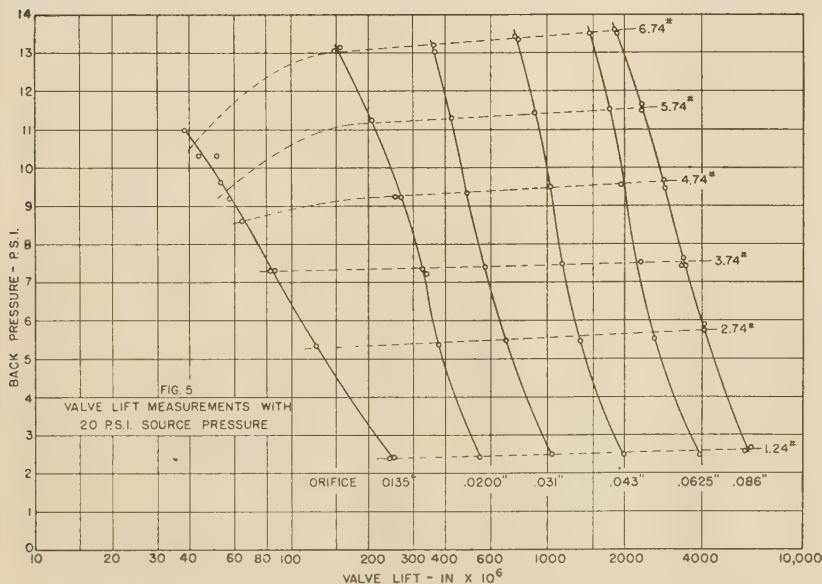


FIG. 5 VALVE-LIFT MEASUREMENTS WITH 20 PSI SOURCE PRESSURE

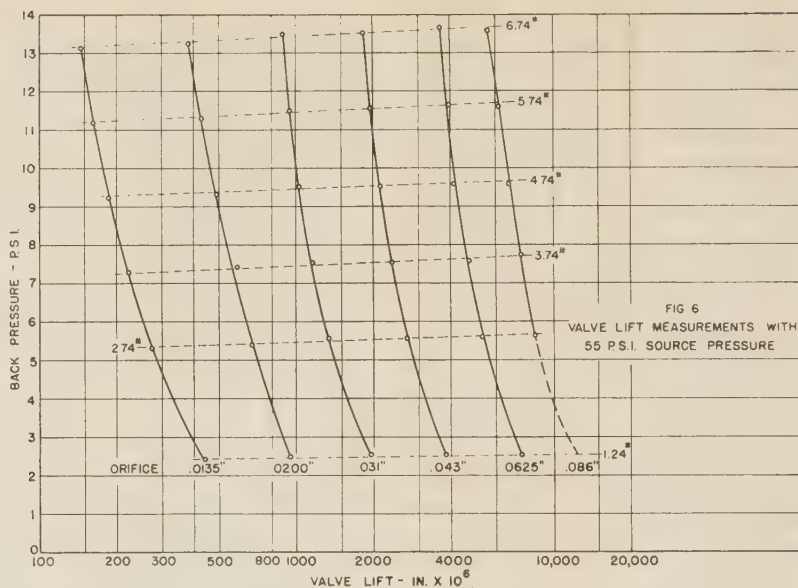


FIG. 6 VALVE-LIFT MEASUREMENTS WITH 55 PSI SOURCE PRESSURE

deflection at each point multiplied by the ring stiffness at the corresponding point.

The valve-lift measurements show that the rate of change of force with deflection is a function of the source pressure and the primary orifice size. With a 15-psi source pressure and the 0.0200-in. orifice, a deflection range of 350 microinches will indicate a load range from 1 lb to 5 lb. If the source pressure and orifice were to be increased to 55 psi and 0.086 in., respectively, the same load range would require a deflection range of 8400 microinches. The average sensitivity in the first case would be 24 times that in the second case.

Two factors mitigate against the use of conditions which would give the maximum possible sensitivity. As explained previously, it is necessary to deflect the ring enough to lift it entirely clear of the gage-ring wall or the readings will be markedly in error. Then too the sensitivity must not be so great as to destroy the ability of the instrument to repeat readings with reasonable accuracy.

When a ring is lifted entirely clear of the wall, a force applied at any point on the inner surface of the ring will cause an increase in the indications of the adjacent measuring units. A more

quantitative test of this condition is to balance the components of the indicated forces perpendicular to a diameter drawn across the ring. If the ring is not resting against the wall, the sum of these components on one side of the diameter should equal the sum of the components on the opposite side. This balance should hold whether the diameter is taken through the ring gap or through any other point on the ring. In Table 1 is shown a series of measurements made on a ring placed with its gap midway between points 1 and 18. The first column gives the observed radial forces at the 18 points. Column 2 shows the components of these forces perpendicular to a diameter drawn through the ring gap. The remaining columns show the components perpendicular to diameters originating at multiples of 20 deg from the gap up to 160 deg. At the bottom of each column are shown the sums of the components on each side of the corresponding diameter and the difference between these sums expressed as a percentage of their mean.

ACCURACY OF INSTRUMENT

As a test of the reproducibility or accuracy of the instrument, a series of measurements was made on a single ring with the gap

TABLE 1 FORCE BALANCE^a

Measuring unit	Radial force, lb	Point of origin of diameter from ring gap								
		0°	20°	40°	60°	80°	100°	120°	140°	160°
1	2.60	0.452	-0.452	-1.300	-1.991	-2.441	-2.600	-2.441	-1.991	-1.300
2	1.85	0.925	0.322	-0.322	-0.925	-1.416	-1.737	-1.850	-1.737	-1.416
3	2.40	1.838	1.200	0.417	-0.417	-1.200	-1.838	-2.253	-2.400	-2.253
4	1.65	1.551	1.265	0.825	0.287	-0.287	-0.825	-1.265	-1.551	-1.650
5	1.35	1.350	1.269	1.035	0.675	0.235	-0.235	-0.675	-1.035	-1.269
6	1.05	0.987	1.050	0.987	0.805	0.525	0.182	-0.182	-0.525	-0.805
7	1.10	0.842	1.034	1.100	1.034	0.842	0.550	0.191	-0.191	-0.550
8	1.55	0.775	1.188	1.456	1.550	1.456	1.188	0.775	0.269	-0.269
9	3.10	0.538	1.550	2.374	2.910	3.100	2.910	2.374	1.550	0.539
10	3.45	-0.600	0.600	1.725	2.641	3.240	3.450	3.240	2.641	1.725
11	2.35	-1.175	-0.408	0.408	1.175	1.800	2.210	2.350	2.210	1.800
12	1.75	-1.340	-0.875	-0.304	0.304	0.875	1.340	1.644	1.750	1.644
13	1.50	-1.410	-1.149	-0.750	-0.260	0.260	0.750	1.149	1.410	1.500
14	1.35	-1.350	-1.268	-1.035	-0.675	-0.235	0.235	0.675	1.035	1.268
15	1.15	-1.080	-1.150	-1.080	-0.881	-0.575	-0.198	0.198	0.575	0.881
16	1.05	-0.805	-0.987	-1.050	-0.987	-0.805	-0.525	-0.182	0.182	0.525
17	1.55	-0.775	-1.187	-1.456	-1.550	-1.456	-1.187	-0.775	-0.269	0.269
18	3.60	-0.626	-1.800	-2.756	-3.380	-3.600	-3.380	-2.756	-1.800	-0.626
		9.258	9.478	10.327	11.381	12.333	12.815	12.596	11.622	10.151
		9.161	9.276	10.053	11.066	12.015	12.525	12.379	11.499	10.138
Per cent deviation		1.05	2.15	2.69	2.81	2.61	2.29	1.74	1.06	0.13

^a Ring No. 13, Pratt & Whitney Aircraft 28356-A; 5.75 in. diam. Ring gage No. 6, 1/16 in. orifices; 22 psi source pressure.

TABLE 2 REPRODUCIBILITY TEST^a

Manometer no.	1'	2'	3'	4'	5'	6'	7'	8'	9'	10'	11'	12'	13'	14'	15'	16'	17'	18'
1	4.2	3.8	4.8	3.6	2.7	2.3	2.1	3.2	6.2	6.7	4.6	3.3	2.8	2.6	2.3	2.3	2.7	4.8
2	4.8	3.7	5.4	3.8	2.9	2.4	2.4	3.3	6.5	6.9	4.7	3.6	3.1	2.8	2.4	2.5	3.0	4.8
3	4.3	3.6	5.1	3.6	2.8	2.3	2.2	3.3	6.2	6.9	4.8	3.4	3.1	2.9	2.4	2.4	2.8	4.9
4	3.8	3.0	4.5	3.5	2.4	2.0	2.0	2.8	5.6	6.7	4.3	3.1	2.6	2.5	2.2	2.0	2.5	4.1
5	4.3	3.4	4.6	3.7	2.9	2.0	2.1	3.1	5.8	6.8	4.7	3.4	3.0	2.7	2.4	2.3	2.6	4.7
6	4.2	3.4	4.9	3.7	2.8	2.2	2.0	3.2	6.2	6.9	5.0	3.4	2.9	2.8	2.3	2.4	2.8	4.4
7	4.3	3.3	4.7	3.7	2.8	2.2	2.2	3.1	5.9	6.8	4.7	3.6	3.0	2.8	2.4	2.3	2.9	4.4
8	4.4	3.3	4.6	3.9	2.9	2.1	2.1	3.1	6.3	6.7	4.9	3.4	3.1	2.7	2.3	2.3	2.7	4.9
9	4.3	3.5	4.7	3.6	2.9	2.3	2.2	3.2	5.9	6.5	4.7	3.6	3.0	2.9	2.3	2.4	2.9	4.6
10	4.1	3.3	4.7	3.7	2.7	2.3	2.2	3.2	5.9	6.9	4.4	3.4	3.1	2.7	2.4	2.3	2.9	4.8
11	4.0	3.1	4.5	3.6	2.6	1.9	2.0	2.9	6.1	6.7	4.8	3.1	2.8	2.6	2.1	2.1	2.6	4.6
12	4.2	3.4	4.4	3.6	2.9	2.2	2.0	3.0	6.1	6.8	4.6	3.5	2.9	2.7	2.3	2.2	2.9	4.5
13	4.2	3.3	4.6	3.4	2.7	2.2	2.0	3.0	5.6	6.9	4.6	3.3	3.0	2.7	2.3	2.2	2.6	4.8
14	4.4	3.3	4.7	3.6	2.6	2.1	2.1	3.0	6.2	6.9	4.9	3.3	2.8	2.8	2.3	2.3	2.7	4.5
15	4.5	3.6	4.7	3.7	3.0	2.2	2.3	3.2	6.0	6.9	5.0	3.6	3.0	2.8	2.5	2.5	2.9	4.6
16	4.2	3.2	4.9	3.6	2.8	2.2	2.0	3.1	5.9	6.8	4.4	3.4	2.8	2.6	2.2	2.3	2.7	5.0
17	4.5	3.5	4.7	4.0	2.9	2.3	2.3	3.2	6.4	7.0	4.8	3.2	3.0	2.8	2.4	2.4	3.0	4.9
18	4.4	3.7	4.7	3.8	3.1	2.5	2.5	3.5	5.9	6.6	4.8	3.5	3.0	2.9	2.6	2.6	3.0	4.7
Total	76.9	61.4	85.5	66.1	50.4	39.7	38.7	56.4	109.0	122.4	84.7	61.1	53.0	49.3	42.1	41.8	50.2	84.0
Average	4.3	3.4	4.7	3.6	2.8	2.2	2.1	3.1	6.0	6.7	4.7	3.4	2.9	2.7	2.3	2.3	2.8	4.6

^a Ring No. 13, Pratt & Whitney Aircraft 28356-A; 5.75 in. diam. Ring gage No. 6, 1/16 in. orifices; 22 psi source pressure. Manometer readings in lb per sq in.

TABLE 3 REPRODUCIBILITY TEST; DEVIATIONS FROM MEANS^a

Manometer no.	1'	2'	3'	4'	5'	6'	7'	8'	9'	10'	11'	12'	13'	14'	15'	16'	17'	18'
1	-0.1	0.4	0.1	0.0	-0.1	0.1	0.0	0.1	0.2	0.0	-0.1	-0.1	-0.1	-0.1	0.0	0.0	-0.1	0.2
2	0.2	0.3	0.7	0.2	0.1	0.2	0.3	0.2	0.5	0.2	0.0	0.2	0.2	0.1	0.1	0.2	0.2	0.2
3	0.0	0.2	0.4	0.0	0.0	0.1	0.1	0.2	0.2	0.2	0.1	0.0	0.2	0.2	0.1	0.1	0.0	0.3
4	-0.5	-0.4	-0.2	-0.1	-0.4	-0.2	-0.1	-0.3	-0.4	0.0	-0.4	-0.3	-0.3	-0.2	-0.1	-0.3	-0.3	-0.5
5	0.0	0.0	-0.1	0.1	0.1	-0.2	0.0	0.0	-0.2	0.1	0.0	0.0	0.1	0.0	0.1	0.0	-0.2	0.1
6	-0.1	0.0	0.2	0.1	0.0	0.0	-0.1	0.1	0.2	0.2	0.3	0.0	0.0	0.1	0.0	0.1	0.0	-0.2
7	0.0	-0.1	0.0	0.1	0.0	0.0	0.1	0.0	-0.1	0.1	0.2	0.3	0.0	0.0	0.1	0.0	0.1	-0.2
8	0.1	-0.1	-0.1	0.3	0.1	-0.1	0.0	0.0	0.3	0.0	0.2	0.0	0.2	0.1	0.1	0.0	-0.1	0.3
9	0.0	0.1	0.0	0.0	0.1	0.1	0.1	0.1	-0.1	-0.2	0.0	0.2	0.1	0.2	0.0	0.1	0.1	0.0
10	-0.2	-0.1	0.0	0.1	-0.1	0.1	0.1	0.1	-0.1	0.2	-0.3	0.0	0.2	0.1	0.1	0.0	0.1	0.2
11	-0.3	-0.3	-0.2	0.0	-0.2	-0.3	-0.1	-0.2	0.1	0.0	0.1	-0.3	-0.1	-0.1	-0.2	-0.2	-0.2	0.0
12	-0.1	0.0	-0.3	0.0	0.1	0.0	-0.1	-0.1	0.1	0.1	-0.1	0.1	0.0	0.0	0.0	-0.1	0.1	-0.1
13	-0.1	-0.1	-0.1	-0.2	-0.1	0.0	-0.1	-0.1	-0.4	0.2	-0.1	-0.1	0.1	0.0	0.0	-0.1	-0.2	0.2
14	0.1	-0.1	0.0	0.0	-0.2	-0.1	0.0	-0.1	0.2	0.2	0.2	-0.1	-0.1	0.1	0.0	0.0	-0.1	-0.1
15	0.2	0.2	0.0	0.1	0.2	0.0	0.2	0.1	0.0	0.2	0.3	0.2	0.1	0.1	0.2	0.2	0.1	0.0
16	-0.1	-0.2	0.2	0.0	0.0	0.0	-0.1	0.0	-0.1	0.1	-0.3	0.0	-0.1	-0.1	-0.1	0.0	-0.1	0.4
17	0.3	0.1	0.0	0.4	0.1	0.1	0.2	0.1	0.4	0.3	0.1	-0.2	0.1	0.1	0.1	0.1	0.2	0.3
18	0.1	0.3	0.0	0.2	0.3	0.3	0.4	0.4	-0.1	-0.1	0.1	0.1	0.1	0.2	0.3	0.3	0.2	0.1

^a Root-mean-square value of all deviations, 4.96 per cent.

successively located between each two adjacent measuring points. In this manner, each unit is used to measure the force at each of 18 points on the ring. The observations are tabulated as shown in Table 2. The numbers in the first column indicate the measuring units and the primed numbers at the column heads indicate points on the ring. Each value in a column then indicates a separate measurement of the force on the same point on the ring. If the assumption be made that the mean of these observations indicates the true value of the force at this point, deviations from this value can be secured by subtraction as shown in Table 3. The root-mean-square value of all the deviations, expressed as a percentage of the average force, is used as a measure of the reproducibility of the instrument. In the case of the ring shown this was 4.96 per cent.

Errors in the operation of the instrument can be caused by improper initial adjustment, variation in the size of the primary orifices, variations in the variable orifices, friction in the valve guides and gage pins, the presence of dirt on the ring or gage-ring wall and variations in the source pressure. By exercising reasonable care in initial adjustment and supplying clean air the instrument will operate with satisfactory accuracy for the selection of rings of a given ring pattern and for production inspection when a given pattern is to be met in manufacture.

One use of the instrument is demonstrated in Fig. 7. This shows the ring pattern of a Caterpillar Diesel ring before and after a run of 486 hr duration in a single-cylinder engine. The engine bore was 5 3/4 in. and the ring was located in the top groove of the piston. This figure shows a high initial tip pressure which was substantially reduced during the test.

The instrument is not limited to a single-size ring as a spacer ring can be placed inside the gage ring to accommodate smaller-diameter piston rings. In the one constructed in this manner, the bore of the gage ring was 5 3/4 in. The spacer ring was made to fit this with a metal-to-metal fit, while the bore was ground to 5 1/2 in. diam. Radial holes were drilled to match those in the

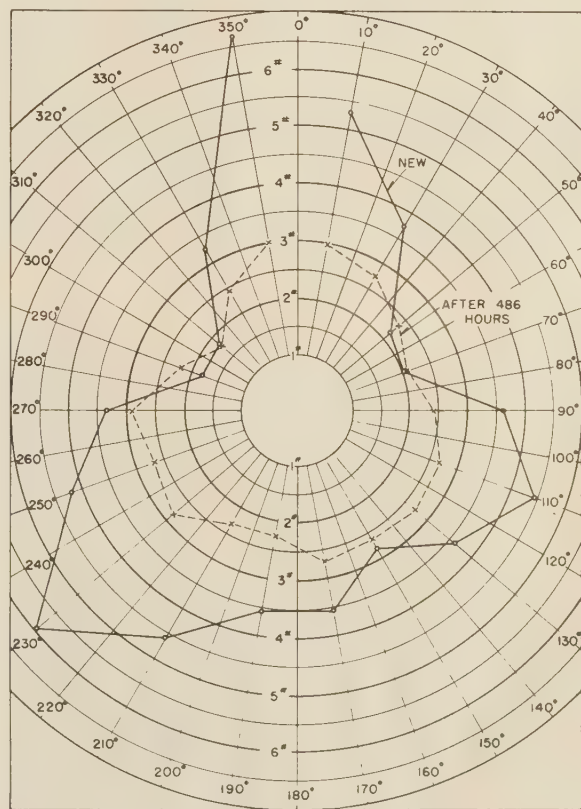


FIG. 7 RING PATTERN OF A CATERPILLAR DIESEL RING BEFORE AND AFTER ENGINE TEST

gage ring. Two sets of pins differing in length by $\frac{1}{8}$ in. were provided since the travel of the measuring units could not accommodate the radial adjustment necessary when changing from one size of ring to the other.

ACKNOWLEDGMENT

The development of this instrument was an outgrowth from suggestions for the need for such a device by members of the Wright Aeronautical Corporation and is based on operating principles proposed by R. J. S. Pigott, Chief Engineer, Gulf Research & Development Company.

BIBLIOGRAPHY

- 1 "Researches on the Piston Ring," by Keikiti Ebihara, 31st rep. of Okōchi Research Laboratory; Scien. Papers of the Inst. of Physical and Chemical Research, Tokyo, vol. 10, no. 182, 1929, pp. 107-185; also U. S. Technical Memorandum, N.A.C.A., no. 1057, Washington, D. C., 1944.
- 2 "Effect of Manufacturing Process on Quality of Piston Rings," by N. Stern, *Automobiltechnische Zeitschrift*, vol. 34, 1931, pp. 89-93, and 177-181.
- 3 "New Piston Ring With Optimum Radial Pressure Distribution," by O. Graf, *Automobiltechnische Zeitschrift*, vol. 34, 1931, pp. 585-586.
- 4 "Faulty Dimensions of Piston Rings," by N. Stern, *Automobiltechnische Zeitschrift*, vol. 34, 1931, pp. 615-617.
- 5 "Piston Ring Progress," by R. R. Teetor and H. M. Bramberry, *S.A.E. Journal*, vol. 31, 1932, pp. 323-326.
- 6 "Measuring Apparatus for Determining Radial Wall Pressure Distribution of Piston Rings," by C. Englisch, *Automobiltechnische Zeitschrift*, vol. 43, 1940, pp. 42-44.
- 7 "Pressure Behind Piston Rings," by O. Steinitz, *Diesel Power*, vol. 18, 1940, pp. 244-245, and 247.
- 8 "Piston-Ring Pressure Distribution," by M. Kuhn, *ATZ, Automobiltechnische Zeitschrift*, vol. 45, 1942, pp. 62-67; translation, U. S. Technical Memorandum, N.A.C.A., no. 1056, Washington, D. C., 1943.
- 9 "Piston Ring Blow-By on High Speed Petrol Engines—Second Report," by C. G. Williams and H. A. Young, *Automobile Engineer*, vol. 32, 1942, pp. 283-288.
- 10 "Methods of Measuring Piston Ring Wall Thrust," by P. Pugh, Royal Aircraft Establishment Technical Note No. Eng. 38, 1942.
- 11 "Photoelastic Measurement of Radial Pressure Distribution Around Piston Rings," by F. W. Bubb, G. C. Mayfield, and R. A. Pepping, 16th Semi-Annual Eastern Photoelasticity Conference Proceedings, Nov. 13 and 14, 1942, pp. 11-15.

Discussion

MICHAEL BEHUN.³ This paper describes a noteworthy contribution to the increasingly important problem of production measurement of piston-ring radial pressure. For quite some time those working with piston rings have been of the opinion that a better method than the measurement of diametral tension was needed to determine the true radial pressure of piston rings. It is felt, however, that further refinements of the instrument and procedure for its application are necessary before it is suitable for use in research on piston rings.

The author has described two methods of preparing the instrument for use, and in that connection the writer would like to mention certain facts. Because the initial setting of the force pins is of such great consequence to the final accuracy of the force measurements, it is important that this initial setting be very carefully considered. The first method of preparation described will result in locating the force pin at the nominal radius when the forces acting on the pin during measurement of piston-ring forces are equal to the forces acting on it during the initial positioning of the force pin. At forces of different magnitudes,

the force pin will not be at the nominal radius because the indicated force, as measured by the back pressure, is a function of the gap created between the disk and the cylindrical chamber.

The second method of preparation described will locate the force pin equidistant from the center of the gage, but the pin will not be located at the nominal radius during measurement of piston-ring forces, because this second method of positioning the force pin initially requires that the piston ring be deflected away from the ring gage whose internal diameter is the nominal diameter.

The author states that all observations are in error by the amount of the deflection at each point multiplied by the ring stiffness at the corresponding point. This statement is true only if the force pin was initially set at the nominal radius. If the second method of preparing the instrument for use is used, then all observations are in error by the amount of deflection at each point from the nominal radius multiplied by the ring stiffness at the corresponding point. If the force pin is not initially set at the nominal radius, this differentiation of deflection must be made because all observations are in error by an amount greater than indicated by the author's statement or the calibration curves.

In regard to the apparent change in the effective area of the disk acted on by the air pressure when larger orifices and higher-source pressures are used, the writer would like to mention the following:

If h is the back pressure, G the area of the fixed orifice, S the area (annular) of the variable orifice, δ_1 and δ_2 the coefficients of contraction for the orifices, σ the air density assumed constant, then

$$\sigma G \sqrt{2g(H-h)\delta_1} = \sigma S \sqrt{2gh\delta_2}$$

and simplifying⁴

$$h = \frac{H}{1 + \frac{\delta_2}{\delta_1} \cdot \frac{S^2}{G^2}}$$

Hence, for a change in orifice size, the effective area in all probability does not change but the ratio of $\frac{\delta_2}{\delta_1}$ likely does.

For the movements of the disk involved during measurement of radial force, it should be noted that the flow of air through an annular orifice at the end of the duct varies almost linearly with the displacement of the disk. This linear relationship, however, holds true only for displacements of the disk greater than some ten thousandths of an inch and less than some thousandths of an inch. Fig. 8 of this discussion is a typical curve for an instrument which operates on the same principle showing the displacement of the disk under different loads. For smaller displacements and for relatively large displacements, the relationship is not linear because of the preponderant presence of an air layer in which the speed varies independently of gap created between the disk and the cylindrical chamber.

Table 1, column 1, of the paper gives the radial forces of 18 points of a 5.75-in.-diam Pratt & Whitney aircraft piston ring, and Table 2 also gives radial forces of 18 points of the same ring. Fig. 9 of this discussion is a plot of the radial forces given in these tables and shows that the force patterns are similar but that the individual forces are of different magnitudes. It is believed that this difference is due to the fact previously mentioned, namely, that in the initial positioning of the force pins the pins were not set at the nominal radius. If the initial positions of the force

³ Mechanical Engineer, Aircraft Engine Research Laboratory, National Advisory Committee for Aeronautics, Cleveland, Ohio.

⁴ "L'amplification pneumatique," by L. Wattebot, *Mécanique*, vol. 21, March-April, 1937, pp. 70-72.

pins had been reset during the time interval between the two sets of measurements of the radial forces of the piston ring and, in either or both instances, if the force pins were not set at the nominal radius, the deflection from the nominal radius of a point on the piston ring during one measurement would be different from the deflection of the same point during the second measurement. It is believed that if all of the indicated forces and the corresponding valve lifts were corrected back to the nominal radius, the true radial forces would be obtained and as a result the two curves in Fig. 9 (on the following page) would be superimposed on each other. Is the author in possession of any data to verify the foregoing discussion, or does he have some other explanation for the large difference between the average forces of the same piston ring?

J. B. MINNICH.⁵ It is felt that this type of pressure-pattern gage can do much to improve the performance of piston rings. This gage has possibilities for use as a production inspection instrument as well as for experimental development. Much has been accomplished to speed the operation of obtaining an approximate pressure pattern but a further improvement could be made to enhance the accuracy. As disclosed in the paper, the weaker sections of a ring are deflected most. It is obvious, therefore, that a ring is not a true circle while being checked. Probably this distortion does not greatly affect pressure-pattern investigation from a comparative viewpoint. The fact that cylinders are often more out of round than the ring while being checked may minimize the error. From an academic standpoint, however, it would seem preferable to check rings while supported as a true circle.

The gage is also incapable of checking points of zero pressure or points which are not light-tight. A section which is not light-tight by 0.0005 in. is not satisfactory for engine operation, but from the author's curves of deflection versus back pressure it can be seen that a definite pressure is obtained by the Pigott gage on rings that are not light-tight. If the gage were capable of indicating the sections of zero or very light pressure its value would be increased. As a production inspection instrument it could then replace the present inspections for tension, circularity, and light-tightness.

As disclosed by the author, some of the mechanical imperfections also affect the results. This has been discovered by using a solid-plate gage for the initial adjustment. Using the solid plate and adjusting all the manometers to the same level, duplicate readings cannot be obtained on a ring when it is rotated. Using a source pressure of 16 lb and adjusting all the manometers to about 12 in., a maximum variation of 1.3 lb between two manometers was required before satisfactory duplication was achieved. The instrument will not remain in good adjustment over a long interval of time when used intermittently. But by using the solid plate as a reference, it is not difficult to reset the apparatus.

One of the most prominent causes of errors was variations caused by friction. When one ring was inserted into the gage many times, as nearly as possible to the same position each time, a maximum variation of 2 lb for one manometer has been observed. The amount of oil on the surface of the ring, the slight variation in surface finish, and the manner in which different personnel would insert the ring would cause variations. By turning on the units in different sequence, it was found that the variations could be effected. The best order of turning on the units was to start opposite the ring gap with the following order: 9-10, 8-11, 7-12, etc. By this means the variations could be greatly reduced and readings duplicated.

To eliminate the chance of disturbing the adjustment of the

⁵ Engineering Department, Wright Aeronautical Corporation, Paterson, N. J.

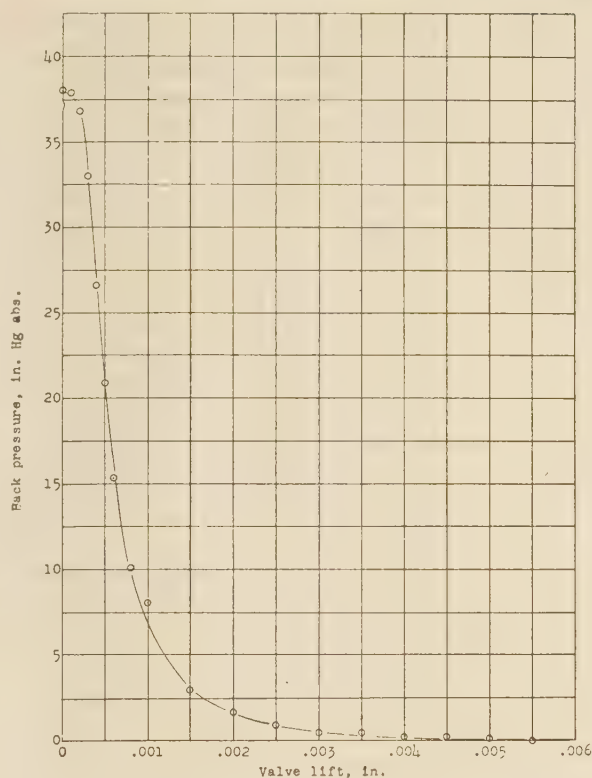


FIG. 8 VALVE-LIFT MEASUREMENTS

individual units and also to eliminate the slow task of turning on the individual valves manually, a piston-type valve was made which would serve as a manifold and turn on the units in the proper order. By incorporating this valve in the gage, we believe that the accuracy and usefulness of the gage have been greatly improved.

C. B. Moore.⁶ It appears that fundamentally the device described in the paper can give an accurate reading only when the piston ring itself has true circularity when compressed to the cylinder diameter. In general, any deviation from circularity of the ring will be indicated at less than its full extent, due to the slight motion required of the contacting pins. It is entirely conceivable that at certain points a ring may have zero pressure against the cylinder wall in actual practice, and yet register a definite pressure with this gage at these points. Experience and familiarity with the use of the gage will no doubt greatly alleviate the seriousness of this shortcoming.

Initially adjusting the zero of the gage by setting to a perfect standard is excellent. No provisions, however, are made for determining the deviation of the diameter of the ring from this standard when pressure measurements are made. It appears accordingly that the ring would not necessarily be measured at the diameter at which it is used when in a cylinder.

Failure of the gage to repeat will therefore be only a part of the error in readings compared to actual operating conditions. It is believed that this failure to repeat can be traced entirely to friction of the valve stem. Further it would seem that the manufacture of the valves would require extreme precision, since the valve movement should theoretically be zero in order to accomplish the intended purpose of the measurement.

⁶ Moore Products Company, Philadelphia, Pa.

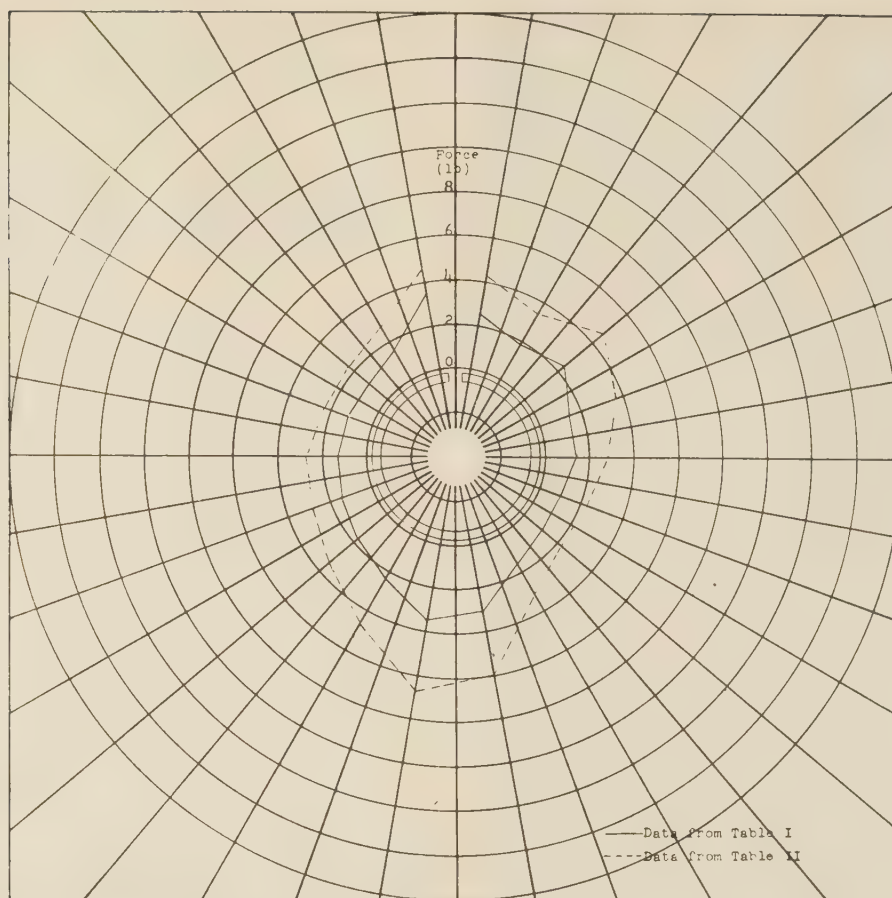


FIG. 9 RING PATTERNS OBTAINED FROM TABLES 1 and 2 of AUTHOR'S PAPER

It is with considerable hesitancy that this discussion has been written, inasmuch as the only constructive suggestion which can be offered is the use of metallic bellows with a leaf spring or other nonfriction member as a guide in order to improve the performance. This suggestion, however, in the writer's opinion has slight constructive merit, as it does not materially aid in achieving the original stated purpose of the device.

AUTHOR'S CLOSURE

The author appreciates the discussion submitted on this paper and the opportunity to present additional experimental evidence which will clarify the points brought out by the discussers.

It is not clear what Mr. Behun had in mind as research on piston rings, but it is the author's belief that any instrument for securing reliable data is suitable for research. The criterion should be "Will the engine respond to differences which the instrument cannot detect?" It is unlikely that the demonstration can ever be made that variations of as much as five per cent in the ring pattern will influence the performance of the ring in the engine.

Mr. Behun also has an incorrect conception of the characteristics of the thrust unit and of its adjustment. The unit is always adjusted with a sensible valve opening when the end of the force pin is in contact with the true circle. Excepting friction, the force on this pin will always be indicated by the manometer pressure. Since a correct measurement cannot be made until the piston ring has everywhere been lifted from contact with the gage

ring, the forces produced by the ring in its altered shape are correctly indicated by the manometers. The amount of deflection at each point will be influenced both by the initial valve opening when the end of the force pin is in contact with the true circle and by the magnitude of the source pressure. It remains true then that each observation is in error by the amount of deflection multiplied by the ring stiffness at that point.

The uncertainty of the magnitude of this deflection error and of the source and amount of the friction error has given rise to serious criticism by these discussers as well as by others who have

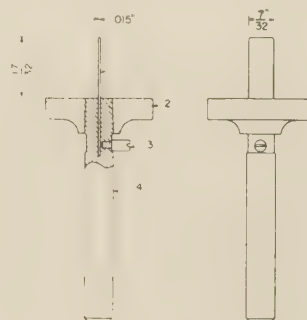


FIG. 10 IMPROVED VALVE

[(1) Reed which supports piston ring; (2) valve head; (3) guide pin; (4) valve stem.]

examined the instrument. The friction error has largely been eliminated by a modification of the valve as shown in Fig. 10. The force pin was replaced by a flexible reed firmly clamped in the slotted end of the valve stem by means of matching tapers in the valve head and on the stem. Any possible air leaks were sealed with De Khotinsky cement. The reed has ample clearance in the hole formerly occupied by the force pin and its end is carefully ground flat in a plane perpendicular to the axis of the valve stem. There is no slippage of the end against the piston ring as its shape is altered and the bending of the reed does not produce tangential forces greater than 0.12 lb.

Tests of the new valve have shown that the root mean square deviation has been substantially reduced with a great reduction in the number of abnormally large deviations. The force balance has also been greatly improved showing that friction no longer plays an important part in the operation of the instrument.

The determination of the magnitude of the deflection error required a more elaborate experimental program. Each of the eighteen thrust units were carefully calibrated to secure curves of valve lift vs. back pressure for different values of source pressure. This was done with a setup similar to that shown in Fig. 3

mitted the determination of the valve opening of each unit for each source pressure and by deducting the initial valve opening, the actual ring deflection was determined.

The valve lift of each thrust unit was then plotted against back pressure as shown in Fig. 12 which gives the curves for units 14 and 18 only. These curves are characteristic of all and show several anomalies which are believed to have little significance. First, the valve opening at low source pressure appears to be less than the initial opening and, second, the apparent rate of deflection of the ring changes abruptly about 0.0002 in. off the wall. Above this range the deflection curve becomes linear with a slope which varies from 0.010 to 0.0008 in. per lb. In general the slope of the straight portion of the curve is least for the points nearest the gap and the average slope of the remaining curves is approximately 0.002 in. per lb.

The assumption is made, at this point, that extrapolation of the straight portion of these curves back to the initial valve opening will show the back pressure which would have been obtained had the measurements been made with the ring constrained on the true circle. Fig. 13 shows the pressure patterns of a ring measured with source pressures of 16 and 18 psi, respectively, and the

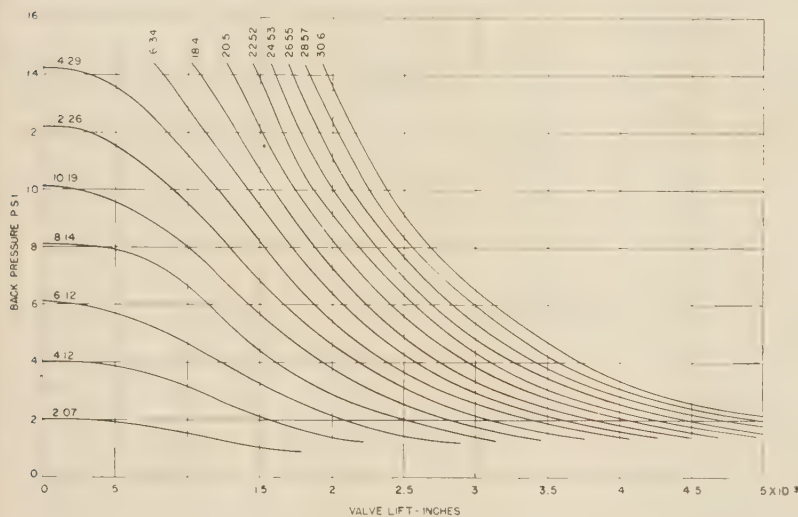


FIG. 11 CALIBRATION CURVES OF THRUST UNITS
(Figure on each curve indicates source pressure.)

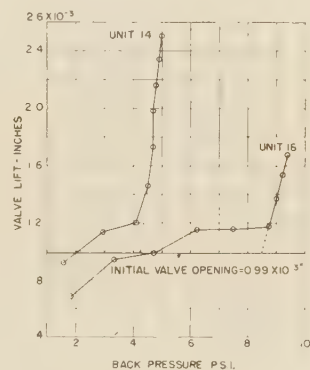


FIG. 12 FORCE DEFLECTION CHARACTERISTICS OF TWO POINTS ON A PISTON RING

with the weight pan replaced by a horizontal pivoted bar resting on the end of the reed. The bar was counterbalanced so that when a movable weight was located at a zero mark, no load was applied to the reed. The force on the reed could be increased to a maximum of 13 lb although in this calibration a maximum of 7 lb was not exceeded.

The calibration curves obtained were similar to those shown in Figs. 4, 5, and 6, the source pressure being the changing parameter rather than the orifice size, since all units had the 0.062-in. diameter orifice. It was found that the valve-lift curves of all eighteen thrust units were quite closely grouped and in order to simplify the work, a single set of calibration curves was drawn representing their average lift characteristics as shown in Fig. 11.

The second step was to assemble the ring gage so that the initial valve opening of each thrust unit was the same. In the case of the example given below, this initial opening was 0.00099 in. A piston ring was then placed in the gage with the gap between units 1 and 18, and a set of observations made at different source pressures. Reference to the calibration curve then per-

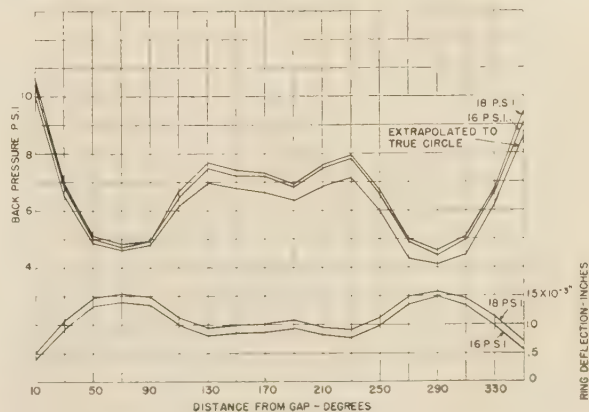


FIG. 13 PRESSURE PATTERN AND DEFLECTION PATTERN OF PISTON RING DURING MEASUREMENT

pattern determined by extrapolating each point back to the true circle. This shows that the deflection error may amount to 0.8 psi or, in terms of force on the ring, 0.4 lb. However, it is possible to secure the true circle pattern in this manner in those cases where it is desirable. For production inspection or selection of rings of like pattern, it would be of no value to make the correction.

The lower two curves of Fig. 13 show the actual deflection of the ring from the true circle. The maximum deflection at the weakest point of the ring was 0.0016 in. Inspection of these curves immediately suggests that by making the gage ring 0.002 in. in diameter oversize and by properly locating the thrust units, the ring would lie very closely on the true circle during measurement and any corrections would be quite small.

Mr. Behun's Fig. 9 is the result of an omission in the preprint. Table 1 gives the radial forces of ring No. 13 while Table 2 gives the manometer readings made during a set of observations on the same ring. Since the deviations in a reproducibility test are reduced to a percentage, it has not been customary to convert the pressure readings to force by dividing by 2. This was not properly indicated in the original reproduction of Table 2.

The author was pleased to receive Mr. Minnich's comments based on his experience with one of these instruments. The suggestion that the gage be modified to permit inspection for light-tightness is entirely feasible and had not previously been considered seriously since it was felt that those interested in the instrument would be equipped with the simple gages for making this inspection. Actually, by following the procedure just outlined for determining the deflection error, it is possible to determine exactly how far a point on the ring lies away from the wall at zero pressure. The procedure would hardly be justified for production inspection, however.

Mr. Moore's suggestion for eliminating friction would undoubtedly serve the purpose but it is believed that it would detract from the simplicity of construction that is so desirable in an instrument of this nature.

There is evidence that the small variations now being observed are due to irregularities of the ring surface and that even a frictionless and deflectionless instrument would not show greatly improved performance.

The author wishes to acknowledge the careful work done by R. S. Wood in determining the deflection errors described.

Application of Controlled Atmospheres to the Processing of Metals

By C. E. PECK,¹ EAST PITTSBURGH, PA.

The development and application of separately controlled atmospheres for use in conjunction with heat-treating processes has been rapid during recent years. By means of controlled atmospheres, finished machine parts which require heat-treatment can be processed without loss of surface hardness during heating, and without further grinding or cleaning. Many other applications in the treatment of metals, such as welding, forging, melting, sintering, and the like, are possible although at present somewhat limited. This paper outlines the principal types of atmospheres and describes briefly the equipment available for producing these atmospheres. A summary is given of the application of these atmospheres to a wide variety of heat-treating processes now in active commercial use.

IN this paper the term "controlled atmospheres" is defined as that produced separately from specific equipment especially designed to make a gas or mixture of gases of a given composition. The development and application of separately controlled atmospheres has grown rapidly for several years, and the uses of these atmospheres are now an important component in a great majority of heat-treating processes where quality control and uniformity of the product are required. It is now possible to control accurately or to prevent entirely the oxidation of practically all of the ferrous and nonferrous metals and their alloy combinations, when these metals are heated to elevated temperatures. On carbon steels and alloy steels it is also possible to control accurately or to prevent the loss of carbon (decarburization) or gain of carbon (carburization) as well as to control accurately the amount of carbon added to the surface of steel (gas carburizing). Because of these developments, large tonnages of metals can be heated without oxidation, and expensive pickling and cleaning costs are eliminated.

In mass production finished machine parts which require heat-treatment can be processed without loss of surface hardness during heating (decarburization) and without further grinding or cleaning. Metals can be furnace-brazed without oxidation. Controlled atmospheres are finding many applications in the sintering and powder-metallurgy fields. In the fields of welding, forging, and melting of metals the use of separately controlled atmospheres is at present quite limited, but future developments may lead to wider uses of atmospheres in these fields of metal-processing.

The purpose of this paper is to outline the principal types of atmospheres and to describe briefly the equipment available for producing these atmospheres. The discussion summarizes the application of these various atmospheres to a wide variety of heat-treating processes now in active commercial use.

The discussion is limited to those atmospheres which are pro-

duced from gaseous sources, such as natural gas, propane, butane, and various types of manufactured gases such as coke-oven gas, carbureted water gas, etc. Gases produced from the dissociation of the anhydrous ammonia are also included in this discussion.

DISCUSSION OF GENERAL COMBUSTION RANGE

Before discussing the principal types of atmospheres, a brief general description will be given covering the complete combustion and cracking range of a fuel gas as related to varying amounts of air mixed with the fuel.

Using methane (CH_4) as an example, the various types of prepared atmospheres which can be made cover the range from complete combustion to partial cracking to complete cracking. The word "combustion" indicates that sufficient heat energy is evolved to generate the desired gas without addition of external heat. The word "cracking" indicates that heat energy must be supplied at a sufficient temperature level to promote the dissociation of the methane when reacting with limited quantities of air.

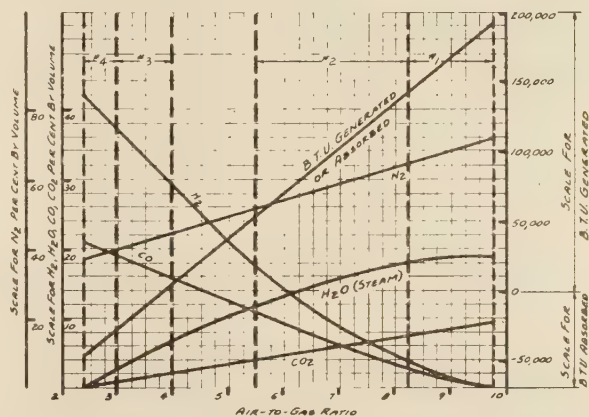


FIG. 1. CURVES SHOWING COMBUSTION PROPERTIES OF METHANE OVER RANGE FROM COMPLETE COMBUSTION TO COMPLETE CRACKING

The range is illustrated by the set of curves shown in Fig. 1. Using methane as the base fuel and mixing it with proper air ratios as indicated on the curve, the variation in approximate gas composition is shown covering the range from complete combustion to complete cracking. At a particular air-to-gas ratio, the approximate amounts of hydrogen, carbon monoxide, carbon dioxide, water vapor, and nitrogen are given. A curve of this type is useful in giving a general picture of what gas composition can be expected over the range from complete combustion to complete cracking. A curve of this type can be calculated for every type of fuel gas commercially available for use in generation of prepared furnace atmospheres.

Between the right-hand side of the curve showing complete combustion and the left-hand side showing complete cracking, the actual atmosphere compositions obtained will depart somewhat from "idealized" composition indicated on the curve for the following reasons:

¹ Industrial Heating Section Engineer, Westinghouse Electric Corporation. Mem. A.S.M.E.

Contributed by the Process Industries Division and presented at the Semi-Annual Meeting, Pittsburgh, Pa., June 19-22, 1944, of THE AMERICAN SOCIETY OF MECHANICAL ENGINEERS.

NOTE: Statements and opinions advanced in papers are to be understood as individual expressions of their authors and not those of the Society.

1 In the partial-combustion range the actual amounts of hydrogen compared to water vapor formed will depend on the design of the gas generator. The same is true for the amount of carbon dioxide compared to the amount of carbon monoxide. The variations are due to size of combustion space, time allowed for reactions, type of catalyst used, temperature level of reaction, etc. All of these factors depend on the individual equipment design.

2 In practical gas analysis the amount of water vapor generated in the reactions is always partially removed by condensing out the steam of combustion down to temperatures and dew points corresponding to normal atmospheric conditions. Per cent water vapor given on the curve is that generated during reaction before any condensation or removal.

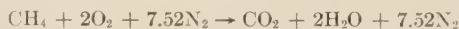
3 At the lower air-to-gas ratios in the partial-combustion range and also on complete cracking range there are small amounts of residual methane. This will show up on actual gas analyses but is not shown on the general curves being discussed here using methane as an example for the available fuel gas.

4 The heat generated or absorbed is shown on the curve. The amount of heat shown represents approximately the heat of generation or heat of absorption required chemically to produce the compositions shown. The heat losses from the generating equipment and the sensible heat corresponding to the temperatures of gases leaving the generating equipment must be subtracted from heat values shown to give net heat generated or absorbed. This has the effect of decreasing the net heat generated and increasing the net heat absorbed and for this reason, the actual air-to-gas ratio on the curve at which heat is neither generated nor absorbed is higher than that indicated on the curve. For a given gas-generator temperature, the increment by which the air-gas ratio is higher depends on heat losses and design of the particular gas equipment.

The following summarizes the important commercial atmospheres produced from either fuel gases or anhydrous ammonia; each atmosphere is briefly described from the standpoint of composition, cost, and equipment required to produce it:

ATMOSPHERE NO. 1: COMPLETELY BURNED FUEL GAS

If any commercially available fuel gas is mixed with the proper amount of air it may be burned under controlled conditions to form CO_2 , H_2O , and N_2 . If this combustion process is carried out with a slight deficiency of air, there is no oxygen present in the resultant atmosphere and small amounts of hydrogen and CO will be present in addition to the gases just given. This resultant atmosphere corresponds to a ratio (assuming methane as the fuel) slightly to the left of the line representing complete combustion shown on curves in Fig. 1.



Similar reactions take place with gaseous fuels containing CO, H_2 , and illuminants or heavier hydrocarbon gases such as propane (C_3H_8), and butane (C_4H_{10}).

A representative composition of prepared gas when burning methane with a slight deficiency of air would be $\text{CO}_2 = 10$ per cent, $\text{CO} = 0.5$ per cent, $\text{H}_2 = 0.5$ per cent, $\text{CH}_4 = 0.0$ per cent, $\text{O}_2 = 0.0$ per cent, $\text{N}_2 = 89$ per cent. Dew point corresponds approximately to room-temperature conditions unless auxiliary drying equipment is used. This atmosphere is inert and non-explosive. This atmosphere can be set with somewhat higher reducing properties, as indicated by the range given by the curve in Fig. 1. This is desirable in many cases in order to overcome effects of impurities in the furnace and on the work being processed.

This atmosphere can be produced for approximately \$0.08

per 1000 cu ft based on assumptions previously mentioned. This particular atmosphere is among the cheapest produced since the minimum of fuel is used owing to the lean mixtures that are involved.

Equipment A. A typical atmosphere generator for producing this gas is shown in Fig. 2. A schematic general arrangement and flow diagram is shown in Fig. 3. The gas-mixing pump draws air through a filter; the air flow automatically regulates the flow of gas to give a predetermined air-to-gas ratio for variable-flow demand. The air and gas, after flowing through visual flowmeters, mix together at a point preceding the pump inlet.

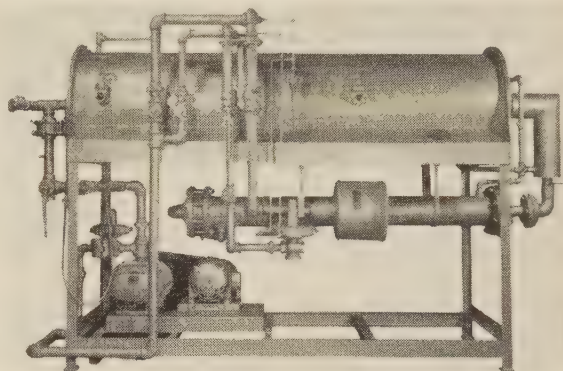


FIG. 2 CONTROLLED-ATMOSPHERE GENERATOR FOR PRODUCING ATMOSPHERES NOS. 1 AND 2, COMPLETELY BURNED OR PARTIALLY BURNED FUEL GAS; EQUIPMENT A

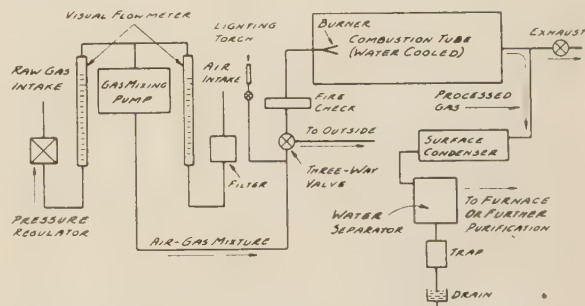


FIG. 3 SCHEMATIC ARRANGEMENT AND FLOW DIAGRAM OF GAS GENERATOR FOR PRODUCING ATMOSPHERES NOS. 1 AND 2, COMPLETELY BURNED OR PARTIALLY BURNED FUEL GAS; EQUIPMENT A

The pump moves the air and gas mixture through the piping system to the fire-check and burner. The temperature of the combustion tube is sufficiently high to ignite the mixture whose combustion is carried quickly to completion in a catalyst-filled refractory bed. This arrangement also insures thorough reaction so that all traces of oxygen are removed. No outside heat is supplied to the combustion tube since its temperature is maintained by the net heat of combustion. The moisture from the products of combustion leaving the exit side of the combustion tube is condensed out of the gas in a surface condenser and separated from the gas in a water separator and a trap. The gas then may be used either in a furnace or further purified before using by drying, scrubbing out CO_2 , or removing small amounts of sulphur.

The gas leaving the water separator is usually saturated with water vapor at a temperature about 10 to 15 deg F higher than the cooling water used in the surface condenser.

ATMOSPHERE No. 1-A: COMPLETELY BURNED FUEL GAS WITH CO₂ AND H₂O REMOVED

This is atmosphere No. 1 with CO₂ and H₂O removed. The reaction required to produce this gas is exactly the same as that outlined for gas No. 1. Fuel gas is burned to almost complete combustion on the reducing side. In this instance, however, the carbon dioxide and the water vapor are completely removed by means of separate auxiliary apparatus used in conjunction with the atmosphere generator described under atmosphere No. 1.

Using methane for the base fuel, a typical composition of this gas would be as follows: CO₂ = 0 per cent, CO = 1/2 per cent, H₂ = 1/2 per cent, O₂ = 0 per cent, CH₄ = 0 per cent, N₂ = 99 per cent. Dew point is -60 F. This gas is inert because of its extremely high nitrogen content. A variation of this composition which is usually somewhat more applicable to commercial furnace conditions consists of CO₂ = 0 per cent, CO = 3 per cent, H₂ = 3 per cent, O₂ = 0 per cent, CH₄ = trace, N₂ = 94 per cent. The gas is still inert but has enough active constituents to overcome oxidizing impurities which enter into the usual furnace application.

This gas is produced at a cost of approximately \$0.20 to \$0.40 per 1000 cu ft. The range in cost is due to the difference between costs of electricity and steam when used for reactivating the carbon-dioxide removal system and the drying system. These costs are based on using methane as the base fuel.

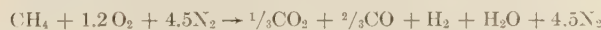
Equipment B. Equipment required to produce this atmosphere consists of an atmosphere generator, the same as that shown in Fig. 2. The gas passes from this unit to the carbon-dioxide re-

moval system which will be described in further detail. From the carbon-dioxide removal system the gas is further dried by means of a combination of refrigerant drying equipment and activated-alumina drying equipment described separately.

Fig. 4 shows the schematic arrangement of the carbon-dioxide removal system. A reproduction of this equipment is shown in Fig. 5. The gas from the generator passes through the absorption tower through special packing material and gives up its carbon dioxide to the liquid which enters at the top of the tower and which trickles down through the packing material. The gas, free of carbon dioxide, collects at the top of the tower and flows through moisture-removal equipment and into the further drying equipment mentioned previously. The remainder of the system consists of a recirculating liquid system which is used to absorb the carbon dioxide and later to be heated up to a point where the carbon dioxide may be driven off. The liquid which is saturated with carbon dioxide collects at the bottom of the stripper column. The liquid trickles down through packing material through which is passing heated steam rising from a boiler located at the base of the stripper column. During this passage the carbon dioxide is driven off and is passed through the top of the tower into a condenser which returns most of the heated steam back to the boiler. The carbon-dioxide gas is discharged to the atmosphere. The absorbing liquid which has collected in the bottom of the column is pumped back again to the top of the absorption tower through the heat exchanger and cooler.

ATMOSPHERE No. 2: PARTIALLY BURNED FUEL GAS

This atmosphere is similar to atmosphere No. 1 except that air-to-gas ratio is smaller, and, hence products of combustion contain appreciable CO and H₂. Sufficient heat is generated to keep these reducing gases forming without adding external heat, but heat generated is considerably less than for atmosphere No. 1 (see curve Fig. 1). For this reason the gas-generating equipment is not self-starting but must first be thoroughly heated up by operating the unit at a lean air-to-gas ratio. After the unit is heated the mixture may be made rich enough to produce atmosphere No. 2 since there is sufficient heat generated to maintain temperature but not heat up the equipment from a cold start. With methane as the fuel the following is a typical reaction at 6 to 1 air-to-gas ratio



For a given air-to-gas ratio, the amount of H₂ compared to H₂O, and the amount of CO compared to CO₂ will vary with the design of equipment used. Efficient catalysts will give higher H₂ and CO and therefore higher reducing properties.

Using a fuel containing practically all methane, a typical composition of this atmosphere would be as follows at a ratio of 6 parts of air to one part of gas: CO₂ = 5 per cent, CO = 10 per cent, H₂ = 15 per cent, CH₄ = 1 per cent, N₂ = 69 per cent, O₂ = 0 per cent. Dew point of gas corresponds to approximately saturation at room-temperature conditions unless auxiliary drying equipment is used. In many applications of this atmosphere it is desirable to dry the gas to dew points of approximately 40 F by using refrigerant-drier equipment illustrated in Fig. 9.

In general, this atmosphere is combustible and therefore air should be thoroughly purged out from any enclosures in which it might be used. Due to its relatively high nitrogen content and correspondingly low Btu content it is not as highly combustible as raw fuel gases, but precautions against creation of explosive mixtures with air should always be taken when handling this gas. Also, any leakage of this gas from furnace openings, etc., should be carried away in efficient ventilation systems because the CO content makes it very toxic. In a great many applica-

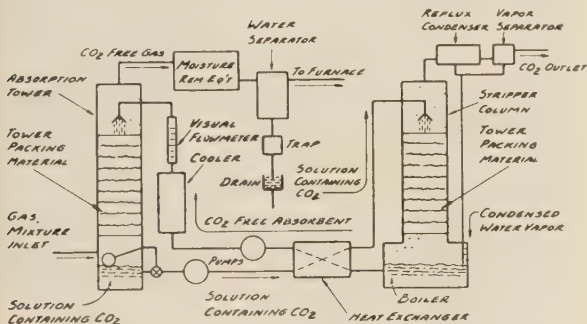


FIG. 4 SCHEMATIC ARRANGEMENT AND FLOW DIAGRAM OF CARBON-DIOXIDE REMOVAL SYSTEM FOR PRODUCING ATMOSPHERES NOS. 1-A AND 2-A; EQUIPMENT B

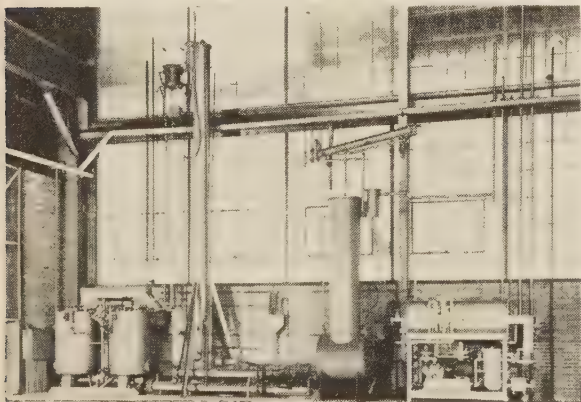


FIG. 5 COMPLETE GAS EQUIPMENT SEQUENCE FOR PRODUCING ATMOSPHERES NOS. 1-A AND 2-A

(Gas generator is followed by carbon-dioxide removal system and activated-alumina drier for thoroughly removing water vapor.)

tions the gas is burned as it issues from the furnace openings so that harmful CO is converted to comparatively harmless CO₂.

Cost of producing this atmosphere differs from that of atmosphere No. 1 in that more raw fuel gas is used. Average costs based on assumptions mentioned in the first part of the paper are from \$0.10 to \$0.12 per 1000 cu ft.

Equipment A. The gas-generating equipment and comments on operation given for atmosphere No. 1 also apply exactly to atmosphere No. 2. Refer to Fig. 2 for equipment and Fig. 3 for schematic arrangement.

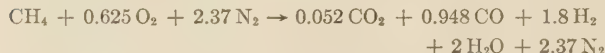
ATMOSPHERE NO. 2-A: PARTIALLY BURNED FUEL GAS WITH CO₂ AND H₂O REMOVED

This atmosphere is the same as atmosphere No. 2 except with CO₂ and H₂O removed.

This gas is produced using the same equipment and the same reaction described for atmosphere No. 1-A. The only difference consists in operating the primary gas generator at a ratio of air to gas which is richer so as to be able to produce the higher reducing properties in the gas.

ATMOSPHERE NO. 3: PARTIALLY REACTED OR CRACKED FUEL GAS

Referring to Fig. 1, the left-hand portion of the curves shows a region between ratios of 5 to 1 and ratios of 2½ to 1 where CO₂ and H₂O are decreasing toward zero, and CO and H₂ are increasing to their maximum values. Atmosphere No. 3 is defined to fall in this region which in general is the region between atmosphere No. 2 which is partially burned fuel gas with some heat generated, and atmosphere No. 4 which is completely reacted fuel gas where heat is required. At 3 to 1 ratio using methane, a typical reaction is



Based on this reaction a typical analysis of this atmosphere would be as follows at a ratio of 3 to 1: CO₂ = 1 per cent, CO = 18 per cent, H₂ = 34 per cent, CH₄ = 1 per cent, O₂ = 0.0 per cent, N₂ = 46 per cent.

Dew point of gas corresponds approximately to saturation at room-temperature conditions. The atmosphere is combustible. As shown on the curve in Fig. 1, this atmosphere can also be produced with lower reducing properties if desired but external heat is still required.

This gas requires some external heat to promote the reactions at a high temperature level. Assuming electricity as the means for supplying this heat, the cost is approximately \$0.15 to \$0.20 per 1000 cu ft, depending on actual air-to-gas ratios used.

Equipment C. The schematic arrangement and description of operation shown for Fig. 3 applies directly to this equipment, the only difference being that the combustion chamber is replaced with an electrically heated catalyst-filled retort chamber. All other auxiliaries are the same. This equipment is shown in Fig. 6.

ATMOSPHERE NO. 4: COMPLETELY REACTED FUEL GAS

This gas is produced from the complete reaction of fuel gas with the proper amount of air to produce an end product consisting of only carbon monoxide and hydrogen and nitrogen from the air. The reaction may be written as follows



This gas corresponds to the extreme left-hand range on the curve, Fig. 1. The carbon dioxide and water vapor are negligible in this range. External heating is required to produce this gas.

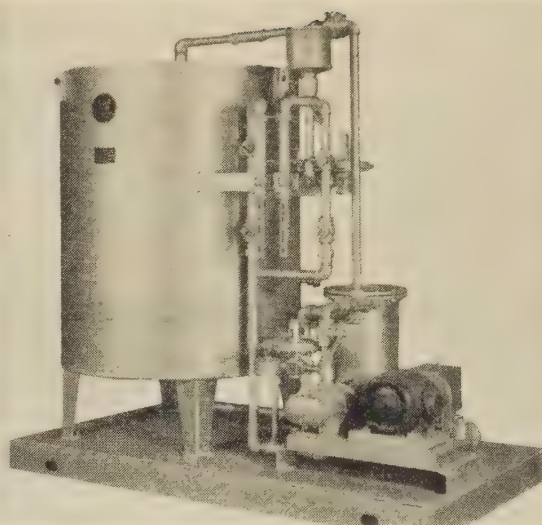


FIG. 6 EQUIPMENT C FOR PRODUCING ATMOSPHERE NO. 3, PARTIALLY REACTED FUEL GAS, OR ATMOSPHERE NO. 4, COMPLETELY REACTED FUEL GAS

Using a fuel gas containing practically all methane, a typical composition of the gas would be as follows: CO₂ = 0 per cent, CO = 19 per cent, H₂ = 40 per cent, CH₄ = 1 per cent, N₂ = 40 per cent. The dew point of this gas would be of the order of —15 F.

The cost of producing this atmosphere using methane as the base fuel is approximately \$0.18 to \$0.25 per 1000 cu ft.

Equipment C. The schematic arrangement and description of operation shown in Fig. 3 applies also to this equipment, the only difference being that the combustion chamber is replaced with an electrically heated catalyst-filled retort. All other auxiliaries are the same. This equipment is shown in Fig. 6; it is the same as that used to produce atmosphere No. 3. The only difference is in the operation which requires a richer air-to-gas ratio.

ATMOSPHERE NO. 5: DISSOCIATED AMMONIA

This gas is produced by the cracking of anhydrous ammonia. This gives a gas very high in hydrogen and with very low dew point.

When the ammonia is thoroughly cracked the composition consists of 75 per cent hydrogen and 25 per cent nitrogen, and the dew point is below —60 F.

This gas is produced at a cost of approximately \$4 per 1000 cu ft, using ammonia in the standard small-size containers. This cost can be cut approximately to one half of this value by using tank-car quantities of ammonia. Approximately 22.1 lb of ammonia are required to produce 1000 cu ft of the dissociated gas.

Equipment D. The equipment for producing this gas is shown in Fig. 7. It consists principally of an electrically heated catalyst-filled retort chamber through which passes the vaporized anhydrous ammonia.

ATMOSPHERE NO. 6: PARTIALLY BURNED DISSOCIATED AMMONIA

This gas is produced by mixing a limited amount of air with dissociated ammonia to produce a pure mixture of hydrogen and nitrogen using a lower hydrogen content than that obtainable with dissociated ammonia. Any proportion of hydrogen compared to nitrogen can be obtained depending on the amount of air mixed with the dissociated ammonia before burning.

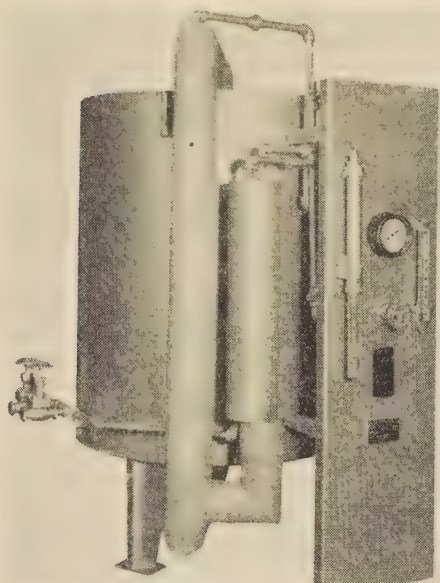


Fig. 7 Equipment D for Producing Atmosphere No. 5, Dissociated Ammonia

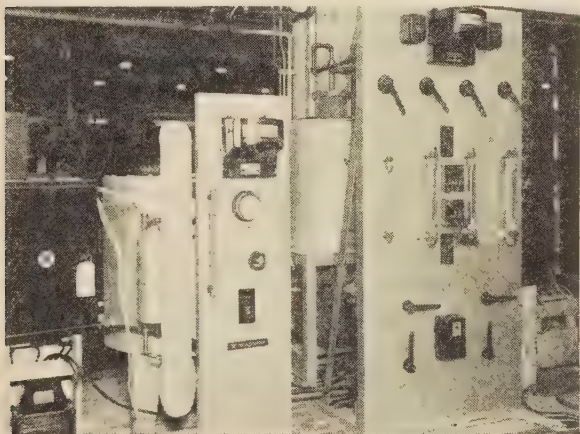


Fig. 8 Equipment E for Producing Atmospheres Nos. 6 and 6-A, Partially or Completely Burned Dissociated Ammonia

A typical composition of this gas is as follows: $H_2 = 20$ per cent, $O_2 = 0$ per cent, $N_2 = 80$ per cent. Dew point corresponds to room-temperature conditions unless auxiliary drying equipment similar to that described under atmosphere No. 2 is used.

A gas containing 20 per cent hydrogen could be produced for approximately \$2.60 per 1000 cu ft, based on small tank quantities of ammonia. This cost would be approximately one half if tank-car ammonia were used.

Equipment E. This equipment is shown in Fig. 8. It consists of two principal parts, the ammonia dissociator such as that described for atmosphere No. 7, and an additional retort chamber used to combust the mixture of air and dissociated ammonia. An advantage of this equipment is that any proportion of hydrogen compared to nitrogen can be produced up to the limits of dissociated ammonia itself. The equipment is also capable of operating at low turnaround values so that no gas is wasted in the process. This is desirable particularly since this gas is much more expensive than the average fuel gas.

ATMOSPHERE No. 6-A: COMPLETELY BURNED DISSOCIATED AMMONIA

This gas is produced by the complete combustion of a mixture of air and dissociated ammonia. A slight deficiency of air is used so that no oxygen results from the combustion process.

This gas consists of a very pure mixture of 99 per cent nitrogen and 1 per cent hydrogen; oxygen = 0 per cent. Dew point corresponds to room-temperature conditions, and further drying must be used if the application requires it.

This gas may be produced at approximately \$2.40 per 1000 cu ft based on small quantities of ammonia or approximately one half of this amount, based on using ammonia from tank cars.

Equipment E. The equipment for producing this atmosphere is exactly the same as that described for atmosphere No. 6.

AUXILIARY EQUIPMENT FOR DRYING ATMOSPHERE GASES

In many applications of atmospheres Nos. 1 and 2 and also of other types of atmospheres it is necessary to dry the gas to lower dew points than those obtained from equipment cooled with



Fig. 9 Equipment F for Partially Drying Gas Atmospheres by Refrigeration to 40 F Dew Point

normal commercial sources of cooling water. Dew points of approximately 40 F can be obtained from cooling the gas by means of refrigerant-drier equipment shown in Fig. 9. The atmosphere gas passes through a system of baffled finned-type cooling coils inside a gastight cabinet. A hermetically sealed refrigerating compressor unit moves refrigerant through the cooling coils. This will be designated as equipment F.

When it is necessary to dry the gas to lower dew points, an activated alumina drier is used. This is shown in Fig. 10. It consists of a dual tower arrangement containing activated alumina for absorbing moisture from the controlled-atmosphere gas. The purpose of the dual arrangement is to provide continuous gas

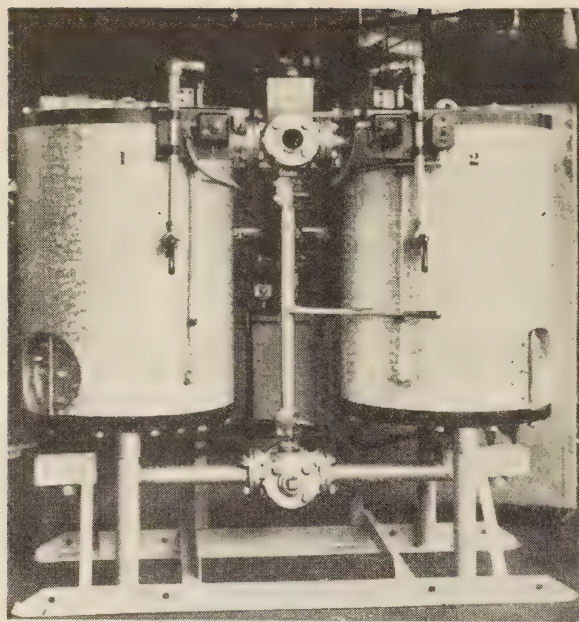


FIG. 10 EQUIPMENT G; ACTIVATED-ALUMINA DRIER FOR REMOVING COMPLETELY MOISTURE FROM GAS ATMOSPHERES

drying while one tower is being reactivated to remove absorbed moisture. This equipment will dry gases to dew points below -60°F if necessary. This will be designated as equipment G.

It may be useful to summarize the equipment combinations necessary to produce the controlled atmospheres previously described.

To produce atmosphere No. 1 (completely burned fuel gas) use equipment A or (A and F) set for complete combustion of fuel gas slightly on the reducing side.

To produce atmosphere No. 1-A (completely burned fuel gas with CO_2 and H_2O removed) use equipment A plus equipments B, F, and G.

To produce atmosphere No. 2 (partially burned fuel gas) use equipment A or (A and F) set for incomplete or partial combustion but not lower than about 55 to 60 per cent of perfect combustion so that sufficient heat will be evolved within the generator itself to keep it going.

To produce atmosphere No. 2-A (partially burned fuel gas with CO_2 and H_2O removed) use equipment A plus equipments B, F, and G.

To produce atmosphere No. 3 (partially reacted fuel gas) use equipment C.

To produce atmosphere No. 4 (completely reacted fuel gas) use equipment C.

To produce atmosphere No. 5 (dissociated ammonia) use equipment D.

To produce atmosphere No. 6 (partially burned dissociated ammonia) use equipments E plus F, and G if drying is required.

To produce atmosphere No. 6-A (completely burned dissociated ammonia) use equipment E plus F, and G if drying is required.

FURNACE EQUIPMENT TO BE USED WITH CONTROLLED ATMOSPHERE

In general, all furnace equipment must be individually analyzed and designed for the particular application of controlled atmosphere required. Atmosphere furnaces are fabricated to be gas-tight. Many schemes are used to minimize the consumption of

prepared atmosphere and to insure positive control of atmosphere flow or circulation inside the furnace structure. When fuel-fired furnaces are used, radiant tubes or muffles are necessary to keep the products of combustion from mixing with the prepared atmospheres. Electric furnaces of the type using resistors may be used without muffles where other factors in the application permit it.

Separately controlled atmospheres are now being widely applied to a variety of popular types of modern furnace equipment such as pusher, roller-hearth, box, bell-type, belt-conveyer, and elevator furnaces.

In general, before any application of separately controlled atmosphere equipment is made to existing furnace equipment, all factors should be carefully analyzed and the experience of equipment manufacturers fully utilized.

The remaining discussion will deal with the applications of the various atmospheres which have been outlined, to various metal processes, particularly those related to annealing, hardening, tempering, and brazing of both nonferrous and ferrous metals. In general, no particular single atmosphere will be universally applicable to all processes related to the heating of metals. The closest approach to a universal heat-treating atmosphere is No. 1-A which consists of a high nitrogen-bearing gas which is oxygen-free and which contains sufficient reducing properties to overcome effect of impurities from the metal being treated and from the brickwork of furnaces in which the metal is treated. The equipment necessary to produce this atmosphere is more expensive than that required for alternate choices of atmospheres which are suitable for a given process and which require less expensive equipment.

The general problem in applying controlled atmospheres to metals usually resolves itself into partial or total prevention of oxidation of the metal surfaces and prevention of metallurgical changes in metal, such as loss of carbon from steel surfaces (decarburization). In some processes the atmosphere is applied purposely to affect the metal structure and composition, such as gas carburizing, where controlled amounts of carbon are added to the steel surface by means of chemical reaction between the metal and the atmosphere surrounding the metal.

ANNEALING NONFERROUS METALS

Copper. This metal may be annealed without oxidation in an atmosphere of steam but this method allows water staining and in many modern installations on wire, strip, and tubing, particularly on finish-annealing, it has been more desirable to use separately controlled atmospheres. Shiny bright surfaces can be obtained by using atmosphere No. 1 (completely burned fuel gas, slightly on the reducing side).

Copper is discolored at elevated temperatures in the presence of extremely small amounts of sulphur compounds, particularly hydrogen sulphide. Manufactured fuel gases such as coke-oven gas or carburized water gas are usually passed through iron-oxide boxes to remove hydrogen sulphide, before being used commercially. This scrubbing operation usually removes hydrogen sulphide to a very small value of 5 grains per 100 cu ft of raw gas. Even though this amount is very small it is sufficient to discolor copper after mixing with air and burning in a gas generator. For this reason further removal is necessary beyond the gas generator.

Complete combustion of the gases in the generator tends to convert most of the sulphur in the fuel gas both organic and inorganic into sulphur dioxide which is carried off in the condensate from the gas generator. The small amounts of hydrogen sulphide are removed by iron-oxide towers on the exit side of the gas generator.

Certain types of copper contain small amounts of oxygen which can react with hydrogen in the controlled atmosphere and

cause embrittlement. In these cases the atmosphere must be set for a bare minimum of hydrogen and carbon monoxide (about $1/2$ to $3/4$ per cent of each) without any free oxygen.

Copper-Nickel Alloys. These alloys may be bright-annealed with the same atmosphere as that used for copper (atmosphere No. 1), and the atmosphere must be entirely free of sulphur. Hydrogen embrittlement in general is not a problem in the case of these alloys so that atmospheres with higher hydrogen and carbon-monoxide contents may be satisfactorily used.

Copper-Zinc Alloys (Brasses). These may be clean-annealed with the same atmosphere as used for copper (atmosphere No. 1). Bright-annealing is not obtained due to volatilization of zinc from the surface of material at elevated temperature. This gives the surface a "clouded" appearance. Volatilization of zinc and subsequent oxidation on the surface of the metal by CO_2 and H_2O in the controlled atmosphere can be greatly retarded by using high nitrogen atmosphere from which CO_2 and H_2O have been removed (atmosphere No. 1-A).

Copper-Silicon Alloys. These may be bright-annealed with high nitrogen atmosphere free from CO_2 and H_2O (atmosphere No. 1-A), as well as being entirely free from traces of sulphur.

Copper-Silver Alloys. These may be bright-annealed with either atmosphere No. 1 or No. 2 but must be absolutely free of any traces of sulphur, or discoloration will occur.

Nickel and Monel Metal. These may be bright-annealed with either atmosphere No. 1 or No. 2 but must be entirely free of sulphur. The metal surfaces, although free of oxide, present a gray or matte finish. Shiny bright surfaces can be obtained by using dissociated ammonia (atmosphere No. 5) or with combusted dissociated ammonia (atmospheres Nos. 6 and 6-A). Inconel which is a high nickel-bearing alloy with chromium and iron can only be bright-annealed in atmospheres Nos. 5, 6, 6-A.

Aluminum and Its Alloys. These can be successfully treated in air atmospheres provided moisture content is relatively low. Completely burned or partially burned and partially dried fuel gases (atmospheres Nos. 1 and 2) can also be successfully used. In this field there is not yet any widespread demand for application of separately prepared controlled atmospheres since prevention of slight surface oxidation is not a serious problem.

Magnesium. This metal can be annealed using atmosphere No. 1 which in general prevents any active or rapid oxidation and thus allows safely against possible combustion of the magnesium at the normal heat-treating temperatures. Air atmospheres with $1/2$ to 1 per cent of sulphur dioxide added are also successfully used.

ANNEALING FERROUS METALS

Low-Carbon Steel. This may be bright-annealed using partially burned fuel gas with generator set to give maximum reducing properties (atmosphere No. 2). In those cases where the available cooling water is over 60 F in temperature the dew point of the gas atmosphere leaving the generator will be over 70 F. In general, atmosphere No. 2 with dew points of over 70 F can cause discoloration of steel due to oxidizing action of excess water vapor as the steel slowly cools down through a temperature range from 1100 F to 700 F. In those cases where cold water is not available the year round it is necessary to supplement the atmosphere with partial drying to dew points of about 40 F. Atmosphere No. 2 is approximately in equilibrium with low-carbon steels at normal annealing temperatures and hence there is no measurable amount of carbon loss or gain from the steel due to chemical combination with the atmosphere surrounding it. This atmosphere is very definitely decarburizing to medium- and high-carbon steels and to various alloy steels and should not be used where decarburization cannot be tolerated.

Medium- and High-Carbon Steels. These can be bright-annealed using atmosphere No. 1-A. This atmosphere is not decarburizing and is practically neutral to a wide range of carbon contents in the steel so that neither carburization nor decarburization takes place. The small amounts of CO and H_2 in the atmosphere are sufficient to react with small amounts of oxidizing impurities on the steel being heated, or react with impurities from furnace brickwork. Long-cycle annealing of alloy carbon steels or high-carbon steels requires an atmosphere that is chemically inactive and which therefore does not react with the carbon in the steel. The high nitrogen content of atmosphere No. 1-A combined with total removal of decarburizing components such as CO_2 and H_2O , results in an atmosphere which is chemically "neutral," and reaction rates with the carbon in the steel are so small that no measurable gain or loss of carbon from steel occurs when steel is heated to annealing temperature and held there for long periods of time.

Alloy Carbon Steels; Tool Steels and High-Speed Steels. These may be annealed on long cycles without oxidation or decarburization using atmosphere No. 1-A. Atmosphere requirements are the same as those just discussed for high-carbon steels.

Stainless Steels. Such steels, including the chrome-nickel-iron alloys and the chrome-iron alloys, can be annealed without heavy oxidation in atmospheres No. 1 and No. 2 and very little oxidation in atmospheres Nos. 1-A, 2-A, 3, and 4. However, if it is desired to bright-anneal these steels it is necessary to use pure dry hydrogen. Immeasurably small amounts of oxygen must be absent from the gas atmosphere, and the bright-annealing to be successful must be done in alloy-steel muffles constructed so that the pure dry atmosphere is maintained without possibility of entrance of the least traces of any oxygen-bearing gases such as O_2 , CO_2 , CO , H_2O . Atmosphere No. 5 (dissociated ammonia) will be suitable. Atmospheres Nos. 6 and 6-A are also suitable provided they are produced from equipment which eliminates all traces of oxygen and water vapor.

HARDENING OF FERROUS METALS

In production finished machined parts of all sizes and descriptions can now be hardened free from oxidation and decarburization. This development is of great significance since uniform quality of work on a large production basis can be realized without subjecting the pieces to further machining, grinding, sandblasting, pickling, or other expensive cleaning operations which formerly were necessary to eliminate scale and soft skin (decarburization) on the work being heat-treated. The atmosphere required to accomplish bright-hardening without decarburization must be very low in CO_2 and water vapor. Atmospheres 1-A and 2-A meet these requirements. However, it is possible to produce an atmosphere which has only very small residual amounts of CO_2 and water vapor by reacting completely the hydrocarbon in the gas to CO and H_2 with a limited amount of air, in the presence of a catalyst at high temperature. This is represented by atmosphere No. 4. A variation of this, where the cracking is not quite so complete, is represented by atmosphere No. 3.

Atmosphere No. 3 is suitable for short-cycle (less than 2 hr) hardening of medium-carbon steels at medium-range hardening temperatures (1400–1450 F) with no oxidation or decarburization.

Atmosphere No. 4 is suitable for hardening of high-carbon steels and alloy carbon steels without oxidation as decarburization. This gas contains no CO_2 and very little water vapor, is nondecarburizing to high-carbon steels, and is particularly applicable to hardening where decarburization cannot be tolerated. This gas can also be set so as to be in "carbon balance" with the steel being heat-treated so that neither carburizing nor decar-

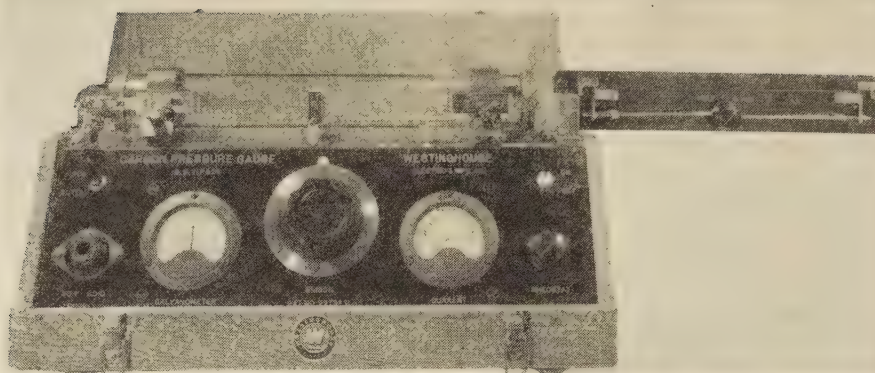


FIG. 11 HOT-WIRE GAGE FOR DETERMINING CARBURIZING POWER OF GAS ATMOSPHERE

burizing takes place. Fig. 11 shows an instrument which has been developed for predicting the approximate carbon content of the steel at which the surrounding atmosphere is in equilibrium. This instrument is known as a "hot-wire gage" and operates on the principle of a measurement of the change in resistance of a low-carbon-steel wire carburized with the surrounding gas atmosphere. The wire is heated by electric current inside a glass tube and is surrounded by the atmosphere being tested. The heated wire absorbs carbon from the gas until it is in equilibrium with the surrounding gas. This process takes place very quickly because of the small cross section of the wire. A change in resistance measured on a potentiometer is calibrated in terms of the carbon content at which the particular gas is in equilibrium with the steel being heat-treated. This instrument is useful on applications where it is desirable to maintain an atmosphere which is in approximate chemical balance with the carbon content of the

steel being hardened so that the steel surface is neither carburized nor decarburized. Atmosphere No. 4 may be produced to give these conditions.

Tool steels and high-speed steels can be successfully hardened without oxidation or decarburization using atmosphere No. 4. The high-carbon high-chromium tool steels can be hardened without decarburization but will be tarnished due to slight oxidation of the chromium. If it is desired to bright-harden these steels it is necessary to use atmosphere No. 5 (dissociated ammonia) inside a special design of alloy-metal muffle furnace.

GAS CARBURIZING

In addition to the developments of controlled atmospheres for prevention of oxidation and decarburization, it is possible to control the rates at which carbon is added to the surface of steel and the distribution and depth through which the carbon dis-

TABLE 1 ATMOSPHERES SUITABLE FOR HEAT-TREATMENT OF DIFFERENT METALS

Material processed	Process	Temperature range, deg F	Time cycle ("long" if over 2 hr)	Required surface	Atmospheres which will give desired results	Atmospheres commonly used
Low-carbon steels.....	Anneal	1200 to 1350	Bright or Clean Annealing	Bright	1A, 2, 2A, 5, 6, 6A	2
Medium-carbon steels.....	Anneal (no decarburization)	1200 to 1450	Long	Bright	1A, 2A, 5, 6, 6A	1A
High-carbon steels.....	Anneal (no decarburization)	1200 to 1450	Long	Bright	1A, 2A, 5, 6, 6A	1A
Alloy steels, medium- and high-carbon.....	Anneal (no decarburization)	1300 to 1600	Long	Bright or clean	1A, 2A, 5, 6, 6A	1A, 2A
High-speed tool steels, including molybdenum high speeds.....	Anneal (no decarburization)	1400 to 1600	Long	Bright or clean	1A, 2A, 5, 6, 6A	1A
Stainless steels, chromium and nickel-chromium.....	Anneal	1800 to 2100	Short and long	Bright	5	5
High-silicon steel, electrical sheet...	Anneal	1900 to 2000	Long	Clean	1A, 6	1A, 6
Copper.....	Anneal	400 to 1200	Long or short	Bright	1	1
Various brasses.....	Anneal	800 to 1350	Long or short	Clean	1	1
Copper-nickel alloys.....	Anneal	800 to 1400	Long or short	Bright	1A, 6	1A
Silicon-copper alloys.....	Anneal	1200 to 1400	Long or short	Bright	1A	1A
Nickel.....	Anneal	1600 to 2000	Long or short	Bright	1, 1A, 2, 2A, 5, 6, 6A	1, 5
Automatic Brazing or Soldering Operations						
Low-carbon steels.....	Copper brazing	2050	Short	Bright	2, 2A, 4, 5, 6	2
Medium- and high-carbon steels...	Copper brazing (no decarburization)	2050	Short	Bright	2A, 4, 5, 6	4
Alloy steels, medium- and high-carbon.....	Copper brazing (no decarburization)	2050	Short	Bright	2A, 4, 5, 6	4
High-carbon, high-chromium steels.....	Copper brazing	2050	Short	Bright	5	5
Stainless steels.....	Copper brazing	2050	Short	Bright	5	5
Copper or brass.....	Phos-Copper brazing or silver soldering	1500 to 1600	Short	Bright	1	1
Bright-Hardening and Tempering						
Medium-carbon steels.....	Hardening	1400 to 1600	Short	Bright or clean	1A, 2A, 4, 5, 6, 6A	4
High-carbon steels.....	Hardening	1400 to 1800	Short	Bright or clean	1A, 2A, 4, 5, 6, 6A	4
Alloy steels, medium- and high-carbon.....	Hardening	1400 to 1800	Short	Bright or clean	1A, 2A, 4, 5, 6, 6A	4
High-speed tool steels, including molybdenum.....	Hardening	1800 to 2400	Short	Bright or clean	1A, 2A, 4, 5, 6, 6A	4
All classes of ferrous metals.....	Tempering or drawing	400 to 1200	Short	Bright or clean	1A, 2	2

perses into the steel. As stated, those gases which contain no CO_2 or water vapor will not remove carbon from steel. A gas with no CO_2 or H_2O vapor is an excellent atmosphere to use as a "base" for adding carbon-bearing gases which will react to add carbon to the steel. With an efficient base or "carrier" gas the amount of carbon-bearing gases which must be added to produce fast soot-free carburizing is relatively small. Methane is by far the most efficient carburizing gas, and small amounts of methane added to a carrier gas containing no CO_2 or water vapor produces a gas very suitable for quick efficient soot-free carburizing. Atmosphere No. 4 is an efficient base or carrier gas. This gas as normally produced has no CO_2 and very small water-vapor content. Due to the presence of CO , H_2 and residual methane in the gas as produced, it already possesses a reasonable carburizing "potential" and the addition of 1 or 2 per cent of methane gives a very active gas for carburizing.

Successful application of these atmospheres for quick clean gas carburizing also requires the use of such atmospheres in furnace equipment which will successfully maintain these atmospheres. Equipment which allows oxygen from the air to infiltrate even in small amounts, will destroy the carburizing potential of the gas, and efficient soot-free gas carburizing is not possible.

ATMOSPHERE FURNACE BRAZING

Nonferrous Metals. Many nonferrous metals can be brazed in protective furnace atmospheres. Copper and copper alloys are brazed using "Phos-Copper" or "Ez-Flow," "Sil-fos," and similar alloys for brazing material. Atmosphere No. 1 is suitable for a great many of these applications. If discoloration is to be prevented all traces of sulphur in the gas must be removed as in the case of bright-annealing copper. Richer gas atmospheres with higher reducing properties are also suitable such as atmospheres Nos. 2, 3, and 4, where hydrogen embrittlement is not a factor.

Ferrous-Metal Brazing. Brazing of steels with copper at 2050 F is a widely used method of joining all types of assemblies. Silver brazing of steels at lower temperatures, such as 1700–1800 F, is finding growing applications. In both instances reducing atmospheres are required. Atmosphere No. 2 (partially burned fuel gas) is applicable when the brazing does not require prevention of decarburization. This is not a problem on low-carbon steels but may be a factor to contend with on medium- and high-carbon steels. Although the average brazing operation requires only a relatively short time at the high temperature, the rates of decarburization are also very rapid at these high temperatures when appreciable CO_2 and water vapor are present such as in atmosphere No. 2.

Where decarburization of the brazed work is to be prevented atmosphere No. 2-A or atmosphere No. 4 should be used. Atmosphere No. 4 is particularly suitable for brazing because the high H_2 and CO content give it very high reducing properties which in general are very desirable for brazing ferrous metals.

Stainless steels and the high-chromium steels require an extremely pure reducing atmosphere. Atmosphere No. 5 is the most suitable, as well as dry, oxygen-free hydrogen.

SINTERING OR POWDER-METALLURGY APPLICATIONS

Controlled atmospheres are necessary in the production of metals and alloys in this rapidly growing field. Brasses, bronzes, etc., are sintered with reducing atmospheres such as atmosphere No. 2, and atmospheres Nos. 3 and 4.

Ferrous alloys and iron, in general, utilize these same atmospheres. Atmospheres Nos. 3 and 4 are particularly useful because of their very high reducing properties.

As in normal ferrous metallurgy these are problems where decarburization must be prevented. Fuel-gas atmospheres, very

low in CO_2 and water vapor, are desirable. Atmospheres Nos. 2-A and 4 fulfill these requirements.

In those cases where oxidation of chrome (such as stainless steels) must be prevented, the pure dry hydrogen and dry hydrogen-nitrogen mixtures must be used. Atmosphere No. 5 (dissociated ammonia) fulfills these requirements.

A summary of the applications of atmospheres to various metals and metal processes is given in Table 1.

CONCLUSION

In conclusion it may be said the field of application of separately prepared controlled atmospheres will continue to expand. As a result of developments in this field many heat-treating processes can be controlled with high precision, quality is improved and is uniform, and large savings result because of elimination of cleaning, finish-machining, grinding, etc. In parallel with the development of controlled atmospheres, the heat-treating-process equipment in which these atmospheres are used has been developed to use these gases properly. The best controlled atmosphere is useless unless the companion equipment in which the metal is processed is designed so as to hold and maintain properly the atmosphere composition which is brought to it.

Continued development, refinement, and improvement of heat-treating equipment are necessary in order to realize fully the benefits of the application of the separately prepared atmosphere.

Discussion

SAM TOUR.² The author has taken a narrow view of the subject which is the title of his paper. He has considered only that portion of the subject for which his company builds special pieces of equipment.

"Combustion" is improperly defined in the paper. It is incorrect to say, "the word 'combustion' indicates that sufficient heat energy is evolved to generate the desired gas without addition of external heat." Properly defined the word "combustion" means the continuous combination of a substance with certain elements, as oxygen, accompanied by the generation of light and heat. The popular conception of the word is rapid oxidation, as of fuel. Coal or wood will combine with oxygen if heated to a kindling temperature. The continuous combining of coal or wood with oxygen in the air is combustion. Similarly, if certain gases are heated to a suitable temperature they will combine with oxygen in the air and combustion will take place.

"Cracking" is improperly defined in the paper. It is incorrect to say "the word 'cracking' indicates that heat energy must be supplied at a sufficient temperature level to promote the dissociation. . . ." Properly defined, the word "cracking" in connection with fuel gases is substantially the same as in connection with petroleum. The cracking process is really destructive distillation or decomposition caused by the application of heat.

The set of curves presented in Fig. 1 of the paper is open to considerable question. The statement is made, "a curve of this type can be calculated for every type of fuel gas commercially available for use in generation of prepared furnace atmospheres." This statement would indicate that the curves given in Fig. 1 have been "calculated." In the following paragraph the author admits that the curves are "idealized." He then goes on to describe how the actual amounts of hydrogen, water vapor, carbon dioxide, and carbon monoxide depend upon space, time, catalyst, and temperature. Since the curves in Fig. 1 are not specific as to these factors of space, time, catalyst, and temperature, it is evident that they were not "calculated" but "thought up."

As a matter of fact, the writer a few years ago presented a

² Sam Tour & Co., Inc., New York, N. Y.

paper² in which the large effect of combustion-chamber temperatures was shown. The following is quoted from that paper:

A large percentage of the controlled atmospheres required for the heat-treatment of steel are those obtained as the result of burning rich mixtures of gas and air. By a rich mixture is meant a mixture in which the amount of air supplied is insufficient for complete combustion of the gas. This is often referred to as "partial combustion" with a deficiency of air. It is in this field that combustion chamber temperatures play their most important role.

Burning city gas and air in the ratios of 1 of air to 1 of gas and 2 of air to 1 of gas, and maintaining combustion-chamber temperatures at various points from 1200 to 2200 F (650 to 1205 C), and making the usual analyses of the products of combustion, the effect of changes in the temperature of the combustion chamber becomes very apparent. The results are shown in Fig. 1 (Fig. 12 of this discussion). It will be noted that as the temperature

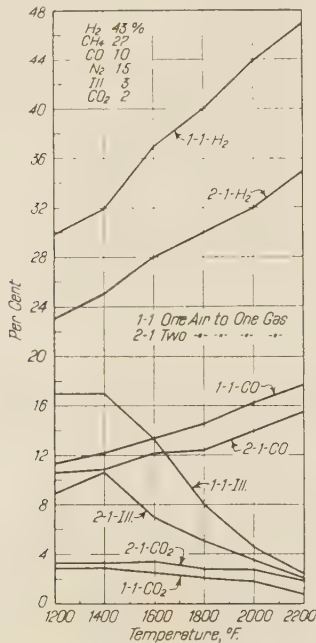


FIG. 12 EFFECT OF CHANGES IN TEMPERATURE OF COMBUSTION CHAMBER; CITY GAS
(Originally Fig. 1 of paper, reference 3, by writer.)

of the combustion chamber is increased, the products of combustion for the same air-to-gas ratio contain less illuminants, slightly less carbon dioxide, considerably more carbon monoxide, and greatly increased quantities of hydrogen. Unfortunately, when this work was done no direct determinations of water-vapor content were made. Due to the large quantities of residual illuminants present in the products of combustion and due to the large quantity of soot and tar formed in burning these rich mixtures at the lower temperatures, it is impossible to calculate the volume relationship between the initial gases and the products of combustion. It is therefore impossible to arrive at a logical basis for the calculation of water-vapor content of the products of combustion. Experience shows that the water-vapor content decreases as the temperature of the combustion chamber increases.

Burning a mixture of propane gas (C_3H_8) and air and maintaining the combustion chamber at various temperatures, and

using an air-gas ratio of 8 of air to 1 of gas, the average analyses of the products of combustion are shown in Fig. 2 (Fig. 13 of this discussion). Here it is seen that the hydrogen content of the products of combustion increases continuously and rapidly as the temperature of the combustion chamber is increased. The percentage of carbon monoxide in the products of combustion increases to a combustion-chamber temperature of around 2000 F. (1095 C), and then decreases. This phenomenon will be referred to later. Illuminants and carbon dioxide both tend to decrease as the combustion-chamber temperature increases.

In the combustion of propane gas we have a base material of known composition, and within certain limits we can calculate

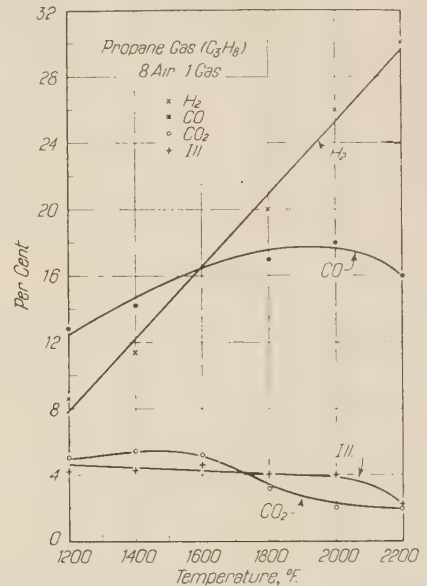


FIG. 13 EFFECT OF CHANGES IN TEMPERATURE OF COMBUSTION CHAMBER; PROPANE GAS (C_3H_8); AVERAGE CURVES
(Originally Fig. 2 of paper, reference 3, by writer.)

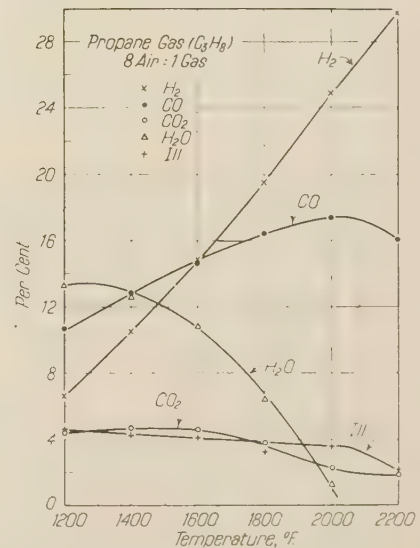


FIG. 14 EFFECT OF CHANGES IN TEMPERATURE OF COMBUSTION CHAMBER; PROPANE GAS (C_3H_8) 8 AIR TO 1 GAS; CORRECTED FOR H_2O
(Originally Fig. 3 of paper, reference 3, by writer.)

² "Furnace Atmosphere Generation," by Sam Tour, TRANS. American Society for Metals, vol. 29, 1941, pp. 693-704.

TABLE 2 COMPARISON OF VARIOUS ATMOSPHERES

No.	CO ₂	CO	H ₂	CH ₄	O ₂	N ₂	H ₂ O	Equipment
1	10	0.5	0.5	0.0	0.0	89.	..	A + F
1-A	0.0	0.5	0.5	0.0	0.0	99.	..	A + B + F + G
	0.0	3.0	3.0	0.0	0.0	94.	..	
2	5.0	10.0	15.0	1.	0.0	69.	..	A + F
2-A	0.0	10.5	16.0	1.	0.0	72.5	..	A + B + F + G
3	1.	18.	34.	1.	0.0	46.	..	C
4	0.	19.	40.	1.	0.0	40.	..	C
5	75.	25.	..	D
6	20.	80.	..	E + F + G
6-A	1.	99.	..	E + F + G

the amount of water vapor present in the products of combustion. The calculation is based on the assumption that for each volume of propane gas which is burned there will be produced three volumes of carbon-monoxide plus carbon-dioxide gases, and four volumes of hydrogen plus water vapor. To the extent that carbon is lost in the formation of illuminants and in the formation of tar, soot, and pitch, the calculated water vapor will be less than the true water-vapor content of the products of combustion. The results shown in Fig. 2, revised and corrected for water-vapor content, are shown in Fig. 3 (Fig. 14 of this discussion). Here the fact that the water-vapor content of the products of combustion decreases rapidly as the temperature of the combustion chamber is increased becomes quite evident.

The decrease in carbon-monoxide content at temperatures above 2000 F (1095 C) is due to the large loss of carbon in the form of coke and carbon particles and heavy oils of the naphthalene type. In many instances the atmosphere desired from an atmosphere generator is one which requires even richer mixtures than the 8 of air to 1 of propane gas covered by the curves in Figs. 2 and 3 (Figs. 13 and 14 of this discussion). With these still richer mixtures the problem of coke deposition in a combustion chamber operating at 2000 F (1095 C) or higher becomes even more accentuated. Continued burning of excessively rich propane gas and air mixtures in a combustion chamber at high temperatures results in loading the combustion chamber with coke and the outlet pipes with tar and naphthalenes.

At low combustion-chamber temperatures the gases are not broken down so completely as to form heavy coke or pitch deposits, but form large quantities of so-called "illuminants," light oil vapors, and soot. The gases coming from the combustion chamber when it is operated at too low a temperature are usually referred to as "smoky." The soot and oil vapors which are carried along rapidly foul the furnace and the work in the furnace. If cooling or cleaning equipment is used to dehydrate the products of combustion, the passageways become coated with soot. Some of the oil vapors are condensed and removed with the condensed water vapor.

Furnace-atmosphere gases carrying large quantities of soot and large quantities of oil vapors are particularly objectionable in metallic-resistor-heated electric furnaces where the gases come in contact with the heating elements. When the current is on the heating elements in an electric metallic resistance furnace are operating at temperatures considerably above the furnace-chamber temperature or the work-temperature control point. As the oil vapors in the atmosphere strike the heating elements they are cracked to form carbon plus lighter vapors or gases such as methane and hydrogen. The carbon residue builds up on the electric heating elements. Within a short time the carbon built up on the heating elements may be sufficient to cause short-circuiting.

It seems evident that a control of the temperature of the combustion chamber is necessary. The combustion chamber should be maintained at a temperature high enough to prevent the excessive formation of soot and oil vapors, but it should not be so high as to cause the formation of coke and heavy tars (end of quote).

For ease of comparison, the various atmospheres which are described by the author have been listed in Table 2 of this discussion.

The author describes atmosphere No. 1, the result of complete combustion, as an inert atmosphere. Here another term is incorrectly used. The term "inert" means neutral or devoid of active chemical properties. The atmosphere in question contains 10 per cent CO₂ and considerable water vapor. Both of these attack steel at elevated temperatures and the atmosphere is not inert. The author fails to point out that, according to his "idealized" curves, this atmosphere as generated contains about 18 per cent of water vapor (steam) which is partially condensed by cooling to room temperature where the water content is still of the order of 2 per cent.

In describing equipment B for removing CO₂ from products of combustion the author fails to mention the chemical used for absorption or the materials necessary for construction of the apparatus in contact with this liquid. Usually "Olamines" are used and corrosion is a problem in the equipment. A much cheaper initial installation cost is possible with a nonregenerating system using cheap caustic as the absorbing medium.

In describing atmosphere No. 2, the author fails to recognize the large effect of combustion-chamber temperature on the amount of H₂ and CO formed. He erroneously refers to "catalysts" as giving higher H₂ and CO. The fact is that temperatures control this and higher temperatures produce higher H₂ and CO.

His estimated cost of production of atmosphere No. 4 at \$0.18 to \$0.25 per 1000 cu ft is rather optimistic. Close to double these figures are more usual.

He describes dissociation of ammonia as "cracking." This is correct. Complicated equipment is shown for generation of atmospheres Nos. 6 and 6-A by ammonia dissociation, followed by combustion. No mention is made of direct combustion of ammonia vapor with air to produce mixtures high in nitrogen. Were such equipment used, the costly dissociator could be eliminated. Ammonia vapor plus air forms a combustible mixture and will burn in a combustion chamber to produce N₂ plus H₂O. Some traces of nitrous oxides are formed and must be scrubbed from the products of combustion of ammonia vapor plus air.

This paper describes "controlled atmospheres" as those produced in equipment separate and distinct from the equipment used for the heating operation. It does not refer to that important line of industrial equipment known as "controlled-atmosphere furnaces." In controlled-atmosphere furnaces, the atmosphere-generating equipment is built into the furnace. Atmospheres equivalent to those described as Nos. 1, 1-A, 2, 2-A, 3, and 4 may all be produced in such built-in generators with suitable auxiliary equipment. Controlled-atmosphere furnaces of the recirculating type are available for this purpose and are discussed by the writer in his review of the art.³

AUTHOR'S CLOSURE

Mr. Tour has pointed out specific limitations on the scope of the material given in the paper. It was purposely limited to a general discussion of separately prepared atmospheres produced from separate equipments. Discussion of atmospheres pro-

duced from built-in equipments, and discussion of atmosphere furnaces were considered beyond the scope of the present paper.

Mr. Tour is probably correct in his comments on definitions used. The present state of the art is such that standardization of terms does not exist, and the definitions given in the paper for "combustion" and "cracking" are those now commonly used by equipment manufacturers and users. Other methods of describing the various atmospheres should also fall into such classifications as the following:

- 1 Completely burned gases.
- 2 Partially burned gases.
- 3 Partially reacted gases.
- 4 Completely reacted gases.

In connection with the composition curve in Fig. 1 of the paper, the compositions given at the left-hand edge and the right-hand edge can be accurately calculated for any fuel gas. The compositions given between these two extremes cannot be calculated but have been determined by values obtained from the operation of properly designed commercial apparatus. In all of this discussion the residual methane is extremely small and the gases are reacted to form the approximate ideal balance between carbon monoxide, carbon dioxide, hydrogen, and water vapor. In all cases the values given on the curve assume temperatures sufficiently high to prevent any excessive formation of carbon in any form and limit the residual methane to very small values.

Mr. Tour's quite complete comments on the effect of temperature on composition are correct and have been substantiated by actual operating experiences. The composition given in the curve, Fig. 1, however, is based on operation of commercial equipment specifically designed so that it will always operate at sufficient temperature level to eliminate practically all carbon deposits and to limit the residual methane to very small amounts.

As Mr. Tour points out, it is important also to consider water-vapor content of the gas. The approximate magnitude of this value is also shown in Fig. 1. In giving specific compositions of the gases throughout the paper, a water-vapor content before partial condensation is not given. The water-vapor content after condensation or drying is the value given since this is the practical value, of interest to the user. However, this does not mean that water vapor is not an important factor in the use and application of gas atmospheres. In a great many cases a water-vapor content is more important in its effects than any of the other constituents in the gas. Here again, however, a more complete discussion of this question was beyond the scope of the present paper.

As pointed out by Mr. Tour, the temperature of operation is more important than the use of a catalyst. However, in the practical design of commercial equipment it has been found that catalysts are essential for speeding up the rates of reactions and thus limiting the physical size of the equipment to reasonable values.

Concerning the removal of carbon dioxide, the chemicals used for this purpose are the ethanolamines. The use of caustic soda is possible, but in general, operating costs for the type of system are high enough to make the use of the ethanolamines more attractive.

Cost figures are based on average cost for natural gas as a fuel, and many of these figures are doubled if expensive manufactured gas is the available fuel.

The ammonia combustion equipment described in the paper could be simplified as pointed out by Mr. Tour, by performing the ammonia cracking and the burning in one operation. However, on the processes justifying this type of equipment, it is not worth while risking a formation of nitrous oxides and it is therefore considered more practical to eliminate these by using separate equipment for dissociating the ammonia.

A Graphical Solution of Windshield Heat Deicing Problems

By H. H. HAUGER, JR.,¹ SANTA MONICA, CALIF.

It is the purpose of this paper to present the problem behind the design of an air-heated double-paneled windshield for aircraft. A windshield ice-prevention nomograph is proposed as a rapid accurate method of making a design analysis of the air-heated windshield. With its use the designer has at his disposal a visual means of determining the relative importance of the variables included within the design, so as to arrive at the optimum solution for a given installation under the conditions imposed. The sample problems analyzed in this paper indicate that the required windshield strength be designed into the inner panel with an outer panel of tempered glass so as to obtain the highest outer-surface temperatures.

INTRODUCTION

UNTIL recently the usefulness of the airplane was somewhat limited due to the formation of ice on various surfaces.

The early air-mail pilot had to turn back or try to fly through the icing weather, bailing out becoming necessary more times than not. Travelers became reluctant to fly in the winter months since the commercial air lines operated only in favorable weather. But the air lines had to maintain regular schedules and overweather flying developed. Even then many flight plans had to be changed in order to avoid icing conditions.

The war has changed this outlook. Military and naval operations must be made regardless of weather conditions. To overcome these difficulties the ice formations on aircraft must either be prevented or removed. Ice may be prevented by taking an ice-free path, although icing conditions might move in unexpectedly. Merely avoiding ice means that many scheduled flights and military missions would have to be canceled. Therefore the only logical way to maintain flight in icing weather would be to remove or prevent ice from forming on certain surfaces, which would seriously affect the flying characteristics of the airplane, by either mechanical, chemical, or thermal means.

The windshield is an example of such a surface since adequate vision must be maintained at all times for successful operation. A mechanical means of removing ice is the windshield wiper which has been used with little success. A chemical anti-icing fluid which reacts with the ice to prevent its adhesion to the glass surface was found to be satisfactory if proper distribution of the fluid over the surface can be maintained. With this type of installation, though, the visibility is impaired by clouding and smear resulting from the use of anti-icing fluids.

Heat is one of the most successful and practical means of preventing the formation of ice. One method is to circulate heated air against the inner surface of the windshield glass, raising the outer surface to a temperature above the freezing point of water. If ice has already formed, the surface under the ice is raised to a

temperature of about 32 F which reduces the adhesion of ice to the glass surface; the air stream then carries the ice away. It is the design of an air-heated double-paneled windshield with which this paper deals exclusively.

AIR-HEATED DOUBLE-PANELED WINDSHIELD

Good vision through the windshield involves a threefold problem: (a) The prevention and removal of ice on the outer surface; (b) prevention and removal of frost or window fog from the inner surface; and (c) removal of rain from the outer surface. An air-heated installation capable of successfully preventing the formation of ice on the outer surface will remove both the frost and the rain. Several windshields of the double-paneled air-heated type have been constructed and tried repeatedly in icing conditions by the National Advisory Committee for Aeronautics. The device appears to be satisfactory and many installations which have given satisfactory service have been made on both commercial and military aircraft (1).²

A typical construction of an air-heated double-paneled windshield is shown in Fig. 1. The outer panel is laminated; a sheet of plastic, such as vinyl, being inserted between two sheets of tempered glass. This laminated panel is needed for structural reasons only, for the windshield must pass satisfactorily an "impact test," in order to demonstrate its ability to withstand collisions with birds during flight. The inner sheet completes the double-panel arrangement, being made from a sheet of plexiglas or its equivalent. The air gap thus formed allows the heated air to be concentrated against the outer panel, thereby improving the heat transfer over that experienced by a single-panel blast-air arrangement. The heated air enters the air gap through an inlet plenum which should be well designed to distribute the flow of air evenly over the windshield surface. The circulating-air exhaust may be either to the outside air or to the cockpit as shown, aiding the cabin-heating system.

The source of heat may be from heat exchangers, employing the waste heat in the engine exhaust, or from internal-combustion heaters located near the windshield. The source of pressure is usually the ram pressure of the airplane. However, a blower is often installed to supply the necessary pressure for defrosting during taxiing, take-off, or landing.

The design complications are now becoming evident. A limited amount of air will be forced through the air gap, the amount being determined by the gap length, gap thickness, and available pressure. A limit is also set on the air temperature allowed to enter the double panel, as there is a definite maximum temperature which the plastic can withstand without deterioration. Often the exhaust from the windshield enters the cockpit just over the pilot's head and to alleviate any discomfort due to this hot-air blast, a restriction is placed on the exhaust-air temperature. Finally, the windshield must be able to remove ice under the worst of flying conditions, which corresponds to the condition resulting in the highest coefficient of heat transfer over the outer surface. For a definite ambient air temperature and windshield size, the average heat-transfer factor for turbulent flow over a flat plate is given in reference (2), as varying directly

² Numbers in parentheses refer to the Bibliography at the end of the paper.

¹ Air Technical Service Command, A.A.F.; formerly Air Conditioning Design Engineer, Douglas Aircraft Company, Inc.

Presented at a meeting of the Aviation Division, Los Angeles, Calif., June 5-9, 1944, of THE AMERICAN SOCIETY OF MECHANICAL ENGINEERS.

NOTE: Statements and opinions advanced in papers are to be understood as individual expressions of their authors and not those of the Society.

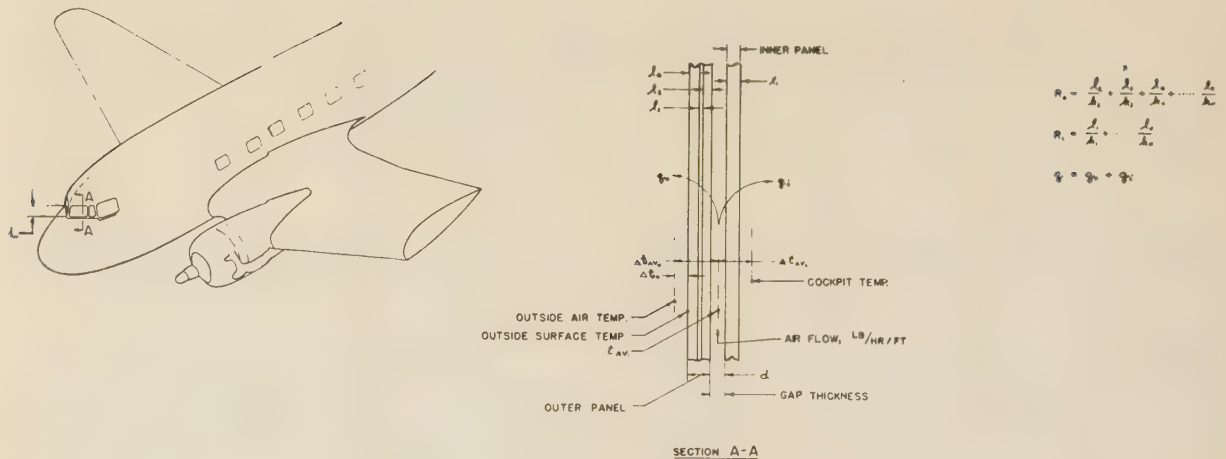


FIG. 1 DETAILS OF AIR-HEATED DOUBLE-PANELED WINDSHIELD

with the 0.8 power of the air velocity and density. Expressed in equation form

$$(\text{Average}) h_0 \propto (V\gamma)^{0.8}$$

It is therefore apparent that the most heat is required at the lowest altitude and the maximum airplane speed.

A moment of reflection will indicate a definite need for a graphical solution to such a design problem. An identical calculation would be required for each proposed structural change. Then for each air flow there is a corresponding gap size which may or may not be a practical size for ease of construction. In time of war there is also a real need for speed in designing. On the other hand, a graphical solution by the use of a nomograph allows a visual means of determining the effect of each variable so as to arrive at the optimum design for a particular installation.

Bearing these factors in mind, the windshield-ice-prevention nomograph, Fig. 2, was prepared. The following nomenclature corresponds to the symbols used in the development of the equations appearing on the nomograph:

NOMENCLATURE

- A = cross-sectional area of gap, sq ft
- b = windshield width, ft
- C_p = specific heat of air at constant pressure, Btu/lb deg F
- d = gap thickness, in.
- D_E = equivalent diameter of air passage between panels, ft
- f = friction factor for air flow, dimensionless
- g = acceleration of gravity, 4.17×10^8 ft per hr per hr
- G = weight flow of air per unit area, lb/(hr)(sq ft)
- h = average convection heat-transfer coefficient on cockpit side of inner panel, Btu/(hr)(sq ft) (deg F)
- h_i = average convection heat-transfer coefficient inside air gap, Btu/(hr) (sq ft) (deg F)
- h_0 = average convection heat-transfer coefficient over outer windshield surface, Btu/(hr) (sq ft) (deg F)
- k = thermal conductivity of each lamination, Btu/(hr) (sq ft) (deg F)/in.
- L = length of windshield parallel to direction of air flow in gap, in.
- l = thickness of each lamination, in.
- ΔP = total pressure drop of air in gap, in. water
- $\Delta P'$ = pressure drop of air in gap per foot of windshield length at sea level, in. water

P = perimeter of gap, ft

q_i = heat transferred through inner panel, Btu/(hr)(sq ft)

q_0 = heat transferred through outer panel, Btu/(hr) (sq ft)

R = Reynolds number, dimensionless

R_i = thermal resistance of inner panel, (deg F) (sq ft)/Btu/hr

R_0 = thermal resistance of outer panel, (deg F) (sq ft)/Btu/hr

T = average temperature of air in gap, deg R

Δt = temperature drop of circulating air in gap, deg F

Δt_{av0} = arithmetic temperature difference between average temperature of air in gap and outside air, deg F

$\Delta t_{av i}$ = arithmetic temperature difference between average temperature of air in gap and cockpit temperature, deg F

t_1 = entering circulating air temperature, deg F

t_2 = leaving circulating air temperature, deg F

U_0 = over-all heat-transfer coefficient across outer panel, Btu/(hr) (sq ft) (deg F)

U_i = over-all heat-transfer coefficient across inner panel, Btu/(hr)(sq ft) (deg F)

v_1 = specific volume of air at entrance and exit, respectively, of a duct, cu ft per lb

W = total air flow to windshield, lb per hr

w = air flow through windshield per foot of windshield width, lb per hr per ft

γ = weight density of air, lb per cu ft

γ_{avg} = average weight density of air in a duct, lb per cu ft

μ = absolute viscosity of air, lb/(hr)(ft)

THERMODYNAMIC ANALYSIS

An analysis of the thermodynamic design of an air-heated double-paneled windshield will now be made. The final equations derived during the course of the following analysis are found in nomographic form in Fig. 2.

Referring to Fig. 1, if the temperature rise of the outer surface over the outside air be denoted as Δt_0 , and if the average heat-transfer coefficient over this surface be denoted as h_0 , then the heat transferred from this surface to the outside air per square foot of surface is given by (3)

$$q_0 = h_0 \Delta t_0 \dots \dots \dots [1]$$

The heat transferred through the outer panel is identical with that as given in Equation [1]; therefore

$$q_0 = U_0 \Delta t_{av} \dots [2]$$

This is Newton's law of heat transfer through a solid wall from one fluid to another. In Equation [2] the arithmetic-mean temperature difference is used in place of the more correct logarithmic-mean temperature difference, introducing an error of less than 4 per cent (4), as will be explained later in the sample problem. The over-all heat-transfer coefficient U_0 is defined as

$$\frac{1}{U_0} = \frac{1}{h_i} + R_0 + \frac{1}{h_o} \dots [3]$$

The thermal resistance to heat transfer, R_0 , for a laminated panel depends on the thickness l , and thermal conductivity k , of each lamination, as

$$R_0 = \frac{l_1}{k_1} + \frac{l_2}{k_2} + \dots \frac{l_n}{k_n} \dots [4]$$

The heat-transfer coefficient inside the gap formed by the two panels is calculated (5) by the equation

$$h_i = 5.56 \times 10^{-4} T^{0.296} \frac{(G)^{0.80}}{D^{0.20}} \dots [5]$$

Although Equation [5] was developed for flow in pipes, it can be applied with reasonable accuracy to small rectangular ducts by the substitution of the equivalent diameter D_E for the pipe diameter D . Letting $w = \frac{W}{b}$, the air flow through the gap per foot of windshield width; then

$$G = \frac{W}{A} = \frac{W}{db} = \frac{12w}{d} \dots [6]$$

By definition the equivalent diameter for a rectangular duct is

$$D_E = \frac{4A}{P} = \frac{4 \times \frac{d}{12} \times b}{\frac{2d}{12} + 2b} \dots [7]$$

Since the gap width is very much smaller than the gap length, slight error will be introduced in dropping the $\left(\frac{2d}{12}\right)$ term from the denominator of the fraction in Equation [7]; therefore

$$D_E = \frac{d}{6} \dots [8]$$

Substituting Equations [6] and [8] into [5]

$$h_i = 5.56 \times 10^{-4} T^{0.296} \frac{\left(\frac{12w}{d}\right)^{0.80}}{\left(\frac{d}{6}\right)^{0.20}} \dots [9]$$

or

$$h_i = 58.1 \times 10^{-4} T^{0.296} \frac{w^{0.80}}{d} \dots [10]$$

Since the available pressure drop through the windshield determines the air flow, an expression will now be developed relating the pressure drop to the air flow and gap thickness.

The well-known Fanning equation for pressure drop in inches of water for a straight duct (3) is

$$\Delta P = 4f \frac{L}{D_E} \frac{G^2}{2g \gamma 5.2} + \frac{G^2}{5.2 \gamma_{av} g} \log_e \frac{v_2}{v_1} \dots [11]$$

Since the change in specific volume of the air as it passes through the windshield is negligible, the second term in the right side of Equation [11] may be omitted. Therefore

$$\Delta P = 4f \frac{L}{D_E} \frac{G^2}{2g \gamma 5.2} \dots [12]$$

Denoting the pressure drop per foot of windshield length as $\Delta P'$

$$\Delta P' = 4f \frac{1}{d} \frac{\left(\frac{12w}{d}\right)^2}{2g \gamma 5.2} \dots [13]$$

The friction factor f is given (3) by

$$f = \frac{0.046}{R^{0.20}} \dots [14]$$

where

$$R = \frac{GD_E}{\mu} = \frac{\frac{d}{12} \frac{w}{6}}{\mu} = \frac{2w}{\mu} \dots [15]$$

The values of γ and μ will be evaluated for sea-level altitude and at an average temperature of 200 deg F, which is the approximate average air temperature in the gap for the majority of the practical windshield designs (6). Therefore

$$\gamma = 0.060 \text{ lb per cu ft, and } \mu = 0.053 \text{ lb/(hr)(ft)}$$

Substituting the value of μ into Equation [15], evaluating the friction factor f , and then replacing f, γ , and g by their numerical values in Equation [13], this equation becomes

$$\Delta P' = 29.65 \times 10^{-8} \frac{w^{1.8}}{d^3} \dots [16]$$

Note that Equation [16] was developed for sea-level altitude and for a windshield length of 1 ft. It will be necessary to correct the chart value of $\Delta P'$ for the design altitude and windshield length under consideration.

It is now necessary to determine the amount of heat transferred into the cockpit through the inner panel, for the total temperature drop in the air passing through the gap depends on the total amount of heat transferred from the double panel. The over-all coefficient of heat transfer is calculated from the equation

$$\frac{1}{U_i} = \frac{1}{h_i} + R_i + \frac{1}{h} \dots [17]$$

The assumption is made that the convection-heat-transfer coefficient, h , on the cockpit side of the inner panel is equal to 1.65 Btu/(hr) (sq ft) (deg F) (7). Then the heat transferred through the inner panel from the air in the gap to the cockpit is

$$q_i = U_i \Delta t_{av} \dots [18]$$

where once again the arithmetic-mean temperature difference rather than the logarithmic-mean temperature difference is used.

Upon equating the total heat lost from the air in the gap to the

NOTE
 1. SAMPLE PROBLEM IS FOR COLUMN 1 OF TABLE
 2. DOTTED LINES INDICATE A TRANSFER OF A VALUE FROM
 ONE SCALE TO ANOTHER
 3. ARROWS MARKED THUS \rightarrow INDICATE STEPS OF SOLUTION

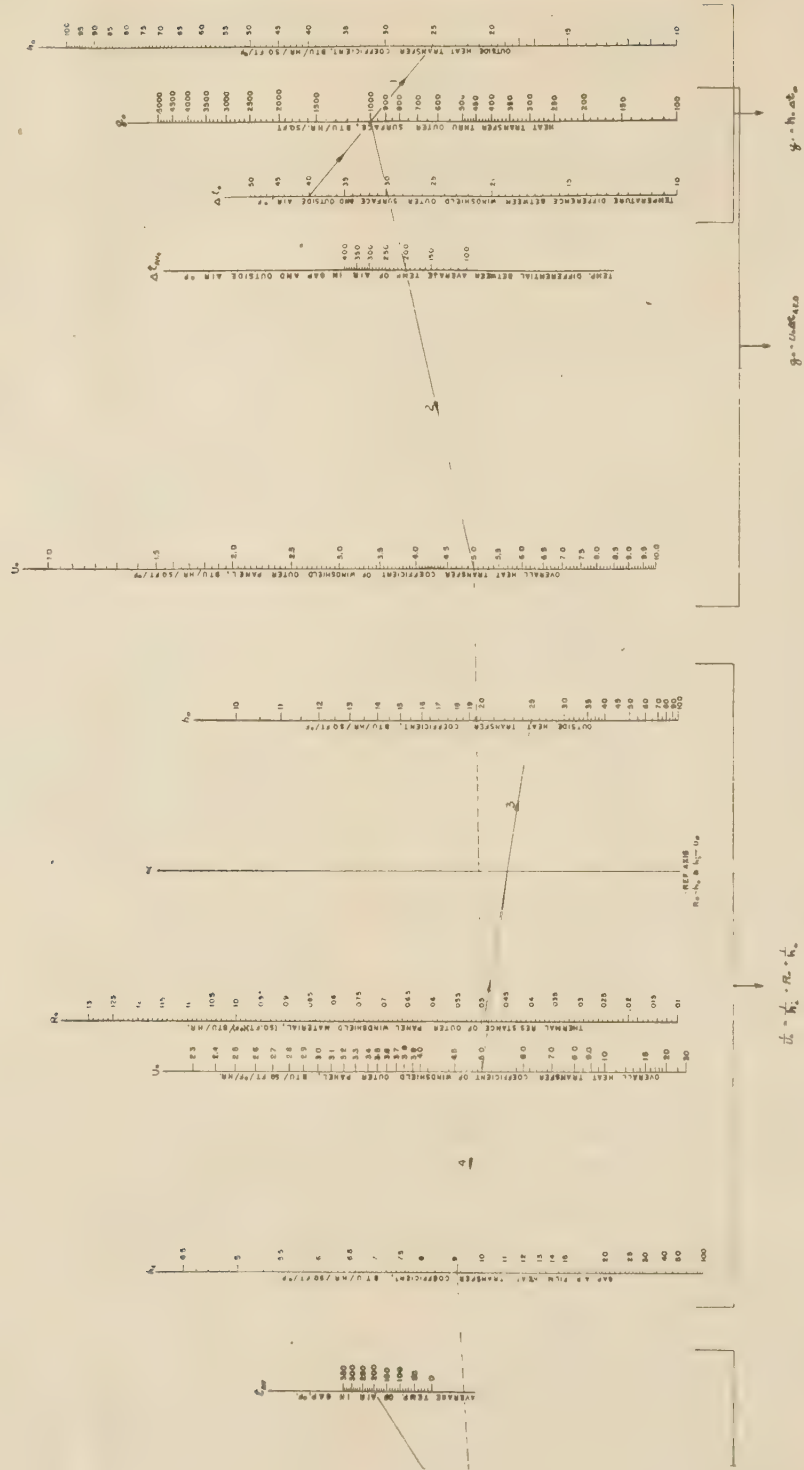
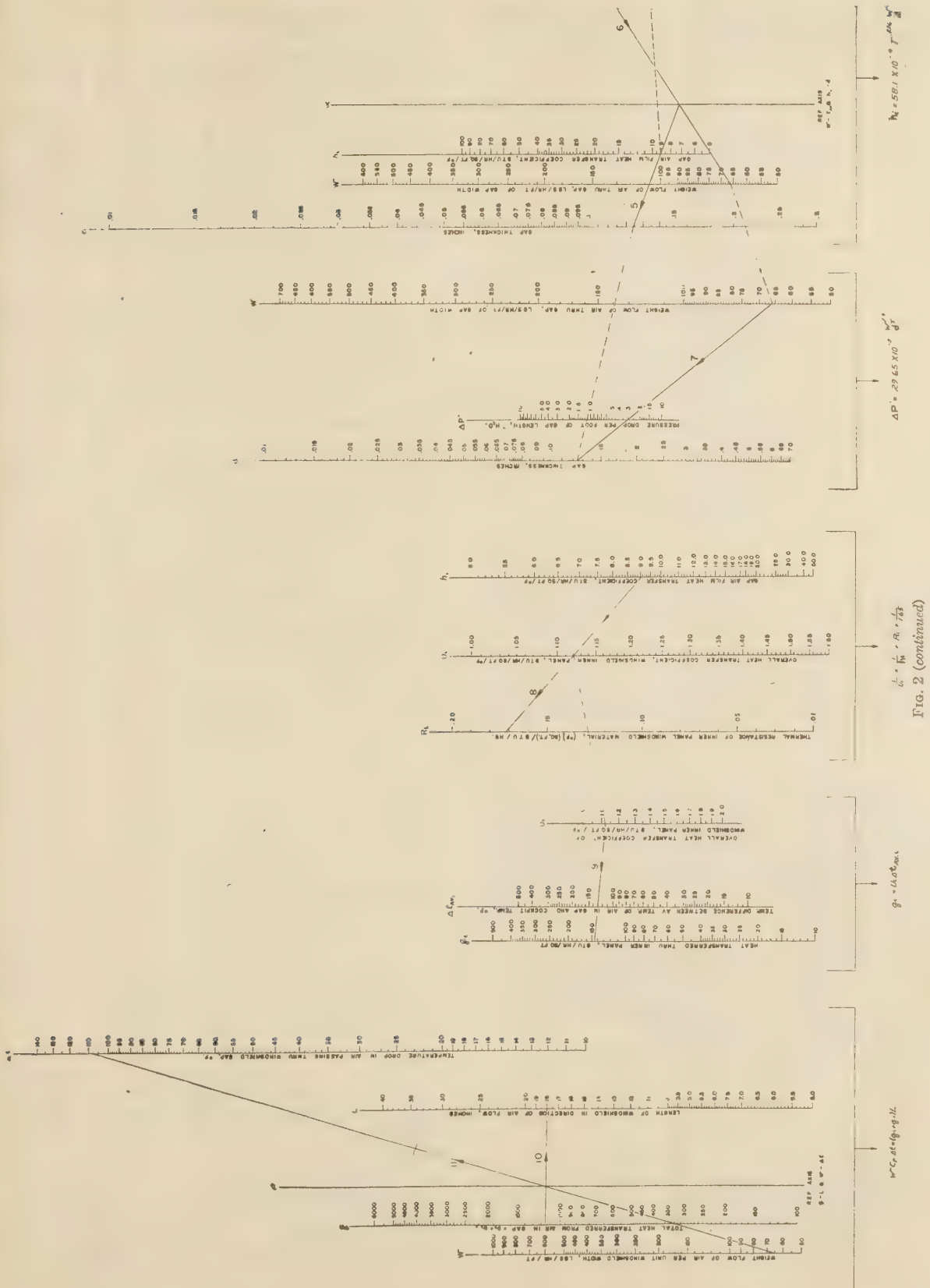


FIG. 2 WINDSHIELD ICE-PREVENTION NOMOGRAPH



total heat transferred through the double panel, the temperature drop in the circulating air can be calculated from

$$\Delta t = \frac{(q_i + q_o) \frac{L}{12}}{w C_p} \dots \dots \dots [19]$$

To recapitulate, the eight fundamental equations derived, which are in nomographic form in Fig. 2, are as follows

$$q_o = h_o \Delta t_o \dots \dots \dots [1]$$

$$q_o = U_o \Delta t_{av} \dots \dots \dots [2]$$

$$\frac{1}{U_o} = \frac{1}{h_i} + R_o + \frac{1}{h_o} \dots \dots \dots [3]$$

$$h_i = 58.1 \times 10^{-4} T^{0.296} \frac{w^{0.80}}{d} \dots \dots \dots [10]$$

$$\Delta P' = 29.65 \times 10^{-8} \frac{w^{1.8}}{d^5} \dots \dots \dots [16]$$

$$\frac{1}{U_i} = \frac{1}{h_i} + R_i + \frac{1}{h} \dots \dots \dots [17]$$

$$q_i = U_i \Delta t_{av} \dots \dots \dots [18]$$

$$\Delta t = \frac{(q_i + q_o) \frac{L}{12}}{w C_p} \dots \dots \dots [19]$$

It would be well to note that any additional surface temperature rise due to the phenomena of kinetic heating has been neglected in this analysis. Kinetic heating has been neglected for three reasons; (a) for speed of best range kinetic heating is a minimum; (b) the temperature rise depends on the specific heat of "wet" air, the value of which is not accurately known since the exact amount of water present in the air under icing conditions is unknown; and (c) the calculated value of the surface temperature by the nomograph will be conservative.

APPLYING THE NOMOGRAPH

In order to illustrate the use of the nomograph, a sample problem will be calculated by use of the eight equations just given and compared to a nomographic solution. However, before the design equations can be applied, certain data relating to materials and dimensions of the windshield, entering-air temperature, leaving-air temperature, air speed, and allowable pressure drop must be known or assumed. For a typical case these data are as follows:

- 1 For the outer panel (refer to Fig. 1)
 $l_1 = 0.125$ in., $k_1 = 7$ Btu/(hr)(sq ft)(deg F)/in. (8)
 $l_2 = 0.020$ in., $k_2 = 1.44$ Btu/(hr)(sq ft) (deg F)/in. (8)
 $l_3 = 0.125$ in., $k_3 = 7$ Btu/(hr)(sq ft) (deg F)/in. (8)
- 2 For the inner panel (refer to Fig. 1)
 $l = 0.250$ in., $k = 1.45$ Btu/hr sq ft deg F/in.
- 3 For the windshield dimensions

$$L = 18 \text{ in.}$$

$$b = 13 \text{ in.}$$

- 4 Entering-air temperature, $t_1 \geq 230$ deg F
- 5 Leaving-air temperature, $t_2 \geq 170$ deg F
- 6 For 25,000 ft altitude, minimum air speed is such that
 $h_o = 25$ Btu/(hr) (sq ft) (deg F); total allowable ΔP
 $= 1.85$ in. water
- 7 For sea level, maximum air speed is such that

$$h_o = 40 \text{ Btu/(hr)(sq ft) (deg F); total allowable } \Delta P$$

$$= 10 \text{ in. water}$$

$$8 \text{ Outside-air temperature} = 0 \text{ deg F}$$

$$9 \text{ Outer-surface temperature to be maintained} = 40 \text{ deg F}$$

$$10 \text{ Cockpit temperature} = 70 \text{ deg F}$$

The problem then resolves itself into finding what value of d in conjunction with w will provide the necessary surface temperature within the allowable pressure drop at 25,000 ft. At this altitude and at minimum speed the ram pressure is the smallest. Then with the gap size set, the maximum required heat input is determined from the maximum speed at sea level.

The solution of this problem proceeds in the following manner:

From Equation [1] at 25,000 ft

$$q_o = 25 \times 40 = 1000 \text{ Btu/hr sq ft}$$

Assume an average temperature of circulating air in gap of 200 F. Then from Equation [2]

$$U_o = \frac{1000}{(200 - 0)} = 5 \text{ Btu/(hr) (sq ft) (deg F)}$$

From Equation [4]

$$R_o = \frac{0.125}{7} + \frac{0.020}{1.44} + \frac{0.125}{7} = 0.0496 \text{ (deg F) (sq ft)/Btu/hr}$$

Therefore from Equation [3]

$$\frac{1}{h_i} = \frac{1}{5} - 0.0496 - \frac{1}{25} = 0.1104$$

$$h_i = 9.05 \text{ Btu/(hr) (sq ft) (deg F)}$$

Now, evaluating Equation [10], for $d = 1/8$ in. (assumption), and solving for w

$$T^{0.296} = (460 + 200)^{0.296} = 6.81$$

$$w^{0.80} = \frac{0.125 \times 9.05 \times 10^4}{58.1 \times 6.81} = 28.6$$

$$w = 66 \text{ lb per hr per ft}$$

Total air flow to the windshield is

$$W = 66 \times \frac{13}{12} = 71.5 \text{ lb per hr}$$

Now from Equation [16]

$$\Delta P' = 29.65 \times 10^{-8} \frac{(66)^{1.8}}{(0.125)^5} = 0.289 \text{ in. water for sea-level altitude}$$

For 25,000 ft altitude, the total pressure drop is

$$\Delta P = \Delta P' \left(\frac{29.92}{11.1} \right) \left(\frac{L}{12} \right)$$

where 29.92 = standard atmospheric pressure at sea level, in. Hg; and 11.1 = standard atmospheric pressure at 25,000 ft, in. Hg.

Solving

$$\Delta P = 0.289 \times 2.69 \times 1.5 = 1.165 \text{ in. water}$$

which is less than that available.

$$\text{Now } R_i = \frac{0.250}{1.45} = 0.1725 \text{ (deg F) (sq ft)/Btu/hr}$$

TABLE 1 DATA FOR SAMPLE PROBLEM SOLUTION FROM NOMOGRAPH, FIG. 2
Windshield length, $L = 18$ in. Windshield width, $b = 13$ in.

Column No.	1	2	3	4	5	6	7	8
Altitude	25000'	25000'	25000'	25000'	25000'	S.L.	S.L.	S.L.
Outside Air Temperature, °F	0	0	0	0	0	0	0	0
Outside Average Heat Transfer Coefficient, h_o	25	25	25	25	25	40	40	40
Surface Temperature To Be Maintained, °F	40	40	40	40	40	40	40	40
Heat Transferred Through Outer Panel, q_o	1000	1000	1000	1000	1000	1600	1600	1600
Average Temperature Of Circulating Air In Gap, t_{av} , °F	200	185	190	180	200	200	205	210
Over-all Coefficient Of Heat Transfer, U_o	5.0	5.4	5.26	5.55	5.0	8.0	7.80	7.63
Thermal Resistance Of Outer Panel, R_o	.0496	.0496	.0496	.0496	.0496	.0496	.0496	.0496
Inside Convection Heat Transfer Coefficient In Gap, h_i	9.05	10.6	10	11.0	9.05	20.5	19.0	17.6
Gap Width, d , in inches	1/8	1/8	5/32	3/32	3/16	1/8	5/32	3/16
Air Flow Per Foot, W	66	82	100	60	110	185	220	250
Pressure Drop Per Foot, $\Delta P'$.29	.42	.35	.60	.23	1.90	1.30	.96
Total Pressure Drop At The Altitude Considered, ΔP	1.17	1.70	1.42	2.43	.927	2.85	1.95	1.44
Thermal Resistance Of Inner Panel, R_i	.1725	.1725	.1725	.1725	.1725	.1725	.1725	.1725
Over-all Coefficient Of Heat Transfer, U_i	1.12	1.14	1.13	1.145	1.126	1.20	1.193	1.190
Heat Transferred Through Inner Panel, q_i	145	132	135	125	145	157	162	170
Total Temperature Drop In Circulating Air, Δt , °F	108	88	70	118	68	60	50	44
Entering Air Temperature, t_1 , °F	254	229	225	239	234	230	230	232
Leaving Air Temperature, t_2 , °F	146	141	155	121	166	170	180	188
Heater Requirement Assuming a 250 °F Rise						12,000	14,300	16,200

and from Equation [17]

$$\frac{1}{U_i} = \frac{1}{9.05} + 0.1725 + \frac{1}{1.65} = 0.8889$$

$$U_i = 1.125 \text{ Btu/(hr) (sq ft) (deg F)}$$

Then by Equation [18], for a cockpit temperature of 70 F

$$q_i = 1.125 (200 - 70) \\ = 146 \text{ Btu/(hr) (sq ft)}$$

The total temperature drop in the gap is, from Equation [19]

$$\Delta t = \frac{(1000 + 146)(1.50)}{66 \times 0.24} = 108.5 \text{ deg F}$$

Hence the entering-air temperature must be

$$t_1 = 200 + \frac{108.5}{2} = 254.2 \text{ deg F}$$

and

$$t_2 = 200 - \frac{108.5}{2} = 145.7 \text{ deg F}$$

It is noticed that the entering-air temperature t_1 is higher than the maximum allowed. Therefore the complete problem

must be recalculated, assuming a lower average gap air temperature until all conditions are satisfied.

The solution for this same problem is shown in Fig. 2 and tabulated in Table 1, column 1. Good agreement is noticed when the chart values are compared with the calculated values.

A simple calculation will show the validity of using the arithmetic-mean rather than the logarithmic-mean temperature difference. Referring to Fig. 3 the temperature difference (Δt_i) between the entering-air temperature and outside-air temperature is 254 deg F, and for the exit condition, $\Delta t_2 = 146$ deg F. From refer-

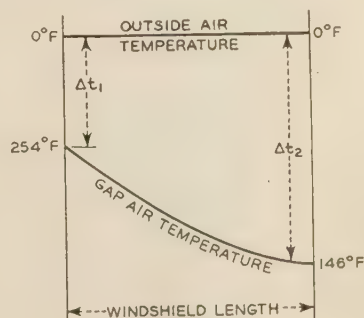


FIG. 3 CURVE OF TEMPERATURE DIFFERENCES

ence (4), the logarithmic-mean temperature difference is given by

$$\Delta t_{LM} = \frac{\Delta t_1 - \Delta t_2}{\log_e \frac{\Delta t_1}{\Delta t_2}} = \frac{254 - 146}{\log_e \frac{254}{146}} = 195 \text{ deg F}$$

The arithmetic-mean temperature difference would be

$$\Delta t_{av0} = \frac{254 - 146}{2} = 200 \text{ deg F}$$

Error = $2\frac{1}{2}$ per cent.

Table 1 has been prepared by the use of the nomograph, Fig. 2, to illustrate one method of determining the correct gap size and air flows. This method is to assume various gap sizes and, in conjunction with the desired outer-surface temperature, solve for the required air flows and circulating-air temperatures. Column 2 is a corrected version of column 1, indicating that the average temperature of the circulating air should be 185 deg F, instead of 200 deg F in order that the design conditions be satisfied. Other gap sizes were then assumed as indicated in columns 3, 4, and 5, and the problem again solved, the results indicating that, at 25,000 ft, a $\frac{3}{32}$ -in. gap is out of the question due to the high

pressure drop but that a $\frac{1}{8}$, $\frac{5}{32}$, or $\frac{3}{16}$ -in. gap may be satisfactory. Columns 6, 7, and 8 prove that at sea level a $\frac{1}{8}$ -in. gap is more to be desired than either of the larger gaps because of the lower heat requirement and lower exit-air temperature from the windshield.

Another method of solving the sample problem, by use of the nomograph, Fig. 2, is to determine the maximum air flows for various gap sizes from the available pressure and to solve for the resulting outer-surface temperature, choosing the gap size which satisfies the design conditions. By this method Table 2 was prepared. Referring to the design requirements of the preceding sample problem, the pressure available at an altitude of 25,000 ft is 1.85 in. of water. This corresponds to a pressure drop at sea level per foot of windshield length of

$$\Delta P' = 1.85 \left(\frac{11.1}{29.92} \right) \left(\frac{12}{18} \right) = 0.457 \text{ in. water}$$

This pressure drop determines the air flow through the windshield which, in turn, determines the outer-surface temperature. In Table 2, column 1 shows that a $\frac{3}{32}$ -in. gap does not give the required 40 deg F surface temperature, but that this temperature rise is realized by a $\frac{1}{8}$, $\frac{5}{32}$, or $\frac{3}{16}$ -in. gap size, as shown by columns 2, 3, and 4.

If the air flow through the windshield were determined by the comparatively large amount of pressure available under sea-level flying conditions, an oversized heating system would result.

TABLE 2 DATA FOR ALTERNATIVE SOLUTION OF PROBLEM
Windshield length, $L = 18$ in. Windshield width, $b = 13$ in.

Column No.	1	2	3	4	5	6	7	8
Altitude	25000'	25000'	25000'	25000'	S.L.	S.L.	S.L.	S.L.
Outside Air Temperature, °F	0	0	0	0	0	0	0	0
Total Pressure Drop At Altitude Considered, ΔP	1.85	1.85	1.85	1.85	2.85	1.95	1.44	2.85
Pressure Drop Per Foot Corrected To Sea Level, ΔP'	.457	.457	.457	.457	1.90	1.30	.95	1.90
Assumed Gap Size, d	3/32	1/8	5/32	3/16	1/8	5/32	3/16	1/8
Air Flow, W PER FOOT	51	86	120	163	185	220	250	185
Average Temperature Of Circulating Air In Gap, t _{av} , °F	175	185	190	190	200	175	210	185
Inside Convection Heat Transfer Coefficient In Gap, h _i	9.9	11.0	11.4	12.2	12.5	13.3	17.6	10.45
Thermal Resistance Of Outer Panel, R _o	.0496	.0496	.0496	.0496	.0496	.0496	.0496	.0357
Outside Average Heat Transfer Coefficient, h _o	25	25	25	25	40	40	40	40
Over-all Coefficient Of Heat Transfer - Outer Panel, U _o	5.21	5.60	5.65	5.80	5.6	5.8	7.63	4.1
Heat Transferred Through Outer Panel, q _o	910	1040	1075	1160	1600	1600	1600	1775
Surface Temperature, °F	36.4	41.6	43	46.4	40	40	40	44.5
Thermal Resistance Of Inner Panel, R _i	.1725	.1725	.1725	.1725	.1725	.1725	.1725	.0496
Over-all Coefficient Of Heat Transfer, Inner Panel, U _i	1.13	1.145	1.148	1.153	1.20	1.193	1.19	1.41
Heat Transferred Through Inner Panel, q _i	116	131	136	150	157	162	170	180
Temperature Drop In Circulating Air, Δt, °F	118	88	64	50	60	50	44	70
Entering Air Temperature, t ₁ , °F	204	209	222	225	230	230	232	230
Leaving Air Temperature, t ₂ , °F	110	141	158	175	170	180	188	160
Heater Requirement Assuming a 250°F Rise					12,000	14,300	16,200	12,000

Hence the maximum required heater capacity should be based on an adequate outer-surface temperature and the gap size as determined by the minimum available pressure at the critical altitude (25,000 ft in this sample problem). A manual or automatic temperature control of the heater-outlet temperature must be provided by utilizing, through a valve or damper, the excess ram pressure at the low altitudes. Thus the maximum heat requirement was determined by method 1 as tabulated in Table 1. Columns 5, 6, and 7 of Table 2 were merely copied from columns 6, 7, and 8 of Table 1.

Another windshield configuration worthy of consideration is to design the required impact strength into the inner windshield panel and to construct the outer panel of one sheet of tempered glass. By this arrangement a higher outer-surface temperature can be maintained due to the decreased thermal resistance of the outer panel. As an example of such a design the sample problem was again solved by the windshield ice-prevention nomograph, assuming that the laminated panel replaces the plexiglas inner panel, and that the outer panel is constructed from a sheet of $\frac{1}{4}$ -in. tempered glass. Referring to column 8 of Table 2, a 4.5-deg F higher surface temperature rise was obtained using the same $\frac{1}{8}$ -in. gap size and air flow, with a further desired reduction in the leaving-air temperature of the circulating air.

CONCLUSION

The paper demonstrates that a logical method of solution for windshield heat deicing problems may be derived from a nomograph. One of its most important features is the saving of time in making a detailed design analysis of such an installation. As quick as two points can be connected with a straightedge the equation is solved with the position of the decimal point already ascertained. Of course a knowledge of the design equations is necessary for a complete understanding of this type of problem, but once the background study is completed, a graphical solution is required to alleviate the monotony of making the same calculation over and over for each proposal.

Inasmuch as the exact heat requirement needed to keep the windshield outer surface at a specified temperature in icing con-

ditions is not accurately known, an installation designed without the benefit of kinetic heating should prove successful in adverse weather. Also, the possibility of constructing the outer panel of tempered glass and designing the required structural strength into the inner panel should not be overlooked because of the increased heat-transmission quality of this type of outer panel. The smallest gap size possible within the limits of the problem is to be desired, as the required heater size and exit-air temperature are kept to a minimum when the windshield is designed as the most efficient heat exchanger possible.

It may therefore be seen that an air-heated windshield is more than just two panes of glass, the gap of which is assumed and to which only the excess air from the cockpit heating system is allowed to be utilized. It is hoped that this windshield ice-prevention nomograph will be of some benefit to the aircraft engineer as a timesaver.

BIBLIOGRAPHY

- 1 "Recent Flight Tests Research on Ice Prevention," by L. Rodert, L. A. Clausing, and W. H. McAvoy, N.A.C.A. ARR, January, 1942.
- 2 "An Investigation of Aircraft Heaters, VIII—A Simplified Method for the Calculation of the Unit Thermal Conductance Over Wings," by R. C. Martinelli, A. G. Guibert, E. H. Morrin, and L. M. K. Boelter, University of California, N.A.C.A. ARR, March, 1943.
- 3 "Heat Transmission," by W. H. McAdams, McGraw-Hill Book Company, Inc., New York, N. Y., second edition, 1942.
- 4 "Applied Heat Transmission," by H. J. Stoeve, McGraw-Hill Book Company, Inc., New York, N. Y., first edition, 1941.
- 5 "An Investigation of Aircraft Heaters, III—Measured and Predicted Performance of Double Tube Heat Exchangers," by R. C. Martinelli, E. B. Weinberg, E. H. Morrin, and L. M. K. Boelter, University of California, N.A.C.A. ARR, October, 1942.
- 6 "An Investigation of Aircraft Heaters, II—Properties of Gases," by Myron Tribus and L. M. K. Boelter, University of California, N.A.C.A. ARR, October, 1942.
- 7 "Thermal Resistance of Air Spaces," by F. B. Rowley and A. B. Algren, A.S.H.V.E. Trans., vol. 35, 1929, p. 165.
- 8 Technical Glass Bulletin No. 8, Pittsburgh Plate Glass Company, Pittsburgh, Pa.

An Acceleration Damper: Development, Design, and Some Applications¹

BY PAUL LIEBER² AND D. P. JENSEN²

An acceleration damper is essentially an impact damper, consisting of a mass particle within a container such that the particle has specified freedom to move relative to the container. The efficiency of the damper depends critically on the freedom of the particle relative to its container. The energy of the mass particle, which is energized by its container, is dissipated in impact. The mechanism and theory of the acceleration damper are discussed and developed in this paper. The theory yields formulas from which the acceleration damper can be designed efficiently for specific application. Theory and procedure for calculating the motion of a mechanical system, as influenced by a given acceleration damper, are developed. Tests were conducted and the agreement between theory and experiment is found to be good. These results show that friction forces acting on the mass particle are detrimental to the efficiency of the damper. Finally, a method for calculating the effect of the acceleration damper on flutter is also developed, which is accompanied by numerical results related to an actual airplane. It is indicated that the acceleration damper may have fundamental and numerous applications, some of which are fatigue, helicopter vibration control, aircraft vibration control in general, and to facilitate flight testing for flutter without endangering aircraft.

NOMENCLATURE

The following nomenclature is used in the paper:

- θ = phase angle between damped system and mass particle
- x = rectilinear co-ordinate of mechanical system, ft
- s = curvilinear co-ordinate of mechanical system, ft
- x_0 = maximum rectilinear amplitude of system, undergoing simple harmonic motion, ft
- d = free path of mass particle in its container, ft
- K = spring constant of schematic mechanical system, lb per ft
- M = mass of schematic mechanical system in slugs
- m = mass of free particle of acceleration damper in slugs
- t = time variable, sec
- ω = frequency of oscillation, radians per sec
- $F_p(t)$ = force exerted on vibrating system by mass particle
- s_0 = maximum curvilinear amplitude of system, ft
- $f(\omega t)$ = unit step function whose periodicity is a function of θ

- T = period of impulse
- $\delta(t - RT)$ = a Dirac function used to represent impulse effect of free particle, and is finite for $t = RT$
- $(x_0\omega - \dot{x})$ = relative velocity of m and M
- $R = (1, 2, 3, \dots, \infty)$
- N = number of impacts per cycle
- $P(t)$ = energy supplied by exciting force $F(t)$ to maintain constant vibration amplitude x_0 or s_0
- \bar{d} = acceleration damping coefficient
- c = viscous damping coefficient

INTRODUCTION

The typical unit of the acceleration damper is essentially an impact damper consisting of a mass particle given freedom to move relative to the periodic motion being damped (see Figs. 4, 5, and 6). In what follows such relative motion will be described by the phase angle θ . The damping force is proportional to the absolute acceleration of the damper. In order to design the acceleration damper efficiently and to apply it effectively, its mechanism is investigated and its effect is quantized by some theoretical and semiempirical considerations set forth in this paper. The efficiency of the damper is a function of the phase angle θ between the motion of the mass particle, and the motion that is being damped by it. It is emphasized that in the acceleration damper each particle moves in a separate channel with purpose of minimizing friction forces on the particle. Dampers containing fine multiparticles in a single container have been compared experimentally to the acceleration damper, and they were found to be relatively inefficient. It is believed that the inefficiency of the multiparticle dampers is caused by the friction forces acting between particles contained therein. This conclusion is borne out in Figs. 11, 12, and 13.

In practice a finite phase angle can be realized by inserting a mass particle in a channel fixed to the moving body, the depth of which exceeds the principal dimension of the particle. The magnitude of the phase angle is determined by the dimensions of the particle, depth of channel, and the amplitude of oscillation. It is independent of frequency. In a sense then, one can represent the effect of the phase angle on the damping unit by an equivalent damping coefficient for a given amplitude of oscillation. The damping coefficient is then a function of the periodic amplitude and is independent of frequency. The theory is developed for rectilinear motion. However, the theoretical results are also applicable to curvilinear motion by replacing the rectilinear amplitude x_0 by the curvilinear amplitude s_0 .

The following applications are indicated and warrant experimental investigation:

- 1 Facilitate flight testing for flutter without endangering aircraft
- 2 Fatigue control of primary and secondary structures
- 3 Reduction of vibration amplitude associated with buffeting
- 4 Control of vibration effects associated with compressibility
- 5 Control of helicopter vibration
- 6 General vibration control.

One of the useful features of this damper is that from its very nature it can be installed to provide a system of uniformly dis-

¹ The material of this paper is based on a Douglas Company Report, Santa Monica 8195, issued April 4, 1944, by co-authors Paul Lieber and D. P. Jensen, and on a Technical Memorandum issued by the company dealing with the solution of a vibration problem.

² Douglas Aircraft Company, Inc., Santa Monica Plant, Santa Monica, Calif.

Contributed by the Aviation and Applied Mechanics Divisions and presented at the Annual Meeting, New York, N. Y., Nov. 27-Dec. 1, 1944, of THE AMERICAN SOCIETY OF MECHANICAL ENGINEERS. Also presented at the Meeting of the A.S.M.E. Aviation Division, Los Angeles, Cal., June 11-14, 1945.

NOTE: Statements and opinions advanced in papers are to be understood as individual expressions of their authors and not those of the Society.

tributed damping forces and thereby have little effect on the modes of oscillation themselves. Since the damping force is a function of absolute acceleration its installation is simple.

This paper considers some theoretical aspects of the acceleration damper itself and gives a formula enabling one to use empirical damping data in theoretical investigations of flutter and vibration phenomena. The elastic rebound between the mass particle and its container is assumed to be zero.

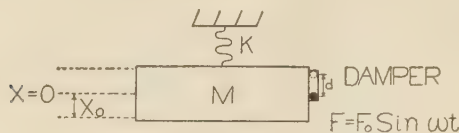


FIG. 1

THEORY

Consider an acceleration damper installed on an inertia elastic system having one degree of freedom, being forced periodically by $F(t)$, such that a steady-state simple harmonic motion is maintained. It is imagined that a power supply $P(t)$ exists, necessary to maintain such motion. The work done by the mass particle on the M and K system in a complete cycle is given by the integral

$$\int_0^{2\pi/\omega} F_p(t) \cdot \frac{dx}{dt} dt = \int_0^{2\pi/\omega} F_p(t) \cdot \dot{x} dt \dots [1]$$

where

$F_p(t)$ = force exerted on vibrating system by mass particle m when in contact with M

ω = frequency of oscillation, radians per sec

x = position of system

x_0 = maximum amplitude of system

t = time variable

M = mass of system

K = spring constant of system

$F_e(t)$ = periodic exciting force

Since M undergoes simple harmonic motion the terms $F_p(t)$ and \dot{x} of the integral in Equation [1] are illustrated graphically in Fig. 2.

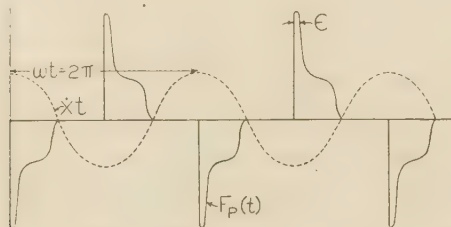


FIG. 2

It is clear that due to the discontinuities in the function $F_p(t)$ the integral in Equation [1] is finite, i.e., $F_p(t)$ is dissipative. In maintaining a constant amplitude of oscillation it is therefore necessary to provide a constant and finite power input $P(t)$ over a cycle.

Since, as will be shown, the effective damping coefficient of an acceleration damper is completely determined for a constant amplitude x_0 by the phase angle θ between the motion of the mass particle m and the mass M , the following analysis is based on steady-state simple harmonic motion. This analysis will bear out the nature of the dissipative forces as well as provide a for-

mula for calculating the efficiency of the damper as a function of the phase angle θ .

Consider the work done by the system of forces acting on the mass M over one cycle

$$\int_0^{2\pi/\omega} Kx\dot{x}dt + \int_0^{2\pi/\omega} M\ddot{x}\dot{x}dt + \int_0^{2\pi/\omega} m\ddot{x}f(\omega t)dt + \sum_R \int_0^{2\pi/\omega} m(x_0\omega - \dot{x})\delta(t - RT)\dot{x}dt = \text{work done per cycle} \dots [2]$$

For a brief discussion of the Dirac function refer to work by Carslaw and Jaeger.³ The effect of the acceleration damper is represented in two integrals in Equation [2]. The integral

$\int_0^{2\pi/\omega} m\ddot{x}f(\omega t)dt$ is the work done by the particle on M after exerting its impact. When the particle is in contact with M , $f(\omega t) = -1$, and when particle is free, $f(\omega t) = 0$. The work exerted by the particle on M upon establishing contact with it is represented by the integral

$$\int_0^{2\pi/\omega} m(x_0\omega - \dot{x})\delta(t - RT)dt$$

if the motion is simple harmonic, then

$$\left. \begin{aligned} x &= x_0 \sin \omega t \\ \dot{x} &= \omega x_0 \cos \omega t \\ \ddot{x} &= -\omega^2 x_0 \sin \omega t \end{aligned} \right\} \dots [3]$$

Substituting Equation [3] in Equation [2] gives

$$K \int_0^{2\pi/\omega} x_0 \sin \omega t \cdot x_0 \omega \cos \omega t dt + M \int_0^{2\pi/\omega} -\omega^2 x_0 \sin \omega t \cdot \omega x_0 \cos \omega t dt + m \int_0^{2\pi/\omega} -\omega^2 x_0 \sin \omega t \cdot \omega x_0 \cos \omega t f(\omega t) dt + m \int_0^{2\pi/\omega} (x_0\omega - x_0\omega \cos \omega t) \cdot \delta(t - RT) x_0 \omega \cos \omega t dt = \left| \int_0^{2\pi/\omega} W \dots [4] \right|$$

work done per cycle.

The first two integrals in Equation [4] vanish and the work done is determined by the remaining integrals whose values depend only on the design and efficiency of the acceleration damper. Equation [4] reduces to

$$-m\omega^2 x_0^2 \int_0^{2\pi/\omega} \sin \omega t \cdot \cos \omega t f(\omega t) dt + m x_0^2 \omega^2 \int_0^{2\pi/\omega} (1 - \cos \omega t) \delta(t - RT) \cos \omega t dt = \left| \int_0^{2\pi/\omega} W \dots [5] \right|$$

The first integral can be readily evaluated for a given phase angle θ since the phase angle completely defines the function $f(\omega t)$ which is illustrated in Fig. 3.

By integrating $\int_0^{2\pi/\omega} \sin \omega t \cdot \cos \omega t f(\omega t) dt$ for a time interval in which $f(\omega t)$ is unity, and which is defined by θ , the contribution of the term $-m\omega^2 x_0^2 \sin \omega t \cdot \cos \omega t f(\omega t) dt$ to $\int_0^{2\pi/\omega} W$ can be readily calculated. It is

$$+ m\omega^2 x_0^2 \left| \int_0^{2\pi/\omega} \frac{1}{2} \sin^2(\omega t) dt \right| = -\frac{m\omega^2 x_0^2}{2} \sin^2 \theta \dots [6]$$

³ "Operational Methods in Applied Mathematics," by H. S. Carslaw and J. C. Jaeger, Oxford University Press, London, England, 1941, appendix 3.

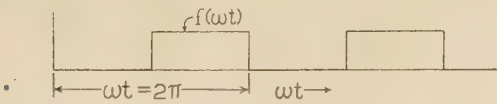


FIG. 3

The contribution of the second term in Equation [5] to the work done can be calculated as follows:

Let
$$(1 - \cos \omega t) \cos \omega t = (\cos \omega t - \cos^2 \omega t) = \mu(t)$$

then the second integral in Equation [5] can be written in the form

$$m x_0^2 \omega^2 \int_0^{2\pi/\omega} \mu(t) \delta(t - RT) dt$$

One of the important properties of a Dirac function defined by the relations

$$\left. \begin{aligned} \delta(x) &= 0, x \leq 0 \\ &= 1/\epsilon, 0 < x < \epsilon \\ &= 0, x \geq \epsilon \end{aligned} \right\} \dots\dots\dots [7]$$

is that for a continuous function $f(t)$

$$\sum_{R=0}^{\infty} \int_{-\infty}^{\infty} f(t) \delta(t - RT) dT = \sum_{R=0}^{\infty} \frac{1}{\epsilon} \int_{RT}^{RT+\epsilon} f(t) dt = \sum_{R=0}^{\infty} f(RT + \phi\epsilon) \dots\dots [8]$$

The integral is finite for

$$t = RT, R = t/T$$

where

$$0 < \phi < 1$$

Since $f(t)$ is a continuous function

$$\lim_{\epsilon \rightarrow 0} \sum_{R=0}^{\infty} f(RT + \phi\epsilon) = \sum_{R=0}^{\infty} f(RT) \dots\dots\dots [9]$$

Letting $f(RT)$ correspond to $\mu(t)$ in the foregoing expression, it follows from Equations [7] and [8] that

$$m x_0^2 \omega^2 \int_0^{2\pi/\omega} \mu(t) \delta(t - RT) dt = m x_0^2 \omega^2 N \mu(RT) \Big|_0^{2\pi/\omega} \dots [10]$$

where N is the number of impacts per cycle. Combining Equations [6] and [10] leads to the following simple expression for the work done by the acceleration damper over one cycle

$$W \Big|_0^{2\pi/\omega} = - \frac{N m \omega^2 x_0^2}{2} \sin^2 \theta + m x_0^2 \omega^2 N \mu(RT) \Big|_0^{2\pi/\omega} \dots [11]$$

where N is equal to the number of hits the mass particle experiences per revolution. The first term in Equation [11] represents the work done by the particle in moving alternately with and leaving the mass M of the system. The second term is the work done by the impact force of the mass particle m on M .

PERIODICITY OF CONTACT

By periodicity of contact is meant the time elapsed between successive contacts of the particle m with M . As a preliminary to calculating the periodicity of contact, consider the time elapsed in which the mass particle m leaves M and re-establishes contact with M ; (if the motion is simple harmonic, i.e., $x = x_0 \sin \omega t$) it is

$$T_{n+1} = \frac{d + \int_{n\pi/\omega}^{T_{n+1}} \dot{x} dt}{x_0 \omega} = \frac{d + x_0 \int_{n\pi/\omega}^{T_{n+1}} \cos \omega t dt}{x_0 \omega} \dots [12]$$

where

- (1) d is the length of the free path of the mass particle m
- (2) the notations n and $n + 1$ are used to denote sequence in terms of an arbitrary cycle n . In particular n could be taken equal to zero

$$T_{n+1} = \frac{d + \int_{n\pi/\omega}^{T_{n+1}} x_0 \sin \omega t}{x_0 \omega} = \frac{d + x_0 \sin \omega T_{n+1}}{x_0 \omega}$$

$$d = x_0 (\omega T_{n+1} - \sin \omega T_{n+1}) = x_0 (\theta_{n+1} - \sin \theta_{n+1}) \dots [13]$$

Equation [13] can be used for designing efficient acceleration dampers, since it gives a simple relationship between a desired angle θ and the depth of channel d in terms of x_0 .

In calculating the periodicity of contact for a constant amplitude it is convenient to consider the following two cases separately:

Case (1): $\theta < 180$ deg

$$T_c = \frac{d + \int_{n\pi/\omega}^{T_{n+1}} \dot{x} dt}{x_0 \omega} + \left[\frac{(n+1)\pi}{\omega} - T_{n+1} \right] \dots [14]$$

where T_c is the periodicity of contact.

But

$$\begin{aligned} \frac{d + \int_{n\pi/\omega}^{T_{n+1}} \dot{x} dt}{x_0 \omega} &= T_{n+1} \\ \therefore T_c &= \frac{(n+1)\pi}{\omega} \dots\dots\dots [15] \end{aligned}$$

Since n is arbitrary, let $n = 0$ in Equation [15]

$$T_c = \frac{\pi}{\omega}$$

That is for $\theta < 180$ deg the particle m will contact M two times per cycle.

Case (2): $\theta > 180$ deg

There exists a phase angle $\theta < 180$ deg for which the work done per impact is equal to that done by a corresponding $\theta > 180$ deg. In other words, for the work done for phase angles $\theta_n > 180$ deg there exists a corresponding phase angle in the first two quadrants for which the work is the same. It follows therefore that the phase angle giving greatest damping efficiency for a single contact can be determined in the first two quadrants, i.e., $\theta < 180$ deg. Furthermore, since for $\theta < 180$ deg the periodicity of contact is 2, and for $\theta > 180$ deg it is less than 2, it follows from Equation [11] that the phase angle corresponding to maximum energy dissipation per cycle must be < 180 deg.

A CRITERION FOR DETERMINING PHASE ANGLE θ , GIVING MAXIMUM DAMPING EFFICIENCY

In the foregoing discussion it was shown that θ_e must be ≤ 180 deg. This simplifies the problem of determining θ_e for a given amplitude of oscillation. Equation [11] can be written in the form

$$W \bigg|_0^{2\pi/\omega} = -\frac{Nm\omega^2 x_0^2}{2} \sin^2 \theta + mx_0^2 \omega^2 N (\cos \omega RT - \cos^2 \omega RT) \quad [16]$$

for $0 < \theta < 180$ deg, then $T_e = \frac{\pi}{\omega}$ (see Equation [15] letting $n=0$).

Since there are two hits per cycle, $N = 2$ and Equation [16] can be written in the form

$$W \bigg|_0^{2\pi/\omega} = -m\omega^2 x_0^2 \sin^2 \theta + 2mx_0^2 \omega^2 (\cos \theta - \cos^2 \theta) = -m\omega^2 x_0^2 (1 - \cos \theta)^2 \dots [17]$$

It is interesting to note that Equation [17] for the work done by the power supply can be arrived at directly by calculating the loss in kinetic energy of the mass particle per impact. It is

$$W = -\frac{1}{2}m(\dot{x}_1 - \dot{x}_2)^2 \dots [17a]$$

where

- \dot{x}_1 = absolute velocity of mass particle m
- \dot{x}_2 = absolute velocity of container

for simple harmonic motion, and considering two impacts per cycle Equation [17a] reduces to

$$W \bigg|_0^{2\pi} = -m\omega^2 x_0^2 (1 - \cos \theta)^2 \dots [17b]$$

which is in agreement with Equation [18].

The reason for using the momentum approach for arriving at Equation [18] is to give a clear step-by-step picture of the mechanism of the acceleration damper and thereby facilitate handling of transient cases, effect of rebound, and extension of theory to modified cases.

The phase angles θ_e giving maximum and minimum damping efficiency can be determined by differentiating Equation [17] with respect to θ and equating the result to zero. Differentiating Equation [17] and equating to zero gives

$$\begin{aligned} \frac{dW}{d\theta} \bigg|_0^{2\pi} &= -m\omega^2 x_0^2 [2 \sin \theta \cos \theta - 4 \sin \theta \cos \theta + 2 \sin \theta] \\ &= -2x_0 m \omega^2 \sin \theta [1 - \cos \theta] = 0 \dots [18] \end{aligned}$$

This is satisfied by $\theta = 0$ and $\theta = \pi$, which corresponds to minimum and maximum damping efficiency, respectively. Applying this result to Equation [13] we obtain $d_e = x_0 \pi$, where d_e is the free path of m corresponding to maximum damping efficiency. Equation [17] shows that the damping efficiency increases continuously from $\theta = 0$ to $\theta = \pi$ and the work done by the particle on the system is always negative. This means that power input is required to maintain a constant amplitude of oscillation.

CALCULATING MOTION OF A SINGLE DEGREE OF FREEDOM UNDER INFLUENCE OF AN ACCELERATION DAMPER

The following development neglects the effect of friction on the motion of the mass particles in the acceleration damper. The

motion can be formally represented by an integral equation of the form

$$x(t) = \int_{t_0}^t f[x(\tau)] d\tau \dots [19]$$

The solution of Equation [19] will be carried out by using step-by-step integration procedure for nonsteady harmonic motion as follows:

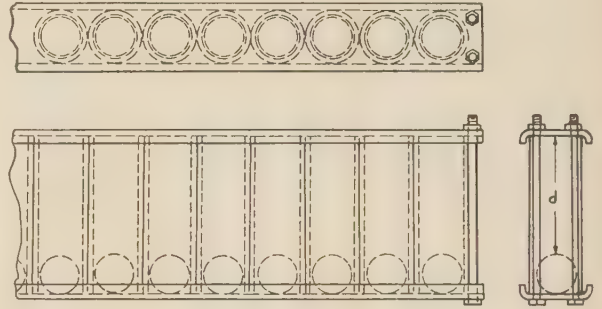


FIG. 4 MULTIUNIT TUBE-TYPE ACCELERATION DAMPER

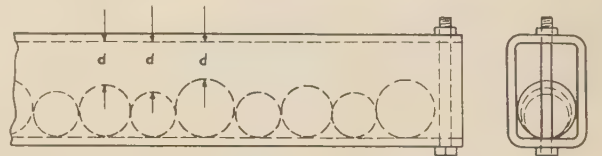


FIG. 5 SINGLE-UNIT RECTANGULAR TUBE-TYPE ACCELERATION DAMPER

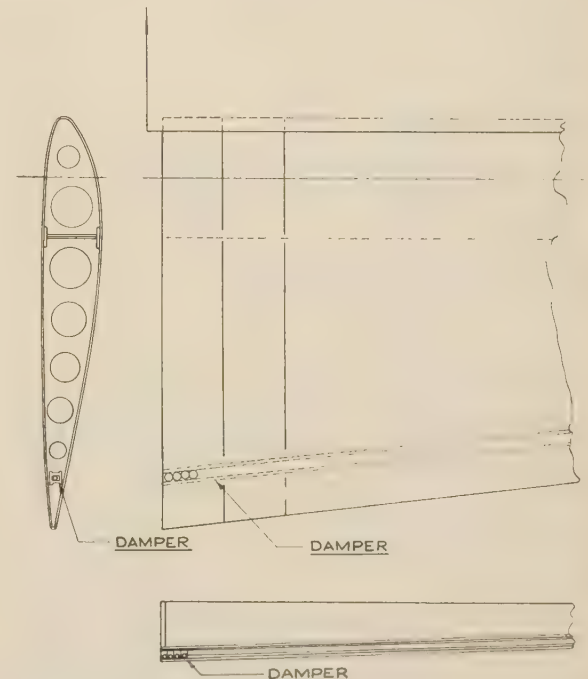


FIG. 6 TYPICAL ACCELERATION-DAMPER INSTALLATION IN A CONTROL SURFACE

Let

$$\begin{aligned}x(t) &= x_0(t) \sin \omega t \\ \frac{1}{2} M \dot{x}_2 &= \frac{1}{2} M (x_0(t) \omega \cos \omega t)^2 \\ \frac{1}{2} K x_2^2 &= \frac{1}{2} K (x_0(t) \sin \omega t)^2\end{aligned}$$

Then using Equation [17a] and substituting $x_1 = x_0 \sin (\omega t + \theta)$ and $x_2 = x_0 \sin \omega t$ the energy $E(t)$ can be expressed as follows

$$E(t) = \frac{1}{2} M (x_0(t) \omega \cos \omega t)^2 + \frac{1}{2} K (x_0(t) \sin \omega t)^2 - \frac{1}{2} M x_0^2(t) \omega^2 (1 - \cos \theta)^2$$

and

$$x_0(t) = \sum_{t_0}^t F[x(\tau)]$$

where

θ is determined by $d = x_0(\theta - \sin \theta)$. (See Equation [13].) From this the logarithmic decrement can be determined and thence the value of c in Equation [22].

Typical designs of the acceleration damper are set forth in Figs. 4, 5, and 6.

SUMMARY OF EXPERIMENTAL RESULTS AND CORRELATION WITH THEORY

In the experiments conducted a cantilever beam was deflected, then released and allowed to vibrate with and without damper units attached, the frequency being controlled by the length of the beam. The converging amplitudes were recorded by means of a seismograph. Figs. 11, 12, 13, and 14 are typical of the numerous recordings obtained in this manner. Fig. 15 shows test results for an acceleration damper installed on a system excited by a simple harmonic force. The effective moment of inertia of the damper used, with respect to the center of rotation, was 15 per cent of the moment of inertia of the system.

In general, the agreement between theory and experiment is good as borne out by Fig. 7, and the numerical results which are given in the next section. The efficiency of the acceleration damper is considered reduced when the friction of the moving mass is increased, as realized when using multiparticles in a single container. This can be seen by comparing Figs. 11, 12, and 13.

The theory relating to flutter has not been experimentally verified and would necessitate flutter wind-tunnel tests.

COMPARISON BETWEEN CALCULATED AND MEASURED LOGARITHMIC DECREMENT AT AN AMPLITUDE OF 0.358 IN. AND A FREQUENCY OF 9.875 RAD/SEC

Refer to Equation [19]

$$\begin{aligned}M &= \frac{7.39}{386} \frac{\text{lb sec}^2}{\text{in.}} & m &= \frac{1.056}{386} \frac{\text{lb sec}^2}{\text{in.}} \\ \omega &= 9.875 \text{ rad/sec}\end{aligned}$$

$x_0(t_1) = 0.358$ and is the maximum amplitude of the beam preceding impact. Then the energy of the beam at impact is

$$\frac{1}{2} \times \frac{7.39}{386} (0.358 \times 9.875)^2 = 0.12$$

and the energy of beam subsequent to impact is

$$0.12 - \frac{1}{2} \times \frac{1.056}{386} \times 0.358^2 \times 9.875^2 \times 4 = 0.05$$

giving

$$\frac{7.39}{772} (x_0(t_2) 9.875)^2 = 0.05$$

then $x_0(t_2) = 0.23$ where $x_0(t_2)$ is the maximum amplitude of the beam following said impact.

The calculated logarithmic decrement is then

$$\log \frac{0.358}{0.23} = 0.39$$

as compared to the measured value

$$\log \frac{0.358}{0.22} = 0.43$$

In the foregoing computations the structural damping of the beam has been neglected, which is consistent with this comparison.

CORRELATION BETWEEN ACCELERATION AND VISCOUS DAMPING

In order to facilitate application of the acceleration damper to specific problems it is convenient to represent its effect by an effective damping coefficient \bar{d} such that when multiplied by the acceleration gives a damping force in phase with the velocity. The effective damping coefficient as defined can be conveniently determined experimentally and theoretically in accordance with the following development: The energy dissipated over a given time interval by an acceleration damper can be expressed in the form

$$-j \int_{t_1}^{t_2} \bar{d} \dot{x} \frac{dx}{dt} dt \dots \dots \dots [20]$$

where $j = \sqrt{-1}$

The problem consists of determining \bar{d} and to ascertain that it adequately represents the damping characteristics of the acceleration damper. In accordance with the following energy criterion, \bar{d} can be readily expressed in terms of a viscous damping coefficient c corresponding to the decay curve obtained for the acceleration damper in the time interval

$$\Delta t = (t_2 - t_1)$$

Proceeding in this manner gives

$$-j \int_{t_1}^{t_2} \bar{d} \dot{x} \dot{x} dt = \int_{t_1}^{t_2} c \dot{x}^2 dt \dots \dots \dots [21]$$

where c is the corresponding viscous damping coefficient. From Equation [21], assuming simple harmonic motion

$$j \bar{d} \int_{t_1}^{t_2} \omega^2 x_0 \sin \omega t \omega x_0 \cos \omega t dt = x_0^2 c \int_{t_1}^{t_2} \omega^2 \cos^2 \omega t dt$$

Since

$$\begin{aligned}j x_0 \sin \omega t &= x_0 \sin (\omega t + 90) = x_0 \cos \omega t \\ \bar{d} \int_{t_1}^{t_2} \omega^2 x_0^2 \cos^2 \omega t dt &= x_0^2 c \int_{t_1}^{t_2} \omega^2 \cos^2 \omega t dt \\ \therefore \bar{d} \omega &= c; \quad \bar{d} = c/\omega \dots \dots \dots [22]\end{aligned}$$

Equation [22] enables one to calculate \bar{d} in terms of the viscous damping coefficient c corresponding to the decay curve of the acceleration damper. Expressions of the form of Equation [20] can be used to represent the damping force of an acceleration damper in the equations of motion of a given system.

INTRODUCTION OF ACCELERATION DAMPING FORCES IN EQUATIONS OF MOTION ENCOUNTERED IN FLUTTER ANALYSIS AND EQUATIONS OF MOTION INVOLVING SIMPLE HARMONIC FORCING FUNCTIONS

As an example, consider the coupled and uncoupled damping forces in the h , α , and β co-ordinates corresponding to an acceleration damper installed near the trailing edge of an aileron,

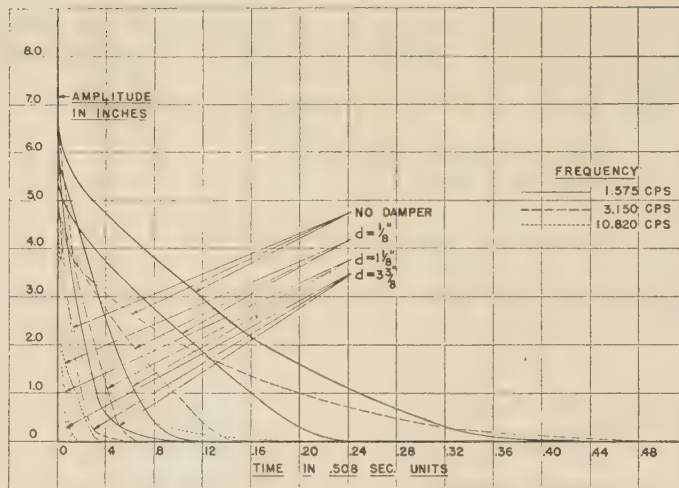


FIG. 7

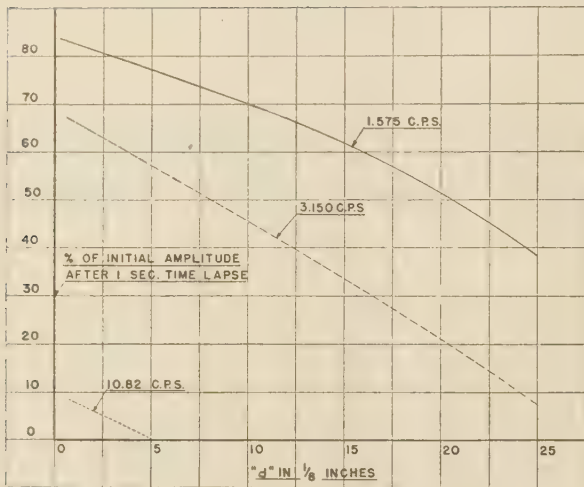


FIG. 8

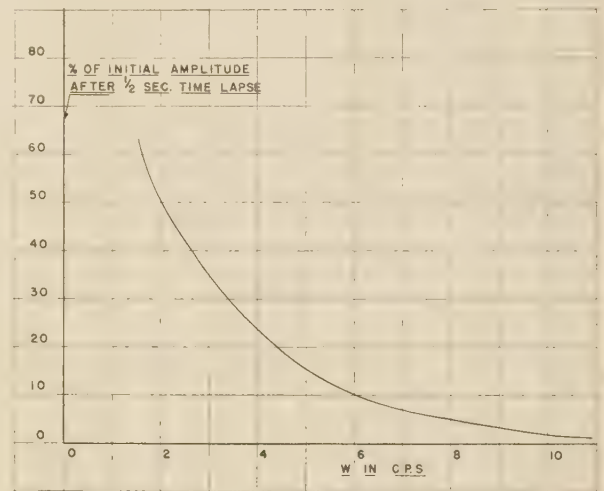


FIG. 9

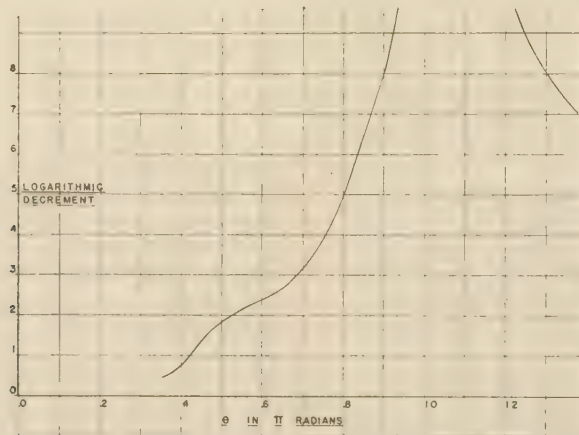


FIG. 10

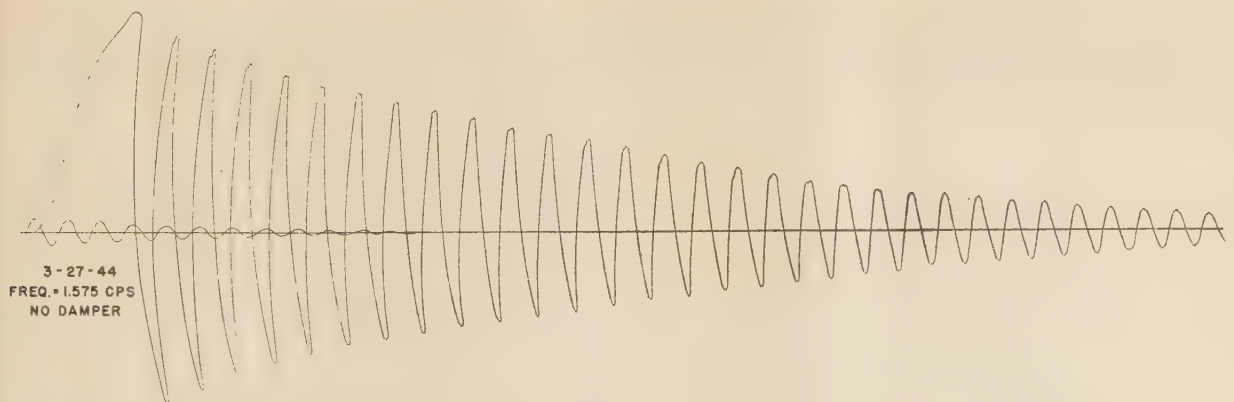


FIG. 11

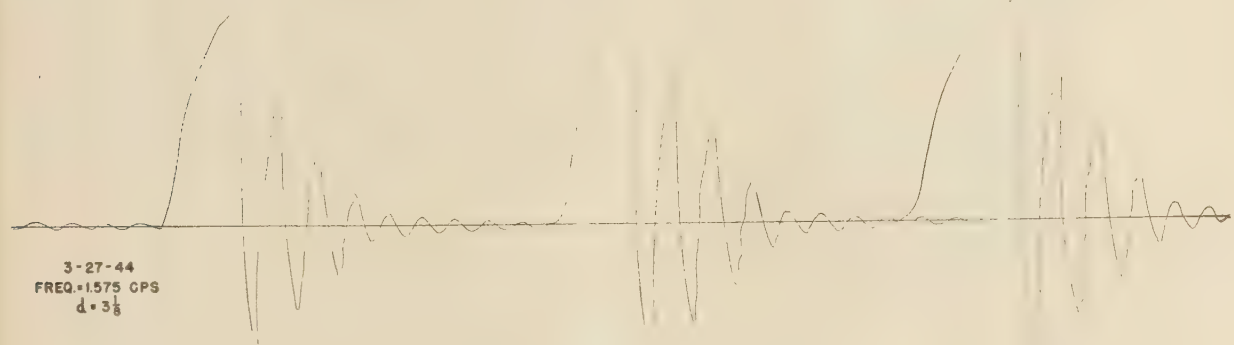


FIG. 12

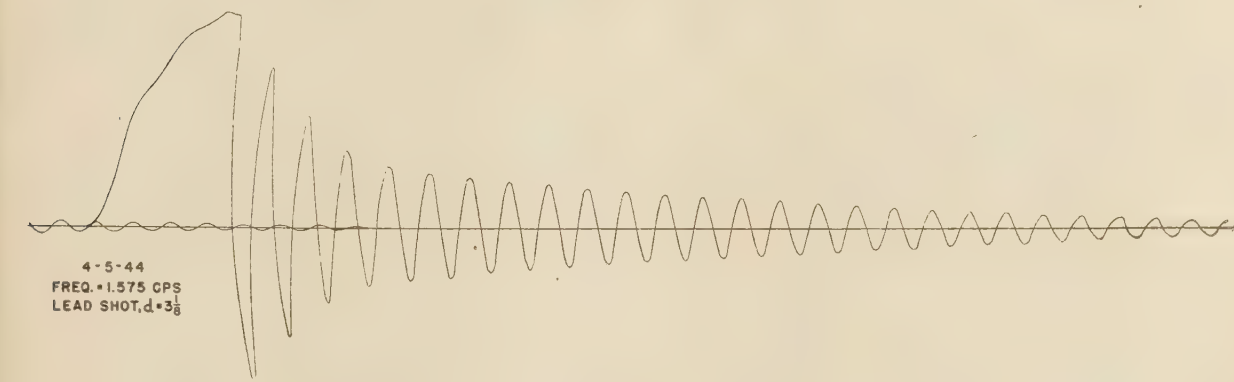


FIG. 13

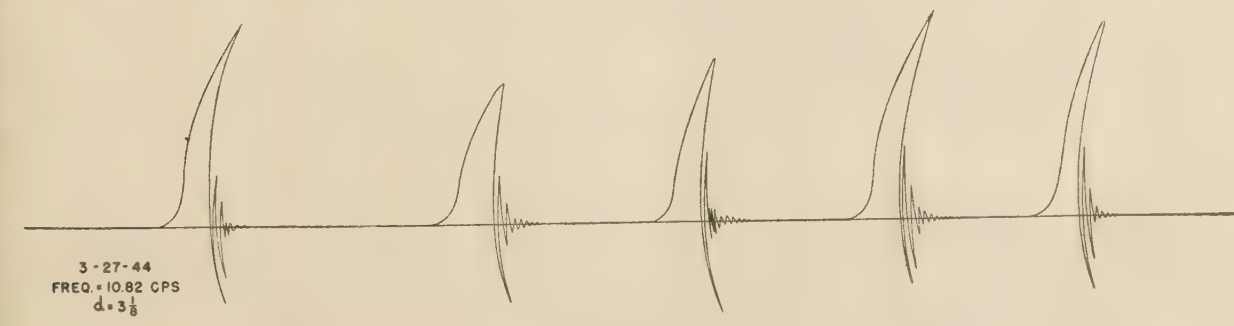


FIG. 14

where h , α , and β are the generalized co-ordinates for the uncoupled bending torsion and control-surface modes, respectively. Let $\bar{d}^{\beta\beta}$ represent the uncoupled acceleration damping coefficient in the β generalized co-ordinate. The coupled and

$\bar{d}^{\alpha\alpha}$ = uncoupled damping coefficient in α
 \bar{d}^{hh} = uncoupled damping coefficient in h
 $\bar{d}^{\beta h}$ = $\bar{d}^{h\beta}$ = coupled damping coefficient between h and β
 $\bar{d}^{\beta\alpha}$ = $\bar{d}^{\alpha\beta}$ = coupled damping coefficient between β and α
 $\bar{d}^{h\alpha}$ = $\bar{d}^{\alpha h}$ = coupled damping coefficient between h and α

In the foregoing development it is assumed that the damper is installed in a control surface. The damping forces corresponding to the set of damping coefficients just given are as follows

$$\left. \begin{aligned} F_{\beta\beta}\ddot{a} &= -j\bar{d}^{\beta\beta}\dot{\beta} & F_{hh}\ddot{a} &= -j\bar{d}^{hh}\dot{h} \\ F_{\alpha\alpha}\ddot{a} &= -j\bar{d}^{\alpha\alpha}\ddot{a} & F_{\alpha\beta}\ddot{a} &= -j\bar{d}^{\alpha\beta}\dot{\beta} \\ F_{h\beta}\ddot{a} &= -j\bar{d}^{h\beta}\dot{\beta} & F_{\alpha h}\ddot{a} &= -j\bar{d}^{\alpha h}\dot{h} \\ F_{\beta h}\ddot{a} &= -j\bar{d}^{h\beta}\dot{h} & F_{h\alpha}\ddot{a} &= -j\bar{d}^{\alpha h}\ddot{a} \\ & & F_{\beta\alpha}\ddot{a} &= -j\bar{d}^{\alpha\beta}\ddot{a} \end{aligned} \right\} \dots [24]$$

Equations [23] and [24] can be readily used in conventional three-dimensional flutter analysis by spanwise integration of the forces in accordance with an energy criterion.⁴ Equation [23] can also be introduced as generalized forces in any system of equations of motion. The effect of the acceleration damper on various flutter modes of an actual airplane has been investigated theoretically by introducing generalized damping forces of the form given by Equation [24]. The results are promising and indicate the damper to be effective, especially for high-speed flutter.

CONCLUSIONS

Some conclusions relating to the acceleration damper are as follows:

- 1 Its application to vibration control for aircraft is promising.
- 2 The agreement between the theory developed herein for the acceleration damper and available test data is good.
- 3 The theory provides an analytical method for designing the acceleration damper efficiently for specific application.
- 4 Results obtained relating to flutter justify experimental research regarding the application of the acceleration damper to flutter control.
- 5 The results arrived at in this paper can be directly applied to curvilinear motion by replacing x_0 by s_0 and x by s .

NOTE: Patents on Acceleration Damper are pending. Use of this damper requires License Agreement.

⁴ "Three-Dimensional Flutter Analysis," by W. M. Bleakney, *Journal of the Aeronautical Sciences*, vol. 9, Dec., 1941, p. 56.

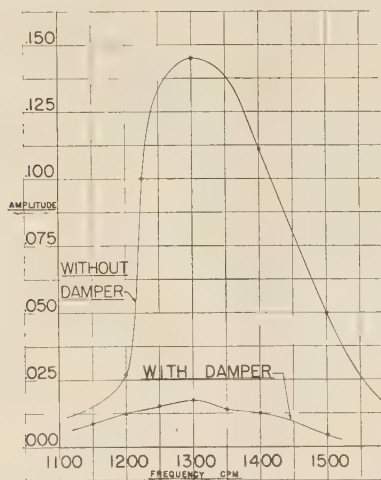


FIG. 15 RESPONSE CURVES TO FORCED VIBRATION

uncoupled coefficients in the generalized co-ordinates, h , α , and β can be expressed in terms of $\bar{d}^{\beta\beta}$ as follows

$$\left. \begin{aligned} \bar{d}^{\alpha\alpha} &= \frac{r_\alpha^2}{r_\beta^2} \cdot \bar{d}^{\beta\beta} \\ \bar{d}^{hh} &= \frac{\bar{d}^{\beta\beta}}{r_\beta^2} & \bar{d}^{\beta\alpha} &= \bar{d}^{\alpha\beta} = \frac{r_\alpha}{r_\beta} \bar{d}^{\beta\beta} \\ \bar{d}^{\beta h} &= \bar{d}^{h\beta} = \frac{\bar{d}^{\beta\beta}}{r_\beta} & \bar{d}^{h\alpha} &= \bar{d}^{\alpha h} = \frac{\bar{d}^{\alpha\alpha}}{r_\alpha} \end{aligned} \right\} \dots [23]$$

where

r_α = distance between damper and elastic axis

r_β = distance between damper and control-surface hinge line

(Owing to travel emergency conditions existing when the second presentation of this paper was made, discussion will be accepted until November 10, 1945)

Heater Designs for the Petroleum Industry

By J. H. RICKERMAN,¹ NEW YORK, N. Y.

Present-day requirements for high-octane aviation fuels and for toluol and benzol fractions for use in the production of munitions increase the need for specialized types of oil heaters. In the past most oil heaters were designed by rule of thumb but this method gave way to more accurate empirical methods while attempts were being made to put the art of design on a sound theoretical basis. The empirical relationships used were derived from correlations of experimental and operating data, and these relationships were satisfactory when used to design heaters of types and service requirements similar to those on which the data were obtained. However, as soon as specialized requirements, such as higher temperatures, increased heat-transfer rates, different box shapes, etc., are involved, the extrapolation of empirical equations and methods becomes hazardous. For this reason strenuous efforts have been made to place all design equations and methods on a theoretical basis, and it is believed that these efforts have yielded satisfactory results. A discussion of these methods of design is the subject of this paper.

OIL heaters may be classified on the basis of the service which they are to perform, namely, as simple heaters in which no chemical conversion of the oil is to take place, and as reaction heaters, typified by cracking furnaces, in which a definite degree of conversion is desired. The basic problems are the same in the two types of heaters with the exception that in the reaction heater there is the additional requirement that the oil must be maintained for a specified time period at a given temperature, or over a given temperature range.

FURNACE SKETCHES

Some of the more recent heater designs which have proved successful in meeting the particular requirements for which they were designed are shown herewith. Fig. 1 shows a simple helical-coil radiant-section furnace which was developed primarily as a low-cost low-efficiency furnace for small duties, preferably not over 10,000,000 Btu per hr. Since a tube cleaner cannot be used on this furnace, its applications should be limited to services in which no coke or scale deposits are expected. However, this type of furnace may also be used where coke is expected if the coke-burning-out procedure is used. By this method the coke deposits are removed by passing air and steam through the coil while firing it sufficiently to start and maintain combustion of the coke. Enough steam is used to keep the combustion temperature under control.

Fig. 2 shows an A-frame furnace which has been found to be a very satisfactory type for a large range of services. Developed originally as a simple heating furnace for duties ranging from 10,000,000 to 30,000,000 Btu per hr, it has since been found suitable for duties as high as 100,000,000 Btu per hr. By routing the oil flow through it properly, this type may also be used as a cracking furnace. Its greatest advantages are (a) lower cost per mil-

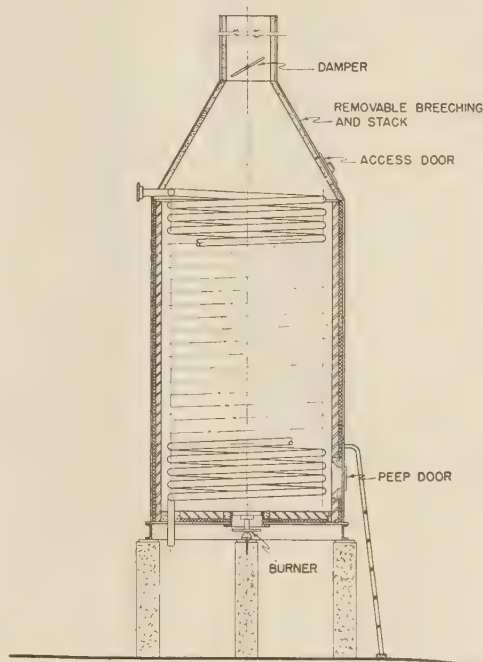


FIG. 1 HELICAL-COIL FURNACE*

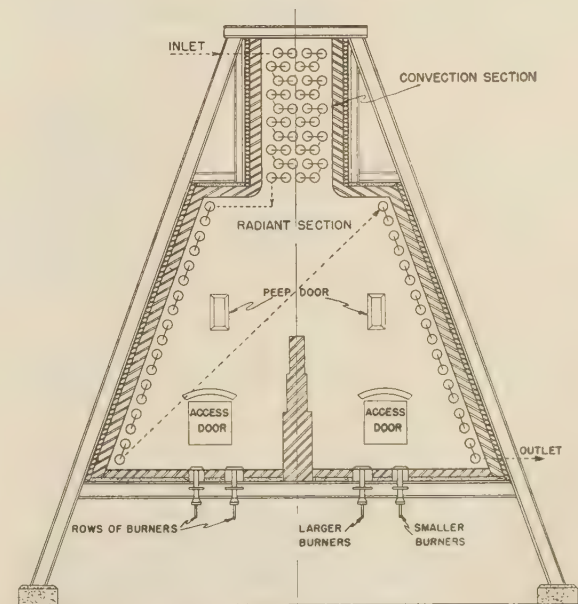


FIG. 2 A-FRAME FURNACE

¹ M. W. Kellogg Company. Mem. A.S.M.E.

Contributed by the Heat Transfer Division and presented at the Semi-Annual Meeting, Pittsburgh, Pa., June 19-22, 1944, of THE AMERICAN SOCIETY OF MECHANICAL ENGINEERS.

NOTE: Statements and opinions advanced in papers are to be understood as individual expressions of their authors and not those of the Society.

lion Btu of duty due largely to its economical use of structural steel, and (b) the fact that two exactly symmetrical streams may be used in parallel.

Fig. 3 shows a rectangular vertical-tube-type furnace which

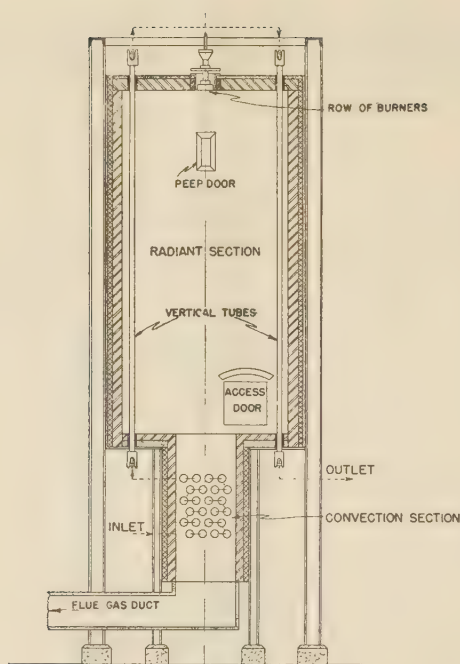


FIG. 3 VERTICAL-TUBE FURNACE

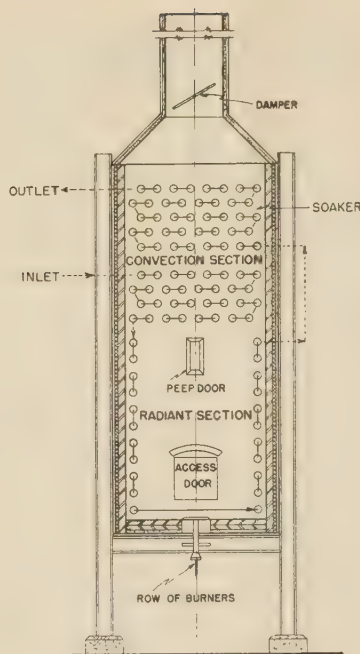


FIG. 4 CONVECTION FURNACE

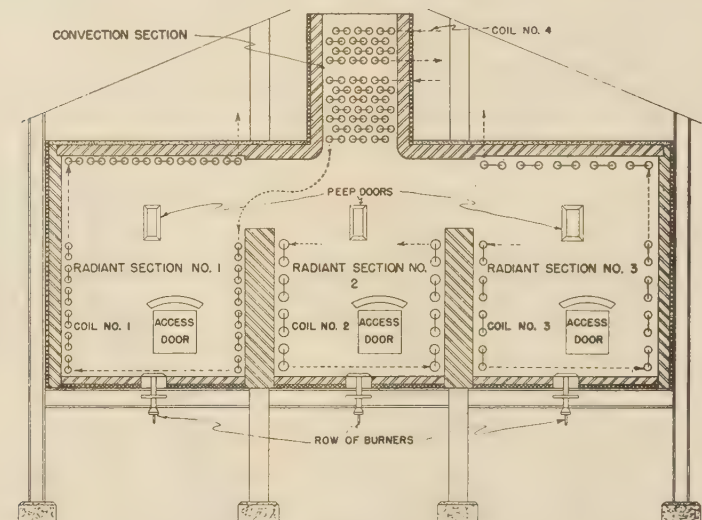


FIG. 5 TRIPLE-RADIANT FLOOR-FIRED FURNACE

offers about the only solution possible when a great number of equal streams of oil are to be heated equally. This type of furnace may be used for practically any service but its higher cost normally limits it to use under the conditions stated. By the use of the proper burners suitably arranged in the roof of the furnace, the heat absorption of each tube will be substantially the same as that of any other so that all the tubes may be connected in parallel.

Fig. 4 shows a convection-type furnace. This furnace has a rather limited field of usefulness. It is particularly suitable only when a large soaking volume at a rather low heat-transfer rate is required. Such a requirement is usually met in gas-pyrolysis or polymerization work. For other services where higher over-all

average rates are required or desired, the furnace will not be satisfactory since the rate of heat transfer in the convection section is low owing to the low flue-gas velocity through it.

In a paper by Rickerman, Lobo, and Baker (1),² several arrangements of the conventional type furnace are shown, both in the single-radiant-section type and the double-radiant-section type. This furnace had been widely used because of its flexibility in variation of size and shape. However, the overhead-convection-section type of furnace, an example of which is shown in Fig. 5 of reference (1), has essentially all the features of the conventional type but it is usually less costly. In the overhead-con-

² Numbers in parentheses refer to the Bibliography at the end of the paper.

vection-section-type furnace the stack may be mounted on the furnace itself thereby eliminating expensive duct work and additional foundations. As a result of eliminating duct work the size of the effective portion of the stack itself may also be considerably reduced. This type of furnace may be built as a single- or multiple-radiant-section type, with or without bridge-walls and may be fired from the walls or from the floor. A triple-radiant-section type, fired from the floor, is shown in Fig. 5 herewith. Here the furnace shows a considerable reduction in first cost over the end-fired type, since, with the use of the floor for burner space, a large number of small burners may be installed with the result that considerably less clearance may safely be used between burners and tubes.

DUTY OR HEAT ABSORPTION

For the simple heater in which no reaction is to take place, the specified conditions such as throughput, gravity, temperatures, pressures, and phase conditions will determine the amount of heat to be absorbed by the oil in its passage through the furnace, or more briefly, the furnace "duty." This duty will consist of the sensible heat plus the heat of vaporization, if any, and may be obtained by use of specific-heat and latent-heat curves, or more conveniently, by means of enthalpy, or total-heat curves.

In the case of the cracking heater, the heat of chemical reaction must also be taken into account and added to the sum of the sensible- and latent-heat duties mentioned. Sometimes it may be found that the heat of reaction is exothermic rather than endothermic, in which event it must of course be subtracted from the other heat duty.

Some laboratory work has been done in an effort to determine the heat of reaction for at least a few typical cracking operations, but the number of variables involved has made it very difficult to obtain a satisfactory correlation. Some approximate correlations have been made based on data obtained from furnace tests and these correlations have been used for such heaters as visbreakers, gas-oil crackers, naphtha reformers, and thermal-polymerization furnaces. Where the character or analysis of the furnace charge and products is accurately known the heat of reaction may be calculated as the difference in the heat of combustion or the heat of formation of the charge and products. However, by this method the heat of reaction is determined as a relatively small difference between two very large total quantities so the stipulation that the analyses be accurately known is an important one.

EFFICIENCY OF FURNACE

Having calculated the furnace duty, the over-all requirements of the oil side of the furnace, or, as it may be considered, the high-temperature-level heat exchanger, are known. The fluid on the other side of the exchanger will consist of flue gas from the combustion of fuel. The flue gas will be available at combustion conditions and may give up its heat to the oil side until its temperature approaches that of the oil to which it is transferring its heat as it leaves the furnace. Therefore, the temperature of the oil in the last pass of the furnace and the closeness of approach of flue gas to oil temperature will practically set the efficiency of the furnace unless other heat-recovery equipment is used. Normally the oil charge will be brought into the furnace at the point where the flue gas is leaving so that with the inlet-oil temperature known and the nearest economical temperature approach fixed, the temperature of the flue gas leaving the furnace may be fixed.

The temperature approach, or difference, will obviously be set by considerations of economy and whether other heat-recovery equipment such as an air preheater, or waste-heat boiler, is to be used. When no external heat-recovery equipment is to be used it has been found that 200 F is about the nearest economi-

cal temperature approach. With low-cost fuel and low oil-inlet temperatures this difference may be as great as 600 to 800 deg F. In general, however, most oil heaters are designed for exit flue-gas temperatures between 700 F and 1100 F, with the majority between 900 F and 1000 F.

The determination of three other factors will completely fix the furnace efficiency, namely, the character of the fuel to be fired in the furnace, the percentage of excess air with which it will be burned, and the radiation loss. In a natural-draft furnace it is possible to burn completely almost any oil or gas fired with 40 per cent excess air, and with care in the design and operation of the furnace even lower percentages may be obtained.

Once the efficiency of the furnace has been determined as outlined, the heat to be liberated in the furnace, i.e., the fuel to be fired, and the quantity and analysis of the flue gas produced may be calculated. Both sides of the high-temperature-level heat-exchanger are then known and the procedure is to determine the heating surface, its arrangement, and the physical dimensions of the furnace.

DETERMINING THE TUBE SIZES

The first dimensions to be decided are those of the tubes. The inside diameter of the tubes will be determined by the allowable or economical pressure drop which may be taken in the coil. In some cases the effective pressure in the cracking coil may have considerable effect on the amount or nature of the thermal decomposition taking place so that a maximum pressure drop may thus be determined. In general, however, economic considerations such as pump cost and horsepower requirements will set the value of the permissible pressure drop.

Of course, until the furnace is finally designed it is not possible to calculate the pressure drop which will obtain with a given tube size, since among other things the number of tubes will not be known. However, a preliminary estimate of the number of tubes required may be made and then an approximation may be made of the pressure drop. This process may be repeated until a suitable internal diameter of tube is determined. It should also be remembered that the oil may if desired flow through several tubes in parallel.

With experience the designer usually will be able to choose an internal tube diameter without making these preliminary pressure-drop estimates. A criterion which may be used as a guide is the oil velocity through the tube, either in terms of "cold-oil velocity," that is, linear velocity of the oil in feet per second, using the density of the oil as liquid at 60 F, or in terms of mass velocity. The cold-oil velocity in most oil heaters will range from about 2 to 10 fps. For vacuum pipe stills the cold-oil velocity may be even lower, some having been designed for about 0.5 fps. For crude heaters and visbreakers the velocity normally ranges from 2 to 5 fps, for gas-oil crackers, naphtha reformers, and polymerization furnaces from 5 to 8 fps, for delayed-coking furnaces, about 7 fps, and for furnaces heating material all in the liquid phase, from 7 to 10 fps. Higher or lower velocities may also be used at an increase in the resulting pressure drop on the one hand and with a poorer inside oil-film heat-transfer coefficient on the other hand. Mass velocities may vary from 100 to 500 lb per sec per sq ft of cross-sectional tube area.

The foregoing discussion is predicated upon the assumption that the highest possible velocity compatible with the allowable pressure drop should be used, since the higher the velocity in the tube the better the inside-film coefficient of heat transfer. This means that for a given maximum allowable tube-metal temperature or for a given maximum allowable oil-film temperature, a higher over-all heat-transfer rate may be used. The upper limit of tube-metal temperature may be set by the tube materials

to be used, or the limit of oil-film temperature may be set so as to avoid coking of the oil film or discoloration of the oil caused by overheating of the film.

Having set the approximate internal diameter of the tubes, an external diameter may be chosen to give a tube thickness appropriate for the pressures and temperatures which will obtain in the tubes.

The length of tube to be used will depend largely on the type of furnace. In general, it has been found that for a given type of furnace it is most economical to use the longest tubes commercially available while at the same time covering the walls and arch of the combustion chamber with tubes. At least two of the dimensions of the combustion chamber, or radiant section, will be determined by the number and size of burners required, so that either the number or length of tubes may be set. If the number of tubes is thus fixed by the box dimensions the length must be calculated from the required heating surface. Alternately, if the length of the tubes is fixed, the number of them must be obtained from the surface. Actually, it is usually necessary to make trial-and-error calculations in order to obtain a well-balanced economical furnace design from the standpoint of the number and length of tubes.

Another point which should be kept in mind is that more intermediate tube supports are required for long tubes than for short, so that the tube length should, if possible, be chosen to take the greatest advantage of the intermediate tube supports which are necessary. Furthermore, it should be remembered that the pressure drop per square foot of heating surface will be less with long tubes since fewer return bends are required.

Normally the tubes chosen will have outside diameters varying from 2 to 6 in. by $\frac{1}{4}$ -in. increments between 2 and 3 in., and by $\frac{1}{2}$ -in. increments between 3 and 6 in. Occasionally smaller tube sizes, iron-pipe-size seamless tubing, or 8-in.-OD tubing are used. Tube thicknesses vary from about $\frac{1}{4}$ to 1 in., the lower limit being set by a nominal corrosion rate, while the upper limit is set by the difficulty of rolling heavier walled tubes into return headers. Over-all tube lengths vary from about 20 ft to 40 ft by 2-ft increments. Shorter lengths may in some instances be used although ordinarily they are uneconomical owing to the increased number of return bends required per square foot of heating surface. Tubes longer than 40 ft may be used if obtainable, or if not obtainable in one piece, two pieces may be butt-welded to make the greater length. Maximum lengths of single-piece tubes will depend on the physical capacity of the tube mill to handle the length, or on the size of the steel billet from which the tube is drawn. A practical limit of tube length may be set by the difficulty of cleaning.

CALCULATING THE RADIANT SECTION

The next step in the design of the heater is to calculate the radiant section or sections. The heat-transfer surface required in each radiant section will depend largely on the heat-transfer rate which is desired in the section. In addition, the percentage of excess air with which the fuel is burned will have an effect. In the Wilson, Lobo, and Hottel (2) empirical radiant-heat-transfer equation for box-type radiant sections these two items are the only variables. This equation has been rather widely used but it is empirical and has a number of limitations. Chief among these is the requirement that the radiant section be of the box type as well as within certain size limits. The box should not vary greatly from a ratio of side dimensions of about 1 to 4, that is, the longest side should not be more than about 4 times as great as the shortest side. Furthermore, the cube root of the internal volume of the radiant section should be within the range of 15 to 25 ft. The average outside tube-metal temperature should be in the range of 700 to 1100 F, while the temperature of

the flue gas leaving the radiant section should be in the range of about 1100 to 1600 F, but in no case should the average metal and exit-gas temperatures be closer than 400 F. In effect, these limitations set the range of radiant-heat-transfer rates between about 4000 and 12,000 Btu per hr per sq ft. The excess air, character of fuel, and distribution of heating surface should also be within the range of the data obtained in the furnace tests used in the derivation of the equation. These data are presented in the original paper (2).

In order to place the design of radiant sections on a sounder basis, a more rational radiant equation was developed by Hottel (3) and modified by Evans and Lobo (4). This equation, having a theoretical basis, should be suitable for use with any radiant section. In it account is taken of most of the variables which affect the heat-transfer rate. The equation is

$$\frac{H}{\alpha A_{cp} \phi} = 0.173 \left[\left(\frac{T_g}{100} \right)^4 - \left(\frac{T_s}{100} \right)^4 \right] + 7 (T_g - T_s) \dots [1]$$

where

H = heat absorbed by radiant surface, Btu per hr

α = factor by which A_{cp} must be reduced to obtain effective cold surface

A_{cp} = area of a cold plane replacing the tubes, sq ft

ϕ = over-all heat-exchange factor

T_g = temperature of flue gas leaving radiant section, deg F abs

T_s = temperature of heat-absorbing surface, deg F abs

As may be seen, Equation [1] is a modified form of the basic Stefan-Boltzmann equation, the modifications consisting of the definition of the effective heating surface αA_{cp} , the inclusion of a factor ϕ to take account of a number of variables, and the addition of an arbitrary factor $7(T_g - T_s)$ to account approximately for convection heat transfer in the radiant section.

The effective heating surface has been defined by Hottel (5, 6) while the over-all exchange factor ϕ is defined by Evans and Lobo (4).

In the nomenclature following Equation [1] T_g is defined as the temperature of the flue gas leaving the radiant section. This definition is true only if the radiant box and the arrangement of the burners in the box are such as to give fairly complete mixing of the flue gas so that the exit gas temperature is also practically the same as the mean gas temperature within the radiant section. For radiant sections in which the products of combustion move substantially in a straight line parallel to the heat-absorbing surface so that the flue gas has a definite temperature gradient from the initial combustion zone to the exit, it is not justifiable to use the exit temperature in the equation. In this case a mean effective radiating temperature must be determined, or the radiant section may be divided into two or more sections and the exit-flue-gas temperature from each section used in the equation when calculating that section. Obviously, with the latter method the proper values of αA_{cp} , ϕ , and T_s , corresponding to the section being calculated, should be used. Term T_s may be taken as the average outside tube-wall temperature in the section under consideration.

Another point which should be noted is that if any of the tubes in the convection section are exposed to direct radiation from the hot products of combustion in the radiant section, this exposed surface must be added to obtain the total effective radiant surface. The over-all heat-transfer rate to the exposed convection surface will then be the sum of this direct radiant rate and the convection rate to be calculated subsequently.

Obviously, the solution of a heat balance using the radiant-section heat absorption, as just calculated, and an allowance for radiation losses should give an exit-flue-gas temperature which

agrees with the assumed radiant-section exit-flue-gas temperature.

Heat-transfer rates commonly used in the radiant sections of oil-heating and cracking furnaces vary from about 5000 to 20,000 Btu per hr per sq ft of exposed outside tube surface. Very low rates may be used in a furnace without a convection section in order that a reasonable furnace efficiency will be obtained. In delayed-coking furnaces and vacuum pipe stills, rates between 5000 and 10,000 are usual while for crude heaters, rates between 10,000 and 12,000 are used. For gas-oil cracking furnaces, naphtha reformers, and polymerization furnaces, rates of from 12,000 to 16,000 are common. Low-temperature reboilers may be designed for rates as high as 20,000 Btu per hr per sq ft. Actually even higher rates than those just outlined are often obtained in practice.

CONVECTION-SECTION DESIGN

With the radiant-section heat absorption calculated, the remaining duty, that to be performed in the convection section, may be obtained by difference from the total, and the oil temperatures into and out of the various divisions of the convection section may be calculated. The heat balance on the flue-gas side for the radiant sections gives the temperature of the flue gas entering the convection section, and subsequent heat balances will give the necessary intermediate flue-gas temperatures.

The length of the tubes in the convection section is usually made the same as those in the radiant section. The width of the convection bank is then set so as to obtain the best heat-transfer rate possible. On the other hand, the flue-gas velocity through the convection bank should not be too high or an excessive draft loss will result and the stack required will be uneconomically large. It has been found through considerable experience that a flue-gas mass velocity of about 0.5 lb per sec per sq ft of minimum free area usually will be satisfactory. "Mass velocities approaching 1.0 will require a stack of such size that the over-all furnace cost may be greater than if a lower velocity were used with the resulting increased heating surface.

With the temperatures known on both sides of the flue-gas-to-oil "heat exchanger," the flue-gas velocity known, and most of the dimensions of the section known, the heat-transfer rates may be calculated. Heat will be transferred by both radiation and convection, in parallel, from the flue gas to the outside surface of the tube and the heat thus transferred will then pass, in series, through the tube wall, any scale or coke deposit, and the inside oil film, to the oil.

The radiant heat transfer consists of "direct" radiation from the hot flue gases and hot refractory walls of the radiant sections, for the first two or three rows of the convection section, (if they are "exposed" to the heat from the radiant section) plus radiation from the hot flue gases passing through the tube bank, and from the hot adjacent refractory walls of the convection section.

The direct radiation to the first rows is included in the radiant-section calculation as previously discussed. The radiation from the hot refractory walls adjacent to the convection tubes may be calculated by an equation for the "wall effect," as given by Monrad (7). The radiation from the hot flue gases passing through the bank may be calculated by the method of Haslam and Hottel (8, 9), using the radiation charts for carbon dioxide and water vapor.

The convection-heat-transfer coefficients may be calculated by the use of Monrad's equation (7), or by the method given by Pierson, et al (10, 11, 12). It is believed that the latter method is the more accurate. In any event, it undoubtedly may be used with a greater degree of assurance in ranges beyond the range of the data upon which the former equation was based. The method which is fully described in the reference articles, con-

sists of a correlation between the Reynolds number and the Nusselt number. In the original article curves are given relating these two numbers, and by their use the convection coefficient may readily be obtained.

SUMMARY OF HEAT-TRANSFER-RATE CALCULATIONS IN CONVECTION SECTION

Summarizing the operations required in calculating the heat-transfer rate in the convection section, the following steps must be taken:

- 1 Assume or by other means fix the total heat to be absorbed in the section under consideration.
- 2 By heat balance, making suitable allowances for radiation losses, calculate the flue-gas and oil temperatures both into and out of the section.
- 3 Calculate the logarithmic-mean temperature difference between the flue gas and oil.
- 4 Calculate the inside-oil-film coefficient in Btu per hour per square foot per deg F. Equations for this coefficient are given by Walker, Lewis, McAdams, and Gilliland (13), by McAdams (14), and others.
- 5 Assume an over-all heat-transfer rate for the section.
- 6 Calculate the average outside tube-metal temperature by adding to the average oil temperature the temperature drop through the oil film, coke deposit (if any expected), and the metal wall of the tube. The latter temperature drop is often neglected since it normally is of small magnitude.
- 7 Determine the amount of radiation in Btu per hour per square foot from the flue gas passing through the tube bank at its average temperature and composition, to the tube walls at their average temperature and surface emissivity by means of the radiation charts for carbon dioxide and water vapor.
- 8 In order to convert it to a coefficient, divide the radiant rate determined under item 7 by the logarithmic-mean temperature difference of item 3.
- 9 Convert to a coefficient the direct radiation, if any (from the radiant section), by dividing it also by the mean temperature difference.
- 10 Calculate the coefficient of convection-heat-transfer rate as outlined previously.
- 11 Add the three coefficients of items 8, 9, and 10 arithmetically, since the total heat flow is the sum of these three components.
- 12 Multiply the over-all outside gas coefficient by Monrad's (7) wall-effect factor to take into account the quantity of radiation from the hot refractory adjacent to the tubes. This result will be the true over-all gas coefficient for the outside surface of the tube.
- 13 Calculate the coefficient of heat transfer through the metal wall of the tubes and convert this to the basis of the outside surface by multiplying by the ratio of average to outside tube diameter.
- 14 Calculate the coefficient of heat transfer through the expected coke deposit, if any, and convert to the outside-surface basis by multiplying by the ratio of inside to outside tube diameter.
- 15 Convert the inside-oil-film coefficient of heat transfer to the outside-surface basis by multiplying by the ratio of inside to outside tube diameter.
- 16 Add the reciprocals of the previous four coefficients. The sum will be the reciprocal of the over-all coefficient.
- 17 Multiply the over-all coefficient of item 16 by the mean temperature difference to obtain the average heat-transfer rate on the outside tube surface. This rate should check the assumed rate rather closely.

18 Obtain the heating surface required by dividing the assumed oil duty for the section by the calculated rate.

Items 13 and 14 of the summary are usually neglected but under certain conditions it may be advisable to include them.

SOAKING SECTIONS

In the discussion thus far only heating surface has been considered and in many of the furnaces to be designed, heating surface is all that is required. In cracking, pyrolysis, polymerization, and some other furnaces, however, some of the tubes will perform a double service. They will absorb heat as well as maintain the oil at approximately a constant temperature or within a definite temperature range for the time required to complete the reaction. These tubes will be in the last part of the coil and this part of the coil is ordinarily termed the "soaking" section or "soaker."

Since over a given temperature range, or at a constant temperature, a definite amount of heat will be required for a definite degree of conversion, it will be necessary to design the furnace so that this heat will be absorbed by the number of tubes required to hold the oil at temperature for the required time. In other words, the number of tubes in the soaking section is fixed by the soaking time required and at the same time the duty of the soaking section is fixed by the heat of reaction required, hence the heat-transfer rate in that section is fixed and the surface must be placed in the furnace so that it receives heat at that rate.

However, a considerable degree of control may in most cases be exercised by the designer over the conditions for which the soaking section is designed. For example, if the heat-transfer rate, necessitated by the desired temperature range, is too high for a consideration of the possibility of coking or for other reasons, it may be feasible to increase the working-temperature range of the soaker section while maintaining the transfer-line temperature constant. This will increase the heat duty to the section but it will increase the time or volume required for cracking to an even greater extent so that the over-all heat-transfer rate in the soaker will decrease. The number of tubes needed will obviously increase considerably. On the other hand, of course, if the heat-transfer rate is too low the temperature rise may be decreased. Other means of control of the design are by changing the outlet temperature of the coil, providing this is possible from a standpoint of economical tube materials and the heat requirements of the fractionating system; or within limits, by changing the effective pressure in the soaking section. This change may be effected in some cases by raising or lowering the coil outlet pressure or by changing the flow through the section in order to change the pressure drop. Obviously, all the inter-related effects of any of these changes must be investigated in order to be sure that in improving one condition, a worse one does not arise at another point.

OTHER CONSIDERATIONS

Burners. In designing the radiant section or combustion chamber, space must, of course, be left available for the required number of burners in the walls or floor. This space should be large enough and the burners so located within the space that they are not too close to tube surfaces, otherwise there will be danger of direct flame impingement on those surfaces. In the case of forced-circulation water heaters, flame impingement can often be tolerated but in most oil heaters it must be strictly avoided.

Pressure Drop. In order to determine the differential pressure required of the furnace-charge pump, the thickness and material of the furnace tubes, and in the case of cracking furnaces,

the amount of soaking time or volume required, it is necessary to calculate the pressure drop through the furnace coil.

The well-known Fanning equation may be used to calculate the pressure drop. This equation in a convenient form is as follows

$$\frac{\Delta P}{\Delta L} = \frac{0.005185 \times f \times G^2 \times v}{D} \dots \dots \dots [2]$$

where

$\Delta P/\Delta L$ = pressure drop per equivalent foot of tubing, psi
 f = dimensionless friction factor, a function of Reynolds number
 G = mass velocity of fluid flowing, lb per sec per sq ft
 v = specific volume of fluid flowing, cu ft per lb
 D = inside diameter of tube, in.

Equation [2] makes no allowance for the pressure drop resulting from a change in the kinetic energy of the fluid. In those cases where a large fraction of the material is vaporized at low pressure (both conditions resulting in a high rate of change of specific volume and therefore of velocity), this pressure loss may be of importance. In order to include this loss the pressure-drop equation has been modified to the following form

$$\frac{\Delta P}{\Delta L} = \left(\frac{0.005185 f G^2 v}{D} \right) \left(\frac{1}{1 - \frac{G^2 v}{4637 P}} \right) \dots \dots \dots [3]$$

where

P = fluid pressure, psia

Other nomenclature as in Equation [2]

The calculation of the pressure drop through the coil consists of a series of trial-and-error steps. If the coil-outlet pressure is fixed, which is usually the case, the pressure drop per foot at the outlet may be calculated directly. With this figure as a guide an estimate may be made of the pressure drop for a given equivalent length of tubing, working toward the inlet of the coil and thus an estimated pressure may be obtained for this new point, ΔL feet from the outlet of the coil. Using the estimated pressure, a new $\Delta P/\Delta L$ should be calculated for this point. The logarithmic mean of the first and second $\Delta P/\Delta L$ values may then be multiplied by the equivalent length between the two points to obtain the calculated pressure drop between the points. This calculated value should check the estimated value rather closely. In this stepwise fashion the pressure drop may be calculated through the coil.

Tube Calculations. Once the temperature and pressure gradients through the coil are known the tube thickness and the tube material may be calculated. Bailey's (15) creep-stress method for calculating tubes is probably the most commonly accepted method at present. In this method the maximum shear stresses in the tube are calculated and compared with allowable shear stresses which will produce a given maximum rate of creep of the tube material.

Flue-Gas Ducts and Stack. After the heater itself has been designed as outlined the flue-gas disposal system must be considered. The simplest is a natural-draft system consisting merely of flue-gas ducts and a stack. Natural draft is used to a much greater extent than forced or induced draft in the petroleum industry. A discussion of the several systems is given by Rickerman, Lobo, and Baker (1).

The purpose of the stack and duct work is two fold; (a) to draw the required amount of combustion air through the burners, and (b) to dispose of the flue gases into the atmosphere so that they are not objectionable. The draft required at the burner throat to insure drawing the proper amount of combustion air through

the burner will depend on the design of the burner itself. However, for those burners designed for natural-draft operation a draft of from 0.10 to 0.20 in. of water will usually be sufficient. Normally, the draft needed at the burners will be used as a starting point in calculating the total draft or stack height required. Another important point which should not be overlooked is that a slight draft should exist throughout the furnace setting for most satisfactory operation.

BIBLIOGRAPHY

- 1 "Fundamentals Involved in the Design of Cracking Furnaces," by J. H. Rickerman, W. E. Lobo, and A. L. Baker, *Oil and Gas Journal*, vol. 36, May 5, 1938, pp. 50-51, and 53-54; vol. 36, May 12, 1938, pp. 141-142, 144, and 146.
- 2 "Heat Transmission in Radiant Sections of Tube Stills," by D. W. Wilson, W. E. Lobo, and H. C. Hottel, *Industrial and Engineering Chemistry*, vol. 24, 1932, pp. 486-493.
- 3 Personal Communication, by H. C. Hottel, 1938.
- 4 "Heat Transfer in the Radiant Section of Petroleum Heaters," by J. E. Evans and W. E. Lobo, *Trans. A.I.Ch.E.*, vol. 35, 1939, pp. 743-778; discussion, vol. 36, 1940, pp. 173-175.
- 5 "Radiant Heat Transmission," by H. C. Hottel, *Mechanical Engineering*, vol. 52, 1930, pp. 699-704.
- 6 "Radiant Heat Transmission Between Surfaces Separated by Non-Absorbing Media," by H. C. Hottel, *Trans. A.S.M.E.*, vol. 53, 1931, paper FSP-53-19b, pp. 265-273.
- 7 "Heat Transmission in Convection Sections of Pipe Stills," by C. C. Monrad, *Industrial and Engineering Chemistry*, vol. 24, 1932, p. 605.
- 8 "Combustion and Heat Transfer," by R. T. Haslam and H. C. Hottel, *Trans. A.S.M.E.*, vol. 50, 1927-1928, paper FSP-50-3.
- 9 "Heat Transmission by Radiation From Non-Luminous Gases," by H. C. Hottel, *Industrial and Engineering Chemistry*, vol. 19, 1927, pp. 888-894.
- 10 "Experimental Investigation of the Influence of Tube Arrangement on Convection Heat Transfer and Flow Resistance in Cross Flow of Gases Over Tube Banks," by O. L. Pierson, *Trans. A.S.M.E.*, vol. 59, 1937, pp. 563-572.
- 11 "Experimental Investigation of Effects of Equipment Size on Convection Heat Transfer and Flow Resistance in Cross Flow of Gases Over Tube Banks," by E. C. Hoge, *Trans. A.S.M.E.*, vol. 59, 1937, pp. 573-581.
- 12 "Correlation and Utilization of New Data on Flow Resistance and Heat Transfer for Cross Flow of Gases Over Tube Banks," by E. C. Grimison, *Trans. A.S.M.E.*, vol. 59, 1937, pp. 583-594.
- 13 "Principles of Chemical Engineering," by W. H. Walker, W. K. Lewis, W. H. McAdams, and E. R. Gilliland, McGraw-Hill Book Company, Inc., New York, N. Y., 1937, third edition, p. 111.
- 14 "Heat Transmission," by W. H. McAdams, McGraw-Hill Book Company, Inc., New York, N. Y., 1942, second edition, pp. 122-168.
- 15 "Creep of Steel Under Simple and Compound Stresses," by R. W. Bailey, *Engineering*, vol. 129, 1930, pp. 265-266 and 327-329.

Discussion

K. W. FLEISCHER.³ It is felt that Mr. Rickerman's paper is a timely and outstanding contribution to all who wish to design tube stills from a more theoretical standpoint. The author should be commended, not only for consolidating so much practical formulation and experience into one treatise, but also for a very sound and workmanlike pattern of approach to a notoriously complicated class of furnace-design problems. Mr. Rickerman's work will no doubt benefit many in the oil-refining industry; and, conceivably, could materially help equipment designers throughout the fast-growing field of "liquid heat-treatment," as involved in rayon, synthetic rubber, food, and all manner of chemical process industries.

However, in connection with techniques of firing radiant sections of tube stills, the author does not refer to one new point of view which promises radical influence on tube-still design.

Mr. Rickerman observes that "burners should not be too close to tube surfaces, otherwise there will be danger of direct flame impingement on those surfaces." He also describes long-standing problems the designer has faced in providing for: large combustion chambers; special tube-burner space relationships; and an average requirement of "40 per cent excess air to burn completely most oils or gases"—all in order to avoid nonuniformities of heating and hot spots on the coils.

Ceramic-cup gas burners are now appearing on the scene which (a) contain the combustion reaction wholly within the cup concavity, (b) may be closely faced (within 10 to 24 in.) of tubes or work without flame impingement or hot spots, and (c) may be distributed in any number and in any desired pattern over any furnace wall or roof surface—so that the heat transfer to any portion (however small or large) of a tube-still coil may be independently manipulated to establish any desired shape of the time-temperature heating curve of the oil. In a 50,000,000-Btu heater as many as 200 burners of this type can be distributed over two walls 40 X 20 ft each—each wall only 1 ft 9 in. from the coil it faces.

It is also possible through this firing method to utilize completely premixed gas-air fuel supplies at any burner pressure from a few ounces to 2 or 3 psi gage. With the normal inspirator-type burner, using gas at the orifice (or spud) at a pressure in the neighborhood of 10 to 15 psi gage as well as an even considerable stack draft, actual pressure drop across the combustion ports could not exceed a few ounces at the most. Thus firing with premixed fuel, at burner pressures measured in pounds, gives greater turndown range, i.e., more individual-burner heat output adjustability than heretofore feasible. Also, it seems that with the multiple-ceramic-concavity firing method, it is no longer necessary to provide for more than 5 or 10 per cent excess air if, indeed, any at all ultimately proves to be necessary. Thus the calculations described by Mr. Rickerman will yield different

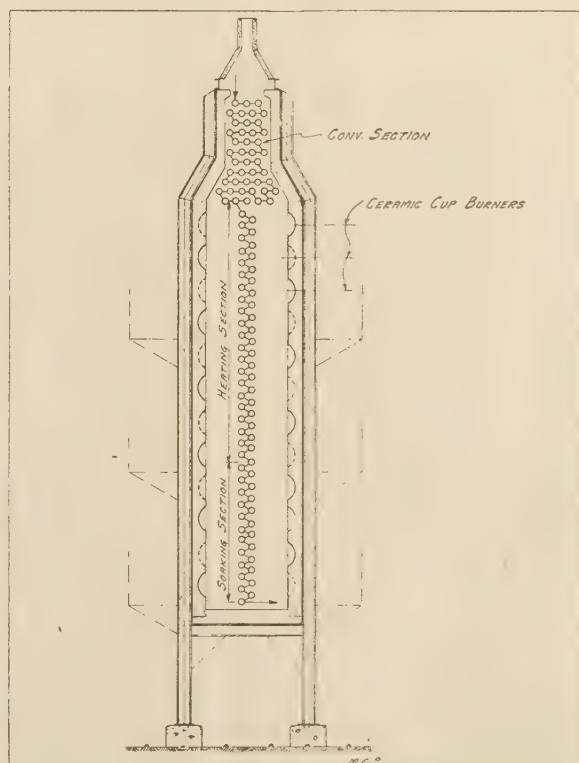


FIG. 6

³ Manager, Liquid Heat-Treating Division, Selsas Corporation of America, Philadelphia, Pa.

heat-transfer results than have been average industry experience to date. Also stacks will become unnecessary.

It is also important to realize that in thermal cracking or other operations in which long soaking times (at given temperatures with carefully balanced small heat inputs) are desired, it is only necessary to throttle the cup burners directed at this coil section—possibly eliminating all necessity for separating soaking chambers from other sections.

Fig. 1 illustrates the considerable simplifications and size reductions of tube-still structures possible with the type of firing described.

AUTHOR'S CLOSURE

In general, Mr. Fleischer's comments on the advantages of short-flame burners are valid, although at the same time it must be pointed out that the *methods* of calculating or designing the furnace do not change at all when such burners are used. The factors or values used in the design equations do change of course, since the equations do take into account all or most of the variables affecting the design.

As to clearances required to avoid flame impingement, obviously they will depend on the expected flame length of the burners used, and experience with the burners under consideration is the best guide to the designer. Nevertheless, it is quite true that by using certain types of burners, such as the ceramic-cup type, or by using a great number of small burners, the flame length is decreased and clearances may accordingly be reduced. The designer must bear in mind the change in over-all furnace cost which may result, on the one hand with a large combustion chamber and a low-cost burner installation, and on the other hand with a

smaller combustion chamber and a high-cost burner installation. He must also keep in mind the auxiliary equipment (such as air blowers) required for some of the special types of burners, and the operating and maintenance cost of both the burners and auxiliary equipment.

Better control of the heating gradient can undoubtedly be obtained by using a large number of small short-flame burners in a small combustion chamber; however, that better control may also entail much closer operational attention in order that the heating gradient may be maintained as desired.

"Turndown ratio" for burners used in the petroleum industry is usually of lesser importance than for burners used in some other industries, except as it enables control of the heating gradient.

The excess air required to burn the fuel is of importance in that it affects the "radiant-section efficiency" or ratio of radiant-section duty to heat liberated and of greater importance, the over-all furnace efficiency. The ceramic-cup burner undoubtedly will operate satisfactorily at lower percentages of excess air than the types of burners commonly used in the petroleum industry.

Mr. Fleischer suggests the elimination of the stack with the furnace which he illustrates. Normally the stack may not be dispensed with because of the second requirement of a stack—that it "dispose of the flue gases into the atmosphere so that they will not be objectionable."

Mr. Fleischer's furnace using the ceramic-cup burners is very interesting and it is felt that this type burner will be used more widely in the future in furnaces of the type shown, or in other arrangements which take advantage of the desirable features of these burners.

Cavitation in Centrifugal Pumps

By A. J. STEPANOFF,¹ PHILLIPSBURG, N. J.

With the introduction of high-head centrifugal pumps of high specific speed, the problem of cavitation became of the utmost importance. As a result, extensive study and experimental work have been done in this field, mostly in connection with hydraulic turbines and with devices without moving parts. In this paper the present state of information on cavitation is presented as it applies to centrifugal pumps, with a method for determining cavitation conditions from velocity considerations. The discussion is illustrated by curves and diagrams. The model test laws as applied to cavitation are deduced, together with their limitations. Theoretical relationships governing cavitation conditions permit establishing means to avoid cavitation, which have been confirmed by experience. A summary of all important conclusions from the recent extensive literature on the subject is presented, and in conclusion, an original explanation is offered of the nature of local high destructive pressures during cavitation and in cases of metal failure by fatigue in the presence of liquids.

INTRODUCTION

IN the last decade no other phase of hydraulic-machinery design and operation has been given so much attention in the technical literature as cavitation. The reason for this has been the use of higher specific speeds, both for hydraulic turbines and centrifugal pumps, with the increased danger of cavitation. To cope with the problem, experimental and theoretical studies of cavitation have been made on hydraulic turbines, centrifugal pumps, and apparatus without moving parts such as Venturi-shaped water conduits. As a result of the study and accumulated experience, modern pumps operating at higher speeds are now safer against cavitation damage than in the recent past. In this paper, an attempt is made to present a summary of the acquired knowledge on cavitation as it applies to centrifugal pumps.

DEFINITION OF CAVITATION

The term "cavitation" refers to conditions within the pump, where, due to a local pressure drop, water-vapor-filled "cavities" are formed, which collapse as soon as such vapor bubbles reach regions of higher pressure on their way through the pump. In order to form such vapor cavities, the pressure first has to drop to the vapor pressure corresponding to the prevailing water temperature. The liberation of air or the formation of air- or gas-filled cavities, however, is not sufficient to produce cavitation, as the effect of air bubbles on the performance and behavior of the pump is different.

Cavitation should be distinguished from "separation," which is a separation of the streamlines from the low-pressure side of the vane and the formation of a turbulent wake behind the vane. Separation is possible only with real viscous fluids, while

cavitation is possible with hypothetical perfect liquids too. Experimentally, separation has been found to be able to exist without cavitation, and cavitation without separation. Although centrifugal fans work on the same principle as centrifugal pumps, the former can have separation while the latter can have both separation and cavitation. Cavitation can appear along stationary parts of a hydraulic machine or along a moving vane, as in the case of centrifugal-pump impellers.

The reduction of the absolute pressure to that of vapor tension may be either general for the whole system or just local which may be realized without a change of the average pressure. The general pressure drop may be produced by (a) an increase in the static lift of the centrifugal pump; (b) a decrease of the atmospheric pressure with a rise in the altitude; (c) a decrease of the absolute pressure on the system, as in the case of pumping from vessels under vacuum; or (d) an increase of the temperature of the pumping liquid, which has the same effect as the decrease of absolute pressure of the system.

The local decrease of pressure is caused by one of the following dynamic means: (a) An increase of velocity by speeding up the pump; (b) a result of separation and contraction (viscosity); and (c) a deviation of streamlines from their normal trajectory, such as takes place in a turn.

Cavitation may also be caused by a sudden starting, and stopping, and recoil of the water column, such as occur during water-hammer phenomena. This type of cavitation is of a transient character and is of slight importance in centrifugal-pump practice.

SIGNS OF CAVITATION

Cavitation is manifested by one or several of the following signs, all of which adversely affect the pump performance and may damage pump parts in severe cases:

(a) *Noise and Vibration.* This is caused by the sudden collapse of vapor bubbles as soon as they reach the high-pressure zones within the pump; the bigger the pump, the bigger the noise and vibration. While these signs of cavitation may appear in the normal operating range of the pump only if the suction head is not sufficient to suppress cavitation, noise and accompanying vibration are present in all pumps to a varying degree when operated at points far removed from the best-efficiency point due to a bad angle of attack at entrance to the impeller. By admitting small amounts of air into the pump suction, noise can be almost completely eliminated. In this way the air serves as a cushion when the vapor bubbles collapse. This method, however, is not often resorted to for elimination of noises in centrifugal pumps, although it is an established procedure with water turbines and large butterfly valves where air is admitted automatically at partial loads (1, 2, 29).² The beneficial effect of air admission to the pump suction under cavitation conditions is not limited to the elimination of noise and mechanical vibration, for the impeller-vane pitting is also reduced if not entirely eliminated, as this is caused by the mechanical shock accompanying the collapse of the vapor bubbles.

(b) *Drop in Head-Capacity and Efficiency Curves.* This appears to a different degree with pumps of different specific speed. With low-specific-speed pumps (up to 1600), the head-capacity, the efficiency, and the bhp curves drop off suddenly

² Numbers in parentheses refer to the Bibliography at the end of the paper.

¹ Development Engineer, Ingersoll-Rand Company. Mem. A.S.M.E.

Contributed by the Hydraulic Division and presented at the Semi-Annual Meeting, Pittsburgh, Pa., June 19-22, 1944, of THE AMERICAN SOCIETY OF MECHANICAL ENGINEERS.

Awarded the First Prize by the Hydraulic Institute, 1942.

NOTE: Statements and opinions advanced in papers are to be understood as individual expressions of their authors and not those of the Society.

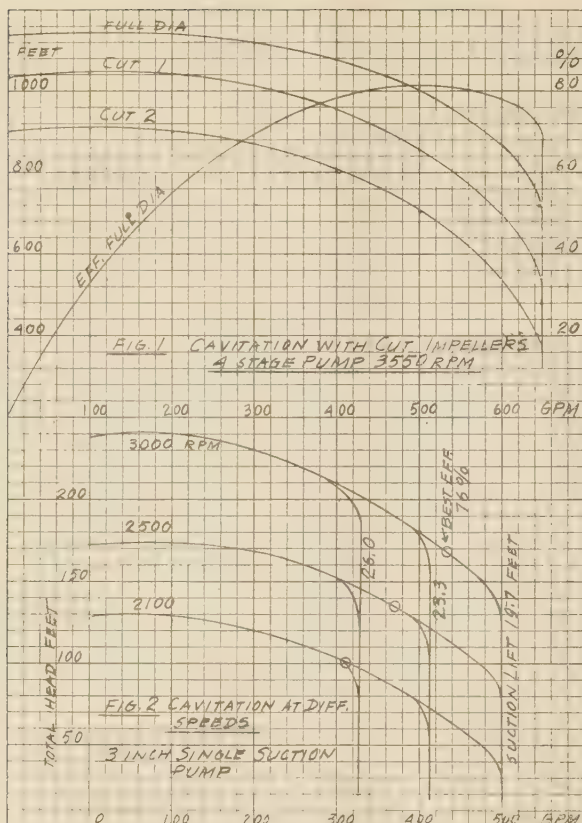


FIG. 1 (Top) CAVITATION WITH CUT IMPELLERS
(Four-stage pump, 3550 rpm.)

FIG. 2 (Bottom) CAVITATION AT DIFFERENT SPEEDS
(Three-inch single-suction pump.)

when cavitation is reached, Figs. 1 and 2. With higher-specific-speed pumps (1500–5000), however, the head-capacity and the efficiency curves begin to drop along the whole range gradually before the point of sudden breakoff is reached, Fig. 3. The degree of drop in the head-capacity and efficiency curves depends on the specific speed and on the suction pressure, increasing for higher specific speed and lower suction pressure.

With high-specific-speed pumps (above 6000) of the propeller type, there is no definite breakoff point on the curves, Fig. 5; instead, there is a gradual drop in the head-capacity and the efficiency curves along the whole range. In these types of pumps, the drop in the efficiency appears before there is a perceptible drop in the head-capacity curve. Therefore a drop in the efficiency is a more reliable criterion of approaching cavitation conditions. Even the objectionable noise may not appear until cavitation has progressed beyond the point where the efficiency becomes unsuited commercially.

Variations in the behavior of pumps of different specific speeds result from differences in impeller design. Low-specific-speed impeller vanes form a definite channel, the length of which depends on the vane angles, the number of vanes, and the ratio of the impeller-eye diameter D_1 to the impeller outside diameter D_2 , Fig. 7. When the pressure at the impeller eye reaches the vapor pressure, usually on the back side of the vane entrance tips, it extends rapidly across the entire width of the channel A–B, Fig. 7(a), with a small increase in capacity and decrease in head. A further drop in the discharge pressure does not

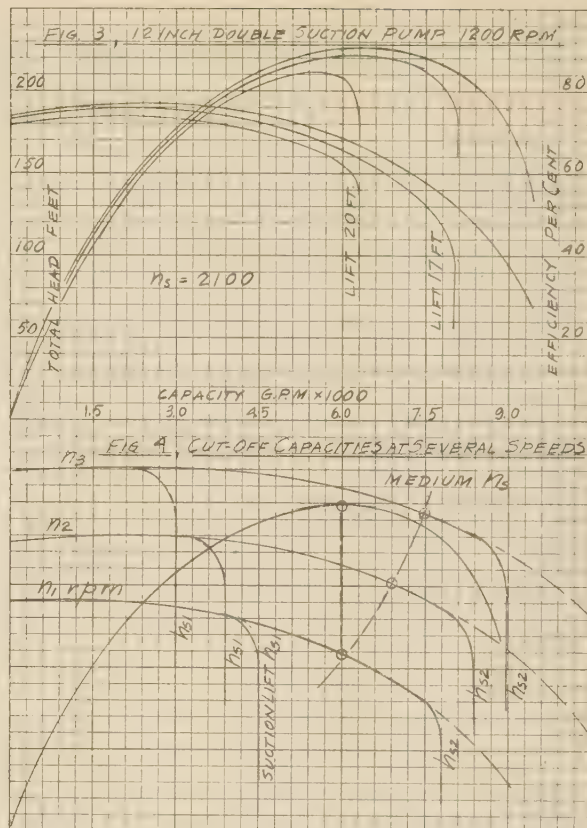


FIG. 3 (Top) CURVES FOR 12-IN. DOUBLE-SUCTION PUMP; 1200 RPM

FIG. 4 (Bottom) CUTOFF CAPACITIES AT SEVERAL SPEEDS

produce any more flow, as the pressure differential moving water to the impeller eye cannot be increased any more. This differential is fixed by the suction pressure outside of the pump, and the vapor pressure across the whole channel between any two vanes at the impeller entrance.

With high-specific-speed impellers, the channel between two vanes is wider and shorter, Fig. 7(b). It requires more drop in head and increase in capacity to extend the vapor-pressure zone

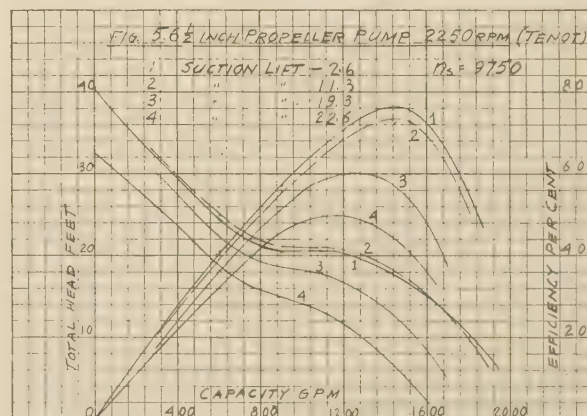


FIG. 5 CURVES FOR 6 1/2-IN. PROPELLER PUMP; 2250 RPM
(Tenot, bibliography reference 19.)

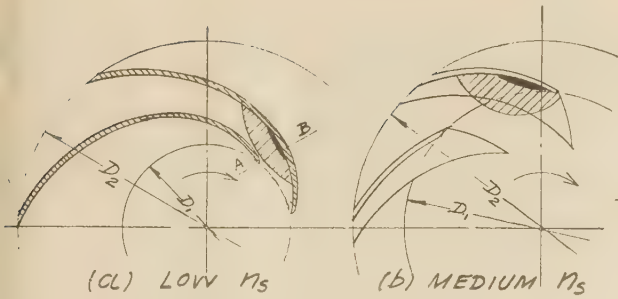


FIG 7, LOW PRESSURE ZONES ON UNDERSIDE OF VANES

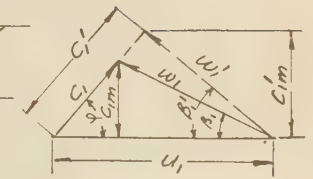
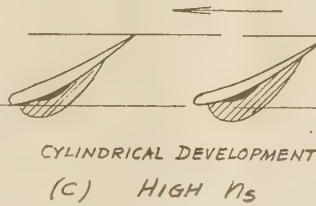


FIG. 6, ENTRANCE TRIANGLE

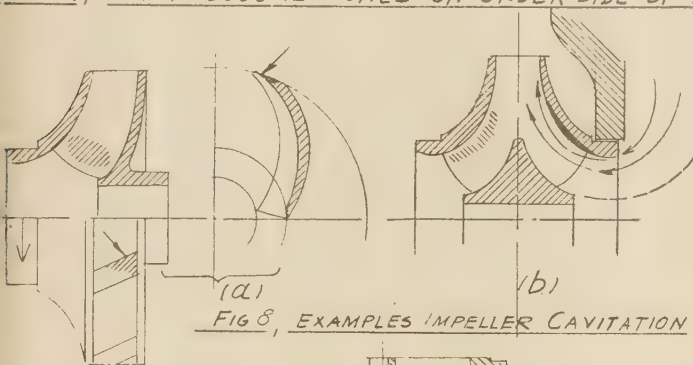


FIG 8, EXAMPLES IMPELLER CAVITATION

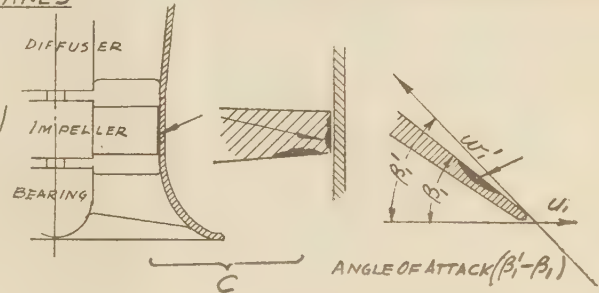


FIG 6(a), VANE TIP

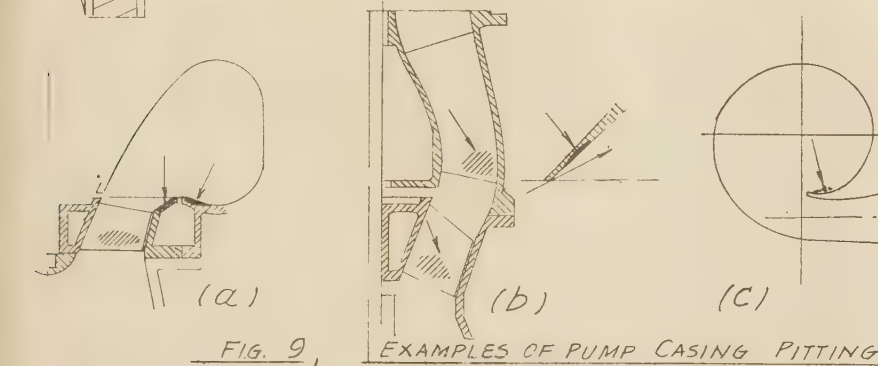


FIG. 9, EXAMPLES OF PUMP CASING PITTING

FIG. 6 ENTRANCE TRIANGLE; FIG. 6(a) VANE TIP; FIG. 7 LOW-PRESSURE ZONES ON UNDERSIDE OF VANES; FIG. 8 EXAMPLES OF IMPELLER CAVITATION; FIG. 9 EXAMPLES OF PUMP-CASING PITTING

across the entire channel. Therefore the drop in the head-capacity curve extends through a wider range before the sudden breakoff occurs. With propeller pumps, the vanes do not overlap, Fig. 7(c). Therefore although the low-pressure zone extends when the pump head is reduced, there are always parts of the channel which remain at pressures higher than the vapor pressure, and the flow through the impeller will steadily increase even though cavitation has definitely set in.

With low- and medium-specific-speed pumps, a reduction in capacity, instead of an increase, is frequently observed at reduced discharge pressure under cavitation conditions, Fig. 13. This is caused by a further increase of the low-pressure zone along the impeller channel, and the expansion of air in the vacuous pockets.

In multistage pumps, cavitation affects only the first stage; therefore the drop in head capacity and efficiency is less pronounced than in a single-stage pump. The cutoff capacity is determined by the first stage.

The drop in the head-capacity and the efficiency curves may begin before the vapor pressure is reached in certain parts of the impeller suction. This is caused by the liberation of air or light

fractions in petroleum oils at reduced pressures in the impeller eye. The absolute pressure in the vacuous pockets is the sum of all the partial pressures of the gases occupying this space, in accordance with Dalton's law of partial pressures.

The drop in the head-capacity and the efficiency curves, due to liberation of free air in the water, is followed by a reduction in the bhp also. This method has been suggested (3) as a means to reduce the head and at the same time save power instead of throttling the pump discharge, as is done ordinarily. Fig. 10 is a reproduction of test results by Siebrecht, showing the head-capacity, efficiency, and bhp curves of a pump with different volumes of air admitted to the pump. The author does not know of any case where this method was employed in actual installations, but a modification of this method whereby the pump suction is throttled instead of the discharge to reduce the head, is frequently employed.

At reduced suction pressures, air or gases begin to be liberated from the liquid, producing a lower head-capacity curve and lower bhp. However, this method is not recommended because if suction-throttling is carried too far, cavitation will start

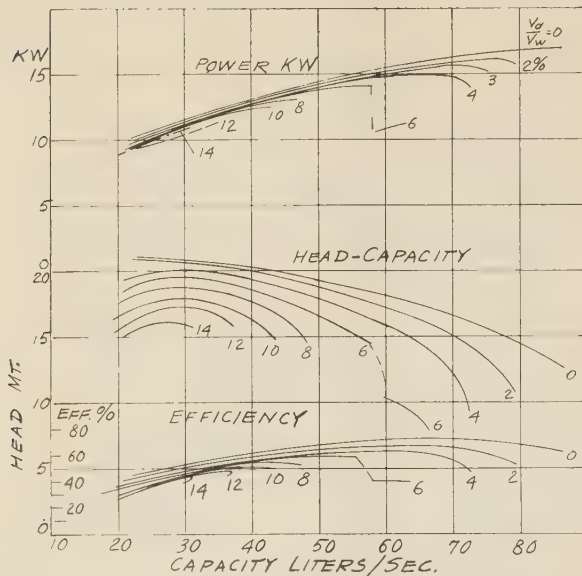


FIG. 10 PERFORMANCE WITH DIFFERENT AIR-WATER RATIO V_L/V_W (SIEBRECHT)

with all its bad effects, i.e., noise, pitting, and vibration. Fig. 11 shows a test of a 5-in. pump with the suction and the discharge throttled. A comparison of the bhp curves, Fig. 11, shows the power saved by suction-throttling (4).

On several occasions, it has been found by careful tests on centrifugal pumps and water turbines, that the efficiency may show a slight increase shortly before cavitation sets in, Fig. 13. This is explained by a reduction of friction at the beginning of separation, just before the disturbing water-hammering begins (5, 9, 12, 22).

(c) *Impeller-Vane Pitting and Corrosion-Fatigue Failure of Metals.* If a pump is operated under cavitating conditions for a sufficient length of time, impeller-vane pitting appears, the amount of metal lost depending on the material in the impeller and the degree of cavitation. Foettinger (5) showed conclusively that vane pitting is caused solely by the mechanical (water-hammer) action of collapsing vapor bubbles, and that electrolytic and chemical action is entirely insignificant in this process. He proved this by producing cavitation in a Venturi made of neutral glass which was pitted in the same manner as the metal in a centrifugal-pump or water-turbine impeller vanes. If electrolytic or chemical reaction is active, it should affect all the parts of the same material and not only the spots subject to cavitation water hammer.

The fact that air or gases may be more active at the instant of liberation has been stated in the past. However, the places affected by pitting are always beyond the low-pressure points

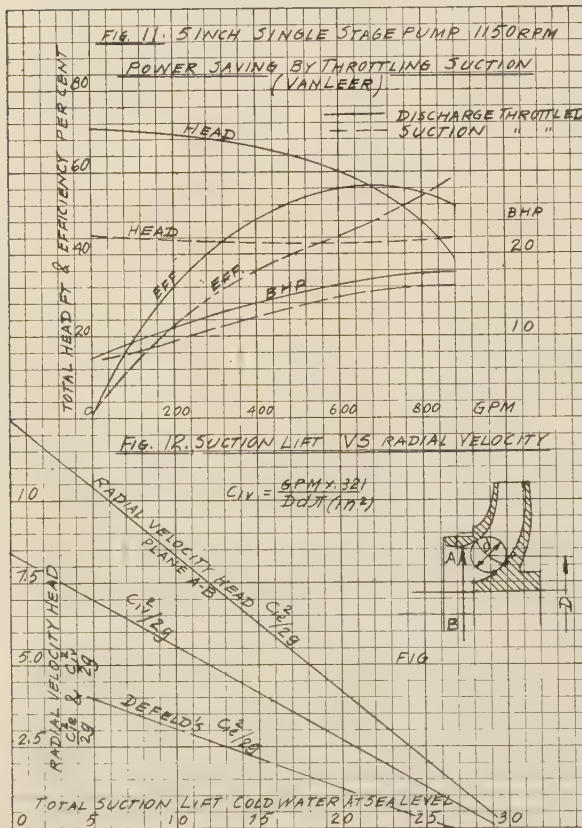


FIG. 11 (Top) CURVES FOR 5-IN. SINGLE-STAGE PUMP; 1150 RPM (Power saving by throttling suction; Van Leer, bibliography reference 4.)

FIG. 12 (Bottom) SUCTION LIFT VERSUS RADIAL VELOCITY

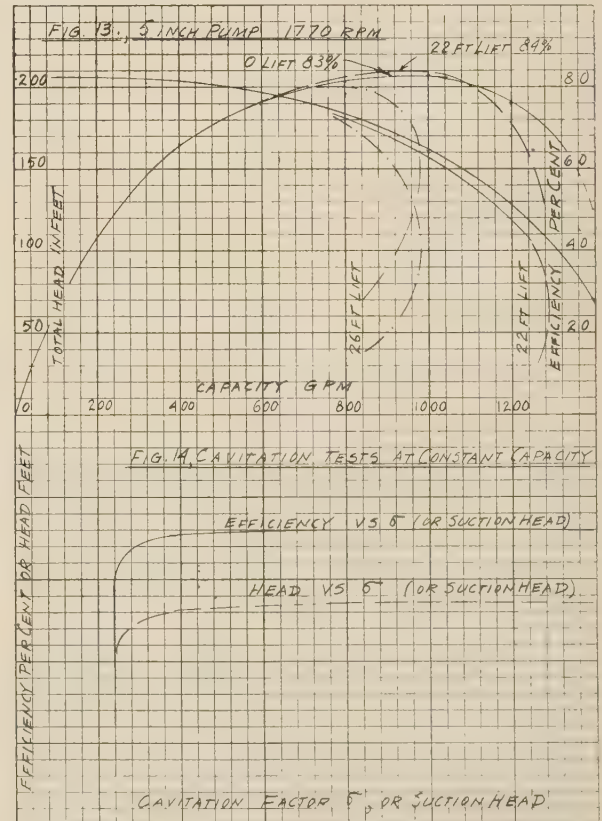


FIG. 13 (Top) CURVES FOR 5-IN. PUMP; 1770 RPM

FIG. 14 (Bottom) CAVITATION TESTS AT CONSTANT CAPACITY

where the vapor bubbles are formed. Another corroboration of the mechanical nature of the metal destruction has been shown by the damage of a lead plate without any loss of weight (6).

By experience it has been found that, when the collapse of vapor bubbles takes place entirely surrounded by the stream of liquid, it is harmless (6). In addition to metal destruction due to the fatigue of the metal surface as a result of repeated water-hammer blows, Poulter (7) has shown that metal particles can be torn off and carried away by liquid penetrating into and escaping from the pores of the metal under successive pressure waves. In that case, more porous materials are most readily affected by such destruction. The degree of destruction depends on the time the specimen is under pressure or the time between two successive pressure waves.

There seems to be no correlation between the hardness and cavitation erosion of metals, but apparently the molecular size and the viscosity of liquids play an important part in cavitation pitting.

Cavitation pitting should be distinguished from "corrosion" and "erosion." The first is caused exclusively by chemical and electrolytic action of the pumped liquids; the second is the wearing away of the metal parts in a pump by foreign bodies carried by the pumped liquids, such as sand, grit, coke, and coal. There is no difficulty in distinguishing between these three kinds of pitting by the appearance of the attacked parts and their location in the water passages of the pump.

Frequencies of hammering were recorded from 600 to 1000 cycles per sec by Hunsaker and up to 2500 cycles per sec by de Haller (8). The intensity of hammering depends on the velocity. Pressures of 300 atm were measured by de Haller. Local pressures confined to very small areas (1.5 mm was the piston area of de Haller's pressure-measuring device) may be considerably higher than those recorded. A satisfactory explanation of how such high pressures may arise in the case of cavitation has been lacking.

In the light of Poulter's investigation (7), it may appear possible that high destructive pressures are derived from the elastic forces of metal parts extending over areas larger than those actually attacked by cavitation. These parts are under fluctuating forces of great magnitude so great that often the whole foundation supporting the pump is set in vibration under cavitation conditions. Under fluctuating stresses, liquid is drawn in

and squeezed from the pores, and it is during this squeezing phase that tremendous pressures may be produced in small restricted areas.

Similar mechanism can be applied as a partial explanation of what is known as "corrosion fatigue" of metals, or metal failure under repeated stresses in the presence of liquids. The "corrosive" effect of water, as compared with oils in the case of "corrosion fatigue," is due to the fact that water molecules are smaller than those of oil; therefore water penetration of metals would be deeper than that of oil; hence the destructive effect on the metal is greater where it is subjected to rapidly fluctuating stresses. This will explain the failure by "corrosion fatigue" of noncorrosive high-chromium steels in the presence of water. Another illustration and proof that the penetration of metals by liquid plays an important part in metal destruction by "corrosion fatigue" is furnished by results of laboratory tests by McKay and Worthington (30). They have found that the endurance limit depends not only on the stress level and the total number of cycles, but also on the frequency of stress reversals. For the same total number of cycles, the low frequency gives much lower endurance limit because more time is allowed for liquid penetration of metal with, consequently, higher destructive pressures developed in the metal pores when the liquid is compressed on the stress reversal.

MATERIALS TO RESIST CAVITATION PITTING

Different materials resist cavitation pitting to a different degree. In addition to the chemical composition, the heat-treatment of metals and also the surface conditions control the amount of material destroyed by cavitation. The behavior of metals under cavitation parallels that under "corrosion-fatigue" conditions. Any notches, nicks, scratches, flaws, or sharp corners on the surface of metals attacked by cavitation accelerate the beginning of pitting. Protective coats do not improve the resistance of metals to cavitation pitting.

H. Schroeter (10) has run tests on different materials under cavitation in a Venturi-shaped conduit built for the purpose. Table 1 gives results of his tests. A velocity of 197 fps was maintained throughout these tests. The accelerated rate of metal destruction can be seen by comparing the amount of metal lost after 15 hr and 44 hr of the same materials. Fig. 15 also shows some materials tested by Schroeter.

Hardening decreases the rate of metal destruction, although

TABLE 1 LOSS OF METAL BY VOLUME, CU MM, BY CAVITATION ACTION (SCHROETER)

Metal	Approximate composition	Volume loss, cu mm	Brinell hardness	Strength, psi
Krupp steels, after 44 hr:				
1 Cast steel.....	63
2 Carbon steel, hardened.....	28
3 HB 6597 annealed.....	27
4 Special nitrided steel.....	25
5 VM annealed.....	Ni, low; Cr, 11-15	22
6 Nirosa cast.....	C, 1.0-2.0 Ni, low; Cr, 24	17
7 HB 6597 case-hardened.....	12
8 VM hardened.....	8
9 HB 6597 hardened.....	6
10 V2A forged.....	C, 0.2; Ni, 7.0; Cr, 20	6
11 WF 100 forged.....	5
12 F 1548 hardened.....	4
Bronzes, after 44 hr:				
1 Manganese bronze.....	76.5	129	79500
2 RG 10 (Krupp).....	Cu, 86; Pb, 10; Sn, 4	42	71	...
3 Aluminum bronze.....	34	148	89500
4 Corrix bronze.....	Cu, 88; Al, 9; Fe, 3	16	106	...
5 DB 16 (Krupp).....	Cu, 84	6	95	...
Bronzes, after 15 hr:				
1 Nickel bronze.....	9.9	139	88000
2 Aluminum bronze.....	8.3	148	89500
3 Manganese bronze.....	7.7	129	79500
4 Aluminum bronze.....	5.1	185	111000
5 DB 12 (Krupp).....	Cu, 88	17	74	...
6 DB 135 (Krupp).....	14	83	...
7 DB 10 (Krupp).....	8	76	...
8 Rg 10 (Krupp).....	Cu, 86; Pb, 12; Sn, 4	4	71	...
9 Corrix bronze.....	Cu, 88; Al, 9.0; Fe, 3.0	1.1	106	...
10 DB 16 (Krupp).....	Cu, 84	0.5	95	...

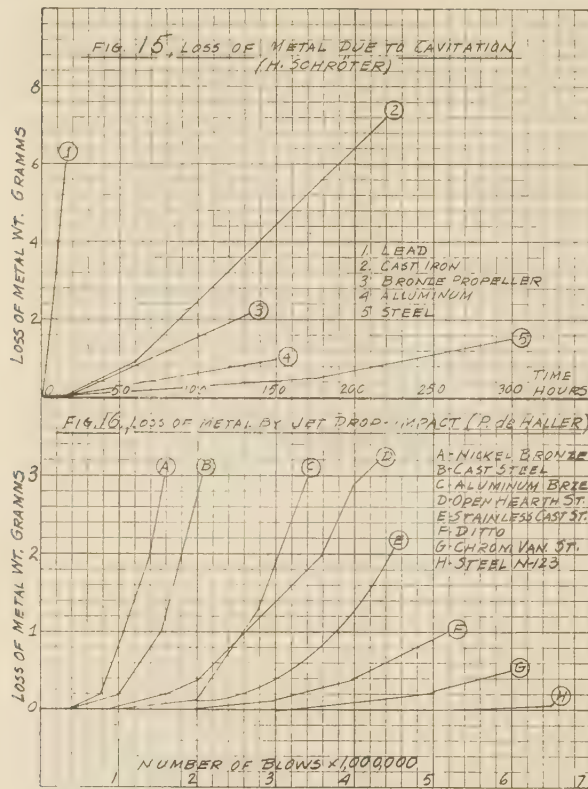


FIG. 15 (Top) LOSS OF METAL DUE TO CAVITATION
(H. Schroeter, bibliography reference 10.)

FIG. 16 (Bottom) LOSS OF METAL BY JET DROP-IMPACT
(de Haller, bibliography reference 8.)

the hardness alone (for different materials) is not a determining factor in so far as resistance to cavitation is concerned.

To prolong the life of runners of large Kaplan turbines working under high heads, (over 50 ft), the turbine manufacturers protect with welded stainless steel the places subject to cavitation pitting (11). Propeller pumps of the same type are not built in sizes justifying such procedure, nor are they operated at such high heads.

Although covering the surface of metals with rubber helps to resist the impact of water-hammering very well, its bond to the metal fails after a short time. No practical method of rubber protection of metals against cavitation has yet been developed. Tests with rubber again corroborate the mechanical nature of cavitation destruction of materials (10).

Schroeter's tests have definitely established the fact that the beginning of cavitation and its extent depends on the velocity of the flow. This must be expected as all the destructive blows by water hammer derive their energy from the kinetic energy of the flow.

P. de Haller (8) has found that there is an analogy between the behavior of various metals during tests with direct drop-impact and cavitation. In both cases the metal destruction is caused by water-hammering. Although the mechanism of water blows against metals is different, their result is quite similar. In a special apparatus resembling a steam-turbine wheel, de Haller ran erosion tests on a number of materials, and his results, reproduced in Fig. 16, are in agreement with those by Schroeter. De Haller's method of testing materials for cavitation resistance requires only a short time to produce cavitation pitting.

Kerr (31) has tested 80 materials for cavitation in sea water in a special vibratory apparatus developed by the Massachusetts Institute of Technology. These tests show that cavitation damage with sea water was slightly greater than with fresh water. It has been found also that temperature of water has a marked effect on the metal loss by cavitation, the loss increasing with temperature. At higher temperatures the amount of air dissolved in water is reduced, thus reducing the cushioning effect of water-hammer blows, at the same time the increased vapor pressure tends to increase the vapor bubble formation.

Mousson (32) has found that loss of metal by cavitation is approximately proportional to vapor pressure. He also demonstrated the beneficial effect of admission of small amounts of air on the metal damage by cavitation. Mousson and Kerr give extensive test data which is useful in selection of materials when cavitation is expected.

EXAMPLES OF METAL ATTACK BY CAVITATION

In pumps of normal design, the lowest pressure occurs on the back side of the impeller vane slightly beyond the suction edge. The cavitation pitting appears somewhat farther upstream where the vapor bubbles collapse, Figs. 8(a), 9(a), 9(b). However, if the pump is operating continuously at a capacity considerably higher than normal, the pitting may appear on the front side of the vane at the suction-vane tips, Fig. 6(a). Cavitation in this case accompanies separation resulting from a bad angle of attack.

Fig. 8(b) shows vane and shroud pitting near the outer shroud, due to lack of streamlining.

Fig. 8(a) shows vane pitting at the impeller discharge caused by the vane's blunt discharge tips.

Fig. 8(c) shows a "marginal" cavitation observed on propeller pumps and also on centrifugal pumps with open impellers. Local high velocity through the clearance, and separation due to a sudden change in direction produce the "marginal" cavitation and pitting. Rounding off of the high-pressure side corners of vanes eliminates the marginal pitting at the expense of increased leakage through the clearance (12).

Fig. 9(a) shows pitting of the volute casing of a propeller pump caused by lack of streamlining.

Fig. 9(b) shows a diffusion-casing vane pitting due to a discrepancy between angles of incoming flow and diffusion vane.

Fig. 9(c) shows pitting of the tongue of a volute casing observed when a pump is operated continuously at capacities above the normal.

Fig. 9(d) is an example of pitting of the baffle in the suction nozzle, permitting excessive prerotation of the flow before it enters the impeller eye.

In general, sudden change in direction, a sudden increase in area, and lack of streamlining are responsible for local pitting of pump parts. This may appear only if the suction pressure is reduced below a certain minimum. On the other hand, pitting of pump parts on the discharge side of the pump has been observed when the pump pressure is not high enough to suppress cavitation.

THEORETICAL RELATIONSHIP AT CAVITATION CONDITIONS

The flow to the impeller of a centrifugal pump is produced by the existing pressure difference between the suction pressure and the pressure established by the flow at the impeller eye. The latter is not uniform at any section of the impeller passages, and even determination of the average pressure inside the impeller presents difficulties. For that reason, the theoretical relationship for the flow through the impeller eye, while easy to establish, does not give a reliable tool for an accurate predetermination of cavitation conditions. An examination of the theoretical

formulas for the flow through the impeller eye, however, enables one to learn the effect of several factors upon cavitation. A study of theoretical relationship has also resulted in the introduction of simplified formulas incorporating experimental coefficients which permit prediction of a pump's behavior as to cavitation if experimental data are available on similar pumps.

Let H_a be the absolute pressure prevailing at the surface of the pump-suction supply. This will be atmospheric pressure if the suction vessel is open to the atmosphere. If the suction is taken from an enclosed vessel, H_a is the absolute pressure in this vessel.

h_s = static head in suction vessel above pump center line.

If it is suction lift, it is negative

h_v = vapor pressure at prevailing water temperature

h_L = head loss in the suction pipe and impeller approach

c_1 = average absolute velocity through impeller eye (Fig. 6)

$\lambda \frac{w_1^2}{2g}$ = local pressure drop below average at point of cavitation.

Here w_1 is average relative velocity at entrance, and λ is an experimental coefficient

This local pressure drop is caused by the difference in pressure on the leading and trailing sides of the vane. When pressure is applied by the vane on water, the water exerts an equal reaction in the opposite direction, which exists as a pressure difference on the two faces of vanes. This is frequently referred to as a "dynamic depression."

Fig. 19 shows a typical pressure distribution inside an impeller channel obtained by Uchimarū (28) under actual operating conditions.

Evidently cavitation starts when

$$H_a + h_s = h_L + h_v + \frac{c_1^2}{2g} + \lambda \frac{w_1^2}{2g} \dots \dots \dots [1]$$

When liquid in the suction vessel is boiling, the pressure in the vessel H_a is equal to the vapor pressure or $H_a = h_v$ and Equation [1] becomes

$$h_s = h_L + \frac{c_1^2}{2g} + \lambda \frac{w_1^2}{2g} \dots \dots \dots [2]$$

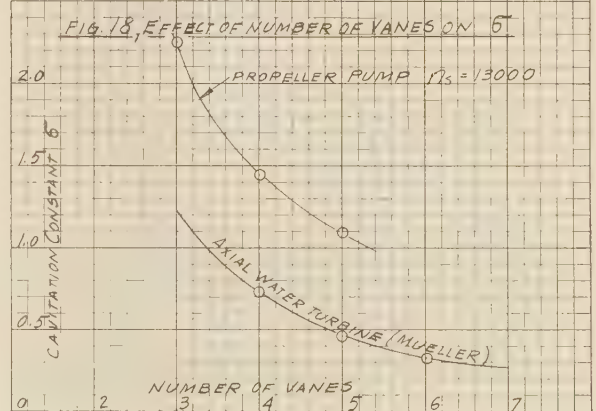
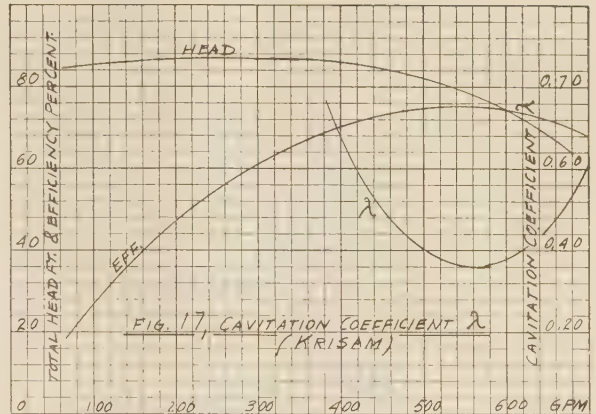


FIG. 17 (Top) CAVITATION COEFFICIENT λ
(Krisam, bibliography reference 13.)

FIG. 18 (Bottom) EFFECT OF NUMBER OF VANES ON σ

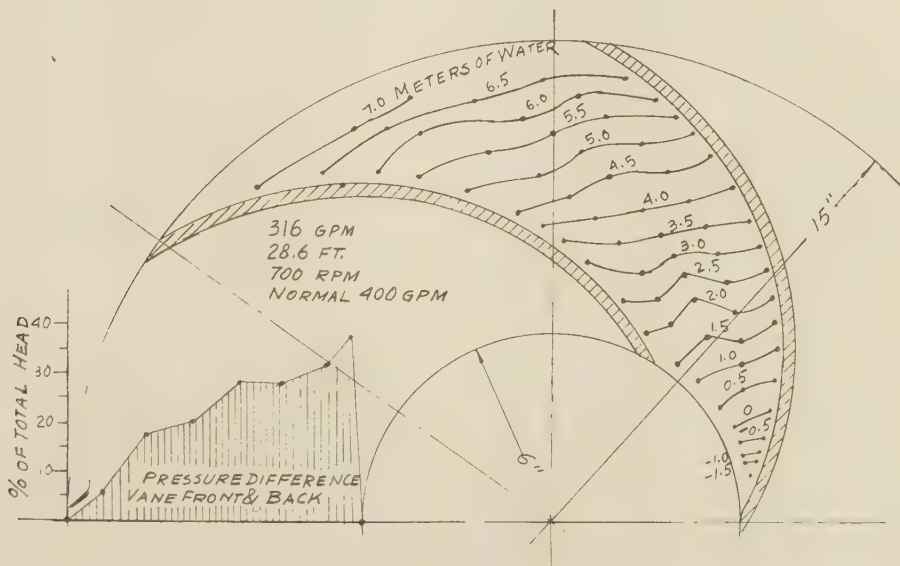


FIG. 19 PRESSURE DISTRIBUTION INSIDE IMPELLER
(Uchimarū, bibliography reference 28.)

meaning that a positive suction head h_s is necessary to produce the flow. To prevent vaporization, an excess of suction head is necessary above h_v .

Equation [1] is not suitable for determining the maximum permissible suction lift for a given pump capacity (c_1 and w_1), because the true value of maximum c_1 is not known, and also because the value of λ varies for pumps of different specific speed. Even for a given pump at constant speed, λ varies with capacity, being a minimum near the best-efficiency point and increasing on both sides of this point. Fig. 17 shows a typical curve of λ variation obtained by Fritz Krisam (13). Similar curves were published by von Widdern (14). The increase of λ on both sides of the best-efficiency point shows the effect of the "angle of attack" Fig. 6(a), between the direction of relative velocity and the vane angle at the impeller entrance.

FACTORS AFFECTING CAVITATION

A study of Equation [1] permits making a number of conclusions which hold in practice, for at cavitation conditions, a change in one term of the equation is always followed by a change in another to satisfy the relationship, thus:

(a) If atmospheric pressure is decreased due to an increased elevation (about 1 ft per 1000 ft of elevation), the pump maximum capacity will decrease (c_1 and w_1 will decrease).

(b) If suction lift is increased ($-h$ greater), or vapor pressure rises due to higher temperature of water, pump maximum capacity will decrease.

(c) Higher suction lifts may be possible with low velocities (c_1 and w_1) or with a minimum loss h_L in the suction pipe.

(d) Note that H_a expressed in feet of liquid depends on the specific gravity of the liquid. Thus when pumping molten salt, (used as a heating medium in the petroleum-refinery process), of specific gravity of 1.75, and the suction vessel under atmospheric pressure, $H_a = 19.4$ ft. Therefore, the danger of cavitation is much greater with heavier liquids (15). Vapor pressure should not be overlooked with liquids different than water.

(e) For given average velocities, c_1 and w_1 , the approach of cavitation is affected by the casing and impeller design as they affect the velocity distribution. Thus pump-suction design permitting more prerotation in the impeller eye will lower the maximum capacity for a fixed suction pressure. Any lack of streamlining in the suction passages of the pump and impellers results in the formation of dead water pockets (separation), increasing local velocities beyond the average or those obtained from the velocity triangle.

(f) With pumps of high specific speed of the straight-propeller type, the beginning of cavitation is indicated by a gradual drop of pump efficiency without any sudden drop in head capacity. In this case a further reduction in the suction pressure extends to the region affected by cavitation, and Equation [1] does not apply, as the vapor pressure is reached locally only; the impeller vanes do not form an entirely enclosed channel, and Bernoulli's equation (Equation [1]) cannot be used.

(g) The presence of gases in the liquid does not affect the validity of Equation [1], except that, according to Dalton's law of partial pressures, the vapor will behave as if it occupied the voids alone, and vaporization will begin at absolute pressure higher than its normal boiling point corresponding to the existing temperature. Petroleum oils represent the most complicated example of that. Being a mixture of different individual hydrocarbons, each having its own vapor pressure, light fractions will vaporize at pressures far above their normal boiling points, but the vaporization will affect only a small portion of the total flowing volume. As a result, the drop in the $Q-H$ curve is more gradual with oils than with water, and the mechanical disturb-

ance is not so violent. The fact that vaporization and condensation during cavitation require a heat exchange, tends to slow down the bubble formation in oils, as compared with water on account of the lower heat conductivity of oil.

(h) When studying cavitation, the suction pressure should be specified or measured at the pump-suction nozzle. In this way the loss in the suction pipe and the entrance loss are eliminated. The loss in the suction nozzle is negligibly small due to a low velocity, short distance, and accelerated flow in a normal nozzle design.

(i) In small pumps of low specific speed, the term $\frac{c_1^2}{2g}$ is pre-dominant in setting up cavitation conditions, and the term $\lambda \frac{w_1^2}{2g}$ is of little significance. In high-specific-speed pumps, approaching propeller-pump type, the term $\lambda \frac{w_1^2}{2g}$ is the controlling factor, $\frac{c_1^2}{2g}$ is of secondary importance. Term $\lambda \frac{w_1^2}{2g}$ depends on the pump head (and hence speed) and number of impeller vanes, decreasing with smaller head or speed and greater number of vanes.

With low-specific-speed pumps, the maximum capacity for a given suction head can be increased by cutting away part of the vanes in the impeller eye and filing the vane tips, thus increasing the available area for c_1 . With propeller pumps, increasing the number of vanes will improve the cavitation conditions of the pump, Fig. 18, for a given submergence, permitting higher head without noise or drop in efficiency.

(j) With low-specific-speed pumps, the maximum absolute velocity c_1 may be reached either at the impeller eye (section A-B, Fig. 12), or at the vane entrance. The actual effective area of both sections is greatly affected by the impeller-approach design. When studying the cavitation test data, both sections should be investigated.

PREDETERMINATION OF CAVITATION CONDITIONS FROM VELOCITY CONSIDERATIONS

From a great number of observations on pumps of low and medium specific speeds (up to 1500), the author has found that for cold water, 70 F, Equation [1] can be simplified to

$$30 - h_s = 2.4 \frac{(c_{1e})^2}{2g}$$

Where c_{1e} is the meridional velocity through the impeller eye at cutoff capacity (plane A-B, Fig. 12) at suction lift h_s taken at the suction nozzle and referred to the pump-shaft center line. The same relationship is represented by a curve in Fig. 12.

A similar curve was plotted for meridional velocities at the vane entrance tips and is shown in Fig. 12. This curve can be expressed by an equation

$$30 - h_s = 3.5 \frac{c_{1e}^2}{2g} \dots \dots \dots [3]$$

Fig. 12 also shows a curve given by Defeld in his book on centrifugal pumps (16). Velocities shown by this curve have been greatly exceeded in modern pumps.

Comparing Equations [2] and [3] with Equation [1], the following remarks can be made:

(a) The difference between the atmospheric pressure $H_a = 34$ and 30 in Equations [2] and [3], or 4 ft, includes 0.85 ft vapor pressure at 70 F water temperature; the loss of head (h_i) in the suction nozzle; local drop in pressure due to uneven velocity distribution in the impeller approach, and a small margin of safety.

(b) The right-hand term in Equation [2] can be expanded as follows

$$2.4 \frac{(c_{1e})^2}{2g} = \frac{c_1^2}{2g} + \lambda \frac{w_1^2}{2g} = \frac{(c_{1e})^2}{2g} \left[\frac{1}{(\sin \alpha)^2} + \frac{\lambda}{(\sin \beta_1)^2} \right] \dots [4]$$

Where α is the absolute velocity angle and β_1 the vane angle at entrance, Fig. 6. Similarly in Equation [3], the right-hand terms can be represented as follows

$$3.5 \frac{(c_{1v})^2}{2g} = \frac{c_1^2}{2g} + \lambda \frac{w_1^2}{2g} = \frac{(c_{1v})^2}{2g} \left[\frac{1}{(\sin \alpha)^2} + \frac{\lambda}{(\sin \beta_1)^2} \right] \left[\frac{1}{\delta^2} \right] \dots [5]$$

Term δ is a contraction coefficient to account for the vane thickness, as this has been disregarded when c_{1v} was calculated.

(c) Since curves in Fig. 12 were plotted for low-specific-speed pumps where the term $\lambda \frac{w_1^2}{2g}$ is of secondary importance, the cutoff capacity is determined by the impeller-eye velocity c_{1e} or c_{1v} and is independent of the impeller diameter or pump speed as long as the cutoff capacity occurs at or near the best-efficiency point, as is shown on Figs. 1 and 2. Similar tests were published by von Widdern (14). Within the specified range for a fixed suction head, the cutoff capacity is independent of the specific speed and is governed by the absolute velocity through the impeller eye. The term $\lambda \frac{w_1^2}{2g}$ is either small or else varies little

with the specific speed, and the term $\lambda \frac{w_1^2}{2g}$ bears an approximately constant ratio to the $c_1^2/2g$, thus leaving the experimental numerical constant in the right-hand terms of Equations [2] and [3] essentially constant.

With pumps of medium and high specific speed, (1500 to 4000), the cutoff capacity will increase somewhat with the speed if the cutoff takes place to the right of the best-efficiency point. The cutoff capacity will decrease at higher speeds if cutoff takes place at capacities smaller than normal, Fig. 4. The reason for this is the variation of the coefficient λ in the term $\lambda \frac{w_1^2}{2g}$.

Fig. 17 shows that is a minimum near the best-efficiency point. When the cutoff takes place at capacities over the normal, the best-efficiency point moves nearer to the cutoff capacity at a higher speed where λ is smaller, and thus $\lambda \frac{w_1^2}{2g}$ is smaller, hence

$\frac{c_1^2}{2g}$ or pump capacity will increase. At partial capacities, the peak efficiency moves away from the cutoff capacity at higher speeds, while λ is increasing and the cutoff capacity is decreasing,

Looking at the same phenomena from a different point of view, it will be noticed that where the cutoff capacity is nearer the peak efficiency at higher speed, the angle of attack of the incoming flow at the impeller entrance is smaller, the extent of separation is reduced at the vane tips, and the effective area available for the flow is increased. Thus at the same suction pressure, a higher capacity is possible at a higher speed. When the cutoff takes place at partial capacity and the best-efficiency point is moving further at a higher speed, the angle of attack is increasing, separation is more pronounced, the effective area is reduced, and the cutoff capacity is lower at a higher speed in this case.

Since the best angle of attack may not coincide with the point of best efficiency, the effect of the angle of attack on the maximum capacity at several speeds may not be apparent if the cutoff capacity is not sufficiently removed from the best-efficiency point.

THOMA'S CAVITATION CONSTANT

The experimental relationship between the impeller-eye velocity at cutoff capacity and the suction pressure gives a satisfactory means for predicting cavitation for low-specific-speed pumps.

For higher-specific-speed pumps this connection becomes inaccurate, and besides with high-specific-speed pumps, the drop in efficiency may appear much sooner than the pump-capacity cutoff. There is no simple way to predict beginning of cavitation in high-specific-speed pumps.

D. Thoma, of Munich, has suggested (17) that the dynamic depression, including the velocity head at the impeller eye, can be expressed as a fraction of the total head, or

$$\frac{c_1^2}{2g} + \lambda \frac{w_1^2}{2} = \Delta h = \sigma H \dots \dots \dots [6]$$

The coefficient σ is determined experimentally. Substituting for the dynamic depression its value in terms of σ and H , Equation [1] takes the form

$$H_a + h_s - h_v = \sigma H \dots \dots \dots [7]$$

or

$$\sigma = \frac{H_a + h_s - h_v}{H} \dots \dots \dots [8]$$

The use of the cavitation coefficient σ became quite general among the water-turbine designers and is coming into wide use by the centrifugal-pump builders. When applied to pumps, the numerator in the expression for Equation [8] represents the absolute pressure at the pump-suction nozzle referred to the pump-shaft center line or to the impeller central plane in a vertical pump.

At about the same time as Thoma, Moody and Rogers (18) offered a cavitation coefficient for hydraulic turbines which is defined as follows

$$K_c = \frac{H_a + h_s - h_v - E_d \frac{c_1^2}{2g}}{H} = \frac{\lambda \frac{w^2}{2g}}{H} \dots \dots \dots [9]$$

where E_d is the draft-tube efficiency. The disadvantage of the Moody coefficient is that it excludes from the absolute pressure at the impeller eye the velocity head at the eye, thus confining the cavitation constant to a definite design of the impeller. The true value of the absolute velocity at the impeller eye is difficult to determine as the direction of this velocity is never certain. Thoma's cavitation coefficient, on the other hand, can be applied to the pumping plant without any reference to the pump or turbine design. The pump or turbine is designed to meet the plant's σ with some degree of safety. Thoma's cavitation constant is generally adopted by the industry; Moody's coefficient is more of academic interest.

The use of the cavitation constant σ is subject to a number of considerations as follows:

(a) For the same pump at different speeds or similar pumps operated at the corresponding points (the same specific speed), all velocities vary as \sqrt{H} , and hence

$$\sigma = \frac{\Delta h}{H} = \text{const.} \dots \dots \dots [10]$$

This presupposes that λ in Equation [5] stays constant. This relationship is the basis of all model testing for cavitation. If σ is determined by test for a certain design, Equation [8] or Equation [10] can be used to determine the required suction head for a given pump total head.

(b) Equation [10] holds only at conditions approaching cavitation while the affinity laws still hold. When cavitation sets in, the laws of similarity are not fulfilled and the relationship, $\sigma = \text{const}$, expressing similarity of conditions as to cavitation becomes approximate only.

(c) Tenot (19) gives the following relationship for the similarity as to cavitation when this has progressed beyond the incipient stage

$$\frac{\sigma_1 - \sigma_c}{\sigma_2 - \sigma_c} = \frac{H_2}{H_1} \dots \dots \dots [11]$$

where σ_c is the critical sigma coefficient which is constant for both model and prototype

$$\sigma_c = \sigma_{c1} = \sigma_{c2}$$

$$\sigma_1 = \frac{\Delta h_1}{H_1} \text{ is sigma for the model}$$

$$\sigma_2 = \frac{\Delta h_2}{H_2} \text{ is sigma for the prototype}$$

Terms H_1 and H_2 are the operating heads of the model and prototype, respectively. Tenot has demonstrated the validity of this relationship by high-speed (1/1,000,000 sec) photography of a small propeller pump, operated at several speeds with different suction heads.

Equation [11] can be transformed as follows

Multiply both sides by $H_2 H_1$

$$\frac{\sigma_1 - \sigma_{c1}}{H_2} = \frac{\sigma_2 - \sigma_{c2}}{H_1}$$

$$(\sigma_1 - \sigma_{c1}) H_1 = (\sigma_2 - \sigma_{c2}) H_2$$

$$\Delta h_1 - \Delta h_{c1} = \Delta h_2 - \Delta h_{c2} \dots \dots \dots [12]$$

Equation [12] shows that for cavitation similarity in two pumps, the absolute pressure at the points of minimum pressure in the impellers is equally removed from the critical pressures (vapor pressure) existing at the incipient cavitation conditions. This means that if two pumps operate at different heads, $H_1 \neq H_2$ but the suction pressures are such that $\sigma_1 = \sigma_2$, the pump with the higher head will have cavitation developed to a smaller degree than that prevailing in the low-head pump.

If both model and prototype are tested at the same head $H_1 = H_2$, then

$$\frac{\sigma_1 - \sigma_c}{\sigma_2 - \sigma_c} = 1$$

$$\sigma_1 = \sigma_2$$

and, evidently, if Equation [11] holds and $H_1 \neq H_2$, $\sigma_1 \neq \sigma_2$.

(d) It has been pointed out already that it is difficult to detect the incipient cavitation, and any σ_c determined as a sigma for the critical cavitation conditions really may represent the state of cavitation progressed sufficiently to be measured by the available testing equipment. Therefore the relationships discussed under (c) are of particular importance.

Again, with wider use of high-specific-speed water turbines and pumps, frequently it becomes uneconomical to provide sufficient submergence to suppress cavitation completely under all operating conditions; therefore unless the heads are reproduced in the model testing the conditions $\sigma_1 = \sigma_2$ will only approximately represent the cavitation similarity. In water-turbine practice, when it is impossible to provide a proper submergence due to high cost of excavation, the runner vanes are protected with stainless steel in the places subject to cavitation pitting (20).

(e) To make the discussion of cavitation more definite, the criterion of incipient cavitation should be stated, i.e., whether it is breaking off of the head-capacity curve, drop in efficiency, noise and vibration, or the pitting of the impeller vane. The drop in efficiency is more general as it applies to pumps, irrespective of the specific speed, and may be found while other signs of cavitation are not yet apparent. Depending on the testing facilities and requirements, a drop of 1 per cent or even just a fraction of a point in the efficiency may be taken to indicate that cavitation has already set in.

During cavitation tests, σ variation is obtained either by changing the suction pressure (mostly by throttling), or by changing the pump speed and, hence the head at the same static suction pressure.

While the first method is simpler to arrange, better results are obtained with the variable-head tests. For laboratory testing, a special testing equipment has been used to a limited extent. With this method the pump suction is taken from a vessel which can be kept under different pressures. With a variable-speed drive, this procedure is ideal for accurate σ determination.

Although the same σ value may be obtained with either low head and low suction pressure (high suction lift), or with high head and correspondingly higher suction head (larger pump or higher speed), the physical aspect of the phenomenon as far as cavitation is concerned is not exactly the same. In the first case, the whole suction pipe is under suction lift, and with low velocities, ample time may be available for air or gases to liberate and accumulate in quantities sufficient to impair the pump efficiency and reduce the head capacity before actual formation of vapor bubbles starts. In the second case the pressure drop is mostly dynamic and is limited to a small part of the impeller passages. Besides, with high velocities through the impeller, the time required for the water particles to cross the low-pressure zone is shorter, and, since in all thermodynamic changes time is an essential factor, the relative volume of vaporization and its effect on the pump performance is smaller for high-head pumps (14).

Even for two similar pumps of different sizes operating at the same head and the same σ value (which in this case means the same suction pressure), the extent of cavitation is not in proportion to the pump size, and the bad effects of cavitation will be less pronounced in the large unit.

The water-turbine experience, where model testing is more frequently resorted to than in the pump industry, tends to indicate the truthfulness of the foregoing deductions. F. H. Rogers suggested (21) that "although cavitation starts at the same value of σ for both model and prototype, the vapor-filled cavities are physically about the same dimensions, if the heads are the same, and hence the entire flow pattern through the large runner is affected to a lesser degree than in the case of the small model."

Although the velocities at similar points in the impellers are the same in both pumps under such conditions, the effect of the curvature of the impeller profile or suction approach on the velocity distribution (the maximum local velocity) is not the same in the small model and large prototype. The centrifugal forces, which are instrumental in the distortion of the velocity distribution along the curved path, are inversely proportional to the radius of curvature; therefore negotiating the curves through the impeller eye and suction approach in a large pump results in lower maximum local velocities, as compared with the average, than in a small model.

(f) There are several ways to represent graphically the results of cavitation tests. In one of them σ is determined for several points on the head-capacity curve and plotted versus specific speed of the same points. Fig. 20 shows curves for two pumps plotted on this basis. These curves give complete cavitation

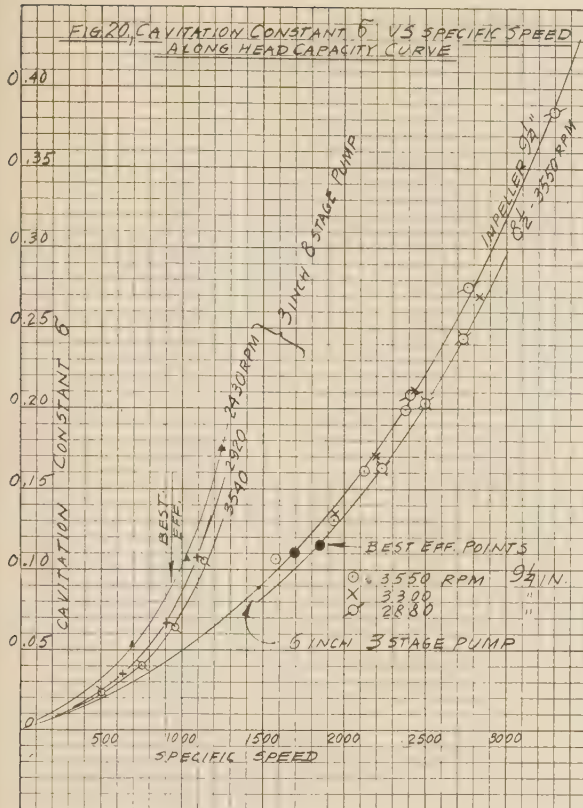


FIG. 20 CAVITATION CONSTANT σ VERSUS SPECIFIC SPEED ALONG HEAD-CAPACITY CURVE

characteristics of the pump, irrespective of size and speed.

In another method, efficiency or head is plotted against sigma or suction head, at a constant speed and capacity, the drop in efficiency and head curves indicating the beginning of cavitation, Fig. 14. These curves give cavitation information for one point on the head-capacity curve, and this method is used mostly for model testing when head-capacity conditions are fixed and safe suction head is determined from model testing.

In water-turbine practice, unit capacity and power are plotted versus sigma. These curves give complete cavitation characteristics for various loads and are independent of head, speed, or size of the unit.

The general trend of sigma variation for the best-efficiency points of pumps of different specific speeds is shown in Fig. 21 and is discussed further under item (i) in this section.

When the plant pumping capacity, head, and suction head are given, the plant σ is fixed. By selecting the proper pump speed, pumps of different specific speed may be used to meet the plant requirements with a desired degree of safety against cavitation. Frequently, the speed is also fixed by the specifications. In that case, the specific speed of the plant is fixed. Only a slight variation in pump design is possible in such a case by placing the operating point to the right or left of the best-efficiency point. The rated normal specific speed of the pump at the best-efficiency point will be different from the plant specific speed, but special designs may be resorted to to obtain the desired degree of safety against cavitation. With pumps of high specific speed, where

the dynamic depression $\lambda \frac{w_1^2}{2g}$ plays an important part in setting

up cavitation conditions, the number of impeller vanes is an effective means of reducing the critical sigma value without changing the specific speed materially, Fig. 18.

(g) The wide variation of σ within the useful range of head capacities is caused partly by the variation of the numerator, representing the dynamic depression, and partly by the variation in the head. In hydraulic turbines where σ has been introduced first, the head is essentially constant. When the load on the turbine varies, the variation in σ is determined entirely by the pressure conditions at the impeller eye. Thoma (23) suggested using the normal head at the best-efficiency point for all points on the head-capacity curve when calculating σ for centrifugal pumps. However, this method has found only limited use in the pump industry.

(h) W. M. White (24) has suggested the use of another factor, "lambda," in addition to sigma. This is defined as

$$\lambda = H_a + h_s - h_v - E_d \frac{c_1^2}{2g} \dots \dots \dots [13]$$

It will be noted that this is nothing else but the numerator from the expression of Moody's cavitation factor K_c , Equation [9], and represents the dynamic depression resulting from the power transmitted by the vanes. It has been pointed out already that the dynamic depression is a predominant factor with the high-specific-speed pumps and varies for different types of pumps along the head-capacity curve. For low-specific-speed pumps, the dynamic depression varies little, therefore λ , as given by Equation [13], will be independent of the head or specific speed. In this case the cavitation conditions can be predicted from the velocity considerations, and the relationships, given in Fig. 12, may be used.

(i) From theoretical considerations, it is possible to establish a relationship between the σ factor and specific speed for best-efficiency points (14, 25)

$$\frac{\sigma_2}{\sigma_1} = \frac{n_2^{4/3}}{n_1} \dots \dots \dots [14]$$

The general trend of σ variation as function of specific speed as found by actually plotting experimental results agrees very well with Equation [14], as is evidenced, for instance, by the curve published by Wislicenus, Watson, and Karassik, reproduced in Fig. 21, which follows exactly this equation. The scatter of the points about an average curve on the original Wislicenus curve is to be expected, as points were obtained with pumps of different design and were not necessarily located at best-efficiency points. For a series of pumps of consistent design, a continuous curve of σ values versus specific speed should be obtained, as all design factors governing cavitation (eye area, number of vanes, etc.) are continuous functions of specific speed. The sigma curve in Fig. 21 can be expressed by the following equations

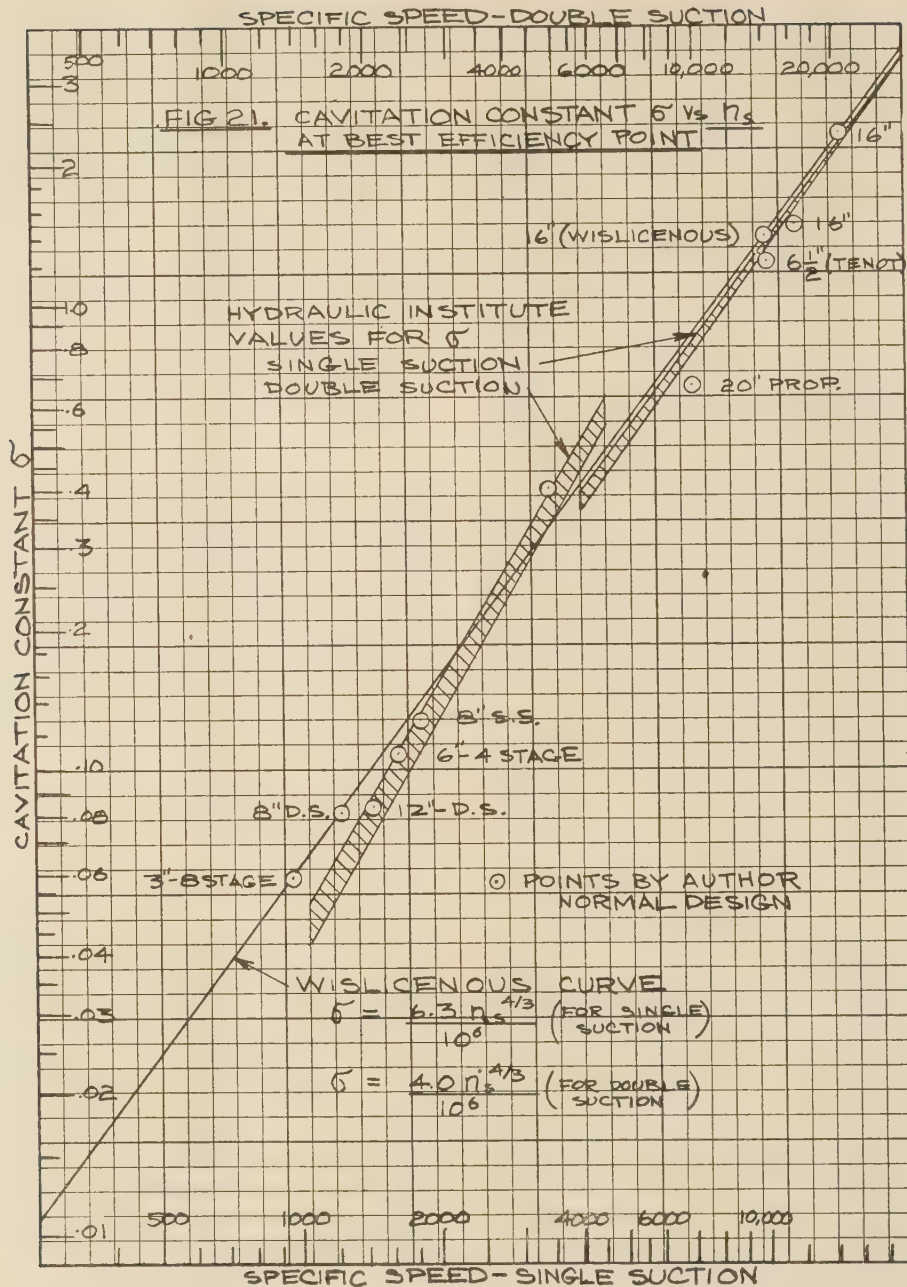
$$\sigma = \frac{6.3n_s^{4/3}}{10^6} \dots \dots \dots [15]$$

for single-suction pumps and

$$\sigma = \frac{4n_s^{4/3}}{10^6} \dots \dots \dots [16]$$

for double-suction pumps.

Fig. 21 also shows sigma values obtained from the Hydraulic Institute charts of the upper limits of specific speeds for double-suction and single-suction pumps. This chart gives a belt of sigma values for several specific speeds rather than a single curve, higher values of sigma applying to lower-head pumps. Such arrangement resulted from the superimposition of performances of pumps of different makes.

FIG. 21 CAVITATION CONSTANT σ VERSUS n_s AT BEST-EFFICIENCY POINT

(j) Attempts have been made to introduce another cavitation criterion in addition to the generally accepted sigma. It is called "suction specific speed" (26, 27), and is defined as

$$S = \frac{\text{Rpm} \sqrt{\text{gpm}}}{\Delta h^{3/4}} \dots \dots \dots [17]$$

The development of Equation [17] is based on the use of similarity relations (affinity laws), at conditions approaching cavitation and do not establish any new relationship between the variables entering into this expression which cannot be determined from the affinity laws or sigma consideration. There is a

fixed connection between the factor S , sigma, and specific speed

$$\frac{n_s}{S} = \sigma^{3/4} \dots \dots \dots [18]$$

Substituting into Equation [18] values of σ from Equations [15] and [16] it is found that

$$S = 7900 = \text{const for single-stage pumps} \dots \dots \dots [19]$$

$$S = 11,200 = \text{const for double-suction pumps} \dots \dots \dots [20]$$

$$\text{Expressing } \sigma \text{ as } \frac{\Delta h}{H} \text{ and } n_s = \frac{\text{rpm} \sqrt{Q}}{H^{1/4}}$$

Equations [15] and [16] can be transformed to

$$\Delta h = (\text{rpm})^{4/3} Q^{2/3} \times \frac{6.3}{10^6} \dots \dots \dots [21]$$

and

$$\Delta h = (\text{rpm})^{4/3} Q^{2/3} \times \frac{4}{10^6} \dots \dots \dots [22]$$

respectively. Note that head H does not appear in Equations [21] and [22], thus indicating that the net positive suction head is independent of the head.

However, this does not mean that the impeller diameter can be cut or extended arbitrarily to obtain any desired head, and expect the relationships, Equations [21] and [22], will hold. For a given head, these equations fix the specific speed and σ values as they appear on curve Fig. 21. This curve applies to pumps of normal design. Evidently if different-specific-speed impellers are obtained by impeller-diameter variation only, the design will not be normal.

(k) When using a model for testing performance and cavitation conditions, the similarity of the model and the prototype should be extended to the suction approach to the impeller and the discharge piping. While this has been fully realized by water-turbine manufacturers, the pump-testing laboratories overlook or underestimate the effects of the suction or discharge piping on the pump performance and behavior as to cavitation.

(l) When applying cavitation data obtained on a small model to the prototype, the suction pressures are usually referred to the impeller-pump center line. However, the points of a minimum pressure may be above this plane of reference, and this distance may be considerably greater on the prototype pump than on the model. Under critical conditions, cavitation may be set up in the larger unit while the model is still free from cavitation.

MEANS TO AVOID OR REDUCE CAVITATION

(a) A knowledge of the cavitation characteristics of pumps is the most important prerequisite of any cavitation-problem study.

(b) Second in importance is the knowledge of existing suction conditions of the plant at the time when the pump selection is made.

(c) An increase of suction-pipe size, reduction of suction-pipe length, elimination of turns, providing a good suction bell, in other words, reduction of losses in the suction pipe, improves the suction conditions of a pump in so far as cavitation is concerned.

(d) An increase in the number of vanes in high-specific-speed pumps, or the removal of parts of the vanes and opening the passages in the impeller eye of low-specific-speed pumps will reduce the minimum suction head to meet fixed head-capacity conditions.

(e) An ample suction-approach area without excessive pre-rotation, a better streamlining of impeller approach, are essential to obtain optimum cavitation characteristics of a pump.

(f) Special materials may be used to reduce the pitting of pump parts due to cavitation, when justified, or if it is impossible to eliminate cavitation by any other means.

(g) The noise and vibration caused by cavitation can be reduced or eliminated by the admission of a small amount of air to the pump suction.

(h) The impeller velocities, impeller-vane load, and head per stage should be low for minimum suction head. All of these factors lead to a bigger pump operated at a low speed, and possibly locating the operating point to the left of the best-efficiency point.

CONCLUSIONS

1 The mechanical nature of cavitation pitting has been established conclusively. Electrolytic and chemical action are of secondary importance or negligible.

2 The suction conditions of the plant should be definitely known when pump selection is made; to avoid cavitation; also, the cavitation characteristics of the pump should be available.

3 The drop in efficiency is the most reliable criterion for detection of cavitation.

4 Cavitation conditions can be predicted for low-specific-speed pumps from the consideration of the velocity through the impeller eye, Fig. 12. For normal design of pumps, sigma can be taken from curve Fig. 21, for any specific speed as an approximation.

5 The law of similarity for cavitation model testing ($\sigma = \text{const}$) holds only for conditions approaching cavitation. When cavitation has progressed to some degree, this relationship is approximate only.

6 The harm caused by cavitation is less pronounced in a large pump than in a small model for the same value of sigma.

7 The presence of gases in liquids does not affect the behavior of pumps as to cavitation, except that vaporization starts at a higher absolute pressure, due to the law of partial pressures. Drop in head capacity may appear earlier on account of liberation of gases of reduced pressure, and the water-hammer effect of collapsing vapor bubbles is cushioned.

8 The life of pump parts can be increased considerably, Figs. 15, 16, by using special materials.

9 Penetration of metals by water under repeated stresses furnishes a logical explanation for the origin of local destructive high pressures found during cavitation, and also in the cases of metal failure by fatigue in presence of liquids.

10 Variation of sigma values with specific speed for normal design of pumps can be represented by the equations

$$\sigma = \frac{6.3 n_s^{4/3}}{10^6} \text{ for single-suction pumps}$$

and

$$\sigma = \frac{4 n_s^{4/3}}{10^6} \text{ for double-suction pumps}$$

Although these relationships have been established experimentally, they have logical theoretical justification.

BIBLIOGRAPHY

- 1 "Hydraulic Turbine Development," by I. A. Winter, Proceedings of the A.S.C.E., vol. 65, 1939, pp. 1553-1589; abstracted in *Mechanical Engineering*, vol. 62, 1940, p. 27.
- 2 "Hydraulic Butterfly Valves," by R. L. Mahon, Trans. A.S.M.E., vol. 54, paper Hyd-54-2, 1932.
- 3 "Untersuchungen Über Regelung von Kreiselpumpen," by W. Siebrecht, *Zeitschrift des Vereines deutscher Ingenieure*, vol. 74, 1930, p. 87.
- 4 "Throttling Suction Changes Pump Characteristic," by B. R. Van Leer, *Power Plant Engineering*, vol. 31, 1927, p. 1133.
- 5 "Untersuchungen Über Kavitation und Korrosion," by H. Foettinger, *Hydraulische Probleme*, V.D.I., Verlag, Berlin, Germany, 1926, p. 14.
- 6 "Cavitation Research," by J. C. Hunsaker, *Mechanical Engineering*, vol. 57, 1935, p. 211.
- 7 "The Mechanism of Cavitation Erosion," by T. C. Poulter, Trans. A.S.M.E., vol. 9, 1942, pp. A-31-A-37.
- 8 "Investigation of Corrosion Phenomena in Water Turbines," by P. de Haller, *Escher-Wyss News*, May-June, 1933, p. 77.
- 9 "Leakage Loss and Axial Thrust in Centrifugal Pumps," by A. J. Stepanoff, Trans. A.S.M.E., vol. 54, paper Hyd 54-5, 1932.
- 10 "Versuche zur Frage der Werkstoffanfressung durch Kavitation," by H. Schroeter, R. Oldenbourg, Munich, 1935.

- 11 "Cavitation of Hydraulic Turbine Runners," by E. B. Sharp, Trans. A.S.M.E., vol. 62, 1940, p. 569.
- 12 "Spalt Kavitation an Schnellaufenden Turbomachines," by Hans Mueller, *Zeitschrift des Vereines deutscher Ingenieure*, vol. 79, 1935, p. 1165.
- 13 "Versuche und Rechnungen zum Kavitations problem der Kreiselpumpen," by Fritz Krisam, Mitteilungen des Institute fur Strömungsmaschinen der Technische Hochschule Karlsruhe, Feb., 1930.
- 14 "On Cavitation in Centrifugal Pumps," by H. Cardinal von Widdern, *Escher-Wyss News*, Jan.-March, 1936, p. 15.
- 15 "Propeller Pumps for Circulation of Molten Salt," by A. J. Stepanoff, *Refiner and Natural Gasoline Manufacturer*, vol. 19, 1940, pp. 474-476.
- 16 "A Practical Treatise on Single and Double Suction Pumps," by Raymond Defeld, Chapman & Hall, Ltd., London, England, 1930, p. 35.
- 17 "Bericht zur Weltkraftkonferenz London 1924," by D. Thoma, *Zeitschrift des Vereines deutscher Ingenieure*, vol. 79, 1935, p. 329.
- 18 "Inter-Relation of Operation and Design of Hydraulic Turbines," by L. F. Moody and F. H. Rogers, *Engineers and Engineering*, vol. 42, 1925, pp. 169-187.
- 19 "Phenomenes de la Cavitation," by M. A. Tenot, *Mémoires de la Societes des Ingenieurs Civils*, May and June, Paris, France, Bulletin 1934, pp. 377-480.
- 20 "Cavitation of Hydraulic Turbine Runners," by R. E. B. Sharp, Trans. A.S.M.E., vol. 62, 1940, p. 569.
- 21 Discussion by F. H. Rogers, Trans. A.S.M.E., vol. 58, 1936, p. 317.
- 22 "Die Kreiselpumpen," by Von C. Pfeleiderer, Julius Springer, Berlin, 1932, p. 241.
- 23 "Verhalten einer Kreiselpumpe beim Betrieb im Hohlzug Bereich," by D. Thoma, *Zeitschrift des Vereines deutscher Ingenieure*, vol. 81, 1937, p. 972.
- 24 "The Construction of the 115,000 Hp Boulder Dam Turbines," by W. M. White, *Mechanical Engineering*, vol. 57, 1935, p. 546.
- 25 Discussion by A. J. Stepanoff, Trans. A.S.M.E., vol. 62, 1940, pp. 158, 164.
- 26 "Cavitation Characteristics of Centrifugal Pumps," by G. E. Wislicenus, R. M. Watson, and I. J. Karassik, Trans. A.S.M.E., vol. 61, 1939, p. 17.
- 27 Discussion by Paul Bergeron, Trans. A.S.M.E., vol. 62, 1940, p. 162.
- 28 "Experimental Research on the Distribution of Water Pressure in a Centrifugal Pump Impeller," by Saichiro Uchimaru, *Journal of the Faculty of Engineering, Tokio University*, vol. 16, 1925.
- 29 "Development of the Automatic Adjustable Blade-Type Propeller Turbine," by R. V. Terry, Trans. A.S.M.E., vol. 63, 1941, pp. 395-409.
- 30 "Prevention of the Failure of Metals Under Repeated Stress," by Battelle Memorial Institute Staff, John Wiley & Sons, Inc., New York, N. Y., 1941, p. 164.
- 31 "Determination of the Relative Resistance to Cavitation Erosion by the Vibratory Method," by S. L. Kerr, Trans. A.S.M.E., vol. 59, 1937, p. 373.
- 32 "Pitting Resistance of Metals Under Cavitation Conditions," by J. M. Mousson, Trans. A.S.M.E., vol. 59, 1937, p. 399.

Testing of Precision-Lathe Spindles

By G. M. EOLEY,¹ COLUMBUS, OHIO

During the war the aircraft industry has demanded the mass production of parts to tolerances previously possible only from the most highly skilled workmanship. In the case of small parts, the tolerances, stated in absolute units, are of the smallest order. This situation led the Bunting Brass and Bronze Company, producer of small bushings, to sponsor research on the design and performance of small precision-lathe spindles, in order that improvements might be made which would result in the production of parts to closer tolerances than had previously been achieved. This paper describes the development and operation of spindle-testing equipment capable of measuring continuously and at any speed changes in the position of the spindle axis relative to the quill as small as one microinch.

THE large demand of the aircraft industry for precision parts at the beginning of the war-production period necessitated mass production to tolerances which were formerly met only with the most highly skilled workmanship.

The smallest tolerances, stated in absolute units, are demanded of small parts. The Bunting Brass and Bronze Company, a producer of small bushings, therefore sponsored research on the performance and design of small precision-lathe spindles, mainly with the object of improving the spindle to the point where it would be suitable for production of parts to closer tolerances than have yet been required.

It was immediately apparent that no means existed for measuring the performance of a lathe spindle apart from the machine, and the only test for performance that was in use was the examination and measurement of parts made using the spindle in the lathe or boring mill. It is obvious that the size and shape of such a part may be affected by many factors outside the spindle, yet the source of errors must be known before steps can be taken to remedy them.

INACCURACIES PRODUCED BY POOR SPINDLE PERFORMANCE

Inaccuracies in the work produced in a lathe originate from "relative" motion between the spindle axis and the work. Instruments which measure vibration of the work or the machine give little information about the spindle, since it is possible that the machine may vibrate as a whole without bad effect on the work, or the source of harmful vibration may not be the spindle.

The spindles tested were to bore smooth round holes or to turn round parts on lathes or boring mills. The quality of such work can be specified in the following terms:

- 1 Size; inside or outside diameter.
- 2 Roundness; the approximation obtained to a true cylinder.
- 3 Straightness; freedom from taper, or the maintenance of required taper.
- 4 Location of hole or boss.
- 5 Smoothness of machined surface.

¹ Physics Department, Battelle Memorial Institute.

Contributed by the Production Engineering Division of THE AMERICAN SOCIETY OF MECHANICAL ENGINEERS and presented at a meeting of the Chicago Section, April 19, 1945.

NOTE: Statements and opinions advanced in papers are to be understood as individual expressions of their authors and not those of the Society.

The role of the spindle in determining these qualities is as follows:

- 1 If the spindle does not rotate always about the same axis there will be a variation in size from place to place on the work.
- 2 If the axis of rotation varies, but in the same or nearly the same pattern upon each revolution, the work will be out of round.
- 3 If the spindle rotates first about one axis and then gradually shifts to rotation about another axis, the work will be tapered.
- 4 If the spindle axis shifts with each new cut, the position of holes bored in a boring mill will vary, or the size of parts turned on a lathe will change.
- 5 If the spindle axis shifts rapidly and vibrates under cutting loads or from other causes, such as inherent roughness in the spindle, the surface cut will be rough. If the spindle axis shifts noncyclically during the revolution, the surface will also be rough.

The last item is ever-increasing in importance because of the smooth surfaces required on machined parts.

SPINDLE-TESTING EQUIPMENT

The testing method adopted was to set up a machine in which the position of the spindle relative to its quill could be measured instantaneously and continuously with a maximum sensitivity better than 1 microinch.



FIG. 1 SPINDLE-TESTING APPARATUS

Spindle Support and Drive. The spindle-testing machine is shown in Fig. 1. The spindle itself is lapped into the cradle shown and is held down by straps pulled up by coil springs. The spindle is driven by a 2-hp induction motor through a variable-speed drive (neither of which is visible in the illustration), and the jackshaft shown at the right of the figure.

The entire spindle mount rests on sponge-rubber pads, and the spindle is connected to the jackshaft through a vibration-absorbing coupling. Vibration of the spindle mount during operation is very small; the measuring equipment is, in any case, unaffected by motions of the entire mount.

The spindle can be driven in the machine at speeds up to 3000 rpm.

Measuring Apparatus. The conditions to be met by the measuring equipment were quite severe. It was required to

measure continuously and at any speed the "position" of the spindle axis relative to the quill. The measurement should not disturb the operation of the spindle in any way. The instrument should measure changes of position as small as 1 microinch in order to detect causes of minute roughness. The sensitivity of the apparatus used was actually limited only by the precision with which the reference surface, whose position was measured, could be lapped to a true cylinder.

Among the most critical of these requirements was that the instrument should measure position, not motion; it had to be sensitive to long-period motions, and to hold its zero over relatively long periods. It had, at the same time, to respond without lag to very rapid movements.

The surface whose position is measured is the cylindrical spindle extension at the front end of the spindle in Fig. 1. This was lapped with a ring lap until further lapping produced no change in its shape; it could then be assumed that it was within 5 microinches of a true cylinder.

The measurement made is of the gap between this cylindrical extension and the two "probes" which can be seen fastened to the spindle cradle one on either side of the machine.

The working end of one of these probes is shown in Fig. 2. The two blocks seen in the end are plates of an electrical condenser. The plates are held on a bakelite block, and the gap between them and the outer brass shield of the probe is filled with sulphur. The whole end of the probe was lapped against a cylinder the same diameter as the spindle extension.

The circuit of one of the two measuring channels is shown in Fig. 3. The condenser shown at C_1 consists of the plates in the end of the probe together with the spindle extension. The capacitance between the two probe plates varies according to changes in spacing between the spindle extension and the probe.

Condenser C_1 is the condenser in the tuned circuit C_1-L_1 of a push-pull Hartley oscillator. The resonant frequency of such a circuit is

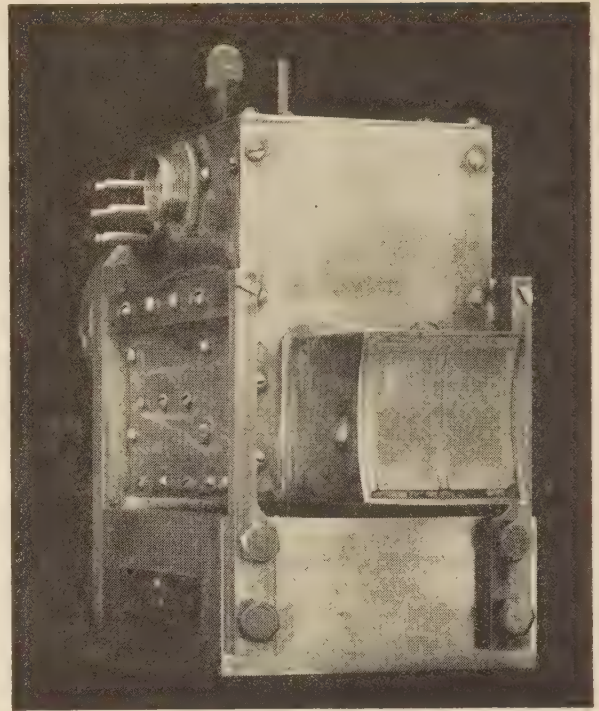


FIG. 2 ONE "PROBE" OF SPINDLE-TESTING APPARATUS

$$F = \frac{1}{2\pi \sqrt{LC}} \quad [1]$$

where L is inductance.

In the tuned circuit L_1-C_1 , the total capacity is composed of a

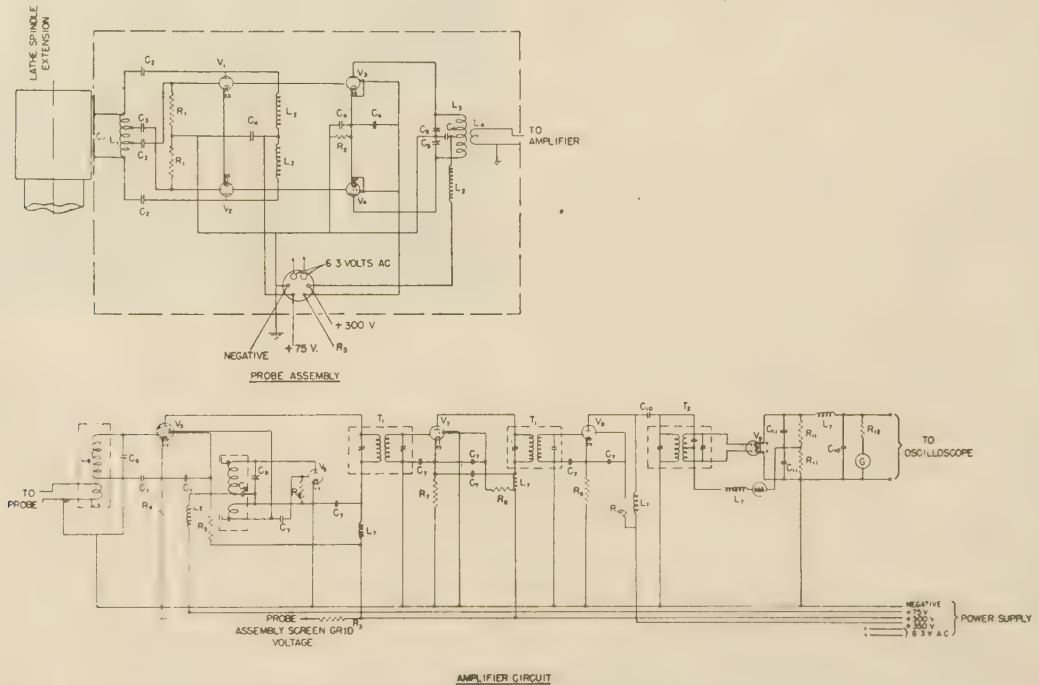


FIG. 3 ELECTRIC MICROMETER CIRCUIT DIAGRAM

stray capacitance C_x and the capacitance C_1 , which is essentially a parallel-plate condenser, in which

$$C_1 = \frac{k}{d}$$

where k is a constant, and d is the spacing between the plates of C_1 and the spindle extension.

If $L = L_1$ and $C = C_x + \frac{k}{d}$ are substituted in Equation [1], differentiation results in the following

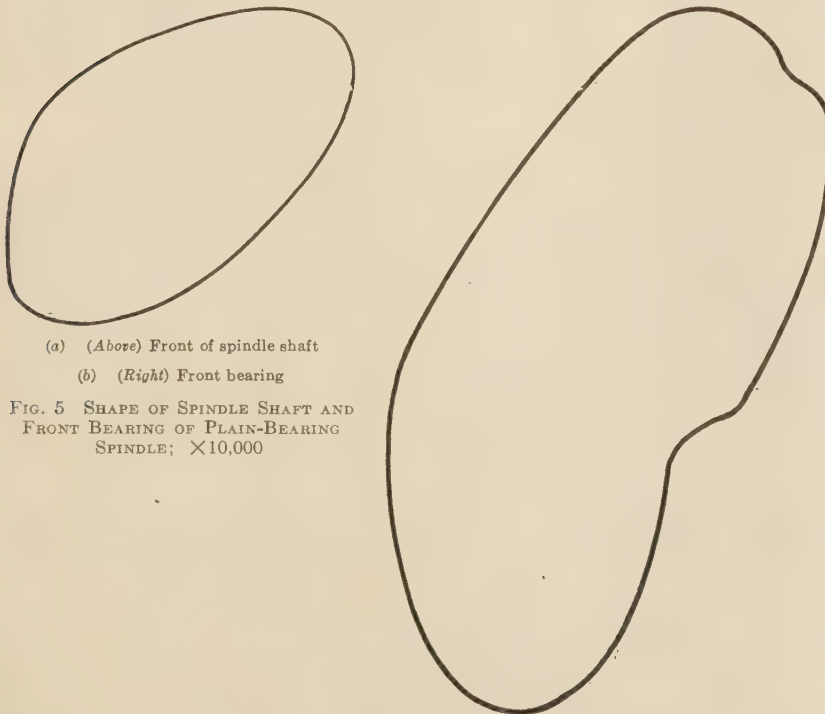
$$\frac{df}{dd} = \frac{kf}{2} \cdot \frac{1}{kd + C_x d^2} \dots \dots \dots [2]$$

The changes in d which it is desired to measure are not more than 1 per cent, so that df/dd is practically inversely proportional to d , while on the other hand the sensitivity of the apparatus can be varied at will by larger changes in d .

The tuned circuit L_1 - C_1 was made resonant at about 3200 kc. The output of the oscillator is fed through the buffer amplifier V_3 and V_4 , which prevents movement of the coupling leads and tuning of the amplifier and mixer from affecting the frequency of the oscillator, to the mixer V_5 . Here the signal is heterodyned with the output of oscillator V_6 , about 2745 kc, and the approximately 465-kc heterodyne signal is selected by the transformer T_1 to be amplified. The voltage of the signal is raised to about 300 volts by the amplifier V_7 and amplifier-limiter V_8 . The signal is then applied to the discriminator tube V_9 .

The discriminator circuit is one which produces a voltage directly proportional to the difference between the applied frequency and the resonant frequency of the discriminator transformer, T_2 . The voltage across the terminals marked "to oscilloscope" is thus proportional to small changes in spacing of the condenser C_1 , which change the frequency of the oscillator V_1 - V_2 and thus the frequency applied to the discriminator.

Tube V_8 was later arranged to operate as a "limiter" amplifier



(a) (Above) Front of spindle shaft
(b) (Right) Front bearing

FIG. 5 SHAPE OF SPINDLE SHAFT AND FRONT BEARING OF PLAIN-BEARING SPINDLE; $\times 10,000$

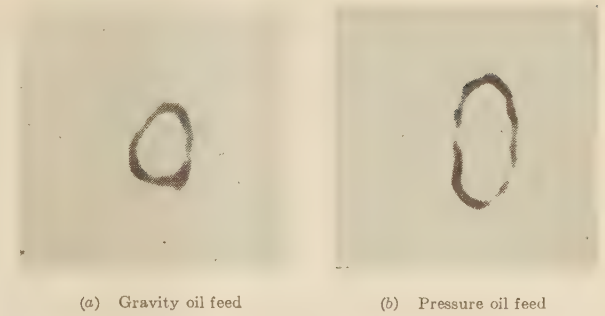


FIG. 4 PATTERNS OF SPINDLE MOTION OF PLAIN-BEARING SPINDLE; $\times 10,000$

and thus prevented changes in amplification in previous stages from affecting the output voltage.

Each of the two channels is entirely independent. The sensitive condensers are placed 90 deg one to the other, so that each is sensitive mainly to motion along one axis of a system of rectangular co-ordinates. The output of each measuring channel is fed directly to one pair of plates of a cathode-ray oscilloscope tube.

The peak output voltage of the discriminator is about 200 volts, so that no direct-current amplification is necessary. Thus the motion of the cathode beam in the oscilloscope is a magnified representation of the motion of a point at the center of the spindle extension. The magnification most often used was $\times 10,000$; although magnifications much greater and much less than this are easily available.

It will be apparent that the center of the spindle extension does not in general coincide with the axis of rotation of the spindle. However, if the spindle axis remains the same during the revolution the center of the spindle extension will move in a circle, and the pattern on the oscilloscope screen will be a circle. Deviations from circularity will indicate changes in axis of rotation of the spindle.

MEASUREMENTS MADE

While the design and performance of lathe spindles are outside the scope of this paper, some examples of the measurements made with the instrument are included.

Fig. 4(a) shows the pattern produced on the oscilloscope screen by the rotation of a simple sleeve-bearing precision-lathe spindle, the lubricant being supplied to it by gravity. The magnification of the original, in terms of spindle movement, was $\times 10,000$, and the pattern shows runout during the revolution of the spindle of about 20×10^{-6} in. Fig. 4(b) is the pattern produced by the same spindle when oil was supplied to it at 40 psi. The runout has increased to about 50×10^{-6} in., apparently on account of nonuniform oil flow through the spindle.

The reasons for this shift are clearly shown in Fig. 5. Fig. 5(a) is a representation of the contour of the front end of the shaft of this spindle. It was obtained by rotating the shaft of the spindle, noting the deflections of

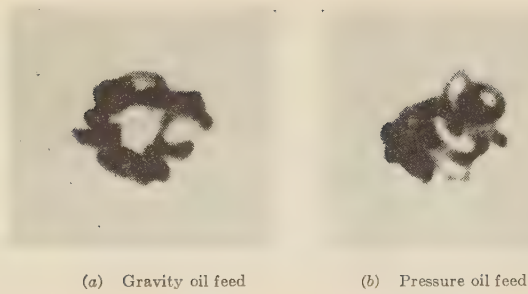


FIG. 6 PATTERNS OF SPINDLE MOTION OF PLAIN-BEARING SPINDLE LOADED BY A SMALL BALL BEARING; $\times 10,000$

the galvanometers of the spindle-testing instrument, and plotting the values obtained. It corresponds exactly with the oscilloscope pattern which would be obtained by rotating the shaft at infinitesimal speed. Fig. 5(b) is the contour of the front bearing of the spindle and was obtained by rotating the shaft while a force was applied to it so that the same surface of the shaft would always be in contact with the bearing.

Figs. 5(a) and 5(b) show that the clearance of the spindle may vary by 2×10^{-4} in. from point to point around the circumference, and that the place having largest clearance will move during the revolution of the shaft; oil under pressure will thus increase the axial shifts of this particular spindle.

In order to study the effect of a vibrating load on the spindle

similar to that which would occur in cutting, a small ball bearing was placed on the spindle extension, the inner race of which moved with the spindle while the outer race was held still by the force of gravity on a small weight attached to it. Fig. 6 shows the oscilloscope patterns produced under such conditions in the plain-bearing spindle both with gravity oil feed and pressure feed. It will be seen that the rigidity of the spindle under such loading is not much affected by oil pressure.

The manner in which the spindle-testing equipment can be used to measure long-time changes in spindle position is shown in Fig. 7. Fig. 7(a) is a double exposure of the oscilloscope patterns before and after a 5-min shutdown of the spindle. The spindle axis has changed about 10^{-4} in. relative to the probes on account of cooling of the machine. A similar double exposure before and after a 1-hr shutdown, Fig. 7(b), shows that a shift of about 3×10^{-4} in. has occurred in this time. This shift, or a greater one, might be cause for rejection of some parts made on a



FIG. 8 PATTERN PRODUCED DURING TWO SUCCESSIVE REVOLUTIONS OF COMBINATION SPINDLE; $\times 10,000$

machine after such a shutdown if the spindle had this performance.

Fig. 8 shows the pattern produced during two successive revolutions of a spindle containing a pair of superprecision combination radial-and-thrust ball bearings in the back end and a plain bearing in the front end. Unlike the plain-bearing spindle, the axis of this spindle does not retrace its path during successive revolutions on account of the ball-bearing races rotating at about one half the rate of the spindle. The precession of the axis of this spindle has an amplitude somewhat greater than 30 microns per revolution, sufficient to produce a roughness quite intolerable on some machined parts.

CONCLUSION

The apparatus described was found very useful in providing information for use in the design of new precision-lathe spindles, and in checking the performance of them after they were built. It is apparent that the same type of circuit may be useful in other cases where measurements of very small changes in position or size are to be made. While the advantages of this design over some other electrical micrometers and strain gages are most apparent where the demand is for an instrument to measure displacements both at very high and zero rates of change, the way in which the frequency-modulation principles used free the equipment from errors caused by changes in amplification is also desirable in other applications.

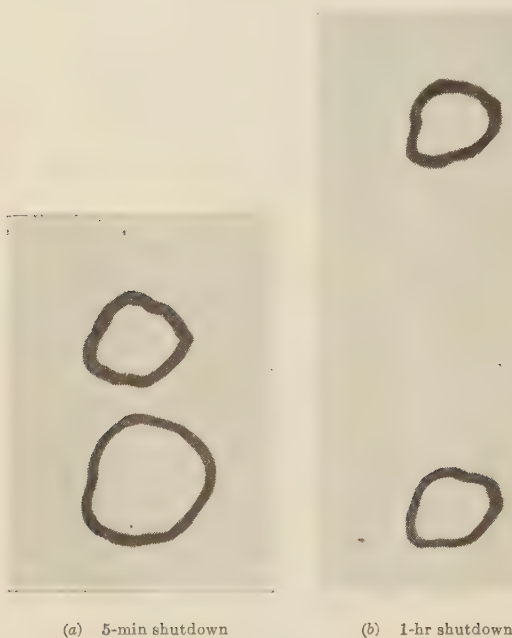


FIG. 7 PATTERNS OF SPINDLE MOTION BEFORE AND AFTER SHUT-DOWN; $\times 10,000$

(Owing to travel emergency conditions existing when this paper was presented, written discussion will be accepted until November 10, 1945.)

Irreversibility in the Theoretical Regenerative Steam Cycle

By R. E. HANSEN,¹ NEW YORK, N. Y.

An irreversible process takes place in the theoretical regenerative steam cycle for power generation when superheat in the steam bled from the turbine is transferred to feedwater. Increase in entropy occurs, as in any irreversible process; this increase can be determined by a simple method of graphic integration, and used in computing additional heat rejection to the condenser. Heat rate of the cycle can then be found with a high degree of accuracy by a simple formula.

NOMENCLATURE

The following nomenclature is used in the paper:

H = enthalpy of steam at point indicated by subscript,
Btu per lb

h = enthalpy of water at point indicated by subscript,
Btu per lb

dp = increase in pressure between adjacent infinitesimal feedwater heaters

s = entropy per pound of steam at point indicated by subscript, Btu per deg F

S = entropy when used to indicate total in system, Btu per deg F

$$\Delta S = \text{total gain in entropy for cycle with 1 lb of steam at throttle, Btu per deg F}$$

T = absolute temperature at point indicated by subscript,
deg F

 v = specific volume of feedwater in heater W_R = work lost during an irreversible process dw = fraction of throttle steam bled at any stage

$(1 - w)$ = quantity of feedwater in any heater, with steam quantity at throttle taken as unity

INTRODUCTION

Analyses of the theoretical regenerative steam cycle have been made in the past, with the purpose of developing procedures for computing heat rate. Methods that have heretofore been presented, however, are laborious and leave much to be desired in the way of simplicity in use. The purpose of the present paper is to show that by computing the increase in entropy which occurs in the cycle, the heat rate may be determined quickly and with a high degree of accuracy.

The theoretical regenerative cycle is one in which steam is expanded adiabatically; a sufficient quantity is bled from the turbine at an infinite number of points to heat feedwater in an infinite number of open (contact) heaters to the temperature at which evaporation occurs. Feed-pump work is done at 100 per cent efficiency. Boiler-plant, pipe-friction, radiation, and generator losses, also temperature differences in conduction, are considered zero, the limit they would approach if size of equipment and insulation were indefinitely large.

The provisions as set forth require that all processes in the

¹ Ebasco Services Incorporated.

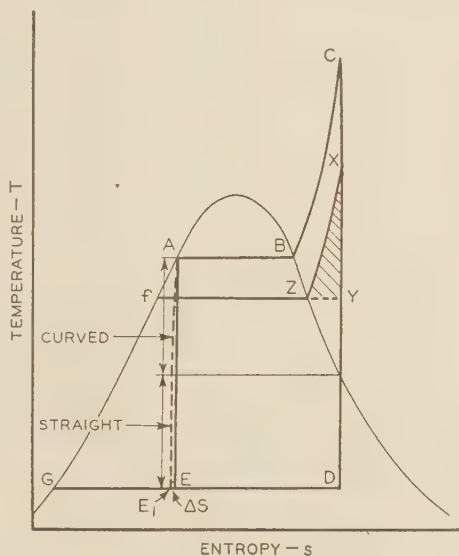
Contributed by the Power Division of THE AMERICAN SOCIETY OF MECHANICAL ENGINEERS and presented before the Metropolitan Section, May 15, 1945, and before the Chicago Section, June, 18, 1945.

NOTE: Statements and opinions advanced in papers are to be understood as individual expressions of their authors and not those of the Society.

cycle be accomplished reversibly except one. Steam bled from the turbine in the superheat region is mixed irreversibly with feedwater, the latter being at the same pressure as the steam but at its saturation temperature. During this irreversible process, an increase in entropy occurs. Usually, engineers are reluctant to utilize the concept of entropy except when it remains constant, but, as will be shown, the quantity is a convenient device, even when it is a variable.

EQUIVALENCE OF REVERSIBLE CYCLES

Steam can theoretically be made to do work in the cycle $ABCDEA$, Fig. 1, condensation being stopped at point E , and wet steam being compressed adiabatically to point A . In the regenerative cycle, steam is completely condensed to point G on the liquid line, steam being bled from several stages in the turbine to heat condensate to point A . If this process of regeneration were strictly reversible, the cycle would then be exactly equivalent to cycle $ABCDEA$, the greater quantity of heat rejected to condensing water per pound of steam going to the

FIG. 1 TEMPERATURE-ENTROPY DIAGRAM FOR THEORETICAL
REGENERATIVE STEAM CYCLE

condenser being exactly compensated by a decrease in the quantity of steam condensed. This is a consequence of Carnot's law that each increment of heat added in a cycle at absolute temperature T_1 and rejected at temperature T_2 is utilized with efficiency $(T_1 - T_2)/T_1$, provided no irreversible processes occur within the cycle. Any cycle in which the pattern of heat input is along line ABC has the same efficiency as the cycle $ABCDEA$, provided only that all heat rejection is at the same temperature and that no irreversible processes are used.

CYCLES WITH VARYING STEAM QUANTITY

To assist in visualizing the cycle, the diagram may be con-

sidered to have a third dimension, i.e., quantity of steam. Any horizontal cross-sectional area of the resulting solid would then represent a total, rather than a unit, quantity of entropy. Rankine cycle, shown by $ABCDGA$, has a constant steam quantity, hence front and rear faces of the solid representing it are plane and parallel, and all vertical sections parallel to the temperature-entropy plane are identical. In the theoretical regenerative cycle, the weight of steam in the turbine diminishes as expansion proceeds from C to D , Fig. 1, and the weight of feedwater increases as it is heated from G to A . The total quantity of entropy represented by any horizontal cross section in Fig. 2 would remain constant below the plane of saturation temperature at the throttle, if a completely reversible regenerative cycle were used, as illustrated by solid lines in Fig. 2. Entropy may here be regarded as transferred from bled steam to feedwater, without increase in total quantity in the system.

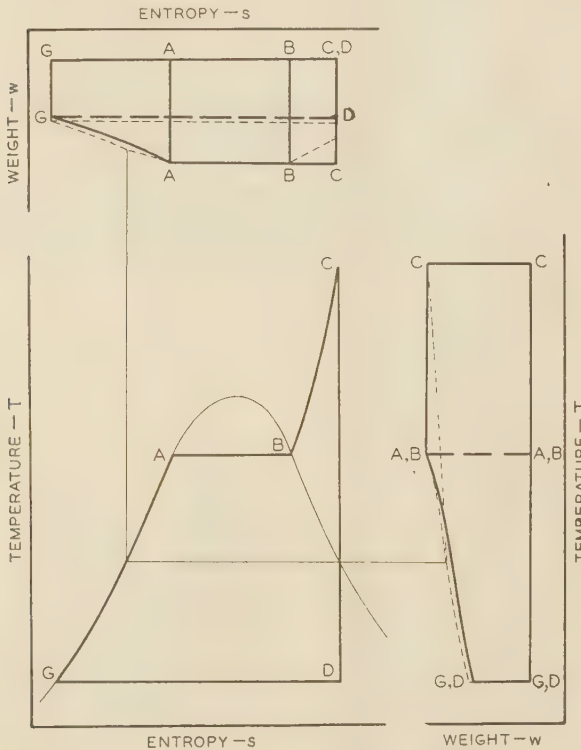


FIG. 2 THREE-DIMENSIONAL DIAGRAM FOR THEORETICAL REGENERATIVE STEAM CYCLE

While, as already indicated, the regenerative cycle cannot be completely represented in a two-dimensional diagram, an equivalent constant-quantity cycle may be depicted. For the reversible regenerative cycle, the width of the equivalent constant-quantity cycle, now representing entropy per unit of steam, is constant. When irreversible processes are used, the additional entropy generated must be taken into account, progressively widening the equivalent diagram, as shown by dotted lines in Figs. 1 and 2. The regenerative cycle with irreversible feed-heating process may therefore be represented on the T - s plane by displacing point E toward the left by an amount ΔS , as at E_1 , where ΔS is the total entropy generated for each pound of throttle steam.

COMPUTING ENTROPY INCREASE

To determine the increase in entropy resulting from the ir-

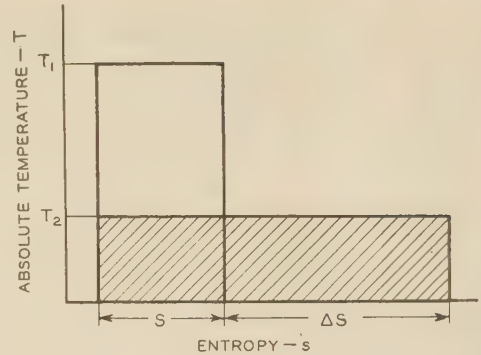


FIG. 3 INCREASE IN ENTROPY WHEN HEAT IS DEGRADED IN TEMPERATURE

reversible process, the first law of thermodynamics is used. Thus if a quantity of heat, represented by an area $T_1 S$ on the temperature-entropy diagram, Fig. 3, is cooled without doing work to temperature T_2 , then the following relation must hold

$$T_1 S = T_2 (S + \Delta S)$$

from which

$$\Delta S = \frac{S(T_1 - T_2)}{T_2} = \frac{W_R}{T_2}$$

where W_R is the quantity of work that could have been generated in a reversible cycle. This may also be expressed differentially, as

$$dS = \frac{dW_R}{T_2} \dots \dots \dots [1]$$

To be reversible, the process of regeneration must be accomplished in such a way that heat passes from one fluid to another at the same temperature. As long as wet steam is bled in infinitesimal steps and gives up its heat in feedwater heaters each operating with zero terminal difference, the process is fully reversible. But when superheated steam is bled and used at constant pressure in the heaters, part of the process is not reversible. This is because heat at temperature higher than saturation passes to water at saturation temperature. To accomplish reversibility in the superheat region, it would be necessary to compress bled steam isothermally to saturation pressure corresponding to its superheat temperature, as from Y to Z in Fig. 1, utilizing the heat rejected in isothermal compression for heating the feedwater. If instead steam is bled at point X where the expansion process has progressed to a pressure equal to that of the saturated steam at feedwater temperature and is cooled irreversibly, work represented by triangle XYZ is lost. Then, from Equation [1]

$$dS = [H_X - h_f - T_f(s_X - s_f)] \frac{dw}{T_f} \dots \dots \dots [2]$$

if dw is the fraction of the throttle steam bled at any stage and subscript f refers to the condition of saturated liquid at the pressure of the bled steam.

The heat balance for the infinitesimal heater is

$$dw(H_X - h_f) = (1 - w) [dh_f - v dp] = (1 - w) T_f ds_f \dots [3]^2$$

Substitution of Equation [3] into Equation [2] yields

$$dS = \left[\frac{H_X - h_f - T_f(s_X - s_f)}{H_X - h_f} \right] (1 - w) ds_f \dots [4]$$

² "Thermodynamic Properties of Steam," by J. H. Keenan and F. G. Keyes, John Wiley & Sons, Inc., New York, N. Y., 1936, Equation [2a], p. 12.

The quantity of steam in the turbine at any temperature $(1 - w)$ is found from the cross-sectional area of the three-dimensional diagram shown in Fig. 2. As stated before, this area remains constant except for the accumulated increase in entropy occurring as regenerative heating proceeds. Such cumulative increase is zero at the throttle, where its rate of increase is greatest, and reaches its maximum value when bled steam becomes saturated, at which point no further increase occurs. It is therefore sufficiently accurate for the purpose of evaluating $1 - w$ to assume the cross-sectional area constant, that is

$$(1 - w) \times (s_x - s_f) = 1 \times (s_c - s_A) \dots [5]$$

The magnitude of inaccuracy resulting from this simplifying assumption is about 1 per cent of ΔS at 3200 psia 1200 F, and much less at lower throttle conditions. The corresponding error in heat rate, computed as will be shown, is less than 2 Btu per kw-hr. Making this substitution and simplifying produces

$$dS = (s_c - s_A) \left[\frac{1}{s_x - s_f} - \frac{T_f}{H_x - h_f} \right] ds_f \dots [6]$$

Equation [6] is integrated between limits of s_f corresponding to the throttle pressure and the point where the expansion curve crosses the saturation line by plotting the values of the bracketed coefficient against s_f as in Fig. 4, and multiplying the area under the curve by the constant term $(s_c - s_A)$; this product is ΔS .

A sample calculation is shown in Table 1 for throttle condi-

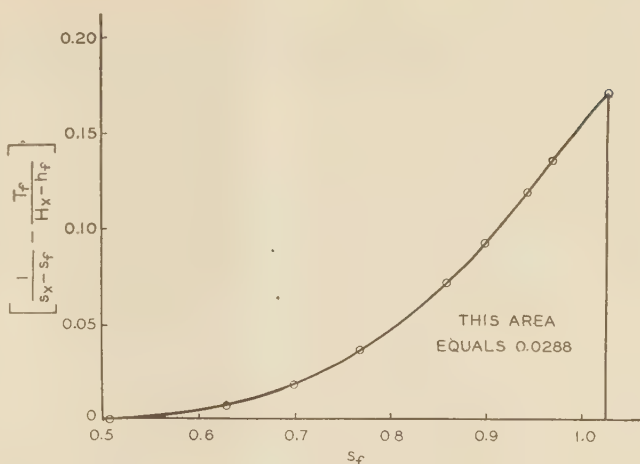


FIG. 4 GRAPHIC INTEGRATION, A STEP IN FINDING ΔS

second paragraph of the present paper. Agreement between those data and heat rates computed by the method now presented is shown in Table 2.

APPLICABILITY OF METHOD

The advantages of computing theoretical cycle heat rates by the new method, as compared with that presented last year, are as follows:

- 1 Less work is involved; only 10 steps are needed in Table 2,

TABLE 1 COMPUTATION OF EXPRESSION IN EQUATION [6] FOR $s_x = 1.5745$, CORRESPONDING TO 3200 PSIA 1200 F

$\left[\frac{1}{s_x - s_f} - \frac{T_f}{H_x - h_f} \right]$									
1 Psia	2 s_f	3 $s_x - (2)$	4 $1.0 \div (3)$	5 T_f	6 H_x	7 h_f	8 (6) - (7)	9 (5) + (8)	10 (4) - (9)
3200	1.0320	0.5425	1.843	1164.8	1569.9	872.4	697.5	1.670	0.173
3000	0.9731	0.6014	1.663	1155.0	1559.3	802.5	756.8	1.526	0.137
2800	0.9459	0.6286	1.591	1144.7	1548.0	770.1	777.9	1.471	0.120
2400	0.9023	0.6722	1.487	1121.8	1523.6	718.4	805.2	1.394	0.093
2000	0.8619	0.7126	1.403	1095.5	1495.6	671.7	823.9	1.330	0.073
1600	0.8196	0.7549	1.323	1064.6	1462.8	624.1	838.7	1.268	0.055
1200	0.7711	0.8034	1.245	1026.9	1422.8	571.7	851.1	1.206	0.039
800	0.7103	0.8637	1.158	977.9	1370.6	509.7	860.9	1.136	0.022
400	0.6214	0.9531	1.049	904.3	1291.3	424.0	867.3	1.043	0.006
141	0.5076	1.0669	0.937	813.3	1193.1	325.4	867.7	0.937	0.000

TABLE 2 COMPUTED HEAT RATES COMPARED WITH PUBLISHED DATA

Steam conditions at throttle		Condenser pressure, In. Hg abs	Value of ΔS	Heat rate, Btu per kw-hr—	
Pressure, psia	Temp, deg F			Computed from ΔS	Selvey and Knowlton, Table 1
3200	1200	1.0	0.0156	5999	5999
850	900	1.0	0.0036	7235	7232
400	700	1.0	0.0014	8229	8222

tions 3200 psia 1200 F, with s_x equal to 1.5745. Values from column 10 are plotted in Fig. 3, and the area, computed as 0.0288, is multiplied by $s_x - s_A = 0.5425$; the product is 0.0156, which is the value of ΔS for use in Equation [7].

HEAT RATES

Heat rate is given as follows:

$$\text{Theoretical heat rate} = \frac{3412.75 (H_c - h_A)}{H_c - h_A - T_E (s_c - s_A + \Delta S)} \dots [7]$$

If ΔS is determined accurately, Equation [7] is exact.

In a paper³ presented last year, Messrs. Selvey and Knowlton gave heat rates accurately computed for a cycle as defined in the

³ "Theoretical Regenerative-Steam-Cycle Heat Rates," by A. M. Selvey and P. H. Knowlton, Trans. A.S.M.E., vol. 66, 1944, pp. 489-512.

compared with 35 in the method described in the previous paper; the nature of the computations is such that slide-rule accuracy will usually be adequate.

2 The integration for ΔS may be performed between different limits on a single curve, such as that in Fig. 4, so that the computation of a few such curves will suffice to give the complete range of values for all commonly used pressures and temperatures. The quantity ΔS , being small compared with $s_D - s_A$, can be obtained with sufficient accuracy by interpolation even though the intervals are quite large.

3 The basis of derivation is concerned only with the fundamental properties of steam and eliminates the need for dealing separately with the work done by the boiler feed pump; attention thus being focused on the essential and limiting factors.

4 Data can be more readily utilized in working with complex cycles in which steam is reheated after partial expansion. In

this case ΔS for partial expansion would be that for the throttle condition minus that for the uncompleted part of the expansion and is added arithmetically to ΔS for additional expansions, each multiplied by the fraction of the original steam remaining at the beginning of expansion.

5 ΔS is independent of back pressure, unless the exhaust is superheated; no back-pressure corrections need be computed.

A complete table of heat rates for the theoretical regenerative cycle having already been published,⁸ the author has not undertaken the computation of exact values of ΔS at this time. Usefulness of such compilation would be largely for special cases; when needed, ΔS can be computed from published theoretical heat rate by means of Equation [7], or by the method just given. To show approximately how quantity varies, however, Fig. 5 is presented. It is based on rough calculations covering pressures up to 3000 psia and temperatures 600 to 1600 F.

NONADIABATIC TURBINE EXPANSION

In applying the method as described to the determination of cycle performance with an actual turbine, the entropy increase due to irreversibility in feedwater heating becomes greater than with the cycle as previously defined. The higher superheat at intermediate bleed points is responsible for this condition, which can be taken accurately into account only by recomputing ΔS , using the actual expansion curve. An additional ΔS value because of irreversibility in turbine expansion can be read from the expansion curve, and the sum of these used to determine the heat rate of another cycle, also having an infinite number of bleed points.

The result under the method indicated would not be the same

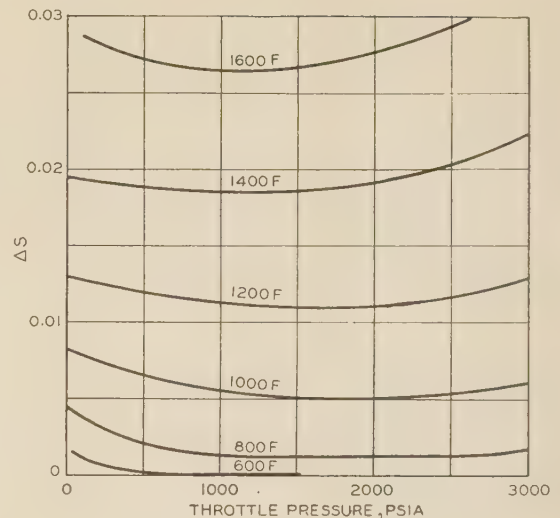


FIG. 5 VARIATION OF ΔS WITH PRESSURE AND TEMPERATURE

as obtained by dividing the heat rate of the theoretical adiabatic cycle by the over-all turbine efficiency, though the difference may be small. It follows that whatever method is used for determining the heat rate of the adiabatic cycle, the entire calculation must be repeated for the nonadiabatic cycle, if exact results are needed.

(Owing to travel emergency conditions existing when this paper was presented, discussion will be accepted until November 10, 1945)

Critical Shearing Stress in Skin-Stressed Boxcar Sides

By V. L. GREEN¹ AND J. J. DRINKA,² MILWAUKEE, WIS.

Developments in boxcar construction are traced through the period of the 1920's and early 1930's, leading to design work by K. F. Nystrom on The Milwaukee Road in which 15-gage side sheets, stiffened by six longitudinals of the lapped type formed integrally with the side sheet, were found to be entirely satisfactory for car-side construction, and accomplished a saving in weight of 600 lb. In order to determine the possibility of further weight reduction without sacrificing strength, a study was made of the elastic stability of various types of car sides, and tests were conducted to correlate the theoretical study with actual test results. This paper includes a discussion of shearing stress in thin-webbed girders, the test procedure, a theoretical analysis of a number of panels tested, and the results obtained for the panels tested.

INTRODUCTION

DURING the late 1920's and early 1930's the trend in boxcar construction was directed from single-sheathed, diagonal-braced construction to the steel-sheathed, wood-lined type of car. The early frame construction was of the truss type and the sheathing was not employed as a part of the load-carrying structure. The steel-sheathed wood-lined cars did not utilize diagonal bracing, and the car structure was therefore similar to a plate girder, the steel side sheets serving as the web of the girder. In this construction the high shear loads at the ends of the beam are transmitted to the supports by the web working in shear. The early steel-sheathed cars utilized rather heavy-gage steel side sheets approximately 0.100 in. thick, and such cars weighed approximately 46,500 lb for cars 40 ft 6 in. in length.

Prior to 1925 the load limit on boxcars was determined on the basis of 110 per cent of the nominal capacity. This method of determining the load limit fixed the maximum lightweight for a 40-ton freight car at 48,000 lb, and for a 50-ton freight car at 59,000 lb. Since the load-carrying capacity of the car was thus definitely determined there was no great advantage in reducing the weight below this maximum light weight. However, in 1925 the procedure for calculating the load limit was modified. The load limit was to be determined by obtaining the difference between the permissible weight at the rail, based on journal size, and the lightweight of the car. Thus weight reduction became of prime importance, as every pound removed from the car structure could be replaced by a pound of tariff-producing lading. Since the weight of the side sheets on a 40-ft 6-in. boxcar with 0.100-in. side sheets was approximately 2735 lb, decreasing the thickness of these sheets was a fertile field for weight reduction, and some boxcars were built with 14-gage (0.075 in.) side sheets stiffened with a few very heavy stiffeners. The weight of the

side sheets on a 40-ft 6-in. boxcar of this type was approximately 2350 lb, a desirable weight reduction. These cars did not collapse and are still in service, but the side sheets developed stress buckles at the bolster panels under heavy loads.

It was decided, nevertheless, that the 14-gage sheets were, if adequately stiffened, suitable for side sheets and K. F. Nystrom of The Milwaukee Road developed a car side utilizing 14-gage sheets with six longitudinal stiffeners of the lapped type formed integrally with the side sheet as shown in Fig. 1. A large number of cars were constructed with this type of side with completely successful results, as the side sheets showed no evidence of the formation of buckles under load. The weight of the side sheets on a 40-ft 6-in. boxcar of this type was 2495 lb, which is 145 lb more than that of the previously discussed inadequately stiffened 14-gage side construction, but is 240 lb less than the weight of the side sheets on a car with 0.100-in. side sheets.

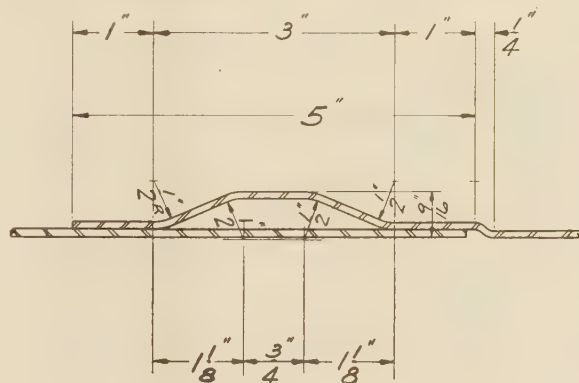


FIG. 1

In order to determine the possibility of accomplishing further weight reduction without sacrificing strength a study was made of the elastic stability of various types of car sides, and a number of tests were conducted to correlate the theoretical study with test results. The following types of side construction were considered in the theoretical analysis:

- 1 A flat, unstiffened side section with 15-gage side sheets.
- 2 A side section consisting of 15-gage side sheets stiffened with two lapped longitudinal ribs.
- 3 Same side section as No. 2 with a 20-gage vertical stiffener added.
- 4 The car-side section previously used on The Milwaukee Road, consisting of a 14-gage side sheet with six lapped, longitudinal stiffeners.
- 5 A side section similar to No. 4 with 14-gage side sheets and six lapped longitudinal stiffeners smaller than those used for No. 4.
- 6 A side section with 15-gage side sheets and six lapped longitudinal stiffeners.
- 7 A side section with 16-gage side sheets and six lapped longitudinal stiffeners.
- 8 A flat unstiffened side section with 0.100-in. side sheets.

¹ Chicago, Milwaukee, St. Paul & Pacific Railroad.

² Chicago, Milwaukee, St. Paul & Pacific Railroad. Jun. A.S.M.E.

Contributed by the Railroad Division and presented at the Annual Meeting, New York, N. Y., Nov. 27-Dec. 1, 1944, of THE AMERICAN SOCIETY OF MECHANICAL ENGINEERS.

NOTE: Statements and opinions advanced in papers are to be understood as individual expressions of their authors and not those of the Society.

Test panels representative of side sections 1 to 5, inclusive, were fabricated and tested to check the analytical results.

This paper will include a discussion of shearing stresses in thin-webbed girders, the test procedure, a theoretical analysis of each panel, and the test results for the panels tested.

SHEARING STRESS IN THIN-WEBBED GIRDERS

The web of a plate girder is a thin plate subjected to shear, compressive, and tensile stresses. The shear and compressive forces tend to buckle the web of the girder.

The plate girders utilized on railway and highway bridges have webs which are thick enough to resist this buckling or have web stiffeners which prevent it. In this type of construction the high shear loads at the ends of the beam and concentrated loads are transmitted to the supports by the web working in shear. The sides of boxcars with heavy side sheets or stiffened thin side sheets are girders of this type.

Other plate girders, for example, those utilized in airplane construction, are not designed to carry the entire load to the support by the shear in the web. A part of the load is carried as shear in the web, and the additional load causes the formation of buckles which permit the web plate to work as a diagonal tension tie. Any stiffeners then act as struts and the load is transmitted as in a truss. The load at which the flat form of equilibrium becomes unstable and the plate begins to buckle is known as the critical load.

The load at which buckle formation begins is dependent on the web thickness and the stiffener strength and spacing. The critical shear or compressive load is proportional to the flexural rigidity of the plate. The resistance to buckling can therefore always be increased by increasing the thickness of the plate, but such a design will not be economical in respect to the weight of material used in deep girders such as boxcar sides. It is generally more economical to keep the side sheets as thin as possible and provide the necessary stability by utilizing posts and longitudinal lapped ribs at stiffeners. The weight of the longitudinal ribs will usually be much less than the additional weight required to provide a plate of adequate thickness.

All boxcar sides must have vertical stiffeners in the form of posts to resist bulging and for other practical reasons. If longitudinal ribs are also used in conjunction with the posts, they must be so located and of such dimensions to prevent buckling of the web. When posts only are used for stiffeners it is possible for buckles to form, allowing the girder to work as a truss as previously mentioned, but if adequate longitudinal ribs are introduced the buckle cannot pass the rib without bending it. Thus the girder has been broken up into rectangular panels bounded by the posts and longitudinal ribs. If the reinforcements are of the lapped-rib variety, it is possible to get the advantage of longitudinal stiffeners and at the same time have the safety factor of being able to go into a tension field if for some reason the unit buckling stress is exceeded. In designing a girder using thin flat sheets or thin sheets stiffened with lapped ribs, a low factor of safety in the neighborhood of 1.5 to 1.25 can be used because buckling of the sheets does not mean immediate failure of the structure since the sheet can go into a diagonal tension field. This will be accompanied by excessive deflection, but the structure will not collapse.

The determination of the spacing of stiffeners, and the size of stiffeners, for a given thickness of web must be based on a study of the elastic stability of the web plate. An excellent discussion of the rational theory of buckling of thin plates is given by S. Timoshenko,³ and the following theory is credited to him.

³ "Theory of Elastic Stability," by S. Timoshenko, McGraw-Hill Book Co., Inc., New York, N. Y., 1936, pp. 324-418.

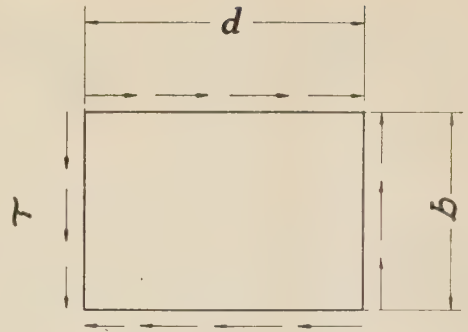


FIG. 2

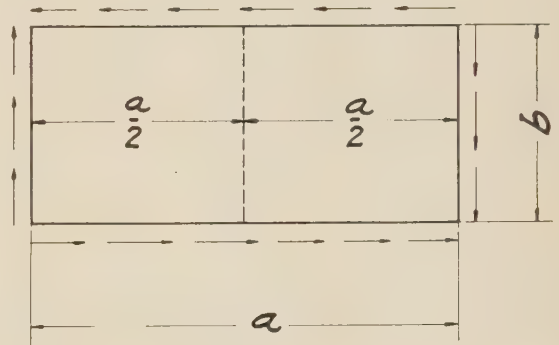


FIG. 3

Near the supports of a beam the shearing force is the most important factor, and the part of the web between the stiffeners may be considered as a rectangular plate subjected to the action of uniform shear, Fig. 2.

In order to facilitate the discussion of the elastic stability of thin webs and stiffened thin-webbed girders the following elementary relationships can be stated. The flexural rigidity of a beam or rib is

$$B = EI$$

and the flexural rigidity of a plate is

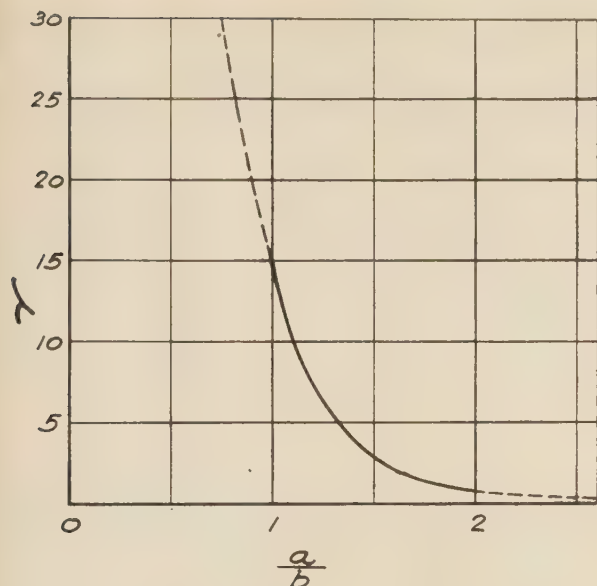
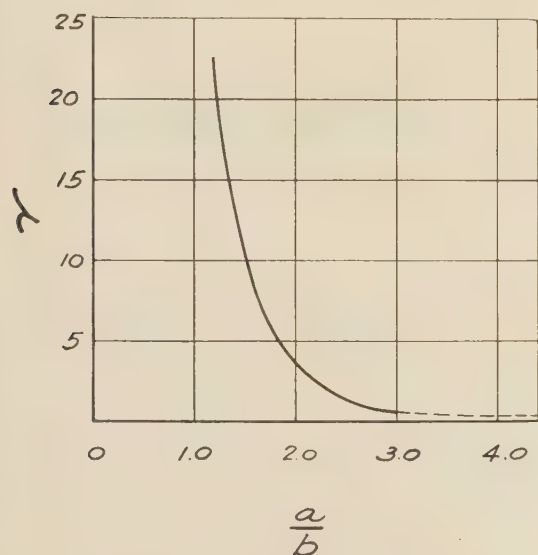
$$D = \frac{Eh^3}{12(1 - \nu^2)}$$

where E is the modulus of elasticity, I is the moment of inertia, h is the plate thickness, and ν is Poisson's ratio.

In the stiffening of simply supported rectangular plates under shearing stresses two cases will be considered, as follows:

1 A simply supported rectangular plate subjected to the action of uniformly distributed shearing stresses, and stiffened by one rib bisecting the plate as shown in Fig. 3. It is known that if the rigidity of the stiffener is not sufficient, the inclined waves of the buckled plate run across the stiffener, and buckling of the plate is accompanied by bending of the rib. By subsequent increases of the rigidity of the rib a condition is reached in which each half of the plate will buckle as a rectangular plate of dimension $a/2$ by b with simply supported edges, and the rib will remain straight. The corresponding limiting values of the flexural rigidity B of the rib can be found from the consideration of strain energy of bending of the plate and of the rib. Values of the ratio γ of the required rib flexural rigidity to the rigidity Da , of the plate if bent into a cylindrical surface are given in Fig. 4.

2 A simply supported rectangular plate of length a and width b submitted to the action of uniformly distributed shearing

FIG. 4 LIMITING VALUES OF RATIO γ FOR CASE OF ONE RIBFIG. 5 LIMITING VALUES OF RATIO γ IN CASE OF TWO RIBS

stresses and divided by two stiffeners into three equal portions $a/3$ by b . Values of the ratio γ of the required rib flexural rigidity to the rigidity, Da , of the plate are given in Fig. 5.

After the value of γ for any specific case is determined from either Fig. 4 or Fig. 5 the required rib flexural rigidity is given by the relationship

$$B = \gamma Da$$

The critical shearing stress for any panel formed by such stiffeners of adequate flexural rigidity can then be determined by the formula

$$\tau_{cr} = \left(5.35 + 4 \frac{b^2}{d^2} \right) \frac{\pi^2 E}{12(1 - \nu^2)} \frac{h^2}{b^2} \dots \dots \dots [1]$$

in which h is the sheet thickness, E is the modulus of elasticity,

ν is Poisson's ratio and b and d are the dimensions of the panel as indicated in Fig. 2.

TEST PROCEDURE

All of the test panels were fabricated with identical posts, side plates, and side-sill upper elements. The panels tested were subjected to a shear load as shown in Fig. 6, applied with a geared jack, and measured with a 0 to 50,000-lb dynamometer. The panels were loaded until attempts to apply additional load resulted only in additional strain of the test panel.

The experimental determination of the exact critical shearing load of a sheet or plate is rather difficult. Theoretically, the critical load is the load at which the flat form of equilibrium becomes unstable and the plate begins to buckle. The exact load at which this occurs is not easily determined. To facilitate the determination of the critical shearing loads of the panels tested the side sheets were carefully observed, and it was noted that in the cases where the panels failed due to buckling of the side sheets, the load was taken by the panels with some lateral movement of the sheet, such as straightening of buckles initially present due to welding, and then a load was reached at which buckles with a definite pattern were formed. The load at which the latter occurred was considered the critical shearing load.

Panel No. 1. This test panel, which consisted of a long narrow 15-gage sheet, stiffened only by the posts, is shown in Fig. 6, the

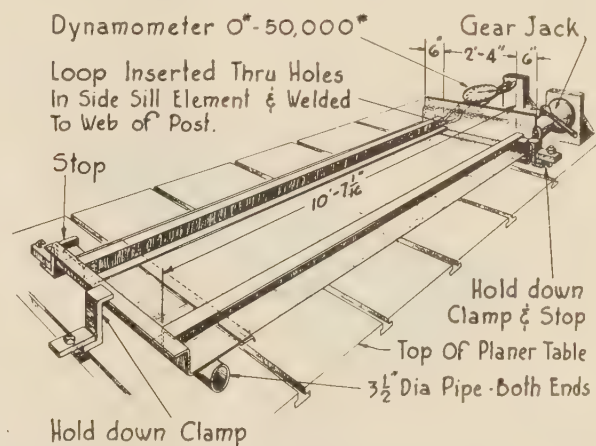


FIG. 6

posts being stiff enough to resist bending when the sheet buckled. The critical shearing stress can be obtained by considering a panel as shown in Fig. 2, with $b = 28$ in., and $d = 113\frac{5}{8}$ in. Applying Equation [1], the critical shearing stress is 870 psi. The effective shear area, consisting of the vertical portion of side plate, the vertical portion of the upper element, and side sheet, is 10.63 sq in. Thus the critical shearing load is

$$Q_{cr} = 10.63 \times 870 = 9250 \text{ lb}$$

The actual test critical shear load of this panel was 12,000 lb.

Panel No. 2. This test panel, consisting of a side section with 15-gage side sheets, and two lapped, longitudinal ribs, is shown in Fig. 7. The flexural rigidity of 15-gage sheet is 827 lb-in.

This test section can be considered as having two ribs dividing the plate into panels with dimensions $a/3$ and b , where $a = 113\frac{5}{8}$ in. and $b = 28$ in. Thus a/b is 4.06. From Fig. 5, $\gamma = 0.37$. Thus the required rib flexural rigidity is

$$B = 0.37 Da = 0.37 (827 \times 113.625) = 34,750 \text{ lb-sq in.}$$

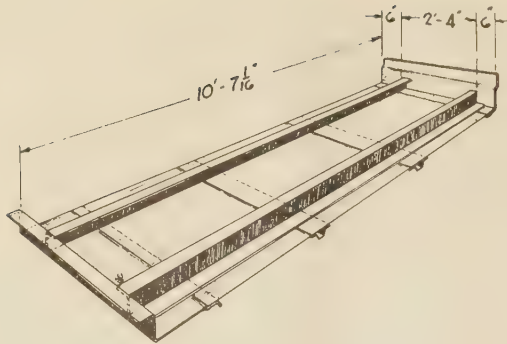


FIG. 7

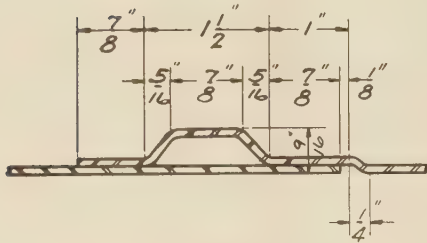


FIG. 8

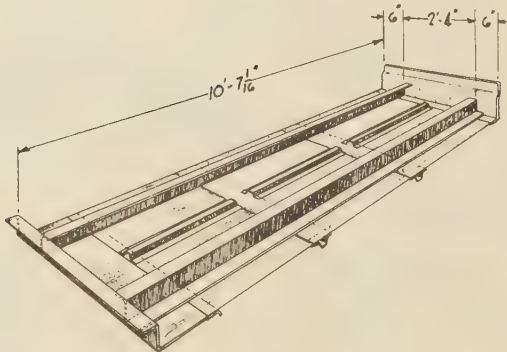


FIG. 9

A cross section of the longitudinal rib is given in Fig. 8. The flexural rigidity of the rib is 466,000 lb-sq in. Thus it is apparent that the section would fail by buckling of the sheet in panels bounded by the posts and the longitudinal ribs, with $b = 28$ in., and $d = 37\frac{1}{2}$ in., Fig. 2. The critical shearing stress is, by Equation [1], 1178 psi. The effective shear area, consisting of the vertical portion of side plate, the vertical portion of the upper element, and the side sheets is 11.14 sq in. Thus the critical shearing load is

$$Q_{cr} = 11.14 \times 1178 = 13,150 \text{ lb}$$

The actual test critical shear load of this panel was 16,500 lb.

Panel No. 3. This test panel was the same panel used for panel No. 2 which has just been discussed, with the addition of vertical stiffeners as shown in Fig. 9. This section can be considered as divided into panels bounded by the longitudinal ribs, the vertical posts, and vertical stiffeners.

For determination of the required longitudinal rib flexural rigidity a unit section with two stiffeners can be considered. The stiffeners divide the unit section into three panels with dimensions $a/3$ and b ; where $a = 113\frac{3}{8}$ in. and $b = 14$ in. Thus a/b

is 8.12. From Fig. 5 it can be seen that the value of γ is even less than that for test No. 2 which did not utilize a vertical stiffener. Thus the required rib flexural rigidity is less than 34,750 lb-sq in. and since the flexural rigidity of the actual longitudinal rib, Fig. 8, is 466,000 lb-sq in., it is apparent that the longitudinal rib is sufficiently rigid. Therefore the sheet will buckle without bending the longitudinal ribs.

In order to determine the flexural rigidity of the vertical stiffener required to prevent bending of the stiffener when the plate buckles, a unit panel with one stiffener can be considered as shown in Fig. 3, with $a = 28$ in. and $b = 37\frac{1}{2}$ in. Thus the ratio a/b is 0.747. From Fig. 4, γ is 30. This value of γ was taken from the broken-line portion in Fig. 4. The dotted portion of this curve is merely an extension of the data given by Timoshenko³ and should be accepted only as an approximation. Considering γ as 30, the required vertical-stiffener flexural rigidity is

$$B = 30 Da = 30 \times 827 \times 28 = 695,000 \text{ lb-sq in.}$$

A cross section of the 20-gage vertical stiffener is given in Fig. 10.

Since the flexural rigidity of this vertical stiffener is only 371,000 lb-sq in. it is apparent that the vertical stiffener will bend when the sheet buckles.

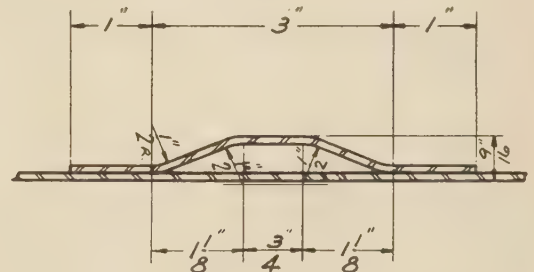


FIG. 10

In order to approximate the critical shearing load for this panel, the critical shearing load of a panel divided as shown for the test panel, but with a vertical stiffener of sufficient rigidity, will be considered. This hypothetical panel can be considered as divided into panels such as that shown in Fig. 2, with $b = 14$ in. and $d = 37\frac{1}{2}$ in. For such a panel the critical shearing stress is, by Equation [1], 3685 psi. The effective shear area is the same as that for test panel No. 2; that is, 11.14 sq in. The critical shearing load is therefore

$$Q_{cr} = 11.14 \times 3685 = 41,100 \text{ lb}$$

However, as previously stated, the vertical stiffener used for this test was not rigid enough to resist bending when the sheet buckles. Failure would therefore occur at some load between the critical shearing load obtained for panel No. 2, which consisted of the same panel without a vertical stiffener, and the critical shearing load of the hypothetical panel discussed which had a sufficiently rigid vertical stiffener. It will be assumed that the additional load-carrying capacity due to the application of the vertical stiffener is in proportion to the ratio of the flexural rigidity of the rib to the required rigidity of the rib. Thus on the basis of this crude assumption, the critical shearing load for panel No. 3 is

$$Q_{cr} = 13,150 + \frac{371,000}{695,000} (41,100 - 13,150) = 28,070 \text{ lb}$$

The actual test critical shear load of this panel was 36,000 lb.

Panel No. 4. This test panel, utilizing 14-gage side sheets and

six longitudinal lapped stiffeners, is shown in Fig. 11. This side section was used on a large number of cars constructed by The Milwaukee Road.

The flexural rigidity of 14-gage (0.075-in.) sheet is 1160 lb-in.

To determine the required longitudinal rib flexural rigidity to cause the panels bounded by the posts and longitudinal ribs to buckle without bending the ribs, a unit panel with one stiffener, Fig. 3, with $a = 31\frac{3}{4}$ in. and $b = 28$ in., can be considered. The ratio a/b is 1.133 and from Fig. 4, γ is 9.15

The required rib flexural rigidity is therefore

$$B = 9.15 Da = 9.15 \times 1160 \times 31.75 = 337,000 \text{ lb-sq in.}$$

If a unit panel, having two stiffeners, is considered having $a = 47\frac{7}{8}$ in. and $b = 28$ in., the ratio a/b is 1.703, and from Fig. 5, γ is 6.80.

The required rib flexural rigidity is therefore

$$B = 6.80 Da = 6.80 \times 1160 \times 47.625 = 376,000 \text{ lb-sq in.}$$

Thus on the basis of a unit section with one stiffener, the required stiffener flexural rigidity is 337,000 lb-sq in. while for a unit section with two stiffeners, the required stiffener flexural rigidity is 376,000 lb-sq in. It can be seen that the required rib rigidity increases slightly as the number of stiffeners increases. Timoshenko³ does not extend the theory regarding the required rib rigidity beyond the case of a panel with two stiffeners. However, for practical cases it will be assumed that the required stiffener flexural rigidity will not be larger than 1.5 times that for a panel with one stiffener. Thus a well-proportioned rib for this test panel should have a rigidity of approximately

$$B = 1.5 \times 337,000 = 505,500 \text{ lb-sq in.}$$

A cross section of the actual rib used on this test panel is given in Fig. 1. The flexural rigidity of this stiffener is 689,000 lb-sq in. The stiffener is therefore conservatively designed, and it is apparent that the panel would fail due to buckling of the sheet in panels with $b = 15\frac{7}{8}$ in. and $d = 28$ in., Fig. 2. Thus the critical shearing stress is, by Equation [1], 4020 psi. The effective shearing area, consisting of the vertical portion of side plate, the vertical portion of upper element, and the side sheets, is 13.86 sq in. and the critical shearing load is therefore

$$Q_{cr} = 13.86 \times 4020 = 55,700 \text{ lb}$$

The actual test critical shear load of this panel was not determined as the posts buckled due to compression at 43,000 lb without buckling the side sheets.

Panel No. 5. This test panel, utilizing 14-gage side sheets, is shown in Fig. 11. The panel is stiffened with six lapped longitudinal ribs smaller than those employed for panel No. 4. Since the spacing of posts and longitudinal ribs is the same for this panel as for panel No. 4, the required longitudinal rib flexural rigidity based on a unit panel with one stiffener is the same as that for panel No. 4, that is, 337,000 lb-sq in. As stated in the discussion of test No. 4 for practical cases with several stiffeners, it is advisable to make the stiffener about 1.5 times the rigidity required on the basis of a calculation for a unit panel with one stiffener, that is, 505,500 lb-sq in. for this panel.

A cross section of the lapped longitudinal stiffener used for this test is given in Fig. 8. The flexural rigidity is 510,000 lb-sq in. This stiffener is therefore well designed, and it is apparent that the longitudinal rib will not bend when the sheet buckles. The sheet will therefore buckle in panels bounded by the posts and longitudinal ribs with $b = 15\frac{7}{8}$ in. and $d = 28$ in., Fig. 2. This is the same as for panel No. 4, and the critical shearing stress based on Equation [1] is again 4020 psi. The effective shear area, consisting of the vertical portion of side plate, the vertical

portion of upper element, and the side sheets, is 13.20 sq in. Thus the critical shearing load is

$$Q_{cr} = 13.20 \times 4020 = 53,000 \text{ lb}$$

The actual test critical shear load of this panel was not determined as the posts buckled due to compression at 43,000 lb without buckling the side sheets.

Panel No. 6. This side section, Fig. 11, with six lapped longitudinal stiffeners of the cross section shown in Fig. 12, was used on 1000 boxcars recently built at the Milwaukee shops. The side sheets were of 15-gage thickness.

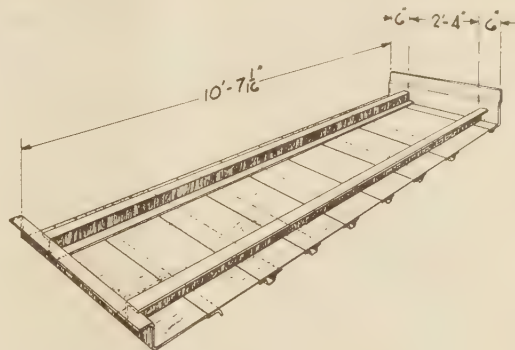


FIG. 11

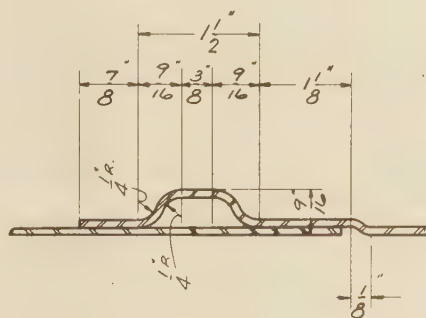


FIG. 12

To determine the required longitudinal-stiffener flexural rigidity, consider a unit panel with one stiffener, Fig. 3, with $a = 31\frac{3}{4}$ in. and $b = 28$ in. Thus the ratio a/b is 1.133 and from Fig. 4, γ is 9.15. Since the flexural rigidity of 15-gage sheet is 827 lb-in. the required longitudinal-stiffener flexural rigidity for a unit panel with one stiffener is

$$B = 9.15 Da = 9.15 (827 \times 31.75) = 240,000 \text{ lb-sq in.}$$

As previously stated, a suitable stiffener for a panel with a multiple number of stiffeners should have a flexural rigidity of approximately 1.5 times that required for a unit panel with one stiffener. Thus a stiffener for this panel should have a flexural rigidity of 360,000 lb-sq in. A cross section of the 15-gage longitudinal stiffener used for this test panel is shown in Fig. 12. The flexural rigidity of this stiffener is 376,800 lb-sq in. Thus the stiffener is well designed and the sheet will buckle in panels with $b = 15\frac{7}{8}$ in. and $d = 28$ in., Fig. 2. The critical shearing stress is, by Equation [1], 3210 psi. Since the effective shearing area, consisting of the vertical portion of the side plate, the vertical portion of the upper element, and the side sheets, is 12.27 sq in., the critical shearing load is

$$Q_{cr} = 12.27 \times 3210 = 39,400 \text{ lb}$$

TABLE 1 SUMMARY OF TESTS AND CALCULATIONS

Panel no.	Description of panel	Analytical critical shear load, lb	Test results Maximum load applied, lb	Critical shear load, lb	Cause of failure	Weight of carset of sheets (40 ft 6 in. box), lb	Weight saved over 0.100-in. sheets, lb	Analytical critical shear load carried per lb of sheet	Factor of safety ^a	Remarks
1	15-gage flat unstiffened side section	9250	28000	12000	Buckling of sheet due shear	1835	900	5.03	0.44 ^b	Load carried beyond 12,000 lb due to development of tension field
2	15-gage side section with two lapped longitudinal stiffeners	13150	25000	16500	Buckling of sheet due shear	1876	859	7.02	0.63 ^b	Load carried beyond 16,500 lb due to development of tension field
3	Same as panel no. 2 with a 20-gage vertical stiffener	28070	43000	36000	Bending of vertical stiffener and buckling sheet	2066	669	13.57	1.34	Shear buckle waves in sheet crossed and bent vertical stiffener
4	14-gage side section with 6 lapped longitudinal stiffeners	55700	43000	Not reached	Buckling of post due to compression	2495	240	22.30	2.65	
5	14-gage side section with 6 lapped longitudinal stiffeners	53000	43000	Not reached	Buckling of post due to compression	2350	385	22.55	2.52	
6	15-gage side section with 6 lapped longitudinal stiffeners	39400	Not tested	Not tested	Not tested	2135	600	18.45	1.88	
7	16-gage side section with 6 lapped longitudinal stiffeners	29050	Not tested	Not tested	Not tested	1910	825	15.20	1.38	
8	0.100-in. flat, unstiffened side section	28050	Not tested	Not tested	Not tested	2735	000	10.25	1.33	

^a Using 21,000 as the maximum shear load at bolster panel.

^b Structure would not collapse due to development of tension fields.

This panel was not tested.

Panel No. 7. This side section is exactly the same as panel No. 6 with the exception that the side sheets were 16 gage. The required longitudinal stiffener flexural rigidity can again be determined on the basis of a unit panel with one stiffener, Fig. 3, with $a = 31\frac{3}{4}$ in. and $b = 28$ in. Thus the ratio of $a/b = 1.133$, and from Fig. 4, γ is 9.15. Since the flexural rigidity of 16-gage sheet is 594 lb-in., the required longitudinal flexural rigidity for a unit panel with one stiffener is

$$B = 9.15 \quad Da = 9.15 (594 \times 31.75) = 172,800 \text{ lb-sq in.}$$

As previously stated, the flexural rigidity of a stiffener for a panel with a multiple number of stiffeners should be approximately 1.5 times that for a unit panel with one stiffener. Thus for this panel the longitudinal stiffener should have a flexural rigidity of 259,200 lb-sq in. The flexural rigidity of the 16-gage stiffener shown in Fig. 12 is 346,500 lb-sq in. Thus it is apparent that the sheet will buckle in panels with $b = 15\frac{7}{8}$ in. and $d = 28$ in., Fig. 2, and the critical shearing stress is, by Equation [1], 2575 psi. Since the shearing area, consisting of the vertical portion of the side plate, the vertical portion of the upper element, and the side sheets, is 11.29 sq in., the critical shearing load for this panel is

$$Q_{cr} = 11.29 \times 2575 = 29,050 \text{ lb}$$

This panel was not tested.

Panel No. 8. This side section consists of a flat, unstiffened 0.100-in. side sheet and is shown in Fig. 6. The critical shearing stress of such a panel can be obtained by considering a panel as shown in Fig. 2, with $b = 28$ in. and $d = 113\frac{3}{8}$ in. Applying Equation [1], the critical shearing stress is 1938 psi. Since the effective shear area, consisting of the vertical portion of the side plate, the vertical portion of the upper element, and the side sheets, is 14.45 sq in., the critical shearing load is

$$Q_{cr} = 14.45 \times 1938 = 28,050 \text{ lb}$$

This panel was not tested.

As previously stated, all of the panels tested were loaded until attempts to apply additional load resulted only in additional strain of the test panel. This additional strain consisted of raising higher sheet buckles in tests Nos. 1 and 2; raising higher sheet buckles and bending vertical stiffeners in test No. 3, and buckling the posts in tests Nos. 4 and 5.

CONCLUSIONS

In an actual car side a great deal more load beyond the critical shearing load can be carried by development of tension fields. Such a tension field is, of course, accompanied by extremely high deflections. These high deflections result in rotation of the doorpost by the side sill and development of high fixed end moments which often result in failure of the doorposts or doorpost attachments in cars with unstiffened side sheets.

The panels tested in tests Nos. 4 and 5 failed at 43,000 lb, due to compressive buckling of the side posts; in actual car construction the shear load is transmitted to the bolster by two posts, and hence a load of 86,000 lb would be required to buckle the posts. Since the actual maximum shear load at the bolster of a 50-ton box or automobile car is 21,000 to 22,000 lb, the post-buckling factor of safety is approximately 4.

The test and analytical results are in reasonably good agreement. The analytical critical shearing loads for the panels which failed due to buckling of the side sheets, are in all cases lower than the actual test critical shearing loads. A part of this difference is undoubtedly due to Vierendeel-truss action of the frame consisting of the upper element, the side posts, and the side plate. It is apparent that a panel designed by the equations discussed in this paper would be suitable for the design loads.

The longitudinal stiffeners were, in all cases, sufficiently large. The longitudinal ribs for test panel No. 2 were, in fact, much larger than necessary as a very small stiffener would have been sufficiently rigid to remain straight while the sheet buckled. It is, however, advisable to make stiffeners more rigid than absolutely necessary, as a panel with ribs with less than the required flexural rigidity would develop tension fields which may be accompanied by permanent bending of the ribs.

An examination of the test results indicates that test panel No. 1 with a flat unstiffened 15-gage side sheet had a critical shear load of 9250 lb. Panel No. 2 with 15-gage side sheets and two longitudinal stiffeners had a critical shear load of 13,150 lb; and panel No. 6 with 15-gage side sheets and six longitudinal stiffeners had a critical shear load of 39,400 lb. Thus the application of two stiffeners increased the carrying capacity of the 15-gage sheet only 3900 lb, while the application of six well-designed ribs increased the carrying capacity 30,150 lb. Therefore it is apparent that a hit-or-miss application of ribs is not necessarily of great advantage and that a girder, stiffened with ribs, must be carefully designed.

Examination of the summary in Table 1 indicates that panel No. 5 is the most efficient panel from the standpoint of critical shearing load carried per pound of sheet. However, the load-carrying capacity of this panel is far greater than that required for a 50-ton boxcar, and for economic reasons either panel No. 6 or panel No. 7 is more desirable. While panel No. 6 has a factor of safety of 1.88 which is higher than required, the added sheet thickness would increase the time required for corrosion to affect seriously the factor of safety.

The critical shearing stresses for all of the test panels were low in comparison to the elastic limit of low-carbon steel. The maximum critical shear stress encountered was the 4000 psi for test panels Nos. 4 and 5. Test panels Nos. 4, 5, 6, and 7 are well designed, and it would be uneconomical to stiffen a panel of the thickness encountered in boxcar construction to the extent required to raise critical shearing stress to that permitted by material strength, although the load-carrying capacity of any of these panels could have been substantially increased by further stiffening. With a given stiffener spacing, the carrying capacity of a panel is proportional to the flexural rigidity of the sheet. Since the flexural rigidity is practically independent of the composition of the steel and is primarily dependent on the plate thickness, the critical shearing load of the panels is not increased by the utilization of high-tensile material.

Discussion

O. W. HOVEY.⁴ We are grateful to the authors for presenting this paper, and to Dr. Nystrom for authorizing the tests which it describes. The ribbed sides of The Milwaukee Road cars have been the subject of much observation and comment, and this paper shows that their use is based on sound structural theory. The paper points out the increased resistance to buckling obtained by the addition of the longitudinal ribs, and the consequent increase in rigidity of the car sides. It also mentions that the ultimate safety of the structure depends on the ability of the sheets to act in diagonal tension, which safety factor is retained by the effective continuity of the sheets across the lapped joints. By introducing longitudinal lapped ribs in the sheets, the posts can be spaced farther apart, or thinner sheets can be used, with consequent reductions in over-all weight. In fact, with this method of construction, the sheets could be considerably thinner than those now applied to The Milwaukee Road cars.

In figuring the required section of the stiffening ribs, some method must be assumed for evaluating the loads which they carry, and thus determining their size. A convenient method is to assume that the shear on the car side at any vertical section is carried by a number of individual panels equal to the number of ribs plus one. As the shear in each of these subpanels has the same value vertically and horizontally, a horizontal traction occurs in opposite directions along the two edges of the rib. As-

suming one side to be in tension and the other in compression, the rib may be figured as a column elastically restrained by its tension side. It has been found that by applying one half of the shear in the subpanel as a column load on the stiffener, a rib of proper size to prevent buckling will be obtained. It should be noted that this load is applied with an eccentricity equal to the distance from the center of the sheet to the neutral axis of the rib. In figuring the properties of the rib, a portion of the sheet is included, the width of this strip being somewhat less than would act without buckling, at the assumed compression unit stress on the rib.

The authors suggest that with the sheet thicknesses and sizes of ribs used in the tests, carbon steel would have resisted the buckling forces as well as high-strength steel. This is true for buckling considerations alone, because elastic-stability values are based upon the modulus of elasticity of the material. It does not hold, however, for ultimate values, because the strength of the rib as a column is a function of the yield strength of the material, and the ultimate shear value of the car side in diagonal tension is a function of the ultimate strength of the material. Thus the high-strength steels afford an increased safety factor, or with their superior corrosion resistance permit lighter sections without any sacrifice in the life expectancy of the car structure.

AUTHOR'S CLOSURE

The authors wish to thank Mr. Hovey for his discussion and for the assistance he has rendered over a period of years during the development of the car sides described in this paper.

Mr. Hovey suggests that the stiffening ribs be considered as columns eccentrically loaded with the shear load on one side as a uniformly distributed compressive load and the shear load on the other side as an elastic restraint. The shear load on each side of the rib is the total vertical shear load carried by the side times the reciprocal of one plus the number of stiffening ribs. Since all of the side panels described in this paper are to be designed to carry the same vertical shear load it is apparent that the stiffeners for panel No. 2 with two stiffeners must, according to the method suggested by Mr. Hovey, carry seven thirds of the load carried by the stiffener on panel No. 6 with six stiffeners. Thus it appears that panel No. 2 requires a larger stiffener than panel No. 6. This is not in agreement with the results obtained by the method given by S. Timoshenko³ which is described and applied in the paper. According to the method given by Timoshenko the stiffener required for Panel No. 2 must have a flexural rigidity of only 34,750 lb-sq in. while that for panel No. 6 must be 360,000 lb-sq in. Since the test results are in reasonably good agreement with the theoretical analysis presented by S. Timoshenko the authors cannot accept the method of designing stiffeners suggested by Mr. Hovey as reliable. The authors believe that if the shear load on one side of the stiffener is considered as a uniformly distributed compressive load on the stiffener as a column, the shear load on the other side of the stiffener which is opposite in direction and equal in magnitude unloads the column rather than provides an elastic restraint. Therefore, the authors recommend that the procedure presented by S. Timoshenko,³ and outlined in the paper, be used for determining the proper size of stiffeners.

The car side section used on The Milwaukee Road is designed to carry the car load limit without buckling of the side sheet and development of tension ties; this keeps the deflection from becoming excessive. However, as stated by Mr. Hovey, a stiffened side section with considerably thinner side sheets than those used on The Milwaukee Road could be designed to carry the required load by permitting the formation of tension ties and the strength of such a side would be dependent upon the yield strength of the side sheet material.

⁴ Development Engineer, Alloys Development Company, Pittsburgh, Pa. Mem. A.S.M.E.

Creep and Relaxation in Rubber Products at Elevated Temperatures

By R. D. ANDREWS,¹ R. B. MESROBIAN,¹ AND A. V. TOBOLSKY¹

The studies reported of creep and relaxation at elevated temperatures suggest possible methods of evaluating deteriorative changes occurring in rubbers. Involving intermittent and continuous relaxation and creep measurements, the new methods seem to be readily amenable to molecular-structural interpretations. The practical value of these measurements, apart from their usefulness in fundamental scientific research, is apparent in cases where service deterioration occurs as a result of creep or relaxation. The usefulness and importance of these measurements of creep, relaxation, and modulus are not limited to the measurement of high-temperature oxidative deterioration in rubbers. The simple way in which they are related to molecular changes in the material being studied should make them very valuable in the study of physical changes in polymeric materials in general, such as cold flow of plastics, drift of rubbers, low-temperature stiffening, permanent set, etc.

THE creep of rubber products under conditions of constant load and their relaxation of stress under conditions of constant extension are interesting and important problems in themselves in many applications involving the use of natural and synthetic rubbers at elevated temperatures. In addition, recent studies of creep and relaxation at elevated temperatures suggest a new approach to the problem of evaluating the deteriorative changes occurring in rubbers. Although conventional aging tests such as the oxygen-bomb test and the Geer oven test have proved their value as standardization methods, the results of these tests are rather difficult to interpret on the basis of fundamental physicochemical concepts. Intermittent and continuous relaxation and creep measurements, on the other hand, seem to be readily amenable to molecular-structural interpretations.

EXPERIMENTAL METHODS

The apparatus used for measurements of relaxation of stress at constant elongation and also of changes of modulus with time ("intermittent relaxation") has been described in a previous paper,² in which illustrations of the apparatus (which was constructed by the Firestone Physics Research Division) are also shown. In principle the apparatus is simply a small beam balance; the rubber samples, which are flat rings (2¹¹/₁₆ in. OD, 2⁵/₁₆ in. ID) died out of cured sheet approximately 0.040 in. thick, are looped around a pulley attached to the short end of the balance beam and are extended from outside the temperature

¹ Frick Chemical Laboratory, Princeton University, Princeton, N. J.

² "Stress Relaxation of Natural and Synthetic Rubber Stocks," by A. V. Tobolsky, I. B. Prettyman, and J. H. Dillon, *Journal of Applied Physics*, vol. 15, 1944, p. 380. Reprinted in *Rubber Chem. Technology*, vol. 17, 1944, p. 551.

Contributed by the Rubber and Plastics Division and presented at the Annual Meeting, New York, N. Y., Nov. 27-Dec. 1, 1944, of THE AMERICAN SOCIETY OF MECHANICAL ENGINEERS.

NOTE: Statements and opinions advanced in papers are to be understood as individual expressions of their authors and not those of the Society.

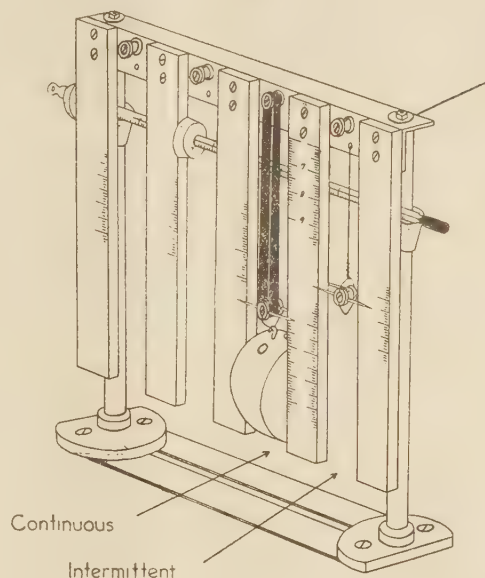


FIG. 1 CREEP APPARATUS

box. The moment exerted by the stretched rubber band on the short lever arm is balanced by suspended weights and a rider on the other arm of the beam. During the experiment the length of the stretched band is maintained constant to within 0.2 per cent, because the long lever arm is allowed to swing over only a small angle on either side of the horizontal position.

Measurement of the change of modulus with time can also be made with this apparatus, and these studies have been called "intermittent relaxation" studies inasmuch as the measurements are made in exactly the same way as the measurements of continuous relaxation of stress, except that the sample is elongated to the fixed length only momentarily at the time of a measurement, remaining unstretched at all other times.³

Measurements of the creep of samples supporting a constant load are made in a very simple way. A frame, shown in Fig. 1, is used, which has four pulleys attached along a crossbar at the top. The samples used are smaller rings (1⁷/₈ in. OD, 1¹/₂ in. ID) died from the same cured sheets as the rings used in the relaxation measurements. Pulleys engage the bands at the bottom also and support the weights which are hollow, cylindrical, copper cans whose weight is adjusted by filling with lead shot.

The samples are extended between sections of meter stick which are held vertically from the top crossbar. Two pairs of phonograph needles are set diametrically into the lower pulley and bracket the adjacent meter sticks, thus serving to indicate the elongation as well as to keep the samples in position.

³ The change of modulus with time can also be measured on creep apparatus ("intermittent creep"), by applying the load to the sample only at intervals when a reading is taken, by the method shown in Fig. 1. This method is in general not as convenient as the "intermittent relaxation" method, however.

THEORETICAL DISCUSSION—CONTINUOUS RELAXATION OF STRESS

According to modern structural concepts, soft vulcanized rubbers are three-dimensional networks of long-chain molecules cross-linked by chemical bonds introduced during the vulcanization. The portions of the network between contiguous cross-linking juncture points are known as network chains. The changes that occur in the properties of rubber due to the effects of heat and exposure to air and light are collectively known as aging. It has been repeatedly demonstrated that aging must be considered a chemical reaction occurring in the presence of oxygen. For this reason the rubber bands used in these studies were made sufficiently thin to allow a homogeneous penetration of oxygen.

The results of the studies of continuous and intermittent relaxation and creep have demonstrated that two competing reactions are responsible for the deteriorative changes occurring in rubbers. One of these reactions is a scission of the network chains of the rubber and the other is a cross-linking reaction. Both these reactions must be intimately related inasmuch as they occur with comparable rates over the entire temperature range. This fact suggests that the activation step for both reactions may well be the same.

The measurement of relaxation of stress at constant extension at elevated temperatures provides a means of isolating the scission reaction inasmuch as cross-links tend to form between molecules which are in a relaxed position and so have no effect on the stress. The decay of stress is presumed to be due to the cutting of some chemical bond in the network chains. According to the most satisfactory theory of rubber elasticity yet available, the stress is proportional to the concentration of network chains (or to the concentration of cross-linkage) in the rubber, and so the rate of decay of stress is proportional to the rate of chain scission.

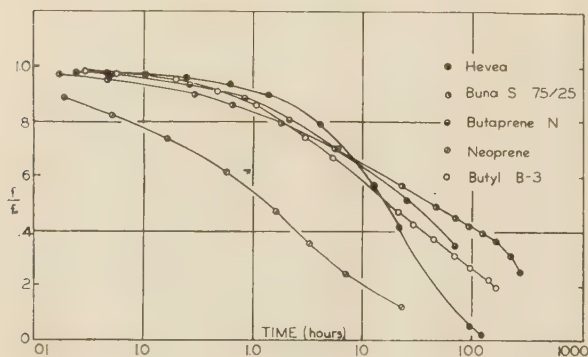


FIG. 2 CONTINUOUS RELAXATION, GUM STOCKS, 100 C, 50 PER CENT ELONGATION

Fig. 2 shows the results of stress-relaxation studies on five different types of rubber. The experiments were carried out at 100 C, and 50 per cent elongation. The ordinate is stress at any given time divided by initial stress, and the abscissa is logarithmic time. For purposes of comparison the same data are replotted in different ways in Figs. 3 and 4.

It is clear from these figures that the different polymers are characterized by quite different relaxation curves. The order of rate of relaxation from the fastest to the slowest is as follows: Neoprene, Hevea, Butyl, Butaprene N, GR-S.

The other facts concerning the relaxation curves are:

1 The rate of relaxation can be slowed a thousandfold by careful exclusion of oxygen.

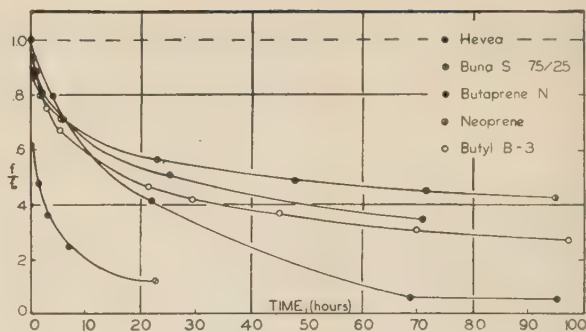


FIG. 3 CONTINUOUS RELAXATION, GUM STOCKS, 100 C, 50 PER CENT ELONGATION

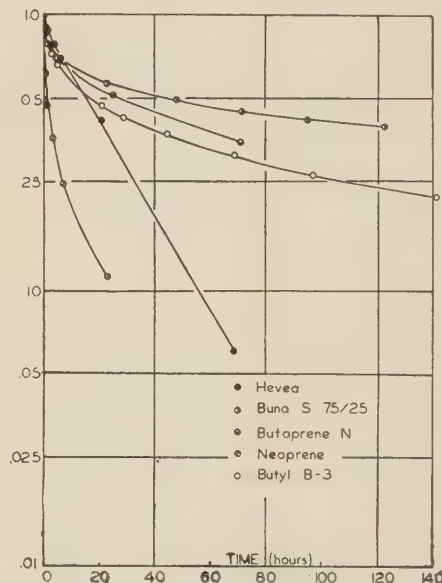


FIG. 4 CONTINUOUS RELAXATION, GUM STOCKS, 100 C, 50 PER CENT ELONGATION

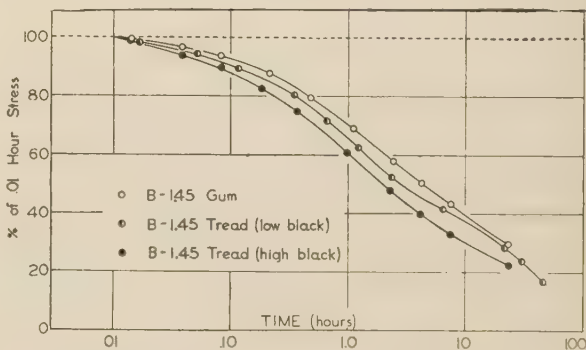


FIG. 5 EFFECT OF CARBON BLACK ON CONTINUOUS RELAXATION BUTYL STOCKS, 120 C, 50 PER CENT ELONGATION

2 The relaxation curves are relatively independent of elongation up to high elongations.

3 The relaxation curves are not markedly altered by the presence of carbon black in the vulcanizate. In certain cases the presence of carbon black has a slight accelerating effect (see Fig. 5); in Neoprene, however, the presence of carbon black decreases the relaxation rate.

4 The relaxation curve for Hevea gum follows a simple exponential decay law. The relaxation curves for other polymers can be fitted by a sum of exponential decay terms.

5 The effect of temperature on the rate of relaxation obeys the Arrhenius law for chemical reactions, namely

$$k' = Ae^{-E/RT} \dots \dots \dots [1]$$

where k' is the specific rate, E is the energy of activation, and A the so-called frequency factor. Fig. 6 shows the dependence of the relaxation curve on temperature for Hevea gum. The calculated energy of activation for relaxation turns out to be 30.4 kcal in this case.

6 The effect of the type of vulcanization (e.g., sulphur versus sulphurless cures) is not as important a factor in the stress-relaxation curve as the polymer type.

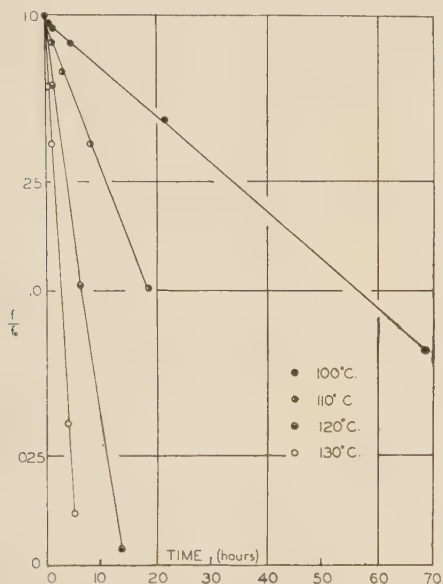


FIG. 6 EFFECT OF TEMPERATURE ON CONTINUOUS RELAXATION RATE, HEVEA GUM, 50 PER CENT ELONGATION

7 The presence of certain antioxidants in the vulcanizate definitely retards the rate of relaxation.

STUDIES OF INTERMITTENT RELAXATION

Figs. 7 and 8 show the results of so-called intermittent relaxation of stress measurements on Hevea and GR-S gum and tread vulcanizates at 130 C. As previously noted, these measurements are nothing more than periodic measurements of the 50 per cent modulus and are plotted in Figs. 7 and 8, in terms of stress at time t divided by stress at zero time. It is to be noted that the intermittent relaxation curve for Hevea shows that the modulus initially decreases. In certain experiments where the rubber bands did not rupture, this initial decrease was followed by a subsequent increase. In the case of GR-S, Fig. 8 shows that the modulus increases with time. In these experiments Butyl rubber shows a continuous modulus decrease, whereas Neoprene and Butaprene N, like GR-S, show a continuous modulus increase.

In terms of molecular concepts, the change of modulus with time measures the "net rate" of cross-linking and scission. For this reason the intermittent relaxation curve never decreases as rapidly as the continuous relaxation curve even when scission

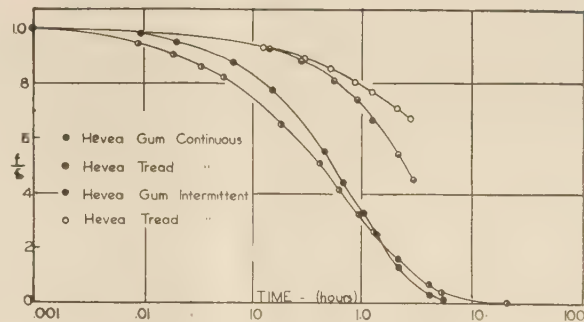


FIG. 7 CONTINUOUS AND INTERMITTENT STRESS RELAXATION, HEVEA STOCKS, 130 C, 50 PER CENT ELONGATION

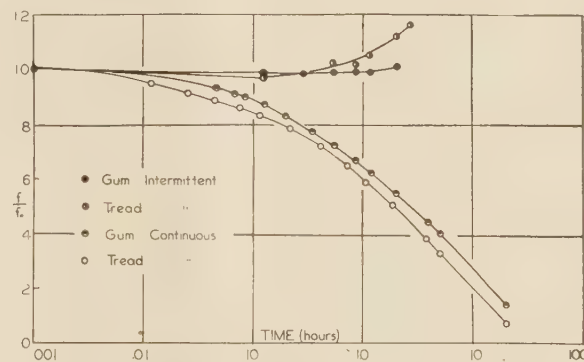


FIG. 8 CONTINUOUS AND INTERMITTENT STRESS RELAXATION, GR-S STOCKS, 130 C, 50 PER CENT ELONGATION

is predominant as in the case of Butyl and Hevea. The rise of modulus with time in the cases of GR-S, Butaprene N, and Neoprene indicates of course that in these rubbers cross-linking is taking place more rapidly than scission.

CREEP STUDIES

Figs. 9 and 10 show the results of creep studies on Hevea gum at 120 C. Here the creep data are plotted in the form of per cent elongation as a function of linear and logarithmic time. It certainly is reasonable to suppose that the same chemical reactions which are responsible for stress relaxation must be responsible also for creep. A theoretical interpretation of these data⁴ has indicated that creep and relaxation should be related as follows

$$\frac{f}{f_0} = \frac{\frac{l_0}{l_u} - \left(\frac{l_u}{l_0}\right)^2}{\frac{l}{l_u} - \left(\frac{l_u}{l}\right)^2} \dots \dots \dots [2]$$

where f/f_0 represents the fraction of original stress at time t in a stress-relaxation experiment, l represents the length at time t in a creep experiment, l_0 the initial length and l_u the unstretched length.

It is therefore useful to define a creep function, " s/s_0 "

$$s/s_0 = \frac{\frac{l_0}{l_u} - \left(\frac{l_u}{l_0}\right)^2}{\frac{l}{l_u} - \left(\frac{l_u}{l}\right)^2} \dots \dots \dots [3]$$

⁴ "Systems Manifesting Superposed Elastic and Viscous Behavior," by A. V. Tobolsky and R. D. Andrews, *Journal of Chemical Physics*, vol. 13, 1945, p. 3.

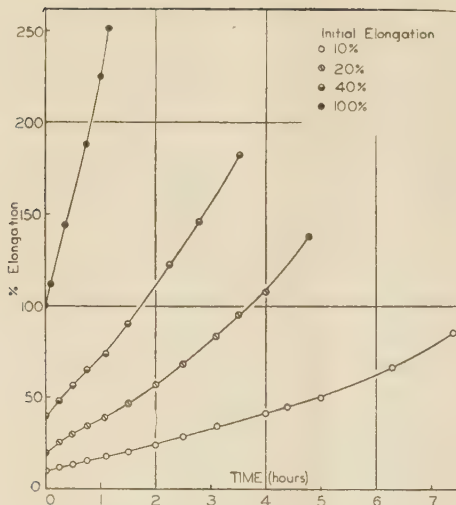


FIG. 9 CREEP OF HEVEA GUM AT DIFFERENT ELONGATIONS, 120 C

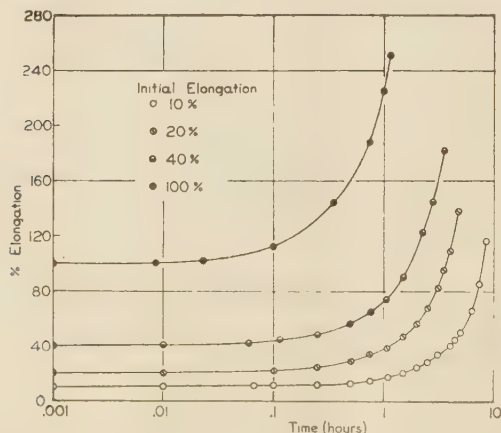


FIG. 10 CREEP OF HEVEA GUM AT DIFFERENT ELONGATIONS, 120 C

Fig. 11 shows the data presented in Figs. 9 and 10, replotted in terms of the creep function against logarithmic time. The relaxation curve at the same temperature is also shown, and it is apparent from these graphs that the creep function is nearly identical with the relaxation function and is largely independent of the initial elongation used in the creep measurement. The same identity of the creep and relaxation functions has been observed for Butyl gum. However, as is shown in Fig. 12, creep is definitely slower than relaxation for GR-S; this is also true for other rubbers which harden rather than soften at elevated temperatures. It has also been observed that the deviation between creep and relaxation is greater in tread stocks than in the corresponding gum stocks. For example, a noticeable deviation between creep and relaxation is observed in Hevea and Butyl tread stocks, though such a deviation does not appear in the gum stocks.

Equation [2] has been derived on the assumption that the observed creep is due only to the scission reaction. This is largely true because at any given moment all cross-links form in a relaxed position. However, as the creep progresses the newly formed cross-linked chains do have a retarding effect. Therefore it is not surprising that in cases where cross-linking is pronounced, the creep function is somewhat slower than the re-

laxation curve. Despite this effect of cross-linking, however, creep curves of different rubber stocks will show the same general differences as the continuous relaxation curves of the same stocks, and so give a general comparison of the rates of oxidative scission in various rubber stocks.

The practical value of these measurements, apart from their usefulness in fundamental scientific research, is immediately apparent in cases where service deterioration occurs as a result of creep or relaxation. It should be remembered, however, that these measurements are carried out on thin samples in which oxidation is homogeneous. When thick samples are to be used in service, these measurements should be made on samples of the same thickness, for the experimental data to have a direct relation to service deterioration. A particularly interesting practical aspect of these studies is that they show (by the great difference between intermittent and continuous relaxation curves) that the failure of rubber products in service at elevated temperatures will depend largely on whether the rubber is subjected to continuous or only to intermittent deformation. Failure will occur more rapidly under continuous deformation, since failure under those circumstances depends primarily on the scission

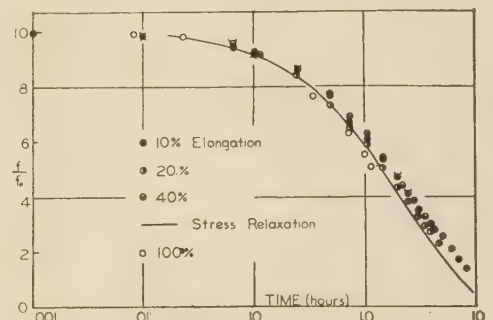


FIG. 11 COMPARISON OF CREEP FUNCTION WITH CONTINUOUS RELAXATION, HEVEA GUM, 120 C

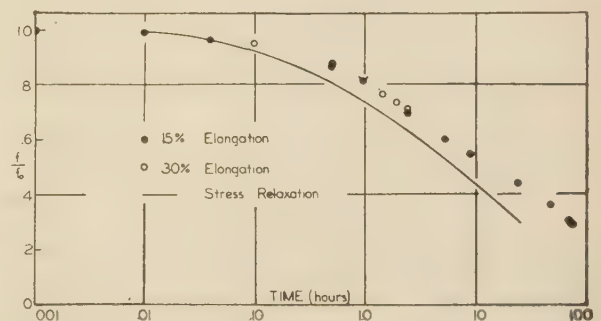


FIG. 12 COMPARISON OF CREEP FUNCTION WITH CONTINUOUS RELAXATION, GR-S Gum, 120 C

reaction; under intermittent deformation, failure will result from the net effect of both reactions, and changes will take place more slowly under these circumstances. The behavior of Neoprene illustrates very well the value of making this distinction. Neoprene relaxes and creeps most rapidly of all the various rubber types studied. However, the modulus of Neoprene changes more slowly with time than is the case with most of the other rubber types (as is seen from comparison of their "intermittent relaxation" curves). Therefore, Neoprene will fail very quickly when under continuous load at high temperatures, but should have a longer service life than most other rubbers when used in ap-

plications which involve only momentary intermittent loading.

The usefulness and importance of these measurements of creep, relaxation, and modulus are by no means limited to the measurement of high-temperature oxidative deterioration in rubbers. The simple way in which they are related to molecular changes in the material being studied should make them very valuable in the study of physical changes in polymeric materials

in general, such as cold flow of plastics, drift of rubbers, low-temperature stiffening,⁴ permanent set, etc., since all these changes in physical properties have their basis in fundamental molecular changes of the type which are reflected in these measurements. Many new applications of these experimental methods will undoubtedly develop with increasing realization of their possibilities.



Investigation of Influence of Ring Size, Bobbin Diameter, and Spindle Speed on Spinning Process, and Their Effect on Over-All Cost of Spinning

BY A. N. SHELDON¹ AND J. J. BLAKE²

From mathematical formulas and data by Dr. Wilhelm Stiel³ the authors have developed a series of charts from which may be predetermined with a fair degree of accuracy, the optimum diameters of ring and bobbin, and speed of spindle, for spinning any size of cotton yarn from any length of staple, carded or combed. The results derived coincide closely with general practice. The use of the charts is explained in some detail by application to specific cases, leading to the prediction of spinning costs under various conditions of spindle speed, ring and bobbin sizes, and the like.

IN so far as the authors are informed, there has never been published in the textile literature any chart from which could be predetermined, with approximate accuracy, the optimum diameter of ring and bobbin and speed of spindle, for spinning any size of cotton yarn from any length of staple, carded or combed. In an attempt to fill this hiatus, the graphs which accompany this text have been prepared. The several curves making up Fig. 1 are derived from mathematical formulas and data developed by Dr. Wilhelm Stiel.³ These have been carefully analyzed and are believed to be correctly deduced and adapted; at any rate, the derivative results appear to coincide rather closely with general practice.

The basic formula is as follows

$$T = \frac{(2 \times 3.14)^2 \times R_r \times G_L \times N_0^2}{g \times F(\phi) \times 61^2}$$

in which

- T = tension in grams
- R_r = ring radius in meters
- G_L = weight of traveler in grams
- N_0 = traveler speed or revolutions per minute
- $g = 9.81$ (acceleration in meters per second)
- $F(\phi)$ = factor, depending on spindle speed, coefficient of traveler friction, and ratio of bobbin to ring diameter

Inspection of the chart will readily demonstrate its utility, but probably an exemplary solution of the formula and a brief description of the use of graphs will facilitate their interpretation.

¹ F. P. Sheldon & Son, Providence, R. I. Mem. A.S.M.E.

² F. P. Sheldon & Son, Providence, R. I.

³ "Textile Electrification," by Wilhelm Stiel, Geo. Routledge and Sons, Ltd., London, Eng., 1933, pp. 178-261.

Contributed by the Textile Division and presented at the Annual Meeting, New York, N. Y., Nov. 27-Dec. 1, 1944, of THE AMERICAN SOCIETY OF MECHANICAL ENGINEERS.

NOTE: Statements and opinions advanced in papers are to be understood as individual expressions of their authors and not those of the Society.

APPLICATION OF EQUATION

For a typical application of the equation, we will consider No. 20's carded yarn spun from 1¹/₁₆-in. cotton, spindle speed 9000 rpm, with 2¹/₄-in. ring, bobbin diameter 1¹/₂ in., and No. 2/0 traveler weighing 0.0518 g. We will also assume a slip of 3 per cent between spindle speed and traveler speed. Adopting these values in the preceding formula, we have

$$R_r = 0.0286$$

$$G_L = 0.0518$$

$$N_0 = 9000 - 270 = 8730$$

These constants supply all of the unknown quantities on the right-hand side of the equation, except $F(\phi)$, which is determined from the charts, Figs. 2 and 3. From the curve in Fig. 2, we ascertain the coefficient of friction between traveler and ring, designated by the letter u , which, for the example chosen, is 0.23. (For complete data on determination of coefficient of traveler friction, refer to an article⁴ by A. Lüdicke.) The vertical line at 9000 rpm spindle speed cuts the curve at point 0.23. Then, having found u , we refer to the corresponding curve, 0.23, Fig. 3, on which the abscissa is graduated into divisions representing the ratio of bobbin diameter to ring diameter. In this instance, $\frac{1/2}{2 1/4} = 0.222$. From this point on the abscissa we raise a perpendicular line until it intersects curve 0.23 and find the corresponding value of $F(\phi)$ on the left-hand margin to be 4.4

We now have all of the quantities to be substituted in the fundamental equation for computing the value of T , as follows

$$T = \frac{(2 \times 3.14)^2 \times 0.0286 \times 0.0518 \times (8730)^2}{9.81 \times 4.4 \times (61)^2} = 27.7 \text{ g}$$

Referring to Fig. 1, for No. 20's yarn, the scale at the right-hand margin denotes various staples of carded K and combed C cottons from which the yarn is spun, while the scale at the left-hand margin shows the safe spinning tension for these staples. The scale at the bottom of the chart gives the ratio of bobbin diameter to ring diameter for the particular condition under consideration.

Suppose, for instance, it is desired to determine the several combinations of ring diameter, bobbin diameter, and spindle speed suitable for commercial 1¹/₁₆-in. carded cotton. From 1¹/₁₆ in. K at the right-hand margin draw a horizontal line to the left-hand margin, indicating a safe tension of 27 to 27.1 g. Any point above this horizontal line indicates an excessive tension, and any point on or below the line, a safe tension to adopt. This line crosses first the curve of 9000 rpm and 1¹/₂-in. bobbin, just

⁴ "A Study of the Ring Spindle" (translation of title), by A. Lüdicke, Dingler's *Polytechnisches Journal*, 1881, pp. 334-345.

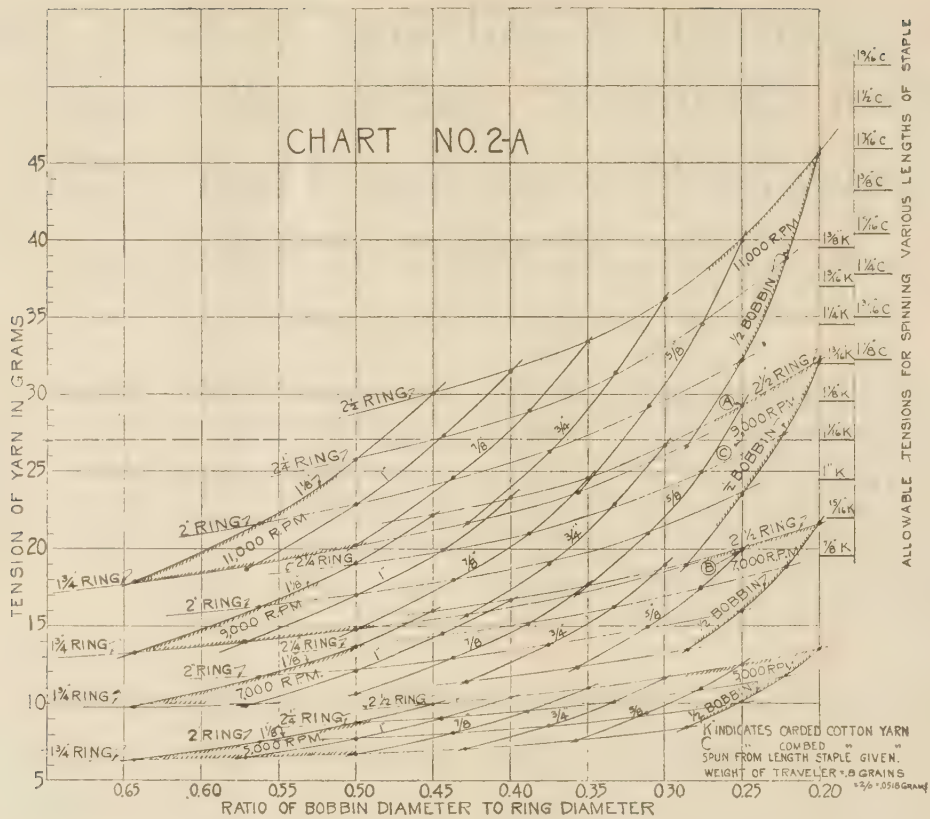


FIG. 1 TENSION 20'S YARN BETWEEN THREAD BOARD AND FRONT ROLLS

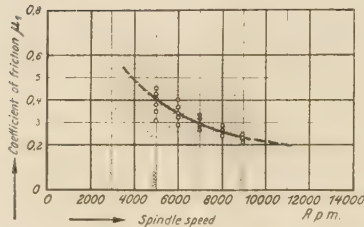
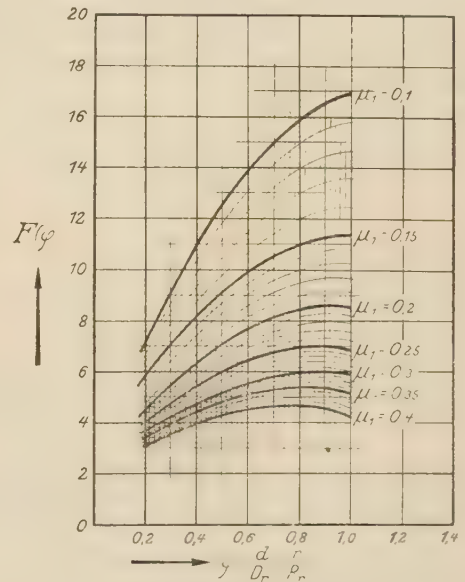


FIG. 2 VALUES OF RING FRICTION ACCORDING TO LÜDCKE

below the $2\frac{1}{4}$ -in. ring, indicating that a $2\frac{1}{4}$ -in. ring, under these conditions, would not be satisfactory. It next crosses the 9000-rpm curve with $\frac{5}{8}$ -in. bobbin just above the $2\frac{1}{4}$ -in. ring, indicating that $2\frac{1}{4}$ -in. is satisfactory. Next it crosses the 11,000-rpm curve with $\frac{1}{2}$ -in. bobbin just above the $1\frac{3}{4}$ -in. ring, and then crosses the 9000-rpm curve with $\frac{3}{4}$ -in. bobbin just above the $2\frac{1}{2}$ -in. ring, indicating that either a $1\frac{3}{4}$ -in. ring at 11,000, or a $2\frac{1}{2}$ -in. ring at 9000 rpm would be satisfactory, with a $\frac{1}{2}$ -in. bobbin in the first, and a $\frac{3}{4}$ -in. bobbin the second instance.

Continuing this line from right to left until it crosses the 11,000-rpm curves with 1-in. and $1\frac{1}{8}$ -in. bobbins, we find that a $2\frac{1}{4}$ -in. ring is slightly too large in the first case but satisfactory in the second.

Next, suppose a spinning frame is already equipped with $2\frac{1}{2}$ -in. rings and $\frac{5}{8}$ -in. bobbins, and it is desired to determine the optimum speed, with $1\frac{1}{16}$ -in. carded staple. First, we drop a vertical line from A (the $2\frac{1}{2}$ -in. ring on the 9000-rpm curve with $\frac{5}{8}$ -in. bobbin) to B (the $2\frac{1}{2}$ -in. ring on the 7000-rpm curve with $\frac{5}{8}$ -in. bobbin) and note its intersection with the horizontal

FIG. 3 $F(\phi)$ AS A FUNCTION OF $\phi = \frac{d}{D_r} = \frac{r}{R_r}$

line through $1\frac{1}{16}$ in. K, at C. Obviously, the suitable speed, with $2\frac{1}{2}$ -in. ring and $\frac{5}{8}$ -in. bobbin, lies between A and B, at point C, which is ascertained by finding the ratio of CB to AB, that is, as 7 is to 9. Since the difference between 9000 and 7000 is 2000,

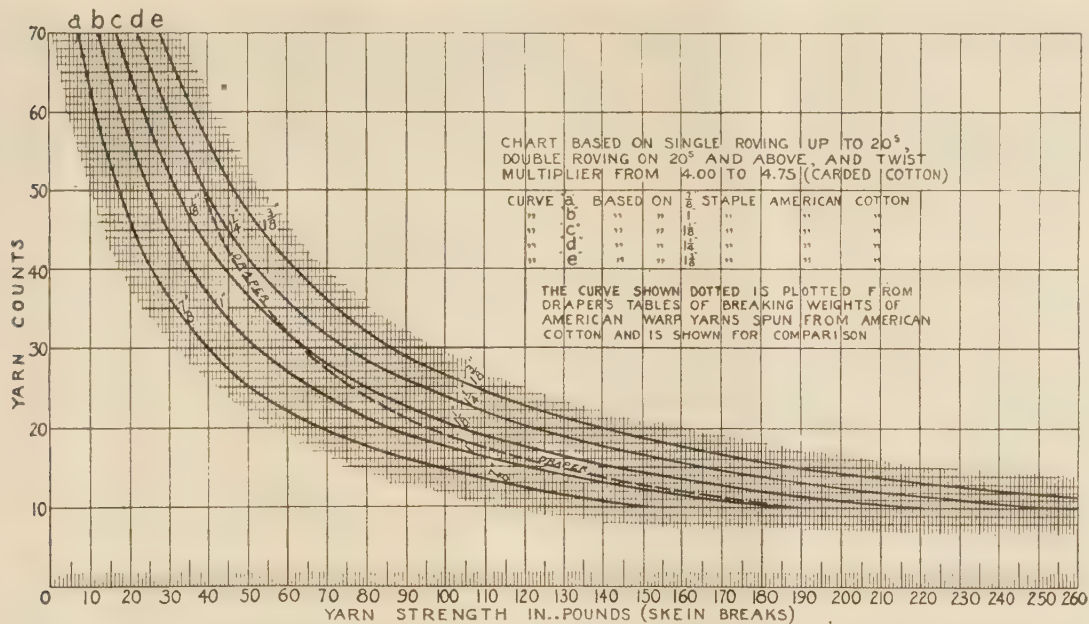


FIG. 4 CHART SHOWING WARP YARN STRENGTH AT 70 PER CENT RELATIVE HUMIDITY COMPUTED FROM FORMULA

$$\frac{1600 (1 \pm 0.11a \pm 0.01b)}{C} = S$$

(C = counts; S = strength in pounds; a = difference in sixteenths of staple over or under 1 in.; use + sign when over, — sign when under; b = difference in number of yarn above or below 28's, use — sign when over 28's and + sign when below.)

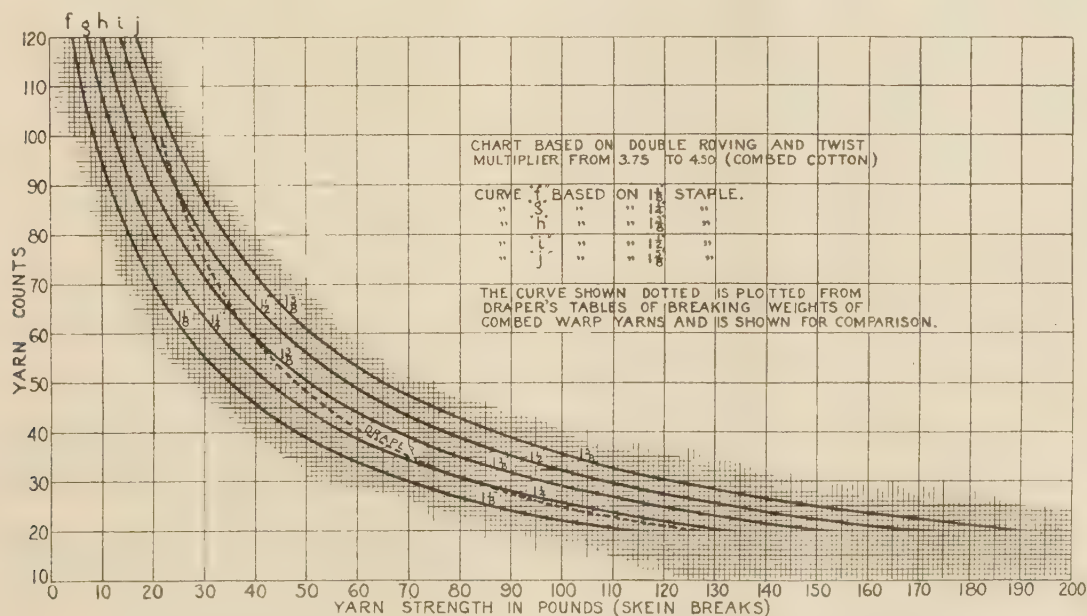


FIG. 5 CHART SHOWING STRENGTH OF COMBED WARP YARN, AT 70 PER CENT HUMIDITY, COMPUTED FROM FORMULA

$$\frac{1750 (1 \pm 0.11a \pm 0.01b)}{C} = S$$

(C = counts; S = strength in pounds; a = difference in sixteenths of staple over 1 in.; b = difference in number of yarn above or below 28's, use — sign when over and + sign when under 28's.)

we add to 7000 the product of $7/9 \times 2000$, or 1555, and find that 8555 rpm is the optimum speed for the conditions imposed

POWER REQUIRED

The horsepower required for each ring size and speed, enumerated in the tabulation which follows, has been carefully computed, according to a formula devised by E. A. Untersee.⁵

$$\text{Hp per spindle} = 0.000284 \times R^{1.42} \times \left(\frac{\text{rev}}{1000} \right)^{1.808}$$

in which R = ring diameter in inches, and rev = speed of spindle per minute.

From subsequent analysis, it is obvious what critical factors are power and fixed charges in the cost of spinning. The conservation of power, in this process, would appear to deserve serious consideration, perhaps by reducing the weight of the spindle through the use of some suitable combination of aluminum and magnesium, perhaps by driving each spindle with an individual motor (similar to the motor drive of rayon spindles), and so eliminate all tapes, tension devices, and cylinders, or by the adoption of both expedients; or by the use of ball-bearing spindles, provided this expedient does not increase fixed charges too much.

With the present mechanism, the power required to drive spinning frames is all dissipated in friction or in heat—more than sufficient to heat the spinning room to a comfortable temperature in winter, even in a northern climate; and which in summer months presents a serious problem in air conditioning. In either case, there is a serious waste of power in the form of heat.

In constructing the chart, Fig. 1, the skein break strength, as determined by our original formulas (charts Figs. 4 and 5), has been divided by 160, to ascertain the corresponding single-strand strength, which in turn has been converted into grams for the scale at the left-hand margin. We realize that this procedure may be subject to criticism, since the average ratio of skein-yarn to single-yarn strength, as determined by numerous tests of a great variety of cottons, is between, say, 100 and 120 to 1, rather than 160 to 1. On the other hand, to insure good running work with a minimum of ends down per hundred spindles per hour, it is necessary to consider the weakest, rather than the average strands, since, obviously, it is the failure of the weakest single strands that controls the result. After reviewing the records of many single-thread and skein break tests, of a wide range of yarns, we have found that dividing the skein break by 160 generally indicates the minimum single-yarn strengths.

In arranging the scale at the left-hand margin of the chart, we have adopted a factor of safety of 10, instead of 14 as suggested by Oertel,⁶ and as used previously by the authors, as it appears from several mill tests that 10 is a conservative factor to use. That is to say, for computing the single-strand strength, we divided the skein break strength, as determined from our formulas, first by 160, and then by 10.

EFFECT ON YARN TENSION OF INCREASING SPEED AND RING SIZE

To show the effect on the yarn tension of increasing the speed and ring size, the following examples will be cited:

Referring to Fig. 1, for No. 20's yarn, it will be observed that increasing the spindle speed from 7000 to 9000 rpm with a $2\frac{1}{4}$ -in. ring and $\frac{5}{8}$ -in. bobbin, the tension is raised from 17.47 to 24.9 g, or 42 per cent; and increasing the speed to 11,000 rpm raises the tension to 34.46 g, or 97 per cent. Again, if the ring size is increased from $1\frac{3}{4}$ in. to 2 in. with $\frac{1}{2}$ -in. bobbin at 9000 rpm, the tension is raised from 18.92 to 23.62 g, or 25 per cent. With a

$2\frac{1}{4}$ -in. ring, the tension is raised to 27.46 g, or 45 per cent, and with a $2\frac{1}{2}$ -in. ring, the tension is raised to 32.15, or 70 per cent.

Obviously, these variations in tension must affect the quality of the yarn produced. If larger packages are desired in order to reduce the number of piecings, they must be acquired with the acceptance of contingent factors more or less undesirable, and the spinner must choose that expedient which fits his particular necessity best.

It is not pretended that the results deduced herein are of absolute validity, but we believe that the graphs and the method by which they are derived are sufficiently consistent with spinning practice to afford a safe guide to a judicious choice of ring sizes, bobbin diameters, spindle speeds, etc., for most conditions occurring in the spinning process.

Also, while the chart, Fig. 1, embraces bobbins of $\frac{1}{2}$ in. diam, we realize that under some circumstances such a small bobbin may be impracticable.

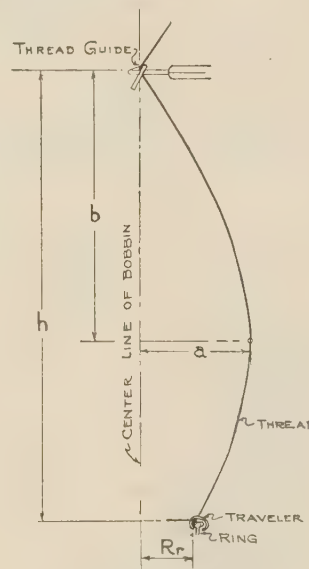


FIG. 6 DIAGRAMMATIC SKETCH AT BALLOON

(Incidentally, the graphs in Fig. 1, if plotted on full logarithmic paper, become straight and parallel lines.)

FACTORS AFFECTING SPINNING FUNCTIONS AND COSTS

To further illustrate the utility of the theoretical conception of this general problem, we will consider No. 20's carded yarn, spun from $1\frac{1}{16}$ -in. staple, and deduce all of the factors affecting the spinning functions and spinning costs.

Prof. George Lindner⁷ has developed a formula proving that the shape of the balloon is a sine curve and from this deduction establishes the equation

$$\frac{h}{b} = \frac{180 - \arcsin \frac{R_r}{a}}{90}$$

See Fig. 6, in which

h = distance from thread guide to bottom layer of thread on bobbin, m

⁵ "The Characteristics and Power Requirements of Spinning Frames," by E. A. Untersee, Trans. A.I.E.E., vol. 59, 1940, pp. 1-4.

⁶ See Reference 3, p. 200.

⁷ "Balloon Shape, Yarn Tension and the Position of the Traveler in the Ring Spinning Machine" (translation of title), by Georg Lindner, *Monatschrift für Textil Industrie*, 1910, pp. 213-216.

TABLE 1 FUNCTIONAL DATA FOR SPINNING NO. 20'S YARN WITH VARIOUS RINGS AND SPEEDS

Ring diam, in.....	1 1/4	1 1/4	1 1/4	1 1/4	1 1/4	1 1/4	2	2 1/4	2 1/4	2 1/4
Bobbin diam, in.....	1 1/2	1 1/2	1 1/2	1 1/2	1 1/2	1 1/2	1 1/2	1 1/2	1 1/2	1 1/2
Gage, in.....	3 3/4	3 3/4	3 3/4	3 3/4	3 3/4	3 3/4	3 3/4	3 3/4	3 3/4	3 3/4
Spindle speed, rpm.....	9000	10000	11000	9000	10000	11000	11000	10000	9000	8000
b in meters.....	0.1621	0.1462	0.1328	0.1621	0.1462	0.1328	0.1328	0.1462	0.1621	0.1814
b in inches.....	10.8	9.73	8.84	10.6	9.58	8.71	8.58	9.25	10.37	11.00
h in meters.....	0.273	0.247	0.224	0.270	0.243	0.221	0.218	0.235	0.264	0.277
Weight of traveler in grams.....	0.0735	0.06229	0.05243	0.0672	0.05587	0.04702	0.04756	0.05360	0.06086	0.05868
Approx weight of traveler in grains.....	1.2	1.0	0.80	1.1	0.85	0.75	0.75	0.85	0.95	0.90
Approx number of travelers.....	2 1/2	1	2/0	1 1/2	1 1/2/0	3/0	3/0	1 1/2/0	1 1/2	1/0
Yarn tension in grams.....	27	27	27	27	27	27	27	27	27	27

TABLE 2 COMPARATIVE COST OF SPINNING NO. 20'S YARN

1-1/16" Cotton - Twist Constant 4.50 - Turns per Inch 20.12
 Production 44,500 lbs. per 80 hr. week - #20's Yarn

Ring Diameter	1-3/4"	1-3/4"	1-3/4"	1-7/8"	1-7/8"	1-7/8"	2"	2-3/16"	2-3/8"	2-3/4"
Bobbin Diameter	1 1/2"	1 1/2"	1 1/2"	1 1/2"	1 1/2"	1 1/2"	5/8"	3/4"	7/8"	1"
Traverse	7-3/4"	6-3/4"	5-3/4"	7-1/2"	6-1/2"	5-3/4"	5-1/2"	6-1/4"	7-3/8"	8"
Gauge	3-3/4"	3-3/4"	3-3/4"	3-3/4"	3-3/4"	3-3/4"	3-3/4"	3-3/4"	4"	4-1/4"
Spindle Speed	9000	10000	11000	9000	10000	11000	11000	10000	9000	8000
Yds. on Bobbin	3538	3055	2562	3969	3391	2961	3339	4200	5932	8736
Sets per Wk.	16.55	21.24	27.56	14.81	19.1	24.0	21.33	15.53	9.94	6.0
Lbs. per Spindle	3.5	3.86	4.20	3.5	3.85	4.23	4.24	3.88	3.51	3.12
No. of Spindles	12714	11528	10595	12714	11528	10595	10595	11528	12678	14262
Cost per Wk.										
Spinning	\$ 254.	\$ 230.	\$ 212.	\$ 254.	\$ 230.	\$ 212.	\$ 212.	\$ 230.	\$ 254.	\$ 285.
Doffing	158.	184.	227.	141.	165.	191.	170.	135.	95.	65.
Winding	300.	347.	424.	270.	313.	359.	321.	258.	186.	131.
	\$ 712.	\$ 761.	\$ 863.	\$ 665.	\$ 708.	\$ 762.	\$ 703.	\$ 623.	\$ 535.	\$ 481.
Day Labor	442.	358.	358.	442.	358.	358.	358.	358.	442.	442.
	\$1154.	\$1119.	\$1221.	\$1107.	\$1066.	\$1120.	\$1061.	\$ 981.	\$ 977.	\$ 923.
Power	424.	461.	504.	462.	512.	558.	614.	640.	650.	731.
	\$1578.	\$1580.	\$1735.	\$1569.	\$1578.	\$1678.	\$1675.	\$1621.	\$1627.	\$1654.
Fixed Chgs.	651.	603.	567.	658.	612.	574.	582.	630.	708.	623.
	\$2229.	\$2163.	\$2292.	\$2227.	\$2190.	\$2252.	\$2257.	\$2251.	\$2335.	\$2477.
Roll Cover., Spdl. Oil, Travelers, etc.	22.	20.	18.	22.	20.	18.	18.	20.	22.	24.
	\$2251.	\$2203.	\$2310.	\$2249.	\$2210.	\$2270.	\$2275.	\$2271.	\$2357.	\$2501.
Air Cond. to 70% R.H.	123.	133.	145.	133.	148.	161.	177.	185.	188.	211.
TOTAL	\$2374.	\$2336.	\$2455.	\$2382.	\$2358.	\$2431.	\$2452.	\$2456.	\$2545.	\$2712.
Add'l Cost for Doffing & Winding with 5/8"										
Bobbin	28.	32.	14.	24.	25.	24.				
TOTAL	\$2402.	\$2368.	\$2469.	\$2406.	\$2383.	\$2455.				

b = distance from thread guide to maximum displacement of balloon, m

R_r = radius of ring, m

a = maximum displacement of balloon, m

He also shows that the yarn tension in grams

$$T = \frac{N_0^2 \times h^2}{61^2 \times N_r} \left(\frac{90}{180 - \arcsin \frac{R_r}{a}} \right)^2$$

which is equivalent to

$$T = \frac{N_0^2 \times b^2}{61^2 \times N_r}$$

in which N_0 = revolutions of traveler per minute, and N_r = counts of yarn, English system.

Having determined T , we can predict the weight in grams of traveler required, from the following formula³

$$G_L = \frac{T \times g \times F(\phi) \times 61^2}{(2 \times 3.14)^2 \times R_r \times N_0^2}$$

We have assumed, in each instance, that a in Fig. 6 equals one half of the gage of spinning frame so that the threads at maximum ballooning theoretically will not collide with each other without separators.

³ Footnote 7, p. 1.

To demonstrate the validity of the foregoing formulas, we have chosen several examples adopting the maximum traveler speed suggested by some of the machinery builders, as follows:

2-in.	ring at 11,000 rpm
2 ³ / ₁₆ -in.	ring at 10,000 rpm
2 ³ / ₈ -in.	ring at 9000 rpm
2 ³ / ₄ -in.	ring at 8000 rpm

and, for comparison, have added

1 ³ / ₄ -in.	ring at 9000, 10,000, and 11,000 rpm
1 ⁷ / ₈ -in.	ring at 9000, 10,000, and 11,000 rpm

The results are given in Table 1.

Based on Table 1, the comparative cost of spinning No. 20's yarn, from 1 ¹/₁₆-in. staple carded, would be as given in Table 2, in which the rate of wages per hour is 55 cents for spinners, 61 cents for doffers, 54 cents for winders, and 48 cents for sweepers, cleaners, oilers, and roving men.

Table 2 suggests that for No. 20's yarn made from 1 ¹/₁₆-in. carded staple, the minimum over-all manufacturing cost is obtained with a spindle speed of 10,000 rpm, 1 ³/₄-in. ring, 1 ¹/₂-in. bobbin, and 6 ³/₄-in. traverse, No. 1 traveler, and 3 ³/₄-in. gage, without separators. With 1 ⁷/₈-in. ring, at the same speed, but with 6 ¹/₂-in. traverse, the cost is only slightly more.

Considered as a group, the use of 1 ³/₄-in. or 1 ⁷/₈-in. rings, at either 9000 or 10,000 rpm, with either 1 ¹/₂-in. or 5 ⁵/₈-in. bobbins, is apparently more economical than these same rings at 11,000 rpm, or than any of the larger rings. Probably with the use of separators the gage for the 1 ³/₄-in. and 1 ⁷/₈-in. rings could be reduced to, maybe, 3 ¹/₄-in. or 3 ¹/₂-in.

At 11,000 rpm for 1 ³/₄-in. and 1 ⁷/₈-in. rings, and at the revolutions per minute specified in the tabulation for 2-in. rings and larger, the critical speed of travelers may be exceeded. Consequently, it might be necessary to reduce these spindle speeds appreciably, which in turn would diminish the production per spindle and so increase the number of spindles, and therefore increase the manufacturing costs above the figures given in Table 2.

It will be noted from the foregoing data that the yarn tension and weight of traveler vary as the square of distance h , provided the speed, ring diameter, and bobbin diameter remain constant. The yarn tension varies as the square of the spindle speed, provided the traverse, diameter of ring and bobbin, and distance b remain constant. Also, for 1 ³/₄-in. and 1 ⁷/₈-in. rings, the traverse can be increased 1 in. for each reduction in spindle speed of 1000 rpm.

Discussion

F. E. BANFIELD, JR.⁹ With nearly half, or about 13,000,000 spindles in place in this country, over 30 years old, the industry is faced with an extensive postwar program of replacement and modernization.

For a number of years, the trend has been toward the use of larger-diameter rings and longer traverses so as to reduce doffing periods, provide longer lengths of yarn with fewer knots or piecings, and thereby obtain greater economy in subsequent operations. These larger packages can be obtained only at some sacrifice in spinning costs as the authors have indicated. Power requirements are increased approximately by the square of the spindle speed. There is a limit to which the speed of travelers can be run efficiently, and as the speeds are increased the number of ends down are also increased. Therefore, there is a limit to the

ring size and speed for a given size and quality of yarn beyond which it is not economical to go. Any savings obtained from larger packages must be weighed carefully against their increased costs.

Reference was made in the paper to the Untersee formula. The object in developing this formula was to provide a means for determining the amount of power that a spinning frame of a given number of spindles, diameter of ring, and spindle speed would require so as to insure the furnishing of the proper size of motor.

Subsequent to working out the formula which the authors have used, Mr. Untersee revised it to include another variable, namely, the yarn size, and at the same time increased the $\frac{(\text{rpm})^{1.8}}{1000}$ to $\frac{(\text{rpm})^{2.04}}{1000}$ as follows:

$$Hp/\text{spindle} = \frac{0.0003055}{4.75\sqrt{S}} \times R^{1.42} \times \frac{(\text{rpm})^{2.04}}{1000}$$

where

S = yarn size

R = ring diameter, in.

rpm = spindle speed

This formula was based on data obtained from a large number of tests made under our supervision, not only at our plant but also supplemented by those made in a number of mills under actual operating conditions. This work was carried out by Untersee over a period of years, during which a considerable amount of data were collected; and experience has shown it to be a safe guide to follow.

It is to be regretted that Mr. Untersee's premature death prevented his work from being carried further along lines of including other variables, such as length of traverse, traveler size, etc. However, the formula he has given us is valuable as far as it goes and it is to be hoped that the work will be continued by others interested in the problem. The use which the authors have made of this formula is comparative. For their purpose it would seem to be quite adequate for, as they point out, they do not pretend that the results deduced are of absolute validity but are sufficiently consistent with spinning practice to afford a safe guide to follow in working out this problem.

It should be pointed out that the power consumption varies considerably from empty to full bobbins. The formula takes into consideration the ring diameter only and is based on the bobbins being full. Therefore, the power required for a complete doff from empty to full bobbins will be less than that derived from the formula.

The writer recommends that consideration be given to carrying this investigation further and believes that it is of sufficient importance to the industry for the Textile Division of the Society to establish a committee for this purpose.

C. H. HARRIGAN,¹⁰ During the last 10 years, the French Ring Spinning Department of the writer's company has made use of improvements such as variable-speed motors, roller-bearing spindles, autolubricated rings, revolving underclearers, balloon controllers synchronized with the ring rail, and our own make of antimarriage (double-spin) preventers, which has made it possible to run many counts and twists of worsted yarn at around 9000 spindle revolutions.

The yarns thus produced are superior to anything previously made here, and the weave shed now demands that all their warp yarns be ring-spun. The mules are now used only for medium counts of yarn that are to be twisted, or for filling.

⁹ Works Manager, Whitin Machine Works, Whitinsville, Mass. Mem. A.S.M.E.

¹⁰ Forstmann Woolen Co., Garfield, N. J.

We have also overcome the old hurdle of maximum traveler speed by using a metal different from the high-carbon steel commonly used in the trade. In this connection, we are running twistors with 4-in. rings at 7500 spindle revolutions, which is about $1\frac{1}{2}$ miles per m, and travelers last at least 40 hr before changing is necessary.

This answers the conception that high spindle speeds are impractical because of traveler trouble. The writer suggests that improvements in the machines to overcome vibration, such as line shaft and pulleys to replace tin cylinders, lighter metal in spindles, antifriction bearings, so made as to prevent oscillation, and mounting of machines on concrete footings might easily make possible 15,000 revolutions spindle speed, since we have already done 12,500 on 3-in. rings (on a 20-spindle trial frame) and made first-class yarn up to 64's metric.

N. M. MITCHELL.¹¹ This subject represents a problem which has confronted mill management from the time ring spinning was invented. In general, spinners and spinning-equipment manufacturers have considered the broad subject one which could best be solved through experimentation.

The activities of industrial and cost engineers in the textile industry require a technical and theoretical approach to the question of what is the proper ring diameter, bobbin size, spindle speed, or traveler for specific counts of yarn, spun from various lengths of staple. In the majority of instances this information is found through analysis of available records covering activities in various mills and experimenting with whatever seems to indicate will best meet the services or requirements for the specific count of yarn under consideration.

Analysis of the present paper indicates the need for giving all factors entering into the formulas extremely careful consideration. The theories presented are generally logical but in practically every instance there is room for criticism from the standpoint of practical spinning operations.

Discussions of the paper with spinners has brought out the opinion that many of the physical and uncontrollable variables normally existent in spinning operations would tend to modify some of the assumptions indicated in the formulas.

There is little to be gained by selecting specific items which have been found controversial in the various tabulations in the paper. The merit in this paper lies in the fact that these progressive and logical steps have been taken, and undoubtedly it was the authors' hope that they would lead the way to further and more detailed investigations which would result in formulas and resultant tables which could be used by the industry as a whole and be found generally acceptable to all concerned.

BRACKETT PARSONS.¹² The question of friction between the traveler and the ring is very important in the tension formula of Dr. Stiel. We find that there is considerable variation in the weight of the traveler used, due to the condition of the ring. On a 21-warp yarn spun from 1-in. middling cotton on a 2-in. ring, $1\frac{1}{16}$ -in. bobbin, 8-in. traverse, at 9000 rpm, warp wind, 4-oz package, $3\frac{1}{2}$ -in-gage frame with separators, we have used travelers from No. 3-0 to No. 7, that is, the ring gradually wears, the friction is reduced, and a heavier traveler is required.

The tension formula ignores the effect of different lengths of traverse. This factor in consideration of spinning tension is almost as important as the bobbin-ring ratio. There is, of course, tension variation from top to bottom of stroke, and it naturally follows that the longer the traverse the greater the variation. We also feel that the quality of the roving, the spinning drafts,

and spinning-frame construction, that is, the stationary or traversing thread guides, affect the tension limit.

In testing the formula on a limited number of yarns that we are running in sizable quantities, we find considerable deviation from the formula. The formula undoubtedly can be revised to conform with more modern practices.

In considering the cost element, there is a wide variation between our various mills, owing to different methods of manufacture caused by the resultant end use of yarn.

R. W. VOSE.¹³ The approach taken by the authors to the problem of the spinning spindle is most comprehensive and should pave the way for developments of considerable engineering and economic importance. Most of the previous work on the subject has been confined to specialized technical aspects, and comparatively little thought has been given to the interweaving of the results of these detailed investigations into a composite whole which would be of direct utility to the machine builder and the textile manufacturer. While the investigations in the fields of dynamics, friction, vibration, lubrication, and aerodynamics as pertaining to the spindle are of technical importance and interest, it is only by their translation into the actual monetary cost of the daily operation of the spinning that any tangible benefits are obtained.

In gathering together the technical data on which to base the development of their thesis, the authors have been forced to draw from widely scattered sources, covering work done over a considerable span of years and by experimenters of differing modes of approach. This has resulted in the inclusion of both theoretical and empirical results, and of results with considerably varying degrees of approximation. As an illustration, it may be pointed out that Lindner's equation for the shape of the balloon, which the authors quote, is derived in the form of sine curve which is a reasonable approximation to the actual balloon only in cases where the balloon is relatively long and narrow. As the balloon widens out, the sine equation loses its validity just as a parabolic equation loses validity for a catenary, and for precisely the same reason. At the present writing it is not possible to give figures for the degree of this approximation in the case of the large balloon, but it would seem worthy of further work since the wide balloon is particularly involved in the fouling of adjacent spindles, and hence governs the spindle spacing. A further defect in Lindner's equation comes from the fact that it is derived on the basis of a two-dimensional curve lying in the plane of the spindle. Actually, a balloon is three-dimensional and its backward slope due to air friction further aggravates the departure from the assumed sine curve.

In numerous earlier treatments of the spinning problem, it has been customary to assume that yarn tension is the limiting factor preventing increases in package size and speed. The authors have followed this same general thought but have quite rightly pointed out that, under a certain range of conditions, the limiting factor may be traveler heating and wear rather than yarn tension. Numerous experiments extending over several years' time, made under the writer's observation, tend to indicate that this question of traveler failure is perhaps sufficiently serious to overbalance entirely the consideration of yarn tension under most practical operating conditions. A series of tests on a variable-speed spinning installation designed to give constant tension did not appear to give the full benefit expected, and it was concluded that traveler wear was the disturbing and controlling factor. Other tests, made for an entirely different purpose, showed no particular correlation between yarn tension and spinning end breakage, and in fact showed that yarn breaks due to tension

¹¹ President, Barnes Textile Associates, Boston, Mass. Mem. A.S.M.E.

¹² Pepperell Manufacturing Company, Boston, Mass.

¹³ Director of Research, Chicopee Manufacturing Corporation, Chicopee Falls, Mass. Mem. A.S.M.E.

alone were probably of relatively rare occurrence except in yarn inherently weak. This of course leads to the question as to whether or not the spinning operation should be adjusted to break out weak yarn, but this a matter beyond the scope of the present discussion.

In regard to the actual tension figures used by the authors, it would seem that the values derived from the skein-break test by calculation were open to some question. Tests made in the writer's laboratory show operating tensions 4 times as high as these, and yet the test was made on a carefully controlled laboratory frame under conditions paralleling operating practice. It would thus seem that, while the use of the skein-break data, figured with an arbitrary factor of safety, might give figures relatively correct, the absolute values might better be determined from actual measurements on the operating spindle. This might lead to extensions of the operating range of speeds or sizes, or both, which would permit distinct economies not shown in the present paper.

An examination of Untersee's equation for power, and a personal acquaintance with some of Mr. Untersee's very excellent experimental work, leads the writer to believe that this equation was intended for empirical design purposes rather than for analysis. One defect, in so far as the present application is concerned, is the lack of the inclusion of the length of traverse as a factor. Obviously, the package weight varies with the traverse and this in turn must affect bearing friction. Another defect, from the theoretical viewpoint, is the lack of separate terms for friction, windage, and yarn drag, each of which may vary as a different power of the radius or of the speed. A preliminary study of the fundamental equation indicates that, with conventional proportions of these variables, the equation given by Untersee may hold approximately but, nevertheless, the separate effect of each of these variables is not fully brought out. Since power is such a serious factor it would seem that the equation describing its variation might well be expanded to place it on a par with the calculation of the other elements entering into the total cost of spinning.

The authors have clearly pointed out the high cost of power in the spinning process, and have made a plea for improved mechanical design in the interests of power conservation. This leads to an analysis of the actual power losses occurring in the spindle. There are three causes, namely, bearing friction in the step, windage of the package, and tension of the yarn resisting the rotation of the spindle. The power taken out of the spindle through the yarn tension is ultimately dissipated in traveler friction and in windage of the balloon. It can be shown that each of the three sources of power loss at the spindle is of the same magnitude, and that the loss in the spindle bearing is the only one capable of direct reduction by machine-design improvements. Experimental spindles utilizing rolling contact bearings seem to show a saving in power in this particular location of about one half, but although the bearings have operated satisfactorily over many months' trial their ultimate life is yet to be determined.

The two remaining items, namely, package windage and yarn tension, would seem to require a completely different method of spinning for their improvement. While windage might conceivably be eliminated by spinning in a vacuum, schemes of this sort seem scarcely practical. In regard to yarn tension, it will be recognized that some amount of tension is necessary to produce a sufficiently firm package, and that as long as this tension is created between the driving spindle and an external drag (namely, the traveler and balloon), the power loss is inescapable. If the tension were supplied through a flyer geared into the driving mechanism of the spindle, this power would be recoverable, but in conventional sizes of spinning spindles it is probable that the friction loss of the added mechanism would render this scheme

impractical. The tension is also required in order to keep the balloon within bounds, as the authors have pointed out through the use of Lindner's equation, and again the elimination of this factor would seem to require inventive genius rather than machine-design ability.

To turn from the engineering aspects of the paper, it may be pointed out that the cost figures of the various operations as quoted by the authors are somewhat out of line with respect to modern mill practice. This is particularly so with regard to the winding operation. However, these matters can be dealt with by relatively straightforward accounting procedures once the engineering fundamentals have been developed, and in any event will vary from one mill to another.

In closing, the writer wishes to compliment the authors for having undertaken this important, but involved, task of correlating the diverse engineering elements of the spinning problem and expressing their result in a form directly usable by the textile industry. The work should prove a guide and an inspiration to those working in the intricacies of mathematical analysis and the delicacies of experimental measurement and those who are prone to forget that their technical results are only part of a broader economic picture.

AUTHORS' CLOSURE

Before discussing the several commentaries relative to the essential features of our thesis, the authors wish to thank each of the contributors for constructive participation and co-operation in preparing this subject for critical analysis, and, in pointing out the limitations of the formulas and the paucity of accurate empirical data, they recognize the need of further careful exploration.

Mr. Vose quite rightly directs attention to the invalidity of the sine curve where the balloon is excessive in proportion to the traverse, but for conditions usually prevailing, perhaps this critical situation seldom exists. His assertion that the "balloon" curve is three-dimensional rather than two, is equally correct—a fact that Lindner recognizes, although, in his analysis of all the forces involved, he considers the effect of windage more or less canceled out by other effects and takes advantage of this circumstance to simplify what would otherwise be a very inconvenient mathematical expression to use.

The question of traveler performance is another element of the spinning process which, as Mr. Vose observes, requires further intensive investigation, particularly when one considers Mr. Harrigan's successful experience with travelers made from a special metal and running 40 hr at 132 fps. In so far as the authors are informed, no one except Honegger,¹⁴ has attempted to confirm Lüdicke's experiments to determine the coefficient of traveler friction, and Honegger's work was, we believe, temporarily discontinued before it was completed.

There is, too, some evidence, confirming Mr. Vose's tests, indicating that spinning end breakages occur, under certain conditions, quite as much from other causes as from excessive tension or weak yarn; for example, the character of the yarn and the fiber from which it is spun.¹⁵

Tests made by Mr. Vose on No. 30's yarn, show a safe operating yarn tension of 4 times the value adopted by the authors; all that we can say is that the tensions we have used appear to agree fairly well with results obtained in usual mill practice.

Turning now to the question of power, we are confronted with one of the most significant factors constituting the over-all cost of spinning, and while Untersee has made a notable contribution

¹⁴ "Tests on Ring Spinning," by E. Honegger, *The Textile Manufacturer*, vol. 61, July, 1935, pp. 267-290.

¹⁵ See Indian Central Cotton Committee Technological Laboratory Bulletin, Series A, No. 36, Jan., 1937, Matunga, Bombay, India.

toward its determination, his formula does not always coincide with actual practice. Therefore, it is to be hoped, as Mr. Banfield suggests, that his work will be continued by others, in such a manner as to show how the power required to operate spinning frames is divided between all of the moving parts of machines covering a wide range of speeds, ring sizes, traverses, regular bearings and antifriction bearings, etc. It is doubtful if spinners realize how much their over-all costs are affected when they increase speed, ring diameter, and traverse. This investigation of power should embrace the application of variable-speed motors and spinning regulators, to ascertain their economic and practical merits.

Mr. Parsons emphasizes the importance of traveler friction and length of traverse. We have already discussed the former factor; and the effect of the latter is comprehended in the following equations

$$\frac{h}{b} = \frac{180 - \arcsin \frac{R_r}{a}}{90}$$

$$T = \frac{N_0^2 \times b^2}{61^2 \times N_s}$$

He also submits a typical example from actual mill practice; viz., No. 21's carded yarn spun from 1-in. middling cotton, 2-in. ring, $\frac{15}{16}$ -in.-diam bobbin, 8-in. traverse, spindle speed 9000 rpm, gage of frame $3\frac{1}{2}$ in., and 4-oz. package. Now referring to yarn chart, Fig. 4 of the paper, we find that the skein breaking strength is $81\frac{3}{4}$ lb, which is equivalent to a safe spinning tension of 23 g, using a factor of safety of 10. Then from the chart, Fig. 2, we find the coefficient of traveler friction to be 0.24, and from the chart, Fig. 3, $F\phi = 6$. Similarly, since the traverse is 8 in., h , the distance from pigtail to bottom layer of yarn on the bobbin would probably be $1\frac{1}{2}$ in. more, or $9\frac{1}{2}$ in., and the sine of the angle obtained by dividing the ring radius by $\frac{1}{2}$ the gage, is 145.15, from which $b = 5.89$ in., or 0.1496 m. Then, substituting the appropriate values in the applicable formula, we find that the theoretical traveler speed is 8961, compared to the actual spindle speed of 9000 rpm and, likewise, the theoretical traveler weight is 0.0624 g, equivalent to a No. 1 traveler which, it will be noted, is about midway between the maximum and minimum weights actually used, that is, No. 7 and No. 3/0.

In this instance, at least, the computed result and practice agrees almost exactly.

Experimental Study of the Flow of Coal in Chutes at Riverside Generating Station

By E. F. WOLF¹ AND H. L. VON HOHENLEITEN,¹ BALTIMORE, MD.

Among the power-plant problems which are gradually being solved, the present study of moving coal from the bunkers to stokers or coal-pulverizing mills is important, for with the use of one boiler only for each turbine generator, the prevention of coal stoppages in chutes is vital. During the war years, the use of coal from lot storage, with consequent moisture absorption, has caused a great deal of ratholing and arching in the bunkers, and frequent stoppages have occurred in the chutes. The experimental investigation, reported, involved a study of the flow and stoppage of coal in a transparent scale model of one of the present chutes; measurements of physical properties of lot coal with relation to possible factors affecting stoppage; development in successive steps of a new design of coal chute in scale-model form. Out of this study a suitable chute design was evolved, now being reproduced full scale for installation and test.

POWER-plant operators have been faced for many years with a number of major equipment problems and since some of the more important mechanical difficulties have been overcome, those of a minor nature are now coming to the front. At the same time the constant improvements in the art of boiler design have magnified some of these minor troubles. Getting coal from the bunker to stoker hoppers or to coal-pulverizing mills has been one of these problems. Heretofore the operator has usually been successful in keeping fairly dry coal flowing through his chutes, or in relieving stoppages due to wet coal by employing air lances and some judicious pounding at points where such stoppages occurred. With the use of one boiler for each turbine generator, the prevention of coal stoppage now assumes major importance.

When the Consolidated Gas Electric Light and Power Company began its expansion program in 1939, it recognized the importance of a trouble-free coal supply and surveyed the field to determine the latest advances in the art of coal-handling and chute design. The chutes installed at the Westport Station extension and at the new Riverside Generating Station represented the best engineering knowledge available up to that time. Chutes, in general, were kept at as steep an angle as possible, flared chutes were employed, and the angles of the sides of hoppers were maintained at 60 deg or steeper. This has resulted in a chute design, which, in general, has performed well with moderately dry coal.

During the winter and early spring of 1943-1944, government regulations of fuel made it necessary to use large amounts of fuel reserves. This led to extensive use of coal from lot storage, which by reason of exposure to weather had absorbed large percentages of moisture. With this wet coal a great amount of ratholing and arching took place in the bunkers and frequent stop-

pages occurred in the chutes from the bunker to the pulverizing mills, especially at the Riverside generating station. It was decided that a thorough study of this problem would be warranted and an experimental program was mapped out and carried through in the following steps:

- 1 Study of the flow and stoppage of coal in a transparent-plastic scale model of one of the present chutes.
- 2 Measurements of physical properties of lot coal to study the cause and factors affecting stoppage.
- 3 The development in successive steps of a new design of coal chute in scale-model form.

The purpose of these experiments was to find a means by which the flow of coal through the chutes could be improved with a minimum of changes. In the redesign of the chutes themselves, extensive structural or mechanical changes could not be contemplated since they would necessitate prolonged outages of plant and their cost would be prohibitive. This decision put certain limitations on the development of a new design and made it impossible therefore to obtain the ultimate in performance.

The experimental work led to designs which in scale form handle, without stoppage, coal of $1\frac{1}{2}$ times as high a moisture content as the model of the existing chute. The final model permits unimpeded flow of coal at a moisture content which ratholes, arches, and sticks in the model of the existing bunker. A full-sized coal chute conforming to the final model design will be placed in operation early this spring and will serve to check results obtained in the laboratory.

STATEMENT OF PROBLEM

It has been observed over a number of years that coal will stick in bunkers and chutes whenever the moisture content exceeds a certain limit for given types of equipment and coal. Stoppages, when using lot-storage coal, have been more frequent at our Riverside plant than at our other plants, principally on account of the method of storing coal at the former location.

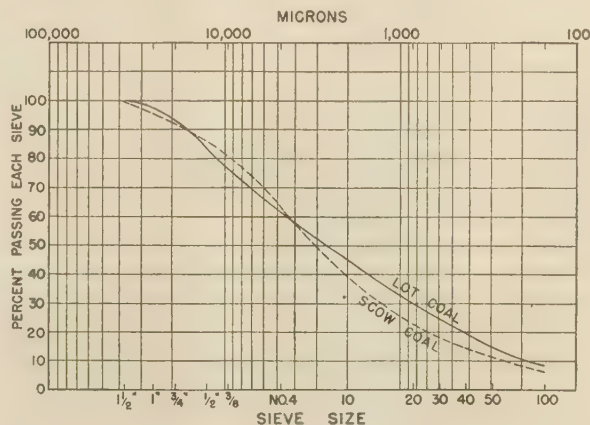


FIG. 1 SIEVE ANALYSES OF COAL
(Representative samples taken from scow deliveries and from Riverside storage lot.)

¹ Consolidated Gas Electric Light and Power Co. of Baltimore.

Contributed by the Fuels and Power Divisions of THE AMERICAN SOCIETY OF MECHANICAL ENGINEERS and presented before the Boston Section on April 12, 1945, and before the Metropolitan Section on May 28, 1945.

NOTE: Statements and opinions advanced in papers are to be understood as individual expressions of their authors and not those of the Society.

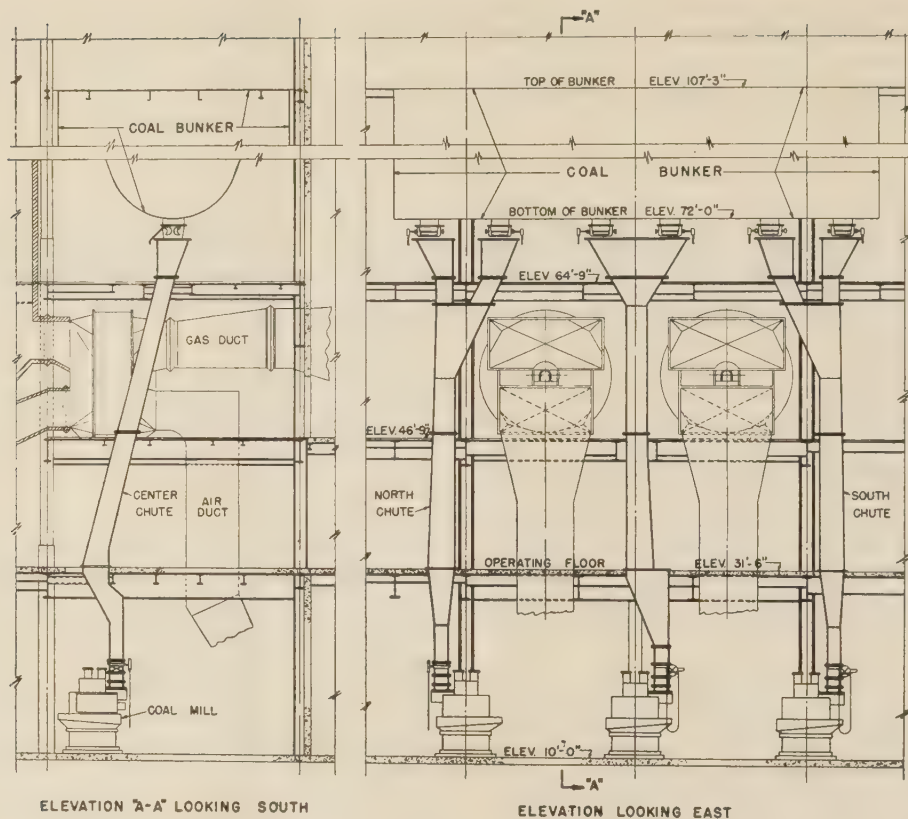


FIG. 2 GENERAL ASSEMBLY OF EXISTING COAL CHUTES AT RIVERSIDE STATION
(Showing main obstructions to possible changes.)

The stocking-out and reclaiming of coal by means of a bulldozer and "carry-all," and the greater degree of compacting that the coal undergoes when stored by this means, is apparently responsible for a higher percentage of fines and, consequently, a greater ability of the coal to retain moisture.

The fuel used at these stations is semibituminous coal produced in District No. 1 from the central Pennsylvania and northern West Virginia regions.

Practical operating experience had indicated that the coal delivered to our plants by barges normally could be relied upon to flow through the chute system with little difficulty in contrast to troubles experienced with lot-stored coal of similar moisture content. It was believed that the explanation for this was to be found in the physical make-up of the coal. Typical sieve analyses plotted in Fig. 1 indicate that the consistency of lot coal is such that approximately 30 per cent by weight is finer than number 20 mesh, and that it contains approximately one third more material of this fineness than scow coal.

Each of the two turbine generators at Riverside Station is served by one 550,000-lb per hr boiler which takes its coal supply from a 990-ton-capacity catenary bunker. The bottom of this bunker is located at elevation 72 and is equipped with six clamshell gates. Three chutes, each fed by two gates, carry the coal to the three pulverizing mills located in the boilerhouse basement at elevation 10, Fig. 2. The center chute, which had proved to be the most troublesome in operation, was selected as the subject for this investigation.

STUDY OF FLOW OF COAL IN SCALE MODEL OF EXISTING CHUTE

Since it was impossible to determine either the exact location

or the nature of each stoppage in the coal chutes at the plant, it was decided to make an exact transparent scale model of one of the existing chutes. This and most of the later models were fabricated from 30-mil sheet pyralin by molding it under boiling water over polished wood templates which conformed to exact inside dimensions. This material is satisfactory for this purpose since it has a coefficient of friction not greatly different from smooth steel plate. The linear scale selected was one tenth full size, which is equivalent to a volume reduction of 1000 to 1. Experiments were conducted with this model using specially prepared coal samples having particle sizes reduced approximately to the linear-scale reduction of the model. Most of the experiments were carried out, however, with coal samples taken directly from lot storage and slightly modified by removal of lumps larger than $1\frac{1}{2}$ in. size. A revolving-table feeder was installed at the outlet of the model to simulate the action of the table feeder at the Riverside plant. Phenomena observed in the actual chutes have been reproduced to a surprising degree in the model with either gradation of coal. Sticking and "hanging up" have occurred in the model at the same location and in the same manner at which sticking could be observed in the prototype.

The authors' previous experience (1, 2)² had demonstrated that a scale model is a useful tool in studying certain power-plant design problems, and careful consideration was given to the reliability of model tests for this specific application. It was recognized that a considerable scale effect exists but, since the components were too numerous and too much subject to variation, no attempt was made to arrive at a mathematical expression of

² Numbers in parentheses refer to the Bibliography at the end of the paper.

the scale factor. While it may be possible to determine such a factor for one part of a system, it seems a hopeless task to establish it for all component parts or to arrive at an over-all scale factor. It was determined, however, that all the phenomena which had been noted in the actual coal chute at an observed moisture content of between 5.5 per cent and 6 per cent occurred in the model between 3.5 per cent and 3.75 per cent moisture content. It is recognized therefore that a scale factor exists but that the scale effect will tend to give model results on the conservative side.

In the operation of the model of the existing chute, the flow of

dry coal was found to be smooth and uniform, which is in accord with service experience. At about 2.5 per cent moisture, the flow became very sluggish along the corner of least slope in the hopper below the operating level (elevation 31 ft 6 in., Fig. 2). Most of the flow occurred in a spiral motion along the opposite vertical corner. The movement of coal from the chute above occurred almost entirely on the side where the hopper below was offset. With further increase in moisture the coal began to rat-hole intermittently by draining entirely from the vertical corner and leaving the remainder of the hopper packed with coal. The observation of these phenomena which have been noted fre-

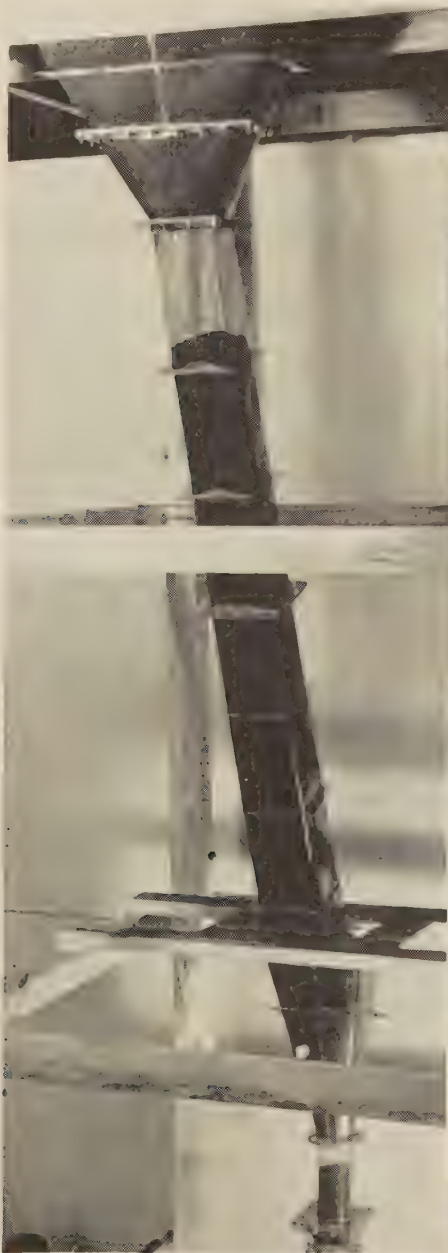
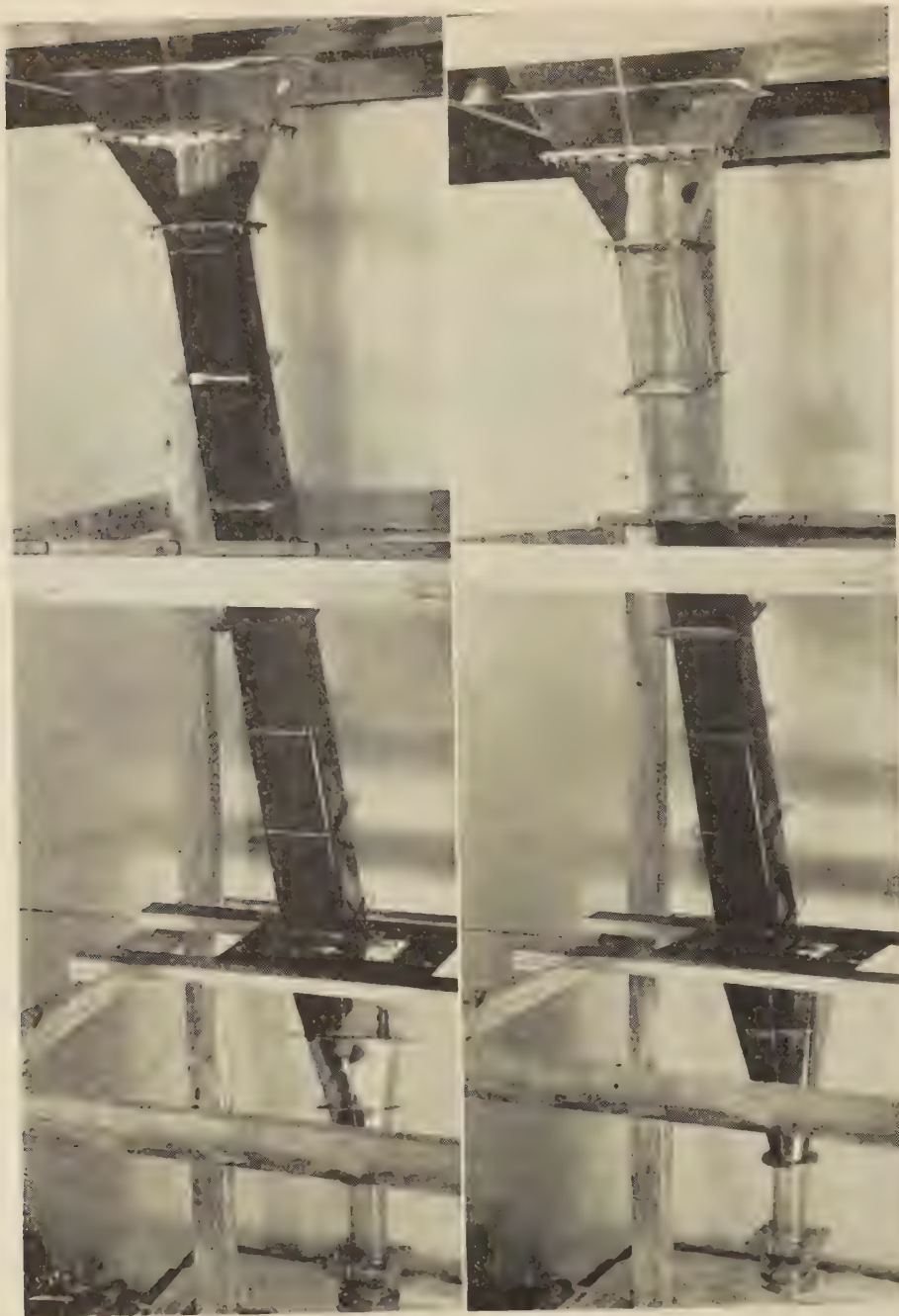


FIG. 3 WEST VIEW OF MODEL OF EXISTING CHUTE
(Stoppage of coal in lower and upper hoppers.)



FIG. 4 WEST VIEW OF MODEL OF LOWER HOPPER
(Arching in hopper and coal gate.)



FIGS. 5 AND 6 STICKING OF COAL IN MODEL OF EXISTING CHUTE

quently in the field, was aided in the model by the use of thin horizontal layers of inert white powder placed at intervals in the coal stream. Two other early points of trouble were the bottom of this hopper and the hopperlike shape simulating the coal gate.

In the range from 3.0 to 3.5 per cent moisture, stoppages occurred in the latter locations and voids began to form in the rectangular tapering chute above the operating floor. With further increase in moisture, flow of coal could be maintained

through the lower hopper by means of scale-sized pokers and air lances, but arching and ratholing then took place at the upper hopper, Figs. 3 to 7, inclusive.

In this chute system, there is a reduction in cross section from a rectangular shape at the top of 41.7 sq ft to a circular shape at the bottom of 1.7 sq ft. This large transition causes the coal to compact, producing the observed stoppages at the bottoms of the hoppers, in corners and at points of change in direction of flow.

PHYSICAL PROPERTIES OF COAL

To determine the cause of the stoppages which were observed in the model and in order to effect improvements in design, it was found necessary to make quantitative measurements of those physical properties which seem to govern the flow of coal. The ratholing, arching, and sticking were found to be closely associated with three mutually interrelated characteristics, namely, moisture content, degree of compacting, and uniformity coefficient. The gradation of the coal affects the amount of moisture which can be retained and also the possible degree of compacting.

Numerous measurements were made with simple laboratory equipment devised for this purpose. The size of specimen was in the range of 20 to 50 lb in most cases. In these discussions the term "loose coal" is being used to indicate that the coal was placed loosely, one scoopful at a time, and every attempt was made to avoid compacting. The term "fully compacted coal" implies that the container was filled with coal and vibrated by mechanical means until no further change in volume could be observed.

Static Angle of Repose. One of the properties which governs the gravity flow of coal is the static angle of repose which is influenced by both moisture content and degree of compacting.

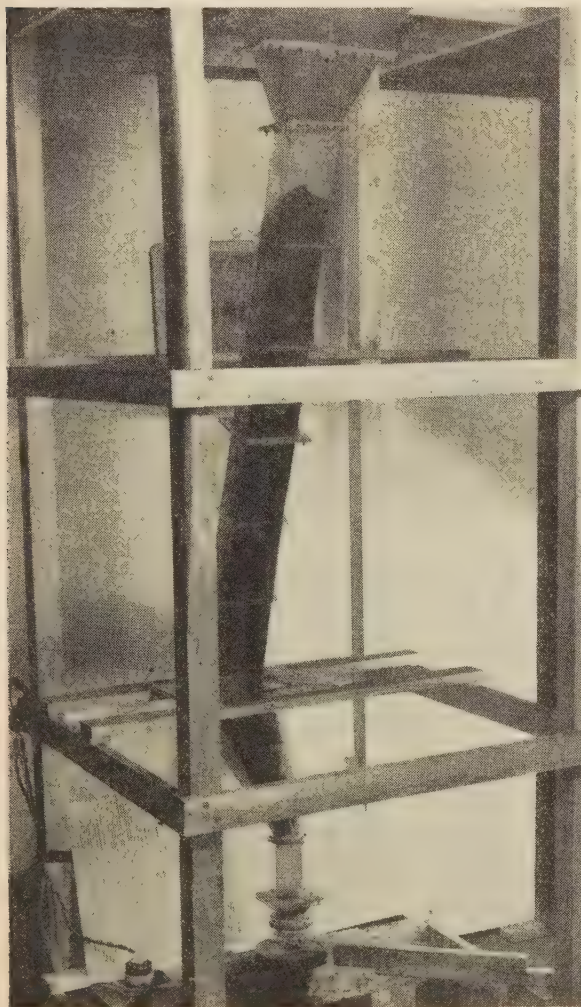
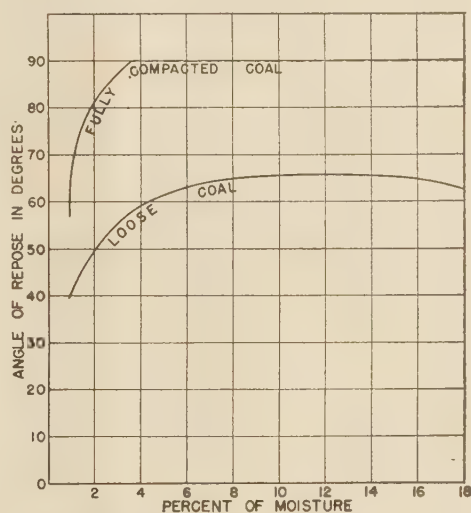
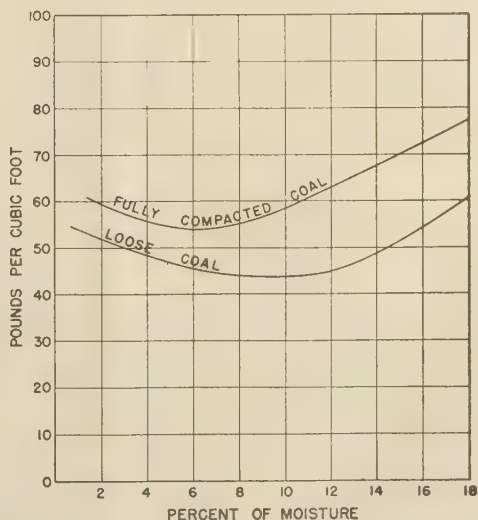


FIG. 7 DIAGONAL VIEW OF EXISTING MODEL

For the determination of this static angle of repose a 12-in. \times 12-in. \times 12-in. metal box with one side hinged at the bottom was used. The box was first filled with loose coal, then the hinged side was dropped, and after all loose coal had fallen away the angle of the cleavage plane was observed. The box was then filled with coal and vibrated until full compactness was reached. Again the side was dropped and the cleavage angle noted. This test was repeated for moisture contents ranging from 1 per cent to 18 per cent and the results are shown in Fig. 8. With fully compacted coal, the angle of repose increases rapidly and reaches 90 deg at 3.6 per cent moisture. Consequently, at this and higher moisture contents, ratholing can occur in hoppers and bunkers. With an increase in moisture content above 3.6 per cent, it was possible to undercut the coal. At higher moisture ranges (above 13 per cent), the wet mass of fully compacted coal had a tendency to bulge out. It may be stated therefore that the angle of repose for these conditions exceeds 90 deg, or, wording it differ-

FIG. 8 EFFECT OF MOISTURE CONTENT OF COAL ON STATIC ANGLE OF REPOSE
(Riverside lot coal.)FIG. 9 EFFECT OF MOISTURE CONTENT ON DENSITY OF COAL
(Measured in 1-cu-ft box.)

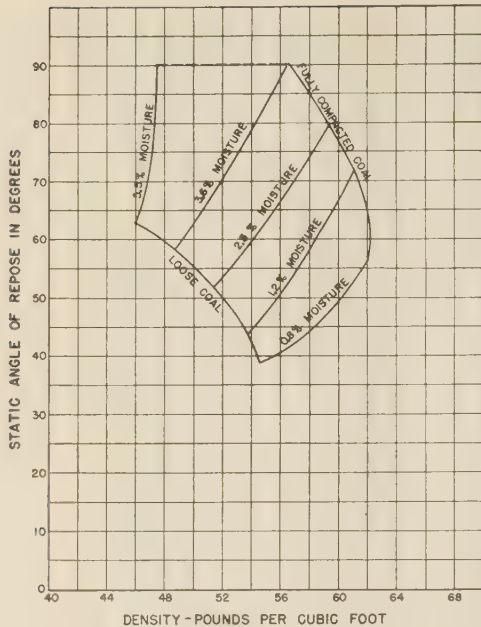


FIG. 10 EFFECT OF MOISTURE AND DEGREE OF COMPACTING ON STATIC ANGLE OF REPOSE

(Degree of compacting is expressed in terms of change in density for coal of five different moisture contents from 0.8 to 5.5 per cent.)

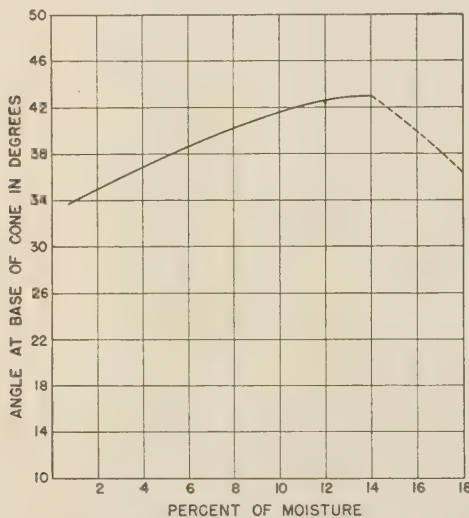


FIG. 11 EFFECT OF MOISTURE CONTENT ON DYNAMIC ANGLE OF REPOSE

ently, reaches negative values. From the investigations mentioned, it is evident that it is important to use the steepest possible angles, preferably 75 deg or more, in the design of coal chutes if moisture contents higher than 3 per cent are to be encountered. All of the tests have indicated that the degree of compactness or density of the coal greatly affects the flow characteristics.

Density of Loose and Fully Compacted Coal With Various Moisture Contents. The 1-cu-ft box used in previous tests was filled repeatedly with coal of various moisture content, and the weight per cubic foot checked. These weights have been plotted for loose and fully compacted coal in Fig. 9. Starting from 1 per cent moisture content, the density of loose coal decreases until

it reaches its lowest value at approximately 7 per cent. Above 7 per cent, it rises until at 15.75 per cent it again reaches the same density as at 1 per cent moisture and continues to rise. Some other granular materials, for instance, sand (3), show this same phenomenon of a point of minimum density at an intermediate moisture content.

Effect of Moisture Content on Degree of Compacting of Coal. To gain a better understanding of the interrelation of moisture content and degree of compacting, additional tests were made, and the information is plotted in Fig. 10. It will be noted that a definite relation exists between the lines on this graph and the information given in Figs. 8 and 9. With very low moisture contents, coal can undergo full compacting without reaching an angle of repose of 90 deg and, consequently, with such coal, ratholing is highly improbable. At 3.6 per cent moisture content and above, there is a definite degree of compacting that can take place before an angle of repose of 90 deg is reached. With increasing moisture content, this margin diminishes.

Dynamic Angle of Repose. The tests described represent the angle of repose under static conditions which will differ from the angle of repose under dynamic conditions. Another series of tests was carried out in which the coal was permitted to fall through a 2-in.-sq opening in the bottom of the 1-cu-ft box. The angle of the cone formed by the loosely falling coal is plotted in Fig. 11.

Angle of Slide of Coal With One Per Cent to 16 Per Cent Moisture Content on Various Metal and Nonmetallic Surfaces. The suita-

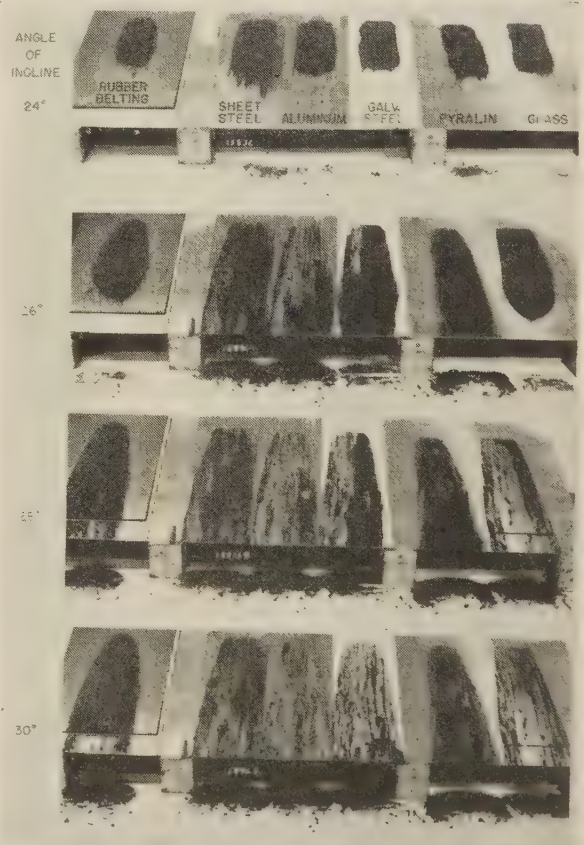


FIG. 12 TEST OF SLIDE ANGLE
(Coal at four positions on six materials.)

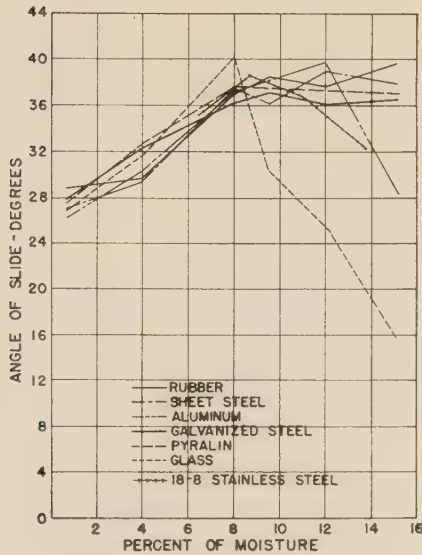


FIG. 13 EFFECT OF MOISTURE CONTENT ON ANGLE OF SLIDE ON PLANE SURFACES
(Data obtained in manner illustrated in Fig. 12.)

bility of various materials for coal chutes was studied. The angle at which coal will slide off these various materials is one indication.

A large plate was arranged in such a fashion that it could be raised slowly from the horizontal position. Various materials were attached to this plate and equal amounts of loose coal carefully placed along the top part of each material, Fig. 12. The angles of slide are plotted in Fig. 13. The variations in slide angle of the materials tested were within 3 deg with coal up to a moisture content of 8 per cent. Above this point the graph shows breaks in the curves for glass, aluminum, and stainless steel. This change in characteristics is apparently due to the formation of a film of moisture on the surface of the material which permits the entire specimen of coal to slide as one mass.

These slide tests represent unrestricted flow with one surface of contact. The influence of three contact surfaces was determined by using channel-shaped metal chutes, Fig. 14. This figure shows that the slide-angle curve for steel also has a maximum value.

A series of experiments was also performed with cylindrical pyralin, glass, and steel tubes to determine the variations between the foregoing conditions and one in which no free surface of coal exists.

Test points have been incorporated on the graph shown in Fig. 15, and an average curve has been drawn to show the trend. It will be noted that the angle of flow increases until it reaches a maximum at 10 per cent moisture and decreases thereafter.

At least three types of flow have been observed in these experiments, which account for the nonuniform behavior in the intermediate moisture ranges, as shown in Fig. 15, and are as follows:

Granular flow, in which there is distinct movement of one particle with respect to the others, occurs with fairly dry coal.

Plug flow, in which the whole column of coal moves as one mass with no apparent relative movement of individual particles, occurs at high moisture contents.

With moisture contents corresponding to the trough of the "density-moisture curve," Fig. 9, there exists a transition type of flow which resembles viscous flow.

The transition from granular flow to plug flow cannot be clearly

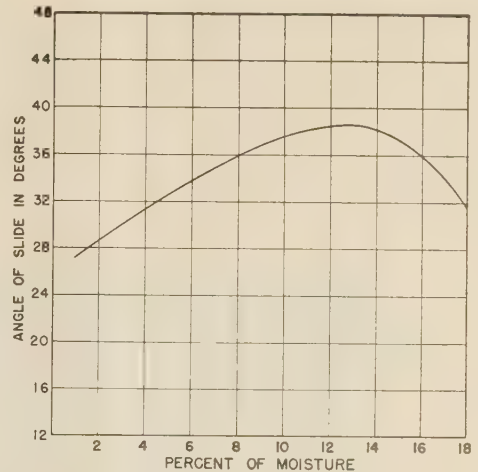


FIG. 14 EFFECT OF MOISTURE CONTENT ON ANGLE OF SLIDE IN CHANNEL
(Measurements made in channel 12 in. wide, 6 in. deep, and 36 in. long, formed from cold-rolled sheet steel. Depth of coal in channel $2\frac{1}{2}$ in.)

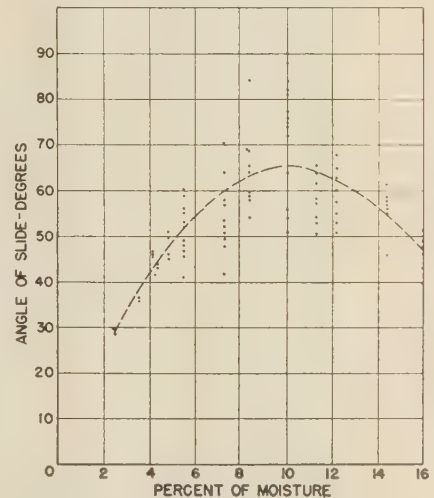


FIG. 15 EFFECT OF MOISTURE CONTENT ON ANGLE OF SLIDE IN STEEL CYLINDER
(Measurements made in 3-in.-diam steel tube, 36 in. long.)

defined and is influenced by the physical composition of coal. In this region of change in type of flow, it was difficult to obtain reproducibility in many tests.

Flow of Coal in Pipes With Uniform and Enlarging Diameters. The wisdom of using pipes with constant increase in cross section in direction of flow (flaring pipes) has been long recognized, and measurements were made to establish the relative merit of a flaring pipe as compared with a pipe of uniform cross section. A piece of smooth steel tubing 9 ft in length and of a uniform 3-in. ID was set up at an angle of 60 deg and paralleled by a pipe of the same length but gradually enlarging from 3 to 4 in. ID. These pipes were carefully filled from the top and the coal was taken away from the bottom by means of a slowly rotating disk. The stoppage occurred in the 3-in. cylindrical pipe at 7 per cent moisture, while the tapering pipe was capable of carrying coal of any moisture content up to the limits of the test (16 per cent).

Effect of Partial Obstructions of Outlets to Coal Chutes. Observations were made on the effect of small obstructions on the

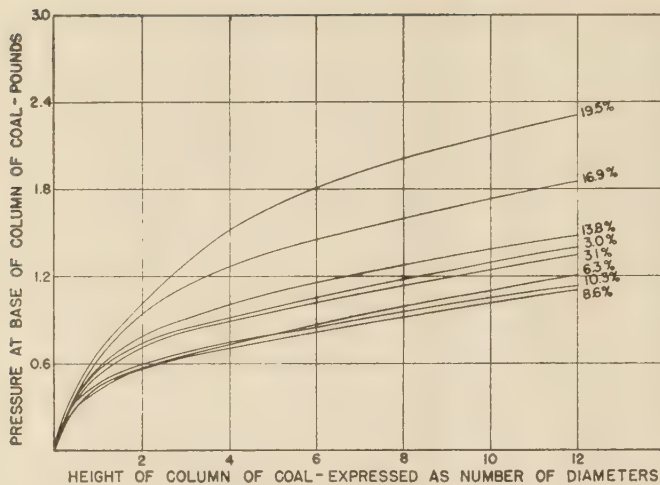


FIG. 16 SIDE-WALL FRICTION TEST

(Pressure at base of column of coal of various moisture contents measured at successive heights in 3-in.-diam steel tube, 36 in. high.)

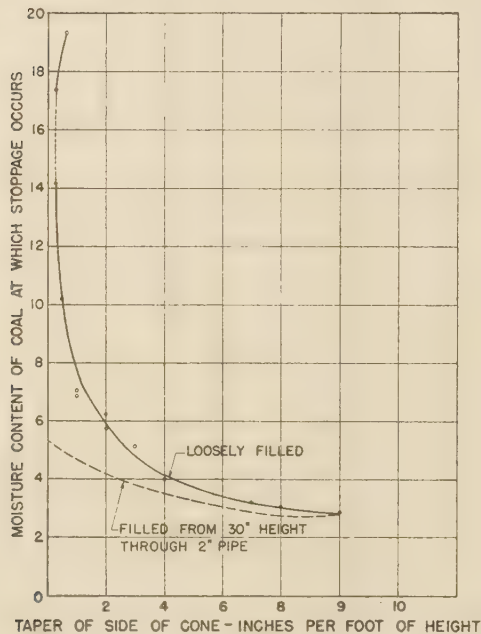


FIG. 17 EFFECT OF TAPER OF CONE ON FLOW OF COAL

(The moisture content at which stoppage occurred was measured in concentric steel cones of varying tapers, 2 in. diam at outlet and 12 in. high.)

angle of slide in cylindrical steel tubes. It was noted that, above 4 per cent moisture content, a very small restriction at the end of a pipe, either in the shape of a small segment, or in the shape of a minute annular ledge, was sufficient to raise the angle of slide to 90 deg, or even to prevent flow in a vertical position. This observation is particularly important since it indicates that a very small projection at a flanged joint can be the cause of stoppage.

Side-Wall Support of Column of Coal by Smooth Cylindrical Pipe. During the model tests, the vertical load that the coal exerted at the bottom of the chute system was measured. It was found to be equal approximately to the weight of a column of coal 1 diam in height. Basic tests were made to determine the influence of a

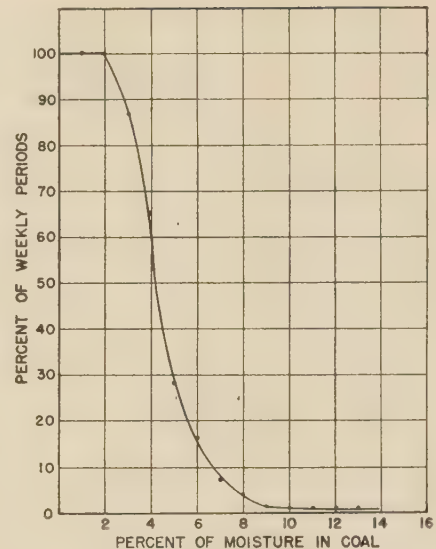


FIG. 18 MOISTURE CONTENT OF COAL USED AT RIVERSIDE PLANT
(Cumulative per cent of weekly periods with moisture content of coal above given amounts.)

given head of coal in producing flow through a chute. For this purpose, a smooth 3-in.-diam steel cylinder, 36 in. long, was arranged vertically in such manner that the bottom of the pipe was suspended over the platform of a scale without actually bearing on it. This pipe was filled in successive steps to varying heights and tests repeated with samples of varying moisture content. At each step the weight of the coal borne by the scale was read to 0.01 lb. The difference between this weight and the total weight of the coal in the pipe represented the support afforded by friction of the wall of the cylinder. It is significant that all curves, plotted in Fig. 16, show a fairly uniform rise up to 1 diam and then flatten out considerably, showing a very small gain in pressure on the bottom from additional height of column. With increasing moisture contents, each successive curve shows lower values and, after having reached minimum values at 8 per cent, begins to rise. This is in close relation with Fig. 9, which shows the change in density of coal with varying moisture contents. With fairly dry coal, approximately 80 per cent of the weight of the 36-in.-high column is carried by static side-wall friction.

Similar experiments were carried out with a flaring pipe, and it was noted that, while the bottom load was greater than for the cylinder, a large part of the load was still carried by side-wall friction and the general trend of curves remained the same. Coal which is confined in a vertical chute will exert a thrust against the side walls and, consequently, create frictional components as long as the angle of the side walls to the horizontal is greater than the static angle of repose of the coal.

Constricting Chutes or Hoppers. In the model of the existing chute as well as in the field, it has been observed that the hoppers were focal points of trouble. For the development of a new design, it became necessary to assemble basic data on the flow of coal through hoppers with various degrees of constriction, shape, and size.

The curve representing the moisture content at stoppage in cones of varying tapers increases rapidly with the increase in steepness of cones, Fig. 17. With the sharp-angle cones it was possible to re-establish flow by further increase in moisture content. The pronounced effect of compacting on the stoppage of coal in hoppers may be seen by a comparison of the two curves in this figure.

A number of eccentric cones with one vertical side were also investigated but it was found that, for equal change in cross section, the concentric cone gave slightly better results.

In order to obtain further indications on the trend of the scale effect, three cones of equal taper (1 in. per ft) but with successively increasing dimensions were also investigated. For this series it was found that a cone having 2 in. ID at the small end, a height of 12 in. and 4 in. ID at the large end would produce stoppage with loose, 7 per cent moisture coal. The next larger cone

with 4-in. base and 8-in. top diam, 24 in. high, stuck at 9 per cent moisture, and the largest cone, varying from 6 in. to 12 in. ID, 36 in. high, failed to function at 11 per cent moisture.

Effect of Addition of Oil and Wetting Agents on Flowing Properties of Coal. The use of admixtures to lubricate the sides of a chute was considered and various experiments were made to establish the effect of oils and wetting agents. No appreciable improvement of practical value was obtained with these admixtures.



FIG. 19 FIRST STEP IN REDESIGN OF HOPPER BELOW OPERATING LEVEL

(Lateral transition in plane of view eliminated; transition normal to view maintained. Coal stuck at bottom of hopper.)

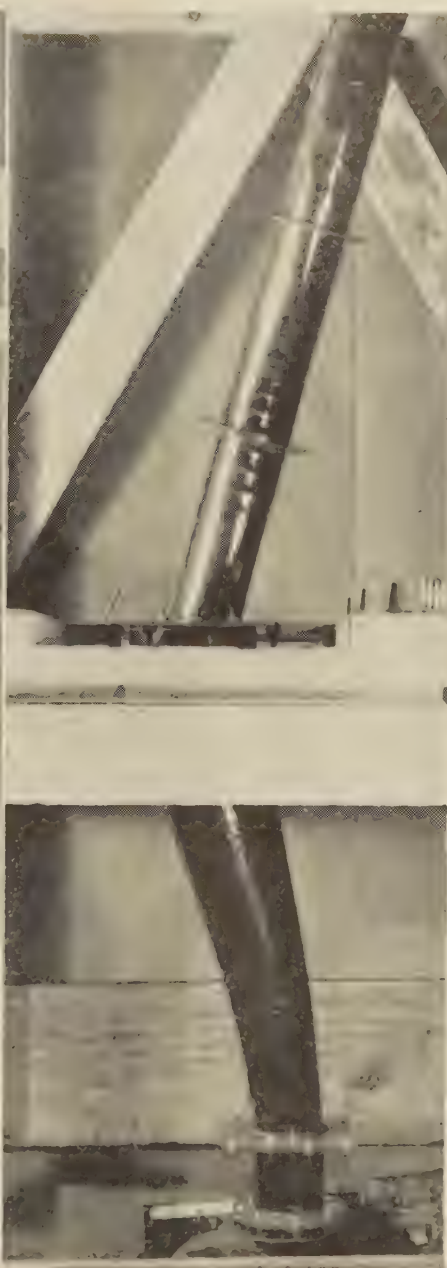


FIG. 20 SECOND STEP IN REDESIGN OF HOPPER BELOW OPERATING LEVEL

(View in direction at right angles to Fig. 19. Lateral transition in one plane only accomplished by streamlining.)

REVISED MODEL DESIGN

With the basic data available as explained, it was decided that improvement to the existing chute system could be accomplished without change in the arrangement and controls of feeders or without alterations of any main structural members or mechanical equipment.

From the shape of the curve showing variations in moisture content of coal during the operating year, Fig. 18, it may be

seen that a moderate improvement in chute performance actually represents a considerable decrease in the number of days in which trouble may be expected. It was with this thought in mind that the redesign of the experimental coal chute was begun.

Successive steps of new design incorporating certain features, to be mentioned, were tried in model form. Essentially these features are intended to approach streamlined flow of the coal similar to the flow of fluids in an efficiently designed system and are:



FIG. 21 "FULLY STREAMLINED" MODEL
(Lateral transition above operating level accomplished by reverse bend in flaring chute.)

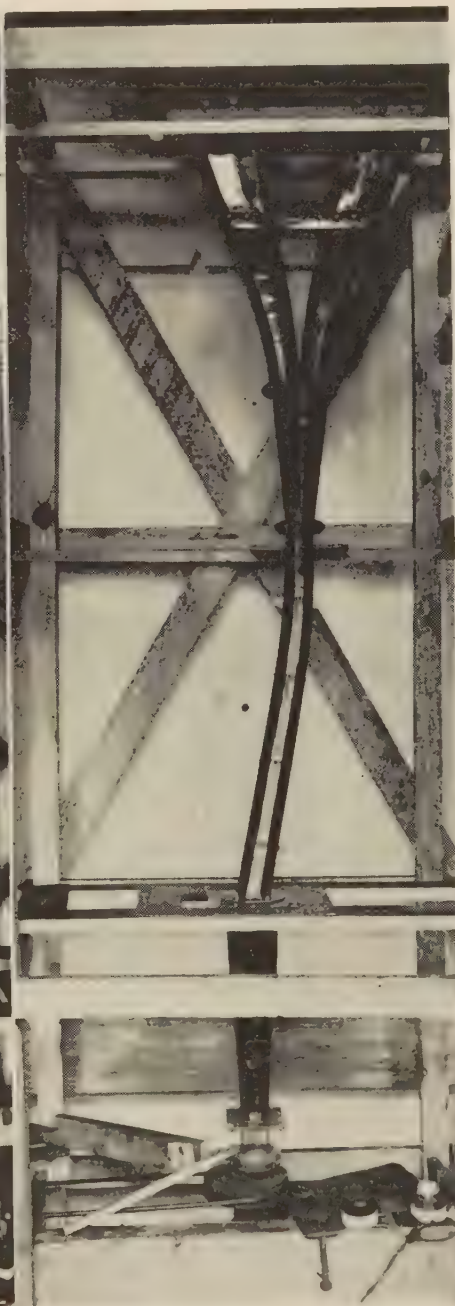


FIG. 22 MODIFIED "STREAMLINED" MODEL
(Lateral transition above operating level accomplished by single bend in flaring chute.)

- 1 Avoidance of sudden constrictions and sharp changes in direction.
- 2 Minimum angles of convergence of lines of flow, preferably approaching zero.
- 3 Minimum practical taper in hoppers.
- 4 Maximum possible angle of inclination with horizontal throughout the system.
- 5 Use of round shapes in preference to square or rectangular shapes.

Since existing space limitations in the plant had to be taken into consideration and the design modified to suit these conditions, it was not possible to apply fully the ideals outlined.

Description of Design Changes as Tested. The first problem encountered was the hopper below the operating floor (elevation 31 ft 6 in., Fig. 2). In the present chute system, this hopper forces the coal into a two-directional lateral transition. This double transition causes the greater part of the hopper space to be inactive. The first changes that were tried were the elimination

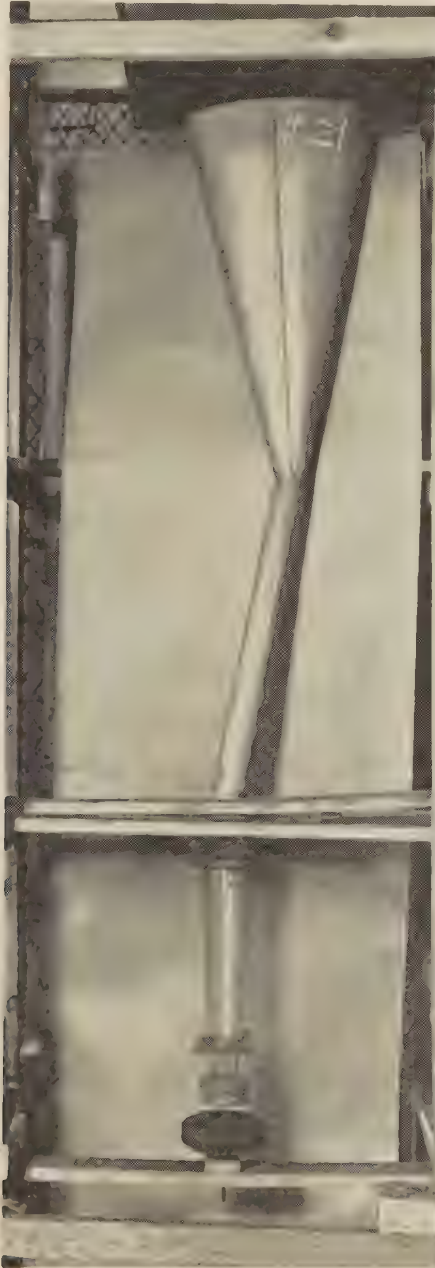


FIG. 23 OVAL CONE HOPPER MODEL

(Showing single cone encompassing both bunker gates and having minimum taper which still clears obstructions. Flow can be restarted only with great difficulty after a stoppage occurs. Upper portion of model made of sheet metal for simplicity of fabrication and strength.)

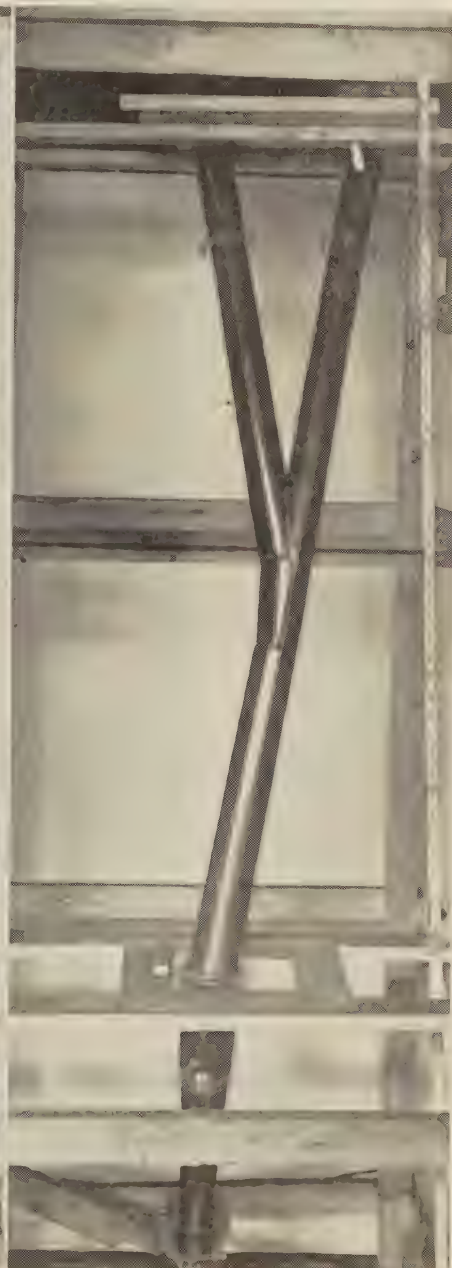


FIG. 24 Y-SHAPED MODEL

(Fabricated from flaring tubes. Use of a symmetrical Y was not possible on account of obstructions. Flow obtained was more rapid in right side than in left. First point of stoppage was at point of convergence.)



FIG. 25 EXAMPLE OF SYMMETRICAL CONICAL HOPPER SECTIONS
(Long cones of slight taper used to accomplish convergence of flow and transition to single pipe. Difficult to relieve stoppages occurring in long cones.)

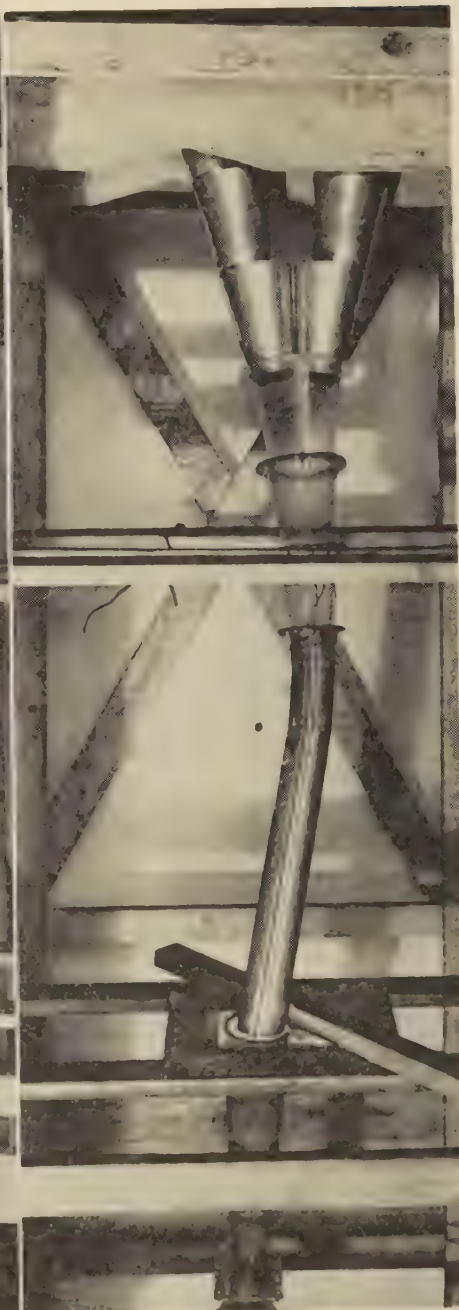


FIG. 26 EXAMPLE OF USE OF OFFSET CONES
(A study to determine behavior of offset cones as a means of accomplishing lateral transition.)

of one transition in the hopper by shifting it to the chutes above, and the use of a conical hopper of small taper, Fig. 19. Further alterations led to a fully streamlined hopper with a lateral transition in one plane only, Fig. 20.

From the underside of the coal bunker to the operating level, the design possibilities were limited by the following facts: The existing coal gates for this system of chutes are spaced 8 ft apart and cannot be changed. The location of the top of the hopper below the operating floor has already been set by virtue of existing structural members and various piping below this floor. In addition to this, there are some main structural members approximately halfway between the operating floor and the bunker.

To accomplish the necessary lateral transition, a number of flared circular sections were tried, first with a reverse bend, Fig. 21, and then with a single bend and straight section, Fig. 22.

Above this section of pipe, the problem still existed of bringing two streams of coal together, and a series of successive shapes led to the development of the completely streamlined model shown in Fig. 21.

Altogether 40 setups were tested covering the full range from a large long hopper section spanning over both bunker gates at the top, Fig. 23, to the extreme of two pipes leading from the coal gates in the most direct manner possible down to the hopper at the operating floor, Fig. 24. These various setups are in part depicted in Figs. 25 to 27, inclusive.

The fully streamlined model which had been assembled and tested to explore the theoretical solution to the problem was not regarded as practical from an engineering standpoint. Since nearly every component part consists of double-curvature shapes, the difficulties encountered in building the model might easily be multiplied in the actual fabrication of a prototype. The model shapes became so sensitive that the slight distortion which the plastic pyralin model underwent during hot humid weather immediately reacted on the ability of the system to carry wet coal. Considerable effort was devoted to the problem of simplifying these shapes to a point where manufacture would be feasible and operating effectiveness would be maintained. The final results of these tests are shown in Figs. 28 and 29, which represent essentially the chute that has been ordered for a full-scale test in the plant at Riverside.

Discussion of Special Shapes and Problems. Several individual problems of interest to the designer were encountered in these tests. In the model of the existing chute, the coal had a tendency to hang up at the transition from the rectangular chute to the hopper below the operating level. This difficulty was especially noticeable where the flow from the rectangular chute was directed against a slanting side of the hopper below. Where this hopper stepped back, permitting the coal to fall away from the end of the chute, less trouble was encountered. This observation led to the development of the "breakaway," which consists of a free space surrounding the lower end of a chute or hopper, thereby permitting the coal flowing from the chute or hopper to break away freely in all directions, Fig. 30. This feature permits a sudden change in direction and has the added advantage of tending to counteract compacting. This device has been employed either wholly or partially in three locations in the new chute system.

The data gained in the cone experiments indicate that the behavior of a separate conical hopper will differ from one incorporated in a chute system. Tests carried out in the development of the new model further indicate that the performance of such a hopper depends on its relative position within a system, since this will govern the amount of compacting the coal undergoes. In general it may be stated that cones of a slight taper, while permitting free flow as an individual unit, show a tendency to compact the coal by their powerful wedge action when they be-

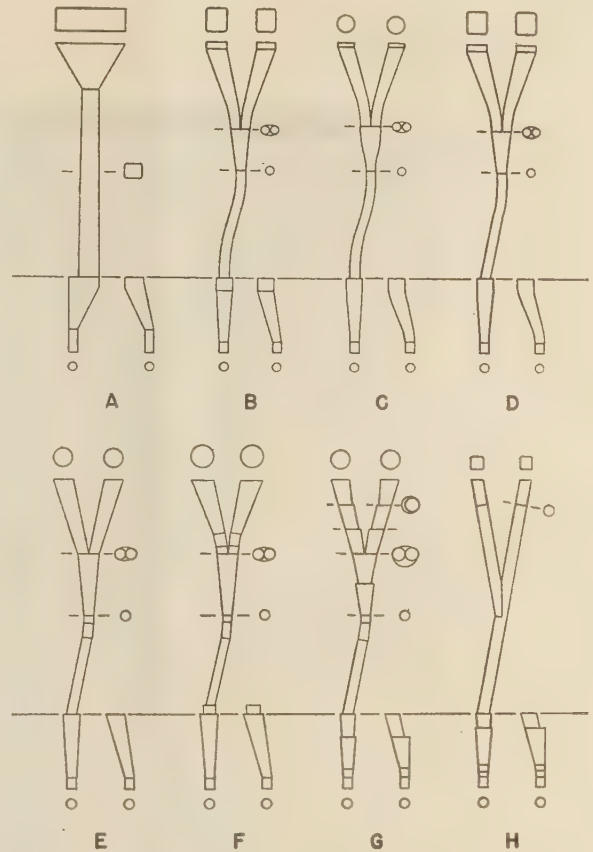


FIG. 27 SCHEMATIC OUTLINE OF VARIOUS TEST ASSEMBLIES

come part of the system, and whenever the ratio of their lengths to smallest diameter exceeds approximately 2. On the other hand, short cones of moderate slope work fairly well as long as the ratio of their lengths to smallest diameter does not exceed 1.5 to 2. Concentric cones have an advantage where it is desired to achieve a reduction in cross section while eccentric cones can be employed effectively where both lateral transition and reduction in area are required. Consequently, both have been employed in the final design.

CONCLUSIONS

The results of observations given in this paper apply to the particular coal tested and, for similar coal the graphs should be interpreted as indicating probable trends, rather than definite values.

The tests have demonstrated that phenomena occurring in a chute system can be reproduced in a scale model.

Application of principles developed in these experiments can lead to improved chute design.

Compaction of coal is one of the most important factors influencing the operation of a solidly filled chute system. An angle of repose of 90 deg may be reached at relatively low moisture contents if the density of coal is increased through impact or wedge action. Since coal must undergo a certain amount of compacting in any composite system, there exists a limit in moisture content at which the chutes can be depended upon to operate without stoppage. The possibility of coal stoppage must be recognized, and therefore the ease of re-establishing flow should be considered in the development of a design.

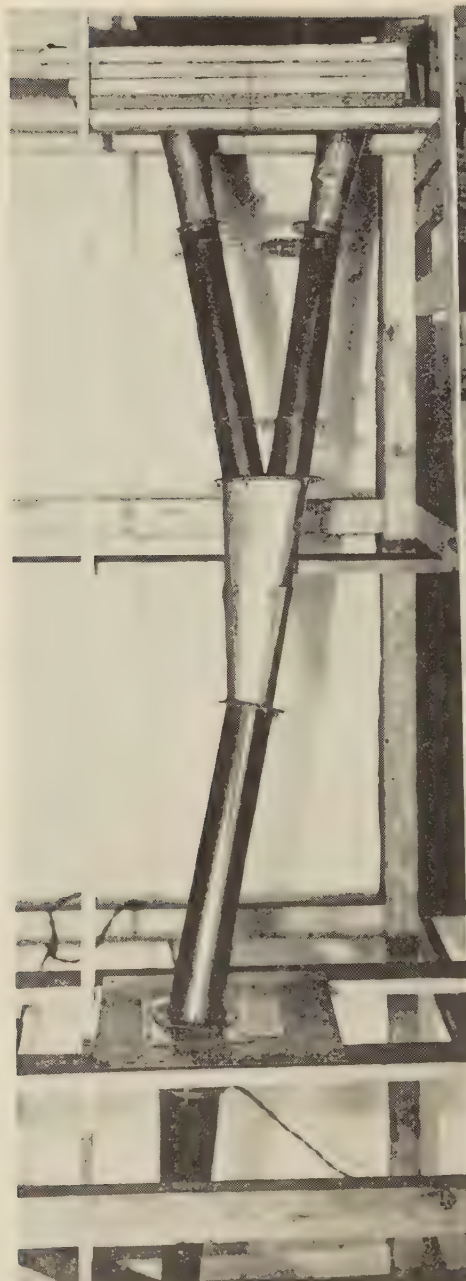


FIG. 28 MODEL OF FINAL DESIGN
(Upper hopper and converging section fabricated from
pyralin-lined tinplate.)

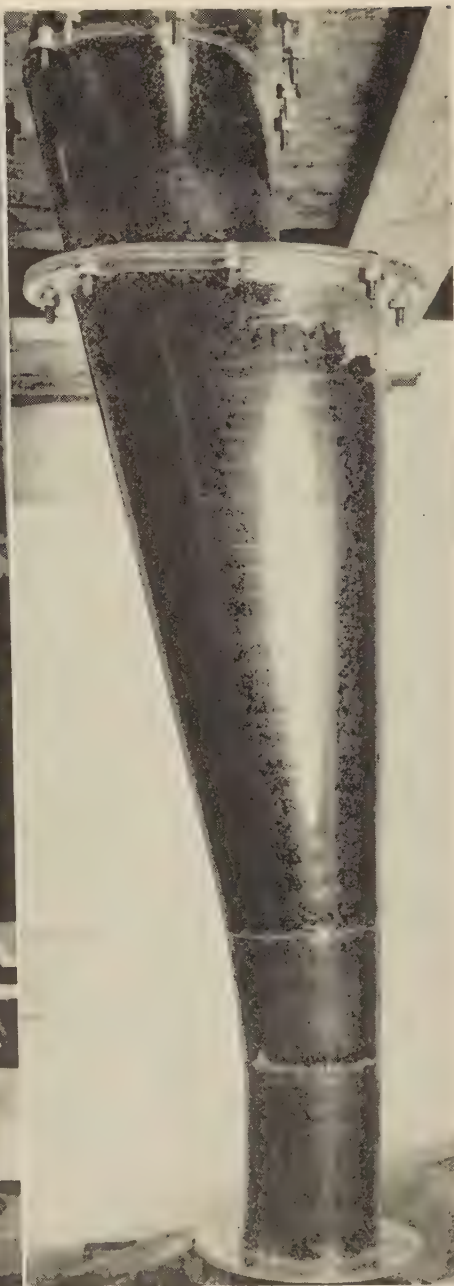


FIG. 29 SIDE VIEW OF FINAL DESIGN HOPPER
BELOW OPERATING LEVEL
(Offset at upper portion was necessitated by obstructions.)

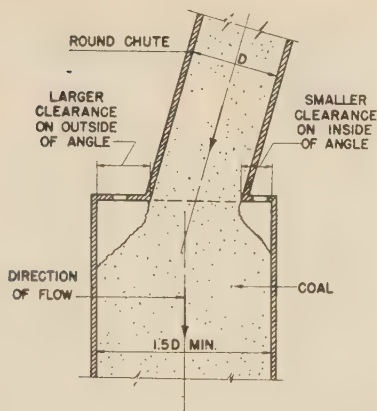


FIG. 30 SCHEMATIC SKETCH OF "BREAKAWAY"
(Typical flow of coal at change in direction.)

It was concluded that the following points should be incorporated in the chute design. The shortest possible path from the coal bunker to the mills should be maintained. Tapered (or uniformly enlarging) round chutes should be used wherever possible. Where two streams of coal must be brought together, this should be accomplished with a minimum angle of convergence. If a sudden change in direction cannot be avoided, the introduction of a "breakaway" to help the coal to realign itself should be utilized. All angles of chutes should be made as steep as possible and reductions in cross section kept to a minimum.

The application of all points mentioned in the foregoing has resulted in a model design which showed sufficient improvement over the model of the existing chute to justify the construction of a full-sized chute for development of actual field experience, Fig. 31.

This investigation has concerned itself entirely with the possibilities of improving flow of coal in an existing chute system and does not take into account the problem of maintaining uninterrupted flow of coal from bunker to chutes, but the latter is now under investigation.

ACKNOWLEDGMENTS

This investigation was carried out under the general direction of Mr. A. L. Penniman, Jr., general superintendent of the Consolidated Gas Electric Light and Power Company of Baltimore. The authors wish to express their appreciation to Messrs. L. Birkhead, G. S. Harris, Dr. P. L. Betz, and members of the operating department for their valuable suggestions. Mr. J. D. Andrew, Jr., of the Babcock & Wilcox Company, gave valued help on special features of the investigation, and Mr. A. D. Stewart of Connery Construction Company assisted with problems concerning fabrication. Messrs. C. V. Moberg, J. D. Miller, R. E. Randall, C. J. Parrish, A. B. Cromer, and other members of the Electric Test and Electric Engineers Departments assisted in conducting the investigation.

BIBLIOGRAPHY

- 1 "Wind-Tunnel Tests to Establish Stack Height for Riverside

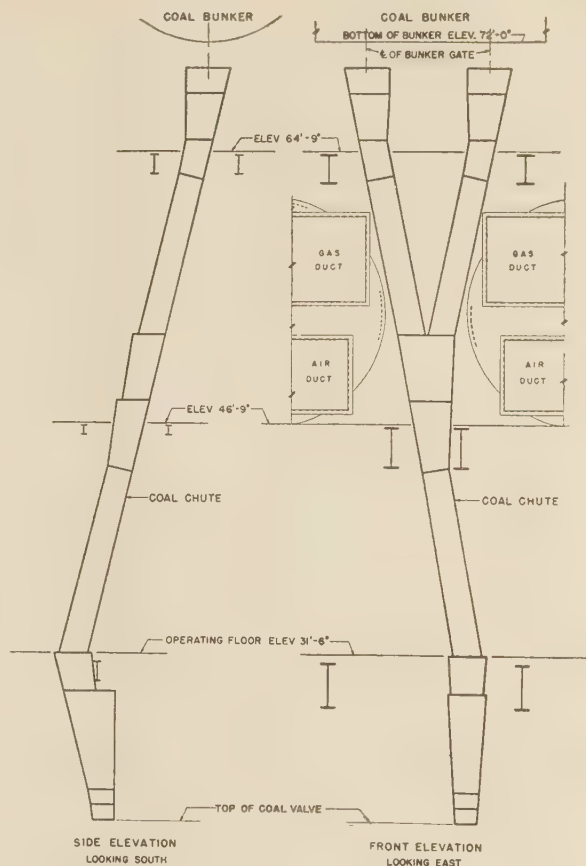


FIG. 31 GENERAL ASSEMBLY OF NEW COAL CHUTE
(Constructed entirely of round or oval sections.)

Generating Station," by H. L. von Hohenleiten and E. F. Wolf, *Trans. A.S.M.E.*, vol. 64, 1942, pp. 671-683.

2 "Scale Models Aid the Engineer," by H. L. von Hohenleiten, *Power*, vol. 83, June, 1939, pp. 326-327.

3 "Design and Control of Concrete Mixture," sixth edition, revised 1936, published by Portland Cement Association, Chicago, Ill., p. 24.

4 "Conveyors and Related Equipment," by W. G. Hudson, John Wiley & Son, New York, N. Y., 1944.

5 "Continuous-Flow Conveyor Elevators Streamline Materials Handling," by W. G. Hudson, *Power*, vol. 88, October, 1944, p. 77-79.

6 "Is Modified Flat Chute Non-Segregating?" by A. J. Stock, *Power*, vol. 88, October, 1944, pp. 101-102.

7 "Coal Segregation in Boiler Plants," by A. J. Stock, *Mechanical Engineering*, vol. 66, 1944, pp. 523-528.

8 "New Coal Chute That Eliminates Stoker-Hopper Segregation Is Easy to Make," by P. B. Richardson and Max R. Boye, *Power*, vol. 88, August, 1943, p. 507.

9 View of Boiler Room of Government Synthetic Rubber Plant of Carbide and Chemicals Corporation, Institute, W. Va., *Power Plant Engineering*, cover, March, 1944.

Heat Transfer From a Baffled-Finned Cylinder to Air

By A. W. LEMMON, JR.,¹ A. P. COLBURN,² AND H. B. NOTTAGE³

Air-cooled aircraft-engine cylinders utilize extensive finned surface to permit maintenance of proper metal temperatures with high rates of heat transfer occurring at high engine power outputs. The process of heat transfer to the flowing air stream differs from that of usual finned tubes not only in size of the cylinder but also because baffles are utilized which force all the air to pass through the fin spaces. Because of this latter difference, data on finned tubes in general do not apply. Therefore, special tests have been carried out to establish the mechanism of heat transfer in this case and to provide a generalization of the data useful for design. The work was carried out at the University of Delaware in conjunction with a Pratt & Whitney Aircraft heat-transfer research program. The experiments were conducted on a typical section of an aluminum finned cylinder barrel. The cylinder was heated by an internal electrical heater. Temperatures were measured not only of the entrance and exit air stream but also at eight points, equally spaced circumferentially, in the base metal. The results were interpreted by comparison with heat-transfer relations for flow inside conduits. The maximum heat-transfer rates were in close agreement with these relations although the average rates were lower owing to the decreased cooling-air velocities over the front and rear fin surfaces outside of the baffled portion of the cylinder. The over-all pressure drop is shown to be about double the estimated frictional resistance; the inlet and exit losses provide an explanation.

NOMENCLATURE

THE following nomenclature is used in the paper:

- A_b = cylinder fin-base area (based on outside diameter of base), sq ft
- A_{os} = cross-sectional area for flow in cylinder fin spaces, sq ft
- A_f = total external heat-transfer surface of cylinder, sq ft
- C = heat capacity of humid air mixture, Btu/(lb)(deg F)
- D_{eq} = equivalent diameter of fin space, ft
- E_{hp} = pumping horsepower
- G = mass velocity, lb/(hr)(sq ft)
- g_c = dimensional constant, 4.169×10^8 ft/hr²
- h = mean surface conductance per unit of A_f , Btu/(hr)(sq ft)(deg F)
- h_z = "local" surface conductance per unit of A_f , Btu/(hr)(sq ft)(deg F)

- P_T = total power loss per unit of A_f , ft-lb/(hr)(sq ft)
- ΔP_{Bi} = baffle pressure drop, in. H₂O (ΔP_{BP} = lb/sq ft)
- t_{avg} = average air temperature across cylinder, deg F
- t_b = average fin-base temperature, deg F
- t_{max} = maximum (rear) fin-base temperature, deg F
- t_1, t_2 , etc. = observed fin-base temperatures, deg F
- Δt_m = arithmetic-mean temperature difference, average fin-base temperature to average air-stream temperature, deg F
- Δt_0 = reference mean temperature difference, deg F ($\Delta t_0 = 100$)
- Δt_r = mean temperature difference ratio, $\Delta t_m / \Delta t_0$
- U = over-all heat-transfer conductance per unit of A_b , Btu/(hr)(sq ft)(deg F)
- U_z = "local" value of U
- W = air flow rate, lb per hr
- ρ = air density, pcf
- ρ_{avg} = air density at average temperature and pressure across cylinder, pcf
- ρ_0 = density of air at 70 F, and 30 in. Hg, pcf ($\rho_0 = 0.0753$)
- ϕ = over-all pressure loss coefficient, Equation [5]
- μ = viscosity of air at average air temperature across cylinder, lb/(hr)(ft)
- NP_r = Prandtl number, $C\mu/k$
- N_{Re} = Reynolds number, $D_{eq}G/\mu$
- N_{St} = Stanton number, h/CG

INTRODUCTION

Problems of designing a fin-and-baffle system to be fitted to cylindrical sections of the size employed as air-cooled aircraft-engine cylinders have recently become of critical importance. Adequate design requires a foundation of fundamental and generalized data from which any desired performance requirements may be met.

Since the publication of earlier preliminary work (2, 4, 7, 8)⁴ along these lines, the general conception of the nature of the processes and problems prevailing in an extended fin-and-baffle system has considerably advanced, and improvements in experimental equipment and techniques have been made. On both of these counts, further experimental studies to permit extending the accuracy and range of the available design data have been needed, together with a broadened fundamental basis for generalizing the behavior of this type of heat-transfer system. Preliminary studies of the problem have suggested that the processes within the fin flow passages, where effectively all of the heat transfer takes place, can be treated most satisfactorily and comprehensively in terms of their relation to the established data on heat transfer in straight tubes or passages; all with due allowance for the effects of the extended-surface boundaries of the passages and the particular nature of the flow system both within the baffle section and at the front and rear points where the stream enters and leaves.

⁴ Numbers in parentheses refer to the Bibliography at the end of the paper.

¹ Research Fellow in Chemical Engineering, University of Delaware, Newark, Del. Present address, National Defense Research Committee, Washington, D. C.

² Professor of Chemical Engineering, University of Delaware. Mem. A.S.M.E.

³ Project Engineer, Pratt and Whitney Aircraft, East Hartford, Conn. Jun. A.S.M.E.

Contributed by the Heat Transfer Division and presented at the Annual Meeting, New York, N. Y., Nov. 27-Dec. 1, 1944, of THE AMERICAN SOCIETY OF MECHANICAL ENGINEERS.

NOTE: Statements and opinions advanced in papers are to be understood as individual expressions of their authors and not those of the Society.

In this paper are presented the results of experimental study and analysis for an actual aluminum-finned section of an aircraft-engine cylinder barrel, fitted with representative baffles and tested under controlled conditions of uniform internal electrical heating and smooth approaching air flow, as well as of visual-flow observations which aid in understanding local effects. These results have been given fundamental study and interpretation, with particular emphasis upon the role and importance of local point-to-point conditions in the heat-transfer and flow processes.

DESCRIPTION OF EXPERIMENTAL ARRANGEMENT

Requirements for the experimental system were based on the need for a flexible assembly yielding reproducible results with a simple operating control. General features decided upon were the following:

- 1 A once-through air-duct system, arranged with a free room-air intake to the test cylinder.
- 2 A test section to contain the cylinder and baffle assembly being studied, arranged for simple removal and adjustment, and with effective heat insulation.
- 3 An electrical heating element to fit snugly within the test cylinder and permit ease of heating control.
- 4 Measurement of the temperature, pressure, and moisture content of the intake air.
- 5 Measurement of the static pressure drop and temperature rise of the air passing across the test cylinder, which latter requires a downstream mixing section to obtain the mixed-mean air temperature, and the use of effective over-all heat insulation.
- 6 Measurement of the temperature pattern about the base of the test cylinder by means of thermocouples installed within the

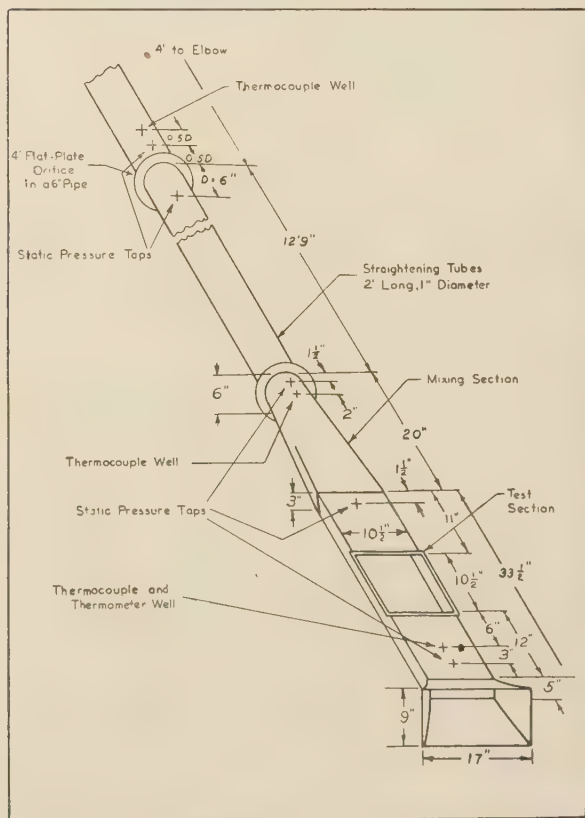


Fig. 1 DIMENSIONED SKETCH OF TEST APPARATUS

base metal, with the junctions and adjacent sections of leads in isothermal zones.

An over-all dimensioned sketch of the duct system constructed, showing the points of static pressure and temperature measurement for the air stream, is given in Fig. 1.

Cylinder and Heater Assembly. Plan dimensions of the finned-cylinder and baffle installations are given in Fig. 2. The baffle was made of sheet metal, held in place by wooden blocks. De-

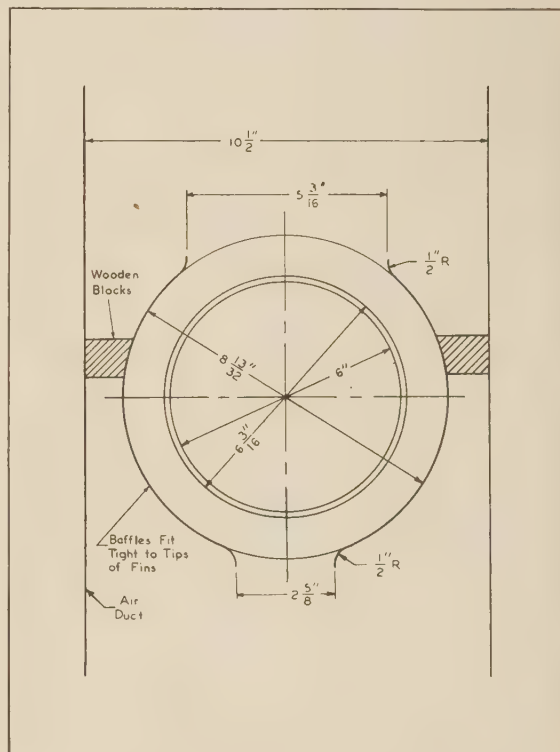


Fig. 2 PLAN VIEW OF FIN-AND-BAFFLE ARRANGEMENT

tailed dimensions of the finned test cylinder are given in Table 1. The fins on the test cylinder were lathe-turned from a forged blank of Alcoa A518-T aluminum, having a nominal thermal conductivity of 99.2 Btu/(hr)(ft)(deg F) at 100 deg C. The alumi-

TABLE 1 GEOMETRICAL DATA ON FINNED TEST CYLINDER

Axial length of test cylinder at fin base, in.....	25/8
Outside diameter of fins, in.....	8 13/32
Root diameter of fins, in.....	6 3/16
Radial width of fins, in.....	17/64
Thickness of cylindrical fin base, in.....	3/32
Fin thickness at tip, in.....	0.02
Fin thickness at root, in.....	0.04
Center-line spacing of fins, in.....	0.141
Number of fins.....	18
Base area of fin-root cylindrical surface (A_b), sq ft.....	0.349
Total fin side-surface area (A_f), sq ft.....	6.67
Cross-sectional area of flow stream between fins, measured on diameter with tight baffles (A_{cs}) sq ft.....	0.0308
Equivalent diameter of fin passages (D_{eq}), in.....	0.202
Equivalent diameter of fin passages (D_{eq}), ft.....	0.01683

TABLE 2 SPECIFICATIONS OF HEATER

Type of wire.....	Chromel "A"
Wire gage.....	B. & S. 18
Number of coils.....	2
Length of wire in each coil, ft.....	55
Length of each close-wound coil, in.....	61
Length of each stretched coil, in.....	87
Resistance of each coil (cold), ohms.....	22.4
Resistance of each coil (400 F), ohms.....	23.0
Amperage of each coil at 250-v rating, amp.....	9.2
Total heat-release rate from heater at maximum output, w.....	4600



FIG. 3 TEST SECTION SHOWING HEATER AND TEST CYLINDER

num machined surface was given a protective anodizing treatment before testing. The baffles were installed in contact with the fin tips.

The method of arranging the heater in the test cylinder is shown in Fig. 3. The heater consisted of two coils of chromel wire, each rated at 2 kw for 250 v. These coils were wound spirally on a core which was built up from 1/2-in. sheets of transite. Larger end disks of transite were attached to this core and fitted tightly to the base section of the test cylinder, so that the uppermost and lowermost fin-side surfaces were exposed to an air stream of slightly less than one half of the cross section between normal consecutive fins. Power for the heater was furnished by two 125-v 3-kw motor generator sets. The generator voltage was controlled through variable-field rheostats. The transite end disks on the heater assembly serve as an effective initial barrier to endwise heat leakage. The entire assembly was completely wrapped in a blanket of 4-in-thick glass wool before testing.

Mixing Unit. The mixing unit was located in the transition duct between the test and metering sections. This consisted of a three-piece disk-and-doughnut section with the disk in the middle, each piece spaced 6 in. from the next. The disk and the holes were each 4 in. diam.

Metering Section. Fig. 1 shows the over-all dimensions of the metering section. The 4-in. orifice in the 6-in. pipe, carefully installed according to the Fluid Meters Report (1) with so-called vena-contracta taps, was considered to have a flow coefficient of 0.684 (including velocity of approach factor) without supplementary calibration.

Instrumentation. The heater power input was determined by a direct-current voltmeter (0–150 v) and ammeter (0–25 amp), both instruments being accurate to 0.5 per cent of full scale deflection. The voltage taps were connected directly to the heater terminals.

The static pressure drop from the room to the tap just before the test section, and the static gage pressure at the metering orifice were read to 0.1 in. on vertical U-tube water manometers. The static pressure drops across both the baffled and sealed-in test cylinder and the metering orifice were obtained with Type-B Uehling draft gages, graduated to 0.01 in., in the range below 1 in. H₂O; and for the higher range, U-tube water manometers were employed, graduated to 0.1 in.

All thermocouples were made from Leeds and Northrup selected, 28-gage iron-constantan duplex-insulated wire. The thermocouple emf's were read on a Leeds and Northrup portable preci-

sion potentiometer, Type 8662. Single thermocouples were employed to measure the air temperature in three locations: (a) Directly beside the intake-air thermometer, as a check thereon; (b) close behind the last "doughnut" of the mixer, with provision for traversing, to determine the mixed-mean heated-air temperature; and (c) in the discharge stream from the metering orifice, to establish the air temperature for calculating the flow rate. Measurements of the metal temperatures in the cylindrical base section of the finned test specimen were accomplished by the use of thermocouples, the junctions of which were installed in the bottom of small holes drilled in axially to the mid-section of the cylinder base from one end. Eight of these thermocouples were installed around the muff, spaced every 45 deg.

EXPERIMENTAL PROCEDURE

Thorough precautions were taken when assembling the heater and finned cylinder to insure a tight fit and seal against all possible air leaks. Room drafts were not allowed during a test, in order to insure constancy of the air source and the surroundings.

Each point required the setting of a heater power and an air-flow rate. Once this was done, conditions were held constant until a steady state was assured. A normal test then consisted of four sets of readings, taken at 5-min intervals, of the inlet and heated-air temperatures, the orifice-air temperature, and of the heater power; and one set of readings of the other variables. The readings taken only once included the metal temperatures, the pressures, and the wet- and dry-bulb temperatures of the inlet air. When making calculations, the readings which were taken four times were averaged for purposes of analysis.

No test point was accepted until its heat balance had been judged satisfactory. All data retained were within the maximum limit of 10 per cent difference between the rate of energy reception by the air stream and the heater power input.

METHODS OF CALCULATION

Air-Flow Correlations. Mass flow rates and Reynolds numbers were calculated from the following relations

$$G = W/A_{cs} \text{ and } N_{Re} = D_{eq}G/\mu$$

The values of μ were taken at the average air temperature across the muff; these values were obtained from the Fluid Meters Report (1).

Pumping horsepower, the total power required to pump air through the muff with negligible kinetic-energy and density changes, is calculated from the relation

$$E_{hp} = \frac{W \Delta P_{BP}}{33,000 \times 60 \rho_{avg}} \dots \dots \dots [1]$$

and since

$$\Delta P_{BP} = 62.3 \Delta P_{Bi/12}$$

$$E_{hp} = 2.62 \times 10^{-6} W \Delta P_{Bi}/\rho_{avg} \dots \dots \dots [2]$$

For purposes of correlation in order to present E_{hp} as a function independent of density, this term is multiplied by the factor $(\rho_{avg}/\rho_0)^2$.

Over-all power loss per unit surface area, also multiplied by $(\rho_{avg}/\rho_0)^2$, is calculated as follows

$$P_T(\rho_{avg}/\rho_0)^2 = \frac{62.3 W \Delta P_{Bi}/\rho_{avg}}{12 \rho_0^2 A_f} \dots \dots \dots [3]$$

The over-all pressure-loss coefficient is evaluated by an expression similar to that for the friction factor in smooth pipes. Since in this study it was not possible to measure the pressure drop

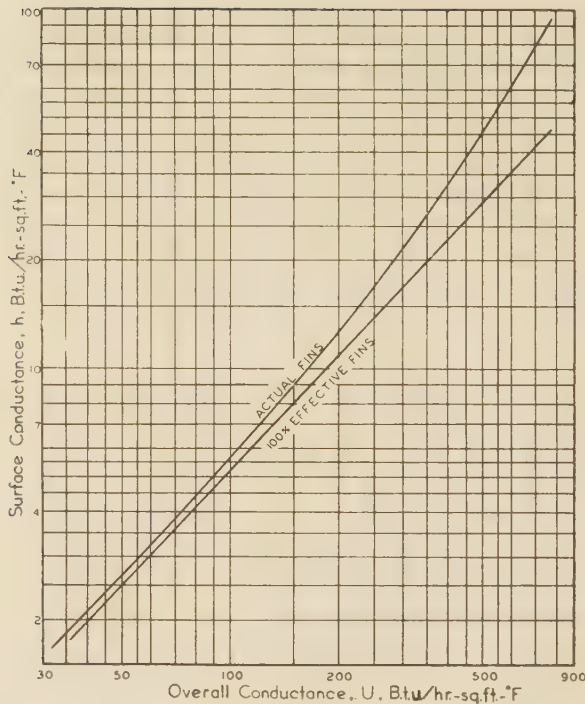


FIG. 4 RELATION BETWEEN SURFACE CONDUCTANCE AND OVER-ALL CONDUCTANCE

due to friction alone, the over-all static pressure drop has been employed for the purpose of obtaining an index of the over-all flow loss which could be compared to the friction factor for flow inside conduits, the friction factor as usual being defined as

$$f/2 = \frac{g_{avg} A_{cs} \Delta P}{G^2 A_f} \quad [4]$$

where ΔP = frictional pressure drop. In this case where only the over-all pressure drop is known, the pressure-loss coefficient is calculated by the analogous equation

$$\phi/2 = \frac{g_c \rho_{avg} A_{cs} \Delta P_{BP}}{G^2 A_f} = 9.95 \times 10^6 \rho_{avg} \Delta P_{BP} / G^2 \dots [5]$$

Heat-Transfer Coefficients. The mean temperature difference used in calculation of the heat-transfer coefficients in this study has been taken as that prevailing between the arithmetic-average metal temperature indicated by the thermocouples in the base of the muff and the average air temperature. The over-all unit heat-transfer conductance U is then calculated by the relation

$$U = Q_s / A_s \Delta t_m \dots [6]$$

Magnitudes of the mean unit surface conductance h are obtained from the over-all conductance according to the method of Harper and Brown (5) for tapered annular fins. Fig. 4 shows the relation between U and h calculated for the dimensions of the test cylinder.

TABLE 3 HEAT-BALANCE DATA

Run no.	Air flow, lb per hr	Air temp rise, deg F	Heat Rates, Btu per Hr			Per cent heat lost
			Electrical input	To air stream	Heat lost	
1	1390	19.6	6714	6617	97	1.45
2	1404	23.5	8568	8028	540	6.30
3	1418	14.5	4936	5000	-64	-1.31
4	1433	8.7	3190	3031	159	4.96
7	1116	15.1	4298	4097	201	4.69
8	990.0	16.0	4097	3852	245	5.98
9	723.6	23.1	4439	4064	375	8.44
10	561.6	13.2	1764	1789	-25	-1.43
11	558.0	19.3	2722	2614	108	3.97
12	547.2	35.2	4856	4684	172	3.56
13	540.0	51.5	6840	6728	112	1.63
14	532.8	68.5	8978	8834	144	1.60
17	1019	7.1	1742	1760	-18	-1.03
18	756.0	9.5	1728	1746	-18	-1.04
19	565.2	12.5	1732	1717	15	2.91
20	392.4	16.1	1681	1526	155	9.20
21	993.6	6.4	1667	1544	123	7.35
22	554.4	12.4	1696	1670	26	1.48
23	381.6	17.6	1678	1786	-108	-6.44
24	982.8	17.7	4532	4230	302	6.67
25	302.0	61.3	4655	4464	191	4.10
26	174.2	102.7	4630	4309	321	6.93

TABLE 4 FIN-BASE TEMPERATURES

Run no.	Fin-base temperature, deg F							
	0°*	45°	90°	135°	180°	225°	270°	315°
1	124.0	120.6	116.1	125.6	159.3	142.0	135.0	124.0
2	133.3	129.1	124.6	138.1	178.6	153.5	144.0	133.4
3	104.6	102.1	98.9	106.5	133.2	120.6	116.5	106.3
4	91.6	89.2	86.4	90.2	110.2	103.6	100.2	92.0
7	111.4	108.8	106.6	113.5	137.4	125.9	120.5	110.6
8	113.8	111.8	110.4	117.1	139.7	128.1	122.3	114.8
9	121.4	119.3	118.8	128.7	153.6	138.8	129.9	122.4
10	95.4	94.6	94.7	99.4	110.9	105.4	101.6	97.0
11	107.8	107.1	108.0	115.0	131.7	122.1	115.0	109.4
12	137.3	136.0	137.3	150.7	180.3	160.2	146.0	139.2
13	164.1	162.1	164.4	183.6	225.7	195.7	173.9	165.4
14	190.2	188.2	192.3	217.6	271.6	231.8	202.6	192.0
17	90.2	88.9	87.4	90.1	102.3	98.8	96.3	91.2
18	92.8	91.7	91.6	95.2	106.8	102.1	98.9	94.1
19	99.1	98.2	99.2	103.8	115.1	109.0	104.8	100.5
20	97.2	97.0	98.8	104.1	115.8	109.1	103.4	99.1
21	87.4	85.9	84.6	87.3	99.2	95.9	93.3	88.6
22	92.3	91.6	92.3	96.7	108.2	102.3	98.1	93.5
23	95.5	95.0	97.3	103.0	115.0	107.3	101.2	96.5
24	113.9	111.5	110.5	118.1	143.6	130.1	122.4	115.0
25	146.0	146.3	155.4	175.1	209.6	183.8	160.1	148.4
26	170.9	172.5	192.7	220.8	256.9	227.0	193.3	172.2

* At upstream center of test cylinder; other angles clockwise from this point.

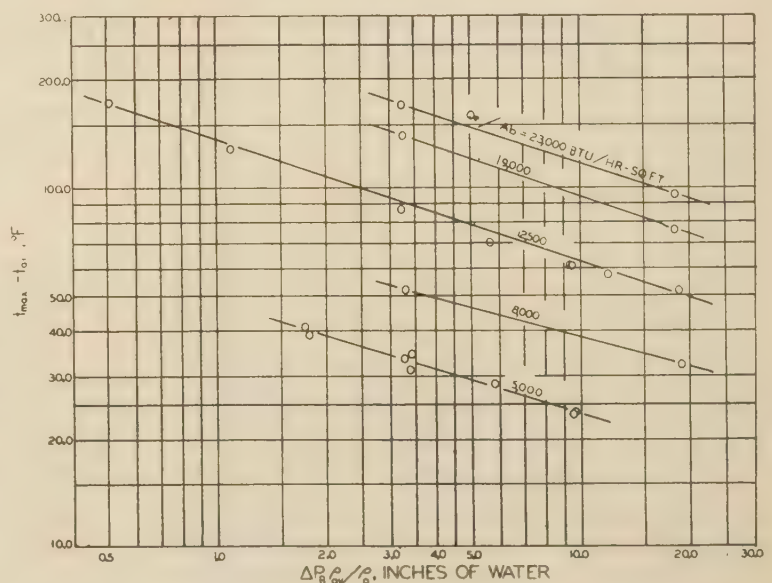


FIG. 5 RELATION OF MAXIMUM METAL TEMPERATURE, BAFFLE PRESSURE DROP, AND HEAT FLUX

TABLE 5 CORRELATION DATA

Run no.	Pressure drop, in. H ₂ O	Average density, pcf	Air-flow rate, lb per hr	Mass velocity, lb/(hr) (sq ft)	Reynolds number	$\Delta P_{Bavg}/\rho$ in. H ₂ O	$PT(p_{avg}/\rho)^{1/2}$ ft-lb/(hr) (sq ft)	$\phi/2$
1	19.43	0.0706	1390	45100	16860	18.29	261662	0.00669
2	19.43	0.0710	1404	45600	17150	18.34	265795	0.00670
3	19.60	0.0714	1418	46050	17420	18.65	272320	0.00655
4	19.68	0.0729	1433	46500	17700	19.00	282129	0.00658
7	12.56	0.0713	1116	35200	13610	11.93	137149	0.00718
8	10.04	0.0712	990.0	32150	12020	9.55	97118	0.00687
9	5.96	0.0714	723.6	23500	8750	5.69	42256	0.00765
10	3.51	0.0727	561.6	18210	6890	3.40	19666	0.00764
11	3.45	0.0716	558.0	18100	6775	3.30	18915	0.00748
12	3.45	0.0723	547.2	17780	6550	3.24	18731	0.00783
13	3.39	0.0695	540.0	17520	6410	3.14	17459	0.00762
14	3.41	0.0687	532.8	17280	6280	3.13	17129	0.00779
17	10.23	0.0728	1019	33050	12500	9.96	104143	0.00677
18	5.92	0.0711	756.0	24600	9260	5.78	43668	0.00690
19	3.54	0.0704	565.2	18370	6880	3.44	19330	0.00733
20	1.84	0.0712	392.4	12710	4760	1.80	7055	0.00805
21	9.80	0.0729	993.6	32200	12200	9.56	97412	0.00684
22	3.36	0.0734	554.4	18000	6810	3.28	18763	0.00756
23	1.79	0.0729	381.6	12390	4680	1.75	6833	0.00844
24	9.82	0.0696	982.8	31900	11980	9.47	92180	0.00669
25	1.24	0.0701	302.0	9790	3590	1.11	3602	0.00900
26	0.57	0.0676	174.2	5650	2020	0.51	921	0.01198

TABLE 5 (Continued) CORRELATION DATA

Run no.	Inlet air, deg F	Heat flux (Q_e/A_b) , Btu/(hr) (sq ft)	Δt_m , deg F	U , Over-all coefficient	h_s , Surface coefficient	$U(\Delta t_p)^{0.18}$	$\frac{h}{CG} (NPr)^{1/2} (\Delta t_p)^{0.18}$	$\frac{h}{C} (\Delta t_p)^{0.18}$
1	80.6	19210	42.9	449	38.3	413	0.00249	137.60
2	75.4	24560	54.4	451	38.3	424	0.00257	142.9
3	74.0	14120	29.8	474	41.8	420	0.00252	141.74
4	73.3	9110	17.7	516	48.1	434	0.00264	150.04
7	80.6	12290	28.6	429	36.6	378	0.00286	123.28
8	82.6	11720	29.2	400	32.3	354	0.00277	109.12
9	81.3	12710	36.2	350	26.4	316	0.00321	92.34
10	79.0	5040	15.0	337	24.9	279	0.00341	75.93
11	80.0	7800	24.4	320	20.6	278	0.00306	67.64
12	82.4	13900	48.4	287	20.0	267	0.00337	73.25
13	81.1	19570	72.5	269	18.3	260	0.00335	71.84
14	78.6	25680	97.9	262	17.4	261	0.00339	71.66
17	78.4	4990	11.2	445	38.0	358	0.00272	110.09
18	78.6	4940	13.3	372	28.9	304	0.00286	86.11
19	82.2	4950	15.2	325	23.9	269	0.00324	72.78
20	77.9	4810	17.1	281	19.4	235	0.00389	60.44
21	76.6	4770	10.5	455	38.4	363	0.00279	110.14
22	75.6	4850	15.1	321	23.5	266	0.00324	71.47
23	74.5	4850	18.1	265	17.9	223	0.00370	56.06
24	79.9	12970	31.8	408	33.3	370	0.00292	114.01
25	72.9	13800	62.0	215	13.2	205	0.00424	50.74
26	71.6	13230	78.0	170	10.1	166	0.00583	40.27

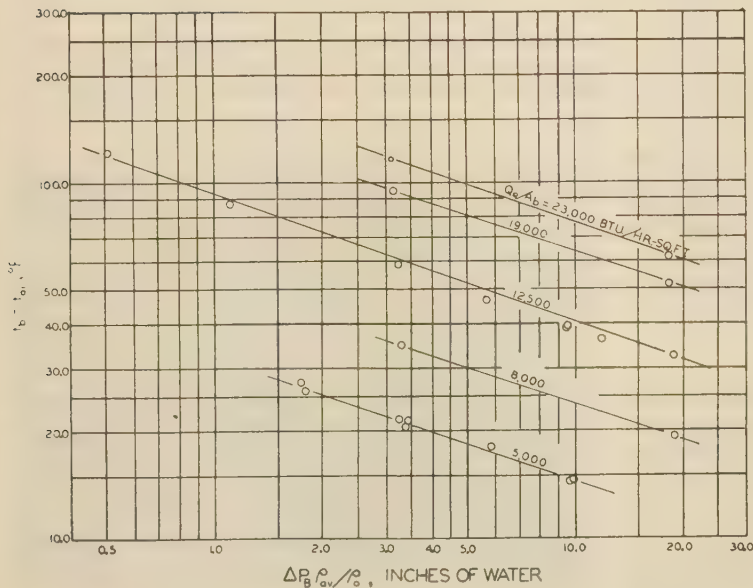


FIG. 6 RELATION OF AVERAGE METAL TEMPERATURE, BAFFLE PRESSURE DROP, AND HEAT FLUX

The so-called "local" values of the unit over-all conductance U_x were calculated on the basis of an assumed uniform heat flux to all sectors of the cylinder and the actual measured fin-base temperature distribution. These local values apply at the various angular positions. Assuming a linear temperature rise of the air through the fin passages, these data then allow the local fin-root-to-air temperature difference to be established, from which the local U_x follows. Fig. 4 then yields the corresponding value of h_x . The values of h_x are average values across the radius of the fin for various angular positions.

The remaining calculations need no further explanation. Complete details are summarized in Tables 3, 4, and 5.

OBSERVED RESULTS

Maximum and Average Base Temperatures. The variation of the maximum (rearmost in these tests) and average temperatures of the fin-base cylindrical section is represented in Figs. 5 and 6, as a function of the over-all static pressure drop across the test section, with the base heat flux as a parameter. The state of

the inlet air is, in this instance, taken into account through the definition of the co-ordinates, that is, the metal temperatures are represented as differences with respect to the initial air temperature, and the air density is included in the adjustment of the pressure drop to standard density by means of the ratio of the average density to the "standard" value chosen. The points as plotted are adjusted to "smoothed" values of heat flux according to the assumption that temperature difference is proportional to heat flux. These curves illustrate the familiar condition of decreasing return, in the form of metal-temperature reduction, as the air-flow rate is increased with the heat-dissipation rate remaining fixed.

Demonstration of Effect of Baffles on Temperature Distribution. In order to illustrate the need for baffles around a finned cylinder of the dimensions tested, if the temperature distribution is to be kept within bounds, reference is made to Fig. 8. Comparative base-temperature distributions are presented for baffled and unbaffled cylinders for a fixed air-inlet temperature and with the over-all heat-dissipation rate being nearly the same. These patterns demonstrate that the air simply will not flow properly around and in-between the relatively deep fins on the rear of the test cylinder without the guiding influence of baffles.

Relation Between Air-Flow Rate and Over-All Static Pressure Drop. While it is the mass flow of air which accomplishes the transfer of heat, it is the over-all total pressure drop which repre-

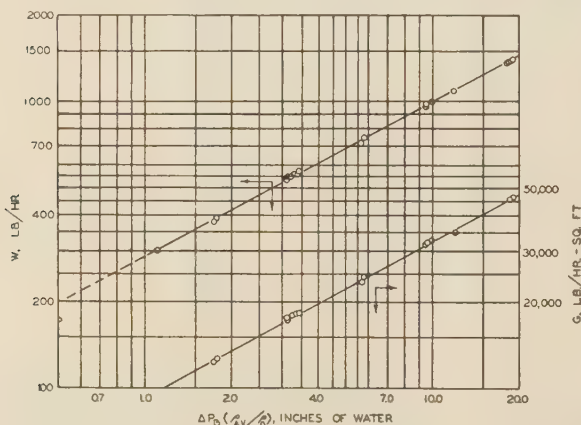


FIG. 7 RELATION BETWEEN AIR-FLOW RATE AND BAFFLE PRESSURE DROP

sents the flow-energy "potential" which must exist in order to cause the flow of air. For these tests the total and static pressure drops are essentially the same. The relation between the flow rate and the static pressure drop thus becomes an important step in establishing or predicting performance. Fig. 7 presents these data on an over-all basis for the test system. The mass velocity through the fin passages is also included because of its fundamental role in characterizing the heat-transfer and flow processes in the fluid stream.

This treatment of the data implies an effective constant density for the air stream at the average temperature and pressure across the test cylinder. It is fully recognized that this approximation has a limited range of validity, and that density variations and component flow losses entering, through, and leaving the fin passages need to be considered in this problem.

Visual Flow Pattern. Before taking up the fundamental correlations, it will be helpful to consider the behavior of the flow stream with respect to the flow problems relating to the temperature patterns presented.

Figs. 9 and 10 present typical flow patterns obtained in a

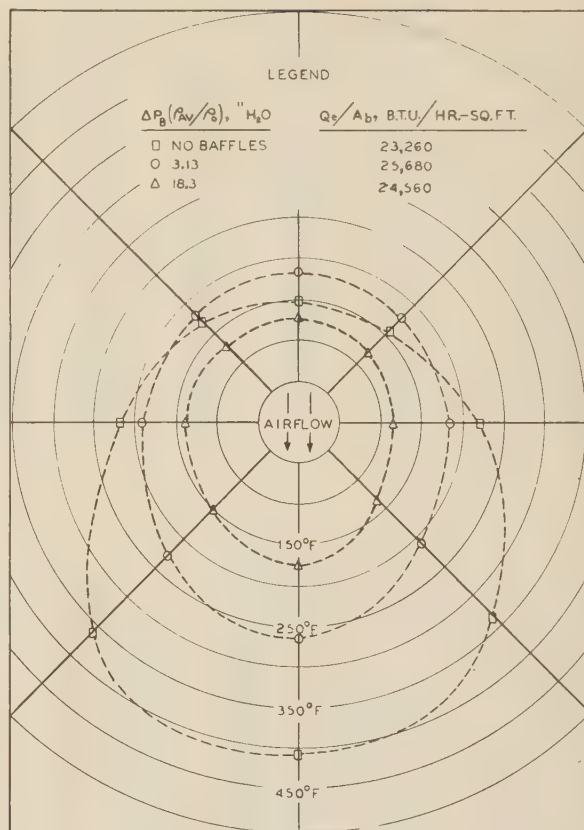


FIG. 8 EFFECT OF BAFFLES ON METAL TEMPERATURES

special visual apparatus with a full-scale installation of a section of the test cylinder. A slurry of aluminum powder in water is employed as the photogenic flow medium. Similarity to the air-flow case is characterized by maintaining comparable magnitudes of the Reynolds number in the fin flow passages.

By comparing the two illustrations, representative of high and low flow rates, it may be observed that no noticeable discontinuities of flow behavior need be expected within the range covered. The difference between water, behaving as an incompressible

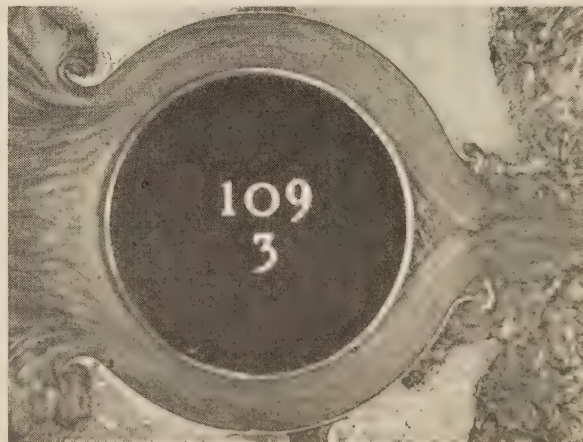


FIG. 9 VISUAL-FLOW PATTERN, REYNOLDS NUMBER OF 3550

fluid, and air, a compressible fluid, is recognized; but this is no handicap for qualitative purposes in the range of air tests covered.

A careful study of the flow pattern will show up such details of interest as: (a) Flow around the entrance lip of the baffle with some separation to be noted; (b) partial stagnation and turning of the flow approaching the cylinder "head-on;" (c) traces of the secondary radial-flow component as the flow develops within the curved passage covered by the baffle; (d) abrupt separation of the flow from the base cylinder near the end of the baffle coverage; (e) the large eddy-stagnant area over the rear of the fins; (f) interaction of the two jets behind the cylinder; and (g) eddy dissipation in the section of abrupt fluid shear as the jet passes through the downstream region of "still" fluid to lose eventually its excess of directed kinetic energy.

Since an effective transfer of heat from a surface by a fluid stream requires a clean and rapid "sweeping" of the surface at all points, the nature of these visual flow patterns would indicate that the finned surfaces of the test cylinder are subjected to particularly unfavorable heat-transfer conditions within the eddy-separation zone over the rear, and to a lesser extent in the stagnation region over the front. These unfavorable conditions are accompanied by related undesirable distortions of the temperature distribution.

FUNDAMENTAL HEAT-TRANSFER AND FLOW CORRELATIONS

Mean Unit Over-All Conductance and Its Variation With Air-Flow Rate and Heat Flux. The mean unit over-all conductance, as calculated in these studies, covers many component influences of local conditions. The approach employed here need not be accepted as final, particularly in regard to the definition of the effective over-all mean temperature difference which has been invoked. The over-all arithmetic mean implies that the cylinder-base temperature is either constant or of linear variation from front to rear, that the rate of heat gain by the cooling air stream is the same for each unit of the circumference swept over from front to rear, that the fin effectiveness has the same value at all points about the cylinder, and that there is no radial variation of air temperature at any point around the cylinder. It is to be recognized that these conditions may be met only to various degrees of approximation in the actual cylinder assembly.

Without more detailed experimentation, it is possible to establish the effect of these approximations only indirectly through calculations and cross-checks of the data correlations. To begin with, under the idealizing postulates the mean over-all conductance would be desired to be a function of the air-flow

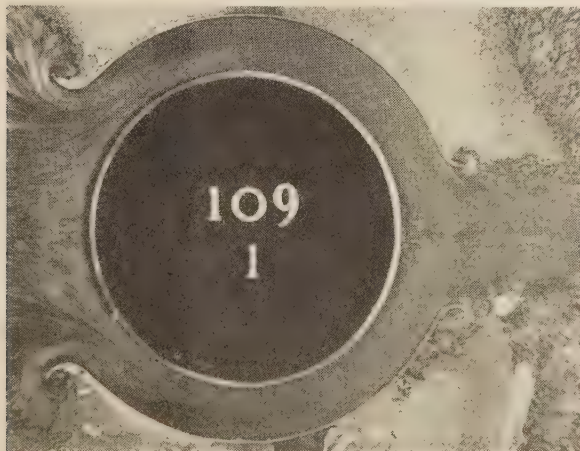


FIG. 10 VISUAL-FLOW PATTERN, REYNOLDS NUMBER OF 13,820

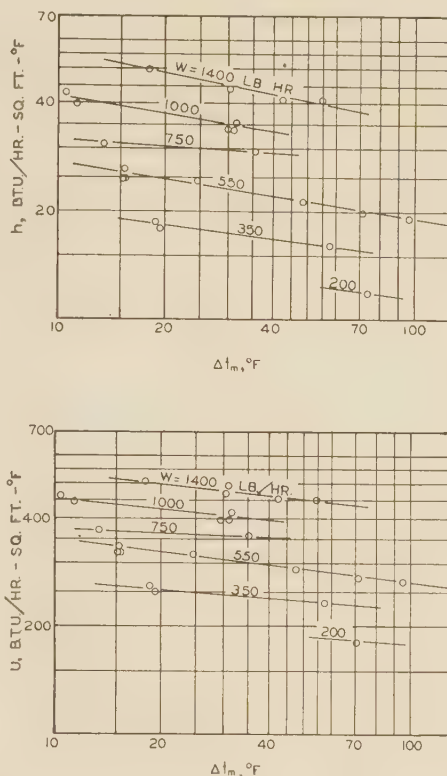


FIG. 11 VARIATION OF HEAT-TRANSFER COEFFICIENT WITH MEAN TEMPERATURE DIFFERENCE

rate and fluid properties only. This thought was investigated through the checking of data obtained at constant heat dissipation and varying air flow by cross-runs at constant air flow and varying heat dissipation. It was determined in this way that the mean over-all conductance, as defined, was a function of both the air-flow and heat-dissipation rates, the fluid properties remaining essentially constant.

Fortunately, the influence of the heat-transfer rate on the over-all conductance was found to be small. It was decided to represent this influence empirically as a correcting function of the mean temperature difference raised to some power, which was found to be -0.10 for these tests. Fig. 11 shows the data on which this observation is based. Thus in all correlations involving the over-all conductance as a function of the air-flow rate, it is necessary to remove the scatter occasioned by different heat-dissipation rates by plotting not the conductance U , alone, but the product $U(\Delta t_m / \Delta t_0)^{0.10}$. The factor Δt_0 is an arbitrary constant reference temperature difference, taken as 100 F. Fig. 12 shows the corrected mean unit over-all conductance represented as a function of the mass velocity in the fin spaces for the test conditions. This unusual effect of temperature difference in turbulent flow points to new factors involved in this type of apparatus. These are believed to include the effects of non-uniformity of flow and temperature in the fin spaces.

Calculated Mean Unit Surface Conductance and Its Variation With Air Flow and Heat Flux. Next, turning to the mean unit surface conductance h , it is expected that similar approximations apply, particularly since the surface conductance is calculated analytically from the over-all conductance. But since the relation between the mean over-all and surface conductance is not one of direct proportionality, the resultant effect would be of a

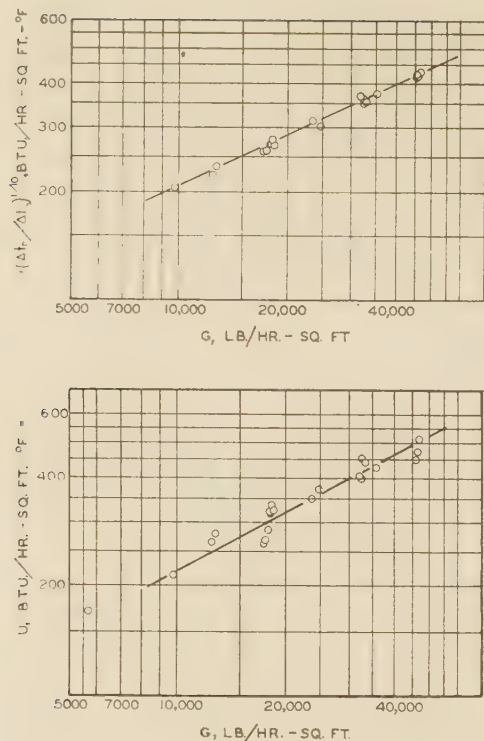


FIG. 12 OVER-ALL HEAT-TRANSFER COEFFICIENT VERSUS MASS VELOCITY

slightly different magnitude in the two cases. In Fig. 11 the same empirical approach is shown, establishing the mean unit surface conductance to be proportional to the -0.16 power of the over-all mean temperature difference employed.

Before discussing the correlation of this calculated conductance, it may be well to consider more closely the method and inherent limitations of its determination. The Harper and Brown (5) procedure is judged to be the most satisfactory analytical means currently available for relating the over-all and surface conductances. But the present data have the limitation of dealing only with mean values. Mean values offer difficulties of generalized extrapolation for systems which are not dominated by fully developed flow and thermal fields. The finned-and-baffled-cylinder studies have flow and thermal fields which are strongly influenced by upstream and entrance-flow conditions, passage curvature, variations in fin-surface temperature, flow separation, and stream interaction at the exit. Large variations locally in the unit surface conductance would be expected under these conditions, so that any mean value would be unfair to the best local performance and overly favorable to the poorest local performance. Preliminary results of analyses dealing with the calculation of local radius-mean conductances will be reported in this paper to support the fundamental inadequacy of over-all mean data.

The mean unit surface conductances inferred from the over-all data, and corrected for the effect of heat flux, are presented in Fig. 13 as a correlation of $N_{St}N_{Pr}^{1/4}(\Delta t_m/\Delta t_0)^{0.16}$ versus N_{Re} . The choice of $\Delta t_0 = 100$ F is seen to make the data correspond with the accepted function for straight passages at a Reynolds number of approximately 4000. Since experimental values of Δt_m varied from 10 F to 98 F, this empirical correction has had the effect of lowering very slightly the test points from the uncorrected level.

These data serve to demonstrate that the mean heat-transfer

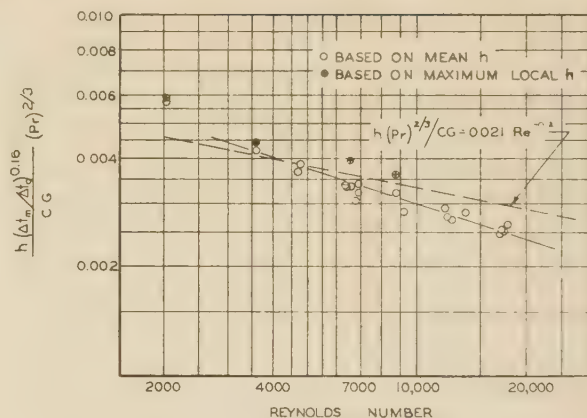


FIG. 13 HEAT TRANSFER FROM A BAFFLED-FINNED CYLINDER COMPARED WITH FLOW INSIDE TUBES

characteristic of the fin passages is similar to that of straight passages, but that at the same time there are differences which are too apparent to be overlooked. An effort was made to explore the possible effect of employing a local surface conductance instead of the over-all mean. Through a procedure to be indicated subsequently, the maximum local surface conductance was estimated for the four representative points shown in Fig. 13. It is seen that these maximum points are more in line with the accepted data for straight passages, so the trend shown by the mean values may be partially explained in terms of the unit surface-conductance distribution being variable with flow conditions.

Relation Between Maximum Unit Surface Conductance and Over-All Power Loss per Unit of Surface Area. Fig. 14 shows the calculated maximum unit surface heat-transfer conductance which occurs at point about halfway through the baffles, as a function of the over-all unit power loss. The comparison of these data with data for heat transfer for flow inside tubes is favorable, which indicates that on the basis of heat transfer from the finned surfaces inside the baffles, no great improvement of the maximum transfer can be expected from subsequent design changes unless some special effects are invoked.

Since the mean-temperature difference is evaluated as a radial mean and is not the over-all circumferential mean, there is not believed to be necessity for the temperature-difference correction which has been shown necessary for the over-all case.

Over-All Pressure-Loss Coefficient. A measure of the extent to which over-all flow losses in the assembly tested were found to exceed those which would occur for isothermal flow through straight tubes (6) is indicated in Fig. 15. As indicated previously, in Equations [4] and [5], the over-all static pressure-drop data have been reduced by an equation equivalent to that defining the friction factor, to establish the "over-all pressure-loss coefficient." By comparing these magnitudes with the accepted friction-factor data for tubes, it becomes immediately apparent that the effects of entrance, internal curvature-induced, frictional, eddying, and separation losses, and the poor flow conditions at the exit are of considerable magnitude.

It may generally be remarked at this juncture that test runs with the fin-passage Reynolds number extending down to about 1000 showed no tendency in the over-all loss to pass through the "dip" region of the friction factor in the transition between laminar and turbulent flow. This indicates that the fin-passage flow is too far under the influence of entrance, exit, and curvature conditions to allow the normal development of true laminar-flow behavior in this test range.

Calculated Local Magnitudes of Unit Surface Conductance. The

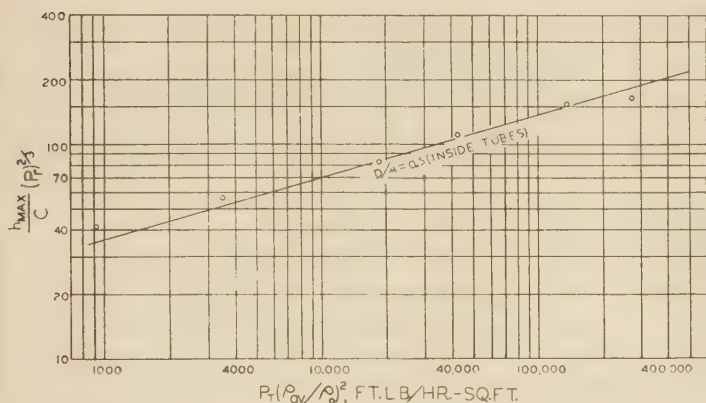


FIG. 14 HEAT TRANSFER AS A FUNCTION OF POWER LOSS PER UNIT SURFACE AREA; COMPARISON OF A BAFFLED-FINNED CYLINDER WITH FLOW INSIDE TUBES

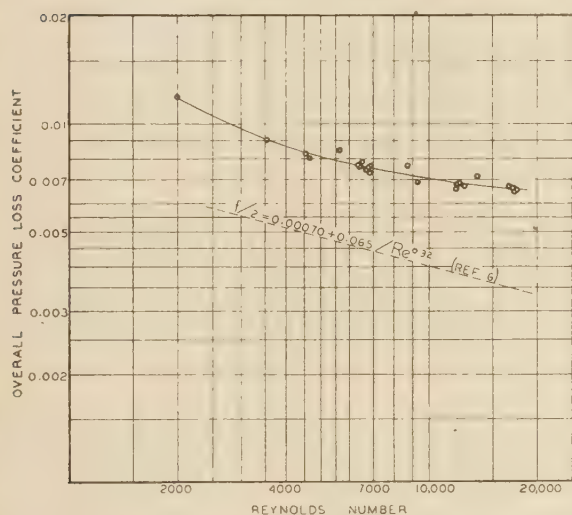


FIG. 15 OVER-ALL PRESSURE-LOSS COEFFICIENT; COMPARISON WITH FRICTION FACTOR FOR FLOW INSIDE TUBES

uniform nature of the electrical heating employed in these tests permits calculations to be made of the local surface conductance for the fins, under the assumption that the rate of heat transfer per unit of circumferential angle is constant around the cylinder. This calls for a linear variation of mean cooling-air temperature from the front to the rear of the cylinder. Then, having the fin-base temperature from direct experimental data, local unit over-all conductances U may be calculated for different positions around the cylinder. From the pattern of these over-all conductances around the cylinder the corresponding local unit surface conductances may be determined according to procedure established for relating U and h , indicated in Fig. 4. The surface conductance thus established is a mean over a radial sector of the fins.

For precise results calculation of circumferential heat conduction would have to be considered. Preliminary estimations indicate that the proportion of such heat flow is small. Consideration of such conduction would result in even lower values of h at the rear of the cylinder.

An example of the air and fin-root metal-temperature distributions for a representative run is shown in Fig. 16. The metal temperatures represent averages from both sides of the cylinder. Fig. 17 presents the distribution of unit over-all conductances for four values of the fin-passage Reynolds number, where the

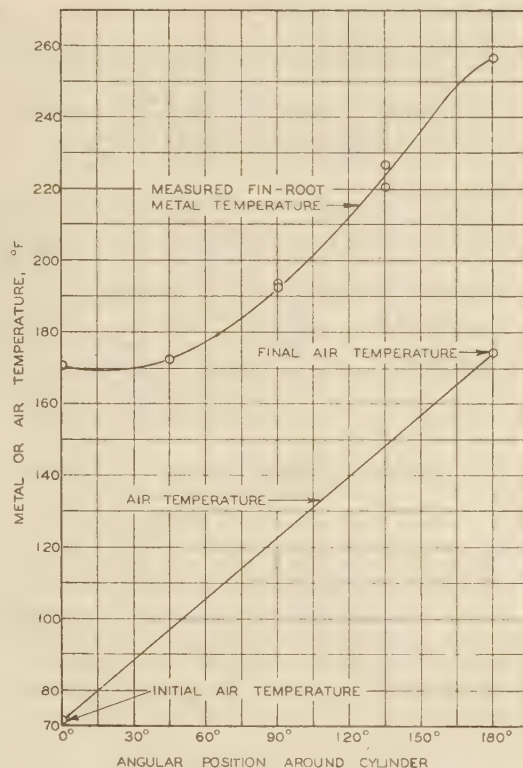


FIG. 16 POINT-TO-POINT TEMPERATURE DISTRIBUTION, RUN 26, $N_{Re} = 2020$

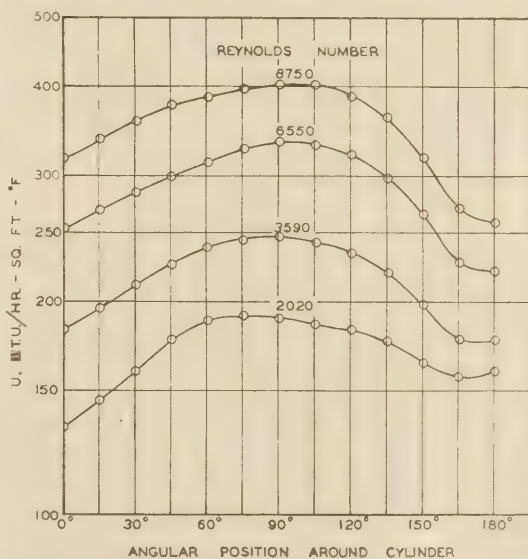


FIG. 17 LOCAL OVER-ALL HEAT-TRANSFER COEFFICIENTS, RUNS 9, 12, 25, AND 26

maximum conductances are observed to range from 30 to 50 per cent above the minimum values. The nature of these variations is quite in accord with the pattern of the flow stream about the cylinder. Corresponding magnitudes of the unit surface conductance are shown in Fig. 18.

In due fairness to the performance of the fin surfaces it is again to be pointed out that the conductances are quite favorably

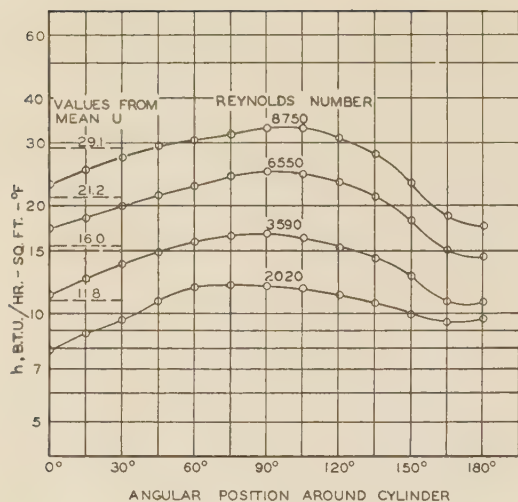


FIG. 18 LOCAL SURFACE HEAT-TRANSFER COEFFICIENTS

high where the flow stream is enclosed by the baffles; and that where the conductances are shown to be low over the unbaffled portions, then the effective Reynolds number for the flow stream in these regions is also low, due to the fact that here the full stream is not passing circumferentially between the fins. A complete adjustment of the data in terms of actual local conditions can be made only with the aid of properly detailed point-to-point experimental studies.

The mean unit surface conductances as previously calculated from the mean unit over-all conductances are also shown in Fig. 18 for reference. The maximum conductances from these curves are those representing the four corresponding points in the general correlation of Fig. 13. These maximum points have been previously noted as representing slightly better performance than the accepted data for straight tubes. It is observed that the angular position of the maximum conductance increases with increasing flow rate, presumably serving as an indication of the influence of the entrance- and exit-flow effects upon the development of the flow within the covered passages.

CONCLUSIONS

- 1 Heat transfer from a finned-and-baffled cylinder of the proportions tested has been found to be generally similar to the behavior of a heat exchanger composed of a set of parallel passages.
- 2 The local patterns of metal temperatures and flow conditions have been emphasized as governing the resultant heat-transfer processes in the fin system.
- 3 The over-all rate of energy loss in the flow stream has been pointed out to be considerably higher than that for frictional dissipation in straight smooth passages, due primarily to the influence of entrance and exit conditions.
- 4 Possible applications of the data obtained to performance problems in engine-cylinder cooling may be developed.

BIBLIOGRAPHY

- 1 "Fluid Meters, Their Theory and Application," by A.S.M.E. Special Research Committee on Fluid Meters, fourth edition, parts 1 and 3, 1937.
- 2 "Heat Transfer From Finned Metal Cylinders in an Air Stream," by Arnold E. Biermann and Benjamin Pinkel, N.A.C.A. Technical Report No. 488, 1934.
- 3 "Heat Transfer by Natural and Forced Convection," by Allan P. Colburn, Purdue University, vol. 26, January, 1942, p. 50.
- 4 "Surface Heat-Transfer Coefficients of Finned Cylinders," by Herman H. Ellerbrock, Jr., and Arnold E. Biermann, N.A.C.A. Technical Report, No. 676, 1939.

5 "Mathematical Equations for Heat Conduction in the Fins of Air-Cooled Engines," by D. R. Harper and W. B. Brown, N.A.C.A. Technical Report No. 158, 1922.

6 "Heat Transmission," by William H. McAdams, McGraw-Hill Book Company, Inc., New York, N. Y., second edition, 1942, p. 119.

7 "Blower Cooling of Finned Cylinders," by Oscar W. Schey and Herman H. Ellerbrock, Jr., N.A.C.A. Technical Report No. 587, 1937.

8 "The Effect of Baffles on the Temperature Distribution and Heat-Transfer Coefficients of Finned Cylinders," by Oscar W. Schey and Vern G. Rollin, N.A.C.A. Technical Report No. 511, 1935.

Discussion

C. M. ASHLEY.⁵ Comments have been made concerning the radial movement of elements of the stream flowing between the fins. The writer believes that this radial movement can be explained by considering the fact that the circumferential movement of the stream in the fin passage constitutes in essence, a portion of a vortex. With initially uniform pressure for all parts of the stream, the velocity of that portion of the stream flowing at the outer portion of the fin will be lower than that flowing at the inner portion with correspondingly higher static pressure. Next to the fin, however, the fluid friction slows down the circumferential velocity, thus permitting the difference of pressure between the inner and outer portions of the fin to become effective, and resulting in an inward flow of fluid along the surface of the fins. In order to balance this there must be an equal outward flow in the main portion of the stream.

G. K. BERNHARDT.⁶ The authors have made a valuable contribution to those concerned with heat transfer from finned surfaces. This paper did not mention how the authors treated the radiation effects. Although these effects should be small, the writer would appreciate a discussion of how they accounted for the radiation between the fin surfaces and from the barrel portion of their muff.

F. A. MCCLINTOCK.⁷ In calculating the local surface conductance, the authors assumed that "the rate of heat transfer per unit of circumferential angle is constant around the cylinder." This assumption seems valid enough for the heat flow to the inside of the muff when radiant heat is used, but if there is a circumferential flow of heat, the flow from the outside of the muff will not be constant around the cylinder. The presence of a circumferential temperature gradient indicates that there must be some circumferential heat flow. The following analysis shows that, for the authors' tests, the local surface conductances are markedly in error because the circumferential flow was neglected, and that an appreciable amount of the heat flow to the rear of the cylinder was carried away by conduction along the walls:

The cylinder height is designated by L and the other symbols are as shown in Fig. 19 of this discussion. Term q is defined as the rate of heat flow per unit area. The mean temperature of the wall T and the rate of heat flow to the inside wall $2\pi r_0 L q_0$ are known. Each side of the cylinder is cooled by the flow of air $W/2$, whose specific heat C_p and initial temperature T_i are known.

For steady-state conditions, the heat efflux from any given section must equal the influx, as follows

$$q_1 r_1 L \Delta \theta + (q_0 + \Delta q_0) L = q_0 r_0 L \Delta \theta + q \theta L \dots [7]$$

By rearranging

⁵ Director of Development, Carrier Corporation, Syracuse, N. Y.

⁶ Experimental Test Engineer, Pratt & Whitney Aircraft, East Hartford, Conn. Jun. A.S.M.E.

⁷ Research Division, United Aircraft Corporation, East Hartford, Conn. Jun. A.S.M.E.

$$\frac{q_{r1}r_1}{q_{r0}r_0} = 1 - \frac{\Delta q_{\theta}t}{\Delta\theta} \dots\dots\dots [7a]$$

The rate of circumferential flow per unit area q_{θ} is equal to the negative of the thermal conductivity of the wall times the temperature gradient

$$q_{\theta} = -k \frac{dT}{r d\theta} \quad \text{and} \quad \Delta q_{\theta} = -k \Delta \frac{dT}{r d\theta} \dots\dots\dots [8]$$

If the temperature gradient is constant from r_0 to r_1 , Equations [7a] and [8] can be combined as follows

$$\frac{q_{r1}r_1}{q_{r0}r_0} = 1 + \frac{kt}{q_{r0}r_0\sigma_m} \frac{\Delta}{\Delta\theta} \left(\frac{dT}{d\theta} \right) \dots\dots\dots [9]$$

where r_m is the log mean radius of a radial section.

As $\Delta\theta$ approaches zero, Equation [9] becomes

$$\frac{q_{r1}r_1}{q_{r0}r_0} = 1 + \frac{kt}{q_{r0}r_0\sigma_m} \frac{d^2T}{d\theta^2} \dots\dots\dots [9a]$$

The term $\frac{q_{r1}r_1}{q_{r0}r_0}$ is unity when the heat flow to the inner wall is equal to that from the outer wall. Therefore the term $\frac{kt}{q_{r0}r_0\sigma_m} \frac{d^2T}{d\theta^2}$ denotes the ratio of net circumferential flow to radial inflow at any section.

Exact evaluation of the terms is difficult for two reasons: (a) The second derivative of temperature with respect to angular position $\frac{d^2T}{d\theta^2}$, depends to a large extent on how the temperature-angle curve is faired. (b) The temperatures and hence the circumferential gradients in the fins are less than those in the base metal, so that if the thickness t includes the fins, the estimated circumferential flow is too high.

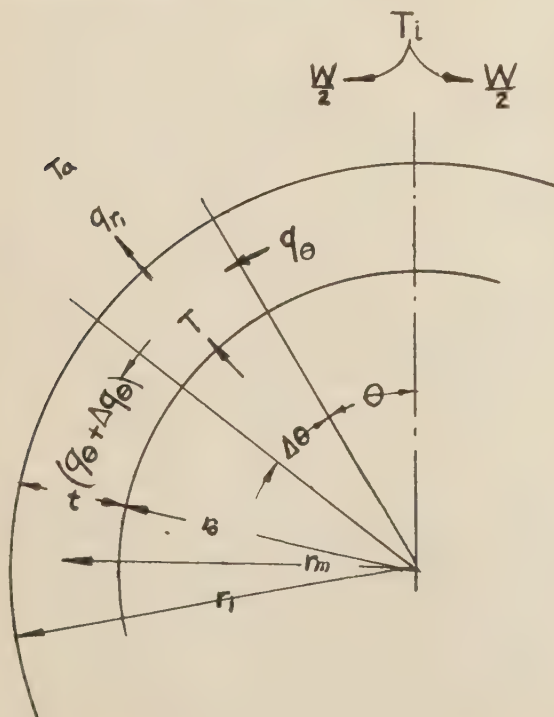


FIG. 19

The run plotted in the authors' Fig. 16, and shown as $R_s = 2020$ in Figs. 17 and 18, is taken as an example. A trigonometric series was fitted to the mean temperatures at the five points, with the condition that the slope was zero at the front and rear of the cylinder. This condition must be satisfied if the second derivative is to be finite at those points. The resulting second derivative was $-151 \text{ deg F/radian}^2$. A power series fitting the same points and conditions gave a second derivative of $-464 \text{ deg F/radian}^2$. If a curve is chosen so that the second derivative is constant between the 135-deg point and the rear of the cylinder, the second derivative has the least possible magnitude, which turns out to be $-108 \text{ deg F/radian}^2$. The trigonometric series is used here because it seems to give the most reasonable result, namely, $-151 \text{ deg F/radian}^2$. The full cross-sectional area of the fins was used in calculating the thickness t , and the log-mean radius r_m . The following values are used in solving Equation [3a] for the circumferential flow:

$$\begin{aligned} k &= 100 \text{ Btu hr}^{-1} \text{ ft}^{-1} \text{ deg F}^{-1} & r_1 &= 0.2578 \text{ ft} \\ q_{r0} &= 13,460 \text{ Btu hr}^{-1} \text{ ft}^{-2} & r_m &= 0.283 \text{ ft} \\ r_0 &= 0.250 \text{ ft} & t &= 0.0275 \text{ ft} \end{aligned}$$

$$\text{Hence } \frac{\text{Circumferential flow}}{\text{Inflow}} = \frac{kt}{q_{r0}r_0\sigma_m} \frac{d^2T}{d\theta^2} = 0.44$$

Because of the assumptions, the ratio may be less, but it is almost certainly over 20 per cent. At other locations on the muff it is even harder to estimate the second derivative accurately, but it may be as much as one third of that at the rear, with resulting circumferential flows of 5 to 10 per cent. Therefore the plot of local surface conductance, Fig. 18 of the paper, may be significantly distorted, especially at the rear of the cylinder. More data would be necessary to determine the actual shape of the surface-conductance plot to see if the surface conductance may be practically constant in the baffled region. In cylinder heads, where the wall thickness is greater, metal conduction may well account for the major part of the cooling.

Circumferential heat flow also makes the air-temperature rise deviate somewhat from a straight line. The air temperature can be calculated as follows

$$T_a = T_i + \int_0^{\theta} \frac{q_{r1}L d\theta}{W/2 C_p} \dots\dots\dots [10]$$

Substituting for q_{r1} from Equation [9a]

$$T_a = T_i + \frac{q_{r0}r_0L\theta}{W/2 C_p} + \frac{ktL}{W/2 C_p r_m} \frac{dT}{d\theta} \dots\dots\dots [11]$$

The last term gives the deviation from a straight-line function, which in this case does not exceed 5 deg F.

R. G. VANDERWEIL.⁸ The illustrations showing the flow characteristics through the baffled fins were taken from water-flow patterns. Were any provisions made to guarantee that this water pattern is actually the same as the pattern resulting by the use of air? If such provisions were made, how did the Reynolds number of the water flow compare with the Reynolds number of the actual air flow?

W. R. WYKOFF.⁹ The authors deserve credit for attempting to break these data down into local heat-transfer functions. It is apparent to those who have attempted to predict cooling performance with data for the type of finned cylinders involved, that over-all data are very restricted as to extrapolation to other

⁸ Office of Consulting Engineer, Chase Brass & Copper Co., Waterbury, Conn.

⁹ Experimental Test Engineer, Pratt & Whitney Aircraft, East Hartford, Conn. Jun. A.S.M.E.

than the original test conditions. It appears necessary to expand approximate point variable analyses of this type, including both component pressure-loss and heat-transfer functions, in order to predict effectively the performance of fin passages over the maximum attained operating range.

The authors have pointed out that over the un baffled portions at the front and rear of the muff, the full air stream does not pass circumferentially between the fins. Also, they have used the mean stream temperature for computing local heat-transfer coefficients in these front and rear regions, as well as in the baffled section. It would appear from observation of the flow patterns, that a rather large radial-temperature gradient exists in the air stream over the un baffled fins. Thus it is felt that the local coefficients over these exposed sections are only equivalent functions and should be so designated by broken lines in Fig. 18.

In Fig. 14 the authors have plotted a local heat-transfer factor against an over-all power loss. In order to rate fairly the heat-transfer surfaces a local power loss should be used. In the calculations reported, baffle entrance and exit losses, which make up an appreciable component of the over-all loss, are included. If these losses were removed, the experimental points shown would fall slightly above the "tube" line. This can be explained perhaps as an effect of the radial "sweeping" component of flow in the fin passages, as noted by the authors.

Furthermore, in regard to the "mean-temperature difference effect" in Fig. 11, what is the interpretation of this? Presumably, any quantity which is properly designated as a "conductance" should be independent of the potential acting.

AUTHORS' CLOSURE

Even beyond the clarification of incidental details in this paper, the authors are appreciative of the opportunity given by the discussers' comments to speak further concerning the basic interpretation of the results released for publication.

Mr. Ashley's comments on the flow behavior in the fin passages are in accord with the expected effects which were observed in the visual study. Still further evidence has been gained from an enlarged scale model, where pressure and velocity distributions could be obtained.

As to Mr. Bernhardt's question on radiation, no analysis of this has been attempted as yet. Radiation would have a small effect on the fin surface-temperature pattern within the fin spaces, and radiant exchange with the surroundings would enter as a small term in the heat balance. Quantitative investigation remains for the future.

Mr. McClintock has brought forth the question of heat conduction in the circumferential direction, which has been skipped over in the published discussion. For purposes of practical judgment, it is unfortunate that run 26, as analyzed in Fig. 16 according to the approximate method adopted by the authors, was the one at the very lowest air-flow rate. At higher rates of air flow and heat transfer Mr. McClintock's Equation [9a] will yield much lower proportions of circumferential conduction.

There exists some question of how closely the idealized cylindrical-shell system of Fig. 19 may be taken as representing a cooling-fin system. While the discussers' comments mention some uncertainty, indeed, it has been the authors' preference to adopt somewhat different analytical procedures for a quantitative study of how much error is introduced through adoption of the simplest one-dimensional concepts for preliminary and entirely practical purposes. The actual system is three-dimensional in its behavior at any point. An initial experimental study of fin and air temperatures over all radial and circumferential-angle positions has shown very interesting temperature patterns, which at once demonstrate the weakness of one-dimensional simplifications. Ana-

lytical studies in two-dimensional co-ordinates (radial and circumferential) lead to a system of partial-differential equations which are basically significant but solvable only by tedious methods. Some preliminary calculations, however, have demonstrated the fundamental importance of the circumferential conduction component over the un baffled portions of the finned cylinder; but, contrary to the implications of Mr. McClintock's numerical results, these calculations have shown that designs of engine-cylinder fins may generally be made to an accuracy compatible with production and assembly tolerances without allowing for the presence of circumferential conduction. Thus for the time being, such refinements will be developed slowly rather than adopted immediately.

The whole broad question of developing basic design procedures with fin-base circumferential temperature distribution as one of the variables remains for future consideration.

In replying to Mr. Vanderweil, the fin-passage Reynolds numbers, based on the mean velocity, were kept within the same range for the air and water tests. Lampblack patterns have been obtained on the fin surfaces with air flow, and these appear to be the same as for the water tests. The greatest inadequacy of the visual pictures in comparison to the actual system lies in another point. This point is that the fin passage in which the photographs were taken was formed by substituting a sheet of plate glass for a fin. This substitution changed the entrance contraction, the cross-sectional form, and the exit contraction of the topmost passage as compared to the others. Justification resides in the fact that the visual studies were employed for qualitative purposes only.

Mr. Wykoff's comments concerning Fig. 18 are appreciated and agreed with. He is also correct in regard to Fig. 14. Data from other tests have allowed independent determination of the frictional loss within the baffle-enclosed passages, which has been shown to be roughly two thirds of the over-all loss.

Then the "mean-temperature-difference effect" of Fig. 11 comes up for further explanation. The authors offer this as nothing more than an empirical result, obtained from the particular test installation, instrumentation, and procedures of data analysis which were employed in these tests. The so-called "conductances" reported are not to be employed for calculations outside of the range of the test results. These preliminary tests simply did not include sufficient internal measurements within the test specimen to allow a more satisfactory analysis of the data. The demonstrated weaknesses of the over-all treatment may serve as an excellent example of how real systems do not usually behave in accord with simple idealizing postulates. The interpretation of Fig. 11 is therefore that the over-all-mean procedure, as applied to the temperature difference and the conductance U , is basically inadequate. This has been known for several years, but the practical slant follows the reply to Mr. McClintock.

Readers will also recognize that the conductance h has been calculated and not directly measured. This leads to the possibility of a small error in the magnitudes reported; but this is no worse than the use of an over-all mean.

By way of further interest to those concerned with applications to design problems, it is hoped that the eventual removal of wartime restrictions will allow release of the very considerable amount of additional data which have been obtained in other more comprehensive studies. The flow-system design problems, in particular, have been entirely neglected in this paper. Yet in some respects, and particularly for low-density air, the flow-loss design requirements may be more critical than those for the over-all heat transfer.

The combined challenges of obtaining improved basic data and extending application design methods to meet all problems encountered in practice are, however, goals within the grasp of continued effort.

Local Coefficients of Heat Transfer for Air Flowing Around a Finned Cylinder

By W. H. McADAMS,¹ R. E. DREXEL,² AND R. H. GOLDEY³

This paper describes an apparatus for measuring local coefficients of heat transfer, hitherto never obtained for a jacketed or baffled-finned cylinder. The inner surface of the vertical cylinder was divided into narrow vertical segments to collect steam condensate, a measure of the local flux. Since the over-all heat balances agreed within a few per cent, local heat balances were used to calculate local air temperatures. Wall temperatures of the base of each segment were measured by calibrated thermocouples, and local coefficients of heat transfer were determined at 11 stations around one half of the cylinder. The results were easily duplicated and the condensate from the undivided side agreed closely with that from the divided side. Average surface coefficients from fins to air agreed satisfactorily with published data. For a given Reynolds number, temperature difference had no effect on the Stanton number.

NOMENCLATURE

The following nomenclature is used in the paper:

- A = area of total air-cooled heat-transfer surface, 12.6 sq ft
 A_b = area at base of fins, 0.686 sq ft
 A_x = local area at base of fins for 1 segment, 0.0312 sq ft
 a = dimensional term $\sqrt{2h/(kx_m)}$, reciprocal feet, in equation for effectiveness
 C = correction factor in Equation [1] for effectiveness, dimensionless
 C_C = for curvature, Fig. 9
 C_T = for taper, Fig. 9
 c_p = specific heat of air, 0.24 Btu per lb per deg F
 D_e = equivalent diameter of gas passage arbitrarily taken as $D_e = 4sw/2(s+w)$, ft
 e = base of natural logarithms
 f' = over-all friction factor, dimensionless, in Fanning equation:

$$\Delta p = \frac{4f'LG^2}{2g_c D_e \rho}$$

 G = mass velocity, lb air/(hr)(sq ft of cross-sectional area of gas passage 90 deg from front of cylinder)
 h = surface coefficient of heat transfer, from surface of fins to air, Btu/(hr)(sq ft)(deg F difference in temperature), from U and Equation [2]
 h_a = based on arithmetic mean Δt
 h_x = based on local Δt

- h_m = based on logarithmic mean Δt
 k = thermal conductivity of fins, Btu/(hr)(sq ft) (deg F/ft)
 L = nominal length of air travel, arbitrarily taken as $\pi(R_b + 0.5w)$, ft
 q = rate of heat transfer for entire finned cylinder, Btu/hr
 q_x = rate for 1 segment having base area A_x
 R = radius, ft
 R_b = radius at base of fins, ft
 s = mean spacing of adjacent fins, ft
 s_b = fin spacing at base of fins, ft
 s_t = fin spacing at tips of fins, ft
 t = local air temperature, deg F
 t_1 = temperature of entering air, deg F
 t_2 = temperature of exit air, deg F
 t_b = local temperature of base of fins, deg F
 t_{bm} = length-mean temperature
 U = apparent coefficient of heat transfer, $U = q/A(t_b - t)$, Btu/(hr)(sq ft of base area) (deg F, base to air)
 U_m = mean value, from Equations [4] and [5]
 U_x = local value, from Equation [3]
 w = width (radial length) of fin, ft
 $w' = w + 0.5x_t$, ft
 x = thickness of fin, ft
 x_m = mean thickness of fin, ft
 x_t = fin thickness at tip, ft
 Δt = temperature difference, deg F
 Δt_a = arithmetic-mean temperature difference
 Δt_m = logarithmic-mean temperature difference
 η = effectiveness of tapered radial fin, dimensionless, from Equation [1]
 η' = approximate effectiveness, $\tanh aw'/aw'$
 μ = viscosity of air at mean bulk temperature, lb/(hr)(ft), equal to $2.42 \times$ centipoises
 ρ = density of air at mean bulk temperature, pounds/cu ft
 $D_e G/\mu$ = Reynolds number
 $h_m/c_p G$ = Stanton number

INTRODUCTION

The finned cylinders of air-cooled engines are provided with external baffles which jacket a portion of each cylinder and cause the air to flow between the fins. It is known that the cooling of the cylinder may be profoundly influenced by factors such as the extent to which the baffles cover the cylinder, the clearance between the baffles and the tips of the fins, and the shape of the baffle at the air entrance and exit. For the important case where the air velocity through the passages between the fins is known, average coefficients of heat transfer for the entire finned cylinder are reported in the literature, but local coefficients are not available.

The purpose of the present study was to develop an apparatus for measuring the local coefficients of heat transfer around a jacketed or baffled-finned cylinder.

¹ Department of Chemical Engineering, Massachusetts Institute of Technology, Cambridge, Mass.

² Department of Chemical Engineering, Massachusetts Institute of Technology. Present address, E. I. du Pont de Nemours & Company, Wilmington, Del.

³ Department of Chemical Engineering, Massachusetts Institute of Technology. Present address, Hotel Miramar, Miami, Fla.

Contributed by the Heat Transfer Division and presented at the Annual Meeting, New York, N. Y., Nov. 27-Dec. 1, 1944, of THE AMERICAN SOCIETY OF MECHANICAL ENGINEERS.

NOTE: Statements and opinions advanced in papers are to be understood as individual expressions of their authors and not those of the Society.

APPARATUS DEVELOPED IN INVESTIGATION

The apparatus developed in this investigation consisted of a special finned heat-transfer surface constructed so that local heat flux could be measured, a blower to draw air through the test section, a boiler to supply steam, and standard orifices. Fig. 1 is a diagrammatic sketch of the apparatus. The cooling air passed through an entrance fairing and then across the baffled-finned cylinder into a mixer after which the air temperature was

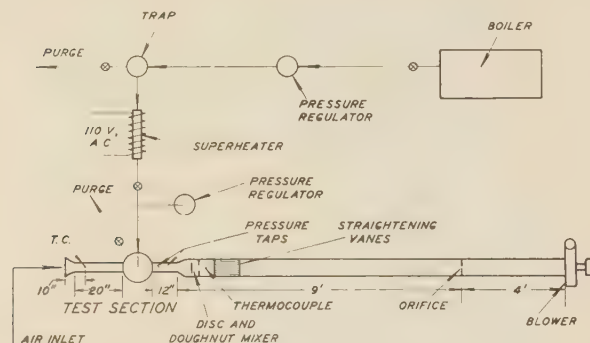


FIG. 1 DIAGRAMMATIC PLAN OF APPARATUS

(Entrance fairing always starts 20 in. from leading edge of fin.)

measured. The ducting between the test section and the mixing section was insulated with hair felt 1 in. thick. After flowing through straightening vanes, the air was metered by a standard orifice and passed to the blower and out to the room. The blower was driven by a 5-hp variable-speed motor.

Steam free from impurities, which would cause dropwise condensation, was generated in a gas-fired boiler at a gage pressure of 15 psi; the pressure was reduced by passing the steam through a regulator. Moisture was removed from the steam in a trap, and the steam was superheated as it passed through an electrically heated section of pipe before entering the test section.

The heat-transfer surface consisted of two aluminum-alloy muffs from an air-cooled airplane engine. The fins of nonuniform

width were machined off and the remainder of the muffs,⁴ Fig. 2, were shrunk onto a vertical steel barrel having the same outside diameter (6.015 in.) as an actual engine cylinder. One side of the barrel was divided into eleven vertical segments, Fig. 3, which collected steam condensate (1).⁵ The equally spaced segments were formed by steel strips silver-soldered into slits cut entirely through the barrel on a milling machine, provided with a dividing head.⁶ A machined ring, Fig. 4, silver-soldered to the division strips and cylinder, collected the condensate which flowed out of the apparatus into 100-cc graduates through $\frac{1}{8}$ -in. copper tubes and U-bends of glass tubing which served as liquid seals.

A cross section of the test section is shown in Fig. 5 and indicates the methods used to prevent heat losses by conduction from both ends of the test section and the precaution taken to collect only the condensate resulting from heat transfer from the finned surface. To prevent heat loss from the top of the test section, the top of the nonfinned portion of the barrel was kept at steam temperature by the steam in the upper chamber made of 8-in. steel pipe. The horizontal glass plate supported by pegs prevented condensate from the top cover from dripping into the collector ring. In the lower steam chamber the condensate lines were bathed in steam to prevent heat losses. The condensate level was kept constant in the drain lines by adjusting the pressure inside the apparatus by means of a needle valve in the inlet steam line and by adjusting the water level in a water seal used as a final pressure regulator. To make certain that conden-

⁴ Each muff had an inside diameter of 5.995 in. and a diameter of 6.188 in. at the base of the fins. Each fin had a width (radial length) of 1.11 in., and the thickness decreased uniformly from 0.040 in. at the base to 0.020 in. at the tip. The center-to-center spacing of fins was 0.141 in.; since the average thickness of each fin was 0.03 in., the average clearance was 0.111 in. The total cross section between the fins was 0.0616 sq ft. The two muffs contained 36 such fins and the total air-cooled surface was 12.6 sq ft. The height of the two muffs was 5.09 in., and the total area at the base of the fins was 0.686 sq ft. Since each segment represents $\frac{1}{22}$ of the total base area, A_2 was 0.0312 sq ft.

⁵ Numbers in parentheses refer to the Bibliography at the end of the paper.

⁶ Drew and Ryan (1) first used this method of measuring local flux and applied it to a bare vertical cylinder placed in the center of a wind tunnel.

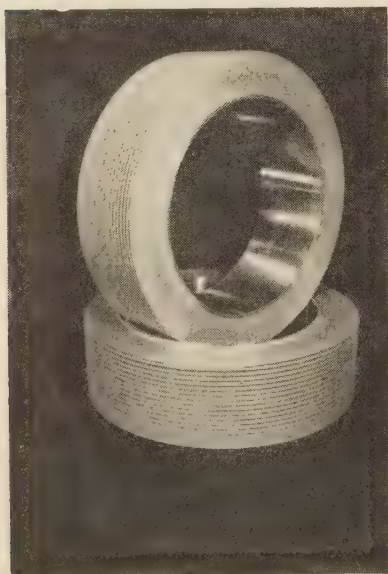


FIG. 2 ALUMINUM-ALLOY MUFFS

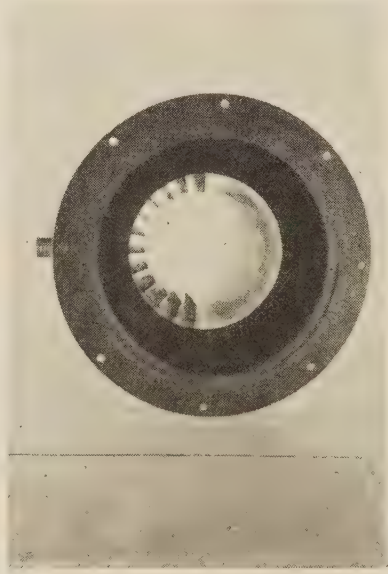


FIG. 3 STEEL BARREL AND DIVISION STRIPS



FIG. 4 COLLECTOR AND DRAINS

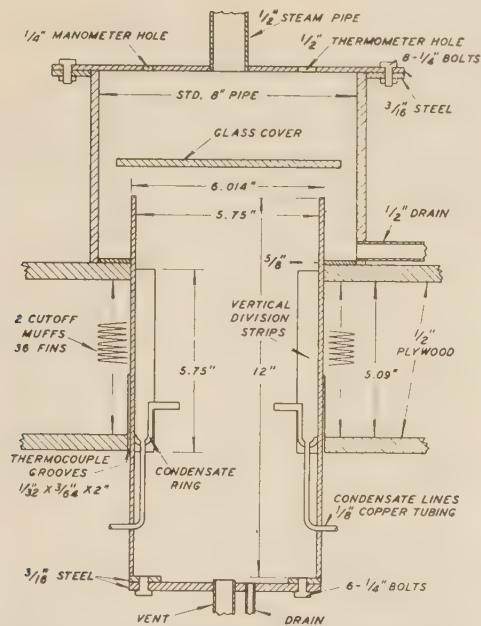


FIG. 5 SECTIONAL ELEVATION OF TEST SECTION

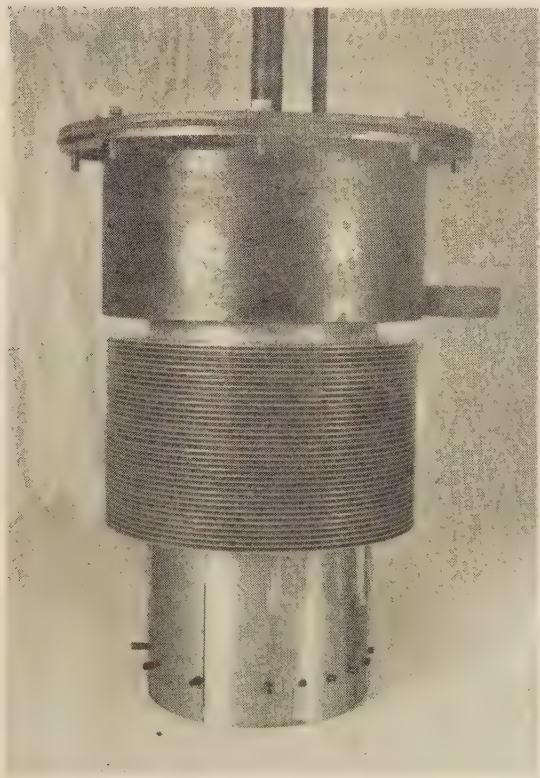


FIG. 6 TEST SECTION WITHOUT JACKET OR BAFFLE
(Air-cooled surface is 12.6 sq ft.)

sate was not overflowing from the collector ring, sight glasses were installed in the top cover of the test section so that frequent observation of the interior of the apparatus could be made; film-type condensation was always obtained. Steam was vented

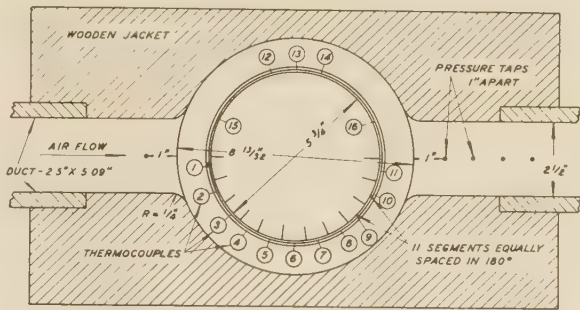


FIG. 7 PLAN VIEW OF TEST SECTION WITH JACKET

(All thermocouples are 2 in. from bottom of lower muff, except No. 12, which is 1/2 in., and No. 14, which is 1 in. Jacket touches tips of fins, and cross-sectional area for air flow is 0.0816 sq ft. Entrance fairing is 5.25 in. long and reduces from a rectangle 7.50 in. wide \times 10 in. high to a rectangle 2.50 in. wide \times 5.09 in. high.)

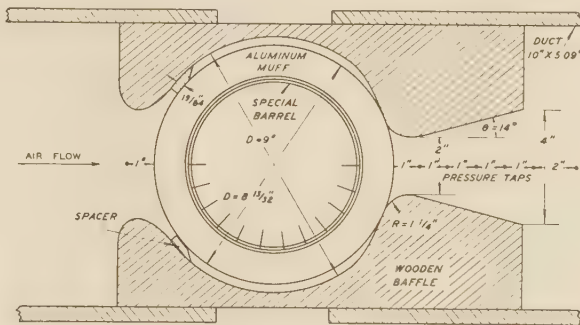


FIG. 8 PLAN VIEW OF TEST SECTION WITH BAFFLE REPLACING JACKET

(Mass velocity of air was arbitrarily based upon total cross-sectional area, 0.0816 sq ft. of air passage, 90 deg from front of cylinder. The entrance fairing is 7 in. long and reduces from a rectangle 16 in. wide \times 11.0 in. high to a rectangle 10 in. wide \times 5.09 in. long.)

from both the upper and lower chambers, to remove noncondensable gases. Fig. 6 shows the test section.

Calibrated thermocouples (No. 30 copper-constantan) were inserted in slots in the base of the bottom muff and cemented in place with "Insalute" cement prior to heating the muffs and shrinking them onto the steel barrel. The thermocouples were connected to a cold junction immersed in an ice bath, and a Leeds and Northrup portable precision potentiometer (Serial No. 347007) by means of a selector switch. A couple was located at the center of each segment 2 in. from the bottom of the lower muff. Thermocouples were also placed in the steel barrel and at different depths in the muff on the undivided side. The locations of thermocouples 1-16 are shown in Fig. 7. Air temperatures were measured by a shielded thermocouple (No. 19) in the inlet stream, by a shielded couple (No. 17) 1 in. behind the trailing edge of the muff, and by a thermocouple (No. 18) after the mixer. Temperatures of the air at the orifice, of the inlet steam, and of the vent steam from the bottom of the apparatus were taken with thermometers.

Static pressures were measured before the test section and before the orifice. Pressure drops across the test section were measured from the pressure tap 1 in. in front of the leading edge of the muff to pressure taps 1, 2, 3, 4, 5, and 7 in., respectively, from the trailing edge of the muff. The pressure drop across the orifice was also measured.

Tests were made with a jacket, Fig. 7, and with a baffle, Fig. 8. To determine whether temperature difference had any effect on the heat-transfer coefficients, the inlet air was preheated in some runs (Series B); heating steam was available at a gage

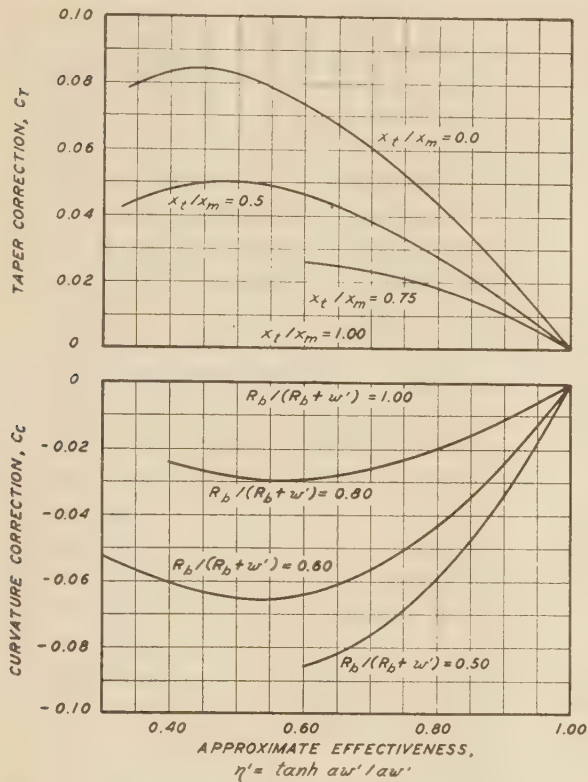


FIG. 9 TAPER AND CURVATURE CORRECTIONS TO BE ADDED TO APPROXIMATE EFFECTIVENESS η' IN OBTAINING TRUE EFFECTIVENESS (Taken from Harper and Brown, reference 3, by courtesy of National Advisory Committee for Aeronautics.)

are combined to give the fin-base temperature. Furthermore, it is known that average surface coefficients, based upon the measured mean temperature of the surface of the fins, often differ from those based upon measured base temperatures and a calculated effectiveness. Consequently, both the correlation of test data and the design procedure based thereon should involve base temperatures and calculated effectiveness, so that any errors due to differences between measured and calculated effectiveness are not involved.

The effectiveness η is defined as the mean temperature difference between the surface of the fins and the air, divided by the temperature difference between the base of the fins and the air, and is given by the following equation for tapered radial fins

$$\eta = \frac{\tanh aw'}{aw'} + C_T + C_C = \eta' + C_T + C_C \dots [1]$$

in which a equals $\sqrt{2h/kx_m}$ and C_T and C_C are corrections for taper and curvature, respectively, taken from Harper and Brown (3) and shown in Fig. 9. It is seen that the effectiveness depends upon the surface coefficient, assumed constant along the radius of the fin, and the dimensions and thermal conductivity of the fin.

The surface coefficient is obtained from the following new equation for tapered radial fins

$$U = \frac{h}{(s + x_m)} \left[\left(2w' + \frac{wx'}{R_b} + \frac{wx_i}{2R_b} \right) \eta + s_b \right] \dots [2]'$$

For a given fin η' , C_T , C_C , and consequently η and U are unique functions of h , and hence a plot of U can be constructed by assuming values of h . The local apparent coefficient U is first calculated from the data by the simple relation

$$U_x = \frac{q_x/A_x}{t_0 - t} \dots [3]$$

and values of h_x are then read directly from the curve of U_x versus h_x , thus avoiding trial-and-error calculations.

RESULTS OF TESTS

All the data for the muff with the jacket or baffle are given in Table 2. Table 3 summarizes calculated values, including average surface coefficients h_m , calculated from

$$U_m = \frac{q/A}{\Delta t_m} \dots [4]$$

based upon the logarithmic-mean apparent temperature difference

$$\Delta t_m = \frac{(t_{bm} - t_1) - (t_{bm} - t_2)}{\ln \frac{t_{bm} - t_1}{t_{bm} - t_2}} \dots [5]$$

LOCAL SURFACE COEFFICIENTS h_x

Runs (Series J) were made at various air-flow rates with the jacket shown in Fig. 7, and similar runs (Series A) were made with the baffle shown in Fig. 8. The results are summarized in Figs. 10 and 11, plotted in terms of local surface coefficients h_x versus the position of the segment; position 0 is at the front and 11 is at the rear. For a given Reynolds number $D_e G/\mu$, for both the jacket and the baffle, the curves of h_x go through a maximum roughly half-way around the cylinder; as the Reynolds number increases, the maximum shifts somewhat nearer the front of the cylinder. For these runs, it is noted that the local surface coefficient of heat transfer from muff to air was always found to be lower in the rear than at the front.⁸

From Figs. 10 and 11 it appears that the local surface coefficients of heat transfer are unduly high for segment 2 (position 1-2) and low for segment 8 (position 7-8). Data for the jacketed cylinder are shown plotted versus location of segment in Fig. 12, which suggests that the contact between the steel barrel and the muff was unusually close in segment 2 and less close in segment 8, which doubtless was caused by high spots on the cement in the grooves on the inner wall of the muff. At segment 8, where the muff temperature and local condensation rate were abnormally low, heat flows circumferentially by conduction in the muff from adjacent segments 7 and 9. If this effect were allowed for, the local coefficients for segments 7 and 9 would decrease and that for 8 would increase, tending to eliminate the dip in the curve of h_x at segment 8.

Tests (Series B) were run on the baffled cylinder to determine the effect of temperature difference on the mean surface coefficient of heat transfer, h_m . The temperature difference was varied by changing the temperature of the inlet air at substantially constant Reynolds number. The data are plotted in Fig.

⁷ Equations [1] and [2] will reduce to the usual approximate equation of reference (4) for a bar fin of constant cross section

$$U = \frac{h}{(s + x_m)} \left[\frac{2}{\alpha} \left(1 + \frac{w}{2R_b} \right) \tanh aw' + s_b \right] \dots [2a]$$

if the sum C_T and C_C is assumed zero and the term $wx_i/2R_b$ is neglected. Although in some cases Equation [2a] will give a result not differing seriously from that obtained from the more rigorous Equations [1] and [2], the latter were used herein.

⁸ In order to simplify Figs. 10 and 11, runs are shown only for alternate Reynolds numbers; intermediate Reynolds numbers (not shown) gave curves of the same shape as those shown.

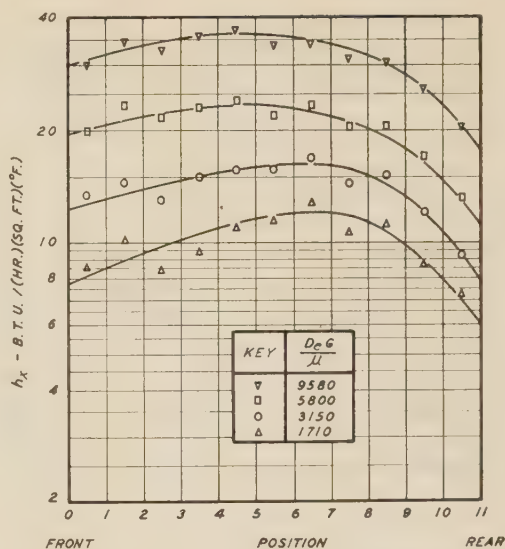
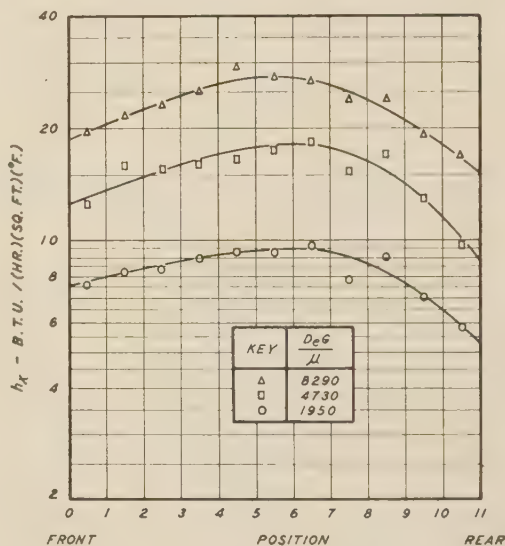
⁷ See footnote 7 at bottom of next column.

TABLE 2 DATA FOR TESTS

Run number	6-J	5-J	4-J	3-J	2-J	1-J	7-J	8-J	5-A	3-A	4-A	1-A	2-A	4-B	2-B	5-B	1-B	3-B
Air rate, lb/hr.	208	288	396	533	728	1390	1390	1620	355	431	1040	1220	1790	1040	1040	1040	1040	1040
Temp exit air, deg F.	188.4	179.0	168.4	162.2	153.7	145.0	134.0	129.7	160.4	153.7	132.5	127.1	119.3	184.6	176.5	163.6	131.4	131.5
Temp inlet air, deg F.	76.2	75.7	75.0	78.3	80.8	79.7	76.2	80.6	77.0	74.0	76.0	75.6	75.9	165.8	152.6	128.6	75.0	74.8
Divided side, cc cond/30 min.	624	817	1018	1202	1464	1707	2101	2287	833	897	1534	1772	2091	557	698	918	1364	1368
Undivided, cc cond/30 min.	627	826	1014	1204	1449	1695	2118	2285	853	910	1578	1762	215	560	706	973	1415	1406
Length of run, min.	90	175	39	80	60	62.5	60	60	1.6	2.0	8.9	11.2	20	9.6	9.6	8.8	8.8	8.8
Δp , cm water	1.0	1.6	2.5	4.2	6.35	11.1	20.2	26.7	1.7	2.2	8.9	11.8	22.3	9.7	9.6	9.3	8.8	8.9
Δt_m , deg F.	205.6	203.2	201.0	198.4	195.5	192.0	186.5	182.9	203.3	200.5	192.2	191.8	184.4	206.1	203.6	200.1	190.7	190.8

TABLE 3 RESULTS OF TESTS

q (air), Btu/hr.	5620	7140	8880	10700	12700	15300	19300	19100	7130	8300	14100	15100	18700	4700	5980	8750	14100	14200
q (steam), Btu/hr.	5300	6950	8580	10240	12320	14620	17840	19200	6920	7670	13200	14900	18100	4770	6060	8410	13400	13500
q (air)/ q (steam)	1.260	1.177	1.283	1.315	1.302	1.462	1.684	0.990	1.023	1.082	1.068	1.013	1.033	0.985	0.987	1.040	1.052	1.032
$D_e G/\mu$	1260	1717	2370	3150	3800	5800	8230	9880	1590	1950	4730	5600	8290	4370	4390	4480	4730	4730
h_m	8.94	10.5	12.1	15.1	18.3	22.4	29.4	30.6	8.07	9.21	16.9	17.5	24.9	16.2	16.3	16.5	16.1	16.2
$h_m/c_p G$	0.0110	0.0093	0.0078	0.0073	0.0064	0.0058	0.0054	0.0049	0.0078	0.0074	0.0055	0.0050	0.0048	0.0053	0.0054	0.0054	0.0053	0.0053
$f^{1/2}/(C_p G)$	0.0220	0.0180	0.0155	0.0143	0.0128	0.0113	0.0102	0.0099	0.0240	0.0210	0.0147	0.0143	0.0126	0.0143	0.0143	0.0144	0.0145	0.0148
$(h_m/c_p G) \div f^{1/2}$	0.50	0.52	0.50	0.51	0.50	0.51	0.53	0.50	0.32	0.35	0.37	0.35	0.38	0.37	0.38	0.37	0.37	0.36

* Adjusted to $D_e G/\mu$ of 4730.FIG. 10 LOCAL SURFACE COEFFICIENTS h_x VERSUS POSITION FOR JACKETED MUFF, FOR SEVERAL REYNOLDS NUMBERSFIG. 11 LOCAL SURFACE COEFFICIENTS h_x VERSUS POSITION FOR BAFFLED MUFF, FOR SEVERAL REYNOLDS NUMBERS

13 and show that $h_m/c_p G$ is independent of Δt_m . Heat balances agreed within a maximum deviation of 7.7 per cent and an average deviation of 3.4 per cent.

Fig. 14 shows the present data for both the jacketed and baffled cylinders, plotted as Stanton numbers, $h_m/c_p G$ versus the Reynolds number, $D_e G/\mu$ based upon the equivalent diameter of the passages between the fins. It is seen that the results with the jacket are higher than those for the baffle, for the same Reynolds number; this would still be the case if the definition of D_e had been based upon the total air passage instead of that between the fins.

The data of reference (2) for an electrically heated muff with a jacket were recalculated by means of Equations [1] and [2] as an approximation, obtaining h_m from U_m based upon an arithmetic-mean temperature difference

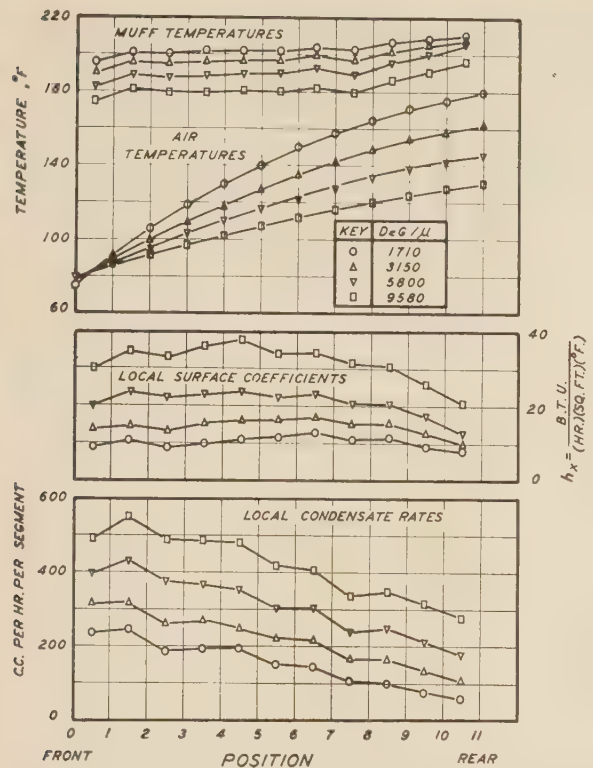


FIG. 12 PLOT OF DATA FOR JACKETED MUFF VERSUS POSITION (Plot shows minor but systematic irregularities of muff temperatures, condensate rates, and local surface coefficients.)

$$\Delta t_a = \frac{(t_{bm} - t_1) + (t_{bm} - t_2)}{2} \dots\dots\dots [6]$$

which is a fair type of mean to use with these data obtained with electric heat. The results are plotted in Fig. 14 and average but little below the present data for a jacketed muff. The present data lie on or above the usual equation for turbulent flow of air in long straight tubes

$$\frac{h_m}{c_p G} = \frac{0.023/(0.74)^{2/3}}{(D_e G / \mu)^{0.2}} \dots\dots\dots [7]$$

given in reference (5); the data of reference (2) shown in Fig. 14 fall on both sides of this equation.

The over-all pressure drops across the test section are reported in the tables, along with the corresponding over-all Fanning friction factors calculated from the data by taking the length of air travel arbitrarily as one half the mean perimeter of a fin. The ratio of the mean Stanton number, $h_m/c_p G$, to one half the over-all friction factor $f'/2$ was found to average 0.51 with the jacket and 0.36 for the baffle, as compared with a value of 1.0 predicted by the Reynolds analogy and 1.22 by the Colburn analogy (5) for turbulent flow of air in long straight tubes.

The jacket gave 20 to 30 per cent greater surface coefficients h_m than the baffle for the same over-all pressure drop, and 22 to 40 per cent greater coefficients for the same power loss per square foot of finned surface.

By measuring local coefficients for each portion of the baffled-finned cylinder it is possible to determine the faults in location and design of baffles, and improvements in baffles can be worked out more readily and on a sounder basis than when measuring only the usual average coefficients of heat transfer for the entire

finned cylinder. Data for other designs and arrangements of baffles have been obtained and may be released in a subsequent paper.

CONCLUSIONS

This study established the following points:

- 1 The data were reproducible.
- 2 Good heat balances were obtained.
- 3 The condensate rates from the divided and undivided halves of the cylinder agreed within 6 per cent.
- 4 In every run with the baffle or jacket tested, the local coefficient of heat transfer from fins to air was low in front, high roughly halfway around the cylinder, and lowest in the rear.
- 5 For a given Reynolds number, the baffle gives a somewhat lower Stanton number than the jacket.
- 6 In terms of average surface coefficients of heat transfer, the data for the jacketed muff of the present study agree well with those of other investigators who determined only average coefficients.
- 7 For a given Reynolds number, temperature difference was varied from 30 to 85 deg F in tests on the baffled cylinder and had no effect on the Stanton number, expressed in terms of the average surface coefficient of heat transfer for the entire cylinder.

ACKNOWLEDGMENT

It is desired to acknowledge the co-operation of the Pratt and Whitney Division of United Aircraft, in donating the muffs.

BIBLIOGRAPHY

- 1 "The Mechanism of Heat Transmission—Distribution of Heat

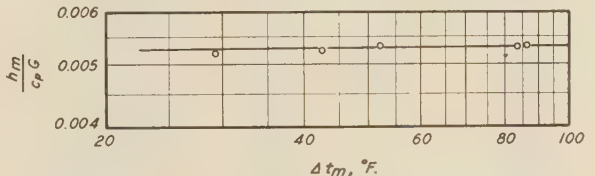


FIG. 13 MEAN STANTON NUMBERS ($h_m/c_p G$) FOR REYNOLDS NUMBER OF 4730, PLOTTED VERSUS TEMPERATURE DIFFERENCE FROM BASE OF FINS TO AIR

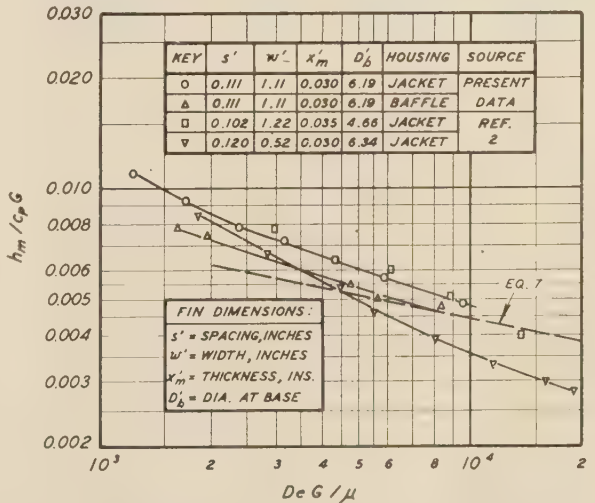


FIG. 14 MEAN STANTON NUMBERS ($h_m/c_p G$) PLOTTED VERSUS REYNOLDS NUMBER ($D_e G / \mu$) FOR PRESENT DATA AND THOSE OF REFERENCE (2) FOR SIMILAR MUFFS (Primes are for dimensions in inches.)

Flow About the Circumference of a Pipe in a Stream of Fluid," by T. B. Drew and W. P. Ryan, *Trans. A.I.Ch.E.*, vol. 26, 1931, pp. 118-147; see also "Heat Transmission About a Cylindrical Pipe at Right Angles to Forced Air Flow," by W. J. Paltz and C. E. Starr, S.B. Thesis in Chemical Engineering, Massachusetts Institute of Technology, 1931.

2 "Surface Heat-Transfer Coefficients of Finned Cylinders," by H. H. Ellerbrock, Jr., and A. E. Biermann, National Advisory Committee for Aeronautics, Report 676, 1939.

3 "Mathematical Equations for Heat Conduction in the Fins of Air-Cooled Engines," by D. R. Harper, 3rd, and W. B. Brown, National Advisory Committee for Aeronautics, Report 158, 1922.

4 "Heat Transfer From Finned Metal Cylinders in an Air Stream," by A. E. Biermann and B. Pinkel, National Advisory Committee for Aeronautics, Report 488, 1934.

5 "A Method of Correlating Forced Convection Heat Transfer Data and a Comparison With Fluid Friction," by A. P. Colburn, *Trans. A.I.Ch.E.*, vol. 29, 1933, pp. 174-210.

Efficiency of Extended Surface

By KARL A. GARDNER,¹ NEW YORK, N. Y.

The work of previous investigators on heat flow through extended surface is briefly reviewed and literature citations are given. General equations are derived for the temperature gradient and fin efficiency in any form of extended surface to which the assumptions listed are applicable. The solution of these equations in terms of Bessel functions is shown to cover practically any form of extended surface whose thickness varies as some power of the distance measured along an axis normal to the basic surface. Curves are presented for the fin efficiency of several forms of straight fins, annular fins, and spines.

NOMENCLATURE

The following nomenclature is used in the paper:

- A = fin surface between origin and point x
- A_f = total surface of one fin
- a = cross-sectional area of fin normal to x axis at point x
- a_b = area of fin base
- c = a constant (Equations [2] and [7])
- h, h_s = heat-transfer coefficient on finned side of extended-surface element
- h_i = heat-transfer coefficient on unfinned side of extended-surface element
- $I_n(u)$ = modified Bessel function of the first kind and order n
- $i = \sqrt{-1}$
- $K_n(u)$ = modified Bessel function of the second kind and order n
- k = thermal conductivity of fin material
- L = length of straight fins
- m = a constant (Equation [2])
- n = a constant, order of Bessel function
- p = a constant (Equation [2])
- q = rate of heat flow through section a
- q_f = total rate of heat flow through entire fin
- q_b = rate of heat flow through basic surface which would be covered by base of fin
- q_1 = rate of heat flow through total basic surface
- q_2 = rate of heat flow through basic plus extended surface
- r = function of u defined following Equation [20]
- u = function of x defined by Equation [7]²
- $w = (x_b - x_s)$ = fin height
- x = distance along axis normal to basic surface²
- y = half thickness of fin at point x
- y_b = half thickness of fin base
- α, β = constants
- $\eta = \phi A_f / a_b$ = fin effectiveness
- θ = temperature difference between fin and surrounding fluid at point x
- θ_b = temperature difference between fin at base and surrounding fluid
- ϕ = fin efficiency

¹ The Griscom-Russell Company.

² Subscripts b and e refer to conditions at base and edge, respectively.

Contributed by the Heat Transfer Division and presented at the Annual Meeting, New York, N. Y., Nov. 27-Dec. 1, 1944, of THE AMERICAN SOCIETY OF MECHANICAL ENGINEERS.

NOTE: Statements and opinions advanced in papers are to be understood as individual expressions of their authors and not those of the Society.

INTRODUCTION

In a conventional heat exchanger heat is transferred from one fluid to another through a metallic wall and, other things being equal, the rate of heat flow is directly proportional to the extent of the wall surface and to the temperature difference between one fluid and the adjacent surface. If thin strips of metal are attached to the basic surface, extending into one of the fluids, the total surface for heat transfer is thereby increased and it might be expected that the rate of heat flow per unit of basic surface would increase in direct proportion. However, the average surface temperature of these strips, by virtue of the temperature gradient through them, tends to approach the temperature of the surrounding fluid so the effective temperature difference is decreased and the net increase of heat flow may be considerably less than would be anticipated on the basis of surface alone.

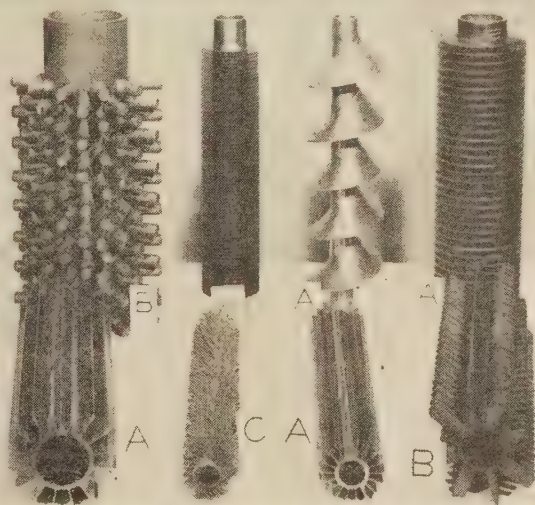


FIG. 1 SOME COMMERCIAL FORMS OF EXTENDED SURFACE
(Samples furnished through the courtesy of A The Griscom-Russell Company, B The Babcock & Wilcox Company, C Thermek Corporation.)

These added heat-conducting strips constitute "extended surface;" they may be of various forms, as shown in Fig. 1. The ratio of the average temperature difference over the extended surface to that over the basic surface is commonly called the "fin efficiency," "fin" being used as a concise generic term for all forms of extended surface. It is the purpose of this paper to derive a general equation for the temperature gradient in fins and to present a solution for fin efficiency which, although not perfectly general, nevertheless includes all the forms previously investigated and several others besides. A secondary purpose is the review and compilation of the significant results of previous investigators.

LITERATURE REVIEW

Some early measurements of the temperature distribution in long metallic rods are available in the experimental determination of the thermal conductivities of iron and copper by Stewart (1).³

³ Numbers in parentheses refer to the Bibliography at the end of the paper.

The iron rod was $\frac{3}{4}$ in. sq \times $4\frac{1}{2}$ ft long, and the copper rod was $\frac{1}{2}$ in. diam \times 7 ft long.

Parsons and Harper (2) derived an equation for the efficiency of straight fins of constant thickness in the course of a paper on airplane-engine radiators. Harper and Brown (3), in connection with air-cooled aircraft engines, investigated straight fins of constant thickness, wedge-shaped straight fins, and annular fins of constant thickness; equations for the fin efficiency of each type were presented and the errors involved in certain of the assumptions were evaluated.

Schmidt (4) covered the same three types of fin from the standpoint of material economy. He stated that the least metal is required for given conditions if the temperature gradient is linear, and showed how the thickness of each type of fin must vary to produce this result. Finding, in general, that the calculated shapes were impractical to manufacture, he proceeded to show the optimum dimensions for straight and annular fins of constant thickness and for wedge-shaped straight fins under given operating conditions.

Murray (5) presented equations for the temperature gradient and the effectiveness of annular fins of constant thickness with a symmetrical temperature distribution around the base of the fin.

A stepwise procedure for calculating the temperature gradient and efficiency for fins whose thickness varies in any manner whatsoever was given by Hausen (6). Curves of both properties for the fins investigated by Schmidt (4) are also included.

The temperature gradient in conical and cylindrical spines was determined by Focke (7) and, independently, by the writer in unpublished work of which this paper is the outcome. Focke, like Schmidt, showed how the spine thickness must vary in order to keep the material requirement to a minimum; he, too, found the result impractical and went on to determine the optimum cylindrical- and conical-spine dimensions.

Avrami and Little (8) derived equations for the temperature gradient in thick-bar fins and showed under what conditions fins might act as insulators on the basic surface. Approximate equations were also given including, as a special case, that of Harper and Brown.

Carrier and Anderson (9) discussed straight fins of constant thickness, annular fins of constant thickness, and annular fins of constant cross-sectional area, presenting equations for the fin efficiency of each. In the latter two cases the solutions are in the form of infinite series.

A rather unusual application of Harper and Brown's equation was made by the writer (10), in considering the ligaments between holes in heat-exchanger tube sheets as fins and thereby estimating the temperature distribution in tube sheets.

The types of extended surface previously investigated, aside from those which may be approximated by Hausen's method, are as follows:

- 1 Straight fins of constant thickness (2, 3, 4, 6, 8, 9).
- 2 Wedge-shaped straight fins (3, 4, 6).
- 3 Annular fins of constant thickness (3, 4, 5, 6, 9).
- 4 Annular fins of constant cross-sectional area (9).
- 5 Cylindrical spines (7).
- 6 Conical spines (7).

MATHEMATICAL TREATMENT—ASSUMPTIONS

The mathematical analysis is based upon the following assumptions, which are essentially those given by Murray (5), but which are common to all previous investigations except that of Avrami and Little (8):

- 1 The heat flow and temperature distribution throughout the fin are independent of time, i.e., the heat flow is steady.
- 2 The fin material is homogeneous and isotropic.

3 There are no heat sources in the fin itself.

4 The heat flow to or from the fin surface at any point is directly proportional to the temperature difference between the surface at that point and the surrounding fluid.

5 The thermal conductivity of the fin is constant.

6 The heat-transfer coefficient is the same over all the fin surface.

7 The temperature of the surrounding fluid is uniform.

8 The temperature of the base of the fin is uniform.

9 The fin thickness is so small compared to its height that temperature gradients normal to the surface may be neglected.

10 The heat transferred through the outermost edge of the fin is negligible compared to that passing through the sides.

Of these assumptions, only 6, 8, 9, and 10 are open to serious question. With some types of fin the heat-transfer coefficient undoubtedly does vary from point to point on the fin, but McAdams and Turner, in a discussion of a paper by Sage (11), show that the use of average coefficients and average conductivity in the theoretical equation for temperature gradient gives good agreement with Stewart's measurements (1). Murray's paper shows how to take account of a nonuniform temperature at the base of annular fins, although it seems reasonable that an average temperature based on the average inside-film coefficient should give sufficiently accurate results for many purposes. The question of temperature variation at the base of the fin is not apt to arise for other types.

The error involved in assumptions 9 and 10 has been investigated by Harper and Brown (3), and Avrami and Little (8), for straight fins of constant thickness; it is very small for most practical forms of extended surface.

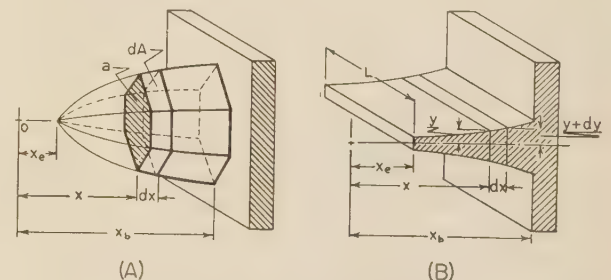


FIG. 2 DIAGRAMS OF (A), GENERALIZED ELEMENT OF EXTENDED SURFACE; (B) STRAIGHT FIN
(Thicknesses are greatly exaggerated.)

APPLICATION OF BESSEL'S DIFFERENTIAL EQUATION

Temperature Gradient. The basic differential equation results from a heat balance on an element of the fin normal to the direction of heat flow, as shown in Fig. 2(a)

$$\frac{d^2\theta}{dx^2} + \left(\frac{1}{a} \frac{da}{dx}\right) \frac{d\theta}{dx} - \left(\frac{h}{ka} \frac{dA}{dx}\right) \theta = 0 \dots \dots \dots [1]$$

In this, θ represents the temperature difference between the fin and the surrounding fluid at a distance x from some reference point. Termwise comparison of this equation (after multiplication by x^2) with the general form of Bessel's equation given by Douglass (12)

$$x^2 \frac{d^2\theta}{dx^2} + [(1-2m)x - 2\alpha x^2] \frac{d\theta}{dx} + [p^2 c^2 x^{2p} + \alpha^2 x^2 + \alpha(2m-1)x + (m^2 - p^2 n^2)] \theta = 0 \dots [2]$$

shows that both have the same form if

$$a = \lambda x^{1-2p} \dots \dots \dots [3]$$

and

$$\frac{dA}{dx} = \mu x^{2p(1-n)-1} \dots \dots \dots [4]$$

where λ and μ are positive constants.

Thus if the cross-sectional area of a fin can be described by Equation [3], and its surface by Equation [4], the solution may be expressed in terms of Bessel functions. The general solution is found by application of the boundary conditions

$$1 \quad \text{When } x = x_b, \theta = \theta_b$$

$$2 \quad \text{When } x = x_e, \frac{d\theta}{dx} = 0 \quad (\text{from assumption 10}).$$

For n equal to zero or an integer

$$\theta = \theta_b \left(\frac{u}{u_b} \right)^n \left[\frac{I_n(u) + \beta K_n(u)}{I_n(u_b) + \beta K_n(u_b)} \right] \dots \dots \dots [5]$$

where

$$\beta = \frac{I_{n-1}(u_e)}{K_{n-1}(u_e)} \dots \dots \dots [6]$$

For n equal to a fraction

$$\theta = \theta_b \left(\frac{u}{u_b} \right)^n \left[\frac{I_n(u) + \beta I_{-n}(u)}{I_n(u_b) + \beta I_{-n}(u_b)} \right] \dots \dots \dots [5a]$$

where

$$\beta = -\frac{I_{n-1}(u_e)}{I_{1-n}(u_e)} \dots \dots \dots [6a]$$

In these equations

$$u = -icx^p = x \sqrt{\frac{h}{ka} \frac{dA}{dx}} \dots \dots \dots [7]$$

and u_b and u_e are found by substituting the values of x , a , and (dA/dx) for the base or edge of the fin, respectively.

Fin Efficiency.⁴ The fin efficiency of extended surface is given by

$$\phi = \frac{\int_0^{A_f} \theta dA}{\theta_b A_f} \dots \dots \dots [8]$$

from which, for n equal to zero or an integer

$$\phi = \frac{2(1-n)}{u_b \left[1 - \left(\frac{u_e}{u_b} \right)^{2(1-n)} \right]} \left[\frac{I_{n-1}(u_b) - \beta K_{n-1}(u_b)}{I_n(u_b) + \beta K_n(u_b)} \right] \dots [9]$$

or, for n equals a fraction,

$$\phi = \frac{2(1-n)}{u_b \left[1 - \left(\frac{u_e}{u_b} \right)^{2(1-n)} \right]} \left[\frac{I_{n-1}(u_b) + \beta I_{1-n}(u_b)}{I_n(u_b) + \beta I_{-n}(u_b)} \right] \dots [9a]$$

Fin Effectiveness.⁴ Another property of extended surface which is often used is the ratio of the heat transferred through the base of a fin to that which would be transferred through the same base area if the fin were not there, the base temperature remaining constant. This ratio is termed the "effectiveness," and it can be simply expressed as a function of the fin efficiency

⁴ The terms "fin efficiency" and "fin effectiveness," in the meanings adopted here have not been consistently adhered to in the English literature; the latter phrase has been used for both ϕ and η . In the German literature, ϕ is called "der Wirkungsgrad."

$$\left(\frac{q_f}{q_b} \right)_{\theta_b = \text{const}} = \eta = \frac{A_f}{a_b} \phi \dots \dots \dots [10]$$

However, in most practical cases, the addition of extended surface to a metal wall changes the base temperature to an extent depending on the heat-transfer coefficients on both sides of the wall. The effectiveness is therefore a misleading indication of the value of extended surface, as comparison with the following more accurate expression will show

$$\frac{q_f}{q_b} = \eta \frac{\left(1 + \frac{h_s}{h_i} \right)}{\left(1 + \eta \frac{h_s}{h_i} \right)} \dots \dots \dots [11]$$

In this, h_s and h_i are the film coefficients on the finned and bare sides of the wall, respectively. Obviously, the advantage of extended surface is greatest when h_s is small compared to h_i .

TYPES OF EXTENDED SURFACE

In the foregoing, general relations have been developed for the temperature gradient and the fin efficiency without inquiring to what types of extended surface they may be applied, other than noting that they must be described by Equations [3] and [4]. For a given fin the exponents of x in these equations are known; there are two exponents, so it is possible to eliminate p between them and to solve for the appropriate value of n .

Space does not permit detailed derivation or discussion of the equations for the various types of extended surface, so the following are submitted without proof:

Straight Fins. The thickness may vary thus

$$y = y_b \left(\frac{x}{x_b} \right)^{\frac{1-2n}{1-n}} \dots \dots \dots [12]$$

The value of u to be used in the temperature-difference and efficiency equations is

$$u = 2(1-n) \left(\frac{x}{x_b} \right)^{\frac{1}{2(1-n)}} \sqrt{\frac{h}{ky_b}} \cdot x_b \dots \dots \dots [13]$$

In these and subsequent equations it is assumed that the square of the slope of the fin sides is negligible compared to unity, which it usually is for thin fins and spines. This assumption is not necessary for $n = 1/2$ and $n = 0$. Equations and curves are given in Fig. 3. Reference to Fig. 2(b) will help in verifying these equations.

Spines—Circular or Regular Polygonal Section.

$$y = y_b \left(\frac{x}{x_b} \right)^{\frac{1-2n}{2-n}} \dots \dots \dots [14]$$

$$u = \frac{2\sqrt{2}(2-n)}{3} \left(\frac{x}{x_b} \right)^{\frac{3}{2(2-n)}} \sqrt{\frac{h}{ky_b}} \cdot x_b \dots \dots \dots [15]$$

The solution is exact for $n = 1/2$ and $n = -1$. Equations and curves are given in Fig. 4.

Annular Fins.

$$y = y_b \left(\frac{x}{x_b} \right)^{\frac{-2n}{1-n}} \dots \dots \dots [16]$$

$$u = (1-n) \left(\frac{x}{x_b} \right)^{\frac{1}{1-n}} \sqrt{\frac{h}{ky_b}} \cdot x_b \dots \dots \dots [17]$$

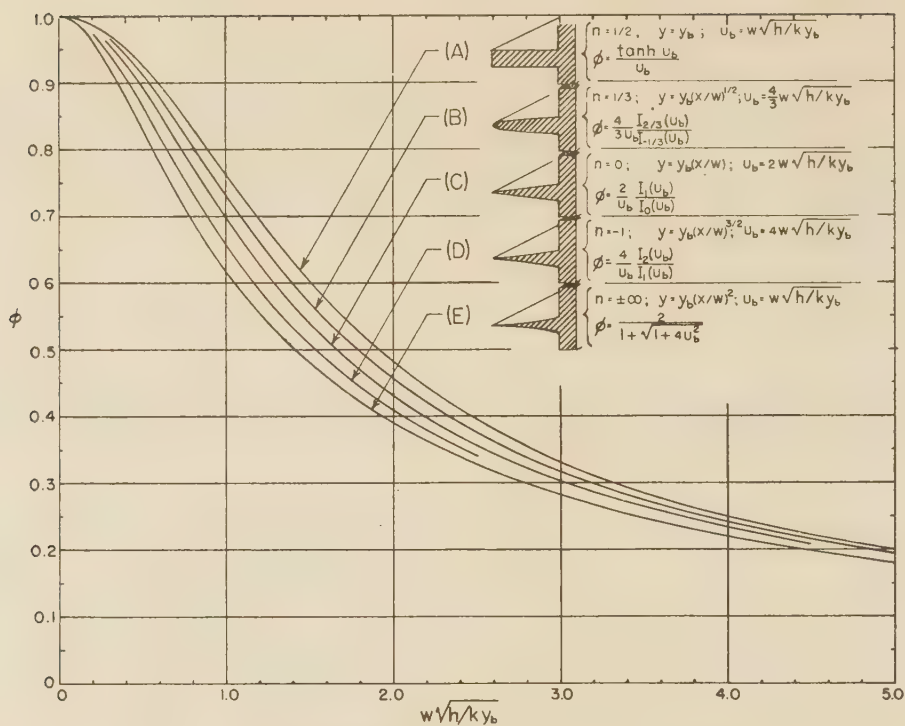


FIG. 3 FIN EFFICIENCY OF SEVERAL TYPES OF STRAIGHT FIN

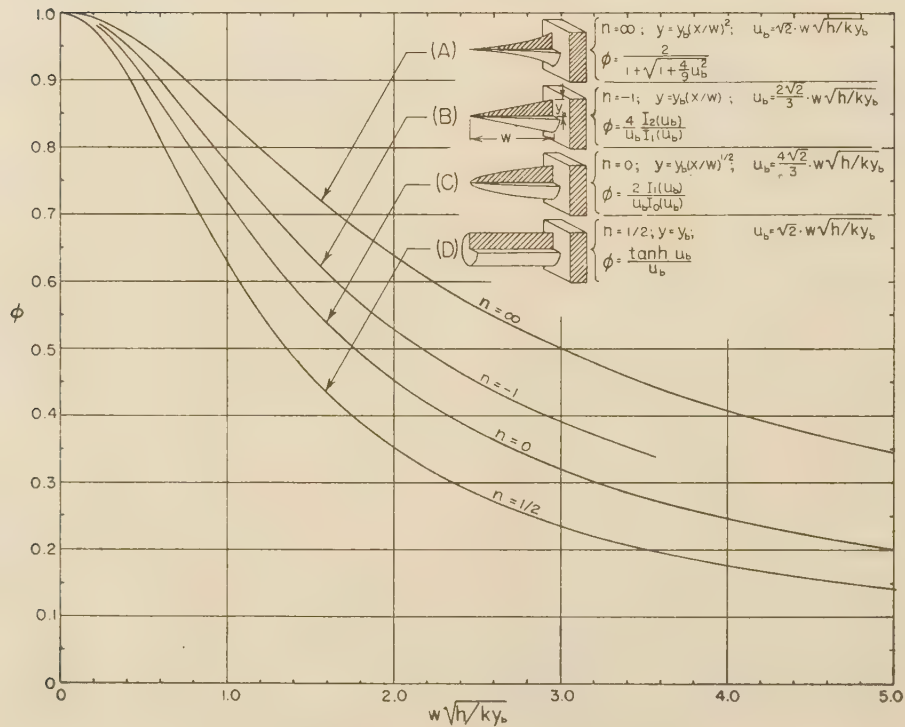
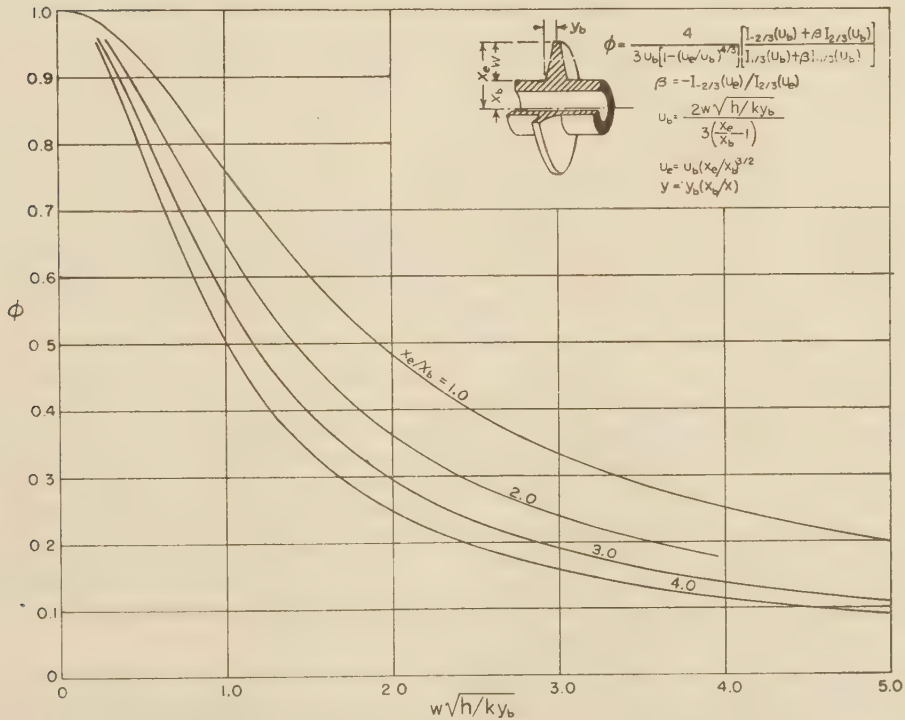
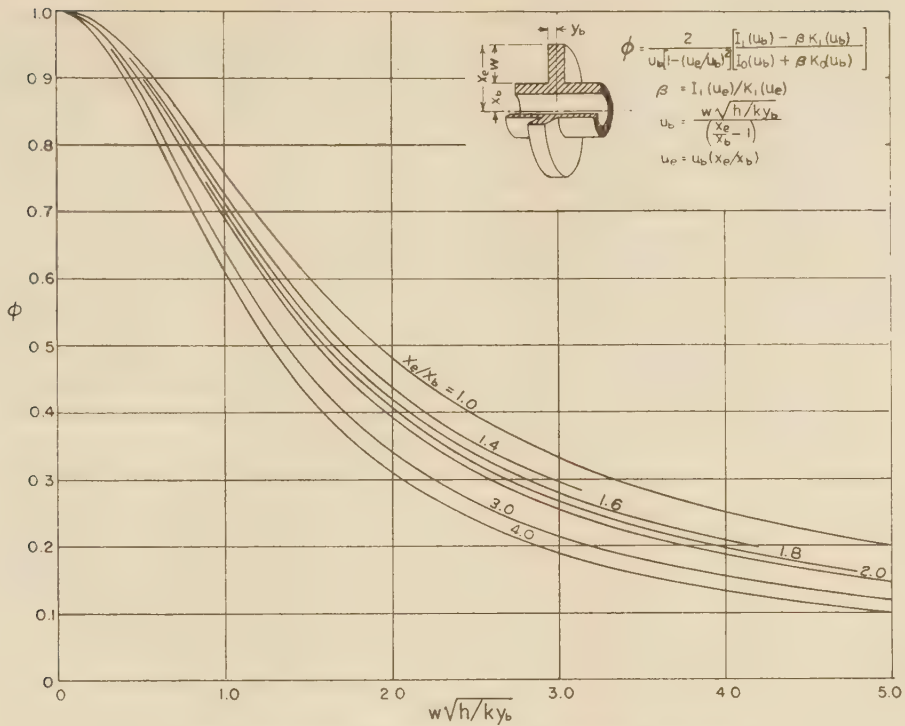


FIG. 4 EFFICIENCY CURVES FOR FOUR TYPES OF SPINE



Equations and curves are shown in Figs. 5 and 6. The solution is exact for $n = 0$.

Three general classes of extended surface have been investigated thus far; straight fins, spines, and annular fins. Other classes might be discussed but the most practical forms have already been included. It will be noted, however, that no straight fin or spine whose thickness varies as the square of the distance along it, can be described in terms of Bessel functions, since n becomes infinite and u is a constant. This case will now be treated for the sake of completeness and to reproduce the results of Schmidt (4), and Focke (7). Termwise comparison of Equation [1] with Euler's differential equation shows that the cross section and surface may vary thus

$$a = \lambda x^{1-2m} \dots\dots\dots [18]$$

and

$$\frac{dA}{dx} = \mu x^{-(1+2m)} \dots\dots\dots [18a]$$

For the case where $x_e = 0$

$$\theta = \theta_b \left(\frac{x}{x_b} \right)^r \dots\dots\dots [19]$$

and

$$\phi = \frac{2}{1 + \sqrt{1 + (u/m)^2}} \dots\dots\dots [20]$$

where

$$r = m [1 - \sqrt{1 + (u/m)^2}]$$

In these equations, u has exactly the same definition as before (Equation [7]) but for this special case, is a constant. The requirement of Schmidt (4) that the temperature gradient be linear to use the minimum material is met if r in Equation [19] equals unity, from which

$$u^2 = (1 - 2m) \dots\dots\dots [21]$$

For straight fins, $(1 - 2m) = 2$, and for regular spines, $(1 - 2m) = 4$, both of which correspond to a thickness varying as the square of the distance from the edge (or tip). In each case the least material is required if

$$\frac{hx_b^2}{ky_b} = 2 \dots\dots\dots [22]$$

GENERALITY OF EQUATIONS

The equations for temperature gradient and fin efficiency derived in this paper are obviously quite general since, by substituting the appropriate value of n , the equations of all previous investigators are readily reproduced. These may be summarized as follows:

$n = 1/2$. This corresponds to the straight fins or spines of constant thickness investigated by Harper and Brown (3), Parsons and Harper (2), Schmidt (4), Focke (7), et al. In the case of spines, the section need not be circular but may be square, triangular, elliptical, or any other shape within the limitations of the assumptions. The same value also describes annular fins whose thickness varies inversely as the square of the distance from the center, although the values of u_b and u_e are not the same as for straight fins or spines. The efficiency is

$$\phi = \frac{\tan h(u_b - u_e)}{(u_b - u_e)} \dots\dots\dots [23]$$

where the expressions for u_b and u_e are given in Figs. 3 and 4.

$n = 0$. This yields the equations for wedge-shaped straight fins and annular fins of constant thickness, as derived by Harper and Brown and Schmidt. Furthermore, the same equations apply to spines whose thickness varies as the square root of the distance from a point at or beyond the tip.

$n = -1$. This represents the conical spines investigated by Focke (7). It also covers straight fins whose thickness varies as the $3/2$ power of the distance from a point at or beyond the edge.

With these three values of n all previous expressions for fin efficiency based on assumptions 1 through 10 are reproduced. Furthermore, the general solution makes it possible to recognize the applicability of the equations for one particular type of fin to other types, e.g., only five different types of fin have been shown previously to be covered by these three values of n , yet it has just been shown that at least seven types can be included. Some other types for which special equations have been developed may also be mentioned.

$n = 1/3$. This corresponds to the annular fins with constant metal area for heat flow, for which Carrier and Anderson gave a solution in terms of infinite series (9). It could also represent straight fins whose thickness varies as the square root of x , and spines whose thickness varies as the fifth root of x .

$n = \infty$. This covers the straight fins of Schmidt (4), and the spines of Focke (7), whose thickness varies as the square of the distance from the edge or tip.

In order to bring the abscissas on all graphs to a common basis, the fin height w has been introduced into the various expressions for u_b and u_e by writing

$$w = \pm(x_b - x_e), \text{ or } w = x_b \text{ if } x_e = 0$$

Aside from this no attempt is made to compare one type of extended surface with another. Straight fins with the same height, base thickness, conductivity, and surface coefficient are comparable one with the other, and the same is true of annular fins. This is so because changing the contour of the sides of such fins has a negligible effect on the surface. Therefore, to some extent Fig. 3 gives an indication of the relative merits of various straight fins, and Figs. 5 and 6, of annular fins. Fig. 4, however, should not be considered as anything more than a means for determining fin efficiency, because the surfaces of the different spines are not the same, e.g., the thorn-shaped spine represented by the highest curve has only one third the surface of the cylindrical spine of the same height and base thickness, represented by the lowest curve in Fig. 4.

ACKNOWLEDGMENT

The author wishes to thank Joseph Price, Vice-President in Charge of Engineering, The Griscom-Russell Company, for permission to publish this paper. The co-operation of the Griscom-Russell Company, The Babcock and Wilcox Company, and the Thermek Corporation in furnishing samples of extended-surface tubing, and the assistance of O. W. Heimberger, Assistant Chief Engineer, the Griscom-Russell Company, and A. C. Mueller, Chemical Engineer, Technical Division, Engineering Department, E. I. du Pont de Nemours and Company, Wilmington, Del., in pointing out references to earlier work are also greatly appreciated.

BIBLIOGRAPHY

- 1 "The Absolute Thermal Conductivities of Iron and Copper," by R. W. Stewart, Philosophical Transactions, Royal Society of London, Eng., vol. 184, series A, 1893, p. 569.
- 2 "Radiators for Aircraft Engines," by S. R. Parsons and D. R. Harper, U. S. Bureau of Standards, Technical Paper no. 211, 1922, pp. 327-330.

3 "Mathematical Equations for Heat Conduction in the Fins of Air-Cooled Engines," by D. R. Harper and W. B. Brown, National Advisory Committee for Aeronautics, Report no. 158, 1922.

4 "Die Wärmeübertragung durch Rippen," by E. Schmidt, *Zeit. V.D.I.*, vol. 70, 1926, pp. 885-889, and 947-951.

5 "Heat Dissipation Through an Annular Disk or Fin of Uniform Thickness," by W. M. Murray, *Journal of Applied Mechanics*, Trans. A.S.M.E., vol. 60, 1938, p. A-78.

6 "Wärmeübertragung durch Rippenrohre," by H. Hausen, *Zeit. V.D.I.*, Beiheft 2, 1940, pp. 55-57.

7 "Die Nadel als Kühlelemente," by R. Focke, *Forschung auf dem Gebiete des Ingenieurwesens*, vol. 13, 1942, pp. 34-42.

8 "Diffusion of Heat Through a Rectangular Bar and the Cooling and Insulating Effect of Fins, I. "The Steady State," by Melvin Avrami and J. B. Little, *Journal of Applied Physics*, vol. 13, 1942, pp. 255-264.

9 "The Resistance to Heat Flow Through Finned Tubing," by W. H. Carrier and S. W. Anderson, *Heating, Piping and Air Conditioning*, vol. 10, 1944, pp. 304-320.

10 "Heat Exchanger Tube Sheet Temperatures," by K. A. Gardner, *Refiner and Natural Gasoline Manufacturer*, vol. 21, 1942, pp. 71-77.

11 "The Value of Extended Heating Surfaces," by C. S. Sage, *Journal of the American Society of Heating and Ventilating Engineers*, vol. 33, 1927, pp. 707-714, and vol. 34, 1928, pp. 385-388.

12 "Applied Mathematics in Chemical Engineering," by T. K. Sherwood and C. E. Reed, McGraw-Hill Book Company, Inc., New York, N. Y., 1939, p. 211.

13 "A Treatise on Bessel Functions and Their Applications to Physics," by A. Gray, G. B. Mathews, and T. M. MacRobert, Macmillan and Company, London, 1931.

14 "Tables of Functions," by E. Jahnke and F. Emde, B. G. Teubner, Leipzig and Berlin, 1938; also Dover Publications, New York, N. Y.

Appendix 1

DETAILS OF DERIVATION OF EQUATIONS

The heat flowing through an element of a fin normal to the basic surface (Fig. 2a) is given by the Fourier equation

$$q = -ka \frac{d\theta}{dx} \dots \dots \dots [24]$$

The heat entering or leaving the sides of the element is

$$-dq = h\theta dA \dots \dots \dots [25]$$

By differentiating Equation [24] and substituting the result into Equation [25], dq is eliminated and Equation [1] is obtained.

If the second terms of Equations [1] (after multiplication through by x^2) and [2] are to be identical, then

$$\frac{x^2}{a} \frac{da}{dx} = (1 - 2m)x - 2\alpha x^2 \dots \dots \dots [26]$$

Integration gives

$$\ln a = (1 - 2m)\ln x - 2\alpha x + \text{const.} \dots \dots \dots [27]$$

or

$$a = \lambda x^{1-2m} e^{-2\alpha x} \dots \dots \dots [27a]$$

From the third terms

$$-\frac{h x^2}{ka} \frac{dA}{dx} = [p^2 c^2 x^{2p} + \alpha^2 x^2 + \alpha(2m-1)x + (m^2 - p^2 n^2)] \dots [28]$$

Introducing a from Equation [27a] and rearranging

$$\frac{dA}{dx} = -\frac{k}{h} \lambda e^{-2\alpha x} x^{-(1+2m)} [p^2 c^2 x^{2p} + \alpha^2 x^2 + \alpha(2m-1)x + (m^2 - p^2 n^2)] \dots [29]$$

Since the surface variation is not a function of k or h , the terms

within the brackets must either be zero or inversely proportional to (k/h) ; α , p , and m occur as exponents so they cannot contain (k/h) . Therefore, $\alpha = 0$, and $m = pn$, leaving c^2 as the only constant involving (k/h) . Substitution of these results into Equations [27a] and [29] gives Equations [3] and [4].

In order to integrate Equation [8] to obtain the fin efficiency, dA must be expressed in terms of u ; from Equations [4] and [7]

$$dA = \nu u^{1-2n} du \dots \dots \dots [30]$$

where all constants have been collected in ν ; then

$$\phi = \frac{\int_{u_b}^{u_s} u^{1-n} [I_n(u) + \beta K_n(u)] du}{u_b^n [I_n(u_b) + \beta K_n(u_b)] \int_{u_b}^{u_s} u^{1-2n} du} \dots \dots [31]$$

Integration of this result to Equation [9] is easily accomplished by reference to the integral formulas of Appendix 2. Similar considerations lead to Equation [9a].

Appendix 2

TABLES AND PROPERTIES OF BESSEL FUNCTIONS

Derivatives:

$$\frac{d}{du} [u^n I_n(u)] = u^n I_{n-1}(u) \quad \frac{d}{du} [u^n K_n(u)] = -u^n K_{n-1}(u)$$

$$\frac{d}{du} [u^{-n} I_n(u)] = u^{-n} I_{n+1}(u) \quad \frac{d}{du} [u^{-n} K_n(u)] = -u^{-n} K_{n+1}(u)$$

$$\frac{d}{du} [I_n(u)] = \frac{n}{u} I_n(u) + I_{n+1}(u) \quad \frac{d}{du} [K_n(u)] = \frac{n}{u} K_n(u) - K_{n+1}(u)$$

Indefinite Integrals:

$$\int u^{n+1} I_n(u) du = u^{n+1} I_{n+1}(u)$$

$$\int \frac{I_n(u)}{u^{n-1}} du = \frac{I_{n-1}(u)}{u^{n-1}}$$

$$\int u^{n+1} K_n(u) du = -u^{n+1} K_{n+1}(u)$$

$$\int \frac{K_n(u)}{u^{n-1}} du = -\frac{K_{n-1}(u)}{u^{n-1}}$$

Identities:

$$I_{-n}(u) = I_n(u) \text{ and } K_{-n}(u) = K_n(u) \text{ if } n = \text{an integer}$$

$$\frac{2n}{u} I_n(u) = I_{n-1}(u) - I_{n+1}(u)$$

$$\frac{2n}{u} K_n(u) = K_{n+1}(u) - K_{n-1}(u)$$

$$I^{1/2}(u) = \sqrt{\frac{2}{\pi u}} \sinh u$$

$$I^{-1/2}(u) = \sqrt{\frac{2}{\pi u}} \cosh u$$

$$I^{3/2}(u) = \sqrt{\frac{2}{\pi u}} \left(\cosh u - \frac{\sinh u}{u} \right)$$

$$I^{-3/2}(u) = \sqrt{\frac{2}{\pi u}} \left(\sinh u - \frac{\cosh u}{u} \right)$$

Tables of Bessel functions are given in the Jahnke-Emde "Tables of Functions" (14), and in "Bessel Functions" by Gray, Mathews, and MacRobert (13). The latter is a treatise on the properties and application of Bessel functions; for more elementary discussion sufficient for many engineering purposes, see Sherwood and Reed (12). The nomenclature used in this paper is that used by Gray, et al. (13). If the Jahnke-Emde tables are used, it will be necessary to substitute $i^{-n}J_n(iu)$ for $I_n(u)$, and $i^{-n}H_n^{(1)}(iu)$ for $K_n(u)$ in the various equations of this paper.

Discussion

G. M. DUSINBERRE.⁵ For all fin problems the writer recommends the "relaxation" method of Southwell. This has been outlined by Emmons.⁶ There is a great advantage of ease and simplicity as compared with the solutions in Bessel functions, and there need be no sacrifice in accuracy. In fact, there may be a gain in accuracy with thick fins and short cylindrical spines, since it is not necessary to make the author's tenth assumption.

In Fig. 5, for example, if $x_e/x_b = 4$, and $w\sqrt{h/ky} = 1$, a rough calculation gives $\phi = 0.605$, neglecting the edge, and this agrees very well with the curve. But if we take account of the edge, we get $\phi = 0.583$.

This agrees with the author's references, that the error in ϕ due to assumption 10 is not large. But the point is, why introduce an error, however small, for the sake of permitting a certain mathematical treatment, when we can avoid that error by the use of a much simpler mathematical treatment?

An inexperienced person, intending to use the author's curves and noting that the edge area was neglected in computing the efficiency, might assume that this area should consequently be neglected in using the curves to estimate the over-all performance of a proposed design. But the edge area may be a considerable fraction of the lateral area. It would add to the usefulness of the paper if the author would clarify this point in his closure.

WALTER GLOYER.⁷ Next to the fin efficiency, the correct spacing of fins is of great importance to the designer. Though this is not within the exact scope of the paper, a few words may be said about it here.

If a maximum of heat per unit area of base surface could be transferred just by an increase in extended surface, then fins placed on close centers would be the ideal solution. Fins have to be spaced, however, in such a manner that adjoining fins do not interfere with each other. Fig. 7 of this discussion represents three adjoining straight fins, showing the so-called boundary layers on the center rib as they develop under flow condition, L being the length of a straight rib in the direction of flow or diameter of a circular rib. Before the fluid stream reaches the leading edge of the fin, its velocity is constant over the whole cross section. After entering the fin section at the leading edge, the velocity field is changed, however. The velocity of the fluid is zero at the fin surface and increases within the boundary layer to the full maximum. Blasius⁸ investigated the velocity field of the boundary layer theoretically and gives for viscous flow the following equation for the thickness of the boundary layer

$$\delta = 5.83 \sqrt{\frac{v \cdot L}{w}}$$

⁵ Department of Mechanical Engineering, Virginia Polytechnic Institute, Blacksburg, Va. Now on duty at U. S. Naval Academy, Annapolis, Md. Mem. A.S.M.E.

⁶ "The Numerical Solution of Heat Conduction Problems," by H. W. Emmons, Trans. A.S.M.E., vol. 65, 1943, pp. 607-615.

⁷ American Locomotive Company, New York, N. Y.

⁸ "Grenzschichten in Flüssigkeiten mit Kleiner Reibung," by H. Blasius, Zeit. für Mathematik und Physik, vol. 56, 1908, pp. 1-37.

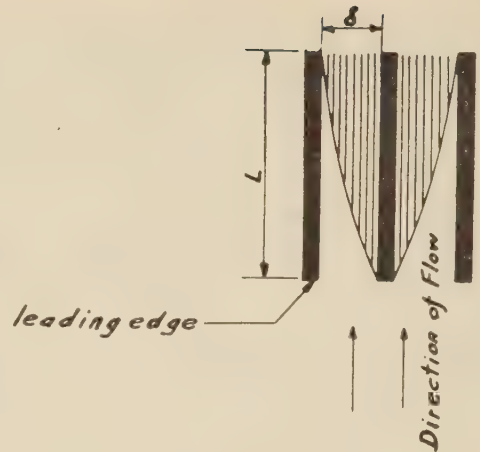


FIG. 7

For turbulent flow von Kármán⁹ determined the boundary-layer thickness from theoretical considerations and gives the following equation

$$\delta = 0.37 L^{1/2} \left(\frac{v}{w} \right)^{1/4}$$

wherein

δ = thickness of boundary layer, cm

v = kinematic viscosity, in stokes, cm^2 per sec

w = fluid velocity outside boundary layer, cm per sec

L = distance from leading edge, cm

If no interference between adjoining ribs would be allowable at all, the distance between them should be twice the thickness of the boundary layer as calculated from the foregoing equations. To clarify this point, Wagener¹⁰ carried through a series of tests on straight ribs with air as the cooling medium. The ribs were of trapezoidal shape, 20 mm high and 20 cm long in the direction of flow. For the tests, the spacing of the ribs as well as the air velocities were varied. Wagener plotted, as shown in Fig. 8, heat transmitted per unit area, time and degrees temperature differential for various air velocities against the spacing of the ribs.

Each resulting curve shows, at a certain spacing, a maximum which swings with decreasing air velocities to a larger spacing. Using a formula of the von Kármán type, Wagener found the most effective spacing to be about 12 per cent larger than the thickness of the boundary layer. These results show that interference between adjoining ribs is slight in the outer regions of the boundary layer. Using his tests as a basis, Wagener recommends a minimum rib spacing of one boundary-layer thickness.

A series of tests similar to Wagener's was conducted at the Langley Memorial Aeronautical Laboratory by Oscar W. Schey and Herman H. Ellerbrock.¹¹ These tests were conducted on finned cylinders. All cylinders had a diameter of 4.5 in., and fins which varied in height, thickness and pitch. The tests were run with air as the cooling medium, and the air velocity was varied between 10 and 130 mph. Schey and Ellerbrock observed the same phenomena as Wagener, but presented no explanation.

⁹ "Über laminare und turbulente Reibung," by T. von Kármán, Zeit. für Angew. Mathematik und Mechanik, vol. 1, 1921, pp. 233-252.

¹⁰ "Der Wärmeübergang an Kühlrippen," by G. Wagener, Beihefte zum Gesundheits Ingenieur, Reihe 1, Heft 24, 1929.

¹¹ "Blower Cooling of Finned Cylinders," by O. W. Schey and H. H. Ellerbrock, Jr., U. S. National Advisory Committee for Aeronautics, Report no. 587, 1937.

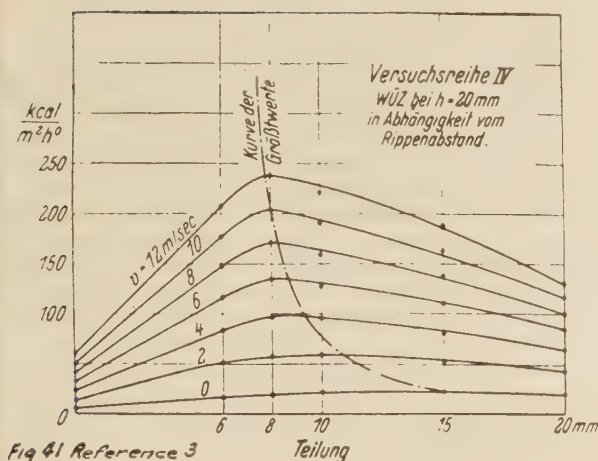


FIG. 8

MAX JAKOB.¹² The author has used an idea of R. D. Douglass to generalize the equations which describe temperature distribution, total heat output, and efficiency of various types of fins. This is presented in such a clear and simple manner as is not often found in the literature on applied mathematics. The paper bristles with Bessel functions; however, an engineer with not more than undergraduate knowledge of calculus and who may never have heard of Bessel functions should be able to operate straightaway with the formulas and one of the tables of Bessel functions referred to in the paper.

According to the outline, contained in the abstract at the beginning of the paper, some forms are excluded from the author's generalization. One of them is the annular fin requiring a minimum of metal, described in E. Schmidt's paper.¹³ Using the author's nomenclature, the profile curve of that fin is represented by the equation

$$y = \frac{h}{6k} \left(2x^2 - 3x_e x + \frac{x_e^3}{x} \right)$$

or

$$a = \frac{2\pi h}{3k} (2x^3 - 3x_e x^2 + x_e^3)$$

which does not satisfy the author's Equation [3].

The differential equations of temperature distribution and heat output of annular fins with triangular or trapezoidal profile do not seem to have been solved exactly as yet, nor are they included in Gardner's generalization, except for the special case where $x \cdot y = \text{const}$.

On the other hand, Gardner's equation covers many cases not dealt with in literature so far. So the generalization in addition to its aesthetic value from a mathematical viewpoint possesses considerable practical value for engineering purposes.

C. F. KAYAN.¹⁴ The excellent treatment of the fin problem by the author leads one to consider comparative methods of analysis by other means. Herein the validity of some of the different assumptions cited by the author and by other workers in

this field might be verified, and possibly the effect of a varying heat-transfer coefficient over the fin surface could be studied. It is believed that the use of a geometrical type of electrical analog could uncover some interesting information along this line. The present paper prompts such a study, with one objective being the determination of isotherms under different conditions of fin shape and of boundary conditions.

H. B. NOTTAGE.¹⁵ The author of this paper is to be complimented for having presented an excellent analytical summary of the extended-surface heat-transfer problem which lends itself very neatly to the treatment of different geometrical contours. With the usual idealizations and boundary conditions being invoked, it is significant to note how Bessel's equation may be employed to represent the different cases. For most practical designs, it would commonly be possible to describe the efficiency of representative fin types, which can be manufactured through ordinary procedures, either in terms of some one or another of the solutions presented or through an approximate interpolation.

Certain considerations beyond the simpler cases remain for future study, however, and it may be helpful to offer a few comments based upon recent experience in similar analyses.

The simplification introduced by the assumption that the heat transfer from the outer edge of the fin tip is negligible, which leads to the author's Equations [6] and [6a], is certainly justifiable for most ordinary problems. However, for precise analyses of large fins, such as those employed on air-cooled engine cylinders, this assumption may be undesirable. The tip-effect correction suggested by Harper and Brown¹⁶ is believed to offer a better approximation.

It may further be worthy of mention to point out that F. D. Bennett has obtained a solution to the case of an annular fin of tapered straight-sided form, described by the sectional contour equation

$$y = y_b - \text{const} (x - x_b)$$

employing the author's nomenclature.

This was accomplished through attacking the difficult differential equation by Picard's method of successive approximations,¹⁷ which is an iteration procedure. The details here are reasonable but tedious, so that there is probably little to recommend for most practical engineering purposes. Harper and Brown suggest an approximate treatment for this type of fin in terms of a taper correction derived for a straight-base fin, and this seems the best simple expedient.

Finally, it may be well to point out an aspect of the fin-design problem which has been dealt with only by inference in this and other recent papers. Fin systems in which the fins are especially wide, and where the fluid medium passes through the interfin passages for an appreciable length, offer important design problems. In these more extended systems the boundary conditions and analytical concepts become more involved than those given here. Point-to-point considerations of the unit surface conductance h , and of the velocity and temperature fields in the fluid become quite important. Compressible fluids make things still more involved.

The fin efficiency then does not remain the constant quantity at all positions along the fin which might be assumed from an application of the simpler analyses. To aid in appreciating the involved features possible, one might visualize this extension of

¹² Consultant in Heat Research, Armour Research Foundation; Research Professor of Mechanical Engineering, Illinois Institute of Technology, Chicago, Ill.; Nonresident Research Professor of Heat Transfer, Purdue University, Lafayette, Ind. Mem. A.S.M.E.

¹³ Reference (4) of author's bibliography.

¹⁴ Assistant Professor, Department of Mechanical Engineering, Columbia University, New York, N. Y. Mem. A.S.M.E.

¹⁵ Project Engineer, Pratt & Whitney Aircraft, East Hartford, Conn. Jun. A.S.M.E.

¹⁶ Reference (3) of author's bibliography.

¹⁷ "The Mathematics of Physics and Chemistry," by H. Margenau and G. M. Murphy, D. Van Nostrand Co., New York, N. Y., 1943, p. 467.

the basic fin problem as a peculiar type of cross-flow heat exchanger, in which a conduction heat stream has replaced one of the fluids. It is believed that analyses of the problems involved in this connection may produce some interesting results, for instance, in the question of a design study to establish fin dimensions for a specified performance.

P. R. TRUMPLER.¹⁸ The use of extended surface in industrial applications is rapidly increasing in scope, and often the economics of a design show great advantages to be gained with large ratios, such as 20 or 30 to 1, of extended to prime surface. Fin efficiency may be a very important factor in such cases.

The problem which the author has solved is idealized, as he has clearly pointed out. In most commercial installations the fin efficiency is 90 per cent or better, and even an appreciable error in determining its value is not serious. It is, however, pertinent to examine the assumptions to find if they are sufficiently close for other applications.

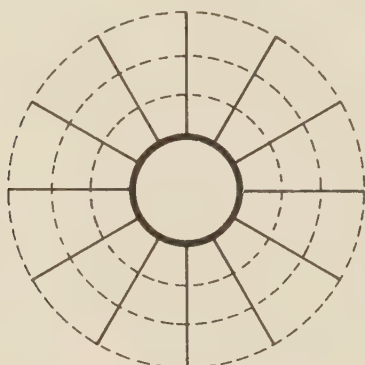


FIG. 9

Let us concern ourselves only with the author's assumptions 6 and 7. With longitudinal or spine fins on tubes, it is apparent that with transfer of sensible heat from a flowing fluid, the longer the fin the wider the variation in film coefficient and the variation in temperature of fluid surrounding the fin. For long fins, however, the efficiency is much more important than for short fins, and it is exactly the condition of long fins that stretches the assumptions.

Next, let us see if the assumptions give a conservative value of fin efficiency in the cases cited. In general, the film coefficient will be less at the base than at the tip of the fin, and the fluid temperature will be closer to the prime-surface temperature near the base than near the tip. The heat load is therefore greater at the tip, and less at the base, than the author's equation would indicate. Thus the calculated fin efficiency is higher than it should be, and we conclude that the calculated values are not conservative.

The possibility of changing assumptions 6 and 7 is not without interest. With much hesitation, the writer proposes a mechanism, as yet untried, to improve the situation for the case of flow parallel to the axis of a finned tube. The flow is channeled into a number of annular spaces separated by membranes as indicated by the dotted lines in Fig. 9 of this discussion. The film coefficients, fluid temperatures, and fin efficiency may be calculated. (The equations for an annulus of differential thickness may be readily set up if the hydraulic diameter is taken as the distance between two adjacent fins at the annular radius.) If the film coefficient at the membranes is taken as infinite, assumption 7

holds. True fluid-temperature conditions exist for membrane-film coefficients which are finite but greater than zero.

The proposed mechanism replaces assumption 6 and permits a conservative assumption in place of 7. It remains to be seen whether the mechanism can be handled mathematically.

In crossflow over finned tube an appreciable variation of film coefficient is to be expected, and the author's values of efficiency must be used with particular care.

With most finned tubes a thermal resistance of appreciable importance is added when the fin is bonded to the tube by pressure contact, solder, or welding. It may be noted that this thermal resistance, often included in the "fin efficiency" of engineering terminology, is not included in the term as used by the author.

AUTHOR'S CLOSURE

It is gratifying to observe the extent of interest in this particular phase of heat transfer apparent in the comments received. Several points requiring amplification are discussed in the following.

In the preparation of this paper it was necessary, due to space limitations, to eliminate certain sections. Among these was that dealing with heat flow through the fin edge, upon which questions are raised by Mr. Nottage and Commander Dusinger. Assumption 10 is not at all necessary to the author's treatment in terms of Bessel functions; it merely simplifies the expressions for β , Equations [6] and [6a], without introducing, in most cases, any significant error. The proper statement of boundary condition 2, following Equation [4], is

$$2(a) \text{ when } x = x_e, \quad \frac{d\theta}{dx} = -\frac{h}{k} \theta$$

from which, for n equal to zero or an integer

$$\beta = \frac{I_{n-1}(u_e) + \frac{1}{p} \sqrt{\frac{ha_e}{k(dA/dx)_e}} I_n(u_e)}{K_{n-1}(u_e) - \frac{1}{p} \sqrt{\frac{ha_e}{k(dA/dx)_e}} K_n(u_e)} \dots \dots [32]$$

or for n equal to a fraction

$$\beta = - \left[\frac{I_{n-1}(u_e) + \frac{1}{p} \sqrt{\frac{ha_e}{k(dA/dx)_e}} I_n(u_e)}{I_{1-n}(u_e) + \frac{1}{p} \sqrt{\frac{ha_e}{k(dA/dx)_e}} I_{-n}(u_e)} \right] \dots \dots [32a]$$

The exact expression for ϕ is

$$\phi = \frac{a_e \theta_e + \int_0^{A_f} \theta dA}{(a_e + A_f) \theta_b} \dots \dots [33]$$

Harper and Brown suggest that substantially the same result may be obtained by considering the fin to be of height, $w + y_e$, instead of w , and using the simpler equations. The fin surface exclusive of the edge area should be used in conjunction with the fin efficiencies presented in this paper. The gain in accuracy by taking the edge area into account may be illusory, since a fin of such dimensions as to make this area an appreciable fraction of the total will probably also violate assumption 9. Professor Kayan's electrical analog seems the simplest solution for such cases.

The variation of film coefficient and ambient temperature which is ignored by assumptions 6 and 7, is probably most appreciable for single annular fins as pointed out by Mr. Nottage. For flow across banks of annular finned tubes, the temperature change over any one film will be considerably less. Although it is

¹⁸ Development Engineer, M. W. Kellogg Company, New York, N. Y. Jun. A.S.M.E.

certainly desirable to know as accurately as possible each of the component parts in the resistance to heat flow through extended surfaces, it should be borne in mind that the *sum* of these resistances (reciprocal heat-transfer coefficients) is the ultimate object. Test data taken to determine film coefficients on extended surface yield an over-all resistance; the outside film resistance sought is obtained by subtracting the other known resistances, among them a metal resistance derived from the fin efficiency. Any error in ϕ due to the assumptions made is therefore reflected in the experimental values of h . However, this resistance ($1/h$) will ordinarily be used in combination with other different internal film and metal resistances. If the latter are based on the same assumptions as used in the original analysis of the test data, much of the error is canceled out in the sum, so that the net effect on over-all heat-transfer coefficient is not so serious as a casual consideration of the points raised by Nottage and Trumpler might suggest.

The author has not had an opportunity to try either of the suggestions for avoiding assumptions 6 and 7 made by Nottage and Trumpler but will add one further suggestion for consideration. If the film coefficient h can be expressed in certain functions of x or θ , Equation [1] can still be solved in many cases, thus eliminating assumption 6.

The ease and speed with which numerical results may be ob-

tained by Southwell's "relaxation" method as recommended by Commander Dusinger is certainly impressive; however, its use seems to be limited to the solution of specific numerical problems. The choice between such a solution and an analytical solution appears to be comparable to a machine-shop problem: A certain operation may require one hour setup time for fifteen minutes of actual machining; by spending eight hours on making a suitable jig the setup time may be reduced to ten minutes. If less than ten parts are to be made it will not pay to make the jig; for any greater number it will. The author believes the fin efficiency curves constitute a well-justified jig for the solution of extended-surface problems.

The digest of the literature on fin spacing contained in Mr. Gloyer's comments is a welcome addition to the symposium on extended surface. So also is Dr. Jakob's inclusion of Schmidt's equations for the most economical annular fin.

Dr. Jakob's comment on annular fins with triangular or trapezoidal profile is partially answered in Mr. Nottage's remarks, although the solution obtained is not claimed to be exact. However, the author has been advised by Dr. G. E. Tate¹⁹ that he has obtained an exact solution in terms of Mathieu or allied functions.

¹⁹ Research Physicist, Foster-Wheeler Corporation, New York, N. Y.

Tube Spacing in Finned-Tube Banks

By S. L. JAMESON,¹ SCHENECTADY, N. Y.

One of the methods used to fulfill application requirements in the design of finned-tube gas coolers for industrial use more adequately is to vary the spacing of the tubes. In the past there has been very little information available on the effect of tube spacing on cooler performance. This paper covers the results of a series of tests made to determine the effect of tube spacing on the pressure drop and the heat-transfer coefficient of air flowing across a bank of helically finned tubes. The tests covered a wide range of tube spacings, both at right angles to air flow and between rows in the direction of air flow. All tests were made on staggered tube rows. The tests showed that tube spacing has a marked effect on air pressure drop, but a negligible effect on the air-side heat-transfer coefficient. The number of fins per linear inch of tube had a similar effect. Baffles in the spaces at the ends of short tube rows were found to be beneficial in minimizing edge effects, the improvement in heat transfer gained by their use more than compensating for the increase in air pressure drop.

NOMENCLATURE

THE following nomenclature is used in the paper:

- A = air-side tube and fin surface, sq ft per linear ft
- B = projected tube perimeter, ft per linear ft
- b = spacing between tube rows in direction of air flow, in.
- c_p = specific heat at constant pressure, Btu/(lb)(deg F)
- d = equivalent diameter of finned tube, ft = $2A/\pi B$
- D = equivalent diameter of tube bundle, as defined by Equation [5], ft
- f = friction factor = $\Delta P \rho g / 2G^2 N$
- g = acceleration due to gravity, ft/hr²
- G = mass velocity, lb/(hr)(sq ft) free area in a row of tubes
- h = true air-film heat-transfer coefficient, Btu/(hr)(sq ft) (deg F)
- H = fin height, ft
- j = heat-transfer factor = $(h/c_p G)(c_p \mu/k)^{2/3}$
- k = thermal conductivity, Btu/(hr)(sq ft)(deg F)/(ft)
- N = cooler depth, rows of tubes in direction of air flow
- Δp = pressure drop over tube bank, in. water
- ΔP = pressure drop over tube bank, psf
- r = diagonal spacing between tubes in successive rows, diameters d
- R = Reynolds number
- s = tube spacing across cooler face, diameters d
- t = fin thickness, ft
- U = over-all heat-transfer coefficient, Btu/(hr)(sq ft) (deg F)
- V = water velocity in tubes, fps
- y = ratio of heat-transfer rate from water to tube at any temperature to that at 90 F average water temperature
- ρ = density, lb per cu ft
- μ = viscosity, (lb)/(hr)(ft)

σ = spacing between fins, ft
 C, n = constants

TEST METHOD

The range of tube diameters and tube spacings tested was made possible by the use of a flexible-duct construction to set up the tube banks. The over-all size of the duct was determined from a study of the capacity of the existing fan and duct equipment, the test banks being made as large as possible in order to make the results more directly applicable to commercial air-cooler design (see Table 1).

TABLE 1 PHYSICAL DATA FOR TUBES AND TEST SECTION

Tubes:					
Diameter of bare tubes, in.....	0.625	0.750	1.00		
Fin:					
Number per linear inch	8.7	7.0	9.05	8.8	7.0
Outside diameter, in.	1.121	1.463	1.737	1.737	1.737
Thickness, in.....	0.010	0.012	0.012	0.012	0.012
Height/2 X spacing	1.133	0.895	1.746	1.751	1.357
Surface, sq ft per ft tube	1.138	0.946	2.049	2.560	2.085
Projected area, sq in./ft tube.....	8.24	8.14	10.19	13.19	13.01
Projected perimeter, ft/ft tube.....	10.3	8.67	14.48	14.54	11.98
Equivalent diameter, ft	0.0702	0.0693	0.0901	0.1119	0.1108
Ratio gas to water-side surface.....	8.25	6.86	12.02	10.85	8.85
Test section:					
Width between side plates, in.....			23 1/2		
Length of tubes, in.....			24		
Centers first to last tube in long row, in.....	22.18	21.80		21.55	
Center outer tube to side of duct, in.....	0.66	0.85		0.975	
Height of baffle in short tube rows, in.....	0.40	0.44		0.44	
Tubes in long tube row	13 to 19	9 to 15		8 to 12	

The initial setup provided for making isothermal pressure-drop tests only. Three to six pressure-drop measurements were made for each tube-bank arrangement, covering about a 10-to-1 range in air flow. Most of these tests were run at room temperature. A few check tests were made at 120 to 140 F.

When it became apparent that there was considerable variation in air pressure drop with tube spacing, the test duct was altered so water could be circulated through the finned tubes and heat-transfer data obtained.

Air-pressure-drop readings were taken during all heat-transfer test runs. In these tests the air temperature drop over the tube banks varied from 10 to 100 deg F. The average air temperature was taken as the arithmetic-mean water temperature plus the log-mean temperature difference between water and air.

All pressure-drop data were corrected to an average air temperature of 120 F, and a pressure of 14.7 psia. Correction factors for test pressure and temperature were based on constant mass-air velocity, assuming that pressure drop varied as the 1.75 power of air velocity. (An error in the assumed value of this coefficient has no effect on the correction factors for pressure, and a negligible effect on the correction factor for temperature, if the factors are based on mass velocity instead of on linear velocity.) These correction factors are given in Fig. 5. There was no appreciable deviation between the results of the isothermal pressure-drop tests and those of the varying temperature tests on a given tube bank.

Heat-transfer test runs on each tube bank were made at the maximum water velocity through the tubes obtainable for each setup, usually about 4 fps, and at approximately 1 fps for each

¹ Engineer, General Electric Company. Jun. A.S.M.E.

Contributed by the Heat Transfer Division and presented at the Annual Meeting, New York, N. Y., Nov. 27-Dec. 1, 1944, of THE AMERICAN SOCIETY OF MECHANICAL ENGINEERS.

NOTE: Statements and opinions advanced in papers are to be understood as individual expressions of their authors and not those of the Society.

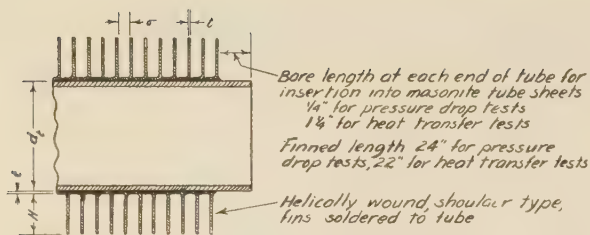


FIG. 1 SKETCH OF FINNED TUBING USED FOR TESTS

of at least two different air flows. In several cases check tests were made at about 2-fps water velocity. Special care was taken to hold the mass-air velocity constant for each set of tests at varying water velocities.

The heat-transfer test data were correlated by plotting

$$1/U \text{ versus } 1/yV^{0.8}$$

The temperature drop through the tube wall is negligible and special care was taken to keep the tubes clean, so the zero intercept of this curve is the reciprocal of the effective air-side heat-transfer coefficient. The "effectiveness factor" of the fins is readily calculated for any effective air-side heat-transfer coefficient, and the true air-side heat-transfer coefficient obtained. This correlation takes into account variations in average water temperature. Variation of average air temperature affects the heat-transfer coefficient about 1 per cent for each 25 deg F and was neglected since the average air temperature was maintained within 15 deg F of the 120 F correlating temperature.

TEST EQUIPMENT AND MEASUREMENTS

The tests were made in a duct system especially designed and constructed for air-flow testing. The general arrangement is shown in Fig. 3.

The air-circulating blower was driven by a direct-current motor with a 10:1 speed range. Fine adjustments in air flow could be obtained by adjustment of a damper in the duct ahead of the blower.

Air flow was measured by rounded-approach nozzles of spun aluminum geometrically similar to nozzles calibrated by the Bureau of Standards. In each test enough nozzles were plugged to make the pressure drop over those in use between 0.5 and 1.0 in. of water. The air pressure drop over the nozzles was measured by an Ellison inclined draft gage with 0.01-in. water scale divisions.

The air pressure drop over the test section was measured by an Ellison draft gage, calibrated in 0.01-in. scale divisions for the first inch of water and 0.1-in. divisions for the next 5 in.

The pressure tap in the inlet duct to the test section was a 1/16-in. hole in a plate flush with the duct wall 12 in. upstream from the coil face. All other pressure taps were 1/4-in. tubes with 1/32-in. holes at intervals over a 4-in. length. These tubes were enclosed in 2 x 2 x 6-in. cages of fine-mesh screen containing a ribbon of screening wound back and forth over the tubes. Tests have shown that this arrangement reads true static pressures, even in the presence of considerable velocities.

Air temperatures were measured with copper-Copnic thermocouples on a thermocouple potentiometer having 1-deg-F scale divisions. The thermocouples and potentiometer were calibrated against laboratory standards and all temperature measurements were corrected for calibration errors. Radiation shields were used on all thermocouples to minimize errors.

The water circulated through the test coil was taken from an overhead tank equipped with an overflow to insure a constant

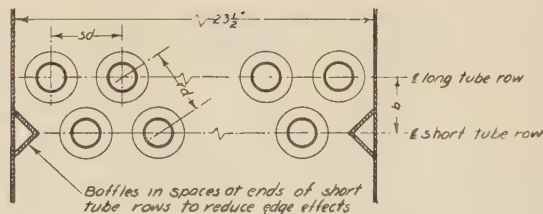


FIG. 2 SKETCH OF TUBE ARRANGEMENT

gravity head. Partial recirculation with make-up water from the city mains was used to maintain constant water temperature to the test section.

Water flow was measured by a sharp-edged orifice, calibrated in place by means of a weigh tank. Colored carbon tetrachloride was used for the manometer fluid in order to magnify the deflection.

Water temperatures were measured by precision-type thermometers inserted directly into the flowing water through packed openings. The thermometer wells were located as close to the test coil as possible and the pipe insulated for a distance of 6 in. on either side of the well. The thermometers were marked in 0.1-deg F scale divisions and were calibrated to 0.01 deg F, against laboratory standards.

The test section consisted of a steel framework to support interchangeable fiberboard tube sheets. Fiberboard side sheets were fastened permanently to the frame. The tubes were standard admiralty-metal condenser tubes wound with copper fins.

The first tests were made for pressure drop over the tube bundle only, and for these tests a length of 1/4 in. was left bare of fins at either end of the tube for insertion into the tube sheets. When the program was extended to include heat-transfer studies the test section was modified so the tubes projected through the tube sheets about 1 in., Fig. 1. Special water headers were made up and connected to the tubes by rubber tubing. Connections between successive rows of tubes in the direction of air flow were also made by rubber tubing. Most of the tests were made with one row of tubes per pass for water flow. The inside of the tubes was carefully cleaned before each test.

RESULTS OF TESTS

Since the tests covered by this paper were made primarily to obtain data for use in the design of cooling equipment for industrial machines, all data were corrected to an average air temperature of 120 F and a pressure of 14.7 psia.

Pressure-Drop Tests. The test results showed the pressure drop over a tube bank of two or more rows depth to be directly proportional to the number of rows of tubes depth. The Fanning equation for flow over a tube bank has therefore been set up as

$$\Delta P = 2fG^2N/\rho g \dots \dots \dots [1]$$

In general, the friction factor is a function of Reynolds number

$$f = C_1 R^{n-2} \dots \dots \dots [2]$$

The pressure drop over a tube bank at a specific pressure and temperature may be expressed as

$$\Delta p = 10^{-7} CG^n \text{ in. water.} \dots \dots \dots [3]$$

For flow through a pipe, the value of n is about 1.8. The value of n for pressure drop over a tube bundle was found to vary from about 1.7 to 1.9 in these tests, the highest values being obtained with a very wide tube spacing across air flow and closely

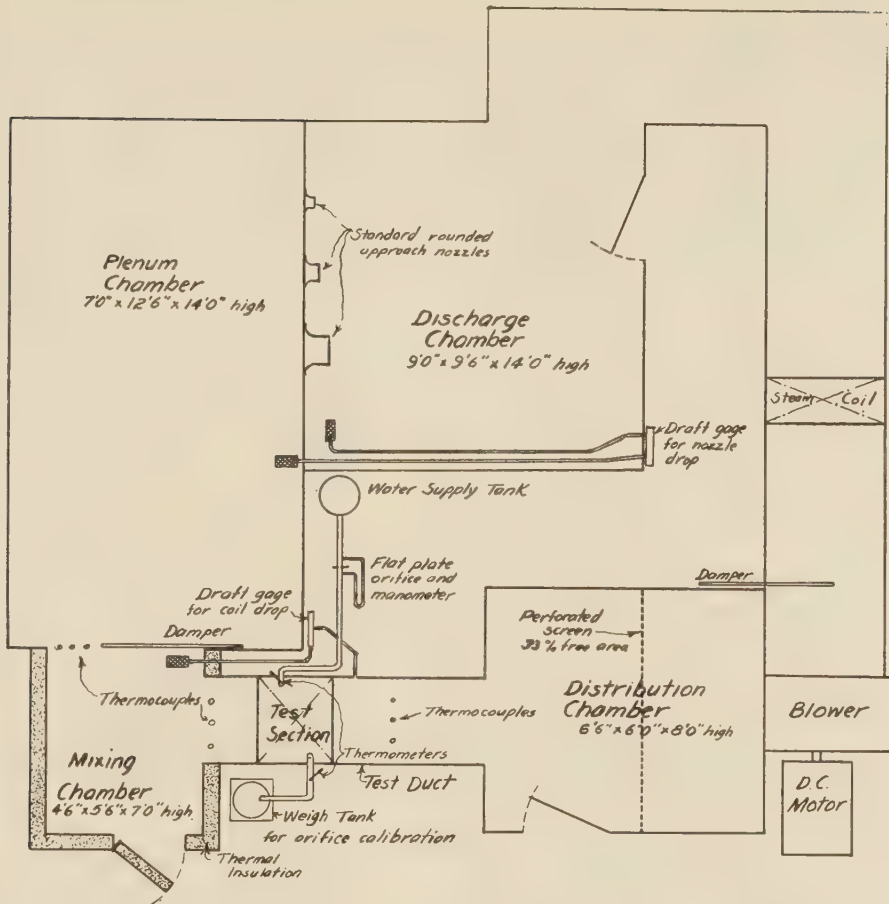


FIG. 3 SKETCH OF TEST DUCT

spaced rows in the direction of air flow. A study of the values of n showed the following:

- (a) An increase in value as tube spacing across the face of the cooler increased.
- (b) A minimum value for the spacing between rows at which the free area through the diagonal openings between two successive rows of tubes equaled that in a single row of tubes.
- (c) A decrease in value as the number of rows of tubes increased.

A possible explanation of these variations is that the pressure drop over a tube bundle is a combination of velocity-head losses, due to the nozzle effect in passing through the minimum spaces between tubes, and frictional losses. The indication from the tests is that the frictional losses would vary as some power of G less than 1.7. The velocity-head loss due to the nozzle effect would vary as the square of G . In the case of close tube spacing, the loss is mostly frictional and the value of n is therefore low. As the tube spacing increases, the frictional component of pressure drop decreases relative to the velocity-head component, and n therefore increases. When the minimum free area through the diagonal openings between two successive rows of tubes equals that in a single row of tubes, the flow path is almost nearly uniform, the velocity head component is a minimum, and the value of n is therefore a minimum.

From the standpoint of obtaining design information and for a general study of the effects of tube spacing it was found con-

venient to use an average value of n for the various tube arrangements. Equation [3] then becomes

$$\Delta p = 10^{-7} C G^{1.75} \dots \dots \dots [4]$$

The values of C for this approximation and the values of n in Equation [3] are given for the various tube arrangements tested in Table 2.

Using the values of C in Equation [4], the curves in Fig. 4 showing the variation of pressure drop with tube spacing were plotted. The variation in pressure drop with tube spacing across the face is nearly enough independent of the spacing between rows to enable using a single curve for each tube diameter for the correction for tube spacing across the cooler face. The same condition holds for the correction for variation of the spacing between rows in the direction of air flow.

The curves for correction factors for tube spacing given in Fig. 5 are based directly on the curves in Fig. 4. The one exception is the curve for variation in spacing between rows for $3/4$ -in. tubes. This curve has been drawn more conservatively than would be indicated by Fig. 4, in order better to line up with the curves for $5/8$ -in. and 1-in. tubes. This may not be completely justified, but from the design standpoint it was felt that any error should be on the conservative side.

The correction factors given in Fig. 5 are adjusted for tube spacing so a single curve of pressure drop versus mass-air velocity may be used for all sizes of finned tubes.

Baffles placed in the spaces at the ends of the short tube rows

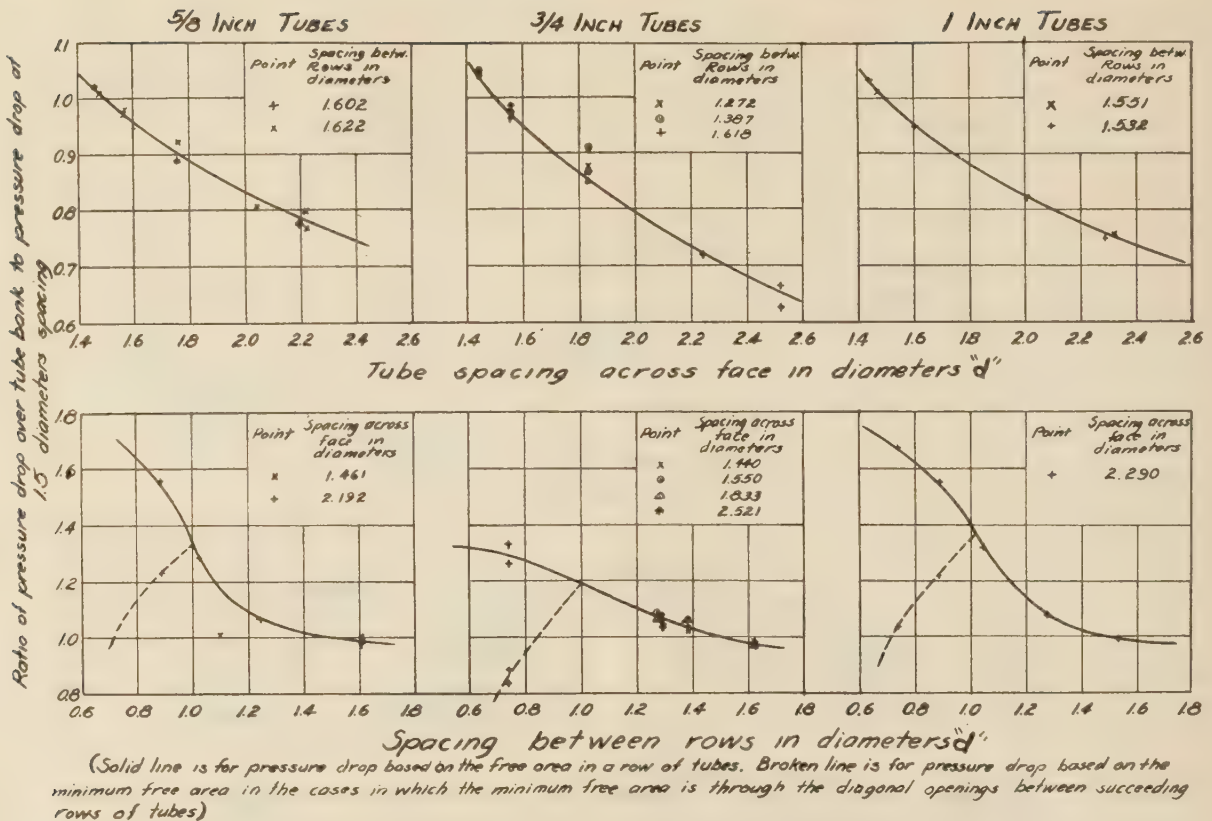


FIG. 4 VARIATION OF PRESSURE DROP WITH TUBE SPACING

(see Fig. 2, and Table 1) were found to be of considerable value in reducing edge effects, particularly in the case of heat transfer. Check tests showed a baffle made up of an angle with the open side laid against the side of the cooler had the same effect as a half-tube. Since an angle-type baffle is convenient from the standpoint of production, most of the tests were made with angle baffles. The effect of the baffles on pressure drop was found to be about as the 1.75 power of the ratio of the free area in a short tube row to the free area in a long tube row.

The correlation between field tests of coolers installed in machines with the pressure drop calculated by the use of the factors given in Fig. 5 has been very good. The deviation has been less than 5 per cent, even with coolers very narrow across air flow and with closely spaced rows in the direction of air flow.

A relation of the form of the Fanning equation which would correlate the data for all the tube sizes and arrangements tested would be of considerable value in predicting the performance of new finned-tube designs and also in improving present designs. Considerable time was spent trying to obtain such a relation, but without complete success.

The following empirical relation for the "equivalent diameter" of a tube bank correlates the data fairly well for tube banks in which the free area in an individual row of tubes is less than that in the diagonal openings between two successive rows of tubes.

$$D = \left[\left(\frac{H}{2\sigma} \right)^{0.4} \left(\frac{1}{2\sqrt{s}-1} + \frac{1}{2\sqrt{r}-1} \right) \right]^4 \dots [5]$$

Equation [2], using this expression becomes

$$f = 1.532 R^{-0.25} \dots [6]$$

Equation [4] becomes

$$\Delta p = 9.56 \times 10^{-9} D^{-0.25} V G^{1.75} \text{ in. water} \dots [7]$$

(This relation applies only for air at 120 F average temperature and 14.7 psia pressure.)

Although these relations are empirical, they cover the usual range of design and give an indication of the effect of some of the variables on pressure drop. The relations should not be used for Reynolds numbers less than 500 or more than 10,000.

Term f is plotted against R in Fig. 6 for the highest and lowest test air flows for all tube arrangements tested in which the minimum free area was that in a single row of tubes.

If the test values of f shown in Fig. 6 are approximated by the broken line, this line reflects the increase in the value of n in Equation [3] with tube spacing. An increase in tube spacing increases the "equivalent diameter" of the tube bank, and therefore the Reynolds number.

Fig. 7 shows a comparison between the friction factor for the tube-spacing tests and the friction factors obtained in tests of larger commercial units. Curves d and e cover tests made at pressures up to 15 psig. The comparative data given are for coolers having the free area through the diagonal openings between two successive rows of tubes greater than that in an individual tube row. Test data on a commercial cooler in which the minimum free area was through the diagonal openings between successive tube rows checked that for model tests on a similar spacing closely, but do not line up with the friction-factor curve. Such coolers are definitely outside the range of application of Equations [5], [6], and [7]. The pressure drop over such coolers may be calculated from Fig. 5, however.

Heat-Transfer Tests. There was no apparent variation in the air-side heat-transfer coefficient with tube spacing in any of the tests made with baffles in the spaces at the ends of the short tube rows. The mass-air velocity used for heat-transfer data was based on the free area in a single row of tubes, regardless of the relative magnitude of the free area in the diagonal openings between successive rows of tubes.

Without the baffles in the spaces at the ends of the short tube rows, the apparent air-side heat-transfer coefficient was lower, especially in the case of tubes spaced close together across air flow. In this case the omission of a tube in the short tube row has a slightly greater percentage effect on the free area.

With the baffles omitted the air at the sides of the cooler is only partially cooled. This has been checked several times by thermocouple traverses across the face of a cooler. This partially cooled air has the effect of lowering the apparent heat-transfer coefficient much more than does the decrease in average mass-air velocity due to the increased free area in the short tube rows. The baffles almost completely eliminated these "edge effects."

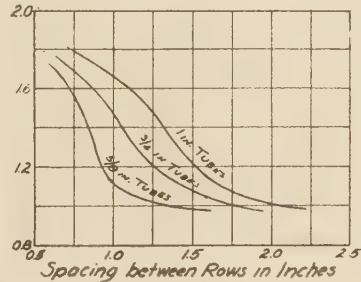
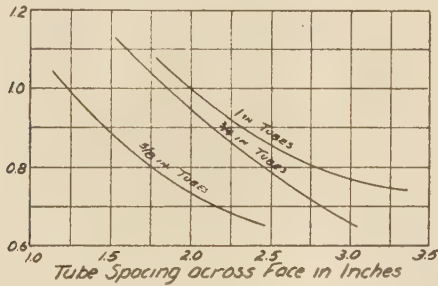
The improvement in heat transfer gained by the use of baffles in the short tube rows more than compensates for the increase in air pressure drop. In addition, the use of baffles makes the heat-transfer coefficient independent of cooler width and of tube spac-

The standard air pressure drop curve is based on.

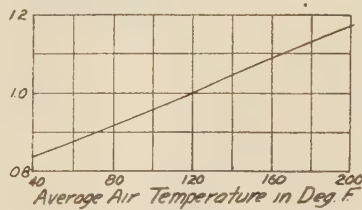
1. Air at 14.7 lb/sq in. abs. pressure and 120°F average temperature.
2. Staggered tube banks.
3. Baffles in the spaces at the ends of the short rows of tubes
4. 9 helically wound fins per lineal inch of tube.

Multiply the pressure drop from the standard curve by the factors given below to determine the pressure drop for an individual design.

1. TUBE SPACING



2. AVERAGE AIR TEMPERATURE



3. AIR PRESSURE

Multiply by $.14.7/\text{pressure in lb./sq. in. abs.}$

4. FINS PER LINEAL INCH OF TUBE

Multiply by $(\text{Number fins per lineal inch}/9)^{0.4}$
(This is about 4% per fin)

5. OMISSION OF BAFFLES IN SHORT TUBE ROWS.

Multiply by $(\text{Free area in long tube row}/\text{Free area in short tube row})^{1.75}$
(This is roughly 0.9 for a 2'6" wide cooler)

NOTES.

1. Correction factors are based on a constant mass air velocity.
2. Use free area in a row of tubes in all cases, even though the free area thru the diagonal openings between successive rows of tubes may be less.

FIG. 5 PRESSURE-DROP CORRECTION FACTORS FOR DESIGN USE
(Air pressure drop over finned-tube banks.)

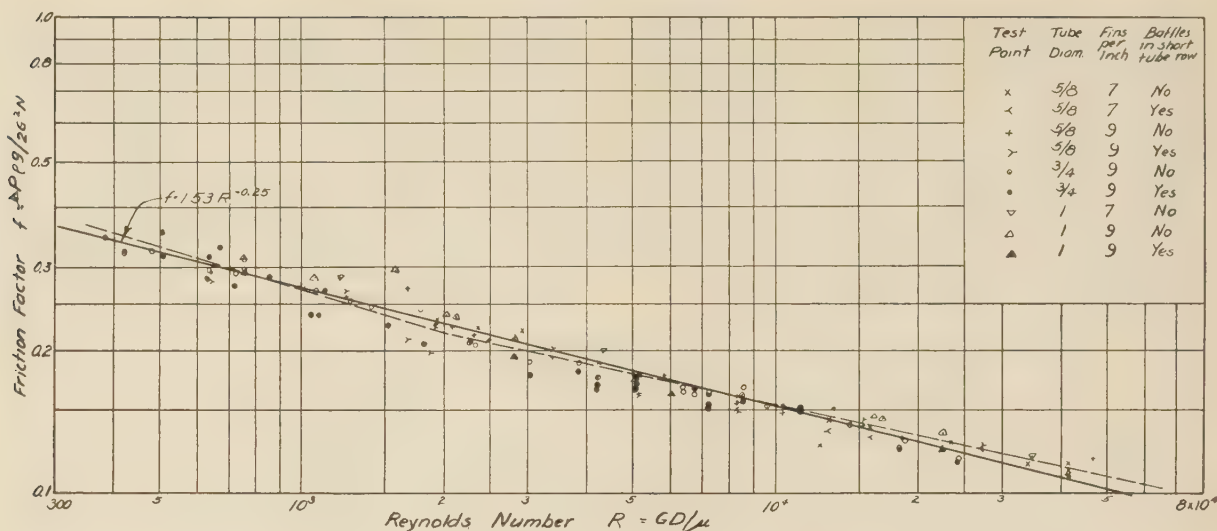


FIG. 6 FRICTION FACTORS FOR TUBE BANKS TESTED
(Points plotted are highest and lowest air-flow test points for each tube arrangement.)

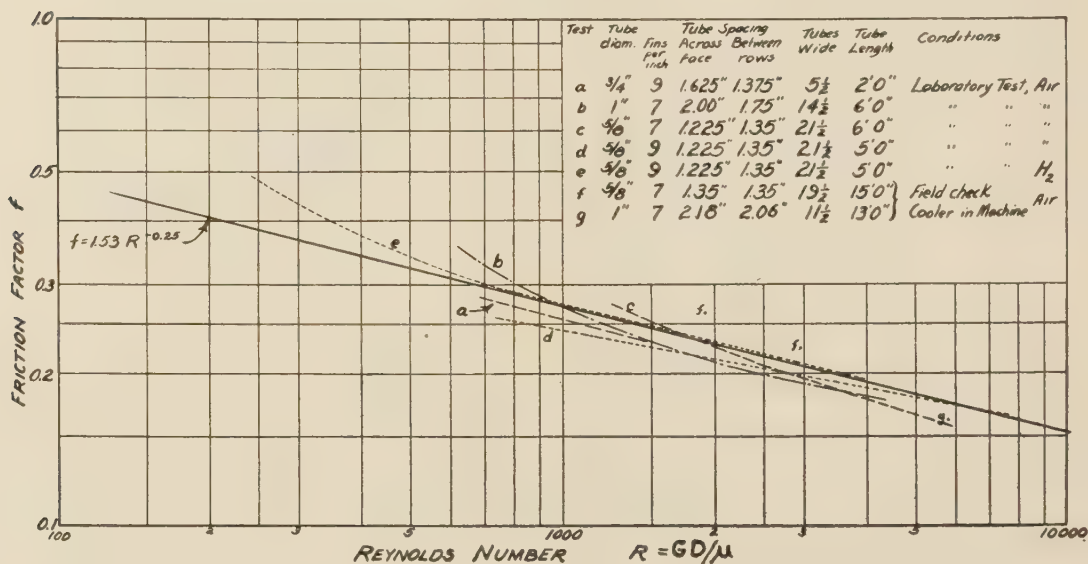


FIG. 7 COMPARISON OF FRICTION FACTOR FROM TUBE-SPACING TESTS WITH TESTS OF COMMERCIAL UNITS

ing. For these reasons baffles are specified for all coolers less than 2 ft in face width and for many wider coolers.

Fig. 8 shows the air-side heat-transfer coefficients obtained for the various tube bundles tested as a function of mass-air velocity.

The dimensionless heat-transfer factor j was plotted against Reynolds number to correlate the tests on various sizes of tubes. The best correlation was obtained using Reynolds number based on the equivalent diameter of an individual tube rather than by using the diameter defined by Equation [5]. The curve of j versus R for all tests made with baffles in the short tube rows is given in Fig. 9.

In all cases the average air-side heat-transfer coefficient decreased as the cooler depth decreased. A study of the results indicated that for a cooler of N rows of tubes depth, $N-1$ rows will have a relative performance of 1.0, and one row will have a relative performance of 0.7. Since most coolers for industrial

equipment are more than four rows of tubes deep, the effect of cooler depth on over-all performance may be neglected in design.

A curve showing the heat-transfer factors obtained in tests of a commercial turbine-generator cooler is also given in Fig. 9. The discrepancy between this curve and the results of the tube-spacing tests is in line with previous model tests. For some unexplained reason tests of sample-size coolers usually give a higher air-side heat-transfer coefficient than is obtained in tests of commercial coolers. On the other hand, pressure-drop data usually check closely.

RELATED DATA AND SUGGESTIONS FOR FUTURE TESTS

There are few data available from other sources on the effects of varying tube spacing in finned-tube banks.

Pierson, Huges, and Grimson have reported on a series of tests on the effect of spacing of bare tubes on heat transfer and pressure

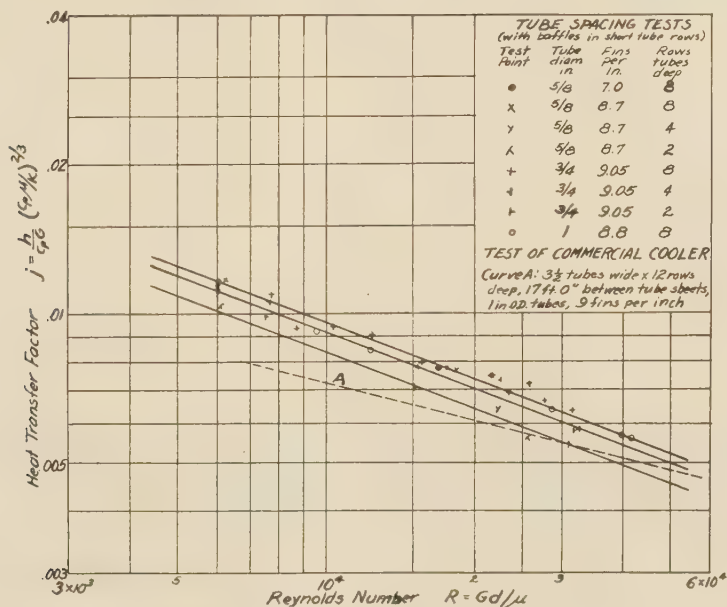
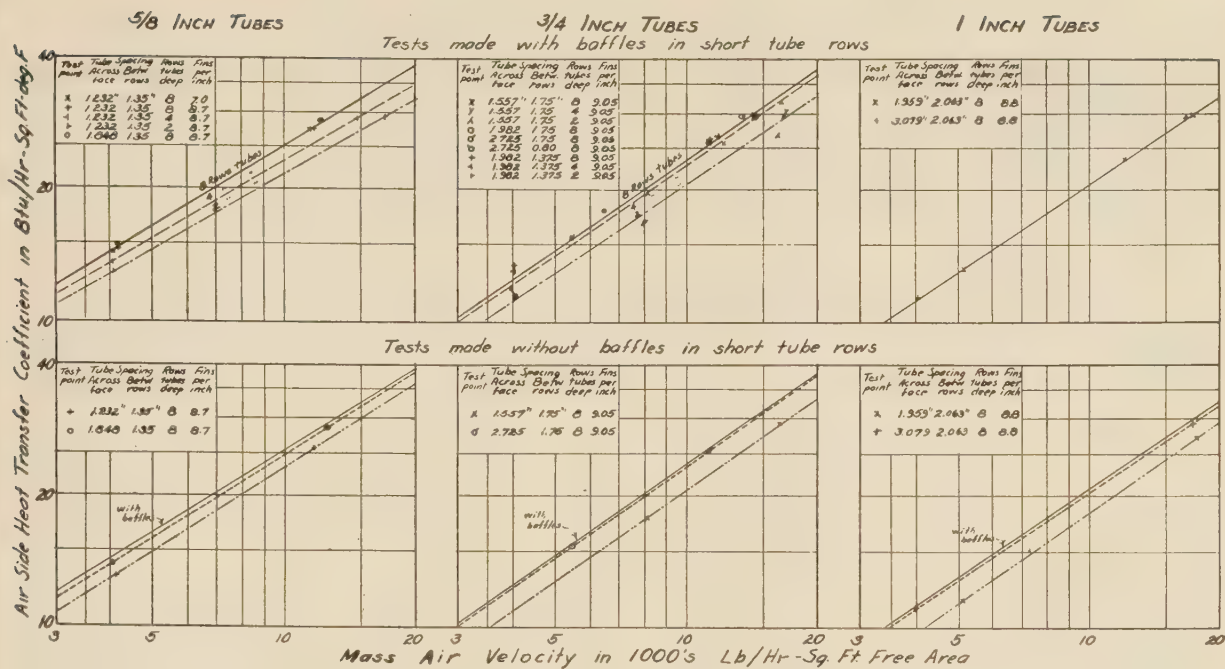


TABLE 2 VALUES OF n IN EQUATION [3], $\Delta p = 10^{-7} CG^n$, AND VALUES OF C IN EQUATION [4], $\Delta p = 10^{-7} CG^{1.75}$

(a) for 5/8 inch O.D. Tube Tests.

Spec. betw. rows, in.	Rows tubes. deep	Values of n , $\Delta p = 10^{-7}CG^n$					Values of C , $\Delta p = 10^{-7}CG^{1.75}$				
		Tube spacing across cooler face in inches									
		1.232	1.304	1.478	1.705	1.848	1.232	1.304	1.478	1.705	1.848

7.0 fins per inch

Without baffles in short tube rows

1.35	8	1.744	1.749	1.749	1.760	1.779	1.647	1.600	1.522	1.350	1.293
1.35	4					1.835					.653
1.35	2					1.877					.304

With baffles in short tube rows

1.35	8	1.757	1.758			1.779	1.720	1.674			1.364
------	---	-------	-------	--	--	-------	-------	-------	--	--	-------

8.7 fins per inch

Without baffles in short tube rows

0.75	8					1.727*					1.779
0.865	8					1.719					1.864
1.05	8					1.759					1.543
1.063	8	1.719					1.931				
1.35	8	1.726		1.756		1.785	1.809		1.600		1.422
1.35	4	1.740					.905				
1.35	2	1.775					.463				
2.00	8					1.809					1.353

With baffles in short tube rows

1.063	8	1.739				1.781	2.099				
1.35	8	1.736		1.769			2.094		1.814		1.586
1.35	4	1.790					.917				
1.35	2	1.832					.466				
	1	1.806					.247				

*Minimum free area in diagonal openings between successive tube rows.

On frontal plane free area:

0.75	8					1.727					2.254
------	---	--	--	--	--	-------	--	--	--	--	-------

drop in crossflow over tube banks in a group of three papers.² An expression similar to that for the "equivalent diameter" of the tube bank used to correlate the finned-tube-spacing tests was of no value in correlating their data for bare tubes. The finned-tube tests do agree with the data for bare tubes in that the variation of heat transfer with tube spacing was small, but that there was considerable variation in air pressure drop. In both cases the pressure drop at a given mass-air velocity decreased with increase in tube spacing.

On the basis of the results of the tests covered by this paper it

² "Experimental Investigation of Influence of Tube Arrangement on Convection Heat Transfer and Flow Resistance in Crossflow of Gases Over Tube Banks," by O. L. Pierson, Trans. A.S.M.E., vol. 59, 1937, pp. 563-572.

"Experimental Investigation of Effects of Equipment Size on Convection Heat Transfer and Flow Resistance in Crossflow of Gases Over Tube Banks," by E. C. Huge, Trans. A.S.M.E., vol. 59, 1937, pp. 573-581.

"Correlation and Utilization of New Data on Flow Resistance and Heat Transfer for Crossflow of Gases Over Tube Banks," by E. D. Grimson, Trans. A.S.M.E., vol. 59, 1937, pp. 583-594.

is suggested that any future tests on the effects of tube spacing be made with half-tubes or baffles in the spaces at the ends of the short tube rows. This gives much more consistent and more generally applicable data.

A wider range of tube diameters and of the number and height of fins would enable a better determination of the effect of tube-design variables and thereby aid in predicting the performance of new designs.

Discussion

A. Y. GUNTER³ and W. A. SHAW.⁴ The author has done an admirable job in the presentation of some usable design data for finned-tube gas coolers.

³ Director of Development, Alco Products Division, American Locomotive Company, New York, N. Y. Mem. A.S.M.E.

⁴ Heat Transfer Engineer, Research and Development Department, Alco Products Division, American Locomotive Company, New York, N. Y. Jun. A.S.M.E.

TABLE 2 (Continued)

(b) for 3/4 inch O.D. Tube Tests.

Spac. betw. rows in.	Rows Tubes deep	Values of $n, \Delta p = 10^{-7}CG^n$					Values of $C, \Delta p = 10^{-7}CG^{1.75}$				
		Tube spacing across cooler face in inches									
		1.557	1.676	1.982	2.422	2.725	1.557	1.676	1.982	2.422	2.725

9.05 fins per inch

Without baffles in short tube rows

0.80	8					1.722*					1.155*
0.80	4					1.753*					.632*
0.80	2					1.780*					.304*
1.162	8					1.731					1.668
1.375	8		1.730	1.753				2.013	1.876		
1.400	8					1.754					1.447
1.500	8	1.737	1.754	1.769			2.127	1.988	1.876		
1.750	8	1.676	1.721	1.750	1.775	1.775	2.056	1.896	1.702	1.458	1.356
1.750	4	1.715					1.000				
1.750	2	1.742					0.497				

With baffles in short tube rows

0.80	8					1.758*					1.323*
1.375	8		1.733	1.771				2.282	2.038		
1.375	4		1.737	1.778				1.098	.969		
1.375	2		1.737	1.775				.533	.481		
1.400	8					1.749					1.600
1.500	8	1.721	1.736	1.745			2.383	2.230	2.013		
1.750	8	1.691	1.710	1.748		1.793	2.396	2.251	1.938		1.434
1.750	4	1.698					1.109				
1.750	2	1.702					.533				
--	1					1.863					.215

*Minimum free area in diagonal openings between successive tube rows.

On frontal plane free area:

0.80	8	Without baffles	1.722	1.742
0.80	4		1.753	.952
0.80	2		1.780	.458
0.80	8	With baffles	1.758	1.997

In a few instances, clarification of certain points seems desirable for a more ready comprehension of the paper:

Under "Nomenclature" in the definitions of r and s , it is suggested that "diameters d " be more specifically stated as being "equivalent diameters, previously defined."

In the tables and in Fig. 2, the "spacing between rows" (shown as b in the figure) should be tied together, with a listing under the nomenclature, to prevent any misinterpretation with rd , the "diagonal spacing."

TABLE 2 (Continued)
(c) for 1 inch O.D. Tube Tests.

Spec. betw. rows, in.	Rows tubes deep	Values of $n, \Delta p = 10^{-7}CG^n$				Values of $C, \Delta p = 10^{-7}CG^{1.75}$			
		Tube spacing across cooler face in inches							
		1.959	2.155	2.694	3.079	1.959	2.155	2.694	3.079

7.0 fins per inch

Without baffles in short tube rows

2.06	8	1.697			1.750	1.720			1.355
------	---	-------	--	--	-------	-------	--	--	-------

8.8 fins per inch

Without baffles in short tube rows

1.00	8				1.725*				1.538*
1.00	4				1.730*				.769*
1.20	8				1.727*				1.805*
1.41	8				1.725				1.948
1.70	8				1.777				1.604
2.06	8	1.717	1.730	1.767	1.781	1.939	1.805	1.601	1.477

With baffles in short tube rows

2.06	8	1.721			1.781	2.122			1.529
------	---	-------	--	--	-------	-------	--	--	-------

*Minimum free area in diagonal openings between successive tube rows.

On frontal plane free area:

1.00	8				1.725				2.485
1.00	4				1.730				1.243
1.20	8				1.727				2.300

A General Correlation of Friction Factors for Various Types of Surfaces in Crossflow

By A. Y. GUNTER¹ AND W. A. SHAW,² NEW YORK, N. Y.

This paper is the elaboration of an unpublished one by the late E. S. Davis and A. Y. Gunter, which was released only to the National Advisory Committee for Aeronautics. The present work, using the friction-factor correlation proposed for bare tubes by Davis and Gunter, demonstrates its merit as a general method for correlating on a single line, pure crossflow friction over both bare and extended surfaces. This result is made possible through the use of an equivalent volumetric hydraulic diameter D_v , in both the Reynolds number and the ordinate, plus configuration ratios of the form $(D_v/S_T)^n$ and $(S_L/S_T)^n$ in the ordinate. Friction factors for bare tubes of diameters from 0.02 in. to 2 in. are included, with transverse and longitudinal pitches ranging from 1.25 to 5 diam. Extended-surface crossflow friction reported on herein covers external round and square cross fins, both meshed and unmeshed, finned cylinders, radiator core-type surface, and one sample of internal wire-mesh fins. It is shown that flat plates and core-type surface with turbulence promoters do not correlate well on the proposed curve.

NOMENCLATURE

The following nomenclature is used in this paper:

- D_p, D_t = pipe or tube diameter, ft (except as noted in tables)
 D_v = volumetric hydraulic diameter = $\frac{4 \times \text{Net free volume}}{\text{Friction surface}}$, ft
 $f'/2$ = half friction factor corrected by viscosity ratio $(\mu/\mu_w)^{0.14}$, dimensionless
 $f''/2$ = half friction factor corrected by viscosity ratio $(\mu/\mu_w)^{0.14}$ and $(D_t/S_T)^{0.4}$, dimensionless
 $f/2$ = half friction factor corrected by viscosity ratio $(\mu/\mu_w)^{0.14}$, $(D_v/S_T)^{0.4}$, and $(S_L/S_T)^{0.4}$, dimensionless
 g = acceleration of gravity = 4.18×10^8 ft/hr per hr
 G = fluid mass velocity (based on minimum net free area), psf per hr
 L = fluid flow length, ft
 n = denotes exponent
 ΔP = pressure drop due to "friction," psf
 S_L = longitudinal pitch = center-to-center distance from tube in one row to nearest tube in next transverse row
 S_T = transverse pitch = center-to-center distance from tube to tube in one transverse row

I = in-line tube arrangement (used in tables)

S = staggered tube arrangement (used in tables)

ϕ = denotes function

μ = absolute viscosity at average main stream temperature, lb per ft per hr

μ_w = absolute viscosity at surface wall temperature, lb per ft per hr

ρ = fluid density, pcf

$(D_v/S_T)^n, (S_L/S_T)^n$ = configuration correction factors, dimensionless

$(\mu/\mu_w)^{0.14}$ = viscosity-ratio correction factor (Sieder and Tate), dimensionless

INTRODUCTION

Up to the present time, correlations of friction factors for pure crossflow over bare tubes have been based on the use of a hydraulic diameter (D_p or D_t), representing the pipe or tube outside diameter in the conventional Reynolds number, i.e., Colburn (1),³ Short (2), Bowman (3), Huge (4), Grimson (5), and others; or some form of equivalent diameter based on perimeter for other types of surfaces, e.g., Norris and Spofford (6).

Sieder and Scott (7) suggested an equivalent hydraulic diameter (D_v), but did not make a usable general correlation. Davis and Gunter (8), in an unpublished paper presented to the N.A.C.A., gave correlations for both heat transfer and pressure drop in crossflow over bare-tube banks. These correlations used D_v in the Reynolds number and in the conventional ordinate, plus correction factors for tube arrangement of the form $(D_v/S_T)^n$ and $(S_L/S_T)^n$.

As far as is known, no one has satisfactorily obtained correlation of bare tubes and conventional extended surface in pure crossflow on one line. Many investigators have taken a limited range and obtained curves describing the results therefrom. It was felt that one curve covering a wide range would be of benefit to all.

The present paper, following the lead of Davis and Gunter (8), proposes a general correlation covering both bare and extended surfaces using the correction factors mentioned. This presumes that fins are relatively smooth, and rows of tubes are three or more in depth in conventional arrangements. In addition, crossflow friction on one arrangement of internal fins is shown to correlate in good agreement on the proposed curve.

It should be pointed out that the following discussions do not take into account baffle effects, and for practical use, these factors should be allowed for, where applicable.

GENERAL DISCUSSION

In the Davis and Gunter paper (8), it was pointed out that most investigators have found that the classic form of the general Fanning equation for flow inside tubes could be adapted to crossflow outside of bare tubes, using tube outside diameter as hydraulic diameter (D_t). Others used perimeter-type hydraulic

³ Numbers in parentheses refer to the Bibliography at the end of the paper.

¹ Director of Development, Alco Products Division, American Locomotive Company. Mem. A.S.M.E.

² Heat Transfer Engineer, Research and Development, Alco Products Division, American Locomotive Company. Jun. A.S.M.E.

Contributed by the Heat Transfer Division and presented at the Annual Meeting, New York, N. Y., Nov. 27-Dec. 1, 1944, of THE AMERICAN SOCIETY OF MECHANICAL ENGINEERS.

NOTE: Statements and opinions advanced in papers are to be understood as individual expressions of their authors and not those of the Society.

diameter for special surfaces. However, these efforts resulted in having a number of friction-factor curves to cover the various tube sizes and arrangements, Fig. 1. The reference paper further demonstrated that a single curve correlation could be made if certain configuration correction factors for the tube bank be included.

It was found necessary to employ three characteristic dimensions in order to determine completely a particular configuration. This meant therefore the introduction of two dimensionless ratios into any correlation involving the form of the general Fanning equation, in order to produce a complete correlation.

It was debated whether a bank might be completely determined by three dimensions in a conventional shell-and-tube exchanger because of the presence of the shell. This, however, was deemed not true because essentially the shell only ends the bank and should be considered only a quantity determining the mass velocity at any point across the bank.

The problem then was to select three characteristic dimensions which would give a consistent correlation of all data. The tube diameter and the pitch both transversely and longitudinally were one possibility for the three configuration dimensions. However, the original work showed that a much more satisfactory correlation could be obtained if the volumetric hydraulic diameter and the longitudinal and transverse pitches be used. The next step was to decide which of these three characteristic dimensions should be employed in the Reynolds number, and which other two should appear solely in the configuration ratios.

Inasmuch as most authors have found it satisfactory to use diameter in the Reynolds number for any particular tube arrangement, it seemed desirable to use volumetric hydraulic diameter in the Reynolds number and to allow the transverse pitch and longitudinal pitch to appear only in the correction ratios. This was later found to be justified by the excellent correlations which were obtained on this basis.

It has been customary for most authors to measure longitudinal pitch as the perpendicular distance from one row of tubes to the next row in the direction of longitudinal flow. However, in order to obtain a correlation which would present data for both staggered and unstaggered tube arrangements on the same line, it was necessary to define the longitudinal pitch as the center-to-center distance from a tube in one row to the nearest tube in the next row transverse to flow.

For equilateral arrangements both in-line and staggered, there is no difference in the configuration definitions and the $(S_L/S_T)^n$ correction factor becomes unity, disappearing from the equation. However, for nonequilateral arrangements, there is a varying degree of difference, depending on whether the layout is rectangular or isosceles. This is illustrated in Fig. 6.

Much uncertainty has existed in the past concerning whether the $f/2$ values vary as a fixed or variable power of the Reynolds number. The present correlation proposed in this paper does not exhibit this variation to any marked degree and the authors have used straight lines as tangents to a short curve in the transition region. The reason for this is the new Reynolds number against which the data were correlated, and the configuration ratios that were introduced.

Various mean temperatures have been employed by authors in evaluating the properties of the fluid flowing over the banks. The possibilities include the use of a film temperature, an average of the wall and main-stream temperature, the average main-stream temperature, or some intermediate combination of these. There are many arguments in favor of the various possibilities. However, the best proof of validity is the experimental data agreement in the final correlation. For this purpose, in this paper the average main-stream temperature has been used, and a correction for the tube-wall temperature is obtained by using the

well-known Sieder and Tate (9) viscosity correction, μ/μ_w . This method appears to give the best correlation and has been well substantiated by checking data on heavy fuel oils and various other petroleum products both for heating and cooling.

The ranges of variables covered in this paper are as follows:

Tube diameter, in.....	0.02 to 2
Reynolds number ($D_e G/\mu$).....	0.01 to 300,000
μ/μ_w	0.015 to 8
Transverse pitch, diam.....	1.25 to 5
Longitudinal pitch, diam.....	1.25 to 5

CORRELATION

The proposed equation for pressure drop in crossflow over both bare and extended-surface tubes is

$$\frac{f}{2} = \frac{\Delta P g D_e \rho}{G^2 L} \left(\frac{\mu}{\mu_w} \right)^{0.14} \left(\frac{D_e}{S_T} \right)^{-0.4} \left(\frac{S_L}{S_T} \right)^{-0.6} = \phi(R)$$

For the viscous range, the function of the Reynolds number is $f/2 = 90 (R)^{-1}$ and in the turbulent region, $f/2 = 0.96 (R)^{-0.14}$.

The transition point from laminar to turbulent flow occurs at a Reynolds number of about 200, although there is a slight curvature with the main straight lines being tangent thereto.

From inspection of the five major curves, Figs. 1 to 5, inclusive, the relative significance of the new correlation will be immediately evident. Fig. 1 shows an attempted correlation using D_e instead of D_e without the correction factors that are proposed in this paper. This figure shows definitely that such a single-line correlation is impossible.

Fig. 2 shows an attempted correlation using D_e in the Reynolds number and ordinate without the two configuration-ratio correction factors. It will be noted again that this correlation is not satisfactory, although better than Fig. 1. However, it shows the merit of using D_e .

Fig. 3 uses D_e in the Reynolds number and in the ordinate, plus one correction factor, namely, $(D_e/S_T)^n$. This is again better than the first two, but still does not take care of wide pitches, especially in the isosceles or rectangular arrangements.

Fig. 4 uses D_e in the Reynolds number and both of the correction ratios in the ordinate. It will be noted that all of the various tube arrangements now fall on a satisfactory single plot.

Fig. 5 shows extended-surface data correlated on the proposed curve which show surprising agreement.

Friction-factor data are shown in Tables 1 and 2.

BARE TUBES

The extensive data of Sieder and Scott (7) available for pressure drop have been used to establish the viscous and part of the turbulent regions. The power of the μ/μ_w ratio is 0.14 in both the viscous and turbulent regions, unlike flow inside tubes. This correction is included in all plots, Figs. 1 to 5, inclusive.

Norris' (6) data on small wires correlate well on the proposed line. This is encouraging, as it establishes the validity of the equation down to a very low value of tube diameter. Huges' (4) data for pressure drop also correlate satisfactorily.

Inasmuch as within the possible range of variation in this case, the average temperature is not of too great importance in pressure-drop calculations, especially on air, it was possible to use the data of Pierson (10) on 38 different arrangements covering transverse- and longitudinal-pitch arrangements from 1.25 to 3 diam, transverse and longitudinal, both staggered and unstaggered. These 38 arrangements provide an excellent basis for the foregoing correlation.

R. P. Wallis (11) has published extensive friction data on two arrangements. The data have apparently been obtained with a very high degree of accuracy. They substantiate the proposed equation quite exactly.

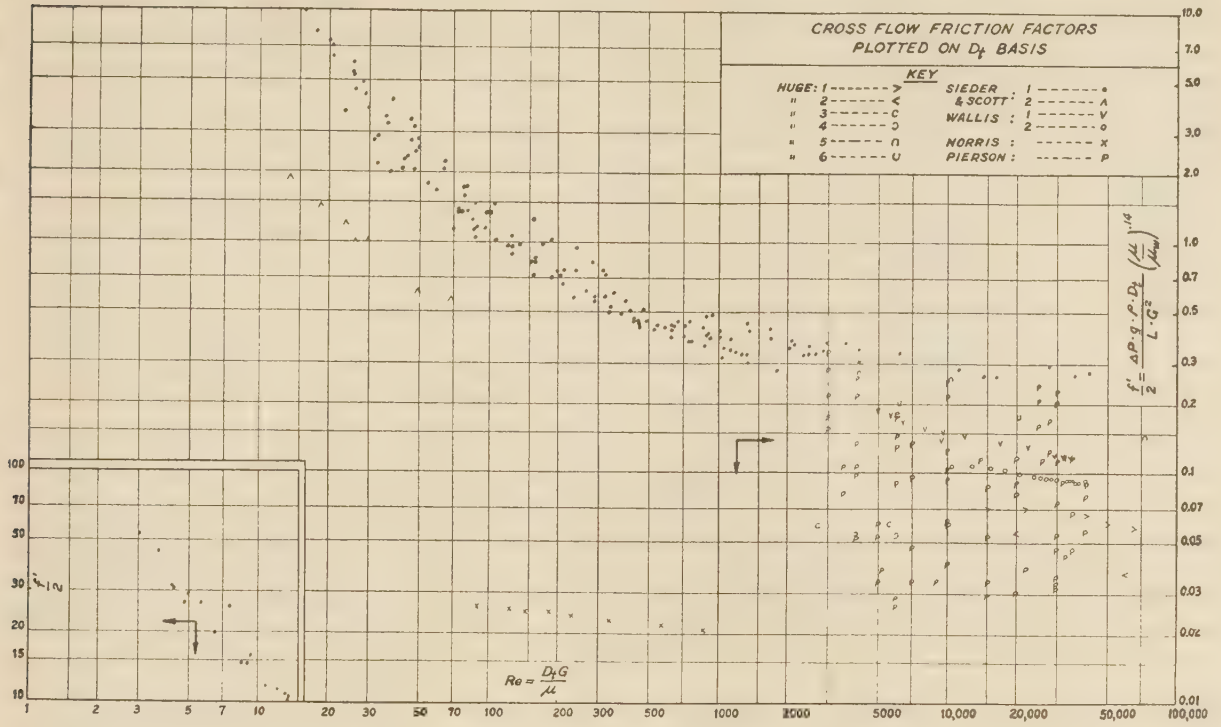


FIG. 1 CROSSFLOW FRICTION FACTORS PLOTTED ON D_i BASIS

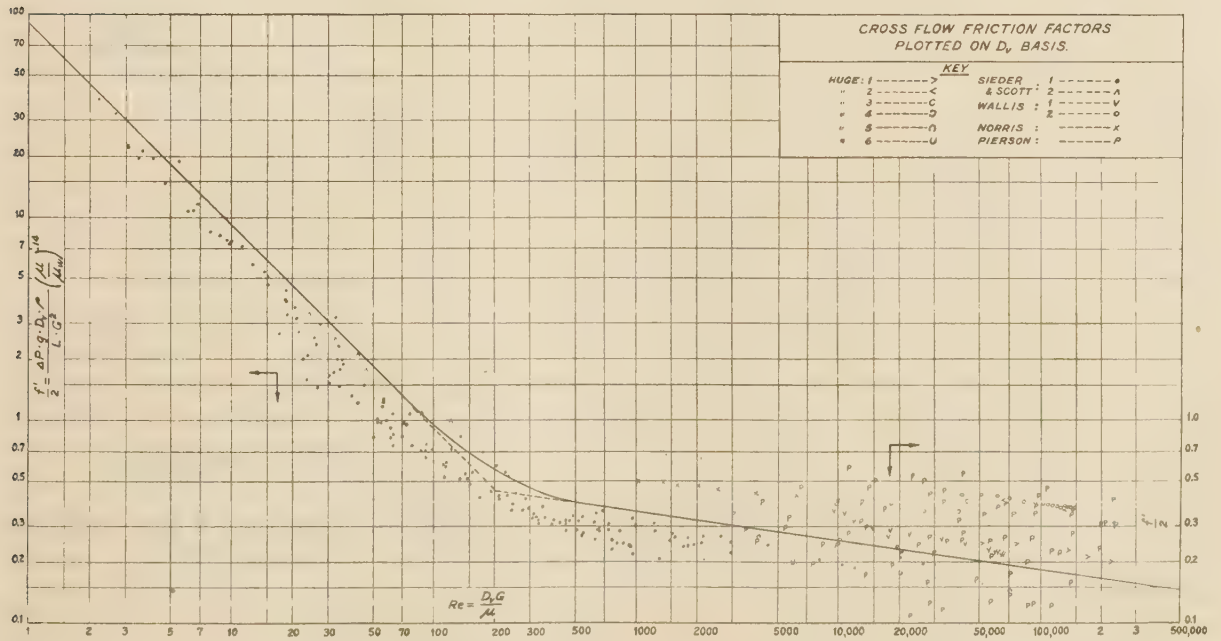


FIG. 2 CROSSFLOW FRICTION FACTORS PLOTTED ON D_o BASIS

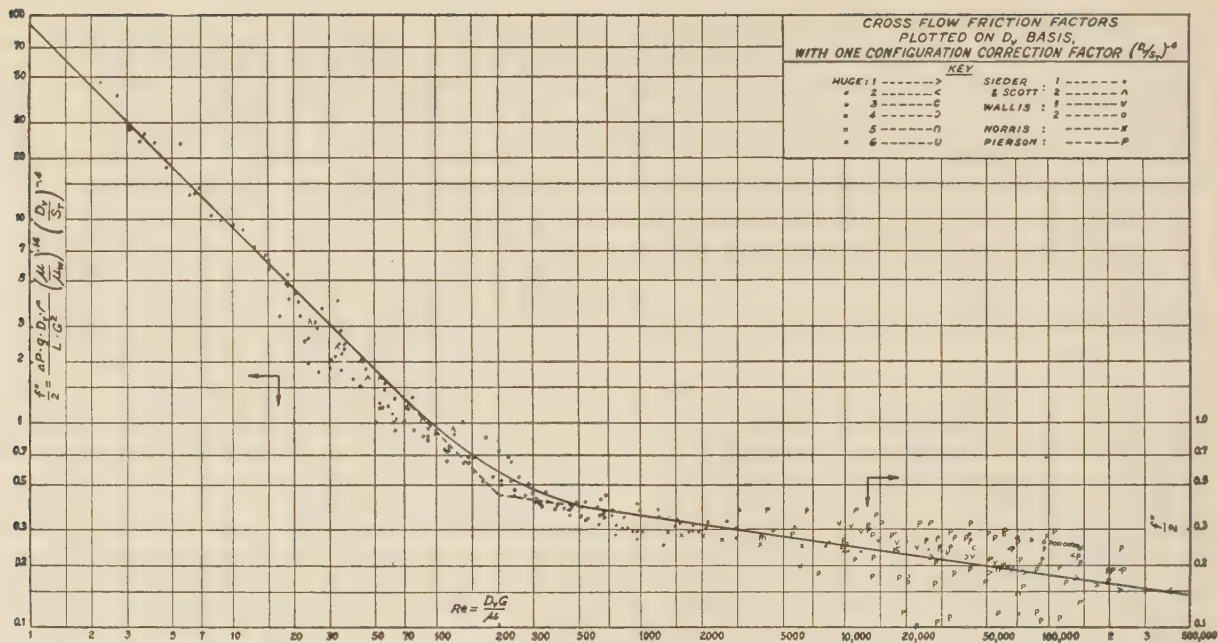


FIG. 3 CROSSFLOW FRICTION FACTORS PLOTTED ON D_o BASIS WITH ONE CONFIGURATION CORRECTION FACTOR, $(D_o/S_T)^{0.6}$

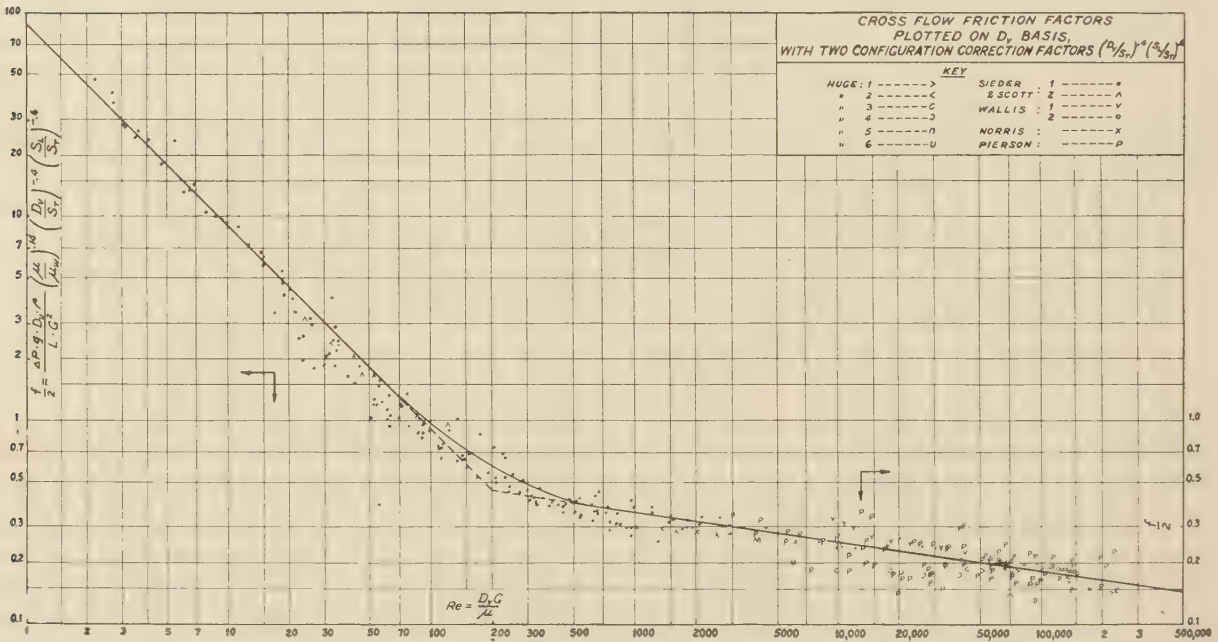


FIG. 4 CROSSFLOW FRICTION FACTORS PLOTTED ON D_o BASIS WITH TWO CONFIGURATION FACTORS, $(D_o/S_T)^{0.6} (S_L/S_T)^{0.6}$

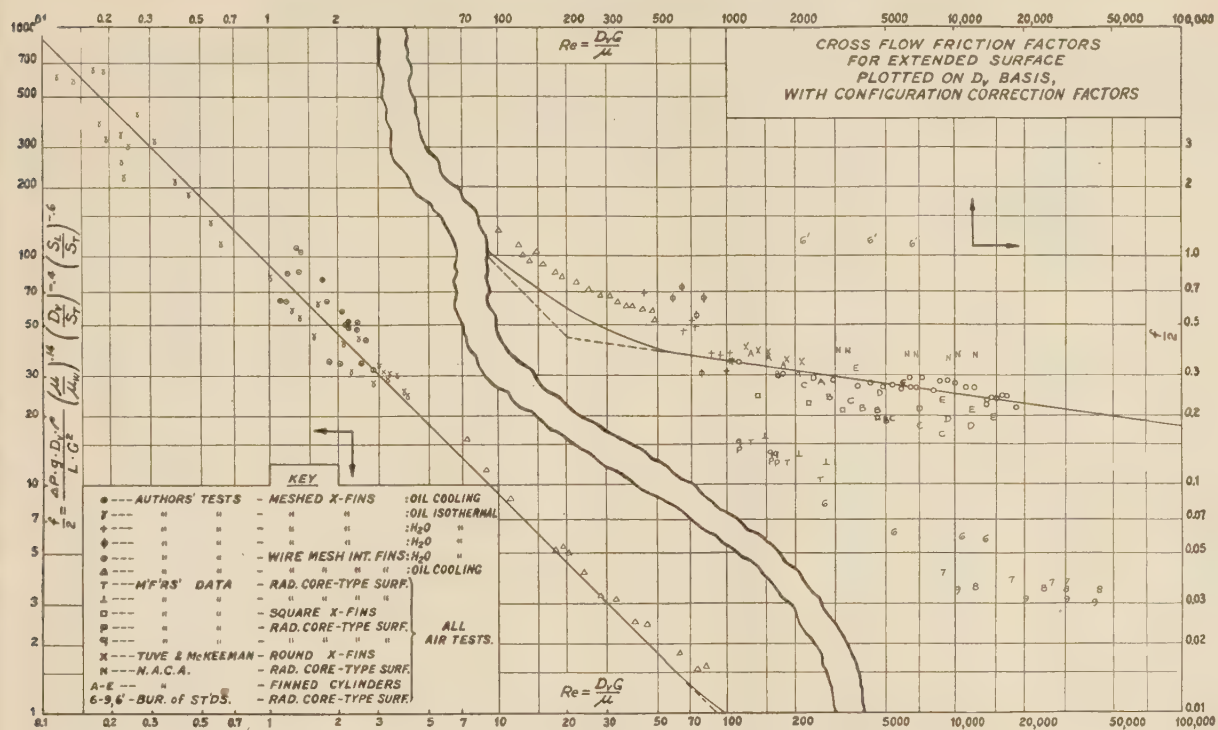


FIG. 5 CROSSFLOW FRICTION FACTORS FOR EXTENDED SURFACE PLOTTED ON D_v BASIS WITH CONFIGURATION CORRECTION FACTORS

TABLE 1. CROSSFLOW FRICTION-FACTOR DATA; BARE TUBES

No.	Ar-range-ment	Source and Material	D_t in.	Basis D_t		D_v ft.	S_L in.	S_T in.	$\left(\frac{D_v}{S_T}\right)^{.4}$	$\left(\frac{S_L}{S_m}\right)^{.6}$	Basis D_v			
				Re	$f'/2$						Re	$f'/2$	$f''/2$	$f'/2$
1	I	Norris	.02	90.3	.0258	.0193	.0625	.0625	1.68	1.0	1,040.	.499	.297	Same
2			or	124.	.0252	or	or	or	-	-	1,385.	.488	.29	as
3		AIR	.04	144.	.0246	.0384	.125	.125	-	-	1,600.	.477	.284	$f''/2$
4			or	184.	.0244	or	or	or	-	-	2,040.	.472	.281	
5			.125	230.	.0235	.115	.375	.375	-	-	2,550.	.455	.271	
6				339.	.0224	-	-	-	-	-	3,930.	.434	.258	
7				567.	.0217	-	-	-	-	-	6,280.	.42	.25	
8				870.	.0206	-	-	-	-	-	10,000.	.398	.237	
9	I	Wallis	.5	37,200.	.0915	.167	1.3	.755	1.48	1.38	149,000.	.366	.247	.179
10				35,900.	.092	-	-	-	-	-	148,000.	.368	.248	.18
11		AIR		35,350.	.0925	-	-	-	-	-	141,000.	.37	.25	.181
12				34,330.	.0927	-	-	-	-	-	137,000.	.371	.251	.182
13				32,950.	.0935	-	-	-	-	-	132,000.	.374	.253	.183
14				31,600.	.093	-	-	-	-	-	127,000.	.372	.252	.183
15				30,100.	.0945	-	-	-	-	-	121,000.	.378	.256	.186
16				28,500.	.095	-	-	-	-	-	114,000.	.38	.257	.186
17				27,050.	.0955	-	-	-	-	-	108,000.	.382	.258	.187
18				25,530.	.0962	-	-	-	-	-	102,000.	.385	.26	.188
19				23,830.	.0972	-	-	-	-	-	95,500.	.389	.263	.191
20				20,650.	.0994	-	-	-	-	-	82,500.	.398	.269	.195
21				17,740.	.103	-	-	-	-	-	71,000.	.412	.278	.202
22				15,250.	.106	-	-	-	-	-	61,000.	.423	.286	.207
23				12,750.	.1075	-	-	-	-	-	51,000.	.43	.29	.21
24				10,140.	.1065	-	-	-	-	-	40,600.	.427	.288	.209
25	S	Wallis	.5	34,600.	.114	.079	.755	.755	1.095	1.0	65,600.	.217	.198	Same
26				34,200.	.115	-	-	-	-	-	64,800.	.218	.199	as
27		AIR		32,700.	.1165	-	-	-	-	-	62,000.	.221	.202	$f''/2$
28				31,700.	.1165	-	-	-	-	-	60,200.	.221	.202	
29				29,100.	.119	-	-	-	-	-	55,200.	.226	.206	
30				22,470.	.129	-	-	-	-	-	42,600.	.244	.223	
31				17,000.	.134	-	-	-	-	-	32,300.	.254	.232	
32				11,890.	.143	-	-	-	-	-	22,600.	.271	.248	
33				9,520.	.149	-	-	-	-	-	18,100.	.282	.258	
34				9,395.	.138	-	-	-	-	-	17,800.	.262	.24	
35				7,920.	.154	-	-	-	-	-	14,800.	.292	.267	
36				6,365.	.168	-	-	-	-	-	12,100.	.318	.291	
37				5,630.	.179	-	-	-	-	-	10,700.	.34	.31	
38				4,990.	.186	-	-	-	-	-	9,460.	.352	.322	

TABLE 1 (Continued) CROSSFLOW FRICTION-FACTOR DATA; BARE TUBES

No.	Ar- range- ment	Source & Material	D _t	Basis D _t		D _v	S _L	S _T	(D _v /S _T) ^{.4}	(S _L /S _T) ^{.6}	Basis D _v			
				Re	$\frac{f'}{2}$						Re	$\frac{f'}{2}$	$\frac{f''}{2}$	$\frac{f}{2}$
39	S	Sieder	.75"	98.2	1.32	.046'	.938"	.938"	.81	1.0	71.4	.965	1.195	Same
40		and		76.8	1.59						56.	1.16	1.44	as
41		Scott		72.6	1.32						53.	.965	1.195	$\frac{f''}{2}$
42				45.6	2.72						33.3	1.98	2.45	
43		FUEL OIL		28.	4.85						20.6	3.54	4.38	
44		16.7° API		15.5	9.81						11.3	7.15	8.85	
45		Isothermal		159.	.845						116.	.616	.765	
46				124.	1.04						90.6	.758	.94	
47				98.4	1.32						71.7	.96	1.19	
48				77.8	1.71						56.7	1.24	1.54	
49				48.4	2.79						35.3	1.95	2.42	
50				25.6	5.95						18.7	4.31	5.35	
51				25.4	5.37						18.5	3.89	4.83	
52				20.7	7.0						15.1	5.06	6.28	
53				17.4	8.08						12.7	5.85	7.25	
54				13.6	10.1						9.9	7.4	9.2	
55				8.48	14.7						6.18	10.65	13.2	
56				47.7	2.43						34.8	1.76	2.18	
57				86.2	1.45						62.8	1.06	1.31	
58				155.	.712						113.	.52	.642	
59				203.	.71						148.	.518	.64	
60				425.	.45						310	.328	.405	
61				333.	.494						243.	.36	.445	
62				233.	.571						170.	.417	.515	
63				452.	.439						330.	.32	.395	
64				289.	.55						211.	.402	.496	
65				338.	.521						246.	.381	.47	
66				377.	.488						275.	.356	.44	
67				428.	.466						312.	.34	.42	
68				484.	.455						353.	.332	.41	
69				864.	.354						630.	.258	.319	
70				706.	.39						515.	.284	.351	
71				624.	.416						455.	.304	.376	
72				540.	.439						394.	.32	.395	
73				455.	.425						332.	.31	.383	

No.	Ar- range- ment	Source & Material	D _t	Basis D _t		D _v	S _L	S _T	(D _v /S _T) ^{.4}	(S _L /S _T) ^{.6}	Basis D _v			
				Re	$\frac{f'}{2}$						Re	$\frac{f'}{2}$	$\frac{f''}{2}$	$\frac{f}{2}$
74	S	Sieder	.75"	1,010.	.389	.046'	.938"	.938"	.81	1.0	735.	.284	.35	Same
75		and Scott		1,270.	.329						928.	.24	.296	as
76				1,145.	.384						635.	.28	.346	
77		KEROSENE		1,015.	.416						740.	.304	.376	$\frac{f''}{2}$
78		31.05° API		852.	.426						622.	.311	.384	
79		Isothermal		669.	.455						483.	.332	.41	
80				2,490.	.356						1,815.	.26	.321	
81				2,080.	.376						1,515.	.274	.338	
82				1,370.	.411						1,000.	.301	.374	
83				1,695.	.384						1,237.	.28	.346	
84				2,040.	.35						1,490.	.256	.316	
85				2,490.	.33						1,815.	.241	.298	
86				2,880.	.34						2,100.	.248	.306	
87				4,090.	.304						2,980.	.222	.274	
88				3,600.	.368						2,630.	.263	.331	
89				2,660.	.33						1,940.	.241	.298	
90				2,150.	.362						1,570.	.264	.326	
91	S	Sieder	.75"	41,400.	.276	.046'	.938"	.938"	.81	1.0	30,200.	.193	.238	Same
92		and Scott		16,400.	.261						12,100.	.189	.234	as
93				35,900.	.268						26,200.	.194	.24	
94		WATER		14,400.	.265						10,500.	.192	.237	$\frac{f''}{2}$
95		Isothermal		27,800.	.292						20,300.	.212	.262	
96				11,100.	.282						8,100.	.204	.25	
97				6,190.	.332						4,510.	.240	.297	
98	S	Sieder	.75"	188.	.7	.046'	.938"	.938"	.81	1.0	137.	.511	.631	Same
99		and Scott		75.5	1.32						55.	.963	1.19	as
100				43.9	2.33						32.	1.7	2.1	
101		FUEL OIL		170.	.98						124.	.715	.883	$\frac{f''}{2}$
102		10.5° API		96.	1.13						70.	.827	1.02	
103		Cooling		135.	.98						98.8	.715	.883	
104				80.	1.34						58.3	.98	1.21	
105				29.6	3.73						21.6	2.72	3.36	
106				78.2	1.72						57.	1.255	1.55	
107				49.	2.56						35.7	1.865	2.3	
108				35.1	3.47						25.6	2.53	3.12	
109				6.52	19.9						4.76	14.55	18.	
110				62.9	2.04						45.9	1.485	1.83	
111				12.15	11.05						8.86	8.07	9.97	

TABLE 1 (Continued) CROSSFLOW FRICTION-FACTOR DATA; BARE TUBES

No.	Arrangement	Source & Material	D_t	Basis D_t		D_v	S_L	S_T	$\left(\frac{D_v}{S_T}\right)^4$	$\left(\frac{S_L}{S_T}\right)^6$	Basis D_v			
				Re	$f'/2$						Re	$f'/2$	$f''/2$	$f''/2$
112	S	Sieder	.75"	35.9	3.24	.046'	.938"	.938"	.81	1.0	26.2	2.36	2.92	Same
113		and		28.8	4.35	-	-	-	-	-	21.	3.17	3.92	as
114		Scott		13.7	10.3	-	-	-	-	-	10.	7.52	9.29	$f''/2$
115				45.	4.39	-	-	-	-	-	32.8	3.2	3.95	
116		FUEL OIL		25.6	5.24	-	-	-	-	-	18.7	3.82	4.71	
117		10.5° API		20.	7.39	-	-	-	-	-	14.6	5.39	6.65	
118		Cooling		9.35	15.8	-	-	-	-	-	6.82	11.55	14.2	
119				5.64	26.4	-	-	-	-	-	4.12	19.3	23.8	
120				4.25	31.3	-	-	-	-	-	3.1	22.8	28.2	
121				46.6	3.15	-	-	-	-	-	34.	2.3	2.84	
122				26.	4.52	-	-	-	-	-	19.	3.3	4.08	
123				10.9	11.6	-	-	-	-	-	7.95	8.45	10.4	
124				4.8	26.7	-	-	-	-	-	3.5	19.5	24.1	
125				4.99	29.	-	-	-	-	-	3.64	21.2	26.2	
126				37.6	4.09	-	-	-	-	-	27.5	2.98	3.64	
127				20.7	6.33	-	-	-	-	-	15.1	4.62	5.7	
128				9.	14.7	-	-	-	-	-	6.57	10.75	13.3	
129				4.27	30.7	-	-	-	-	-	3.12	22.4	27.7	
130				13.1	10.55	-	-	-	-	-	9.55	7.7	9.52	
131				7.55	25.9	-	-	-	-	-	5.5	18.9	23.4	
132				3.7	44.5	-	-	-	-	-	2.7	32.5	40.1	
133				3.06	52.4	-	-	-	-	-	2.23	38.2	47.1	
134	S	Sieder	.75"	2,360.	.325	.046'	.938"	.938"	.81	1.0	1,730.	.237	.292	Same
135		and		1,690.	.42	-	-	-	-	-	1,230.	.306	.378	as
136		Scott		1,340.	.445	-	-	-	-	-	977.	.325	.4	$f''/2$
137				2,960.	.369	-	-	-	-	-	2,160.	.269	.332	
138		KEROSENE		4,090.	.342	-	-	-	-	-	2,980.	.25	.308	
139		31.05° API		886.	.475	-	-	-	-	-	646.	.346	.426	
140		Heating		902.	.4	-	-	-	-	-	664.	.292	.36	
141				640.	.433	-	-	-	-	-	468.	.316	.389	
142				713.	.436	-	-	-	-	-	520.	.318	.392	
143				1,045.	.315	-	-	-	-	-	762.	.23	.284	
144	S	Sieder	.75"	26.	.99	.111'	1.18"	1.18"	1.05	1.0	46.2	1.77	1.685	Same
145		and		18.3	1.41	-	-	-	-	-	32.6	2.51	2.39	as
146		Scott		29.6	.995	-	-	-	-	-	52.7	1.77	1.685	$f''/2$
147				68.	.56	-	-	-	-	-	121.	.995	.948	
148		FUEL OIL		48.9	.606	-	-	-	-	-	86.8	1.08	1.03	
149		12.8° API		23.7	1.19	-	-	-	-	-	42.2	2.12	2.02	
150		Heating		13.6	1.87	-	-	-	-	-	24.2	3.32	3.16	
151	S	Sieder	.75"	105.	1.47	.046'	.938"	.938"	.81	1.0	76.7	1.075	1.325	Same
152		and		157.5	.809	-	-	-	-	-	115.	.59	.729	as
153		Scott		120.	.96	-	-	-	-	-	87.7	.7	.865	$f''/2$
154				86.4	1.02	-	-	-	-	-	63.	.745	.92	
155		FUEL OIL		36.8	1.99	-	-	-	-	-	26.9	1.455	1.79	
156		16.7° API		32.4	2.16	-	-	-	-	-	23.7	1.58	1.95	
157		Heating		198.5	.746	-	-	-	-	-	145.	.545	.674	
158				263.	.611	-	-	-	-	-	192.	.446	.551	
159				392.	.555	-	-	-	-	-	286.	.405	.5	
160				318.	.576	-	-	-	-	-	232.	.421	.52	
161				156.	.82	-	-	-	-	-	114.	.598	.737	
162				208.	.658	-	-	-	-	-	151.5	.48	.581	
163				581.	.425	-	-	-	-	-	424.	.31	.382	
164				744.	.371	-	-	-	-	-	543.	.271	.334	
165	S	Sieder	.75"	1,800.	.28	.046'	.938"	.938"	.81	1.0	1,315.	.205	.253	Same
166		and		1,320.	.327	-	-	-	-	-	965.	.239	.296	as
167		Scott		747.	.372	-	-	-	-	-	545.	.272	.338	$f''/2$
168				321.	.723	-	-	-	-	-	234.	.527	.65	
169		FUEL OIL		311.	.756	-	-	-	-	-	227.	.553	.683	
170		25.4° API		1,335.	.3	-	-	-	-	-	974.	.219	.27	
171		Cooling		1,190.	.336	-	-	-	-	-	870.	.245	.305	
172				1,050.	.349	-	-	-	-	-	765.	.255	.314	
173				620.	.389	-	-	-	-	-	453.	.284	.352	
174				281.	.818	-	-	-	-	-	205.	.597	.73	
175				1,125.	.341	-	-	-	-	-	822.	.249	.308	
176				915.	.386	-	-	-	-	-	667.	.282	.347	
177				524.	.419	-	-	-	-	-	382.	.306	.378	
178				240.	.945	-	-	-	-	-	175.	.69	.849	
179				880.	.393	-	-	-	-	-	542.	.287	.354	
180				748.	.455	-	-	-	-	-	545.	.333	.41	
181				410.	.501	-	-	-	-	-	299.	.366	.452	
182				187.	1.114	-	-	-	-	-	136.5	.833	1.02	
183				626.	.438	-	-	-	-	-	457.	.32	.394	
184				441.	.454	-	-	-	-	-	322.	.331	.408	
185				288.	.576	-	-	-	-	-	210.	.421	.52	
186				125.5	.959	-	-	-	-	-	91.6	.7	.86	
187				472.	.51	-	-	-	-	-	345.	.373	.46	
188				348.	.6	-	-	-	-	-	254.	.439	.54	
189				212.	.756	-	-	-	-	-	155.	.552	.68	
190				940.	.486	-	-	-	-	-	685.	.355	.442	

TABLE 1 (Continued) CROSSFLOW FRICTION-FACTOR DATA; BARE TUBES

No.	Ar- range- ment	Source & Material	D_t in.	Basis D_t		D_v ft.	S_L in.	S_T in.	$(\frac{D_v}{S_T})^{.4}$	$(\frac{S_L}{S_T})^{.6}$	Basis D_v			
				Re	$f'/2$						Re	$f'/2$	$f''/2$	$f/2$
191	S	Sieder & Scott	.75"	238.	.75	.046	.938	.938	.81	1.0	174.	.547	.672	Same
192		Scott		155.	1.25	-	-	-	-	-	113.	.914	1.12	as
193		(Same)		63.9	2.21	-	-	-	-	-	46.6	1.615	2.0	$f''/2$
194	S	Sieder & Scott	.75	107.	1.02	.046	.938	.938	.81	1.0	78.	.746	.926	Same
195		Scott		87.4	1.15	-	-	-	-	-	63.7	.84	1.04	as
196				69.5	1.12	-	-	-	-	-	50.7	.82	1.01	$f''/2$
197		FUEL OIL		41.4	2.07	-	-	-	-	-	30.2	1.51	1.86	
198		11.7° API		84.	1.24	-	-	-	-	-	61.3	.902	1.11	
199		Heating		73.	1.38	-	-	-	-	-	53.3	1.01	1.24	
200				58.2	1.67	-	-	-	-	-	42.5	1.22	1.5	
201				46.9	2.02	-	-	-	-	-	34.2	1.47	1.81	
202				31.1	2.74	-	-	-	-	-	22.7	2.0	2.5	
203				53.9	1.795	-	-	-	-	-	39.3	1.31	1.63	
204				42.4	2.26	-	-	-	-	-	30.9	1.65	2.06	
205				32.6	2.85	-	-	-	-	-	23.8	2.08	2.58	
206				23.4	3.66	-	-	-	-	-	17.1	2.67	3.33	
207				152.	.818	-	-	-	-	-	111.	.597	.74	
208				125.	.886	-	-	-	-	-	91.5	.647	.816	
209				84.8	1.12	-	-	-	-	-	61.8	.817	1.0	
210	I	Huge	2.0	15,000.	.07	.575	4.0	3.5	1.31	1.08	51,800.	.244	.185	.171
211				22,000.	.07	-	-	-	-	-	76,000.	.244	.185	.171
212		AIR		40,000.	.066	-	-	-	-	-	138,000.	.229	.174	.161
213		Heating		50,000.	.061	-	-	-	-	-	172,500.	.212	.16	.148
214				65,000.	.058	-	-	-	-	-	224,000.	.202	.153	.142
215	S	"	2.0	60,000.	.0367	1.1	6.33	4.0	1.61	1.32	400,000.	.245	.152	.115
216				35,000.	.0467	-	-	-	-	-	232,000.	.312	.193	.146
217				20,000.	.0547	-	-	-	-	-	133,000.	.365	.226	.171
218				10,000.	.06	-	-	-	-	-	66,500.	.40	.248	.188
219	S	"	.5	1,500.	.0587	.276	1.58	1.0	1.61	1.316	9,950.	.37	.242	.183
220				2,750.	.0587	-	-	-	-	-	18,300.	.39	.242	.183
221				5,600.	.06	-	-	-	-	-	43,800.	.398	.247	.187
222	I	"	.5	4,000.	.0534	.276	1.5	1.0	1.61	1.28	26,600.	.354	.22	.172
223				6,000.	.0534	-	-	-	-	-	39,800.	.354	.22	.172
224	S	"	2.0	71,500.	.147	.163	2.78	2.5	.996	1.068	70,800.	.146	.1465	.137
225				10,200.	.256	-	-	-	-	-	10,100.	.254	.255	.239
226				4,080.	.272	-	-	-	-	-	4,040.	.269	.27	.252
227	I	"	.5	6,120.	.20	.041	.625	.625	.996	1.0	6,000.	.198	.199	.199
228				20,400.	.176	-	-	-	-	-	20,200.	.174	.175	.175
229	I	Pierson	.31"	5,000.	.0334	.268	.93	.93	1.645	1.0	52,000.	.348	.212	.212
230				7,000.	.0334	-	-	-	-	-	72,800.	.348	.212	.212
231		AIR		9,000.	.0334	-	-	-	-	-	93,600.	.348	.212	.212
232		Heating		20,000.	.03	-	-	-	-	-	208,000.	.312	.19	.19
233	"	"	"	5,200.	.038	.171	.62	.93	1.38	0.79	34,400.	.252	.183	.231
234				10,000.	.04	-	-	-	-	-	66,000.	.264	.191	.242
235				30,000.	.035	-	-	-	-	-	198,000.	.232	.168	.212
236	"	"	"	6,000.	.0266	.121	.465	.93	1.19	0.66	28,200.	.125	.105	.159
237				30,000.	.0332	-	-	-	-	-	141,000.	.157	.132	.2
238				15,000.	.0292	-	-	-	-	-	70,500.	.138	.111	.175
239	"	"	"	6,000.	.0288	.096	.388	.93	1.09	0.592	22,600.	.108	.1	.167
240				15,000.	.0336	-	-	-	-	-	56,500.	.127	.1165	.197
241				30,000.	.032	-	-	-	-	-	113,000.	.121	.111	.1875
242	"	"	"	5,000.	.06	.171	.93	.62	1.61	1.27	33,000.	.396	.246	.194
243				10,000.	.06	-	-	-	-	-	66,000.	.396	.246	.194
244				30,000.	.0467	-	-	-	-	-	198,000.	.308	.191	.1505
245	"	"	"	5,000.	.053	.106	.62	.62	1.33	1.0	20,500.	.218	.164	.164
246				10,000.	.062	-	-	-	-	-	41,000.	.255	.192	.192
247				30,000.	.054	-	-	-	-	-	123,000.	.222	.167	.167
248	"	"	"	7,000.	.0479	.072	.465	.62	1.14	0.84	19,600.	.134	.1175	.14
249				33,000.	.0439	-	-	-	-	-	92,500.	.123	.108	.129
250	"	"	"	15,000.	.0528	.056	.388	.62	1.03	0.752	32,700.	.115	.112	.149
251				40,000.	.056	-	-	-	-	-	87,500.	.122	.1185	.1575
252	"	"	"	7,000.	.0967	.121	.93	.465	1.57	1.51	33,000.	.456	.291	.193
253				15,000.	.0868	-	-	-	-	-	70,500.	.409	.26	.172
254				30,000.	.0734	-	-	-	-	-	141,000.	.346	.22	.146
255	"	"	"	4,000.	.098	.073	.62	.465	1.28	1.19	11,200.	.274	.214	.18
256				10,000.	.094	-	-	-	-	-	28,000.	.263	.206	.173
257				20,000.	.09	-	-	-	-	-	56,000.	.252	.197	.166
258	"	"	"	40,000.	.093	.039	.465	.465	1.09	1.0	74,500.	.173	.159	.159
259				10,000.	.103	-	-	-	-	-	18,600.	.192	.176	.176
260				4,000.	.106	-	-	-	-	-	7,450.	.197	.181	.181
261	"	"	"	10,000.	.125	.036	.388	.465	.97	.9	13,800.	.172	.177	.197
262				20,000.	.115	-	-	-	-	-	27,600.	.159	.164	.182
263	"	"	"	4,000.	.133	.099	.93	.388	1.55	1.69	15,100.	.502	.324	.191
264				28,000.	.123	-	-	-	-	-	106,000.	.464	.299	.177
265	"	"	"	6,000.	.18	.057	.62	.388	1.25	1.33	13,100.	.392	.314	.236
266				28,000.	.17	-	-	-	-	-	61,000.	.371	.296	.223

TABLE 1 (Continued) CROSSFLOW FRICTION-FACTOR DATA; BARE TUBES

No.	Ar-range-ment	Source & Material	D _t in.	Basis D _t		D _v ft.	S _L in.	S _T in.	(D _v /S _T)*.4	(S _L /S _T)*.6	Basis D _v			
				Re	f'/2						Re	f'/2	f''/2	f/2
267	I	Pierson	.31	4,000.	.214	.036	.465	.388	1.04	1.12	5,520.	.296	.285	.254
268		AIR		10,000.	.214	-	-	-	-	-	13,800.	.296	.285	.254
269		Heating		30,000.	.201	-	-	-	-	-	41,400.	.276	.266	.298
270	I	"	"	4,000.	.258	.026	.388	.388	.91	1.0	3,940.	.252	.278	.278
271		"	"	10,000.	.25	-	-	-	-	-	9,850.	.244	.268	.268
272		"	"	30,000.	.226	-	-	-	-	-	29,600.	.221	.243	.243
273	S	"	"	3,000.	.154	.097	.952	.388	1.55	1.71	11,300.	.58	.374	.218
274		"	"	7,000.	.134	-	-	-	-	-	26,400.	.505	.326	.19
275		"	"	26,000.	.113	-	-	-	-	-	98,000.	.425	.274	.16
276	"	"	"	25,000.	.16	.056	.65	.388	1.25	1.36	52,300.	.347	.278	.204
277		"	"	3,000.	.215	-	-	-	-	-	6,500.	.467	.374	.275
278	"	"	"	3,000.	.28	.036	.505	.388	1.04	1.17	4,180.	.39	.375	.32
279		"	"	25,000.	.206	-	-	-	-	-	34,900.	.288	.277	.236
280	"	"	"	3,000.	.336	.026	.434	.388	.91	1.07	3,030.	.34	.374	.349
281		"	"	25,000.	.24	-	-	-	-	-	25,200.	.242	.266	.248
282	"	"	"	6,000.	.09	.122	.96	.465	1.58	1.54	28,600.	.43	.272	.177
283		"	"	20,000.	.08	-	-	-	-	-	95,500.	.382	.242	.157
284	"	"	"	6,000.	.13	.073	.661	.465	1.28	1.235	17,000.	.368	.288	.234
285		"	"	32,000.	.092	-	-	-	-	-	90,500.	.26	.203	.164
286	"	"	"	3,000.	.173	.049	.522	.465	1.09	1.07	5,700.	.329	.302	.282
287		"	"	30,000.	.112	-	-	-	-	-	57,000.	.213	.195	.182
288	"	"	"	35,000.	.117	.036	.451	.465	.97	.982	48,800.	.163	.168	.171
289		"	"	6,000.	.176	-	-	-	-	-	8,360.	.246	.254	.258
290	"	"	"	3,500.	.08	.171	.98	.62	1.61	1.315	23,200.	.53	.329	.25
291		"	"	35,000.	.0468	-	-	-	-	-	232,000.	.31	.193	.147
292	"	"	"	3,500.	.105	.106	.693	.62	1.33	1.07	14,300.	.472	.355	.332
293		"	"	35,000.	.067	-	-	-	-	-	143,000.	.274	.206	.193
294	"	"	"	40,000.	.0798	.073	.557	.62	1.15	.94	113,000.	.226	.197	.21
295		"	"	14,000.	.113	-	-	-	-	-	39,600.	.32	.278	.296
296	"	"	"	6,000.	.144	.056	.496	.62	1.03	.874	13,000.	.314	.305	.35
297		"	"	40,000.	.091	-	-	-	-	-	86,800.	.198	.192	.22
298	"	"	"	4,000.	.052	.268	1.04	.93	1.65	1.07	41,400.	.541	.328	.306
299		"	"	22,000.	.0387	-	-	-	-	-	229,000.	.402	.244	.228

TABLE 2 CROSSFLOW FRICTION DATA; EXTENDED SURFACE

No.	Ar-range-ment	Source and Material	D _t	Basis D _t		D _v	S _L	S _T	(D _v /S _T)*.4	(S _L /S _T)*.6	Basis D _v			
				Re	f'/2						Re	f'/2	f''/2	f/2
300	S	Authors' Tests	-	-	-	.0265'	.1094'	.1094'	.566	1.0	2.62	24.2	42.7	Same
301						-	-	-	-	-	2.46	29.1	51.4	as
302	Meshed	NOTE:				-	-	-	-	-	2.22	27.2	48.0	f''/2
303	Round	OIL				-	-	-	-	-	1.79	35.6	62.8	
304	X-fins	Cooling				-	-	-	-	-	1.32	61.1	108.0	
305		These Tests				-	-	-	-	-	2.84	17.9	31.6	
306		Not Evaluated				-	-	-	-	-	2.54	19.2	33.9	
307		on				-	-	-	-	-	2.24	28.8	50.9	
308		D _t Basis				-	-	-	-	-	2.20	28.0	49.5	
309						-	-	-	-	-	2.44	26.9	47.5	
310						-	-	-	-	-	1.35	47.9	84.5	
311						-	-	-	-	-	2.07	32.5	57.4	
312						-	-	-	-	-	1.71	44.5	78.6	
313						-	-	-	-	-	1.38	69.0	104.0	
314						-	-	-	-	-	2.06	19.0	33.6	
315						-	-	-	-	-	1.83	19.6	34.6	
316						-	-	-	-	-	1.20	35.6	62.8	
317						-	-	-	-	-	1.145	35.9	63.4	
318						-	-	-	-	-	1.205	47.5	83.8	
319	S	Authors' Tests	"	"	"	.0265'	.1094'	.1094'	.566	1.0	.548	79.3	140.0	Same
320						-	-	-	-	-	.495	90.0	159.0	as
321	Meshed					-	-	-	-	-	.613	63.5	112.0	f''/2
322	Round	OIL				-	-	-	-	-	.440	104.5	184.6	
323	X-fins	Isothermal				-	-	-	-	-	.386	120.0	212.0	
324						-	-	-	-	-	.262	235.0	416.0	
325						-	-	-	-	-	.312	178.5	315.	
326						-	-	-	-	-	.187	366.	645.	
327						-	-	-	-	-	.169	375.	660.	
328						-	-	-	-	-	3.33	17.	30.	
329						-	-	-	-	-	2.46	24.7	43.6	
330						-	-	-	-	-	1.62	34.6	61.2	
331						-	-	-	-	-	.24	172.	304.	
332						-	-	-	-	-	.23	125.	221.	
333						-	-	-	-	-	.193	185.	327.	
334						-	-	-	-	-	.222	144.	254.	
335						-	-	-	-	-	.221	193.	341.	
336						-	-	-	-	-	.180	214.	378.	

TABLE 2 (Continued) CROSS FLOW FRICTION DATA; EXTENDED SURFACE

No.	Ar-range-ment	Source and Material	(Basis D_t)				S_L	S_T	$(\frac{D_v}{S_T})^{.4}$	$(\frac{S_L}{S_T})^{.6}$	(Basis D_v)			
			D_t	$(\frac{Re}{2})$	$\frac{f'}{2}$	D_v					$(\frac{Re}{2})$	$\frac{f''}{2}$	$\frac{f'''}{2}$	$\frac{f''''}{2}$
337	S	Authors' Tests	-	-	-	.0265'	.1094'	.1094'	.566	1.0	.139	330.	583.	Same
338											.116	349.	616.	as $\frac{f''}{2}$
339	Meshed	OIL Isothermal	NOTE: These Tests Not Evaluated on D_t Basis.				-	-	-	-	2.26	17.5	30.9	
340	Round						-	-	-	-	2.81	15.75	27.8	
341	X-fins						-	-	-	-	2.91	17.85	31.5	
342							-	-	-	-	3.14	17.5	30.9	
343							-	-	-	-	3.28	16.25	28.7	
344							-	-	-	-	3.21	16.85	29.8	
345							-	-	-	-	3.6	16.9	29.9	
346							-	-	-	-	3.88	14.15	25.	
347							-	-	-	-	3.94	13.7	24.2	
348							-	-	-	-	1.01	45.6	80.2	
349							-	-	-	-	1.25	32.4	57.3	
350							-	-	-	-	1.35	30.3	53.5	
351							-	-	-	-	1.56	25.3	44.7	
352							-	-	-	-	2.11	23.6	41.7	
353							-	-	-	-	3.0	18.35	32.4	
354	S	Authors' Tests	-	-	-	.0265'	.1094'	.1094'	.566	1.0	1,025.	.212	.375	Same
355							-	-	-	-	923.	.208	.367	as $\frac{f''}{2}$
356	Meshed	WATER Isothermal					-	-	-	-	636.	.264	.465	
357	Round						-	-	-	-	848.	.211	.372	
358	X-fins						-	-	-	-	1,065.	.197	.348	
359							-	-	-	-	1,010.	.178	.315	
360							-	-	-	-	704.	.296	.521	
361							-	-	-	-	439.	.385	.68	
362							-	-	-	-	1,060.	.195	.345	
363							-	-	-	-	729.	.276	.486	
364							-	-	-	-	575.	.361	.637	
365							-	-	-	-	648.	.4	.707	
366							-	-	-	-	765.	.172	.504	
367							-	-	-	-	733.	.304	.537	
368							-	-	-	-	800.	.321	.65	
369	Wire	Authors' Tests	-	-	-	.0220'	.0104'	.0104'	1.35	1.0	14,000.	.3175	.235	Same
370	Mesh						-	-	-	Assumed	15,150.	.32	.237	as $\frac{f''}{2}$
371	In-						-	-	-	-	16,150.	.331	.245	
372	ternal	WATER					-	-	-	-	16,900.	.326	.2415	
373	Fins	Isothermal					-	-	-	-	18,700.	.296	.219	
374							-	-	-	-	13,950.	.301	.223	

No.	Ar-range-ment	Source and Material	(Basis D_t)				S_L	S_T	$(\frac{D_v}{S_T})^{.4}$	$(\frac{S_L}{S_T})^{.6}$	(Basis D_v)			
			D_t	$(\frac{Re}{2})$	$\frac{f'}{2}$	D_v					$(\frac{Re}{2})$	$\frac{f''}{2}$	$\frac{f'''}{2}$	$\frac{f''''}{2}$
375	Wire	Authors' Tests	-	-	-	.0220'	.0104'	.0104'	1.35	1.0	14,650.	.322	.238	Same
376	Mesh						-	-	-	Assumed	10,100.	.374	.277	as $\frac{f''}{2}$
377	Internal	WATER Isothermal	NOTE: These Tests Not Evaluated On D_t Basis				-	-	-	-	11,300.	.36	.266	
378	Fins						-	-	-	-	12,320.	.356	.264	
379							-	-	-	-	1,135.	.456	.338	
380							-	-	-	-	1,760.	.413	.306	
381							-	-	-	-	2,900.	.389	.288	
382							-	-	-	-	3,740.	.364	.270	
383							-	-	-	-	4,260.	.375	.278	
384							-	-	-	-	4,800.	.362	.268	
385							-	-	-	-	5,300.	.373	.276	
386							-	-	-	-	5,810.	.361	.2675	
387							-	-	-	-	6,400.	.358	.267	
388							-	-	-	-	6,780.	.365	.269	
389							-	-	-	-	6,310.	.394	.292	
390							-	-	-	-	7,230.	.396	.294	
391							-	-	-	-	8,150.	.344	.255	
392							-	-	-	-	8,780.	.379	.281	
393							-	-	-	-	9,350.	.390	.289	
394	Wire	Authors' Tests	-	-	-	.0220'	.0104'	.0104'	1.35	1.0	488.	.715	.53	Same
395	Mesh						-	-	-	Assumed	471.	.775	.576	as $\frac{f''}{2}$
396	Internal	OIL Cooling					-	-	-	-	427.	.798	.591	
397	Fins						-	-	-	-	388.	.812	.602	
398							-	-	-	-	366.	.82	.608	
399							-	-	-	-	332.	.852	.631	
400							-	-	-	-	309.	.91	.676	
401							-	-	-	-	280.	.912	.676	
402							-	-	-	-	250.	.967	.718	
403							-	-	-	-	221.	1.03	.762	
404							-	-	-	-	190.	1.09	.608	
405							-	-	-	-	177.	1.155	.856	
406							-	-	-	-	158.6	1.26	.934	
407							-	-	-	-	137.5	1.285	.952	
408							-	-	-	-	129.	1.353	1.002	
409							-	-	-	-	149.	1.403	1.04	
410							-	-	-	-	123.	1.53	1.135	
411							-	-	-	-	101.	1.765	1.3	

TABLE 2 (Continued) CROSSFLOW FRICTION DATA; EXTENDED SURFACE

No.	Ar- range- ment	Source and Material	D _t	(Basis D _t)		D _v	S _L	S _T	(D _v S _T) ^{.4}	(S _L S _T) ^{.6}	(Basis D _v)			
				(Re 2)	(f' 2)						(Re 2)	(f' 2)	(Re 2)	(f' 2)
412	Radiator	Manufac-	NOTE: These tests not evaluated on D _t Basis.			.0137'	-	.052'	.586	1.0	1,280.	.0895	.1525	Same
413	Core-(A)	turers'				-	-	-	-	Assumed	1,830.	.074	.126	as
414	Type	Data				-	-	-	-	since	2,570.	.0619	.1055	f'' 2
415	Surface	AIR				.0156'	-	-	.618	indeter- minate	1,460.	.10	.162	
416	(B)					-	-	-	-		2,080.	.0822	.133	
417						-	-	-	-		2,730.	.0767	.124	
418	Square	Manufac-	"			.024'	.198'	.198'	.43	1.0	1,360.	.1055	.245	Same
419	X-fins	turers'				-	-	-	-	-	2,260.	.0972	.226	as
420		Data				-	-	-	-	-	3,180.	.0912	.212	f'' 2
421		AIR				-	-	-	-	-	4,530.	.0856	.199	
422	Radiator	Manufac-				.0152'	-	.0364'	.705	1.0	1,120.	.10	.142	Same
423	Core-(I)	turers'	"			-	-	-	-	Assumed	1,570.	.0895	.127	as
424	Type	Data				-	-	-	-	since	1,620.	.0882	.125	f'' 2
425	Surface	AIR				.0152'	-	.0364'	.705	indeter- minate	1,120.	.1065	.151	
426	(II)					-	-	-	-	-	1,570.	.0955	.1355	
427						-	-	-	-	-	1,620.	.0952	.135	
428	Round	Tube	"			.0297'	-	.1354'	.545	1.0	1,227.	.2165	.397	Same
429	X-fins					-	One	-	-	Assumed	1,380.	.208	.382	as
430		AIR				-	row	-	-	because	1,533.	.204	.374	f'' 2
431						-	Deep	-	-	only one	1,840.	.189	.347	
432						-	-	-	-	row deep	2,150.	.186	.3415	
433	Radiator	N.A.C.A.	"			.0207'	.0417'	.0834'	.574	.66	3,390.	.144	.251	.38
434	Core-					-	-	-	-	-	6,770.	.141	.246	.372
435	Type	AIR				-	-	-	-	-	10,200.	.140	.244	.369
436	Surface					-	-	-	-	-	3,080.	.1453	.255	.386
437						-	-	-	-	-	6,160.	.140	.244	.369
438			"			-	-	-	-	-	9,270.	.1342	.234	.355
439						-	-	-	-	-	12,300.	.139	.242	.366
440	Finned	N.A.C.A.				.00364'	-	.591'	.130	1.0	1,280.	.0489	.376	Same
441	Cylinders					-	Single	-	-	Assumed	1,540.	.0468	.36	as
442	(A)	AIR				-	Cylinder	-	-	because	1,795.	.0432	.333	f'' 2
443					-	in	-	-	of	2,050.	.0398	.306		
444					-	Shroud	-	-	Shroud	2,560.	.0365	.281		
445	(B)		"			.00784'	-	.591'	.176	Effect	1,650.	.0542	.308	"
446						-	-	-	-	-	2,760.	.0423	.240	
447						-	-	-	-	-	3,870.	.0384	.218	
448						-	-	-	-	-	4,430.	.0354	.201	
449						-	-	-	-	-	4,980.	.0342	.194	
No.	Ar- range- ment	Source and Material	D _t	(Basis D _t)		D _v	S _L	S _T	(D _v S _T) ^{.4}	(S _L S _T) ^{.6}	(Basis D _v)			
				(Re 2)	(f' 2)						(Re 2)	(f' 2)	(f'' 2)	(f' 2)
450	Finned		NOTE: These tests not evaluated on D _t Basis.			.0124'	Single	.591'	.213	1.0	2,190.	.0578	.271	Same
451	Cylinders	N.A.C.A.				-	Cylinder	-	-	Assumed	3,500.	.049	.230	as
452	(C)	AIR				-	in	-	-	because	5,250.	.0418	.196	f'' 2
453						-	Shroud	-	-	of	7,000.	.0384	.180	
454						-	-	-	-	Shroud	8,760.	.0352	.165	
455	(D)		"			.0163'	-	.591'	.237	Effect	2,880.	.0697	.294	"
456						-	-	-	-	-	4,800.	.0593	.250	
457						-	-	-	-	-	6,910.	.0503	.212	
458						-	-	-	-	-	9,220.	.0462	.195	
459						-	-	-	-	-	11,500.	.0425	.1795	
460	(E)		"			.0207'	-	.591'	.280	-	3,650.	.0835	.321	"
461						-	-	-	-	-	5,850.	.0707	.272	
462						-	-	-	-	-	8,770.	.0603	.232	
463						-	-	-	-	-	11,700.	.0551	.212	
464						-	-	-	-	-	14,600.	.051	.196	
465	Radiator	Bureau of	"			.033'	Flat	.0208'	1.22	1.0	2,700.	.0983	.081	"
466	Core-Type	Standards				-	Plate	-	-	Assumed	5,400.	.0738	.0605	
467	Surface					-	Tubes	-	-	since	10,800.	.0718	.0588	
468	(E-6)	AIR				-	-	-	-	inde-	13,500.	.0697	.0671	
469	(E-7)					.0543'	Flat	.0312'	1.248	terminate	8,900.	.0514	.0412	"
470			"			-	Plate	-	-	-	17,800.	.0477	.0382	
471						-	Tubes	-	-	-	26,600.	.0467	.0374	
472						-	-	-	-	-	31,100.	.0464	.0372	
473	(E-8)					.076'	Flat	.0417'	1.27	-	12,450.	.0455	.0358	
474						-	Plate	-	-	-	24,800.	.0446	.0351	
475			"			-	Tubes	-	-	-	31,000.	.0446	.0351	
476						-	-	-	-	-	43,500.	.0446	.0351	
477	(E-9)					.127'	Flat	.0625'	1.33	-	10,400.	.0457	.0344	"
478						-	Plate	-	-	-	20,800.	.0418	.0314	
479						-	Tubes	-	-	-	31,200.	.0417	.0313	
480			"			-	-	-	-	-	41,500.	.0402	.0302	
481	(F-6)					.0266'	.0417'	.0834'	.634	.66	2,170.	.498	.785	1.19
482						-	-	-	-	-	4,340.	.498	.785	1.19
483					-	-	-	-	-	6,610.	.437	.69	1.146	

Friction data of Carrier, Allen, Soule, Dehn, Reiher, and Reitschel for a great variety of tube arrangements have also been used to establish the equation, but are not shown.

There are certain discrepancies and deviations from the proposed main line in the data of Pierson. However, the magnitude of these deviations is in general not more than 10 or 15 per cent. Another point of importance is that no other authors have found friction factors which increase with Reynolds number, which is reported over limited ranges by both Pierson and Hoge. Lindmark, in his discussion of this paper, pointed this out and stated that he found no such increase in experiments he conducted. A certain amount of these deviations may be accounted for by the fact that entrance and exit losses are contained in the over-all pressure drop reported by these authors.

Jakob (12) proposed two equations of rather complex form for the correlation of Pierson's data. It appears that the present

equation is simpler to use, and probably more accurate as it is substantiated by data from many other sources.

EXTENDED SURFACE

Fig. 5 illustrates how extended surface, both external and internal, will plot on this same proposed correlation.

It will be noted that some forms of extended surface, namely, flat plates and fins with turbulence promoters, do not correlate well on the suggested curve as would be expected.

McAdams (13), Colburn (14), Norris and Streid (15), and many others have pointed out that flat plates and turbulence promoters will produce different flow characteristics. Flat plates show low $f/2$ values, and turbulence promoters give high values. The published and authors' data included in the paper bear out these conclusions.

The authors' data on meshed round-cross-fin tubes (eight $1/4$ -in.

fin per in.) with no turbulence promoters, Figs. 6(h) and 7(a), show good agreement with the proposed correlation. They cover both heavy lubricating-oil and water tests.

The N.A.C.A. tests on finned airplane-engine cylinders (16), Fig. 6n, in an air stream show ≈ 20 per cent, which is well in line. These results are encouraging, since fin heights are 1.22 in. and spacing varies from 0.057 to 0.166 in.

Authors' results on one sample of internal-fin tubes, Fig. 7b, show good correlation. This is especially interesting, since the tests represent a combination of cross- and internal-tube flow.

Tuve and McKeeman's tests on unmeshed cross-fin tubes (17), Fig. 6g, (for only one row), show agreement within 15 per cent, on the proposed curve.

For comparative purposes, data from the Bureau of Standards reports (18, 19), on various types of aircraft nose radiators, are included. These data show flat plates some 80 per cent low, and round tubes and flat plates with turbulence promoters approximately 300 per cent high for friction factors on the suggested basis.

In addition, manufacturers' data on flat-tube core-type radiators are included to show that where not too much turbulence-promoter effect is present, these too correlate on the curve within ~ 60 per cent.

Reference to Table 2 will show that for the factor $(S_L/S_T)^n$, as applied to some of the extended-surface samples, assumptions of unity were made in certain instances.

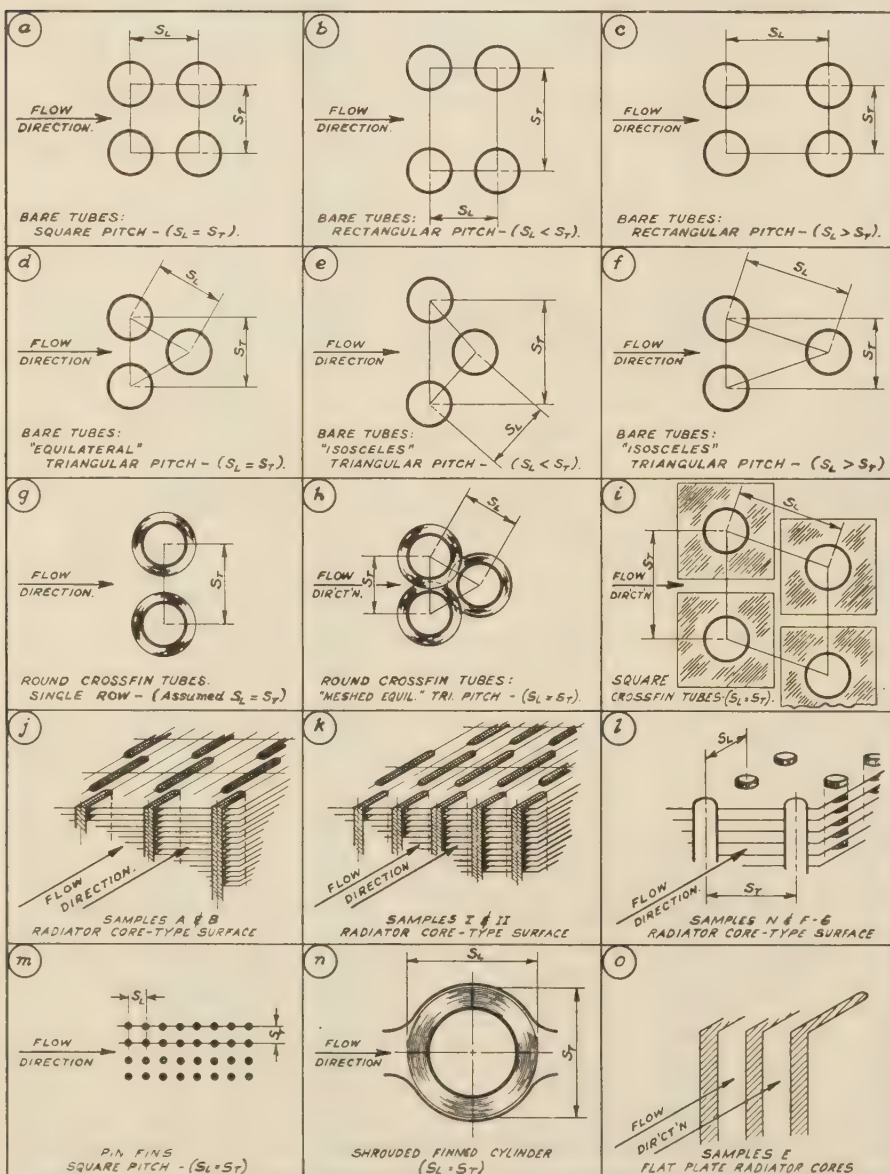


FIG. 6 VARIOUS TYPES OF CROSSFLOW SURFACES

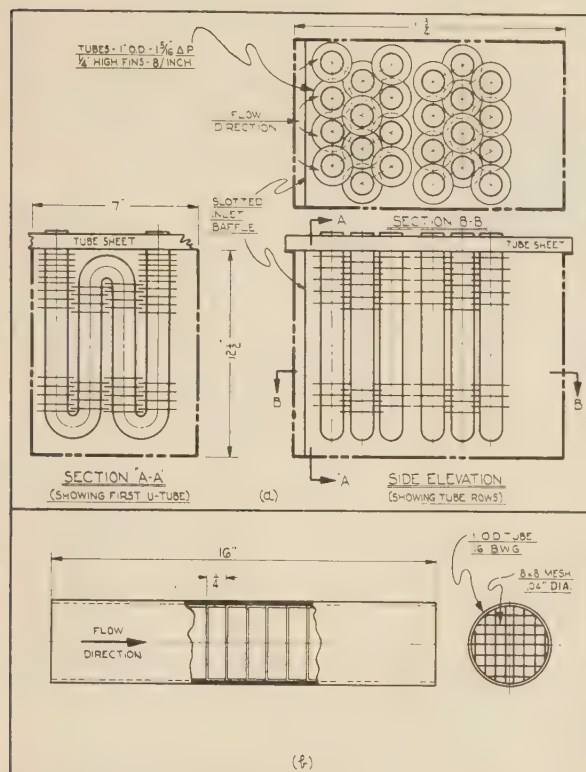


FIG. 7 AUTHORS' TEST SAMPLES
 (a, External meshed round cross fins.
 b, Internal wire-mesh fins.)

In the case of the wire-mesh internal fins, Fig. 7b (Tests No. 369-411), an 8×8 screen wire mesh was used for the inserts. It was reasoned that the symmetrical spacing of the cross-wires at 0.125 in. centers was the equivalent of equilateral pitch in a conventional tube bank; hence the use of $(S_L/S_T)^{0.6} = 1$.

For the various samples of radiator core-type surface, using flat tubes with relatively smooth plate-type fins, the evaluation of the configuration ratio was deemed indeterminate. Since these samples were included solely for comparative purposes, the factor was taken as unity.

Tu ve and McKeeman's tests on round cross-fin tubes, un-meshed, were for only one row deep in the direction of flow. While no finite value of S_L is determinable for this arrangement, it was assumed that sufficient exit turbulence was present to give at least some of the effect of additional rows. Therefore, $(S_L/S_T)^{0.6}$ was assumed as 1 for the plot.

With the shrouded-finned cylinders reported on by the N.A.C.A., a variation of the foregoing is found. In this case, the single "tube" is surrounded by a close-fitting baffle just clearing the outer periphery of the fins, Fig. 6n. It was felt that this produced the effect of an equilateral tube arrangement, and therefore, the configuration factor would become unity.

CONCLUSIONS

1 The use of D_e and the configuration factors proposed herein is recommended for a general correlation of pure crossflow friction on a single curve.

2 This same type of correlation can be applied to heat transfer, although demonstration of this is beyond the scope of the present paper.

3 It has been shown that certain types of extended surface, approximating conventional tube arrangements, correlate well on the general plot. This statement is qualified by the assumption that fins are relatively smooth and tubes are disposed in three or more rows deep, transverse to flow. It is admitted that where flat-plate or turbulence-promoter effects become significant, the suggested correlation does not apply.

4 It should be pointed out that additional data for the viscous range, on a greater variety of tube sizes and surface arrangements, are needed to establish more definitely this portion of the plot. This will be evident from an inspection of Figs. 1 to 5.

ACKNOWLEDGMENT

The authors wish to take this opportunity of crediting their late colleague, Mr. E. S. Davis, with his full due for the original mathematical analysis which formed the basis for the correlation revealed herein.

As in the unpublished reference work, appreciation is expressed to Messrs. E. N. Sieder and N. A. Scott, Jr., of Foster-Wheeler Corporation for making available extensive original crossflow data, and to Mr. R. H. Norris for his courtesy in supplying exact values of his published data.

In addition, the authors must acknowledge their debt to the National Advisory Committee for Aeronautics, the Bureau of Standards, and to all the other investigators whose published data were made free use of in this paper.

Finally, thanks are due to Mr. C. P. Byrne, who carried out most of the authors' test work; and to Miss B. L. Samson and Mrs. D. G. Davis for their efforts in working up the test calculations, tabulations, and plots.

Appendix

As mentioned previously, the present paper incorporates data from many diverse sources. The basic bare-tube plots are taken directly from the published data of various investigators, as set forth in the Bibliography. Some of the extended-surface plots are from published data; the rest from private manufacturers' data made available for this work, and from actual authors' tests. The last specifically are the external meshed cross-fin plots and those for the internal wire-mesh fins.

Meshed Cross Fins. The meshed-cross-fin-surface sample tested is detailed in Fig. 7a. Conventional spiral cross-fin tubes (1 in. OD with $1\frac{1}{2}$ -in.-OD fins, 0.012 in. in thickness, 8 per in.), were arranged on $1\frac{1}{16}$ -in. triangular pitch with fins intermeshed, as shown, in two nests of three rows each. The open tube ends were rolled into a tube sheet in the conventional manner, with the return bends disposed as shown. This assembly was enclosed in a rectangular box-type shell with suitable inlet and outlet nozzles at the narrow ends for installation in the test setup piping. A slotted baffle plate was placed at the inlet end of the test section to insure proper distribution of the entering fluid over the full face of the tube bundle.

Cooling and isothermal test runs, Table 2 (No. 300-368), for both lube oil and water were made to fill in as complete a range of the curve as possible. It will be noted that the oil tests fall along the viscous portion of the line, with those for water in the turbulent region.

Internal Wire-Mesh Fins. The internal wire-mesh fin-tube sample tested is shown in Fig. 7b. This was a 1-in. OD, No. 16 Bwg copper tube with tinned wire-mesh inserts (8×8 mesh, 0.04-in.-diam wire), disposed inside throughout its length. The test sample was then installed with suitable entrance and exit straightening tubes in the piping setup, and the water and oil tests run as listed in Table 2 (No. 369-411).

ADDENDA

It is recognized that the admirable work of Chilton and Genereaux (20) was seemingly overlooked in the presentation of the present correlation. It must be explained that, while the data of all the investigators covered by these authors were utilized to establish the new recommended curve, preprint deadline limitations prohibited a direct comparison with this earlier work.

BIBLIOGRAPHY

- 1 "A Method of Correlating Forced-Convection Heat-Transfer Data and a Comparison With Fluid Friction," by A. P. Colburn, Trans. American Institute of Chemical Engineers, vol. 29, 1933, pp. 174-210.
- 2 "A Review of Heat-Transfer Coefficients and Friction Factors for Tubular Heat Exchangers," by B. E. Short, Trans. A.S.M.E., vol. 64, 1942, pp. 779-785.
- 3 "Investigation of Heat Transfer Rates on the External Surface of Baffled Tube Banks," by R. A. Bowman, in "Heat Transfer," A.S.M.E. unpublished papers, no. 28, 1936, pp. 75-81.
- 4 "Experimental Investigation of Effects of Equipment Size on Convection Heat Transfer and Flow Resistance in Crossflow of Gases Over Tube Banks," by E. C. Hoge, Trans. A.S.M.E., vol. 59, 1937, pp. 573-581.
- 5 "Correlation and Utilization of New Data on Flow Resistance and Heat Transfer for Crossflow of Gases Over Tube Banks," by E. D. Grimison, Trans. A.S.M.E., vol. 59, 1937, pp. 583-594.
- 6 "High-Performance Fins for Heat Transfer," by R. H. Norris and W. A. Spofford, Trans. A.S.M.E., vol. 64, 1942, pp. 489-496.
- 7 "Fluid Friction at Parallel and Right Angles to Tubes and Tube Bundles," by E. N. Sieder and N. A. Scott, Jr., A.S.M.E. unpublished papers, No. 83, 1932.
- 8 "Heat Transfer and Pressure Drop in Crossflow Over Bare Tube Banks," by E. S. Davis and A. Y. Gunter, unpublished paper released only to N.A.C.A., 1943.
- 9 "Heat Transfer and Pressure Drop of Liquids in Tubes," by E. N. Sieder and G. E. Tate, *Industrial and Engineering Chemistry*, vol. 28, 1936, pp. 1429-1435.
- 10 "Experimental Investigation of the Influence of Tube Arrangement on Convection Heat Transfer and Flow Resistance in Crossflow of Gases Over Tube Banks," by O. L. Pierson, Trans. A.S.M.E., vol. 59, 1937, pp. 563-572.
- 11 "Resistance to Flow Through Nests of Tubes," by R. Pendenis Wallis and C. M. White, *Engineering*, vol. 146, 1938, pp. 605-607, 665-666, and 723-725.
- 12 "Discussion of Pierson, Hoge, and Grimison Papers," by Max Jakob, Trans. A.S.M.E., vol. 60, 1938, pp. 384-386.
- 13 "Heat Transmission," by W. H. McAdams, McGraw-Hill Book Company, Inc., New York, N. Y., 1942, pp. 123-124, 197-198.
- 14 "Heat Transfer by Natural and Forced Convection," by A. P. Colburn, Purdue University, Engineering Experiment Station, Research Series No. 84, Jan., 1942, pp. 38-40, 51.
- 15 "Laminar-Flow Heat-Transfer Coefficients for Ducts," by R. H. Norris and D. D. Streid, Trans. A.S.M.E., vol. 62, 1940, pp. 525-533.
- 16 "Blower Cooling of Finned Cylinders," by O. W. Schey and H. H. Ellerbrock, Jr., U. S. N.A.C.A., Report No. 587, 1937, p. 269.
- 17 "Heat Transfer From Direct and Extended Surfaces With Forced Air Circulation," by G. L. Tuve and C. A. McKeeman, Trans. American Society of Heating and Ventilating Engineers, vol. 40, No. 997, 1934, pp. 427-442.
- 18 "Radiators for Aircraft Engines," by S. R. Parsons and D. R. Harper 3rd, U. S. Bureau of Standards, Technical Paper No. 211, 1922, pp. 369-371, 391-392.
- 19 "Heat Dissipation and Other Properties of Radiators," by H. C. Dickinson, W. S. James, and R. V. Kleinschmidt, N.A.C.A. Report No. 63, 1919.
- 20 "Pressure Drop Across Tube Banks," by T. H. Chilton and R. P. Genereaux, Trans. American Institute of Chemical Engineers, vol. 29, 1933, pp. 161-173.

Discussion

D. F. BOUCHER⁴ AND C. E. LAPPLE.⁴ The authors have undertaken the formulation of a generalized method for estimat-

⁴ Engineering Department, Experimental Station, E. I. du Pont de Nemours & Co., Wilmington, Del.

ing pressure drop across tube banks, a field in which a large amount of conflicting data are available and in which correlation is sorely needed. The advantages claimed for the proposed method are that it attempts to combine the data for tubes of both plain and extended surfaces in a single empirical correlation, and that the same method of representation is applied to the streamline- and turbulent-flow regimes, as well as to staggered and in-line tube arrangements.

An empirical generalization of this type is a useful design tool and has much to recommend it. However, as is usually the case in such instances, a certain sacrifice in accuracy is entailed. For banks of plain tubes, the accuracy is fairly good in the range of spacings commonly used in practice but becomes progressively worse as more extreme spacings are approached. Unfortunately, this is not made clear by the authors since their plots ascribe almost one half of all the points plotted to an arrangement tested by Sieder and Scott, while each of the two Wallis-White arrangements is given considerably more weight than each of the numerous arrangements tested by Hoge and Pierson. Figs. 8 and 9 of this discussion show all the available data on pressure drop for turbulent flow across plain tube banks on the authors' method of presentation, giving equal weight to each arrangement reported. It is apparent that the deviation of the data from the line proposed by the authors is as much as three- to fourfold as compared with less than twofold indicated by their Fig. 4. This greater deviation is due to the additional data of Allen, Andreas, Brandt and Dingler, Carlson and Hurt, Dehn, Jauernick, Reiher, Rietschel, Soule, and ter Linden, as well as some of Pierson's and Hoge's data that had not been included in the original presentation by the authors.

Their line for streamline flow appears to be based on isothermal data for only a single arrangement. All other points are based on heating and cooling runs. In view of the uncertainty as to the proper interpretation of data for banks in which heat transfer occurs, it would hardly appear justifiable to use them for the fundamental correlation, particularly when isothermal data are available. The isothermal correlation should then be used to determine the proper way to handle data for the case of heat transfer.

Fig. 10 of this discussion has been prepared to compare the available isothermal data on the basis of the authors' method of presentation. The points shown represent all the isothermal streamline data originally reported by Sieder and Scott as well as some additional data obtained by Sieder and reported by the authors. All of the data represent staggered equilateral tube-bank arrangements. By reference to the original Sieder-Scott method of presentation, subsequently adopted by Chilton and Genereaux for the streamline region, it becomes apparent that the authors' method does not give as good a representation of the data.

It is to be expected that the effect of tube spacing will be different for turbulent and for streamline flow. In one case, kinetic energy or inertia forces are predominant, while in the other shear or frictional forces are controlling. It is only by pure coincidence that tube spacing can affect each to the same degree. The fact that the authors obtained a fairly good correlation for both streamline and turbulent flow would appear to indicate that an equal effect is closely approximated. However, it should be pointed out that the available data for streamline flow, while copious, cover a very limited range of spacings (two staggered equilateral and no in-line arrangements). Consequently, acceptance of the possibility of a single correlation for both regions must be made with considerable reservation until more data become available.

In the case of the Wallis-White staggered arrangement, the authors apparently used a value of D_o of 0.079 ft, whereas it

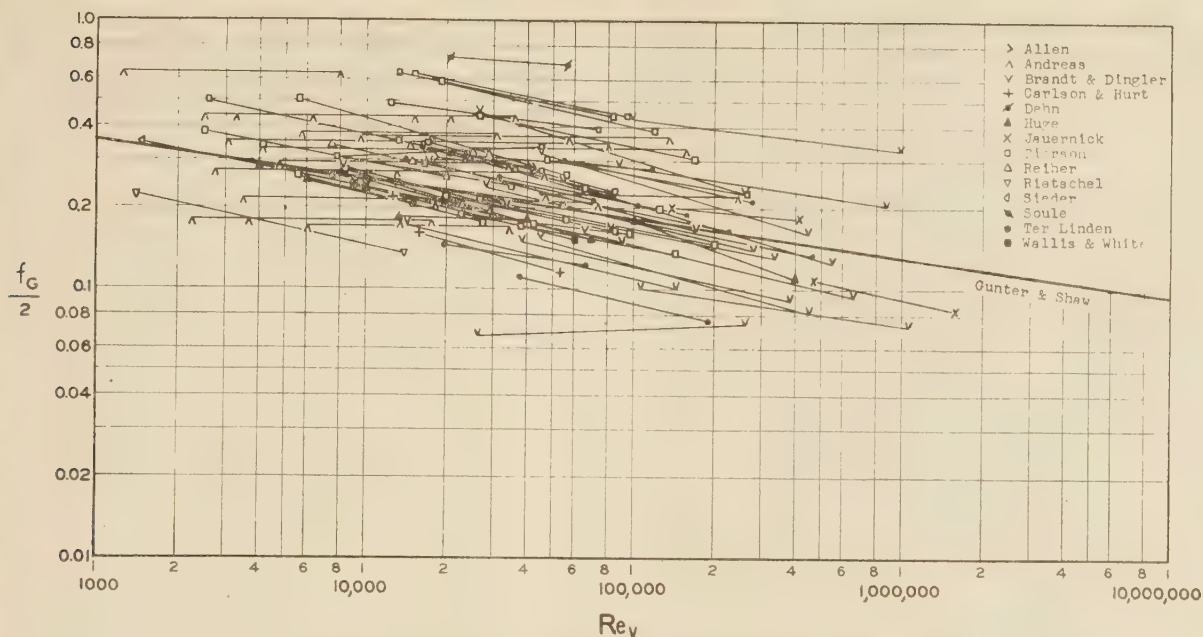


FIG. 8 COMPARISON OF TURBULENT-FLOW DATA FOR STAGGERED ARRANGEMENTS
(Gunter-Shaw method of representation.)

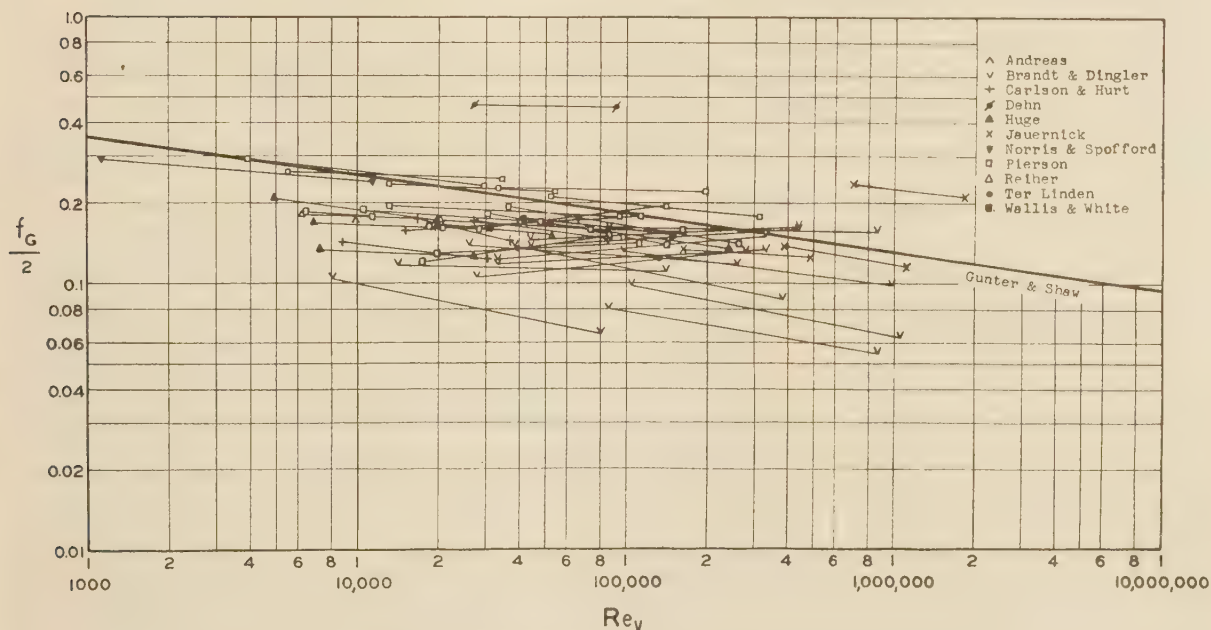


FIG. 9 COMPARISON OF TURBULENT-FLOW DATA FOR IN-LINE ARRANGEMENTS
(Gunter-Shaw method of representation.)

should have been 0.0625 ft, which results in their friction factors being high by 25 per cent. The original calculations of the Sieder-Scott data reported by the authors also contained some errors, which, when rectified, resulted in most of the values originally reported for Reynolds numbers, $D_o G/\mu$, less than 20 being shifted to a Reynolds number tenfold higher. The corrected values are given in Fig. 10 of this discussion. (See page 658).

Summarizing, it would appear that the effect of tube spacing

is considerably more complex than the authors' method would imply. The foregoing discussion largely represents excerpts from a forthcoming review paper on the same subject. This paper will compare the various methods that have been proposed for the representation of data on pressure drop across plain tube banks, using all available data. It will be shown that other methods are considerably more accurate and simpler to employ for design calculations in the case of plain tube banks than that

proposed by the authors. Extended surfaces have not been considered, since data are considered still too meager to permit any critical comparison.

S. L. JAMESON.⁶ The equation for pressure drop in crossflow proposed by the authors is very interesting, both from the degree of correlation they have obtained, and from the ease with which it may be used in design. However, a study of data on the effect of tube spacing in staggered banks of helically finned tubes⁶ indicates that the equation requires further study and refinement before it can be generally used.

In Figs. 11 and 12 of this discussion, friction factors are plotted against Reynolds number, as defined by the authors, for the highest and lowest test air flows for the arrangements reported.⁶ In all cases the friction factor is calculated on the basis of the free area in a single row of tubes, regardless of the relative free area through the diagonal openings between successive tube rows.

Fig. 11 shows the friction factors for various 3/4-in. tube arrangements as calculated from the authors' equation. The points diverge widely from their curve, and show definite trends of divergence with variation of either the tube spacing across the face of the tube bank, or of variation of the spacing between tube rows.

The authors' equation revised by interchanging S_L and S_T gave a much better correlation of the friction factors for crossflow over finned-tube banks. The revised equation is

$$\frac{f}{2} = \frac{\Delta P g D_{ep}}{G^2 L} \left(\frac{\mu}{\mu_w} \right)^{0.14} \left(\frac{D_p}{S_L} \right)^{-0.4} \left(\frac{S_T}{S_L} \right)^{-0.8} = \phi(R)$$

All symbols are as defined by the authors. The friction factors

⁶ Construction Engineering Division, General Electric Company, Schenectady, N. Y. Mem. A.S.M.E.

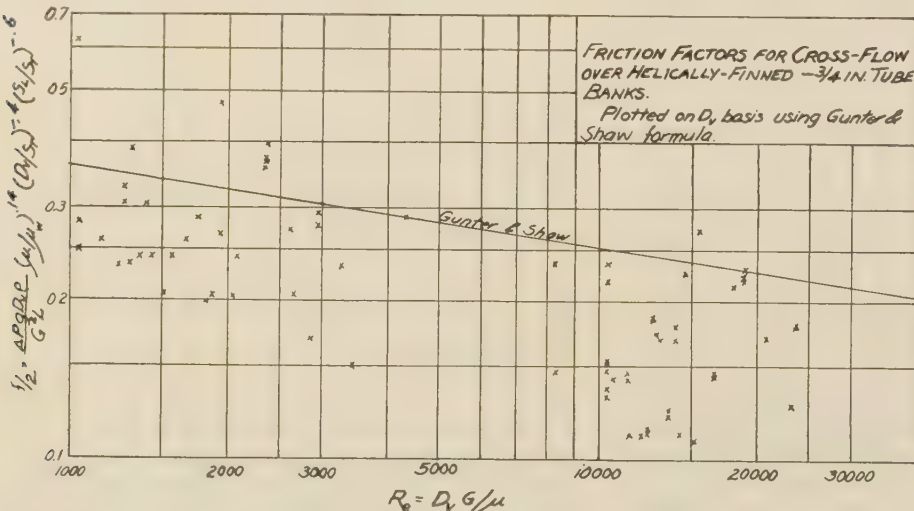


FIG. 11 FRICTION FACTORS FOR CROSSFLOW OVER HELICALLY FINNED 3/4-IN. TUBE BANKS (Plotted on D_p basis using Gunter and Shaw formula.)

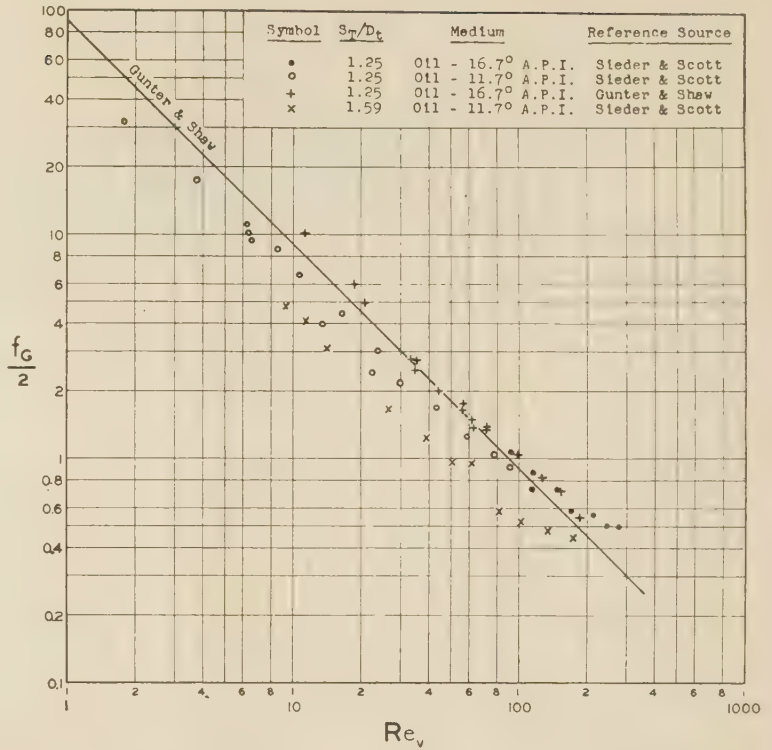


FIG. 10 COMPARISON OF STREAMLINE-FLOW DATA ON GUNTER-SHAW METHOD OF REPRESENTATION

for all tube arrangements tested⁶ are plotted against Reynolds number in Fig. 12. The equation of the curve approximating the data is $f/2 = 1.69 (R)^{-0.26}$.

A factor to correct air pressure drop for tube spacing in a finned-tube bank is very useful in design (see Fig. 5 of the writer's paper⁶). Factors based on constant air-mass velocity, pressure, and temperature are plotted in Fig. 13 of this discussion. The factors calculated from the revised equation given previously

check the test results satisfactorily. The factors calculated using the original relation of the authors show about double the test correction for tube spacing across the face of the tube bundle, and a decrease in pressure drop with a decrease in spacing between rows, rather than an increase as found in the tests.

The revised equation indicates about double the effect of change in number of fins on pressure drop as was obtained in tests of finned-tube banks.

The revised equation correlates the data for cross-

⁶ "Tube Spacing in Finned Tube Banks," by S. L. Jameson, Trans. A.S.M.E., vol. 67, 1945, pp. 633-642.

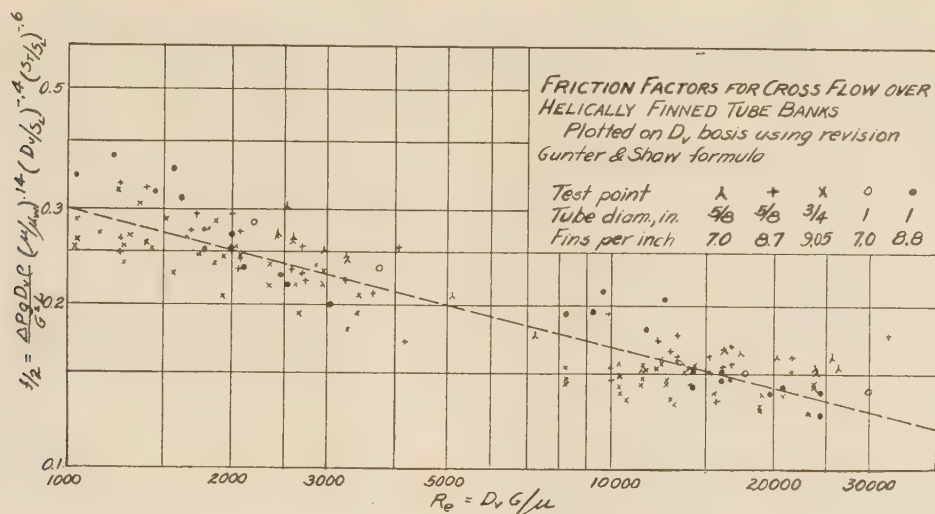


FIG. 12 FRICTION FACTORS FOR CROSSFLOW OVER HELICALLY FINNED TUBE BANKS
(Plotted on D_v basis using revision Gunter and Shaw formula.)

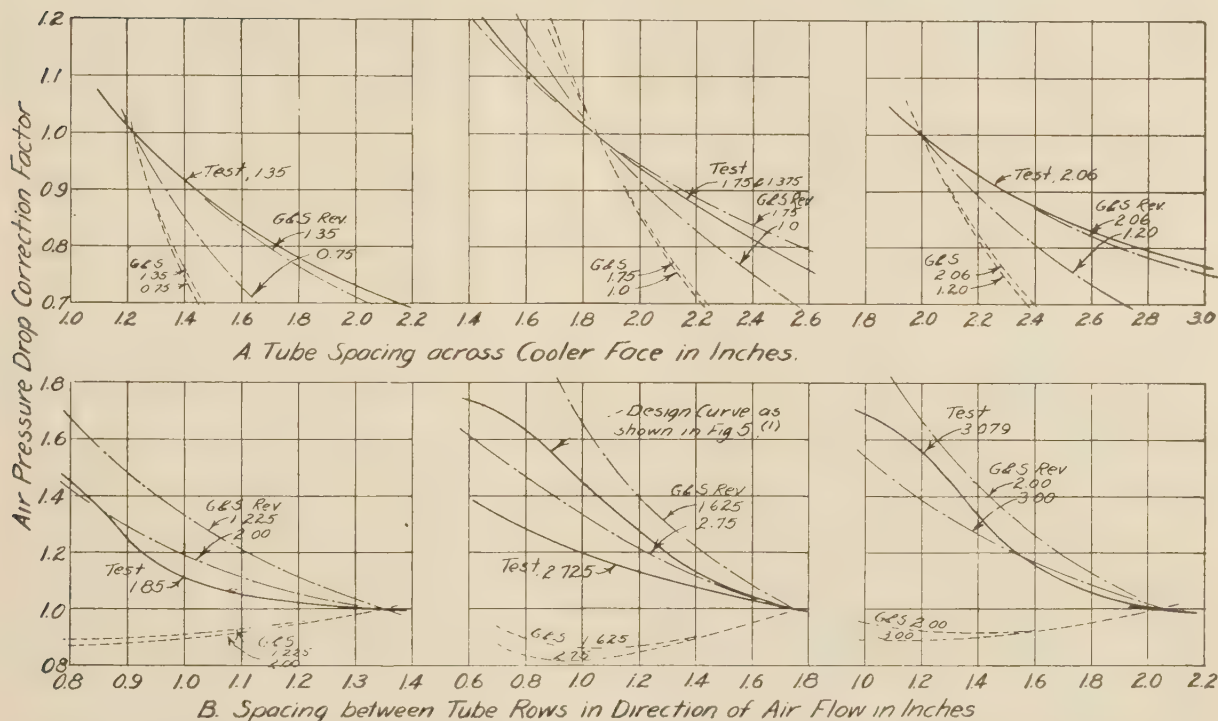


FIG. 13 FACTORS TO CORRECT AIR PRESSURE DROP FOR TUBE SPACING IN BANKS OF HELICALLY FINNED TUBES

(Correction factors are based on constant air-mass velocity and on $f/2$ varying as $Re^{-0.25}$. Curves are designated as follows: G&S factors based on Gunter & Shaw equation. G&S Rev.: Factors based on a revision of Gunter & Shaw equation. Test: Factors based on actual test data. Figures: In curves A, spacing between rows; in curves B, tube spacing across cooler face.)

flow across banks of helically finned tubes much better than does the original equation of the authors, but both require much study and revision before they may be applied to all types of surface in crossflow.

AUTHORS' CLOSURE

The authors appreciate the contribution, by Messrs. Boucher and Lapple and Mr. Jameson, of some thought-provoking discussion material on the subject paper. Although their comments

seemingly refute certain parts of the over-all correlation these are welcome, since it is only by constructive criticism that progress can be made in a field in which, admittedly, such advances are desirable.

With regard to the Boucher and Lapple comments, it is agreed that some over-all accuracy is lost in attempting a crossflow friction correlation which presumes to take care of both staggered and in-line, bare and extended-surface tubes; at the same time it is observed that a single curve covering both streamline and

turbulent flow is most advantageous for practical engineering application. It might be well to point out that a majority of the additional data cited by Messrs. Boucher and Lapple fall outside the "conventional arrangement" limitations imposed by the paper, and that "single cylinder" effects predominate.

Further, as originally mentioned under "Bare Tubes" in the paper, "friction data of Carrier, Allen, Soule, Dehn, Reiher and Reitschel. . . . (were) used to establish the correlation but are not shown." Recheck of this material against discussers' Figs. 8 and 9 reveals inconsistencies of their plots here. The reference to Pierson's and Huger's data "not included" is refuted by the statement that a majority of the minimum and maximum cases of these investigators were reported on in the paper while random tests of the remainder were made to check the validity of the correlation, but were not published.

With regard to the streamline region of the curve, it is unfortunate that only two tube arrangements were available. However, a number of extended-surface arrangements were applied which confirm this portion of the plot, in good agreement with the bare-tube data. Moreover, from a practical standpoint, the authors have used a large number of heating and cooling streamline flow tests which fall on the suggested line, using the well-known Sieder and Tate μ/μ_w viscosity correction ratio. Conclusion 4 of the paper admitted this scarcity of variety in the data available for this range of the correlation, and thereby justified the foregoing procedures. In any case, the authors' curve is found to be more conservative than that of Chilton and Genereaux (20).

In this connection, critical study was made of the evaluation of the final ΔP values as produced by the two methods. As a result it may be stated that the Chilton and Genereaux correlation gives calculated results for the Seider and Scott isothermal data, for example, with average deviation of approximately -20 per cent, as against approximately +10 per cent for the new correlation recommended by the authors. Since practical applications always countenance a certain amount of safety factor, and since, in the final analysis, it is the ultimate values of ΔP which should carry the most weight in establishing the validity of a correlation against actual results, it is felt that the proposed curve is more acceptable in this regard.

In Mr. Sieder's published discussion of the Chilton and Genereaux paper (20) he indicated that the use of two individual plots, covering streamline and turbulent flow, might be confusing and that there definitely is a gradual transition from one type of flow to the other, which is lost in the separate curve presentation. From a practical standpoint as brought out previously, a single curve is also very desirable for commercial use. For these reasons the development of the present correlation was undertaken.

The authors must admit to an error in the published value of D_e for the Wallis-White staggered arrangement, (Line No. 25-38, Table 1). The corresponding in-line data, however, are correctly shown. Further reference to the original plots of authors' Fig. 4 and corrected replots of these data in discussers' Fig. 8 will show that the 20 per cent discrepancy reported by the latter is of minor significance. Whereas the incorrect plotting first fell some 10 per cent above the recommended line, the true replotted positions these points an approximately equivalent amount below. The net result of this shift does not warrant any change in the published curve.

With regard to the tenfold correction reported by the discussers

in certain of the Sieder and Scott data for Reynolds numbers originally less than 20, the authors cannot identify the tests referred to, only one run having been located which contained such a change. In addition, four points appear to have been omitted from Boucher and Lapple's Fig. 10 which fall on the published line at Reynolds numbers between 6 through 20.

With reference to Mr. Jameson's discussion, there are several items which warrant comment. In the first place, his reproduction of the authors' basic line as given in Fig. 11 is not strictly correct, being slightly high for the turbulent region shown (compare with Figs. 4 and 5). Moreover, it is to be noted that Fig. 11 is restricted to but one tube size, $3/4$ in. A more complete plotting by the authors, including the $5/8$ -inch and 1-in. tube data shown in Fig. 12 transposed to original basis, falls both above and below the published curve, which represents a good average of these plots (see Fig. 14).

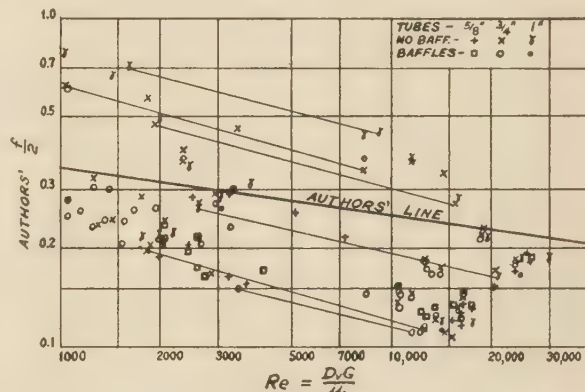


FIG. 14 COMPARISON OF JAMESON FINNED-TUBE DATA WITH TURBULENT REGION OF AUTHORS' RECOMMENDED LINE

It must be pointed out that a minimum of three rows was stipulated as the lower limit of accuracy for the recommended correlation. Since some of Mr. Jameson's work was on one or two rows, it might be expected that these points would plot low, which they do.

As to the suggested revision of the basic equation by interchanging S_L and S_T , the authors cannot subscribe to this as a definitely established, recommended revision of the proposed general correlation. Application of this reversal to bare-tube data destroys the alignment there; hence for general correlation of both bare and extended surfaces, the original published version of the equation and correlation is preferred, at least for the present. The interchanged factor idea, is, however, most interesting, and as a demonstration of possible future work toward refinement of the basic correlation for more over-all accuracy, has much to recommend it.

It is believed that when heat transfer and pressure drop can each be correlated on a single line for both turbulent and streamline flow, using dimensionless correction factor ratios, this is a major advance in crossflow analysis.

Further development of the basic equation must consider the following groups of surfaces—round bare tubes and single cylinders, round tubes plus flat plates (crossfin tubes), and flat tubes plus flat plates (core-type surface).

Air-Cooled Steam Condensers

By R. A. BOWMAN,¹ PHILADELPHIA, PA.

In connection with the rehabilitation of the war-torn areas of the world, there is a great need for power plants which can be moved from one location to another without difficulty, and which can be put into operation in a short period of time. In some of the locations where these power plants must operate, cooling water will be unavailable, or obtainable only at a great premium. To take care of such cases, a number of power trains have been built to use air as a cooling medium rather than water. The trains in general have been widely described. The present paper is devoted to a more complete description of the condensers and to a report on their operation.

POWER trains are expected to operate at temperatures varying from 40 F below zero to +95 F. The primary purpose of the condenser is to recover condensate and not to reduce the heat rate of the plant by the production of vacuum. Back-pressure operation was chosen for design conditions because the condenser size and power requirements of the blowers would be excessive if a vacuum of any magnitude is to be maintained. At lower air temperatures or at partial loads, vacuum will, of course, be practical, and a single-stage ejector is supplied to take advantage of these conditions.

DETAILS OF CONDENSER AND OPERATING CONSIDERATIONS.

The condenser for a 5000-kw power train is placed on two cars, each car containing eight separate condenser sections, air for which is supplied by four propeller-type blowers. Fig. 1 is a general view of the condenser cars. Steam is supplied to the cars through a manifold from the turbine, connecting to a pair of longitudinal steam ducts running the length of the car. The condenser sections are set on these ducts so that steam enters them from the bottom, is condensed, and the condensate drains back into the ducts from which it is removed by a condensate pump. This counterflow relationship between steam and condensate was chosen because it not only serves to heat and deaerate the condensate but also prevents its freezing.

The condensing sections themselves consist of ten rows of finned tubes, mounted vertically. Each section contains 370 tubes, giving 5625 sq ft of finned surface, or a total of 90,000 sq ft for the train. The face area of each section is 42.5 sq ft. The dimensions of the tubes are given in Fig. 2. They are arranged on a 2-in. staggered pitch. The tubes are constructed of steel, with steel fins, and the tube assembly is galvanized inside and out. Steel was chosen for the material because it is adequate for the service and was more available at the time the design was prepared than were the copper-base alloys.

In all condensing apparatus where the latent heat of steam is transferred to a cooling fluid as sensible heat, there will be variations in the condensing capacity of different sections of the condenser. In order to supply each part of the condenser with the steam it requires, it is necessary either to provide a varying

pressure drop to the different parts, or to arrange the flow paths so that they will have the proper resistance to limit the steam to that required by the condensing surface. In the ordinary surface condenser this can be accomplished in a natural manner by arrangement of tubes and tube plates. In those cases where the steam is inside of the tubes, nothing can be done to vary the resistance of the individual flow paths, but resistances can be added in the form of orifices to bring about a balance in the steam-flow paths.

A section through the individual condensing unit is shown in Fig. 3, illustrating the method used in this air-cooled condenser to provide balanced steam flows. The tube bank is divided into five separate groups, each group comprising two rows of tubes. The first four of these groups exhaust into the fifth group through orifices. The fifth group of tubes serves as a final condensing section, or what is frequently called an "air-cooler section." The orifices limit the amount of steam which any group can supply to the air cooler, and in order to pass the total steam required by the air-cooler section it is necessary that steam be supplied through all the other four groups of tubes, giving an adequate balance of steam flows.

The requirement that the condenser operate satisfactorily at a temperature of -40 F makes it imperative that every possible precaution be taken to prevent freezing inside the condenser. The greatest danger of freezing arises in those areas which, because of poor distribution or light loading, are not fully supplied with steam. Fortunately, the design which leads to efficient use of the condenser surface by supplying steam to all the tubes in accordance with their capacity to condense it, also serves to keep all areas warm and free from ice.

AVOIDING DIFFICULTIES AT LOW TEMPERATURES

Under conditions of light load and cold air the vacuum determined from heat-transfer considerations will exceed that produced by the ejector, and the condenser will begin to fill with air until the point is reached at which the remaining surface supplied with steam is just sufficient to satisfy the heat-transfer equation. As soon as a tube fills with air its temperature will drop approximately to that of the air outside the tube. If this temperature is below the freezing point the condensate which is formed within the tube or flows into it from other sections will freeze. The first tubes in which this will occur are those in the air-cooler section; but since this section is located on the air-discharge side, the air will have been warmed up to a temperature above 32 F in almost all cases. Any reduction in load occurring after the air-cooler section has been blanked off will introduce air at the top of the tubes in the first row where danger of freezing is great.

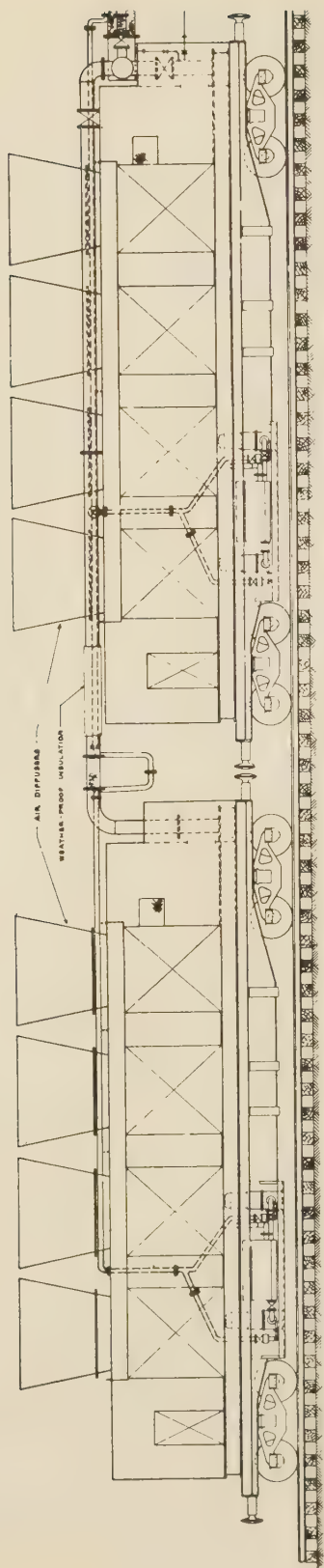
Each section of the condenser is supplied with a distant-reading thermometer, the bulb of which is located in the top of the center tube of the first row. Since this thermometer bulb is located at a point where freezing is most likely to occur, the operator is given a reliable guide on the danger of ice formation. The operating instructions of the train state that when the temperature as measured by this thermometer falls below 150 F, the amount of air circulated should be reduced by closing down one or more blowers.

In the case of extremely low temperatures and very light loads, it is possible that even with only one car in service and one

¹ Manager, Condenser Engineering, Westinghouse Electric Corporation. Mem. A.S.M.E.

Contributed by the Heat Transfer Division and presented at the Annual Meeting, New York, N. Y., Nov. 27-Dec. 1, 1944, of THE AMERICAN SOCIETY OF MECHANICAL ENGINEERS.

NOTE: Statements and opinions advanced in papers are to be understood as individual expressions of their authors and not those of the Society.



CONDENSER CAR #1

CONDENSER CAR #2

FIG. 1 GENERAL ARRANGEMENT OF CONDENSER CARS

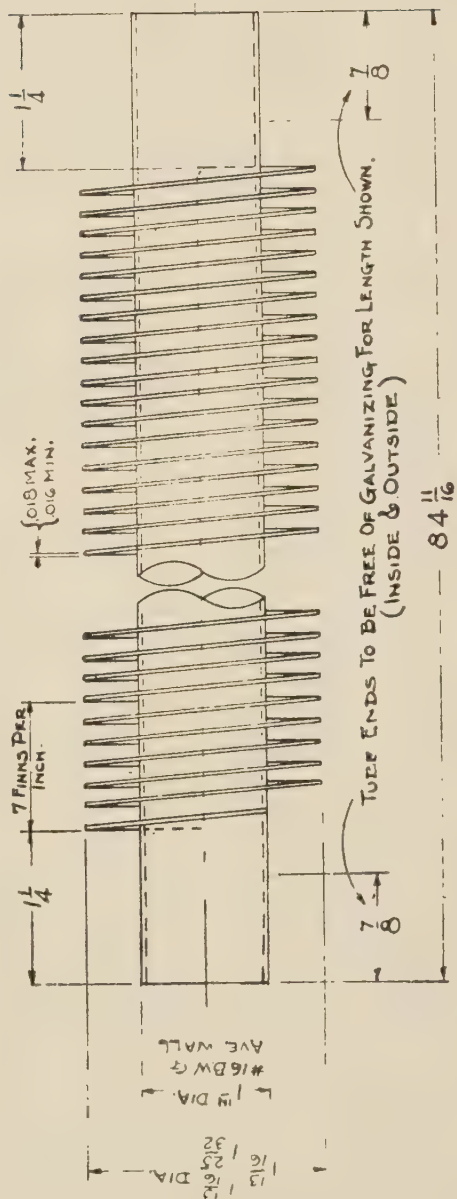


FIG. 2 DIMENSION DETAILS OF FINNED STEEL TUBES

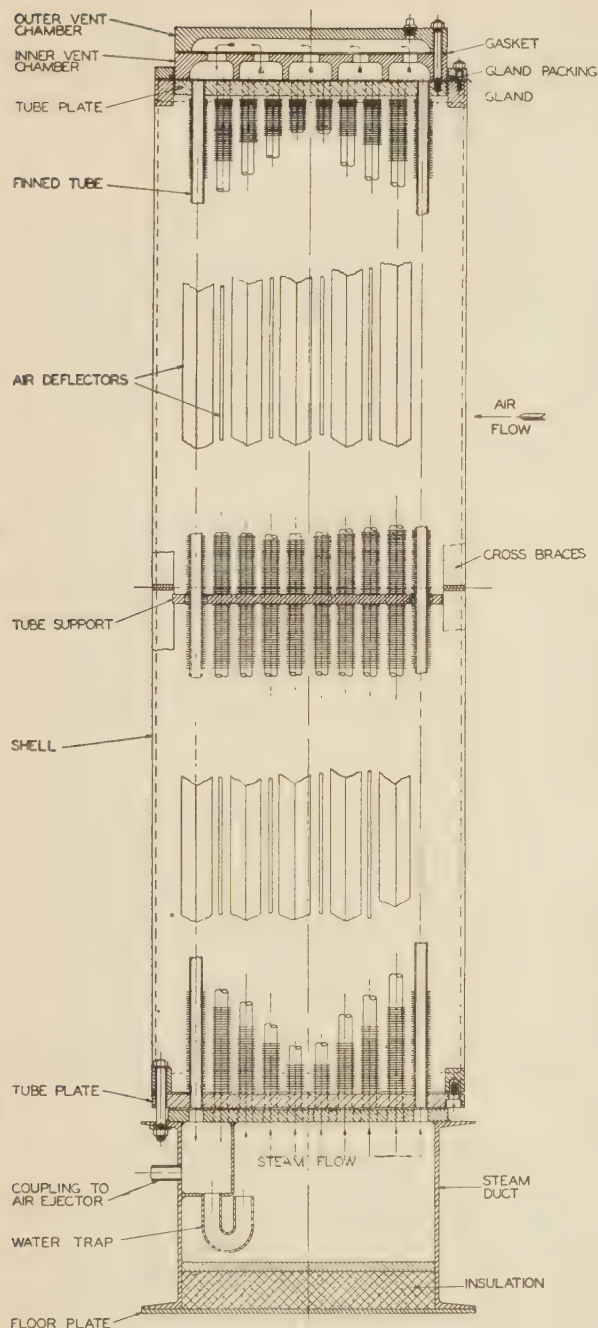


FIG. 3 SECTION THROUGH CONDENSING UNIT

CONDENSER TESTS CONDUCTED

At the time the entire train was tested, readings were made on the condenser. The purpose of these tests was to determine the amount of heat which could be transferred by the condenser under design conditions and were limited to this objective. Time was not available to run tests under carefully controlled conditions or to develop careful instrumentation. Test data were obtained on the following items:

- 1 Ambient temperature.
- 2 Barometer.
- 3 Air temperature leaving condenser.
- 4 Steam temperature.
- 5 Steam flow to the condenser.
- 6 Air-pressure drop through condenser.

The temperatures were measured with glass thermometers, except for the temperature of the air leaving the condenser which was measured by means of thermocouples. The steam pressure in the duct was measured with a mercury column, the pressure drop through the condenser with a water column, and the amount of steam flowing with a calibrated commercial flowmeter at the boiler. The test results are given in Table 1.

TABLE 1 TEST RESULTS ON CONDENSER

Test no.	1	2	3
Ambient temperature, deg F	94.25	86.8	70.3
Barometer, in. Hg.	28.95	28.93	28.86
Air temperature from condenser, deg F	202.2	184.2	171.3
Steam temperature, deg F	225.4	217.2	202.4
Steam condensed, lb per hr.	79860	78640	78140
Air-pressure drop, in. H ₂ O	2.4	2.53	2.64
Heat load, Btu per hr.	75,330,000	74,360,000	75,830,000
Heat-transfer rate	13.4	11.7	12.0
Face velocity, psi per hr.	4300	4700	4640

Tests on the air-cooled condenser for the power train indicate that such a condenser is entirely practical where conditions justify its use. It has the advantage that no water is required for cooling and can be put into operation without connection to an outside source of cooling medium. Because of the poor heat-transfer properties and the low specific heat of air, such a condenser in general requires higher auxiliary power, greater investment, and higher back pressure on the turbine than would the usual water-cooled condenser. For this reason it is not likely to find many profitable applications in the power-generation field, and its use will be confined to those extreme conditions where water is not available, and the increased cost and reduced operating efficiencies can be justified.

Discussion

S. KOPP.² The air-cooled steam condenser described by the author is an interesting application of extended heat-transfer surface to meet a wartime need in the power-generation field. As mentioned by the author, only in rare cases will such condensers be used in peacetime for this purpose. The power requirements for the blowers is high, although this could be reduced by increasing the amount of heat-transfer surface.

At the present time several companies are manufacturing standardized air-cooled heat exchangers which are being used in those sections where water is scarce or may only be obtained at a premium. Several of these installations are quite large and justify their installation from an economical standpoint. The writer knows of one case where the cost of installing a water line plus the cost of a cooling tower alone far exceeded the total cost of an air-cooled heat exchanger.

² American Locomotive Company, Alco Products Division, New York, N. Y. Mem. A.S.M.E.

blower operating on that car, the temperature as read on the thermometer will still tend to fall to a dangerous degree. To provide for such an eventuality condensers are equipped with cover plates which can be used to cover a part of the surface of each section to reduce the cooling area and amount of air flowing.

The air-removal system from the sections consists of a manifold running along the car, connected to the air off-take from each section. This manifold delivers the air to the suction of a single-stage ejector which in turn is served by an air-cooled after condenser.

Heat Transfer Through Tubes With Integral Spiral Fins

BY D. L. KATZ,¹ K. O. BEATTY, JR.,¹ AND A. S. FOUST¹

Heat-transfer data are presented for a group of tubes having integral spiral fins. The group includes tubes with a range of from 4 to 24 fins per in. and from 0.05 to 0.38 in. fin height. Seven series of measurements were made, using steam, air, water, and oil as fluids. The data are compared, when possible, with theoretical equations which apply to the particular heat transfer. The performance of tubes with the extended surface is compared in all cases with that of plain tubes tested under similar conditions.

NOMENCLATURE

The following nomenclature is used in the paper:

- A_0 = outside area of tube, sq ft per ft
- A_1 = inside area of tube, sq ft per ft
- c_p = heat capacity of fluid, Btu per lb per deg F
- D_0 = diameter of tube over fins, in.
- D_1 = inside diameter of tube, in.
- D_E = equivalent diameter or diameter of a plain tube which has the same longitudinal cross section as the finned tube (including fins)
- D' = inside diameter of outside wall of annulus minus D_E of inner tube
- G = mass velocity, lb per sq ft per sec
- h = film coefficient, Btu per hr per deg F per sq ft
- k = thermal conductivity, Btu (ft per hr per deg F per sq ft)
- L = length of tube, ft
- q = rate of heat transfer, Btu per hr
- Δt = logarithmic-mean temperature difference
- U_0 = over-all heat-transfer coefficient, Btu per hr per deg F per sq ft outside surface
- U_L = over-all heat-transfer coefficient, Btu per hr per deg F per ft length of tube
- V = velocity, fpm, V_{\max} = velocity at minimum cross section
- μ = viscosity, lb per ft sec

INTRODUCTION

Heat-transfer measurements have been made on eighteen tubes with integral spiral fins and two plain tubes. The tubes were made of copper and were either of $1/2$ or $5/8$ in. nominal diameter with actual dimensions as given in Table 1. Fig. 1 shows the nature of the integral spiral fins which are formed from a plain thick-walled tube. With the exception of tubes Nos. 13, 14, and 24, the fins have a small uniform taper; the tip of the fin is from 60 to 80 per cent as thick as the base. Fig. 1(a) shows the nature and magnitude of corrugations inside the tubes.

Seven groups of heat-transfer measurements were made with steam, air, water, and a mineral oil as fluids, as follows:

Series A: Heat transfer from steam inside single horizontal tubes to air in forced convection outside.

¹ Department of Engineering Research, University of Michigan, Ann Arbor, Mich.

Contributed by the Heat Transfer Division and presented at the Annual Meeting, New York, N. Y., Nov. 27-Dec. 1, 1944, of THE AMERICAN SOCIETY OF MECHANICAL ENGINEERS.

NOTE: Statements and opinions advanced in papers are to be understood as individual expressions of their authors, and not those of the Society.

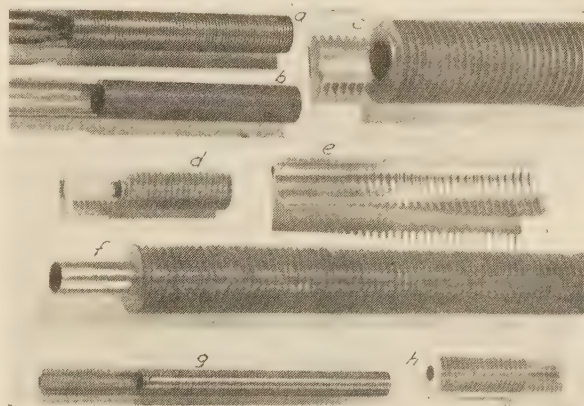


FIG. 1 INTEGRAL SPIRAL-FINNED TUBING

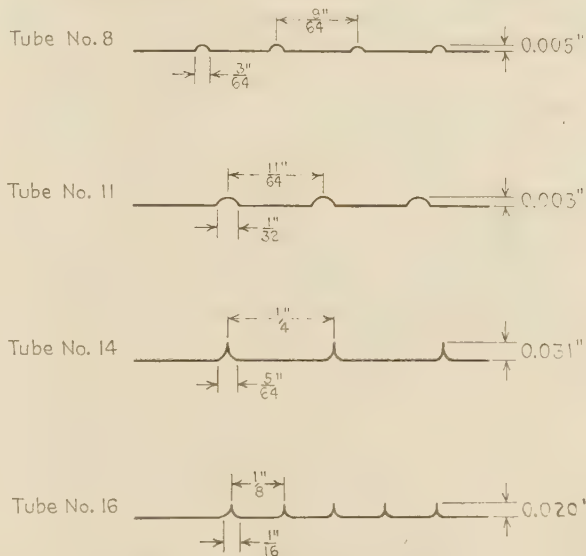


FIG. 1(a) DIMENSIONS OF CORRUGATIONS ON INSIDE OF TYPICAL TUBES

Series B: Heat transfer from steam inside banks of vertical tubes to air in forced convection outside.

Series C: Heat transfer between cold water inside single horizontal tubes and humid air in forced convection outside.

Series D: Heat transfer between water inside single horizontal tubes and steam outside.

Series E: Heat transfer between steam inside single horizontal tubes and water in annular space outside.

Series F: Heat transfer between water inside single horizontal tubes and hot oil in annular space outside.

Series G: Heat transfer between steam inside single horizontal tubes and oil in annular space outside.

TABLE 1 DIMENSIONS OF TUBES TESTED

Tube no.	Fins per in.	Fin height, in.	A_0 ft ² per ft	A_1 ft ² per ft	Root diam., in.	Inside diam., in.	Outside fin diam., in.	Fin thickness, in.	DE , in. ^a	Face depth of duct during Series A, in.
1	16.1	0.050	0.46	0.144	0.640	0.550	0.740	0.016	0.666	1.25
4	24	0.044	0.556	0.143	0.628	0.548	0.717	0.012	0.654	1.00
7	None	0	0.163	0.143	0.625	0.547			0.625	1.00
8	7.5	0.228	0.964	0.147	0.662	0.562	1.115	0.020	0.730	1.50
9	None	0	0.131	0.110	0.500	0.422			0.500	1.00
10	7.7	0.335	1.46	0.141	0.620	0.540	1.291	0.024	0.744	1.291
11	5.8	0.300	1.01	0.142	0.622	0.542	1.223	0.024	0.706	1.223
12	8.1	0.320	1.47	0.148	0.640	0.564	1.280	0.024	0.764	1.280
13	4.0	0.123	0.281	0.106	0.481	0.404	0.725	0.035 ^b	0.515	1.50
14	4.0	0.235	0.505	0.111	0.500	0.424	0.970	0.032	0.560	1.50
15	3.9	0.380	0.81	0.111	0.500	0.424	1.260	0.027	0.580	1.50
16	8.0	0.285	1.28	0.149	0.645	0.569	1.215	0.024	0.754	1.215
22	8.33	0.166	0.617	0.114	0.503	0.436	0.835	0.024	0.569	1.215
23	9.00	0.119	0.471	0.113	0.492	0.432	0.730	0.022	0.539	1.215
24	3.8	0.157	0.336	0.102	0.500	0.390	0.815	0.037	0.544	1.215
25	3.8	0.286	0.594	0.104	0.518	0.398	1.090	0.032	0.588	1.09
26	3.8	0.316	0.66	0.104	0.518	0.398	1.150	0.032	0.595	1.15
27	5.8	0.250	0.74	0.111	0.510	0.424	1.010	0.027	0.588	1.01
28	6.0	0.141	0.43	0.115	0.521	0.441	0.840	0.027	0.567	1.01
29	6.0	0.347	1.09	0.116	0.525	0.445	1.220	0.024	0.625	1.22

^a DE is the diameter of a plain tube which has the same longitudinal cross section as the finned tube (including fins).

^b Estimated.

NOTE: A_0 = outside area. A_1 = inside area.

Over-all coefficients of heat transfer were measured in all cases. The results for Series A, B, and C have been correlated by generally accepted methods and are presented as correlation curves. The experimental data for the remaining series have been tabulated, since no complete correlation has been found.

SERIES A HEAT TRANSFER FROM STEAM INSIDE SINGLE HORIZONTAL TUBES TO AIR IN FORCED CONVECTION OUTSIDE

Single tubes 3 ft long were placed in a horizontal position as shown in Fig. 2. Air blown normal to the axis of the tube was controlled by vanes which had a spacing at the position of the tube as listed in Table 1. Calming was accomplished by six vertical vanes 16 in. long, as indicated in Fig. 2. Inlet- and outlet-air temperatures were measured by mercury-in-glass thermometers.

Steam was admitted to the inside of the tubes at 10 psig, and the condensate was collected in a calibrated tank. Care was exercised that noncondensable gases did not accumulate in the condensate receiver.

The observed rate of steam condensation, corrected for radiation losses, was used to calculate the rate of heat transfer. The air rate on a weight basis was calculated from the measured rise in air temperature and the heat-transfer rate.

Over-all coefficients of heat transfer are expressed either as U_L or U_0 , as calculated from the following equations

$$U_L = \frac{q}{L\Delta t} = \frac{\text{Btu}}{(\text{hr})(\text{deg F})(\text{ft})} \dots \dots \dots [1]$$

$$U_0 = \frac{q}{LA_0\Delta t} = \frac{\text{Btu}}{(\text{hr})(\text{deg F})(\text{sq ft})} \dots \dots \dots [2]$$

where q = heat-transfer rate, Btu per hr

L = length of tube, ft

A_0 = sq ft of outside tube surface per ft of length

Δt = logarithmic-mean temperature difference between steam and air

The relation between the two coefficients is

$$U_L = U_0 A_0 \dots \dots \dots [3]$$

From the data obtained, correlations have been developed between the heat-transfer coefficient U_0 , and the air velocity at the minimum free cross section, V_{\max} . Air velocity is expressed in feet per minute of standard air defined at 70 F, 29.92 in. mercury barometer, and 50 per cent relative humidity. At these conditions, the specific volume of air is 13.5 cu ft per lb. In calculating the minimum free cross section, allowance is made for the longitudinal cross-sectional area of the tube, including the fins.

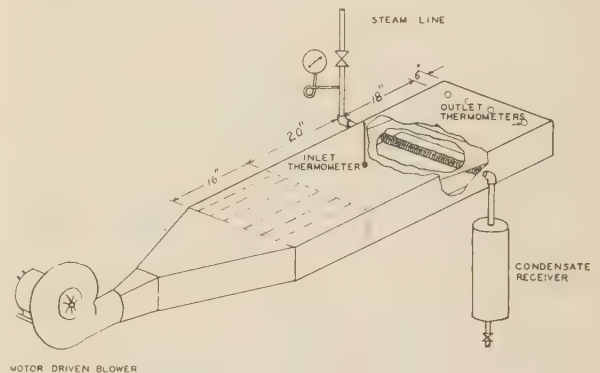


FIG. 2 APPARATUS USED FOR HEAT-TRANSFER MEASUREMENTS ON SINGLE TUBES

(Section through duct and top vane to show tube.)

The correlations for the data on the tubes of Table 1 are presented in Figs. 3, 4, and 5, as plots on logarithmic co-ordinates. Fig. 3 includes the data for tubes having outside-surface areas in excess of 0.65 sq ft per ft. Fig. 4 shows the data for tubes having outside-surface areas less than 0.65 sq ft per ft. In each figure, the tubes included range from those having 4 to those having 9 fins per in. The straight line in Fig. 3 has the equation

$$U_0 = 0.229 V_{\max}^{0.63} \dots \dots \dots [4]$$

In Fig. 4 the straight line drawn corresponds to

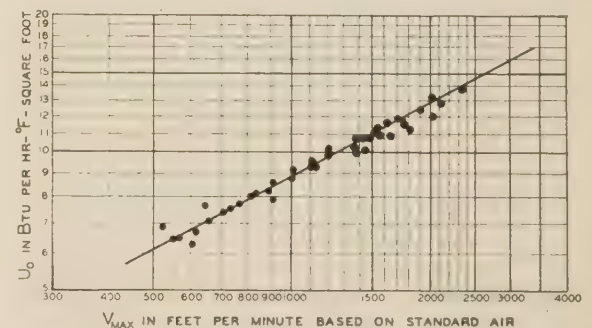


FIG. 3 OVER-ALL COEFFICIENTS OF HEAT TRANSFER FOR SINGLE TUBES AGAINST AIR VELOCITY AT MINIMUM FREE CROSS SECTION (Data for tubes Nos. 10, 12, 15, 16, 26, 27, and 29.)

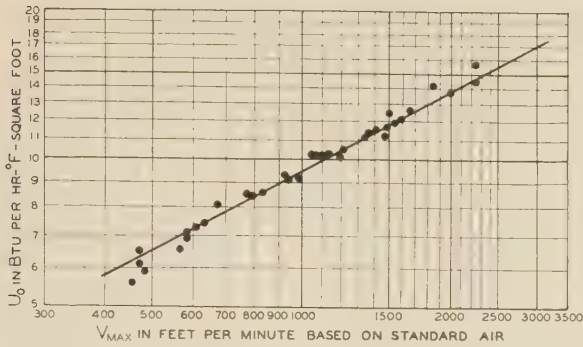


FIG. 4 OVER-ALL COEFFICIENTS OF HEAT TRANSFER FOR SINGLE TUBES AGAINST AIR VELOCITY AT MINIMUM FREE CROSS SECTION (Data for tubes Nos. 11, 22, 23, 24, 25, and 28.)

$$U_0 = 0.244 V_{\max}^{0.53} \dots \dots \dots [5]$$

Both groups of data agree within approximately ± 7 per cent with a single line drawn in between the two lines shown. This line has the equation

$$U_0 = 0.236 V_{\max}^{0.53} \dots \dots \dots [6]$$

Fig. 5 contains the data on the two low-finned tubes Nos. 1 and 4 and the plain tubes, Nos. 7 and 9. Equation [6] is plotted as a dashed line for comparison. The extended surface of the fins for the tubes in Figs. 3 and 4 is slightly more effective per square foot than the surface of the plain tube. The tubes 1 and 4 are low-fin tubes having 16 and 24 fins per in. The curves show

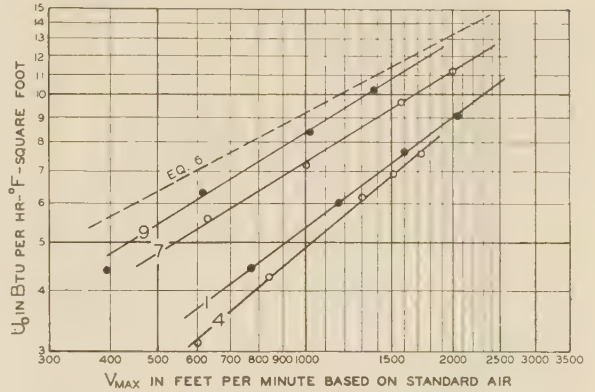


FIG. 5 OVER-ALL COEFFICIENTS OF HEAT TRANSFER FOR SINGLE TUBES AGAINST AIR VELOCITY AT MINIMUM FREE CROSS SECTION (Data for tube numbers as labeled on curves.)

that the increase in surface produced by the fins does not cause a proportionate increase in the heat-transfer coefficient per foot of length. This is probably because the fins are too close together to permit free passage of air between them.

In Fig. 6 certain of the data have been plotted as U_L , the heat-transfer coefficient per foot of length, against the air velocity at minimum free cross section. This figure illustrates the wide differences in fin heights and fin pitches of the tubes tested. The consequent variations in outside tube surface per foot of length make great differences in the heat-transfer coefficients, based on the length of the tube.

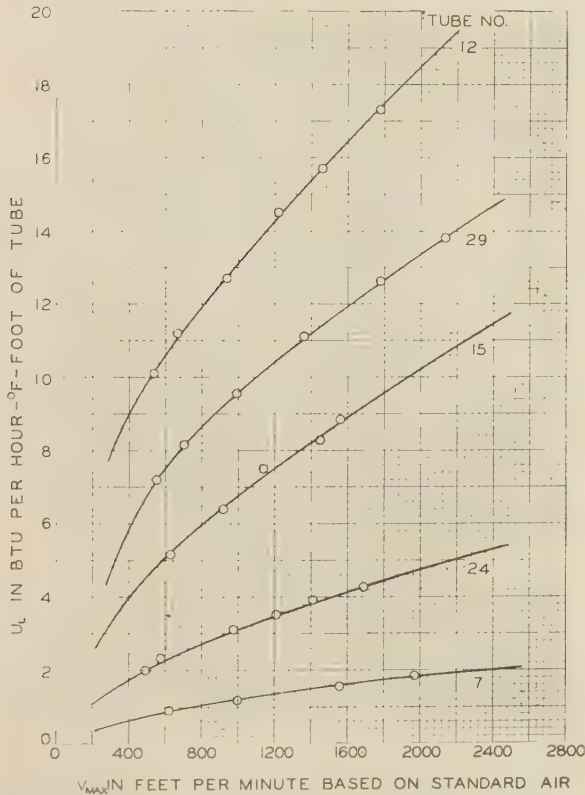


FIG. 6 HEAT-TRANSFER COEFFICIENTS PER FOOT FOR TYPICAL TUBES FROM THOSE TESTED

SERIES B HEAT TRANSFER FROM STEAM INSIDE BANKS OF VERTICAL TUBES TO AIR IN FORCED CONVECTION OUTSIDE

One single row of 12 tubes and one double-row unit were used for heat-transfer measurements on banks of tubes. The dimensions of the units and of the finned tubes used in them are given in Table 2. Fig. 7 is a sketch of the apparatus used in testing the two finned-tube units. The units were set with tubes vertical in a duct of cross section equal to the face dimensions of the unit. Measurements of steam condensed and air-temperature rise were made at a variety of constant air velocities for each of several different steam pressures. Steam pressures used were 5, 25, 50, 75, 100, and 125 psig. Face air velocities were varied from 200 to 750 fpm, based on standard air.

Calculations of the data were made in the same manner as with single tubes. The calculated values of U_0 are plotted against V_{\max} , on logarithmic co-ordinates in Fig. 8. No distinction has been made between points obtained at various steam pressures,

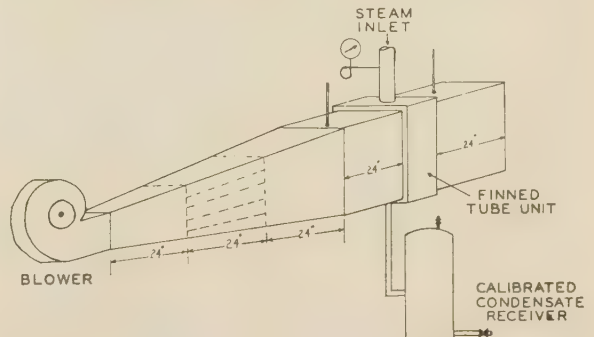


FIG. 7 APPARATUS USED IN TESTING FINNED-TUBE UNITS

TABLE 2 DIMENSIONS OF UNITS TESTED
SINGLE-ROW UNIT

Dimensions:

Face, in. high \times in. wide.....	24.5 \times 17.6
Face area, sq ft.....	3.0
Minimum free area, sq ft.....	1.55
Number of tubes.....	12
Number of rows.....	1
Total length of tubes, ft.....	24.5
Total heat-transfer area, sq ft.....	25.95
Center-to-center tube spacing, in.....	1.41

Data on tube in single-row unit:

N = 5.80 fins per in.
H = 0.314 in. = fin height
A_o = 1.056 sq ft per ft = outside tube surface
D = 0.622 in. = root diam of tube
D_o = 1.250 in. = outside fin diam
DE = 0.709 in.

DOUBLE-ROW UNIT

Dimensions:

Face, in. high \times in. wide.....	24.5 \times 17.6
Face area, sq ft.....	3.0
Minimum free area, sq ft.....	1.461
Number of tubes.....	24
Number of rows.....	2
Total length of tubes, ft.....	49
Total heat-transfer area, sq ft.....	75
Tube arrangement.....	Staggered 2 rows, 1.5 in.
Center line to center line.....	12 tubes, 1.41 in., center to center in each row

Data on tube in double-row unit:

N = 7.80 fins per in.
H = 0.347 in. = fin height
A_o = 1.056 sq ft per ft = outside tube surface
D = 0.621 in. = root diam of tube
D_o = 1.315 in. = outside fin diam
DE = 0.751 in.

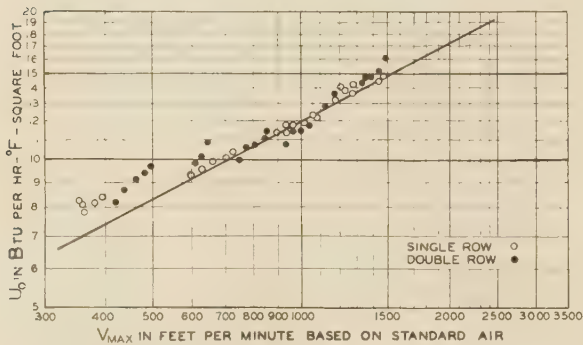


FIG. 8 OVER-ALL COEFFICIENTS OF HEAT TRANSFER FOR TUBE BANKS AGAINST AIR VELOCITY AT MINIMUM FREE CROSS SECTION

since no trend was observed. The straight line in the figure has the equation

$$U_0 = 0.308 V_{\max}^{0.53} \quad [7]$$

A comparison of this equation with Equation [6] for similar single tubes shows that the heat-transfer coefficients at a given air velocity are approximately 30 per cent higher when the tubes are arranged in banks than when they are used singly. This increase is probably caused by a greater turbulence of the air around the tubes in banks, or could be attributed partially to the layer of condensate accumulating inside the horizontal tube. The effect of turbulence has been observed by other investigators^{2,3} between a single row and a bank of several rows with plain tubes. It appears that a single row of finned tubes causes turbulence equivalent to several rows of plain tubes and that only minor increases in turbulence occur with added rows of finned tubes. When tubes are to be used vertically in banks, the coefficient

² "Correlation and Utilization of New Data on Flow Resistance and Heat Transfer for Crossflow of Gases Over Tube Banks," by E. D. Grimson, Trans. A.S.M.E., vol. 59, 1937, pp. 583-594.

³ "Heat Transmission," by W. H. McAdams, second edition, McGraw-Hill Book Company, Inc., New York, N. Y., 1942, p. 228.

should be estimated from the solid line in Fig. 8 and not from Fig. 3 or 4.

SERIES C HEAT TRANSFER BETWEEN COLD WATER INSIDE SINGLE HORIZONTAL TUBES AND HUMID AIR IN FORCED CONVECTION OUTSIDE

Measurements of heat transfer between humid air and cold water were made, using the apparatus in Fig. 2, with modifications. Air entering the blower was conditioned to 80 F, with 50 per cent relative humidity, and held constant. Water cooled to 40 F was circulated through the tube at a velocity of about 200 fpm in the tube. Actual water rates were determined by a calibrated orifice, and the rise in water temperature was measured by Beckmann thermometers in the inlet and outlet streams.

Wet- and dry-bulb temperatures of the inlet air and dry-bulb temperature of the outlet air were measured by mercury-in-glass

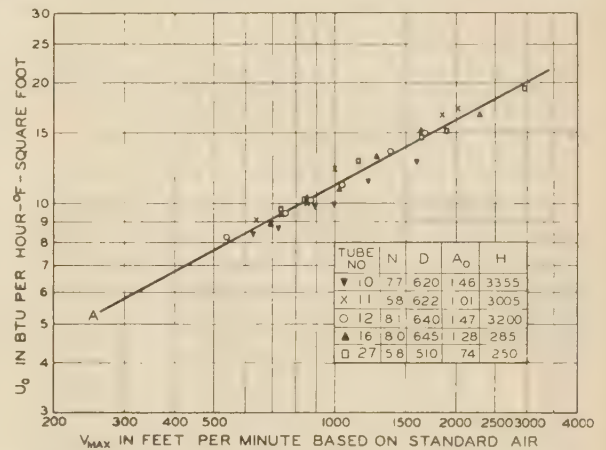


FIG. 9 OVER-ALL HEAT-TRANSFER COEFFICIENTS, HUMID AIR TO COLD WATER FOR TUBES WITH EIGHT HIGH FINS PER INCH

thermometers. The rate of heat transfer was computed from the measurements on the water side. The air rate was computed by a heat balance, assuming the air to have been cooled and dehumidified according to the "contact-mixture theory."⁴ This method was considered more reliable than wet-bulb measurements on the outlet air because of the possibility of condensate from the tube being entrained in the air stream.

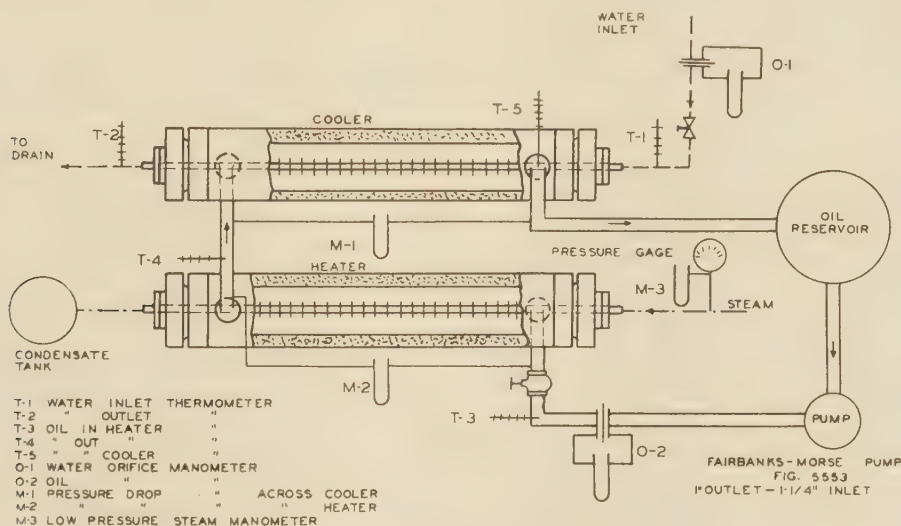
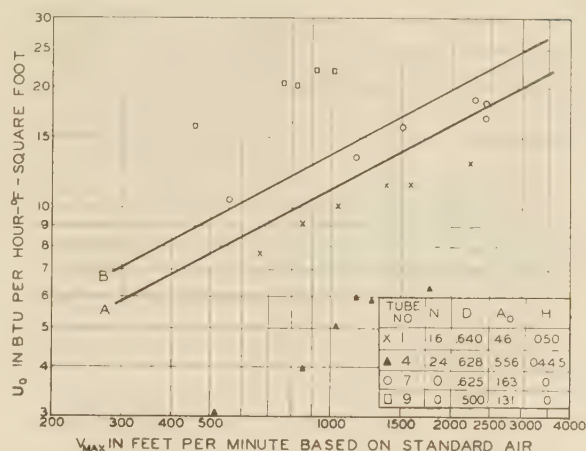
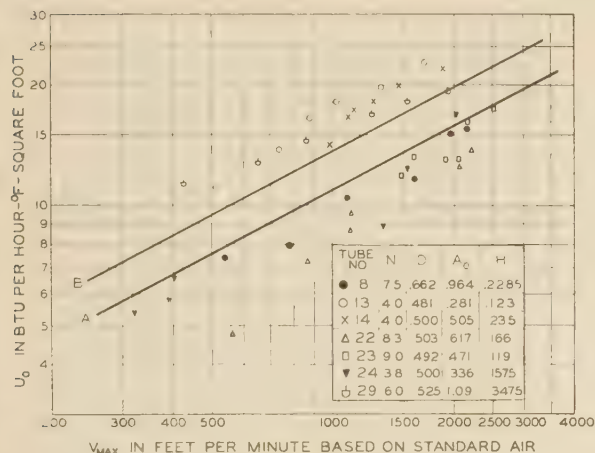
The over-all coefficients of heat transfer were computed using Equation [2]. The results for five high-finned tubes which follow the same curve A are given in Fig. 9. A similar curve was drawn for tubes Nos. 15, 25, 26, and 28. It is shown in Fig. 10, as curve B, which figure also includes curve A of Fig. 9 and the data for seven individual tubes. Fig. 11 is a comparison of the plain tubes, the low-finned tubes and the curves A and B. The equations for curves A and B are as follows

$$\text{Curve A } U_0 = 0.286 V_{\max}^{0.53} \quad [8]$$

$$\text{Curve B } U_0 = 0.353 V_{\max}^{0.53} \quad [9]$$

In calculating the minimum free cross section of the duct to obtain V_{\max} in feet per minute of standard air, allowance was made for a condensate film approximately 0.01 in. thick covering the entire outer tube surface in addition to the longitudinal cross section of the dry tube.

⁴ "Contact Mixture Analogy Applied to Heat Transfer With Mixtures of Air and Water Vapor," by W. H. Carrier, Trans. A.S.M.E., vol. 59, 1937, p. 49.



The fin shape, height, and pitch appear to have considerably more effect on the heat-transfer coefficients of the tubes when they are wet than when dry. In general, the large number of fins per inch give lower coefficients with the extreme effect shown by tube No. 4 with 24 fins (0.044 in. high) per inch, Fig. 11. No explanation can be given for the high coefficients for plain tube No. 9. It should be appreciated that the temperature rise measured for the water was lowest for the plain tubes and rose with increased surface for the finned tubes.

SERIES D HEAT TRANSFER BETWEEN WATER INSIDE SINGLE HORIZONTAL TUBES AND STEAM OUTSIDE

The last four series of tests were made using variations of the apparatus shown in Fig. 12. For Series D, the cooler section only was used with water flow as indicated in Fig. 12, and steam at 25 psig in the annular space outside the tube with condensate going to a calibrated receiver.

The experimental data and calculated coefficients are given in Table 3. The over-all coefficient is composed of the steam-film coefficient on the outside which should remain substantially

constant, the copper resistance, and the water-film coefficient on the inside, which should vary as the 0.8 power of the Reynolds number. It was possible to select steam-film coefficients for the outside by the Wilson method,^{5,6} which give straight lines of slope equal to 0.8 for the water-film coefficient as plotted in Fig. 13. For many of the tubes no constant value for the resistance of the steam film plus the metal resistance could be found which would give straight lines in Fig. 13. A possible explanation could be that dropwise condensation occurred during the early runs at low water velocity and filmwise condensation gradually set in. In several cases the over-all coefficient was reduced for an increased water velocity, although further increase in water velocity always gave a net increase in the coefficient.

For all finned tubes the water-film coefficient was greater than that predicted by the Dittus-Boelter type equation recommended by McAdams⁷

⁵ "Basis for Rational Design of Heat-Transfer Apparatus," by E. E. Wilson, Trans. A.S.M.E., vol. 37, 1915, p. 47.

⁶ Reference 3, p. 272.

⁷ Ibid., 3, p. 168.

TABLE 3 DATA ON FINNED TUBES; WATER INSIDE, STEAM OUTSIDE

TUBE NO.	WATER TEMPERATURE INLET °F	WATER TEMPERATURE OUTLET °F	LN MEAN ΔT °F	WATER VELOCITY FT/SEC	STEAM CONDENSED LBS/HR	HEAT TRANSFERRED BTU/HR	COEFFICIENT BTU PER °F PER SQ FT	PER °F PER FT
1	112.2	136.4	70.4	1.65	57.4	49000	47700	89.9
4	112.2	121.6	146.8	3.94	8.4	37500	80100	113.0
4	112.2	116.6	176.0	4.36	14.4	104400	100600	142.9
4	112.2	111.3	212.2	4.43	187.2	124800	124000	163.5
4	112.2	106.6	254.6	4.52	352.0	142200	141000	184.0
4	112.2	101.6	297.6	4.59	632.0	198000	196000	212.0
4	112.2	96.6	340.6	4.65	106.6	29600	29400	190.0
4	112.2	91.6	383.6	4.70	131.1	32000	31800	202.0
4	112.2	86.6	426.6	4.75	181.1	43200	43000	234.0
7	112.2	129.7	62.5	1.65	58.9	34600	34400	59.5
7	112.2	124.7	67.5	3.57	44.6	38500	48700	76.5
7	112.2	119.7	72.5	6.46	78.9	51600	71600	102.5
7	112.2	114.7	77.5	9.34	85.4	53500	43500	105.0
8	112.2	143.4	79.9	1.95	63.3	53800	53700	89.8
8	112.2	138.4	74.9	3.94	103.3	98000	98000	137.0
8	112.2	133.4	69.9	5.93	156.0	124000	117000	167.0
8	112.2	128.4	64.9	7.92	208.7	160000	149000	208.0
8	112.2	123.4	59.9	9.91	261.4	196000	185000	249.0
8	112.2	118.4	54.9	11.90	314.1	232000	221000	290.0
8	112.2	113.4	49.9	13.89	366.8	268000	257000	331.0
8	112.2	108.4	44.9	15.88	419.5	304000	293000	372.0
8	112.2	103.4	39.9	17.87	472.2	340000	329000	413.0
8	112.2	98.4	34.9	19.86	524.9	376000	365000	454.0
8	112.2	93.4	29.9	21.85	577.6	412000	401000	495.0
8	112.2	88.4	24.9	23.84	630.3	448000	437000	536.0
8	112.2	83.4	19.9	25.83	683.0	484000	473000	577.0
8	112.2	78.4	14.9	27.82	735.7	520000	509000	618.0
8	112.2	73.4	9.9	29.81	788.4	556000	545000	659.0
8	112.2	68.4	4.9	31.80	841.1	592000	581000	700.0
8	112.2	63.4	-0.1	33.79	893.8	628000	617000	741.0
8	112.2	58.4	-5.1	35.78	946.5	664000	653000	782.0
8	112.2	53.4	-10.1	37.77	999.2	700000	689000	823.0
8	112.2	48.4	-15.1	39.76	1051.9	736000	725000	864.0
8	112.2	43.4	-20.1	41.75	1104.6	772000	761000	905.0
8	112.2	38.4	-25.1	43.74	1157.3	808000	797000	946.0
8	112.2	33.4	-30.1	45.73	1210.0	844000	833000	987.0
8	112.2	28.4	-35.1	47.72	1262.7	880000	869000	1028.0
8	112.2	23.4	-40.1	49.71	1315.4	916000	905000	1069.0
8	112.2	18.4	-45.1	51.70	1368.1	952000	941000	1110.0
8	112.2	13.4	-50.1	53.69	1420.8	988000	977000	1151.0
8	112.2	8.4	-55.1	55.68	1473.5	1024000	1013000	1192.0
8	112.2	3.4	-60.1	57.67	1526.2	1060000	1049000	1233.0
8	112.2	-1.6	-65.1	59.66	1578.9	1100000	1085000	1274.0
8	112.2	-6.6	-70.1	61.65	1631.6	1140000	1121000	1315.0
8	112.2	-11.6	-75.1	63.64	1684.3	1180000	1157000	1356.0
8	112.2	-16.6	-80.1	65.63	1737.0	1220000	1193000	1397.0
8	112.2	-21.6	-85.1	67.62	1789.7	1260000	1229000	1438.0
8	112.2	-26.6	-90.1	69.61	1842.4	1300000	1265000	1479.0
8	112.2	-31.6	-95.1	71.60	1895.1	1340000	1301000	1520.0
8	112.2	-36.6	-100.1	73.59	1947.8	1380000	1337000	1561.0
8	112.2	-41.6	-105.1	75.58	2000.5	1420000	1373000	1602.0
8	112.2	-46.6	-110.1	77.57	2053.2	1460000	1409000	1643.0
8	112.2	-51.6	-115.1	79.56	2105.9	1500000	1445000	1684.0
8	112.2	-56.6	-120.1	81.55	2158.6	1540000	1481000	1725.0
8	112.2	-61.6	-125.1	83.54	2211.3	1580000	1517000	1766.0
8	112.2	-66.6	-130.1	85.53	2264.0	1620000	1553000	1807.0
8	112.2	-71.6	-135.1	87.52	2316.7	1660000	1589000	1848.0
8	112.2	-76.6	-140.1	89.51	2369.4	1700000	1625000	1889.0
8	112.2	-81.6	-145.1	91.50	2422.1	1740000	1661000	1930.0
8	112.2	-86.6	-150.1	93.49	2474.8	1780000	1697000	1971.0
8	112.2	-91.6	-155.1	95.48	2527.5	1820000	1733000	2012.0
8	112.2	-96.6	-160.1	97.47	2580.2	1860000	1769000	2053.0
8	112.2	-101.6	-165.1	99.46	2632.9	1900000	1805000	2094.0
8	112.2	-106.6	-170.1	101.45	2685.6	1940000	1841000	2135.0
8	112.2	-111.6	-175.1	103.44	2738.3	1980000	1877000	2176.0
8	112.2	-116.6	-180.1	105.43	2791.0	2020000	1913000	2217.0
8	112.2	-121.6	-185.1	107.42	2843.7	2060000	1949000	2258.0
8	112.2	-126.6	-190.1	109.41	2896.4	2100000	1985000	2299.0
8	112.2	-131.6	-195.1	111.40	2949.1	2140000	2021000	2340.0
8	112.2	-136.6	-200.1	113.39	3001.8	2180000	2057000	2381.0
8	112.2	-141.6	-205.1	115.38	3054.5	2220000	2093000	2422.0
8	112.2	-146.6	-210.1	117.37	3107.2	2260000	2129000	2463.0
8	112.2	-151.6	-215.1	119.36	3159.9	2300000	2165000	2504.0
8	112.2	-156.6	-220.1	121.35	3212.6	2340000	2201000	2545.0
8	112.2	-161.6	-225.1	123.34	3265.3	2380000	2237000	2586.0
8	112.2	-166.6	-230.1	125.33	3318.0	2420000	2273000	2627.0
8	112.2	-171.6	-235.1	127.32	3370.7	2460000	2309000	2668.0
8	112.2	-176.6	-240.1	129.31	3423.4	2500000	2345000	2709.0
8	112.2	-181.6	-245.1	131.30	3476.1	2540000	2381000	2750.0
8	112.2	-186.6	-250.1	133.29	3528.8	2580000	2417000	2791.0
8	112.2	-191.6	-255.1	135.28	3581.5	2620000	2453000	2832.0
8	112.2	-196.6	-260.1	137.27	3634.2	2660000	2489000	2873.0
8	112.2	-201.6	-265.1	139.26	3686.9	2700000	2525000	2914.0
8	112.2	-206.6	-270.1	141.25	3739.6	2740000	2561000	2955.0
8	112.2	-211.6	-275.1	143.24	3792.3	2780000	2597000	2996.0
8	112.2	-216.6	-280.1	145.23	3845.0	2820000	2633000	3037.0
8	112.2	-221.6	-285.1	147.22	3897.7	2860000	2669000	3078.0
8	112.2	-226.6	-290.1	149.21	3950.4	2900000	2705000	3119.0
8	112.2	-231.6	-295.1	151.20	4003.1	2940000	2741000	3160.0
8	112.2	-236.6	-300.1	153.19	4055.8	2980000	2777000	3201.0
8	112.2	-241.6	-305.1	155.18	4108.5	3020000	2813000	3242.0
8	112.2	-246.6	-310.1	157.17	4161.2	3060000	2849000	3283.0
8	112.2	-251.6	-315.1	159.16	4213.9	3100000	2885000	3324.0
8	112.2	-256.6	-320.1	161.15	4266.6	3140000	2921000	3365.0
8	112.2	-261.6	-325.1	163.14	4319.3	3180000	2957000	3406.0
8	112.2	-266.6	-330.1	165.13	4372.0	3220000	2993000	3447.0
8	112.2	-271.6	-335.1	167.12	4424.7	3260000	3029000	3488.0
8	112.2	-276.6	-340.1	169.11	4477.4	3300000	3065000	3529.0
8	112.2	-281.6	-345.1	171.10	4530.1	3340000	3101000	3570.0
8	112.2	-286.6	-350.1	173.09	4582.8	3380000	3137000	3611.0
8	112.2	-291.6	-355.1	175.08	4635.5	3420000	3173000	3652.0
8	112.2	-296.6	-360.1	177.07	4688.2	3460000	3209000	3693.0
8	112.2	-301.6	-365.1	179.06	4740.9	3500000	3245000	3734.0
8	112.2	-306.6	-370.1	181.05	4793.6	3540000	3281000	3775.0
8	112.2	-311.6	-375.1	183.04	4846.3	3580000	3317000	3816.0
8	112.2	-316.6	-380.1	185.03	4899.0	3620000	3353000	3857.0
8	112.2	-321.6	-385.1	187.02	4951.7	3660000	3389000	3898.0
8	112.2	-326.6	-390.1	189.01	5004.4	3700000	3425000	3939.0
8	112.2	-331.6	-395.1	191.00	5057.1	3740000	3461000	3980.0
8	112.2	-336.6	-400.1	192.99	5109.8	3780000	3497000	4021.0
8	112.2	-341.6	-405.1	194.98	5162.5	3820000	3533000	4062.0
8	112.2	-346.6	-410.1	196.97	5215.2	3860000	3569000	4103.0
8	112.2	-351.6	-415.1	198.96	5267.9	3900000	3605000	4144.0
8	112.2	-356.6	-420.1	200.95	5320.6	3940000	3641000	4185.0
8	112.2	-361.6	-425.1	202.94	5373.3	3980000	3677000	4226.0
8	112.2	-366.6	-430.1	204.93	5426.0	4020000	3713000	4267.0
8	112.2	-371.6	-435.1	206.92	5478.7	4060000	3749000	4308.0
8	112.2	-376.6	-440.1	208.91	5531.4	4100000	3785000	4349.0
8	112.2	-381.6	-445.1	210.90	5584.1	4140000	3821000	4390.0
8	112.2	-386.6	-450.1	212.89	5636.8	4180000	3857000	4431.0
8	112.2	-391.6	-455.1	214.88	5689.5	4220000	3893000	4472.0
8	112.2	-396.6	-460.1	216.87	5742.2	4260000	3929000	4513.0
8	112.2	-401.6	-465.1	218.86	5794.9	4300000	3965000	4554.0
8	112.2	-406.6	-470.1	220.85	5847.6	4340000	4001000	4595.0
8	112.2	-411.6	-475.1	222.84	5900.3	4380000	4037000	4636.0
8	112.2	-416.6	-480.1	224.83				

TABLE 4 DATA ON FINNED TUBES; WATER OUTSIDE, STEAM INSIDE

TUBE NO.	WATER INLET TEMP. °F	WATER OUTLET TEMP. °F	WATER MEAN TEMP. °F	WATER VELOCITY LB/HR	STEAM CONDENS. LB/HR	HEAT TRANSFERED BTU/HR	STEAM BURNER BTU/HR	COEFFICIENT BTU/HR-FT ² -°F	PER FT
1	144	124	134	179.8	16.3	173,300	173,300	2.88	2.88
2	144	124	134	179.8	16.3	173,300	173,300	2.88	2.88
3	144	124	134	179.8	16.3	173,300	173,300	2.88	2.88
4	144	124	134	179.8	16.3	173,300	173,300	2.88	2.88
5	144	124	134	179.8	16.3	173,300	173,300	2.88	2.88
6	144	124	134	179.8	16.3	173,300	173,300	2.88	2.88
7	144	124	134	179.8	16.3	173,300	173,300	2.88	2.88
8	144	124	134	179.8	16.3	173,300	173,300	2.88	2.88
9	144	124	134	179.8	16.3	173,300	173,300	2.88	2.88
10	144	124	134	179.8	16.3	173,300	173,300	2.88	2.88
11	144	124	134	179.8	16.3	173,300	173,300	2.88	2.88
12	144	124	134	179.8	16.3	173,300	173,300	2.88	2.88
13	144	124	134	179.8	16.3	173,300	173,300	2.88	2.88
14	144	124	134	179.8	16.3	173,300	173,300	2.88	2.88
15	144	124	134	179.8	16.3	173,300	173,300	2.88	2.88
16	144	124	134	179.8	16.3	173,300	173,300	2.88	2.88
17	144	124	134	179.8	16.3	173,300	173,300	2.88	2.88
18	144	124	134	179.8	16.3	173,300	173,300	2.88	2.88
19	144	124	134	179.8	16.3	173,300	173,300	2.88	2.88
20	144	124	134	179.8	16.3	173,300	173,300	2.88	2.88
21	144	124	134	179.8	16.3	173,300	173,300	2.88	2.88
22	144	124	134	179.8	16.3	173,300	173,300	2.88	2.88
23	144	124	134	179.8	16.3	173,300	173,300	2.88	2.88
24	144	124	134	179.8	16.3	173,300	173,300	2.88	2.88
25	144	124	134	179.8	16.3	173,300	173,300	2.88	2.88
26	144	124	134	179.8	16.3	173,300	173,300	2.88	2.88
27	144	124	134	179.8	16.3	173,300	173,300	2.88	2.88
28	144	124	134	179.8	16.3	173,300	173,300	2.88	2.88
29	144	124	134	179.8	16.3	173,300	173,300	2.88	2.88
30	144	124	134	179.8	16.3	173,300	173,300	2.88	2.88
31	144	124	134	179.8	16.3	173,300	173,300	2.88	2.88
32	144	124	134	179.8	16.3	173,300	173,300	2.88	2.88
33	144	124	134	179.8	16.3	173,300	173,300	2.88	2.88
34	144	124	134	179.8	16.3	173,300	173,300	2.88	2.88
35	144	124	134	179.8	16.3	173,300	173,300	2.88	2.88
36	144	124	134	179.8	16.3	173,300	173,300	2.88	2.88
37	144	124	134	179.8	16.3	173,300	173,300	2.88	2.88
38	144	124	134	179.8	16.3	173,300	173,300	2.88	2.88
39	144	124	134	179.8	16.3	173,300	173,300	2.88	2.88
40	144	124	134	179.8	16.3	173,300	173,300	2.88	2.88
41	144	124	134	179.8	16.3	173,300	173,300	2.88	2.88
42	144	124	134	179.8	16.3	173,300	173,300	2.88	2.88
43	144	124	134	179.8	16.3	173,300	173,300	2.88	2.88
44	144	124	134	179.8	16.3	173,300	173,300	2.88	2.88
45	144	124	134	179.8	16.3	173,300	173,300	2.88	2.88
46	144	124	134	179.8	16.3	173,300	173,300	2.88	2.88
47	144	124	134	179.8	16.3	173,300	173,300	2.88	2.88
48	144	124	134	179.8	16.3	173,300	173,300	2.88	2.88
49	144	124	134	179.8	16.3	173,300	173,300	2.88	2.88
50	144	124	134	179.8	16.3	173,300	173,300	2.88	2.88
51	144	124	134	179.8	16.3	173,300	173,300	2.88	2.88
52	144	124	134	179.8	16.3	173,300	173,300	2.88	2.88
53	144	124	134	179.8	16.3	173,300	173,300	2.88	2.88
54	144	124	134	179.8	16.3	173,300	173,300	2.88	2.88
55	144	124	134	179.8	16.3	173,300	173,300	2.88	2.88
56	144	124	134	179.8	16.3	173,300	173,300	2.88	2.88
57	144	124	134	179.8	16.3	173,300	173,300	2.88	2.88
58	144	124	134	179.8	16.3	173,300	173,300	2.88	2.88
59	144	124	134	179.8	16.3	173,300	173,300	2.88	2.88
60	144	124	134	179.8	16.3	173,300	173,300	2.88	2.88
61	144	124	134	179.8	16.3	173,300	173,300	2.88	2.88
62	144	124	134	179.8	16.3	173,300	173,300	2.88	2.88
63	144	124	134	179.8	16.3	173,300	173,300	2.88	2.88
64	144	124	134	179.8	16.3	173,300	173,300	2.88	2.88
65	144	124	134	179.8	16.3	173,300	173,300	2.88	2.88
66	144	124	134	179.8	16.3	173,300	173,300	2.88	2.88
67	144	124	134	179.8	16.3	173,300	173,300	2.88	2.88
68	144	124	134	179.8	16.3	173,300	173,300	2.88	2.88
69	144	124	134	179.8	16.3	173,300	173,300	2.88	2.88
70	144	124	134	179.8	16.3	173,300	173,300	2.88	2.88
71	144	124	134	179.8	16.3	173,300	173,300	2.88	2.88
72	144	124	134	179.8	16.3	173,300	173,300	2.88	2.88
73	144	124	134	179.8	16.3	173,300	173,300	2.88	2.88
74	144	124	134	179.8	16.3	173,300	173,300	2.88	2.88
75	144	124	134	179.8	16.3	173,300	173,300	2.88	2.88
76	144	124	134	179.8	16.3	173,300	173,300	2.88	2.88
77	144	124	134	179.8	16.3	173,300	173,300	2.88	2.88
78	144	124	134	179.8	16.3	173,300	173,300	2.88	2.88
79	144	124	134	179.8	16.3	173,300	173,300	2.88	2.88
80	144	124	134	179.8	16.3	173,300	173,300	2.88	2.88
81	144	124	134	179.8	16.3	173,300	173,300	2.88	2.88
82	144	124	134	179.8	16.3	173,300	173,300	2.88	2.88
83	144	124	134	179.8	16.3	173,300	173,300	2.88	2.88
84	144	124	134	179.8	16.3	173,300	173,300	2.88	2.88
85	144	124	134	179.8	16.3	173,300	173,300	2.88	2.88
86	144	124	134	179.8	16.3	173,300	173,300	2.88	2.88
87	144	124	134	179.8	16.3	173,300	173,300	2.88	2.88
88	144	124	134	179.8	16.3	173,300	173,300	2.88	2.88
89	144	124	134	179.8	16.3	173,300	173,300	2.88	2.88
90	144	124	134	179.8	16.3	173,300	173,300	2.88	2.88
91	144	124	134	179.8	16.3	173,300	173,300	2.88	2.88
92	144	124	134	179.8	16.3	173,300	173,300	2.88	2.88
93	144	124	134	179.8	16.3	173,300	173,300	2.88	2.88
94	144	124	134	179.8	16.3	173,300	173,300	2.88	2.88
95	144	124	134	179.8	16.3	173,300	173,300	2.88	2.88
96	144	124	134	179.8	16.3	173,300	173,300	2.88	2.88
97	144	124	134	179.8	16.3	173,300	173,300	2.88	2.88
98	144	124	134	179.8	16.3	173,300	173,300	2.88	2.88
99	144	124	134	179.8	16.3	173,300	173,300	2.88	2.88
100	144	124	134	179.8	16.3	173,300	173,300	2.88	2.88

coefficient must have been in excess of the 3060 Btu per hr per deg F per sq ft.

SERIES F HEAT TRANSFER BETWEEN WATER INSIDE SINGLE HORIZONTAL TUBES AND HOT OIL IN ANNULAR SPACE OUTSIDE

The apparatus in Fig. 12 was used with measurements for Series F on the cooler. The 37-deg A.P.I. mineral-seal oil had viscosities of 3.20 centipoise at 100 F, and 1.03 centipoise at 210 F. The boiling range was from 525 F at 10 per cent to 644 F at 90 per cent with a 50 per cent temperature of 568 F. Two sets of heat-transfer data were taken, one for an annulus with a diameter 2.073 in. for the inside diameter of the outer pipe, and the other for an annulus of 1.583 in. The data are given in Tables 5 and 6.

The measurements on plain tubes Nos. 7 and 9 are the usual over-all coefficients for the inside wall of an annulus. In the case of finned tubes, the spiral fins affect the path of the oil through the annulus.

Water-film coefficients inside the tube under conditions similar to these were computed in Series E. These water-film coefficients and the assumption that the resistance of the copper may be neglected were used along with the over-all coefficients to compute film coefficients for the oil in the annulus.

A comparison between the experimental coefficients and those calculated by Nusselt-type equation, Equation [10], requires equivalent diameters for the annuli. A procedure for plain tubes is to use the difference between the inside and outside diameters of the annulus. For the finned tubes, the inside diameter of the annulus has been taken as equal to D_E . For the twelve tubes which gave essentially straight lines for the water-film coefficients in Fig. 13, a plot was made of the product of hD' versus Reynolds

number, Figs. 15 and 16. If the Prandtl number $(\frac{c_p \mu}{k})$ and the thermal conductivity k are assumed to be constant over the small temperature range used, Equation [10] may be simplified as shown by Equation [11]

$$hD' = 0.023 \left(\frac{c_p \mu}{k} \right)^{0.4} k \left(\frac{DG}{\mu} \right)^{0.8} = b \left(\frac{DG}{\mu} \right)^{0.8} \dots [11]$$

By using average values for c_p , μ , and k (Prandtl number =

TABLE 5 DATA ON FINNED TUBES; OIL OUTSIDE, WATER INSIDE

TUBE NO.	WATER TEMPERATURE		WATER INLET TEMPERATURE		WATER MEAN TEMPERATURE		WATER VELOCITY		HEAT TRANSFERED		COEFFICIENT		
	INLET	OUTLET	INLET	OUTLET	INLET	OUTLET	INLET	OUTLET	INLET	OUTLET	BTU PER SQ. FT. PER DEG. F.	PER FT.	
	°C	°C	°C	°C	°C	°C	MIN	MIN	°C	°C			
1	13.39	26.92	7.63	68.05	6.46	2.87	119.5	1.3	30.0	146.00	143.96	71.9	33.6
2	13.39	25.71	8.41	68.05	6.46	2.87	119.5	1.3	30.0	146.00	143.96	71.9	33.6
3	13.39	21.68	8.41	67.94	11.1	2.83	117.2	1.4	46.0	67.00	70.00	41	19.3
4	13.39	22.16	2.81	67.90	8.02	4.48	117.0	1.8	22.9	44.60	44.60	27.1	12.7
5	13.39	27.71	7.63	68.05	6.46	2.87	119.5	1.3	30.0	146.00	143.96	71.9	33.6
6	17.40	25.67	6.28	68.05	6.46	2.87	119.5	1.3	30.0	146.00	143.96	71.9	33.6
7	17.40	24.76	7.20	68.05	6.46	2.87	119.5	1.3	30.0	146.00	143.96	71.9	33.6
8	17.40	24.76	7.20	68.05	6.46	2.87	119.5	1.3	30.0	146.00	143.96	71.9	33.6
9	17.40	24.76	7.20	68.05	6.46	2.87	119.5	1.3	30.0	146.00	143.96	71.9	33.6
10	17.40	24.76	7.20	68.05	6.46	2.87	119.5	1.3	30.0	146.00	143.96	71.9	33.6
11	17.40	24.76	7.20	68.05	6.46	2.87	119.5	1.3	30.0	146.00	143.96	71.9	33.6
12	17.40	24.76	7.20	68.05	6.46	2.87	119.5	1.3	30.0	146.00	143.96	71.9	33.6
13	17.40	24.76	7.20	68.05	6.46	2.87	119.5	1.3	30.0	146.00	143.96	71.9	33.6
14	17.40	24.76	7.20	68.05	6.46	2.87	119.5	1.3	30.0	146.00	143.96	71.9	33.6
15	17.40	24.76	7.20	68.05	6.46	2.87	119.5	1.3	30.0	146.00	143.96	71.9	33.6
16	17.40	24.76	7.20	68.05	6.46	2.87	119.5	1.3	30.0	146.00	143.96	71.9	33.6
17	17.40	24.76	7.20	68.05	6.46	2.87	119.5	1.3	30.0	146.00	143.96	71.9	33.6
18	17.40	24.76	7.20	68.05	6.46	2.87	119.5	1.3	30.0	146.00	143.96	71.9	33.6
19	17.40	24.76	7.20	68.05	6.46	2.87	119.5	1.3	30.0	146.00	143.96	71.9	33.6
20	17.40	24.76	7.20	68.05	6.46	2.87	119.5	1.3	30.0	146.00	143.96	71.9	33.6
21	17.40	24.76	7.20	68.05	6.46	2.87	119.5	1.3	30.0	146.00	143.96	71.9	33.6
22	17.40	24.76	7.20	68.05	6.46	2.87	119.5	1.3	30.0	146.00	143.96	71.9	33.6
23	17.40	24.76	7.20	68.05	6.46	2.87	119.5	1.3	30.0	146.00	143.96	71.9	33.6
24	17.40	24.76	7.20	68.05	6.46	2.87	119.5	1.3	30.0	146.00	143.96	71.9	33.6
25	17.40	24.76	7.20	68.05	6.46	2.87	119.5	1.3	30.0	146.00	143.96	71.9	33.6
26	17.40	24.76	7.20	68.05	6.46	2.87	119.5	1.3	30.0	146.00	143.96	71.9	33.6
27	17.40	24.76	7.20	68.05	6.46	2.87	119.5	1.3	30.0	146.00	143.96	71.9	33.6
28	17.40	24.76	7.20	68.05	6.46	2.87	119.5	1.3	30.0	146.00	143.96	71.9	33.6
29	17.40	24.76	7.20	68.05	6.46	2.87	119.5	1.3	30.0	146.00	143.96	71.9	33.6
30	17.40	24.76	7.20	68.05	6.46	2.87	119.5	1.3	30.0	146.00	143.96	71.9	33.6
31	17.40	24.76	7.20	68.05	6.46	2.87	119.5	1.3	30.0	146.00	143.96	71.9	33.6
32	17.40	24.76	7.20	68.05	6.46	2.87	119.5	1.3	30.0	146.00	143.96	71.9	33.6
33	17.40	24.76	7.20	68.05	6.46	2.87	119.5	1.3	30.0	146.00	143.96	71.9	33.6
34	17.40	24.76	7.20	68.05	6.46	2.87	119.5	1.3	30.0	146.00	143.96	71.9	33.6
35	17.40	24.76	7.20	68.05	6.46	2.87	119.5	1.3	30.0	146.00	143.96	71.9	33.6
36	17.40	24.76	7.20	68.05	6.46	2.87	119.5	1.3	30.0	146.00	143.96	71.9	33.6
37	17.40	24.76	7.20	68.05	6.46	2.87	119.5	1.3	30.0	146.00	143.96	71.9	33.6
38	17.40	24.76	7.20	68.05	6.46	2.87	119.5	1.3	30.0	146.00	143.96	71.9	33.6
39	17.40	24.76	7.20	68.05	6.46	2.87	119.5	1.3	30.0	146.00	143.96	71.9	33.6
40	17.40	24.76	7.20	68.05	6.46	2.87	119.5	1.3	30.0	146.00	143.96	71.9	33.6
41	17.40	24.76	7.20	68.05	6.46	2.87	119.5	1.3	30.0	146.00	143.96	71.9	33.6
42	17.40	24.76	7.20	68.05	6.46	2.87	119.5	1.3	30.0	146.00	143.96	71.9	33.6
43	17.40	24.76	7.20	68.05	6.46	2.87	119.5	1.3	30.0	146.00	143.96	71.9	33.6
44	17.40	24.76	7.20	68.05	6.46	2.87	119.5	1.3	30.0	146.00	143.96	71.9	33.6
45	17.40	24.76	7.20	68.05	6.46	2.87	119.5	1.3	30.0	146.00	143.96	71.9	33.6
46	17.40	24.76	7.20	68.05	6.46	2.87	119.5	1.3	30.0	146.00	143.96	71.9	33.6
47	17.40	24.76	7.20	68.05	6.46	2.87	119.5	1.3	30.0	146.00	143.96	71.9	33.6
48	17.40	24.76	7.20	68.05	6.46	2.87	119.5	1.3	30.0	146.00	143.96	71.9	33.6
49	17.40	24.76	7.20	68.05	6.46	2.87	119.5	1.3	30.0	146.00	143.96	71.9	33.6
50	17.40	24.76	7.20	68.05	6.46	2.87	119.5	1.3	30.0	146.00	143.96	71.9	33.6
51	17.40	24.76	7.20	68.05	6.46	2.87	119.5	1.3	30.0	146.00	143.96	71.9	33.6
52	17.40	24.76	7.20	68.05	6.46	2.87	119.5	1.3	30.0	146.00	143.96	71.9	33.6
53	17.40	24.76	7.20	68.05	6.46	2.87	119.5	1.3	30.0	146.00	143.96	71.9	33.6
54	17.40	24.76	7.20	68.05	6.46	2.87	119.5	1.3	30.0	146.00	143.96	71.9	33.6
55	17.40	24.76	7.20	68.05	6.46	2.87	119.5	1.3	30.0	146.00	143.96	71.9	33.6
56	17.40	24.76	7.20	68.05	6.46	2.87	119.5	1.3	30.0	146.00	143.96	71.9	33.6
57	17.40	24.76	7.20	68.05	6.46	2.87	119.5	1.3	30.0	146.00	143.96	71.9	33.6
58	17.40	24.76	7.20	68.05	6.46	2.87	119.5	1.3	30.0	146.00	143.96	71.9	33.6
59	17.40	24.76	7.20	68.05	6.46	2.87	119.5	1.3	30.0	146.00	143.96	71.9	33.6
60	17.40	24.76	7.20	68.05	6.46	2.87	119.5	1.3	30.0	146.00	143.96	71.9	33.6
61	17.40	24.76	7.20	68.05	6.46	2.87	119.5	1.3	30.0	146.00	143.96	71.9	33.6
62	17.40	24.76	7.20	68.05	6.46	2.87	119.5	1.3	30.0	146.00	143.96	71.9	33.6
63	17.40	24.76	7.20	68.05	6.46	2.87	119.5	1.3	30.0	146.00	143.96	71.9	33.6
64	17.40	24.76	7.20	68.05	6.46	2.87	119.5	1.3	30.0	146.00	143.96	71.9	33.6
65	17.40	24.76	7.20	68.05	6.46	2.87	119.5	1.3	30.0	146.00	143.96	71.9	33.6
66	17.40	24.76	7.20	68.05	6.46	2.87	119.5	1.3	30.0	146.00	143.96	71.9	33.6
67	17.40	24.76	7.20	68.05	6.46	2.87	119.5	1.3	30.0	146.00	143.96	71.9	33.6
68	17.40	24.76	7.20	68.05	6.46	2.87	119.5	1.3	30.0	146.00	143.96	71.9	33.6
69	17.40	24.76	7.20	68.05	6.46	2.87	119.5	1.3	30.0	146.00	143.96	71.9	33.6
70	17.40	24.76	7.20	68.05	6.46	2.87	119.5	1.3	30.0	146.00	143.96	71.9	33.6
71	17.40	24.76	7.20	68.05	6.46	2.87	119.5	1.3	30.0	146.00	143.96	71.9	33.6
72	17.40	24.76	7.20	68.05	6.46	2.87	119.5	1.3	30.0	146.00	143.96	71.9	33.6
73	17.40	24.76	7.20	68.05	6.46	2.87	119.5	1.3	30.0	146.00	143.96	71.9	33.6
74	17.40	24.76	7.20	68.05	6.46	2.87	119.5	1.3	30.0	146.00	143.96	71.9	33.6
75	17.40	24.76	7.20	68.05	6.46	2.87	119.5	1.3	30.0	146.00	143.96	71.9	33.6
76	17.40	24.76	7.20	68.05	6.46	2.87	119.5	1.3	30.0	146.00	143.96	71.9	33.6
77	17.40	24.76	7.20	68.05	6.46	2.87	119.5	1.3	30.0	146.00	143.96	71.9	33.6
78	17.40	24.76	7.20	68.05	6.46	2.87	119.5	1.3	30.0	146.00	143.96	71.9	33.6
79	17.40	24.76	7.20	68.05	6.46	2.87	119.5	1.3	30.0	146.00	143.96	71.9	33.6
80	17.40	24.76	7.20	68.05	6.46	2.87	119.5	1.3	30.0	146.00	143.96	71.9	33.6
81	17.40	24.76	7.20	68.05	6.46	2.87	119.5	1.3	30.0	146.00	143.96	71.9	33.6
82	17.40	24.76	7.20	68.05	6.46	2.87	119.5	1.3	30.0	146.00	143.96	71.9	33.6
83	17.40	24.76	7.20	68.05	6.46	2.87	119.5	1.3	30.0	146.00	143.96	71.9	33.6
84	17.40	24.76	7.20	68.05	6.46	2.87	119.5	1.3	30.0	146.00	143.96	71.9	33.6
85	17.40	24.76	7.20	68.05	6.46	2.87	119.5	1.3	30.0	146.00	143.96	71.9	33.6
86	17.40	24.76	7.20	68.05	6.46	2.87	119.5	1.3	30.0	146.00	143.96	71.9	33.6
87	17.40	24.76	7.20	68.05	6.46	2.87	119.5	1.3	30.0	146.00	143.96	71.9	33.6
88	17.40	24.76	7.20	68.05	6.46	2.87	119.5	1.3	30.0	146.00	143.96	71.9	33.6
89	17.40	24.76	7.20	68.05	6.46	2.87	119.5	1.3	30.0	146.00	143.96	71.9	33.6
90	17.40	24.76	7.20	68.05	6.46	2.87	119.5	1.3	30.0	146.00	143.		

TABLE 6 DATA ON FINNED TUBES; OIL OUTSIDE, WATER INSIDE

TUBE NO.	WATER INLET TEMP. °C	WATER OUTLET TEMP. °C	WATER FLOW RATE LBS./HR.	WATER INLET TEMP. °F	WATER OUTLET TEMP. °F	WATER FLOW RATE GPM.	WATER VELOCITY FT./SEC.	WATER REYNOLDS NUMBER	WATER PRANDTL NUMBER	WATER FILM COEFFICIENT BTU/HR. SQ. FT. °F	WATER HEAT TRANSFER BTU/HR.	WATER LOSS PERCENT	WATER LOSS PERCENT
1	16.42	24.61	10.19	61.56	76.30	2.99	116.5	13.9	91.0	15,300	1,520.0	31.3	41.4
4	16.30	23.23	12.05	61.14	73.81	3.19	113.9	14.0	92.5	20,300	1,640.0	106.2	53.2
7	16.30	23.23	12.05	61.14	73.81	3.19	113.9	14.0	92.5	17,800	1,670.0	104.4	49.8
9	16.30	23.23	12.05	61.14	73.81	3.19	113.9	14.0	92.5	11,000	1,650.0	105.1	39.7
13	16.30	23.23	12.05	61.14	73.81	3.19	113.9	14.0	92.5	3,570	1,670.0	106.2	16.1
14	16.30	23.23	12.05	61.14	73.81	3.19	113.9	14.0	92.5	2,500	1,670.0	106.2	16.1
15	16.30	23.23	12.05	61.14	73.81	3.19	113.9	14.0	92.5	1,500	1,670.0	106.2	16.1
16	16.30	23.23	12.05	61.14	73.81	3.19	113.9	14.0	92.5	1,000	1,670.0	106.2	16.1
17	16.30	23.23	12.05	61.14	73.81	3.19	113.9	14.0	92.5	500	1,670.0	106.2	16.1
18	16.30	23.23	12.05	61.14	73.81	3.19	113.9	14.0	92.5	250	1,670.0	106.2	16.1
19	16.30	23.23	12.05	61.14	73.81	3.19	113.9	14.0	92.5	125	1,670.0	106.2	16.1
20	16.30	23.23	12.05	61.14	73.81	3.19	113.9	14.0	92.5	62.5	1,670.0	106.2	16.1
21	16.30	23.23	12.05	61.14	73.81	3.19	113.9	14.0	92.5	31.25	1,670.0	106.2	16.1
22	16.30	23.23	12.05	61.14	73.81	3.19	113.9	14.0	92.5	15.625	1,670.0	106.2	16.1
23	16.30	23.23	12.05	61.14	73.81	3.19	113.9	14.0	92.5	7.8125	1,670.0	106.2	16.1
24	16.30	23.23	12.05	61.14	73.81	3.19	113.9	14.0	92.5	3.90625	1,670.0	106.2	16.1
25	16.30	23.23	12.05	61.14	73.81	3.19	113.9	14.0	92.5	1.953125	1,670.0	106.2	16.1
26	16.30	23.23	12.05	61.14	73.81	3.19	113.9	14.0	92.5	0.9765625	1,670.0	106.2	16.1
27	16.30	23.23	12.05	61.14	73.81	3.19	113.9	14.0	92.5	0.48828125	1,670.0	106.2	16.1
28	16.30	23.23	12.05	61.14	73.81	3.19	113.9	14.0	92.5	0.244140625	1,670.0	106.2	16.1
29	16.30	23.23	12.05	61.14	73.81	3.19	113.9	14.0	92.5	0.1220703125	1,670.0	106.2	16.1
30	16.30	23.23	12.05	61.14	73.81	3.19	113.9	14.0	92.5	0.06103515625	1,670.0	106.2	16.1
31	16.30	23.23	12.05	61.14	73.81	3.19	113.9	14.0	92.5	0.030517578125	1,670.0	106.2	16.1
32	16.30	23.23	12.05	61.14	73.81	3.19	113.9	14.0	92.5	0.0152587890625	1,670.0	106.2	16.1
33	16.30	23.23	12.05	61.14	73.81	3.19	113.9	14.0	92.5	0.00762939453125	1,670.0	106.2	16.1
34	16.30	23.23	12.05	61.14	73.81	3.19	113.9	14.0	92.5	0.003814697265625	1,670.0	106.2	16.1
35	16.30	23.23	12.05	61.14	73.81	3.19	113.9	14.0	92.5	0.0019073486328125	1,670.0	106.2	16.1
36	16.30	23.23	12.05	61.14	73.81	3.19	113.9	14.0	92.5	0.00095367431640625	1,670.0	106.2	16.1
37	16.30	23.23	12.05	61.14	73.81	3.19	113.9	14.0	92.5	0.000476837158203125	1,670.0	106.2	16.1
38	16.30	23.23	12.05	61.14	73.81	3.19	113.9	14.0	92.5	0.0002384185791015625	1,670.0	106.2	16.1
39	16.30	23.23	12.05	61.14	73.81	3.19	113.9	14.0	92.5	0.00011920928955078125	1,670.0	106.2	16.1
40	16.30	23.23	12.05	61.14	73.81	3.19	113.9	14.0	92.5	5.96e-05	1,670.0	106.2	16.1
41	16.30	23.23	12.05	61.14	73.81	3.19	113.9	14.0	92.5	2.98e-05	1,670.0	106.2	16.1
42	16.30	23.23	12.05	61.14	73.81	3.19	113.9	14.0	92.5	1.49e-05	1,670.0	106.2	16.1
43	16.30	23.23	12.05	61.14	73.81	3.19	113.9	14.0	92.5	7.45e-06	1,670.0	106.2	16.1
44	16.30	23.23	12.05	61.14	73.81	3.19	113.9	14.0	92.5	3.72e-06	1,670.0	106.2	16.1
45	16.30	23.23	12.05	61.14	73.81	3.19	113.9	14.0	92.5	1.86e-06	1,670.0	106.2	16.1
46	16.30	23.23	12.05	61.14	73.81	3.19	113.9	14.0	92.5	9.3e-07	1,670.0	106.2	16.1
47	16.30	23.23	12.05	61.14	73.81	3.19	113.9	14.0	92.5	4.65e-07	1,670.0	106.2	16.1
48	16.30	23.23	12.05	61.14	73.81	3.19	113.9	14.0	92.5	2.32e-07	1,670.0	106.2	16.1
49	16.30	23.23	12.05	61.14	73.81	3.19	113.9	14.0	92.5	1.16e-07	1,670.0	106.2	16.1
50	16.30	23.23	12.05	61.14	73.81	3.19	113.9	14.0	92.5	5.8e-08	1,670.0	106.2	16.1
51	16.30	23.23	12.05	61.14	73.81	3.19	113.9	14.0	92.5	2.9e-08	1,670.0	106.2	16.1
52	16.30	23.23	12.05	61.14	73.81	3.19	113.9	14.0	92.5	1.45e-08	1,670.0	106.2	16.1
53	16.30	23.23	12.05	61.14	73.81	3.19	113.9	14.0	92.5	7.25e-09	1,670.0	106.2	16.1
54	16.30	23.23	12.05	61.14	73.81	3.19	113.9	14.0	92.5	3.62e-09	1,670.0	106.2	16.1
55	16.30	23.23	12.05	61.14	73.81	3.19	113.9	14.0	92.5	1.81e-09	1,670.0	106.2	16.1
56	16.30	23.23	12.05	61.14	73.81	3.19	113.9	14.0	92.5	9.05e-10	1,670.0	106.2	16.1
57	16.30	23.23	12.05	61.14	73.81	3.19	113.9	14.0	92.5	4.52e-10	1,670.0	106.2	16.1
58	16.30	23.23	12.05	61.14	73.81	3.19	113.9	14.0	92.5	2.26e-10	1,670.0	106.2	16.1
59	16.30	23.23	12.05	61.14	73.81	3.19	113.9	14.0	92.5	1.13e-10	1,670.0	106.2	16.1
60	16.30	23.23	12.05	61.14	73.81	3.19	113.9	14.0	92.5	5.65e-11	1,670.0	106.2	16.1
61	16.30	23.23	12.05	61.14	73.81	3.19	113.9	14.0	92.5	2.82e-11	1,670.0	106.2	16.1
62	16.30	23.23	12.05	61.14	73.81	3.19	113.9	14.0	92.5	1.41e-11	1,670.0	106.2	16.1
63	16.30	23.23	12.05	61.14	73.81	3.19	113.9	14.0	92.5	7.05e-12	1,670.0	106.2	16.1
64	16.30	23.23	12.05	61.14	73.81	3.19	113.9	14.0	92.5	3.52e-12	1,670.0	106.2	16.1
65	16.30	23.23	12.05	61.14	73.81	3.19	113.9	14.0	92.5	1.76e-12	1,670.0	106.2	16.1
66	16.30	23.23	12.05	61.14	73.81	3.19	113.9	14.0	92.5	8.8e-13	1,670.0	106.2	16.1
67	16.30	23.23	12.05	61.14	73.81	3.19	113.9	14.0	92.5	4.4e-13	1,670.0	106.2	16.1
68	16.30	23.23	12.05	61.14	73.81	3.19	113.9	14.0	92.5	2.2e-13	1,670.0	106.2	16.1
69	16.30	23.23	12.05	61.14	73.81	3.19	113.9	14.0	92.5	1.1e-13	1,670.0	106.2	16.1
70	16.30	23.23	12.05	61.14	73.81	3.19	113.9	14.0	92.5	5.5e-14	1,670.0	106.2	16.1
71	16.30	23.23	12.05	61.14	73.81	3.19	113.9	14.0	92.5	2.75e-14	1,670.0	106.2	16.1
72	16.30	23.23	12.05	61.14	73.81	3.19	113.9	14.0	92.5	1.37e-14	1,670.0	106.2	16.1
73	16.30	23.23	12.05	61.14	73.81	3.19	113.9	14.0	92.5	6.85e-15	1,670.0	106.2	16.1
74	16.30	23.23	12.05	61.14	73.81	3.19	113.9	14.0	92.5	3.42e-15	1,670.0	106.2	16.1
75	16.30	23.23	12.05	61.14	73.81	3.19	113.9	14.0	92.5	1.71e-15	1,670.0	106.2	16.1
76	16.30	23.23	12.05	61.14	73.81	3.19	113.9	14.0	92.5	8.55e-16	1,670.0	106.2	16.1
77	16.30	23.23	12.05	61.14	73.81	3.19	113.9	14.0	92.5	4.27e-16	1,670.0	106.2	16.1
78	16.30	23.23	12.05	61.14	73.81	3.19	113.9	14.0	92.5	2.14e-16	1,670.0	106.2	16.1
79	16.30	23.23	12.05	61.14	73.81	3.19	113.9	14.0	92.5	1.07e-16	1,670.0	106.2	16.1
80	16.30	23.23	12.05	61.14	73.81	3.19	113.9	14.0	92.5	5.35e-17	1,670.0	106.2	16.1
81	16.30	23.23	12.05	61.14	73.81	3.19	113.9	14.0	92.5	2.67e-17	1,670.0	106.2	16.1
82	16.30	23.23	12.05	61.14	73.81	3.19	113.9	14.0	92.5	1.34e-17	1,670.0	106.2	16.1
83	16.30	23.23	12.05	61.14	73.81	3.19	113.9	14.0	92.5	6.7e-18	1,670.0	106.2	16.1
84	16.30	23.23	12.05	61.14	73.81	3.19	113.9	14.0	92.5	3.35e-18	1,670.0	106.2	16.1
85	16.30	23.23	12.05	61.14	73.81	3.19	113.9	14.0	92.5	1.67e-18	1,670.0	106.2	16.1
86	16.30	23.23	12.05	61.14	73.81	3.19	113.9	14.0	92.5	8.35e-19	1,670.0	106.2	16.1
87	16.30	23.23	12.05	61.14	73.81	3.19	113.9	14.0	92.5	4.17e-19	1,670.0	106.2	16.1
88	16.30	23.23	12.05	61.14	73.81	3.19	113.9	14.0	92.5	2.09e-19	1,670.0	106.2	16.1
89	16.30	23.23	12.05	61.14	73.81	3.19	113.9	14.0	92.5	1.04e-19	1,670.0	106.2	16.1
90	16.30	23.23	12.05	61.14	73.81	3.19	113.9	14.0	92.5	5.2e-20	1,670.0	106.2	16.1
91	16.30	23.23	12.05	61.14	73.81	3.19	113.9	14.0	92.5	2.6e-20	1,670.0	106.2	16.1
92	16.30												

relations between temperature of fluids, velocity of fluids, viscosity of fluids, etc., and the film coefficient, in the course of their tests?

AUTHORS' CLOSURE

The authors appreciate the comments by Messrs. Ashley, Paugh, and Vanderweil.

Mr. Ashley states that his experience shows that the high coefficient noted at low air velocities in Fig. 8 may be "accounted for by the fact that these are in streamline flow." At 600 fpm the Reynolds number is approximately 3300, a value normally considered to be in the critical region between viscous and turbulent flow. However, because of the doubt as to the proper value of D to use in calculating the Reynolds number for banks of finned tubes and because other independent data available to the authors showed a straight line for the data down to a velocity of 380 fpm, we were reluctant to interpret the data below 600 fpm as being in the viscous region. It is quite possible that the data are in the transition region between viscous and turbulent flow at velocities of 300 to 500 fpm.

In regard to Mr. Ashley's second point, steam was always taken from a line at 125 psi gage and throttled directly to the unit. Since many of the tests were run at low pressures such as 5, 25, and 50 lb per sq in. gage it was felt that this throttling gave adequate assurance of dry steam entering the unit at least

for the lower pressures. Concerning the uniformity of air velocities and the accuracy of the temperature measurements, vanes were present as shown in the sketches of this paper but which were not present on the preprint. Pitot-tube traverses made of the air stream leaving the unit were used to check the general accuracy of the heat balance. The thermometer was placed in several positions before selecting the one used. The outlet thermometer was always shielded to avoid errors due to radiation. The inlet thermometer was not shielded in the tests reported in the paper but a correction was made based on similar tests with and without a shielded inlet thermometer.

Mr. Vanderweil asked about film coefficients. In the case of heating air with steam in series *A* and *B*, the steam film resistance is so low that the over-all coefficient is substantially equal to the air film coefficient. In such cases the over-all coefficient is used directly for design purposes without investigating the detail of the film coefficient. In other cases such as series *E* and *F* an understanding of the data requires that the over-all coefficient be broken down into the film coefficient for the two sides of the heat-transfer surface. It may be possible to vary these film coefficients independently and so no general correlation is available for over-all coefficients but only for the film coefficients. The viscosity, velocity, and density of the flowing fluids were correlated with the film coefficient for the cases of oil and water in series *E* and *F*.

Heat Transfer and Pressure Loss in Small Commercial Shell-and-Finned-Tube Heat Exchangers

By R. M. ARMSTRONG,¹ DOWNINGTOWN, PA.

Preliminary results are submitted covering heat transfer and pressure loss for fluids flowing through the shells of small shell and finned-tube heat exchangers in crossflow. These results are compared to the calculated performance of similar exchangers with bare tubes, and the comparisons noted. It is brought out that this type of exchanger can now be applied to duties where finned tubes heretofore have not been used, namely, where over-all heat-transfer rates for bare-tube service would be from about 25 to 250 Btu/(hr)(sq ft)(deg F). It is also pointed out that this type unit is not suitable for many services. Actual field experiences are related.

NOMENCLATURE

The following nomenclature is used in the paper:

- A_s = cross-sectional area for flow across tubes, sq ft
- c = specific heat of fluid at constant pressure and average temperature
- D_s = inside diameter of shell, ft
- d_o = outside diameter of tube, ft
- F = MTD correction factor for pass, from TEMA Standards (p. 20)
- G_s = mass velocity through shell, lb/(hr)(sq ft)
- h_m = heat-transfer rate through metal wall of tube, Btu/(hr)(sq ft)(deg F)
- h_s = film heat-transfer rate on shell side, Btu/(hr)(sq ft)(deg F)
- $h_{s,d}$ = scale heat-transfer rate on shell side, Btu/(hr)(sq ft)(deg F)
- h_t = film heat-transfer rate on tube side, Btu/(hr)(sq ft)(deg F)
- $h_{t,d}$ = scale heat-transfer rate on tube side, Btu/(hr)(sq ft)(deg F)
- J = dimensionless number $\left(\frac{h_s}{cG_s} \right) \left(\frac{c\mu}{k} \right)^{2/3}$
- K = pass correction factor, from TEMA Standards, p. 20
- k = thermal conductivity of fluid at average temperature, Btu/(hr)(sq ft)(deg F/ft)
- n = number of tubes in shell of heat exchanger
- R = pass correction factor, from TEMA Standards (p. 20)
- S = baffle spacing, ft
- U = over-all heat-transfer rate, Btu/(hr)(sq ft)(deg F)
- W = pounds fluid flowing through shell per hour
- μ = viscosity of fluid at average temperature, lb/(hr)(ft)
- μ_w = viscosity of fluid at wall temperature, lb/(hr)(ft)

INTRODUCTION

Several years ago a new type of finned tube, extruded from the

¹ Downingtown Iron Works, Inc.

Contributed by the Heat Transfer Division and presented at the Annual Meeting, New York, N. Y., Nov. 27-Dec. 1, 1944, of THE AMERICAN SOCIETY OF MECHANICAL ENGINEERS.

NOTE: Statements and opinions advanced in papers are to be understood as individual expressions of their authors and not those of the Society.

base metal itself and with low ratio of outside to inside surface, became available for use in heat exchangers. It was decided to consider the application of this tube to shell-and-tube exchangers for crossflow and liquid-to-liquid service, since the compact nature of the tube made it possible to get about 3 times as much outside surface with the finned tube as with a bare tube, in a given shell diameter. No published data were available for heat transfer to baffled banks of finned tubes and experiments were begun to obtain such data.

Some advantages and disadvantages were rather obvious from the examination of the tube, details of which are shown in Figs. 1 and 2. These are as follows:

Advantages:

(a) Low ratio of outside to inside surface, about 3.5 to 1. Most previous finned tubes for similar service had run from 7 or 10 to 1. The low ratio makes possible the use of the tube for higher film heat-transfer rates.

(b) Low metal resistance, due to very low fin height, absence of any metal-to-metal bond. The calculated metal-wall resistance for this type tube runs about 0.0004 for admiralty metal, compared to as much as 0.015 for steel, and 0.006 for admiralty in high-ratio tubes with a bond.

(c) Mechanically the tube is stable and due to low outside diameter gives a large amount of surface per unit of volume. The tube is so built that it can be withdrawn from a bundle and otherwise handled the same as a bare tube.

Disadvantages:

(a) The most obvious and immediate disadvantage is the danger of fouling of the space between the fins, greatly reducing the outside area in contact with the fluid.

(b) The fins are thin and subject to attack by corrosion if the fluid and metal used are not entirely suited to each other. Fortunately, several metal choices are available.

(c) Many services are not suitable for finned-tube work under any circumstances, particularly high-efficiency operations like steam condensing where the compensating effect of finned surface is not needed and therefore is an unnecessary expense.

One of the questions which immediately arises from a heat-transfer and pressure-loss standpoint is whether or not the finned surface gives results qualitatively the same as a bare tube, if coefficients are based on the outside finned area, as they are in this paper. Experiments on this score are still continuing and this paper reports only a small portion of the work done to date, but the following statements can be made at this time, and some preliminary data are shown to bear out the statements:

1 The shell-side heat-transfer film coefficient, based on the outside finned area, is at the very least equal to the rate which would be obtained at a like Reynolds number with bare tube, at a Reynolds number of 300 or higher, using the nomenclature and units given in this paper. Fig. 5 shows experimental results from a set of tests on 8.5-centipose oil. At Reynolds numbers materially above 300 the experimental results are seen to be materially higher than those predicted by bare-tube data.

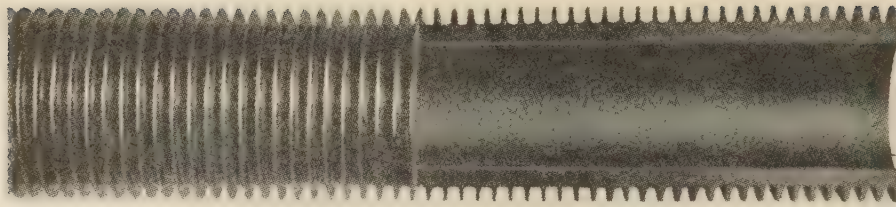


FIG. 1 SECTION OF TUBE USED IN EXPERIMENTS

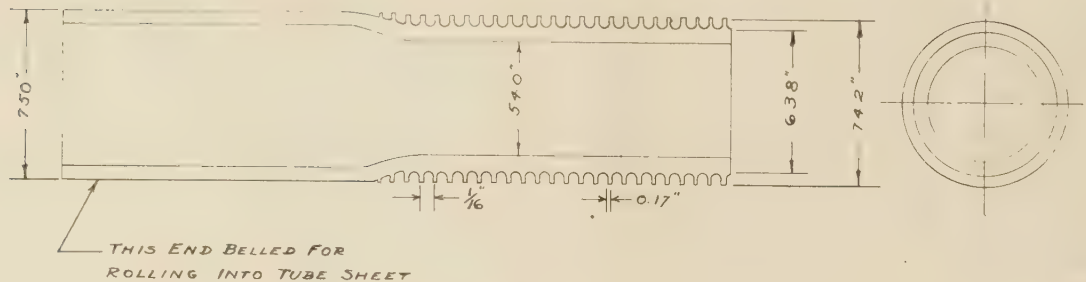


FIG. 2 DIMENSIONS OF TUBE USED

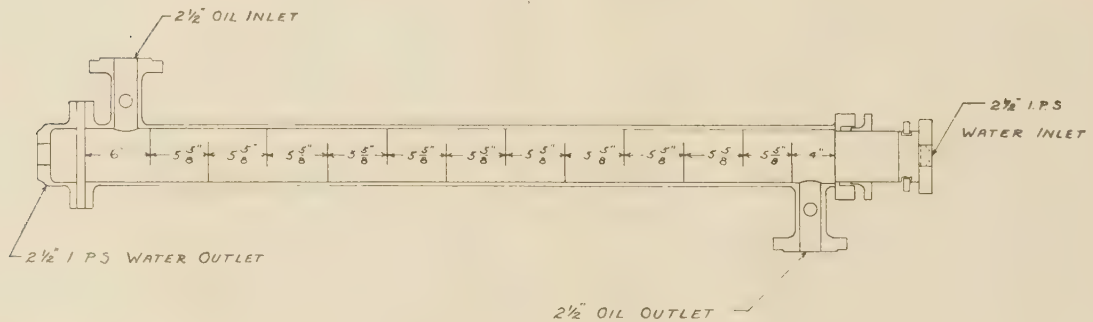


FIG. 3 TEST HEAT EXCHANGER

2 The crossflow friction is undoubtedly greater for the finned tube than for a bare tube. Determination of the friction loss for finned-tube bundles has been run on a research project concurrently with bare-tube bundles. While finned tubes show greater losses, other features of bundle design are vastly more important in determining the over-all pressure loss, so that the effect of the finned surface alone does not represent more than a small percentage of the total.

TEST PROCEDURE

The heat-transfer data shown in Fig. 5 were developed in tests on a 5-in.-shell-size unit with 6-ft.-long finned tubes. This is a full-size standardized unit developed for finned-tube work. The tests reported here were run with an oil in the shell of about 8.5 centipoises average viscosity at the test conditions. The test unit is shown in Fig. 3. Baffle height was 3.68 in.

The oil was pumped in a closed circuit, Fig. 4, through the exchanger and into a reservoir where it was heated. The water for cooling came in from the supply main and was discharged to the sewer after passing through the tubes.

The quantities of oil and water were measured by calibrated orifices to which were attached 36-in. mercury manometers. The temperatures were measured at the points marked *T* in Fig. 4 by the use of $1/16$ deg F thermometers with 15-in. scales. The pressure loss of oil flowing through the shell was measured using a

36-in. mercury manometer with taps in the shell nozzles, as shown in Fig. 4.

Unfortunately, it was found that the capacity of the system was considerably greater than had been anticipated, and as a result the water velocity going through the tubes was neces-

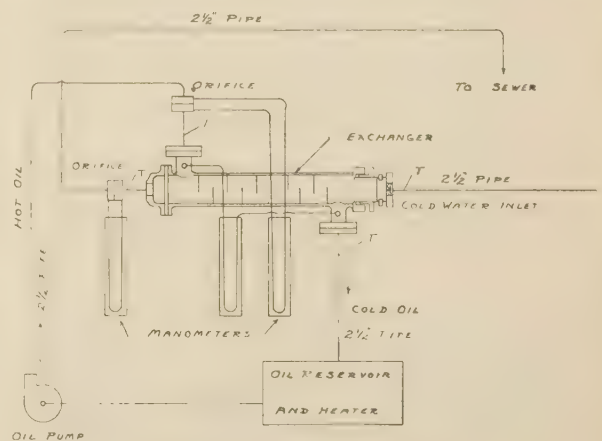


FIG. 4 TEST ARRANGEMENTS AND FLOW PATTERNS

sarily slow as the water temperature was low and there was no available means of heating the water at that time.

The over-all heat-transfer rate was calculated from the test results, based on total outside finned surface. The individual film rates were calculated from the curves given by the TEMA Standards (page 42). Then the metal-wall resistance and the water-film resistance were subtracted from the over-all measured resistance, and the remainder was taken as the oil-side resistance. This method is somewhat conservative in one respect as it makes no allowance whatsoever for fouling, and the tests took up a sufficient period of time so that it is likely some fouling actually did occur. The method of figuring water-film resistance by the TEMA curves, however, we feel to be conservative on the other side, as we found a number of tests, not reported here, where the calculated water-film resistance alone was greater than the over-all resistance as measured. These were mostly at very low water-flow rates.

In several instances we have noted that when cooling a fluid with water in the tubes at low velocity, obviously higher results are obtained than would be predicted by TEMA curves (page 42). Some of this is undoubtedly due to natural convection, as suggested by Dr. A. C. Mueller, and could perhaps be evaluated further by suggested methods.² However, from an entirely practical viewpoint there are also other factors, notably possibility of fouling, which would counteract this factor somewhat for the purposes for which these tests were made.

The agreement of the heat balances was quite good throughout and since in all but two or three cases the water heat balance was the lower and in general considered the more reliable, it was used as a basis of figuring.

DISCUSSION OF RESULTS OF TESTS

The results shown in Fig. 5, as plotted with $\frac{d_o G_s}{\mu}$ versus J are based on a diameter of tube taken on a weighted basis referred to

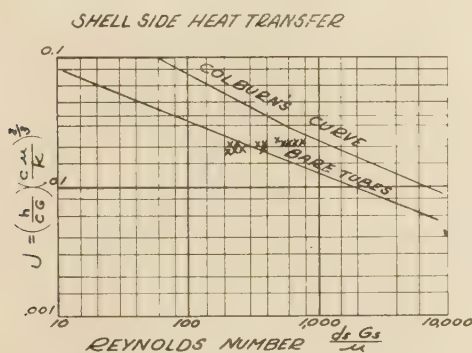


FIG. 5 HEAT-TRANSFER-RATE CURVES, BARE VERSUS FINNED TUBES

the outside area of fin across which the flow occurs. The outside diameter of the fin is 0.742 in., and the diameter at the base of the fin 0.638 in. The weighted outside diameter works out to be 0.656 in., or somewhat below the mean of outside diameter and inside diameter.

The area for flow on which G is based is determined by the formula

$$G_s = \frac{W}{S \left(D_s - d_s \sqrt{\frac{4n}{\pi}} \right)}$$

This is a modified form of the equation suggested by Bowman,³ and the main difference is that the so-called leakage factor is eliminated. These data have been plotted both with and without the leakage factor and just as good agreement is obtained without the factor as with it. Since the area is much simpler to handle without the factor the modified form is used.

It will be seen that the data fall well underneath the "Colburn curve" reported in Bowman's paper, but they fall partly above and partly below a conservative line drawn through the lower area of experimental points on Bowman's plot.

Considerable plotting of experimental points on a plot of this type for both bare- and finned-tube data, using the modified form of G , will show that the line given falls in the lower area of the majority of points and for this reason the author considers it a fair comparison against which to consider the finned-tube data reported herewith.

Evidence is shown that in the small shell unit with finned tubing, the flow is not entirely the same as in a larger unit. The shell-side fluid does not have time to straighten out into pure crossflow before it is again broken into eddy currents and turbulence. As a result, we should expect the performance of the unit tested to be better than the performance of the same tube in a larger shell where the crossflow distance is materially larger. The relatively low performance at low Reynolds numbers indicates that basically the finned tube does not exert a 100 per cent quality of surface efficiency when compared to bare tube in pure crossflow. The lesser slope of the curve we feel indicates that when the flow is reversed at frequent intervals and a good deal of the flow is quite turbulent in nature, the performance is greater than would be predicted by normal bare-tube rating methods.

Field experience with this type of unit has indicated that if the flow conditions are such that the Reynolds number always exceeds 300 on the shell side, calculated as indicated here, the performance of the exchanger can be conservatively calculated by holding to the bare-tube performance as shown on the curve.

As further indication of field performance, in the Appendix are data and calculations resulting from a spot check on the performance of a 16-in-shell-diam by 8-ft-tube-length compressed-air aftercooler which had been in operation about 6 months at the time of test. Unfortunately, this test was run with an extremely low water velocity in the tubes, only 0.287 fps. This was far below the design conditions and resulted in a very low over-all heat-transfer coefficient. However, the actual observed rate of 15 Btu/(hr)(sq ft)(deg F) was slightly below the calculated performance for a bare 5/8-in.-OD, 18-gage, copper tube under the identical conditions, namely, 16.4 Btu/(hr)(sq ft)(deg F), and we should point out that in calculating the MTD, which is almost off the scale on the correction curves, the highest possible value was taken. As this was on the flat part of the curve, it could easily be as much as 25 per cent on the conservative side. This amount would be reflected by an increased actual rate on the test unit, and in this case the actual rate would be greater than the calculated rate for the bare tube.

To give an idea of how this works out in practice Example 1 is given in which the film coefficients are the same on the bare tube

² "The Effect of Free Convection on Viscous Heat Transfer in Horizontal Tubes," by D. Q. Kern and D. F. Othmer, Trans. of American Institute of Chemical Engineers, vol. 39, 1943, pp. 517-555.

³ "Investigation of Heat Transfer Rates on the External Surface of Baffled Tube Banks," by R. A. Bowman, A.S.M.E., Miscellaneous Papers, 1934.

EXAMPLE 1 EFFECT OF RATIO OF OUTSIDE TO INSIDE AREAS OF TUBES

Size	BASIC DATA	
	Bare tubes 5/8-in. \times 18-gage admiralty	Finned tubes 5/8-in. nominal, 16 fins per in., admiralty
Ratio outside to inside surface.....	1.19	3.5
Shell-side-film rate.....	50	50
Tube-side-film rate.....	400	400
Fouling, both sides.....	1000	1000

CALCULATION OF HEAT-TRANSFER RATE

Resistance, shell film.....	0.02000	0.02000
Resistance, shell fouling.....	0.00100	0.00100
Metal-wall resistance.....	0.00002	0.00040
Resistance, tube fouling.....	0.00119	0.00350
Resistance, tube film.....	0.00298	0.00875
Total resistance.....	0.02519	0.03365
Over-all heat-transfer rate.....	39.7	29.7

as on the finned tube, showing the effect of the ratio of outside to inside areas.

While the bare-tube coefficient is $1/3$ greater than that of the finned tube, the amount of surface on the finned tube is roughly 3 times as great, resulting in a net gain of volume inside the exchanger of about 2 to 1. As an example, in the case cited, if the same size shell is used then the length of the finned-tube unit will be roughly one half the length of the bare-tube unit. If the baffle pitch must be substantially the same on both, then the pressure loss in the finned unit, while somewhat higher per baffle, will likely be less over-all since fewer baffles would be required.

The finned unit works out most advantageously when the inside coefficient is fairly high, and at least 2 or 3 times as great as the outside coefficient.

COMPARISON OF RESULTS IN PRACTICE

To gain some impression of how the heat-transfer rates compare in practice, refer to Fig. 6 which shows a plot of test results on

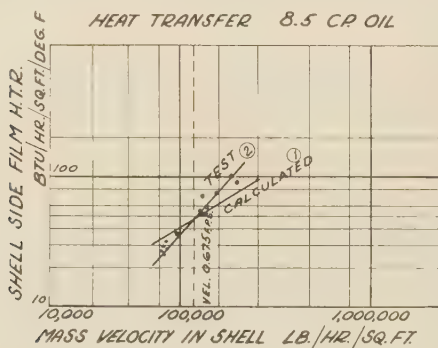


FIG. 6 COMPARISON OF OIL-FILM HEAT-TRANSFER RATES, BARE VERSUS FINNED TUBES

(Curve 1: Calculated rate for $5/8$ -in.-OD bare tube in conventional shell-and-tube exchanger.
Curve 2: Test results for 5-in. shell unit 19 finned tubes, $5/8$ -in. baffle spacing; effective tube length 6 ft; baffle height 3.68 in.)

the 5-in. exchanger against calculated bare-tube results for the same conditions. This shows that at relatively low flow rates the finned tube has a lower shell-side heat-transfer rate, while when the flow exceeds what is about 1 fps, the rate catches the bare tube and begins to pull away. From a practical viewpoint it is desirable to have at least a velocity of 1 fps to keep the surface swept clean and also to get a high enough film factor so that the unit as a whole is economical. We feel therefore that the policy of rating the finned-tube unit with an outside film coefficient equal to that used for the bare tube, with velocities of at least 1 fps, is conservative and so it has worked out in practice.

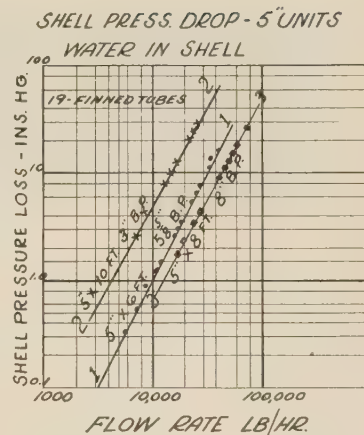


FIG. 7 SHELL-SIDE PRESSURE LOSS IN 5-IN. UNIT WITH WATER IN SHELL

(Curve 1: 5-in. \times 6-ft unit, $5/8$ -in. baffle pitch; baffle height 3.68 in.
Curve 2: 5-in. \times 10-ft. unit, 3-in. baffle pitch; baffle height 3.68 in.
Curve 3: 5-in. \times 8-ft unit, 8-in. baffle pitch, with reduced segment cut; baffle height 3.25 in.)

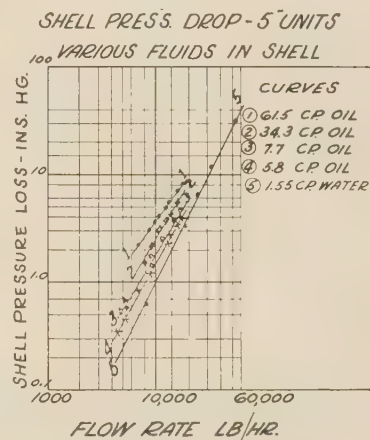


FIG. 8 SHELL-SIDE PRESSURE LOSS IN 5-IN. UNIT WITH VARIOUS FLUIDS IN SHELL
(Baffle height, 3.68 in.)

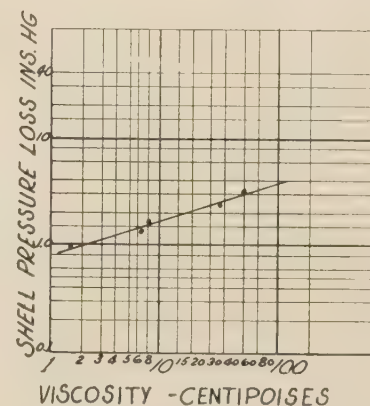


FIG. 9 EFFECT OF VISCOSITY ON PRESSURE LOSS IN 5-IN. SHELL
(Baffle height, 3.68 in.)

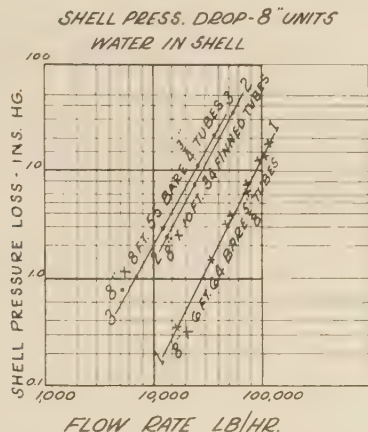


FIG. 10 SHELL-SIDE PRESSURE LOSS IN 8-IN. UNIT WITH WATER IN SHELL

(Curve 1: 8-in. \times 6-ft unit, 64 tubes $\frac{3}{4}$ in. OD on $\frac{15}{16}$ -in. triangular pitch, 7-in. baffle pitch, bare tubes; baffle height, 5.44 in.
Curve 2: 8-in. \times 10-ft unit, 34 finned tubes $\frac{3}{4}$ in. OD on $\frac{15}{16}$ -in. triangular pitch, $2\frac{1}{2}$ -in. baffle pitch; baffle height, 5.66 in.
Curve 3: 8-in. \times 8-ft unit, 55 bare tubes $\frac{3}{4}$ in. OD on $\frac{15}{16}$ -in. triangular pitch, 2-in. baffle pitch; baffle height, 5.38 in.)

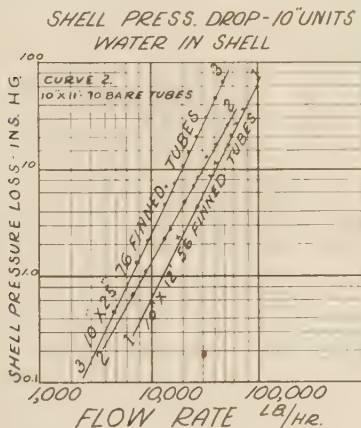


FIG. 11 SHELL-SIDE PRESSURE LOSS IN 10-IN. UNIT WITH WATER IN SHELL

(Curve 1: 10-in. \times 12-ft unit, 56 finned tubes $\frac{3}{4}$ in. OD on $\frac{15}{16}$ -in. triangular pitch, 3-in. baffle pitch; baffle height, 6.625 in.
Curve 2: 10-in. \times 11-ft unit, 70 bare tubes, $\frac{3}{4}$ in. OD on $\frac{15}{16}$ -in. triangular pitch, $2\frac{1}{2}$ -in. baffle pitch; baffle height, 7.18 in.
Curve 3: 10-in. \times 25-in. unit, 76 finned tubes, $\frac{3}{4}$ in. OD on $\frac{15}{16}$ -in. triangular pitch, 1-in. baffle pitch; baffle height, 7.25 in.)

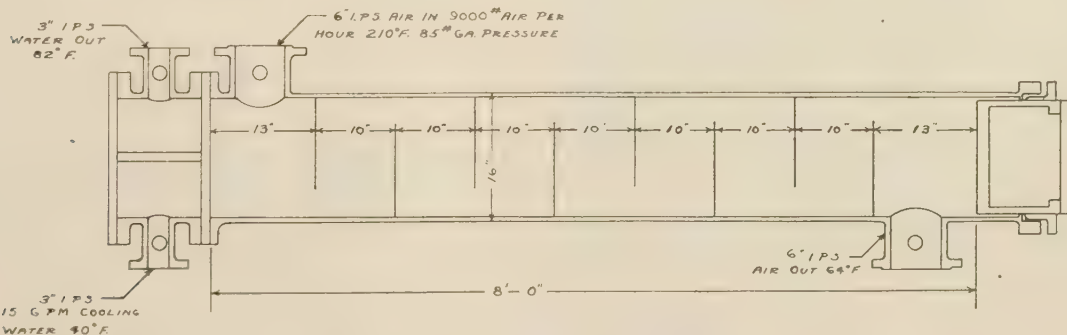


FIG. 12 TEST AIR AFTERCOOLER WITH FINNED-TUBE BUNDLE

PRESSURE LOSS IN SHELL SIDE

To pass on to the subject of pressure loss in the shell side, we report here the results of a series of tests on small heat exchangers with both finned and bare tubes. We can say that the results of these tests on small units agree rather well with a much more extensive set of tests on units of larger size and widely varying description as to tube size, pitch, baffle spacing, etc.

At the outset we can state briefly that it seems rather obvious that one of the main factors in determining the pressure loss of a fluid through a baffled shell is the relation of the actual flow area to the by-pass or clearance area. The clearance area is the summation of cracks between tube and baffle and between the baffle and the shell. On close baffle pitches with normal tolerances, as recommended by the TEMA and the WPB, the amount of crack area may easily almost equal the normal flow area. In such cases our tests have shown that the pressure loss calculated without regard to by-pass area may be as much as 800 per cent high when the equipment is new and the effect of fouling has not come into play. There are several methods now in use to compensate for the effect of this by-pass area. None of these methods, however, can be any more accurate than the shop tolerances and in general we find variations from one exchanger to another are enough to upset seriously any exact method of compensating for by-pass area. Also we can state definitely that the relation of the baffle (segment-cut) flow to crossflow may have a serious effect on the over-all friction loss. This effect is so much greater than the surface effect of the finned tube that while the finned tube does have a greater friction loss, it is only a small part of the over-all drop in most cases. The shell inside diameter of the experimental unit was 5.047 in., baffle outside diameter was exactly 5 in., and baffle holes were $\frac{49}{64}$ in.

The tests, Figs. 7, 8, 9, 10, 11, show actual pressure-loss measurements taken with water and with oil flowing through the shells of the heat exchangers tested. The manometer taps were located in the nozzles of the exchangers tested at an average distance of about 3 in. from the shell.

The effect of baffle height is clearly shown in Fig. 7. On curves 1 and 3 the number of baffles in the shell was almost the same, namely, 11 and 12. The tube length was 2 ft greater on 3 than on 1, or 33 per cent. Yet, by merely cutting the baffle height from 3.68 in. to 3.25 in. the friction loss was reduced in the face of the greater length. We cannot account for the slight variation in slope, although we do find from time to time that there will be some such minor differences in test results.

The effect of viscosity on pressure loss is indicated in Figs. 8 and 9, first showing that the lines, while at slightly different slope with higher viscosities, in general follow the same pattern. Fig. 9 shows the effect of viscosity taken at one flow rate. The test

points are in remarkably close agreement and we feel that the effect of viscosity on the particular exchanger tested is definitely greater than the effect on a larger unit of bare-tube design. The segment flow of oil passing along the tube perpendicular to the fins, introduces a considerable drag that would not be found in a bare-tube unit and it is possible that this effect increases with the viscosity.

Figs. 10 and 11 are given to show the trend in pressure-loss measurements on 8-in. and 10-in. units and to indicate that in general the same slope applies. The results shown were all taken on new and clean units.

From a practical standpoint we can state that finned-type shell-and-tube heat exchangers of this type have been in commercial use for the following purposes:

- Cooling quench oil.
- Cooling lubricating oil on Diesel engines.
- Cooling circulating oil on hydraulic presses.
- Cooling of air and compressed gases.
- Cooling and condensation of organic vapors.
- Condensation and subcooling of propane.
- Vaporization of organic solvents.
- Cooling of jacket water on Diesel engines.

To date, the performance of the finned tube in the services listed has been satisfactory when designed in accordance with the recommended procedure mentioned before.

As an example of field conditions, a metal-quench-bath oil cooler which had been in operation about 6 months on a continuous system, with oil temperatures varying from 50 F to 200 F, was taken apart and cleaned. Sludge had formed between the fins on the major portion of the bundle, but the edges of the fins were quite visible. On the baffles and tie rods the sludge had bridged over completely, indicating that the finned surface does not offer a firm footing for the sludge. The oil was about 0.9 specific gravity and 100 SSU at 100 F. The fouled performance was about 33 per cent of clean performance. The bundle was removed, sludge cleaned off by pouring solvent over the bundle, then a water hose stream removed most of the foreign material. The bundle was blown clean with compressed air and reinstalled, all in a period of approximately 2 hr. When reconnected the cooler gave approximately new performance.

Quenching-oil duty is relatively dirty and, in our opinion, about as dirty an application as should be considered for this type of finned surface.

CONCLUSION

The availability of a new low-ratio (3.5 to 1) finned tube of extruded manufacture opens a new field of application for liquid-to-liquid heat transfer for finned tubing.

Preliminary experimental results indicate that the surface is active at all points and that the heat-transfer rate from the fluid to the outside of the finned tube is in general somewhat better than that to the bare tube. It is felt that a conservative practice is to base designs on film-heat-transfer rates used for bare tubes for like service, using a minimum Reynolds number of 300.

The resistance to pressure loss is somewhat greater than the corresponding loss to a bare-tube bundle of the same dimensions, but other factors of design are very much more important in determining the pressure loss in a given unit.

Commercial heat exchangers incorporating finned tubes of the type described, are in service on several types of duty. Field experience with these has been satisfactory.

It is recommended that in the interest of furthering the application of finned tubes to industrial heat transfer, extreme care be applied in choosing the type to be used. Finned tubes of

TABLE 1 HEAT-TRANSFER TESTS—OIL IN SHELL TO WATER INSIDE TUBES OF 5-IN. X 6-FT FINNED UNIT

BASIC DATA									
External surface, sq ft.....	57	16.3	0.0069	59%	0.49	0.855			
Internal surface, sq ft.....	57	16.3	0.0069	59%	0.49	0.855			
Crossflow area between baffles, sq ft.....	57	16.3	0.0069	59%	0.49	0.855			
Baffle pitch, in. center to center.....	57	16.3	0.0069	59%	0.49	0.855			
Oil specific heat, at 150 F.....	57	16.3	0.0069	59%	0.49	0.855			
Oil specific gravity, at 150 F.....	57	16.3	0.0069	59%	0.49	0.855			
TABULATED DATA									
Pressure loss through shell, in. Hg.....	Temp oil entering, deg F.....	Temp oil leaving, deg F.....	Temp drop, deg F.....	Viscosity (cp) oil at avg temp, deg F.....	Water flow rate, gpm.....	Temp water entering, deg F.....	Temp water leaving, deg F.....	Temp rise, deg F.....	Heat bal—ance—oil, Btu per hr.....
1.6	177	135.3	41.7	7.6	18.8	36.2	61.2	25	235000
2.92	169	132.2	36.8	8.2	18.4	36.4	62	25.6	234000
3.6	168	127.7	40.3	8.5	19.3	36.2	50	15.2	141000
1.68	175.3	127.7	47.6	8.45	19.3	36.2	50	13.8	129300
1.55	172	124.7	47.3	8.77	19.3	36.2	49.2	13.5	130000
1.53	169.7	122.2	47.5	8.77	15.8	36.2	51.7	15.5	127000
1.40	174.8	125.4	49.4	8.3	15.8	36	50.8	14.8	123000
1.44	170	122.6	47.4	8.55	15.8	36	50	14	120800
1.28	170.4	128.7	41.7	8.33	15.8	35.8	57.6	21.8	191200
2.7	169.4	129.4	40	8.4	15.8	35.8	58.4	22.6	191000
2.65	162	125.6	36.4	9.24	15.8	35.8	56.6	20.8	170500
3.45	164	135.6	28.4	8.3	13.8	36.8	67	30.2	208500
4.5	160.6	133.4	27.2	8.68	13.8	36.8	65.8	29.4	220500
3.7	152	127.8	24.2	9.75	13.8	36.2	62.6	26.4	196500
4.6	152	127.8	24.2	9.75	13.8	36.2	62.6	26.4	196500
Oil flow rate, lb per sec.....	Temp oil entering, deg F.....	Temp oil leaving, deg F.....	Temp drop, deg F.....	Viscosity (cp) oil at avg temp, deg F.....	Water flow rate, gpm.....	Temp water entering, deg F.....	Temp water leaving, deg F.....	Temp rise, deg F.....	Heat bal—ance—oil, Btu per hr.....
2.92	177	135.3	41.7	7.6	18.8	36.2	61.2	25	235000
3.6	169	132.2	36.8	8.2	18.4	36.4	62	25.6	234000
1.68	175.3	127.7	47.6	8.45	19.3	36.2	50	15.2	141000
1.55	172	124.7	47.3	8.77	19.3	36.2	49.2	13.5	130000
1.53	169.7	122.2	47.5	8.77	15.8	36.2	51.7	15.5	127000
1.40	174.8	125.4	49.4	8.3	15.8	36	50.8	14.8	123000
1.44	170	122.6	47.4	8.55	15.8	36	50	14	120800
1.28	170.4	128.7	41.7	8.33	15.8	35.8	57.6	21.8	191200
2.7	169.4	129.4	40	8.4	15.8	35.8	58.4	22.6	191000
2.65	162	125.6	36.4	9.24	15.8	35.8	56.6	20.8	170500
3.45	164	135.6	28.4	8.3	13.8	36.8	67	30.2	208500
4.5	160.6	133.4	27.2	8.68	13.8	36.8	65.8	29.4	220500
3.7	152	127.8	24.2	9.75	13.8	36.2	62.6	26.4	196500
4.6	152	127.8	24.2	9.75	13.8	36.2	62.6	26.4	196500
Oil viscosity, tested, SSU at 210 F.....	Temp oil entering, deg F.....	Temp oil leaving, deg F.....	Temp drop, deg F.....	Viscosity (cp) oil at avg temp, deg F.....	Water flow rate, gpm.....	Temp water entering, deg F.....	Temp water leaving, deg F.....	Temp rise, deg F.....	Heat bal—ance—oil, Btu per hr.....
Oil viscosity, tested, SSU at 100 F.....	177	135.3	41.7	7.6	18.8	36.2	61.2	25	235000
Number of tubes.....	169	132.2	36.8	8.2	18.4	36.4	62	25.6	234000
Counterflow	175.3	127.7	47.6	8.45	19.3	36.2	50	15.2	141000
Single pass both sides.....	172	124.7	47.3	8.77	19.3	36.2	49.2	13.5	130000
Water-side viscosity correction $(\frac{Z}{Z_w})^{0.14}$	169.7	122.2	47.5	8.77	15.8	36.2	51.7	15.5	127000
Film resistance inside tube plus metal resistance, $\frac{1}{h_m} + \frac{1}{h_o}$	174.8	125.4	49.4	8.3	15.8	36	50.8	14.8	123000
Film resistance outside tube, $\frac{1}{h_o}$	170	122.6	47.4	8.55	15.8	36	50	14	120800
Film heat-transfer rate inside tubes.....	170.4	128.7	41.7	8.33	15.8	35.8	57.6	21.8	191200
Film heat-transfer rate on oil side.....	169.4	129.4	40	8.4	15.8	35.8	58.4	22.6	191000
Film heat-transfer rate on water side.....	162	125.6	36.4	9.24	15.8	35.8	56.6	20.8	170500
Over-all heat-transfer rate, U, deg F.....	164	135.6	28.4	8.3	13.8	36.8	67	30.2	208500
MTD, deg F.....	160.6	133.4	27.2	8.68	13.8	36.8	65.8	29.4	220500
deg F.....	152	127.8	24.2	9.75	13.8	36.2	62.6	26.4	196500
deg F.....	152	127.8	24.2	9.75	13.8	36.2	62.6	26.4	196500
deg F.....	152	127.8	24.2	9.75	13.8	36.2	62.6	26.4	196500
deg F.....	152	127.8	24.2	9.75	13.8	36.2	62.6	26.4	196500
deg F.....	152	127.8	24.2	9.75	13.8	36.2	62.6	26.4	196500
deg F.....	152	127.8	24.2	9.75	13.8	36.2	62.6	26.4	196500
deg F.....	152	127.8	24.2	9.75	13.8	36.2	62.6	26.4	196500
deg F.....	152	127.8	24.2	9.75	13.8	36.2	62.6	26.4	196500
deg F.....	152	127.8	24.2	9.75	13.8	36.2	62.6	26.4	196500
deg F.....	152	127.8	24.2	9.75	13.8	36.2	62.6	26.4	196500
deg F.....	152	127.8	24.2	9.75	13.8	36.2	62.6	26.4	196500
deg F.....	152	127.8	24.2	9.75	13.8	36.2	62.6	26.4	196500
deg F.....	152	127.8	24.2	9.75	13.8	36.2	62.6	26.4	196500
deg F.....	152	127.8	24.2	9.75	13.8	36.2	62.6	26.4	196500
deg F.....	152	127.8	24.2	9.75	13.8	36.2	62.6	26.4	196500
deg F.....	152	127.8	24.2	9.75	13.8	36.2	62.6	26.4	196500
deg F.....	152	127.8	24.2	9.75	13.8	36.2	62.6	26.4	196500
deg F.....	152	127.8	24.2	9.75	13.8	36.2	62.6	26.4	196500
deg F.....	152	127.8	24.2	9.75	13.8	36.2	62.6	26.4	196500
deg F.....	152	127.8	24.2	9.75	13.8	36.2	62.6	26.4	196500
deg F.....	152	127.8	24.2	9.75	13.8	36.2	62.6	26.4	196500
deg F.....	152	127.8	24.2	9.75	13.8	36.2	62.6	26.4	196500
deg F.....	152	127.8	24.2	9.75	13.8	36.2	62.6	26.4	196500
deg F.....	152	127.8	24.2	9.75	13.8	36.2	62.6	26.4	196500
deg F.....	152	127.8	24.2	9.75	13.8	36.2	62.6	26.4	196500
deg F.....	152	127.8	24.2	9.75	13.8	36.2	62.6	26.4	196500
deg F.....	152	127.8	24.2	9.75	13.8	36.2	62.6	26.4	196500
deg F.....	152	127.8	24.2	9.75	13.8	36.2	62.6	26.4	196500
deg F.....	152	127.8	24.2	9.75	13.8	36.2	62.6	26.4	196500
deg F.....	152	127.8	24.2	9.75	13.8	36.2	62.6	26.4	196500
deg F.....	152	127.8	24.2	9.75	13.8	36.2	62.6	26.4	196500
deg F.....	152	127.8	24.2	9.75	13.8	36.2	62.6	26.4	196500
deg F.....	152	127.8	24.2	9.75	13.8	36.2	62.6	26.4	196500
deg F.....	152	127.8	24.2	9.75	13.8	36.2	62.6	26.4	196500
deg F.....	152	127.8	24.2	9.75	13.8	36.2	62.6	26.4	196500
deg F.....	152	127.8	24.2	9.75	13.8	36.2	62.6	26.4	196500
deg F.....	152	127.8	24.2	9.75	13.8	36.2	62.6	26.4	196500
deg F.....	152	127.8	24.2	9.75	13.8	36.2	62.6	26.4	196500
deg F.....	152	127.8	24.2	9.75	13.8	36.2	62.6	26.4	196500
deg F.....	152	127.8	24.2	9.75	13.8	36.2	62.6	26.4	196500
deg F.....	152	127.8	24.2	9.75	13.8	36.			

low ratio and close fin spacing should not be used where the fouling is severe, or where the fluid is definitely corrosive to the tube metal available. There are a number of applications where the finned tube is not mathematically desirable, principally where the film rate on the finned side is equal to or greater than the film rate on the plain side.

Appendix

Tables 1, 2, and 3 make up the Appendix.

TABLE 2 CALCULATIONS FOR HEAT-TRANSFER CURVE.

$$\frac{DG_s}{\mu} \text{ VERSUS } \left(\frac{h}{cG_s} \right) \left(\frac{c\mu}{k} \right)^{2/3}$$

BASIC DATA

c = specific heat, taken at 0.49 (from TEMA Standards)
 D = tube diameter 0.0547 ft
 G_s = shell-side mass velocity, lb/(hr)(sq ft). Leakage factor omitted
 k = thermal conductivity, taken at 0.074 Btu/(hr)(sq ft)(deg F/ft) (from TEMA Standards)
 μ = viscosity at average body temperature, lb/(hr)(ft)

TABULATED DATA

G	μ	$\frac{DG_s}{\mu}$	$\left(\frac{c\mu}{k} \right)^{2/3}$	h_s	$\frac{h_s}{cG_s}$	J
157200	18.4	468	24.5	71.95	0.000932	0.0228
194000	19.85	535	25.8	77.5	0.000815	0.0210
90500	19.6	253	25.6	33.1	0.000748	0.0192
83500	20.5	223	26.5	31.3	0.000765	0.0203
83500	21.2	216	27.1	29.35	0.000716	0.0194
78600	20.1	214	26.1	29.20	0.000758	0.0198
77500	20.7	205	26.6	28.25	0.000745	0.0198
77500	20.9	203	26.7	26.50	0.000698	0.01865
140000	20.2	379	26.2	52.1	0.000760	0.01990
145500	20.3	393	26.25	55.30	0.000775	0.0204
142800	22.4	348	28	51.3	0.000735	0.0206
242300	20.1	660	26.1	100.0	0.000838	0.0219
242300	21.0	645	26.8	98.0	0.000806	0.0216
248000	24.6	551	29.8	87.7	0.000723	0.0216

J = dimensionless number $\left(\frac{h_s}{cG_s} \right) \left(\frac{c\mu}{k} \right)^{2/3}$

TABLE 3 PERFORMANCE DATA AND CALCULATIONS FOR 16-IN-SHELL \times 8-FT-TUBE-LENGTH FINNED-TUBE AIR AFTER-COOLER; AIR IN SHELL, WATER IN TUBES

BASIC DATA

Number of tubes	154
Length of tubes, ft	8
Outside surface, sq ft	616
Inside surface, sq ft	176
Arrangement	Air-single pass Water-two pass
Baffle pitch, in	10
Area for crossflow over tubes, sq ft	0.443
Water quantity, gpm	15.0
Water temperature:	
Entering, deg F	40
Leaving, deg F	82
Air quantity, lb per hr	9000
Air temperature:	
Entering, deg F	210
Leaving, deg F	64

CALCULATIONS

Greater temperature difference	Lesser temperature difference
210	64
82	40
128	24

Uncorrected MTD..... 62 deg F
 To correct MTD refer to pass-correction plot (TEMA Standards, p. 20)

$$K = \frac{42}{170} = 0.247$$

$$R = \frac{146}{42} = 3.47$$

F is on flat of curve. The most conservative estimate gives F as a maximum value of 0.55

Corrected MTD = $62 \times 0.55 = 34.1$ deg F

Heat load = $15 \times 500 \times 42 = 315,000$ Btu per hr

Heat-transfer rate = $\frac{315,000}{34.1 \times 616} = 15.0$ Btu/(hr)(sq ft)(deg F)

Discussion

R. G. VANDERWEIL.⁴ It seems quite encouraging that this paper gives the designing engineer a chance to compare test data with actual data taken on commercial heat-transfer equipment. As to the use of finned and unfinned surfaces, the writer would like to complement the author's statements with the following:

It seems that the only criterion not only in selecting between finned or unfinned tubes, but also in selecting the fin spacing, thickness, and the width of the fin, is the ratio of the two film coefficients f_i/f_o .

In this connection, the writer would like to know if tests have been carried out with one fin arrangement only, or by any chance a second set of tubes with fins of less thickness and pitch but of the same width has been tested? Finally, it would be interesting to know how the over-all heat output of exchangers compares if shells of the same over-all dimensions are used and provided with prime surface in one case and with finned tubes in another.

AUTHOR'S CLOSURE

It should be emphasized that the tests were made on equipment of commercial scale and may not entirely agree with tests on single tubes or tests made under conditions which might be different from commercial practice.

It is suggested by Mr. London that there may be a break in the curve in Fig. 5 resulting in a change of slope, at the point where there may be a change-over from viscous flow to turbulent flow. The available data are found to be so scattered, however, that there is no clear-cut line, and frankly at this time we feel that the accuracy of the test data reported so far in the literature would not allow that much refinement.

The tests reported cover only one type of finned tube. This type is the only type tested and was chosen for a combination of mechanical and thermal reasons. It is a question of using an available tube which has desirable features mechanically and which for a number of uses is also suitable thermally. To cover a wide range of applications different ratios can be employed, but testing these goes beyond the scope of this paper.

Mr. Donahue suggests that the data be plotted using the Nusselt method rather than Dr. Colburn's method which has been used. This may well give a better agreement and it is regretted that the time to do this has not been available.

The tests were made using comparatively clean city water, which is not thought to have had much tendency toward fouling in the time the tests were run. The orifices were calibrated by separate calibration runs during which the fluid discharged was actually weighed.

The question has been raised whether the type of finned tube used has given difficulty from cutting tube walls at the baffle or tube support due to vibration. So far in normal crossflow service we have seen no evidence of this—certainly no greater tendency on the part of this tube than on a bare tube. Most duties have been with close baffle pitches where the tendency toward extreme vibration is considerably curbed.

Again it must be stressed that this report is preliminary in nature and is only a first indication of what may be expected from shell-and-finned-tube exchangers of this type. A number of these are in commercial service and so far have proved satisfactory.

⁴ Office of Consulting Engineer, Chase Brass & Copper Company, Waterbury, Conn.

Heat-Transfer Coefficients and Other Data on Individual Serrated-Finned Surface

By E. A. SCHRYBER,¹ BROOKLYN, N. Y.

The purpose of this paper is to provide data on the serrated (segmented) type of finned surface; also to show the ease of fabrication and the flexibility of sizes, i.e., the ability to alter the ratio of secondary to prime surface without difficulty.

THE individual serrated-finned surface under discussion is made from relatively thin flat metal strip. As the finned surface is wound around the tube, each individual fin takes the shape, roughly, of the letter L. The foot of the L is the shoulder of the fin and is used to secure a bond between the fin and the tube wall. The thickness, width, and length of the fin may vary to suit the need, but the general appearance and method of manufacture remain the same. The shoulder, or base, of the finned surface is continuous and is wound around the tube in a helical manner. The individual fins, being perpendicular to the shoulder, are caused by this winding operation to stand out from the tube in much the same manner as spokes from the hub of a wheel. Each individual fin is given a slight twist so that its flat surfaces do not follow the helical wind but lie in planes parallel to all other fins and perpendicular to the axis of the tube. These details are indicated in Fig. 1.

With the serrated form of tube surface, no material is removed in forming the fins. The total width of all the fins in one row will therefore substantially equal the circumference of the tube. The fin height times the circumference of the tube, doubled to cover the area of both sides of the fin, plus the area of the fin edges, will substantially total the area of one row of fins. Where the same fin length is used, larger- or smaller-diameter tubes will have a surface area directly in proportion to the diameter of the tube. Changing the number of rows of fins per inch of tube or using longer or shorter fins will give a wide range of ratios of secondary to prime surface.

It is not the purpose of this paper to go into a lengthy discussion of the relative value of individual serrated surface compared with other surface designs. Considerable work has been done by others, among them the interesting paper by Norris and Spofford.² Evidence has frequently been presented that the design of extended surface greatly influences its over-all heat transfer per square foot of surface and per foot of tube length. Extensive laboratory tests³ were made to establish the performance data for the surface under discussion. An all-copper tube, solder-bonded, was used, having a $\frac{5}{8}$ -in. tube, $1\frac{1}{2}$ in. diam over the fins, 7 rows of fins per inch. The results, together with a description of the test apparatus and procedure, follow.

¹ Extended Surface, Inc.

² "High-Performance Fins for Heat Transfer," by R. H. Norris and W. A. Spofford, Trans. A.S.M.E., vol. 64, July, 1942, pp. 489-495.

³ These tests were made in the laboratory of The Pennsylvania State College under the personal supervision of H.A. Everett and F. C. Stewart, and the results presented in a private report from which the data herewith are abstracted.

Contributed by the Heat Transfer Division and presented at the Annual Meeting, New York, N. Y., Nov. 27-Dec. 1, 1944, of THE AMERICAN SOCIETY OF MECHANICAL ENGINEERS.

NOTE: Statements and opinions advanced in papers are to be understood as individual expressions of their authors and not those of the Society.

DETAILS OF TEST SETUP

The construction details of the test setup should be carefully noted, Figs. 2 and 3. They were selected to give the nearest approach to basic data and take into consideration the fact that units of this sort are sensitive to installation details, such as rounded versus sharp edges, and forced versus induced convection. Air was drawn through the test section, thence through the calibrated bellmouth orifice, by which the quantity of air was measured, then through an exhaust fan which was operated at various speeds. Air temperatures were taken by thermocouples ahead and behind the heater section, all shielded by aluminum foil to minimize radiation errors. The flow of air was measured at the bellmouth orifice by a pitot tube.

Three assembly units were tested. The first was a single row of 15 vertical tubes, each 2 ft long, assembled on $1\frac{1}{2}$ -in. centers. The gross duct area was practically 4 sq ft (2 ft \times 2 ft) where occupied by the coil. The second assembly consisted of two rows, each identical to the single-row section, but placed with the second row slightly offset so that the center line of the rear row of tubes was at the mid-point of the front row (known as staggered arrangement). The third test assembly consisted of three rows of tubes, all identical, and also assembled in a staggered arrangement.

Table 1 gives the important dimensions of the units tested.

TABLE 1 UNIT DIMENSIONS

	Unit 1	Unit 2	Unit 3
Tube inside diameter, in.	0.575	0.575	0.575
Tube outside diameter, in.	0.652	0.652	0.652
Outside diameter extended surface, in.	1.5	1.5	1.5
Thickness extended surface, in.	0.010	0.010	0.010
No. of fins per inch.	7	7	7
Numbers of rows.	1	2	3
Number of tubes per row.	15	15	15
Air-side area, sq ft per ft tube.	1.245	1.245	1.245
Air-side area of unit, sq ft.	37.4	74.8	112.2
Steam-side area of unit, sq ft.	4.51	9.02	13.53
Ratio air-side to steam-side area.	8.29	8.29	8.29
Approach-face area, sq ft.	3.9	3.9	3.9
Net area between tubes, sq ft.	2.03	2.03	2.03
Length of tubes, ft.	2	2	2

Three sets of curves represent the results of these tests. Only the over-all coefficient of heat transfer and pressure-drop⁴ curves are shown here, Figs. 4 and 5. Equations for the heat-transfer curves are as follows:

$$\text{Row (1)} \quad U = 0.165 G^{0.523}$$

$$\text{Rows (2)} \quad U = 0.143 G^{0.542}$$

$$\text{Rows (3)} \quad U = 0.0838 G^{0.6}$$

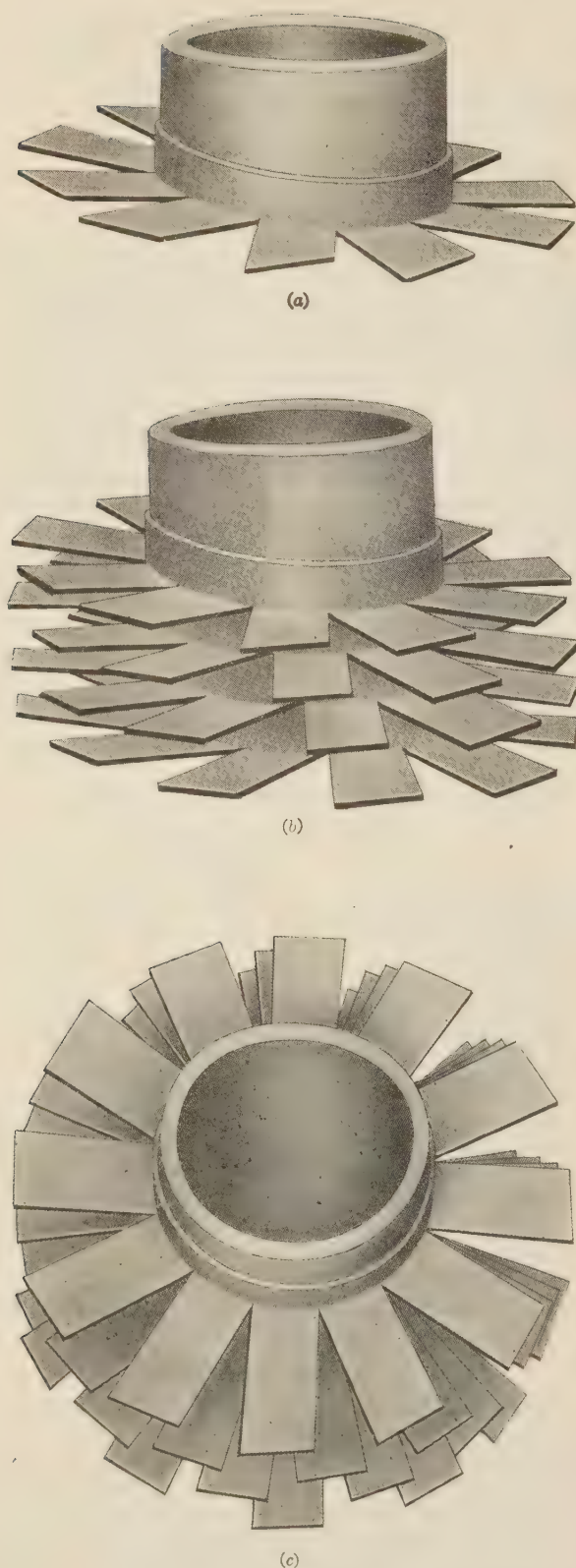
$$U = \text{Btu per hr per sq ft total air-side area per deg F, L.T.D.}$$

$$G = \text{lb air per hr per sq ft net or free area}$$

CONDUCTING THE TESTS

As the test runs were being conducted, a check was made from time to time of the heat balance between the air-temperature rise and the steam condensed. As this balance was found to be in accord, within reasonable test limits, the tests were recorded and

⁴ The schematic drawing of the test layout, Fig. 3, shows an ordinary slant gage as the device for determining the pressure drop through the test sections. However, to insure utmost accuracy, a manometer calibrated in thousandths of an inch was used to determine the exact pressure drop as shown on the curves.



checked using the air-temperature rise to calculate the total Btu transfer. Special care was taken to limit heat losses so that the heat taken up by the air would equal the heat given up by the steam.

Reference to the schematic drawing of the test apparatus, Fig. 3, will show five thermocouples, connected in series, ahead of the test section to measure the temperature of the incoming air. Behind the test section are nine thermocouples, connected in three series of three each, to measure leaving-air temperature. There is an air-mixing and straightening chamber about 4 ft long immediately behind the test section, at the discharge end of which was placed the nine thermocouples. Checking one series of thermocouples against another, on the discharge side, indicated an even temperature distribution at this point.

Attention is called to the fact that but one-, two-, and three-row assemblies were tested. The primary objective of these tests was to ascertain the heat-transfer characteristics and pressure-drop characteristics of the surface design. The results of these tests therefore are not directly comparable with tests of multi-row assemblies.

METHOD OF MANUFACTURE

To build the individual serrated-finned-surface tube, a simple but complete machine designed solely for this purpose is used. The bare tube is fed into the side of the machine and reels of fin stock are fed from the rear. The turning and forward progression of the tube, the serrating and bending of the fin stock, the winding of the fin stock on the tube, are all accomplished simultaneously and synchronized. The use of wider or narrower fin stock will result in longer or shorter fins, but the fabricating operation remains the same. Also, by winding the fins at a greater or lesser number of turns per inch the ratio of prime to secondary surface can be altered at will.

Securing the fins to the tube is accomplished in one of two ways. Either the tube, as it passes through the winding operation, now progresses through a fluxing and soldering bath, or the shoulder of the fins is welded to the tube by continuous electric-resistance welding simultaneously with the winding operation. All nonferrous metals can be easily bonded by the soldering method. Capillary attraction causes the solder to flow under the shoulder of the fin creating a metallic bond with an area far greater than the cross-sectional area of the fin itself. Most metals can be readily resistance-welded by known techniques and some of the more difficult metals to weld, including aluminum and copper, are now being welded, and commercially acceptable welding techniques are being developed. The joining of metals by welding, as it applies to extended-surface tubes, opens a new field for this product. Subzero temperatures, as well as very high temperatures, can be handled without thought to bond rupture or disintegration. This development of the resistance-welding method of securing a bond is a substantial improvement over metallic or mechanical bonds.

For the handling of corrosive fluids or gases on either side of the tube, bimetal extended-surface tubes can be fabricated by the welding method to the great advantage of the coil designer. Combinations of bimetal tubes using steel, copper, monel metal, cupronickel, admiralty metal, etc., can be fabricated. In this manner the most durable and satisfactory metal surface, either inside or on the outside of the tube, can be presented to the destructive action of many commonly handled materials, such as hot oil, ammonia, acid or alkaline solutions, many corrosive gases, etc. Fin materials would be the same as the outside surface of the tube thereby presenting a corrosion-resistant surface with a welded bond. The structure of the bond would be such that durability, and full flow of heat through this important point could be expected.

FIG. 1 DETAILS OF SERRATED-FINNED TYPE OF TUBE SURFACE

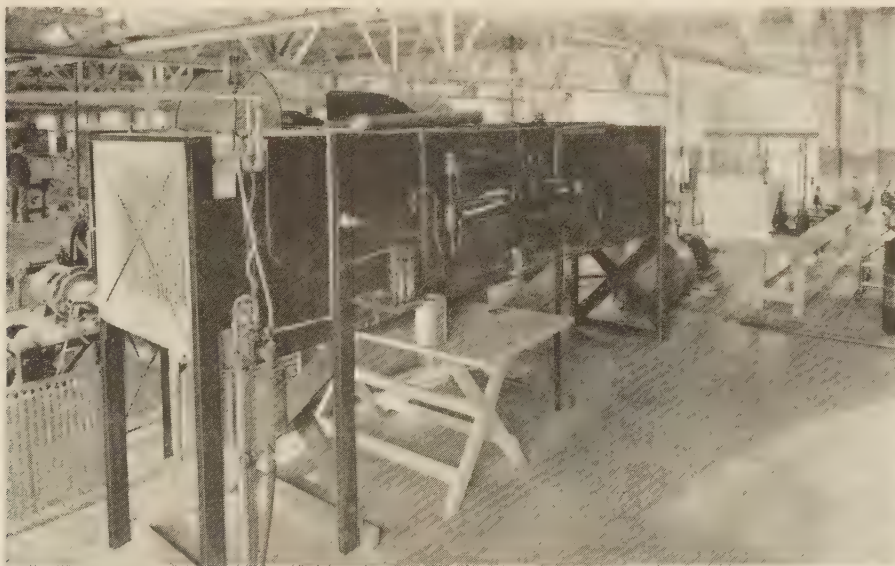


FIG. 2 VIEW OF TEST APPARATUS SET UP IN LABORATORY

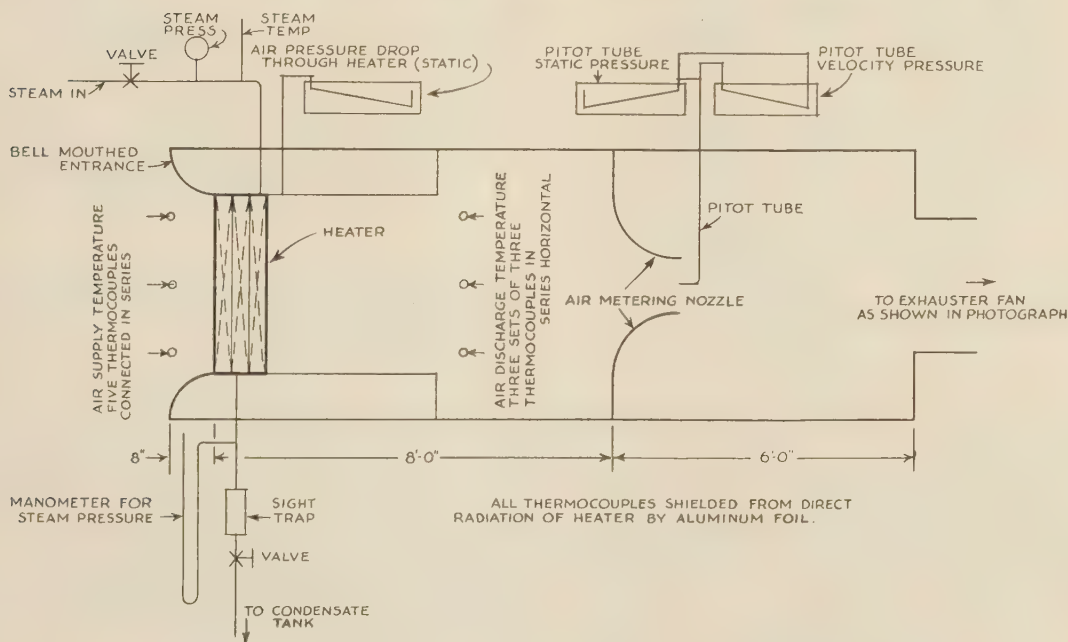


FIG. 3 SCHEMATIC DIAGRAM OF TEST APPARATUS

SPECIAL APPLICATIONS

Distinct and apart from the foregoing tests has been the application of individual serrated-finned surface in tube-within-tube heat exchangers. In this application the V-shaped openings between the individual fins form a definitely controllable and computable free opening in direction of flow. Full test data on the performance of this surface in such applications is not presently available. While the surface arrangements are not directly comparable, the paper by Gunter and Shaw⁵ shows the value of many

short surfaces, instead of long continuous-surface arrangements, in direction of flow. Of similar character is the application of extended-surface tubes in standard shell-and-tube heat exchangers. Their definite worth is being demonstrated in many installations; however, their comparatively recent widespread use is handicapped by the lack of generally acceptable data except for specific applications.

Individual segmented-finned surface, because of its high heat-transfer coefficient, is economical to use. If higher values of U are obtained per square foot of outside surface, it is axiomatic that economy of surface, and therefore economy of metal used, will result. For full commercial realization of this economy of de-

⁵ "Heat Transfer, Pressure Drop, and Fouling Rates of Liquids for Continuous and Noncontinuous Longitudinal Fins," by A. Y. Gunter and W. A. Shaw, Trans. A.S.M.E., vol. 64, 1942, pp. 795-802.

OVERALL COEFFICIENT HEAT TRANSFER VS
POUNDS OF AIR PER HOUR PER SQ. FT. NET AREA
DRAW THROUGH FAN STEAM 5 POUNDS GAGE

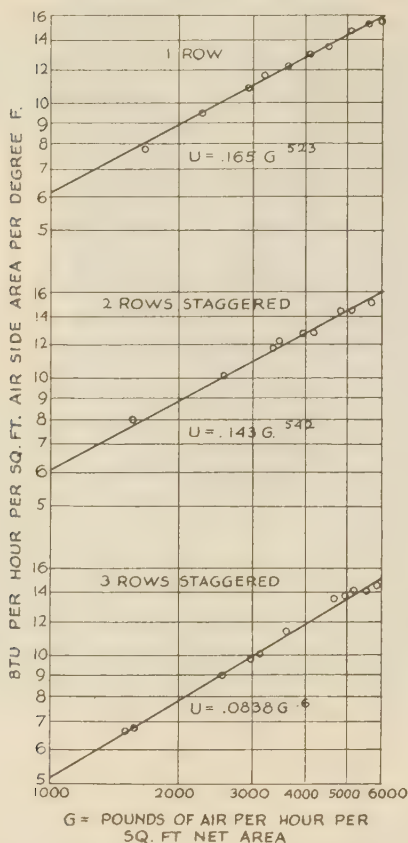


FIG. 4 OVER-ALL COEFFICIENT OF HEAT TRANSFER VERSUS POUNDS OF AIR PER HOUR PER SQUARE FOOT NET AREA DRAW THROUGH FAN
(Steam 5 lb per sq. in. gage.)

sign, it is necessary that it be coupled to economy of manufacture. Rapid automatic single-purpose machines, building the tube in one operation, complete the team of engineering and technological progress. Individual segmented-finned surface which can be made with a wide range of fin lengths, with a wide range of fin spacings per inch and wound on any size of tube, is therefore an extended-surface tube, the design of which gives use and manufacturing economy.

Discussion

R. G. VANDERWEIL.* Is it possible to apply successfully the soldering and welding equipment mentioned to narrowly spaced fins, say $1/16$ in. spacing, of a height of 1 to 2 in.? Another question arises in connection with the application of the flux: We have found that the flux applied between fin and tube will accumu-

* Office of Consulting Engineer, Chase Brass & Copper Company, Waterbury, Conn.

PRESSURE DROP THROUGH HEATER VS POUNDS OF AIR PER HOUR PER SQ. FT. NET AREA ISOTHERMAL FLOW 80° AIR DRAW THROUGH FAN

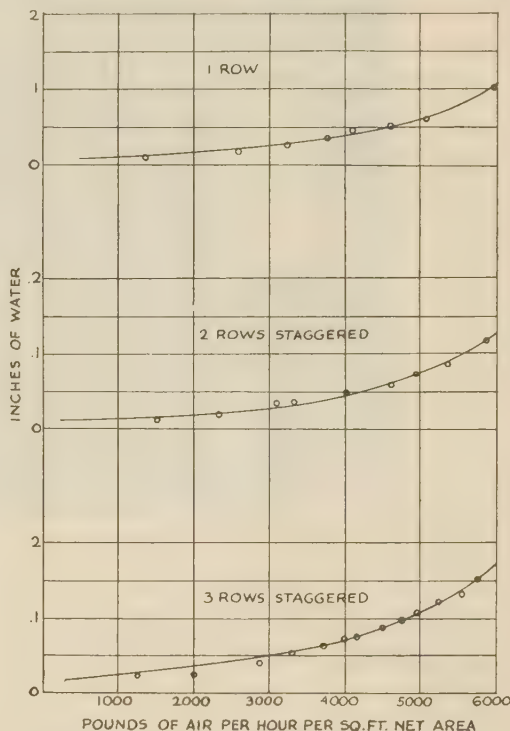


FIG. 5 PRESSURE DROP THROUGH HEATER VERSUS POUNDS OF AIR PER HOUR PER SQUARE FOOT NET AREA
(Isothermal flow, 80 F air draw through fan.)

late at certain spots in the joint and thus decrease the effectiveness of the bond. This is particularly true for fins of small spacing and where no openings were provided to accommodate the exit of the flux from the joint.

AUTHOR'S CLOSURE

In reply to the questions by Mr. Vanderweil, the fabrication of narrowly spaced fins, both solder-bonded and welded, has been done experimentally. However, there is a practical difficulty; the foot of the fin strip must be strong enough to stand the stress of fabrication and is usually not less than $7/16$ in. wide. Therefore, the building of tubes of more than 8 rows of fins per inch necessitates a partial overlapping of the fin shoulder. This overlapping brings up new problems and the fabrication of very narrowly spaced fins has not been done in normal production. The height of the fin is of no consequence.

It has been the practice to use an aqueous mixture of ammonium chloride and zinc chloride, together with a wetting agent, in mild solution as a flux. This is jetted on the tube after the winding operation, and thoroughly wets all exterior surfaces. The surface between the tube wall and the fin shoulder is wetted by capillary attraction. The molten solder, applied immediately after and in like manner, apparently flushes off all acid residue. No evidence of acid inclusion has yet been found.

Disk Extended Surfaces for High Heat-Absorption Rates

By G. E. TATE¹ AND JOHN CARTINHOUR,² NEW YORK, N. Y.

Four types of disk-on-tube extended-surface heat exchangers are discussed in this paper, i.e., interlocking cast-iron sections of nine disks each; die-cast aluminum-alloy disks each with shroud and hub; two surfaces die-pressed from wrought-iron sheet, each with a flue; and one a sixteen-pronged star. Data for both the cast-iron and aluminum surfaces were obtained from tests of full-sized economizers in conjunction with boiler tests, while data on the wrought-iron disks were obtained from laboratory studies. Details are given of the testing procedure, and the results in terms of effectiveness of the various surfaces are analyzed and correlated.

THE advantages of using extended surfaces in commercial-sized heat exchangers have long been generally recognized. Convenient proportions, greater compactness, fewer pressure joints, ease of arranging counterflow of the heat-exchanging fluids, and ease of achieving equal flows in the parallel circuits being traversed are the principal advantages realized. A requisite of commercial heat exchangers, unless their use is to be restricted to clean fluids, is provision for cleaning the heat-exchanging surfaces with ease and speed. A type of extended surface having these features is the disk-on-tube, four varieties of which are illustrated in Figs. 1 to 3, inclusive.

TYPES OF HEAT-ABSORBING SURFACES

The first variety, Fig. 1, consists of interlocking cast-iron sections of nine disks each, shrunk onto steel tubes. Sand molds are used in the casting process. The internal surface, which is to be in contact with the tube, is broached to a diameter slightly less than that of the tube; the joint faces are finished on semiautomatic machines. The external surface requires neither machining nor finishing. The contact between tube and cast-iron section, after the latter is shrunk on, has a thermal resistance of the order of 0.002 deg F hr/Btu per ft length of finned tube. This value includes the resistance of the hub metal.

This form of extended surface has been most frequently applied to superheaters and economizers for stationary and marine boilers, waste-heat boilers, and oil heaters. Another interesting application is to gas coolers for chemical processes where the resistance of cast iron to highly corrosive gases is utilized. For example, cast-iron surface is advantageously used in the sulphur-dioxide coolers required after the initial sulphur-burning step of the contact process of making sulphuric acid. Here the primary function of the heat exchanger is to cool the reactant mixture of gases to the temperature required for the next step; the conservation of useful heat is a valuable secondary function.

The second type, Fig. 2, consists of individually die-cast aluminum-alloy disks, each having a shroud and hub. The

2" x 4 1/8" CAST IRON GILLED RING

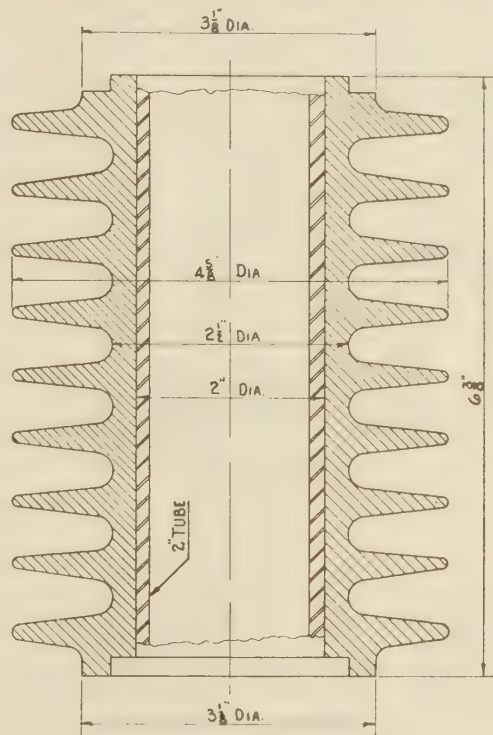


FIG. 1

accuracy of the casting and the condition of its surface are such as to require no machining. In assembly a hydraulic ram is used to force each disk, the internal diameter of which is less than the outer diameter of the tube, onto the tube and against the preceding disk. As may be seen from the assembly figure, the tip of the shroud of the preceding disk is encased in a groove in the leading end (gill) of the disk being put in place. At the same time, the steel hoop ring is forced onto the hub underneath the shroud. Tubes of particularly close tolerance are used in order to insure good contact between hub and tube.

Under service conditions the hoop ring and tube expand less than the aluminum hub, on account of the lower coefficient of thermal expansion of steel. The function of the hoop ring is to hold the aluminum hub in good thermal contact with the tube. The thermal resistance of this contact, including the metal of the hub, is approximately 0.002 deg F hr/Btu per ft length of finned tube. This value represents a mean of extensive tests wherein test elements 1 ft long and comprising 22 disks are heated in a 9-kw electric furnace. The element is in effect the heating surface of a natural-circulation boiler, and the heat absorbed is obtained from the measured electric power as well as from the steam pro-

¹ Research Physicist, Foster Wheeler Corporation.

² Engineer, Foster Wheeler Corporation.

Contributed by the Heat Transfer Division and presented at the Annual Meeting, New York, N. Y., Nov. 27-Dec. 1, 1944, of THE AMERICAN SOCIETY OF MECHANICAL ENGINEERS.

NOTE: Statements and opinions advanced in papers are to be understood as individual expressions of their authors and not those of the Society.

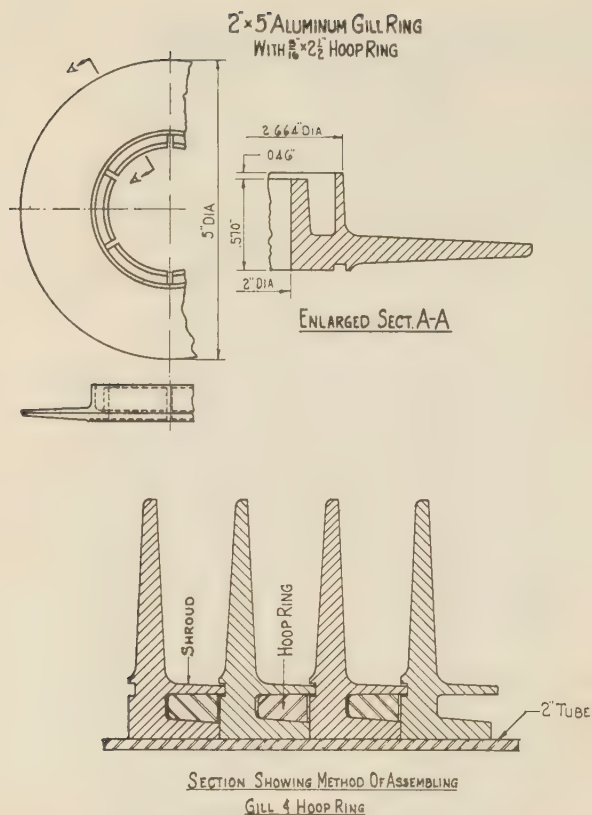


FIG. 2

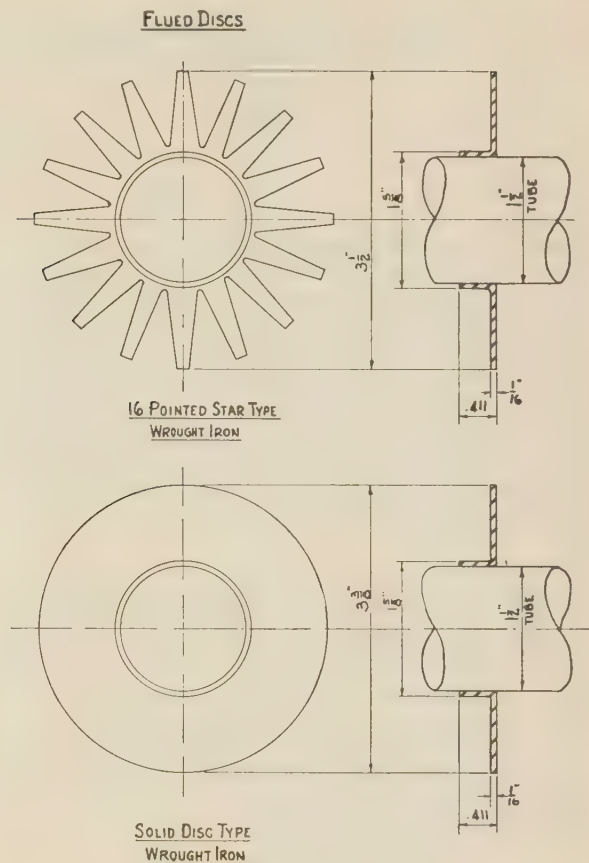


FIG. 3

duced. The temperature of the disks, hubs, and tube are measured with thermocouples.

The aluminum disk was developed for application to economizers of marine boilers where space and weight are of primary importance. Its use obviously is not limited to this application. A limit to the maximum, feasible, heat-absorption rate does exist, however, as the tips of the disks must be kept below the softening temperature (approximately 1000 F). By means of the theoretical formulas of Schmidt (1),³ which relate the temperature drop, fin tip to base, to the heat-absorption rate, the theoretically safe maximum rate of heat absorption can be expressed as a function of tube temperature. In actual service a heat-absorption rate of 43,000 Btu/hr per ft length of 2-in. tube has been reached with a tube temperature of 480 F, without impairment of the tips of the disks.

The third and fourth surfaces are formed from wrought-iron sheet by a series of die-press operations. The resulting shape is a disk with a flue. In one case portions of the disk are cut out by stamping, leaving a sixteen-pronged "star." Wrought iron is used because of its thermal conductivity and ductility. These disks are then attached to the tube by seam-welding the flues to the tubes by means of automatic welding machines. Fusion between the metal of the flue and that of the tube takes place over approximately 50 per cent of the flue width. The thermal resistance of the flue, including the weld, is found to be less than 0.002 deg F hr/Btu per ft length of finned tube. These disks are used in economizers where weight and space are at a premium.

³ Numbers in parentheses refer to the Bibliography at the end of the paper.

TAKING TEST DATA

The data for both the cast-iron and aluminum surfaces were obtained from tests of full-sized economizers in conjunction with tests of the boilers proper. The flue-gas temperature ranged between 1150 F maximum at the inlet and 200 F minimum at the outlet; the inlet feedwater temperature ranged between 150 F minimum and 410 F maximum. In the aluminum-ring-economizer tests the fuel was oil, while for the cast iron several types of coal are included, as well as oil.

It is recognized that the accuracy of some of the data is not of a high order. True average gas temperatures are difficult to measure on large-scale equipment, particularly at the inlets of economizers placed close to the boiler outlet, where little mixing of the gas has taken place. Radiation losses from thermocouples also add to the difficulty. Hence a selection from the data obtained over a period of several years was made, using the heat balance as a criterion in judging the accuracy of the temperature measured with thermocouples. Only tests in which the feedwater flow, the fuel-consumption rate, the fuel analysis, and the flue-gas analysis were accurately determined are included.

The data presented on the wrought-iron disks were obtained by laboratory tests of air heaters, wherein room air passing over the fins was heated by steam condensing inside the tubes. Finned elements 1 ft long were arranged in staggered rows, four elements in each of the five rows, on $4\frac{1}{8}$ -in. equilateral centers. Dummy half-elements were used at each end of alternate rows in order to effect the same flow pattern around the end elements as obtained about the middle ones. The tubes were vertical in order to

insure free drainage of the condensate. The temperature of the air was measured by means of thermometers in regions where the air was well mixed. Standard orifices were used to meter the air. The heat absorbed by the air was in good agreement with the heat given up by the steam, as calculated from the measured quantity of condensate, steam pressure and temperature, and condensate temperature.

The results of the laboratory tests have been compared with tests on economizers used to cool the flue gas from boilers with the feedwater, and substantial agreement was found. The data from the laboratory tests are presented in preference to those from full-sized economizers for two reasons:

- 1 Absence of soot.
- 2 Small variation of thermal properties of the air over the small temperature range obtaining.

As a matter of interest results of a test of unflued disks $4\frac{3}{4}$ in. diam and $\frac{1}{16}$ in. thick, silver-soldered to 2-in. tubes, have been included. Five staggered rows, each of three tubes 1 ft long, comprised the air heater. The tubes were on $5\frac{1}{4}$ -in. centers.

From the over-all coefficients of heat transfer from the gas to the water U' , the corresponding coefficient of heat transfer from gas to fin surface h , was computed by means of the relation

$$1/h = 1/U' - (S_1 + S_2)\Sigma R$$

Here ΣR is the sum of the following thermal resistances: Fluid inside tube to inner tube wall; the rust layer on this surface; the tube wall itself; contact between tube and flue, or hub; flue or hub; disk. No allowance for soot deposits on the fin and flue surface was made in the case of the full-sized economizers, because of the arbitrary assumptions that would be involved.

In calculating the resistance of the inner fluid, also that of the tube wall, the ample data of various investigators (2) were utilized. The resistance of the rust deposit was calculated from its measured thickness on the assumption that the deposit was porous and therefore the thermal conductivity was equal to that of the water filling the pores.

The method of measuring the thermal resistance of the contact between tubes and aluminum hub, together with that of the hub, in the electric furnace has been described previously. This method was applied to the shrunk-on cast-iron elements and to the wrought-iron disks having their flues welded to the tubes. In the latter case a more rapid test by electrical means was also employed, wherein a current of 200 amp was passed into the periphery of one disk, and the voltage drops along the flue and across to tube were explored by means of a probe and a precision millivoltmeter. The electrical resistivity of the flue material was

HEAT TRANSFER COEFFICIENTS

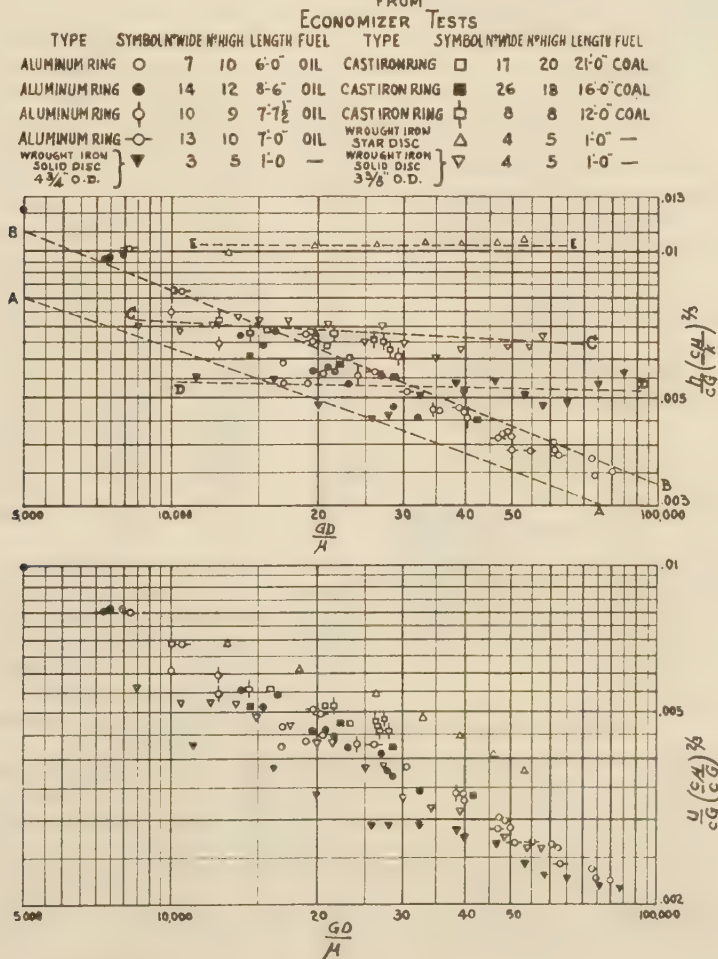


FIG. 4

measured, using specimens machined to accurate dimensions, and the thermal conductivity was deduced approximately by means of data available in the literature (3).

The average value of the ratio, length of path to cross-sectional area of path, was calculated from the electrical resistance and resistivity. The shape factor so obtained, when divided by the thermal conductivity, gave the thermal resistance. However, before comparing with the results of the first method (measured temperatures and heat-absorption rate), an allowance had to be made for the heat absorbed by the flue direct from the gas. When this was done the results of the two methods were found to be comparable.

Probably a more satisfactory electrical method, except from the standpoint of routine tests of full-sized elements, would be to surround a disk and flue with mercury, thus providing an anode analogous to the gas from which heat is transferred in the thermal case. In this manner the resistance from anode to the tube, or including it, could be obtained from the measured current, voltage drop, and resistivity of the fin material. If the flue were cut away the resistance of the disk alone could be obtained; thus the adequacy of the theoretical treatment of variously shaped disks could be checked.

Values of the thermal resistance of the disks were calculated by means of theoretical formulas derived by Harper and Brown (4). A graphical representation of disk resistance and effectiveness, based on the foregoing theoretical analysis, is shown in Fig. 5. Here h is the heat-transfer coefficient from gas to fin surface, U that from gas to base of disk, and M is

$$2k_{eff} \sqrt{D_1}/\sqrt{D_2} (D_2 - D_1)^2$$

M/h and M/U are dimensionless. The derivation is discussed in the Appendix.

In the case of a disk and shroud, e.g., Fig. 2, we have in effect two fins of unequal dimensions in parallel. If we assume that the values of the coefficients of heat transfer from gas to fin surface are the same for both disk and shroud, the respective heat flows are

$$Q_1 = ehS_1 \times \text{temperature drop from gas to hub}$$

$$Q_2 = EhS_2 \times \text{temperature drop from gas to hub}$$

Defining U and U' by the relation

$$Q_1 + Q_2 = U(S_1 + S_2) \times \text{temperature drop gas to hub} \\ = U'(S_1 + S_2) \times \text{temperature drop gas to water}$$

$$\text{we obtain } \frac{1}{U'} - (R_s + R_r + R_w + R_e)(S_1 + S_2) = \frac{1}{U}$$

$$= \frac{1}{h} \frac{S_1 + S_2}{eS_1 + ES_2}$$

Treating the shroud as a strip, receiving heat on one side only, its effectiveness e , was calculated from the well-known hyperbolic-tangent formula, and the disk effectiveness E was read from Fig. 5; so a plot of

$$\frac{1}{U'} \text{ versus } \frac{1}{h} \frac{S_1 + S_2}{eS_1 + ES_2}$$

was prepared. From this subsidiary graph values of h , corresponding to test values of U' , were easily computed.

CORRELATION OF TEST DATA

The values of h calculated in the manner described were incorporated into the dimensionless group $(h/cG)(c\mu/k)^{2/3}$, and plotted against Reynolds number DG/μ , as shown in Fig. 4. Here the mass flow of the gas G is that through the minimum area available. The equivalent diameter D , used in Re is that of a

THERMAL RESISTANCE OF DISC FINS

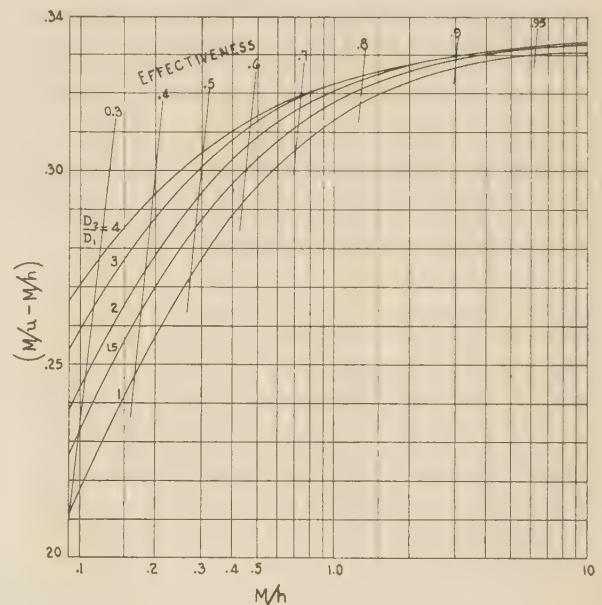


Fig. 5

cylinder having the same projected area as the finned tube. It was chosen somewhat arbitrarily. The particular grouping of the heat-transfer factors used here is preferred because the diameter, the choice of which is to be substantiated, appears only in the abscissa.

Values of U were plotted in the same manner, as shown in the lower plot of Fig. 4. In Table 1 the various resistances, the

TABLE 1 RESISTANCES, DIMENSIONS, AND THERMAL CONDUCTIVITIES OF VARIOUS SURFACES

Surface	Cast iron	Aluminum	3 ³ / ₈ -In. wrought iron	4 ³ / ₈ -In. wrought iron	Star
D_1	0.208	0.225	0.134	0.167	0.134
D_2	0.387	0.417	0.282	0.396	0.292
D	0.275	0.282	0.158	0.201	0.158
S	3.10	4.50	3.29	6.50	2.16
d_1	0.139	0.139	0.100	0.146	0.100
d_2	0.167	0.167	0.125	0.167	0.150
R_r	0.0023	0.0035	0	0	0
R_T	0.0030	0.0045	0.0039	0.0046	0.0026
R_e	0.0060	0.0090	0.0061	0.0070	0.0040
kT	29	87	36	36	36
kT	29	29	29	29	29
t_F	0.0207	0.0117	0.0052	0.0052	0.0052

sum of which was subtracted from the over-all resistance in obtaining U , are listed together with pertinent dimensions and thermal conductivities. U was chosen in preference to the over-all heat-transfer coefficient U' , in order to show the characteristic performance of the various disks unencumbered by the particular resistances which are imposed by the inner fluid and its conduit and which have no general relation to the convective process occurring at the external surface.

The temperature at which the thermal properties of the gas were evaluated was the arithmetic average of the gas and fin temperatures at inlet and outlet. The viscosity and thermal conductivity of the flue gas were assumed to be the same as those of air. The specific heat was calculated from the known composition of the gas, using current values of specific heats derived from spectroscopic data (5).

It will be noted in Fig. 4 that the surface heat-transfer coefficients h of the cast-iron and aluminum disks are fairly con-

sistent, and that they are approximately represented by curve *B-B*. This curve, which is drawn for purpose of comparison, represents a rough average of the results obtained by Pierson (6) for banks of staggered bare tubes. Curve *A-A*, also shown for comparison, represents average values for single bare tubes (7). The scattering of the points is attributable to experimental inaccuracy, due chiefly to nonuniform temperature distribution in the gas stream to and from large-scale apparatus, and to the deposition of soot on the fin surface. The rate and character of the soot deposits are believed to depend on the nature of the ash in the fuel, the concentration of solid carbonaceous matter in the gas, the gas temperature, and its velocity. The tendency of the points to converge to a single curve at the higher flows is considered to have a basis in reality; for it is a common observation that much less soot is blown free by the soot blowers at the end of tests at high gas flows than at the end of tests of the same duration at low rates of flow.

A notable feature of the surface heat-transfer group in the case of the solid wrought-iron disks, lines *C-C* and *D-D* in Fig. 4, is its independence of Reynolds number over the range covered in the tests. Any alternate choice of mean of disk and tube diameter would merely displace the points to right or left, parallel to the axis of the abscissa, while leaving their ordinates unchanged. Obviously, the ordinates of the points represented by *C-C* and *D-D* require a factor in order to merge with one or the other extremity of *B-B*, after suitable modification of the abscissa as well.

In the case of the star disks, disposition of the disk surface in the form of prongs apparently increases the turbulence in the bank of finned tubes to such a degree that the heat-transfer group, line *E-E*, is increased by 50 per cent. The heat absorbed per unit length of finned tube is nearly the same for the star disks with segments cut out as for the solid disk of the same diameter.

The effect is similar to that found by Norris and Spofford (8) for strip fins. If their method of correlation is applied to the prongs of the star disks, using 0.56 in. as the average perimeter of a prong, the test points form a nearly horizontal line. The middle of this line is approximately the point of intersection with the sloping line representing their results. An alternate procedure is to divide the perimeter of the prongs by π , and seek a way of averaging this and the tube diameter. In view of the complex nature of the flow, however, probably no such simple parameter would suffice.

Two undoubtedly important factors are tube spacing and fin spacing. The data presented here are too meager to warrant any conclusions. However, the persistence of eddies from one row to the next and their penetration of the passageway between adjacent fins are undoubtedly involved. A possible basis for extending the correlation to cover further data may be:

1 Incorporation of the square root of the ratio, fin-passageway width to height, into the heat-transfer group.

2 Use of some implicit function of tube diameter and pitch, together with fin spacing and height, such as hydraulic diameter, in the expression for Reynolds number.

3 Use of the ratio of tube pitch to diameter as a separate explicit parameter.

The first two are suggested by the results of Ellerbrock and Biermann (9) on single-finned cylinders.

No account has been taken of the variation of h locally over the surface of a disk. In the case of single-finned cylinders, considerable variation was found by Biermann and Pintel (10). If the thermal resistance of a disk is appreciably affected by this variation, as well as the average value of h , allowance for this might change the slope of lines *C-C* and *D-D*.

Appendix

NOMENCLATURE

The following nomenclature is used in this paper.

- R_F = resistance of fin, (deg F)(hr)/Btu
 R_s = resistance, fluid inside tube to inner tube wall, (deg F)(hr)/Btu
 R_R = resistance of rust on inner tube wall, (deg F)(hr)/Btu
 R_T = resistance of tube wall, (deg F)(hr)/Btu
 R_c = resistance of contact and hub of disk, (deg F)(hr)/Btu
 h_i = heat-transfer coefficient, fluid inside tube to inner tube wall, Btu/(hr)(sq ft)(deg F)
 h = coefficient of heat transfer, gas to fin surface, Btu/(hr)(sq ft)(deg F)
 U = heat-transfer coefficient, gas to base of disk, Btu/(hr)(sq ft)(deg F)
 U' = over-all heat-transfer coefficient, gas to fluid inside tube, Btu/(hr)(sq ft)(deg F)
 S_1 = surface of flue per foot length of tube, sq ft per ft
 S_2 = surface of disk per foot length of tube, sq ft per ft
 $S = S_1 + S_2$
 E = effectiveness of fin
 e = effectiveness of flue
 k_F = thermal conductivity of disk metal, Btu/(hr)(ft)(deg F)
 k_T = thermal conductivity of tube metal, Btu/(hr)(ft)(deg F)
 k_G = thermal conductivity of gas, Btu/(hr)(ft)(deg F)
 μ = viscosity of gas, lb/(hr)(ft)
 c = specific heat of gas at constant pressure
 G = mass flow of gas, lb/(hr)(sq ft)
 W = weight flow of fluid per tube, lb/hr
 D = equivalent diameter of surface, ft
 D_1 = inner diameter of disk, ft
 D_2 = outer diameter of disk, ft
 d_1 = inner diameter of tube, ft
 d_2 = outer diameter of tube, ft
 t_1 = thickness of fin at D_1 , ft
 t_2 = thickness of fin at D_2 , ft
 t_F = mean fin thickness, ft

THERMAL RESISTANCE OF DISK FINNS

The heat balance for a differential element of volume of a disk, neglecting temperature gradients in all directions except the radial, is for steady flow

$$d \left(2\pi k r z \frac{d\theta}{dr} \right) = 4\pi h \theta r \sqrt{1 + \frac{1}{4} \left(\frac{dz}{dr} \right)^2} dr \dots \dots [1]$$

Here θ is the temperature difference between gas and the surface of the disk at radius r , z is the thickness at radius r , k is the thermal conductivity of the disk material, and h the surface coefficient of convective heat transfer.

If the disk is tapered, and its thickness varies with radius according to

$$z = z_1 \frac{r_1^{2m}}{r} \dots \dots \dots [2]$$

Equation [1] assumes the form

$$\frac{d^2\theta}{dx^2} + \frac{1-2m}{x} \frac{d\theta}{dx} - \lambda^2 x^{2m} \theta = 0 \dots \dots \dots [3]$$

where

$$x \equiv \frac{r}{r_1} \text{ and } \lambda^2 \equiv \frac{2hr_1^2}{kz_1} \left[1 + \frac{m^2 z_1^2}{r_1^2 x^{4m+2}} \right]^{1/2} \text{Mean} \dots \dots [4]$$

Use of the mean value of the radical in Equation [1] is justifiable where $\frac{z_1}{r_1}$ is small compared to x .

The solution of Equation [3] is

$$\theta = x^m \left[AI \frac{m}{m+1} \left(\frac{\lambda}{m+1} x^{m+1} \right) + BK \frac{m}{m+1} \left(\frac{\lambda}{m+1} x^{m+1} \right) \right] \dots \dots \dots [5]$$

where A and B are integration constants to be determined from the boundary conditions

$$\left. \begin{aligned} \theta &= \theta_1 \text{ when } x = x_1 = 1 \\ \frac{d\theta}{dx} &= 0 \text{ when } x = x_2 \\ -2\pi z_1 r_1 k \frac{d\theta}{dx} &= 2\pi U \theta_1 \int_{r_1}^{r_2} r \sqrt{1 + \frac{1}{4} \left(\frac{dz}{dr} \right)^2} dr \end{aligned} \right\} \dots [6]$$

when $x = x_1$

Here $I \frac{m}{m+1}$ and $K \frac{m}{m+1}$ are modified Bessel functions of first and second kind, respectively, and order $\frac{m}{m+1}$.

The case $m = 0$ has been treated by Harper and Brown (4), and Schmidt (1), who used Hankel's notation for the Bessel functions. The case $m = 1/2$ was treated by Carrier and Anderson (11) without identification of the series obtained as solutions.

In the case $m = 0$, i.e., a disk of constant thickness, the disk effectiveness E , is found to be (in the notation employed here)

$$E = \frac{U}{h} = \frac{2}{(x_2^2 - 1)\lambda} \frac{I_1(\lambda x_2) K_1(\lambda) - I_1(\lambda) K_1(\lambda x_2)}{I_0(\lambda x_2) K_0(\lambda) + I_0(\lambda) K_1(\lambda x_2)} \dots [7]$$

Ten-place tables of the I and K functions of integral order are given by Gray and Mathews (12). By means of these the numerator in Equation [7] can be calculated with precision more than ample for our purpose.

A graphical representation of Equation [7] in a form frequently convenient is shown in Fig. 5. Use of the parameter

$$M = \frac{k z_1}{2(r_2 - r_1)^2} \sqrt{\frac{r_1}{r_2}} = \frac{2k z_1}{(D_2 - D_1)^2} \sqrt{\frac{D_1}{D_2}}$$

effects a merger of the individual curves at large values of the abscissa M/h , to a degree of accuracy exceeding that required for most purposes. This parameter M involves the dimensions of the disk and the thermal conductivity of its material. Values of the ordinate were obtained from Equation [7] and the relation

$$\frac{M}{U} - \frac{M}{h} = \frac{1 - E}{E} \frac{M}{h} \dots \dots \dots [8]$$

Lines of constant disk effectiveness E were drawn by plotting $\frac{1 - E}{E} \frac{M}{h}$ as ordinate, assigning decimal values successively to E .

As r_1 becomes very large, while $(r_2 - r_1)$ remains small in comparison, the influence of curvature diminishes, and as a limit we approach the strip fin of height $(r_2 - r_1)$. The equation of the curve denoted by $D_2/D_1 = 1$ in Fig. 5 is easily derived from the usual hyperbolic-tangent formula for effectiveness, together with Equation [8], yielding

$$\frac{M}{U} - \frac{M}{h} = \sqrt{M/h} \coth \sqrt{\frac{h}{M}} - \frac{M}{h} \dots \dots [9]$$

The chart may be used directly in calculating the unit resistance $\left(\frac{1}{U} - \frac{1}{h} \right)$, of a disk when h , k , and the dimensions are specified.

When U instead of h is specified, a subsidiary plot with M/U as abscissa is more convenient, and is easily constructed. Correction for the heat flow into the edge of the disk may be made approximately by adding one half the disk thickness to $(r_2 - r_1)$, following the procedure of Harper and Brown.

In the case of a disk having a parabolic profile, $m = 1$ in Equation [4], the Bessel functions of Equation [5] are of order $1/2$ and reduce to hyperbolic functions, yielding

$$\theta = A \cosh (\lambda x^2/2) + B \sinh (\lambda x^2/2) \dots \dots \dots [10]$$

and

$$E = \frac{U}{h} = \frac{2 \tanh \{ \lambda (x_2^2 - 1)/2 \}}{\lambda (x_2^2 - 1)} \dots \dots \dots [11]$$

after determination of A and B by means of the boundary conditions Equations [6]. By assigning to M the value

$$M = \frac{2k z_1 z_2}{(r_2 - r_1)^2 (\sqrt{z_1} + \sqrt{z_2})^2} \left(1 - \frac{z_1^2 + z_2^2}{4r_1^2 z_1} \right)$$

the curve labeled $D_2/D_1 = 1$ may be used for the parabolic disk.

Correction for the temperature gradients other than radial was treated by Harper and Brown and shown to be small in ordinary cases. In the case examined in detail by them M/h had the value 0.2967, and the correction to effectiveness 0.6 per cent.

The corresponding correction to be added to $\left(\frac{M}{U} - \frac{M}{h} \right)$ amounts to 1 per cent.

No account was taken of the local variation of h over the disk surface. An influence as great as that due to curvature and shape would be anticipated.

BIBLIOGRAPHY

- 1 "Wärmeübertragung Durch Rippen," by E. Schmidt, *Zeitschrift des Vereines deutscher Ingenieure*, vol. 70, 1926, p. 947.
- 2 "Heat Transmission," by W. H. McAdams, McGraw-Hill Book Company, Inc., New York, N. Y., second edition, 1942, p. 180.
- 3 "Further Measurements of the Thermal and Electrical Conductivity of Iron at High Temperatures," by R. W. Powell, *Proceedings of the Philosophical Society*, vol. 51, 1939, pp. 407-418.
- 4 "Mathematical Equations for Heat Conduction in the Fins of Air-Cooled Engines," by D. R. Harper and W. B. Brown, N.A.C.A. Report No. 158, 1923, pp. 679-703.
- 5 "Spezifische Wärme, Enthalpie, Entropy und Dissoziation Technischer Gase," by E. Justi, J. Springer, Berlin, 1938, pp. 143-147.
- 6 "Experimental Investigation of the Influence of Tube Arrangement on Convection Heat Transfer and Flow Resistance in Cross-flow of Gases Over Tube Banks," by O. L. Pierson, *Trans. A.S.M.E.*, vol. 59, 1937, pp. 563-572.
- 7 "Heat Transmission," by W. H. McAdams, McGraw-Hill Book Company, Inc., New York, N. Y., 1942, p. 221.
- 8 "High-Performance Fins for Heat Transfer," by R. H. Norris and W. A. Spofford, *Trans. A.S.M.E.*, vol. 64, 1942, pp. 489-495.
- 9 "Surface Heat Transfer Coefficients of Finned Cylinders," by H. H. Ellerbrock and A. Biermann, N.A.C.A. Report No. 676, 1939, pp. 1-14.
- 10 "Heat Transfer From Finned Metal Cylinders in an Air Stream," by A. E. Biermann and B. Pinkel, N.A.C.A. Report No. 488, 1934, pp. 1-22.
- 11 "The Resistance to Heat Flow Through Finned Tubing," by W. H. Carrier and S. W. Anderson, *A.S.H.V.E. Journal section of Heating Piping and Air Conditioning*, May, 1944, pp. 304-318.
- 12 "A Treatise on Bessel Functions," by A. Gray and G. B. Mathews, The Macmillan Co., New York, N. Y., 1931.

Heat-Flux Pattern in Fin Tubes Under Radiation

By A. R. MUMFORD¹ AND E. M. POWELL,² NEW YORK, N. Y.

In this paper data are presented showing heat-flux patterns as indicated by temperature-drop curves from field measurements and from an electrical analogy in the laboratory. Data of this kind may become of some importance if the use of tube-surface temperatures in furnace-testing technique is successfully developed.

SEVERAL examples of the use of surface temperatures to indicate the heat-flux variation around the circumference of a tube have appeared in technical publications. Although this method is fascinating and gives promise of producing data which will aid in a more complete understanding of what is going on in the furnace and at the walls, it is apparent that the variations caused by slag deposits in coal-fired furnaces are of such magnitude that many more data than are at present available will be required before we can say with assurance that this condition or that condition represents the normal at a given location and rating.

Fig. 1 shows a plan section through a furnace having a slagging bottom and fired tangentially with pulverized coal. The furnace walls are made up of finned tubes, one of which, as indicated, was selected for the measurement of surface temperatures. A section of the finned tubes used in the construction of the walls of this furnace is shown in Fig. 1. Thermocouples were installed at several points around the circumference of the tube at an elevation of approximately 13 ft from the floor of the furnace. The method of installing the thermocouples for measuring the surface temperatures of tubes has been described by C. G. R. Humphreys.³ When couples were installed on the back of the tubes in a position not exposed to furnace gases or ash, the temperatures indicated were within a degree or two of the saturation temperature corresponding to the boiler pressure. It is therefore probable that this method of surface-temperature measurement provides a means which can be expected to be accurate within 0.5 per cent of the indicated temperature.

Fig. 2 gives a number of curves showing the difference between the tube-surface temperature and the saturation temperature around the exposed semicircumference of that tube at intervals after the unit was lit-off. Curve *a* represents the condition shortly after lighting-off when the load was less than $1/2$ normal. Only a small amount of coal had been burned up to that time, and it is probable that the tube surface was clean and exposed. The temperature elevation varies about 50 F with the peak to the right of the normal to the wall. Fourteen hours later the boiler was operating at about 90 per cent of normal and no lancing had been done. Some ash had accumulated on the

surface because the surface temperature of the metal had dropped as shown on curve *b*, in spite of the fact that the rate of heat release in the furnace had doubled. It may be significant that the greater drop in surface temperature occurred in the right quadrant of the tube. At least, from an examination of the geometry of the furnace, noting the direction of the fuel stream and the point of highest heat intensity, this quadrant is the point at which we would expect ash to deposit.

Curve *c* represents the conditions about 6 days after the boiler was lit. The load was normal but apparently a fairly uniform coating of ash had accumulated which reduced the rate of heat transfer to such a point that the surface temperature of the tube was only 60–70 F above saturation.

Curve *d* represents conditions a week after the unit was lit-off,

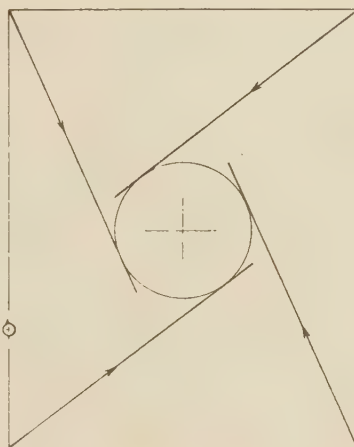


FIG. 1 PLAN SECTION THROUGH PULVERIZED-COAL-FIRED FURNACE

with only routine lancing and with a load of about 90 per cent of normal. This curve is of particular interest because of the small variation around the circumference. The evidence of these observations would indicate that the normal temperatures would be higher in the right quadrant.

Six days later, or 13 days after lighting-off, the conditions are represented by curve *e*. These surface temperatures are the lowest observations at full load and indicate the existence of a heavy coating of slag with more heat being transmitted through the right quadrant. This curve represents the condition immediately preceding a thorough lancing of the walls.

Curve *f* represents conditions immediately after the wall had been lanced. The largest temperature drop, and probably the largest rate of heat transfer, exists in the right-hand quadrant. The comparatively low drop which is shown at 30 deg from the face of the wall in the left-hand quadrant is probably due to the continued adherence of some insulating slag in this region.

PERIOD PRECEDING AND FOLLOWING LANCING OF FURNACE WALL

A more detailed examination of the period immediately pre-

¹ Research and Development Department, Combustion Engineering Company, Inc. Fellow A.S.M.E.

² Engineering Department, Combustion Engineering Company, Inc.

³ "Thermocouples for Furnace-Tube-Surface Temperature Measurements," by C. G. R. Humphreys, *Combustion*, vol. 16, 1944, pp. 53–55.

Contributed by the Heat Transfer Division and presented at the Annual Meeting, New York, N. Y., Nov. 27–Dec. 1, 1944, of THE AMERICAN SOCIETY OF MECHANICAL ENGINEERS.

NOTE: Statements and opinions advanced in papers are to be understood as individual expressions of their authors and not those of the Society.

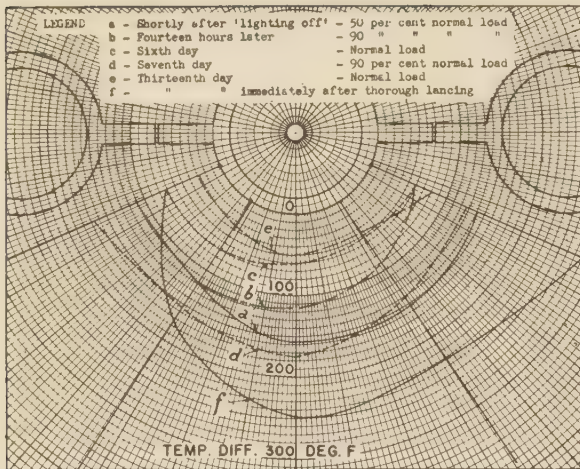


FIG. 2 CURVES SHOWING TEMPERATURE DIFFERENCES BETWEEN TUBE SURFACE AND SATURATION TEMPERATURE AROUND SEMI-CIRCUMFERENCE

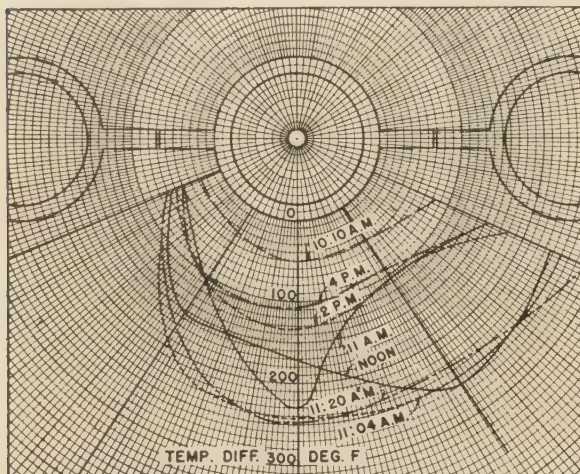


FIG. 3 TEMPERATURE DIFFERENCES FOR PERIOD PRECEDING AND FOLLOWING LANCING OF WALL

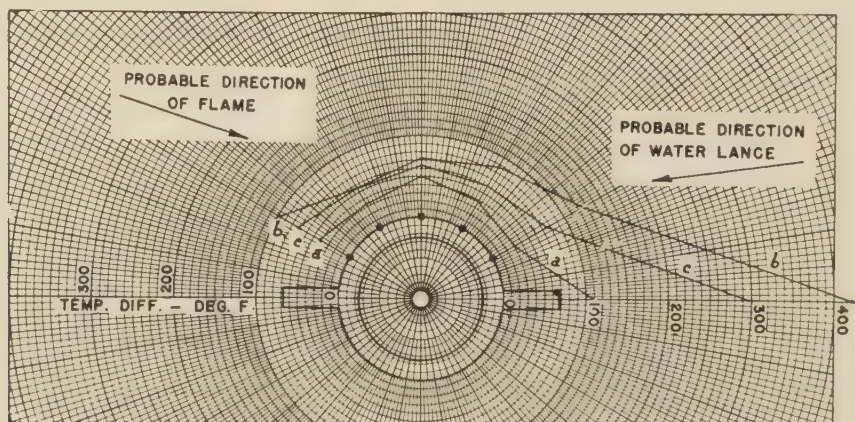


FIG. 4 TEMPERATURE DIFFERENCES AT VARIOUS TIMES ON CIRCUMFERENCE OF TUBE AND AT EXTREMITY OF FIN

ceding and following the lancing of the wall is shown in Fig. 3. The wall in the region of this particular tube was lanced between 11 a.m. and 11:20 a.m. and the changes in heat transfer are indicated by the temperature differences. At 10:10 a.m. before lancing, the average temperature difference was 50 F, being somewhat lower in the left quadrant. At 11 a.m. at the start of lancing, the temperature difference through the tube wall on a normal to the plane of the furnace wall increased to 230 F with lesser increases at other points. If the rate of heat transfer is taken as proportional to the temperature drop, then the rate at the front face of the tube immediately after lancing is 4.7 times that before lancing. At 11:04 a.m. what is indicated as the cleanest condition was reached, and this was practically unchanged at 11:20 a.m. when the lancing had been completed. At noon, 2 p.m., and 4 p.m., the rate of accumulation of the insulating layer of ash is indicated by a decreasing temperature difference. A better appreciation of the changes taking place will be realized by noting the location of this tube in Fig. 1 with relation to the approaching coal stream and the zone of highest heat intensity off the right quadrant and the lance coming from the left.

In Figs. 2 and 3 zero of the temperature scale is at the tube surface. The elevation within the furnace at which these temperatures were taken is in the zone of high heat release and slag deposits and therefore, although these temperatures are not representative of the entire furnace, they do serve as a good indication of the variations which can take place in the zone of intense heat transfer during operation. Conclusive study of the heat-flux pattern in a finned tube would require the collection of field data, not only over a long period in a coal-fired furnace, but over many areas of the furnace in which insulating layers of slag are or are not deposited.

In Fig. 4 are plotted several curves which show the temperature differences which existed at various times on the circumference of the tube and at the extremity of one fin. The temperature scale is the same as used in Figs. 2 and 3. The variations of surface temperature are most pronounced at the tip of the fin and on the tube wall adjacent to the fin. Except for the general rise after 11:30 a.m., the variations in the right quadrant were comparatively small, but in the left quadrant were so great that the most feasible explanation is the dropping off of a fairly dense layer of slag. The method of presentation does not take into consideration the fact that the metal thickness between the measuring point and the internal fluid is greater by 1 in. for the fin-temperature point. If it were certain that the entire fin had been exposed, a heat flux proportional to the tempera-

ture drop per inch of metal could have been assumed, but with the available data there was no assurance of this, consequently no attempt at correction was made.

Obviously, the variations occurring in this zone of the furnace preclude any short-time study of heat-flux patterns by field measurements in a coal-fired furnace. The opinion should be emphasized that the conditions shown in Figs. 2, 3, and 4 are not representative of the entire furnace, but only of the flowing-slag zone of a slagging-bottom pulverized-coal furnace. The condition at other furnace-wall areas is known to be less variable. Evidence of the variation to be expected in different areas of the furnace has been given by H. Kreisinger and R. C. Patterson.⁴ The variable conditions in the slag zone, however, will set the requirements for the testing period because the slag zone is about 10 per cent of the furnace area.

LABORATORY STUDY OF HEAT-FLUX PATTERNS

The laboratory approach to the problem of heat-flux pattern in finned tubes under radiation permits a determination of temperature drops by analogy and therefore the determination of heat-flux patterns without the interference of ash deposits. Fig. 5 shows a test setup used for the purpose of studying flux patterns with particular emphasis on the flow of heat from the base of the fin through the tube wall. On a sheet of high-resistance alloy

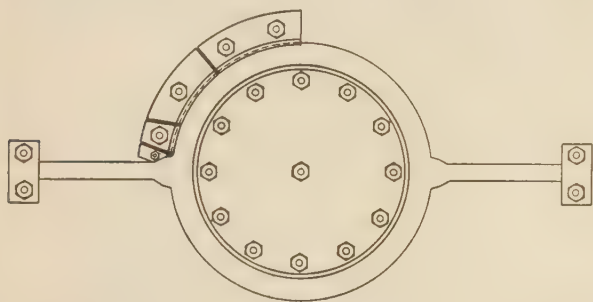


Fig. 5 DIAGRAM OF APPARATUS FOR PRODUCING VOLTAGE DROPS ACROSS SIMULATED FINNED-TUBE WALL

cut in the shape of a section of a finned tube, a number of radial and circumferential lines were machine-scribed. Electric currents were passed through the sheet in such values that were comparable to the heat flow by radiation. By taking voltage drop, amperes, and electrical conductivity as equivalent to temperature drop, quantity of heat per unit of time, and thermal conductivity, respectively, temperature drops could be computed from the electrical measurements. Voltage drops were measured at the intersections of the scribed lines and the analogous temperatures computed.

Fig. 6 shows the calculated temperature distribution at the base of a fin $\frac{1}{4}$ in. \times 1 in. long on a 4-in. \times 0.380-in. tube, and Fig. 7 shows the distribution at the base of a fin $\frac{1}{4}$ in. \times $\frac{17}{16}$ in. long on the same tube. In each case the current flow was adjusted to be equivalent to a uniform rate of heat transmission for the tube and fin of approximately 50,000 Btu per hr per sq ft. The electrical resistance between the inner face of the tube and the inside contact plate was uniform and corresponded to a thermal conductivity of approximately 3500 Btu per hr per sq ft per deg F temperature difference. Other sources have indicated this to be somewhat low.

The distribution of heat-flux density imposed in the form of

⁴ "Heat Transfer of Water-Cooled Furnace Walls," by H. Kreisinger and R. C. Patterson, Trans. A.S.M.E., vol. 66, 1944. Bound at back of volume in pamphlet entitled "Furnace Performance Factors," pp. 71-78.

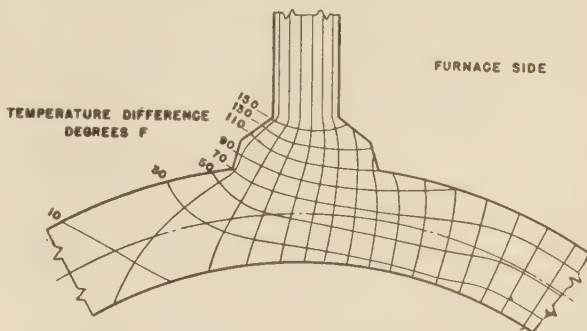


Fig. 6 TEMPERATURE DISTRIBUTION AND HEAT FLOW AT BASE OF $\frac{1}{4}$ -IN. \times 1-IN. FIN

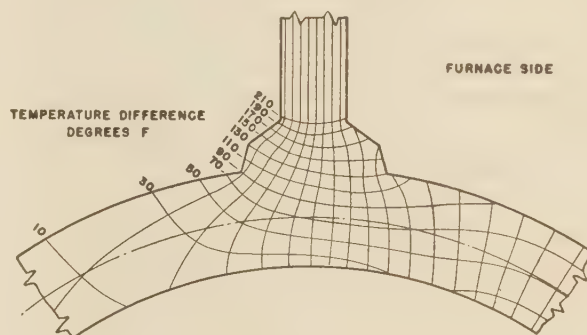


Fig. 7 TEMPERATURE DISTRIBUTION AND HEAT FLOW AT BASE OF $\frac{1}{4}$ -IN. \times $\frac{17}{16}$ -IN. FIN

current flow was uniform on the circumferential part of the tube and the weld of the fin. The heat picked up by the fin was represented by current flow from the end of the fin only. An examination of the two figures makes it quite apparent that the only marked difference in temperature drop occurs in the region of the fin, and the greatest temperature drops occur with the largest fin. The influence of the fin and the heat it picks up is to change the direction of heat flow from radial to a combination of radial and circumferential. The isotherms, instead of being circumferential, dip radially more and more as the circumferential distance increases at or near the fin. Back of the fin, in the region where no heat is being added to the tube, the heat flow extends almost 45 deg but the magnitude is very small after about 15 deg have been passed. The fanning out of the lines of flow of the heat, i.e., normal to the isotherms, is clearly indicated by the movement of the peak of the temperature-difference curves from the line of the fin forward toward the exposure. This forward shift reaches a maximum at the inner face of the tube.

For the experiments uniform radial absorption has been assumed around the semicircumference of the tube. This is seldom realized in actual practice, the rate usually being less near the base of the fin. This factor would tend to reduce the heat concentration ahead of the base of the fin and the temperature difference calculated at that point.

The use of tube-surface-temperature measurements in furnace technique has been discussed elsewhere. It does not seem out of place, however, to indicate that under conditions of parallel radiation at any degree of incidence, a fin tube will have greater exposure than one of a group of tangent tubes because of their spacing, and at some angles the area of the fin will be very important in fixing the heat-flux pattern through the tube because of its proportion to the total.

Heat Transfer and Pressure Drop of Liquids in Double-Pipe Fin-Tube Exchangers

By B. DE LORENZO¹ AND E. D. ANDERSON,² ELYRIA, OHIO

This paper presents data on the fin side of standard commercial-size longitudinally finned double-pipe exchangers. Three fin-tube sizes were investigated in heating and cooling for both heat transfer and pressure drop. The data indicate that the transition between laminar and turbulent flow begins at $R < 400$ for both heat transfer and pressure drop, corroborating results reported by previous investigators. Methods of evaluating heat-transfer coefficients and pressure drop for liquids inside tubes are applicable for liquids in the fin side of finned double-pipe exchangers. For values of R up to 4000 (approximately), recommended curves for fin-side heat transfer give higher coefficients than the values obtained, by the procedure outlined by the Tubular Exchanger Manufacturers Association for liquids flowing in tubes. A method is presented for determining the weighted average temperature of the outside surface of the fin tube to be used in evaluating μ_w in the viscosity gradient correction μ/μ_w .

NOMENCLATURE

The following nomenclature is used in this paper:

- $A = (A_f + A_i)$ = total fin-side surface area, sq ft
 A_o = net free cross-sectional area for flow on fin side, sq ft
 A_f = surface area of fins only, sq ft
 A_i = inside surface area of tube, sq ft
 A_t = outside surface area of tube only, sq ft
 b = height of fin (see Fig. 2e), ft
 c = specific heat of fluid, Btu/(lb)(deg F)
 $D_e = 4A_o/\psi$ = equivalent hydraulic diameter of fin side, ft
 D' = inside fin-tube diameter, in.
 f = friction factor in Fanning equation, dimensionless
 G = mass velocity of fluid, lb/(sq ft)(hr)
 g = acceleration due to gravity = 4.17×10^8 ft/(hr)(hr)
 h_d = reciprocal of fouling resistance (see Fig. 4), Btu/(hr)(sq ft)(deg F)
 h_f and h_{fd} = fin-side film coefficient based on A_i , clean and fouled, respectively, Btu/(hr)(sq ft)(deg F)
 h_{fi} and h_{fdi} = fin-side film coefficient referred to A_i , corrected for weighted fin effectiveness, clean and fouled, respectively, (see Fig. 4), Btu/(hr)(sq ft)(deg F)
 h_i = tube-side film coefficient, based on A_i , clean, Btu/(hr)(sq ft)(deg F)
 h_r = reciprocal of tube-wall resistance, Btu/(hr)(sq ft)(deg F)
 $j = \frac{h_f}{cG} \left(\frac{c\mu}{k} \right)^{1/4} \left(\frac{\mu}{\mu_w} \right)^{-0.14} = \text{Colburn's } (1)^3 \text{ heat transfer}$

factor modified by Sieder and Tate's (2) viscosity correction, dimensionless

- k and k_f = thermal conductivity of fin-side fluid and of fin material, respectively, Btu/(hr)(sq ft)(deg F/ft)
 L = length of fin section (see Fig. 2), ft
 L_e = total equivalent length of fin side (see Fig. 6), ft
 Q = total quantity of heat transferred, Btu per hr
 Δp = pressure drop of fin-side fluid, psf
 $R = DeG/\mu$ = Reynolds number, dimensionless
 t = average temperature of fin-side fluid, deg F
 T = average temperature of fluid inside tubes, deg F
 T_i = average temperature of tube wall, (see Equation [7]), deg F
 T_w = weighted average temperature of fin surface and tube-wall surface, defined by Equation [8], deg F
 U_i = over-all heat-transfer coefficient (clean), based on A_i , Btu/(hr)(sq ft)(deg F log MTD)
 V = linear velocity of fin-side fluid (at A_o), fph
 V' = linear velocity of water inside fin tube, (see Equation [2]), fps
 δ = fin thickness (see Fig. 2), ft
 η = effectiveness factor of fin surface only (see Fig. 4), dimensionless
 η' = total weighted effectiveness of fin and tube surface, (see Fig. 4), dimensionless
 μ = viscosity of fin-side fluid, evaluated at t , lb/(ft)(hr)
 μ_w = viscosity of fin-side fluid, evaluated at T_w , lb/(ft)(hr)
 ψ = total wetted perimeter of fin side (fins plus outside of tube, plus inner surface of shell pipe), ft
 ρ = density of fin-side fluid evaluated at t , lb per cu ft
 ϕ = viscosity ratio = $(\mu/\mu_w)^{0.28}$ and $(\mu/\mu_w)^{0.14}$ for pressure drop in laminar and turbulent flow, respectively (see Fig. 6), dimensionless

INTRODUCTION

Double-pipe heat exchangers, having longitudinal fins attached to the outside of the inner pipe, have come into more and more general use in recent years as the advantages of this type of exchanger have become better known. The most frequently used form of the double-pipe exchanger is the "hairpin" section. This design permits easy connection of the number of sections required to perform the desired heat-transfer duty into a compact bank.

Generally speaking, the best application of the longitudinally finned double-pipe hairpin exchanger is in transferring heat between two fluids having unequal heat-transfer characteristics; the fluid having the higher rate of heat transfer flows through the innermost tube, and the fluid with the lower heat-transfer rate flows through the space between the two tubes, i.e., the fin, or shell side. Fig. 1 illustrates a typical installation of this type of exchanger. The bank consists of 20 hairpin sections arranged 5 in parallel by 4 in series. This unit is used for cooling gasoline. Water, used as the cooling medium, passes through the inner tube, the gasoline flows through the fin side.

Longitudinally finned double-pipe hairpin exchangers have

³ Numbers in parentheses refer to the Bibliography at the end of the paper.

¹ Manager, Heat Transfer Department, Brown Fintube Company.
² Design Engineer, Brown Fintube Company.

Contributed by the Heat Transfer Division and presented at the Annual Meeting, New York, N. Y., Nov. 27-Dec. 1, 1944, of THE AMERICAN SOCIETY OF MECHANICAL ENGINEERS.

NOTE: Statements and opinions advanced in papers are to be understood as individual expressions of their authors and not those of the Society.

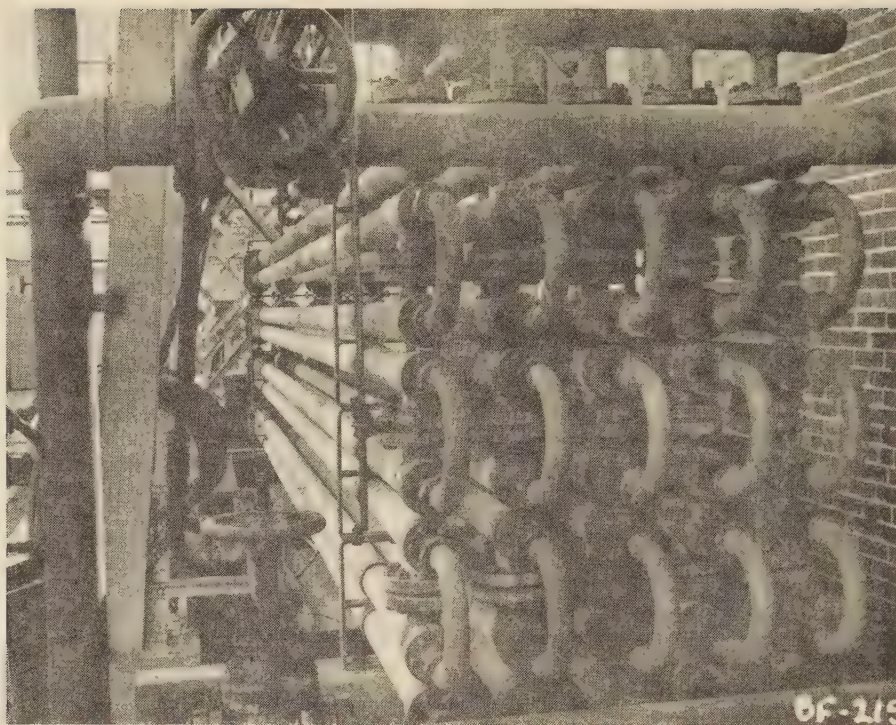


FIG. 1 GASOLINE COOLER CONSISTING OF 20 FINNED HAIRPIN SECTIONS

also been used extensively, and to great advantage, in transferring heat between two fluids having similar heat-transfer characteristics. In these cases the tube-side fluid generally flows at high velocity, utilizing the maximum allowable pressure drop, so as to secure the best coefficient possible, while the fin-side fluid may flow at moderate velocities. Also, in effecting transfers between fluids having unequal transfer characteristics, it is entirely feasible to pass the fluid having the lower heat-transfer properties through the center tube (in cases where the characteristics of the fluid makes this desirable) by using removable turbulence promoters on the inside of the tube. These turbulence promoters increase the tube-side heat-transfer coefficient at the expense of a higher pressure drop (3).

Since the ratio of the total outside fin surface A_f to the inside tube surface A_t is generally 5 to 1 and greater, the fin-side coefficient may be considerably lower than the tube-side coefficient, yet, when the factor of relative surface area is introduced, the fin-side coefficient, corrected for the weighted fin effectiveness, may amount to a higher value than the value secured on the tube side.

The primary purpose of this paper is to make available to engineers practical proved methods for evaluating the film heat-transfer coefficients and pressure drops of liquids flowing in the fin side of standard commercial-size longitudinally finned double-pipe heat exchangers. With the exception of the excellent pioneer paper by Gunter and Shaw (4), design data on double-pipe fin-tube exchangers are nonexistent. To provide these data a series of tests was made on standard hairpin exchangers manufactured by the authors' company.

It is not the intention of this paper to present a theoretical analysis of the data reported; nor to make comparisons with extended-surface-heat-transfer and pressure-drop data reported by other investigators. It is, rather, the object of this paper to pre-

sent the results obtained clearly and concisely for not only experienced design engineers but also for operating personnel.

TEST APPARATUS AND PROCEDURE

The test apparatus consisted of three standard double-pipe hairpin heat exchangers of the type described, and shown in Fig. 2 (a). One exchanger was used as a heater and two as coolers, see Fig. 3. The entire equipment including the heater, both coolers, and all connecting piping was covered with 1-in.-thick standard insulation to minimize heat loss.

Tests were run on exchangers using three different fin tubes (see Table 1), shown in Fig. 2(b), (c), and (d). Each hairpin consisted of two identical standard Brown resistance-welded fin tubes, taken at random from production runs and having 24, 28, and 36 longitudinal low-carbon-steel fins, $\frac{1}{2}$ in. high \times 0.035 in. thick and 20 ft long, integrally bonded by overlapping spot welds, Fig. 2 (e). The fin channels were evenly spaced around the perimeter of $1\frac{1}{2}$ -in. I.P.S. standard-weight seamless steel tubing. These fin tubes were welded to 180-deg steel return bends thus forming hairpins having a total 40-ft of fin length. The shells of the double-pipe heat exchangers consisted of two 3-in. I.P.S. standard-weight steel pipes welded to a housing which encloses the 180-deg return bend of the finned hairpin.

Table 1 gives areas, surface ratios, and other physical data of the three different fin-tube hairpins tested.

The fluids used in the tests were S.A.E. 40 and 50 lube oils and 43 deg API kerosene. These fluids, in all cases, were circulated through the finned or shell side of the exchanger. Saturated steam, at pressures ranging from 10 to 100 psig, was used as the heating medium inside the fin tubes of the heater. City water flowing through the fin tubes countercurrent to the flow of the oil on the fin side was used as the cooling medium in the coolers. Flow rates, of both lube oils and water, were measured with

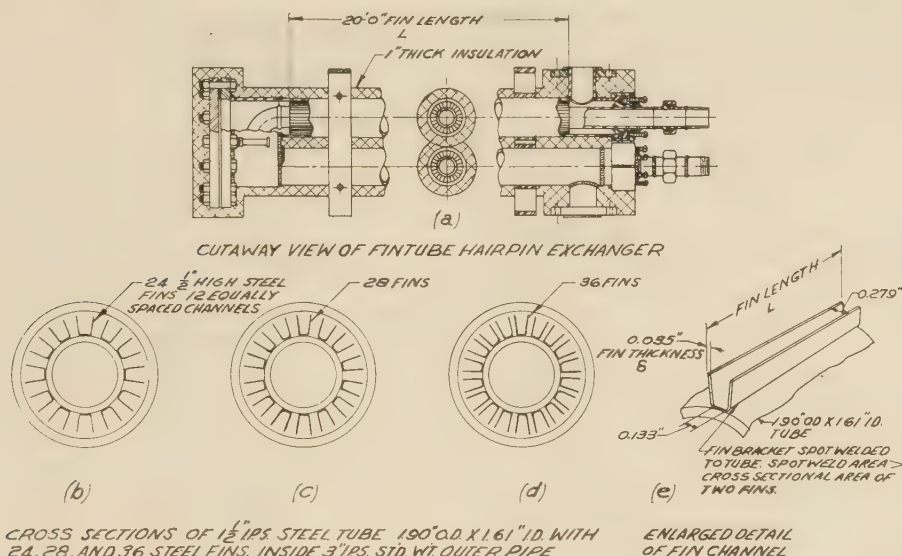


FIG. 2 DETAILS OF DOUBLE-PIPE LONGITUDINALLY FINNED HAIRPIN EXCHANGER AND THREE SIZES OF FIN TUBES TESTED

TABLE 1 PHYSICAL DATA OF FIN-TUBE HAIRPIN SECTIONS TESTED (SEE FIG. 2)

No. of fins.....	24	28	36
Net free area fin side, A_c , sq ft.....	0.0285	0.0280	0.0275
Hydraulic diameter, D_e , ft.....	0.0346	0.0308	0.0251
Ratios:			
Fin length L			
Hydraulic diameter, \bar{D}_e	578	650	797
Fin surface only A_f	0.800	0.824	0.858
Total fin-tube external surface, \bar{A}			
Tube external surface A_t	0.200	0.176	0.142
Total fin-tube external surface, \bar{A}			
Total fin-tube external surface, \bar{A}			
Fin-tube internal surface A_i	5.93	6.72	8.30
Total fin-side surface per hairpin section, sq ft	101	114	141

calibrated displacement-type flowmeters. No flowmeter was used to measure the kerosene, as the kerosene flow rates exceeded the capacity of the meter. It was possible, however, to determine the kerosene flow rate by a heat-and-material balance on the coolers, as a flowmeter was always used to measure the water rate. Temperatures were taken with standard A.S.T.M. mercury-bulb glass thermometers located in thermowells. Check thermowells were installed at several points, and, as a further check, the thermometers were interchanged at intervals. Pressure drops across the heater and each cooler were measured by differential mercury manometers. Pressure taps were located in the inlet and outlet nozzles, thus the pressure drop obtained included end losses. No calming sections were used as all the tests were made with standard commercial-size hairpin sections.

In all runs the oil tested was pumped from the storage tank, through the heater and the two coolers in series, and back to the storage tank, as shown in Fig. 3. Each test run lasted from 15 to 20 min after equilibrium was attained. Readings were taken at 5-min intervals. Flow rates and inlet temperatures of the two lube oils were varied over wide limits to obtain the maximum spread of Reynolds numbers for each oil. Steam temperatures and water flow rates were also varied for a fixed oil-flow rate so that a wider range of film temperatures could be investigated. Heat balances to within 5 per cent were obtained in the different tests.

Of the three fin-tube sizes tested, the Reynolds numbers have the greatest spread on the runs made with the fin tubes having 28

fins. Runs with R up to 1000 were made with refined S.A.E. 40 and 50 lube oils and above 1000 with commercial kerosene. The fin tubes with 24 fins were tested in the range from $R = 20$ to 800 using refined S.A.E. 40 lube oil. Only a few runs were made with the tubes having 36 fins, and the same S.A.E. 40 lube oil was used. The heat-transfer and pressure-drop results of all the runs covered by this paper are shown in Figs. 5 and 6, respectively. The range of the Prandtl number was from a minimum of 11.0 to a maximum of 1625. L/D ratios are given in Table 1.

The over-all heat-transfer coefficient was obtained by dividing the total heat transferred by the log MTD and the total inside surface of the fin tubes

$$U_i = \frac{Q}{(\log \text{MTD})(A_i)} \quad [1]$$

For the steam-side coefficient, the value $h_i = 2500$ was used, as this figure was considered to be in line with field operation. For heating lube oil, a maximum deviation of 4 per cent would result by assuming steam-condensing coefficients ranging from

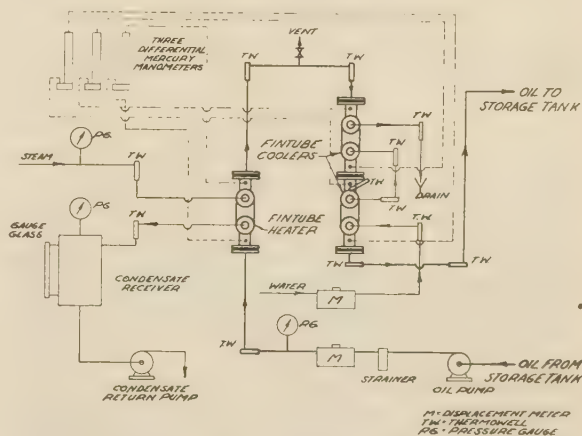


FIG. 3 FLOW DIAGRAM OF TEST UNIT

1500 to 5000 Btu/(hr)(sq ft)(deg F). For heating light fluids such as kerosene, with Reynolds numbers over 1000 where the fin-side coefficient would be higher than that for heating lube oil, the deviation would be greater. The water-side coefficient was calculated by the equation as given by McAdams (5).

$$h_i = \frac{150(1 + 0.011T)(V')^{0.8}}{(D')^{0.2}} \quad [2]$$

The fin-side film coefficient h_{fi} for the three sizes of fin tubes tested was then calculated readily from the equation

$$\frac{1}{U_i} = \frac{1}{h_i} + \frac{1}{h_t} + \frac{1}{h_{fi}} \quad [3]$$

and the curves shown in Fig. 4 which employ the Harper and Brown (6) method of computing fin efficiency.

EVALUATION OF T_w

The term μ_w as used in this paper to correlate the heat-transfer and pressure-drop data, denotes the viscosity of the fin-side fluid evaluated at the weighted average temperature of the finned surface and the outside bare surface of the tube, herein designated by T_w . No satisfactory method for evaluating T_w for tubes having extended surface could be found in the available literature. Consequently, the method for determining T_w illustrated subsequently and the values obtained by using this method were used in calculating the results reported in this paper.

The derivation of the equation for T_w is based on a heat balance between the fluid inside the tubes and the fluid on the fin side, and the corresponding surfaces. Thus when the hot fluid is inside the fin tubes and the cold fluid in the shell side, the heat transferred per unit area of inside tube surface can be defined by the equation

$$\frac{Q}{A_i} = h_i(T - T_i) \quad [4]$$

also

$$h_i(T - T_i) = h_f \eta' (T_i - t) A / A_i \quad [5]$$

and again

$$h_i(T - T_i) = h_f(T_w - t) A / A_i \quad [6]$$

Solving Equation [5] for T_i

$$T_i = \frac{h_i T + h_f \eta' t A / A_i}{h_i + h_f \eta' A / A_i} \quad [7]$$

Substituting the expression for T_i in Equation [6] and solving for T_w it is found that

$$T_w = \frac{\eta' h_i (T - t)}{h_i + h_f \eta' A / A_i} + t \quad [8]$$

When the cold fluid is in the inside of the fin tube and the hot fluid is on the fin side, it is found that Equation [8] is the same and can therefore be used for both heating and cooling.

In the foregoing derivation the assumption is made that there is no temperature gradient across the tube wall of the fin tube. This was a reasonable assumption as the equation for T_w would be more complicated if this assumption were not made and the effect on T_w would be small.

Temperature T_w is evaluated by successive approximations of h_f and finding the corresponding η' . All the other terms in Equation [8] are either known or are previously calculated. Generally, a first approximation suffices, as an error in T_w is

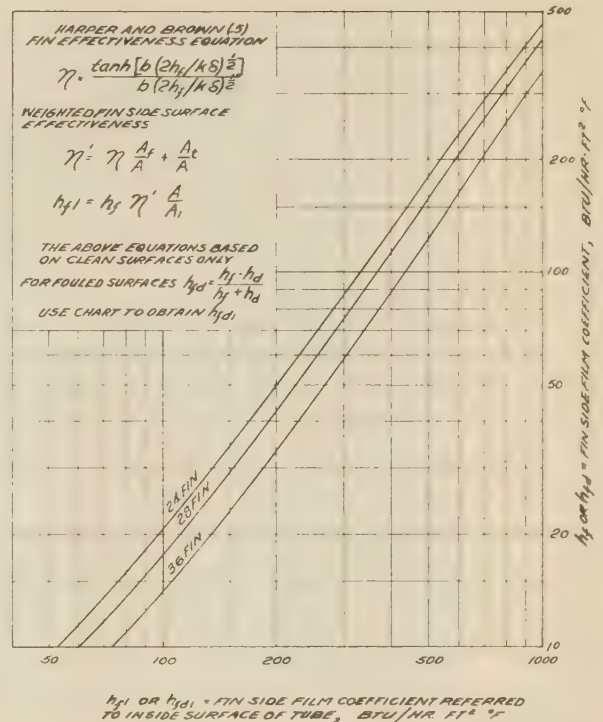


FIG. 4 FIN-SIDE FILM COEFFICIENTS CORRECTED FOR FIN-SIDE SURFACE EFFECTIVENESS REFERRED TO INSIDE SURFACE OF TUBE

greatly reduced when the corresponding μ_w is raised to the fractional power of 0.14 or 0.25.

HEAT-TRANSFER RESULTS

The heat-transfer data were correlated by the Colburn (1) heat-transfer factor j , modified by Sieder and Tate's (2) viscosity correction $(\mu/\mu_w)^{-0.14}$ giving the dimensionless expression

$$j = \frac{h_f}{cG} \left(\frac{c\mu}{k} \right)^{1/4} \left(\frac{\mu}{\mu_w} \right)^{-0.14} \quad [9]$$

The reason for using this method of correlation is that one curve can be used for heating and cooling for each fin-tube size. Also the same method was used by other investigators (4, 7), reporting data on heat transfer for extended surface.

The results for the 24- and 28-fin fin tubes plotted in Fig. 5 show that good agreement is obtained between heating and cooling in the range of R covered, indicating that this method of correlation is valid.

The results of the heat-transfer data obtained for the 36-fin fin tubes are not shown in Fig. 5, since only a few runs were made with this fin-tube size. A sufficient number of tests were made on this fin tube to determine the slope of the curve plotted for these data. The results obtained were in accord with the findings reported for the 24- and 28-fin fin tubes, when allowance was made for the higher L/D ratio for the 36-fin fin tube.

Inspection of the plotted results for the 28-fin fin-tube tests shown in Fig. 5 indicates that the transition between laminar and turbulent flow begins between $R = 200$ to 300. This is also indicated, to a lesser extent, by the results of the 24-fin fin-tube tests also shown in Fig. 5. Additional runs, not reported in this paper, made with other fin-tube sizes also gave similar results; i.e., the transition began at $R < 300$.

This phenomenon was also observed by Gunter and Shaw (4),

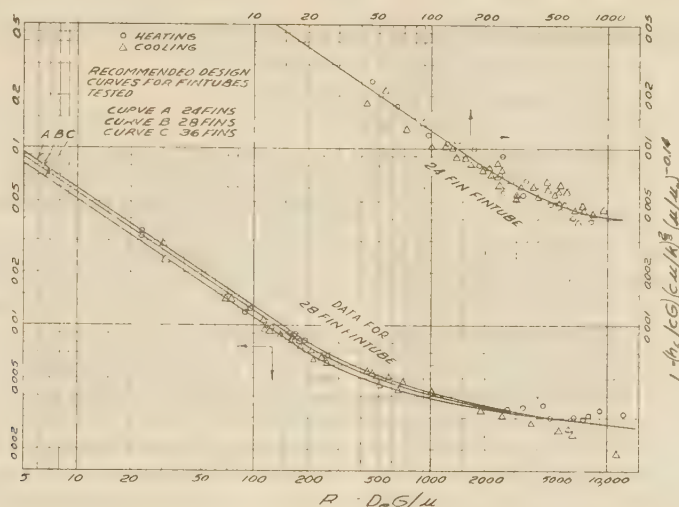


FIG. 5 HEAT TRANSFER ON FIN SIDE OF LONGITUDINALLY FINNED DOUBLE PIPES

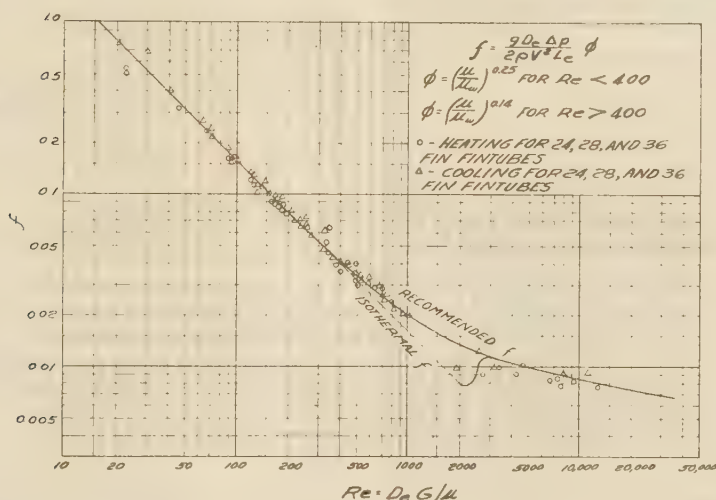


FIG. 6 PRESSURE DROP IN FIN SIDE OF LONGITUDINALLY FINNED DOUBLE PIPES

who reported the results of numerous tests heating oils in a similar double-pipe exchanger, using smaller fin tubes. They point out the analogy that an increase in the friction factor f normally increases the heat-transfer coefficient h . The pressure-drop results reported in this paper (see Fig. 6) show an increase in f over that normally expected for the isothermal f for circular ducts at Reynolds numbers ranging from 400 to 3000. In view of this it is not surprising to expect a break in the heat-transfer curve at around $R = 300$ to 400.

The data presented here are based on clean surfaces. For design purposes fouling rates as recommended by T.E.M.A. (8) should be used.

PRESSURE-DROP RESULTS

The pressure-drop data obtained were evaluated by the general isothermal Fanning equation, modified by adding the Sieder and Tate (2) function $(\mu/\mu_w)^{0.25}$ in the laminar-flow region and $(\mu/\mu_w)^{0.14}$ in turbulent flow, to make it applicable for both heating and cooling liquids. The pressure-drop results are shown in Fig. 6 for all three sizes of fin tubes tested.

Sieder and Tate (2) found that the friction factor for liquids inside tubes in nonisothermal flow would fall on the isothermal f when multiplied by $1.1(\mu/\mu_w)^{0.25}$ and $1.02(\mu/\mu_w)^{0.14}$ in the laminar- and turbulent-flow regions, respectively. In this paper better correlation was obtained by omitting the constants 1.1 and 1.02.

Since the pressure taps were located in the inlet and outlet nozzles of each hairpin section, Fig. 3, end and return-bend housing losses were included. It was found that these losses could be adjusted by increasing the actual length from 40 to 45 ft equivalent fin length.

Fig. 6 shows excellent agreement between the isothermal line and the plotted results for $R < 400$. Between $R = 400$ to 1000 the results obtained are slightly higher than the isothermal curve, indicating that the transition between laminar and turbulent flow may start at $R = 300$ to 400. At R between 3000 and 12,000 the data are again in good agreement with the isothermal curve.

Originally the data were plotted using $(\mu/\mu_w)^{0.25}$ and $(\mu/\mu_w)^{0.14}$ for $R < 2100$ and $R > 2100$, respectively. It was found, how-

ever, the correlation for heating and cooling was improved by using the factor $(\mu/\mu_w)^{0.14}$ for all values of R above 400. This finding provides an additional argument that the transition between a laminar and turbulent flow, for liquids flowing in the fin side, begins at a Reynolds number considerably below 2100. Both the heat-transfer and pressure-drop results substantiate this point.

CONCLUSIONS

1 Heat transfer on the fin side of longitudinally finned double-pipe exchangers for both heating and cooling is correlated by the conventional j factor corrected by μ/μ_w for viscosity gradient.

2 Correlation of the pressure drop for three sizes of fin tubes tested in both heating and cooling was in excellent agreement with isothermal pressure drop for values of R below 400 and also for R above 3000. In the range of R between 400 and 3000, pressure drop was greater than that predicted by the conventional Fanning equation.

3 The breaks in both the heat-transfer and pressure-drop curves indicate that transition between laminar and turbulent flow begins at $R < 400$.

4 It has been found that the usual methods for evaluating heat transfer and pressure drop for liquids inside tubes are applicable for liquids in the fin side of finned double-pipe exchangers. The equivalent diameter used in both cases was the hydraulic diameter, $D_e = 4A_c/\psi$.

BIBLIOGRAPHY

- 1 "A Method of Correlating Forced-Convection Heat-Transfer Data and a Comparison With Fluid Friction," by A. P. Colburn, Trans. American Institute of Chemical Engineers, vol. 29, 1933, pp. 174-210.
- 2 "Heat Transfer and Pressure Drop of Liquids in Tubes," by E. N. Sieder and G. E. Tate, *Industrial and Engineering Chemistry*, vol. 28, 1936, pp. 1429-1435.
- 3 "Heat Transfer and Pressure Drop in Empty, Baffled, and Packed Tubes," Part III—Relationship Between Heat Transfer and Pressure Drop," by A. P. Colburn and W. J. King, Trans. American Institute of Chemical Engineers, vol. 26, 1931, pp. 196-207.
- 4 "Heat Transfer, Pressure Drop, and Fouling Rates of Liquids for Continuous and Noncontinuous Longitudinal Fins," by A. Y. Gunter and W. A. Shaw, Trans. A.S.M.E., vol. 64, 1942, pp. 795-802.
- 5 "Heat Transmission," second edition, by W. H. McAdams, McGraw-Hill Book Company, Inc., New York, N. Y., 1942, p. 183.
- 6 "Mathematical Equations for Heat Conduction in the Fins of Air-Cooled Engines," by D. R. Harper, 3rd, and W. B. Brown, U. S. Technical Report no. 158, National Advisory Committee for Aeronautics, 1922.
- 7 "Laminar-Flow Heat-Transfer Coefficients for Ducts," by R. H. Norris and D. D. Streid, Trans. A.S.M.E., vol. 62, 1940, pp. 525-533.

8 "Standards of Tubular Exchanger Manufacturers Association," 1941 edition, published by T.E.M.A., Inc., 366 Madison Avenue, New York, N. Y.

Discussion

A. Y. GUNTER⁴ AND W. A. SHAW.⁵ The authors are to be complimented on their paper covering double-pipe longitudinal fin-tube heat exchangers.

After accounting for slightly different methods of obtaining T_w and fin effectiveness, their data on heat-transfer and friction factors check very well with the results published in a previous paper by the writers.⁶

It is gratifying to note that these data cover a much wider range than the writers' previously published material and should be of added benefit to design engineers in this field of equipment rating.

It is suggested that a table giving the range of variables covered in their tests be provided so that the extent of accurate application of the data will be made known to all concerned.

AUTHORS' CLOSURE

The table below gives the range of variables covered in the tests reported.

G from 63,800 to 665,000

R from 7.5 to 12,800

$\frac{C\mu}{k}$ from 11.0 to 1625

$\frac{\mu}{\mu_w}$ from 0.274 to 3.45

A statement on the effect of using an assumed value of 2500 Btu/(hr) (sq ft) (deg F) for the condensing steam coefficient has been added to the text of the paper. It must be remembered that the tests reported were made on hairpin sections having 20 ft 0 in. continuous fin. For shorter fin lengths an adjustment must be made for the change in $\frac{L}{D_e}$ ratio.

⁴ Director of Development, Alco Products Division of the American Locomotive Company, New York, N. Y. Mem. A.S.M.E.

⁵ Development Engineer, Alco Products Division of the American Locomotive Company, New York, N. Y. Jun. A.S.M.E.

⁶ Refer to authors' bibliography (4).

Numerical Methods for Transient Heat Flow

By G. M. DUSINBERRE,¹ BLACKSBURG, VA.

This paper deals with the application of numerical methods for the solution of heat-conduction problems, their generality being extended in the following ways: (a) A modulus is developed by choice of which the worker may proceed most rapidly to a solution, or may proceed more slowly and with greater precision; (b) criteria are developed for the choice of modulus to insure convergence. This is most important at a convective surface; (c) a method is developed for handling k and c when these properties vary independently with temperature. A comprehensive Appendix gives the derivations, and the use of equations and charts is demonstrated by typical examples.

NOMENCLATURE

THE following nomenclature is used in the paper:

- k = conductivity
- c = specific heat
- ρ = density
- t = time
- Δt = a small finite time interval
- x, y, z = space co-ordinates
- Δx = a small finite distance
- T = temperature
- T' = temperature after an interval Δt
- h = surface coefficient of heat transmission
- M = modulus relating Δx and Δt
- N = the ratio $h\Delta x/k$
- F = a coefficient
- C = a temperature change
- p = a ratio of specific heats
- q = a ratio of conductivities

GENERAL

The conventional treatment of heat conduction problems, since the time of Fourier, has been by analytical attack on the general equation

$$\frac{\partial}{\partial x} k_x \frac{\partial T}{\partial x} + \frac{\partial}{\partial y} k_y \frac{\partial T}{\partial y} + \frac{\partial}{\partial z} k_z \frac{\partial T}{\partial z} = c\rho \frac{\partial T}{\partial t} \dots [1]$$

This is quite unmanageable as it stands. Fortunately, the variation of k with orientation and temperature, and of c with temperature, are often negligible within the required accuracy of a particular problem, so these properties are taken as constant. It is generally necessary also to impose certain simplifications on the boundary conditions. Under these assumptions a literature has grown up, too extensive and too familiar for detailed reference. Solutions arrived at in this way are known, somewhat strangely, as "exact" solutions.

Recently some attention has been given to numerical and graphical methods. A few of the more accessible references are

¹ Department of Mechanical Engineering, Virginia Polytechnic Institute. Mem. A.S.M.E.

Contributed by the Heat Transfer Division and presented at the Annual Meeting, New York, N. Y., Nov. 27-Dec. 1, 1944, of THE AMERICAN SOCIETY OF MECHANICAL ENGINEERS.

NOTE: Statements and opinions advanced in papers are to be understood as individual expressions of their authors and not those of the Society.

given in the bibliography (1, 2, 3).² These treat generally of the simpler cases. There remains then a wide range of engineering problems for which no analytical solution exists, or for which the analytical solution is intolerably complex. Many of these yield to the method of analogous electrical circuits (4), but the necessary apparatus may not be available when and where needed. Numerical methods can be used by any engineer at any time.

We extend the generality of these methods in the following ways:

- (a) A modulus is developed, by choice of which the worker may proceed most rapidly to a solution, or may proceed more slowly and with greater precision.
- (b) Criteria are developed for the choice of modulus to insure convergence. This is most important at a convective surface.
- (c) A method is developed for handling k and c when these properties vary independently with temperature.

Derivations will be found in the Appendix. The use of the equations and charts will be demonstrated by examples.

EXAMPLE 1 ILLUSTRATING FLEXIBILITY OF NUMERICAL METHOD

Example 1 is set up to illustrate the flexibility of the numerical method. A relatively complex situation is analyzed by a combination of simple procedures. The assumptions are to be taken as merely typical and perhaps not the most accurate that might be made.

A large cast-iron slab 1 in. thick lies on a bed of insulating material. Slab and surroundings are at 100 F. A large copper slab 2 in. thick, having been heated uniformly to 400 F, is placed on the iron slab and sprayed with water at 100 F.

Required. The cooling curves at $1/2$ -in. intervals in the two slabs, down to a surface temperature of 300 F.

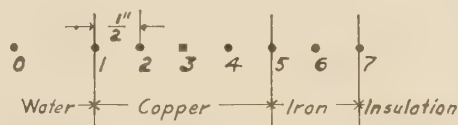


FIG. 1 REFERENCE POINTS FOR EXAMPLE 1

Assumptions. Edge effects may be neglected, making the flow one-dimensional. Surface resistance between the slabs is negligible. Conduction from iron to surroundings is negligible. The following values of metal properties may be assumed as constant: Copper, $k = 218$, $c = 0.094$, $\rho = 556$; Iron, $k = 27$, $c = 0.118$, $\rho = 442$. The surface coefficient h may be assumed 500 at 400 F, 700 at 350 F, and 900 at 300 F.

Solution. Reference points are as designated in Fig. 1. The following preliminary calculations are made, the derivation and significance of which are given in the Appendix:

$$\frac{M_{Cu}}{M_{Fe}} = \frac{0.094 \times 556 \times 27}{0.118 \times 442 \times 218} = 0.124$$

$$N_{max} = \frac{900}{24 \times 218} = 0.172$$

$$2N + 2 = 2.34 < 3$$

² Numbers in parentheses refer to the Bibliography at the end of the paper.

Choosing

$$M_{Cu} = 3, M_{Fe} = 3/0.124 = 24.2$$

$$\Delta t = \frac{0.094 \times 556}{3 \times 218 \times 24 \times 24} = 0.000139 \text{ hr} = 0.5 \text{ sec}$$

$$\text{Initial } T_s = \frac{400 \times 0.094 \times 556 + 100 \times 0.118 \times 442}{0.094 \times 556 + 0.118 \times 442} = 250 \text{ F}$$

sec	0	1	2	3	4	5	6	7
$F_{n-1,n}$		0.064				0.333	0.041	0.091
$F_{n,n}$		0.269				0.626	0.918	0.918
$F_{n+1,n}$		0.667				0.041	0.041	—
0	0	100	400	400	400	250	100	100
			6A			133	10	8
			107A	1200B	1200B	156	92	92
			267A			4	4	—
1	0.5	100	380	400	400	350	293	106
			6			117	12	9
			102	1180	1150	1043	98	92
			267			4	4	—
2	1.0	100	375	393	383	348	304	114
			0.089C	9		118	12	10
			0.244C	91	1151	1124	1035	104
			0.667C	262		5	4	—
3	1.5	D	362	384	375	345	311	120
								103

Notes: A. We add $F_{n-1,n}$, $F_{n,n}$, and $F_{n+1,n}$ to get T_i . The same "weighting" procedure is used at points 5, 6, and 7.
 B. We add T_i , T_s and T_b and divide by 3 to get T_s . This "averaging" procedure is used at points 3 and 4.
 C. T_i having reached 375, we change $F_{n-1,n}$ and $F_{n,n}$.
 D. Remaining work omitted, for brevity.

FIG. 2 SAMPLE WORK SHEET FOR EXAMPLE 1

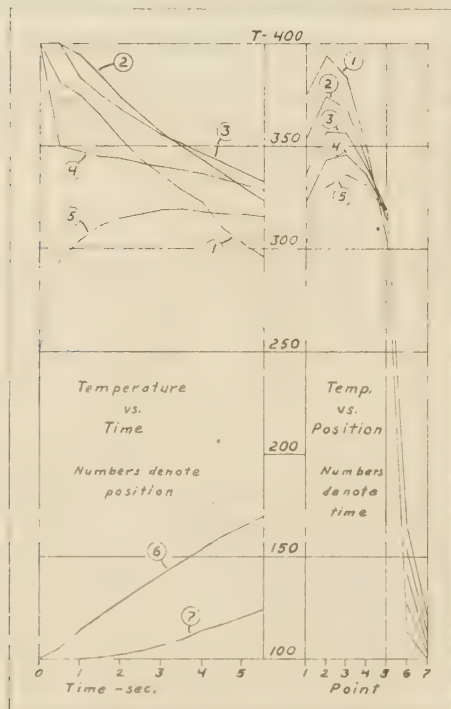


FIG. 3 TEMPERATURE CURVES FOR EXAMPLE 1

An "averaging" procedure is available for points 2, 3, and 4. Coefficients used for other points are calculated and entered on the work sheet, Fig. 2. Additional coefficients for point 1 are given in Table 1.

TABLE 1 COEFFICIENTS FOR EXAMPLE 1

T_1	h	N	F_{n1}	F_{n11}	F_{n11}
400—375	500	0.096	0.064	0.269	0.667
375—325	700	0.134	0.089	0.244	0.667
325—300	900	0.172	0.114	0.218	0.667

The calculations are then performed according to the work sheet. Results are shown graphically in Fig. 3.

EXAMPLE 2, ILLUSTRATING PROCEDURE WHEN k VARIES WITH TEMPERATURE

Example 2 is chosen to illustrate the procedure when k varies with temperature, and because an experimental solution is available for check. This is the subject of a paper by Bradley and Ernst (5).

A furnace is operated cyclically, on 8 hr and off 16 hr. During operation the hot-side temperature is as near 1900 F as possible. The ambient temperature is 100 F. The furnace wall is laid up with a single course of brick, headed to the fire, giving a thickness of 9 in.

Required. The time-temperature curves for the outer surface and three interior points of the wall, and an estimate of the daily heat loss when the furnace has reached an equilibrium cycle.

Assumptions. The $T-k$ relation for the brick is given in Table 2, and $c = 0.23$, constant. Strictly, we should assume the furnace airtight with no heat losses from the interior while secured, or else assume a rate of air leakage. But to permit a closer comparison of results we use the experimentally measured fire-side surface temperatures as "feed-in." The same was done with the electric analyzer, as described in reference (5). A rough steady-state analysis shows that the outer surface temperature will rise less than 100 deg F above the ambient, so the fluctuation here will not be great. We estimate h to be 2.4 and assume that its variation can be neglected.

TABLE 2 SAMPLE CALCULATIONS FOR FIG. 5

T	k^*	q	$q\Delta T$	$\sum_{100}^T q\Delta T$
100	94	...
200	96	94
300	98	190
400	0.99	1.000	101	288
500	104	389
600	1.04	1.050	107	493
700	110	600
800	1.11	1.121	114	710
900	118	824
1000	1.19	1.202	123	942
1100	127	1065
1200	1.29	1.303	135	1192
1300	139	1327
1400	1.42	1.434	148	1466
1500	153	1614
1600	1.56	1.576	162	1767
1700	170	1929
1800	1.73	1.747	179	2099
1900	189	2278
2000	1.91	1.929	189	2467

* Conductivity was reported on a "per-inch" basis.

Solution. Δx has been set at $1/4$, the length of the brick, 0.1875 ft. We designate reference points as in Fig. 4. Preliminary calculations are as follows:

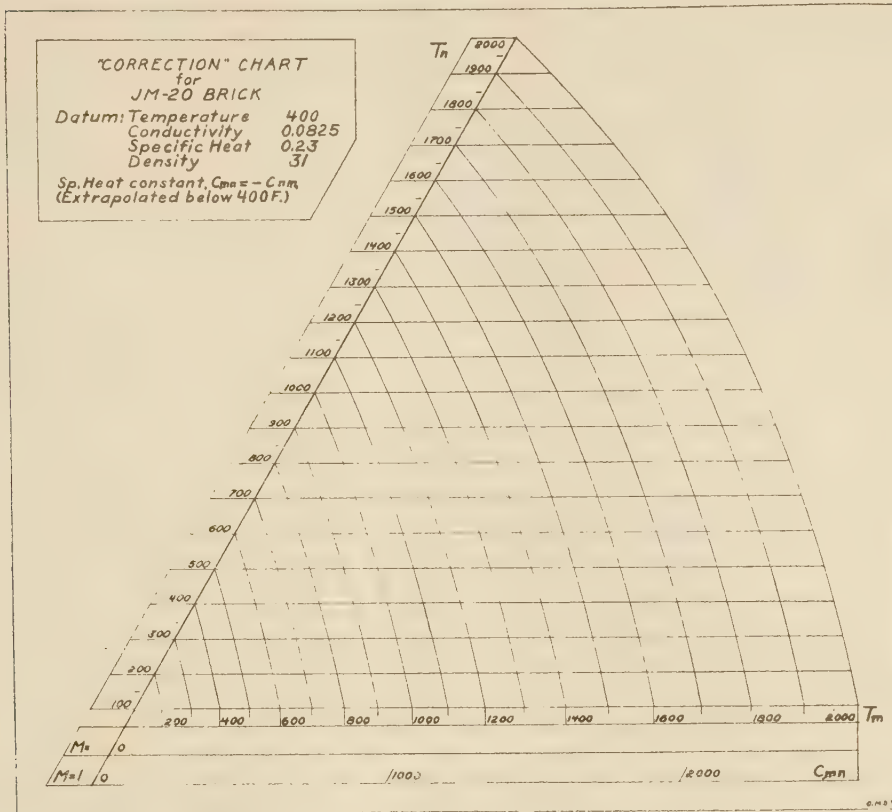


FIG. 5 CORRECTION CHART FOR JM-20 BRICK



FIG. 4 REFERENCE POINTS FOR EXAMPLE 2

$$q_{mn \max} = q_{1,900,100} = 2278/1800 = 1.264$$

$$M \geq 2 \times 1.264 = 2.53$$

Steady-state analysis shows $T_2 \leq 800$ F, and

$$q_{21 \max} = q_{800,100} = 710/700 = 1.014$$

$$M \geq 3 \times 1.014 = 3.04$$

$$N = \frac{2.4 \times 0.1875}{0.0825} = 5.45$$

$$M \geq 2(5.45 + 1) = 12.90$$

The conditions are such that we can disregard the last restriction. Choosing $M = 3.04$

$$\Delta t = \frac{0.23 \times 31 \times 0.1875^2}{3.04 \times 0.0825} = 1 \text{ hr}$$

We have a previously prepared "correction" chart for the material, Fig. 5. We convert this to the chosen modulus, drawing the diagonal lines shown in Fig. 6. The chart now shows, for an interior point, the change during Δt due to the temperature at an

adjacent point. For the outer surface we calculate the auxiliary diagonal lines at the lower left.

Starting with the initial distribution and taking T_5 from the experimental data, we calculate the succeeding temperatures. The results for three days are shown in Fig. 7. The fourth day was practically a repetition of the third, showing that an equilibrium cycle had been reached.

The complete work sheet is too long for reproduction but we show for example how the temperatures for the 58th hour are obtained. At the 57th hour we have

Point.....	0	1	2	3	4	5
Temperature.....	100	175	620	1075	1440	1500

Using Fig. 6 we find the "corrections" for each point

$-C_{01}$	C_{21}	$-C_{12}$	$C_{22} = -C_{23}$	$C_{42} = -C_{24}$	C_{54}
60	65	150	175	160	30

These values are entered directly on the work sheet, Fig. 8.

If we were not using experimental data for point 5 and wished to assume no air leakage, we should use $C_{45} = -2C_{54}$, whence $T_5 = 1440$.

The calculated heat flow for the equilibrium cycle is 3430 Btu per sq ft per day. From the experimental curves the figure is 3350. This agreement should be satisfactory for most purposes.

A slight overshooting can be observed at several points in Fig. 7. This will occur when the temperature changes rapidly, especially with a minimum M . When greater precision is required, the remedy is to use a larger M , and the cost is extra work. In this problem it could be foreseen that the T_4 curve would

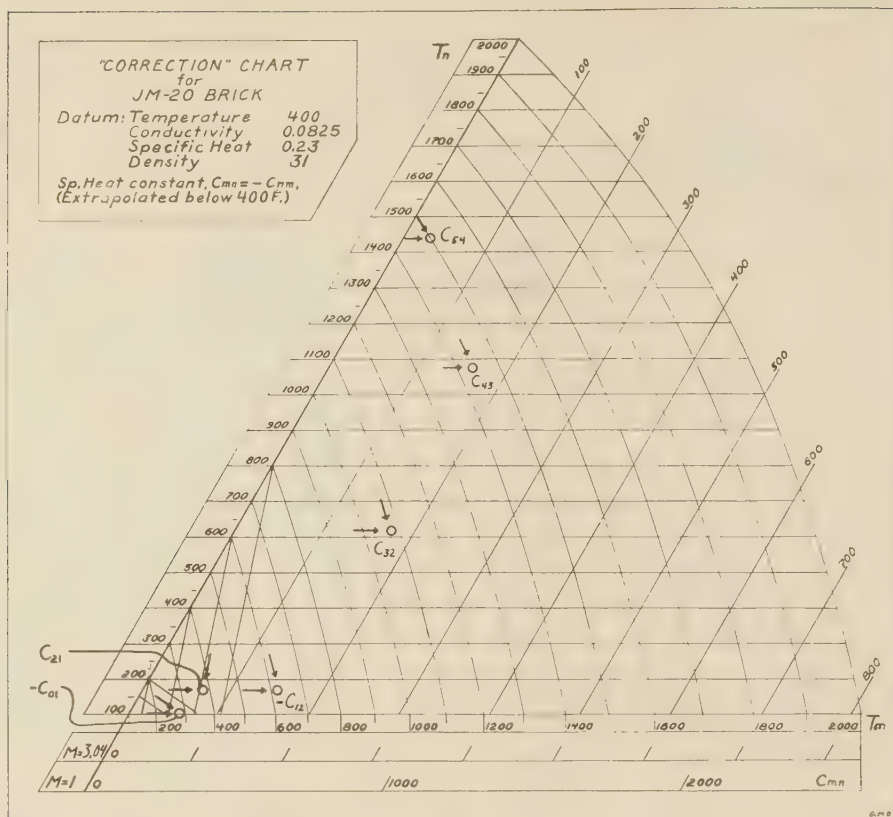


FIG. 6 CORRECTION CHART AS USED FOR EXAMPLE 2

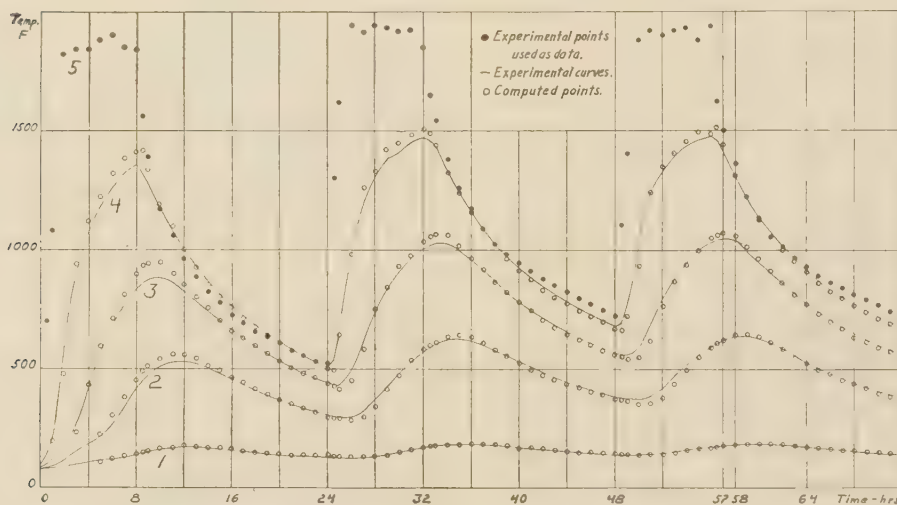


FIG. 7 TEMPERATURE CURVES FOR EXAMPLE 2

Time	Point	0	1	2	3	4	5
57	Temperature	100	175	620	1075	1440	1500
	$C_{n+1,n}$		65	175	160	30	
	$C_{n-1,n}$		-60	-150	-125	-160	
	C_{total}		5	25	-15	-130	
58	Temperature	100	180	645	1060	1310	1360

FIG. 8 SAMPLE WORK SHEET FOR EXAMPLE 2

overshoot at the beginning and end of the heating period, so half-intervals were used as shown in Fig. 7.

CONCLUSION

These examples have shown the use of a number of the procedures outlined in the Appendix. Many other combinations are possible, permitting investigation of a wide range of heat-transfer problems. Applications suggest themselves especially in metal-

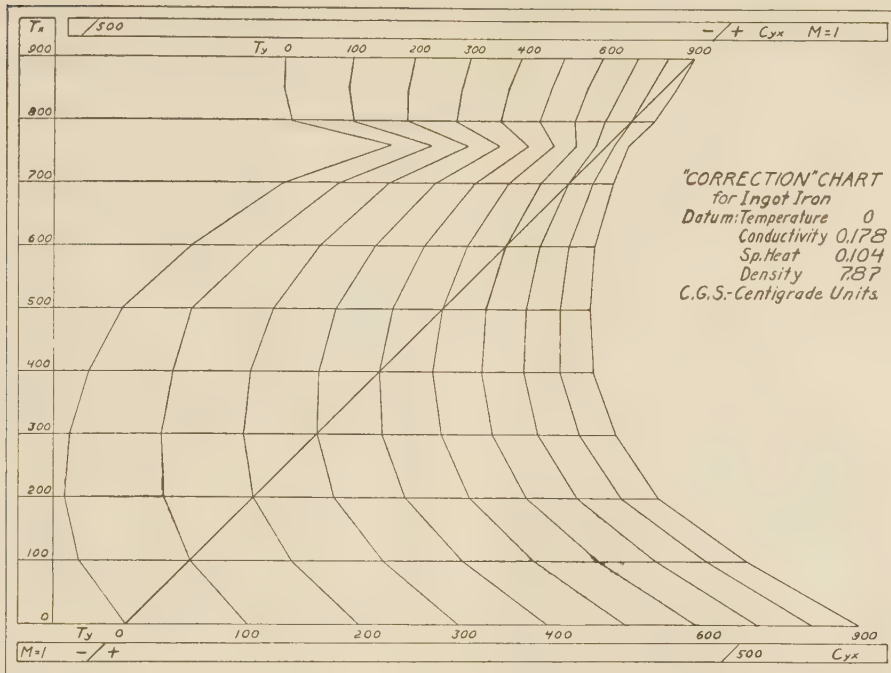


FIG. 9 CORRECTION CHART FOR INGOT IRON

lurgical processes where k , c , and h vary greatly. Fig. 9 is exhibited to show the form the correction chart may take for a metal in which k has a range of about 4:1 and c about 3:1.

ACKNOWLEDGMENTS

The author is grateful to his associates, H. G. Elrod, Jr., and C. M. Fowler for continued interest, criticism, and advice, and to Dr. C. B. Bradley of Johns-Manville Research Laboratory for furnishing the large-scale chart from which Fig. 7 was drawn.

Appendix

1 Regarding k and c as constant for the present, and flow as one-dimensional, we consider Fig. 10 an element of the material centered at 2. The dimension Δx has some small value consistent with the practical requirements of the problem. The element 2 is insulated except where it adjoins element 1, which is no larger than 2. At time t the temperatures are T_1 and T_2 and the gradient is $(T_1 - T_2) / \Delta x$.

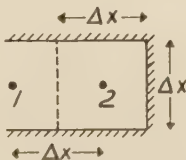


FIG. 10 ONE ADJACENT ELEMENT

We now make three important assumptions:

- A time interval Δt can be chosen sufficiently small that there is negligible error in using the initial gradient $(T_1 - T_2) / \Delta x$ to compute the heat flow during this interval.
- Time interval Δt is sufficiently small that there is negligible error in neglecting the effect on 2 of any region beyond 1.
- Δx is sufficiently small that there is negligible error in

using the temperature at point 2 to compute the heat capacity of the element 2.

Under these assumptions we can write the following heat balance

$$k \Delta t (T_1 - T_2) = c \rho \Delta x^2 (T'_2 - T_2) \dots \dots \dots [2]$$

We introduce a modulus defined as

$$M = c \rho \Delta x^2 / k \Delta t \dots \dots \dots [3]$$

Then Equation [2] becomes

$$T_1 - T_2 = M (T'_2 - T_2) \dots \dots \dots [4]$$

Under our assumptions, T'_2 cannot, in any Δt , attain a value more than half way between the initial values T_1 and T_2 ; that is

$$T'_2 - T_2 \leq \frac{1}{2} (T_1 - T_2) \text{ and } M \geq 2 \dots \dots \dots [5]$$

This is the first criterion for a valid numerical procedure.

2 Now consider element 2 as lying between two similar elements, Fig. 11. The heat flow from 3 is additive to that from 1, and

$$(T_1 - T_2) + (T_3 - T_2) = M (T'_2 - T_2) \dots \dots \dots [6]$$

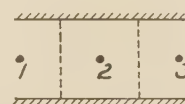


FIG. 11 TWO ADJACENT ELEMENTS

We may put this in three different forms as follows

$$T'_2 = \frac{T_1 + (M - 2)T_2 + T_3}{M} \dots \dots \dots [7]$$

This defines what we may call an "averaging" procedure.

It is the quickest and most convenient since it involves only two arithmetical steps for each computed point, namely, one addition and one division.

Or

$$T'_2 = F_{12}T_1 + F_{22}T_2 + F_{32}T_3 \dots [8]$$

in which

$$F_{12} = F_{22} = 1/M \quad F_{22} = (M - 2)/M \quad \Sigma F = 1 \dots [9]$$

This defines a "weighting" procedure. It involves three multiplications and one addition.

Or

$$T'_2 = T_2 + C_{12} + C_{32} \dots [10]$$

in which

$$C_{12} = (T_1 - T_2)/M \quad C_{32} = (T_3 - T_2)/M \dots [11]$$

This defines a "correction" procedure. It involves two subtractions, two multiplications, and an algebraic addition. However, the work can be simplified by the use of a chart, and this is our best recourse when thermal properties vary with temperature.

In Equation [7], if we give M its low limiting value of 2, we get the Schmidt³ formula, $T'_2 = (T_1 + T_3)/2$. This says that the temperature at a point depends upon the previous temperatures at adjacent points but not upon its own previous temperature.⁴ Starting with a constant temperature in the material, this method gives rise to a stepwise time-temperature plot, though by "cranking-in" the initial calculation from an analytical solution, this can be avoided (1, 2). The choice of modulus 3 gives $T'_2 = (T_1 + T_2 + T_3)/3$, which is about as convenient as the Schmidt formula and has a number of advantages.

A further justification of Equation [5] can be had from Equation [8]. If $M < 2$, then $F_{22} < 0$, which says that T'_2 depends on T_2 in a negative sense. Intuitively, this seems absurd. No formal proof can be offered here,⁵ but it would appear that we may take as a general criterion

$$F_{nn} \geq 0 \dots [12]$$

3 At a surface where convection occurs, the reference points may be disposed as in Fig. 12 (a) or (b). Formulas may be developed for (b), and these have certain advantages, but as we are generally interested in the surface temperature, we confine attention here to (a).

The point 0 in Fig. 13 is taken in the adjacent medium at some distance where the gradient normal to the surface has become negligible. We make use of a surface coefficient h which is to include the effect of convection and radiation. Temperature T_0 and h may vary, so long as they may be regarded constant over any Δt . Under our assumptions the heat balance is

$$k \Delta t (T_2 - T_1) + h \Delta x \Delta t (T_0 - T_1) = c \rho \Delta x^2 (T'_1 - T_1)/2 \dots [13]$$

We define a "Nusselt number"

$$N = h \Delta x / k \dots [14]$$

Introducing M and N

$$(T_2 - T_1) + N(T_0 - T_1) = \frac{M}{2} (T'_1 - T_1) \dots [15]$$

³ Max Jakob (Trans. A.S.M.E., vol. 65, 1943, p. 613) states that the method should be credited to L. Binder.

⁴ After the calculation is under way, the temperature at a point does depend on the value at the second preceding time interval.

⁵ In a paper under preparation, C. M. Fowler undertakes a formal mathematical investigation of the convergence of these methods.

If $T_0 = T_1$, a very common initial condition, then

$$T'_1 - T_1 \leq \frac{2}{3} (T_2 - T_1) \text{ and } M \geq 3 \dots [16]$$

If we write Equation [15] in the form of Equation [8]

$$F_{21} = 2/M, \quad F_{01} = 2N/M, \quad \text{and } F_{11} = (M - 2N - 2)/M \dots [17]$$

Then if we are to meet the condition of Equation [12]

$$M \geq 2N + 2 \dots [18]$$

In choosing M , we should be guided by whichever of Equations [16] or [18] is more restrictive, using of course the largest N which occurs in the problem.

If N is large, observance of these criteria may be inconvenient. Provided the surface temperature does not fluctuate much from the steady-state value (but not otherwise), a permissible approximation is to jump at once to the steady-state relations (1)

$$F_{21} = 1/(N + 1), \quad F_{11} = 0, \quad F_{01} = N/(N + 1) \dots [19]$$

At a well-insulated surface h , N , and F_{01} may approximate zero.

4 In a heterogeneous wall, Fig. 14, materials 2 and 4 have different properties. Time interval Δt must be the same for all layers. If it is convenient to choose

$$\Delta x_2 / \Delta x_4 = \sqrt{k_2 c_4 \rho_4 / k_4 c_2 \rho_2}$$

then the same modulus applies in both regions. But Equation [3] allows more freedom in treating such cases. For ex-

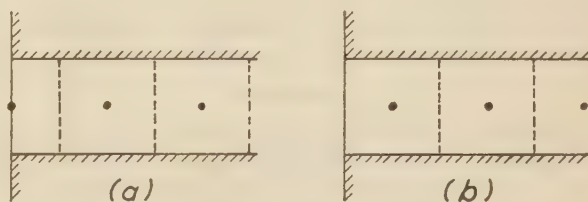


FIG. 12 TWO POSSIBLE REFERENCE SYSTEMS

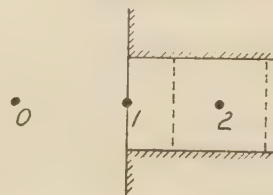


FIG. 13 A CONVECTIVE SURFACE



FIG. 14 A HETEROGENEOUS WALL

ample, if we wish to keep Δx the same in both regions it is only necessary that

$$M_2/M_4 = c_2 \rho_2 k_4 / c_4 \rho_4 k_2$$

We choose M for the region in which it is lowest and use an averaging procedure here, and weighting procedures elsewhere. In this case, for point 3, the weighting formulas become

$$F_{23} = 2k_2/(k_2M_2 + k_4M_4), \quad F_{43} = 2k_4/(k_2M_2 + k_4M_4), \\ F_{23} = 1 - F_{33} - F_{43} \dots [20]$$

If two materials at different temperatures are placed in good thermal contact, the initial T_2 may be taken as a weighted mean with respect to $c\rho \Delta x$ in the two regions, by conservation of energy. If there is an appreciable interface resistance, the surfaces are treated under section 3.

A homogeneous material may be treated under varying Δx and M if we wish to study changes more closely in certain regions.

5 Sensible heat may be absorbed within the material by a phase change or chemical reaction and may be produced by these phenomena and by electrical means. In the last case it is only necessary to add, at each point involved, the temperature rise during each Δt , which is the energy supplied divided by the heat capacity of the element.

Where a latent heat exists, temperature changes are delayed. When the calculated temperature at a point passes the phase-change temperature, we subtract the excess, making an account of it, and continue the calculation using the phase-change temperature. When our account of excess degrees reaches the value L/c we discontinue the account and use the computed temperature.

6 Weighting equations are readily derived for the effectively one-dimensional radial flow in a long cylinder, Fig. 15. $M \geq 4$ and $F_{mn} \neq F_{nm}$, etc. The uniform Δx shown may be preferable to a possible logarithmic spacing when we are interested in gradients near the surface.

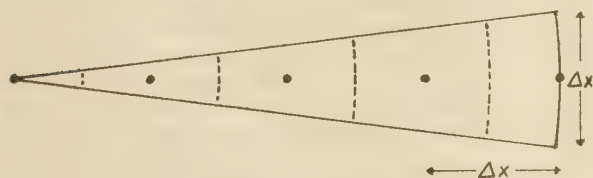


FIG. 15 REFERENCE POINTS IN A CYLINDER

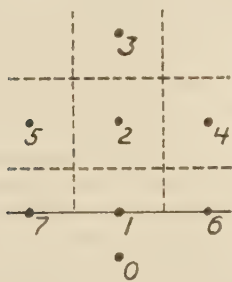


FIG. 16 A TWO-DIMENSIONAL SYSTEM

7 From Fig. 16 we can derive equations for two-dimensional flow. For the interior, $M \geq 4$ and preferably $M = 5$. There is no great additional difficulty in allowing for a k variable with orientation.

8 We now take up methods useful when k and c vary independently with temperature. Inspection of Equation [1] shows that the concept of diffusivity is not applicable here, which is why we have not introduced it.

In order to continue the use of the modulus already developed, it is convenient to select a datum temperature to which the subscript d refers.

Then

$$M = c_d \rho \Delta x^2 / k_d \Delta t \quad p_n = c_n / c_d \quad q_n = k_n / k_d \dots [21]$$

Referring to Fig. 11, the heat balance is now

$$k_{12} \Delta t (T_1 - T_2) + k_{22} \Delta t (T_2 - T_2) = c_2 \rho \Delta x^2 (T'_2 - T_2) \dots [22]$$

Double subscripts here indicate a mean value. Using Equations [21]

$$q_{12}(T_1 - T_2) + q_{22}(T_2 - T_2) = p_2 M (T'_2 - T_2) \dots [23]$$

If we put this in the form of Equation [10], then, corresponding to Equation [11]

$$C_{12} = q_{12}(T_1 - T_2) / p_2 M \text{ and } C_{22} = q_{22}(T_2 - T_2) / p_2 M \dots [24]$$

These formulas are the basis of the "correction" chart. The trouble of computing and plotting this chart may be justified by the fact that it can be used for any problem with the material to which it refers.

Any C_{mn} can be taken as

$$\left[\frac{1}{M} \right] \cdot \left[\frac{1}{p_n} \right] \cdot [q_{mn}(T_m - T_n)]$$

The last factor amounts to

$$\int_n^m \frac{k dT}{k_d}$$

If the $T - k$ relation is expressed by a table, we integrate numerically; if by an equation, we can integrate formally. In either case, construct a table of this factor over the required range of T_m, T_n . Introduce the second factor by dividing each entry by p_n . This gives a table of C_{mn} to modulus 1. Plot (a) horizontal straight lines of T_n to a uniform scale, (b) straight lines of C_{mn} to a uniform scale, inclined about 30 deg to the right of the vertical, and (c) curves of T_m inclined to the left and non-uniform. Erase the C_{mn} lines and the chart is like Fig. 5 or 9. It can be converted to any desired modulus by drawing new diagonal lines to the appropriate scale.

Table 2 shows part of the calculations for Fig. 5. The $T - k$ data are from reference (5). In this case c is constant, p drops out, and $C_{nm} = -C_{mn}$, so only half the chart need be drawn.

9 For a convective surface the equations are analogous to those derived in Section 3. We redefine N as $h \Delta x / k_d$. As before, we must give attention to the maximum N occurring in the problem, and also to the maximum q/p ratio. Referring to Fig. 13

$$C_{21} = 2q_{21}(T_2 - T_1) / p_1 M \quad C_{01} = 2N(T_0 - T_1) / p_1 M \dots [25]$$

C_{21} at a surface is then double the value from the chart.

Criteria corresponding to Equations [16] and [18] are

$$M \geq 3(q_{21}/p_1) \quad M \geq 2(N + q_{21})/p_1 \dots [26]$$

Steady-state approximations corresponding to Equation [19] are

$$C_{21} = q_{21}(T_2 - T_1) / (N + q_{21}) \quad C_{01} = N(T_0 - T_1) / (N + q_{21}) \dots [27]$$

If conditions are nearly steady at a surface, we can plot the results as auxiliary lines on the correction chart. Otherwise we must tabulate.

BIBLIOGRAPHY

- 1 "Heat Transmission," by W. H. McAdams, McGraw-Hill Book Company, Inc., New York, N. Y., 1942, pp. 39-43.
- 2 "Applied Mathematics in Chemical Engineering," by T. K. Sherwood and C. E. Reed, McGraw-Hill Book Company, Inc., New York, N. Y., 1939, pp. 241-255.
- 3 "The Numerical Solution of Heat-Conduction Problems," by H. W. Emmons, Trans. A.S.M.E., vol. 65, 1943, pp. 607-615.

4 "A Method for Determining Unsteady-State Heat Transfer by Means of an Electrical Analogy," by V. Paschakis and H. D. Baker, *Trans. A.S.M.E.*, vol. 64, 1942, pp. 105-112.

5 "Analyzing Heat Flow in Cyclic Furnace Operation," by C. B. Bradley and C. E. Ernst, *Mechanical Engineering*, vol. 65, 1943, pp. 125-129 and 527-530.

Discussion

C. M. FOWLER.⁶ The author's two representative problems seem to dispose of the practical side of the theoretically unsolved cases where both thermal properties and transfer coefficients are functions of temperature.

The writer has had occasion to study heat flow through steel specimens for the purpose of determining hardness distributions throughout specimens after quenching, and to his knowledge, the work done so far on this problem has been confined to cases where transfer coefficients and thermal properties are assumed constant over the quenching range, with no account being taken of heats of phase change in the steel. It is the writer's opinion that the numerical study of the heat flow in, say, a circular cylinder or slab taking into account the variable properties mentioned would be of real value in making more accurate predictions of "after-quench" hardness distributions of these specimens.

In the actual mechanics involved in solving a problem, the author develops a restrictive criterion for the modulus, $M = 2$, Equation [5]. For all practical purposes this is true. However, the assumptions used in deriving this criterion are actually more restrictive than necessary for many problems, and in a paper under preparation the writer has shown that in some cases M may be as low as 1 which, as the author points out, is intuitively absurd. It appears to the writer that most of the criteria developed for both the modulus and the surface transfer coefficient N have been demonstrated under conditions more restricted than those actually called for in the problems under consideration.

The writer would also be very much interested in seeing some problems worked out involving a phase change such as the author suggests in the Appendix, Section 5.

W. A. HADLEY.⁷ It would appear to the writer that the method described in the paper would be even more useful in evaluating unsteady-state diffusional processes, such as drying, carburization of steel, etc., than heat transfer. In general, most diffusional processes are not steady state and must be analyzed mathematically by making untrue but simplifying assumptions. It would appear that the paper offers every engineer a simple but powerful tool whose use will permit him to analyze closely diffusional processes which he could only approximate before.

Will the author please verify this contention?

VICTOR PASCHAKIS.⁸ The numerical method is a powerful tool and any paper which attempts to make this tool more acceptable is to be welcomed.

In studying the paper the writer notes in particular the following observations of the author:

1 That "... under our assumptions T'_2 cannot in any Δt attain a value more than halfway between the initial values T_1 and T_2 . . ." Whereas this statement is certainly correct, it would help the reader unfamiliar with the basis of this method if this point would be clarified.

⁶ Department of Marine Engineering, United States Naval Academy, Annapolis, Md.

⁷ Ensign, U.S.N.R., Department of Marine Engineering, United States Naval Academy, Annapolis, Md. Jun. A.S.M.E.

⁸ Research Associate, Department of Mechanical Engineering, Columbia University, New York, N. Y.

2 At another point the author states, "intuitively it seems absurd that T'_2 should depend on T_2 in a negative sense." Probably one could establish a reasoning from which such a dependence could be calculated and therefore the formal proof which is forthcoming will be of high interest.

3 In Fig. 3 curve 4 on the left side shows a remarkable discontinuity at approximately 0.8 sec. This discontinuity has either to be attributed to too coarse a lumping or to an error in the procedure. Clarification of this point would be helpful.

The author mentions the electric-analogy method in which the writer is particularly interested. He states, "the necessary apparatus may not be available when and where needed. Numerical methods can be used by any engineer at any time." It is the opinion of the writer that each method (numerical and electric analogy) has its useful applications. The fact that a "heat-and-mass-flow analyzer" is available in only one or two places does not appear to be a legitimate reason against the method. For all cases where the electric method is a more powerful tool it should be applied, and when the numerical method is better, it should be applied. It appears that the refinements presented in the paper make the last part of the author's statement a bit doubtful. The rules and procedure become so complicated that many engineers in the field may not have the time to familiarize themselves with the necessary steps. Moreover, it appears to the writer that the electric-analogy method has unusual educational values in showing the observer, on instruments, what is going on in the pieces subject to heat flow.

Finally it should be noted that the numerical method and the electric-analogy method have in common the necessity of lumping. But the electric method does not in most instances call for any lumping of time, and in those cases where lumping of time is required it is never an entire lumping. The numerical method is of course based entirely upon lumping in time as well as in space, which is obviously a disadvantage as against the analogy method.

In the presentation, the author brought up the problem of constant properties of materials, and in problems dealing with metals, the desirability of working with the actual specific-heat and conductivity curves which show a temperature dependency.

The writer feels that the practicing engineer will by and large make use only of such engineering knowledge as is reduced to charts and graphs or to material available in handbooks. Often he has not the time to work out numerically any type of problem.

Now, if curves with dimensionless parameters should be used, the introduction of changing properties increases the necessary number of charts very considerably. For example, in quenching the introduction of each phase change adds three parameters to those necessary for representation in dimensionless units. The consequence is the necessity of a vast number of charts too unwieldy for use. For many purposes the charts with constant properties, as for example those by Gurney and Lurie, are sufficient.

This of course should not imply that it is not desirable to have methods which permit the solution of problems considering the change of properties, but it is the opinion of the writer that such methods will be more helpful to the research worker than to the practicing engineer and that it is most important to help the latter by development of easily usable curves and charts.

AUTHOR'S CLOSURE

Lieutenant Fowler's discussion is welcome in supporting the author's opinion that the methods may be of use in metallurgical research. The phase change of principal interest to Lieutenant Fowler, and perhaps to other metallurgists, is that occurring in steel around 723 C. There are many examples of this; for a

recent one we may cite a paper by Hess.⁹ By the numerical method, good qualitative agreement has been obtained with experimental heating and cooling curves. Better quantitative results depend on better determinations of physical properties. If merely a mean value of specific heat is used, the true shape of the curves is not obtained. When qualitative agreement does not exist, quantitative accuracy can be only accidental.

Where temperature changes are small and the principal phenomenon is freezing, the author recommends the analysis of London and Seban.¹⁰

Lieutenant Fowler suggests that the criteria for choice of modulus are unduly restrictive, and it is to be hoped that his studies on this subject will be published soon. In the meantime, the author can only say that, in practice, observance of the criteria will avoid divergence and the oscillating type of convergence. The worst one gets is a poor result at the first computed point, such as occurs in Fig. 3 of the paper, at 0.5 sec at point 4. This was noted by Professor Paschkis. If this is not satisfactory for the purpose at hand, the remedy is to use a closer network or a larger modulus.

Mr. Hadley's discussion is welcome, as it brings out the point that these methods may be used for any physical situation which gives rise to the same form of differential equation. The treatment of diffusion, however, involves some features which are worth illustrating by an example.

The problem chosen¹¹ concerns the drying of clay slabs. We have the following data and notation:

Diffusivity, D	0.4 sq cm per hr
Density (bone dry), ρ	1.55 g per cc
Initial concentration, T_0	0.27 g per g
Drying rate, α	0.20 g per sq cm hr
Half-thickness of slab, L	0.4 cm
Equilibrium concentration, T_{se}	0.05 g per g

The constant drying rate α will obtain until the surface concentration reaches the equilibrium value. We are required to find the time at which that will occur, and also the average concentration at that time.

We express T_0 and T_{se} on a volume basis as 0.418 and 0.078 g per cc, respectively. We choose reference point 1 at the surface, 3 at the center line, and 2 halfway between. Then $\Delta x = 0.2$ cm. If $M = 3$, $\Delta t = \Delta x^2 / DM = 0.04 / 0.4 \times 3 = 1/30$ hr. For points 2 and 3 the formulas are: $T'_2 = (T_1 + T_2 + T_3)/3$ and $T'_3 = (2T_2 + T_3)/3$.

The treatment of the surface point is somewhat different, as we use the ideas of section 5 of the Appendix, rather than section 3. Considering the effect of the interior alone, we would have the formula $T'_1 = (T_1 + 2T_2)/3$. We use this, but concurrently we have the effect of the constant drying rate. Applying this to the half-element at the surface, and calling the result ΔT , we have: $\Delta T = \alpha \Delta t / \frac{1}{2} \Delta x = 0.2 \times 2 / 0.2 \times 30 = 0.067$ g per cc.

We are now ready to calculate Table 3 of this closure. In the numerical work, all concentrations are multiplied by 1000 to avoid decimals.

By interpolation, the time of reaching the equilibrium concentration at the surface is $(16 + 7/17)/30 = 0.55$ hr. The solution given in the reference¹¹ is 0.545 hr.

When $T_1 = 0.078$, $T_2 = 0.153$, and $T_3 = 0.178$. The mean value, $T_e = 0.141$ g per cc $= 0.091$ g per g. The reference solution is 0.094 g per g.

⁹ "Fuel-Fired Techniques and Their Possibilities," by F. O. Hess, *Mechanical Engineering*, vol. 67, 1945, p. 442.

¹⁰ "Rate of Ice Formation," by A. L. London and R. A. Seban, *Trans. A.S.M.E.*, vol. 65, 1943, p. 771.

¹¹ "Principles of Chemical Engineering," by W. H. Walker, W. K. Lewis, W. H. McAdams, and E. R. Gilliland, McGraw-Hill Book Company, Inc., New York, N. Y., 1937, p. 656.

TABLE 3

Δt	T_1	T_2	T_3	Δt	T_1	T_2	T_3
0	418	418	418	4	289	364	388
					1017	1041	1116
	67				339		
1	351	418	418	5	272	347	372
(a)	1187	1187			966	991	1066
(b)	396				322		
(c)	67				67		
2	329	396	418	6	255	330	355
	1121	1143	1210	(d)	170	170	170
	374						
	67						
3	307	381	403	16	85	160	185
	1069	1091	1065		405	430	505
	356			(e)	135		
	67				67		
4	289	364	388	17	68	143	168

NOTES: (a) On this line we enter $T_1 + 2T_2$, $T_1 + T_2 + T_3$, and $2T_2 + T_3$.
(b) We divide the entries on line (a) by 3. The result for column 1 is entered on this line. The results for the other columns are final and are entered below.

(c) We subtract 0.067 here, at every time interval.

(d) Here we observe that a parabolic distribution has been established and each T decreases by 0.017 during each time interval. So we can jump to the 16th interval by subtracting 0.170 from each T .

(e) The given equilibrium concentration at the surface is reached between the 16th and 17th intervals.

But now, assuming no vapor forms in the material, suppose we want to go on and find the time required to bring the center-line concentration down to 0.70 g per g $= 0.109$ g per cc. To do this analytically requires shifting to a new formula. But we can do it numerically merely by continuing the calculation with a fixed value of T_1 , as in Table 4. The solution is 22/30 hr.

As a final illustration, suppose the equilibrium concentration is less than 0.078 g per cc, so that it is possible to go below this value. But suppose this figure represents a concentration below which we do not wish to go. Then the lines such as (c) in Table 4 give the drying rates which we must maintain in order to get this result. In other words, the method enables the prediction of a schedule for controlled drying.

TABLE 4

Δt	T_1	T_2	T_3	Δt	T_1	T_2	T_3
16	85	160	185	19	78	120	137
(a)	405	430	505		318	335	377
(b)	135				106		
(c)	57				28		
17	78	143	168	20	78	112	126
	364	389	454		302	316	350
	121				101		
	43				23		
18	78	130	151	21	78	105	117
	338	359	411		288	300	327
	113				96		
	35				18		
19	78	120	137	22	78	100	109

NOTES: (a) and (b). These lines are obtained as before.

(c) The value of T_1 being fixed by equilibrium, we get this line by subtraction. It shows the rate at which drying will actually proceed, under the assumptions.

It adds to the paper to have a discussion by Professor Paschkis who has done so much with the electrical analyzer. In reply to his comments, we note first that if elements 1 and 2 are brought in contact and isolated, the steady-state temperature will be the weighted average of the initial temperatures, and each element can approach this steady-state temperature from only one direction.

As to T'_2 depending on T_2 in a negative sense, this would amount to saying that the hotter a body is at a given instant, the colder it must be at some selected future instant.

The discontinuity in Fig. 3 of the paper has been noted in reply to Lieutenant Fowler's discussion. It is due, not to error in the calculations, which are easily verified, but to the crude "lumping" chosen to make the example simple.

Professor Paschkis states that "lumping in time... is obviously a disadvantage as against the analogy method." The author is unable to agree. If a method can be made "sufficiently" accurate for the engineering purpose at hand, then no further refinement is

necessary or justified. If it cannot be made sufficiently accurate, then it must be discarded upon that ground, and not for any hypothetical reason.

As to what constitutes "sufficient" accuracy, that is a matter of engineering judgment. A good engineer will use all refinements which the job demands and will skip any refinements which the job does not warrant. In fact, many problems in heat conduction are too complicated for any sort of analysis and are best solved by trial-and-error experiment.

Finally, in favor of the numerical method, there is a sort of accuracy not subject to reasoning. This lies simply in human fallibility—the chance of making a mistake. The author finds that in simple arithmetic, which is all that this method demands, it is hard to make a mistake and easy to detect and remedy one when made. The opposite is true when working with parameters which have no obvious physical significance, or with the series which arise in analytical solutions.

An Electrical Geometrical Analogue for Complex Heat Flow

By C. F. KAYAN,¹ NEW YORK, N. Y.

Through the medium of the resistance concept, the general similarity of "contour maps" for heat flow and electrical flow may be visualized. The electrical analogy permits ready study of simple and complex heat-flow conditions which, because of distorted temperature conditions, would defy orthodox mathematical or graphical analysis. Internal-temperature lines (isotherms) obtained by relatively simple equipment with a geometrical type of analyzer are shown for one complex case of flow conditions.

PREVIOUS ELECTRICAL ANALOGIES

USE of the electrical analogy to study heat flow for different shapes is not new. Herein electrical potential differences (voltages) are equivalent to the thermal (temperatures). Because of ready manipulation and prospect of accurate measurements, the electrical analogy is regarded as a very useful tool. Whereas the electrical-conduction effect is more usually thought of in this connection, still it is not the only electrical effect available; for example, electrical capacity for steady-flow studies has also been used. But the electrical-conduction effect so well parallels the heat-conduction effect that in terms of the so-called resistance concept, inherently involving Ohm's law of electrical flow extended to heat flow, the problem of flow may be readily visualized.

Langmuir, Adams, and Meikle (1)² in 1913 described the use of an electrical bath in a shallow tank for model study of different heat-flow shapes, as, for example, a thick corner. Here the inside and outside surfaces of a thick corner in two-dimensional heat flow were represented in the model by metal corners forming the vertical walls of the tank. Beyond the corner for each wall were set up boundary partitions; these and the tank bottom were made of nonconducting material. A conducting liquid electrolyte represented the single isotropic homogeneous material of the heat-flow corner. With an alternating-current electrical potential established between the parallel wall electrodes, the equivalent of steady-state heat-flow conditions between constant-temperature walls was set up. By means of an electrical probe, isopotential lines representing isothermal lines in the solid body could be established. This was truly a geometrical heat-flow analogue. The same type of analysis for two-dimensional flow could be made by replacing the liquid bath by a solid conductor of uniform electrical characteristics, using thin metal or other conductive sheet cut to the pattern desired, with isopotential electrodes connected at the boundary for isothermal conditions. This has been used by many as a simplification of the Langmuir liquid bath. With direct-current electrical flow established between boundary edges, isopotentials could be probed and

plotted to represent conditions for a simple homogeneous material between isothermal surfaces.

Another form of electrical analogue, the network analyzer, primarily devised for transient heat flow, was described by Paschkis and Baker (2) in 1942. Here the heat-flow path, whether one-, two-, or three-dimensional, was represented by a number of electrical resistors arranged in the form of built-up network to simulate through the resistance concept the thermal resistance of the original heat-flow form. A direct-current electrical-potential difference established across the boundaries of the network set up the flow conditions equivalent to the heat-flow conditions. The network type of analogue also permitted handling of transient conditions. This was truly the outstanding point basic to the design. Here heat-storage effects of solid-wall structures were simulated by electrical condensers which could be charged or discharged, during a transient process. For steady flow the condensers were not required.

Of additional interest is the electrical analogue as based on conductive sheet. This has been used to some extent for flow analysis by different experimenters, principally foreign. It has received scant attention in the American literature, more in the European literature; particularly recent work by Bruckmayer (3) has come to light and should be cited. Using metallic foil to represent a wall of composite material between isopotential boundaries, Bruckmayer cut the sheet to include straight thin strips of foil to represent a layer of insulating material. This was a step in the right direction, but it obviously had limited application and could handle only simple cases of one-dimensional flow between isothermal faces, without surface-boundary effects, such as due to air "films."

Finally should also be mentioned, in passing, the heat-flow version of the Southwell relaxation method, the numerical procedure of Emmons (4). This is often cited by its proponents as having preferential features over the analogical methods. It is a useful tool. For certain work it has admitted advantages, but since it does not fall into the classification of electrical analogies, it will not be discussed any further here.

The geometrical analogue of the Langmuir type, whether fluid or solid, has the advantage of simplicity in obtaining the direct geometrical patterns occurring in flow; it has certain shortcomings: (a) Limitation to a single homogeneous material between the two potential levels; (b) requirement of isopotential boundary-surface wall conditions. There are also some practical objections to working with a bath. On the other hand, the network type of analyzer has the advantage of full utilization of the resistance concept with extension to multiple materials in a complex heat-flow path. It is very flexible. It has the advantage of permitting change of physical properties readily, and above all of being able to handle transient conditions, which is its particularly outstanding feature. However, its equipment is admittedly extensive and since it is not a direct geometrical analyzer, the determination of the geometrical pattern of isothermals is not readily made.

PRESENT GEOMETRICAL ANALYZER

To meet some of these shortcomings, the present electrical "analogizer" employing conductive sheet has been devised. It is

¹ Department of Mechanical Engineering, Columbia University. Mem. A.S.M.E.

² Numbers in parentheses refer to the Bibliography at the end of the paper.

Contributed by the Heat Transfer Division and presented at the Annual Meeting, New York, N. Y., Nov. 27-Dec. 1, 1944, of THE AMERICAN SOCIETY OF MECHANICAL ENGINEERS.

NOTE: Statements and opinions advanced in papers are to be understood as individual expressions of their authors and not those of the Society.

of the geometrical type and primarily for steady-state one- and two-dimensional studies. It permits inclusion of fluid boundary conditions for multiple homogeneous materials in the heat-flow path. Thus it is not limited to isothermal conditions at the boundary walls, and to one single material. Broadly considered, it is founded on the basic principles of the electrical analogy; equivalent temperature conditions for a heat-flow path can be determined through analysis of an electrical flow path in which the component resistances have the same relationship between themselves as the thermal resistances. In both types of flow the potential difference is equal to the product of flow rate and resistance.

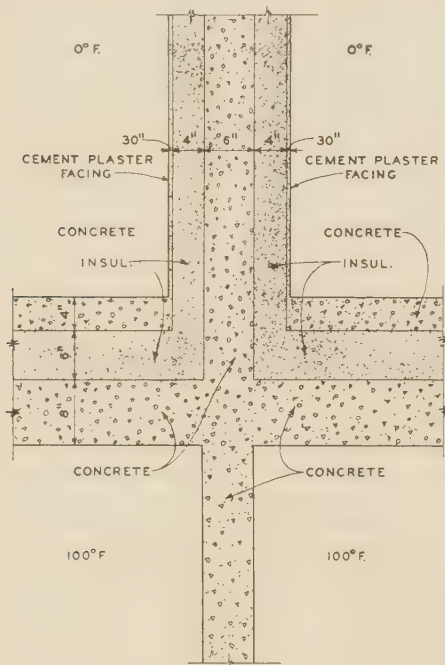


FIG. 1 CROSS SECTION OF BUILDING STRUCTURE

The analogger is best understood by considering a particular case. Fig. 1 represents conditions for a given building structure. One set of rooms is at 0 F, another at 100 F, with a concrete floor between the two temperature zones, and a concrete wall between the adjoining rooms at one given temperature. The floor and the cold wall in addition carry insulation as indicated, with concrete surface added for physical protection. Dimensions are indicated in the figure. Since opposite conditions are similar (mirrored), only one side need be analyzed as set up by the center line. (This is equivalent to considering perfect insulation at the center-line boundary.) It is desired to obtain the steady-state internal-temperature lines, as well as the underside floor and wall-surface temperatures in the 100 F room, to study possible condensation under humid conditions.

The boundary condition produced by the still air in both rooms is readily interpreted through the "film" concept of heat transfer, added and coupled to the resistance concept. Considering resistances on the unit-area basis, the air boundary resistance R_a , deg F/[Btu/(ft²)(hr)], may be defined as

$$R_a = \frac{1}{h_a} \quad [1]$$

where h_a = air-side surface conductance, Btu/(ft²)(hr)(deg F). The resistance R_w , deg F/[Btu/(ft²)(hr)], of the wall material is

$$R_w = \frac{L_w}{k_w} \quad [2]$$

where

L_w = thickness of wall material, ft

k_w = thermal conductivity of wall material, Btu/(ft²)(hr)(deg F/ft)

Thus for a given value of h_a there is a corresponding value of resistance R_a . For a given conductivity of wall material, there is some equivalent length or thickness L_e of material that would give the same resistance R_e to heat transfer as the air boundary

$$R_a = \frac{1}{h_a} = R_e = \frac{L_e}{k_w} \quad [3]$$

thus

$$L_e = \frac{k_w}{h_a} \text{ ft.} \quad [4]$$

Hence if there were involved only an air boundary and a wall thickness, the equivalent electrical resistances to represent the conditions would be proportional to L_e and L_w . For conductive sheet of uniform unit resistance therefore these resistances could be represented by proportional lengths directly on the sheet. This takes care of the fluid boundary conditions, in terms of equivalent length of solid material to produce the same resistance effect. (Though not so apparent, the same general result would be produced by direct consideration in terms of the resistance concept.)

The next point to be considered is the problem of insulation, or of different materials in the heat-flow path. Considering the solid wall as the basic material in the problem, lengths of the actual heat-flow path are directly represented on the conductive sheet. However, insulation in the geometrical electrical analogy requires increased unit resistance in the sheet material to represent increased thermal resistance: this is brought about by modifying the electrical characteristics of the sheet.

The effective electrical unit resistance of a given section may readily be altered by cutting the sheet carefully into a mesh pattern (perforating). This alteration may be made in progressive steps during an investigation, thus covering different values of equivalent thermal resistance in insulation, and enabling progressive study as well as interpolation for exact value. One type of mesh that may readily be used is the square mesh shown in Fig. 2 with progressive alteration. The transverse (edge-to-edge) resistance of mesh sheet as compared with equivalent solid sheet increases as the amount of cutout area increases. The resistance characteristics may be determined by direct comparative electrical measurements. (For a 1-in. nominal mesh, 0.80-in.-square holes and 0.20-in. web, the resistance ratio was measured and averaged about 4.6.) Of course it is essential that one continuous sheet be used and that the webs of the mesh be in no way cut through. It is further to be noted that the mesh may be adjusted to handle material with differing conductivities depending on the direction of heat flow, as, for example, in wood with-the-grain vs. across-the-grain conductivity.

DETAILS OF CONSTRUCTION FOR MODEL

Based on the principles outlined, a geometrical model representing the insulated structure in Fig. 1 has been constructed and is shown in Fig. 3, with its electrical connections for the one-half section of the symmetrical layout. In accordance with the geometrical-model requirements, the proportions are to scale; as a matter of fact the model is full size and of the actual structure dimensions. It is made from one large continuous sheet of metalized paper.

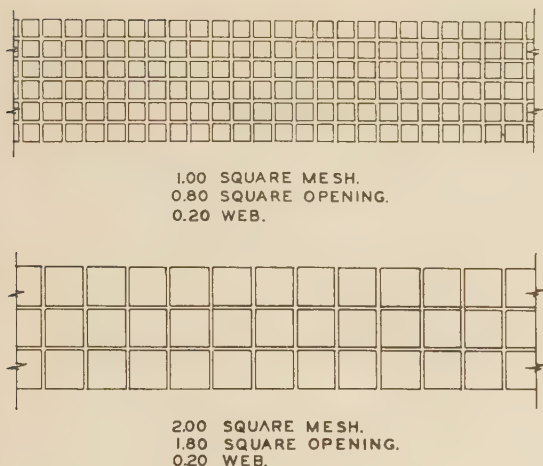


FIG. 2 TYPES OF MESH

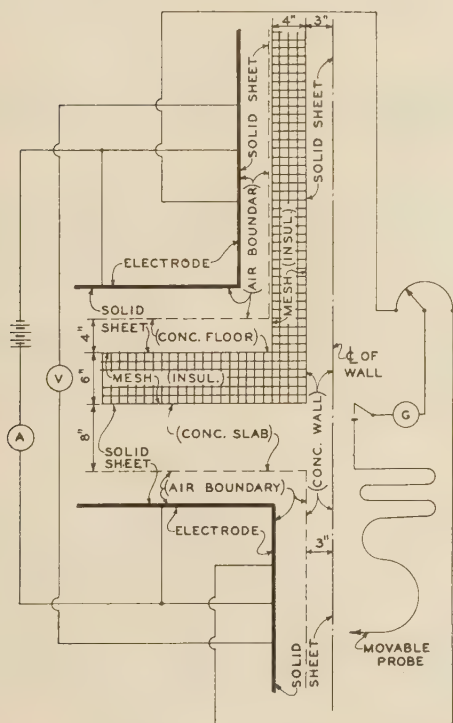


FIG. 3 EXPERIMENTAL SETUP

In addition to the dimensions shown in Fig. 1, the following basic data have been assumed for the problem: h_a , representing still air, has been taken at 1.65 Btu/(ft²)(hr)(deg F) for all of the air boundaries. This could readily be varied for different conditions. The conductivity of the concrete floor and wall, taken as equal, has been assumed as 0.50 Btu/(ft²)(hr)(deg F/ft). Thus

$$L_e = \frac{k_w}{h_a} = \frac{0.50}{1.65} = 0.303 \text{ ft} = 3.63 \text{ in.}$$

Using continuous metallized conductive sheet for the geometrical model, one edge of the conductive sheet is assumed to represent the center line of the wall, Fig. 3. The wall proper as

the basic material is represented by a 3-in. width on the sheet as measured from the center-line edge. As shown at the bottom, an additional 3.63 in. represents the air-boundary effect on the bare concrete wall. The 4 in. of interposed insulation on the upper wall are represented by a 4-in. strip of modified sheet as produced by cutting a mesh pattern in the original sheet. To account for the 0.30 in. of concrete facing as well as the air boundary, the additional solid material beyond the insulation on the upper wall is 3.93 in. Similar treatment is arranged for the floor conditions, 6 in. of insulation being represented by 6 in. of modified sheet, the floor slab and air boundary together represented by 7.63 in. of solid sheet. The treatment for the different parts is clearly shown in the diagram. An electrode making good line contact with the sheet is fastened down at the limiting positions as shown. Thus isopotential conditions are established for the air. Electrical connections are made according to the diagram. Direct current from a storage battery supplies the electrical needs, the voltage required being relatively small, a matter of a few volts. Proportional electrical potentials over the entire field are obtained using the slide wire, a detecting galvanometer for balance, and a probe for point contact at different locations.

The results are best illustrated by a "contour map" of relative electrical potentials with equivalent temperatures shown. Thus the 90 per cent isopotential line (0.900) is equivalent, for an overall value of $\Delta t = 100 \text{ F}$ to $100 \times 0.900 = 90 \text{ F}$. Fig. 4 represents such a contour map for the 1-in. mesh, that is, for insulation having a resistance ratio of about 4.6, i.e., $k_{ins} = 0.109 \text{ Btu}/(\text{ft}^2)(\text{hr})(\text{deg F}/\text{ft})$.

It must be pointed out that the method is dependent on the uniformity of the sheet electrical conductivity in all directions. This has been a problem and various materials have been studied from this point of view. In addition, an analysis by this method can be no better than the original assumed data and physical properties. Also receiving further consideration is the requirement that the resistance ratio for mesh in all directions should be the same. This is somewhat dependent upon the accuracy of cutting and duplicating the mesh. Present investigations show

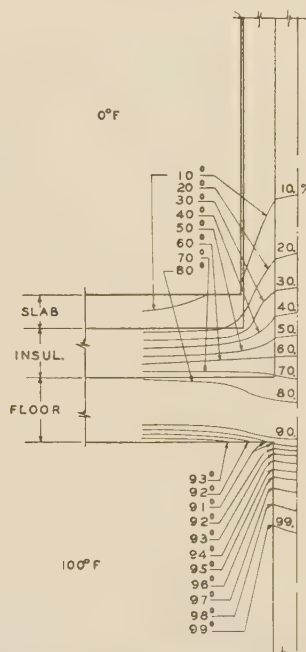


FIG. 4 STRUCTURE ISOOTHERMS

an apparent deviation of less than 5 per cent. It should further be noted that the model for multiple thermal conditions may also be built up by using different component materials such as sheet of different unit resistance, with or without mesh. Experimental studies are also being continued, for comparative purposes, on the application of the fluid model to this type of problem.

MULTIPLE MATERIALS BY TANK METHOD

The extension of the geometrical analogy in steady-state flow, to cover fluid boundary resistances as well as multiple materials of different relative conductivity, has been undertaken for the tank (electrolyte) method and will be reported on in detail at another time. Here the solid boundaries of the structure are associated with a thermal-film resistance. This is represented by tank-wall electrodes, having electrical resistances interposed between them and the electrical potentials representing the fluid temperature levels.

The problem of altering the electrical resistance of the liquid bath according to the fixed pattern of the actual structure is quite important and accordingly has been studied in detail. The liquid bath, it must be remembered, is conductive by virtue of its behavior as an electrolyte. Salt solutions such as NaCl, etc., take care of this requirement. But for different unit resistances in different parts of the tank, in effect a different material must be present. This can be realized to some measure by using sand or other porous material for the more resistive sections of a structure, the electrolyte penetrating the porous material in its fixed location.

More promising results have been obtained in another manner. The goal in the ideal is to have material combinations whose proportional resistances can be adjusted at will, to cover different physical characteristics of structural materials. The use of a solidified-jelly bath (about 1 in. deep) with different amounts of dissolved salt is proposed for this purpose. The jelly is liquid at temperatures somewhat above atmospheric, and different amounts of salt may be dissolved in it while it is in the liquid form.

As a practical operation, different material combinations may readily be made up by using plain salt solution against a solid-jelly mass. Different shape configurations may be cut out of the solidified-jelly mass to conform to the actual structure shapes. The jelly, a semirigid solid mass, is still soft enough to permit the penetration of an exploring potential probe.

Fig. 5 shows alternating-current results (potential versus length of path) for a test cell originally containing one solid-jelly mass between its end electrodes, as well as the results with the middle-third solid section cut out and replaced by a liquid electrolyte of different conductivity from the solid. The sharp change of slope clearly shows the differing possibilities in the analysis of complex flow systems.

The present method offers possibility in handling numerous complex flow problems in different fields of stable flow on a simple basis. One problem of interest in this connection is that of extended surface.

Another is that of diffusion. Still another is involved in some aspects of fluid flow. The equipment required is not complex, and the general advantage of geometrical similarity to actual configurations makes it an attractive working tool.

ACKNOWLEDGMENTS

Acknowledgment is hereby made to different associates of the author who have so generously co-operated on various aspects of the problem; to Prof. J. A. Balmford of the Electrical Engineering Department at Columbia University for his continued advice

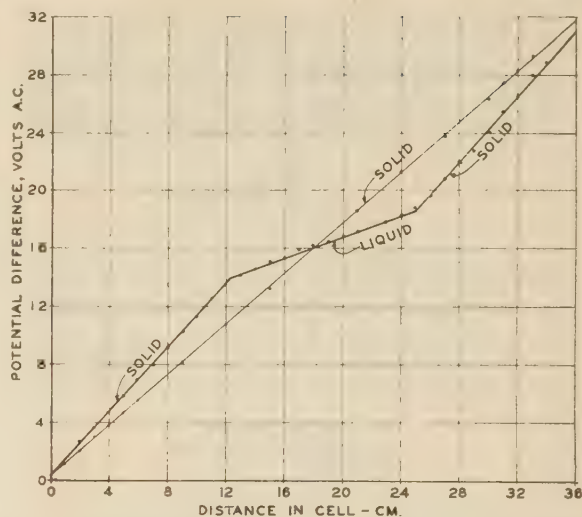


FIG. 5 POTENTIAL DIFFERENCE VERSUS LENGTH FOR ALL-SOLID AND SOLID-LIQUID SYSTEM

and co-operation on electrical details; and to Mr. Harvey W. Bell, Consulting Engineer, Yonkers, N. Y., for his help in preparing the mesh patterns in the test sheet.

BIBLIOGRAPHY

- 1 "Flow of Heat Through Furnace Walls," by I. Langmuir, E. Q. Adams, and F. S. Meikle, Trans. American Electrochemical Society, vol. 24, 1913, pp. 53-84.
- 2 "A Method for Determining Unsteady State Heat Transfer by Means of an Electrical Analogy," by V. Paschakis and H. D. Baker, Trans. A.S.M.E., vol. 64, 1942, pp. 105-110.
- 3 "Elektrische Modellversuche zur Lösung wärmetechnischer Aufgaben," by F. Bruckmayer, *Archiv für Wärmewirtschaft und Dampfkesselwesen*, vol. 20, 1939, pp. 23-25.
- 4 "The Numerical Solutions of Heat Conduction Problems," by H. W. Emmons, Trans. A.S.M.E., vol. 65, 1943, pp. 607-615.

Discussion

G. M. DUSINBERRE.³ The writer has favored the "relaxation" method for solution of most steady-state heat-conduction problems. But where the geometry is complex, a close network is needed and the work becomes rather tedious. Also, if a plot of the isotherms is required, we must interpolate over the network. Though this last step is not difficult, the electrical analogue avoids the necessity for it. Thus the ingenious methods developed by the author have certain definite advantages in this field of application.

One may question the accuracy of the use of a thick layer of isotropic conducting material to represent the effect of a convective air film. The model permits a heat transfer parallel to the surface, equally with the normal direction, and this would not appear to be correct for the actual film.

MAX JAKOB.⁴ The paper under discussion shows that the possibilities to develop or modify analogy methods for heat-flow determination are not exhausted as yet. However, the author

³ Department of Mechanical Engineering, Virginia Polytechnic Institute, Blacksburg, Va. Now on duty at U. S. Naval Academy, Annapolis, Md. Mem. A.S.M.E.

⁴ Consultant in Heat Research, Armour Research Foundation, and Research Professor of Mechanical Engineering, Illinois Institute of Technology, Chicago, Ill.; Nonresident Research Professor of Heat Transfer, Purdue University, Lafayette, Ind. Mem. A.S.M.E.

seems to have overlooked that Awberry and Schofield^{5, 6, 7} have previously used the electric resistance of a thin metal sheet, cut geometrically similar to the cross-sectional area of a wall, to find the thermal resistance of that wall. An ingenious modification of this method is also due to Schofield.^{6, 7} Since the flow and equipotential lines cross each other perpendicularly, he measured the electrical resistance of the model in the direction of the equipotential lines of the original in cases where the resistance along the flow lines of the original was much smaller than perpendicular to them and would have been difficult to measure exactly.

In general, the writer would prefer continuous sheets of different thickness to mesh sheets. An advantage of the model method with solid sheets, compared to the relaxation method, is the perfect geometrical similarity between object and model, whereas a web approaches geometrical similarity less well than the ideal web used in the relaxation method. However, if local differences in the thermal resistance of a wall are to be imitated, this may be done efficiently by punching holes of appropriate size at corresponding places of the model. A wall built up from hollow bricks would be such a case although the merit of the method should be greatest when irregular and singular differences in the resistance are to be imitated. The change of thermal conductivity of the material of a wall with temperature through the wall may also be dealt with in this way.

In addition to the previous electrical analogies quoted in the paper, the writer would like to mention that he used a magnetic analogue⁸ as early as 1914. An electromagnet was made having a core of sheets which were cut to size so that the poles imitated the shape of the surface of the object. Cardboard, cut geometrically similar to the cross-sectional area of the object, was placed between the magnet poles and covered with iron filings. The magnetic-force lines formed by the iron filings, after excitation of the magnet, imitated the thermal flow lines and were used to determine the heat conduction.

VICTOR PASCHKIS.⁹ The author should be commended for bringing into literature a tool which is so frequently used today but of which little has been written in American literature.

The use of electrical analogy between heat flow and electric current for the analysis of steady-state problems, based on a geometrically similar model, has undergone a long development between its inception by Langmuir and the present status. It may be of interest to review briefly some of the intermediate steps. In so doing it should be kept in mind that the analogy holds for any field to which the Laplace equation may be applied.

In 1922 N. N. Pavlovski (Leningrad) applied this method to a study of the flow of water under hydraulic constructions. Also in 1922 Puppini (Bologna) used electric models for the same purpose.¹⁰

In 1933, C. B. Biezeno and J. J. Koch described the application of the geometric analogue to stress analysis.¹¹ This method was

⁵ "Effect of Shape on Heat-Loss Through Insulation," by J. H. Awberry and F. H. Schofield, 5th International Congress on Refrigeration, 1928.

⁶ "The Heat-Loss From a Plate Embedded in an Insulating Wall," by F. H. Schofield, *Philosophical Magazine*, series 7, vol. 10, 1930, pp. 480-500.

⁷ "The Heat-Loss From a Cylinder Embedded in an Insulating Wall," by F. H. Schofield, *Philosophical Magazine*, series 7, vol. 12, 1931, p. 329.

⁸ "American Heat Flow Measurements Using the Twin-Plate Method," by Max Jakob, *Zeitschrift für die gesamte Kälte-Industrie*, vol. 29, 1922, pp. 83-87.

⁹ Research Associate, Department of Mechanical Engineering, Columbia University, New York, N. Y.

¹⁰ "Modelli Elettrici per lo Studio Della Acqua Filtranti," by Puppini, Bologna, *Monitore Tecnico*, vol. 28, 1922, p. 209.

¹¹ Über einige Beispiele zur elektrischen Spannungsbestimmung," by C. B. Biezeno and J. J. Koch, *Ingenieur Archiv*, vol. 4, 1933, pp. 384-393.

again described by H. Meyer and F. Tank.¹² In 1937, B. Finzi-Contini (Milan) published an article on the application of this method to heat flow.¹³

In the same year C. L. Beuken (Maastricht, Netherlands) published some work on development based on Langmuir's tank method.¹⁴ Finzi-Contini and Beuken, apparently working independently of each other, developed a method allowing the introduction of boundary conductance. The continuous electrode as applied by Langmuir is replaced by a number of individual electrodes, each connected with a resistor which may be equal if the boundary conductance is to be assumed constant or can by the trial-and-error method be adjusted to the potential at the electrode; it then simulates a temperature dependency of the boundary conductance. It should be noted that Finzi-Contini mentions work with India ink, with mixtures of carbon and graphite, and with a gelatin containing electrically conducting powders. Without giving details, he states that these methods did not give so good a result. He also tried to reproduce different conductivities by applying tanks of different depths but found that if the depths were too different the analogy to heat flow was no longer close enough; or to be more precise, replacing change of conductivity by change of cross section is permissible only within limits.

The author mentions meshing in order to represent a higher thermal resistivity. His method is a definite improvement as against Bruckmayer. From Bruckmayer's paper it would appear that the conductivity perpendicular and parallel to the direction of main heat flow are not the same, at least in the "cork part." Kayan's method provides for equal conductivity in both directions of flow. Bruckmayer's method may be simpler and may be acceptable if conductivity in one direction can be neglected. Otherwise Kayan's method seems preferable. Bruckmayer uses copper connectors for introducing the current to the tinfoil and places the tinfoil and the copper connectors on linoleum, and finally the entire assembly on a board. By bolting the metal to the board he claims to get intimate contact between copper and tin.

It may be of interest to note that Bruckmayer¹⁵ recently described the application of his method for a problem quite closely related to that dealt with in the paper, namely, the investigation of thermal short circuits in refrigerated spaces.

The author points out two dangers inherent in the geometric-analogy method. One is the possibility of uneven thickness of resistivity of the metallized paper. It is mentioned that the resistivity across the paper was measured in length and width and that the difference was 5 per cent. If irregularities do occur, it is not sufficient to measure over-all resistance in two or three directions, because a local change in thickness at critical points may spoil the entire measurements. The other is the necessity of cutting the perforations very accurately. In the example mentioned, the web was 0.2 in. wide; a change in thickness of 0.02 in., which certainly is within possibility, would cause an error of 10 per cent. It appears dangerous to represent high resistivity by a material of low resistivity using very small cross sections.

The author of the present paper mentions also the "heat and

¹² "Über ein verbessertes elektrisches Verfahren zur Auswertung der Gleichung $\Delta \phi = 0$ und Seine Anwendung Bei Photoelastischen Untersuchungen," by H. Meyer and F. Tank, *Helvetica Physica Acta*, vol. 8, 1935, pp. 315-317.

¹³ "Un modello elettrico," by B. Finzi-Contini, Milan, *Il Politecnico*, vol. 85, Sept., 1937, pp. 291-298.

¹⁴ "Die Wärmeströmung durch die Ecken von Ofenwandungen," by C. L. Beuken, *Wärme- und Kältetechnik*, vol. 39, 1937, issue 7, p. 1.

¹⁵ "Elektrisches Modellmessverfahren zur Wärmebrücken im Kühlraumbau," by F. Bruckmayer, *Zeitschrift des Vereines deutscher Ingenieure*, vol. 88, May 13, 1944, pp. 270-272.

mass flow analyzer" at Columbia University and gives a brief description of it. The network analyzer and the geometric analyzer both have their useful fields of application. For investigations of one single problem probably the use of the geometric analyzer is less expensive, provided the necessary measuring equipment is available and provided the afore-mentioned difficulties can be overcome. If, however, a series of investigations has to be carried out with only minor changes either in properties or in geometry, then the circuit set up on the network analyzer (heat and mass flow analyzer) remains almost the same and the only necessary changes are settings of the resistors. In that case work on this type of equipment would appear preferable because the actual measurements are at least as fast on the network analyzer as on the geometric analyzer and the change of setting of resistors is certainly faster than the preparing of new geometric analogues.

In comparing the two methods of electrical analogy it should be kept in mind that the accuracy of the elements of the circuit in the case of the lumped (network) method is easily measurable and not subject to change from one experiment to the next, whereas in the geometric-analogy method the accuracy (even thickness and precise cutting) has to be ascertained in every case anew.

R. G. VANDERWEIL.¹⁶ We made a thorough investigation as to the behavior of building structures heated by tubes (panel heating); and the time required for building and testing the panels would have been reduced to a fraction if the panels could have been "cut out of paper," and the readings taken in volts. There is one point, however, the writer would like to note. The boundary layer in this system is replaced by a layer of "building material" of constant thickness (author's equation)

$$L_e = k_w/h_a \dots \dots \dots [4]$$

Now, we have found in tests that the equivalent thickness of the actual boundary layer does not only vary with the average surface conductance of the film h_a , but also with the direction of the heat flow near the surface of the slab. Wherever the heat flow at the slab surface is essentially perpendicular to this surface Equation [4] of the paper is in excellent agreement with panel test results, but at points where the heat-flow lines within the panel intersect the slab surface under an angle much smaller than

90 deg, the actual equivalent thickness of the boundary layer seems to be smaller than the computed thickness L_e . Applied to Fig. 3 of the paper, this would indicate that all readings along the center part of ceiling and floor will be in good agreement with actual conditions but readings taken near the intersection of ceiling and wall as well as floor and wall may be off for 10 per cent or more. By comparing the measurements on the actual slab and on the electrical analogue it may be possible to compensate for this inaccuracy by changing the thickness L_e near the corner.

AUTHOR'S CLOSURE

The author wishes to acknowledge, with appreciation, the contributions of the discussers, particularly those of Dr. Max Jakob and Dr. V. Paschakis in providing the additional citations for amplification of the brief list of fundamental references given in the paper. They round out the history of the electrical analogy for the American literature.

As pointed out directly at the beginning of the author's paper, the general method is not new and stems from the Langmuir development cited. However, the additional references, dealing in the main with relatively simple cases, serve to emphasize the point brought out in the paper that the present treatment was particularly devised to meet some of the shortcomings of earlier electrical analogies, i.e., to permit "geometrical" analysis of complex cases involving multiple materials and also boundary conditions.

Commander Dusinger properly brings up a point on which the author gave some considerable thought, having been of the same opinion as to the possibility of crossflow in the boundary material, particularly at the corners. Nevertheless, upon slitting the conductive sheet at the corners after the final experiments, no perceptible changes in values could be detected, with the conclusion therefore that whereas the possibility of crossflow still exists, no ultimately great error need be expected.

Likewise the point of Mr. Vanderweil, with respect to the non-uniform character of the film conductance h_a , has merit. In the paper the value was assumed constant over the surface, and through the use of a constant value for L_e a fixed distance was assigned as the corresponding value of wall resistance. It is suggested that if more specific information is available for the variation of h_a over the surface, the variation may be handled by using the correspondingly varying value of L_e along the surface.

Finally, the author has pointed out the need for care in dealing with the conductive sheet method. Dr. Paschakis's observations, in concurring with the author's viewpoint, serve to emphasize the need for diligent procedure in using the described analogue.

¹⁶ Office of Consulting Engineer, Chase Brass & Copper Company, Waterbury, Conn.

Index to Mechanical Engineering

Volume 67, January—December, 1945

(A) denotes Abstract; (AC) Author's Closure; (BR) Book Review; (C) Correspondence; (D) Discussion; (Ed) Editorial; (P) Photograph

A

ABERDEEN PROVING GROUND Supersonic wind tunnel laboratory.....	827
ABRASIVES Some recent developments in engineering materials.....	334
Use of modern coated abrasives in wood-working industries.....	387
ADAMS, ARTHUR S. Stevens honors three A.S.M.E. members	620
ADHESIVES. <i>See also</i> Glue, Plywood. Controlling moisture content in wood and glued test samples.....	475
Glues for metals.....	337
Bibliography.....	342
Some recent developments in engineering materials.....	334
Bibliography.....	342
Use and evaluation of some specialty adhesives.....	380
ADMINISTRATION The elements of administration (BR)...	140
AGRICULTURE Factors conditioning innovations in agriculture.....	180
Steel silo (A).....	856
AINSWORTH, W. E. Tool control practiced at the Puget Sound Navy Yard (AC).....	534
AIR Thermodynamic properties of air (BR)...	685
AIR BRAKES Air-brake developments (D).....	859
Load-compensating air brakes.....	511
AIR COMPRESSOR Free piston.....	852
Installation, operation, and maintenance (BR).....	865
AIR CONDITIONING An all-year gas air-conditioning unit....	171
AIRCRAFT. <i>See also</i> Air Transportation, Airplanes, Aviation, Jet Propulsion. Air-cargo problems.....	572
Aircraft armament (BR).....	616
Aircraft organization.....	548
Air filters for aircraft engines.....	704
Aviation power plants.....	550
Gas turbines and jet propulsion.....	275
Helicopters.....	312
Plastics in aircraft design.....	548
Radial aircraft engines discussed.....	875
Rocket motor.....	546
Standardization tomorrow?.....	729
Supersonic wind-tunnel laboratory.....	827
Superspeed aircraft (A).....	852
AIR FILTERS Carburetor air filters for aircraft engines.	704
AIRPLANES. <i>See also</i> Aircraft, Aviation. Aircraft armament (BR).....	616
Contemporary jet-propulsion gas turbines for aircraft.....	707
Effect of ventilation rate on cabin temperature.....	668
Jet-propelled (P).....	566
Magnesium design considerations and applications.....	468
Magnesium in aircraft (D).....	766
Standardization tomorrow?.....	729
AIR TRANSPORTATION Air-cargo handling.....	463
Air transport command air-cargo problems.....	572 (D)
Postwar air transportation.....	225
The next twenty-five years in aviation..	309
ALEXANDERSON, E. F. W. Edison medal awarded.....	143
ALFORD, J. S. The gas turbine in aviation.....	803
ALLEN, CHARLES M. Honorary membership, 1944 (P).....	54
ALLEN, F. B. Discussion of hydraulic materials transportation.....	825
ALLER, W. FAY Dressing grinding wheels (AC).....	681

ISSUE	PAGE
NUMBERS	
January	1-88
February	89-152
March	153-220
April	221-292 *
May	293-364
June	365-432
July	433-496
August	497-564
September	565-628
October	629-696
November	697-784
December	785-880

ALLOYS. <i>See also</i> Nonferrous Metals, Steel. Aluminum.....	190
Bibliography.....	196
Dependence on stress of damping capacity of alloys.....	33
Lithium (A).....	835
Magnesium.....	191
Bibliography.....	197
Magnesium in aircraft (D).....	766
Magnesium in aircraft design.....	468
Nickel.....	123
Bibliography.....	128, 195, 198
Some recent developments in engineering materials.....	101
1—Ferrous metals.....	107
Bibliography.....	107
2—Nonferrous metals.....	190
Bibliography.....	196
ALUMINUM Some recent developments in engineering materials.....	190
Bibliography.....	196
AMERICAN BUREAU OF SHIPPING Elects officers.....	559
AMERICAN-CANADIAN INDUSTRIAL MISSION London conference.....	79
AMERICAN ENGINEERING COUNCIL 25 years of Washington, D. C., section..	353
AMERICAN INSTITUTE OF CONSULTING ENGINEERS Elects officers.....	280
Plan to promote postwar employment....	360
AMERICAN INSTITUTE OF ELECTRICAL ENGINEERS Electrical engineers elect officers....	289, 544
AMERICAN INSTITUTE OF MINING AND METALLURGICAL ENGINEERS Officers for 1945.....	78
AMERICAN MANAGEMENT ASSOCIATION Gantt Medal award.....	58, 78, 849
AMERICAN ROCKET SOCIETY.....	867
AMERICAN SOCIETY FOR METALS Officers elected.....	868
AMERICAN SOCIETY OF CIVIL ENGINEERS Public Information Service inaugurated..	870
W. N. Carey named secretary.....	486
AMERICAN SOCIETY OF HEATING AND VENTILATING ENGINEERS Establishes Allen Memorial Library....	626
AMERICAN SOCIETY OF LUBRICATION ENGINEERS Organization meeting in Chicago.....	144
AMERICAN SOCIETY OF MECHANICAL ENGINEERS Applied Mechanics Division meetings. 67, Appointments.....	60, 62
Awards. <i>See</i> Honors and Awards. Boiler Code. <i>See</i> Boiler Code. Budget 1945-1946.....	543
Business meeting, 1944.....	59
Annual, 1945.....	770

AMERICAN SOCIETY OF MECHANICAL ENGINEERS (continued) Semi-annual, 1945.....	419
Committees Boiler Code Committee Alternate rules.....	39, 41
Dinner.....	484
Committee personnel list sent on request.....	143
Consultative Committee.....	39
Education and training for the industries.....	66
Elevator Safety Code Committee meeting.....	350
Engineers' consultative.....	39
Executive Committee actions 206, 279, 350, 422, 483, 543, 544, 619, 687, 781,	867
Finance Committee report, 1943-1944.....	44
Forest Protection Committee.....	157, 279
Gas Turbine Committee study course.....	688
Joint Conference.....	41
Management.....	66
Manufacturing Engineering Committee Meetings and Program.....	350
Membership development.....	68
National Security Committee.....	545
Nominating Committee.....	867
Personnel list sent on request.....	59, 72
Power Test Codes.....	143
Research.....	63
Safety.....	62, 67
Standardization Committees.....	65
Technical Committees.....	64, 867
War Committees.....	39
Council Chicago meeting.....	543
Council at Annual Meeting, 1944.....	60, 61
Executive Committee actions.....	206, 279, 350, 422, 483, 543, 544, 619, 687, 781, 867
New members.....	54
Regional conferences representatives.....	350
Report for 1944.....	39
Divisions at 1944 Annual Meeting.....	62
Exposition exhibit.....	71
Fiftieth anniversary.....	354
Heat Transfer Division (Ed).....	92
Its development, objectives, and operation.....	130
Sessions at 1944 Annual Meeting.....	68
Los Angeles meeting.....	548
Industrial Instruments and Regulators Division.....	67, 548
Management Division objectives.....	484
Meetings Annual Meeting, 1945.....	687, 769
Annual Meeting, 1944.....	50
Aviation war conference, Los Angeles.....	348, 546
Business meeting, annual, 1944.....	559
Annual, 1945.....	770
Semi-annual, 1945.....	419
Calendar of meetings.....	150
Cincinnati fall meeting.....	618, 775
"Convention by mail" planned in O.D.T. ban on national meetings... Council. <i>See</i> A.S.M.E. Council. Detroit section joint meeting with E.I.C.....	872
Fall meeting, 1945.....	618, 775
Keep programs alive (Ed).....	223
Los Angeles aviation war conference.....	348, 546
National meetings.....	40
National meetings postponed.....	207
Professional Divisions meetings.....	40
Semi-annual meeting, 1945, Chicago.....	419, 539, 542
Spring meeting, 1945, Boston.....	142
Members Co-operation.....	866
Membership Candidates.....	87, 152, 220, 292, 364, 431, 495, 564, 628, 695, 783, 879
Honorary, 1944.....	40, 53, 57, 58
Honorary, 1945.....	780
How to buy life membership.....	362
Membership statistics.....	43
Memorial Biographies, 1945, sent on request.....	696
Necrology.....	43, 60, 88, 152, 220, 292, 432, 496, 564, 628, 784, 880
News.....	70, 142, 206, 279, 348, 419, 483, 539, 618, 687, 769, 866

AMERICAN SOCIETY OF MECHANICAL ENGINEERS (continued)

Officers	
Nominated for 1945-1946.....	72, 78, 551
Treasurers (Ed).....	3
Oil and Gas Power Division National Conference, Milwaukee, Wis.....	144
Pension plan.....	350, 362
President nominated 1945-1946.....	552
President's page.....	73, 145, 209, 281, 352, 421, 487, 545, 621, 693, 774, 871
Process Industries Division	
Session at 1944 Annual Meeting.....	68
Publications	
Bibliography on cutting of metals.....	622
Cost performance data on oil and automotive-Diesel engines, 1943.....	622
Index to 1944 MECHANICAL ENGINEERING available.....	151
Keep programs alive (Ed).....	223
1945 Memorial Biographies.....	696
Mechanical Catalog and Directory, 1946.....	687
Power test codes.....	622
Supplements on instruments and apparatus.....	622
Sixty-year index of technical papers	
Technical programs (Ed).....	295
Regional conferences.....	350
Sections	
Meetings.....	88, 148, 219, 290, 362, 695, 781, 879
News.....	81, 82, 146, 211, 282, 353, 425, 488, 559, 624, 687, 777, 872, 879
Sections delegates.....	59
Section delegates conference.....	70
Service men.....	50, 60
Standards	
Condensing steam turbine generators	
Student branches, news, 84, 148, 215, 285, 357, 428, 491, 560, 625, 690, 779, 876	
Washington, D. C., Section 25th Anniversary.....	353
Woman's Auxiliary Annual meeting.....	80
AMERICAN SOCIETY OF REFRIGERATING ENGINEERS	
Officers for 1945.....	81
AMERICAN SOCIETY OF TOOL ENGINEERS	
Elects officers.....	424
AMERICAN STANDARDS ASSOCIATION	
Broadens its scope.....	870
Officers for 1945.....	144
Safety color code.....	424
AMERICAN WELDING SOCIETY	
Honorary members elected.....	849
Officers elected.....	869
AMMUNITION. See Ordnance, Bomb-Testing, Firearms.	
ANDERSON, ROBERT L.	
Receives Octave Chanute medal.....	431
ANTIFRICTION BEARINGS. See Bearings.	
APPLIED MECHANICS DIVISION A.S.M.E.	
Aviation war conference.....	548, 550
ARCHIBALD, F. R.	
Carbide milling of steel.....	659
ARMITAGE, J. B.	
Radial rake angles in face milling	
1—Continuation of an investigation on cutter characteristics.....	403
2—Toolwear, chip formation, and cutting speed in carbide-steel milling	
3—Milling cutters with double radial rake angles.....	507
Discussion (AC).....	862
ARMY	
Armed forces and engineering college cooperation (C).....	612
ARMY ENGINEERING	
Engineers into battle.....	591
ARMY ORDNANCE. See also Ordnance.	
Ordnance supply system.....	789
ATOM SMASHING	
W. L. Laurence articles (A).....	674
ATOMIC ENERGY	
Atomic by-products.....	748
ATOMIC ENGINEERING	
Engineering aids atom smashing (A).....	674
Atomic engineering?.....	672
More fundamentals (Ed).....	632
ATOMIC POWER	
A. H. Compton address at Chicago Association of Commerce (Ed).....	850
AUTOMOBILES	
Vibration investigation.....	723
AUYER, E. L.	
Contemporary jet-propulsion gas turbines for aircraft.....	707
AVIATION. See also Aircraft, Airplanes, Air Transportation.	
Air cargo handling.....	683
Aviation power plants (BR).....	275, 550, (A) 679
Gas turbine in aviation.....	803
Los Angeles aviation war conference, 348, 546	

AVIATION (continued)

Recent developments in engineering materials.....	101, 190, 267, 334
Safety in air and rail travel.....	536
Supersonic wind tunnel dedicated.....	423
The next twenty-five years in aviation.....	309
Various jet propulsion units (A).....	679
25 years of Aviation Division (Ed).....	436
War conference.....	348, 546
Young engineer's avocation (A).....	679

AWARDS. See Honors and Awards.

B

BACHMAN, JANET E.	
Obituary.....	367
BAILEY, ALEX D.	
Elected President (P).....	51
See President's page.	
Speaks at Chicago section.....	211
BAILEY, E. G.	
Enough and to spare (BR).....	140
Honorary member, I.M.E.....	485
BAKER, M. D.	
Boiler water treatment (AC).....	858
BALL AND ROLLER BEARINGS. See Antifric-tion Bearings.	
BALLANTYNE, W. M. H.	
Surface finish (C).....	862
BALLEISEN, C. E.	
Principles of firearms (BR).....	482
BALLISTICS	
Supersonic wind tunnel laboratory.....	827
BARKLEY, J. F.	
War problem of increasing utilization of small anthracite.....	457
Discussion.....	758
BARLOW, H. W.	
Elected dean at Texas A.&M.....	143
BARNES, G. M.	
Aircraft armament (BR).....	616
Supersonic wind-tunnel laboratory.....	827
BATT, W. L.	
A.B.C. Standards Conference (Ed).....	699
Address on national policy.....	79
Batt and Dodd head A.M.A.....	619
BAUSCH, CARL L.	
Diamond tools (BR).....	204
BEAMS	
Glued-laminated arches.....	813
BEARCE, W. D.	
Safety in air and rail travel (C).....	536
BEARINGS	
Diesel-engine bearings.....	297
Evaluating ball- and roller-bearing greases in electric motors.....	645
Grease lubrication of ball-bearing motors and generators.....	639
BECK, C. E.	
Supercharged Diesel engines (D).....	860
BEITLER, SAMUEL R.	
Biography (P).....	552, 553
BELKNAP, JOHN H.	
To head engineering at Rochester.....	289
BELL, LAWRENCE D.	
Receives Guggenheim Medal.....	81
BENDING TESTS	
Bending tests of wooden beams.....	814
BERNER, LEO	
Welding engineering must be based on exact science (D).....	680
BETTY, B. B.	
Some engineering properties of nickel and high-nickel alloys.....	123
BEVERIDGE, W. H.	
Full employment in a free society (BR).....	480
BISHOP, ROBERT L.	
A policy for full employment (BR).....	480
BLACK, ARCHIBALD	
Magnesium in aircraft (D).....	766
Some recent developments in engineering materials	
1—Ferrous metals.....	101
2—Nonferrous metals.....	190
3—Synthetics, fuels, lubricants.....	267
4—Glass, wood, glues, miscellaneous materials, and processes.....	334
Discussion (AC).....	614
BLACK, JOHN D.	
Factors conditioning innovations in agriculture.....	180
BOHUSLAV, HANS	
Supercharged Diesel engines (D).....	859
BOILER	
Boiler-water treatment.....	857
BOILER (continued)	
Fabrication costs of boilers, tanks, and pressure vessels.....	247, (D) 614
Handling and burning fuels on board American ships.....	161
Installing 52-ton boiler.....	323
Intercrystalline cracking.....	834
Locomotive boiler feedwater treatment.....	515
Marine boiler firing.....	161
Marine boiler installation (P).....	323
BOILER AND PRESSURE VESSEL INSPECTORS National Board Convention.....	484
BOILER CODE COMMITTEE OF A.S.M.E.	
Alternate rules.....	39, 41
Boiler code committee holds dinner.....	484
E. R. Fish honored.....	143
BOILER CODE OF A.S.M.E.	
Interpretations.....	137, 202, 346, 418, 538, 617, 863
Proposed provisions for use of noncode materials.....	863
Proposed revisions and addenda.....	139, 203, 346, 538, 617, 863
BOLTS AND NUTS	
Loosening by vibration of threaded fastenings.....	798
BOMB TESTING	
Supersonic wind tunnel laboratory.....	827
BONDI, A.	
Viscosity-temperature coefficient (D).....	201
BOOK REVIEWS	
Aircraft armament.....	616
Budgeting for management control.....	767
Business leadership in the large corporation.....	685
Chemistry of coal utilization.....	767
Diamond tools.....	204
Economic maturity and business prosperity.....	836
Education for what?.....	324
Elements of administration.....	140
Engineering preview.....	537
Enough and to spare.....	140
Establishing and operating a metalworking shop.....	615
Full employment in a free society.....	480
Gas turbines and jet propulsion for aircraft.....	275
How to tell progress from reaction: roads to industrial democracy.....	199
Management at the bargaining table.....	610
Management of inspection and quality control.....	616
Modern gas turbine.....	275
Occupational accident prevention.....	684
Policy for full employment.....	480
Postwar federal taxes.....	32
Postwar fiscal requirements, federal, state, and local.....	744
Principio to Wheeling.....	416
Principles of firearms.....	482
Production, jobs, and taxes.....	32
Sampling inspection tables.....	276
Soundings in the literature of management (A).....	676
The builders of the bridge—the story of John Roebling and his son.....	481
The coming age of rocket power.....	686
The elements of administration.....	140
The road to serfdom.....	199
Thermodynamic properties of air.....	685
The valley and its people.....	277
Twentieth-century engineering.....	415
BOOKS RECEIVED IN ENGINEERING SOCIETIES LIBRARY.....	141, 205, 277, 416, 482, 537, 617, 768, 865
BORING, M. M.	
A reply from industry to the colleges... ..	504
BOULTON, B. C.	
Standardization tomorrow?.....	729
BOYER, R. L.	
Design aspects of supercharged Diesel engines.....	392
Supercharged Diesel engines (AC).....	860
BRADY, GEORGE S.	
Plant layout.....	331
BRAKES. See also Railroad Brakes.	
Air-brake developments (D).....	859
BRIDGES	
The builders of the bridge (BR).....	481
BRIEFING THE RECORD	
Abstracts and comments.....	673, 746, 849
BRISSON, N. H.	
Tool control at Puget Sound Navy Yard (D).....	533
BRITISH WAR PRODUCTION	
Compilation by London Times (A).....	850
Production rates (A).....	676
BROWN, J. CALVIN	
Biography (P).....	552, 553
BROWN, W. T.	
Utilizing small sizes of anthracite (D).....	758

- BRUCHIS, LOUIS
Aircraft armament (BR)..... 616
- BUCKINGHAM, EARLE
Receives Worcester Reed Warner Medal (P)..... 55, 56
- BURD, EDWARD G.
Receives A.S.M.E. Medal (P)..... 55, 56
- BUDGETING
Budgeting for management control (BR) 767
- BULLOCK, W. E.
Milling cast iron with carbides..... 647
- BURNETT, R. S.
Controlling moisture content in wood and glued test samples..... 475
- C**
- CAIN, B. S.
Gas-turbine locomotives (D)..... 407
- CAMPBELL, LEVIN H., JR.
Contribution to ordnance research and development by technical associations. Honorary membership, 1944 (P)..... 54, 57
- CAMS
An analytical method of cam design.... 523
- CANADIAN ENGINEERS
Contribution to victory..... 839
- CANNING MACHINES
Storage of war materials..... 752
- CARBIDES. *See also* Metal Cutting.
Bibliography..... 274
Milling cast iron with carbides..... 647
Some recent developments in engineering materials..... 192
Bibliography..... 197
- CARBURETORS
Carburetor air filters for aircraft engines. 704
- CAREY, WILLIAM N.
Named secretary A.S.C.E..... 486
- CARVER, W. B.
An analytical method of cam design.... 523
- CAST IRON. *See also* Iron, Steel.
Milling cast iron with carbides..... 647
Bibliography..... 107, 658
- CASTING
Die-casting materials and practices. 193.
Making standard cast models in rubber molds..... 385
- CATALYTIC CRACKING
Hot-catalyst elevators..... 635
- CEMENTED CARBIDES. *See* Carbides.
- CENTRIFUGAL CASTING
Making standard cast models in rubber molds..... 385
- CHAPIN, EARL
Principio to Wheeling (BR)..... 416
- CHARLTON, EDWARD J.
Trends in the use of welded machinery parts..... 109
- CHEN, K. Y.
How can China be industrialized?..... 398
- CHICAGO TECHNICAL SOCIETIES
War production conference..... 361
- CHICK, ALTON C.
Biography..... 556
- CHINA
China's steel industry..... 670
How can China be industrialized?..... 398
- CITIZENSHIP
Citizenship (C)..... 764
The engineer's status in the community. 401
- CLAPP, PAUL S.
Anson Marston medal..... 626
- CLENDENIN, J. D.
Utilizing small sizes of anthracite (D)... 758
- CLEPPER, HENRY
Foresters request co-operation in protection of woodlands..... 157
- CLUETT, S. L.
Wins Longstreth Medal..... 351
- COAL. *See also* Fuel.
Chemistry of coal utilization (BR)..... 767
Proximate analyses of various coals..... 161
War problem of increasing utilization of small anthracite..... 457 (D) 758
- CODES. *See* Boiler Code, Safety Engineering.
- COES, HAROLD V.
Budgeting for management control (BR) 767
- COLLECTIVE BARGAINING. *See* Industrial Relations.
- COLLES, GEORGE WETMORE
Duodecimal system (D)..... 682
- COLOR CODE
New A.S.A. color code completed..... 688
- COLVIN, CHARLES H.
Elected president of the Institute of the Aeronautical Sciences..... 208
President of I.A.S..... 210
- COMBUSTION. *See also* Coal, Fuel.
Paths to smoke abatement..... 520
Utilizing small sizes of anthracite (D)... 758
War problem of increasing utilization of small anthracite..... 457
- COMMITTEE FOR ECONOMIC DEVELOPMENT
Joint engineering society participation in the program of the Committee for Economic Development (C.E.D.)..... 620
Text for C.E.D. (Ed)..... 631
- COMMITTEES OF A.S.M.E.
Personnel list sent on request..... 143
- COMPRESSORS. *See also* Air Compressors.
Operating experience with the gas turbine 594
- COMPTON, A. H.
Address on atomic power..... 850
Receives Washington award..... 208
- COOKE, MORRIS L.
Science knocks at the door of American politics..... 569
- CORROSION
Boiler-water treatment..... 857
Corrosion of bearing alloys..... 299
Intercrystalline cracking..... 834
Recent developments in engineering materials..... 341
- COST ANALYSIS
Fabrication costs of boilers, tanks, and pressure vessels..... 247
- COTTRELL, ROBERT BOYD
Developments in the freight-car truck... 517
- COUNCIL OF A.S.M.E. *See* A.S.M.E. Council.
Report..... 39
- COWING, GUY R.
Upper management in training..... 21
- CRAWFORD, DONALD M.
On engineering writing..... 607
- CREEP OF METALS
Dependence on stress of damping capacity of alloys..... 33
Loosening by vibration of threaded fastenings..... 798
- CREESE, JAMES
Named president of Drexel..... 692
- CULLMORE, ALLAN R.
Normal lives for the disabled (BR)..... 204
Reconnaissance (BR)..... 537
Small business is big business (BR).... 615
- CYCLOTRACTORS
Power and transport (A)..... 675
- CYCLOTRON MAGNET
Engineering aids atom smashing (A).... 674
- D**
- DAMPING. *See also* Vibration.
Damping capacity of alloys..... 33
- DAVIES, C. E.
Labram and the "Long Cecil"..... 530
- DE GARMO, E. PAUL
Applying engineering principles to design of welded joints (D)..... 536
Engineering is a more exact science than welding (C)..... 136
Increasing productive machine time... 584
Welding engineering must be based on exact science (D)..... 680
- DENIG, FRED
Utilizing small sizes of anthracite (D)... 759
- DESIGN
Developing creative engineers..... 843
Society of industrial designers formed... 485
- DEVENEY, W. T.
Utilizing small sizes of anthracite (D)... 760
- DIAMONDS
Diamond cutting tools..... 369
Diamond tools (BR)..... 204
- DIE CASTING
Materials and practices..... 193
Bibliography..... 197
- DIESEL-DRIVEN COMPRESSOR
Free-piston air compressor..... 852
- DIESEL ENGINES
Design aspects of supercharged Diesel engines..... 392
Diesel-engine bearings..... 297
"Diesel facts" booklet available..... 694
Discussed by engineers at meeting in Cleveland..... 420
Supercharged Diesel engines (D)..... 859
- DISTRIBUTION
Engineers' role in distribution..... 244
- DODD, ALVIN E.
Batt and Dodd head A.M.A..... 619
- DODGE, H. F.
Sampling inspection tables (BR)..... 276
- DONHAM, W. B.
Education for responsible living (BR)... 324
- DRAFTING
American war standards for drawing and drafting-room practice..... 361
Drafting-room practices to be co-ordinated..... 495
- DRANDELL, J.
Charles T. Main Award..... 867
- DUBIN, E. A.
Glued-laminated arches with sawed laminations..... 813
- DUFFUS, R. L.
The Valley and its people (BR)..... 277
- DUNN, GANO
Engineers' role in distribution..... 244
Honorary member A.S.M.E..... 143
Honorary membership, 1944 (P)..... 54, 57
- DUODECIMALS
Do-Metric system (A)..... 675
Duodecimal system (C)..... 682
History (Ed)..... 500
- DURAND, W. F.
Honored by President Truman..... 753
Receives Carty Medal..... 420
- E**
- EBAUGH, N. C.
Armed Forces and engineering colleges should continue to co-operate (C).... 612
- ECONOMICS
Economic maturity and business prosperity (BR)..... 836
Enough and to spare (BR)..... 140
How can China be industrialized?..... 398
PMH (A)..... 676
Policy for full employment (BR)..... 480
- EDITORIALS
A few short weeks..... 567
A National Science Foundation..... 787
A.C. standards conference..... 699
Aid to science..... 700
America needs engineers..... 367
A.S.M.E. Heat Transfer Division..... 92
A.S.M.E. technical programs..... 295
An improved catalog..... 499
Aviation engineers' anniversary..... 368
Janet E. Bachman..... 367
Education our common interest..... 224
E.C.P.D. poses problems..... 155
Engineers into battle..... 568
50 years of X ray..... 296
Fighting forest fires..... 223
William B. Gregory..... 155
High production..... 568
Industry's influence..... 499
It makes sense..... 223
Keep programs alive..... 223
Metric system..... 500
More fundamentals..... 632
Moving day..... 788
Professional engineering..... 92
Charles F. Scott..... 91
George T. Seabury..... 435
Sets an example..... 368
Text for C.E.D..... 631
Training for management..... 3
Treasurers..... 3
25 years of Aviation Division..... 436
Victory..... 4
Visual aids..... 295
- EDUCATION. *See also* Industrial Training.
Aid to science (Ed)..... 700
America needs engineers (Ed)..... 367
A.S.M.E. committee on education and training for the industries..... 66
An experiment in management education..... 19, (D) 682
An improved catalog (Ed)..... 499
Armed Forces and engineering colleges should continue to co-operate (C).... 612
Developing creative engineers..... 843
Education for what? (BR)..... 324
Education our common interest (Ed).... 224
E.C.P.D. objectives..... 77
E.C.P.D. to accredit technical institutes. 79
Engineers in training..... 134
Engineers of tomorrow..... 5
Industrial..... 66
Industry's influence (Ed)..... 499
More fundamentals (Ed)..... 632
National Science Foundation (Ed).... 787
Reconnaissance (BR)..... 537

EDUCATION (continued)					
Reply from industry to the colleges.....	504				
Requirements (A).....	746				
Scholarships for foreign students at Michigan Tech.....	287				
Soundings in the literature of management (A).....	677				
U. S. naval postgraduate school.....	623				
Upper management training.....	21				
Visual aids (Ed).....	295				
EIPORT, H. E.					
Cost of fabricating boilers and pressure vessels (C).....	614				
EISLER, CHARLES					
Elected president of the R. W. M. A.....	290				
ELECTRIC MOTORS					
Evaluating ball- and roller-bearing greases in electric motors.....	645				
Grease lubrication of ball-bearing motors and generators.....	639				
ELECTRIC POWER					
A. I. E. E. report on electric power distribution for industrial plants.....	210				
ELECTRICAL IGNITION					
Aircraft internal-combustion heaters.....	715				
Discussion.....	547				
ELECTRICAL PRECISION MEASUREMENT					
I. I. T. to establish laboratory.....	362				
ELECTRICAL PROPERTIES OF ALLOYS					
Nickel alloys.....	123				
ELECTRONIC BLOWTORCH					
Hurls radar beams (P).....	824				
ELECTRONIC TUBES					
Winding grids (P).....	294				
ELECTROPLATING					
Some recent developments in engineering materials.....	334				
ELEVATORS					
Safety code for elevators.....	550				
ELLIS, DANIEL S.					
Biography.....	557				
Manager of A. S. M. E. (P).....	54				
EMPLOYMENT					
A. I. C. E. postwar plan.....	360				
A policy for full employment (BR).....	480				
Employment of handicapped people.....	234				
Engineering Societies Personnel Service, Inc., men and positions available.....	86, 151, 218, 291, 363, 430, 494, 563, 627, 694, 782,	878			
Engineers' salaries.....	353				
Industrial jobs for returning veterans.....	14				
Job placement reference (BR).....	864				
Letters applying for a job.....	847				
Office of scientific personnel.....	77				
Plan to promote postwar employment.....	360				
Problem of returning service man.....	12				
Postwar employment of veterans.....	9				
Veteran re-employment.....	17, 809				
ENGINEERING					
American Engineering Council.....	353				
Armed Forces and engineering-college co-operation (C).....	612				
Atomic engineering.....	672				
Creative engineering and patents.....	633				
Engineering aids atom smashing (A).....	674				
Engineers of tomorrow.....	5				
Engineering preview (BR).....	537				
E. C. P. D. poses problems (Ed).....	135				
Interprofessional institute.....	137				
Professional engineering (Ed).....	537				
Reconnaissance (BR).....	537				
The creative mind and victory.....	238				
Twentieth-century engineering (BR).....	415				
ENGINEERING EDUCATION. See Education.					
ENGINEERING FOUNDATION					
Annual Report 1943-1944.....	75				
Objectives.....	41				
ENGINEERING INSTITUTE OF CANADA					
Joint meeting with Detroit Section.....	872				
Rehabilitation and personnel services.....	430				
ENGINEERING MATERIALS					
Mechanical properties and uses of wool felt.....	93				
Recent developments (with Bibliographies).....					
1—Ferrous metals.....	101				
2—Nonferrous metals.....	190				
3—Synthetic fuels and lubricants.....	267				
4—Glasses, woods, glue, miscellaneous materials.....	334				
Malleable iron.....	613				
ENGINEERING SOCIETIES					
An American society of engineers.....	735				
Interprofessional institute (C).....	137				
Sets an example (Ed).....	368				
Professional-mindedness and the young engineer.....	866				
Survey of co-operative councils.....	477				
Technical societies council formed at Kansas City.....	623				
ENGINEERING SOCIETIES COMMITTEE ON WAR PRODUCTION					
First conference on war production and planning.....	206				
ENGINEERING SOCIETIES LIBRARY					
1944 Annual report.....	78				
Books received.....	865				
141, 205, 277, 416, 482, 537, 617, 768, Report on Orinoco-Casiquiare-Negro Waterway.....	877				
ENGINEERING SOCIETIES PERSONNEL SERVICE, INC.					
Men and positions available.....	86, 151, 218, 291, 363, 430, 494, 563, 627, 694, 782,	878			
ENGINEERING STANDARDS. See also Standards.					
Conference on unification of engineering standards.....	776				
ENGINEERING WRITING					
On engineering writing.....	607				
ENGINEERS					
Canadian engineers' contribution to victory.....	839				
Definitions.....	751				
Developing creative engineers.....	843				
Engineer officers.....	100				
Engineering writing.....	607				
Engineer's duty as a citizen.....	421				
Engineers in management.....	332				
Engineers into battle.....	591				
Engineers into battle (Ed).....	568				
Engineers in training.....	134				
Engineers of tomorrow.....	5				
Engineers' role in distribution.....	244				
A message to each engineer from the chairman of E. C. P. D.....	344				
Professional-mindedness and the young engineer.....	866				
Registration law of Pennsylvania.....	867				
Salaries.....	353				
Science knocks at the door of American politics.....	569				
The engineer's status in the community.....	401				
Training for industry (Ed).....	499				
Twenty-five years of Washington, D. C., section.....	353				
ENGINEERS' ADVISORY SERVICES					
A. S. C. E. public information service.....	870				
Engineers' consultative committee.....	39				
See Engineering Societies Personnel Service					
ENGINEERS COUNCIL FOR PROFESSIONAL DEVELOPMENT					
A message to each engineer from the chairman of E. C. P. D.....	344				
E. C. P. D. poses problems (Ed).....	155				
Officers elected.....	870				
Project No. 56, committees.....	77				
Reading list for junior engineers available.....	289				
ENGINEERS SOCIETY OF WESTERN PENNSYLVANIA					
Proceedings of water conference available.....	559				
ENGINES. See also Diesel Engines.					
Aircraft engines (A).....	854				
Aircraft engine carburetor air filter.....	704				
Welded parts.....	109				
ENNIS, W. D.					
Treasurer A. S. M. E. 1935-1944 (P).....	63				
ERICKSON, J. W.					
Undergraduate Student Award.....	867				
ESHBACH, O. W.					
To head Washington award commission.....	144				
EVANS, M. J.					
Experiment in management education (D).....	682				
		F			
FABIES, VIRGIL M.					
An American society of engineers.....	735				
FAN					
Thermo-control fan (A).....	836				
FARMING					
Innovations in agriculture.....	180				
Steel silo (A).....	856				
FARR, RICHARD S.					
Carburetor air filters for aircraft engines.....	704				
FEEDWATER					
Boiler-water treatment.....	857				
Feedwater treatment for locomotive use.....	515				
FELLER, E. W.					
Air compressors (BR).....	865				
FELT					
Mechanical properties and uses of wool felt.....	93				
FIELD, MICHAEL					
Milling cast iron with carbides.....	647				
FILTERS					
Carburetor air filters for aircraft engines.....	704				
FINANCE					
Fiscal requirements in 1949 (BR).....	744				
FINDLEY, W. N.					
Receives Charles B. Dudley medal.....	754				
FIREARMS. See also Ordnance.					
Labram and the "Long Cecil".....	530				
Principles of firearms (BR).....	482				
FIRE-FIGHTING EQUIPMENT					
Adapting army equipment to forest-fire fighting.....	437				
FIRE PREVENTION					
Foresters request co-operation in protection of woodlands.....	157, (Ed)	223			
Joint A. S. M. E.-S. A. F. Committee on forest-fire prevention.....	290				
1945 National fire codes available.....	289				
FISH, E. R.					
Honored by A. S. M. E. Boiler Code Committee.....	143				
FLANDERS, RALPH E.					
Awarded Hoover Medal (P).....	55, 58				
FLEMING, A. P. M.					
Knights Bachelor honor.....	219				
FLOYD, T. N.					
Electrical ignition for aircraft internal-combustion heaters.....	715				
FLUID FLOW					
Fluid flow study of locomotive firebox design.....	586				
FLUID FRICTION					
A. S. H. V. E. laboratory studies air-duct friction.....	429				
FOOTE, AVERY					
Effect of ventilation rate on cabin temperature.....	668				
FORESTRY					
Adapting army equipment to forest-fire fighting.....	437				
Fighting forest fires (Ed).....	223				
Foresters request co-operation in protection of woodlands.....	157				
FOWLE, FRANK F.					
Receives Octave Chanute medal.....	431				
FRANZ, FREDERICK					
Applying engineering principles to design of welded joints (D).....	536				
FRARY, FRANCIS C.					
Awarded Perkin Medal.....	849				
FREEMAN, RALPH E.					
Postwar federal taxes (BR).....	32				
FUEL. See also Coal.					
Fuel consumption of aircraft.....	803				
Handling and burning fuels on board American ships.....	161				
Increasing utilization of small anthracite.....	457, (D)	758			
Some recent developments in engineering materials.....	267				
Three papers on fuel economics available.....	494				
FURNAS, C. C.					
The next twenty-five years in aviation.....	309				
FUSES. See Ordnance.					
FUEL OIL					
Handling and burning fuels on U. S. ships.....	161				
		G			
GABOR, HARRY W.					
Occupational accident prevention (BR).....	684				
GAGG, RUDOLPH F.					
Biography (P).....	554				
GAILLARD, JOHN					
Inspection and quality control (BR).....	616				
GANTT MEDAL					
1944 Award to Lillian Gilbreth and Frank Gilbreth.....	58				
1945 Award to John M. Hancock.....	849				
GAS TURBINES. See also Locomotives.					
As propulsion equipment for axial air compressors.....	594				
Aviation gas turbines and jet propulsion.....	549				
Contemporary jet-propulsion gas turbines for aircraft.....	707				
Courses in gas turbines outlined by A. S. M. E. Committee.....	688				
Gas-turbine test code.....	867				
Gas turbines (A).....	747				
Gas turbines and jet propulsion for aircraft (BR).....	275				
Gas turbines (BR).....	677				
High-temperature gas-turbine power plants.....	229				
New C. E. aircraft power plant (A).....	855				
Next 25 years in aviation.....	311				
Operating experience with the gas turbine.....	594				

GAS TURBINES (continued)			HAMMOND, H. P.			HONORS AND AWARDS (continued)		
Soderberg comments on Elliott develop- ment (A).....	677		Awarded Lamme Medal.....	626		American honorary fellow of I.A.S.....	210	
The gas turbine in aviation.....	803		HAMMOND, NELSON B.			A.S.M.E. awards.....	289	
The modern gas turbine (BR).....	275		Receives Undergraduate Student Award (P).....	53, 55		A.S.M.E. awards at Annual Meeting 1944.....	53	
Thermodynamic properties of air.....	685		HANCOCK, JOHN M.			A.S.M.E. honorary membership, 1944.....	40, 53, 57, 58	
GATES, ROBERT M.			Awarded Gantt Medal.....	849		1945.....	780	
Engineers of tomorrow.....	5		HANDICAPPED WORKERS			A.S.M.E. Medals, 1945.....	780	
President A.S.M.E. (P).....	50, 51, 52		Hiring handicapped people.....	234		A.S.M.E. Medal awarded to E. G. Budd 1944 (P).....	55, 56	
GEMANT, ANDREW			It makes sense (Ed).....	223		American Welding Society honorary members.....	849	
Dependence on stress of damping capacity of alloys.....	33		Normal lives for the disabled (BR).....	204		Annual awards for student papers.....	218	
GENERATORS			HANKISON, L. E.			Anson Marston Medal.....	626	
Grease lubrication of ball-bearing motors and generators.....	639		Boiler-water treatment (AC).....	858		Chanute Medal.....	431	
GEOGRAPHICAL PROSPECTING			HARMS, CARL			Charles B. Dudley Medal.....	754	
The Gulf Marsh buggy.....	501		Supercharged Diesel engines (D).....	859		Chas. T. Main Award.....	33	
GERMANY			HARR, W. H.			Daniel Guggenheim Medal awarded, 1944.....	81	
Control of German industry (A).....	754		Budgeting for management control (BR).....	767		Daniel Guggenheim Medal, 1945.....	754	
GESCHELIN, JOSEPH			HARRIS, H. R.			Dunn and Jewett honored.....	143	
Tool control at Puget Sound Navy Yard (D).....	533		Air transport command air-cargo prob- lems.....	572		W. F. Durand receives Carty Medal.....	420	
GILBRETH, FRANK B.			HARRISON, W. H.			Edison Medal awarded.....	143	
Awarded Gantt Medal (posthumously).....	58		Receives Hoover Medal.....	753, 807		Elliott Cresson Medal.....	361	
GILBRETH, LILLIAN M.			HAVERSTICK, J. S.			Exceptional Civilian Service Award.....	144, 430	
Awarded Gantt Medal (P).....	55, 58		High-temperature gas-turbine power plants.....	229		Fifty-year members.....	52	
GILLMOR, R. E.			HAYEK, F. A.			E. R. Fish honored.....	143	
Addresses war-production conference.....	206		Road to serfdom (BR).....	109		Gantt Medal award, 1944.....	58	
The creative mind and victory.....	238		HAYNES, G. P.			Gantt Medal award, 1945.....	849	
GLASS			Handling and burning fuels on board American ships.....	161		Gold Medal of the Institution of Loco- motive Engineers (England).....	351	
Milled glass fibers.....	752		HEAT TRANSFER			Holley Medal awarded to C. L. Norden.....	53	
Some recent developments in engineering materials.....	334		Thermodynamic properties of air (BR).....	685		Honorary fellowship in I.A.S. 1911.....	210	
Bibliography.....	341		Time-temperature relationships in work- pieces.....	445		Honorary memberships A.S.M.E. 1911.....	40, 53, 57, 58	
GLUE. See also Adhesives, Plywood.			HEAT TRANSFER DIVISION OF A.S.M.E.			1945.....	780	
Controlling moisture content in glued test samples.....	475		Objectives and operation.....	130		Hoover Medal award 1944 and 1945.....	58, 753, 867	
Metal glues.....	337		Sessions at Los Angeles.....	547, 548		Illuminating Engineering Society Medal Institution of Mechanical Engineers hon- orary members.....	288, 485	
Recent developments in engineering ma- terials.....	334		HEAT-TREATMENT			James Clayton lecture delivered by F. Whittle.....	850	
GLUED-LAMINATED CONSTRUCTION. See also Plywood.			Fuel-fired techniques and their possibili- ties.....	442		Institute of Aeronautical Sciences awards.....	210	
Glued-laminated arches with sawed lami- nations.....	813		High-frequency induction heating.....	448		James Douglas Award.....	207	
GODWIN, DAVID P.			High-speed heating (D).....	451		James Watt Medal.....	849	
Foresters request co-operation in protec- tion of woodlands.....	157		Bibliography.....	452		John Fritz Medal award.....	288	
GOFF, JOHN A.			Modern methods in the heat-treatment of steel.....	549		Jewett research fellowships awarded.....	420	
Thermodynamic properties of air (BR).....	685		Time-temperature relationships in work- pieces.....	445		John J. Carty Medal and award.....	210	
GOLAND, MARTIN			HEATERS			John Jeffries award.....	868	
Receives Spirit of St. Louis Junior Award (P).....	53, 55		Electrical ignition for aircraft internal- combustion heaters.....	715		Sir John Kennedy Medal award.....	361	
GOLDEN, CLINTON S.			HEATING			John A. Penton Medal.....	289	
Problem of returning service man from labor viewpoint.....	12		Effect of ventilation rate on airplane cabin temperature.....	608		J. E. Johnson, Jr., Award.....	351	
GOODIER, J. N.			HEINRICH, H. W.			Joseph H. Linnard Prize.....	361	
Loosening by vibration of threaded fastenings.....	798		Basic principles of supervision.....	701		Lamme Medal award.....	288	
GORDON, M.			HELANDER, LINN			1945.....	626	
How to tell progress from reaction (BR).....	199		Biography (P).....	554		Lawrence Sperry Award.....	210	
GORSELINE, DONALD			HELICOPTERS			Lincoln Agricultural Award.....	424	
Job placement reference (BR).....	864		Discussed at Annual Meeting.....	67		Lincoln arc-welding foundation offers new awards.....	431	
GOVERNMENT			The next 25 years in aviation.....	312		Lincoln Medal award.....	869	
Citizenship (C).....	764		HERSCHMAN, HARRY K.			Longstreth Medal.....	351	
Science knocks at the door of American politics.....	569		Replica method for evaluating finish of a metal surface.....	119		Melville Medal.....	53	
GRAF, SAMUEL H.			HERSEY, M. D.			Octave Chanute Award.....	210	
Biography (P).....	558		Viscosity of lubricants under high pres- sure.....	820		Ordnance Award.....	60	
GRANT, EUGENE L.			HESS, FREDERIC O.			Orville Wright honored.....	144	
Sampling inspection tables (BR).....	276		Fuel-fired techniques and their possibili- ties.....	442		Perkin Medal awarded to F. C. Frary.....	849	
GRAPHICAL METHODS			HESS, WENDELL F.			Rice Lecturers.....	61	
Nomographs for analysis of metal-cutting processes.....	737		Elected president of A.W.S.....	849		Robert M. Losey Award.....	210	
GRAVES, B. P.			HIGGINS, EDWIN M.			Robert W. Hunt Medal.....	289	
Dressing grinding wheels (D).....	681		Grease lubrication of ball-bearing motors and generators.....	639		Rumford Medal awarded.....	142	
GREENE, ARTHUR M., JR.			HILL, L. H.			Spirit of St. Louis Junior Award.....	53	
Twentieth-century engineering (BR).....	415		Management at the bargaining table (BR).....	610		Spirit of St. Louis Medal.....	53	
GREGORY, WM. B.			HILL, PHILIP			Stevens Honor Award.....	287	
Obituary.....	155		Collective bargaining at Whiting refinery (C).....	536		Stevens honors three A.S.M.E. members.....	620	
GRINDING WHEELS			HIMMELRIGHT, CARL			Stevens Institute powder-metallurgy medal.....	289	
Dressing grinding wheels (D).....	681		Indicated principles of postwar machin- ing.....	473		Sylvanus Albert Reed Award.....	210	
GRINTER, L. E.			HINDLE, N. F.			Undergraduate Student Award.....	53, 55	
Engineering preview (BR).....	537		Engineering materials (C).....	613		Warner Medal.....	53	
GRODINSKI, PAUL			HISLOP, T. W.			Washington Award.....	208	
Diamond cutting tools.....	369		Feedwater treatment for locomotive use.....	515		James Watt International Medal.....	207	
Correction.....	766		HOAGLAND, F. O.			HOOK, C. R.		
Diamond tools (BR).....	204		Tool control at Puget Sound Navy Yard (D).....	533		Management at the bargaining table.....	610	
GROVES, H. M.			HOLDEN, PAUL E.			HOPKINS, R. F.		
Production, jobs, and taxes.....	32		Business leadership in the large corpora- tion (BR).....	685		Viscosity of lubricants under high pres- sure.....	820	
GUHL, H. C.			HOLLERAN, LESLIE G.			HOUSTON, L. W.		
Hot-forming of phenolic laminates.....	175		The builders of the bridge (BR).....	481		Elected president of Rensselaer.....	80	
GUNS. See Firearms, Ordnance.			HOLMES, H. N.			Stevens honors three A.S.M.E. members.....	620	
HAMILTON, W. S. H.			Engineering preview (BR).....	537		HUMPTON, W. G.		
Gas-turbine locomotives (D).....	407		HONORS AND AWARDS			Boiler Code Committee certificate of award.....	867	
			American Foundrymen's Association awards.....	361		HUNSAKER, J. C.		
						Honorary member, I.M.E.....	485	
						HYDRAULICS		
						Hydraulic materials transportation.....	825	
						IGNITION		
						Electrical ignition for aircraft internal- combustion heaters.....	715	

ILLUMINATING ENGINEERING SOCIETY					
Award to P. S. Millar.....	688	JET PROPULSION (continued)			
INDIANA ENGINEERING COUNCIL		G. E. propjet (A).....	855	LEE, EVERETT S.	
Annual meeting.....	81	Jet-propelled airplanes.....	547	A message to each engineer from the	344
INDUCTION		Jets.....	678	chairman of E.C.P.D.....	
Bibliography.....	196	N.A.C.A. announces new supersonic wind		LEHMBERG, W. H.	
INDUCTION HEATING		tunnel for jet-propulsion research.....	619	Mechanical properties and uses of wool	93
High-frequency induction heating.....	448	Next 25 years in aviation.....	311	LEWIS, GEORGE W.	
INDUSTRIAL DEVELOPMENT		Power plant for jet-propelled planes (P).....	611	Receives Spirit of St. Louis medal, 1944	55
Branch plants (A).....	746	"Shooting Star" (P).....	566	(P).....	
China's steel industry.....	670	Various power units (A).....	679	LIBRARY. See Engineering Societies Li-	
Control of German industry (A).....	754	JEWETT, FRANK B.		brary.....	
How can China be industrialized?.....	398	Honorary member A.S.M.E.....	143	LINCOLN, J. F.	
INDUSTRIAL MISSION TO LONDON, Report...	79	JOHNSON, GERALD		Engineering is a more exact science than	
INDUSTRIAL RELATIONS		Product planning.....	330	welding (C).....	137
A reply from industry to the colleges...	504	JOHNSON, MELVIN M., JR.		Welding electrode standards (C).....	535
Collective bargaining at Whiting refinery		Principles of firearms (BR).....	482	LINDQUIST, DAVID L.	
(C).....	536	JURAN, J. M.		Obituary.....	280
Experiment in management education...	19	Management of inspection and quality		LISKA, JOHN W.	
Industrial jobs for returning veterans...	14	control (BR).....	616	Advances in rubber during 1944.....	262
Management rights and collective bar-		The elements of administration (BR)...	140	LITHIUM	
gaining (BR).....	610			Production.....	196, 198, (A) 855
Problem of returning service man from				LOCAL SECTIONS. See American Society of	
labor viewpoint.....	12			Mechanical Engineers, Sections.	
Veteran re-employment.....	17			LOCOMOTIVE	
INDUSTRIAL PRODUCTIVITY				Firebox construction.....	253
High production (Ed).....	568			Fluid-flow study of locomotive firebox de-	
INDUSTRIAL TRAINING		KATES, EDGAR J.		sign.....	586
A.S.M.E. committee.....	66	Biography.....	555	Gas-turbine locomotives (D).....	407
Basic principles of supervision for safe and		KAYE, JOSEPH		Steam-turbine driven.....	875
efficient production.....	701	Thermodynamic properties of air (BR)...	685	LOCOMOTIVE BOILERS	
Experiment in management education...	19	KEENAN, J. H.		Feedwater treatment.....	515
Upper management in training.....	21	Thermodynamic properties of air (BR)...	685	LOGGING	
Visual aids (Ed).....	295	KELLOGG, MORRIS W.		Preplanning of logging operations for	
INDUSTRIAL TRUCKS		Stevens honors three A.S.M.E. members.	620	minimum costs.....	325
Material-handling aids in modern produc-		KELSEY, BENJAMIN S.		LOVELY, JOHN E.	
tion.....	235	Receives Octave Chanute award.....	210	Biography.....	558
INDUSTRY		KENNEDY, ROBERT E.		Vice-president of A.S.M.E. (P).....	54
A reply from industry to the colleges...	504	Awarded Joseph S. Seaman Medal.....	361	LOWE, T. A.	
Engineers in training (Ed).....	499	KENNEY, L. H.		Engineers into battle.....	591
How can China be industrialized?.....	398	Honored by Brazil.....	620	LOWRY, STEWART M.	
Liaison with engineering.....	7	KENNICOTT, W. L.		Industrial jobs for returning veterans...	14
INFORMATION SERVICE		Mounting solid cemented-carbide cutting		LUBRICANTS	
American Society of Civil Engineers'		blades mechanically.....	241	A.S.A. standard for oils and greases....	430
public information service.....	870	KERR, A. J.		Evaluating ball- and roller-bearing greases	
Engineers' Consultative Committee.....	39	Biography.....	557	in electric motors.....	645
See Engineering Societies Personnel Ser-		Manager of A.S.M.E. (P).....	54	Silicones.....	271, 274
vice.....		KERRICK, J. H.		Some recent developments in engineering	
INSPECTION		Utilizing small sizes of anthracite (D)...	760	materials.....	267
Inspection and quality control (BR)...	616	KIMBALL, D. S.		Viscosity of lubricants under high pressure	820
Sampling inspection tables (BR).....	276	Honored by Cornell alumni.....	869	Bibliography.....	823
INSTITUTE OF THE AERONAUTICAL SCIENCES		KIMMEL, LEWIS H.		LUBRICATION	
Awards.....	210	Postwar fiscal requirements (BR).....	744	Grease lubrication of ball-bearing motors	
INSTITUTE OF RADIO ENGINEERS		KLINE, G. M.		and generators.....	639
Elects officers.....	78	Advances in plastics during 1944.....	255	Grease lubrication of motor ball and	
Inaugurates building fund campaign.....	208	KNICKERBOCKER, IRVING		roller bearings.....	645
INSTITUTION OF MECHANICAL ENGINEERS		Education for what? (BR).....	324	LUCHT, FRED W.	
Frank Whittle, R.A.F., delivers first		KOPF, J. L.		A study of some fundamentals when face-	
James Clayton lecture.....	850	Appointed assistant treasurer A.S.M.E.		milling steel with carbides—the radial	
History.....	100	(P).....	63	rake angle.....	185
INSTRUMENT SOCIETY OF AMERICA				Radial rake angles in face milling (D)...	861
National Instrument Society formed....	486			Tool control at Puget Sound Navy Yard	
INSULATION				(D).....	533
Recent developments in engineering				LUMINESCENT MATERIALS	
materials.....	334			Bibliography.....	343
Silicones.....	271, 274			LUPKE, PAUL, JR.	
INTERCRYSTALLINE CRACKING				Making standard cast models in rubber	
Silica-sodium hydroxide ratio in boiler				molds.....	385
failure.....	834			LYNE, L. F., JR.	
INVENTION. See also Patents.		LABOR		Metropolitan representative for license of	
Creative engineering and patents.....	633	Materials handling survey.....	83	enemy patents.....	71
Developing creative engineers.....	843	Output in agriculture and manufacturing...	181		
Navy Dept.—25 invention problems....	207	Problem of returning service man from			
IRON. See also Cast Iron, Steel.		labor viewpoint.....	12		
Ordinance, A.S.T.M. specifications (C)...	613	LABRAM, GEORGE			
IRON AND STEEL INDUSTRY		Labram and the "Long Cecil".....	530		
Pageant of steel (BR).....	416	LAMINATED ARCHES			
		Glued-laminated arches with sawed lami-			
		nations.....	813		
		LAMINATED METALS			
		Some recent developments in engineering			
		materials.....	190		
		Bibliography.....	196		
		LAMINATES			
		Hot-forming of phenolic laminates.....	175		
		LANCHESTER, R. W.			
		Receives 1945 James Watt Medal.....	207		
		LAND, EMORY S.			
		Honorary membership, 1944.....	57		
		LANDIS, J. N.			
		Biography.....	355		
		LANDRY, BERTRAND A.			
		Chemistry of coal utilization (BR).....	767		
		LARKIN, DAVID			
		Biography.....	558		
		Vice-president of A.S.M.E. (P).....	54		
		LATRENCE, W. L.			
		Atom smashing articles (A).....	674		
		LEAF, WALTER			
		Fluid-flow study of locomotive firebox de-			
		sign.....	586		

MAGNESIUM (continued)					
Some recent developments in engineering materials.....	191				
Bibliography.....	197				
MALLEABLE IRON					
Recent developments in engineering materials (C).....	613				
MALLICK, R. W.					
Three-dimensional plant-layout models.....	383				
MANAGEMENT					
Aircraft organization.....	548				
Aircraft quality control.....	547				
A.S.M.E. committee.....	66				
A.S.M.E. management division.....	484				
An experiment in management education (D).....	682				
Basic principles of supervision.....	701				
Bibliography (BR).....	676				
Budgeting for management control (BR).....	767				
Business leadership in the large corporation (BR).....	685				
Engineers in management.....	352				
Engineers' role in distribution.....	244				
Experiment in management education.....	682				
Factors conditioning innovations in agriculture.....	180				
Increasing productive machine time.....	584				
Management congress proposed.....	39				
Management of inspection and quality control (BR).....	616				
Management rights and collective bargaining (BR).....	610				
Soundings in the literature of management (A).....	676				
Stevens initiates seminars for executives.....	494				
Training for management (Ed).....	21				
Upper management in training.....	330				
What the engineer can do in a small plant.....	330				
MANUFACTURING					
Manufacturing Engineering Committee, A.S.M.E.....	350				
MARINE BOILER FIRING. See also Boilers.					
Handling and burning fuels on board American ships.....	161				
MARINE TURBINE					
Elliott development (A).....	677				
MARKETING					
Engineers' role in distribution.....	244				
MARSH BUGGY					
The Gulf marsh buggy.....	501				
MASON, D. M.					
Veteran re-employment.....	17				
MASON, M. A.					
Receives exceptional civilian service award.....	430				
MATERIALS. See Engineering Materials					
MATERIALS HANDLING					
Air-cargo handling.....	463, 572, (D) 683				
Army Ordnance Depot problem.....	789				
Hot-catalyst elevators.....	635				
Hydraulic materials transportation.....	825				
Material-handling aids in modern production.....	235				
Society formed.....	870				
MATHEMATICS					
Duodecimals (A).....	675				
Duodecimal system (C).....	682				
MATERIALS TESTING					
Controlling moisture content in wood and glued test samples.....	475				
MATHER, K. F.					
Enough and to spare (BR).....	140				
MATHE, JOHN C.					
Magnesium design considerations and applications.....	468				
MATTHEWS, DON M.					
Preplanning of logging operations for minimum costs.....	325				
MAY, E. C.					
Pageant of steel (BR).....	416				
MCCARTHY, EDMUND					
Utilizing small sizes of anthracite (D).....	761				
MCCOLLUM, C. E.					
Postwar air transportation.....	225				
MCCONVILLE, H. A.					
Evaluating ball- and roller-bearing greases in electric motors.....	615				
MCCRUMM, J. D.					
Electrical ignition for aircraft internal-combustion heaters.....	715				
MCEACHRON, K. B., JR.					
A reply from industry to the colleges.....	504				
McEWAN, THOMAS S.					
Biography.....	556				
Vice-President of A.S.M.E. (P).....	54				
MCGREGOR, DOUGLAS					
Management rights and collective bargaining (BR).....	610				
MCCNAUGHTON, A. G. L.					
Canadian engineers' contribution to victory.....	839				
MEDALS. See Honors and Awards.					
MEETINGS. See American Society of Mechanical Engineers.					
MERCHANT M. EUGENE					
Nomographs for analysis of metal-cutting processes.....	737				
MERCIER, STANLEY M.					
Hot-catalyst elevators.....	635				
MERRIFIELD, A. L.					
Controlling moisture content in wood and glued test samples.....	475				
METAL. See also Engineering Materials.					
Damping capacity of alloys.....	33				
Bibliography.....	38				
Engineering properties of nickel.....	123				
Glues for metals.....	337				
Bibliography.....	342				
Indium.....	196				
Lithium.....	196, 198, (A) 855				
Magnesium design considerations and applications.....	468				
Recent developments in engineering materials.....	101, 190, 613				
Bibliography.....	107, 196, 343				
Laminated.....	194				
Metals engineering in aviation.....	549				
Surface finishing.....	119				
<i>See also Surface Finish.</i>					
METAL CUTTING. See also Machine Shop					
Practice, Milling.....	622				
Bibliography available.....	659				
Carbide milling of steel.....	343				
Machinability studies, Bibliography.....	340, 647				
Milling cast iron with carbides.....	192				
Cemented carbides.....	197				
Bibliography.....	241				
Cemented carbide cutting blades.....	681				
Dressing grinding wheels (A).....	473				
Indicated principles of postwar machining.....	647				
Milling cast iron with carbides.....	658				
Bibliography.....	241				
Mounting solid cemented-carbide cutting blades mechanically.....	737				
Nomographs for analysis of metal-cutting processes.....	403				
Radial rake angles in face milling.....	453				
1—Continuation of an investigation on cutter characteristics.....	507				
2—Tool wear, chip formation, and cutting speed in carbide steel milling.....	861				
3—Milling cutters with double radial rake angles.....	575				
Discussion.....	185				
Studies on the machinability of carbon and alloy steels.....	675, 682				
Study of some fundamentals when face-milling steel with carbides—the radial rake angle.....	500				
METALLURGY. See Powder Metallurgy					
METALWORKING					
Establishing and operating a metalworking shop (BR).....	615				
METHODS ENGINEERING					
Shop equipment and the engineer.....	332				
METRIC SYSTEM					
Duodecimals (A).....	675, 682				
History (Ed).....	500				
MEYER, A. W.					
Carbide milling of steel.....	659				
MILLAR P. S.					
Awarded I.E.S. Medal.....	688				
MILLER, RALPH H.					
Gas-turbine locomotives (D).....	409				
Supercharged Diesel engines (D).....	860				
MILLET, M. A.					
Heat-stabilized compressed wood—(Stay-pak).....	25				
MILLING. See also Metal Cutting.					
Milling cast iron with carbides.....	647				
Bibliography.....	658				
MILLING CUTTERS. See Metal Cutting.					
MINING					
Hydraulic materials transportation.....	825				
MODELS					
Fluid flow study of locomotive-firebox design.....	586				
Making standard cast models in rubber molds.....	385				
Three-dimensional plant-layout models.....	383				
MOELLER, CARL H.					
Material-handling aids in modern production.....	235				
MOODY, A. M. G.					
High-temperature gas-turbine power plants.....	229				
MOODY, L. F.					
Awarded Cresson Medal.....	361				
MOORE, JAMES R.					
Some aspects of shipbuilding during world war II.....	319				
MORTENSEN, S. H.					
Awarded Lamme Medal.....	288				
MOTOR					
Grease lubrication of ball-bearing motors and generators.....	639				
Rocket, Jato unit.....	546				
MOTOR VEHICLES					
The Gulf Marsh buggy.....	501				
Vibration investigation.....	723				
MUDGE, W. A.					
Some engineering properties of nickel and high-nickel alloys.....	123				
MUIR, R. C.					
Experiment in management education.....	19				
Discussion.....	682, 683				
MULLIE, W. R.					
An experiment in management education (D).....	682				
MULLER, LLOYD E.					
A vibration investigation.....	723				
MYER, W. H.					
Establishing and operating a metalworking shop (BR).....	615				

N

NATIONAL ADVISORY COMMITTEE FOR AERONAUTICS	
Aeronautical Research policy.....	210
NATIONAL BOARD OF BOILER AND PRESSURE VESSEL INSPECTORS	
Dinner meeting with Boiler Code Committee of A.S.M.E.....	484
NATIONAL EXPOSITION OF POWER AND MECHANICAL ENGINEERING	
Sixteenth exposition.....	71
NATIONAL RESEARCH COUNCIL	
Chemistry of coal utilization (BR).....	767
NAVY. See also Marine.	
Navy Department submits 25 invention problems.....	207
Navy establishes research laboratories at Penn State.....	622
Tool control at Puget Sound Navy Yard.....	533
(D).....	
NEWELL, W. S.	
Heads naval architects.....	144
NEWKIRK, D. L.	
Utilizing small sizes of anthracite (D).....	761
NEWMAN, L. L.	
Utilizing small sizes of anthracite (D).....	763
NEWTON, J. S.	
Gas-turbine locomotives (D).....	408
NICKEL. See also Metal.	
Engineering properties of nickel and high-nickel alloys.....	123
Bibliography.....	129
NOMOGRAPHS. See Graphical Methods.	
Nomographs for analysis of metal-cutting processes.....	737
NONFERROUS METALS	
Dependence on stress of damping capacity of alloys.....	33
Some engineering properties of nickel and high-nickel alloys.....	123
Some recent developments in engineering materials.....	190
2—Nonferrous metals and alloys.....	196
Bibliography.....	
NORDEN, CARL L.	
Receives Holley Medal, (P).....	55, 56
NOTTAGE, H. B.	
Joins staff of A.S.H.V.E.....	624
NYSTROM, K. F.	
High-speed passenger-car trucks.....	313

O

OFFICE OF SCIENTIFIC PERSONNEL	
Project No. 83.....	77
OIL BURNERS	
Handling and burning fuels on board American ships.....	161
OLDENBURGER, RUFUS	
Engineering preview (BR).....	537
ORDNANCE	
Aircraft armament (BR).....	616
A.S.M.E. receives Distinguished Service Award.....	39
Army Ordnance depot problem.....	789
Contribution to ordnance research and development by technical associations.....	23
Dodge-Romig tables.....	169, 276
Gen. L. H. Campbell addresses students.....	84
Labram and the "Long Cecil".....	530

ORDNANCE (<i>continued</i>)	
Malleable iron specifications.....	613
Ordnance supply system. 1—Army Ordnance depot problem.....	789
Principles of firearms (BR).....	482
Proximity fuse (A).....	752
Supersonic wind-tunnel laboratory.....	827
Volumetric pouring machine—a development for mine, projectile, and bomb loading.....	599
ORDNANCE AWARD	
Col. Walsh's address.....	60
OVESEN, HENRIK	
China's steel industry.....	670
P	
PACK, HARRY S.	
Air-cargo handling.....	463
PAGE, FREDERICK HANDLEY	
Honorary fellowship in I.A.S.....	210
PASCHALL, A. L.	
More mud in the water (C).....	613
PASCHIS, VICTOR	
Time-temperature relationships in workpieces.....	445
PATENTS	
Creative engineering and patents.....	633
Developing creative engineers.....	843
Enemy-owned U. S. patents now available.....	290
Lists of patents available for licensing.....	626
Metropolitan representative for license of enemy patents.....	71
Navy Department submits 25 invention problems.....	207
Second report on the American patent system.....	200
Third report of the National Patent Planning Commission.....	743
PATTERSON, MOREHEAD	
Engineers' role in distribution.....	244
PEARCE, SIR (STANDEN) LEONARD	
Honorary member of The American Society of Mechanical Engineers.....	58, 144
PENDRAY, G. E.	
The coming age of rocket power (BR)...	686
PETERSON, C. G.	
Air-cargo handling (D).....	683
PETROLEUM PIPE LINES	
Operation Pluto, the story of the English Channel pipe line.....	527
PETROLEUM REFINING	
Hot-catalyst elevators.....	635
Operating experience with the gas turbine.....	594
PEW, ARTHUR E., JR.	
Operating experience with the gas turbine.....	594
PHILLIPS, WILLIAM H.	
Receives Lawrence Sperry award.....	210
PIASKOWSKI, FRED M.	
Receives Charles T. Main award (P)...	53, 55
PIERCE, H. C.	
An all-year gas air-conditioning unit....	171
PIGORS, PAUL	
Road maps to freedom (BR).....	199
PIPE AND FITTINGS	
Pipe coupling.....	753
PLANNING. <i>See also</i> Postwar Planning.	
Increasing productive machine time.....	584
Industrial jobs for returning veterans....	14
Joint engineering society participation in the program of the Committee for Economic Development (C.E.D.).....	620
Plan to promote postwar employment....	360
Third report of the National Patent Planning Commission.....	743
PLANT LAYOUT. <i>See also</i> Power Plants.	
Plant layout.....	331
Three-dimensional plant-layout models..	383
PLASTICS	
Advances in plastics during 1944.....	255
Bibliography.....	258
Aircraft design.....	548
New nonflammable thermoset plastic....	752
Plastic foam.....	752
Some recent developments in engineering materials.....	267
Bibliography.....	273
PLESSET, E. H.	
Electrical ignition for aircraft internal-combustion heaters.....	715

PLESSET, M. S.	
Electrical ignition for aircraft internal-combustion heaters.....	715
PLYWOOD	
Bibliography.....	342
Controlling moisture content in wood and glued test samples.....	475
Heat-stabilized compressed wood—(Stay-pak).....	25
Some recent developments in engineering materials.....	334
POLARIZED LIGHT	
Study of fluid flow in firebox design....	589
POSTWAR PLANNING	
Air-cargo transportation.....	282
Air transportation.....	225
A.I.C.E. plan for postwar employment....	360
Controlling productive capacity in postwar Germany.....	41
POTTER, A. A.	
Acting president of Purdue.....	485
Address, 25th Anniversary of General Motors Institute.....	400
Creative engineering and patents.....	633
Second report on the American patent system.....	200
Third report of the national patent planning commission.....	743
POWDER METALLURGY	
Discussion.....	84
Sectional carbide molds.....	748
Some recent developments in engineering materials.....	334
Bibliography.....	343
POWER	
Cyclotrons (A).....	675
POWER PLANT	
Airplane power plant (A).....	855
Aviation power plants.....	550
Gas-turbine, high-temperature.....	229
Bibliography.....	233
Gas turbine in aviation.....	803
Jet propulsion (BR).....	275, 611
Plant layout.....	331
POWERS, EDWARD M.	
Appointed to N.A.C.A.....	626
PRATT, E. A.	
To direct A.S.A. Inter-American development.....	290
PRESSURE INDICATOR	
Pressure-sensitive device (A).....	753
PRESIDENT'S PAGE OF A.S.M.E.....	73, 145, 209, 281, 352, 421, 487, 545, 621, 693, 774, 871
PRESSURE VESSELS	
Cost of fabricating boilers and pressure vessels (D).....	614
Fabrication costs of boilers, tanks, and pressure vessels.....	247
PRODUCT DESIGN	
Product planning.....	330
PRODUCT INSPECTION	
Maintaining scientific tolerances by inspection.....	168
PRODUCTION	
Britain's production rates (AB).....	676
Canadian engineers' contribution to victory.....	839
PROPELLER FAN MANUFACTURERS ASSOCIATION	
Elects officers.....	351
PROXIMITY FUSE	
V.T. fuse (A).....	752
PROPIET	
Airplane power plant (A).....	855
PUFFER, S. R.	
The gas turbine in aviation.....	803
PUMPS	
Fuel oil.....	161
Hydraulic materials transportation.....	825
Portable (P).....	157
Radial hydraulic pump (A).....	856
PURCELL, T. E.	
Boiler-water treatment (D).....	857
Q	
QUALITY CONTROL. <i>See also</i> Product Inspection.	
Inspection and quality control (BR)....	616
Sampling inspection tables (BR).....	276
QUAYLE, L. A.	
Volumetric pouring machine—a development for mine, projectile, and bomb loading.....	599
QUINN, B. E.	
An analytical method of cam design....	523

R

RAGSDALE, E. J. W.	
Gas-turbine locomotives (D).....	409
RAILROAD. <i>See also</i> Locomotive.	
Developments discussed.....	356
Freight-car truck.....	517
Locomotive firebox construction.....	253
Locomotive firebox design.....	586
RAILROAD BRAKES	
Load-compensating air brakes.....	511
RAILROAD CARS	
Developments in the freight-car truck...	517
High-speed passenger-car trucks.....	313
RE-EMPLOYMENT. <i>See also</i> Employment.	
Industrial jobs for returning veterans....	14
Postwar employment of veterans.....	9
Problem of returning service man from labor viewpoint.....	12
Veteran re-employment.....	17
REFRACTORY MATERIALS	
Recent developments.....	341
Bibliography.....	343
REFRIGERATION	
Absorption principle.....	172
REHABILITATION	
Small business is big business (BR)....	615
REICHELDERFER, F. W.	
Receives Robert M. Losey award.....	210
RESEARCH	
A few short weeks (Ed).....	567
Aid to science (Ed).....	700
A.S.M.E. Research Committee.....	62, 67
Brown to expand engineering laboratory.	287
General Motors announces proposed technical center.....	623
I.I.T. organizes mechanics laboratory....	287
Institute of industrial research established at Louisville.....	287
N.A.C.A. presents research policy.....	210
National Science Foundation (Ed).....	787
Navy establishes research laboratories at Penn State.....	622
Postwar collegiate research.....	756
Predoctoral Fellowships.....	756
Supersonic wind tunnel laboratory.....	827
U. of Maryland announces Martin gift for aeronautics.....	287
Valedictory (Ed).....	4
RETTALIATA, J. T.	
A gas-turbine road locomotive (AC)....	411
To head M.E. department at I.I.T.....	624
RICARDO, H. R.	
Awarded Rumford Medal.....	142
They help to make engineer officers....	100
RICE, WILLIAM B.	
Maintaining scientific tolerances by inspection.....	168
RIFLING	
Labram and the "Long Cecil".....	530
RIGHTER, R. W.	
Tool control at Puget Sound Navy Yard (D).....	534
ROBERDS, WESLEY M.	
High-frequency induction heating.....	448
ROBERT, JAMES M.	
Biography.....	559
ROBERTSON, ANDREW	
New I.M.E. president.....	486
ROBINSON, ERNEST L.	
Receives Melville Medal (P).....	55
ROCKET MOTOR	
Jato unit.....	546
ROCKETS	
The coming age of rocket power (BR)...	686
Proximity fuse.....	752
ROE, JOSEPH W.	
Pageant of steel (BR).....	416
ROEBLING, JOHN A.	
Biography (BR).....	481
ROEBLING, WASHINGTON	
Biography (BR).....	481
ROMIG, H. G.	
Sampling inspection tables (BR).....	276
ROSE, WILLIAM C.	
Postwar employment of veterans.....	9
ROWLAND, C. A., JR.	
Adapting army equipment to forest-fire fighting.....	437
ROWLAND, FLOYD	
Budgeting for management control (BR)...	767
RUBBER. <i>See also</i> Synthetic Rubber.	
Advances in rubber during 1944.....	262
Bibliography.....	264

S

SAFETY ENGINEERING			SOCIETY FOR PROMOTION OF ENGINEERING		STORAGE	
A.S.A. safety color code.....	424, 688		Education		Balanced pressure barrier.....	752
New war standard to protect X-ray users.....	623		Meetings.....	494, 868	STREAMER, A. C.	
1945 National Fire Codes available.....	289		SODERBERG, C. RICHARD		President of N.E.M.A.....	71
Occupational accident prevention (BR).....	684		Gas turbines (A).....	677	STRICKER, ADAM K., JR.	
SALISBURY, J. KENNETH			Gas turbines and jet propulsion for air- craft (BR).....	275	Receives exceptional civilian service award.....	144
Gas-turbine locomotives (D).....	409		Receives Joseph H. Linnard Prize.....	351	SUPA, MICHAEL	
SANDING. See Woodworking.			The coming age of rocket power (BR).....	686	Hiring handicapped people.....	234
SANFORD, FRANK			The modern gas turbine (BR).....	275	SUPERCHARGING	
A survey of co-operative councils.....	477		SOLDERING		Design aspects of supercharged Diesel en- gines.....	392
SAVAGE, P. S.			Timless solders, bibliography.....	193, 197	SUPERSONIC RESEARCH	
Utilizing small sizes of anthracite (D)....	763		SPARK PLUGS		Supersonic wind-tunnel laboratory.....	827
SAWYER, R. TOM			Electrical ignition for aircraft internal- combustion heaters.....	715	SUPERVISION. See Industrial Training.	
Modern gas turbine (BR).....	275		SPENCER, H. C.		SURFACE FINISH	
SCHMIDT, A. O.			Engineering preview (BR).....	537	Less mud in the water (C).....	862
Radial rake angles in face milling			SPRABAGEN, W.		More mud in the water (C).....	613
1—Continuation of an investigation on			Appointed director of Welding Research		Replica method for evaluating finish of a metal surface.....	119
cutter characteristics.....	403		Council.....	485	Some recent developments in engineering materials.....	190
2—Tool wear, chip formation, and cut- ting speed in carbide steel milling.....	453		STAMM, A. J.		Bibliography.....	197
3—Milling cutters with double radial rake angles.....	507		Heat-stabilized compressed wood—(Stay- pak).....	25	Surface-finish analyzer.....	748
SCHOENFELD, D. M.			STANDARDS		SURFACE HARDENING	
Handling and burning fuels on board American ships.....	161		A.B.C. standards conference (Ed).....	699	High-frequency induction heating.....	448
SCHOESSOW, G. J.			Aircraft parts.....	729	SWEENEY, R. J.	
Cost of fabricating boilers and pressure vessels (D).....	614		A.S.M.E.—A.I.E.E. preferred standards for condensing steam turbine generators	360	Loosening by vibration of threaded fast- enings.....	798
SCIENCE			A.S.M.E. Standardization committees.....	64, 867	SYNTHETIC RUBBER	
A National Science Foundation.....	787		A.S.A. broadens its scope.....	870	Advances in rubber during 1944.....	262
SCOTT, CHARLES F.			A.S.A. standard for oils and greases.....	430	Bibliography.....	264
Engineers in training.....	134		American war standards for drawing and drafting-room practice.....	361	Making standard cast models in rubber molds.....	385
Obituary (Ed).....	91		College instruction in standardization.....	549	Some recent developments in engineering materials.....	267
SCREW THREADS			Conference on unification of engineering standards.....	776	Bibliography.....	272
W. L. Batt reports on screw thread prac- tice.....	79		Drafting-room practices to be co-ordi- nated.....	495	Synthetic rubber in automotive chassis..	353
International Conference on screw threads to be held at Ottawa.....	483		Drafting-room standards.....	361	SYNTHETIC SAPPHIRES AND SPINELS	
Loosening by vibration of threaded fast- enings.....	798		Filler metal specifications (C).....	765	Physical constants.....	274
SEABURY, GEORGE T.			International Conference on screw threads to be held at Ottawa.....	483		
Obituary.....	435, 485		Machine parts.....	79		
SEBORG, R. M.			New guide and specifications for iron and steel arc-welding electrodes.....	622		
Heat-stabilized compressed wood—(Stay- pak).....	25		New A.S.A. color code completed.....	688		
SECTIONS OF A.S.M.E.			Joint U. S.-Canadian mission.....	79		
See American Society of Mechanical En- gineers			Policy committee report, Secretary of Commerce.....	781		
SEELEY, L. E.			Safety color code submitted.....	424	TANKS	
To be dean of University of New Hamp- shire.....	542		Screw threads, W. L. Batt report.....	79	Fabrication costs of boilers, tanks, and pressure vessels.....	247
SEYMOUR, WILLIAM			Standards advisory committee meets.....	290	TAPPING	
War problems of increasing utilization of small anthracite.....	457		Steam turbine, A.S.M.E.-A.I.E.E. stand- ards available.....	360	Blind-hole tapping (A).....	747
Discussion.....	758		Stoker Manufacturers Association Tech- nical Manual available.....	289	TAXATION	
SHELL LOADING. See also Ordnance.			Technical sessions at 1944 Annual Meet- ing.....	64	Postwar federal taxes (BR).....	32
Volumetric pouring machine—a develop- ment for mine, projectile, and bomb loading.....	599		Tentative standards (C).....	613	TECHNICAL INSTITUTES	
SHERMAN, RALPH A.			Welding-electrode standards (C).....	535	Accrediting.....	79
Paths to smoke abatement.....	520		STATISTICAL METHODS		TENNESSEE VALLEY AUTHORITY	
SHIPBUILDING			Maintaining scientific tolerances by in- spection.....	168	The Valley and its people (BR).....	277
Some aspects of shipbuilding during world war II.....	319		STEAM TURBINES		THEISINGER, W. G.	
SHIPS			A.S.M.E.-A.I.E.E. preferred standards for condensing steam turbine generators	360	Fabrication costs of boilers, tanks, and pressure vessels.....	247
Handling and burning fuels on board American ships.....	161		STEEL. See also Iron and Steel, Metal, Steel		THERMODYNAMICS	
SIDLER, P. R.			Alloys, Welding.....	659	Thermodynamic properties of air (BR)..<	685
Gas-turbine locomotives for main-line service (AC).....	412		Carbide milling of steel.....	670	THIELSCHER, H. G.	
SILICONES			China's steel industry.....	103	Manager of A.S.M.E. (P).....	54
Bibliography.....	271, 274		Hardenability calculations.....	107	TICHVINSKY, L. M.	
SILLCOX, L. K.			Bibliography.....	107	Diesel-engine bearings.....	297
Receives gold medal of Institution of Locomotive Engineers (England).....	351		Leaded.....	575	TOLERANCES	
SILLO			Machinability of carbon and alloy steels..<	630	Maintaining scientific tolerances by in- spection.....	168
Steel silo (A).....	856		Slag-free sample (P).....		TOOL ENGINEERING	
SIMON, ARTHUR			Some recent developments in engineering materials.....	101	Tool control at Puget Sound Navy Yard (D).....	533
Interprofessional institute (C).....	137		1—Ferrous metals.....	190	TOOLS	
SMITH, E. D.			2—Nonferrous metals.....	343	Carbide milling of steel.....	659
Letters applying for a job.....	847		Bibliography.....	107, 196	Diamond tools (BR).....	204
SMITH, G. G.			Welded parts.....	109	TOWNSEND, J. R.	
Gas turbines and jet propulsion for air- craft (BR).....	275		STEEL ALLOYS. See also Alloys.		Heads A.S.T.M.....	620
Gas-turbine locomotives (D).....	410		Bending data.....	469	TRANSPORTATION	
SMITH, R. B.			Dependence on stress of damping capac- ity of alloys.....	33	Safety in air and rail travel (C).....	536
Receives Joseph H. Linnard prize.....	351		Some recent developments in engineering materials.....	101	TRIBUS, MYRON	
SMOKE			1—Ferrous metals.....	190	Effect of ventilation rate on cabin tem- perature.....	668
Paths to smoke abatement.....	520		2—Nonferrous metals.....	196	TROWBRIDGE, THOMAS	
Smoke density determination.....	867		Bibliography.....	107	Use of modern coated abrasives in wood- working industries.....	387
SOCIAL RELATIONS			Studies on the machinability of carbon and alloy steels.....	575	TRUCKS. See Railroad Cars.	
Education for what? (BR).....	324		STEINMAN, D. B.		TUCKER, D. S.	
Road maps to freedom (BR).....	199		The builders of the bridge (BR).....	481	Economic maturity and business prosper- ity (BR).....	836
SOCIETY OF CHEMICAL INDUSTRY			STEVENSON, A. R., JR.		Fiscal requirements in 1949.....	744
Perkin Medal awarded.....	849		A reply from industry to the colleges.....	501	TUCKER, J. MACK	
			Biography.....	552	Editor of "Refrigeration abstracts".....	208
			STEWART, C. D.		TULL, M. G.	
			Load-compensating air brakes.....	511	Tool control at Puget Sound Navy Yard (D).....	534
			STOKERS		TULLO, A. M.	
			Handling and burning fuels on board American ships.....	161	Shop equipment and the engineer.....	332
			New S.M.A. "Technical manual".....	289		

T

TUPHOLME, C. H. S. Twentieth century engineering (BR).....	415
TURBINES. <i>See</i> Gas Turbines, Steam Turbines.	
New aircraft power plant (A).....	855
TURBOCHARGING. <i>See</i> Supercharging.	
TURBOCOMPRESSORS Operating experience with the gas turbine.....	594
TURBOSUPERCHARGER First aviation gas turbine.....	550
Gas turbine in aviation.....	803
TURCK, FENTON B. Engineers' role in distribution.....	244

U

UNIONS. <i>See</i> Industrial Relations.	
UNITED ENGINEERING TRUSTEES J. P. H. Perry elected president.....	849
Report for 1943-1944.....	74
URWICK, L. Elements of Administration (BR).....	140

V

VALENTINE, WILLARD L. Editor of "Science".....	849
VAN ALLYN, K. Job placement reference (BR).....	861
VAN LEER, BLAKE R. Elected chairman of Georgia ports authority.....	485
VAN PELT, J. R., JR. To head Battelle's research education program.....	361
VENTILATION Effect of ventilation rate on airplane cabin temperature.....	668
VETERAN EMPLOYMENT. <i>See</i> Employment, Re-employment.	
VIBRATION Applications of supersonic vibration.....	340
Bibliography.....	343
Dependence on stress of damping capacity of alloys.....	33
Bibliography.....	38
Loosening by vibration of threaded fastenings.....	798
Testing experimental motorcars.....	723
VISCOSITY Viscosity of lubricants under high pressure.....	820
Bibliography.....	823
VON KÁRMÁN, THEODORE Atomic engineering.....	672

W

WALKER, EDWARD Cost of fabricating boilers and pressure vessels (D).....	146
---	-----

WALTERS, J. E. President of Alfred University.....	624
WAR EFFORT O.P.R.D. solicits projects.....	289
WAR PRODUCTION A.S.M.E. Committee on War Production Canadian engineers' contribution to victory.....	39
WARNER, D. F. Contemporary jet-propulsion gas turbines for aircraft.....	839
WARNER, EDWARD PEARSON American honorary fellow of I.A.S.....	707
WATSON, R. M. Air compressors (BR).....	210
WEAR Radial rake angles in face milling.....	865
WEHMER, FRED Use and evaluation of some specialty adhesives.....	453
WEICK, FRED E. Receives Sylvanus Albert Reed Award..	380
WEIGHTS AND MEASURES The metric system (Ed).....	210
WEIR, C. D. Inter-crystalline cracking.....	500
WELDING Applying engineering principles to design of welded joints (C).....	834
Clad steel plate, cost.....	535
Cost of fabricating boilers and pressure vessels (C).....	254
Engineering is a more exact science than welding (C).....	614
Filler metal specifications (C).....	136
Foreign welding terms.....	765
New guide and specifications for iron and steel arc-welding electrodes.....	81
Resistance welding manufacturers association awards.....	622
Trends in the use of welded machinery parts.....	870
Welding-electrode standards (C).....	109
Welding engineering must be based on exact science (C).....	535
WELDING RESEARCH COUNCIL W. Sparagen appointed director.....	680
WESTERN SOCIETY OF ENGINEERS Celebrates 75th anniversary.....	485
WHIRL, S. F. Boiler-water treatment (D).....	81
WHITTINGHAM, HAROLD Receives John Jeffries award.....	857
WHITTLE, FRANK Delivers James Clayton Lecture of I.M.E. Honorary member I.M.E.....	210
WILCOCK, DONALD F. Viscosity-temperature coefficient (AC).....	850
WILLARD, JOHN A. Preplanning of logging operations for minimum costs.....	288
WILLIAMS, EDWARD E. Biography (P).....	325
WILLIAMS, S. V. Cost of fabricating boilers and pressure vessels (D).....	551
WILLISTON, A. L. An experiment in management education (D).....	615
	683

WIND TUNNELS

N.A.C.A. announces new supersonic wind tunnel for jet-propulsion research.....	619
Supersonic wind tunnel dedicated at Aberdeen proving ground.....	423
Supersonic wind-tunnel laboratory.....	827

WITHINGTON, SIDNEY

Gas-turbine locomotives (D).....	411
----------------------------------	-----

WITTMAN, G. P.

Studies on the machinability of carbon and alloy steels.....	575
--	-----

WOOD. *See also* Plywood.

A cubic inch of wood.....	261
Glued-laminated arches with sawed laminations.....	813
Heat-stabilized compressed wood.....	25
Logging operations for minimum cost.....	325
Properties of.....	261
Some recent developments in engineering materials.....	334

WOOD PRODUCTS

Sawdust uses.....	751
-------------------	-----

WOODLAND PROTECTION

Proposed committee.....	157
-------------------------	-----

WOODWORKING. *See also* Adhesives, Plywood.

Use of modern coated abrasives in wood-working industries.....	387
--	-----

WOOL

Mechanical properties and uses of wool felt.....	92
--	----

WOOLRICH, W. R.

The Valley and its people (BR).....	277
-------------------------------------	-----

WESTERN SOCIETY OF ENGINEERS

Elects officers.....	485
----------------------	-----

WRIGHT, ORVILLE

Honorary member, British I.M.E.....	144
-------------------------------------	-----

WRIGHT, ROY V.

Address at engineers' forum.....	873
----------------------------------	-----

The engineer's status in the community..	401
--	-----

WRIGHT, T. P.

Receives Daniel Guggenheim medal.....	754
---------------------------------------	-----

X-Y-Z

X RAYS

50 years of X ray (Ed).....	296
New war standard to protect X-ray users.	623
Welding boilers and pressure vessels.....	614

YARNALL, D. ROBERT

Biography.....	552
----------------	-----

President of A.S.M.E.....	551
---------------------------	-----

President's page.....	871
-----------------------	-----

YOST, EDNA

Normal lives for the disabled (BR).....	204
---	-----

YOUNG, J. F.

Developing creative engineers.....	843
------------------------------------	-----

ZELLER, HOWARD

Utilizing small sizes of anthracite (D)...	764
--	-----

ZLATIN, NORMAN

Nomographs for analysis of metal-cutting processes.....	737
---	-----

ZSUFFA, LESLIE

Return to civilian life.....	673
------------------------------	-----

Index to A.S.M.E. Transactions

Volume 67, 1945

The A.S.M.E. Transactions for 1945 was issued monthly. Four of the twelve issues are the *Journal of Applied Mechanics*, the page numbers of which are preceded by the letter A.

The Society Records for the year 1945 appeared as supplements, one in February, 1945, the Memorial Biographies in October, 1945, and the index section in January, 1946. The page numbers for these supplements are designated by the symbol RI, and the February supplement contains its own index. (AC) denotes author's closure; (BR) book review; (D) discussion of a paper.

A

ABBOTT, CHARLES CARROLL. Obituary.....	RI-47
ABÉ KEIICHI. Obituary.....	RI-47
ACOUSTICS	
Stabilizing a suction-relief valve.....	87
ADLER, ALPHONSE ANDREW. Obituary.....	RI-47
AERODYNAMICS. <i>See also</i> Flow of Fluids.	
AIR. <i>See</i> Gases, Instruments—Measuring.	
AIRCRAFT	
Flutter of a uniform cantilever wing.....	A-197
Graphical method for the evaluation of principal strains from normal strains.....	A-209
Parallel columns with lateral supports.....	A-253
Stresses in a reinforced monocoque cylinder under concentrated symmetric transverse loads (D).....	A-187
AIRPLANES	
An acceleration damper: development, design, and some applications.....	523
An analytical theory of landing-shock effects on an airplane considered as an elastic body (D).....	A-186
Effect of aeration on gear-pump delivery and lubrication ceiling.....	123
Fatigue tests of airplane generator brackets with special reference to failure of screw fastenings.....	A-113
Bibliography.....	A-119
AIRPLANE WINDSHIELDS	
Graphical solution of windshield heating problems.....	513
AIRPLANE WINGS. <i>See also</i> Flutter.	
New method of calculating natural modes of coupled bending-torsion vibration of beams.....	61
Structural efficiency of wing covers.....	A-8
The flutter of a uniform cantilever wing.....	A-197
ALECK, B. J.	
The effects of web deformation on the torsion of I-beams (D).....	A-125
ALEXANDROFF, W. A.	
Influence of applying cutting fluids at different temperatures when turning steel (D).....	222
ALLOYS. <i>See</i> Aluminum.	
Application of controlled atmospheres to the processing of metals.....	501
ALUMINUM	
Methods of joining aluminum-alloy products.....	1
AMERICAN SOCIETY OF MECHANICAL ENGINEERS	
Awards.....	RI-40
Committee personnel index.....	RI-5
Council.....	RI-5
Honorary members.....	RI-43
Past-Presidents, Treasurers, and Secretaries.....	RI-44
Publications	
Biographies.....	RI-87
Boiler Construction Code.....	RI-88
Books on special subjects.....	RI-89
Indexes.....	RI-87
Memorial Biographies.....	RI-47
Papers presented at meetings.....	RI-87
Power Test Codes.....	RI-88
Professional Divisions.....	RI-10
Research, index.....	RI-88
Safety Codes.....	RI-89
Sections.....	RI-15
Society Records.....	RI-1
Standards.....	RI-1
Student Branches.....	RI-23
Technical Committee publications.....	RI-87
Woman's auxiliary.....	RI-39
ANDERSON, E. D.	
Heat transfer and pressure drop of liquids in double-pipe fin-tube exchangers.....	697
ANDERSON, HENRY CLAY. Obituary.....	RI-48
ANDERSON, ROBERT MARSHALL. Obituary.....	RI-48
ANDREWS, R. D.	
Creep and relaxation in rubber products at elevated temperatures.....	569

ISSUE	PAGE NUMBERS
January	1-68
February	69-140
April	141-216
May	217-308
July	309-404
August	405-512
October	513-600
November	601-718

Journal of Applied Mechanics

March	A - 1-A-64
June	A - 65-A-128
September	A-129-A-196
December	A-197-A-264

ANGUS, R. W.	
Prediction of centrifugal-pump performance (D).....	440
Water-hammer analysis by LaPlace-Mellin transformation (D).....	369
Water-hammer problems in connection with the design of hydroelectric plants (D).....	389
ARMSTRONG, R. M.	
Heat transfer and pressure loss in small commercial shell and finned-tube heat exchangers.....	675
ARMY ORDNANCE	
Electric turret-traversing mechanism for tanks.....	A-228
ASHLEY, C. M.	
Heat transfer from a baffled-finned cylinder to air (D).....	610
Heat transfer through tubes with integral spiral fins (D).....	673
AUTOMATIC CONTROL	
Electrical-analogy method for fundamental investigations in automatic control.....	81
Electronic-type instruments for industrial processes.....	393
Stabilizing a suction-relief valve.....	87
AVIATION. <i>See also</i> Aircraft, Airplanes.	
Effect of aeration on gear-pump delivery and lubrication ceiling.....	123

B

BAGLEY, G. D.	
Economic thickness of thermal insulation for intermittent operation (D).....	100
BAKER, M. D.	
History of potassium boiler-water treatment at Springdale.....	317
BAKHMETEFF, B. A.	
Water-hammer analysis by LaPlace-Mellin transformation (D).....	369
BANFIELD, F. E., JR.	
Investigation of influence of ring size, bobbin diameter, and spindle speed on spinning process, and their effect on over-all cost of spinning (D).....	580
BARCLAY, K. M.	
Use of anthracite fines in by-product coke production.....	405
BARNES, H. GORDON. Obituary.....	RI-48
BARS	
Dynamics of an elastic bar.....	A-101
BARSTOW, FRANCIS LORING. Obituary.....	RI-48

BARTON, M. V.	
Effects of web deformation on the torsion of I-beams (D).....	A-123
Shrink-fit stresses and deformations (D).....	A-182
BATES, L. W.	
10,000-Kw railway-mounted mobile steam power plant for U. S. Navy Department, Bureau of Yards and Docks (D).....	165
BAUDRY, R. A.	
Some thermal effects in oil-ring journal bearings.....	117
BAUM, KARL P., JR. Obituary.....	RI-49
BEAMS	
Design of beams of long span and low specific strength.....	A-156
New method of calculating natural modes of coupled bending-torsion vibration of beams.....	61
The effects of web deformation on the torsion of I-beams (D).....	A-125
BEARINGS	
Heat effects in lubricating films (D).....	A-126
Some thermal effects in oil-ring journal bearings.....	117
Bibliography.....	122
BEATTY, K. O., JR.	
Heat transfer through tubes with integral spiral fins.....	665
BEAUSOLEIL, RAYMOND J. Obituary.....	RI-49
BEHREND, ERNST RICHARD. Obituary.....	RI-49
BEHUN, MICHAEL	
A pneumatic piston-ring gage for radial-pressure measurement (D).....	496
BEITLER, S. R.	
Piping arrangements for acceptable flow-meter accuracy (D).....	357
BENDING TESTS	
Bending of curved thin tubes.....	A-1
The effect of transverse shear deformation on the bending of elastic plates.....	A-69
Bibliography.....	A-77
BERGREN, W. P.	
Economic thickness of thermal insulation for intermittent operation (D).....	101
BERK, A. A.	
Embrittlement cracking in waters containing potassium salts.....	329
BERNHARDT, G. K.	
Heat transfer from a baffled-finned cylinder to air (D).....	610
BERRY, C. HAROLD	
Thermodynamic charts (BR).....	A-263
BESKIN, LEON	
Bending of curved thin tubes.....	A-1
BIGGS, L. R.	
10,000-Kw railway-mounted mobile steam power plant for U. S. Navy Department, Bureau of Yards and Docks.....	141
BINDER, R. C.	
Direct analysis of mechanical wave filters.....	A-129
BIOMECHANICS	
Locomotor mechanics and occupation... ..	167
BLACK, P. H.	
Lubrication characteristics of involute spur gears; a theoretical investigation (D).....	185
BLAKE, J. J.	
Investigation of influence of ring size, bobbin diameter, and spindle speed on spinning process, and their effect on over-all cost of spinning.....	575
BLOWERS	
Presentation of centrifugal-compressor performance in terms of nondimensional relationships.....	483
BOILER	
10,000-Kw railway-mounted mobile steam power plant for U. S. Navy Department, Bureau of Yards and Docks... ..	141

- BOILER CODE**
Boiler nozzles and valve inlets for maximum-capacity safety valves..... 133
- BOILER CODE COMMITTEES**
A.S.M.E. committee personnel..... RI-38
- BOILER DRUMS**
Stresses in a cylindrical shell due to nozzle or pipe connection..... A-107
- BOILER FEEDWATER.** *See also* Feedwater Treatment.
Carry-over in locomotive boilers..... 197
Bibliography..... 205
- BOILER FURNACES**
External corrosion of furnace-wall tubes
1—History and occurrence..... 279
2—Significance of sulphate deposits and sulphur trioxide in corrosion mechanism..... 289
- BOILER SCALE.** *See* Feedwater Treatment.
- BOILER TESTS**
Carry-over in locomotive boilers..... 197
- BOMER, EDGAR THOMAS.** Obituary..... RI-50
- BOOK REVIEWS**
Handbuch der Werkstoffprüfung..... A-127
How to solve it..... A-263
Materials and processes..... A-127
Mathematical and physical principles of engineering analysis..... A-128
Methods of advanced calculus..... A-63
Reine metallie..... A-63
Society for Experimental Stress Analysis, Proceedings, vol. 1..... A-63
Proceedings, vol. 2..... A-264
The modern gas turbine..... A-196
Thermodynamic charts..... A-263
Vibration analysis..... A-128
What are cosmic rays?..... A-196
- BORDEN, M. M.**
The coefficient of Herschel type cast-iron Venturi meters (D)..... 342
- BOSSEST, CHARLES PHILIP.** Obituary..... RI-50
- BOSTON, O. W.**
A thermal-balance method and mechanical investigation for evaluating machinability..... 225
Influence of applying cutting fluids at different temperatures when turning steel..... 217
- BOUCHER, D. F.**
A general correlation of friction factors for various types of surfaces in crossflow (D)..... 656
- BOWMAN, R. A.**
Air-cooled steam condensers..... 661
- BOYD, JOHN**
The friction properties of various lubricants at high pressures..... 51
- BRADLEY, C. B.**
Economic thickness of thermal insulation for intermittent operation..... 93
- BRAZING**
Methods of joining aluminum-alloy products..... 13
- BRECKENRIDGE, LESTER PAIGE.** Obituary..... RI-50
- BRIDGMAN, P. W.**
The friction properties of various lubricants at high pressures (D)..... 56
- BROWN, HARRY CLEOPHAS.** Obituary..... RI-51
- BROWN, R. J.**
Balancing of rotating apparatus—II (D). A-59
- BROWN, WILLIAM CLINTON.** Obituary..... RI-51
- BUCKLING**
Critical shearing stress in skin-stressed boxcar sides..... 561
Inelastic buckling of variable-section columns..... A-163
- BUCKWALTER, T. V.**
Fatigue strength of 5/16-in.-diam shafts as related to design of large parts..... A-149
- BUENTING, OTTO WILHELM.** Obituary..... RI-51
- BURGER, CHARLES BERNARD.** Obituary..... RI-51
- BURWELL, J. T., JR.**
Lubrication characteristics of involute spur gears; a theoretical investigation (D)..... 185
The friction properties of various lubricants at high pressures (D)..... 56
- C**
- CALORIMETER**
Thermal balance method for evaluating machinability..... 225
- CAMPBELL, CHARLES ALBERT.** Obituary..... RI-52
- CARMAN, E. P.**
Ignition through fuel beds on traveling- or chain-grate stokers..... 425
- CARR, R. A.**
Carry-over in locomotive boilers (D).... 205
- CARRY-OVER**
Carry-over in locomotive boilers..... 197
Bibliography..... 205
- CARSWELL, T. S.**
Effect of some environmental conditions on the mechanical properties of cellulose acetate and cellulose nitrate plastic sheets..... 23
- CARTER, W. A.**
Coefficient of Herschel type cast-iron Venturi meters (D)..... 342
Piping arrangements for acceptable flow-meter accuracy (D)..... 357
- CARTINHOOR, JOHN**
Disk extended surfaces for high heat-absorption rates..... 687
- CAVITATION**
Cavitation in centrifugal pumps..... 539
- CHAMBERLAIN, PAUL MELLE.** Obituary..... RI-52
- CHAPMAN, KENNETH BRYANT.** Obituary..... RI-52
- CHARLES, CARL LUDWIG.** Obituary..... RI-53
- CHRISTOPH, JOSEPH BENEDICT.** Obituary..... RI-53
- CHURCH, W. H.**
A study of the theory of axial-flow pumps (D)..... 463
- CHUTES.** *See* Coal Handling.
- CLENDENIN, J. D.**
Use of anthracite fines in by-product coke production..... 405
- COAL**
Blending coals reflects greater uniformity of product..... 417
The missing data on coal sampling..... 69
Bibliography..... 79
Use of anthracite fines in by-product coke production..... 405
Bibliography..... 415
- COAL HANDLING**
Experimental study of the flow of coal in chutes at Riverside Generating Station. 585
- COAL PROCESSING**
Blending coals reflects greater uniformity of product..... 417
- COAL TESTING**
The missing data on coal sampling..... 69
Bibliography..... 79
- CODES**
A.S.M.E., Index..... RI-87
- COKE**
Use of anthracite fines in coke production..... 405
Bibliography..... 415
- COLBURN, A. P.**
Heat transfer from a baffled-finned cylinder to air..... 601
- COLUMNS**
Inelastic buckling of variable-section columns..... A-165
- COMBUSTION**
Ignition through fuel beds on traveling- or chain-grate stokers..... 425
- COMMITTEES OF A.S.M.E.**
Personnel lists..... RI-5
- COMPRESSORS**
Presentation of centrifugal-compressor performance in terms of nondimensional relationships..... 483
- CONCORDIA, C.**
Network- and differential-analyzer solution of torsional oscillation problems involving nonlinear springs..... A-43
Discussion..... A-194
- CONE, HUTCHINSON INGHAM.** Obituary..... RI-53
- CONNELL, FRANK GILL.** Obituary..... RI-54
- CONTERMAN, FRED A.** Obituary..... RI-55
- CONTROL**
Electrical-analogy method for fundamental investigations in automatic control..... 81
- CONTROLLED ATMOSPHERES.** *See* Heat-Treatment.
- COOGAN, C. H., JR.**
Nozzles for supersonic flow without shock fronts (D)..... A-260
- CORCORAN, JAMES L.**
Boiler nozzles and valve inlets for maximum-capacity safety valves (D).... 139
- COREY, R. C.**
External corrosion of furnace-wall tubes
1—History and occurrence..... 279
2—Significance of sulphate deposits and sulphur trioxide in corrosion mechanism..... 289
- CORNELIUS, HENRY ROBERT.** Obituary..... RI-55
- CORROSION.** *See also* Embrittlement, Feed-water.
External corrosion of furnace-wall tubes
1—History and occurrence..... 279
2—Significance of sulphate deposits and sulphur trioxide in corrosion mechanism..... 289
- COSMIC RAYS**
What are cosmic rays? (BR)..... A-196
- CREEP**
Creep and relaxation in rubber products at elevated temperatures..... 569
Creep properties of molded phenolic plastics at elevated temperatures..... 253
Bibliography..... 258
- CREEP OF METALS**
New machines for creep and creep-rupture tests..... 111
Bibliography..... 116
- CRINER, H. E.**
A new device for the solution of transient-vibration problems by the method of electrical-mechanical analogy..... A-135
- CRISSEY, CLARENCE PHILIP.** Obituary..... RI-55
- CROSS, B. J.**
External corrosion of furnace-wall tubes
1—History and occurrence..... 279
2—Significance of sulphate deposits and sulphur trioxide in corrosion mechanism..... 289
- CURTISS, NATHAN ALFRED.** Obituary..... RI-55
- CUTTING FLUIDS.** *See* Metal Cutting.
- CYLINDERS**
Heat transfer from a baffled-finned cylinder to air..... 601
Local coefficients of heat transfer for air flowing around a finned cylinder..... 613
- D**
- DALL, A. H.**
Relation of surface-roughness readings to actual surface profile (D)..... 194
- DALLAS, JOHN.** Obituary..... RI-56
- DAMPING.** *See* Vibration.
- DAVENPORT, WILLIAM SIMEON.** Obituary..... RI-56
- DAVIS, CHARLES ETHAN.** Obituary..... RI-56
- DAVIS, E. A.**
Yielding and fracture of medium-carbon steel under combined stress..... A-13
- DAVIS, WILLIAM J., JR.** Obituary..... RI-57
- DEHART, R. C.**
Moment-distribution analysis for three-dimensional pipe structures (AC)..... A-190
- DEICING**
Graphical solution of windshield heat deicing problems..... 513
- DEJUHASZ, K. J.**
Forced and free motion of a mass on an air spring (D)..... A-175
- DEL MAR, B. E.**
Presentation of centrifugal-compressor performance in terms of nondimensional relationships..... 483
- DELMONTE, JOHN**
Elastic properties of plastic materials.... 477
- DE LORENZO, B.**
Heat transfer and pressure drop of liquids in double-pipe fin-tube exchangers..... 697
- DEMICHEAL, D. J.**
Measurement of dynamic stress and strain in tensile-test specimen (AC)..... A-124
- DICKEY, DONALD EDGAR.** Obituary..... RI-57
- DICKEY, P. S.**
Electronic-type instruments for industrial processes..... 393
- DICKINSON, EDGAR DRURY.** Obituary..... RI-57
- DIEHL, AMBROSE NEVIN.** Obituary..... RI-58
- DIEMER, HUGO.** Obituary..... RI-59
- DIESEL ENGINES**
Optimum compression ratios for a high-speed Diesel engine..... 471
- DISKS.** *See* Rotors, Turbines.
- DOERING, WALTER CHARLES.** Obituary..... RI-59
- DONNELL, L. H.**
Basic mechanics of the metal-cutting process (D)..... A-257
- DONOVAN, A. E.**
Structural efficiency of wing covers..... A-8
- DOTY, PAUL.** Obituary..... RI-59
- DREXEL, R. E.**
Local coefficients of heat transfer for air flowing around a finned cylinder..... 613

- DRILLING**
A thermal-balance method and mechanical investigation for evaluating machinability..... 225
- DRINKA, J. J.**
Critical shearing stress in skin-stressed boxcar sides..... 561
- DRUCKER, D. C.**
A new design criterion for wire rope..... A-33
- DUBOSQUE, FRANCIS LEBRUN.** Obituary..RI-61
- DUSINBERRE, G. M.**
An electrical geometrical analogue for complex heat flow (D)..... 713
Efficiency of extended surface (D)..... 628
Numerical methods for transient heat flow..... 703
- DYNAMICS.** See Railroad Trains.
- E**
- ECKMAN, D. P.**
Electrical-analogy method for fundamental investigations in automatic control..... 81
- EJECTORS**
The theory of ejectors.....A-170
- ELECTRIC ANALOGY**
An electrical geometrical analogue for complex heat flow..... 713
Economic thickness of thermal insulation for intermittent operation..... 93
Electrical-analogy method for fundamental investigations in automatic control..... 81
Heat-flux pattern in fin tubes under radiation..... 693
New device for the solution of transient-vibration problems by the method of electrical-mechanical analogy.....A-135
- ELECTRIC MACHINERY**
10,000-Kw railway-mounted mobile steam power plant for U. S. Navy Department, Bureau of Yards and Docks 141
- ELECTRIC TRAVERSING MECHANISM**
Electric turret-traversing mechanism for tanks.....A-228
- ELECTRONICS**
Electronic-type instruments for industrial processes..... 393
- ELLENWOOD, F. O.**
Thermodynamic charts (BR).....A-263
- ELLIOTT, GEORGE FREDERICK.** Obituary..RI-61
- ELROD, H. G., JR.**
The theory of ejectors.....A-170
- EMBRITTELEMENT.** See also Corrosion.
Embrittlement cracking in waters containing potassium salts..... 329
- EMMONS, H. W.**
Nozzles for supersonic flow without shock fronts (D).....A-260
- EMSWILER, JOHN EDWARD.** Obituary.....RI-61
- ENGINES**
Optimum compression ratios for a high-speed Diesel engine..... 471
- ENGINEERING**
Mathematical and physical principles of engineering analysis (BR).....A-128
- ENGVALI, HARRY**
Lubrication characteristics of involute spur gears; a theoretical investigation (D)..... 186
- ERICKSON, E. C. O.**
Properties and development of papreg—a high-strength laminated paper plastic.. 267
- ERNST, C. E.**
Economic thickness of thermal insulation for intermittent operation..... 93
- EXLINE, P. G.**
A pneumatic piston-ring gage for radial-pressure measurement..... 491
Heat effects in lubricating films (D).....A-126
Investigation of cross-spring pivot (D).... A-62
- F**
- FALLS, E. K.**
Boiler nozzles and valve inlets for maximum-capacity safety valves..... 133
- FANS**
A simplified method of determining hoop stresses in fan rotors..... A-65
- FATIGUE.** See Metal Testing—Fatigue.
- FEEDWATER TREATMENT**
Carry-over in locomotive boilers..... 197
Bibliography..... 205
Embrittlement cracking in waters containing potassium salts..... 329
Experience with potassium treatment at Windsor Station..... 325
Experience with sodium and potassium chemicals for boiler-water conditioning at Montaup Electric..... 335
History of potassium boiler-water treatment at Springdale..... 317
Silica deposition in steam turbines..... 309
- FEHR, R. O.**
Measurement of dynamic stress and strain in tensile-test specimen (AC).....A-124
Measurement of the damping of engineering materials during flexural vibration at elevated temperatures (AC).....A-181
- FERGUSON, FERGUS RICHARD.** Obituary..RI-61
- FIELD, DAVID PORTER.** Obituary.....RI-62
- FINNEGAN, THOMAS**
History of potassium boiler-water treatment at Springdale (D)..... 321
- FINS.** See Heat Transfer, Cylinders, Tubes.
- FISH, M. J.**
Moment-distribution analysis for three-dimensional pipe structures (D).....A-188
- FISHER, J. C.**
Tension tests at constant true strain rates.....A-217
- FLEISCHER, K. W.**
Heater designs for the petroleum industry (D)..... 537
- FLEISCHMANN, LIONEL**
Balancing of rotating apparatus—II (AC).....A-60
- FLINT, BERTRAM PIERPONT.** Obituary..RI-62
- FLOW OF FLUIDS**
A general correlation of friction factors for various types of surfaces in crossflow.. 643
An instrument for indicating amount of gas in gas-liquid mixtures..... 399
Experimental investigation of turbulence diffusion—a factor in transportation of sediment in open-channel flow.....A-91
Bibliography.....A-100
Heat transfer and pressure drop of liquids in double-pipe fin-tube exchangers..... 697
Heat transfer and pressure loss in small commercial shell and finned-tube heat exchangers..... 675
Nozzles for supersonic flow without shock fronts (D).....A-260
Presentation of centrifugal-compressor performance in terms of nondimensional relationships..... 483
Temperature measurements in high-velocity air streams.....A-25
Tube spacing in finned-tube banks..... 633
- FLUID METERS**
Piping arrangements for acceptable flow-meter accuracy..... 345
The coefficient of Herschel type cast-iron Venturi meters..... 339
- FLUTTER**
An acceleration damper; development, design, and some applications..... 523
Flutter of a uniform cantilever wing.....A-197
- FOAMING.** See Boiler Tests, Feedwater.
- FOLEY, G. M.**
Testing of precision-lathe spindles..... 553
- FOLSOM, R. G.**
A study of the theory of axial-flow pumps (D)..... 463
- FORDYCE, JOHN RISON.** Obituary.....RI-62
- FOSHEE, HOWARD L., JR.** Obituary.....RI-63
- FOSTER, H. H.**
Optimum compression ratios for a high-speed Diesel engine (D)..... 474
- FOUST, A. S.**
Heat transfer through tubes with integral spiral fins..... 665
- FOWLER, C. M.**
Numerical methods for transient heat flow (D)..... 710
- FOWLER, F. H., JR.**
On fatigue failure under triaxial static and fluctuating stresses and a statistical explanation of size effect..... 213
- FOX, MERRITT LIDDLE.** Obituary.....RI-63
- FRANKLIN, BENJAMIN ALVEY.** Obituary..RI-63
- FRANKLIN, PHILIP**
Methods of advanced calculus (BR).... A-63
- FREEZING RATES**
Experimental confirmation of water freezing rates..... 39
Bibliography..... 44
- FREYSCHMIDT, CURT.** Obituary.....RI-63
- FRICTION.** See Flow of Fluids.
Investigation of friction and wear under quasi-hydrodynamic conditions..... 45
The friction properties of various lubricants at high pressure..... 51
- FUEL.** See Coal, Coke, Oil.
Ignition through fuel beds on traveling-chain-grate stokers..... 425
- FUEL GAS**
Application of controlled atmospheres to the processing of metals..... 501
- FULLER, D. D.**
Lubrication characteristics of involute spur gears; a theoretical investigation (D)..... 186
The friction properties of various lubricants at high pressures (D)..... 57
- FURNACE.** See Boiler.
- G**
- GAGES—PRESSURE.** See Instruments—Pressure.
- GAILUS, W. J.**
Creep properties of molded phenolic plastics at elevated temperatures..... 253
- GARDNER, KARL A.**
Efficiency of extended surface..... 621
Variable heat-transfer rate correction in multipass exchangers, shell-side film controlling..... 31
- GAS TURBINES**
The modern gas turbine (BR).....A-196
- GASES.** See also Instruments—Measuring.
An instrument for indicating amount of gas in gas-liquid mixtures..... 399
Application of controlled atmospheres to the processing of metals..... 501
Temperature measurements in high-velocity air streams.....A-25
- GATCOMBE, E. K.**
The friction properties of various lubricants at high pressures (D)..... 58
Lubrication characteristics of involute spur gears; a theoretical investigation.. 177
- GEARS**
Distribution of tooth load along a pinion A-78
Load distribution of reduction gears.... A-87
Lubrication characteristics of involute spur gears; a theoretical investigation.. 177
Bibliography..... 185
- GESCHELIN, JOSEPH**
Basic mechanics of the metal-cutting process (D).....A-257
Influence of applying cutting fluids at different temperatures when turning steel (D)..... 223
- GIACOMINI, ALFRED WILLIAM.** Obituary..RI-64
- GIBSON, GEORGE HERBERT.** Obituary.....RI-64
- GILBERT, W. W.**
A thermal-balance method and mechanical investigation for evaluating machinability..... 225
Influence of applying cutting fluids at different temperatures when turning steel.. 217
- GITHENS, THOMAS F.**
Helical taper reamers milled with constant helix angle..... 303
- GLOYER, WALTER**
Efficiency of extended surface (D)..... 628
- GLUED JOINTS**
Shear strength of glue joints as affected by wood surfaces and pressures..... 104
- GOLAND, MARTIN**
Structural efficiency of wing covers..... A-8
The flutter of a uniform cantilever wing..A-197
- GOLDBY, R. H.**
Local coefficients of heat transfer for air flowing around a finned cylinder..... 613
- GOODIER, J. N.**
An analytical theory of landing-shock effects on an airplane considered as an elastic body (D).....A-186
Effect of web deformation on the torsion of I-beams (AC).....A-126
Structural efficiency of wing covers..... A-8
- GRABOWSKI, H. A.**
Silica deposition in steam turbines..... 309
A graphic resolution of strain.....A-211
- GRAPHICAL METHODS.** See Electric Analogy.
A graphical method for the evaluation of principal strains from normal strains..A-209
Determining water-hammer pressure in pipes..... 383
Graphical solution of windshield heat deicing problems..... 513

GRAPHICAL SYMBOLS AND CHARTS

A.S.M.E. publication..... RI-88

GRAPHITIZATION OF STEEL PIPING

Bound in 1945 volume of the Transactions of the A.S.M.E. Also in the back of the 1944 volume of the Transactions with Forging of Steel Shells and Furnace Performance Factors.

GREEN, V. L.
Critical shearing stress in skin-stressed boxcar sides..... 561GREEN, W. P.
Optimum compression ratios for a high-speed Diesel engine..... 471GREENBERG, H. J.
Forced and free motion of a mass on an air spring (D)..... A-178

GUEBLAUM, DAVID. Obituary..... RI-64

GUNTER, A. Y.

A general correlation of friction factors for various types of surfaces in crossflow..... 643

Heat transfer and pressure drop of liquids in double-pipe fin-tube exchangers (D)..... 702

Tube spacing in finned-tube banks (D)..... 640

GYROSCOPE

Electric turret-traversing mechanism for tanks..... A-235

H

HADLEY, W. A.
Numerical methods for transient heat flow (D)..... 710HAGG, A. C.
Heat effects in lubricating films (AC)..... A-126

HAMILTON, JAMES. Obituary..... RI-64

HAMMER, ALEXANDER

Lubrication characteristics of involute spur gears; a theoretical investigation (D)..... 186

HAMMERSMITH, GEORGE WILLIAM. Obituary..... RI-64

HANKISON, L. E.

History of potassium boiler-water treatment at Springdale..... 317

HANSEN, R. E.

Irreversibility in the theoretical regenerative steam cycle..... 557

HARRIGAN, C. H.

Investigation of influence of ring size, bobbin diameter, and spindle speed on spinning process, and their effect on over-all cost of spinning (D)..... 580

HARTMANN, E. C.

Methods of joining aluminum-alloy products..... 1

HEAT EXCHANGERS See Heat Transfer

HEAT TRANSFER

An electrical geometrical analogue for complex heat flow..... 713

Disk extended surfaces for high heat-absorption rates..... 687

Economic thickness of thermal insulation for intermittent operation..... 93

Efficiency of extended surface..... 621

Graphical solution of windshield heat-deicing problems..... 513

Heat-flux pattern in fin tubes under radiation..... 693

Heat transfer and pressure drop of liquids in double-pipe fin-tube exchangers..... 697

Heat transfer and pressure loss in small commercial shell-and-finned-tube heat exchangers..... 675

Heat-transfer coefficients and other data on individual serrated-finned surface..... 683

Heat transfer from a baffled-finned cylinder to air..... 601

Heat transfer through tubes with integral spiral fins..... 531

Heater designs for the petroleum industry..... 531

Local coefficients of heat transfer for air flowing around a finned cylinder..... 613

Numerical methods for transient heat flow..... 703

Some thermal effects in oil-ring journal bearings..... 117

Tube spacing in finned-tube banks..... 633

Variable heat-transfer rate correction in multipass exchangers, shell-side film controlling..... 31

Bibliography..... 38

HEAT-TREATMENT

Application of controlled atmospheres to the processing of metals..... 501

HEATERS

Heater designs for the petroleum industry..... 531

HERSEY, MAYO D.

The friction properties of various lubricants at high pressures (D)..... 58

Lubrication characteristics of involute spur gears; a theoretical investigation (D)..... 187

HIERSCH, F. A.

Balancing of rotating apparatus—I (D)..... A-58

HIGGINS, GEORGE FREDERICK. Obituary..... RI-64

HIRST, G. W. C.

Shrink-fit stresses and deformations (D)..... A-183

HOFF, N. J.

A graphic resolution of strain..... A-211

Stresses in a reinforced monocoque cylinder under concentrated symmetric transverse loads (AC)..... A-187

HOGLUND, G. O.

Methods of joining aluminum-alloy products..... 1

HORGER, O. J.

Fatigue strength of 5/16-in.-diam shafts as related to design of large parts..... A-149

HORNFECK, A. J.

Electronic-type instruments for industrial processes..... 393

HORVAY, G.

Static and dynamic spring constants, and the appropriate lumped constants of vibrating shaft systems (AC)..... A-56

HOTTEL, H. C.

Temperature measurements in high-velocity air streams..... A-25

HOUGH, DAVID LEAVITT. Obituary..... RI-65

HOUGHTON, BERT. Obituary..... RI-65

HOVEY, O. W.

Critical shearing stress in boxcar sides (D)..... 567

HUSON, WINFIELD SCOTT. Obituary..... RI-66

HUTCHINSON, CARY TALCOTT. Obituary..... RI-67

HUTCHISON, MILLER REESE. Obituary..... RI-66

HYDRAULICS. See also Flow of Fluids.

A study of the theory of axial-flow pumps..... 451

Water-hammer analysis by the Laplace-Melin transformation..... 361

Water-hammer problems in connection with the design of hydroelectric plants..... 377

I

Ice

Experimental confirmation of predicted water-freezing rates..... 39

Graphical solution of windshield heat-deicing problems..... 513

IMHOFF, C. E.

Silica deposition in steam turbines (D)..... 314

IMPACT. See Metal Testing—Impact.

INDUSTRIAL PROCESSES

Electronic type instruments for industrial processes..... 393

INSTRUMENTS—MEASURING

An instrument for indicating the amount of gas in gas-liquid mixtures..... 399

Electronic-type instruments for industrial processes..... 393

Relation of surface-roughness readings to actual surface profile..... 189

Testing of precision-lathe spindles..... 553

INSTRUMENTS—PRESSURE

A pneumatic piston-ring gage for radial-pressure measurement..... 491

INSTRUMENTS—TEMPERATURE

Temperature measurements in high-velocity air streams..... A-25

INSULATION

Economic thickness of thermal insulation for intermittent operation..... 93

Bibliography..... 100

J

JAKOB, MAX

An electrical geometrical analogue for complex heat flow (D)..... 716

Efficiency of extended surface (D)..... 629

JACKSON, J. R.

Carry-over in locomotive boilers (D)..... 206

JAMESON, S. L.

A general correlation of friction factors for various types of surfaces in crossflow (D)..... 658

Tube spacing in finned-tube banks..... 633

JASPER, T. McLEAN

Influence of rate of strain and temperature on yield stresses of mild steel (D)..... A-186

JENSEN, D. P.

An acceleration damper: development, design, and some applications..... 523

JOHNSON, WALTER C.

Mathematical and physical principles of engineering analysis (BR)..... A-128

JOURNAL BEARINGS

Thermal effects in oil-ring journal bearing..... 117

Bibliography..... 122

K

KALITINSKY, A.

Temperature measurements in high-velocity air streams..... A-25

KANE, J. R.

Static and dynamic spring constants, and the appropriate lumped constants of vibrating shaft systems (D)..... A-55

KATZ, D. L.

Heat transfer through tubes with integral spiral fins..... 665

KAUFMAN, C. E.

Embrittlement cracking in waters containing potassium salts (D)..... 333

KAYAN, C. F.

An electrical geometrical analogue for complex heat flow..... 713

Efficiency of extended surface (D)..... 629

KEENAN, JOSEPH H.

The modern gas turbine (BR)..... A-196

Nozzles for supersonic flow without shock fronts (D)..... A-261

KELLER, E. G.

An analytical theory of landing-shock effects on an airplane considered as an elastic body (AC)..... A-187

KENNARD, E. H.

Forced and free motion of a mass on an air spring (D)..... A-177

KERRICK, J. H.

Ignition through fuel beds on traveling-chain-grate stokers (D)..... 436

KING, W. J.

Optimum compression ratios for a high-speed Diesel engine (D)..... 475

KNOWLTON, FREDERICK KIRK. Obituary..... RI-67

KOOISTRA, L. F.

Stresses in a cylindrical shell due to nozzle or pipe connection..... A-107

KOPP, S.

Air-cooled steam condensers (D)..... 663

KORNFIELD, ALFRED EPHRAIM. Obituary..... RI-67

KREISINGER, HENRY

Ignition through fuel beds on traveling-chain-grate stokers (D)..... 436

KROON, R. P.

Balancing of rotating apparatus (AC)..... A-61

KYLE, PETER E.

Materials and processes (BR)..... A-127

L

LAKE, G. F.

A simplified method of determining hoop stresses in fan rotors..... A-65

LAMINATES

Properties and development of papreg—a high-strength laminated paper plastic..... 267

LANDRY, B. A.

The missing data on coal sampling..... 69

LANGER, B. F.

Measurement of torque transmitted by rotating shafts..... A-39

LANGHAAR, H. L.

Parallel columns with common lateral supports..... A-253

LAPPLE, C. E.

A general correlation of friction factors for various types of surfaces in crossflow (D)..... 656

LARSEN, R. G.

Investigation of friction and wear under quasi-hydrodynamic conditions..... 45

LAWTON, T. S., JR.

Effect of some environmental conditions on the mechanical properties of cellulose acetate and cellulose nitrate plastic sheets..... 23

Effect of some environmental conditions on the permanence of cellulose-acetate and cellulose-nitrate sheet plastics..... 259

LEFSCHETZ, SOLOMON	
Forced and free motion of a mass on an air spring (D).....	A-178
LEMMON, A. W., JR.	
Heat transfer from a baffled-finned cylinder to air.....	601
LETTELLIER, Z.	
Influence of applying cutting fluids at different temperatures when turning steel (D).....	222
LEWIS, FRANK M.	
Load distribution of reduction gears.....	A-87
LIEBER, PAUL	
An acceleration damper: development, design, and some applications.....	523
LOCOMOTIVE BOILERS	
Carry-over in locomotive boilers.....	197
10,000-Kw railway-mounted steam power plant for U. S. Navy Department, Bureau of Yards and Docks.....	141
LOCOMOTOR MECHANICS	
Locomotor mechanics and occupation....	167
LONDON, A. L.	
Experimental confirmation of predicted water-freezing rates.....	39
LOSS, HENRIK VON ZERNIKOW. Obituary.....	RI-68
LOWRY, GEORGE ARCHIBALD. Obituary.....	RI-68
LOWY, R.	
A study of the theory of axial-flow pumps (D).....	463
Measurement of dynamic stress and strain in tensile-test specimen (D).....	A-123
LUBAHN, J. D.	
The effect of triaxiality on the technical cohesive strength of steels.....	A-241
LUBRICATION	
Effect of aeration on gear-pump delivery and lubrication ceiling.....	123
Heat effects in lubricating films (D).....	A-126
Instrument for indicating the amount of gas in gas-liquid mixtures.....	399
Investigation of friction and wear under quasi-hydrodynamic conditions.....	45
Lubrication characteristics of involute spur gears; a theoretical investigation.	177
Some thermal effects in oil-ring journal bearings.....	117
Bibliography.....	122
LUBRICANTS	
The friction properties of various lubricants at high pressure.....	51
Bibliography.....	58
LUCHT, F. W.	
Basic mechanics of the metal-cutting process (D).....	A-257
Helical taper reamers milled with constant helix angle (D).....	307
Influence of applying cutting fluids at different temperatures when turning steel (D).....	223
LUND, NELS BIRGER. Obituary.....	RI-68
LUNDGREN, EDWIN	
10,000-Kw railway-mounted mobile steam power plant for U. S. Navy Department, Bureau of Yards and Docks.....	141

M

MACGREGOR, C. W.	
Tension tests at constant true strain rates.....	A-217
MACHINABILITY. See Metal Cutting.	
MACHT, M. L.	
Effect of some environmental conditions on the permanence of cellulose-acetate and cellulose-nitrate sheet plastics (D).....	265
MACKAY, C. O.	
Thermodynamic charts (BR).....	A-263
MACKIN, G. E.	
Properties and development of papreg—a high-strength laminated paper plastic.....	267
MANAGEMENT	
Locomotor mechanics and occupation....	167
MANJOINE, M. J.	
Influence of rate of strain and temperature on yield stresses of mild steel (AC).....	A-186
New machines for creep and creep-rupture tests.....	111
MARINE ENGINES	
Static and dynamic spring constants and the appropriate lumped constants of vibrating shaft systems.....	A-55
MARTELOTTI, M. E.	
Analysis of the milling process, Part II—down milling.....	233

MARTIN, C. R.	
Water-hammer problems in connection with the design of hydroelectric plants (D).....	389
MASON, H. L.	
Stabilizing a suction-relief valve (D).....	91
MASON, WILLIAM HORATIO. Obituary.....	RI-69
MATERIALS TESTING. See also Metal Testing.	
Creep properties of molded phenolic plastics at elevated temperatures.....	253
Effect of some environmental conditions on the permanence of cellulose-acetate and cellulose-nitrate sheet plastics.....	259
Handbook of material testing (BR).....	A-127
MATHEMATICS	
An analytical theory of landing-shock effects on an airplane considered as an elastic body (D).....	A-186
Application of the Fourier method to the solution of certain boundary problems in the theory of elasticity (D).....	A-185
Mathematical and physical principles of engineering analysis (BR).....	A-128
Methods of advanced calculus (BR).....	A-63
Water-hammer analysis by the LaPlace-Mellin transformation.....	361
MAXWELL, J. W.	
Shear strength of glue joints as affected by wood surfaces and pressures.....	104
MAWHINNEY, M. H.	
Economic thickness of thermal insulation for intermittent operation (D).....	100
MCDAMAS, W. H.	
Local coefficients of heat transfer for air flowing around a finned cylinder.....	613
MCCANN, G. D.	
A new device for the solution of transient-vibration problems by the method of electrical-mechanical analogy.....	A-135
MCCLELLAND, JOHN THOMAS. Obituary.....	RI-69
MCCLEINTOCK, F. A.	
Heat transfer from a baffled-finned cylinder to air (D).....	610
MCCOY, V. E.	
Carry-over in locomotive boilers (D)....	207
MCCUTCHAN, ARTHUR	
Moment-distribution analysis for three-dimensional pipe structures (D).....	A-188
MCKEE, R. E.	
Influence of applying cutting fluids at different temperatures when turning steel.....	217
MERCHANT, M. E.	
Basic mechanics of the metal-cutting process (AC).....	A-258
MESROBIAN, R. B.	
Creep and relaxation in rubber products at elevated temperatures.....	569
METAL	
Application of controlled atmospheres to the processing of metals.....	501
Materials and processes (BR).....	A-127
Pure metals (BR).....	A-63
Tension tests at constant true strain rates.....	A-211
Bibliography.....	A-226
METAL CUTTING. See also Milling.	
Analysis of the milling process, part II—down milling.....	233
Basic mechanics of the metal cutting process (D).....	A-257
Influence of applying cutting fluids at different temperatures when turning steel.....	217
METAL CUTTING	
Thermal-balance method and mechanical investigation for evaluating machinability.....	225
Bibliography.....	232
METAL FATIGUE	
On fatigue failure under triaxial static and fluctuating stresses and a statistical explanation of size effect.....	213
METAL PROCESSING	
Application of controlled atmospheres to the processing of metals.....	501
METAL TESTING	
Handbook of material testing (BR)....	A-127
Influence of rate of strain and temperature on yield stresses of mild steel (D).....	A-186
METAL TESTING—CREEP	
New machines for creep and creep-rupture tests.....	111
METAL TESTING—FATIGUE	
Cumulative damage in fatigue.....	A-159
Fatigue failure under triaxial static and fluctuating stresses and a statistical explanation of size effect.....	213
Fatigue strength of 5/4-in-diam shafts as related to design of large parts.....	A-149

METAL TESTING—FATIGUE (continued)	
Fatigue tests of airplane generator brackets with special reference to failure of screw fastenings.....	A-113
Bibliography.....	A-119
Measurement of dynamic stress and strain in tensile-test specimen (D).....	A-123
METALLURGY	
Materials and processes (BR).....	A-127
METERS. See also Instruments, Flow of Fluids, Fluid Meters.	
Coefficient of Herschel type cast-iron Venturi meters.....	339
MIKINA, S. J.	
Electric-turret-traversing mechanism for tanks.....	A-228
MILLER, M. A.	
Methods of joining aluminum-alloy products.....	1
MILLER, RALPH	
Optimum compression ratios for a high-speed Diesel engine (D).....	475
MILLING. See also Metal Cutting.	
Analysis of the milling process, part II—down milling.....	233
Helical taper reamers milled with constant helix angle.....	303
MINER, I. O.	
The coefficient of Herschel type cast-iron Venturi meters (D).....	342
MINER, MILTON A.	
Cumulative damage in fatigue.....	A-159
MINNICH, J. B.	
A pneumatic piston-ring gage for radial-pressure measurements (D).....	497
MITCHELL, N. M.	
Investigation of influence of ring size, bobbin diameter, and spindle speed on spinning process, and their effect on over-all cost of spinning (D).....	581
MODELS	
Experimental study of the flow of coal in chutes at Riverside Generating Station.....	585
MOODY, A. M. G.	
Axial vibration of turbine disks.....	A-48
MOODY, L. F.	
A study of the theory of axial-flow pumps (D).....	464
Water-hammer problems in connection with the design of hydroelectric plants (D).....	390
MOORE, C. B.	
A pneumatic piston-ring gage for radial-pressure measurements (D).....	497
MOSS, SANFORD A.	
Nozzles for supersonic flow without shock fronts (D).....	A-262
MOTION STUDY. See Time and Motion Study.	
MUENGER, J. R.	
The friction properties of various lubricants at high pressures (D).....	59
MUMFORD, A. R.	
Heat-flux pattern in fin tubes under radiation.....	693
MURPHY, GLENN	
A graphical method for the evaluation of principal strains from normal strains.....	A-209
MYKLESTAD, N. O.	
New method of calculating natural modes of coupled bending-torsion vibration of beams.....	61
Vibration analysis (BR).....	A-128

N

NASON, H. K.	
Effect of some environmental conditions on the mechanical properties of cellulose acetate and cellulose nitrate plastic sheets.....	23
Effect of some environmental conditions on the permanence of cellulose-acetate and cellulose-nitrate sheet plastics....	259
NAVY	
U. S. Navy railway-mounted steam power plants.....	141
NEIFERT, H. R.	
Fatigue strength of 5/4-in-diam shafts as related to design of large parts.....	A-149
NEKERVIS, R. J.	
Investigation of friction and wear under quasi-hydrodynamic conditions (D)...	50
NEWTON, R. E.	
Stresses in a reinforced monocoque cylinder under concentrated symmetric transverse loads (D).....	A-187

- NONDIMENSIONAL COEFFICIENTS.** *See* Flow of Fluids.
- NONFERROUS METALS AND ALLOYS**
 A thermal-balance method and mechanical investigation for evaluating machinability..... 225
 Methods of joining aluminum-alloy products..... 1
- NOTTAGE, H. B.**
 Efficiency of extended surface (D)..... 629
 Heat transfer from a baffled-finned cylinder to air..... 601
- NOZZLES**
 Nozzles for supersonic flow without shock fronts (D)..... A-260
 Boiler nozzles and valve inlet for maximum-capacity safety valves..... 133
- NUNN, PAUL N.** Obituary..... RI-69
- O**
- OLDACRE, W. H.**
 Basic mechanics of the metal-cutting process (D)..... A-258
 Influence of applying cutting fluids at different temperatures when turning steel (D)..... 224
- OPATOWSKI, I.**
 Design of beams of long span and low specific strength..... A-156
- ORNANCE**
 Electric turret-traversing mechanism for tanks..... A-228
- ORMONDOYD, J.**
 How to solve it (BR)..... A-263
 Static and dynamic spring constants, and the appropriate lumped constants of vibrating shaft systems (AC)..... A-56
 What are cosmic rays? (BR)..... A-196
- OSCILLATION.** *See* Vibration.
- OSTERMANN, R. M.**
 Carry-over in locomotive boilers (D)..... 207
- P**
- PARDOE, W. S.**
 Piping arrangements for acceptable flow-meter accuracy (D)..... 357
 The coefficient of Herschel type cast-iron Venturi meters..... 339
- PARISH, WILLIAM FRANCIS.** Obituary..... RI-70
- PARKER, E. R.**
 Measurement of dynamic stress and strain in tensile-test specimen (AC)..... A-124
- PARKS, G. U.**
 Experience with sodium and potassium chemicals for boiler-water conditioning at Montau Electric..... 335
- PARSONS, BRACKETT**
 Investigation of influence of ring size, bobbin diameter, and spindle speed on spinning process, and their effect on over-all cost of spinning (D)..... 581
- PASCHKEIS, VICTOR**
 An electrical geometrical analogue for complex heat flow (D)..... 717
 Electrical-analogy method for fundamental investigations in automatic control (D)..... 86
 Economic thickness of thermal insulation for intermittent operation..... 93
 Numerical methods for transient heat flow (D)..... 710
- PAUGH, C. T.**
 Heat transfer through tubes with integral spiral fins (D)..... 673
- PECK, C. E.**
 Application of controlled atmospheres to the processing of metals..... 501
- PERNICK, A.**
 Distribution of tooth load along a pinion..... A-78
- PERRY, G. L.**
 Investigation of friction and wear under quasi-hydrodynamic conditions..... 45
- PERRY, HAROLD SLAUSON.** Obituary..... RI-70
- PERRY, R. L.**
 Economic thickness of thermal insulation for intermittent operations (D)..... 101
- PETERSON, G. S.**
 An instrument for indicating the amount of gas in gas-liquid mixtures..... 399
- PETERSON, R. E.**
 On fatigue failure under triaxial static and fluctuating stresses and a statistical explanation of size effect (D)..... 215
- PETROLEUM REFINING**
 Heater designs for the petroleum industry..... 531
- PHYSICS**
 Mathematical and physical principles of engineering analysis (BR)..... A-128
- PICKETT, GERALD**
 Application of the Fourier method to the solution of certain boundary problems in the theory of elasticity (AC)..... A-186
- PIGOTT, R. J. S.**
 Piping arrangements for acceptable flow-meter accuracy (D)..... 360
 Prediction of centrifugal-pump performance..... 439
- PIKE, E. W.**
 Measurement of the damping of engineering materials during flexural vibration at elevated temperatures (D)..... A-180
- PIPE**
 Moment-distribution analysis for three-dimensional pipe structures (D)..... A-188
 Water-hammer problems in connection with the design of hydroelectric plants..... 377
- PIPE CONNECTIONS**
 Stresses in a cylindrical shell due to nozzle or pipe connection..... A-107
- PIPING.** *See also* Graphitization.
 Piping arrangements for acceptable flow-meter accuracy..... 345
- PISTON RINGS**
 A pneumatic piston-ring gage for radial-pressure measurement..... 491
- PIVOTS**
 Investigation of cross-spring pivot (D)..... A-62
- PLACE, P. B.**
 Carry-over in locomotive boilers (D)..... 210
- PLASTICITY**
 Yielding and fracture of medium-carbon steel under combined stress..... A-13
- PLASTICS**
 Creep properties of molded phenolic plastics at elevated temperatures..... 253
 Bibliography..... 258
 Effect of some environmental conditions on the mechanical properties of cellulose acetate and cellulose nitrate plastic sheets..... 23
 Bibliography..... 29
 Effect of some environmental conditions on the permanence of cellulose-acetate and cellulose-nitrate sheet plastics..... 259
 Elastic properties of plastic materials..... 477
 Materials and processes (BR)..... A-127
 Properties and development of papreg—a high-strength laminated paper plastic..... 267
 Bibliography..... 277
- PLATES**
 The effect of transverse shear deformation on the bending of elastic plates..... A-69
- POLYA, G.**
 How to solve it (BR)..... A-263
- PORITSKY, H.**
 Distribution of tooth load along a pinion..... A-78
 Shrink-fit stresses and deformations (D)..... A-183
- POWELL, E. B.**
 History of potassium boiler-water treatment at Springdale (D)..... 322
- POWELL, E. M.**
 Heat-flux pattern in fin tubes under radiation..... 693
- POWER PLANTS—HYDROELECTRIC**
 Water-hammer problems in connection with the design of hydroelectric plants..... 377
- POWER PLANTS—STEAM**
 10,000-Kw railway-mounted mobile steam power plant for U. S. Navy Department, Bureau of Yards and Docks..... 141
- POWNALL, W. A.**
 Carry-over in locomotive boilers (D)..... 208
- PRAGER, W.**
 Forced and free motion of a mass on an air spring (D)..... A-178
- PRESSURE DROP.** *See* Flow of Fluids.
- PRINDLE, EDWIN JAY.** Obituary..... RI-71
- PROFILOMETER.** *See* Roughness Indicators.
- PROHL, M. A.**
 General method for calculating critical speeds of flexible rotors..... A-142
- PUMPS—AXIAL FLOW**
 A study of the theory of axial-flow pumps..... 415
- PUMPS—CENTRIFUGAL**
 Cavitation in centrifugal pumps..... 539
 Prediction of centrifugal-pump performance..... 439
- PUMPS—GEAR**
 Effect of aeration on gear-pump delivery and lubrication ceiling..... 123
- PURCELL, T. E.**
 Embrittlement cracking in waters containing potassium salts (D)..... 333
- R**
- RABINOVITZ, JACK**
 Moment-distribution analysis for three-dimensional pipe structures (D)..... A-188
- RAILROAD CARS**
 Critical shearing stress in skin-stressed boxcar sides..... 561
 10,000-Kw railway-mounted mobile steam power plant for U. S. Navy Department, Bureau of Yards and Docks..... 141
- RAILROAD TRAINS**
 Dynamics of an elastic bar..... A-101
- RANKIN, A. W.**
 Shrink-fit stresses and deformations (AC)..... A-184
- RATZEL, R. A.**
 Helical taper reamers milled with constant helix angle (D)..... 307
- REAMERS**
 Helical taper reamers milled with constant helix angle..... 303, (D) 307
- REED, RALPH JOHN.** Obituary..... RI-72
- REFRIGERATION**
 Experimental confirmation of predicted water-freezing rates..... 39
 Bibliography..... 44
- REID, W. T.**
 External corrosion of furnace-wall tubes
 1—History and occurrence..... 279
 2—Significance of sulphate deposits and sulphur trioxide in corrosion mechanism..... 289
 Ignition through fuel beds on traveling-or chain-grate stokers..... 425
- REISSNER, ERIC**
 Application of the Fourier method to the solution of certain boundary problems in the theory of elasticity (D)..... A-185
 The effect of transverse shear deformation on the bending of elastic plates..... A-69
- RELAXATION.** *See* Rubber.
- RESIN-BONDING**
 Methods of joining aluminum-alloy products..... 1
- RICE, HOWARD C.** Obituary..... RI-72
- RICH, G. R.**
 Water-hammer analysis by the LaPlace-Mellin transformation..... 361
- RICKERMAN, J. H.**
 Heater designs for the petroleum industry..... 531
- RIDDELL, JOHN TATE, JR.** Obituary..... RI-72
- RINGS**
 Stresses in a reinforced monocoque cylinder under concentrated symmetric transverse loads (D)..... A-187
- RITTER, HENRY.** Obituary..... RI-72
- RIVETING**
 Methods of joining aluminum-alloy products..... 1
- ROBERTS, J. F.**
 Water-hammer analysis by LaPlace-Mellin transformation (D)..... 370
- ROBERTSON, B. P.**
 The friction properties of various lubricants at high pressures..... 51
- ROBERTSON, J. M.**
 Measurement of the damping of engineering materials during flexural vibration at elevated temperatures (D)..... A-180
- ROBINSON, C. S. L.**
 Network- and differential-analyzer solution of torsional oscillation problems involving nonlinear springs (D)..... A-194
- ROGERS, N. E.**
 Embrittlement cracking in waters containing potassium salts..... 329
- ROPE**
 A new design criterion for wire rope..... A-33
 Bibliography..... A-38
- ROTORS.** *See also* Turbines.
 A simplified method of determining hoop stresses in fan rotors..... A-65
 Balancing of rotating apparatus (D)..... A-58
 General method for calculating critical speeds of flexible rotors..... A-142
- ROUGHNESS INDICATORS**
 Relation of surface-roughness readings to actual surface profile..... 189

RUBBER	
Creep and relaxation in rubber products at elevated temperatures.....	569
RUEGG, CLEMENT. Obituary.....	RI-73
RYAN, J. L.	
Carry-over in locomotive boilers (D)....	208

S

SACHS, GEORGE	
Handbook of material testing (BR).....	A-127
Pure metals (BR).....	A-63
The effect of triaxiality on the technical cohesive strength of steels.....	A-241
SAFETY VALVES. See Valves.	
SCHABTACH, CARL	
Measurement of the damping of engineering materials during flexural vibration at elevated temperatures (AC).....	A-181
SCHIEREN, GEORGE ARTHUR. Obituary....	RI-73
SCHMELTZER, JOHN EMILE. Obituary....	RI-73
SCHMIDT, A. O.	
A thermal-balance method and mechanical investigation for evaluating machinability.....	225
SCHOESSOW, G. J.	
Stresses in a cylindrical shell due to nozzle or pipe connection.....	A-107
SCHRYBER, E. A.	
Heat-transfer coefficients and other data on individual serrated-finned surface..	683
SCHWEITZER, P. H.	
Effect of aeration on gear-pump delivery and lubrication ceiling.....	123
Optimum compression ratios for a high-speed Diesel engine (D).....	475
SCOTT, RICHARD SELLMAN. Obituary.....	RI-74
SCOTT, WALTER WINTHROP. Obituary....	RI-74
SCREWS	
Fatigue tests of airplane generator brackets with special reference to failure of screw fastenings.....	A-113
SEBAN, R. A.	
Experimental confirmation of predicted water-freezing rates.....	39
SEDERHOLM, EDWARD THEODOR. Obituary.....	RI-75
SENIFF, R. W.	
Carry-over in locomotive boilers (D)....	209
SHAFTS	
Balancing of rotating apparatus (D).....	A-58
Fatigue strength of 5/16-in-diam shafts as related to design of large parts.....	A-149
General method for calculating critical speeds of flexible rotors.....	A-142
Measurement of torque transmitted by rotating shafts.....	A-39
Static and dynamic spring constants, and the appropriate lumped constants of vibrating shaft systems (D).....	A-55
SHANNON, DON H. Obituary.....	RI-75
SHAPIRO, A. H.	
Nozzles for supersonic flow without shock fronts (AC).....	A-262
SHAW, W. A.	
A general correlation of friction factors for various types of surfaces in cross-flow.....	643
Heat transfer and pressure drop of liquids in double-pipe fin-tube exchangers (D).....	702
Tube spacing in finned-tube banks (D)...	640
SHEETS, H. E.	
A study of the theory of axial-flow pumps (D).....	465
SHELDON, A. N.	
Investigation of influence of ring size, bobbin diameter, and spindle speed on spinning process, and their effect on over-all cost of spinning.....	575
SHELLS	
Stresses in a cylindrical shell due to nozzle or pipe connection.....	A-107
SHERMAN, RALPH A.	
Ignition through fuel beds on traveling- or chain-grate stokers.....	437
SHRINK FITS	
Shrink-fit stresses and deformations (D).....	A-182
SHRIVER, HARRY T. Obituary.....	RI-75
SILICA DEPOSITS. See Feedwater Treatment, Steam Turbines.	
SMITH, AUGUSTUS PARKER. Obituary.....	RI-75
SMITH, EDWARD JOSEPH. Obituary.....	RI-75
SMITH, ED S.	
Stabilizing a suction-relief valve.....	87

SNELLING, GORDON A. Obituary.....	RI-76
SNYDER, GEORGE T. Obituary.....	RI-76
SOCIETY FOR EXPERIMENTAL STRESS ANALYSIS	
Experimental stress analysis (BR).....	A-63
Proceedings, vol. 1.....	A-264
Proceedings, vol. 2.....	A-264
SODERBERG, C. RICHARD	
Vibration analysis (BR).....	A-128
SOLDERING	
Methods of joining aluminum-alloy products.....	16
SOMERS, J. C.	
Carry-over in locomotive boilers (D)....	209
SOUTHERN, GILBERT WALLHEAD. Obituary.....	RI-76
SPICER, CLARENCE WINFRED. Obituary....	RI-76
SPINDLES	
Testing of precision-lathe spindles.....	553
SPINNING. See Textile Industry.	
SPIRO, WALTER J. Obituary.....	RI-77
SPREngle, R. E.	
Piping arrangements for acceptable flow-meter accuracy.....	45
SPRINGS	
Network- and differential-analyzer solution of torsional oscillation problems involving nonlinear springs.....	A-43
Discussion.....	A-194
STANDARDS	
A.S.M.E. American Standards index....	RI-87
STANTON, A. LENNOX. Obituary.....	RI-77
STEAM	
Irreversibility in the theoretical regenerative steam cycle.....	557
STEAM CONDENSERS	
Air-cooled steam condensers.....	661
STEAM SEPARATORS	
Carry-over in locomotive boilers.....	197
STEAM TURBINES	
History of potassium boiler-water treatment at Springdale.....	317
Silica deposition in steam turbines.....	309
STEEL	
Effect of triaxiality on the technical cohesive strength of steels.....	A-241
Tension tests at constant true strain rates.....	A-217
STEINDLER, A.	
Locomotor mechanics and occupation....	167
STEPANOFF, A. J.	
A study of the theory of axial-flow pumps (D).....	465
Cavitation in centrifugal pumps.....	539
STILLWELL, R. F.	
Blending coals reflects greater uniformity of product.....	417
STOKERS	
Ignition through fuel beds on traveling- or chain-grate stokers.....	425
STRAINS. See Stresses and Strains.	
STRAUB, F. G.	
Silica deposition in steam turbines.....	309
STRESS ANALYSIS	
Experimental stress analysis.....	A-264
STRESSES AND STRAINS	
A new design criterion for wire rope....	A-33
A simplified method of determining hoop stresses in fan rotors.....	A-65
Bending of curved thin tubes.....	A-1
Critical shearing stress in skin-stressed boxcar sides.....	561
Graphic resolution of strain.....	A-211
Graphical method for the evaluation of principal strains from normal strains..	A-209
Measurement of dynamic stress and strain in tensile-test specimen (D).....	A-123
On fatigue failure under triaxial static and fluctuating stresses and statistical explanation of size effect.....	213
Proceedings of the Society for Experimental Stress Analysis, Vol. 1 (BR).....	A-63
Vol. 2 (BR).....	A-264
Shrink-fit stresses and deformations (D).....	A-182
Stresses in a cylindrical shell due to nozzle or pipe connection.....	A-107
Stresses in a reinforced monocoque cylinder under concentrated symmetric transverse loads (D).....	A-187
Structural efficiency of wing covers.....	A-8
Tension tests at constant true strain rates.....	A-217
The effect of transverse shear deformation on the bending of elastic plates... A-69	
Yielding and fracture of medium-carbon steel under combined stress.....	A-13
STROWGER, E. B.	
Water-hammer problems in connection with the design of hydroelectric plants.	377

STUCHELL, R. M.	
Economic thickness of thermal insulation for intermittent operation (D).....	101
SUPERSONIC FLOW	
Nozzles for supersonic flow without shock fronts (D).....	A-260
SURFACE FINISH	
Relation of surface-roughness readings to actual surface profile.....	189
SUSSHOLZ, B.	
Forced and free motion of a mass on an air spring (AC).....	A-178
SUTTON, A. D.	
Distribution of tooth load along a pinion..	A-78
SWEET, J. E.	
Thermodynamic charts (BR).....	A-263
SWEETSER, WILLIAM JORDAN. Obituary....	RI-78
TACHAU, H.	
A new design criterion for wire rope....	A-33
TANK TURRETS	
Electric turret-traversing mechanism for tanks.....	A-228
TARASOV, L. P.	
Relation of surface-roughness readings to actual surface profile.....	189
TATE, G. E.	
Disk extended surfaces for high heat-absorption rates.....	687
TAUBE, HARRY ROBERT. Obituary.....	RI-78
TELFAR, DAVID	
Creep properties of molded phenolic plastics at elevated temperatures.....	253
TEMPERATURE MEASUREMENT. See Instruments—Temperature.	
TENSION TESTS. See Stress.	
Tension tests at constant true strain rates.....	A-217
TEXTILE INDUSTRY	
Investigation of influence of ring size, bobbin diameter, and spindle speed on spinning process, and their effect on over-all cost of spinning.....	575
THERMOCOUPLES. See Instruments—Temperature.	
THERMODYNAMICS	
Irreversibility in the theoretical regenerative steam cycle.....	557
THOMA, DIETER. Obituary.....	RI-78
TIME AND MOTION STUDY	
Locomotor mechanics and occupation....	167
TOLBSKY, A. V.	
Creep and relaxation in rubber products at elevated temperatures.....	569
TORQUE	
Network- and differential-analyzer solution of torsional oscillation problems involving nonlinear springs.....	A-43
Measurement of torque transmitted by rotating shafts.....	A-39
TOUR, SAM	
Application of controlled atmospheres to the processing of metals (D).....	509
TROLLER, T. H.	
A study of the theory of axial-flow pumps (D).....	468
TROWBRIDGE, AMASA. Obituary.....	RI-76
TRUMPLER, P. R.	
Efficiency of extended surface (D).....	630
TUBES	
A general correlation of friction factors for various types of surfaces in cross-flow.....	643
Bending of curved thin tubes.....	A-1
Disk extended surfaces for high heat-absorption rates.....	687
Heat-flux pattern in fin tubes under radiation.....	693
Heat-transfer coefficients and other data on individual serrated-finned surface..	683
Heat transfer through tubes with integral spiral fins.....	665
Tube spacing in finned-tube banks.....	633
Yielding and fracture of medium carbon steel under combined stress.....	A-13
TURBINES	
Axial vibration of turbine disks.....	A-48
TURBOGENERATORS	
10,000-Kw railway-mounted mobile steam power plant for U. S. Navy Department, Bureau of Yards and Docks....	141
TURBULENCE. See Flow of Fluids.	

TURRET-TRAVERSING MECHANISM

- Electric turret-traversing mechanism for tanks.....A-228

V

VALVES

- Boiler nozzles and valve inlets for maximum-capacity safety valves..... 133
Bibliography..... 139
Stabilizing a suction-relief valve..... 87

VAN ARKEL

- Reine metallie (BR)..... A-63

VANDERWEIL, R. G.

- An electrical geometrical analogue for complex heat flow (D)..... 718
Heat transfer and pressure loss in small commercial shell-and-finned-tube heat exchangers (D)..... 681

- Heat-transfer coefficients and other data on individual serrated-finned surface (D)..... 686
Heat transfer from a baffled-finned cylinder to air (D)..... 611

- Heat transfer through tubes with integral spiral fins (D)..... 673

VAN DRIEST, E. R.

- Experimental investigation of turbulence diffusion—a factor in transportation of sediment in open-channel flow..... A-91

- VIALI, WILLIAM ANGELL. Obituary.....RI-79

VIBRATION

- A new device for the solution of transient-vibration problems by the method of electrical-mechanical analogy..... A-135
An acceleration damper: development, design, and some applications..... 523

- Axial vibration of turbine disks..... A-48
Direct analysis of mechanical wave filters..... A-129

- Forced and free motion of a mass on an air spring (D)..... A-175
General method for calculating critical speeds of flexible rotors..... A-142

- Measurement of the damping of engineering materials during flexural vibration at elevated temperatures (D)..... A-180

- Network- and differential-analyzer solution of torsional oscillation problems involving nonlinear springs..... A-43

- Network- and differential-analyzer solution of torsional oscillation problems involving nonlinear springs (D)..... A-194

- New method of calculating natural modes of coupled bending-torsion vibration of beams..... 61

- Stabilizing a suction-relief valve..... 87
Static and dynamic spring constants, and the appropriate lumped constants of vibrating lumped shaft systems (D).... A-55

- Vibration analysis (BR)..... A-128

VON HOHENLEITEN, H. L.

- Experimental study of the flow of coal in chutes at Riverside Generating Station..... 585

VOSE, R. W.

- Investigation of influence of ring size, bobbin diameter, and spindle speed on spinning process, and their effect on over-all cost of spinning (D)..... 581

W

- WAGNER, JAMES JOHN. Obituary.....RI-79

WAHL, A. M.

- Experimental stress analysis (BR)..... A-264
Fatigue tests of airplane generator brackets with special reference to failure of screw fastenings..... A-113

- Mathematical and physical principles of engineering analysis (BR)..... A-128
Proceedings of the Society for Experimental Stress Analysis, Vol. 1 (BR). A-63

- Vol. 2 (BR)..... 264

WALSH, B. R.

- An instrument for indicating the amount of gas in gas-liquid mixtures..... 399

WANNAMAKER, W. H.

- Electrical-analogy method for fundamental investigations in automatic control..... 81

WARD, MORGAN

- Methods of advanced calculus (BR).... A-63

WARREN, C. E.

- A new device for the solution of transient-vibration problems by the method of electrical-mechanical analogy..... A-135

WATER FREEZING

- Experimental confirmation of predicted water-freezing rates..... 39

WATER HAMMER

- Water-hammer analysis by the LaPlace-Mellin transformation..... 361
Water-hammer problems in connection with the design of hydroelectric plants. 377

WATSON, R. M.

- Prediction of centrifugal-pump performance (D)..... 447

WATTENDORF, F. L.

- A study of the theory of axial-flow pumps (D)..... 468

WAVE FILTERS—MECHANICAL. See Vibration.

WEAR

- Investigation of friction and wear under quasi-hydrodynamic conditions..... 45

WEBB, W. L.

- Experience with potassium treatment at Windsor Station..... 325

WEEKS, W. L.

- Effect of aeration on gear-pump delivery and lubrication ceiling (D)..... 132

WELDING

- Methods of joining aluminum-alloy products..... 1

WHIRL, S. F.

- Embrittlement cracking in waters containing potassium salts (D)..... 333

WIKANDER, O. R.

- Dynamics of an elastic bar..... A-101

WILLIAMS, ARTHUR

- Carry-over in locomotive boilers..... 197

WILLIAMSON, D. E.

- Investigation of cross-spring pivot (D).... A-62
Relation of surface-roughness readings to actual surface profile (D)..... 195

WILSON, H. R.

- Economic thickness of thermal insulation (D)..... 102

WIRE ROPE

- A new design criterion for wire rope.... A-33
Bibliography..... A-38

WISLICIENUS, G. F.

- A study of the theory of axial-flow pumps. 451

WOLCOTT, HENRY AUGUSTUS. Obituary...RI-80

WOLF, E. F.

- Experimental study of the flow of coal in chutes at Riverside Generating Station..... 585

WOOD

- Shear strength of glue joints as affected by wood surfaces and pressures..... 104

WOOD, F. M.

- Water-hammer analysis by LaPlace-Mellin transformation (D)..... 370

WOOD, FREDERICK WILLIAM. Obituary...RI-80

WRIGHT, C. C.

- Use of anthracite fines in by-product coke production..... 405

WRIGHT, JAMES WILLIAM. Obituary....RI-81

WYKOFF, W. R.

- Heat transfer from a baffled-finned cylinder to air (D)..... 611

Y

YODER, J. D.

- History of potassium boiler-water treatment at Springdale (D)..... 323

YORGIADES, A. J.

- Measurement of the damping of engineering materials during flexural vibration at elevated temperatures (D)..... A-180

YOUNG, DANA

- Inelastic buckling of variable-section columns..... A-165

YOUNG, GILBERT AMOS. Obituary.....RI-81

- YOUNG, W. E.
Investigation of cross-spring pivot (AC). A-62

Z

- ZEBINE, ABRAHAM SIDNEY. Obituary....RI-81